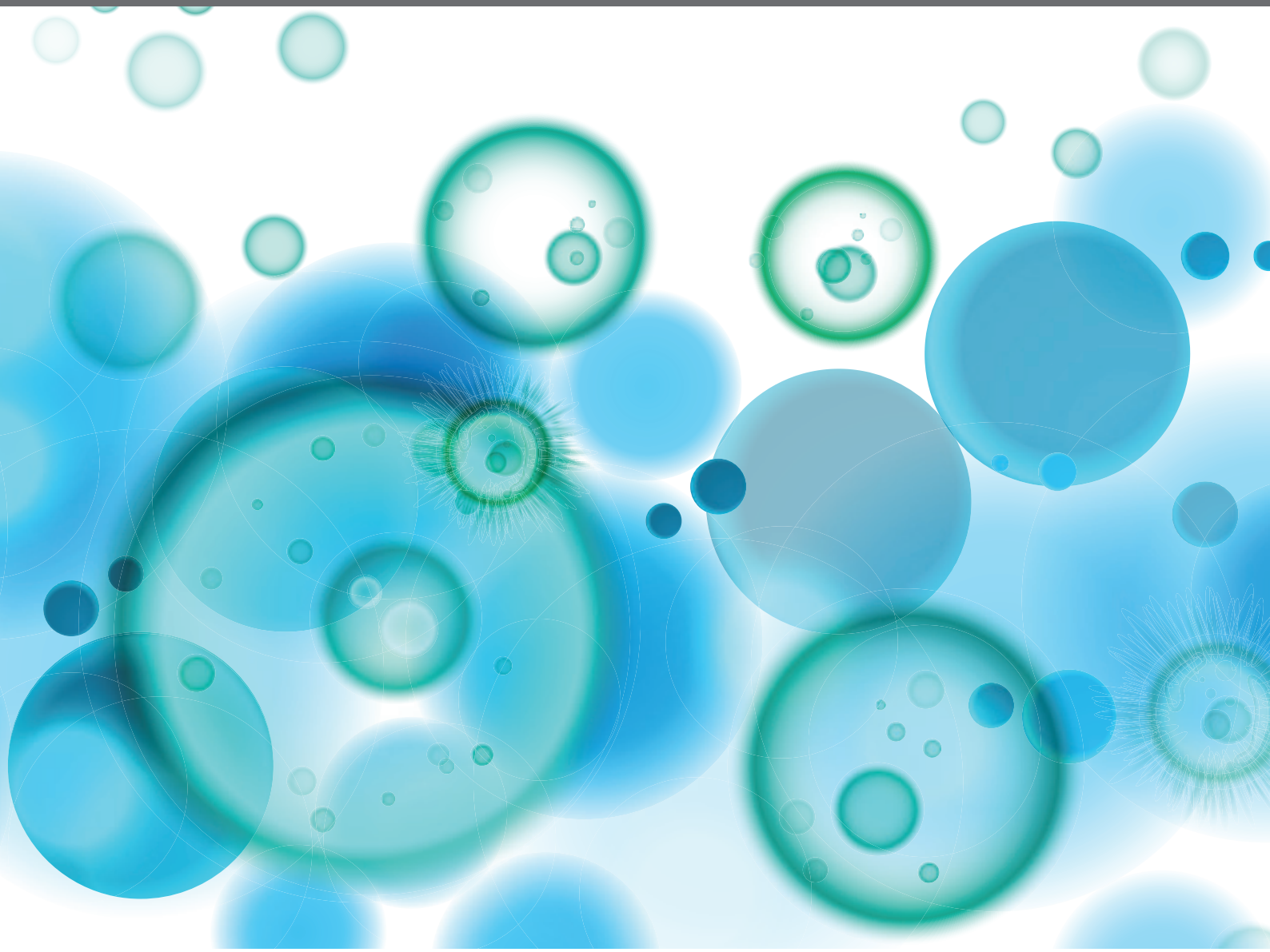
THE MONONUCLEAR PHAGOCYTE SYSTEM IN INFECTIOUS DISEASE

EDITED BY: Geanncarlo Lugo-Villarino, Céline Cougoule, Etienne Meunier
Yoann Rombouts, Christel Vérollet and Luciana Balboa
PUBLISHED IN: Frontiers in Immunology and Frontiers in Microbiology



frontiers Research Topics



frontiers

Frontiers Copyright Statement

© Copyright 2007-2019 Frontiers Media SA. All rights reserved.

All content included on this site, such as text, graphics, logos, button icons, images, video/audio clips, downloads, data compilations and software, is the property of or is licensed to Frontiers Media SA ("Frontiers") or its licensees and/or subcontractors. The copyright in the text of individual articles is the property of their respective authors, subject to a license granted to Frontiers.

The compilation of articles constituting this e-book, wherever published, as well as the compilation of all other content on this site, is the exclusive property of Frontiers. For the conditions for downloading and copying of e-books from Frontiers' website, please see the Terms for Website Use. If purchasing Frontiers e-books from other websites or sources, the conditions of the website concerned apply.

Images and graphics not forming part of user-contributed materials may not be downloaded or copied without permission.

Individual articles may be downloaded and reproduced in accordance with the principles of the CC-BY licence subject to any copyright or other notices. They may not be re-sold as an e-book.

As author or other contributor you grant a CC-BY licence to others to reproduce your articles, including any graphics and third-party materials supplied by you, in accordance with the Conditions for Website Use and subject to any copyright notices which you include in connection with your articles and materials.

All copyright, and all rights therein, are protected by national and international copyright laws.

The above represents a summary only. For the full conditions see the Conditions for Authors and the Conditions for Website Use.

ISSN 1664-8714
ISBN 978-2-88963-057-8
DOI 10.3389/978-2-88963-057-8

About Frontiers

Frontiers is more than just an open-access publisher of scholarly articles: it is a pioneering approach to the world of academia, radically improving the way scholarly research is managed. The grand vision of Frontiers is a world where all people have an equal opportunity to seek, share and generate knowledge. Frontiers provides immediate and permanent online open access to all its publications, but this alone is not enough to realize our grand goals.

Frontiers Journal Series

The Frontiers Journal Series is a multi-tier and interdisciplinary set of open-access, online journals, promising a paradigm shift from the current review, selection and dissemination processes in academic publishing. All Frontiers journals are driven by researchers for researchers; therefore, they constitute a service to the scholarly community. At the same time, the Frontiers Journal Series operates on a revolutionary invention, the tiered publishing system, initially addressing specific communities of scholars, and gradually climbing up to broader public understanding, thus serving the interests of the lay society, too.

Dedication to Quality

Each Frontiers article is a landmark of the highest quality, thanks to genuinely collaborative interactions between authors and review editors, who include some of the world's best academicians. Research must be certified by peers before entering a stream of knowledge that may eventually reach the public - and shape society; therefore, Frontiers only applies the most rigorous and unbiased reviews.
Frontiers revolutionizes research publishing by freely delivering the most outstanding research, evaluated with no bias from both the academic and social point of view. By applying the most advanced information technologies, Frontiers is catapulting scholarly publishing into a new generation.

What are Frontiers Research Topics?

Frontiers Research Topics are very popular trademarks of the Frontiers Journals Series: they are collections of at least ten articles, all centered on a particular subject. With their unique mix of varied contributions from Original Research to Review Articles, Frontiers Research Topics unify the most influential researchers, the latest key findings and historical advances in a hot research area! Find out more on how to host your own Frontiers Research Topic or contribute to one as an author by contacting the Frontiers Editorial Office: researchtopics@frontiersin.org

THE MONONUCLEAR PHAGOCYTE SYSTEM IN INFECTIOUS DISEASE

Topic Editors:
Geanncarlo Lugo-Villarino, Institut de Pharmacologie et de Biologie Structurale, IPBS, Université de Toulouse, CNRS, UPS, France
Céline Cougoule, Institut de Pharmacologie et de Biologie Structurale, IPBS, Université de Toulouse, CNRS, UPS, France
Etienne Meunier, Institut de Pharmacologie et de Biologie Structurale, IPBS, Université de Toulouse, CNRS, UPS, France
Yoann Rombouts, Institut de Pharmacologie et de Biologie Structurale, IPBS, Université de Toulouse, CNRS, UPS, France
Christel Vérollet, Institut de Pharmacologie et de Biologie Structurale, IPBS, Université de Toulouse, CNRS, UPS, France
Luciana Balboa, IMEX-CONICET, Academia Nacional de Medicina, Buenos Aires, Argentina

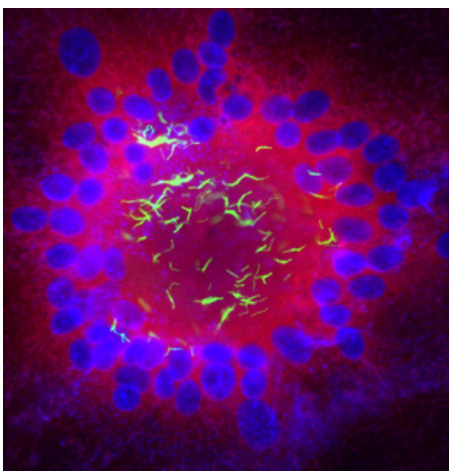


Image: Karine Pingris and Christel Vérollet
"Human multi-nucleated giant cell co-infected with HIV-1 (red) and Mycobacterium tuberculosis (green)" by Karine Pingris and Christel Vérollet

The Mononuclear Phagocyte System (MPS) of vertebrates is composed of monocytes, macrophages and dendritic cells. Together, they form part of the first line of immune defense against a variety of pathogens (bacteria, fungi, parasites and viruses), and thus play an important role in maintaining organism homeostasis. The mode of transmission, type of replication and mechanism of disease-causing differ significantly for each pathogen, eliciting a unique immune response in the host. Within this context, the MPS acts as both the sentinel and tailor of the immune system.

As sentinels, MPS cells are found in blood and within tissues throughout the body to patrol against pathogenic insult. The strategy to detect 'microbial non-self' relies on MPS to recognize conserved microbial products known as

'pathogen-associated molecular pattern' (PAMPs). PAMPs recognition represents a checkpoint in the response to pathogens and relies on conserved 'pattern recognition receptors' (PRRs). Upon PRR engagement, MPS mount a cell-autonomous attack that includes the internalization and compartmentalization of intracellular pathogens into toxic compartments that promote destruction. In parallel, MPS cells launch an inflammatory response composed of a cellular arm and soluble factors to control extracellular pathogens. In cases when innate immunity fails to eliminate the invading microbe, MPS serves as a tailor to generate adaptive immunity for pathogen eradication and generation of "memory" cells, thus ensuring enhanced protection against re-infection. Indeed, MPS cell functions comprise the capture, process, migration and delivery of antigenic information to lymphoid organs, where type-1 immunity is tailored against intracellular microbes and type-2 immunity against extracellular pathogens. However, this potent adaptive immunity is also a double-edge sword that can cause aberrant inflammatory disorders, like autoimmunity or chronic inflammation. For this reason, MPS also tailors tolerance immunity against unwanted inflammation. Successful clearance of the microbe results in its destruction and proper collection of debris, resolution of inflammation and tissue healing for which MPS is essential.

Reciprocally, as part of the evolutionary process taking place in all organisms, microbes evolved strategies to circumvent the actions bestowed by MPS cells. Multiple pathogens modulate the differentiation, maturation and activation programs of the MPS, as an efficient strategy to avoid a dedicated immune response. Among the most common evasion strategies are the subversion of phagocytosis, inhibition of PRR-mediated immunity, resistance to intracellular killing by reactive oxygen and nitrogen species, restriction of phagosome maturation, modulation of cellular metabolism and nutrient acquisition, regulation of cell death and autophagy, and modulation of pro-inflammatory responses and hijacking of tolerance mechanisms, among others.

The tenet of this eBook is that a better understanding of MPS in infection will yield insights for development of therapeutics to enhance antimicrobial processes or dampen detrimental inflammation for the host's benefit. We believe that contributions to this topic will serve as a platform for discussion and debate about relevant issues and themes in this field. Our aim is to bring expert junior and senior scientists to address recent progress, highlight critical knowledge gaps, foment scientific exchange, and establish conceptual frameworks for future MPS investigation in the context of infectious disease.

Citation: Lugo-Villarino, G., Cougoule, C., Meunier, E., Rombouts, Y., Vérollet, C., Balboa, L., eds. (2019). The Mononuclear Phagocyte System in Infectious Disease. Lausanne: Frontiers Media. doi: 10.3389/978-2-88963-057-8

Table of Contents

10 ***Editorial: The Mononuclear Phagocyte System in Infectious Disease***
Geanncarlo Lugo-Villarino, Céline Cougoule, Etienne Meunier, Yoann Rombouts, Christel Vérollet and Luciana Balboa

INTRODUCTION TO MPS BIOLOGY AND FUNCTION

16 ***Control of Phagocytosis by Microbial Pathogens***
Eileen Uribe-Querol and Carlos Rosales

39 ***Autophagy Proteins in Phagocyte Endocytosis and Exocytosis***
Christian Münz

46 ***Macrophage Autophagy and Bacterial Infections***
Aïcha Bah and Isabelle Vergne

55 ***Bruton's Tyrosine Kinase: An Emerging Key Player in Innate Immunity***
Alexander N. R. Weber, Zsofia Bittner, Xiao Liu, Truong-Minh Dang, Markus Philipp Radsak and Cornelia Brunner

61 ***Efferocytosis of Pathogen-Infected Cells***
Niloofar Karaji and Quentin J. Sattentau

71 ***A 17-kDa Fragment of Lactoferrin Associates With the Termination of Inflammation and Peptides Within Promote Resolution***
Aviv Lutaty, Soaad Soboh, Sagie Schif-Zuck, Orly Zeituni-Timor, Ran Rostoker, Malgorzata J. Podolska, Christine Schauer, Martin Herrmann, Luis E. Muñoz and Amiram Ariel

86 ***Monocytic Myeloid-Derived Suppressor Cells in Chronic Infections***
Anca Dorhoi and Nelita Du Plessis

101 ***E-Selectin Ligands in the Human Mononuclear Phagocyte System: Implications for Infection, Inflammation, and Immunotherapy***
Mariana Silva, Paula A. Videira and Robert Sackstein

118 ***Podosomes, but not the Maturation Status, Determine the Protease-Dependent 3D Migration in Human Dendritic Cells***
Céline Cougoule, Claire Lastrucci, Romain Guiet, Rémi Mascarau, Etienne Meunier, Geanncarlo Lugo-Villarino, Olivier Neyrolles, Renaud Poincloux and Isabelle Maridonneau-Parini

130 ***The Peyer's Patch Mononuclear Phagocyte System at Steady State and During Infection***
Clément Da Silva, Camille Wagner, Johnny Bonnardel, Jean-Pierre Gorvel and Hugues Lelouard

147 ***New Insights Into the Immunobiology of Mononuclear Phagocytic Cells and Their Relevance to the Pathogenesis of Cardiovascular Diseases***
Liliana Maria Sanmarco, Natalia Eberhardt, Nicolás Eric Ponce, Roxana Carolina Cano, Gustavo Bonacci and Maria Pilar Aoki

167 ***Understanding the Cellular Origin of the Mononuclear Phagocyte System Sheds Light on the Myeloid Postulate of Immune Paralysis in Sepsis***
Lionel Franz Poulin, Corentin Lasseaux and Mathias Chamaillard

181 ***Type I IFNs are Required to Promote Central Nervous System Immune Surveillance Through the Recruitment of Inflammatory Monocytes Upon Systemic Inflammation***
Javier María Peralta Ramos, Claudio Bussi, Emilia Andrea Gaviglio, Daniela Soledad Arroyo, Natalia Soledad Baez, Maria Cecilia Rodriguez-Galan and Pablo Iribarren

MPS BIOLOGY IN DIFFERENTINFECTIOUS DISEASES TUBERCULOSIS DISEASE

194 ***Monocyte Subsets: Phenotypes and Function in Tuberculosis Infection***
Pavithra Sampath, Kadar Moideen, Uma Devi Ranganathan and Ramalingam Bethunaickan

202 ***Macrophage Heterogeneity in the Immunopathogenesis of Tuberculosis***
Mohlopheni J. Marakalala, Fernando O. Martinez, Annette Plüddemann and Siamon Gordon

217 ***The C-Type Lectin Receptor DC-SIGN has an Anti-Inflammatory Role in Human M(IL-4) Macrophages in Response to* Mycobacterium tuberculosis**
Geanncarlo Lugo-Villarino, Anthony Troegeler, Luciana Balboa, Claire Lastrucci, Carine Duval, Ingrid Mercier, Alan Bénard, Florence Capilla, Talal Al Saati, Renaud Poincloux, Ivanela Kondova, Frank A. W. Verreck, Céline Cougoule, Isabelle Maridonneau-Parini, Maria del Carmen Sasiain and Olivier Neyrolles

232 ***Formation of Foamy Macrophages by Tuberculous Pleural Effusions is Triggered by the Interleukin-10/Signal Transducer and Activator of Transcription 3 Axis Through ACAT Upregulation***
Melanie Genoula, José Luis Marín Franco, Maeva Dupont, Denise Kviatcovsky, Ayelén Milillo, Pablo Schierloh, Eduardo Jose Moraña, Susana Poggi, Domingo Palmero, Dulce Mata-Espinosa, Erika González-Domínguez, Juan Carlos León Contreras, Paula Barrionuevo, Bárbara Rearte, Marlina Olyissa Córdoba Moreno, Adriana Fontanals, Agostina Crotta Asis, Gabriela Gago, Céline Cougoule, Olivier Neyrolles, Isabelle Maridonneau-Parini, Carmen Sánchez-Torres, Rogelio Hernández-Pando, Christel Vérollet, Geanncarlo Lugo-Villarino, María del Carmen Sasiain and Luciana Balboa

249 ***Suppressor of Cytokine Signaling 3 in Macrophages Prevents Exacerbated Interleukin-6-Dependent Arginase-1 Activity and Early Permissiveness to Experimental Tuberculosis***
Erik Schmok, Mahin Abad Dar, Jochen Behrends, Hanna Erdmann, Dominik Rückerl, Tanja Endermann, Lisa Heitmann, Manuela Hessmann, Akihiko Yoshimura, Stefan Rose-John, Jürgen Scheller, Ulrich Emil Schaible, Stefan Ehlers, Roland Lang and Christoph Hölscher

265 ***The Macrophage: A Disputed Fortress in the Battle Against* Mycobacterium tuberculosis**
Christophe J. Queval, Roland Brosch and Roxane Simeone

276 ***Macrophage–Bacteria Interactions—A Lipid-Centric Relationship***
Ooiean Teng, Candice Ke En Ang and Xue Li Guan

293 ***Mycobacterial Phenolic Glycolipids Selectively Disable TRIF-Dependent TLR4 Signaling in Macrophages***
Reid Oldenburg, Veronique Mayau, Jacques Prandi, Ainhoa Arbues, Catherine Astarie-Dequeker, Christophe Guilhot, Catherine Werts, Nathalie Winter and Caroline Demangel

305 ***Lipoarabinomannan Decreases Galectin-9 Expression and Tumor Necrosis Factor Pathway in Macrophages Favoring* Mycobacterium tuberculosis *Intracellular Growth***
Leslie Chávez-Galán, Lucero Ramon-Luing, Claudia Carranza, Irene Garcia and Isabel Sada-Ovalle

321 **Mycobacterium tuberculosis *Modulates miR-106b-5p to Control Cathepsin S Expression Resulting in Higher Pathogen Survival and Poor T-Cell Activation***
David Pires, Elliott M. Bernard, João Palma Pombo, Nuno Carmo, Catarina Fialho, Maximiliano Gabriel Gutierrez, Paulo Bettencourt and Elsa Anes

334 ***Iron- and Hepcidin-Independent Downregulation of the Iron Exporter Ferroportin in Macrophages During* Salmonella *Infection***
Alexandra Willemetz, Sean Beatty, Etienne Richer, Aude Rubio, Anne Auriac, Ruth J. Milkereit, Olivier Thibaudeau, Sophie Vaulont, Danielle Malo and François Canonne-Hergaux

345 ***Type I Interferons in the Pathogenesis of Tuberculosis: Molecular Drivers and Immunological Consequences***
Meg L. Donovan, Thomas E. Schultz, Taylor J. Duke and Antje Blumenthal

361 **De Novo *Fatty Acid Synthesis During Mycobacterial Infection is a Prerequisite for the Function of Highly Proliferative T Cells, but not for Dendritic Cells or Macrophages***
Philipp Stüve, Lucía Minarrieta, Hanna Erdmann, Catharina Arnold-Schrauf, Maxine Swallow, Melanie Guderian, Freyja Krull, Alexandra Hölscher, Peyman Ghorbani, Jochen Behrends, Wolf-Rainer Abraham, Christoph Hölscher, Tim D. Sparwasser and Luciana Berod

383 ***Proteomics of* Mycobacterium *Infection: Moving Towards a Better Understanding of Pathogen-Driven Immunomodulation***
Eik Hoffmann, Arnaud Machelart, Ok-Ryul Song and Priscille Brodin

391 ***Reinforcing the Functionality of Mononuclear Phagocyte System to Control Tuberculosis***
Susanta Pahari, Gurpreet Kaur, Shikha Negi, Mohammad Aqdas, Deepjyoti K. Das, Hilal Bashir, Sanpreet Singh, Mukta Nagare, Junaid Khan and Javed N. Agrewala

408 ***Antimycobacterial and Anti-inflammatory Mechanisms of Baicalin via Induced Autophagy in Macrophages Infected With* Mycobacterium tuberculosis**
Qingwen Zhang, Jinxia Sun, Yuli Wang, Weigang He, Lixin Wang, Yuejuan Zheng, Jing Wu, Ying Zhang and Xin Jiang

423 ***Cytokine Biomarkers Associated With Human Extra-Pulmonary Tuberculosis Clinical Strains and Symptoms***
Paulo Ranaivomanana, Mihaja Raberahona, Sedera Rabarioelina, Ysé Borella, Alice Machado, Mamy J. De Dieu Randria, Rivo A. Rakotoarivelo, Voahangy Rasolofo and Niaina Rakotosamimanana

434 ***Bovine WC1^{+} and WC1^{neg} γ δ T Lymphocytes Influence Monocyte Differentiation and Monocyte-Derived Dendritic Cell Maturation During In Vitro Mycobacterium avium Subspecies paratuberculosis Infection***
Monica M. Baquero and Brandon L. Plattner

HIV AND OTHER VIRAL DISEASES

445 ***Myeloid Cell Interaction With HIV: A Complex Relationship***
Vasco Rodrigues, Nicolas Ruffin, Mabel San-Roman and Philippe Benaroch

461 ***Role of Monocyte/Macrophages During HIV/SIV Infection in Adult and Pediatric Acquired Immune Deficiency Syndrome***
Kristen M. Merino, Carolina Allers, Elizabeth S. Didier and Marcelo J. Kuroda

477 ***Interaction Between Macrophage Migration Inhibitory Factor and CD74 in Human Immunodeficiency Virus Type I Infected Primary Monocyte-Derived Macrophages Triggers the Production of Proinflammatory Mediators and Enhances Infection of Unactivated CD4^{+} T Cells***
César Trifone, Jimena Salido, María Julia Ruiz, Lin Leng, María Florencia Quiroga, Horacio Salomón, Richard Bucala, Yanina Ghiglione andGabriela Turk

497 ***Mechanisms for Cell-to-Cell Transmission of HIV-1***
Lucie Bracq, Maorong Xie, Serge Benichou and Jérôme Bouchet

511 ***Tunneling Nanotubes: Intimate Communication Between Myeloid Cells***
Maeva Dupont, Shanti Souriant, Geanncarlo Lugo-Villarino, Isabelle Maridonneau-Parini and Christel Vérollet

517 ***Retroviruses as Myeloid Cell Riders: What Natural Human Siglec-1 "Knockouts" Tell us About Pathogenesis***
Javier Martinez-Picado, Paul J. McLaren, Amalio Telenti and Nuria Izquierdo-Useros

523 ***Functional Analysis of Phagocyte Activity in Whole Blood From HIV/Tuberculosis-Infected Individuals Using a Novel Flow Cytometry-Based Assay***
Ankur Gupta-Wright, Dumizulu Tembo, Kondwani C. Jambo, Elizabeth Chimbayo, Leonard Mvaya, Shannon Caldwell, David G. Russell and Henry C. Mwandumba

532 ***Defective Phagocytic Properties of HIV-Infected Macrophages: How Might They be Implicated in the Development of Invasive* Salmonella *Typhimurium?***
Gabrielle Lê-Bury and Florence Niedergang

544 ***Perturbation of Intracellular Cholesterol and Fatty Acid Homeostasis During Flavivirus Infections***
Joao Palma Pombo and Sumana Sanyal

551 ***Functional Impairment of Mononuclear Phagocyte System by the Human Respiratory Syncytial Virus***
Karen Bohmwald, Janyra A. Espinoza, Raúl A. Pulgar, Evelyn L. Jar and Alexis M. Kalergis

563 ***M(IL-4) Tissue Macrophages Support Efficient Interferon-Gamma Production in Antigen-Specific CD8^{+} T Cells With Reduced Proliferative Capacity***
Rylend Mulder, Andra Banete, Kyle Seaver and Sameh Basta

575 ***Enhanced Replication of Virulent Newcastle Disease Virus in Chicken Macrophages is Due to Polarized Activation of Cells by Inhibition of TLR7***
Pingze Zhang, Zhuang Ding, Xinxin Liu, Yanyu Chen, Junjiao Li, Zhi Tao, Yidong Fei, Cong Xue, Jing Qian, Xueli Wang, Qingmei Li, Tobias Stoeger, Jianjun Chen, Yuhai Bi and Renfu Yin

FUNGAL AND PARASITIC DISEASES

588 ***Helminth Infections: Recognition and Modulation of the Immune Response by Innate Immune Cells***
Claudia Cristina Motran, Leonardo Silvane, Laura Silvina Chiapello, Martin Gustavo Theumer, Laura Fernanda Ambrosio, Ximena Volpini, Daiana Pamela Celias and Laura Cervi

600 ***The Mannose Receptor in Regulation of Helminth-Mediated Host Immunity***
Irma van Die and Richard D. Cummings

609 ***African Trypanosomiasis-Associated Anemia: The Contribution of the Interplay Between Parasites and the Mononuclear Phagocyte System***
Benoit Stijlemans, Patrick De Baetselier, Stefan Magez, Jo A. Van Ginderachter and Carl De Trez

624 ***Trypanosomatid Infections: How do Parasites and Their Excreted–Secreted Factors Modulate the Inducible Metabolism of L-Arginine in Macrophages?***
Philippe Holzmuller, Anne Geiger, Romaric Nzoumbou-Boko, Joana Pissarra, Sarra Hamrouni, Valérie Rodrigues, Frédéric-Antoine Dauchy, Jean-Loup Lemesre, Philippe Vincendeau and Rachel Bras-Gonçalves

638 ***Mammalian Target of Rapamycin Inhibition in* Trypanosoma cruzi-*Infected Macrophages Leads to an Intracellular Profile That is Detrimental for Infection***
Jorge David Rojas Márquez, Yamile Ana, Ruth Eliana Baigorrí, Cinthia Carolina Stempin and Fabio Marcelo Cerban

653 ***All*-Trans *Retinoic Acid Promotes an M1- to M2-Phenotype Shift and Inhibits Macrophage-Mediated Immunity to* Leishmania major**
Natália S. Vellozo, Sâmara T. Pereira-Marques, Mariela P. Cabral-Piccin, Alessandra A. Filardy, Flávia L. Ribeiro-Gomes, Thaís S. Rigoni, George A. DosReis and Marcela F. Lopes

664 ***Infection of Human Macrophages by* Leishmania infantum *is Influenced by Ecto-Nucleotidases***
Nalu Teixeira de Aguiar Peres, Luana Celina Seraphim Cunha, Meirielly Lima Almeida Barbosa, Márcio Bezerra Santos, Fabrícia Alvise de Oliveira, Amélia Maria Ribeiro de Jesus and Roque Pacheco de Almeida

672 ***Heme-Oxygenase-1 Expression Contributes to the Immunoregulation Induced by* Fasciola hepatica *and Promotes Infection***
Paula Carasi, Ernesto Rodríguez, Valeria da Costa, Sofía Frigerio, Natalie Brossard, Verónica Noya, Carlos Robello, Ignacio Anegón and Teresa Freire

687 **Anaplasma phagocytophilum-*Related Defects in CD8, NKT, and NK Lymphocyte Cytotoxicity***
Diana G. Scorpio, Kyoung-Seong Choi and J. Stephen Dumler

695 ***The Complexity of Fungal ß-Glucan in Health and Disease: Effects on the Mononuclear Phagocyte System***
Giorgio Camilli, Guillaume Tabouret and Jessica Quintin

704 ***Combination of Classifiers Identifies Fungal-Specific Activation of Lysosome Genes in Human Monocytes***
João P. Leonor Fernandes Saraiva, Cristina Zubiria-Barrera, Tilman E. Klassert, Maximilian J. Lautenbach, Markus Blaess, Ralf A. Claus, Hortense Slevogt and Rainer König

714 ***P17, an Original Host Defense Peptide From Ant Venom, Promotes Antifungal Activities of Macrophages Through the Induction of C-Type Lectin Receptors Dependent on LTB4-Mediated PPARγ Activation***
Khaddouj Benmoussa, Hélène Authier, Mélissa Prat, Mohammad AlaEddine, Lise Lefèvre, Mouna Chirine Rahabi, José Bernad, Agnès Aubouy, Elsa Bonnafé, Jérome Leprince, Bernard Pipy, Michel Treilhou and Agnès Coste

ALTERNATIVE AND NOVEL MODELS

729 ***Macrophage–Microbe Interactions: Lessons From the Zebrafish Model***
Nagisa Yoshida, Eva-Maria Frickel and Serge Mostowy

737 ***A Model of Superinfection of Virus-Infected Zebrafish Larvae: Increased Susceptibility to Bacteria Associated With Neutrophil Death***
Laurent Boucontet, Gabriella Passoni, Valéry Thiry, Ludovico Maggi, Philippe Herbomel, Jean-Pierre Levraud and Emma Colucci-Guyon

752 ***Eat Prey, Live:* Dictyostelium discoideum *as a Model for Cell-Autonomous Defenses***
Joe Dan Dunn, Cristina Bosmani, Caroline Barisch, Lyudmil Raykov, Louise H. Lefrançois, Elena Cardenal-Muñoz, Ana Teresa López-Jiménez and Thierry Soldati

782 ***Humans in a Dish: The Potential of Organoids in Modeling Immunity and Infectious Diseases***
Nino Iakobachvili and Peter J. Peters

frontiers in Immunology

EDITORIAL
published: 26 June 2019
doi: 10.3389/fimmu.2019.01443

Editorial: The Mononuclear Phagocyte System in Infectious Disease

Geanncarlo Lugo-Villarino[1,2]*, *Céline Cougoule*[1,2], *Etienne Meunier*[1], *Yoann Rombouts*[1], *Christel Vérollet*[1,2] *and Luciana Balboa*[2,3]

[1] CNRS, UPS, Institut de Pharmacologie et de Biologie Structurale, IPBS, Université de Toulouse, Toulouse, France, [2] International Associated Laboratory, CNRS "IM-TB/HIV" (1167), Toulouse, France, [3] IMEX-CONICET, Academia Nacional de Medicina, Buenos Aires, Argentina

Keywords: monocytes, macrophages, dendritic cells, infection, pathogen, microbe, inflammation

Editorial on the Research Topic

The Mononuclear Phagocyte System in Infectious Disease

The term "Mononuclear Phagocyte System" (MPS) was introduced by van Furth and Cohn in 1968 to describe a group of leukocytes that shared phenotypic features (e.g., a single nucleus) and biological functions (e.g., phagocytosis) (1). This term served originally to characterize bone marrow progenitors, blood monocytes, and tissue macrophages, under the assumption that it was a linear progression from progenitor to monocyte, and from monocyte to macrophage. Upon the discovery of dendritic cells (DC) in 1973 by the late Nobel Laureate, Ralph Steinman, and subsequent inclusion of this cell type as part of MPS in the late 1970s, the term "MPS" undertook a specialized function for processing and presenting antigen to activate lymphocytes (2). Monocytes, DCs, and macrophages became referred to as antigen-presenting cells (APC). Today, beyond serving as primordial APCs, these cells are also known to play roles in thermogenesis, tissue development, and organ function, maintenance of homeostasis, microbiota interactions, innate immunity against pathogens, inflammation and its resolution, and wound healing and tissue repair, among others (3). Also, it is now clear that monocytes, DCs and macrophages, are not homogenous populations (4). Recent conceptual advances concerning the MPS ontogeny and development have shattered the traditional view of DCs and macrophages as linear derivates and functional variations of monocytes (5). It is predicted that the incorporation of new technologies (e.g., mass cytometry, single-cell RNA sequencing) along with the progress in imaging capacities, will continue to unveil cellular heterogeneity and behavior in different tissues, differentiation trajectories, and the identification of novel immune functions, within the mouse and human MPS (5). Therefore, as the MPS field continues its unrelenting progress, it is important to regularly revisit the MPS conceptual framework in health and disease.

This is precisely what we accomplished through the collection of articles in this research topic entitled "The Mononuclear Phagocyte System in Infectious Disease". As its title indicates, there are a total of 60 articles (26 original research and 34 literature reviews) written by 379 authors and published within this eBook dealing with multiple aspects of host-pathogen interaction. The tenet of this article collection is that a better understanding of MPS in infection will yield insights for development of therapeutics to enhance antimicrobial processes or dampen detrimental inflammation, for the benefit of the host. We believe that the contributions made to this topic will serve as a platform for discussion and debate about relevant issues and themes in this field.

OPEN ACCESS

Edited and reviewed by:
Ian Marriott,
University of North Carolina at Charlotte, United States

***Correspondence:**
Geanncarlo Lugo-Villarino
lugo@ipbs.fr

Specialty section:
This article was submitted to Microbial Immunology, a section of the journal Frontiers in Immunology

Received: *22 April 2019*
Accepted: *10 June 2019*
Published: *26 June 2019*

Citation:
Lugo-Villarino G, Cougoule C, Meunier E, Rombouts Y, Vérollet C and Balboa L (2019) Editorial: The Mononuclear Phagocyte System in Infectious Disease. Front. Immunol. 10:1443. doi: 10.3389/fimmu.2019.01443

INTRODUCTION TO MPS BIOLOGY AND FUNCTION

For didactic purposes, we begin this collection with a series of "introductory" articles where readers can find general informations about MPS biology and functions in the context of infectious and inflammatory diseases.

Addressing cell-intrinsic functions, Uribe-Querol and Rosales discuss the influence on phagocytosis by microbial pathogens. Following an overview of phagocytosis and the antimicrobial factors employed by MPS, they summarize the microbial strategies used to inhibit phagocytosis at the level of ingestion, phagosome formation, and maturation, including microbial escape from these vesicles. Münz takes on autophagy in the context of viral infection. He describes recent evidence for how autophagy proteins regulate endocytosis and exocytosis in MPS cell activation, viral replication, and antigen presentation. Reciprocally, Bah and Vergne focus on autophagy in the context of bacterial infections. They discuss multiple functions of autophagy proteins in conferring cell defense against bacteria, and discuss how some pathogenic bacteria manipulate autophagy. Together, these authors argue that a better understanding of autophagy proteins might yield new therapeutic approaches against pathogenic infections. In terms of factors involved in the inflammatory response against pathogens, Weber et al. cast light on Bruton's tyrosine kinase (BTK). Beyond its central role as a mediator of B cell receptor signaling, BTK is crucial in the recognition of infectious agents, cellular maturation, and recruitment, and inflammasome regulation. Thus, it will be beneficial to improve our understanding of BTK biology not only as a kinase, but also as a scaffold protein, within the MPS. As a final point in cell-intrinsic properties, Karaji and Sattentau take on the efferocytosis of pathogen-infected cells, which is the process of clearing of unwanted cells by MPS. After a description of pathogen-triggered cell death and the signals inducing efferocytosis, they discuss how it controls different pathogenic infections and generates immune responses. Conversely, pathogens have evolved ingenious strategies to subvert efferocytosis, thus opening avenues to block immune evasion and pathogen persistence. The importance of efferocytosis in the resolution of inflammation is highlighted in the study by Lutati et al., who identified a neutrophil-derived glycoprotein lactoferrin (Lf) that triggers resolution-phase macrophages. Indeed, they demonstrate that Lf promotes the conversion of pro-inflammatory into pro-resolution macrophages that have enhanced efferocytotic capacity to clear apoptotic neutrophils.

We continue our introductory articles to address pathophysiological aspects of the MPS. Dorhoi and Du Plessis take on the monocytic-like myeloid-derived suppressor cells (M-MDSC), which inhibit innate and adaptive immune cell activation, proliferation, viability, trafficking, and cytokine production, to promote peripheral tolerance against unwanted inflammation during pathogenic infection. However, M-MDSC also serve as reservoirs for pathogens favoring their survival and limiting optimal host responses, highlighting the need to better understand their genesis and biological functions in chronic infections. Silva et al. focus on the role of E-Selectin ligands to home blood-borne MPS cells into infection sites. Insights to the structural and functional properties of E-Selectin ligands in MPS cells are likely to improve the efficiency of immune responses and ameliorate immunopathology derived from chronic inflammation. Within the context of cell migration, Cougoule et al. reveal the importance of podosomes (actin-rich structures found specifically on the basal membrane of MPS cells) for the capacity of human DCs to penetrate dense microenvironments. This study describes the influence of pathogen-derived signals on podosome formation and dynamics, thus dictating the mode of migration of DCs toward infectious sites. Da Silva et al. provide an overview on Peyer's patch MPS in health and disease. This includes MPS cell diversity and specificity, anatomical localization, functions, interaction with microbiota and generation of humoral immunity, and their role in multiple infectious contexts.

Recent advances in MPS biology in the cardiovascular system is the subject for the review by Sanmarco et al. MPS cells play roles in cardiac inflammation and infection, such as in Chagas cardiomyopathy, viral myocarditis, bacterial infections, sterile inflammation, among other disorders. The authors highlight the importance of dissecting the signaling pathways and molecules modulating MPS functions during infection. Lastly, Poulin et al. tackle the myeloid postulate of immune paralysis in sepsis by focusing on the well-known disappearance of circulating DCs. Beyond the description of the DC ontogeny and functions, they discuss about novel myelopoiesis-based therapeutic targeting MPS cells in sepsis. As described above, sometimes infection may lead to uncontrolled inflammation causing immunopathology. In their study, Peralta-Ramos et al. address the role of type-I interferons (IFN-I) in establishing and developing neuroinflammatory diseases. Upon systemic inflammatory challenge, they show that IFN-I promotes the recruitment of inflammatory monocytes into the brain, which subsequently induces local T cell activation leading to immunopathology.

MPS BIOLOGY IN DIFFERENT INFECTIOUS DISEASES

This section addresses the interaction of human and mouse MPS with different types of pathogens: bacterial, viral, fungal, and parasitic.

Tuberculosis Disease

Reflecting the expertise contained within our editorial group, we provide a robust collection of articles that address MPS cell interaction with *Mycobacterium tuberculosis* (Mtb), the etiological agent responsible for tuberculosis. Within the context of cell heterogeneity, Sampath et al. discuss how monocyte subsets participate as effector and cell targets contributing to the control and pathogenesis of Mtb, respectively. Likewise, Marakalala et al. review macrophage heterogeneity in Mtb tropism, granuloma formation and maintenance, activation and product secretion during infection, foam cell formation, and

caseation, among other aspects. Contrary to classical activation of pro-inflammatory macrophages with IFNγ, there are other immune signals that activate macrophages toward alternative phenotypes, such as interleukin (IL)-4, IL-10, and IL-6. In their study, Lugo-Villarino et al. address the role of the C-type lectin receptor (CLR) DC-SIGN, a marker for IL-4-activated macrophages, in the response against Mtb. While this CLR helps Mtb to parasitize macrophages, they describe a parallel role as a molecular switch to turn off the pro-inflammatory response to prevent unwanted immunopathology associated to tuberculosis. Using an acellular fraction of tuberculous pleural effusions as a physiological source of local factors released during Mtb infection, Genoula et al. characterize how the IL-10/STAT3 axis induces foam cell differentiation by activating the enzyme acyl CoA:cholesterol acyl transferase, contributing to our understanding of how alterations of the host metabolic pathways may favor pathogen persistence. Excessive activation toward a macrophage subset may often lead to susceptibility to pathogen invasion or immunopathological disorders. Employing a mouse model targeting the deletion of the suppressor of cytokine signaling 3 (SOCS3) specifically in macrophages, Schmok et al. demonstrate how SOCS3 prevents macrophage activation driven by IL-6, increasing susceptibility to Mtb replication in lung macrophage.

Continuing with the interaction between macrophages and Mtb, Queval et al. review the molecular events governing the bacilli survival, and how it is able to transform macrophages into survival and dissemination vessels. One of these aspects is the regulation of metabolism that is critical in shaping macrophage activation and immune functions. Teng et al. write about mycobacterial lipid-based tactics to manipulate host metabolism. They address the emerging roles of lipids in the complex host–pathogen relationship, and discuss recent methodologies used to assess lipid dynamics during infection (Teng et al.). Within this context, Oldenburg et al. report how mycobacterial phenolic glycolipids (PGL) decrease the TLR-4-dependent signaling cascade, resulting in the low production of pro-inflammatory signals in macrophages. The authors show that PGL-1 targets the posttranscriptional decrease of TIR-domain-containing adapter-inducing interferon-β (TRIF) protein level, an important component of the TLR-4 signaling pathway. Likewise, Chavez-Galán et al. describe how Lipoarabinomannan affects the T-cell immunoglobulin and mucin domain 3 (TIM3)/galectin (GAL)9 pathway by targeting GAL9 expression. This is important because the interaction between TIM3 and GAL9 was shown to promote microbicidal activity against Mtb. Another strategy used by Mtb is to control the activity of host lysosomal cathepsins in macrophages. Pires et al. demonstrate that Mtb upregulates miRNAs such as miR-106b-5p, which binds to the 3′-untranslated region of the mRNA for cathepsin S, thus preventing its protein expression and consequently increasing Mtb survival.

Beyond tuberculosis, we include a study on "nutritional immunity" in the context of *Salmonella enterica* serovar Typhimurium infection. This is a host defense strategy against infection that relies on the sequestration of essential molecules, such as iron, to prevent pathogen growth. However, pathogens evolved counter strategies to deal with nutritional immunity. In their study, Willemetz et al. demonstrate that *Salmonella* modulates macrophage iron homeostasis to favor its access to high intracellular content of iron by downregulating the iron exporter ferroportin (FPN). Intriguingly, FPN is repressed through an iron and hepcidin-independent mechanism, suggesting the cellular iron is indispensable for the growth of *Salmonella* inside the macrophages (Willemetz et al.). It will be interesting to find out whether this is a general host response observed with other intracellular pathogens infection, such as Mtb.

As we move forward in understanding the host and Mtb interactions, there are various aspects that require further refinement. For example, Donovan et al. address the role of IFN-I in tuberculosis. In their review, the authors argue the need to identify the myeloid source for IFN-I production during Mtb infection *in vivo*; characterize the roles for individual members of the IFN-I family; and define whether blood gene expression signatures in active tuberculosis are a natural consequence of Mtb infection in humans or an indication of disease susceptibility. Another field requiring further elucidation is MPS immunometabolism. Using novel genetic mouse models to delete acetyl-CoA carboxylase (ACC) 1 and 2 specifically in DCs, macrophage or T lymphocytes, Stuve et al. clearly demonstrate that MPS cells do not require these enzymes for the control of mycobacteria infection. By contrast, targeted deletion in T cells results in susceptibility to Mtb. One novel approach to more deeply investigate how Mtb modulates the host response is to perform mass spectrometry (MS)-based proteomics on infected cells. Specifically, Hoffmann et al. summarize the progress made in determining the protein composition of mycobacteria-containing vacuoles, which has already shown, for example, how Mtb prevents the fusion of late endosomes and lysosomal compartments. The authors argue this approach will promote the development of novel host-directed therapies, particularly against the emergent drug-resistant Mtb strains. Likewise, Pahari et al. propose different strategies in their review to reinforce the functional aspects of the MPS to achieve better control of Mtb. They discuss multiple molecules to boost the innate immune system to enhance the emergent field of immunotherapeutics. For instance, Zhang et al. show in their study that the herbal medicine, baicalin, induces autophagy activation in Mtb-infected macrophages leading to a better control of intracellular Mtb. At the same time, baicalin also regulates the inflammasome-dependent activation of IL-1β, suggesting this herbal medicine also controls unnecessary inflammation derived from infection (Zhang et al.). An area that requires improvement is the assessment of biomarkers according to the different states of disease progression and severity. In their study, Ranaivomanana et al. provide a biomarker signature that is different between patients with pulmonary and extrapulmonary tuberculosis, and they correlate it in human macrophages infected *in vitro* with clinical strains representative for each tuberculosis disease type. Finally, inter-species comparisons are helpful not only to advance our understanding of the MPS, but also necessary to deal with infectious diseases afflicting in domestic animals. In bovines, the *Mycobacterium avium* subspecies *paratuberculosis* (*Map*)

causes a chronic intestinal infection known as paratuberculosis, which leads to significant economic loss to livestock industries. One of the problems is that early host-pathogen interactions in bovines remain poorly understood. In their study, Baquero and Plattner report that γδ T cells influence differentiation, maturation, and functional aspects of bovine monocytes during *Map* infection. The authors argue that modulation of the γδ T cells/MPS axis represents a viable vaccination/therapeutic strategy to generate a strong adaptive immunity to counteract paratuberculosis in bovines (Baquero and Plattner).

Collectively, this series of articles promote the importance of MPS in the tuberculosis context, and it highlights its therapeutic potential yet to be exploited to control this disease.

HIV and Other Viral Diseases

Reflecting another area of expertise within our editorial group, the following article collection addresses MPS cell interaction with the human immunodeficiency virus (HIV). We start with a review article by Rodrigues et al., who provide an in-depth description of HIV-macrophage interaction during the various stages of the virus life cycle. This is complemented by another review article from Merino et al. discussing the contribution of monocytes and macrophages to the infection and progression of HIV and SIV, a closely related HIV-like virus that causes disease similar to AIDS in monkeys and apes. The macrophage interaction with HIV is important because it influences the adaptive immune response. Trifone et al. demonstrate the role of macrophage migration inhibitory factor (MIF)/CD74 axis in HIV pathogenesis. They show that HIV-1 infection of $CD74^+$ macrophages results in a pro-inflammatory environment in the presence of MIF, which predisposes unactivated $CD4^+$ T cells to HIV-1 infection (Trifone et al.).

Another way the MPS participates in HIV pathogenesis is through cell-to-cell transmission of the virus, including through interactions with lymphocytes. In their review, Bracq et al. provide a description of the different mechanisms that occur during cell-to-cell transmission of HIV, such as intercellular structures and membrane protrusions, immunological synapses, efferocytosis of dying cells, and cell-to-cell fusion. Concerning intercellular structures and membrane protrusions, Dupont et al. focus their review on tunneling nanotubes (TNT), which are long membranous dynamic structures and a novel route for cell-to-cell communication. They argue TNT serve as major "corridors" for viral to spread efficiently to bystander cells and remain undetected by the immune system (Dupont et al.). As a strategy to hijack cell-to-cell communication between MPS cells, Martinez-Picado et al. write about the lectin receptor Siglec-1/CD169 that facilitates the binding of HIV-1 without internalization and, consequently, the infection of bystander cells. In their review, they discuss how working with human cohorts lacking Siglec-1 provides a unique understanding of the role this receptor plays in viral pathogenesis *in vivo*.

An important issue of HIV-positive patients is their susceptibility of co-infection with other pathogens. For example, patients living with HIV are more likely to die from tuberculosis than HIV-negative people. Addressing this issue, Gupta-Wright et al. developed a flow cytometry-based fluorescent reporter of phagosomal oxidase activity to demonstrate impaired superoxide burst activity in the phagocytes of hospitalized HIV-positive patients with tuberculosis. The authors promote the use of this assay to assess the immune competence of co-infected patients in clinical settings, including the activation state of MPS cells. Another complication in HIV-positive patients is susceptibility to opportunistic pathogens such as non-typhoidal *Salmonella enterica* serovar Typhimurium, which is the most common cause of bacterial bloodstream infections in these patients. In their review, Lê-Bury and Niedergang describe how macrophage function is impaired upon HIV infection, discuss factors that make invasive Salmonella Typhimurium specific for HIV pathogenesis, and provide reasons for why these bacteria are well-suited to invade the HIV-infected host.

This section closes with an overall look at the MPS in the context of other viral infections. Pombo and Sanyal review different mechanisms of altering lipid metabolic pathways during infection by flaviviruses, and they focus on cholesterol and fatty acid biosynthesis. Intriguingly, these events can promote an advantage for invading viruses to support replication, and thus they can be modulated for the benefit of the host as a mean to fight infection. Since the Human Respiratory Syncytial Virus (hRSV) is responsible for bronchiolitis, pneumonia, recurrent wheezing and asthma, Bohmwald et al. provide a review on the role of the lung MPS during hRSV infection and their involvement in its pathogenesis. This is critical given that hRSV causes functional impairment of the MPS. Next, Mulder et al. use the Lymphocytic Choriomeningitis Virus (LCMV), of the family Arenaviridae, an etiological agent for human acute aseptic meningitis and grippe-like infections, to understand how different macrophage subsets are able to control viral infection and activate the adaptive immune response in the mouse model. In their study, they show that IL-4-activated macrophages do not support $CD8^+$ T-cell proliferation and effector functions during virus infection, as opposed to other macrophages activated by stimuli such as IFN-γ, for example. As part of the inter-species comparisons included in this eBook, Zhang et al. assess the impact of virulent Newcastle Disease Virus (NDV) infection in the macrophage compartment in chickens. Indeed, NDV causes Newcastle disease that is highly contagious and fatal in birds that dramatically affects the global domestic poultry production. The authors describe that the macrophage compartment becomes susceptible to viral replication due to inhibition of TLR-7-dependent signaling, which is avoided by pre-treatment with TLR-7 ligand (Zhang et al.).

Together, this series of articles promote the importance of MPS in viral infection, highlighting the need to better understand the interaction of MPS cells with viruses and the mechanisms involved in viral subversion and evasion strategies.

Fungal and Parasitic Diseases

This eBook continues with an overall perspective of the MPS in the context of parasite and fungal infection. Human parasites are divided into endoparasites (cause infection inside the body) and ectoparasites (cause infection superficially within the skin). Parasitic worms (helminths) are endoparasites

that infect ∼24% of the entire human population. For this reason, Motran et al. provide a discussion of the recognition and modulation of the MPS during helminth infections. In particular, they address excretory-secretory products resulting from helminth recognition by DCs and macrophages. With regards to recognition of helminths, van Die and Cummings shed light on the macrophage Mannose Receptor (MR) in the MPS to that shapes the immune responses to these parasites, and they deliver an overview of the structural aspects of this receptor along with important functional implications. Another endoparasite that afflicts the human population and affects the MPS is *African trypanosomosis*, which causes a debilitating disease known as "sleeping sickness." In their review, Stijlemans et al. deliver a discussion of how factors derived from this parasite and the MPS contribute to trypanosomosis-associated anemia development, along with intervention strategies partially targeting the MPS to alleviate this disease. This is complemented by another review by Holzmuller et al., who focus on how trypanosomatid excreted-secreted or host molecules affect the metabolic balance between nitric oxide synthase/arginase in the activation of macrophages, and their overall impact on the pathogenesis of this disease. Within the metabolic context, Rojas-Márquez et al. report that *Trypanosoma cruzi*, the causative agent for Chagas' disease, is controlled inside macrophages by the activation of the NLRP3 inflammasome and reactive oxygen species (ROS) production. Interestingly, they show that the metabolic checkpoint kinase mammalian target of rapamycin (mTOR) is activated by *T. cruzi* infection and it negatively regulates the NLRP3 activation, and its pharmacological inhibition restores the microbicidal properties of macrophages against this parasite (Rojas-Márquez et al.).

Leishmaniasis is a disease caused by protozoa endoparasites of the *Leishmania* order, affecting 4–12 million people in the world. It is manifested at the cutaneous, mucocutaneous or visceral level. In the context of cutaneous Leishmaniasis caused by *L. major*, Vellozo et al. show that, while this parasite promotes the pro-inflammatory activation of anti-parasitic macrophages, the all-trans retinoic acid (ATRA) therapy prevents this differentiation rendering susceptibility in the host. This is important because the ATRA treatment has been proposed as a therapy to differentiate immature myeloid cells into macrophages to boost immunity against tumors, suggesting an increased risk for endoparasite infections in such patients. In the context of visceral Leishmaniasis caused by *L. infantum*, Peres et al. address the role of Ecto-nucleotidases in the infection of human macrophages. They demonstrate ecto-nucleotidase activity of *L. infantum* is directly associated with infectivity of macrophages, which is blocked using antibodies targeting this enzyme, opening new therapeutic avenues against Leishmaniasis and other trypanosomitides infections (Peres et al.). Other forms of endoparasite are parasitic flukes, such as liver fluke disease that is caused by *Fasciola hepatica*. In their study, Carasi et al. investigate the role of heme-oxygenase-1 (HO-1) in the immunoregulation of DCs by *F. hepatica*. They show that the HO-1 expression favors this parasite infection, resulting in increased clinical signs and liver damage. This is associated with the upregulation of IL-10 that down-modulates the activation of DCs and macrophages. Indeed, the authors demonstrate that enzymatic inhibition of HO-1 leads to a decrease of IL-10 and an increase in the resistance of mice against infection, indicating that *F. hepatica* employs HO-1 to subvert the MPS (Carasi et al.).

Finally, ectoparasites can also be a burden to the human population even in developed countries. For example, tick-transmitted *Anaplasma phagocytophilum* is responsible for human granulocytic anaplasmosis, which is the third most common human vector-borne infection in USA causing lethality in 1% of patients. Here, Scorpio et al. report that impaired cytotoxicity against *A. phagocytophilum* is associated with a defect in APCs that express MHC class I and interact with innate and adaptive immune cells during infection, inferring that parasite-derived products may alter the MPS functions to circumvent $CD8^+$ T cell cytotoxicity.

This section concludes with a brief overview of the role of MPS in mycosis, which are a public health problem afflicting humans; there is an estimated 1.6 million people who die each year of fungal infections. To understand the host-fungi interactions, fundamental research has turned partially toward the use of fungal cell wall polysaccharides due to their immunogenicity properties and potential to be therapeutic compounds in infectious disease. In their review, Camili et al. write about the complexity of MPS interaction with β-glucan, the most abundant fungal cell wall polysaccharide. It is argued that a better understanding of the biochemical and immunogenicity properties of the different fungal β-glucans (isolated from different sources) will be necessary to uncover novel cellular and molecular mechanisms of action, and to improve a rational use in the future as an adjuvant or therapeutic agent. One of the problems with blood stream fungal infection is the lack of an appropriate and rapid treatment. This is the main issue addressed by Leonor Fernades-Saraiva et al., who developed a combined classifier approach with distinct differential gene expression profiles across multiple studies to generate an exclusive lysosome-related gene expression as a blood monocyte-specific footprint for fungal infections. This is crucial because it is specific for fungal (as opposed to bacterial) infection and it may allow its rapid identification in the patient's blood. Within the context of therapeutic perspectives, Benmoussa et al. identify a novel compound P17, derived from ant venom, with the capacity to modulate macrophage differentiation toward an anti-fungal phenotype characterized by a signaling pathway dependent on the peroxisome proliferator-activated receptor gamma (PPARγ), Dectin-1 and MR receptors.

Taken in concert, while the MPS plays a key role in controlling and generating immunity against parasitic and fungal infections, these pathogens have also evolved strategies to circumvent and subvert the MPS. Understanding this complexity represents an opportunity for diagnostic, prevention, and therapeutic advances.

ALTERNATIVE AND NOVEL MODELS

In this section, we offer a wider perspective of the MPS with a series of articles describing alternative animal and cellular models to highlight different approaches, limitations, and advantages to

better define MPS functional properties that can be exploited for therapeutic and vaccination purposes.

With regard to animal models, the zebrafish (*Danio rerio*) model symbolizes complementarity with the human and mouse models. This is a unique platform to study the MPS interaction with pathogens *in vivo*, ranging from the single cell level to the whole organism. Advantages include: non-invasive real-time visualization of the MPS system, chemical and genetic tractability, and this model is a natural host of a great number of pathogens of bacteria, virus, parasite and fungal origin, among others. In their review, Yoshida et al. argue why zebrafish are a unique model to study macrophage-microbe interactions, focusing on recent developments in the context of bacterial and fungal infection. Furthermore, Boucontet et al. promote zebrafish as a model of superinfection with a virus (i.e., Sindbis virus) and a bacterium (i.e., Shigella). In their study, they uncover a virus-induced hyper-susceptibility to bacterial infection that is associated with defects in neutrophil functions. Thus, zebrafish offer an alternative model to better understand this phenomenon, and a platform for drug-testing and therapeutic-development to restore the host immunity (Boucontet et al.).

In terms of cellular models, use of the soil dwelling, social amoeba *Dictyostelium discoideum*, is already making important contributions to our understanding of cell-autonomous mechanisms in MPS cells. Dunn et al. provide a review of the advantages and relevance of *D. discoideum* to study the antimicrobial functions of phagocytosis and autophagy, and the microbial properties of the phagosome. Reciprocally, they also discuss microbial interference with these defenses, and address a variety of conserved microbial restriction factors in *D. discoideum* that are relevant to the mammalian MPS. Another cellular model likely to make an impact is that of embryonic derived, self-renewing human tissue-resident macrophages (Max Planck Institute, MPI cells), which mimic lung alveolar macrophages. In their study, Woo et al. perform characterization of the responses of MPI cells to Mtb infection, including recognition and ingestion of live Mtb, bacterial intracellular replication, induction of pro- and anti-inflammatory cytokines, microbicidal activity and elimination of bacteria, and accumulation of lipid droplets in the cytoplasm upon lipoprotein exposure. The authors conclude that MPI cells are a tractable cell model for tuberculosis research that will enhance our understanding of human alveolar macrophages (Woo et al.). Finally, Iakobachvili and Peters provide an outlook on the "Organoid Revolution" that is currently taking place in all fields of biology. They explain organoid technology, describe its current impact in infectious diseases, and discuss how it may be used to study MPS biology in infection (Iakobachvili and Peters). Altogether, these cellular models are compliant with the 3Rs (Replace, Reduce, Refine) initiative to reduce the use of animals to study the MPS, and provide a context to study cell-autonomous defenses independent of other immune responses.

SUMMARY

We compiled expertise of scientists of all career stages and from 23 countries and five continents to address recent progress, highlight critical knowledge gaps, foment scientific exchange, and establish conceptual frameworks for future MPS investigation in the context of infectious disease. We hope that the present MPS conceptual framework will enhance the reader's knowledge within the infectious disease context, and inspire new lines of investigation to further fuel the progress in this field.

AUTHOR CONTRIBUTIONS

GL-V wrote manuscript. CC, EM, YR, CV, and LB edited and contributed to the organization of the editorial article.

ACKNOWLEDGMENTS

We are grateful for the warm reception that this research topic has received from the scientific community; to all 379 authors who contributed to its success; to all review editors whose expertise significantly improved the quality of each manuscript submitted; to the associate editors, in particular Dr. Christoph Hölscher, who gave a timely helping hand in conflict-of-interest cases; and for all people involved in the collective effort and candid discussions necessary to create this topic and eBook.

REFERENCES

1. Lasser A. The mononuclear phagocytic system: a review. *Hum pathol.* (1983) 14:108–26. doi: 10.1016/S0046-8177(83)80239-1
2. Viehmann SF, Bohner AMC, Kurts C, Brahler S. The multifaceted role of the renal mononuclear phagocyte system. *Cell immunol.* (2018) 330:97–104. doi: 10.1016/j.cellimm.2018.04.009
3. Jenkins SJ, Hume DA. Homeostasis in the mononuclear phagocyte system. *Trends immunol.* (2014) 35:358–67. doi: 10.1016/j.it.2014.06.006
4. Chow A, Brown BD, Merad M. Studying the mononuclear phagocyte system in the molecular age. *Nat rev Immunol.* (2011) 11:788–98. doi: 10.1038/nri3087
5. Haniffa M, Bigley V, Collin M. Human mononuclear phagocyte system reunited. *Sem cell dev biol.* (2015) 41:59–69. doi: 10.1016/j.semcdb.2015.05.004

Conflict of Interest Statement: The authors declare that the research was conducted in the absence of any commercial or financial relationships that could be construed as a potential conflict of interest.

Copyright © 2019 Lugo-Villarino, Cougoule, Meunier, Rombouts, Vérollet and Balboa. This is an open-access article distributed under the terms of the Creative Commons Attribution License (CC BY). The use, distribution or reproduction in other forums is permitted, provided the original author(s) and the copyright owner(s) are credited and that the original publication in this journal is cited, in accordance with accepted academic practice. No use, distribution or reproduction is permitted which does not comply with these terms.

frontiers in Immunology

REVIEW
published: 24 October 2017
doi: 10.3389/fimmu.2017.01368

Control of Phagocytosis by Microbial Pathogens

*Eileen Uribe-Querol[1] and Carlos Rosales[2]**

[1] División de Estudios de Posgrado e Investigación, Facultad de Odontología, Universidad Nacional Autónoma de México, Mexico City, Mexico, [2] Departamento de Inmunología, Instituto de Investigaciones Biomédicas, Universidad Nacional Autónoma de México, Mexico City, Mexico

Phagocytosis is a fundamental process of cells to capture and ingest foreign particles. Small unicellular organisms such as free-living amoeba use this process to acquire food. In pluricellular organisms, phagocytosis is a universal phenomenon that all cells are able to perform (including epithelial, endothelial, fibroblasts, etc.), but some specialized cells (such as neutrophils and macrophages) perform this very efficiently and were therefore named professional phagocytes by Rabinovitch. Cells use phagocytosis to capture and clear all particles larger than 0.5 μm, including pathogenic microorganisms and cellular debris. Phagocytosis involves a series of steps from recognition of the target particle, ingestion of it in a phagosome (phagocytic vacuole), maturation of this phagosome into a phagolysosome, to the final destruction of the ingested particle in the robust antimicrobial environment of the phagolysosome. For the most part, phagocytosis is an efficient process that eliminates invading pathogens and helps maintaining homeostasis. However, several pathogens have also evolved different strategies to prevent phagocytosis from proceeding in a normal way. These pathogens have a clear advantage to perpetuate the infection and continue their replication. Here, we present an overview of the phagocytic process with emphasis on the antimicrobial elements professional phagocytes use. We also summarize the current knowledge on the microbial strategies different pathogens use to prevent phagocytosis either at the level of ingestion, phagosome formation, and maturation, and even complete escape from phagosomes.

Keywords: macrophage, neutrophil, bacteria, infection, inflammation, phagosome maturation, phagolysosome

OPEN ACCESS

Edited by:
Elsa Anes,
Universidade de Lisboa, Portugal

Reviewed by:
Anthony George Tsolaki,
Brunel University London, United Kingdom
Carmen Judith Serrano,
Instituto Mexicano del Seguro Social, Mexico

****Correspondence:***
Carlos Rosales
carosal@unam.mx

Specialty section:
This article was submitted to Microbial Immunology, a section of the journal Frontiers in Immunology

Received: *13 August 2017*
Accepted: *05 October 2017*
Published: *24 October 2017*

Citation:
Uribe-Querol E and Rosales C (2017) Control of Phagocytosis by Microbial Pathogens. Front. Immunol. 8:1368. doi: 10.3389/fimmu.2017.01368

INTRODUCTION

Phagocytosis, in pluricellular organisms, is a complex process for the ingestion and elimination of pathogens. It is also important for elimination of apoptotic cells, and for maintaining tissue homeostasis (1, 2). All cells may, to some extent, perform phagocytosis; however, in mammals, phagocytosis is the hallmark of specialized cells including monocytes, macrophages, dendritic cells, osteoclasts, eosinophils, and polymorphonuclear neutrophils—these cells are collectively referred to as professional phagocytes (3). Professional phagocytes eliminate microorganisms and present them to cells of the adaptive immune system. Phagocytosis can be divided into several main steps: (i) microbial recognition, (ii) phagosome formation, and (iii) phagolysosome maturation.

Phagocytosis initiates with the recognition and ingestion of microbial pathogens larger than 0.5 μm into a plasma membrane-derived vesicle, known as phagosome. This recognition is achieved through several receptors that recognize precise molecular patterns associated with microorganisms. These receptors then trigger signaling cascades that induce phagocytosis. Receptors on phagocytes

can be divided into non-opsonic or opsonic receptors. Non-opsonic receptors can directly identify pathogen-associated molecular patterns (PAMPs) on the surface of the microorganisms. Opsonic receptors bind to host-produced molecules called opsonins. These molecules bind to microorganisms and mark them for ingestion. Opsonins include antibodies, complement, fibronectin, mannose-binding lectin, and milk fat globulin (lactadherin) (4).

After receptor engagement, the plasma membrane covers the microorganism to be ingested and closes at the distal end, forming a vacuole where the microorganism is internalized (**Figure 1**). This vacuole, the early phagosome, then fuses with endocytic vesicles and at the same time secretory vesicles are separated from it, transforming the early phagosome into a late phagosome. This dynamic process consists of sequential fusion and fission events between the new phagosome and endosomes, and it is known as "the kiss-and-run" model (5). Later, the intermediary phagosome turns into a microbicidal vacuole, the phagolysosome, by fusing with lysosomes and changing its membrane and interior characteristics through a process named phagolysosome maturation (6). The results of this process are remodeling of the membrane, progressive acidification of the phagosome, and creation of an oxidative and degradative milieu (7, 8) (**Figure 2**).

The phagocytic process is usually very efficient and concludes with the destruction of the microorganism ingested. Nevertheless, several pathogens possess various anti-phagocytic strategies, which allow them to survive and escape phagocytes. These strategies can be directed to any step of the phagocytic process. However, most microorganisms interfere with phagosome maturation since the phagolysosome is the most destructive organelle. It is the purpose of this review to highlight the multiple anti-microbial effectors of professional phagocytes and to describe how various microbial pathogens hinder phagocytosis to continue the course of their infection.

INITIATION OF PHAGOCYTOSIS

Microbial Recognition

The first step in phagocytosis is the detection of a microorganism by phagocytes. Microbial pathogens are recognized directly by receptors that bind PAMPs or indirectly by receptors that bind opsonins. Receptors that directly bind PAMPs are known as pattern-recognition receptors and among these receptors, we find lectin-like recognition molecules, such as CD169 and CD33; C-type lectins, such as Dectin-2, Monocyte-INducible C-type LEctin (Mincle), or DNGR-1; scavenger receptors (26), such as scavenger receptor A, which detects lipopolysaccharide (LPS) on some Gram-negative bacteria (27), and on *Neisseria meningitidis* (27); and Dectin-1, which is a receptor for fungal beta-glucan (28, 29). Mannose receptors bind to mannan (30), and CD14 binds to LPS-binding protein (31). Toll-like receptors (TLRs), although recognize microorganisms, do not function as phagocytic receptors (32), however, they can cooperate with other non-opsonic receptors to stimulate phagocytosis (33).

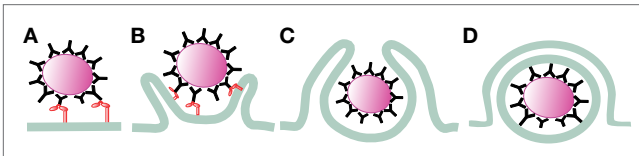


FIGURE 1 | Initiation of phagocytosis. After receptor engagement **(A)** (2), the plasma membrane covers the microorganism to be ingested **(B)** (9, 10) and closes at the distal end **(C)** (11, 12), forming a vacuole where the microorganism is internalized **(D)**.

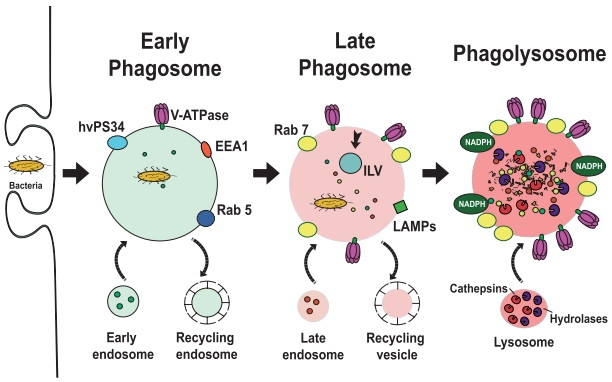


FIGURE 2 | Phagosome maturation. The new phagosome quickly develops the characteristics of early endosomes, through a series of fusion and fission events with sorting and recycling endosomes (5, 6). *The early phagosome* is marked by the presence of the small GTPase Rab5 (13, 14), early endosome antigen 1 (EEA1) (15), and the class III PI-3K human vacuolar protein-sorting 34 (hvPS34) (16). The early phagosome also becomes a little acidic (pH 6.1–6.5) by the action of V-ATPase accumulating on its membrane (17, 18). *The late phagosome* is marked by the presence of Rab7 (19–21) and lysosomal-associated membrane proteins (LAMPs) (22, 23). Proteins that will be recycled are separated in sorting (recycling) vesicles, while proteins intended for degradation are eliminated in intraluminal vesicles (ILVs), directed into the lumen of the phagosome (24). The lumen of the late phagosome gets more acidic (pH 5.5–6.0), due to the action of more V-ATPase molecules on the membrane. *Phagolysosomes* are formed when late phagosomes fuse with lysosomes. Phagolysosomes are acidic (pH 5–5.5) and contain many degradative enzymes, including various cathepsins, proteases, lysozymes, and lipases. Other microbicidal component of the phagosome is the NADPH oxidase that generates reactive oxygen species (25).

Opsonins are soluble molecules that bind to microorganisms, marking them for phagocytosis. Antibody [immunoglobulin (Ig)] molecules and complement components are important opsonins that induce efficient phagocytosis (2). The most studied opsonic phagocytic receptors are the Fc receptors (FcRs), and the complement receptors (CRs), respectively (34). FcγRs bind to the constant (Fc) portion of IgG (35–38), while FcαRs bind IgA antibodies (39). CRs, such as CR3, bind to iC3b deposited on the microorganism after complement activation (40). Crosslinking of FcγR on the surface of cells activates efficient phagocytosis and other effector functions. These effector functions, such as activation of the oxidative burst, cell degranulation, antibody-dependent cell-mediated cytotoxicity, and activation of genes for production of cytokines and chemokines, are aimed toward the destruction of pathogens and the induction of an inflammatory response that is beneficial during infections (37, 41, 42). CRs, such as the integrin $\alpha_M\beta2$ (also known as CD11b/CD18, CR3,

or Mac-1), bind the complement component iC3b deposited on pathogens to promote phagocytosis (34, 43).

Phagosome Formation

After phagocyte receptors engage a microorganism, signaling events are triggered to initiate phagocytosis. Important changes in membrane remodeling and the actin cytoskeleton take place leading to the formation of pseudopods that cover the microorganism. Lipids associate and dissociate from the membrane of phagosomes in an orderly fashion (44), and the small GTPases Rho, Rac, and cell division cycle 42 (Cdc42), which are important regulators of the actin cytoskeleton, get activated and recruited to the forming phagosome (9, 10). At the point of contact, a depression of the membrane (the phagocytic cup) is formed. Then, F-actin polymerization allows formation of pseudopods that surround the target microorganism and within few minutes, the membrane protrusions fuse at the distal end (11, 12, 45) to seal the new phagosome (**Figure 1**).

PHAGOSOME MATURATION

The new phagosome rapidly changes its membrane composition and its contents, to become a microbicidal vacuole, the phagolysosome. This process is known as phagosome maturation. The mechanism for transferring endocytosed material from endosomes to lysosomes is complex and not completely described. Four hypotheses have been proposed to explain the process of phagolysosome formation [reviewed in Ref. (46, 47)]. These include a maturation model where the endosome turns into a lysosome (48), a vesicular transport model where vesicles carry cargo from the endosome to the lysosome (49), a kiss-and-run model where endosomes and lysosomes engage in repeated transient fusions (50) and a direct fusion model where endosomes and lysosomes completely fuse giving rise to a hybrid compartment from which lysosomes reform (51, 52). Experimental evidence suggests that both the kiss-and-run and the complete fusion models contribute to the mechanism for delivery of endocytosed particles to the lysosome (53). The coordinated activities of endosomal sorting complex required for transport, homotypic fusion and vacuole protein sorting, and soluble *N*-ethylmaleimide-sensitive factor-attachment protein receptor protein complexes on the different vesicle membranes are required for efficient delivery of endocytosed macromolecules to lysosomes [reviewed in Ref. (54, 55)]. Phagosome maturation can be divided into three main stages, namely the early phagosome, the late phagosome, and the phagolysosome, as described later.

Early Phagosome

The new phagosome quickly develops the characteristics of early endosomes, through a series of fusion and fission events with endosomes (5, 6). The early phagosome is marked by the presence of the small GTPase Rab5 (13, 14). This membrane GTPase regulates the fusion events between the phagosome and early endosomes by recruiting early endosome antigen 1 (EEA1) (15). Rab5 also recruits the class III PI-3K human vacuolar protein-sorting 34, which in turn, generates phosphatidylinositol 3-phosphate (16). This lipid then promotes recruitment of other proteins involved in phagosome maturation, including Rab7, a marker of late endosomes (19, 20). The early phagosome also becomes a little acidic (pH 6.1–6.5) by the action of V-ATPase accumulating on its membrane and also by transient fusions with more acidic vesicles (56). This V-ATPase translocates protons (H^+) into the lumen of the phagosome using cytosolic ATP as an energy source (17, 18) (**Figure 2**).

Late Phagosome

As maturation continues, Rab5 is lost, and Rab7 appears on the membrane. Rab7 mediates the fusion of the phagosome with late endosomes (21). At the same time, proteins that will be recycled are separated in sorting (recycling) vesicles, while proteins intended for degradation are eliminated in intraluminal vesicles, directed into the lumen of the phagosome (24). Furthermore, the lumen of the late phagosome gets more acidic (pH 5.5–6.0), due to the action of more V-ATPase molecules on the membrane (17) (**Figure 2**). Rab7 also recruits other proteins to the membrane. One such protein is Rab-interacting lysosomal protein (RILP), which brings the phagosome in contact with microtubules (57, 58), and lysosomes (57, 58). In addition, lysosomal-associated membrane proteins (LAMPs) and luminal proteases (cathepsins and hydrolases) are incorporated from fusion with late endosomes (7, 59) (**Figure 2**). LAMPs are a family of heavily glycosylated proteins that accumulate on the lysosomal membrane. They all contain a conserved intracytoplasmic tyrosine-based lysosome-targeting motif YXXφ (where φ represents a bulky hydrophobic residue) that directs the trafficking of the molecule through an endosome/lysosome pathway (60). LAMPs are fundamental in regulating membrane fusion events (61) and are required for fusion of lysosomes with phagosomes (22, 23).

Phagolysosome

The late phagosomes gradually fuse with lysosomes, to become phagolysosomes, the definitive microbicidal organelles (**Figure 2**) (47, 53, 62). Phagolysosomes possess many sophisticated mechanisms directed to eliminate and degrade microorganisms. They are acidic (pH 5–5.5) thanks to the large number of V-ATPase molecules on their membrane (18) and contain many degradative enzymes, including various cathepsins, proteases, lysozymes, and lipases (17). Other microbicidal components of the phagosome are scavenger molecules, such as lactoferrin that sequesters the iron required by some bacteria (63), and the NADPH oxidase that generates superoxide $\left(O_2^-\right)$ (25), and other reactive oxygen species (ROS) (64, 65) (**Figure 2**). Although the low pH is clearly microbicidal, it is important to note that phagosome acidification is highly regulated. The lysosomal pH may cycle between acidic and neutral conditions, allowing for the optimal activity of the different hydrolases (66). Within the hybrid degradative vesicle (phagolysosome) (46), most of these enzymes are active at pH 5–5.5; while in primary lysosomes that function as storage vesicles, the lower pH of 4.5 induces enzyme aggregation and inactivation (66).

ANTIMICROBIAL EFFECTORS

The phagolysosome is the definitive antimicrobial organelle. The arsenal at its disposal is large and complex. The major destructive strategies will be presented next.

pH

The most distinctive characteristic of phagolysosomes is their low pH. During the maturation process, the membrane of the phagosome accumulates more and more active molecules of V-ATPase. The molecular complex of this ATPase translocates protons (H^+) into the lumen of the phagosome using cytosolic ATP as an energy source (17, 18) (**Figure 3**). The acidic content of the phagosome creates an adverse environment for most microorganisms. The low pH disrupts the normal metabolism of many bacteria and fungi and prevents the use of several essential microbial nutrients (67). In addition, the low pH is required for the activation of many hydrolytic enzymes, which will degrade the ingested pathogen. The V-ATPase also favors the generation superoxide (O_2^-) (25) by neutralizing the negative charges generated by the NADPH oxidase and by combining O_2^- with H^+ to generate other ROS (**Figure 3**) (as discussed later).

Reactive Oxygen and Nitrogen Species

In addition to an acid environment, the phagolysosome can concentrate ROS to destroy microorganisms. Production of ROS is achieved by the NADPH oxidase (NOX2) on the membrane of phagosomes (68, 69, 84). The relevance of this antimicrobial mechanism is evident in patients with chronic granulomatous disease, who have mutations that result in malfunction of the NADPH oxidase. These patients suffer from severe recurrent infections that can cause death in many cases (85, 86). The NADPH oxidase is an enzymatic complex formed by two transmembrane proteins, CYBB (cytochrome *b*-245 heavy chain/gp91-phox) and CYBA (cytochrome *b*-245 light chain/p22-phox), that upon activation bring together three cytosolic components: NCF-4 (neutrophil cytosol factor 4/p40-phox), NCF-1 (neutrophil cytosol factor 1/p47-phox), and NCF-2 (neutrophil cytosol factor 2/p67-phox) (69, 87) (**Figure 3**). In addition, Rac1 and Rac2 are also required for efficient activation of the enzyme complex (70, 71). The oxidase transfers electrons from cytosolic NADPH to molecular oxygen to generate O_2^- inside the phagosome (25). In the acid conditions of the phagosome, O_2^- quickly dismutate into H_2O_2, which can then produce hydroxyl radicals (OH^-) by a Fenton reaction (88) catalyzed by iron released from proteins in the phagosome (89). Also, myeloperoxidase can transform H_2O_2 into hypochlorous acid and chloramines (65) (**Figure 3**). In addition, O_2^- can also react with nitric oxide (NO) to form peroxynitrite ($ONOO^-$), both of which are highly reactive agents. The various forms of ROS are together efficient antimicrobial agents because they can damage proteins, lipids, and DNA of microorganisms in the phagosome (89).

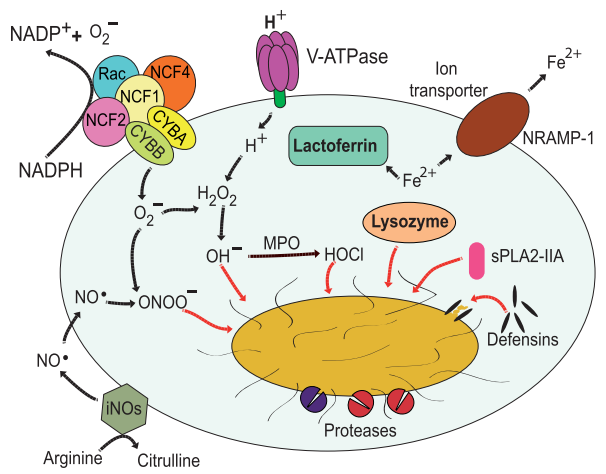


FIGURE 3 | Antimicrobial effectors inside the phagolysosome. The most distinctive characteristic of phagolysosomes is their low pH. The V-ATPase translocates protons (H^+) into the lumen of the phagosome (17, 18). The NADPH oxidase is an enzymatic complex formed by two transmembrane proteins, such as CYBB and CYBA, and three cytosolic components: NCF-4, NCF-1, and NCF-2 (68, 69). Rac is also required for efficient activation of the enzyme complex (70, 71). Myeloperoxidase (MPO) can transform H_2O_2 into hypochlorous acid (65). Nitric oxide radicals ($NO^·$) are produced by the inducible nitric oxide synthase 2 (iNOS) (72), and $NO^·$ reacts with O_2^- to form peroxynitrite ($ONOO^-$) (73, 74). Lactoferrin captures Fe^{2+} that is essential for bacterial growth (75), and the transporter natural resistance-associated macrophage protein 1 (NRAMP-1) takes Fe^{2+} out of the phagosome (76). Defensins are antimicrobial peptides that form multimeric ion-permeable channels on bacteria (77, 78). Cathepsins are lysosomal proteases (79, 80). Lysozyme (81, 82) degrades peptidoglycan, a primary building block of the cell wall of bacteria, and the type IIA secreted phospholipase A2 (sPLA2-IIA) (83) degrades anionic phospholipids such as phosphatidylglycerol, the main phospholipid component of bacterial membranes.

In addition to ROS, phagocytes, such as macrophages, can also generate nitrogen-based radicals or reactive nitrogen species (RNS) that contribute to microbial destruction. Nitric oxide radicals ($NO^·$) are produced by the inducible nitric oxide synthase 2 (iNOS or NOS2) (72). This enzyme is not present in the resting phagocyte and is only produced in response to proinflammatory agonists (90). NOS2 catalyzes the conversion of L-arginine and oxygen into L-citrulline and $NO^·$ (**Figure 3**). Contrary to O_2^-, $NO^·$ is produced on the cytoplasmic side of phagosomes, but it can diffuse across membranes and accumulate inside the phagosome (91). As mentioned earlier, once inside the phagosome, $NO^·$ can react with O_2^- to generate the highly toxic peroxynitrite ($ONOO^-$) that can alter proteins and DNA of ingested microorganisms (73, 74). Also, $NO^·$ can directly impair bacterial enzymes and affect microbial growth (92).

Nutrient Capture

Not only the low pH and the oxidative conditions are used to harm the ingested pathogen but also a series of enzymes and peptides are delivered into the phagosome to limit its growth. Microbial growth can be limited by reducing the amount of essential nutrients inside the phagosome. Nutrients are eliminated from the phagosome by special capture molecules delivered into the phagosome or by transporters present on the phagosome membrane. Perhaps, lactoferrin is the best characterized capture molecule that prevents growth of some bacteria (75). Lactoferrin is a non-heme Fe^{2+}-binding glycoprotein present in the specific granules of neutrophils (93), and it can be delivered into the phagolysosome. In there, lactofferin captures Fe^{2+} that is essential for bacterial growth (75, 94) (**Figure 3**). Other metals, such as Mn^{2+}, are also important for microbial growth. Thus, during maturation, phagosomes become gradually depleted of Fe^{2+} and Mn^{2+} by the action the transporter natural resistance-associated

macrophage protein 1 (NRAMP-1; also known as SlC11A1) (76) (**Figure 3**). NRAMP-1 is a membrane protein present on phagolysosomes that transports divalent cations, such as Fe^{2+}, Zn^{2+}, and Mn^{2+} out of the phagolysosome. This transporter requires H^+ ions to function, thus NRAMP-1 is more efficient in the acid environment of the phagolysosome (76). Removal of these metal ions prevents microbial growth. However, some microorganisms present a mechanism to counteract the phagocyte function and retain these nutrients (see next section). Microorganisms secrete siderophores, specialized molecules that capture Fe^{2+} and target it for pathogen use (95). The phagocyte in turn presents yet another strategy to control microbial growth. The phagocyte protein lipocalin binds selectively catechol type siderophores expressed by some bacteria, such as *Escherichia coli* and *Mycobacterium tuberculosis*. Consequently, the Fe^{2+}-loaded siderophore is still sequestered from the bacteria (96, 97).

Microorganism Destruction

As described earlier, the phagolysosome interior is an inhospitable environment for most microorganisms. Enzymes and peptides delivered to the phagolysosome have potent antimicrobial effects by destroying the different components of the microbial cell.

Antimicrobial peptides are small (<10 kDa), cationic, and amphipathic polypeptides, often broadly classified based on structure (82, 98). In phagocytes, the main types include defensins (disulfide-stabilized peptides) (77, 78) and cathelicidins (α-helical or extended peptides) (99). Defensins are subdivided into α and β groups and are stored in primary granules of neutrophils. These peptides disrupt the integrity of pathogens by attaching to negatively charged molecules on their membrane. Defensins form multimeric ion-permeable channels that cause membrane permeabilization on both Gram-positive and Gram-negative bacteria (100) (**Figure 3**). Cathelicidins are stored in secondary granules of neutrophils as inactive precursors. They are then converted into active antimicrobial peptides in the lumen of the phagosome by elastase (99), a primary granule enzyme (93). Active cathelicidins permeabilize the cell wall and inner membrane of Gram-positive bacteria (100). In particular, the cathelicidin LL-37 (hCAP) has drawn particular attention because of its multiple functions. Not only LL-37 works as a broad-spectrum antibiotic but also it has potent chemotactic and immunomodulatory properties (101). Neutrophil-produced LL-37 can be internalized by macrophages (102) and can induce phagocytosis of IgG-opsonized Gram-negative and Gram-positive bacteria by these phagocytes (103). LL-37 also promotes leukotriene B4 and thromboxane A2 generation by human monocyte-derived macrophages (104), thus regulating the inflammation response during infections. Recently, it was also found that macrophages could also produce LL-37. Mice deficient in the Cramp (cathelicidin-related antimicrobial peptide) gene, the murine functional homolog of human LL-37, had increased susceptibility to *M. tuberculosis*; and macrophages from these mice were unable to control *M. tuberculosis* growth in an *in vitro* infection model (105).

Among the many degradative enzymes, the cathepsins are perhaps the most extensively characterized group of lysosomal proteases. These are cysteine proteases that play a direct role in microbial killing by inducing the disruption of bacterial membranes (**Figure 3**). For example, cathepsins L and K were found to be involved in phagocytosis and non-oxidative killing of *Staphylococcus aureus* (80), while cathepsin D controlled *Listeria monocytogenes* intracellular growth (79), probably by degrading the pore-forming toxin listeriolysin O of *L. monocytogenes* and thus preventing bacterial escape from the phagosome (see next section).

The phagolysosome also contains many lysosomal hydrolases, which help destroy ingested pathogens (106). An important enzyme of this group is lysozyme, an antibacterial protein that can be expressed and secreted by several cell types (81, 82). Lysozyme degrades peptidoglycan, a primary building block of the cell wall of bacteria (**Figure 3**). By breaking the bonds between *N*-acetylmuramic acid and *N*-acetyl-D-glucosamine, lysozyme disrupts the peptidoglycan integrity (107), and then other enzymes can complete the lysis of bacterial cells. One such enzyme is the type IIA secreted phospholipase A2 (sPLA2-IIA) (**Figure 3**), which exhibits potent antimicrobial activity against Gram-positive and Gram-negative bacteria (83). This remarkable property is due to the unique preference of sPLA2-IIA for anionic phospholipids such as phosphatidylglycerol, the main phospholipid component of bacterial membranes. The importance of this mechanism is highlighted by the fact that transgenic mice overexpressing human sPLA2-IIA are resistant to infection by *S. aureus*, *E. coli*, and *Bacillus anthracis*, the etiological agent of anthrax (83). Thus, antimicrobial peptides and degradative enzymes work together in the lumen of the phagolysosome to completely degrade most phagocytized microorganisms (**Figure 3**).

MICROBIAL CONTROL OF PHAGOCYTOSIS

The discussion presented earlier clearly shows that phagocytosis is an efficient process (1, 2, 4, 108, 109) that culminates with the generation of the phagolysosome and its very harsh environment for most microorganisms (6). Therefore, it is not surprising that many successful pathogens have evolved multiple strategies to prevent and/or inhibit phagocytosis (110, 111). These strategies include prevention of phagocytosis, interference of phagosome maturation, resistance to phagolysosome contents, and even physical escape from the phagosome. Our knowledge comes mainly from studies of important extracellular and intracellular pathogens, such as *S. aureus* (112–114), *M. tuberculosis* (115–117), and *L. monocytogenes* (118, 119). However, many other microbial pathogens also have tactics for interfering with phagocytosis. The mechanisms for controlling phagocytosis employed by these model pathogens, as we understand them today, will be described next. In addition, information available on microbial control of phagocytosis by some other pathogens will also be presented.

Prevention of Phagocytosis

The best way to escape from the destructive power of phagocytosis would be just to prevent ingestion by phagocytes from happening. Some pathogens try just to do that by producing substances that extracellularly intoxicate phagocytes. *S. aureus* can secrete various membrane damaging toxins that will

cause cell lysis and death. These toxins include the leukocidins (120) (named this way because they can kill leukocytes) and α-hemolysin (121) (**Figure 4**). Although there are different leukocidins, they all are dimer proteins (e.g., LukAB, LukED, HlgAB, HlgCB, and LukSF-PV) that induce membrane permeability by the formation of octameric β-barrel pores on the cell membrane (120, 122, 123). Interestingly, leukocidins do not attack any membrane indiscriminately. They must bind first to specific membrane receptors, and therefore, only cells with these receptors are targeted for intoxication (124, 125). For example, LukE binds to the chemokine receptor CCR5 on macrophages, marking these cells for lysis by the active leukocidin LukED (124, 126). Similarly, LukA binds only to the CD11b subunit of the CR Mac-1, which is expressed on both macrophages and neutrophils (125) (**Figure 4**). The α-hemolysin is another toxin from *S. aureus* that also forms pores on the membrane of macrophages. It uses phagocyte protein ADAM10 (a disintegrin and metalloproteinase domain-containing protein 10) as a receptor (127, 128), and then it assembles into a β-barrel pore of seven identical monomers across the cell membrane (129, 130) (**Figure 4**).

Phagocytosis is most efficient when microorganisms have been opsonized by antibodies or complement. Microorganisms have also evolved mechanisms to prevent opsonization. The first strategy displayed by *S. aureus* to block opsonization is simply to degrade opsonins. Some staphylococcal proteases seem capable of directly attacking opsonins. However, a more efficient instrument for this function is the protein staphylokinase, a bacterial plasminogen activator that converts host plasminogen to the active serine protease plasmin. Activated plasmin can then degrade IgG or C3b on the bacterial surface (139) (**Figure 4**). Another mechanism is to capture the opsonin, so that it does not bind to the bacteria. *S. aureus* Protein A is a well-known protein expressed on the bacterial cell wall. Protein A specifically binds to the Fc region of IgG, preventing the antibody from engaging FcγRs. In consequence, phagocytosis is effectively blocked (131) (**Figure 4**). In addition, Protein A can obstruct complement activation by the classical pathway, since the Fc portion of IgG is no longer accessible to the complement component C1q. This will result in less deposition of C3b on the bacteria (140). In addition to Protein A, most *S. aureus* strains express the Staphylococcal binder of IgG (Sbi) protein, which also binds to the Fc portion of IgG (132–134) (**Figure 4**). Inhibition of complement activation is an important strategy also used by *Staphylococcus*. The secreted metalloprotease aureolysin functions as an effective C3 convertase. Aureolysin cuts C3 in the α-chain at a different cleavage site from the C3 convertase, leaving C3a′ and C3b′ fragments (135). Unfortunately, the aureolysin-generated C3b′ fragment is rapidly degraded and not deposited on the bacteria (**Figure 4**). In addition, the staphylococcal complement inhibitor, a 10-kDa protein, can inhibit complement activation and efficiently prevent phagocytosis and killing of staphylococci (136) (**Figure 4**). As if all this were not enough, *S. aureus* can also hide the C3b deposited on its surface. The bacteria secrete the extracellular fibrinogen binding protein (Efb), which binds the serum protein fibrinogen (137). In this way, the bacterium creates a proteinaceous shield that covers the surface bound opsonin and prevents phagocytosis (137, 138) (**Figure 4**). This impressive array of anti-phagocytic effectors has been described for individual molecules. However, there is not enough information on when and how bacteria decide to use each one of them. The external elements that regulate the expression of each factor are not known. Novel techniques, such as expression profiling, should bring new light into these topics, as discussed later.

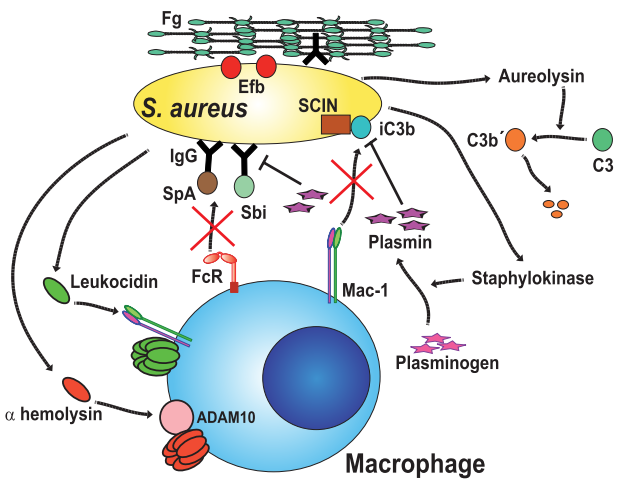


FIGURE 4 | *Staphylococcus aureus* blocks opsonic phagocytosis. *S. aureus* secrete toxins, leukocidins (120, 125) and α-hemolysin (121), which induce membrane permeability by forming pores on the cell membrane. To be fully active, leukocidin A binds to the complement receptor Mac-1 (125), while α-hemolysin binds to protein ADAM10 (a disintegrin and metalloproteinase domain-containing protein 10) (127, 128). Staphylokinase converts host plasminogen to the active serine protease plasmin, which in turn degrades IgG or iC3b on the bacteria (127, 129). Protein A (SpA) (131) and staphylococcal binder of IgG (Sbi) protein specifically bind to the Fc region of IgG (132–134), blocking Fc receptor (FcR) engagement and activation. Aureolysin functions as a C3 convertase, leaving non-functional C3b′ fragments (135). Also, the staphylococcal complement inhibitor (SCIN) prevents complement activation on the bacteria (136). Finally, the extracellular fibrinogen binding protein (Efb) binds the serum protein fibrinogen (Fg), creating a proteinaceous shield that covers surface-bound opsonins (137, 138).

Another way to prevent ingestion by phagocytes from happening is to inactivate the cell machinery that creates the phagosome around the microorganism. Some pathogens have developed strategies to prevent actin polymerization and thus avoiding phagocytosis (141). The role of the actin cytoskeleton is fundamental for constructing a phagocytic cup and then extending membrane protrusions around the target particle. The small GTPase Rho family (10) controls formation of F-actin fibers required for phagocytosis. The GTPases Rho, Rac1, and Cdc42 act as molecular switches alternating between an active (GTP-bound) state and an inactive (GDP-bound) state (142, 143). For activation, they need to release GDP and replace it with GTP. This action is catalyzed by guanine nucleotide exchange factors (GEFs). Later, GTP is hydrolyzed to GDP returning the GTPase to its inactive state. This last step is enhanced through interactions with GTPase-activating proteins (GAPs). During phagocytosis, these GTPases are activated and recruited to the forming phagosome, where they activate nucleation-promoting factors such as

Wiskott–Aldrich Syndrome protein (WASp) (144). WASp, in turn activates the actin-related protein 2/3 (Arp2/3) complex for actin polymerization (145, 146). As the new actin fibers grow, the plasma membrane is forced out, extending the membrane as pseudopodia around the particle to be ingested. Due to their central role in controlling actin dynamics, these small GTPases are the chosen target of some bacterial toxins. These toxins can alter the activity of the GTPases through covalent modifications or regulation of the nucleotide state. For example, the bacterium *Clostridium difficile*, which causes pseudomembranous colitis and is responsible for many cases of nosocomial antibiotic-associated diarrhea, produces two glycosylating exotoxins. Toxin A and toxin B modify Rho by glycosylation and inactivate its function. Rho inactivation causes disorganization of actin reducing phagocyte cell migration and phagocytosis (147). Similarly, the bacterium *Photorhabdus asymbiotica*, an emerging pathogen in humans, produces a toxin (PaTox) that tyrosine glycosylates Rho causing its inactivation. PaTox actions result in actin disassembly and inhibition of phagocytosis (148).

Another group of bacterial toxins regulate the nucleotide state and thus the function of the GTPases by functioning as GAPs or GEFs. For example, the enteropathogenic bacteria *Yersinia* spp. have type III secretion systems that inject Rho GAP toxins into cells. One such toxin (virulence factor) is YopO, which prevents Rac activation and in consequence prevents phagocytosis (149). Similarly, the Gram-negative bacteria *Pseudomonas aeruginosa*, an opportunistic pathogen that causes life-threatening infections in cystic fibrosis patients, burn victims, and immunosuppressed individuals, produces the type III virulence factor ExoS that is injected into cells. ExoS is a Rho GAP for Rho, Rac, and Cdc42 that causes the reorganization of the actin cytoskeleton by inhibition of Rac and Cdc42, and actin stress fiber formation by inhibition of Rho (150). An additional example recently described of pathogens disrupting Rho GTPase function comes from the opportunistic bacteria *Burkholderia cenocepacia* that has a propensity to infect cystic fibrosis patients. *B. cenocepacia* was shown to disrupt Rac and Cdc42 activation through perturbation of GEF function. Inactive Rac and Cdc42 led to inhibition of phagocyte function (151).

Besides bacteria, several fungal pathogens also display mechanisms for evading phagocytosis. *Candida albicans*, a commensal ascomycete, is part of the normal microbiota associated with mucosal tissues. It causes opportunistic infections, known as thrush, on superficial mucosas, and systemic infections, named candidiasis. *C. albicans* is normally phagocytized by macrophages, but it can decrease being recognized by phagocytes with a thick cell wall. The cell wall antigen, β-glucan is hidden among mannoproteins, thus reducing phagocytosis (152). In addition, *C. albicans* can limit phagocyte chemotaxis during transition from the yeast to the hyphal forms (153). Another fungus, *Aspergillus fumigatus*, also can mask antigenic proteins and carbohydrates to avoid recognition by phagocytes. RodA hydrophobin is a hydrophobic protein expressed on the surface of *A. fumigatus* conidia. This hydrophobin efficiently prevents recognition and phagocytosis (154). Similarly, the yeast basidiomycete *Cryptococcus neoformans* can also avoid recognition by macrophages. The basidiospores of *C. neoformans* produce a polysaccharide coat (capsule) that forms a thick barrier from phagocytes (155). This capsule can also be shed to prevent macrophage detection and phagocytosis (155). In addition, *C. neoformans* secretes antiphagocytic protein 1, a protein that binds to CR Mac-1 and inhibits phagocytosis (156).

Interference with Phagosome Maturation

Once a microorganism is ingested, it will be exposed to the very harsh environment of the phagolysosome. Thus, many pathogens present strategies directed to avoid the formation of this final antimicrobial organelle. Phagosome maturation can be blocked at different points and there are examples of pathogens blocking acidification, reducing activation of the NADPH oxidase, and preventing phagosome to lysosome fusion. Perhaps the most studied example of inhibition of phagosome maturation occurs in *M. tuberculosis*. The first report was published more than 40 years ago (157), and since then several mycobacterial factors interfering with the process have been found, such as mannose-capped lipoarabinomannan (ManLAM), phosphatidyl-*myo*-inositol-mannosides (PIMs) (115, 158, 159), and trehalose-6,6′-dimycolate (TDM) (160).

As mentioned earlier, one of the earlier features of phagosome maturation is the rapid and gradual acidification of the phagosome. The number of V-ATPase molecules increases on the phagosome membrane as the maturation process takes place. The low pH directly affects many pathogens (67), and it is also required for the activation of many hydrolytic enzymes. In the case of *M. tuberculosis*, acidification is inhibited by preventing the accumulation of V-ATPase on the phagosome membrane (161) (**Figure 5**). Although the complete mechanism is unknown, the *M. tuberculosis* secreted protein tyrosine phosphatase (PtpA) plays an important role. PtpA binds to subunit H of the macrophage vacuolar V-ATPase (162), and then it dephosphorylates human vacuolar protein sorting 33B (VPS33B) (163), leading to subsequent exclusion of the V-ATPase from the phagosome (**Figure 5**).

The Gram-positive bacteria *Streptococcus pyogenes* blocks the V-ATPase activity through expression of surface proteins regulated by the virulence factor Mga (a transcription factor) (181). Similarly, *Rhodococcus equi*, Gram-positive bacteria that cause severe pneumonia in horses, and the dimorphic fungus *Histoplasma capsulatum* are also able to maintain a non-acidic phagosome by excluding the V-ATPase (182, 183) (**Figure 6**). Other pathogens can avoid acidification of phagosomes, including *Yersenia pestis*, the Gram-negative bacteria causing bubonic plague (184), and *C. albicans* (185), by mechanisms not completely described.

Phagosome maturation is also inhibited by interfering with the proper accumulation of molecules responsible for vesicle fusion, thus keeping the new phagosome with characteristics of an early phagosome. *M. tuberculosis* blocks phagosome maturation at a stage between the expression of Rab5 and Rab7, by preventing the delivery of the molecule EEA1 to the membrane (165) (**Figure 5**). This effect is mediated in part by the action of nucleoside diphosphate kinase (Ndk), which exhibits GAP activity toward Rab5 and Rab7. Ndk inactivates both Rab5 and Rab7 thus preventing

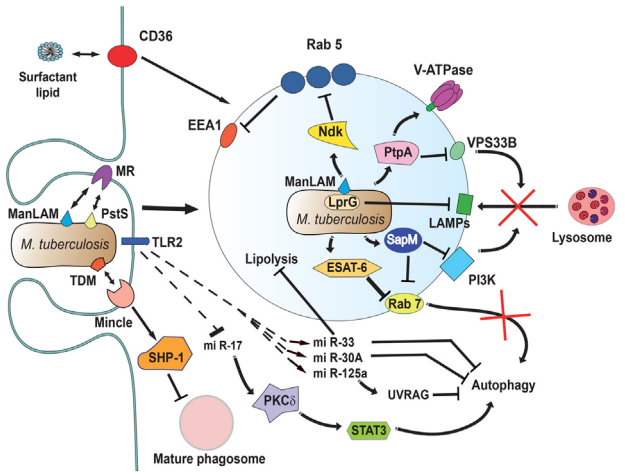


FIGURE 5 | *Mycobacterium tuberculosis* interferes with phagosome maturation. *M. tuberculosis* inhibits acidification by preventing the accumulation of V-ATPase on the phagosome membrane (161), in part through the action of protein tyrosine phosphatase (PtpA) (162). PtpA also dephosphorylates human vacuolar protein sorting 33B (VPS33B) leading to the inhibition of phagosome-lysosome fusion (163). The nucleoside diphosphate kinase (Ndk) is a GAP for Rab5, and by inactivating this GTPase (164), it prevents recruitment of early endosome antigen 1 (EEA1) to the membrane (165). The lipoprotein LprG increases the surface-expression of mannose-capped lipoarabinomannan (ManLAM) (166) and can directly bind to lysosomal-associated membrane proteins (LAMPs) to modulate the traffic machinery of the cell (167, 168). Also, ManLAM (169) and the adhesin PstS-1 (170) bind the mannose receptor, which is involved in the lysosome fusion machinery by an unknown mechanism (171). The mycobacterial glycolipid TDM binds the receptor Monocyte-INducible C-type LEctin (Mincle) (172), activating the SH2-domain-containing inositol polyphosphate 5′ phosphatase (SHP-1) to interfere with phagosome maturation (160). The virulence factor early secretory antigenic target-6 (ESAT-6) inhibits recruitment of Rab7 to the phagosome membrane, preventing autophagy-mediated degradation (173). Also, the secretory acid phosphatase (SapM) direct binds to Rab7 (174) and prevents autophagosome-lysosome fusion (174). In addition, SapM can block the effects of phosphotidylinositol 3-kinase (PI3K) present on phagosomes (158). Upon infection, mycobacteria induce upregulation of several microRNAs (miRNAs) (175–177) and downregulation of others (178) to block autophagy. miR-125a targets UV radiation resistance-associated gene (UVRAG) (176) to block autophagy, while miR-17 activates a protein kinase Cδ (PKCδ)/signal transducer and activator of transcription 3 (STAT3) pathway to regulate autophagy (178). The miR-33 also inhibits fatty acid oxidation to support bacterial replication by a mechanism not yet described (177). How *M. tuberculosis* alters cell signaling to control miRNAs is not known, but the initial signal might come from TLR2 (176, 179). Finally, the scavenger receptor CD36 participates in surfactant lipid uptake by alveolar macrophages, and *M. tuberculosis* exploits this function for growth (180).

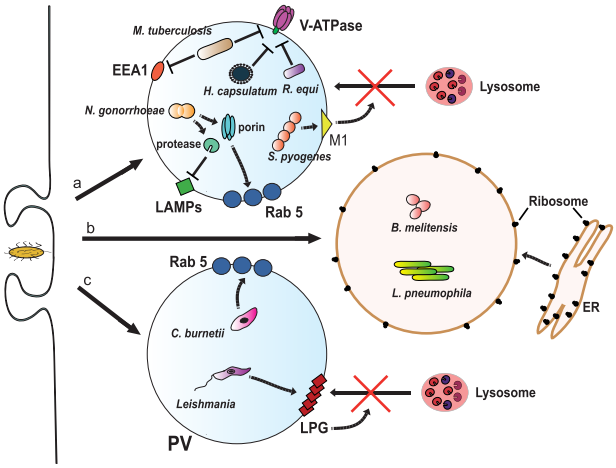


FIGURE 6 | Inhibition of phagosome maturation. (a) Several pathogens, such as *Mycobacterium tuberculosis* (161), *Histoplasma capsulatum* (182), and *Rhodococcus equi* (183) inhibit acidification by preventing the accumulation of V-ATPase on the phagosome membrane. *M. tuberculosis* also blocks early endosome antigen 1 (EEA1) on the membrane (165), while *Neisseria gonorrhoeae* express a porin that induces large amounts of Rab5 (186) and also proteases that digest lysosomal-associated membrane proteins (LAMPs) (187). Another bacteria, *Streptococcus pyogenes*, express the virulence factor M1, which regulates vesicle trafficking (188). Each of these actions effectively will block lysosome fusion to the phagosome. (b) Other pathogens, such as *Legionella pneumophila* (189, 190) and *Brucella melitensis* (191), induce the rapid association of the phagosome with the endoplasmic reticulum (ER). (c) The bacteria *Coxiella burnetti* (192, 193), and the parasite *Leishmania* reside inside a phagolysosome-like vesicle known as parasitophorous vacuole (PV) that concentrates Rab5 on the membrane. *Leishmania* promastigotes also insert lipophosphoglycan (LPG) into the phagosome membrane (194). These actions, in consequence, prevent lysosome fusion (195).

recruitment of their respective effectors EEA1 and RILP and in consequence inhibits phagosome maturation and fusion with lysosomes (164) (**Figure 5**). This blockage also involves ManLAM (171), and it seems to require binding of ManLAM to the mannose receptor (169). Recently, the adhesin PstS-1, a 38-kDa mannosylated glycolipoprotein, was also found to bind the mannose receptor (170) (**Figure 5**). The connection between the mannose receptor and the lysosome fusion machinery is obscure. Because, capping of the ManLAM with mannose receptor was necessary during phagocytosis to maintain the blockade (169), it seems that the initial engagement of the mannose receptor directs, in an unclear manner, *M. tuberculosis* to a selective initial phagosomal niche, where other molecules can be excluded. Also, Mincle was recently identified as a receptor for the mycobacterial glycolipid TDM (172). Recruitment of Mincle by TDM coupled to IgG-opsonized beads during FcγR-mediated phagocytosis interfered with phagosome maturation (160). This inhibition involved the SH2-domain-containing inositol polyphosphate 5′ phosphatase (SHP-1) and the FcγRIIb (160), strongly suggesting an inhibitory downstream signaling of Mincle during phagosome formation (**Figure 5**). Without EEA1, delivery of the V-ATPase or enzymes such as cathepsin D does not take place (196). Therefore, the *M. tuberculosis*-containing phagosome is kept with a pathogen-friendly environment (**Figure 5**). Other microorganisms can also arrest phagosome maturation at early stages. For example, the Gram-negative bacteria *Neisseria gonorrhoeae* express a porin that induces phagosomes to keep larger amounts of Rab5 and low levels of Rab7 (186) (**Figure 6**). In addition, this bacterium also secretes proteases that digest LAMPs (187) (**Figure 6**). As mentioned earlier, LAMPs are fundamental for fusion of lysosomes to phagosomes (22), thus its degradation prevents formation of a mature phagolysosome (187). Similarly, the Gram-negative bacteria *Legionella pneumophila* intercepts vesicular traffic from

endoplasmic reticulum (ER) (189) to create an organelle that allows the bacteria to have access to cysteine for survival (190) (**Figure 6**). This bacterium is the cause of Legionnaires' disease, a severe form of pneumonia. When the bacteria are phagocytized, the phagosome is rapidly associated with mitochondria and the rough ER, thus getting decorated with ribosomes (197). This effect seems to be mediated by DotA, a bacterial product that is part of the type IV secretion system (T4SS) transporter. T4SS exports various bacterial effector proteins, including RalF, a GEF for the phagocyte ADP-ribosylation factor (ARF1) (198). Active ARF1 promotes vesicle traffic between the ER and the Golgi (199). Therefore, the ER-like phagosome does not get acidic and it does not fuse with lysosomes. Another example of phagosomes fusing with the ER is found in the Gram-negative bacteria *Brucella melitensis* (**Figure 6**). This bacterium is the etiological agent of brucellosis, a zoonotic infection that can cause muscle pain, fever, weight loss, and fatigue in people, but can also induce abortion and infertility in animals. In the macrophage cell line J774, *B. melitensis* alters vesicle trafficking (200) to create a modified phagosome known as a *Brucella*-containing vacuole (BCV) that fuses with the ER (191) (**Figure 6**). The mechanism for creating a BCV is not completely known, but it involves several virulence factors such as VirB, an element of the bacterial type III secretion system (191), and cyclic β-1,2-glucan, a cell wall component (201).

Since the phagolysosome is the most harmful organelle for microorganisms, many pathogens have mechanisms to prevent fusion of lysosomes with the phagosome. The best-known example is again *M. tuberculosis* that avoids lysosome fusion by maintaining an early phagosome (115) (**Figure 5**). The mechanism for this effect is multifactorial and complex. We only have a partial understanding of it with the identification of some key virulent factors involved. One such virulent factor is the lipoprotein LprG, which binds to lipoglycans, such as lipoarabinomannan (LAM), increasing the surface expression of LAM (166). A *M. tuberculosis* null mutant for LprG (Mtb ΔlprG) had lower levels of surface-exposed LAM and impaired phagosome–lysosome fusion (167). How LprG prevents phagosome–lysosome fusion is only partially known. It is possible that its effect is indirect *via* Ndk, which inactivates both Rab5 and Rab7 (164), or is direct by binding to LAMP-3 and modulating the traffic machinery in the host cell (168) (**Figure 5**). One more virulent factor is PtpA which, as mentioned earlier, dephosphorylates VPS33B, a regulator of membrane fusion events and leads to inhibition of phagosome–lysosome fusion (163) (**Figure 5**). Another way *M. tuberculosis* prevents phagosome–lysosome fusion involves inhibition of Rab7 recruitment to prevent autophagy-mediated degradation. The maturation of mycobacteria-containing autophagosomes into autolysosomes requires recruitment of Rab7, but this is blocked by the virulence factor early secretory antigenic target-6 (ESAT-6) (173) (**Figure 5**). Again, the molecular events for this blockage are not known. However, for another virulence factor of *M. tuberculosis*, the secretory acid phosphatase (SapM) the inhibition of autophagosome-lysosome fusion (202) is achieved *via* direct binding to Rab7 (174). Molecularly, Rab7 is blocked by SapM through its cytoplasmic domain preventing its involvement in autophagosome–lysosome fusion (174) (**Figure 5**). In addition, SapM is known to dephosphorylate phosphotidylinositol 3-phosphate present on phagosomes (158). This phospholipid is also required for membrane fusion events, thus SapM also prevents lysosome fusion in this manner (**Figure 5**).

Mycobacterium tuberculosis has also evolved other ways to prevent autophagy from happening. One recently described way is the activation or inhibition of cell host microRNAs (miRNAs). Upon infection, macrophages increased several miRNAs and inhibited pathways involved in autophagy. These miRNAs include miR-30A (175), miR-33 (177), and miR-125a (176) (**Figure 5**). At the same time, another miRNA, miR-17, is downregulated with the same result, blockage of autophagy (178). The signaling pathways affected by these miRNAs are only beginning to be described. For example, miR-125a targets UV radiation resistance-associated gene (UVRAG) (176) to block autophagy, while miR-17 activates a PKCδ/STAT3 pathway to regulate autophagy (178). Thus, inhibition of miR-17 leads also to reduce autophagy (**Figure 5**). How *M. tuberculosis* usurps cell host signaling pathways to alter expression of these miRNAs is not known. It seems, however, that the initial signal for this comes from TLRs (176) (**Figure 5**).

Similarly, *S. pyogenes* can also prevent lysosome fusion by expressing the virulence factor M1, which regulates vesicle trafficking (188) (**Figure 6**). M1 can also inhibit activation of the nuclear factor κB and in consequence reduce the macrophage inflammatory response (188). The Gram-negative bacteria *Coxiella burnetti*, the causative agent of Q fever, resides inside a large phagolysosome-like vesicle known as parasitophorous vacuole (192). This modified phagosome concentrates Rab5 on the membrane and avoids lysosome fusion (193) (**Figure 6**). The fungi *A. fumigatus* (203) and the parasitic protozoa *Leishmania* (204) seem also able to avoid being killed by macrophages by preventing fusion between phagosomes and lysosomes. In the case of *A. fumigatus*, the molecule dihydroxynaphthalene–melanin on the surface of the pathogen has been reported as responsible for altering vesicle fusion events (205). For *Leishmania*, the promastigote is efficiently internalized by receptor-mediated phagocytosis (204). Complement and mannose receptors participate in macrophage ingestion (195). Once internalized, promastigotes insert lipophosphoglycan (LPG) into the phagosome membrane. LPG inhibits depolymetization of F-actin (194), and in consequence prevents lysosome fusion (195) (**Figure 6**). This allows enough time for the promastigote to transform into the other life-cycle form, the amastigote, which can then replicate inside the phagosome.

Resistance to Phagolysosome Contents

In addition to preventing phagolysosome formation, pathogens also possess various mechanisms to resist the microbial components found in the phagolysosome lumen. A prominent example is *S. aureus* that can resist the lytic effect of lysozyme on the cell wall peptidoglycan. These bacteria express the enzyme *O*-acetyltransferase A (OatA), which causes O-acetylation of the peptidoglycan. This modification makes the peptidoglycan resistant to the muramidase activity of lysozyme (206, 207) (**Figure 7**). *S. aureus* also can block the action of antimicrobial peptides. First, the enzyme staphylokinase directly binds α-defensins, blocking almost completely their bactericidal effect (208) (**Figure 7**).

Second, bacteria alter the composition of its membrane. Phosphatidylglycerol is modified with L-lysine, causing a reduction in the negative charge of the membrane (209). In addition, the cell wall is also modified by incorporation of teichoic acids and lipoteichoic acids (210), making it more positively charged. These modifications reduce interaction of α-defensins with the bacterial surface. Third, the metalloprotease aureolysin can degrade LL-37, an antimicrobial peptide with potent activity against staphylococci (211) (**Figure 7**).

Also, several pathogens express urease, an enzyme that catalyzes the hydrolysis of urea to form ammonia, resulting in the pH neutralization of the phagosome (**Figure 7**). Important examples of microorganisms using this strategy to survive in the phagosome are *S. aureus* (218), *Helicobacter pylori*, bacteria known for causing gastric and duodenal ulcers (221), *C. neoformans* (222), and *Coccidioides posadasii* (223).

The oxidative environment of the phagolysosome is also very damaging to most microorganisms. Yet, some pathogens have evolved ways to fight back the effects of ROS and RNS. For example, *S. aureus* has the golden pigment staphyloxanthin, which works as an antioxidant and prevents damage from peroxide (212) (**Figure 7**). Also, the protein SOK (surface factor promoting resistance to oxidative killing), that is expressed on the bacteria surface, was recently described as a virulence factor that blocks the effects of ROS (224). In addition, *S. aureus* express the enzymes super oxide dismutases, sodA and sodM, which convert O_2^- into H_2O_2 (213), and the enzyme catalase (KatA), which breaks down H_2O_2 into oxygen and water (214, 215) (**Figure 7**). A phagocytized bacterium has also to prevent the effects of iNOS-derived RNS. *S. aureus* can detect $NO^·$ by the two component system SsrAB (225), which regulates the expression of the gene hmp coding for a flavohemoglobin that functions as an $NO^·$ scavenger (216, 217) (**Figure 7**).

Similarly, *M. tuberculosis* can resist in various ways the microbicidal components within the phagolysosome. A novel glycosylated and surface-localized lipoprotein, Lprl can inhibit the lytic activity of lysozyme (226) (**Figure 8**). Also, at least two proteins have been found to prevent the formation of ROS by inhibiting the NADPH oxidase. The type I NADH dehydrogenase (NDH-1) blocks ROS production to inhibit tumor necrosis factor alpha (TNF-α)-mediated host cell apoptosis (227) (**Figure 8**), while the enhanced intracellular survival (eis) gene product (Eis) abrogates production of both ROS and proinflammatory cytokines leading to arrest in apoptosis. These effects seem to depend on the *N*-acetyltransferase domain of the Eis protein

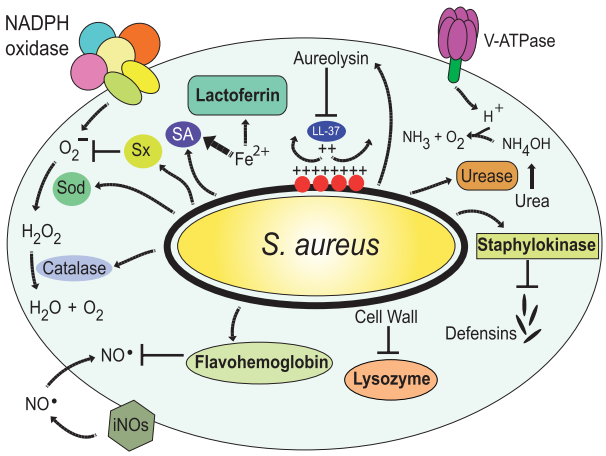


FIGURE 7 | Resistance of *Staphylococcus aureus* to phagolysosome contents. The bacteria *S. aureus* modifies the composition of its cell wall to resist the action of lysozyme (206, 207) and alters the composition of its membrane, with L-lysine and lipoteichoic acids, to reduce the negative charge of the membrane (209, 210); thus resisting antimicrobial peptides, such as the cathelicidin LL-37. Also, it secretes staphylokinase and aureolysin to block α-defensins and LL-37, respectively (208, 211). In addition, *S. aureus* has the golden pigment staphyloxanthin (Sx), which works as an antioxidant (212), two super oxide dismutases (Sod) (213), and a catalase (214, 215) that together protect against reactive oxygen species. In addition, flavohemoglobin functions as an $NO^·$ scavenger (216, 217). The bacterial urease catalyzes the hydrolysis of urea to form ammonia, resulting in pH neutralization (218). Finally, *S. aureus* produces siderophores (SA) (219, 220) that trap enough Fe^{2+} to allow bacterial survival.

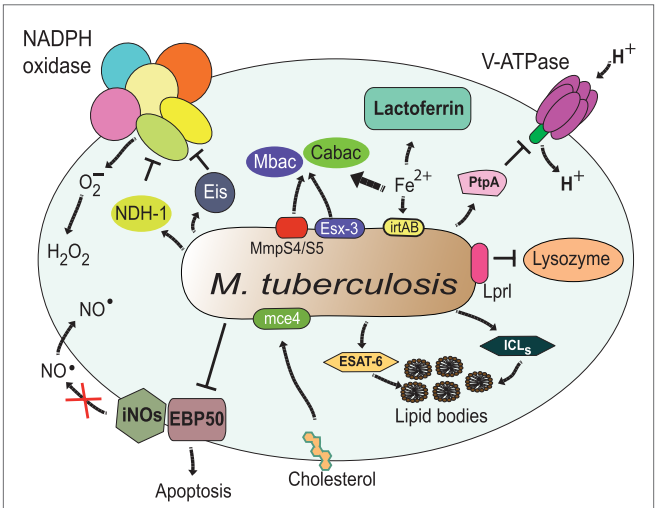


FIGURE 8 | Resistance of *Mycobacterium tuberculosis* to phagolysosome contents. *M. tuberculosis* inhibits acidification by preventing the accumulation of V-ATPase on the phagosome membrane (161), in part through the action of protein tyrosine phosphatase (PtpA) (162). The bacterial lipoprotein, LprI, can inhibit the lytic activity of lysozyme (226). The secretion system Esx-3 (230, 231) and the MmpS4/S5 transporters (232) are required for biosynthesis and secretion of the siderophores mycobactins (Mbac) and carboxymycobactins (Cabac), which seize Fe^{2+} from host proteins, such as lactoferrin (233). Then, the transporter system irtAB takes Fe^{2+} from Fe^{2+}-carboxymycobactin into the bacterium (234, 235). The type I NADH dehydrogenase (NDH-1) (227) and the Eis protein (228) inhibit the NADPH oxidase, preventing formation of ROS. Also, *M. tuberculosis* prevents the generation of $NO^·$ and apoptosis by interfering with EBP50, a scaffolding protein that controls the recruitment of iNOS at the membrane of phagosomes (229). In addition, *M. tuberculosis* alters the phagosome to divert host lipids for its own benefit through mce4, a cholesterol import system (236), and through accumulation of lipid bodies *via* the early secretory antigenic target-6 (ESAT-6) (237). The enzymes isocitrate lyases (ICLs) allow bacteria survival on even (acetate) and odd (propionate) chain fatty acids in lipid bodies (238).

(228) (**Figure 8**). In both cases, apoptosis is inhibited, but the mechanisms are different. In the case of NDH-1, apoptosis is dependent on caspase-3 and caspase-8 (227), while for Eis, apoptosis seems to be caspase independent (228). *M. tuberculosis* can also block RNS by interfering with EBP50, a scaffolding protein that controls the recruitment of iNOS at the membrane of phagosomes in macrophages. Interestingly, overexpression of EBP50 by a recombinant lentivirus had no effect on the iNOS recruitment to *M. tuberculosis*-containing phagosomes, but significantly increased the generation of $NO^{\cdot}$ and the level of apoptosis in macrophages (229). The EBP50-induced apoptosis was $NO^{\cdot}$-dependent and mediated by Bax and caspase-3 (229) (**Figure 8**). The mechanism for iNOS inhibition is not completely elucidated, but it seems to involve both having less iNOS on the membrane and blocking its enzymatic activity. The way *M. tuberculosis* prevents EBP50 functions remains a mystery.

Other pathogens are also known to display similar mechanisms against ROS and RNS. *Streptococcus agalactiae* (Group B *Streptococcus*) is an important cause of pneumonia and meningitis in neonatal humans (239). *S. agalactiae* expresses a superoxide dismutase (SodA), an orange carotenoid pigment, and glutathione. The latter two compounds functions as ROS scavengers (240, 241). *H. pylori* can also express a superoxide dismutase (SodB) (242), a catalase (KatA) (243), and the arginase RocF, which transforms the iNOS substrate arginine into urea (244, 245). Similarly, the yeast *C. albicans* expresses a copper and zinc containing superoxide dismutase (Sod1) (246), and a catalase (Cta1p) (247, 248), while *H. capsulatum* also secretes two catalases, CatB and CatP (249). The fungus *C. neoformans* produces a superoxide dismutase (250) and covers itself in a thick polysaccharide and melanin capsule that absorbs ROS (251). Also, the dimorphic fungus *Blastomyces dermatitidis* seems to be able to inhibit the enzyme iNOS to prevent the production of RNS (252). In all these pathogens, the expression of these enzymes and virulent factors effectively reduces the levels of ROS and RNS within the phagosome. Yet, very little is known about the mechanisms that induce expression of these virulent factors in each pathogen and the molecular details by which they inhibit NADPH oxidase and iNOS enzymes.

Resistance to Nutrient Capture

The phagolysosome is a place where microbial nutrients are eliminated to arrest pathogen growth. As mentioned earlier, divalent cations, such as Fe^{2+}, Zn^{2+}, and Mn^{2+}, are actively transported out of the phagolysosome (76). In response to this, several microorganisms have evolved mechanisms to retain these important nutrients. One strategy to acquire Fe^{2+} relies on the production of siderophores, which are low-molecular weight Fe^{2+}-binding molecules of extremely high affinity, that remove Fe^{2+} from host proteins, such as hemoglobin, and transferrin (233). *S. aureus* produces two citrate-based siderophores, staphyloferrin A (SA) and staphyloferrin B (SB) (219, 220) (**Figure 7**). Together, SA and SB can trap enough Fe^{2+} to allow bacterial survival. These siderophores are very efficient because they avoid detection by the phagocyte siderophore-binding protein lipocalin (96, 97). In addition, *S. aureus* is also able to acquire Mn^{2+} through the action of Mn^{2+} transporters encoded by the bacterial gene loci *mntABC* and *mntH* (253). In *M. tuberculosis*, two groups of siderophores, mycobactins and carboxymycobactins, exist to overcome Fe^{2+} deficiency. The type VII secretion system Esx-3 contributes to siderophore production and release from these bacteria (230, 231) (**Figure 8**). Recently, another siderophore export system was identified in *M. tuberculosis*. The MmpS4 and MmpS5 transporters are required for biosynthesis and secretion of siderophores (**Figure 8**). Because a *M. tuberculosis* mutant lacking the mmpS4 and mmpS5 genes did not grow under low Fe^{2+} conditions and experienced Fe^{2+} starvation even under high-Fe^{2+} conditions, it seems that these transporters are the primary source of siderophores in mycobacteria (232). The importance of siderophore synthesis for Fe^{2+} acquisition is clear, but Fe^{2+} must find a way back into the bacteria. In *M. tuberculosis* an ABC transporter system, irtAB (product of the genes irtA and irtB), has been described for efficient utilization of Fe^{2+} from Fe^{2+} carboxymycobactin (**Figure 8**). Inactivation of the irtAB system decreases the ability of *M. tuberculosis* to survive Fe^{2+}-deficient conditions (234, 235). Similarly, other microorganisms such as *A. fumigatus* (254) and *H. capsulatum* (255) can produce siderophores for Fe^{2+} capture.

Intracellular bacteria have also evolved various means to take nutrients from the host cell. Lipids are important building blocks for bacterial membrane formation and an energy source (256). Upon infection, *M. tuberculosis* alters the phagosome to divert host lipids for its own benefit. A virulent factor was identified within the gene cluster, mce4, because it was specifically required for bacterial survival during prolonged infection. It was found that mce4 encodes a cholesterol import system that enables these bacteria to derive both carbon and energy from this lipid in host membranes (236) (**Figure 8**). Also, mycobacteria-infected macrophages acquire a "foamy" phenotype characterized by the accumulation of lipid bodies, which serve as source of nutrients. This foamy phenotype is caused by bacterial manipulation of host cellular metabolism to divert the glycolytic pathway toward ketone body synthesis (237). This deregulation results in feedback activation of the anti-lipolytic G protein-coupled receptor GPR109A, causing changes in lipid homeostasis and accumulation of lipid bodies in the cell. ESAT-6, a secreted *M. tuberculosis* virulence factor, mediates the enforcement of this feedback loop *via* an unknown mechanism (237) (**Figure 8**). Another strategy used by *M. tuberculosis* to exploit host lipids involves the bacterial enzymes isocitrate lyases (ICLs). These ICLs are catalytically bifunctional isocitrate and methylisocitrate lyases that allow bacteria survival on even (acetate) and odd (propionate) chain fatty acids (238) (**Figure 8**). Moreover, the miR-33 induced by *M. tuberculosis* also inhibited fatty acid oxidation to support bacterial growth by a mechanism not yet described (177) (**Figure 5**). In addition, *M. tuberculosis* has yet another strategy to acquire lipids even from outside the cell in the lung environment. Alveolar macrophages are not only responsible for phagocytosis of these bacteria but also for catabolizing lung surfactant, a lipid–protein complex that lines the alveolar spaces. Recently, it was found that the scavenger receptor CD36 is redistributed to the macrophage cell membrane following exposure to surfactant lipids and participated in surfactant lipid uptake by these cells (180) (**Figure 5**). These macrophages also supported better bacterial growth in a CD36-dependent manner (180). Thus, it seems that

CD36 mediates surfactant lipid uptake by human macrophages and that *M. tuberculosis* exploits this function for growth.

Physical Escape from the Phagosome

In addition to resisting all the microbial effectors within a phagolysosome, several pathogens such as *C. neoformans*, *L. monocytogenes*, or *M. tuberculosis* can also completely escape from it. By getting out of the phagosome, these microorganisms can in the cytoplasm travel to other cell sites and finally leave the host cell.

As mentioned earlier, the fungus *C. neoformans* is well equipped to replicate inside the phagosome. In addition, it can subsequently escape the cell by a non-lytic tactic known as vomocytosis (257, 258). Vomocytosis allows for the pathogen escape leaving the phagocytic cell alive (259). Although the molecular details of vomocytosis are not completely described, the process involves an exocytic fusion of the phagosome with the plasma membrane, thus releasing the fungus (259) (**Figure 9**). Vomocytosis also involves microtubules, but apparently not actin polymerization. Nevertheless, the formation of dynamic actin cages ("actin flashes") around the phagosome is observed in many cases. These actin structures actually prevent vomocytosis. Yet, fungus strains with high rates of vomocytosis induce more actin flashes, suggesting that these flashes are a reaction from the cell to contain the phagosome. Still, at the end, the fungal phagosome is fused with the cell membrane and the pathogen is liberated (259). Also, the secreted phospholipase B1 (PLB_1) is required for vomocytosis (260). It is thought that PLB_1 helps permeabilizing the fungal phagosome to neutralize its lumen and

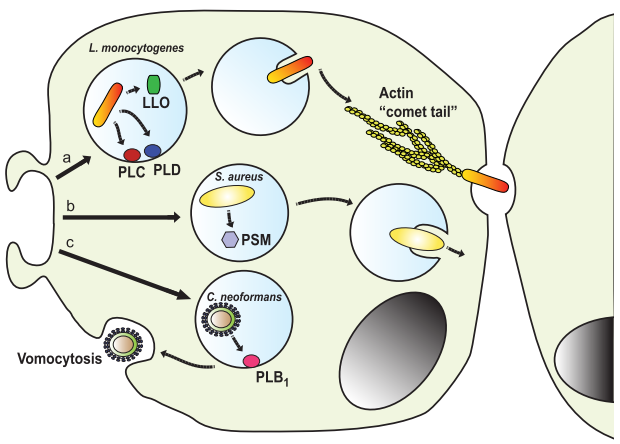


FIGURE 9 | Escape from the phagosome. Several pathogens escape from the phagosome to persist in the less harsh environment of the cytoplasm. (a) The intracellular pathogen *Listeria monocytogenes* uses its virulent factor listeriolysin O (LLO) (264) and phospholipases (PLC and PLD) (265) to escape the phagosome. Once in the cytosol, the bacterium is propelled by the formation of actin "comet tails" that push it across the cell, allowing it to transfer between cells (266–268). (b) *Staphylococcus aureus* can escape from neutrophil phagosomes (269) by producing phenol soluble modulins (PSM), which are peptides with lytic activity toward many mammalian cells (270). (c) The fungus *Cryptococcus neoformans* escapes the cell by vomocytosis (257, 258). Here, the phagosome fuses with the cell membrane with assistance of the secreted phospholipase B1 (PLB_1) (260), leaving the pathogen free and the phagocytic cell alive.

to allow nutrients to come in (111, 261). Although vomocytosis is a unique escape function known only for cryptococci, a similar process has recently been described for *C. albicans* (262) and *Candida krusei* (263).

Another intracellular pathogen capable of escaping from the phagosome and then from the infected cell is *L. monocytogenes* (268). This bacterium uses its virulent factor listeriolysin O (LLO) to escape the phagosome (264) (**Figure 9**). LLO is a pore-forming toxin that permeabilizes the phagosome membrane. It is a potent toxin capable of also degrading the cell membrane, thus its expression and activity are strictly regulated. LLO expression is limited to the intraphagosomal phase of the bacteria, where it is induced by the low pH and high Ca^{2+} conditions of the phagosome (264). Also, LLO activation requires cooperation of host factor such as GILT (γ-inducible lysosomal thiol reductase) (271). In addition, several phospholipases are activated to completely degrade the phagosomal membrane and allow the bacterial escape (265). Once in the cytosol, the bacterium is propelled by the formation of actin tails that push it across the cell. This process is known as "actin rocketing" and it is initiated by the *Listeria* surface protein ActA (266, 267) (**Figure 9**). The actin fibers pushing the bacteria are called "comet tails" and propel the bacteria with enough force, allowing it to transfer between cells (268). In the same way, the Gram-negative bacteria *Shigella flexneri* can disrupt the phagosome membrane and escape into the cytosol (272), where it induces "comet tails" similar to *Listeria*. The bacterial protein IscA induces activation of N-WASp to initiate actin polymerization by the complex Arp2/3 (273). The actin "comet tails" then propel the bacteria across the cytosol and into neighboring cells. Bacteria from the genus *Rickettsia* are obligate intracellular pathogens that can also escape phagosomes. *Rickettsia* uses a secreted phospholipase A2 to disturb the phagosome membrane (274). Once in the cytosol, *Rickettsia* produce actin tails that allow them direct cell to cell transfer. The bacterial protein RickA is able to activate the Arp2/3 complex to initiate actin polymerization (275). Another microorganism that seems capable of phagosome escaping from neutrophils but not macrophages is *S. aureus* (269). These bacteria produce phenol soluble modulins (PSMs), which are peptides with lytic activity toward many mammalian cells (270). In particular, the α-PSM was found to induce a strong destruction of neutrophils after phagocytosis, allowing the escape of the phagocytized bacteria (276) (**Figure 9**).

Other bacteria, such as *M. tuberculosis* (277) and *Mycobacterium marinum* (278), can also escape phagosomes. After escaping the phagosome into the cytosol, *M. marinum* is able to move around by actin-mediated propulsion (279). The *M. marinum* actin tail formation involves activation of WASp proteins (280) and requires a functional region of difference 1 (RD1) loci (281). This RD1 locus encodes for a secretion system called the ESAT-6 system-1 (ESX-1) or type VII secretion system, which can induce pore formation on host-cell membranes (282). Thus, it was thought that all mycobacteria could escape from phagosomes using the pore-forming activity of ESX-1. However, this has to be formally proven experimentally. *M. tuberculosis* could be found in increasing numbers in the cytosol of dendritic cells and macrophages when infection was allowed to proceed beyond 2 days in culture (283), and the presence of cytosolic bacteria was also shown to

occur *in vivo* (284). Therefore, there is no doubt about the capacity of mycobacteria to escape into the cytosol but the significance of this phenomenon is still a matter of debate. A simple idea is that bacteria need to leave the phagosome to replicate and then leave the cell. However, bacilli escape the phagosome at later times of infection and this is followed by cell lysis and release of bacilli (278). In consequence, escaping from the vacuole is not a requirement for either survival or growth of *M. tuberculosis* (285). Instead, it was proposed that the escape from the vacuole represents a transient state that could be critical to the rapid expansion of the bacterial population (285). If this is the case, then escaping from the phagosome is just an important step in the pathology that accompanies progression of tuberculosis infection to active disease. How, mycobacteria kill the cell to allow its release is not clear. Yet, recently, it was reported that the *M. tuberculosis* protein Rv3903c (channel protein with necrosis-inducing toxin, CpnT) is required for survival and cytotoxicity of *M. tuberculosis* in macrophages (286). CpnT consists of an N-terminal channel domain that is used for uptake of nutrients across the outer membrane and a secreted toxic C-terminal domain. This secreted portion is also named tuberculosis-necrotizing toxin (287). It can, in the cytosol of mycobacteria-infected macrophages, hydrolyze the essential coenzyme NAD(+) and induce cell necrosis. However, the mechanism for this cell lysis remains to be elucidated. Clearly, CpnT has a dual function in *M. tuberculosis*. It is used for uptake of nutrients within the phagosome and for induction of host cell lysis in the cytosol. The regulation of CpnT functions becomes then a topic of important research for controlling *M. tuberculosis* infections. Another *M. tuberculosis* virulence factor has also been found to participate in phagosome escape. The unique cell wall lipid phthiocerol dimycocerosates greatly augmented the bacteria escape from its intracellular vacuole (288), by a process not well understood. The mechanism for phagosome lysis is clearly complex as indicated by the fact that host molecules are also recruited by the bacteria to aid in its escape. Activation of host cytosolic phospholipase A2 rapidly led to phagosome lysis for bacteria moving into the cytoplasm of the host cell (116).

NOVEL THERAPEUTIC OPPORTUNITIES

The study of the many mechanisms used by microbial pathogens to control phagocytosis provides opportunity for detecting novel potential targets of clinical intervention. Promising therapeutic approaches will be designed based on our new understanding of the tactics pathogens use to interfere with phagocytosis. For example, studies with miRNA in mycobacteria infections identified TLR2 as a potential target to prevent the blockage of phagosome maturation (179) (**Figure 5**). Recently, it was also found by gene expression profiling of human macrophages treated with glucocorticoids and/or IFN-γ that glucocorticoids, in contrast to IFN-γ, failed to trigger expression and phagolysosome recruitment of V-ATPase (289). This explained the increased risk for mycobacterial infections associated with the use of glucocorticoids. Moreover, this group also found that giving imatinib, a tyrosine kinase inhibitor, to glucocorticoid-treated macrophages induced lysosome acidification and antimicrobial activity without reversing the anti-inflammatory effects of glucocorticoids (289). Thus, an improved therapy would be to administer glucocorticoids together with drugs that induce phagosome acidification. In another recent report, a phagosome maturation assay using confocal microscopy in THP-1-derived macrophages infected with an attenuated *M. tuberculosis* strain was used to test the effects of Saxifragifolin D, a traditional Chinese medicine (290). Saxifragifolin D (a pentacyclic triterpenoid compound first isolated from the rockjasmine *Androsace umbellata*) reduced the inhibition of phagosome maturation. Using assays of this type, new potential drugs can be tested for future therapies.

Another potential therapeutic approach would be to modulate macrophage function to improve their antimicrobial potential against bacterial infections. The feasibility of such an approach has been suggested in a recent report of macrophage phagocytosis of *L. monocytogenes* (291). In this study, the engagement of receptor T cell immunoglobulin mucin-3 (Tim-3) on macrophages inhibited phagocytosis of *L. monocytogenes* by blocking nuclear erythroid 2-related factor 2 (Nrf2) signaling. In contrast, inhibition of Tim-3 augmented phagocytosis (291). Thus, modulating the Tim-3 pathway to alter macrophage function is a promising tool for treating infectious diseases, such as *Listeria* infections.

Phagocytosis of opsonized particles is, in general, more efficient and more efficacious in eliminating microorganisms. The idea to generate opsonizing antibodies for controlling infections is another promising area of opportunity for novel therapeutics. The value of this approach has been suggested in studies where opsonizing antibodies improve elimination of bacteria. In a study with five apparently healthy Indian donors having high titers of serum antibodies against *M. tuberculosis* cell membrane antigens, it was found that phagocytosis and killing of bacilli by the donor macrophages was significantly enhanced following their opsonization with antibody-rich, heat-inactivated autologous sera (292). Another study showed that antibodies directed at the R domain of *S. aureus* secreted coagulase could trigger phagocytosis and killing of staphylococci (293). This coagulase activates host prothrombin and generates fibrin fibers that cover the bacteria and prevent phagocytosis. These antibodies directed the fibrin-covered bacteria to phagocytes and also protected mice against lethal bloodstream infections caused by methicillin-resistant *S. aureus* isolates (293). Yet, another study, showed that a monoclonal antibody (mAb) directed at the Protein A could protect neonatal mice against *S. aureus* sepsis and create protective immunity against subsequent staphylococcal infection (294). A humanized version of this mAb was developed, and it is proposed as a potential new therapy for *S. aureus*-induced sepsis and meningitis in very-low-birth-weight infants (294). These reports encourage the development of novel vaccines that favor the formation of opsonizing antibodies against bacterial antigens to activate phagocyte innate immunity.

FUTURE DIRECTIONS

Phagocytosis is a fundamental biological process (109) that in multicellular organisms is required for proper homeostasis and for fighting infections (1, 2). Therefore, it is not surprising that many microbial pathogens have mechanisms to counteract phagocytosis. As we have discussed here, for some model

pathogens, namely *S. aureus* (295), *M. tuberculosis* (117), and *L. monocytogenes* (119), particular virulence factors that affect phagocytosis have been identified and to some extent the way they work is described. For many other microbial pathogens, their tactics for interfering with phagocytosis are only beginning to be defined. Despite the tremendous amount of published studies on microbial phagocytosis or knowledge on microbial control of this biological process is still incipient and fragmented. We know that some pathogens block phagocytosis at one step or another, but no information is available on how this blockage is accomplished. Some molecules have been identified but their mechanisms of action are not yet described. Future research will serve to fill these gaps and will provide clues on how to improve antimicrobial therapeutics.

An important element for future research is the implementation of novel techniques. Great advances have been achieved by application of proteomics analysis to phagosomes formed under different infection conditions (296). Earlier studies on *M. tuberculosis* phagosomes with high-resolution two-dimensional gel electrophoresis and mass spectrometry revealed unique bacterial proteins associated with the intracellular stage of the bacteria (297). The effect of a particular protein of the phagocytic machinery identified by proteomics can then also be tested by RNA-mediated interference (298). By comparing the protein profile of phagosomes formed with virulent and avirulent variants of a pathogen, relevant molecules for pathogenesis can be identified. For example, comparing phagosomes containing highly virulent *L. pneumophila* to phagosomes with avirulent *L. hackeliae* revealed a lack of Rho GDP-dissociation inhibitor (RhoGDI) in *L. pneumophila* replicative phagosomes (299). Similarly, comparing macrophage phagosomes formed after triggering different receptors, it was found that phagosome outcome was regulated by the individual receptors triggered for phagocytosis (300). This is in agreement with recent findings that indicate particular FcRs promote particular cell responses on neutrophil phagocytes (42). Thus, phagocytosis is clearly modified according to the receptor involved. We have a good understanding on how opsonic phagocytic receptors signal, but very little is known about the signaling pathways activated by other phagocytic receptors. This is an area of research that needs much further exploration in the future.

Other techniques that have been instrumental for our present understanding of phagocytosis are fluorescence microscopy coupled to particular probes to measure phagosome pH (301), to describe phospholipid dynamics during phagosome formation (302), and to quantify antibody-dependent phagocytosis (303). Together with these, the use of confocal microscopy coupled to fluorescence resonance energy transfer-based assays has been helpful to investigate the mechanisms of *L. monocytogenes* for phagosome escaping (304). Equally important, the use of novel microbial readouts of bacterial fitness have been developed to probe the host cell environments that promote or control bacterial growth (305). In particular, *M. tuberculosis* strains that express GFP under certain environmental signals relevant to the infection status of the macrophage, permitted identify infected phagocytes and demonstrated that bacteria in immune-activated phagocytes presented higher drug tolerance than bacteria in resting phagocytes (306). These assays will be very useful in future studies on phagocytosis of other microbial pathogens. To implement these assays, the proper fluorescent probes will need to be developed.

During phagocytosis, both the phagocyte and the microorganism adapt to fight and overcome each other. These changes, important to the final outcome of an infection, can be studied by modern techniques such as transcriptional analysis *via* RNA sequencing (RNA-seq). Changes in pathogen phenotype under various conditions are revealed when the total transcriptome is analyzed. For example, it is known that cigarette smoke predisposes exposed individuals to respiratory infections by enhancing the virulence of pathogenic bacteria. A recent study on the effect of cigarette smoke on *S. aureus* gene expression using RNA-seq revealed that these bacteria increased twofold the expression of protein A with the consequent reduction in phagocytosis (307). A similar comparative transcriptome study with RNA-seq of *Brucella melitensis* grown in normal-medium culture and in acid-medium (pH 4.4) culture revealed that 113 genes were differentially expressed. Among these genes, a two-component response regulator gene in the transcriptional regulation pathway was identified as important for acid resistance and virulence of *Brucella* (308). Also, an analysis of RNA-seq data from *in vivo* and *in vitro* cultures of *Cryptococcus gattii* identified highly expressed genes and pathways of amino acid metabolism that would enable these bacteria to survive and proliferate *in vivo* (309). Hence, particular genes expressed under particular conditions can be identified as potential therapeutic targets for controlling infections. Likewise, changes in cell phenotype can be analyzed by RNA-seq. For example, increased susceptibility to bacterial pneumonia is found after influenza infections. A recent RNA-seq analysis of alveolar macrophages revealed that the virus infection caused a reduction in the phagocytic receptor MARCO. This effect could be reversed after IFNγ treatment of monocyte-derived macrophages and THP-1 macrophages. Moreover, treatment with sulforaphane or SC79, activators of Nrf2 and Akt, respectively, caused increased MARCO expression and MARCO-dependent phagocytosis (310). Therefore, a promising strategy for controlling postinfluenza bacterial pneumonia would be to increase MARCO expression by targeting Nrf2 and Akt signaling in alveolar macrophages. Another example of RNA-seq analysis of macrophages in two different conditions, namely infection with virulent or avirulent strains of *M. tuberculosis*, revealed extensive remodeling of alternative splicing in macrophage transcriptome (311). This led to considerable increase in truncated/non-translatable variants of several genes with a decline in the corresponding protein levels. The product of one such gene, RAB8B that is required for phagosome maturation, was reduced due to elevated levels of truncated RAB8B variants in cells with virulent mycobacteria (311). Alternative splicing is a new mechanism that *M. tuberculosis* uses to control macrophages. The molecular details of this mechanism are not known and will certainly become an area of interesting research in the near future.

We have described phagocytosis as a general model based mainly on macrophages. However, there are important differences among diverse types of phagocytes and even between phenotypes of the same phagocyte. As indicated earlier, environmental cues can alter the functioning of a phagocyte, and no much is known

about the mechanisms involved in these cell changes. Hence, this is an area of great interest, as shown by some recent studies. Metabolic conditions can alter macrophage function (312), and in the case of diabetes mellitus it was found that phagocytosis was reduced (313). This disease is also associated with increased tuberculosis risk and severity. Recently, it was also reported that alveolar murine macrophages from diabetic mice have a reduced expression of MARCO (314). The lack of this receptor could be the reason for inefficient phagocytosis in diabetic cells. Future research should determine whether other phagocytic receptors are also altered in diabetic macrophages. Nothing is known about the metabolic mechanisms that control phagocyte receptor expression.

The role of other phagocytes besides macrophages in controlling some intracellular bacterial infections is just beginning to be appreciated. For example, neutrophils also participate in controlling *M. tuberculosis* by autophagy (315) and are mobilized from the bone marrow to perform phagocytosis and secrete antimicrobial factors against *L. monocytogenes* (119). In addition, other cells such as dendritic cells can also perform phagocytosis by mechanisms that are different from those of macrophages (316). The particular role of these various phagocytic cells in different infection settings will also become an area of fruitful research in the future.

Macrophages not only perform phagocytosis of microbial pathogens but also ingest dead and dying host cells. The process of engulfing apoptotic cells is called efferocytosis, and it has an important role in the resolution of inflammation (317). Although efferocytosis of *M. tuberculosis*-infected cells leads to pathogen destruction, efferocytosis of *Leishmania*-infected neutrophils may promote infection (318). Understanding how macrophages, neutrophils, and dendritic cells process pathogens within a dying cell is another area for future research. Discoveries in this field should lead to novel therapeutics that simultaneously suppress inflammation and promote pathogen clearance.

CONCLUSION

Elimination of pathogens by macrophages and neutrophils is an essential function of our innate defenses. These phagocytic leukocytes clear microorganisms from tissues *via* phagocytosis. Once inside the phagocyte, the microorganism is destroyed by a series of degrading mechanisms inside the phagosome. Despite this, many pathogens have evolved means to prevent phagocytosis or to resist its effects inside the phagocytic cells. Thus, these pathogens remain a considerable health threat. We have presented the main mechanisms phagocytes have for eliminating microbes and then we discussed the strategies used by some pathogens to interfere with each step of the phagocytic process. Our list of pathogens is not complete, since there are many microorganisms capable of resisting phagocytosis in ways, we do not completely recognize. Technical advances have allowed us to make significant advances toward understanding the molecular details of the interaction between some pathogens and phagocytes, but important questions remain. Future research in this area will certainly bring us interesting surprises that will help us conceive novel therapeutic approaches that could render pathogens more susceptible to phagocyte attack.

AUTHOR CONTRIBUTIONS

CR and EU-Q both equally conceived the issues, which formed the content of the manuscript, prepared the figures, and wrote the manuscript.

FUNDING

Research in the authors' laboratory was supported by grant 254434 from Consejo Nacional de Ciencia y Tecnología (CONACyT), Mexico.

REFERENCES

1. Lim JJ, Grinstein S, Roth Z. Diversity and versatility of phagocytosis: roles in innate immunity, tissue remodeling, and homeostasis. *Front Cell Infect Microbiol* (2017) 7:191. doi:10.3389/fcimb.2017.00191
2. Rosales C, Uribe-Querol E. Phagocytosis: a fundamental process in immunity. *Biomed Res Int* (2017) 2017:9042851. doi:10.1155/2017/9042851
3. Rabinovitch M. Professional and non-professional phagocytes: an introduction. *Trends Cell Biol* (1995) 5:85–7. doi:10.1016/S0962-8924(00)88955-2
4. Flannagan RS, Jaumouillé V, Grinstein S. The cell biology of phagocytosis. *Annu Rev Pathol* (2012) 7:61–98. doi:10.1146/annurev-pathol-011811-132445
5. Desjardins M. Biogenesis of phagolysosomes: the 'kiss and run' hypothesis. *Trends Cell Biol* (1995) 5:183–6. doi:10.1016/0962-8924(95)80001-W
6. Levin R, Grinstein S, Canton J. The life cycle of phagosomes: formation, maturation, and resolution. *Immunol Rev* (2016) 273:156–79. doi:10.1111/imr.12439
7. Fairn G, Grinstein S. How nascent phagosomes mature to become phagolysosomes. *Trends Immunol* (2012) 33:397–405. doi:10.1016/j.it.2012.03.003
8. Canton J, Khezri R, Glogauer M, Grinstein S. Contrasting phagosome pH regulation and maturation in human M1 and M2 macrophages. *Mol Biol Cell* (2014) 25:3330–41. doi:10.1091/mbc.E14-05-0967
9. Hoppe AD, Swanson JA. Cdc42, Rac1, and Rac2 display distinct patterns of activation during phagocytosis. *Mol Biol Cell* (2004) 15:3509–19. doi:10.1091/mbc.E03-11-0847
10. Mao Y, Finnemann SC. Regulation of phagocytosis by Rho GTPases. *Small GTPases* (2015) 6:89–99. doi:10.4161/21541248.2014.989785
11. Araki N, Hatae T, Furukawa A, Swanson JA. Phosphoinositide-3-kinase-independent contractile activities associated with Fcγ-receptor-mediated phagocytosis and macropinocytosis in macrophages. *J Cell Sci* (2003) 116:247–57. doi:10.1242/jcs.00235
12. Dart AE, Tollis S, Bright MD, Frankel G, Endres RG. The motor protein myosin 1G functions in FcγR-mediated phagocytosis. *J Cell Sci* (2012) 125:6020–9. doi:10.1242/jcs.109561
13. Kitano M, Nakaya M, Nakamura T, Nagata S, Matsuda M. Imaging of Rab5 activity identifies essential regulators for phagosome maturation. *Nature* (2008) 453:241–5. doi:10.1038/nature06857
14. Gutierrez MG. Functional role(s) of phagosomal Rab GTPases. *Small GTPases* (2013) 4:148–58. doi:10.4161/sgtp.25604
15. Christoforidis S, McBride HM, Burgoyne RD, Zerial M. The Rab5 effector EEA1 is a core component of endosome docking. *Nature* (1999) 397:621–5. doi:10.1038/17618
16. Vieira OV, Botelho RJ, Rameh L, Brachmann SM, Matsuo T, Davidson HW, et al. Distinct roles of class I and class III phosphatidylinositol 3-kinases in phagosome formation and maturation. *J Cell Biol* (2001) 155:19–25. doi:10.1083/jcb.200107069

17. Kinchen JM, Ravichandran KS. Phagosome maturation: going through the acid test. *Nat Rev Mol Cell Biol* (2008) 9:781–95. doi:10.1038/nrm2515
18. Marshansky V, Futai M. The V-type H^+-ATPase in vesicular trafficking: targeting, regulation and function. *Curr Opin Cell Biol* (2008) 20:415–26. doi:10.1016/j.ceb.2008.03.015
19. Araki N, Johnson MT, Swanson JA. A role for phosphoinositide 3-kinase in the completion of macropinocytosis and phagocytosis by macrophages. *J Cell Biol* (1996) 135:1249–60. doi:10.1083/jcb.135.5.1249
20. Vieira OV, Bucci C, Harrison RE, Trimble WS, Lanzetti L, Gruenberg J, et al. Modulation of Rab5 and Rab7 recruitment to phagosomes by phosphatidylinositol 3-kinase. *Mol Cell Biol* (2003) 23:2501–14. doi:10.1128/MCB.23.7.2501-2514.2003
21. Rink J, Ghigo E, Kalaidzidis Y, Zerial M. Rab conversion as a mechanism of progression from early to late endosomes. *Cell* (2005) 122:735–49. doi:10.1016/j.cell.2005.06.043
22. Huynh KK, Eskelinen EL, Scott CC, Malevanets A, Saftig P, Grinstein S. LAMP proteins are required for fusion of lysosomes with phagosomes. *EMBO J* (2007) 26:313–24. doi:10.1038/sj.emboj.7601511
23. Beertsen W, Willenborg M, Everts V, Zirogianni A, Podschun R, Schröder B, et al. Impaired phagosomal maturation in neutrophils leads to periodontitis in lysosomal-associated membrane protein-2 knockout mice. *J Immunol* (2008) 180:475–82. doi:10.4049/jimmunol.180.1.475
24. Hanson PI, Roth R, Lin Y, Heuser JE. Plasma membrane deformation by circular arrays of ESCRT-III protein filaments. *J Cell Biol* (2008) 180:389–402. doi:10.1083/jcb.200707031
25. Babior BM. NADPH oxidase. *Curr Opin Immunol* (2004) 16:42–7. doi:10.1016/j.coi.2003.12.001
26. Canton J, Neculai D, Grinstein S. Scavenger receptors in homeostasis and immunity. *Nat Rev Immunol* (2013) 13:621–34. doi:10.1038/nri3515
27. Peiser L, Gough PJ, Kodama T, Gordon S. Macrophage class A scavenger receptor-mediated phagocytosis of *Escherichia coli*: role of cell heterogeneity, microbial strain, and culture conditions in vitro. *Infect Immun* (2000) 68:1953–63. doi:10.1128/IAI.68.4.1953-1963.2000
28. Herre J, Marshall AS, Caron E, Edwards AD, Williams DL, Schweighoffer E, et al. Dectin-1 uses novel mechanisms for yeast phagocytosis in macrophages. *Blood* (2004) 104:4038–45. doi:10.1182/blood-2004-03-1140
29. Dambuza IM, Brown GD. C-type lectins in immunity: recent developments. *Curr Opin Immunol* (2015) 32:21–7. doi:10.1016/j.coi.2014.12.002
30. Ezekowitz RA, Sastry K, Bailly P, Warner A. Molecular characterization of the human macrophage mannose receptor: demonstration of multiple carbohydrate recognition-like domains and phagocytosis of yeasts in Cos-1 cells. *J Exp Med* (1990) 172:1785–94. doi:10.1084/jem.172.6.1785
31. Schiff DE, Kline L, Soldau K, Lee JD, Pugin J, Tobias PS, et al. Phagocytosis of Gram-negative bacteria by a unique CD14-dependent mechanism. *J Leukoc Biol* (1997) 62:786–94.
32. Kawai T, Akira S. Toll-like receptors and their crosstalk with other innate receptors in infection and immunity. *Immunity* (2011) 34:637–50. doi:10.1016/j.immuni.2011.05.006
33. Iwasaki A, Medzhitov R. Control of adaptive immunity by the innate immune system. *Nat Immunol* (2015) 16:343–53. doi:10.1038/ni.3123
34. Rosales C. Fc receptor and integrin signaling in phagocytes. *Signal Transduct* (2007) 7:386–401. doi:10.1002/sita.200700141
35. Nimmerjahn F, Ravetch J. Antibodies, Fc receptors and cancer. *Curr Opin Immunol* (2007) 19:239–45. doi:10.1016/j.coi.2007.01.005
36. Powell MS, Hogarth PM. Fc receptors. *Adv Exp Med Biol* (2008) 640:22–34. doi:10.1007/978-0-387-09789-3_3
37. Rosales C, Uribe-Querol E. Antibody-Fc receptor interactions in antimicrobial functions. *Curr Immunol Rev* (2013) 9:44–55. doi:10.2174/1573395511309010006
38. Rosales C, Uribe-Querol E. Fc receptors: cell activators of antibody functions. *Adv Biosci Biotechnol* (2013) 4:21–33. doi:10.4236/abb.2013.44A004
39. Bakema JE, Ganzevles SH, Fluitsma DM, Schilham MW, Beelen RH, Valerius T, et al. Targeting FcαRI on polymorphonuclear cells induces tumor cell killing through autophagy. *J Immunol* (2011) 187:726–32. doi:10.4049/jimmunol.1002581
40. van Lookeren Campagne M, Wiesmann C, Brown EJ. Macrophage complement receptors and pathogen clearance. *Cell Microbiol* (2007) 9:2095–102. doi:10.1111/j.1462-5822.2007.00981.x
41. Nimmerjahn F, Ravetch JV. FcγRs in health and disease. *Curr Top Microbiol Immunol* (2011) 350:105–25. doi:10.1007/82_2010_86
42. Rosales C. Fcγ receptor heterogeneity in leukocyte functional responses. *Front Immunol* (2017) 8:280. doi:10.3389/fimmu.2017.00280
43. Tohyama Y, Yamamura H. Complement-mediated phagocytosis – the role of Syk. *IUBMB Life* (2006) 58:304–8. doi:10.1080/15216540600746377
44. Flannagan R, Grinstein S. The application of fluorescent probes for the analysis of lipid dynamics during phagocytosis. *Methods Mol Biol* (2010) 591:121–34. doi:10.1007/978-1-60761-404-3_7
45. Swanson JA, Johnson MT, Beningo K, Post P, Mooseker M, Araki N. A contractile activity that closes phagosomes in macrophages. *J Cell Sci* (1999) 112:307–16.
46. Luzio JP, Pryor PR, Bright NA. Lysosomes: fusion and function. *Nat Rev Mol Cell Biol* (2007) 8:622–32. doi:10.1038/nrm2217
47. Pryor PR, Luzio JP. Delivery of endocytosed membrane proteins to the lysosome. *Biochim Biophys Acta* (2009) 1793:615–24. doi:10.1016/j.bbamcr.2008.12.022
48. Mullins C, Bonifacino JS. The molecular machinery for lysosome biogenesis. *Bioessays* (2001) 23:333–43. doi:10.1002/bies.1048
49. Vida T, Gerhardt B. A cell-free assay allows reconstitution of Vps33p-dependent transport to the yeast vacuole/lysosome. *J Cell Biol* (1999) 146:85–98. doi:10.1083/jcb.146.1.85
50. Storrie B, Desjardins M. The biogenesis of lysosomes: is it a kiss and run, continuous fusion and fission process? *Bioessays* (1996) 18:895–903. doi:10.1002/bies.950181108
51. Bright NA, Reaves BJ, Mullock BM, Luzio JP. Dense core lysosomes can fuse with late endosomes and are re-formed from the resultant hybrid organelles. *J Cell Sci* (1997) 110:2027–40.
52. Mullock BM, Bright NA, Fearon CW, Gray SR, Luzio JP. Fusion of lysosomes with late endosomes produces a hybrid organelle of intermediate density and is NSF dependent. *J Cell Biol* (1998) 140:591–601. doi:10.1083/jcb.140.3.591
53. Bright NA, Gratian MJ, Luzio JP. Endocytic delivery to lysosomes mediated by concurrent fusion and kissing events in living cells. *Curr Biol* (2005) 15:360–5. doi:10.1016/j.cub.2005.01.049
54. Luzio JP, Gray SR, Bright NA. Endosome-lysosome fusion. *Biochem Soc Trans* (2010) 38:1413–6. doi:10.1042/BST0381413
55. Luzio JP, Hackmann Y, Dieckmann NM, Griffiths GM. The biogenesis of lysosomes and lysosome-related organelles. *Cold Spring Harb Perspect Biol* (2014) 6:a016840. doi:10.1101/cshperspect.a016840
56. Steinberg BE, Huynh KK, Grinstein S. Phagosomal acidification: measurement, manipulation and functional consequences. *Biochem Soc Trans* (2007) 35:1083–7. doi:10.1042/BST0351083
57. Jordens I, Fernandez-Borja M, Marsman M, Dusseljee S, Janssen L, Calafat J, et al. The Rab7 effector protein RILP controls lysosomal transport by inducing the recruitment of dynein-dynactin motors. *Curr Biol* (2001) 11:1680–5. doi:10.1016/S0960-9822(01)00531-0
58. Harrison RE, Bucci C, Vieira OV, Schroer TA, Grinstein S. Phagosomes fuse with late endosomes and/or lysosomes by extension of membrane protrusions along microtubules: role of Rab7 and RILP. *Mol Cell Biol* (2003) 23:6494–506. doi:10.1128/MCB.23.18.6494-6506.2003
59. Canton J. Phagosome maturation in polarized macrophages. *J Leukoc Biol* (2014) 96:729–38. doi:10.1189/jlb.1MR0114-021R
60. Guarnieri FG, Arterburn LM, Penno MB, Cha Y, August JT. The motif Tyr-X-X-hydrophobic residue mediates lysosomal membrane targeting of lysosome-associated membrane protein 1. *J Biol Chem* (1993) 268:1941–6.
61. Schwake M, Schröder B, Saftig P. Lysosomal membrane proteins and their central role in physiology. *Traffic* (2013) 14:739–48. doi:10.1111/tra.12056
62. Luzio JP, Parkinson MD, Gray SR, Bright NA. The delivery of endocytosed cargo to lysosomes. *Biochem Soc Trans* (2009) 37:1019–21. doi:10.1042/BST0371019
63. Masson PL, Heremans JF, Schonne E. Lactoferrin, an iron-binding protein in neutrophilic leukocytes. *J Exp Med* (1969) 130:643–58. doi:10.1084/jem.130.3.643
64. Minakami R, Sumimotoa H. Phagocytosis-coupled activation of the superoxide-producing phagocyte oxidase, a member of the NADPH oxidase (nox) family. *Int J Hematol* (2006) 84:193–8. doi:10.1532/IJH97.06133
65. Nauseef WM. Myeloperoxidase in human neutrophil host defence. *Cell Microbiol* (2014) 16:1146–55. doi:10.1111/cmi.12312

66. Pillay CS, Elliott E, Dennison C. Endolysosomal proteolysis and its regulation. *Biochem J* (2002) 363:417–29. doi:10.1042/bj3630417
67. Jabado N, Jankowski A, Dougaparsad S, Picard V, Grinstein S, Gros P. Natural resistance to intracellular infections: natural resistance-associated macrophage protein 1 (Nramp1) functions as a pH-dependent manganese transporter at the phagosomal membrane. *J Exp Med* (2000) 192:1237–48. doi:10.1084/jem.192.9.1237
68. Panday A, Sahoo MK, Osorio D, Batra S. NADPH oxidases: an overview from structure to innate immunity-associated pathologies. *Cell Mol Immunol* (2015) 12:5–23. doi:10.1038/cmi.2014.89
69. El-Benna J, Hurtado-Nedelec M, Marzaioli V, Marie JC, Gougerot-Pocidalo MA, Dang PM. Priming of the neutrophil respiratory burst: role in host defense and inflammation. *Immunol Rev* (2016) 273:180–93. doi:10.1111/imr.12447
70. Abo A, Pick E, Hall A, Totty N, Teahan CG, Segal AW. Activation of the NADPH oxidase involves the small GTP-binding protein p21rac1. *Nature* (1991) 353:668–70. doi:10.1038/353668a0
71. Knaus UG, Heyworth PG, Evans T, Curnutte JT, Bokoch GM. Regulation of phagocyte oxygen radical production by the GTP-binding protein Rac 2. *Science* (1991) 254:1512–5. doi:10.1126/science.1660188
72. Bogdan C, Röllinghoff M, Diefenbach A. The role of nitric oxide in innate immunity. *Immunol Rev* (2000) 173:17–26. doi:10.1034/j.1600-065X.2000.917307.x
73. Richardson AR, Soliven KC, Castor ME, Barnes PD, Libby SJ, Fang FC. The base excision repair system of *Salmonella enterica* serovar typhimurium counteracts DNA damage by host nitric oxide. *PLoS Pathog* (2009) 5:e1000451. doi:10.1371/journal.ppat.1000451
74. Richardson AR, Payne EC, Younger N, Karlinsey JE, Thomas VC, Becker LA, et al. Multiple targets of nitric oxide in the tricarboxylic acid cycle of *Salmonella enterica* serovar typhimurium. *Cell Host Microbe* (2011) 10:33–43. doi:10.1016/j.chom.2011.06.004
75. Ward PP, Uribe-Luna S, Conneely OM. Lactoferrin and host defense. *Biochem Cell Biol* (2002) 80:95–102. doi:10.1139/o01-214
76. Cellier MF, Courville P, Campion C. Nramp1 phagocyte intracellular metal withdrawal defense. *Microbes Infect* (2007) 9:1662–70. doi:10.1016/j.micinf.2007.09.006
77. Zhao L, Lu W. Defensins in innate immunity. *Curr Opin Hematol* (2014) 21:37–42. doi:10.1097/MOH.0000000000000005
78. Suarez-Carmona M, Hubert P, Delvenne P, Herfs M. Defensins: "simple" antimicrobial peptides or broad-spectrum molecules? *Cytokine Growth Factor Rev* (2015) 26:361–70. doi:10.1016/j.cytogfr.2014.12.005
79. del Cerro-Vadillo E, Madrazo-Toca F, Carrasco-Marín E, Fernandez-Prieto L, Beck C, Leyva-Cobián F, et al. Cutting edge: a novel nonoxidative phagosomal mechanism exerted by cathepsin-D controls *Listeria monocytogenes* intracellular growth. *J Immunol* (2006) 176:1321–5. doi:10.4049/jimmunol.176.3.1321
80. Müller S, Faulhaber A, Sieber C, Pfeifer D, Hochberg T, Gansz M, et al. The endolysosomal cysteine cathepsins L and K are involved in macrophage-mediated clearance of *Staphylococcus aureus* and the concomitant cytokine induction. *FASEB J* (2014) 28:162–75. doi:10.1096/fj.13-232272
81. Miyauchi J, Sasadaira H, Watanabe K, Watanabe Y. Ultrastructural immunocytochemical localization of lysozyme in human monocytes and macrophages. *Cell Tissue Res* (1985) 242:269–77. doi:10.1007/BF00214539
82. Ganz T. Antimicrobial polypeptides. *J Leukoc Biol* (2004) 75:34–8. doi:10.1189/jlb.0403150
83. Wu Y, Raymond B, Goossens PL, Njamkepo E, Guiso N, Paya M, et al. Type-IIA secreted phospholipase A2 is an endogenous antibiotic-like protein of the host. *Biochimie* (2010) 92:583–7. doi:10.1016/j.biochi.2010.01.024
84. Behe P, Segal AW. The function of the NADPH oxidase of phagocytes, and its relationship to other NOXs. *Biochem Soc Trans* (2007) 35:1100–3. doi:10.1042/BST0351100
85. Goldblatt D. Recent advances in chronic granulomatous disease. *J Infect* (2014) 69:S32–5. doi:10.1016/j.jinf.2014.07.013
86. Roos D. Chronic granulomatous disease. *Br Med Bull* (2016) 118:50–63. doi:10.1093/bmb/ldw009
87. El-Benna J, Dang PM, Gougerot-Pocidalo MA, Marie JC, Braut-Boucher F. p47phox, the phagocyte NADPH oxidase/NOX2 organizer: structure, phosphorylation and implication in diseases. *Exp Mol Med* (2009) 41:217–25. doi:10.3858/emm.2009.41.4.058
88. Winterbourn CC. Toxicity of iron and hydrogen peroxide: the Fenton reaction. *Toxicol Lett* (1995) 82-83:969–74. doi:10.1016/0378-4274(95)03532-X
89. Lam GY, Huang J, Brumell JH. The many roles of NOX2 NADPH oxidase-derived ROS in immunity. *Semin Immunopathol* (2010) 32:415–30. doi:10.1007/s00281-010-0221-0
90. Fang FC. Antimicrobial reactive oxygen and nitrogen species: concepts and controversies. *Nat Rev Microbiol* (2004) 2:820–32. doi:10.1038/nrmicro1004
91. Webb JL, Harvey MW, Holden DW, Evans TJ. Macrophage nitric oxide synthase associates with cortical actin but is not recruited to phagosomes. *Infect Immun* (2001) 69:6391–400. doi:10.1128/IAI.69.10.6391-6400.2001
92. Grosser MR, Weiss A, Shaw LN, Richardson AR. Regulatory requirements for *Staphylococcus aureus* nitric oxide resistance. *J Bacteriol* (2016) 198:2043–55. doi:10.1128/JB.00229-16
93. Häger M, Cowland JB, Borregaard N. Neutrophil granules in health and disease. *J Intern Med* (2010) 268:25–34. doi:10.1111/j.1365-2796.2010.02237.x
94. Ward PP, Paz E, Conneely OM. Multifunctional roles of lactoferrin: a critical overview. *Cell Mol Life Sci* (2005) 62:2540–8. doi:10.1007/s00018-005-5369-8
95. Luo M, Fadeev EA, Groves JT. Mycobactin-mediated iron acquisition within macrophages. *Nat Chem Biol* (2005) 1:149–53. doi:10.1038/nchembio717
96. Goetz DH, Holmes MA, Borregaard N, Bluhm ME, Raymond KN, Strong RK. The neutrophil lipocalin NGAL is a bacteriostatic agent that interferes with siderophore-mediated iron acquisition. *Mol Cell* (2002) 10:1033–43. doi:10.1016/S1097-2765(02)00708-6
97. Flo TH, Smith KD, Sato S, Rodriguez DJ, Holmes MA, Strong RK, et al. Lipocalin 2 mediates an innate immune response to bacterial infection by sequestrating iron. *Nature* (2004) 432:917–21. doi:10.1038/nature03104
98. Yount NY, Yeaman MR. Peptide antimicrobials: cell wall as a bacterial target. *Ann N Y Acad Sci* (2013) 1277:127–38. doi:10.1111/nyas.12005
99. Kościuczuk EM, Lisowski P, Jarczak J, Strzałkowska N, Jóźwik A, Horbańczuk J, et al. Cathelicidins: family of antimicrobial peptides. A review. *Mol Biol Rep* (2012) 39:10957–70. doi:10.1007/s11033-012-1997-x
100. Lehrer RI, Lu W. α-Defensins in human innate immunity. *Immunol Rev* (2012) 245:84–112. doi:10.1111/j.1600-065X.2011.01082.x
101. Fabisiak A, Murawska N, Fichna J. LL-37: cathelicidin-related antimicrobial peptide with pleiotropic activity. *Pharmacol Rep* (2016) 68:802–8. doi:10.1016/j.pharep.2016.03.015
102. Tang X, Basavarajappa D, Haeggström JZ, Wan M. P2X7 receptor regulates internalization of antimicrobial peptide LL-37 by human macrophages that promotes intracellular pathogen clearance. *J Immunol* (2015) 195:1191–201. doi:10.4049/jimmunol.1402845
103. Wan M, van der Does AM, Tang X, Lindbom L, Agerberth B, Haeggström JZ. Antimicrobial peptide LL-37 promotes bacterial phagocytosis by human macrophages. *J Leukoc Biol* (2014) 95:971–81. doi:10.1189/jlb.0513304
104. Wan M, Soehnlein O, Tang X, van der Does AM, Smedler E, Uhlén P, et al. Cathelicidin LL-37 induces time-resolved release of LTB4 and TXA2 by human macrophages and triggers eicosanoid generation in vivo. *FASEB J* (2014) 28:3456–67. doi:10.1096/fj.14-251306
105. Gupta S, Winglee K, Gallo R, Bishai WR. Bacterial subversion of cAMP signalling inhibits cathelicidin expression, which is required for innate resistance to *Mycobacterium tuberculosis*. *J Pathol* (2017) 242:52–61. doi:10.1002/path.4878
106. Schröder BA, Wrocklage C, Hasilik A, Saftig P. The proteome of lysosomes. *Proteomics* (2010) 10:4053–76. doi:10.1002/pmic.201000196
107. Ganz T, Lehrer RI. Antimicrobial peptides of leukocytes. *Curr Opin Hematol* (1997) 4:53–8. doi:10.1097/00062752-199704010-00009
108. Botelho RJ, Grinstein S. Phagocytosis. *Curr Biol* (2011) 21:R533–8. doi:10.1016/j.cub.2011.05.053
109. Gordon S. Phagocytosis: an immunobiologic process. *Immunity* (2016) 44:463–75. doi:10.1016/j.immuni.2016.02.026
110. Flannagan RS, Cosío G, Grinstein S. Antimicrobial mechanisms of phagocytes and bacterial evasion strategies. *Nat Rev Microbiol* (2009) 7:355–66. doi:10.1038/nrmicro2128
111. Smith LM, May RC. Mechanisms of microbial escape from phagocyte killing. *Biochem Soc Trans* (2013) 41:475–90. doi:10.1042/BST20130014
112. Spaan AN, Surewaard BG, Nijland R, van Strijp JA. Neutrophils versus *Staphylococcus aureus*: a biological tug of war. *Annu Rev Microbiol* (2013) 67:629–50. doi:10.1146/annurev-micro-092412-155746

113. Flannagan RS, Heit B, Heinrichs DE. Antimicrobial mechanisms of macrophages and the immune evasion strategies of *Staphylococcus aureus*. *Pathogens* (2015) 4:826–68. doi:10.3390/pathogens4040826
114. Lacoma A, Cano V, Moranta D, Regueiro V, Domínguez-Villanueva D, Laabei M, et al. Investigating intracellular persistence of *Staphylococcus aureus* within a murine alveolar macrophage cell line. *Virulence* (2017) 1–15. doi:10.1080/21505594.2017.1361089
115. Vergne I, Gilleron M, Nigou J. Manipulation of the endocytic pathway and phagocyte functions by *Mycobacterium tuberculosis* lipoarabinomannan. *Front Cell Infect Microbiol* (2015) 4:187. doi:10.3389/fcimb.2014.00187
116. Jamwal SV, Mehrotra P, Singh A, Siddiqui Z, Basu A, Rao KV. Mycobacterial escape from macrophage phagosomes to the cytoplasm represents an alternate adaptation mechanism. *Sci Rep* (2016) 6:23089. doi:10.1038/srep23089
117. Awuh JA, Flo TH. Molecular basis of mycobacterial survival in macrophages. *Cell Mol Life Sci* (2017) 74:1625–48. doi:10.1007/s00018-016-2422-8
118. Arnett E, Vadia S, Nackerman CC, Oghumu S, Satoskar AR, McLeish KR, et al. The pore-forming toxin listeriolysin O is degraded by neutrophil metalloproteinase-8 and fails to mediate *Listeria monocytogenes* intracellular survival in neutrophils. *J Immunol* (2014) 192:234–44. doi:10.4049/jimmunol.1301302
119. Witter AR, Okunnu BM, Berg RE. The essential role of neutrophils during infection with the intracellular bacterial pathogen *Listeria monocytogenes*. *J Immunol* (2016) 197:1557–65. doi:10.4049/jimmunol.1600599
120. Alonzo F III, Torres VJ. The bicomponent pore-forming leucocidins of *Staphylococcus aureus*. *Microbiol Mol Biol Rev* (2014) 78:199–230. doi:10.1128/MMBR.00055-13
121. Berube BJ, Bubeck Wardenburg J. *Staphylococcus aureus* α-toxin: nearly a century of intrigue. *Toxins (Basel)* (2013) 5:1140–66. doi:10.3390/toxins5061140
122. Yamashita K, Kawai Y, Tanaka Y, Hirano N, Kaneko J, Tomita N, et al. Crystal structure of the octameric pore of staphylococcal γ-hemolysin reveals the β-barrel pore formation mechanism by two components. *Proc Natl Acad Sci U S A* (2011) 108:17314–9. doi:10.1073/pnas.1110402108
123. Badarau A, Rouha H, Malafa S, Logan DT, Håkansson M, Stulik L, et al. Structure-function analysis of heterodimer formation, oligomerization, and receptor binding of the *Staphylococcus aureus* bi-component toxin LukGH. *J Biol Chem* (2015) 290:142–56. doi:10.1074/jbc.M114.598110
124. Alonzo F III, Kozhaya L, Rawlings SA, Reyes-Robles T, DuMont AL, Myszka DG, et al. CCR5 is a receptor for *Staphylococcus aureus* leukotoxin ED. *Nature* (2013) 493:51–5. doi:10.1038/nature11724
125. DuMont AL, Yoong P, Day CJ, Alonzo F III, McDonald WH, Jennings MP, et al. *Staphylococcus aureus* LukAB cytotoxin kills human neutrophils by targeting the CD11b subunit of the integrin Mac-1. *Proc Natl Acad Sci U S A* (2013) 110:10794–9. doi:10.1073/pnas.1305121110
126. Reyes-Robles T, Alonzo F III, Kozhaya L, Lacy DB, Unutmaz D, Torres VJ. *Staphylococcus aureus* leukotoxin ED targets the chemokine receptors CXCR1 and CXCR2 to kill leukocytes and promote infection. *Cell Host Microbe* (2013) 14:453–9. doi:10.1016/j.chom.2013.09.005
127. Wilke GA, Bubeck Wardenburg J. Role of a disintegrin and metalloprotease 10 in *Staphylococcus aureus* alpha-hemolysin-mediated cellular injury. *Proc Natl Acad Sci U S A* (2010) 107:13473–8. doi:10.1073/pnas.1001815107
128. Becker RE, Berube BJ, Sampedro GR, DeDent AC, Bubeck Wardenburg J. Tissue-specific patterning of host innate immune responses by *Staphylococcus aureus* α-toxin. *J Innate Immun* (2014) 6:619–31. doi:10.1159/000360006
129. Song L, Hobaugh MR, Shustak C, Cheley S, Bayley H, Gouaux JE. Structure of staphylococcal alpha-hemolysin, a heptameric transmembrane pore. *Science* (1996) 274:1859–66. doi:10.1126/science.274.5294.1859
130. Sugawara T, Yamashita D, Kato K, Peng Z, Ueda J, Kaneko J, et al. Structural basis for pore-forming mechanism of staphylococcal α-hemolysin. *Toxicon* (2015) 108:226–31. doi:10.1016/j.toxicon.2015.09.033
131. Sulica A, Medesan C, Laky M, Onică D, Sjöquist J, Ghetie V. Effect of protein A of *Staphylococcus aureus* on the binding of monomeric and polymeric IgG to Fc receptor-bearing cells. *Immunology* (1979) 38:173–9.
132. Zhang L, Jacobsson K, Vasi J, Lindberg M, Frykberg L. A second IgG-binding protein in *Staphylococcus aureus*. *Microbiology* (1998) 144:985–91. doi:10.1099/00221287-144-4-985
133. Smith EJ, Visai L, Kerrigan SW, Speziale P, Foster TJ. The Sbi protein is a multifunctional immune evasion factor of *Staphylococcus aureus*. *Infect Immun* (2011) 79:3801–9. doi:10.1128/IAI.05075-11
134. Smith EJ, Corrigan RM, van der Sluis T, Gründling A, Speziale P, Geoghegan JA, et al. The immune evasion protein Sbi of *Staphylococcus aureus* occurs both extracellularly and anchored to the cell envelope by binding lipoteichoic acid. *Mol Microbiol* (2012) 83:789–804. doi:10.1111/j.1365-2958.2011.07966.x
135. Laarman AJ, Ruyken M, Malone CL, van Strijp JA, Horswill AR, Rooijakkers SH. *Staphylococcus aureus* metalloprotease aureolysin cleaves complement C3 to mediate immune evasion. *J Immunol* (2011) 186:6445–53. doi:10.4049/jimmunol.1002948
136. Rooijakkers SH, Wu J, Ruyken M, van Domselaar R, Planken KL, Tzekou A, et al. Structural and functional implications of the alternative complement pathway C3 convertase stabilized by a staphylococcal inhibitor. *Nat Immunol* (2009) 10:721–7. doi:10.1038/ni.1756
137. Ko YP, Kuipers A, Freitag CM, Jongerius I, Medina E, van Rooijen WJ, et al. Phagocytosis escape by a *Staphylococcus aureus* protein that connects complement and coagulation proteins at the bacterial surface. *PLoS Pathog* (2013) 9:e1003816. doi:10.1371/journal.ppat.1003816
138. Kuipers A, Stapels DA, Weerwind LT, Ko YP, Ruyken M, Lee JC, et al. The *Staphylococcus aureus* polysaccharide capsule and Efb-dependent fibrinogen shield act in concert to protect against phagocytosis. *Microbiology* (2016) 162:1185–94. doi:10.1099/mic.0.000293
139. Rooijakkers SH, van Wamel WJ, Ruyken M, van Kessel KP, van Strijp JA. Anti-opsonic properties of staphylokinase. *Microbes Infect* (2005) 7:476–84. doi:10.1016/j.micinf.2004.12.014
140. Laky M, Sjöquist J, Moraru I, Gheţie V. Mutual inhibition of the binding of C1q and protein A to rabbit IgG immune complexes. *Mol Immunol* (1985) 22:1297–302. doi:10.1016/0161-5890(85)90049-5
141. Anes E. Acting on actin during bacterial infection, cytoskeleton – structure, dynamics, function and disease. In: Jimenez-Lopez JC, editor. *Biochemistry, Genetics and Molecular Biology*. Rijeka, Croacia: InTech d.o.o. (2017). p. 257–78.
142. Hall A. Rho family GTPases. *Biochem Soc Trans* (2012) 40:1378–82. doi:10.1042/BST20120103
143. Biro M, Munoz MA, Weninger W. Targeting Rho-GTPases in immune cell migration and inflammation. *Br J Pharmacol* (2014) 171:5491–506. doi:10.1111/bph.12658
144. Higgs HN, Pollard TD. Activation by Cdc42 and PIP(2) of Wiskott-Aldrich Syndrome protein (WASp) stimulates actin nucleation by Arp2/3 complex. *J Cell Biol* (2000) 150:1311–20. doi:10.1083/jcb.150.6.1311
145. Marchand JB, Kaiser DA, Pollard TD, Higgs HN. Interaction of WASP/Scar proteins with actin and vertebrate Arp2/3 complex. *Nat Cell Biol* (2001) 3:76–82. doi:10.1038/35050590
146. Pollard TD, Cooper JA. Actin, a central player in cell shape and movement. *Science* (2009) 326:1208–12. doi:10.1126/science.1175862
147. Jank T, Giesemann T, Aktories K. Rho-glucosylating *Clostridium difficile* toxins A and B: new insights into structure and function. *Glycobiology* (2007) 17:15R–22R. doi:10.1093/glycob/cwm004
148. Jank T, Bogdanović X, Wirth C, Haaf E, Spoerner M, Böhmer KE, et al. A bacterial toxin catalyzing tyrosine glycosylation of Rho and deamidation of Gq and Gi proteins. *Nat Struct Mol Biol* (2013) 20:1273–80. doi:10.1038/nsmb.2688
149. Groves E, Rittinger K, Amstutz M, Berry S, Holden DW, Cornelis GR, et al. Sequestering of Rac by the *Yersinia* effector YopO blocks Fcγ receptor-mediated phagocytosis. *J Biol Chem* (2010) 285:4087–98. doi:10.1074/jbc.M109.071035
150. Krall R, Sun J, Pederson KJ, Barbieri JT. In vivo Rho GTPase-activating protein activity of *Pseudomonas aeruginosa* cytotoxin ExoS. *Infect Immun* (2002) 70:360–7. doi:10.1128/IAI.70.1.360-367.2002
151. Flannagan RS. *Burkholderia cenocepacia* infection: disruption of phagocyte immune functions through Rho GTPase inactivation. *Cell Adh Migr* (2012) 6:297–301. doi:10.4161/cam.20487
152. Wheeler RT, Kombe D, Agarwala SD, Fink GR. Dynamic, morphotype-specific *Candida albicans* beta-glucan exposure during infection and drug treatment. *PLoS Pathog* (2008) 4:e1000227. doi:10.1371/journal.ppat.1000227
153. Brothers KM, Gratacap RL, Barker SE, Newman ZR, Norum A, Wheeler RT. NADPH oxidase-driven phagocyte recruitment controls *Candida albicans* filamentous growth and prevents mortality. *PLoS Pathog* (2013) 9:e1003634. doi:10.1371/journal.ppat.1003634
154. Aimanianda V, Bayry J, Bozza S, Kniemeyer O, Perruccio K, Elluru SR, et al. Surface hydrophobin prevents immune recognition of airborne fungal spores. *Nature* (2009) 460:1117–21. doi:10.1038/nature08264

155. Bose I, Reese AJ, Ory JJ, Janbon G, Doering TL. A yeast under cover: the capsule of *Cryptococcus neoformans*. *Eukaryot Cell* (2003) 2:655–63. doi:10.1128/EC.2.4.655-663.2003
156. Stano P, Williams V, Villani M, Cymbalyuk ES, Qureshi A, Huang Y, et al. App1: an antiphagocytic protein that binds to complement receptors 3 and 2. *J Immunol* (2009) 182:84–91. doi:10.4049/jimmunol.182.1.84
157. Armstrong JA, Hart PD. Response of cultured macrophages to *Mycobacterium tuberculosis*, with observations on fusion of lysosomes with phagosomes. *J Exp Med* (1971) 134:713–40. doi:10.1084/jem.134.3.713
158. Vergne I, Chua J, Lee HH, Lucas M, Belisle J, Deretic V. Mechanism of phagolysosome biogenesis block by viable *Mycobacterium tuberculosis*. *Proc Natl Acad Sci U S A* (2005) 102:4033–8. doi:10.1073/pnas.0409716102
159. Russell DG. *Mycobacterium tuberculosis* and the intimate discourse of a chronic infection. *Immunol Rev* (2011) 240:252–68. doi:10.1111/j.1600-065X.2010.00984.x
160. Patin EC, Geffken AC, Willcocks S, Leschczyk C, Haas A, Nimmerjahn F, et al. Trehalose dimycolate interferes with FcγR-mediated phagosome maturation through Mincle, SHP-1 and FcγRIIB signalling. *PLoS One* (2017) 12:e0174973. doi:10.1371/journal.pone.0174973
161. Sturgill-Koszycki S, Schlesinger PH, Chakraborty P, Haddix PL, Collins HL, Fok AK, et al. Lack of acidification in *Mycobacterium* phagosomes produced by exclusion of the vesicular proton-ATPase. *Science* (1994) 263:678–81. doi:10.1126/science.8303277
162. Wong D, Bach H, Sun J, Hmama Z, Av-Gay Y. *Mycobacterium tuberculosis* protein tyrosine phosphatase (PtpA) excludes host vacuolar-H^+-ATPase to inhibit phagosome acidification. *Proc Natl Acad Sci U S A* (2011) 108:19371–6. doi:10.1073/pnas.1109201108
163. Bach H, Papavinasasundaram KG, Wong D, Hmama Z, Av-Gay Y. *Mycobacterium tuberculosis* virulence is mediated by PtpA dephosphorylation of human vacuolar protein sorting 33B. *Cell Host Microbe* (2008) 3:316–22. doi:10.1016/j.chom.2008.03.008
164. Sun J, Wang X, Lau A, Liao TY, Bucci C, Hmama Z. Mycobacterial nucleoside diphosphate kinase blocks phagosome maturation in murine RAW 264.7 macrophages. *PLoS One* (2010) 5:e8769. doi:10.1371/journal.pone.0008769
165. Fratti RA, Backer JM, Gruenberg J, Corvera S, Deretic V. Role of phosphatidylinositol 3-kinase and Rab5 effectors in phagosomal biogenesis and mycobacterial phagosome maturation arrest. *J Cell Biol* (2001) 154:631–44. doi:10.1083/jcb.200106049
166. Gaur RL, Ren K, Blumenthal A, Bhamidi S, González-Nilo FD, Jackson M, et al. LprG-mediated surface expression of lipoarabinomannan is essential for virulence of *Mycobacterium tuberculosis*. *PLoS Pathog* (2014) 10:e1004376. doi:10.1371/journal.ppat.1004376
167. Shukla S, Richardson ET, Athman JJ, Shi L, Wearsch PA, McDonald D, et al. *Mycobacterium tuberculosis* lipoprotein LprG binds lipoarabinomannan and determines its cell envelope localization to control phagolysosomal fusion. *PLoS Pathog* (2014) 10:e1004471. doi:10.1371/journal.ppat.1004471
168. Vázquez CL, Bianco MV, Blanco FC, Forrellad MA, Gutierrez MG, Bigi F. *Mycobacterium bovis* requires P27 (LprG) to arrest phagosome maturation and replicate within bovine macrophages. *Infect Immun* (2017) 85:e00720–16. doi:10.1128/IAI.00720-16
169. Kang PB, Azad AK, Torrelles JB, Kaufman TM, Beharka A, Tibesar E, et al. The human macrophage mannose receptor directs *Mycobacterium tuberculosis* lipoarabinomannan-mediated phagosome biogenesis. *J Exp Med* (2005) 202:987–99. doi:10.1084/jem.20051239
170. Esparza M, Palomares B, García T, Espinosa P, Zenteno E, Mancilla R. PstS-1, the 38-kDa *Mycobacterium tuberculosis* glycoprotein, is an adhesin, which binds the macrophage mannose receptor and promotes phagocytosis. *Scand J Immunol* (2015) 81:46–55. doi:10.1111/sji.12249
171. Welin A, Winberg ME, Abdalla H, Särndahl E, Rasmusson B, Stendahl O, et al. Incorporation of *Mycobacterium tuberculosis* lipoarabinomannan into macrophage membrane rafts is a prerequisite for the phagosomal maturation block. *Infect Immun* (2008) 76:2882–7. doi:10.1128/IAI.01549-07
172. Ishikawa E, Ishikawa T, Morita YS, Toyonaga K, Yamada H, Takeuchi O, et al. Direct recognition of the mycobacterial glycolipid, trehalose dimycolate, by C-type lectin Mincle. *J Exp Med* (2016) 206:2879–88. doi:10.1084/jem.20091750
173. Chandra P, Ghanwat S, Matta SK, Yadav SS, Mehta M, Siddiqui Z, et al. *Mycobacterium tuberculosis* inhibits Rab7 recruitment to selectively modulate autophagy flux in macrophages. *Sci Rep* (2015) 5:16320. doi:10.1038/srep16320
174. Hu D, Wu J, Wang W, Mu M, Zhao R, Xu X, et al. Autophagy regulation revealed by SapM-induced block of autophagosome-lysosome fusion via binding Rab7. *Biochem Biophys Res Commun* (2015) 461:401–7. doi:10.1016/j.bbrc.2015.04.051
175. Chen Z, Wang T, Liu Z, Zhang G, Wang J, Feng S, et al. Inhibition of autophagy by miR-30A induced by *Mycobacteria tuberculosis* as a possible mechanism of immune escape in human macrophages. *Jpn J Infect Dis* (2015) 68:420–4. doi:10.7883/yoken.JJID.2014.466
176. Kim JK, Yuk JM, Kim SY, Kim TS, Jin HS, Yang CS, et al. MicroRNA-125a inhibits autophagy activation and antimicrobial responses during mycobacterial infection. *J Immunol* (2015) 194:5355–65. doi:10.4049/jimmunol.1402557
177. Ouimet M, Koster S, Sakowski E, Ramkhelawon B, van Solingen C, Oldebeken S, et al. *Mycobacterium tuberculosis* induces the miR-33 locus to reprogram autophagy and host lipid metabolism. *Nat Immunol* (2016) 17:677–86. doi:10.1038/ni.3434
178. Kumar R, Sahu SK, Kumar M, Jana K, Gupta P, Gupta UD, et al. MicroRNA 17-5p regulates autophagy in *Mycobacterium tuberculosis*-infected macrophages by targeting Mcl-1 and STAT3. *Cell Microbiol* (2016) 18:679–91. doi:10.1111/cmi.12540
179. Gu X, Gao Y, Mu DG, Fu EQ. miR-23a-5p modulates mycobacterial survival and autophagy during *Mycobacterium tuberculosis* infection through TLR2/MyD88/NF-κB pathway. *Exp Cell Res* (2017) 354:71–7. doi:10.1016/j.yexcr.2017.03.039
180. Dodd CE, Pyle CJ, Glowinski R, Rajaram MV, Schlesinger LS. CD36-mediated uptake of surfactant lipids by human macrophages promotes intracellular growth of *Mycobacterium tuberculosis*. *J Immunol* (2016) 197:4727–35. doi:10.4049/jimmunol.1600856
181. Nordenfelt P, Grinstein S, Bjorck L, Tapper H. V-ATPase-mediated phagosomal acidification is impaired by *Streptococcus pyogenes* through Mga-regulated surface proteins. *Microbes Infect* (2012) 14:1319–29. doi:10.1016/j.micinf.2012.08.005
182. Strasser JE, Newman SL, Ciraolo GM, Morris RE, Howell ML, Dean GE. Regulation of the macrophage vacuolar ATPase and phagosome-lysosome fusion by *Histoplasma capsulatum*. *J Immunol* (1999) 162:6148–54.
183. Toyooka K, Takai S, Kirikae T. *Rhodococcus equi* can survive a phagolysosomal environment in macrophages by suppressing acidification of the phagolysosome. *J Med Microbiol* (2005) 54:1007–15. doi:10.1099/jmm.0.46086-0
184. Pujol C, Klein KA, Romanov GA, Palmer LE, Cirota C, Zhao Z, et al. *Yersinia pestis* can reside in autophagosomes and avoid xenophagy in murine macrophages by preventing vacuole acidification. *Infect Immun* (2009) 77:2251–61. doi:10.1128/IAI.00068-09
185. Fernández-Arenas E, Bleck CK, Nombela C, Gil C, Griffiths G, Diez-Orejas R. *Candida albicans* actively modulates intracellular membrane trafficking in mouse macrophage phagosomes. *Cell Microbiol* (2009) 11:560–89. doi:10.1111/j.1462-5822.2008.01274.x
186. Mosleh IM, Huber LA, Steinlein P, Pasquali C, Gunther D, Meyer TF. *Neisseria gonorrhoeae* porin modulates phagosome maturation. *J Biol Chem* (1998) 273:35332–8. doi:10.1074/jbc.273.52.35332
187. Binker MG, Cosen-Binker LI, Terebiznik MR, Mallo GV, McCaw SE, Eskelinen EL, et al. Arrested maturation of *Neisseria*-containing phagosomes in the absence of the lysosome-associated membrane proteins, LAMP-1 and LAMP-2. *Cell Microbiol* (2007) 9:2153–66. doi:10.1111/j.1462-5822.2007.00946.x
188. Hertzen E, Johansson L, Wallin R, Schmidt H, Kroll M, Rehn AP, et al. M1 protein-dependent intracellular trafficking promotes persistence and replication of *Streptococcus pyogenes* in macrophages. *J Innate Immun* (2010) 2:534–45. doi:10.1159/000317635
189. Kagan JC, Roy CR. *Legionella* phagosomes intercept vesicular traffic from endoplasmic reticulum exit sites. *Nat Cell Biol* (2002) 4:945–54. doi:10.1038/ncb883
190. Ewann F, Hoffman PS. Cysteine metabolism in *Legionella pneumophila*: characterization of an L-cystine-utilizing mutant. *Appl Environ Microbiol* (2006) 72:3993–4000. doi:10.1128/AEM.00684-06
191. Celli J, de Chastellier C, Franchini DM, Pizarro-Cerda J, Moreno E, Gorvel JP. *Brucella* evades macrophage killing via VirB-dependent sustained

interactions with the endoplasmic reticulum. *J Exp Med* (2003) 198:545–56. doi:10.1084/jem.20030088
192. Ghigo E, Colombo MI, Heinzen RA. The *Coxiella burnetii* parasitophorous vacuole. *Adv Exp Med Biol* (2012) 984:141–69. doi:10.1007/978-94-007-4315-1_8
193. Graham JG, MacDonald LJ, Hussain SK, Sharma UM, Kurten RC, Voth DE. Virulent *Coxiella burnetii* pathotypes productively infect primary human alveolar macrophages. *Cell Microbiol* (2013) 15:1012–25. doi:10.1111/cmi.12096
194. Holm A, Tejle K, Magnusson KE, Descoteaux A, Rasmusson B. *Leishmania donovani* lipophosphoglycan causes periphagosomal actin accumulation: correlation with impaired translocation of PKCα and defective phagosome maturation. *Cell Microbiol* (2001) 3:439–47. doi:10.1046/j.1462-5822.2001.00127.x
195. Rodriguez NE, Gaur Dixit U, Allen LA, Wilson ME. Stage-specific pathways of *Leishmania infantum chagasi* entry and phagosome maturation in macrophages. *PLoS One* (2011) 6:e19000. doi:10.1371/journal.pone.0019000
196. Fratti RA, Chua J, Deretic V. Induction of p38 mitogen-activated protein kinase reduces early endosome autoantigen 1 (EEA1) recruitment to phagosomal membranes. *J Biol Chem* (2003) 278:46961–7. doi:10.1074/jbc.M305225200
197. Horwitz MA. Formation of a novel phagosome by the Legionnaires' disease bacterium (*Legionella pneumophila*) in human monocytes. *J Exp Med* (1983) 158:1319–31. doi:10.1084/jem.158.4.1319
198. Coers J, Monahan C, Roy CR. Modulation of phagosome biogenesis by *Legionella pneumophila* creates an organelle permissive for intracellular growth. *Nat Cell Biol* (1999) 1:451–3. doi:10.1038/15687
199. Nagai H, Kagan JC, Zhu X, Kahn RA, Roy CR. A bacterial guanine nucleotide exchange factor activates ARF on *Legionella* phagosomes. *Science* (2002) 295:679–82. doi:10.1126/science.1067025
200. Arenas GN, Grilli DJ, Samartino LE, Magadan J, Mayorga LS. *Brucella* alters endocytic pathway in J774 macrophages. *Virulence* (2010) 1:376–85. doi:10.4161/viru.1.5.12861
201. Arellano-Reynoso B, Lapaque N, Salcedo S, Briones G, Ciocchini AE, Ugalde R, et al. Cyclic β-1,2-glucan is a *Brucella* virulence factor required for intracellular survival. *Nat Immunol* (2005) 6:618–25. doi:10.1038/ni1202
202. Puri RV, Reddy PV, Tyagi AK. Secreted acid phosphatase (SapM) of *Mycobacterium tuberculosis* is indispensable for arresting phagosomal maturation and growth of the pathogen in guinea pig tissues. *PLoS One* (2013) 8:e70514. doi:10.1371/journal.pone.0070514
203. Morton CO, Bouzani M, Loeffler J, Rogers TR. Direct interaction studies between *Aspergillus fumigatus* and human immune cells; what have we learned about pathogenicity and host immunity? *Front Microbiol* (2012) 3:413. doi:10.3389/fmicb.2012.00413
204. Sacks D, Sher A. Evasion of innate immunity by parasitic protozoa. *Nat Immunol* (2002) 3:1041–7. doi:10.1038/ni1102-1041
205. Thywissen A, Heinekamp T, Dahse HM, Schmaler-Ripcke J, Nietzsche S, Zipfel PF, et al. Conidial dihydroxynaphthalene melanin of the human pathogenic fungus *Aspergillus fumigatus* interferes with the host endocytosis pathway. *Front Microbiol* (2011) 2:96. doi:10.3389/fmicb.2011.00096
206. Bera A, Herbert S, Jakob A, Vollmer W, Gotz F. Why are pathogenic staphylococci so lysozyme resistant? The peptidoglycan O-acetyltransferase OatA is the major determinant for lysozyme resistance of *Staphylococcus aureus*. *Mol Microbiol* (2005) 55:778–87. doi:10.1111/j.1365-2958.2004.04446.x
207. Herbert S, Bera A, Nerz C, Kraus D, Peschel A, Goerke C, et al. Molecular basis of resistance to muramidase and cationic antimicrobial peptide activity of lysozyme in staphylococci. *PLoS Pathog* (2007) 3:e102. doi:10.1371/journal.ppat.0030102
208. Jin T, Bokarewa M, Foster T, Mitchell J, Higgins J, Tarkowski A. *Staphylococcus aureus* resists human defensins by production of staphylokinase, a novel bacterial evasion mechanism. *J Immunol* (2004) 172:1169–76. doi:10.4049/jimmunol.172.2.1169
209. Peschel A, Jack RW, Otto M, Collins LV, Staubitz P, Nicholson G, et al. *Staphylococcus aureus* resistance to human defensins and evasion of neutrophil killing via the novel virulence factor MprF is based on modification of membrane lipids with L-lysine. *J Exp Med* (2001) 193:1067–76. doi:10.1084/jem.193.9.1067
210. Weidenmaier C, Peschel A. Teichoic acids and related cell-wall glycopolymers in Gram-positive physiology and host interactions. *Nat Rev Microbiol* (2008) 6:276–87. doi:10.1038/nrmicro1861
211. Sieprawska-Lupa M, Mydel P, Krawczyk K, Wojcik K, Puklo M, Lupa B, et al. Degradation of human antimicrobial peptide LL-37 by *Staphylococcus aureus*-derived proteinases. *Antimicrob Agents Chemother* (2004) 48:4673–9. doi:10.1128/AAC.48.12.4673-4679.2004
212. Liu GY, Essex A, Buchanan JT, Datta V, Hoffman HM, Bastian JF, et al. *Staphylococcus aureus* golden pigment impairs neutrophil killing and promotes virulence through its antioxidant activity. *J Exp Med* (2005) 202:209–15. doi:10.1084/jem.20050846
213. Ballal A, Manna AC. Regulation of superoxide dismutase (sod) genes by SarA in *Staphylococcus aureus*. *J Bacteriol* (2009) 191:3301–10. doi:10.1128/JB.01496-08
214. Mandell GL. Catalase, superoxide dismutase, and virulence of *Staphylococcus aureus*. In vitro and in vivo studies with emphasis on staphylococcal-leukocyte interaction. *J Clin Invest* (1975) 55:561–6. doi:10.1172/JCI107963
215. Cosgrove K, Coutts G, Jonsson IM, Tarkowski A, Kokai-Kun JF, Mond JJ, et al. Catalase (KatA) and alkyl hydroperoxide reductase (AhpC) have compensatory roles in peroxide stress resistance and are required for survival, persistence, and nasal colonization in *Staphylococcus aureus*. *J Bacteriol* (2007) 189:1025–35. doi:10.1128/JB.01524-06
216. Gonçalves VL, Nobre LS, Vicente JB, Teixeira M, Saraiva LM. Flavohemoglobin requires microaerophilic conditions for nitrosative protection of *Staphylococcus aureus*. *FEBS Lett* (2006) 580:1817–21. doi:10.1016/j.febslet.2006.02.039
217. Richardson AR, Dunman PM, Fang FC. The nitrosative stress response of *Staphylococcus aureus* is required for resistance to innate immunity. *Mol Microbiol* (2006) 61:927–39. doi:10.1111/j.1365-2958.2006.05290.x
218. Bore E, Langsrud S, Langsrud O, Rode TM, Holck A. Acid-shock responses in *Staphylococcus aureus* investigated by global gene expression analysis. *Microbiology* (2007) 153:2289–303. doi:10.1099/mic.0.2007/005942-0
219. Beasley FC, Vines ED, Grigg JC, Zheng Q, Liu S, Lajoie GA, et al. Characterization of staphyloferrin A biosynthetic and transport mutants in *Staphylococcus aureus*. *Mol Microbiol* (2009) 72:947–63. doi:10.1111/j.1365-2958.2009.06698.x
220. Cheung J, Beasley FC, Liu S, Lajoie GA, Heinrichs DE. Molecular characterization of staphyloferrin B biosynthesis in *Staphylococcus aureus*. *Mol Microbiol* (2009) 74:594–608. doi:10.1111/j.1365-2958.2009.06880.x
221. Schwartz JT, Allen LA. Role of urease in megasome formation and *Helicobacter pylori* survival in macrophages. *J Leukoc Biol* (2006) 79:1214–25. doi:10.1189/jlb.0106030
222. Johnston SA, May RC. *Cryptococcus* interactions with macrophages: evasion and manipulation of the phagosome by a fungal pathogen. *Cell Microbiol* (2013) 15:403–11. doi:10.1111/cmi.12067
223. Mirbod-Donovan F, Schaller R, Hung CY, Xue J, Reichard U, Cole GT. Urease produced by *Coccidioides posadasii* contributes to the virulence of this respiratory pathogen. *Infect Immun* (2006) 74:504–15. doi:10.1128/IAI.74.1.504-515.2006
224. Malachowa N, Kohler PL, Schlievert PM, Chuang ON, Dunny GM, Kobayashi SD, et al. Characterization of a *Staphylococcus aureus* surface virulence factor that promotes resistance to oxidative killing and infectious endocarditis. *Infect Immun* (2011) 79:342–52. doi:10.1128/IAI.00736-10
225. Kinkel TL, Roux CM, Dunman PM, Fang FC. The *Staphylococcus aureus* SrrAB two-component system promotes resistance to nitrosative stress and hypoxia. *MBio* (2013) 4:e00696–13. doi:10.1128/mBio.00696-13
226. Sethi D, Mahajan S, Singh C, Lama A, Hade MD, Gupta P, et al. Lipoprotein LprI of *Mycobacterium tuberculosis* acts as a lysozyme inhibitor. *J Biol Chem* (2016) 291:2938–53. doi:10.1074/jbc.M115.662593
227. Miller JL, Velmurugan K, Cowan MJ, Briken V. The type I NADH dehydrogenase of *Mycobacterium tuberculosis* counters phagosomal NOX2 activity to inhibit TNF-alpha-mediated host cell apoptosis. *PLoS Pathog* (2010) 6:e1000864. doi:10.1371/journal.ppat.1000864
228. Shin DM, Jeon BY, Lee HM, Jin HS, Yuk JM, Song CH, et al. *Mycobacterium tuberculosis* eis regulates autophagy, inflammation, and cell death through redox-dependent signaling. *PLoS Pathog* (2010) 6:e1001230. doi:10.1371/journal.ppat.1001230
229. Guo Y, Deng Y, Huang Z, Luo Q, Peng Y, Chen J, et al. EBP50 induces apoptosis in macrophages by upregulating nitric oxide production to eliminate intracellular *Mycobacterium tuberculosis*. *Sci Rep* (2016) 6:18961. doi:10.1038/srep18961

230. Serafini A, Boldrin F, Palù G, Manganelli R. Characterization of a *Mycobacterium tuberculosis* ESX-3 conditional mutant: essentiality and rescue by iron and zinc. *J Bacteriol* (2009) 191:6340–4. doi:10.1128/JB.00756-09
231. Siegrist MS, Steigedal M, Ahmad R, Mehra A, Dragset MS, Schuster BM, et al. Mycobacterial Esx-3 requires multiple components for iron acquisition. *MBio* (2014) 5:e01073–14. doi:10.1128/mBio.01073-14
232. Wells RM, Jones CM, Xi Z, Speer A, Danilchanka O, Doornbos KS, et al. Discovery of a siderophore export system essential for virulence of *Mycobacterium tuberculosis*. *PLoS Pathog* (2013) 9:e1003120. doi:10.1371/journal.ppat.1003120
233. Beasley FC, Marolda CL, Cheung J, Buac S, Heinrichs DE. *Staphylococcus aureus* transporters Hts, Sir, and Sst capture iron liberated from human transferrin by staphyloferrin A, staphyloferrin B, and catecholamine stress hormones, respectively, and contribute to virulence. *Infect Immun* (2011) 79:2345–55. doi:10.1128/IAI.00117-11
234. Rodriguez GM, Smith I. Identification of an ABC transporter required for iron acquisition and virulence in *Mycobacterium tuberculosis*. *J Bacteriol* (2006) 188:424–30. doi:10.1128/JB.188.2.424-430.2006
235. Ryndak MB, Wang S, Smith I, Rodriguez GM. The *Mycobacterium tuberculosis* high-affinity iron importer, IrtA, contains an FAD-binding domain. *J Bacteriol* (2010) 192:861–9. doi:10.1128/JB.00223-09
236. Pandey AK, Sassetti CM. Mycobacterial persistence requires the utilization of host cholesterol. *Proc Natl Acad Sci U S A* (2008) 105:4376–80. doi:10.1073/pnas.0711159105
237. Singh V, Jamwal S, Jain R, Verma P, Gokhale R, Rao KV. *Mycobacterium tuberculosis*-driven targeted recalibration of macrophage lipid homeostasis promotes the foamy phenotype. *Cell Host Microbe* (2012) 12:669–81. doi:10.1016/j.chom.2012.09.012
238. Eoh H, Rhee KY. Methylcitrate cycle defines the bactericidal essentiality of isocitrate lyase for survival of *Mycobacterium tuberculosis* on fatty acids. *Proc Natl Acad Sci U S A* (2014) 111:4976–81. doi:10.1073/pnas.1400390111
239. Vornhagen J, Adams Waldorf KM, Rajagopal L. Perinatal group B streptococcal infections: virulence factors, immunity, and prevention strategies. *Trends Microbiol* (2017). doi:10.1016/j.tim.2017.05.013
240. Maisey HC, Doran KS, Nizet V. Recent advances in understanding the molecular basis of group B *Streptococcus* virulence. *Expert Rev Mol Med* (2008) 10:e27. doi:10.1017/S1462399408000811
241. Rajagopal L. Understanding the regulation of group B streptococcal virulence factors. *Future Microbiol* (2009) 4:201–21. doi:10.2217/17460913.4.2.201
242. Borlace GN, Keep SJ, Prodoehl MJ, Jones HF, Butler RN, Brooks DA. A role for altered phagosome maturation in the long-term persistence of *Helicobacter pylori* infection. *Am J Physiol Gastrointest Liver Physiol* (2012) 303:G169–79. doi:10.1152/ajpgi.00320.2011
243. Basu M, Czinn SJ, Blanchard TG. Absence of catalase reduces long-term survival of *Helicobacter pylori* in macrophage phagosomes. *Helicobacter* (2004) 9:211–6. doi:10.1111/j.1083-4389.2004.00226.x
244. Gobert AP, McGee DJ, Akhtar M, Mendz GL, Newton JC, Cheng Y, et al. *Helicobacter pylori* arginase inhibits nitric oxide production by eukaryotic cells: a strategy for bacterial survival. *Proc Natl Acad Sci U S A* (2001) 98:13844–9. doi:10.1073/pnas.241443798
245. Gobert AP, Wilson KT. The immune battle against *Helicobacter pylori* infection: NO offense. *Trends Microbiol* (2016) 24:366–76. doi:10.1016/j.tim.2016.02.005
246. Hwang CS, Rhie GE, Oh JH, Huh WK, Yim HS, Kang SO. Copper- and zinc-containing superoxide dismutase (Cu/ZnSOD) is required for the protection of *Candida albicans* against oxidative stresses and the expression of its full virulence. *Microbiology* (2002) 148:3705–13. doi:10.1099/00221287-148-11-3705
247. Enjalbert B, MacCallum DM, Odds FC, Brown AJ. Niche-specific activation of the oxidative stress response by the pathogenic fungus *Candida albicans*. *Infect Immun* (2007) 75:2143–51. doi:10.1128/IAI.01680-06
248. Mayer FL, Wilson D, Hube B. *Candida albicans* pathogenicity mechanisms. *Virulence* (2013) 4:119–28. doi:10.4161/viru.22913
249. Holbrook ED, Smolnycki KA, Youseff BH, Rappleye CA. Redundant catalases detoxify phagocyte reactive oxygen and facilitate *Histoplasma capsulatum* pathogenesis. *Infect Immun* (2013) 81:2334–46. doi:10.1128/IAI.00173-13
250. Brown SM, Campbell LT, Lodge JK. *Cryptococcus neoformans*, a fungus under stress. *Curr Opin Microbiol* (2007) 10:320–5. doi:10.1016/j.mib.2007.05.014
251. Zaragoza O, Chrisman CJ, Castelli MV, Frases S, Cuenca-Estrella M, Rodriguez-Tudela JL, et al. Capsule enlargement in *Cryptococcus neoformans* confers resistance to oxidative stress suggesting a mechanism for intracellular survival. *Cell Microbiol* (2008) 10:2043–57. doi:10.1111/j.1462-5822.2008.01186.x
252. Rocco NM, Carmen JC, Klein BS. *Blastomyces dermatitidis* yeast cells inhibit nitric oxide production by alveolar macrophage inducible nitric oxide synthase. *Infect Immun* (2011) 79:2385–95. doi:10.1128/IAI.01249-10
253. Kehl-Fie TE, Zhang Y, Moore JL, Farrand AJ, Hood MI, Rathi S, et al. MntABC and MntH contribute to systemic *Staphylococcus aureus* infection by competing with calprotectin for nutrient manganese. *Infect Immun* (2013) 81:3395–405. doi:10.1128/IAI.00420-13
254. Schrettl M, Haas H. Iron homeostasis – Achilles' heel of *Aspergillus fumigatus*? *Curr Opin Microbiol* (2011) 14:400–5. doi:10.1016/j.mib.2011.06.002
255. Inglis DO, Voorhies M, Hocking Murray DR, Sil A. Comparative transcriptomics of infectious spores from the fungal pathogen *Histoplasma capsulatum* reveals a core set of transcripts that specify infectious and pathogenic states. *Eukaryot Cell* (2013) 12:828–52. doi:10.1128/EC.00069-13
256. Vromman F, Subtil A. Exploitation of host lipids by bacteria. *Curr Opin Microbiol* (2014) 17:38–45. doi:10.1016/j.mib.2013.11.003
257. Alvarez M, Casadevall A. Phagosome extrusion and host-cell survival after *Cryptococcus neoformans* phagocytosis by macrophages. *Curr Biol* (2006) 16:2161–5. doi:10.1016/j.cub.2006.09.061
258. Nicola AM, Robertson EJ, Albuquerque P, Derengowski Lda S, Casadevall A. Nonlytic exocytosis of *Cryptococcus neoformans* from macrophages occurs in vivo and is influenced by phagosomal pH. *MBio* (2011) 2:e00167–11. doi:10.1128/mBio.00167-11
259. Johnston SA, May RC. The human fungal pathogen *Cryptococcus neoformans* escapes macrophages by a phagosome emptying mechanism that is inhibited by Arp2/3 complex-mediated actin polymerisation. *PLoS Pathog* (2010) 6:e1001041. doi:10.1371/journal.ppat.1001041
260. Chayakulkeeree M, Johnston SA, Oei JB, Lev S, Williamson PR, Wilson CF, et al. SEC14 is a specific requirement for secretion of phospholipase B1 and pathogenicity of *Cryptococcus neoformans*. *Mol Microbiol* (2011) 80:1088–101. doi:10.1111/j.1365-2958.2011.07632.x
261. Smith LM, Dixon EF, May RC. The fungal pathogen *Cryptococcus neoformans* manipulates macrophage phagosome maturation. *Cell Microbiol* (2015) 17:702–13. doi:10.1111/cmi.12394
262. Bain JM, Lewis LE, Okai B, Quinn J, Gow NA, Erwig LP. Non-lytic expulsion/exocytosis of *Candida albicans* from macrophages. *Fungal Genet Biol* (2012) 49:677–8. doi:10.1016/j.fgb.2012.01.008
263. García-Rodas R, González-Camacho F, Rodríguez-Tudela JL, Cuenca-Estrella M, Zaragoza O. The interaction between *Candida krusei* and murine macrophages results in multiple outcomes, including intracellular survival and escape from killing. *Infect Immun* (2011) 79:2136–44. doi:10.1128/IAI.00044-11
264. Schnupf P, Portnoy DA. Listeriolysin O: a phagosome-specific lysin. *Microbes Infect* (2007) 9:1176–87. doi:10.1016/j.micinf.2007.05.005
265. Goldfine H, Wadsworth SJ, Johnston NC. Activation of host phospholipases C and D in macrophages after infection with *Listeria monocytogenes*. *Infect Immun* (2000) 68:5735–41. doi:10.1128/IAI.68.10.5735-5741.2000
266. Kocks C, Gouin E, Tabouret M, Berche P, Ohayon H, Cossart P. *L. monocytogenes*-induced actin assembly requires the actA gene product, a surface protein. *Cell* (1992) 68:521–31. doi:10.1016/0092-8674(92)90188-I
267. Pistor S, Gröbe L, Sechi AS, Domann E, Gerstel B, Machesky LM, et al. Mutations of arginine residues within the 146-KKRRK-150 motif of the ActA protein of *Listeria monocytogenes* abolish intracellular motility by interfering with the recruitment of the Arp2/3 complex. *J Cell Sci* (2000) 113:3277–87.
268. Portnoy DA, Auerbuch V, Glomski IJ. The cell biology of *Listeria monocytogenes* infection: the intersection of bacterial pathogenesis and cell-mediated immunity. *J Cell Biol* (2002) 158:409–14. doi:10.1083/jcb.200205009
269. Wang R, Braughton KR, Kretschmer D, Bach TH, Queck SY, Li M, et al. Identification of novel cytolytic peptides as key virulence determinants for community-associated MRSA. *Nat Med* (2007) 13:1510–4. doi:10.1038/nm1656
270. Peschel A, Otto M. Phenol-soluble modulins and staphylococcal infection. *Nat Rev Microbiol* (2013) 11:667–73. doi:10.1038/nrmicro3110
271. Singh R, Jamieson A, Cresswell P. GILT is a critical host factor for *Listeria monocytogenes* infection. *Nature* (2008) 455:1244–7. doi:10.1038/nature07344

272. Marteyn B, Gazi A, Sansonetti P. *Shigella*: a model of virulence regulation in vivo. *Gut Microbes* (2012) 3:104–20. doi:10.4161/gmic.19325
273. Egile C, Loisel TP, Laurent V, Li R, Pantaloni D, Sansonetti PJ, et al. Activation of the CDC42 effector N-WASP by the *Shigella flexneri* IcsA protein promotes actin nucleation by Arp2/3 complex and bacterial actin-based motility. *J Cell Biol* (1999) 146:1319–32. doi:10.1083/jcb.146.6.1319
274. Walker DH, Feng HM, Popov VL. Rickettsial phospholipase A2 as a pathogenic mechanism in a model of cell injury by typhus and spotted fever group rickettsiae. *Am J Trop Med Hyg* (2001) 65:936–42. doi:10.4269/ajtmh.2001.65.936
275. Gouin E, Egile C, Dehoux P, Villiers V, Adams J, Gertler F, et al. The RickA protein of *Rickettsia conorii* activates the Arp2/3 complex. *Nature* (2004) 427:457–61. doi:10.1038/nature02318
276. Surewaard BG, de Haas CJ, Vervoort F, Rigby KM, DeLeo FR, Otto M, et al. Staphylococcal alpha-phenol soluble modulins contribute to neutrophil lysis after phagocytosis. *Cell Microbiol* (2013) 15:1427–37. doi:10.1111/cmi.12130
277. Myrvik QN, Leake ES, Wright MJ. Disruption of phagosomal membranes of normal alveolar macrophages by the H37Rv strain of *Mycobacterium tuberculosis*. A correlate of virulence. *Am Rev Respir Dis* (1984) 129:322–8.
278. Simeone R, Bobard A, Lippmann J, Bitter W, Majlessi L, Brosch R, et al. Phagosomal rupture by *Mycobacterium tuberculosis* results in toxicity and host cell death. *PLoS Pathog* (2012) 8:e1002507. doi:10.1371/journal.ppat.1002507
279. Stamm LM, Morisaki JH, Gao LY, Jeng RL, McDonald KL, Roth R, et al. *Mycobacterium marinum* escapes from phagosomes and is propelled by actin-based motility. *J Exp Med* (2003) 198:1361–8. doi:10.1084/jem.20031072
280. Stamm LM, Pak MA, Morisaki JH, Snapper SB, Rottner K, Lommel S, et al. Role of the WASP family proteins for *Mycobacterium marinum* actin tail formation. *Proc Natl Acad Sci U S A* (2005) 102:14837–42. doi:10.1073/pnas.0504663102
281. Gao LY, Guo S, McLaughlin B, Morisaki H, Engel JN, Brown EJ. A mycobacterial virulence gene cluster extending RD1 is required for cytolysis, bacterial spreading and ESAT-6 secretion. *Mol Microbiol* (2004) 53:1677–93. doi:10.1111/j.1365-2958.2004.04261.x
282. Smith J, Manoranjan J, Pan M, Bohsali A, Xu J, Liu J, et al. Evidence for pore formation in host cell membranes by ESX-1-secreted ESAT-6 and its role in *Mycobacterium marinum* escape from the vacuole. *Infect Immun* (2008) 76:5478–87. doi:10.1128/IAI.00614-08
283. van der Wel N, Hava D, Houben D, Fluitsma D, van Zon M, Pierson J, et al. *M. tuberculosis* and *M. leprae* translocate from the phagolysosome to the cytosol in myeloid cells. *Cell* (2007) 129:1287–98. doi:10.1016/j.cell.2007.05.059
284. Simeone R, Sayes F, Song O, Gröschel MI, Brodin P, Brosch R, et al. Cytosolic access of *Mycobacterium tuberculosis*: critical impact of phagosomal acidification control and demonstration of occurrence in vivo. *PLoS Pathog* (2015) 6:e1004650. doi:10.1371/journal.ppat.1004650
285. Russell DG. The ins and outs of the *Mycobacterium tuberculosis*-containing vacuole. *Cell Microbiol* (2016) 18:1065–9. doi:10.1111/cmi.12623
286. Danilchanka O, Sun J, Pavlenok M, Maueröder C, Speer A, Siroy A, et al. An outer membrane channel protein of *Mycobacterium tuberculosis* with exotoxin activity. *Proc Natl Acad Sci U S A* (2014) 111:6750–5. doi:10.1073/pnas.1400136111
287. Sun J, Siroy A, Lokareddy RK, Speer A, Doornbos KS, Cingolani G, et al. The tuberculosis necrotizing toxin kills macrophages by hydrolyzing NAD. *Nat Struct Mol Biol* (2015) 22:672–8. doi:10.1038/nsmb.3064
288. Quigley J, Hughitt VK, Velikovsky CA, Mariuzza RA, El-Sayed NM, Briken V. The cell wall lipid PDIM contributes to phagosomal escape and host cell exit of *Mycobacterium tuberculosis*. *MBio* (2017) 8:e00148–17. doi:10.1128/mBio.00148-17
289. Steiger J, Stephan A, Inkeles MS, Realegeno S, Bruns H, Kröll P, et al. Imatinib triggers phagolysosome acidification and antimicrobial activity against *Mycobacterium bovis* bacille Calmette-Guérin in glucocorticoid-treated human macrophages. *J Immunol* (2016) 197:222–32. doi:10.4049/jimmunol.1502407
290. Zhou J, Xu R, Du XZ, Zhou XD, Li Q. Saxifragifolin D attenuates phagosome maturation arrest in *Mycobacterium tuberculosis*-infected macrophages via an AMPK and VPS34-dependent pathway. *AMB Express* (2017) 7:11. doi:10.1186/s13568-016-0317-6
291. Wang Z, Sun D, Chen G, Li G, Dou S, Wang R, et al. Tim-3 inhibits macrophage control of *Listeria monocytogenes* by inhibiting Nrf2. *Sci Rep* (2017) 7:42095. doi:10.1038/srep42095
292. Kumar SK, Singh P, Sinha S. Naturally produced opsonizing antibodies restrict the survival of *Mycobacterium tuberculosis* in human macrophages by augmenting phagosome maturation. *Open Biol* (2015) 5:150171. doi:10.1098/rsob.150171
293. Thomer L, Emolo C, Thammavongsa V, Kim HK, McAdow ME, Yu W, et al. Antibodies against a secreted product of *Staphylococcus aureus* trigger phagocytic killing. *J Exp Med* (2016) 213:293–301. doi:10.1084/jem.20150074
294. Thammavongsa V, Rauch S, Kim HK, Missiakas DM, Schneewind O. Protein A-neutralizing monoclonal antibody protects neonatal mice against *Staphylococcus aureus*. *Vaccine* (2015) 33:523–6. doi:10.1016/j.vaccine.2014.11.051
295. McGuinness WA, Kobayashi SD, DeLeo FR. Evasion of neutrophil killing by *Staphylococcus aureus*. *Pathogens* (2016) 5:E32. doi:10.3390/pathogens5010032
296. Herweg JA, Hansmeier N, Otto A, Geffken AC, Subbarayal P, Prusty BK, et al. Purification and proteomics of pathogen-modified vacuoles and membranes. *Front Cell Infect Microbiol* (2015) 5:48. doi:10.3389/fcimb.2015.00048
297. Mattow J, Siejak F, Hagens K, Becher D, Albrecht D, Krah A, et al. Proteins unique to intraphagosomally grown *Mycobacterium tuberculosis*. *Proteomics* (2006) 6:2485–94. doi:10.1002/pmic.200500547
298. Stuart LM, Boulais J, Charriere GM, Hennessy EJ, Brunet S, Jutras I, et al. A systems biology analysis of the *Drosophila* phagosome. *Nature* (2007) 445:95–101. doi:10.1038/nature05380
299. Shevchuk O, Batzilla C, Hägele S, Kusch H, Engelmann S, Hecker M, et al. Proteomic analysis of *Legionella*-containing phagosomes isolated from *Dictyostelium*. *Int J Med Microbiol* (2009) 299:489–508. doi:10.1016/j.ijmm.2009.03.006
300. Dill BD, Gierlinski M, Härtlova A, Arandilla AG, Guo M, Clarke RG, et al. Quantitative proteome analysis of temporally resolved phagosomes following uptake via key phagocytic receptors. *Mol Cell Proteomics* (2015) 14:1334–49. doi:10.1074/mcp.M114.044594
301. Canton J, Grinstein S. Measuring phagosomal pH by fluorescence microscopy. *Methods Mol Biol* (2017) 1519:185–99. doi:10.1007/978-1-4939-6581-6_12
302. Steinberg B, Magalhaes M, Grinstein S. Expression of genetically encoded fluorescent probes to monitor phospholipid dynamics in live neutrophils. *Methods Mol Biol* (2014) 1124:269–77. doi:10.1007/978-1-62703-845-4_17
303. Lu SM, Grinstein S, Fairn GD. Quantitative live-cell fluorescence microscopy during phagocytosis. *Methods Mol Biol* (2017) 1519:79–91. doi:10.1007/978-1-4939-6581-6_6
304. Quereda JJ, Sachse M, Balestrino D, Grenier T, Fredlund J, Danckaert A, et al. Assessing vacuolar escape of *Listeria monocytogenes*. *Methods Mol Biol* (2017) 1535:173–95. doi:10.1007/978-1-4939-6673-8_11
305. Tan S, Yates RM, Russell DG. *Mycobacterium tuberculosis*: readouts of bacterial fitness and the environment within the phagosome. *Methods Mol Biol* (2017) 1519:333–47. doi:10.1007/978-1-4939-6581-6_23
306. Liu Y, Tan S, Huang L, Abramovitch RB, Rohde KH, Zimmerman MD, et al. Immune activation of the host cell induces drug tolerance in *Mycobacterium tuberculosis* both in vitro and in vivo. *J Exp Med* (2016) 213:213. doi:10.1084/jem.20151248
307. Kulkarni R, Caskey J, Singh SK, Paudel S, Baral P, Schexnayder M, et al. Cigarette smoke extract-exposed methicillin-resistant *Staphylococcus aureus* regulates leukocyte function for pulmonary persistence. *Am J Respir Cell Mol Biol* (2016) 55:586–601. doi:10.1165/rcmb.2015-0397OC
308. Liu Q, Liu X, Yan F, He Y, Wei J, Zhang Y, et al. Comparative transcriptome analysis of *Brucella melitensis* in an acidic environment: identification of the two-component response regulator involved in the acid resistance and virulence of *Brucella*. *Microb Pathog* (2016) 91:92–8. doi:10.1016/j.micpath.2015.11.007
309. Ferrareze PAG, Streit RSA, Santos PRD, Santos FMD, Almeida RMC, Schrank A, et al. Transcriptional analysis allows genome reannotation and reveals that *Cryptococcus gattii* VGII undergoes nutrient restriction during infection. *Microorganisms* (2017) 5:E49. doi:10.3390/microorganisms5030049
310. Wu M, Gibbons JG, DeLoid GM, Bedugnis AS, Thimmulappa RK, Biswal S, et al. Immunomodulators targeting MARCO expression improve resistance to postinfluenza bacterial pneumonia. *Am J Physiol Lung Cell Mol Physiol* (2017) 313:L138–53. doi:10.1152/ajplung.00075.2017

311. Kalam H, Fontana MF, Kumar D. Alternate splicing of transcripts shape macrophage response to *Mycobacterium tuberculosis* infection. *PLoS Pathog* (2017) 13:e1006236. doi:10.1371/journal.ppat.1006236
312. O'Neill LA, Pearce EJ. Immunometabolism governs dendritic cell and macrophage function. *J Exp Med* (2016) 213:15–23. doi:10.1084/jem.20151570
313. Lecube A, Pachón G, Petriz J, Hernández C, Simó R. Phagocytic activity is impaired in type 2 diabetes mellitus and increases after metabolic improvement. *PLoS One* (2011) 6:e23366. doi:10.1371/journal.pone.0023366
314. Martinez N, Ketheesan N, West K, Vallerskog T, Kornfeld H. Impaired recognition of *Mycobacterium tuberculosis* by alveolar macrophages from diabetic mice. *J Infect Dis* (2016) 214:1629–37. doi:10.1093/infdis/jiw436
315. Kimmey JM, Huynh JP, Weiss LA, Park S, Kambal A, Debnath J, et al. Unique role for ATG5 in neutrophil-mediated immunopathology during *M. tuberculosis* infection. *Nature* (2015) 528:565–9. doi:10.1038/nature16451
316. Rengarajan M, Hayer A, Theriot JA. Endothelial cells use a formin-dependent phagocytosis-like process to internalize the bacterium *Listeria monocytogenes*. *PLoS Pathog* (2016) 12:e1005603. doi:10.1371/journal.ppat.1005603
317. Greenlee-Wacker MC. Clearance of apoptotic neutrophils and resolution of inflammation. *Immunol Rev* (2016) 273:357–70. doi:10.1111/imr.12453
318. Martin CJ, Peters KN, Behar SM. Macrophages clean up: efferocytosis and microbial control. *Curr Opin Microbiol* (2014) 17:17–23. doi:10.1016/j.mib.2013.10.007

Conflict of Interest Statement: The authors declare that this research was conducted in the absence of any commercial or financial relationships that could be construed as a potential conflict of interest.

Copyright © 2017 Uribe-Querol and Rosales. This is an open-access article distributed under the terms of the Creative Commons Attribution License (CC BY). The use, distribution or reproduction in other forums is permitted, provided the original author(s) or licensor are credited and that the original publication in this journal is cited, in accordance with accepted academic practice. No use, distribution or reproduction is permitted which does not comply with these terms.

frontiers in Immunology

MINI REVIEW
published: 22 September 2017
doi: 10.3389/fimmu.2017.01183

Autophagy Proteins in Phagocyte Endocytosis and Exocytosis

*Christian Münz**

Viral Immunobiology, Institute of Experimental Immunology, University of Zürich, Zürich, Switzerland

Autophagy was initially described as a catabolic pathway that recycles nutrients of cytoplasmic constituents after lysosomal degradation during starvation. Since the immune system monitors products of lysosomal degradation *via* major histocompatibility complex (MHC) class II restricted antigen presentation, autophagy was found to process intracellular antigens for display on MHC class II molecules. In recent years, however, it has become apparent that the molecular machinery of autophagy serves phagocytes in many more membrane trafficking pathways, thereby regulating immunity to infectious disease agents. In this minireview, we will summarize the recent evidence that autophagy proteins regulate phagocyte endocytosis and exocytosis for myeloid cell activation, pathogen replication, and MHC class I and II restricted antigen presentation. Selective stimulation and inhibition of the respective functional modules of the autophagy machinery might constitute valid therapeutic options in the discussed disease settings.

Keywords: major histocompatibility complex, LC3-associated phagocytosis, IL-1, Epstein–Barr virus, varicella zoster virus, poliovirus, coxsackievirus

OPEN ACCESS

Edited by:
Geanncarlo Lugo-Villarino, UMR5089 Institut de Pharmacologie et de Biologie Structurale (IPBS), France

Reviewed by:
Lilliana Radoshevich, Institut Pasteur, France
Mathias Faure, Claude Bernard University Lyon 1, France

***Correspondence:**
Christian Münz
christian.muenz@uzh.ch

Specialty section:
This article was submitted to Microbial Immunology, a section of the journal Frontiers in Immunology

Received: *26 July 2017*
Accepted: *07 September 2017*
Published: *22 September 2017*

Citation:
Münz C (2017) Autophagy Proteins in Phagocyte Endocytosis and Exocytosis. Front. Immunol. 8:1183. doi: 10.3389/fimmu.2017.01183

INTRODUCTION

Autophagy is a group of at least three pathways that deliver cytoplasmic constituents for lysosomal degradation (1). While microautophagy and chaperone-mediated autophagy directly operate at the late endosomal or lysosomal membrane for cytosolic substrate engulfment or translocation, respectively, macroautophagy assembles double-membrane surrounded vesicles *de novo*, which are then transported to lysosomes. For this autophagosome generation and delivery to lysosomes, autophagy-related gene (*atg*) products are essential, the first 15 of these were identified by Yoshinori Ohsumi in 1993 (2) and formed the basis of the molecular machinery of macroautophagy that led to his Nobel Prize in 2016. These Atgs are organized in complexes that integrate metabolic cues to regulate macroautophagy and modify membranes by lipid phosphorylation and ubiquitin-like protein conjugation to lipids, which result in autophagosome formation and substrate recruitment. The Atg1/ULK1 complex is regulated through phosphorylation by mammalian target of rapamycin (mTOR) inhibition and AMP-activated protein kinase (AMPK) activation. These two pathways sense nutrient or growth factor depletion *via* decreased mTOR activity and low-energy levels, resulting in elevated AMP concentration, and *via* increased AMPK activity. Atg1/ULK1 in turn phosphorylates Atg6/Beclin-1, a regulatory subunit of the VPS34 type III phosphatidylinositol 3-kinase (PI3K) complex. The resulting phosphoinositide mark on membranes serves as the landing platform for WIPI proteins that recruit *via* Atg16L1 binding the machinery to conjugate Atg8/LC3 to phosphatidylethanolamine, which might mediate both the fusion of additional membranes to this site for double-membrane elongation to a cup-shaped isolation membrane, resulting in fusion of these double membranes to autophagosomes, and substrate recruitment into the autophagosome (3–6).For this purpose, yeast Atg8 and its six mammalian orthologs LC3A, B, C, GABARAP, GABARAP-L1, and GABARAP-L2

are first processed by Atg4 to expose a *C*-terminal glycine for the ubiquitin-like conjugation reaction, which is then executed by the E1-like enzyme Atg7, the E2-like enzyme Atg3 and the E3-like enzyme Atg12-Atg5/Atg16L1. This enzymatic cascade leads to Atg8/LC3 coupling to the outer and inner autophagosome membrane. While some of these Atg8 orthologs have membrane fusion activity on their own, they recruit substrates often through intermediaries that contain LC3-interacting regions (LIRs) (6). These include proteins that get exposed on damaged organelles, such as mitochondria (7), and others that bridge ubiquitinated substrates, such as protein aggregates and cytosolic bacteria with LC3 (8, 9). The latter include sequestosome/p62, NBR1, NDP52, and optineurin and are often investigated as prototypic macroautophagy substrates. The completed autophagosome loses much of its LC3 from the outer membrane by deconjugation by Atg4, but retains some to facilitate transport along microtubules *via* FYCO1 and NDP52 recruitment (10, 11) and lysosome fusion *via* binding to PLEKHM1 (12). The much higher affinity of the PLEKHM1 LIR for GABARAPs might, however, indicate that these cytosolic functions are executed by Atg8 orthologs that do not belong to the LC3 subfamily (13). HOPS complex and Rab7 recruitment then prepare for lysosome fusion, which is executed by the SNAREs syntaxin17, SNAP29, and VAMP8 (14). This leads to lysosomal degradation of not only the autophagosome cargo but also the inner autophagosomal membrane including the Atg8/LC3 molecules that are still coupled to it. Therefore, Atg8/LC3 turnover, especially of its lipidated form LC3-II, serves also as a measure of macroautophagy. This modular format of the macroautophagy machinery lends itself to membrane modifications during cell biological processes that are distinct from macroautophagy. For example, the cascade of ULK1 and VPS34 complexes can put phosphoinositide marks on non-isolation membranes and the cascade of VPS34 and Atg8 lipidation complexes can label non-autophagosomal membranes with Atg8/LC3 (15, 16). While these modules are successively used by macroautophagy to restrict intracellular pathogens, like bacteria and viruses (17–19), and to degrade intracellular proteins for major histocompatibility complex (MHC) class II restricted antigen presentation, during anti-viral immune responses and $CD4^+$ T cell education (20, 21), individual modules are used in alternative pathways, including proviral roles in infectious viral particle release, restriction of phagocytosed bacteria, secretion of inflammatory mediators, and presentation of phagocytosed antigens on MHC molecules (22–29). The characteristics and functional roles of the respective pathways will be discussed in this minireview.

Atg PROTEINS IN LC3-ASSOCIATED PHAGOCYTOSIS (LAP)

The most prominent of these alternative pathways is probably LAP. It was originally reported in 2007 that Atg8/LC3 can also be conjugated to phagosomal membranes, especially after the uptake of particulate toll-like receptor (TLR) ligands (**Figure 1**) (25). For example, the yeast cell wall component zymosan is often used for these assays (25, 29, 30). Apart from TLRs, a handful of other receptors seem to trigger LAP. These include

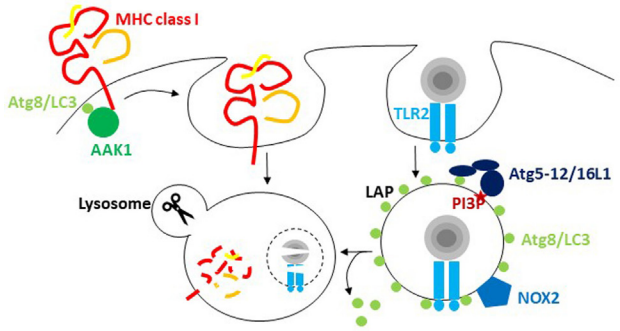


FIGURE 1 | The macroautophagy machinery regulates endocytosis. Atg8/LC3 lipidation facilitates the internalization of receptors from the cell surface *via* recruitment of components of clathrin-mediated endocytosis. For major histocompatibility complex (MHC) class I internalization, recruitment of adaptor-associated kinase 1 (AAK1) facilitates MHC class I internalization and degradation in lysosomes. During LC3-associated phagocytosis (LAP), endocytosed cargo that engages receptors like TLR2 stimulates the conjugation and/or maintenance of Atg8/LC3 lipidation on the cytosolic side of the phagosome. PI3 phosphorylation recruits the Atg8/LC3 conjugation machinery, including Atg5, 12, and 16L1, to these phagosomes, and NADPH oxidase 2 (NOX2)-dependent reactive oxygen species (ROS) production is required for LAP. Atg8/LC3 conjugation to phagosomes regulates their fusion with lysosomes.

the C-type lectin Dectin-1, Fc receptors during the uptake of antibody opsonized targets and receptors for apoptotic whole cells or cell fragments (30–33). During LAP, Atg8/LC3 gets conjugated to the cytosolic side of the phagosomal membrane and dissociates before phagosome fusion with lysosomes (25, 29). The VPS34 complex including Beclin-1 and the Atg lipidation machinery but not the ULK1 complex is required for this Atg8/LC3 lipidation (29, 34). Instead reactive oxygen species (ROS) production by the NADPH oxidase 2 (NOX2) is either required for Atg8/LC3 lipidation or maintenance of Atg8/LC3 on the phagosomal membrane (29, 34). This also probably explains earlier findings that suggested ROS production by NOX2 being required for the recruitment of autophagosomes to endocytosed *Salmonella* bacteria (24). Furthermore, Rubicon, a negative regulator of autophagosome fusion with lysosomes, seems to be required for LAP (34, 35). In contrast to the role of Rubicon during autophagosome maturation, LAP vesicles have been reported to fuse with lysosomes more rapidly than LC3-negative phagosomes in mouse macrophages (25, 34, 36). This enhanced maturation might result from accelerated transport along microtubules *via* FYCO1 recruitment by Atg8/LC3 binding (36). However, in other cell types, namely human macrophages as well as conventional and plasmacytoid dendritic cells (DCs), LAP phagosomes might not rapidly fuse with lysosomes, but rather retain phagocytosed cargo for delayed delivery to lysosomes and to endogenous TLR, like TLR9, containing vesicles (29, 31). However, why and how phagosomes use the Atg8/LC3 membrane tag to regulate their phagosome trafficking needs further investigations. This regulation seems to increase MHC class II restricted antigen presentation and to decrease inflammation. LAP deficiency compromised extracellular antigen presentation

on MHC class II molecules to CD4+ T cells (29, 30). Also *in vivo*, CD4+ T cell responses to herpes simplex virus (HSV) infection and ovalbumin containing apoptotic splenocyte injection were compromised in the absence of Atg5 in DCs (28). In addition, cross-presentation of antigens of *Aspergillus*, *Chlamydia*, and human cytomegalovirus on MHC class I molecules was found to be inhibited by Atg deficiency (37–39). In macrophages, the dominant phenotype of Atg deficiency is a hyperinflammatory phenotype (40), probably originating to a large extent from mitochondrial ROS-mediated inflammasome activation in the absence of macroautophagy of damaged mitochondria (41). Interestingly, aging of mice with macrophage deficiencies of Atg7, Atg5, Beclin-1, NOX2, or Rubicon developed signs of hyperinflammatory disease, while this phenotype was far less pronounced in mice with ULK1 and FIP200 deficiencies in macrophages (35). These findings suggested that LAP, but not classical macroautophagy, protects wild-type mice from this aging-related hyperinflammation. In addition, the development of lupus-like anti-DNA immune complex deposition in kidneys and elevated pro-inflammatory cytokine titers were detected. Surprisingly, the increase in inflammasome-dependent IL-1β production was quite pronounced, but the mechanism of LAP-mediated inflammasome regulation remains unclear. Instead, deficient LAP-mediated apoptotic cell clearance might be mainly responsible for the observed hyperinflammatory phenotypes, and indeed, the investigated parameters were similar to mice lacking apoptotic cell clearance due to deficiency of the TIM4 receptor in their macrophages. Thus, the VPS34 and LC3 lipidation complexes of the macroautophagy machinery seem to modify phagosomes for improved antigen presentation and inhibition of hyperinflammation.

Atg PROTEINS IN RECEPTOR INTERNALIZATION AND MHC CLASS I ANTIGEN PRESENTATION

In addition to this role of Atg8/LC3 lipidation in influencing phagosome fate, recent studies have suggested that recruitment of the receptor internalization machinery can also benefit from Atg8/LC3 binding (**Figure 1**). In pioneering studies, Alzheimer precursor protein (APP) was shown to be degraded by an ULK1, Atg6/Beclin-1, and Atg5-dependent mechanism (42). The internalization of APP that is required for this degradation is mediated by clathrin-dependent phagocytosis, which requires the adaptor protein 2 (AP2) complex. AP2α1 was identified as a Atg8/LC3 interactor by the same group (43). It contains a LIR motif, and mutating it abolished efficient APP internalization and degradation. Furthermore, phosphorylation or the APP-degrading enzyme presenelin 1 facilitated APP degradation, possibly by syntaxin 17-mediated fusion with lysosomes (44, 45). Thus, Atg8/LC3-mediated AP2 recruitment and syntaxin 17-mediated fusion with lysosomes seem to cause efficient degradation of APP and its *C*-terminal fragment from the cell membrane. However, AP2 recruitment to Atg8/LC3 does not seem to be the only connection of the autophagic machinery to clathrin-mediated endocytosis. A LIR motif was also detected in the clathrin heavy chain itself (6). However, it remains unclear what functional consequences this has beyond the biochemical interaction. Finally, as a third component of clathrin-mediated endocytosis that might depend on the macroautophagy machinery for its efficient recruitment to cell membrane receptors, the adaptor-associated kinase 1 (AAK1) was recently identified as an Atg8/LC3 interactor and contains predicted LIR motifs (46). AAK1 phosphorylates the μ subunit of the AP2 complex for more efficient clathrin-dependent internalization but might also facilitate clathrin-independent endocytosis (47, 48). In Atg5- or Atg7-deficient mouse DCs, MHC class I surface levels were increased, while B and T cells in the same mice showed no differences in MHC class I surface levels *in vivo* (46). This increased surface expression resulted from diminished internalization, and AAK1 was not efficiently recruited to MHC class I molecules in Atg5- or Atg7-deficient DCs. This resulted in increased CD8+ T cell stimulation *in vitro* and elevated CD8+ T cell responses to influenza A virus (IAV) and lymphocytic choriomeningitis virus infection *in vivo*, as well as improved immune control of IAV. However, not only classical MHC class I molecules are affected by diminished clathrin-dependent receptor internalization in the absence of Atg8/LC3 lipidation but also the non-classical MHC class I molecule CD1d gets stabilized on the cell surface of Atg5-deficient DCs (49). These non-classical MHC class I molecules present glycolipids to NKT cells (50). The increased CD1d surface stabilization in the absence of Atg-dependent internalization led to increased NKT cell stimulation *in vitro* and *in vivo* (49). Furthermore, the NKT cell-dependent pathogen *Sphingomonas paucimobilis* was more efficiently restricted in mice with Atg5 deficiency in their DCs. These studies suggest that Atg/LC3 lipidation assists clathrin-mediated phagocytosis by recruiting different components of the respective endocytic pathway to the cell membrane.

Atg PROTEINS IN INFLAMMATORY MEDIATOR AND ANTIGEN RELEASE

The above-described pathways still utilize Atg proteins for lysosomal degradation, albeit not through intracellular delivery, but degradation of endocytosed cargo and surface receptors. However, as a non-catabolic function of the macroautophagy machinery, it was noted that antigen release for efficient cross-presentation on MHC class I molecules requires Atgs in antigen donor cells (51, 52). This role during unconventional secretion was first demonstrated for IAV-infected cells or tumor cells in these two initial studies. The respective vesicles, which might be related to Atg8/LC3 containing exosomes that originate from multivesicular bodies (53), can be forced to be released in higher numbers by inhibiting lysosomal degradation and to incorporate defective ribosomal products by proteasome inhibition (54, 55). Therefore, they have been coined defective ribosomal products-containing autophagosome-rich blebs (DRibbles). Moreover, they contain some TLR and NOD2 agonists to activate antigen-presenting cells, at the same time as they transfer antigen (56). These formulations have been used to vaccinate mice against a variety of tumor challenges (57–60). Thus, autophagic cargo gets

released from transformed and infected cells in vesicles that can be efficiently taken up and activate antigen-presenting cells to induce antitumor immune responses.

These findings point toward unconventional ER targeting signal peptide-independent secretion by the autophagic machinery. Indeed, acyl coenzyme A-binding protein has been described to be secreted by yeast and ameba in an autophagy-dependent fashion (61, 62). This secretion is Golgi reassembly and stacking protein (GRASP) dependent. Similarly, the secretion of caspase-processed IL-1β is also dependent on Atgs in mammalian cells (**Figure 2**) (26, 27). It is worthwhile pointing out that the net outcome of Atg deficiency in myeloid cells as a major source of inflammasome-dependent IL-1β release is usually hyperinflammation (40) and that IL-1β usually leaves these cells during pyroptosis *via* gasdermin-dependent cell lysis (63, 64). However, in cells in which mature IL-1β is expressed without inflammasome activation and pyroptosis, IL-1β is released in a GRASP- and Atg-dependent fashion that involves the SNAREs Sec22b, syntaxin 3 and 4, as well as SNAPs 23 and 29 for membrane fusion (65). The cell type and physiological condition under which such Atg-dependent IL-1β secretion, however, occurs still needs to be identified. Additional cargo for this unconventional secretion pathway includes ferritin (65), HMGB1 (66), and secretory lysosomes (67). These studies suggest that Atg proteins support unconventional secretion, but how substrates are selected for this secretion versus degradation by autophagy still needs to be characterized.

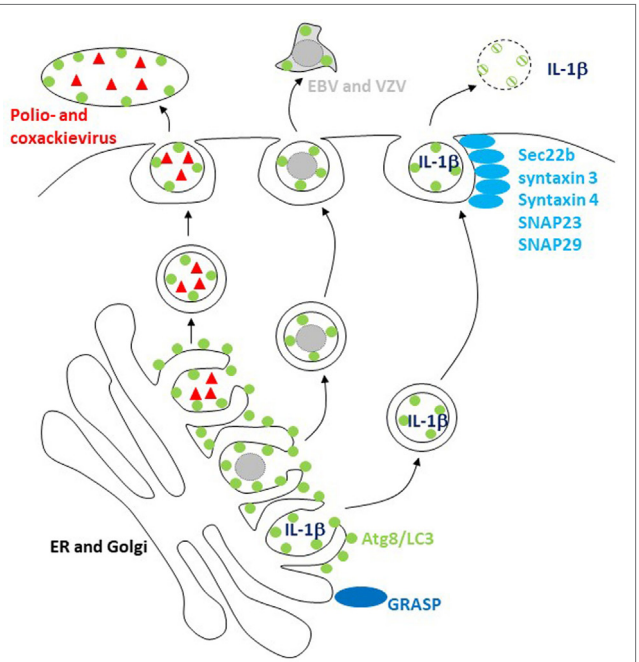


FIGURE 2 | The macroautophagy machinery supports unconventional exocytosis. Atg8/LC3-conjugated membranes facilitate the release of packages of picornaviruses (poliovirus and coxsackievirus) and of herpesviruses [varicella zoster virus (VZV) and Epstein–Barr virus (EBV)]. Unconventional ER targeting signal peptide-independent secretion of caspase-processed IL-1β also required Atg8/LC3 lipidation for release. Golgi reassembly and stacking proteins (GRASPs) and the SNAREs Sec22b, syntaxin 3 and 4, and SNAPs 23 and 29 are involved in this release and fusion of Atg8/LC3-coupled membranes with the cell membrane.

Atg PROTEINS IN VIRAL RELEASE

Viruses might be able to teach us how Atg-dependent secretion versus degradation can be regulated, because a number of them seem to harness Atg8/LC3-coupled membranes for their release (16). The first virus that was found to stabilize Atg8/LC3-associated membranes was a picornavirus, i.e., poliovirus (68). The release of poliovirus was dependent on these structures (69), and it was proposed that viral RNA replication and capsid assembly occurs in Atg8/LC3-coated double-membrane-surrounded vesicles, which then fuse with the cell membrane after acidification (70). Although poliovirus and related picornaviruses are non-enveloped, it was recently observed that they are released from cells in packages of multiple viral particles enveloped in a lipidated Atg8/LC3-positive membrane (**Figure 2**), topologically similar to the inner autophagosome membrane (23). Similarly, the closely related picornavirus coxsackievirus B is also released in packages that are surrounded with LC3-II-containing membranes (71). These packages might explain why coxsackievirus B spreads efficiently through cultures of cells with an intact macroautophagy machinery (72). This benefit for viral dissemination could result from protection by the surrounding Atg8/LC3-coupled membrane and its phosphatidylserine (PS) content in the outer membrane leaflet, which allows for efficient uptake by phagocytes *via* scavenger receptors that usually clear apoptotic cells (23). Indeed, ER and Golgi membranes seem to have substantial amounts of PS in both inner and outer leaflet, and sampling from this source of autophagic membranes might endow viruses with an envelope lipid composition that is beneficial for infection *via* clearance pathways for apoptotic cells (73).

Herpesviruses might also use this pathway for envelope acquisition. They acquire their second and final envelope from ER and Golgi membranes in the cytosol (74). Indeed, a γ-herpesvirus, i.e., Epstein–Barr virus (EBV), was found to stabilize Atg8/LC3-coupled membranes during lytic replication (22, 75). Loss of Atg proteins inhibited the release of infectious EBV particles (22, 75), and viral DNA was trapped in the cytosolic fraction (22). Similar to poliovirus packages, lipidated Atg8/LC3 enriched with EBV particle purification from the supernatant of virus replicating (**Figure 2**), but not latently EBV genome carrying cells (22). Furthermore, Atg8/LC3 could be observed in purified virus particles by immunoelectron microscopy (22). However, EBV is not the only herpesvirus that seems to use autophagic membranes. The α-herpesvirus varicella zoster virus (VZV) also exits cells with Atg8/LC3-coated membranes, and its replication is inhibited by Atg silencing (76, 77). It is worthwhile noting that apart from EBV and VZV, α- and γ-herpesviruses contain also members, namely HSV and Kaposi sarcoma-associated herpesvirus (KSHV), which instead of utilizing Atg-dependent membranes inhibit their generation (78–80). Even though these viruses are closely related, their differences on cellular tropism might dictate why HSV and KSHV rather inhibit, while VZV and EBV utilize autophagic membranes during replication.

As a last example for redirecting autophagic membranes to the cell surface, influenza A virus (IAV) infection will be discussed. IAV infection also accumulated Atg8/LC3-conjugated membranes upon infection (81–83). Autophagosomes did not fuse with lysosomes upon IAV infection, but instead accumulated around the nucleus, and Atg8/LC3-positive membranes were rerouted to the cell membrane (81, 82). Both accumulation and rerouting are caused by matrix protein 2 (MP2) of IAV. MP2 contains a LIR motif that is required for Atg8/LC3-positive membrane accumulation on the cell surface (82), and MP2 proton channel activity contributes to the block in lysosome fusion and perinuclear accumulation of autophagosomes (83). This autophagic membrane rerouting provides sufficient membranes for filamentous budding of IAV, which increases the stability of the resulting IAV particles, possibly *via* changing the membrane composition of the IAV envelope (82). However, Atg8/LC3 itself is not incorporated into infectious IAV particles. Nevertheless, Atg proteins seem to be used by viruses to select membranes for their envelopes to improve viral transmission.

CONCLUSION AND OUTLOOK

Macroautophagy uses a membrane remodeling machinery of Atg proteins to form autophagosomes around cargo that is destined for lysosomal degradation. This machinery acts in a modular format for activation of PI3K activity by phosphorylation *via* ULK1, for PI3P deposition on membranes, which is then used for the recruitment of the Atg8/LC3 lipidation machinery. These modules of autophagosome formation can be used in other membrane remodeling pathways, in which substrates need to be recruited to lipid bilayers *via* PI3P or Atg8/LC3. For example, LAP uses only the PI3K and Atg8/LC3 lipidation modules. Future research will need to unravel how the Atg modules are distributed to the different tasks and how the resulting membrane marks result in different cell biological outcomes. A detailed understanding might allow us to harness Atg proteins for therapeutic approaches against infectious diseases, cancer, neurodegeneration, hyperinflammatory diseases, and aging.

AUTHOR CONTRIBUTIONS

The author confirms being the sole contributor of this work and approved it for publication.

ACKNOWLEDGMENTS

The research in my laboratory is supported by grants from the Swiss National Science Foundation (310030_162560 and CRSII3_160708), Cancer Research Switzerland (KFS-4091-02-2017), SPARKS (15UOZ01), Sobek Foundation, the Swiss MS Society, and the clinical research priority programs on multiple sclerosis ($KFSP^{MS}$) and human hemato-lymphatic diseases ($KFSP^{HHLD}$) of the University of Zürich.

REFERENCES

1. Mizushima N, Yoshimori T, Ohsumi Y. The role of Atg proteins in autophagosome formation. *Annu Rev Cell Dev Biol* (2011) 27:107–32. doi:10.1146/annurev-cellbio-092910-154005
2. Tsukada M, Ohsumi Y. Isolation and characterization of autophagy-defective mutants of *Saccharomyces cerevisiae*. *FEBS Lett* (1993) 333(1–2):169–74. doi:10.1016/0014-5793(93)80398-E
3. Nakatogawa H, Ichimura Y, Ohsumi Y. Atg8, a ubiquitin-like protein required for autophagosome formation, mediates membrane tethering and hemifusion. *Cell* (2007) 130(1):165–78. doi:10.1016/j.cell.2007.05.021
4. Weidberg H, Shpilka T, Shvets E, Abada A, Shimron F, Elazar Z. LC3 and GATE-16 N termini mediate membrane fusion processes required for autophagosome biogenesis. *Dev Cell* (2011) 20(4):444–54. doi:10.1016/j.devcel.2011.02.006
5. Weidberg H, Shvets E, Elazar Z. Biogenesis and cargo selectivity of autophagosomes. *Annu Rev Biochem* (2011) 80:125–56. doi:10.1146/annurev-biochem-052709-094552
6. Rogov V, Dotsch V, Johansen T, Kirkin V. Interactions between autophagy receptors and ubiquitin-like proteins form the molecular basis for selective autophagy. *Mol Cell* (2014) 53(2):167–78. doi:10.1016/j.molcel.2013.12.014
7. Wei Y, Chiang WC, Sumpter R Jr, Mishra P, Levine B. Prohibitin 2 is an inner mitochondrial membrane mitophagy receptor. *Cell* (2017) 168(1–2):224–38.e10. doi:10.1016/j.cell.2016.11.042
8. Wild P, Farhan H, McEwan DG, Wagner S, Rogov VV, Brady NR, et al. Phosphorylation of the autophagy receptor optineurin restricts *Salmonella* growth. *Science* (2011) 333:228–33. doi:10.1126/science.1205405
9. Thurston TL, Ryzhakov G, Bloor S, von Muhlinen N, Randow F. The TBK1 adaptor and autophagy receptor NDP52 restricts the proliferation of ubiquitin-coated bacteria. *Nat Immunol* (2009) 10(11):1215–21. doi:10.1038/ni.1800
10. Pankiv S, Alemu EA, Brech A, Bruun JA, Lamark T, Overvatn A, et al. FYCO1 is a Rab7 effector that binds to LC3 and PI3P to mediate microtubule plus end-directed vesicle transport. *J Cell Biol* (2010) 188(2):253–69. doi:10.1083/jcb.200907015
11. Verlhac P, Gregoire IP, Azocar O, Petkova DS, Baguet J, Viret C, et al. Autophagy receptor NDP52 regulates pathogen-containing autophagosome maturation. *Cell Host Microbe* (2015) 17(4):515–25. doi:10.1016/j.chom.2015.02.008
12. McEwan DG, Popovic D, Gubas A, Terawaki S, Suzuki H, Stadel D, et al. PLEKHM1 regulates autophagosome-lysosome fusion through HOPS complex and LC3/GABARAP proteins. *Mol Cell* (2015) 57(1):39–54. doi:10.1016/j.molcel.2014.11.006
13. Rogov VV, Stolz A, Ravicahandran AC, Rios-Szwed DO, Suzuki H, Kniss A, et al. Structural and functional analysis of the GABARAP interaction motif (GIM). *EMBO Rep* (2017) 18(8):1382–96. doi:10.15252/embr.201643587
14. Itakura E, Kishi-Itakura C, Mizushima N. The hairpin-type tail-anchored SNARE syntaxin 17 targets to autophagosomes for fusion with endosomes/lysosomes. *Cell* (2012) 151(6):1256–69. doi:10.1016/j.cell.2012.11.001
15. Münz C. Autophagy beyond intracellular MHC class II antigen presentation. *Trends Immunol* (2016) 37(11):755–63. doi:10.1016/j.it.2016.08.017
16. Paul P, Münz C. Autophagy and mammalian viruses: roles in immune response, viral replication, and beyond. *Adv Virus Res* (2016) 95:149–95. doi:10.1016/bs.aivir.2016.02.002
17. Gutierrez MG, Master SS, Singh SB, Taylor GA, Colombo MI, Deretic V. Autophagy is a defense mechanism inhibiting BCG and *Mycobacterium tuberculosis* survival in infected macrophages. *Cell* (2004) 119(6):753–66. doi:10.1016/j.cell.2004.11.038
18. Nakagawa I, Amano A, Mizushima N, Yamamoto A, Yamaguchi H, Kamimoto T, et al. Autophagy defends cells against invading group A *Streptococcus*. *Science* (2004) 306(5698):1037–40. doi:10.1126/science.1103966
19. Orvedahl A, Sumpter R Jr, Xiao G, Ng A, Zou Z, Tang Y, et al. Image-based genome-wide siRNA screen identifies selective autophagy factors. *Nature* (2011) 480(7375):113–7. doi:10.1038/nature10546
20. Paludan C, Schmid D, Landthaler M, Vockerodt M, Kube D, Tuschl T, et al. Endogenous MHC class II processing of a viral nuclear antigen after autophagy. *Science* (2005) 307(5709):593–6. doi:10.1126/science.1104904
21. Nedjic J, Aichinger M, Emmerich J, Mizushima N, Klein L. Autophagy in thymic epithelium shapes the T-cell repertoire and is essential for tolerance. *Nature* (2008) 455(7211):396–400. doi:10.1038/nature07208

22. Nowag H, Guhl B, Thriene K, Romao S, Ziegler U, Dengjel J, et al. Macroautopphagy proteins assist Epstein Barr virus production and get incorporated into the virus particles. *EBioMedicine* (2014) 1(2–3):116–25. doi:10.1016/j.ebiom.2014.11.007
23. Chen YH, Du W, Hagemeijer MC, Takvorian PM, Pau C, Cali A, et al. Phosphatidylserine vesicles enable efficient en bloc transmission of enteroviruses. *Cell* (2015) 160(4):619–30. doi:10.1016/j.cell.2015.01.032
24. Huang J, Canadien V, Lam GY, Steinberg BE, Dinauer MC, Magalhaes MA, et al. Activation of antibacterial autophagy by NADPH oxidases. *Proc Natl Acad Sci U S A* (2009) 106(15):6226–31. doi:10.1073/pnas.0811045106
25. Sanjuan MA, Dillon CP, Tait SW, Moshiach S, Dorsey F, Connell S, et al. Toll-like receptor signalling in macrophages links the autophagy pathway to phagocytosis. *Nature* (2007) 450(7173):1253–7. doi:10.1038/nature06421
26. Dupont N, Jiang S, Pilli M, Ornatowski W, Bhattacharya D, Deretic V. Autophagy-based unconventional secretory pathway for extracellular delivery of IL-1beta. *EMBO J* (2011) 30(23):4701–11. doi:10.1038/emboj.2011.398
27. Zhang M, Kenny S, Ge L, Xu K, Schekman R. Translocation of interleukin-1beta into a vesicle intermediate in autophagy-mediated secretion. *Elife* (2015) 4:e11205. doi:10.7554/eLife.11205
28. Lee HK, Mattei LM, Steinberg BE, Alberts P, Lee YH, Chervonsky A, et al. In vivo requirement for Atg5 in antigen presentation by dendritic cells. *Immunity* (2010) 32(2):227–39. doi:10.1016/j.immuni.2009.12.006
29. Romao S, Gasser N, Becker AC, Guhl B, Bagajic M, Vanoaica LD, et al. Essential autophagy proteins stabilize pathogen containing phagosomes for prolonged MHC class II antigen processing. *J Cell Biol* (2013) 203(5):757–66. doi:10.1083/jcb.201308173
30. Ma J, Becker C, Lowell CA, Underhill DM. Dectin-1-triggered recruitment of light chain 3 protein to phagosomes facilitates major histocompatibility complex class II presentation of fungal-derived antigens. *J Biol Chem* (2012) 287(41):34149–56. doi:10.1074/jbc.M112.382812
31. Henault J, Martinez J, Riggs JM, Tian J, Mehta P, Clarke L, et al. Noncanonical autophagy is required for type I interferon secretion in response to DNA-immune complexes. *Immunity* (2012) 37(6):986–97. doi:10.1016/j.immuni.2012.09.014
32. Martinez J, Almendinger J, Oberst A, Ness R, Dillon CP, Fitzgerald P, et al. Microtubule-associated protein 1 light chain 3 alpha (LC3)-associated phagocytosis is required for the efficient clearance of dead cells. *Proc Natl Acad Sci U S A* (2011) 108(42):17396–401. doi:10.1073/pnas.1113421108
33. Florey O, Kim SE, Sandoval CP, Haynes CM, Overholtzer M. Autophagy machinery mediates macroendocytic processing and entotic cell death by targeting single membranes. *Nat Cell Biol* (2011) 13(11):1335–43. doi:10.1038/ncb2363
34. Martinez J, Malireddi RK, Lu Q, Cunha LD, Pelletier S, Gingras S, et al. Molecular characterization of LC3-associated phagocytosis reveals distinct roles for Rubicon, NOX2 and autophagy proteins. *Nat Cell Biol* (2015) 17(7):893–906. doi:10.1038/ncb3192
35. Martinez J, Cunha LD, Park S, Yang M, Lu Q, Orchard R, et al. Noncanonical autophagy inhibits the autoinflammatory, lupus-like response to dying cells. *Nature* (2016) 533(7601):115–9. doi:10.1038/nature17950
36. Ma J, Becker C, Reyes C, Underhill DM. Cutting edge: FYCO1 recruitment to dectin-1 phagosomes is accelerated by light chain 3 protein and regulates phagosome maturation and reactive oxygen production. *J Immunol* (2014) 192(4):1356–60. doi:10.4049/jimmunol.1302835
37. De Luca A, Iannitti RG, Bozza S, Beau R, Casagrande A, D'Angelo C, et al. $CD4^+$ T cell vaccination overcomes defective cross-presentation of fungal antigens in a mouse model of chronic granulomatous disease. *J Clin Invest* (2012) 122(5):1816–31. doi:10.1172/JCI60862
38. Fiegl D, Kagebein D, Liebler-Tenorio EM, Weisser T, Sens M, Gutjahr M, et al. Amphisomal route of MHC class I cross-presentation in bacteria-infected dendritic cells. *J Immunol* (2013) 190(6):2791–806. doi:10.4049/jimmunol.1202741
39. Dasari V, Rehan S, Tey SK, Smyth MJ, Smith C, Khanna R. Autophagy and proteasome interconnect to coordinate cross-presentation through MHC class I pathway in B cells. *Immunol Cell Biol* (2016) 94(10):964–74. doi:10.1038/icb.2016.59
40. Saitoh T, Fujita N, Jang MH, Uematsu S, Yang BG, Satoh T, et al. Loss of the autophagy protein Atg16L1 enhances endotoxin-induced IL-1beta production. *Nature* (2008) 456(7219):264–8. doi:10.1038/nature07383
41. Zhou R, Yazdi AS, Menu P, Tschopp J. A role for mitochondria in NLRP3 inflammasome activation. *Nature* (2011) 469(7329):221–5. doi:10.1038/nature09663
42. Tian Y, Bustos V, Flajolet M, Greengard P. A small-molecule enhancer of autophagy decreases levels of Abeta and APP-CTF via Atg5-dependent autophagy pathway. *FASEB J* (2011) 25(6):1934–42. doi:10.1096/fj.10-175158
43. Tian Y, Chang JC, Fan EY, Flajolet M, Greengard P. Adaptor complex AP2/PICALM, through interaction with LC3, targets Alzheimer's APP-CTF for terminal degradation via autophagy. *Proc Natl Acad Sci U S A* (2013) 110(42):17071–6. doi:10.1073/pnas.1315110110
44. Bustos V, Pulina MV, Bispo A, Lam A, Flajolet M, Gorelick FS, et al. Phosphorylated Presenilin 1 decreases beta-amyloid by facilitating autophagosome-lysosome fusion. *Proc Natl Acad Sci U S A* (2017) 114(27):7148–53. doi:10.1073/pnas.1705240114
45. Bustos V, Pulina MV, Kelahmetoglu Y, Sinha SC, Gorelick FS, Flajolet M, et al. Bidirectional regulation of Abeta levels by Presenilin 1. *Proc Natl Acad Sci U S A* (2017) 114(27):7142–7. doi:10.1073/pnas.1705235114
46. Loi M, Muller A, Steinbach K, Niven J, Barreira da Silva R, Paul P, et al. Macroautophagy proteins control MHC class I levels on dendritic cells and shape anti-viral $CD8^+$ T cell responses. *Cell Rep* (2016) 15(5):1076–87. doi:10.1016/j.celrep.2016.04.002
47. Conner SD, Schmid SL. Identification of an adaptor-associated kinase, AAK1, as a regulator of clathrin-mediated endocytosis. *J Cell Biol* (2002) 156(5):921–9. doi:10.1083/jcb.200108123
48. Henderson DM, Conner SD. A novel AAK1 splice variant functions at multiple steps of the endocytic pathway. *Mol Biol Cell* (2007) 18(7):2698–706. doi:10.1091/mbc.E06-09-0831
49. Keller CW, Loi M, Ewert S, Quast I, Theiler R, Gannage M, et al. The autophagy machinery restrains iNKT cell activation through CD1d1 internalization. *Autophagy* (2017) 13(6):1025–36. doi:10.1080/15548627.2017.1297907
50. Chandra S, Kronenberg M. Activation and function of iNKT and MAIT cells. *Adv Immunol* (2015) 127:145–201. doi:10.1016/bs.ai.2015.03.003
51. Uhl M, Kepp O, Jusforgues-Saklani H, Vicencio JM, Kroemer G, Albert ML. Autophagy within the antigen donor cell facilitates efficient antigen cross-priming of virus-specific $CD8^+$ T cells. *Cell Death Differ* (2009) 16(7):991–1005. doi:10.1038/cdd.2009.8
52. Li Y, Wang LX, Yang G, Hao F, Urba WJ, Hu HM. Efficient cross-presentation depends on autophagy in tumor cells. *Cancer Res* (2008) 68(17):6889–95. doi:10.1158/0008-5472.CAN-08-0161
53. Pallet N, Sirois I, Bell C, Hanafi LA, Hamelin K, Dieude M, et al. A comprehensive characterization of membrane vesicles released by autophagic human endothelial cells. *Proteomics* (2013) 13(7):1108–20. doi:10.1002/pmic.201200531
54. Yi Y, Zhou Z, Shu S, Fang Y, Twitty C, Hilton TL, et al. Autophagy-assisted antigen cross-presentation: autophagosome as the argo of shared tumor-specific antigens and DAMPs. *Oncoimmunology* (2012) 1(6):976–8. doi:10.4161/onci.20059
55. Li Y, Hahn T, Garrison K, Cui ZH, Thorburn A, Thorburn J, et al. The vitamin E analogue alpha-TEA stimulates tumor autophagy and enhances antigen cross-presentation. *Cancer Res* (2012) 72(14):3535–45. doi:10.1158/1538-7445.AM2012-3535
56. Xing Y, Cao R, Hu HM. TLR and NLRP3 inflammasome-dependent innate immune responses to tumor-derived autophagosomes (DRibbles). *Cell Death Dis* (2016) 7(8):e2322. doi:10.1038/cddis.2016.206
57. Twitty CG, Jensen SM, Hu HM, Fox BA. Tumor-derived autophagosome vaccine: induction of cross-protective immune responses against short-lived proteins through a p62-dependent mechanism. *Clin Cancer Res* (2011) 17(20):6467–81. doi:10.1158/1078-0432.CCR-11-0812
58. Li Y, Wang LX, Pang P, Cui Z, Aung S, Haley D, et al. Tumor-derived autophagosome vaccine: mechanism of cross-presentation and therapeutic efficacy. *Clin Cancer Res* (2011) 17(22):7047–57. doi:10.1158/1078-0432.CCR-11-0951
59. Ren H, Zhao S, Li W, Dong H, Zhou M, Cao M, et al. Therapeutic antitumor efficacy of B cells loaded with tumor-derived autophagasomes vaccine (DRibbles). *J Immunother* (2014) 37(8):383–93. doi:10.1097/CJI.0000000000000051
60. Yu G, Li Y, Cui Z, Morris NP, Weinberg AD, Fox BA, et al. Combinational immunotherapy with Allo-DRibble vaccines and anti-OX40 co-stimulation leads to generation of cross-reactive effector T cells and tumor regression. *Sci Rep* (2016) 6:37558. doi:10.1038/srep37558

61. Duran JM, Anjard C, Stefan C, Loomis WF, Malhotra V. Unconventional secretion of Acb1 is mediated by autophagosomes. *J Cell Biol* (2010) 188(4): 527–36. doi:10.1083/jcb.200911154
62. Manjithaya R, Anjard C, Loomis WF, Subramani S. Unconventional secretion of *Pichia pastoris* Acb1 is dependent on GRASP protein, peroxisomal functions, and autophagosome formation. *J Cell Biol* (2010) 188(4):537–46. doi:10.1083/jcb.200911149
63. Kayagaki N, Stowe IB, Lee BL, O'Rourke K, Anderson K, Warming S, et al. Caspase-11 cleaves gasdermin D for non-canonical inflammasome signalling. *Nature* (2015) 526(7575):666–71. doi:10.1038/nature15541
64. Shi J, Zhao Y, Wang K, Shi X, Wang Y, Huang H, et al. Cleavage of GSDMD by inflammatory caspases determines pyroptotic cell death. *Nature* (2015) 526(7575):660–5. doi:10.1038/nature15514
65. Kimura T, Jia J, Kumar S, Choi SW, Gu Y, Mudd M, et al. Dedicated SNAREs and specialized TRIM cargo receptors mediate secretory autophagy. *EMBO J* (2017) 36(1):42–60. doi:10.15252/embj.201695081
66. Thorburn J, Horita H, Redzic J, Hansen K, Frankel AE, Thorburn A. Autophagy regulates selective HMGB1 release in tumor cells that are destined to die. *Cell Death Differ* (2009) 16(1):175–83. doi:10.1038/cdd.2008.143
67. DeSelm CJ, Miller BC, Zou W, Beatty WL, van Meel E, Takahata Y, et al. Autophagy proteins regulate the secretory component of osteoclastic bone resorption. *Dev Cell* (2011) 21(5):966–74. doi:10.1016/j.devcel.2011.08.016
68. Dales S, Eggers HJ, Tamm I, Palade GE. Electron microscopic study of the formation of poliovirus. *Virology* (1965) 26:379–89. doi:10.1016/0042-6822(65)90001-2
69. Jackson WT, Giddings TH Jr, Taylor MP, Mulinyawe S, Rabinovitch M, Kopito RR, et al. Subversion of cellular autophagosomal machinery by RNA viruses. *PLoS Biol* (2005) 3(5):e156. doi:10.1371/journal.pbio.0030156
70. Richards AL, Jackson WT. Intracellular vesicle acidification promotes maturation of infectious poliovirus particles. *PLoS Pathog* (2012) 8(11):e1003046. doi:10.1371/journal.ppat.1003046
71. Robinson SM, Tsueng G, Sin J, Mangale V, Rahawi S, McIntyre LL, et al. Coxsackievirus B exits the host cell in shed microvesicles displaying autophagosomal markers. *PLoS Pathog* (2014) 10(4):e1004045. doi:10.1371/journal.ppat.1004045
72. Bird SW, Maynard ND, Covert MW, Kirkegaard K. Nonlytic viral spread enhanced by autophagy components. *Proc Natl Acad Sci U S A* (2014) 111(36):13081–6. doi:10.1073/pnas.1401437111
73. Altan-Bonnet N. Lipid tales of viral replication and transmission. *Trends Cell Biol* (2017) 27(3):201–13. doi:10.1016/j.tcb.2016.09.011
74. Johnson DC, Baines JD. Herpesviruses remodel host membranes for virus egress. *Nat Rev Microbiol* (2011) 9(5):382–94. doi:10.1038/nrmicro2559
75. Granato M, Santarelli R, Farina A, Gonnella R, Lotti LV, Faggioni A, et al. EBV blocks the autophagic flux and appropriates the autophagic machinery to enhance viral replication. *J Virol* (2014) 88(21):12715–26. doi:10.1128/JVI.02199-14
76. Buckingham EM, Carpenter JE, Jackson W, Grose C. Autophagy and the effects of its inhibition on varicella-zoster virus glycoprotein biosynthesis and infectivity. *J Virol* (2014) 88(2):890–902. doi:10.1128/JVI.02646-13
77. Buckingham EM, Jarosinski KW, Jackson W, Carpenter JE, Grose C. Exocytosis of varicella-zoster virions involves a convergence of endosomal and autophagy pathways. *J Virol* (2016) 90(19):8673–85. doi:10.1128/JVI.00915-16
78. Orvedahl A, Alexander D, Talloczy Z, Sun Q, Wei Y, Zhang W, et al. HSV-1 ICP34.5 confers neurovirulence by targeting the Beclin 1 autophagy protein. *Cell Host Microbe* (2007) 1:23–35. doi:10.1016/j.chom.2006.12.001
79. Pattingre S, Tassa A, Qu X, Garuti R, Liang XH, Mizushima N, et al. Bcl-2 antiapoptotic proteins inhibit Beclin 1-dependent autophagy. *Cell* (2005) 122(6):927–39. doi:10.1016/j.cell.2005.07.002
80. Lee JS, Li Q, Lee JY, Lee SH, Jeong JH, Lee HR, et al. FLIP-mediated autophagy regulation in cell death control. *Nat Cell Biol* (2009) 11(11):1355–62. doi:10.1038/ncb1980
81. Gannage M, Dormann D, Albrecht R, Dengjel J, Torossi T, Ramer PC, et al. Matrix protein 2 of influenza A virus blocks autophagosome fusion with lysosomes. *Cell Host Microbe* (2009) 6(4):367–80. doi:10.1016/j.chom.2009.09.005
82. Beale R, Wise H, Stuart A, Ravenhill BJ, Digard P, Randow F. A LIR motif in influenza A virus M2 is required for virion stability. *Cell Host Microbe* (2014) 5(2):239–47. doi:10.1016/j.chom.2014.01.006
83. Ren Y, Li C, Feng L, Pan W, Li L, Wang Q, et al. Proton channel activity of influenza A virus matrix protein 2 contributes to autophagy arrest. *J Virol* (2015) 90(1):591–8. doi:10.1128/JVI.00576-15

Conflict of Interest Statement: The author declares that the research was conducted in the absence of any commercial or financial relationships that could be construed as a potential conflict of interest.

Copyright © 2017 Münz. This is an open-access article distributed under the terms of the Creative Commons Attribution License (CC BY). The use, distribution or reproduction in other forums is permitted, provided the original author(s) or licensor are credited and that the original publication in this journal is cited, in accordance with accepted academic practice. No use, distribution or reproduction is permitted which does not comply with these terms.

frontiers in Immunology

MINI REVIEW
published: 06 November 2017
doi: 10.3389/fimmu.2017.01483

Macrophage Autophagy and Bacterial Infections

*Aïcha Bah and Isabelle Vergne**

Institut de Pharmacologie et de Biologie Structurale, UMR 5089 CNRS—Université de Toulouse, Toulouse, France

Autophagy is a well-conserved lysosomal degradation pathway that plays key roles in bacterial infections. One of the most studied is probably xenophagy, the selective capture and degradation of intracellular bacteria by lysosomes. However, the impact of autophagy goes beyond xenophagy and involves intensive cross-talks with other host defense mechanisms. In addition, autophagy machinery can have non-canonical functions such as LC3-associated phagocytosis. In this review, we intend to summarize the current knowledge on the many functions of autophagy proteins in cell defenses with a focus on bacteria–macrophage interaction. We also present the strategies developed by pathogens to evade or to exploit this machinery in order to establish a successful infection. Finally, we discuss the opportunities and challenges of autophagy manipulation in improving therapeutics and vaccines against bacterial pathogens.

Keywords: autophagy, macrophage, bacteria, pathogen, phagocytosis, xenophagy, inflammation

OPEN ACCESS

Edited by:
Luciana Balboa, Consejo Nacional de Investigaciones Científicas y Técnicas (CONICET), Argentina

Reviewed by:
Roberta Olmo Pinheiro, Oswaldo Cruz Foundation, Brazil
Elsa Anes, Universidade de Lisboa, Portugal

***Correspondence:**
Isabelle Vergne
isabelle.vergne@ipbs.fr

Specialty section:
This article was submitted to Microbial Immunology, a section of the journal Frontiers in Immunology

Received: *13 September 2017*
Accepted: *23 October 2017*
Published: *06 November 2017*

Citation:
Bah A and Vergne I (2017) Macrophage Autophagy and Bacterial Infections. Front. Immunol. 8:1483. doi: 10.3389/fimmu.2017.01483

INTRODUCTION

Macroautophagy, hereafter referred to as autophagy, is a lysosomal degradative process that participates in cellular homeostasis by enabling the removal of defective organelles, protein aggregates, or intracellular microorganisms (1). The process is highly regulated by multiple signaling pathways and orchestrated by more than 30 autophagy-related (Atgs) proteins organized in several functional units (2). Upon autophagy activation, Atgs, serine/threonine kinase ULK1, and Beclin-1, in association with Atg14 and type III phosphatidylinositol 3-kinase Vps34, promote the formation of a cup-shaped isolation membrane to engulf the cargo (1). Through concomitant activity of two ubiquitin-like conjugation systems, the covalent linkage of Atg12 with Atg5/Atg16L1 and LC3 lipidation with phosphatidylethanolamime, the isolation membrane elongates into a double-membrane vesicle, called autophagosome. The autophagosome then fuses with lysosomes to form an autolysosome in which the engulfed cargo is degraded. This latter step is mediated by a second Beclin-1 complex, lysosomal-associated membrane protein 1 (LAMP1), and a fusion machinery including SNARE syntaxin-17.

In addition to its role in cellular homeostasis, autophagy is essential to immunity. The autophagy machinery targets intracellular pathogens for degradation, modulates inflammation, and participates in adaptive immune responses (3–5). Here, we review the many functions of autophagy in bacterial infections with a focus on macrophages, the first line of host defenses, and the replicative niche of numerous pathogens.

AUTOPHAGY MACHINERY IN MACROPHAGE ANTIBACTERIAL DEFENSES

Bacteria induce autophagy mainly *via* their pathogen-associated molecular patterns (PAMPs) and pathogen-induced damage-associated molecular patterns (DAMPs) (4, 5). Cell surface recognition and cytosolic sensing of these molecules result in signaling cascades that promote rapid and

localized autophagy machinery recruitment. Autophagy can further be regulated by several transcriptional factors such as NFkappaB and TFEB to promote expression of different autophagy genes and thus prolong autophagy activation (6, 7). Depending on PAMP/DAMP nature and localization, autophagy can selectively capture bacteria, such event is called xenophagy, damaged organelles, and other signaling platforms activated during the infection (4, 5). Furthermore, Atgs proteins have non-autophagic functions essential for innate immunity against bacteria (**Figure 1**).

Xenophagy

In macrophages, xenophagy has mainly been characterized during *Mycobacterium tuberculosis* infection but the mechanism is quite similar in epithelial cells infected with *Salmonella typhimurium* (8). *M. tuberculosis* through its ESX-1 secretion system damages the phagosomal membrane and access the cytosol (9). Cytosolic sensor c-GAS recognizes bacterial DNA, which results in ubiquitination of the bacterium or its phagosome by ubiquitin ligases Parkin and Smurf1 (10–12). Subsequently, ubiquitin chains bind to autophagy adaptors, such as p62 and NDP52, which recruit LC3 to deliver *M. tuberculosis* into an autophagosome. Damaged phagosome can also be targeted by autophagy *via* the recognition of host glycan present on the phagosomal lumen by cytosolic lectins of the galectin family (8, 13). Additionally, in human macrophages, immunity-related GTPase family M protein participates in xenophagy by promoting mitochondrial reactive oxygen species (ROS)

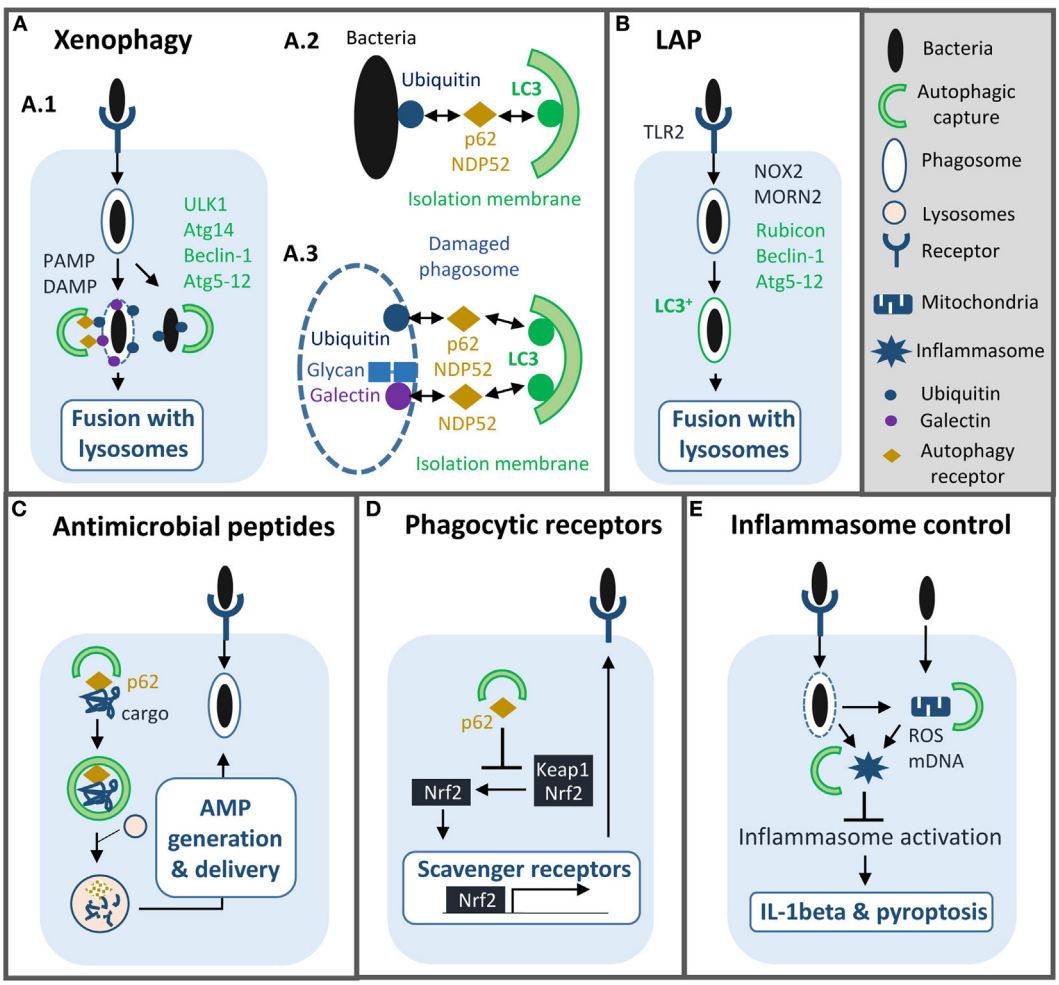


FIGURE 1 | Roles of autophagy machinery in macrophage antibacterial defenses. Autophagy machinery plays several functions in innate immunity to bacterial infection such as: **(A)** xenophagy: selective capture and lysosomal degradation of cytosolic and vacuolar pathogens. Xenophagy requires formation of an autophagosome and depends on ULK1, autophagy-related (Atg)14, Beclin-1, Atg5-12, and autophagy receptor proteins such as p62 (A.1). Bacterial compartment is captured by autophagosome either *via* ubiquitination (A.2, 3) or host glycan recognition by galectins (A.3). **(B)** LC3-associated phagocytosis (LAP): LC3 is conjugated onto the membrane of phagosome containing bacteria to promote fusion with lysosome. LAP depends on Rubicon, Beclin-1, and Atg5-12. **(C)** Induction of autophagy enables production and delivery of antimicrobial peptides to bacterial compartments. **(D)** Autophagy machinery reduces the expression of scavenger receptors to limit phagocytosis of some intracellular pathogens. **(E)** Autophagy controls inflammation by limiting inflammasome activation. PAMP, pathogen-associated molecular pattern; DAMP, damage-associated molecular pattern; AMP, antimicrobial peptide; ROS, reactive oxygen species; mDNA, mitochondrial DNA.

production and recruiting autophagy machinery after PAMP exposure (14, 15).

Ultimately, autophagosome sends bacteria to lysosome for degradation (5, 8). In parallel, autophagy can also generate and deliver antimicrobial peptides to bacterial compartment to enhance killing (16, 17). Several, *in vitro*, studies have shown that xenophagy reduces intracellular survival of *M. tuberculosis*, however, its role, *in vivo*, is unclear (9, 12). Mice with monocyte-derived cells and neutrophils lacking Atg5 are more susceptible to *M. tuberculosis*, but not those lacking other Atgs such as Beclin-1 or Atg14, suggesting that autophagy is not involved in controlling the infection (9, 18, 19). Nonetheless, separate studies suggest that autophagy may play a role in a latter chronic phase of infection and/or that *M. tuberculosis* may inhibit the process *in vivo* (12, 20). As we will discuss below, *M. tuberculosis* and other pathogens have developed multiple strategies to block autophagy and some of them have been relevant *in vivo*.

LC3-Associated Phagocytosis (LAP)

Aside from xenophagy, a non-canonical autophagy process named LAP is known to play an important role in antibacterial defenses (21, 22). Upon phagocytosis, particles or pathogens that engage surface receptors, such as toll-like receptors, Fcgamma receptors or Dectin-1, trigger LC3 conjugation directly onto the phagosomal membrane and independently of autophagosome formation (23–25). In contrast to canonical autophagy, this process does not require ULK1 or Beclin-1/Atg14 complexes but instead relies on Beclin-1/Rubicon complex and NADPH oxidase-2 (NOX2) activation (25, 26). Rubicon activates phosphatidylinositol 3-phosphate (PI3P) synthesis, which in turn, stimulates ROS production. PI3P and ROS then promote recruitment of the two ubiquitin-like conjugation systems to trigger LC3 conjugation. Another protein MORN2 has recently been implicated in that pathway, however, its action mechanism is unknown (27).

In several instances, LC3 conjugation onto the phagosome enhances the fusion between phagosome and lysosomes. Consequently, macrophages with defects in LAP pathway are less efficient in controlling intracellular growth of various bacteria such as *Legionella pneumophila*, *Staphylococcus aureus*, *M. tuberculosis*, *M. bovis* BCG, and *Listeria monocytogenes* (27, 28). Importantly, *in vivo* studies have shown that Rubicon-deficient mice have greater bacterial load and are more susceptible to *L. monocytogenes* infection (28). Another important function of LAP is to assist antigen presentation *via* MHC class II molecules, thus to bridge innate to adaptive immunity (24, 29). Of note, in some specific contexts, LC3 conjugation delays or does not affect at all phagosome maturation suggesting that LC3 alone is not sufficient to boost fusion with lysosomes (29, 30).

Autophagy machinery can also regulate phagocytosis indirectly by altering surface expression of phagocytic receptors. Lack of Atg protein Atg7 in macrophages results in upregulation of two class A scavenger receptors, MARCO and MSR1 that facilitate phagocytosis of *M. bovis* BCG and *M. tuberculosis* (31). Autophagy-deficient cells accumulate p62, which promotes dissociation of transcription factor nuclear erythroid-related factor 2 from Keap1 and then its translocation into the nucleus to mediate expression of these receptors. Notably, in another instance, autophagy deficiency can lead to reduced phagocytosis depending on the nature of the bacteria (32).

Inflammation Dampening

Although inflammation is central to control bacterial infection, excessive inflammatory responses can lead to host tissue injury, and disease progression. Numerous studies have demonstrated the importance of autophagy in inflammation regulation in infectious and non-infectious settings, the interested readers can refer to recent reviews for a comprehensive view on this subject (3, 5). Here, we will only discuss on the beneficial role of autophagy machinery in modulating inflammation in a context of bacterial infections and macrophages. One key role of autophagy is the down-regulation of inflammasome activation through multiple mechanisms (33, 34). *Pseudomonas aeruginosa* infection results in mitochondrial damage that leads to NLRC4 inflammasome. Elimination of damaged mitochondria *via* autophagy, i.e., mitophagy, limits inflammasome activation both *in vitro* and *in vivo* (35). Similarly, in a *P. aeruginosa* septic model, $atg7^{fl/fl}$ mice have an enhanced susceptibility to infection with important neutrophil infiltration and severe lung damage. Loss of Atg7 in alveolar macrophages results in upregulation of IL-1beta and pyroptosis (36). Besides mitophagy, autophagy can also restrain inflammasome activation by capturing inflammasome subunits (37, 38). Lastly, autophagy can prevent non-canonical caspase-11 inflammasome activation by targeting *S. typhimurium* and thus limiting LPS release into the cytosol (39).

Finally, mechanisms and levels of autophagy dependent greatly on macrophage microenvironment. While IL-4, IL-13, and IL-10 appear to inhibit autophagy, proinflammatory cytokines such as IFNgamma, IL-1beta, and TNFalpha, activate this process (40). Specifically, IFNgamma-mediated xenophagy requires additionally ubiquilin-1 and guanylate-binding proteins 1 and 7 to promote recruitment of autophagy proteins p62 and Atg4B (41, 42). On another hand, the presence of vitamin D in serum enhances significantly macrophage autophagy *via* expression of cathelicidin antimicrobial peptide (43). Specific T cells can also stimulate autophagic activity in *M. tuberculosis*-infected human macrophages (44). Finally, microbiota may influence autophagy response too, as recently, probiotic *Bacillus amyloliquefaciens* has been shown to upregulate autophagy genes in macrophages, which lead to enhanced *Escherichia coli* killing (45).

BACTERIAL PATHOGENS EVADE AUTOPHAGY

Intracellular bacterial pathogens have developed a wide array of tactics to counterbalance macrophage antibacterial defenses and autophagy is no exception (46). Most of the uncovered strategies are directed against xenophagy and target different steps of the process (**Figure 2**).

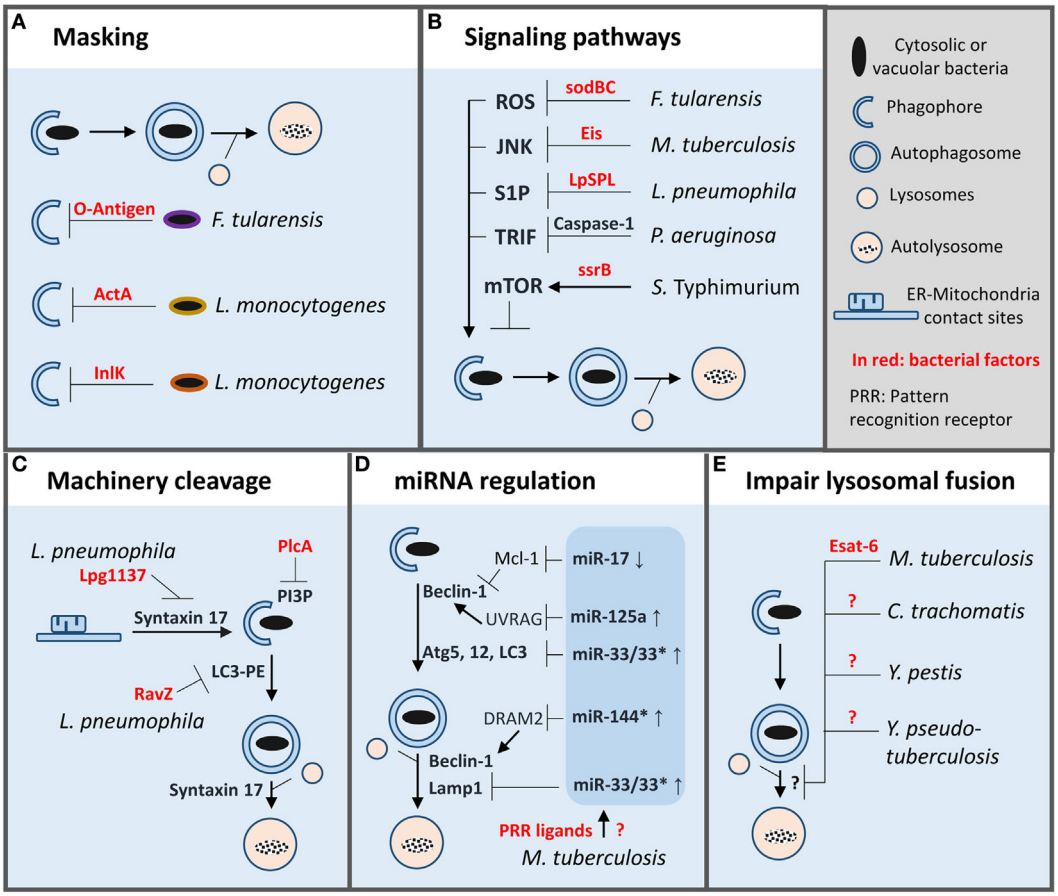


FIGURE 2 | Autophagy evasion strategies adopted by bacterial pathogens inside macrophages. To evade autophagy in macrophages bacterial pathogens have developed a wide array of strategies such as: **(A)** masking of microbial surface to avoid recognition. **(B)** Manipulation of macrophage signaling pathways involved in autophagy regulation. **(C)** Direct cleavage of autophagy proteins or signaling lipid. **(D)** Limitation of autophagy machinery expression or function by miRNA regulation. **(E)** Inhibition of autophagosomes/lysosome fusion. PI3P, phosphatidylinositol 3-phosphate; LC3-PE, LC3 lipidated with phosphatidylethanolamine.

Masking Bacterial Surface to Prevent Recognition

Cytosolic *L. monocytogenes* avoids recognition by autophagy machinery by secreting two virulence factors ActA and InlK (47, 48). These factors promote recruitment of host proteins, actin, and major vault protein, respectively, to form a protective coat that masks the bacteria. *Francisella tularensis* disguises itself directly by producing a surface polysaccharide, the O-antigen, which prevents cytosolic sensing of the pathogen and thus xenophagy (49). Importantly, cytosolic O-antigen mutants are killed by Atg5-dependent autophagy inside murine macrophages.

Regulation of Signaling Pathways Involved in Autophagy Initiation

In macrophages, *S. typhimurium* prevents autophagy by activating mTOR, a master repressor of autophagy (50, 51). Two mechanisms seem to be at play, first, the degradation of the energy sensor, Sirt1/AMPK complex, which negatively regulates mTOR resulting in autophagy activation and, second, the recruitment of non-receptor tyrosine kinase focal adhesion kinase (FAK), an activator of Akt/mTOR pathway. SsrB, a response regulator of a two-component system involved in the regulation of SPI2 encoded virulence factors, promotes AMPK down-regulation (50). Notably, *in vivo*, macrophages deficient in FAK are more efficient in clearing *S. typhimurium* infection than their wild-type counterpart (51).

Conversely, some pathogens can inhibit signaling pathways that promote autophagy. *M. tuberculosis* secretes an *N*-acetyltransferase, Eis, to target JNK-dependent autophagy; however, it does not seem to be sufficient to affect intracellular growth (52, 53). In addition, *M. tuberculosis* limits LAP by inhibiting NADPH oxidase recruitment onto its phagosome, which favors pathogen intracellular growth *in vitro* and *in vivo* (54). Interestingly, antioxidant enzymes SodB and SodC of *F. tularensis* prevent ROS-induced xenophagy and possibly LAP (55). Further, vacuolar *L. pneumophila* translocates a sphingosine-1 phosphate lyase into the cytosol to alter sphingosine metabolism implicated in autophagy activation (56). Lastly, some pathogens can take advantage of negative feedback regulatory circuits present in macrophages to target autophagy. *P. aeruginosa* infection

leads to NLRC4-dependent caspase-1 activation which results in cleavage of TRIF, an important mediator of TLR4-induced autophagy (57). Importantly, *in vivo*, preventing TRIF cleavage restores autophagy and bacterial clearance.

Cleavage of Autophagy Machinery

L. pneumophila can also block autophagy directly by secreting two specific proteases. First, Lpg1137 targets ER-mitochondria contact sites to cleave syntaxin-17, a key SNARE protein implicated in autophagosome formation (58, 59). On another hand, RavZ, a cysteine protease, cleaves phosphatidylethanolamine-conjugated LC3 to produce a permanent unlipidated form of LC3 that is inadequate for the formation of autophagosomes (60). Another example is *L. monocytogenes*, which secretes phospholipase PlcA to degrade PI3P, a key lipid produced by Beclin-1 complex, and involved in LC3 lipidation (48, 61).

Regulation of miRNA (miR) Targeting Autophagy Machinery

Besides post-translational modification, autophagy can also be modulated at a post-transcriptional level *via* expression of various small non-coding RNAs (miR). *M. tuberculosis* thwarts autophagy by inducing expression of miR-33 which down-regulates expression of several autophagy proteins along the pathway (Atg5, Atg12, LC3, and LAMP1) (62). Remarkably, mice with hematopoietic miR-33 deficiency have a superior capacity to control *M. tuberculosis* infection. Another miR induced by *M. tuberculosis*, is miR-125a, which targets UVRAG in complex with Beclin-1 to inhibit autophagy and thus promote pathogen intracellular survival inside macrophages (63). Interestingly, miR-33 and miR-125a can be induced by PRR ligands isolated from *M. tuberculosis* (62, 63). Expression of these miR may be a normal negative feedback loop present in host cells to prevent excessive autophagy, which *M. tuberculosis* exploits to its advantage. Additionally, *M. tuberculosis* upregulates miR-144* to reduce expression of DRAM2, a recently discovered autophagy protein, that promotes activation of a second Beclin-1 complex involved in autophagosome maturation (64). Finally, *M. tuberculosis* can down-regulate miR-17, which targets Mcl-1, an inhibitor of Beclin-1 complex involved in autophagy initiation (65).

Blockade of Autophagosome–Lysosome Fusion

As mentioned above, *M. tuberculosis* can block autophagosome maturation *via* miR-144*, although, the bacterial factor(s) involved in that process remain to be identified (65). Separate studies have shown that Esat-6, an important *M. tuberculosis* virulence factor, plays also a role in blocking autophagosome maturation in macrophages as well as in dendritic cells (66, 67). The action mechanism of Esat-6 is unknown but might be mediated, in part, by miR modulation (68). Several other bacterial pathogens can impair autophagosome maturation for survival or growth in macrophages such as *Chlamydia trachomatis*, *Yersinia pestis*, *Y. pseudotuberculosis*, but like for *M. tuberculosis* the underlying molecular mechanisms are unknown (69–71). Furthermore, it is unclear whether these mechanisms applied to both xenophagy and LAP.

AUTOPHAGY MACHINERY FAVORS BACTERIAL PATHOGENS

Nutrient and Membrane Acquisition

While some pathogens neutralize autophagy to replicate intracellularly, others exploit autophagy or some autophagy proteins to acquire nutrients and remodel their vacuoles. *Y. pseudotuberculosis* inhibits autophagosome maturation; however, it relies on autophagosome formation for its growth in macrophages (71). An early study has shown that exogenous autophagy activation promotes the development of *Coxiella*-replicative vacuole (72). In macrophages and epithelial cells, *C. burnetti* resides in an large acidified compartment, which fuses with mature autophagosomes *via* Cig2, a type IV secretion system effector (73, 74). Interestingly, *in vivo*, Cig2 reduces host tolerance to *C. burnetti* infection without affecting bacterial load (74).

Brucella abortus subverts ULK1 and Beclin-1 complexes to remodel its ER-derived vacuole into a compartment with autophagic properties (75). Nonetheless, this conversion is independent of the two ubiquitin-like conjugation systems, Atg5-12 and LC3. This selective manipulation of autophagy proteins is important for *Brucella* lifecycle and cell-to-cell spreading. Similarly, *M. marinum*, a species closely related to *M. tuberculosis*, uses autophagy machinery to promote bacterial egress from its natural host, *Dictyostelium*, a macrophage-like unicellular organism (76). How *Brucella* and *M. marinum* manipulate autophagy proteins to favor transmission is still unknown.

Some pathogens have a more complex relationship with autophagy in a sense that they can evade, as outlined above, or exploit autophagy depending on the infection stages or the type of autophagy. At early stage, vacuolar *Legionella* interacts with autophagy pathway and seems to rely on autophagosome for survival in permissive macrophages (77). Similarly, cytosolic *F. tularensis* triggers an Atg5-independent autophagy pathway to acquire nutrients and replicate while avoiding xenophagy (78). The molecular differences between these two autophagy-related pathways, one that favors bacterial growth and the other promotes killing, definitely call for further investigation. Finally, immediately after entering macrophages, *L. monocytogenes* manipulates LAP to form spacious non-acidified *Listeria*-containing phagosomes (SLAPs) which are believed to participate in persistent infection (79, 80). Low expression of virulent factor, Listeriolysin O, appears to play a role in SLAP formation whereas high-expression triggers bacterial escape into the cytosol (80).

Inflammation Dampening

One example is *Vibrio parahaemolyticus*, which limits NLRC4 inflammasome-mediated IL-1beta production by activating macrophage autophagy *via* a type III secretion effector, VopQ (81). Other bacteria seem to benefit from the autophagy machinery in a more passive way. For example,

Atg16L1-deficient mice clear more efficiently uropathogenic *E. coli* (UPEC) and *Citrobacter rodentium* than wild-type controls (82–84). The improved protection against *C. rodentium* is associated with an enhanced immune response dependent on monocytes; however, it does not rely on a cell-intrinsic role of Atg16L1 in myeloid cells (84). In contrast, loss of Atg16L1 in macrophages is responsible for the phenotype observed during UPEC infection (83). Atg16L1-deficient macrophages, infected with UPEC, activate more NLRP3/Caspase-1 inflammasome, and IL-1beta production. Importantly, *in vivo*, IL-1beta neutralization reduces the capacity of Atg16L1-deficient mice to control UPEC infection. Testing other autophagy proteins will be essential to confirm the role of autophagy entire pathway in that process.

AUTOPHAGY IN HOST-DIRECTED THERAPY (HDT) AND VACCINE

Host-Directed Therapy

In the past few years, a number of studies have highlighted the potential of targeting autophagy for the control of bacterial infections. FDA-approved drugs with proautophagy activity, such as statin, gefitinib, carbamazepine, and metformin, have been shown to limit *M. tuberculosis* growth in mice model of infection (85–88). Similarly, rapamycin enhances clearance of *P. aeruginosa* and *B. cepacia*, *in vivo*, in addition to reducing lung inflammation (89, 90). However, these drugs can module several other cellular functions, so it is unclear whether their action, *in vivo*, is mediated by autophagy. Another difficulty is the seemingly opposing effects of a same drug depending on the infection settings. Indeed, while rapamycin induces *M. tuberculosis* killing in macrophages, it promotes bacterial survival in endothelial cells and in HIV-coinfected macrophages (91–93). The only compound tested, *in vivo* that specifically activates autophagy is a small cell permeant peptide, TAT-Beclin-1 (94). This designed peptide has been shown to improve outcome of chikungunya and West Nile virus infections in mice, thus it would be a good candidate to test in the context of bacterial infection. However, one has to bear in mind that some pathogens use autophagy to thrive in host cells and other can either evade or exploit this pathway according to the infection stage. Therefore, a detailed knowledge of the role(s) of autophagy and its molecular mechanisms for each bacterial pathogen is mandatory to develop more specific autophagy modulators, as well as, the availability of relevant preclinical models to evaluate the efficacy of these compounds.

Vaccine

Manipulation of autophagy in antigen-presenting cells including macrophages holds also great promise in vaccine development. Autophagy plays an important role in antigen processing and MHC presentation (95). Studies already indicate that boosting autophagy can enhance antigen presentation and vaccine efficacy. For instance, mice immunized with BCG-infected dendritic cells treated with mTOR inhibitor, rapamycin, have greater Th1-mediated protection after being challenged with *M. tuberculosis* (96). Recently, BCG*ΔureC::hly*, a live vaccine with improved immunogenicity and in clinical trial phase II, has been shown to enhance xenophagy (97). However, the importance, *in vivo*, of phagocyte autophagy in vaccine enhanced-efficacy is unclear as both cited strategies trigger other cellular pathways.

CONCLUSION

Macrophage autophagy is central to host defenses against bacterial infections, sending intracellular pathogens to lysosomes for degradation while controlling inflammation to limit host damages. Since novel functions for autophagy proteins have emerged in various physiological and pathological situations, it is likely that further contributions of autophagy machinery to macrophage biology will be unveiled in the context of bacterial infection (98, 99). On the other hand, pathogens have found multiple subterfuges to manipulate this machinery in order to persist or proliferate, still, their action mechanisms and significance *in vivo* are far from being thoroughly understood. A more comprehensive and integrated view of bacteria-autophagy interplay will definitely help in designing more specific HDT and vaccine based on autophagy modulation.

AUTHOR CONTRIBUTIONS

IV and AB reviewed the relevant literature and wrote the manuscript. IV prepared and AB revised the figures. IV and AB have read and approved the final manuscript.

ACKNOWLEDGMENTS

We apologize to colleagues whose work could not be cited due to space limitation. The work in the authors' laboratories was supported by EU FP7 Marie Curie Career Integration Grant 293416 (IV), EU Horizon 2020 TBVAC2020 under grant agreement No. 643381 (IV), and Horizon 2020 COST action TRANSAUTOPHAGY (CA15138).

REFERENCES

1. Ktistakis NT, Tooze SA. Digesting the expanding mechanisms of autophagy. *Trends Cell Biol* (2016) 26(8):624–35. doi:10.1016/j.tcb.2016.03.006
2. Ravikumar B, Sarkar S, Davies JE, Futter M, Garcia-Arencibia M, Green-Thompson ZW, et al. Regulation of mammalian autophagy in physiology and pathophysiology. *Physiol Rev* (2010) 90(4):1383–435. doi:10.1152/physrev.00030.2009
3. Cadwell K. Crosstalk between autophagy and inflammatory signalling pathways: balancing defence and homeostasis. *Nat Rev Immunol* (2016) 16(11):661–75. doi:10.1038/nri.2016.100
4. Shibutani ST, Saitoh T, Nowag H, Munz C, Yoshimori T. Autophagy and autophagy-related proteins in the immune system. *Nat Immunol* (2015) 16(10):1014–24. doi:10.1038/ni.3273
5. Deretic V, Kimura T, Timmins G, Moseley P, Chauhan S, Mandell M. Immunologic manifestations of autophagy. *J Clin Invest* (2015) 125(1):75–84. doi:10.1172/JCI73945
6. van der Vaart M, Korbee CJ, Lamers GE, Tengeler AC, Hosseini R, Haks MC, et al. The DNA damage-regulated autophagy modulator DRAM1 links mycobacterial recognition via TLR-MYD88 to autophagic defense [corrected]. *Cell Host Microbe* (2014) 15(6):753–67. doi:10.1016/j.chom.2014.05.005

7. Pastore N, Brady OA, Diab HI, Martina JA, Sun L, Huynh T, et al. TFEB and TFE3 cooperate in the regulation of the innate immune response in activated macrophages. *Autophagy* (2016) 12(8):1240–58. doi:10.1080/15548627.2016.1179405
8. Gomes LC, Dikic I. Autophagy in antimicrobial immunity. *Mol Cell* (2014) 54(2):224–33. doi:10.1016/j.molcel.2014.03.009
9. Watson RO, Manzanillo PS, Cox JS. Extracellular *M. tuberculosis* DNA targets bacteria for autophagy by activating the host DNA-sensing pathway. *Cell* (2012) 150(4):803–15. doi:10.1016/j.cell.2012.06.040
10. Watson RO, Bell SL, MacDuff DA, Kimmey JM, Diner EJ, Olivas J, et al. The cytosolic sensor cGAS detects *Mycobacterium tuberculosis* DNA to induce type I interferons and activate autophagy. *Cell Host Microbe* (2015) 17(6):811–9. doi:10.1016/j.chom.2015.05.004
11. Manzanillo PS, Ayres JS, Watson RO, Collins AC, Souza G, Rae CS, et al. The ubiquitin ligase parkin mediates resistance to intracellular pathogens. *Nature* (2013) 501(7468):512–6. doi:10.1038/nature12566
12. Franco LH, Nair VR, Scharn CR, Xavier RJ, Torrealba JR, Shiloh MU, et al. The ubiquitin ligase Smurf1 functions in selective autophagy of *Mycobacterium tuberculosis* and anti-tuberculous host defense. *Cell Host Microbe* (2017) 21(1):59–72. doi:10.1016/j.chom.2016.11.002
13. Chauhan S, Kumar S, Jain A, Ponpuak M, Mudd MH, Kimura T, et al. TRIMs and galectins globally cooperate and TRIM16 and galectin-3 co-direct autophagy in endomembrane damage homeostasis. *Dev Cell* (2016) 39(1):13–27. doi:10.1016/j.devcel.2016.08.003
14. Singh SB, Ornatowski W, Vergne I, Naylor J, Delgado M, Roberts E, et al. Human IRGM regulates autophagy and cell-autonomous immunity functions through mitochondria. *Nat Cell Biol* (2010) 12(12):1154–65. doi:10.1038/ncb2119
15. Chauhan S, Mandell MA, Deretic V. IRGM governs the core autophagy machinery to conduct antimicrobial defense. *Mol Cell* (2015) 58(3):507–21. doi:10.1016/j.molcel.2015.03.020
16. Ponpuak M, Davis AS, Roberts EA, Delgado MA, Dinkins C, Zhao Z, et al. Delivery of cytosolic components by autophagic adaptor protein p62 endows autophagosomes with unique antimicrobial properties. *Immunity* (2010) 32(3):329–41. doi:10.1016/j.immuni.2010.02.009
17. Alonso S, Pethe K, Russell DG, Purdy GE. Lysosomal killing of *Mycobacterium* mediated by ubiquitin-derived peptides is enhanced by autophagy. *Proc Natl Acad Sci U S A* (2007) 104(14):6031–6. doi:10.1073/pnas.0700036104
18. Castillo EF, Dekonenko A, Arko-Mensah J, Mandell MA, Dupont N, Jiang S, et al. Autophagy protects against active tuberculosis by suppressing bacterial burden and inflammation. *Proc Natl Acad Sci U S A* (2012) 109(46):E3168–76. doi:10.1073/pnas.1210500109
19. Kimmey JM, Huynh JP, Weiss LA, Park S, Kambal A, Debnath J, et al. Unique role for ATG5 in neutrophil-mediated immunopathology during *M. tuberculosis* infection. *Nature* (2015) 528(7583):565–9. doi:10.1038/nature16451
20. Saini NK, Baena A, Ng TW, Venkataswamy MM, Kennedy SC, Kunnath-Velayudhan S, et al. Suppression of autophagy and antigen presentation by *Mycobacterium tuberculosis* PE_PGRS47. *Nat Microbiol* (2016) 1(9):16133. doi:10.1038/nmicrobiol.2016.133
21. Galluzzi L, Baehrecke EH, Ballabio A, Boya P, Bravo-San Pedro JM, Cecconi F, et al. Molecular definitions of autophagy and related processes. *EMBO J* (2017) 36(13):1811–36. doi:10.15252/embj.201796697
22. Mitchell G, Isberg RR. Innate immunity to intracellular pathogens: balancing microbial elimination and inflammation. *Cell Host Microbe* (2017) 22(2):166–75. doi:10.1016/j.chom.2017.07.005
23. Sanjuan MA, Dillon CP, Tait SW, Moshiach S, Dorsey F, Connell S, et al. Toll-like receptor signalling in macrophages links the autophagy pathway to phagocytosis. *Nature* (2007) 450(7173):1253–7. doi:10.1038/nature06421
24. Ma J, Becker C, Lowell CA, Underhill DM. Dectin-1-triggered recruitment of light chain 3 protein to phagosomes facilitates major histocompatibility complex class II presentation of fungal-derived antigens. *J Biol Chem* (2012) 287(41):34149–56. doi:10.1074/jbc.M112.382812
25. Huang J, Canadien V, Lam GY, Steinberg BE, Dinauer MC, Magalhaes MA, et al. Activation of antibacterial autophagy by NADPH oxidases. *Proc Natl Acad Sci U S A* (2009) 106(15):6226–31. doi:10.1073/pnas.0811045106
26. Martinez J, Malireddi RK, Lu Q, Cunha LD, Pelletier S, Gingras S, et al. Molecular characterization of LC3-associated phagocytosis reveals distinct roles for Rubicon, NOX2 and autophagy proteins. *Nat Cell Biol* (2015) 17(7):893–906. doi:10.1038/ncb3192
27. Abnave P, Mottola G, Gimenez G, Boucherit N, Trouplin V, Torre C, et al. Screening in planarians identifies MORN2 as a key component in LC3-associated phagocytosis and resistance to bacterial infection. *Cell Host Microbe* (2014) 16(3):338–50. doi:10.1016/j.chom.2014.08.002
28. Yang CS, Lee JS, Rodgers M, Min CK, Lee JY, Kim HJ, et al. Autophagy protein Rubicon mediates phagocytic NADPH oxidase activation in response to microbial infection or TLR stimulation. *Cell Host Microbe* (2012) 11(3):264–76. doi:10.1016/j.chom.2012.01.018
29. Romao S, Gasser N, Becker AC, Guhl B, Bajagic M, Vanoaica D, et al. Autophagy proteins stabilize pathogen-containing phagosomes for prolonged MHC II antigen processing. *J Cell Biol* (2013) 203(5):757–66. doi:10.1083/jcb.201308173
30. Cemma M, Grinstein S, Brumell JH. Autophagy proteins are not universally required for phagosome maturation. *Autophagy* (2016) 12(9):1440–6. doi:10.1080/15548627.2016.1191724
31. Bonilla DL, Bhattacharya A, Sha Y, Xu Y, Xiang Q, Kan A, et al. Autophagy regulates phagocytosis by modulating the expression of scavenger receptors. *Immunity* (2013) 39(3):537–47. doi:10.1016/j.immuni.2013.08.026
32. Jacquel A, Obba S, Boyer L, Dufies M, Robert G, Gounon P, et al. Autophagy is required for CSF-1-induced macrophagic differentiation and acquisition of phagocytic functions. *Blood* (2012) 119(19):4527–31. doi:10.1182/blood-2011-11-392167
33. Harris J, Lang T, Thomas JPW, Sukkar MB, Nabar NR, Kehrl JH. Autophagy and inflammasomes. *Mol Immunol* (2017) 86:10–5. doi:10.1016/j.molimm.2017.02.013
34. Saitoh T, Akira S. Regulation of inflammasomes by autophagy. *J Allergy Clin Immunol* (2016) 138(1):28–36. doi:10.1016/j.jaci.2016.05.009
35. Jabir MS, Hopkins L, Ritchie ND, Ullah I, Bayes HK, Li D, et al. Mitochondrial damage contributes to *Pseudomonas aeruginosa* activation of the inflammasome and is downregulated by autophagy. *Autophagy* (2015) 11(1):166–82. doi:10.4161/15548627.2014.981915
36. Pu Q, Gan C, Li R, Li Y, Tan S, Li X, et al. Atg7 deficiency intensifies inflammasome activation and pyroptosis in *Pseudomonas* sepsis. *J Immunol* (2017) 198(8):3205–13. doi:10.4049/jimmunol.1601196
37. Shi CS, Shenderov K, Huang NN, Kabat J, Abu-Asab M, Fitzgerald KA, et al. Activation of autophagy by inflammatory signals limits IL-1beta production by targeting ubiquitinated inflammasomes for destruction. *Nat Immunol* (2012) 13(3):255–63. doi:10.1038/ni.2215
38. Kimura T, Jain A, Choi SW, Mandell MA, Schroder K, Johansen T, et al. TRIM-mediated precision autophagy targets cytoplasmic regulators of innate immunity. *J Cell Biol* (2015) 210(6):973–89. doi:10.1083/jcb.201503023
39. Meunier E, Dick MS, Dreier RF, Schurmann N, Kenzelmann Broz D, Warming S, et al. Caspase-11 activation requires lysis of pathogen-containing vacuoles by IFN-induced GTPases. *Nature* (2014) 509(7500):366–70. doi:10.1038/nature13157
40. Harris J. Autophagy and cytokines. *Cytokine* (2011) 56(2):140–4. doi:10.1016/j.cyto.2011.08.022
41. Sakowski ET, Koster S, Portal Celhay C, Park HS, Shrestha E, Hetzenecker SE, et al. Ubiquilin 1 promotes IFN-gamma-induced xenophagy of *Mycobacterium tuberculosis*. *PLoS Pathog* (2015) 11(7):e1005076. doi:10.1371/journal.ppat.1005076
42. Kim BH, Shenoy AR, Kumar P, Das R, Tiwari S, MacMicking JD. A family of IFN-gamma-inducible 65-kD GTPases protects against bacterial infection. *Science* (2011) 332(6030):717–21. doi:10.1126/science.1201711
43. Yuk JM, Shin DM, Lee HM, Yang CS, Jin HS, Kim KK, et al. Vitamin D3 induces autophagy in human monocytes/macrophages via cathelicidin. *Cell Host Microbe* (2009) 6(3):231–43. doi:10.1016/j.chom.2009.08.004
44. Petruccioli E, Romagnoli A, Corazzari M, Coccia EM, Butera O, Delogu G, et al. Specific T cells restore the autophagic flux inhibited by *Mycobacterium tuberculosis* in human primary macrophages. *J Infect Dis* (2012) 205(9):1425–35. doi:10.1093/infdis/jis226
45. Wu Y, Wang Y, Zou H, Wang B, Sun Q, Fu A, et al. Probiotic *Bacillus amyloliquefaciens* SC06 induces autophagy to protect against pathogens

in macrophages. *Front Microbiol* (2017) 8:469. doi:10.3389/fmicb.2017.00469
46. Mitchell G, Chen C, Portnoy DA. Strategies used by bacteria to grow in macrophages. *Microbiol Spectr* (2016) 4(3):1–22. doi:10.1128/microbiolspec.MCHD-0012-2015
47. Dortet L, Mostowy S, Samba-Louaka A, Gouin E, Nahori MA, Wiemer EA, et al. Recruitment of the major vault protein by InlK: a *Listeria monocytogenes* strategy to avoid autophagy. *PLoS Pathog* (2011) 7(8):e1002168. doi:10.1371/journal.ppat.1002168
48. Mitchell G, Ge L, Huang Q, Chen C, Kianian S, Roberts MF, et al. Avoidance of autophagy mediated by PlcA or ActA is required for *Listeria monocytogenes* growth in macrophages. *Infect Immun* (2015) 83(5):2175–84. doi:10.1128/IAI.00110-15
49. Case ED, Chong A, Wehrly TD, Hansen B, Child R, Hwang S, et al. The *Francisella* O-antigen mediates survival in the macrophage cytosol via autophagy avoidance. *Cell Microbiol* (2014) 16(6):862–77. doi:10.1111/cmi.12246
50. Ganesan R, Hos NJ, Gutierrez S, Fischer J, Stepek JM, Daglidu E, et al. *Salmonella typhimurium* disrupts Sirt1/AMPK checkpoint control of mTOR to impair autophagy. *PLoS Pathog* (2017) 13(2):e1006227. doi:10.1371/journal.ppat.1006227
51. Owen KA, Meyer CB, Bouton AH, Casanova JE. Activation of focal adhesion kinase by *Salmonella* suppresses autophagy via an Akt/mTOR signaling pathway and promotes bacterial survival in macrophages. *PLoS Pathog* (2014) 10(6):e1004159. doi:10.1371/journal.ppat.1004159
52. Shin DM, Jeon BY, Lee HM, Jin HS, Yuk JM, Song CH, et al. *Mycobacterium tuberculosis* eis regulates autophagy, inflammation, and cell death through redox-dependent signaling. *PLoS Pathog* (2010) 6(12):e1001230. doi:10.1371/journal.ppat.1001230
53. Kim KH, An DR, Song J, Yoon JY, Kim HS, Yoon HJ, et al. *Mycobacterium tuberculosis* Eis protein initiates suppression of host immune responses by acetylation of DUSP16/MKP-7. *Proc Natl Acad Sci U S A* (2012) 109(20):7729–34. doi:10.1073/pnas.1120251109
54. Koster S, Upadhyay S, Chandra P, Papavinasasundaram K, Yang G, Hassan A, et al. *Mycobacterium tuberculosis* is protected from NADPH oxidase and LC3-associated phagocytosis by the LCP protein CpsA. *Proc Natl Acad Sci U S A* (2017) 114(41):E8711–20. doi:10.1073/pnas.1707792114
55. Rabadi SM, Sanchez BC, Varanat M, Ma Z, Catlett SV, Melendez JA, et al. Antioxidant defenses of *Francisella tularensis* modulate macrophage function and production of proinflammatory cytokines. *J Biol Chem* (2016) 291(10):5009–21. doi:10.1074/jbc.M115.681478
56. Rolando M, Escoll P, Nora T, Botti J, Boitez V, Bedia C, et al. *Legionella pneumophila* S1P-lyase targets host sphingolipid metabolism and restrains autophagy. *Proc Natl Acad Sci U S A* (2016) 113(7):1901–6. doi:10.1073/pnas.1522067113
57. Jabir MS, Ritchie ND, Li D, Bayes HK, Tourlomousis P, Puleston D, et al. Caspase-1 cleavage of the TLR adaptor TRIF inhibits autophagy and beta-interferon production during *Pseudomonas aeruginosa* infection. *Cell Host Microbe* (2014) 15(2):214–27. doi:10.1016/j.chom.2014.01.010
58. Hamasaki M, Furuta N, Matsuda A, Nezu A, Yamamoto A, Fujita N, et al. Autophagosomes form at ER-mitochondria contact sites. *Nature* (2013) 495(7441):389–93. doi:10.1038/nature11910
59. Arasaki K, Mikami Y, Shames SR, Inoue H, Wakana Y, Tagaya M. *Legionella* effector Lpg1137 shuts down ER-mitochondria communication through cleavage of syntaxin 17. *Nat Commun* (2017) 8:15406. doi:10.1038/ncomms15406
60. Choy A, Dancourt J, Mugo B, O'Connor TJ, Isberg RR, Melia TJ, et al. The *Legionella* effector RavZ inhibits host autophagy through irreversible Atg8 deconjugation. *Science* (2012) 338(6110):1072–6. doi:10.1126/science.1227026
61. Tattoli I, Sorbara MT, Yang C, Tooze SA, Philpott DJ, Girardin SE. Listeria phospholipases subvert host autophagic defenses by stalling pre-autophagosomal structures. *EMBO J* (2013) 32(23):3066–78. doi:10.1038/emboj.2013.234
62. Ouimet M, Koster S, Sakowski E, Ramkhelawon B, van Solingen C, Oldebeken S, et al. *Mycobacterium tuberculosis* induces the miR-33 locus to reprogram autophagy and host lipid metabolism. *Nat Immunol* (2016) 17(6):677–86. doi:10.1038/ni.3434
63. Kim JK, Yuk JM, Kim SY, Kim TS, Jin HS, Yang CS, et al. MicroRNA-125a inhibits autophagy activation and antimicrobial responses during mycobacterial infection. *J Immunol* (2015) 194(11):5355–65. doi:10.4049/jimmunol.1402557
64. Kim JK, Lee HM, Park KS, Shin DM, Kim TS, Kim YS, et al. miR144* inhibits antimicrobial responses against *Mycobacterium tuberculosis* in human monocytes and macrophages by targeting the autophagy protein DRAM2. *Autophagy* (2017) 13(2):423–41. doi:10.1080/15548627.2016.1241922
65. Kumar R, Sahu SK, Kumar M, Jana K, Gupta P, Gupta UD, et al. MicroRNA 17-5p regulates autophagy in *Mycobacterium tuberculosis*-infected macrophages by targeting Mcl-1 and STAT3. *Cell Microbiol* (2016) 18(5):679–91. doi:10.1111/cmi.12540
66. Chandra P, Ghanwat S, Matta SK, Yadav SS, Mehta M, Siddiqui Z, et al. *Mycobacterium tuberculosis* inhibits RAB7 recruitment to selectively modulate autophagy flux in macrophages. *Sci Rep* (2015) 5:16320. doi:10.1038/srep16320
67. Romagnoli A, Etna MP, Giacomini E, Pardini M, Remoli ME, Corazzari M, et al. ESX-1 dependent impairment of autophagic flux by *Mycobacterium tuberculosis* in human dendritic cells. *Autophagy* (2012) 8(9):1357–70. doi:10.4161/auto.20881
68. Kumar M, Sahu SK, Kumar R, Subuddhi A, Maji RK, Jana K, et al. MicroRNA let-7 modulates the immune response to *Mycobacterium tuberculosis* infection via control of A20, an inhibitor of the NF-kappaB pathway. *Cell Host Microbe* (2015) 17(3):345–56. doi:10.1016/j.chom.2015.01.007
69. Yasir M, Pachikara ND, Bao X, Pan Z, Fan H. Regulation of chlamydial infection by host autophagy and vacuolar ATPase-bearing organelles. *Infect Immun* (2011) 79(10):4019–28. doi:10.1128/IAI.05308-11
70. Pujol C, Klein KA, Romanov GA, Palmer LE, Cirota C, Zhao Z, et al. *Yersinia pestis* can reside in autophagosomes and avoid xenophagy in murine macrophages by preventing vacuole acidification. *Infect Immun* (2009) 77(6):2251–61. doi:10.1128/IAI.00068-09
71. Moreau K, Lacas-Gervais S, Fujita N, Sebbane F, Yoshimori T, Simonet M, et al. Autophagosomes can support *Yersinia pseudotuberculosis* replication in macrophages. *Cell Microbiol* (2010) 12(8):1108–23. doi:10.1111/j.1462-5822.2010.01456.x
72. Gutierrez MG, Vazquez CL, Munafo DB, Zoppino FC, Beron W, Rabinovitch M, et al. Autophagy induction favours the generation and maturation of the *Coxiella*-replicative vacuoles. *Cell Microbiol* (2005) 7(7):981–93. doi:10.1111/j.1462-5822.2005.00527.x
73. Winchell CG, Steele S, Kawula T, Voth DE. Dining in: intracellular bacterial pathogen interplay with autophagy. *Curr Opin Microbiol* (2016) 29:9–14. doi:10.1016/j.mib.2015.09.004
74. Kohler LJ, Reed Sh C, Sarraf SA, Arteaga DD, Newton HJ, Roy CR. Effector protein Cig2 decreases host tolerance of infection by directing constitutive fusion of autophagosomes with the *Coxiella*-containing vacuole. *MBio* (2016) 7(4):e1127–1116. doi:10.1128/mBio.01127-16
75. Starr T, Child R, Wehrly TD, Hansen B, Hwang S, Lopez-Otin C, et al. Selective subversion of autophagy complexes facilitates completion of the *Brucella* intracellular cycle. *Cell Host Microbe* (2012) 11(1):33–45. doi:10.1016/j.chom.2011.12.002
76. Gerstenmaier L, Pilla R, Herrmann L, Herrmann H, Prado M, Villafano GJ, et al. The autophagic machinery ensures nonlytic transmission of mycobacteria. *Proc Natl Acad Sci U S A* (2015) 112(7):E687–92. doi:10.1073/pnas.1423318112
77. Amer AO, Byrne BG, Swanson MS. Macrophages rapidly transfer pathogens from lipid raft vacuoles to autophagosomes. *Autophagy* (2005) 1(1):53–8. doi:10.4161/auto.1.1.1589
78. Steele S, Brunton J, Ziehr B, Taft-Benz S, Moorman N, Kawula T. *Francisella tularensis* harvests nutrients derived via ATG5-independent autophagy to support intracellular growth. *PLoS Pathog* (2013) 9(8):e1003562. doi:10.1371/journal.ppat.1003562
79. Lam GY, Cemma M, Muise AM, Higgins DE, Brumell JH. Host and bacterial factors that regulate LC3 recruitment to *Listeria monocytogenes* during the early stages of macrophage infection. *Autophagy* (2013) 9(7):985–95. doi:10.4161/auto.24406
80. Birmingham CL, Canadien V, Kaniuk NA, Steinberg BE, Higgins DE, Brumell JH. Listeriolysin O allows *Listeria monocytogenes* replication in macrophage vacuoles. *Nature* (2008) 451(7176):350–4. doi:10.1038/nature06479

81. Higa N, Toma C, Koizumi Y, Nakasone N, Nohara T, Masumoto J, et al. *Vibrio parahaemolyticus* effector proteins suppress inflammasome activation by interfering with host autophagy signaling. *PLoS Pathog* (2013) 9(1):e1003142. doi:10.1371/journal.ppat.1003142
82. Wang C, Mendonsa GR, Symington JW, Zhang Q, Cadwell K, Virgin HW, et al. Atg16L1 deficiency confers protection from uropathogenic *Escherichia coli* infection in vivo. *Proc Natl Acad Sci U S A* (2012) 109(27):11008–13. doi:10.1073/pnas.1203952109
83. Symington JW, Wang C, Twentyman J, Owusu-Boaitey N, Schwendener R, Nunez G, et al. ATG16L1 deficiency in macrophages drives clearance of uropathogenic *E. coli* in an IL-1beta-dependent manner. *Mucosal Immunol* (2015) 8(6):1388–99. doi:10.1038/mi.2015.7
84. Marchiando AM, Ramanan D, Ding Y, Gomez LE, Hubbard-Lucey VM, Maurer K, et al. A deficiency in the autophagy gene Atg16L1 enhances resistance to enteric bacterial infection. *Cell Host Microbe* (2013) 14(2):216–24. doi:10.1016/j.chom.2013.07.013
85. Parihar SP, Guler R, Khutlang R, Lang DM, Hurdayal R, Mhlanga MM, et al. Statin therapy reduces the *Mycobacterium tuberculosis* burden in human macrophages and in mice by enhancing autophagy and phagosome maturation. *J Infect Dis* (2014) 209(5):754–63. doi:10.1093/infdis/jit550
86. Stanley SA, Barczak AK, Silvis MR, Luo SS, Sogi K, Vokes M, et al. Identification of host-targeted small molecules that restrict intracellular *Mycobacterium tuberculosis* growth. *PLoS Pathog* (2014) 10(2):e1003946. doi:10.1371/journal.ppat.1003946
87. Schiebler M, Brown K, Hegyi K, Newton SM, Renna M, Hepburn L, et al. Functional drug screening reveals anticonvulsants as enhancers of mTOR-independent autophagic killing of *Mycobacterium tuberculosis* through inositol depletion. *EMBO Mol Med* (2015) 7(2):127–39. doi:10.15252/emmm.201404137
88. Singhal A, Jie L, Kumar P, Hong GS, Leow MK-S, Paleja B, et al. Metformin as adjunct antituberculosis therapy. *Sci Transl Med* (2014) 6(263):263ra159. doi:10.1126/scitranslmed.3009885
89. Junkins RD, Shen A, Rosen K, McCormick C, Lin TJ. Autophagy enhances bacterial clearance during *P. aeruginosa* lung infection. *PLoS One* (2013) 8(8):e72263. doi:10.1371/journal.pone.0072263
90. Abdulrahman BA, Khweek AA, Akhter A, Caution K, Kotrange S, Abdelaziz DH, et al. Autophagy stimulation by rapamycin suppresses lung inflammation and infection by *Burkholderia cenocepacia* in a model of cystic fibrosis. *Autophagy* (2011) 7(11):1359–70. doi:10.4161/auto.7.11.17660
91. Gutierrez MG, Master SS, Singh SB, Taylor GA, Colombo MI, Deretic V. Autophagy is a defense mechanism inhibiting BCG and *Mycobacterium tuberculosis* survival in infected macrophages. *Cell* (2004) 119(6):753–66. doi:10.1016/j.cell.2004.11.038
92. Lerner TR, de Souza Carvalho-Wodarz C, Repnik U, Russell MR, Borel S, Diedrich CR, et al. Lymphatic endothelial cells are a replicative niche for *Mycobacterium tuberculosis*. *J Clin Invest* (2016) 126(3):1093–108. doi:10.1172/JCI83379
93. Andersson AM, Andersson B, Lorell C, Raffetseder J, Larsson M, Blomgran R. Autophagy induction targeting mTORC1 enhances *Mycobacterium tuberculosis* replication in HIV co-infected human macrophages. *Sci Rep* (2016) 6:28171. doi:10.1038/srep28171
94. Shoji-Kawata S, Sumpter R, Leveno M, Campbell GR, Zou Z, Kinch L, et al. Identification of a candidate therapeutic autophagy-inducing peptide. *Nature* (2013) 494(7436):201–6. doi:10.1038/nature11866
95. Munz C. Autophagy proteins in antigen processing for presentation on MHC molecules. *Immunol Rev* (2016) 272(1):17–27. doi:10.1111/imr.12422
96. Jagannath C, Lindsey DR, Dhandayuthapani S, Xu Y, Hunter RL Jr, Eissa NT. Autophagy enhances the efficacy of BCG vaccine by increasing peptide presentation in mouse dendritic cells. *Nat Med* (2009) 15(3):267–76. doi:10.1038/nm.1928
97. Saiga H, Nieuwenhuizen N, Gengenbacher M, Koehler AB, Schuerer S, Moura-Alves P, et al. The recombinant BCG DeltaureC::hly vaccine targets the AIM2 inflammasome to induce autophagy and inflammation. *J Infect Dis* (2015) 211(11):1831–41. doi:10.1093/infdis/jiu675
98. Kenific CM, Wittmann T, Debnath J. Autophagy in adhesion and migration. *J Cell Sci* (2016) 129(20):3685–93. doi:10.1242/jcs.188490
99. Ponpuak M, Mandell MA, Kimura T, Chauhan S, Cleyrat C, Deretic V. Secretory autophagy. *Curr Opin Cell Biol* (2015) 35:106–16. doi:10.1016/j.ceb.2015.04.016

Conflict of Interest Statement: The authors declare that the research was conducted in the absence of any commercial or financial relationships that could be construed as a potential conflict of interest.

Copyright © 2017 Bah and Vergne. This is an open-access article distributed under the terms of the Creative Commons Attribution License (CC BY). The use, distribution or reproduction in other forums is permitted, provided the original author(s) or licensor are credited and that the original publication in this journal is cited, in accordance with accepted academic practice. No use, distribution or reproduction is permitted which does not comply with these terms.

frontiers in Immunology

MINI REVIEW
published: 08 November 2017
doi: 10.3389/fimmu.2017.01454

Bruton's Tyrosine Kinase: An Emerging Key Player in Innate Immunity

Alexander N. R. Weber[1], Zsofia Bittner[1], Xiao Liu[1], Truong-Minh Dang[1], Markus Philipp Radsak[2] and Cornelia Brunner[3]*

[1] Department of Immunology, Interfaculty Institute for Cell Biology, University of Tübingen, Tübingen, Germany, [2] Department of Internal Medicine III, University Medical Center of the Johannes Gutenberg-University Mainz, Mainz, Germany, [3] Department of Otorhinolaryngology, Ulm University Medical Center, Ulm, Germany

Bruton's tyrosine kinase (BTK) was initially discovered as a critical mediator of B cell receptor signaling in the development and functioning of adaptive immunity. Growing evidence also suggests multiple roles for BTK in mononuclear cells of the innate immune system, especially in dendritic cells and macrophages. For example, BTK has been shown to function in Toll-like receptor-mediated recognition of infectious agents, cellular maturation and recruitment processes, and Fc receptor signaling. Most recently, BTK was additionally identified as a direct regulator of a key innate inflammatory machinery, the NLRP3 inflammasome. BTK has thus attracted interest not only for gaining a more thorough basic understanding of the human innate immune system but also as a target to therapeutically modulate innate immunity. We here review the latest developments on the role of BTK in mononuclear innate immune cells in mouse versus man, with specific emphasis on the sensing of infectious agents and the induction of inflammation. Therapeutic implications for modulating innate immunity and critical open questions are also discussed.

Keywords: Bruton's tyrosine kinase, macrophage, dendritic cell, Toll-like receptor, NLRP3 inflammasome, ibrutinib, X-linked agammaglobulinemia

OPEN ACCESS

Edited by:
Geanncarlo Lugo-Villarino, UMR5089 Institut de Pharmacologie et de Biologie Structurale (IPBS), France

Reviewed by:
Pradip Sen, Institute of Microbial Technology (CSIR), India
Isabella Quinti, Sapienza Università di Roma, Italy
Amir Feisal Merican Bin Aljunid Merican, University of Malaya, Malaysia

****Correspondence:***
Alexander N. R. Weber
alexander.weber@uni-tuebingen.de

Specialty section:
This article was submitted to Microbial Immunology, a section of the journal Frontiers in Immunology

Received: *10 August 2017*
Accepted: *18 October 2017*
Published: *08 November 2017*

Citation:
Weber AN, Bittner Z, Liu X, Dang T-M, Radsak MP and Brunner C (2017) Bruton's Tyrosine Kinase: An Emerging Key Player in Innate Immunity. Front. Immunol. 8:1454. doi: 10.3389/fimmu.2017.01454

INTRODUCTION

Since the first description of X-linked agammaglobulinemia (XLA, OMIM entry 300300) (1) and the identification of Bruton's tyrosine kinase (*BTK*) as its genetic cause (2), BTK has been widely characterized as a critical mediator of B cell receptor (BCR) signaling and thus adaptive immunity (3). In the murine *Btk*-mutated (R28C) X-linked immunodeficiency (*Xid)* mutant strain CBA/N (4) B cell numbers and functionality are reduced but detectable [e.g., unaffected B-1b cell levels (5)]. In contrast, in humans BTK's pivotal role is highlighted by the fact that a wide spectrum of *BTK* loss-of-function mutations [reviewed by Ref. (6) and documented in the 'BTKbase' database] lead to an almost complete absence of peripheral B cells and antibodies in XLA. BTK catalytic activity typically drives the activation of at least three key signaling pathways, phospholipase C, phosphatidalyinositol-3-kinase/Akt and NF-κB, giving B cells a very strong survival signal upon BCR engagement. Totaling a molecular weight of approximately 77 kDa, BTK also contains an N-terminal Pleckstrin homology domain that binds membrane phosphatidylinositol (3,4,5)-trisphosphate (PIP_3), and Tec homology, Src homology (SH) 3, and SH2 domains involved in

protein-protein interactions. Y223 and Y551 represent two critical tyrosine phosphorylation sites in the SH3 and kinase domain (7). Y551 is phosphorylated by the kinases Syk or Lyn during BCR signaling and promotes the catalytic activity of BTK and subsequent Y223 autophosphorylation. The strong dependence of malignant B cells on BTK activity for survival (3), made BTK a key target for the development of small molecule inhibitors (8) in B cell malignancies. Nevertheless, BTK is being increasingly studied for its role in myeloid and other innate immune cells (**Figure 1**). Here, we summarize the emerging multi-faceted roles of this versatile and therapeutically tractable kinase in innate immunity.

BTK IN INFECTION AND DANGER RECOGNITION BY CELL SURFACE RECEPTORS IN INNATE IMMUNE CELLS

Although innate immune contributions for BTK in *in vivo* infection models with *Btk* gene knockout or *Xid* mice have to be interpreted with care (see below), a role for BTK/Btk in the sensing of multiple microbes has been reported: Sensing and antimicrobial responses to *Listeria monocytogenes* (9), *Staphylococcus aureus* (10), dengue virus (11), and *Aspergillus fumigatus* (12) were shown to depend on BTK. This effect may in part be due to BTK's involvement in the sensing of microbes *via* multiple Toll-like receptors (TLRs)—TLR2 (13, 14), TLR3 (11), TLR4 (14, 15), TLR7/8 (14, 16, 17), and TLR9 (9, 17, 18) on human and mouse macrophages and dendritic cells (DC). However, some TLR studies, especially those involving XLA patients, have been contradictory with regard to specific TLRs requiring BTK (19). Potentially, the functional requirements for BTK function during B cell development are higher, leading to an XLA phenotype in a broader range of mutations and thus patients; conversely, it seems that for TLR signaling only certain BTK mutations may cause a significant impairment of signaling. Within the vast spectrum of BTK mutations reported in XLA patients the functional impact can oftentimes not adequately be predicted. On a postreceptor level, BTK is thought to interface with canonical TLR pathways at the level of the TLR/MyD88 bridging adaptor Mal/TIRAP, one suggested direct BTK substrate (15, 20, 21) apart from TLR3 (11). TLR-dependent BTK-activation promotes NF-κB and interferon-regulatory factor-dependent transcription of inflammatory cytokines and interferons (IFNs) (15, 17). BTK was also linked with the cytosolic nucleic acid sensor DDX41 (11) and promoted its cooperation with the important IFN response regulator STING. BTK also operates downstream of the myeloid receptor TREM-1 for cytokine production (22, 23). On a more global immunoregulatory level, downregulation of innate immune-related genes and an upregulation of oxidative

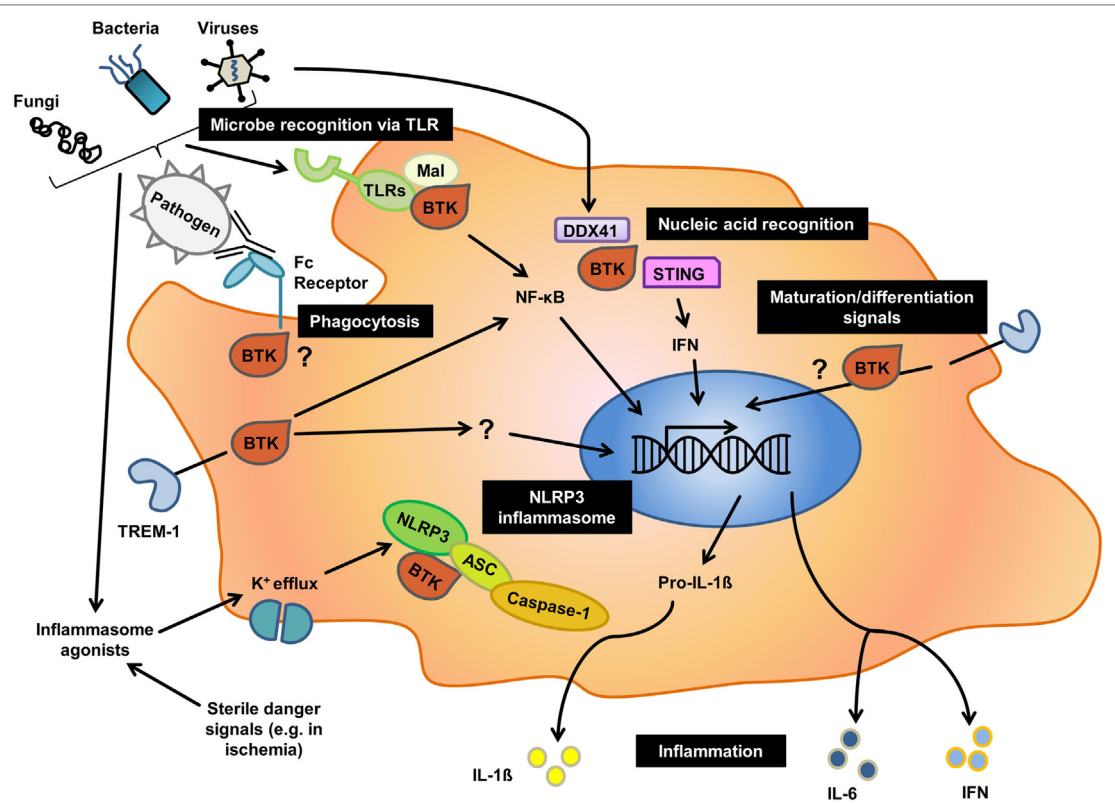


FIGURE 1 | Overview of the different roles of Bruton's tyrosine kinase (BTK) in innate immunity. Black boxes indicate major cellular processes for which an involvement of BTK has been reported in human or mice, or both. As outlined in the text, for processes such as phagocytosis there is contradictory evidence illustrating that the nature of function-modifying mutations, cellular context and species may have a profound effect on the role of BTK in a given process.

phosphorylation and apoptosis-related genes was observed in XLA patients (24). In contrast to these proimmune innate functions of BTK, the kinase was also shown to negatively regulate TLR-induced cytokine release from primary human innate immune cells (25). Moreover, in other DC studies, hepatocyte growth factor (HGF) as well as T cell Ig and mucin protein-3 (TIM-3)-induced BTK function blocked NF-κB activity (26, 27). In phagocytosis BTK was found essential for the clearance of infectious agents by mouse macrophages (12, 28); for humans, both data supporting a requirement for BTK in phagocytosis (24, 29, 30) as well as data arguing for a redundant role of BTK in this process (19, 31) have been reported based on studies of cells from XLA patients. Off-target effects in studies involving BTK inhibitors and the aforementioned unpredictability of naturally occurring BTK mutations or gene alterations[1] are likely to contribute to these controversial findings. The breadth of this multifaceted body of evidence certainly highlights the complexity of BTK function and regulation. Specific mutation site, receptor pathway, cell type and species are thus important factors, rendering the more systematic exploration of BTK's role in innate immunity a formidable challenge.

BTK IN THE MATURATION, RECRUITMENT AND FUNCTION OF INNATE IMMUNE CELLS

Given its role in B cell development, a role for BTK in the development of myeloid cells, which depends on many cues provided by cell surface receptors (32), is not surprising. Interestingly, in mice GM-CSF receptor α-chain expression was required for macrophage maturation and survival. In mice, Btk deficiency also correlated with reduced monocyte/macrophage numbers (33) but favored granulopoiesis (34, 35). However, these granulocytes were immature, had inefficient granule function and impaired recruitment of neutrophils to sites of sterile inflammation. Similarly, in humans BTK seems to be implicated in the maturation of neutrophils, since in XLA patients, who are frequently neutropenic, neutrophils were arrested at the myelocyte/promyelocyte stage (36–38). Conversely, Marron et al. (19) and Cavaliere et al. (31) suggested that BTK is dispensable for human neutrophil function; Honda et al. (39) even found an increased TLR or tumor necrosis factor receptor-induced ROS production of XLA neutrophils, albeit at higher levels of neutrophil apoptosis. Although DC numbers in *Btk*-deficient animals were unaffected, these DC had defects in maturation and DC-mediated antigen presentation (40). In human DC, the aforementioned HGF- and TIM-3-induced BTK-mediated NF-κB inhibition impaired DC activation as well as maturation leading to impaired CpG-induced anti-tumor responses (26, 27).

[1]Gross deletion within the *BTK* genomic locus could affect not only expression and function of BTK itself but also that of adjacent genes like *TIMM8A*, the genetic cause of the Mohr-Tranebjærg syndrome (MTS, OMIM entry 304700), a neurodegenerative disorder leading to sensorineural deafness. Additionally, beside isolated *BTK*-deficiency (XLA OMIM entry 300300), patients were reported with growth hormone deficiency (GHD) associated with mutations within the BTK gene (XLH-GHD, OMIM entry 307200). The reason for GHD in XLA remains obscure.

In tumor infiltrating macrophages BTK was found to exert immune-inhibitory and tumor-promoting effects (41, 42). In contrast, inhibition of Btk activity promoted DC maturation and $CD4^+$ T cell activating functions (43, 44). Together, these data suggest BTK may serve as an important target for immunomodulatory-based anticancer therapy. The unexpected description of (so far) cancer-specific alternative isoforms, p65 and p80, in breast (45), brain (46), prostate (47), gastric (48), and colon cancer (49) as well as reports for a role of BTK in NK cells (50), and platelets (51) also deserve mention and warrant further research.

BTK AND THE NLRP3 INFLAMMASOME

The NLRP3 inflammasome, a multiprotein complex involving NLRP3, the adaptor ASC and the proteolytic enzyme, caspase-1, has recently emerged as a key molecular machinery for the processing and thus activation of bioactive IL-1β (52, 53) and a major pathophysiological regulator in infection, myocardial infarction, stroke, Alzheimer's and diabetes (53). Reports by us (10) and others (54) recently identified BTK as a direct regulator in NLRP3 inflammasome activation (**Figure 2**): Ito et al. demonstrated that BTK was critically required for NLRP3 inflammasome-dependent IL-1β release from murine macrophages. BTK physically interacted with NLRP3 and its adaptor ASC, resulting in the induction of ASC oligomerization and caspase-1 activation in a kinase activity-dependent manner *in vitro*. In both studies, BTK was rapidly phosphorylated upon NLRP3 activation. We additionally observed that inflammasome activity was impaired in PBMC from XLA patients, suggesting that a genetic inflammasome deficiency may contribute to the immunocompromised

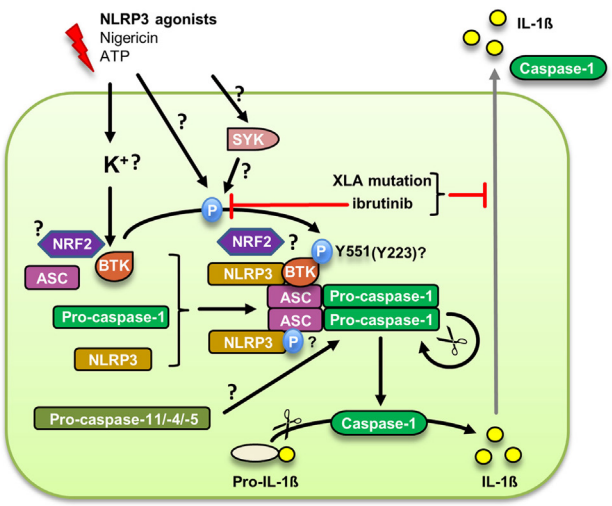


FIGURE 2 | Bruton's tyrosine kinase (BTK) regulation of the canonical NLRP3 inflammasome. Upon an upstream signal potentially linked to membrane integrity or K^+ efflux, BTK is phosphorylated at Y551, presumably by Syk, and subsequently is activated. The supposed phosphorylation of ASC promotes inflammasome assembly and caspase-1 autoproteolytic activation leading to the cleavage and secretion of mature IL-1β. Whether BTK also plays a role in the alternative NLRP3 inflammasome dependent on caspase-11 remains to be investigated.

XLA phenotype. Pharmacological BTK inhibitors *in vivo* affected *S. aureus* clearance in mice and IL-1β release in cancer patients, which was associated with a reduced ability of isolated PBMC to secrete IL-1β. Excessive IL-1β release in PBMC from Muckle-Wells Syndrome MWS (OMIM entry 191900) patients could also be blocked by BTK inhibitors (10). In a brain ischemia/reperfusion *in vivo* model Btk was activated in infiltrating macrophages/neutrophils, and Btk inhibition protected against brain injury (54). In combination, these results warrant the exploration of BTK inhibition as a strategy to target the NLRP3 inflammasome therapeutically. Mechanistically, the emerging role of NRF2, a protein shown separately to interact with both BTK (55) and NLRP3 (56), will also be interesting to study further. Likewise, the observed link with caspase-11 (33) may indicate an additional role for BTK in the non-canonical NLRP3 inflammasome that depends on caspase-11 in mice and caspase-4/-5 in humans for intracellular LPS sensing (57)—a notion intriguing for further study.

THERAPEUTIC OPPORTUNITIES IN INNATE IMMUNITY

Undoubtedly, the existence of and first clinical data for an FDA-approved BTK inhibitor, ibrutinib (also known as PCI-32765), in oncology (8) make preclinical and translational research into BTK's innate functions highly interesting, for example in arthritis (30), thromboinflammation (51), or in ischemic stroke, as aforementioned (52, 54). Compared to other strategies proposed to target the pathologically relevant NLRP3 inflammasome/IL-1 axis—for example, the inhibitor MCC950, whose target is however unknown (58), or IL-1 blockade which only neutralizes the inflammatory potential of certain inflammasome-dependent mediators—targeting NLRP3 *via* BTK is highly intriguing since BTK is a well-known (if incompletely understood) molecular target with inhibitors approved or in clinical trials. In cancer immunotherapies, first results on BTK inhibition modulating DC and subsequent $CD4^+$ T cell activation (43) or upregulation of the inhibitory receptor TIM-3 on DCs are also noteworthy (59). On the other hand, targeting BTK with ibrutinib causes significant immunosuppression associated with an increased risk of infections (60) indicating that BTK dependent innate immunity is severely impaired (23). In addition, leukostasis as well as bleeding complications have been reported indicating that BTK inhibition by ibrutinib also affects leukocyte adhesion and platelet functions in a clinically relevant way (51, 61). Increased rates of atrial fibrillation (62) as a non-immune adverse event in patients receiving ibrutinib advises caution when exploring the novel opportunities of BTK blockade in various disease entities. Potentially, transient use of inhibitors, e.g., only during phases of acute adverse inflammation (e.g., shortly after ischemic brain or heart injury), may nevertheless offer advantageous therapeutic windows in non-chronic diseases. Nonetheless, much further work will be required to safely harness the potential of BTK for treating additional innate immune-related disorders.

OPEN QUESTIONS AND OUTLOOK

Although much progress on deciphering the molecular function of BTK in various innate cell types has been made, specific BTK interactors and substrates in the different aforementioned processes have to be studied more systematically as highlighted by the many apparent controversies. Additionally, whether BTK functions as a *bona fide* kinase or more as a scaffold protein requires clarification, e.g., in the NLRP3 inflammasome process. In cell lines, well-characterized loss and gain of function mutants of BTK may be useful tools (22). Conditional and/or inducible gain- or loss-of-function mouse alleles, which surprisingly have not been described, will be essential for innate immunologists to meaningfully study BTK further *in vivo* and to exclude confounding effects from impaired B cell function, e.g., in *in vivo* infection studies. Furthermore, conditional alleles would help flesh out cell-specific and hematopoietic roles of BTK more precisely. The resulting *in vivo* mouse models should complement urgently needed additional studies on human BTK that may help to solve some of the apparent discrepancies between human and murine studies and decipher some of the profound complexity surrounding BTK. Such vital research could be done within ongoing studies in the cancer field or of *ex vivo* studies on biomaterial from healthy volunteers or XLA patients. Concomitant and standardized kinase and expression level assays conducted on XLA samples may help to gauge the penetrance and severity of naturally occurring variants better and, by incorporating these results, may allow drawing more generally valid conclusions from these patient studies.

In conclusion, BTK has emerged as a key node in many immunological signaling networks in innate immunity, some of which have profound therapeutic potential. Future efforts in both academia and industry may help to explore and subsequently harness the potential of this intriguing yet highly complex kinase for innate immunity. This may offer therapeutic opportunities comparable or potentially exceeding those already envisaged for oncology.

AUTHOR CONTRIBUTIONS

All authors collected and analyzed data, AW coordinated the study and drafted the manuscript, and all authors contributed toward and approved the final manuscript.

FUNDING

This work was supported by the German Research Foundation (DFG)-funded CRC 685 "Immunotherapy" and CRC/TR 156 "The skin as a sensor and effector organ orchestrating local and systemic immune responses," the Else-Kröner-Fresenius Stiftung, the University of Tübingen, and the University Hospital Tübingen (Fortüne Grant 2310-0-0 to XL and AW).

REFERENCES

1. Bruton OC. Agammaglobulinemia. *Pediatrics* (1952) 9:722–8.
2. Vetrie D, Vorechovsky I, Sideras P, Holland J, Davies A, Flinter F, et al. The gene involved in X-linked agammaglobulinaemia is a member of the src family of protein-tyrosine kinases. *Nature* (1993) 361:226–33. doi:10.1038/361226a0
3. Woyach JA, Johnson AJ, Byrd JC. The B-cell receptor signaling pathway as a therapeutic target in CLL. *Blood* (2012) 120:1175–84. doi:10.1182/blood-2012-02-362624
4. Rawlings DJ, Saffran DC, Tsukada S, Largaespada DA, Grimaldi JC, Cohen L, et al. Mutation of unique region of Bruton's tyrosine kinase in immunodeficient XID mice. *Science* (1993) 261:358–61. doi:10.1126/science.8332901
5. Riggs J, Howell K, Matechin B, Matlack R, Pennello A, Chiasson R. X-chromosome-linked immune-deficient mice have B-1b cells. *Immunology* (2003) 108:440–51. doi:10.1046/j.1365-2567.2003.01624.x
6. Valiaho J, Smith CI, Vihinen M. BTKbase: the mutation database for X-linked agammaglobulinemia. *Hum Mutat* (2006) 27:1209–17. doi:10.1002/humu.20410
7. Wahl MI, Fluckiger AC, Kato RM, Park H, Witte ON, Rawlings DJ. Phosphorylation of two regulatory tyrosine residues in the activation of Bruton's tyrosine kinase via alternative receptors. *Proc Natl Acad Sci U S A* (1997) 94:11526–33. doi:10.1073/pnas.94.21.11526
8. Wilson WH, Young RM, Schmitz R, Yang Y, Pittaluga S, Wright G, et al. Targeting B cell receptor signaling with ibrutinib in diffuse large B cell lymphoma. *Nat Med* (2015) 21:922–6. doi:10.1038/nm.3884
9. Koprulu AD, Kastner R, Wienerroither S, Lassnig C, Putz EM, Majer O, et al. The tyrosine kinase Btk regulates the macrophage response to *Listeria monocytogenes* infection. *PLoS One* (2013) 8:e60476. doi:10.1371/journal.pone.0060476
10. Liu X, Pichulik T, Wolz OO, Dang TM, Stutz A, Dillen C, et al. Human NACHT, LRR, and PYD domain-containing protein 3 (NLRP3) inflammasome activity is regulated by and potentially targetable through Bruton tyrosine kinase. *J Allergy Clin Immunol* (2017) 140:1054–67.e10. doi:10.1016/j.jaci.2017.01.017
11. Lee KG, Xu S, Kang ZH, Huo J, Huang M, Liu D, et al. Bruton's tyrosine kinase phosphorylates toll-like receptor 3 to initiate antiviral response. *Proc Natl Acad Sci U S A* (2012) 109:5791–6. doi:10.1073/pnas.1119238109
12. Herbst S, Shah A, Mazon Moya M, Marzola V, Jensen B, Reed A, et al. Phagocytosis-dependent activation of a TLR9-BTK-calcineurin-NFAT pathway co-ordinates innate immunity to *Aspergillus fumigatus*. *EMBO Mol Med* (2015). doi:10.15252/emmm.201404556
13. Horwood NJ, Page TH, Mcdaid JP, Palmer CD, Campbell J, Mahon T, et al. Bruton's tyrosine kinase is required for TLR2 and TLR4-induced TNF, but not IL-6, production. *J Immunol* (2006) 176:3635–41. doi:10.4049/jimmunol.176.6.3635
14. Taneichi H, Kanegane H, Sira MM, Futatani T, Agematsu K, Sako M, et al. Toll-like receptor signaling is impaired in dendritic cells from patients with X-linked agammaglobulinemia. *Clin Immunol* (2008) 126:148–54. doi:10.1016/j.clim.2007.10.005
15. Jefferies CA, Doyle S, Brunner C, Dunne A, Brint E, Wietek C, et al. Bruton's tyrosine kinase is a Toll/interleukin-1 receptor domain-binding protein that participates in nuclear factor kappaB activation by Toll-like receptor 4. *J Biol Chem* (2003) 278:26258–64. doi:10.1074/jbc.M301484200
16. Sochorova K, Horvath R, Rozkova D, Litzman J, Bartunkova J, Sediva A, et al. Impaired toll-like receptor 8-mediated IL-6 and TNF-alpha production in antigen-presenting cells from patients with X-linked agammaglobulinemia. *Blood* (2007) 109:2553–6. doi:10.1182/blood-2006-07-037960
17. Li YF, Lee KG, Ou X, Lam KP. Bruton's tyrosine kinase and protein kinase C micro are required for TLR7/9-induced IKKalpha and IRF-1 activation and interferon-beta production in conventional dendritic cells. *PLoS One* (2014) 9:e105420. doi:10.1371/journal.pone.0105420
18. Lougaris V, Baronio M, Vitali M, Tampella G, Cattalini M, Tassone L, et al. Bruton tyrosine kinase mediates TLR9-dependent human dendritic cell activation. *J Allergy Clin Immunol* (2014) 133:1644–50.e4. doi:10.1016/j.jaci.2013.12.1085
19. Marron TU, Rohr K, Martinez-Gallo M, Yu J, Cunningham-Rundles C. TLR signaling and effector functions are intact in XLA neutrophils. *Clin Immunol* (2010) 137:74–80. doi:10.1016/j.clim.2010.06.011
20. Gray P, Dunne A, Brikos C, Jefferies CA, Doyle SL, O'neill LA. MyD88 adapter-like (Mal) is phosphorylated by Bruton's tyrosine kinase during TLR2 and TLR4 signal transduction. *J Biol Chem* (2006) 281:10489–95. doi:10.1074/jbc.M508892200
21. Semaan N, Alsaleh G, Gottenberg JE, Wachsmann D, Sibilia J. Etk/BMX, a Btk family tyrosine kinase, and Mal contribute to the cross-talk between MyD88 and FAK pathways. *J Immunol* (2008) 180:3485–91. doi:10.4049/jimmunol.180.5.3485
22. Ormsby T, Schlecker E, Ferdin J, Tessarz AS, Angelisova P, Koprulu AD, et al. Btk is a positive regulator in the TREM-1/DAP12 signaling pathway. *Blood* (2011) 118:936–45. doi:10.1182/blood-2010-11-317016
23. Stadler N, Hasibeder A, Aranda Lopez P, Teschner D, Desuki A, Kriege O, et al. The Bruton tyrosine kinase inhibitor ibrutinib abrogates triggering receptor on myeloid cells 1 mediated neutrophil activation. *Haematologica* (2017) 102:e191–4. doi:10.3324/haematol.2016.152017
24. Mirsafian H, Ripen AM, Leong WM, Chear CT, Bin Mohamad S, Merican AF. Transcriptome profiling of monocytes from XLA patients revealed the innate immune function dysregulation due to the BTK gene expression deficiency. *Sci Rep* (2017) 7:6836. doi:10.1038/s41598-017-06342-5
25. Marron TU, Martinez-Gallo M, Yu JE, Cunningham-Rundles C. Toll-like receptor 4-, 7-, and 8-activated myeloid cells from patients with X-linked agammaglobulinemia produce enhanced inflammatory cytokines. *J Allergy Clin Immunol* (2012) 129:184–90.e1–4. doi:10.1016/j.jaci.2011.10.009
26. Singhal E, Kumar P, Sen P. A novel role for Bruton's tyrosine kinase in hepatocyte growth factor-mediated immunoregulation of dendritic cells. *J Biol Chem* (2011) 286:32054–63. doi:10.1074/jbc.M111.271247
27. Maurya N, Gujar R, Gupta M, Yadav V, Verma S, Sen P. Immunoregulation of dendritic cells by the receptor T cell Ig and mucin protein-3 via Bruton's tyrosine kinase and c-Src. *J Immunol* (2014) 193:3417–25. doi:10.4049/jimmunol.1400395
28. Jongstra-Bilen J, Puig Cano A, Hasija M, Xiao H, Smith CI, Cybulsky MI. Dual functions of Bruton's tyrosine kinase and Tec kinase during Fcgamma receptor-induced signaling and phagocytosis. *J Immunol* (2008) 181:288–98. doi:10.4049/jimmunol.181.1.288
29. Amoras AL, Kanegane H, Miyawaki T, Vilela MM. Defective Fc-, CR1- and CR3-mediated monocyte phagocytosis and chemotaxis in common variable immunodeficiency and X-linked agammaglobulinemia patients. *J Investig Allergol Clin Immunol* (2003) 13:181–8.
30. Di Paolo JA, Huang T, Balazs M, Barbosa J, Barck KH, Bravo BJ, et al. Specific Btk inhibition suppresses B cell- and myeloid cell-mediated arthritis. *Nat Chem Biol* (2011) 7:41–50. doi:10.1038/nchembio.481
31. Cavaliere FM, Prezzo A, Bilotta C, Iacobini M, Quinti I. The lack of BTK does not impair monocytes and polymorphonuclear cells functions in X-linked agammaglobulinemia under treatment with intravenous immunoglobulin replacement. *PLoS One* (2017) 12:e0175961. doi:10.1371/journal.pone.0175961
32. Nagai Y, Garrett KP, Ohta S, Bahrun U, Kouro T, Akira S, et al. Toll-like receptors on hematopoietic progenitor cells stimulate innate immune system replenishment. *Immunity* (2006) 24:801–12. doi:10.1016/j.immuni.2006.04.008
33. Melcher M, Unger B, Schmidt U, Rajantie IA, Alitalo K, Ellmeier W. Essential roles for the Tec family kinases Tec and Btk in M-CSF receptor signaling pathways that regulate macrophage survival. *J Immunol* (2008) 180:8048–56. doi:10.4049/jimmunol.180.12.8048
34. Fiedler K, Sindrilaru A, Terszowski G, Kokai E, Feyerabend TB, Bullinger L, et al. Neutrophil development and function critically depend on Bruton tyrosine kinase in a mouse model of X-linked agammaglobulinemia. *Blood* (2011) 117:1329–39. doi:10.1182/blood-2010-04-281170
35. Volmering S, Block H, Boras M, Lowell CA, Zarbock A. The neutrophil Btk signalosome regulates integrin activation during sterile inflammation. *Immunity* (2016) 44:73–87. doi:10.1016/j.immuni.2015.11.011
36. Kozlowski C, Evans DI. Neutropenia associated with X-linked agammaglobulinaemia. *J Clin Pathol* (1991) 44:388–90. doi:10.1136/jcp.44.5.388
37. Farrar JE, Rohrer J, Conley ME. Neutropenia in X-linked agammaglobulinemia. *Clin Immunol Immunopathol* (1996) 81:271–6. doi:10.1006/clin.1996.0188
38. Winkelstein JA, Marino MC, Lederman HM, Jones SM, Sullivan K, Burks AW, et al. X-linked agammaglobulinemia: report on a United States registry

of 201 patients. *Medicine (Baltimore)* (2006) 85:193–202. doi:10.1097/01.md.0000229482.27398.ad
39. Honda F, Kano H, Kanegane H, Nonoyama S, Kim ES, Lee SK, et al. The kinase Btk negatively regulates the production of reactive oxygen species and stimulation-induced apoptosis in human neutrophils. *Nat Immunol* (2012) 13:369–78. doi:10.1038/ni.2234
40. Kawakami Y, Inagaki N, Salek-Ardakani S, Kitaura J, Tanaka H, Nagao K, et al. Regulation of dendritic cell maturation and function by Bruton's tyrosine kinase via IL-10 and Stat3. *Proc Natl Acad Sci U S A* (2006) 103:153–8. doi:10.1073/pnas.0509784103
41. Gunderson AJ, Kaneda MM, Tsujikawa T, Nguyen AV, Affara NI, Ruffell B, et al. Bruton tyrosine kinase-dependent immune cell cross-talk drives pancreas cancer. *Cancer Discov* (2016) 6:270–85. doi:10.1158/2159-8290.CD-15-0827
42. Ping LY, Ding N, Shi YF, Feng LX, Li J, Liu YL, et al. The Bruton's tyrosine kinase inhibitor ibrutinib exerts immunomodulatory effects through regulation of tumor-infiltrating macrophages. *Oncotarget* (2017) 8:39218–29. doi:10.18632/oncotarget.16836
43. Natarajan G, Oghumu S, Terrazas C, Varikuti S, Byrd JC, Satoskar AR. A Tec kinase BTK inhibitor ibrutinib promotes maturation and activation of dendritic cells. *Oncoimmunology* (2016) 5:e1151592. doi:10.1080/2162402X.2016.1151592
44. Natarajan G, Terrazas C, Oghumu S, Varikuti S, Dubovsky JA, Byrd JC, et al. Ibrutinib enhances IL-17 response by modulating the function of bone marrow derived dendritic cells. *Oncoimmunology* (2016) 5:e1057385. doi:10.1080/2162402X.2015.1057385
45. Eifert C, Wang X, Kokabee L, Kourtidis A, Jain R, Gerdes MJ, et al. A novel isoform of the B cell tyrosine kinase BTK protects breast cancer cells from apoptosis. *Genes Chromosomes Cancer* (2013) 52:961–75. doi:10.1002/gcc.22091
46. Wei L, Su YK, Lin CM, Chao TY, Huang SP, Huynh TT, et al. Preclinical investigation of ibrutinib, a Bruton's kinase tyrosine (Btk) inhibitor, in suppressing glioma tumorigenesis and stem cell phenotypes. *Oncotarget* (2016) 7:69961–75. doi:10.18632/oncotarget.11572
47. Kokabee L, Wang X, Sevinsky CJ, Wang WL, Cheu L, Chittur SV, et al. Bruton's tyrosine kinase is a potential therapeutic target in prostate cancer. *Cancer Biol Ther* (2015) 16:1604–15. doi:10.1080/15384047.2015.1078023
48. Wang JD, Chen XY, Ji KW, Tao F. Targeting Btk with ibrutinib inhibit gastric carcinoma cells growth. *Am J Transl Res* (2016) 8:3003–12.
49. Grassilli E, Pisano F, Cialdella A, Bonomo S, Missaglia C, Cerrito MG, et al. A novel oncogenic BTK isoform is overexpressed in colon cancers and required for RAS-mediated transformation. *Oncogene* (2016) 35:4368–78. doi:10.1038/onc.2015.504
50. Bao Y, Zheng J, Han C, Jin J, Han H, Liu Y, et al. Tyrosine kinase Btk is required for NK cell activation. *J Biol Chem* (2012) 287:23769–78. doi:10.1074/jbc.M112.372425
51. Murthy P, Durco F, Miller-Ocuin JL, Takedai T, Shankar S, Liang X, et al. The NLRP3 inflammasome and Bruton's tyrosine kinase in platelets co-regulate platelet activation, aggregation, and in vitro thrombus formation. *Biochem Biophys Res Commun* (2017) 483:230–6. doi:10.1016/j.bbrc.2016.12.161
52. Broderick L, De Nardo D, Franklin BS, Hoffman HM, Latz E. The inflammasomes and autoinflammatory syndromes. *Annu Rev Pathol* (2015) 10:395–424. doi:10.1146/annurev-pathol-012414-040431
53. Dubois H, Wullaert A, Lamkanfi M. General strategies in inflammasome biology. *Curr Top Microbiol Immunol* (2016) 397:1–22. doi:10.1007/978-3-319-41171-2_1
54. Ito M, Shichita T, Okada M, Komine R, Noguchi Y, Yoshimura A, et al. Bruton's tyrosine kinase is essential for NLRP3 inflammasome activation and contributes to ischaemic brain injury. *Nat Commun* (2015) 6:7360. doi:10.1038/ncomms8360
55. Vijayan V, Baumgart-Vogt E, Naidu S, Qian G, Immenschuh S. Bruton's tyrosine kinase is required for TLR-dependent heme oxygenase-1 gene activation via Nrf2 in macrophages. *J Immunol* (2011) 187:817–27. doi:10.4049/jimmunol.1003631
56. Garstkiewicz M, Strittmatter GE, Grossi S, Sand J, Fenini G, Werner S, et al. Opposing effects of Nrf2 and Nrf2-activating compounds on the NLRP3 inflammasome independent of Nrf2-mediated gene expression. *Eur J Immunol* (2017) 47:806–17. doi:10.1002/eji.201646665
57. Schmid-Burgk JL, Gaidt MM, Schmidt T, Ebert TS, Bartok E, Hornung V. Caspase-4 mediates non-canonical activation of the NLRP3 inflammasome in human myeloid cells. *Eur J Immunol* (2015) 45:2911–7. doi:10.1002/eji.201545523
58. Coll RC, Robertson AA, Chae JJ, Higgins SC, Munoz-Planillo R, Inserra MC, et al. A small-molecule inhibitor of the NLRP3 inflammasome for the treatment of inflammatory diseases. *Nat Med* (2015) 21:248–55. doi:10.1038/nm.3806
59. Gujar R, Maurya N, Yadav V, Gupta M, Arora S, Khatri N, et al. c-Src suppresses dendritic cell antitumor activity via T cell Ig and mucin protein-3 receptor. *J Immunol* (2016) 197:1650–62. doi:10.4049/jimmunol.1600104
60. Williams AM, Baran AM, Meacham PJ, Feldman MM, Valencia HE, Newsom-Stewart C, et al. Analysis of the risk of infection in patients with chronic lymphocytic leukemia in the era of novel therapies. *Leuk Lymphoma* (2017) 11:1–8. doi:10.1080/10428194.2017.1347931
61. Kamel S, Horton L, Ysebaert L, Levade M, Burbury K, Tan S, et al. Ibrutinib inhibits collagen-mediated but not ADP-mediated platelet aggregation. *Leukemia* (2015) 29:783–7. doi:10.1038/leu.2014.247
62. Wiczer TE, Levine LB, Brumbaugh J, Coggins J, Zhao Q, Ruppert AS, et al. Cumulative incidence, risk factors, and management of atrial fibrillation in patients receiving ibrutinib. *Blood Adv* (2017) 1:1739–48. doi:10.1182/bloodadvances.2017009720

Conflict of Interest Statement: The authors declare that the research was conducted in the absence of any commercial or financial relationships that could be construed as a potential conflict of interest.

Copyright © 2017 Weber, Bittner, Liu, Dang, Radsak and Brunner. This is an open-access article distributed under the terms of the Creative Commons Attribution License (CC BY). The use, distribution or reproduction in other forums is permitted, provided the original author(s) or licensor are credited and that the original publication in this journal is cited, in accordance with accepted academic practice. No use, distribution or reproduction is permitted which does not comply with these terms.

frontiers in Immunology

REVIEW
published: 22 December 2017
doi: 10.3389/fimmu.2017.01863

Efferocytosis of Pathogen-Infected Cells

*Niloofar Karaji and Quentin J. Sattentau**

The Sir William Dunn School of Pathology, The University of Oxford, Oxford, United Kingdom

The prompt and efficient clearance of unwanted and abnormal cells by phagocytes is termed efferocytosis and is crucial for organism development, maintenance of tissue homeostasis, and regulation of the immune system. Dying cells are recognized by phagocytes through pathways initiated *via* "find me" signals, recognition *via* "eat me" signals and down-modulation of regulatory "don't eat me" signals. Pathogen infection may trigger cell death that drives phagocytic clearance in an immunologically silent, or pro-inflammatory manner, depending on the mode of cell death. In many cases, efferocytosis is a mechanism for eliminating pathogens and pathogen-infected cells; however, some pathogens have subverted this process and use efferocytic mechanisms to avoid innate immune detection and assist phagocyte infection. In parallel, phagocytes can integrate signals received from infected dying cells to elicit the most appropriate effector response against the infecting pathogen. This review focuses on pathogen-induced cell death signals that drive infected cell recognition and uptake by phagocytes, and the outcomes for the infected target cell, the phagocyte, the pathogen and the host.

Keywords: phagocytosis, efferocytosis, cell death, pathogen, bacteria, virus, parasite, inflammation

OPEN ACCESS

Edited by:
Christel Vérollet, UMR5089 Institut de Pharmacologie et de Biologie Structurale (IPBS), France

Reviewed by:
Mark Marsh, University College London, United Kingdom
Philippe Benaroch, Centre national de la recherche scientifique (CNRS), France
Serge Benichou, Centre national de la recherche scientifique (CNRS), France

***Correspondence:**
Quentin J. Sattentau
quentin.sattentau@path.ox.ac.uk

Specialty section:
This article was submitted to Microbial Immunology, a section of the journal Frontiers in Immunology

Received: *02 October 2017*
Accepted: *07 December 2017*
Published: *22 December 2017*

Citation:
Karaji N and Sattentau QJ (2017) Efferocytosis of Pathogen-Infected Cells. Front. Immunol. 8:1863. doi: 10.3389/fimmu.2017.01863

INTRODUCTION

To maintain and protect themselves, multicellular organisms remove dead and dying cells arising during normal tissue development and function (1) or triggered by infection or sterile inflammation (2). At steady state, even within tissues with high constitutive rates of apoptosis, the number of detectable apoptotic cells is relatively low, indicating a high rate of removal (3–5). Efficient clearance is vital for the constant removal of approximately 10^6 cells/s undergoing apoptosis in various tissues in adult humans (6). Phagocytosis is defined as engulfment of particulate matter of >0.5–1 μm (7, 8) and is mediated by both professional and non-professional phagocytic cell types. Professional phagocytes are primarily macrophages and immature dendritic cells (DCs) resident in multiple tissues and tissue-infiltrating monocytes, neutrophils, and eosinophils. Non-professional phagocytes such as epithelial cells of mammary epithelium (9) and astrocytes in the brain (10) can also capture and engulf material including dying cells that are present in close proximity within tissue. "Efferocytosis" is a term describing the engulfment by phagocytes of dying and dead cells and their debris (11, 12) and demonstrates features of both conventional phagocytosis and the fluid-phase uptake mechanism macropinocytosis (13–15), resulting in uptake into "spaceous phagosomes" (15). However, although the term efferocytosis distinguishes recognition and engulfment of dead and dying cells from phagocytosis of other objects (12, 16), we are unaware of specific mechanistic differences that discriminate between the two processes. Efferocytosis is mediated by a variety of interactions between the phagocyte and its dying target cell that show substantial redundancy and many soluble and cell surface receptor–ligand interactions defined for phagocytosis are used in efferocytosis (described in more detail below). The initial definition of efferocytosis related to clearance of apoptotic cells (15), but this has more recently been widened to include other modes of cell death (17, 18).

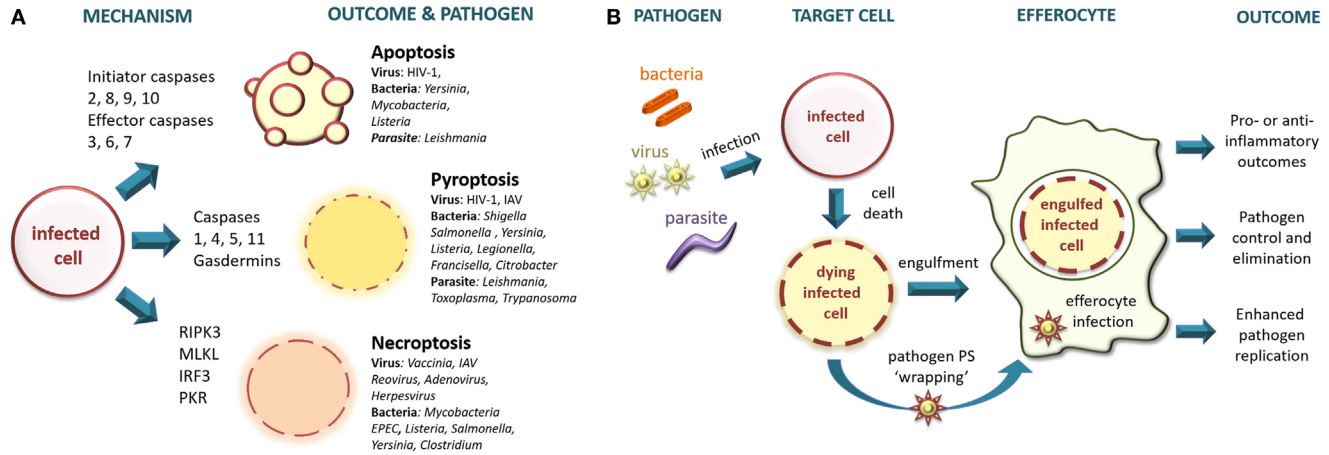


FIGURE 1 | **(A)** Intracellular pathogens trigger regulated modes of cell death. Intracellular bacteria, viruses, and parasites infect target cells triggering different cell death pathways. Apoptosis is a non-inflammatory type of cell death in which the cellular contents remain membrane enclosed, whereas pyroptosis and necroptosis result in compromised membrane integrity leading to the release of intracellular contents that are pro-inflammatory. RIPK3, receptor-interacting protein kinase 3; MLKL, mixed lineage kinase domain-like; IRF3, interferon regulatory factor-3; PKR, protein kinase R; IAV, influenza A virus; EPEC, enteropathogenic *Escherichia coli*. **(B)** Pathogen infection modulates efferocytic outcomes. Intracellular bacteria, viruses, and parasites infect target cells inducing apoptosis. Dying target cells expose eat me signals and may down-modulate don't eat me signals, leading to uptake and engulfment by efferocytes. Alternatively, the pathogen may escape from the infected cell wrapped in phosphatidylserine (PS)-containing membrane to deploy "apoptotic mimicry" for entry into the efferocyte. Efferocytosis may eliminate the pathogen, or may allow the pathogen to infect the efferocyte in a Trojan-horse type maneuver. The efferocyte will initiate anti-inflammatory or pro-inflammatory signaling depending upon the combined presence of immune-silencing signals (e.g., PS) and pro-inflammatory pathogen-associated molecular patterns and damage-associated molecular patterns.

Cell death has been broadly categorized into accidental (necrosis) and regulated (including apoptosis, pyroptosis, and necroptosis) (17). Accidental cell death occurs during severe physical or chemical insult, such as membrane shearing and rupture *via* extremes of pressure, temperature, osmolarity, pH, or exposure to agents such as detergents and bacterial toxins, and is insensitive to pharmacologic or genetic manipulation. Because accidental cell death results in uncontrolled release of cell contents including damage-associated molecular patterns (DAMPs), it is pro-inflammatory (19, 20). Regulated modes of cell death are implicated in post-embryonic ontogeny, tissue homeostasis, and during infection and immune responses, have a genetically programmed component, and can be modulated by altering pro- and anti-death signals (17). Pathogen infection is variously associated with all forms of regulated cell death (**Figure 1A**) and necrosis, and the type of cell death induced is directly linked to the type of infecting pathogen, its life cycle and its pathogen-associated molecular patterns (PAMPs) recognized by pattern recognition receptors (PRRs).

PATHOGEN-TRIGGERED CELL DEATH

Apoptosis is a caspase-dependent programmed form of regulated cell death resulting in a series of well-characterized morphologic and molecular changes culminating in membrane blebbing, DNA fragmentation and expression of signals designed to attract phagocytes and trigger engulfment and disposal of the apoptotic cargo (17). Apoptotic cells that are not rapidly efferocytosed become late apoptotic cells with a phenotype related to that of necrosis and are pro-inflammatory (21, 22). Apoptosis may be triggered in various cell types by a variety of pathogens, including intracellular bacteria (23), parasites (24), and viruses (25). Despite having evolved in part as a mechanism to limit pathogen replication and spread, apoptosis may have been subverted to contribute to pathogen survival and disease pathogenesis as discussed below. Pyroptosis is a regulated mode of cell death triggered principally by infection with intracellular pathogens (26, 27) and is linked to inflammasome activation driving caspase-1 or non-canonical caspase-11-triggering of the pore-forming effector gasdermin family (28, 29). Since pyroptosis results in plasma membrane permeabilization and eventual rupture with release of cytoplasmic contents, it has pro-inflammatory outcomes similar to accidental cell death and necroptosis. Necroptosis is triggered by infection with a variety of intracellular pathogens including viruses and bacteria (30, 31). Similar to pyroptosis, necroptosis is also a pro-inflammatory mode of regulated cell death initiated by cell surface receptors but is triggered in a caspase-independent RIPK3-dependent manner and may be modulated by caspase-8 activation toward apoptosis (17). Non-canonical forms of necroptosis activated by IRF3 and PKR-dependent pathways have also been described (31). The different modes of pathogen-initiated cell death and their mechanisms have been recently reviewed [e.g., Ref. (27, 30–33)] and so will not be further discussed here but are summarized in **Figure 1A** with some examples of pathogens implicated.

EFFEROCYTIC SIGNALS

Phagocytes engage apoptotic cells *via* a defined set of markers termed "apoptotic cell-associated molecular patterns" or ACAMPs

(16). ACAMPs include externalized phosphatidylserine, calreticulin, and modified carbohydrates that are recognized by a set of specific receptors and bridging molecules and will be described briefly below. Efferocytosis of dead and dying cells can be divided into four distinct stages (34, 35): (i) Detection of the target cell by release of chemotactic "find me" signals (36, 37) that include lysophosphatidylcholine, CX3CL1 (fractalkine), nucleotides adenosine triphosphate and uridine 5′ triphosphate, and sphingosine 1-phosphate (38–41). (ii) Exposure of "eat me" signals (42, 43), of which phosphatidylserine (PS) exposure on the outer leaflet of the plasma membrane is the best characterized, and although initially described in the context of apoptosis, appears to be shared between all modes of cell death (43–47). However, whereas PS externalization during apoptosis is mediated enzymatically, it becomes accessible during pyroptosis and necroptosis *via* membrane permeabilization. Eat me signaling is counter-balanced by expression levels of "don't eat me" cell surface molecules such as CD47 (48, 49). Many eat me signals are recognized directly by phagocyte receptors such as members of the T-cell immunoglobulin domain and mucin domain (TIM) family, complement receptors CR3 and CR4, scavenger receptors SRA and CD36, mannose receptor (MR) and integrins α5β3 and α5β5, whereas others require bridging molecules such as collectins, complement C1q, mannose binding lectin, pentraxin3, ficolins, thrombospondin, and milk fat globule protein (MFG-8) for their recognition (18, 42, 50, 51). (iii) Following recognition of eat me signals, receptors such as antibody Fc (52) and complement (53) receptors signal to the cytoskeleton and are directly phagocytic, whereas others such as TIM-4 (54) are implicated only in tethering the target cell. However, a phagocyte will integrate signals from multiple receptors to inform the outcome of whether or not to engulf the target cell (12, 34, 55). (iv) Cellular material is fully internalized *via* cytoskeletal rearrangement of the plasma membrane (5, 12, 35) with processing of the engulfed cell usually (5, 55), but not exclusively (56), leading to its elimination within a phagolysosome-type compartment (57, 58). During the target cell recognition process, phagocytes may further evaluate the target's chemical composition to estimate the threat posed by its contents and form such as size (59), geometry (60), and topography (61). This assessment determines (i) whether engulfment occurs or is replaced with, for example, neutrophil NETosis, an anti-microbial cell death mechanism whereby neutrophils eject chromatin extracellular traps (62); (ii) the fate of the target cell within the phagocyte; and (iii) whether the clearance process is immunologically silent, such as the efferocytosis of apoptotic cells (11, 63), or stimulates an inflammatory response such as the engulfment of most pathogens, pathogen-infected cells, and necrotic cells (8, 19, 20).

This review will not further consider find me and eat me signals involved in recognition and uptake of dead and dying cells, or the downstream signaling and cytoskeletal changes leading to phagocytic uptake, topics that have been very comprehensively reviewed recently (4, 6, 12, 16, 63–67). Instead, we will highlight recent discoveries regarding phagocyte recognition of cell death triggered by microbial infection and outcomes for the pathogen and infected target cell, the phagocyte, and the host.

PATHOGEN INFECTION DRIVING CELL DEATH AND EFFEROCYTOSIS

Infection by intracellular pathogens may lead to cell death by any of the regulated pathways described earlier (see **Figure 1A**), or by necrotic cell death in the case of some lytic infections. Microbial induction of regulated death is generally considered to be a mechanism evolved to reduce or prevent pathogen replication and spread (33). The beneficial outcomes for the host of pathogen-triggered cell death may comprise: (i) removal of the intracellular environment required for survival and replication; (ii) direct antipathogen effects of released intracellular components; (iii) initiation of an anti-microbial inflammatory response by release of DAMPs and PAMPs; and (iv) uptake and presentation of pathogen antigens by antigen-presenting cells. Induction of cell death may itself be sufficient to reduce and control pathogen replication or may be assisted or mediated by efferocytic mechanisms as has been described for several bacterial and viral pathogens (14). Conversely, some pathogens may use efferocytic mechanisms to invade the phagocyte in a "Trojan-horse" type of manoeuver and thereby perpetuate or enhance replication and dissemination (14, 68). These outcomes are discussed in more detail below and summarized in **Figure 1B**.

EFFEROCYTOSIS IN PATHOGEN CONTROL AND ITS SUBVERSION BY PATHOGENS

Bacterial Infection

Gram-negative intracellular pathogenic bacteria including the Enterobacteriaceae *Shigella* (69, 70) and *Salmonella* (71) were initially proposed to induce apoptosis in infected macrophages. However, more recently, this view has been modified to take into account features of pyroptotic cell death including caspase-1 and inflammasome activation (26, 72, 73). Virulent strains of many gram-negative intracellular bacteria have evolved to evade pyroptotic cell death, for example, *Shigella* inhibition of caspase-4 activation (74), testifying to its importance as an innate immune antibacterial mechanism (26, 75, 76). Using an attenuated strain of *Salmonella typhimurium* that constitutively expresses flagellin and, therefore, activates NLRC4, Jorgensen et al. demonstrated that infected pyroptotic macrophages form "pore-induced intracellular traps" that capture bacteria within cellular debris without killing them (77). The bacterium-containing cell debris is then cleared by efferocytic neutrophils that are attracted by find me and eat me signals and kill the bacteria in a ROS-dependent manner (72, 77). Although apoptotic cell death of human monocytes or macrophages infected with wild-type (78–80) or attenuated (81) *Mycobacterium tuberculosis* is associated with reduced bacterial survival, the mechanism was until recently unclear. Apoptosis may impart some cell-intrinsic anti-*M. tuberculosis* activity to macrophages by enclosing the bacilli within apoptotic membrane vesicles, but efferocytosis appears to be an important adjunct mechanism to clear viable bacteria associated with apoptotic macrophages (82, 83). Efferocytosis of apoptotic *M. tuberculosis*-infected macrophages by uninfected macrophages results in

their trafficking to a degradative phagolysosomal compartment (83). Similarly, in the zebrafish model, apoptotic *Mycobacterium marinum*-infected granulomatous macrophages were engulfed by neutrophils resulting in their death by oxidative-burst exposure (84). Not only does efferocytosis reduce mycobacterial viability in human cells but also allows cross-presentation by DC of mycobacterial antigens for MHC class-I and CD1 presentation to $CD8^+$ T cells in mice, reinforcing adaptive anti-bacterial immunity (85). The importance of macrophage apoptosis as an anti-mycobacterial mechanism contrasts with the finding that some virulent forms of *M. tuberculosis* have evolved to divert apoptotic cell death toward a programmed necrotic pathway, which fails to inhibit bacterial growth and allows bacterial release from the disrupted cell, promoting pathogen dissemination (79, 81, 86, 87). Thus, the type of cell death induced directly influences the outcome for the pathogen.

Bacteria may use efferocytic pathways to escape from elimination or to assist their dissemination using Trojan-horse-type mechanisms in which dying cells carrying viable bacteria are engulfed leading to infection of the efferocyte. After the uptake of *M. marinum* by zebrafish macrophages, the infected macrophage undergoes apoptotic cell death. These apoptotic, infected macrophages are engulfed by other healthy macrophages, driving dissemination of infection *via* efferocytosis to increase granuloma burden and seed secondary granulomas in a manner dependent on the RD1 virulence factor (88). Eat me signals potentially involved in efferocytic mycobacterial infected cell uptake have been partially defined. Blocking of human macrophage cell surface MR using anti-MR antibody or pre-incubation with competitive soluble sugars (mannan and GlcNAc) (89), or blocking TIM-4 (83) significantly reduced the uptake of apoptotic *M. tuberculosis*-infected macrophages by uninfected macrophages. TIM-4 is also implicated in the subversion of efferocytic mechanisms by the gram-positive bacterial pathogen *Listeria monocytogenes*. The bacterium is phagocytosed by macrophages but avoids elimination by escaping the phagosome using the pore-forming toxin listeriolysin O (LLO) and recruits actin to drive cell-to-cell spread (90). The bacterium wraps itself in vesicles derived from the LLO-damaged host cell plasma membrane that exposes PS, which are in turn recognized by TIM-4 on healthy macrophages, leading to bacterial uptake and infection of a new host cell (91). Infection of a mouse strain lacking TIM-4 expression resulted in impaired bacterial growth, thus emphasizing its role *in vivo*. An efferocytic Trojan-horse mechanism of dissemination using neutrophils as a cellular vector is proposed for *Chlamydia pneumoniae* (92) and *Yersinia pestis* (93). In mice, both bacteria are initially phagocytosed by neutrophils at the site of inoculation, but the bacteria survive and, in the case of *Y. pestis*, replicate within the neutrophils. Subsequent infected neutrophil apoptosis and PS exposure triggered efferocytosis by macrophages, which were permissive for replication of both bacteria but elicited an anti-inflammatory cytokine response, potentially limiting anti-bacterial activity (92, 93). Macrophage recognition of *C. pneumoniae* in the context of apoptotic cells was shown to be important for bacterial replication, since inhibition of efferocytosis using annexin-V reduced macrophage infection (92).

Viral Infection

There is limited work on the role of efferocytosis in controlling viral replication. Influenza A virus infection of HeLa cells resulted in their apoptosis and rapid efferocytic engulfment and transit into phagosome-like structures within murine alveolar macrophages (94). The outcome of this was to limit viral release in the culture, suggesting that this may be a mechanism for suppressing replication *in vivo* (95). Of interest, the authors demonstrated that the eat me signals implicated in this efferocytic uptake were a combination of plasma membrane PS exposure and desialylation of surface glycans on the infected cells (96), consistent with other studies suggesting that loss of cell surface sialic acid during apoptosis is a novel eat me signal (97).

Recently, Baxter et al. observed that recognition and uptake of HIV-1-infected $CD4^+$ T cells by human monocyte-derived macrophages led to enhanced macrophage infection when compared to incubation of these cells with cell-free virus (98). Macrophage infection by this cell-to-cell route was high multiplicity allowing robust infection even by weakly-macrophage–tropic viral strains (98). Although infected apparently healthy cells were weakly selectively captured, the strongest eat me signal came from dying HIV-1-infected cells, implying efferocytic signals. However inhibitors of PS–receptor interactions and other apoptotic cell death recognition receptor–ligand interactions failed to significantly reduce infected T-cell uptake, suggesting alternative signals that have yet to be defined (98). Macrophage phagocytosis of simian immunodeficiency virus-infected $CD4^+$ T cells occurs in the macaque model, suggesting that this mode of viral spread may have *in vivo* relevance for immunodeficiency viruses, although it is unclear if the macrophages were productively infected or simply harbored infected efferocytosed cells (99, 100). This raises the general caveat that phagocytes may take up pathogen-infected cells giving the appearance of infection but without necessarily undergoing productive infection themselves (68). Thus, astrocytes, long proposed to undergo an atypical HIV-1 infection in the brain but which lack the primary HIV-1 receptor CD4, are phagocytic and engulf dying HIV-1-infected cells leading to markers of viral infection but are resistant to viral entry and infection (101). Finally, in an interesting twist to this paradigm, human papilloma virus (HPV) appears to have subverted efferocytosis to facilitate viral persistence *in vivo*. Efferocytosis of HPV-infected cervical cancer cells by primary human fibroblasts (102) led to expression of the HPV E6 gene within the fibroblasts and elicitation of a tumorigenic phenotype with implications for viral persistence (103).

While not formally efferocytosis, apoptotic cell mimicry achieved by the incorporation of PS into viral envelopes is a related phenomenon that has been described as enhancing infectivity for several enveloped virus families (104, 105) including HIV-1 (106), vaccinia virus (107), and lentiviral vectors pseudotyped with multiple viral envelope glycoproteins (105, 108). Non-enveloped picornaviruses also use this strategy, effected by wrapping themselves in PS-containing vesicles during cellular exit (109, 110). PS incorporated into the viral envelope during budding is recognized by a multitude of PS receptors on the target cell including TIM-1 and TIM-4 and TAM tyrosine kinase receptors TYRO3, AXL, and MER (11, 105, 108, 111) and may be

further enhanced by bridging molecules such as MFG-E8 (105). Apoptotic mimicry has the major advantage of compromising pro-inflammatory programs by activating anti-inflammatory signaling cascades, which would otherwise trigger innate and adaptive immune responses against the invading virus, reducing viral replication *in vivo* (112). This immune evasion strategy is also used to good effect by parasites (see below).

Parasite Infection

Leishmania infection is transmitted to man by the sandfly, recruits a rapid neutrophil influx to the site of parasite entry, and replicates primarily within macrophages. The *Leishmania major* inoculum consists of a mixture of apoptotic and viable parasites, and depletion of apoptotic parasites reduces *in vivo* infectivity in a mouse model, proposed to be a consequence of loss of the anti-inflammatory TGF-β signal imparted on macrophages by the PS-expressing parasites (113). Using intravital microscopy of infected sandfly bites in mouse ear, it was observed that neutrophils are rapidly recruited to the site of the bite and engulf the parasites, many of which remain viable and infectious (114). *Leishmania* uptake by neutrophils can delay or accelerate neutrophil death in a manner dependent upon the experimental system. *In vitro* studies demonstrate that apoptosis of neutrophils is delayed for up to 2 days by *L. major* infection, thereby potentially serving as intracellular survival vectors for the parasites, during which time the neutrophils release MIP-1β, which attracts monocytes and macrophages (115). However, by contrast with *in vitro* studies, *Leishmania*-infected neutrophils analyzed *ex vivo* showed enhanced expression of PS, indicating accelerated apoptosis and potentially serving as an eat me signal for macrophage and DC uptake (116). Regardless of the underlying mechanism, macrophages may then efferocytose-infected apoptotic neutrophils becoming infected themselves in the process, the Trojan-horse mechanism (113). An alternative scenario, imaged by intravital microscopic analysis, is that rather than carrying parasites into the macrophage by efferocytosis, neutrophils may release viable parasites into regions densely populated by macrophages for subsequent macrophage engulfment and infection (114). Interestingly, in this study, depletion of neutrophils reduced *L. major* infection in mice (114), consistent with the idea that efferocytosis of apoptotic neutrophils imprinted an anti-inflammatory TGF-β signal on the neutrophils, preventing effective parasite elimination (115). A similar finding was also obtained when apoptotic neutrophils were engulfed by *L. major*-infected macrophages that produced the anti-inflammatory mediators TGF-β and prostaglandin PGE2 (117). However, these results must be evaluated in the context of the strain of mouse, the species of parasite, and the timing of macrophage encounter with apoptotic neutrophils in comparison with their encounter with the parasite. By contrast with the BALB/c mice used in the study above, engulfment of neutrophils by *L. major*-infected macrophages from parasite-resistant C57BL/6 mice reduced parasite load, concomitant with the secretion of TNF that most likely antagonized the anti-inflammatory signals released by uptake of apoptotic neutrophils (117, 118). Moreover, parasite killing may be parasite species dependent, since neutrophils from parasite-susceptible BALB/c mice triggered macrophage killing of *Leishmania amazonensis* and *Leishmania braziliensis* (119, 120). Finally, efferocytosis of apoptotic neutrophils by macrophages from resistant C57BL/6 mice 3 days prior to encounter with *L. major* led to enhanced permissivity to the parasite (121), a result that contrasts with studies in which infection took place prior to neutrophil exposure. Thus, in summary, whether efferocytosis of dying neutrophils results in advantageous or deleterious consequences for the parasite is complex and context dependent.

Trypanosma cruzi infection induces lymphocyte apoptosis in both experimentally infected mice (122, 123) and infected humans (124), and disease severity correlated with the degree of *ex vivo* apoptosis observed (124, 125). Mouse experiments support the concept that phagocyte uptake of apoptotic T lymphocytes results in the establishment of an anti-inflammatory response dictated by TGF-β and prostaglandin PGE2 that fuels parasite persistence and disease (126). Treatment of *T. cruzi* infected mice with inhibitors of apoptosis reversed the anti-inflammatory phenotype and reduced *ex vivo* parasite replication (123, 127), consistent with efferocytosis of apoptotic cells reducing macrophage anti-parasite activity and enhancing parasite persistence and disease.

IMMUNE CONSEQUENCES OF INFECTED CELL EFFEROCYTOSIS

The outcome for the phagocyte of engulfment of an infected dying cell is influenced both by the infecting pathogen and by the mode of death elicited in the target cell. PS exposed on apoptotic cells delivers an anti-inflammatory signal that is associated with defined receptor and signaling pathways and the production of regulatory cytokines such as TGF-β and IL-10 (11, 66) and is essential for rapid removal of apoptotic cells to avoid inflammatory and potential autoimmune consequences (19, 63). However, this is in the context of uninfected cells undergoing homeostatic apoptosis and immune-silent clearance. As described earlier, pathogen infection may induce more pro-inflammatory types of cell death *via* release of DAMPs and components of the pathogen present within the infected dying cell act as PAMPs to signal a pro-inflammatory response through PRRs (128). Thus, the phagocyte must integrate the pro- and anti-inflammatory signals to initiate the appropriate outcome, resulting in pathogen containment or clearance. Due to this complexity, experiments to probe the effects of specific pathogen infections of target cells on phagocyte pro- and anti-inflammatory programs are challenging to design and interpret. However, some information is available, particularly with regard to outcomes of efferocytosis of bacterial infection in the context of apoptotic cells. Torchinsky et al. (129) demonstrated that the combination of apoptotic and TLR-4-based signals presented to DCs by apoptotic neutrophils or B cells associated or not with *E. coli* or LPS triggered the release of TGF-β and IL-23 in the context of IL-6, a cytokine pattern, which favors the induction of Th17 effector Th cells. Th17 cells secrete the cytokine IL-17, which is important for the recruitment of neutrophils to resolve bacterial infections, and the combination of apoptotic cells and bacterial PAMPs was optimal for Th17 induction in the context of the model *Citrobacter rodentium* infection of mouse gut (129). LPS alone failed to induce biologically active TGF-β and also

induced high levels of IL-12, favoring a Th1-type response rather than Th17-type response, an outcome that would be suboptimal for extracellular bacterial clearance. Similarly, comparison of DC-mediated efferocytosis of an uninfected or *E. coli*-infected macrophage line induced to undergo apoptosis resulted in distinct outcomes (130). DC efferocytosis of infected apoptotic cells showed increased CD86 and CCR7 expression associated with an enhanced migratory capacity compared to uninfected apoptotic cells and enhanced production of IL-6, TGF-β, and IL-23, indicative of Th17 differentiation capacity (130). This again suggests that combination of pathogen and dying cells integrates signals to elicit the most appropriate immune outcome to control the specific pathogen. However, infection associated with apoptosis may also lead to misdirected adaptive immunity resulting in autoimmune outcomes. Thus, using apoptotic B cells infected with *L. monocytogenes*, Campisi et al. showed that the combination of stimuli present within the phagocyte resulted in presentation of self-antigens in the context of a pro-inflammatory environment (131). Using an *in vivo* murine model, this translated into Th17-induced colitis in the context of a *C. rodentium* bacterial infection, confirming the potentially deleterious effects of co-presentation of apoptotic and inflammatory infection signals by DC.

The most obvious implication of efferocytic uptake of virally infected dying cells is in cross-presentation, since $CD8^+$ T-cell priming against viral infections requires access of viral antigens to the MHC class-I processing and presentation apparatus. While viruses that infect antigen-presenting cells do this directly by cytoplasmic expression of their antigens, induction of immune responses to viruses that do not productively infect DCs rely upon efferocytosis of infected apoptotic cells followed by cross-presentation. The first demonstration of this was in the context of influenza virus infection of monocytes that led to their apoptosis and uptake by DCs, driving efficient CD8 T-cell priming against influenza antigens (132). Since then, multiple studies have reported on cross-presentation of viral antigens by efferocytic uptake of dying cells infected with vaccinia virus, HTLV-1, measles virus, CMV, and EBV (133, 134). Similar observations have been made for a series of intracellular bacterial pathogens including *L. monocytogenes* and *M. tuberculosis* (133). Although much of the cell biology of cross-presentation has been defined, what remains to be addressed is how the combination of cell death and pathogen-triggered signals influence the outcome of cross-presentation, as for example has been dissected for T-helper cell responses (128). The restriction factor SAMHD1 renders DC relatively resistant to HIV-1 infection and limits DC activation and antigen presentation (135). However, as recently demonstrated by Silvin et al. (136), DCs are heterogeneous with respect to viral infection and, while $CD1c^+$ DCs are sensitive to HIV-1 and influenza virus infection resulting in DC death, $CD141^+$ DCs are resistant. The authors provide evidence that in the absence of direct infection, $CD141^+$ DC acquires viral antigen by efferocytosis of dying virus-infected cells including $CD1c^+$ DC, allowing efficient cross-presentation. Also relevant to cross-presentation of infected dying cells, cells dying by necroptosis, rather than by necrosis or apoptosis, trigger a RIPK1-dependent NFκB transcriptional program-directing release of inflammatory cytokines that enhance cross-priming of $CD8^+$ T cells by DC (137). Although the cells in this instance were not infected, the relationship between this mechanism and infections driving necroptosis is obvious and raises questions regarding the ability of pathogens to modulate or suppress NFκB activation and other pro-inflammatory programs in dying cells. HIV-1 infection is a weak trigger of type-I interferon responses in macrophages, considered in part to result from "shielding" of viral nucleic acid PAMPs from intracellular sensors (138, 139), although early entry events can elicit low interferon levels (140). HIV-1 infection of $CD4^+$ T cells leads to their death by apoptosis (141) during productive infection or pyroptosis during abortive infection (142), and *in vivo*, there is likely to be a combination of these types of death associated with infection. Using model *in vitro* systems, Lepelley et al. showed that HIV-1-infected $CD4^+$ T cells elicit robust type-I interferon release from plasmacytoid DCs that is partially elicited by TLR-7 sensing of viral RNA (143) but potentially also by DAMPs released from infected dying T cells. Thus, cell-associated viral PAMPs appear to elicit a stronger innate immune anti-viral response than the virus alone.

CONCLUDING REMARKS

It is evident that efferocytosis is both an essential element of tissue homeostasis and a mechanism for elimination of intracellular pathogens. However, as described earlier, subversion of efferocytic mechanisms *via* (i) the Trojan-horse type of strategy, (ii) cell-free microorganisms expressing or hijacking PS-containing membrane, and (iii) triggering of anti-inflammatory programs in macrophages by efferocytosis of apoptotic cells contributes to immune evasion and pathogen persistence. Therapeutic intervention in efferocytic pathways may well be a rational approach to reducing infection by certain pathogens, but care must of course be exercised to avoid perturbing the fine balance between homeostasis and deleterious inflammation. *In vitro* studies demonstrated a reduction in HIV-1 infectivity of macrophages in the presence of soluble recombinant annexin-V, suggesting a mechanism to target this viral reservoir (144). The anti-PS monoclonal antibody Bavituximab has been used in a number of clinical trials as an anti-cancer agent, and its use in targeting viral infections such as HIV-1 (145), Pichinde virus (as a model for Lassa fever virus), and CMV (146) has been investigated. Aside from directly targeting pathogen replication, chronic infections such as HIV-1 (147) and HCV (148) are associated with long-term inflammatory outcomes that predispose to disease even in the context of suppressive anti-viral regimens. Chronic inflammation in HIV-1 infection is linked to acute inflammatory events in the gut-associated lymphoid tissue (GALT) initiated by massive HIV-1 infection and death of $CD4^+$ T cells (149) that predispose this tissue to translocation of microbial products from the lumen (150). Excessive $CD4^+$ T-cell apoptotic death may saturate GALT efferocytic capacity driving neglect of apoptotic cells by phagocytes leading to secondary necrosis, a type of cell death associated with tissue infiltration of monocytes and neutrophils that may mediate further tissue damage and is linked to chronic inflammatory autoimmune conditions (22). Moreover, abortive HIV-1 infection of tissue $CD4^+$ T cells has been implicated in pyroptotic cell death (142), which might directly promote pro-inflammatory

programs in phagocytes. Whether modulating efferocytosis in conditions such as this may influence the inflammatory outcome is a question that requires attention. Very recently, it has been demonstrated that efferocytosis during drosophila development can reprogram macrophages *via* JNK signaling to increased expression of the damage receptor Draper for robust responses to subsequent tissue injury or infection (151). This type of priming leading to innate immune "memory" deserves further investigation and may potentially be targeted for either anti-pathogen or anti-inflammatory outcomes in the clinic.

AUTHOR CONTRIBUTIONS

NK and QS conceptualized the article. NK wrote and revised the first draft. NK and QS revised and edited subsequent drafts.

FUNDING

The authors acknowledge funding by the Medical Research Council UK and the Edward Penley Abraham Trust, The Sir William Dunn School of Pathology.

REFERENCES

1. Baehrecke EH. How death shapes life during development. *Nat Rev Mol Cell Biol* (2002) 3(10):779–87. doi:10.1038/nrm931
2. Shi C, Pamer EG. Monocyte recruitment during infection and inflammation. *Nat Rev Immunol* (2011) 11(11):762–74. doi:10.1038/nri3070
3. Scott RS, McMahon EJ, Pop SM, Reap EA, Caricchio R, Cohen PL, et al. Phagocytosis and clearance of apoptotic cells is mediated by MER. *Nature* (2001) 411(6834):207–11. doi:10.1038/35075603
4. Elliott MR, Ravichandran KS. The dynamics of apoptotic cell clearance. *Dev Cell* (2016) 38(2):147–60. doi:10.1016/j.devcel.2016.06.029
5. Zent CS, Elliott MR. Maxed out macs: physiologic cell clearance as a function of macrophage phagocytic capacity. *FEBS J* (2017) 284(7):1021–39. doi:10.1111/febs.13961
6. Ravichandran KS. Find-me and eat-me signals in apoptotic cell clearance: progress and conundrums. *J Exp Med* (2010) 207(9):1807–17. doi:10.1084/jem.20101157
7. Gordon S. Phagocytosis: an immunobiologic process. *Immunity* (2016) 44(3):463–75. doi:10.1016/j.immuni.2016.02.026
8. Underhill DM, Goodridge HS. Information processing during phagocytosis. *Nat Rev Immunol* (2012) 12(7):492–502. doi:10.1038/nri3244
9. Monks J, Smith-Steinhart C, Kruk ER, Fadok VA, Henson PM. Epithelial cells remove apoptotic epithelial cells during post-lactation involution of the mouse mammary gland. *Biol Reprod* (2008) 78(4):586–94. doi:10.1095/biolreprod.107.065045
10. Loov C, Mitchell CH, Simonsson M, Erlandsson A. Slow degradation in phagocytic astrocytes can be enhanced by lysosomal acidification. *Glia* (2015) 63:1997–2009. doi:10.1002/glia.22873
11. Birge RB, Boeltz S, Kumar S, Carlson J, Wanderley J, Calianese D, et al. Phosphatidylserine is a global immunosuppressive signal in efferocytosis, infectious disease, and cancer. *Cell Death Differ* (2016) 23(6):962–78. doi:10.1038/cdd.2016.11
12. Henson PM. Cell removal: efferocytosis. *Annu Rev Cell Dev Biol* (2017) 33:127–44. doi:10.1146/annurev-cellbio-111315-125315
13. Hoffmann PR, deCathelineau AM, Ogden CA, Leverrier Y, Bratton DL, Daleke DL, et al. Phosphatidylserine (PS) induces PS receptor-mediated macropinocytosis and promotes clearance of apoptotic cells. *J Cell Biol* (2001) 155(4):649–59. doi:10.1083/jcb.200108080
14. Martin CJ, Peters KN, Behar SM. Macrophages clean up: efferocytosis and microbial control. *Curr Opin Microbiol* (2014) 17:17–23. doi:10.1016/j.mib.2013.10.007
15. deCathelineau AM, Henson PM. The final step in programmed cell death: phagocytes carry apoptotic cells to the grave. *Essays Biochem* (2003) 39:105–17. doi:10.1042/bse0390105
16. Kumar S, Birge RB. Efferocytosis. *Curr Biol* (2016) 26(13):R558–9. doi:10.1016/j.cub.2016.01.059
17. Galluzzi L, Bravo-San Pedro JM, Vitale I, Aaronson SA, Abrams JM, Adam D, et al. Essential versus accessory aspects of cell death: recommendations of the NCCD 2015. *Cell Death Differ* (2015) 22(1):58–73. doi:10.1038/cdd.2014.137
18. Poon IKH, Lucas CD, Rossi AG, Ravichandran KS. Apoptotic cell clearance: basic biology and therapeutic potential. *Nat Rev Immunol* (2014) 14(3):166–80. doi:10.1038/nri3607
19. Blander JM. The many ways tissue phagocytes respond to dying cells. *Immunol Rev* (2017) 277(1):158–73. doi:10.1111/imr.12537
20. Yatim N, Cullen S, Albert ML. Dying cells actively regulate adaptive immune responses. *Nat Rev Immunol* (2017) 17(4):262–75. doi:10.1038/nri.2017.9
21. Poon IKH, Hulett MD, Parish CR. Molecular mechanisms of late apoptotic/necrotic cell clearance. *Cell Death Differ* (2010) 17(3):381–97. doi:10.1038/cdd.2009.195
22. Sachet M, Liang YY, Oehler R. The immune response to secondary necrotic cells. *Apoptosis* (2017) 22:1189–204. doi:10.1007/s10495-017-1413-z
23. Divangahi M, Chen M, Gan H, Desjardins D, Hickman TT, Lee DM, et al. *Mycobacterium tuberculosis* evades macrophage defenses by inhibiting plasma membrane repair. *Nat Immunol* (2009) 10(8):899–906. doi:10.1038/ni.1758
24. Decote-Ricardo D, Nunes MP, Morrot A, Freire-de-Lima CG. Implication of apoptosis for the pathogenesis of *Trypanosoma cruzi* infection. *Front Immunol* (2017) 8:518. doi:10.3389/fimmu.2017.00518
25. Yu X, He S. The interplay between human herpes simplex virus infection and the apoptosis and necroptosis cell death pathways. *Virol J* (2016) 13:77. doi:10.1186/s12985-016-0528-0
26. Jorgensen I, Miao EA. Pyroptotic cell death defends against intracellular pathogens. *Immunol Rev* (2015) 265(1):130–42. doi:10.1111/imr.12287
27. Man SM, Karki R, Kanneganti TD. Molecular mechanisms and functions of pyroptosis, inflammatory caspases and inflammasomes in infectious diseases. *Immunol Rev* (2017) 277(1):61–75. doi:10.1111/imr.12534
28. Shi J, Zhao Y, Wang K, Shi X, Wang Y, Huang H, et al. Cleavage of GSDMD by inflammatory caspases determines pyroptotic cell death. *Nature* (2015) 526(7575):660–5. doi:10.1038/nature15514
29. Kayagaki N, Stowe IB, Lee BL, O'Rourke K, Anderson K, Warming S, et al. Caspase-11 cleaves gasdermin D for non-canonical inflammasome signalling. *Nature* (2015) 526(7575):666–71. doi:10.1038/nature15541
30. Brault M, Oberst A. Controlled detonation: evolution of necroptosis in pathogen defense. *Immunol Cell Biol* (2017) 95(2):131–6. doi:10.1038/icb.2016.117
31. Sridharan H, Upton JW. Programmed necrosis in microbial pathogenesis. *Trends Microbiol* (2014) 22(4):199–207. doi:10.1016/j.tim.2014.01.005
32. Jorgensen I, Rayamajhi M, Miao EA. Programmed cell death as a defence against infection. *Nat Rev Immunol* (2017) 17(3):151–64. doi:10.1038/nri.2016.147
33. Stephenson HN, Herzig A, Zychlinsky A. Beyond the grave: when is cell death critical for immunity to infection? *Curr Opin Immunol* (2016) 38:59–66. doi:10.1016/j.coi.2015.11.004
34. Hochreiter-Hufford A, Ravichandran KS. Clearing the dead: apoptotic cell sensing, recognition, engulfment, and digestion. *Cold Spring Harb Perspect Biol* (2013) 5(1):a008748–008748. doi:10.1101/cshperspect.a008748
35. Fond AM, Ravichandran KS. Clearance of dying cells by phagocytes: mechanisms and implications for disease pathogenesis. *Adv Exp Med Biol* (2016) 930:133–49. doi:10.1007/978-3-319-39406-0
36. Peter C, Wesselborg S, Lauber K. Molecular suicide notes: last call from apoptosing cells. *J Mol Cell Biol* (2010) 2(2):78–80. doi:10.1093/jmcb/mjp045
37. Kroemer G. Dying cell recognition shapes the pathophysiology of cell death. *Cell Death Differ* (2016) 23(6):913–4. doi:10.1038/cdd.2016.30
38. Lauber K, Bohn E, Kröber SM, Xiao Y-J, Blumenthal SG, Lindemann RK, et al. Apoptotic cells induce migration of phagocytes via caspase-3-mediated release of a lipid attraction signal. *Cell* (2003) 113(6):717–30. doi:10.1016/S0092-8674(03)00422-7

39. Truman LA, Ford CA, Pasikowska M, Pound JD, Wilkinson SJ, Dumitriu IE, et al. CX3CL1/fractalkine is released from apoptotic lymphocytes to stimulate macrophage chemotaxis. *Blood* (2008) 112(13):5026–36. doi:10.1182/blood-2008-06-162404
40. Elliott MR, Chekeni FB, Trampont PC, Lazarowski ER, Kadl A, Walk SF, et al. Nucleotides released by apoptotic cells act as a find-me signal to promote phagocytic clearance. *Nature* (2009) 461(7261):282–6. doi:10.1038/nature08296
41. Gude DR, Alvarez SE, Paugh SW, Mitra P, Yu J, Griffiths R, et al. Apoptosis induces expression of sphingosine kinase 1 to release sphingosine-1-phosphate as a "come-and-get-me" signal. *FASEB J* (2008) 22(8):2629–38. doi:10.1096/fj.08-107169
42. Li W. Eat-me signals: keys to molecular phagocyte biology and "appetite" control. *J Cell Physiol* (2012) 227(4):1291–7. doi:10.1002/jcp.22815
43. Segawa K, Nagata S. An apoptotic 'Eat Me' signal: phosphatidylserine exposure. *Trends Cell Biol* (2015) 25(11):639–50. doi:10.1016/j.tcb.2015.08.003
44. Wang Q, Imamura R, Motani K, Kushiyama H, Nagata S, Suda T. Pyroptotic cells externalize eat-me and release find-me signals and are efficiently engulfed by macrophages. *Int Immunol* (2013) 25(2):363–72. doi:10.1093/intimm/dxs161
45. Zargarian S, Shlomovitz I, Erlich Z, Hourizadeh A, Ofir-Birin Y, Croker BA, et al. Phosphatidylserine externalization, "necroptotic bodies" release, and phagocytosis during necroptosis. *PLoS Biol* (2017) 15(6):e2002711. doi:10.1371/journal.pbio.2002711
46. Hirt UA, Leist M. Rapid, noninflammatory and PS-dependent phagocytic clearance of necrotic cells. *Cell Death Differ* (2003) 10(10):1156–64. doi:10.1038/sj.cdd.4401286
47. Brouckaert G, Kalai M, Krysko DV, Saelens X, Vercammen D, Ndlovu MN, et al. Phagocytosis of necrotic cells by macrophages is phosphatidylserine dependent and does not induce inflammatory cytokine production. *Mol Biol Cell* (2004) 15(3):1089–100. doi:10.1091/mbc.E03-09-0668
48. Brown GC, Neher JJ. Eaten alive! Cell death by primary phagocytosis: 'phagoptosis'. *Trends Biochem Sci* (2012) 37(8):325–32. doi:10.1016/j.tibs.2012.05.002
49. Gardai SJ, Bratton DL, Ogden CA, Henson PM. Recognition ligands on apoptotic cells: a perspective. *J Leukoc Biol* (2006) 79(5):896–903. doi:10.1189/jlb.1005550
50. Park SY, Kim IS. Engulfment signals and the phagocytic machinery for apoptotic cell clearance. *Exp Mol Med* (2017) 49(5):e331. doi:10.1038/emm.2017.52
51. Biermann M, Maueroder C, Brauner JM, Chaurio R, Janko C, Herrmann M, et al. Surface code – biophysical signals for apoptotic cell clearance. *Phys Biol* (2013) 10(6):065007. doi:10.1088/1478-3975/10/6/065007
52. Anderson CL, Shen L, Eicher DM, Wewers MD, Gill JK. Phagocytosis mediated by three distinct Fc gamma receptor classes on human leukocytes. *J Exp Med* (1990) 171(4):1333–45. doi:10.1084/jem.171.4.1333
53. Ross GD, Reed W, Dalzell JG, Becker SE, Hogg N. Macrophage cytoskeleton association with CR3 and CR4 regulates receptor mobility and phagocytosis of iC3b-opsonized erythrocytes. *J Leukoc Biol* (1992) 51(2):109–17.
54. Park S-Y, Jung M-Y, Lee S-J, Kang K-B, Gratchev A, Riabov V, et al. Stabilin-1 mediates phosphatidylserine-dependent clearance of cell corpses in alternatively activated macrophages. *J Cell Sci* (2009) 122(18):3365–73. doi:10.1242/jcs.049569
55. Green DR, Oguin TH, Martinez J. The clearance of dying cells: table for two. *Cell Death Differ* (2016) 23(6):915–26. doi:10.1038/cdd.2015.172
56. Overholtzer M, Mailleux AA, Mouneimne G, Normand G, Schnitt SJ, King RW, et al. A nonapoptotic cell death process, entosis, that occurs by cell-in-cell invasion. *Cell* (2007) 131(5):966–79. doi:10.1016/j.cell.2007.10.040
57. Flannagan RS, Jaumouille V, Grinstein S. The cell biology of phagocytosis. *Annu Rev Pathol* (2012) 7:61–98. doi:10.1146/annurev-pathol-011811-132445
58. Pauwels AM, Trost M, Beyaert R, Hoffmann E. Patterns, receptors, and signals: regulation of phagosome maturation. *Trends Immunol* (2017) 38(6):407–22. doi:10.1016/j.it.2017.03.006
59. Brewer JM, Pollock KGJ, Tetley L, Russell DG. Vesicle size influences the trafficking, processing, and presentation of antigens in lipid vesicles. *J Immunol* (2004) 173(10):6143–50. doi:10.4049/jimmunol.173.10.6143
60. Doshi N, Mitragotri S. Macrophages recognize size and shape of their targets. *PLoS One* (2010) 5(4):e10051. doi:10.1371/journal.pone.0010051
61. Champion JA, Mitragotri S. Role of target geometry in phagocytosis. *Proc Natl Acad Sci U S A* (2006) 103(13):4930–4. doi:10.1073/pnas.0600997103
62. Branzk N, Lubojemska A, Hardison SE, Wang Q, Gutierrez MG, Brown GD, et al. Neutrophils sense microbe size and selectively release neutrophil extracellular traps in response to large pathogens. *Nat Immunol* (2014) 15(11):1017–25. doi:10.1038/ni.2987
63. Greenlee-Wacker MC. Clearance of apoptotic neutrophils and resolution of inflammation. *Immunol Rev* (2016) 273(1):357–70. doi:10.1111/imr.12453
64. Medina CB, Ravichandran KS. Do not let death do us part: 'find-me' signals in communication between dying cells and the phagocytes. *Cell Death Differ* (2016) 23(6):979–89. doi:10.1038/cdd.2016.13
65. Ravichandran KS. Beginnings of a good apoptotic meal: the find-me and eat-me signaling pathways. *Immunity* (2011) 35(4):445–55. doi:10.1016/j.immuni.2011.09.004
66. Penberthy KK, Ravichandran KS. Apoptotic cell recognition receptors and scavenger receptors. *Immunol Rev* (2016) 269(1):44–59. doi:10.1111/imr.12376
67. Kinchen JM, Ravichandran KS. Journey to the grave: signaling events regulating removal of apoptotic cells. *J Cell Sci* (2007) 120(Pt 13):2143–9. doi:10.1242/jcs.03463
68. Sattentau QJ, Stevenson M. Macrophages and HIV-1: an unhealthy constellation. *Cell Host Microbe* (2016) 19:304–10. doi:10.1016/j.chom.2016.02.013
69. Zychlinsky A, Prevost MC, Sansonetti PJ. *Shigella flexneri* induces apoptosis in infected macrophages. *Nature* (1992) 358(6382):167–9. doi:10.1038/358167a0
70. Hilbi H, Moss JE, Hersh D, Chen Y, Arondel J, Banerjee S, et al. *Shigella*-induced apoptosis is dependent on caspase-1 which binds to IpaB. *J Biol Chem* (1998) 273(49):32895–900. doi:10.1074/jbc.273.49.32895
71. Monack DM, Raupach B, Hromockyj AE, Falkow S. *Salmonella typhimurium* invasion induces apoptosis in infected macrophages. *Proc Natl Acad Sci U S A* (1996) 93(18):9833–8. doi:10.1073/pnas.93.18.9833
72. Miao EA, Leaf IA, Treuting PM, Mao DP, Dors M, Sarkar A, et al. Caspase-1-induced pyroptosis is an innate immune effector mechanism against intracellular bacteria. *Nat Immunol* (2010) 11(12):1136–42. doi:10.1038/ni.1960
73. Suzuki T, Franchi L, Toma C, Ashida H, Ogawa M, Yoshikawa Y, et al. Differential regulation of caspase-1 activation, pyroptosis, and autophagy via Ipaf and ASC in *Shigella*-infected macrophages. *PLoS Pathog* (2007) 3(8):e111. doi:10.1371/journal.ppat.0030111
74. Kobayashi T, Ogawa M, Sanada T, Mimuro H, Kim M, Ashida H, et al. The *Shigella* OspC3 effector inhibits caspase-4, antagonizes inflammatory cell death, and promotes epithelial infection. *Cell Host Microbe* (2013) 13(5):570–83. doi:10.1016/j.chom.2013.04.012
75. Cunha LD, Zamboni DS. Subversion of inflammasome activation and pyroptosis by pathogenic bacteria. *Front Cell Infect Microbiol* (2013) 3:76. doi:10.3389/fcimb.2013.00076
76. Bleriot C, Lecuit M. The interplay between regulated necrosis and bacterial infection. *Cell Mol Life Sci* (2016) 73(11–12):2369–78. doi:10.1007/s00018-016-2206-1
77. Jorgensen I, Zhang Y, Krantz BA, Miao EA. Pyroptosis triggers pore-induced intracellular traps (PITs) that capture bacteria and lead to their clearance by efferocytosis. *J Exp Med* (2016) 213(10):2113–28. doi:10.1084/jem.20151613
78. Oddo M, Renno T, Attinger A, Bakker T, MacDonald HR, Meylan PR. Fas ligand-induced apoptosis of infected human macrophages reduces the viability of intracellular *Mycobacterium tuberculosis*. *J Immunol* (1998) 160(11):5448–54.
79. Behar SM, Martin CJ, Booty MG, Nishimura T, Zhao X, Gan HX, et al. Apoptosis is an innate defense function of macrophages against *Mycobacterium tuberculosis*. *Mucosal Immunol* (2011) 4(3):279–87. doi:10.1038/mi.2011.3
80. Keane J, Balcewicz-Sablinska MK, Remold HG, Chupp GL, Meek BB, Fenton MJ, et al. Infection by *Mycobacterium tuberculosis* promotes human alveolar macrophage apoptosis. *Infect Immun* (1997) 65(1):298–304.
81. Molloy A, Laochumroonvorapong P, Kaplan G. Apoptosis, but not necrosis, of infected monocytes is coupled with killing of intracellular bacillus Calmette-Guerin. *J Exp Med* (1994) 180(4):1499–509. doi:10.1084/jem.180.4.1499
82. Fratazzi C, Arbeit RD, Carini C, Remold HG. Programmed cell death of *Mycobacterium avium* serovar 4-infected human macrophages prevents the mycobacteria from spreading and induces mycobacterial growth inhibition by freshly added, uninfected macrophages. *J Immunol* (1997) 158(9):4320–7.

83. Martin CJ, Booty MG, Rosebrock TR, Nunes-Alves C, Desjardins DM, Keren I, et al. Efferocytosis is an innate antibacterial mechanism. *Cell Host Microbe* (2012) 12(3):289–300. doi:10.1016/j.chom.2012.06.010
84. Yang C-T, Cambier CJ, Davis JM, Hall CJ, Crosier PS, Ramakrishnan L. Neutrophils exert protection in the early tuberculous granuloma by oxidative killing of mycobacteria phagocytosed from infected macrophages. *Cell Host Microbe* (2012) 12(3):301–12. doi:10.1016/j.chom.2012.07.009
85. Schaible UE, Winau F, Sieling PA, Fischer K, Collins HL, Hagens K, et al. Apoptosis facilitates antigen presentation to T lymphocytes through MHC-I and CD1 in tuberculosis. *Nat Med* (2003) 9(8):1039–46. doi:10.1038/nm906
86. Duan L, Gan H, Golan DE, Remold HG. Critical role of mitochondrial damage in determining outcome of macrophage infection with *Mycobacterium tuberculosis*. *J Immunol* (2002) 169(9):5181–7. doi:10.4049/jimmunol.169.9.5181
87. Amaral EP, Ribeiro SC, Lanes VR, Almeida FM, de Andrade MR, Bomfim CC, et al. Pulmonary infection with hypervirulent mycobacteria reveals a crucial role for the P2X7 receptor in aggressive forms of tuberculosis. *PLoS Pathog* (2014) 10(7):e1004188. doi:10.1371/journal.ppat.1004188
88. Davis JM, Ramakrishnan L. The role of the granuloma in expansion and dissemination of early tuberculous infection. *Cell* (2009) 136(1):37–49. doi:10.1016/j.cell.2008.11.014
89. Garcia-Aguilar T, Espinosa-Cueto P, Magallanes-Puebla A, Mancilla R. The mannose receptor is involved in the phagocytosis of mycobacteria-induced apoptotic cells. *J Immunol Res* (2016) 2016:1–14. doi:10.1155/2016/3845247
90. Kocks C, Gouin E, Tabouret M, Berche P, Ohayon H, Cossart P. *L. monocytogenes*-induced actin assembly requires the actA gene product, a surface protein. *Cell* (1992) 68(3):521–31. doi:10.1016/0092-8674(92)90188-I
91. Czuczman MA, Fattouh R, van Rijn JM, Canadien V, Osborne S, Muise AM, et al. *Listeria monocytogenes* exploits efferocytosis to promote cell-to-cell spread. *Nature* (2014) 509(7499):230–4. doi:10.1038/nature13168
92. Rupp J, Pfleiderer L, Jugert C, Moeller S, Klinger M, Dalhoff K, et al. *Chlamydia pneumoniae* hides inside apoptotic neutrophils to silently infect and propagate in macrophages. *PLoS One* (2009) 4(6):e6020. doi:10.1371/journal.pone.0006020
93. Spinner JL, Winfree S, Starr T, Shannon JG, Nair V, Steele-Mortimer O, et al. *Yersinia pestis* survival and replication within human neutrophil phagosomes and uptake of infected neutrophils by macrophages. *J Leukoc Biol* (2014) 95(3):389–98. doi:10.1189/jlb.1112551
94. Shiratsuchi A, Kaido M, Takizawa T, Nakanishi Y. Phosphatidylserine-mediated phagocytosis of influenza A virus-infected cells by mouse peritoneal macrophages. *J Virol* (2000) 74(19):9240–4. doi:10.1128/JVI.74.19.9240-9244.2000
95. Fujimoto I, Pan J, Takizawa T, Nakanishi Y. Virus clearance through apoptosis-dependent phagocytosis of influenza A virus-infected cells by macrophages. *J Virol* (2000) 74(7):3399–403. doi:10.1128/JVI.74.7.3399-3403.2000
96. Watanabe Y, Shiratsuchi A, Shimizu K, Takizawa T, Nakanishi Y. Role of phosphatidylserine exposure and sugar chain desialylation at the surface of influenza virus-infected cells in efficient phagocytosis by macrophages. *J Biol Chem* (2002) 277(20):18222–8. doi:10.1074/jbc.M201074200
97. Meesmann HM, Fehr E-M, Kierschke S, Herrmann M, Bilyy R, Heyder P, et al. Decrease of sialic acid residues as an eat-me signal on the surface of apoptotic lymphocytes. *J Cell Sci* (2010) 123(Pt 19):3347–56. doi:10.1242/jcs.066696
98. Baxter AE, Russell RA, Duncan CJ, Moore MD, Willberg CB, Pablos JL, et al. Macrophage infection via selective capture of HIV-1-infected CD4+ T cells. *Cell Host Microbe* (2014) 16(6):711–21. doi:10.1016/j.chom.2014.10.010
99. Calantone N, Wu F, Klase Z, Deleage C, Perkins M, Matsuda K, et al. Tissue myeloid cells in SIV-infected primates acquire viral DNA through phagocytosis of infected T cells. *Immunity* (2014) 41(3):493–502. doi:10.1016/j.immuni.2014.08.014
100. Deleage C, Wietgrefe SW, Del Prete G, Morcock DR, Hao XP, Piatak M Jr, et al. Defining HIV and SIV reservoirs in lymphoid tissues. *Pathog Immun* (2016) 1(1):68–106. doi:10.20411/pai.v1i1.100
101. Russell RA, Chojnacki J, Jones DM, Johnson E, Do T, Eggeling C, et al. Astrocytes resist HIV-1 fusion but engulf infected macrophage material. *Cell Rep* (2017) 18(6):1473–83. doi:10.1016/j.celrep.2017.01.027
102. Hermetet F, Jacquin E, Launay S, Gaiffe E, Couturier M, Hirchaud F, et al. Efferocytosis of apoptotic human papillomavirus-positive cervical cancer cells by human primary fibroblasts. *Biol Cell* (2016) 108(7):189–204. doi:10.1111/boc.201500090
103. Gaiffe E, Pretet JL, Launay S, Jacquin E, Saunier M, Hetzel G, et al. Apoptotic HPV positive cancer cells exhibit transforming properties. *PLoS One* (2012) 7(5):e36766. doi:10.1371/journal.pone.0036766
104. Amara A, Mercer J. Viral apoptotic mimicry. *Nat Rev Microbiol* (2015) 13(8):461–9. doi:10.1038/nrmicro3469
105. Morizono K, Chen IS. Role of phosphatidylserine receptors in enveloped virus infection. *J Virol* (2014) 88(8):4275–90. doi:10.1128/JVI.03287-13
106. Callahan MK, Popernack PM, Tsutsui S, Truong L, Schlegel RA, Henderson AJ. Phosphatidylserine on HIV envelope is a cofactor for infection of monocytic cells. *J Immunol* (2003) 170(9):4840–5. doi:10.4049/jimmunol.170.9.4840
107. Mercer J, Helenius A. Vaccinia virus uses macropinocytosis and apoptotic mimicry to enter host cells. *Science* (2008) 320(5875):531–5. doi:10.1126/science.1155164
108. Jemielity S, Wang JJ, Chan YK, Ahmed AA, Li W, Monahan S, et al. TIM-family proteins promote infection of multiple enveloped viruses through virion-associated phosphatidylserine. *PLoS Pathog* (2013) 9(3):e1003232. doi:10.1371/journal.ppat.1003232
109. Chen YH, Du W, Hagemeijer MC, Takvorian PM, Pau C, Cali A, et al. Phosphatidylserine vesicles enable efficient en bloc transmission of enteroviruses. *Cell* (2015) 160(4):619–30. doi:10.1016/j.cell.2015.01.032
110. Feng Z, Hensley L, McKnight KL, Hu F, Madden V, Ping L, et al. A pathogenic picornavirus acquires an envelope by hijacking cellular membranes. *Nature* (2013) 496(7445):367–71. doi:10.1038/nature12029
111. Gu L, Sims B, Krendelchtchikov A, Tabengwa E, Matthews QL. Differential binding of the HIV-1 envelope to phosphatidylserine receptors. *Biochim Biophys Acta* (2017) 1859(10):1962–6. doi:10.1016/j.bbamem.2017.06.007
112. Bhattacharyya S, Zagorska A, Lew ED, Shrestha B, Rothlin CV, Naughton J, et al. Enveloped viruses disable innate immune responses in dendritic cells by direct activation of TAM receptors. *Cell Host Microbe* (2013) 14(2):136–47. doi:10.1016/j.chom.2013.07.005
113. van Zandbergen G, Bollinger A, Wenzel A, Kamhawi S, Voll R, Klinger M, et al. *Leishmania* disease development depends on the presence of apoptotic promastigotes in the virulent inoculum. *Proc Natl Acad Sci U S A* (2006) 103(37):13837–42. doi:10.1073/pnas.0600843103
114. Peters NC, Egen JG, Secundino N, Debrabant A, Kimblin N, Kamhawi S, et al. In vivo imaging reveals an essential role for neutrophils in leishmaniasis transmitted by sand flies. *Science* (2008) 321(5891):970–4. doi:10.1126/science.1159194
115. van Zandbergen G, Klinger M, Mueller A, Dannenberg S, Gebert A, Solbach W, et al. Cutting edge: neutrophil granulocyte serves as a vector for *Leishmania* entry into macrophages. *J Immunol* (2004) 173(11):6521–5. doi:10.4049/jimmunol.173.11.6521
116. Ribeiro-Gomes FL, Peters NC, Debrabant A, Sacks DL. Efficient capture of infected neutrophils by dendritic cells in the skin inhibits the early anti-*Leishmania* response. *PLoS Pathog* (2012) 8(2):e1002536. doi:10.1371/journal.ppat.1002536
117. Ribeiro-Gomes FL, Otero AC, Gomes NA, Moniz-De-Souza MC, Cysne-Finkelstein L, Arnholdt AC, et al. Macrophage interactions with neutrophils regulate *Leishmania major* infection. *J Immunol* (2004) 172(7):4454–62. doi:10.4049/jimmunol.172.7.4454
118. Ribeiro-Gomes FL, Moniz-de-Souza MC, Alexandre-Moreira MS, Dias WB, Lopes MF, Nunes MP, et al. Neutrophils activate macrophages for intracellular killing of *Leishmania major* through recruitment of TLR4 by neutrophil elastase. *J Immunol* (2007) 179(6):3988–94. doi:10.4049/jimmunol.179.6.3988
119. de Souza Carmo EV, Katz S, Barbieri CL. Neutrophils reduce the parasite burden in *Leishmania* (*Leishmania*) *amazonensis*-infected macrophages. *PLoS One* (2010) 5(11):e13815. doi:10.1371/journal.pone.0013815
120. Novais FO, Santiago RC, Bafica A, Khouri R, Afonso L, Borges VM, et al. Neutrophils and macrophages cooperate in host resistance against *Leishmania braziliensis* infection. *J Immunol* (2009) 183(12):8088–98. doi:10.4049/jimmunol.0803720
121. Filardy AA, Pires DR, Nunes MP, Takiya CM, Freire-de-Lima CG, Ribeiro-Gomes FL, et al. Proinflammatory clearance of apoptotic neutrophils induces an IL-12(low)IL-10(high) regulatory phenotype in macrophages. *J Immunol* (2010) 185(4):2044–50. doi:10.4049/jimmunol.1000017
122. Lopes MF, da Veiga VF, Santos AR, Fonseca ME, DosReis GA. Activation-induced CD4+ T cell death by apoptosis in experimental Chagas' disease. *J Immunol* (1995) 154(2):744–52.

123. Cabral-Piccin MP, Guillermo LV, Vellozo NS, Filardy AA, Pereira-Marques ST, Rigoni TS, et al. Apoptotic CD8 T-lymphocytes disable macrophage-mediated immunity to *Trypanosoma cruzi* infection. *Cell Death Dis* (2016) 7:e2232. doi:10.1038/cddis.2016.135
124. Rodrigues V Jr, Agrelli GS, Leon SC, Silva Teixeira DN, Tostes S Jr, Rocha-Rodrigues DB. Fas/Fas-L expression, apoptosis and low proliferative response are associated with heart failure in patients with chronic Chagas' disease. *Microbes Infect* (2008) 10(1):29–37. doi:10.1016/j.micinf.2007.09.015
125. Chaves AT, de Assis Silva Gomes Estanislau J, Fiuza JA, Carvalho AT, Ferreira KS, Fares RC, et al. Immunoregulatory mechanisms in Chagas disease: modulation of apoptosis in T-cell mediated immune responses. *BMC Infect Dis* (2016) 16:191. doi:10.1186/s12879-016-1523-1
126. Freire-de-Lima CG, Nascimento DO, Soares MB, Bozza PT, Castro-Faria-Neto HC, de Mello FG, et al. Uptake of apoptotic cells drives the growth of a pathogenic trypanosome in macrophages. *Nature* (2000) 403(6766):199–203. doi:10.1038/35003208
127. Silva EM, Guillermo LV, Ribeiro-Gomes FL, De Meis J, Nunes MP, Senra JF, et al. Caspase inhibition reduces lymphocyte apoptosis and improves host immune responses to *Trypanosoma cruzi* infection. *Eur J Immunol* (2007) 37(3):738–46. doi:10.1002/eji.200636790
128. Torchinsky MB, Garaude J, Blander JM. Infection and apoptosis as a combined inflammatory trigger. *Curr Opin Immunol* (2010) 22(1):55–62. doi:10.1016/j.coi.2010.01.003
129. Torchinsky MB, Garaude J, Martin AP, Blander JM. Innate immune recognition of infected apoptotic cells directs T(H)17 cell differentiation. *Nature* (2009) 458(7234):78–82. doi:10.1038/nature07781
130. Penteado LA, Dejani NN, Verdan FF, Orlando AB, Nino VE, Dias FN, et al. Distinctive role of efferocytosis in dendritic cell maturation and migration in sterile or infectious conditions. *Immunology* (2017) 151(3):304–13. doi:10.1111/imm.12731
131. Campisi L, Barbet G, Ding Y, Esplugues E, Flavell RA, Blander JM. Apoptosis in response to microbial infection induces autoreactive TH17 cells. *Nat Immunol* (2016) 17(9):1084–92. doi:10.1038/ni.3512
132. Albert ML, Sauter B, Bhardwaj N. Dendritic cells acquire antigen from apoptotic cells and induce class I-restricted CTLs. *Nature* (1998) 392(6671):86–9. doi:10.1038/32183
133. Kurts C, Robinson BW, Knolle PA. Cross-priming in health and disease. *Nat Rev Immunol* (2010) 10(6):403–14. doi:10.1038/nri2780
134. van Montfoort N, van der Aa E, Woltman AM. Understanding MHC class I presentation of viral antigens by human dendritic cells as a basis for rational design of therapeutic vaccines. *Front Immunol* (2014) 5:182. doi:10.3389/fimmu.2014.00182
135. Laguette N, Sobhian B, Casartelli N, Ringeard M, Chable-Bessia C, Segeral E, et al. SAMHD1 is the dendritic- and myeloid-cell-specific HIV-1 restriction factor counteracted by Vpx. *Nature* (2011) 474(7353):654–7. doi:10.1038/nature10117
136. Silvin A, Yu CI, Lahaye X, Imperatore F, Brault JB, Cardinaud S, et al. Constitutive resistance to viral infection in human CD141+ dendritic cells. *Sci Immunol* (2017) 2(13):eaai8071. doi:10.1126/sciimmunol.aai8071
137. Yatim N, Jusforgues-Saklani H, Orozco S, Schulz O, Barreira da Silva R, Reis e Sousa C, et al. RIPK1 and NF-kappaB signaling in dying cells determines cross-priming of CD8(+) T cells. *Science* (2015) 350(6258):328–34. doi:10.1126/science.aad0395
138. Rasaiyaah J, Tan CP, Fletcher AJ, Price AJ, Blondeau C, Hilditch L, et al. HIV-1 evades innate immune recognition through specific cofactor recruitment. *Nature* (2013) 503(7476):402–5. doi:10.1038/nature12769
139. Lahaye X, Satoh T, Gentili M, Cerboni S, Conrad C, Hurbain I, et al. The capsids of HIV-1 and HIV-2 determine immune detection of the viral cDNA by the innate sensor cGAS in dendritic cells. *Immunity* (2013) 39(6):1132–42. doi:10.1016/j.immuni.2013.11.002
140. Decalf J, Desdouits M, Rodrigues V, Gobert FX, Gentili M, Marques-Ladeira S, et al. Sensing of HIV-1 entry triggers a type I interferon response in human primary macrophages. *J Virol* (2017) 91(15):e00147-17. doi:10.1128/JVI.00147-17
141. Cooper A, García M, Petrovas C, Yamamoto T, Koup RA, Nabel GJ. HIV-1 causes CD4 cell death through DNA-dependent protein kinase during viral integration. *Nature* (2013) 498(7454):376–9. doi:10.1038/nature12274
142. Doitsh G, Galloway NLK, Geng X, Yang Z, Monroe KM, Zepeda O, et al. Cell death by pyroptosis drives CD4 T-cell depletion in HIV-1 infection. *Nature* (2014) 505:509–14. doi:10.1038/nature12940
143. Lepelley A, Louis S, Sourisseau M, Law HK, Pothlichet J, Schilte C, et al. Innate sensing of HIV-infected cells. *PLoS Pathog* (2011) 7(2):e1001284. doi:10.1371/journal.ppat.1001284
144. Munoz LE, Franz S, Pausch F, Furnrohr B, Sheriff A, Vogt B, et al. The influence on the immunomodulatory effects of dying and dead cells of Annexin V. *J Leukoc Biol* (2007) 81(1):6–14. doi:10.1189/jlb.0306166
145. Moody MA, Liao HX, Alam SM, Scearce RM, Plonk MK, Kozink DM, et al. Anti-phospholipid human monoclonal antibodies inhibit CCR5-tropic HIV-1 and induce beta-chemokines. *J Exp Med* (2010) 207(4):763–76. doi:10.1084/jem.20091281
146. Soares MM, King SW, Thorpe PE. Targeting inside-out phosphatidylserine as a therapeutic strategy for viral diseases. *Nat Med* (2008) 14(12):1357–62. doi:10.1038/nm.1885
147. Taiwo B, Barcena L, Tressler R. Understanding and controlling chronic immune activation in the HIV-infected patients suppressed on combination antiretroviral therapy. *Curr HIV/AIDS Rep* (2013) 10(1):21–32. doi:10.1007/s11904-012-0147-3
148. Naggie S. Hepatitis C virus, inflammation, and cellular aging: turning back time. *Top Antivir Med* (2017) 25(1):3–6.
149. Brenchley JM, Schacker TW, Ruff LE, Price DA, Taylor JH, Beilman GJ, et al. CD4+ T cell depletion during all stages of HIV disease occurs predominantly in the gastrointestinal tract. *J Exp Med* (2004) 200(6):749–59. doi:10.1084/jem.20040874
150. Brenchley JM, Price DA, Schacker TW, Asher TE, Silvestri G, Rao S, et al. Microbial translocation is a cause of systemic immune activation in chronic HIV infection. *Nat Med* (2006) 12(12):1365–71. doi:10.1038/nm1511
151. Weavers H, Evans IR, Martin P, Wood W. Corpse engulfment generates a molecular memory that primes the macrophage inflammatory response. *Cell* (2016) 165(7):1658–71. doi:10.1016/j.cell.2016.04.049

Conflict of Interest Statement: The authors declare that the research was conducted in the absence of any commercial or financial relationships that could be construed as a potential conflict of interest.

Copyright © 2017 Karaji and Sattentau. This is an open-access article distributed under the terms of the Creative Commons Attribution License (CC BY). The use, distribution or reproduction in other forums is permitted, provided the original author(s) or licensor are credited and that the original publication in this journal is cited, in accordance with accepted academic practice. No use, distribution or reproduction is permitted which does not comply with these terms.

frontiers in Immunology

ORIGINAL RESEARCH
published: 28 March 2018
doi: 10.3389/fimmu.2018.00644

A 17-kDa Fragment of Lactoferrin Associates With the Termination of Inflammation and Peptides Within Promote Resolution

*Aviv Lutaty[1,2], Soaad Soboh[1,2], Sagie Schif-Zuck[1,2], Orly Zeituni-Timor[1,2], Ran Rostoker[1,2], Malgorzata J. Podolska[3], Christine Schauer[3], Martin Herrmann[3], Luis E. Muñoz[3] and Amiram Ariel[1,2]**

[1] The Laboratory for Molecular Pathways in the Resolution of Inflammation, The Department of Biology, University of Haifa, Haifa, Israel, [2] The Department of Human Biology, University of Haifa, Haifa, Israel, [3] Friedrich-Alexander-University Erlangen-Nürnberg (FAU), Department of Internal Medicine 3—Rheumatology and Immunology, Universitätsklinikum Erlangen, Erlangen, Germany

During the resolution of inflammation, macrophages engulf apoptotic polymorphonuclear cells (PMN) and can accumulate large numbers of their corpses. Here, we report that resolution phase macrophages acquire the neutrophil-derived glycoprotein lactoferrin (Lf) and fragments thereof *in vivo* and *ex vivo*. During the onset and resolving phases of inflammation in murine peritonitis and bovine mastitis, Lf fragments of 15 and 17 kDa occurred in various body fluids, and the murine fragmentation, accumulation, and release were mediated initially by neutrophils and later by efferocytic macrophages. The 17-kDa fragment contained two bioactive tripeptides, FKD and FKE that promoted resolution phase macrophage conversion to a pro-resolving phenotype. This resulted in a reduction in peritoneal macrophage numbers and an increase in the CD11b^{low} subset of these cells. Moreover, FKE, but not FKD, peptides enhanced efferocytosis of apoptotic PMN, reduced TNFα and interleukin (IL)-6, and increased IL-10 secretion by lipopolysaccharide-stimulated macrophages *ex vivo*. In addition, FKE promoted neutrophil-mediated resolution at high concentrations (100 μM) by enhancing the formation of cytokine-scavenging aggregated NETs (tophi) at a low cellular density. Thus, PMN Lf is processed, acquired, and "recycled" by neutrophils and macrophages during inflammation resolution to generate fragments and peptides with paramount pro-resolving activities.

Keywords: resolution of inflammation, lactoferrin, macrophages, efferocytosis, NETosis

OPEN ACCESS

Edited by:
Céline Cougoule, Centre National de la Recherche Scientifique (CNRS), France

Reviewed by:
Werner Solbach, University of Lübeck, Germany
Lucy V. Norling, Barts and The London School of Medicine and Dentistry, United Kingdom

****Correspondence:***
Amiram Ariel
amiram@research.haifa.ac.il

Specialty section:
This article was submitted to Microbial Immunology, a section of the journal Frontiers in Immunology

Received: *23 August 2017*
Accepted: *14 March 2018*
Published: *28 March 2018*

Citation:
Lutaty A, Soboh S, Schif-Zuck S, Zeituni-Timor O, Rostoker R, Podolska MJ, Schauer C, Herrmann M, Muñoz LE and Ariel A (2018) A 17-kDa Fragment of Lactoferrin Associates With the Termination of Inflammation and Peptides Within Promote Resolution. Front. Immunol. 9:644. doi: 10.3389/fimmu.2018.00644

INTRODUCTION

The clearance of apoptotic cells is essential for proper development, homeostasis, and the termination of immune responses (1, 2). The engulfment of apoptotic polymorphonuclear cells (PMN) by macrophages during the resolution of inflammation, in particular, is considered to be a hallmark and a major fate-determining event for these cells (3–6). The phagocytosis of apoptotic cells and

Abbreviations: aggNETs, aggregated neutrophil extracellular traps; ATP, adenosine triphosphate; BMEC, bovine mammary gland epithelial cells; CID, collision-induced dissociation; ELISA, enzyme-linked immunosorbent assay; FCS, fetal calf serum; IgG, immunoglobulin G; IL, interleukin; ISF, interstitial fluid; LBs, latex beads; Lf, lactoferrin; LFPs, lactoferrin peptides; LPS, lipopolysaccharide; LN, lymph nodes; MCP-1, monocyte chemotactic protein-1; NF-κB, nuclear factor kappa B; PMA, phorbol myristate acetate; PMN, polymorphonuclear cells; PPI, post-peritonitis initiation; PVDF, polyvinylidene difluoride; RIPA, radioimmunoprecipitation assay; ROS, reactive oxygen species; SDS-PAGE, sodium dodecyl sulfate-polyacrylamide gel electrophoresis; TGFβ, tumor growth factor β; TNFα, tumor necrosis factor α.

phagolysosome maturation reportedly result in the degradation of the apoptotic cell content (7). However, neutrophil-derived defensins were preserved and transferred from engulfed apoptotic PMN to the phagolysosomes in the engulfing macrophage (8). Here, they limit the intracellular growth of *Mycobacterium tuberculosis*. It has been shown that CD11b^{low} macrophages emerge during the resolution of inflammation (9). These satiated phagocytes engulf high numbers of apoptotic PMN and consecutively migrate to spleen and inguinal lymph nodes (LN) (9).

Lactoferrin (Lf), an iron-binding glycoprotein from the transferrin family with a molecular weight of 78 kDa, is found in various body fluids like milk, colostrum, saliva, tears, mucus secretions, as well as in neutrophil secondary granules (10). Neutrophil degranulation is the main source of Lf in blood (11). Lf is endowed with a plethora of biological functions, including antimicrobial, antiviral, antiparasite, anti-inflammatory, and anticancer activities (12). Lf-binding proteins have been detected on the surfaces of various cells, including neutrophils, monocytes, and peritoneal macrophages (13, 14), as well as on the surfaces of various microorganisms (15). Lf is an important pro-resolving mediator when it is released from apoptotic neutrophils, *i.e.*, it blocks the directed migration of neutrophils and eosinophils (16, 17). The region(s) of Lf responsible for its bactericidal properties is still elusive, although the primary sequences of human Lf and bovine Lf are known, and the molecular structure of this protein has been studied by X-ray crystallography. Numerous studies found that pepsin-digested Lf has a stronger antimicrobial activity than the native protein. A peptide fragment of Lf that exerts antimicrobial activity is referred to as lactoferricin (18). Komine et al. reported that cleavage by the neutrophil-borne serine proteases elastase and/or proteinase 3 of human or bovine Lf generated several bioactive oligopeptides (19, 20). One of these oligopeptides (PGQRDLLFKDSAL) promoted the secretion of pro-inflammatory cytokines and chemokines [interleukin (IL)-6, IL-8, tumor necrosis factor α (TNFα), and monocyte chemotactic protein-1 (MCP-1)] by bovine mammary epithelial cells, whereas its human homolog induced the production of IL-6, MCP-1, and IL-8. In addition, it activated nuclear factor kappa B (NF-κB) in human oral epithelial HSC-2 cells (20). An additional sequence (FKDCHLA) that also contains an FKD motif showed similar pro-inflammatory properties (20), whereas its bovine counterpart (FKECHLA) was inactive (19). Hence, Lf can be cleaved into bioactive peptides that display activities different from the established antibacterial properties.

Recent reports have indicated that the accumulation of neutrophils in high density *in vivo* or *in vitro* and their activation with monosodium urate (MSU) crystals leads to the generation of aggregated neutrophil extracellular traps (aggNETs) in a reactive oxygen species-dependent manner (21). These tophus-like structures promote the degradation of inflammatory cytokines through cleavage by associated serine proteases (21). However, especially in glandular tissues, aggNETs may carry the risk to occlude ducts and secondarily precipitate inflammatory reactions (22). Lf and adenosine triphosphate enhanced aggNETs formation in low-density neutrophil cultures (21). This suggests that Lf and serine proteases cooperate in the resolution of inflammation.

Here, we report that murine resolution phase macrophages contain truncated forms of Lf that are generated by aged/senescent PMN and are acquired following their engulfment. In turn, distinct shorter fragments of Lf are found in body fluids during the inflammatory and resolving phases of both murine peritonitis and bovine mastitis. A resolution-associated fragment of Lf contained two tripeptides that modulated *in vivo* pro-resolving properties of macrophages as well as the formation of aggNETs. These results suggest that macrophages acquire Lf from senescent PMN, process it to shorter bioactive peptides, and fragments thereof release them in a temporal manner. These peptides in turn promote pro-resolving actions of neutrophils and macrophages, as needed.

MATERIALS AND METHODS

Reagents

The following reagents were purchased as detailed: acrylamide/bis-acrylamide, fibronectin, lipopolysaccharide (LPS) (from *Escherichia coli*, clone 055:B5), staurosporine, TEMED, Tween-20, the neutrophil elastase inhibitor silevestat, and zymosan A from Sigma-Aldrich; clodronate from Liposoma BV; anti-goat horseradish peroxidase-conjugated immunoglobulin G (IgG) and anti-rabbit horseradish peroxidase-conjugated IgG from Jackson Immuno Research Laboratories; WesternBright™ ECL from Advansta, fetal calf serum (FCS), L-glutamine, penicillin–streptomycin, RPMI 1640 and trypan blue from Biological Industries, Kibbutz Beit Haemek; goat anti-mouse CD11b (M-19) polyclonal IgG and rabbit anti-human Lf (H-65) polyclonal IgG from SantaCruz Biotechnology; FITC-conjugated anti-mouse Gr-1, PE-conjugated anti-mouse F4/80, PerCP-conjugated anti-mouse CD11b, APC-conjugated anti-mouse CXCR4 (clone BL6-146508) and enzyme-linked immunosorbent assay (ELISA) kits for TNFα, IL-6, IL-12, and IL-10 from Biolegend; cycloheximide (CHX) from Cayman Chemical; PE selection kit was purchased from Stem Cell Technologies; and Protease Inhibitors Cocktail was purchased from Roche. FKD and FKE peptides were organically synthesized by GL Biochem (Shanghai) Ltd.

Murine Peritonitis

Male C57BL/6 mice (6–8 weeks from Harlan Biotech, protocol approved by the Committee of Ethics, The Technion, authorization no. IL-065-04-2010) were injected intraperitoneally (i.p.) with sterile zymosan A (1 mg/ml in PBS). At 24 or 66 h post-peritonitis initiation (PPI), mice were euthanized using isoflurane, and peritoneal exudates were collected by lavaging with 5 ml of sterile PBS. In some experiments, mice challenged with zymosan A for 42 h or unchallenged were injected i.p. with pre-made liposomal clodronate (1 or 0.1 mg/mouse, respectively) or empty liposomes. Then, unchallenged mice were injected with zymosan A. After additional 24 h, peritoneal fluids and spleens were collected from all mice and analyzed for leukocyte subsets by flow cytometry and by Western blotting for Lf as indicated below. Clodronate treatment resulted in an 84% reduction in peritoneal macrophages and no significant changes in the percentage of splenic macrophages. In other experiments, vehicle, FKD, or FKE peptides (50 μM) were injected i.p. at 48 h PPI,

and peritoneal exudates were recovered at 66 h. Macrophages from the exudates were evaluated for CD11b expression, their apoptotic PMN content, and reprogrammed cytokine secretion as detailed below.

Apoptosis Induction

Jurkat T cells (1×10^6 cell/ml) were cultured in culture media (RPMI 1640 supplemented with 10% FCS, 2 mM L-glutamine, 100 μg/ml streptomycin, and 100 U/ml penicillin) under a humidified 5% CO_2 atmosphere at 37°C. Apoptosis was induced by staurosporine (1 μM) for 4 h. PMN cells were isolated from peritoneal exudates 24 h PPI and incubated (1×10^6 cell/ml) in culture media under a humidified 5% CO_2 atmosphere at 37°C for 16–24 h or for 4 h with roscovitine (10 μM) to promote apoptosis. After culturing, each cell type was collected, and the percentage of apoptotic cells was detected using MEBCYTO apoptosis kit (MBL). In some experiments, PMNs were treated with protease inhibitor (diluted 1:25), CHX (30 mM), or silevestat (40 nM), concomitantly with roscovitine and then analyzed for Lf content by Western blotting. In some experiments, the neutrophils were stained for CXCR4 and Annexin V and analyzed by flow cytometry.

Apoptotic Cell Engulfment *Ex Vivo*

Neutrophils or macrophages were isolated from peritoneal exudates 24 or 66 h after zymosan A injection, respectively, using EasySep® Selection Kit following the manufacturer's instructions (Stem Cells Technologies Inc.) with primary antibodies directed against Ly-6G and F4/80, respectively. Then, macrophages were incubated with either apoptotic Jurkat T cells or senescent PMNs (1:5 ratio) for 24 h. Next, unbound cells were washed with PBS and the adherent cells were lysed with radioimmunoprecipitation assay (RIPA) buffer containing protease inhibitor cocktail for 20 min on ice, followed by centrifugation (15,000 RPM, 4°C) for 15 min and collection of supernatants.

Interstitial Fluids (ISFs) From Lymphoid Organs

Inguinal LN and spleens were harvested from mice 24 or 66 h PPI. The organs were mechanically dissociated and strained through a 100-μm nylon mesh (Beckton-Dickinson) to produce a single cell suspension, followed by separation of cells from ISF by centrifugation (1,200 RPM for 5 min). Then, red blood cells were lysed using RBC Lysis Buffer (biological industries), and both fluids and cells were saved at −20°C for further analysis. ISFs were added with a sample buffer and analyzed by Western blotting for Lf.

Mastitis Milk Sample Preparation

Milk samples were obtained from three different dairy cow farms. Samples were taken from cows undergoing resolving or non-resolving *E. coli*-induced mastitis or from healthy cows based on farmer's criteria. The farmers' criteria for resolving mastitis were high somatic cell counts and a swollen and red udder that resolved to a healthy state within 7–10 days. The milk initially became watered-down but later restored normal complexion. Non-resolving mastitis had the same diagnosis parameters initially, but instead of resolving, the milk became bloody and the udder became painful upon touching and eventually clogged. In order to separate the cellular and fat fraction from the aqueous fraction, samples were centrifuged at 1,200 RPM for 5 min (cellular fraction), and the supernatants were incubated overnight at 4°C to solidify the fat fraction. Then, the fat fraction was mechanically peeled from samples and sample buffer was added to the samples. Equal milk volumes were analyzed by Western blotting for Lf.

Purification of Lf-Derived Fragments

Mastitis milk samples from day 5 of resolving mastitis were defatted by centrifugation at $2,000 \times g$ for 30 min at 4°C. The pH of the skim milk was adjusted to 4.6 with 5 N HCl and the milk was centrifuged at $10,000 \times g$ for 1 h to remove the casein precipitate. The whey was then passed through a 0.45-mm filter (Millipore) to completely remove the casein precipitate and its pH was readjusted to 6.0 with 1 N NaOH. The immunoglobulin in the whey was removed by ammonium sulfate precipitation (48%). After passing through a 0.45-mm filter, the solution in the whey was replaced with 0.005 M sodium phosphate buffer (pH 6.0) using dialysis bag (33 mm cellulose membrane, 12–14 kDa cutoff, Sigma-Aldrich). Dialysis was performed in two repetitions, for 5 h and consequently overnight with stirring in a high volume of 0.005 M sodium phosphate buffer (pH 6.0) at 4°C. Then, the samples were loaded into a heparin affinity column (Affi-gel Heparin gel, Bio-Rad), washed and eluted by a stepwise elution with increasing salt concentrations (0.005 M sodium phosphate buffer; pH 6.0, containing 0.1, 0.3, or 0.5 M NaCl). The proteins were then collected at the 0.5 M NaCl fraction, and its content was assessed by sodium dodecyl sulfate-polyacrylamide gel electrophoresis (SDS-PAGE) followed by Coomassie Blue staining and Western blotting for Lf (SantaCruz).

Western Blotting

Isolated cells were washed with PBS and lysed in RIPA buffer containing Protease Inhibitors Cocktail (1:25 dilution, Roche). Cell lysates, ISF, milk samples or isolated Lf derivatives were added with a sample buffer, run by SDS-PAGE (7.5 or 10%), and then transferred to a polyvinylidene difluoride membrane. The membranes were blocked with 5% BSA and probed with primary rabbit anti-mouse Lf polyclonal IgG (SantaCruz). Next, the membranes were blotted with appropriate secondary antibodies (1:10,000 dilution, 1 h at room temperature, Jackson ImmunoResearch) conjugated with horseradish peroxidase. Membranes were developed with WesternBright™ ECL kit (Advansta) and analyzed using Luminescent Image Analyzer LAS-4000 (Fujifilm Corporation) and "Image Reader LAS-4000" software (Fujifilm Corporation). Densitometric analysis was performed using TotalLab TL100 (nonlinear dynamics) image analysis software.

Lf Fragment Sequencing

The Coomassie-stained bands corresponding to the 15- and 17-kDa fragments of bovine Lf from milk samples were proteomically analyzed at the Smoler Proteomics Center, The Technion,

Israel, according to the following protocol: the proteins in each sample were denatured in 8 M urea, reduced with 3 mM DTT (60°C for 30 min), and modified with 10 mM iodoacetamide in 100 mM ammonium bicarbonate (room temperature for 30 min). The urea was diluted to 2 M, and the sample was trypsinized in 10 mM ammonium bicarbonate containing trypsin (modified trypsin; Promega) at a 1:50 enzyme-to-substrate ratio, overnight at 37°C. A second step of trypsinization was performed by adding another portion of trypsin and incubation at 37°C for 4 h. Mass spectrometry was done according to the following protocol: the resulting peptides were desalted using C18 tips (homemade), dried, and re-suspended in 50 mM Hepes (pH 6.4). Labeling by dimethylation was done in the presence of 100 mM $NaCBH_3$ (Sterogene 1 M), by adding light formaldehyde (35% Frutarom, 12.3 M) to one of the samples and heavy formaldehyde (20% w/w, Cambridge Isotope Laboratories, 6.5 M) to the other sample to a final concentration of 200 mM. After 1-h incubation at room temperature, the pH was raised to 8 and the reaction was incubated for 1 h. Neutralization was done with 25 mM ABC for 30 min, and equal amounts of the light and heavy peptides were mixed, cleaned on C18, and re-suspended in 0.1% formic acid. The peptides were resolved by reverse-phase chromatography on 0.075 × 200-mm fused silica capillaries (J&W) packed with Reprosil reversed phase material (Dr. Maisch GmbH, Germany). The peptides were eluted with linear 90-min, gradients of 5–45% and 15 min at 95% acetonitrile with 0.1% formic acid in water at flow rates of 0.25 µl/min. Mass spectrometry was performed by an ion-trap mass spectrometer (Orbitrap, Thermo) in a positive mode using repetitively full MS scan followed by collision-induced dissociation (CID) of the seven most dominant ions selected from the first MS scan.

The mass spectrometry data were analyzed using the Sequest 3.31 software (J. Eng and J. Yates, University of Washington and Finnigan, San Jose) searching against the bovine part of the NCBI-NR database. Peptide quantities were calculated as area under the pick using the PepQuant algorithm from Bioworks.

Sequence Alignment

Sequences from the identified peptides were aligned relative to full-length Lf using STRAP, Interactive Structure based Sequence Alignment Program,[1] along with PubMed protein database.[2] For an illustration of the complete isolation and sequencing procedure, please see Figure S2 in Supplementary Material.

Macrophage CD11b Expression

Peritoneal exudates were recovered from mice 66 h PPI following treatment for 18 h with vehicle, FKD, or FKE peptides. The cells were enumerated and immune-stained for Gr-1, F4/80, and CD11b and analyzed by flow cytometry (FACSCanto II) for leukocyte subtypes. $F4/80^+$ macrophages were analyzed for the expression of CD11b as previously (9).

[1] www.bioinformatics.org/strap/.

[2] www.ncbi.nlm.nih.gov/pubmed/.

In Vivo Efferocytosis

Peritoneal macrophages from Section "Macrophage CD11b Expression" were isolated using F4/80-directed magnetic beads, and 150×10^3 cells were plated in an 8-well glass chamber slide (Nunc) for 2 h in 150-µl culture medium. Then, medium was aspirated, and unbound cells were washed gently with PBS. Adherent cells were subsequently fixed (200 µl of 4% paraformaldehyde, 5% sucrose, 15 min). Next, the cells were washed in PBS and stained (overnight, 4°C) with 200 µl of CF488A-conjugated phalloidin (5 U/ml from Biotium), for F-actin. Next, cells were washed three times with PBS and stained for nuclear DNA in 200 µl of Hoechst (20 µg/ml, 5 min, from Invitrogen), and rinsed with PBS. Then, the chambers were removed, mounted with Fluoromount G, and visualized under a Nikon A1 confocal microscope. The number of engulfed apoptotic cells per macrophage was scored, as well as the percentage of non-engulfing macrophages. The results were obtained from eight mice and 503–592 macrophages per treatment.

Macrophage Cytokine Secretion

Peritoneal macrophages from Section "Macrophage CD11b Expression" were isolated and then treated with LPS (1 µg/ml, 24 h) or vehicle. Then, culture media were collected and its cytokine content was determined by standard ELISA for TNFα, IL-6, IL-10, or IL-12.

Regulation of aggNETs Formation

All analyses of material derived from human subjects were performed in full agreement with institutional guidelines and with the approval of the Ethical Committee of the University Hospital Erlangen (permit number 193 13B). Peripheral blood PMNs (>95% neutrophils) were separated from mononuclear cells by density gradient centrifugation on Lymphoflot (Bio-Rad, Hercules, CA, USA) and cleared from contaminating erythrocytes by short hypotonic lysis. PMNs were incubated at a low cell density (5×10^6 cells/ml) with 50 pg/cell MSU crystals and/or 10–100 µM Lf (Sigma-Aldrich) and/or 10–100 µM FKD or FKE peptides and 1 µg/ml propidium iodide solution in RPMI (Thermo Fisher Scientific) without serum supplementation for 3 h at 37°C and 5% CO_2. NET aggregation was stopped by adding 1% paraformaldehyde to cell cultures for 20 min. NET aggregates were filtrated through a 40-µM mesh, and macrophotographs of captured material with UVB transillumination were made with a Nikon D700 reflex camera.

Data Analysis

Experimental data were analyzed by Student's *t*-test or ANOVA followed by Tukey's *post hoc* analysis. *p*-values of ≤0.05 were designated as statistically significant. Results are presented as average ± SEM.

RESULTS

Resolution Phase Macrophages Acquire Lf From Senescent PMN

During the resolution of inflammation, macrophages engulf apoptotic PMN and consecutively migrate to lymphoid organs

(9, 23). Macrophages acquire granular defensins from neutrophils that had undergone apoptosis and "recycle" it for antimicrobial activity (8). Lf is a major constituent of neutrophils secondary granules. We hypothesized that Lf is acquired by macrophages once they engulf senescent PMN. To test this, we incubated neutrophils with resolution phase macrophages from the peritoneum *ex vivo* and quantified their levels of Lf. Apoptotic Jurkat T cells, latex beads (LBs), IgG-opsonized LB (oLB), and anti-CD11b antibodies were used as phagocytosis and CD11b crosslinking controls, respectively. The results in **Figure 1A** show that macrophages contained only a single 50-kDa band immunoreactive with anti-Lf antibodies. Incubation with aging/senescent

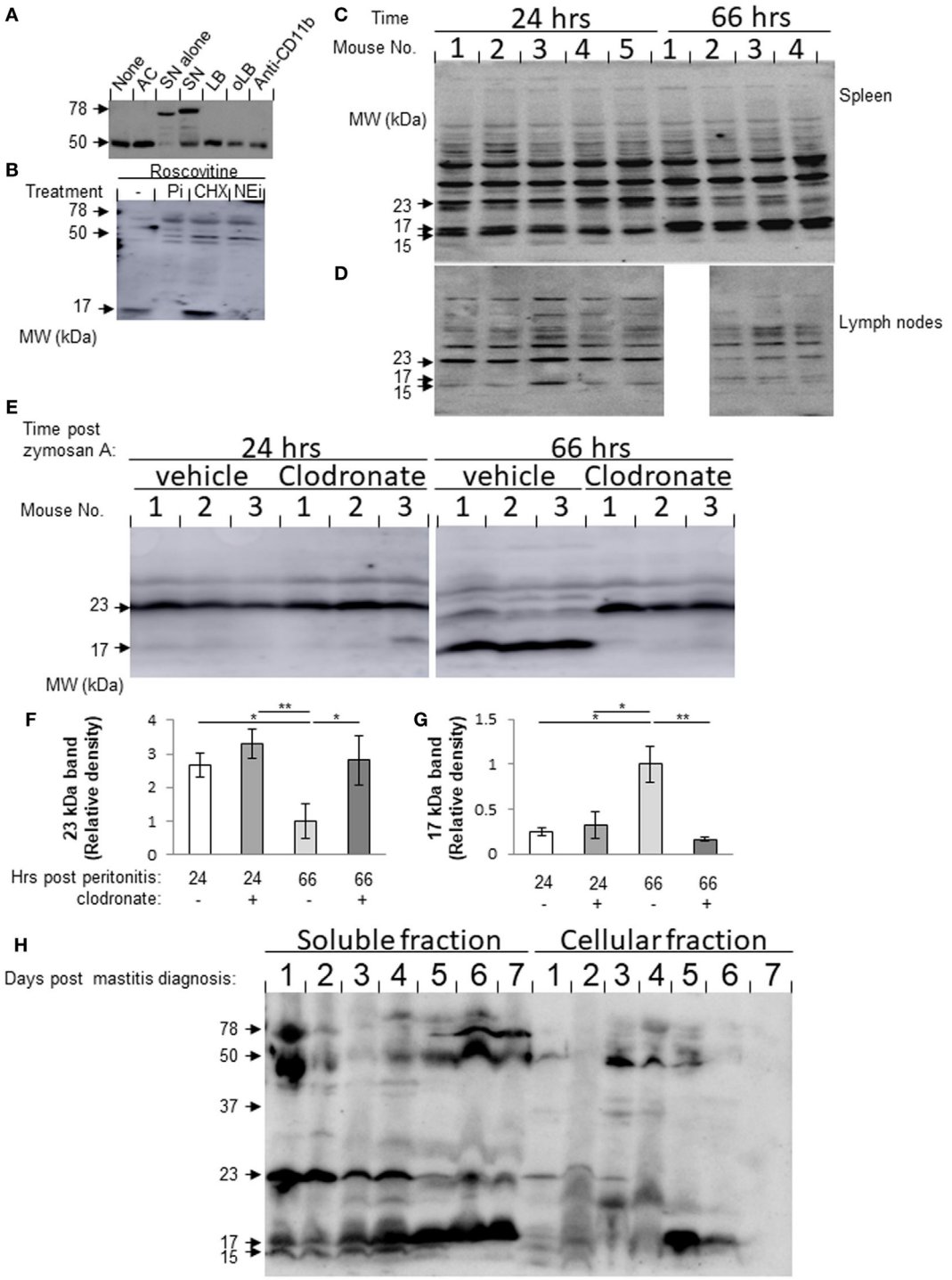


FIGURE 1 | Continued

FIGURE 1 | **(A,B)** Lactoferrin (Lf) fragments accumulate in macrophages following incubation with senescent neutrophils. **(A)** Peritoneal macrophages were recovered 66 h post zymosan A-induced (1 mg/mouse) peritonitis initiation and incubated with apoptotic Jurkat cells (AC), senescent peritoneal neutrophils (SN), latex beads (LBs), IgG-opsonized LB (oLB), or anti-CD11b monoclonal antibodies as indicated. After 24 h, unbound cells were washed and macrophages were recovered. Then, the cells were lysed, and equal amounts of protein extract were blotted for Lf. Protein extracts from apoptotic neutrophils were also analyzed as indicated. Results are representative from three independent experiments (cells were pooled from three to five mice). **(B)** Peritoneal neutrophils were recovered 24 h PPI and treated with roscovitine (10 μM) alone or with protease inhibitor cocktail (Pi), cycloheximide (CHX), or the neutrophil elastase inhibitor, silevestat (NEi) for 20 h. Then, neutrophils were lysed, and their protein content was immunoblotted for Lf [results are representative from three experiments (cells were pooled from three to five mice)]. **(C,D)** Lf fragments are found in interstitial fluids (ISFs) of spleen and inguinal lymph nodes (LN) during peritonitis. Spleen **(C)** and inguinal LN **(D)** were harvested 24 and 66 h after initiation of peritonitis (n = 4–5) and mashed in equal volumes of PBS employing a nylon grid. Equal amounts of ISF protein were run by 10% sodium dodecyl sulfate-polyacrylamide gel electrophoresis (SDS–PAGE), followed by Western blotting for Lf. Results are representative blots from three experiments. **(E–G)** Peritoneal resolution phase macrophages are essential for the differential production of splenic Lf fragments. Mice were injected intraperitoneally (i.p.) with clodronate-containing or empty liposomes 42 h PPI or before the initiation of peritonitis. After additional 24 h, the spleens were recovered and mashed in equal volumes of PBS employing a nylon grid. Equal amounts of ISF protein were run by 12% SDS-PAGE, followed by Western blotting for Lf. Results are a representative blot **(E)** and averages of densitometric analysis of the 23- **(F)** and 17 **(G)**-kDa bands from three experiments (n = 3–6 mice per group). **/*indicate statistically significant differences of $P \leq 0.01$/$P \leq 0.05$, respectively, by ANOVA with Tukey *post hoc* analysis. **(H)** Lf fragments are found in dairy cow milk during the onset and resolution of mastitis. Milk samples from dairy cows with mastitis (days 1–7) were defatted and separated into soluble and cellular fractions by centrifugation. The cellular fraction was lysed and the cytoplasmic proteins were recovered. Equal amounts of protein from both fractions were analyzed by Western blotting for Lf. Results show representative blots from three sample sets taken daily from three different cows.

neutrophils resulted in the appearance of an additional 78-kDa protein similar to the major band corresponding to neutrophil-borne Lf. Interestingly, the expression of the 50-kDa band in macrophages was not significantly modulated by incubation with apoptotic Jurkat cells or other phagocytic targets, such as LB and oLB. Crosslinking of CD11b did not modulate Lf levels in resolution phase macrophages either. To determine whether Lf fragmentation already takes place in PMN or whether Lf is expressed *de novo* in PMN, the recovered cells were treated with roscovitine in the presence of a general protease inhibitor cocktail, an elastase inhibitor (silevestat), or CHX. The results in **Figure 1B** indicate that roscovitine treatment enhanced Lf fragmentation to shorter fragments than 50 kDa already in unengulfed PMN. A fragment of 17 kDa was especially evident in apoptotic PMN. Moreover, both protease inhibitors significantly abrogated the generation of the 17-kDa Lf fragment, whereas CHX increased this Lf fragment levels. It was previously shown that senescent neutrophils express CXCR4 and migrate to the BM once they age through CXCL12 gradients (24). Of interest, the aging of peritoneal neutrophils *ex vivo* resulted in membrane expression of both annexin V and CXCR4 on most cells after 24 h (Figure S1 in Supplementary Material), and this was enhanced by roscovitine at 4 h, but not at 24 h. This indicates that aging PMNs have features of both apoptotic and senescent neutrophils. Altogether, these results indicate that Lf was processed, at least partially, in neutrophils during the apoptotic process, and consequently Lf and its fragments were acquired by resolution phase macrophages following the phagocytosis of apoptotic cells. Thus, macrophages can acquire Lf and its fragments from senescing neutrophils following their engulfment and maintain it as distinct fragments.

Resolution-Associated Fragments of Lf Are Present in Murine Draining LN and Spleen as Well as Bovine Udder

Next, we analyzed whether Lf fragments can be detected in lymphoid tissues during inflammation and its resolution, since macrophages that engulf apoptotic PMN tend to adopt the CD11b^{low} phenotype and migrate to lymphoid organs (9). To this end, we collected ISFs from meshed inguinal LN and spleens 24 and 66 h post initiation of murine peritonitis. Our results in **Figures 1C,D** show three specific bands corresponding to Lf fragments that were detected in both spleen and LN with molecular weights of 23, 17 and 15 kDa. Notably, the 23-kDa fragment was present at a higher amount during the inflammatory phase of the response (24 h) in comparison to the resolution phase (66 h) in both organs. The 15-kDa fragment showed a similar trend in the LN but did not reduce during the resolution phase in the spleen. Importantly, the 17-kDa fragment of Lf showed the opposite trend in both spleen and LNs. Essentially, its levels were significantly increased during the resolution phase compared to the inflammatory phase of peritonitis. To determine whether processing and/or release by peritoneal macrophages is key to determining the different fragments of Lf present at the spleen, we depleted peritoneal macrophages using clodronate 24 h prior to spleen recovery. Our results (**Figures 1E–G**) indicate that the depletion of resident macrophages did not affect the levels of either the 23- or 17-kDa fragments of Lf in the ISF at 24 h PPI. However, the depletion of resolution phase macrophages significantly reduced the levels of the 17-kDa fragment and increased the levels of the 23-kDa fragment at 66 h PPI. Thus, our results suggest that the inflammatory 23-kDa fragment of Lf is produced primarily by other cells, while the resolution phase-associated 17-kDa fragment is acquired and released by peritoneal macrophages that engulf PMN and migrate to the spleen.

Lactoferrin is a major component of milk and plays a key role in innate immune defense. We aimed to determine whether Lf fragments are also present in bovine milk during mastitis and its resolution, since neutrophils and macrophages increased in bovine milk during inflammation (25, 26). Our previous results determined that Lf fragments are accumulating in macrophages. Therefore, we sought to determine whether Lf fragments are also present in bovine milk during mastitis and its resolution. To this end, protein samples from the soluble and cellular fractions of bovine milk were collected daily during resolving mastitis (Figure S2 in Supplementary Material for Methodology; **Figure 1H**). As controls, milk samples were also collected from non-resolving mastitis as well as from healthy cows (Figure

S3 in Supplementary Material). Our results indicate a similar fragmentation pattern for murine and bovine Lf. Moreover, during spontaneous resolution of mastitis, the amounts of the 17-kDa fragment of soluble Lf increase from day 1 until day 7. Concomitantly, the amounts of the 23- and 15-kDa fragments of Lf were decreased during the transition from the inflammatory phase to the resolving phase. The full-length 78-kDa Lf and its 50-kDa fragment are evident only at the beginning of the inflammatory episode (day 1) and during the late resolution phase of mastitis (days 6 and 7), while during the course of early inflammation, its levels are very low. Importantly, the 50- and 17-kDa fragments of Lf were also found in the cellular fraction of the milk from resolving mastitis, albeit in kinetics that preceded the soluble fraction by 24 h. This suggested that the soluble fragments originated in leukocytes that infiltrated into the infected udder. In non-resolving mastitis, the prevalence of Lf fragments was different from that of resolving mastitis. Only the 50-kDa fragment is evident in non-resolving mastitis, and

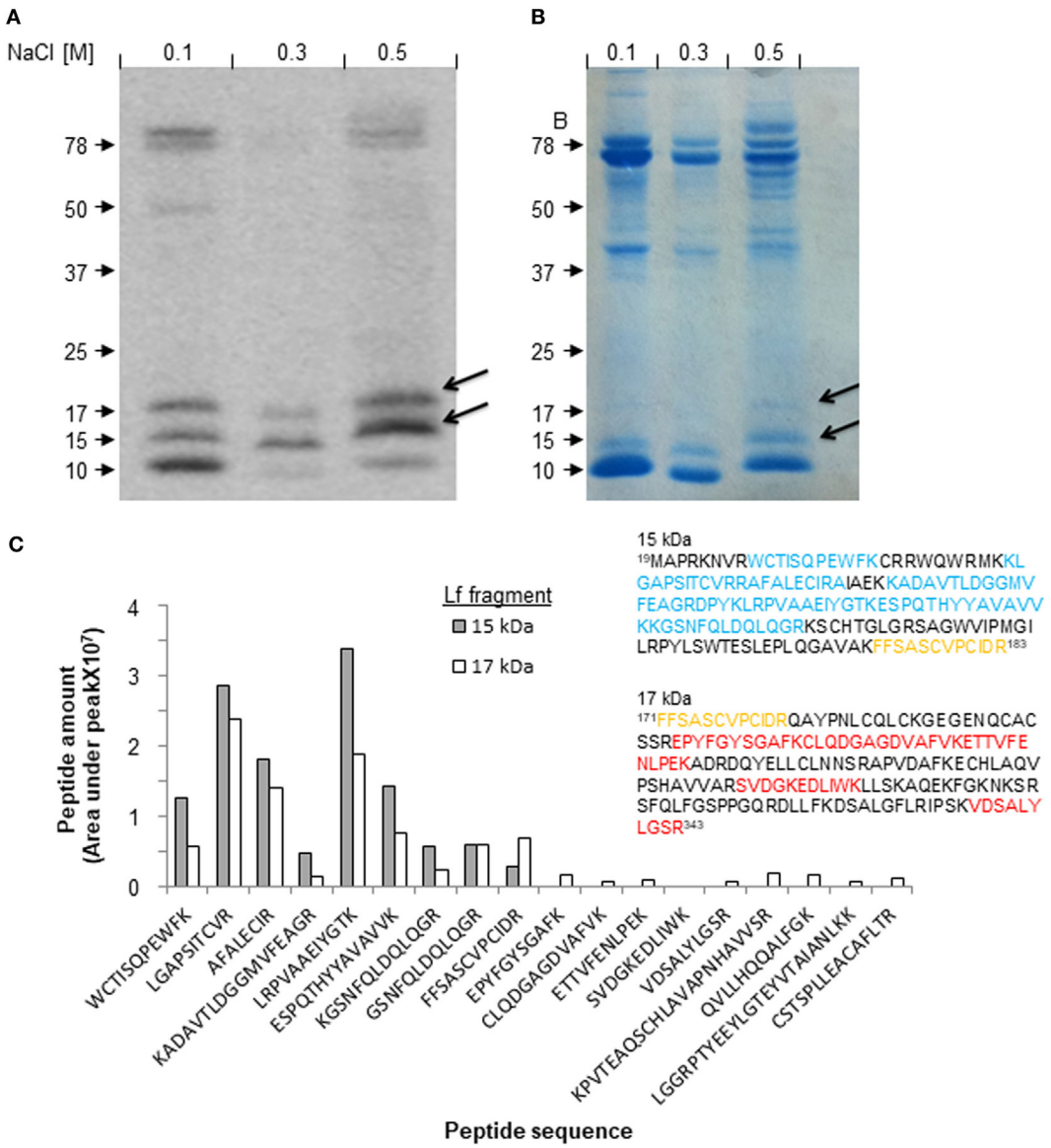


FIGURE 2 | Isolation and identification of lactoferrin (Lf)-derived fragments from udders with resolving inflammation. Milk samples from cows with mastitis (day 5, early phase of resolution) were defatted and run on heparin gel columns. The bound proteins and fragments were eluted stepwise with 0.005 M sodium phosphate buffer (pH 6.0) containing 0.1, 0.3, or 0.5 M NaCl. The recovered protein samples were run on 10% sodium dodecyl sulfate-polyacrylamide gel electrophoresis (SDS-PAGE) followed with Western blotting for Lf **(A)**, and Coomassie Brilliant Blue staining for total protein content **(B)**. The bands corresponding to the 15- and 17-kDa fragments of Lf were excised from the gel and analyzed by LC-MS-MS. Quantification of the frequency of each fragment was provided by analysis of area under the peak. The indicated fragments were aligned using STRAP software against the full-length Lf sequence taken from the PubMed database. Then, each peptide was associated with the corresponding fragment of 15 or 17 kDa (inset, highlighted in blue and red, respectively). One common peptide present in both fragments is highlighted in orange **(C)**.

its levels in the milk increased with time. Altogether, our findings indicate that Lf undergoes a distinct proteolytic processing during inflammation and its resolution in various organs and mammals, and that a leukocyte-derived 17-kDa fragment accumulates in various immune-active organs during the resolution of inflammation.

Isolation of Lf-Derived Fragments and Determination of Their Amino Acid Sequences

Next, we isolated the 17-kDa fragment of Lf from milk collected during the resolution of mastitis and determined its amino acid sequence, to identify novel resolution-associated molecules. To this end, milk samples from day 5 of mastitis were prepared and loaded on heparin liquid-gel columns. After washing of unbound material, the eluted products were run on 10% SDS-PAGE, blotted by anti-Lf antibodies, and visualized by Coomassie Brilliant Blue staining (**Figures 2A,B**). The bands at 17 and 15 kDa were identified as Lf fragments by Western blotting and therefore were excised from the gel and used for amino acid sequencing using mass spectrometry. No other small Lf-derived fragments were detected in our isolated proteins, suggesting that the other fragments found in bovine milk do not bind heparin. The proteomic analysis of the 15- and 17-kDa fragments of Lf resulted in a series of peptides with relative quantities (**Figure 2C**) that were aligned to the amino acid sequence of full-length bovine Lf as well as to Lf sequences from eight other species taken from the PubMed database. These species include *Homo sapiens*, *Mus musculus*, and two subgroups of the bovine family: *Bos indicus* and *Bos taurus*. Alignment, amino acid coloring, frame shift, and amino acid numbering were done using the STRAP software (Figure S4 in Supplementary Material). Our analysis was based on the notion that our anti-Lf antibody was generated against a peptide comprising amino acids 146–210, and therefore this portion of Lf should be included in both the 15- and 17-kDa fragments. Our results revealed that the 15-kDa fragment was composed of eight peptides that encompassed amino

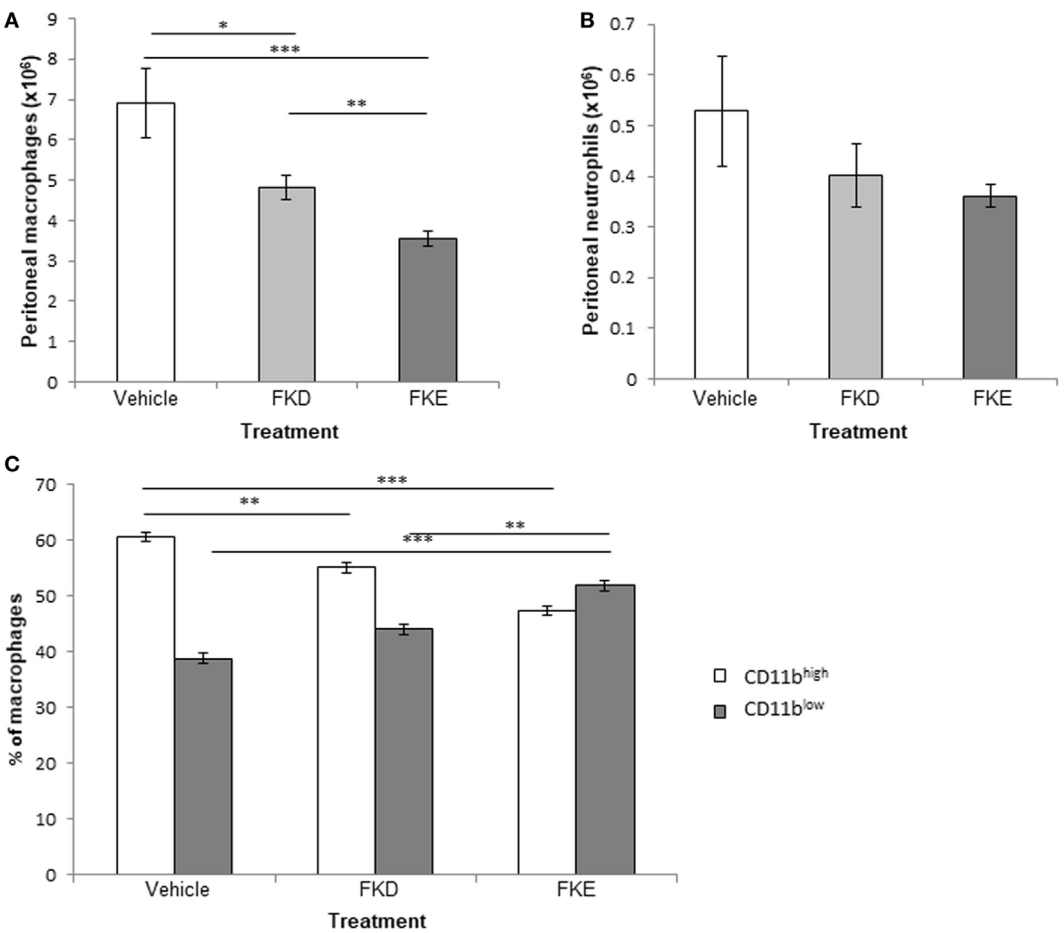


FIGURE 3 | Lactoferrin (Lf)-derived peptides promote macrophage conversion to the CD11b^{low} phenotype. Mice undergoing peritonitis for 48 h were injected intraperitoneally (i.p.) with PBS, FKE, or FKD peptides (50 μM each). After additional 18 h, peritoneal exudates were recovered and the cells were enumerated. Then, exudate cells were immunostained for Ly-6G, F4/80, and CD11b and analyzed by flow cytometry. The numbers of macrophages **(A)** and neutrophils **(B)**, and the percentages of CD11b^{high} and CD11b^{low} macrophages **(C)** are presented. Results are averages ± SEM from three independent experiments ($n = 4$ per group). ***/**/*indicate statistically significant differences of $P \leq 0.005$/$P \leq 0.01$/$P \leq 0.05$, respectively, by ANOVA with Tukey *post hoc* analysis.

acids 19–183 (including the peptides ^{27}WCTISQPEWFK^{38}, ^{47}KLGAPSITCVRRAFALECIRA^{68}, ^{72}KADAVTLD^{80}, ^{80}GGM VFEAGRD^{90}, ^{90}PYKLRPVAAE^{100}, ^{100}IYGTKESPQT^{110}, ^{110}HYY AVAVVKK^{120}, ^{120}GSNFQLDQLQGR^{132}, and ^{171}FFSASCVPCI DR^{183}). Most of these peptides also appeared with similar frequencies in the 17-kDa fragment analysis (probably due to dispersion of the 15-kDa band and inaccuracies in the excision process). However, a second molecular species was also evident. This fragment ranged from amino acids 171–343 (including the peptides ^{171}FFSASCVPCIDR^{183}, ^{206}EPYFGYSGAF^{216}, ^{217}CLQDGAGDVAFVK^{230}, ^{231}ETTVFENLPEK^{241}, ^{278}SVDGKE DLIWK^{289}, and ^{333}VDSALYLGSR^{343}; **Figure 2C**, insert). These designated amino acid sequences matched in predicted molecular weights to 15 and 17 kDa, respectively. Notably, another Lf peptide that was not detected by Western blotting was identified using mass spectrometry within the 17-kDa band. This fragment from the C-lobe of Lf (containing peptides ^{598}PVTEAQSCHLAVAPNHAVVSR^{619}, ^{627}QVLLHQQALFGK^{639}, ^{669}LGGRPTYEEYL-GTEYVTAIANLKK^{693}, and ^{693}CSTSPLLEA CAFLTR^{708}) was not further pursued as it is not known whether it is associated exclusively with the resolution phase of inflammation. Thus, we conclude that the 15- and 17-kDa fragments differ from one another, for the most part, with a short overlapping region in the domain that is recognized by the anti-Lf antibodies (**Figure 2C**, highlighted in orange).

The Lf-Derived Peptides FKE and FKD Promote *In Vivo* Macrophage Conversion to the Pro-Resolving CD11b^{low} Phenotype

Previously, Komine et al. (19) identified four peptides in serine protease-digested bovine Lf: FKECHLA, VPSHAVVAR, FQLFGSP, and PGQRDLLFKDSAL (designated pep1–4, respectively). All peptides are located within the 17-kDa Lf fragment (Figure S4 in Supplementary Material, underlined) and showed that pep4 had an enhanced pro-inflammatory effect in terms of cytokine and chemokine secretion in a bovine mammary gland epithelial cell line (19), while pep1–3 were devoid of activity. Other results from the same group (20) showed that the human homolog of pep1 contains an FKDCHLA sequence, induced pro-inflammatory cytokines and chemokines (IL-8, IL-6, and MCP-1), and activated NF-κB in the HSC-2 cell line. The human homolog of pep 4 (SGQKDLLFKDSAI) was active as well. Thus, we suggest that the difference in immunemodulatory properties between bovine pep4 and pep1 could be due to the replacement of a single aspartate by glutamate (D → E). As a result, the active consensus sequence changes from phenylalanine–lysine–aspartate (FKD) to phenylalanine–lysine–glutamate (FKE; Figure S4 in Supplementary Material, inside the red frame) and results in loss of activity under their experimental setting. Since our results indicate that both peptides are present in the 17-kDa Lf-derived fragment that accumulates during the resolution of inflammation in various species and models, we determined whether these peptides exert anti-inflammatory and pro-resolving actions and whether the FKD and FKE peptides differ in this respect. To this end, FKD and FKE peptides (50 μM) were injected i.p. to mice undergoing peritonitis for 48 h. After additional 18 h, peritoneal exudates from these mice were recovered, and the properties of the leukocytes collected were determined. Our results (**Figures 3A,B**) indicate that FKD, and to a higher extent FKE, reduced peritoneal macrophage and PMN numbers (0.7- and 0.51-fold of PBS for macrophages, 0.77- and 0.69-fold of control for PMN, respectively), although the latter reduction was not statistically significant. Importantly, the conversion of macrophages from the reparative CD11b^{high} phenotype to the pro-resolving CD11b^{low} phenotype (9, 27) in the peritoneum was upregulated by FKD and to a higher extent by FKE peptides (**Figure 3C**; 1.13- and 1.33-fold of PBS, respectively).

FKE Peptides Promote Macrophage Efferocytosis

It was previously shown that macrophage conversion to the CD11b^{low} phenotype can be induced by apoptotic PMN uptake (9). Hence, we examined the impact of Lf peptides on efferocytosis *in vivo*. Our results in **Figures 4A–C** indicate that FKE increased efferocytosis, while FKD reduced it (1.17- and 0.57-fold of PBS, respectively). These responses were primarily due to a

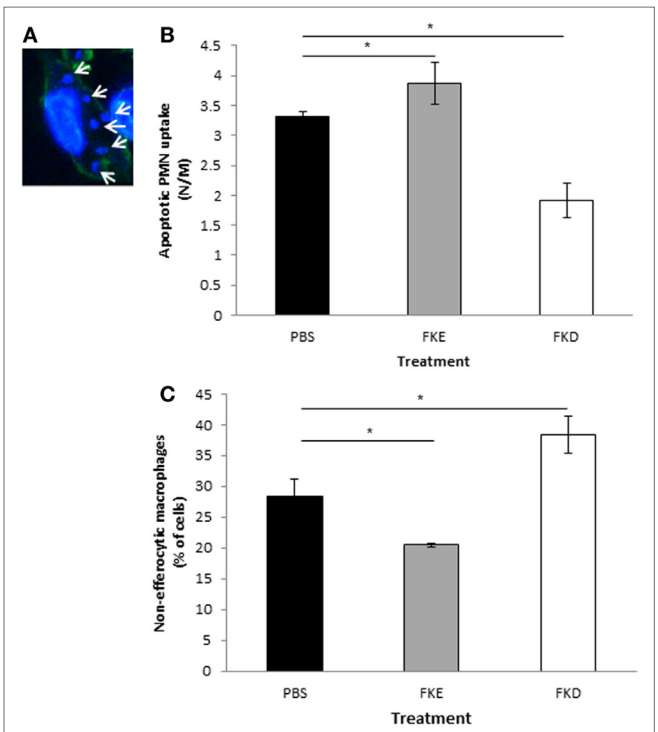


FIGURE 4 | FKE peptides promote macrophage efferocytosis. Mice undergoing peritonitis for 48 h were injected intraperitoneally (i.p.) with PBS, FKE, or FKD peptides (50 μM each). After additional 18 h, peritoneal macrophages were isolated and stained with CF488A-conjugated phalloidin and Hoechst. Slides were visualized under a Nikon A1 confocal microscope and nuclei of engulfed polymorphonuclear cells (PMN) were enumerated [see **(A)** for a representative image]. Results show the average number of engulfed apoptotic PMN per macrophage **(B)** and the percentage of macrophages that did not engulf apoptotic PMN **(C)**. Results are averages ± SEM from three independent experiments ($n = 4$ per group). *indicate statistically significant differences of $P \leq 0.05$ by ANOVA with Tukey *post hoc* analysis.

decrease in non-efferocytic macrophages following FKE treatment, while the percentage of these macrophages was increased by FKD (0.72- and 1.35-fold of PBS, respectively). Thus, FKE, but not FKD, peptides enhance the uptake of apoptotic PMN by resolution phase macrophages.

FKE Peptides Promote Macrophage Reprogramming

The uptake of apoptotic cells promotes macrophage reprogramming and results in a reduced secretion of pro-inflammatory cytokines and an increased secretion of anti-inflammatory/reparative cytokines upon exposure to bacterial agents (5). Hence, we examined whether Lf peptides can affect macrophage reprogramming and cytokine secretion upon LPS stimulation. Our results indicate that FKE exposure *in vivo* reduced TNFα and IL-6 secretion by LPS-stimulated resolution phase macrophages [(**Figures 5A,B**); 0.79- and 0.81-fold of PBS, respectively]. FKD peptides, on the other hand, increased the secretion of these inflammatory cytokines from LPS-stimulated resolution phase macrophages [(**Figures 5A,B**); 1.66- and 1.2-fold of PBS, respectively]. Notably, IL-10 secretion was induced by FKE, but not by FKD [(**Figure 5C**); 1.72- and 0.98-fold of PBS, respectively], whereas both peptides reduced IL-12 secretion but not in a statistically significant manner (**Figure 5D**). Thus, FKE, but not FKD, seems to promote macrophage reprogramming during resolving inflammation.

Lf-Derived Peptides Enhance MSU-Induced aggNETs Formation

The resolution of neutrophilic inflammation was recently shown to be associated with the formation of cytokine-scavenging aggNETs displaying a tophus texture (21). Since Lf promotes human

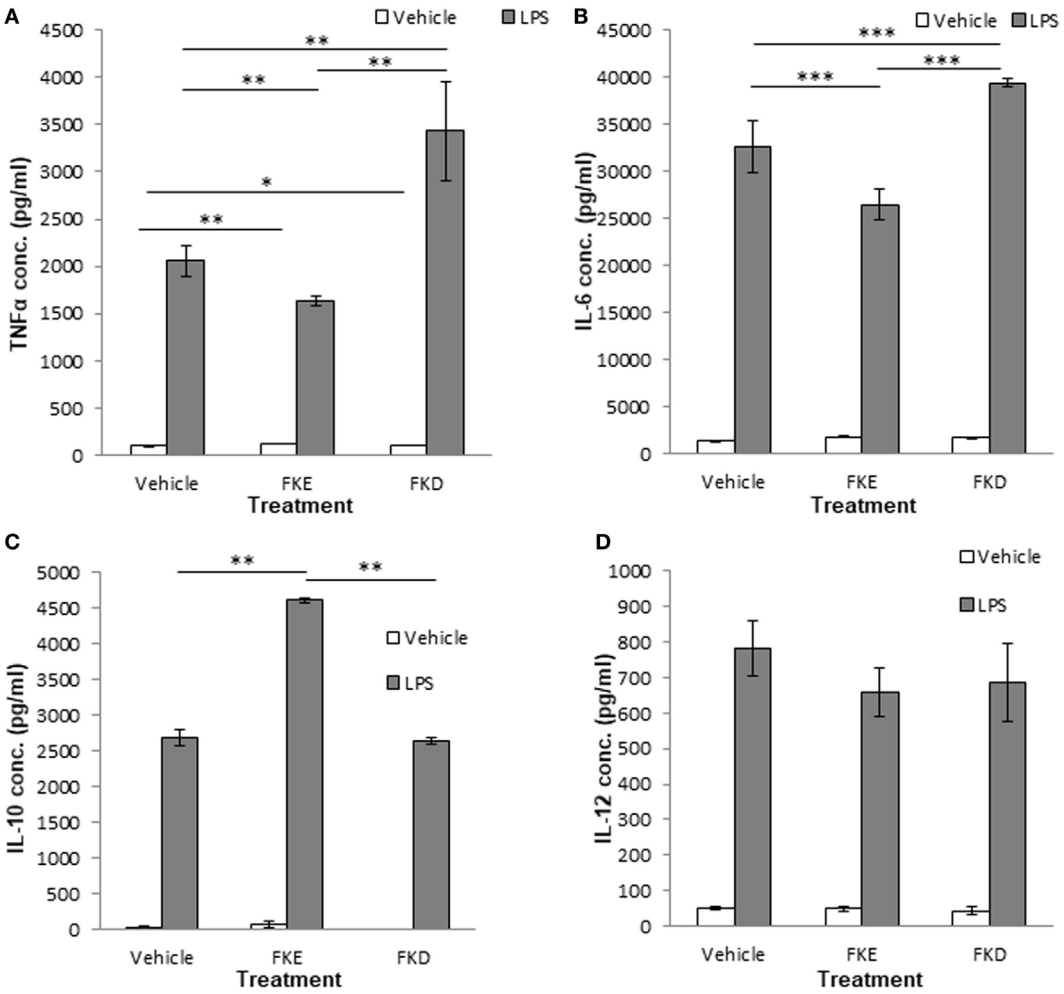


FIGURE 5 | FKE peptides promote macrophage reprogramming. Mice undergoing peritonitis for 48 h were injected intraperitoneally (i.p.) with PBS, FKE, or FKD peptides (50 μM each). After additional 24 h, peritoneal macrophages were isolated and incubated *ex vivo* with lipopolysaccharide (LPS) (1 μg/ml, 24 h) or vehicle. Then, culture media were collected and its content of tumor necrosis factor α (TNFα) **(A)**, interleukin (IL)-6 **(B)**, IL-10 **(C)**, and IL-12 **(D)** was determined by standard enzyme-linked immunosorbent assay. Results are representative **(A,D)** and averages ± SEM **(B,C)** from three experiments ($n = 4$ per group). ***/**/*indicate statistically significant differences of $P \leq 0.005$/$P \leq 0.01$/$P \leq 0.05$, respectively, by ANOVA with Tukey *post hoc* analysis.

neutrophil aggregation at low density, we determined whether Lf, Lf peptides (LFPs), or combinations of these agents also promote aggNETs formation. To this end, we added FKE or FKD peptides alone or together with full-length Lf to MSU crystals in NETs formation and aggregation assays. Our results show that treatment with FKE enhanced MSU-induced aggNETs formation at 100 μM, whereas FKD did it to a lower and nonstatistically significant manner (**Figure 6A**). Full-length Lf reduced MSU-induced aggNETs formation in a concentration-dependent (but not statistically significant) manner at 30–100 μM (**Figure 6B**). Surprisingly, this effect was enhanced by FKE and FKD peptides (at 100 μM) in a statistically significant manner (compared to MSU alone; **Figure 6B**). Notably, FKD (at 30 μM) and FKE (at 100 μM) modulated MSU-induced aggNETs formation in a significantly different manner than Lf (**Figure 6C**), suggesting that the fragmentation of Lf is necessary for it to enhance the resolution of inflammation through aggNETs formation. We conclude that LFP enhances aggNETs formation by human neutrophils and thus contributes to the resolution of inflammation.

DISCUSSION

Rapid engulfment of senescent PMN by macrophages during the resolution phase of inflammation causes the accumulation of stodgy cellular remnants in phagolysosomes that is congruent with the satiation of the engulfing macrophages (9). Macrophages have developed specific molecular mechanisms to cope with this burden (28). We hypothesized that Lf, a major neutrophil constituent that contains several proteolytic peptides with variable actions, can be processed during neutrophil apoptosis into bioactive fragments that accumulate in the engulfing macrophages. These will in turn be released and regulate both inflammation and its resolution. Since macrophages are emigrating from inflammatory and resolving tissues to remote sites (9, 23, 29), they can release Lf-derived products either locally or at their final destination. Our results in **Figure 1** indicate that a truncated form of Lf with 50 kDa is to be found in resolution phase macrophages and that the latter can acquire Lf from apoptotic PMN but not from engulfment of other apoptotic cells or phagocytic targets. Our results indicate that Lf and its fragments found in these macrophages are not expressed *de novo*, but rather accumulating following efferocytosis. The Lf is cleaved in either PMN or macrophages to yield smaller fragments of 23, 17, and 15 kDa, which can robustly be found in murine ISFs from spleen and inguinal LN and in the udder of cows inflicted by mastitis. Importantly, we also detected these Lf fragments in macrophages or immune cells collected at inflammatory sites. Of particular interest, the Lf fragments showed different kinetics. The 23- and 15-kDa fragments were associated with the inflammatory phase, while the 17-kDa fragment increased during the resolving phase of inflammation. Moreover, the levels of splenic 17-kDa fragment were reduced upon peritoneal macrophage depletion during the resolution

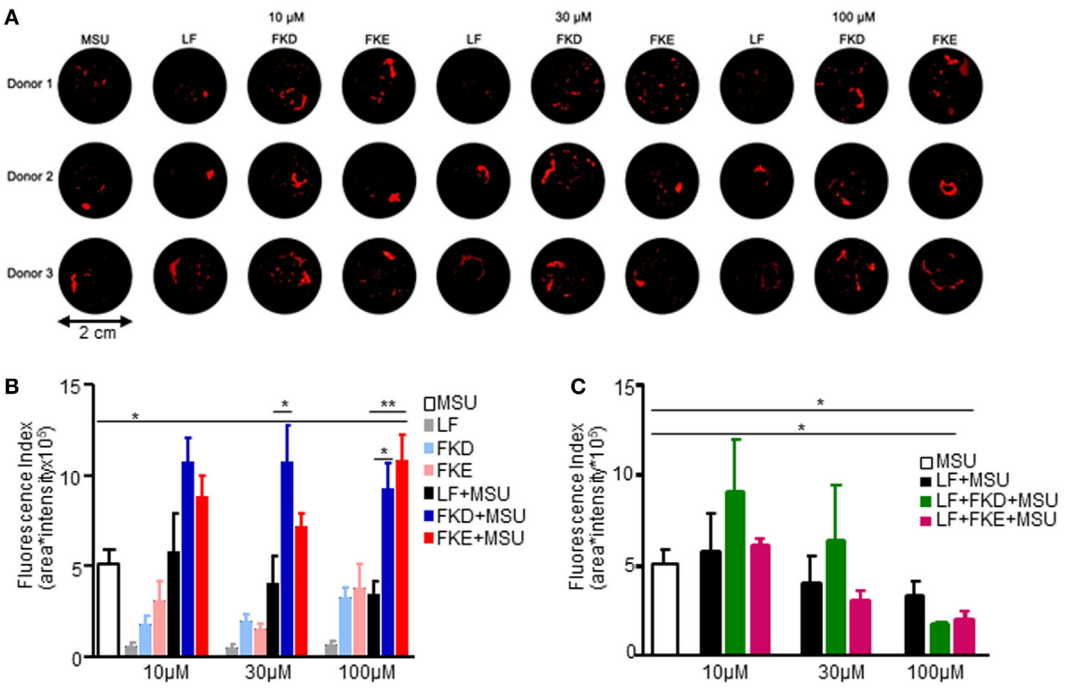


FIGURE 6 | Lactoferrin (Lf)-derived peptides induce aggregated neutrophil extracellular traps (aggNETs) formation. Human polymorphonuclear cells (PMN) from three healthy donors were freshly isolated from peripheral blood and seeded in a final cell density of 5×10^6 cells/ml. PMNs were incubated with 50 pg/cell monosodium urate crystals (MSU) and/or 10–100 μM Lf (LF) and/or 10–100 μM FKD or FKE peptides and 1 μg/ml propidium iodide solution. NET aggregation was stopped by fixation and aggNETs formed were filtrated through a 40-μM mesh. Macrophotographs with UVB transillumination were captured with a Nikon D700 reflex camera **(A)**. Averages ± SEM of fluorescence values from three independent donors of the images of control, MSU, and MSU + Lf **(B)** and MSU + FKD/FKE peptides at the indicated concentrations **(C)**. **/*indicate statistically significant differences of $P \leq 0.01$/$P \leq 0.05$, respectively, by ANOVA with Tukey *post hoc* analysis.

phase, whereas the levels of the 23-kDa fragment were increased. Thus, apoptotic PMN and efferocytic macrophages processed Lf, and the later cells released its fragments in a spatially and temporally regulated manner during the inflammatory responses. Since the inflammatory 23- and 15-kDa fragments of Lf were not found in apoptotic PMN, it is not clear whether they are generated by diversion of the proteolytic cascade in PMN that were engulfed, the efferocytic macrophages themselves or cleavage of secreted Lf at local or remote sites.

Notably, during bacterial infection, a Lf fragment with 22 kDa was previously described in bovine and human samples (19, 20). This fragment contained four peptides generated by the

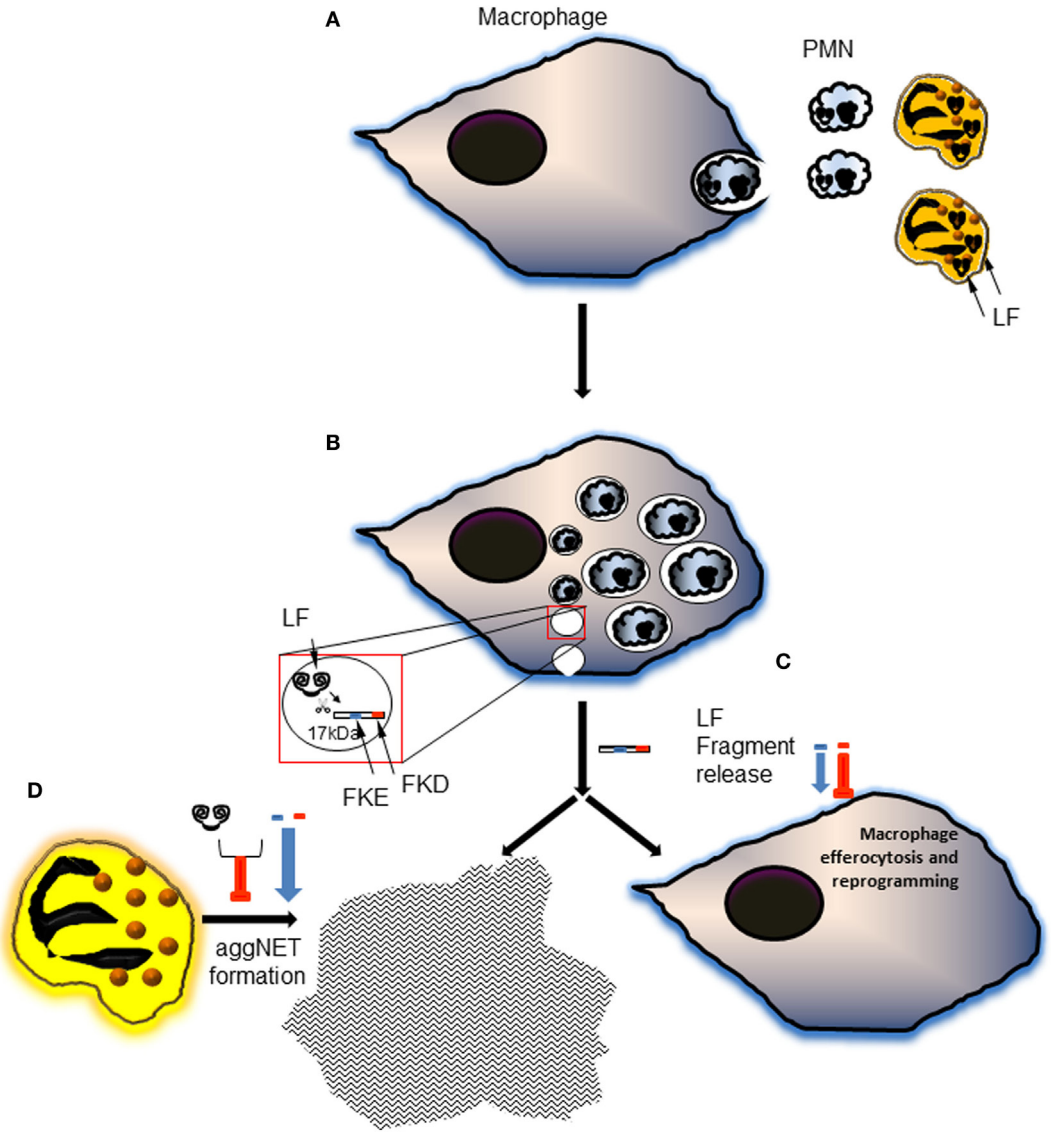


FIGURE 7 | A schematic illustration of the proposed model of generation and action of lactoferrin (Lf) fragments and peptides during the resolution of inflammation. **(A)** During inflammation and its resolution, neutrophils undergo apoptosis and get engulfed by macrophages. This process is accompanied by neutrophil elastase-mediated cleavage of Lf and generation of the 17-kDa fragment. **(B)** The engulfed polymorphonuclear cell (PMN) corpses traffic to the phagolysosome where most of their cellular components are hydrolyzed. Lf fragments are accumulating in resolution phase macrophages during the inflammatory and resolving phases of the response. 15- and 17-kDa fragments were produced during the inflammatory phase and the resolution of inflammation, respectively. The 17-kDa Lf fragment is released and possibly undergoes further processing to shorter peptides containing the tripeptides FKE and FKD. **(C)** Both peptides enhance macrophage conversion to the CD11b^{low} phenotype, whereas FKE peptides enhance macrophage efferocytosis *in vivo*. FKE peptides also promote macrophage reprogramming *in vivo* culminating in a reduced secretion of tumor necrosis factor α (TNFα) and interleukin (IL)-6, and an increased secretion of IL-10 upon exposure to LPS. **(D)** Lf peptides also promote the generation of pro-resolving aggregated neutrophil extracellular traps (aggNETs) in monosodium urate (MSU)-activated human neutrophils, while Lf fails to do so. Intriguingly, when combined with full-length Lf, Lf peptides enhance its inhibition of aggNETs formation following MSU exposure. Altogether, these findings suggest that Lf undergoes specific proteolytic processing to yield functional fragments that are released and "recycled". These fragments contain bioactive peptides with anti-inflammatory and pro-resolving properties that orchestrate the resolution of neutrophil-driven inflammation.

serine proteases elastase and proteinase 3. One of these peptides with the sequences PGQRDLLFKDSAL/SGQKDLLFKDSAI in bovine and human Lf, respectively, induced cytokine and chemokine secretion in epithelial cells. Another peptide present in human Lf, FKDCHLA, induced inflammatory cytokine secretion, while its bovine homolog FKECHLA was inactive. It seems that the FKD tripeptide present in the first three peptides might account for their activity while the replacement of aspartic acid (D) to glutamic acid (E) results in the abortion of the stimulatory activity. Hence, we examined whether FKE or FKD peptides can shift resolution indices *in vivo*. Our previous studies (9) showed that a distinct subset of pro-resolving macrophages designated $CD11b^{low}$ macrophages were converted from $CD11b^{high}$ ones upon satiated efferocytosis of apoptotic PMN. These macrophages produced reduced levels of inflammatory cytokines and increased levels of tumor growth factor β (TGFβ) in comparison to their $CD11b^{high}$ counterparts. Earlier studies have shown that the uptake of apoptotic cells by monocyte/macrophage leads to their reprogramming that is accompanied by a reduced inflammatory cytokine production and increased IL-10 and TGFβ secretion (30, 31). Our current results indicate that FKE, and to a lesser degree FKD, reduced macrophage numbers in the peritoneum while increasing the percentage of $CD11b^{low}$ macrophages (**Figure 3**). In addition, FKE peptides promoted efferocytosis of apoptotic PMN (**Figure 4**) and reduced TNFα and IL-6 secretion while increasing IL-10 secretion by resolution phase macrophages in response to LPS, while FKD peptides exerted opposite actions (**Figure 5**). Altogether, our findings suggest that peptides present within the resolution-associated fragment of Lf can modulate resolution phase macrophage reprogramming toward a pro-resolving phenotype, with FKE having superior actions to FKD.

Lactoferrin has previously been shown to enhance MSU-induced aggregation of neutrophils at a low cellular density in PBS (21), but to limit phorbol myristate acetate-induced NET formation due to its positively charged amino acids (32). These apparently conflicting results can be explained by the activity of Lf in different *in vitro* conditions. In the presence of culture media like RPMI, full-length Lf has no effect on the formation of aggNETs induced by MSU crystals. Importantly, the FKE peptide, and to a lesser degree FKD, enhanced the pro-resolving action of MSU in promoting aggNETs formation even in low neutrophil densities (**Figure 6**). Both peptides had a significantly different impact than the parent protein, but surprisingly exerted an inhibitory effect on aggNETs formation when applied together with full-length Lf. Thus, LFP promoted human neutrophil-mediated resolution of inflammation by enhancing the generation of aggNETs, while full-length Lf failed to do so. These findings suggest that Lf cleavage and disposal of its positive charge are essential for its promotion of aggNETs formation (see **Figure 7** for illustration).

In sum, the current report unveils the generation and release of Lf-derived fragments temporally changing during the initiation and resolution of inflammation. The fragment that is prevalent during the resolution phase contains bioactive peptides that promote pro-resolving actions of human neutrophils and macrophages most likely through binding to surface receptors and intracellular signaling. These findings improve our understanding of the molecular aspects of resolving inflammation and may lead to novel Lf-based therapies for inflammatory conditions.

DATA AVAILABILITY STATEMENT

The mass spectrometry proteomics data have been deposited to the ProteomeXchange Consortium *via* the PRIDE [1] partner repository with the dataset identifier PXD009190.

ETHICS STATEMENT

Experiments were approved by the Committee of Ethics, The Technion, authorization no. IL-065-04-2010.

AUTHOR CONTRIBUTIONS

AL isolated macrophages and ISF from murine peritonitis, and protein extracts from milk samples, *in vivo* LFP experiments, performed flow cytometry analysis, and drafted the manuscript. SS performed clodronate depletion, isolated fluids and cells, analyzed samples by flow cytometry and Western blotting, stained and scored for efferocytosis, and measured cytokine secretion. SS-Z assisted in various aspects of the experimental design and experimentation. OT performed Western blotting of milk samples. RR performed the senescent PMN engulfment assays. LM and MP performed the aggNETs experiments. LM, MH, and CS assisted in designing the aggNETs experiments and analyzing the results. AA designed the study, assisted in analyzing the data, and wrote the manuscript.

FUNDING

The study was partially funded by the Israel Science Foundation: grants No. 534/09 and No. 678/13, by the Rosetrees Trust and the Wolfson Family Charitable Trust, by the German Research Foundation (DFG) grants SFB1181-C3 and KFO257, and by Ardea Biosciences, Inc.

SUPPLEMENTARY MATERIAL

The Supplementary Material for this article can be found online at https://www.frontiersin.org/articles/10.3389/fimmu.2018.00644/full#supplementary-material.

FIGURE S1 | Senescent peritoneal neutrophils are primarily apoptotic with CXCR4 expression. Mice were injected with zymosan A (1 mg/mouse, i.p.), and neutrophils were isolated from peritoneal exudates at 4 h post-peritonitis initiation (PPI), and incubated with roscovitine (10 μM) or vehicle for 4–24 h. Next, the neutrophils were immunostained for FITC-annexin V and PE-CXCR4 and analyzed by flow cytometry. Results are representative dot plots **(A)** and averages ± SEM **(B)** from five to six independent experiments. ***/*indicate statistically significant differences of $P \leq 0.005$/$P \leq 0.05$, respectively, by ANOVA with Tukey *post hoc* analysis.

FIGURE S2 | Lactoferrin (Lf) fragment isolation and identification. Mastitis milk samples from dairy farms **(A,B)** were processed to separate the cellular and fat fractions from the aqueous fraction [**(C–F)**, see Section "Materials and Methods" for details] and to prepare them for isolation of Lf peptides. To reduce the amount of low-molecular weight constituents, the samples were dialyzed (cutoff of 12–14 kDa). Then, Lf fragments were isolated on heparin columns **(G,H)**. After

stepwise elution with increasing NaCl concentrations, the samples were run on sodium dodecyl sulfate-polyacrylamide gel electrophoresis (SDS-PAGE) and the gel was stained with Coomassie Blue **(I)**. Afterward, the 15- and 17-kDa bands were excised, digested, and analyzed by MS-MS mass spectrometry **(J,K)**. The peptides contained in the fragments were identified and aligned in comparison to full-length Lf from various species **(L)**. Adding quantitative properties of the MS-MS analysis and the known immunogenic epitope in both fragments allowed the determination of the fragment boundaries. The alignment of the various Lf species and the reports by Komine et al. allowed us to predict potentially bioactive peptides present in the 17-kDa fragment of bovine Lf. These peptides were synthesized and purchased from GL Biochem (Shanghai) Ltd. **(M)**.

FIGURE S3 | The 17- and 15-kDa fragments of lactoferrin (Lf) are absent in non-resolving and healthy dairy cow milk. Milk samples from none-resolving mastitis-inflicted dairy cows (days 1–4) or healthy (H) cows were separated into soluble and cellular fractions by centrifugation. The cellular fraction was lysed, and the cytoplasmic proteins were recovered. Equal amounts of protein from both fractions were analyzed by Western blotting for Lf. Results show representative blots from two sample sets taken daily from two different cows.

FIGURE S4 | Alignment of the identified lactoferrin (Lf)-derived fragments to full-length Lf originated from different species. Protein bands corresponding to the 15- and 17-kDa fragments of Lf were sequenced using trypsin cleavage and mass spectrometry analysis. The sequences of the resulting peptides were aligned and compared to full-length Lf from nine species: *Capra hircus*, *Equus caballus*, *Ovis aries*, *Sus scrofa*, *Camelus dromedarius*, *Bos indicus*, *Bos taurus*, *Homo sapiens*, and *Mus musculus*, using STRAP software. Highlighted in yellow and in bright purple are peptides corresponding to the 15- and 17-kDa fragments, respectively. Positions 1–19 of all sequences (excluding *E. caballus*) serve as a signal peptide, and therefore amino acid numbering starts from the 19th amino acid. Peptides produced by serine proteases and reported by Komine et al. (FKECHLA, VPSHAVVAR, FQLFGSP, and PGQRDLLFKDSAL from bovine Lf) are underlined. The sequences in the red frame indicate the minimal consensus sequences in the 17-kDa fragment that were predicted to be bioactive.

REFERENCES

1. Henson PM. Dampening inflammation. *Nat Immunol* (2005) 6:1179–81. doi:10.1038/ni1205-1179
2. Poon IK, Lucas CD, Rossi AG, Ravichandran KS. Apoptotic cell clearance: basic biology and therapeutic potential. *Nat Rev Immunol* (2014) 14:166–80. doi:10.1038/nri3607
3. Serhan CN, Savill J. Resolution of inflammation: the beginning programs the end. *Nat Immunol* (2005) 6:1191–7. doi:10.1038/ni1276
4. Rossi AG, Sawatzky DA, Walker A, Ward C, Sheldrake TA, Riley NA, et al. Cyclin-dependent kinase inhibitors enhance the resolution of inflammation by promoting inflammatory cell apoptosis. *Nat Med* (2006) 12:1056–64. doi:10.1038/nm1468
5. Ariel A, Serhan CN. New lives given by cell death: macrophage differentiation following their encounter with apoptotic leukocytes during the resolution of inflammation. *Front Immunol* (2012) 3:4. doi:10.3389/fimmu.2012.00004
6. Ortega-Gomez A, Perretti M, Soehnlein O. Resolution of inflammation: an integrated view. *EMBO Mol Med* (2013) 5:661–74. doi:10.1002/emmm.201202382
7. Hochreiter-Hufford A, Ravichandran KS. Clearing the dead: apoptotic cell sensing, recognition, engulfment, and digestion. *Cold Spring Harb Perspect Biol* (2013) 5:a008748. doi:10.1101/cshperspect.a008748
8. Tan BH, Meinken C, Bastian M, Bruns H, Legaspi A, Ochoa MT, et al. Macrophages acquire neutrophil granules for antimicrobial activity against intracellular pathogens. *J Immunol* (2006) 177:1864–71. doi:10.4049/jimmunol.177.3.1864
9. Schif-Zuck S, Gross N, Assi S, Rostoker R, Serhan CN, Ariel A. Saturated-efferocytosis generates pro-resolving CD11b(low) macrophages: modulation by resolvins and glucocorticoids. *Eur J Immunol* (2011) 41:366–79. doi:10.1002/eji.201040801
10. Ward PP, Paz E, Conneely OM. Multifunctional roles of lactoferrin: a critical overview. *Cell Mol Life Sci* (2005) 62:2540–8. doi:10.1007/s00018-005-5369-8
11. Iyer S, Lonnerdal B. Lactoferrin, lactoferrin receptors and iron metabolism. *Eur J Clin Nutr* (1993) 47:232–41.
12. Vogel HJ. Lactoferrin, a bird's eye view. *Biochem Cell Biol* (2012) 90:233–44. doi:10.1139/o2012-016
13. Van Snick JL, Masson PL. The binding of human lactoferrin to mouse peritoneal cells. *J Exp Med* (1976) 144:1568–80. doi:10.1084/jem.144.6.1568
14. Kobayashi S, Abe Y, Inanami O, Oda S, Yamauchi K, Hankanga C, et al. Oral administration of bovine lactoferrin upregulates neutrophil functions in a dog with familial beta2-integrin-related neutrophil dysfunction. *Vet Immunol Immunopathol* (2011) 143:155–61. doi:10.1016/j.vetimm.2011.05.027
15. Schryvers AB, Bonnah R, Yu RH, Wong H, Retzer M. Bacterial lactoferrin receptors. *Adv Exp Med Biol* (1998) 443:123–33. doi:10.1007/978-1-4757-9068-9_15
16. Bournazou I, Pound JD, Duffin R, Bournazos S, Melville LA, Brown SB, et al. Apoptotic human cells inhibit migration of granulocytes *via* release of lactoferrin. *J Clin Invest* (2009) 119:20–32. doi:10.1172/JCI36226
17. Bournazou I, Mackenzie KJ, Duffin R, Rossi AG, Gregory CD. Inhibition of eosinophil migration by lactoferrin. *Immunol Cell Biol* (2010) 88:220–3. doi:10.1038/icb.2009.86
18. Wakabayashi H, Takase M, Tomita M. Lactoferricin derived from milk protein lactoferrin. *Curr Pharm Des* (2003) 9:1277–87. doi:10.2174/1381612033454829
19. Komine Y, Kuroishi T, Kobayashi J, Aso H, Obara Y, Kumagai K, et al. Inflammatory effect of cleaved bovine lactoferrin by elastase on staphylococcal mastitis. *J Vet Med Sci* (2006) 68:715–23. doi:10.1292/jvms.68.715
20. Komine K, Kuroishi T, Ozawa A, Komine Y, Minami T, Shimauchi H, et al. Cleaved inflammatory lactoferrin peptides in parotid saliva of periodontitis patients. *Mol Immunol* (2007) 44:1498–508. doi:10.1016/j.molimm.2006.09.003
21. Schauer C, Janko C, Munoz LE, Zhao Y, Kienhofer D, Frey B, et al. Aggregated neutrophil extracellular traps limit inflammation by degrading cytokines and chemokines. *Nat Med* (2014) 20:511–7. doi:10.1038/nm.3547
22. Leppkes M, Maueroder C, Hirth S, Nowecki S, Gunther C, Billmeier U, et al. Externalized decondensed neutrophil chromatin occludes pancreatic ducts and drives pancreatitis. *Nat Commun* (2016) 7:10973. doi:10.1038/ncomms10973
23. Angsana J, Chen J, Liu L, Haller CA, Chaikof EL. Efferocytosis as a regulator of macrophage chemokine receptor expression and polarization. *Eur J Immunol* (2016) 46(7):1592–9. doi:10.1002/eji.201546262
24. Martin C, Burdon PC, Bridger G, Gutierrez-Ramos JC, Williams TJ, Rankin SM. Chemokines acting *via* CXCR2 and CXCR4 control the release of neutrophils from the bone marrow and their return following senescence. *Immunity* (2003) 19:583–93. doi:10.1016/S1074-7613(03)00263-2
25. Hebert A, Sayasith K, Senechal S, Dubreuil P, Lagace J. Demonstration of intracellular *Staphylococcus aureus* in bovine mastitis alveolar cells and macrophages isolated from naturally infected cow milk. *FEMS Microbiol Lett* (2000) 193:57–62. doi:10.1016/S0378-1097(00)00455-9
26. Sordillo LM, Streicher KL. Mammary gland immunity and mastitis susceptibility. *J Mammary Gland Biol Neoplasia* (2002) 7:135–46. doi:10.1023/A:1020347818725
27. Sugimoto MA, Ribeiro ALC, Costa BRC, Vago JP, Lima KM, Carneiro FS, et al. Plasmin and plasminogen induce macrophage reprogramming and regulate key steps of inflammation resolution *via* annexin A1. *Blood* (2017) 129:2896–907. doi:10.1182/blood-2016-09-742825
28. Park D, Han CZ, Elliott MR, Kinchen JM, Trampont PC, Das S, et al. Continued clearance of apoptotic cells critically depends on the phagocyte Ucp2 protein. *Nature* (2011) 477:220–4. doi:10.1038/nature10340
29. Bellingan GJ, Caldwell H, Howie SE, Dransfield I, Haslett C. *In vivo* fate of the inflammatory macrophage during the resolution of inflammation: inflammatory macrophages do not die locally, but emigrate to the draining lymph nodes. *J Immunol* (1996) 157:2577–85.
30. Voll RE, Herrmann M, Roth EA, Stach C, Kalden JR, Girkontaite I. Immunosuppressive effects of apoptotic cells. *Nature* (1997) 390:350–1. doi:10.1038/37022
31. Fadok VA, Bratton DL, Konowal A, Freed PW, Westcott JY, Henson PM. Macrophages that have ingested apoptotic cells *in vitro* inhibit proinflammatory

cytokine production through autocrine/paracrine mechanisms involving TGF-beta, PGE2, and PAF. *J Clin Invest* (1998) 101:890–8. doi:10.1172/JCI1112

32. Okubo K, Kamiya M, Urano Y, Nishi H, Herter JM, Mayadas T, et al. Lactoferrin suppresses neutrophil extracellular traps release in inflammation. *EBioMedicine* (2016) 10:204–15. doi:10.1016/j.ebiom.2016.07.012

Conflict of Interest Statement: The authors declare a potential conflict of interest and state it below. Patent applications in which AA, AL, and SS-Z are inventors were approved for the data presented in the manuscript: 1. Lactoferrin Fragments And Use Thereof (US 20140162377). 2. Synthetic Anti-Inflammatory Peptides and Use Thereof (WO 2014174517A1).

Copyright © 2018 Lutaty, Soboh, Schif-Zuck, Zeituni-Timor, Rostoker, Podolska, Schauer, Herrmann, Muñoz and Ariel. This is an open-access article distributed under the terms of the Creative Commons Attribution License (CC BY). The use, distribution or reproduction in other forums is permitted, provided the original author(s) and the copyright owner are credited and that the original publication in this journal is cited, in accordance with accepted academic practice. No use, distribution or reproduction is permitted which does not comply with these terms.

frontiers in Immunology

REVIEW
published: 04 January 2018
doi: 10.3389/fimmu.2017.01895

Monocytic Myeloid-Derived Suppressor Cells in Chronic Infections

Anca Dorhoi[1,2,3]* *and Nelita Du Plessis*[4]*

[1] Institute of Immunology, Bundesforschungsinstitut für Tiergesundheit, Friedrich-Loeffler-Institut (FLI), Insel Riems, Germany, [2] Faculty of Mathematics and Natural Sciences, University of Greifswald, Greifswald, Germany, [3] Department of Immunology, Max Planck Institute for Infection Biology, Berlin, Germany, [4] Division of Molecular Biology and Human Genetics, Department of Biomedical Sciences, Faculty of Medicine and Health Sciences, SAMRC Centre for Tuberculosis Research, DST and NRF Centre of Excellence for Biomedical TB Research, Stellenbosch University, Tygerberg, South Africa

OPEN ACCESS

Edited by:
Geanncarlo Lugo-Villarino, UMR5089 Institut de Pharmacologie et de Biologie Structurale (IPBS), France

Reviewed by:
Leslie Chavez-Galan, National Institute of Respiratory Diseases, Mexico
Simona Stäger, Institut national de la recherche scientifique (INRS), Canada
Prabir Ray, University of Pittsburgh School of Medicine, United States

***Correspondence:**
Anca Dorhoi
anca.dorhoi@fli.de;
Nelita Du Plessis
nelita@sun.ac.za

Specialty section:
This article was submitted to Microbial Immunology, a section of the journal Frontiers in Immunology

Received: 13 September 2017
Accepted: 11 December 2017
Published: 04 January 2018

Citation:
Dorhoi A and Du Plessis N (2018) Monocytic Myeloid-Derived Suppressor Cells in Chronic Infections. Front. Immunol. 8:1895. doi: 10.3389/fimmu.2017.01895

Heterogeneous populations of myeloid regulatory cells (MRC), including monocytes, macrophages, dendritic cells, and neutrophils, are found in cancer and infectious diseases. The inflammatory environment in solid tumors as well as infectious foci with persistent pathogens promotes the development and recruitment of MRC. These cells help to resolve inflammation and establish host immune homeostasis by restricting T lymphocyte function, inducing regulatory T cells and releasing immune suppressive cytokines and enzyme products. Monocytic MRC, also termed monocytic myeloid-derived suppressor cells (M-MDSC), are *bona fide* phagocytes, capable of pathogen internalization and persistence, while exerting localized suppressive activity. Here, we summarize molecular pathways controlling M-MDSC genesis and functions in microbial-induced non-resolved inflammation and immunopathology. We focus on the roles of M-MDSC in infections, including opportunistic extracellular bacteria and fungi as well as persistent intracellular pathogens, such as mycobacteria and certain viruses. Better understanding of M-MDSC biology in chronic infections and their role in antimicrobial immunity, will advance development of novel, more effective and broad-range anti-infective therapies.

Keywords: myeloid-derived suppressor cells, infection, inflammation, tuberculosis, human immunodeficiency virus, *Staphylococcus*, viral hepatitis

INTRODUCTION

Mononuclear myeloid cells encompass various phagocyte populations exerting distinct functions during infection. From progenitors and immature myeloid cells (IMC) to mature and polarized phagocytes, subsets of myeloid regulatory cells (MRC) have been described. These populations include regulatory dendritic cells (DCs), regulatory and alternatively activated macrophages (M2-like macrophages), tumor-associated macrophages (TAM), and a unique mixture of heterogeneous cells coined myeloid-derived suppressor cells (MDSC) (1). This nomenclature indicates their origin and ability to suppress T-cell immunity (2). MDSC comprise morphologically distinct subsets, monocyte-like [monocytic MDSC (M-MDSC)] and neutrophil-like (PMN-MDSC) cells. Phenotypically, M-MDSC are HLA-DR$^{-/low}$CD11b^{+}CD33$^{+/high}$CD14^{+}CD15^{-} in humans and Gr-1$^{dim/+}$CD11b^{+}Ly6C^{+}Ly6G^{-} in mice (2). Several studies report on CD11b^{+}Ly6C$^{+/dim}$Ly6G^{int} murine M-MDSC, a phenotype that requires further validation in additional disease models and

in-depth characterization (3, 4). These cells have biochemical features characteristic of the myeloid lineage, notably abundance of products downstream of arginase 1 (ARG1), inducible nitric oxide synthase (iNOS), indoleamine dioxygenase (IDO), and cyclooxygenase (COX1) (2, 5). Unequivocal phenotypic markers for MDSC have not been identified so far, implying that cells can only be classified as MDSC upon demonstration of their lymphocyte suppressive function. This suggests that MDSC are likely underreported, particularly in conditions characterized by expansion of myeloid cells such as in infectious diseases.

Most of the information on MDSC emerges from cancer research where MDSC are associated with poor disease outcome. However, reports on myeloid suppressor cells in infection date back four decades. "Natural suppressor" cells were identified in spleens of experimentally infected animals following systemic delivery of mycobacteria, notably the vaccine strain *Mycobacterium bovis* Bacille Calmette–Guérin (BCG) (6). Although research on suppressor cells in cancers has flourished since then, studies in infectious diseases lagged behind. Cancer and infection share several pathophysiological features, including the non-resolving inflammation (7), which often triggers emergency hematopoiesis and expansion of MDSC (8). Given such similarities and encouraged by progress made in cancer biology, recent investigations found MDSC in communicable diseases (9–12), uncovered their interactions with microbes and emphasized critical roles in disease pathogenesis. This review focuses on M-MDSC and discusses their genesis during infection as well as interactions with immune cells, elaborating on targets and mechanisms of suppression. We will mostly describe M-MDSC biology in infections caused by *M. tuberculosis*, *Staphylococcus aureus*, hepatitis viruses [hepatitis B virus (HBV), hepatitis C virus (HCV)], and human immunodeficiency viruses (HIV) and to a lesser extent fungi and parasites (**Box 1**). We will use the term MDSC to refer to the total MDSC population, without further subset phenotype characterization. For studies using monocytic subsets, within the MDSC pool, we will use the acronym M-MDSC.

BOX 1 | Chronic infections associated with monocytic myeloid-derived suppressor cells (M-MDSC).

Monocytic myeloid-derived suppressor cells have been reported in various infections caused by bacterial and viral agents, many of them causing diseases highly relevant for the public health. Key points about the pathogen and the respective disease are presented in the following. *M. tuberculosis* is a Gram-positive bacterium and represents the etiologic agent of human tuberculosis (TB). TB primarily affects the lungs of millions of people, and is among the top 10 causes of death worldwide (13). Infection with *M. tuberculosis* frequently leads to latent TB, bacteria being contained within tissue lesions, but not eliminated. Such individuals, estimated at one-third of global population, are at risk of developing active TB upon immune suppression. *S. aureus* is a Gram-positive bacterium that often colonizes the human skin and nose (14). It is the leading cause of skin and soft tissue infections, pneumonia, osteomyelitis, endocarditis, and septicemia. Such conditions can manifest as acute and often long-lasting, frequently nosocomial-associated diseases, which are often resistant to antibiotics. Increased antimicrobial resistance characterizes current clinical isolates of *M. tuberculosis* and *S. aureus*. This results in significant therapy failures and economic burdens because of refractoriness to canonical chemotherapy (15). HCV and HBV are single-stranded RNA (*Flaviviridae*) and double-stranded DNA (*Hepatdnaviridae*) viruses, respectively, which cause chronic infection of the liver leading to end-stage liver disease in the absence of therapy. Prevalence of HCV and HBV in human population is high, reaching 70 million and 250 million chronic cases, respectively (16). HIV, encompassing HIV-1 and HIV-2, are lentiviruses belonging to the *Retroviridae* family that cause the acquired-immune deficiency syndrome (AIDS). AIDS affects more than 35 million people worldwide and the virus causes lytic infection of immune cells, primarily CD4+ lymphocytes (17). Often AIDS leads to reactivation of latent TB and such a comorbidity results in high death tolls (13).

GENESIS OF M-MDSC IN INFECTIOUS DISEASES

Expansion of M-MDSC occurs in various infectious diseases. Accumulating evidence indicate that oncogenic viruses, including HBV (18) and HCV (19–22), retroviruses, notably HIV (23, 24), simian immunodeficiency virus (SIV) (25, 26), and mouse immunodeficiency virus LP-BM (27), as well as Gram-positive bacteria, such as mycobacteria (28–30), staphylococci (31–33), enterotoxigenic bacilli (34), and Gram-negative pathogens, such as klebsiellae (35), trigger generation of M-MDSC. Fluctuation of this MDSC subset during anti-infective therapy was demonstrated in patients undergoing canonical TB chemotherapy (29), further strengthening the notion that disease progression in chronic infections is associated with expansion of M-MDSC. For some microbes, precise microbial cues and corresponding host pathways triggering M-MDSC generation or reprogramming of monocytes into M-MDSC have been elucidated (**Figure 1**). However, to date, for most infections, expansion of M-MDSC is explained solely by generation of inflammatory mediators during the course of the disease. Cytokines (IL-1 family members, IL-6, TNF, IL-10), lipid mediators (prostaglandin E2, PGE2), and growth factors (GM-CSF) foster generation of M-MDSC by promoting emergency myelopoiesis, skewing differentiation of progenitors into monocytes and DCs (STAT3/STAT5 activation) and promoting survival of M-MDSC (TGF-β, MCL-1-related anti-apoptotic A1) (36–40) (**Figure 1**). Just like in cancer, M-MDSC and populations containing M-MDSC are detectable at the site of pathology; e.g., in infected lungs in TB (29, 30, 41), pneumonia caused by *Francisella tularensis* (42), and influenza A virus (43, 44), in liver during HBV infection (45, 46), in skin and prosthetic bone implants during *S. aureus* colonization (32, 47, 48), and systemically in AIDS and sepsis (23, 24, 49). M-MDSC have also been detected in bone marrow and spleen, e.g., in TB (50), indicating their origin.

Microbial Signatures and Microbial Sensors Trigger M-MDSC Genesis

Pathogen Sensors Involved in Generation of M-MDSC

Microbial signatures are detected by non-clonally distributed innate receptors termed pattern recognition receptors (PRR). PRR are grouped in families and the founder toll-like receptors (TLR) have been best characterized so far. TLR are present on the plasma membrane and within endosomes and are activated by diverse microbial structures, including lipids [e.g., TLR-4

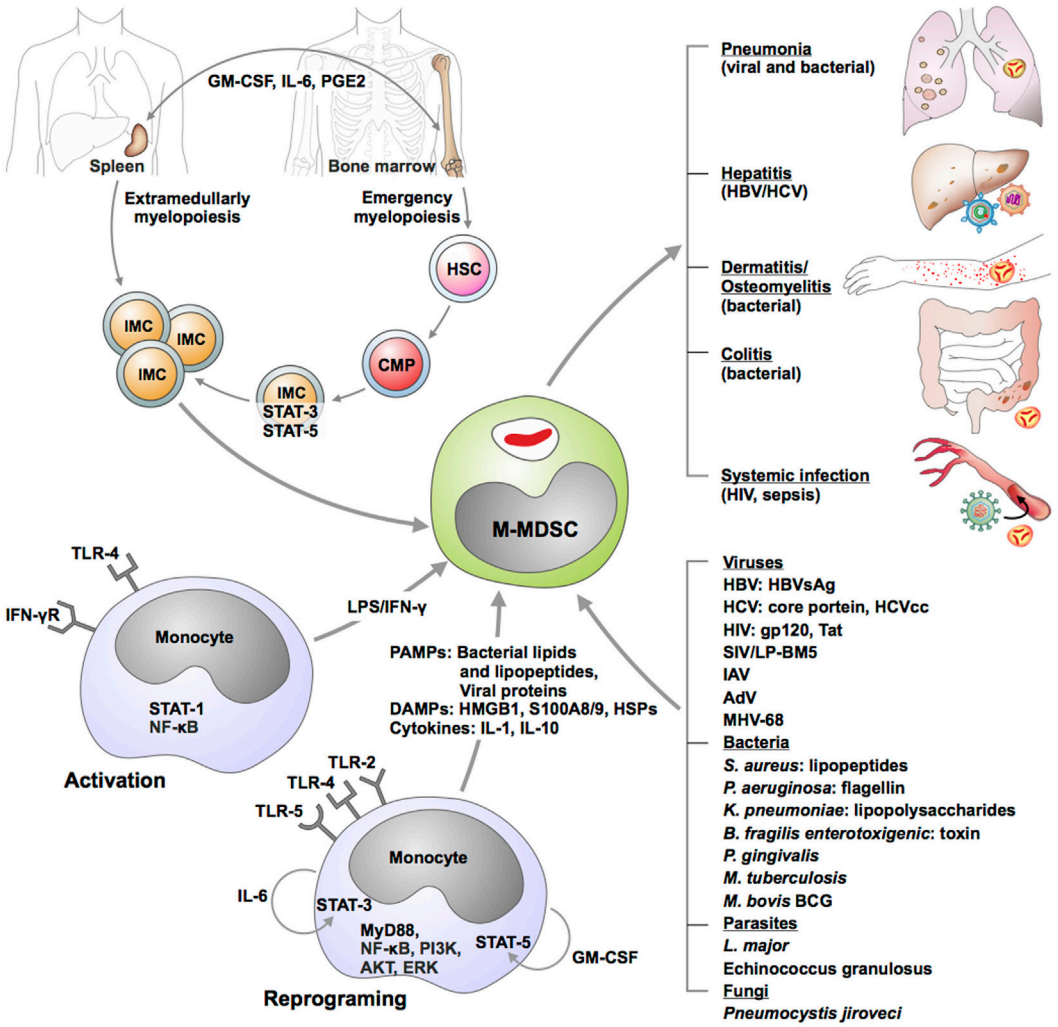


FIGURE 1 | Genesis of monocytic myeloid-derived suppressor cells (M-MDSC) during infectious diseases. Hypothetical models were derived from *ex vivo* results, correlative studies in animal models as well as clinical observations. Immature myeloid cells (IMC) are generated either in bone marrow or in spleen as a consequence of emergency myelopoiesis. Growth factors, cytokines, and lipids promote progression of hematopoietic stem cells (HSC) toward common myeloid progenitor (CMP) development and subsequent IMC genesis. Combination of cytokines as well as direct stimulation of selected microbial receptors by various microorganisms may activate or reprogram circulating monocytes toward M-MDSC. M-MDSC are recruited in various organs where they exert suppressive function and modulate manifestations and outcome of the disease. Abbreviations: AdV, adenovirus; AKT, protein kinase B; ERK, extracellular signal-regulated kinase; GM-CSF, granulocyte-macrophage colony stimulating factor; gp120, glycoprotein 120; HBV, hepatitis B virus; HBVsAg, HBV soluble antigen; HCV, hepatitis C virus; HIV, human immunodeficiency virus; IAV, influenza A virus; IFN-γ, interferon gamma; IL-6, interleukin 6; LPS, lipopolysaccharide; LP-BM5, virus murine acquired-immune deficiency syndrome (AIDS); MHV-68, murine herpesvirus 68; MyD88, myeloid differentiation primary response gene 88; NF-κB, nuclear factor "kappa-light-chain-enhancer" of activated B-cells; PI3K, phosphatidylinositide 3-kinase; PGE2, prostaglandin E2; STAT, signal transducer and activator of transcription; SIV, simian immunodeficiency virus; tat, trans-activator of transcription; TLR, toll-like receptor.

senses lipopolysaccharide (LPS)], lipoproteins (e.g., TLR-2 senses acylated peptides) and proteins (e.g., TLR-5 senses flagellin). Generally, microbial-derived cognates of TLR-2 and -4 induce M-MDSC (20, 32, 51–53). LPS, which is the major cell wall component of Gram-negative bacteria, triggers proliferation of HSC (40) and induces M-MDSC upon pulmonary instillation or subsequent infection with *Salmonella* spp. or *Klebsiella pneumonia* (35, 51). Stimulation of human monocytes with TLR-4 agonists reprograms the cells into M-MDSC in a process dependent on STAT-3 activation (54). Crosstalk between TLR/MyD88 and JAK2/STAT5 pathways following receptor activation by LPS and GM-CSF is critical for M-MDSC generation (35, 51). The adaptor MyD88, which converges signals from multiple TLR, has also been implicated in generation of MDSC during polymicrobial sepsis (55). TLR-4 appears dispensable for sepsis-induced suppression of T cells (55) thereby indicating that IL-1, which binds IL-1R upstream of MyD88, conditions MDSC differentiation.

Several bacterial and viral agonists of TLR-2 promote M-MDSC differentiation from monocytes and in certain instances precise signaling pathways have been identified. *S.*

aureus lipopeptides activate TLR2/6 dimers in skin cells for IL-6 production which in turn promote local MDSC accumulation (32). HCV reprograms monocytes into M-MDSC by stimulating TLR-2. More precisely, HCV core proteins or HCV cell culture-derived virions trigger TLR-2/PI3K/AKT/STAT3 pathway and this leads to cytokine production, notably IL-10 and TNF-α, and monocyte differentiation into MDSC (19–21). By contrast, TLR-3 ligation restricts HCV and LPS-induced M-MDSC differentiation (19, 52). Nonetheless, vesicular stomatitis virus activation of TLR-3 induces MDSC expansion (56). Alike TLR-3, TLR-7 activation by influenza virus blocks MDSC, including M-MDSC, accumulation in infected lungs (44). Both TLR-3 and -7 are located in endosomes. Whether signal compartmentalization, notably at the cell membrane or within endosomes, is critical for MDSC genesis remains to be established. Very little information exists on the roles of cytosolic PRR, such as nod-like receptors and AIM-like receptors, in monocyte reprogramming or M-MDSC generation. Moreover, many pathogens, notably mycobacteria, simultaneously stimulate multiple PRR (57) and the net outcome of such innate recognition on M-MDSC in TB awaits clarification.

Host alarmins that activate PRR have also been implicated in MDSC generation. S100A proteins, high-mobility-group-protein B1 and heat-shock proteins bind the receptor for advanced glycation products (RAGE), TLR-2, and TLR-4. In cancer and autoimmune diseases, these ligands have been associated with increased dynamics of MDSC, including M-MDSC (58–60). Just like microbial-derived PRR agonists, alarmins may induce cytokine release, such as IL-6 and subsequent autocrine or paracrine differentiation of immature mononuclear cells toward MDSC (61). In chronic infections, for instance, in TB patients, S100A8/9 proteins are abundant in the lung (62). These alarmins besides driving recruitment of MDSC (63) bind RAGE and subsequently upregulate ARG1, a key suppressive enzyme in M-MDSC (2). Since tissue damage often occurs during microbial insult, PRR stimulation by host-derived danger molecules along with microbial-derived agonists could contribute to the regulation of MRC. Similarly, synergy between microbial products, such as LPS, and inflammatory cytokines, notably IFN-γ, restricts differentiation of DCs and fosters genesis of M-MDSC in the bone marrow (64).

Microbial Factors Required for M-MDSC Genesis

For many microbes, the precise pathways required for M-MDSC genesis are not known. Mycobacteria induce accumulation of such cells irrespective of key virulence features, notably the type VII secretion system. M-MDSC have been reported for both *M. tuberculosis* and the vaccine BCG (29, 30, 50, 65). Mycobacterial glycolipids appear sufficient to induce these regulatory monocytes, as indicated by the presence of MDSC in animals inoculated with complete Freund's adjuvant (66). In contrast to mycobacteria, non-colitogenic bacteria and oncogenic gut species (*Fusobacterium nucleatum*, pks$^+$ *Escherichia coli*) do not trigger M-MDSC, whereas enterotoxigenic *Bacillus fragilis* employs the toxin to prime epithelial cells for IL-17 and M-MDSC expansion (34). HIV and SIV infection triggers accumulation of M-MDSC in the blood and their reduction in the bone marrow, which correlates with plasma viral loads and disease progression (25, 49). Several HIV viral factors promote expansion of the M-MDSC or reprogramming of monocytes. Human monocytes stimulated with HIV gp120 (23, 24) and/or with Tat proteins (54) acquire T-cell suppressive activity. This differentiation requires autocrine release of IL-6 and activation of STAT-3 (23, 54). HBV surface antigen similarly triggers differentiation of human monocytes toward M-MDSC in an autocrine manner depending on activation of the kinase ERK and the transcription factor STAT-3 (18). The necessity of specific kinases, such as ERK (18) and AKT (19, 20) for microbial-induced M-MDSC generation resembles kinase signatures of MDSC in cancer (67). Similarly, STAT-3 is required for M-MDSC in cancer (68) as well as during infection with HIV (23, 54), HCV (20, 22), and stimulation with bacterial LPS (54). For many bacterial (*Mycobacterium* spp., *F. tularensis*, *Porphyromonas gingivalis*) (29, 30, 42, 50, 69) and viral pathogens [vaccinia virus, lymphocoriomeningitis virus (LCMV), MCMV, murine gamma virus, LP-BM5] (70–72), and protozoa (*Leishmania* spp.)(73, 74), the host pathways or microbial signatures required for M-MDSC genesis are still undefined.

Inflammation Drives M-MDSC Generation during Infection

A common denominator in infection and cancer biology is the inflammation. Whereas physiological inflammation protects the host and restores homeostasis, in exuberant acute infections and chronic processes, inflammation often becomes pathologic and leads to disease manifestation. In such a scenario, inflammation-induced pathology becomes life-threatening. M-MDSC are primarily associated with chronic infections; however, they have been also reported in acute infectious diseases. Genesis of this myeloid regulatory subset is uncoupled from a specific phase of an infectious process. For instance, *F. tularensis* triggers IMC with M-MDSC features during acute, but not sub-acute, non-lethal infection (42). In polymicrobial sepsis M-MDSC are present early, as well as at late stages of sepsis, during the suppressive phase (55, 75). In infection with the LCMV, acute strains (Armstrong) do not induce M-MDSC, whereas chronic strains (Clone 13) induce suppressive myeloid cells (71).

Certain transcription factors and inflammatory mediators are critical for generation of MRC in infections. These requirements resemble those observed for MDSC in cancer (63). In sepsis, myeloid specific deletion of the myeloid differentiation-related transcription factor nuclear factor I-A, or deletion of the transcription factor C/EBPβ, result in reduction of MDSC, including M-MDSC (76, 77). Pro-inflammatory cytokines, notably IL-6, TNF-α, and IL-1, drive generation of MDSC in various infection models. In viral infections, including HIV (23) and HBV (18), IL-6 reprograms monocytes into suppressor cells. The same cytokine drives accumulation of M-MDSC in *S. aureus* skin infection and into the lungs subsequent to LPS instillations (32, 35). TNF promotes differentiation of MDSC in chronic inflammation (37, 78), likely through membrane expression of TNFR2, as shown in sterile inflammation (79). TNF signaling contributes to M-MDSC generation in HCV infection (19) and

regulates M-MDSC dynamics and activity also in murine mycobacterial infection (80). Besides cytokines, pro-inflammatory lipids such as the eicosanoid PGE2 are highly abundant in the TB-susceptible mouse strain C3HeB/FeJ (81) and these animals also accumulate M-MDSC (41). Interestingly, application of a COX2 inhibitor which lowers PGE2 levels rescues C3HeB/FeJ from TB lethality (81), thereby suggesting that this lipid may be critical for genesis of host-detrimental MDSC in TB. In addition, PGE2 positively regulates enzymatic pathways critical for the suppressive function of the MDSC, including iNOS, IDO1, and IL-10. COX2 crosstalks with the IL-1/IL-1R pathway, as well as with IFN I pathway, which has been revealed in TB and flu (82, 83). The positive cross-regulation between COX2 and IL-1 may affect M-MDSC genesis. IL-1/IL-1R pathway drives accumulation of M-MDSC in BCG-vaccinated mice (65). IL-1β also regulates PMN-MDSC generation by itself and during fungal disease (84). Activation of specific inflammasomes for release of bioactive IL-1β has not yet been related to MDSC induction during infectious diseases. However, the NLRP3 inflammasome drives MDSC accumulation in cancer (85). To what extent key inflammatory molecules, including IL-1β and the downstream inflammasome platforms, may affect generation and accumulation of M-MDSC in other chronic infections than TB remains to be established.

As a corollary, various stimuli trigger M-MDSC generation and expansion during microbial insult. Additional pathways will likely be uncovered as the research into M-MDSC in infection expands. Recent studies indicate that GM-CSF licenses monocytes for suppressive activity upon further stimulation with PRR agonists or cytokines (86). Such a two-step process likely occurs during infection. Furthermore, fate-mapping studies are imperative to elucidate whether bone marrow or extramedullary myelopoiesis are unique sites for M-MDSC expansion or whether this myeloid subset can self-maintain *in situ*, at the site of the infection. Furthermore, the signals triggering recruitment of M-MDSC at the site of the pathology require further elucidation. Panoply of chemokines and alarmins are generated during infection. These, along with factors known to drive MDSC accumulation in cancer may be essential for MDSC dynamics in infected tissue. For instance, both PGE2 and TGF-β upregulate CXCR2 and CXCR4 expression in M-MDSC in cancers and they may be critical for the accumulation of such cells toward CXCL12 or CCL2 gradients at the site of infection, as it has been demonstrated in tumors (63, 87–89).

M-MDSC IN PATHOPHYSIOLOGY OF CHRONIC INFECTIONS

M-MDSC Immunosuppressive Mechanisms and Cellular Interactions

Myeloid regulatory cells regulate host immunity through interaction with immune and non-immune cells (90) (**Figure 2**). This link is typically bi-directional: e.g., T-cells also regulate MRC expansion and activity, to induce tissue healing and remodeling (91, 92). Here, we describe current information on monocytic MDSC immunosuppressive machinery and interaction with archetypal immune cells (**Table 1**).

T Cells

Immunosuppression by MDSC has the potential to inhibit innate and adaptive immune cell activation, proliferation, viability, trafficking, and cytokine production. M-MDSC utilize a variety of suppressive mechanisms and likely differ in their ability to initiate antigen-specific versus non-specific suppression (126, 127). Each immune suppressive function is determined by the type of MRC, the microenvironmental components and the state of T-cell activation, favoring the probability that non-specific and antigen-specific suppressive mechanisms may coincide. Although not the focus of this review, as an example, PMN-MDSC can present peptides to T cells, but their low expression of major histocompatibility complex (MHC) II and costimulatory molecules, suggest they might only affect CD8 T-cell responses in an antigen-specific manner, as reported during retrovirus infection (128). This idea is supported by reports on MDSC-mediated inhibition of antigen-specific CD8 T-cell responses in tumors, likely due to the MHC I-restricted nature of cancer MDSC (2, 127, 129, 130). In infection, antigen-specific immunosuppression of CD8 T cells by M-MDSC is restricted to polymicrobial sepsis (131), HCV (21), HBV (46), murine encephalomyelitis virus (132), SIV and HIV infections (26), and LCMV infection (71). Data on the effect of MDSC on CD4 T helper cell (TH) subsets during infectious diseases are limited, but do exist as a result of the MHC-independent suppressive effects of MDSC in the context of HCV (21), HIV (24), and murine encephalomyelitis virus infection (132). During BCG-induced pleurisy, transmembrane TNF on M-MDSC restricts proliferation of CD4 T cells *via* interaction with lymphocyte-expressed TNFR2 (80). Results on MDSC interaction with TH17 and TH2 polarized CD4 T cells are contradictory and reports exist of mainly PMN-MDSC-mediated induction and suppression of TH17 responses in cancer, autoimmunity and infection (133–138), likely indicating that the combination of mediators present in the microenvironment determines the final outcome. In turn, TH1 and TH2 are involved in the expansion and activation of MDSC in cancer and also hepatitis (137, 139). Interestingly, recent findings suggest that CD1d-restricted natural killer T cells can convert immunosuppressive murine-MDSC into immune stimulating APCs following influenza virus infection, *via* their interaction with CD40 (140).

Regulatory T cells (Treg) are equally important components of the host immunoregulatory network. Data suggest reciprocal regulation of MDSC and Treg through mechanisms involving presence of IL-10, TGF-β, IL-4Rα, p47phox, PD-L1, TGF-β, and CD40–CD40L interactions, ARG1 induction and CCR-5-mediated recruitment (91, 126, 141–144). Interactions between total MDSC and Treg in cancer are well described (145, 146) with Treg depletion reducing MDSC immunosuppression by lowering their expression of PD-L1 and IL-10 production (147). Evidence of interaction in non-cancerous models, including type-1 diabetes, cardiac allograft and airway hyper-responsiveness, also exist (148–150). More specifically, the induction of Treg by M-MDSC, has also been described during HIV infection and shown to contribute to host immunosuppression (23, 49, 54). Data by O'Connor suggest reciprocal crosstalk between M-MDSC and Treg during LP-BM5-induced murine AIDS. Here, M-MDSC subsets display

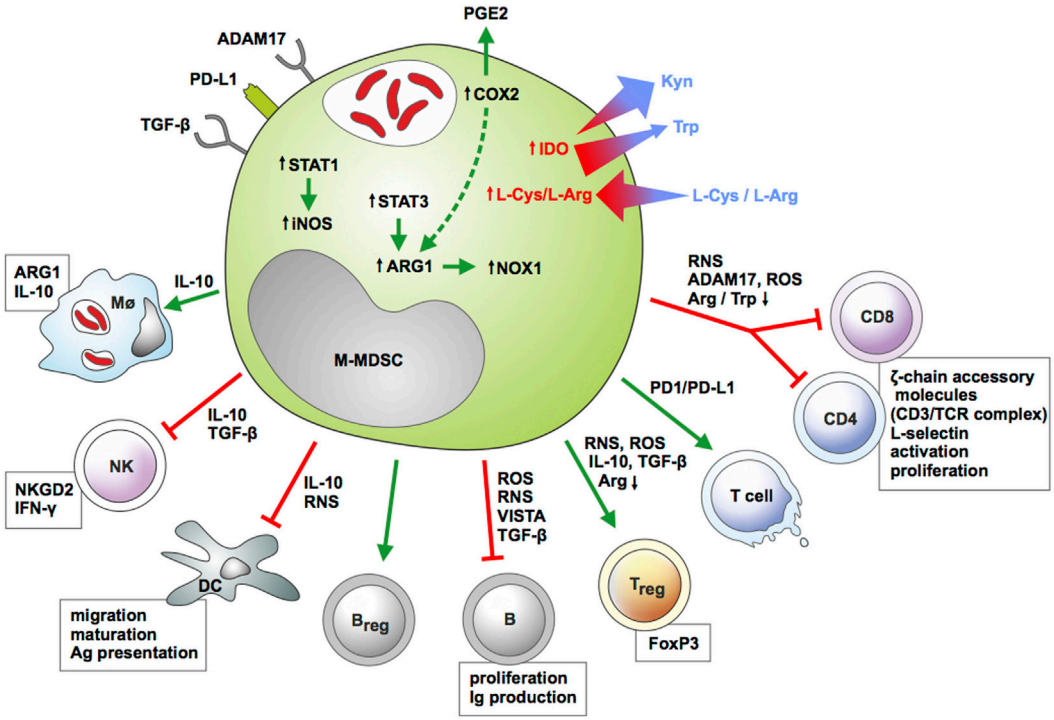


FIGURE 2 | Features of monocytic myeloid-derived suppressor cells (M-MDSC) and their interactions with immune cells during infection. M-MDSC express membrane-bound inhibitory receptors and upregulate enzymatic pathways [inducible nitric oxide synthase (iNOS), ARG1, COX2, IDO] conferring suppressive activity toward multiple myeloid and lymphoid cell subsets. The key function of M-MDSC is suppression of T-cell immunity. M-MDSC restrict proliferation and release of cytokines by effector CD4 and CD8 lymphocytes and induce apoptotic cell death in these cells. In addition, these myeloid regulatory cells induce regulatory T and B cells, while limiting antibody release and proliferation of conventional B cells. M-MDSC alter activity of NK cells and antigen-presenting cells (APCs) and induce polarization of macrophages toward a regulatory phenotype. Color-coded arrows indicate induction/activation (green) or suppression (red), and molecules employed by M-MDSC for such effects are highlighted. Size- and color-coded arrows indicate gradient fluxes for selected essential amino acids. Boxes indicate cellular functions or pathways modulated by M-MDSC. Abbreviations: ADAM17, ADAM metallopeptidase domain 17; ARG1, arginase 1; CD, cluster of differentiation; COX2, cyclooxygenase 2; DC, dendritic cell; IDO1, indoleamine dioxygenase 1; IFN-γ, interferon gamma; IL-10, interleukin 10; iNOS, inducible nitric oxide synthase; Kyn, kynurenine; L-Arg, L-arginine; L-Cys, L-cysteine; MΦ, macrophage; NK, natural killer cell; NKGD2, killer cell lectin like receptor K1; NOX1, NADPH oxidase 1; PGE2, prostaglandin E2, PD-L1, programmed-death ligand 1; RNS, reactive nitrogen species; ROS, reactive oxygen species; STAT, signal transducer and activator of transcription; TGF-β, transforming growth factor beta; Trp, tryptophan; VISTA, V-domain Ig suppressor of T-cell Activation.

differential suppression of T- and B-cells, thereby indicating functionally overlapping, but distinguishable, immunosuppressive effects (27, 95). Incubation of M-MDSC from peripheral blood of HIV-1-infected individuals, even those on antiretroviral therapy with undetectable viremia, with CD4 T cells from healthy individuals, significantly increased differentiation of Foxp3 Treg, whereas depletion of MDSC significantly increased IFN-γ production by CD4 T cells (54).

B Cells

Information on MDSC interaction with B-cells only recently started to accumulate. In autoimmune disease, M-MDSC inhibit B-cell proliferation and antibody production *via* an iNOS and a PGE2-induced pathway (151). However, opposing data demonstrated that the total MDSC population promotes proliferation and differentiation of immunoglobulin-A-producing immunosuppressive plasma B-cells *via* cell contact in mouse tumor models (152). In infectious diseases, M-MDSC suppressed B-cell responsiveness to retroviral infection in mice *via* iNOS and the negative immune checkpoint regulator V-domain Ig Suppressor of T-cell Activation (VISTA) (72, 93).

Myeloid Cells

Data on MDSC interaction with myeloid cells, such as DC, neutrophils, and macrophages in infectious diseases, are equally restricted, with reports mainly revealing that their inhibitory effects are exacerbated by cross-regulation with macrophages at tumor sites. In lung infections, such as *Pneumocystis* pneumonia (PcP), M-MDSC expressing PD-L1 are induced and impair alveolar macrophage (AM) phagocytic activity while increasing AM expression of PD-1 (153). MDSC interaction with neutrophils has been described in mice infected with *K. pneumoniae* or challenged with LPS, demonstrating that MDSC efferocytose infected, apoptotic neutrophils (35). Furthermore, M-MDSC suppress DC maturation, antigen uptake, migration, and TH1 cytokine production following administration of a DC vaccine for malignant melanoma (154). Similar findings were reported following LPS stimulation and in hepatocellular carcinoma,

TABLE 1 | Impact of monocytic myeloid-derived suppressor cells (M-MDSC) on infectious disease outcome and their immunosuppressive effects.

Microbial organism	Context of M-MDSC investigation	Major outcome; immunosuppressive effect	Reference
Viruses			
Immunodeficiency virus [human immunodeficiency viruse (HIV), simian immunodeficiency virus, LP-BM5]	M-MDSC and total MDSC	Host detrimental; suppress T-cell and B-cell responses, express inducible nitric oxide synthase (iNOS), and produce reactive oxygen species (ROS), ARG-1, IL-10, induce Treg	Gama et al. (26); Vollbrecht et al. (49); Qin et al. (24); Green et al. (93); Garg and Spector (23); Sui et al. (94); Wang et al. (54); O'Connor et al. (95); du Plessis et al. (28); Sui et al. (25); Garg et al. (96); Dross et al. (97)
Cytomegalovirus (CMV)	M-MDSC-like	Host detrimental; impair T-cell expansion, slowing viral clearance	Daley-Bauer et al. (70)
Hepatitis C virus (HCV)	M-MDSC and total MDSC	Host detrimental; suppress CD4 T-cell and NK cell function, increase Treg	Tacke et al. (21); Salem et al. (98); Zeng et al. (99); Nonnenman et al. (100); Ning et al. (101); Goh et al. (102); Ren et al. (22); Lei et al. (103); Pang et al. (19); Ren et al. (104)
Hepatitis B virus (HBV)	M-MDSC and total MDSC	Host detrimental; express IL-10, suppress T-cell function, promote disease chronicity	Chen et al. (45); Huang et al. (105); Kondo et al. (106)
Viral coinfection (HIV/CMV, HCV/HIV)		Host detrimental; impair T-cell function, accelerate disease progression	Lei et al. (103); Garg et al. (96); Tumino et al. (107)
Bacteria			
Staphylococcus aureus	M-MDSC and PMN-MDSC	Host detrimental; suppress T-cell function, express ARG-1, iNOS, IL-10, exacerbate disease, promote disease chronicity	Skabytska et al. (32); Heim et al. (108); Heim et al. (47, 48); Tebartz et al. (33); Peng et al. (31)
Francisella tularensis	Total MDSC	Host detrimental; reduced phagocytosis, reduced survival	Periasamy et al. (42)
Mycobacteria spp.	M-MDSC and total MDSC	Host beneficial/detrimental; suppress T-cell function; express ARG-1 and iNOS, impaired pathogen killing; TNF-dependent suppression of CD4 T cells	Dietlin et al. (109); Martino et al. (65); Obregón-Henao et al. (41); Knaul et al. (30); Tsiganov et al. (50); Yang et al. (110); du Plessis et al. (28); Chavez-Galan et al. (80)
Klebsiella pneumoniae	M-MDSC and PMN-MDSC	Host beneficial/detrimental; pro-resolving, express ARG-1, IL-10/impair phagocytosis/killing	Poe et al. (35); Ahn et al. (3); Chakraborty et al. (4)
Helicobacter pylori	M-MDSC	Host detrimental; suppress protective TH1 development.	Zhuang et al. (111)
Polymicrobial sepsis	M-MDSC and total MDSC	Host beneficial/detrimental; suppress T-cell function, express nitric oxide and pro-inflammatory cytokines (early) and ARG-1, IL-10, and TGF-β (late)	Delano et al. (55); Sander et al. (112); Brudecki et al. (75); McPeak et al. (76, 77)
Escherichia coli	M-MDSC	Host detrimental; suppress T-cell activation, innate immunity, impair bacterial uptake and increase disease severity, infection susceptibility	Bernsmeier et al. (52)
Protozoa			
Leishmania spp.	M-MDSC and total MDSC	Host beneficial/detrimental; species-specificity, suppress CD4 T-cell proliferation, improved killing of parasites	Pereira et al. (73); Schmid et al. (74); Ribeiro-Gomes et al. (113); Bandyopadhyay et al. (114); Hammami et al. (115)
Trypanosoma cruzi	M-MDSC and PMN-MDSC	Host beneficial/detrimental; dependent on MDSC subset, express ROS, NO, suppress CD8 T-cell proliferation	Goni et al. (116); Cuervo et al. (117); Arocena et al. (118)
Toxoplasma gondii	Total MDSC	Host protective; express NO, control parasite replication	Voisin et al. (119); Dunay et al. (120)
Helminths			
Schistosoma spp.	Total MDSC	Not evaluated; express ROS, suppress T-cell responses	Yang et al. (121)
Echinnococcus granulosus	Total MDSC	Not evaluated; association with increased Treg and impaired T-cell L-selectin	Pan et al. (122)
Nippostrongylus brasiliensis	M-MDSC and PMN-MDSC	Host beneficial/detrimental; dependent on MDSC subset, express TH2 cytokines, reduce parasite burden (PMN-MDSC)	Saleem et al. (123)
Heligmosomoides polygyrus bakeri	Total MDSC	Host detrimental; suppress CD4 T-cell proliferation, increase parasite burden, and promote chronic infection	Valanparambil et al. (124, 125)

M-MDSC are studied as a purified cell population or as part of the total MDSC population to measure their impact on the host control of infectious pathogens.

where both MDSC subsets reduced expression ofMHC II, stimulatory molecules on DC, and cytokine production (64, 155). It stands to reason that these MDSC-induced modifications, affecting DC-mediated activation of T cells and antigen uptake, could also be effective in infectious diseases and warrant further investigation.

Natural Killer (NK) Cells

Reports on MDSC-mediated impairment of NK cell function emanate mainly from the cancer field. NK cells are critical to the innate immune system, exhibit cytotoxic and cytolytic functions, and target pathogens and malignant cells. In tumors, M-MDSC and also a population containing M-MDSC, inhibit cytotoxic activity and cytokine production by NK cells through cell contact-dependent mechanisms involving membrane-bound TGF-β and NKp30 ligand (156–158). NK cell-mediated suppression by total HLA-DR^{lo}CD33^{+}CD11b^{lo} MDSC has also been reported in chronic HCV infection and it is mediated *via* an ARG1-dependent inhibition of mammalian target of rapamycin (102).

Kinetics, Interference with Immunity, and Impact on Disease Outcome

The immune inhibitory functions of M-MDSC have extensive consequences on disease outcome (**Table 1**). According to current understanding, the class of pathogen and the immune mediators present, collectively determine pathogen persistence versus clearance. M-MDSC have versatile roles in infection, with either beneficial or detrimental outcomes for the host depending on the pathogen and the course of infection. During long-lasting infections, MDSC may even exhibit dual roles depending on the disease stage. E.g., M-MDSC are host-protective in certain fulminant acute infections by restricting immunopathology (35, 112, 159). During late sepsis, the immature total MDSC population aggravates disease (76, 77, 160). M-MDSC may, however, be harmful in acute infection with intracellular microbes, notably francisellae (42). Alternatively, M-MDSC may be detrimental to the host, irrespective of the phase of the disease, as reported in AIDS (25). By limiting anti-viral immunity early, these regulatory monocytes foster disease progression, while provoking disease exacerbation during the chronic HIV infection.

Viruses

Viral infections are known for their induction of pro-inflammatory mediators associated with the generation of MDSC. E.g., M-MDSC are increased in both clinical and experimental viral infections, such as HIV, SIV, and LP-BM5 (25–27, 49, 93, 94). During these retroviral infections, increased levels of M-MDSC are likely detrimental to disease outcome and facilitate pathogen survival, when considering the TH1 immunosuppressive effect and correlation to viral load and CD4 T-cell count (24, 49, 54, 95). Interestingly, HIV infection-mediated expansion of M-MDSC in peripheral blood mononuclear cells may also negatively affect containment of other concurrent infections, as reported for cytomegalovirus (CMV) infection (96). Recruitment of M-MDSC-like cells were also reported for murine CMV mono-infection and shown to impair viral clearance (70). Information on MDSC in HCV infections has been variable, but largely provides evidence of unfavorable effects on host protective immunity (19, 22, 104). Increased MDSC frequencies positively correlate with HCV viral load and decreased CD8 T-cell function (21, 99). Reports show that elevated levels of immature Lin^{-}HLA-DR^{-}CD33^{+} CD11b^{+} MDSC, consisting of M-MDSC and PMN-MDSC, in chronic HCV-infected patients, decline following successful IFN-α treatment (98), while treatment-naive HCV-infected individuals show significantly increased liver- and circulating MDSC frequencies compared to treated and uninfected individuals (99, 161). Nonetheless, other *in vivo* investigations failed to show significant MDSC elevations or an association with viral load (100). Ning et al. also provided evidence of increased M-MDSC in HCV-infected patients; however, this was correlated with age and not viral load, suggesting that the immune response caused by viral replication, rather than the virus itself, is responsible for increased M-MDSC (101). HBV infections are also associated with induction of MDSC. HLA-DR$^{-/low}$CD14^{+} M-MDSC occur at higher frequency in peripheral blood of chronic HBV-infected patients and suppress HBV-specific CD8 T-cell cytotoxicity (105). Suppressive MDSC are also increased in murine HBV infection (45) and drive CD8 T-cell exhaustion *via* their crosstalk with γδT-cells (46). M-MDSC accumulate during viral coinfections, but frequencies appear to be similar with those observed in mono-infections (103). E.g., elevated number of MDSC were reported for HCV/HIV (103) and shown to regulate excessive IFN-γ production in HIV/CMV coinfected individuals (96).

Bacteria

Bacterial infections are often associated with excessive inflammation or low-grade chronic production of pro-inflammatory cytokines and chemokines known to induce the expansion and activation of MDSC. E.g., chronic *S. aureus* infection in mice is sustained by M-MDSC and PMN-MDSC expressing ARG1, iNOS, and IL-10 which foster an immunosuppressive environment and impair monocyte/macrophage responsiveness (33, 47, 48, 108). Similarly, during infections with intracellular bacteria, such as *F. tularensis,* MDSC frequencies correlate with the extent of tissue pathology, loss of pulmonary function, and host mortality (42). Several reports demonstrate that inoculation of mice with BCG or infection with *M. tuberculosis* induce M-MDSC that diminish pathogen control and promote disease lethality (50, 65, 109). Obregón-Henao provided new evidence, demonstrating accumulation of ARG1-producing MDSC in *M. tuberculosis*-infected mice (41). Similar findings were reported in human TB, with increased immunosuppressive M-MDSC in TB patients and individuals with recent exposure to TB patients (28, 110). More recently, a protective role of M-MDSC in early stages of BCG-induced pleurisy was reported (80). This effect has been linked to TNF-dependent suppression of CD4+ T-cell inflammation. MDSC were also highly induced following infection with a clinical isolate of multidrug-resistant *K. pneumoniae*. These M-MDSC express anti-inflammatory surface markers and displayed compromised phagocytic abilities (3). Impairment of IL-10 production from total MDSC inhibited resolution of *K. pneumoniae*-induced inflammation (4). *H. pylori*-mediated inflammation of the gastric mucosa also promoted an influx of M-MDSC that countered host protective TH1 immune responses (111). In addition, MDSC gradually increase after polymicrobial sepsis (75–77), with M-MDSC mainly promoting sepsis-induced mortality early during infection (75).

Fungi

TH17-polarized immunity is generally required for protection against fungal infections; however, fungi modulate host

immunity by inducing immunosuppressive MDSC which could also benefit the host by reducing hyperinflammatory responses (84). The majority of studies only report the induction of PMN-MDSC following infection with pathogenic fungi, such as *Candida albicans* and *Aspergillus fumigatus* (84, 162). In line with this, treatment of mice with yeast-derived antigens, such as β-glucan specific to dectin-1, reduced accumulation of PMN-MDSC but not M-MDSC and significantly decreased tumor burden (163).

Protozoa

Induction of potent TH1 immunity is generally sufficient to protect the host against debilitating protozoal expansion and pathology. While MDSC are typically detrimental to diseases requiring a robust host protective TH1 response, MDSC induction could in fact be beneficial during infections triggering inflammation-mediated tissue damage. For example, chronic and acute protozoan infections with *L. major* or *Trypanosoma cruzi*, mediate induction of M-MDSC which protect against pathology and parasite load, despite suppression of T-cell proliferation (73, 116, 118), although contradictory evidence have been reported (117). Similar results were shown in a mouse model of *Toxoplasma gondii* infection, where the total MDSC population induced hyporesponsiveness and were required for resistance against the pathogen (119). Corroborating work demonstrated that the absence of cells resembling total MDSC during acute *T. gondii* infection resulted in extensive intestinal necrosis due to the host TH1 inflammatory response (119, 120). More recent data on *L. donovani* provided evidence of the expansion of myeloid cells, likely a combination of M-MDSC and PMN-MDSC, in the spleens of infected BALB/c and C57BL/6 mice. These cells exhibit TH1 immunosuppressive features and their immunosuppressive capacity is reduced following soluble leishmanial antigen vaccination (114, 115).

Helminths

Helminths characteristically cause stable, long-term infections with severe host immunomodulatory consequences, such as triggering TH2 host immune polarization. Several helminth species and their excretory/secretory products induce accumulation of M-MDSC, including *Schistosoma* spp. (121), *Echinnococcus granulosus* (122), and *Nippostrongylus brasiliensis* (123). Important work in a mouse model of *Heligmosomoides polygyrus bakeri* infection revealed the induction of a MDSC subset, likely comprising M-MDSC and PMN-MDSC, with TH2 immunosuppressive capabilities that exacerbate infection and worm burden (124, 125). Another important consideration during helminth infections is the host protective effect of MDSC-mediated suppression of TH1 immunity and induction of TH2 immunity. E.g., MDSC mediate enhanced pathogen clearance in a model of *N. brasiliensis* infection, although this appears to be specific to the granulocytic subset and might increase host susceptibility to diseases requiring TH1 for protection (123).

Monocytic myeloid-derived suppressor cells have been investigated only in a number of infections. In some circumstances, this MRC subset emerges as a regulator of disease pathogenesis. Based on depletion studies in animal models and correlative studies in humans undergoing anti-infective therapy, M-MDSC have both host-destructive and -protective roles. They promote establishment and progression of HIV/SIV (24, 25, 49), LCMV (71), staphylococcal prosthetic complications (33, 48, 108), and TB (29, 30) (**Table 1**). On the contrary, several studies indicate that this MRC subset protects from immunopathology, particularly in certain acute bacterial infections (35) and in protozoal infection (73), but also at distinct stages of viral infection with vaccinia virus (164). In such circumstances, M-MDSC contribute to resolution of inflammation or prevent disease flares. Such dual roles may correlate with biology of M-MDSC, notably their interaction with pathogens.

Phagocytic M-MDSC Harboring Pathogens

Subcellular compartmentalization of microbes within M-MDSC, as well as how pathogens modulate cell death patterns or metabolic features of these monocytic cells have not been fully elucidated. Since MDSC are phagocytes, an alternative function of M-MDSC is as a reservoir for invading pathogens. Initial evidence of impaired pathogen elimination came from a mouse model showing that mycobacteria, notably BCG, are phagocytosed by $CD11b^{+}Ly6C^{int}Ly6G^{-}$ MDSC (65). Despite NO production, they were unable to kill *M. bovis* or the nonpathogenic *M. smegmatis* and suppressed T-cell activation. More recent data demonstrate that murine MDSC, induced following *M. tuberculosis* infection, display dose-dependent phagocytic and endocytic capabilities (30). Considering that *M. tuberculosis* survival in phagocytes is attributed to host-derived lipids, and since these serve as their primary carbon source *via* the glyoxylate shunt, it is tempting to speculate that MDSC provide niche for pathogen persistence. This assumption is supported by the finding that MDSC highly express complement receptor-3 CD11b and receptors for oxidized lipid (oxLDL)-uptake (CD36 and LOX-1) (165), which assist *M. tuberculosis* engulfment (166, 167). MDSC-resembling cells were shown to contain microbes, such as *Escherichia coli* and *L. major* (52, 55, 73, 113).

Other investigators report on defects in MDSC phagocytic potential under conditions of persistent stimulation or chronic inflammation (168). M-MDSC displayed reduced uptake of *F. tularensis* in comparison to naïve bone marrow-derived macrophages or AM (42) and poor phagocytic/killing potential of *K. pneumoniae* (3). MDSC may also impair the phagocytic potential of other innate cells. For example, the phagocytic ability of AM is significantly reduced in the presence of MDSC from PcP-infected mice. These adverse effects on AM are dependent on MDSC expressing PD-L1 and induction of PD-1 expression in AM during PcP infection (153, 169). Nonetheless, others failed to show any significant impact of MDSC on macrophage phagocytic potential (170).

Besides harboring bacterial pathogens, M-MDSC may support replication of viruses. Retroviruses, including SIV (25), LP-BM5 (93), and HIV (24) have been detected within this monocytic subset in macaques, mice, and humans, respectively. M-MDSC may traffic and interact with lymphocytes and thereby contribute to viral spread, besides limiting functionality of T lymphocytes.

CONCLUSION AND OUTLOOK

Many open questions and challenges for MDSC research remain. In particular, evidence on human MDSC subset characterization and their place in the spectrum of the myeloid lineage are still conflicting. In mice, TAM differentiation from M-MDSC may be accomplished to some extent based on positivity of TAM for F4/80 and their low or negative expression of Ly6C along with higher transcript levels for IRF8, M-CSF, and reduced ER-stress markers (2, 36, 171, 172). A detailed comparison between activated tissue macrophages and M-MDSC has not been conclusively conducted in infection. Lineage-tagging studies and phenotype stability are currently lacking and, therefore, tracing M-MDSC development in infection is either hypothetical or based on *ex vivo* observations and extrapolations from cancer models. Furthermore, a detailed understanding of the pathogen- and host-derived signals modulating MDSC induction and function will assist in the development of their therapeutic application. Specifically, the factors mediating suppression of host immunity in an antigen-specific manner need to be better understood to exploit drugs inhibiting MDSC in infections where these cells favor pathogen survival or limit optimal host responses. Moreover, pathogen responses, including stress and adaptation, to M-MDSC have not been investigated yet.

Although several therapeutic approaches involving re-purposed agents, mostly all-trans retinoic acid, effectively reverse MDSC immunosuppressive features in murine infection models of TB (30) and sepsis (173) as well as in few *ex vivo* human studies in HBV (18), comprehensive human clinical studies are required to systematically assess the safety, efficacy, dose, and timing of such interventions. Same rationale may improve vaccination in case of live vaccine, notably BCG and viral vector-based vaccines against HIV, known to trigger M-MDSC (65, 94). Furthermore, considering the diagnostic and prognostic potential of MDSC in the cancer field, these myeloid regulatory subsets should be considered for their potential role in biomarker development for infectious diseases.

AUTHOR CONTRIBUTIONS

All authors listed have made a substantial, direct, and intellectual contribution to the work, and approved it for publication.

ACKNOWLEDGMENTS

The authors thank Helga Keßler and Helena Kuivaniemi for the editorial assistance and Diane Schad for assistance with the graphics work. AD acknowledges the European Cooperation in Science and Technology program "Mye-EUNITER"; NDP acknowledges the "ICIDR" Biology and Biosignatures of Anti-Tuberculosis Treatment Response (NIH U01 AI115619).

REFERENCES

1. Gabrilovich DI, Bronte V, Chen SH, Colombo MP, Ochoa A, Ostrand-Rosenberg S, et al. The terminology issue for myeloid-derived suppressor cells. *Cancer Res* (2007) 67(1):425. doi:10.1158/0008-5472
2. Bronte V, Brandau S, Chen SH, Colombo MP, Frey AB, Greten TF, et al. Recommendations for myeloid-derived suppressor cell nomenclature and characterization standards. *Nat Commun* (2016) 7:12150. doi:10.1038/ncomms12150
3. Ahn D, Peñaloza H, Wang Z, Wickersham M, Parker D, Patel P, et al. Acquired resistance to innate immune clearance promotes *Klebsiella pneumoniae* ST258 pulmonary infection. *JCI Insight* (2016) 1(17):e89704. doi:10.1172/jci.insight.89704
4. Chakraborty K, Raundhal M, Chen BB, Morse C, Tyurina YY, Khare A, et al. The mito-DAMP cardiolipin blocks IL-10 production causing persistent inflammation during bacterial pneumonia. *Nat Commun* (2017) 8:13944. doi:10.1038/ncomms13944
5. Talmadge JE, Gabrilovich DI. History of myeloid-derived suppressor cells. *Nat Rev Cancer* (2013) 13(10):739–52. doi:10.1038/nrc3581
6. Bennett JA, Rao VS, Mitchell MS. Systemic bacillus Calmette-Guerin (BCG) activates natural suppressor cells. *Proc Natl Acad Sci U S A* (1978) 75(10):5142–4. doi:10.1073/pnas.75.10.5142
7. Nathan C, Ding A. Nonresolving inflammation. *Cell* (2010) 140(6):871–82. doi:10.1016/j.cell.2010.02.029
8. Strauss L, Sangaletti S, Consonni FM, Szebeni G, Morlacchi S, Totaro MG, et al. RORC1 regulates tumor-promoting "emergency" granulo-monocytopoiesis. *Cancer Cell* (2015) 28(2):253–69. doi:10.1016/j.ccell.2015.07.006
9. Ost M, Singh A, Peschel A, Mehling R, Rieber N, Hartl D. Myeloid-derived suppressor cells in bacterial infections. *Front Cell Infect Microbiol* (2016) 6:37. doi:10.3389/fcimb.2016.00037
10. Goh C, Narayanan S, Hahn YS. Myeloid-derived suppressor cells: the dark knight or the joker in viral infections? *Immunol Rev* (2013) 255(1):210–21. doi:10.1111/imr.12084
11. Ray A, Chakraborty K, Ray P. Immunosuppressive MDSCs induced by TLR signaling during infection and role in resolution of inflammation. *Front Cell Infect Microbiol* (2013) 3:52. doi:10.3389/fcimb.2013.00052
12. O'Connor MA, Rastad JL, Green WR. The role of myeloid-derived suppressor cells in viral infection. *Viral Immunol* (2017) 30(2):82–97. doi:10.1089/vim.2016.0125
13. WHO. *Global Tuberculosis Report 2016*. World Health Organization (2016). Available from: http://www.who.int/tb/publications/global_report/en/
14. Thammavongsa V, Kim HK, Missiakas D, Schneewind O. Staphylococcal manipulation of host immune responses. *Nat Rev Microbiol* (2015) 13(9):529–43. doi:10.1038/nrmicro3521
15. O'Neill J. *Tackling Drug-resistance Infections Globally: Final Report and Recommendations. Review on Antimicrobial Resistance*. (2016). Available from: https://amr-review.org/sites/default/files/160518_Final%20paper_with%20cover.pdf
16. WHO. *Global Hepatitis Report 2017*. World Health Organization (2017). Available from: http://www.who.int/hepatitis/publications/global-hepatitis-report2017/en/
17. WHO. *HIV/AIDS Fact Sheet*. World Health Organization (2017). Available from: http://www.who.int/mediacentre/factsheets/fs360/en/
18. Fang Z, Li J, Yu X, Zhang D, Ren G, Shi B, et al. Polarization of monocytic myeloid-derived suppressor cells by hepatitis B surface antigen is mediated via ERK/IL-6/STAT3 signaling feedback and restrains the activation of T cells in chronic hepatitis B virus infection. *J Immunol* (2015) 195(10):4873–83. doi:10.4049/jimmunol.1501362
19. Pang X, Song H, Zhang Q, Tu Z, Niu J. Hepatitis C virus regulates the production of monocytic myeloid-derived suppressor cells from peripheral blood mononuclear cells through PI3K pathway and autocrine signaling. *Clin Immunol* (2016) 164:57–64. doi:10.1016/j.clim.2016.01.014
20. Zhai N, Li H, Song H, Yang Y, Cui A, Li T, et al. Hepatitis C virus induces MDSCs-like monocytes through TLR2/PI3K/AKT/STAT3 signaling. *PLoS One* (2017) 12(1):e0170516. doi:10.1371/journal.pone.0170516
21. Tacke RS, Lee HC, Goh C, Courtney J, Polyak SJ, Rosen HR, et al. Myeloid suppressor cells induced by hepatitis C virus suppress T-cell responses through the production of reactive oxygen species. *Hepatology* (2012) 55(2):343–53. doi:10.1002/hep.24700
22. Ren JP, Zhao J, Dai J, Griffin JW, Wang L, Wu XY, et al. Hepatitis C virus-induced myeloid-derived suppressor cells regulate T-cell differentiation and

function via the signal transducer and activator of transcription 3 pathway. *Immunology* (2016) 148(4):377–86. doi:10.1111/imm.12616
23. Garg A, Spector SA. HIV type 1 gp120-induced expansion of myeloid derived suppressor cells is dependent on interleukin 6 and suppresses immunity. *J Infect Dis* (2014) 209(3):441–51. doi:10.1093/infdis/jit469
24. Qin A, Cai W, Pan T, Wu K, Yang Q, Wang N, et al. Expansion of monocytic myeloid-derived suppressor cells dampens T cell function in HIV-1-seropositive individuals. *J Virol* (2013) 87(3):1477–90. doi:10.1128/jvi.01759-12
25. Sui Y, Frey B, Wang Y, Billeskov R, Kulkarni S, McKinnon K, et al. Paradoxical myeloid-derived suppressor cell reduction in the bone marrow of SIV chronically infected macaques. *PLoS Pathog* (2017) 13(5):e1006395. doi:10.1371/journal.ppat.1006395
26. Gama L, Shirk EN, Russell JN, Carvalho KI, Li M, Queen SE, et al. Expansion of a subset of CD14highCD16negCCR2low/neg monocytes functionally similar to myeloid-derived suppressor cells during SIV and HIV infection. *J Leukoc Biol* (2012) 91(5):803–16. doi:10.1189/jlb.1111579
27. O'Connor MA, Fu WW, Green KA, Green WR. Subpopulations of M-MDSCs from mice infected by an immunodeficiency-causing retrovirus and their differential suppression of T- vs B-cell responses. *Virology* (2015) 485:263–73. doi:10.1016/j.virol.2015.07.020
28. du Plessis N, Jacobs R, Gutschmidt A, Fang Z, van Helden PD, Lutz MB, et al. Phenotypically resembling myeloid derived suppressor cells are increased in children with HIV and exposed/infected with *Mycobacterium tuberculosis*. *Eur J Immunol* (2017) 47(1):107–18. doi:10.1002/eji.201646658
29. du Plessis N, Loebenberg L, Kriel M, von Groote-Bidlingmaier F, Ribechini E, Loxton AG, et al. Increased frequency of myeloid-derived suppressor cells during active tuberculosis and after recent *Mycobacterium tuberculosis* infection suppresses T-cell function. *Am J Respir Crit Care Med* (2013) 188(6):724–32. doi:10.1164/rccm.201302-0249OC
30. Knaul JK, Jorg S, Oberbeck-Mueller D, Heinemann E, Scheuermann L, Brinkmann V, et al. Lung-residing myeloid-derived suppressors display dual functionality in murine pulmonary tuberculosis. *Am J Respir Crit Care Med* (2014) 190(9):1053–66. doi:10.1164/rccm.201405-0828OC
31. Peng KT, Hsieh CC, Huang TY, Chen PC, Shih HN, Lee MS, et al. *Staphylococcus aureus* biofilm elicits the expansion, activation and polarization of myeloid-derived suppressor cells in vivo and in vitro. *PLoS One* (2017) 12(8):e0183271. doi:10.1371/journal.pone.0183271
32. Skabytska Y, Wolbing F, Gunther C, Koberle M, Kaesler S, Chen KM, et al. Cutaneous innate immune sensing of toll-like receptor 2–6 ligands suppresses T cell immunity by inducing myeloid-derived suppressor cells. *Immunity* (2014) 41(5):762–75. doi:10.1016/j.immuni.2014.10.009
33. Tebartz C, Horst SA, Sparwasser T, Huehn J, Beineke A, Peters G, et al. A major role for myeloid-derived suppressor cells and a minor role for regulatory T cells in immunosuppression during *Staphylococcus aureus* infection. *J Immunol* (2015) 194(3):1100–11. doi:10.4049/jimmunol.1400196
34. Thiele Orberg E, Fan H, Tam AJ, Dejea CM, Destefano Shields CE, Wu S, et al. The myeloid immune signature of enterotoxigenic *Bacteroides fragilis*-induced murine colon tumorigenesis. *Mucosal Immunol* (2017) 10(2):421–33. doi:10.1038/mi.2016.53
35. Poe SL, Arora M, Oriss TB, Yarlagadda M, Isse K, Khare A, et al. STAT1-regulated lung MDSC-like cells produce IL-10 and efferocytose apoptotic neutrophils with relevance in resolution of bacterial pneumonia. *Mucosal Immunol* (2013) 6(1):189–99. doi:10.1038/mi.2012.62
36. Kumar V, Patel S, Tcyganov E, Gabrilovich DI. The nature of myeloid-derived suppressor cells in the tumor microenvironment. *Trends Immunol* (2016) 37(3):208–20. doi:10.1016/j.it.2016.01.004
37. Zhao X, Rong L, Zhao X, Li X, Liu X, Deng J, et al. TNF signaling drives myeloid-derived suppressor cell accumulation. *J Clin Invest* (2012) 122(11):4094–104. doi:10.1172/JCI64115
38. Sinha P, Clements VK, Fulton AM, Ostrand-Rosenberg S. Prostaglandin E2 promotes tumor progression by inducing myeloid-derived suppressor cells. *Cancer Res* (2007) 67(9):4507–13. doi:10.1158/0008-5472.CAN-06-4174
39. Haverkamp JM, Smith AM, Weinlich R, Dillon CP, Qualls JE, Neale G, et al. Myeloid-derived suppressor activity is mediated by monocytic lineages maintained by continuous inhibition of extrinsic and intrinsic death pathways. *Immunity* (2014) 41(6):947–59. doi:10.1016/j.immuni.2014.10.020
40. Massberg S, Schaerli P, Knezevic-Maramica I, Kollnberger M, Tubo N, Moseman EA, et al. Immunosurveillance by hematopoietic progenitor cells trafficking through blood, lymph, and peripheral tissues. *Cell* (2007) 131(5):994–1008. doi:10.1016/j.cell.2007.09.047
41. Obregón-Henao A, Henao-Tamayo M, Orme IM, Ordway DJ. Gr1intCD11b+ myeloid-derived suppressor cells in *Mycobacterium tuberculosis* infection. *PLoS One* (2013) 8(11):e80669. doi:10.1371/journal.pone.0080669
42. Periasamy S, Avram D, McCabe A, MacNamara KC, Sellati TJ, Harton JA. An immature myeloid/myeloid-suppressor cell response associated with necrotizing inflammation mediates lethal pulmonary tularemia. *PLoS Pathog* (2016) 12(3):e1005517. doi:10.1371/journal.ppat.1005517
43. De Santo C, Salio M, Masri SH, Lee LY, Dong T, Speak AO, et al. Invariant NKT cells reduce the immunosuppressive activity of influenza A virus-induced myeloid-derived suppressor cells in mice and humans. *J Clin Invest* (2008) 118(12):4036–48. doi:10.1172/jci36264
44. Jeisy-Scott V, Davis WG, Patel JR, Bowzard JB, Shieh WJ, Zaki SR, et al. Increased MDSC accumulation and Th2 biased response to influenza A virus infection in the absence of TLR7 in mice. *PLoS One* (2011) 6(9):e25242. doi:10.1371/journal.pone.0025242
45. Chen S, Akbar SM, Abe M, Hiasa Y, Onji M. Immunosuppressive functions of hepatic myeloid-derived suppressor cells of normal mice and in a murine model of chronic hepatitis B virus. *Clin Exp Immunol* (2011) 166(1):134–42. doi:10.1111/j.1365-2249.2011.04445.x
46. Kong X, Sun R, Chen Y, Wei H, Tian Z. γδT cells drive myeloid-derived suppressor cell-mediated CD8+ T cell exhaustion in hepatitis B virus-induced immunotolerance. *J Immunol* (2014) 193(4):1645–53. doi:10.4049/jimmunol.1303432
47. Heim CE, Vidlak D, Kielian T. Interleukin-10 production by myeloid-derived suppressor cells contributes to bacterial persistence during *Staphylococcus aureus* orthopedic biofilm infection. *J Leukoc Biol* (2015) 98(6):1003–13. doi:10.1189/jlb.4VMA0315-125RR
48. Heim CE, Vidlak D, Scherr TD, Hartman CW, Garvin KL, Kielian T. IL-12 promotes myeloid-derived suppressor cell recruitment and bacterial persistence during *Staphylococcus aureus* orthopedic implant infection. *J Immunol* (2015) 194(8):3861–72. doi:10.4049/jimmunol.1402689
49. Vollbrecht T, Stirner R, Tufman A, Roider J, Huber RM, Bogner JR, et al. Chronic progressive HIV-1 infection is associated with elevated levels of myeloid-derived suppressor cells. *AIDS* (2012) 26(12):F31–7. doi:10.1097/QAD.0b013e328354b43f
50. Tsiganov EN, Verbina EM, Radaeva TV, Sosunov VV, Kosmiadi GA, Nikitina IY, et al. Gr-1dimCD11b+ immature myeloid-derived suppressor cells but not neutrophils are markers of lethal tuberculosis infection in mice. *J Immunol* (2014) 192(10):4718–27. doi:10.4049/jimmunol.1301365
51. Arora M, Poe SL, Oriss TB, Krishnamoorthy N, Yarlagadda M, Wenzel SE, et al. TLR4/MyD88-induced CD11b+Gr-1 int F4/80+ non-migratory myeloid cells suppress Th2 effector function in the lung. *Mucosal Immunol* (2010) 3(6):578–93. doi:10.1038/mi.2010.41
52. Bernsmeier C, Triantafyllou E, Brenig R, Lebosse FJ, Singanayagam A, Patel VC, et al. CD14+CD15-HLA-DR- myeloid-derived suppressor cells impair antimicrobial responses in patients with acute-on-chronic liver failure. *Gut* (2017). doi:10.1136/gutjnl-2017-314184
53. Van Rompaey N, Le Moine A. Myeloid-derived suppressor cells: characterization and expansion in models of endotoxemia and transplantation. *Methods Mol Biol* (2011) 677:169–80. doi:10.1007/978-1-60761-869-0_12
54. Wang L, Zhao J, Ren JP, Wu XY, Morrison ZD, Elgazzar MA, et al. Expansion of myeloid-derived suppressor cells promotes differentiation of regulatory T cells in HIV-1+ individuals. *AIDS* (2016) 30(10):1521–31. doi:10.1097/qad.0000000000001083
55. Delano MJ, Scumpia PO, Weinstein JS, Coco D, Nagaraj S, Kelly-Scumpia KM, et al. MyD88-dependent expansion of an immature GR-1(+)CD11b(+) population induces T cell suppression and Th2 polarization in sepsis. *J Exp Med* (2007) 204(6):1463–74. doi:10.1084/jem.20062602
56. Liu C, Zhang C, Lu H, Cai J, Wang Z, Chen J, et al. Poly(I:C) induce bone marrow precursor cells into myeloid-derived suppressor cells. *Mol Cell Biochem* (2011) 358(1–2):317–23. doi:10.1007/s11010-011-0982-3
57. Dorhoi A, Kaufmann SH. Perspectives on host adaptation in response to *Mycobacterium tuberculosis*: modulation of inflammation. *Semin Immunol* (2014) 26(6):533–42. doi:10.1016/j.smim.2014.10.002
58. Bunt SK, Clements VK, Hanson EM, Sinha P, Ostrand-Rosenberg S. Inflammation enhances myeloid-derived suppressor cell cross-talk by

signaling through toll-like receptor 4. *J Leukoc Biol* (2009) 85(6):996–1004. doi:10.1189/jlb.0708446
59. Cheng P, Corzo CA, Luetteke N, Yu B, Nagaraj S, Bui MM, et al. Inhibition of dendritic cell differentiation and accumulation of myeloid-derived suppressor cells in cancer is regulated by S100A9 protein. *J Exp Med* (2008) 205(10):2235–49. doi:10.1084/jem.20080132
60. Thaxton JE, Liu B, Zheng P, Liu Y, Li Z. Deletion of CD24 impairs development of heat shock protein gp96-driven autoimmune disease through expansion of myeloid-derived suppressor cells. *J Immunol* (2014) 192(12):5679–86. doi:10.4049/jimmunol.1302755
61. Chalmin F, Ladoire S, Mignot G, Vincent J, Bruchard M, Remy-Martin JP, et al. Membrane-associated Hsp72 from tumor-derived exosomes mediates STAT3-dependent immunosuppressive function of mouse and human myeloid-derived suppressor cells. *J Clin Invest* (2010) 120(2):457–71. doi:10.1172/jci40483
62. Gopal R, Monin L, Torres D, Slight S, Mehra S, McKenna KC, et al. S100A8/A9 proteins mediate neutrophilic inflammation and lung pathology during tuberculosis. *Am J Respir Crit Care Med* (2013) 188(9):1137–46. doi:10.1164/rccm.201304-0803OC
63. Gabrilovich DI, Ostrand-Rosenberg S, Bronte V. Coordinated regulation of myeloid cells by tumours. *Nat Rev Immunol* (2012) 12(4):253–68. doi:10.1038/nri3175
64. Greifenberg V, Ribechini E, Rossner S, Lutz MB. Myeloid-derived suppressor cell activation by combined LPS and IFN-gamma treatment impairs DC development. *Eur J Immunol* (2009) 39(10):2865–76. doi:10.1002/eji.200939486
65. Martino A, Badell E, Abadie V, Balloy V, Chignard M, Mistou MY, et al. Mycobacterium bovis bacillus Calmette-Guerin vaccination mobilizes innate myeloid-derived suppressor cells restraining in vivo T cell priming via IL-1R-dependent nitric oxide production. *J Immunol* (2010) 184(4):2038–47. doi:10.4049/jimmunol.0903348
66. Wang Z, Jiang J, Li Z, Zhang J, Wang H, Qin Z. A myeloid cell population induced by Freund adjuvant suppresses T-cell-mediated antitumor immunity. *J Immunother* (2010) 33(2):167–77. doi:10.1097/CJI.0b013e3181bed2ba
67. Gato-Canas M, Martinez de Morentin X, Blanco-Luquin I, Fernandez-Irigoyen J, Zudaire I, Liechtenstein T, et al. A core of kinase-regulated interactomes defines the neoplastic MDSC lineage. *Oncotarget* (2015) 6(29):27160–75. doi:10.18632/oncotarget.4746
68. Gabrilovich DI, Nagaraj S. Myeloid-derived suppressor cells as regulators of the immune system. *Nat Rev Immunol* (2009) 9(3):162–74. doi:10.1038/nri2506
69. Su L, Xu Q, Zhang P, Michalek SM, Katz J. Phenotype and function of myeloid-derived suppressor cells induced by *Porphyromonas gingivalis* infection. *Infect Immun* (2017) 85(8):e00213-17. doi:10.1128/IAI.00213-17
70. Daley-Bauer LP, Wynn GM, Mocarski ES. Cytomegalovirus impairs antiviral CD8+ T cell immunity by recruiting inflammatory monocytes. *Immunity* (2012) 37(1):122–33. doi:10.1016/j.immuni.2012.04.014
71. Norris BA, Uebelhoer LS, Nakaya HI, Price AA, Grakoui A, Pulendran B. Chronic but not acute virus infection induces sustained expansion of myeloid suppressor cell numbers that inhibit viral-specific T cell immunity. *Immunity* (2013) 38(2):309–21. doi:10.1016/j.immuni.2012.10.022
72. Rastad JL, Green WR. Myeloid-derived suppressor cells in murine AIDS inhibit B-cell responses in part via soluble mediators including reactive oxygen and nitrogen species, and TGF-beta. *Virology* (2016) 499:9–22. doi:10.1016/j.virol.2016.08.031
73. Pereira WF, Ribeiro-Gomes FL, Guillermo LV, Vellozo NS, Montalvao F, Dosreis GA, et al. Myeloid-derived suppressor cells help protective immunity to *Leishmania major* infection despite suppressed T cell responses. *J Leukoc Biol* (2011) 90(6):1191–7. doi:10.1189/jlb.1110608
74. Schmid M, Zimara N, Wege AK, Ritter U. Myeloid-derived suppressor cell functionality and interaction with *Leishmania major* parasites differ in C57BL/6 and BALB/c mice. *Eur J Immunol* (2014) 44(11):3295–306. doi:10.1002/eji.201344335
75. Brudecki L, Ferguson DA, McCall CE, El Gazzar M. Myeloid-derived suppressor cells evolve during sepsis and can enhance or attenuate the systemic inflammatory response. *Infect Immun* (2012) 80(6):2026–34. doi:10.1128/IAI.00239-12
76. McPeak MB, Youssef D, Williams DA, Pritchett C, Yao ZQ, McCall CE, et al. Myeloid cell-specific knockout of NFI-A improves sepsis survival. *Infect Immun* (2017) 85(4):e00066-17. doi:10.1128/IAI.00066-17
77. McPeak MB, Youssef D, Williams DA, Pritchett CL, Yao ZQ, McCall CE, et al. Frontline science: myeloid cell-specific deletion of Cebpb decreases sepsis-induced immunosuppression in mice. *J Leukoc Biol* (2017) 102(2):191–200. doi:10.1189/jlb.4HI1216-537R
78. Sade-Feldman M, Kanterman J, Ish-Shalom E, Elnekave M, Horwitz E, Baniyash M. Tumor necrosis factor-alpha blocks differentiation and enhances suppressive activity of immature myeloid cells during chronic inflammation. *Immunity* (2013) 38(3):541–54. doi:10.1016/j.immuni.2013.02.007
79. Polz J, Remke A, Weber S, Schmidt D, Weber-Steffens D, Pietryga-Krieger A, et al. Myeloid suppressor cells require membrane TNFR2 expression for suppressive activity. *Immun Inflamm Dis* (2014) 2(2):121–30. doi:10.1002/iid3.19
80. Chavez-Galan L, Vesin D, Uysal H, Blaser G, Benkhoucha M, Ryffel B, et al. Transmembrane tumor necrosis factor controls myeloid-derived suppressor cell activity via TNF receptor 2 and protects from excessive inflammation during BCG-induced pleurisy. *Front Immunol* (2017) 8:999. doi:10.3389/fimmu.2017.00999
81. Vilaplana C, Marzo E, Tapia G, Diaz J, Garcia V, Cardona PJ. Ibuprofen therapy resulted in significantly decreased tissue bacillary loads and increased survival in a new murine experimental model of active tuberculosis. *J Infect Dis* (2013) 208(2):199–202. doi:10.1093/infdis/jit152
82. Coulombe F, Divangahi M. Targeting eicosanoid pathways in the development of novel anti-influenza drugs. *Expert Rev Anti Infect Ther* (2014) 12(11):1337–43. doi:10.1586/14787210.2014.966082
83. Mayer-Barber KD, Andrade BB, Oland SD, Amaral EP, Barber DL, Gonzales J, et al. Host-directed therapy of tuberculosis based on interleukin-1 and type I interferon crosstalk. *Nature* (2014) 511(7507):99–103. doi:10.1038/nature13489
84. Rieber N, Singh A, Oz H, Carevic M, Bouzani M, Amich J, et al. Pathogenic fungi regulate immunity by inducing neutrophilic myeloid-derived suppressor cells. *Cell Host Microbe* (2015) 17(4):507–14. doi:10.1016/j.chom.2015.02.007
85. van Deventer HW, Burgents JE, Wu QP, Woodford RM, Brickey WJ, Allen IC, et al. The inflammasome component NLRP3 impairs antitumor vaccine by enhancing the accumulation of tumor-associated myeloid-derived suppressor cells. *Cancer Res* (2010) 70(24):10161–9. doi:10.1158/0008-5472.CAN-10-1921
86. Ribechini E, Hutchinson JA, Hergovits S, Heuer M, Lucas J, Schleicher U, et al. Novel GM-CSF signals via IFN-γR/IRF-1 and AKT/mTOR license monocytes for suppressor function. *Blood* (2017) 1:947–60. doi:10.1182/bloodadvances.2017006858
87. Condamine T, Ramachandran I, Youn JI, Gabrilovich DI. Regulation of tumor metastasis by myeloid-derived suppressor cells. *Annu Rev Med* (2015) 66:97–110. doi:10.1146/annurev-med-051013-052304
88. Yang L, Huang J, Ren X, Gorska AE, Chytil A, Aakre M, et al. Abrogation of TGF beta signaling in mammary carcinomas recruits Gr-1+CD11b+ myeloid cells that promote metastasis. *Cancer Cell* (2008) 13(1):23–35. doi:10.1016/j.ccr.2007.12.004
89. Zhang H, Li Z, Wang L, Tian G, Tian J, Yang Z, et al. Critical role of myeloid-derived suppressor cells in tumor-induced liver immune suppression through inhibition of NKT cell function. *Front Immunol* (2017) 8:129. doi:10.3389/fimmu.2017.00129
90. Zhang S, Ma X, Zhu C, Liu L, Wang G, Yuan X. The role of myeloid-derived suppressor cells in patients with solid tumors: a meta-analysis. *PLoS One* (2016) 11(10):e0164514. doi:10.1371/journal.pone.0164514
91. Lee C-R, Kwak Y, Yang T, Han JH, Park S-H, Ye MB, et al. Myeloid-derived suppressor cells are controlled by regulatory T cells via TGF-β during murine colitis. *Cell Rep* (2016) 17(12):3219–32. doi:10.1016/j.celrep.2016.11.062
92. Pinton L, Solito S, Damuzzo V, Francescato S, Pozzuoli A, Berizzi A, et al. Activated T cells sustain myeloid-derived suppressor cell-mediated immune suppression. *Oncotarget* (2016) 7(2):1168–84. doi:10.18632/oncotarget.6662
93. Green KA, Cook WJ, Green WR. Myeloid-derived suppressor cells in murine retrovirus-induced AIDS inhibit T- and B-cell responses in vitro that are used to define the immunodeficiency. *J Virol* (2013) 87(4):2058–71. doi:10.1128/jvi.01547-12

94. Sui Y, Hogg A, Wang Y, Frey B, Yu H, Xia Z, et al. Vaccine-induced myeloid cell population dampens protective immunity to SIV. *J Clin Invest* (2014) 124(6):2538–49. doi:10.1172/jci73518
95. O'Connor MA, Vella JL, Green WR. Reciprocal relationship of T regulatory cells and monocytic myeloid-derived suppressor cells in LP-BM5 murine retrovirus-induced immunodeficiency. *J Gen Virol* (2016) 97(2):509–22. doi:10.1099/jgv.0.000260
96. Garg A, Trout R, Spector SA. Human immunodeficiency virus type-1 myeloid derived suppressor cells inhibit cytomegalovirus inflammation through interleukin-27 and B7-H4. *Sci Rep* (2017) 7:44485. doi:10.1038/srep44485
97. Dross SE, Munson PV, Kim SE, Bratt DL, Tunggal HC, Gervassi AL, et al. Kinetics of myeloid-derived suppressor cell frequency and function during Simian Immunodeficiency Virus infection, combination antiretroviral therapy, and treatment interruption. *J Immunol* (2017) 198(2):757–66. doi:10.4049/jimmunol.1600759
98. Salem ML, Zidan A-AA, Abou Senna M, Abou Al-Azm AR, Albatei H, Aldemelaawy M, et al. Frequencies of circulating myeloid derived suppressor cells and dendritic cells in Egyptian patients with chronic Hepatitis C Virus infection undergoing treatment with IFN-α-based therapy. *J Immunother Cancer* (2013) 1(1):248. doi:10.1186/2051-1426-1-s1-p248
99. Zeng Q-L, Yang B, Sun H-Q, Feng G-H, Jin L, Zou Z-S, et al. Myeloid-derived suppressor cells are associated with viral persistence and downregulation of TCR ζ chain expression on CD8(+) T cells in chronic hepatitis C patients. *Mol Cells* (2014) 37(1):66–73. doi:10.14348/molcells.2014.2282
100. Nonnenmann J, Stirner R, Roider J, Jung MC, Schrödl K, Bogner JR, et al. Lack of significant elevation of myeloid-derived suppressor cells in peripheral blood of chronically hepatitis C virus-infected individuals. *J Virol* (2014) 88(13):7678–82. doi:10.1128/JVI.00113-14
101. Ning G, She L, Lu L, Liu Y, Zeng Y, Yan Y, et al. Analysis of monocytic and granulocytic myeloid-derived suppressor cells subsets in patients with hepatitis C virus infection and their clinical significance. *Biomed Res Int* (2015) 2015:8. doi:10.1155/2015/385378
102. Goh CC, Roggerson KM, Lee HC, Golden-Mason L, Rosen HR, Hahn YS. Hepatitis C virus-induced myeloid-derived suppressor cells suppress NK cell IFN-gamma production by altering cellular metabolism via arginase-1. *J Immunol* (2016) 196(5):2283–92. doi:10.4049/jimmunol.1501881
103. Lei AH, Yang Q, Cai WP, Liu YF, Lan Y, Qin AP, et al. Clinical significance of myeloid-derived suppressor cells in human immunodeficiency virus-1/hepatitis C virus-coinfected patients. *Scand J Immunol* (2016) 83(6):438–44. doi:10.1111/sji.12429
104. Ren JP, Wang L, Zhao J, Wang L, Ning SB, El Gazzar M, et al. Decline of miR-124 in myeloid cells promotes regulatory T-cell development in hepatitis C virus infection. *Immunology* (2017) 150(2):213–20. doi:10.1111/imm.12680
105. Huang A, Zhang B, Yan W, Wang B, Wei H, Zhang F, et al. Myeloid-derived suppressor cells regulate immune response in patients with chronic hepatitis B virus infection through PD-1-induced IL-10. *J Immunol* (2014) 193(11):5461–9. doi:10.4049/jimmunol.1400849
106. Kondo Y, Shimosegawa T. Significant roles of regulatory T cells and myeloid derived suppressor cells in Hepatitis B Virus persistent infection and Hepatitis B Virus-related HCCs. *Int J Mol Sci* (2015) 16(2):3307–22. doi:10.3390/ijms16023307
107. Tumino N, Casetti R, Fabbri G, Cimini E, Romanelli A, Turchi F, et al. In HIV/HCV co-infected patients T regulatory and myeloid-derived suppressor cells persist after successful treatment with directly acting antivirals. *J Hepatol* (2017) 67(2):422–4. doi:10.1016/j.jhep.2017.03.036
108. Heim CE, Vidlak D, Scherr TD, Kozel JA, Holzapfel M, Muirhead DE, et al. Myeloid-derived suppressor cells contribute to *Staphylococcus aureus* orthopedic biofilm infection. *J Immunol* (2014) 192(8):3778–92. doi:10.4049/jimmunol.1303408
109. Dietlin TA, Hofman FM, Lund BT, Gilmore W, Stohlman SA, van der Veen RC. Mycobacteria-induced Gr-1+ subsets from distinct myeloid lineages have opposite effects on T cell expansion. *J Leukoc Biol* (2007) 81(5):1205–12. doi:10.1189/jlb.1006640
110. Yang B, Wang X, Jiang J, Zhai F, Cheng X. Identification of CD244-expressing myeloid-derived suppressor cells in patients with active tuberculosis. *Immunol Lett* (2014) 158(1–2):66–72. doi:10.1016/j.imlet.2013.12.003
111. Zhuang Y, Cheng P, Liu XF, Peng LS, Li BS, Wang TT, et al. A pro-inflammatory role for Th22 cells in *Helicobacter pylori*-associated gastritis. *Gut* (2015) 64(9):1368–78. doi:10.1136/gutjnl-2014-307020
112. Sander LE, Sackett SD, Dierssen U, Beraza N, Linke RP, Muller M, et al. Hepatic acute-phase proteins control innate immune responses during infection by promoting myeloid-derived suppressor cell function. *J Exp Med* (2010) 207(7):1453–64. doi:10.1084/jem.20091474
113. Ribeiro-Gomes FL, Roma EH, Carneiro MB, Doria NA, Sacks DL, Peters NC. Site-dependent recruitment of inflammatory cells determines the effective dose of *Leishmania major*. *Infect Immun* (2014) 82(7):2713–27. doi:10.1128/IAI.01600-13
114. Bandyopadhyay S, Bhattacharjee A, Banerjee S, Halder K, Das S, Paul Chowdhury B, et al. Glycyrrhizic acid-mediated subdual of myeloid-derived suppressor cells induces antileishmanial immune responses in a susceptible host. *Infect Immun* (2015) 83(12):4476–86. doi:10.1128/IAI.00729-15
115. Hammami A, Abidin BM, Charpentier T, Fabie A, Duguay AP, Heinonen KM, et al. HIF-1alpha is a key regulator in potentiating suppressor activity and limiting the microbicidal capacity of MDSC-like cells during visceral leishmaniasis. *PLoS Pathog* (2017) 13(9):e1006616. doi:10.1371/journal.ppat.1006616
116. Goni O, Alcaide P, Fresno M. Immunosuppression during acute *Trypanosoma cruzi* infection: involvement of Ly6G (Gr1(+))CD11b(+)immature myeloid suppressor cells. *Int Immunol* (2002) 14(10):1125–34. doi:10.1093/intimm/dxf076
117. Cuervo H, Guerrero NA, Carbajosa S, Beschin A, De Baetselier P, Girones N, et al. Myeloid-derived suppressor cells infiltrate the heart in acute *Trypanosoma cruzi* infection. *J Immunol* (2011) 187(5):2656–65. doi:10.4049/jimmunol.1002928
118. Arocena AR, Onofrio LI, Pellegrini AV, Carrera Silva AE, Paroli A, Cano RC, et al. Myeloid-derived suppressor cells are key players in the resolution of inflammation during a model of acute infection. *Eur J Immunol* (2014) 44(1):184–94. doi:10.1002/eji.201343606
119. Voisin M-B, Buzoni-Gatel D, Bout D, Velge-Roussel F. Both expansion of regulatory GR1(+) CD11b(+) myeloid cells and anergy of T lymphocytes participate in hyporesponsiveness of the lung-associated immune system during acute toxoplasmosis. *Infect Immun* (2004) 72(9):5487–92. doi:10.1128/IAI.72.9.5487-5492.2004
120. Dunay IR, Damatta RA, Fux B, Presti R, Greco S, Colonna M, et al. Gr1(+) inflammatory monocytes are required for mucosal resistance to the pathogen *Toxoplasma gondii*. *Immunity* (2008) 29(2):306–17. doi:10.1016/j.immuni.2008.05.019
121. Yang Q, Qiu H, Xie H, Qi Y, Cha H, Qu J, et al. A *Schistosoma japonicum* infection promotes the expansion of myeloid-derived suppressor cells by activating the JAK/STAT3 pathway. *J Immunol* (2017) 198(12):4716–27. doi:10.4049/jimmunol.1601860
122. Pan W, Zhou HJ, Shen YJ, Wang Y, Xu YX, Hu Y, et al. Surveillance on the status of immune cells after *Echinnococcus granulosus* protoscoleces infection in Balb/c mice. *PLoS One* (2013) 8(3):e59746. doi:10.1371/journal.pone.0059746
123. Saleem SJ, Martin RK, Morales JK, Sturgill JL, Gibb DR, Graham L, et al. Cutting edge: mast cells critically augment myeloid-derived suppressor cell activity. *J Immunol* (2012) 189(2):511–5. doi:10.4049/jimmunol.1200647
124. Valanparambil RM, Tam M, Gros PP, Auger JP, Segura M, Gros P, et al. IRF-8 regulates expansion of myeloid-derived suppressor cells and Foxp3+ regulatory T cells and modulates Th2 immune responses to gastrointestinal nematode infection. *PLoS Pathog* (2017) 13(10):e1006647. doi:10.1371/journal.ppat.1006647
125. Valanparambil RM, Tam M, Jardim A, Geary TG, Stevenson MM. Primary *Heligmosomoides polygyrus* bakeri infection induces myeloid-derived suppressor cells that suppress CD4+ Th2 responses and promote chronic infection. *Mucosal Immunol* (2017) 10(1):238–49. doi:10.1038/mi.2016.36
126. Huang B, Pan PY, Li Q, Sato AI, Levy DE, Bromberg J, et al. Gr-1+CD115+ immature myeloid suppressor cells mediate the development of tumor-induced T regulatory cells and T-cell anergy in tumor-bearing host. *Cancer Res* (2006) 66(2):1123–31. doi:10.1158/0008-5472.can-05-1299
127. Gabrilovich DI, Velders MP, Sotomayor EM, Kast WM. Mechanism of immune dysfunction in cancer mediated by immature Gr-1+ myeloid cells. *J Immunol* (2001) 166(9):5398–406. doi:10.4049/jimmunol.166.9.5398
128. Drabczyk-Pluta M, Werner T, Hoffmann D, Leng Q, Chen L, Dittmer U, et al. Granulocytic myeloid-derived suppressor cells suppress virus-specific CD8+ T cell responses during acute Friend retrovirus infection. *Retrovirology* (2017) 14(1):42. doi:10.1186/s12977-017-0364-3

129. Kusmartsev S, Nefedova Y, Yoder D, Gabrilovich DI. Antigen-specific inhibition of CD8+ T cell response by immature myeloid cells in cancer is mediated by reactive oxygen species. *J Immunol* (2004) 172(2):989–99. doi:10.4049/jimmunol.172.2.989
130. Nagaraj S, Gabrilovich DI. Myeloid-derived suppressor cells. *Adv Exp Med Biol* (2007) 601:213–23. doi:10.1007/978-0-387-72005-0_22
131. Lai D, Qin C, Shu Q. Myeloid-derived suppressor cells in sepsis. *Biomed Res Int* (2014) 2014:8. doi:10.1155/2014/598654
132. Bowen JL, Olson JK. Innate immune CD11b+Gr-1+ cells, suppressor cells, affect the immune response during Theiler's virus-induced demyelinating disease. *J Immunol* (2009) 183(11):6971–80. doi:10.4049/jimmunol.0902193
133. Yi H, Guo C, Yu X, Zuo D, Wang XY. Mouse CD11b+Gr-1+ myeloid cells can promote Th17 cell differentiation and experimental autoimmune encephalomyelitis. *J Immunol* (2012) 189(9):4295–304. doi:10.4049/jimmunol.1200086
134. Hammerich L, Warzecha KT, Stefkova M, Bartneck M, Ohl K, Gassler N, et al. Cyclic adenosine monophosphate-responsive element modulator alpha overexpression impairs function of hepatic myeloid-derived suppressor cells and aggravates immune-mediated hepatitis in mice. *Hepatology* (2015) 61(3):990–1002. doi:10.1002/hep.27571
135. Obermajer N, Wong JL, Edwards RP, Chen K, Scott M, Khader S, et al. Induction and stability of human Th17 cells require endogenous NOS2 and cGMP-dependent NO signaling. *J Exp Med* (2013) 210(7):1433–45. doi:10.1084/jem.20121277
136. Yazawa T, Shibata M, Gonda K, Machida T, Suzuki S, Kenjo A, et al. Increased IL-17 production correlates with immunosuppression involving myeloid-derived suppressor cells and nutritional impairment in patients with various gastrointestinal cancers. *Mol Clin Oncol* (2013) 1(4):675–9. doi:10.3892/mco.2013.134
137. Deng Z, Rong Y, Teng Y, Zhuang X, Samykutty A, Mu J, et al. Exosomes miR-126a released from MDSC induced by DOX treatment promotes lung metastasis. *Oncogene* (2017) 36(5):639–51. doi:10.1038/onc.2016.229
138. Park MJ, Lee SH, Kim EK, Lee EJ, Park SH, Kwok SK, et al. Myeloid-derived suppressor cells induce the expansion of regulatory B cells and ameliorate autoimmunity in the sanroque mouse model of systemic lupus erythematosus. *Arthritis Rheumatol* (2016) 68(11):2717–27. doi:10.1002/art.39767
139. Cripps JG, Wang J, Maria A, Blumenthal I, Gorham JD. Type 1 T helper cells induce the accumulation of myeloid-derived suppressor cells in the inflamed Tgfb1 knockout mouse liver. *Hepatology* (2010) 52(4):1350–9. doi:10.1002/hep.23841
140. Mussai F, De Santo C, Cerundolo V. Interaction between invariant NKT cells and myeloid-derived suppressor cells in cancer patients: evidence and therapeutic opportunities. *J Immunother* (2012) 35(6):449–59. doi:10.1097/CJI.0b013e31825be926
141. Pan PY, Ma G, Weber KJ, Ozao-Choy J, Wang G, Yin B, et al. Immune stimulatory receptor CD40 is required for T-cell suppression and T regulatory cell activation mediated by myeloid-derived suppressor cells in cancer. *Cancer Res* (2010) 70(1):99–108. doi:10.1158/0008-5472.can-09-1882
142. Schlecker E, Stojanovic A, Eisen C, Quack C, Falk CS, Umansky V, et al. Tumor-infiltrating monocytic myeloid-derived suppressor cells mediate CCR5-dependent recruitment of regulatory T cells favoring tumor growth. *J Immunol* (2012) 189(12):5602–11. doi:10.4049/jimmunol.1201018
143. Serafini P, Mgebroff S, Noonan K, Borrello I. Myeloid-derived suppressor cells promote cross-tolerance in B-cell lymphoma by expanding regulatory T cells. *Cancer Res* (2008) 68(13):5439–49. doi:10.1158/0008-5472.can-07-6621
144. Yang R, Cai Z, Zhang Y, Yutzy WH, Roby KF, Roden RB. CD80 in immune suppression by mouse ovarian carcinoma-associated Gr-1+CD11b+ myeloid cells. *Cancer Res* (2006) 66(13):6807–15. doi:10.1158/0008-5472.can-05-3755
145. Hoechst B, Ormandy LA, Ballmaier M, Lehner F, Kruger C, Manns MP, et al. A new population of myeloid-derived suppressor cells in hepatocellular carcinoma patients induces CD4(+)CD25(+)Foxp3(+) T cells. *Gastroenterology* (2008) 135(1):234–43. doi:10.1053/j.gastro.2008.03.020
146. Fujimura T, Ring S, Umansky V, Mahnke K, Enk AH. Regulatory T cells stimulate B7-H1 expression in myeloid-derived suppressor cells in ret melanomas. *J Invest Dermatol* (2012) 132(4):1239–46. doi:10.1038/jid.2011.416
147. Yang Z, Zhang B, Li D, Lv M, Huang C, Shen GX, et al. Mast cells mobilize myeloid-derived suppressor cells and Treg cells in tumor microenvironment via IL-17 pathway in murine hepatocarcinoma model. *PLoS One* (2010) 5(1):e8922. doi:10.1371/journal.pone.0008922
148. Deshane J, Zmijewski JW, Luther R, Gaggar A, Deshane R, Lai JF, et al. Free radical-producing myeloid-derived regulatory cells: potent activators and suppressors of lung inflammation and airway hyperresponsiveness. *Mucosal Immunol* (2011) 4(5):503–18. doi:10.1038/mi.2011.16
149. Nakamura T, Nakao T, Ashihara E, Yoshimura N. Myeloid-derived suppressor cells recruit CD4(+)/foxp3(+) regulatory T cells in a murine cardiac allograft. *Transplant Proc* (2016) 48(4):1275–8. doi:10.1016/j.transproceed.2015.10.060
150. Yin B, Ma G, Yen CY, Zhou Z, Wang GX, Divino CM, et al. Myeloid-derived suppressor cells prevent type 1 diabetes in murine models. *J Immunol* (2010) 185(10):5828–34. doi:10.4049/jimmunol.0903636
151. Crook KR, Jin M, Weeks MF, Rampersad RR, Baldi RM, Glekas AS, et al. Myeloid-derived suppressor cells regulate T cell and B cell responses during autoimmune disease. *J Leukoc Biol* (2015) 97(3):573–82. doi:10.1189/jlb.4A0314-139R
152. Xu X, Meng Q, Erben U, Wang P, Glauben R, Kuhl AA, et al. Myeloid-derived suppressor cells promote B-cell production of IgA in a TNFR2-dependent manner. *Cell Mol Immunol* (2017) 14(7):597–606. doi:10.1038/cmi.2015.103
153. Lei GS, Zhang C, Lee CH. Myeloid-derived suppressor cells impair alveolar macrophages through PD-1 receptor ligation during *Pneumocystis* pneumonia. *Infect Immun* (2015) 83(2):572–82. doi:10.1128/iai.02686-14
154. Poschke I, Mao Y, Adamson L, Salazar-Onfray F, Masucci G, Kiessling R. Myeloid-derived suppressor cells impair the quality of dendritic cell vaccines. *Cancer Immunol Immunother* (2012) 61(6):827–38. doi:10.1007/s00262-011-1143-y
155. Hu C-E, Gan J, Zhang R-D, Cheng Y-R, Huang G-J. Up-regulated myeloid-derived suppressor cell contributes to hepatocellular carcinoma development by impairing dendritic cell function. *Scand J Gastroenterol* (2011) 46(2):156–64. doi:10.3109/00365521.2010.516450
156. Hoechst B, Voigtlaender T, Ormandy L, Gamrekelashvili J, Zhao F, Wedemeyer H, et al. Myeloid derived suppressor cells inhibit natural killer cells in patients with hepatocellular carcinoma via the NKp30 receptor. *Hepatology* (2009) 50(3):799–807. doi:10.1002/hep.23054
157. Li H, Han Y, Guo Q, Zhang M, Cao X. Cancer-expanded myeloid-derived suppressor cells induce anergy of NK cells through membrane-bound TGF-beta 1. *J Immunol* (2009) 182(1):240–9. doi:10.4049/jimmunol.182.1.240
158. Mao Y, Sarhan D, Steven A, Seliger B, Kiessling R, Lundqvist A. Inhibition of tumor-derived prostaglandin-e2 blocks the induction of myeloid-derived suppressor cells and recovers natural killer cell activity. *Clin Cancer Res* (2014) 20(15):4096–106. doi:10.1158/1078-0432.ccr-14-0635
159. Derive M, Bouazza Y, Alauzet C, Gibot S. Myeloid-derived suppressor cells control microbial sepsis. *Intensive Care Med* (2012) 38(6):1040–9. doi:10.1007/s00134-012-2574-4
160. Martire-Greco D, Rodriguez-Rodrigues N, Castillo LA, Vecchione MB, de Campos-Nebel M, Cordoba Moreno M, et al. Novel use of all-trans-retinoic acid in A model of lipopolysaccharide-immunosuppression to decrease the generation of myeloid-derived suppressor cells by reducing the proliferation of CD34+ precursor cells. *Shock* (2017) 48(1):94–103. doi:10.1097/shk.0000000000000812
161. Liu G, Bi Y, Shen B, Yang H, Zhang Y, Wang X, et al. SIRT1 limits the function and fate of myeloid-derived suppressor cells in tumors by orchestrating HIF-1alpha-dependent glycolysis. *Cancer Res* (2014) 74(3):727–37. doi:10.1158/0008-5472.can-13-2584
162. Singh A, Lelis F, Braig S, Schäfer I, Hartl D, Rieber N. Differential regulation of myeloid-derived suppressor cells by *Candida* species. *Front Microbiol* (2016) 7:1624. doi:10.3389/fmicb.2016.01624
163. Albeituni SH, Ding C, Liu M, Hu X, Luo F, Kloecker G, et al. Yeast-derived particulate β-glucan treatment subverts the suppression of myeloid-derived suppressor cells by inducing PMN-MDSC apoptosis and M-MDSC differentiation to APC in cancer. *J Immunol* (2016) 196(5):2167–80. doi:10.4049/jimmunol.1501853
164. Fortin C, Huang X, Yang Y. NK cell response to vaccinia virus is regulated by myeloid-derived suppressor cells. *J Immunol* (2012) 189(4):1843–9. doi:10.4049/jimmunol.1200584
165. Hossain F, Al-Khami AA, Wyczechowska D, Hernandez C, Zheng L, Reiss K, et al. Inhibition of fatty acid oxidation modulates immunosuppressive

functions of myeloid-derived suppressor cells and enhances cancer therapies. *Cancer Immunol Res* (2015) 3(11):1236–47. doi:10.1158/2326-6066.cir-15-0036

166. Dodd CE, Pyle CJ, Glowinski R, Rajaram MV, Schlesinger LS. CD36-mediated uptake of surfactant lipids by human macrophages promotes intracellular growth of *Mycobacterium tuberculosis*. *J Immunol* (2016) 197(12):4727–35. doi:10.4049/jimmunol.1600856
167. Philips JA, Rubin EJ, Perrimon N. *Drosophila* RNAi screen reveals CD36 family member required for mycobacterial infection. *Science* (2005) 309(5738):1251–3. doi:10.1126/science.1116006
168. Youn JI, Collazo M, Shalova IN, Biswas SK, Gabrilovich DI. Characterization of the nature of granulocytic myeloid-derived suppressor cells in tumor-bearing mice. *J Leukoc Biol* (2012) 91(1):167–81. doi:10.1189/jlb.0311177
169. Zhang C, Lei GS, Shao S, Jung HW, Durant PJ, Lee CH. Accumulation of myeloid-derived suppressor cells in the lungs during *Pneumocystis* pneumonia. *Infect Immun* (2012) 80(10):3634–41. doi:10.1128/iai.00668-12
170. Lacotte S, Slits F, Orci LA, Meyer J, Oldani G, Delaune V, et al. Impact of myeloid-derived suppressor cell on Kupffer cells from mouse livers with hepatocellular carcinoma. *Oncoimmunology* (2016) 5(11):e1234565. doi:10.1080/2162402X.2016.1234565
171. Condamine T, Kumar V, Ramachandran IR, Youn JI, Celis E, Finnberg N, et al. ER stress regulates myeloid-derived suppressor cell fate through TRAIL-R-mediated apoptosis. *J Clin Invest* (2014) 124(6):2626–39. doi:10.1172/JCI74056
172. Thevenot PT, Sierra RA, Raber PL, Al-Khami AA, Trillo-Tinoco J, Zarreii P, et al. The stress-response sensor chop regulates the function and accumulation of myeloid-derived suppressor cells in tumors. *Immunity* (2014) 41(3):389–401. doi:10.1016/j.immuni.2014.08.015
173. Martire-Greco D, Landoni VI, Chiarella P, Rodriguez-Rodrigues N, Schierloh P, Rearte B, et al. All-trans-retinoic acid improves immunocompetence in a murine model of lipopolysaccharide-induced immunosuppression. *Clin Sci (Lond)* (2014) 126(5):355–65. doi:10.1042/cs20130236

Conflict of Interest Statement: The authors declare that the research was conducted in the absence of any commercial or financial relationships that could be construed as a potential conflict of interest.

Copyright © 2018 Dorhoi and Du Plessis. This is an open-access article distributed under the terms of the Creative Commons Attribution License (CC BY). The use, distribution or reproduction in other forums is permitted, provided the original author(s) or licensor are credited and that the original publication in this journal is cited, in accordance with accepted academic practice. No use, distribution or reproduction is permitted which does not comply with these terms.

frontiers in Immunology

REVIEW
published: 19 January 2018
doi: 10.3389/fimmu.2017.01878

E-Selectin Ligands in the Human Mononuclear Phagocyte System: Implications for Infection, Inflammation, and Immunotherapy

Mariana Silva[1,2†], Paula A. Videira[3,4†] and Robert Sackstein[1,2,5*]*

[1] Department of Dermatology, Harvard Skin Disease Research Center, Brigham and Women's Hospital, Harvard Medical School, Boston, MA, United States, [2] Program of Excellence in Glycosciences, Harvard Medical School, Boston, MA, United States, [3] UCIBIO, Departamento Ciências da Vida, Faculdade de Ciências e Tecnologia, Universidade NOVA de Lisboa, Lisboa, Portugal, [4] Professionals and Patient Associations International Network (CDG & Allies – PPAIN), Faculdade de Ciências e Tecnologia, Universidade NOVA de Lisboa, Lisboa, Portugal, [5] Department of Medicine, Brigham and Women's Hospital, Harvard Medical School, Boston, MA, United States

OPEN ACCESS

Edited by:
Yoann Rombouts,
UMR5089 Institut de Pharmacologie et de Biologie Structurale (IPBS), France

Reviewed by:
Michael Hickey,
Monash University, Australia
Luciana Barros Arruda,
Universidade Federal do Rio de Janeiro, Brazil

***Correspondence:**
Paula A. Videira
p.videira@fct.unl.pt;
Robert Sackstein
rsackstein@rics.bwh.harvard.edu

[†]Co-first authorship.

Specialty section:
This article was submitted to Microbial Immunology, a section of the journal Frontiers in Immunology

Received: 30 September 2017
Accepted: 08 December 2017
Published: 19 January 2018

Citation:
Silva M, Videira PA and Sackstein R (2018) E-Selectin Ligands in the Human Mononuclear Phagocyte System: Implications for Infection, Inflammation, and Immunotherapy. Front. Immunol. 8:1878. doi: 10.3389/fimmu.2017.01878

The mononuclear phagocyte system comprises a network of circulating monocytes and dendritic cells (DCs), and "histiocytes" (tissue-resident macrophages and DCs) that are derived in part from blood-borne monocytes and DCs. The capacity of circulating monocytes and DCs to function as the body's first-line defense against offending pathogens greatly depends on their ability to egress the bloodstream and infiltrate inflammatory sites. Extravasation involves a sequence of coordinated molecular events and is initiated by E-selectin-mediated deceleration of the circulating leukocytes onto microvascular endothelial cells of the target tissue. E-selectin is inducibly expressed by cytokines (tumor necrosis factor-α and IL-1β) on inflamed endothelium, and binds to sialofucosylated glycan determinants displayed on protein and lipid scaffolds of blood cells. Efficient extravasation of circulating monocytes and DCs to inflamed tissues is crucial in facilitating an effective immune response, but also fuels the immunopathology of several inflammatory disorders. Thus, insights into the structural and functional properties of the E-selectin ligands expressed by different monocyte and DC populations is key to understanding the biology of protective immunity and the pathobiology of several acute and chronic inflammatory diseases. This review will address the role of E-selectin in recruitment of human circulating monocytes and DCs to sites of tissue injury/inflammation, the structural biology of the E-selectin ligands expressed by these cells, and the molecular effectors that shape E-selectin ligand cell-specific display. In addition, therapeutic approaches targeting E-selectin receptor/ligand interactions, which can be used to boost host defense or, conversely, to dampen pathological inflammatory conditions, will also be discussed.

Keywords: mononuclear phagocyte, HCELL, E-selectin ligand, cell migration, E-selectin, sialyl Lewis X

INTRODUCTION

The mononuclear phagocyte system (MPS) comprises monocytes, dendritic cells (DC), and tissue-resident macrophages. MPS cells have specialized phagocytic capabilities, and antigen processing and presenting functions, thereby initiating the immune response and linking innate and adaptive immune systems (1). In addition to their role as key sentinels and regulators of immunity,

mononuclear phagocytes are also involved in several pathological inflammatory conditions, including autoimmune diseases, infection, cancer, and abnormal wound healing processes (2). To access inflammatory sites, circulating monocytes and DCs must first engage the vascular endothelial barrier against the prevailing forces of hemodynamic shear, a process that occurs *via* adhesive interactions between vascular E-selectin and its glycan counter-receptors (E-selectin ligands) on the circulating cells (3). This initial contact results in tethering and slow rolling of the cells along the endothelial surface at velocities well below that of blood flow (4). E-selectin-mediated slow rolling is a vital step in this cascade of events as it allows intimate contact between MPS cells and the inflamed endothelium, and the recognition of inflammatory molecules within the milieu (3). Consequently, a greater knowledge of how E-selectin ligand display is elaborated by different types of circulating monocytes and DCs is key to understanding the physiological and pathological events associated with the MPS. In this review, we will provide information on the structural biology and operation of the wide variety of E-selectin-binding glycoconjugates expressed by circulating MPS cells (i.e., blood monocyte and non-tissue-resident DC populations) in light of their impact on pathology and potential therapies. Furthermore, we will discuss the molecular basis of the biosynthesis of these glycoconjugates, and how such knowledge can frame novel strategies to inhibit or enforce trafficking of MPS cells.

MONONUCLEAR PHAGOCYTE FAMILY: HETEROGENEITY AND MIGRATORY CAPABILITIES

Monocytes

Monocytes constitute a heterogeneous cell population, comprising approximately 5–10% of total peripheral blood leukocytes. These cells arise from granulocyte–macrophage progenitors in the bone marrow and are subsequently released into peripheral blood, where they circulate for several days (5). At steady state (i.e., without any inflammatory cue), monocytes can enter non-lymphoid tissues, and there they either retain their blood monocytic behavior (6), or generate the immediate precursors of "monocyte-derived macrophages and DCs," which constitute a small portion of tissue-resident macrophage and DC populations (7–9). On the other hand, under inflammatory conditions, monocytes transmigrate into injured tissues, where they then directly mediate antimicrobial activity or, depending on the local biochemical milieu, differentiate into inflammatory macrophages or monocyte-derived DCs (moDCs) (10) (**Figure 1**). Circulating

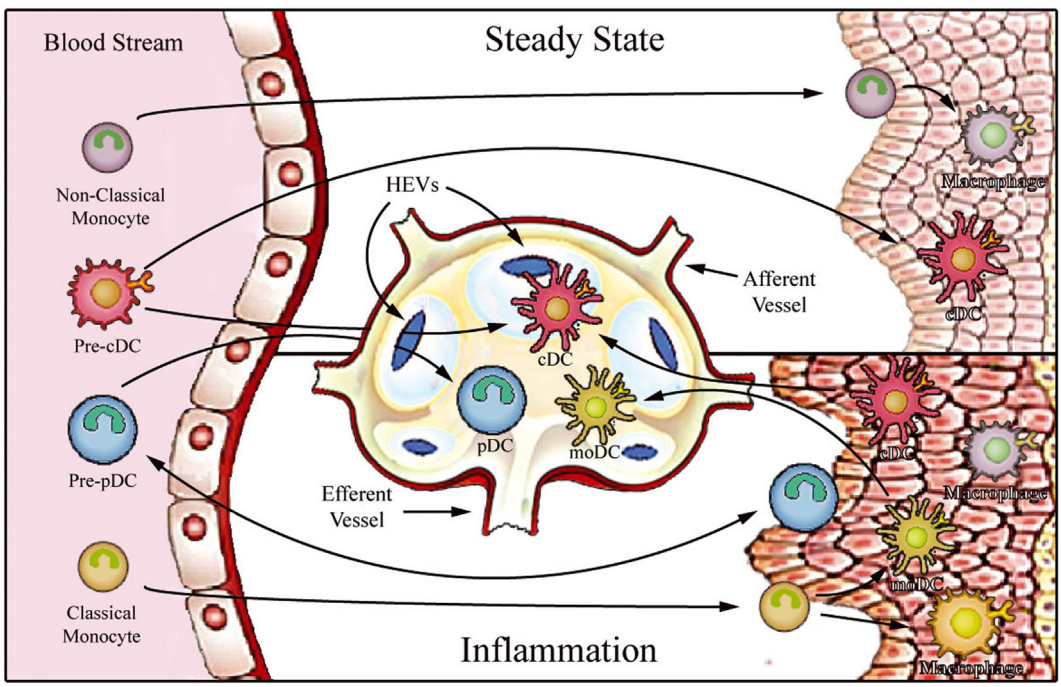


FIGURE 1 | Proposed model for migration of human monocytes and dendritic cell (DC) progenitors into tissues in steady-state and inflammatory conditions. After differentiation in the bone barrow, precursors of DCs and monocytes enter the blood stream and are distributed to lymphoid organs [through high endothelial venules (HEV)] and to various peripheral tissues. In steady state, non-classical monocytes are preferentially recruited into the resting vasculature, where they patrol the endothelium and may contribute to the maintenance of tissue-resident macrophage and DC populations. Conventional DCs (cDCs) recirculate between peripheral tissues and lymphoid organs (migratory cDCs), participating in the induction of peripheral tolerance, or reside in the lymphoid organs (lymphoid-resident cDCs). By contrast, plasmacytoid DCs (pDCs) mostly populate lymphoid tissues (lymphoid-resident pDCs) and lack migratory ability under steady-state conditions. Upon inflammation, classical monocytes, cDCs, and pDCs are recruited to affected tissues. After antigen uptake and differentiation into fully functional mature DCs, monocyte-derived DCs (moDCs), and cDCs enter draining lymph nodes *via* afferent lymphatics. pDCs can only access reactive lymph nodes from the blood stream *via* HEVs.

monocytes, thus, function as a systemic reservoir of tissue-resident myeloid cells (11, 12).

There are three subsets of human monocytes, each of which display different functional and migratory abilities and can be distinguished based on their expression of specific chemokine receptors, CD14 [the lipopolysaccharide (LPS) receptor], and CD16 (Fcγ RIII) (13). "Classical" monocytes ($CD14^{++}CD16^{-}$), which account for about 90% of circulating monocytes in healthy individuals, express high levels of the C-C chemokine receptor type 2 (CCR2), display high phagocytic and myeloperoxidase activities, generate reactive oxygen species, and produce inflammatory cytokines, such as interleukin (IL)-1β, IL-6, and tumor necrosis factor (TNF)-α (14). On the other hand, the "non-classical" monocytes ($CD14^{+}CD16^{++}$) comprise a population that exhibits low phagocytic and myeloperoxidase activities (15, 16). Importantly, while classical monocytes are recruited preferentially to distressed tissues (17), non-classical monocytes are recruited to non-inflamed areas, where they patrol the microvasculature *via* the CX3C chemokine receptor 1 (CX3CR1) and leukocyte function-associated antigen (LFA)-1, monitoring the luminal surface of resting endothelium for signs of tissue damage or infection (18–20). In addition, non-classical monocytes are mainly responsive to virus-associated signals, *via* toll-like receptors (TLRs) 7 and 8, whereas classical monocytes respond mostly to bacteria-associated signals (21). An intermediate subset of monocytes, characterized as $CD14^{++}CD16^{+}$, is viewed as being a transitional population between classical and non-classical monocyte subsets, displaying significant production of TNF-α and IL-1β, but low peroxidase activity (16, 22). While the migratory ability of the intermediate subset is controversial, they express the chemokine receptor CCR2, a feature supporting their ability to infiltrate sites of inflammation (23). Still, overall, the intermediate monocyte population reportedly displays weaker ability to migrate across resting endothelium compared to the other two monocytic subsets (24).

Dendritic Cells

Dendritic cells are the antigen-presenting cells par excellence, showing a unique capacity to initiate immune responses. These specialized antigen-presenting cells constitute a unique leukocyte population that display high morphological and functional heterogeneity (25). DCs can be originated from common myeloid or lymphoid precursors and are divided into two main groups: conventional DCs (cDCs) and plasmacytoid DCs (pDCs) (26). After being released into the bloodstream, they are distributed to lymphoid organs (lymph nodes, spleen, and thymus) and various peripheral tissues. DC function is intrinsically related to their anatomical localization, and, therefore, a stringent DC functional-anatomical classification needs to be defined (**Figure 1**). At steady state, DCs are found to be immature (as indicated by high phagocytic and endocytic capacity and low expression of MHC and costimulatory molecules) and can be classified as either migratory or lymphoid-resident DCs (27, 28). Migratory DCs serve as immune sentinels screening peripheral tissues for signals of danger. They can also capture apoptotic cells or self-antigens in non-inflamed tissues and, after entering lymph nodes *via* afferent lymphatics, present these to T cells in the lymph nodes, thus playing a key role in antigen-mediated peripheral tolerance (29–31). On the other hand, lymphoid-resident DCs differentiate within lymphoid organs directly from blood DC precursors, and they function to continuously survey blood or lymph (27, 32). Both cDC and pDC hematopoietic progenitors contribute to the lymphoid-resident DC pool, whereas most migratory DCs arise from blood cDCs (33). Under infection or sterile inflammatory circumstances, both circulating cDCs and classical monocytes enter inflamed tissues, where they capture antigens and differentiate into highly functional mature DCs. The mature DCs migrate to the lymph nodes *via* the afferent lymph, initiating T cell-mediated immune responses.

In addition to cDCs and pDCs, a distinct subset of DCs are derived from monocytes (known as "moDCs") which are considered to be "inflammatory DCs"; these cells prominently produce TNF-α, nitric oxide, and IL-23, and are potent inducers of TH17 cells (34–37). Interestingly, although pDCs are believed to be absent from peripheral tissues under steady-state conditions, a number of recent publications reported pDC extravasation into some inflamed tissues, where they secrete large amounts of type I interferon (38–42). In contrast to cDCs, pDCs do not enter reactive secondary lymphoid organs after trafficking from peripheral tissue *via* afferent lymphatics; instead, they apparently migrate directly from the bloodstream *via* high endothelial venules (HEVs) by an E-selectin-dependent mechanism (43–47).

Macrophages

Macrophages are a heterogeneous and versatile population of tissue-resident cells, mostly originating from self-renewing embryo-derived progenitors and from blood monocytes that have colonized tissues (48, 49). They exist virtually in every tissue throughout the body, where they survey for potential signs of infection/danger and perform phagocytic clearance of dying cells (50). In addition, macrophages play a role in adaptive immunity through antigen presentation and production of cytokines (51, 52).

There are two main macrophage subsets, the M1 and the M2 macrophages, with distinct responses to environmental signals. The M1 subset produces high amounts of pro-inflammatory cytokines and reactive oxygen and nitrogen species, thus playing a crucial role in Th1 polarization and promotion of cellular immunity. M2 macrophages are characterized by their ability to stimulate humoral immune responses, fight extracellular parasite infections, and promote tissue repair, angiogenesis, and tumor progression (53, 54). Whereas the major function of macrophages is to fight infections and kill target cells, they do not typically display hematogenous migration, nor leave sites of tissue injury (11, 55).

MPS Extravasation Cascade: The Multistep Model

Recruitment of circulating cells from blood to inflamed tissue involves a sequential and coordinated series of molecular actions mediated by adhesive interactions between circulating sentinels and endothelial cells in post-capillary venules (56). Here, we review the molecular effectors that regulate the initial phagocyte–endothelial binding interactions, which are essential for transendothelial migration of blood monocytes and DCs to sites of injury.

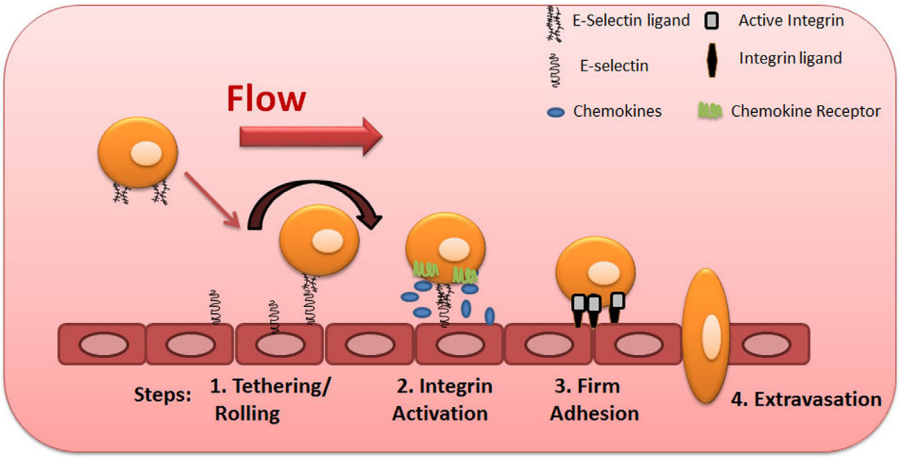


FIGURE 2 | Multistep model of circulating blood cell adhesion and migration along the vascular endothelium. Cells make adhesive contacts onto the inflamed endothelial surface through engagement of their sialofucosylated glycan determinants to vascular E-selectin (Step 1—tethering and rolling). Subsequent engagement of chemokine receptors leads to integrin activation (Step 2) and firm adhesion of leukocytes to endothelium (Step 3), allowing their transmigration (Step 4).

To initiate the extravasation process, circulating phagocytes establish low-affinity and reversible interactions (tethering) on target endothelial cells, achieving low velocity "rolling" adhesive interactions (Step 1, **Figure 2**). Rolling exposes these cells to chemokines that are immobilized by glycosaminoglycans on the endothelial surface, and, in turn, facilitates engagement of G-protein-coupled chemokine receptors (GPCRs) expressed on the mononuclear phagocyte cell surface (Step 2, **Figure 2**), with resultant G-protein-driven integrin activation (3, 57). Activated integrins on phagocytes, principally very late activation protein 4 and LFA-1, bind to their respective endothelial receptors vascular cell adhesion molecule-1 and intercellular adhesion molecule-1 (ICAM-1), leading to firm adhesion of MPS cells on the endothelium (Step 3, **Figure 2**) (3, 57). The binding of activated integrins then allows diapedesis into the tissue (Step 4, **Figure 2**). Two distinct mechanisms enable diapedesis: (1) transient dismantling of endothelial junctions (paracellular migration) or (2) migration through individual endothelial cells (transcellular migration) (58, 59).

Although several cell-associated proteins are specialized at mediating the first step of cell migration, the selectins and their ligands are the most potent effectors of tethering and rolling adhesive interactions. These molecules are responsible for the initial low-affinity binding interactions of leukocytes on endothelial layer (60), a property related to the unique biophysics of lectin–carbohydrate interactions under fluid shear conditions.

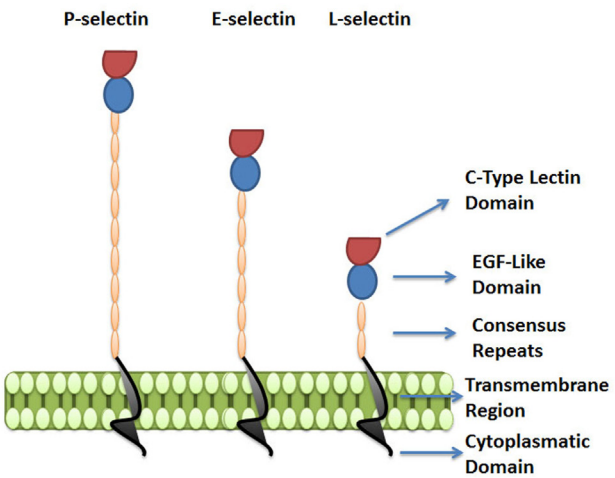


FIGURE 3 | The selectin family. Selectins are a family of three carbohydrate-binding proteins: P-selectin, expressed on activated platelets and endothelial cells, E-selectin expressed on activated endothelial cells, and L-selectin expressed on leukocytes. The figure represents the five domains shared by selectins: C-type lectin domain, epidermal growth factor-like domain (EGF), a varying number of short consensus repeats having homology to complement regulatory proteins, a transmembrane region, and a cytoplasmatic domain.

SELECTINS AND THEIR GLYCOCONJUGATE LIGANDS

The Selectin Family

The selectins are a family of three carbohydrate-binding proteins that can be expressed on endothelial cells, leukocytes and platelets (**Figure 3**). Due to their requirement of calcium ions for binding, all three selectins, E-selectin (CD62E), P-selectin (CD62P), and L-selectin (CD62L), belong to the C-type lectin family (61). Selectins share a common structure of five different domains: an *N*-terminal carbohydrate recognition domain (CRD), an epidermal growth factor-like domain (EGF), a varying number of short consensus repeats that have homology to complement regulatory domains ("CRs" of which there are 2, 6, and 9 within L-, E-, and P-selectin, respectively), a transmembrane region, and a C-terminal cytoplasmatic domain (**Figure 3**) (62–64). While the CRD and EGF domains are highly homologous between the three selectins, the structure

of the transmembrane and cytoplasmic portions, as well as the extracellular CR domains are not conserved across the selectins, resulting in structural diversity and varying molecular weights between selectins (61, 65).

Despite sharing common elements, the three selectins have different functions in diverse pathological and physiological processes and vary in their distribution and binding kinetics.

The biology of L-selectin was first elucidated by use of an *in vitro* assay in which suspensions of lymphocytes were overlaid onto lymph node sections (66). This assay then allowed for creation of mAb that could interrupt this binding, such as the mAb known as "MEL-14" described by Gallatin and coworkers (67) in 1983, and thereafter led investigators to cloning of this structure (62). L-selectin is highly expressed on hematopoietic stem cells and mature leukocytes, including all myeloid cells, subsets of natural killer cells, *naïve* T and B cells, and central memory T cells. When leukocytes are activated, cell surface levels of L-selectin are down-regulated by proteolytic cleavage *via* metalloprotease-dependent shedding of the extracellular domain (61, 68, 69).

P-selectin was described in 1984 by McEver and coworkers (70, 71) and Furie and coworkers (72) as a glycoprotein expressed on the cell surface of activated platelets. P-selectin is constitutively expressed by circulating platelets and endothelial cells, where it is stored in α-granules and Weibel–Palade bodies, respectively. Because it can be expressed on endothelial cells, P-selectin together with E-selectin (described below) are known as the "vascular selectins." Following pro-inflammatory stimulus by molecules such as thrombin or histamine, P-selectin is rapidly translocated from the granules to the cell surface by fusion of intracellular storage compartments with the plasma membrane. In murine endothelial cells, inflammatory mediators, such as TNF-α, IL-1β, and LPS, induce P-selectin mRNA transcription, which requires the cooperative binding of the nuclear factor κ-light chain-enhancer of activated B cells (NF-κB) and activating transcription factor-2 (ATF-2) to their response elements within the P-selectin promoter (73–75). However, importantly, the promoter of P-selectin in humans and other primates lacks binding sites for NF-κB and ATF-2 (76). For this reason, in human endothelial cells, the only vascular selectin inducibly expressed by TNF-α, LPS, and IL-1β is E-selectin (77).

E-selectin was first reported by Bevilacqua and coworkers (63, 78) in 1980s as a leukocyte adhesion molecule on activated endothelial cells. Skin and bone marrow microvessels express E-selectin constitutively (79), however, in other tissues, endothelial cells do not constitutively express E-selectin but its expression is strongly upregulated by inflammatory cytokines, such as TNF-α and IL-1β. These cytokines potently induce transient transcription (within hours of exposure) of E-selectin mRNA in both human and mouse endothelial cells (80). Cytokine-dependent activation of E-selectin is mediated by NF-κB binding to regulatory domains in the E-selectin promoter (81). Functionally, E-selectin slows leukocyte rolling to much lower velocities than do either L- or P-selectin, favoring subsequent leukocyte arrest (4, 82). This capacity, along with the inability of human endothelial cells to upregulate P-selectin in the presence of IL-1β and TNF-α, is why E-selectin is considered to be the most important selectin for cell trafficking to sites of inflammation in humans, and it plays a critical role in the recruitment of immune effectors to target inflammatory sites.

The Carbohydrate E-Selectin Ligands

E-selectin recognizes a range of structurally diverse glycan epitopes expressed by human leukocytes that typically contain α(1,3)-fucose (Fuc) and α(2,3)-sialic acid (Sia) modification(s) on a lactosamine backbone [consisting of galactose (Gal) linked to *N*-acetylglucosamine (GlcNAc)], as shown in **Figure 4** (79). The terminal tetrasaccharide known as sialyl Lewis X (sLe^x—Siaα2-3Galβ1-4(Fucα1-3)GlcNAc) is the prototypical E-selectin-binding determinant (83–85). Some sLe^x-variant structures can also exhibit E-selectin binding activity, namely an internally fucosylated sLe^x-variant (VIM-2) and other polylactosamine structures, in which Fuc modifications occur at more than one GlcNAc residue along the polylactosamine chain (tri-fucosyl-sialyl Lewis^x and di-fucosyl-sialyl Lewis^x) (86–88). In addition, other glycan structures that are not natively expressed on leukocytes exhibit E-selectin binding activity, namely the sLe^x isomer, sialyl Lewis a (sLe^a—Siaα2-3Galβ1-3(Fucα1-4)GlcNAc) (89), some sulfated derivatives of Le^x and Le^a (3′-sulfo-Le^x and 3′-sulfo-Le^a, respectively) (90, 91), and a fucosylated glycoform of LacdiNac that displays a terminal *N*-acetylgalactosamine (GalNAc) instead of Sia (GalNAc-Lewis x) (92).

Glycosyltransferases Involved in the Biosynthesis of Selectin–Carbohydrate-Binding Determinants

E-selectin binding determinants are typically displayed at the end of *O*-glycans, *N*-glycans, or glycolipid precursor structures, and require the coordinated and sequential action of specific glycosyltransferases localized within the lumen of the Golgi apparatus. Assembly of sLe^x is driven by the terminal addition of Sia (to Gal) and of Fuc (to GlcNAc) through the action of α(2,3)-sialyltransferases and α(1,3)-fucosyltransferases (FTs), respectively, on type 2 lactosamine (LacNAc) chains (i.e., Gal connected to GlcNAc through a β(1,4)-linkage) (**Figure 4**) (93, 94). The sialylated forms of Lewis antigens are synthesized by the action of the α(2,3)-sialyltransferases (ST3Gal isoenzymes). These enzymes transfer Sia residues to the Gal on the LacNAc chain, exclusively acting prior to fucosylation (95, 96). There are six members of the α(2,3)-sialyltransferase family (ST3Gal-I–ST3Gal-VI), but only ST3Gal-III, ST3Gal-IV, and ST3Gal-VI are reported to sialylate lactosamine chains (97). Importantly, ST3Gal-III exhibits preference for type 1 lactosamine chain acceptors (wherein Gal is connected to GlcNAc through a β(1,3)-linkage), whereas ST3Gal-IV and ST3Gal-VI preferentially act on type 2 polylactosamine chains (98–100). When Type 1 lactosamines are decorated with Sia in α(2,3)-linkage to Gal and with Fuc in β(1,3)-linkage to GlcNAc, this tetrasaccharide is known as sialyl Lewis A (sLe^A).

So far, six human FTs have been found to catalyze the addition of Fuc at α(1,3) linkage to GlcNAc with a type 2 lactosamine—FTIII, FTIV, FTV, FTVI, FTVII, and FTIX. Each enzyme exhibits specificity for acceptor substrates and,

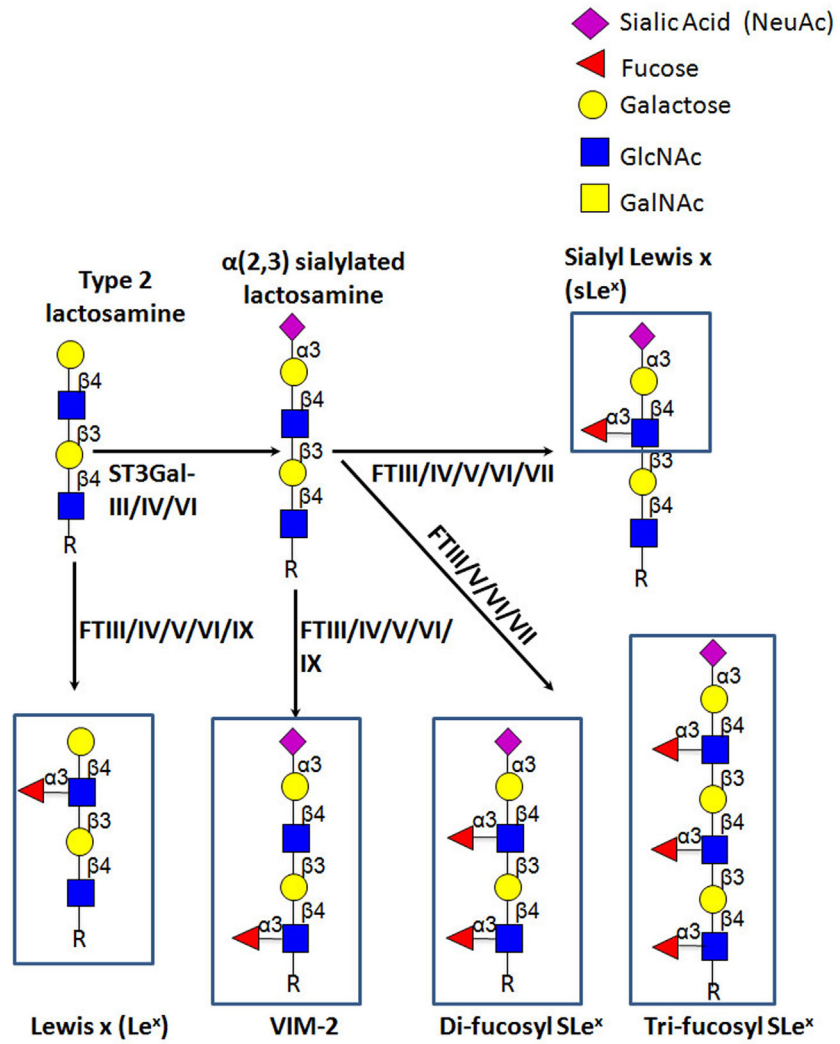


FIGURE 4 | Schematic representation of biosynthesis of the E-selectin ligand determinants. The α(2,3)-sialyltransferases, ST3Gal-III, -IV, and -VI, terminate the elongation of both *O*- and *N*-glycans by creating sialylated type 2 lactosamine chains. These can be further fucosylated by the action of the specific fucosyltransferases, yielding different Lewis-related structures that display E-selectin binding activity.

therefore, has the ability to generate distinct fucosylated structures (101, 102). Particularly, FTIII and FTV are unique in that they exhibit both α(1,3) and α(1,4) FT activity on both sialylated and unsialylated type 2 and type 1 lactosamines thereby creating (s)Le^x and (s)Le^a epitopes, respectively (103, 104). On the other hand, FTIV and FTVI fucosylate both sialylated and unsialylated type 2 lactosamine chains, with FTIV creating VIM-2 and Le^x (105, 106) and, modestly, sLe^x determinants (107, 108), and FTVI creating these structures as well as di-fucosyl-sLe^x (108–110). Uniquely, FTVII can only act on sialylated type 2 lactosamines, yielding sLe^x and di/tri-fucosyl-sLe^x-structures (111, 112), whereas FTIX is known to synthesize mostly Le^x (101, 106).

Most of the reports that assess the role of the different glycosyltransferases involved in selectin ligand biosynthesis in leukocytes have been performed using knock-out mouse models, with a small proportion of these studies using human leukocytes or human hematopoietic cell lines. Concerning the role of the α(2,3)-sialyltransferases, murine studies suggest that ST3Gal-IV and ST3Gal-VI collaborate together in murine E-selectin ligand biosynthesis, with ST3Gal-IV having an important role in the regulation of E-selectin-dependent rolling velocity (113, 114). Interestingly, ST3Gal-III does not seem to contribute to the synthesis of murine E-selectin ligand moieties, since deficiency of this enzyme did not affect E-selectin ligand expression or activity on murine leukocytes (113). Surprisingly, ST3Gal-IV is reportedly the only human α(2,3)-sialyltransferase involved in the biosynthesis of E-selectin ligands in human myeloid leukocytes, since ST3Gal-IV-silenced HL-60 cells (a human promyelocytic cell line), and neutrophils derived from stable ST3Gal-IV knockdown hematopoietic stem cells fail to engage in tethering and rolling interactions on E-selectin-bearing

substrates (115). In case of α(1,3)-FTs, studies demonstrate that mostly FTVII, and to a lesser extent FTIV, are the key murine α(1,3) FTs that mediate leukocyte selectin ligand biosynthesis. In fact, murine leukocytes lacking FTVII show poor adhesive contacts with E- and P-selectin, indicating that this FT plays a prominent role in murine E-selectin ligand biosynthesis (116, 117). However, others reported that FTIV is crucial for slow murine leukocyte rolling velocity (118, 119). Importantly, E-selectin binding activity conferred by murine FTIV, but not by FTVII, apparently occurs mainly on glycolipids rather than glycoproteins (120). Conversely, in human leukocytes, there is evidence that FTVII, FTIV, and FTIX could each act in synthesis of E-selectin ligand determinants (121). Notably, the mouse genome encodes only FTIV, FTVII, and FTIX (122), whereas primates possess an additional three FT gene products—FTIII, FTV, and FTIV. These additional FTs provide for a much wider capacity to create sLe^X; in addition, the expression of FTIII and FTV in primates uniquely drives creation of sLe^A determinants. Human circulating monocytes express all the α(1,3)-FTs, with the exception of FTV, heightening the potential for variability in glycoconjugates bearing sLe^x among human and mouse cells (123). Notably, sLe^A is not expressed on any primate leukocytes as these cells do not synthesize Type 1 lactosamines (3).

Other glycosyltransferases involved in the biosynthesis of sLe^x have also been studied for their relevance in generating functional selectin ligands (**Figure 5**). Regarding sLe^x presentation on O-glycans, one study reported that leukocytes from mice deficient in the enzyme required for initiation of *O*-glycosylation, ppGalNAcT-1, showed impaired recruitment during inflammation due to a significant reduction in E- and

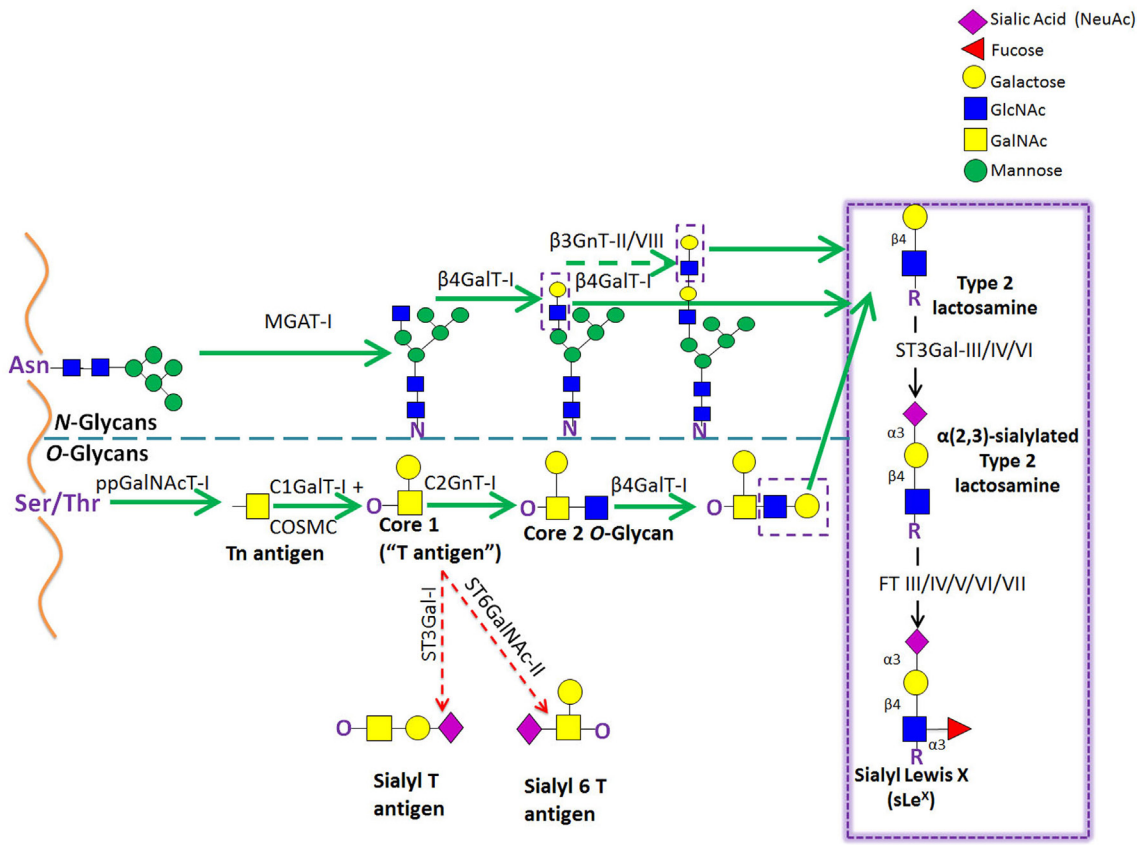


FIGURE 5 | Schematic representation of the biosynthetic pathways leading to glycoprotein synthesis: O-linked and N-linked glycosylation. The *O*-glycosylation process is characterized by a stepwise sugar addition that occurs in the Golgi apparatus and involves a broad array of enzymes. This synthesis is initiated by one of the *N*-acetylgalactosaminyltransferase (ppGalNAcTs) family members, forming the Tn antigen. After the first sugar [*N*-acetylgalactosamine (GalNAc)] addition, Tn is typically elongated by Core 1 β(1,3)galactosyltransferase (Core1GalT or T synthase, whose Golgi expression requires the activity of its chaperone COSMC), creating the "Core 1" *O*-glycan (also known as "T antigen"). Core 1 is then further lengthened by C2GnT-I, which adds an *N*-acetylglucosamine (GlcNAc) to the GalNAc, forming the "Core 2" *O*-glycan structure. Alternatively, Core 1 sialylation, by ST3Gal-I or ST6GalNAc-II [forming sialyl-T (sT) or sialyl-6T (s6T) antigens, respectively] stops Core 2 formation. In contrast to *O*-glycosylation, the *N*-glycosylation process requires the production of an oligosaccharide precursor (GlcNAc2Man5) in the cytoplasmic face of the endoplasmic reticulum (ER) membrane. This glycan flipped in the ER lumen and is then transferred en block from a lipid donor to the Asn residue of a newly synthesized protein within the ER lumen, and then further processed in the Golgi compartment. Biosynthesis of hybrid and complex glycans is initiated by the action of MGAT-I, which adds a GlcNAc residue to the mannose (Man) present on the α(1,3)-arm of the Man5GlcNAc2 structure. Repetitive additions of galactose (Gal) and GlcNAc by β(1/4)GalT and β(1,3)GnT enzymes, respectively, can further elongate Core 2 *O*-glycan and hybrid- and complex-type *N*-glycan structures, creating the lactosaminyl type 2 chains that serve as acceptors for terminal sialofucosylation reactions.

P-selectin ligand levels (124). Mice lacking the *O*-glycan core 1 β3galactosyltransferase (C1GalT-I) showed dramatic loss of leukocyte rolling on E-selectin and, consequently, these leukocytes did not transmigrate into inflamed tissues (125). Transgenic mouse studies, where the O-glycan core 2 β6-*N*-acetylglucosaminyltransferase-I (C2GnT-I) was knocked out, also showed reduced E-selectin and P-selectin binding activity of leukocytes under static and shear-based rolling assays, with impaired leukocyte recruitment to sites of inflammation (126–128). In agreement, in human moDCs, the downregulation of C2GnT-I, with concurrent upregulation of ST3Gal-I and GalNAc α(2,6)sialyltransferase (ST6GalNAc)-II, results in a loss of the core 2 structures required for O-glycan display of sLe^x (**Figure 5**) (129). Furthermore, studies using HL-60 cells have revealed that the ST6GalNAc-II overexpression abrogates sLe^x cell surface display and reduces the number of adherent cells to E-selectin under flow conditions, reinforcing the notion that there exists a competition between ST6GalNAc-II and C2GnT-I for core 1 acceptors, affecting the biosynthesis of sLe^x-bearing core 2-*O*-glycan structures (**Figure 5**) (130). Interestingly, in mice, knockout of one of the β(1,4)galactosyltransferases (of the family of five isoenzymes) involved in Type 2 lactosamine synthesis, β(1,4)galactosyltransferase-I (β(1,4)GalT-I), showed reduced inflammatory responses and impaired P-selectin binding activity; however, the contribution of this enzyme in the synthesis of E-selectin counter-receptors remains to be elucidated (131).

One study has recently evaluated the contributions of *N*-glycans, *O*-glycans and glycosphingolipids (GSLs) to E-selectin binding by human myeloid cells under physiological flow conditions (132). To address this issue, *O*-glycan and GSL synthesis was abolished by, respectively, knocking-out the core 1 Gal transferase chaperone, i.e., the C1GalT-I-specific Molecular Chaperone (COSMC), β1,2 GlcNAc-transferase (MGAT-I), and UDP-glucose ceramide glucosyltransferase (UGCG). Notably, these studies indicate that while *O*-glycans are indispensable for myeloid cell binding to L- and P-selectins, *N*-glycans play the major role in the initial myeloid cell recruitment into E-selectin-bearing substrates, with *O*-glycans playing a more modest role. In addition, both glycolipids and *N*-glycans are responsible for the slowing down of rolling velocities that precede firm arrest (132).

Most studies that have assessed biologic modulators of E-selectin ligands in leukocytes have been performed using human and murine T cells. An array of cytokines has been shown to regulate E-selectin ligand expression *via* upregulation or downregulation of specific glycosyltrasferases that control sLe^x expression. Specifically, IL-2, IL-7, IL-15, and IL-12 increase the expression of glycosyltransferases involved in the biosynthesis of E-selectin ligand determinants, whereas IL-4 has the opposite effect (133). This selectin ligand upregulation in T cells in response to cytokine signaling was shown to be dependent on Th1 transcription factor T-bet (134) and on STAT4-mediated pathways (135). Interestingly, human myeloid cells treated with granulocyte-colony stimulating factor (G-CSF) show increased cell surface expression of E-selectin ligands associated with significant increases in gene expression of the glycosyltransferases ST3Gal-IV, FTIV, and FTVII (136).

E-SELECTIN LIGAND ACTIVITY DISPLAYED BY CIRCULATING MPS SUBSETS

Among the cells of MPS, human circulating monocytes and, to a lesser extent, human blood cDCs and moDCs are the most comprehensively analyzed group in terms of E-selectin ligand activity. In our studies, human classical monocytes ($CD14^{++}CD16^{-}$) showed significantly higher levels of sLe^x determinants as compared to intermediate monocytes ($CD14^{++}CD16^{+}$), whereas non-classical monocytes ($CD14^{+}CD16^{++}$) were almost devoid of sLe^x expression (123). Another study compared the trafficking capacity of human monocyte subsets by analyzing their ability to bind to activated endothelial monolayers, and commensurately, classical monocytes showed noticeably higher capability of adhering to reactive endothelium than did non-classical/intermediate monocytes (137). In agreement with human studies, murine classical monocytes ($Ly\text{-}6C^{hi}$) exhibit greater binding to E-selectin under flow conditions and express higher levels of the scaffolds that bear sLe^x determinants compared to non-classical monocytes ($Ly\text{-}6C^{lo}$) (138, 139). This differential pattern of E-selectin ligand display is in agreement with the specific migratory requirements among the monocyte subsets: classical monocytes are typically recruited to inflamed lesions (138, 139), whereas non-classical monocytes migrate to non-inflamed endothelium (14) upon which they patrol healthy tissues in a LFA-1-dependent manner (19). Indeed, although the first observations of non-classical monocytes were made in non-inflamed skin blood vessels (19), these cells were further described in the microvasculature of kidney under steady-state conditions (20). The patrolling profile that these cells exhibit is independent of the activation state of the endothelium, since non-classical monocytes constitutively scavenge the luminal side of non-reactive endothelium (18). Therefore, their ability to bind to endothelium seems to be independent of E-selectin receptor/ligand interactions, but, instead, appears critically regulated by LFA-1 expression and its interaction with endothelial ICAM (19, 20). Notably, although selectins play a major role in the initial adhesive contacts with endothelium surfaces, integrins can also support tethering and rolling events under flow conditions, albeit with less potency than do selectins (140, 141).

Multiple adhesion molecules are involved in monocyte attachment to endothelium. While E-selectin receptor/ligand interactions prominently mediate Step 1 events in transmigration for all leukocytes, L-selectin-dependent binding interaction have also been observed to potently mediate human peripheral blood monocyte binding to activated vascular endothelium under shear stress (142–144). Thus, even though the majority of the reports indicates that initial monocyte adhesion to activated endothelial cells is most critically dependent on E-selectin receptor/ligand interactions (123, 145–150), distinct interactions were also reported by other authors. The differences have to do with differences in the leukocyte populations under study, variations in the assay conditions employed (i.e., shear stress levels employed, rotatory shear versus fluid shear conditions, temperature, etc.), differences in the adhesion metrics (i.e., number of adhered cells, number of rolling cells, rolling velocity measurements,

etc) altogether compounded by the innate biologic differences between mice and human cells, could alternatively emphasize the contribution(s) of other adhesion molecules.

Concerning DCs, human blood cDCs express high levels of sLe^x determinants, which allow them to tether and roll on E-selectin under flow conditions (151, 152). Importantly, in *in vivo* intravital microscopy studies, human blood cDCs adoptively transferred into mice were observed to roll along resting murine skin endothelium and extravasate at sites of inflammation (151). Notably, human moDCs significantly express sLe^x, especially on *O*-glycan structures. Upon maturation of moDCs with the TLR4 ligand, LPS, sLe^x expression is downregulated due to decreased C2GnT-I expression and upregulation of ST6GalNAc-II and ST3Gal-I (129). Biologically, these observations suggest that sLe^x is less relevant for transendothelial migration of TLR4-induced-mature moDCs, or that maturation is a step that follows transendothelial migration. By contrast, IFN-γ-induced maturation of moDCs leads to an upregulation of C2GnT-I, resulting in increased expression of core 2 *O*-glycan substrates for sLe^x decoration (153). These features suggest that sLe^x-bearing core 1-derived (or core 2) *O*-glycans are required for human moDC migration and are modulated according to specific maturation stimuli. Human pDCs also express sLe^x, allowing their recruitment to some inflamed tissues (38, 39, 154) and to reactive lymph nodes (43), a process believed to be mediated by the expression of E-selectin in HEVs (45, 47).

GLYCOCONJUGATE STRUCTURES THAT DISPLAY E-SELECTIN LIGAND DETERMINANTS IN CIRCULATING MPS CELLS

Several diverse and structurally singular glycostructures with E-selectin binding activity have been identified on human classical monocytes or human blood DCs. Human classical monocytes greatly display sLe^x decorations on an array of protein scaffolds, consisting of P-selectin glycoprotein ligand-1 (PSGL-1), CD43 and CD44, and GSLs (123), whereas human circulating DCs appear to display sLe^x solely on PSGL-1 (129, 155).

Cutaneous Lymphocyte Antigen

The cutaneous lymphocyte antigen (CLA) is the E-selectin-reactive glycoform of PSGL-1. PSGL-1 is a transmembrane 240-kDa homodimeric, mucin-like glycoprotein expressed on leukocytes (and, reportedly, on some activated endothelial cells) that plays a crucial role in the homing of leukocytes into inflamed tissue (156, 157). E-selectin binding activity of PSGL-1 is conferred by sialylated and fucosylated core 2-based-*O*-glycans that are cluster-distributed along the stalk region of the PSGL-1 extracellular domain (158). A number of studies have identified PSGL-1 as one of the several scaffolds expressed by human classical monocytes displaying E-selectin-binding activity (123, 155). On the other hand, PSGL-1 is the only known scaffold that presents sLe^x determinants on human circulating cDCs (151, 155) and moDCs (129). Yet, Silva et al. observed that although PSGL-1 is essential for P- and L-selectin recognition by human moDCs under fluid shear conditions, it is not mandatory for tethering to E-selectin (153). Moreover, there are reports that extravasation of murine immature DC to inflamed tissues requires both E- and P-selectin, but not PSGL-1 (159). Together, these data suggest the expression of ligands for E-selectin in addition to CLA by human and murine DCs. Still, PSGL-1 is the dominant ligand for P- and L- selectin and is the only known glycoprotein that binds all three selectins (160, 161). Accordingly, circulating monocytes that have already bound to E-selectin on inflamed endothelium can also interact with L-selectin expressed by other circulating monocytes/DCs *via* PSGL-1 and support their secondary capture, potentiating mononuclear phagocyte recruitment to sites of inflammation (162).

Hematopoietic Cell E- and L-Selectin Ligand

HCELL is a sialofucosylated glycoform of CD44 that exhibits potent E-selectin (and L-selectin) binding activity. CD44 is a transmembrane protein that exists in a wide variety of protein isoforms due to alternative splicing and extensive post-translational modifications (with molecular weight ranging from 80 to 220 kDa). CD44 is expressed by most mammalian cells, where it serves as the principal receptor for hyaloronic acid and participates in a broad range of cellular activities, including lymphocyte activation, leukocyte trafficking, hematopoiesis, cell growth and survival, and tumor dissemination (163). Post-translational modifications along with extensive alternative splicing allow the formation of multiple protein isoforms, expressed in a tissue-specific manner (164, 165). The standard protein isoform of CD44 (CD44s or CD44H) is encoded by mRNA transcripts comprising exons 1–5 and 16–20 ("s1–s5 and s6–s10"). CD44s is ubiquitously expressed by mammalian cells and is the form most often displayed by hematopoietic-lineage cells. In addition to CD44s, non-hematopoietic cells characteristically display CD44 variant isoforms contain peptide products of variant exons (exons "v2–v10") in addition to the standard exon peptide products.

CD44 post-translational modifications include the addition of different glycan structures, namely glycosaminoglycans, and *N*- and *O*-glycan substitutions (166). While previous studies indicated that HCELL was only expressed by human hematopoietic stem and progenitor cells (HSPCs) (167, 168), and some hematologic (167, 169) and solid malignancies (170), HCELL was recently reported to be expressed by classical human monocytes (123). Importantly, for human HSPCs, the sLe^x determinant is exclusively displayed on *N*-glycan lactosamines on CD44s, but classical monocytes express sLe^x on *O*-glycans of CD44s (123). Because of its ability to engage E- and L-selectin under relatively high fluid shear conditions (i.e., in excess of 20 dynes/cm^2 shear stress), HCELL is considered the most potent L- and E-selectin ligand expressed on mammalian cells (167, 171).

CD43E

CD43, also known as sialophorin or leukosialin, is a cell surface glycoprotein expressed by nearly all hematopoietic cells and is involved in several important processes, including cell development, activation, survival, and migration (172–176). Glycosylation

of CD43 molecules with either core 1 or core 2 *O*-glycan structures produces the ~115 and ~135 kDa glycoforms, respectively (177). Recently, we reported that human classical monocytes display E-selectin binding activity on CD43 (123). CD43 that displays sLe^x and binds E-selectin is known as "CD43E" and this protein harbors sLe^x on *O*-glycans (178).

Glycosphingolipids

In contrast to results in mouse leukocytes, reports using human cells have suggested that sialofucosylated determinants displayed on lipid scaffolds can mediate adhesion to E-selectin under static and flow conditions. In native human leukocytes and in the myelocytic leukemia cell line HL-60, the glycolipid structures that display ability to bind to E-selectin consist of sialylated lactosylceramides decorated with internal fucosylated GlcNAc structures (myeloglycans) (86, 87, 179). It has been reported that the disruption of myeloglycan biosynthesis *via* knockdown of ceramide glucosyltransferase (UGCG) in HL-60 cells disturbed stable cell rolling and impaired transmigration across inflamed endothelial cells (180). Finally, human classical monocytes treated with a broadly active protease did not show a complete abrogation of sLe^x staining, suggesting that although the majority of sialofucosylated moieties required for E-selectin binding are preferentially expressed on proteins rather than lipids, a considerable amount of sialofucosylated determinants are present on glycolipids (123).

PATHOPHYSIOLOGICAL IMPORTANCE OF THE SELECTINS

Due to its crucial role in the transmigration of specific myeloid populations to sites of inflammation, the selectin/selectin–ligand axis is involved in the development of many acute and chronic inflammatory conditions (181, 182). In fact, cutaneous inflammatory disorders, such as allergic contact dermatitis (183), atopic dermatitis (184–188), and psoriasis (183, 184, 189–191), are known to be promoted by the upregulation of selectins on dermal microvasculature. Specifically, P- and E-selectins are upregulated in skin lesions of cutaneous inflammatory patients, which enables inflammatory mononuclear phagocyte infiltration with subsequent release of soluble cytotoxic mediators, T cell activation, and destruction of the dermal layer of skin (154, 192–194). Atherosclerosis is another chronic inflammatory disease in which the recruitment of monocytes into selectin-expressing endothelial beds constitutes a key molecular event in the pathogenesis of the disease (195). Both E-and P-selectins are expressed on human arterial luminal endothelial cells of atherosclerotic plaques (195, 196), and mouse studies have shown that E-selectin and/or P-selectin deficiency substantially reduces the formation of atherosclerotic plaques, suggesting an overlapping function of these two selectins in the development of atherosclerotic lesions (197, 198). Murine classical monocytes ($Ly6C^{hi}$) preferentially migrate into activated endothelium and infiltrate developing atheromas to become atherosclerotic macrophages, inflammatory DCs, or foam cells (139). Indeed, murine classical monocytes display high levels of PSGL-1 and higher binding affinity to E-/P-selectin expressing cells than do the non-classical patrolling monocytes, which might explain why they are preferentially recruited to sites of endothelial inflammation and thrombosis (138).

Inflammatory bowel disease (199–202), multiple sclerosis (203, 204), rheumatoid arthritis (205–207), and type 1 diabetes (208, 209) are other examples of inflammatory diseases in which upregulated E-/P-selectin expression in tissue microvasculature drives myeloid cell recruitment crucial for the development of the disease. Increased E-selectin expression and mononuclear phagocyte infiltration have been similarly observed in cases of transplantation rejection, including human renal (210, 211), lung (212–214), and cardiac (215–217) rejection and in acute graft versus host disease (218–221). Recruitment of inflammatory classical monocytes (222, 223) and pDCs (38, 41, 224) to tumor-cell-activated endothelium has also been reported to be dependent on E-selectin expression, which can lead to an inhibition of the tumor-specific immune defense response and induction of tolerance (225, 226). Some studies have also indicated that inflammatory monocytes license extravasation of tumor cells *via* the induction of E-selectin-dependent adhesive interactions (222).

THERAPEUTIC STRATEGIES TARGETING THE SELECTIN/SELECTIN–LIGAND AXIS

The critical role of selectins and their ligands in the pathogenesis of many inflammatory conditions makes them potential molecular targets for therapy and, therefore, several strategies have been developed to interfere with this biology (182, 227, 228). One strategy relies on the development of pan-selectin competitive inhibitors that inhibit leukocyte/endothelial cell interaction and, therefore, cell recruitment to affected inflammatory or metastatic tissues. One example is the molecule Bimosiamose (Encysive Pharmaceuticals), a sLe^x mimetic that showed clinical efficacy in both asthma and psoriasis (229, 230). Other examples of pan-selectin inhibitors include sLe^x-peptides (231), sLe^x-bearing liposomes (232) or heparin oligosaccharides (233, 234). Also, GMI-127 and GMI-1271, E-selectin antagonists developed by GlycoMimetics based on the bioactive conformation of sLe^x in the carbohydrate-binding domain of E-selectin, have been used in treatment of sickle cell crisis (ClinicalTrials.gov Identifier: NCT00911495) and as an adjuvant for chemotherapy of hematological malignancies, including multiple myeloma and acute myeloid leukemia (NCT02811822, NCT02306291). In addition, an alternative approach involves the inhibition of the selectin ligand synthesis, either by interfering with the expression of key glycosyltransferases involved in sLe^x biosynthesis (235), or by using fluorinated analogs of Sia and/or Fuc residues (232, 236) that inhibit sLe^x synthesis. Finally, competing antibodies that bind to vascular E- and P-selectins and/or to selectin ligands expressed on the leukocyte cell surface constitute alternative methods that have been explored to prevent inflammatory exacerbation (182, 228). Indeed, a soluble form of PSGL-1 linked to the Fc portion of human IgG1 (PSGL-1-Ig) has been shown to inhibit leukocyte rolling in several disease models in mice (237–240).

On the other hand, the disruption of the selectin–leukocyte interaction has been reported to trigger severe immune-deficiency

by disruption of immunosurveillance (241). Leukocyte adhesion deficiency Type II is a rare genetic disorder characterized by defective neutrophil and monocyte migration caused by a mutation in a GDP-Fuc transporter gene (242). This mutation leads to the formation of glycans that lack fucosylation, resulting in impaired leukocyte rolling and consequent leukocytosis and recurrent infections (242, 243). To overcome deficient cellular rolling, our lab developed a FT-driven sLe^x biosynthesis approach to enforce cell surface expression of E-selectin ligands while preserving cell viability, called glycosyltransferase-programmed stereosubstitution (GPS) (244, 245). This platform uses optimized reaction conditions, which enables the efficient α(1,3)-fucosylation of underfucosylatated sialylated type 2 lactosamine acceptors (Siaα2-3Galβ1-4GlcNAc), *via* a soluble α(1,3) FT, installing expression of sLe^x (Siaα2-3Galβ1-4GlcNAcα1-3Fuc) (3). GPS has been used to improve the recruitment of a variety of human and mouse cells into E-selectin-bearing endothelial beds, driving cell migration into bone marrow and inflammatory sites (123, 178, 208, 244, 246–248).

CONCLUDING REMARKS

Specific migratory routes and distinct localization in steady and inflammatory conditions of the different human MPS subsets suggests that they play differential roles in immunity. These cells are operational in multiple beneficial processes, including immediate antimicrobial host defense, activation of the adaptive immune system, and tissue healing processes. However, they may also contribute to the pathobiology of several inflammatory conditions. A better understanding of the molecular basis of glycosylation-dependent creation of E-selectin ligands could yield the development of novel therapeutic approaches for inflammatory diseases, or, alternatively, could yield enhanced ability to infiltrate sites where immunity is needed (e.g., tumors or infection). To our knowledge, only a limited number of studies have analyzed the functional and structural biology of the full spectrum of E-selectin ligands expressed by different circulating human MPS subsets. Future work will be required to address this issue and to elucidate how custom-modified expression of these homing receptors can be achieved to preferentially influence the specific migratory routes of the different subsets of circulating MPS cells.

AUTHOR CONTRIBUTIONS

All authors listed have made a substantial, direct, and intellectual contribution to the work and approved it for publication.

ACKNOWLEDGMENTS

We thank Dr. Nandini Mondal and Kyle Martin for their helpful review of the manuscript.

FUNDING

This work was supported by the National Institutes of Health National Heart Lung Blood Institute grant PO1 HL107146 (Program of Excellence in Glycosciences) (RS), and by the Team Jobie Fund (RS) and the Faye Geronemus Leukemia Research Fund (RS). INclude Fulbright Commission fellowship (to PAV).

REFERENCES

1. Haniffa M, Bigley V, Collin M. Human mononuclear phagocyte system reunited. *Semin Cell Dev Biol* (2015) 41:59–69. doi:10.1016/j.semcdb.2015.05.004
2. Chow A, Brown BD, Merad M. Studying the mononuclear phagocyte system in the molecular age. *Nat Rev Immunol* (2011) 11(11):788–98. doi:10.1038/nri3087
3. Sackstein R. Glycosyltransferase-programmed stereosubstitution (GPS) to create HCELL: engineering a roadmap for cell migration. *Immunol Rev* (2009) 230(1):51–74. doi:10.1111/j.1600-065X.2009.00792.x
4. Kunkel EJ, Ley K. Distinct phenotype of E-selectin-deficient mice. E-selectin is required for slow leukocyte rolling in vivo. *Circ Res* (1996) 79(6):1196–204. doi:10.1161/01.RES.79.6.1196
5. van Furth R, Cohn ZA. The origin and kinetics of mononuclear phagocytes. *J Exp Med* (1968) 128(3):415–35. doi:10.1084/jem.128.3.415
6. Jakubzick C, Gautier EL, Gibbings SL, Sojka DK, Schlitzer A, Johnson TE, et al. Minimal differentiation of classical monocytes as they survey steady-state tissues and transport antigen to lymph nodes. *Immunity* (2013) 39(3):599–610. doi:10.1016/j.immuni.2013.08.007
7. Epelman S, Lavine KJ, Beaudin AE, Sojka DK, Carrero JA, Calderon B, et al. Embryonic and adult-derived resident cardiac macrophages are maintained through distinct mechanisms at steady state and during inflammation. *Immunity* (2014) 40(1):91–104. doi:10.1016/j.immuni.2013.11.019
8. Bain CC, Scott CL, Uronen-Hansson H, Gudjonsson S, Jansson O, Grip O, et al. Resident and pro-inflammatory macrophages in the colon represent alternative context-dependent fates of the same Ly6Chi monocyte precursors. *Mucosal Immunol* (2013) 6(3):498–510. doi:10.1038/mi.2012.89
9. Rivollier A, He J, Kole A, Valatas V, Kelsall BL. Inflammation switches the differentiation program of Ly6Chi monocytes from antiinflammatory macrophages to inflammatory dendritic cells in the colon. *J Exp Med* (2012) 209(1):139–55. doi:10.1084/jem.20101387
10. Serbina NV, Jia T, Hohl TM, Pamer EG. Monocyte-mediated defense against microbial pathogens. *Annu Rev Immunol* (2008) 26:421–52. doi:10.1146/annurev.immunol.26.021607.090326
11. Gordon S, Taylor PR. Monocyte and macrophage heterogeneity. *Nat Rev Immunol* (2005) 5(12):953–64. doi:10.1038/nri1733
12. Shi C, Pamer EG. Monocyte recruitment during infection and inflammation. *Nat Rev Immunol* (2011) 11(11):762–74. doi:10.1038/nri3070
13. Stansfield BK, Ingram DA. Clinical significance of monocyte heterogeneity. *Clin Transl Med* (2015) 4:5. doi:10.1186/s40169-014-0040-3
14. Geissmann F, Jung S, Littman DR. Blood monocytes consist of two principal subsets with distinct migratory properties. *Immunity* (2003) 19(1):71–82. doi:10.1016/S1074-7613(03)00174-2
15. Ziegler-Heitbrock L, Ancuta P, Crowe S, Dalod M, Grau V, Hart DN, et al. Nomenclature of monocytes and dendritic cells in blood. *Blood* (2010) 116(16):e74–80. doi:10.1182/blood-2010-02-258558
16. Kratofil RM, Kubes P, Deniset JF. Monocyte conversion during inflammation and injury. *Arterioscler Thromb Vasc Biol* (2016) 37(1):35–42. doi:10.1161/ATVBAHA.116.308198
17. Ziegler-Heitbrock L, Hofer TP. Toward a refined definition of monocyte subsets. *Front Immunol* (2013) 4:23. doi:10.3389/fimmu.2013.00023
18. Thomas G, Tacke R, Hedrick CC, Hanna RN. Nonclassical patrolling monocyte function in the vasculature. *Arterioscler Thromb Vasc Biol* (2015) 35(6):1306–16. doi:10.1161/ATVBAHA.114.304650
19. Auffray C, Fogg D, Garfa M, Elain G, Join-Lambert O, Kayal S, et al. Monitoring of blood vessels and tissues by a population of monocytes with patrolling behavior. *Science* (2007) 317(5838):666–70. doi:10.1126/science.1142883

20. Carlin LM, Stamatiades EG, Auffray C, Hanna RN, Glover L, Vizcay-Barrena G, et al. Nr4a1-dependent Ly6C(low) monocytes monitor endothelial cells and orchestrate their disposal. *Cell* (2013) 153(2):362–75. doi:10.1016/j.cell.2013.03.010
21. Cros J, Cagnard N, Woollard K, Patey N, Zhang SY, Senechal B, et al. Human CD14dim monocytes patrol and sense nucleic acids and viruses via TLR7 and TLR8 receptors. *Immunity* (2010) 33(3):375–86. doi:10.1016/j.immuni.2010.08.012
22. Yang J, Zhang L, Yu C, Yang XF, Wang H. Monocyte and macrophage differentiation: circulation inflammatory monocyte as biomarker for inflammatory diseases. *Biomark Res* (2014) 2(1):1. doi:10.1186/2050-7771-2-1
23. Passos S, Carvalho LP, Costa RS, Campos TM, Novais FO, Magalhaes A, et al. Intermediate monocytes contribute to pathologic immune response in *Leishmania braziliensis* infections. *J Infect Dis* (2015) 211(2):274–82. doi:10.1093/infdis/jiu439
24. Tolouei Semnani R, Moore V, Bennuru S, McDonald-Fleming R, Ganesan S, Cotton R, et al. Human monocyte subsets at homeostasis and their perturbation in numbers and function in filarial infection. *Infect Immun* (2014) 82(11):4438–46. doi:10.1128/IAI.01973-14
25. Lin KW, Jacek T, Jacek R. Dendritic cells heterogeneity and its role in cancer immunity. *J Cancer Res Ther* (2006) 2(2):35–40. doi:10.4103/0973-1482.25847
26. Ishikawa F, Niiro H, Iino T, Yoshida S, Saito N, Onohara S, et al. The developmental program of human dendritic cells is operated independently of conventional myeloid and lymphoid pathways. *Blood* (2007) 110(10):3591–660. doi:10.1182/blood-2007-02-071613
27. Shortman K, Naik SH. Steady-state and inflammatory dendritic-cell development. *Nat Rev Immunol* (2007) 7(1):19–30. doi:10.1038/nri1996
28. Boltjes A, van Wijk F. Human dendritic cell functional specialization in steady-state and inflammation. *Front Immunol* (2014) 5:131. doi:10.3389/fimmu.2014.00131
29. Hawiger D, Inaba K, Dorsett Y, Guo M, Mahnke K, Rivera M, et al. Dendritic cells induce peripheral T cell unresponsiveness under steady state conditions in vivo. *J Exp Med* (2001) 194(6):769–79. doi:10.1084/jem.194.6.769
30. Huang FP, Platt N, Wykes M, Major JR, Powell TJ, Jenkins CD, et al. A discrete subpopulation of dendritic cells transports apoptotic intestinal epithelial cells to T cell areas of mesenteric lymph nodes. *J Exp Med* (2000) 191(3):435–44. doi:10.1084/jem.191.3.435
31. Matsuno K, Ezaki T, Kudo S, Uehara Y. A life stage of particle-laden rat dendritic cells in vivo: their terminal division, active phagocytosis, and translocation from the liver to the draining lymph. *J Exp Med* (1996) 183(4):1865–78. doi:10.1084/jem.183.4.1865
32. Crespo HJ, Lau JT, Videira PA. Dendritic cells: a spot on sialic Acid. *Front Immunol* (2013) 4:491. doi:10.3389/fimmu.2013.00491
33. Segura E, Valladeau-Guilemond J, Donnadieu MH, Sastre-Garau X, Soumelis V, Amigorena S. Characterization of resident and migratory dendritic cells in human lymph nodes. *J Exp Med* (2012) 209(4):653–60. doi:10.1084/jem.20111457
34. Segura E, Amigorena S. Inflammatory dendritic cells in mice and humans. *Trends Immunol* (2013) 34(9):440–5. doi:10.1016/j.it.2013.06.001
35. Segura E, Amigorena S. Identification of human inflammatory dendritic cells. *Oncoimmunology* (2013) 2(5):e23851. doi:10.4161/onci.23851
36. Serbina NV, Salazar-Mather TP, Biron CA, Kuziel WA, Pamer EG. TNF/iNOS-producing dendritic cells mediate innate immune defense against bacterial infection. *Immunity* (2003) 19(1):59–70. doi:10.1016/S1074-7613(03)00171-7
37. Mathan TS, Figdor CG, Buschow SI. Human plasmacytoid dendritic cells: from molecules to intercellular communication network. *Front Immunol* (2013) 4:372. doi:10.3389/fimmu.2013.00372
38. Salio M, Cella M, Vermi W, Facchetti F, Palmowski MJ, Smith CL, et al. Plasmacytoid dendritic cells prime IFN-gamma-secreting melanoma-specific CD8 lymphocytes and are found in primary melanoma lesions. *Eur J Immunol* (2003) 33(4):1052–62. doi:10.1002/eji.200323676
39. Hartmann E, Wollenberg B, Rothenfusser S, Wagner M, Wellisch D, Mack B, et al. Identification and functional analysis of tumor-infiltrating plasmacytoid dendritic cells in head and neck cancer. *Cancer Res* (2003) 63(19):6478–87.
40. Zou W, Machelon V, Coulomb-L'Hermin A, Borvak J, Nome F, Isaeva T, et al. Stromal-derived factor-1 in human tumors recruits and alters the function of plasmacytoid precursor dendritic cells. *Nat Med* (2001) 7(12):1339–46. doi:10.1038/nm1201-1339
41. Vermi W, Bonecchi R, Facchetti F, Bianchi D, Sozzani S, Festa S, et al. Recruitment of immature plasmacytoid dendritic cells (plasmacytoid monocytes) and myeloid dendritic cells in primary cutaneous melanomas. *J Pathol* (2003) 200(2):255–68. doi:10.1002/path.1344
42. Conrad C, Meller S, Gilliet M. Plasmacytoid dendritic cells in the skin: to sense or not to sense nucleic acids. *Semin Immunol* (2009) 21(3):101–9. doi:10.1016/j.smim.2009.01.004
43. Cella M, Jarrossay D, Facchetti F, Alebardi O, Nakajima H, Lanzavecchia A, et al. Plasmacytoid monocytes migrate to inflamed lymph nodes and produce large amounts of type I interferon. *Nat Med* (1999) 5(8):919–23. doi:10.1038/11360
44. Banchereau J, Pulendran B, Steinman R, Palucka K. Will the making of plasmacytoid dendritic cells in vitro help unravel their mysteries? *J Exp Med* (2000) 192(12):F39–44. doi:10.1084/jem.192.12.F39
45. Yoneyama H, Matsuno K, Zhang Y, Nishiwaki T, Kitabatake M, Ueha S, et al. Evidence for recruitment of plasmacytoid dendritic cell precursors to inflamed lymph nodes through high endothelial venules. *Int Immunol* (2004) 16(7):915–28. doi:10.1093/intimm/dxh093
46. Yrlid U, Cerovic V, Milling S, Jenkins CD, Zhang J, Crocker PR, et al. Plasmacytoid dendritic cells do not migrate in intestinal or hepatic lymph. *J Immunol* (2006) 177(9):6115–21. doi:10.4049/jimmunol.177.9.6115
47. Diacovo TG, Blasius AL, Mak TW, Cella M, Colonna M. Adhesive mechanisms governing interferon-producing cell recruitment into lymph nodes. *J Exp Med* (2005) 202(5):687–96. doi:10.1084/jem.20051035
48. Ginhoux F, Greter M, Leboeuf M, Nandi S, See P, Gokhan S, et al. Fate mapping analysis reveals that adult microglia derive from primitive macrophages. *Science* (2010) 330(6005):841–5. doi:10.1126/science.1194637
49. Sieweke MH, Allen JE. Beyond stem cells: self-renewal of differentiated macrophages. *Science* (2013) 342(6161):1242974. doi:10.1126/science.1242974
50. Hoefsmit EC. Macrophages, Langerhans cells, interdigitating and dendritic accessory cells: a summary. *Adv Exp Med Biol* (1982) 149:463–8. doi:10.1007/978-1-4684-9066-4_65
51. Gordon S, Plüddemann A, Martinez Estrada F. Macrophage heterogeneity in tissues: phenotypic diversity and functions. *Immunol Rev* (2014) 262(1):36–55. doi:10.1111/imr.12223
52. Kindt TJ, Goldsby RA, Osborne BA. Overview of the immune system. *Kuby Immunology*, Chapter 1, 6th ed. New York, United States: WH Freeman & Company (2007). 574 p.
53. Mosser DM, Edwards JP. Exploring the full spectrum of macrophage activation. *Nat Rev Immunol* (2008) 8(12):958–69. doi:10.1038/nri2448
54. Italiani P, Boraschi D. From monocytes to M1/M2 macrophages: phenotypical vs. functional differentiation. *Front Immunol* (2014) 5:514. doi:10.3389/fimmu.2014.00514
55. Ferenbach D, Hughes J. Macrophages and dendritic cells: what is the difference? *Kidney Int* (2008) 74(1):5–7. doi:10.1038/ki.2008.189
56. Butcher EC. Leukocyte-endothelial cell recognition: three (or more) steps to specificity and diversity. *Cell* (1991) 67(6):1033–6. doi:10.1016/0092-8674(91)90279-8
57. Ley K, Laudanna C, Cybulsky MI, Nourshargh S. Getting to the site of inflammation: the leukocyte adhesion cascade updated. *Nat Rev Immunol* (2007) 7(9):678–89. doi:10.1038/nri2156
58. Vestweber D. Novel insights into leukocyte extravasation. *Curr Opin Hematol* (2012) 19(3):212–7. doi:10.1097/MOH.0b013e3283523e78
59. Jacobs PP, Sackstein R. CD44 and HCELL: preventing hematogenous metastasis at step 1. *FEBS Lett* (2011) 585(20):3148–58. doi:10.1016/j.febslet.2011.07.039
60. Lawrence MB, Kansas GS, Kunkel EJ, Ley K. Threshold levels of fluid shear promote leukocyte adhesion through selectins (CD62L,P,E). *J Cell Biol* (1997) 136(3):717–27. doi:10.1083/jcb.136.3.717
61. Tedder TF, Steeber DA, Chen A, Engel P. The selectins: vascular adhesion molecules. *FASEB J* (1995) 9(10):866–73.
62. Tedder TF, Isaacs CM, Ernst TJ, Demetri GD, Adler DA, Disteche CM. Isolation and chromosomal localization of cDNAs encoding a novel human lymphocyte cell surface molecule, LAM-1. Homology with the mouse lymphocyte homing receptor and other human adhesion proteins. *J Exp Med* (1989) 170(1):123–33. doi:10.1084/jem.170.1.123
63. Bevilacqua MP, Stengelin S, Gimbrone MA Jr, Seed B. Endothelial leukocyte adhesion molecule 1: an inducible receptor for neutrophils related to

complement regulatory proteins and lectins. *Science* (1989) 243(4895):1160–5. doi:10.1126/science.2466335
64. Johnston GI, Cook RG, McEver RP. Cloning of GMP-140, a granule membrane protein of platelets and endothelium: sequence similarity to proteins involved in cell adhesion and inflammation. *Cell* (1989) 56(6):1033–44. doi:10.1016/0092-8674(89)90636-3
65. Lasky LA. Selectin-carbohydrate interactions and the initiation of the inflammatory response. *Annu Rev Biochem* (1995) 64:113–39. doi:10.1146/annurev.bi.64.070195.000553
66. Stamper HB Jr, Woodruff JJ. Lymphocyte homing into lymph nodes: in vitro demonstration of the selective affinity of recirculating lymphocytes for high-endothelial venules. *J Exp Med* (1976) 144(3):828–33. doi:10.1084/jem.144.3.828
67. Gallatin WM, Weissman IL, Butcher EC. A cell-surface molecule involved in organ-specific homing of lymphocytes. *Nature* (1983) 304(5921):30–4. doi:10.1038/304030a0
68. Smalley DM, Ley K. L-selectin: mechanisms and physiological significance of ectodomain cleavage. *J Cell Mol Med* (2005) 9(2):255–66. doi:10.1111/j.1582-4934.2005.tb00354.x
69. Rosen SD. Ligands for L-selectin: homing, inflammation, and beyond. *Annu Rev Immunol* (2004) 22:129–56. doi:10.1146/annurev.immunol.21.090501.080131
70. McEver RP, Martin MN. A monoclonal antibody to a membrane glycoprotein binds only to activated platelets. *J Biol Chem* (1984) 259(15):9799–804.
71. Stenberg PE, McEver RP, Shuman MA, Jacques YV, Bainton DF. A platelet alpha-granule membrane protein (GMP-140) is expressed on the plasma membrane after activation. *J Cell Biol* (1985) 101(3):880–6. doi:10.1083/jcb.101.3.880
72. Hsu-Lin S, Berman CL, Furie BC, August D, Furie B. A platelet membrane protein expressed during platelet activation and secretion. Studies using a monoclonal antibody specific for thrombin-activated platelets. *J Biol Chem* (1984) 259(14):9121–6.
73. Sanders WE, Wilson RW, Ballantyne CM, Beaudet AL. Molecular cloning and analysis of in vivo expression of murine P-selectin. *Blood* (1992) 80(3):795–800.
74. Pan J, Xia L, Yao L, McEver RP. Tumor necrosis factor-alpha- or lipopolysaccharide-induced expression of the murine P-selectin gene in endothelial cells involves novel kappaB sites and a variant activating transcription factor/cAMP response element. *J Biol Chem* (1998) 273(16):10068–77. doi:10.1074/jbc.273.16.10068
75. Sperandio M. Selectins and glycosyltransferases in leukocyte rolling in vivo. *FEBS J* (2006) 273(19):4377–89. doi:10.1111/j.1742-4658.2006.05437.x
76. Pan J, Xia L, McEver RP. Comparison of promoters for the murine and human P-selectin genes suggests species-specific and conserved mechanisms for transcriptional regulation in endothelial cells. *J Biol Chem* (1998) 273(16):10058–67. doi:10.1074/jbc.273.16.10058
77. Yao L, Setiadi H, Xia L, Laszik Z, Taylor FB, McEver RP. Divergent inducible expression of P-selectin and E-selectin in mice and primates. *Blood* (1999) 94(11):3820–8.
78. Bevilacqua MP, Pober JS, Mendrick DL, Cotran RS, Gimbrone MA. Identification of an inducible endothelial-leukocyte adhesion molecule. *Proc Natl Acad Sci U S A* (1987) 84(24):9238–42. doi:10.1073/pnas.84.24.9238
79. Sackstein R. Glycoengineering of HCELL, the human bone marrow homing receptor: sweetly programming cell migration. *Ann Biomed Eng* (2012) 40(4):766–76. doi:10.1007/s10439-011-0461-8
80. Vestweber D, Blanks JE. Mechanisms that regulate the function of the selectins and their ligands. *Physiol Rev* (1999) 79(1):181–213.
81. Lewis H, Kaszubska W, DeLamarter JF, Whelan J. Cooperativity between two NF-kappa B complexes, mediated by high-mobility-group protein I(Y), is essential for cytokine-induced expression of the E-selectin promoter. *Mol Cell Biol* (1994) 14(9):5701–9. doi:10.1128/MCB.14.9.5701
82. Ley K, Allietta M, Bullard DC, Morgan S. Importance of E-selectin for firm leukocyte adhesion in vivo. *Circ Res* (1998) 83(3):287–94. doi:10.1161/01.RES.83.3.287
83. Phillips ML, Nudelman E, Gaeta FC, Perez M, Singhal AK, Hakomori S, et al. ELAM-1 mediates cell adhesion by recognition of a carbohydrate ligand, sialyl-Lex. *Science* (1990) 250(4984):1130–2. doi:10.1126/science.1701274
84. Tyrrell D, James P, Rao N, Foxall C, Abbas S, Dasgupta F, et al. Structural requirements for the carbohydrate ligand of E-selectin. *Proc Natl Acad Sci U S A* (1991) 88(22):10372–6. doi:10.1073/pnas.88.22.10372
85. Munro JM, Lo SK, Corless C, Robertson MJ, Lee NC, Barnhill RL, et al. Expression of sialyl-Lewis X, an E-selectin ligand, in inflammation, immune processes, and lymphoid tissues. *Am J Pathol* (1992) 141(6):1397–408.
86. Handa K, Stroud MR, Hakomori S. Sialosyl-fucosyl poly-LacNAc without the sialosyl-Lex epitope as the physiological myeloid cell ligand in E-selectin-dependent adhesion: studies under static and dynamic flow conditions. *Biochemistry* (1997) 36(41):12412–20. doi:10.1021/bi971181t
87. Stroud MR, Handa K, Salyan ME, Ito K, Levery SB, Hakomori S, et al. Monosialogangliosides of human myelogenous leukemia HL60 cells and normal human leukocytes. 2. Characterization of E-selectin binding fractions, and structural requirements for physiological binding to E-selectin. *Biochemistry* (1996) 35(3):770–8. doi:10.1021/bi952461g
88. Nimrichter L, Burdick MM, Aoki K, Laroy W, Fierro MA, Hudson SA, et al. E-selectin receptors on human leukocytes. *Blood* (2008) 112(9):3744–52. doi:10.1182/blood-2008-04-149641
89. Ugorski M, Laskowska A. Sialyl Lewis(a): a tumor-associated carbohydrate antigen involved in adhesion and metastatic potential of cancer cells. *Acta Biochim Pol* (2002) 49(2):303–11.
90. Yuen CT, Bezouska K, O'Brien J, Stoll M, Lemoine R, Lubineau A, et al. Sulfated blood group Lewis(a). A superior oligosaccharide ligand for human E-selectin. *J Biol Chem* (1994) 269(3):1595–8.
91. Yuen CT, Lawson AM, Chai W, Larkin M, Stoll MS, Stuart AC, et al. Novel sulfated ligands for the cell adhesion molecule E-selectin revealed by the neoglycolipid technology among O-linked oligosaccharides on an ovarian cystadenoma glycoprotein. *Biochemistry* (1992) 31(38):9126–31. doi:10.1021/bi00153a003
92. Grinnell BW, Hermann RB, Yan SB. Human protein C inhibits selectin-mediated cell adhesion: role of unique fucosylated oligosaccharide. *Glycobiology* (1994) 4(2):221–5. doi:10.1093/glycob/4.2.221
93. Lowe JB. Glycan-dependent leukocyte adhesion and recruitment in inflammation. *Curr Opin Cell Biol* (2003) 15(5):531–8. doi:10.1016/j.ceb.2003.08.002
94. Lowe JB. Glycosylation in the control of selectin counter-receptor structure and function. *Immunol Rev* (2002) 186:19–36. doi:10.1034/j.1600-065X.2002.18603.x
95. Dall'Olio F, Chiricolo M. Sialyltransferases in cancer. *Glycoconj J* (2001) 18(11–12):841–50. doi:10.1023/A:1022288022969
96. Cazet A, Julien S, Bobowski M, Burchell J, Delannoy P. Tumour-associated carbohydrate antigens in breast cancer. *Breast Cancer Res* (2010) 12(3):204. doi:10.1186/bcr2577
97. Harduin-Lepers A, Vallejo-Ruiz V, Krzewinski-Recchi MA, Samyn-Petit B, Julien S, Delannoy P. The human sialyltransferase family. *Biochimie* (2001) 83(8):727–37. doi:10.1016/S0300-9084(01)01301-3
98. Sasaki K, Watanabe E, Kawashima K, Sekine S, Dohi T, Oshima M, et al. Expression cloning of a novel Gal beta (1-3/1-4) GlcNAc alpha 2,3-sialyltransferase using lectin resistance selection. *J Biol Chem* (1993) 268(30):22782–7.
99. Kitagawa H, Paulson JC. Cloning of a novel alpha 2,3-sialyltransferase that sialylates glycoprotein and glycolipid carbohydrate groups. *J Biol Chem* (1994) 269(2):1394–401.
100. Okajima T, Fukumoto S, Miyazaki H, Ishida H, Kiso M, Furukawa K, et al. Molecular cloning of a novel alpha2,3-sialyltransferase (ST3Gal VI) that sialylates type II lactosamine structures on glycoproteins and glycolipids. *J Biol Chem* (1999) 274(17):11479–86. doi:10.1074/jbc.274.17.11479
101. de Vries T, Knegtel RM, Holmes EH, Macher BA. Fucosyltransferases: structure/function studies. *Glycobiology* (2001) 11(10):119R–28R. doi:10.1093/glycob/11.10.119R
102. Mollicone R, Reguigne I, Kelly RJ, Fletcher A, Watt J, Chatfield S, et al. Molecular basis for Lewis alpha(1,3/1,4)-fucosyltransferase gene deficiency (FUT3) found in Lewis-negative Indonesian pedigrees. *J Biol Chem* (1994) 269(33):20987–94.
103. Kukowska-Latallo JF, Larsen RD, Nair RP, Lowe JB. A cloned human cDNA determines expression of a mouse stage-specific embryonic antigen and the Lewis blood group alpha(1,3/1,4)fucosyltransferase. *Genes Dev* (1990) 4(8):1288–303. doi:10.1101/gad.4.8.1288
104. Weston BW, Nair RP, Larsen RD, Lowe JB. Isolation of a novel human alpha (1,3)fucosyltransferase gene and molecular comparison to the human Lewis blood group alpha (1,3/1,4)fucosyltransferase gene. Syntenic, homologous, nonallelic genes encoding enzymes with distinct acceptor substrate specificities. *J Biol Chem* (1992) 267(6):4152–60.

105. Lowe JB, Kukowska-Latallo JF, Nair RP, Larsen RD, Marks RM, Macher BA, et al. Molecular cloning of a human fucosyltransferase gene that determines expression of the Lewis x and VIM-2 epitopes but not ELAM-1-dependent cell adhesion. *J Biol Chem* (1991) 266(26):17467–77.
106. Nakayama F, Nishihara S, Iwasaki H, Kudo T, Okubo R, Kaneko M, et al. CD15 expression in mature granulocytes is determined by alpha 1,3-fucosyltransferase IX, but in promyelocytes and monocytes by alpha 1,3-fucosyltransferase IV. *J Biol Chem* (2001) 276(19):16100–6. doi:10.1074/jbc.M007272200
107. Goelz S, Kumar R, Potvin B, Sundaram S, Brickelmaier M, Stanley P. Differential expression of an E-selectin ligand (SLex) by two Chinese hamster ovary cell lines transfected with the same alpha (1,3)-fucosyltransferase gene (ELFT). *J Biol Chem* (1994) 269(2):1033–40.
108. Barthel SR, Wiese GK, Cho J, Opperman MJ, Hays DL, Siddiqui J, et al. Alpha 1,3 fucosyltransferases are master regulators of prostate cancer cell trafficking. *Proc Natl Acad Sci U S A* (2009) 106(46):19491–6. doi:10.1073/pnas.0906074106
109. De Vries T, Palcic MP, Schoenmakers PS, Van Den Eijnden DH, Joziasse DH. Acceptor specificity of GDP-Fuc:Gal beta 1 – >4GlcNAc-R alpha 3-fucosyltransferase VI (FucT VI) expressed in insect cells as soluble, secreted enzyme. *Glycobiology* (1997) 7(7):921–7. doi:10.1093/glycob/7.7.921
110. Weston BW, Smith PL, Kelly RJ, Lowe JB. Molecular cloning of a fourth member of a human alpha (1,3)fucosyltransferase gene family. Multiple homologous sequences that determine expression of the Lewis x, sialyl Lewis x, and difucosyl sialyl Lewis x epitopes. *J Biol Chem* (1992) 267(34):24575–84.
111. Britten CJ, van den Eijnden DH, McDowell W, Kelly VA, Witham SJ, Edbrooke MR, et al. Acceptor specificity of the human leukocyte alpha3 fucosyltransferase: role of FucT-VII in the generation of selectin ligands. *Glycobiology* (1998) 8(4):321–7. doi:10.1093/glycob/8.4.321
112. Sasaki K, Kurata K, Funayama K, Nagata M, Watanabe E, Ohta S, et al. Expression cloning of a novel alpha 1,3-fucosyltransferase that is involved in biosynthesis of the sialyl Lewis x carbohydrate determinants in leukocytes. *J Biol Chem* (1994) 269(20):14730–7.
113. Ellies LG, Sperandio M, Underhill GH, Yousif J, Smith M, Priatel JJ, et al. Sialyltransferase specificity in selectin ligand formation. *Blood* (2002) 100(10):3618–25. doi:10.1182/blood-2002-04-1007
114. Yang WH, Nussbaum C, Grewal PK, Marth JD, Sperandio M. Coordinated roles of ST3Gal-VI and ST3Gal-IV sialyltransferases in the synthesis of selectin ligands. *Blood* (2012) 120(5):1015–26. doi:10.1182/blood-2012-04-424366
115. Mondal N, Buffone A, Stolfa G, Antonopoulos A, Lau JT, Haslam SM, et al. ST3Gal-4 is the primary sialyltransferase regulating the synthesis of E-, P-, and L-selectin ligands on human myeloid leukocytes. *Blood* (2015) 125(4):687–96. doi:10.1182/blood-2014-07-588590
116. Maly P, Thall A, Petryniak B, Rogers CE, Smith PL, Marks RM, et al. The alpha(1,3)fucosyltransferase Fuc-TVII controls leukocyte trafficking through an essential role in L-, E-, and P-selectin ligand biosynthesis. *Cell* (1996) 86(4):643–53. doi:10.1016/S0092-8674(00)80137-3
117. Smithson G, Rogers CE, Smith PL, Scheidegger EP, Petryniak B, Myers JT, et al. Fuc-TVII is required for T helper 1 and T cytotoxic 1 lymphocyte selectin ligand expression and recruitment in inflammation, and together with Fuc-TIV regulates naive T cell trafficking to lymph nodes. *J Exp Med* (2001) 194(5):601–14. doi:10.1084/jem.194.5.601
118. Homeister JW, Thall AD, Petryniak B, Malý P, Rogers CE, Smith PL, et al. The alpha(1,3)fucosyltransferases FucT-IV and FucT-VII exert collaborative control over selectin-dependent leukocyte recruitment and lymphocyte homing. *Immunity* (2001) 15(1):115–26. doi:10.1016/S1074-7613(01)00166-2
119. Weninger W, Ulfman LH, Cheng G, Souchkova N, Quackenbush EJ, Lowe JB, et al. Specialized contributions by alpha(1,3)-fucosyltransferase-IV and FucT-VII during leukocyte rolling in dermal microvessels. *Immunity* (2000) 12(6):665–76. doi:10.1016/S1074-7613(00)80217-4
120. Huang MC, Laskowska A, Vestweber D, Wild MK. The alpha (1,3)-fucosyltransferase Fuc-TIV, but not Fuc-TVII, generates sialyl Lewis X-like epitopes preferentially on glycolipids. *J Biol Chem* (2002) 277(49):47786–95. doi:10.1074/jbc.M208283200
121. Buffone A, Mondal N, Gupta R, McHugh KP, Lau JT, Neelamegham S. Silencing α1,3-fucosyltransferases in human leukocytes reveals a role for FUT9 enzyme during E-selectin-mediated cell adhesion. *J Biol Chem* (2013) 288(3):1620–33. doi:10.1074/jbc.M112.400929
122. Kaneko M, Kudo T, Iwasaki H, Ikehara Y, Nishihara S, Nakagawa S, et al. Alpha1,3-fucosyltransferase IX (Fuc-TIX) is very highly conserved between human and mouse; molecular cloning, characterization and tissue distribution of human Fuc-TIX. *FEBS Lett* (1999) 452(3):237–42. doi:10.1016/S0014-5793(99)00640-7
123. Silva M, Fung RKF, Donnelly CB, Videira PA, Sackstein R. Cell-specific variation in E-selectin ligand expression among human peripheral blood mononuclear cells: implications for immunosurveillance and pathobiology. *J Immunol* (2017) 198(9):3576–87. doi:10.4049/jimmunol.1601636
124. Tenno M, Ohtsubo K, Hagen FK, Ditto D, Zarbock A, Schaerli P, et al. Initiation of protein O glycosylation by the polypeptide GalNAcT-1 in vascular biology and humoral immunity. *Mol Cell Biol* (2007) 27(24):8783–96. doi:10.1128/MCB.01204-07
125. Yago T, Fu J, McDaniel JM, Miner JJ, McEver RP, Xia L. Core 1-derived O-glycans are essential E-selectin ligands on neutrophils. *Proc Natl Acad Sci U S A* (2010) 107(20):9204–9. doi:10.1073/pnas.1003110107
126. Ellies LG, Tsuboi S, Petryniak B, Lowe JB, Fukuda M, Marth JD. Core 2 oligosaccharide biosynthesis distinguishes between selectin ligands essential for leukocyte homing and inflammation. *Immunity* (1998) 9(6):881–90. doi:10.1016/S1074-7613(00)80653-6
127. Sperandio M, Thatte A, Foy D, Ellies LG, Marth JD, Ley K. Severe impairment of leukocyte rolling in venules of core 2 glucosaminyltransferase-deficient mice. *Blood* (2001) 97(12):3812–9. doi:10.1182/blood.V97.12.3812
128. Snapp KR, Heitzig CE, Ellies LG, Marth JD, Kansas GS. Differential requirements for the O-linked branching enzyme core 2 beta1-6-N-glucosaminyltransferase in biosynthesis of ligands for E-selectin and P-selectin. *Blood* (2001) 97(12):3806–11. doi:10.1182/blood.V97.12.3806
129. Julien S, Grimshaw MJ, Sutton-Smith M, Coleman J, Morris HR, Dell A, et al. Sialyl-Lewis(x) on P-selectin glycoprotein ligand-1 is regulated during differentiation and maturation of dendritic cells: a mechanism involving the glycosyltransferases C2GnT1 and ST3Gal I. *J Immunol* (2007) 179(9):5701–10. doi:10.4049/jimmunol.179.9.5701
130. Lo CY, Antonopoulos A, Gupta R, Qu J, Dell A, Haslam SM, et al. Competition between core-2 GlcNAc-transferase and ST6GalNAc-transferase regulates the synthesis of the leukocyte selectin ligand on human P-selectin glycoprotein ligand-1. *J Biol Chem* (2013) 288(20):13974–87. doi:10.1074/jbc.M113.463653
131. Asano M, Nakae S, Kotani N, Shirafuji N, Nambu A, Hashimoto N, et al. Impaired selectin-ligand biosynthesis and reduced inflammatory responses in beta-1,4-galactosyltransferase-I-deficient mice. *Blood* (2003) 102(5):1678–85. doi:10.1182/blood-2003-03-0836
132. Stolfa G, Mondal N, Zhu Y, Yu X, Buffone A Jr, Neelamegham S. Using CRISPR-Cas9 to quantify the contributions of O-glycans, N-glycans and glycosphingolipids to human leukocyte-endothelium adhesion. *Sci Rep* (2016) 6:30392. doi:10.1038/srep30392
133. Wagers AJ, Waters CM, Stoolman LM, Kansas GS. Interleukin 12 and interleukin 4 control T cell adhesion to endothelial selectins through opposite effects on alpha1, 3-fucosyltransferase VII gene expression. *J Exp Med* (1998) 188(12):2225–31. doi:10.1084/jem.188.12.2225
134. Underhill GH, Zisoulis DG, Kolli KP, Ellies LG, Marth JD, Kansas GS. A crucial role for T-bet in selectin ligand expression in T helper 1 (Th1) cells. *Blood* (2005) 106(12):3867–73. doi:10.1182/blood-2005-03-0984
135. Lim YC, Xie H, Come CE, Alexander SI, Grusby MJ, Lichtman AH, et al. IL-12, STAT4-dependent up-regulation of CD4(+) T cell core 2 beta-1,6-n-acetylglucosaminyltransferase, an enzyme essential for biosynthesis of P-selectin ligands. *J Immunol* (2001) 167(8):4476–84. doi:10.4049/jimmunol.167.8.4476
136. Dagia NM, Gadhoum SZ, Knoblauch CA, Spencer JA, Zamiri P, Lin CP, et al. G-CSF induces E-selectin ligand expression on human myeloid cells. *Nat Med* (2006) 12(10):1185–90. doi:10.1038/nm1470
137. Chimen M, Yates CM, McGettrick HM, Ward LS, Harrison MJ, Apta B, et al. Monocyte subsets coregulate inflammatory responses by integrated signaling through TNF and IL-6 at the endothelial cell interface. *J Immunol* (2017) 198(7):2834–43. doi:10.4049/jimmunol.1601281
138. An G, Wang H, Tang R, Yago T, McDaniel JM, McGee S, et al. P-selectin glycoprotein ligand-1 is highly expressed on Ly-6Chi monocytes and a major determinant for Ly-6Chi monocyte recruitment to sites of atherosclerosis in mice. *Circulation* (2008) 117(25):3227–37. doi:10.1161/CIRCULATIONAHA.108.771048

139. Swirski FK, Libby P, Aikawa E, Alcaide P, Luscinskas FW, Weissleder R, et al. Ly-6Chi monocytes dominate hypercholesterolemia-associated monocytosis and give rise to macrophages in atheromata. *J Clin Invest* (2007) 117(1):195–205. doi:10.1172/JCI29950
140. Alon R, Kassner PD, Carr MW, Finger EB, Hemler ME, Springer TA. The integrin VLA-4 supports tethering and rolling in flow on VCAM-1. *J Cell Biol* (1995) 128(6):1243–53. doi:10.1083/jcb.128.6.1243
141. Berlin C, Bargatze RF, Campbell JJ, von Andrian UH, Szabo MC, Hasslen SR, et al. alpha 4 integrins mediate lymphocyte attachment and rolling under physiologic flow. *Cell* (1995) 80(3):413–22. doi:10.1016/0092-8674(95)90491-3
142. Spertini O, Luscinskas FW, Gimbrone MA Jr, Tedder TF. Monocyte attachment to activated human vascular endothelium in vitro is mediated by leukocyte adhesion molecule-1 (L-selectin) under nonstatic conditions. *J Exp Med* (1992) 175(6):1789–92. doi:10.1084/jem.175.6.1789
143. Luscinskas FW, Kansas GS, Ding H, Pizcueta P, Schleiffenbaum BE, Tedder TF, et al. Monocyte rolling, arrest and spreading on IL-4-activated vascular endothelium under flow is mediated via sequential action of L-selectin, beta 1-integrins, and beta 2-integrins. *J Cell Biol* (1994) 125(6):1417–27. doi:10.1083/jcb.125.6.1417
144. Luscinskas FW, Ding H, Tan P, Cumming D, Tedder TF, Gerritsen ME. L- and P-selectins, but not CD49d (VLA-4) integrins, mediate monocyte initial attachment to TNF-alpha-activated vascular endothelium under flow in vitro. *J Immunol* (1996) 157(1):326–35.
145. Carlos T, Kovach N, Schwartz B, Rosa M, Newman B, Wayner E, et al. Human monocytes bind to two cytokine-induced adhesive ligands on cultured human endothelial cells: endothelial-leukocyte adhesion molecule-1 and vascular cell adhesion molecule-1. *Blood* (1991) 77(10):2266–71.
146. Leeuwenberg JF, Jeunhomme TM, Buurman WA. Role of ELAM-1 in adhesion of monocytes to activated human endothelial cells. *Scand J Immunol* (1992) 35(3):335–41. doi:10.1111/j.1365-3083.1992.tb02866.x
147. Wojciak-Stothard B, Williams L, Ridley AJ. Monocyte adhesion and spreading on human endothelial cells is dependent on Rho-regulated receptor clustering. *J Cell Biol* (1999) 145(6):1293–307. doi:10.1083/jcb.145.6.1293
148. Chen L, Zhao Q, Wang XL, You R, Zhang YH, Ji H, et al. ZLJ-6, a novel COX/5-LOX inhibitor, attenuates TNF-alpha-induced endothelial E-selectin, ICAM-1 and VCAM-1 expression and monocyte-endothelial interactions via a COX/5-LOX-independent mechanism. *Vascul Pharmacol* (2011) 55(5–6):135–42. doi:10.1016/j.vph.2011.07.003
149. Burns MP, DePaola N. Flow-conditioned HUVECs support clustered leukocyte adhesion by coexpressing ICAM-1 and E-selectin. *Am J Physiol Heart Circ Physiol* (2005) 288(1):H194–204. doi:10.1152/ajpheart.01078.2003
150. Gerszten RE, Garcia-Zepeda EA, Lim YC, Yoshida M, Ding HA, Gimbrone MA Jr, et al. MCP-1 and IL-8 trigger firm adhesion of monocytes to vascular endothelium under flow conditions. *Nature* (1999) 398(6729):718–23. doi:10.1038/19546
151. Robert C, Fuhlbrigge RC, Kieffer JD, Ayehunie S, Hynes RO, Cheng G, et al. Interaction of dendritic cells with skin endothelium: a new perspective on immunosurveillance. *J Exp Med* (1999) 189(4):627–36. doi:10.1084/jem.189.4.627
152. Srinivas U, Larsson M, Lundblad A, Forsum U. E-selectin involvement in in vitro adhesion of blood dendritic cells to human umbilical cord endothelial cells. *Scand J Immunol* (1993) 38(3):273–8. doi:10.1111/j.1365-3083.1993.tb01725.x
153. Silva Z, Tong Z, Cabral MG, Martins C, Castro R, Reis C, et al. Sialyl Lewisx-dependent binding of human monocyte-derived dendritic cells to selectins. *Biochem Biophys Res Commun* (2011) 409(3):459–64. doi:10.1016/j.bbrc.2011.05.026
154. Bangert C, Friedl J, Stary G, Stingl G, Kopp T. Immunopathologic features of allergic contact dermatitis in humans: participation of plasmacytoid dendritic cells in the pathogenesis of the disease? *J Invest Dermatol* (2003) 121(6):1409–18. doi:10.1111/j.1523-1747.2003.12623.x
155. Kieffer JD, Fuhlbrigge RC, Armerding D, Robert C, Ferenczi K, Camphausen RT, et al. Neutrophils, monocytes, and dendritic cells express the same specialized form of PSGL-1 as do skin-homing memory T cells: cutaneous lymphocyte antigen. *Biochem Biophys Res Commun* (2001) 285(3):577–87. doi:10.1006/bbrc.2001.5230
156. McEver RP, Moore KL, Cummings RD. Leukocyte trafficking mediated by selectin-carbohydrate interactions. *J Biol Chem* (1995) 270(19):11025–8. doi:10.1074/jbc.270.19.11025
157. Laszik Z, Jansen PJ, Cummings RD, Tedder TF, McEver RP, Moore KL. P-selectin glycoprotein ligand-1 is broadly expressed in cells of myeloid, lymphoid, and dendritic lineage and in some nonhematopoietic cells. *Blood* (1996) 88(8):3010–21.
158. Moore KL, Eaton SF, Lyons DE, Lichenstein HS, Cummings RD, McEver RP. The P-selectin glycoprotein ligand from human neutrophils displays sialylated, fucosylated, O-linked poly-N-acetyllactosamine. *J Biol Chem* (1994) 269(37):23318–27.
159. Pendl GG, Robert C, Steinert M, Thanos R, Eytner R, Borges E, et al. Immature mouse dendritic cells enter inflamed tissue, a process that requires E- and P-selectin, but not P-selectin glycoprotein ligand 1. *Blood* (2002) 99(3):946–56. doi:10.1182/blood.V99.3.946
160. Moore KL. Structure and function of P-selectin glycoprotein ligand-1. *Leuk Lymphoma* (1998) 29(1–2):1–15. doi:10.3109/10428199809058377
161. Somers WS, Tang J, Shaw GD, Camphausen RT. Insights into the molecular basis of leukocyte tethering and rolling revealed by structures of P- and E-selectin bound to SLe(X) and PSGL-1. *Cell* (2000) 103(3):467–79. doi:10.1016/S0092-8674(00)00138-0
162. Lim YC, Snapp K, Kansas GS, Camphausen R, Ding H, Luscinskas FW. Important contributions of P-selectin glycoprotein ligand-1-mediated secondary capture to human monocyte adhesion to P-selectin, E-selectin, and TNF-alpha-activated endothelium under flow in vitro. *J Immunol* (1998) 161(5):2501–8.
163. Ponta H, Sherman L, Herrlich PA. CD44: from adhesion molecules to signalling regulators. *Nat Rev Mol Cell Biol* (2003) 4(1):33–45. doi:10.1038/nrm1004
164. Lesley J, Hyman R, Kincade PW. CD44 and its interaction with extracellular matrix. *Adv Immunol* (1993) 54:271–335. doi:10.1016/S0065-2776(08)60537-4
165. Goodison S, Urquidi V, Tarin D. CD44 cell adhesion molecules. *Mol Pathol* (1999) 52(4):189–96. doi:10.1136/mp.52.4.189
166. Sackstein R. The biology of CD44 and HCELL in hematopoiesis: the 'step 2-bypass pathway' and other emerging perspectives. *Curr Opin Hematol* (2011) 18(4):239–48. doi:10.1097/MOH.0b013e3283476140
167. Dimitroff CJ, Lee JY, Rafii S, Fuhlbrigge RC, Sackstein R. CD44 is a major E-selectin ligand on human hematopoietic progenitor cells. *J Cell Biol* (2001) 153(6):1277–86. doi:10.1083/jcb.153.6.1277
168. Sackstein R. The bone marrow is akin to skin: HCELL and the biology of hematopoietic stem cell homing. *J Invest Dermatol* (2004) 122(5):1061–9. doi:10.1111/j.0022-202X.2004.09301.x
169. Sackstein R, Dimitroff CJ. A hematopoietic cell L-selectin ligand that is distinct from PSGL-1 and displays N-glycan-dependent binding activity. *Blood* (2000) 96(8):2765–74.
170. Hanley WD, Burdick MM, Konstantopoulos K, Sackstein R. CD44 on LS174T colon carcinoma cells possesses E-selectin ligand activity. *Cancer Res* (2005) 65(13):5812–7. doi:10.1158/0008-5472.CAN-04-4557
171. Burdick MM, Chu JT, Godar S, Sackstein R. HCELL is the major E- and L-selectin ligand expressed on LS174T colon carcinoma cells. *J Biol Chem* (2006) 281(20):13899–905. doi:10.1074/jbc.M513617200
172. Stockton BM, Cheng G, Manjunath N, Ardman B, von Andrian UH. Negative regulation of T cell homing by CD43. *Immunity* (1998) 8(3):373–81. doi:10.1016/S1074-7613(00)80542-7
173. McEvoy LM, Jutila MA, Tsao PS, Cooke JP, Butcher EC. Anti-CD43 inhibits monocyte-endothelial adhesion in inflammation and atherogenesis. *Blood* (1997) 90(9):3587–94.
174. Fanales-Belasio E, Zambruno G, Cavani A, Girolomoni G. Antibodies against sialophorin (CD43) enhance the capacity of dendritic cells to cluster and activate T lymphocytes. *J Immunol* (1997) 159(5):2203–11.
175. Hamad M, Mosley RL, Wang J, Klein JR. Stimulation via the CD43 coreceptor augments T cell proliferation during the early phase of antigen-induced activation. *Dev Comp Immunol* (1996) 20(1):77–82. doi:10.1016/0145-305X(95)00037-T
176. Mody PD, Cannon JL, Bandukwala HS, Blaine KM, Schilling AB, Swier K, et al. Signaling through CD43 regulates CD4 T-cell trafficking. *Blood* (2007) 110(8):2974–82. doi:10.1182/blood-2007-01-065276
177. Barran P, Fellinger W, Warren CE, Dennis JW, Ziltener HJ. Modification of CD43 and other lymphocyte O-glycoproteins by core 2 N-acetylglucosaminyltransferase. *Glycobiology* (1997) 7(1):129–36. doi:10.1093/glycob/7.1.129

178. Merzaban JS, Burdick MM, Gadhoum SZ, Dagia NM, Chu JT, Fuhlbrigge RC, et al. Analysis of glycoprotein E-selectin ligands on human and mouse marrow cells enriched for hematopoietic stem/progenitor cells. *Blood* (2011) 118(7):1774–83. doi:10.1182/blood-2010-11-320705
179. Tiemeyer M, Swiedler SJ, Ishihara M, Moreland M, Schweingruber H, Hirtzer P, et al. Carbohydrate ligands for endothelial-leukocyte adhesion molecule 1. *Proc Natl Acad Sci U S A* (1991) 88(4):1138–42. doi:10.1073/pnas.88.4.1138
180. Mondal N, Stolfa G, Antonopoulos A, Zhu Y, Wang SS, Buffone A Jr, et al. Glycosphingolipids on human myeloid cells stabilize E-selectin-dependent rolling in the multistep leukocyte adhesion cascade. *Arterioscler Thromb Vasc Biol* (2016) 36(4):718–27. doi:10.1161/ATVBAHA.115.306748
181. Angiari S. Selectin-mediated leukocyte trafficking during the development of autoimmune disease. *Autoimmun Rev* (2015) 14(11):984–95. doi:10.1016/j.autrev.2015.06.006
182. Barthel SR, Gavino JD, Descheny L, Dimitroff CJ. Targeting selectins and selectin ligands in inflammation and cancer. *Expert Opin Ther Targets* (2007) 11(11):1473–91. doi:10.1517/14728222.11.11.1473
183. Das PK, de Boer OJ, Visser A, Verhagen CE, Bos JD, Pals ST. Differential expression of ICAM-1, E-selectin and VCAM-1 by endothelial cells in psoriasis and contact dermatitis. *Acta Derm Venereol Suppl (Stockh)* (1994) 186:21–2.
184. Czech W, Schöpf E, Kapp A. Soluble E-selectin in sera of patients with atopic dermatitis and psoriasis – correlation with disease activity. *Br J Dermatol* (1996) 134(1):17–21. doi:10.1111/j.1365-2133.1996.tb07833.x
185. Hirai S, Kageshita T, Kimura T, Tsujisaki M, Okajima K, Imai K, et al. Soluble intercellular adhesion molecule-1 and soluble E-selectin levels in patients with atopic dermatitis. *Br J Dermatol* (1996) 134(4):657–61. doi:10.1111/j.1365-2133.1996.tb06965.x
186. Kowalzick L, Kleinheinz A, Neuber K, Weichenthal M, Köhler I, Ring J. Elevated serum levels of soluble adhesion molecules ICAM-1 and ELAM-1 in patients with severe atopic eczema and influence of UVA1 treatment. *Dermatology* (1995) 190(1):14–8. doi:10.1159/000246627
187. Morita H, Kitano Y, Kawasaki N. Elevation of serum-soluble E-selectin in atopic dermatitis. *J Dermatol Sci* (1995) 10(2):145–50. doi:10.1016/0923-1811(95)96802-T
188. Wakita H, Sakamoto T, Tokura Y, Takigawa M. E-selectin and vascular cell adhesion molecule-1 as critical adhesion molecules for infiltration of T lymphocytes and eosinophils in atopic dermatitis. *J Cutan Pathol* (1994) 21(1):33–9. doi:10.1111/j.1600-0560.1994.tb00688.x
189. Krasowska D, Pietrzak A, Lecewicz-Torun B. Serum level of sELAM-1 in psoriatic patients correlates with disease activity. *J Eur Acad Dermatol Venereol* (1999) 12(2):140–2. doi:10.1111/j.1468-3083.1999.tb01004.x
190. Kowalzick L, Neuber K, Weichenthal M, Köhler I, Ring J. Elevated serum-soluble ELAM-1 levels in patients with severe plaque-type psoriasis. *Arch Dermatol Res* (1994) 286(7):414–6. doi:10.1007/BF00371802
191. Wakita H, Takigawa M. E-selectin and vascular cell adhesion molecule-1 are critical for initial trafficking of helper-inducer/memory T cells in psoriatic plaques. *Arch Dermatol* (1994) 130(4):457–63. doi:10.1001/archderm.1994.01690040061008
192. Singh TP, Zhang HH, Borek I, Wolf P, Hedrick MN, Singh SP, et al. Monocyte-derived inflammatory Langerhans cells and dermal dendritic cells mediate psoriasis-like inflammation. *Nat Commun* (2016) 7:13581. doi:10.1038/ncomms13581
193. Steinhoff M, Steinhoff A, Homey B, Luger TA, Schneider SW. Role of vasculature in atopic dermatitis. *J Allergy Clin Immunol* (2006) 118(1):190–7. doi:10.1016/j.jaci.2006.04.025
194. Wollenberg A, Wagner M, Gunther S, Towarowski A, Tuma E, Moderer M, et al. Plasmacytoid dendritic cells: a new cutaneous dendritic cell subset with distinct role in inflammatory skin diseases. *J Invest Dermatol* (2002) 119(5):1096–102. doi:10.1046/j.1523-1747.2002.19515.x
195. Davies MJ, Gordon JL, Gearing AJ, Pigott R, Woolf N, Katz D, et al. The expression of the adhesion molecules ICAM-1, VCAM-1, PECAM, and E-selectin in human atherosclerosis. *J Pathol* (1993) 171(3):223–9. doi:10.1002/path.1711710311
196. O'Brien KD, McDonald TO, Chait A, Allen MD, Alpers CE. Neovascular expression of E-selectin, intercellular adhesion molecule-1, and vascular cell adhesion molecule-1 in human atherosclerosis and their relation to intimal leukocyte content. *Circulation* (1996) 93(4):672–82. doi:10.1161/01.CIR.93.4.672
197. Collins RG, Velji R, Guevara NV, Hicks MJ, Chan L, Beaudet AL. P-Selectin or intercellular adhesion molecule (ICAM)-1 deficiency substantially protects against atherosclerosis in apolipoprotein E-deficient mice. *J Exp Med* (2000) 191(1):189–94. doi:10.1084/jem.191.1.189
198. Dong ZM, Chapman SM, Brown AA, Frenette PS, Hynes RO, Wagner DD. The combined role of P- and E-selectins in atherosclerosis. *J Clin Invest* (1998) 102(1):145–52. doi:10.1172/JCI3001
199. Pooley N, Ghosh L, Sharon P. Up-regulation of E-selectin and intercellular adhesion molecule-1 differs between Crohn's disease and ulcerative colitis. *Dig Dis Sci* (1995) 40(1):219–25. doi:10.1007/BF02063969
200. Lazaris AC, Dicoglou C, Tseleni-Balafouta S, Paraskevakou H, Davaris PS. In situ expression of E-selectin and intercellular adhesion molecule-1 in chronic inflammatory diseases of the gastrointestinal tract. *APMIS* (1999) 107(9):819–27. doi:10.1111/j.1699-0463.1999.tb01477.x
201. Vainer B, Nielsen OH, Horn T. Expression of E-selectin, sialyl Lewis X, and macrophage inflammatory protein-1alpha by colonic epithelial cells in ulcerative colitis. *Dig Dis Sci* (1998) 43(3):596–608. doi:10.1023/A:1018875410987
202. Rugtveit J, Brandtzaeg P, Halstensen TS, Fausa O, Scott H. Increased macrophage subset in inflammatory bowel disease: apparent recruitment from peripheral blood monocytes. *Gut* (1994) 35(5):669–74. doi:10.1136/gut.35.5.669
203. Zhao J, Gao Y, Cheng C, Yan M, Wang J. Upregulation of β-1,4-galactosyltransferase I in rat spinal cord with experimental autoimmune encephalomyelitis. *J Mol Neurosci* (2013) 49(3):437–45. doi:10.1007/s12031-012-9824-3
204. King IL, Dickendesher TL, Segal BM. Circulating Ly-6C+ myeloid precursors migrate to the CNS and play a pathogenic role during autoimmune demyelinating disease. *Blood* (2009) 113(14):3190–7. doi:10.1182/blood-2008-07-168575
205. Chapman PT, Jamar F, Keelan ET, Peters AM, Haskard DO. Use of a radiolabeled monoclonal antibody against E-selectin for imaging of endothelial activation in rheumatoid arthritis. *Arthritis Rheum* (1996) 39(8):1371–5. doi:10.1002/art.1780390815
206. Ishikawa H, Nishibayashi Y, Kita K, Ohno O, Imura S, Hirata S. Adhesion molecules in the lymphoid cell distribution in rheumatoid synovial membrane. *Bull Hosp Jt Dis* (1993) 53(2):23–8.
207. Kinne RW, Brauer R, Stuhlmuller B, Palombo-Kinne E, Burmester GR. Macrophages in rheumatoid arthritis. *Arthritis Res* (2000) 2(3):189–202. doi:10.1186/ar86
208. Abdi R, Moore R, Sakai S, Donnelly CB, Mounayar M, Sackstein R. HCELL expression on murine MSC licenses pancreatotropism and confers durable reversal of autoimmune diabetes in NOD mice. *Stem Cells* (2015) 33(5):1523–31. doi:10.1002/stem.1948
209. Martin AP, Rankin S, Pitchford S, Charo IF, Furtado GC, Lira SA. Increased expression of CCL2 in insulin-producing cells of transgenic mice promotes mobilization of myeloid cells from the bone marrow, marked insulitis, and diabetes. *Diabetes* (2008) 57(11):3025–33. doi:10.2337/db08-0625
210. Brockmeyer C, Ulbrecht M, Schendel DJ, Weiss EH, Hillebrand G, Burkhardt K, et al. Distribution of cell adhesion molecules (ICAM-1, VCAM-1, ELAM-1) in renal tissue during allograft rejection. *Transplantation* (1993) 55(3):610–5. doi:10.1097/00007890-199303000-00027
211. Magil AB. Monocytes/macrophages in renal allograft rejection. *Transplant Rev* (2009) 23(4):199–208. doi:10.1016/j.trre.2009.06.005
212. Shreeniwas R, Schulman LL, Narasimhan M, McGregor CC, Marboe CC. Adhesion molecules (E-selectin and ICAM-1) in pulmonary allograft rejection. *Chest* (1996) 110(5):1143–9. doi:10.1378/chest.110.5.1143
213. Rothman A, Mann D, Behling CA, McGraw M, Seslar S, Shiu P, et al. Increased expression of endoarterial vascular cell adhesion molecule-1 mRNA in an experimental model of lung transplant rejection: diagnosis by pulmonary arterial biopsy. *Transplantation* (2003) 75(7):960–5. doi:10.1097/01.TP.0000057530.32397.6D
214. Gelman AE, Okazaki M, Sugimoto S, Li W, Kornfeld CG, Lai J, et al. CCR2 regulates monocyte recruitment as well as CD4 T1 allorecognition after lung transplantation. *Am J Transplant* (2010) 10(5):1189–99. doi:10.1111/j.1600-6143.2010.03101.x
215. Ferran C, Peuchmaur M, Desruennes M, Ghoussoub JJ, Cabrol A, Brousse N, et al. Implications of de novo ELAM-1 and VCAM-1 expression in human cardiac allograft rejection. *Transplantation* (1993) 55(3):605–9. doi:10.1097/00007890-199303000-00026

216. Morel O, Ohlmann P, Epailly E, Bakouboula B, Zobairi F, Jesel L, et al. Endothelial cell activation contributes to the release of procoagulant microparticles during acute cardiac allograft rejection. *J Heart Lung Transplant* (2008) 27(1):38–45. doi:10.1016/j.healun.2007.09.031
217. Salama M, Andrukhova O, Roedler S, Zuckermann A, Laufer G, Aharinejad S. Association of CD14+ monocyte-derived progenitor cells with cardiac allograft vasculopathy. *J Thorac Cardiovasc Surg* (2011) 142(5):1246–53. doi:10.1016/j.jtcvs.2011.07.032
218. Norton J, Sloane JP, al-Saffar N, Haskard DO. Vessel associated adhesion molecules in normal skin and acute graft-versus-host disease. *J Clin Pathol* (1991) 44(7):586–91. doi:10.1136/jcp.44.7.586
219. Norton J, Sloane JP, al-Saffar N, Haskard DO. Expression of adhesion molecules in human intestinal graft-versus-host disease. *Clin Exp Immunol* (1992) 87(2):231–6. doi:10.1111/j.1365-2249.1992.tb02980.x
220. Reddy P. Pathophysiology of acute graft-versus-host disease. *Hematol Oncol* (2003) 21(4):149–61. doi:10.1002/hon.716
221. Nishiwaki S, Terakura S, Ito M, Goto T, Seto A, Watanabe K, et al. Impact of macrophage infiltration of skin lesions on survival after allogeneic stem cell transplantation: a clue to refractory graft-versus-host disease. *Blood* (2009) 114(14):3113–6. doi:10.1182/blood-2009-03-209635
222. Hauselmann I, Roblek M, Protsyuk D, Huck V, Knopfova L, Grassle S, et al. Monocyte induction of E-selectin-mediated endothelial activation releases VE-cadherin junctions to promote tumor cell extravasation in the metastasis cascade. *Cancer Res* (2016) 76(18):5302–12. doi:10.1158/0008-5472.CAN-16-0784
223. Hoos A, Protsyuk D, Borsig L. Metastatic growth progression caused by PSGL-1-mediated recruitment of monocytes to metastatic sites. *Cancer Res* (2014) 74(3):695–704. doi:10.1158/0008-5472.CAN-13-0946
224. Schettini J, Mukherjee P. Physiological role of plasmacytoid dendritic cells and their potential use in cancer immunity. *Clin Dev Immunol* (2008) 2008:106321. doi:10.1155/2008/106321
225. Harimoto H, Shimizu M, Nakagawa Y, Nakatsuka K, Wakabayashi A, Sakamoto C, et al. Inactivation of tumor-specific CD8(+) CTLs by tumor-infiltrating tolerogenic dendritic cells. *Immunol Cell Biol* (2013) 91(9):545–55. doi:10.1038/icb.2013.38
226. Conrad C, Gregorio J, Wang YH, Ito T, Meller S, Hanabuchi S, et al. Plasmacytoid dendritic cells promote immunosuppression in ovarian cancer via ICOS costimulation of Foxp3(+) T-regulatory cells. *Cancer Res* (2012) 72(20):5240–9. doi:10.1158/0008-5472.CAN-12-2271
227. Ludwig RJ, Schön MP, Boehncke WH. P-selectin: a common therapeutic target for cardiovascular disorders, inflammation and tumour metastasis. *Expert Opin Ther Targets* (2007) 11(8):1103–17. doi:10.1517/14728222.11.8.1103
228. Fuhlbrigge RC, Weishaupt C. Adhesion molecules in cutaneous immunity. *Semin Immunopathol* (2007) 29(1):45–57. doi:10.1007/s00281-007-0065-4
229. Beeh KM, Beier J, Meyer M, Buhl R, Zahlten R, Wolff G. Bimosiamose, an inhaled small-molecule pan-selectin antagonist, attenuates late asthmatic reactions following allergen challenge in mild asthmatics: a randomized, double-blind, placebo-controlled clinical cross-over-trial. *Pulm Pharmacol Ther* (2006) 19(4):233–41. doi:10.1016/j.pupt.2005.07.004
230. Friedrich M, Bock D, Philipp S, Ludwig N, Sabat R, Wolk K, et al. Pan-selectin antagonism improves psoriasis manifestation in mice and man. *Arch Dermatol Res* (2006) 297(8):345–51. doi:10.1007/s00403-005-0626-0
231. Stahn R, Schäfer H, Kernchen F, Schreiber J. Multivalent sialyl Lewis x ligands of definite structures as inhibitors of E-selectin mediated cell adhesion. *Glycobiology* (1998) 8(4):311–9. doi:10.1093/glycob/8.4.311
232. Dimitroff CJ, Kupper TS, Sackstein R. Prevention of leukocyte migration to inflamed skin with a novel fluorosugar modifier of cutaneous lymphocyte-associated antigen. *J Clin Invest* (2003) 112(7):1008–18. doi:10.1172/JCI19220
233. Nelson RM, Cecconi O, Roberts WG, Aruffo A, Linhardt RJ, Bevilacqua MP. Heparin oligosaccharides bind L- and P-selectin and inhibit acute inflammation. *Blood* (1993) 82(11):3253–8.
234. Ludwig RJ, Alban S, Bistrian R, Boehncke WH, Kaufmann R, Henschler R, et al. The ability of different forms of heparins to suppress P-selectin function in vitro correlates to their inhibitory capacity on bloodborne metastasis in vivo. *Thromb Haemost* (2006) 95(3):535–40. doi:10.1267/THRO06030535
235. Schön MP. Inhibitors of selectin functions in the treatment of inflammatory skin disorders. *Ther Clin Risk Manag* (2005) 1(3):201–8.
236. Rillahan CD, Brown SJ, Register AC, Rosen H, Paulson JC. High-throughput screening for inhibitors of sialyl- and fucosyltransferases. *Angew Chem Int Ed Engl* (2011) 50(52):12534–7. doi:10.1002/anie.201105065
237. Scalia R, Hayward R, Armstead VE, Minchenko AG, Lefer AM. Effect of recombinant soluble P-selectin glycoprotein ligand-1 on leukocyte-endothelium interaction in vivo. Role in rat traumatic shock. *Circ Res* (1999) 84(1):93–102. doi:10.1161/01.RES.84.1.93
238. Hayward R, Campbell B, Shin YK, Scalia R, Lefer AM. Recombinant soluble P-selectin glycoprotein ligand-1 protects against myocardial ischemic reperfusion injury in cats. *Cardiovasc Res* (1999) 41(1):65–76. doi:10.1016/S0008-6363(98)00266-1
239. Kyriakides C, Austen W, Wang Y, Favuzza J, Moore FD, Hechtman HB. Endothelial selectin blockade attenuates lung permeability of experimental acid aspiration. *Surgery* (2000) 128(2):327–31. doi:10.1067/msy.2000.108216
240. Hayward R, Lefer AM. Acute mesenteric ischemia and reperfusion: protective effects of recombinant soluble P-selectin glycoprotein ligand-1. *Shock* (1999) 12(3):201–7. doi:10.1097/00024382-199909000-00006
241. Etzioni A, Frydman M, Pollack S, Avidor I, Phillips ML, Paulson JC, et al. Brief report: recurrent severe infections caused by a novel leukocyte adhesion deficiency. *N Engl J Med* (1992) 327(25):1789–92. doi:10.1056/NEJM199212173272505
242. Karsan A, Cornejo CJ, Winn RK, Schwartz BR, Way W, Lannir N, et al. Leukocyte adhesion deficiency type II is a generalized defect of de novo GDP-fucose biosynthesis. Endothelial cell fucosylation is not required for neutrophil rolling on human nonlymphoid endothelium. *J Clin Invest* (1998) 101(11):2438–45. doi:10.1172/JCI905
243. Etzioni A, Harlan JM, Pollack S, Phillips LM, Gershoni-Baruch R, Paulson JC. Leukocyte adhesion deficiency (LAD) II: a new adhesion defect due to absence of sialyl Lewis X, the ligand for selectins. *Immunodeficiency* (1993) 4(1–4):307–8.
244. Sackstein R, Merzaban JS, Cain DW, Dagia NM, Spencer JA, Lin CP, et al. Ex vivo glycan engineering of CD44 programs human multipotent mesenchymal stromal cell trafficking to bone. *Nat Med* (2008) 14(2):181–7. doi:10.1038/nm1703
245. Sackstein R. Engineering cellular trafficking via glycosyltransferase-programmed stereosubstitution. *Ann N Y Acad Sci* (2012) 1253:193–200. doi:10.1111/j.1749-6632.2011.06421.x
246. Dykstra B, Lee J, Mortensen LJ, Yu H, Wu ZL, Lin CP, et al. Glycoengineering of E-selectin ligands by intracellular versus extracellular fucosylation differentially affects osteotropism of human mesenchymal stem cells. *Stem Cells* (2016) 34(10):2501–11. doi:10.1002/stem.2435
247. Pachon-Pena G, Donnelly C, Ruiz-Canada C, Katz A, Fernandez-Veledo S, Vendrell J, et al. A glycovariant of human CD44 is characteristically expressed on human mesenchymal stem cells. *Stem Cells* (2017) 35(4):1080–92. doi:10.1002/stem.2549
248. Merzaban JS, Imitola J, Starossom SC, Zhu B, Wang Y, Lee J, et al. Cell surface glycan engineering of neural stem cells augments neurotropism and improves recovery in a murine model of multiple sclerosis. *Glycobiology* (2015) 25(12):1392–409. doi:10.1093/glycob/cwv046

Conflict of Interest Statement: According to the National Institutes of Health policies and procedures, the Brigham and Women's Hospital has assigned intellectual property rights regarding HCELL and GPS to the inventor (RS), who may benefit financially if the technology is licensed. RS's ownership interests were reviewed and are managed by the Brigham and Women's Hospital and Partners HealthCare in accordance with their conflict of interest policy. All other authors declare no competing financial interests.

Copyright © 2018 Silva, Videira and Sackstein. This is an open-access article distributed under the terms of the Creative Commons Attribution License (CC BY). The use, distribution or reproduction in other forums is permitted, provided the original author(s) or licensor are credited and that the original publication in this journal is cited, in accordance with accepted academic practice. No use, distribution or reproduction is permitted which does not comply with these terms.

frontiers in Immunology

ORIGINAL RESEARCH
published: 30 April 2018
doi: 10.3389/fimmu.2018.00846

Podosomes, But Not the Maturation Status, Determine the Protease-Dependent 3D Migration in Human Dendritic Cells

Céline Cougoule, Claire Lastrucci†, Romain Guiet†, Rémi Mascarau, Etienne Meunier, Geanncarlo Lugo-Villarino, Olivier Neyrolles, Renaud Poincloux and Isabelle Maridonneau-Parini**

Institut de Pharmacologie et de Biologie Structurale, IPBS, Université de Toulouse, CNRS, UPS, Toulouse, France

Dendritic cells (DC) are professional Antigen-Presenting Cells scattered throughout antigen-exposed tissues and draining lymph nodes, and survey the body for pathogens. Their ability to migrate through tissues, a 3D environment, is essential for an effective immune response. Upon infection, recognition of Pathogen-Associated Molecular Patterns (PAMP) by Toll-like receptors (TLR) triggers DC maturation. Mature DC (mDC) essentially use the protease-independent, ROCK-dependent amoeboid mode *in vivo,* or in collagen matrices *in vitro*. However, the mechanisms of 3D migration used by human immature DC (iDC) are still poorly characterized. Here, we reveal that human monocyte-derived DC are able to use two migration modes in 3D. In porous matrices of fibrillar collagen I, iDC adopted the amoeboid migration mode. In dense matrices of gelled collagen I or Matrigel, iDC used the protease-dependent, ROCK-independent mesenchymal migration mode. Upon TLR4 activation by LPS, mDC-LPS lose the capacity to form podosomes and degrade the matrix along with impaired mesenchymal migration. TLR2 activation by Pam_3CSK_4 resulted in DC maturation, podosome maintenance, and efficient mesenchymal migration. Under all these conditions, when DC used the mesenchymal mode in dense matrices, they formed 3D podosomes at the tip of cell protrusions. Using PGE_2, known to disrupt podosomes in DC, we observed that the cells remained in an immature status and the mesenchymal migration mode was abolished. We also observed that, while CCL5 (attractant of iDC) enhanced both amoeboid and mesenchymal migration of iDC, CCL19 and CCL21 (attractants of mDC) only enhanced mDC-LPS amoeboid migration without triggering mesenchymal migration. Finally, we examined the migration of iDC in tumor cell spheroids, a tissue-like 3D environment. We observed that iDC infiltrated spheroids of tumor cells using both migration modes. Altogether, these results demonstrate that human DC adopt the mesenchymal mode to migrate in 3D dense environments, which relies on their capacity to form podosomes independent of their maturation status, paving the way of further investigations on *in vivo* DC migration in dense tissues and its regulation during infections.

Keywords: dendritic cells, podosomes, 3D migration, toll-like receptor, maturation

OPEN ACCESS

Edited by:
Pierre Guermonprez, King's College London, United Kingdom

Reviewed by:
Alessandra Cambi, Radboud University Nijmegen, Netherlands
Andrew Mark Jackson, University of Nottingham, United Kingdom

****Correspondence:***
Céline Cougoule
celine.cougoule@ipbs.fr;
Isabelle Maridonneau-Parini
isabelle.maridonneau-parini@ipbs.fr

†Present address:
Claire Lastrucci, Centre for Genomic Regulation, Barcelona Institute of Science and Technology, Barcelona, Spain;
Romain Guiet, Bioimaging and Optics Platform, Faculty of Life Sciences, École Polytechnique Fédérale de Lausanne (EPFL), Lausanne, Switzerland

Specialty section:
This article was submitted to Antigen Presenting Cell Biology, a section of the journal Frontiers in Immunology

Received: *10 November 2017*
Accepted: *05 April 2018*
Published: *30 April 2018*

Citation:
Cougoule C, Lastrucci C, Guiet R, Mascarau R, Meunier E, Lugo-Villarino G, Neyrolles O, Poincloux R and Maridonneau-Parini I (2018) Podosomes, But Not the Maturation Status, Determine the Protease-Dependent 3D Migration in Human Dendritic Cells. Front. Immunol. 9:846. doi: 10.3389/fimmu.2018.00846

INTRODUCTION

Dendritic cells (DC) are professional phagocytic and antigen-presenting cells, which populate the skin, mucosal surfaces, and most organs of the body (1, 2). They scan their environment in search for antigens, collect antigenic materials, and transport them via lymphatic vessels to draining lymph nodes where they trigger T lymphocyte activation and the onset of the adaptive immune response (2). Yet, while DC functions rely on their ability to migrate in tissues, the mechanisms underlying DC migration in three-dimensional (3D) environments are not completely understood.

Immature DC (iDC) have been shown *in vivo* to patrol randomly in tissues, such as the gut and the skin, constantly sampling the interstitium for potential pathogen entry (3, 4). Using micro-channels as an *in vitro* model of constrained migration, iDC alternate phases of rapid migration with phases of arrest, corresponding to random scanning of the environment and antigen capture (5–7).

During infection, Toll-like receptors (TLRs) mediate cellular responses to a large variety of pathogens (viruses, bacteria, and parasites) by inducing DC activation and maturation. DC maturation is characterized by changes in the surface expression pattern of CC-chemokine receptors. A decrease in the expression of CCR5, which is highly abundant in iDC and involved in their recruitment to the site of inflammation, is accompanied by an increase in the expression of CCR7 that is required for mature DC (mDC) migration toward its ligands CCL19 and CCL21 expressed by lymphatic vessels (2, 8–13). mDC also upregulate protein surface expression of antigen-presenting and co-stimulatory molecules for a proper activation of the T cell responses. Regarding the mechanisms of mDC migration, data from *in vivo* approaches and *in vitro* 3D collagen models showed that the so-called "amoeboid" migration mode, which refers to crawling amoeba, are used in porous environments. The amoeboid mode is integrin and protease independent, it involves cell contractility induced by activation of RhoA, the Rho-associated protein kinase ROCK and myosin II, and it is characterized by a round cell shape (1, 14–21).

Podosomes are adhesion cell structures, which are formed constitutively by macrophages, DC, and osteoclasts (22). The known podosome functions are cell adhesion, substrate rigidity sensing, and matrix degradation (22–28). In addition, podosomes and their cancer cell counterpart, invadopodia, are involved in the protease-dependent cell migration that takes place in dense 3D-environments. This mode is integrin-dependent and ROCK-independent. It is characterized by an elongated and protrusive cell shape, and it involves proteolytic degradation of the extracellular matrix (ECM) mediated by podosomes in macrophages and osteoclasts precursors (29–31). This migration mode is called mesenchymal migration. Interestingly, while TLR4-mediated human DC maturation by LPS induces the loss of podosomes (32–34), the TLR2-mediated maturation by Pam_3CSK_4 maintains podosome formation and stability (34), suggesting that DC migration capacity may be differentially regulated by TLR activation.

Therefore, in the present study, we hypothesized that the migration capacity of DC in 3D environments could be influenced by the architecture of the matrix, the cell maturation status, and the presence/absence of podosomes. We report that human monocyte-derived DC display amoeboid 3D migration in porous matrices of fibrillar collagen I, independent of their maturation status. We demonstrate that both iDC and mDC can adopt the mesenchymal migration mode to infiltrate 3D dense environments, a process that relies on their capacity to form podosomes.

MATERIALS AND METHODS

Dendritic Cell Differentiation and Activation

Human monocytes were obtained from blood donors (Etablissement Français de Sang, EFS, Toulouse). For this report, written informed consents were obtained from all the donors under EFS contract n°21/PLER/TOU/IPBS01/2013-0042. According to articles L1243-4 and R1243-61 of the French Public Health Code, the contract was approved by the French Ministry of Science and Technology (agreement number AC 2009-921). All subjects gave written informed consent in accordance with the Declaration of Helsinki. Monocyte-derived macrophages and DC were differentiated as previously described (29, 35). Briefly, purified $CD14^+$ monocytes were seeded in 24-well plates (5×10^5 cells/well) with RPMI 1640 supplemented with 10% FCS, human IL-4 (Miltenyi Biotec) at 20 ng/mL, and human GM-CSF (Miltenyi Biotec) at 10 ng/mL. Cells were allowed to differentiate for 5–7 days. Fresh culture medium was added at day 3 of differentiation. For DC activation, cells were stimulated overnight with either LPS (from *Escherichia coli* O111:B4, Sigma-Aldrich) at 10 ng/mL, Pam_3CSK_4 (Synthetic triacylated lipoprotein, Invivogen) at 100 ng/mL, or PGE_2 (Prostaglandin E2, kindly provided by Agnès Coste (PharmaDev, Toulouse)) at 5 μM, then harvested and used for the following assays. We also used ultra-pure LPS (from *Escherichia coli* O111:B4, Invivogen) and obtained similar results as those obtained with LPS from Sigma.

Flow Cytometry

Immature DC, mDC-LPS, mDC-Pam_3CSK_4 and, iDC treated with PGE_2 were harvested by gentle flushing with 1 mL of culture medium, centrifuged for 5 min at 340 g, incubated in staining buffer (PBS, 2 mM EDTA, 0.5% FBS) with a 1:100 dilution of Human TruStain FcX (Biolegend) for 5 min at room temperature. Cells were then stained in cold staining buffer for 25 min with fluorophore-conjugated antibodies (APC-Cy7 labeled anti-HLA-DR (clone: L243, 1/400), PE labeled anti-CD80 (clone: 2D10, 1/200), PerCP-Cy5.5 labeled anti-CD86 (clone: IT2.2, 1/400), Pacific Blue labeled anti-PD-L1 (clone: 29E.2A3, 1/400), PerCP-Cy5.5 labeled anti-CCR5 (clone: J418J1, 1/400), and PE labeled anti-CCR7 (clone: G043H7, 1/400)) from Biolegend. After staining, the cells were washed with cold staining buffer, centrifuged twice for 5 min at 340 g at 4°C, and analyzed by flow cytometry using LSR-II flow cytometer (BD Biosciences) and the associated BD FACSDiva software. Data were then analyzed using the FlowJo 7.6.5 software (TreeStar).

3D Migration Assay

Fibrillar (2.15 or 4 mg/mL) and gelled (5.15 mg/mL) collagen I, and Matrigel were prepared as previously described (29). Matrices

(100 µL) were polymerized for 1 h and 30 min, respectively, in Transwell Invasion Chambers (BD Falcon) within 24-well companion plates. The viscoelasticity parameters of these matrices have been measured previously (29, 36). Matrigel, gelled collagen I at 5.15 mg/mL and fibrillar collagen I at 4 mg/mL display comparable viscoelasticity, while fibrillar collagen I at 2.15 mg/mL displays lower viscoelasticity. iDC, mDC-LPS, mDC-Pam_3CSK_4, and iDC treated with PGE_2 (5×10^3/transwell) were seeded on top of matrices. Migration experiments were conducted for 24–72 h, and the percentage of migrating cells, the distance of migration, and the number of membrane protrusions were quantified as described (29, 37). For live cell imaging of 3D migration (see Video S2 in Supplementary Material), pictures at the matrix surface and at 300 µm below the surface were recorded every 10 min during 13.5 h, using the 10× objective of an inverted video microscope (Leica DMIRB, Leica Microsystems, Deerfield, IL, USA) equipped with an incubator chamber to maintain constant temperature and CO_2 levels. The chemokines CCL5, CCL19, and CCL21 (Immunotools) were added in the bottom chamber at 20 ng/mL. The mixture of protease inhibitors (PI mix) comprises E64c (100 µM), GM6001 (5 µM), aprotinin (0.04 TIU/mL), leupeptin (6 µM), and pepstatin (2 µM) (29). Y27632 was used at 20 µM. DMSO at the concentration of PI mix was used as a control in all experiments.

Fluorescence Microscopy

Glass coverslips were coated with fibronectin (10 µg/mL, Sigma Aldrich) in PBS for 1 h at 37°C. Cells were seeded on fibronectin-coated coverslips (3×10^5/well in 24-well plate), left to adhere for 1–3 h and stimulated as indicated. DC were then fixed and stained with anti-Vinculin (Sigma-Aldrich) and Texas-Red-coupled phalloidin as previously described (38) and imaged using the 60×1.4 objective on an FV1000 confocal microscope (Olympus). The number of cells displaying podosomes was counted using a Leica DM-RB fluorescence microscope on least 100 cells per experimental conditions.

3D Podosome Staining and Imaging

At the end of migration experiments, matrices were fixed with 3.7% (w/v) paraformaldehyde (PFA) and 15 mM sucrose for 45 min at room temperature. PFA was quenched with 50 mM NH_4Cl for 5 min. Cells embedded in matrices were permeabilized with PBS–Triton X-100 0.1% supplemented with 3% (w/v) BSA to perform saturation at the same time for 1 h. Afterward, cells were stained anti-vinculin (Sigma-Aldrich) and secondary AlexaFluor 488-coupled secondary antibody, phalloidin-Texas Red (Invitrogen) and DAPI (0.5 mg/mL; Sigma-Aldrich). Cells were imaged using an Olympus/Andor CSU-X1 spinning disk with a 60× objective.

Scanning Electron Microscopy

Scanning electron microscopy (SEM) observations were performed as previously described (39, 40). Briefly, at the end of the 3D migration assay, cells and matrices were fixed in 2.5% glutaraldehyde/3.7% PFA/0.1M sodium cacodylate (pH 7.4) and dehydrated in a series of increasing ethanol. Critical point was dried using carbon dioxide in a Leica EMCPD300. After coating with gold, cells were examined with an FEI Quanta FEG250 scanning electron microscope.

Tumor Cells and Spheroid Culture

Spheroids were generated as previously described (36). Briefly, 24-well tissue culture plates were coated with 500 µL of 2% agar per well. The human breast tumor cell line SUM159PT (10^3 cells/20 µL) was plated in the lid of tissue culture plates. After 7 days, each spheroid was transferred into wells with 500 µL culture medium. Preliminary studies have established that after 20–24 days of culture, spheroids reached a diameter of ~400 µm. DC staining was performed using the cell-live permeant probe CellTracker Red CMPTX (Molecular Probes, Invitrogen) at 0.5 µM in PBS, as described by the manufacturer. DC at day 7 of differentiation were distributed (10^4 cells) into agar-coated wells containing a single spheroid and co-incubated for 3 days. Formalin-fixed spheroids stained with DAPI were imaged in chambers (CoverWell PCI-1.0; Grace Bio-Labs, Bend, OR) using a Zeiss LSM710 microscope (10× objective, NA 0.3, voxel size 1.3 µm × 1.3 µm × 5.5 µm) with a multiphoton source at 715 nm (coherent Chameleon) for z-stack acquisition of DAPI and CellTracker fluorescence. With the cell counter plugin of ImageJ software (National Institutes of Health, Bethesda, MD, USA), CellTracker-stained DC associated to spheroids were counted. DC were classified "out of spheroids" when located in the first line of nuclei, and "inside" when entering the first line of nuclei. At least three spheroids per condition were used.

Statistics

A Wilcoxon matched-paired signed rank test was used for statistical analyses performed using GraphPad Prism 6.0 (GraphPad Software Inc.). The $P < 0.05$ was considered significant.

RESULTS

Immature DC Adopt Either the Amoeboid or the Mesenchymal Migration Mode, and Form Podosomes Depending on the Matrix Architecture

To study the 3D migration ability of human monocyte-derived DC, we used different matrices presenting distinct architectures that were polymerized in transwells as thick layers (>1 mm) (29). Fibrillar collagen I is a porous matrix used to mimic classical stromal/interstitial ECM, and Matrigel is a dense matrix composed of a mixture of ECM proteins particularly rich in laminin and collagen IV (**Figure 1A**) (41). Since Matrigel and fibrillar collagen I have distinct biochemical compositions, we also used collagen I polymerized as a dense gel, called gelled collagen I, which displays a dense architecture and viscoelasticity parameters similar to Matrigel (**Figure 1A**). As shown in **Figure 1B**, iDC migrated in fibrillar collagen I, Matrigel and, to a lower extent, in gelled collagen I. iDC, imaged inside gelled collagen I and Matrigel, displayed an elongated cell shape with long protrusions (Videos S1 and S2 in Supplementary Material; **Figure 1C**). In fibrillar collagen I, iDC displayed a round cell shape (Video S1 in Supplementary

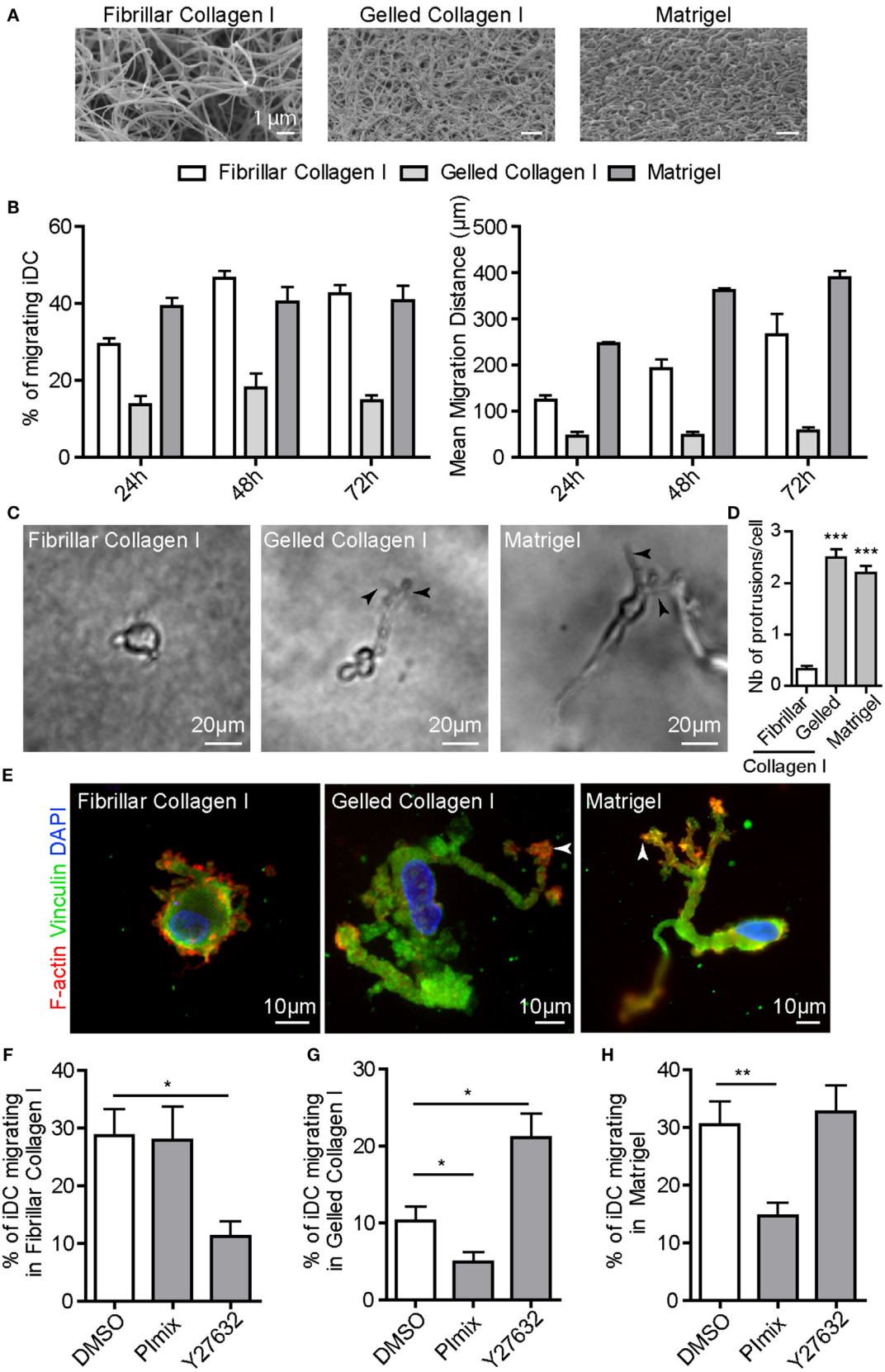


FIGURE 1 | Continued

FIGURE 1 | Immature DC (iDC) adopt either the amoeboid or the mesenchymal migration mode depending on the matrix architecture. iDC were seeded on top of a thick layer of fibrillar or gelled collagen I, or Matrigel polymerized in culture transwell inserts. **(A)** Scanning electron microscopy pictures revealing the porous (fibrillar collagen I) *versus* dense (gelled collagen I and Matrigel) architecture of the matrix. **(B)** The percentage of migrating cells and the mean migration distance of iDC in fibrillar, gelled collagen I or Matrigel were measured. Results are expressed as mean ± SEM of at least three independent experiments. **(C)** Bright field images of iDC within matrices were taken using an inverted video microscope and illustrate the round cell morphology in fibrillar collagen I and the elongated and protrusive cell morphology in gelled collagen I and Matrigel. **(D)** Quantification of the number of membrane protrusions per cells. Results are expressed as mean ± SEM of at least 100 cells counted per conditions. **(E)** After migration in matrices in Transwell inserts for 24 h, samples were fixed, permeabilized, and stained with anti-vinculin (green), phalloidin Texas-Red (red) and DAPI (blue). iDC form 3D podosomes, F-actin-, vinculin-enriched structures at the tip of membrane protrusions when migrating in dense matrices of gelled collagen I and Matrigel (arrowheads). **(F–H)**, The percentage of iDC migrating in fibrillar collagen I **(F)**, gelled collagen I **(G)** or Matrigel **(H)** was measured in control or drug-treated cells (PImix or Y27632). Results are expressed as mean ± SEM of at least three independent experiments.

Material; **Figure 1C**). The number of cells forming membrane protrusions and the number of membrane protrusions per cell were quantified. More than 90% of iDC migrating in gelled collagen I and Matrigel form membrane protrusions (mean of two to three protrusions per cell), while cells in fibrillar collagen I had occasional protrusions (**Figure 1D**).

Next, we examined whether iDC migrating in dense matrices form 3D podosomes, as these structures are instrumental for matrix remodeling and protease-dependent migration (26, 29, 30, 42). Cell staining in dense matrices revealed that the tips of membrane protrusions were enriched in F-actin and vinculin (**Figure 1E**), indicative of the presence of 3D podosomes. When iDC migrated inside fibrillar collagen I, they did not form 3D podosomes as observed with F-actin and vinculin at the subcortical area (**Figure 1E**).

To further characterize the migration mode of iDC, we used the ROCK inhibitor Y27632 or a mix of protease inhibitors [PImix (29)], which inhibit the amoeboid and mesenchymal migration modes, respectively. In the presence of Y27632, iDC migration in fibrillar collagen I was strongly inhibited, whereas it was not affected by PImix (**Figure 1F**). Since Matrigel and fibrillar collagen I have distinct viscoelasticity parameters, we also used fibrillar collagen I at 4 mg/mL, which displays similar viscoelasticity parameters as Matrigel but the same porous architecture as fibrillar collagen I at 2.15 mg/mL (29). Using this matrix, we showed that iDC migration was inhibited by Y27632 (43 + 1.2% *versus* 1.6 + 2.4%, $P = 0{,}0022$). On the contrary, while Y27632 did not affect cell migration in gelled collagen I and Matrigel, PImix significantly reduced it (**Figures 1G,H**). We verified that podosomes displayed a proteolytic activity on gelatin-FITC coated glass coverslips (Figures S1A–D in Supplementary Material) that was markedly reduced in the presence of PImix (Figures S1C,D in Supplementary Material). As previously reported (43), protease inhibitors induced podosome dissolution (Figures S1A,B in Supplementary Material). By contrast, Y27632 did not affect podosome formation and matrix degradation activity (Figures S1A–D in Supplementary Material).

Taking together the results on the cell shape, the effect of inhibitors and the formation of 3D podosomes, we conclude that iDC use the amoeboid migration mode in porous matrices of fibrillar collagen I and the mesenchymal migration mode in dense matrices of gelled collagen I and Matrigel. Thus, iDC adapt their migration mode to the architecture rather than the composition of the 3D matrix. As these results are comparable to those obtained with human monocyte-derived macrophages (26, 29), we decided to compare the 3D migration capacity of these two cell types that form podosomes [Figure S2A in Supplementary Material (23, 27, 29)]. Macrophages and iDC were differentiated from monocytes isolated from the same donors. The percentage of macrophages and iDC migrating in fibrillar collagen I was similar, but macrophages covered a longer distance than DC at 24 h (Figure S2B in Supplementary Material). In Matrigel, iDC displayed a higher capacity to infiltrate the matrix compared to macrophages (percentage of migrating cells and migration distance) during the first 24 h; however, both cell types migrated equally after 3 days (Figure S2C in Supplementary Material). Therefore, macrophages and iDC display similar ability to migrate in both types of matrix.

Podosomes, Rather Than the Maturation Status, Determine the Ability of DC to Perform Mesenchymal 3D Migration

Next, we investigated the influence of DC maturation on the 3D migration capacity. iDC were stimulated by LPS (TLR4 agonist) or Pam_3CSK_4 (TLR2 lipopeptide agonist) to generate mDC-LPS or mDC-Pam_3CSK_4. LPS- and Pam_3CSK_4-induced DC maturation was confirmed by the up-regulation of maturation markers at the cell surface, such as HLA-DR, CD80, CD86 and PD-L1 (Figures S3A,B in Supplementary Material). On top of porous fibrillar collagen I, both iDC, mDC-LPS and mDC-Pam_3CSK_4 exhibited a round cell shape with large membrane ruffles and blebs, as shown by SEM (**Figure 2A**). They efficiently infiltrated the matrix and covered a similar migration distance (**Figure 2C**). SEM pictures of Matrigel revealed that iDC and mDC-Pam_3CSK_4 remodeled the matrix by forming infiltrating holes, while mDC-LPS failed to do so (**Figure 2B**). In line with these observations, unlike mDC-LPS that did not infiltrate Matrigel or gelled collagen I, iDC and mDC-Pam_3CSK_4 infiltrated dense matrices and covered a similar migration distance (**Figure 2C**). Similar to iDC, mDC-Pam_3CSK_4 displayed a round cell shape in fibrillar collagen I and an elongated cell shape in dense matrices (Video S3 in Supplementary Material).

Of note, we observed that LPS treatment triggered DC maturation along with podosome dissolution (32–34). By contrast, podosomes were maintained when DC maturation was induced by Pam_3CSK_4 (34). These previous observations were confirmed in **Figures 2D,E**. iDC and mDC-Pam_3CSK_4 formed 3D podosomes in gelled collagen I (**Figure 2F**) and membrane protrusions in dense matrices (**Figure 2G**). Altogether, these results suggest that the ability of DC to migrate in dense matrices is independent of their maturation status, but it relies on the capacity to form podosomes.

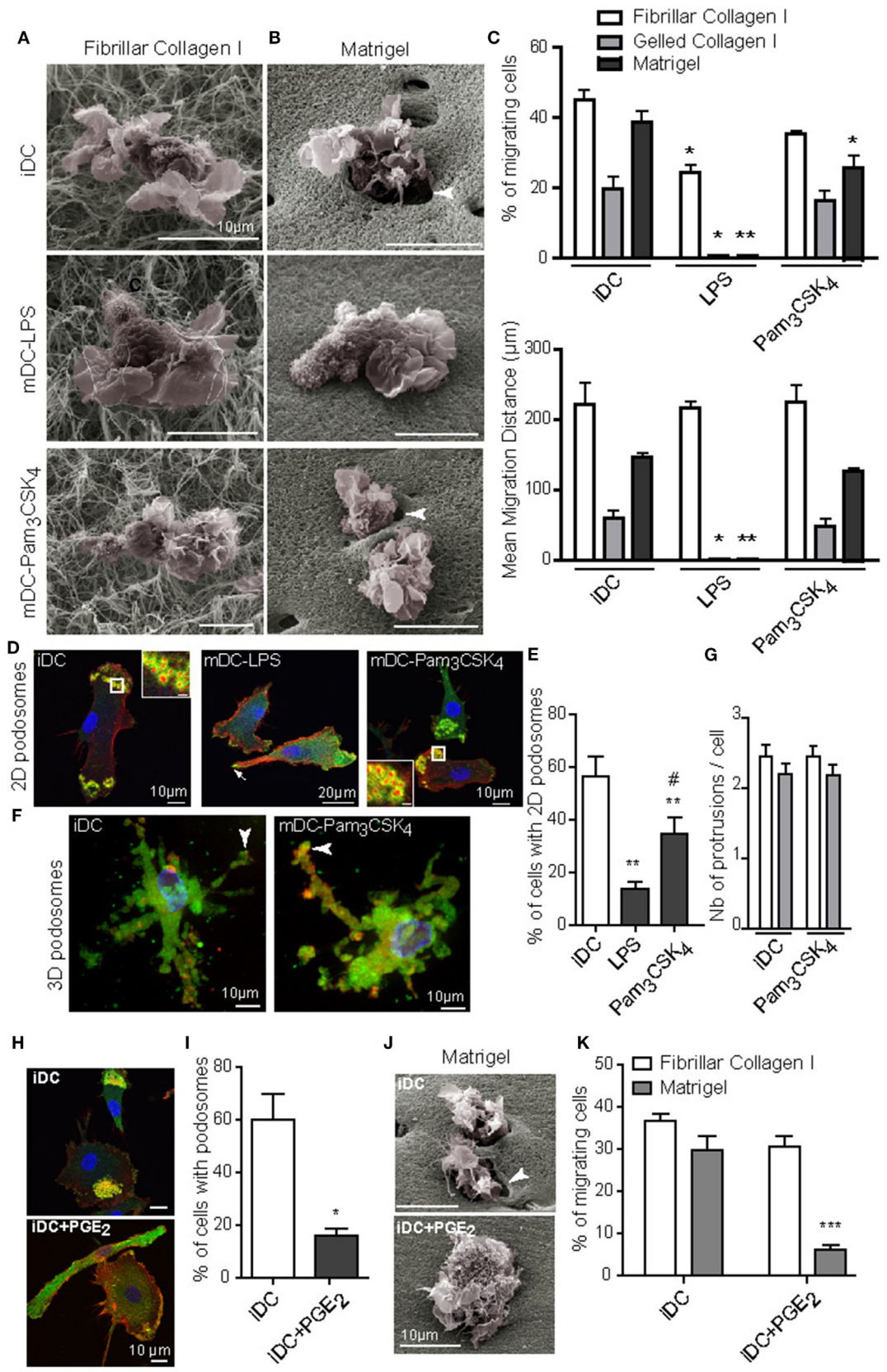


FIGURE 2 | Continued

FIGURE 2 | TLR4 and PGE_2, but not TLR2, activation induced podosome dissolution and abolished 3D mesenchymal migration of dendritic cells (DC). Immature DC (iDC) were left untreated or stimulated with LPS (10 ng/mL) or Pam_3CSK_4 (100 ng/mL) for 16 h. **(A,B)**, Morphology of cells and interaction with the surrounding matrix of fibrillar collagen I **(A)** or Matrigel **(B)** were visualized by scanning electron microscopy. Note the presence of holes in the matrix around iDC and mature DC (mDC)-Pam_3CSK_4 penetrating Matrigel (arrowheads), which were not seen in mDC-LPS. **(C)** The percentage of migrating cells and the mean migration distance in fibrillar, gelled collagen I or Matrigel, were measured after 24 h. Results are expressed as mean ± SEM of at least three independent experiments. **(D)** 2D podosomes were stained with an anti-vinculin Ab (green), phalloidin Texas-Red to detect F-actin (red), and DAPI to stain nuclei (blue) (scale bar inset: 2 μm). **(E)** The percentage of cells forming 2D podosomes was quantified. Results are expressed as mean ± SEM of seven independent experiments. **(F)** 3D podosomes of iDC and mDC-Pam_3CSK_4 in gelled collagen I were stained with an anti-vinculin Ab (green), phalloidin Texas-Red to detect F-actin (red), and DAPI to stain nuclei (blue). **(G)** The number of membrane protrusions per cell was quantified in gelled collagen I (white) and Matrigel (gray). **(H–K)**, iDC were left untreated or treated with PGE_2 (5 μM) for 16 h. **(H)** Podosomes were stained with an anti-vinculin Ab (green), phalloidin Texas-Red to detect F-actin (red), and DAPI to stain nuclei (blue). **(I)** the percentage of cells forming 2D podosomes was quantified. Results are expressed as mean ± SEM of seven independent experiments. **(J)** Morphology of cells and interaction with the surrounding matrix of Matrigel were visualized by scanning electron microscopy. Note the presence of holes in the matrix around iDC (arrowhead), which were not seen in iDC + PGE_2. **(K)** The percentage of cells migrating in fibrillar collagen I or Matrigel was measured after 24 h. Results are expressed as mean ± SEM of at least three independent experiments. $^*P < 0.05$; $^{**}P < 0.01$; $^{***}P < 0.001$ compared to iDC condition. $^{\#}P < 0.05$ compared to mDC-LPS condition.

To further characterize the role of podosomes in DC mesenchymal migration, we looked for a way to trigger podosome dissolution without inducing DC maturation. To address this question, PGE_2 was used as a potent inducer of podosome dissolution (44), and thus we examined whether it modifies the DC maturation status. PGE_2 did not induce DC maturation, as the cell surface expression of HLA-DR, CD80, and CD86 remained unchanged compared to iDC (Figure S3B in Supplementary Material), and we confirmed its capacity to disrupt podosomes (**Figures 2H,I**). When PGE_2-treated iDC were seeded on top of matrices, we observed that both matrix proteolysis and migration in Matrigel were impaired without affecting amoeboid migration in fibrillar collagen I (**Figures 2J,K**).

Collectively, these results indicate that the presence of podosomes, rather than the maturation status of DC, determines the ability to migrate in dense 3D environments.

CC-Chemokines Regulate 3D Migration of DC

Since mDC-LPS migration in Matrigel is impaired, we next investigated whether it could be restored by chemokines. Upon TLR4 activation by LPS, the expression pattern of CC-chemokine receptors was modified with decreased expression of CCR5 and enhanced expression of CCR7 (Figure S4A in Supplementary Material), as previously described (8). Consequently, we used CCL5 or a combination of CCL19 and CCL21, as ligands for CCR5 and CCR7, respectively. In fibrillar collagen I, the percentage of migrating cells and the distance covered by iDC and mDC-LPS were enhanced by CCL5 and the combination of CCL19 and CCL21, respectively (**Figure 3A**). Under the influence of chemokines, both iDC and mDC-LPS exhibited the characteristic amoeboid round cell shape in fibrillar collagen I (**Figure 3B**), and their migration capacity was inhibited by Y27632 (Figures S4E,F in Supplementary Material). In Matrigel, however, CCL5 strongly increased the 3D migration and the distance covered by iDC, while CCL19 and CCL21 had no effect on these cells (**Figure 3C**). CCL5 also enhanced iDC migration in gelled collagen I (Figure S4B in Supplementary Material), and the percentage of migrating iDC under the influence of CCL5 was inhibited by PImix in Matrigel and gelled collagen I (Figures S4G–H in Supplementary Material). Importantly, none of these cytokines triggered mDC-LPS migration in Matrigel. Under the influence of CCL5, iDC displayed an elongated cell shape in Matrigel while mDC-LPS remained on top of the matrix (**Figure 3D**). Finally, we did not observe any influence of these chemokines on the capacity of iDC and mDC-LPS to degrade the matrix (Figures S4C,D in Supplementary Material).

Due to the switch in CC-chemokine receptor expression pattern, we observed that the amoeboid migration of iDC and mDC-LPS is, as expected, influenced by CCR5 and CCR7 ligands, respectively. While the mesenchymal migration of iDC is influenced by CCL5, CCL19 and CCL21 failed to trigger mDC-LPS infiltration in Matrigel. We infer that this is likely due to the dissolution of podosomes induced by LPS resulting in mDC-LPS inability to degrade the matrix.

Immature DC Use Both Migration Modes in Tumor Cell Spheroids

To examine the migration of iDC in a tissue-like 3D environment, we used spheroids of the breast carcinoma cell line SUM159PT, which secrete several ECM proteins including fibronectin, laminin, and collagen IV (36). DC were stained with CellTracker and co-cultured with spheroids in the presence of DMSO (vehicle), the pan-matrix metalloprotease inhibitor GM6001 (a component of PImix), or Y27632. After 3 days of co-culture, iDC infiltrated in spheroids were visualized using multiphoton microscopy (**Figure 4A**) and quantified. As shown in **Figure 4B**, iDC efficiently infiltrated tumor spheroids and both GM6001 and Y27632 significantly decreased the percentage of iDC inside spheroids (**Figure 4B**). Therefore, iDC are able to use both the mesenchymal and amoeboid modes in a complex tissue-like environment.

DISCUSSION

This study extends our knowledge on the migration ability of human DC in 3D environments and its modulation during TLR-induced DC maturation. We report the following novel findings: (1) both iDC and mDC use the amoeboid mode to migrate in porous 3D collagen I; (2) only DC forming podosomes migrate in dense environments, independent of their maturation status or the presence of chemokines; and (3) iDC use both the mesenchymal and amoeboid migration modes to infiltrate tumor cell spheroids.

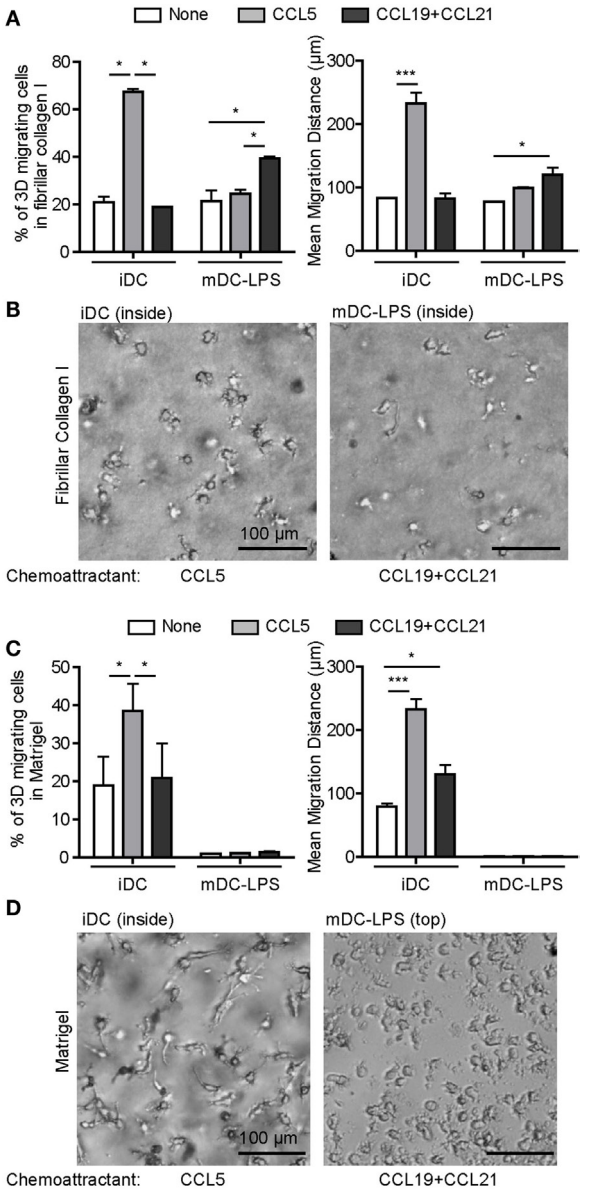


FIGURE 3 | Chemokines regulate three-dimensional (3D) migration of dendritic cells (DC). **(A)** Immature DC (iDC) and mature DC (mDC)-LPS were seeded on top of a matrix of fibrillar collagen I and the percentage of migrating cells (left) or the mean migration distance (right) were monitored after 6 h, when none (white), CCL5 (gray), or a mixture of CCL19 and CCL21 (black) were added in the lower chamber as chemoattractant. Results are expressed as mean ± SEM of three independent experiments. *$P < 0.05$; ***$P < 0.001$ compared to iDC condition. **(B)** Bright field images of iDC and mDC-LPS within the matrix of fibrillar collagen I were taken using an inverted video microscope and illustrate the round cell morphology in response to CCL5 or a mixture of CCL19 and CCL21 chemokines, respectively. **(C)** iDC and mDC-LPS were seeded on top of Matrigel and the percentage of 3D migrating cells (left) or the mean migration distance (right) were monitored after 6 h, when none (white), CCL5 (gray), or a mix of CCL19 and CCL21 (black) were added in the lower chamber as chemoattractant. Results are expressed as mean ± SEM of three independent experiments. *$P < 0.05$; ***$P < 0.001$. **(D)** Bright field images of iDC within Matrigel were taken using an inverted video microscope and illustrate the elongated cell morphology in response to CCL5, while mDC-LPS remained on top of the matrix under the influence of CCL19 and CCL21 chemokines.

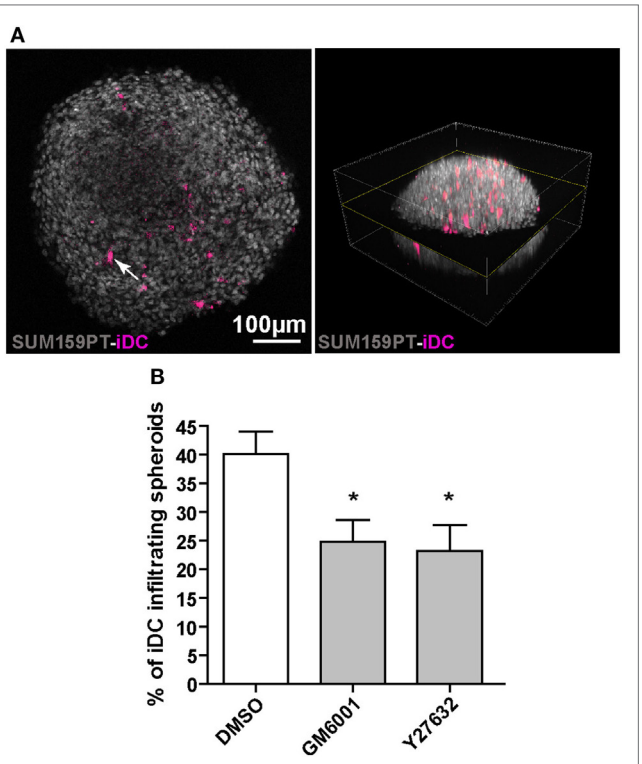


FIGURE 4 | Immature dendritic cells (iDC) adopt both amoeboid and mesenchymal three-dimensional (3D) migration in tumor spheroids. SUM159PT cell spheroids were coincubated for 3 days with CellTracker-stained DC, with or without drugs. **(A)** Multiphoton acquisition of DAPI stained spheroids (gray) infiltrated by CellTracker-stained iDC (purple). A spheroid cross-section (left) set in the 3D spheroid reconstitution is shown (right). The arrow indicates a CellTracker-stained iDC located inside the spheroid. **(B)** Quantification of iDC infiltration into spheroids, with or without inhibitors. Results are expressed as the percentage of iDC inside spheroids (100% corresponds to iDC inside plus iDC at the periphery). Results are expressed as mean ± SEM of five independent experiments. *$P < 0.05$.

Our first attempt was to investigate the migration capacity of iDC and the influence of TLR-induced maturation in 3D environments using different matrices with distinct architectures (29). We observed that, independent of their maturation status, DC adopt the amoeboid mode to migrate in porous collagen I as characterized by ROCK dependency and round cell shape. Hence, both iDC and mDC behave like other leukocytes, namely monocytes, T lymphocytes, macrophages, and neutrophils (14, 18, 29, 38, 45) with the 3D amoeboid mode as a common feature to migrate in porous 3D environments.

We demonstrate that, independent of their maturation status, DC migrate in dense matrices if they form podosomes as examined in 2D and 3D settings. Both the TLR4 and TLR2 agonists, LPS and Pam_3CKS_4, respectively, induce DC maturation. However, although LPS triggers podosome dissolution and loss of the mesenchymal migration capacity, Pam_3CKS_4 maintains podosomes and mesenchymal migration in dense matrices. These results suggest that in the context of infectious diseases, activation of distinct TLR triggers DC maturation with distinct impact on podosome formation and matrix degradation capacity. Using PGE_2, which is synthesized downstream of

LPS stimulation and mediates podosome dissolution (44, 46), we showed that it maintained DC in an immature state and abolished migration in Matrigel concomitantly to podosome disruption. In contrast to the TLR4 signaling pathway, PGE_2 is not produced upon TLR2 stimulation (47), and thus podosomes are maintained. Due to the unique ability of DC to dissolve their podosomes, this study further supports the critical role of these cell structures in 3D migration in dense environments. We also report that when DC form podosomes in 2D, they form 3D podosomes during migration in dense 3D environments, as previously described in macrophages (29, 30, 36). Altogether, these data provide evidence that when DC form podosomes, they have the dual 3D migration ability, using the amoeboid mode in a porous matrix and the mesenchymal mode in a dense environment.

Among leukocytes, only macrophages and osteoclast precursors perform mesenchymal migration, which is functionally linked to their capacity to form podosomes (26, 29, 31, 37, 38, 42, 48). Macrophages that form podosomes (in 2D and 3D environments) are able to degrade, ingest, and compact the matrix to form tunnels and create paths allowing migration into dense matrix (26, 30). Interestingly, gene deletion or knockdown of podosome effectors such as Hck, WASp, or Filamin A translate in reduced podosome stability, ECM proteolysis and mesenchymal migration without any effect on amoeboid migration (39, 49, 50). Conversely, the HIV-1 protein Nef, which stabilizes podosomes and increases their proteolytic activity, enhances the mesenchymal migration of human macrophages (37). Thus, a pathogen able to modify podosome formation and function alters the 3D migration of its host cell in dense matrices (37). A few other studies described the influence of pathogens on podosomes and the consequences on DC migration mainly studied in 2D. In 2D, the influence of podosomes on cell migration is likely related to their adhesion property rather than to their proteolytic activity. Gram-positive *versus* Gram-negative bacteria have distinct effects on podosomes. Gram-negative bacteria, such as *Neisseria meningitidis or Salmonella enteritidis*, induce podosome dissolution in DC associated with enhanced migration on 2D surface in a LPS- and TLR4-dependent manner (34). Gram-positive bacteria, such as *Staphylococcus aureus* or *Streptococcus pneumoniae*, maintain podosomes and do not influence 2D migration of DC (34). Infection of human DC with the parasite *Toxoplasma gondii* induces a rapid dissolution of podosomes (51, 52) and enhanced amoeboid 3D migration in fibrillar collagen I (53). Finally, *Helicobacter pylori* is able to induce podosome formation in cells devoid of podosomes. Hepatocytes infected with *H. pylori* form podosomes, degrade the matrix, and exhibit diminished 2D cell migration (54). Altogether, these data show that several pathogens target podosomes with potential consequences on cell adhesion, matrix degradation, and cell migration, likely influencing tissue immunopathology and activation of the adaptive immune response.

Although podosomes in macrophages and DC are involved in mesenchymal migration, they exhibit distinct behaviors in response to protease inhibitors. The presence of protease inhibitors in the culture medium disrupted podosomes in DC, as previously observed with a cathepsin B inhibitor (43), but they exhibited no effect on podosomes in macrophages (29). Thus, proteases in macrophages and DC are involved in the proteolytic activity of podosomes toward the ECM and regulate podosome dynamics only in DC. Additional comparative experiments are required to further characterize specific properties of podosomes between macrophages and DC.

Chemokines, together with the switch in CC–chemokine receptor expression operating during DC maturation, tightly regulate DC migration (2). Here, we observed that chemokines enhanced the 3D migration capacities of DC and the migration distance in both dense and porous matrices, but none of them modulated their matrix degradation capacities. In addition, when DC are devoid of podosomes, chemokines are unable to trigger mesenchymal migration. Thus, chemokine receptors do not directly govern the 3D migration mode used by DC, but they facilitate their intrinsic migratory capacities. In response to CCL19, the small Rho-GTPase Cdc42 is essential for an efficient unipolar and directional migration of mDC-LPS both *in vivo* and *in vitro* in a 3D collagen matrix (16), likely explaining the increased distance covered by DC in matrices. Moreover, PGE_2 induced during TLR4-mediated maturation of DC plays a critical role in CCR7 expression and signaling for an efficient migration of mDC-LPS toward CCL19 and CCL21 (55–57). Our results are in line with these previous studies since CCR7 expression is up-regulated and the amoeboid migration of mDC-LPS is enhanced in response to CCL19 and CCL21, probably facilitating the amoeboid migration to lymph nodes (1). The dual capacity of CCL5 to enhance both amoeboid and mesenchymal migration in iDC suggests that activation of CCR5 might support cell migration in all types of matrix architecture. Whether common or distinct molecular mechanisms are involved downstream of CCR5 activation to stimulate both migration modes remains to be determined.

The role of proteases in DC migration has been already reported showing that the Matrix Metallo-Proteases MT1-MMP and MMP9 regulate CCL5-induced iDC migration (58, 59). Interestingly, MT1-MMP localizes on podosome protrusions in iDC where it mediates ECM degradation (60–63). Moreover, MMP9 and MMP2 activities are also involved in Langerhans and dermal DC emigration from *ex vivo* murine and human epidermis (64). However, in these studies, it was not investigated whether cells form podosomes and exhibit the characteristics of mesenchymal motility. In tumor cell spheroids, we found that the pan-MMP inhibitor reduced cell infiltration, indicating that MMPs are involved in mesenchymal migration used by DC to infiltrate a tissue-like environment.

In vivo, existence of podosomes in myeloid cells and their role in 3D migration have not been formally demonstrated, but correlations have been provided between the capacity of cells to form podosomes in 2D and their migration capacity *in vivo.* In the past, we showed that deficiency of the tyrosine kinase Hck in macrophages reduces podosome stability and mesenchymal migration *in vitro*, which correlated with impaired migration of macrophages in the peritoneal cavity during inflammation (39, 49). Conversely, the HIV-1 protein Nef, which increases the podosome stability and mesenchymal migration *in vitro,*

enhances the recruitment of macrophages in tumors in Nef-transgenic mice (37). Here, we showed that iDC infiltration in tumor cell spheroids was in part dependent on MMP activity, suggesting that DC might use proteases, probably through podosome formation, to migrate in tumors. Interestingly, abolition of tumor cell-secreted PGE_2 enhanced conventional DC1 infiltration in tumors, and this was associated with tumor rejection (65). Although the impact of PGE_2 on the actin cytoskeleton was not addressed, we hypothesize that tumor-derived PGE_2, by partly disrupting podosomes, may prevent protease-dependent DC accumulation and immune-dependent tumor rejection. *In vivo*, conventional DC subsets (cDC1and cDC2) and monocyte-derived DC have a different ontogeny (66) and functions (2, 67, 68). Whether these DC subsets share the capacity to form podosomes and migrate in 3D in a protease-dependent manner remains to be explored.

In conclusion, DC adapt their migration mode to the matrix architecture: in a matrix with large pores, they use the amoeboid mode; in a matrix with a low porosity, they use the mesenchymal mode. Interestingly, we demonstrate that mesenchymal migration relies on the capacity to form podosomes and not on the DC maturation status. It is likely that differential regulation of podosome maintenance or dissolution during DC activation has consequences on DC migration in tissues and immune responses during infections and cancer.

ETHICS STATEMENT

For this report, written informed consents were obtained from all the donors under EFS contract n°21/PLER/TOU/IPBS01/2013-0042. According to articles L1243-4 and R1243-61 of the French Public Health Code, the contract was approved by the French Ministry of Science and Technology (agreement number AC 2009-921). All subjects gave written informed consent in accordance with the Declaration of Helsinki.

AUTHOR CONTRIBUTIONS

CC and IMP designed the study; EM, GLV, RP, and ON provided reagents and expertize; CC, CL, RG, RM, GLV, and RP performed experiments; CC and IMP wrote the manuscript, all authors provided a final approval of the version to be published.

ACKNOWLEDGMENTS

The authors acknowledge Drs. Sylvie Guerder, Agnès Coste, and Gareth Jones for fruitful scientific discussions; Stéphanie Dauvillier from TRI Imaging facility for technical assistance with confocal microscopy; and Isabelle Fourqueaux (TRI imaging facility, CMEAB, Toulouse) for her help with sample preparation for scanning electron microscopy. This work was supported by CNRS, University of Toulouse, Agence Nationale de la Recherche (ANR14-CE11-0020-02), la Fondation pour la Recherche Médicale (FRM DEQ2016 0334894, DEQ20160334902 and AJE20151034460), INSERM Plan Cancer, IDEX-UNITI 2014, Fondation Toulouse Cancer, Human Frontier Science Program (RGP0035/2016) and ATIP-AVENIR.

SUPPLEMENTARY MATERIAL

The Supplementary Material for this article can be found online at https://www.frontiersin.org/articles/10.3389/fimmu.2018.00846/full#supplementary-material.

FIGURE S1 | **(A)** iDC were left untreated or treated with PImix or Y27632 for 16 h, and stained with phalloidin Texas-Red to detect F-actin (red) to reveal podosomes and DAPI to stain nuclei (blue). **(B)** The percentage of cells forming podosomes was quantified. *$p < 0.05$. **(C)** iDC seeded on gelatin-FITC-coated glass coverslips were left untreated or treated with PImix or Y27632 for 16 h. Cells were stained with phalloidin Texas-Red to detect F-actin (red) and DAPI to stain nuclei (blue). Dark areas correspond to gelatin-FITC degradation. **(D)** The percentage gelatin-FITC matrix degradation was quantified. Results are expressed as mean ± SEM of at least three independent experiments. ***$p < 0.001$ (related to **Figure 1**).

FIGURE S2 | **(A)** Macrophages and iDC were stained with an anti-vinculin Ab (green), phalloidin Texas-Red to detect F-actin (red) revealing podosomes, and DAPI to stain nuclei (blue). **(B)** The percentage of migrating cells and the mean migration distance of macrophages and iDC migrating in fibrillar collagen I were measured. Results are expressed as mean ± SEM of three independent experiments. **(C)** The percentage of migrating cells and the mean migration distance of macrophages and iDC in Matrigel were measured. Results are expressed as mean ± SEM of three independent experiments. **$p < 0.01$; ***$p < 0.001$ compared to iDC condition (related to **Figure 1**).

FIGURE S3 | **(A)** Histograms showing the MFI of cell-surface maturation markers in iDC and mDC-Pam_3CSK_4. Results are expressed as mean ± SEM of 10 independent experiments. *$p < 0.05$; **$p < 0.01$; ***$p < 0.001$ compared to iDC condition. **(B)** Histograms showing the MFI of cell-surface maturation markers in iDC, mDC-LPS, and iDC+PGE_2. Results are expressed as mean ± SEM of 10 independent experiments. **$p < 0.01$; ***$p < 0.001$ compared to iDC condition (related to **Figure 2**).

FIGURE S4 | **(A)** Histograms showing the MFI of cell-surface CCR5 or CCR7 in iDC and mDC-LPS. Results are expressed as mean ± SEM of 10 independent experiments. **$p < 0.01$; ***$p < 0.001$ compared to iDC condition. **(B)** The percentage of iDC migrating in gelled collagen I was monitored after 24 h when none (white) or CCL5 (grey) was added in the lower chamber as chemoattractant. Results are expressed as mean + SEM of three independent experiments. **$p < 0.01$ compared to none condition. **(C)** quantification of gelatin-FITC degradation by iDC and mDC-LPS left untreated or treated with either CCL5 or CCL19 and CCL21 for 16 h. **(D)** iDC and mDC-LPS seeded on gelatin-FITC-coated glass coverslips were left untreated or stimulated with either CCL5 or CCL19 and CCL21 for 16 h. Cells were stained with phalloidin Texas-Red to detect F-actin (red) and DAPI to stain nuclei (blue). Dark areas correspond to gelatin-FITC degradation. **(E)** The percentage of iDC migrating in fibrillar collagen I was measured when none (white) or CCL5 (grey) was added in the lower chamber as chemoattractant, in control or drug-treated cells (PImix or Y27632). Results are expressed as mean ± SEM of at least three independent experiments. *$p < 0.05$ compared to DMSO condition. **(F)** The percentage of mDC-LPS migrating in fibrillar collagen I was measured when none (white) or CCL19 and CCL21 (grey) were added in the lower chamber as chemoattractant, in control or drug-treated cells (PImix or Y27632). Results are expressed as mean ± SEM of at least three independent experiments. *$p < 0.05$ compared to DMSO condition. **(G)** The percentage of iDC migrating in Matrigel was measured when none (white) or CCL5 (grey) was added in the lower chamber as chemoattractant, in control or drug-treated cells (PImix or Y27632). Results are expressed as mean ± SEM of at least three independent experiments. *$p < 0.05$; **$p < 0.01$ compared to DMSO condition. **(H)** The percentage of iDC migrating in gelled collagen I was measured when none (white) or CCL5 (grey) was added in the lower chamber as chemoattractant, in control or drug-treated cells (PImix or Y27632). Results are expressed as mean ± SEM of at least three independent experiments (related to **Figure 3**).

VIDEO S1 | Immature dendritic cell migrating in 3D matrices. iDC were seeded in transwells filled with fibrillar collagen I, gelled collagen I or Matrigel. z-series of

images were acquired after 24 h of migration at the surface of the matrices and at several depth (until 660 µm, 30 µm intervals) into the matrix.

VIDEO S2 | Immature dendritic cells migrating in Matrigel. Time-lapse every 10 min during 13.5 h, using the 10× objective of an inverted video microscope.

VIDEO S3 | mDC-Pam_3CSK_4 migrating in 3D matrices. mDC-Pam_3CSK_4 were seeded in transwells filled with fibrillar collagen I, gelled collagen I or Matrigel. z-series of images were acquired after 24 h of migration at the surface of the matrices and at several depth (until 420 µm, 30 µm intervals) into the matrices.

REFERENCES

1. Lammermann T, Germain RN. The multiple faces of leukocyte interstitial migration. *Semin Immunopathol* (2014) 36:227–51. doi:10.1007/s00281-014-0418-8
2. Worbs T, Hammerschmidt SI, Forster R. Dendritic cell migration in health and disease. *Nat Rev Immunol* (2017) 17:30–48. doi:10.1038/nri.2016.116
3. Ng LG, Hsu A, Mandell MA, Roediger B, Hoeller C, Mrass P, et al. Migratory dermal dendritic cells act as rapid sensors of protozoan parasites. *PLoS Pathog* (2008) 4:e1000222. doi:10.1371/journal.ppat.1000222
4. Farache J, Koren I, Milo I, Gurevich I, Kim KW, Zigmond E, et al. Luminal bacteria recruit CD103+ dendritic cells into the intestinal epithelium to sample bacterial antigens for presentation. *Immunity* (2013) 38:581–95. doi:10.1016/j.immuni.2013.01.009
5. Faure-Andre G, Vargas P, Yuseff MI, Heuze M, Diaz J, Lankar D, et al. Regulation of dendritic cell migration by CD74, the MHC class II-associated invariant chain. *Science* (2008) 322:1705–10. doi:10.1126/science.1159894
6. Chabaud M, Heuze ML, Bretou M, Vargas P, Maiuri P, Solanes P, et al. Cell migration and antigen capture are antagonistic processes coupled by myosin II in dendritic cells. *Nat Commun* (2015) 6:7526. doi:10.1038/ncomms8526
7. Vargas P, Chabaud M, Thiam HR, Lankar D, Piel M, Lennon-Dumenil AM. Study of dendritic cell migration using micro-fabrication. *J Immunol Methods* (2016) 432:30–4. doi:10.1016/j.jim.2015.12.005
8. Sallusto F, Schaerli P, Loetscher P, Schaniel C, Lenig D, Mackay CR, et al. Rapid and coordinated switch in chemokine receptor expression during dendritic cell maturation. *Eur J Immunol* (1998) 28:2760–9. doi:10.1002/(SICI)1521-4141(199809)28:09<2760::AID-IMMU2760>3.0.CO;2-N
9. Sozzani S, Allavena P, D'amico G, Luini W, Bianchi G, Kataura M, et al. Differential regulation of chemokine receptors during dendritic cell maturation: a model for their trafficking properties. *J Immunol* (1998) 161:1083–6.
10. Randolph GJ, Angeli V, Swartz MA. Dendritic-cell trafficking to lymph nodes through lymphatic vessels. *Nat Rev Immunol* (2005) 5:617–28. doi:10.1038/nri1670
11. Schumann K, Lammermann T, Bruckner M, Legler DF, Polleux J, Spatz JP, et al. Immobilized chemokine fields and soluble chemokine gradients cooperatively shape migration patterns of dendritic cells. *Immunity* (2010) 32:703–13. doi:10.1016/j.immuni.2010.04.017
12. Platt AM, Randolph GJ. Dendritic cell migration through the lymphatic vasculature to lymph nodes. *Adv Immunol* (2013) 120:51–68. doi:10.1016/B978-0-12-417028-5.00002-8
13. Weber M, Hauschild R, Schwarz J, Moussion C, De Vries I, Legler DF, et al. Interstitial dendritic cell guidance by haptotactic chemokine gradients. *Science* (2013) 339:328–32. doi:10.1126/science.1228456
14. Wolf K, Muller R, Borgmann S, Brocker EB, Friedl P. Amoeboid shape change and contact guidance: T-lymphocyte crawling through fibrillar collagen is independent of matrix remodeling by MMPs and other proteases. *Blood* (2003) 102:3262–9. doi:10.1182/blood-2002-12-3791
15. Lämmermann T, Bader B, Monkley S, Worbs T, Wedlich-Söldner R, Hirsch K, et al. Rapid leukocyte migration by integrin-independent flowing and squeezing. *Nature* (2008) 453:51–5. doi:10.1038/nature06887
16. Lammermann T, Renkawitz J, Wu X, Hirsch K, Brakebusch C, Sixt M. Cdc42-dependent leading edge coordination is essential for interstitial dendritic cell migration. *Blood* (2009) 113:5703–10. doi:10.1182/blood-2008-11-191882
17. Lammermann T, Sixt M. Mechanical modes of 'amoeboid' cell migration. *Curr Opin Cell Biol* (2009) 21:636–44. doi:10.1016/j.ceb.2009.05.003
18. Sabeh F, Shimizu-Hirota R, Weiss SJ. Protease-dependent versus -independent cancer cell invasion programs: three-dimensional amoeboid movement revisited. *J Cell Biol* (2009) 185:11–9. doi:10.1083/jcb.200807195
19. Vigl B, Aebischer D, Nitschke M, Iolyeva M, Rothlin T, Antsiferova O, et al. Tissue inflammation modulates gene expression of lymphatic endothelial cells and dendritic cell migration in a stimulus-dependent manner. *Blood* (2011) 118:205–15. doi:10.1182/blood-2010-12-326447
20. Nitschke M, Aebischer D, Abadier M, Haener S, Lucic M, Vigl B, et al. Differential requirement for ROCK in dendritic cell migration within lymphatic capillaries in steady-state and inflammation. *Blood* (2012) 120:2249–58. doi:10.1182/blood-2012-03-417923
21. Vargas P, Barbier L, Saez PJ, Piel M. Mechanisms for fast cell migration in complex environments. *Curr Opin Cell Biol* (2017) 48:72–8. doi:10.1016/j.ceb.2017.04.007
22. Linder S, Wiesner C. Tools of the trade: podosomes as multipurpose organelles of monocytic cells. *Cell Mol Life Sci* (2015) 72:121–35. doi:10.1007/s00018-014-1731-z
23. Calle Y, Burns S, Thrasher AJ, Jones GE. The leukocyte podosome. *Eur J Cell Biol* (2006) 85:151–7. doi:10.1016/j.ejcb.2005.09.003
24. Labernadie A, Thibault C, Vieu C, Maridonneau-Parini I, Charrière G. Dynamics of podosome stiffness revealed by atomic force microscopy. *Proc Natl Acad Sci U S A* (2010) 107:21016–21. doi:10.1073/pnas.1007835107
25. Labernadie A, Bouissou A, Delobelle P, Balor S, Voituriez R, Proag A, et al. Protrusion force microscopy reveals oscillatory force generation and mechanosensing activity of human macrophage podosomes. *Nat Commun* (2014) 5:5343. doi:10.1038/ncomms6343
26. Maridonneau-Parini I. Control of macrophage 3D migration: a therapeutic challenge to limit tissue infiltration. *Immunol Rev* (2014) 262:216–31. doi:10.1111/imr.12214
27. Wiesner C, Le-Cabec V, El Azzouzi K, Maridonneau-Parini I, Linder S. Podosomes in space: macrophage migration and matrix degradation in 2D and 3D settings. *Cell Adh Migr* (2014) 8:179–91. doi:10.4161/cam.28116
28. Bouissou A, Proag A, Bourg N, Pingris K, Cabriel C, Balor S, et al. Podosome force generation machinery: a local balance between protrusion at the core and traction at the ring. *ACS Nano* (2017) 11:4028–40. doi:10.1021/acsnano.7b00622
29. Van Goethem E, Poincloux R, Gauffre F, Maridonneau-Parini I, Le Cabec V. Matrix architecture dictates three-dimensional migration modes of human macrophages: differential involvement of proteases and podosome-like structures. *J Immunol* (2010) 184:1049–61. doi:10.4049/jimmunol.0902223
30. Van Goethem E, Guiet R, Balor S, Charriere GM, Poincloux R, Labrousse A, et al. Macrophage podosomes go 3D. *Eur J Cell Biol* (2011) 90:224–36. doi:10.1016/j.ejcb.2010.07.011
31. Verollet C, Gallois A, Dacquin R, Lastrucci C, Pandruvada SN, Ortega N, et al. Hck contributes to bone homeostasis by controlling the recruitment of osteoclast precursors. *FASEB J* (2013) 27:3608–18. doi:10.1096/fj.13-232736
32. Burns S, Thrasher AJ, Blundell MP, Machesky L, Jones GE. Configuration of human dendritic cell cytoskeleton by Rho GTPases, the WAS protein, and differentiation. *Blood* (2001) 98:1142–9. doi:10.1182/blood.V98.4.1142
33. West MA, Wallin RP, Matthews SP, Svensson HG, Zaru R, Ljunggren HG, et al. Enhanced dendritic cell antigen capture via toll-like receptor-induced actin remodeling. *Science* (2004) 305:1153–7. doi:10.1126/science.1099153
34. van Helden SF, Van Den Dries K, Oud MM, Raymakers RA, Netea MG, Van Leeuwen FN, et al. TLR4-mediated podosome loss discriminates gram-negative from gram-positive bacteria in their capacity to induce dendritic cell migration and maturation. *J Immunol* (2010) 184:1280–91. doi:10.4049/jimmunol.0900764
35. Troegeler A, Lastrucci C, Duval C, Tanne A, Cougoule C, Maridonneau-Parini I, et al. An efficient siRNA-mediated gene silencing in primary human monocytes, dendritic cells and macrophages. *Immunol Cell Biol* (2014) 92:699–708. doi:10.1038/icb.2014.39
36. Guiet R, Van Goethem E, Cougoule C, Balor S, Valette A, Al Saati T, et al. The process of macrophage migration promotes matrix metalloproteinase-independent invasion by tumor cells. *J Immunol* (2011) 187:3806–14. doi:10.4049/jimmunol.1101245

37. Verollet C, Souriant S, Bonnaud E, Jolicoeur P, Raynaud-Messina B, Kinnaer C, et al. HIV-1 reprograms the migration of macrophages. *Blood* (2015) 125:1611–22. doi:10.1182/blood-2014-08-596775
38. Cougoule C, Van Goethem E, Le Cabec V, Lafouresse F, Dupre L, Mehraj V, et al. Blood leukocytes and macrophages of various phenotypes have distinct abilities to form podosomes and to migrate in 3D environments. *Eur J Cell Biol* (2012) 91:938–49. doi:10.1016/j.ejcb.2012.07.002
39. Cougoule C, Le Cabec V, Poincloux R, Al Saati T, Mege JL, Tabouret G, et al. Three-dimensional migration of macrophages requires Hck for podosome organization and extracellular matrix proteolysis. *Blood* (2010) 115:1444–52. doi:10.1182/blood-2009-04-218735
40. Lastrucci C, Benard A, Balboa L, Pingris K, Souriant S, Poincloux R, et al. Tuberculosis is associated with expansion of a motile, permissive and immunomodulatory CD16(+) monocyte population via the IL-10/STAT3 axis. *Cell Res* (2015) 25:1333–51. doi:10.1038/cr.2015.123
41. LeBleu VS, Macdonald B, Kalluri R. Structure and function of basement membranes. *Exp Biol Med (Maywood)* (2007) 232:1121–9. doi:10.3181/0703-MR-72
42. Jevnikar Z, Mirkovic B, Fonovic UP, Zidar N, Svajger U, Kos J. Three-dimensional invasion of macrophages is mediated by cysteine cathepsins in protrusive podosomes. *Eur J Immunol* (2012) 42:3429–41. doi:10.1002/eji.201242610
43. Calle Y, Carragher NO, Thrasher AJ, Jones GE. Inhibition of calpain stabilises podosomes and impairs dendritic cell motility. *J Cell Sci* (2006) 119:2375–85. doi:10.1242/jcs.02939
44. van Helden SF, Krooshoop DJ, Broers KC, Raymakers RA, Figdor CG, Van Leeuwen FN. A critical role for prostaglandin E2 in podosome dissolution and induction of high-speed migration during dendritic cell maturation. *J Immunol* (2006) 177:1567–74. doi:10.4049/jimmunol.177.3.1567
45. Nourshargh S, Hordijk PL, Sixt M. Breaching multiple barriers: leukocyte motility through venular walls and the interstitium. *Nat Rev Mol Cell Biol* (2010) 11:366–78. doi:10.1038/nrm2889
46. van Helden SF, Oud MM, Joosten B, Peterse N, Figdor CG, Van Leeuwen FN. PGE2-mediated podosome loss in dendritic cells is dependent on actomyosin contraction downstream of the RhoA-Rho-kinase axis. *J Cell Sci* (2008) 121:1096–106. doi:10.1242/jcs.020289
47. Salvi V, Vaira X, Gianello V, Vermi W, Bugatti M, Sozzani S, et al. TLR signalling pathways diverge in their ability to induce PGE2. *Mediators Inflamm* (2016) 2016:5678046. doi:10.1155/2016/5678046
48. Gui P, Labrousse A, Van Goethem E, Besson A, Maridonneau-Parini I, Le Cabec V. Rho/ROCK pathway inhibition by the CDK inhibitor p27(kip1) participates in the onset of macrophage 3D-mesenchymal migration. *J Cell Sci* (2014) 127:4009–23. doi:10.1242/jcs.150987
49. Guiet R, Verollet C, Lamsoul I, Cougoule C, Poincloux R, Labrousse A, et al. Macrophage mesenchymal migration requires podosome stabilization by filamin A. *J Biol Chem* (2012) 287:13051–62. doi:10.1074/jbc.M111.307124
50. Park H, Dovas A, Hanna S, Lastrucci C, Cougoule C, Guiet R, et al. Tyrosine phosphorylation of Wiskott-Aldrich syndrome protein (WASP) by Hck regulates macrophage function. *J Biol Chem* (2014) 289:7897–906. doi:10.1074/jbc.M113.509497
51. Weidner JM, Kanatani S, Hernandez-Castaneda MA, Fuks JM, Rethi B, Wallin RP, et al. Rapid cytoskeleton remodelling in dendritic cells following invasion by *Toxoplasma gondii* coincides with the onset of a hypermigratory phenotype. *Cell Microbiol* (2013) 15:1735–52. doi:10.1111/cmi.12145
52. Olafsson EB, Varas-Godoy M, Barragan A. *Toxoplasma gondii* infection shifts dendritic cells into an amoeboid rapid migration mode encompassing podosome dissolution, secretion of TIMP-1, and reduced proteolysis of extracellular matrix. *Cell Microbiol* (2018) 20(3). doi:10.1111/cmi.12808
53. Kanatani S, Uhlen P, Barragan A. Infection by *Toxoplasma gondii* induces amoeboid-like migration of dendritic cells in a three-dimensional collagen matrix. *PLoS One* (2015) 10:e0139104. doi:10.1371/journal.pone.0139104
54. Le Roux-Goglin E, Varon C, Spuul P, Asencio C, Megraud F, Genot E. Helicobacter infection induces podosome assembly in primary hepatocytes in vitro. *Eur J Cell Biol* (2012) 91:161–70. doi:10.1016/j.ejcb.2011.11.003
55. Scandella E, Men Y, Legler DF, Gillessen S, Prikler L, Ludewig B, et al. CCL19/CCL21-triggered signal transduction and migration of dendritic cells requires prostaglandin E2. *Blood* (2004) 103:1595–601. doi:10.1182/blood-2003-05-1643
56. Legler DF, Krause P, Scandella E, Singer E, Groettrup M. Prostaglandin E2 is generally required for human dendritic cell migration and exerts its effect via EP2 and EP4 receptors. *J Immunol* (2006) 176:966–73. doi:10.4049/jimmunol.176.2.966
57. Yen JH, Kocieda VP, Jing H, Ganea D. Prostaglandin E2 induces matrix metalloproteinase 9 expression in dendritic cells through two independent signaling pathways leading to activator protein 1 (AP-1) activation. *J Biol Chem* (2011) 286:38913–23. doi:10.1074/jbc.M111.252932
58. Chabot V, Reverdiau P, Iochmann S, Rico A, Senecal D, Goupille C, et al. CCL5-enhanced human immature dendritic cell migration through the basement membrane in vitro depends on matrix metalloproteinase-9. *J Leukoc Biol* (2006) 79:767–78. doi:10.1189/jlb.0804464
59. Yang MX, Qu X, Kong BH, Lam QL, Shao QQ, Deng BP, et al. Membrane type 1-matrix metalloproteinase is involved in the migration of human monocyte-derived dendritic cells. *Immunol Cell Biol* (2006) 84:557–62. doi:10.1111/j.1440-1711.2006.01465.x
60. West MA, Prescott AR, Chan KM, Zhou Z, Rose-John S, Scheller J, et al. TLR ligand-induced podosome disassembly in dendritic cells is ADAM17 dependent. *J Cell Biol* (2008) 182:993–1005. doi:10.1083/jcb.200801022
61. Gawden-Bone C, Zhou Z, King E, Prescott A, Watts C, Lucocq J. Dendritic cell podosomes are protrusive and invade the extracellular matrix using metalloproteinase MMP-14. *J Cell Sci* (2010) 123:1427–37. doi:10.1242/jcs.056515
62. Wiesner C, Faix J, Himmel M, Bentzien F, Linder S. KIF5B and KIF3A/KIF3B kinesins drive MT1-MMP surface exposure, CD44 shedding, and extracellular matrix degradation in primary macrophages. *Blood* (2010) 116:1559–69. doi:10.1182/blood-2009-12-257089
63. Baranov M, Ter Beest M, Reinieren-Beeren I, Cambi A, Figdor CG, Van Den Bogaart G. Podosomes of dendritic cells facilitate antigen sampling. *J Cell Sci* (2014) 127:1052–64. doi:10.1242/jcs.141226
64. Ratzinger G, Stoitzner P, Ebner S, Lutz MB, Layton GT, Rainer C, et al. Matrix metalloproteinases 9 and 2 are necessary for the migration of Langerhans cells and dermal dendritic cells from human and murine skin. *J Immunol* (2002) 168:4361–71. doi:10.4049/jimmunol.168.9.4361
65. Zelenay S, Van Der Veen AG, Bottcher JP, Snelgrove KJ, Rogers N, Acton SE, et al. Cyclooxygenase-dependent tumor growth through evasion of immunity. *Cell* (2015) 162:1257–70. doi:10.1016/j.cell.2015.08.015
66. Guilliams M, Ginhoux F, Jakubzick C, Naik SH, Onai N, Schraml BU, et al. Dendritic cells, monocytes and macrophages: a unified nomenclature based on ontogeny. *Nat Rev Immunol* (2014) 14:571–8. doi:10.1038/nri3712
67. Hansen M, Andersen MH. The role of dendritic cells in cancer. *Semin Immunopathol* (2017) 39:307–16. doi:10.1007/s00281-016-0592-y
68. Keirsse J, Van Damme H, Van Ginderachter JA, Laoui D. Exploiting tumor-associated dendritic cell heterogeneity for novel cancer therapies. *J Leukoc Biol* (2017) 102:317–24. doi:10.1189/jlb.4MR1116-466R

Conflict of Interest Statement: The authors declare that the research was conducted in the absence of any commercial or financial relationships that could be construed as a potential conflict of interest.

Copyright © 2018 Cougoule, Lastrucci, Guiet, Mascarau, Meunier, Lugo-Villarino, Neyrolles, Poincloux and Maridonneau-Parini. This is an open-access article distributed under the terms of the Creative Commons Attribution License (CC BY). The use, distribution or reproduction in other forums is permitted, provided the original author(s) and the copyright owner are credited and that the original publication in this journal is cited, in accordance with accepted academic practice. No use, distribution or reproduction is permitted which does not comply with these terms.

frontiers in Immunology

REVIEW
published: 02 October 2017
doi: 10.3389/fimmu.2017.01254

The Peyer's Patch Mononuclear Phagocyte System at Steady State and during Infection

*Clément Da Silva[1], Camille Wagner[1], Johnny Bonnardel[2], Jean-Pierre Gorvel[1] and Hugues Lelouard[1]**

[1] Aix-Marseille University, CNRS, INSERM, CIML, Marseille, France, [2] Laboratory of Myeloid Cell Ontogeny and Functional Specialisation, VIB Inflammation Research Center, Ghent, Belgium

The gut represents a potential entry site for a wide range of pathogens including protozoa, bacteria, viruses, or fungi. Consequently, it is protected by one of the largest and most diversified population of immune cells of the body. Its surveillance requires the constant sampling of its encounters by dedicated sentinels composed of follicles and their associated epithelium located in specialized area. In the small intestine, Peyer's patches (PPs) are the most important of these mucosal immune response inductive sites. Through several mechanisms including transcytosis by specialized epithelial cells called M-cells, access to the gut lumen is facilitated in PPs. Although antigen sampling is critical to the initiation of the mucosal immune response, pathogens have evolved strategies to take advantage of this permissive gateway to enter the host and disseminate. It is, therefore, critical to decipher the mechanisms that underlie both host defense and pathogen subversive strategies in order to develop new mucosal-based therapeutic approaches. Whereas penetration of pathogens through M cells has been well described, their fate once they have reached the subepithelial dome (SED) remains less well understood. Nevertheless, it is clear that the mononuclear phagocyte system (MPS) plays a critical role in handling these pathogens. MPS members, including both dendritic cells and macrophages, are indeed strongly enriched in the SED, interact with M cells, and are necessary for antigen presentation to immune effector cells. This review focuses on recent advances, which have allowed distinguishing the different PP mononuclear phagocyte subsets. It gives an overview of their diversity, specificity, location, and functions. Interaction of PP phagocytes with the microbiota and the follicle-associated epithelium as well as PP infection studies are described in the light of these new criteria of PP phagocyte identification. Finally, known alterations affecting the different phagocyte subsets during PP stimulation or infection are discussed.

Keywords: mucosal immunity, Peyer's patch, dendritic cells, macrophages, M cells, microbiota, IgA, bacterial and viral infections

OPEN ACCESS

Edited by:
Christel Vérollet, UMR5089 Institut de Pharmacologie et de Biologie Structurale (IPBS), France

Reviewed by:
Dhanansayan Shanmuganayagam, University of Wisconsin-Madison, United States
Sunil Joshi, Old Dominion University, United States

****Correspondence:***
Hugues Lelouard
lelouard@ciml.univ-mrs.fr

Specialty section:
This article was submitted to Microbial Immunology, a section of the journal Frontiers in Immunology

Received: *27 July 2017*
Accepted: *20 September 2017*
Published: *02 October 2017*

Citation:
Da Silva C, Wagner C, Bonnardel J, Gorvel J-P and Lelouard H (2017) The Peyer's Patch Mononuclear Phagocyte System at Steady State and during Infection. Front. Immunol. 8:1254. doi: 10.3389/fimmu.2017.01254

INTRODUCTION

In mammals, the gastrointestinal mucosa is the largest surface of interaction with the external environment. This ensures an efficient absorption of nutrients, electrolytes, and water but concomitantly it exposes the body to environmental threats through the ingestion of contaminated food or drinks. Thus, the gut represents a privileged site of entry for various pathogen agents,

such as protozoa, bacteria, viruses, toxins, or prion. Different mechanisms of defense exist to protect the body integrity against these threats. The efficient and size-selective shield provided by the mucus layer and the glycocalyx above the villous epithelium favors the uptake of small diffusible molecules while preventing microorganisms from reaching the epithelium. Protection is also ensured through secretion of antimicrobial compounds and innate polyreactive and antigen-specific secretory immunoglobulin A (sIgA) in the intestinal lumen. Finally, the intestinal epithelium forms a physical barrier between the lumen and the *lamina propria*. However, pathogens, such as *Salmonella* and *Shigella*, can survive challenging environmental conditions, disrupt the mucus and the continuity of the epithelial barrier, and penetrate the epithelium to reach interstitial tissues (1). It is, therefore, important for the mucosal immune system to be aware of the presence of pathogens as soon as possible. A simple way to achieve this objective is to provide a facilitated access to the gut luminal content toward the mucosal surface at restricted areas distributed regularly along the gastrointestinal tract. The mammal small intestine possesses such specific sentinel sites marked by the presence of lymphoid follicles. Peyer's patches (PPs) are the most important of these monitoring sites since they are constituted of several clustered B-cell follicles forming domes interspersed with T-cell zones termed interfollicular regions (IFR). While villi are specialized for absorption of nutrients, PPs are dedicated to the sampling of foreign material and to the induction of mucosal immune responses (2–4). Due to the low number of mucus-secreting goblet cells and lack of polymeric immunoglobulin receptor expression in the follicle-associated epithelium (FAE), PP have a reduced mucus layer and no IgA secretion, respectively, which may favor interaction with pathogens (5, 6). Moreover, the FAE is characterized by the presence of specialized epithelial cells termed M cells, which lack a typical brush border and possess a thin glycocalyx that give a better accessibility to large particulate antigens (7–12). The underlying stromal cell network ensures at least in part this specialization of the FAE. Thus, subepithelial stromal cells express high amounts of the cytokine RANKL, which is necessary to both the production of the chemokine CCL20 by the FAE and the development of M cells (13, 14). The latter display specific carbohydrates and receptors that are used as binding sites by pathogens (15–22). Following their adherence to M cells, particulate antigens are rapidly transported from the lumen to the subepithelial dome (SED) or to an invagination of the basolateral membrane of M cells forming a pocket in which phagocytes, T and B cells reside. Importantly, the presence of M cells is critical for the sampling of both commensals and pathogens (17, 23–25). Once delivered into the basolateral pocket or in the SED, uptake, degradation, and presentation of antigens by the mononuclear phagocyte system (MPS), i.e., macrophages (MF) and dendritic cells (DCs), are key steps to induce a mucosal immune response. During infection, subepithelial phagocytes are, therefore, involved both in PP innate defense and in the initiation of the mucosal immune response (11). However, the role of each phagocyte subpopulation in infection has remained elusive due to an absence of consensual phenotype markers for each subset. Studies have indeed pointed out the substantial overlap in several key surface markers between MF and DC (e.g., CD11c, CD11b, SIRPα, and the major histocompatibility complex class II, MHCII) (26). Thus, until very recently, the characterization of MF in PP has been hampered by the lack of reliable markers. Finally, each dome of a given PP is surrounded by villi, thus preventing an easy discrimination of phagocytes from dome and dome-associated villus (DAV). Although IFRs are located on the sides of each dome, we, hereafter, refer FAE, SED, follicle, and IFR-located phagocytes jointly as dome phagocytes by opposition with DAV phagocytes.

In this review, we focus on recent advances, which have allowed distinguishing the different dome mononuclear phagocyte subsets. We provide an overview of their phenotype, distribution, ontogeny, lifespan, transcriptional profile, and function. We then consider some PP functional studies in the context of these new criteria to propose an identification of implicated dome phagocytes. Finally, we discuss alterations affecting the different phagocyte subsets upon PP stimulation or infection.

DIVERSITY AND SPECIFICITY OF THE PP MPS

Recent progresses in the characterization of PP MPS have demonstrated that dome DC and MF display unique characteristics very distinct from their DAV counterparts (**Table 1**).

Dome Conventional DC

Mouse common DC precursor (CDP)-derived DC, also called conventional DC (cDC), comprise two major subsets, which have been first identified through the expression of either CD8α (cDC1) or CD11b (cDC2) in addition to CD11c and MHCII (27, 28). Recently, more reliable, specific, and cross-species conserved markers for cDC1, such as XCR1 and Clec9a, have been identified (29–34). Similarly, SIRPα is a more widely distributed marker of cDC2 than CD11b, although shared with MF (35). Both cDC1 and cDC2 are present in domes (**Figure 1**) (36, 37). In addition, a third cDC subset, termed double negative cDC (DN cDC), which neither expresses CD11b nor CD8α, has been described in PP (37, 38). However, DN cDC have been recently identified as belonging to the cDC2 subset (**Figure 1**). They indeed share key surface markers with cDC2, such as SIRPα and Clec4a4, and, unlike cDC1, do not depend on Batf3 for their differentiation (39, 40). In addition, the transcriptional programs of $CD11b^+$ and DN cDC are very close from each other. Notably, $CD11b^+$ cDC express more MHCII at their surface and higher levels of key maturation marker genes such as *Stat4, Ccr7, Ccl22, Socs2*, and *Il6* than DN cDC (40). Moreover, the latter are able to express CD11b upon *in vitro* culture and are recruited in PP before $CD11b^+$ cDC (40). Therefore, it is assumed that DN and $CD11b^+$ dome cDC represent immature and mature homeostatic differentiation stages of cDC2, respectively. Dome cDC2 encompass actually a developmental continuum of cells with gradual surface acquisition of CCR7, CD11b, EpCAM, JAM-A, and MHCII and decrease of CD24 expression (40). Importantly, dome cDC2 are distinct from DAV cDC2 (**Table 1**). Thus, the latter display more CD11b and less SIRPα at their surface than

TABLE 1 | Peyer's patch (PP) phagocyte subsets at steady state.

PP subset	Phenotype[a]	Minimal markers[b] for LSM of WT mouse[c,d]	Renewal rate	Reference
DN cDC2	CD11c^{hi}MHCII^{+}**SIRPα^{+}CD11b^{-}**BST2^{-}MerTK^{-}CD8α^{-}CX$_3$CR1^{-}CD101^{-}	SED: **CD11c, SIRPα**, MerTK/lysozyme	Fast	(38, 40)
CD11b^{+} cDC2	CD11c^{hi}MHCII^{hi}**SIRPα^{+}CD11b^{int}**BST2^{-}MerTK^{-}CD8α^{-}CX$_3$CR1^{-}CD101^{-}	IFR: **CD11c, SIRPα,** MerTK,/lysozyme	Fast	(38, 40)
CD8α^{+}cDC1	CD11c^{hi}MHCII^{hi}CD8α^{+}**XCR1^{+}SIRPα^{-}**BST2^{-}MerTK^{-}CD11b^{-} CX$_3$CR1^{-}CD101^{-}	IFR: **CD11c,** SIRPα	Fast	(38, 40)
Plasmacytoid DC	CD11c^{int}MHCII^{+}SIRPα^{int}**BST2^{hi}**B220^{+}MerTK^{-}CD11b^{-}CX$_3$CR1^{-}CD101^{-}	IFR: **BST2**	Unknown	(44, 50), this review
LysoDC	CD11c^{hi}MHCII^{hi}SIRPα^{hi}CD11b^{hi}**BST2^{int}MerTK^{+}lysozyme^{+}CX$_3$CR1^{+}CD4^{+}**TIM4^{-}F4/80^{-}	SED, F: **CD11c, MerTK/lysozyme**, CD4	Fast	(39, 42)
TIM-4^{-} LysoMac	CD11c^{hi}MHCII^{lo}SIRPα^{hi}CD11b$^{int\ to\ hi}$**BST2^{int}MerTK^{+}lysozyme^{+}CX$_3$CR1^{+}CD4^{+}TIM4^{-}**F4/80^{-}	SED, F: **CD11c, MerTK/lysozyme, CD4**, TIM-4	Slow	(39)
TIM-4^{+} LysoMac	CD11c^{hi}MHCII^{lo}SIRPαhiCD11b^{hi}**BST2^{int}MerTK^{+}lysozyme^{+}CX$_3$CR1^{+}CD4^{+}TIM4^{+}**F4/80^{-}	IFR, F: **CD11c, MerTK/lysozyme, TIM-4**	Slow	(39)
TBM	**CD11c^{-}**MHCII^{-}CD11b^{-}SIRPα^{+}**MerTK^{+}lysozyme^{+}CX$_3$CR1^{+}CD4^{+}TIM4^{+}**F4/80^{-}	GC: **MerTK/lysozyme, TIM-4**, CD11c	Unknown	(39, 42)
Main DAV conventional DC	CD11c^{hi}MHCII^{hi}SIRPα^{int}CD11b^{hi}MerTK^{-}**CD101^{+}**CX$_3$CR1^{-}CD8α^{-}	DAV: **CD11c, CD101**	Fast	(39, 40)
Main DAV MF	CD11c^{hi}MHCII^{hi}SIRPα^{int}CD11b^{hi}**MerTK^{+}CX$_3$CR1^{+}F4/80^{+}**lysozyme^{-}CD8α^{-}CD101^{-}	DAV: **CD11c, MerTK/F4/80**	Slow	(39, 40)

Gray background, common dendritic cell precursor-derived cells; white background, monocyte-derived cells (TBM may also be derived from embryonic precursors).

[a]In bold, main distinctive markers of each subset.

[b]The main location is indicated and together with the expression (bold) or not (regular) of each marker it allows the discrimination of the given subset by LSM.

[c]The most efficient surface marker panel to discriminate PP phagocyte subsets by flow cytometry up to now is CD11c, MHCII, SIRPα, BST2, CD4, TIM-4, XCR1, CD11b, CD101.

[d]In Cx$_3$cr1-GFP (monocyte-derived cell labeling) or Zbtb46-GFP (conventional DC labeling) transgenic mice, MerTK or lysozyme staining can be omitted.

LSM, laser scanning microscopy; SED, subepithelial dome; IFR, interfollicular region; GC, germinal center; DAV, dome-associated villus; DN cDC2, double-negative cDC2; TBM, tingible-body macrophages; MF, macrophages; WT, wild type.

dome cDC2. Moreover, most of them express CD101 whereas dome cDC2 do not (40).

Dome MF

Unlike villous MF, identification of dome MF has remained unsolved for decades due to the lack of expression of classic macrophage markers such as F4/80 (EMR1), sialoadhesin (Siglec1/CD169), Mannose Macrophage Receptor (MMR/CD206), or Fc Gamma Receptor I (FcGRI/CD64) (39). Moreover, a substantial overlap of key surface markers, such as CD11c, CD11b, MHCII, and SIRPα, exists between MF and cDC (26). By the past, this has led to a great confusion concerning location and functions of both dome phagocyte populations. However, recent works managed distinguishing dome cDC from monocyte-derived cells (**Table 1**) (39–41). The latter encompass dome MF and the monocyte-derived DC termed LysoDC (**Figure 1**). Most dome monocyte-derived cells express CD11c, CD11b, SIRPα, BST2, CX_3CR1, MerTK, and lysozyme (**Table 1**). BST2 and lysozyme expression are hallmarks of dome monocyte-derived cells since DAV MF express little or none of these molecules (39, 42). Thus, CD11c^{+} dome MF have been termed LysoMac by analogy with LysoDC and by opposition to villous MF, which do not express lysozyme. LysoMac are strongly autofluorescent large long-lived cells, which depend on the growth factor M-CSF to develop (39). They express CD4 but only low levels of MHCII. They encompass two main subsets based on the expression of the phosphatidylserine receptor TIM-4 (**Figure 1**) (39).

Tingible-body macrophages (TBM), which also display TIM-4 at their surface, form a third dome macrophage subset (39). Like LysoMac, TBM express MerTK, CX_3CR1, SIRPα, lysozyme, and CD4 but typically lack CD11c, CD11b, and MHCII expression (**Table 1**) (39, 42). BST2 expression in TBM has not been investigated so far. Although easily detectable *in situ* through the presence of many internalized apoptotic bodies, they have been poorly characterized and their origin, either circulating monocytes, embryonic precursors or both, is unknown. In addition to these subsets, PP contain a layer of poorly described serosal/muscularis MF, which, depending on their location, express or not CD169 (see below) (39).

LysoDC

LysoDC are short-lived monocyte-derived DC (**Figure 1**; **Table 1**) (39). Unlike LysoMac, they are weakly autofluorescent, express very high levels of MHCII, but no CD4, and are strongly dependent on CCR2, the chemokine receptor that allows monocyte egress from the bone marrow (39). Morphologically, they are large stellate motile cells (42, 43). Upon stimulation with the TLR7 agonist R848, they secrete IL-6 and TNF but no IL-10 (**Table 2**) (39). So far, no equivalent of LysoDC has been described in villous *lamina propria.* LysoDC are present in mouse, rat, and human PP (42). Thus, these phagocytes seem to be specific of PP and maybe of isolated lymphoid follicles in several species including humans.

Plasmacytoid DC

Although PP plasmacytoid DCs (pDCs) share BST2 expression with monocyte-derived cells, they constantly express higher levels

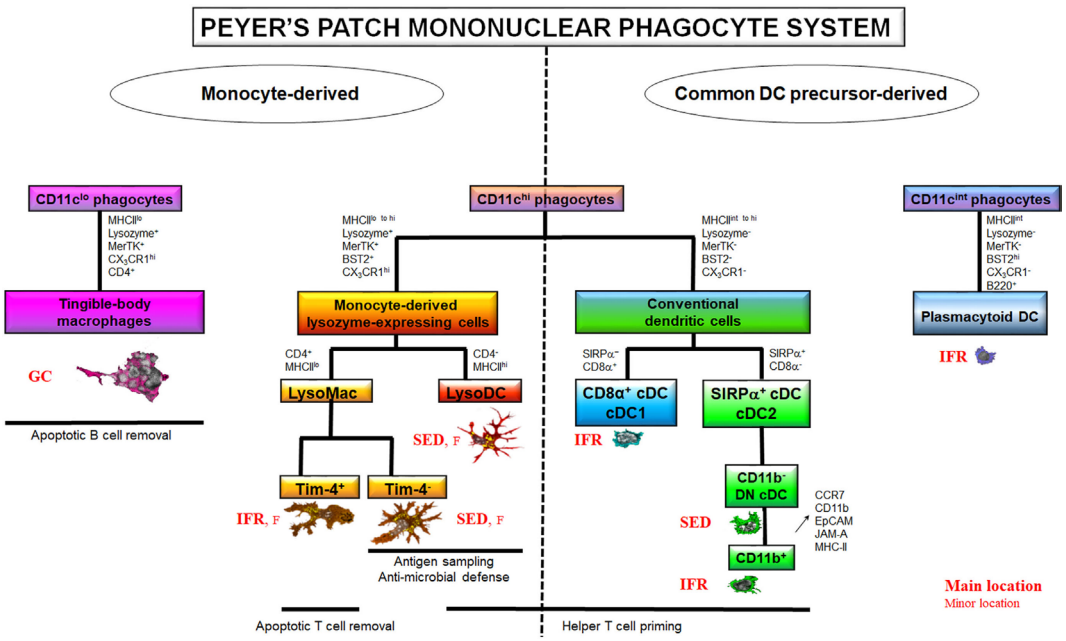


FIGURE 1 | The Peyer's patch (PP) mononuclear phagocyte system (MPS). The PP MPS encompasses two large families of cells based on their origin, the common DC precursor (CDP)-derived and the monocyte-derived phagocytes. The CDP-derived cells comprise CD11c^{hi} conventional DC (cDC) and CD11c^{int} plasmacytoid DC. Among cDC, cDC1 are CD8α^{+} but SIRPα^{-} whereas cDC2 are SIRPα^{+} but CD8α^{-}. cDC2 exist in several stages of differentiation among which the two extremes are the so-called double negative (DN) cDC2, which do not express CD11b, and the CD11b^{+} cDC2. CD11b^{+} cDC2 derive from DN cDC2 through the upregulation of CCR7, CD11b, EpCAM, JAM-A, and MHCII. CDP-derived cells are mainly located in the T cell zones, i.e., interfollicular regions (IFR), at the exception of DN cDC2, which transit through the subepithelial dome (SED). cDC excel in helper T cell priming but are poorly phagocytic. On the contrary, CD11c^{hi} monocyte-derived cells are strongly phagocytic. They also display a broad range of antimicrobial defense mechanisms. CD11c^{hi} monocyte-derived cells encompass two main subsets based on their phenotype, lifespan, and ability to prime T cells: macrophages (MF) and the monocyte-derived dendritic cell (DC) termed LysoDC. LysoDC are CD4^{-}MHCII^{hi} short-lived SED-located DC with helper T cell priming ability. CD11c^{hi} MF, also called LysoMac, are CD4^{+}MHCII^{lo} long-lived cells without any helper T cell priming ability. TIM-4^{-} LysoMac are mainly located in the SED whereas TIM-4^{+} LysoMac are mainly located in the IFR. A third type of MF, termed tingible-body macrophages, reside in the germinal center (GC) of the follicle (F) where they are involved in apoptotic B cell removal. Unlike other PP MF, they do not express CD11c. Although shown on the monocyte-derived cell part of the diagram, it is currently unknown whether they truly derive from monocytes or whether they self-renew from embryonic precursors. Adapted from Ref. (39).

TABLE 2 | Functions of dome phagocyte subsets.

Peyer's patch subset	Antigen sampling activity	Apoptotic cell removal	Cytokine production	T cell priming and polarization	IgA production induction	Reference
Double-negative cDC2 (DN cDC2)	Unknown	Unknown	(*)	(*)	*In vivo* candidate	(38, 39, 89, 90)
CD11b^{+} cDC2	Unknown	Unknown	IL-6	IL-6	*In vivo* candidate	(38, 39, 89, 90)
CD8α^{+} cDC1	Unknown	Unknown	IL-12 p70	IFNγ	No	(38, 39, 89, 90)
Plasmacytoid DC	Unknown	Unknown	IL-12 p70, No type I IFN	IL-17	*In vitro*, not *in vivo*	(44, 45, 87, 88)
LysoDC	Microspheres, *Salmonella*, sIgA-IC	Follicle-associated epithelium (FAE) cells	IL-6, TNF	IFNγ, IL-6, TNF	*In vivo* candidate	(39, 42, 43, 101)
TIM4^{-} LysoMac	Microspheres, *Salmonella*, prion, sIgA-IC	FAE cells	ND	No priming	*In vivo* candidate	(39, 42, 90, 101, 131)
TIM^{+}4^{+} LysoMac	Unknown	T cells	ND	No priming	No	(39)
Tingible-body macrophages	Unknown	Germinal center B cells	ND	ND	No	(39, 42)

(*)Upon maturation, DN cDC2 may give rise to CD11b^{+} cDC2 and acquire their functional attributes, i.e., IL-6 production and T cell polarization for IL-6 production.
Grey background, common dendritic cell precursor-derived cells; white background, monocyte-derived cells.
sIgA-IC, secretory immunoglobulin A immune complex; ND, not determined.

of BST2 and lower levels of CD11c and SIRPα than LysoDC and LysoMac (**Table 1**) (39, 40). One can also distinguish PP pDC from monocyte-derived cells, thanks to their B220 expression. PP pDCs are distinct from pDCs isolated from other tissues by their inability to secrete abundant type I IFN in response to the TLR9 agonist CpG (**Table 2**) (44). Expression of the mucosal migratory receptor CCR9 and of the specific transcriptional regulator of the pDC lineage E2-2 is also reduced in PP pDCs

as compared to other pDCs (45). Like other pDCs, PP pDCs are derived from the CDP and are induced by Flt3L, but their recruitment also requires type I IFN/STAT1 signaling (45). This type I IFN conditioning of PP pDC could favor the production of the inflammatory cytokines IL-6, IL-23, and TNF instead of type I IFNs (45).

ANATOMIC LOCALIZATION OF PP PHAGOCYTE SUBSETS AT STEADY STATE

Each region of the dome, i.e., FAE, SED, follicle, germinal center (GC), and IFR, is populated with specific subsets of phagocytes (**Figure 2**).

FAE and SED

Subepithelial phagocytes are mainly composed of CD11c$^+$ CD11b$^+$ cells (37, 40, 42). Due to the expression of both surface markers, these cells were initially thought to be cDC2. However, these subepithelial CD11c$^+$CD11b$^+$ cells also express CX_3CR1 and lysozyme and belong to the monocyte-derived family of phagocytes, i.e., LysoDC and LysoMac (40). Both represent actually two-third of subepithelial phagocytes with increasing ratio while reaching the upper part of the dome (**Figure 2**). By contrast, the SED contains few cDC, mainly DN cDC2 (JAM-A$^-$CCR7$^-$CD11b$^-$SIRPα$^+$ cDC), which are rather located in the lower part of the dome (**Figure 3**) (40). Both subepithelial LysoDC and DN cDC2 can penetrate the FAE and strongly interact with M cells, whereas LysoMac remain mainly located in the SED (40). Heterogeneity in dome macrophage-associated phenotype is tightly linked to their different anatomic localization within PP (**Figure 2**). This suggests that these phenotype differences reflect an important regional specialization of macrophage functions. Thus, subepithelial LysoMac do not express TIM-4 (39).

Follicle and GC

Conventional DCs are generally absent from the follicle and from the GC. The upper part of the follicle comprises exclusively scattered LysoDC and TIM-4$^-$ LysoMac, whereas in its lower part, TIM-4$^+$ LysoMac replace TIM-4$^-$ LysoMac (39). Finally, TBM are the only phagocytes of the GC.

Interfollicular Regions

Interfollicular regions contain mainly cDC1 (SIRPα$^-$ cDC), CD11b$^+$ cDC2 (JAM-A$^+$CCR7$^+$CD11b$^+$SIRPα$^+$ cDC), and scattered TIM-4$^+$ LysoMac (**Figures 2** and **3**) (39, 40). Of note, by microscopy, CD11b staining is not detectable in interfollicular CD11b$^+$ cDC2 and TIM-4$^+$ LysoMac due to its low levels of expression in these cells (40). Only LysoDC and subepithelial TIM-4$^-$ LysoMac actually stain for CD11b in the dome. Since interfollicular cDC (cDC1 and CD11b$^+$ cDC2) express CCR7 whereas subepithelial cDC (DN cDC2) do not (**Figure 3B**), the former are likely recruited through the specific expression of CCL19 and CCL21 in the IFR whereas the latter are likely recruited in the SED through their expression of CCR6 and secretion of CCL20 by the FAE (37, 40, 46–49). Surprisingly, interfollicular TIM-4$^+$ LysoMac do not express CCR7, indicating that another factor may be involved in their addressing to the IFR (40). Interestingly, a layer of these MF surrounds the IFR, thus forming border guards of the T cell zone. Finally, CD169 is only expressed by MF located at the base of the IFR toward the serosa, including serosal/muscularis MF (39).

BST2 has been extensively used to identify pDC in different mouse organs including PP (44, 50). Based on this marker,

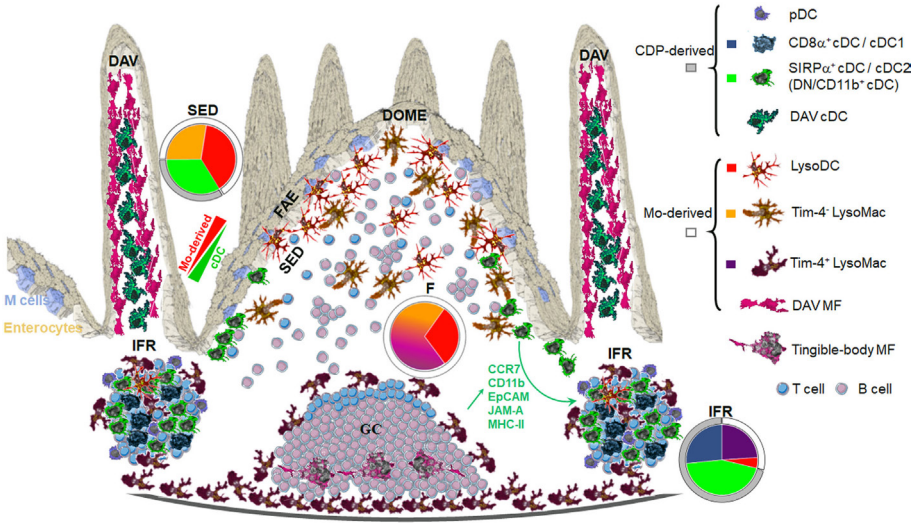


FIGURE 2 | Anatomic localization of Peyer's patch (PP) phagocyte subpopulations. Origin and shape of each PP phagocyte subset is displayed on the right. Color codes correspond to colors displayed in pie charts. The latter show in each region of the dome the distribution of PP phagocyte subsets at the exception of plasmacytoid DC (pDC). FAE, follicle-associated epithelium; SED, subepithelial dome; F, follicle; IFR, interfollicular region; DAV, dome-associated villus; MF, macrophages. Adapted from Ref. (40).

pDCs were first supposed to be located in the SED and in the IFR (44, 50). However, PP monocyte-derived cells express BST2 at steady state (**Figure 4A**) (39). Moreover, stimuli that trigger interferon responses induce BST2 expression in several cell types (51). We, therefore, decided to re-investigate pDC location. We found that pDCs are mainly located in the IFR but not in the SED where BST2 is weakly displayed by monocyte-derived cells (**Figure 4B**).

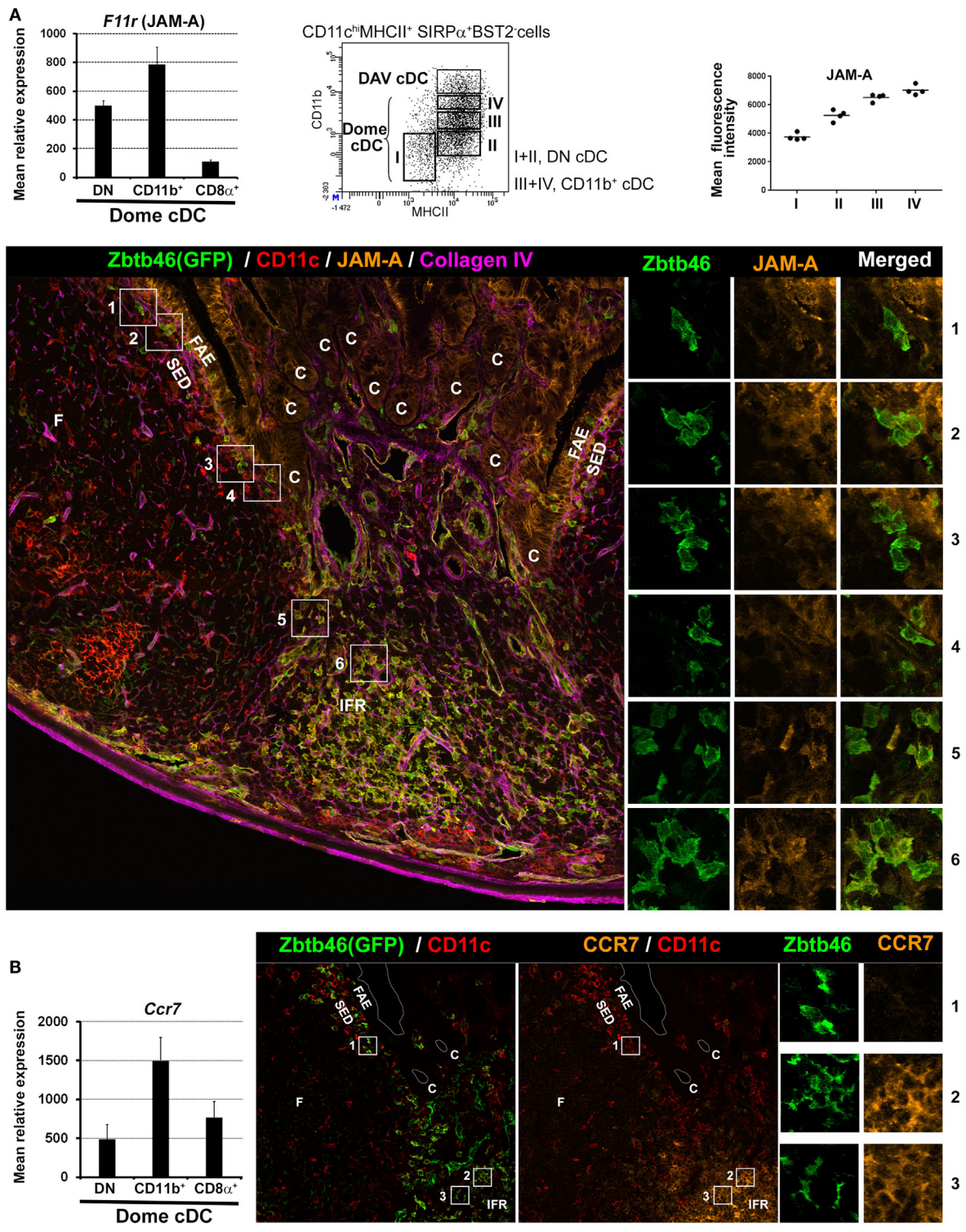


FIGURE 3 | Continued

FIGURE 3 | Continued
Location of dome double negative (DN) and CD11b$^+$ cDC2 based on JAM-A and CCR7 expression. **(A)** Left panel: normalized mean relative expression ± SD of *F11r* (JAM-A) in dome conventional DC (cDC) subsets. Mid-panel: identification of four developmental stages of dome cDC2 based on CD11b and MHCII surface expression. Stage I, CD11b$^-$MHCII^{lo}; Stage II, CD11b$^-$MHCII^{int}; Stage III, CD11b^{lo}MHCII^{hi}; Stage IV, CD11b^{int}MHCII^{hi}. Right panel: mean fluorescence intensity of JAM-A in the four developmental stages of dome cDC2. JAM-A expression increases from stage I (DN cDC2) to stage IV (CD11b$^+$ cDC2). Lower panel: confocal microscopy projection of a *Zbtb46*-GFP$^{-/+}$ mouse Peyer's patch (PP) section stained for EGFP (green), CD11c (red), JAM-A (orange), and collagen IV (magenta). Higher magnifications of the numbered boxed area are shown on the right. cDC (CD11c$^+$GFP$^+$ cells) are mainly located in the IFR. However, some of them are located in the SED with a progressive decrease in numbers while reaching the upper part of the dome. Like LysoDC, they can penetrate into the follicle-associated epithelium (FAE). Subepithelial cDC2 (boxed area 1–4) express no or faint levels of JAM-A (stage I or II of dome cDC2; DN cDC2) whereas interfollicular cDC2 (boxed area 5 and 6) express it (stage III or IV of dome cDC2; CD11b$^+$ cDC2). **(B)** Left panel: normalized mean relative expression ± SD of *Ccr7* in dome cDC subsets. Right panel: confocal microscopy projection of a *Zbtb46*-GFP$^{-/+}$ mouse PP section stained for EGFP (green), CD11c (red), and CCR7 (orange). Higher magnifications of the numbered boxed area are shown on the right. Subepithelial cDC2 (boxed area 1) do not express CCR7 (DN cDC2) whereas interfollicular cDC2 (boxed area 2 and 3) do (CD11b$^+$ cDC2). Parts of **(A,B)** are adapted from Ref. (40).

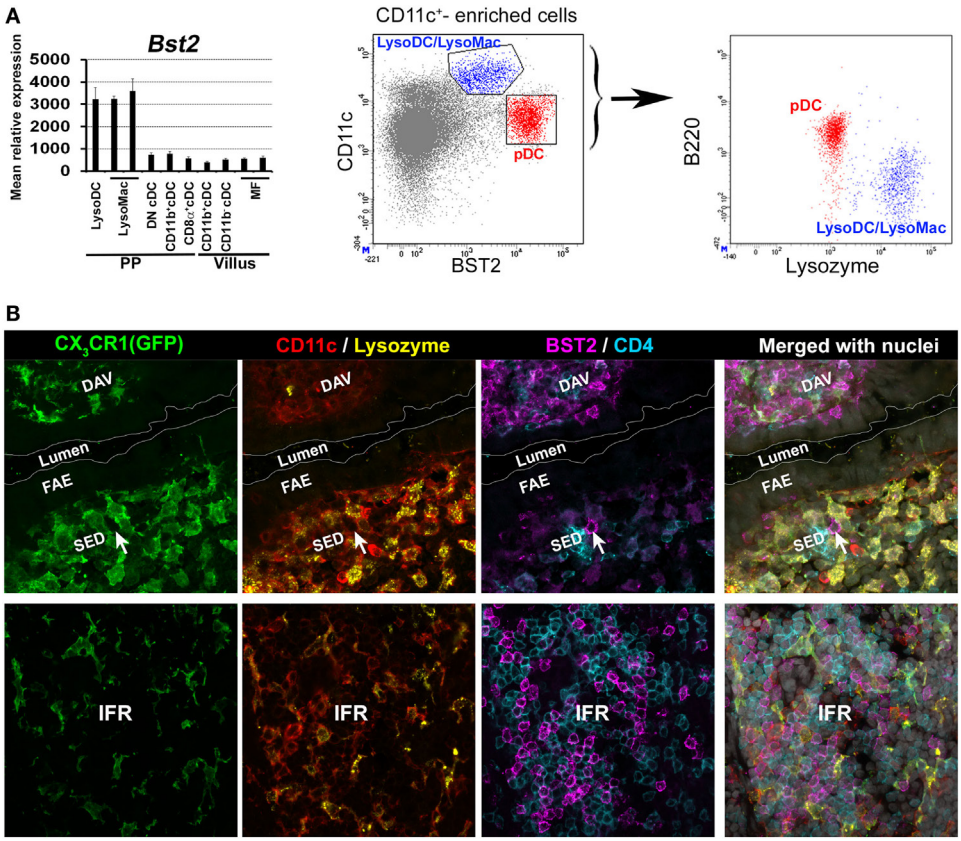


FIGURE 4 | Location of plasmacytoid DC (pDC) in Peyer's patch (PP). **(A)** Left panel: normalized mean relative expression ± SD of *Bst2* in intestinal phagocytes based on Immgen database (139) and on the PP phagocyte microarray data deposited to NCBI GEO under accession numbers GSE94380 and GSE65514 (39, 40). Expression of *Bst2* by LysoDC and LysoMac is shown. Right panel: in PP, monocyte-derived cells (CD11c^{hi}B220$^-$lysozyme$^+$ in blue), i.e., LysoDC and LysoMac, express lower levels of BST2 than pDC (CD11c^{int}B220$^+$lysozyme$^-$ in red). **(B)** Confocal microscopy projection of CX_3CR1-EGFP$^{-/+}$ mouse PP sections stained for EGFP (green), CD11c (red), lysozyme (yellow), CD4 (blue), and BST2 (magenta). Upper panel: BST2 is strongly expressed by cells of the dome-associated villus (DAV) but only weakly by LysoDC and LysoMac (CX_3CR1^+CD11c$^+$lysozyme$^+$ cells) in the subepithelial dome (SED). A single putative pDC (arrow) strongly stained for BST2 is located in the SED. Lower panel: unlike the SED, the IFR is enriched in pDC. **(A)** is adapted from Ref. (39).

FUNCTIONS OF PP PHAGOCYTE SUBSETS

Interaction with the FAE and Antigen Sampling Activity

The preferential uptake of luminal particulate antigens in PP as compared to villi first relies on the specific characteristics of the FAE (5–10, 52). Some of these properties, such as low levels of mucin expression, altered surface glycosylation, and lack of secretion of antimicrobial proteins, depend on IL-22 signaling inhibition through the production of IL-22 binding protein (IL-22BP) by CD11c$^+$CD11b$^+$MHCII$^+$ cells of the SED (53). Thereby, IL-22BP promotes microbial uptake into PP by influencing the FAE transcriptional program. Unfortunately, the markers used to identify IL-22BP-secreting cells do not allow distinguishing cDC

from monocyte-derived cells (53). In order to better characterize these IL-22BP-secreting phagocytes, we decided to interrogate the gene expression database of dome CD11c^{hi} phagocytes (NCBI GEO accession numbers GSE94380 and GSE65514) for IL-22BP transcripts (*Il22ra2*). *Il22ra2* was enriched in LysoDC and TIM-4$^-$ LysoMac as compared to cDC (**Figure 5A**). These results, together with the preferential location of LysoDC and TIM-4$^-$ LysoMac in the SED, support their role in the secretion of IL-22BP, which in turn inhibits IL-22 signaling, alters the FAE transcriptional program, and favors the internalization of both commensal and pathogenic bacteria (53).

In addition to this strong influence on FAE global characteristics, monocyte-derived cells and especially LysoDC maintain privileged interaction with M cells. Thus, LysoDC are able to extend dendrites through M cell specific transcellular pores to gain access to the lumen (**Figure 6**) (43). The cell adhesion molecules EpCAM and JAM-A are recruited at the M cell pore-forming membrane but neither the tight junction proteins ZO-1 and occludin nor the adherens junction proteins E-cadherin and β-catenin. Therefore, the formation of these M cell transcellular pores does not alter the integrity of the epithelial barrier. JAM-A is also enriched at the trans-M cell dendrite (TMD) membrane, which may favor homotypic interaction. In addition, there is a strong recruitment of filamentous actin in TMD in agreement with their high level of motility. These TMD scan indeed rapidly the surface of M cells and attract particulate antigens and bacteria from the lumen to capture them (43). Since blockade of the M cell-specific chemokine CCL9 drastically reduces the number of CD11c$^+$CD11b$^+$ cells in the SED and since LysoDC strongly express its receptor CCR1, it is tempting to speculate

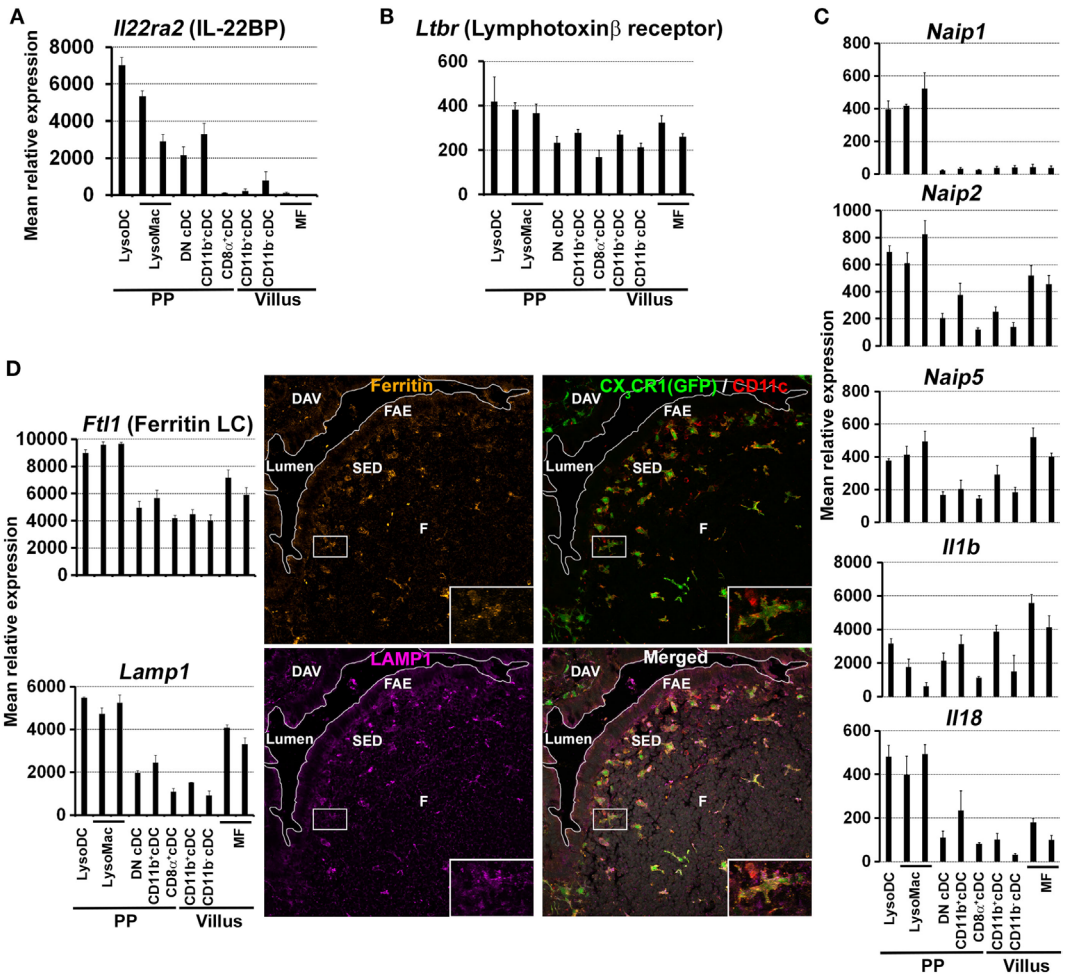


FIGURE 5 | Expression of defined markers by Peyer's patch (PP) phagocyte subpopulations. **(A–D)** Normalized mean relative expression ± SD of *Il22ra2*, *Ltbr*, *Naip1*, *Naip2*, *Naip5*, *Il1b*, *Il18*, *Ftl1*, and *Lamp1* in intestinal phagocytes based on Immgen database (139) and on the PP phagocyte microarray data deposited to NCBI GEO under accession numbers GSE94380 and GSE65514 (39, 40). **(A)** In the gut, *Il22ra2* [IL-22 binding protein (IL-22BP)] is mainly expressed by LysoDC and TIM-4$^-$ LysoMac. **(B)** In PP, *Ltbr* (lymphotoxin β receptor) is mainly expressed by LysoDC, LysoMac and, to a lesser extent, conventional DC (cDC). **(C)** Enrichment of some members of the NAIP/NLRC4 inflammasome pathway (*Naip1*, *Naip2*, *Naip5*, *Il1b*, and *Il18*) in LysoDC and LysoMac. Note that *Naip1* is only expressed by dome monocyte-derived cells. **(D)** Left panel: in the gut, LysoDC and LysoMac express higher levels of *Ftl1* (ferritin light chain) and *Lamp1* than other phagocytes. Right panel: labeling of a PP section shows enrichment of ferritin and LAMP1 expression in LysoDC and LysoMac of the subepithelial dome (SED) and of the follicle (F). Inserts: higher magnification of the boxed area showing one LysoDC strongly stained for ferritin and LAMP1.

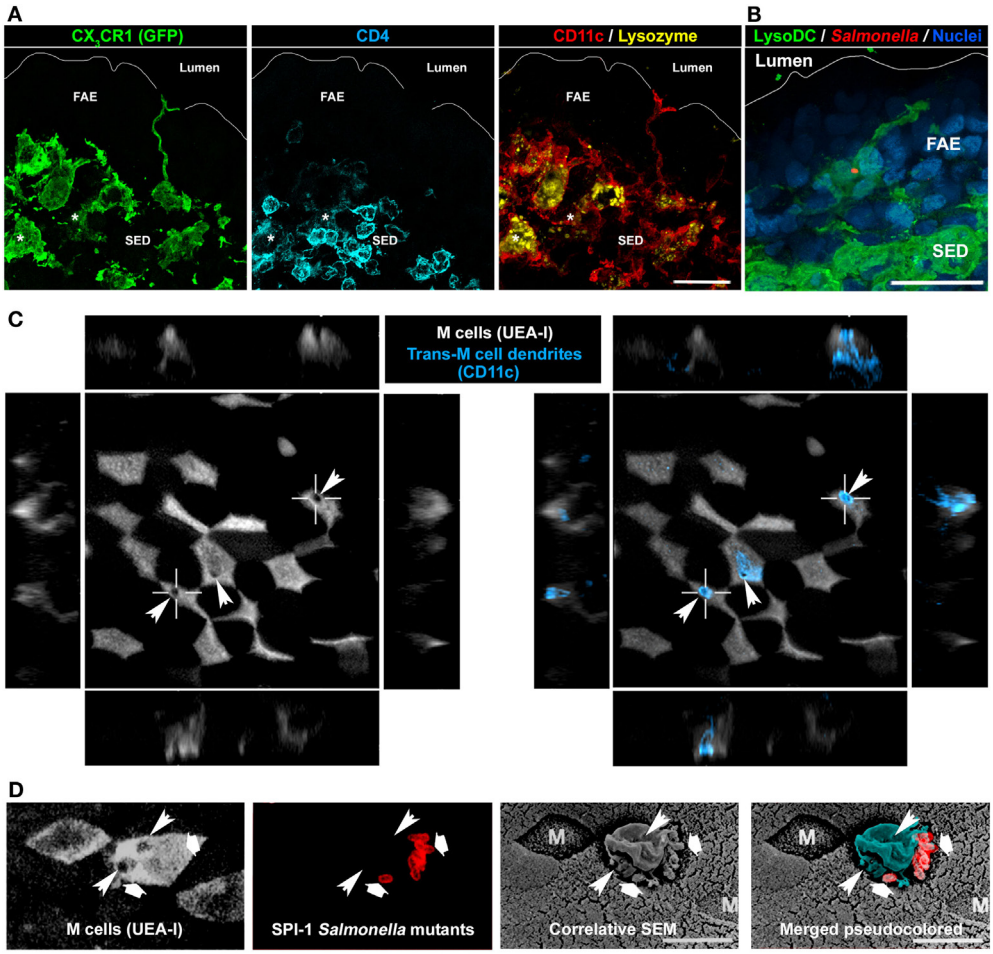


FIGURE 6 | Involvement of LysoDC trans-M cell dendrites in the sampling of *Salmonella typhimurium*. **(A)** A CX_3CR1-deficient LysoDC (GFP in place of CX_3CR1 in green; CD11c in red; lysozyme in yellow) extends a dendrite through the follicle-associated epithelium (FAE) to reach the lumen. In addition to CX_3CR1, CD11c, and lysozyme, LysoMac (*) stain for CD4 (blue). **(B)** 2 h postoral infection, a *Salmonella* (red) is taken up by a LysoDC (green) extending a dendrite into an uninfected FAE. **(C)** M cell transcellular pores (arrowheads), through which trans-M cell dendrites (CD11c in blue) cross the FAE, are highlighted by circular holes in the UEA-I cell surface staining. **(D)** By correlative scanning electron microscopy (SEM), *Salmonella* (second and last panels in red, large arrows) are located at the periphery of a protrusion (pseudocolored in blue) arising from an M cell. Circular holes (thin arrowheads) in the UEA-I cell surface staining indicate the presence of M cell transcellular pores. **(B,C)** are adapted from Ref. (43), **(D)** is adapted from Ref. (110).

that the degree of interaction between M cell and LysoDC is regulated through the release control of this chemokine by M cells (39, 49).

Although LysoDC are the main TMD-forming phagocytes, subepithelial LysoDC and TIM-4$^-$ LysoMac equally internalize particulate antigens (**Table 2**) (39). This suggests that, at least at steady state, the main route of particulate antigen sampling across the FAE is mediated through M cell transcytosis rather than by TMD. The lack of particulate antigen uptake by subepithelial cDC (DN cDC2) *in vivo* is in agreement first with their low number in this region and second with *in vitro* microparticle uptake assays showing a much more efficient phagocytic activity of LysoDC and LysoMac as compared to dome cDC (40, 42). Interestingly, in addition to transporting luminal antigens in their basolateral pocket or in the SED, M cells constitutively release on their basal side microvesicles, which are taken up by subepithelial $CD11c^+CD11b^+CX_3CR1^+$ cells, i.e., LysoDC and TIM-4$^-$ LysoMac (54). Finally, monocyte-derived cells and M cell cooperation extend beyond cell death since the former engulf dying M cells (**Table 2**) (42). In summary, particulate antigen uptake in the SED is mainly performed by subepithelial monocyte-derived cells and occurs through at least four distinct mechanisms, which all involve M cells: (i) M cell-mediated transcytosis; (ii) M cell microvesicle shedding; (iii) formation of TMD; (iv) dying M cell phagocytosis.

Innate Defense Functions

LysoDC and LysoMac have been first identified through their strong expression of the antibacterial compound lysozyme (42). Then, they have been distinguished from dome cDC by their surface expression of the host antiviral restriction factor BST2 (39). This suggests that, in addition to playing a primary role in antigen sampling, this family of dome phagocytes are strongly involved in the innate defense of PP. Analysis of their transcriptional profile

confirmed this assumption (39). Dome monocyte-derived cells display indeed a strong antibacterial and antiviral gene signature as compared to cDC. This includes genes encoding for viral and bacterial-associated molecular pattern recognition molecules such as toll-like receptors (TLRs), NAIPs, STING, DAI, and RIG-I. Several pathways of antiviral and antibacterial defense such as replication inhibition, metal sequestration, NLRC4 inflammasome formation, and detoxification mechanisms are also upregulated in monocyte-derived cells as compared to cDC. Therefore, LysoDC and LysoMac, but not cDCs, display strong innate defense mechanisms against both viral and bacterial infections (**Figure 1**).

Priming of T Cells

Conventional DC have been long recognized as the most efficient professional antigen-presenting cells to initiate an antigen-specific immune response through the priming of both naïve $CD4^+$ and $CD8^+$ T cells (55). Upon activation, cDC initiate a process of differentiation, also termed maturation, which involves an important genetic reprogramming (56, 57). This induces profound phenotypic, morphological, and functional changes, which allow their migration to lymph node T cell zones and their antigen presentation and naïve T cell priming ability. Depletion of $CD11c^+$ phagocytes showed that in PP they are involved both in the retention of interfollicular naive helper T cells and in their priming following antigen feeding (58, 59). Most dome cDC reside in the IFR and, therefore, do not require to migrate to encounter naïve T cells (40). Although it may be convenient and secure to rapidly prime naïve T cells, it raises indubitably the question of antigen acquisition. It could be, however, hypothesized that, after acquisition of soluble antigens or transfer of particulate antigens from monocyte-derived cells, DN cDC2 upregulate CCR7 and downregulate CCR6 to rapidly shuttle from the SED to the IFR. Their constant migratory activity would thus lead to the apparent underrepresentation of cDC in the SED where most of the luminal antigen sampling activity is performed (39, 40). By contrast, LysoDC, which are highly efficient in particulate antigen sampling, are mainly located in the SED and, to some extent, in the follicle but their migration to the T cell zone or their ability to prime T cells *in vivo* in the SED remain pending issues (39, 42, 43).

In vitro, unlike LysoMac, both dome cDC and LysoDC are able to induce naïve antigen-specific T helper cell proliferation (**Table 2**) (39). This is in line with the fact that, upon TLR7 stimulation, LysoDC upregulate MHCII and the co-stimulatory molecules CD40 and CD86 whereas LysoMac do not. Both cDC1 and LysoDC prime naïve antigen-specific T helper cells for IFNγ production. LysoDC also induce the production of IL-6, a property shared with cDC2 (**Table 2**).

Interaction with the Microbiota and Induction of the Mucosal Humoral Immune Response

Peyer's patches are the primary site of antigen-specific sIgA-secreting cell induction (3, 4, 60–64). Production of sIgA is rapidly induced upon microbial colonization and strongly reduced in germ-free animals (65). Moreover, sIgA coating of the microbiota plays a critical role in its diversification (66–68). Interestingly, sIgA predominantly target specific members of the microbiota, especially those residing in the small intestine and those considered as pathobionts (69–71). Therefore, microbiota influences the mucosal immune system, which in turn regulates symbiont diversity and stability (72, 73). Among commensal bacteria that profoundly influence the mucosal immune system in mouse, segmented filamentous bacteria (SFB) play a privileged role, through induction of Th17 cells and IgA-secreting cells (74–76). This SFB-induced immune response largely depends on the stimulation of PPs and isolated lymphoid follicles (77). Interestingly, specific members of the microbiota, including SFB, colonize PPs (77–80). Moreover, M cells are able to transport different defined commensal bacteria, which induce distinct M cell transcriptional programs (81). This sampling of gut microbiota through M cell-mediated pathways is crucial to initiate mucosal sIgA production (25). Thus, it is tempting to speculate that microbiota members capable of inducing strong humoral immune responses are those that strongly interact with the FAE. Once translocated in the SED, SFBs are internalized by $CD11c^{int}CD11b^+$ and $CD11c^{hi}CD11b^+$ phagocytes (82). Other IgA-inducer commensals, especially *Alcaligenes* species, reside inside $CD11c^+$ cells within isolated lymphoid follicles, PP, and mesenteric lymph nodes (MLN) of mice and humans (79, 80, 83). PP $CD11c^+$ phagocytes are known to carry commensal bacteria through a CCR7-dependent mechanism to the MLN, which are required to restrict commensal-loaded $CD11c^+$ phagocytes to the mucosal compartment but are dispensable for IgA induction (84). However, the accurate identification of the $CD11c^+$ phagocyte subset(s), which sample(s) and carry(ies) commensal bacteria, remains currently unknown.

In vitro, the role of PP phagocytes in IgA class switching has long been recognized (85, 86). More recently, it has been shown that PP and MLN pDC efficiently promote IgA class switch recombination through their expression of membrane-bound BAFF (B-cell activating factor) and APRIL (a proliferation-inducing ligand) independently of any T-cell or microbial stimulus (**Table 2**) (87). However, a recent pDC depletion study showed that pDCs are dispensable for intestinal IgA production *in vivo* (88). $CD11c^{hi}CD11b^+B220^-$ phagocytes have also been implicated in the differentiation of naïve B cells into sIgA-secreting cells *in vitro* (89). It remains, however, to establish whether these $CD11c^{hi}CD11b^+B220^-$ phagocytes are LysoDC, LysoMac, or dome $CD11b^+$ cDC2 and to confirm their function *in vivo*. The role of each dome phagocyte subset in sIgA-secreting cell commitment *in vivo* is indeed not well-established (**Table 2**). However, efficient IgA class switching requires interaction of $CCR6^+$ B cells with lymphotoxin-dependent $CD11c^{hi}MHCII^+CD11b^+$ phagocytes in the SED (90). Since lymphotoxin β receptor transcripts (*Ltbr*) are expressed by monocyte-derived cells and, to a lesser extent, by cDC (**Figure 5B**), it remains to establish whether these $CD11c^{hi}MHCII^+CD11b^+$ phagocytes correspond to $CD11b^+$ cDC2, LysoDC, or LysoMac. Nevertheless, the sampling activity and the anatomic localization of the different phagocyte subsets as described above would argue for LysoDC/LysoMac rather than for $CD11b^+$ cDC2 involvement.

The lymphotoxin required to maintain these phagocytes in the SED could be mainly provided by subepithelial innate lymphoid cells type 3 (ILC3) (90). However, a recent report indicates that microbiota-derived butyrate suppresses ILC3 in terminal ileal PP, rendering their role in subepithelial phagocyte maintenance unlikely at least in this part of the gut (91). Lack of CCR6 expression by B cells or RANKL expression deficiency in subepithelial stromal cells, which results in inhibition of CCL20 production by the FAE, prevents B cells migration into the SED, precludes their interaction with $CD11c^{hi}MHCII^{+}CD11b^{+}$ phagocytes and finally inhibits IgA class switching and bacteria-specific sIgA production (14, 90). The integrin complex αvβ8 expressed by $CD11c^{hi}MHCII^{+}CD11b^{+}$ phagocytes could directly activate TGFβ during the interaction of these phagocytes with $CCR6^{+}$ B cells and promote IgA class switching (90). In summary, induction of commensal bacteria-specific sIgA-secreting cells is a complex process involving many different cell types: (i) subepithelial stromal cells producing RANKL for the formation of M cells and for the production of CCL20, which recruits $CCR6^{+}$ B cell and DN cDC2 into the SED; (ii) M cells for antigen sampling; (iii) lymphotoxin-producing cells for the maintenance of $CD11c^{hi}MHCII^{+}CD11b^{+}$ phagocytes; (iv) $CD11c^{hi}MHCII^{+}CD11b^{+}$ phagocytes for activation of $CCR6^{+}$ B cells.

Regulation of the Adaptive Immune Response

Tingible-body macrophages are critical in the removal of apoptotic B cells during the selection process that occurs in the GC (**Table 2**) (92). Defect in this scavenging function leads to secondary necrosis, release of noxious molecules and pro-inflammatory signals, and is linked to autoantibody production and autoimmune disease development. This scavenging function requires the expression of the apoptotic receptor MerTK by TBM and of the soluble bridging molecule MFG-E8 by follicular DC, the GC stromal cells involved in the shaping of the B cell response (93–96). A number of other factors and receptors, such as TIM-4, have also been implicated in this process and their deficiency leads to autoimmunity, too (92). Therefore, although some of these molecules may have redundant roles, they may also function together to be more efficient in apoptotic cell removal through several mechanisms, thus preventing the arising of autoimmunity (97).

Like TBM, interfollicular MF express the apoptotic cell receptor TIM-4 and are located in a region of effector cell priming (39). Although the function of these $TIM\text{-}4^{+}$ LysoMac remains elusive, they are thus likely to participate to the clearance of dying T cells like TBM contribute to the removal of dying B cells. Interestingly, TIM-4 deficiency leads to not only B cell but also T cells hyperactivity (98). Moreover, TIM-4 functions have been linked to the control of the adaptive immune response and tolerance through the removal of antigen-specific T cells (99, 100). Concerning PP phagocytes, while LysoDC interact with and prime naïve helper T cells *in vitro*, in the same conditions LysoMac phagocytize them, supporting their role in the removal of T cells (**Table 2**) (39). Thus, the location of $TIM\text{-}4^{+}$ LysoMac in the T cell zone correlates well with a possible function in the removal of some naïve T cells during their priming process. Therefore, TBM and $TIM\text{-}4^{+}$ LysoMac could perform a crucial role in PP adaptive immune response regulation at the level of GC and IFR, respectively.

PP PHAGOCYTES IN INFECTION

Sensing and Uptake of Immune Complexes

Innate polyreactive and antigen-specific sIgA are secreted by *lamina propria* plasma cells and transported through the epithelium by the polymeric immunoglobulin receptor to be finally released in the lumen. During infection, sIgA recognize and bind pathogens, thus participating to their clearance through a process called immune exclusion. Interestingly, M cells express on their surface dectin-1 and Siglec-F, which can serve as sIgA receptors allowing the uptake of luminal sIgA immune complexes (101). Since uptake of sIgA-coated bacteria persists in PP of dectin-1-deficient mice, Siglec-F expression may be sufficient to mediate sIgA binding to M cells (102). In the SED, sIgA immune complexes are associated with $CD11c^{+}CD11b^{+}CX_3CR1^{+}MHCII^{+}$ cells, i.e., LysoDC and/or $TIM\text{-}4^{-}$ LysoMac (101). Entry of IgA-coated bacteria into PP does not require CX_3CR1 expression (102). However, this does not preclude a potential role of TMD in sIgA immune complex uptake since CX_3CR1 is not involved in TMD formation (**Figure 6A**) (39). Finally, this mechanism of immune complex sampling ensures the constant monitoring of sIgA-coated antigens present in the gut, including both pathogens and symbionts (103, 104). Through this process, new antigen-specific IgA-secreting cells could be produced to allow a better exclusion of pathogens.

Bacterial Infection: The Case of *Salmonella*

Salmonella enterica is an enteroinvasive bacterium typically acquired by ingestion of contaminated water or food. In the absence of dysbiosis, the primary invasion sites of *Salmonella enterica* serovar Typhimurium, the murine model of systemic salmonellosis, are PP of the distal ileum and cecal patches (105, 106). Through their fimbrial FimH adhesin, *Salmonella Typhimurium* are able to bind to the GP2 molecules expressed at the surface of M cells (17). Then, they use their *Salmonella* pathogenicity island 1 (SPI-1) type III secretion system to deliver effector proteins, which reorganize the cytoskeleton and allow the translocation of bacteria through M cells by inducing membrane ruffling (17, 107, 108). However, even SPI-1 and FimH *Salmonella* mutants or GP2-deficient mice show, to some extent, bacterial translocation into PP (17, 102, 109–111). One possible mechanism for this residual penetration could be transcytosis mediated by M cells, as observed with inert particles (13, 112, 113). Alternatively, these bacteria could be directly sampled by TMD (**Figure 6**) (43). *Salmonella Typhimurium* indeed induce TMD that rapidly internalize bacteria before retracting back to the SED (43). As soon as 2 h after oral infection, bacteria are present in LysoDC extending dendrites into the FAE in absence of any

bacterial invasion of epithelial cells (**Figure 6B**). Interestingly, similar trans-M cell passages of uncharacterized leukocytes have been observed by electron microscopy using rabbit intestinal loop models of *Streptococcus pneumoniae* and *Vibrio cholerae* infection (114, 115). TMD are, therefore, infection-inducible and transient processes, which allow a fast M cell-regulated uptake of luminal material by immunocompetent cells. Such mechanism of sampling may notably avoid risks of massive penetration by pathogens. A typical feature of TMD formation is the appearance of a circular hole at the M cell apical membrane (**Figure 6C**). Interestingly, correlative scanning electron microscopy studies of PP in mouse intestinal loop infected with SPI-1 *Salmonella* mutants, which are unable to induce epithelial cell apical membrane ruffling, have highlighted the formation of membrane protrusions above M cell surface circular holes (**Figure 6D**) (109, 110). Therefore, these protrusions, which do not express the M cell marker UEA-I but bind bacteria, are likely TMD.

Once translocated by M cells or internalized by TMD, *Salmonella Typhimurium* are predominantly found in subepithelial lysozyme-expressing cells, i.e., TIM-4$^-$ LysoMac and/or LysoDC (**Table 2**) (42). Importantly, these phagocytes express genes involved in innate defense against *Salmonella* (39). These genes notably include *Naip1*, *Naip2*, and *Naip5*, which encode cytosolic receptors for the needle and inner rod proteins of the type III secretion system and for flagellin, respectively (**Figure 5C**) (116). Upon recognition of their ligands, NAIP proteins co-oligomerize with the adaptor NLRC4 to form an inflammasome complex and to recruit and activate caspase-1, which in turn process IL-1β and IL-18 into their active form. Interestingly, monocyte-derived cells express high levels of *Il1b* and *Il18*, indicating that, upon inflammasome activation, they may secrete large amounts of these pro-inflammatory cytokines (**Figure 5C**). Despite the expression of all these defense genes, it is currently unknown whether TIM-4$^-$ LysoMac and/or LysoDC are able to kill internalized *Salmonella* and die from pyroptosis upon inflammasome activation or whether bacteria have evolved strategies to survive, replicate inside, and kill these phagocytes.

Invasion of PP by *Salmonella* also induces the CCR6-dependent recruitment of CD11c$^+$ cells in the SED and the FAE, probably through the release of CCL20 by the latter (117). As mentioned above, CCL20 is indeed specifically expressed by the FAE, thanks to its contact with RANKL-producing stromal cells (14). Among PP CD11c$^+$ phagocytes, CCR6 expression is restricted to cDC2, and more specifically, DN cDC2 (40, 118). Thus, *Salmonella* induce the recruitment of DN cDC2 in the SED and the FAE. CCR6 expression also promotes the activation of *Salmonella*-specific T cells upon infection (117). Whether this activation relies on the cooperation between monocyte-derived cells that internalize bacteria and DN cDC2, which are recruited to the SED, remains to establish. Interestingly, upon inflammasome activation, pyroptosis of monocyte-derived cells could lead to the release of bacterial antigens and presentation of the latter to T cells by cDC2 as demonstrated in *in vitro* models using mouse bone marrow-derived DC and MF (119). However, since CCR6 is expressed by many other PP immune cell types and is involved in many cellular processes such as B cell migration in the SED and M cell differentiation, it remains to establish whether CCR6$^+$ DN cDC2 are directly involved in activation of *Salmonella*-specific T cells upon infection (90, 118, 120–122).

Viral Infection: Reovirus and Norovirus

Reovirus enters the host through intestinal M cells and lack of M cells prevents from productive infection (18, 23, 123). Similarly, norovirus infection is reduced in M cell-deficient mice (23). Thus, M cells represent preferential entry sites for viruses, in addition to enteropathogenic bacteria. Although noroviruses have a tropism for DC and MF, their precise target following transport through M cells is currently unknown (124, 125). Unlike norovirus, reovirus preferentially replicates within the FAE (126). Interestingly, CD11c$^+$ cells of the SED internalize reovirus-infected apoptotic FAE cells (127). As mentioned above, lysozyme-expressing CD11c$^+$ cells, i.e., LysoDC and TIM-4$^-$ LysoMac, internalize apoptotic FAE cells (**Table 2**), suggesting their involvement in apoptotic epithelial cell-derived viral antigen handling (42). Importantly, PP CD11c$^+$ cells from infected mice are able to process and present viral antigens from apoptotic cells to activate reovirus-primed T cells (127). Finally, initiation of an anti-reovirus immune response characterized by the production of virus-specific sIgA and cytotoxic T cells occurs in PP.

Prion Infection

Infectious prions are proteins with an abnormal conformation, which, upon conversion of the normally folded endogenous cellular prion protein and spreading to the central nervous system, lead to neurodegenerative diseases. Natural infection occurs mainly by oral consumption of prion-contaminated food. After oral exposure, uptake of infectious prions by M cells and their accumulation and replication upon follicular DCs in small intestine PP are essential for the efficient spread of disease to the brain (128, 129). CD11c$^+$ cells are also required for the early stage of PP infection (130). In the SED, infectious prions are located in cells enriched for ferritin and LAMP1 but not MHCII (131). To better characterize these subepithelial phagocytes, we examined the expression of ferritin and LAMP1 transcripts in the gene expression database of dome phagocytes. We found that these transcripts are enriched in LysoDC and LysoMac as compared to cDC (**Figure 5D**). We also confirmed by immunostaining of PP sections the increased expression of ferritin and LAMP1 inside subepithelial LysoDC and LysoMac (CD11c$^+$CX$_3$CR1$^+$ cells) as compared to other cells (**Figure 5D**). Since LysoDC express high levels of MHCII, this rather supports a role of TIM-4$^-$ LysoMac in the transmission of infectious prion (**Table 2**). Another population of infectious prion-loaded CD11b$^+$ phagocytes is located in the subfollicular area of PP (132). These subfollicular phagocytes are absent from uninfected animals, which suggests that TIM-4$^-$ LysoMac could migrate from the SED to this subfollicular area upon infection. Interestingly, CXCR5 expression deletion in CD11c$^+$ cells delays accumulation of infectious prion upon follicular DC and impedes oral prion disease pathogenesis (133). This suggests that CXCR5 could allow migration of CD11c$^+$ phagocytes from the SED to the follicle or subfollicular

area, which would promote spreading of infectious prion to follicular DC. However, when we interrogated the gene expression database of dome phagocytes, we did not find significant CXCR5 expression in any CD11c$^+$ phagocytes. Therefore, identity of CD11c$^+$CXCR5$^+$ cells in PP as well as the mechanism of transfer of infectious prion from TIM-4$^-$ LysoMac to follicular DC remain pending issues.

Behavior of PP Phagocytes upon Infection

Our knowledge on the alteration induced by pathogens on PP phagocyte populations is scarce. What we know relies mainly on stimulation of PP with pathogen-derived compounds or mimetics. Thus, the cholera toxin induces the migration of CD11c$^+$ cells into the FAE. Several TLR ligands induce similar CD11c$^+$ cell relocation (112, 134–136). This is in line with the recruitment of DN cDC2 and formation of TMD observed shortly after *Salmonella* infection (43, 117). Thus, the first event that occurs upon pathogen detection is an increase of the sampling activity by recruitment in the FAE of both DN cDC2 and LysoDC. Then, SED-located CD11c$^+$ cells are thought to migrate from the SED to the IFR in order to prime naïve T cells. Microsphere-loaded CD11c$^+$ cells usually located in the SED are indeed observed in the IFR after cholera toxin or *Salmonella Typhimurium*-induced stimulation (137). Moreover, systemic injection of soluble *Toxoplasma gondii* tachyzoite antigen leads to a loss of CD11c$^+$CD11b$^+$ cells in the SED combined with the recruitment of CD11c$^+$CD11b$^+$ cells in the IFR (37). Actually, all activated dome cDC are located in the IFR as exemplified by their specific expression of CD83, CD86, CD205, CCL22, and CCR7 (40). Finally, the number of interfollicular cDC increase in the IFR of R848-fed animals (40, 138). However, this is at least in part due to interfollicular cDC1 number increase and to DAV cDC2 recruitment through a TNF-dependent pathway (40). The respective contribution of DAV and SED cDC2 to the migratory pool of interfollicular cDC is currently unknown, as well as their role in the induction of the mucosal immune response. Nevertheless, DAV and SED cDC recruitment in the IFR upon stimulation may allow in a single region the presentation of antigens sampled both in DAV and in SED. Since uptake of pathogens is facilitated in the FAE as compared to villous epithelium (11, 25, 42, 43), such mechanism of antigen sorting could help the mucosal immune system to discriminate between innocuous and harmful matters. Whether other stimuli than R848 induce similar recruitment of DAV cDC in the IFR is, however, currently unknown. If so, the current model of PP phagocyte activation will have to be modified to include DAV cDC as an integral part of the process.

CONCLUDING REMARKS

Although PP phagocytes are now well characterized, many efforts have to be done in order to understand the role of each phagocyte population in the mucosal immune response initiation during enteric infection. Importantly, to assess carefully these functions, a convenient and well-established panel of markers should be used in the different research laboratories in order to clearly identify each subset and avoid confusion between them. Here, we propose two panels of markers, one for microscopy and one for flow cytometry, which allow distinguishing each PP subset including DAV cDC and DAV MF (**Table 1**). These panels undoubtedly identify each subset of PP phagocytes and in the future should help clarify their functions in the initiation of the mucosal immune response.

AUTHOR CONTRIBUTIONS

HL wrote the manuscript. CDS, CW, JB, and J-PG gave feedback and revised the manuscript.

ACKNOWLEDGMENTS

We thank Mark A. Jepson for sharing data and opinion with us. We acknowledge the CIML histology, cytometry, and mouse house facilities. We thank the PICSL imaging facility of the CIML (ImagImm), member of the national infrastructure France-BioImaging supported by the French National Research Agency (ANR-10-INBS-04). The project leading to this publication has received funding from Excellence Initiative of Aix-Marseille University—A*MIDEX, a French "Investissements d'Avenir" programme. The studies performed by the authors were supported by institutional grants from INSERM, CNRS, and Aix-Marseille University to the CIML. CDS is supported by the FRM fellowship FDT20160434982.

REFERENCES

1. Sperandio B, Fischer N, Sansonetti PJ. Mucosal physical and chemical innate barriers: lessons from microbial evasion strategies. *Semin Immunol* (2015) 27(2):111–8. doi:10.1016/j.smim.2015.03.011
2. Jung C, Hugot JP, Barreau F. Peyer's patches: the immune sensors of the intestine. *Int J Inflam* (2010) 2010:823710. doi:10.4061/2010/823710
3. Suzuki K, Kawamoto S, Maruya M, Fagarasan S. GALT: organization and dynamics leading to IgA synthesis. *Adv Immunol* (2010) 107:153–85. doi:10.1016/b978-0-12-381300-8.00006-x
4. Reboldi A, Cyster JG. Peyer's patches: organizing B-cell responses at the intestinal frontier. *Immunol Rev* (2016) 271(1):230–45. doi:10.1111/imr.12400
5. Bhalla DK, Owen RL. Cell renewal and migration in lymphoid follicles of Peyer's patches and cecum – an autoradiographic study in mice. *Gastroenterology* (1982) 82(2):232–42.
6. Pappo J, Owen RL. Absence of secretory component expression by epithelial cells overlying rabbit gut-associated lymphoid tissue. *Gastroenterology* (1988) 95(5):1173–7. doi:10.1016/0016-5085(88)90347-2
7. Frey A, Giannasca KT, Weltzin R, Giannasca PJ, Reggio H, Lencer WI, et al. Role of the glycocalyx in regulating access of microparticles to apical plasma membranes of intestinal epithelial cells: implications for microbial attachment and oral vaccine targeting. *J Exp Med* (1996) 184(3):1045–59. doi:10.1084/jem.184.3.1045
8. Mabbott NA, Donaldson DS, Ohno H, Williams IR, Mahajan A. Microfold (M) cells: important immunosurveillance posts in the intestinal epithelium. *Mucosal Immunol* (2013) 6(4):666–77. doi:10.1038/mi.2013.30
9. Ohno H. Intestinal M cells. *J Biochem* (2016) 159(2):151–60. doi:10.1093/jb/mvv121
10. Owen RL, Jones AL. Epithelial cell specialization within human Peyer's patches: an ultrastructural study of intestinal lymphoid follicles. *Gastroenterology* (1974) 66(2):189–203.

11. Schulz O, Pabst O. Antigen sampling in the small intestine. *Trends Immunol* (2013) 34(4):155–61. doi:10.1016/j.it.2012.09.006
12. Bockman DE, Cooper MD. Pinocytosis by epithelium associated with lymphoid follicles in the bursa of Fabricius, appendix, and Peyer's patches. An electron microscopic study. *Am J Anat* (1973) 136(4):455–77. doi:10.1002/aja.1001360406
13. Knoop KA, Kumar N, Butler BR, Sakthivel SK, Taylor RT, Nochi T, et al. RANKL is necessary and sufficient to initiate development of antigen-sampling M cells in the intestinal epithelium. *J Immunol* (2009) 183(9):5738–47. doi:10.4049/jimmunol.0901563
14. Nagashima K, Sawa S, Nitta T, Tsutsumi M, Okamura T, Penninger JM, et al. Identification of subepithelial mesenchymal cells that induce IgA and diversify gut microbiota. *Nat Immunol* (2017) 18(6):675–82. doi:10.1038/ni.3732
15. Clark MA, Jepson MA, Simmons NL, Booth TA, Hirst BH. Differential expression of lectin-binding sites defines mouse intestinal M-cells. *J Histochem Cytochem* (1993) 41(11):1679–87. doi:10.1177/41.11.7691933
16. Giannasca PJ, Giannasca KT, Falk P, Gordon JI, Neutra MR. Regional differences in glycoconjugates of intestinal M cells in mice: potential targets for mucosal vaccines. *Am J Physiol* (1994) 267(6 Pt 1):G1108–21.
17. Hase K, Kawano K, Nochi T, Pontes GS, Fukuda S, Ebisawa M, et al. Uptake through glycoprotein 2 of FimH(+) bacteria by M cells initiates mucosal immune response. *Nature* (2009) 462(7270):226–30. doi:10.1038/nature08529
18. Helander A, Silvey KJ, Mantis NJ, Hutchings AB, Chandran K, Lucas WT, et al. The viral sigma1 protein and glycoconjugates containing alpha2-3-linked sialic acid are involved in type 1 reovirus adherence to M cell apical surfaces. *J Virol* (2003) 77(14):7964–77. doi:10.1128/JVI.77.14.7964-7977.2003
19. Lelouard H, Reggio H, Mangeat P, Neutra M, Montcourrier P. Mucin-related epitopes distinguish M cells and enterocytes in rabbit appendix and Peyer's patches. *Infect Immun* (1999) 67(1):357–67.
20. Lelouard H, Reggio H, Roy C, Sahuquet A, Mangeat P, Montcourrier P. Glycocalyx on rabbit intestinal M cells displays carbohydrate epitopes from Muc2. *Infect Immun* (2001) 69(2):1061–71. doi:10.1128/IAI.69.2.1061-1071.2001
21. Clark MA, Hirst BH, Jepson MA. M-cell surface beta1 integrin expression and invasin-mediated targeting of *Yersinia pseudotuberculosis* to mouse Peyer's patch M cells. *Infect Immun* (1998) 66(3):1237–43.
22. Nakato G, Hase K, Suzuki M, Kimura M, Ato M, Hanazato M, et al. Cutting edge: *Brucella abortus* exploits a cellular prion protein on intestinal M cells as an invasive receptor. *J Immunol* (2012) 189(4):1540–4. doi:10.4049/jimmunol.1103332
23. Gonzalez-Hernandez MB, Liu T, Payne HC, Stencel-Baerenwald JE, Ikizler M, Yagita H, et al. Efficient norovirus and reovirus replication in the mouse intestine requires microfold (M) cells. *J Virol* (2014) 88(12):6934–43. doi:10.1128/jvi.00204-14
24. Kanaya T, Hase K, Takahashi D, Fukuda S, Hoshino K, Sasaki I, et al. The Ets transcription factor Spi-B is essential for the differentiation of intestinal microfold cells. *Nat Immunol* (2012) 13(8):729–36. doi:10.1038/ni.2352
25. Rios D, Wood MB, Li J, Chassaing B, Gewirtz AT, Williams IR. Antigen sampling by intestinal M cells is the principal pathway initiating mucosal IgA production to commensal enteric bacteria. *Mucosal Immunol* (2016) 9(4):907–16. doi:10.1038/mi.2015.121
26. Cerovic V, Bain CC, Mowat AM, Milling SW. Intestinal macrophages and dendritic cells: what's the difference? *Trends Immunol* (2014) 35(6):270–7. doi:10.1016/j.it.2014.04.003
27. Vremec D, Shortman K. Dendritic cell subtypes in mouse lymphoid organs: cross-correlation of surface markers, changes with incubation, and differences among thymus, spleen, and lymph nodes. *J Immunol* (1997) 159(2):565–73.
28. Guilliams M, Ginhoux F, Jakubzick C, Naik SH, Onai N, Schraml BU, et al. Dendritic cells, monocytes and macrophages: a unified nomenclature based on ontogeny. *Nat Rev Immunol* (2014) 14(8):571–8. doi:10.1038/nri3712
29. Sancho D, Mourao-Sa D, Joffre OP, Schulz O, Rogers NC, Pennington DJ, et al. Tumor therapy in mice via antigen targeting to a novel, DC-restricted C-type lectin. *J Clin Invest* (2008) 118(6):2098–110. doi:10.1172/jci34584
30. Huysamen C, Willment JA, Dennehy KM, Brown GD. CLEC9A is a novel activation C-type lectin-like receptor expressed on BDCA3+ dendritic cells and a subset of monocytes. *J Biol Chem* (2008) 283(24):16693–701. doi:10.1074/jbc.M709923200
31. Caminschi I, Proietto AI, Ahmet F, Kitsoulis S, Shin Teh J, Lo JC, et al. The dendritic cell subtype-restricted C-type lectin Clec9A is a target for vaccine enhancement. *Blood* (2008) 112(8):3264–73. doi:10.1182/blood-2008-05-155176
32. Dorner BG, Dorner MB, Zhou X, Opitz C, Mora A, Guttler S, et al. Selective expression of the chemokine receptor XCR1 on cross-presenting dendritic cells determines cooperation with CD8+ T cells. *Immunity* (2009) 31(5):823–33. doi:10.1016/j.immuni.2009.08.027
33. Crozat K, Guiton R, Contreras V, Feuillet V, Dutertre CA, Ventre E, et al. The XC chemokine receptor 1 is a conserved selective marker of mammalian cells homologous to mouse CD8alpha+ dendritic cells. *J Exp Med* (2010) 207(6):1283–92. doi:10.1084/jem.20100223
34. Bachem A, Guttler S, Hartung E, Ebstein F, Schaefer M, Tannert A, et al. Superior antigen cross-presentation and XCR1 expression define human CD11c+CD141+ cells as homologues of mouse CD8+ dendritic cells. *J Exp Med* (2010) 207(6):1273–81. doi:10.1084/jem.20100348
35. Gurka S, Hartung E, Becker M, Kroczek RA. Mouse conventional dendritic cells can be universally classified based on the mutually exclusive expression of XCR1 and SIRPalpha. *Front Immunol* (2015) 6:35. doi:10.3389/fimmu.2015.00035
36. Anjuere F, Martin P, Ferrero I, Fraga ML, del Hoyo GM, Wright N, et al. Definition of dendritic cell subpopulations present in the spleen, Peyer's patches, lymph nodes, and skin of the mouse. *Blood* (1999) 93(2):590–8.
37. Iwasaki A, Kelsall BL. Localization of distinct Peyer's patch dendritic cell subsets and their recruitment by chemokines macrophage inflammatory protein (MIP)-3alpha, MIP-3beta, and secondary lymphoid organ chemokine. *J Exp Med* (2000) 191(8):1381–94. doi:10.1084/jem.191.8.1381
38. Iwasaki A, Kelsall BL. Unique functions of CD11b+, CD8 alpha+, and double-negative Peyer's patch dendritic cells. *J Immunol* (2001) 166(8):4884–90. doi:10.4049/jimmunol.166.8.4884
39. Bonnardel J, Da Silva C, Henri S, Tamoutounour S, Chasson L, Montanana-Sanchis F, et al. Innate and adaptive immune functions of Peyer's patch monocyte-derived cells. *Cell Rep* (2015) 11(5):770–84. doi:10.1016/j.celrep.2015.03.067
40. Bonnardel J, Da Silva C, Wagner C, Bonifay R, Chasson L, Masse M, et al. Distribution, location, and transcriptional profile of Peyer's patch conventional DC subsets at steady state and under TLR7 ligand stimulation. *Mucosal Immunol* (2017). doi:10.1038/mi.2017.30
41. Bonnardel J, Da Silva C, Masse M, Montanana-Sanchis F, Gorvel JP, Lelouard H. Gene expression profiling of the Peyer's patch mononuclear phagocyte system. *Genom Data* (2015) 5:21–4. doi:10.1016/j.gdata.2015.05.002
42. Lelouard H, Henri S, De Bovis B, Mugnier B, Chollat-Namy A, Malissen B, et al. Pathogenic bacteria and dead cells are internalized by a unique subset of Peyer's patch dendritic cells that express lysozyme. *Gastroenterology* (2010) 138(1):173–84.e1–3. doi:10.1053/j.gastro.2009.09.051
43. Lelouard H, Fallet M, de Bovis B, Meresse S, Gorvel JP. Peyer's patch dendritic cells sample antigens by extending dendrites through M cell-specific transcellular pores. *Gastroenterology* (2012) 142(3):592–601.e3. doi:10.1053/j.gastro.2011.11.039
44. Contractor N, Louten J, Kim L, Biron CA, Kelsall BL. Cutting edge: Peyer's patch plasmacytoid dendritic cells (pDCs) produce low levels of type I interferons: possible role for IL-10, TGFbeta, and prostaglandin E2 in conditioning a unique mucosal pDC phenotype. *J Immunol* (2007) 179(5):2690–4. doi:10.4049/jimmunol.179.5.2690
45. Li HS, Gelbard A, Martinez GJ, Esashi E, Zhang H, Nguyen-Jackson H, et al. Cell-intrinsic role for IFN-alpha-STAT1 signals in regulating murine Peyer patch plasmacytoid dendritic cells and conditioning an inflammatory response. *Blood* (2011) 118(14):3879–89. doi:10.1182/blood-2011-04-349761
46. Gunn MD, Tangemann K, Tam C, Cyster JG, Rosen SD, Williams LT. A chemokine expressed in lymphoid high endothelial venules promotes

the adhesion and chemotaxis of naive T lymphocytes. *Proc Natl Acad Sci U S A* (1998) 95(1):258–63. doi:10.1073/pnas.95.1.258
47. Ngo VN, Tang HL, Cyster JG. Epstein-Barr virus-induced molecule 1 ligand chemokine is expressed by dendritic cells in lymphoid tissues and strongly attracts naive T cells and activated B cells. *J Exp Med* (1998) 188(1):181–91. doi:10.1084/jem.188.1.181
48. Willimann K, Legler DF, Loetscher M, Roos RS, Delgado MB, Clark-Lewis I, et al. The chemokine SLC is expressed in T cell areas of lymph nodes and mucosal lymphoid tissues and attracts activated T cells via CCR7. *Eur J Immunol* (1998) 28(6):2025–34. doi:10.1002/(SICI)1521-4141(199806)28:06<2025::AID-IMMU2025>3.0.CO;2-C
49. Zhao X, Sato A, Dela Cruz CS, Linehan M, Luegering A, Kucharzik T, et al. CCL9 is secreted by the follicle-associated epithelium and recruits dome region Peyer's patch CD11b+ dendritic cells. *J Immunol* (2003) 171(6):2797–803. doi:10.4049/jimmunol.171.6.2797
50. Asselin-Paturel C, Brizard G, Pin JJ, Briere F, Trinchieri G. Mouse strain differences in plasmacytoid dendritic cell frequency and function revealed by a novel monoclonal antibody. *J Immunol* (2003) 171(12):6466–77. doi:10.4049/jimmunol.171.12.6466
51. Blasius AL, Giurisato E, Cella M, Schreiber RD, Shaw AS, Colonna M. Bone marrow stromal cell antigen 2 is a specific marker of type I IFN-producing cells in the naive mouse, but a promiscuous cell surface antigen following IFN stimulation. *J Immunol* (2006) 177(5):3260–5. doi:10.4049/jimmunol.177.5.3260
52. Owen RL, Pierce NF, Apple RT, Cray WC Jr. M cell transport of *Vibrio cholerae* from the intestinal lumen into Peyer's patches: a mechanism for antigen sampling and for microbial transepithelial migration. *J Infect Dis* (1986) 153(6):1108–18. doi:10.1093/infdis/153.6.1108
53. Jinnohara T, Kanaya T, Hase K, Sakakibara S, Kato T, Tachibana N, et al. IL-22BP dictates characteristics of Peyer's patch follicle-associated epithelium for antigen uptake. *J Exp Med* (2017) 214(6):1607–18. doi:10.1084/jem.20160770
54. Sakhon OS, Ross B, Gusti V, Pham AJ, Vu K, Lo DD. M cell-derived vesicles suggest a unique pathway for trans-epithelial antigen delivery. *Tissue Barriers* (2015) 3(1–2):e1004975. doi:10.1080/21688370.2015.1004975
55. Banchereau J, Steinman RM. Dendritic cells and the control of immunity. *Nature* (1998) 392(6673):245–52. doi:10.1038/32588
56. Dalod M, Chelbi R, Malissen B, Lawrence T. Dendritic cell maturation: functional specialization through signaling specificity and transcriptional programming. *EMBO J* (2014) 33(10):1104–16. doi:10.1002/embj.201488027
57. Manh TP, Alexandre Y, Baranek T, Crozat K, Dalod M. Plasmacytoid, conventional, and monocyte-derived dendritic cells undergo a profound and convergent genetic reprogramming during their maturation. *Eur J Immunol* (2013) 43(7):1706–15. doi:10.1002/eji.201243106
58. Fahlen-Yrlid L, Gustafsson T, Westlund J, Holmberg A, Strombeck A, Blomquist M, et al. CD11c(high)dendritic cells are essential for activation of CD4+ T cells and generation of specific antibodies following mucosal immunization. *J Immunol* (2009) 183(8):5032–41. doi:10.4049/jimmunol.0803992
59. Obata T, Shibata N, Goto Y, Ishikawa I, Sato S, Kunisawa J, et al. Critical role of dendritic cells in T cell retention in the interfollicular region of Peyer's patches. *J Immunol* (2013) 191(2):942–8. doi:10.4049/jimmunol.1200636
60. Craig SW, Cebra JJ. Peyer's patches: an enriched source of precursors for IgA-producing immunocytes in the rabbit. *J Exp Med* (1971) 134(1):188–200. doi:10.1084/jem.134.1.188
61. Gutzeit C, Magri G, Cerutti A. Intestinal IgA production and its role in host-microbe interaction. *Immunol Rev* (2014) 260(1):76–85. doi:10.1111/imr.12189
62. Husband AJ, Gowans JL. The origin and antigen-dependent distribution of IgA-containing cells in the intestine. *J Exp Med* (1978) 148(5):1146–60. doi:10.1084/jem.148.5.1146
63. Lycke NY, Bemark M. The role of Peyer's patches in synchronizing gut IgA responses. *Front Immunol* (2012) 3:329. doi:10.3389/fimmu.2012.00329
64. Macpherson AJ, Geuking MB, Slack E, Hapfelmeier S, McCoy KD. The habitat, double life, citizenship, and forgetfulness of IgA. *Immunol Rev* (2012) 245(1):132–46. doi:10.1111/j.1600-065X.2011.01072.x
65. Benveniste J, Lespinats G, Salomon J. Serum and secretory IgA in axenic and holoxenic mice. *J Immunol* (1971) 107(6):1656–62.
66. Kawamoto S, Maruya M, Kato LM, Suda W, Atarashi K, Doi Y, et al. Foxp3(+) T cells regulate immunoglobulin a selection and facilitate diversification of bacterial species responsible for immune homeostasis. *Immunity* (2014) 41(1):152–65. doi:10.1016/j.immuni.2014.05.016
67. Reikvam DH, Derrien M, Islam R, Erofeev A, Grcic V, Sandvik A, et al. Epithelial-microbial crosstalk in polymeric Ig receptor deficient mice. *Eur J Immunol* (2012) 42(11):2959–70. doi:10.1002/eji.201242543
68. Wei M, Shinkura R, Doi Y, Maruya M, Fagarasan S, Honjo T. Mice carrying a knock-in mutation of Aicda resulting in a defect in somatic hypermutation have impaired gut homeostasis and compromised mucosal defense. *Nat Immunol* (2011) 12(3):264–70. doi:10.1038/ni.1991
69. Bunker JJ, Flynn TM, Koval JC, Shaw DG, Meisel M, McDonald BD, et al. Innate and adaptive humoral responses coat distinct commensal bacteria with immunoglobulin A. *Immunity* (2015) 43(3):541–53. doi:10.1016/j.immuni.2015.08.007
70. Kau AL, Planer JD, Liu J, Rao S, Yatsunenko T, Trehan I, et al. Functional characterization of IgA-targeted bacterial taxa from undernourished Malawian children that produce diet-dependent enteropathy. *Sci Transl Med* (2015) 7(276):276ra24. doi:10.1126/scitranslmed.aaa4877
71. Palm NW, de Zoete MR, Cullen TW, Barry NA, Stefanowski J, Hao L, et al. Immunoglobulin A coating identifies colitogenic bacteria in inflammatory bowel disease. *Cell* (2014) 158(5):1000–10. doi:10.1016/j.cell.2014.08.006
72. Macpherson AJ, Koller Y, McCoy KD. The bilateral responsiveness between intestinal microbes and IgA. *Trends Immunol* (2015) 36(8):460–70. doi:10.1016/j.it.2015.06.006
73. Pabst O, Cerovic V, Hornef M. Secretory IgA in the coordination of establishment and maintenance of the microbiota. *Trends Immunol* (2016) 37(5):287–96. doi:10.1016/j.it.2016.03.002
74. Gaboriau-Routhiau V, Rakotobe S, Lecuyer E, Mulder I, Lan A, Bridonneau C, et al. The key role of segmented filamentous bacteria in the coordinated maturation of gut helper T cell responses. *Immunity* (2009) 31(4):677–89. doi:10.1016/j.immuni.2009.08.020
75. Ivanov II, Atarashi K, Manel N, Brodie EL, Shima T, Karaoz U, et al. Induction of intestinal Th17 cells by segmented filamentous bacteria. *Cell* (2009) 139(3):485–98. doi:10.1016/j.cell.2009.09.033
76. Klaasen HL, Van der Heijden PJ, Stok W, Poelma FG, Koopman JP, Van den Brink ME, et al. Apathogenic, intestinal, segmented, filamentous bacteria stimulate the mucosal immune system of mice. *Infect Immun* (1993) 61(1):303–6.
77. Lecuyer E, Rakotobe S, Lengline-Garnier H, Lebreton C, Picard M, Juste C, et al. Segmented filamentous bacterium uses secondary and tertiary lymphoid tissues to induce gut IgA and specific T helper 17 cell responses. *Immunity* (2014) 40(4):608–20. doi:10.1016/j.immuni.2014.03.009
78. Jepson MA, Clark MA, Simmons NL, Hirst BH. Actin accumulation at sites of attachment of indigenous apathogenic segmented filamentous bacteria to mouse ileal epithelial cells. *Infect Immun* (1993) 61(9):4001–4.
79. Obata T, Goto Y, Kunisawa J, Sato S, Sakamoto M, Setoyama H, et al. Indigenous opportunistic bacteria inhabit mammalian gut-associated lymphoid tissues and share a mucosal antibody-mediated symbiosis. *Proc Natl Acad Sci U S A* (2010) 107(16):7419–24. doi:10.1073/pnas.1001061107
80. Sonnenberg GF, Monticelli LA, Alenghat T, Fung TC, Hutnick NA, Kunisawa J, et al. Innate lymphoid cells promote anatomical containment of lymphoid-resident commensal bacteria. *Science* (2012) 336(6086):1321–5. doi:10.1126/science.1222551
81. Lapthorne S, Macsharry J, Scully P, Nally K, Shanahan F. Differential intestinal M-cell gene expression response to gut commensals. *Immunology* (2012) 136(3):312–24. doi:10.1111/j.1365-2567.2012.03581.x
82. Morikawa M, Tsujibe S, Kiyoshima-Shibata J, Watanabe Y, Kato-Nagaoka N, Shida K, et al. Microbiota of the small intestine is selectively engulfed by phagocytes of the lamina propria and Peyer's patches. *PLoS One* (2016) 11(10):e0163607. doi:10.1371/journal.pone.0163607
83. Fung TC, Bessman NJ, Hepworth MR, Kumar N, Shibata N, Kobuley D, et al. Lymphoid-tissue-resident commensal bacteria promote members of the IL-10 cytokine family to establish mutualism. *Immunity* (2016) 44(3):634–46. doi:10.1016/j.immuni.2016.02.019

84. Macpherson AJ, Uhr T. Induction of protective IgA by intestinal dendritic cells carrying commensal bacteria. *Science* (2004) 303(5664):1662–5. doi:10.1126/science.1091334
85. Spalding DM, Griffin JA. Different pathways of differentiation of pre-B cell lines are induced by dendritic cells and T cells from different lymphoid tissues. *Cell* (1986) 44(3):507–15. doi:10.1016/0092-8674(86)90472-1
86. Spalding DM, Williamson SI, Koopman WJ, McGhee JR. Preferential induction of polyclonal IgA secretion by murine Peyer's patch dendritic cell-T cell mixtures. *J Exp Med* (1984) 160(3):941–6. doi:10.1084/jem.160.3.941
87. Tezuka H, Abe Y, Asano J, Sato T, Liu J, Iwata M, et al. Prominent role for plasmacytoid dendritic cells in mucosal T cell-independent IgA induction. *Immunity* (2011) 34(2):247–57. doi:10.1016/j.immuni.2011.02.002
88. Moro-Sibilot L, This S, Blanc P, Sanlaville A, Sisirak V, Bardel E, et al. Plasmacytoid dendritic cells are dispensable for noninfectious intestinal IgA responses in vivo. *Eur J Immunol* (2016) 46(2):354–9. doi:10.1002/eji.201545977
89. Sato A, Hashiguchi M, Toda E, Iwasaki A, Hachimura S, Kaminogawa S. CD11b+ Peyer's patch dendritic cells secrete IL-6 and induce IgA secretion from naive B cells. *J Immunol* (2003) 171(7):3684–90. doi:10.4049/jimmunol.171.7.3684
90. Reboldi A, Arnon TI, Rodda LB, Atakilit A, Sheppard D, Cyster JG. IgA production requires B cell interaction with subepithelial dendritic cells in Peyer's patches. *Science* (2016) 352(6287):aaf4822. doi:10.1126/science.aaf4822
91. Kim SH, Cho BH, Kiyono H, Jang YS. Microbiota-derived butyrate suppresses group 3 innate lymphoid cells in terminal ileal Peyer's patches. *Sci Rep* (2017) 7(1):3980. doi:10.1038/s41598-017-02729-6
92. Rahman ZS. Impaired clearance of apoptotic cells in germinal centers: implications for loss of B cell tolerance and induction of autoimmunity. *Immunol Res* (2011) 51(2–3):125–33. doi:10.1007/s12026-011-8248-4
93. Hanayama R, Tanaka M, Miyasaka K, Aozasa K, Koike M, Uchiyama Y, et al. Autoimmune disease and impaired uptake of apoptotic cells in MFG-E8-deficient mice. *Science* (2004) 304(5674):1147–50. doi:10.1126/science.1094359
94. Khan TN, Wong EB, Soni C, Rahman ZS. Prolonged apoptotic cell accumulation in germinal centers of Mer-deficient mice causes elevated B cell and CD4+ Th cell responses leading to autoantibody production. *J Immunol* (2013) 190(4):1433–46. doi:10.4049/jimmunol.1200824
95. Kranich J, Krautler NJ, Heinen E, Polymenidou M, Bridel C, Schildknecht A, et al. Follicular dendritic cells control engulfment of apoptotic bodies by secreting Mfge8. *J Exp Med* (2008) 205(6):1293–302. doi:10.1084/jem.20071019
96. Rahman ZS, Shao WH, Khan TN, Zhen Y, Cohen PL. Impaired apoptotic cell clearance in the germinal center by Mer-deficient tingible body macrophages leads to enhanced antibody-forming cell and germinal center responses. *J Immunol* (2010) 185(10):5859–68. doi:10.4049/jimmunol.1001187
97. Nishi C, Toda S, Segawa K, Nagata S. Tim4- and MerTK-mediated engulfment of apoptotic cells by mouse resident peritoneal macrophages. *Mol Cell Biol* (2014) 34(8):1512–20. doi:10.1128/mcb.01394-13
98. Rodriguez-Manzanet R, Sanjuan MA, Wu HY, Quintana FJ, Xiao S, Anderson AC, et al. T and B cell hyperactivity and autoimmunity associated with niche-specific defects in apoptotic body clearance in TIM-4-deficient mice. *Proc Natl Acad Sci U S A* (2010) 107(19):8706–11. doi:10.1073/pnas.0910359107
99. Albacker LA, Karisola P, Chang YJ, Umetsu SE, Zhou M, Akbari O, et al. TIM-4, a receptor for phosphatidylserine, controls adaptive immunity by regulating the removal of antigen-specific T cells. *J Immunol* (2010) 185(11):6839–49. doi:10.4049/jimmunol.1001360
100. Albacker LA, Yu S, Bedoret D, Lee WL, Umetsu SE, Monahan S, et al. TIM-4, expressed by medullary macrophages, regulates respiratory tolerance by mediating phagocytosis of antigen-specific T cells. *Mucosal Immunol* (2013) 6(3):580–90. doi:10.1038/mi.2012.100
101. Rochereau N, Drocourt D, Perouzel E, Pavot V, Redelinghuys P, Brown GD, et al. Dectin-1 is essential for reverse transcytosis of glycosylated SIgA-antigen complexes by intestinal M cells. *PLoS Biol* (2013) 11(9):e1001658. doi:10.1371/journal.pbio.1001658
102. Fransen F, Zagato E, Mazzini E, Fosso B, Manzari C, El Aidy S, et al. BALB/c and C57BL/6 mice differ in polyreactive IgA abundance, which impacts the generation of antigen-specific IgA and microbiota diversity. *Immunity* (2015) 43(3):527–40. doi:10.1016/j.immuni.2015.08.011
103. Kadaoui KA, Corthesy B. Secretory IgA mediates bacterial translocation to dendritic cells in mouse Peyer's patches with restriction to mucosal compartment. *J Immunol* (2007) 179(11):7751–7. doi:10.4049/jimmunol.179.11.7751
104. Rol N, Favre L, Benyacoub J, Corthesy B. The role of secretory immunoglobulin A in the natural sensing of commensal bacteria by mouse Peyer's patch dendritic cells. *J Biol Chem* (2012) 287(47):40074–82. doi:10.1074/jbc.M112.405001
105. Carter PB, Collins FM. The route of enteric infection in normal mice. *J Exp Med* (1974) 139(5):1189–203. doi:10.1084/jem.139.5.1189
106. Hohmann AW, Schmidt G, Rowley D. Intestinal colonization and virulence of *Salmonella* in mice. *Infect Immun* (1978) 22(3):763–70.
107. Clark MA, Jepson MA, Simmons NL, Hirst BH. Preferential interaction of *Salmonella typhimurium* with mouse Peyer's patch M cells. *Res Microbiol* (1994) 145(7):543–52. doi:10.1016/0923-2508(94)90031-0
108. Jones BD, Ghori N, Falkow S. *Salmonella typhimurium* initiates murine infection by penetrating and destroying the specialized epithelial M cells of the Peyer's patches. *J Exp Med* (1994) 180(1):15–23. doi:10.1084/jem.180.1.15
109. Clark MA, Hirst BH, Jepson MA. Inoculum composition and *Salmonella* pathogenicity island 1 regulate M-cell invasion and epithelial destruction by *Salmonella typhimurium*. *Infect Immun* (1998) 66(2):724–31.
110. Clark MA, Reed KA, Lodge J, Stephen J, Hirst BH, Jepson MA. Invasion of murine intestinal M cells by *Salmonella typhimurium* inv mutants severely deficient for invasion of cultured cells. *Infect Immun* (1996) 64(10):4363–8.
111. Martinoli C, Chiavelli A, Rescigno M. Entry route of *Salmonella typhimurium* directs the type of induced immune response. *Immunity* (2007) 27(6):975–84. doi:10.1016/j.immuni.2007.10.011
112. Chabot S, Wagner JS, Farrant S, Neutra MR. TLRs regulate the gatekeeping functions of the intestinal follicle-associated epithelium. *J Immunol* (2006) 176(7):4275–83. doi:10.4049/jimmunol.176.7.4275
113. Pappo J, Ermak TH. Uptake and translocation of fluorescent latex particles by rabbit Peyer's patch follicle epithelium: a quantitative model for M cell uptake. *Clin Exp Immunol* (1989) 76(1):144–8.
114. Owen RL, Heyworth MF. Lymphocyte migration from Peyer's patches by diapedesis through M cells into the intestinal lumen. *Adv Exp Med Biol* (1985) 186:647–54.
115. Regoli M, Borghesi C, Bertelli E, Nicoletti C. A morphological study of the lymphocyte traffic in Peyer's patches after an in vivo antigenic stimulation. *Anat Rec* (1994) 239(1):47–54. doi:10.1002/ar.1092390106
116. Vance RE. The NAIP/NLRC4 inflammasomes. *Curr Opin Immunol* (2015) 32:84–9. doi:10.1016/j.coi.2015.01.010
117. Salazar-Gonzalez RM, Niess JH, Zammit DJ, Ravindran R, Srinivasan A, Maxwell JR, et al. CCR6-mediated dendritic cell activation of pathogen-specific T cells in Peyer's patches. *Immunity* (2006) 24(5):623–32. doi:10.1016/j.immuni.2006.02.015
118. Kucharzik T, Hudson JT III, Waikel RL, Martin WD, Williams IR. CCR6 expression distinguishes mouse myeloid and lymphoid dendritic cell subsets: demonstration using a CCR6 EGFP knock-in mouse. *Eur J Immunol* (2002) 32(1):104–12. doi:10.1002/1521-4141(200201)32:1<104::AID-IMMU104>3.0.CO;2-C
119. Yrlid U, Wick MJ. *Salmonella*-induced apoptosis of infected macrophages results in presentation of a bacteria-encoded antigen after uptake by bystander dendritic cells. *J Exp Med* (2000) 191(4):613–24. doi:10.1084/jem.191.4.613
120. Ebisawa M, Hase K, Takahashi D, Kitamura H, Knoop KA, Williams IR, et al. CCR6hiCD11c(int) B cells promote M-cell differentiation in Peyer's patch. *Int Immunol* (2011) 23(4):261–9. doi:10.1093/intimm/dxq478
121. Lugering A, Floer M, Westphal S, Maaser C, Spahn TW, Schmidt MA, et al. Absence of CCR6 inhibits CD4+ regulatory T-cell development and M-cell formation inside Peyer's patches. *Am J Pathol* (2005) 166(6):1647–54. doi:10.1016/S0002-9440(10)62475-3

122. Westphal S, Lugering A, von Wedel J, von Eiff C, Maaser C, Spahn T, et al. Resistance of chemokine receptor 6-deficient mice to *Yersinia enterocolitica* infection: evidence of defective M-cell formation in vivo. *Am J Pathol* (2008) 172(3):671–80. doi:10.2353/ajpath.2008.070393
123. Wolf JL, Rubin DH, Finberg R, Kauffman RS, Sharpe AH, Trier JS, et al. Intestinal M cells: a pathway for entry of reovirus into the host. *Science* (1981) 212(4493):471–2. doi:10.1126/science.6259737
124. Karst SM, Wobus CE. A working model of how noroviruses infect the intestine. *PLoS Pathog* (2015) 11(2):e1004626. doi:10.1371/journal.ppat.1004626
125. Wobus CE, Karst SM, Thackray LB, Chang KO, Sosnovtsev SV, Belliot G, et al. Replication of Norovirus in cell culture reveals a tropism for dendritic cells and macrophages. *PLoS Biol* (2004) 2(12):e432. doi:10.1371/journal.pbio.0020432
126. Bass DM, Trier JS, Dambrauskas R, Wolf JL. Reovirus type I infection of small intestinal epithelium in suckling mice and its effect on M cells. *Lab Invest* (1988) 58(2):226–35.
127. Fleeton MN, Contractor N, Leon F, Wetzel JD, Dermody TS, Kelsall BL. Peyer's patch dendritic cells process viral antigen from apoptotic epithelial cells in the intestine of reovirus-infected mice. *J Exp Med* (2004) 200(2):235–45. doi:10.1084/jem.20041132
128. Donaldson DS, Kobayashi A, Ohno H, Yagita H, Williams IR, Mabbott NA. M cell-depletion blocks oral prion disease pathogenesis. *Mucosal Immunol* (2012) 5(2):216–25. doi:10.1038/mi.2011.68
129. Donaldson DS, Sehgal A, Rios D, Williams IR, Mabbott NA. Increased abundance of M cells in the gut epithelium dramatically enhances oral prion disease susceptibility. *PLoS Pathog* (2016) 12(12):e1006075. doi:10.1371/journal.ppat.1006075
130. Raymond CR, Aucouturier P, Mabbott NA. In vivo depletion of CD11c+ cells impairs scrapie agent neuroinvasion from the intestine. *J Immunol* (2007) 179(11):7758–66. doi:10.4049/jimmunol.179.11.7758
131. Kujala P, Raymond CR, Romeijn M, Godsave SF, van Kasteren SI, Wille H, et al. Prion uptake in the gut: identification of the first uptake and replication sites. *PLoS Pathog* (2011) 7(12):e1002449. doi:10.1371/journal.ppat.1002449
132. Takakura I, Miyazawa K, Kanaya T, Itani W, Watanabe K, Ohwada S, et al. Orally administered prion protein is incorporated by m cells and spreads into lymphoid tissues with macrophages in prion protein knockout mice. *Am J Pathol* (2011) 179(3):1301–9. doi:10.1016/j.ajpath.2011.05.058
133. Bradford BM, Reizis B, Mabbott NA. Oral prion disease pathogenesis is impeded in the specific absence of CXCR5-expressing dendritic cells. *J Virol* (2017) 91(10). doi:10.1128/jvi.00124-17
134. Anosova NG, Chabot S, Shreedhar V, Borawski JA, Dickinson BL, Neutra MR. Cholera toxin, *E. coli* heat-labile toxin, and non-toxic derivatives induce dendritic cell migration into the follicle-associated epithelium of Peyer's patches. *Mucosal Immunol* (2008) 1(1):59–67. doi:10.1038/mi.2007.7
135. Chabot SM, Chernin TS, Shawi M, Wagner J, Farrant S, Burt DS, et al. TLR2 activation by proteosomes promotes uptake of particulate vaccines at mucosal surfaces. *Vaccine* (2007) 25(29):5348–58. doi:10.1016/j.vaccine.2007.05.029
136. Chabot SM, Shawi M, Eaves-Pyles T, Neutra MR. Effects of flagellin on the functions of follicle-associated epithelium. *J Infect Dis* (2008) 198(6):907–10. doi:10.1086/591056
137. Shreedhar VK, Kelsall BL, Neutra MR. Cholera toxin induces migration of dendritic cells from the subepithelial dome region to T- and B-cell areas of Peyer's patches. *Infect Immun* (2003) 71(1):504–9. doi:10.1128/IAI.71.1.504-509.2003
138. Yrlid U, Milling SW, Miller JL, Cartland S, Jenkins CD, MacPherson GG. Regulation of intestinal dendritic cell migration and activation by plasmacytoid dendritic cells, TNF-alpha and type 1 IFNs after feeding a TLR7/8 ligand. *J Immunol* (2006) 176(9):5205–12. doi:10.4049/jimmunol.176.9.5205
139. Heng TS, Painter MW. The immunological genome project: networks of gene expression in immune cells. *Nat Immunol* (2008) 9(10):1091–4. doi:10.1038/ni1008-1091

Conflict of Interest Statement: The authors declare that the research was conducted in the absence of any commercial or financial relationships that could be construed as a potential conflict of interest.

Copyright © 2017 Da Silva, Wagner, Bonnardel, Gorvel and Lelouard. This is an open-access article distributed under the terms of the Creative Commons Attribution License (CC BY). The use, distribution or reproduction in other forums is permitted, provided the original author(s) or licensor are credited and that the original publication in this journal is cited, in accordance with accepted academic practice. No use, distribution or reproduction is permitted which does not comply with these terms.

frontiers in Immunology

REVIEW
published: 09 January 2018
doi: 10.3389/fimmu.2017.01921

New Insights into the Immunobiology of Mononuclear Phagocytic Cells and Their Relevance to the Pathogenesis of Cardiovascular Diseases

*Liliana Maria Sanmarco[1,2], Natalia Eberhardt[2], Nicolás Eric Ponce[1,3], Roxana Carolina Cano[1,4], Gustavo Bonacci[1,2] and Maria Pilar Aoki[1,2]**

[1] Departamento de Bioquímica Clínica, Facultad de Ciencias Químicas, Universidad Nacional de Córdoba, Córdoba, Argentina, [2] Centro de Investigaciones en Bioquímica Clínica e Inmunología (CIBICI), Consejo Nacional de Investigaciones Científicas y Tecnológicas (CONICET), Córdoba, Argentina, [3] Laboratorio de Neuropatología Experimental, Instituto de Investigación Médica Mercedes y Martín Ferreyra (INIMEC), Consejo Nacional de Investigaciones Científicas y Tecnológicas (CONICET), Universidad Nacional de Córdoba, Córdoba, Argentina, [4] Consejo Nacional de Investigaciones Científicas y Tecnológicas (CONICET), Universidad Católica de Córdoba, Unidad Asociada Área Ciencias Agrarias, Ingeniería, Ciencias Biológicas y de la Salud, Facultad de Ciencias Químicas, Córdoba, Argentina

Macrophages are the primary immune cells that reside within the myocardium, suggesting that these mononuclear phagocytes are essential in the orchestration of cardiac immunity and homeostasis. Independent of the nature of the injury, the heart triggers leukocyte activation and recruitment. However, inflammation is harmful to this vital terminally differentiated organ with extremely poor regenerative capacity. As such, cardiac tissue has evolved particular strategies to increase the stress tolerance and minimize the impact of inflammation. In this sense, growing evidences show that mononuclear phagocytic cells are particularly dynamic during cardiac inflammation or infection and would actively participate in tissue repair and functional recovery. They respond to soluble mediators such as metabolites or cytokines, which play central roles in the timing of the intrinsic cardiac stress response. During myocardial infarction two distinct phases of monocyte influx have been identified. Upon infarction, the heart modulates its chemokine expression profile that sequentially and actively recruits inflammatory monocytes, first, and healing monocytes, later. In the same way, a sudden switch from inflammatory macrophages (with microbicidal effectors) toward anti-inflammatory macrophages occurs within the myocardium very shortly after infection with *Trypanosoma cruzi*, the causal agent of Chagas cardiomyopathy. While in sterile injury, healing response is necessary to stop tissue damage; during an intracellular infection, the anti-inflammatory milieu in infected hearts would promote microbial persistence. The balance of mononuclear phagocytic cells seems to be also dynamic in atherosclerosis influencing plaque initiation and fate. This review summarizes the participation of mononuclear phagocyte system in cardiovascular diseases, keeping in mind that the immune system evolved to promote the reestablishment of tissue homeostasis following infection/injury, and that the effects of different mediators could modulate the magnitude and quality of the immune response. The knowledge of the effects triggered by diverse mediators would serve to identify new therapeutic targets in different cardiovascular pathologies.

Keywords: macrophages, monocytes, Chagas disease, atherosclerosis, oxidative stress, interleukin-6, oxidized phospholipids, purinergic signaling

OPEN ACCESS

Edited by:
Luciana Balboa, Academia Nacional de Medicina (CONICET), Argentina

Reviewed by:
Debora Decote-Ricardo, Universidade Federal Rural do Rio de Janeiro, Brazil
Ricardo Silvestre, Instituto de Pesquisa em Ciências da Vida e da Saúde (ICVS), Portugal

***Correspondence:**
Maria Pilar Aoki
paoki@fcq.unc.edu.ar

Specialty section:
This article was submitted to Microbial Immunology, a section of the journal Frontiers in Immunology

Received: *15 September 2017*
Accepted: *14 December 2017*
Published: *09 January 2018*

Citation:
Sanmarco LM, Eberhardt N, Ponce NE, Cano RC, Bonacci G and Aoki MP (2018) New Insights into the Immunobiology of Mononuclear Phagocytic Cells and Their Relevance to the Pathogenesis of Cardiovascular Diseases. Front. Immunol. 8:1921. doi: 10.3389/fimmu.2017.01921

INTRODUCTION

Cardiovascular diseases are the leading causes of worldwide morbidity and mortality. In consequence, understanding the precise contribution of the mechanisms involved in cardiovascular tissue injury and repair is of prominent importance. In this sense, increasing evidences reveal that innate immune response plays a critical and complex role throughout the acute inflammation and regenerative process triggered after cardiac or vascular injury. As such, leukocytosis and monocytosis have been associated with cardiovascular diseases in numerous epidemiological studies, prompting speculation on the functional importance of these cells (1). The goal of this review is to summarize the complex immunobiology of mononuclear phagocytic cells and their relevance to the pathogenesis of cardiovascular diseases, highlighting the effect of major immune modulators.

Origin

In the last decade, important advances in the knowledge of macrophage origin have triggered an essential conceptual progress in the mononuclear phagocyte system field. Parabiosed mice and genetic fate-mapping experiments have revealed that the majority of resident macrophages in healthy tissues are established from the yolk sac and fetal liver before birth (2–4). This cellular compartment locally self-maintains throughout life within the tissue and is independent from the hematopoietic input. On the other hand, during adulthood tissue-infiltrating macrophages can develop from circulating monocytes. The recruitment of monocytes is associated with pathological, but also with homeostatic response. Macrophages derived from monocytes display a short lifespan, although exceptions have also been reported. Embryonic- and adult-derived macrophages generally coexist in a given tissue, and their respective number correlates with the origin and records of their tissue of residence. Seminal experiments have demonstrated that embryonic- and monocyte-derived macrophages make different functional contributions in homeostatic conditions or following challenge. In this sense, Levine and coworkers have revealed that embryonic-derived macrophages are clue for cardiac recovery after injury (5). Their results suggest that targeting specific macrophage lineages could have important therapeutic implications in order to improve treatments for heart diseases.

Adult resident macrophage compartments seem to be independent from monocyte recruitment in a given tissue, as was demonstrated by parabiotic experiments. Monocyte compartments of the parabionts reach, with time, considerable chimerism in the joined circulation. However, tissue macrophages failed to equilibrate even after several months of parabiosis, suggesting the absence of an ongoing steady-state contribution of bone marrow-derived cells to adult tissue macrophage compartments (3). Furthermore, recruited monocytes are short-lived effector cells in tissues and assumed different roles that have yet to be better defined; emerging reports suggest, for example, that monocytes can promote angiogenesis and arteriogenesis (6). In addition, it was recently reported that inflammatory Ly6C^{high} monocytes persist during the steady state without commitment toward macrophage or dendritic cell (DC) fates and might contribute to antigen transport toward lymph nodes (7). Remarkably, macrophage effector function also needs to be tailored to its tissue of residence, an adaptation that is driven by the local microenvironment and by the inflammatory history of a given tissue.

Phenotypes and Functions of Monocytes

Monocytes/macrophages are very plastic cells and can acquire distinct phenotypes and activation states under the influence of different microenvironments. Although several authors have shown that macrophages treated with different stimuli display altered phenotypes or functional capacities, many of these studies are limited considering that they compare only one particular activation state with non-polarized macrophages. Although macrophage activation was initially seen as a dichotomy between classically and alternatively activated states, it is now clear that the spectrum of macrophage activation states is much more diverse.

Monocytes develop in steady state in the bone marrow from hematopoietic precursors, and they enter the circulation *via* CCR2 receptor. In mice, circulating monocytes are phenotypically and functionally heterogeneous and can be defined according to Ly6C expression marker (**Figure 1**). In mice, during steady-state conditions, about 50–60% of circulating monocytes belongs to the Ly6C^{high} CCR2^{high} CX3CR1^{low} CD62L^{+} subset. These inflammatory or classical monocytes have a relatively short-circulating lifespan and are preferentially recruited to injured/inflamed tissues where they maturate to macrophages. The remaining non classical (Ly6C^{low} CCR2^{low} CX3CR1^{high} CD62L^{-}) subset patrols blood vessels and accumulates at low numbers in the steady state (8). The number of Ly6C^{high} monocytes rises during inflammation, at expenses of enhanced monocytopoiesis in the bone marrow and spleen (1, 9–11). Regarding the origin, evidence shows that monocyte subpopulations do not arise from separate progenitors, but rather convert from the Ly6C^{high} to Ly6C^{low} subset (12) (**Figure 1**).

In humans, circulating monocytes can be segregated into three major subsets based on the expression of CD14 and CD16 (13). Over the past decades, human circulating monocytes had been separated into two subpopulations based on CD16 expression, the CD14^{+} CD16^{-} and CD14^{+} CD16^{+} monocyte subsets (hereby designated as CD16^{-} and CD16^{+}, respectively). A new nomenclature defines three monocyte populations, where the minor CD16^{+} subset is further separated into two subpopulations (**Figure 2**). The intermediate subset expresses relatively high levels of CD14 coupled with low CD16 expression (CD14^{++} CD16^{+}), while the non-classical subset expresses low levels of CD14 with

Abbreviations: AGE, advanced glycation end-products; APCP, adenosine 5′α,β-methylene-diphosphate; CCR2, chemokine (C–C motif) receptor 2; CD39, ectonucleoside triphosphate diphosphohydrolase-1 enzyme; CD73, ecto-5′-nucleotidase enzyme; CVB3, enteroviral coxsackievirus B group type 3; DC, dendritic cells; HMGB1, high-mobility group box-1 protein; IL, interleukin; iNOS, inducible nitric oxide synthase; KO, knock out; LDL, low-density lipoprotein; LDLR, low-density lipoprotein receptor; Ly6C, lymphocyte antigen 6 complex; Mhem, hemorrhage-associated macrophages; NADPH, nicotinamide adenine dinucleotide phosphate; NF-κB, pro-inflammatory signaling pathways; NO, nitric oxide; NO_2-FAs, nitro-fatty acids; oxLDL, oxidized low-density lipoprotein; oxPL, oxidized phospholipids; PBMC, peripheral blood mononuclear cells; PKM2, pyruvate kinase M2; PRRs, pattern-recognition receptor; RONS, reactive oxygen and nitrogen species; SR, scavenger receptor; TLR, toll-like receptor; WHO, World Health Organization.

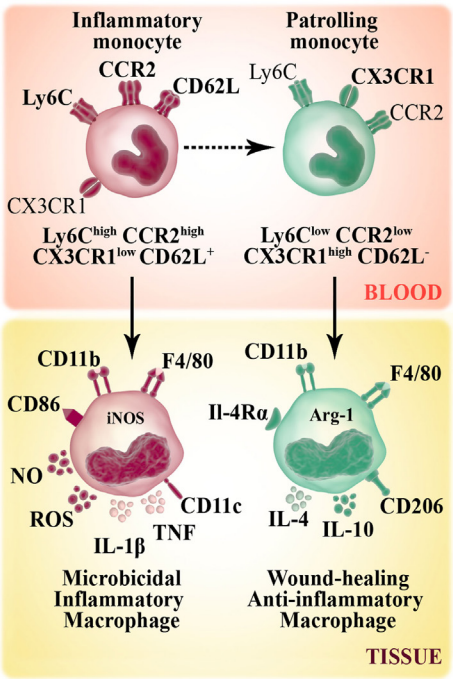


FIGURE 1 | Murine monocyte and macrophage subsets. Murine monocytes develop from a common myeloid progenitor and leave the bone marrow through the chemokine receptor CCR2. In bloodstream, circulating monocytes are phenotypically and functionally heterogeneous. Non-classical monocytes (Ly6C^{low} CCR2^{low} CX3CR1^{high} CD62L^{-}) patrol the vasculature and accumulate at low numbers in the steady state. Inflammatory or classical (Ly6C^{high} CCR2^{high} CX3CR1^{low} CD62L^{+}) monocytes have a relatively short-circulating lifespan and preferentially accumulate in inflammatory sites where they give rise to inflammatory M1 macrophages (F4/80^{+} CD11b^{+} CD86^{+} CD206^{-}). M1 macrophage subset has high microbicidal capacity due to their ability to produce inflammatory cytokines [TNF, IL-1β], reactive oxygen species (ROS) secretion and the expression of iNOS enzyme that metabolizes arginine to arginine-derived killer molecule NO. Non-classical monocytes can be recruited to tissue and differentiate to M2 macrophages (F4/80^{+} CD11b^{+} CD86^{-} CD206^{+}), which secrete anti-inflammatory cytokines (IL-10, IL-4) and contribute to tissue repair mechanisms.

high expression of CD16 (CD14^{+} CD16^{++}). The subset with high CD14 and no CD16 expression, termed classical subset (CD14^{++} CD16^{-}), constitute approximately 85–90% of human monocytes in the peripheral blood. Several studies have demonstrated that circulating CD16^{+} monocytes are found in large numbers in patients with inflammation processes (14) and infectious diseases (15, 16).

Analyses based on hierarchical clustering of gene expression profiles of human monocyte subsets have been a matter of debate. Cros et al. reported that the classical and intermediate subpopulations were most closely related among the subsets, while the most distant was the non-classical subset (17). However, other independent groups described that both CD16^{+} subpopulations are more closely related (18, 19). Indeed, the number of genes that were significantly different between both CD16^{+} subsets was the lowest among the three subpopulations. Until now, there is poor agreement on the effector functions of the three monocyte subsets. In this sense, it was reported that TNF is produced mainly by CD16^{+} monocytes (intermediate and non-classical subsets) (20, 21). However, recent results have evidenced that TNF is produced by the three subsets. While Cros et al. (17) described that non-classical monocytes were poor producers of several cytokines [TNF, interleukin (IL)-1β, CCL2, IL-10, IL-8, IL-6, and CCL3] in response to LPS, other reports showed that the stimulation of intermediate subset with LPS produced the most TNF, IL-1β, and IL-6. In agreement, others also showed that intermediate monocytes produced the most TNF and IL-1β upon treatment with LPS and that this subset is the highest producer of TNF when cocultured with pre-activated T cells (22). In addition, Wong et al. (18) showed that non-classical monocytes upon LPS stimulation produced the highest levels of TNF and IL-1β, while equivalent amounts of IL-6 and IL-8 were produced by all three subsets. Other reports also recognized non-classical monocyte population as the greatest producer of TNF (21). Hence, it seems that non-classical monocytes constitute the subset capable of producing inflammatory cytokines in response to TLR ligands. There are also controversies on which monocyte subset is the major producer of the anti-inflammatory cytokine IL-10. In this sense, although it was demonstrated that intermediate monocytes produced the most IL-10 in response to LPS and zymosan (23), some recent reports showed that classical monocytes produced the most IL-10 (17, 18, 24). Further studies are necessary to clarify this relevant question.

Phenotypes and Functions of Macrophages

Several studies on macrophage biology have focused on the particular functions that these cells acquire after tissue accumulation. Macrophages are highly plastic and can adapt to environmental stimuli, displaying either a classically activated (M1) or alternatively activated (M2) profile, which represent extremes of a spectrum of functional phenotypes (25, 26). M1 macrophages are activated by pro-inflammatory Th1 cytokines and LPS. Besides being antigen-presenting cells, the M1 subset shows an enhanced microbicidal capacity attributable to the production of reactive oxygen species (ROS) (such as hydrogen peroxide, superoxide, nitric oxide (NO), and peroxynitrite) and inflammatory cytokines (TNF, IL-1β, IL-12, and IL-23). On the other extreme, M2 macrophages are activated by Th2 cytokines (IL-4 and IL-13) or by anti-inflammatory mediators (IL-10), enhancing the arginase activity and mannose receptor (CD206) expression, to promote wound healing and reduce Th1 response. However, the M2 subset development can also be detrimental to host tissue, leading to fibrosis when their matrix-enhancing activity is not regulated (27). Although embryonic and monocyte-derived macrophages likely are on a continuum spectrum that lies between (and outside of) the M1 and M2 classifications, the terminology nevertheless has been helpful in order to elucidate macrophage heterogeneity. When Ly6C^{high} monocytes are recruited to atherosclerotic lesions, they mature to F4/80^{+} macrophages. In a persistent inflammatory environment, these Ly6C^{high} monocyte-derived macrophages contribute to oxidative stress and are inflammatory

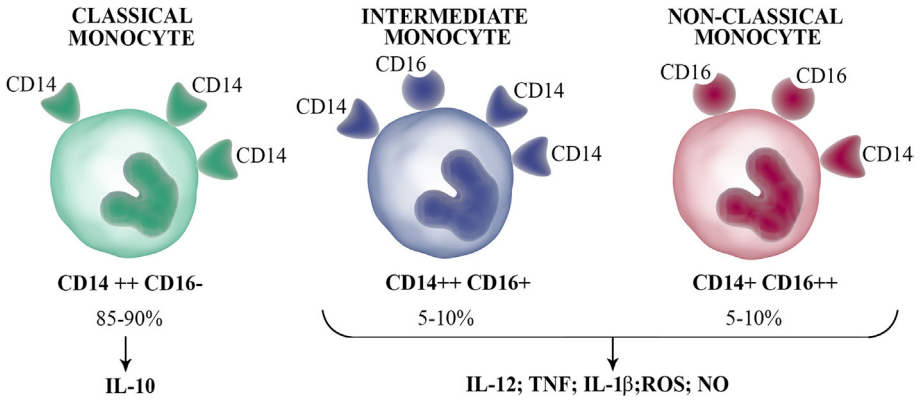


FIGURE 2 | Human circulating monocyte subsets. Human blood monocytes can be separated into three subsets according to the CD16 and CD14 expression: classical monocytes ($CD14^{++}$ $CD16^{-}$), which represent the majority of circulating monocytes produce the anti-inflammatory IL-10 upon stimulation; intermediate monocytes ($CD14^{++}$ $CD16^{+}$); and non-classical monocytes ($CD14^{+}$ $CD16^{++}$), which secrete inflammatory cytokines such as IL-1β, IL-12, TNF, and antimicrobial molecules [nitric oxide (NO) and reactive oxygen species (ROS)].

by producing IL-1β and TNF (9). In this respect, $Ly6C^{high}$ monocyte-derived cells are M1 macrophages. In the setting of inflammation resolution, M1 macrophages are replaced by M2 repairing macrophages. Although it has been proposed that M1 to M2 conversion occurs locally (28–30), M2 macrophages also could derive from non-classical and less inflammatory $Ly6C^{low}$ monocytes (12). Otherwise, M2 macrophages may arise through direct differentiation of $Ly6C^{high}$ monocytes in a microenvironment that favors wound healing. This option should be further explored because it is enticing for potential therapeutic reasons.

Cardiac resident macrophages coexpress M1 and M2 markers suggesting no specific polarization (31). However, within myocardium macrophages respond to systemic Th2 environment induced by helminth parasites infection, adopting an M2 phenotype associated with enhanced fibrosis. In this model, the increased amount of cardiac macrophages relies on recruitment of $Ly6C^{high}CCR2^{+}$ monocytes instead of IL-4-induced expansion. In this sense, Jenkins et al. have shown that IL-4 and IL-13 through IL-4Rα not only activate macrophages but also cause proliferative expansion of resident macrophages (32, 33). Moreover, IL-33 also induces macrophages proliferation, but in an IL-4Rα-signaling-independent manner (34), suggesting that the number and activation state of cardiac macrophages largely depend on mediators locally produced.

RELEVANCE TO CARDIOVASCULAR PATHOLOGIES

Mononuclear phagocytes are becoming increasingly recognized as key cells in the initiation and propagation of cardiac injury and remodeling. This growing body of evidence should prompt cardiovascular researchers to explore new therapeutic targets. Because of their functional and phenotypic versatility, manipulating specific macrophage subsets may spare key and vital cardiovascular functions, such as tissue repair and defense against pathogens, while preventing specific deleterious effects that contribute to adverse cardiac remodeling or atherosclerotic plaque formation.

Infections

Chagas Cardiomyopathy

Chagas disease is caused by *Trypanosoma cruzi* infection and constitutes a major public health problem in Latin America due to its prevalence, morbidity, and mortality. The World Health Organization (WHO) classifies it as a neglected tropical disease, and has recently estimated that 6–7 million people worldwide are infected, and about 7,000 people annually die (35). The cardiomyopathy represents the most frequent and serious complication of Chagas disease, affecting about 30–40% of infected individuals. In consequence, Chagas myocarditis is the most common form of infectious cardiomyopathy worldwide.

The clinical course of the disease is divided into acute and chronic phases. During the acute phase, which lasts 2–4 months, the infective trypomastigote form is in the bloodstream and invades target cells, where it replicates as amastigote form. This stage is followed by a life-long chronic phase, in which parasites are cleared from the circulation but persist for years within the myocardium among other target tissues. Nowadays, it is widely accepted that the persistence of parasites in target tissues coupled with an unbalanced immune response is a necessary and sufficient condition for the development of the cardiomyopathy (36–39).

In response to the infection, macrophages are one of the main infiltrating leukocytes arriving early to the myocardium (40) and they remain as an important immune cell population in heart explants from patients with severe advanced chronic Chagas disease (41). Interestingly, selective depletion of macrophages causes a significant increment in the number of amastigote nests within cardiomyocytes, suggesting a crucial role for macrophages in the resistance to this infection (42). Even though several antiparasitic roles of these cells in Chagas disease has been further documented, the functional characterization of resident and

infiltrating macrophages in infected myocardium has not been widely studied until very recently. In this sense, we have described the kinetics of macrophage populations during the acute and chronic phase of *T. cruzi* infection in BALB/c and C57BL/6 cardiac tissue (43, 44). In both mouse strains, macrophages with M1 phenotype ($CD45^+$ $F4/80^+$ $CD11b^+$ $CD86^+$ $CD206^-$) predominate only at short times postinfection [4 days postinfection (dpi)], but then macrophages are rapidly polarized toward M2 phenotype ($CD45^+$ $F4/80^+$ $CD11b^+$ $CD86^-$ $CD206^+$), which remains sustained during the acute and chronic phase (90 dpi). The sudden shift in cardiac M1/M2 ratio correlates with the changes in local cytokine milieu. These works evidence that alternatively activated macrophages are the main cardiac cell subset throughout the infection. Alternative macrophages provide protection against overwhelming cardiac inflammation, but they also interfere with the activation of M1 macrophages and its microbicidal function, promoting parasite persistence. The sustained M2 profile is promoted, at least in part, by the action of IL-6 (44).

In order to stablish the possible mechanisms by which cardiac M1 macrophages shift toward M2 profile quickly after infection, we focused on purinergic signaling. The ecto-5′-nucleotidase (CD73) enzyme is part of the purinergic system and together with ectonucleoside triphosphate diphosphohydrolase-1 (CD39) metabolize, in a step-wise manner, the extracellular ATP into adenosine (ADO). ADO has a regulating role on macrophage functions associated with M1 profile, such as suppression of chemokines and pro-inflammatory cytokines production, impairment of inducible nitric oxide synthase (iNOS) activity and induction of anti-inflammatory IL-10 production (45). CD73 is the rate-limiting enzyme in the ADO generation and it is expressed by immune and parenchymal cells (46). We showed that pharmacological inhibition of CD73 enzymatic activity with ADO 5′α,β-methylene-diphosphate (APCP) during the early acute phase enhances the number of M1 cardiac macrophages over the M2 subset and increases cardiac levels of NO, IL-6, TNF, and IL-1β in infected BALB/c mice (**Figure 3A**). These APCP-induced changes result in a concomitant reduction of cardiac parasite load during the acute phase and, as a direct consequence, improve the outcome of chronic cardiomyopathy (43). The study demonstrates that the polarization of cardiac macrophages is strongly influenced by the products of extracellular ATP metabolism and that the manipulation of this pathway could provide new approaches to reduce Chagas heart pathology.

In response to different cardiac injuries, soluble mediators are key players since they drive the immune response and the reestablishment of homeostasis. In this sense, IL-6 cytokine is suddenly and continuously produced by cardiomyocytes and neighboring cells after different pathological stimuli, suggesting that this cytokine is clue for the heart's intrinsic stress response system. We and others have reported that IL-6-deficient (IL6KO) mice succumb to *T. cruzi* infection very early during the acute phase (44, 47, 48). By analyzing immune mechanism that could explain the lethal effect observed in the absence of this cytokine, we discovered that IL-6 negatively regulates inflammasome activation and, consequently, IL-1β-induced NO production, and that excessive oxidative stress accounts for the increased mortality of infected IL6KO mice (44). We also found that IL-6 promotes the establishment of M2 cardiac macrophage profile during infection and induces *in vivo* and *in vitro* expression of the enzyme CD39 on macrophages, suggesting that IL-6 could promote a shift from an ATP driven pro-inflammatory environment to an anti-inflammatory milieu induced by ADO (44) (**Figure 3B**). Considering that IL-6 is a therapeutic target in individuals with different inflammatory diseases (49), our results provide the basis

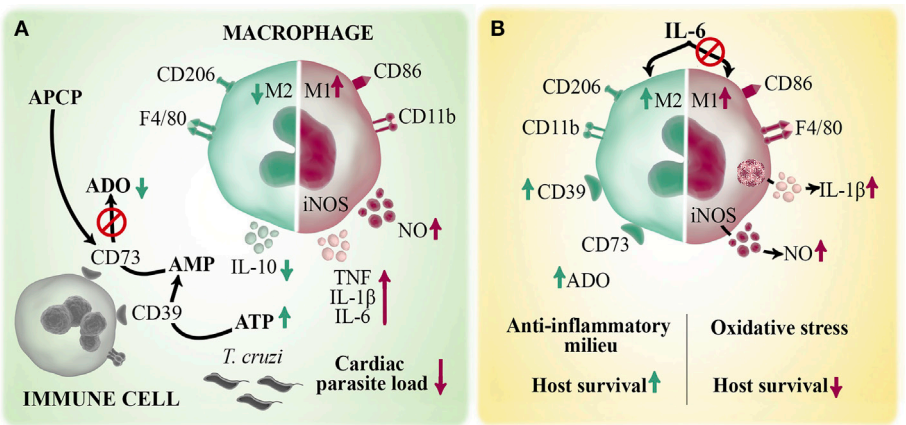


FIGURE 3 | Role of macrophages in the immune response against *Trypanosoma cruzi* infection. Macrophages are the main infiltrating cells arriving to the myocardium early after *T. cruzi* infection. Different mediators can regulate the magnitude and quality of the cardiac immune response by modulating macrophages activation. **(A)** ATP is released by infected/injured cells and hydrolyzed by two ectoenzymes, CD39 and CD73, to the immunoregulatory metabolite ADO. Pharmacological inhibition of CD73 activity with APCP enhances M1 over M2 macrophage phenotype and increases the local production of TNF, IL-1β, IL-6, and NO and diminished IL-10 levels. **(B)** IL-6 is a pleiotropic cytokine that contributes to the establishment of cardiac M2 macrophage profile during *T. cruzi* infection by inducing an anti-inflammatory microenvironment and augmented CD39 expression. Deficiency of IL-6 (IL6KO mice) dysregulates inflammasome activation with a consequent increases in IL1-β-induced NO production. The excessive oxidative stress and exacerbated pro-inflammatory immune response cause the lethal effect observed in infected IL6KO mice.

for understanding why blocking IL-6 in certain clinical situations does not represent an effective treatment; instead triggering pro-inflammatory adverse events.

In agreement with the results obtained with the mouse experimental model, the culture of *in vitro*-infected peripheral blood mononuclear cells obtained from control human donors with IL-6 blunted *T. cruzi*-induced nitration of cytotoxic T-cell subpopulation and increased their survival. The nitration of surface proteins on T cells is a consequence of NO and superoxide anion reaction which generates peroxynitrite. Furthermore, the blockade of IL-6 in these cultures with an IL-6 neutralizing antibody increased the frequency of *T. cruzi*-induced nitration of $CD8^+$ T cells as a consequence of elevated NO production. In line with these results, leukocytes from chronic Chagas patients show increased NO production concomitant with significant tyrosine nitration mainly in $CD8^+$ T cells compared with seronegative patients. Superficial tyrosine nitration on cytotoxic cells is concomitant with impaired effector functions and lower capacity for activation but also it is associated with a significant fall in the number of circulating $CD8^+$ T cells (50). Altogether, the results suggest that $CD8^+$ T cell functionality decreases in the setting of human Chagas disease, but this under-responsiveness could be reverted by the pleiotropic actions of IL-6, which functions as a survival factor for this population and improves its effector functions. Strikingly, the parasite has evolved strategies to counteract IL-6-dependent signaling through the specific cleavage of its receptor, the gp130 chain (51).

In contrast to the antioxidant properties of IL-6, IFN-γ enhances iNOS expression in infected macrophages resulting in the killing of intracellular parasites. Strikingly, IL-17A-stimulated macrophages control replication in a comparable level to IFN-γ treatment (52). The IL-17 stimulation alters the uptake pathway of trypomastigotes promoting phagocytosis over active invasion of macrophages. Phagocytosis of trypomastigotes enhances the number of internalized parasite and prolongs its residency in the endosomal/lisosomal compartment. A recent report demonstrates that IL-17-mediated direct protection of infected macrophages involves the NADPH oxidase activation and ROS production (53). In concordance, mice deficient in IL-23 (IL23p19KO), a potent inducer of IL-17A production, show enhanced parasitemia and a greater susceptibility to acute *T. cruzi* infection compared with infected WT mice. Moreover, IL-17AKO mice seemed to be even more susceptible to *T. cruzi* infection than IL23p19KO mice. The fact that the treatment of macrophages with IL-17A plus IFN-γ is more efficient to eliminate the parasite compared with single-cytokine stimulation, might explain the higher mortality ratio in IL23p19KO and IL-17AKO mice even though the Th1 immune response, measured by IFN-γ production and the iNOS expression, is not impaired during the infection in both KO mice (52). Finally, correlation analysis in Chagas disease patients demonstrates that high IL-17 serum levels are associated with better cardiac function (54–56).

After reaching the cytosol in macrophages, *T. cruzi* is recognized by innate receptor NLRP3, a member of nod-like receptor family (57). Infected mice deficient in IL-1β receptor, ASC, or caspase-1 are defective in NO production and exhibit an enhanced cardiac parasitism and mortality (58). Furthermore, the weak IL-1β production in NLRP3KO macrophages is compensated by an enhanced ROS production that mediates an effective parasite killing, indicating that NLRP3 modulates NADPH oxidase/ROS levels (59). Moreover, these low levels of IL-1β and the partial survival of infected NLRP3KO mice suggest that another Nod-like receptor might be activating inflammasome during infection.

Following cardiac injury, immune cell infiltration and fibroblasts migration trigger tissue remodeling, that is largely dependent on matrix metalloproteinases (MMPs) activity. Immunohistochemistry analysis revealed that vascular wall and infiltrating leukocytes are the cellular source of MMP-2 and MMP-9, which are increased in cardiac tissue during the acute phase of *T. cruzi* infection. As expected, treatment with MMP inhibitors reduces myocarditis in infected mice (60). In Chagas disease patients, T cells, neutrophils and monocytes are source of MMP-2 and MMP-9. *In vitro* stimulation with *T. cruzi*-derived antigens induces higher MMP-2 and MMP-9 expression in monocyte from patients with cardiac clinical forms of Chagas disease compared with those from non-infected patients (61). Recent reports showed a significant positive correlation between the levels of MMP-9, IL-1β and TNF, but a negative correlation between MMP-2 levels and these inflammatory cytokines and a positive correlation with IL-10 expression in serum from chronic Chagas disease patients (61, 62). These results suggest that MMP-9 may be related to inflammation and cardiomyopathy development; meanwhile, MMP-2 would be associated with regulation of chronic inflammatory process. Other study indicated that MMP-2 and MMP-9 levels peaks in plasma from patients clinically asymptomatic with an abnormal ECG (an early indicator of cardiac disease) and progressively augmented in patients with advancing Chagas cardiomyopathy. Although MMPs are strongly associated with several inflammatory diseases, the data suggested that MMP-2 and MMP-9 plasmatic levels could be used as early biomarkers of cardiac disease (63).

It is widely accepted that *T. cruzi* modulate apoptosis of different target cells in order to evade the immune response. In this sense, Freire-de-Lima and coworkers demonstrated that phagocytic removal of apoptotic T lymphocytes by infected-macrophages exacerbate parasite replication by driving its differentiation toward an M2-like phenotype concomitant with TGF-β, IL-10, and PGE2 production (64, 65). TGF-β promotes in macrophages the L-arginine metabolism by arginase to synthesize polyamines which functions as a growth factor for parasites (66). Another work found that blocking apoptosis of $CD8^+$ T cells in cocultures, infected macrophages increase NO levels and M1 features leading to restrict intracellular parasite growth (67). In addition, while coculture of apoptotic neutrophils induce an M2-like phenotype in infected macrophages, live neutrophils *via* elastase induce M1 macrophages with NO and TNF production that allow to control *T. cruzi* replication (68). Further studies in human cells are needed to validate these findings.

Similar to others cardiac pathologies, cardiomyocyte apoptosis seems to be determinant of Chagas disease progression. In this sense, it was found that infection induces apoptosis of cardiomyocytes (69, 70). In contrast, several reports demonstrated that *T. cruzi* induces anti-apoptotic effect on cardiac cell (51, 71–75).

Indeed, it is plausible to think that cardiac cell exposure to pro-inflammatory milieu may precondition the heart tissue to protect cardiomyocytes from a massive apoptosis (76). This hypothesis is clinically supported by experiments performed by Metzger et al. The authors described that apoptotic cells are increased in the myocardium from Chagas disease patients with severe heart failure. However, the apoptotic cells are not cardiomyocytes, and the majority of $TUNEL^+$ cells are also $CD68^+$ (human macrophage marker) (77), similar results also being observed by other researchers (78). Related to this, an intense Bcl-2 expression is induced in cardiomyocytes during the acute phase of the experimental infection, likely establishing a higher threshold to apoptosis in this cell type (73).

Although enthusiastic researchers have suggested the therapeutic use of apoptosis inhibitors as an attractive choice for adjuvant therapy during the chronic phase (79), the effects of apoptosis modulation on the outcome of chronic cardiomyopathy requires further studies.

Viral Myocarditis

The cardiotropic viruses that cause myocarditis in humans include enteroviruses, adenoviruses, influenza viruses, cytomegaloviruses, parvoviruses, and herpes viruses. Although most of these viruses commonly cause only mild upper respiratory or gastrointestinal complications in most individuals, a few infected people develop cardiac clinical symptoms (80). The enteroviral coxsackievirus B group type 3 (CVB3), adenoviruses parvovirus B19, and human herpes virus 6 are frequently observed in myocarditis biopsies. The most common viral myocarditis is caused by CVB3 infection. It affects about 5–20% of world population, and yet lacks efficient treatments. Although acute viral myocarditis is self-limiting in most individuals, in others develop chronic myocarditis, progressive cardiac fibrosis, dilated cardiomyopathy, heart failure, and even death (81–83). Strong clinical and experimental evidence has demonstrated that two main mechanisms are involved in pathogenesis of CVB3-induced myocarditis, first a direct viral injury to cardiac cells during the acute stage of infection and second, the excessive pro-inflammatory immune response against CVB3 which can subsequently evolve to a chronic autoimmune cardiac pathology in some susceptible patients (80).

Monocytes/macrophages represent one of the major infiltrating inflammatory cells in CVB3-induced myocarditis. It was reported that cardiac CCL2 levels are significantly enhanced at 1 dpi and peak at 4 dpi and hence closely involved in CVB3-induced myocarditis initiation, by attracting monocytes. CCL2 incidence in viral myocarditis was even more evident after blocking CCL2 activity *in vivo,* since those infected mice exhibit reduced myocardial cell infiltration, decreased serum CK-MB levels and increased host survival (82).

Other study showed that *in vivo* CVB3 infection also triggers the production of galectin-3 (a β-galactoside binding lectin) in cardiac macrophages during acute and chronic phases. Abrogation of galectin-3 expression or its pharmacological inhibition does not affect viral titers but reduce acute myocarditis and chronic fibrosis, suggesting a critical role of galectin 3-producing macrophages in the induction of fibrosis subsequent to CVB3 infection.

Studies in experimental murine infection with CVB3 have been widely employed as a model of human enteroviral infection and they have significantly contributed to the understanding of the immunological mechanisms underlying acute and chronic viral inflammatory heart disease. Strikingly, male, but not female, mice infected with CVB3 present a severe myocarditis with a pathological process resembling human disease. Although similar viral infection titers have been detected in patients of both genders, the estimated incidence of myocarditis in men is twofold increase or more than in women (84, 85).

Experimental approaches assessing the differential susceptibility against CVB3 infection between male and female mice have greatly contributed to the knowledge of the etiopathological mechanisms of this viral myocarditis. During the early acute infection, cardiac tissue from male and female mice presents high levels of IFN-γ and IL-4, respectively. Consistently, male cardiac macrophages express M1 markers; meanwhile, female cardiac macrophages polarize toward M2 phenotype (86, 87). Employing adoptive transfer experiments of *in vitro* IFN-γ-induced M1 macrophages, the authors demonstrated this pro-inflammatory subset is responsible for myocardial inflammation and damage after CVB3 infection (86).

It is important to highlight that IL-10 has a protective role during virus-induced cardiac fibrotic process by inhibiting fibroblast collagen synthesis (85, 88). As counterpoint, male infected mice exhibit a reduced frequency of cardiac monocytic-myeloid-derived suppressor cell (MDSC) subset and regulatory T cells, which negatively correlates with the severity of cardiac fibrosis induced by CVB3 infection. Although it was reported that myocardial infiltrating immune cells have a different cell composition in both mouse genders, how this difference affects macrophage functions and the development of CVB3-induced myocarditis needs further studies. In this sense, infiltrating NK cells could have a role in the physiopathology of the disease. Kinetic studies of myocardial infiltrate revealed that NK cells arrive together with macrophages and the synergistic action of sex hormones and CVB3 infection contribute to NK cells differential cytokine production (87).

On the other hand, it was reported that CVB3 can efficiently induce endoplasmic reticulum (ER) stress in infected cardiomyocytes and, in turn, stressed myocardial cells transfer the ER stress to macrophages *via* some unknown soluble molecules and facilitate the pro-inflammatory phenotype. In concordance, an *in vivo* pharmacological treatment with ER stress inhibitor induces a substantial reduction of pro-inflammatory cytokines in macrophages, diminishes CK-MB serum levels, relieves myocardial inflammation and improves cardiac functions. Moreover, adoptive transfer experiments of ER stress-inhibited macrophages into infected mice also alleviate viral-myocarditis together with an increase in mice survival, confirming the pathological role of ER stressed macrophages in CVB3-induced myocarditis (89). Other work showed that CVB3 infection in cardiac cells induces ROS production and alters potassium efflux, triggering NLRP3 inflammasome activation in infected cardiomyocytes (90). Therefore, all these studies indicate that the cardiac environment that shape macrophages polarization has a key role in the outcome of CVB3-induced heart disease.

Bacterial Infections

Mononuclear phagocytic cells are essential in cardiac immunity to several myocarditis-related to bacterial infections. Lyme disease is a long-term infection caused by *Borrelia burgdorferi* spirochetes. Its most severe complications are myocarditis and inflammatory arthritis of the lower bearing joints. An important difference between arthritis and myocarditis is the distribution of phagocytes within the lesions; while polymorphonuclear leukocytes are more prevalent in the joint, macrophages are the predominant infiltrating cells in infected hearts (91). The severity of Lyme myocarditis is controlled by CD11c integrin, because CD11cKO mice caused increased cardiac MCP-1 production and consequently, increased macrophage infiltration. The loss of this integrin generates an impaired macrophage immune response leading to an aggravated Lyme disease (92). Similarly, in absence of CCR2, the receptor that induces monocyte recruitment to the site of infection, resistant CCR2KO mice had augmented bacterial heart burden compared with WT counterpart (C57BL/6) suggesting a reduced clearance of the bacteria. In contrast, deficiency of CCR2 in sensitive mice strain CCR2KO (C3H) produced severe inflammation with increased presence of polymorphonuclear cells but decreased *B. burgdorferi* burden in comparison with WT (C3H/HeJ) mice. The less efficient spirochete clearance from hearts of WT C3H mice compared with CCR2KO C3H mice suggests an impaired recruitment or function of macrophages in C3H mice, which may contribute to the susceptibility of this animal strain to *B. burgdorferi* infection (93). Nevertheless, there were no differences in cardiac macrophage polarization of C3H sensitive strain, with similar number of M1 and M2 subtype macrophages at the peak of inflammation (94).

Regarding cytokine production, there are several reports showing that IFN-γ is a key cytokine that modulates the immune response to *B. burgdorferi,* particularly the macrophage activation and functions. Sabino and coworkers proposed that IFN-γ influence the composition of cardiac leukocyte infiltrates. They found that *B. burgdorferi* and IFN-γ synergistically enhance the secretion of mononuclear cell chemoattractants such as CXCL9 and CXCL10, decrease those for neutrophils (CXCL1 and CXCL2), and, in consequence, this modifies the nature of the cellular infiltration (95). Additionally, the production of IFN-γ by iNKT cells enhance the bacterial recognition and activation of macrophages as evidenced by augmented TNF and IL-6 production, leading to an increased phagocytic activity (91). Importantly, IFN-γ is produced in lesions of Lyme patient myocarditis and its levels positively correlate with the severity of the pathology.

Considering innate receptors, it was reported that mice deficient in the intracellular adapter molecule myeloid differentiation antigen 88 (MyD88KO), which is required for several TLR-induced inflammatory responses had 250-fold higher pathogen burden than WT mice. In agreement, *in vitro* experiment confirmed that MyD88KO macrophages phagocytize spirochetes but degrade them more slowly than WT macrophages (96). In accordance, Hawley et al. demonstrated that CR3KO-mediated spirochete internalization requires the participation of CD14 molecule as an accessory receptor and showed that CR3/CD14-mediated phagocytosis generates a pro-inflammatory macrophage phenotype in response to bacterial invasion (97). On the other hand, several reports demonstrate key roles for the intracellular innate receptor Nod2. In *B. burgdorferi* infection context, Nod2-deficient mice resulted in increased myocarditis compared with control mice. Although Nod2 induces inflammatory milieu in *in vitro* models of *B. burgdorferi* infection, BMDM upon a prolonged stimulation of Nod2 no longer respond in the same manner. Indeed, prolonged exposure to the Nod2 ligand results in suppression of pro-inflammatory responses. The authors theorize that the dual role of Nod2 signaling in the inflammatory response may be associated with the chronicity of the infection (98). In the same way, Zlotnikov et al. revealed that a high fat diet-induced obesity (DIO) in a murine model of Lyme disease was associated with systemic suppression of innate immune response. The hearts of DIO-infected mice presented significantly elevated inflammation and increased bacterial burden due to an impaired bacterial uptake and pro-inflammatory cytokine production by macrophages and this effect became more pronounced as infection progressed (99). All these data together substantiate the importance of macrophages in the immune response against this pathogen, but also the dual role that they can play in order to control the infection or perpetuate the inflammation state.

Other bacterial infection in which macrophages play a key role on disease outcome is poststreptococcal myocarditis. *Streptococcus pneumoniae* is capable of invading the heart soon after the development of bacteremia. The pneumococcus is the responsible of the community-acquired pneumonia and sometimes it may worsen by producing the invasive pneumococcal disease that injures the heart. Macrophages have been postulated as inducers of heart-reactive T cells due to their capacity to transfer the inflammatory lesions into normal recipient mice when they are pulsed with group A streptococcus extract (SAE) resulting in an increased serum CK levels, an enzyme that is released in the bloodstream after inflammatory cardiac muscle injury. SAE pulsed macrophages may present to T cells an antigenic determinant characteristic to rheumatogenic streptococci that cross-reacts with a normal component of the heart tissue (100). In accordance, group A streptococcal M proteins had the ability to stimulate human PBMC to proliferate and induce cytotoxic T cells against cultured human heart cells (101). The results suggest a critical role for monocytes/macrophages as antigen-presenting cells in the outcome of heart damage after infection.

More recent studies have proposed that *S. pneumoniae* forms discrete pneumococcus-filled micro lesions in the myocardium during invasive pneumococcal disease (102) generating direct tissue damage. The pneumococci within cardiac micro lesions produce pneumolysin, a cholesterol-dependent pore-forming toxin, which kills cardiomyocytes and macrophages due to pneumolysin-induced necroptosis. This precludes the generation of an effective immune response and perpetuates cardiac damage (103). These reports bring to light that macrophages are crucial for innate immune response to bacterial infections and that the alteration of their functions can alter the outcome of the disease.

Sterile Inflammation

Although inflammation is the process in which components of the innate immune system respond to an injury or infection, inflammatory response can also be triggered in absence of infection by a

process known as *sterile inflammation*. This type of inflammation is implicated in the development of a variety of clinical conditions such as atherosclerosis, cardiac injury, neurodegenerative and metabolic disorders. Unlike microbial-induced inflammation, sterile inflammation is activated by endogenous danger-associated molecular patterns (DAMPs) released as a consequence of cellular injury and/or inflammation, such as oxidized low-density lipoprotein (oxLDL), oxidized phospholipids (oxPLs), amyloid β or uric-acid crystals (104, 105). This sterile inflammatory response induces recruitment of neutrophils and monocytes leading to production of pro-inflammatory cytokines and chemokines, mainly IL-18 and IL-1β in a caspase-1-dependent manner. As mentioned above, monocytes subsets (classical, intermediate, and non-classical) extensively participate in the response to infectious disease; however, their role in sterile inflammation in cardiac ischemia-reperfusion injury and atherosclerosis is still not well understood. Myocardial ischemia-reperfusion injury is a condition that involved cardiomyocytes death affecting contractibility and loss of heart function as a result of a vascular occlusion and loss of tissue irrigation. While different pathways contributed to limit the damage, the inflammatory response in the ischemic heart can be detrimental (106).

The knowledge gained on the origin of resident cardiac macrophages has greatly improved the therapeutic potential of macrophage manipulation in the context of sterile inflammation. Considering that adult mammalian heart contains two macrophage pools which include: Ly6C^{low} MHC-II^{low} and MHC-II^{high} (CCR2^{-}) representing embryonically established macrophages and the second pool and much less abundant derived from blood Ly6C^{high} CCR2^{+} monocytes. Altered homeostasis induced by transient depletion (chemically) of monocytes and macrophages population in heart shown proliferation of CCR2^{-} resident macrophages and recruitment of Ly6C^{high} CCR2^{+} monocytes from blood to contribute to tissue macrophages repopulation (107). Thus, after myocardial injury and knowing that NLRP3 inflammasome activation impair tissue regeneration, blockage of CCR2 abolishes ischemic damage. This concept suggests that blockage of CCR2^{+} monocytes influx or recruitment during cardiac ischemia-reperfusion will be protective, while a strategy of depletion of resident macrophages (CCR2^{-}) abolished that protection. In the same way, Marchetti et al. applied a pharmacological inhibitory strategy for NLRP3 inflammasome in a mouse model of myocardial injury. They found that in acute myocardial infarction (MI) with reperfusion and in a model of non-ischemic injury induced with doxorubicin, the inhibition of NLRP3 inflammasome cause a significantly reduction of infarct size and preserved systolic function (108).

The understanding of circulating monocytes and cardiac macrophage biology under physiology and disease condition may help discover new mechanisms to target specific subset population of macrophage that impact in cardiac cytoprotective pathways.

Atherosclerosis

Atherosclerosis is the result of lipid accumulation and chronic inflammation in the arterial wall where macrophage plays a central role in the development and progression of plaque formation (**Figure 4**). Thus, transmigration of monocytes into

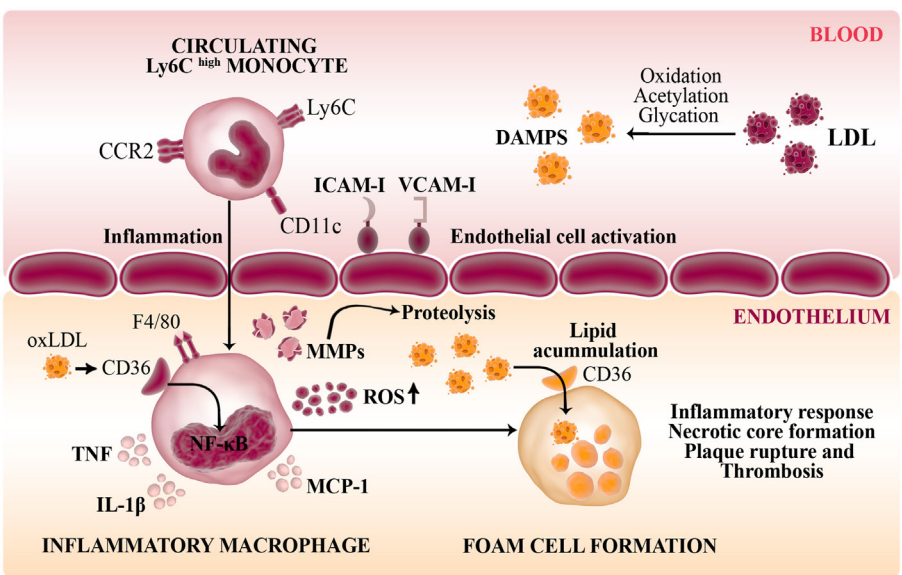


FIGURE 4 | Role of macrophages in the pathogenesis of atherosclerosis. Disturbance of normal vascular physiology is characterized by endothelial activation which stimulates the expression of endothelial adhesion molecules (VCAM-1, ICAM-1) to favor the passage of inflammatory monocytes to the subendothelium. Modified LDL and other DAMPS are recognized by pattern-recognition receptors such as CD36 (scavenger receptor-B) in infiltrating macrophages. Thus, these innate cells are transformed into lipid-laden foam cells in the vasculature intima. The activation of NF-κB in response to ox-LDL induce the secretion of inflammatory cytokines (IL-1β, TNF), NO, MCP-1, and macrophage-derived matrix metalloproteinases (MMPs) that degrade the extracellular matrix generating a maladaptative inflammatory response and contribute to plaque formation.

the subendothelial space, lipid uptake (oxLDL) and foam cell differentiation are key step in atherogenesis. The maintenance of a healthy endothelium regulates the precise balance in vascular homeostasis between vasoconstriction and vasodilation, trombogenesis and fibrinolysis, cellular migration and proliferation (109). Disturbance of normal vascular physiology is characterized by endothelial activation, which may be caused by infection or by cardiovascular risk factor such as hyperlipidemia (pathophysiologic). Thus, pro-inflammatory mediators (IL-1β, TNF, and MCP-1) induce a deleterious effect on NO bioavailability increasing ROS which stimulate the expression of endothelial adhesion molecules (VCAM-1, ICAM-1) to favor the passage of monocytes to the subendothelium and promoting their differentiation into macrophages (110).

In atherosclerosis, circulating low-density lipoprotein (LDL) molecules undergoes modifications mainly oxidation, acetylation and glycation that alter the normal metabolism of lipoprotein to promote cytotoxic damage on endothelial cells and macrophages. There is a broad spectrum of mediators that induce LDL oxidation from enzymatic (lipoxygenase and cyclooxygenase) to non-enzymatic reactions (free radicals and oxidants). Some of these reactions have differential selectivity for LDL components as occur with ROS that oxidize predominantly the lipid portion of LDL or the neutrophil myeloperoxidase that oxidize the protein portion (Apo B) of LDL by action of hypochlorous acid byproducts (111, 112).

In this inflammatory milieu, other biomolecules, in addition to LDL, such as lipids and proteins are target of oxidation and nitration reactions generating new species that may affect the fate of the plaque development and limit or exacerbate the inflammatory state. Thus, nitro-fatty acids (NO_2-FAs) are the product of the reaction of unsaturated fatty acids and nitrogen-derived species (NO and nitrites) (113). Administration of NO_2-FA in a mice model of atherosclerosis (ApoEKO) exhibited anti-inflammatory and protective actions, decelerating the development of the atheroma plaque, affecting oxLDL uptake and foam cell formation in macrophages (114).

Modified LDLs are recognized and internalized in macrophages by pattern-recognition receptor (PRR) which includes scavenger receptor (SR) and toll-like receptor (TLR). SRs bind diverse ligands and contribute to the clearance of foreign or modified particles. Regarding to macrophage cholesterol metabolism, CD36 (SR-B) and SR-A1 mediate internalization of oxLDL and transform these cells into cholesterol-laden foam cells in the vasculature intima. Exploration in experimental models evidenced that CD36-deficient macrophages exhibited a reduced uptake of oxLDL; further study in ApoE/CD36 double mutant mice described the reduction of the size of atherosclerotic plaque (115, 116). These results emphasized the role of CD36 as a pro-atherogenic receptor in the vasculature and cardiovascular disease. However, discrepancy on CD36 implication as pro- or anti-atherogenic has been raised by other studies in which described advanced atherogenesis in LDLR/CD36 double mutant mice or less macrophage accumulation but increased aortic lesions in ApoE/CD36 double KO (117). The inconsistency of this result may be in part explained by the different experimental model and animal background employed. Besides the discrepancy on CD36 function in atheroma plaque formation the binding of oxLDL stimulates pro-inflammatory signaling pathways (NF-κB) in macrophage contributing to maintain the chronic inflammatory state generated during the onset of atherosclerosis disease.

In atherosclerosis, the recognition of the subsets of recruited monocytes that differentiate into macrophages in the atheroma plaque may be relevant to design new strategies to treat pathological inflammatory process. During the development of atheroma plaque, the recruitment of monocytes are drawn from the $Ly6C^{high}$ circulating subset (precursor of M1 macrophages) but after treatment and control of hyperlipidemia a rapid reduction of plaque inflammation and regression was exhibited, characterized by decrease number of macrophages and the relative increase in markers of M2 macrophages state. Rahman et al. described in a model of aortic arch transplantation that plaque regression is characterized by recruitment of $Ly6C^{high}$ circulating monocytes and the posterior polarization to M2 phenotype (118). This result is contrary to the prevailing paradigm about M2 macrophages recruitment in plaque regression and the authors promote the strategy of M2 macrophage accumulation in atherosclerotic lesions to stimulate plaque regression. Consistent results were obtained in mice treated with IL-13 and IL-4 (promote M2 polarization) which describe protective effects in plaque progression in mice (119).

Summing up, the data obtained clearly illustrate the clue role that mononuclear phagocytic cells play in the development of the atherosclerotic pathology, further molecular mechanisms involved in plaque formation are described in the next chapter.

SIGNALING PATHWAYS AND MOLECULES MODULATING CARDIOVASCULAR IMMUNE RESPONSE

Cytokines and Chemokines

Macrophages are major contributors to the inflammatory response in the setting of cardiovascular diseases. They secrete diverse pro-inflammatory mediators (including cytokines, chemokines, ROS and nitrogen species, among others), and MMPs and they eventually die by necrosis or apoptosis. Dying macrophages release their lipid contents, which lead to the development of a pro-thrombotic necrotic core. The necrotic core is, in turn, a clue component of unstable plaques and contributes to their rupture and the consequent intravascular blood clot that causes MI and stroke. The main effect of cytokines/chemokines released by macrophages is the recruitment of different innate and adaptive immune cell populations into the atherosclerotic lesions (120, 121), thereby amplifying the inflammatory environment. For example, different inflammatory mediators such as IL-1, TNF and IFN-γ increase the expression of MCP-1 in macrophages (120, 122). Also, under inflammatory conditions macrophages produce different enzymes such as MMPs, cathepsins and serine proteases that degrade the extracellular matrix of the atherosclerotic plaque contributing to the pathogenesis of atherosclerosis (123). In this sense, IL-1 and TNF increase the expression of numerous MMPs, such as MMP-9, and their activity contribute to unstable plaque morphology (123).

While initial reports indicated that IFN-γ prevented macrophage foam cell formation (124), subsequent studies demonstrate that this cytokine promotes foam cell formation through diverse mechanisms: enhancing the uptake of oxLDL/AcLDL through SRs (122, 125), diminishing efflux of cholesterol *via* inhibition of ABCA-1 transporter and ApoE expression (126, 127) and increasing ACAT-1 levels (126) in macrophage-derived foam cells. For example, it was recently reported that the axis IFN-γ/STAT1 mediates the uptake of acLDL/oxLDL by human macrophages in an extracellular signal-regulated kinase (ERK)-dependent signaling (125). The activity of IFN-γ as a pro-foam cell mediator has been supported by several *in vivo* studies (128).

Since IFN-γ was identified as a pro-foam cell cytokine, different authors evaluated the effect of other pro-inflammatory cytokines. Studies using a murine macrophage cell line have shown that TNF inhibits the expression of SRs and the uptake of oxLDL (129). Regarding additional mechanisms, more recent evidence has suggested that TNF promotes foam cell formation *in vitro* by reducing the mRNA expression of ABCA-1/ABCG-1 (130), and intracellular lipid catabolism (131), and by enhancing the expression of ACAT-1 and the accumulation of cholesteryl ester (132). However, the role for TNF remains controversial since other studies have shown that TNF enhances ABCA-1 expression and the efflux of cholesterol in peritoneal macrophages stimulated with ApoA–I (133, 134) and since evidences from studies performed in murine models are also contentious (128).

Regarding anti-inflammatory cytokines, it has been demonstrated that TGF-β decreases CD36/SR-A expression and the uptake of oxLDL in human macrophages (135, 136). Additional data emphasized this anti-foam cell effect by showing that TGF-β downregulates CD36/SR-BI mRNA levels in peritoneal macrophages (137) and increases ApoA–I and HDL-stimulated cholesterol efflux and ABCA-1 gene transcription in foam cells (138). Argmann et al. (139) demonstrated that TGF-β1 decreases LPL expression/activity and cholesteryl ester accumulation with a coincident increase in the expression of ABCG-1 in murine macrophages. Recently, it was reported that TGF-β diminishes LPL gene transcription (140) and increases the expression of ApoE (141). Moreover, other group has shown that $CD4^+$ $CD25^+$ regulatory T cells use TGF-β1 to inhibit the uptake of oxLDL and the expression of CD36/SR-A mRNA (142). These mechanisms evidence an anti-foam cell role for TGF-β1, although it is important to stress that TGF-β may promote development either of anti-atherosclerotic regulatory T cells or of T-helper 17 (Th17) cells, depending on factors in the local milieu. Therefore, TGF-β signaling in T cells could promote stabilization of atherosclerotic plaques through an IL-17-dependent pathway.

The effect of IL-10 on plaque formation has also been reported. This anti-inflammatory mediator downregulates the CD36 SR expression (143) and, in consequence, decreases the accumulation of cholesterol in human macrophages (144). In addition, two independent groups have reported anti-foam cell activity of IL-10. Indeed, they found that IL-10 enhances the uptake and efflux of cholesterol by human macrophages *in vitro* and reduces foam cell formation and atherosclerotic plaque progression *in vivo* (145, 146). Altogether, the results suggest that IL-10 counteract atherogenesis.

Besides M1 and M2 macrophage profiles, additional phenotypes have been described within atherosclerotic lesion and they have become a topic of increasing relevance. In areas of hemorrhage, macrophages respond adaptively to heme acquiring an activation status that was designated hemorrhage-associated macrophages (Mhem). *In vitro* human blood-derived monocytes are induced to Mhem by stimulation with hemoglobin–haptoglobin complexes and it is dependent on an autocrine action of secreted IL-10 (147, 148). This macrophage profile prevents foam cell formation and has antioxidant functions. Other study showed that oxPL products that accumulate in atherosclerotic lesions induce another phenotype designated as Mox. Data indicate that Mox macrophages are characterized by high expression of heme oxygenase-1 and it comprises approximately 30% of all macrophages in established atherosclerotic lesions in experimental models (149). In addition, CXCL4, a chemokine released by activated platelet, was demonstrated to prevent monocytes/macrophages apoptosis and promote its differentiation into a phenotype called "M4" ($MMP7^+$ $S100A8^+$ $CD68^+$). M4 macrophage was described in human coronary atherosclerotic plaques *ex vivo* and postmortem (150, 151). The prevalence of this macrophage subset is higher in patients with severe coronary artery disease and there is a significant correlation between the accumulation of M4 macrophages within the intima and plaque destabilization, which is independent of the overall number of macrophages in the vascular wall (150).

Recently, several groups have published that IL-17A-stimulated macrophages are suggested to constitute a new macrophage population. Barin et al. (152) showed that IL-17A induces activation of primary macrophages in a unique profile of cytokines and chemokines, including IL-12p70, GM-CSF, IL-3, IL-9, CCL4 and CCL5, that can be distinguished from previously characterized macrophage activation states. Moreover, another work showed that IL-17A induces a pro-inflammatory transcriptome in human monocytes/macrophages, including cytokines such as IL-1α and IL-6, chemokines like CCL2, CCL8, CCL20, CXCL1, CXCL2 and CXCL6, genes involved in oxidative stress, upregulation of CD14, CD163 levels and downregulation of genes associated with T cell costimulation. By comparing the entire transcriptomes of M1, M2 and M4 macrophages, authors confirm that IL-17A-treated macrophages are a unique polarization subset (153). On the other hand, it was reported that IL-17 also can strongly amplifies human monocytes/macrophages differentiation toward M2c profile, making it resistant to apoptosis and promoting its MerTK-dependent clearance of apoptotic bodies (154). M2c cells ($CD14^{bright}$ $CD16^+$ $CD163^+$ $MerTK^+$) are a subset of alternatively activated macrophages induced by M-CSF plus IL-10 or glucocorticoids and they are involved in inflammation resolution through phagocytosis of early apoptotic neutrophils and anti-inflammatory cytokines production (155). In contrast with the mentioned effects of IL-17, authors demonstrated that both IFN-γ/Th1 environment and IL-4-chronic exposure impair glucocorticoid and IL-10-induced M2c macrophage differentiation and also alters phagocytosis function of stablished M2c macrophages by reducing MerTK levels and promoting its apoptosis. Thus, this work indicates that Th17 environment orchestrates the resolution

of innate inflammation through expansion of M2c regulatory macrophages.

An important point to note is that in a predominantly Th17 environment, monocytes/macrophages have a key role in the IL-17-induced inflammatory responses. In an experimental murine autoimmune myocarditis (EAM) model, the genetic ablation of IL-17RA alters the recruitment of monocytes/macrophages, which is the most numerous component of the inflammatory infiltrate and it is implicated in the cardiac damage (152). In concordance, other work shows that IL-17A promotes cardiac infiltration of Ly6C^{high} monocytes by inducing fibroblasts to produce high levels of cytokines and chemokines. Particularly, GM-CSF production by IL-17-stimulated cardiac fibroblasts drives differentiation of infiltrating monocytes into an even more inflammatory phenotype which further intensifies the myocarditis. Experiments performed in IL17RAKO mice or depletion of Ly6C^{high} monocytes/macrophages demonstrates the involvement of these innate cells in the inflammatory dilated cardiomyopathy (156). On the other hand, in an advanced atherosclerotic model in ApoEKO mice, *in vivo* IL-17A blocking markedly prevents atherosclerotic lesion progression and improves its stability by reducing inflammatory burden and monocyte infiltration (153). Moreover, the CCL2 and CCL5 production were significantly reduced in those IL-17A mAb-treated mice. *In vitro* experiments demonstrated that IL-17A induces adhesion of human monocytes, adhesion and rolling of platelets on endothelial cells. Other studies performed in early stages of atherosclerosis demonstrate that IL-17/IL-17RA axis has a pro-atherogenic role by promoting early monocyte recruitment into plaque through CCL5 production, endothelial VCAM-1 expression and increasing CXCL1 expression on the vessel lumen (157–159).

Purinergic Signaling

Purinergic system has been recognized as a main pathway to regulate immune response and it is critical to prevent the collateral damage produced by the exacerbation of the immune response in several diseases including cardiac pathologies. In normal conditions, ATP is localized intracellularly where it is the main source of energy for cell functions and it accomplishes indispensable functions in cellular metabolism such as proliferation, migration, motility, biosynthesis and contraction functions within the cardiomyocytes. In addition to its metabolic function, ATP also acts as an important signaling molecule when it is released to the extracellular compartment. After it is released, the extracellular ATP hydrolysis is governed by the activity of two membrane ectoenzymes, the CD39 that catalyzes the phosphohydrolysis of ATP to ADO monophosphate (AMP) and CD73 that hydrolyzes AMP into ADO and inorganic phosphate (45). CD39 and CD73 expression on immune and vascular cells and their enzymatic activities play decisive role in the regulation of the magnitude and duration of purinergic signals that modulate cellular function in an autocrine or paracrine manner (160). These effects are mediated by two types of nucleotide/nucleoside receptors: P1 receptors activated by extracellular ADO and P2 receptors activated by ATP and other nucleotides such as ADP and AMP. The first group includes 4 ADO receptors (ADORA 1, ADORA 2A, ADORA 2B, and ADORA 3), and the second group includes several P2X and P2Y subtypes of receptors (161).

Purinergic signaling is highly described in tumoral context (162) and in autoimmune diseases (163) but poorly studied in the context of cardiac pathologies. Given the high production rate of ATP and the turnover required to maintain its continuous mechanical work, disruption of heart tissue generates the release of high amounts of ATP to the extracellular space. Bonner et al. have reported that cardiomyocytes and erythrocytes do not detectably express the ATP catabolic machinery, but coronary endothelial cells were highly positive for CD39 under basal conditions and a low proportion of these cells express CD73. Furthermore, they stated that resident cardiac APCs and monocytes were the responsible of the first step of ATP degradation in the heart after ischemic injury because they were highly positive for the CD39 while CD73 was absent. Likewise, the dephosphorylating step of AMP to immunosuppressive ADO seems to take place on T lymphocytes and granulocytes because CD73 was mainly expressed in those populations (164).

In contrast to the pro-inflammatory action of ATP, ADO exhibits diverse immunoregulatory roles. Bonner and coworkers found that macrophages stimulated through ADORA 2A and ADORA 2B receptors with ADO undergo M2 phenotype in infarcted mice. In addition, in CD73KO mice there was augmented expression of microbicidal M1 genes, while the expression of M2 genes like arginase-1, IL-10, and TGF-β decreased. This monocyte imbalance toward inflammatory Ly6C^{high}-expressing monocytes in mice lacking CD73 had been related to adverse myocardial healing and ventricular dilatation after MI (165). Furthermore, Haskó et al. reported that ADO diminish the oxidative burst by downregulating NO production and inhibit TNF release from monocytes and macrophages (166). A parallel mechanism has also been reported by Cain group in murine isquemia/reperfusion model where ADO pretreatment decreased myocardial TNF production (167). There is strong evidence that ADO can modulate leukocyte adhesion to vascular endothelium *in vivo*. In this sense, Koszalka et al. demonstrated that ADO is an important endogenous pathway to modulate the inflammatory vascular response. After a period of ischemia-reperfusion, they observed significant increase of leukocyte adherence to the vascular endothelium only in the CD73 mutant (168). It has also been suggested that purinergic signals play a role in cellular migration. Analysis of atherosclerotic lesions of P2Y6 KO mice revealed fewer macrophages, diminished RNA expression of IL-6 and VCAM-1, suggesting that deficiency in this ATP receptor limits atherosclerosis and plaque inflammation (169). Recently, it was reported that lack of P2X7 receptor resolute plaque destabilization by inhibiting inflammasome activation and consequently ameliorates experimental atherosclerosis. ATP binding to P2 receptors is crucial to NLRP3 assembly and the subsequent IL-1β release. P2X7 null mice had decreased amount of macrophages in the wound and, in consequence, smaller and less inflamed atherosclerotic lesions than respective control animals (170). Altogether, the data indicate that purinergic signaling can modulate macrophage polarization and infiltration; and that ADO is a key metabolite in suppressing inflammation following injury or infection.

In addition, ADO induces the production of vascular endothelial growth factor (VEGF) in human macrophages, associated with increased hypoxia inducible factor-1α (HIF-1α) expression, the main transcriptional inducer of VEGF in hypoxic milieu. VEGF promotes blood vessel formation, induces cell proliferation and initiates immune cell migration to stimulate vasculogenesis and angiogenesis (171). On the other hand, extracellular ATP contributes to tissue repair by the stimulation of P2X7 receptor and release of the pro-angiogenic factor VEGF (172). Summing up, activation of purinergic receptors in macrophages can promote wound healing and may be targeted to improve cardiac repair mechanisms.

Metabolism

The heart changes its substrate preferences throughout the life, under physiological or pathological conditions. This metabolic flexibility allows it to adapt to environmental changes. However, shifts in fuel selectivity can become detrimental in the pathological heart (173).

Pathological cardiac hypertrophy is a common consequence of several cardiovascular diseases and is a maladaptive response to chronic stress, sometimes resulting in cardiac failure. Pathological hypertrophy involves a shift in fuel metabolism from fatty-acid oxidation to enhanced reliance on glucose. Increased glucose utilization is characterized by upregulation of glucose uptake and glycolysis concomitant with no change or a decrease in glucose oxidation, resulting in uncoupling of glucose uptake/oxidation metabolism. Nowadays, it is accepted that changes in mitochondrial function and cardiac metabolism precede heart dysfunction, indicating that metabolic remodeling is an early event in the development of cardiac diseases.

Recent interest in understanding the impact of these fundamental metabolic changes on immune cell differentiation and function has yielded numerous studies examining the pathways and metabolites involved in driving protective immune responses. A key question that has emerged is whether differential metabolic activity (i.e., use of glycolysis versus mitochondrial respiration) is coincident with differentiation or if it is a direct driver of alterations in immune cell differentiation and function. Classically activated macrophages that promote inflammation utilize glycolysis and glutamine metabolism to generate large quantities of succinate which enhances inflammation and IL-1β production (174). In contrast, macrophages that play a role in tissue healing and inflammatory resolution increase mitochondrial lipid oxidation (175). A key differentiator between these metabolic phenotypes may arise in the mitochondria, where rather than engaging in conventional electron transport, altered electron flow through the succinate dehydrogenase complex promotes ROS generation and inflammation (176). Enhanced glycolysis in coronary artery disease patients drives mitochondrial ROS production, resulting in pyruvate kinase M2 (PKM2) assembly and translocation to the nucleus. It then phosphorylates and activates STAT3 to promote the production of the cytokines IL-1β and IL-6 (177). Indeed, the increased activation of glycolytic pathway was associated with epigenetic changes in monocyte-derived macrophages describing a new mechanism to explain trained immunity in human innate immune cells (178).

Diabetes is a major risk factor for cardiovascular diseases (179). As such it may lead to heart failure indirectly, by promoting the development of coronary artery disease. However, it is now known that diabetes may cause heart failure also by eliciting a direct detrimental impact on the myocardium leading to the development of cardiac hypertrophy, diastolic and systolic dysfunction (180). The clinical condition associated with the spectrum of cardiac abnormalities induced by diabetes is termed diabetic cardiomyopathy. High glucose levels and dyslipidemia directly induce the upregulation and secretion of cytokines, chemokines and adhesion molecules in immune cells by modulating multiple signaling pathways that converge toward NF-κB signaling (181–183). Activation of the renin–angiotensin–aldosterone system and accumulation of advanced glycation end-products (AGE) and DAMPs molecules like extracellular high-mobility group box-1 protein (HMGB1), also represent key mechanisms that mediate inflammatory response in the diabetic heart primarily by acting TLRs (184–186). Following these initial molecular events, leukocytes infiltrate the myocardium and perpetuate the inflammatory process through secretion of cytokines and pro-fibrotic factors and by increasing the production of ROS. Mediators resulting from this inflammatory cascade, in turn, modulate specific intracellular signaling mechanisms in cardiac cells causing hypertrophy, mitochondrial dysfunction, ER stress and cell death fibroblast proliferation and collagen production. In addition, inflammatory factors may affect myocardial metabolic processes and interfere with cardiomyocyte contractile properties. These abnormalities together promote the development of diabetic cardiomyopathy.

Diabetes-associated metabolic derangements can directly induce cytokine expression and release from cardiac cells. It was previously shown that hyperglycemia augmented the expression of HMGB1 in isolated cardiomyocytes, macrophages and cardiac fibroblasts, thereby activating the MAPK and NF-κB pathways and by inducing TNF and IL-6 secretion (187). Inhibition of HMGB1 decreased myocardial inflammation and fibrosis in a murine model of type 1 diabetes and protected diabetic animals in response to postinfarction remodeling (187, 188).

An increase in circulating lipids may also contribute to cardiac inflammation in diabetes. Fatty acids activate TLR4 that strongly promotes inflammation through the NF-κB pathway (189). Mice with a TLR4 gene deletion demonstrate improved cardiac function and reduced cardiac intracellular lipid accumulation in response to streptozotocin-induced diabetes (190). Fatty acids induce the subsequent expression of IL-6, TNF and IL-1, which can be reversed by peroxisome proliferator-activated receptor-γ, β/δ (PPAR-b/d) (191). Previous work showed that hyperglycemia and high circulating levels of lipids promote inflammation through the activation of protein kinase C (PKC), which activates MAPK pathway thereby inactivating IkB (192).

The challenge to improve cardiovascular disorders therapy by modulating metabolic pathways must take into account potential off-target effects on other cells and tissues. In these sense, by exploiting the intrinsic capacity of monocytes and macrophages to take up foreign particles, the use of nanoparticle formulations might be one option to achieve targeting specificity (193).

Oxidative Stress

Oxygen is the molecular source of the production of several molecules that damage vital tissues. Reactive oxygen and nitrogen species (RONS) are continuously produced as by-products of the reaction leading to energy production through the mitochondrial and microsomal electron-transport chains. In phagocytes, the oxidative bursts and enzyme systems such as xanthine oxidase and cytochrome P-450 oxidase are the endogenous sources of RONS. While physiological levels of RONS are crucial for cell function, excessive RONS levels trigger oxidative stress. Oxidative stress may damage clues molecules (proteins, lipids, DNA) and could, eventually, conducted to cell death. To prevent oxidative stress, antioxidants have evolved to protect biological systems against RONS-induced damage. Oxidative stress resulting from uncontrolled production of RONS that exceeds the antioxidant capacity, exacerbate atherosclerosis; since it induces endothelial dysfunction by impairing the bioactivity of endothelial NO and promotes leukocyte adhesion, enhances inflammation and thrombosis.

Numerous reports demonstrated that increased oxidative stress is associated with disturbances in cardiovascular diseases. In this sense, it was reported an overproduction of superoxide anion by cardiac dysfunctional mitochondria or increased production of RONS from non-mitochondrial sources in experimental models of type 1 diabetes (194, 195). The augmented production of RONS induces maladaptive cardiac response causing cardiac cells death contributing to cardiovascular disease (196). An excessive oxidative stress has been associated with increased cardiac cell apoptosis, as was evidenced by $TUNEL^+$ cells and caspase 3 activation in *T. cruzi*-infected cardiac tissue (44). In this sense, high oxidative state has been associated with amplified lipid and DNA damage and the consequent cardiac cell injury and death. Therapeutic treatment that promotes RONS regulation have been shown to be effective in reducing cardiovascular dysfunction.

It is known that increased oxidative stress induces modifications of LDL, generating DAMPs that are detected by TLRs on different immune cell populations, mainly monocytes/macrophages. A variety of mechanisms mediated by enzymatic (such as 12/15-lipoxygenase and myeloperoxidase) or no-enzymatic redox reaction (such as RONS) boost LDL oxidation in the artery wall. The level of LDL oxidation modulates the immune system, when cells were treated with low oxLDL, the expression level of CD86, a marker for M1 macrophages, increases compared with that in cells treated with high oxLDL. In contrast, the expression level of the marker for M2 macrophages, CD206, significantly increases in cells treated with high oxLDL compared with that in cells treated with native LDL or low oxLDL. These results indicate that the degree of LDL oxidation affects the differentiation of monocytes into different subtypes of macrophages (197). Further research is needed to assess the functional consequences of oxidation processes on human macrophage behavior.

CONCLUSION AND PERSPECTIVES

The crucial role of mononuclear phagocyte system in homeostasis and inflammation described herein makes it a potential therapeutic target for a variety of cardiovascular diseases. However, most of our current knowledge on monocyte/macrophage phenotypes and functions is derived from studies performed in murine models and, as such, requires clinical translation and validation in human cells. Understanding macrophage activation in such settings using high-resolution, single-cell and deep phenotyping approaches will provide the basis for therapeutic proposals directed to target specific subsets while sparing others.

AUTHOR CONTRIBUTIONS

LS, NE, NP, RC, GB, and MA wrote the revision. NE and MA design the figures. NE helped to perform the figures. LS and MA critically revised the manuscript.

ACKNOWLEDGMENTS

The authors wish to thank Agustín Losso for figure design and realization. This work was supported by Secretaría de Ciencia y Tecnología, Universidad Nacional de Córdoba (113/17), Agencia Nacional de Promoción Científica y Tecnológica (ANPCyT) Fondo para la Investigación Científica y Tecnológica (PICT 2013-2885 and 2015-1130), Consejo Nacional de Investigaciones Científicas y Técnicas (CONICET) (PIP11220120100620), and by Ministerio de Ciencia y Tecnología, Gobierno de la Provincia de Córdoba (1143/10). MA and GB are members of the scientific career from the Consejo Nacional de Investigaciones Científicas y Técnicas de la República Argentina (CONICET). LS thanks CONICET for the fellowships granted. NP and NE thank fellowship granted from ANPCyT-FONCyT.

REFERENCES

1. Swirski FK, Libby P, Aikawa E, Alcaide P, Luscinskas FW, Weissleder R, et al. Ly-6Chi monocytes dominate hypercholesterolemia-associated monocytosis and give rise to macrophages in atheromata. *J Clin Invest* (2007) 117(1): 195–205. doi:10.1172/JCI29950
2. Schulz C, Gomez Perdiguero E, Chorro L, Szabo-Rogers H, Cagnard N, Kierdorf K, et al. A lineage of myeloid cells independent of Myb and hematopoietic stem cells. *Science* (2012) 336(6077):86–90. doi:10.1126/science.1219179
3. Hashimoto D, Chow A, Noizat C, Teo P, Beasley MB, Leboeuf M, et al. Tissue-resident macrophages self-maintain locally throughout adult life with minimal contribution from circulating monocytes. *Immunity* (2013) 38(4):792–804. doi:10.1016/j.immuni.2013.04.004
4. Wynn TA, Chawla A, Pollard JW. Macrophage biology in development, homeostasis and disease. *Nature* (2013) 496(7446):445–55. doi:10.1038/nature12034
5. Lavine KJ, Epelman S, Uchida K, Weber KJ, Nichols CG, Schilling JD, et al. Distinct macrophage lineages contribute to disparate patterns of cardiac recovery and remodeling in the neonatal and adult heart. *Proc Natl Acad Sci U S A* (2014) 111(45):16029–34. doi:10.1073/pnas.1406508111
6. Avraham-Davidi I, Yona S, Grunewald M, Landsman L, Cochain C, Silvestre JS, et al. On-site education of VEGF-recruited monocytes improves their

performance as angiogenic and arteriogenic accessory cells. *J Exp Med* (2013) 210(12):2611–25. doi:10.1084/jem.20120690
7. Jakubzick C, Gautier EL, Gibbings SL, Sojka DK, Schlitzer A, Johnson TE, et al. Minimal differentiation of classical monocytes as they survey steady-state tissues and transport antigen to lymph nodes. *Immunity* (2013) 39(3):599–610. doi:10.1016/j.immuni.2013.08.007
8. Geissmann F, Manz MG, Jung S, Sieweke MH, Merad M, Ley K. Development of monocytes, macrophages, and dendritic cells. *Science* (2010) 327(5966):656–61. doi:10.1126/science.1178331
9. Robbins CS, Chudnovskiy A, Rauch PJ, Figueiredo JL, Iwamoto Y, Gorbatov R, et al. Extramedullary hematopoiesis generates Ly-6C(high) monocytes that infiltrate atherosclerotic lesions. *Circulation* (2012) 125(2):364–74. doi:10.1161/CIRCULATIONAHA.111.061986
10. Leuschner F, Rauch PJ, Ueno T, Gorbatov R, Marinelli B, Lee WW, et al. Rapid monocyte kinetics in acute myocardial infarction are sustained by extramedullary monocytopoiesis. *J Exp Med* (2012) 209(1):123–37. doi:10.1084/jem.20111009
11. Tacke F, Alvarez D, Kaplan TJ, Jakubzick C, Spanbroek R, Llodra J, et al. Monocyte subsets differentially employ CCR2, CCR5, and CX3CR1 to accumulate within atherosclerotic plaques. *J Clin Invest* (2007) 117(1):185–94. doi:10.1172/JCI28549
12. Nahrendorf M, Swirski FK. Monocyte and macrophage heterogeneity in the heart. *Circ Res* (2013) 112(12):1624–33. doi:10.1161/CIRCRESAHA.113.300890
13. Hilgendorf I, Swirski FK. Making a difference: monocyte heterogeneity in cardiovascular disease. *Curr Atheroscler Rep* (2012) 14(5):450–9. doi:10.1007/s11883-012-0274-8
14. Mizuno K, Toma T, Tsukiji H, Okamoto H, Yamazaki H, Ohta K, et al. Selective expansion of CD16highCCR2-subpopulation of circulating monocytes with preferential production of haem oxygenase (HO)-1 in response to acute inflammation. *Clin Exp Immunol* (2005) 142(3):461–70. doi:10.1111/j.1365-2249.2005.02932.x
15. Fingerle-Rowson G, Auers J, Kreuzer E, Fraunberger P, Blumenstein M, Ziegler-Heitbrock LH. Expansion of CD14+CD16+ monocytes in critically ill cardiac surgery patients. *Inflammation* (1998) 22(4):367–79. doi:10.1023/A:1022316815196
16. Horelt A, Belge KU, Steppich B, Prinz J, Ziegler-Heitbrock L. The CD14+CD16+ monocytes in erysipelas are expanded and show reduced cytokine production. *Eur J Immunol* (2002) 32(5):1319–27. doi:10.1002/1521-4141(200205)32:5<1319::AID-IMMU1319>3.0.CO;2-2
17. Cros J, Cagnard N, Woollard K, Patey N, Zhang SY, Senechal B, et al. Human CD14dim monocytes patrol and sense nucleic acids and viruses via TLR7 and TLR8 receptors. *Immunity* (2010) 33(3):375–86. doi:10.1016/j.immuni.2010.08.012
18. Wong KL, Tai JJ, Wong WC, Han H, Sem X, Yeap WH, et al. Gene expression profiling reveals the defining features of the classical, intermediate, and nonclassical human monocyte subsets. *Blood* (2011) 118(5):e16–31. doi:10.1182/blood-2010-12-326355
19. Zawada AM, Rogacev KS, Rotter B, Winter P, Marell RR, Fliser D, et al. SuperSAGE evidence for CD14++CD16+ monocytes as a third monocyte subset. *Blood* (2011) 118(12):e50–61. doi:10.1182/blood-2011-01-326827
20. Frankenberger M, Sternsdorf T, Pechumer H, Pforte A, Ziegler-Heitbrock HW. Differential cytokine expression in human blood monocyte subpopulations: a polymerase chain reaction analysis. *Blood* (1996) 87(1):373–7.
21. Belge KU, Dayyani F, Horelt A, Siedlar M, Frankenberger M, Frankenberger B, et al. The proinflammatory CD14+CD16+DR++ monocytes are a major source of TNF. *J Immunol* (2002) 168(7):3536–42. doi:10.4049/jimmunol.168.7.3536
22. Rossol M, Kraus S, Pierer M, Baerwald C, Wagner U. The CD14(bright) CD16+ monocyte subset is expanded in rheumatoid arthritis and promotes expansion of the Th17 cell population. *Arthritis Rheum* (2012) 64(3):671–7. doi:10.1002/art.33418
23. Skrzeczynska-Moncznik J, Bzowska M, Loseke S, Grage-Griebenow E, Zembala M, Pryjma J. Peripheral blood CD14high CD16+ monocytes are main producers of IL-10. *Scand J Immunol* (2008) 67(2):152–9. doi:10.1111/j.1365-3083.2007.02051.x
24. Smedman C, Ernemar T, Gudmundsdotter L, Gille-Johnson P, Somell A, Nihlmark K, et al. FluoroSpot analysis of TLR-activated monocytes reveals several distinct cytokine-secreting subpopulations. *Scand J Immunol* (2012) 75(2):249–58. doi:10.1111/j.1365-3083.2011.02641.x
25. Biswas SK, Mantovani A. Macrophage plasticity and interaction with lymphocyte subsets: cancer as a paradigm. *Nat Immunol* (2010) 11(10):889–96. doi:10.1038/ni.1937
26. Sica A, Mantovani A. Macrophage plasticity and polarization: in vivo veritas. *J Clin Invest* (2012) 122(3):787–95. doi:10.1172/JCI59643
27. Tidball JG, Villalta SA. Regulatory interactions between muscle and the immune system during muscle regeneration. *Am J Physiol Regul Integr Comp Physiol* (2010) 298(5):R1173–87. doi:10.1152/ajpregu.00735.2009
28. Arnold L, Henry A, Poron F, Baba-Amer Y, van Rooijen N, Plonquet A, et al. Inflammatory monocytes recruited after skeletal muscle injury switch into antiinflammatory macrophages to support myogenesis. *J Exp Med* (2007) 204(5):1057–69. doi:10.1084/jem.20070075
29. Egawa M, Mukai K, Yoshikawa S, Iki M, Mukaida N, Kawano Y, et al. Inflammatory monocytes recruited to allergic skin acquire an anti-inflammatory M2 phenotype via basophil-derived interleukin-4. *Immunity* (2013) 38(3):570–80. doi:10.1016/j.immuni.2012.11.014
30. Ramachandran P, Pellicoro A, Vernon MA, Boulter L, Aucott RL, Ali A, et al. Differential Ly-6C expression identifies the recruited macrophage phenotype, which orchestrates the regression of murine liver fibrosis. *Proc Natl Acad Sci U S A* (2012) 109(46):E3186–95. doi:10.1073/pnas.1119964109
31. Mylonas KJ, Jenkins SJ, Castellan RF, Ruckerl D, McGregor K, Phythian-Adams AT, et al. The adult murine heart has a sparse, phagocytically active macrophage population that expands through monocyte recruitment and adopts an 'M2' phenotype in response to Th2 immunologic challenge. *Immunobiology* (2015) 220(7):924–33. doi:10.1016/j.imbio.2015.01.013
32. Jenkins SJ, Ruckerl D, Cook PC, Jones LH, Finkelman FD, van Rooijen N, et al. Local macrophage proliferation, rather than recruitment from the blood, is a signature of TH2 inflammation. *Science* (2011) 332(6035):1284–8. doi:10.1126/science.1204351
33. Jenkins SJ, Ruckerl D, Thomas GD, Hewitson JP, Duncan S, Brombacher F, et al. IL-4 directly signals tissue-resident macrophages to proliferate beyond homeostatic levels controlled by CSF-1. *J Exp Med* (2013) 210(11):2477–91. doi:10.1084/jem.20121999
34. Jackson-Jones LH, Ruckerl D, Svedberg F, Duncan S, Maizels RM, Sutherland TE, et al. IL-33 delivery induces serous cavity macrophage proliferation independent of interleukin-4 receptor alpha. *Eur J Immunol* (2016) 46(10):2311–21. doi:10.1002/eji.201646442
35. WHO. *Chagas Disease (American Trypanosomiasis)*. (2017). Available at: http://www.who.int/mediacentre/factsheets/fs340/en/
36. Gutierrez FR, Guedes PM, Gazzinelli RT, Silva JS. The role of parasite persistence in pathogenesis of Chagas heart disease. *Parasite Immunol* (2009) 31(11):673–85. doi:10.1111/j.1365-3024.2009.01108.x
37. Machado FS, Tyler KM, Brant F, Esper L, Teixeira MM, Tanowitz HB. Pathogenesis of Chagas disease: time to move on. *Front Biosci (Elite Ed)* (2012) 4:1743–58. doi:10.2741/e495
38. Marin-Neto JA, Cunha-Neto E, Maciel BC, Simoes MV. Pathogenesis of chronic Chagas heart disease. *Circulation* (2007) 115(9):1109–23. doi:10.1161/CIRCULATIONAHA.106.624296
39. Tarleton RL. Parasite persistence in the aetiology of Chagas disease. *Int J Parasitol* (2001) 31(5–6):550–4. doi:10.1016/S0020-7519(01)00158-8
40. Melo RC. Acute heart inflammation: ultrastructural and functional aspects of macrophages elicited by *Trypanosoma cruzi* infection. *J Cell Mol Med* (2009) 13(2):279–94. doi:10.1111/j.1582-4934.2008.00388.x
41. Arguello RJ, Vigliano C, Cabeza-Meckert P, Viotti R, Garelli F, Favaloro LE, et al. Presence of antigen-experienced T cells with low grade of differentiation and proliferative potential in chronic Chagas disease myocarditis. *PLoS Negl Trop Dis* (2014) 8(8):e2989. doi:10.1371/journal.pntd.0002989
42. Melo RC, Machado CR. *Trypanosoma cruzi*: peripheral blood monocytes and heart macrophages in the resistance to acute experimental infection in rats. *Exp Parasitol* (2001) 97(1):15–23. doi:10.1006/expr.2000.4576
43. Ponce NE, Sanmarco LM, Eberhardt N, Garcia MC, Rivarola HW, Cano RC, et al. CD73 inhibition shifts cardiac macrophage polarization toward a microbicidal phenotype and ameliorates the outcome of experimental chagas cardiomyopathy. *J Immunol* (2016) 197(3):814–23. doi:10.4049/jimmunol.1600371

44. Sanmarco LM, Ponce NE, Visconti LM, Eberhardt N, Theumer MG, Minguez AR, et al. IL-6 promotes M2 macrophage polarization by modulating purinergic signaling and regulates the lethal release of nitric oxide during *Trypanosoma cruzi* infection. *Biochim Biophys Acta* (2017) 1863(4):857–69. doi:10.1016/j.bbadis.2017.01.006
45. Antonioli L, Pacher P, Vizi ES, Hasko G. CD39 and CD73 in immunity and inflammation. *Trends Mol Med* (2013) 19(6):355–67. doi:10.1016/j.molmed.2013.03.005
46. Forte G, Sorrentino R, Montinaro A, Luciano A, Adcock IM, Maiolino P, et al. Inhibition of CD73 improves B cell-mediated anti-tumor immunity in a mouse model of melanoma. *J Immunol* (2012) 189(5):2226–33. doi:10.4049/jimmunol.1200744
47. Gao W, Pereira MA. Interleukin-6 is required for parasite specific response and host resistance to *Trypanosoma cruzi*. *Int J Parasitol* (2002) 32(2):167–70. doi:10.1016/S0020-7519(01)00322-8
48. Arocena AR, Onofrio LI, Pellegrini AV, Carrera Silva AE, Paroli A, Cano RC, et al. Myeloid-derived suppressor cells are key players in the resolution of inflammation during a model of acute infection. *Eur J Immunol* (2014) 44(1):184–94. doi:10.1002/eji.201343606
49. Hunter CA, Jones SA. IL-6 as a keystone cytokine in health and disease. *Nat Immunol* (2015) 16(5):448–57. doi:10.1038/ni.3153
50. Sanmarco LM, Visconti LM, Eberhardt N, Ramello MC, Ponce NE, Spitale NB, et al. IL-6 improves the nitric oxide-induced cytotoxic CD8+ T cell dysfunction in human chagas disease. *Front Immunol* (2016) 7:626. doi:10.3389/fimmu.2016.00626
51. Hashimoto M, Nakajima-Shimada J, Aoki T. *Trypanosoma cruzi* post-transcriptionally up-regulates and exploits cellular FLIP for inhibition of death-inducing signal. *Mol Biol Cell* (2005) 16(8):3521–8. doi:10.1091/mbc.E04-12-1051
52. Erdmann H, Rossnagel C, Bohme J, Iwakura Y, Jacobs T, Schaible UE, et al. IL-17A promotes macrophage effector mechanisms against *Trypanosoma cruzi* by trapping parasites in the endolysosomal compartment. *Immunobiology* (2013) 218(6):910–23. doi:10.1016/j.imbio.2012.10.005
53. Cai YH, Ma ZJ, Lu XY, He EL, You MY. Study on the effect and mechanism of the dysfunction of CD4(+) T cells in the disease process of chronic cardiac failure. *Asian Pac J Trop Med* (2016) 9(7):682–7. doi:10.1016/j.apjtm.2016.05.006
54. Guedes PM, Gutierrez FR, Silva GK, Dellalibera-Joviliano R, Rodrigues GJ, Bendhack LM, et al. Deficient regulatory T cell activity and low frequency of IL-17-producing T cells correlate with the extent of cardiomyopathy in human Chagas' disease. *PLoS Negl Trop Dis* (2012) 6(4):e1630. doi:10.1371/journal.pntd.0001630
55. Magalhaes LM, Villani FN, Nunes Mdo C, Gollob KJ, Rocha MO, Dutra WO. High interleukin 17 expression is correlated with better cardiac function in human Chagas disease. *J Infect Dis* (2013) 207(4):661–5. doi:10.1093/infdis/jis724
56. Sousa GR, Gomes JA, Damasio MP, Nunes MC, Costa HS, Medeiros NI, et al. The role of interleukin 17-mediated immune response in Chagas disease: high level is correlated with better left ventricular function. *PLoS One* (2017) 12(3):e0172833. doi:10.1371/journal.pone.0172833
57. Gonçalves VM, Matteucci KC, Buzzo CL, Miollo BH, Ferrante D, Torrecilhas AC, et al. NLRP3 controls *Trypanosoma cruzi* infection through a caspase-1-dependent IL-1R-independent NO production. *PLoS Negl Trop Dis* (2013) 7(10):e2469. doi:10.1371/journal.pntd.0002469
58. Silva GK, Costa RS, Silveira TN, Caetano BC, Horta CV, Gutierrez FRS, et al. Apoptosis-associated Speck–like protein containing a caspase recruitment domain inflammasomes mediate IL-1β response and host resistance to *Trypanosoma cruzi* infection. *J Immunol* (2013) 191(6):3373–83. doi:10.4049/jimmunol.1203293
59. Dey N, Sinha M, Gupta S, Gonzalez MN, Fang R, Endsley JJ, et al. Caspase-1/ASC inflammasome-mediated activation of IL-1β–ROS–NF-κB pathway for control of *Trypanosoma cruzi* replication and survival is dispensable in NLRP3−/− macrophages. *PLoS One* (2014) 9(11):e111539. doi:10.1371/journal.pone.0111539
60. Gutierrez FR, Lalu MM, Mariano FS, Milanezi CM, Cena J, Gerlach RF, et al. Increased activities of cardiac matrix metalloproteinases matrix metalloproteinase (MMP)-2 and MMP-9 are associated with mortality during the acute phase of experimental *Trypanosoma cruzi* infection. *J Infect Dis* (2008) 197(10):1468–76. doi:10.1086/587487
61. Medeiros NI, Fares RC, Franco EP, Sousa GR, Mattos RT, Chaves AT, et al. Differential expression of matrix metalloproteinases 2, 9 and cytokines by neutrophils and monocytes in the clinical forms of Chagas disease. *PLoS Negl Trop Dis* (2017) 11(1):e0005284. doi:10.1371/journal.pntd.0005284
62. Fares RC, Gomes Jde A, Garzoni LR, Waghabi MC, Saraiva RM, Medeiros NI, et al. Matrix metalloproteinases 2 and 9 are differentially expressed in patients with indeterminate and cardiac clinical forms of Chagas disease. *Infect Immun* (2013) 81(10):3600–8. doi:10.1128/IAI.00153-13
63. Bautista-Lopez NL, Morillo CA, Lopez-Jaramillo P, Quiroz R, Luengas C, Silva SY, et al. Matrix metalloproteinases 2 and 9 as diagnostic markers in the progression to Chagas cardiomyopathy. *Am Heart J* (2013) 165(4):558–66. doi:10.1016/j.ahj.2013.01.001
64. Freire-de-Lima CG, Nascimento DO, Soares MB, Bozza PT, Castro-Faria-Neto HC, de Mello FG, et al. Uptake of apoptotic cells drives the growth of a pathogenic trypanosome in macrophages. *Nature* (2000) 403(6766):199–203. doi:10.1038/35003208
65. Freire-de-Lima CG, Xiao YQ, Gardai SJ, Bratton DL, Schiemann WP, Henson PM. Apoptotic cells, through transforming growth factor-beta, coordinately induce anti-inflammatory and suppress pro-inflammatory eicosanoid and NO synthesis in murine macrophages. *J Biol Chem* (2006) 281(50):38376–84. doi:10.1074/jbc.M605146200
66. D'Avila H, Freire-de-Lima CG, Roque NR, Teixeira L, Barja-Fidalgo C, Silva AR, et al. Host cell lipid bodies triggered by *Trypanosoma cruzi* infection and enhanced by the uptake of apoptotic cells are associated with prostaglandin E(2) generation and increased parasite growth. *J Infect Dis* (2011) 204(6):951–61. doi:10.1093/infdis/jir432
67. Cabral-Piccin MP, Guillermo LV, Vellozo NS, Filardy AA, Pereira-Marques ST, Rigoni TS, et al. Apoptotic CD8 T-lymphocytes disable macrophage-mediated immunity to *Trypanosoma cruzi* infection. *Cell Death Dis* (2016) 7:e2232. doi:10.1038/cddis.2016.135
68. Luna-Gomes T, Filardy AA, Rocha JDB, Decote-Ricardo D, LaRocque-de-Freitas IF, Morrot A, et al. Neutrophils increase or reduce parasite burden in *Trypanosoma cruzi*-infected macrophages, depending on host strain: role of neutrophil elastase. *PLoS One* (2014) 9(3):e90582. doi:10.1371/journal.pone.0090582
69. de Souza EM, Araujo-Jorge TC, Bailly C, Lansiaux A, Batista MM, Oliveira GM, et al. Host and parasite apoptosis following *Trypanosoma cruzi* infection in in vitro and in vivo models. *Cell Tissue Res* (2003) 314(2):223–35. doi:10.1007/s00441-003-0782-5
70. Tostes S Jr, Bertulucci Rocha-Rodrigues D, de Araujo Pereira G, Rodrigues V Jr. Myocardiocyte apoptosis in heart failure in chronic Chagas' disease. *Int J Cardiol* (2005) 99(2):233–7. doi:10.1016/j.ijcard.2004.01.026
71. Aoki MP, Guinazu NL, Pellegrini AV, Gotoh T, Masih DT, Gea S. Cruzipain, a major *Trypanosoma cruzi* antigen, promotes arginase-2 expression and survival of neonatal mouse cardiomyocytes. *Am J Physiol Cell Physiol* (2004) 286(2):C206–12. doi:10.1152/ajpcell.00282.2003
72. Aoki MP, Cano RC, Pellegrini AV, Tanos T, Guinazu NL, Coso OA, et al. Different signaling pathways are involved in cardiomyocyte survival induced by a *Trypanosoma cruzi* glycoprotein. *Microbes Infect* (2006) 8(7):1723–31. doi:10.1016/j.micinf.2006.02.010
73. Ponce NE, Cano RC, Carrera-Silva EA, Lima AP, Gea S, Aoki MP. Toll-like receptor-2 and interleukin-6 mediate cardiomyocyte protection from apoptosis during *Trypanosoma cruzi* murine infection. *Med Microbiol Immunol* (2012) 201(2):145–55. doi:10.1007/s00430-011-0216-z
74. Ponce NE, Carrera-Silva EA, Pellegrini AV, Cazorla SI, Malchiodi EL, Lima AP, et al. *Trypanosoma cruzi*, the causative agent of Chagas disease, modulates interleukin-6-induced STAT3 phosphorylation via gp130 cleavage in different host cells. *Biochim Biophys Acta* (2013) 1832(3):485–94. doi:10.1016/j.bbadis.2012.12.003
75. Petersen CA, Krumholz KA, Carmen J, Sinai AP, Burleigh BA. *Trypanosoma cruzi* infection and nuclear factor kappa B activation prevent apoptosis in cardiac cells. *Infect Immun* (2006) 74(3):1580–7. doi:10.1128/IAI.74.3.1580-1587.2006
76. Smith RM, Lecour S, Sack MN. Innate immunity and cardiac preconditioning: a putative intrinsic cardioprotective program. *Cardiovasc Res* (2002) 55(3):474–82. doi:10.1016/S0008-6363(02)00288-2

77. Metzger M, Higuchi ML, Brito T. Lack of apoptosis of cardiomyocytes in chronic chagasic myocarditis. *Virchow's Archiv* (2001) 439(6):352–9. doi:10.1007/BF02698641
78. Rossi MA, Souza AC. Is apoptosis a mechanism of cell death of cardiomyocytes in chronic chagasic myocarditis? *Int J Cardiol* (1999) 68(3):325–31. doi:10.1016/S0167-5273(98)00375-1
79. Decote-Ricardo D, Nunes MP, Morrot A, Freire-de-Lima CG. Implication of apoptosis for the pathogenesis of *Trypanosoma cruzi* infection. *Front Immunol* (2017) 8:518. doi:10.3389/fimmu.2017.00518
80. Corsten MF, Schroen B, Heymans S. Inflammation in viral myocarditis: friend or foe? *Trends Mol Med* (2012) 18(7):426–37. doi:10.1016/j.molmed.2012.05.005
81. Yue Y, Gui J, Ai W, Xu W, Xiong S. Direct gene transfer with IP-10 mutant ameliorates mouse CVB3-induced myocarditis by blunting Th1 immune responses. *PLoS One* (2011) 6(3):e18186. doi:10.1371/journal.pone.0018186
82. Yue Y, Gui J, Xu W, Xiong S. Gene therapy with CCL2 (MCP-1) mutant protects CVB3-induced myocarditis by compromising Th1 polarization. *Mol Immunol* (2011) 48(4):706–13. doi:10.1016/j.molimm.2010.11.018
83. Jaquenod De Giusti C, Ure AE, Rivadeneyra L, Schattner M, Gomez RM. Macrophages and galectin 3 play critical roles in CVB3-induced murine acute myocarditis and chronic fibrosis. *J Mol Cell Cardiol* (2015) 85:58–70. doi:10.1016/j.yjmcc.2015.05.010
84. Woodruff JF. Viral myocarditis. A review. *Am J Pathol* (1980) 101(2):425–84.
85. Su N, Yue Y, Xiong S. Monocytic myeloid-derived suppressor cells from females, but not males, alleviate CVB3-induced myocarditis by increasing regulatory and CD4(+)IL-10(+) T cells. *Sci Rep* (2016) 6:22658. doi:10.1038/srep22658
86. Li K, Xu W, Guo Q, Jiang Z, Wang P, Yue Y, et al. Differential macrophage polarization in male and female BALB/c mice infected with coxsackievirus B3 defines susceptibility to viral myocarditis. *Circ Res* (2009) 105(4):353–64. doi:10.1161/CIRCRESAHA.109.195230
87. Liu L, Yue Y, Xiong S. NK-derived IFN-gamma/IL-4 triggers the sexually disparate polarization of macrophages in CVB3-induced myocarditis. *J Mol Cell Cardiol* (2014) 76:15–25. doi:10.1016/j.yjmcc.2014.07.021
88. Cao Y, Xu W, Xiong S. Adoptive transfer of regulatory T cells protects against Coxsackievirus B3-induced cardiac fibrosis. *PLoS One* (2013) 8(9):e74955. doi:10.1371/journal.pone.0074955
89. Zhang H, Yue Y, Sun T, Wu X, Xiong S. Transmissible endoplasmic reticulum stress from myocardiocytes to macrophages is pivotal for the pathogenesis of CVB3-induced viral myocarditis. *Sci Rep* (2017) 7:42162. doi:10.1038/srep42162
90. Wang Y, Gao B, Xiong S. Involvement of NLRP3 inflammasome in CVB3-induced viral myocarditis. *Am J Physiol Heart Circ Physiol* (2014) 307(10):H1438–47. doi:10.1152/ajpheart.00441.2014
91. Olson CM, Bates TC, Izadi H, Radolf JD, Huber SA, Boyson JE, et al. Local production of IFN-γ by invariant NKT cells modulates acute Lyme carditis. *J Immunol* (2009) 182(6):3728–34. doi:10.4049/jimmunol.0804111
92. Guerau-de-Arellano M, Alroy J, Bullard D, Huber BT. Aggravated Lyme carditis in CD11a−/− and CD11c−/− mice. *Infect Immun* (2005) 73(11):7637–43. doi:10.1128/IAI.73.11.7637-7643.2005
93. Montgomery RR, Booth CJ, Wang X, Blaho VA, Malawista SE, Brown CR. Recruitment of macrophages and polymorphonuclear leukocytes in Lyme carditis. *Infect Immun* (2007) 75(2):613–20. doi:10.1128/IAI.00685-06
94. Lasky CE, Olson RM, Brown CR. Macrophage polarization during murine Lyme borreliosis. *Infect Immun* (2015) 83(7):2627–35. doi:10.1128/IAI.00369-15
95. Sabino GJ, Hwang SJ, McAllister SC, Mena P, Furie MB. Interferon-γ influences the composition of leukocytic infiltrates in murine Lyme carditis. *Am J Pathol* (2011) 179(4):1917–28. doi:10.1016/j.ajpath.2011.06.029
96. Liu N, Montgomery RR, Barthold SW, Bockenstedt LK. Myeloid differentiation antigen 88 deficiency impairs pathogen clearance but does not alter inflammation in *Borrelia burgdorferi*-infected mice. *Infect Immun* (2004) 72(6):3195–203. doi:10.1128/IAI.72.6.3195-3203.2004
97. Hawley KL, Olson CM, Iglesias-Pedraz JM, Navasa N, Cervantes JL, Caimano MJ, et al. CD14 cooperates with complement receptor 3 to mediate MyD88-independent phagocytosis of *Borrelia burgdorferi*. *Proc Natl Acad Sci U S A* (2012) 109(4):1228–32. doi:10.1073/pnas.1112078109
98. Petnicki-Ocwieja T, DeFrancesco AS, Chung E, Darcy CT, Bronson RT, Kobayashi KS, et al. Nod2 suppresses *Borrelia burgdorferi* mediated murine Lyme arthritis and carditis through the induction of tolerance. *PLoS One* (2011) 6(2):e17414. doi:10.1371/journal.pone.0017414
99. Zlotnikov N, Javid A, Ahmed M, Eshghi A, Tang TT, Arya A, et al. Infection with the Lyme disease pathogen suppresses innate immunity in mice with diet-induced obesity. *Cell Microbiol* (2017) 19(5):e12689. doi:10.1111/cmi.12689
100. Dos Reis G, Gaspar M, Barcinski M. Immune recognition in the streptococcal carditis of mice: the role of macrophages in the generation of heart-reactive lymphocytes. *J Immunol* (1982) 128(4):1514–21.
101. Kotb M, Courtney H, Dale J, Beachey E. Cellular and biochemical responses of human T lymphocytes stimulated with streptococcal M proteins. *J Immunol* (1989) 142(3):966–70.
102. Brown AO, Mann B, Gao G, Hankins JS, Humann J, Giardina J, et al. *Streptococcus pneumoniae* translocates into the myocardium and forms unique microlesions that disrupt cardiac function. *PLoS Pathog* (2014) 10(9):e1004383. doi:10.1371/journal.ppat.1004383
103. Gilley RP, González-Juarbe N, Shenoy AT, Reyes LF, Dube PH, Restrepo MI, et al. Infiltrated macrophages die of pneumolysin-mediated necroptosis following pneumococcal myocardial invasion. *Infect Immun* (2016) 84(5):1457–69. doi:10.1128/IAI.00007-16
104. Lucas K, Maes M. Role of the toll like receptor (TLR) radical cycle in chronic inflammation: possible treatments targeting the TLR4 pathway. *Mol Neurobiol* (2013) 48(1):190–204. doi:10.1007/s12035-013-8425-7
105. Sheedy FJ, Grebe A, Rayner KJ, Kalantari P, Ramkhelawon B, Carpenter SB, et al. CD36 coordinates NLRP3 inflammasome activation by facilitating intracellular nucleation of soluble ligands into particulate ligands in sterile inflammation. *Nat Immunol* (2013) 14(8):812–20. doi:10.1038/ni.2639
106. Takahashi M. NLRP3 inflammasome as a novel player in myocardial infarction. *Int Heart J* (2014) 55(2):101–5. doi:10.1536/ihj.13-388
107. Epelman S, Lavine KJ, Beaudin AE, Sojka DK, Carrero JA, Calderon B, et al. Embryonic and adult-derived resident cardiac macrophages are maintained through distinct mechanisms at steady state and during inflammation. *Immunity* (2014) 40(1):91–104. doi:10.1016/j.immuni.2013.11.019
108. Marchetti C, Toldo S, Chojnacki J, Mezzaroma E, Liu K, Salloum FN, et al. Pharmacologic inhibition of the NLRP3 inflammasome preserves cardiac function after ischemic and nonischemic injury in the mouse. *J Cardiovasc Pharmacol* (2015) 66(1):1–8. doi:10.1097/FJC.0000000000000247
109. Brown RA, Shantsila E, Varma C, Lip GY. Current understanding of atherogenesis. *Am J Med* (2017) 130(3):268–82. doi:10.1016/j.amjmed.2016.10.022
110. Mizuno Y, Jacob RF, Mason RP. Inflammation and the development of atherosclerosis. *J Atheroscler Thromb* (2011) 18(5):351–8. doi:10.5551/jat.7591
111. Delporte C, Boudjeltia KZ, Noyon C, Furtmuller PG, Nuyens V, Slomianny MC, et al. Impact of myeloperoxidase-LDL interactions on enzyme activity and subsequent posttranslational oxidative modifications of apoB-100. *J Lipid Res* (2014) 55(4):747–57. doi:10.1194/jlr.M047449
112. Yamaguchi Y, Haginaka J, Morimoto S, Fujioka Y, Kunitomo M. Facilitated nitration and oxidation of LDL in cigarette smokers. *Eur J Clin Invest* (2005) 35(3):186–93. doi:10.1111/j.1365-2362.2005.01472.x
113. Bonacci G, Baker PR, Salvatore SR, Shores D, Khoo NK, Koenitzer JR, et al. Conjugated linoleic acid is a preferential substrate for fatty acid nitration. *J Biol Chem* (2012) 287(53):44071–82. doi:10.1074/jbc.M112.401356
114. Rudolph TK, Rudolph V, Edreira MM, Cole MP, Bonacci G, Schopfer FJ, et al. Nitro-fatty acids reduce atherosclerosis in apolipoprotein E-deficient mice. *Arterioscler Thromb Vasc Biol* (2010) 30(5):938–45. doi:10.1161/ATVBAHA.109.201582
115. Febbraio M, Guy E, Silverstein RL. Stem cell transplantation reveals that absence of macrophage CD36 is protective against atherosclerosis. *Arterioscler Thromb Vasc Biol* (2004) 24(12):2333–8. doi:10.1161/01.ATV.0000148007.06370.68
116. Guy E, Kuchibhotla S, Silverstein R, Febbraio M. Continued inhibition of atherosclerotic lesion development in long term Western diet fed CD36o/apoEo mice. *Atherosclerosis* (2007) 192(1):123–30. doi:10.1016/j.atherosclerosis.2006.07.015
117. Moore KJ, Kunjathoor VV, Koehn SL, Manning JJ, Tseng AA, Silver JM, et al. Loss of receptor-mediated lipid uptake via scavenger receptor A or CD36 pathways does not ameliorate atherosclerosis in hyperlipidemic mice. *J Clin Invest* (2005) 115(8):2192–201. doi:10.1172/JCI24061

118. Rahman K, Vengrenyuk Y, Ramsey SA, Vila NR, Girgis NM, Liu J, et al. Inflammatory Ly6Chi monocytes and their conversion to M2 macrophages drive atherosclerosis regression. *J Clin Invest* (2017) 127(8):2904–15. doi:10.1172/JCI75005
119. Wolfs IM, Stoger JL, Goossens P, Pottgens C, Gijbels MJ, Wijnands E, et al. Reprogramming macrophages to an anti-inflammatory phenotype by helminth antigens reduces murine atherosclerosis. *FASEB J* (2014) 28(1):288–99. doi:10.1096/fj.13-235911
120. Charo IF, Taubman MB. Chemokines in the pathogenesis of vascular disease. *Circ Res* (2004) 95(9):858–66. doi:10.1161/01.RES.0000146672.10582.17
121. Zernecke A, Shagdarsuren E, Weber C. Chemokines in atherosclerosis: an update. *Arterioscler Thromb Vasc Biol* (2008) 28(11):1897–908. doi:10.1161/ATVBAHA.107.161174
122. McLaren JE, Ramji DP. Interferon gamma: a master regulator of atherosclerosis. *Cytokine Growth Factor Rev* (2009) 20(2):125–35. doi:10.1016/j.cytogfr.2008.11.003
123. Newby AC. Metalloproteinase expression in monocytes and macrophages and its relationship to atherosclerotic plaque instability. *Arterioscler Thromb Vasc Biol* (2008) 28(12):2108–14. doi:10.1161/ATVBAHA.108.173898
124. Geng YJ, Hansson GK. Interferon-gamma inhibits scavenger receptor expression and foam cell formation in human monocyte-derived macrophages. *J Clin Invest* (1992) 89(4):1322–30. doi:10.1172/JCI115718
125. Li N, McLaren JE, Michael DR, Clement M, Fielding CA, Ramji DP. ERK is integral to the IFN-gamma-mediated activation of STAT1, the expression of key genes implicated in atherosclerosis, and the uptake of modified lipoproteins by human macrophages. *J Immunol* (2010) 185(5):3041–8. doi:10.4049/jimmunol.1000993
126. Panousis CG, Zuckerman SH. Interferon-gamma induces downregulation of Tangier disease gene (ATP-binding-cassette transporter 1) in macrophage-derived foam cells. *Arterioscler Thromb Vasc Biol* (2000) 20(6):1565–71. doi:10.1161/01.ATV.20.6.1565
127. Brand K, Mackman N, Curtiss LK. Interferon-gamma inhibits macrophage apolipoprotein E production by posttranslational mechanisms. *J Clin Invest* (1993) 91(5):2031–9. doi:10.1172/JCI116425
128. Kleemann R, Zadelaar S, Kooistra T. Cytokines and atherosclerosis: a comprehensive review of studies in mice. *Cardiovasc Res* (2008) 79(3):360–76. doi:10.1093/cvr/cvn120
129. Hsu HY, Twu YC. Tumor necrosis factor-alpha-mediated protein kinases in regulation of scavenger receptor and foam cell formation on macrophage. *J Biol Chem* (2000) 275(52):41035–48. doi:10.1074/jbc.M003464200
130. Khovidhunkit W, Moser AH, Shigenaga JK, Grunfeld C, Feingold KR. Endotoxin down-regulates ABCG5 and ABCG8 in mouse liver and ABCA1 and ABCG1 in J774 murine macrophages: differential role of LXR. *J Lipid Res* (2003) 44(9):1728–36. doi:10.1194/jlr.M300100-JLR200
131. Persson J, Nilsson J, Lindholm MW. Interleukin-1beta and tumour necrosis factor-alpha impede neutral lipid turnover in macrophage-derived foam cells. *BMC Immunol* (2008) 9:70. doi:10.1186/1471-2172-9-70
132. Lei L, Xiong Y, Chen J, Yang JB, Wang Y, Yang XY, et al. TNF-alpha stimulates the ACAT1 expression in differentiating monocytes to promote the CE-laden cell formation. *J Lipid Res* (2009) 50(6):1057–67. doi:10.1194/jlr.M800484-JLR200
133. Gerbod-Giannone MC, Li Y, Holleboom A, Han S, Hsu LC, Tabas I, et al. TNFalpha induces ABCA1 through NF-kappaB in macrophages and in phagocytes ingesting apoptotic cells. *Proc Natl Acad Sci U S A* (2006) 103(9):3112–7. doi:10.1073/pnas.0510345103
134. Edgel KA, Leboeuf RC, Oram JF. Tumor necrosis factor-alpha and lymphotoxin-alpha increase macrophage ABCA1 by gene expression and protein stabilization via different receptors. *Atherosclerosis* (2010) 209(2):387–92. doi:10.1016/j.atherosclerosis.2009.10.019
135. Han J, Hajjar DP, Tauras JM, Feng J, Gotto AM Jr, Nicholson AC. Transforming growth factor-beta1 (TGF-beta1) and TGF-beta2 decrease expression of CD36, the type B scavenger receptor, through mitogen-activated protein kinase phosphorylation of peroxisome proliferator-activated receptor-gamma. *J Biol Chem* (2000) 275(2):1241–6. doi:10.1074/jbc.275.2.1241
136. Draude G, Lorenz RL. TGF-beta1 downregulates CD36 and scavenger receptor A but upregulates LOX-1 in human macrophages. *Am J Physiol Heart Circ Physiol* (2000) 278(4):H1042–8. doi:10.1152/ajpheart.2000.278.4.H1042
137. Singh NN, Ramji DP. The role of transforming growth factor-beta in atherosclerosis. *Cytokine Growth Factor Rev* (2006) 17(6):487–99. doi:10.1016/j.cytogfr.2006.09.002
138. Panousis CG, Evans G, Zuckerman SH. TGF-beta increases cholesterol efflux and ABC-1 expression in macrophage-derived foam cells: opposing the effects of IFN-gamma. *J Lipid Res* (2001) 42(5):856–63.
139. Argmann CA, Van Den Diepstraten CH, Sawyez CG, Edwards JY, Hegele RA, Wolfe BM, et al. Transforming growth factor-beta1 inhibits macrophage cholesteryl ester accumulation induced by native and oxidized VLDL remnants. *Arterioscler Thromb Vasc Biol* (2001) 21(12):2011–8. doi:10.1161/hq1201.099426
140. Irvine SA, Foka P, Rogers SA, Mead JR, Ramji DP. A critical role for the Sp1-binding sites in the transforming growth factor-beta-mediated inhibition of lipoprotein lipase gene expression in macrophages. *Nucleic Acids Res* (2005) 33(5):1423–34. doi:10.1093/nar/gki280
141. Singh NN, Ramji DP. Transforming growth factor-beta-induced expression of the apolipoprotein E gene requires c-Jun N-terminal kinase, p38 kinase, and casein kinase 2. *Arterioscler Thromb Vasc Biol* (2006) 26(6):1323–9. doi:10.1161/01.ATV.0000220383.19192.55
142. Lin J, Li M, Wang Z, He S, Ma X, Li D. The role of CD4+CD25+ regulatory T cells in macrophage-derived foam-cell formation. *J Lipid Res* (2010) 51(5):1208–17. doi:10.1194/jlr.D000497
143. Rubic T, Lorenz RL. Downregulated CD36 and oxLDL uptake and stimulated ABCA1/G1 and cholesterol efflux as anti-atherosclerotic mechanisms of interleukin-10. *Cardiovasc Res* (2006) 69(2):527–35. doi:10.1016/j.cardiores.2005.10.018
144. Mei CL, Chen ZJ, Liao YH, Wang YF, Peng HY, Chen Y. Interleukin-10 inhibits the down-regulation of ATP binding cassette transporter A1 by tumour necrosis factor-alpha in THP-1 macrophage-derived foam cells. *Cell Biol Int* (2007) 31(12):1456–61. doi:10.1016/j.cellbi.2007.06.009
145. Han X, Kitamoto S, Lian Q, Boisvert WA. Interleukin-10 facilitates both cholesterol uptake and efflux in macrophages. *J Biol Chem* (2009) 284(47):32950–8. doi:10.1074/jbc.M109.040899
146. Han X, Kitamoto S, Wang H, Boisvert WA. Interleukin-10 overexpression in macrophages suppresses atherosclerosis in hyperlipidemic mice. *FASEB J* (2010) 24(8):2869–80. doi:10.1096/fj.09-148155
147. Boyle JJ, Harrington HA, Piper E, Elderfield K, Stark J, Landis RC, et al. Coronary intraplaque hemorrhage evokes a novel atheroprotective macrophage phenotype. *Am J Pathol* (2009) 174(3):1097–108. doi:10.2353/ajpath.2009.080431
148. Boyle JJ. Heme and haemoglobin direct macrophage Mhem phenotype and counter foam cell formation in areas of intraplaque haemorrhage. *Curr Opin Lipidol* (2012) 23(5):453–61. doi:10.1097/MOL.0b013e328356b145
149. Kadl A, Meher AK, Sharma PR, Lee MY, Doran AC, Johnstone SR, et al. Identification of a novel macrophage phenotype that develops in response to atherogenic phospholipids via Nrf2. *Circ Res* (2010) 107(6):737–46. doi:10.1161/CIRCRESAHA.109.215715
150. Erbel C, Wolf A, Lasitschka F, Linden F, Domschke G, Akhavanpoor M, et al. Prevalence of M4 macrophages within human coronary atherosclerotic plaques is associated with features of plaque instability. *Int J Cardiol* (2015) 186:219–25. doi:10.1016/j.ijcard.2015.03.151
151. Gleissner CA, Shaked I, Erbel C, Bockler D, Katus HA, Ley K. CXCL4 downregulates the atheroprotective hemoglobin receptor CD163 in human macrophages. *Circ Res* (2010) 106(1):203–11. doi:10.1161/CIRCRESAHA.109.199505
152. Barin JG, Baldeviano GC, Talor MV, Wu L, Ong S, Quader F, et al. Macrophages participate in IL-17-mediated inflammation. *Eur J Immunol* (2012) 42(3):726–36. doi:10.1002/eji.201141737
153. Erbel C, Akhavanpoor M, Okuyucu D, Wangler S, Dietz A, Zhao L, et al. IL-17A influences essential functions of the monocyte/macrophage lineage and is involved in advanced murine and human atherosclerosis. *J Immunol* (2014) 193(9):4344–55. doi:10.4049/jimmunol.1400181
154. Zizzo G, Cohen PL. IL-17 stimulates differentiation of human anti-inflammatory macrophages and phagocytosis of apoptotic neutrophils in response to IL-10 and glucocorticoids. *J Immunol* (2013) 190(10):5237–46. doi:10.4049/jimmunol.1203017
155. Zizzo G, Hilliard BA, Monestier M, Cohen PL. Efficient clearance of early apoptotic cells by human macrophages requires M2c polarization

and MerTK induction. *J Immunol* (2012) 189(7):3508–20. doi:10.4049/jimmunol.1200662
156. Wu L, Ong S, Talor MV, Barin JG, Baldeviano GC, Kass DA, et al. Cardiac fibroblasts mediate IL-17A-driven inflammatory dilated cardiomyopathy. *J Exp Med* (2014) 211(7):1449–64. doi:10.1084/jem.20132126
157. Butcher MJ, Gjurich BN, Phillips T, Galkina EV. The IL-17A/IL-17RA axis plays a proatherogenic role via the regulation of aortic myeloid cell recruitment. *Circ Res* (2012) 110(5):675–87. doi:10.1161/CIRCRESAHA.111.261784
158. Erbel C, Chen L, Bea F, Wangler S, Celik S, Lasitschka F, et al. Inhibition of IL-17A attenuates atherosclerotic lesion development in apoE-deficient mice. *J Immunol* (2009) 183(12):8167–75. doi:10.4049/jimmunol.0901126
159. Smith E, Prasad KM, Butcher M, Dobrian A, Kolls JK, Ley K, et al. Blockade of interleukin-17A results in reduced atherosclerosis in apolipoprotein E-deficient mice. *Circulation* (2010) 121(15):1746–55. doi:10.1161/CIRCULATIONAHA.109.924886
160. Corriden R, Insel PA. Basal release of ATP: an autocrine-paracrine mechanism for cell regulation. *Sci Signal* (2010) 3(104):re1. doi:10.1126/scisignal.3104re1
161. Yegutkin GG. Nucleotide- and nucleoside-converting ectoenzymes: important modulators of purinergic signalling cascade. *Biochim Biophys Acta* (2008) 1783(5):673–94. doi:10.1016/j.bbamcr.2008.01.024
162. Allard B, Longhi MS, Robson SC, Stagg J. The ectonucleotidases CD39 and CD73: novel checkpoint inhibitor targets. *Immunol Rev* (2017) 276(1):121–44. doi:10.1111/imr.12528
163. Dong K, Gao ZW, Zhang HZ. The role of adenosinergic pathway in human autoimmune diseases. *Immunol Res* (2016) 64(5–6):1133–41. doi:10.1007/s12026-016-8870-2
164. Bonner F, Borg N, Burghoff S, Schrader J. Resident cardiac immune cells and expression of the ectonucleotidase enzymes CD39 and CD73 after ischemic injury. *PLoS One* (2012) 7(4):e34730. doi:10.1371/journal.pone.0034730
165. Bonner F, Borg N, Jacoby C, Temme S, Ding Z, Flogel U, et al. Ecto-5'-nucleotidase on immune cells protects from adverse cardiac remodeling. *Circ Res* (2013) 113(3):301–12. doi:10.1161/CIRCRESAHA.113.300180
166. Hasko G, Pacher P, Deitch EA, Vizi ES. Shaping of monocyte and macrophage function by adenosine receptors. *Pharmacol Ther* (2007) 113(2):264–75. doi:10.1016/j.pharmthera.2006.08.003
167. Cain BS, Meldrum DR, Dinarello CA, Meng X, Banerjee A, Harken AH. Adenosine reduces cardiac TNF-alpha production and human myocardial injury following ischemia-reperfusion. *J Surg Res* (1998) 76(2):117–23. doi:10.1006/jsre.1998.5304
168. Koszalka P, Ozuyaman B, Huo Y, Zernecke A, Flogel U, Braun N, et al. Targeted disruption of cd73/ecto-5'-nucleotidase alters thromboregulation and augments vascular inflammatory response. *Circ Res* (2004) 95(8):814–21. doi:10.1161/01.RES.0000144796.82787.6f
169. Stachon P, Peikert A, Michel NA, Hergeth S, Marchini T, Wolf D, et al. P2Y6 deficiency limits vascular inflammation and atherosclerosis in mice. *Arterioscler Thromb Vasc Biol* (2014) 34(10):2237–45. doi:10.1161/ATVBAHA.114.303585
170. Stachon P, Heidenreich A, Merz J, Hilgendorf I, Wolf D, Willecke F, et al. P2X7 deficiency blocks lesional inflammasome activity and ameliorates atherosclerosis in mice. *Circulation* (2017) 135(25):2524–33. doi:10.1161/CIRCULATIONAHA.117.027400
171. Ernens I, Leonard F, Vausort M, Rolland-Turner M, Devaux Y, Wagner DR. Adenosine up-regulates vascular endothelial growth factor in human macrophages. *Biochem Biophys Res Commun* (2010) 392(3):351–6. doi:10.1016/j.bbrc.2010.01.023
172. Hill LM, Gavala ML, Lenertz LY, Bertics PJ. Extracellular ATP may contribute to tissue repair by rapidly stimulating purinergic receptor X7-dependent vascular endothelial growth factor release from primary human monocytes. *J Immunol* (2010) 185(5):3028–34. doi:10.4049/jimmunol.1001298
173. Neubauer S. The failing heart – an engine out of fuel. *N Engl J Med* (2007) 356(11):1140–51. doi:10.1056/NEJMra063052
174. Tannahill GM, Curtis AM, Adamik J, Palsson-McDermott EM, McGettrick AF, Goel G, et al. Succinate is an inflammatory signal that induces IL-1beta through HIF-1alpha. *Nature* (2013) 496(7444):238–42. doi:10.1038/nature11986
175. Vats D, Mukundan L, Odegaard JI, Zhang L, Smith KL, Morel CR, et al. Oxidative metabolism and PGC-1beta attenuate macrophage-mediated inflammation. *Cell Metab* (2006) 4(1):13–24. doi:10.1016/j.cmet.2006.05.011
176. Mills EL, Kelly B, Logan A, Costa AS, Varma M, Bryant CE, et al. Succinate dehydrogenase supports metabolic repurposing of mitochondria to drive inflammatory macrophages. *Cell* (2016) 167(2):457–70.e13. doi:10.1016/j.cell.2016.08.064
177. Shirai T, Nazarewicz RR, Wallis BB, Yanes RE, Watanabe R, Hilhorst M, et al. The glycolytic enzyme PKM2 bridges metabolic and inflammatory dysfunction in coronary artery disease. *J Exp Med* (2016) 213(3):337–54. doi:10.1084/jem.20150900
178. Arts RJW, Carvalho A, La Rocca C, Palma C, Rodrigues F, Silvestre R, et al. Immunometabolic pathways in BCG-induced trained immunity. *Cell Rep* (2016) 17(10):2562–71. doi:10.1016/j.celrep.2016.11.011
179. Kahn SE, Cooper ME, Del Prato S. Pathophysiology and treatment of type 2 diabetes: perspectives on the past, present, and future. *Lancet* (2014) 383(9922):1068–83. doi:10.1016/S0140-6736(13)62154-6
180. Boudina S, Abel ED. Diabetic cardiomyopathy revisited. *Circulation* (2007) 115(25):3213–23. doi:10.1161/CIRCULATIONAHA.106.679597
181. Frieler RA, Mortensen RM. Immune cell and other noncardiomyocyte regulation of cardiac hypertrophy and remodeling. *Circulation* (2015) 131(11):1019–30. doi:10.1161/CIRCULATIONAHA.114.008788
182. Mann DL. Innate immunity and the failing heart: the cytokine hypothesis revisited. *Circ Res* (2015) 116(7):1254–68. doi:10.1161/CIRCRESAHA.116.302317
183. Prabhu SD, Frangogiannis NG. The biological basis for cardiac repair after myocardial infarction: from inflammation to fibrosis. *Circ Res* (2016) 119(1):91–112. doi:10.1161/CIRCRESAHA.116.303577
184. Mann DL. The emerging role of innate immunity in the heart and vascular system: for whom the cell tolls. *Circ Res* (2011) 108(9):1133–45. doi:10.1161/CIRCRESAHA.110.226936
185. Sciarretta S, Paneni F, Palano F, Chin D, Tocci G, Rubattu S, et al. Role of the renin-angiotensin-aldosterone system and inflammatory processes in the development and progression of diastolic dysfunction. *Clin Sci* (2009) 116(6):467–77. doi:10.1042/CS20080390
186. Yan SF, Ramasamy R, Naka Y, Schmidt AM. Glycation, inflammation, and RAGE: a scaffold for the macrovascular complications of diabetes and beyond. *Circ Res* (2003) 93(12):1159–69. doi:10.1161/01.RES.0000103862.26506.3D
187. Volz HC, Seidel C, Laohachewin D, Kaya Z, Muller OJ, Pleger ST, et al. HMGB1: the missing link between diabetes mellitus and heart failure. *Basic Res Cardiol* (2010) 105(6):805–20. doi:10.1007/s00395-010-0114-3
188. Wang WK, Wang B, Lu QH, Zhang W, Qin WD, Liu XJ, et al. Inhibition of high-mobility group box 1 improves myocardial fibrosis and dysfunction in diabetic cardiomyopathy. *Int J Cardiol* (2014) 172(1):202–12. doi:10.1016/j.ijcard.2014.01.011
189. Kim F, Pham M, Luttrell I, Bannerman DD, Tupper J, Thaler J, et al. Toll-like receptor-4 mediates vascular inflammation and insulin resistance in diet-induced obesity. *Circ Res* (2007) 100(11):1589–96. doi:10.1161/CIRCRESAHA.106.142851
190. Dong B, Qi D, Yang L, Huang Y, Xiao X, Tai N, et al. TLR4 regulates cardiac lipid accumulation and diabetic heart disease in the nonobese diabetic mouse model of type 1 diabetes. *Am J Physiol Heart Circ Physiol* (2012) 303(6):H732–42. doi:10.1152/ajpheart.00948.2011
191. Alvarez-Guardia D, Palomer X, Coll T, Serrano L, Rodriguez-Calvo R, Davidson MM, et al. PPARbeta/delta activation blocks lipid-induced inflammatory pathways in mouse heart and human cardiac cells. *Biochim Biophys Acta* (2011) 1811(2):59–67. doi:10.1016/j.bbalip.2010.11.002
192. Itani SI, Ruderman NB, Schmieder F, Boden G. Lipid-induced insulin resistance in human muscle is associated with changes in diacylglycerol, protein kinase C, and IkappaB-alpha. *Diabetes* (2002) 51(7):2005–11. doi:10.2337/diabetes.51.7.2005
193. Tang J, Baxter S, Menon A, Alaarg A, Sanchez-Gaytan BL, Fay F, et al. Immune cell screening of a nanoparticle library improves atherosclerosis therapy. *Proc Natl Acad Sci U S A* (2016) 113(44):E6731–40. doi:10.1073/pnas.1609629113
194. Saraiva RM, Minhas KM, Zheng M, Pitz E, Treuer A, Gonzalez D, et al. Reduced neuronal nitric oxide synthase expression contributes to cardiac oxidative stress and nitroso-redox imbalance in ob/ob mice. *Nitric oxide* (2007) 16(3):331–8. doi:10.1016/j.niox.2006.12.001

195. Li SY, Yang X, Ceylan-Isik AF, Du M, Sreejayan N, Ren J. Cardiac contractile dysfunction in Lep/Lep obesity is accompanied by NADPH oxidase activation, oxidative modification of sarco(endo)plasmic reticulum Ca2+-ATPase and myosin heavy chain isozyme switch. *Diabetologia* (2006) 49(6):1434–46. doi:10.1007/s00125-006-0229-0
196. Kwon SH, Pimentel DR, Remondino A, Sawyer DB, Colucci WS. H(2)O(2) regulates cardiac myocyte phenotype via concentration-dependent activation of distinct kinase pathways. *J Mol Cell Cardiol* (2003) 35(6):615–21. doi:10.1016/S0022-2828(03)00084-1
197. Seo JW, Yang EJ, Yoo KH, Choi IH. Macrophage differentiation from monocytes is influenced by the lipid oxidation degree of low density lipoprotein. *Mediators Inflamm* (2015) 2015:235797. doi:10.1155/2015/235797

Conflict of Interest Statement: The authors declare that the research was conducted in the absence of any commercial or financial relationships that could be construed as a potential conflict of interest.

Copyright © 2018 Sanmarco, Eberhardt, Ponce, Cano, Bonacci and Aoki. This is an open-access article distributed under the terms of the Creative Commons Attribution License (CC BY). The use, distribution or reproduction in other forums is permitted, provided the original author(s) or licensor are credited and that the original publication in this journal is cited, in accordance with accepted academic practice. No use, distribution or reproduction is permitted which does not comply with these terms.

frontiers in Immunology

REVIEW
published: 24 April 2018
doi: 10.3389/fimmu.2018.00823

Understanding the Cellular Origin of the Mononuclear Phagocyte System Sheds Light on the Myeloid Postulate of Immune Paralysis in Sepsis

Lionel Franz Poulin, Corentin Lasseaux and Mathias Chamaillard*

Univ. Lille, CNRS, INSERM, CHU Lille, Institut Pasteur de Lille, U1019 – UMR 8204 – CIIL – Center for Infection and Immunity of Lille, Lille, France

OPEN ACCESS

Edited by:
Etienne Meunier, UMR5089 Institut de Pharmacologie et de Biologie Structurale (IPBS), France

Reviewed by:
Marc DALOD, Centre national de la recherche scientifique (CNRS), France
Paul Fisch, Universitätsklinikum Freiburg, Germany

****Correspondence:***
Lionel Franz Poulin
lionel.poulin@cnrs.fr

Specialty section:
This article was submitted to Microbial Immunology, a section of the journal Frontiers in Immunology

Received: *22 September 2017*
Accepted: *04 April 2018*
Published: *24 April 2018*

Citation:
Poulin LF, Lasseaux C and Chamaillard M (2018) Understanding the Cellular Origin of the Mononuclear Phagocyte System Sheds Light on the Myeloid Postulate of Immune Paralysis in Sepsis. Front. Immunol. 9:823. doi: 10.3389/fimmu.2018.00823

Sepsis, in essence, is a serious clinical condition that can subsequently result in death as a consequence of a systemic inflammatory response syndrome including febrile leukopenia, hypotension, and multiple organ failures. To date, such life-threatening organ dysfunction remains one of the leading causes of death in intensive care units, with an increasing incidence rate worldwide and particularly within the rapidly growing senior population. While most of the clinical trials are aimed at dampening the overwhelming immune response to infection that spreads through the bloodstream, based on several human immunological investigations, it is now widely accepted that susceptibility to nosocomial infections and long-term sepsis mortality involves an immunosuppressive phase that is characterized by a decrease in some subsets of dendritic cells (DCs). Only recently substantial advances have been made in terms of the origin of the mononuclear phagocyte system that is now likely to allow for a better understanding of how the paralysis of DCs leads to sepsis-related death. Indeed, the unifying view of each subset of DCs has already improved our understanding of the pivotal pathways that contribute to the shift in commitment of their progenitors that originate from the bone marrow. It is quite plausible that this anomaly in sepsis may occur at the single level of DC-committed precursors, and elucidating the immunological basis for such a derangement during the ontogeny of each subset of DCs is now of particular importance for restoring an adequate cell fate decision to their vulnerable progenitors. Last but not least, it provides a direct perspective on the development of sophisticated myelopoiesis-based strategies that are currently being considered for the treatment of immunosenescence within different tissue microenvironments, such as the kidney and the spleen.

Keywords: dendritic cell, monocytes, ontogeny, sepsis, endotoxemia

Abbreviations: DC(s), dendritic cell(s); cDC, conventional DC; pre-cDC, precursor of cDCs; pDC, plasmacytoid dendritic cell; IFN, interferon; LPS, lipopolysaccharide; MDP, macrophage and DC progenitor; CDP, cDC precursor; cMoP, common monocyte progenitor; MHC-II, major histocompatibility complex class II; BM, bone marrow; Mo-APC, monocyte-derived antigen presenting cells; Mo-DC, monocyte-derived dendritic cell.

INTRODUCTION

Where Do We Stand in Regard to the Ontogeny of Dendritic Cells?

The mononuclear phagocyte system has been initially formulated by the late 1960. It consists of a network of cells, comprising monocytes, macrophages, and dendritic cells (DCs) that are disseminated throughout the organism. These cells are characterized by their morphology, their phenotypic characteristics (including phagocytic activity), and their roles in orchestrating the immune system. The majority of their committed progenitors are quiescent at homeostasis, although their very high proliferative potential provides them with the capacity to continuously maintain their numbers. Significant progresses in system biology have been made only recently in regard to understanding of the ontogeny and the function of mononucleated cells (referred to as myelopoiesis). This led to the discovery of committed precursors for adult-derived monocytes, conventional, plasmacytoid, or monocyte-derived dendritic cells (Mo-DCs), which are primarily described in the present perspective article. For more details on the embryonically derived phagocytes, we direct the reader to the following outstanding review (1).

Macrophage and DC precursor cells (referred to as MDP) does not constitute a homogeneous population but rather consists in a mixture of progenitors committed either to the DC lineage or the monocyte/macrophage lineage when they are transferred into the bone marrow (BM) of hosts that have previously been irradiated (2, 3). While less is known about the ontogeny of monocytes, macrophages, and DCs in humans than in mice, recent studies have allowed a link to be made with what has been observed in animal models. Notably, a homolog of murine MDP has been identified based on the *in vitro* differentiation of human $CD34^+$ hematopoietic progenitors into type 1 conventional DC (cDC1) (4). There has since been a concerted effort to identify precursors restricted to either cDCs or those derived from the monocytic lineage. MDP express M-CSF-R (or CD115) and the Flt3 receptor (CD135), which are receptors for cytokines that play important roles in the development of monocytes or DCs, respectively. It is likely that the commitment shift of MDP depends on the balance between signals linked to the activation of these receptors (5). This hypothesis is bolstered by the fact that the expression of M-CSF-R decreases in the precursors of cDCs and plasmacytoid DCs (pDCs), although it is not detectable in mature cells. Conversely, Flt3 is not found in the precursors restricted to the monocytic lineage (6, 7). Signaling by the aforementioned growth factors could induce changes at the level of the expression of certain transcription factors. For example, the hematopoietic transcription factors PU.1 and MAFB (for MAF BZIP Transcription Factor B) are crucial for the development of DCs or monocytes, respectively, and they could be implicated in engagement in one of these lineages (8).

Apart from the MDP, the precursor CDP stands for common DC progenitor (**Figure 1**). Like the MDP, it expresses M-CSF-R and Flt3 (9–11). The CDP on the one hand generates pDCs, and on the other hand generates pre-cDCs, which are the direct circulating precursors of the cDCs in tissues. In parallel, other teams have elegantly shown that, as is the case with mice, the generation of cDC1 and cDC2 by common DC progenitor (hCDP) occurs by production of a circulating progenitor, namely the hPre-cDC, which is incapable of generating pDCs (12). Like their murine homologs, hPre-cDCs are heterogeneous and they comprise various fractions already committed to become cDC1 or cDC2 (13–15). Pre-cDCs leave the BM via blood circulation and then penetrate into lymphoid and non-lymphoid tissues in order to differentiate into cDCs (9–11). The factors that influence the differentiation of pre-cDCs into cDC1 or DC2 are still unknown. However, it appears that this decision is taken at the CDP stage, which can already exhibit a transcriptional signature similar to cDC1 or cDC2. Moreover, the pre-cDC population appears to be heterogeneous, comprising a mixture of pre-cDC1 and pre-cDC2 in mice (16) and in humans (15).

More recently, a progenitor restricted to monocytes and derived directly from MDP was identified and designated as cMoP, for common monocyte progenitor (**Figure 1**). It differs phenotypically from MDP by the loss of Flt3 expression. Consequently, cMoPs differentiate into monocytes and their descendants, but they do not generate cDCs (7). The development of cMoPs into monocytes also takes place as monoblast and then as pro-monocyte stages. They are characterized by the expression of stem cell antigen 1 (Sca-1) and they undergo very fast turn-over in the BM (20, 21). The monocytes generated in this manner then migrate from the BM to the tissues where they differentiate depending on the microenvironment (22). Furthermore, a recent study has shown that the generation of human monocytes by hMDP occurs by production of restricted precursors referred to as cMoPs (23), as in mice (7).

These novel concepts are not yet set in stone, however, as the single cell genomic era is already leading to refinements in ontogeny of each subsets of DCs and macrophages. For instance, Helft and colleagues recently demonstrated that human cDC1 are derived more efficiently from the multipotent lymphoid progenitor than from the common myeloid progenitor (CMP) (24). In parallel, it is proposed that the MDP does not constitute a homogeneous population but rather consists in a mixture of progenitors committed either to the DC lineage or the monocyte/macrophage lineage, with no or only very few individual cells able to yield both cell lineages in their progeny (25, 26).

The Myeloid Enigma of Sepsis-Related Mortality

Monocytopoiesis is a dynamic process that occurs in the BM as well as in other organs as an adaption to several physiological stresses that varies over time, while emergency myelopoiesis refers to the rapid generation of myeloid effector cells in response to purified lipopolysaccharide (LPS) (27). A hallmark of septicemia is a profound decrease of circulating DCs, which is also an indicator of a poor prognosis for septic patients (28–30). Two main types of murine models of sepsis or acute inflammation are generally used. On the one hand, the model of peritoneal or intravenous injection of purified endotoxins constitutes a simple model of acute inflammation. On the other hand, the other widely used murine sepsis model is based on cecal ligature and puncture (CLP). This chirurgical model induces intestinal bacterial translocation into the peritoneal cavity, generating a

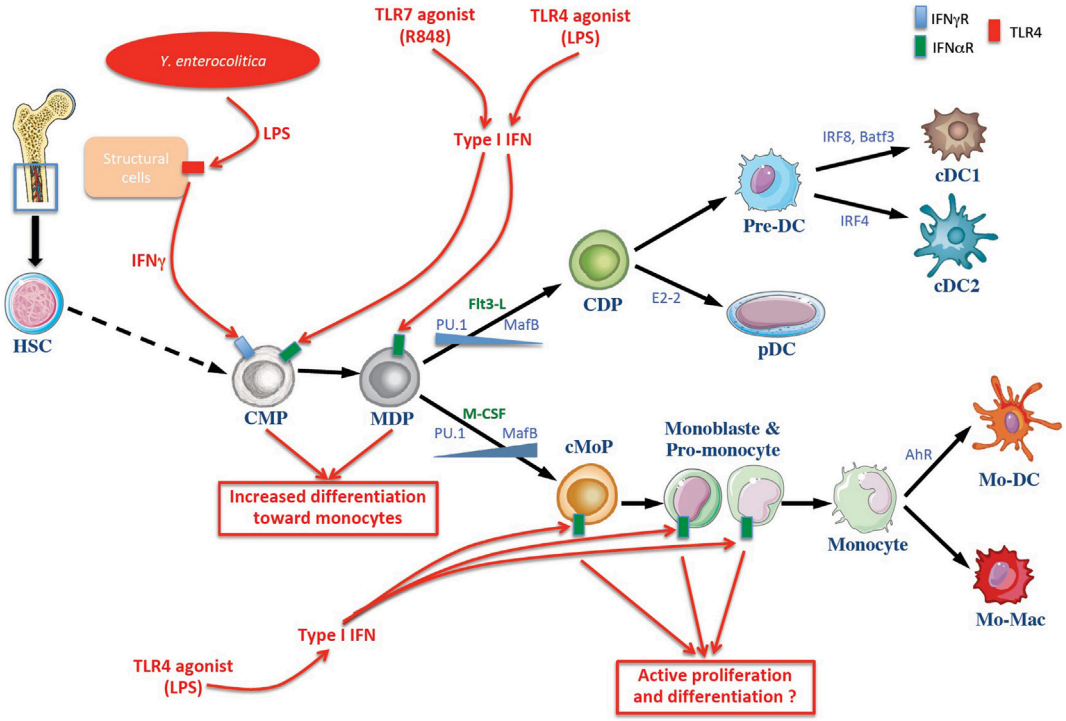


FIGURE 1 | Schematic overview of dendritic cell (DC) and monocytes generation at homeostasis and in systemic infection or endotoxemia murine models. The common myeloid progenitor (CMP) derived from hematopoietic stem cells (HSCs) in the bone marrow and can give rise to the monocyte and DC progenitor (MDP) which in turn differentiates into the DC or monocytic lineages. The differentiation toward DC and monocytes is influenced by cytokines and growth factors (noted in green), notably Flt3-L and M-CSF. Transcription factors involved in cell's fate choice are noted in blue. Infectious stimuli (in red) can affect this process. Lipopolysaccharides (LPS) of the Gram negative bacilli *Yersinia enterocolitica* are sensed by radio-resistant cells that produce IFNγ, inducing a selective differentiation of myeloid progenitors toward the monocytic lineage (monocytopoiesis) at the expense of conventional DC (cDC) (17). Moreover, R848 and LPS induce the production of type I IFN involved in the differentiation of myeloid progenitors toward the monocytic lineage (18, 19). cDC, conventional dendritic cell; CDP, common dendritic cell progenitor; Pre-DC, precursor of cDCs; pDC, plasmacytoide DC; cMoP, common monocyte progenitor; Mo-DC, monocyte-derived dendritic cells, Mo-Mac, monocyte-derived macrophages; IFNγ, interferon γ; TLR toll-like receptor.

systemic infection and massive inflammation. Meanwhile, the extent to which murine models adequately reflect the complexity of human sepsis or acute inflammation is a matter of debate (31, 32). Although differences in TLR distribution among the various mononuclear phagocyte subsets exist between humans and mice (33), the latter are widely used to understand part of these complex disorders.

In order for this emergency myelopoiesis to be induced, TLR4 needs to be expressed by the radiation-resistant cells of the host. These cells then produce the growth factor G-CSF, which is sufficient to induce this phenomenon (34). G-CSF can also be produced following activation of inflammasomes, which depends on the cytokines IL-1beta and IL-1alpha, thereby inducing emergency myelopoiesis (35, 36). A recent study has also provided evidence for the production of IL-3 by B lymphocytes in a murine model of septicemia. This IL-3 allows for a significant increase in the production of monocytes and neutrophils, which are involved in systemic inflammatory respiratory syndrome (SIRS) and the "cytokine storm." Furthermore, an elevated level of IL-3 in serum is predictive of a poor prognosis in septic patients (37). The hematopoietic progenitors can hence be indirectly activated in case of severe infection, so as to reorient the production of cells toward the myeloid lineage. However, the mechanisms causing this decrease in DCs during sepsis remain unclear, possibly encompassing both enhanced cell death of at least some subsets of DCs (and their defective reconstitution from their progenitor cells, e.g., originated from cMop and/or pre-cDC). Using the recently accepted nomenclature (38), we herein discuss the potential mechanisms causing this decrease in some DCs during sepsis that is linked to long-term sepsis-related mortality, especially in elderly and diabetic populations. In addition to studies of DCs in sepsis and endotoxemia models, we also review the contribution of macrophages, as these phagocytes have sometimes been incorrectly classified as Mo-DCs with the use of non-discriminating markers (38), such as CD64.

Monocytes

Monocytes are circulating hematopoietic cells generated in the BM, with a very short half-life that does not exceed a few days. In mice, they are generally divided into two subpopulations that are distinguished based on the expression of Ly6C surface molecules (39). Ly6C^{hi} monocytes, or inflammatory monocytes, are rapidly recruited at sites of infection and inflammation in a CCR2 chemokine-dependent manner. Once inside tissues, diverse

signals from the microenvironment can induce an increase in phagocytosis, the production of cytokines, antimicrobial activity, and antigen presentation by the cells, thereby inducing a phenotype that is sometimes very similar to that of macrophages or DCs (22, 40). Ly6C^{low} monocytes, also called patrolling monocytes, are less common than inflammatory monocytes, and they express the CX3C chemokine receptor 1 (CX3CR1) also known as the G-protein coupled receptor 13 (GPR13) or fractalkine receptor. Indeed it appears that their main function is to ensure endothelial integrity, by patrolling in the lumen of the blood vessels along the endothelium (41). These cells are the product of the differentiation of Ly6C^{hi} blood monocytes at homeostasis (42). Ly6C^{low} monocytes could hence be considered as macrophages of the vascular system (22, 40). Two monocyte populations are also present in humans, and they correlate with those found in mice (43, 44). However, they are not distinguished based on the same surface markers as in mice. Rather, they are distinguished by the expression of the LPS CD14 coreceptor and of the CD16 receptor for crystalizable fragments of antibody. Human CD14^{+}CD16^{-} monocytes appear to be the homologs of the murine Ly6C^{hi} population, while the CD14^{+}CD16^{+} population appears to be analogous to the murine Ly6C^{low} population (22, 40, 41). During polymicrobial sepsis, inflammatory monocytes prevent renal damage in a CX3CR1-dependent adhesion mechanism (45) and a decrease in circulating patrolling monocytes is associated with unfavorable outcome (46). While reactivity to the subsequent endotoxin challenge is enhanced by muramyldipedtide, it remains to be determined whether the anaphylactic reactions are influenced by the muramyldipeptide-induced conversion of Ly6C^{hi} toward Ly6C^{low} monocytes (47) or by other mechanisms involved in leukocyte binding and adhesion.

Macrophages

Adult-derived macrophages have been assumed to be the progeny of monocytes in tissues (48). However, although monocytes can indeed generate macrophages under certain conditions, circulating monocytes do not appear to be the main source of these cells. With the aim of simplifying nomenclatures, Martin Guilliams and his collaborators recently proposed that the use of the term "macrophage" should be restricted to mononucleated phagocytes of embryonic origin (49). Indeed, recent studies have shown that the majority of macrophages residing in the brain, the liver, the lungs, and even the spleen are derived from embryonic precursors in the vitellin vesicle and in the fetal liver. These macrophages disseminate to the various tissues of the body once the blood circulation becomes established, and they are maintained there by proliferating locally throughout the individual's lifetime (42, 50–57). These embryonic macrophages can be progressively displaced by blood-derived monocytes. For instance, the intestinal macrophages that are of embryonic origin are replaced by the differentiation of blood monocytes that are recruited into tissues several weeks after birth (58). Moreover, monocytes constitute a major source of tissue macrophages already at steady state, including the skin (59) and the oral mucosa (60), and this phenomenon is amplified by inflammatory and/or aging processes in a range of organs such as the intestine (61), the heart (62, 63), the peritoneal cavity (64), and the liver (65, 66). Hotchkiss et al. reported that the number of splenic macrophages is not reduced in septic and trauma patients (67). These observations still need to be investigated with up-to-date markers to decipher the exact changes in the mononuclear phagocytes at the subset level. Indeed, the identification of splenic macrophages with CD14 is not sufficient.

Monocyte-Derived Antigen-Presenting cells

Upon homeostasis in certain tissues such as the kidney, or in case of either infection or inflammation, numerous studies have shown that some DCs and macrophages are two sides of the same coin, as they both are derived from monocytes. These cells will hence be referred to here as monocyte-derived antigen-presenting cells (Mo-APCs). The cells derived from monocytes can express high levels of major histocompatibility complex class II (MHC-II) and CD11c, and they can migrate and efficiently present Ag to T lymphocytes (59). Certain studies have also shown their efficacy at cross-presentation of Ag, although these cells appear to use different intracellular components than cDC1 to achieve this (68–71). As suggested by their cross-presenting activity, like cDC1, APCs derived from monocytes have been implicated in cytotoxic Th1 responses (72, 73). However, like cDC2, Mo-APCs have also been reported to induce Th2 and Th17 types of responses (74–76). Depending on the context, Mo-APCs could develop functions similar to those of the various populations of cDCs. However, the lack of markers to discriminate these cells from cDCs, macrophages, or active monocytes greatly complicates the study of Mo-APCs. A study has shown the presence of MHC-II^{+}CD11c^{+} cells derived from monocytes in skeletal muscles under conditions of homeostasis. The intramuscular administration of alum adjuvant induced a very pronounced increase in the representation of these cells and the simultaneous administration of LPS greatly increased their capacity to migrate to lymph nodes and the spleen. These cells are capable of presenting Ag to naive T lymphocyte by normal as well as cross-presentation. They are characterized by the expression of inducible nitric oxide synthase (iNOS) and of the Fc receptor CD64 (FcγRI), which are not expressed by cDCs and pDCs (69). The CD64 marker can also be used to distinguish CDP-derived cells from monocyte-derived cells at the level of the intestine and the skin under homeostatic or inflammatory conditions in mice (59, 61), but not at the level of the kidney (77). The immunoglobulin FcεRI receptor has also recently been reported to be expressed by Mo-APCs in mice and in humans (70, 74), and on human cDC2 (15, 78, 79), it appears that Fc receptors are mainly restricted to phagocytes of monocytic origin (80), thereby they may facilitate their identification in conjunction with other discriminative traits (80). Improvements in the characterization of these cells within distinct tissue microenvironments will undoubtedly increase our knowledge of their biology and presumably provide an explanation for the poor clinical impact of past investigations regarding each DC subsets in sepsis. Despite these limitations, Kassianos et al. demonstrated that human Mo-APCs are the major subsets responsive to *Escherichia coli* in terms of inflammatory cytokine secretion, antigen presentation to CD8^{+} T cells, and phagocytosis (33).

Dendritic Cells

Dendritic cells are the main antigen-presenting cells (APCs) of the organism. They are characterized by the expression of

MHC-II, integrin CD11c, and the transcription factor Zbtb46 (sometimes referred to as zDC) (81–83). However, these markers are also expressed by certain macrophages or other cells that are derived from monocytes. Generally, a distinction is made between cDCs, plasmacytoid (pDCs), which are present in the basal state, and DCs derived from monocytes (Mo-DCs), which are recruited extensively in case of inflammation (6). cDCs are found in the vast majority of lymphoid and non-lymphoid tissues. The term "conventional" refers to DCs that are non-plasmacytoid and that are not derived from monocytes but from a precursor restricted to these cells. cDCs induce either immunity or tolerance toward the Ag that they present to lymphocytes (6). There is a general consensus that there are two populations of cDCs, namely cDC1 and cDC2, which are endowed with distinct functional specialization and thus play complementary roles in the shaping of immune responses (6, 49, 83, 84). Numerous studies have shown a dramatic decrease in DCs during septicemia. Integrin CD11c is often used as a marker of DCs, although it is also expressed to a varying degree by other cell populations such as certain macrophages, neutrophils, and lymphocytes (**Table 1**). A dramatic decrease in $CD11c^+$ cells in the periphery has been observed over the first days of a murine model of polymicrobial sepsis (85–90), and in the BM (91) (**Table 2**). Wen and colleagues found that there was a significant reduction in the percentage of $CD11c^+CD11b^+MHCII^{hi}$ cells in lung and spleen from 3 to 14 days post-CLP procedure in comparison to sham mice (86). They also noted a decrease in the percentage of lung $CD11c^+CD11b^+$ and $CD11c^+B220^+$ cells at days 2 and 8 in post-CLP mice infected by *S. mansoni* eggs, which was associated with a diminished ability of lung $CD11c^+$ cells to produce IL12p70 after TLR agonist stimulation (88).

In order to evaluate the impact of septicemia on different populations of DCs, Flohé and his collaborators used a mouse CLP model, and they distinguished $CD11c^+$ cells on the basis of expression of CD8 (expressed by cDC1) and CD4 (expressed by cDC2), from double-negative cells that might be cDC precursors, for example (108). In light of this, the observed loss of DCs at 36 h postoperative to the procedure was due to the $CD8^+$ and $CD4^+$ populations, while the total number of double-negative cells itself was increased in this model (94). Another CLP study has also provided evidence for a depletion of DCs from the local mesenteric and systemic inguinal lymph nodes, with a preferential loss of cDC1 expressing CD8, which was associated with increased apoptosis (92). This splenic cDC1 loss was maintained up to 5 days post-CLP procedure, and the cells repopulated the spleen at day-7 post-CLP procedure in an NF-kB signaling-dependent pathway (90).

It hence appears that, in mice, polymicrobial septicemia induces a specific depletion of certain DC populations of the lymphoid organs. Some populations may be depleted more so than others, as has been observed in the spleen with an increase in the $CD4^-$ $CD8^-$ population, for which the exact link with cDC1 and cDC2 is not known (94, 108). In keeping with a less-mature phenotype of this double-negative population, when cell proliferation was measured, during a CLP procedure, by BrdU incorporation after 4 days, these cells had a significantly higher BrdU content compared to sham control mice (91). The double-negative splenic cells were differently affected according to the model selected. Thus, they were not affected after CLP, although they were significantly increased after LPS or Pam3CSK4 injection (95).

TABLE 1 | Different markers used to distinguishe mouse and human phagocytes.

Subset	Phenotype		Reference
	Mouse (spleen)	**Human (blood or ascites)**	
cDC1	$MHC\text{-}II^{hi}$ $CD11c^{hi}$ $Clec9^+$ $XCR1^+$ $CD8^+$ $CD4^-$ $CD24^+$ $CD64^-$	$HLA\text{-}DR^+$ $CD11c^+$ $Clec9^+$ $XCR1^+$ $CD141^+$ $CD14^-$ $CD16^-$	(4, 7, 100–103)
cDC2	$MHC\text{-}II^{hi}$ $CD11c^{hi}$ $CD11b^+$ $SIRP\alpha^+$ $CD8^-$ $CD4^+$ $CD64^-$	$HLA\text{-}DR^+$ $CD11c^+$ $CD11b^+$ $CD1a^+$ $CD1c^+$ $CD14^-$ $CD16^-$	(4, 72, 102, 103)
pDC	$CD11c^{int}$ $SiglecH^+$ $B220^+$	$HLA\text{-}DR^+$ $CD123^+$ $CD303^+$ $CD11c^-$ Axl^- $CD2^-$	(4, 11, 102, 104, 105)
Mo-DC	$MHC\text{-}II^+$ $CD11c^+$ $CCR2^+$ $CD64^+$	$HLA\text{-}DR^+$ $CD11c^+$ $CD1a^+$ $CD1c^-$ $CD141^-$	(53, 63, 102, 103, 106, 107)
Mo-Mac	$CD64^+$ $F4/80^+$ $MERTK^+$	$HLA\text{-}DR^\pm$ $CD16^+$	(53, 63, 103, 106, 107)

Type 1 Conventional DC

Type 1 conventional DCs are characterized by the expression of TLR3 that is required for sensing of viral RNA, and by a greater capacity for secretion of the cytokine IL-12p70 following their activation. This cytokine allows for differentiation of type 1 T helper cells (Th1) implicated in cytotoxic anti-viral and anti-tumor immunity (100, 109, 110), and promotes $CD4^+$ T helper cells for $CD8^+$ responses (101). This subpopulation of cDCs has also been reported to be efficient in terms of a particular mechanism of antigen presentation that is called "cross-presentation", which allows these cells that are constitutively resistant to viral infection to acquire exogenous antigens from the infectious agent (111). This cross-presentation process consists of the processing of exogenous antigens into peptides and their loading onto MHC-I molecules so as to be presented to $CD8^+$ T cells. This process is called cross-priming if it results in their activation (112, 113). In humans, a very similar population has been reported to be present in the blood and in the spleen, expressing CLEC9A, as do their murine homologs (4, 114–117) (**Table 1**). Overall, the data in humans suggest that cDC1 excels at cross-presentation of cell-associated antigens (115, 118–122) or of antigens that are delivered to late endosomes/lysosomes (123, 124). However, the data in mice show that other DC subsets are also capable of cross-presentation, provided that they have been properly stimulated (125, 126). Meanwhile, this function could depend on a number of variables such as the type of antigen, its intracellular route of delivery, and the accompanying adjuvant signal sensed by the DCs. cDC1 cells are more effective in regard to this function in specific pathophysiological contexts including viral infections or tumor development/treatment (127–129). During LPS-induced endotoxemia in mice, a reduced cross-priming activity of splenic cDC1 (130) correlates with a prominent loss of splenic

TABLE 2 | Comparison of cell numbers for mononuclear phagocytes populations in murine models of polymicrobial sepsis, systemic inflammation, or endotoxemia.

Reference	Model	Organ	pDC	Total CD11c$^+$ cells	Monocytes and derivatives	cDC1-like	cDC2-like	DN
(85)	CLP	Spleen, peritoneum	?	↘	?	?	?	?
(92)	CLP	Lymph nodes	?	↘	?	?	?	?
(84)	CLP	Spleen	?	↘	?	?	?	?
(93)	CLP	Lung	?	↘	?	?	?	?
(88)	CLP	Lung	↘	?	?	?	↘	?
(86)	CLP	Spleen, lung	?	↘	?	?	?	?
(94)	CLP	Spleen	?	↘	?	↘	↘	✖
(91)	CLP	Spleen, bone marrow	?	↘	?	↘	↘	✖
(89)	CLP	Spleen	?	↘	?	↘	↘	↗
(95)	CLP	Spleen	?	↘	?	↘	↘	✖
	LPS injection		?	↘	?	✖	↘	↗
	P3CSK4 injection		?	↘	?	↗	↘	↗
(96)	*Escherichia coli* infection	Spleen	?	↘	?	↘	↘	↘
	LPS injection		?	↘	?	↘	↘	↘
(97)	*Yersinia enterocolitica* infection	Spleen	?	?	↗	?	?	?
(98)	LPS injection	Spleen	?	?	?	↘	✖	?
(99)	LPS injection	Spleen	?	?	↗	↘	↘	?

Down or up arrows mean that the cell number is decreased or increased compared to controls, respectively. The cross means that the cell number is not significantly changed compared to controls. Cell numbers described here were measured within 24 h after injection for endotoxemia models or within a week after infection or surgery for CLP and systemic infection models. cDC1-like cells correspond to CD8$^+$ or CD11b$^-$ DCs. cDC2-like cells correspond to CD11b$^+$ or CD4$^+$ DC. CLP, cecal ligation and puncture; pDC, plasmacytoid dendritic cells; cDC, conventionnal DC; DN, double negative DC for CD4 and CD8 markers; LPS, lipopolysaccharides.

cDC1, defined as CD8$^+$ DCs, which is glucocorticoid dependent (98). Indeed, endogenous glucocorticoids blunt LPS-induced inflammation and they promote tolerance by suppressing cDC1 IL-12 production. In the absence of glucocorticoid signaling in CD11c-expressing cells, LPS treatment induces higher serum levels of IL-12, type I IFN, TNF-α, and IFN-γ (98). In terms of epigenomic reprogramming, the inflammatory function of TNF is potentiated by type I IFN by prevention of the silencing of genes encoding inflammatory molecules in human macrophages (131). A similar decrease in mouse splenic cDC1 has also been observed after CLP procedures (89, 95). However, injection of different PAMPs induced various effects on cDC numbers. Indeed, LPS does significantly affect splenic cDC1 numbers within 2 days after LPS injection (96), which is followed by a cDC1 number recovery (95, 96) (**Table 2**). On the other hand, Pam3CSK4 does induce an increase in cDC1 cells after 4 days (95) (**Table 2**). Like their mouse counterpart (114, 132), human blood cDC1 cells were found to not express or very low level of TLR4 and they failed to ingest *E. coli* (33). It remains to be investigated whether these differences are still maintained in human lymphoid and non-lymphoid tissues during sepsis and endotoxemia.

cDC2

By contrast, cDC2 are often characterized by the expression of integrin CD11b and SIRPα (also referred to as CD172a) (80), and in the spleen as CD4$^+$CD8$^-$ cells (**Table 1**). They are found in lymphoid and non-lymphoid tissues, and they predominate over the cDC1 population in nearly all tissues. The development and maintenance of cDC2 appear to be dependent, for example, on the IRF4 transcription factor (102, 103, 133) and the activation of Notch-2 receptors (134). This population of cDCs appears to be more efficient than the cDC1 in terms of the interaction with CD4$^+$ T lymphocyte and the polarization of helper T lymphocytes, particularly for Th2 and Th17, which are implicated in immune responses toward extracellular pathogens and the regulation of immunity (74, 133, 135–137). However, the heterogeneity of CD11b$^+$ cells has greatly complicated the study of this population. Indeed, distinguishing cDC2 from macrophages and cells derived from monocytes is difficult as they can express numerous markers that they have in common. To date, it has hence been difficult to assign them non-overlapping immunological properties as well as to establish their dependence on specific transcription factors. New markers have recently been described to assist with the discrimination between cDC2 and macrophages and the cells derived from monocytes in various tissues, such as the lungs, muscles, and the intestines. A decrease in splenic cDC2 has been observed in CLP models (91, 94, 95), associated with a decrease in proliferation of the residual cells (91) (**Table 2**). Proper definition of cDC2 cells in various species and tissues, and in various acute inflammatory models and human samples to define their decline in numbers and alteration of their function, still needs to be investigated with the improved definition of the markers (**Table 1**). Indeed it has been proposed a set of markers to define properly cDC2, and cDC1, across species and tissues (38), and the new refinements by single cell approaches would need to be taken into account to further study cDC2 cell modulations during sepsis and endotoxemia (15, 79, 138).

Plasmacytoid DCs

Already in the first papers describing their discovery more than 15 years ago, human and mouse pDCs have been shown to lack any antigen presenting functions at steady state but to acquire it upon proper stimulation. Relative to human pDCs that do not express CD11c, mouse pDCs may express intermediate, not low, levels of this marker. While mouse and human pDCs have been found to express Siglec-H or Blood Dendritic Cell Antigen 2 (BDCA-2) markers, respectively, they are not sufficient to characterize them, since they are also expressed on subsets of macrophages in mouse

(16, 139) and of pre-cDCs in human (15, 79). pDCs are found in blood, as well as peripheral lymphoid and non-lymphoid tissues. The main function of pDCs is the rapid and pronounced release of type 1 IFN in case of viral infection, due to activation of TLR7 and TLR9 by viral nucleic acids (140). Despite their role in secreting type I IFNs during endotoxemia, pDCs may also be critically involved in regulating endotoxemia through their function in cross-priming and cross-presentation of antigen to T cells (141–143). While the inability to present antigens of steady state human pDC is widely accepted since their discoveries, measuring this function necessitates both to properly purify pDC ensuring lack of contamination by other DCs (15, 79) and also to segregate pDC according to their different activation states that may be linked to distinct functional specialization (138, 144). Indeed, a proper preparation of pDC from human blood can be reached by studying Lin^- (by using these markers: CD14, CD16, CD19, CD20 and CD56), $CD123^+HLA\text{-}DR^+AXL^-CD11c^-$ cells (**Table 1**) (15, 79, 138, 144). As few studies have investigated pDC during endotoxemia and sepsis (**Table 2**) (88), there is a need to revisit the role of pDCs during endotoxemia and sepsis. In the future, these refinements to ensure proper purification of pDCs should allow for a better delineation of the roles of these various populations in immunological processes, such as sepsis (61, 69, 74, 102, 132).

Toward the Identification of Novel Myelopoiesis-Based Therapeutic Targets in Sepsis

The different types of mononuclear phagocytes might be affected during sepsis by a reduction in their number, by cell death or precursor fate mechanisms, or by their resolutive functions. Numerous studies have shown that immune cell death contributes to immunosuppression and damage to organs during the development of septicemia (145). Apoptosis appears to at least partially explain the loss of DCs observed in a murine model of septicemia (146). For instance, sera from sepsis patients has been shown to induce death of circulating $CD11c^+$ $CD123^-$ DCs, $CD14^+$ monocytes and of *in vitro* generated monocyte-derived DCs (147). However, the markers used do not allow the subset specificity to be determined. Moreover, the potentially lowered survival of pDC needs to be evaluated with more specific markers that preclude pre-DC contamination (15, 79). This programmed cell death is in part due to the engagement of some TLRs (89, 96, 148). For instance, cDC1 apoptosis in the spleen within 48 h following live *E. coli* injection is TLR4- and TRIF-dependent (96). Furthermore, phagocytosis of apoptotic cells by DCs renders them tolerogenic. Immunosuppression induced by an endotoxic shock is restrained by the expression of an anti-apoptotic protein by DCs, or by an increase in their number and their activation state by treatment with Flt3L (106, 107, 149). In conclusion, the increase in apoptotic cells with septicemia could contribute to immunosuppression by, on the one hand, the loss of effector cells, and, on the other hand, the induction of tolerance (150).

In addition to death-mediated modulation of the mononuclear phagocyte system, these cells can also be affected by their functions. For instance, during sepsis, monocytes are reprogrammed to enhance protective functions such as anti-microbial functions, which are dependent on hypoxia inducible factor-1α (151). In contrast to this beneficial modulation, the mononuclear phagocyte system can also be modulated during the course of sepsis to promote immunosuppression. For instance, the mononuclear phagocyte system might lose the ability to drive a suitable adaptive immune response. DCs of septic patients, for example, exhibit a decrease in the expression of HLA-DR, thereby reducing their capacity to interact with T lymphocytes (152). Similarly, DCs of septic mice also exhibit a decrease in the expression of MHC-II (91). Moreover, numerous studies in humans as well as in mice have provided evidence for a pronounced decrease in the production of pro-inflammatory cytokines such as IL-12 or TNF by septic DCs stimulated by several PAMPs, while DC dysfunction during sepsis is partly mimicked by the TLR2 agonist Pam3CSK4, rather than the TLR4 agonist LPS (95). Conversely, their capacity to produce the anti-inflammatory cytokines IL-10 or TGF-β is significantly increased (86, 94, 152, 153). Like DCs, monocytes isolated from the blood of septic patients exhibit decreased expression of HLA-DR molecules and lower production of the pro-inflammatory cytokine IL-12 following stimulation after an increase in the production of the anti-inflammatory cytokine IL-10. A high concentration of IL-10 is particularly associated with a poor prognosis for septic patients (93). In the same way, human blood cDC2 produced immunoregulatory molecules, such as IDO, upregulated PD-L1 (a ligand of the inhibitory co-receptor PD1 on T cells), produced high levels of IL-10, and were immunosuppressive in response to *E. coli* (33). Similarly, PD-1 or PD-L1 was expressed at higher levels in septic shock patients (154), and their functional blockade by antibodies restored monocyte functions (155). In terms of helper T cell (Th) polarization, in mice it appears that the interaction between septic DCs and $CD4^+$ T lymphocytes induces preferential polarization of the latter toward a Th2 type or T regulatory profile (86, 91, 153, 156). In addition, GM-CSF-derived BM DCs from CLP- and Pam3CSK4-treated mice were less effective *in vivo* at Th1 priming compared to GM-CSF-derived DCs from LPS-treated mice (95). It is possible that the loss of the capacity to induce Th1 responses is due, at least in part, to a specific loss of cDC1 which appear to be crucial for the development of such responses (92, 94, 107, 112, 113). Although progress has been made in this regard, the exact molecular mechanism of such functional difference remains unclear. Moreover, it has been reported that the failure of DCs generated by post-septic mice to produce IL-12 with the CLP model was observed at least 6 weeks after this process. This failure to produce IL-12 appears to be due to epigenetic changes induced at the level of promoters for genes coding for this cytokine (86). In summary, these long lasting events might occur in myeloid progenitors as DCs are short lived. Future molecular investigations should consider their epigenetic regulation.

In contrast to modulation of the mononuclear phagocyte system at a functional level, sepsis may affect the developmental fate of myeloid progenitor cells. Monocytes can also acquire phenotypic and functional characteristics of DCs, although the factors influencing this differentiation are still unknown. In keeping with the high level of plasticity of monocytes, the differentiation of these cells depends on local mediators such as cytokines, PAMPs,

or DAMPs (76, 157). Some of these cytokines are induced by these danger signals, such as type I IFN. Indeed, type I IFN gives rise to Mo-APCs by acting through the IFNAR receptor on direct monocyte progenitors (**Figure 1**) (18). Similar to DAMPs, microbiota-dependent metabolites affect the balance between Mo-DCs and macrophages. For instance, aryl hydrocarbon receptor (AHR) ligands, derived either from dietary food intake or from tryptophan catabolism at the mucosal barrier, shift the monocyte cell fate toward monocyte-derived DCs in a PRDM1- (also known as BLIMP1) and IRF4-dependent manner (99, 158). It appears that activation of IRF4 allows monocytes to differentiate into Mo-DC while it remains controversial that only monocytes re-expressing Flt3 can generate Mo-APCs (71, 99, 159). It might be of interest to understand the molecular mechanism of how reprogramming of each monocytes impacts their subsequent ability to differentiate into either DCs or macrophages within different microenvironment. In summary, the generation of monocytes at the expense of cDCs could limit the availability of innate immune effector cells that can counter the infection, and this process might be involved in the immunosuppression in septic animals and patients.

Recent studies have shown that hematopoietic progenitors themselves express PRR, such as TLR (160, 161). They can hence theoretically directly detect PAMP and react as a consequence. *In vitro* culture experiments of murine and human HSC stimulated by agonists of TLR have shown their preferential differentiation into phagocytes at the expense of cells of the lymphoid lineage (161–164). Furthermore, experiments with parabiotics have elegantly demonstrated that a low number of HSC continuously enter the blood circulation before returning to the BM (165). This phenomenon could allow HSC to locally generate effector cells, directly after encountering a circulating microorganism and in a way that is tailored to the molecular signature of the invading pathogens (166).

Type I IFNs can have an effect on hematopoiesis *in vivo*, particularly by induction of the proliferation of quiescent HSC following injection of the TLR3 agonist polyinosinic: poly cytidylic acid (poly I:C) into mice (167). However, excessive signaling by type 1 IFNs, induced for example by a deficiency in the negative regulator IRF-2, leads to attenuation of HSC proliferation over time, as evidenced by the low capacity of these hematopoietic cells to repopulate following transplantation (168, 169). Additionally, chronic administration of poly I:C induces a selective depletion of WT hematopoietic stem cells (HSCs) in chimeric mice with WT: *Ifnar1*$^{-/-}$ BM cells. Excessive proliferation could, as a matter of fact, induce a state of attenuation of the function of stem cells by differentiation, senescence, or also apoptosis, thereby decreasing the risk of malignant transformation and of perturbation of the tolerogenic tissue architecture (167, 170). This attenuation of stem cells could, over time, lead to leukopenias and hematopoietic anomalies. There is still scant documentation regarding the influence of the infectious context on the potential for differentiation of myeloid precursors. In addition to their roles in regard to HSC, type 1 IFNs are involved in the differentiation of common myeloid precursors into macrophages, following the direct activation of TLR7 of these cells by R848 (19). Also, a study has shown that the precursor cells of common DC progenitors express several TLR in mice, including TLR4. *In vitro* activation of these TLR induces a reduction in the expression of the chemokine receptor CXCR4, which is involved in the retention of CDPs in the BM. *In vitro* activation of the TLR of CDP also induces an increase in the expression of the chemokine receptor CCR7, which is involved in migration of DCs toward the lymphoid organs. When these active CDP were transferred to mice, they were preferentially found at the level of lymph nodes rich in agonists of TLR, subsequent to local TLR agonist injection, where they underwent differentiation. As the various populations of DCs were not studied in detail in this study, it is hence not possible to draw conclusions regarding the potential selective differentiation of stimulated CDP (160). However, a study has shown that the *in vitro* differentiation by the cytokine GM-CSF of hematopoietic cells derived from CLP septic mice induced the generation of DCs with an immunosuppressive phenotype, aggravating the susceptibility to secondary infections with *Pseudomonas aeruginosa* when they were injected into post-CLP septic mice (91, 171). Conversely, the injection of DCs derived *in vitro* from the BM of healthy mice considerably increased the resistance of septic mice to secondary infections (171). Similarly, when injected intratracheally at day-5 after CLP surgery, cultures of DCs isolated from mouse BM with GM-CSF and IL-4 protected recipient mice from *Aspergilus fumigatus*-induced death (153). The exact contribution of each DC subset in cultures of mouse BM with GM-CSF remains to be investigated, as *in vitro* generated CD11c^{+}MHC II^{+} cells are a heterogeneous population of cells, with some resembling macrophages more than DCs (172).

Similarly, IL-4 may favor monocyte development toward monocyte-derived DCs to the detriment of monocyte-derived macrophages (99, 172). Aside from a role for IL-4 in the ontogenic shift between DCs and macrophages, IL-4 plays an important role at the functional level as it is required for optimal cross-priming by GM-CSF-induced Mo-DCs (71). A side-by-side comparison of these *in vitro* generated DC subsets in the protection of septic mice needs to be undertaken. Moreover, the contribution of *in vitro* generated cDC1 and cDC2 needs to be investigated by using cultures of mouse BM with Flt3L (173). Finally, supplementation of mouse BM cultures with GM-CSF and IL-4 should be studied so as to determine the contribution of each DCsubset in the resolution of sepsis. As done recently in a cancer model, and because *in vitro* generated DCs might lack environmental cues, the benefit of directly *ex vivo* extracted DC in sepsis models might be of interest (174). Despite this comparison between *in vitro* and *ex vivo* generated DC subsets, their ability to reach the organs of interest, such as lung-draining lymph nodes in the case of intratracheally injected cells, remains to be verified in each sepsis model (153). Meanwhile, limitations of diphtheria toxin-mediated models of cell type depletion have been described such as for DC targeting in CD11c-hDTR mice where many other cell types are affected (175). This implies performing complementation studies with each DC subset obtained *in vitro* or *ex vivo*, for proper interpretation of the phenotype of diphtheria toxin-treated mice. For instance, adoptive transfer of GM-CSF-derived DCs into DC depleted mice prevents CLP-induced mortality (176).

It hence appears that DCs generated during septicemia have different effects compared to those produced under homeostatic conditions, and that they are involved in the immunosuppression observed in septic patients. In various models of bacterial

infection, the chemokine CCR2 receptor-dependent mobilization of monocytes is crucial for the control of the pathology. Pasquevich and his collaborators have recently shown that the infection of mice with Gram-negative *Y. enterocolitica* bacilli induces a selective differentiation of myeloid progenitors toward the monocytic lineage (monocytopoiesis) at the expense of cDCs. This process depends on the activation of TLR4 and on the production and the detection of IFN-γ by non-hematopoietic cells (17).

CONCLUDING REMARKS

The word "Septicemia" is of Greek origin and it means blood putrefaction. Aside from septicemia, sepsis is a medical term defined as "life-threatening organ dysfunction due to a dysregulated host response to infection" (97, 104, 177). Sepsis is a common and lethal syndrome for which no specific treatments exist (105). In the United States, severe sepsis has been shown to occur in about 2% of patients admitted to hospital. The number of cases in the United States exceeds 750,000 per year and was recently reported to be increasing. Whereas the estimated annual economic burden of this condition is about € 2 billion, the lifetime therapeutic management of sepsis is still far from optimal. Sepsis develops when an initial immune response to an endotoxin derived from an infectious agent becomes amplified and deregulated, leading to persistent inflammation and, in the most severe cases, multiorgan failure and death. Sepsis is often thought to result from systemic invasion of the bloodstream by pathogenic organisms. However, several lines of evidence have converged in support of the notion that it also develops in the absence of any invading pathogens as a consequence of tissue injury and/or unrestrained translocation of commensals. Roquilly et al. showed that resolution of the primary infection changed the local lung environment, which led to the development of tolerogenic DCs and macrophages that contributed to immune suppression (178).

As a conceptual framework, we herein propose that sepsis-mediated mononuclear phagocyte system deregulation might occur at the mononuclear phagocyte precursor level. Therefore, strategies aiming to restore the differentiation of DCs, and maintenance of their physiological functions (178) could be beneficial in the treatment of sepsis. However, it remains to be clearly established whether these tolerogenic cells have been biased in their development at the precursor level in a specific environment, such as the kidney. Such a precursor effect is supported by the fact that the impaired capacity of antigen presentation through MHCII molecules lasts for 21 days or more after recovery from the primary infection, which exceeds the short lifetime of DCs. Moreover, if BM precursors are affected by the primary infection, their degree of resilience needs to be measured in the framework of the new paradigm of infection memory (179).

It is worth noting that similar inflammatory pathways that are required for host protection against infectious agents can also be induced in response to sterile tissue damage (180). For instance, type I interferons and TNF cooperatively induce signals to epigenetically reprogram macrophages, thereby rendering them more sensitive to weak signals, such as responses to LPS, while also making them resistant to suppression by IL-10 (131). In other words, the hematopoietic cells integrate infection marks with deleterious consequences and they are then reinitialized differently in a subsequent challenge. It remains to be investigated whether the epigenetic reprogramming of the mononuclear phagocyte system and their precursors may influence long-term disease outcomes. Indeed, new technologies such as single cell RNA sequencing, epigenomic approaches such as ATAC-seq, mass cytometry, and mass histology may improve our knowledge regarding the developmental and functional changes that affect mononuclear phagocytes during various inflammatory conditions such as sepsis and endotoxemia. The availability of different conditional mice to deplete specific genes or subsets would shed light on their specific requirements during sepsis and endotoxemia situations.

Overall, these data indicate functional changes in various populations of myeloid cells over the course of septicemia. However, these results also suggest that sepsis could induce modulations of myeloid cells in terms of the overall populations; promoting the production, survival, differentiation, or proliferation of certain cells at the expense of others. These results therefore suggest that therapeutic strategies aimed at maintaining the number and the functions of the mononuclear phagocyte system, in particular DCs, are likely to limit the immunosuppressive state that is commonly found during septicemia and infectious situations (178).

AUTHOR CONTRIBUTIONS

LFP, CL, and MC wrote the manuscript, gave feedback and revised the manuscript.

FUNDING

This work was supported by grants from the Fondation pour la Recherche Médicale (DEQ20130326475) for M.C. LFP also received a fellowship from the ATIP-Avenir program. CL received of a PhD fellowship funded by the INSERM, the Nord-Pas de Calais Regional Council, and the "Association pour la Recherche sur le Cancer" cancer charity.

REFERENCES

1. Ginhoux F, Guilliams M. Tissue-resident macrophage ontogeny and homeostasis. *Immunity* (2016) 44:439–49. doi:10.1016/j.immuni.2016.02.024
2. Fogg DK, Sibon C, Miled C, Jung S, Aucouturier P, Littman DR, et al. A clonogenic bone marrow progenitor specific for macrophages and dendritic cells. *Science* (2006) 311:83–7. doi:10.1126/science.1117729
3. Auffray C, Fogg DK, Narni-Mancinelli E, Senechal B, Trouillet C, Saederup N, et al. CX3CR1+ CD115+ CD135+ common macrophage/DC precursors and the role of CX3CR1 in their response to inflammation. *J Exp Med* (2009) 206:595–606. doi:10.1084/jem.20081385
4. Poulin LF, Salio M, Griessinger E, Anjos-Afonso F, Craciun L, Chen JL, et al. Characterization of human DNGR-1+ BDCA3+ leukocytes as putative equivalents of mouse CD8alpha+ dendritic cells. *J Exp Med* (2010) 207:1261–71. doi:10.1084/jem.20092618
5. Schmid MA, Kingston D, Boddupalli S, Manz MG. Instructive cytokine signals in dendritic cell lineage commitment. *Immunol Rev* (2010) 234:32–44. doi:10.1111/j.0105-2896.2009.00877.x
6. Merad M, Sathe P, Helft J, Miller J, Mortha A. The dendritic cell lineage: ontogeny and function of dendritic cells and their subsets in the steady state and the inflamed setting. *Annu Rev Immunol* (2013) 31:563–604. doi:10.1146/annurev-immunol-020711-074950

7. Hettinger J, Richards DM, Hansson J, Barra MM, Joschko AC, Krijgsveld J, et al. Origin of monocytes and macrophages in a committed progenitor. *Nat Immunol* (2013) 14:821–30. doi:10.1038/ni.2638
8. Bakri Y, Sarrazin S, Mayer UP, Tillmanns S, Nerlov C, Boned A, et al. Balance of MafB and PU.1 specifies alternative macrophage or dendritic cell fate. *Blood* (2005) 105:2707–16. doi:10.1182/blood-2004-04-1448
9. Naik SH, Metcalf D, van Nieuwenhuijze A, Wicks I, Wu L, O'Keeffe M, et al. Intrasplenic steady-state dendritic cell precursors that are distinct from monocytes. *Nat Immunol* (2006) 7:663–71. doi:10.1038/ni1340
10. Naik SH, Sathe P, Park HY, Metcalf D, Proietto AI, Dakic A, et al. Development of plasmacytoid and conventional dendritic cell subtypes from single precursor cells derived in vitro and in vivo. *Nat Immunol* (2007) 8:1217–26. doi:10.1038/ni1522
11. Onai N, Obata-Onai A, Schmid MA, Ohteki T, Jarrossay D, Manz MG. Identification of clonogenic common Flt3+M-CSFR+ plasmacytoid and conventional dendritic cell progenitors in mouse bone marrow. *Nat Immunol* (2007) 8:1207–16. doi:10.1038/ni1518
12. Lee J, Breton G, Oliveira TY, Zhou YJ, Aljoufi A, Puhr S, et al. Restricted dendritic cell and monocyte progenitors in human cord blood and bone marrow. *J Exp Med* (2015) 212:385–99. doi:10.1084/jem.20141442
13. Breton G, Lee J, Zhou YJ, Schreiber JJ, Keler T, Puhr S, et al. Circulating precursors of human CD1c+ and CD141+ dendritic cells. *J Exp Med* (2015) 212:401–13. doi:10.1084/jem.20141441
14. Breton G, Zheng S, Valieris R, Tojal da Silva I, Satija R, Nussenzweig MC. Human dendritic cells (DCs) are derived from distinct circulating precursors that are precommitted to become CD1c+ or CD141+ DCs. *J Exp Med* (2016) 213:2861–70. doi:10.1084/jem.20161135
15. See P, Dutertre CA, Chen J, Günther P, McGovern N, Irac SE, et al. Mapping the human DC lineage through the integration of high-dimensional techniques. *Science* (2017) 356. doi:10.1126/science.aag3009
16. Schlitzer A, Sivakamasundari V, Chen J, Sumatoh HR, Schreuder J, Lum J, et al. Identification of cDC1- and cDC2-committed DC progenitors reveals early lineage priming at the common DC progenitor stage in the bone marrow. *Nat Immunol* (2015) 16:718–28. doi:10.1038/ni.3200
17. Pasquevich KA, Bieber K, Günter M, Grauer M, Pötz O, Schleicher U, et al. Innate immune system favors emergency monopoiesis at the expense of DC-differentiation to control systemic bacterial infection in mice. *Eur J Immunol* (2015) 45:2821–33. doi:10.1002/eji.201545530
18. Lasseaux C, Fourmaux MP, Chamaillard M, Poulin LF. Type I interferons drive inflammasome-independent emergency monocytopoiesis during endotoxemia. *Sci Rep* (2017) 7:16935. doi:10.1038/s41598-017-16869-2
19. Buechler MB, Akilesh HM, Hamerman JA. Cutting edge: direct sensing of TLR7 ligands and type I IFN by the common myeloid progenitor promotes mTOR/PI3K-dependent emergency myelopoiesis. *J Immunol* (2016) 197:2577–82. doi:10.4049/jimmunol.1600813
20. Serbina NV, Hohl TM, Cherny M, Pamer EG. Selective expansion of the monocytic lineage directed by bacterial infection. *J Immunol* (2009) 183:1900–10. doi:10.4049/jimmunol.0900612
21. Takahashi K, Naito M, Takeya M. Development and heterogeneity of macrophages and their related cells through their differentiation pathways. *Pathol Int* (1996) 46:473–85. doi:10.1111/j.1440-1827.1996.tb03641.x
22. Ginhoux F, Jung S. Monocytes and macrophages: developmental pathways and tissue homeostasis. *Nat Rev Immunol* (2014) 14:392–404. doi:10.1038/nri3671
23. Kawamura S, Onai N, Miya F, Sato T, Tsunoda T, Kurabayashi K, et al. Identification of a human clonogenic progenitor with strict monocyte differentiation potential: a counterpart of mouse cMoPs. *Immunity* (2017) 46:835–48.e4. doi:10.1016/j.immuni.2017.04.019
24. Helft J, Anjos-Afonso F, van der Veen AG, Chakravarty P, Bonnet D, Reis E Sousa C. Dendritic cell lineage potential in human early hematopoietic progenitors. *Cell Rep* (2017) 20:529–37. doi:10.1016/j.celrep.2017.06.075
25. Onai N, Ohteki T. Bipotent or oligopotent? A macrophage and DC progenitor revisited. *Immunity* (2014) 41:5–7. doi:10.1016/j.immuni.2014.07.004
26. Sathe P, Metcalf D, Vremec D, Naik SH, Langdon WY, Huntington ND, et al. Lymphoid tissue and plasmacytoid dendritic cells and macrophages do not share a common macrophage-dendritic cell-restricted progenitor. *Immunity* (2014) 41:104–15. doi:10.1016/j.immuni.2014.05.020
27. Manz MG, Boettcher S. Emergency granulopoiesis. *Nat Rev Immunol* (2014) 14:302–14. doi:10.1038/nri3660
28. Grimaldi D, Louis S, Pène F, Sirgo G, Rousseau C, Claessens YE, et al. Profound and persistent decrease of circulating dendritic cells is associated with ICU-acquired infection in patients with septic shock. *Intensive Care Med* (2011) 37:1438–46. doi:10.1007/s00134-011-2306-1
29. Guisset O, Dilhuydy MS, Thiébaut R, Lefèvre J, Camou F, Sarrat A, et al. Decrease in circulating dendritic cells predicts fatal outcome in septic shock. *Intensive Care Med* (2007) 33:148–52. doi:10.1007/s00134-006-0436-7
30. Elsayh KI, Zahran AM, Lotfy Mohamad I, Aly SS. Dendritic cells in childhood sepsis. *J Crit Care* (2013) 28(881):e887–813. doi:10.1016/j.jcrc.2013.05.007
31. Takao K, Miyakawa T. Genomic responses in mouse models greatly mimic human inflammatory diseases. *Proc Natl Acad Sci U S A* (2015) 112:1167–72. doi:10.1073/pnas.1401965111
32. Seok J, Warren HS, Cuenca AG, Mindrinos MN, Baker HV, Xu W, et al. Genomic responses in mouse models poorly mimic human inflammatory diseases. *Proc Natl Acad Sci U S A* (2013) 110:3507–12. doi:10.1073/pnas.1222878110
33. Kassianos AJ, Hardy MY, Ju X, Vijayan D, Ding Y, Vulink AJ, et al. Human CD1c (BDCA-1)+ myeloid dendritic cells secrete IL-10 and display an immuno-regulatory phenotype and function in response to *Escherichia coli*. *Eur J Immunol* (2012) 42:1512–22. doi:10.1002/eji.201142098
34. Boettcher S, Ziegler P, Schmid MA, Takizawa H, van Rooijen N, Kopf M, et al. Cutting edge: LPS-induced emergency myelopoiesis depends on TLR4-expressing nonhematopoietic cells. *J Immunol* (2012) 188:5824–8. doi:10.4049/jimmunol.1103253
35. Suzuki A, Takahashi T, Okuno Y, Tsuyuoka R, Fukumoto M, Nakamura K, et al. IL-1 production as a regulator of G-CSF and IL-6 production in CSF-producing cell lines. *Br J Cancer* (1992) 65:515–8. doi:10.1038/bjc.1992.106
36. Dubois CM, Neta R, Keller JR, Jacobsen SE, Oppenheim JJ, Ruscetti F. Hematopoietic growth factors and glucocorticoids synergize to mimic the effects of IL-1 on granulocyte differentiation and IL-1 receptor induction on bone marrow cells in vivo. *Exp Hematol* (1993) 21:303–10.
37. Weber GF, Chousterman BG, He S, Fenn AM, Nairz M, Anzai A, et al. Interleukin-3 amplifies acute inflammation and is a potential therapeutic target in sepsis. *Science* (2015) 347:1260–5. doi:10.1126/science.aaa4268
38. Guilliams M, Dutertre CA, Scott CL, McGovern N, Sichien D, Chakarov S, et al. Unsupervised high-dimensional analysis aligns dendritic cells across tissues and species. *Immunity* (2016) 45:669–84. doi:10.1016/j.immuni.2016.08.015
39. Geissmann F, Jung S, Littman DR. Blood monocytes consist of two principal subsets with distinct migratory properties. *Immunity* (2003) 19:71–82. doi:10.1016/S1074-7613(03)00174-2
40. Shi C, Pamer EG. Monocyte recruitment during infection and inflammation. *Nat Rev Immunol* (2011) 11:762–74. doi:10.1038/nri3070
41. Cros J, Cagnard N, Woollard K, Patey N, Zhang SY, Senechal B, et al. Human CD14dim monocytes patrol and sense nucleic acids and viruses via TLR7 and TLR8 receptors. *Immunity* (2010) 33:375–86. doi:10.1016/j.immuni.2010.08.012
42. Yona S, Kim KW, Wolf Y, Mildner A, Varol D, Breker M, et al. Fate mapping reveals origins and dynamics of monocytes and tissue macrophages under homeostasis. *Immunity* (2013) 38:79–91. doi:10.1016/j.immuni.2012.12.001
43. Ziegler-Heitbrock L, Ancuta P, Crowe S, Dalod M, Grau V, Hart DN, et al. Nomenclature of monocytes and dendritic cells in blood. *Blood* (2010) 116:e74–80. doi:10.1182/blood-2010-02-258558
44. Vu Manh TP, Elhmouzi-Younes J, Urien C, Ruscanu S, Jouneau L, Bourge M, et al. Defining mononuclear phagocyte subset homology across several distant warm-blooded vertebrates through comparative transcriptomics. *Front Immunol* (2015) 6:299. doi:10.3389/fimmu.2015.00299
45. Chousterman BG, Boissonnas A, Poupel L, Baudesson de Chanville C, Adam J, Tabibzadeh N, et al. Ly6Chigh monocytes protect against kidney damage during sepsis via a CX3CR1-dependent adhesion mechanism. *J Am Soc Nephrol* (2016) 27:792–803. doi:10.1681/ASN.2015010009
46. Gainaru G, Papadopoulos A, Tsangaris I, Lada M, Giamarellos-Bourboulis EJ, Pistiki A, et al. Increases in inflammatory and CD14(dim)/CD16(pos)/CD45(pos) patrolling monocytes in sepsis: correlation with final outcome. *Crit Care* (2018) 22:56. doi:10.1186/s13054-018-1977-1
47. Lessard AJ, LeBel M, Egarnes B, Préfontaine P, Thériault P, Droit A, et al. Triggering of NOD2 receptor converts inflammatory Ly6C(high) into Ly6C(low) monocytes with patrolling properties. *Cell Rep* (2017) 20:1830–43. doi:10.1016/j.celrep.2017.08.009

48. Geissmann F, Manz MG, Jung S, Sieweke MH, Merad M, Ley K. Development of monocytes, macrophages, and dendritic cells. *Science* (2010) 327:656–61. doi:10.1126/science.1178331
49. Guilliams M, Ginhoux F, Jakubzick C, Naik SH, Onai N, Schraml BU, et al. Dendritic cells, monocytes and macrophages: a unified nomenclature based on ontogeny. *Nat Rev Immunol* (2014) 14:571–8. doi:10.1038/nri3712
50. Aziz A, Soucie E, Sarrazin S, Sieweke MH. MafB/c-Maf deficiency enables self-renewal of differentiated functional macrophages. *Science* (2009) 326:867–71. doi:10.1126/science.1176056
51. Schulz C, Gomez Perdiguero E, Chorro L, Szabo-Rogers H, Cagnard N, Kierdorf K, et al. A lineage of myeloid cells independent of Myb and hematopoietic stem cells. *Science* (2012) 336:86–90. doi:10.1126/science.1219179
52. Ginhoux F, Greter M, Leboeuf M, Nandi S, See P, Gokhan S, et al. Fate mapping analysis reveals that adult microglia derive from primitive macrophages. *Science* (2010) 330:841–5. doi:10.1126/science.1194637
53. Naito M, Hasegawa G, Takahashi K. Development, differentiation, and maturation of Kupffer cells. *Microsc Res Tech* (1997) 39:350–64. doi:10.1002/(SICI)1097-0029(19971115)39:4<350::AID-JEMT5>3.0.CO;2-L
54. Alliot F, Godin I, Pessac B. Microglia derive from progenitors, originating from the yolk sac, and which proliferate in the brain. *Brain Res Dev Brain Res* (1999) 117:145–52. doi:10.1016/S0165-3806(99)00113-3
55. Guilliams M, De Kleer I, Henri S, Post S, Vanhoutte L, De Prijck S, et al. Alveolar macrophages develop from fetal monocytes that differentiate into long-lived cells in the first week of life via GM-CSF. *J Exp Med* (2013) 210:1977–92. doi:10.1084/jem.20131199
56. Zigmond E, Samia-Grinberg S, Pasmanik-Chor M, Brazowski E, Shibolet O, Halpern Z, et al. Infiltrating monocyte-derived macrophages and resident kupffer cells display different ontogeny and functions in acute liver injury. *J Immunol* (2014) 193:344–53. doi:10.4049/jimmunol.1400574
57. Hoeffel G, Chen J, Lavin Y, Low D, Almeida FF, See P, et al. C-Myb(+) erythro-myeloid progenitor-derived fetal monocytes give rise to adult tissue-resident macrophages. *Immunity* (2015) 42:665–78. doi:10.1016/j.immuni.2015.03.011
58. Bain CC, Bravo-Blas A, Scott CL, Perdiguero EG, Geissmann F, Henri S, et al. Constant replenishment from circulating monocytes maintains the macrophage pool in the intestine of adult mice. *Nat Immunol* (2014) 15:929–37. doi:10.1038/ni.2967
59. Tamoutounour S, Guilliams M, Montanana Sanchis F, Liu H, Terhorst D, Malosse C, et al. Origins and functional specialization of macrophages and of conventional and monocyte-derived dendritic cells in mouse skin. *Immunity* (2013) 39:925–38. doi:10.1016/j.immuni.2013.10.004
60. Capucha T, Mizraji G, Segev H, Blecher-Gonen R, Winter D, Khalaileh A, et al. Distinct murine mucosal langerhans cell subsets develop from pre-dendritic cells and monocytes. *Immunity* (2015) 43:369–81. doi:10.1016/j.immuni.2015.06.017
61. Tamoutounour S, Henri S, Lelouard H, de Bovis B, de Haar C, van der Woude CJ, et al. CD64 distinguishes macrophages from dendritic cells in the gut and reveals the Th1-inducing role of mesenteric lymph node macrophages during colitis. *Eur J Immunol* (2012) 42:3150–66. doi:10.1002/eji.201242847
62. Molawi K, Wolf Y, Kandalla PK, Favret J, Hagemeyer N, Frenzel K, et al. Progressive replacement of embryo-derived cardiac macrophages with age. *J Exp Med* (2014) 211:2151–8. doi:10.1084/jem.20140639
63. Epelman S, Lavine KJ, Beaudin AE, Sojka DK, Carrero JA, Calderon B, et al. Embryonic and adult-derived resident cardiac macrophages are maintained through distinct mechanisms at steady state and during inflammation. *Immunity* (2014) 40:91–104. doi:10.1016/j.immuni.2013.11.019
64. Bain CC, Hawley CA, Garner H, Scott CL, Schridde A, Steers NJ, et al. Long-lived self-renewing bone marrow-derived macrophages displace embryo-derived cells to inhabit adult serous cavities. *Nat Commun* (2016) 7:ncomms11852. doi:10.1038/ncomms11852
65. Blériot C, Dupuis T, Jouvion G, Eberl G, Disson O, Lecuit M. Liver-resident macrophage necroptosis orchestrates type 1 microbicidal inflammation and type-2-mediated tissue repair during bacterial infection. *Immunity* (2015) 42:145–58. doi:10.1016/j.immuni.2014.12.020
66. Scott CL, Zheng F, De Baetselier P, Martens L, Saeys Y, De Prijck S, et al. Bone marrow-derived monocytes give rise to self-renewing and fully differentiated Kupffer cells. *Nat Commun* (2016) 7:10321. doi:10.1038/ncomms10321
67. Hotchkiss RS, Tinsley KW, Swanson PE, Grayson MH, Osborne DF, Wagner TH, et al. Depletion of dendritic cells, but not macrophages, in patients with sepsis. *J Immunol* (2002) 168:2493–500. doi:10.4049/jimmunol.168.5.2493
68. Cheong C, Matos I, Choi JH, Dandamudi DB, Shrestha E, Longhi MP, et al. Microbial stimulation fully differentiates monocytes to DC-SIGN/CD209(+) dendritic cells for immune T cell areas. *Cell* (2010) 143:416–29. doi:10.1016/j.cell.2010.09.039
69. Langlet C, Tamoutounour S, Henri S, Luche H, Ardouin L, Grégoire C, et al. CD64 expression distinguishes monocyte-derived and conventional dendritic cells and reveals their distinct role during intramuscular immunization. *J Immunol* (2012) 188:1751–60. doi:10.4049/jimmunol.1102744
70. Segura E, Albiston AL, Wicks IP, Chai SY, Villadangos JA. Different cross-presentation pathways in steady-state and inflammatory dendritic cells. *Proc Natl Acad Sci U S A* (2009) 106:20377–81. doi:10.1073/pnas.0910295106
71. Briseño CG, Haldar M, Kretzer NM, Wu X, Theisen DJ, Kc W, et al. Distinct transcriptional programs control cross-priming in classical and monocyte-derived dendritic cells. *Cell Rep* (2016) 15:2462–74. doi:10.1016/j.celrep.2016.05.025
72. Leon B, Lopez-Bravo M, Ardavin C. Monocyte-derived dendritic cells formed at the infection site control the induction of protective T helper 1 responses against *Leishmania*. *Immunity* (2007) 26:519–31. doi:10.1016/j.immuni.2007.01.017
73. Ji Q, Castelli L, Goverman JM. MHC class I-restricted myelin epitopes are cross-presented by Tip-DCs that promote determinant spreading to CD8(+) T cells. *Nat Immunol* (2013) 14:254–61. doi:10.1038/ni.2513
74. Plantinga M, Guilliams M, Vanheerswynghels M, Deswarte K, Branco-Madeira F, Toussaint W, et al. Conventional and monocyte-derived CD11b(+) dendritic cells initiate and maintain T helper 2 cell-mediated immunity to house dust mite allergen. *Immunity* (2013) 38:322–35. doi:10.1016/j.immuni.2012.10.016
75. Siddiqui KR, Laffont S, Powrie F. E-cadherin marks a subset of inflammatory dendritic cells that promote T cell-mediated colitis. *Immunity* (2010) 32:557–67. doi:10.1016/j.immuni.2010.03.017
76. Segura E, Amigorena S. Inflammatory dendritic cells in mice and humans. *Trends Immunol* (2013) 34:440–5. doi:10.1016/j.it.2013.06.001
77. Schraml BU, van Blijswijk J, Zelenay S, Whitney PG, Filby A, Acton SE, et al. Genetic tracing via DNGR-1 expression history defines dendritic cells as a hematopoietic lineage. *Cell* (2013) 154:843–58. doi:10.1016/j.cell.2013.07.014
78. Segura E, Touzot M, Bohineust A, Cappuccio A, Chiocchia G, Hosmalin A, et al. Human inflammatory dendritic cells induce Th17 cell differentiation. *Immunity* (2013) 38:336–48. doi:10.1016/j.immuni.2012.10.018
79. Villani AC, Satija R, Reynolds G, Sarkizova S, Shekhar K, Fletcher J, et al. Single-cell RNA-seq reveals new types of human blood dendritic cells, monocytes, and progenitors. *Science* (2017) 356. doi:10.1126/science.aah4573
80. Guilliams M, Bruhns P, Saeys Y, Hammad H, Lambrecht BN. The function of Fcgamma receptors in dendritic cells and macrophages. *Nat Rev Immunol* (2014) 14:94–108. doi:10.1038/nri3666
81. Meredith MM, Liu K, Darrasse-Jeze G, Kamphorst AO, Schreiber HA, Guermonprez P, et al. Expression of the zinc finger transcription factor zDC (Zbtb46, Btbd4) defines the classical dendritic cell lineage. *J Exp Med* (2012) 209:1153–65. doi:10.1084/jem.20112675
82. Satpathy AT, KC W, Albring JC, Edelson BT, Kretzer NM, Bhattacharya D, et al. Zbtb46 expression distinguishes classical dendritic cells and their committed progenitors from other immune lineages. *J Exp Med* (2012) 209:1135–52. doi:10.1084/jem.20120030
83. Satpathy AT, Wu X, Albring JC, Murphy KM. Re(de)fining the dendritic cell lineage. *Nat Immunol* (2012) 13:1145–54. doi:10.1038/ni.2467
84. Sichien D, Lambrecht BN, Guilliams M, Scott CL. Development of conventional dendritic cells: from common bone marrow progenitors to multiple subsets in peripheral tissues. *Mucosal Immunol* (2017) 10:831–44. doi:10.1038/mi.2017.8
85. Ding Y, Chung CS, Newton S, Chen Y, Carlton S, Albina JE, et al. Polymicrobial sepsis induces divergent effects on splenic and peritoneal dendritic cell function in mice. *Shock* (2004) 22:137–44. doi:10.1097/01.shk.0000131194.80038.3f
86. Wen H, Dou Y, Hogaboam CM, Kunkel SL. Epigenetic regulation of dendritic cell-derived interleukin-12 facilitates immunosuppression after a

severe innate immune response. *Blood* (2008) 111:1797–804. doi:10.1182/blood-2007-08-106443
87. Tinsley KW, Grayson MH, Swanson PE, Drewry AM, Chang KC, Karl IE, et al. Sepsis induces apoptosis and profound depletion of splenic interdigitating and follicular dendritic cells. *J Immunol* (2003) 171:909–14. doi:10.4049/jimmunol.171.2.909
88. Wen H, Hogaboam CM, Gauldie J, Kunkel SL. Severe sepsis exacerbates cell-mediated immunity in the lung due to an altered dendritic cell cytokine profile. *Am J Pathol* (2006) 168:1940–50. doi:10.2353/ajpath.2006.051155
89. Pène F, Courtine E, Ouaaz F, Zuber B, Sauneuf B, Sirgo G, et al. Toll-like receptors 2 and 4 contribute to sepsis-induced depletion of spleen dendritic cells. *Infect Immun* (2009) 77:5651–8. doi:10.1128/IAI.00238-09
90. Courtine E, Pène F, Cagnard N, Toubiana J, Fitting C, Brocheton J, et al. Critical role of cRel subunit of NF-kappaB in sepsis survival. *Infect Immun* (2011) 79:1848–54. doi:10.1128/IAI.00021-11
91. Pastille E, Didovic S, Brauckmann D, Rani M, Agrawal H, Schade FU, et al. Modulation of dendritic cell differentiation in the bone marrow mediates sustained immunosuppression after polymicrobial sepsis. *J Immunol* (2011) 186:977–86. doi:10.4049/jimmunol.1001147
92. Efron PA, Martins A, Minnich D, Tinsley K, Ungaro R, Bahjat FR, et al. Characterization of the systemic loss of dendritic cells in murine lymph nodes during polymicrobial sepsis. *J Immunol* (2004) 173:3035–43. doi:10.4049/jimmunol.173.5.3035
93. Hotchkiss RS, Monneret G, Payen D. Immunosuppression in sepsis: a novel understanding of the disorder and a new therapeutic approach. *Lancet Infect Dis* (2013) 13:260–8. doi:10.1016/S1473-3099(13)70001-X
94. Flohé SB, Agrawal H, Schmitz D, Gertz M, Flohé S, Schade FU. Dendritic cells during polymicrobial sepsis rapidly mature but fail to initiate a protective Th1-type immune response. *J Leukoc Biol* (2006) 79:473–81. doi:10.1189/jlb.0705413
95. Bruns S, Pastille E, Wirsdorfer F, Frisch M, Flohe SB. Lipopeptides rather than lipopolysaccharide favor the development of dendritic cell dysfunction similar to polymicrobial sepsis in mice. *Inflamm Res* (2013) 62:627–36. doi:10.1007/s00011-013-0616-1
96. De Trez C, Pajak B, Brait M, Glaichenhaus N, Urbain J, Moser M, et al. TLR4 and toll-IL-1 receptor domain-containing adapter-inducing IFN-beta, but not MyD88, regulate *Escherichia coli*-induced dendritic cell maturation and apoptosis in vivo. *J Immunol* (2005) 175:839–46. doi:10.4049/jimmunol.175.2.839
97. Seymour CW, Liu VX, Iwashyna TJ, Brunkhorst FM, Rea TD, Scherag A, et al. Assessment of clinical criteria for sepsis: for the Third International Consensus Definitions for Sepsis and Septic Shock (Sepsis-3). *JAMA* (2016) 315:762–74. doi:10.1001/jama.2016.0288
98. Li CC, Munitic I, Mittelstadt PR, Castro E, Ashwell JD. Suppression of dendritic cell-derived IL-12 by endogenous glucocorticoids is protective in LPS-induced sepsis. *PLoS Biol* (2015) 13:e1002269. doi:10.1371/journal.pbio.1002269
99. Goudot C, Coillard A, Villani AC, Gueguen P, Cros A, Sarkizova S, et al. Aryl hydrocarbon receptor controls monocyte differentiation into dendritic cells versus macrophages. *Immunity* (2017) 47:582–96.e6. doi:10.1016/j.immuni.2017.08.016
100. Edelson BT, KC W, Juang R, Kohyama M, Benoit LA, Klekotka PA, et al. Peripheral CD103+ dendritic cells form a unified subset developmentally related to CD8alpha+ conventional dendritic cells. *J Exp Med* (2010) 207:823–36. doi:10.1084/jem.20091627
101. Eickhoff S, Brewitz A, Gerner MY, Klauschen F, Komander K, Hemmi H, et al. Robust anti-viral immunity requires multiple distinct T cell-dendritic cell interactions. *Cell* (2015) 162:1322–37. doi:10.1016/j.cell.2015.08.004
102. Schlitzer A, McGovern N, Teo P, Zelante T, Atarashi K, Low D, et al. IRF4 transcription factor-dependent CD11b+ dendritic cells in human and mouse control mucosal IL-17 cytokine responses. *Immunity* (2013) 38:970–83. doi:10.1016/j.immuni.2013.04.011
103. Williams JW, Tjota MY, Clay BS, Vander Lugt B, Bandukwala HS, Hrusch CL, et al. Transcription factor IRF4 drives dendritic cells to promote Th2 differentiation. *Nat Commun* (2013) 4:2990. doi:10.1038/ncomms3990
104. Singer M, Deutschman CS, Seymour CW, Shankar-Hari M, Annane D, Bauer M, et al. The Third International Consensus Definitions for Sepsis and Septic Shock (Sepsis-3). *JAMA* (2016) 315:801–10. doi:10.1001/jama.2016.0287
105. Cohen J, Vincent JL, Adhikari NK, Machado FR, Angus DC, Calandra T, et al. Sepsis: a roadmap for future research. *Lancet Infect Dis* (2015) 15:581–614. doi:10.1016/S1473-3099(15)70112-X
106. Wysocka M, Montaner LJ, Karp CL. Flt3 ligand treatment reverses endotoxin tolerance-related immunoparalysis. *J Immunol* (2005) 174:7398–402. doi:10.4049/jimmunol.174.11.7398
107. Strother RK, Danahy DB, Kotov DI, Kucaba TA, Zacharias ZR, Griffith TS, et al. Polymicrobial sepsis diminishes dendritic cell numbers and function directly contributing to impaired primary CD8 T cell responses in vivo. *J Immunol* (2016) 197:4301–11. doi:10.4049/jimmunol.1601463
108. Torres D, Köhler A, Delbauve S, Caminschi I, Lahoud MH, Shortman K, et al. IL-12p40/IL-10 producing preCD8alpha/Clec9A+ dendritic cells are induced in neonates upon *Listeria monocytogenes* infection. *PLoS Pathog* (2016) 12:e1005561. doi:10.1371/journal.ppat.1005561
109. del Rio ML, Bernhardt G, Rodriguez-Barbosa JI, Forster R. Development and functional specialization of CD103+ dendritic cells. *Immunol Rev* (2010) 234:268–81. doi:10.1111/j.0105-2896.2009.00874.x
110. Hochrein H, Shortman K, Vremec D, Scott B, Hertzog P, O'Keeffe M. Differential production of IL-12, IFN-alpha, and IFN-gamma by mouse dendritic cell subsets. *J Immunol* (2001) 166:5448–55. doi:10.4049/jimmunol.166.9.5448
111. Silvin A, Yu CI, Lahaye X, Imperatore F, Brault JB, Cardinaud S, et al. Constitutive resistance to viral infection in human CD141+ dendritic cells. *Sci Immunol* (2017) 2. doi:10.1126/sciimmunol.aai8071
112. den Haan JM, Bevan MJ. Constitutive versus activation-dependent cross-presentation of immune complexes by CD8(+) and CD8(-) dendritic cells in vivo. *J Exp Med* (2002) 196:817–27. doi:10.1084/jem.20020295
113. Hildner K, Edelson BT, Purtha WE, Diamond M, Matsushita H, Kohyama M, et al. Batf3 deficiency reveals a critical role for CD8alpha+ dendritic cells in cytotoxic T cell immunity. *Science* (2008) 322:1097–100. doi:10.1126/science.1164206
114. Robbins SH, Walzer T, Dembélé D, Thibault C, Defays A, Bessou G, et al. Novel insights into the relationships between dendritic cell subsets in human and mouse revealed by genome-wide expression profiling. *Genome Biol* (2008) 9:R17. doi:10.1186/gb-2008-9-1-r17
115. Bachem A, Güttler S, Hartung E, Ebstein F, Schaefer M, Tannert A, et al. Superior antigen cross-presentation and XCR1 expression define human CD11c+CD141+ cells as homologues of mouse CD8+ dendritic cells. *J Exp Med* (2010) 207:1273–81. doi:10.1084/jem.20100348
116. Poulin LF, Reyal Y, Uronen-Hansson H, Schraml BU, Sancho D, Murphy KM, et al. DNGR-1 is a specific and universal marker of mouse and human Batf3-dependent dendritic cells in lymphoid and nonlymphoid tissues. *Blood* (2012) 119:6052–62. doi:10.1182/blood-2012-01-406967
117. Haniffa M, Shin A, Bigley V, McGovern N, Teo P, See P, et al. Human tissues contain CD141hi cross-presenting dendritic cells with functional homology to mouse CD103+ nonlymphoid dendritic cells. *Immunity* (2012) 37:60–73. doi:10.1016/j.immuni.2012.04.012
118. Crozat K, Guiton R, Contreras V, Feuillet V, Dutertre CA, Ventre E, et al. The XC chemokine receptor 1 is a conserved selective marker of mammalian cells homologous to mouse CD8alpha+ dendritic cells. *J Exp Med* (2010) 207:1283–92. doi:10.1084/jem.20100223
119. Segura E, Durand M, Amigorena S. Similar antigen cross-presentation capacity and phagocytic functions in all freshly isolated human lymphoid organ-resident dendritic cells. *J Exp Med* (2013) 210:1035–47. doi:10.1084/jem.20121103
120. Jongbloed SL, Kassianos AJ, McDonald KJ, Clark GJ, Ju X, Angel CE, et al. Human CD141+ (BDCA-3)+ dendritic cells (DCs) represent a unique myeloid DC subset that cross-presents necrotic cell antigens. *J Exp Med* (2010) 207:1247–60. doi:10.1084/jem.20092140
121. Balan S, Ollion V, Colletti N, Chelbi R, Montanana-Sanchis F, Liu H, et al. Human XCR1+ dendritic cells derived in vitro from CD34+ progenitors closely resemble blood dendritic cells, including their adjuvant responsiveness, contrary to monocyte-derived dendritic cells. *J Immunol* (2014) 193:1622–35. doi:10.4049/jimmunol.1401243
122. Deauvieau F, Ollion V, Doffin AC, Achard C, Fonteneau JF, Verronese E, et al. Human natural killer cells promote cross-presentation of tumor cell-derived antigens by dendritic cells. *Int J Cancer* (2015) 136:1085–94. doi:10.1002/ijc.29087
123. Cohn L, Chatterjee B, Esselborn F, Smed-Sörensen A, Nakamura N, Chalouni C, et al. Antigen delivery to early endosomes eliminates the superiority of

human blood BDCA3+ dendritic cells at cross presentation. *J Exp Med* (2013) 210:1049–63. doi:10.1084/jem.20121251
124. Flinsenberg TW, Compeer EB, Koning D, Klein M, Amelung FJ, van Baarle D, et al. Fcgamma receptor antigen targeting potentiates cross-presentation by human blood and lymphoid tissue BDCA-3+ dendritic cells. *Blood* (2012) 120:5163–72. doi:10.1182/blood-2012-06-434498
125. Desch AN, Gibbings SL, Clambey ET, Janssen WJ, Slansky JE, Kedl RM, et al. Dendritic cell subsets require cis-activation for cytotoxic CD8 T-cell induction. *Nat Commun* (2014) 5:4674. doi:10.1038/ncomms5674
126. Neubert K, Lehmann CH, Heger L, Baranska A, Staedtler AM, Buchholz VR, et al. Antigen delivery to CD11c+CD8- dendritic cells induces protective immune responses against experimental melanoma in mice in vivo. *J Immunol* (2014) 192:5830–8. doi:10.4049/jimmunol.1300975
127. Nierkens S, Tel J, Janssen E, Adema GJ. Antigen cross-presentation by dendritic cell subsets: one general or all sergeants? *Trends Immunol* (2013) 34:361–70. doi:10.1016/j.it.2013.02.007
128. Alloatti A, Rookhuizen DC, Joannas L, Carpier JM, Iborra S, Magalhaes JG, et al. Critical role for Sec22b-dependent antigen cross-presentation in antitumor immunity. *J Exp Med* (2017) 214:2231–41. doi:10.1084/jem.20170229
129. Sánchez-Paulete AR, Cueto FJ, Martínez-López M, Labiano S, Morales-Kastresana A, Rodríguez-Ruiz ME, et al. Cancer immunotherapy with immunomodulatory anti-CD137 and anti-PD-1 monoclonal antibodies requires BATF3-dependent dendritic cells. *Cancer Discov* (2016) 6:71–9. doi:10.1158/2159-8290.CD-15-0510
130. Wilson NS, Behrens GM, Lundie RJ, Smith CM, Waithman J, Young L, et al. Systemic activation of dendritic cells by toll-like receptor ligands or malaria infection impairs cross-presentation and antiviral immunity. *Nat Immunol* (2006) 7:165–72. doi:10.1038/ni1300
131. Park SH, Kang K, Giannopoulou E, Qiao Y, Kang K, Kim G, et al. Type I interferons and the cytokine TNF cooperatively reprogram the macrophage epigenome to promote inflammatory activation. *Nat Immunol* (2017) 18:1104–16. doi:10.1038/ni.3818
132. Gautier EL, Shay T, Miller J, Greter M, Jakubzick C, Ivanov S, et al. Gene-expression profiles and transcriptional regulatory pathways that underlie the identity and diversity of mouse tissue macrophages. *Nat Immunol* (2012) 13:1118–28. doi:10.1038/ni.2419
133. Gao Y, Nish SA, Jiang R, Hou L, Licona-Limón P, Weinstein JS, et al. Control of T helper 2 responses by transcription factor IRF4-dependent dendritic cells. *Immunity* (2013) 39:722–32. doi:10.1016/j.immuni.2013.08.028
134. Lewis KL, Caton ML, Bogunovic M, Greter M, Grajkowska LT, Ng D, et al. Notch2 receptor signaling controls functional differentiation of dendritic cells in the spleen and intestine. *Immunity* (2011) 35:780–91. doi:10.1016/j.immuni.2011.08.013
135. Tussiwand R, Everts B, Grajales-Reyes GE, Kretzer NM, Iwata A, Bagaitkar J, et al. Klf4 expression in conventional dendritic cells is required for T helper 2 cell responses. *Immunity* (2015) 42:916–28. doi:10.1016/j.immuni.2015.04.017
136. Persson EK, Uronen-Hansson H, Semmrich M, Rivollier A, Hägerbrand K, Marsal J, et al. IRF4 transcription-factor-dependent CD103(+)CD11b(+) dendritic cells drive mucosal T helper 17 cell differentiation. *Immunity* (2013) 38:958–69. doi:10.1016/j.immuni.2013.03.009
137. Sun CM, Hall JA, Blank RB, Bouladoux N, Oukka M, Mora JR, et al. Small intestine lamina propria dendritic cells promote de novo generation of Foxp3 T reg cells via retinoic acid. *J Exp Med* (2007) 204:1775–85. doi:10.1084/jem.20070602
138. Alcántara-Hernández M, Leylek R, Wagar LE, Engleman EG, Keler T, Marinkovich MP, et al. High-dimensional phenotypic mapping of human dendritic cells reveals interindividual variation and tissue specialization. *Immunity* (2017) 47:1037–50.e6. doi:10.1016/j.immuni.2017.11.001
139. Swiecki M, Wang Y, Riboldi E, Kim AH, Dzutsev A, Gilfillan S, et al. Cell depletion in mice that express diphtheria toxin receptor under the control of SiglecH encompasses more than plasmacytoid dendritic cells. *J Immunol* (2014) 192:4409–16. doi:10.4049/jimmunol.1303135
140. Reizis B, Bunin A, Ghosh HS, Lewis KL, Sisirak V. Plasmacytoid dendritic cells: recent progress and open questions. *Annu Rev Immunol* (2011) 29:163–83. doi:10.1146/annurev-immunol-031210-101345
141. Mouriès J, Moron G, Schlecht G, Escriou N, Dadaglio G, Leclerc C. Plasmacytoid dendritic cells efficiently cross-prime naive T cells in vivo after TLR activation. *Blood* (2008) 112:3713–22. doi:10.1182/blood-2008-03-146290
142. Zhang H, Gregorio JD, Iwahori T, Zhang X, Choi O, Tolentino LL, et al. A distinct subset of plasmacytoid dendritic cells induces activation and differentiation of B and T lymphocytes. *Proc Natl Acad Sci U S A* (2017) 114:1988–93. doi:10.1073/pnas.1610630114
143. Hoeffel G, Ripoche AC, Matheoud D, Nascimbeni M, Escriou N, Lebon P, et al. Antigen crosspresentation by human plasmacytoid dendritic cells. *Immunity* (2007) 27:481–92. doi:10.1016/j.immuni.2007.07.021
144. Alculumbre SG, Saint-André V, Di Domizio J, Vargas P, Sirven P, Bost P, et al. Diversification of human plasmacytoid predendritic cells in response to a single stimulus. *Nat Immunol* (2018) 19:63–75. doi:10.1038/s41590-017-0012-z
145. Pinheiro da Silva F, Nizet V. Cell death during sepsis: integration of disintegration in the inflammatory response to overwhelming infection. *Apoptosis* (2009) 14:509–21. doi:10.1007/s10495-009-0320-3
146. Peck-Palmer OM, Unsinger J, Chang KC, McDonough JS, Perlman H, McDunn JE, et al. Modulation of the Bcl-2 family blocks sepsis-induced depletion of dendritic cells and macrophages. *Shock* (2009) 31:359–66. doi:10.1097/SHK.0b013e31818ba2a2
147. Raffray L, Douchet I, Augusto JF, Youssef J, Contin-Bordes C, Richez C, et al. Septic shock sera containing circulating histones induce dendritic cell-regulated necrosis in fatal septic shock patients. *Crit Care Med* (2015) 43:e107–16. doi:10.1097/CCM.0000000000000879
148. Zhang L, Cardinal JS, Pan P, Rosborough BR, Chang Y, Yan W, et al. Splenocyte apoptosis and autophagy is mediated by interferon regulatory factor 1 during murine endotoxemia. *Shock* (2012) 37:511–7. doi:10.1097/SHK.0b013e318249cfa2
149. Gautier EL, Huby T, Saint-Charles F, Ouzilleau B, Chapman MJ, Lesnik P. Enhanced dendritic cell survival attenuates lipopolysaccharide-induced immunosuppression and increases resistance to lethal endotoxic shock. *J Immunol* (2008) 180:6941–6. doi:10.4049/jimmunol.180.10.6941
150. Kushwah R, Wu J, Oliver JR, Jiang G, Zhang J, Siminovitch KA, et al. Uptake of apoptotic DC converts immature DC into tolerogenic DC that induce differentiation of Foxp3+ Treg. *Eur J Immunol* (2010) 40:1022–35. doi:10.1002/eji.200939782
151. Shalova IN, Lim JY, Chittezhath M, Zinkernagel AS, Beasley F, Hernández-Jiménez E, et al. Human monocytes undergo functional re-programming during sepsis mediated by hypoxia-inducible factor-1alpha. *Immunity* (2015) 42:484–98. doi:10.1016/j.immuni.2015.02.001
152. Poehlmann H, Schefold JC, Zuckermann-Becker H, Volk HD, Meisel C. Phenotype changes and impaired function of dendritic cell subsets in patients with sepsis: a prospective observational analysis. *Crit Care* (2009) 13:R119. doi:10.1186/cc7969
153. Benjamim CF, Lundy SK, Lukacs NW, Hogaboam CM, Kunkel SL. Reversal of long-term sepsis-induced immunosuppression by dendritic cells. *Blood* (2005) 105:3588–95. doi:10.1182/blood-2004-08-3251
154. Patera AC, Drewry AM, Chang K, Beiter ER, Osborne D, Hotchkiss RS. Frontline science: defects in immune function in patients with sepsis are associated with PD-1 or PD-L1 expression and can be restored by antibodies targeting PD-1 or PD-L1. *J Leukoc Biol* (2016) 100:1239–54. doi:10.1189/jlb.4HI0616-255R
155. Guignant C, Lepape A, Huang X, Kherouf H, Denis L, Poitevin F, et al. Programmed death-1 levels correlate with increased mortality, nosocomial infection and immune dysfunctions in septic shock patients. *Crit Care* (2011) 15:R99. doi:10.1186/cc10112
156. Faivre V, Lukaszewicz AC, Alves A, Charron D, Payen D, Haziot A. Human monocytes differentiate into dendritic cells subsets that induce anergic and regulatory T cells in sepsis. *PLoS One* (2012) 7:e47209. doi:10.1371/journal.pone.0047209
157. Dominguez PM, Ardavin C. Differentiation and function of mouse monocyte-derived dendritic cells in steady state and inflammation. *Immunol Rev* (2010) 234:90–104. doi:10.1111/j.0105-2896.2009.00876.x
158. Lamas B, Richard ML, Leducq V, Pham HP, Michel ML, Da Costa G, et al. CARD9 impacts colitis by altering gut microbiota metabolism of tryptophan into aryl hydrocarbon receptor ligands. *Nat Med* (2016) 22:598–605. doi:10.1038/nm.4102
159. Menezes S, Melandri D, Anselmi G, Perchet T, Loschko J, Dubrot J, et al. The heterogeneity of Ly6Chi monocytes controls their differentiation into

iNOS+ macrophages or monocyte-derived dendritic cells. *Immunity* (2016) 45:1205–18. doi:10.1016/j.immuni.2016.12.001
160. Schmid MA, Takizawa H, Baumjohann DR, Saito Y, Manz MG. Bone marrow dendritic cell progenitors sense pathogens via toll-like receptors and subsequently migrate to inflamed lymph nodes. *Blood* (2011) 118:4829–40. doi:10.1182/blood-2011-03-344960
161. Nagai Y, Garrett KP, Ohta S, Bahrun U, Kouro T, Akira S, et al. Toll-like receptors on hematopoietic progenitor cells stimulate innate immune system replenishment. *Immunity* (2006) 24:801–12. doi:10.1016/j.immuni.2006.04.008
162. De Luca K, Frances-Duvert V, Asensio MJ, Ihsani R, Debien E, Taillardet M, et al. The TLR1/2 agonist PAM(3)CSK(4) instructs commitment of human hematopoietic stem cells to a myeloid cell fate. *Leukemia* (2009) 23:2063–74. doi:10.1038/leu.2009.155
163. Sioud M, Floisand Y, Forfang L, Lund-Johansen F. Signaling through toll-like receptor 7/8 induces the differentiation of human bone marrow CD34+ progenitor cells along the myeloid lineage. *J Mol Biol* (2006) 364:945–54. doi:10.1016/j.jmb.2006.09.054
164. Sioud M, Floisand Y. TLR agonists induce the differentiation of human bone marrow CD34+ progenitors into CD11c+ CD80/86+ DC capable of inducing a Th1-type response. *Eur J Immunol* (2007) 37:2834–46. doi:10.1002/eji.200790042
165. Wright DE, Wagers AJ, Gulati AP, Johnson FL, Weissman IL. Physiological migration of hematopoietic stem and progenitor cells. *Science* (2001) 294:1933–6. doi:10.1126/science.1064081
166. Massberg S, Schaerli P, Knezevic-Maramica I, Köllnberger M, Tubo N, Moseman EA, et al. Immunosurveillance by hematopoietic progenitor cells trafficking through blood, lymph, and peripheral tissues. *Cell* (2007) 131:994–1008. doi:10.1016/j.cell.2007.09.047
167. Essers MA, Offner S, Blanco-Bose WE, Waibler Z, Kalinke U, Duchosal MA, et al. IFNalpha activates dormant haematopoietic stem cells in vivo. *Nature* (2009) 458:904–8. doi:10.1038/nature07815
168. Sato S, Sugiyama M, Yamamoto M, Watanabe Y, Kawai T, Takeda K, et al. Toll/IL-1 receptor domain-containing adaptor inducing IFN-beta (TRIF) associates with TNF receptor-associated factor 6 and TANK-binding kinase 1, and activates two distinct transcription factors, NF-kappa B and IFN-regulatory factor-3, in the toll-like receptor signaling. *J Immunol* (2003) 171:4304–10. doi:10.4049/jimmunol.171.8.4304
169. Passegue E, Wagers AJ, Giuriato S, Anderson WC, Weissman IL. Global analysis of proliferation and cell cycle gene expression in the regulation of hematopoietic stem and progenitor cell fates. *J Exp Med* (2005) 202:1599–611. doi:10.1084/jem.20050967
170. Orford KW, Scadden DT. Deconstructing stem cell self-renewal: genetic insights into cell-cycle regulation. *Nat Rev Genet* (2008) 9:115–28. doi:10.1038/nrg2269
171. Pène F, Zuber B, Courtine E, Rousseau C, Ouaaz F, Toubiana J, et al. Dendritic cells modulate lung response to *Pseudomonas aeruginosa* in a murine model of sepsis-induced immune dysfunction. *J Immunol* (2008) 181:8513–20. doi:10.4049/jimmunol.181.12.8513
172. Helft J, Böttcher J, Chakravarty P, Zelenay S, Huotari J, Schraml BU, et al. GM-CSF mouse bone marrow cultures comprise a heterogeneous population of CD11c(+)MHCII(+) macrophages and dendritic cells. *Immunity* (2015) 42:1197–211. doi:10.1016/j.immuni.2015.05.018
173. Naik SH, Proietto AI, Wilson NS, Dakic A, Schnorrer P, Fuchsberger M, et al. Cutting edge: generation of splenic CD8+ and CD8- dendritic cell equivalents in Fms-like tyrosine kinase 3 ligand bone marrow cultures. *J Immunol* (2005) 174:6592–7. doi:10.4049/jimmunol.174.11.6592
174. Laoui D, Keirsse J, Morias Y, Van Overmeire E, Geeraerts X, Elkrim Y, et al. The tumour microenvironment harbours ontogenically distinct dendritic cell populations with opposing effects on tumour immunity. *Nat Commun* (2016) 7:13720. doi:10.1038/ncomms13720
175. van Blijswijk J, Schraml BU, Reis e Sousa C. Advantages and limitations of mouse models to deplete dendritic cells. *Eur J Immunol* (2013) 43:22–6. doi:10.1002/eji.201243022
176. Scumpia PO, McAuliffe PF, O'Malley KA, Ungaro R, Uchida T, Matsumoto T, et al. CD11c+ dendritic cells are required for survival in murine polymicrobial sepsis. *J Immunol* (2005) 175:3282–6. doi:10.4049/jimmunol.175.5.3282
177. Shankar-Hari M, Phillips GS, Levy ML, Seymour CW, Liu VX, Deutschman CS, et al. Developing a new definition and assessing new clinical criteria for septic shock: for the Third International Consensus Definitions for Sepsis and Septic Shock (Sepsis-3). *JAMA* (2016) 315:775–87. doi:10.1001/jama.2016.0289
178. Roquilly A, McWilliam HEG, Jacqueline C, Tian Z, Cinotti R, Rimbert M, et al. Local modulation of antigen-presenting cell development after resolution of pneumonia induces long-term susceptibility to secondary infections. *Immunity* (2017) 47:135–47.e5. doi:10.1016/j.immuni.2017.06.021
179. Naik S, Larsen SB, Gomez NC, Alaverdyan K, Sendoel A, Yuan S, et al. Inflammatory memory sensitizes skin epithelial stem cells to tissue damage. *Nature* (2017) 550:475–80. doi:10.1038/nature24271
180. Lukens JR, Gross JM, Kanneganti TD. IL-1 family cytokines trigger sterile inflammatory disease. *Front Immunol* (2012) 3:315. doi:10.3389/fimmu.2012.00315

Conflict of Interest Statement: The authors declare that the research was conducted in the absence of any commercial or financial relationships that could be construed as a potential conflict of interest.

Copyright © 2018 Poulin, Lasseaux and Chamaillard. This is an open-access article distributed under the terms of the Creative Commons Attribution License (CC BY). The use, distribution or reproduction in other forums is permitted, provided the original author(s) and the copyright owner are credited and that the original publication in this journal is cited, in accordance with accepted academic practice. No use, distribution or reproduction is permitted which does not comply with these terms.

frontiers in Immunology

ORIGINAL RESEARCH
published: 04 December 2017
doi: 10.3389/fimmu.2017.01666

Type I IFNs Are Required to Promote Central Nervous System Immune Surveillance through the Recruitment of Inflammatory Monocytes upon Systemic Inflammation

*Javier María Peralta Ramos, Claudio Bussi†, Emilia Andrea Gaviglio†, Daniela Soledad Arroyo, Natalia Soledad Baez, Maria Cecilia Rodriguez-Galan and Pablo Iribarren**

Centro de Investigación en Bioquímica Clínica e Inmunología (CIBICI-CONICET), Departamento de Bioquímica Clínica, Facultad de Ciencias Químicas, Universidad Nacional de Córdoba, Córdoba, Argentina

OPEN ACCESS

Edited by:
Luciana Balboa, Consejo Nacional de Investigaciones Científicas y Técnicas (CONICET), Argentina

Reviewed by:
Mario M. D'Elios, University of Florence, Italy
Beatrix Schumak, University of Bonn, Germany

***Correspondence:**
Pablo Iribarren
piribarr@fcq.unc.edu.ar

†These authors have contributed equally to the present work.

Specialty section:
This article was submitted to Microbial Immunology, a section of the journal Frontiers in Immunology

Received: *15 August 2017*
Accepted: *14 November 2017*
Published: *04 December 2017*

Citation:
Peralta Ramos JM, Bussi C, Gaviglio EA, Arroyo DS, Baez NS, Rodriguez-Galan MC and Iribarren P (2017) Type I IFNs Are Required to Promote Central Nervous System Immune Surveillance through the Recruitment of Inflammatory Monocytes upon Systemic Inflammation. Front. Immunol. 8:1666. doi: 10.3389/fimmu.2017.01666

Brain-resident microglia and peripheral migratory leukocytes play essential roles in shaping the immune response in the central nervous system. These cells activate and migrate in response to chemokines produced during active immune responses and may contribute to the progression of neuroinflammation. Herein, we addressed the participation of type I–II interferons in the response displayed by microglia and inflammatory monocytes to comprehend the contribution of these cytokines in the establishment and development of a neuroinflammatory process. Following systemic lipopolysaccharide (LPS) challenge, we found glial reactivity and an active recruitment of $CD45^{hi}$ leukocytes close to $CD31^{+}$ vascular endothelial cells in circumventricular organs. Isolated $CD11b^{+}$ $CD45^{hi}$ $Ly6C^{hi}$ $Ly6G^{-}$-primed inflammatory monocytes were able to induce T cell proliferation, unlike $CD11b^{+}$ $CD45^{lo}$ microglia. Moreover, *ex vivo* re-stimulation with LPS exhibited an enhancement of T cell proliferative response promoted by inflammatory monocytes. These myeloid cells also proved to be recruited in a type I interferon-dependent fashion as opposed to neutrophils, unveiling a role of these cytokines in their trafficking. Together, our results compares the phenotypic and functional features between tissue-resident vs peripheral recruited cells in an inflamed microenvironment, identifying inflammatory monocytes as key sentinels in a LPS-induced murine model of neuroinflammation.

Keywords: microglia, inflammatory monocytes, inflammation, lipopolysaccharide, interferons

INTRODUCTION

Immunological surveillance of the central nervous system (CNS) is dynamic, specific, and tightly regulated. During neuroinflammation, the blood–brain barrier (BBB) might get disrupted, enabling peripheral immune cells to gain access to the brain parenchyma. Brain-resident microglia encounter myeloid immune cells that have been primed in the periphery, establishing an interplay that could lead to the development and worsening of this inflammatory process with a detrimental outcome (1, 2).

Systemic injection of the endotoxin lipopolysaccharide (LPS), a cell wall component of Gram-negative bacteria and a canonical ligand for toll-like receptor 4 (TLR4), has been widely used as an inflammatory model (3–14). These peripherally applied stimuli leads to a cytokine-storm that signals to the brain, inducing a decline in BBB integrity and triggering an immune response within it.

Tissue-resident microglia represent the first line of defense against invading pathogens and modulate neuroinflammation. Despite being extremely long-lived, microglia exhibit considerable self-renewal (15) and are highly active surveillants of the CNS under steady-state conditions (16). Peripheral blood-derived monocytes consist of two functional subsets, a patrolling CX_3CR1^{hi} $CCR2^{-}$ subset and an inflammatory CX_3CR1^{lo} $CCR2^{+}$ subset (17) with the ability to migrate to inflamed tissues and differentiate into dendritic cells (18) or microglia under defined conditions (19, 20).

Current knowledge in neuroimmunology remains scarce. The recognition of a lymphatic drainage system of the CNS has drawn attention to the meninges and the choroid plexus, challenging the established basic assumptions of the CNS immune privilege (21, 22). In this regard, type I and II interferon (IFN-a/b and IFN-g) pathways have proved to be part of an elaborate cytokine network regulating the migration of immune cells through these CNS gateways (23), seemingly yielding opposite effects.

There is growing evidence that systemic inflammatory events can have devastating effects in the brain (4, 24, 25) due to their impact in the progression of several CNS disorders (11, 26), such as autoimmune and neurodegenerative diseases in which leukocyte recruitment is a key feature. Understanding the impact of systemic inflammation in myeloid cell trafficking into the CNS and the underlying mechanisms involved in this process is determining.

In our study, we shed light on the differential roles of microglia and inflammatory monocytes (27, 28) and contributed to elucidate the participation of type I–II interferons during the immune response elicited by these tissue-resident versus peripheral recruited cells in a lipopolysaccharide (LPS)-induced murine model of neuroinflammation.

MATERIALS AND METHODS

Animals and LPS Administration

Wild-type (WT) C57BL/6 mice were originally obtained from School of Veterinary, National University of La Plata. IFN-$g^{-/-}$ (B6.129S7-Ifngtm1Ts/J strain) mice were obtained from The Jackson Laboratory and $IFNAR^{-/-}$ (Ifnar1tm1Ag strain) mice were kindly provided by Institut Pasteur. Between 8- and 12-week-old male mice were maintained in the specific pathogen-free barrier facilities at the School of Chemical Sciences animal facility, where all experiments were done in compliance with the procedures outlined in the "Guide for the Care and Use of Laboratory Animals" (NIH Publication No. 86-23, 1985). The experimental protocols were approved by the Institutional Animal Care and Use Committee (IACUC). Our animal facility obtained NIH animal welfare assurance (No. A5802-01, OLAW, NIH, US).

Lipopolysaccharide from *Escherichia coli* 055:B5 (purified by gel-filtration chromatography) was purchased from Sigma-Aldrich and freshly dissolved in sterile saline prior to intraperitoneal (i.p.) injection. Mice were treated with either vehicle or 40 µg of LPS (1,6 mg/kg) for four consecutive days to induce neuroinflammation, following an injection scheme modified from Cardona et al. (5).

Isolation of Immune Cells from Mice Brains

Twelve hours post the last i.p. injection, mice were weighed and deeply anesthetized with a ketamine/xylazine cocktail according to their weight. Immune cells were isolated from whole brain homogenates as follows. Briefly, mice were transcardially perfused with ice-cold PBS (Gibco), and brains were collected in DMEM (Gibco) supplemented with sodium pyruvate (Gibco) and a penicillin, streptomycin, and glutamine cocktail (Gibco), gently disaggregated mechanically and resuspended in PBS containing 3 mg/mL collagenase D (Roche Diagnostics) plus 10 µg/mL DNAse (Sigma-Aldrich) for an enzymatically homogenization. After this incubation, brain homogenates were filtered in 40-µm pore size cell strainers (BD Biosciences), centrifuged 8 min at 1,800 rpm, washed with PBS, and resuspended in 6 mL of 38% isotonic Percoll® (GE Healthcare) before a 25-min centrifugation at 800*g* without neither acceleration nor brake. Myelin and debris were discarded. Cell pellets containing total brain immune cells were collected, washed with DMEM supplemented with 10% fetal bovine serum (Gibco), and cell viability was determined by trypan blue exclusion using a Neubauer's chamber. Finally, cells were labeled for subsequent flow cytometric analysis or cell sorting.

Flow Cytometric Analysis and Cell Sorting

Surface staining of single-cell suspension of isolated brain immune cells was performed using standard protocols and analyzed on a FACS Canto II (BD Biosciences) or sorted on a FACS Aria III (BD Biosciences). Sort gates were defined based on the expression of CD11b, CD45, Ly6C, and Ly6G as follows: microglial cells, $CD11b^{+}$ $CD45^{lo}$; neutrophils, $CD11b^{+}$ $CD45^{hi}$ $Ly6C^{+}$ $Ly6G^{+}$; inflammatory monocytes, $CD11b^{+}$ $CD45^{hi}$ $Ly6C^{hi}$ $Ly6G^{-}$. Data analysis was conducted using FCS express (*De Novo* Software). The following antibodies were used in the procedure: monoclonal anti-mouse CD11b APC (BioLegend, clone M1/70), CD11b FITC (BD Pharmingen, clone M1/70), CD45 APC-Cy7 (BioLegend, clone 30-F11), CD11c PerCP (BD Pharmingen, clone N418), Ly6C PE-Cy7 (BD Pharmingen, clone AL-21), Ly6G PE (BD Pharmingen, clone 1A8), I-A/I-E Alexa Fluor 647 (BioLegend, clone M5/114.15.2), FcεRI PE-Cy7 (eBioscience, clone MAR-1), CCR2 (Abcam, clone E68), or polyclonal anti-mouse CX_3CR1 (Abcam) plus Alexa Fluor 488 (Molecular Probes) antibody or isotype control antibodies (BD Pharmingen, APC, clone R35-95; PerCP/PE, clone A95-1; PE-Cy7, clone G155-178). The assessment of intracellular expression of chemokine receptors was performed according to the Cytofix/Cytoperm™ fixation/permeabilization solution kit (BD Biosciences) manufacturer's instructions. Briefly, cells were surface-labeled as mentioned

above. Then, samples were fixed and permeabilized for 20 min at 4°C with Fixation/Permeabilization solution and washed with BD Perm/Wash buffer™. Next, cells were incubated with BD Perm/Wash buffer™ containing monoclonal anti-mouse CCR2 (Abcam, clone E68) or polyclonal anti-mouse CX_3CR1 (Abcam). Finally, samples were washed with BD Perm/Wash buffer™ and resuspended in the same buffer containing Alexa Fluor 488 antibody (Molecular Probes).

Ex Vivo Suppression Assays

Microglial cells or inflammatory monocytes isolated from endotoxemic mice, stimulated or not with a LPS (100 ng/mL) plus interferon gamma (IFN-g, 20 ng/mL) (Peprotech) cocktail were cocultured with splenocytes derived from naïve control mice and previously stained with CFSE (4 μM) (Molecular Probes), at a 1:1 ratio (1×10^5 cell/mL). For mitogenic-induced cell proliferation, cocultures were maintained for 72 h in round-bottom 96-well plates in the presence or absence of Concanavalin A (Con A, 5 μg/mL) (Sigma-Aldrich) in RPMI (Gibco) supplemented with 10% fetal bovine serum (Gibco). Cells were then harvested and stained with CD4 APC (BD Pharmingen, clone RM4-5) and CD8 PE (BD Pharmingen, clone 53-6.7) and analyzed as mentioned above.

Reverse Transcription of mRNA and Quantification by Real-time PCR

Brain homogenates or isolated cells were incubated with TRIzol® (Invitrogen), then RNA was extracted according to the manufacturer's instructions and stored at −80°C. Total RNA was quantified using a Synergy HT spectrophotometer (BioTek) and 1 μg was treated with DNAse (Sigma-Aldrich) and reverse-transcribed using the High-Capacity cDNA Reverse Transcription Kit (Applied Biosystems) and following the manufacturer's protocol. Real-time PCR was performed on a StepOnePlus™ real-time PCR system (Applied Biosystems) using SYBR® Green real-time PCR master mix (Applied Biosystems), and relative quantification (RQ) was calculated by using StepOne™ software V2.2.2, based on the equation $RQ = 2^{-\Delta\Delta Ct}$, where Ct is the threshold cycle to detect fluorescence. Ct data were normalized to the internal standard HPRT1. Primer sequences were as follows: CCL2, sense: CCC ACT CAC CTG CTA CT, anti-sense: TCT GGA CCC ATT CCT TCT TG; CCR2, sense: GTG TGA TTG ACA AGC ACT TAG ACC, anti-sense: GGA GAG ATA CCT TCG GAA CTT CTC; CX_3CL1, sense: CGA AAT GCG AAA TCA TGT GCG AC, anti-sense: GAC TCC TGG TTT AGC TGA TAG CG; CX_3CR1: GGA CTC ACT ACC TCA GCC, anti-sense: TCC GGT TGT TCA TGG AGT TGG; CXCL1, sense: CAC CTC AAG AAC ATC CAG AGC, anti-sense: GGT CGC GAG GCT TGC CTT GA; CXCR2, sense: CTG GCA TGC CCT CTA TTC TGC, anti-sense: GCT GGT CAT CTT ATA CAA CGG G; IFN-b, sense: TTA CAC TGC CTT TGC CAT CC, anti-sense: ACT GTC TGC TGG AGT TCA T; IFNAR, sense: CGA GGC GAA GTG GTT AAA A, anti-sense: ACG GAT CAA CCT CAT TCC AC; HPRT1, sense: TCA GTC AAC GGG GGA CAT AAA, anti-sense: GGG GCT GTA CTG CTT AAC CAG.

H&E Staining and Immunofluorescence

Twelve hours post the last i.p. injection, mice were weighed and deeply anesthetized with a ketamine/xylazine cocktail according to their weight. Animals were transcardially perfused once with ice-cold PBS (Gibco) and then with 4% paraformaldehyde. Brains were collected in 4% paraformaldehyde for an additional 24 h post-fixation and incubated in 20% sucrose for 24 h more.

For H&E staining, brains were embedded in paraffin, cut into 10 μm sections of thickness using a Shandon Cryotome E cryostat (Thermo Scientific), and mounted on Starfrost® adhesive slides (Knittel Glass). Then, sections were immersed in hematoxylin and rinsed in distilled water. Next, slides were immersed in eosin and rinsed three times with 95% isopropilic alcohol. Following that, sections were quickly rinsed in a combined solution of xylene and ethanol and twice in xylene. Finally, slides were mounted with a drop of Canada balsam and analyzed under an Eclipse TE 2000-Ulight microscope (Nikon) with an ACT-2U digital camera (Nikon) attached to it to capture the images.

For immunofluorescence, brains were embedded in Tissue-Tek® optimal cutting temperature compound (Sakura), cut into 10 μm sections of thickness using a Shandon Cryotome E cryostat (Thermo Scientific), and mounted on Starfrost® adhesive slides (Knittel Glass). Sections were rehydrated with blocking buffer (10% BSA, 0.3% Triton in TBS), rinsed with TBS (Gibco), and incubated overnight at 4°C with the corresponding dilutions of the antibodies CD45 (BioLegend, clone 30-F11), CD31 (Santa Cruz, clone M-20), or glial fibrillary acidic protein (Abcam, clone GF5) in blocking buffer. After several rinses, sections were incubated with Alexa Fluor 488 (Molecular Probes), Alexa Fluor 546 (Molecular Probes), or Alexa Fluor 633 (Molecular Probes) antibodies and counterstained with DAPI. Slides were analyzed under a FV1000 laser scanning confocal fluorescence microscope (Olympus).

Statistical Analysis

Results are expressed as mean ± SEM. Data distribution was assumed to be normal, but this was not formally tested for all experiments. All statistical analyses were performed using Prism® 7.0 (GraphPad software). Means between two groups were compared with unpaired *t*-test. Means between three or more groups were compared with two-way analysis of variance followed by a Tuckey's *post hoc* test. Statistical significance levels were set as follows: * if $p < 0.05$, ** if $p < 0.01$, and *** if $p < 0.001$.

RESULTS

Systemic LPS Challenge Induces Glial Activation and Recruitment of Peripheral $CD11b^+$ $CD45^{hi}$ $Ly6C^{hi}$ $Ly6G^-$ Cells into the CNS

To assess neuroinflammation and to establish the cellular players involved in this process after a systemic LPS challenge, we evaluated glial activation and the recruitment of peripheral

immune cells to the CNS through a flow cytometry multiparametric gating analysis strategy (Figure S1 in Supplementary Material).

For this purpose, we took advantage of the differential expression of the myeloid surface antigen CD11b and the pan-leukocyte marker CD45 in tissue-resident microglial cells ($CD11b^{+}$ $CD45^{lo}$) and peripheral recruited immune cells ($CD11b^{+/-}$ $CD45^{hi}$) (**Figures 1A–C**). Following LPS stimulation and based on these selection criteria, we found no changes in the absolute number but a decrease in the frequency of microglial cells due to the overwhelming recruitment of peripheral leukocytes. This effect upon LPS injection was accompanied by a marked weight loss, probably due to the development of sickness behavior (**Figure 1D**). To characterize the phenotypic features of the leukocyte trafficking to the CNS, we identified neutrophils ($CD11b^{+}$ $CD45^{hi}$ $Ly6C^{+}$ $Ly6G^{+}$) and inflammatory monocytes ($CD11b^{+}$ $CD45^{hi}$ $Ly6C^{hi}$ $Ly6G^{-}$) as the major population of CNS-associated phagocytes in LPS-treated mice (**Figures 2A,B**) among innate myeloid $CD11b^{+}$ $CD45^{hi}$ leukocytes.

Correspondingly, we noticed an increase in the recruitment of professional antigen presenting dendritic cells ($CD11b^{+}$ $CD45^{hi}$ $CD11c^{+}$ $Ly6C^{-}$ $Ly6G^{-}$) and of a distinctive subset, derived from monocytes that differentiate *in situ* under inflammatory circumstances, termed inflammatory dendritic cells ($CD11b^{+}$ $CD45^{hi}$ $CD11c^{+}$ $Ly6C^{+}$ $Fc\epsilon RI^{+}$) (**Figures 2A,B**). Furthermore, we found $CD11b^{-}$ $CD45^{hi}$ T ($Ly6C^{+}$) and B-like ($Ly6C^{-}$) cells (**Figures 2A,B**). Our results clearly show that an inflammogen, such as LPS, promotes the redistribution of the

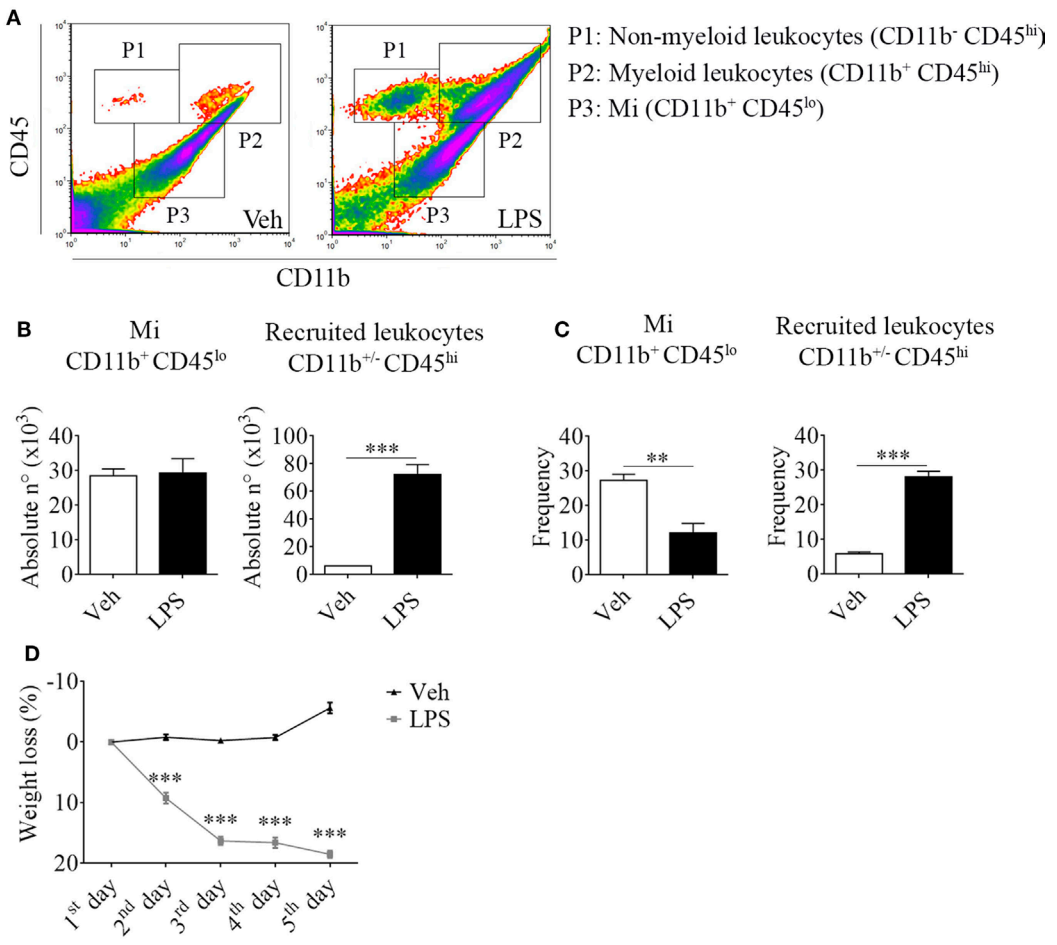


FIGURE 1 | Lipopolysaccharide (LPS) stimulation induces the recruitment of peripheral $CD11b^{+/-}$ $CD45^{hi}$ cells to the central nervous system. Mice were treated i.p. with either vehicle or 40 µg of LPS (1,6 mg/kg) for four consecutive days to induce neuroinflammation. Twelve hours post the last injection, mice were euthanized and immune cells were isolated from whole brain homogenates and labeled for subsequent flow cytometric analysis. **(A)** Representative CD45 vs CD11b flow cytometry density-plots illustrating the gating analysis strategy employed. P1: $CD11b^{-}$ $CD45^{hi}$ lymphoid recruited leukocytes; P2: $CD11b^{+}$ $CD45^{hi}$ myeloid recruited leukocytes; P3: $CD11b^{+}$ $CD45^{lo}$ microglial cells. **(B)** Absolute number and **(C)** frequency of $CD11b^{+}$ $CD45^{lo}$ microglial cells, $CD11b^{+/-}$ $CD45^{hi}$ recruited leukocytes, $CD11b^{+}$ $CD45^{hi}$ $Ly6C^{+}$ $Ly6G^{+}$ neutrophils, and $CD11b^{+}$ $CD45^{hi}$ $Ly6C^{hi}$ $Ly6G^{-}$ inflammatory monocytes, were assessed by flow cytometry. The percentage of these two last populations corresponding when gated in $CD11b^{+}$ $CD45^{hi}$. Results are representative of at least three independent experiments (n = 3–4 animals per group). **(D)** Mice weight loss following the i.p. administration scheme with vehicle or 40 µg of LPS (1.6 mg/kg) for four consecutive days to induce neuroinflammation. Results are representative of at least three independent experiments (n = 3–20 animals per group). Data are expressed as mean ± SEM. Mi, microglial cells; PMN, neutrophils; Inf Mo, inflammatory monocytes.

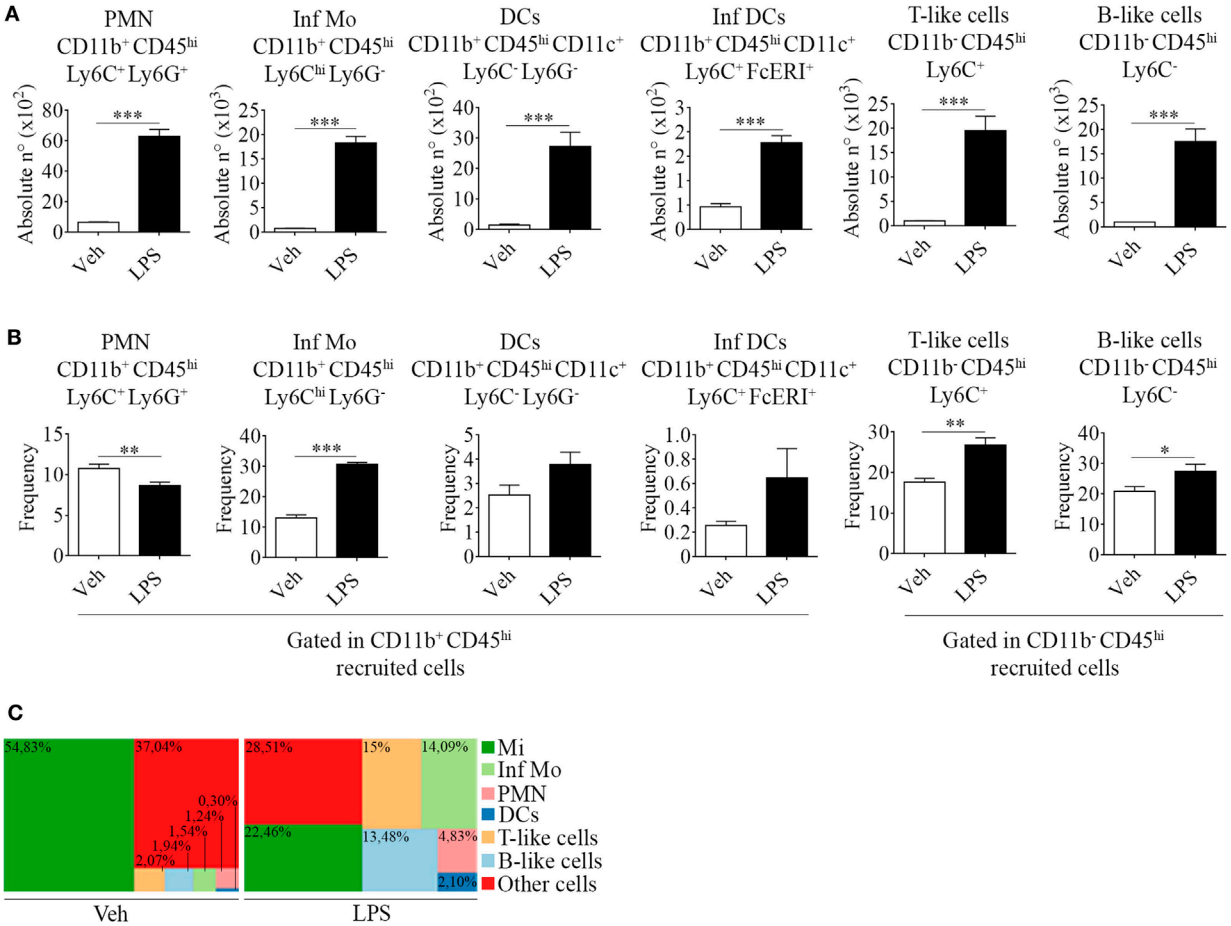


FIGURE 2 | Phenotypic features of immune cells involved in neuroinflammation in the brain from endotoxemic mice. Mice were treated i.p. with either vehicle or 40 µg of lipopolysaccharide (LPS) (1,6 mg/kg) for four consecutive days to induce neuroinflammation. Twelve hours post the last injection, mice were euthanized and immune cells were isolated from whole brain homogenates and labeled for subsequent flow cytometric analysis. **(A)** Absolute number and **(B)** frequency of CD11b$^+$ CD45^{hi} CD11c$^+$ Ly6C$^-$ Ly6G$^-$ dendritic cells, CD11b$^+$ CD45^{hi} CD11c$^+$ Ly6C$^+$ FcεRI$^+$ inflammatory dendritic cells, CD11b$^-$ CD45^{hi} Ly6C$^+$ T-like, and CD11b$^+$ CD45^{hi} Ly6C$^-$ B-like lymphocytes, was assessed by flow cytometry. The percentages shown correspond to populations gated as CD11b$^+$ CD45^{hi}. Results are representative of at least two independent experiments (n = 3–4 animals per group). **(C)** Representative hierarchical tree map comparing vehicle vs LPS frequency of resident and peripheral populations previously analyzed by flow cytometry. Results are representative of at least three independent experiments (n = 3–4 animals per group). Data are expressed as mean ± SEM. Mi, microglial cells; Inf Mo, inflammatory monocytes; PMN, neutrophils; DCs, dendritic cells; Inf DCs, inflammatory dendritic cells; other cells, neurons, astrocytes, oligodendrocytes.

frequencies of different populations of leukocytes recruited to the CNS when compared to those of neuronal or glial populations (**Figure 2C**).

Recent findings have revealed a role for circumventricular organs as gateways in the trafficking of peripheral leukocytes to the CNS. By virtue of this, we next assessed neuroinflammation and determined the location of the leukocytes recruited to the brain by both immunohistochemistry and immunofluorescence. Hematoxylin and eosin staining revealed recruitment of leukocytes in choroid plexus of endotoxemic mice (**Figure 3A**), confirming the involvement of this site in the immune surveillance of the brain. As mentioned above, when using confocal microscopy, we exploited both the morphology and the mild expression of the cluster of differentiation CD45 in star-shaped brain-resident microglial cells to distinguish them from rounded peripheral leukocytes bearing a high expression of this marker. Thus, systemic LPS induced microglial and astrocytic reactivity as shown by the shrinkage and thickening of glial processes and promoted the recruitment of inflammatory leukocytes, particularly close to vascular CD31-expressing endothelial cells in circumventricular organs (**Figure 3B**). Our results exhibited no infiltration of immune cells into the brain parenchyma but remain in the perivascular compartment, suggesting that at least under these circumstances, there may be no signals in the microenvironment to do so.

LPS Stimulation Modulates CCR2 and CX_3CR1 Expression in Tissue-Resident CD11b$^+$ CD45^{lo} and Peripheral CD11b$^+$ CD45^{hi} Ly6C^{hi} Ly6G$^-$ Cells

Chemokines and their receptors are active players inducing the access of myeloid cells to the CNS. To better understand microglial activation and the selective migration of inflammatory

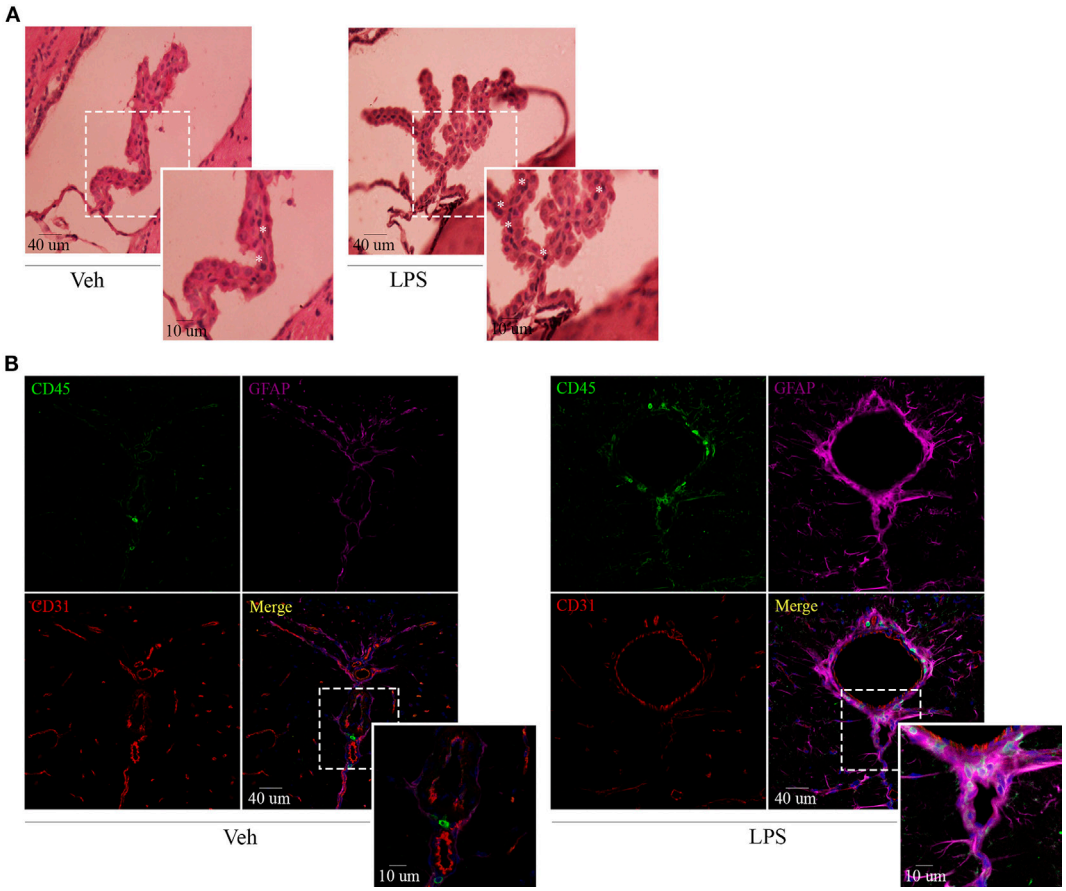


FIGURE 3 | Lipopolysaccharide (LPS) challenge induces glial activation and recruitment of leukocytes to CVOs. Mice were treated i.p. with either vehicle or 40 µg of LPS (1,6 mg/kg) for four consecutive days to induce neuroinflammation. Twelve hours post the last injection, mice were euthanized and brains collected. **(A)** H&E micrographs of the choroid plexus. Scale bars, 40 µm (main panels), 13 µm (inset). The asterisks denote recruited leukocytes. Results are representative of at least two independent experiments (n = 3–4 animals per group). **(B)** Confocal micrographs of CVOs depicting cluster of differentiation (CD45)-low microglial cells and high recruited leukocytes (upper-left, green), glial fibrillary acidic protein-positive astrocytes (upper-right, false-colored magenta), and cluster of differentiation (CD31)-positive endothelial cells (lower-left, red). DAPI counterstain (blue) shows nucleus. Scale bars, 40 µm (main panels), 13 µm (inset). Results are representative of at least three independent experiments (n = 3–4 animals per group).

monocytes following a LPS challenge, we next assessed the status of CCL2/CCR2 and CX_3CL1/CX_3CR1 axes.

Systemic LPS conversely modulated these chemokine/receptor axes, as determined by an increase in CCL2 and CCR2 gene expression levels but a decrease in both CX_3CL1 and CX_3CR1 in total bulk brains from LPS-treated mice when compared to their vehicle-treated counterparts (**Figure 4A**). Subsequently, we performed surface and intracellular staining of chemokine receptors CCR2 and CX_3CR1 in tissue-resident microglia and peripheral inflammatory monocytes to further characterize the response exerted by LPS in these populations. Thereby, we noticed an increase in the absolute number of CCR2 surface-bearing microglia (**Figures 4B,C** and Figure S2 in Supplementary Material) and CX_3CR1^+ inflammatory monocytes (**Figures 4D,E** and Figure S2 in Supplementary Material) after LPS systemic administration. These results imply a positive feedback between the unhindered recruitment of $CCR2^+$ cells and the exacerbation of inflammation through the downregulation of inhibitory CX_3CL1 and CX_3CR1, as shown by quantitative real-time PCR. Likewise, flow cytometry assays showed that despite not always promoting the expression of either CCR2 or CX_3CR1 in the surface of microglia and inflammatory monocytes, LPS upregulates the expression of both chemokine receptors intracellularly in these populations.

Plasticity of LPS-Primed Inflammatory $CD11b^+$ $CD45^{hi}$ $Ly6C^{hi}$ $Ly6G^-$ Cells in the Regulation of T Cell Proliferation

To date, several studies have described invading blood-derived monocytes as highly mobile and inflammatory, whereas resident microglia have been characterized as active motile CNS myeloid cells that function as the first line of defense against invading pathogens. Therefore, we addressed the hypothesis that inflammatory monocytes and microglia could be playing different roles in neuroinflammation by either promoting or suppressing T cell proliferative response.

To tackle this issue, we performed a proliferation assay in which CNS isolated inflammatory monocytes or microglia were

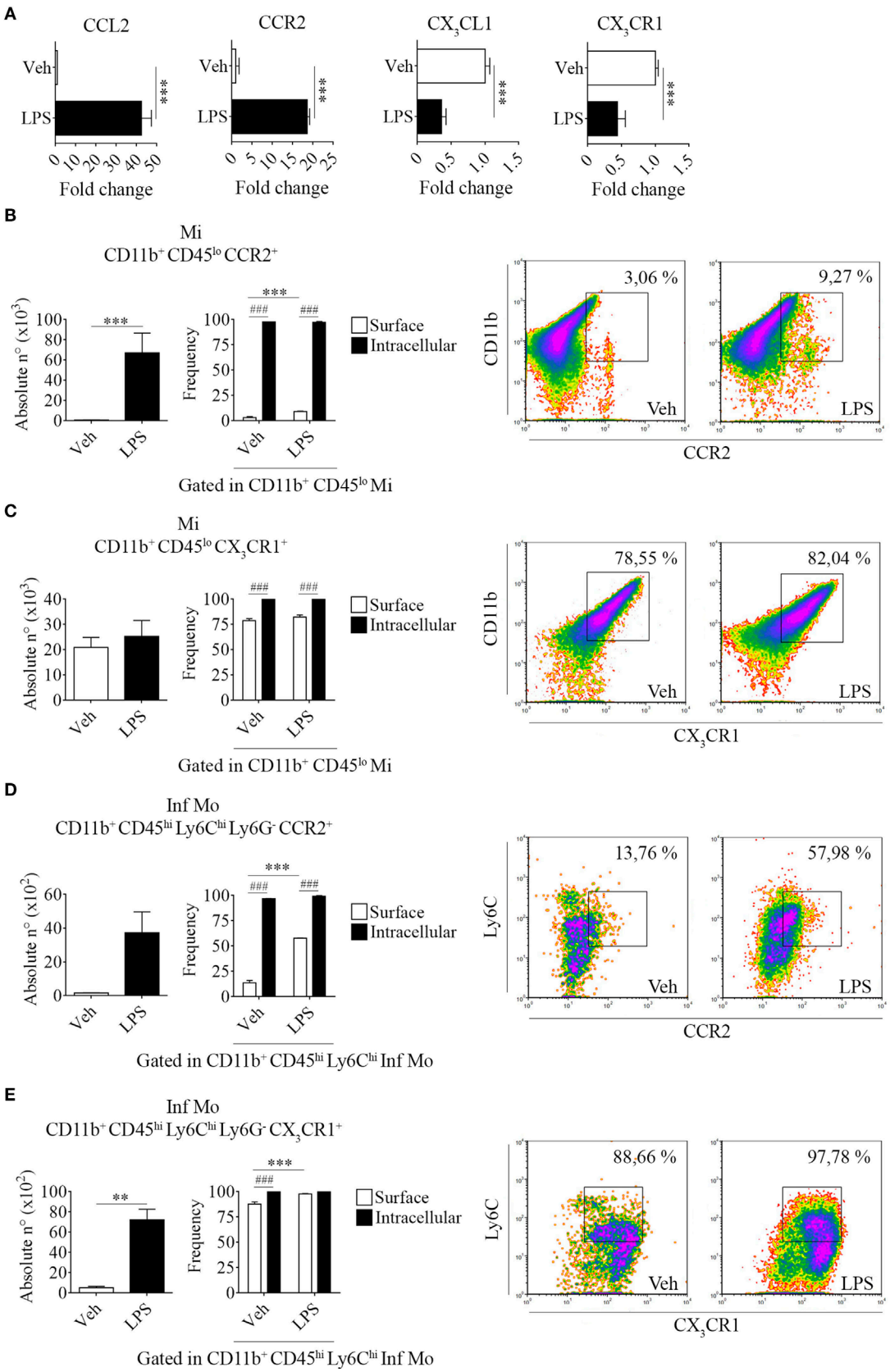


FIGURE 4 | Continued

FIGURE 4 | Continued
Increase of brain-resident CD11b$^+$ CD45^{lo} and peripheral CD11b$^+$ CD45^{hi} Ly6C^{hi} Ly6G$^-$ cells bearing CCR2 and CX$_3$CR1 in lipopolysaccharide (LPS)-treated mice. Mice were treated i.p. with either vehicle or 40 µg of LPS (1,6 mg/kg) for four consecutive days to induce neuroinflammation. Twelve hours post the last injection, mice were euthanized and RNA extracted from whole brain homogenates cells or immune cells isolated and labeled for subsequent flow cytometric analysis. **(A)** Gene expression analysis by real-time PCR of CCL2, CX$_3$CL1 and CCR2, CX$_3$CR1 in total bulk brain. Results are representative of at least two independent experiments (n = 3 animals per group). Relative quantification (RQ) was calculated based on the equation RQ = $2^{-\Delta\Delta Ct}$, where Ct is the threshold cycle to detect fluorescence. Ct data were normalized to the internal standard HPRT1. **(B,D)** Absolute number and **(C,E)** frequency of CD11b$^+$ CD45^{lo} microglial cells and CD11b$^+$ CD45^{hi} Ly6C^{hi} Ly6G$^-$ inflammatory monocytes expressing CCR2 and CX$_3$CR1, was assessed by flow cytometry. The percentage of these populations corresponding when gated in CD11b$^+$ CD45^{lo} or CD11b$^+$ CD45^{hi} Ly6C^{hi}, respectively. Representative density-plots illustrate the gating analysis strategy employed. Results are representative of two independent experiments (n = 3–6 animals per group). Data are expressed as mean ± SEM. Mi, microglial cells; Inf Mo, inflammatory monocytes.

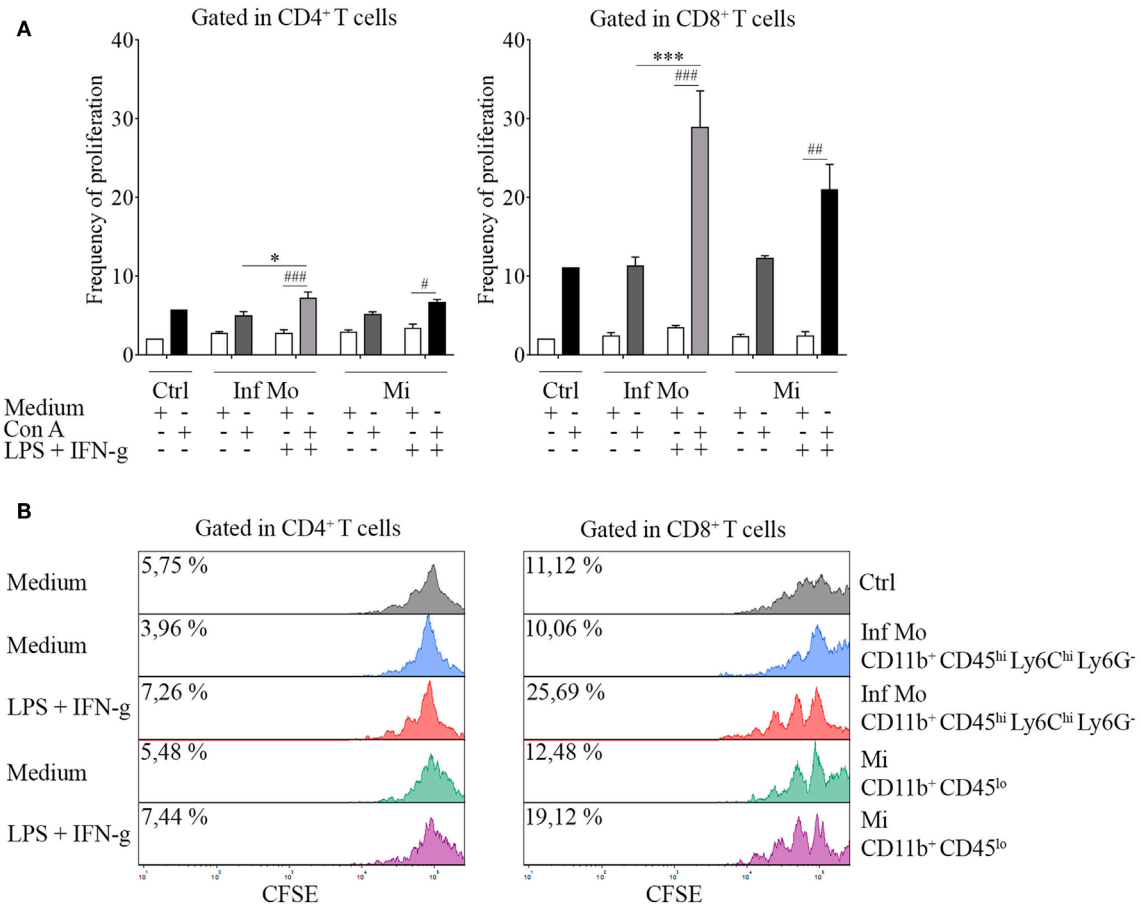


FIGURE 5 | Immune function of inflammatory CD11b$^+$ CD45^{hi} Ly6C^{hi} Ly6G$^-$ cells isolated after a systemic lipopolysaccharide (LPS) challenge. Mice were treated i.p. with either vehicle or 40 µg of LPS (1,6 mg/kg) for four consecutive days to induce neuroinflammation. Twelve hours post the last injection, mice were euthanized and immune cells were isolated from whole brain homogenates and labeled for subsequent cell sorting. **(A)** *In vivo* LPS-primed CD11b$^+$ CD45^{hi} Ly6C^{hi} Ly6G$^-$ inflammatory monocytes or CD11b$^+$ CD45^{lo} microglial cells isolated by cell sorting from a pool of mice brains were cocultured with CFSE (4 µM)-labeled naïve splenocytes at a 1:1 ratio (1 × 10^5 cell/mL) in the presence or absence of concanavalin A (Con A) (5 µg/mL). Cells from endotoxemic mice were challenged or not *ex vivo* with LPS (100 ng/mL) plus IFN-g (20 ng/mL) cocktail prior to the coculture. T cell frequency of proliferation was examined after 72 h by CFSE dilution through flow cytometry. Results are representative of two independent experiments combined (n = 17–20 animals). **(B)** Representative stacked histograms depicting CFSE dilution. Data are expressed as mean ± SEM. Ctrl, control; Inf Mo, inflammatory monocytes; Mi, microglial cells.

cocultured with naïve splenocytes in the presence or not of Con A. Interestingly, we found that LPS-primed inflammatory monocytes were able to induce T cell proliferation unlike microglia, in an increasing ratio-dependent manner (data not shown). To gain insight into this mechanism, we sought to test if peripheral isolated inflammatory monocytes and tissue-resident microglia might have functional plasticity by exposing or not these cells to a repeated *ex vivo* LPS challenge in addition with IFN-g as a combination of multiple activation signals prior to the coculture. Surprisingly, boosting of the cells showed an enhancement of T cell proliferation by inflammatory monocytes when compared to the single stimulation condition (**Figure 5A**), as pictured by the representative CFSE dilution stacked histograms (**Figure 5B**). These results demonstrate monocytes and microglia are sensitive

to pro-inflammatory re-stimulation and could differentially regulate T cell subsets multiplication, as suggested by $CD4^+$ T cell weakened proliferative response in comparison with the $CD8^+$ T cell proliferation.

Type I IFNs Are Required to Promote $CD11b^+$ $CD45^{hi}$ $Ly6C^{hi}$ $Ly6G^-$ Cell Recruitment to the CNS in Endotoxemic Mice

Recent studies proposed IFNs as crucial mediators in brain function but many questions regarding the role of these molecules in the CNS remain unanswered yet. We appealed to our previously described flow cytometric analysis strategy to delve deeper in the understanding of these cytokines and evaluate whether if they could be participating in the modulation of neuroinflammation.

Following a systemic challenge with LPS, we did not find any variation in the absolute number of microglia but a decrease in the absolute number of recruited peripheral leukocytes in IFNs deficient mice strains compared to WT mice. This effect upon LPS injection in KO mice was accompanied by a reduced weight loss (Figure S3 in Supplementary Material), probably correlating with the observed decline in the immune cell recruitment to their CNS. Unexpectedly, we found LPS favored the recruitment of peripheral inflammatory monocytes rather than neutrophils in animals devoid of IFN-g. Moreover, inflammatory monocytes proved to be recruited to the CNS in a type I IFN-dependent fashion as opposed to neutrophils, as shown by the impairment in their recruitment in IFN-a/b receptor knockout ($IFNAR^{-/-}$) brains (**Figures 6A,B**). In this sense, only LPS-challenged WT mice showed an increase in the recruitment of peripheral major histocompatibility class II (MHC II)-expressing inflammatory monocytes (Figure S4 in Supplementary Material). In order to clarify the underlying mechanism whereby peripheral inflammatory monocytes lacking the type I IFN receptor could mildly migrate to the CNS upon a systemic LPS administration, we then set out to identify the molecular mediator involved in this response. Thus, we separately isolated microglia, neutrophils and inflammatory monocytes and assessed the gene expression of several chemokine/receptor axes considered critical for the trafficking of these cells to the brain. As depicted by the representative gene array chart (**Figure 6C**), the increase in CCL2 gene expression levels in inflammatory monocytes suggest a redundant function for the recruitment of these cells. Indeed, the upregulation of CX_3CL1 in neutrophils (**Figures 6C,D**) implies a crosstalk of this chemokine with type I IFNs as well as a requirement of both mediators for a proper immune cell entry to the CNS under inflammatory circumstances.

DISCUSSION

The results presented identify inflammatory monocytes as gatekeepers of CNS immune surveillance (29) upon a LPS peripheral challenge, as determined by the augmentation of their recruitment when compared to other immune cell populations. This is in agreement with Cazareth et al. (12), which shows an enhanced migration of inflammatory monocytes but neither trafficking of neutrophils nor T and B lymphocytes to the CNS by means of a similar flow cytometry approach, following a single and acute systemic administration of LPS. On the contrary, the finding of a consistent recruitment of these latter cells in our experimental settings demonstrates that the outcome of a proposed model varies depending on the dose and timing regime of LPS exposure. Several studies have described the design of LPS models to assess the implications of central or peripheral inflammation in the development of a less-common neurodegenerative condition such as prion disease (4, 11, 26) or even to induce and mimic features of Alzheimer's (8) and Parkinson's disease (7) in naïve animals. Noteworthy, Ruiz-Valdepenas et al. (9) showed by intravital microscopy increased extravasation of dextran after a single moderate dose of LPS so it is certainly likely that in our neuroinflammation model this inflammogen would be gaining access, via BBB breakdown, to the parenchyma and activating directly to brain cells.

Similar to previous reports during pathogenic inflammation in experimental autoimmune encephalomyelitis (30, 31), we determined the presence of a peculiar subset of dendritic cells, termed inflammatory dendritic cells, in inflamed brains from endotoxemic mice. However, we particularly used FcεRI to characterize these cells, to date probably the best phenotypic marker to distinguish inflammatory dendritic cells from other myeloid cells and avoid giving a mistaken identity (18). Inflammatory dendritic cells characterize for being absent from steady-state tissues and differentiate, as well as microglia (19, 20), from monocytes during inflammation. This would at least partially explain the presence of these cells, as revealed here, in spite of the fact that LPS could actually block the conversion of inflammatory monocytes into dendritic cells *in vivo* (3).

Recent findings support the idea of leukocyte trafficking under physiological and pathological circumstances along circumventricular organs that function as gateways in the CNS such as the choroid plexus (32), a unique neuroimmunological interface positioned to integrate the signals received from the parenchyma with signals coming from circulating immune cells (33–35). Accordingly, we found recruitment but no infiltration of leukocytes in this site along with microglial and astrocytic reactivity after systemic inflammation evoked by LPS as revealed by both the retraction of their processes and enlargement of their cell bodies, which are classic traits of glial activation (5, 16, 36). It should be pointed out that our criteria for the use of the term infiltration was not that given by numerous works as a synonym of recruitment, but the phenomenon by which the cells can invade the parenchyma after their entry through the vessels. This is clearly not only a semantic problem, since the incorrect use of the term may lead to a misunderstanding of the results.

Myeloid cells recruitment to the CNS is a shared characteristic between several autoimmune and neurodegenerative diseases. Chemokine receptors CCR2 and CX_3CR1 are both essential for myeloid cell trafficking and localization of migrating leukocytes (17, 37) to the perivascular space (2, 38, 39). In this sense and consisting with previous observations (12), we found brain CCL2 production together with CCR2-expressing inflammatory monocytes would ease the selective migration of these cells to the CNS

(20, 40–42) following a LPS challenge. Moreover, downregulation of cerebral CX_3CL1 and its receptor CX_3CR1 would amplify this response, unleashing microglia pro-inflammatory role by removing the inhibition exerted by CX_3CL1 (5, 43, 44).

Unlike microglia, LPS priming of isolated inflammatory monocytes led to an induction of T cell proliferative response (45). Despite *ex vivo* re-stimulation with LPS and IFN-g, a potent stimulus for the induction of T cell-suppressive nitric oxide

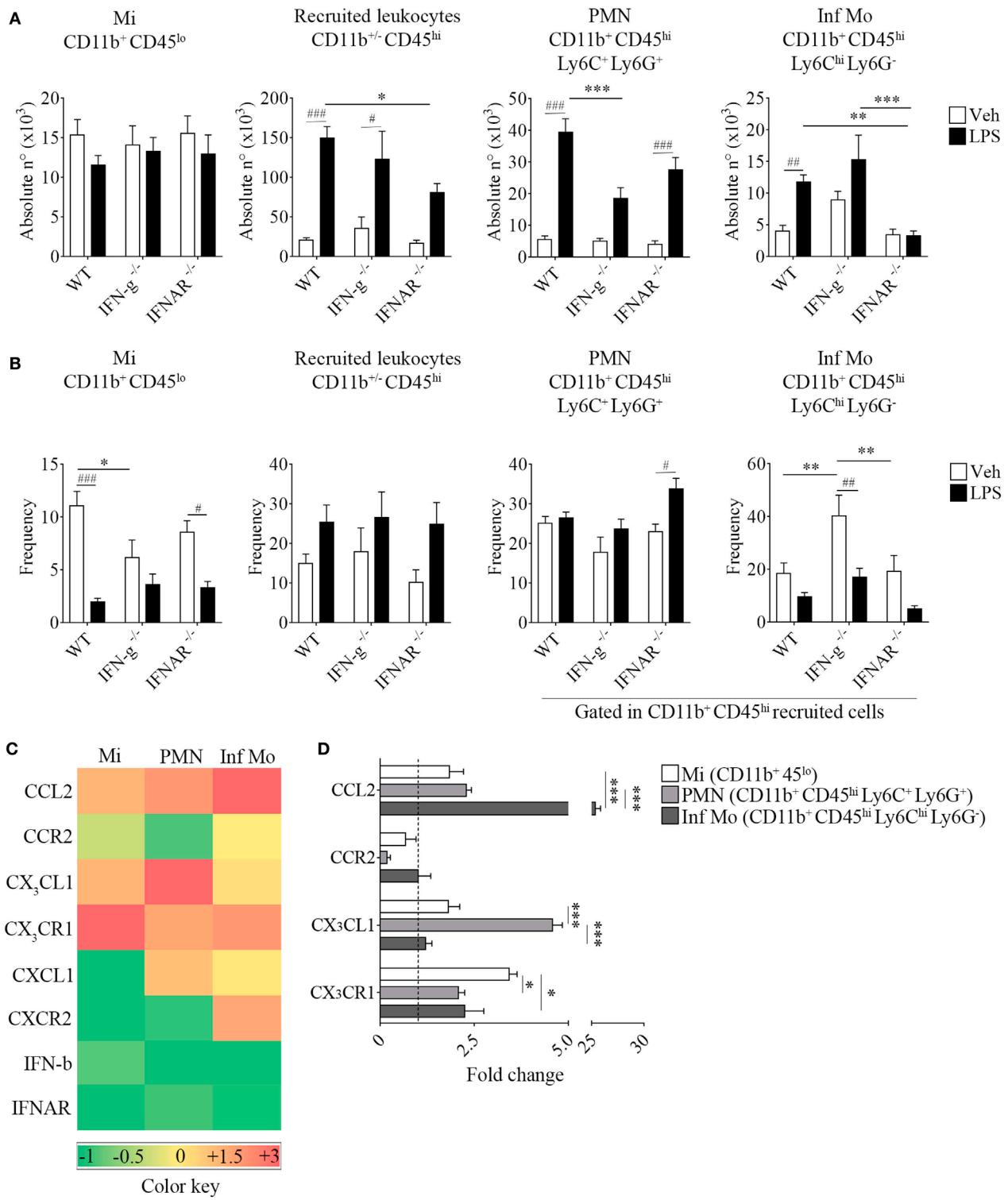


FIGURE 6 | Continued

FIGURE 6 | Continued
Impaired recruitment of inflammatory CD11b$^+$ CD45^{hi} Ly6C^{hi} Ly6G$^-$ cells in IFNAR$^{-/-}$ endotoxemic mice. Mice were treated i.p. with either vehicle or 40 μg of lipopolysaccharide (LPS) (1,6 mg/kg) for four consecutive days to induce neuroinflammation. Twelve hours post the last injection, mice were euthanized and immune cells were isolated from whole brain homogenates and labeled for subsequent flow cytometric analysis or cell sorting. **(A)** Absolute number and **(B)** frequency of CD11b$^+$ CD45^{lo} microglial cells, CD11b$^{+/-}$ CD45^{hi} recruited leukocytes, CD11b$^+$ CD45^{hi} Ly6C$^+$ Ly6G$^+$ neutrophils, and CD11b$^+$ CD45^{hi} Ly6C^{hi} Ly6G$^-$ inflammatory monocytes derived from wild-type (WT), IFN-g$^{-/-}$, and IFNAR$^{-/-}$ mice, were assessed by flow cytometry. Results are an average of three independent experiments (n = 3–4 animals per group) for each knockout mice strain. **(C)** Heat map rendering the gene expression analysis (fold increase) by real-time PCR of CCL2, CX_3CL1, CXCL1, IFN-b and CCR2, CX_3CR1, CXCR2, IFNAR of LPS-primed CD11b$^+$ CD45^{lo} microglial cells, CD11b$^+$ CD45^{hi} Ly6C$^+$ Ly6G$^+$ neutrophils and CD11b$^+$ CD45^{hi} Ly6C^{hi} Ly6G$^-$ inflammatory monocytes isolated from a pool of endotoxemic WT vs IFNAR$^{-/-}$ mice brains. Relative quantification (RQ) was calculated based on the equation $RQ = 2^{-\Delta\Delta Ct}$, where Ct is the threshold cycle to detect fluorescence. Ct data were normalized to the internal standard HPRT1. Results are representative of two independent experiments (n = 9–17 animals per group). **(D)** Further comparison between CCL2, CX_3CL1 and CCR2, CX_3CR1 gene expression of LPS-primed CD11b$^+$ CD45^{lo} microglial cells, CD11b$^+$ CD45^{hi} Ly6C$^+$ Ly6G$^+$ neutrophils, and CD11b$^+$ CD45^{hi} Ly6C^{hi} Ly6G$^-$ inflammatory monocytes from WT (dashed line) vs IFNAR$^{-/-}$ mice. Data are expressed as mean ± SEM. Mi, microglial cells; PMN, neutrophils; Inf Mo, inflammatory monocytes.

(46, 47), inflammatory monocytes showed responsiveness in the enhancement of T cell proliferation. Zhu et al. (48) clearly showed that CNS isolated inflammatory monocytes could switch their function (49) from antigen presentation to T suppression depending on their activation state and therefore, their ability to produce nitric oxide. In this regard, LPS-treated inflammatory monocytes exhibited an activation threshold higher enough to differentially modulate CD4$^+$ (50) and CD8$^+$ T cell subsets but not to promote T cell suppression. Besides, the surprisingly functional incompetence of tissue-resident microglia to favor T cell proliferation, which contrasts with other studies done in experimental autoimmune encephalomyelitis (51), highlights the role of peripheral inflammatory monocytes to elicit an appropriate immune response within the CNS in endotoxemic mice.

Type I IFN-mediated recruitment of inflammatory monocytes confirms the importance of these cytokines to orchestrate the trafficking of these cells (52–55) to the CNS (40, 56, 57) and reveals an unknown interaction with CX_3CL1 to exert its role. Janova et al. (13) recently described an essential function for TLR4 co-receptor CD14 in microglial sensing of CNS damage (6, 10) and further characterized a loop by which IFN-b signaling limits CXCL1 overproduction, thereby modulating myeloid recruitment. Even though CXCL1 appear to be dispensable for neutrophils (14), this could partially explain the reason why these cells still migrate to the CNS albeit type I IFN deficiency.

Although experimental procedures to distinguish properly between microglia and monocytes in CNS impose practical limitations, the results presented here compares the phenotypic and functional features between these tissue-resident vs peripheral recruited cells in LPS-induced neuroinflammation, identifying inflammatory monocytes as key surveillants of the CNS and potential targets for immunotherapy.

ETHICS STATEMENT

All experiments were done in compliance with the procedures outlined in the "Guide for the Care and Use of Laboratory Animals" (NIH Publication No. 86-23, 1985). The experimental protocols were approved by the Institutional Animal Care and Use Committee (IACUC). Our animal facility obtained NIH animal welfare assurance (No. A5802-01, OLAW, NIH, US).

AUTHOR CONTRIBUTIONS

JPR conceived and designed the research study, performed the experiments, analyzed data, and wrote the manuscript; CB, EG, and DA performed the experiments and analyzed the data; NB performed the experiments; CRG conceived and designed the research; PI conceived and designed the research study and wrote the manuscript; all authors reviewed the manuscript before submission.

ACKNOWLEDGMENTS

The authors thank Alejandra Romero for cell culture assistance; Fabricio Navarro, Diego Luti, Carolina Florit, Victoria Blanco, and Ivanna Novotny-Núñez for animal care and Pilar Crespo and Paula Abadie for cell sorting technical support.

FUNDING

This work was supported in part by Secretaría de Ciencia y Tecnología from Universidad Nacional de Córdoba (SECyT), Agencia Nacional de Promoción Científica y Tecnológica (ANPCyT), Fondo para la Investigación Científica y Tecnológica (FONCyT), and Consejo Nacional de Investigaciones Científicas y Técnicas (CONICET).

SUPPLEMENTARY MATERIAL

The Supplementary Material for this article can be found online at http://www.frontiersin.org/article/10.3389/fimmu.2017.01666/full#supplementary-material.

FIGURE S1 | Gating strategy sequence applied for the flow cytometric analysis and cell sorting. Mice were treated i.p. with 40 μg of lipopolysaccharide (LPS) (1,6 mg/kg) for four consecutive days to induce neuroinflammation. Twelve hours post the last injection, mice were euthanized and immune cells were isolated from whole brain homogenates and labeled for subsequent flow cytometric analysis or cell sorting. **(A)** FSC vs SSC, FSC-W vs FSC-H, and SSC-W vs SSC-H flow cytometry density-plots illustrating the gating analysis strategy employed to exclude cell doublets. **(B)** Hierarchical gate view depicting the strategy sequence adopted to assess the phenotypic features of immune cells. Representative rectangle gates were used in all cases for statistical purpose rather than for selection of a cell population.

FIGURE S2 | Two-step intracellular staining Ctrl. Mice were treated i.p. with 40 µg of lipopolysaccharide (LPS) (1,6 mg/kg) for four consecutive days to induce neuroinflammation. Twelve hours post the last injection, mice were euthanized and immune cells isolated and labeled for subsequent flow cytometric analysis. CD11b/Ly6C vs Alexa Fluor 488 flow cytometry density-plots illustrating the secondary antibody control from the intracellular labeling of CCR2 and CX_3CR1. Representative rectangle gates were used in all cases for statistical purpose rather than for selection of a cell population.

FIGURE S3 | Weight loss comparison between wild-type (WT), IFN-g$^{-/-}$, and IFNAR$^{-/-}$ mice strains following LPS stimulation. Weight loss was assessed in WT, IFN-g$^{-/-}$, and IFNAR$^{-/-}$ mice following the i.p. administration scheme with vehicle or 40 µg of lipopolysaccharide (LPS) (1,6 mg/kg) for four consecutive days to induce neuroinflammation. Results are an average of three independent experiments (n = 3–4 animals per group) for each knockout mice strain. Data are expressed as mean ± SEM. Statistical significance levels were set as follows: ### if $p < 0.001$ (WT-Veh, IFN-g$^{-/-}$ Veh, and IFNAR$^{-/-}$ Veh vs WT-LPS, IFN-g$^{-/-}$ LPS, and IFNAR$^{-/-}$ LPS), *** if $p < 0.001$ (WT-LPS vs IFN-g$^{-/-}$ LPS), [a] if $p < 0.001$ (WT-LPS vs IFNAR$^{-/-}$ LPS).

FIGURE S4 | Major histocompatibility class II (MHC II) expression comparison between brain-resident CD11b^{+} CD45^{lo} vs peripheral CD11b^{+} CD45^{hi} Ly6C^{+} Ly6G^{+} and CD11b^{+} CD45^{hi} Ly6C^{hi} Ly6G^{-} cells in LPS-treated WT, IFN-g$^{-/-}$, and IFNAR$^{-/-}$ mice strains. Mice were treated i.p. with either vehicle or 40 µg of lipopolysaccharide (LPS) (1,6 mg/kg) for four consecutive days to induce neuroinflammation. Twelve hours post the last injection, mice were euthanised and immune cells were isolated from whole brain homogenates and labelled for subsequent flow cytometric analysis. **(A)** Absolute number and **(B)** mean fluorescence intensity (MFI) of CD11b^{+} CD45^{lo} MHC II^{+} microglial cells, CD11b^{+} CD45^{hi} Ly6C^{+} Ly6G^{+} MHC II^{+} neutrophils and CD11b^{+} CD45^{hi} Ly6C^{hi} Ly6G^{-} MHC II^{+} inflammatory monocytes derived from WT, IFN-g$^{-/-}$ and IFNAR$^{-/-}$ mice, was assessed by flow cytometry. Results are an average of three independent experiments (n = 3–4 animals per group) for each knock-out mice strain. Data are expressed as mean ± SEM.

REFERENCES

1. Ousman SS, Kubes P. Immune surveillance in the central nervous system. *Nat Neurosci* (2012) 15(8):1096–101. doi:10.1038/nn.3161
2. Prinz M, Priller J. The role of peripheral immune cells in the CNS in steady state and disease. *Nat Neurosci* (2017) 20(2):136–44. doi:10.1038/nn.4475
3. Rotta G, Edwards EW, Sangaletti S, Bennett C, Ronzoni S, Colombo MP, et al. Lipopolysaccharide or whole bacteria block the conversion of inflammatory monocytes into dendritic cells in vivo. *J Exp Med* (2003) 198(8):1253–63. doi:10.1084/jem.20030335
4. Cunningham C, Wilcockson DC, Campion S, Lunnon K, Perry VH. Central and systemic endotoxin challenges exacerbate the local inflammatory response and increase neuronal death during chronic neurodegeneration. *J Neurosci* (2005) 25(40):9275–84. doi:10.1523/JNEUROSCI.2614-05.2005
5. Cardona AE, Pioro EP, Sasse ME, Kostenko V, Cardona SM, Dijkstra IM, et al. Control of microglial neurotoxicity by the fractalkine receptor. *Nat Neurosci* (2006) 9(7):917–24. doi:10.1038/nn1715
6. Zhou H, Lapointe BM, Clark SR, Zbytnuik L, Kubes P. A requirement for microglial TLR4 in leukocyte recruitment into brain in response to lipopolysaccharide. *J Immunol* (2006) 177(11):8103–10. doi:10.4049/jimmunol.177.11.8103
7. Qin L, Wu X, Block ML, Liu Y, Breese GR, Hong JS, et al. Systemic LPS causes chronic neuroinflammation and progressive neurodegeneration. *Glia* (2007) 55(5):453–62. doi:10.1002/glia.20467
8. Lee JW, Lee YK, Yuk DY, Choi DY, Ban SB, Oh KW, et al. Neuro-inflammation induced by lipopolysaccharide causes cognitive impairment through enhancement of beta-amyloid generation. *J Neuroinflammation* (2008) 5:37. doi:10.1186/1742-2094-5-37
9. Ruiz-Valdepenas L, Martinez-Orgado JA, Benito C, Millan A, Tolon RM, Romero J. Cannabidiol reduces lipopolysaccharide-induced vascular changes and inflammation in the mouse brain: an intravital microscopy study. *J Neuroinflammation* (2011) 8(1):5. doi:10.1186/1742-2094-8-5
10. Melief J, Koning N, Schuurman KG, Van De Garde MD, Smolders J, Hoek RM, et al. Phenotyping primary human microglia: tight regulation of LPS responsiveness. *Glia* (2012) 60(10):1506–17. doi:10.1002/glia.22370
11. Cunningham C. Microglia and neurodegeneration: the role of systemic inflammation. *Glia* (2013) 61(1):71–90. doi:10.1002/glia.22350
12. Cazareth J, Guyon A, Heurteaux C, Chabry J, Petit-Paitel A. Molecular and cellular neuroinflammatory status of mouse brain after systemic lipopolysaccharide challenge: importance of CCR2/CCL2 signaling. *J Neuroinflammation* (2014) 11:132. doi:10.1186/1742-2094-11-132
13. Janova H, Bottcher C, Holtman IR, Regen T, van Rossum D, Gotz A, et al. CD14 is a key organizer of microglial responses to CNS infection and injury. *Glia* (2016) 64(4):635–49. doi:10.1002/glia.22955
14. Reber LL, Gillis CM, Starkl P, Jonsson F, Sibilano R, Marichal T, et al. Neutrophil myeloperoxidase diminishes the toxic effects and mortality induced by lipopolysaccharide. *J Exp Med* (2017) 214(5):1249–58. doi:10.1084/jem.20161238
15. Tay TL, Mai D, Dautzenberg J, Fernandez-Klett F, Lin G, Sagar, et al. A new fate mapping system reveals context-dependent random or clonal expansion of microglia. *Nat Neurosci* (2017) 20(6):793–803. doi:10.1038/nn.4547
16. Nimmerjahn A, Kirchhoff F, Helmchen F. Resting microglial cells are highly dynamic surveillants of brain parenchyma in vivo. *Science* (2005) 308(5726):1314–8. doi:10.1126/science.1110647
17. Geissmann F, Jung S, Littman DR. Blood monocytes consist of two principal subsets with distinct migratory properties. *Immunity* (2003) 19(1):71–82. doi:10.1016/s1074-7613(03)00174-2
18. Segura E, Amigorena S. Inflammatory dendritic cells in mice and humans. *Trends Immunol* (2013) 34(9):440–5. doi:10.1016/j.it.2013.06.001
19. Mildner A, Schmidt H, Nitsche M, Merkler D, Hanisch UK, Mack M, et al. Microglia in the adult brain arise from Ly-6ChiCCR2+ monocytes only under defined host conditions. *Nat Neurosci* (2007) 10(12):1544–53. doi:10.1038/nn2015
20. Getts DR, Terry RL, Getts MT, Muller M, Rana S, Shrestha B, et al. Ly6c+ "inflammatory monocytes" are microglial precursors recruited in a pathogenic manner in West Nile virus encephalitis. *J Exp Med* (2008) 205(10):2319–37. doi:10.1084/jem.20080421
21. Aspelund A, Antila S, Proulx ST, Karlsen TV, Karaman S, Detmar M, et al. A dural lymphatic vascular system that drains brain interstitial fluid and macromolecules. *J Exp Med* (2015) 212(7):991–9. doi:10.1084/jem.20142290
22. Louveau A, Smirnov I, Keyes TJ, Eccles JD, Rouhani SJ, Peske JD, et al. Structural and functional features of central nervous system lymphatic vessels. *Nature* (2015) 523(7560):337–41. doi:10.1038/nature14432
23. Deczkowska A, Baruch K, Schwartz M. Type I/II interferon balance in the regulation of brain physiology and pathology. *Trends Immunol* (2016) 37(3):181–92. doi:10.1016/j.it.2016.01.006
24. Ransohoff RM, Engelhardt B. The anatomical and cellular basis of immune surveillance in the central nervous system. *Nat Rev Immunol* (2012) 12(9):623–35. doi:10.1038/nri3265
25. Peelaerts W, Bousset L, Van der Perren A, Moskalyuk A, Pulizzi R, Giugliano M, et al. alpha-Synuclein strains cause distinct synucleinopathies after local and systemic administration. *Nature* (2015) 522(7556):340–4. doi:10.1038/nature14547
26. Perry VH, Newman TA, Cunningham C. The impact of systemic infection on the progression of neurodegenerative disease. *Nat Rev Neurosci* (2003) 4(2):103–12. doi:10.1038/nrn1032
27. Yamasaki R, Lu H, Butovsky O, Ohno N, Rietsch AM, Cialic R, et al. Differential roles of microglia and monocytes in the inflamed central nervous system. *J Exp Med* (2014) 211(8):1533–49. doi:10.1084/jem.20132477
28. Ritzel RM, Patel AR, Grenier JM, Crapser J, Verma R, Jellison ER, et al. Functional differences between microglia and monocytes after ischemic stroke. *J Neuroinflammation* (2015) 12:106. doi:10.1186/s12974-015-0329-1
29. Shi C, Pamer EG. Monocyte recruitment during infection and inflammation. *Nat Rev Immunol* (2011) 11(11):762–74. doi:10.1038/nri3070
30. Greter M, Helft J, Chow A, Hashimoto D, Mortha A, Agudo-Cantero J, et al. GM-CSF controls nonlymphoid tissue dendritic cell homeostasis but is

dispensable for the differentiation of inflammatory dendritic cells. *Immunity* (2012) 36(6):1031–46. doi:10.1016/j.immuni.2012.03.027
31. Ji Q, Castelli L, Goverman JM. MHC class I-restricted myelin epitopes are cross-presented by Tip-DCs that promote determinant spreading to CD8(+) T cells. *Nat Immunol* (2013) 14(3):254–61. doi:10.1038/ni.2513
32. Ransohoff RM, Kivisakk P, Kidd G. Three or more routes for leukocyte migration into the central nervous system. *Nat Rev Immunol* (2003) 3(7):569–81. doi:10.1038/nri1130
33. Shechter R, Miller O, Yovel G, Rosenzweig N, London A, Ruckh J, et al. Recruitment of beneficial M2 macrophages to injured spinal cord is orchestrated by remote brain choroid plexus. *Immunity* (2013) 38(3):555–69. doi:10.1016/j.immuni.2013.02.012
34. Baruch K, Deczkowska A, David E, Castellano JM, Miller O, Kertser A, et al. Aging. Aging-induced type I interferon response at the choroid plexus negatively affects brain function. *Science* (2014) 346(6205):89–93. doi:10.1126/science.1252945
35. Baruch K, Kertser A, Porat Z, Schwartz M. Cerebral nitric oxide represses choroid plexus NFkappaB-dependent gateway activity for leukocyte trafficking. *EMBO J* (2015) 34(13):1816–28. doi:10.15252/embj.201591468
36. Dickens AM, Tovar YRLB, Yoo SW, Trout AL, Bae M, Kanmogne M, et al. Astrocyte-shed extracellular vesicles regulate the peripheral leukocyte response to inflammatory brain lesions. *Sci Signal* (2017) 10(473):eaai7696. doi:10.1126/scisignal.aai7696
37. Dal-Secco D, Wang J, Zeng Z, Kolaczkowska E, Wong CH, Petri B, et al. A dynamic spectrum of monocytes arising from the in situ reprogramming of CCR2+ monocytes at a site of sterile injury. *J Exp Med* (2015) 212(4):447–56. doi:10.1084/jem.20141539
38. Ransohoff RM. Chemokines and chemokine receptors: standing at the crossroads of immunobiology and neurobiology. *Immunity* (2009) 31(5):711–21. doi:10.1016/j.immuni.2009.09.010
39. Prinz M, Priller J. Tickets to the brain: role of CCR2 and CX3CR1 in myeloid cell entry in the CNS. *J Neuroimmunol* (2010) 224(1–2):80–4. doi:10.1016/j.jneuroim.2010.05.015
40. D'Mello C, Le T, Swain MG. Cerebral microglia recruit monocytes into the brain in response to tumor necrosis factoralpha signaling during peripheral organ inflammation. *J Neurosci* (2009) 29(7):2089–102. doi:10.1523/JNEUROSCI.3567-08.2009
41. Saederup N, Cardona AE, Croft K, Mizutani M, Cotleur AC, Tsou CL, et al. Selective chemokine receptor usage by central nervous system myeloid cells in CCR2-red fluorescent protein knock-in mice. *PLoS One* (2010) 5(10):e13693. doi:10.1371/journal.pone.0013693
42. Hammond MD, Taylor RA, Mullen MT, Ai Y, Aguila HL, Mack M, et al. CCR2+ Ly6C(hi) inflammatory monocyte recruitment exacerbates acute disability following intracerebral hemorrhage. *J Neurosci* (2014) 34(11):3901–9. doi:10.1523/JNEUROSCI.4070-13.2014
43. Ransohoff RM, Cardona AE. The myeloid cells of the central nervous system parenchyma. *Nature* (2010) 468(7321):253–62. doi:10.1038/nature09615
44. Limatola C, Ransohoff RM. Modulating neurotoxicity through CX3CL1/CX3CR1 signaling. *Front Cell Neurosci* (2014) 8:229. doi:10.3389/fncel.2014.00229
45. Braun M, Vaibhav K, Saad N, Fatima S, Brann DW, Vender JR, et al. Activation of myeloid TLR4 mediates T lymphocyte polarization after traumatic brain injury. *J Immunol* (2017) 198(9):3615–26. doi:10.4049/jimmunol.1601948
46. Gabrilovich DI, Nagaraj S. Myeloid-derived suppressor cells as regulators of the immune system. *Nat Rev Immunol* (2009) 9(3):162–74. doi:10.1038/nri2506
47. Condamine T, Gabrilovich DI. Molecular mechanisms regulating myeloid-derived suppressor cell differentiation and function. *Trends Immunol* (2011) 32(1):19–25. doi:10.1016/j.it.2010.10.002
48. Zhu B, Kennedy JK, Wang Y, Sandoval-Garcia C, Cao L, Xiao S, et al. Plasticity of Ly-6C(hi) myeloid cells in T cell regulation. *J Immunol* (2011) 187(5):2418–32. doi:10.4049/jimmunol.1100403
49. Shalova IN, Lim JY, Chittezhath M, Zinkernagel AS, Beasley F, Hernandez-Jimenez E, et al. Human monocytes undergo functional re-programming during sepsis mediated by hypoxia-inducible factor-1alpha. *Immunity* (2015) 42(3):484–98. doi:10.1016/j.immuni.2015.02.001
50. Waschbisch A, Schroder S, Schraudner D, Sammet L, Weksler B, Melms A, et al. Pivotal role for CD16+ monocytes in immune surveillance of the central nervous system. *J Immunol* (2016) 196(4):1558–67. doi:10.4049/jimmunol.1501960
51. Wlodarczyk A, Lobner M, Cedile O, Owens T. Comparison of microglia and infiltrating CD11c(+) cells as antigen presenting cells for T cell proliferation and cytokine response. *J Neuroinflammation* (2014) 11:57. doi:10.1186/1742-2094-11-57
52. Jia T, Leiner I, Dorothee G, Brandl K, Pamer EG. MyD88 and Type I interferon receptor-mediated chemokine induction and monocyte recruitment during *Listeria monocytogenes* infection. *J Immunol* (2009) 183(2):1271–8. doi:10.4049/jimmunol.0900460
53. Uyangaa E, Kim JH, Patil AM, Choi JY, Kim SB, Eo SK. Distinct upstream role of type I IFN signaling in hematopoietic stem cell-derived and epithelial resident cells for concerted recruitment of Ly-6Chi monocytes and NK cells via CCL2-CCL3 cascade. *PLoS Pathog* (2015) 11(11):e1005256. doi:10.1371/journal.ppat.1005256
54. Sammicheli S, Kuka M, Di Lucia P, de Oya NJ, De Giovanni M, Fioravanti J, et al. Inflammatory monocytes hinder antiviral B cell responses. *Sci Immunol* (2016) 1(4):eaah6789. doi:10.1126/sciimmunol.aah6789
55. Lee AJ, Chen B, Chew MV, Barra NG, Shenouda MM, Nham T, et al. Inflammatory monocytes require type I interferon receptor signaling to activate NK cells via IL-18 during a mucosal viral infection. *J Exp Med* (2017) 214(4):1153–67. doi:10.1084/jem.20160880
56. Prinz M, Schmidt H, Mildner A, Knobeloch KP, Hanisch UK, Raasch J, et al. Distinct and nonredundant in vivo functions of IFNAR on myeloid cells limit autoimmunity in the central nervous system. *Immunity* (2008) 28(5):675–86. doi:10.1016/j.immuni.2008.03.011
57. Wolf Y, Shemer A, Polonsky M, Gross M, Mildner A, Yona S, et al. Autonomous TNF is critical for in vivo monocyte survival in steady state and inflammation. *J Exp Med* (2017) 214(4):905–17. doi:10.1084/jem.20160499

Conflict of Interest Statement: The authors declare that the research was conducted in the absence of any commercial or financial relationships that could be construed as a potential conflict of interest.

Copyright © 2017 Peralta Ramos, Bussi, Gaviglio, Arroyo, Baez, Rodriguez-Galan and Iribarren. This is an open-access article distributed under the terms of the Creative Commons Attribution License (CC BY). The use, distribution or reproduction in other forums is permitted, provided the original author(s) or licensor are credited and that the original publication in this journal is cited, in accordance with accepted academic practice. No use, distribution or reproduction is permitted which does not comply with these terms.

frontiers in Immunology

MINI REVIEW
published: 30 July 2018
doi: 10.3389/fimmu.2018.01726

Monocyte Subsets: Phenotypes and Function in Tuberculosis Infection

*Pavithra Sampath[1], Kadar Moideen[2], Uma Devi Ranganathan[1] and Ramalingam Bethunaickan[1]**

[1] Department of Immunology, National Institute for Research in Tuberculosis, Chennai, India, [2] International Center of Excellence in Research, National Institute for Research in Tuberculosis, National Institutes for Health, Chennai, India

Monocytes are critical defense components that play an important role in the primary innate immune response. The heterogeneous nature of monocytes and their ability to differentiate into either monocyte-derived macrophages or monocyte-derived dendritic cells allows them to serve as a bridge between the innate and adaptive immune responses. Current studies of monocytes based on immunofluorescence, single-cell RNA sequencing and whole mass spectrometry finger printing reveals different classification systems for monocyte subsets. In humans, three circulating monocyte subsets are classified based on relative expression levels of CD14 and CD16 surface proteins, namely classical, intermediate and non-classical subsets. Transcriptomic analyses of these subsets help to define their distinct functional properties. Tuberculosis (TB) is a disease instigated by the deadly pathogen *Mycobacterium tuberculosis.* Current research on monocytes in TB has indicated that there are alterations in the frequency of intermediate and non-classical subsets suggesting their impact in bacterial persistence. In this review, we will focus on these monocyte subsets, including their classification, frequency distribution, cytokine profiles, role as a biomarker and will comment on future directions for understanding the salient phenotypic and functional properties relevant to TB pathogenesis.

Keywords: monocyte subsets, CD14$^+$ monocytes, CD16$^+$ monocytes, biomarkers for tuberculosis, monocyte to lymphocyte ratio, monocyte signatures, *Mycobacterium tuberculosis*

OPEN ACCESS

Edited by:
Geanncarlo Lugo-Villarino, UMR5089 Institut de Pharmacologie et de Biologie Structurale (IPBS), France

Reviewed by:
Masaaki Miyazawa, Kindai University, Japan
Werner Solbach, Universität zu Lübeck, Germany

****Correspondence:***
Ramalingam Bethunaickan
bramalingam@gmail.com, ramalingam.b@nirt.res.in

Specialty section:
This article was submitted to Microbial Immunology, a section of the journal Frontiers in Immunology

Received: *13 December 2017*
Accepted: *12 July 2018*
Published: *30 July 2018*

Citation:
Sampath P, Moideen K, Ranganathan UD and Bethunaickan R (2018) Monocyte Subsets: Phenotypes and Function in Tuberculosis Infection. Front. Immunol. 9:1726. doi: 10.3389/fimmu.2018.01726

INTRODUCTION

Mononuclear cells (monocytes/macrophages) are professional phagocytes that are highly skilled in defense against many pathogens including *Mycobacterium tuberculosis* (MTB). In MTB infection, the phenomenon of granuloma formation helps to isolate organisms and prevent their dissemination, besides, providing a niche for the survival of MTB without damage over long periods of time. Monocytes also participate in many other processes such as homeostasis, tumor surveillance, tissue repair, microbial resistance, maintenance of tissue integrity, apoptosis, necrosis, autophagy, etc. Advances in subset classification of mononuclear cells, their phenotypic and functional properties, and their modulation during disease conditions has stimulated research on identifying monocyte-derived biomarkers for diagnostic and treatment purposes.

CIRCULATING MONOCYTES AND THEIR SUBSETS

Human monocytes are bone marrow-derived leukocytes that circulate in the blood and can differentiate into monocyte-derived macrophages and monocyte-derived dendritic cells that govern innate and adaptive immune responses (1). These cells are heterogeneous in nature and exhibit

high plasticity. Subset identification of monocytes is based on the relative expression of CD14 [co-receptor for toll-like receptor 4 (TLR4) and mediates lipopolysaccharide (LPS) signaling] and CD16 (Fc gamma receptor IIIa). Flow cytometric phenotyping has identified three different populations of monocytes namely, classical ($CD14^{++}$, $CD16^{-}$), intermediate ($CD14^{+}$, $CD16^{+}$), and non-classical ($CD14^{+}$, $CD16^{++}$) monocytes (2). The three monocyte subsets are phenotypically and functionally different. Earlier studies carried out by Murdoch et al. (3) and Venneri et al. (4) clearly identified two distinct populations of $CD16^{+}$ (intermediate and non-classical) monocytes based on the surface expression and function of the Tie-2 marker. In addition, expression of Slan (6-sulfo LacNac) further distinguished the non-classical and intermediate monocyte subsets (5). However, the function of intermediate population is still not defined with some reports suggesting that they are related to the classical subset and others suggesting that they are related to the non-classical subset. Classical monocytes comprise about 80–95% of circulating monocytes. These cells are highly phagocytic and are known to be important scavenger cells. Intermediate monocytes comprise about 2–8% of circulating monocytes. Their functions include production of reactive oxygen species (ROS), antigen presentation, participating in the proliferation and stimulation of T cells, inflammatory responses, and angiogenesis. Non-classical monocytes comprise about 2–11% of circulating monocytes. They are mobile in nature and patrol the endothelium in search of injury. They can have pro-inflammatory behavior and secrete inflammatory cytokines in response to infection. These cells are also involved in antigen presentation and T cell stimulation (6, 7). Phenotypic and functional differences of these subsets are listed in **Table 1**.

Subsets of monocytes have also been characterized and classified by various functional studies. Smedman et al. classified monocyte subsets into two groups based on cytokine induction by lipoteichoic acid and LPS; one larger population of cells secreting interleukin (IL)-1beta, IL-6, TNF-alpha, and CCL4 and a second smaller population of cells secreting GM-CSF, IL-10, and IL-12 p40 (31). Gren et al. using single-cell PCR gene expression identified 22 genes that are expressed by the classical population, 8 that characterize the intermediate population, and 6 that distinguish the non-classical population (32). Resting and activated monocyte subsets can be effectively distinguished using whole cell mass spectrometry fingerprinting (33). All these studies provide a platform to study further key details about monocyte phenotype and function, their behavior during disease and their interactions with pathogens.

FUNCTIONAL ROLE OF MONOCYTE SUBSETS DEFINED BY TRANSCRIPTOMICS AND PROTEOMICS

Transcriptomic, and proteomic studies can help to decode the functional variation within monocyte subsets. Classical monocytes mainly promote antimicrobial activity by characteristic upregulation of myeloperoxidase (MPO), lysozyme C precursor (LYZ), S100 calcium binding protein A9 (S100A9), eosinophil cationic protein precursor (RNase3), phospholipase B domain containing 1 (PLBD1), and Cathepsin G (CTSG), at both mRNA and protein levels (13, 34). Expression of pro-inflammatory mediators, particularly, S100A12, S100A9, and S100A8 is a hallmark of this subset, but other stimuli can potentially mediate even tissue repair functions, such as wound healing, angiogenesis, and coagulation (6, 13). Non-classical monocytes exhibit upregulation in the mRNA levels of heme oxygenase 1 (HMOX1), Villin 2 (VIL2), and Src family kinases constituting hemopoietic cell kinase (HCK) and tyrosine-protein kinase Lyn (LYN) and protein levels of actin related proteins (ARP2 and ARP3), HCK and LYN. These proteins phosphorylate the immunoreceptor tyrosine-based activation motif (ITAM) of Fc receptors leading to recruitment of downstream genes necessary for cytoskeletal remodeling suggesting a role for this macrophage subset in Fc receptor-mediated phagocytosis (34). In addition, upregulation of Rho GTPases, RhoC, and RhoF with their activators; guanine nucleotide exchange factors (VAV2 and ARH GEF18) and downstream effectors such as phosphatidylinositol-5-phosphate 4-kinase, type II, alpha (PIP5K2A) and protein kinase N1 (PKN1) suggests that they undergo cytoskeletal rearrangement (6, 13). Non-classical subset do not secrete ROS or cytokines in response to cell-surface toll-like receptors. However, they secrete TNF-alpha, IL-1beta, and CCL3 in response to virus and immune complex containing nucleic acids *via* the MyD88–MEK pathway (26). In depth proteome analysis further supports the established functions of classical and non-classical monocyte subsets (35).

A recent study performed by Villani et al. (14) defines the heterogeneity of intermediate monocyte subset based on single-cell RNA sequencing. They identified four monocyte subpopulations namely, Mono 1 (representing mostly the classical monocytes and some intermediate monocytes), Mono 2 (containing a major proportion of non-classical monocytes together with some intermediate monocytes), Mono 3, and Mono 4. These two newly identified Mono 3 and Mono 4 populations represent a major proportion of intermediate monocyte subsets and have unique expression of a set of genes along with co-expression of Mono 1 markers. Mono 3 subset expresses a unique combination of genes that affect cell cycle, differentiation, and trafficking, including MAX dimerization protein 1 (MXD1), C-X-C motif chemokine receptor 1 (CXCR1), C-X-C motif chemokine receptor 2 (CXCR2), and vascular non-inflammatory molecule 2 (VNN2). Mono 4 subset expresses a cytotoxic gene signature resembling that of natural killer dendritic cells including perforin 1, granulysin, and cathepsin W. Thus, it is evident that the earlier identified intermediate monocyte subset is highly heterogeneous in nature.

MONOCYTES IN TUBERCULOSIS (TB)

Current research focusing on monocytes and their subsets in TB has found that $CD16^{+}$ monocytes are expanded in TB infection (36). Perturbation of this subset defines the severity of TB. Expansion of $CD16^{+}$ monocytes is reversed with anti-TB treatment (37) suggesting this expansion is caused by microbial or host components (36). By contrast, tuberculin skin test (TST) positive individuals express higher $CD14^{+}$ $CD16^{+}$ monocyte subset than

TABLE 1 | Phenotypic and functional differences of classical ($CD14^{++}$, $CD16^{-}$), intermediate ($CD14^{++}$, $CD16^{+}$), and non-classical monocyte ($CD14^{+}$, $CD16^{++}$) subsets.

		Classical	Intermediate	Non-classical	Reference
1	Approximate proportions of total monocytes	80–95%	2–11%	2–8%	Chimen et al. (7) Yang et al. (8) Wong et al. (9) Shantsila et al. (10) Ziegler-Heitbrock (11) Passlick et al. (12)
2	Size	18 μm	Intermediate	14 μm	Anbazhagan et al. (13)
3	Differentiation potential	Few macrophages and mostly dendritic cells	Non-homogenous population having the potential to differentiate into some macrophages and occasional cells with dendrites	Mostly macrophages	Villani et al. (14) Boyette et al. (15)
4	Surface markers and gene signatures	$CD14^{++}$ $CD16^{-}$	$CD14^{++}$ $CD16^{+}$	$CD14^{+}$ $CD16^{++}$	
	ACE	+	++	+	Boyette et al. (15)
	CCR1	+++	+	+/–	Ziegler-Heitbrock (16)
	CCR2	+++	+/–	–	Stansfield and Ingram (17)
	CCR5	++	+++	+/–	Anbazhagan et al. (13)
	CD1d	+++	++	+/–	Hijdra et al. (18)
	CD9	+++	++	+/–	Wong et al. (9)
	CD11a	+	+	++	Tallone et al. (19)
	CD11b	+++	+++	+/–	Wong et al. (6)
	CD11c	+/–	+	+++	Zawada et al. (20)
	CD32	+	+++	++	Rogacev et al. (21)
	CD33	+++	++	+/–	Ulrich et al. (22)
	CD36	+++	++	+/–	Ingersoll et al. (23)
	CD40	+/–	+++	++	Sunderkotter et al. (24)
	CD43	–	+	++	Ancuta et al. (25)
	CD47	++	+++	++	
	CD54	+	+++	++	
	CD62L	+	++	–	
	CD64	+++	+++	+/–	
	CD80	+	+++	+/–	
	CD86	+	+++	++	
	CD97	+	++	+++	
	CD99	+++	+	+/–	
	CD115	+	++	+++	
	CD123	+/–	++	+++	
	CD163	++	+++	+/–	
	CD294	+/–	++	+++	
	CLEC4D	+++	+/–	–	
	CLEC5A	+++	+/–	–	
	CLEC10a	+/–	++	+/–	
	CXCR1	+++	+/–	–	
	CXCR2	+++	+/–	–	
	CXCR4	+++	++	+/–	
	CX3CR1	+/–	++	+++	
	GFRα2	+/–	+++	+	
	HLA-ABC	++	+++	+	
	HLA-DR	+/–	+++	++	
	IL13Rα1	+++	+/–	–	
	MHCII	+	++	+	
	PSGL-1	++	+	+	
	P2RX1	+/–	++	+++	
	Siglec10	+/–	+	+++	
	SIRPα	+	++	+++	
	SLAN	+	+/–	+++	
	Tie2	–	+	+/–	
	TNFR1	+	+++	+	
	TNFR2	+	++	+++	
5	Preferred response to LPS	IL-10, G-CSF, CCL2, CCL5, IL-6, IL-8, TNF-alpha	IL-6, IL-8, TNF-alpha	TNF-alpha, IL-1beta, IL-6, IL-8, CCL3 (in response to virus rather than LPS)	Boyette et al. (15) Wong et al. (9) Cros et al. (26)

(*Continued*)

TABLE 1 | Continued

		Classical	Intermediate	Non-classical	Reference
6	Gene signature derived functions	Superior phagocytosis, high MPO activity, high antibody-dependent cell-mediated cytotoxicity, increased skin homing potential, wound healing, coagulation, tissue repair, pro-inflammatory (S-100 proteins), scavenger receptors, C-type lectin receptors, anti-apoptosis, proliferative, response to various stimuli, antibacterial, more plasticity	T cell proliferation and stimulation, superior ROS production, angiogenesis (Tie-2 subpopulation), MHC class II presentation and processing, cell differentiation	T cell proliferation and stimulation (SLAN subpopulation), patrolling behavior *in vivo*, better in Fc receptor-mediated phagocytosis, cytoskeletal rearrangement, complement components, pro-apoptosis, anti-proliferative, negative regulation of transcription, antiviral response, pro-angiogenic behavior	Lastrucci et al. (27) Anbazhagan et al. (13) Wong et al. (9) Wong et al. (6) Robbins and Swirski (28) Cros et al. (26) Martinez (29) Mobley et al. (30)
			Present tetanus toxoid and other particulate antigens, produce reactive nitrogen intermediates, increased gut homing potential, increased expression of pro-inflammatory genes and co-stimulatory molecules		

IL, interleukins; TNF, tumor necrosis factor; G-CSF, granulocyte colony-stimulating factor; CCL, C-C motif chemokine ligand; MPO, myeloperoxidase; CXCR1, C-X-C motif chemokine receptor 1; CXCR2, C-X-C motif chemokine receptor 2; LPS, lipopolysaccharide; ROS, reactive oxygen species.

either active TB patients or healthy TST negative controls, suggesting that these cells constitute an innate protective mechanism against TB in such individuals (38). This finding has, however, not been well-reproduced. For example Castano et al. (36), did not find significant differences in the monocyte subpopulations between TST-positive individuals and TB patients except for higher CD11b and low HLA-DR surface marker expression in non-classical monocytes.

Castano et al. (36) focused on the differences among the three monocyte subsets between TB patients and healthy individuals. In their study, the percentage of intermediate and non-classical monocytes was increased and classical monocyte was decreased in TB patients. There was also an alteration in the profile of monocyte subsets in TB patients. Classical monocytes and intermediate monocytes of TB patients exhibited a lower expression of CD11b and CCR5 and higher expression of CD80, CD86, non-specific esterase (NSE), and CCR2 when compared with healthy individuals. In addition, intermediate monocytes showed higher expression of CD40 and CD68. $CD16^+$ monocytes did not differentiate into macrophages due to limited expression of maturation and differentiation markers such as CD11b, CD11c, CD33, and CD36 (36). Non-classical monocytes of TB patients exhibited a lower expression of CD11c, CD33, CD36, HLA-DR, and CCR5 and higher expression of CD11b, CD40, CD80, NSE, and CCR2. These studies suggest a potential role of intermediate monocytes in T cell activation, proliferation, and antigen presentation.

When compared to $CD16^+$ monocytes, $CD16^-$ (classical) monocytes confer anti-mycobacterial immune responses during TB infection such as enhanced *in vitro* migration in response to mycobacterial derivatives, higher production of ROS, higher lung migration index, and induction of strong pulmonary infiltration. It has been suggested that immediate infiltration of these subsets to the infection site and the production of ROS results in reduction of bacterial growth. By contrast, $CD16^+$ monocytes are involved in promoting bacterial resilience (39). This subset induces a minimal level of respiratory burst and is unresponsive at early stages of infection due to the lack of chemokine receptors (CCR2) necessary for the migration of this subset to the infection site. Similarly, earlier studies have reported that $CD16^+$ subset upregulates CCR2 expression during disease severity which aims to improve their migration ability toward the infection (40). Upregulation of CD11b within $CD16^+$ monocytes suggests a possible way for intracellular survival of MTB and the loss of HLA-DR confers inefficient antigen presentation potency which leads to disease severity (41). Differential induction of a response to purified protein derivative (PPD) and MTB has been displayed by monocytes obtained from PPD skin test-positive individuals and active TB patients. PPD could induce apoptosis in both groups of subjects, whereas induction with MTB resulted in necrosis only among active TB patients, suggesting that apoptosis can influence the protective ability of the host (42).

Studies carried out by Balboa et al. (43), revealed that $CD16^+$ monocytes from active TB patients have a poor capability to differentiate into functional dendritic cells due to high level of phosphorylated p38 MAP kinase. They have also reported differences in the dendritic cell profile among healthy (DC $SIGN^{high}$ and $CD1a^+$) and active TB (DC $SIGN^{low}$ and $CD86^{high}$) subjects. This impairs their differentiation of monocytes to monocyte-derived dendritic cells and their antigen-presenting cell functions (44) resulting in a decrease in their ability to mount strong adaptive responses toward infection.

Mycobacterium tuberculosis has the ability to modulate the macrophage response and induce the secretion of anti-inflammatory cytokines such as IL-10 thereby modulating the differentiation of $CD14^+$ $CD16^-$ monocytes toward the M2 activation program ($CD16^+CD163^+MerTK^+pSTAT3^+$) in a STAT3-dependent manner. This leads to enhanced protease-dependent motility making them permissive for intracellular MTB survival with reduced ability to produce pro-inflammatory cytokines (27).

CYTOKINE PROFILE OF MONOCYTES DURING TB INFECTION

Only limited studies have focused on the cytokine expression of monocytes and their subsets during TB infection. Upon MTB infection, $CD16^-$ monocytes produce IL-10 which results in a

higher frequency of CD16$^+$ monocytes. Adoptive transfer studies of CD16$^+$ and CD16$^-$ monocytes within SCID/Beige mice infected with MTB showed that mice receiving CD16$^-$ monocytes produce higher IL-10 and TGF-beta and mice receiving CD16$^+$ monocytes produced higher TNF-alpha. CD16$^-$ monocytes exhibit both pro- and anti-inflammatory cytokine production besides leukocyte recruitment under infectious conditions, whereas, CD16$^+$ monocytes induce IL-1beta production and leukocyte recruitment under non-infectious conditions (39). In work by Castano et al. (36), classical monocytes produce less TNF-alpha and more IL-10 whereas intermediate and non-classical monocytes produce less IL-10 and more TNF-alpha. CD16$^+$ monocytes are involved in promoting the disease, but *in vitro* production of TNF-alpha by these cells helps to control TB infection. In addition, differential cytokine production by CD16$^+$ monocytes was observed in response to live vs. dead MTB. Dead MTB induced lower TNF-alpha and IL-8 compared to live MTB as a result of differences in their cell wall structure and components (45). However, it is still not known which subset of CD16$^+$ monocytes is actually producing TNF-alpha.

MONOCYTE TO LYMPHOCYTE RATIO (ML RATIO)

Monocyte to lymphocyte ratio is considered an important criterion to determine the immune efficiency of an individual during infectious conditions and is easily quantified in the peripheral blood. During MTB infection, there have been evolving reports suggesting that an increased ratio of monocytes to lymphocytes in comparison with healthy donors denotes the severity of active TB. A high ML ratio may also serve as an indicator of the effectiveness of anti-TB treatment (46) since it normalizes following treatment. Studies by La Manna et al. (47) and Wang et al. (48) suggest that the ML ratio can also be used as a marker to predict the risk of developing active TB. A study by Rakotosamimanana et al. (49), suggested that TST along with ML ratio may predict the risk for the development of TB in contacts. *In vitro* studies performed by Naranbhai et al. (50) showed that ML ratio is related to MTB growth and thereby related to the stage of TB. Naranbhai et al. (51) performed a study of ML ratio in 3–4 month infants and found that an elevated ML ratio is directly correlated with the increased risk for the development of TB before 2 years of age. Though ML ratio seems to be a well-suited prognostic marker in defining the risk for TB as well as the efficiency of treatment, the reliability of this marker remains to be confirmed and it is not known whether it correlates with any other diseases or inflammatory conditions. Further prospective studies in larger cohorts will help to define the role of ML ratio in TB prognosis and management.

BIOMARKERS

Biomarkers are considered to be a critical component of management of all diseases including TB. Biomarkers are the key factors that can help in determining disease stage, early diagnosis, predicting the behavior of pathogens within the host immune system, and the response of host immune cells toward the pathogen and the disease. Biomarkers may also help to determine treatment and to protect from future complications. Numerous transcriptomic approaches have revealed biomarkers for TB expressed by monocytes. ML ratio as discussed in the previous section can also be considered as a biomarker for TB. Some of the biomarkers identified by the researchers for TB are described in **Table 2**.

Although many biomarkers for TB based on monocytes have been suggested are available, they need to be validated in larger patient cohorts. In addition, the cost, time, and the conditions for performing reproducible assays need to be established so that they can be used in rural areas where TB is endemic. These are challenging considerations that will require much future work.

CURRENT RESEARCH GAPS AND FUTURE RESEARCH

Although many studies exploring monocytes and their subsets have been performed in TB, further studies on monocyte subsets, particularly CD16$^+$ intermediate monocytes are still needed to fill the gaps in knowledge.

- Limited studies have been performed that investigate the role of CD16$^+$ monocyte subsets in TB. Animal studies may be helpful to correlate their function and phenotype with respect to disease progression and protection.
- Recent studies have documented perturbation of the CD16 intermediate monocyte subset upon infection with MTB, suggesting that this cell type favors the intracellular survival of MTB. More studies are needed to document the dysfunction of this subset with reference to their differentiation ability, antigen recognition potency, migration behavior, phagocytic properties, immunostimulation, autophagy, apoptosis, metabolic program, and the mechanism of pathogen clearance. These studies will be helpful to develop newer host directed therapies.
- Although IL-10 contribute to the expansion of CD16$^+$ monocytes, other factors such as the antigenic components of MTB (secreted and membrane bound antigens) and the host environment (antigen presentation), can favor the expansion of CD16$^+$ monocytes. More work is needed to identify the factors involved in the expansion of CD16$^+$ monocytes in established mycobacterial infection.
- Molecular profiling of sorted monocyte subsets of infected patients will be helpful to identify their unique functions. Exploring the phenotype and function of monocyte subsets in granulomas through *in vivo* animal studies could provide the clues about the intracellular survival of MTB and help to decipher the pathophysiology of TB. Newer techniques such as CyTOF and MALDI-TOF could be employed to identify additional phenotypes within sorted monocyte subsets. Single-cell transcriptomic studies involving RNAseq, miRNome, and/or epigenetic profiling needs to be performed in order to understand the functional roles and transcriptional regulation of the different subsets.
- Metabolomic profiles of classical and non-classical monocytes have been very well studied. Substantial insights into the underlying mechanisms of metabolic switches within intermediate

TABLE 2 | List of identified biomarkers based on monocytes for tuberculosis (TB).

Biomarkers	Signature	Functions	Expressed by	Able to	Reference
FPR1	Formyl peptide receptor 1	Pro-inflammatory, antimicrobial defense	Professional phagocytes		Jacobsen et al. (52)
Combination of CD64, LTF, and RaB33a	CD64 Fc gamma receptor Ia	Induce phagocytosis, respiratory burst and antibody-dependent cell-mediated cytotoxicity in monocytes, macrophages, and granulocytes	Monocytes	Discriminate active TB, latent TB infection, and healthy status	
	LTF Lactoferrin is a transport molecule with high affinity for iron	Modulates the host response by competing with the microbes for iron			
	Rab33a Member of Ras-associated small GTPase family	Regulates intracellular trafficking			
mCD14 receptor	Membrane bound CD14 receptor—55 kD glycoprotein	Pattern recognition receptor for *Mycobacterium* tuberculosis components such as LAM and lipoproteins	Monocytes	Biomarker for active TB	Druszczynska et al. (53)
HMBG1	High mobility group box 1 protein also known as Amphoterin	Pro-inflammatory cytokine, serves as DAMP to alert the innate immune system by recruiting inflammatory cells during disease condition, acts as an immune adjuvant to trigger the response of T cells, dendritic cells, and endothelial cells	Monocytes	Biomarker for active TB	Zeng et al. (54)
IL26	Member of interleukin-10 cytokine family	Inhibitory effect on anti-mycobacterial activity	Monocytes	Susceptible gene for TB	Guerra-Laso et al. (55)
CD163	Monocyte/macrophage specific glycoprotein	Scavenger receptor	Monocytes	Biomarker for TB disease progression and monitor treatment efficacy	Lastrucci et al. (27)

monocyte subsets may provide novel tools to identify their cellular function during mycobacterial infection. Drugs inducing metabolic switches can be tested for the treatment of TB.

- Studies of monocyte-related biomarkers in patients of different ethnicities should be encouraged. Previously reported biomarkers need to be validated in larger clinical cohorts including extra pulmonary TB and other infectious or inflammatory conditions in order to delineate their specificity.

CONCLUSION

Our review describes the phenotypic and functional variations within monocyte subsets, with reference to mycobacterial infection. With further understanding, we may be able to identify a possible mechanism for the intracellular survival of MTB and to decipher the clues behind the host immune response that influences TB pathogenesis. Current knowledge gaps and suggested future research on monocyte subsets also include better definition of biomarkers for early diagnosis or prognosis of disease and exploration of newer host directed therapies to combat mycobacterial infection.

AUTHOR CONTRIBUTIONS

PS and RB: drafting and revising the article, concept and design. KM: contributed to writing. UR: revision of the article; concept and design.

ACKNOWLEDGMENTS

The authors would like to sincerely thank Dr. Anne Davidson, Investigator, Feinstein Institute for Medical Research, New York, USA, for critical reading of the manuscript. PS work has been supported by DST INSPIRE fellowship and RB's work has been supported by the DBT Ramalingaswami Fellowship, Ministry of Science and Technology, Government of India.

REFERENCES

1. Guilliams M, Ginhoux F, Jakubzick C, Naik SH, Onai N, Schraml BU, et al. Dendritic cells, monocytes and macrophages: a unified nomenclature based on ontogeny. *Nat Rev Immunol* (2014) 14(8):571–8. doi:10.1038/nri3712
2. Ziegler-Heitbrock L, Ancuta P, Crowe S, Dalod M, Grau V, Hart DN, et al. Nomenclature of monocytes and dendritic cells in blood. *Blood* (2010) 116(16):e74–80. doi:10.1182/blood-2010-02-258558
3. Murdoch C, Tazzyman S, Webster S, Lewis CE. Expression of Tie-2 by human monocytes and their responses to angiopoietin-2. *J Immunol* (2007) 178(11):7405–11. doi:10.4049/jimmunol.178.11.7405
4. Venneri MA, De Palma M, Ponzoni M, Pucci F, Scielzo C, Zonari E, et al. Identification of proangiogenic TIE2-expressing monocytes (TEMs) in human peripheral blood and cancer. *Blood* (2007) 109(12):5276–85. doi:10.1182/blood-2006-10-053504
5. Hofer TP, Zawada AM, Frankenberger M, Skokann K, Satzl AA, Gesierich W, et al. Slan-defined subsets of CD16-positive monocytes: impact of granulomatous inflammation and M-CSF receptor mutation. *Blood* (2015) 126(24):2601–10. doi:10.1182/blood-2015-06-651331
6. Wong KL, Tai JJ, Wong WC, Han H, Sem X, Yeap WH, et al. Gene expression profiling reveals the defining features of the classical, intermediate, and nonclassical human monocyte subsets. *Blood* (2011) 118(5):e16–31. doi:10.1182/blood-2010-12-326355

7. Chimen M, Yates CM, McGettrick HM, Ward LS, Harrison MJ, Apta B, et al. Monocyte subsets coregulate inflammatory responses by integrated signaling through TNF and IL-6 at the endothelial cell interface. *J Immunol* (2017) 198(7):2834–43. doi:10.4049/jimmunol.1601281
8. Yang J, Zhang L, Yu C, Yang XF, Wang H. Monocyte and macrophage differentiation: circulation inflammatory monocyte as biomarker for inflammatory diseases. *Biomark Res* (2014) 2(1):1. doi:10.1186/2050-7771-2-1
9. Wong KL, Yeap WH, Tai JJ, Ong SM, Dang TM, Wong SC. The three human monocyte subsets: implications for health and disease. *Immunol Res* (2012) 53(1–3):41–57. doi:10.1007/s12026-012-8297-3
10. Shantsila E, Wrigley B, Tapp L, Apostolakis S, Montoro-Garcia S, Drayson MT, et al. Immunophenotypic characterization of human monocyte subsets: possible implications for cardiovascular disease pathophysiology. *J Thromb Haemost* (2011) 9(5):1056–66. doi:10.1111/j.1538-7836.2011.04244.x
11. Ziegler-Heitbrock HW. Definition of human blood monocytes. *J Leukoc Biol* (2000) 67(5):603–6. doi:10.1002/jlb.67.5.603
12. Passlick B, Flieger D, Ziegler-Heitbrock HW. Identification and characterization of a novel monocyte subpopulation in human peripheral blood. *Blood* (1989) 74(7):2527–34.
13. Anbazhagan K, Duroux-Richard I, Jorgensen C, Apparailly F. Transcriptomic network support distinct roles of classical and non-classical monocytes in human. *Int Rev Immunol* (2014) 33(6):470–89. doi:10.3109/08830185.2014.902453
14. Villani AC, Satija R, Reynolds G, Sarkizova S, Shekhar K, Fletcher J, et al. Single-cell RNA-seq reveals new types of human blood dendritic cells, monocytes, and progenitors. *Science* (2017) 356(6335):eaah4573. doi:10.1126/science.aah4573
15. Boyette LB, Macedo C, Hadi K, Elinoff BD, Walters JT, Ramaswami B, et al. Phenotype, function, and differentiation potential of human monocyte subsets. *PLoS One* (2017) 12(4):e0176460. doi:10.1371/journal.pone.0176460
16. Ziegler-Heitbrock L. Blood monocytes and their subsets: established features and open questions. *Front Immunol* (2015) 6:423. doi:10.3389/fimmu.2015.00423
17. Stansfield BK, Ingram DA. Clinical significance of monocyte heterogeneity. *Clin Transl Med* (2015) 4:5. doi:10.1186/s40169-014-0040-3
18. Hijdra D, Vorselaars AD, Grutters JC, Claessen AM, Rijkers GT. Phenotypic characterization of human intermediate monocytes. *Front Immunol* (2013) 4:339. doi:10.3389/fimmu.2013.00339
19. Tallone T, Turconi G, Soldati G, Pedrazzini G, Moccetti T, Vassalli G. Heterogeneity of human monocytes: an optimized four-color flow cytometry protocol for analysis of monocyte subsets. *J Cardiovasc Trans Res* (2011) 4(2):211–9. doi:10.1007/s12265-011-9256-4
20. Zawada AM, Rogacev KS, Rotter B, Winter P, Marell RR, Fliser D, et al. SuperSAGE evidence for CD14++CD16+ monocytes as a third monocyte subset. *Blood* (2011) 118(12):e50–61. doi:10.1182/blood-2011-01-326827
21. Rogacev KS, Seiler S, Zawada AM, Reichart B, Herath E, Roth D, et al. CD14++CD16+ monocytes and cardiovascular outcome in patients with chronic kidney disease. *Eur Heart J* (2011) 32(1):84–92. doi:10.1093/eurheartj/ehq371
22. Ulrich C, Heine GH, Seibert E, Fliser D, Girndt M. Circulating monocyte subpopulations with high expression of angiotensin-converting enzyme predict mortality in patients with end-stage renal disease. *Nephrol Dial Transplant* (2010) 25(7):2265–72. doi:10.1093/ndt/gfq012
23. Ingersoll MA, Spanbroek R, Lottaz C, Gautier EL, Frankenberger M, Hoffmann R, et al. Comparison of gene expression profiles between human and mouse monocyte subsets. *Blood* (2010) 115(3):e10–9. doi:10.1182/blood-2009-07-235028
24. Sunderkotter C, Nikolic T, Dillon MJ, Van Rooijen N, Stehling M, Drevets DA, et al. Subpopulations of mouse blood monocytes differ in maturation stage and inflammatory response. *J Immunol* (2004) 172(7):4410–7. doi:10.4049/jimmunol.172.7.4410
25. Ancuta P, Rao R, Moses A, Mehle A, Shaw SK, Luscinskas FW, et al. Fractalkine preferentially mediates arrest and migration of CD16+ monocytes. *J Exp Med* (2003) 197(12):1701–7. doi:10.1084/jem.20022156
26. Cros J, Cagnard N, Woollard K, Patey N, Zhang SY, Senechal B, et al. Human CD14dim monocytes patrol and sense nucleic acids and viruses via TLR7 and TLR8 receptors. *Immunity* (2010) 33(3):375–86. doi:10.1016/j.immuni.2010.08.012
27. Lastrucci C, Benard A, Balboa L, Pingris K, Souriant S, Poincloux R, et al. Tuberculosis is associated with expansion of a motile, permissive and immunomodulatory CD16+ monocyte population via the IL-10/STAT3 axis. *Cell Res* (2015) 25(12):1333–51. doi:10.1038/cr.2015.123
28. Robbins CS, Swirski FK. The multiple roles of monocyte subsets in steady state and inflammation. *Cell Mol Life Sci* (2010) 67(16):2685–93. doi:10.1007/s00018-010-0375-x
29. Martinez FO. The transcriptome of human monocyte subsets begins to emerge. *J Biol* (2009) 8(11):99. doi:10.1186/jbiol206
30. Mobley JL, Leininger M, Madore S, Baginski TJ, Renkiewicz R. Genetic evidence of a functional monocyte dichotomy. *Inflammation* (2007) 30(6):189–97. doi:10.1007/s10753-007-9036-0
31. Smedman C, Ernemar T, Gudmundsdotter L, Gille-Johnson P, Somell A, Nihlmark K, et al. Fluorospot analysis of TLR-activated monocytes reveals several distinct cytokine-secreting subpopulations. *Scand J Immunol* (2011) 75(2):249–58. doi:10.1111/j.1365-3083.2011.02641.x
32. Gren ST, Rasmussen TB, Janciauskiene S, Håkansson K, Gerwien JG, Grip O. A single-cell gene-expression profile reveals inter-cellular heterogeneity within human monocyte subsets. *PLoS One* (2015) 10(12):e0144351. doi:10.1371/journal.pone.0144351
33. Portevin D, Pflüger V, Otieno P, Brunisholz R, Vogel G, Daubenberger C. Quantitative whole-cell MALDI-TOF MS fingerprints distinguishes human monocyte sub-populations activated by distinct microbial ligands. *BMC Biotechnol* (2015) 15:24. doi:10.1186/s12896-015-0140-1
34. Zhao C, Zhang H, Wong WC, Sem X, Han H, Ong SM, et al. Identification of novel functional differences in monocyte subsets using proteomic and transcriptomic methods. *J Proteome Res* (2009) 8(8):4028–38. doi:10.1021/pr900364p
35. Segura V, Valero ML, Cantero L, Muñoz J, Zarzuela E, García F, et al. In-depth proteomic characterization of classical and non-classical monocyte subsets. *Proteomes* (2018) 6(1):8. doi:10.3390/proteomes6010008
36. Castano D, Garcia LF, Rojas M. Increased frequency and cell death of CD16+ monocytes with *Mycobacterium tuberculosis* infection. *Tuberculosis (Edinb)* (2011) 91:348–60. doi:10.1016/j.tube.2011.04.002
37. Sanchez MD, Garcia Y, Montes C, Paris SC, Rojas M, Barrera LF, et al. Functional and phenotypic changes in monocytes from patients with tuberculosis are reversed with treatment. *Microbes Infect* (2006) 8(9–10):2492–500. doi:10.1016/j.micinf.2006.06.005
38. Barcelos W, Sathler-Avelar R, Martins-Filho OA, Carvalho BN, Guimaraes TM, Miranda SS, et al. Natural killer cell subpopulations in putative resistant individuals and patients with active *Mycobacterium tuberculosis* infection. *Scand J Immunol* (2008) 68(1):92–102. doi:10.1111/j.1365-3083.2008.02116.x
39. Balboa L, Barrios-Payan J, Gonzalez-Dominguez E, Lastrucci C, Lugo-Villarino G, Mata-Espinoza D, et al. Diverging biological roles among human monocyte subsets in the context of tuberculosis infection. *Clin Sci (Lond)* (2015) 129(4):319–30. doi:10.1042/CS20150021
40. Balboa L, Romero MM, Basile JI, Sabio y García CA, Schierloh P, Yokobori N, et al. Paradoxical role of CD16+CCR2+CCR5+ monocytes in tuberculosis: efficient APC in pleural effusion but also mark disease severity in blood. *J Leukoc Biol* (2011) 90(1):69–75. doi:10.1189/jlb.1010577
41. Malik ZA, Denning GM, Kusner DJ. Inhibition of Ca (2+) signaling *by Mycobacterium tuberculosis* is associated with reduced phagosome-lysosome fusion and increased survival within human macrophages. *J Exp Med* (2000) 191(2):287–302. doi:10.1084/jem.191.2.287
42. Gil DP, León LG, Correa LI, Maya JR, París SC, García LF, et al. Differential induction of apoptosis and necrosis in monocytes from patients with tuberculosis and healthy control subjects. *J Infect Dis* (2004) 189(11):2120–8. doi:10.1086/386369
43. Balboa L, Romero MM, Laborde E, Sabio Y Garcia CA, Basile JI, Schierloh P, et al. Impaired dendritic cell differentiation of CD16-positive monocytes in tuberculosis: role of p38 MAPK. *Eur J Immunol* (2013) 43:335–47. doi:10.1002/eji.201242557
44. Lugo-Villarino G, Neyrolles O. Dressed not to kill: CD16+ monocytes impair immune defense against tuberculosis. *Eur J Immunol* (2013) 43(2):327–30. doi:10.1002/eji.201243256
45. Shimada K, Takimoto H, Yano I, Kumazawa Y. Involvement of mannose receptor in glycopeptidolipid-mediated inhibition of phagosome-lysosome fusion. *Microbiol Immunol* (2006) 50:243.e51. doi:10.1111/j.1348-0421.2006.tb03782.x

46. Iqbal S, Ahmed U, Zaidi SBH. Monocyte lymphocyte ratio as a possible prognostic marker in antituberculous therapy. *J Rawalpindi Med Coll (JRMC)* (2014) 18(2):178–81.
47. La Manna MP, Orlando V, Dieli F, Di Carlo P, Cascio A, Cuzzi G, et al. Quantitative and qualitative profiles of circulating monocytes may help identifying tuberculosis infection and disease stages. *PLoS One* (2017) 12(2):e0171358. doi:10.1371/journal.pone.0171358
48. Wang J, Yin Y, Wang X, Pei H, Kuai S, Gu L, et al. Ratio of monocytes to lymphocytes in peripheral blood in patients diagnosed with active tuberculosis. *Braz J Infect Dis* (2015) 19(2):125–31. doi:10.1016/j.bjid.2014.10.008
49. Rakotosamimanana N, Richard V, Raharimanga V, Gicquel B, Doherty TM, Zumla A, et al. Biomarkers for risk of developing active tuberculosis in contacts of TB patients: a prospective cohort study. *Eur Respir J* (2015) 46(4):1095–103. doi:10.1183/13993003.00263-2015
50. Naranbhai V, Fletcher HA, Tanner R, O'Shea MK, McShane H, Fairfax BP, et al. Distinct transcriptional and anti-mycobacterial profiles of peripheral blood monocytes dependent on the ratio of monocytes: lymphocytes. *EBioMedicine* (2015) 2(11):1619–26. doi:10.1016/j.ebiom.2015.09.027
51. Naranbhai V, Kim S, Fletcher H, Cotton MF, Violari A, Mitchell C, et al. The association between the ratio of monocytes: lymphocytes at age 3 months and risk of tuberculosis (TB) in the first two years of life. *BMC Med* (2014) 12:120. doi:10.1186/s12916-014-0120-7
52. Jacobsen M, Repsilber D, Gutschmidt A, Neher A, Feldmann K, Mollenkopf HJ, et al. Candidate biomarkers for discrimination between infection and disease caused by *Mycobacterium tuberculosis*. *J Mol Med (Berl)* (2007) 85(6):613–21. doi:10.1007/s00109-007-0157-6
53. Druszczynska M, Wlodarczyk M, Janiszewska-Drobinska B, Kielnierowski G, Zawadzka J, Kowalewicz-Kulbat M, et al. Monocyte signal transduction receptors in active and latent tuberculosis. *Clin Dev Immunol* (2013) 2013:851452. doi:10.1155/2013/851452
54. Zeng JC, Xiang WY, Lin DZ, Zhang JA, Liu GB, Kong B. Elevated HMGB1-related interleukin-6 is associated with dynamic responses of monocytes in patients with active pulmonary tuberculosis. *Int J Clin Exp Pathol* (2015) 8(2):1341–53.
55. Guerra-Laso JM, Raposo-García S, Garcia-Garcia S, Diez-Tascon C, Rivero-Lezcano OM. Microarray analysis of *Mycobacterium* tuberculosis-infected monocytes reveals IL26 as a new candidate gene for tuberculosis susceptibility. *Immunology* (2015) 144(2):291–301. doi:10.1111/imm.12371

Conflict of Interest Statement: The authors declare that the research was conducted in the absence of any commercial or financial relationships that could be construed as a potential conflict of interest.

Copyright © 2018 Sampath, Moideen, Ranganathan and Bethunaickan. This is an open-access article distributed under the terms of the Creative Commons Attribution License (CC BY). The use, distribution or reproduction in other forums is permitted, provided the original author(s) and the copyright owner(s) are credited and that the original publication in this journal is cited, in accordance with accepted academic practice. No use, distribution or reproduction is permitted which does not comply with these terms.

frontiers in Microbiology

REVIEW
published: 23 May 2018
doi: 10.3389/fmicb.2018.01028

Macrophage Heterogeneity in the Immunopathogenesis of Tuberculosis

Mohlopheni J. Marakalala[1], *Fernando O. Martinez*[2,3], *Annette Plüddemann*[4] *and Siamon Gordon*[5,6]*

[1] Division of Immunology, Department of Pathology, Institute of Infectious Disease and Molecular Medicine, University of Cape Town, Cape Town, South Africa, [2] Faculty of Health and Medical Sciences, University of Surrey, Guildford, United Kingdom, [3] Botnar Research Centre, NDORMS, University of Oxford, Oxford, United Kingdom, [4] Nuffield Department of Primary Care Health Sciences, University of Oxford, Oxford, United Kingdom, [5] Graduate Institute of Biomedical Sciences, College of Medicine, Chang Gung University, Taoyuan City, Taiwan, [6] Sir William Dunn School of Pathology, University of Oxford, Oxford, United Kingdom

Macrophages play a central role in tuberculosis, as the site of primary infection, inducers and effectors of inflammation, innate and adaptive immunity, as well as mediators of tissue destruction and repair. Early descriptions by pathologists have emphasized their morphological heterogeneity in granulomas, followed by delineation of T lymphocyte-dependent activation of anti-mycobacterial resistance. More recently, powerful genetic and molecular tools have become available to describe macrophage cellular properties and their role in host-pathogen interactions. In this review we discuss aspects of macrophage heterogeneity relevant to the pathogenesis of tuberculosis and, conversely, lessons that can be learnt from mycobacterial infection, with regard to the immunobiological functions of macrophages in homeostasis and disease.

Keywords: macrophage, immunopathogenesis, tuberculosis, pulmonary, macrophage heterogeneity4, *Mycobacterium tuberculosis*

OPEN ACCESS

Edited by:
Geanncarlo Lugo-Villarino, UMR5089 Institut de Pharmacologie et de Biologie Structurale (IPBS), France

Reviewed by:
Larry Schlesinger, The Ohio State University, United States
Roi Avraham, Weizmann Institute of Science, Israel

***Correspondence:**
Siamon Gordon
siamon.gordon@path.ox.ac.uk

Specialty section:
This article was submitted to Microbial Immunology, a section of the journal Frontiers in Microbiology

Received: *22 February 2018*
Accepted: *01 May 2018*
Published: *23 May 2018*

Citation:
Marakalala MJ, Martinez FO, Plüddemann A and Gordon S (2018) Macrophage Heterogeneity in the Immunopathogenesis of Tuberculosis. Front. Microbiol. 9:1028. doi: 10.3389/fmicb.2018.01028

INTRODUCTION

Tuberculosis (TB), caused by the bacterial pathogen *Mycobacterium tuberculosis* (MTB), is an airborne infection that primarily affects the lungs, and remains a major global health problem responsible for 1.5 million deaths annually (WHO)[1]. Upon inhalation, MTB organisms seed the alveolar space in the lung, where they are captured by alveolar macrophages. This is followed by an early inflammatory response, induced by both bacterial and host factors, which results in recruitment of leukocytes from neighboring blood vessels to the site of infection. These include monocytes which differentiate into various populations of tissue macrophages, such as epithelioid cells, foamy macrophages and multinucleated Langhans giant cells, to create macrophage-rich granulomatous lesions (Taylor et al., 2006; Volkman et al., 2010). Initially, granulomas are cellular aggregates of the different macrophages and other innate immune cells surrounded by fibroblasts (Ulrichs et al., 2004; Ehlers and Schaible, 2012; Guirado and Schlesinger, 2013). With the onset of adaptive immunity, granulomas acquire a more solid, intact structure with a lymphocytic cuff composed of T and B cells at their periphery. Later in infection, granulomas can undergo complex remodeling. For reasons not yet fully understood, the solid granuloma can accumulate necrotic damage that results in the formation of caseum at the center. Necrotic granulomas may undergo

[1]WHO. World Health Organization Tuberculosis Fact sheet. http://www.who.int/mediacentre/factsheets/fs104/en/index.html. In, (January 2018).

liquefaction to form cavitary lesions, giving the bacteria access to nearby airways and thus the ability to spread (Russell et al., 2010) within the lung and elsewhere within the body.

Granulomas have been assigned wide-ranging functions, some of which also depend on the animal model studied. In zebrafish, for example, granulomas have been depicted as vehicles that help spread the pathogen to other sites within the organism (Ramakrishnan, 2012). Different investigators have described granulomas as a successful method of sequestering a chronic pathogen (Saunders and Cooper, 2000; Nathan, 2016). However, if containment fails, granulomas may simply become structures that provide nutrients and a niche for the bacteria to replicate without immune restriction (Peyron et al., 2008).

Macrophages are the predominant host cells implicated in entry, growth and restriction within the infected host. Both MTB and macrophages are heterogeneous in metabolic activity and their interaction determines the outcome of infection. Before considering various aspects of the host-pathogen response to infection, we summarize present understanding of the heterogeneous origin, differentiation and activation of monocytes and tissue macrophages, the dispersed organ known as the Mononuclear Phagocyte System (MPS).

HETEROGENEITY OF MACROPHAGES AND PATHOGENS

There has been a paradigm shift in our understanding of the origin, differentiation, distribution and properties of the cells of the MPS (Ginhoux and Guilliams, 2016; Gordon and Plüddemann, 2017). Almost all current knowledge is based on studies in the mouse, and, although not identical in detail, the broad outlines are likely to be similar in the human. The main shift in our thinking arises from discovery of the mixed origins of mouse macrophages from yolk sac and fetal liver precursors during development, and postnatally from bone marrow. Embryo-derived "monocytes" and macrophages seed tissue resident macrophages throughout the body, turning over slowly at local sites where they persist throughout adult life. As required, e.g., in the gut (Bujko et al., 2018), tissue-resident macrophages are replenished from bone marrow hematopoietic stem cells (HSC), to a variable extent in different organs.

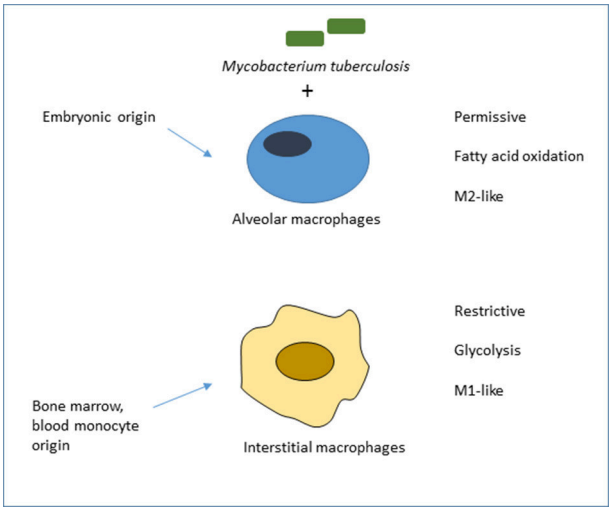


FIGURE 1 | Ontogeny of mouse lung macrophages shapes the outcome of initial MTB infection *in vivo*. Adapted from Huang et al. (2018), who compared the role of alveolar macrophages (AM), of embryonic origin, with mainly monocytic, bone marrow-derived interstitial macrophages (IM) in acute infection of mice by fluorescent MTB reporter strains. Bacilli in AM, deriving energy from fatty acid oxidation, grew more readily than IM, which were actively glycolytic, more restrictive and expressed M1-like rather than M2-like markers of macrophage activation. The authors favored a model of pre-programming, linked to ontogeny, rather than adaptation to the distinct local microenvironment. There is suggestive, but no direct, evidence in humans that alveolar and other tissue-resident macrophages are of embryonic origin. This conclusion is based on transplantation studies of donor and recipient macrophages in skin (Bigley et al., 2011) and small intestine (Bujko et al., 2018), and evidence of local turnover in lung rather than bone marrow origin. It is not known which plasma membrane receptors mediate uptake of MTB in this *in vivo* model. Alveolar macrophages in the mouse express low levels of F4/80 and of CD11b, and high levels of several plasma membrane receptors: lectins such as the mannose receptor (CD206), and the Scavenger Receptor AI/II and MARCO, which are involved in the uptake of inhaled particles such as MTB (Gordon et al., 2014a). Other widely studied lectins expressed by lung macrophages include the FcRgamma-coupled receptors Dectin-2, Mincle and MCL, as well as Dectin-1, Mannose Receptor and DC-SIGN (Marakalala and Ndlovu, 2017).

Bone marrow-derived monocytes are themselves heterogeneous within the circulation, where they can remain, enter tissues constitutively or be recruited in response to a variety of sterile or infectious stimuli. They are loosely described as inflammatory, elicited or recruited monocyte-derived macrophages, and are known to display markedly different properties to those of tissue-resident macrophages. In response to poorly understood local environmental stimuli, e.g., in the lung, liver, gut, brain and skin, these macrophage populations adopt different tissue-specific phenotypes (Lavin et al., 2014), which can influence the outcome of MTB infection. As described below and shown schematically in **Figure 1**, Russell and colleagues have used a pulmonary infection model in the mouse to establish for the first time, the importance of the distinction between embryonic and bone marrow origin of lung macrophages in determining the outcome of initial infection by MTB (Huang et al., 2018).

Abbreviations: Adam-17, disintegrin and metalloproteinase17; ADCC, antibody-dependent cellular cytotoxicity, ALOX-5; arachidonate 5-lipoxygenase; APC, Antigen presenting cell, BCG, Bacille Calmette Guerin; COX 1/2 cyclooxygenase 1/2; CTL, C-type lectin; DC, dendritic cell, DC-SIGN, dendritic cell-specific intercellular adhesion molecule-3-non integrin; FcR, Fc Receptor; HAART, Highly active antiretroviral therapy; HSC, haemopoietic stem cells; IRIS, immune reconstitution inflammatory syndrome; IgG, Immunoglobulin G; i-RHOM2, inactive rhomboid protein2; LTA4H, Leukotriene A4 hydrolase; LTB, leukotriene B; LXA4, lipoxin A4; ManLam, mannose-capped lipoarabinomannan; MARCO, macrophage receptor with collagenous domain; MCL, macrophage C-type lectin; Mincle, macrophage inducible Ca++-dependent lectin; Mm, mycobacterium marinum; MPS, mononuclear phagocyte system; MTB, mycobacterium tuberculosis; NLR, nod-like receptor; N-Ramp, natural resistance associated macrophage protein; PGE2, prostaglandin E2; PPAR, peroxisome proliferator activated receptor; SP-A, Surfactant protein-A; SR-A, Scavenger receptor A; STING, stimulator of interferon genes; TB, tuberculosis; TNF, tumor necrosis factor; TLR, Toll-like receptor; TRegs, regulatory T lymphocytes.

Recent population and single cell analysis of macrophages, *in situ* and *ex vivo*, illustrate the extensive heterogeneity of plasma membrane receptor (Gordon and Plüddemann, 2017) and biosynthetic gene expression (Lavin et al., 2014), of macrophages in the steady state and in various intracellular infection models. In addition, macrophages in different organs express distinct tissue-specific phenotypes, as well as canonical genes shared by macrophages in different tissues (e.g., Lavin et al., 2014). Intriguingly, phagocytosis of apoptotic cells downregulates inflammatory responses irrespective of tissue macrophage location (reviewed in Gordon and Plüddemann, 2018). Conversely, Avraham and colleagues have shown that pathogen cell-to-cell variability drives Type 1 Interferon production by individual macrophages in a Salmonella model; this was ascribed to PhoPQ activity in the population of invading bacteria that modified LPS in a subset of organisms (Avraham et al., 2015). Similarly, Saliba et al. (2017) demonstrated by single–cell RNA-seq analysis that heterogeneity of bacterial growth rate in individual macrophages could be correlated with different macrophage gene expression profiles.

Similar variability in both pathogens and macrophages could give rise to marked heterogeneity in susceptibility or resistance to TB encounters at body surfaces such as lung, skin and gut, in serosal cavities e.g., the pleura, pericardium and peritoneum (Rosas et al., 2014; Okabe and Medzhitov, 2016; Wang and Kubes, 2016), and within the blood or lymphatic circulation (Gordon et al., 2014b). At present, we know little about the impact of microbial heterogeneity and local and regional diversity of macrophages, on the initiation, dissemination and outcome of TB, well described in the early pathology literature. The mixed origin of MPS populations is further enhanced by mobilization from tissue reservoirs such as the spleen (Swirski et al., 2009) or the peritoneal cavity (Wang and Kubes, 2016), and by dynamic modulation of a spectrum of different cellular phenotypes, loosely described as "activation." Organ-specific properties clearly relevant to pulmonary infection include the role of GM-CSF in alveolar macrophage development (Guilliams et al., 2013), their interactions with surfactant proteins and lipids (Hussell and Bell, 2014), as well as impact of the oxygen-rich environment and inhaled particulates. Moreover, the bone marrow, gut, liver and brain, for example, contain multiple subpopulations of resident macrophages, with different, but still largely undefined tissue-specific properties which will affect their response to MTB; these include differences in metabolism, microbicidal/microbistatic activity, persistence, latency and reactivation of infection. In addition, the presence of other micro-organisms, whether commensals or pathogens, can have a profound impact on macrophage-mycobacterial interactions. This is well illustrated in HIV/AIDS, a major co-pathogen of Tuberculosis, but subtler interactions with organisms in the microbiome of the gut, skin and lung, for example, and with antibiotics need further study. A particular illustration of genomic diversity of MTB as a result of spread within the lung as well as to extra-pulmonary tissues was provided by analysis of HIV-associated Tuberculosis at autopsy in subjects who had received minimal antitubercular treatment (Lieberman et al., 2016). Selection in individual patients resulted in co-existence of substrains for long periods, giving rise to repeated dissemination within, rather than new infections between individuals. It is not known whether this can also occur in the absence of AIDS.

In the present review we focus on macrophage properties relevant to the pathogenesis of tuberculosis during both innate and adaptive immunity to infection; further references can be found in recent multi-author volumes published by the American Society of Microbiology (Gordon, 2017; Jacobs et al., 2018); individual chapters are available in Microbiology Spectrum. We do not cover the role of polymorphonuclear leukocytes(PMN) and Dendritic cells(DC), except in passing. **Box 1** summarizes the role of T lymphocytes in granuloma formation and macrophage effector functions. The potential roles of B lymphocytes and humoral responses including antibodies are beyond the scope of this review.

MTB TROPISM FOR MACROPHAGES, ENTRY AND RESPONSES

The microbiology of MTB is under intense study, with emphasis on its metabolism, growth and unique constituents, such as complex surface glycolipids (Jackson, 2014), known to influence cellular infection. Although to a great extent tropic for macrophages and DC, it is clear that other cell types such as adipocytes are also infectible by MTB, as discussed below. Neutrophils can and do take up MTB, whether opsonized or not, and may die by pyroptosis as well as apoptosis. Human neutrophils which undergo MTB-induced necrosis can be ingested by macrophages (Dallenga et al., 2017) and MTB also replicates within necrotic human macrophages (Lerner et al., 2017, 2018). Recent studies have reported that activated macrophages can generate extracellular traps (METOSIS), comparable to, but distinct from NETOSIS (Doster et al., 2017).

Although there have been many attempts to identify the macrophage plasma membrane receptors responsible for MTB tropism, we still lack a clear understanding of the role of particular receptors and their heterogeneous expression by different tissue macrophage populations. This can be due to receptor redundancy, the low affinity of individual receptors, variable expression by different macrophages, *in vivo*, including species differences, and the presence of opsonins, rather than direct receptor-mediated uptake. The lectin-like mannose receptor (CD206) recognizes ManLam on MTB; its role in MTB uptake has been studied in considerable detail by Schlesinger and his colleagues (Kang et al., 2005). Other lectins that play a possible role in MTB infection of macrophages (Wilson et al., 2015; Rajaram et al., 2017) including Mincle (Ishikawa et al., 2009) and MCL; Beta2 integrins (CD11b/CD18) and Scavenger receptors such as MARCO and CD36, have also been implicated (Dodd et al., 2016). Siglecs (Crocker et al., 2007) expressed by a variety of immune cells, including macrophages, are sialic acid recognition sensors; desialylation of complex glycoconjugates can expose galactosyl residues, ligands for galectins (Sundblad et al., 2017). Identification of the contribution of particular receptors is complicated by the role of many of these macrophage surface receptors in clearance of apoptotic and necrotic cell targets, which are abundant in MTB infection and may even serve as

BOX 1 | Adaptive immunity.

The adaptive immune response, mainly comprised of antigen specific CD4+ cells, plays a critical role in the outcome of M. tuberculosis infection (Jasenosky et al., 2015). For robust control of the infection, T cells need to arrive timeously at the right site where they can interact with heterogeneous subpopulations of DCs, derived from circulating monocyte precursors and mature monocytes in blood (Austyn, 2016; Villani et al., 2017). Monocytes, essential effector cells in adaptive as well as innate immunity, are themselves heterogeneous and contribute to granuloma supply and demand at the core of the necrotic granuloma (Randolph, 2015; Pagan and Ramakrishnan, 2018). Apoptosis facilitates antigen presentation to T lymphocytes through MHC-I and CD1 on antigen presenting cells (APC) (Schaible et al., 2003). Typically, MTB- specific T cells become detectable at least 3 weeks after infection. In many TB models, establishment of the T cell immune response coincides with the arrest of bacterial replication (Flynn, 2006), indicating a significant role of adaptive immune T cell dependent—macrophage interactions in TB control. Two CD4+ T cell phenotypes essential for MTB control are Th1 and Th17 responses. Th1 immunity is characterized by the release of IFN-γ that activates macrophage microbicidal activities. IFN-γ is essential for anti-mycobacterial defense in mice (Flynn et al., 1993), and polymorphisms in the IFNG gene are associated with MTB infection risk and disease progression in humans (Rossouw et al., 2003). Th17 differentiation is driven by IL-23, and is characterized by the release of IL-17, which is critical for early recruitment of neutrophils to the site of infection (Freches et al., 2013). IL-17 has been shown to be required for protection against TB in mice infected with a hyper-virulent clinical isolate *M. tuberculosis* HN878 strain. Mice deficient in this cytokine had significantly higher bacillary burdens and less organized granulomas (Gopal et al., 2014). At excessive levels, however, IL-17 promotes tissue pathology and inflammation, suggesting that tight regulation of this cytokine is required during infection (Das and Khader, 2017). Foxp3+ T regulatory cells (Tregs) dampen Th1 immunity through inhibition of inflammatory cytokines by IL-10. Treg frequencies are higher in peripheral blood and at disease sites of patients with active TB, where they suppress production of MTB-specific IFNγ by Th1 cells *ex vivo* (Marin et al., 2010); too much expansion of these cells may result in impaired immunity.

The role of Th2 responses in TB infection is controversial. Mice deficient in IL-4, IL-4Rα, or STAT6 on a C57BL/6 background display disease outcomes similar to wild-type mice infected with MTB (North, 1998; Flynn and Chan, 2001; Jung et al., 2002). However, IL-4 seems to be detrimental in a BALB/c mouse background, with its deletion resulting in more protection against TB infections. Also, antibody neutralization of IL-4 on this background provides protection against chronic TB infection. Mechanisms associated with the detrimental role of Th2 cytokines remain unclear, but may stem from their ability to inhibit Th1 factors such as TNF, required to control bacterial replication (Hernandez-Pando et al., 2004). IL-4 is expressed in human surgically-derived lung tissues (Stanton et al., 2003), although its function in humans has not been established. Over-expression of another Th2 cytokine, IL-13, in mice, results in susceptibility to TB infection characterized by enhanced collagen deposition and enhanced lung pathology with necrotizing granulomas (Heitmann et al., 2014). These studies suggest that the IL-4/IL-13 axis drives pathological damage. A recent report by Minutti et al. (2017) has identified SP-A in the lung as a tissue-specific amplifier of IL-4-dependent macrophage proliferation and activation.

In granulomas, T cells constitute a larger part of the outermost layer. However, it is poorly understood how CD4+ T cells or IFNgamma penetrate lung lesions to access macrophage-rich areas at the centers. The Kaufmann laboratory has shown that chronic infection in both mice and humans is associated with the development of lymphoid follicle-like structures at the periphery of granulomas to orchestrate local host defense in the lung (Ulrichs and Kaufmann, 2006; Kahnert et al., 2007). They identified two layers surrounding the necrotic centers; the first, an inner layer that comprised CD68+ APCs and large cells, including epithelioid and Langhans giant cells. This layer also contained the bacilli, and CD4+ and CD45RO+ memory cells. The second layer was the outer area of the lesions, characterized by infiltration of B and T cells. This outer-most layer was enriched with CD8+ T cells, largely absent in the inner layer (Ulrichs and Kaufmann, 2006). Thus CD4+ and CD8+ T cells seem to exhibit distinct spatial distribution in a granuloma structure.

The importance of CD8 T cells in the long-term control of infection has been demonstrated using several mouse strains deficient in CD8 T cells due to different gene deletions (Lin and Flynn, 2015), but little is known about colocalisation of CD8 T cells and macrophages in granulomas. Depletion of this subset of cells in TB-infected mice results in an increased bacterial burden (van Pinxteren et al., 2000). The requirement for CD8 T cells was also shown in macaque models of TB, with some research indicating that the depletion of CD8 T cells in BCG-vaccinated macaques results in compromised control of MTB infection (Chen et al., 2009). Although more research is required in humans, data from macaques support the importance of CD8 cells in TB (Lin and Flynn, 2015). Other T cell subsets involved in immune responses to MTB infections and potential interactions with macrophage subpopulations include γδ T, innate lymphoid cells, NK and CD1-restricted CD4/CD8 double negative T cells (Jasenosky et al., 2015; Ndlovu and Marakalala, 2016).

The role of B cells and antibodies in TB remains largely unclear (Achkar et al., 2015); antibodies mediate potent effector mechanisms through macrophage Fc and Complement receptors and activation of their microbicidal mechanisms.

potential Trojan horses for infection. These include Phosphatidyl Serine (PS) recognition molecules MerTK, axl (prominent in alveolar macrophages), their opsonic cofactors such as Gas and protein S, as well as other opsonins such as lactadherin (MFGE8), annexin, calreticulin, SP-A, and C1Q (Gordon and Plüddemann, 2018). Known MTB ligands for Mincle and MARCO include trehalose dimycolate (TDM, cord factor). Mincle together with MCL engages TDM to induce production of inflammatory cytokines such as IL-6, TNF, and IL-1beta (Ishikawa et al., 2009; Miyake et al., 2013). Dectin-2, DC-SIGN, and Mannose Receptor all recognize mannose-capped lipoarabinomannan (ManLAM) on the surface of MTB (Yonekawa et al., 2014; Marakalala and Ndlovu, 2017). Dectin-1, a major receptor of fungal beta-glucans that signals through the adaptor molecule CARD9, which is essential for tuberculosis control in the mouse (Dorhoi et al., 2010), has also been demonstrated to recognize an unknown ligand on the surface of MTB. This may differ from the well characterized beta-glucan ligand for Dectin-1 on fungi; such a ligand has been detected in selected tumor cells, and may be masked by N-glycans (Chiba et al., 2014).

Macrophage receptor-TB interactions result in activation of numerous cellular responses (Marakalala and Ndlovu, 2017). These molecules, however, are largely redundant in the *in vivo* control of chronic TB infection in mice and nor is it known which receptors are responsible for MTB uptake by the different macrophage subpopulations in granulomas, in situ, and for their resultant responses. For example, Dectin-1 knockout mice mount the same immune response as wild-type mice (Marakalala et al., 2011), whereas Dectin-2 has not yet been studied in an MTB *in vivo* model. MCL seems to drive a moderate protective role, while contradictory results have been reported for Mincle and DC-SIGN (Marakalala and Ndlovu, 2017). Future research should explore potential cooperation (Bezbradica et al., 2014) between individual CLRs, their synergy with other receptors

such as TLRs and potential scaffold proteins in lipid rafts, and how this might affect the outcome of TB disease *in vivo*. Studies in human populations should confirm or identify novel dominant or recessive genetic susceptibility to MTB infection and BCG.

Macrophages express a range of plasma membrane and endosomal receptors for uptake of MTB components; exchange of mycobacterial and host-derived lipids is considered further below. Contrasting results have been reported on the role of TLRs in TB. TLR-2 and TLR-4, for example, have been shown to play a role in the long-term control of *M. tuberculosis* (Jo, 2008). Some studies, however, have reported that TLR2/4/9–/– triple knockout mice mount the same T cell mediated immune response compared with WT mice after infection with MTB (Holscher et al., 2008). Macrophages and other myeloid leukocytes express activatory and inhibitory FcR for IgG, as well as CR3 and other regulatory receptors for complement and antibody-coated immune complexes; these play a potentially important role in their endocytic and cytotoxic responses. Cytosolic sensors of MTB constituents and nucleic acids have been shown to play an important role in macrophage responses to MTB infection. For example, the nucleotide-binding oligomerization domain protein NOD2 has been shown to synergize with TLR-2 for the production of pro-inflammatory cytokines in response to live MTB (Jo, 2008). Another widely studied cytosolic sensor is the NLRP3 inflammasome, which induces IL-1beta processing and pyroptosis through caspase-1. Mishra et al have linked the NLRP3 inflammasome with lung pathology in TB infection, which can be regulated by NO (Mishra et al., 2013). Another report, however, has demonstrated that the inflammasome is not linked to the disease outcome (Walter et al., 2010). The recognition of MTB DNA will be described below after first considering the membrane dynamics and fate of the MTB phagosome in macrophages.

D'Arcy Hart and colleagues (Goren et al., 1976) first reported that MTB inhibited phagosome-lysosome fusion and acidification within the vacuolar compartment in which they resided after uptake, an important evasion mechanism for this intracellular pathogen. The question of entry to the cytosol by mycobacterial constituents and potential antigens for CD8 cytotoxic T lymphocytes has been under considerable debate for some years. It is likely that macrophage activation by CD4 T lymphocyte- and NK–dependent Interferon gamma overcomes both the fusion and acidification block. Macrophages are not only active endocytic and phagocytic cells, but also highly regulated secretory cells (Nathan, 2012), characterized by extensive membrane flow, selective intracellular fusion of vesicular membranes, fission and recycling (Tan and Russell, 2015). It is not known in detail how membrane traffic is selectively altered by MTB, and the impact of autocrine and paracrine effects of cytokines such as TNFalpha must also be kept in mind (Caldwell et al., 2014). Small GTPases play an important role in regulating intracellular survival of Mycobacteria in mouse macrophages; there are significant species differences in this regard (Gazzinelli et al., 2014). Another, genetic, difference in mouse susceptibility to infection relates to N-Ramp1 (Natural resistance-associated macrophage protein,1), a member of a metal ion transporter family at the interface between the phagolysosomal compartment and the cytosol (Buschman and Skamene, 2001; Blackwell et al., 2003). Recent studies with other Gram negative and Gram positive bacteria have described a role for a family of Copper-binding molecules (Burstein et al., 2005; Phillips-Krawczak et al., 2015) which participate in cytosolic multi-protein complexes and interact with the phagocytic pathway, lysosomal biogenesis and inflammasome activation. Their role in MTB infection has not been defined. Russell (Tan and Russell, 2015), Grinstein (Fairn et al., 2009), and their colleagues have made important contributions to studying acidification mechanisms in macrophages, and their role in anti-TB drug development, which requires screening within living macrophages and not in isolation. The interaction of MTB and the autophagy pathway (Deretic and Klionsky, 2018) has also attracted considerable attention, bearing on macrophage death and its role in immune activation and pathogenesis, as well as on mycobacterial survival and latency. Live imaging of spatiotemporal dynamics of MTB phagosomes has revealed that effective control of MTB replication in IFN-γ activated macrophages requires appropriate spaciousness of proteolytic phagosomes whose generation and membrane integrity are maintained by a Rab20-dependent membrane traffic pathway (Schnettger et al., 2017). Further studies on the proteome of isolated phagosomes from infected and uninfected cells as well as super resolution and intravital microscopy will help to clarify the complex interplay between the macrophage and its infectious cargo (Mahamed et al., 2017; Schnettger et al., 2017).

Intracellular bacteria, viruses and parasites have evolved a variety of different strategies to survive within macrophages; TB provides a particularly challenging infection model of great interest to cell biologists, microbiologists and immunologists. Although there has been an explosion of knowledge bearing on cytosolic sensing and intracellular signaling mechanisms of bacterial membrane molecules (NLRs) and nucleic acids (RIG-I, STING), the recognition of mycobacterial constituents by these intracytoplasmic protein complexes remains largely unknown. Direct detection of cytosolic MTB DNA by cGAS has been demonstrated by Watson et al. (2015). Unlike Listeria monocytogenes which produces the STING agonist cyclic-di-AMP, cGAS (cyclic GMP-AMP synthase) is required to activate type1 interferon by cytosolic DNA of MTB and Legionella pneumophila, via the STING/TBK/IRF3 pathway. Human genetic auto-inflammatory syndromes and mouse genetic models should have much to teach us in this regard.

GRANULOMA FORMATION IN THE LUNG

Alveolar macrophage infection is an important and well-studied initiator of granuloma formation. As noted above, they are exposed via the airway to MTB, which they capture and sense through plasma membrane, endosomal and cytosolic receptors. They generate antigens and interact with DC, which are required to activate naïve T lymphocytes, although macrophages can activate primed T cells (Austyn, 2016). Alveolar macrophages communicate with local epithelial cells to maintain gas exchange

and set the threshold and the appropriate quality of the immune response. Macrophage populations in the lung are heterogeneous in their initial embryonic and subsequent bone marrow origin; monocyte recruitment to the lung is enhanced by exposure to particulates and pollutants that reach the lower airways (Torrelles and Schlesinger, 2017). As described above and in **Figure 1**, Russell and colleagues have demonstrated that ontogeny contributes to the interaction and outcome of initial MTB infection in the mouse (Huang et al., 2018). The authors favor a pre-programmed model ascribed to developmental origin, rather than responses to different local microenvironments. The receptors that mediate acute infection in this *in vivo* model were not defined. Apart from exposure to local surfactant proteins, potential opsonins and high levels of oxygen in the microenvironment are other macrophage modifying factors. Surfactant proteins A and D contribute to innate immunity outside the lung as well as within the alveolar space and may also contribute to extra-pulmonary TB (Ujma et al., 2017). The lung contains other specialized populations such as interstitial macrophages, that are not directly exposed to exogenous alveolar stimuli; these include intra-epithelial macrophages and DCs, found mostly in larger airways, and macrophage populations in the pleural cavity (Gordon et al., 2014a; McClean and Tobin, 2016). Alveolar macrophages undergo tissue imprinting in the lung as a result of their unique environment and exposure to infectious agents via the airways (Hussell and Bell, 2014). Other cells that are involved in the early response to TB infection are PMNs, which are the first defensive cells to be recruited to tissue during infection. PMNs have been reported to be the most abundant infected cells in the airways, sputum and BAL from patients with active TB.

Heterogeneity in TB Granulomas

The overall composition and fate of granulomas have been briefly described above, with emphasis on the heterogeneity of macrophage origin, anatomic location and phenotypes. Here we consider heterogeneity of MTB-induced granulomas in the lung. Recent data in human disease and primate models have shown that infected individuals contain a heterogeneous mixture of granulomas in various histologic states, with varying degree of immune activation, macrophage immune-phenotypes and the ability to control bacterial replication (Stanton et al., 2003; Kim et al., 2010; Lin et al., 2014; Gideon et al., 2015). Also, some important immune pathways seem to be distinctly enriched in specific regions within granulomas (Marakalala et al., 2016). This body of research suggests that disease-driving processes are compartmentalized within individual granulomas, and that these spatial processes may be linked to the clinical outcome. Our understanding of granuloma organization has come mostly from histopathology, which assesses structure by the abundance of various cell-types (Ulrichs et al., 2004; Gideon et al., 2015). Histological analyses of human TB have provided evidence for morphologic heterogeneity among pulmonary alveolar macrophages, foam cell formation, epithelioid cells and multinucleated giant cells (**Figure 2**; Dannenberg and Rook, 1994). Distinct phenotypes and activation status of macrophages in human pulmonary granulomas have also been demonstrated by immunohistochemistry with a panel of antibodies (Stanton et al., 2003). However, more research is still required for better understanding of macrophage differentiation, cell-to-cell interactions, heterogeneity and functions within various compartments of TB granulomas.

With the availability of new advanced techniques, research on the role of granulomas in TB has received considerable attention recently, with many advanced genome-wide approaches explored to give a better molecular characterization of the macrophage-rich structures. Using a combination of laser microdissection and microarray analysis of human lung tissues, a study by Kim et al. (2010) demonstrated that genes involved in lipid sequestration and metabolism were highly expressed in caseous granulomas. Immunohistochemical analysis of the tissue confirmed the upregulation of proteins involved in lipid metabolism in cells surrounding the caseum, including adipophilin, acyl-CoA synthetase long-chain family member 1 and saposin C.

In a similar approach, Marakalala et al. (2016) utilized proteomics and mass spectrometric imaging to characterize spatial organization of inflammatory pathways within human granulomas. The centers of the granulomas were concentrated with pro-inflammatory and antibacterial signatures whereas the cellular peripheries were enriched with anti-inflammatory, tissue-preserving mediators (Marakalala et al., 2016). A similar phenomenon has been shown in granulomas from macaques, in which spatial delineation and inflammatory cell programmes were organized around distinct subsets of macrophages (Mattila et al., 2013). These studies suggest that local balance of pro- and anti-inflammatory responses may determine the fate of individual granulomas, which collectively influence the host response (Marakalala et al., 2016). The model proposed by these studies may also help to explain the heterogeneity that is often observed in TB granulomas, even within the same host, as differences in inflammatory responses probably contribute to diverse granuloma structures and functions (Cadena et al., 2017). In macaques, Lin et al demonstrated that the majority of granulomas begin with a single bacterium (Lin et al., 2014). The authors observed variability in bacterial killing within individual granulomas that was independent of host status. These findings established that local events at granuloma level are likely to influence the clinical outcome of infection. To understand the repertoire of the adaptive immune system in various granulomas, Subbian et al. examined lung granulomas from patients with chronic pulmonary TB (Subbian et al., 2015). The study revealed significant variability in T cell density and fibrosis. Gideon et al reported variability in different factors even within the same macaque (Gideon et al., 2015). These factors included the total numbers and phenotypes of T cells, the numbers and heterogeneity of macrophages and a wide range of cytokine profiles and bacterial burdens within each granuloma. The majority of these T cells produced only a single cytokine; dominant cytokines included IFNγ, interleukin-2 (IL-2), Tumor Necrosis Factor (TNF), IL-10, and IL-17. These findings suggest that granuloma heterogeneity and spatial organization of cellular and humoral host responses at granuloma level should be taken into account when designing host-directed therapies that limit lung pathology.

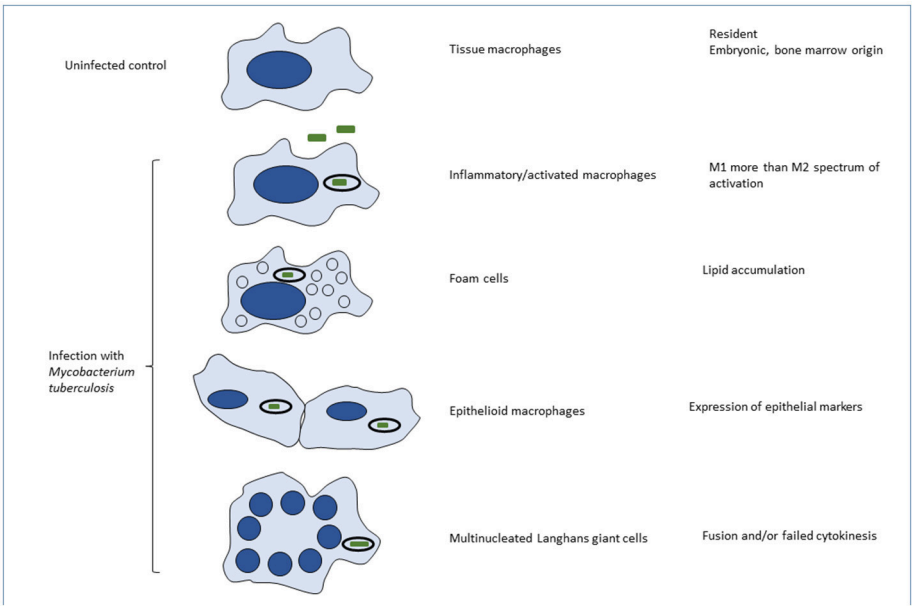


FIGURE 2 | Phenotypic heterogeneity of macrophages induced by MTB infection *in vivo*. Macrophages are able to undergo remarkable variations in their phenotype *in vivo*, yet the mechanisms are poorly understood. This is partly the result of species variation, inadequacy of defined *in vitro* conditions to mimic *in vivo* phenotypes, limited population and single cell analysis of cells in situ or after extraction, *ex vivo*, and above all, the complexity and heterogeneity of the mixed populations present in tissues. Variables that have been characterized to some extent, include: ontogeny (embryonic or bone marrow origin); steady state and physiological conditions in different organs and microenvironments; sterile injury and acute or chronic infections such as MTB; cell recruitment, phagocytosis and activation by different exogenous and endogenous stimuli; and cell death by apoptosis, necrosis or pyroptosis. In many situations the macrophage phenotype covers a spectrum of responses, rather than binary alternatives. Their characterization is morphological, utilizing combinations of marker antigens, signatures of gene expression, and, where known, functional differences. The text provides examples of the different phenotypes illustrated here. The impact of macrophage phenotype on MTB infection, and conversely, of MTB infection on macrophage functions is barely understood.

Epithelioidisation of Macrophages Within Granulomas

Macrophages can undergo a series of morphological changes characterized by cytoplasm expansion and interlocking between membranes of neighboring cells. Macrophages undergoing this histological transformation have always been termed epithelioid cells (Dannenberg and Rook, 1994), although their significance in granuloma functions remains unclear. Recent work by Cronan et al. has meticulously described molecular underpinnings of macrophage epithelialization within granulomas (Cronan et al., 2016). Using a zebrafish model, immunofluorescence and live imaging techniques, the authors showed that as macrophages create junctions with each other to form a tuberculous granuloma, they express and deploy adherens components. The macrophages expressed proteins that are typically associated with epithelial cells, including desmosomal proteins (desmoplakin, desmoglein, and desmocollin), adherens junction proteins (E-cadherin, plakoglobin, α-, β-, and δ- catenin), and tight junction pathways (ZO-1 and ZO-2). Proteins corresponding to these genes have been identified in a proteomic survey of granulomas from humans infected with MTB (Marakalala et al., 2016). A significant finding from the study by Cronan and colleagues is the observation of epithelial markers in the epithelioid cells of granulomas. Taken together, these studies underpin epithelioidisation of tissue macrophages as a fundamental process in granuloma development and the ability to control infection in zebrafish and humans.

MACROPHAGE ACTIVATION: GENE EXPRESSION AND PHENOTYPE MODULATION

BCG has provided a potent adjuvant to study for its own sake as a vaccine, as well as providing a tool to induce innate and adaptive immune activation of macrophages. Mackaness and colleagues performed now-classic studies on the role of BCG administration in mice, in order to induce enhanced resistance, not only to BCG, but also non-specifically to an unrelated challenge, e.g., Listeria monocytogenes, and vice versa (Carter, 2014). Building on earlier pioneering discoveries by Koch and Ehrlich, as well as Metchnikoff, the Mackaness group confirmed that this mechanism, now termed "Classical macrophage activation," was cellular and not humoral in origin. Subsequent studies identified Interferon gamma as the major cytokine produced by specific CD4 T lymphocytes or by innate NK cells. The role of IL-12 and IL-18, and various cytokine receptors on macrophages was elucidated by several investigators; these studies complemented the discovery by Casanova (Casanova and Abel, 2017), Holland (Wu and Holland, 2016) and others

of primary immunodeficient patients unable to control BCG infection after immunization with live BCG or after infection by relatively avirulent organisms. Studies by Nathan (Nathan, 2013) and others established that the induction of inducible nitric oxide synthase (i-NOS) and generation of antimicrobial nitrogen-based radicals, combined with oxygen radicals generated by the respiratory burst, contributed to anti-microbial resistance in mice. After some technical issues, the role of NO in human infection by MTB was confirmed. Subsequent microarray analysis by several research groups revealed a signature of gene expression in mouse and humans after IFN gamma activation of macrophages, distinct from the "alternative activation" signature induced by the Th2 cytokines IL-4 and IL-13, acting through the common IL-4R alpha chain receptor. Nathan's group also documented potent metabolic anti-oxidant defenses in macrophages. Vitamin D induces antimicrobial peptides and autophagy in monocyte/macrophages and promotes resolution of inflammation in TB patients (Fabri et al., 2011; Coussens et al., 2012). Glucocorticosteroids have potent inhibitory effects on inflammation, monocyte recruitment and activation of macrophages by MTB.

There is evidence that TB infection in humans induces IL-4 gene expression in macrophages (Stanton et al., 2003), possibly mediated by TLR involvement, the spectrum of gene activation that is upregulated indicates a more mixed activation signature than in laboratory mouse strains. The initial binary classification of M1- and M2-types of macrophage activation by IFN gamma and IL4/13 respectively has been refined to a broader spectrum of activation, in which individual markers are replaced by a signature of a group of genes, many of which overlap with altered gene expression by other defined stimuli. Alternative activation of macrophages has been implicated in tissue repair and fibrosis; whether this plays a role, together with transforming growth factor beta, in Tuberculosis-induced fibrosis remains to be elucidated. Although Th2 cytokines readily induce macrophage cell-cell fusion *in vitro* and *in vivo*, the mechanism of Langhans giant cell formation (**Figure 2**), a characteristic feature of human tuberculosis, remains obscure. Interferon gamma by itself does not promote fusion *in vitro*, but may contribute to macrophage fusion in combination with ligation of uncharacterized macrophage plasma membrane glycoproteins (Sakai et al., 2012), GM-CSF and fusogenic MTB (Puissegur et al., 2007) and host lipids. An alternative mechanism, DNA injury and failure of cytokinesis has been proposed to account for multinuclear giant cell (MNGC) formation in tuberculosis (Herrtwich et al., 2016). The functional significance of Langhans giant cell formation, especially in relation to interactions with MTB, remains unclear, Studies on IL-4 induced MNGC have revealed enhanced clearance of large particulates and systemic amyloid deposits *in vivo*; this was associated with selective activation of CR3 function, as a result of cell fusion (Milde et al., 2015). Recent revival of interest in macrophage metabolism has provided evidence that classically and alternatively activated macrophages utilize glycolysis and oxidative phosphorylation, respectively (O'Neill and Pearce, 2016), as their main source of energy. Shi et al have reported that infection with MTB induces the Warburg effect in mouse lungs (Shi et al., 2015). Gleason, O'Neill and Keane have shown that enhanced aerobic glycolysis in human alveolar macrophages is required to control intracellular bacillary replication (Gleeson et al., 2016).

As an adjuvant, BCG has been utilized to boost anti-cancer immunity, with some success in bladder cancer after local administration (Alexandroff et al., 1999). This could benefit combination therapy with antibody-based checkpoint therapy targeting T lymphocyte co-stimulatory receptors. Extending earlier findings that BCG could prime macrophage activation, Netea and colleagues (Arts et al., 2018) have used BCG as one of their protocols to induce "trained immunity," ascribed to epigenetic mechanisms. Yeast particles, taken up by macrophages through the beta-glucan receptor, Dectin-1, which signals through syk and Card9, provides a similar priming function. As information accumulates from GWAS and SNP studies, other genes than those mentioned above and the MHC complex may be found to contribute to human macrophage activation.

PROTEIN SECRETION BY ACTIVATED MACROPHAGES: ROLE IN PATHOGENESIS OF TUBERCULOSIS

It is only since the early 70's, from the description of lysozyme secretion by mouse macrophages in cell culture (Gordon et al., 1974), that it was recognized that macrophages are not only professional phagocytes, but also highly active secretory cells. Mature macrophages do not accumulate preformed proteins in granules as do granulocytes, for immediate release in acute inflammation. Low molecular metabolites derived from oxygen during the respiratory burst and from preformed lipids during acute inflammation can be rapidly generated from arachidonates in the plasma membrane, but proteins are newly synthesized, consistent with their required functions in prolonged inflammation, as well as in tissue homeostasis. Macrophages produce a large variety of proteins in relatively small amounts, e.g., all components of the complement cascade, potentially significant in their immediate local environment. Lysozyme is constitutively released by macrophages in culture, although its production is greatly enhanced by chronic inflammation and activation, as seen by in situ hybridization in BCG granulomas (Chung et al., 1988). It is highly cationic, will bind to host negatively charged proteoglycans, but enzymatic activity seems restricted to bacterial wall rather than host substrates, directly or after exposure, eg through complement lysis, as in MTB. It is lost from plasma by filtration through the kidney (MW 14 Kd), but can be elevated by increased numbers of macrophages, as well as enhanced output per cell, as in tuberculosis.

Activated macrophages produce neutral proteinases such as urokinase, elastase, collagenases and other metalloproteinases, implicated in fibrinolysis, tissue remodeling and degradation. Caspases are released as a result of inflammasome activation; recent studies have demonstrated a range of caspase functions unrelated to cell death (Shrestha and Megeney, 2012). As part of inflammatory regulation, macrophages also release alpha 1 antitrypsin and alpha 2 macroglobulin to inhibit proteolytic

activity. More restricted cleavage can activate proenzymes, e.g., Angiotensin-converting enzyme (ACE) (Bernstein et al., 2013), or inactivate components of plasma protein cascades, e.g., by carboxypeptidase action, a macrophage-specific enzyme (Mahoney et al., 2001). The protein cross-linking enzyme Transglutaminase 2, a conserved feature of alternative activation of macrophages (Martinez et al., 2013), has been implicated in MTB restriction by macrophages (Palucci et al., 2017), as well as in fibrosis. FXIIIA, a distinct transglutaminase, also expressed by macrophages, displays similar properties (McGovern et al., 2014). Macrophages can release a large number of proinflammatory (e.g., Type I interferon, TNF alpha, Interleukin 1 beta, IL-12, IL-18, IL-6) and anti-inflammatory cytokines (IL-10 and TGFbeta), and a range of CC, CXC and CX3C chemokines, as well as expressing their receptors. Growth factors which macrophages produce, and respond to, include M-CSF, GM-CSF and Erythropoietin, as well as releasing vascular endothelial and fibroblast growth factors.

Release of TNF alpha from the plasma membrane is mediated by ADAM 17, a metalloproteinase; surface TNF is an essential ingredient of granuloma formation (Fremond et al., 2005) and may play a role in contact-dependent killing of viable, TB-infected macrophages (Mahamed et al., 2017), whereas secreted TNF may be important in catabolism and weight loss, with IL-6 (Flint et al., 2016). Recent findings by McIlwain et al (McIlwain et al., 2012) and the Freeman group (Christova et al., 2013) have shown that a Rhomboid family of multispan transmembrane molecules, of which i-Rhom 2 is specific for macrophages, are essential for Adam17- dependent release of TNF alpha from the macrophage plasma membrane, and may also contribute to chaperone activity in ER transport and in lysosomal stability. Taken together, it is clear that macrophage secretory activity plays a major role in granuloma formation and function. To establish which macrophage genes are expressed at the single cell level, both as message and protein, it will be necessary to examine samples of TB-infected tissue *in situ* and *ex vivo*. It will also be necessary to relate macrophage activities within and among granulomas and to characterize heterogeneity of macrophage sources and functions of different products within lesions.

TYPE I INTERFERON AND TUBERCULOSIS

Macrophages are an important source of Type 1 Interferon in inflammation. Studies by Berry et al. (2010) identified a whole blood transcriptional signature in active TB patient cohorts from the United Kingdom and South Africa. The signature was dominated by IFNα/β-inducible genes, which were overexpressed in neutrophils. It is likely that blood and activated tissue macrophages are a major source of type I IFN as well, since the type I IFN gene profile also correlated with the extent of radiographic disease. Interestingly, the whole blood IFN signature was diminished with successful TB treatment, suggesting an association of the interferons with disease severity. Additional studies have verified the potential detrimental role of type I IFNs in TB (McNab et al., 2015).

A recent study by Zak et al investigated blood RNA expression to predict progression from latent tuberculosis infection to active disease (Zak et al., 2016). In the study, latently infected South African adolescents were followed for 2 years. Blood samples from latent infections that converted to active disease were analyzed by RNA sequencing to identify genes that were differentially expressed in comparison to the controls who did not convert. A 16-gene signature was identified and validated using quantitative real-time PCR (Zak et al., 2016). Interestingly, the signature comprised interferon-inducible genes previously identified as expressed in active tuberculosis (Berry et al., 2010). This confirms that type I interferon signatures can be exploited to predict disease progression in point of care testing.

MACROPHAGE EICOSANOIDS AND TUBERCULOSIS

Macrophages are a major source of Arachidonate metabolites which have been shown to be important regulators of inflammation and the outcome of tuberculosis and granuloma formation (**Figure 3**). Although the mechanisms driving type I IFN-mediated disease progression are still poorly understood, a few studies have suggested suppression of pro-inflammatory cytokines and Th-1 immunity as a major factor. A study by Mayer-Barber and colleagues demonstrated a detrimental role for type I IFNs in TB infection in mice (Mayer-Barber et al., 2014); inhibition of IFNalpha/beta reversed the detrimental effects of type I IFNs. This response was dependent on the induction of prostaglandin E2 (PGE2). Direct administration of this prostanoid resulted in the control of bacterial infection through inhibition of type I IFNs (Mayer-Barber et al., 2014). This study indicated the importance of type I IFNs and manipulation of the eicosanoid balance as a target for host- directed therapies.

Studies in mice and zebrafish models have linked the eicosanoid pathways with various modes of macrophage death. Virulent MTB H37Rv has been shown to drive macrophage necrosis through the production of lipoxin A4 (LXA4), which inhibits prostanoid synthesis and promotes mitochondrial inner membrane perturbations. In contrast, prostaglandin E2 (PGE2) suppressed inner mitochondrial membrane damage and inhibited macrophage necrosis in macrophages. Furthermore, mice deficient in prostaglandin E2 synthase (PGES) had higher lung bacillary loads compared with wild type mice, indicating the protective role of prostaglandin E2 against mycobacterial infections in the lung (Chen et al., 2008). ALOX5 knockout mice, which cannot produce LXA4, undergo more apoptosis with enhanced MTB-specific T cell responses (Divangahi et al., 2010), and are more resistant to MTB infection (Bafica et al., 2005), suggesting detrimental effects of LXA4 during infection. On the other hand, mice deficient in COX-2 are more susceptible to MTB infection, confirming an important role for prostanoids (Mayer-Barber et al., 2014).

Using a zebrafish model, Tobin and co-workers studied the contribution of eicosanoid mediators in response to *Mycobacterium marinum* (Mm) infection (Tobin et al., 2010, 2012). The authors identified a critical role for the enzyme

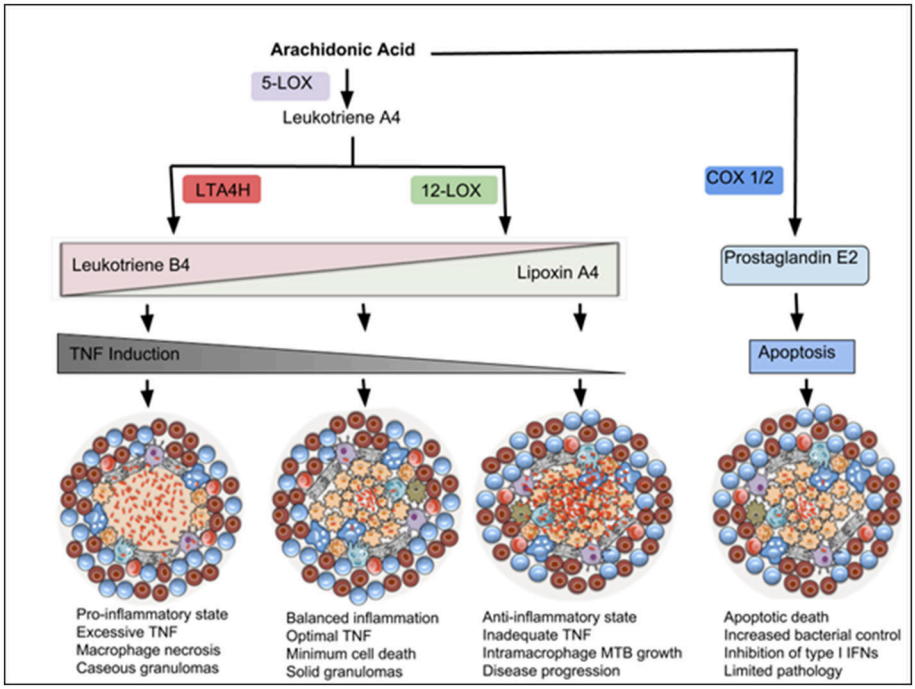


FIGURE 3 | Eicosanoids drive inflammatory responses that modulate macrophage cell death and TB disease outcome. Arachidonic Acid (AA) can be metabolized by 5-LOX to produce Leukotriene A4 (LTA4), which is a precursor of Leukotriene B4 (produced via an enzyme LTA4H) or Lipoxin A4 (produced via 12-LOX). Leukotriene B4 (LTB4) induces pro-inflammatory responses and TNF expression, which in excess, promotes macrophage necrosis and granuloma caseation. Lipoxin A4 (LXA4) is anti-inflammatory and associated with TNF deficiency and increased intra-macrophage bacterial growth. Balanced amounts of these pro- and anti-inflammatory lipid mediators are required for optimal control of cell death and disease progression. AA can also be metabolized by COX-1/2 to produce Prostaglandin E2, which induces macrophage apoptosis and promotes antimicrobial activities.

Leukotriene A4 Hydrolase (LTA4H) in determining susceptibility of zebrafish to infection. LTA4H is responsible for production of Leukotriene B4, a pro-inflammatory eicosanoid that induces the transcription of TNF. Excess LTA4H in Mm-infected zebrafish led to early reduction of bacterial growth inside macrophages. However, bacterial restriction was rapidly followed by macrophage necrosis, which enabled bacterial replication in the permissive extracellular milieu (Tobin et al., 2010, 2012). These results suggest that LTA4H, through TNF production, can dually mediate resistance and susceptibility to mycobacterial infection (Roca and Ramakrishnan, 2013). Its absence leads to TNF deficiency, resulting in increased bacterial growth intracellularly, while its overexpression leads to excessive production of TNF resulting in macrophage necrosis (**Figure 3**; Tobin et al., 2012; Roca and Ramakrishnan, 2013). In human tuberculous granulomas, LTA4H is abundant in necrotic regions, where it colocalises with TNF (Marakalala et al., 2016). In humans, the genetic status of LTA4H has been shown to be critical for disease outcome in TB meningitis patients. Patients who are homozygous for low or high LTA4H expression alleles developed severe TB meningitis with reduced survival, while those heterozygous for intermediate LTA4H expression controlled the infection (Tobin et al., 2012). These findings confirm a need for balance in inflammatory responses, much of it orchestrated by metabolic changes in activated macrophages.

MACROPHAGE FOAM CELL FORMATION AND CASEATION

Foam cell formation and caseation are hallmarks of human tuberculosis, yet their genesis, lipid composition, and significance for outcome remain poorly understood. Caseation could be due to cell death, resulting from mycobacterial toxicity and/or an exuberant host immune response, as well as altered lipid metabolism. Possible mechanisms include mobilization from lipid stores, endocytosis and deposition in macrophages, enhanced synthesis, locally and systemically, and/or failure to degrade accumulated lipids in macrophages. Macrophage foam cells form readily after uptake of various protein-bound lipids by a range of scavenger receptors, e.g., SR-A, CD36 and LDL receptors (Neyen and Gordon, 2014). Lipid droplets arise by synthesis and export from the endoplasmic reticulum to the cytosol, before becoming bound by vesicle membranes (**Figure 2**). Macrophage synthesis, uptake and exchange of lipids are regulated by transcription factors such as PPAR gamma and cytokines released by T lymphocytes and adipocytes (Daniel et al., 2011; Ouimet et al., 2016; Cambier et al., 2017). Foam cells in mouse granuloma models have been shown to express Wnt 6, involved in macrophage arginase1 induction and proliferation (Schaale et al., 2013). In addition to MTB-macrophage interactions, there seems to be an axis

of interactions among MTB, macrophages and adipocytes, eg multinucleated macrophages are closely associated with adipocytes in white adipose tissue crown-like structures (Touton cells) and there is evidence that MTB can infect adipocytes (Neyrolles et al., 2006; Agarwal et al., 2016). Lipids derived from intracellular bacteria and/or plasma are potentially fusogenic, contributing in addition to host cytokines to Langhans giant cell formation. At a systemic level there is an association between TB and diabetes, cachexia is a characteristic feature of advanced TB, possibly mediated by TNF (originally named cachectin) and IL-6, and there is more than a superficial resemblance between caseation and atheroma, a hallmark of non-infective atherosclerosis. Recent studies have drawn attention to cholesterol (Huang et al., 2018) and oxysterol metabolism (Lu et al., 2017) in immune cells and of phenolic glycolipids in experimental mycobacterial infection (Cambier et al., 2017). Huang et al. have stressed the capacity of MTB to access and degrade fatty acids and sterols in order to survive within macrophages. To gain a better understanding of prolonged host-pathogen interactions in chronic TB, it will be necessary to perform lipidomic analysis of the heterogeneous macrophage populations as well as MTB, ideally, *in vivo*, and at the single cell level.

CONCLUSIONS

Tuberculosis has been well documented as a clinical and pathological entity, yet many aspects of the disease remain unclear; while its rich natural history provides unique opportunities for fundamental and applied research. Since the nineteenth century it has been known that macrophages are an integral component of its pathogenesis and sequelae. In this review we have shown how cellular and molecular advances have generated new insights into the role of macrophages and, conversely how tuberculosis research continues to provide a wealth of theoretical and practical problems for study of macrophage immunobiology. Although we are beginning to understand the phenotypic distinction between tissue- resident yolk sac-derived and inflammatory bone marrow- derived macrophages in the mouse, this concept needs validation in humans; moreover, we do not know the impact of specific organ localization as well as origin on macrophage- MTB interactions. The extensive heterogeneity of macrophage populations *in vivo*, revealed by population and single cell analysis, mandates exquisite selectivity to target particular subsets of infected cells, without collateral injury to the host, as emphasized by Srivastava et al. (2014). Furthermore, the associated caseation and fibrosis, hallmark complications of the human disease, are poorly expressed in experimental models and *in vitro*; distinctions between the immune response to TB in humans and in animal models are emphasized by Scriba et al. (2017). Further progress will depend on access to human tissue from patients, the development of sensitive methods to study small amounts of tissue in situ, ideally by non-invasive methods over the course of the disease, and validation with *in vitro* models of human cells as well as development of new animal models that mimic the disease in humans. Shorter courses and more effective drug treatment of patients will be achieved by high throughput screening within macrophages to identify novel mycobacterial targets. The role of macrophages in granuloma and giant cell formation, epitheliodisation, caseation and fibrosis, all associated with TB, requires further investigation.

Study of tuberculous granulomas should promote understanding of other granulomatous diseases such as sarcoidosis and autoimmune destructive conditions such as Granulomatosis with polyangiitis, formerly called Wegener's granulomatosis. The co-epidemic of TB with HIV-1/AIDS, characteristically treated as a T cell failure, also involves macrophage dysfunction, as a viral reservoir, but especially when successful HAART restores CD4 T lymphocyte function, resulting in the Immune reconstitution inflammatory syndrome (IRIS) (Bell et al., 2017). Corticosteroid treatment, usually associated with increased risk in TB treatment, may be of benefit in preventing this outcome.

Apart from its remaining, but limited value as a vaccine, BCG offers a useful starting point to probe macrophage functions as an immunological adjuvant, in non-tuberculous intracellular infections and in selected cancer therapy. Recent benefits from BCG administration have been ascribed to imprinting haematopoietic stem cells in bone marrow to generate daughter macrophages with enhanced antimycobacterial effector function (Kaufmann et al., 2018). Dissection of the BCG genome should reveal new immunomodulatory prospects, without side effects resulting from unbridled macrophage activation. Perhaps most exciting will be to utilize such information in host-directed and combination therapy of drug-resistant Tuberculosis (Reiche et al., 2017), for example, targeting DNA replication and repair for the development of novel therapeutics against TB (Guler and Brombacher, 2015).

AUTHOR CONTRIBUTIONS

SG conceived and wrote the manuscript. MM wrote the manuscript and produced the figure. FM wrote the manuscript. AP reviewed and revised the manuscript.

FUNDING

Wellcome Trust (MM, 206751/Z/17/Z), SA Medical Research Council (SAMRC) SIR grant (MM), The SA National Research Foundation (MM), SAMRC with funding from SA Department of Health (MM).

ACKNOWLEDGMENTS

We are grateful for stimulating discussions with colleagues.

REFERENCES

Achkar, J. M., Chan, J., and Casadevall, A. (2015). B cells and antibodies in the defense against *Mycobacterium tuberculosis* infection. *Immunol. Rev.* 264, 167–181. doi: 10.1111/imr.12276

Agarwal, P., Pandey, P., Sarkar, J., and Krishnan, M. Y. (2016). Mycobacterium tuberculosis can gain access to adipose depots of mice infected via the intra-nasal route and to lungs of mice with an infected subcutaneous fat implant. *Microb. Pathog.* 93, 32–37. doi: 10.1016/j.micpath.2016.01.004

Alexandroff, A. B., Jackson, A. M., O'Donnell, M. A., and James, K. (1999). BCG immunotherapy of bladder cancer: 20 years on. *Lancet* 353, 1689–1694. doi: 10.1016/s0140-6736(98)07422-4

Arts, R. J. W., Moorlag, S.J.C.F.M., Novakovic, B., Li, Y., Wang, S. Y., Oosting, M., et al. (2018). BCG vaccination protects against experimental viral infection in humans through the induction of cytokines associated with trained immunity. *Cell Host Microbe* 23, 89–100.e5. doi: 10.1016/j.chom.2017.12.010

Austyn, J. M. (2016). Dendritic cells in the immune system-history, lineages, tissues, tolerance, and immunity. *Microbiol. Spectr.* 4, 1–50. doi: 10.1128/microbiolspec.MCHD-0046-2016

Avraham, R., Haseley, N., Brown, D., Penaranda, C., Jijon, H. B., Trombetta, J. J., et al. (2015). Pathogen cell-to-cell variability drives heterogeneity in host immune responses. *Cell* 162, 1309–1321. doi: 10.1016/j.cell.2015.08.027

Bafica, A., Scanga, C. A., Serhan, C., Machado, F., White, S., Sher, A., et al. (2005). Host control of *Mycobacterium tuberculosis* is regulated by 5-lipoxygenase-dependent lipoxin production. *J. Clin. Invest.* 115, 1601–1606. doi: 10.1172/jci23949

Bell, L., Peyper, J. M., Garnett, S., Tadokera, R., Wilkinson, R., Meintjes, G., et al. (2017). TB-IRIS: proteomic analysis of *in vitro* PBMC responses to *Mycobacterium tuberculosis* and response modulation by dexamethasone. *Exp. Mol. Pathol.* 102, 237–246. doi: 10.1016/j.yexmp.2017.02.008

Bernstein, K. E., Ong, F. S., Blackwell, W. L., Shah, K. H., Giani, J. F., Gonzalez-Villalobos, R. A., et al. (2013). A modern understanding of the traditional and nontraditional biological functions of angiotensin-converting enzyme. *Pharmacol. Rev.* 65, 1–46. doi: 10.1124/pr.112.006809

Berry, M. P., Graham, C. M., McNab, F. W., Xu, Z., Bloch, S. A., Oni, T., et al. (2010). An interferon-inducible neutrophil-driven blood transcriptional signature in human tuberculosis. *Nature* 466, 973–977. doi: 10.1038/nature09247

Bezbradica, J. S., Rosenstein, R. K., DeMarco, R. A., Brodsky, I., and Medzhitov, R. (2014). A role for the ITAM signaling module in specifying cytokine-receptor functions. *Nat. Immunol.* 15, 333–342. doi: 10.1038/ni.2845

Bigley, V., Haniffa, M., Doulatov, S., Wang, X. N., Dickinson, R., McGovern, N., et al. (2011). The human syndrome of dendritic cell, monocyte, B and NK lymphoid deficiency. *J. Exp. Med.* 208, 227–234. doi: 10.1084/jem.20101459

Blackwell, J. M., Searle, S., Mohamed, H., and White, J. K. (2003). Divalent cation transport and susceptibility to infectious and autoimmune disease: continuation of the Ity/Lsh/Bcg/Nramp1/Slc11a1 gene story. *Immunol. Lett.* 85, 197–203. doi: 10.1016/S0165-2478(02)00231-6

Bujko, A., Atlasy, N., Landsverk, O. J. B., Richter, L., Yaqub, S., Horneland, R., et al. (2018). Transcriptional and functional profiling defines human small intestinal macrophage subsets. *J. Exp. Med.* 215, 441–458. doi: 10.1084/jem.20170057

Burstein, E., Hoberg, J. E., Wilkinson, A. S., Rumble, J. M., Csomos, R. A., Komarck, C. M., et al. (2005). COMMD proteins, a novel family of structural and functional homologs of MURR1. *J. Biol. Chem.* 280, 22222–22232. doi: 10.1074/jbc.M501928200

Buschman, E., and Skamene, E. (2001). From Bcg/Lsh/Ity to Nramp1: three decades of search and research. *Drug Metab. Dispos.* 29(4 Pt 2), 471−473.

Cadena, A. M., Fortune, S. M., and Flynn, J. L. (2017). Heterogeneity in tuberculosis. *Nat. Rev. Immunol.* 17, 691–702. doi: 10.1038/nri.2017.69

Caldwell, A. B., Cheng, Z., Vargas, J. D., Birnbaum, H. A., and Hoffmann, A. (2014). Network dynamics determine the autocrine and paracrine signaling functions of TN. *Genes Dev. F.* 28, 2120–2133. doi: 10.1101/gad.244749.114

Cambier, C. J., O'Leary, S. M., O'Sullivan, M. P., Keane, J., and Ramakrishnan, L. (2017). Phenolic glycolipid facilitates mycobacterial escape from microbicidal tissue-resident macrophages. *Immunity* 47, 552–565.e4. doi: 10.1016/j.immuni.2017.08.003

Carter, P. B. (2014). George Bellamy Mackaness. 20 August 1922 — 4 March 2007. *Biogr. Mems Fell. R. Soc.* 60, 277–298. doi: 10.1098/rsbm.2014.0017

Casanova, J. L., and Abel, L. (2017). Human genetics of infectious diseases: unique insights into immunological redundancy. *Semin. Immunol.* 36, 1–12. doi: 10.1016/j.smim.2017.12.008

Chen, C. Y., Huang, D., Wang, R. C., Shen, L., Zeng, G., Yao, S., et al. (2009). A critical role for CD8 T cells in a nonhuman primate model of tuberculosis. *PLoS Pathog.* 5:e1000392. doi: 10.1371/journal.ppat.1000392

Chen, M., Divangahi, M., Gan, H., Shin, D. S., Hong, S., Lee, D. M., et al. (2008). Lipid mediators in innate immunity against tuberculosis: opposing roles of PGE2 and LXA4 in the induction of macrophage death. *J. Exp. Med.* 205, 2791–2801. doi: 10.1084/jem.20080767

Chiba, S., Ikushima, H., Ueki, H., Yanai, H., Kimura, Y., Hangai, S., et al. (2014). Recognition of tumor cells by Dectin-1 orchestrates innate immune cells for anti-tumor responses. *Elife* 3:e04177. doi: 10.7554/eLife.04177

Christova, Y., Adrain, C., Bambrough, P., Ibrahim, A., and Freeman, M., (2013). Mammalian iRhoms have distinct physiological functions including an essential role in TACE regulation. *EMBO Rep.* 14, 884–890. doi: 10.1038/embor.2013.128

Chung, L. P., Keshav, S., and Gordon, S. (1988). Cloning the human lysozyme cDNA: inverted Alu repeat in the mRNA and in situ hybridization for macrophages and Paneth cells. *Proc. Natl. Acad. Sci. U.S.A.* 85, 6227–6231.

Coussens, A. K., Wilkinson, R. J., Hanifa, Y., Nikolayevskyy, V., Elkington, P. T., Islam, K., et al. (2012). Vitamin D accelerates resolution of inflammatory responses during tuberculosis treatment. *Proc. Natl. Acad. Sci. U.S.A.* 109, 15449–15454. doi: 10.1073/pnas.1200072109

Crocker, P. R., Paulson, J. C., and Varki, A. (2007). Siglecs and their roles in the immune system. *Nat. Rev. Immunol.* 7, 255–266. doi: 10.1038/nri2056

Cronan, M. R., Beerman, R. W., Rosenberg, A. F., Saelens, J. W., Johnson, M. G., Oehlers, S. H., et al. (2016). Macrophage epithelial reprogramming underlies mycobacterial granuloma formation and promotes infection. *Immunity* 45, 861–876. doi: 10.1016/j.immuni.2016.09.014

Dallenga, T., Repnik, U., Corleis, B., Eich, J., Reimer, R., Griffiths, G. W., et al. (2017). *M. tuberculosis*-induced necrosis of infected neutrophils promotes bacterial growth following phagocytosis by macrophages. *Cell Host Microbe* 22, 519–530.e3. doi: 10.1016/j.chom.2017.09.003

Daniel, J., Maamar, H., Deb, C., Sirakova, T. D., and Kolattukudy, P. E. (2011). *Mycobacterium tuberculosis* uses host triacylglycerol to accumulate lipid droplets and acquires a dormancy-like phenotype in lipid-loaded macrophages. *PLoS Pathog.* 7:e1002093. doi: 10.1371/journal.ppat.1002093

Dannenberg, A. M., and Rook, G. A. W. (1994). "Pathogenesis of pulmonary tuberculosis: an interplay of tissue-damaging and macrophage-activating immune responses—dual mechanisms that control bacillary multiplication," in *Tuberculosis: Pathogenesis, Protection, and Control*, ed B. R. Bloom (Washington, DC: American Society for Microbiology), 459–483.

Das, S., and Khader, S. (2017). Yin and yang of interleukin-17 in host immunity to infection. *F1000Res.* 6:741. doi: 10.12688/f1000research.10862.1

Deretic, V., and Klionsky, D. J. (2018). Autophagy and inflammation: a special review issue. *Autophagy* 14, 178–180. doi: 10.1080/15548627.2017.1412229

Divangahi, M., Desjardins, D., Nunes-Alves, C., Remold, H. G., and Behar, S. M. (2010). Eicosanoid pathways regulate adaptive immunity to *Mycobacterium tuberculosis*. *Nat. Immunol.* 11, 751–758. doi: 10.1038/ni.1904

Dodd, C. E., Pyle, C. J., Glowinski, R., Rajaram, M. V., and Schlesinger, L. S. (2016). CD36-Mediated Uptake of Surfactant Lipids by Human Macrophages Promotes Intracellular Growth of *Mycobacterium tuberculosis*. *J. Immunol.* 197, 4727–4735. doi: 10.4049/jimmunol.1600856

Dorhoi, A., Desel, C., Yeremeev, V., Pradl, L., Brinkmann, V., Mollenkopf, H. J., et al. (2010). The adaptor molecule CARD9 is essential for tuberculosis control. *J. Exp. Med.* 207, 777–792. doi: 10.1084/jem.20090067

Doster, R. S., Rogers, L. M., Gaddy, J. A., and Aronoff, D. M. (2017). Macrophage extracellular traps: a scoping review. *J. Innate Immun.* 10, 3–13. doi: 10.1159/000480373

Ehlers, S., and Schaible, U. E. (2012). The granuloma in tuberculosis: dynamics of a host-pathogen collusion. *Front. Immunol.* 3:411. doi: 10.3389/fimmu.2012.00411

Fabri, M., Stenger, S., Shin, D. M., Yuk, J. M., Liu, P. T., Realegeno, S., et al. (2011). Vitamin D is required for IFN-gamma-mediated

antimicrobial activity of human macrophages. *Sci. Transl. Med.* 3:104ra102. doi: 10.1126/scitranslmed.3003045

Fairn, G. D., Gershenzon, E., and Grinstein, S. (2009). "Membrane trafficking during phagosome formation and maturation," in *Phagocyte-Pathogen Interactions: Macrophages and the Host Response to Infection*, ed D. G. Russelland and S. Gordon (Washington, DC: ASM Press), 209–223.

Flint, T. R., Janowitz, T., Connell, C. M., Roberts, E. W., Denton, A. E., Coll, A. P., et al. (2016). Tumor-Induced IL-6 Reprograms Host Metabolism to Suppress Anti-tumor Immunity. *Cell Metab.* 24, 672–684. doi: 10.1016/j.cmet.2016.10.010

Flynn, J. L. (2006). Lessons from experimental Mycobacterium tuberculosis infections. *Microbes Infect.* 8, 1179–1188. doi: 10.1016/j.micinf.2005.10.033

Flynn, J. L., and Chan, J. (2001). Immunology of tuberculosis. *Annu. Rev. Immunol.* 19, 93–129. doi: 10.1146/annurev.immunol.19.1.93

Flynn, J. L., Chan, J., Triebold, K. J., Dalton, D. K., Stewart, T. A., and Bloom, B. R. (1993). An essential role for interferon gamma in resistance to Mycobacterium tuberculosis infection. *J. Exp. Med.*, 178, 2249–2254.

Freches, D., Korf, H., Denis, O., Havaux, X., Huygen, K., and Romano, M. (2013). Mice genetically inactivated in interleukin-17A receptor are defective in long-term control of *Mycobacterium tuberculosis* infection. *Immunology* 140, 220–231. doi: 10.1111/imm.12130

Fremond, C., Allie, N., Dambuza, I., Grivennikov, S. I., Yeremeev, V., Quesniaux, V. F., et al. (2005). Membrane TNF confers protection to acute mycobacterial infection. *Respir. Res.* 6:136. doi: 10.1186/1465-9921-6-136

Gazzinelli, R. T., Mendonça-Neto, R., Lilue, J., Howard, J., and Sher, A. (2014). Innate resistance against *Toxoplasma gondii*: an evolutionary tale of mice, cats, and men. *Cell Host Microbe* 15, 132–138. doi: 10.1016/j.chom.2014.01.004

Gideon, H. P., Phuah, J., Myers, A. J., Bryson, B. D., Rodgers, M. A., Coleman, M. T., et al. (2015). Variability in tuberculosis granuloma T cell responses exists, but a balance of pro- and anti-inflammatory cytokines is associated with sterilization. *PLoS Pathog.* 11:e1004603. doi: 10.1371/journal.ppat.1004603

Ginhoux, F., and Guilliams, M. (2016). Tissue-Resident Macrophage Ontogeny and Homeostasis. *Immunity* 44, 439–449. doi: 10.1016/j.immuni.2016.02.024

Gleeson, L. E., Sheedy, F. J., Palsson-McDermott, E. M., Triglia, D., O'Leary, S. M., O'Sullivan, M. P., et al. (2016). Cutting edge: *Mycobacterium tuberculosis* induces aerobic glycolysis in human alveolar macrophages that is required for control of intracellular bacillary replication. *J. Immunol.* 196, 2444–2449. doi: 10.4049/jimmunol.1501612

Gopal, R., Monin, L., Slight, S., Uche, U., Blanchard, E., Fallert Junecko, B. A., et al. (2014). Unexpected role for IL-17 in protective immunity against hypervirulent *Mycobacterium tuberculosis* HN878 infection. *PLoS Pathog.* 10:e1004099. doi: 10.1371/journal.ppat.1004099

Gordon, S. (2017). *Myeloid Cells in Health and Disease. A Synthesis*. Washington DC: ASM Press.

Gordon, S., and Plüddemann, A. (2017). Tissue macrophages: heterogeneity and functions. *BMC Biol.* 15:53. doi: 10.1186/s12915-017-0392-4

Gordon, S., and Plüddemann, A. (2018). Macrophage clearance of apoptotic cells: a critical assessment. *Front. Immunol.* 9:127. doi: 10.3389/fimmu.2018.00127

Gordon, S., Plüddemann, A., and Martinez Estrada, F. (2014a). Macrophage heterogeneity in tissues: phenotypic diversity and functions. *Immunol. Rev.* 262, 36–55. doi: 10.1111/imr.12223

Gordon, S., Plüddemann, A., and Mukhopadhyay, S. (2014b). Sinusoidal immunity: macrophages at the lymphohematopoietic interface. *Cold Spring Harb. Perspect. Biol.* 7:a016378. doi: 10.1101/cshperspect.a016378

Gordon, S., Todd, J., and Cohn, Z. A. (1974). *In vitro* synthesis and secretion of lysozyme by mononuclear phagocytes. *J. Exp. Med.* 139, 1228–1248.

Goren, M. B., D'Arcy Hart, P., Young, M. R., and Armstrong, J. A. (1976). Prevention of phagosome-lysosome fusion in cultured macrophages by sulfatides of *Mycobacterium tuberculosis*. *Proc. Natl. Acad. Sci. U.S.A.* 73, 2510–2514

Guilliams, M., De Kleer, I., Henri, S., Post, S., Vanhoutte, L., De Prijck, S., et al. (2013). Alveolar macrophages develop from fetal monocytes that differentiate into long-lived cells in the first week of life via GM-CSF. *J. Exp. Med.* 210, 1977–1992. doi: 10.1084/jem.20131199

Guirado, E., and Schlesinger, L. S. (2013). Modeling the Mycobacterium tuberculosis Granuloma - the Critical Battlefield in Host Immunity and Disease. *Front. Immunol.* 4:98. doi: 10.3389/fimmu.2013.00098

Guler, R., and Brombacher, F. (2015). Host-directed drug therapy for tuberculosis. *Nat. Chem. Biol.* 11, 748–751. doi: 10.1038/nchembio.1917

Heitmann, L., Abad Dar, M., Schreiber, T., Erdmann, H., Behrends, J., McKenzie, A. N., et al. (2014). The IL-13/IL-4Ralpha axis is involved in tuberculosis-associated pathology. *J. Pathol.* 234, 338–350. doi: 10.1002/path.4399

Hernandez-Pando, R., Aguilar, D., Hernandez, M. L., Orozco, H., and Rook, G. (2004). Pulmonary tuberculosis in BALB/c mice with non-functional IL-4 genes: changes in the inflammatory effects of TNF-alpha and in the regulation of fibrosis. *Eur. J. Immunol.* 34, 174–183. doi: 10.1002/eji.200324253

Herrtwich, L., Nanda, I., Evangelou, K., Nikolova, T., Horn, V., Sagar, E., et al. and Triantafyllopoulou, A. (2016). DNA damage signaling instructs polyploid macrophage fate in granulomas. *Cell* 167, 1264–1280.e18. doi: 10.1016/j.cell.2016.09.054

Holscher, C., Reiling, N., Schaible, U. E., Holscher, A., Bathmann, C., Korbel, D., et al. (2008). Containment of aerogenic Mycobacterium tuberculosis infection in mice does not require MyD88 adaptor function for TLR2,−4 and−9. *Eur. J. Immunol.* 38, 680–694. doi: 10.1002/eji.200736458

Huang, L., Nazarova, E. V., Tan, S., Liu, Y., and Russell, D. G. (2018). Growth of Mycobacterium tuberculosis *in vivo* segregates with host macrophage metabolism and ontogeny. *J. Exp. Med.* 215, 1135–1152. doi: 10.1084/jem.20172020

Hussell, T., and Bell, T. J. (2014). Alveolar macrophages: plasticity in a tissue-specific context. *Nat. Rev. Immunol.* 14, 81–93. doi: 10.1038/nri3600

Ishikawa, E., Ishikawa, T., Morita, Y. S., Toyonaga, K., Yamada, H., Takeuchi, O., et al. (2009). Direct recognition of the mycobacterial glycolipid, trehalose dimycolate, by C-type lectin Mincle. *J. Exp. Med.*, 206, 2879–2888. doi: 10.1084/jem.20091750

Jackson, M. (2014). The mycobacterial cell envelope-lipids. *Cold Spring Harb. Perspect. Med.* 4, 1–22. doi: 10.1101/cshperspect.a021105

Jacobs, W. R., McShane, H., Mizrahi, V., and Orme, I. M. (2018). *Tuberculosis and the Tubercle Bacillus*. Washington, DC: ASM Press.

Jasenosky, L. D., Scriba, T. J., Hanekom, W. A., and Goldfeld, A. E. (2015). T cells and adaptive immunity to *Mycobacterium tuberculosis* in humans. *Immunol. Rev.* 264, 74–87. doi: 10.1111/imr.12274

Jo, E. K. (2008). Mycobacterial interaction with innate receptors: TLRs, C-type lectins, and NLRs. *Curr. Opin. Infect. Dis.*, 21, 279–286. doi: 10.1097/QCO.0b013e3282f88b5d

Jung, Y. J., LaCourse, R., Ryan, L., and North, R. J. (2002). Evidence inconsistent with a negative influence of T helper 2 cells on protection afforded by a dominant T helper 1 response against *Mycobacterium tuberculosis* lung infection in mice. *Infect. Immun.* 70, 6436–6443. doi: 10.1128/IAI.70.11.6436-6443.2002

Kahnert, A., Höpken, U. E., Stein, M., Bandermann, S., Lipp, M., and Kaufmann, S. H. (2007). *Mycobacterium tuberculosis* triggers formation of lymphoid structure in murine lungs. *J. Infect. Dis.* 195, 46–54. doi: 10.1086/508894

Kang, P. B., Azad, A. K., Torrelles, J. B., Kaufman, T. M., Beharka, A., Tibesar, E., et al. (2005). The human macrophage mannose receptor directs Mycobacterium tuberculosis lipoarabinomannan-mediated phagosome biogenesis. *J. Exp. Med.* 202, 987–999. doi: 10.1084/jem.20051239

Kaufmann, E., Sanz, J., Dunn, J. L., Khan, N., Mendonça, L. E., Pacis, A., et al. (2018). BCG Educates Hematopoietic Stem Cells to Generate Protective Innate Immunity against Tuberculosis. *Cell* 172, 176–190.e19. doi: 10.1016/j.cell.2017.12.031

Kim, M. J., Wainwright, H. C., Locketz, M., Bekker, L. G., Walther, G. B., Dittrich, C., et al. (2010). Caseation of human tuberculosis granulomas correlates with elevated host lipid metabolism. *EMBO Mol. Med.* 2, 258–274. doi: 10.1002/emmm.201000079

Lavin, Y., Winter, D., Blecher-Gonen, R., David, E., Keren-Shaul, H., Merad, M., et al. (2014). Tissue-resident macrophage enhancer landscapes are shaped by the local microenvironment. *Cell*, 159, 1312–1326. doi: 10.1016/j.cell.2014.11.018

Lerner, T. R., Borel, S., Greenwood, D. J., Repnik, U., Russell, M. R., Herbst, S., et al. (2017). Mycobacterium tuberculosis replicates within necrotic human macrophages. *J. Cell Biol.* 216, 583–594. doi: 10.1083/jcb.201603040

Lerner, T. R., Queval, C. J., Fearns, A., Repnik, U., Griffiths, G., and Gutierrez, M. G. (2018). Phthiocerol dimycocerosates promote access to the cytosol and

intracellular burden of *Mycobacterium tuberculosis* in lymphatic endothelial cells. *BMC Biol.* 16:1. doi: 10.1186/s12915-017-0471-6

Lieberman, T. D., Wilson, D., Misra, R., Xiong, L. L., Moodley, P., Cohen, T., et al. (2016). Genomic diversity in autopsy samples reveals within-host dissemination of HIV-associated *Mycobacterium tuberculosis*. *Nat. Med.* 22, 1470–1474. doi: 10.1038/nm.4205

Lin, P. L., and Flynn, J. L. (2015). CD8 T cells and Mycobacterium tuberculosis infection. *Semin. Immunopathol.* 37, 239–249. doi: 10.1007/s00281-015-0490-8

Lin, P. L., Ford, C. B., Coleman, M. T., Myers, A. J., Gawande, R., Ioerger, T., et al. (2014). Sterilization of granulomas is common in active and latent tuberculosis despite within-host variability in bacterial killing. *Nat. Med.* 20, 75–79. doi: 10.1038/nm.3412

Lu, E., Dang, E. V., McDonald, J. G., and Cyster, J. G. (2017). Distinct oxysterol requirements for positioning naive and activated dendritic cells in the spleen. *Sci. Immunol.* 2:eaal5237. doi: 10.1126/sciimmunol.aal5237

Mahamed, D., Boulle, M., Ganga, Y., Mc Arthur, C., Skroch, S., Oom, L., et al. (2017). Intracellular growth of *Mycobacterium tuberculosis* after macrophage cell death leads to serial killing of host cells. *Elife* 6:e22028. doi: 10.7554/eLife.22028

Mahoney, J. A., Ntolosi, B., DaSilva, R. P., Gordon, S., and McKnight, A. J. (2001). Cloning and characterization of CPVL, a novel serine carboxypeptidase, from human macrophages. *Genomics* 72, 243–251. doi: 10.1006/geno.2000.6484

Marakalala, M. J., and Ndlovu, H. (2017). Signaling C-type lectin receptors in antimycobacterial immunity. *PLoS Pathog.* 13:e1006333. doi: 10.1371/journal.ppat.1006333

Marakalala, M. J., Guler, R., Matika, L., Murray, G., Jacobs, M., Brombacher, F., et al. (2011). The Syk/CARD9-coupled receptor Dectin-1 is not required for host resistance to *Mycobacterium tuberculosis* in mice. *Microbes Infect.* 13, 198–201. doi: 10.1016/j.micinf.2010.10.013

Marakalala, M. J., Raju, R. M., Sharma, K., Zhang, Y. J., Eugenin, E. A., Prideaux, B., et al. (2016). Inflammatory signaling in human tuberculosis granulomas is spatially organized. *Nat. Med.* 22, 531–538. doi: 10.1038/nm.4073

Marin, N. D., París, S. C., Vélez, V. M., Rojas, C. A., Rojas, M., and Garcia, L. F. (2010). Regulatory T cell frequency and modulation of IFN-gamma and IL-17 in active and latent tuberculosis. *Tuberculosis (Edinb)* 90, 252–261. doi: 10.1016/j.tube.2010.05.003

Martinez, F. O., Helming, L., Milde, R., Varin, A., Melgert, B. N., Draijer, C., et al. (2013). Genetic programs expressed in resting and IL-4 alternatively activated mouse and human macrophages: similarities and differences. *Blood* 121, e57–e69. doi: 10.1182/blood-2012-06-436212

Mattila, J. T., Ojo, O. O., Kepka-Lenhart, D., Marino, S., Kim, J. H., Eum, S. Y., et al. (2013). Microenvironments in tuberculous granulomas are delineated by distinct populations of macrophage subsets and expression of nitric oxide synthase and arginase isoforms. *J. Immunol.* 191, 773–784. doi: 10.4049/jimmunol.1300113

Mayer-Barber, K. D., Andrade, B. B., Oland, S. D., Amaral, E. P., Barber, D. L., Gonzales, J., et al. (2014). Host-directed therapy of tuberculosis based on interleukin-1 and type I interferon crosstalk. *Nature* 511, 99–103. doi: 10.1038/nature13489

McClean, C. M., and Tobin, D. M. (2016). Macrophage form, function, and phenotype in mycobacterial infection: lessons from tuberculosis and other diseases. *Pathog. Dis.* 74:ftw068. doi: 10.1093/femspd/ftw068

McGovern, N., Schlitzer, A., Gunawan, M., Jardine, L., Shin, A., Poyner, E., et al. (2014). Human dermal CD14(+) cells are a transient population of monocyte-derived macrophages. *Immunity* 41, 465–477. doi: 10.1016/j.immuni.2014.08.006

McIlwain, D. R., Lang, P. A., Maretzky, T., Hamada, K., Ohishi, K., Maney, S. K., et al. (2012). iRhom2 regulation of TACE controls TNF-mediated protection against Listeria and responses to LPS. *Science* 335, 229–232. doi: 10.1126/science.1214448

McNab, F., Mayer-Barber, K., Sher, A., Wack, A., and O'Garra, A. (2015). Type I interferons in infectious disease. *Nat. Rev. Immunol.* 15, 87–103. doi: 10.1038/nri3787

Milde, R., Ritter, J., Tennent, G. A., Loesch, A., Martinez, F. O., Gordon, S., et al. (2015). Multinucleated giant cells are specialized for complement-mediated phagocytosis and large target destruction. *Cell Rep.* 13, 1937–1948. doi: 10.1016/j.celrep.2015.10.065

Minutti, C. M., Jackson-Jones, L. H., García-Fojeda, B., Knipper, J. A., Sutherland, T. E., Logan, N., et al. (2017). Local amplifiers of IL-4Ralpha-mediated macrophage activation promote repair in lung and liver. *Science* 356, 1076–1080. doi: 10.1126/science.aaj2067

Mishra, B. B., Rathinam, V. A., Martens, G. W., Martinot, A. J., Kornfeld, H., Fitzgerald, K. A., et al. (2013). Nitric oxide controls the immunopathology of tuberculosis by inhibiting NLRP3 inflammasome-dependent processing of IL-1beta. *Nat. Immunol.* 14, 52–60. doi: 10.1038/ni.2474

Miyake, Y., Toyonaga, K., Mori, D., Kakuta, S., Hoshino, Y., Oyamada, A., et al. (2013). C-type lectin MCL is an FcRgamma-coupled receptor that mediates the adjuvanticity of mycobacterial cord factor. *Immunity* 38, 1050–1062. doi: 10.1016/j.immuni.2013.03.010

Nathan, C. (2012). Secretory products of macrophages: twenty-five years on. *J. Clin. Invest.* 122, 1189–1190. doi: 10.1172/JCI62930

Nathan, C. (2013). A journey in science: promise, purpose, privilege. *Mol. Med.* 19, 305–313. doi: 10.2119/molmed.2013.00063

Nathan, C. (2016). Macrophages' choice: take it in or keep it out. *Immunity* 45, 710–711. doi: 10.1016/j.immuni.2016.10.002

Ndlovu, H., and Marakalala, M. J. (2016). Granulomas and Inflammation: host-directed therapies for tuberculosis. *Front. Immunol.* 7:434. doi: 10.3389/fimmu.2016.00434

Neyen, C. D., and Gordon, S. (2014). *Macrophages in Lipid and Immune Homeostasis.* Wiley Online Library.

Neyrolles, O., Hernández-Pando, R., Pietri-Rouxel, F., Fornès, P., Tailleux, L., Barrios Payán, J. A., et al. (2006). Is adipose tissue a place for Mycobacterium tuberculosis persistence? *PLoS ONE* 1:e43. doi: 10.1371/journal.pone.0000043

North, R. J. (1998). Mice incapable of making IL-4 or IL-10 display normal resistance to infection with Mycobacterium tuberculosis. *Clin. Exp. Immunol.* 113, 55–58.

Okabe, Y., and Medzhitov, R. (2016). Tissue biology perspective on macrophages. *Nat. Immunol.* 17, 9–17. doi: 10.1038/ni.3320

O'Neill, L. A., and Pearce, E. J. (2016). Immunometabolism governs dendritic cell and macrophage function. *J. Exp. Med.* 213, 15–23. doi: 10.1084/jem.20151570

Ouimet, M., Koster, S., Sakowski, E., Ramkhelawon, B., van Solingen, C., Oldebeken, S., et al. (2016). Mycobacterium tuberculosis induces the miR-33 locus to reprogram autophagy and host lipid metabolism. *Nat. Immunol.* 17, 677–686. doi: 10.1038/ni.3434

Pagan, A. J., and Ramakrishnan, L. (2018). The formation and function of granulomas. *Annu. Rev. Immunol.* 36, 639–665. doi: 10.1146/annurev-immunol-032712-100022

Palucci, I., Matic, I., Falasca, L., Minerva, M., Maulucci, G., De Spirito, M., et al. (2017). Transglutaminase type 2 plays a key role in the pathogenesis of Mycobacterium tuberculosis infection. *J. Intern. Med.* 283, 303–313. doi: 10.1111/joim.12714

Peyron, P., Vaubourgeix, J., Poquet, Y., Levillain, F., Botanch, C., Bardou, F., et al. (2008). Foamy macrophages from tuberculous patients' granulomas constitute a nutrient-rich reservoir for *M. tuberculosis* persistence. *PLoS Pathog.* 4:e1000204. doi: 10.1371/journal.ppat.1000204

Phillips-Krawczak, C. A., Singla, A., Starokadomskyy, P., Deng, Z., Osborne, D. G., Li, H., et al. (2015). COMMD1 is linked to the WASH complex and regulates endosomal trafficking of the copper transporter ATP7A. *Mol. Biol. Cell* 26, 91–103. doi: 10.1091/mbc.E14-06-1073

Puissegur, M. P., Lay, G., Gilleron, M., Botella, L., Nigou, J., Marrakchi, H., et al. (2007). Mycobacterial lipomannan induces granuloma macrophage fusion via a TLR2-dependent, ADAM9- and beta1 integrin-mediated pathway. *J. Immunol.* 178, 3161–3169. doi: 10.4049/jimmunol.178.5.3161

Rajaram, M. V. S., Arnett, E., Azad, A. K., Guirado, E., Ni, B., Gerberick, A. D., et al. (2017). *M. tuberculosis*-initiated human mannose receptor signaling regulates macrophage recognition and vesicle trafficking by FcRgamma-Chain, Grb2, and SHP-1. *Cell Rep.* 21, 126–140. doi: 10.1016/j.celrep.2017.09.034

Ramakrishnan, L. (2012). Revisiting the role of the granuloma in tuberculosis. *Nat. Rev. Immunol.* 12, 352–366. doi: 10.1038/nri3211

Randolph, G. J. (2015). Macrophage supply and demand at the core of the necrotic granuloma. *Cell Host Microbe* 18, 3–4. doi: 10.1016/j.chom.2015.06.014

Reiche, M. A., Warner, D. F., and Mizrahi, V. (2017). Targeting DNA replication and repair for the development of novel therapeutics against tuberculosis. *Front. Mol. Biosci.* 4:75. doi: 10.3389/fmolb.2017.00075

Roca, F. J., and Ramakrishnan, L. (2013). TNF dually mediates resistance and susceptibility to mycobacteria via mitochondrial reactive oxygen species. *Cell* 153, 521–534. doi: 10.1016/j.cell.2013.03.022

Rosas, M., Davies, L. C., Giles, P. J., Liao, C. T., Kharfan, B., Stone, T. C., et al. (2014). The transcription factor Gata6 links tissue macrophage phenotype and proliferative renewal. *Science* 344, 645–648. doi: 10.1126/science.1251414

Rossouw, M., Nel, H. J., Cooke, G. S., van Helden, P. D., and Hoal, E. G. (2003). Association between tuberculosis and a polymorphic NFkappaB binding site in the interferon gamma gene. *Lancet* 361, 1871–1872. doi: 10.1016/s0140-6736(03)13491-5

Russell, D. G., Barry, C. E. III., and Flynn, J. L. (2010). Tuberculosis: what we don't know can, and does, hurt us. *Science* 328, 852–856. doi: 10.1126/science.1184784

Sakai, H., Okafuji, I., Nishikomori, R., Abe, J., Izawa, K., Kambe, N., et al. (2012). The CD40-CD40L axis and IFN-gamma play critical roles in Langhans giant cell formation. *Int. Immunol.* 24, 5–15. doi: 10.1093/intimm/dxr088

Saliba, A. E., C Santos, S., and Vogel, J. (2017). New RNA-seq approaches for the study of bacterial pathogens. *Curr. Opin. Microbiol.* 35, 78–87. doi: 10.1016/j.mib.2017.01.001

Saunders, B. M., and Cooper, A. M. (2000). Restraining mycobacteria: role of granulomas in mycobacterial infections. *Immunol. Cell Biol.* 78, 334–341. doi: 10.1046/j.1440-1711.2000.00933.x

Schaale, K., Brandenburg, J., Kispert, A., Leitges, M., Ehlers, S., and Reiling, N. (2013). Wnt6 is expressed in granulomatous lesions of *Mycobacterium tuberculosis*-infected mice and is involved in macrophage differentiation and proliferation. *J. Immunol.* 191, 5182–5195. doi: 10.4049/jimmunol.1201819

Schaible, U. E., Winau, F., Sieling, P. A., Fischer, K., Collins, H. L., Hagens, K., et al. (2003). Apoptosis facilitates antigen presentation to T lymphocytes through MHC-I and CD1 in tuberculosis. *Nat. Med.* 9, 1039–1046. doi: 10.1038/nm906

Schnettger, L., Rodgers, A., Repnik, U., Lai, R. P., Pei, G., Verdoes, M., et al. (2017). A Rab20-dependent membrane trafficking pathway controls *M. tuberculosis* replication by regulating phagosome spaciousness and integrity. *Cell Host Microbe* 21, 619–628.e5. doi: 10.1016/j.chom.2017.04.004

Scriba, T. J., Coussens, A. K., and Fletcher, H. A. (2017). Human immunology of tuberculosis. *Microbiol. Spectr.* 5, 1–24. doi: 10.1128/microbiolspec.TBTB2-0016-2016

Shi, L., Salamon, H., Eugenin, E. A., Pine, R., Cooper, A., and Gennaro, M. L. (2015). Infection with *Mycobacterium tuberculosis* induces the Warburg effect in mouse lungs. *Sci. Rep.* 5:18176. doi: 10.1038/srep18176

Shrestha, A., and Megeney, L. A. (2012). The non-death role of metacaspase proteases. *Front. Oncol.* 2:78. doi: 10.3389/fonc.2012.00078

Srivastava, S., Ernst, J. D., and Desvignes, L. (2014). Beyond macrophages: the diversity of mononuclear cells in tuberculosis. *Immunol. Rev.* 262, 179–192. doi: 10.1111/imr.12217

Stanton, L. A., Fenhalls, G., Lucas, A., Gough, P., Greaves, D. R., Mahoney, J. A., et al. (2003). Immunophenotyping of macrophages in human pulmonary tuberculosis and sarcoidosis. *Int. J. Exp. Pathol.* 84, 289–304. doi: 10.1111/j.0959-9673.2003.00365.x

Subbian, S., Tsenova, L., Kim, M. J., Wainwright, H. C., Visser, A., Bandyopadhyay, N., et al. (2015). Lesion-specific immune response in granulomas of patients with pulmonary tuberculosis: a pilot study. *PLoS ONE* 10:e0132249. doi: 10.1371/journal.pone.0132249

Sundblad, V., Morosi, L. G., Geffner, J. R., and Rabinovich, G. A. (2017). Galectin-1: a jack-of-all-trades in the resolution of acute and chronic inflammation. *J. Immunol.* 199, 3721–3730. doi: 10.4049/jimmunol.1701172

Swirski, F. K., Nahrendorf, M., Etzrodt, M., Wildgruber, M., Cortez-Retamozo, V., Panizzi, P., et al. (2009). Identification of splenic reservoir monocytes and their deployment to inflammatory sites. *Science* 325, 612–616. doi: 10.1126/science.1175202

Tan, S., and Russell, D. G. (2015). Trans-species communication in the Mycobacterium tuberculosis-infected macrophage. *Immunol. Rev.* 264, 233–248. doi: 10.1111/imr.12254

Taylor, J. L., Hattle, J. M., Dreitz, S. A., Troudt, J. M., Izzo, L. S., Basaraba, R. J., et al. (2006). Role for matrix metalloproteinase 9 in granuloma formation during pulmonary Mycobacterium tuberculosis infection. *Infect. Immun.* 74, 6135–6144. doi: 10.1128/iai.02048-05

Tobin, D. M., Roca, F. J., Oh, S. F., McFarland, R., Vickery, T. W., Ray, J. P., et al. (2012). Host genotype-specific therapies can optimize the inflammatory response to mycobacterial infections. *Cell* 148, 434–446. doi: 10.1016/j.cell.2011.12.023

Tobin, D. M., Vary, J. C. Jr., Ray, J. P., Walsh, G. S., Dunstan, S. J., Bang, N. D., et al. (2010). The lta4h locus modulates susceptibility to mycobacterial infection in zebrafish and humans. *Cell* 140, 717–730. doi: 10.1016/j.cell.2010.02.013

Torrelles, J. B., and Schlesinger, L. S. (2017). Integrating Lung Physiology, Immunology, and Tuberculosis. *Trends Microbiol.* 25, 688–697. doi: 10.1016/j.tim.2017.03.007

Ujma, S., Horsnell, W. G., Katz, A. A., Clark, H. W., and Schäfer, G. (2017). Non-pulmonary immune functions of surfactant proteins A and D. *J. Innate Immun.* 9, 3–11. doi: 10.1159/000451026

Ulrichs, T., and Kaufmann, S. H. (2006). New insights into the function of granulomas in human tuberculosis. *J. Pathol.* 208, 261–269. doi: 10.1002/path.1906

Ulrichs, T., Kosmiadi, G. A., Trusov, V., Jörg, S., Pradl, L., Titukhina, M., et al. (2004). Human tuberculous granulomas induce peripheral lymphoid follicle-like structures to orchestrate local host defence in the lung. *J. Pathol.* 204, 217–228. doi: 10.1002/path.1628

van Pinxteren, L. A., Cassidy, J. P., Smedegaard, B. H., Agger, E. M., and Andersen, P. (2000). Control of latent *Mycobacterium tuberculosis* infection is dependent on CD8 T cells. *Eur. J. Immunol.* 30, 3689–3698. doi: 10.1002/1521-4141(200012)30:12<3689::AID-IMMU3689>3.0.CO;2-4

Villani, A. C., Satija, R., Reynolds, G., Sarkizova, S., Shekhar, K., Fletcher, J., et al. (2017). Single-cell RNA-seq reveals new types of human blood dendritic cells, monocytes, and progenitors. *Science* 356, 284–296. doi: 10.1126/science.aah4573

Volkman, H. E., Pozos, T. C., Zheng, J., Davis, J. M., Rawls, J. F., and Ramakrishnan, L. (2010). Tuberculous granuloma induction via interaction of a bacterial secreted protein with host epithelium. *Science* 327, 466–469. doi: 10.1126/science.1179663

Walter, K., Holscher, C., Tschopp, J., and Ehlers, S. (2010). NALP3 is not necessary for early protection against experimental tuberculosis. *Immunobiology* 215, 804–811. doi: 10.1016/j.imbio.2010.05.015

Wang, J., and Kubes, P. (2016). A reservoir of mature cavity macrophages that can rapidly invade visceral organs to affect tissue repair. *Cell* 165, 668–678. doi: 10.1016/j.cell.2016.03.009

Watson, R. O., Bell, S. L., MacDuff, D. A., Kimmey, J. M., Diner, E. J., Olivas, J., et al. (2015). The cytosolic sensor cGAS detects *Mycobacterium tuberculosis* DNA to induce type I interferons and activate autophagy. *Cell Host Microbe* 17, 811–819. doi: 10.1016/j.chom.2015.05.004

Wilson, G. J., Marakalala, M. J., Hoving, J. C., van Laarhoven, A., Drummond, R. A., Kerscher, B., et al. (2015). The C-type lectin receptor CLECSF8/CLEC4D is a key component of anti-mycobacterial immunity. *Cell Host Microbe* 17, 252–259. doi: 10.1016/j.chom.2015.01.004

Wu, U. I., and Holland, S. M. (2016). A genetic perspective on granulomatous diseases with an emphasis on mycobacterial infections. *Semin. Immunopathol.* 38, 199–212. doi: 10.1007/s00281-015-0552-y

Yonekawa, A., Saijo, S., Hoshino, Y., Miyake, Y., Ishikawa, E., Suzukawa, M., et al. (2014). Dectin-2 is a direct receptor for mannose-capped lipoarabinomannan of mycobacteria. *Immunity* 41, 402–413. doi: 10.1016/j.immuni.2014.08.005

Zak, D. E., Penn-Nicholson, A., Scriba, T. J., Thompson, E., Suliman, S., Amon, L. M., et al. (2016). A blood RNA signature for tuberculosis disease risk: a prospective cohort study. *Lancet* 387, 2312–2322. doi: 10.1016/s0140-6736(15)01316-1

Conflict of Interest Statement: The authors declare that the research was conducted in the absence of any commercial or financial relationships that could be construed as a potential conflict of interest.

Copyright © 2018 Marakalala, Martinez, Plüddemann and Gordon. This is an open-access article distributed under the terms of the Creative Commons Attribution License (CC BY). The use, distribution or reproduction in other forums is permitted, provided the original author(s) and the copyright owner are credited and that the original publication in this journal is cited, in accordance with accepted academic practice. No use, distribution or reproduction is permitted which does not comply with these terms.

frontiers in Immunology

ORIGINAL RESEARCH
published: 12 June 2018
doi: 10.3389/fimmu.2018.01123

The C-Type Lectin Receptor DC-SIGN Has an Anti-Inflammatory Role in Human M(IL-4) Macrophages in Response to *Mycobacterium tuberculosis*

Geanncarlo Lugo-Villarino[1,2,3]†, Anthony Troegeler[1,2,3†], Luciana Balboa[2,3,4], Claire Lastrucci[1,2,3,5], Carine Duval[1], Ingrid Mercier[1], Alan Bénard[1,6], Florence Capilla[7], Talal Al Saati[7], Renaud Poincloux[1], Ivanela Kondova[8], Frank A. W. Verreck[8], Céline Cougoule[1,2,3], Isabelle Maridonneau-Parini[1,2,3], Maria del Carmen Sasiain[2,3,4] and Olivier Neyrolles[1,2,3]*

[1] Institut de Pharmacologie et de Biologie Structurale, IPBS, Université de Toulouse, CNRS, UPS, Toulouse, France, [2] International Associated Laboratory (LIA) CNRS "IM–TB/HIV" (1167), Toulouse, France, [3] International Associated Laboratory (LIA) CNRS "IM–TB/HIV" (1167), Buenos Aires, Argentina, [4] IMEX-CONICET, Academia Nacional de Medicina, Buenos Aires, Argentina, [5] Centre for Genomic Regulation, Barcelona, Spain, [6] Department of Surgery, University, Hospital Erlangen, Friedrich-Alexander, University Erlangen-Nürnberg, Erlangen, Germany, [7] INSERM/UPS/US006 CREFRE, CHU Purpan, Toulouse, France, [8] Biomedical Primate Research Centre, Rijswijk, Netherlands

OPEN ACCESS

Edited by:
Steffen Stenger, Universitätsklinikum Ulm, Germany

Reviewed by:
Hridayesh Prakash, All India Institute of Medical Sciences, India
Masaaki Miyazawa, Kindai University, Japan

***Correspondence:**
Geanncarlo Lugo-Villarino
lugo@ipbs.fr

†These authors have contributed equally to this work.

Specialty section:
This article was submitted to Microbial Immunology, a section of the journal Frontiers in Immunology

Received: *06 December 2017*
Accepted: *03 May 2018*
Published: *12 June 2018*

Citation:
Lugo-Villarino G, Troegeler A, Balboa L, Lastrucci C, Duval C, Mercier I, Bénard A, Capilla F, Al Saati T, Poincloux R, Kondova I, Verreck FAW, Cougoule C, Maridonneau-Parini I, Sasiain MdC and Neyrolles O (2018) The C-Type Lectin Receptor DC-SIGN Has an Anti-Inflammatory Role in Human M(IL-4) Macrophages in Response to Mycobacterium tuberculosis. Front. Immunol. 9:1123. doi: 10.3389/fimmu.2018.01123

DC-SIGN (CD209/CLEC4L) is a C-type lectin receptor (CLR) that serves as a reliable cell-surface marker of interleukin 4 (IL-4)-activated human macrophages [M(IL-4)], which historically represent the most studied subset within the M2 spectrum of macrophage activation. Although DC-SIGN plays important roles in *Mycobacterium tuberculosis* (Mtb) interactions with dendritic cells, its contribution to the Mtb–macrophage interaction remains poorly understood. Since high levels of IL-4 are correlated with tuberculosis (TB) susceptibility and progression, we investigated the role of DC-SIGN in M(IL-4) macrophages in the TB context. First, we demonstrate that DC-SIGN expression is present both in $CD68^+$ macrophages found in tuberculous pulmonary lesions of non-human primates, and in the $CD14^+$ cell population isolated from pleural effusions obtained from TB patients (TB-PE). Likewise, we show that DC-SIGN expression is accentuated in M(IL-4) macrophages derived from peripheral blood $CD14^+$ monocytes isolated from TB patients, or in macrophages stimulated with acellular TB-PE, arguing for the pertinence of DC-SIGN-expressing macrophages in TB. Second, using a siRNA-mediated gene silencing approach, we performed a transcriptomic analysis of DC-SIGN-depleted M(IL-4) macrophages and revealed the upregulation of pro-inflammatory signals in response to challenge with Mtb, as compared to control cells. This pro-inflammatory gene signature was confirmed by RT-qPCR, cytokine/chemokine-based protein array, and ELISA analyses. We also found that inactivation of DC-SIGN renders M(IL-4) macrophages less permissive to Mtb intracellular growth compared to control cells, despite the equal level of bacteria uptake. Last, at the molecular level, we show that DC-SIGN interferes negatively with the pro-inflammatory response and control of Mtb intracellular growth mediated by another CLR, Dectin-1 (CLEC7A). Collectively, this study highlights a dual role for DC-SIGN as, on the one hand, being a host factor granting advantage for Mtb to parasitize macrophages and, on the other hand, representing a molecular switch to turn off the pro-inflammatory response in these cells to prevent potential immunopathology associated to TB.

Keywords: macrophages, *Mycobacterium tuberculosis*, DC-SIGN, C-type lectin receptors, anti-inflammatory

INTRODUCTION

According to the latest World Health Organization (WHO) report, tuberculosis (TB) is the largest killer among communicable diseases (WHO Annual report 2017). In 2016, there were an estimated 1.7 million deaths due to TB, making it the leading cause of death worldwide due to a single infectious agent, *Mycobacterium tuberculosis* (Mtb). In general, it is estimated that one quarter of the human population could be latently infected with Mtb (1). The bacillus may be active either after infection or through the reactivation of latent infection, which occurs in approximately 5% of infected people. During latency, for which there are no pathological or contagious conditions, Mtb is contained within elaborated aggregates of immune cells that are called granulomas, the hallmark of TB (2, 3). It is thought that a dedicated immune response is responsible for the formation and maintenance of granulomas, which will ultimately determine the outcome of the disease (2, 4). However, there is a strong need to better understand the factors that define an efficient immune response both during the early and late phases of Mtb infection in order to facilitate potential targets for preventive and therapeutic purposes.

Macrophages are considered key players during the early and late stages of Mtb infection (5). These sentinel cells are strategically located in secondary lymphoid organs and multiple mucosal sites, such as lung alveolar and interstitial space. At such, macrophages recognize and internalize Mtb and, consequently, modulate the inflammatory response to shape their microenvironment (e.g., granulomas) and the adaptive immune response against this pathogen. Interestingly, these cells display a high degree of tissue heterogeneity within the broad spectrum of pro- (M1) and anti-inflammatory (M2) programs of activation that manifest intracellular pathogen resistance and permissiveness, respectively (6). Macrophages may also serve as long-lived pathogen tissue reservoirs and contribute to TB pathogenesis (6–9). Remarkably, Mtb influences the differentiation, maturation, and activation of macrophages, resulting in the circumvention of the immune system and augmented persistence in the host (6–8, 10). This capacity of Mtb to modulate the host pro-inflammatory response and seize the anti-inflammatory mechanisms has generated a keen interest to investigate how this pathogen manipulates the process of macrophage activation.

The initial interaction with Mtb is thought to be crucial for macrophage activation and the eventual disease outcome. Pattern recognition receptors (PRRs) expressed in macrophages determine the binding, internalization, and fate of the bacillus' intracellular lifestyle. Among the various PRR families that recognize Mtb, the C-type lectin receptors (CLR) are known to contribute to the control or persistence of this pathogen within macrophages (11–13). The CLR family includes collectins, selectins, endocytic and phagocytic receptors, and proteoglycans. CLRs are calcium-dependent glycan-binding proteins exhibiting similarities in the structures of the carbohydrate-recognition domain (CRD), which in turn recognize the carbohydrates expressed on the surface of Mtb including glycolipids [e.g., phosphatidyl-*myo*-inositol mannoside (PIM)], glycoglycans [e.g., lipoarabinomannan (LAM)], polysaccharides (e.g., α-glucan) and glycoproteins (e.g.,19 kDa antigen). In recent years, our understanding of the interactions of mycobacterial ligands with CLRs has advanced considerably, specifically in membrane-anchored phagocytic receptors such as the mannose receptor MRC1 (CD206/CLEC13D), Dectin-1 (CLEC7A) and Dectin-2 (CLEC6A), Mincle (CLEC4E), and Dendritic Cell-Specific Intercellular adhesion molecule-3-Grabbing Non-integrin (DC-SIGN/CD209/CLEC4L) (11–15). In general terms, the activation of these receptors by Mtb leads to downstream effects like endocytosis, oligomerization, intracellular trafficking, and signal transduction. Emerging evidence points out that signaling pathways triggered by these CLRs converge in a limited set of synergistic or antagonistic interactions with other PRRs and with each other, giving rise to a phenomenon known as signaling crosstalk. Interestingly, Mtb has evolved the capacity to subvert CLR signaling crosstalk to increase its survival and fitness within macrophages (5, 11, 15).

Studies by others and us identified and characterized DC-SIGN as a key receptor for Mtb in human dendritic cells and alveolar macrophages (14, 16–20). This CLR is a transmembrane receptor that possesses one single extracellular CRD (at the C-terminus) capable of recognizing mannose-containing molecules such as those present in mycobacterial Man-LAM (mannose-capped LAM), lipomannan (LM), arabinomannan, glycoproteins (e.g., 19, 38, and 45 kDa antigens), PIMs, and α-glucan, among others. Its functional cytoplasmic domain (at the N-terminus) contains different motifs that are crucial for endocytosis/phagocytosis, intracellular trafficking, and signal transduction (11). In the case of Mtb, it was shown that DC-SIGN is targeted by the mycobacterial ManLAM to induce the immunosupressive mediator interleukin-10 (IL-10) and counteract the toll-like receptor-4 (TLR-4)-dependent pro-inflammatory response (14). In this manner, the bacillus prevents the proper activation of dendritic cells given that IL-10 inhibits the expression of co-stimulatory molecules (e.g., CD86) and production of IL-12, which are essential for the activation of type-1 immunity best represented by T-helper 1 (Th1) cells. Of note, the hijacking of IL-10 production *via* DC-SIGN in dendritic cells seems to be a general evasion strategy by various pathogens like *Mycobacterium leprae*, *Helicobacter pylori,* and *Candida albicans*, among others (14).

Until recently, the expression of DC-SIGN was thought to be exclusive to human dendritic cells. In fact, this CLR is also expressed in human alveolar macrophages and some lymphocyte populations (19, 21). In particular, DC-SIGN is a reliable cell-surface marker in human macrophages activated with interleukin 4 (IL-4) [M(IL-4)], which is historically the most representative subset within the M2 spectrum of macrophage activation (22, 23). While the role of M(IL-4) macrophages has not been explored in in the TB context, high levels of type-2 inflammatory signals, such as IL-4, are correlated to TB susceptibility and progression (10). Reciprocally, the predominant type-2 inflammatory environment shifts toward type-1 immune signals [e.g., interferon-γ (IFNγ)] upon successful treatment of pulmonary TB. This is important because, in comparison to IFNγ, IL-4 renders macrophages less microbicidal against intracellular bacterial infections (6, 24). Furthermore, our group has also reported that DC-SIGN expression is induced specifically in alveolar macrophages of patients with active TB (19), suggesting a major role for this CLR in the interaction between macrophages and Mtb.

In this study, we provide for the first-time evidence supporting the anti-inflammatory role of DC-SIGN in the M(IL-4) macrophage response to Mtb. We report that DC-SIGN expression is accentuated in macrophages under different contexts using samples from TB patients, or in tuberculous pulmonary lesions of non-human primates (NHP), arguing for the pertinence of DC-SIGN-expressing macrophages in TB pathology. In the absence of this CLR, M(IL-4) macrophages displayed a pro-inflammatory signature upon challenge with Mtb, and acquired a better ability to control the intracellular growth of this pathogen. Finally, while there are no major changes in the production of IL-10, we demonstrate that DC-SIGN interferes negatively with the activation of M(IL-4) macrophages triggered by Dectin-1.

MATERIALS AND METHODS

Ethics Statement for Non-Human Primate Samples

The NHP study protocol was done to comply with the EC Directive 86/609/EEC, approved by the local independent ethics committee prior to the start of the study, and executed under Dutch law on animal experiments (agreement number DEC#579). The endpoint for any particular animal was based either by signs of severe disease (humane endpoint criteria, referring to animal condition by adverse body weight development, respiratory capacity, and animal behavior) or by protocol, which limited the follow-up time to 1-year postinfection.

Non-Human Primate Handling

The NHP samples were prepared from animals that were used for vaccine research and development purposes, as previously described (25). Briefly, healthy young adult female rhesus macaques (*Macaca mulatta*), all captive-bred for research purposes and of homogeneous breeding background, were challenged with 500 colony forming units (CFU) of Mtb strain Erdman K01 (prepared and provided under an agreement between WHO and CBER/FDA with assistance of Aeras), which was administered by intra-bronchial instillation under sedation. At endpoint, the animals were sedated, euthanized and submitted to macroscopic lung pathology scoring, as previously published (26).

Histological Analyses on Non-Human Primate Samples

The gross pathological findings were assessed and described by an experienced veterinary pathologist while blinded for treatment as previously described (25). Representative lung biopsies were collected and fixed in 10% neutral buffered formalin and embedded in paraffin for long-term storage. Tissue sections were stained with hematoxylin and eosin (HE) for histomorphological analysis. Histopathological scoring of TB lesions in NHP was determined using a worksheet in which TB disease from lung biopsies was described (25, 26). Immunohistochemical staining was performed on paraffin-embedded tissue sections using the following monoclonal primary antibodies: CD68 (clone:KP1, Dako), DC-SIGN (clone 120612, R&D System), CD163 (clone 10D6, Leica/Novocastra), and MerTK (clone: Y323, Abcam). After incubation with primary antibodies, sections were stained with biotin-conjugated polyclonal anti-mouse or -rabbit immunoglobulin antibodies followed by the streptavidin-biotin-peroxidase complex (ABC) method (Vector Laboratories), and then were counterstained with hematoxylin. Slides were scanned with the Panoramic 250 Flash II (3DHISTECH). For confocal microscopy, samples were stained with primary antibodies as described above and followed by anti-mouse IgG isotype specific or anti-rabbit IgG antibodies labeled with Alexa488 and Alexa555 (Molecular Probes). Samples were mounted with Prolong® Antifade reagent (Molecular Probes) and examined using a 40×/0.95N.A. objective of an Olympus FV1000 confocal microscope.

Ethics Statement for Human Samples

Blood samples from healthy subjects (HS) or TB patients were provided by the Blood Transfusion Service, Hospital Fernandez, Buenos Aires (agreement number CEIANM-52-5-2012), or the Hospital F. J. Muñiz, Buenos Aires (protocol number: NIN-1671-12). Pleural effusions (PE) were obtained by therapeutic thoracentesis by physicians at the Hospital F. J. Muñiz (Buenos Aires). The research was carried out in accordance with the Declaration of Helsinki (2013) of the World Medical Association and was approved by the Ethics Committees of the Hospital F. J. Muñiz and the Academia Nacional de Medicina de Buenos Aires (protocol number: NIN-1671-12). Written informed consent was obtained before sample collection. The diagnosis of TB pleurisy was based on a positive Ziehl–Nielsen staining or Lowestein–Jensen culture from PE and/or histopathology of pleural biopsy and was further confirmed by an Mtb-induced IFN-γ response and an ADA-positive test (27). Mononuclear cells from peripheral blood (PB) and PE were isolated by Ficoll-Hypaque gradient centrifugation (Pharmacia, Uppsala, Sweden), as described previously (25, 28).

Likewise, monocytes from HS were isolated from buffy coat provided by Etablissement Français du Sang, Toulouse, under contract 21/PLER/TOU/IPBS01/2013-0042. According to articles L1243-4 and R1243-61 of the French Public Health Code, the contract was approved by the French Ministry of Science and Technology (agreement number AC 2009-921). Donors signed and provided written informed consents before sample collection.

Preparation of Pool of Sera and Tuberculous PE

The cell-free supernatant from tuberculous PE and sera was transferred into new plastic tubes, further centrifuged at 12,000 *g* for 10 min and aliquots were stored at −80°C. Pools were prepared by mixing same amounts of eight individual PE or serum. The pools were de-complemented at 56°C for 30 min, and filtered by 0.22 μm in order to remove any remaining debris or residual bacteria.

Preparation of Human Monocyte-Derived Macrophages From HS and TB Patients

Monocytes from HS or TB patients were isolated and differentiated into macrophages as previously described (25, 28). Briefly, purified $CD14^+$ monocytes from HS were differentiated for

5–7 days in RPMI-1640 medium (GIBCO), 10% fetal bovine serum (FBS, Sigma-Aldrich), and human recombinant macrophage colony-stimulating factor (M-CSF, Peprotech) at 10 ng/mL. The cell medium was renewed every 3 or 4 days. Thereafter, macrophages were treated with IL-4 (Peprotech) at 20 ng/mL to induce the M(IL-4) program, 10% v/v of a pool of sera from HS or TB patients, or of acellular fraction of TB PE for 48 h. Untreated cells under differentiation with M-CSF only were considered as part of the M(M-CSF) program.

Alternatively, monocyte isolation and purification was done as previously published (29). Succinctly, following Ficoll gradient enrichment, monocytes were purified using positive selection with anti-CD14 microbeads and MACS separation columns (Miltenyi Biotec), according to manufacturer's instructions. For macrophage differentiation, monocytes were allowed to adhere to glass coverslips (VWR international) in 6-well or 24-well plates (Thermo Scientific), at 1.5×10^6 and 3×10^5 cells/well, respectively, for 2 h at 37°C in warm RPMI-1640 medium (GIBCO). The medium was then supplemented to a final concentration of 10% FBS (Sigma-Aldrich) and human recombinant M-CSF (Peprotech) at 20 ng/ml, and the cells were allowed to differentiate for 5 days. The cell medium was renewed at day 3 or 4 of culture. At day 5, macrophages were activated for 48 h with 1 μg/ml of lipopolysaccharide (LPS, Invivogen) and 2.5 ng/ml of IFN-γ (Miltenyi Biotec) to induce the M(LPS + IFN-γ) program, and with 20 ng/ml of IL-4 (Miltenyi Biotec) for the M(IL-4) program.

Flow Cytometry

Cells from TB patients and related controls from HS (2×10^5 cells) were labeled as described above and acquired in a FACSAria II cytometer (BD Biosciences). The monocyte–macrophage population was gated according to its forward scatter (FSC) and size scatter (SSC) proprieties. The percentage of positive cells and the median fluorescence intensity (MFI) were analyzed using FCS Express V3 software (De Novo Software, Los Angeles, CA, USA). In the context of macrophage activation programs, the CLR expression was analyzed by flow cytometry using antibodies (general dilution of 1:400) against DC-SIGN and Dectin-1 from R&D Systems, and MRC1 from BD Pharmingen (San Diego, CA, USA). Concerning the cellular content in PE fluid from TB patients, DC-SIGN expression was also analyzed by flow cytometry in mononuclear cells, gating within the $CD14^+$ population and using human anti-DC-SIGN (R&D Systems).

Alternatively, the antibody staining of macrophages was performed as previously described (29). Adherent cells were collected using the Cell Dissociation Buffer according to manufacturer's instructions (Life Technologies), centrifuged for 5 min at 340 *g* at 4°C, and then stained in cold FACS buffer (PBS pH 7.2, 5% BSA) for 25 min with the indicated fluorophore-conjugated antibodies using a general dilution of 1:400. The antibodies were the following: CD16 (FCGR3A), PD-L1 (CD274), CD11b (MAC-1) and CD14 from Biolegend; CD163 (SCARI1), CD86 (B7-2), CD64 (FCGR1A), CD36 (SCARB3), CD11c (ITGAX), IL-7R (CD127), MRC1, and DC-SIGN from BD Biosciences; MerTK (Tyro12) from R&D system, and HLA-DR from Santa Cruz Biotechnology. In parallel, we also performed the staining with the corresponding isotype control antibody. Afterward, the cells were washed with cold FACS buffer, centrifuged for 5 min at 340 *g* at 4°C, and analyzed by flow cytometry using LSR-II flow cytometer (BD Biosciences). Data was then acquired and analyzed using the FlowJo 7.6.5 software.

siRNA Silencing of DC-SIGN and Dectin-1

The siRNA gene silencing in human primary macrophages was performed using the forward transfection approach, as previously described (29). Briefly, macrophages differentiated at day 5 were transfected using the lipid-based HiPerfect system (Qiagen) and an ON-TARGETplus SMARTpool siRNA targeting DC-SIGN (siDC-SIGN) and Dectin-1 (siDectin-1), or a non-targeting siRNA (siControl) (Dharmacon), at a final concentration of siRNA at 200 nM. Of note, for the simultaneous inactivation of two genes, the working siRNA concentration combined for DC-SIGN and Dectin-1 did not exceed the final concentration of 200 nM, as previously published (29, 30). After 6 h, RPMI-1640 medium supplemented with M-CSF (10 ng/ml) was added to each well, and the cells were allowed to recuperate overnight. The following day, IL-4 (20 ng/ml) was added to the transfected macrophages in order to induce the M(IL-4) program along with the CLR expression for an additional 72 h (or as indicated). The inactivation for DC-SIGN and Dectin-1 was confirmed by flow cytometry in non-permeabilized cells at the indicated time points post-transfection. Cell viability was determined by using the Annexin-V-FITC kit designed for flow cytometry. Cell viability was defined as cells negative for either Annexin-V-FITC and/or propidium iodide. For the upregulation of co-stimulatory molecules, control and DC-SIGN-depleted M(IL-4) macrophages were stimulated with LPS (1 μg/ml) for 24 h, and the cell-surface marker expression was assessed by flow cytometry.

Blocking and Stimulation of DC-SIGN and Dectin-1 Receptors

Human macrophages were differentiated at day 5, and activated with IL-4 (20 ng/ml) for additional 48 h. At day 7, the M(IL-4) macrophages were washed with warmed RPMI-1640 medium supplemented with M-CSF (10 ng/ml) and pre-incubated for 30 min with 10 μg/ml blocking antibodies specific to either Dectin-1 (MAB1859, R&D Systems) or DC-SIGN (ab13847, abcam), or both. As a control, M(IL-4) macrophages were incubated with an irrevelevant antibody (Ab-Control). For efficient stimulation of Dectin-1, M(IL-4) macrophages were treated with cytochalasin D (1 μg/ml, C8273, SIGMA) in combination with purified β-glucan from Saccharomyces cerevisiae (10 μg/ml, G5011, SIGMA), as previously described (31); for DC-SIGN, cells were stimulated with 10 μg/ml of ManLAM (kindly provided by Dr. Jerome Nigou, IPBS/CNRS); and for TLR-4, cells were stimulated with 1 μg/ml of LPS. After 24 h, the supernatants were collected and stored at −80°C until further use for ELISA analysis.

Mtb Strain, Culture, and Preparation for Infection

All manipulation with Mtb (H37Rv strain) was performed in a dedicated BSL-3 laboratory. Mtb was cultured at 37°C

in Middlebrook 7H9 medium (Difco) supplemented with 10% albumin-dextrose-catalase (Difco) and 0.05% Tween-80 (Sigma-Aldrich). For infection, exponentially growing Mtb was centrifuged (2,000 *g*) for 15 min, and resuspended in 1x phosphate buffered saline (PBS). Clumps were dissociated by passages through a 26-G needle, and then resuspended in RPMI-1640 containing 10% FBS. The mycobacterial concentration was determined by measuring optical density at 600 nm [OD_{600}]. For binding experiments, the GFP-expressing Mtb (H37Rv) strain was generated and cultivated as previously published (20).

RNA Extraction and Transcriptomic Analysis

Control and DC-SIGN-depleted M(IL-4) macrophages (approximately 1.5 million cells) were infected with Mtb at a multiplicity of infection (MOI) of 3 bacteria to 1 cell in RPMI-1640 with 10% FBS for 4 h. The cells were then washed twice with 1x PBS. At this point, the cells were either treated with TRIzol Reagent (Invitrogen) to harvest at 4 h postinfection (*p.i.*) and stored at −80°C, or cultured with RPMI-1640 with 10% FBS overnight. The procedure with the TRIzol reagent was repeated the following day to harvest at 18 h *p.i.* and stored at −80°C. Total RNA was extracted from the TRIzol samples using the RNeasy mini kit (Qiagen). The amount and purity of RNA (absorbance at 260/280 nm) was measured with the Nanodrop ND-1000 apparatus (Thermo Scientific). Complementary DNA was reverse transcribed from 1 µg total RNA with Moloney murine leukemia virus reverse transcriptase (Invitrogen) using random hexamer oligonucleotides for priming, according to the manufacturer's protocol. The microarray analysis was done using the Agilent Human GE 4 × 44 v2 (single color), as previously described (32). Briefly, the hybridization was performed with 2 µg Cy3-cDNA and the hybridization kit (Roche NimbleGen). According to manufacturer's protocol, the samples were incubated for 5 min at 65°C, and 5 min at 42°C before loading for 17 h at 42°C. After washing, the microarrays were scanned with MS200 microarray scanner (Roche NimbleGen). Using Feature Extraction software, the Agilent raw files were extracted and then processed through Bioconductor (version 3.1) in the R statistical environment (version 3.2.0). A careful assessment of the quality of the hybridization, evaluation of the sampling method and normalization of the expression values was done as previously published (32). We then obtained the differentially expressed genes (DEGs) between control and DC-SIGN-depleted M(IL-4) macrophages at each time point after Mtb infection based on false discovery rate (*t*-test, $P < 0.1$) and a threshold of twofold change in the comparison between the two conditions. The normalized values for the entire microarray analysis and the determined DEGs are provided in Tables S1–S3 in Supplementary Material. Finally, DEGs were analyzed with QIAGEN's Ingenuity® Pathway Analysis (IPA®, QIAGEN Redwood City, www.qiagen.com/ingenuity).

qRT-PCR Analysis

The amplification of RNA was performed with an ABI Prism 7500 Sequence Detector (Applied Biosystems) using the PCR SYBR Green sequence detection system (Eurogentec, Seraing, Belgium). Primers are listed in Table S4 in Supplementary Material. Data were analyzed using the software supplied with the Sequence Detector (Applied Biosystems). The mRNA content was normalized to the metastatic lymph node protein 51 (MLN51) mRNA and quantified using the ΔΔCt method.

Semi-Quantitative Cytokine/Chemokine Antibody Array Assay and Quantitative ELISA

Control and DC-SIGN-depleted M(IL-4) macrophages were infected with Mtb at MOI of 3. Supernatants were harvested at 4 and 18 h p.i., centrifuged (2,000 *g*) for 10 min, passed through filters (0.22 µm pores) and stored at −80°C. With the use of the Human Cytokine Antibody Array C Series 1000 (RayBiotech), we assessed the supernatant content in terms of cytokine and chemokines following the manufacturer's instructions, as previously described (33). We used Amersham Hyperfilm ECL (GE Healthcare) to detect individual signals, and the GS-800 calibrated densitometer (Bio-Rad) to quantify these signals. As instructed, the positive control signal on each array was used to normalize the rest of the detected signals. In parallel, cytokine quantification was measured in cell supernatants by ELISA using kits from BD Bioscience (TNFα, IL-6, and IL-10), according to manufacturer's instructions.

Binding and Phagocytosis of Mtb

As previously described (19), control and DC-SIGN-depleted M(IL-4) macrophages were infected with the GFP-expressing Mtb strain, at a MOI of 5 for 4 h, at either 4°C or 37°C, in order to assess binding and phagocytosis, respectively. Cells were then washed with 1× PBS (without calcium and magnesium), collected using the Cell Dissociation Buffer, centrifuged for 5 min at 340 *g* at 4°C, fixed with 4% PFA for 2 h, washed with 1× PBS and resuspended in FACS buffer. Cells were then analyzed by flow cytometry.

Measurement of Mtb Intracellular Growth

Macrophages were washed with PBS and then infected with Mtb at a MOI of 0.2 bacteria/cell in RPMI-1640 with 10% FBS for 4 h. Cells were then washed twice with 1x PBS before addition of RPMI-1640/10% FBS. At the indicated time points, the cells were lysed in 0.01% Triton X-100 (Sigma-Aldrich), and serial dilutions of the lysates were plated onto 7H11-Oleic Albumin Dextrose Catalase (Difco) agar medium for CFU scoring.

Statistical Analyses

Two-tailed Wilcoxon (matched-paired test) was applied to compare the M(IL-4) macrophage population under two conditions (siControl versus siDC-SIGN). Two-tailed unpaired *t*-test (parametric) was applied on data sets with a normal distribution, whereas one-tailed unpaired Mann–Whitney (nonparametric) was done for data not showing a normal distribution and where the outcome was already expected, as indicated for each figure legend. $P < 0.05$ was considered as the level of statistical significance.

RESULTS

DC-SIGN-Expressing Macrophages Are Present in Pulmonary Lesions of NHP Infected With Mtb

Tuberculous granulomas have organized microenvironments that presumably balance the antimicrobial functions to control bacteria growth and anti-inflammatory properties to limit pathology in the lung (34). Recently, others and we have detected the high abundance of an M2-like macrophage population in tuberculous granulomas in the context of pulmonary lesions of NHPs with severe TB (25, 35). Here, we further investigated whether DC-SIGN-expressing macrophages are present in these samples derived from Mtb-infected rhesus macaques, which displayed different levels of lung pathology. In samples from NHPs exhibiting a low pathological score in lungs, immunohistochemical analyses revealed the low presence of $CD68^+$ macrophages and DC-SIGN-expressing cells in areas where leukocyte infiltrate was also detected by HE staining (**Figure 1A**). By contrast, in samples from animals characterized by a high lung pathological score, we observed not only the characteristic necrotic lung granuloma and $CD68^+$ macrophages abundantly infiltrating the interstitial lung tissue, but also the increased number of DC-SIGN-expressing cells in these areas (**Figure 1A**). To determine whether DC-SIGN is expressed by M2 macrophages in the context of tuberculous granulomas, we also performed an additional staining for CD163 and MerTK, two strong markers of M2 macrophages. As shown for **Figure 1B**, DC-SIGN-expressing cells localized at the granuloma periphery and alveoli, where $CD163^+$ and $MerTK^+$ macrophages are also found. Importantly, co-localization analysis revealed the presence of cells positive for DC-SIGN within $CD68^+$ ($41 \pm 20\%$, $n = 893$ counted cells) and $CD163^+$ ($27 \pm 3\%$, $n = 754$ counted cells) macrophage populations (**Figure 1C**). These analyses demonstrate that the environment generated during pulmonary TB is associated with enhanced DC-SIGN expression in $CD68^+$ and $CD163^+$ macrophages, which become accentuated in NHPs with severe TB as previously described (25).

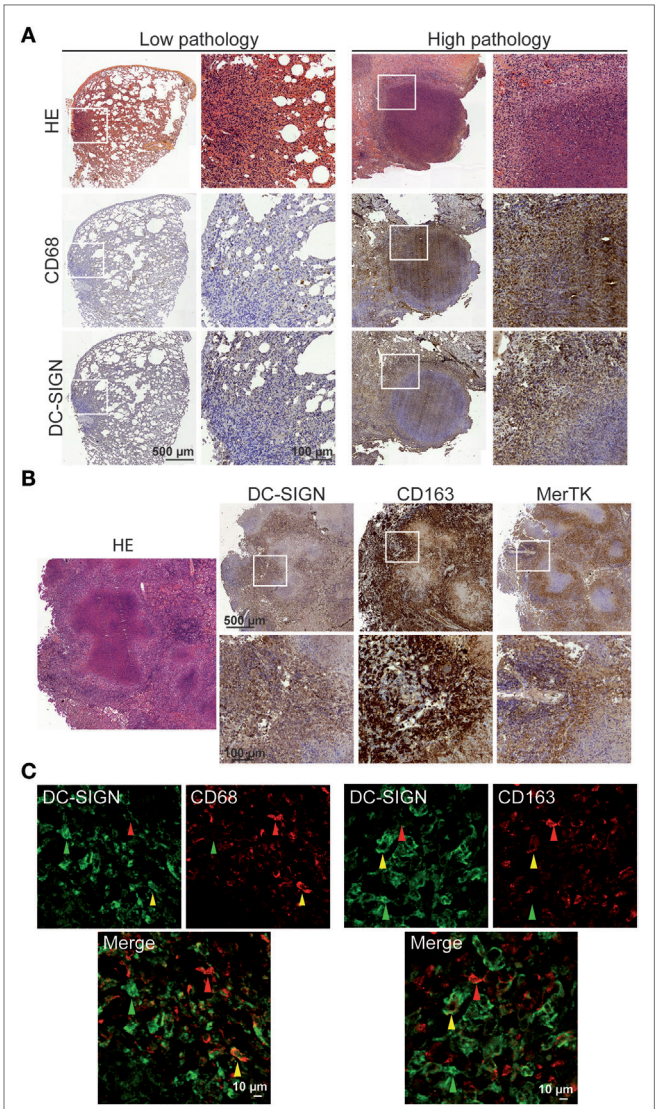


FIGURE 1 | DC-SIGN-expressing macrophages are present in pulmonary lesions of non-human primates (NHP) infected with Mtb. **(A)** Representative immunohistochemical images illustrating the distribution of CD68 (middle row) and DC-SIGN (bottom row), among areas where leukocyte infiltration (top row) is detected by hematoxylin and eosin (HE), in pulmonary tissue and granulomas of NHP with very mild (left columns) and severe (right columns) pathology. **(B)** Representative immunohistochemical images illustrating the distribution of DC-SIGN, CD163, and MerTK in areas where leukocyte infiltration is detected by HE, such as in granulomas of NHP with severe pathology. **(C)** *Left panel*: immunostaining of DC-SIGN (green: Alexa-488) and CD68 (red: Alexa-555) in lung tissue of NHP with severe pathology; *right panel*: immunostaining of DC-SIGN (green: Alexa-488) and CD163 (red: Alexa-555) in lung tissue of NHP with severe pathology. Green arrow points out a cell positive for DC-SIGN only; red arrow a cell positive for CD68 or CD163 only; and yellow arrow for a cell positive for both DC-SIGN and CD68/CD163. Scale bar = 10 µm.

Human Tuberculosis-Associated Microenvironment Induces DC-SIGN Expression in Macrophages

Our group previously reported that, in lungs, DC-SIGN expression is induced specifically in alveolar macrophages of patients with active TB (19). Using samples obtained from patients with active TB, we expanded our assessment of DC-SIGN expression in the context of macrophage activation. First, we isolated and differentiated monocytes from HS or TB patients into macrophages. Macrophages were activated toward the M(IL-4) program and the expression of DC-SIGN was measured by flow cytometry analysis. Our results revealed that, unlike unactivated macrophages [M(M-CSF)], DC-SIGN expression was accentuated in M(IL-4) macrophages and with a higher tendency (albeit not significant) in TB patients (**Figure 2A**). Second, we induced the activation of macrophages (derived from HS monocytes) with cell-free supernatants from sera or PE from TB patients (TB-S and TB-PE, respectively). We noticed that while sera from either HS or TB patients failed to induce DC-SIGN expression, TB-PE significantly increased the cell-surface level for this CLR (**Figure 2B**). Last, we measured

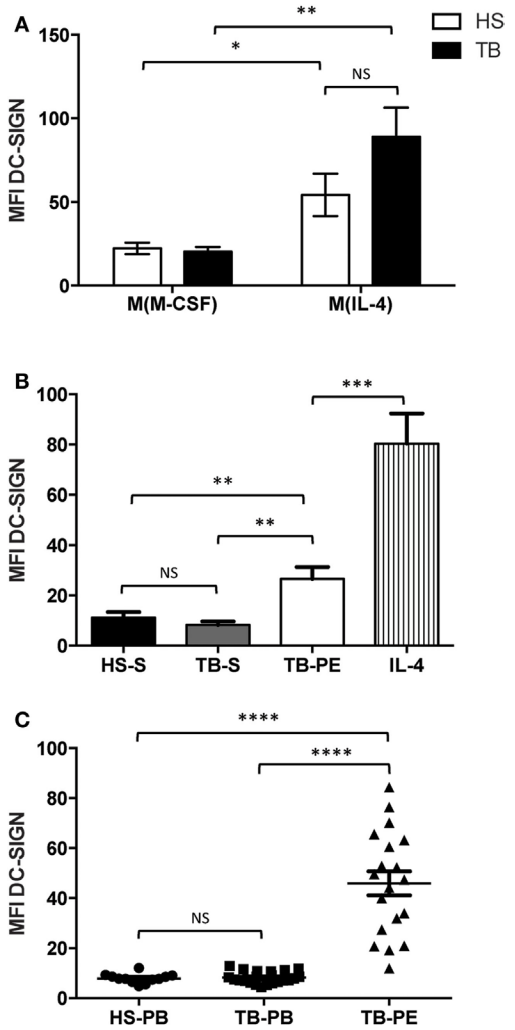


FIGURE 2 | Human tuberculosis-associated microenvironment induces DC-SIGN expression in macrophages. **(A)** DC-SIGN expression is induced in M(IL-4) macrophages from TB patients. Freshly isolated monocytes from healthy subjects (HS, white) and TB patients (TB, black) were differentiated into macrophages using M-CSF. At day 5, the cells were activated with IL-4 (20 ng/ml) for 48 h to induce the M(IL-4) macrophage program. Otherwise, macrophages were kept under M-CSF to fully establish the M(M-CSF) program. The cells were harvested and the DC-SIGN expression was analyzed by flow cytometry. Vertical bar graphs depicting the median fluorescent intensity (MFI) of DC-SIGN expression in the different cell populations. Results are expressed as mean ± SD (n = 10 donors). **(B)** DC-SIGN expression is induced by pleural fluid from TB patients. Freshly isolated monocytes from HS were differentiated into macrophages using M-CSF. At day 5, the cells were activated for 48 h with sera from HS (HS-S, black) and TB patients (TB-S, gray), acellular pleural fluid from TB patients (TB-PE, white), and IL-4 (20 ng/ml, vertical stripes). The cells were harvested and the DC-SIGN expression was analyzed by flow cytometry. Vertical bar graphs depicting the MFI of DC-SIGN expression in the different cell populations. Results are expressed as mean ± SD (n = 13 donors). **(C)** DC-SIGN-expressing macrophages are present in the pleural cavity of TB patients. Mononuclear cells were isolated either from peripheral blood from HS (HS-PB) and TB patients (TB-PB), or from the pleural effusions from TB patients (TB-PE), and the expression of DC-SIGN was analyzed on the CD14$^+$ population by flow cytometry. Results are expressed as vertical scatter plots showing the MFI of DC-SIGN for each population; each individual symbol represents a single donor. Two-tailed t-test (unpaired/parametric): $^*P < 0.05$, $^{**}P < 0.01$, $^{***}P < 0.001$, $^{****}P < 0.0001$, NS = not significant.

DC-SIGN expression directly in the CD14$^+$ cell population present in the circulation or PE of TB patients. We failed to observe the presence of DC-SIGN-expressing CD14$^+$ blood monocytes in either HS or TB patients. Strikingly, however, we detected DC-SIGN highly expressed in all CD14$^+$ monocyte/macrophages collected in TB-PE (**Figure 2C**). Altogether, these results demonstrate that TB-associated environments are capable to induce DC-SIGN expression in the context of human macrophage activation.

Depletion of DC-SIGN Expression Does Not Affect Cell Viability nor the Establishment of the M(IL-4) Macrophage Program

In the context of the most commonly studied *in vitro* programs of human macrophage activation [i.e., M(LPS + IFNγ) and M(IL-4)], DC-SIGN is a reliable cell-surface marker for M(IL-4) macrophages (22, 23). To confirm this, we differentiated freshly isolated CD14$^+$ monocytes from healthy donors into macrophages. We activated macrophages toward M(IL-4) and M(LPS + IFNγ), and then assessed the cell-surface marker profile of these cell populations by flow cytometry. While we noticed that expression of DC-SIGN and other markers varies dramatically between donors (in terms of MFI), we still detected a significantly higher cell-surface expression of DC-SIGN in M(IL-4) in comparison to M(LPS + IFNγ) macrophages (Figure S1A in Supplementary Material). Its expression was accompanied by that of Dectin-1 and MRC1, a *bona fide* M(IL-4) macrophage marker (22). We also observed a higher expression (albeit not significant) of CD11b and CD36 in M(IL-4) compared to M(LPS + IFNγ) cells (Figure S1A in Supplementary Material). By contrast, M(LPS + IFNγ) were distinguished by significant elevated levels of CD64, CD86, and PD-L1 (Figure S1A in Supplementary Material). These results confirm that DC-SIGN is exclusively expressed in M(IL-4) macrophages, thus making it an ideal cell model to study the role of this CLR in human macrophages.

With the aim to examine the role of DC-SIGN in the activation of the M(IL-4) program, we made use of a lipid-based siRNA-mediated gene silencing protocol we recently developed (29, 30). Macrophages were transfected with siRNA targeting this CLR (siDC-SIGN) or with non-targeting scrambled siRNA control (siControl), and these cells were then stimulated with IL-4 to activate the M(IL-4) program. As expected, while the MFI of DC-SIGN expression augmented under 72 h treatment with IL-4 in control cells, the induction of DC-SIGN was minimal in cells transfected with siRNA targeting this CLR (Figure S1B in Supplementary Material). In addition, cell viability was not affected after depletion of DC-SIGN for 72 h post-transfection (Figure S1B in Supplementary Material). Similar results in terms of DC-SIGN depletion and cell viability were obtained at 96, 120, and 144 h post-transfection (data not shown). Importantly, we noticed that DC-SIGN-depleted macrophages differentiate normally toward the M(IL-4) program (Figure S2A in Supplementary Material), and up-regulate co-stimulatory receptors when challenged with LPS (Figure S2B in Supplementary Material), as compared to control cells. Therefore, the inactivation of DC-SIGN in M(IL-4)

macrophages appears to have no major consequences at steady state conditions or in response to LPS challenge.

The Pro-Inflammatory Response of M(IL-4) Macrophages Against Mtb Is Regulated by DC-SIGN

To explore the role of DC-SIGN in the M(IL-4) macrophage response to Mtb, we performed a genome-wide transcriptome analysis of cells expressing DC-SIGN (siControl) or not (siDC-SIGN) challenged with Mtb at different time points. In general, DC-SIGN-depleted M(IL-4) macrophages displayed a broad DEG profile when compared to control cells. At 4 h postinfection (*p.i.*), we observed that the majority of genes that are upregulated in DC-SIGN-depleted M(IL-4) macrophages are of pro-inflammatory nature, such as interferon alpha inducible protein (*IFI27*), *IL-6*, Oncostatin M (*OSM*), *CXCL1*, *IL-17RB,* and *IL-1β*, among others (Tables S1 and S2 in Supplementary Material). By contrast, we observed very few genes downregulated in DC-SIGN-depleted M(IL-4) macrophages, including *FCER1A* (*FcERI*), *CD1B*, *CCL17* (*TARC*), and DC-SIGN, among others (Tables S1 and S2 in Supplementary Material). At 18 h *p.i.*, the pro-inflammatory tendency is further accentuated in the DEG that becomes upregulated in DC-SIGN-depleted M(IL-4) macrophages (Figure S3A and Tables S1 and S3 in Supplementary Material). For example, Ingenuity pathway analysis indicated that the DEG in these cells formed a network centered on NF-κB, a master transcription factor that regulates the pro-inflammatory response against infection (Figure S3A and Table S1 in Supplementary Material). Similar to 4 h *p.i.*, there were few genes that were downregulated in in DC-SIGN-depleted M(IL-4) macrophages when compared to control cells at 18 h *p.i.*, including DC-SIGN (Figure S3A and Tables S1 and S3 in Supplementary Material). Importantly, we confirmed the higher expression of the pro-inflammatory genes, and the downregulation of DC-SIGN, at 18 h *p.i.* by qPCR analysis (**Figure 3A**). Of note, the mRNA expression of *IL-10* was not affected significantly in the absence of DC-SIGN (**Figure 3A**).

At the protein level, we performed a dedicated antibody-based membrane array to assess the cytokine and chemokine content in the culture medium collected from DC-SIGN-depleted and control M(IL-4) macrophages at 18 h *p.i.* with Mtb. Again, we observed the shift toward a pro-inflammatory profile in DC-SIGN-depleted M(IL-4) macrophages as they secreted more IL-6, TNF, and CXCL1, among other cytokines and chemokines, compared to the supernatant content from siControl cells (**Figure 3B**). By contrast, the secretion of anti-inflammatory factors such as vascular endothelial growth factor A (VEGFA), thrombopoietin (THPO), TNF receptor superfamily member 10C (TNFRSF10C/TRAIL-R3) and 10D (TNFRSF10D/TRAIL-R4), among others, was downregulated in the absence of DC-SIGN (**Figure 3B**). Finally, we validated by ELISA analysis the high level of both IL-6 and TNF in the supernatant content of DC-SIGN-depleted M(IL-4) macrophages in comparison to that of control cells (**Figure 3C**). Similar to RNA levels, we observed no differences in the secretion of IL-10 in the absence of DC-SIGN, as measured both by the antibody-based membrane arrays and ELISA (**Figures 3B,C**).

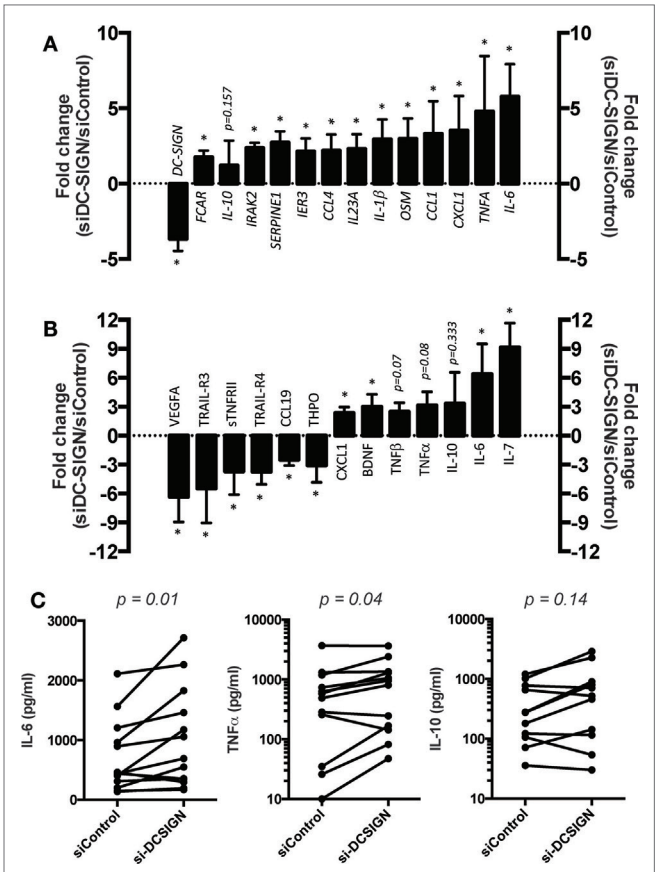


FIGURE 3 | DC-SIGN regulates the pro-inflammatory response by M(IL-4) macrophages against Mtb. Human monocytes were differentiated into macrophages using M-CSF. At day 5, macrophages were transfected with siRNA targeting DC-SIGN (siDC-SIGN) or a non-targeting siRNA (siControl). The following day, the cells were activated with IL-4 (20 ng/ml) for 48 h to induce M(IL-4) program. The cells were then infected with Mtb at multiplicity of infection (MOI) of 3 bacteria to 1 cell. At 18 h *p.i.*, the cells were harvested and their supernatant collected. Assessment of **(A)** gene mRNA expression by qRT-PCR analysis, and **(B)** cytokine and chemokine content by semi-quantitative antibody array. Vertical bar graphs illustrate the fold change of mRNA/protein levels in siDC-SIGN over siControl macrophages; "0" was set arbitrarily to represent no change. Results are expressed as mean ± SD (n = 4 donors). One-tailed Mann–Whitney (unpaired/nonparametric): $^*P < 0.05$. **(C)** Assessment of cytokines by ELISA analysis. Results are expressed as before-and-after plot for the indicated genes (n = 11 donors). Each circle within the plots represents a single donor. Two-tailed Wilcoxon (matched-paired/nonparametric): $P < 0.05$ was considered as the level of statistical significance.

Collectively, these results suggest that the expression of DC-SIGN restrain the pro-inflammatory capacity of M(IL-4) macrophages in response to Mtb.

Inactivation of DC-SIGN Expression in M(IL-4) Macrophages Reduces the Intracellular Mtb Burden

While macrophages from the M2 spectrum of activation are associated with intracellular pathogen permissivity (6), it was previously shown that activation of human macrophages with

IL-4 enhances the microbicidal capacity against Mtb in a dose-dependent manner (24). To assess the role of DC-SIGN in the control Mtb intracellular growth, we first conducted flow cytometry-based experiments using a fluorescent Mtb strain (H37Rv-eGFP) to determine the capacity of M(IL-4) macrophages to bind and internalize the bacillus when DC-SIGN is inactivated. To our surprise, we noticed that both parameters were equally performed by control and DC-SIGN-depleted M(IL-4) macrophages (**Figure 4A**). Next, we carried out the CFU assays. At 4 h *p.i.,* we confirmed that DC-SIGN-depleted M(IL-4) macrophages displayed normal levels of bacteria internalization compared to control cells (**Figure 4B**). However, when DC-SIGN is depleted, Mtb intracellular growth is better restricted at day 3, 5, and 7 *p.i.* compared to control M(IL-4) macrophages (**Figure 4B**). These results indicate that the expression of DC-SIGN renders M(IL-4) more permissive to intracellular growth by Mtb.

DC-SIGN Interferes Negatively With the Activation of M(IL-4) Macrophages Triggered by Dectin-1 in Response to Mtb

Dectin-1 is an important CLR expressed in human dendritic cells that activates a pro-inflammatory response distinguished by IL-6, TNF, IL-23, and IL-1β, against Mtb (36). Using our siRNA-mediated gene silencing method (29), we inactivated the expression of Dectin-1 in M(IL-4) macrophages and confirmed its pro-inflammatory role in the response to challenge with Mtb, as reflected by the decrease of IL-6 secretion (as an example of the pro-inflammatory response) at 18 *p.i.* (**Figure 5A**; Figure S4 in Supplementary Material). Importantly, simultaneous inactivation of Dectin-1 and DC-SIGN resulted in a similar IL-6 secretion as Dectin-1 inactivation alone, indicating that the high levels observed for this cytokine in DC-SIGN-depleted

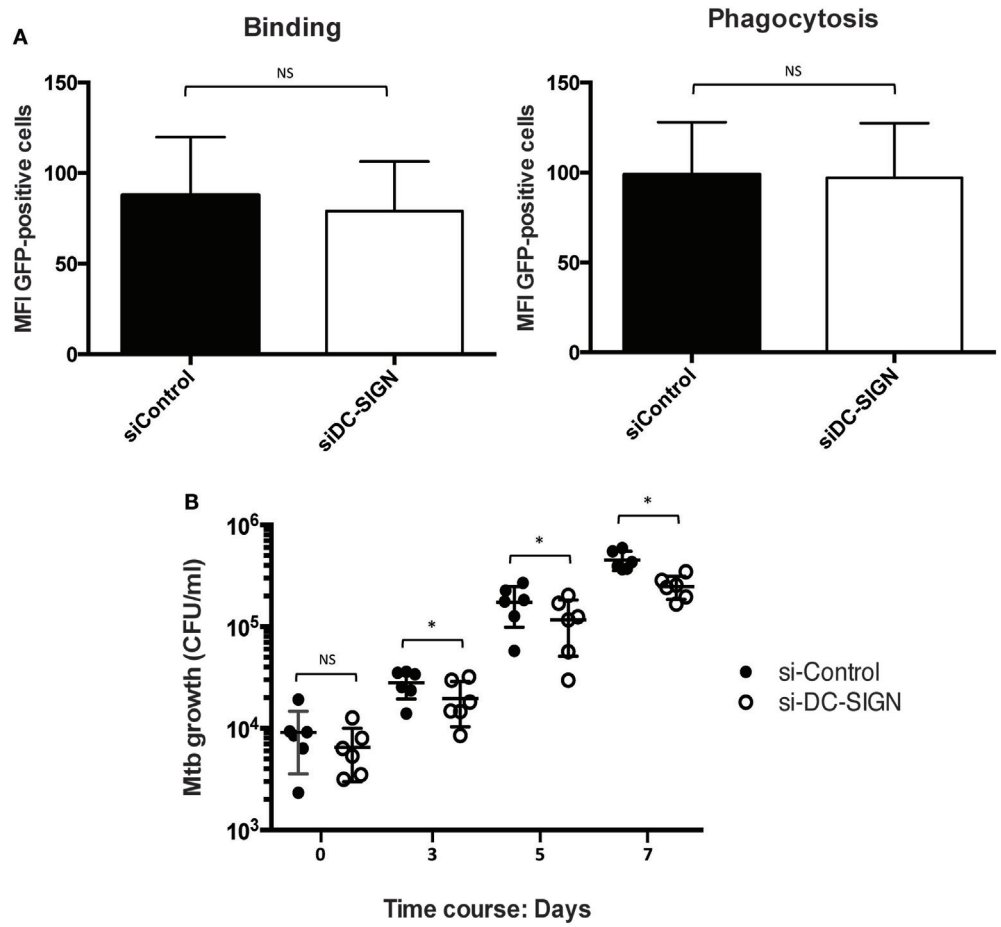


FIGURE 4 | Different roles for DC-SIGN in the M(IL-4) macrophage–Mtb interaction. Human monocytes were differentiated into macrophages using M-CSF. At day 5, macrophages were transfected with siRNA targeting DC-SIGN (siDC-SIGN, white) or a non-targeting siRNA (siControl, black). The following day, the cells were activated for 48 h with IL-4 (20 ng/ml) to induce M(IL-4) program. **(A)** DC-SIGN expression in M(IL-4) macrophages is redundant for the binding and internalization of Mtb. Control and DC-SIGN-depleted macrophages were tested for the capacity to bind (at 4°C, left) or phagocytose (at 37°C, right) the Mtb strain expressing GFP during 4 h of challenge. Bar graphs illustrate the median fluorescent intensity (MFI) of cells positive for GFP, as measured by flow cytometry analysis. Results are expressed as mean ± SD ($n = 4$ donors). NS, not significant. **(B)** DC-SIGN influences the capacity of M(IL-4) macrophages to control the Mtb intracellular burden. The cells were infected with Mtb (MOI of 0.2 bacteria to 1 cell) and the intracellular growth of the bacteria was followed at 4 h (day 0), 72 h (day 3), 120 h (day 5), and 168 h (day 7), as measured by colony forming unit (CFU) assays. Results are expressed as vertical scatter plots showing the CFU scoring per ml; each circle represents a single donor. Two-tailed Wilcoxon (matched-paired/nonparametric): $^*P < 0.05$; NS, not significant.

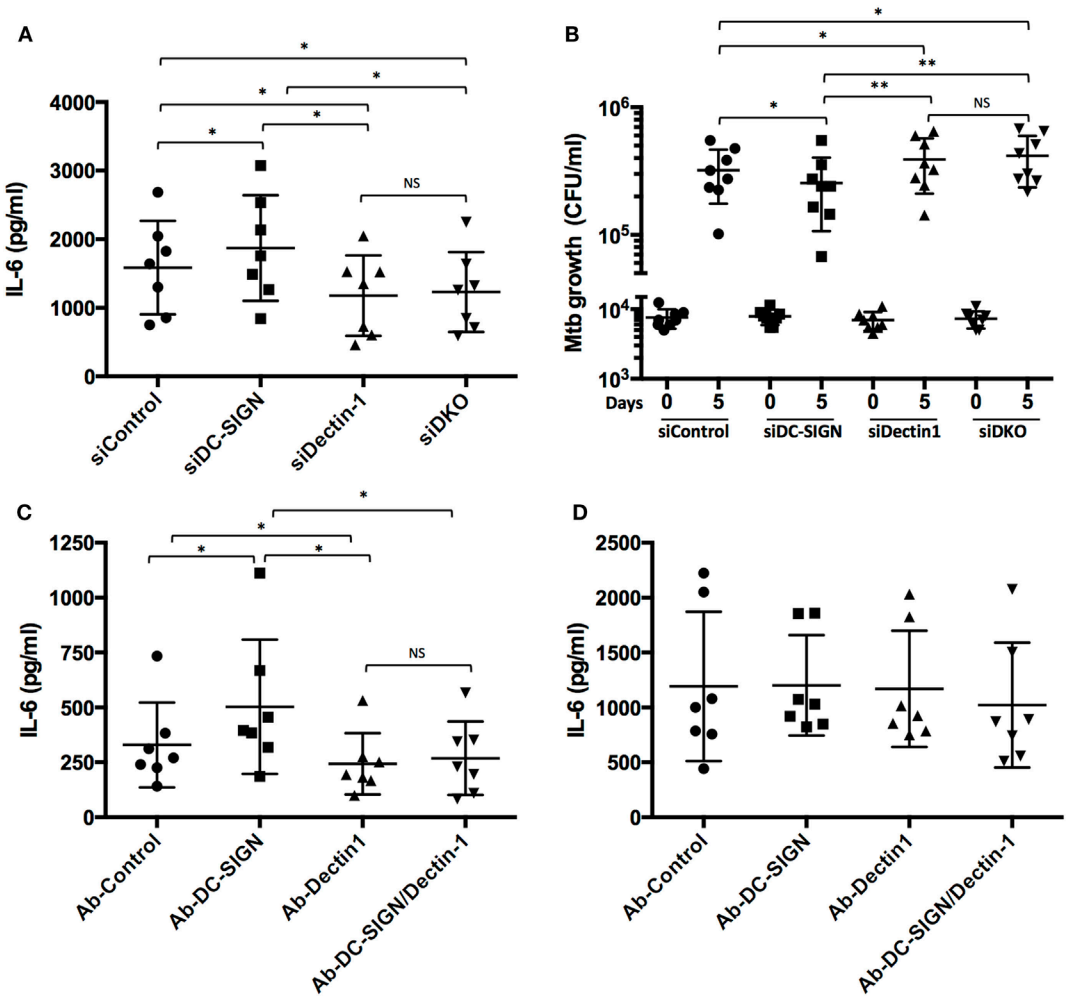


FIGURE 5 | DC-SIGN interferes negatively with the activation of M(IL-4) macrophages triggered by Dectin-1. Human monocytes were differentiated into macrophages using M-CSF. At day 5, the macrophages were transfected with siRNA targeting DC-SIGN (siDC-SIGN, squares) and Dectin-1 (siDectin-1, upward triangle), both siRNAs (siDKO, downward triangle), or a non-targeting siRNA (siControl, circles). The following day, the cells were activated with IL-4 (20 ng/ml) for 48 h to induce M(IL-4) program and the C-type lectin receptor expression. **(A)** Assessment of IL-6 secretion by ELISA analysis. The cells were infected with Mtb at MOI of 3 bacteria to 1 cell. At 18 h *p.i.*, the supernatant from these cells was collected. Results are expressed as vertical scatter plots, and as mean ± SD ($n = 7$ donors). **(B)** Assessment of Mtb intracellular growth by colony forming unit (CFU) assay. The cells were infected with Mtb (MOI of 0.2 bacteria to 1 cell), and the intracellular growth of the bacteria was followed at 4 h (day 0, left) or 120 h (day 5, right). Results are expressed as vertical scatter plots, and as mean ± SD ($n = 8$ donors). Two-tailed Wilcoxon (matched-paired/nonparametric): $^*P < 0.05$, $^{**}P < 0.01$; NS, not significant. **(C,D)** Upon differentiation until day 5, macrophages were then activated with IL-4 for 48 h. Prior to stimulation, M(IL-4) macrophages were pre-treated for 30 min with blocking antibodies for either DC-SIGN or Dectin-1, or both. An irrelevant antibody was used as a control. M(IL-4) macrophages were then treated with either **(C)** cytochalasin D (1 μg/ml), β-glucan (10 μg/ml) and ManLAM (10 μg/ml), or **(D)** LPS (1 μg/ml) and ManLAM (10 μg/ml). After 24 h, the supernatants were collected and the production of IL-6 was measured by for ELISA analysis.

M(IL-4) macrophages are dependent on the Dectin-1 signaling pathway (**Figure 5A**; Figure S4 in Supplementary Material). By contrast, the production of IL-10 was not affected by the inactivation of either DC-SIGN or Dectin-1 (Figure S5A in Supplementary Material). In terms of bacterial burden, we found that Dectin-1 depletion rendered the M(IL-4) macrophages more susceptible to Mtb growth (**Figure 5B**; Figure S4 in Supplementary Material). Moreover, simultaneous inactivation of both CLRs fully reversed the lower CFU counts observed when DC-SIGN is inactivated alone, suggesting that Dectin-1 depletion is dominant over that of DC-SIGN (**Figure 5B**; Figure S4 in Supplementary Material).

To better understand the potential crosstalk between these receptors in the generation of a pro-inflammatory response (e.g., IL-6 production), we employed the use of the ligands β-glucan and ManLAM to stimulate specifically Dectin-1 and DC-SIGN, respectively. As a control for macrophage activation, we used LPS as the ligand for TLR-4. As illustrated in the **Figures 5C,D**, we noticed that the stimulation of M(IL-4) macrophages with β-glucan and ManLAM induces the production

of IL-6, albeit to a lower level than that obtained with LPS and ManLAM. Interestingly, while the use of a blocking antibody targeting DC-SIGN resulted in the upregulation of IL-6 after stimulation with β-glucan and ManLAM (**Figure 5C**), it failed to do so upon stimulation with LPS and ManLAM (**Figure 5D**). As expected, the use of a blocking antibody targeting the Dectin-1 receptor diminished the production of IL-6 induced by β-glucan and ManLAM (**Figure 5C**), but it had no effect on the production driven by the stimulation with LPS and ManLAM (**Figure 5D**). Likewise, simultaneous blocking of DC-SIGN and Dectin-1 resulted in a diminished production of IL-6 upon stimulation only with by β-glucan and ManLAM (**Figure 5C**), and not with LPS and ManLAM (**Figure 5D**). Of note, the crosstalk between DC-SIGN and Dectin-1 is specific for IL-6 because the production of the anti-inflammatory IL-10 was not affected (Figures S5B,C in Supplementary Material).

Altogether, these findings support a role of DC-SIGN in interfering negatively with the pro-inflammatory response triggered by Dectin-1 during Mtb infection of M(IL-4) macrophages.

DISCUSSION

This study highlights a dual role for DC-SIGN as, on the one hand, being a host factor granting advantage for Mtb to parasitize macrophages and, on the other hand, representing a molecular switch to turn off the pro-inflammatory response in these cells to potentially prevent potential immunopathology associated to TB. Notwithstanding, there are some limitations to this study that should be considered in the interpretation of results and derived conclusions. First, while our siRNA-mediated gene silencing protocol is effective in primary macrophages, without altering cell viability or biological functions (29), the expression of DC-SIGN is not totally abrogated. Prior to infection with Mtb, macrophages transfected with the siRNA targeting DC-SIGN still continue to express this CLR (albeit at minimal levels) upon activation with IL-4, ranging between 5 and 25% compared to control cells. Second, working with human primary macrophages introduces a high degree of biological variance compared to experiments done with human cell lines (e.g., THP-1) or bone marrow derived macrophages from congenic mice. Third, among membrane-anchored CLRs, there is a well-known functional redundancy that might cooperate in a coordinated immune response in favor or against Mtb infection (11, 37). Last, the context for which DC-SIGN is activated should be taken into account, as this CLR can mediate both immunosuppression and immunity (38). Indeed, there are multiple studies supporting the immunosuppressive role of DC-SIGN in macrophages during inflammatory contexts, including in autoimmunity and, just recently, in allotransplantation acceptance (38–40). Likewise, DC-SIGN is well known to play a pro-inflammatory role by enhancing the antigen-presentation process in human dendritic cells and inducing a strong activation of $CD4^+$ and $CD8^+$ T cells (41, 42). In the case of M(IL-4) macrophages, our findings on DC-SIGN should be taken within the immunosuppression context given that the nature of these cells is that of wound healers and tissue remodelers (22). In spite of these limitations, our study dealing with primary human cells in a TB context provides relevant data improving our knowledge on DC-SIGN.

We first described the presence of DC-SIGN-expressing macrophages in the pleural cavity of patients and in the lung tissue of NHP with active TB. The identification of a human$CD14^+$ macrophage population displaying high cell-surface levels of DC-SIGN, MRC1, and CD163, is supported by our previous finding describing the presence of the $CD16^{hi}CD163^{hi}MerTK^{hi}$ immunosuppressive macrophages in the pleural cavity of patients with active TB (25), and by our first report on DC-SIGN-expressing alveolar macrophages isolated from the bronchoalveolar lavage in patients with pulmonary TB (19). This suggests that a TB-associated environment favors the presence of macrophages with an M2-marker signature, including DC-SIGN expression. Interestingly, IL-4 is one of the most detected cytokines in TB PE, and thus making probably the responsible signal to induce DC-SIGN expression in cells at this site (43). IL-13 is another cytokine that is present in the pleural cavity of active TB patients (44), and that is probably responsible for the mediating DC-SIGN expression in macrophages since its signaling pathway is considered to be equivalent to that of IL-4 (22). At the pulmonary tissue level, while we detected DC-SIGN-expressing cells with a morphology typical of dendritic cells and lymphocytes (likely B cells), there were also numerous DC-SIGN-expressing cells which also co-express the macrophage marker CD68 and CD163. This is supported by previous reports describing the presence of M2-like cells in the context of tuberculous granulomas structures (25, 34, 35). Beyond the TB context, $CD68^+$ macrophages expressing DC-SIGN were preferentially detected in granuloma lesions in lepromatous leprosy (45), as well as in granuloma-like structures in pathological conditions of dermatological diseases, like granuloma annulare and necrobiosis lipoidica (46). Altogether, these findings confirmed the presence of DC-SIGN-expressing macrophages in different contexts of active TB, which may not be able to mount an appropriate type-1 immune response against Mtb infection, and thus may likely contribute to the pathogenesis of this disease. While limited, these findings provide an important association between the abundance of DC-SIGN expressing macrophages and active TB, and they highlight the need to establish whether these cells actually play a pathophysiological role in this disease.

We demonstrated that DC-SIGN regulates the pro-inflammatory response of M(IL-4) macrophages during Mtb infection. Indeed, this inflammatory profile closely resembles the common response of macrophages to bacterial infections involving the upregulation of genes typical within the spectrum of M1 macrophages (6). If excessive or prolonged, the M1 macrophage response could then be deleterious for the host in terms of tissue damage or organ failure, as demonstrated during *E. coli* infection in baboon experimental peritonitis (47). In addition, a recent study in human microglia supports the immunosuppressive role for DC-SIGN in macrophages against inflammatory insults (40). Garcia-Vallejo et al. elegantly demonstrated that this CLR interacts with fucosylated glycans on myelin oligodendrocyte glycoprotein resulting in the synergistic upregulation of the TLR4-dependent production of the anti-inflammatory cytokine

IL-10 in these macrophages. However, to our surprise, the IL-10 production appears not to be responsible for the dysregulation of pro-inflammatory signals in M(IL-4) macrophages. In human dendritic cells, the activation of DC-SIGN with mycobacterial ManLAM (or agonist antibodies) leads to the synergetic increase of IL-10 if it coincides with TLR4 stimulation with bacterial LPS (17, 48). Based on this well-established crosstalk, we expected the levels of IL-10 to be significantly lower in DC-SIGN-depleted M(IL-4) macrophages compared to control cells, and thus explaining the tilting toward a pro-inflammatory nature. It is likely that human M(IL-4) macrophages differ from dendritic cells (and other cells) in this respect. This is supported by our previous study showing that DC-SIGN does not potentiate IL-10 secretion in LPS-stimulated alveolar macrophages from TB patients, which highly expressed this CLR along with TLR4 (19). Moreover, another key study using humanized DC-SIGN mice demonstrated the anti-inflammatory role of this CLR in macrophages conferring protection against autoimmunity in intravenous immunoglobulin therapy, which is dependent on IL-4 and IL-33 but not IL-10 (39). It is worth mentioning that the physiological role of TLR4 remains to be proven in the context of TB. While Mtb-derived compounds can activate TLR4 *in vitro* (49, 50), it does not appear to affect the *in vivo* immune response against Mtb, as demonstrated in the mouse model (51, 52). Beyond IL-10, we showed a downregulation of protein levels involved in angiogenesis and vascularization (e.g., VEGFA), thrombopoiesis (e.g., THPO), and anti-apoptosis factors (e.g., TRAIL-R3, TRAIL-R4), in the absence of DC-SIGN during Mtb infection. These results infer a decrease of homeostatic functions such as tissue repair and remodeling, which are hallmark functional properties of M(IL-4) macrophages (22, 53, 54), and they support an immunosuppressive role for DC-SIGN in M(IL-4) macrophages that seems independent on the potentiation of IL-10 production, which may represent yet another way for Mtb to control NF-κB-driven pro-inflammatory signals.

We determined that DC-SIGN expression in M(IL-4) macrophages affects their capacity to control the Mtb burden. To our knowledge, this is the first time that deficiency of DC-SIGN in human cells is shown to directly improve the control of bacterial load in the context of infection. This improved control of Mtb burden is neither due to defects in the differentiation or activation of M(IL-4) macrophages, nor due to deficient bacterial recognition or intake by these cells, in the absence of DC-SIGN. In terms of binding, we were greatly surprised that DC-SIGN-depleted M(IL-4) macrophages were able to bind and phagocytose Mtb at the same level as control cells. In the context of DC-SIGN-expressing alveolar macrophages from TB patients, and of the human monocytic cell line expressing DC-SIGN (THP-1:DC-SIGN), we convincingly demonstrated in the past that this CLR contributed majorly to the binding and infection of these cells by Mtb (19). However, one postulate governing M(IL-4) macrophages is the acquisition of an entirely different phagocytic receptor repertoire compared to other macrophages and cell types (22). In addition to DC-SIGN, these cells are characterized by MRC1, MSR1 (macrophage scavenger receptor 1), Dectin-1, DCIR (CLEC4A), DCL-1 (CLEC13A), MGL (CLEC10A), CD36, MS4A4A (CD20-L1), and CD23 (CLEC4J), among others. Thus, it is most likely that the absence of DC-SIGN is compensated by the high abundance of these receptors in M(IL-4) macrophages unlike other cells. Recently, we described that human DC-SIGN-depleted M(IL-4) macrophages became resistant to *Leishmania infantum* infection (30). This improved control of parasite infection was dependent on the high production of IL-1β in macrophages lacking DC-SIGN. In fact, we demonstrated that DC-SIGN downregulated the mRNA expression of *LTA4H* (leukotriene A4 hydrolase), whose enzymatic activity is critical for LTB4 (leukotriene B4) synthesis, and consequently, for the caspase-1-dependent production of IL-1β. In the TB context, this is not the case for DC-SIGN. While we confirmed a significant augmentation of the *IL-1β* mRNA, we did not observe a change in the levels of IL-1β and LTB4 proteins, nor in the *LTA4H* mRNA expression, in DC-SIGN-depleted M(IL-4) macrophages at 18 h *p.i.* (data not shown). Furthermore, there were no changes in mRNA expression of antimicrobial peptides (based on the transcriptomic data), the production of reactive oxygen species, nor in the autophagy flux, between DC-SIGN-depleted and control M(IL-4) macrophages at 18 h *p.i.* (data not shown). Therefore, we inferred there might be alternative microbicidal mechanisms affected by DC-SIGN expression in M(IL-4) macrophages to control the bacilli intracellular burden.

Finally, we shed light on the capacity of DC-SIGN to regulate the pro-inflammatory response and control of bacterial burden driven by Dectin-1. Both CLRs are expressed favorably in M(IL-4) macrophages. Our results demonstrate that Dectin-1 plays a pro-inflammatory and microbicidal role against Mtb. This is in agreement with the fact that Dectin-1 is an ITAM (immunoreceptor tyrosine-based activation motif) immunoreceptor with the capacity to engage a pro-inflammatory response upon engagement with its ligand, including through the activation NFκβ-dependent transcription profile (13). In the context of TB, Dectin-1-depleted mice exhibit reduction of bacterial burden in the lungs, but there are no differences in lung pathology score, cytokine levels, or survival (55). However, in human dendritic cells, Dectin-1 is clearly partially responsible for the pro-inflammatory response against Mtb infection, specifically in the induction of the Th1/Th17 immune response (36, 56). In the case of DC-SIGN, our results propose a role for this CLR to interfere negatively in the pro-inflammatory response to Mtb that is dependent on Dectin-1. The signaling crosstalk between Dectin-1 and DC-SIGN has been reported in the recent past (30, 36, 57). While this crosstalk can be synergistic such as in the case of prostaglandin 2 (PGE_2) production in human dendritic cells, where these receptors are shown to even bind together (57), it can also be the opposite. In Mtb and *L. infantum* infection, DC-SIGN interferes negatively with the production of pro-inflammatory signals triggered by Dectin-1 in human dendritic cells and M(IL-4) macrophages, respectively (30, 36). In this study, while we cannot exclude contribution of other PRRs (e.g., TLR-2), we propose that the pro-inflammatory signature and improved control of Mtb burden in the absence of DC-SIGN must be mainly contributed by Dectin-1. Whether this signaling crosstalk can be translated to other human macrophage subsets expressing both CLRs remains to be confirmed.

In conclusion, most of what we know about DC-SIGN in the field of host–pathogen interaction mainly derives from the work done in human dendritic cells. While both dendritic cells and macrophages perform similar functions, these cells are thought to have different roles in the context of TB. On the one hand, dendritic cells are known as the professional antigen-presenting cell because they possess a great capacity to pick up and process antigens, migrate to secondary lymphoid organs, and present antigenic information to tailor an adaptive immune response against Mtb. On the other hand, macrophages are considered to be the premier effector because they are the first leukocyte to encounter Mtb in the alveolar space and activate the innate immune response to contain and eliminate this pathogen at the site of infection. Our present study brings into focus the anti-inflammatory role of DC-SIGN in M(IL-4) macrophages. Since type-2 inflammatory signals (e.g., IL-4, IL-13) are correlated with TB susceptibility and progression, we believe that DC-SIGN expression in these macrophages is of pertinence and consequence to TB pathogenesis. Indeed, these findings support the notion that Mtb hijacks the immunosuppressive aspects of DC-SIGN to invade and persist in M(IL-4) macrophages and, at the same time, modulate the local inflammatory response by these cells in its favor. Future studies shall focus on the identification of endogenous ligands targeting DC-SIGN to trigger the wound healing and tissue remodeling activity of M(IL-4) macrophages for the benefit of the patient in lung inflammatory disease. Furthermore, we believe these results can be extrapolated from the context of TB into parasitology, as M(IL-4) macrophages are considered as essential effector cells in parasite eradication (22). All things considered, beyond the role of DC-SIGN in macrophages, this study also points toward the need to investigate the pathophysiological impact of IL4 and other type-2 immune signals in the TB context, which remains unknown.

ETHICS STATEMENT

Ethics Statement for Non-Human Primate Samples: In the Netherlands, the NHP study protocol was done to comply with the EC Directive 86/609/EEC, approved by the local independent ethics committee prior to the start of the study, and executed under Dutch law on animal experiments (agreement number DEC#579). The endpoint for any particular animal was based either by signs of severe disease (human endpoint criteria, referring to animal condition by adverse body weight development, respiratory capacity and animal behavior) or by protocol, which limited the follow-up time to 1-year postinfection. Ethic Statement for Human Samples: In Argentina, blood samples from HS or TB patients were provided by the Blood Transfusion Service, Hospital Fernandez, Buenos Aires (agreement number CEIANM-52-5-2012), or the Hospital F. J. Muñiz, Buenos Aires (protocol number: NIN-1671-12). PE were obtained by therapeutic thoracentesis by physicians at the Hospital F. J. Muñiz (Buenos Aires). The research was carried out in accordance with the Declaration of Helsinki (2013) of the World Medical Association, and was approved by the Ethics Committees of the Hospital F. J. Muñiz and the Academia Nacional de Medicina de Buenos Aires (protocol number: NIN-1671-12). Written informed consent was obtained before sample collection. The diagnosis of TB pleurisy was based on a positive Ziehl–Nielsen staining or Lowestein–Jensen culture from PE and/or histopathology of pleural biopsy, and was further confirmed by an Mtb-induced IFN-γ response and an ADA-positive test (27). Mononuclear cells from PB and PE were isolated by Ficoll-Hypaque gradient centrifugation (Pharmacia, Uppsala, Sweden), as described previously (25, 28). In France, monocytes from HS were isolated from buffy coat provided by Etablissement Français du Sang, Toulouse, under contract 21/PLER/TOU/IPBS01/2013-0042. According to articles L1243-4 and R1243-61 of the French Public Health Code, the contract was approved by the French Ministry of Science and Technology (agreement number AC 2009-921). Donors signed and provided written informed consents before sample collection.

AUTHOR CONTRIBUTIONS

Conceptualization and methodology: GL-V, AT, LB, CL, CC, and ON. Software: IM. Investigation: GL-V, AT, LB, CL, CD, IM, AB, FC, TS, RP, IK, and CC. Resources: FV, IM-P, MS, and ON. Writing: GL-V and ON. Visualization: TS, CC, and RP. Supervision: GL-V and ON. Corresponding author: GL-V.

ACKNOWLEDGMENTS

We acknowledge P. Constant and F. Levillan, and the BSL3 facilities at IPBS including the newly created multi-pathogen laboratory; the flow cytometry facility and personnel at TRI-IPBS, in particular C. Bordier; J. Nigou for providing reagents; and I. Vergne for expertise and technical support provided in the assessment of autophagy. We greatly thank D. Hudrisier, C. Gutierrez, C. Vérollet, B. Raynaud, M. Dupont, L. Bernard, and C. A. Spinner, for critical reading of the manuscript and helpful comments.

FUNDING

This work was supported in part by ECOS-Sud (A14S01), *Laboratoire International Associé* (LIA, No. 1167), the *Centre National de la Recherche Scientifique*, the *Université Paul Sabatier*, the *Agence Nationale de la Recherche* (ANR 2010–01301, ANR14–CE11–0020–02, ANR16–CE13–0005–01, ANR–11–EQUIPEX–0003), the *Fondation pour la Recherche Médicale* (DEQ2016 0334894; DEQ2016 0334902), the *Fondation Bettencourt–Schueller*, and the Argentinean National Agency of Promotion of Science and Technology (PICT-2015-0055). FV acknowledges support from Aeras (Rockville, MD, USA). GL-V acknowledges support by FRM (SPF20110421334).

SUPPLEMENTARY MATERIAL

The Supplementary Material for this article can be found online at https://www.frontiersin.org/articles/10.3389/fimmu.2018.01123/full#supplementary-material.

REFERENCES

1. Houben RM, Dodd PJ. The global burden of latent tuberculosis infection: a re-estimation using mathematical modelling. *PLoS Med* (2016) 13:e1002152. doi:10.1371/journal.pmed.1002152
2. Dorhoi A, Reece ST, Kaufmann SH. For better or for worse: the immune response against *Mycobacterium tuberculosis* balances pathology and protection. *Immunol Rev* (2011) 240:235–51. doi:10.1111/j.1600-065X.2010.00994.x
3. Ernst JD. The immunological life cycle of tuberculosis. *Nat Rev Immunol* (2012) 12:581–91. doi:10.1038/nri3259
4. O'Garra A, Redford PS, McNab FW, Bloom CI, Wilkinson RJ, Berry MP. The immune response in tuberculosis. *Annu Rev Immunol* (2013) 31:475–527. doi:10.1146/annurev-immunol-032712-095939
5. Rajaram MV, Ni B, Dodd CE, Schlesinger LS. Macrophage immunoregulatory pathways in tuberculosis. *Semin Immunol* (2014) 26:471–85. doi:10.1016/j.smim.2014.09.010
6. Benoit M, Desnues B, Mege JL. Macrophage polarization in bacterial infections. *J Immunol* (2008) 181:3733–9. doi:10.4049/jimmunol.181.6.3733
7. Lugo-Villarino G, Neyrolles O. Manipulation of the mononuclear phagocyte system by *Mycobacterium tuberculosis*. *Cold Spring Harb Perspect Med* (2014) 4:a018549. doi:10.1101/cshperspect.a018549
8. Mege JL, Mehraj V, Capo C. Macrophage polarization and bacterial infections. *Curr Opin Infect Dis* (2011) 24:230–4. doi:10.1097/QCO.0b013e328344b73e
9. Wynn TA, Chawla A, Pollard JW. Macrophage biology in development, homeostasis and disease. *Nature* (2013) 496:445–55. doi:10.1038/nature12034
10. Lugo-Villarino G, Verollet C, Maridonneau-Parini I, Neyrolles O. Macrophage polarization: convergence point targeted by *Mycobacterium tuberculosis* and HIV. *Front Immunol* (2011) 2:43. doi:10.3389/fimmu.2011.00043
11. Lugo-Villarino G, Hudrisier D, Tanne A, Neyrolles O. C-type lectins with a sweet spot for *Mycobacterium tuberculosis*. *Eur J Microbiol Immunol* (2011) 1:25–40. doi:10.1556/EuJMI.1.2011.1.6
12. Robinson MJ, Sancho D, Slack EC, LeibundGut-Landmann S, Reis e Sousa C. Myeloid C-type lectins in innate immunity. *Nat Immunol* (2006) 7:1258–65. doi:10.1038/ni1417
13. Sancho D, Reis e Sousa C. Signaling by myeloid C-type lectin receptors in immunity and homeostasis. *Ann Rev Immunol* (2012) 30:491–529. doi:10.1146/annurev-immunol-031210-101352
14. van Kooyk Y, Geijtenbeek TB. DC-SIGN: escape mechanism for pathogens. *Nat Rev Immunol* (2003) 3:697–709. doi:10.1038/nri1182
15. Yonekawa A, Saijo S, Hoshino Y, Miyake Y, Ishikawa E, Suzukawa M, et al. Dectin-2 is a direct receptor for mannose-capped lipoarabinomannan of mycobacteria. *Immunity* (2014) 41:402–13. doi:10.1016/j.immuni.2014.08.005
16. Geijtenbeek TB, Van Vliet SJ, Koppel EA, Sanchez-Hernandez M, Vandenbroucke-Grauls CM, Appelmelk B, et al. Mycobacteria target DC-SIGN to suppress dendritic cell function. *J Exp Med* (2003) 197:7–17. doi:10.1084/jem.20021229
17. Gringhuis SI, den Dunnen J, Litjens M, van der Vlist M, Geijtenbeek TB. Carbohydrate-specific signaling through the DC-SIGN signalosome tailors immunity to *Mycobacterium tuberculosis*, HIV-1 and *Helicobacter pylori*. *Nat Immunol* (2009) 10:1081–8. doi:10.1038/ni.1778
18. Neyrolles O, Gicquel B, Quintana-Murci L. Towards a crucial role for DC-SIGN in tuberculosis and beyond. *Trends Microbiol* (2006) 14:383–7. doi:10.1016/j.tim.2006.07.007
19. Tailleux L, Pham-Thi N, Bergeron-Lafaurie A, Herrmann JL, Charles P, Schwartz O, et al. DC-SIGN induction in alveolar macrophages defines privileged target host cells for mycobacteria in patients with tuberculosis. *PLoS Med* (2005) 2:e381. doi:10.1371/journal.pmed.0020381
20. Tailleux L, Schwartz O, Herrmann JL, Pivert E, Jackson M, Amara A, et al. DC-SIGN is the major *Mycobacterium tuberculosis* receptor on human dendritic cells. *J Exp Med* (2003) 197:121–7. doi:10.1084/jem.20021468
21. Garcia-Vallejo JJ, van Kooyk Y. The physiological role of DC-SIGN: a tale of mice and men. *Trends Immunol* (2013) 34:482–6. doi:10.1016/j.it.2013.03.001
22. Martinez FO, Helming L, Gordon S. Alternative activation of macrophages: an immunologic functional perspective. *Annu Rev Immunol* (2009) 27:451–83. doi:10.1146/annurev.immunol.021908.132532
23. Murray PJ, Allen JE, Biswas SK, Fisher EA, Gilroy DW, Goerdt S, et al. Macrophage activation and polarization: nomenclature and experimental guidelines. *Immunity* (2014) 41:14–20. doi:10.1016/j.immuni.2014.06.008
24. Vogt G, Nathan C. In vitro differentiation of human macrophages with enhanced antimycobacterial activity. *J Clin Invest* (2011) 121:3889–901. doi:10.1172/JCI57235
25. Lastrucci C, Benard A, Balboa L, Pingris K, Souriant S, Poincloux R, et al. Tuberculosis is associated with expansion of a motile, permissive and immunomodulatory CD16(+) monocyte population via the IL-10/STAT3 axis. *Cell Res* (2015) 25:1333–51. doi:10.1038/cr.2015.123
26. Lin PL, Rodgers M, Smith L, Bigbee M, Myers A, Bigbee C, et al. Quantitative comparison of active and latent tuberculosis in the cynomolgus macaque model. *Infect Immun* (2009) 77:4631–42. doi:10.1128/IAI.00592-09
27. Light RW. Update on tuberculous pleural effusion. *Respirology* (2010) 15:451–8. doi:10.1111/j.1440-1843.2010.01723.x
28. Balboa L, Romero MM, Basile JI, Sabio y Garcia CA, Schierloh P, Yokobori N, et al. Paradoxical role of CD16+CCR2+CCR5+ monocytes in tuberculosis: efficient APC in pleural effusion but also mark disease severity in blood. *J Leukoc Biol* (2011) 90:69–75. doi:10.1189/jlb.1010577
29. Troegeler A, Lastrucci C, Duval C, Tanne A, Cougoule C, Maridonneau-Parini I, et al. An efficient siRNA-mediated gene silencing in primary human monocytes, dendritic cells and macrophages. *Immunol Cell Biol* (2014) 92:699–708. doi:10.1038/icb.2014.39
30. Lefevre L, Lugo-Villarino G, Meunier E, Valentin A, Olagnier D, Authier H, et al. The C-type lectin receptors dectin-1, MR, and SIGNR3 contribute both positively and negatively to the macrophage response to *Leishmania infantum*. *Immunity* (2013) 38:1038–49. doi:10.1016/j.immuni.2013.04.010
31. Camilli G, Eren E, Williams DL, Aimanianda V, Meunier E, Quintin J. Impaired phagocytosis directs human monocyte activation in response to fungal derived β-glucan particles. *Eur J Immunol* (2018). doi:10.1002/eji.201747224
32. Troegeler A, Mercier I, Cougoule C, Pietretti D, Colom A, Duval C, et al. C-type lectin receptor DCIR modulates immunity to tuberculosis by sustaining type I interferon signaling in dendritic cells. *Proc Natl Acad Sci U S A* (2017) 114:E540–9. doi:10.1073/pnas.1613254114
33. Wang C, Peyron P, Mestre O, Kaplan G, van Soolingen D, Gao Q, et al. Innate immune response to *Mycobacterium tuberculosis* Beijing and other genotypes. *PLoS One* (2010) 5:e13594. doi:10.1371/journal.pone.0013594
34. Lugo-Villarino G, Hudrisier D, Benard A, Neyrolles O. Emerging trends in the formation and function of tuberculosis granulomas. *Front Immunol* (2013) 3:405. doi:10.3389/fimmu.2012.00405
35. Mattila JT, Ojo OO, Kepka-Lenhart D, Marino S, Kim JH, Eum SY, et al. Microenvironments in tuberculous granulomas are delineated by distinct populations of macrophage subsets and expression of nitric oxide synthase and arginase isoforms. *J Immunol* (2013) 191:773–84. doi:10.4049/jimmunol.1300113
36. Zenaro E, Donini M, Dusi S. Induction of Th1/Th17 immune response by *Mycobacterium tuberculosis*: role of dectin-1, mannose receptor, and DC-SIGN. *J Leukoc Biol* (2009) 86:1393–401. doi:10.1189/jlb.0409242
37. Court N, Vasseur V, Vacher R, Fremond C, Shebzukhov Y, Yeremeev VV, et al. Partial redundancy of the pattern recognition receptors, scavenger receptors, and C-type lectins for the long-term control of *Mycobacterium tuberculosis* infection. *J Immunol* (2010) 184:7057–70. doi:10.4049/jimmunol.1000164
38. Garcia-Vallejo JJ, van Kooyk Y. DC-SIGN: the strange case of Dr. Jekyll and Mr. Hyde. *Immunity* (2015) 42:983–5. doi:10.1016/j.immuni.2015.05.021
39. Anthony RM, Kobayashi T, Wermeling F, Ravetch JV. Intravenous gammaglobulin suppresses inflammation through a novel T(H)2 pathway. *Nature* (2011) 475:110–3. doi:10.1038/nature10134
40. Garcia-Vallejo JJ, Ilarregui JM, Kalay H, Chamorro S, Koning N, Unger WW, et al. CNS myelin induces regulatory functions of DC-SIGN-expressing, antigen-presenting cells via cognate interaction with MOG. *J Exp Med* (2014) 211:1465–83. doi:10.1084/jem.20122192
41. Tacken PJ, de Vries IJ, Gijzen K, Joosten B, Wu D, Rother RP, et al. Effective induction of naive and recall T-cell responses by targeting antigen to human dendritic cells via a humanized anti-DC-SIGN antibody. *Blood* (2005) 106:1278–85. doi:10.1182/blood-2005-01-0318
42. Unger WW, van Beelen AJ, Bruijns SC, Joshi M, Fehres CM, van Bloois L, et al. Glycan-modified liposomes boost CD4+ and CD8+ T-cell responses by targeting DC-SIGN on dendritic cells. *J Control Release* (2012) 160:88–95. doi:10.1016/j.jconrel.2012.02.007

43. Aoe K, Hiraki A, Murakami T, Murakami K, Makihata K, Takao K, et al. Relative abundance and patterns of correlation among six cytokines in pleural fluid measured by cytometric bead array. *Int J Mol Med* (2003) 12:193–8. doi:10.3892/ijmm.12.2.193
44. Chen K, Feng PH, Chang CC, Chen TT, Chuang HC, Lee CN, et al. Novel biomarker analysis of pleural effusion enhances differentiation of tuberculous from malignant pleural effusion. *Int J Gen Med* (2016) 9:183–9. doi:10.2147/IJGM.S100237
45. Soilleux EJ, Sarno EN, Hernandez MO, Moseley E, Horsley J, Lopes UG, et al. DC-SIGN association with the Th2 environment of lepromatous lesions: cause or effect? *J Pathol* (2006) 209:182–9. doi:10.1002/path.1972
46. Torocsik D, Bardos H, Hatalyak Z, Dezso B, Losonczy G, Paragh L, et al. Detection of factor XIII-A is a valuable tool for distinguishing dendritic cells and tissue macrophages in granuloma annulare and necrobiosis lipoidica. *J Eur Acad Dermatol Venereol* (2014) 28:1087–96. doi:10.1111/jdv.12290
47. Mehta A, Brewington R, Chatterji M, Zoubine M, Kinasewitz GT, Peer GT, et al. Infection-induced modulation of m1 and m2 phenotypes in circulating monocytes: role in immune monitoring and early prognosis of sepsis. *Shock* (2004) 22:423–30. doi:10.1097/01.shk.0000142184.49976.0c
48. Gringhuis SI, den Dunnen J, Litjens M, van Het Hof B, van Kooyk Y, Geijtenbeek TB. C-type lectin DC-SIGN modulates toll-like receptor signaling via Raf-1 kinase-dependent acetylation of transcription factor NF-kappaB. *Immunity* (2007) 26:605–16. doi:10.1016/j.immuni.2007.03.012
49. Means TK, Wang S, Lien E, Yoshimura A, Golenbock DT, Fenton MJ. Human toll-like receptors mediate cellular activation by *Mycobacterium tuberculosis*. *J Immunol* (1999) 163:3920–7.
50. Takeuchi O, Takeda K, Hoshino K, Adachi O, Ogawa T, Akira S. Cellular responses to bacterial cell wall components are mediated through MyD88-dependent signaling cascades. *Int Immunol* (2000) 12:113–7. doi:10.1093/intimm/12.1.113
51. Holscher C, Reiling N, Schaible UE, Holscher A, Bathmann C, Korbel D, et al. Containment of aerogenic *Mycobacterium tuberculosis* infection in mice does not require MyD88 adaptor function for TLR2, -4 and -9. *Eur J Immunol* (2008) 38:680–94. doi:10.1002/eji.200736458
52. Reiling N, Holscher C, Fehrenbach A, Kroger S, Kirschning CJ, Goyert S, et al. Cutting edge: toll-like receptor (TLR)2- and TLR4-mediated pathogen recognition in resistance to airborne infection with *Mycobacterium tuberculosis*. *J Immunol* (2002) 169:3480–4. doi:10.4049/jimmunol.169.7.3480
53. Mantovani A, Biswas SK, Galdiero MR, Sica A, Locati M. Macrophage plasticity and polarization in tissue repair and remodelling. *J Pathol* (2013) 229:176–85. doi:10.1002/path.4133
54. Mosser DM, Edwards JP. Exploring the full spectrum of macrophage activation. *Nat Rev Immunol* (2008) 8:958–69. doi:10.1038/nri2448
55. Marakalala MJ, Guler R, Matika L, Murray G, Jacobs M, Brombacher F, et al. The Syk/CARD9-coupled receptor dectin-1 is not required for host resistance to *Mycobacterium tuberculosis* in mice. *Microbes Infect* (2011) 13:198–201. doi:10.1016/j.micinf.2010.10.013
56. van de Veerdonk FL, Teirlinck AC, Kleinnijenhuis J, Kullberg BJ, van Crevel R, van der Meer JW, et al. *Mycobacterium tuberculosis* induces IL-17A responses through TLR4 and dectin-1 and is critically dependent on endogenous IL-1. *J Leukoc Biol* (2010) 88:227–32. doi:10.1189/jlb.0809550
57. Valera I, Fernandez N, Trinidad AG, Alonso S, Brown GD, Alonso A, et al. Costimulation of dectin-1 and DC-SIGN triggers the arachidonic acid cascade in human monocyte-derived dendritic cells. *J Immunol* (2008) 180:5727–36. doi:10.4049/jimmunol.180.8.5727

Conflict of Interest Statement: The authors declare that the research was conducted in the absence of any commercial or financial relationships that could be construed as a potential conflict of interest.

Copyright © 2018 Lugo-Villarino, Troegeler, Balboa, Lastrucci, Duval, Mercier, Bénard, Capilla, Al Saati, Poincloux, Kondova, Verreck, Cougoule, Maridonneau-Parini, Sasiain and Neyrolles. This is an open-access article distributed under the terms of the Creative Commons Attribution License (CC BY). The use, distribution or reproduction in other forums is permitted, provided the original author(s) and the copyright owner are credited and that the original publication in this journal is cited, in accordance with accepted academic practice. No use, distribution or reproduction is permitted which does not comply with these terms.

frontiers in Immunology

ORIGINAL RESEARCH
published: 09 March 2018
doi: 10.3389/fimmu.2018.00459

Formation of Foamy Macrophages by Tuberculous Pleural Effusions Is Triggered by the Interleukin-10/Signal Transducer and Activator of Transcription 3 Axis through ACAT Upregulation

*Melanie Genoula[1,2,3], José Luis Marín Franco[1,2,3†], Maeva Dupont[2,3,4†], Denise Kviatcovsky[1,2,3], Ayelén Milillo[5], Pablo Schierloh[1,2,3], Eduardo Jose Moraña[6], Susana Poggi[6], Domingo Palmero[6], Dulce Mata-Espinosa[7], Erika González-Domínguez[8], Juan Carlos León Contreras[7], Paula Barrionuevo[5], Bárbara Rearte[5], Marlina Olyissa Córdoba Moreno[5], Adriana Fontanals[9], Agostina Crotta Asis[10], Gabriela Gago[10], Céline Cougoule[2,3,4], Olivier Neyrolles[2,3,4], Isabelle Maridonneau-Parini[2,3,4], Carmen Sánchez-Torres[8], Rogelio Hernández-Pando[7], Christel Vérollet[2,3,4†], Geanncarlo Lugo-Villarino[2,3,4†], María del Carmen Sasiain[1,2,3†] and Luciana Balboa[1,2,3]**

[1] Laboratorio de Inmunología de Enfermedades Respiratorias, Instituto de Medicina Experimental (IMEX)-CONICET, Academia Nacional de Medicina, Buenos Aires, Argentina, [2] International Associated Laboratory (LIA) CNRS IM-TB/HIV (1167), Toulouse, France, [3] International Associated Laboratory (LIA) CNRS IM-TB/HIV (1167), Buenos Aires, Argentina, [4] Institut de Pharmacologie et de Biologie Structurale, Université de Toulouse, CNRS, UPS, Toulouse, France, [5] Laboratorio de Fisiología de los Procesos Inflamatorios, Instituto de Medicina Experimental (IMEX)-CONICET, Academia Nacional de Medicina, Buenos Aires, Argentina, [6] Instituto Prof. Dr. Raúl Vaccarezza, Hospital de Infecciosas Dr. F. J. Muñiz, Buenos Aires, Argentina, [7] Sección de Patología Experimental, Departamento de Patología, Instituto Nacional de Ciencias Médicas y Nutrición Salvador Zubirán, Mexico City, Mexico, [8] Departamento de Biomedicina Molecular, Centro de Investigación y de Estudios Avanzados del Instituto Politécnico Nacional, Mexico City, Mexico, [9] Fundación Instituto Leloir, CABA, Buenos Aires, Argentina, [10] Laboratory of Physiology and Genetics of Actinomycetes, Instituto de Biología Molecular y Celular de Rosario (IBR-CONICET), Facultad de Ciencias Bioquímicas y Farmacéuticas, Universidad Nacional de Rosario, Rosario, Argentina

The ability of *Mycobacterium tuberculosis* (Mtb) to persist in its human host relies on numerous immune evasion strategies, such as the deregulation of the lipid metabolism leading to the formation of foamy macrophages (FM). Yet, the specific host factors leading to the foamy phenotype of Mtb-infected macrophages remain unknown. Herein, we aimed to address whether host cytokines contribute to FM formation in the context of Mtb infection. Our approach is based on the use of an acellular fraction of tuberculous pleural effusions (TB-PE) as a physiological source of local factors released during Mtb infection. We found that TB-PE induced FM differentiation as observed by the increase in lipid bodies, intracellular cholesterol, and expression of the scavenger receptor CD36, as well as the enzyme acyl CoA:cholesterol acyl transferase (ACAT). Importantly, interleukin-10 (IL-10) depletion from TB-PE prevented the augmentation of all these parameters. Moreover, we observed a positive correlation between the levels of IL-10 and the number of lipid-laden $CD14^+$ cells among the pleural cells in TB patients, demonstrating that FM differentiation occurs within the pleural environment. Downstream of IL-10 signaling, we

OPEN ACCESS

Edited by:
Christoph Hölscher, Forschungszentrum Borstel (LG), Germany

Reviewed by:
Peter Murray, Max Planck Institute of Biochemistry (MPG), Germany
Joseph E. Qualls, Cincinnati Children's Research Foundation, United States
Robin James Flynn, University of Liverpool, United Kingdom

***Correspondence:**
Luciana Balboa
luciana_balboa@hotmail.com

†These authors have contributed equally to this work.

Specialty section:
This article was submitted to Microbial Immunology, a section of the journal Frontiers in Immunology

Received: *30 November 2017*
Accepted: *20 February 2018*
Published: *09 March 2018*

Citation:
Genoula M, Marín Franco JL, Dupont M, Kviatcovsky D, Milillo A, Schierloh P, Moraña EJ, Poggi S, Palmero D, Mata-Espinosa D, González-Domínguez E, León Contreras JC, Barrionuevo P, Rearte B, Córdoba Moreno MO, Fontanals A, Crotta Asis A, Gago G, Cougoule C, Neyrolles O, Maridonneau-Parini I, Sánchez-Torres C, Hernández-Pando R, Vérollet C, Lugo-Villarino G, Sasiain MdC and Balboa L (2018) Formation of Foamy Macrophages by Tuberculous Pleural Effusions Is Triggered by the Interleukin-10/Signal Transducer and Activator of Transcription 3 Axis through ACAT Upregulation. Front. Immunol. 9:459. doi: 10.3389/fimmu.2018.00459

noticed that the transcription factor signal transducer and activator of transcription 3 was activated by TB-PE, and its chemical inhibition prevented the accumulation of lipid bodies and ACAT expression in macrophages. In terms of the host immune response, TB-PE-treated macrophages displayed immunosuppressive properties and bore higher bacillary loads. Finally, we confirmed our results using bone marrow-derived macrophage from IL-10$^{-/-}$ mice demonstrating that IL-10 deficiency partially prevented foamy phenotype induction after Mtb lipids exposure. In conclusion, our results evidence a role of IL-10 in promoting the differentiation of FM in the context of Mtb infection, contributing to our understanding of how alterations of the host metabolic factors may favor pathogen persistence.

Keywords: ACAT, interleukin-10, foamy macrophages, lipids, signal transducer and activator of transcription 3, tuberculosis

INTRODUCTION

Tuberculosis (TB) is a highly contagious disease caused by *Mycobacterium tuberculosis* (Mtb) infection. Even though the treatment of the disease has been standardized for a while, TB still remains one of the top 10 causes of death worldwide with 10.4 million new cases and 1.3 million deaths from TB among HIV-negative people in 2016 (1). Chronic host–pathogen interaction in TB leads to extensive metabolic remodeling in both the host and the pathogen (2). In fact, the success of Mtb as a pathogen derives from its efficient adaptation to the intracellular milieu of human macrophages. An important strategy to reach this metabolic adaptation is the promotion of lipid body accumulation by the host macrophage leading to foamy macrophages (FM) differentiation. The formation of lipid-laden macrophages is caused by infectious agents through deregulation in the balance between the influx and efflux of lipids. Key for the biogenesis of lipid bodies is the enzyme acyl CoA:cholesterol acyltransferase (ACAT), which represents an ideal target for pathogens (3).

Lipid body accumulation within leukocytes is a common feature in both clinical and experimental infections, especially in mycobacterial infections (4, 5). Mtb infection leads to the induction of FM, a process which is promoted by several mycobacterial lipids (6–8). This event enables the fusion between Mtb-containing phagosomes and lipid bodies resulting in an abundant supply of lipids for the pathogen (7), allowing Mtb to switch into a dormancy phenotype and to become tolerant to several front-line antibiotics (9). For this reason, lipid bodies are considered to be a secure niche for Mtb conferring protection from bactericidal mechanisms, such as respiratory burst (10). Moreover, the presence of FM within granulomatous structures was demonstrated in both experimentally infected animals and patients, especially in individuals developing secondary TB (5, 11). Therefore, FM may play a central role in mycobacterial persistence and reactivation (12, 13).

Concerning the impact of FM on the host immunity against Mtb, it was shown that human macrophages exposed to lipids prior to Mtb infection failed to produce TNF-α and to clear the infection (14, 15). Taking into account that FM generated prior to Mtb infection impair the host immune response, there is a keen interest to identify the host-derived cytokines released at the site of Mtb infection, and to understand how these signals contribute to FM differentiation and alter host defense against Mtb. In this regard, it is well known that different activation programs in macrophages driven by pro or anti-inflammatory cytokines are associated to changes in the lipid metabolism (16). Therefore, it is likely that host cytokines produced in response to Mtb infection contribute to lipids turnover promoting FM formation, and consequently lead to Mtb persistence.

In this work, we report that a TB-associated microenvironment induces FM differentiation program dependent partially on the interleukin-10 (IL-10)/signal transducer and activator of transcription 3 (STAT3) axis through ACAT upregulation. Our approach was to model a genuine TB-associated microenvironment by employing a physiological relevant sample derived from active TB patients, such as the acellular fraction of tuberculous pleural effusions (TB-PE). Indeed, TB-PE are manifested in up to 30% of patients with TB, and they are caused by the spread of Mtb into the pleural space and subsequent local inflammation and recruitment of leukocytes (17). Based on this, we show that the acquisition of the foamy phenotype with immunosuppressive properties involves high IL-10 release, low TNF-α production, impaired Th1 activation, and high bacillary loads. We also confirmed that IL-10-deficiency in bone marrow-derived macrophages (BMDM) prevented partially foamy phenotype induction upon exposure to Mtb lipids. In conclusion, our results provide evidence for a role of IL-10 in promoting foamy differentiation of macrophages in the context of Mtb infection.

MATERIALS AND METHODS

Bacterial Strain and Antigens

Mycobacterium tuberculosis H37Rv strain was grown at 37°C in Middlebrook 7H9 medium (Difco) supplemented with 10% albumin-dextrose-catalase (Difco) and 0.05% Tween-80 (Sigma-Aldrich). The Mtb γ-irradiated H37Rv strain (NR-49098) and its total lipids' preparation (NR-14837) were obtained from BEI Resource, USA.

Preparation of Human Monocyte-Derived Macrophages (MDM)

Buffy coats from healthy donors were prepared at *Centro Regional de Hemoterapia Garrahan* (Buenos Aires, Argentina) according to institutional guidelines (resolution number CEIANM-664/07). Informed consent was obtained from each donor before blood collection. Peripheral blood mononuclear cells were obtained by Ficoll gradient separation on Ficoll-Paque (GE Healthcare). Then, monocytes were purified by centrifugation on a discontinuous Percoll gradient (Amersham) as previously described (18). After that, monocytes were allowed to adhere to 24-well plates (Costar) at 5×10^5 cells/well for 1 h at 37°C in warm RPMI-1640 medium (GIBCO). The cells were then washed with warm PBS twice. The final purity was checked by fluorescence-activated cell sorting analysis using an anti-CD14 monoclonal antibody (mAb) and was found to be >90%. The medium was then supplemented to a final concentration of 10% fetal bovine serum (FBS, Sigma-Aldrich) and human recombinant Macrophage Colony-Stimulating Factor (M-CSF, Peprotech) at 10 ng/ml. Cells were allowed to differentiate for 5–7 days.

Preparation of Pleural Effusion (PE) Pools

Pleural effusions were obtained by therapeutic thoracentesis by physicians at the *Hospital F. J Muñiz* (Buenos Aires, Argentina). The research was carried out in accordance with the Declaration of Helsinki (2013) of the World Medical Association, and was approved by the Ethics Committees of the *Hospital F. J Muñiz* and the *Academia Nacional de Medicina de Buenos Aires* (protocol number: NIN-1671-12). Written informed consent was obtained before sample collection. We collected a total of 43 PE samples which were classified according to their etiology, being 38 of them associated to TB (TB-PE) and 5 to heart failure (HF-PE). Individual samples of confirmed TB patients were used for correlation analysis. A group of samples ($n = 10$) were pooled and used for *in vitro* assays to treat macrophages. The selection of these samples was based merely on practical reasons, involving those samples that have been collected earlier through the course of this study. The diagnosis of TB pleurisy was based on a positive Ziehl–Nielsen stain or Lowestein–Jensen culture from PE and/or histopathology of pleural biopsy, and was further confirmed by an Mtb-induced IFN-γ response and an ADA-positive test (19). Exclusion criteria included a positive HIV test, and the presence of concurrent infectious diseases or non-infectious conditions (cancer, diabetes, or steroid therapy). None of the patients had multidrug-resistant TB. Those PE samples derived from patients with pleural transudates secondary to heart failure (HF-PE, $n = 5$) were employed to prepare a second pool of PE, used as control of non-infectious inflammatory PE. The PE were collected in heparin tubes and centrifuged at 300 *g* for 10 min at room temperature without brake. The cell-free supernatant was transferred into new plastic tubes, further centrifuged at 12,000 *g* for 10 min and aliquots were stored at −80°C. After having the diagnosis of the PE, pools were prepared by mixing same amounts of individual PE associated to a specific etiology. The pools were decomplemented at 56°C for 30 min, and filtered by 0.22 µm in order to remove any remaining debris or residual bacteria.

FM Induction

Macrophages were plated on glass coverslips within a 24-well tissue culture plate (Costar) at a density of 5×10^5 cells/ml per well with or without 20% v/v of PE, 10 µg/ml of Mtb lipids (BEI resources) or infected with Mtb (MOI 2:1) for 24 h. When indicated, cells were pre-incubated with either Cucurbitacin I (50–100 nM, Sigma-Aldrich), or the STAT3 inhibitor Stattic (1–20 µM, Sigma-Aldrich), or the ACAT inhibitor Sandoz 58-035 (5–50 µg/ml, Sigma-Aldrich) for 2 h prior TB-PE addition and for further 24 h during TB-PE incubation. DMSO alone was used as control. Alternatively, cells were treated with recombinant human IL-10 (Peprotech) at the indicated doses. Foam cell formation was followed by Oil Red O (ORO) staining (Sigma-Aldrich) as previously described (20) at 37°C for 1–5 min, and washed with water three times. For the visualization of the lipid bodies, slides were prepared using the aqueous mounting medium Poly-Mount (Polysciences), observed *via* light microscope (Leica) and finally photographed using the Leica Application Suite software. Alternatively, after fixation, cells were labeled with 1 µg/ml of BODIPY 493/503 (Life technologies) for 15 min in order to visualize the lipid bodies by green fluorescence emission using a confocal microscope (Olympus BX51).

Infection of Human Macrophages with Mtb

Infections were performed in the biosafety level 3 laboratory at the *Unidad Operativa Centro de Contención Biológica, ANLIS-MALBRAN* (Buenos Aires), according to the biosafety institutional guidelines. Macrophages seeded on glass coverslips within a 24-well tissue culture plate (Costar) at a density of 5×10^5 cells/ml were infected with Mtb H37Rv strain at a MOI of 2:1 during 1 h at 37°C. Then, extracellular bacteria were removed gently by washing with pre-warmed PBS, and cells were cultured in RPMI-1640 medium supplemented with 10% FBS and gentamicin (50 µg/ml) for 24 h. The glass coverslips were fixed with PFA 4% and stained with ORO, as was previously described.

Quantification of Total Cholesterol

Total cholesterol was determined in TB-PE or cell lysates using the *Colestat Enzimatico kit* according to manufacturer instructions (Wiener Lab, Argentina). This assay is based in Trinder reaction in which cholesterol in the sample is quantified by enzymatic hydrolysis of cholesterol esters (21).

Lipid Analysis

Total lipids were extracted from the same number of macrophages with methanol/chloroform (2:1 v/v) as described by Bligh and Dyer (22). After extraction, lipids were dried and analyzed by thin layer chromatography on silica gel 60 F254 plates (Merck), using hexane/diethyl ether/acetic acid (75:25:1, v/v/v) as the developing solvent. Chemical staining with Cu-phosphoric was used for detection.

Phenotypic Characterization by Flow Cytometry

Macrophages were centrifuged for 7 min at 1,200 rpm and then stained for 40 min at 4°C with fluorophore-conjugated antibodies

FITC-anti-CD36 (clone 5-271), PerCP.Cy5.5-anti-CD14 (clone HCD14), PE-anti-CD163 (clone GHI/61), FITC-anti-CD206 (clone C068C2) (Biolegend), FITC-anti-HLA-DR (clone G46-6), or PE-anti-CD274 (clone MIH1) (BD Biosciences), and in parallel, with the corresponding isotype control antibody. After staining, the cells were washed with PBS 1×, centrifuged and analyzed by flow cytometry using FACSCalibur cytometer (BD Biosciences). The median fluorescence intensity were analyzed using FCS Express V3 software (*De Novo* Software, Los Angeles, CA, USA). The mean of the median fluorescence intensities (MFI) of the independent assays were used for comparisons between experimental conditions.

Soluble Cytokine Determinations

The amounts of human TNF-α, IL-1β, IL-10, IL-6, IFN-γ, and IL-4 were measured by ELISA, according to manufacturers' instructions kits (TNF-α, IL-4, and IFN-γ Ready-SET-Go!™ Kits from eBioscience; IL-10, IL-1β, and IL-6 ELISA MAX™ Deluxe Kits from Biolegend). The detection limit was 3 pg/ml for TNF-α; 8 pg/ml for IL-10 and IL-6; 6.25 pg/ml for IFN-γ and IL-4; and 15.6 pg/ml for IL-1β. Murine TNF-α and IL-10 were measured by ELISA, according to manufacturer's instructions (OptEIA™ Set kits from BD Bioscience) with a detection limit at 30 pg/ml.

Cytokine Depletions of PE

Tuberculosis-PE were incubated with 10 µg/ml of the following neutralizing antibodies for 1 h at 4°C for the specific depletion of IL-10 (αIL-10, clone 19F1; Biolegend), IL-6 (αIL-6, clone MQ2-13A5; BD Bioscience), IL-1β (αIL-1β, clone 8516.311; SIGMA), or TNF-α (αTNF-α, clone MAb1; Biolegend). Then, 100 µl/ml of Protein G Sepharose beads (Amersham) were added and incubated for 1 h at 4°C. Finally, TB-PE were centrifuged at 12,000 *g* to remove antibody-bead complexes and then filtered (0.22-µm pores) before use. IFN-γ depletion was performed by incubating TB-PE for 2 h in sterile 96-well plates that had been coated with the capture antibody provided by the Human IFN-γ ELISA Kit (BD Bioscience). In all cases, depletions were controlled by ELISA.

Electron Microscopy

Macrophages exposed (or not) to TB-PE, and depleted (or not) for IL-10, were prepared for transmission electron microscopy study. For this purpose, cells were centrifuged at 6,000 rpm for 1 min, fixed in 1% glutaraldehyde dissolved in 0.1 M cacodylate buffer (pH 7); post-fixed in 2% osmium tetroxide; dehydrated with increasing concentrations of ethanol and gradually infiltrated with Epon resin (Pelco). Thin sections were contrasted with uranyl acetate and lead citrate (Electron Microscopy Sciences, Fort Washington, PA, USA) and examined with a FEI Tecnai transmission electron microscope (Hillsboro, OR, USA). For morphometry, 30 cells from each condition were randomly selected and digitalized at 40,000× magnification. Then the area of lipid electron dense vacuoles per cell were measured and compared in each experimental group by automated morphometry.

Proliferation of Antimycobacterial CD4 T Cells Induced by Macrophages

We purified and maintained CD4 T cells from blood derived from healthy PPD^+ donors as previously demonstrated (23). In parallel, we cultured autologous monocytes to generate macrophages and exposed them or not to TB-PE 20% v/v for 24 h. The next day, the medium was replaced, and macrophages were loaded with mycobacterial antigens by adding γ-irradiated Mtb at 2 bacteria to 1 macrophage ratio for further 24 h. Thereafter, the medium was replaced and autologous carboxyfluorescein succinimidyl ester (CFSE)-labeled CD4 T cells (Invitrogen) were added at a ratio of 10 lymphocytes to 1 macrophage for 5 days, as detailed previously (24). To determine IFN-γ production among proliferating CD4 T cells ($CFSE^{low}$), brefeldin A (5 µg/ml; Sigma Chemical Co.) was added 4 h prior the end of the coculture to block cytokine secretion. Thereafter, CFSE-labeled lymphocytes were first stained with anti-CD4-PerCP-Cy5.5 mAbs (eBioscience), then fixed with 0.5% PFA for 15 min. Second, cells were permeabilized with 500 µl Perm2 (Becton Dickinson, Cockysville, MD, USA) for 10 min and incubated with anti-IFN-γ-PE mAb (Invitrogen, CA, USA). Cells were gated according to its FSC and side scatter (SSC) properties analyzed on FACScan (Becton Dickinson). In order to gate out dead lymphocytes, the gate of CD4 T cells with increased SSC and low FSC was excluded (25). Isotype matched controls were used to determine auto-fluorescence and non-specific staining. Analysis was performed using the FCS Express (*De Novo* Software) and results were expressed as percentages of $IFN\text{-}\gamma^{pos}/CFSE^{low}/CD4^{pos}$ T cells induced by the different macrophage populations. To complement these results, the amounts of IFN-γ released in the supernatant throughout the coculture were determined by ELISA according to the manufacturer's kit indications (BD Bioscience).

Measurement of Bacterial Intracellular Growth in Macrophages by Colony Forming Unit (CFU) Assay

Macrophages exposed (or not) to TB-PE, were infected with H37Rv Mtb strain at a MOI of 1 bacteria/cell in triplicates. After 2 h, extracellular bacteria were removed by gently washing four times with pre-warmed PBS. At 4 h and days 3, 6, and 10, cells were lysed in 0.1% SDS and neutralized with 20% Bovine Serum Albumine in Middlebrook 7H9 broth. Serial dilutions of the lysates were plated in triplicate, onto 7H11-Oleic Albumin Dextrose Catalase (OADC, Difco) agar medium for CFU scoring at 21 days later.

Western Blots

Macrophages were treated (or not) with TB-PE. Following the different experimental treatments, cells were lysed in ice-cold buffer consisting of 150 mM NaCl, 10 mM Tris, 5 mM EDTA, 1% SDS, 1% Triton X-100, 1% sodium deoxycholate, gentamicin/streptomycin, 0.2% azide plus a cocktail of protease inhibitors (Sigma-Aldrich). Lysates were incubated on ice for 3 h and cleared by centrifugation for 15 min at 14,000 rpm at 4°C. Protein concentrations were determined using the

BCA protein assay (Pierce). Equal amounts of protein (40 μg) were then resolved on a 10% SDS-PAGE. Proteins were then transferred to Hybond-ECL nitrocellulose membranes (Amersham) for 2 h at 100 V and blocked with 1% BSA-0.05% Tween-20 for 1 h at room temperature. Membranes were then probed with primary anti-human ACAT (1:200 dilution, SOAT; Santa Cruz) or anti-human pY705-STAT3 (1:1,000 dilution, Cell Signaling Technology, clone D3A7) overnight at 4°C. After extensive washing, blots were incubated with a HRP-conjugated goat anti-rabbit IgG Ab (1:5,000 dilution; Santa Cruz Biotechnology) or HRP-conjugated goat anti-mouse IgG Ab (1:2,000 dilution; Santa Cruz Biotechnology) for 1 h at room temperature. Immunoreactivity was detected using ECL Western Blotting Substrate (Pierce). Protein bands were visualized using Kodak Medical X-Ray General Purpose Film. For internal loading controls, membranes were stripped by incubating in buffer consisting of 1.5% Glycine, 0.1% SDS, 1% Tween-20, pH 2.2 for 10 min twice, extensively washed and then reprobed with anti-β-actin (1:2,000 dilution; ThermoFisher, clone AC-15) or anti-STAT3 Ab (1:1,000 dilution; Cell Signaling Technology, clone D1A5). Results from Western blot were analyzed by densitometric analysis (Image J software).

Immunostaining

Macrophages were plated on glass coverslips and were treated with or without 20% v/v of TB-PE for 24 h. Cells were fixed with PFA 4% for 20 min at room temperature and then PFA was quenched with 50 mM NH_4Cl for 2 min. Cells were rinsed in PBS once and then were labeled with 1 μg/ml of BODIPY 493/503 (Life technologies) for 15 min before permeabilization with PBS-Triton X-100 0.1% for 10 min. Cells were then incubated with PBS-BSA 3% w/v for 30 min prior to overnight incubation at 4°C with primary anti-human pY705-STAT3 (dilution 1/100, Cell Signaling Technology, Clone D3A7). Cells were then washed and incubated with Goat anti-Mouse IgG, AlexaFluor 555 (dilution 1/1,000, Cell Signaling Technology) for 1 h at room temperature. Cells were extensively washed and then incubated for 10 min with DAPI in PBS-BSA 1% (500 ng/ml, Sigma-Aldrich). Finally, slides were mounted and visualized with a Leica DM-RB fluorescence microscope.

Mice

Wild-type (WT) BALB/c and IL-10 knockout (IL-10 KO) (C.129P2(B6)-IL-10 tm1Cgn/J) BALB/c male mice (8–12 weeks old), were obtained from the Leloir Institute Foundation. Animals were bred and housed in accordance with the guidelines established by the Institutional Animal Care and Use Committee of Institute of Experimental Medicine (IMEX)-CONICET-ANM. All animal procedures were shaped to the principles set forth in the Guide for the Care and Use of Laboratory Animals (26).

Generation of BMDMs

Femurs and tibia from WT and IL-10 KO mice were removed after euthanasia and the bones were flushed with RPMI-1640 medium by using syringes and 25-Gauge needles. The cellular suspension was centrifuged and the red blood cells were removed. The BMDMs were obtained by culturing the cells with RPMI-1640 medium containing L-glutamine, pyruvate, β-mercaptoethanol (all from Sigma-Aldrich), 10% FCS and 20 ng/ml of murine recombinant M-CSF (Biolegend) at 37°C in a humidified incubator for 7–8 days. Differentiated BMDMs were re-plated into 24-well tissue culture plates in complete medium prior to cell stimulation with Mtb lipids for 24 h. Alternatively, recombinant murine IL-10 (Peprotech) at 10 ng/ml was added to the cultures for 24 h.

Statistical Analysis

All values are presented as mean and SEM of a number of independent experiments. Independent experiments are defined as those performed with macrophages derived from monocytes isolated independently from different donors. As most of our datasets did not pass the normality tests, non-parametric tests were applied. Comparisons between more than two paired data sets were made using the Friedman test followed by Dunn's Multiple Comparison Test. Comparisons between two paired experimental conditions were made using the two-tailed Wilcoxon Signed Rank. Correlation analyses were determined using the Spearman's rank test. For all statistical comparisons, a p value < 0.05 was considered significant.

RESULTS

Tuberculous PE Fluids Induce Lipid Bodies Accumulation in Macrophages

It has been demonstrated that Mtb induces a lipid-rich foam cell phenotype in host macrophages (6–8, 27), possibly *via* TLR2 and TLR6 activation (28). Moreover, merely isolated lipids from Mtb were able to induce the foamy phenotype (7, 27). Based on this knowledge, we aimed to determine whether soluble factors found in physiological samples derived from active TB patients could promote the generation of FM. To this end, we treated human M-CSF-driven macrophages with cell-free preparations of PE derived from patients with tuberculosis (TB-PE) in order to mimic a genuine microenvironment derived during Mtb infection. According to the pattern of staining of neutral lipids with ORO, we observed that TB-PE treatment induced lipid bodies accumulation in macrophages to the same extent as Mtb infection or exposure to Mtb-derived lipids (**Figure 1A**). We also demonstrated that the formation of lipid bodies was specific for TB-PE treatment in comparison to PE from patients with heart failure (HF-PE) (**Figure 1B**). Moreover, biochemical analysis of the lipids recovered from macrophages identified higher abundance of cholesteryl esters and triacylglycerols in TB-PE-treated macrophages in comparison to control or HF-PE-treated macrophages (**Figure 1C**). Additionally, unlike HF-PE, the treatment with TB-PE resulted in an increase of the total intracellular cholesterol content (**Figure 1D**) and a twofold increase of CD36 expression (**Figure 1E**). Therefore, soluble factors released during pleural Mtb infection induced lipid body accumulation in human macrophages that typically confirm the FM phenotype.

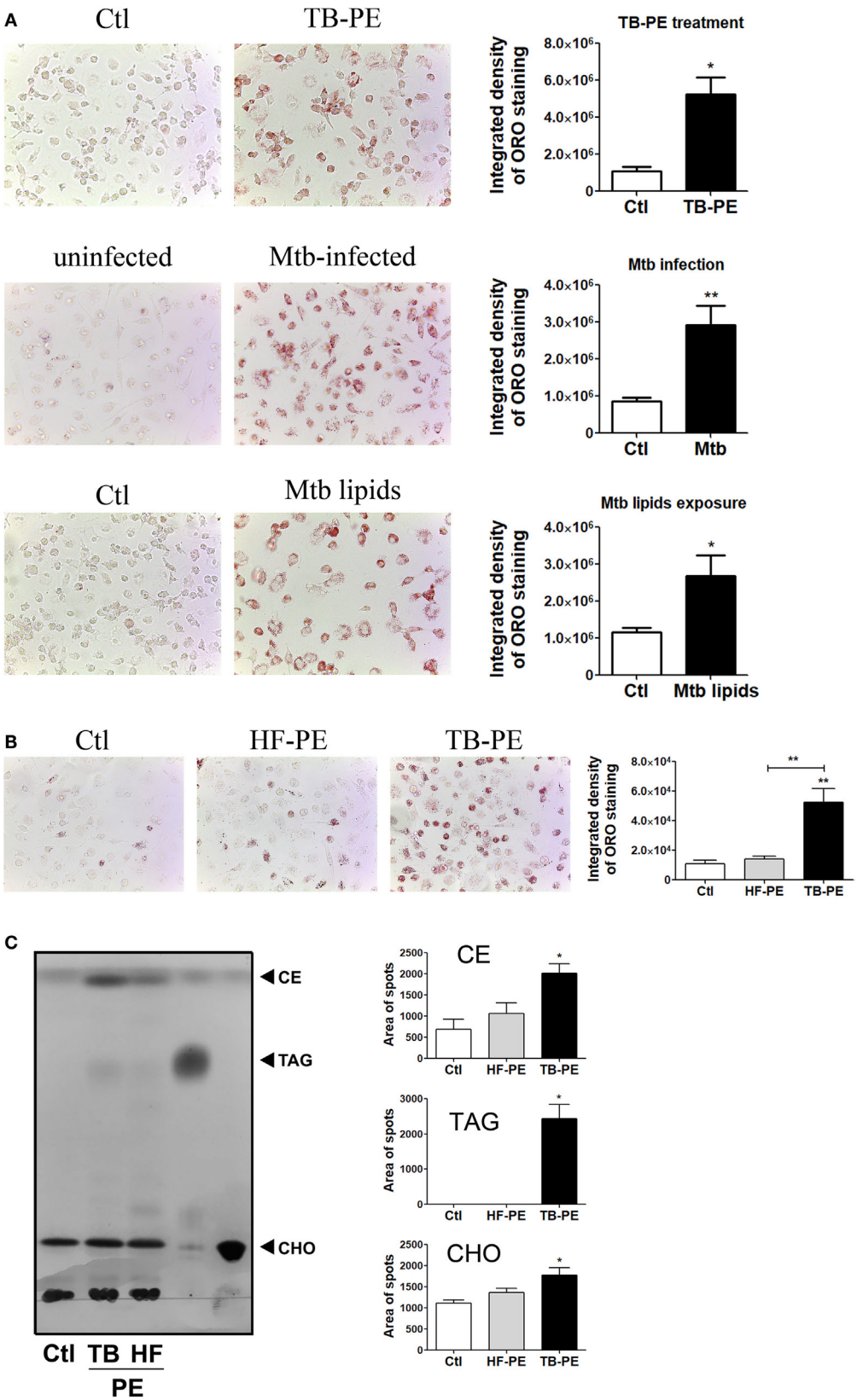


FIGURE 1 | Continued

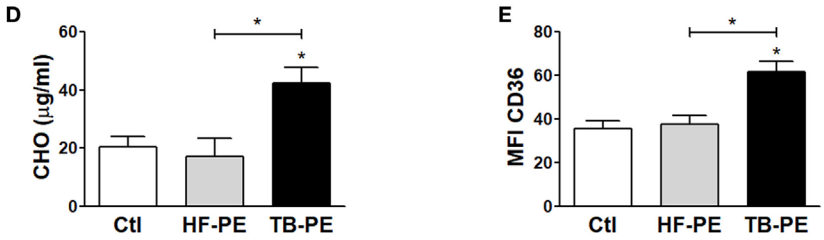


FIGURE 1 | Tuberculous pleural effusions (TB-PE) induce lipid bodies accumulation in macrophages. **(A)** Human monocyte-derived macrophages (MDM) were treated either with TB-PE or with *Mycobacterium tuberculosis* (Mtb) lipids, or infected with Mtb H37Rv for 24 h and then stained with Oil Red O (ORO). Representative images are shown in left panels (40× magnification) and the integrated density of ORO staining is shown in right panels. Values are expressed as means ± SEM of six independent experiments, considering five microphotographs per experiment. Wilcoxon signed rank test: $^{*}p < 0.05$. **(B)** MDM were treated with TB-PE or PE from heart failure patients (HF-PE) and stained with ORO ($n = 5$). **(C)** Left panel shows a representative thin layer chromatographic analysis of lipids from MDM treated or not with either TB-PE or HF-PE. Total lipids were extracted from untreated MDM (lane 1), TB-PE-treated MDM (lane 2), HF-PE-treated MDM (lane 3), and the standard lipids triacylglycerol (TAG, lane 4) and free cholesterol (CHO, lane 5). Cholesterol esters (CE) are also indicated. Right panels depict the area of spots for CE, TAG, and CHO in control and TB-PE or HF-PE treated MDM ($n = 4$). **(D)** Intracellular total cholesterol (CHO) content in MDM exposed or not to TB-PE or HF-PE measured by an enzymatic method ($n = 5$). **(E)** Mean fluorescence intensity (MFI) of CD36 cell-surface expression in MDM exposed or not to TB-PE or HF-PE measured by flow cytometry ($n = 5$). **(B–E)** Friedman test followed by Dunn's Multiple Comparison Test: $^{*}p < 0.05$; $^{**}p < 0.01$ for TB-PE vs Ctl or as depicted by lines.

FM Induced by Tuberculous PE Display Immunosuppressive Properties

In order to assess whether the differentiation into FM induced by TB-PE may have a negative impact on the development of the antimycobacterial response, we determined phenotype and functions of TB-PE-induced FM. As observed in **Figure 2A**, macrophages treated with TB-PE displayed a higher expression of anti-inflammatory markers such as CD163, mannose receptor or CD206 (MRC1), and PD-L1, and a lower expression of the MHC class II cell-surface receptor, HLA-DR. In accordance with the acquisition of this anti-inflammatory profile, TB-PE-induced FM secreted higher levels of IL-10 and lower levels of TNF-α upon stimulation with irradiated *Mycobacterium tuberculosis* (iMtb) than untreated cells (**Figure 2B**). In order to assess the effect of TB-PE treatment on the presentation of mycobacterial antigens, macrophages were treated with or without TB-PE for 24 h, washed and stimulated with iMtb for further 24 h. Thereafter, cells were washed and cocultured with autologous CFSE-labeled CD4 T cells derived from healthy PPD positive subjects for 5 days. Based on the CFSE labeling of CD4 T cells, while TB-PE-treated macrophages did not induce differential levels of proliferation of antimycobacterial CD4 T cells (**Figure 2C**), they promoted differential distribution of the IFN-γ producing clones (**Figure 2D**). In particular, those macrophages treated with TB-PE induced lower percentages of IFN-γ producing clones (**Figure 2D**) and a lower release of IFN-γ (**Figure 2E**), as compared to untreated macrophages in response to iMtb stimulation. Of note, IL-4 and IL-17 contents were undetectable in these assays (data not shown). Therefore, the activation of Ag-specific IFN-γ-producing CD4 T cells was impaired when macrophages were exposed to TB-PE, suggesting that the accumulation of lipid bodies is accompanied by a reduced capacity to activate antimycobacterial Th1 cells.

Next, we assessed whether the treatment with TB-PE had an impact on the control of the bacillary load. To accomplish this, macrophages were treated with TB-PE for 24 h, washed and infected with Mtb. Although no differences were observed in the uptake of the mycobacteria as judged by the scoring of the CFU at 4 h post-infection (**Figure 2F**), a significant increase in the bacillary load was observed in TB-PE-treated macrophages at later time points (**Figure 2G**). Therefore, FM induced by TB-PE are more susceptible to Mtb intracellular growth.

IL-10 Promotes Accumulation of Lipid Bodies in Macrophages under TB-PE Treatment

In order to evaluate the host factors involved in promoting the accumulation of lipid bodies by TB-PE, we depleted different cytokines known to be highly present in this fluids (29, 30), including IL-10, TNF-α, IL-1β, IL-6, and IFN-γ. We then evaluated the ability of these depleted-PE to induce the foamy phenotype in macrophages. The depletion of each individual cytokine was confirmed by ELISA (Figure S1A in Supplementary Material). Interestingly, only the depletion of IL-10 from TB-PE was capable of preventing lipid bodies accumulation (**Figure 3A**). This result was also confirmed by labeling the cells with Bodipy staining (Figure S1B in Supplementary Material). In addition, macrophages exposed to IL-10-depleted TB-PE showed a reduction of intracellular cholesterol content and CD36 cell-surface expression in comparison to those cells treated with non-depleted or depleted of any other cytokines (**Figures 3B,C**). In line with these results, the addition of recombinant IL-10 to the IL-10-depleted TB-PE restored the acquisition of the foamy phenotype in a dose-dependent manner (**Figure 3D**). Of note, the addition of IL-10 in the absence of TB-PE did not induce the foamy phenotype (**Figure 3D**). Thereafter, we determined the presence of the lipidic vacuoles by electron microscopy in macrophages treated with TB-PE depleted (or not) of IL-10. As it is shown in **Figure 3E**, while untreated macrophages showed numerous pseudopodia and empty cytoplasmic vacuoles, TB-PE-treated macrophages displayed electron dense lipid osmiophilic vacuoles,

which correspond to lipid bodies. Interestingly, macrophages treated with IL-10-depleted TB-PE showed smaller-sized lipidic vacuoles than those exposed to non-depleted TB-PE. These results indicate that the IL-10 present in TB-PE is a key host factor promoting the lipid-laden phenotype in the presence of exogenous lipids.

IL-10 Levels Correlate with FM Abundance in PE

In order to evaluate whether IL-10 level is associated to the acquisition of the foamy phenotype in the course of a Mtb natural infection, we assessed the levels of IL-10 and total cholesterol in individual preparations of TB-PE, and the numbers of FM found

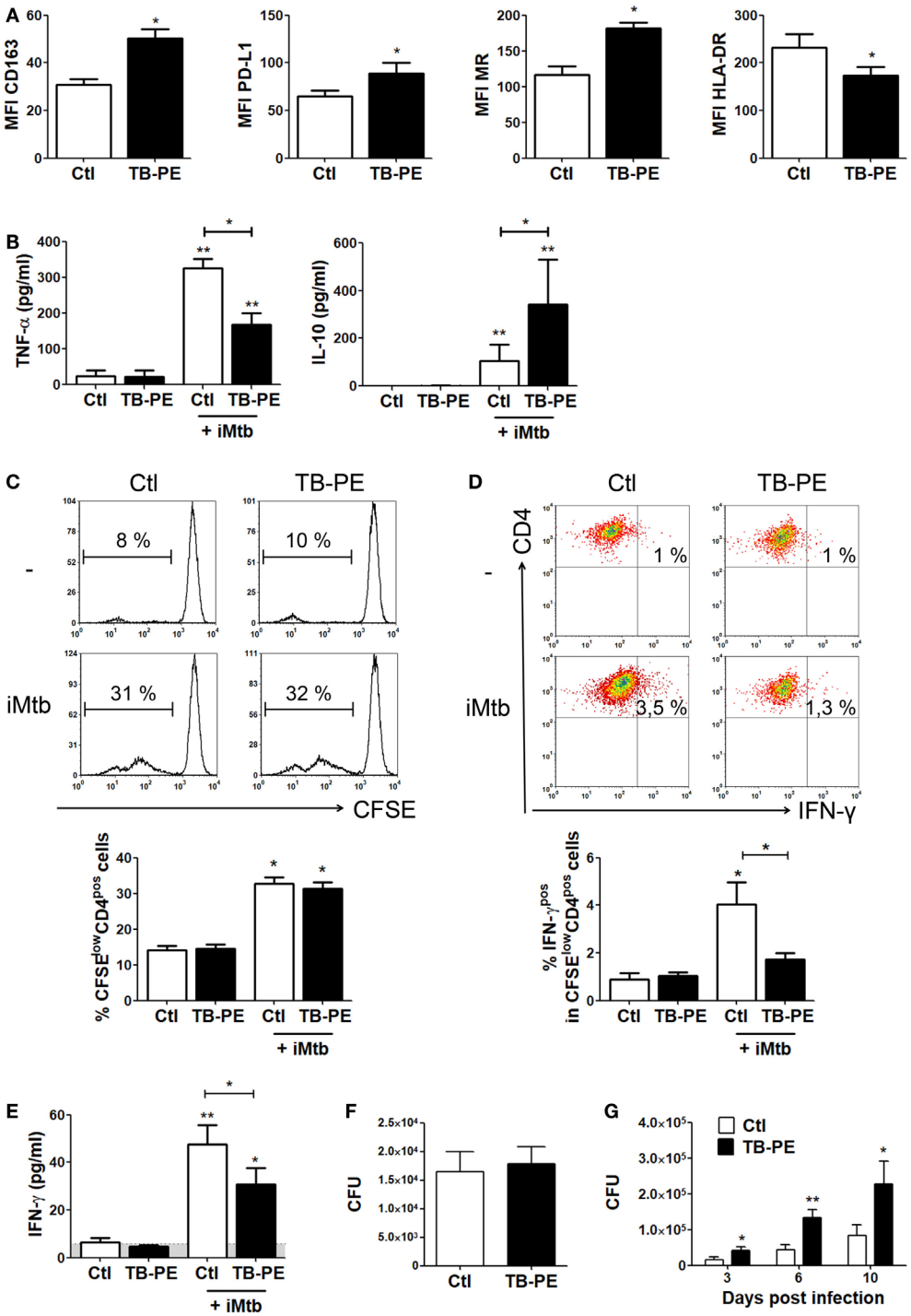


FIGURE 2 | Continued

FIGURE 2 | Macrophages treated with tuberculous pleural effusion (TB-PE) display immunosuppressive properties. **(A)** Mean fluorescence intensity (MFI) of CD163, PDL-1, MR, and HLA-DR measured by flow cytometry in human monocyte-derived macrophages (MDM) exposed or not to TB-PE ($n = 5$). Wilcoxon signed rank test: $^{*}p < 0.05$. **(B)** Levels of secreted IL-10 and TNF-α by MDM exposed or not to TB-PE in response to irradiated *Mycobacterium tuberculosis* (iMtb) measured by ELISA ($n = 5$). Friedman test followed by Dunn's Multiple Comparison Test: $^{*}p < 0.05$; $^{**}p < 0.01$, for iMtb-stimulated vs unstimulated, or as indicated in the graph. **(C–E)** MDM from healthy PPD^{+} donors exposed or not to TB-PE for 24 h, were stimulated or not with iMtb for 24 h and then used as antigen presenting cells (APC) in autologous proliferation assays. Cocultures were performed with autologous carboxyfluorescein succinimidyl ester (CFSE)-labeled CD4 T cells at a ratio of 10 T cells: 1MDM. **(C)** Representative histograms showing CFSE labeling in CD4^{pos} T cells activated by macrophages exposed (or not) to TB-PE, loaded (or not) with iMtb. Right panel shows the quantification of the percentages of proliferating CD4^{pos} T cells (CFSE^{low}/CD4^{pos} cells) in each condition. Loaded vs unloaded with iMtb: $^{*}p \leq 0.05$ ($n = 4$). **(D)** Representative dot plots showing CD4 and IFN-γ expression among CFSE^{low}/CD4^{pos} T cells activated by MDM exposed (or not) to TB-PE, loaded (or not) with iMtb. Right panel shows the quantification of the percentages of proliferating IFN-γ-producing CD4^{pos} T cells (IFN-γ^{pos}/CFSE^{low}/CD4^{pos} T cells) in each condition ($n = 4$). Friedman test followed by Dunn's Multiple Comparison Test: $^{*}p < 0.05$, for iMtb-stimulated vs unstimulated, or as indicated in the graph. **(E)** The amounts of IFN-γ released throughout the coculture were determined by ELISA. Friedman test followed by Dunn's Multiple Comparison Test: $^{*}p < 0.05$; $^{**}p < 0.01$, for iMtb-stimulated vs unstimulated, or as indicated in the graph. **(F)** Bacillary loads in MDM treated (or not) with TB-PE, washed, and infected with *Mycobacterium tuberculosis* (Mtb) strain H37Rv for 4 h ($n = 6$). Wilcoxon signed rank test. **(G)** Intracellular colony forming units were determined at different time points in MDM treated with TB-PE for 24 h, washed and infected with Mtb ($n = 10$). Wilcoxon signed rank test: $^{*}p < 0.05$; $^{**}p < 0.01$; $^{***}p < 0.001$ for TB-PE treated vs Ctl.

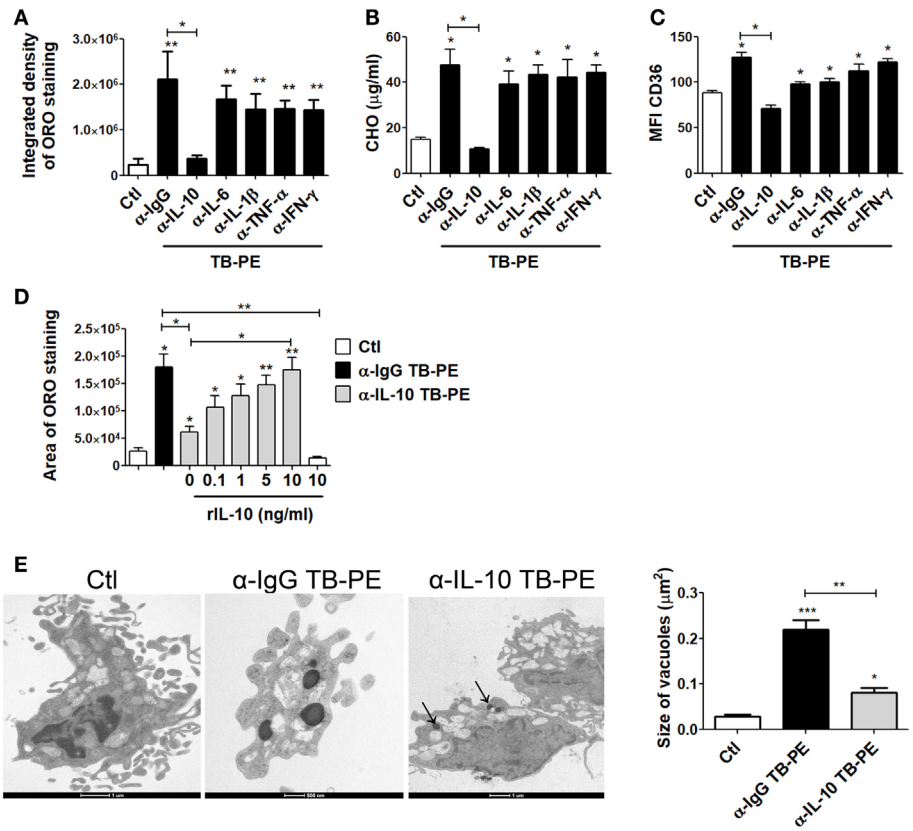
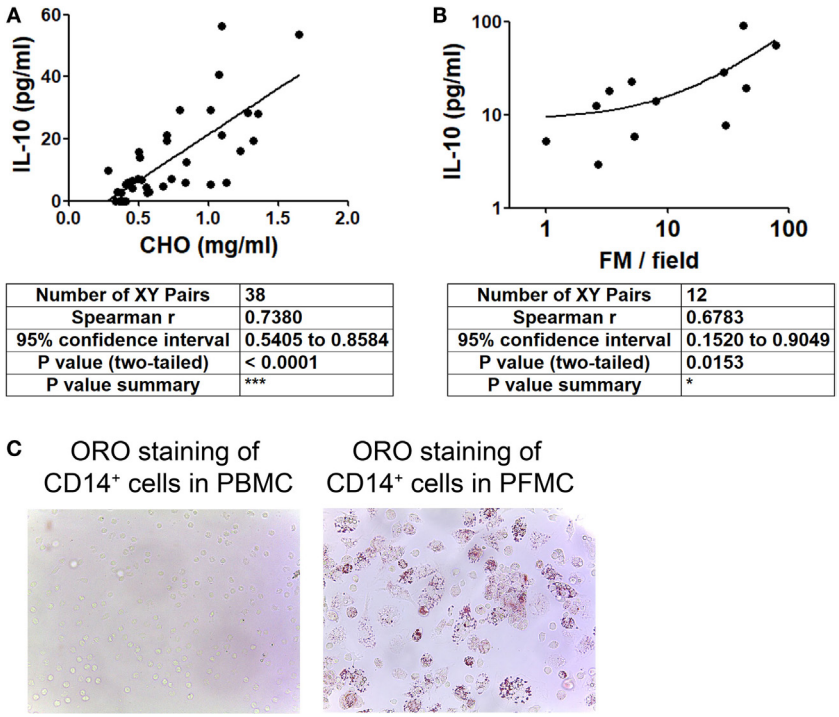


FIGURE 3 | Interleukin-10 (IL-10) promotes lipid bodies accumulation in macrophages treated with tuberculous pleural effusion (TB-PE). **(A–C)** Human monocyte-derived macrophages (MDM) were treated with TB-PE depleted or not for different cytokines for 24 h and **(A)** lipid bodies' content was measured by Oil Red O (ORO) staining ($n = 4$). **(B)** Intracellular cholesterol (CHO) content measured by an enzymatic method ($n = 4$) was determined. **(C)** Mean fluorescence intensity (MFI) of CD36 cell-surface expression was measured by flow cytometry ($n = 4$). **(D)** MDM were treated (or not) with TB-PE depleted or not of IL-10 in the presence of different amounts of recombinant human IL-10 (rIL-10) for 24 h and lipid bodies content was measured by ORO staining ($n = 6$). **(E)** Representative electron microscopy micrographs of MDM treated with TB-PE depleted or not of IL-10. White asterisks indicate large electron dense osmiophilic vacuoles and arrows point small sized ones. Morphometric study of the area per vacuole in each condition is shown ($n = 14$). **(A–E)** Friedman test followed by Dunn's Multiple Comparison Test: $^{*}p < 0.05$; $^{**}p < 0.01$; $^{***}p < 0.001$ for experimental condition vs Ctl or as depicted by lines.

within the pleural fluids mononuclear cells (PFMC). We found that levels of IL-10 and total cholesterol were positively correlated (**Figure 4A**), unlike other cytokines such as IFN-γ, IL-6, TNF-α, and IL-1β (Figure S2 in Supplementary Material). Noticeably, there was also a positive correlation between the level of IL-10 and the number of FM among the PFMC (**Figure 4B**). Moreover, lipid-laden CD14^{+} cells were found in the pleural compartment but not in paired peripheral blood (**Figure 4C**). These results



Number of XY Pairs	38
Spearman r	0.7380
95% confidence interval	0.5405 to 0.8584
P value (two-tailed)	< 0.0001
P value summary	***

Number of XY Pairs	12
Spearman r	0.6783
95% confidence interval	0.1520 to 0.9049
P value (two-tailed)	0.0153
P value summary	*

FIGURE 4 | Cholesterol levels and foamy macrophages (FM) are associated with interleukin-10 (IL-10) amounts present in tuberculous pleural effusion (TB-PE). **(A,B)** Correlation analysis between the levels of IL-10 and **(A)** the cholesterol content (n = 38) or **(B)** the number of lipid-laden CD14+ cells within the pleural fluids mononuclear cells (PFMC) (n = 12) found in individual preparations of TB-PE. In B log-10 scale for both axes is used. Linear regression lines are shown. Spearman's rank test. **(C)** Representative image of ORO staining of CD14+ cells isolated from paired peripheral blood mononuclear cells (PBMC) and PFMC is shown (40× magnification).

support the idea that IL-10 potentiates the acquisition of the foamy program in human macrophages in the context of a natural infection.

IL-10 Deficiency Prevents the Foamy Phenotype in BMDM

To confirm the role of IL-10 in the differentiation of FM, we evaluated whether BMDM derived from IL-10-knock out (KO) mice could indeed become FM after the treatment with lipids from Mtb. First, we determined IL-10 production in M-CSF-derived BMDM from WT mice stimulated with mycobacterial lipids for 24 h. As shown in **Figure 5A**, unlike the undetectable level of TNF-α (data not shown), BMDM secreted IL-10 in response to mycobacterial lipid-stimulation. Second, we compared whether BMDM derived from WT or IL-10-KO mice differed in their propensity to accumulate lipid bodies in response to Mtb-derived lipids. As illustrated in **Figures 5B,C**, IL-10-deficiency prevented the foamy phenotype induced by Mtb lipids, which in turn could be partially reverted by the addition of exogenous IL-10. In agreement with our previous results, exogenous IL-10 did not induce the foamy phenotype in the absence of the source of lipids in BMDM. These results obtained in murine macrophages confirm those obtained in human TB-PE-treated macrophages, demonstrating the key role of IL-10 in favor of the differentiation program toward foamy cells.

The IL-10/STAT3 Axis Is Involved in the FM Differentiation Induced by TB-PE

Considering the role of IL-10 in promoting the differentiation of macrophages into FM, and that STAT3 is a pivotal transcriptional factor induced by IL-10 (31, 32), we studied the contribution of STAT3 activation in the induction of the foamy phenotype by measuring its phosphorylated form (pSTAT3). First, we determined that STAT3 was activated in TB-PE-treated macrophages detecting its phosphorylated form by western blot and immunofluorescence microscopy (**Figures 6A,B**). As depicted in **Figure 6B** FM induced by TB-PE showed nuclear localization of STAT3 phosphorylated on tyrosine 705, reflecting STAT3 activation. Importantly, pharmacological inhibition of STAT3 with Stattic (or with cucurbitacin I) prevented the accumulation of lipid bodies in macrophages in a dose-dependent manner (**Figure 6C**; Figures S3A,B in Supplementary Material). Therefore, the enhancement of FM differentiation driven by IL-10 is mediated by STAT3.

IL-10 Enhances ACAT Expression in TB-PE-Treated Macrophages Leading to FM Differentiation

In order to elucidate the mechanism by which IL-10 promotes FM differentiation, we assessed the expression of ACAT, which is central for the biogenesis of lipid bodies by converting free- into

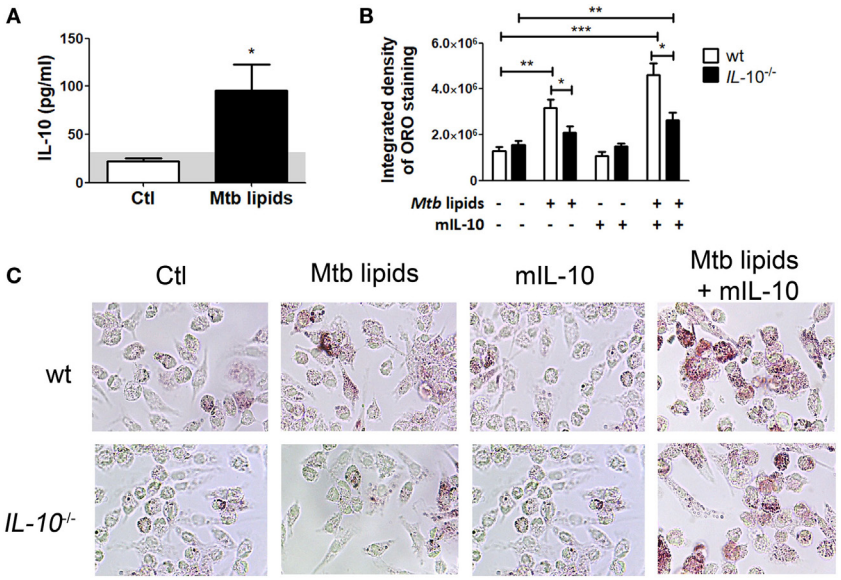


FIGURE 5 | Interleukin-10 (IL-10) deficiency reduces lipid bodies accumulation in bone marrow-derived mouse macrophages (BMDM) in response to *Mycobacterium tuberculosis* (Mtb) lipids. **(A)** BMDM from wt mice were treated or not with Mtb lipids for 24 h and the levels of secreted IL-10 were measured by ELISA ($n = 5$) Wilcoxon signed rank test: $^{*}p < 0.05$. **(B,C)** BMDM from wt or *IL-10*$^{-/-}$ mice were treated or not with Mtb lipids in the presence or not of recombinant murine IL-10 for 24 h and then stained with Oil Red O (ORO). The integrated density of ORO staining **(B)** and representative images **(C)** are shown ($n = 6$). Friedman test followed by Dunn's Multiple Comparison Test: $^{*}p < 0.05$; $^{**}p < 0.01$; $^{***}p < 0.001$ as depicted by lines.

esterified-cholesterol that are eventually packed inside the lipid droplets (33). We first showed that the foamy phenotype induced by TB-PE was dependent on ACAT activity, as judged both by the increase of ACAT expression after TB-PE treatment (**Figure 7A**), and by the blocking of the accumulation of lipid bodies in the presence of Sandoz, a specific inhibitor of ACAT (**Figure 7B**). Noticeably, the inhibition of ACAT lead to reduced amounts of both cholesteryl esters and triacylglycerols in TB-PE-treated macrophages (**Figure 7C**), confirming the involvement of ACAT in FM formation upon TB-PE treatment. We then assessed ACAT expression in IL-10-depleted TB-PE and we found that its expression was reduced in the absence of IL-10 (**Figure 7A**). In agreement with this result, ACAT induction by TB-PE was abolished when STAT3 activity was inhibited (**Figure 7D**). Therefore, the IL-10/STAT3 axis activated by TB-PE enhances FM differentiation through the upregulation of ACAT expression, leading to an increased biogenesis and accumulation of lipid bodies.

Based on our findings, we propose a model for the modulation of FM in the context of a physiologically relevant microenvironment promoted by Mtb infection for which the axis IL-10/STAT3 induces the accumulation of lipid bodies *via* ACAT upregulation. This in turn is accompanied by an increase of CD36 and the acquisition of immunosuppressive properties, such as a reduced induction of antimycobacterial Th1 clones, an enhanced production of IL-10 and a more permissive phenotype for bacillary growth (**Figure 8**).

DISCUSSION

Tuberculosis, as a chronic condition, entails the establishment of extensive metabolic remodeling in both host and pathogen. One of the consequences of this adaptation is the formation of FM. Since FM have been associated with the bacilli persistence and tissue pathology (6, 8, 12, 27, 34), we aimed to determine which host factors may contribute to enlarge the pool of FM in TB. In this sense, we used the acellular fraction of TB-PE to mimic those soluble factors released locally during Mtb infection. Although pleural disease due to *Mtb* is generally categorized as extra-pulmonary, there is an intimate anatomic relationship between the pleura and the pulmonary parenchyma (35, 36). Current literature supports the notion that TB-PE is the consequence of a direct local infection with a cascade of events, including an immunological response, instead of the result of a pure delayed hypersensitivity reaction, as previously thought (37). Even though we cannot state that macrophages infiltrating the pleural cavity will reproduce with fidelity those macrophages in the infected alveolar space or lung interstitial tissue, we can affirm that TB-PE represents microenvironment from a human respiratory cavity that is impacted by the infection. To our knowledge, this is the first time that such a complex but physiologically relevant human sample has been used in order to study the biology of FM. Using this *in vitro* model, we demonstrated that the acellular fraction of TB-PE induces the accumulation of lipid bodies in human macrophages. Moreover, our finding was validated by the detection of lipid-laden CD14^{+} cells isolated directly from the mononuclear cells of the PE, providing physiological relevance to our *in vitro* model. Taking into account that tuberculous PE has, if any, very few bacilli content (38), and that it displays high cholesterol content, we infer that in our model the source of lipids feeding the lipid bodies in the macrophages are likely host-derived components instead of mycobacterial ones.

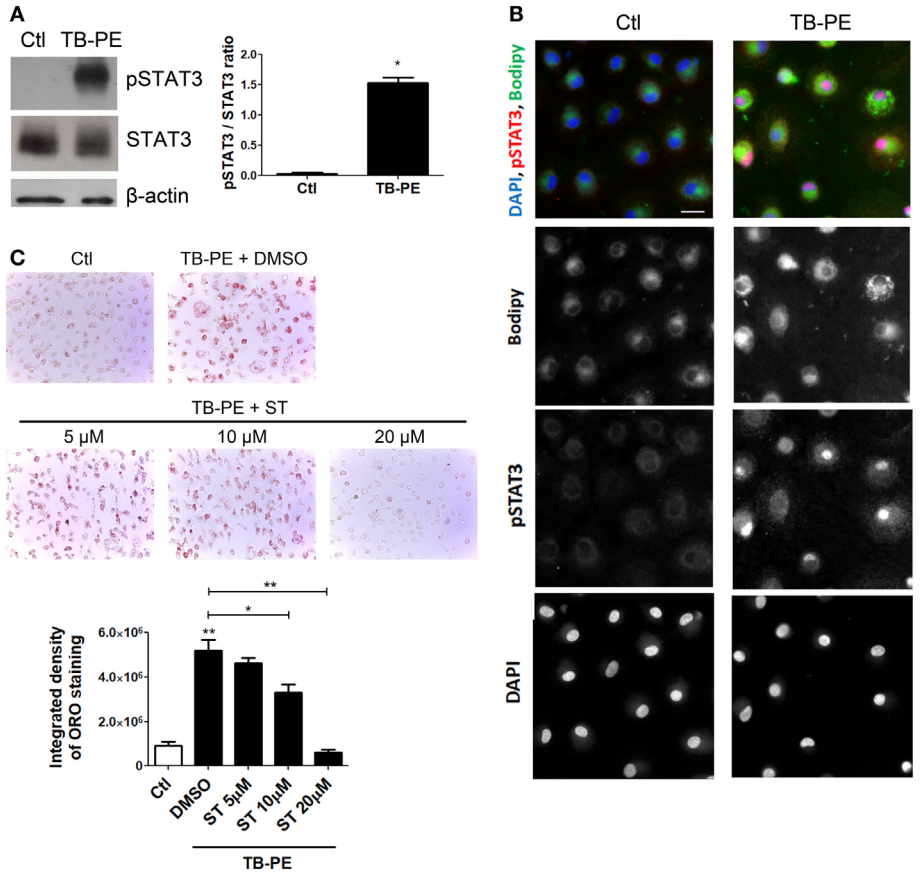


FIGURE 6 | Signal transducer and activator of transcription 3 (STAT3) activation enhances lipid bodies accumulation induced by treatment of macrophages with tuberculous pleural effusion (TB-PE). **(A)** Analysis of p705-STAT3, STAT3, and β-actin protein expression level by western Blot (left panel) and quantification (right panel; $n = 4$) in human monocyte-derived macrophages (MDM) treated with TB-PE for 24 h. Wilcoxon signed rank test: $^{*}p < 0.05$ **(B)** MDM were treated or not with TB-PE for 24 h and then were fixed, labeled with Bodipy 493/503 (green), permeabilized, and stained for p705-STAT3 (Red) and DAPI (blue). Representative images are shown. Scale bar, 10 μm. **(C)** MDM were treated or not with different concentrations of Stattic (STAT3 inhibitor, ST) for 2 h and then exposed or not to TB-PE for 24 h. Lipid bodies' content was determined by Oil red O (ORO) staining ($n = 6$). Representative images are shown and the integrated density of ORO staining is shown. Friedman test followed by Dunn's Multiple Comparison Test: $^{*}p < 0.05$; $^{**}p < 0.01$ for TB-PE treated vs Ctl, or as depicted by lines.

Although lipid bodies were qualified as passive organelles involved in lipid storage, it became clear that these organelles play a central role in several inflammatory (e.g., atherosclerosis) or chronic infectious diseases (e.g., TB) (8, 13). In this work, we provide evidence that FM differentiation induced by TB-PE is potentiated by IL-10 in association with the acquisition immunosuppressive properties, impairing the activation of antimycobacterial Th1 clones, producing the anti-inflammatory cytokine IL-10 and bearing higher bacillary loads. This is in line with previous reports characterizing the immunosuppressive profile in macrophages activated by the IL-10/STAT3 signaling pathway (39, 40). In this study, we show that FM formation depends (albeit partially) on the IL-10/STAT3 axis, and thus establishing an association between both processes (accumulation of lipid bodies and immunosuppression). Within this context, we observed that both processes are enhanced by the IL-10/STAT3 signaling pathway, arguing for likelihood of two independent outcomes emanating from the same signaling axis (**Figure 8**). Of note, it has been reported that the synthetic glucocorticoid dexamethasone can upregulate ACAT expression promoting formation of FM (41). Although there are extensive reports demonstrating transcriptional interactions between STAT3 and glucocorticoids leading to repression or synergism of target genes (42), it is interesting to notice that both IL-10 and glucocorticoids can polarize macrophages into an immunoregulatory profile (43). Based on that, we propose that the establishment of a foamy phenotype is accompanied by the acquisition of immunosuppressive properties.

It should be mentioned that Stattic is not an inhibitor completely specific for STAT3 (44). In this regard, a desirable goal is the discrimination between STAT3 and STAT1 involvement because both transcription factors can be activated by IL-10 (albeit at different levels), and because of their high degree of homology, particularly in their SH2 domains (44). Under our experimental conditions, unlike the strong activation of STAT3, we did not observe the phosphorylation of STAT1

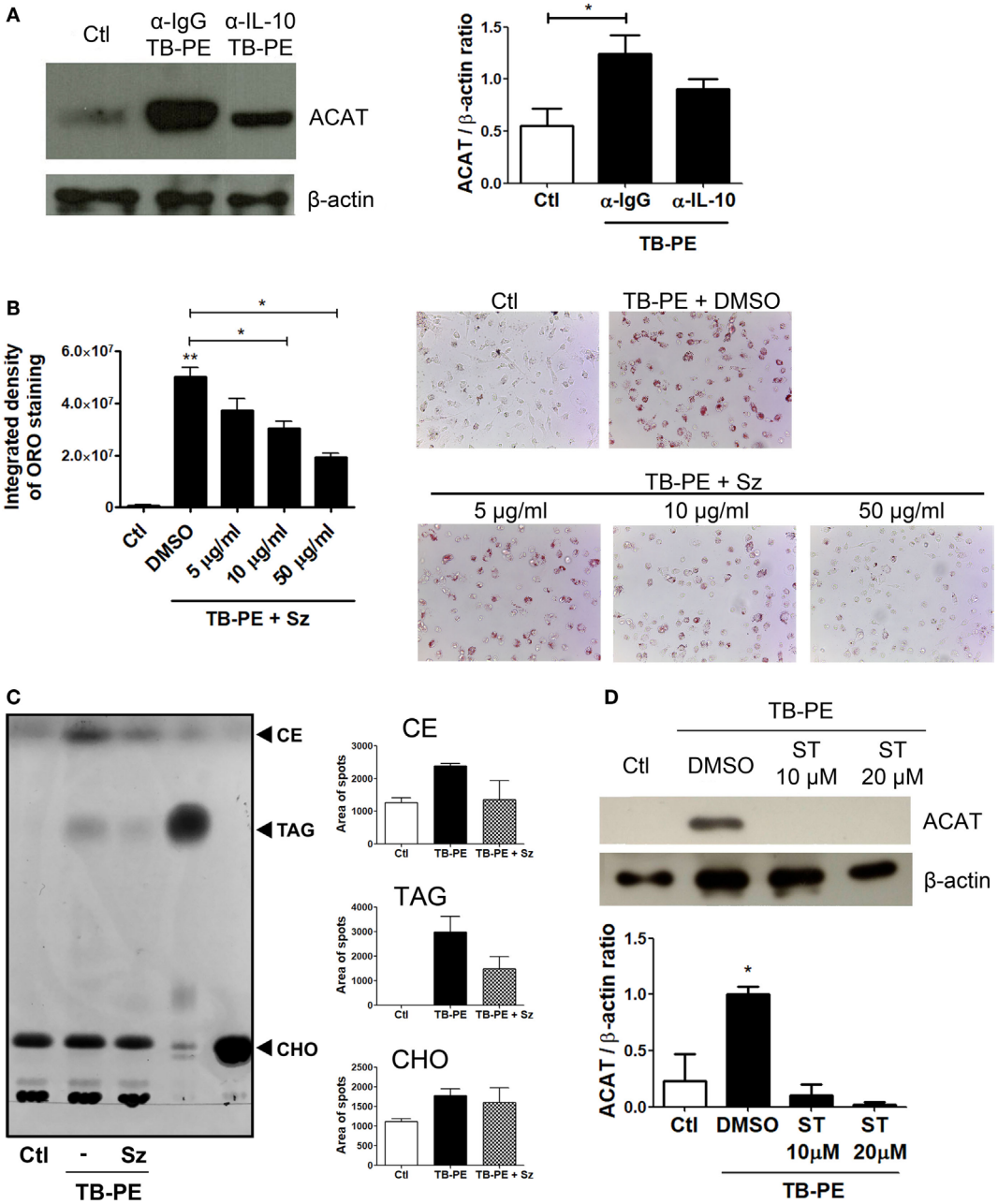


FIGURE 7 | The interleukin-10 (IL-10)/signal transducer and activator of transcription 3 (STAT3) axis promotes foamy macrophage formation through ACAT upregulation. **(A)** Analysis of ACAT and β-actin protein expression level by western Blot (left panel) and quantification (right panel; $n = 5$) in human monocyte-derived macrophages (MDM) treated with tuberculous pleural effusion (TB-PE) for 24 h depleted or not for IL-10. **(B)** MDM were treated or not with different concentrations of Sandoz (Sz, ACAT inhibitor) for 1 h, exposed or not to TB-PE for 24 h, and then stained with Oil Red O (ORO). The Integrated density and representative images are shown ($n = 6$). **(A,B)** Friedman test followed by Dunn's Multiple Comparison Test: $^*p < 0.05$; $^{**}p < 0.01$ for TB-PE treated vs Ctl, or as depicted by lines. **(C)** Thin layer chromatographic analysis of lipids from MDM treated or not with TB-PE in the presence or not of Sz. Total lipids were extracted from untreated MDM (lane 1), TB-PE-treated MDM (lane 2), TB-PE-treated MDM in the presence of Sz (lane 3), and the standard lipids triacylglycerol (TAG, lane 4) and cholesterol (CHO, lane 5). Cholesterol esters (CE) are also indicated. Right panels depict the area of spots for CE, TAG, and CHO in control and TB-PE in the presence or not of Sz treated MDM ($n = 2$). **(D)** Analysis of ACAT and β-actin protein expression level by Western Blot (left panel) and quantification (right panel; $n = 3$) in MDM treated or not with different concentrations of Stattic (ST) for 2 h and then exposed or not to TB-PE for 24 h. Friedman test followed by Dunn's Multiple Comparison Test: $^*p < 0.05$ for TB-PE treated vs Ctl.

in macrophages treated with TB-PE (data not shown and **Figure 6**). Likewise, the depletion of IFN-γ (a STAT1 activating cytokine) from TB-PE did not prevent the accumulation lipid bodies in macrophages (**Figures 3A–C**). Therefore, we consider that our experimental model is dependent of STAT3 instead of STAT1.

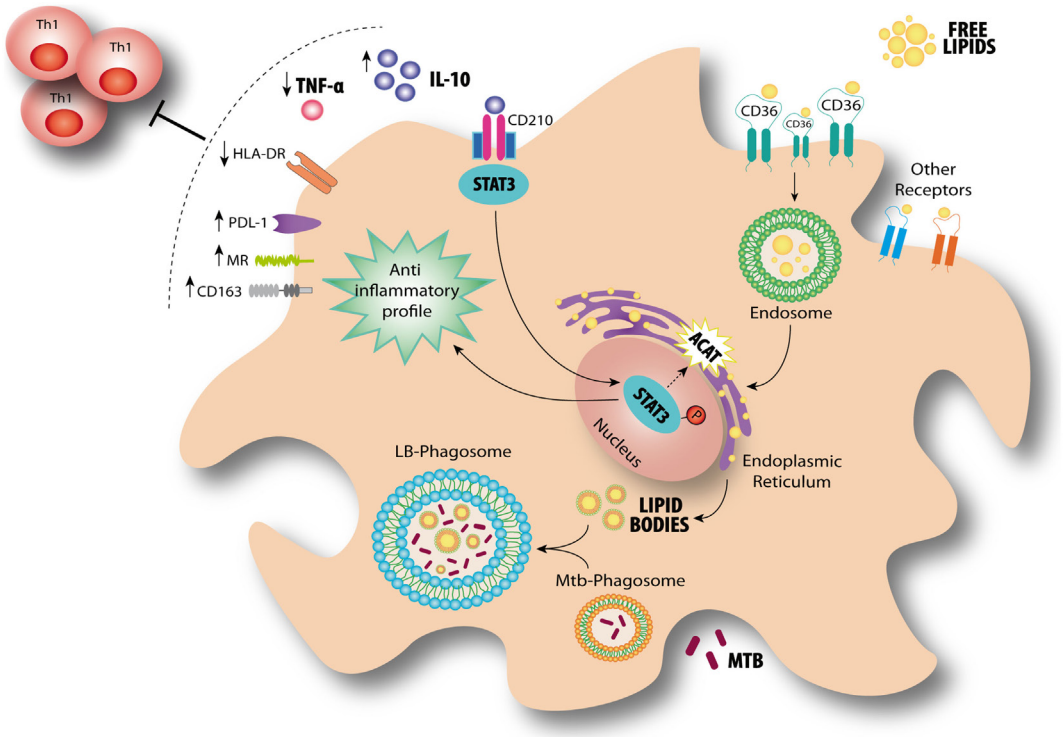


FIGURE 8 | Interleukin-10 (IL-10) promotes foamy macrophage (FM) formation in an IL-10/signal transducer and activator of transcription 3 (STAT3)-dependent manner in tuberculosis (TB). According to our results, FM induced by pleural effusion from TB patients display immunosuppressive properties such as high IL-10 release, low TNF-α production, impaired Th1 activation, and high bacillary loads. At the same time, lipid bodies' accumulation is enhanced by IL-10/STAT3 axis through an increase of CD36 cell-surface expression levels and ACAT expression. It has been demonstrated that *Mycobacterium tuberculosis* (Mtb)-containing phagosomes migrate toward these lipid bodies and engulf them (7). This mechanism ensures protection from microbicidal pathways and allows persistence of the bacilli inside host. Our results provide additional mechanisms by which the environment created by the infection context drives the FM differentiation even in the absence of the pathogen.

Our findings are in agreement with previous reports that demonstrated that macrophages exposed to lipids displayed impaired immune functions. Particularly, FM generated *in vitro* by the incubation with acetylated LDL displayed a reduced expression of pro-inflammatory genes (45). In addition, the ligation of the pregnane X receptor in human macrophages, which was associated to foamy formation, resulted in the impairment of the secretion of pro-inflammatory cytokines, phagolysosomal fusion and apoptosis (46). Moreover, a recent study showed that the treatment of human macrophages with surfactant lipids resulted in the reduction of TNF-α release and the enhancement of Mtb growth (14). Likewise, cholesterol-exposed THP1 macrophages failed both to produce TNF-α in response to Mtb and to clear the infection (15). To the best of our knowledge, we provide the first evidence that FM display a reduced ability to activate a recall Th1 response of specific antimycobacterial T cell clones. Therefore, we propose that FM significantly subvert the host immune response by impairing both the innate and the adaptive immune branches, and we predict a close relationship between lipid exposure, foamy phenotype acquisition and immunosuppressive properties.

Our study also provides additional mechanisms by which the environment created during infection can drive the foamy differentiation even in the absence of a direct contact with the pathogen. On the one hand, Mtb-infected macrophages can acquire a foamy phenotype as demonstrated in this study and several others (6–9, 27). Indeed, the accumulation of lipid bodies within infected cells has undesirable effects for the host, such as the protection of the pathogen against microbicidal mechanisms (10) and the acquisition of a dormancy phenotype, which confers tolerance to several front-line antibiotics (9). On the other hand, uninfected macrophages can also be driven into foamy cells by IL-10 and a source of lipids. These uninfected lipid-rich cells abrogate the host innate and adaptive cellular defense mechanisms, and when infected, they become a niche favoring pathogen persistence. In the latter case, we infer that uninfected individuals suffering from a lipid dysbalance may bear an enlarged pool of lipid-rich cells that potentially increase the susceptibility, persistence and/or progression of TB. In fact, diabetes and obesity have been associated with TB disease progression (47, 48), and even asymptomatic dyslipidemia was correlated to a reduced antimycobacterial activity (15).

In the past, most reports focused on assessing the impact of certain cytokines in the accumulation of lipid bodies in macrophages within the context of atherosclerosis; FM were proposed to cause the formation of atheroma (49). In fact, IL-1β

and TNF-α are known to impede neutral lipid turnover in THP-1 cells loaded with lipoproteins (50), and these pro-inflammatory cytokines can decrease the efflux of lipids in J774 murine macrophages (51). In addition, IL-10 was shown to regulate lipid metabolism in human macrophages loaded with acetylated and oxidized LDL by increasing both cholesterol uptake and efflux resulting in a net increase in cholesterol content (52, 53). Considering that both pro- and anti-inflammatory cytokines were associated to the accumulation of lipid bodies, we evaluated in this study the effect of depleting several cytokines from TB-PE on the FM formation. In our hands, unlike the depletion of IL-10, the foamy phenotype induced by TB-PE was not altered by depletion of IL-1β, TNF-α, IL-6 or IFN-γ, pointing toward a specific role of IL-10 in promoting FM formation in the context of the pleural infection. Moreover, anti-inflammatory cytokines such as IL-4 and IL-13 were shown to alter lipid metabolism in macrophages through the activation of the lipid-activated nuclear receptors PPARγ (54), which mediates accumulation of lipid bodies (55, 56). Yet, we dismiss a potential role for IL-4 in our model given that its level was undetectable in TB-PE samples (data not shown).

In summary, our present study provides insights into the mechanisms by which host factors can enhance FM formation in macrophages. This knowledge may contribute to the identification of host molecular pathways that could be modulated to the benefit of the patient. Besides, the complementation of the conventional anti-TB therapy with host-directed therapies is desirable in order to achieve shorter treatment times, reduction in lung damage caused by the disease, and lower risk of relapse or reinfection. In this regard, a better understanding of the molecular mechanisms underlying host–pathogen interactions could provide a rational basis for the development of effective anti-TB therapeutics.

ETHICS STATEMENT

Human samples: The research was carried out in accordance with the Declaration of Helsinki (2013) of the World Medical Association, and was approved by the Ethics Committees of the Hospital F. J Muñiz and the Academia Nacional de Medicina de Buenos Aires (protocol number: NIN-1671-12). Written informed consent was obtained before sample collection. Mice samples: Animals were bred and housed in accordance with the guidelines established by the Institutional Animal Care and Use Committee of Institute of Experimental Medicine (IMEX)-CONICET-ANM. All animal procedures were shaped to the principles set forth in the Guide for the Care and Use of Laboratory Animals (NIH, 1996).

AUTHOR CONTRIBUTIONS

MG designed experiments; MG, JF, MD, DK, AM, DM-E, EG-D, and CC performed experiments and analyzed data; BR, AF, and MM performed experiments with mice; EM, SP, and DP collected and provided TB samples; AA and GG performed TLC determinations; JC and RH-P performed ME determinations; PS, PB, ON, IM-P, CS-T, CC, and RH-P supervised experiments and wrote sections of the manuscript; CV, GL-V, MS, and LB contributed to conception and design of the study, supervised experiments, and wrote the manuscript. All authors contributed to manuscript revision, read, and approved the submitted version.

ACKNOWLEDGMENTS

The authors thank Federico Fuentes for his technical assistance. This work was supported by the Argentinean National Agency of Promotion of Science and Technology (PICT-2015-0055), the Argentinean National Council of Scientific and Technical Investigations (CONICET, PIP 112-2013-0100202), the Alberto J. Roemmers Fundation (2016), the bilateral cooperation programs ECOS-Sud (A14S01) and CONACYT/CONICET, the National Council for Science and Technology Mexico (CONACyT FC 2015-1/115), the Centre National de la Recherche Scientifique, the Agence Nationale de la Recherche (ANR 2010-01301, ANR14-CE11-0020-02, ANR16-CE13-0005-01, ANR-11-EQUIPEX-0003), the University of Toulouse, and the Fondation pour la Recherche Médicale (www.frm.org, grants DEQ20160334902 to ON and DEQ20160334894 to IM-P). The funders had no role in study design, data collection, and analysis, decision to publish, or preparation of the manuscript.

SUPPLEMENTARY MATERIAL

The Supplementary Material for this article can be found online at http://www.frontiersin.org/articles/10.3389/fimmu.2018.00459/full#supplementary-material.

FIGURE S1 | Interleukin-10 (IL-10) promotes lipid bodies' accumulation in TB-PE-treated macrophages. **(A)** TB-PE were incubated with neutralizing antibodies for 1 h (4°C) for the depletion of IL-10, IL-6, IL-1β, or TNF-α, and then, Protein G Sepharose beads were added and incubated for 1 h (4°C). Finally, TB-PE was centrifuged at 12,000 × *g* to remove antibody-bead complexes. In the case of IFN-γ depletion, it was performed by incubating TB-PE for 2 h in sterile 96-well plates that had been coated with the capture antibody provided by the human IFN-γ ELISA Kit. In all cases, depletions were controlled by ELISA. **(B)** Human monocyte-derived macrophages were treated with TB-PE depleted or not of IL-10 for 24 h and then, cells were labeled with BODIPY 493/503 to visualize the lipid bodies by green fluorescence emission. The left panels are DIC images of the same field.

FIGURE S2 | Correlation between cholesterol levels and different cytokines present in TB-PE. Correlation analysis between the levels of IL-6, IL-1β, TNF-α, or IFN-γ and the cholesterol content found in individual preparations of TB-PE (n = 23–24).

FIGURE S3 | Signal transducer and activator of transcription 3 (STAT3) activation enhances lipid bodies accumulation by TB-PE. **(A)** Immunoblot images of p705-STAT3, STAT3, and β-actin (left panel); quantification of p705-STAT3 vs STAT3 on macrophages treated or not with Static (20 μM) or cucurbitacin (100 nM) for 2 h and then exposed or not to TB-PE for 24 h (right panel; n = 3). **(B)** Macrophages were treated or not with different concentrations of cucurbitacin for 2 h and then were exposed or not to TB-PE for 24 h. Lipid bodies' content was assessed by Oil Red O (ORO) staining. The results are shown like the integrated density of ORO staining (n = 6) (*$p \leq 0.05$).

REFERENCES

1. World Health Organization. *Global Tuberculosis Report 2017*. Geneva: World Health Organization (2017). 76 p.
2. Russell DG, VanderVen BC, Lee W, Abramovitch RB, Kim MJ, Homolka S, et al. *Mycobacterium tuberculosis* wears what it eats. *Cell Host Microbe* (2010) 8(1):68–76. doi:10.1016/j.chom.2010.06.002
3. Getz GS, Reardon CA. The mutual interplay of lipid metabolism and the cells of the immune system in relation to atherosclerosis. *Clin Lipidol* (2014) 9(6):657–71. doi:10.2217/clp.14.50
4. D'Avila H, Melo RC, Parreira GG, Werneck-Barroso E, Castro-Faria-Neto HC, Bozza PT. *Mycobacterium bovis* bacillus Calmette-Guerin induces TLR2-mediated formation of lipid bodies: intracellular domains for eicosanoid synthesis in vivo. *J Immunol* (2006) 176(5):3087–97. doi:10.4049/jimmunol.176.5.3087
5. Cardona PJ, Llatjos R, Gordillo S, Diaz J, Ojanguren I, Ariza A, et al. Evolution of granulomas in lungs of mice infected aerogenically with *Mycobacterium tuberculosis*. *Scand J Immunol* (2000) 52(2):156–63. doi:10.1046/j.1365-3083.2000.00763.x
6. Kim MJ, Wainwright HC, Locketz M, Bekker LG, Walther GB, Dittrich C, et al. Caseation of human tuberculosis granulomas correlates with elevated host lipid metabolism. *EMBO Mol Med* (2010) 2(7):258–74. doi:10.1002/emmm.201000079
7. Peyron P, Vaubourgeix J, Poquet Y, Levillain F, Botanch C, Bardou F, et al. Foamy macrophages from tuberculous patients' granulomas constitute a nutrient-rich reservoir for *M. tuberculosis* persistence. *PLoS Pathog* (2008) 4(11):e1000204. doi:10.1371/journal.ppat.1000204
8. Russell DG, Cardona PJ, Kim MJ, Allain S, Altare F. Foamy macrophages and the progression of the human tuberculosis granuloma. *Nat Immunol* (2009) 10(9):943–8. doi:10.1038/ni.1781
9. Daniel J, Maamar H, Deb C, Sirakova TD, Kolattukudy PE. *Mycobacterium tuberculosis* uses host triacylglycerol to accumulate lipid droplets and acquires a dormancy-like phenotype in lipid-loaded macrophages. *PLoS Pathog* (2011) 7(6):e1002093. doi:10.1371/journal.ppat.1002093
10. Singh V, Jamwal S, Jain R, Verma P, Gokhale R, Rao KV. *Mycobacterium tuberculosis*-driven targeted recalibration of macrophage lipid homeostasis promotes the foamy phenotype. *Cell Host Microbe* (2012) 12(5):669–81. doi:10.1016/j.chom.2012.09.012
11. Ridley DS, Ridley MJ. Rationale for the histological spectrum of tuberculosis. A basis for classification. *Pathology* (1987) 19(2):186–92. doi:10.3109/00313028709077132
12. Hunter RL, Jagannath C, Actor JK. Pathology of postprimary tuberculosis in humans and mice: contradiction of long-held beliefs. *Tuberculosis* (2007) 87(4):267–78. doi:10.1016/j.tube.2006.11.003
13. Santucci P, Bouzid F, Smichi N, Poncin I, Kremer L, De Chastellier C, et al. Experimental models of foamy macrophages and approaches for dissecting the mechanisms of lipid accumulation and consumption during dormancy and reactivation of tuberculosis. *Front Cell Infect Microbiol* (2016) 6:122. doi:10.3389/fcimb.2016.00122
14. Dodd CE, Pyle CJ, Glowinski R, Rajaram MV, Schlesinger LS. CD36-mediated uptake of surfactant lipids by human macrophages promotes intracellular growth of *Mycobacterium tuberculosis*. *J Immunol* (2016) 197(12):4727–35. doi:10.4049/jimmunol.1600856
15. Asalla S, Mohareer K, Banerjee S. Small molecule mediated restoration of mitochondrial function augments anti-mycobacterial activity of human macrophages subjected to cholesterol induced asymptomatic dyslipidemia. *Front Cell Infect Microbiol* (2017) 7:439. doi:10.3389/fcimb.2017.00439
16. Martinez FO, Gordon S, Locati M, Mantovani A. Transcriptional profiling of the human monocyte-to-macrophage differentiation and polarization: new molecules and patterns of gene expression. *J Immunol* (2006) 177(10):7303–11. doi:10.4049/jimmunol.177.10.7303
17. Ferrer J. Pleural tuberculosis. *Eur Respir J* (1997) 10(4):942–7.
18. Pascutti MF, Rodriguez AM, Falivene J, Giavedoni L, Drexler I, Gherardi MM. Interplay between modified vaccinia virus Ankara and dendritic cells: phenotypic and functional maturation of bystander dendritic cells. *J Virol* (2011) 85(11):5532–45. doi:10.1128/JVI.02267-10
19. Light RW. Update on tuberculous pleural effusion. *Respirology* (2010) 15(3):451–8. doi:10.1111/j.1440-1843.2010.01723.x
20. Xu S, Huang Y, Xie Y, Lan T, Le K, Chen J, et al. Evaluation of foam cell formation in cultured macrophages: an improved method with Oil Red O staining and DiI-oxLDL uptake. *Cytotechnology* (2010) 62(5):473–81. doi:10.1007/s10616-010-9290-0
21. Trinder P. Determination of glucose in blood using glucose oxidase with an alternative oxygen acceptor. *Ann Clin Biochem* (1969) 6(1):24–7. doi:10.1177/000456326900600108
22. Bligh EG, Dyer WJ. A rapid method of total lipid extraction and purification. *Can J Biochem Physiol* (1959) 37(8):911–7. doi:10.1139/o59-099
23. Balboa L, Kviatcovsky D, Schierloh P, Garcia M, de la Barrera S, Sasiain MDC. Monocyte-derived dendritic cells early exposed to *Mycobacterium tuberculosis* induce an enhanced T helper 17 response and transfer mycobacterial antigens. *Int J Med Microbiol* (2016) 306(7):541–53. doi:10.1016/j.ijmm.2016.06.004
24. Balboa L, Romero MM, Laborde E, Sabio YGCA, Basile JI, Schierloh P, et al. Impaired dendritic cell differentiation of CD16-positive monocytes in tuberculosis: role of p38 MAPK. *Eur J Immunol* (2013) 43(2):335–47. doi:10.1002/eji.201242557
25. Swat W, Ignatowicz L, Kisielow P. Detection of apoptosis of immature CD4+8+ thymocytes by flow cytometry. *J Immunol Methods* (1991) 137(1):79–87. doi:10.1016/0022-1759(91)90396-W
26. National Institutes of Health. *Guide for the Care and Use of Laboratory Animals*. Bethesda, MD: National Institutes of Health Publication (1996).
27. Podinovskaia M, Lee W, Caldwell S, Russell DG. Infection of macrophages with *Mycobacterium tuberculosis* induces global modifications to phagosomal function. *Cell Microbiol* (2013) 15(6):843–59. doi:10.1111/cmi.12092
28. Mattos KA, D'Avila H, Rodrigues LS, Oliveira VG, Sarno EN, Atella GC, et al. Lipid droplet formation in leprosy: toll-like receptor-regulated organelles involved in eicosanoid formation and *Mycobacterium leprae* pathogenesis. *J Leukoc Biol* (2010) 87(3):371–84. doi:10.1189/jlb.0609433
29. Schierloh P, Landoni V, Balboa L, Musella RM, Castagnino J, Morana E, et al. Human pleural B-cells regulate IFN-gamma production by local T-cells and NK cells in a *Mycobacterium tuberculosis*-induced delayed hypersensitivity reaction. *Clin Sci* (2014) 127(6):391–403. doi:10.1042/CS20130769
30. Yang L, Hu YJ, Li FG, Chang XJ, Zhang TH, Wang ZT. Analysis of cytokine levers in pleural effusions of tuberculous pleurisy and tuberculous empyema. *Mediators Inflamm* (2016) 2016:3068103. doi:10.1155/2016/3068103
31. Lang R. Tuning of macrophage responses by Stat3-inducing cytokines: molecular mechanisms and consequences in infection. *Immunobiology* (2005) 210(2–4):63–76. doi:10.1016/j.imbio.2005.05.001
32. Murray PJ. Understanding and exploiting the endogenous interleukin-10/STAT3-mediated anti-inflammatory response. *Curr Opin Pharmacol* (2006) 6(4):379–86. doi:10.1016/j.coph.2006.01.010
33. Pol A, Gross SP, Parton RG. Review: biogenesis of the multifunctional lipid droplet: lipids, proteins, and sites. *J Cell Biol* (2014) 204(5):635–46. doi:10.1083/jcb.201311051
34. Russell DG. *Mycobacterium tuberculosis* and the intimate discourse of a chronic infection. *Immunol Rev* (2011) 240(1):252–68. doi:10.1111/j.1600-065X.2010.00984.x
35. Dutt AK, Stead WW. Treatment of extrapulmonary tuberculosis. *Semin Respir Infect* (1989) 4(3):225–31.
36. Seibert AF, Haynes J Jr, Middleton R, Bass JB Jr. Tuberculous pleural effusion. Twenty-year experience. *Chest* (1991) 99(4):883–6. doi:10.1378/chest.99.4.883
37. Vorster MJ, Allwood BW, Diacon AH, Koegelenberg CF. Tuberculous pleural effusions: advances and controversies. *J Thorac Dis* (2015) 7(6):981–91. doi:10.3978/j.issn.2072-1439.2015.02.18
38. Klimiuk J, Krenke R, Safianowska A, Korczynski P, Chazan R. Diagnostic performance of different pleural fluid biomarkers in tuberculous pleurisy. *Adv Exp Med Biol* (2015) 852:21–30. doi:10.1007/5584_2014_105
39. Hutchins AP, Diez D, Miranda-Saavedra D. Genomic and computational approaches to dissect the mechanisms of STAT3's universal and cell type-specific functions. *JAKSTAT* (2013) 2(4):e25097. doi:10.4161/jkst.25097
40. Lastrucci C, Benard A, Balboa L, Pingris K, Souriant S, Poincloux R, et al. Tuberculosis is associated with expansion of a motile, permissive and immunomodulatory CD16(+) monocyte population via the IL-10/STAT3 axis. *Cell Res* (2015) 25(12):1333–51. doi:10.1038/cr.2015.123
41. Yang L, Yang JB, Chen J, Yu GY, Zhou P, Lei L, et al. Enhancement of human ACAT1 gene expression to promote the macrophage-derived foam cell

formation by dexamethasone. *Cell Res* (2004) 14(4):315–23. doi:10.1038/sj.cr.7290231
42. Langlais D, Couture C, Balsalobre A, Drouin J. The Stat3/GR interaction code: predictive value of direct/indirect DNA recruitment for transcription outcome. *Mol Cell* (2012) 47(1):38–49. doi:10.1016/j.molcel.2012.04.021
43. Murray PJ, Allen JE, Biswas SK, Fisher EA, Gilroy DW, Goerdt S, et al. Macrophage activation and polarization: nomenclature and experimental guidelines. *Immunity* (2014) 41(1):14–20. doi:10.1016/j.immuni.2014.06.008
44. Schust J, Sperl B, Hollis A, Mayer TU, Berg T. Stattic: a small-molecule inhibitor of STAT3 activation and dimerization. *Chem Biol* (2006) 13(11):1235–42. doi:10.1016/j.chembiol.2006.09.018
45. da Silva RF, Lappalainen J, Lee-Rueckert M, Kovanen PT. Conversion of human M-CSF macrophages into foam cells reduces their proinflammatory responses to classical M1-polarizing activation. *Atherosclerosis* (2016) 248:170–8. doi:10.1016/j.atherosclerosis.2016.03.012
46. Bhagyaraj E, Nanduri R, Saini A, Dkhar HK, Ahuja N, Chandra V, et al. Human xenobiotic nuclear receptor PXR augments *Mycobacterium tuberculosis* survival. *J Immunol* (2016) 197(1):244–55. doi:10.4049/jimmunol.1600203
47. Hanrahan CF, Golub JE, Mohapi L, Tshabangu N, Modisenyane T, Chaisson RE, et al. Body mass index and risk of tuberculosis and death. *AIDS* (2010) 24(10):1501–8. doi:10.1097/QAD.0b013e32833a2a4a
48. Kumar NP, Moideen K, Sivakumar S, Menon PA, Viswanathan V, Kornfeld H, et al. Tuberculosis-diabetes co-morbidity is characterized by heightened systemic levels of circulating angiogenic factors. *J Infect* (2017) 74(1):10–21. doi:10.1016/j.jinf.2016.08.021
49. Randolph GJ. Mechanisms that regulate macrophage burden in atherosclerosis. *Circ Res* (2014) 114(11):1757–71. doi:10.1161/CIRCRESAHA.114.301174
50. Persson J, Nilsson J, Lindholm MW. Interleukin-1beta and tumour necrosis factor-alpha impede neutral lipid turnover in macrophage-derived foam cells. *BMC Immunol* (2008) 9:70. doi:10.1186/1471-2172-9-70
51. Khovidhunkit W, Moser AH, Shigenaga JK, Grunfeld C, Feingold KR. Endotoxin down-regulates ABCG5 and ABCG8 in mouse liver and ABCA1 and ABCG1 in J774 murine macrophages: differential role of LXR. *J Lipid Res* (2003) 44(9):1728–36. doi:10.1194/jlr.M300100-JLR200
52. Halvorsen B, Waehre T, Scholz H, Clausen OP, von der Thusen JH, Muller F, et al. Interleukin-10 enhances the oxidized LDL-induced foam cell formation of macrophages by antiapoptotic mechanisms. *J Lipid Res* (2005) 46(2):211–9. doi:10.1194/jlr.M400324-JLR200
53. Han X, Kitamoto S, Lian Q, Boisvert WA. Interleukin-10 facilitates both cholesterol uptake and efflux in macrophages. *J Biol Chem* (2009) 284(47):32950–8. doi:10.1074/jbc.M109.040899
54. Almeida PE, Carneiro AB, Silva AR, Bozza PT. PPARgamma expression and function in mycobacterial infection: roles in lipid metabolism, immunity, and bacterial killing. *PPAR Res* (2012) 2012:383829. doi:10.1155/2012/383829
55. Ahluwalia PK, Pandey RK, Sehajpal PK, Prajapati VK. Perturbed microRNA expression by *Mycobacterium tuberculosis* promotes macrophage polarization leading to pro-survival foam cell. *Front Immunol* (2017) 8:107. doi:10.3389/fimmu.2017.00107
56. Vosper H, Patel L, Graham TL, Khoudoli GA, Hill A, Macphee CH, et al. The peroxisome proliferator-activated receptor delta promotes lipid accumulation in human macrophages. *J Biol Chem* (2001) 276(47):44258–65. doi:10.1074/jbc.M108482200

Conflict of Interest Statement: Authors declare that the submitted work was carried out in the absence of personal, professional, or financial relationships that could potentially be construed as a conflict of interest.

Copyright © 2018 Genoula, Marín Franco, Dupont, Kviatcovsky, Milillo, Schierloh, Moraña, Poggi, Palmero, Mata-Espinosa, González-Domínguez, León Contreras, Barrionuevo, Rearte, Córdoba Moreno, Fontanals, Crotta Asis, Gago, Cougoule, Neyrolles, Maridonneau-Parini, Sánchez-Torres, Hernández-Pando, Vérollet, Lugo-Villarino, Sasiain and Balboa. This is an open-access article distributed under the terms of the Creative Commons Attribution License (CC BY). The use, distribution or reproduction in other forums is permitted, provided the original author(s) and the copyright owner are credited and that the original publication in this journal is cited, in accordance with accepted academic practice. No use, distribution or reproduction is permitted which does not comply with these terms.

frontiers in Immunology

ORIGINAL RESEARCH
published: 10 November 2017
doi: 10.3389/fimmu.2017.01537

Suppressor of Cytokine Signaling 3 in Macrophages Prevents Exacerbated Interleukin-6-Dependent Arginase-1 Activity and Early Permissiveness to Experimental Tuberculosis

*Erik Schmok[1], Mahin Abad Dar[1], Jochen Behrends[1], Hanna Erdmann[1], Dominik Rückerl[1], Tanja Endermann[1], Lisa Heitmann[1], Manuela Hessmann[1], Akihiko Yoshimura[2], Stefan Rose-John[3,4], Jürgen Scheller[5], Ulrich Emil Schaible[6], Stefan Ehlers[4,7,8], Roland Lang[9] and Christoph Hölscher[1,4]**

[1] Infection Immunology, Research Center Borstel, Borstel, Germany, [2] Department of Microbiology and Immunology, Graduate School of Medicine, Keio University, Tokyo, Japan, [3] Department of Biochemistry, Christian-Albrechts-University, Kiel, Germany, [4] Cluster of Excellence Inflammation-at-Interfaces (Borstel-Kiel-Lübeck-Plön), Kiel, Germany, [5] Medical Faculty, Institute of Biochemistry and Molecular Biology II, Heinrich-Heine-University, Düsseldorf, Germany, [6] Cellular Microbiology, Research Center Borstel, Borstel, Germany, [7] Microbial Inflammation Research, Research Center Borstel, Borstel, Germany, [8] Molecular Inflammation Medicine, Christian-Albrechts-University, Kiel, Germany, [9] Institute of Clinical Microbiology, Immunology and Hygiene, University Hospital Erlangen, Friedrich-Alexander-University Erlangen-Nuremberg, Erlangen, Germany

OPEN ACCESS

Edited by:
Geanncarlo Lugo-Villarino, UMR5089 Institut de Pharmacologie et de Biologie Structurale (IPBS), France

Reviewed by:
Robin James Flynn, University of Liverpool, United Kingdom
Arnold H. Zea, LSU Health Sciences Center New Orleans, United States

***Correspondence:**
Christoph Hölscher
choelscher@fz-borstel.de

Specialty section:
This article was submitted to Microbial Immunology, a section of the journal Frontiers in Immunology

Received: *08 August 2017*
Accepted: *27 October 2017*
Published: *10 November 2017*

Citation:
Schmok E, Abad Dar M, Behrends J, Erdmann H, Rückerl D, Endermann T, Heitmann L, Hessmann M, Yoshimura A, Rose-John S, Scheller J, Schaible UE, Ehlers S, Lang R and Hölscher C (2017) Suppressor of Cytokine Signaling 3 in Macrophages Prevents Exacerbated Interleukin-6-Dependent Arginase-1 Activity and Early Permissiveness to Experimental Tuberculosis. Front. Immunol. 8:1537. doi: 10.3389/fimmu.2017.01537

Suppressor of cytokine signaling 3 (SOCS3) is a feedback inhibitor of interleukin (IL)-6 signaling in macrophages. In the absence of this molecule, macrophages become extremely prone to an IL-6-dependent expression of arginase-1 (Arg1) and nitric oxide synthase (NOS)2, the prototype markers for alternative or classical macrophage activation, respectively. Because both enzymes are antipodean macrophage effector molecules in *Mycobacterium tuberculosis* (*Mtb*) infection, we assessed the relevance of SOCS3 for macrophage activation during experimental tuberculosis using macrophage-specific SOCS3-deficient (LysM^{cre}SOCS3$^{loxP/loxP}$) mice. Aerosol infection of LysM^{cre}SOCS3$^{loxP/loxP}$ mice resulted in remarkably higher bacterial loads in infected lungs and exacerbated pulmonary inflammation. This increased susceptibility to *Mtb* infection was accompanied by enhanced levels of both classical and alternative macrophage activation. However, high Arg1 expression preceded the increased induction of NOS2 and at early time points of infection mycobacteria were mostly found in cells positive for Arg1. This sequential activation of Arg1 and NOS2 expression in LysM^{cre}SOCS3$^{loxP/loxP}$ mice appears to favor the initial replication of *Mtb* particularly in Arg1-positive cells. Neutralization of IL-6 in *Mtb*-infected LysM^{cre}SOCS3$^{loxP/loxP}$ mice reduced arginase activity and restored control of mycobacterial replication in LysM^{cre}SOCS3$^{loxP/loxP}$ mice. Our data reveal an unexpected role of SOCS3 during experimental TB: macrophage SOCS3 restrains early expression of Arg1 and helps limit *Mtb* replication in resident lung macrophages, thereby limiting the growth of mycobacteria. Together, SOCS3 keeps IL-6-dependent divergent macrophage responses such as *Nos2* and *Arg1* expression under control and safeguard protective macrophage effector mechanisms.

Keywords: ***Mycobacterium tuberculosis*, suppressor of cytokine signaling proteins, mice, knockout, macrophages, arginase I**

INTRODUCTION

Infection with *Mycobacterium tuberculosis* (*Mtb*) remains a major health threat worldwide (1). The family of suppressor of cytokine signaling (SOCS)-proteins includes eight members (2). These molecules are feedback inhibitors of janus kinases (JAK) signaling pathways downstream of cytokine receptors. During cytokine signaling, SOCS proteins are induced *via* signal transducers and activators of transcription (STAT) molecules and in a negative feedback loop regulate and terminate STAT signaling. Importantly, these proteins determine which STAT factors are activated after cytokine receptor ligation and which downstream signaling events are induced. In particular, suppressor of cytokine signaling 3 (SOCS3) is involved in the regulation of gp130-mediated signaling pathways (3–5). gp130 is a common cytokine receptor chain and is responsible in cooperation with individual receptor subunits—for the recognition of many cytokines, the most important of which is interleukin (IL)-6 (6). In the absence of SOCS3 in macrophages, IL-6 is able to mediate both anti- and pro-inflammatory effects (4, 5, 7). These effects are mediated *via* prolonged STAT3 or STAT1 signaling leading to IL-10- or interferon-gamma (IFN-γ)-like responses, respectively. Eventually, this aberrant gp130-mediated signaling in the absence of macrophage SOCS3 lead to an uncontrolled classical macrophages activation (4). Additionally, a knock down of SOCS3 shifts the activation of macrophages toward an alternative phenotype at the same time (8). Consequently, SOCS3 is essential for regulating the specificity of IL-6 signaling in macrophages.

Macrophages are the main host and effector cells in *Mtb* infection. In experimental animal models, control of mycobacterial replication is strictly dependent on the IL-12-instructed development and infiltration of CD4$^+$ T helper type 1 (Th1) cells into the lung (9). The secretion of IFN-γ by Th1 cells eventually induces the so-called classically activated macrophages to express effector molecules central to the anti-mycobacterial immune response such as the inducible nitric oxide synthase (NOS)2 and LRG-47, a member of the 47-kilodalton p47 guanosine triphosphatase family (10, 11). On the other hand, a Th2 immune response induces the arginase-1 (Arg1) expressing so-called alternatively activated macrophages, which counteract protective anti-mycobacterial macrophage effector mechanisms (12–14).

Hence, the activation state of macrophages is critical for the control of mycobacterial growth. *Mtb*-infected macrophages express *Socs3* in a MyD88-dependent manner (15) and during experimental tuberculosis (TB), *Socs3* is induced in lungs of infected mice (13). Previously, SOCS3 in macrophages has been implicated in promoting the IL-12-dependent development of Th1 cells in experimental *Toxoplasma gondii* (16) and *Mtb* (15) infection. To further assess the role of macrophage SOCS3 in experimental TB, we analyzed macrophage responses in macrophage-specific SOCS3-deficient (LysM^{cre}SOCS3$^{loxP/loxP}$) mice (5) and give evidence that in the absence of macrophage SOCS3, IL-6 promotes susceptibility to *Mtb* infection by the early induction of Arg1 in resident macrophages. Our study implicates that SOCS3 additionally act as an underappreciated critical component to prevent mycobacterial growth in macrophages.

RESULTS

Macrophage-Specific SOCS3-Deficient Mice Are Highly Susceptible to *Mtb* Infection

To evaluate the effect of macrophage SOCS3 on the outcome of experimental TB, we infected LysM^{cre}SOCS3$^{loxP/loxP}$ mice (deficient for SOCS3 in macrophages) and cre-negative littermates. Bacterial loads were determined at different time-points following aerosol *Mtb* infection. Compared to SOCS3$^{loxP/loxP}$ mice, bacterial loads in lungs of LysM^{cre}SOCS3$^{loxP/loxP}$ mice were significantly enhanced 21 and 25 days after infection (**Figure 1A**) confirming the high susceptibility of these mice shown by Carow et al. (15).

Infiltration of Macrophages and Granulocytes in the Lungs of *Mtb*-Infected LysM^{cre}SOCS3$^{loxP/loxP}$ Mice Is Increased

We next assessed the pathological consequences of macrophage-specific SOCS3 deficiency during experimental TB. After 23 days of infection, the total number of cells infiltrating the lungs of *Mtb*-infected LysM^{cre}SOCS3$^{loxP/loxP}$ mice was increased threefold when compared to SOCS3$^{loxP/loxP}$ mice (data not shown). The main cell types progressively infiltrating the lungs of macrophage-specific SOCS3-deficient mice were predominantly CD11b$^+$ macrophages and granulocytes (**Figure 1B**). Twenty-three days after *Mtb* infection, their numbers were approximately 3- and 10-fold increased as compared to SOCS3$^{loxP/loxP}$ mice, respectively (**Figure 1C**). By contrast, the absolute number of CD4$^+$ T cells was comparable in the lungs of both SOCS3$^{loxP/loxP}$ and LysM^{cre}SOCS3$^{loxP/loxP}$ mice (**Figure 1C**). Histopathological analysis of lungs taken from LysM^{cre}SOCS3$^{loxP/loxP}$ mice confirmed an enhanced inflammatory cell influx (**Figure 1D**). Organized granuloma formation was absent in cre-positive SOCS3$^{loxP/loxP}$ mice until day 28 (**Figure 1D**; H&E staining) and this enhanced inflammatory environment alongside the mycobacterial overgrowth (**Figure 1D**; ZN staining) led to accelerated death of these mice (**Figure 1E**).

Inflammatory Immune Responses Are Severely Altered in *Mtb*-Infected LysM^{cre}SOCS3$^{loxP/loxP}$ Mice

To examine why mycobacteria growth was not controlled in LysM^{cre}SOCS3$^{loxP/loxP}$ mice, the induction of pro- and anti-inflammatory cytokines in lung homogenates after *Mtb* infection was characterized by determining the concentrations of IL-6, tumor necrosis factor (TNF), IL-10, IFN-γ, and IL-12/IL-23p40 in a cytometric bead array (CBA) (**Figure 2A**). Compared to SOCS3$^{loxP/loxP}$ mice, the production of IL-6, TNF, and IL-10 was significantly elevated in the lungs of LysM^{cre}SOCS3$^{loxP/loxP}$ mice after *Mtb* infection whereas the amount of IFN-γ was comparable in both cre-negative and cre-positive SOCS3$^{loxP/loxP}$ mice (**Figure 2A**). In striking contrast, during the course of experimental TB the expression of IL-12/IL-23p40 was significantly reduced in macrophage-specific SOCS3-deficient mice when compared to infected SOCS3$^{loxP/loxP}$ mice (**Figure 2A**). Because IL-12 is required to promote a protective Th1 immune response

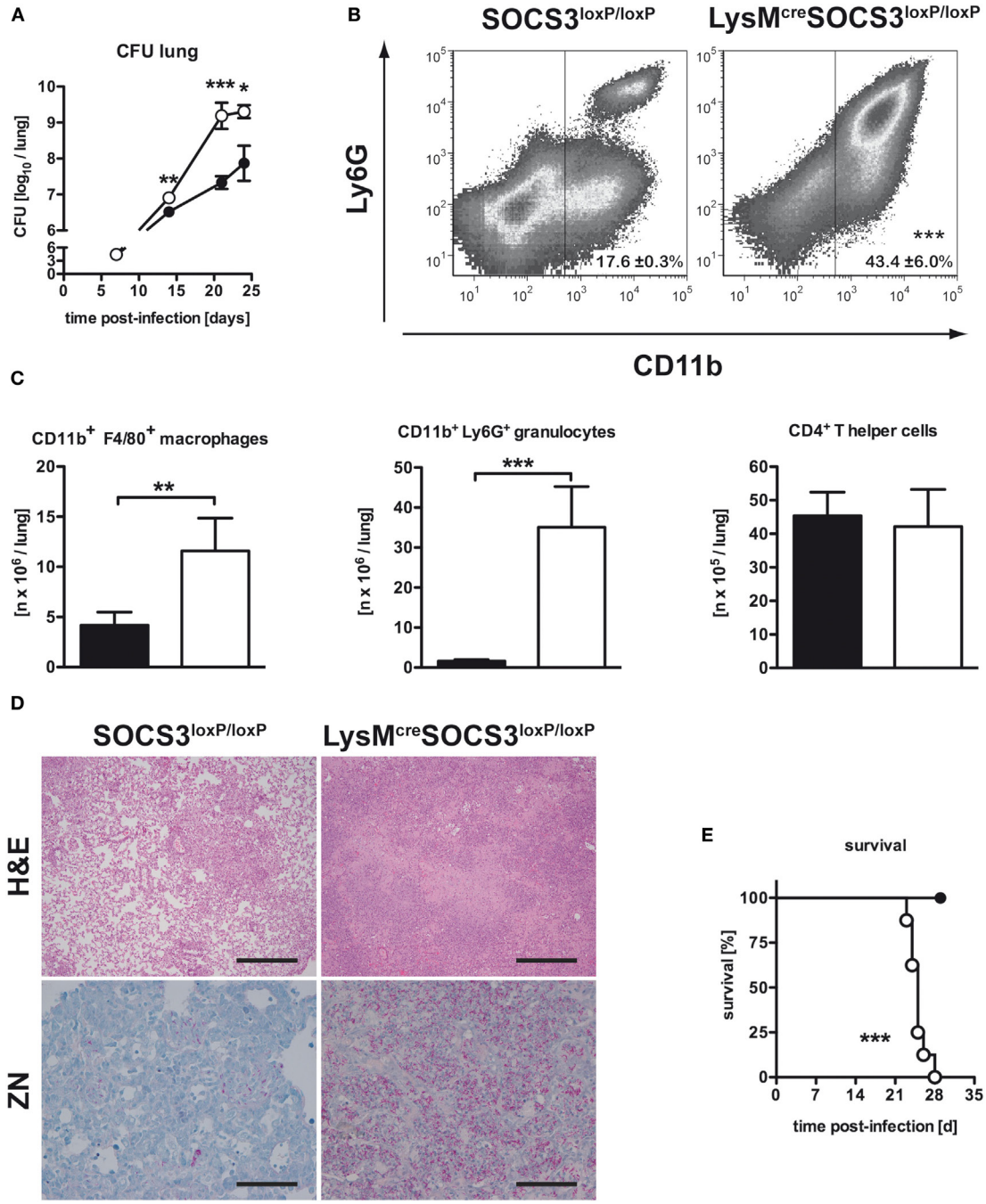


FIGURE 1 | Macrophage-specific suppressor of cytokine signaling 3 (SOCS3)-deficient mice were highly susceptible to *Mtb* infection. Cre-negative SOCS3$^{loxP/loxP}$ control mice (black symbols) and LysM^{cre}SOCS3$^{loxP/loxP}$ mice (white symbols) were infected with approximately 1,000 CFU *Mtb via* the aerosol route and lungs were isolated at the indicated time points. **(A)** For mycobacterial colony enumeration assays, aseptically removed lungs were weighed, transferred into PBS containing a proteinase inhibitor cocktail and homogenized. Tenfold serial dilutions of organ homogenates were plated and colonies were counted 3 weeks later. One experiment representative of three performed is shown. **(B,C)** At 23 days of infection, perfused lungs were digested and single-cell suspensions were analyzed by flow cytometry for surface expression of CD11b and Ly6G **(B)**. **(C)** After automated cell counting and flow cytometry of CD11b$^+$ F4/80$^+$ macrophages, CD11b$^+$ Ly6G$^+$ granulocytes, and CD4$^+$ T cells, absolute numbers of these cell populations were calculated. Data represent means ± SD of at least five mice per group. One experiment representative of two performed is shown. Statistical analysis was performed as described in experimental procedures defining differences between SOCS3$^{loxP/loxP}$ and LysM^{cre}SOCS3$^{loxP/loxP}$ mice as significant (***$p < 0.001$; **$p < 0.01$). **(D)** Hematoxylin/eosin (H&E, original magnification 100×; scale bar = 1 mm) and Ziehl–Neelsen staining (ZN, original magnification 400×; scale bar = 0.25 mm) of sections from formalin-fixed and paraffin-embedded lungs isolated from mice after 27 days of infection. **(E)** Survival of 10 infected mice per group was monitored. Animals that lost more than 25% of their original body weight were sacrificed. Statistical analysis was performed as described in experimental procedures defining differences between SOCS3$^{loxP/loxP}$ and LysM^{cre}SOCS3$^{loxP/loxP}$ mice as significant (***$p \leq 0.001$).

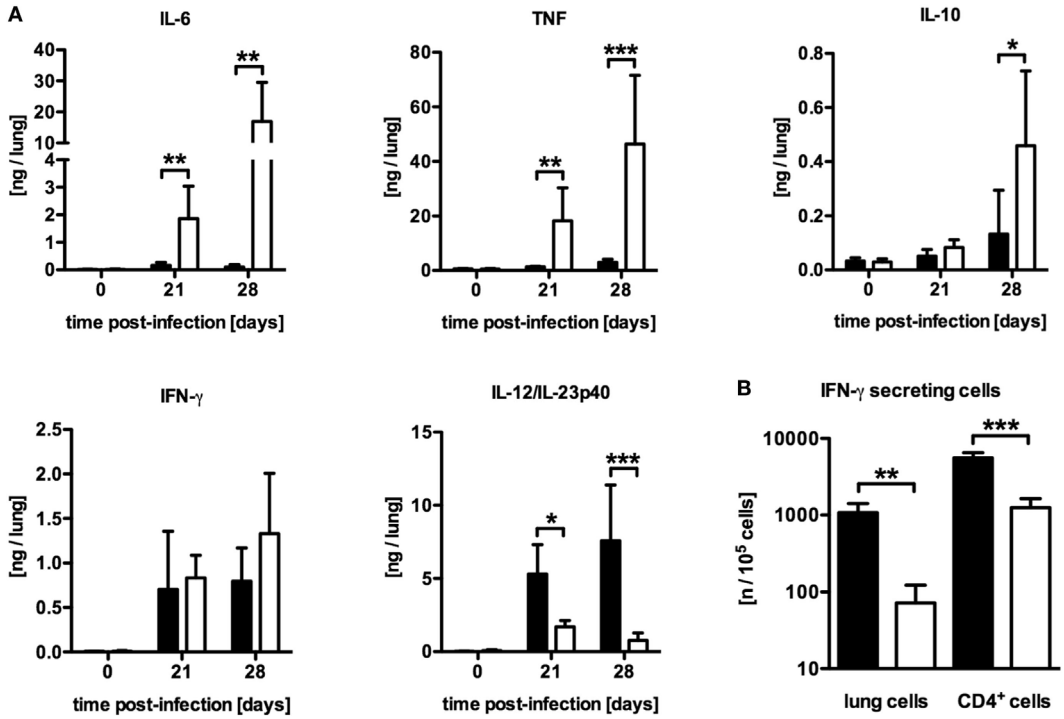


FIGURE 2 | Differentially expressed inflammatory immune responses in *Mtb*-infected LysM^{cre}SOCS3$^{loxP/loxP}$ mice. Cre-negative SOCS3$^{loxP/loxP}$ control mice (black symbols) and LysM^{cre}SOCS3$^{loxP/loxP}$ mice (white symbols) were infected with approximately 1,000 CFU *Mtb via* the aerosol route and lungs were isolated at the indicated time points. **(A)** Cytokine levels were measured by cytometric bead array (CBA) in lung homogenates and the quantity of cytokines per lung was calculated based on the ratio of lung to sample weight. **(B)** At 23 days of infection, perfused lungs were digested and single-cell suspensions, as well as enriched CD4$^+$ T cells, were restimulated with ESAT-6$_{1–20}$. The frequency of IFN-γ-producing cells was determined by an ELISPOT assay. Data represent means ± SD of at least five mice per group. One experiment representative of two performed is shown. Statistical analysis was performed as described in experimental procedures defining differences between SOCS3$^{loxP/loxP}$ and LysM^{cre}SOCS3$^{loxP/loxP}$ mice as significant (*$p \leq 0.05$; **$p \leq 0.01$; ***$p \leq 0.001$).

(17), we next investigated the frequency of antigen-specific IFN-γ-producing cells using whole cell suspensions or purified CD4$^+$ T cells from lungs of infected animals in an ELISPOT assay (**Figure 2B**). On day 21 of *Mtb* infection, the frequency of IFN-γ-producing CD4$^+$ T cells was significantly reduced in the lungs of *Mtb*-infected LysM^{cre}SOCS3$^{loxP/loxP}$ mice (**Figure 2B**). Taken together, these data show a dysregulation of pro- and anti-inflammatory cytokine production in LysM^{cre}SOCS3$^{loxP/loxP}$ mice during *Mtb* infection.

Our results are in line with previous studies addressing the impact of a macrophage-specific SOCS3 deficiency on the outcome of experimental toxoplasmosis (16) and TB (15) which implicated the reduced IL-12/IL-23 production and subsequent impaired Th1 immune response to be involved in the impaired control of *Mtb* infection in LysM^{cre}SOCS3$^{loxP/loxP}$ mice.

NOS2 and Arg1 Are Elevated in *Mtb*-Infected LysM^{cre}SOCS3$^{loxP/loxP}$ Mice but Arg1 Expression Precedes That of NOS2

Based on *in vitro* experiments, Carow et al. excluded impaired macrophages effector functions as a cause for the increased susceptibility of *Mtb*-infected LysM^{cre}SOCS3$^{loxP/loxP}$ mice (15). The IFN-γ-dependent induction of the effector molecule NOS2 and subsequent production of reactive nitrogen intermediates (RNI) in classically activated macrophages, which are toxic to intracellular *Mtb*, is required for control of mycobacterial growth (10). Hence, the reduced frequency of Th1 cells in LysM^{cre}SOCS3$^{loxP/loxP}$ mice might also result in a diminished induction of this enzyme. To evaluate whether a modulated expression of *Nos2* accounts for the increased susceptibility of *Mtb*-infected LysM^{cre}SOCS3$^{loxP/loxP}$ mice, we determined the expression of *Nos2* and the production of RNI in lung homogenates of infected mice (**Figure 3A**). Quantitative real time (qRT)-PCR revealed that 21 and 28 days after *Mtb* infection *Nos2* was considerably induced in lungs of SOCS3$^{loxP/loxP}$ mice (**Figure 3A**). However, *Nos2* expression was even higher in lung homogenates of infected LysM^{cre}SOCS3$^{loxP/loxP}$ mice. To determine the NOS2-dependent production of RNI during experimental TB we quantified the production of nitrate in lung homogenates from SOCS3$^{loxP/loxP}$ and LysM^{cre}SOCS3$^{loxP/loxP}$ mice (**Figure 3A**). In uninfected mice, low amounts of nitrate were detected in lung homogenates. After infection with *Mtb*, the production of nitrates increased in SOCS3$^{loxP/loxP}$ mice. In lung homogenates of infected LysM^{cre}SOCS3$^{loxP/loxP}$ mice, nitrate levels were significantly increased by threefold compared to littermate controls. Therefore, it appears that if the increased susceptibility of LysM^{cre}SOCS3$^{loxP/loxP}$ mice to experimental TB cannot be attributed to an impaired expression and function of NOS2, other

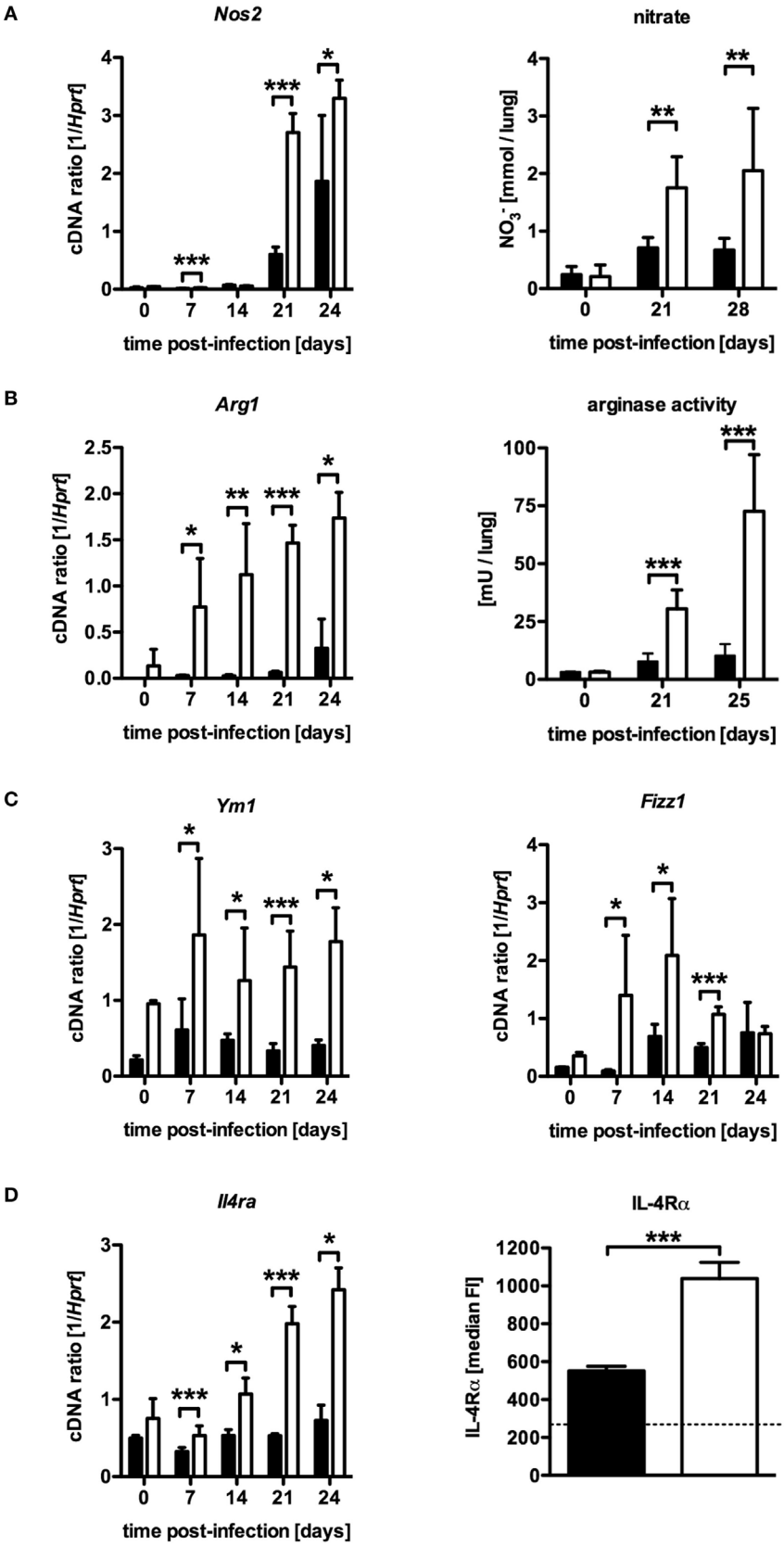


FIGURE 3 | Continued

FIGURE 3 | Continued
Elevated NOS2 and arginase activity in *Mtb*-infected LysM^{cre}SOCS3$^{loxP/loxP}$ mice. Cre-negative SOCS3$^{loxP/loxP}$ control mice (black symbols) and LysM^{cre}SOCS3$^{loxP/loxP}$ mice (white symbols) were infected with approximately 1,000 CFU *Mtb via* the aerosol route and lungs were isolated at the indicated time points. **(A)** Gene expression of *Nos2* in lung homogenates was determined by qRT-PCR. To detect RNI, NO_3 was converted into NO_2 after deproteination of homogenates. Following the addition of Griess reagents, the content of NO_2 was determined by photometric measurement. **(B)** Gene expression of *Arg1* in lung homogenates was determined by qRT-PCR. To determine arginase activity, the enzyme was activated and arginine hydrolysis was conducted after the addition of L-arginine. The reaction was stopped and the urea concentration was determined as a degree of arginase activity. **(C)** Gene expression of *Ym1* and *Fizz1* in lung homogenates was determined by qRT-PCR. **(D)** Gene expression of *Il4ra* in lung homogenates and surface expression of the IL-4Rα was determined by qRT-PCR and flow cytometry of CD11b$^+$ F4/80$^+$ macrophages, respectively. Data represent means ± SD of at least five mice per group. One experiment representative of 2 performed is shown. Statistical analysis was performed as described in experimental procedures defining differences between SOCS3$^{loxP/loxP}$ and LysM^{cre}SOCS3$^{loxP/loxP}$ mice as significant (**$p \leq 0.01$; ***$p \leq 0.001$).

mechanisms may overwrite this normally protective response. Induction of *Nos2* can be counter-regulated by a concomitant Arg1 enzyme activity (12, 13). Arg1, a marker of alternative activation, hydrolyzes L-arginine to urea and L-ornithine and has been discussed to regulate RNI production in macrophages through depletion of L-arginine, the substrate for NOS2 (18, 19). Additionally, Arg1-dependent production of polyamines may promote growth of intracellular pathogens (20, 21). Therefore, we speculated that in LysM^{cre}SOCS3$^{loxP/loxP}$ mice, an increased arginase activity in the lungs modulates protective effector mechanisms against *Mtb* usually exerted by classically activated macrophages. A kinetic quantification of gene expression in lung homogenates revealed that *Arg1* is only moderately induced in lungs of SOCS3$^{loxP/loxP}$ mice during the course of *Mtb* infection (**Figure 3B**). By contrast, *Arg1* expression in LysM^{cre}SOCS3$^{loxP/loxP}$ mice was highly induced early during *Mtb* infection. Accordingly, arginase activity in lungs of LysM^{cre}SOCS3$^{loxP/loxP}$ mice was also strikingly elevated when compared to enzyme activity in lungs of infected SOCS3$^{loxP/loxP}$ mice (**Figure 3B**). Importantly, high *Arg1* gene expression precedes the increased gene expression of *Nos2* (**Figures 3A,B**).

The expression of *Nos2* in infected tissue characterizes classical macrophage activation, which is required for protective macrophage effector responses. By contrast, alternatively activated macrophages are defined by tissue expression of *Arg1* and other markers, such as *Ym1*, *Fizz1*, and the IL-4Rα-subunit especially during pulmonary inflammation (22). To evaluate whether SOCS3 deficiency generally intensify alternative macrophage activation during *Mtb* infection, gene and surface expression of different markers were quantified by qRT-PCR in lung homogenates and flow cytometry of single-cell suspensions, respectively (**Figures 3C,D**). Interestingly, LysM^{cre}SOCS3$^{loxP/loxP}$ mice constitutively expressed elevated levels of *Ym1* and *Fizz1* in lung homogenates (**Figure 3C**). Whereas in SOCS3$^{loxP/loxP}$ mice, *Ym1* and *Fizz1* were only marginally stimulated after *Mtb* infection, gene expression of these markers for alternative macrophage activation was highly induced in lung homogenates of *Mtb*-infected LysM^{cre}SOCS3$^{loxP/loxP}$ mice. During the course of infection, the expression of these markers was significantly increased in LysM^{cre}SOCS3$^{loxP/loxP}$ mice compared to SOCS3$^{loxP/loxP}$ animals. To further evaluate alternative macrophage activation in LysM^{cre}SOCS3$^{loxP/loxP}$ mice during experimental TB, we also quantified expression of *Il4ra* by qRT-PCR in lung homogenates and on the single-cell level by flow cytometric analysis of IL-4Rα expression on CD11b$^+$ F4/80$^+$ lung cells (**Figure 3D**). Before infection, gene expression was similarly low in both SOCS3$^{loxP/loxP}$ and LysM^{cre}SOCS3$^{loxP/loxP}$ mice. After infection with *Mtb*, only LysM^{cre}SOCS3$^{loxP/loxP}$ mice showed *Il4ra* gene expression levels that were significantly different from a basal expression in SOCS3$^{loxP/loxP}$ mice. On day 23 of experimental TB, surface expression of the IL-4Rα was significantly increased on macrophages in single lung cell suspensions of LysM^{cre}SOCS3$^{loxP/loxP}$ mice when compared to the surface expression on macrophages from infected SOCS3$^{loxP/loxP}$ mice. Our results so far indicate that during *Mtb* infection SOCS3 is involved in regulating early alternative macrophage activation.

Because we found that *Nos2* and *Arg1* are highly expressed in the absence of macrophage SOCS3 but *Arg1* precedes the expression of *Nos2*; we considered that, in LysM^{cre}SOCS3$^{loxP/loxP}$ mice, most bacteria might initially and preferentially multiply in *Arg1*-expressing cells. We, therefore, conducted double staining of mycobacteria and NOS2 or Arg1 in lung sections of LysM^{cre}SOCS3$^{loxP/loxP}$ mice 1 week after infection with *Mtb*. In SOCS3$^{loxP/loxP}$ mice, NOS2- and Arg1-expressing cells were not detectable at this early time point (data not shown) reflecting the low gene expression of both enzymes (see **Figures 3A,B**). In lungs of LysM^{cre}SOCS3$^{loxP/loxP}$ mice, 1 week after infection *Arg1* precedes *Nos2* gene expression (see **Figures 3A,B**) and accordingly Arg1-positive cells were abundant (**Figure 4A**), whereas NOS2-positive cells were hardly detectable (**Figure 4B**). Importantly, at this early time point, mycobacteria were mostly found in Arg1-expressing cells. Together, these results indicate that in *Mtb*-infected LysM^{cre}SOCS3$^{loxP/loxP}$ mice an early exacerbated arginase activity favors the initial replication of *Mtb* particularly in *Arg1*-expressing cells.

In the Absence of Macrophage SOCS3, *Mtb* Infects Increasingly Arg1-Expressing Resident Macrophages

Having shown that in the absence of macrophage SOCS3 *Mtb* evades in early appearing Arg1-expressing cells, we next analyzed the fate of mycobacteria in different types of macrophages during the course of infection *in vivo*. A defective recruitment of CD11b^{med}F4/80^{med} infiltrating macrophages in the lungs of infected mice is associated with susceptibility to *Mtb* (23). The examination of resident CD11b^{hi}F4/80^{hi} and infiltrating CD11b^{med}F4/80^{med} macrophages in lungs of *Mtb*-infected SOCS3$^{loxP/loxP}$ and LysM^{cre}SOCS3$^{loxP/loxP}$ mice (as defined in the representative plot in **Figure 5A**) revealed a comparable frequency in both strains

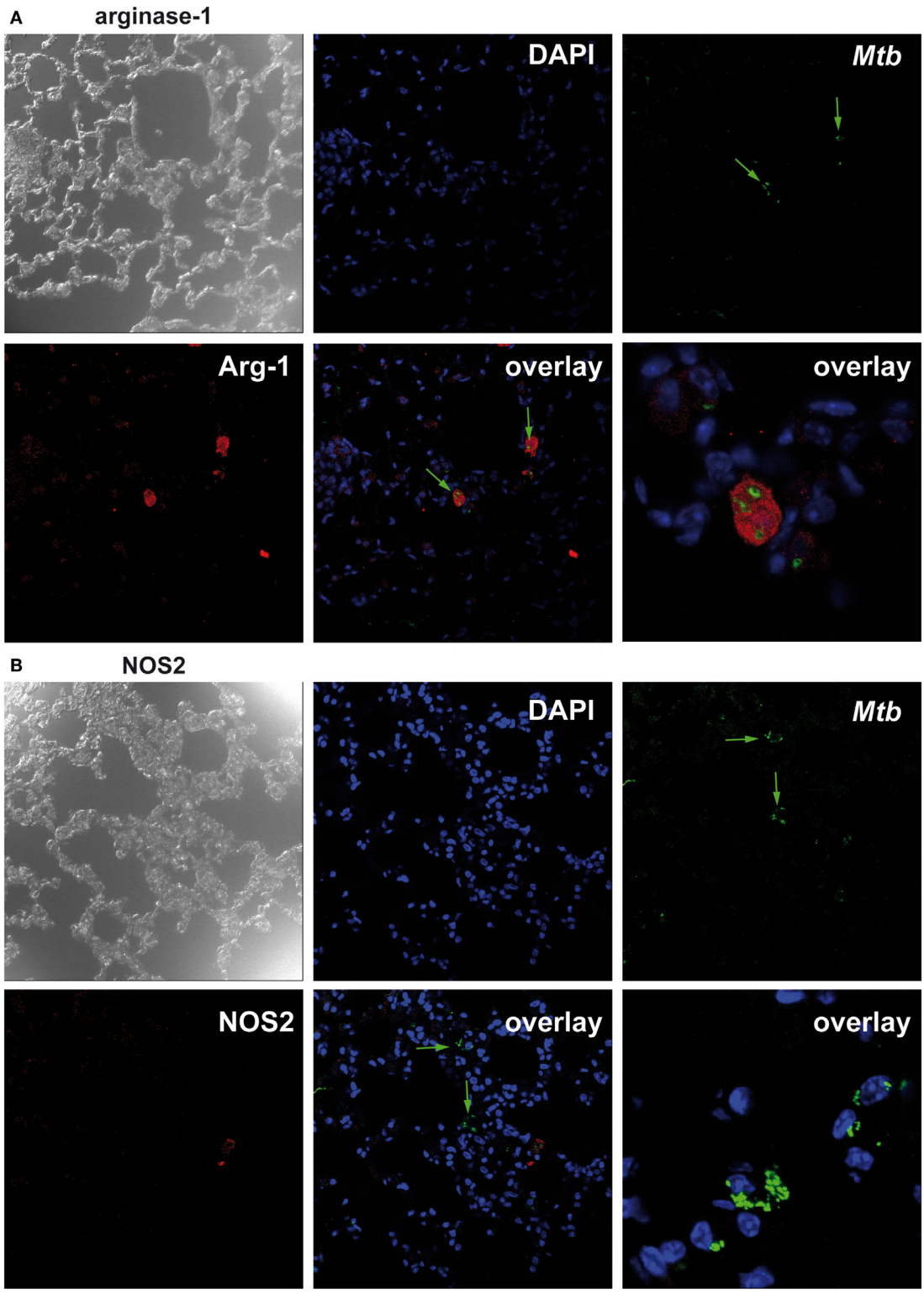


FIGURE 4 | Suppressor of cytokine signaling 3 (SOCS3) deficiency in macrophages favors the initial replication of *Mtb* in arginase-1 (Arg1)-expressing cells. Cre-negative SOCS3$^{loxP/loxP}$ control mice and LysM^{cre}SOCS3$^{loxP/loxP}$ mice were infected with approximately 1,000 CFU *Mtb via* the aerosol route and lungs were isolated 1 week later. After antigen retrieval and blocking, deparaffinized formalin-fixed lung sections were incubated with goat anti-Arg1 antibody or rabbit anti-NOS2 antibody. Sections were subsequently incubated with rabbit anti-goat IgG-biotin or goat anti-rabbit IgG-biotin, respectively, followed by an incubation with Streptavidin-Cy5. Finally, sections were co-stained with rabbit anti-*Mtb*-FITC and DAPI. Co-localization of *Mtb* and **(A)** Arg1 or **(B)** NOS2 was determined by confocal microscopy. Data represent representative photomicrographs of at least five mice per group.

with a relative proportion of approximately 45–60% infiltrating macrophages and approximately 10% resident macrophages (**Figure 5A**). Infection of experimental mice with recombinant *Mtb* expressing mCherry enabled us to track bacteria in these cell types by flow cytometry (representative plot in **Figure 5B**). However, because *Mtb*^{mCherry} was less virulent than wild-type *Mtb*, lungs were isolated on day 36 after infection. Whereas in lungs of SOCS3$^{loxP/loxP}$ mice, *Mtb* was predominantly found in infiltrating

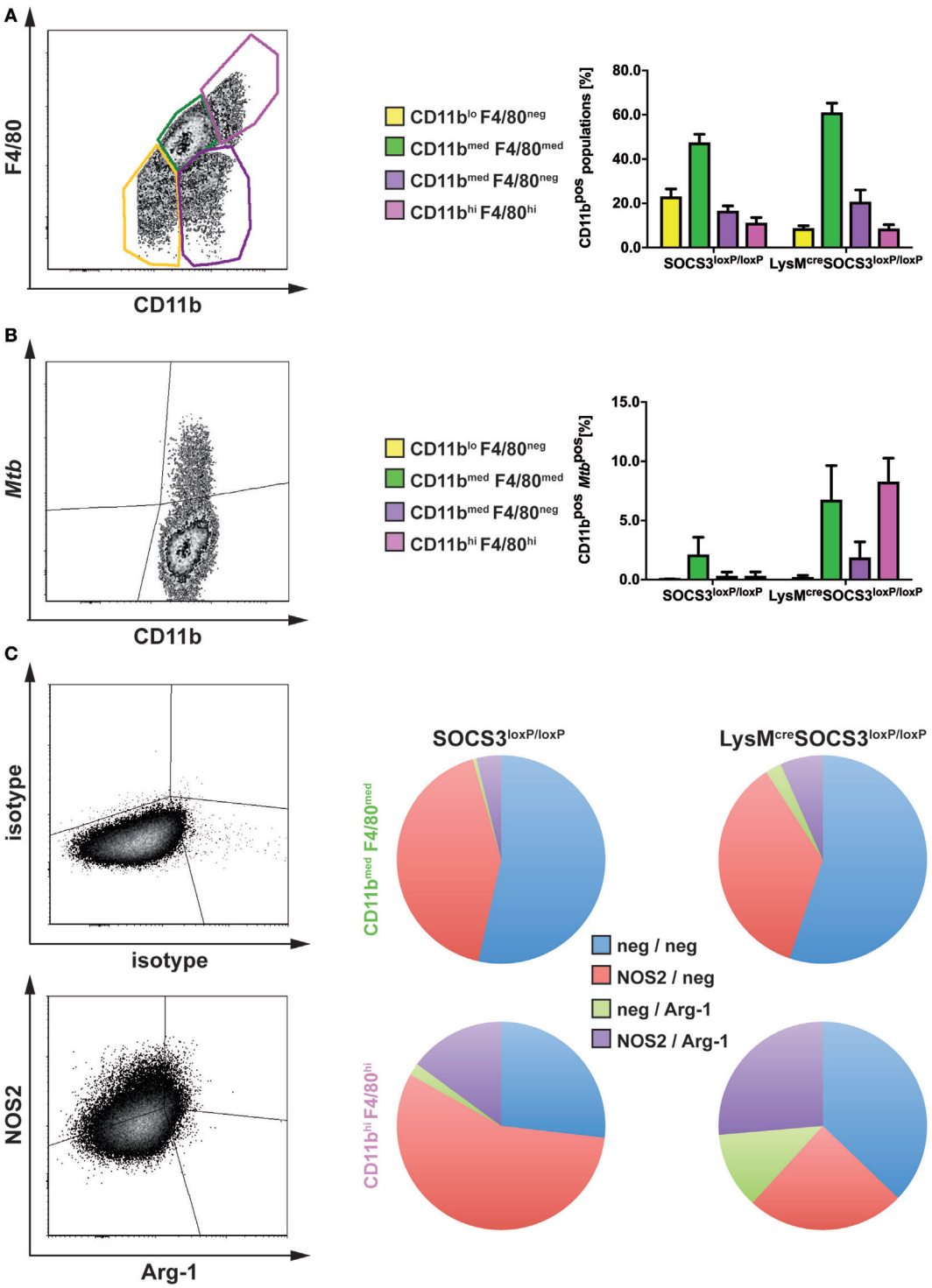


FIGURE 5 | Continued

FIGURE 5 | Continued
In the absence of macrophage suppressor of cytokine signaling 3 (SOCS3), *Mtb* infects increasingly arginase-1 (Arg1)-expressing resident macrophages. Cre-negative SOCS3$^{loxP/loxP}$ control mice and LysM^{cre}SOCS3$^{loxP/loxP}$ mice were infected with approximately 1,000 CFU *Mtb* **(A,C)** or *Mtb*^{mCherry} **(B)** *via* the aerosol route. At 21 or 36 days of infection, respectively, perfused lungs were digested and single-cell suspensions were analyzed by flow cytometry for surface expression of CD11b, F4/80, *Mtb*^{mCherry}, and intracellular NOS2 and Arg1. **(A,B)** For flow cytometric analysis of surface markers, single-cell suspensions of lungs were incubated with an anti-FcγRIII/II monoclonal antibody and stained with optimal concentrations of anti-CD11b and anti-F4/80. **(A)** Characterization of different macrophage populations (as defined in the representative plot) in SOCS3$^{loxP/loxP}$ and LysM^{cre}SOCS3$^{loxP/loxP}$ mice based on surface expression of CD11b and F4/80. **(B)** The presence of *Mtb* in the macrophage populations defined in **(A)**. **(C)** For intracellular staining of NOS2 and Arg1 in CD11b^{med} F4/80^{med} and CD11b^{hi} F4/80^{hi} cells isolated from lungs of SOCS3$^{loxP/loxP}$ and LysM^{cre}SOCS3$^{loxP/loxP}$ mice, single-cell suspensions of lungs were stained for surface markers before permeabilization. Staining of NOS2 and Arg1 was performed using optimal concentrations of anti-NOS2 and anti-Arg1 antibodies. Appropriate isotype controls were used. Data represent means ± SD of three to five mice per group. In **(A and C)**, one experiment representative of two performed is shown.

macrophages, in LysM^{cre}SOCS3$^{loxP/loxP}$ mice mycobacteria were detectable not only in infiltrating CD11b^{med}F4/80^{med} but also, to the same extent, in resident CD11b^{hi}F4/80^{hi} cells (**Figure 5B**).

We next determined the relative expression of NOS2 and Arg1 by intracellular staining of both enzymes in resident CD11b^{hi}F4/80^{hi} and infiltrating CD11b^{med}F4/80^{med} macrophages in lungs of *Mtb*-infected SOCS3$^{loxP/loxP}$ and LysM^{cre}SOCS3$^{loxP/loxP}$ mice (**Figure 5C**). Most of the infiltrating macrophages in lungs of both SOCS3$^{loxP/loxP}$ and LysM^{cre}SOCS3$^{loxP/loxP}$ mice were found negative for both, NOS2 and Arg1 or expressed only NOS2. Very few CD11b^{med}F4/80^{med} cells expressed Arg1 alone or both, NOS2 and Arg1 (**Figure 5C**). Approximately 50% of resident CD11b^{hi}F4/80^{hi} macrophages in lungs of SOCS3$^{loxP/loxP}$ animals were found single positive for NOS2, about 20% were double positive for NOS2, and Arg-1 and 25% double negative. A small proportion expressed Arg1 only. By contrast, in lungs of LysM^{cre}SOCS3$^{loxP/loxP}$ mice the frequencies of Arg1-positive and Arg1/NOS2-positive but also that of Arg1/NOS2-negative CD11b^{hi}F4/80^{hi} cells increased at the cost of a decreased relative amount of NOS2-positive cells (**Figure 5C**).

Together, the absence of SOCS3 is associated with an uncontrolled expression of Arg1 and concomitant enhanced replication of *Mtb* in lung macrophages during experimental TB.

IL-6 Contributes to Alternative Macrophage Activation and Subsequent Susceptibility and Pathology in *Mtb*-Infected LysM^{cre}SOCS3$^{loxP/loxP}$ Mice

Suppressor of cytokine signaling 3 is involved in the regulation of gp130-mediated IL-6 signaling and suppresses the induction and maintenance of STAT1- and STAT3-dependent downstream effects (4, 5). We, therefore, determined whether IL-6-dependent signaling was causally involved in the increased susceptibility of LysM^{cre}SOCS3$^{loxP/loxP}$ mice during *Mtb* infection *in vivo*. To this end, we neutralized IL-6 by using a monoclonal anti-IL-6 antibody *in vivo*. During experimental TB, IL-6 neutralization had no effect on bacterial loads in lungs of C57LB/6 mice (**Figure 6A**). In contrast, neutralization of IL-6-dependent signals significantly reduced CFU in lungs of LysM^{cre}SOCS3$^{loxP/loxP}$ mice infected for 21 and 28 days with *Mtb*. However, bacterial loads in lungs from anti-IL-6-treated cre-positive SOCS3$^{loxP/loxP}$ mice were still increased compared to infected SOCS3$^{loxP/loxP}$ mice. IL-6 neutralization also greatly ameliorated pathology in LysM^{cre}SOCS3$^{loxP/loxP}$ mice infected with *Mtb* for 28 days (**Figure 6B**). The reduced expression of *Il12b* and *Ifng* in lung homogenates of *Mtb*-infected LysM^{cre}SOCS3$^{loxP/loxP}$ mice could only partially be restored by treatment with anti-IL-6 (**Figure 6C**). Because we show here that macrophage-specific SOCS3 deficiency promotes IL-6-induced classical and alternative macrophage activation during experimental TB *in vivo*, we next assessed whether IL-6 neutralization affected macrophage activation in the lungs of *Mtb*-infected mice. Treatment of C57BL/6 mice with anti-IL-6 had neither an effect on classical macrophage activation (measured by *Nos2* gene expression and nitrate production in lung homogenates; **Figure 6D**) nor on alternative macrophage activation (determined by *Ym1*, *Fizz1*, *Arg1* gene expression, and arginase activity in lung homogenates; **Figures 6E,F**). IL-6 neutralization reduced classical macrophage activation only to some extent with significantly decreased levels of RNI in lung homogenates of LysM^{cre}SOCS3$^{loxP/loxP}$ mice 21 after *Mtb* infection (**Figure 6D**). In infected SOCS3-deficient mice anti-IL-6 mAb treatment had no effect on gene expression of *Ym1* and *Fizz1* (**Figure 6E**) but IL-6 neutralization significantly reduced *Arg1* gene expression and arginase activity in lung homogenates of LysM^{cre}SOCS3$^{loxP/loxP}$ mice that were infected with *Mtb* for 21 and 28 days (**Figure 6F**).

Together, these results demonstrate that SOCS3 prevents an IL-6-dependent dysregulated state of macrophage activation *in vivo* that promotes mycobacterial growth.

DISCUSSION

Reduced expression of SOCS3 has been associated with recurrent and pulmonary disease in TB patients, respectively (24, 25). For the model of experimental TB, Carow et al. convincingly showed that the control of an IL-6-mediated inhibition of IL-12 secretion by SOCS3 in macrophages contributes to the protective effect of SOCS3 (15).

Our results corroborate these findings and additionally show that a lack of macrophage-specific expression of SOCS3 results in a profound susceptibility to *Mtb* infection. The defect in controlling mycobacterial growth might be explained by the impaired IL-12/23p40 production and the decreased frequency of IFN-γ-producing Th1 cells in LysM^{cre}SOCS3$^{loxP/loxP}$ mice. This reduced Th1 immune response is in line with reports showing SOCS3 to be responsible for preventing IL-6-dependent suppression of IL-12/23p40 in macrophages and, consequently, for mediating protective Th1 immune responses against *Mtb* (15) or *T. gondii* infection (16).

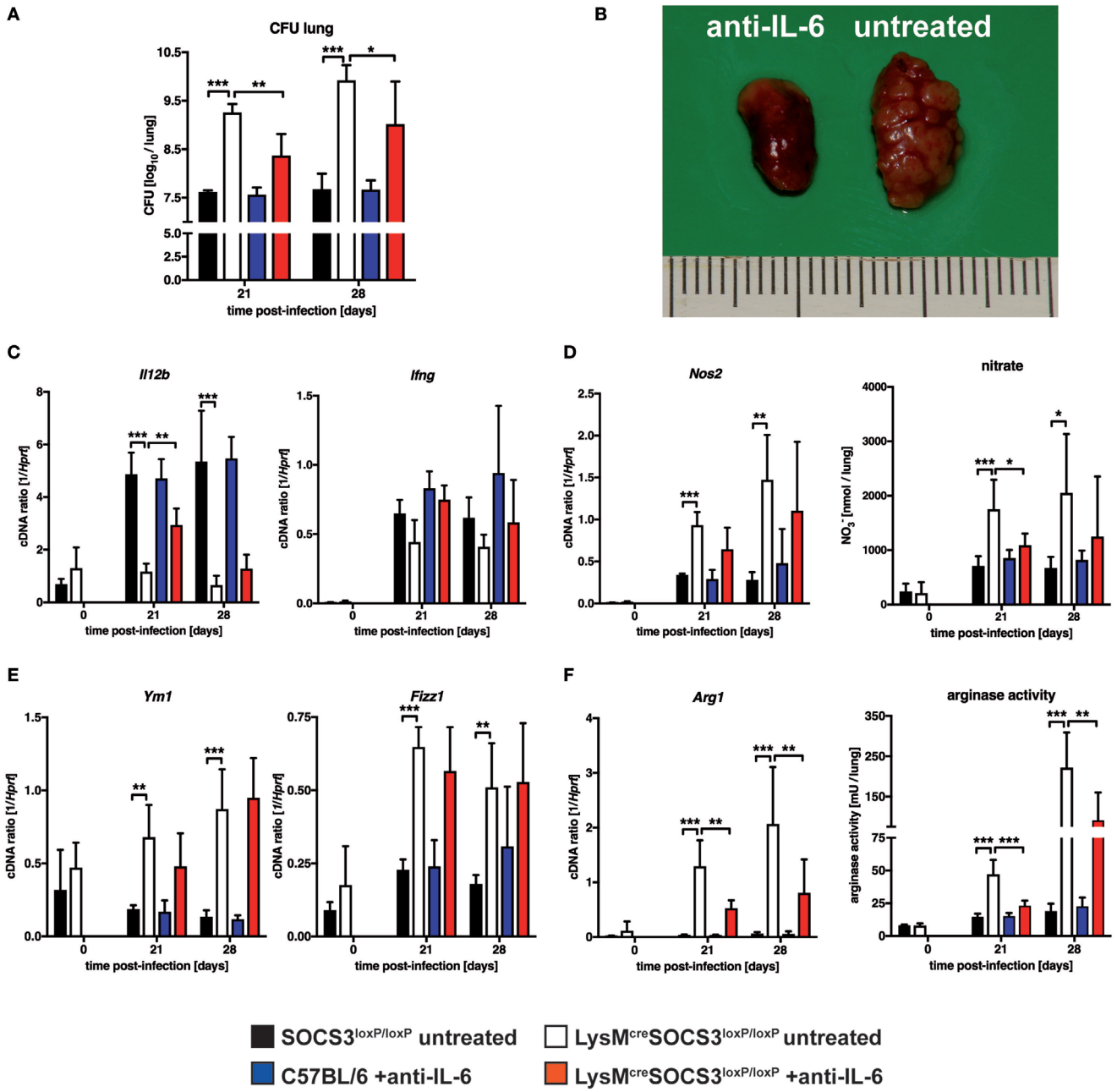


FIGURE 6 | Interleukin (IL)-6-dependent macrophage responses, susceptibility and pathology in *Mtb*-infected LysM^{cre}SOCS3$^{loxP/loxP}$ mice. Control (C57BL/6 and Cre-negative SOCS3$^{loxP/loxP}$) mice and LysM^{cre}SOCS3$^{loxP/loxP}$ mice were infected with approximately 1,000 CFU *Mtb via* the aerosol route. Two groups, C57BL/6 and LysM^{cre}SOCS3$^{loxP/loxP}$ mice, were i.p. injected twice a week with 250 µg of a monoclonal rat anti-mouse IL-6 antibody. Two other groups of cre-negative SOCS3$^{loxP/loxP}$ and LysM^{cre}SOCS3$^{loxP/loxP}$ mice were left untreated. Lungs were removed at the indicated time points. **(A)** For mycobacterial colony enumeration assays, aseptically removed lungs were weighed, transferred into PBS containing a proteinase inhibitor cocktail and homogenized. Tenfold serial dilutions of organ homogenates were plated and colonies were counted three weeks later. **(B)** At 28 days of infection, photographs of removed lungs were taken. **(C)** Gene expression of *Il12b* and *Ifng* in lung homogenates was determined by qRT-PCR. **(D)** Gene expression of *Nos2* in lung homogenates was determined by qRT-PCR. To detect RNI, NO_3 was converted into NO_2 after deproteination of homogenates. Following the addition of Griess reagents, the content of NO_2 was determined by photometric measurement. **(E)** Gene expression of *Ym1* and *Fizz1* in lung homogenates was determined by qRT-PCR **(F)** Gene expression of *Arg1* was determined by qRT-PCR. To determine arginase activity, the enzyme was activated and arginine hydrolysis was conducted after the addition of L-arginine. The reaction was stopped and the urea concentration was determined as a degree of arginase activity. Data represent means ± SD of at least five mice per group. Statistical analysis was performed as described in experimental procedures defining differences between control and LysM^{cre}SOCS3$^{loxP/loxP}$ mice or untreated and treated animals as significant (*$p \leq 0.05$; **$p \leq 0.01$; ***$p \leq 0.001$).

However, our study is the first to reveal that the increased susceptibility of LysM^{cre}SOCS3$^{loxP/loxP}$ mice to *Mtb* infection is associated with strongly elevated levels of both pro- and anti-inflammatory cytokines. Such a dysbalanced inflammatory reaction is likely a direct consequence of the macrophage-specific SOCS3 deletion. SOCS3 binds to the gp130 receptor chain and regulates downstream STAT3-mediated signaling events (26). As a feedback inhibitor of cytokine signaling pathways, it plays a prominent role in limiting and terminating cytokine-induced mechanisms during inflammatory diseases (27–30). When this feedback mechanism is missing, the cytokine response by macrophages is uncontrolled as observed in *Mtb*-infected LysM^{cre}SOCS3$^{loxP/loxP}$ mice of the present study. Moreover, the specificity of IL-6 signaling is lost in the absence of macrophage SOCS3 and IL-6 induces aberrant STAT1-dependent pro-inflammatory (IFN-γ-like) and STAT3-mediated anti-inflammatory (IL-10-like) responses (3–5). This regulatory function of SOCS3 is also reflected in *Mtb*-infected LysM^{cre}SOCS3$^{loxP/loxP}$ mice of the present study by the concomitantly elevated levels of NOS2 [preferentially induced by IFN-γ/STAT1-mediated signals (31)] and Arg1 as well as the IL-4Rα [both induced to some extent by IL-10/STAT3-dependent signals (32, 33)], respectively.

In light of these findings, macrophage-specific SOCS3 appears necessary to ensure a balanced inflammatory immune response during experimental TB. The absence of SOCS3 in macrophages has detrimental consequences after infection with *Mtb* because excessive cytokine production exacerbated inflammation-induced lung pathology. The present study revealed an elevated infiltration of macrophages and granulocytes into the lungs of *Mtb*-infected LysM^{cre}SOCS3$^{loxP/loxP}$ mice resulting in a very rapid loss of functional alveolar space and subsequent early death presumably due to respiratory failure. Hence, macrophage SOCS3 efficiently controls potentially detrimental inflammation-induced pathology early after *Mtb* infection.

Deficiency in macrophage SOCS3 resulted in an utterly immunocompromised phenotype characterized by a strikingly enhanced susceptibility to *Mtb* infection, even in the face of a heightened overall inflammatory response. The exacerbated bacterial loads in LysM^{cre}SOCS3$^{loxP/loxP}$ mice might be a consequence of the strikingly increased neutrophil infiltration because susceptibility to *Mtb* infection has previously been attributed to enhanced granulocyte recruitment (34). Hence, we cannot rule out a direct effect of the enhanced granulocyte infiltration on the outcome of experimental TB in these mice. The early defect in controlling mycobacterial growth might also be explained by the impaired IL-12/23p40 production and the decreased frequency of IFN-γ-producing Th1 cells in LysM^{cre}SOCS3$^{loxP/loxP}$ mice (15). Yet, after infection with *Mtb* the expression of *Nos2* and the production of RNI were rather elevated in the absence of macrophage SOCS3. Therefore, the inability of LysM^{cre}SOCS3$^{loxP/loxP}$ mice to restrict mycobacterial growth appears not to be based on a malfunction of these classically activated macrophages. Th2 cytokines, such as IL-4, IL-10, and IL-13, are potent mediators of alternative macrophage activation that counteract protective functions induced in classically activated macrophages (12, 13, 19, 21). However, in the present study, Th2 cytokines could hardly be detected in both, SOCS3$^{loxP/loxP}$ and LysM^{cre}SOCS3$^{loxP/loxP}$ mice (data not shown) but analysis of activation markers such as NOS2 (for classical macrophage activation) and *Fizz1*, *Ym1*, *Il4ra*, or *Arg1* (for alternative macrophage activation) revealed that in *Mtb*-infected LysM^{cre}SOCS3$^{loxP/loxP}$ mice both phenotypes are significantly enhanced as compared to cre-negative SOCS3$^{loxP/loxP}$ mice. Hence, the increased susceptibility of LysM^{cre}SOCS3$^{loxP/loxP}$ mice to *Mtb* infection was associated with an elevated alternative macrophage activation.

We and others have shown that Arg1 in alternatively activated macrophages subverts effector mechanisms against intracellular *Mtb* (12, 13, 19). However, the underlying mechanism induced by Arg1 that is key to a decreased control of mycobacterial growth in macrophages is not fully understood. Classical macrophage activation plays a central role in combating infection with *Mtb* through IFN-γ-induced expression of effector molecules such as the NOS2-dependent production of RNI (35). The production of RNI might be counter-regulated by *Arg1* expression as both *Arg1* and *Nos2* share L-arginine as substrate (18). Hence, substrate depletion by either enzyme might be one regulatory mechanism in macrophages. Though *Mtb* infection induced exacerbated arginase activity in the absence of macrophage SOCS3, RNI production was not reduced. This argues against Arg1-mediated depletion of L-arginine to be a crucial factor for the susceptibility of *Mtb*-infected LysM^{cre}SOCS3$^{loxP/loxP}$ mice. After *Mtb* infection, SOCS3-deficient mice expressed increased amounts of both NOS2 and Arg1. It appears that two distinct macrophage populations, classically activated and alternatively activated, are induced by *Mtb* infection in the absence of macrophage SOCS3. Whereas classically activated cells are able to control mycobacterial growth by NOS2 expression and subsequent production of RNI, arginase activity in alternatively activated macrophages may support the replication of *Mtb* in a compartmentalized fashion. Because in *Mtb*-infected LysM^{cre}SOCS3$^{loxP/loxP}$ mice an elevated arginase activity precedes the increased induction of NOS2 mycobacteria were mostly found in Arg1-expressing cells at early time points of infection. This differential expression of Arg1 and NOS2 appears to favor the initial replication of *Mtb* particularly in Arg1-expressing cells. In our study, *Mtb* predominantly infected infiltrating macrophages. In LysM^{cre}SOCS3$^{loxP/loxP}$ mice, however, mycobacteria were detectable not only in infiltrating but also to a similar extent in resident cells. Moreover, whereas infiltrating macrophages of both SOCS3$^{loxP/loxP}$ and LysM^{cre}SOCS3$^{loxP/loxP}$ mice displayed a similar expression pattern of Arg1 and NOS2, SOCS3-deficient resident macrophages consisted of increased proportions of Arg1-expressing cells. Given that alternatively activated macrophages (measured by the gene expression of *Arg1*, *Ym1*, and *Fizz1*) are already present in the lungs of LysM^{cre}SOCS3$^{loxP/loxP}$ mice before infection these mice appear to be constitutively permissive for *Mtb*. As a consequence, the hyperinflammatory phenotype of LysM^{cre}SOCS3$^{loxP/loxP}$ mice may have been expedited by this initial susceptibility. Together, SOCS3 restrains an uncontrolled early expression of Arg1 and is necessary for controlling infection of lung macrophages during experimental TB.

Suppressor of cytokine signaling proteins have been shown to have multiple functions in shaping macrophage responses. However, not much is known about the specific impact of SOCS molecules on classical and alternative macrophage activation.

Whereas SOCS1 has been described to be crucial for IL-4-induced *Arg1* expression (36), SOCS3 is involved in promoting classical activation (8). Classical macrophage activation is mostly facilitated by the IFN-γ–STAT1 pathway but alternative macrophage activation and *Arg1* expression is mainly induced by the Th2 cytokines IL-4 and IL-13 *via* STAT6- or IL-10 through STAT3-mediated signals (22, 37). Our *in vivo* study confirms previous *in vitro* findings that after IL-6 ligation SOCS3 deficiency results in the preferential induction of STAT1-dependent responses of classical macrophage activation such as the expression of *Nos2* (4). Various markers of alternative macrophage activation including *Arg1* appear to be differentially induced by IL-4/IL-13 and IL-10. IL-4Rα-mediated signals promote full alternative activation. By contrast, IL-10 directly induces *Il4ra* (thereby indirectly enhancing IL-4/IL-13-dependent alternative activation) and *Arg1* but not other markers expressed by alternatively activated macrophages (33). In addition to IL-4, IL-13, and IL-10, IL-6 has recently been shown to specifically induce *Arg1* in macrophages (38). Because SOCS3 regulates signaling at the gp130 receptor chain, the expression of IL-6-induced genes such as *Arg1* is enhanced in SOCS3-deficient macrophages (38). The present *in vivo* study shows for the first time that after infection with *Mtb* the absence of macrophage SOCS3 resulted in exacerbated alternative macrophage activation with strikingly increased levels of *Fizz1*, *Ym1*, *Il4ra*, and *Arg1*.

We cannot formally exclude that the reduced IL-12 expression and subsequent impaired Th1 immune response account for the uncontrolled alternative macrophage activation in *Mtb*-infected LysM^{cre}SOCS3$^{loxP/loxP}$ mice. It was shown during experimental toxoplasmosis that supplementation with recombinant IL-12 corrects the susceptible phenotype in macrophage-specific SOCS3-deficient animals (16). Along this line, Carow et al. failed to increase the already enhanced bacterial loads in *Mtb*-infected LysM^{cre}SOCS3$^{loxP/loxP}$ mice by depleting CD4 T cells and concluded that macrophage SOCS3 does not directly impair innate effector responses (15). In our hands, however, injection of IL-12 did not ameliorate the course of *Mtb* infection in LysM^{cre}SOCS3$^{loxP/loxP}$ mice (Figure S1 in Supplementary Material) which may imply that macrophage-specific SOCS3 deficiency does indeed affect effector mechanisms against *Mtb* in macrophages. Although Carow et al. showed that SOCS3-deficient macrophages were in fact able to restrict the growth of *Mtb* in response to IFN-γ, they did not analyze the effect of IL-6 on the expression of *Arg1* and mycobacterial growth in LysM^{cre}SOCS3$^{loxP/loxP}$ macrophages (15). However, during *Mtb* infection the key player in the absence of macrophage SOCS3 is IL-6. *In vitro*, SOCS3 has been shown to prevent the development of alternative macrophage activation and the addition of IL-6 to SOCS3-deficient macrophages increases the expression of *Arg1* (8, 38) (data not shown). Hence, by way of an abnormal gp130-dependent signal transduction in SOCS3-deficient macrophages, the presence of IL-6 may still directly affect effector mechanisms of macrophages against *Mtb*. Our hypothesis is supported by experiments of the present study in which depletion of IL-6 in *Mtb*-infected LysM^{cre}SOCS3$^{loxP/loxP}$ mice resulted in a significant reduction of bacterial loads and lung pathology. This was accompanied by a reduced expression and activity of Arg1 rather than by a corrected Th1 immune response. Interestingly, IL-6 depletion had no effect on gene expression of *Ym1* and *Fizz1* corroborating previous findings that IL-6 specifically mediates the STAT3-dependent expression of *Arg1* in the first place (38). However, we could exclude that the differential induction of *Ym1* and *Fizz1* is mediated through STAT6 because inhibition of IL-6 also reduces gene expression levels of *Il4ra* (data not shown). Hence, these markers for alternative macrophage activation may be indirectly induced after *Mtb* infection by the hyperinflammatory phenotype in the absence of macrophage SOCS3. Together, our *in vivo* study revealed that SOCS3 is also key in specifically controlling IL-6-mediated *Arg1* expression in macrophages.

We interpret our findings to indicate that in experimental *Mtb* infection SOCS3 does not act in a predetermined, biased way. In addition to promoting protective Th1 immune responses, SOCS3 also keeps IL-6-dependent divergent macrophage responses such as *Nos2* and *Arg1* expression under control. As a consequence, if macrophage SOCS3 is absent preferential replication of mycobacteria in *Arg1*-expressing macrophages and a dysbalanced inflammatory response result in early death. The early appearance of these permissive macrophages is not controlled due to the impaired Th1 immune response. In addition, SOCS3 deficiency allows the immediate exacerbation of Arg1 expression in *Mtb*-infected macrophages. As a consequence, macrophage-specific SOCS3 is essential to eventually safeguard protective macrophage effector mechanisms.

MATERIALS AND METHODS

Ethics Statement

All animal experiments performed were in accordance with the German Animal Protection Law and were approved by the Animal Research Ethics Board of the Ministry of Environment, Kiel, Germany.

Mice

SOCS3$^{loxP/loxP}$ mice were backcrossed 10 generations to C57BL/6 under specific-pathogen-free conditions at the Technical University of Munich (Germany) and the University of Erlangen (Germany). Mating with LysM^{cre} mice on the C57BL/6 genetic background produced LysM^{cre}SOCS3$^{loxP/loxP}$ and cre-negative SOCS3$^{loxP/loxP}$ littermates. In addition, in some experiments, C57BL/6 mice (Charles River, Sulzfeld, Germany) were used as controls.

Infection with *Mtb*

Mycobacterium tuberculosis H37rv or recombinant *Mtb*^{mCherry} (39) were grown in Middlebrook 7H9 broth (Difco, Detroit, MI, USA) supplemented with Middlebrook OADC enrichment medium (Life Technologies, Gaithersburg, MI, USA), 0.002% glycerol, and 0.05% Tween 80. Midlog phase cultures were harvested, aliquoted, and frozen at −80°C. After thawing, viable cell counts were determined by plating serial dilutions of the cultures on Middlebrook 7H10 agar plates followed by incubation at 37°C. Before infection of experimental animals, stock solutions of *Mtb* were diluted in sterile distilled water to a

defined concentration and pulmonary infection was performed using an inhalation exposure system (Glas-Col, Terre-Haute, IN, USA).

Colony Enumeration Assay and Histology

Bacterial loads in lungs were evaluated at 3 and 4 weeks of infection. Lungs were removed aseptically, weighed, and transferred into PBS containing a proteinase inhibitor cocktail (Roche Diagnostics, Mannheim, Germany) and homogenized using the FastPrep™ System (MP Biomedicals, Solon, OH, USA). Tenfold serial dilutions of organ homogenates were plated onto Middlebrook 7H10 (Life Technologies, Darmstadt, Germany) agar plates containing 5% glycerine (Applichem, Darmstadt, Germany) and 10% heat-inactivated bovine serum (Biowest, Nuaillé, France) and incubated at 37°C for 21 days.

For histology, one lung lobe per mouse was fixed in 4% formalin-PBS, set in paraffin blocks, and sectioned (2–3 µm). Histopathological analyses were performed using standard protocols for hematoxylin/eosin staining. Acid-fast bacilli were detected using a modified Ziehl–Neelsen protocol. For the immunohistochemical detection of Arg1 and NOS2 (Upstate, Lake Placid, NY, USA) tissue sections were deparaffinized and pressure cooked in 10 mM citrate buffer, pH 6. After peroxidase quenching with 3% H_2O_2/TBS and blocking with 3% BSA, sections were incubated with primary antibodies against Arg1 (Santa Cruz Biotechnology, Santa Cruz, CA, USA) or NOS2 (Upstate) overnight followed by the incubation with HRP-conjugated goat-anti-rabbit secondary antibody (Dianova, Hamburg, Germany). Development was performed by using Elite ABC Kit (Vector, Burlingame, CA, USA) and diaminobenzidine (Vector).

Quantitative Real Time PCR

Weighed lung samples before and at different time points of infection with *Mtb*, were homogenized in 4 M guanidinium-isothiocyanate buffer and total RNA was extracted by acid phenol extraction. cDNA was obtained using murine moloney leukemia virus (MMLV) reverse transcriptase (Superscript II, Invitrogen, Karlsruhe, Germany) and oligo-dT (12–18mer; Sigma) as a primer. Quantitative PCR was performed on a Light Cycler (Roche). Data were analyzed employing the "2nd Derivate Maximum method" and "Standard Curve method" using hypoxanthine-guanine phosphoribosyl transferase (*Hprt*) as a housekeeping gene to calculate the level of gene expression in relation to *Hprt*. The following primer and probe sets were employed: *Arg1*: sense 5′-CCT GAA GGA ACT GAA AGG AAA-3′, antisense 5′-TTG GCA GAT ATG CAG GGA GT-3′, probe 5′-TTC TTC TG-3′; *Fizz1*: sense 5′-TAT GAA CAGATG GGC CTC CT-3′, antisense 5′-GGC AGT TGC AAG TAT CTC CAC-3′, probe 5′-GGC AGG AG-3′; *Hprt*: sense 5′-TCC TCC TCA GAC CGC TTT T-3′, antisense 5′-CCT GGT TCA TCA TCG CTA ATC-3′, probe 5′-AGT CCA G-3′; *ifng*: sense 5′-ATC TGG AGG AAC TGG CAA AA-3′, antisense 5′-TTC AAG ACT TCA AAG AGT CTG AGG TA-3′, probe 5′-CAGAGCCA-3′; *Il4ra*: sense 5′-GAG TGG AGT CCT AGC ATC ACG-3′, antisense 5′-CAG TGG AAG GCG CTG TAT C-3′, probe 5′-CTT CCA GC-3′; *Il12b*: sense 5′-ATC GTT TTG CTG GTG TCT CC-3′, antisense 5′-GGA GTC CAG TCC ACC TCT ACA-3′, probe 5′-AGC TGG AG-3′; *Nos2*: sense 5′-CTT TGC CAC GGA CGA GAC-3′, antisense 5′-TCA TTG TAC TCT GAG GGC TGA C-3′, probe 5′-AGG CAG AG-3′; *Ym1*: sense 5′-GAA CAC TGA GCT AAA AAC TCT CCT G-3′, antisense 5′-GAG ACC ATG GCA CTG AAC G-3′, probe 5′-GGA GGA TG-3′.

Quantification of Cytokine Production

The concentrations of cytokines in lung homogenates from uninfected and infected mice were determined by a cytometric bead array (CBA) (BD Biosciences, Heidelberg, Germany) as described (40). IL-6 was analyzed using a CBA mouse-flex-set (BD Biosciences). To determine TNF, IL-12/IL-23p40, IL-10, and IFN-γ, beads were conjugated with purified antibodies (BD Bisosiences) using a functional-bead-conjugation buffer set following the manufacturer's instructions (BD Biosciences). The quantity of cytokines per lung was calculated based on the ratio of lung to sample weight.

Arginase Activity and Nitrate Production in Lung Homogenates

To determine arginase activity in murine tissue, weighed pieces of organs were homogenized in 100 µl of 0.1% Triton X-100 (Sigma) containing a protease inhibitor cocktail (Roche). 50 µl of 10 mM $MnCl_2$ (Merck, Darmstadt, Germany) and 50 mM Tris–HCl (Merck) were added to all samples and the enzyme was activated by heating for 10 min at 55°C. Arginine hydrolysis was conducted by incubating 25 µl of the activated lysate with 25 µl of 0.5 M L-arginine (Merck) at 37°C for 60 min. The reaction was stopped with 400 µl of H_2SO_4 (96%)/H_3PO_4 (85%)/H_2O (1/3/7, v/v/v). As a degree of arginase activity, the urea concentration was measured at 540 nm after addition of 25 µl α-isonitrosopropiophenone (Sigma; dissolved in 100% ethanol) followed by heating at 95°C for 45 min. One unit of arginase activity is defined as the amount of enzyme that catalyzes the formation of 1 µmol urea/min. To detect RNI in uninfected and infected mice, lung homogenates were collected at different time points. After deproteination of homogenates using Micron YM-30 centrifugal filters (Millipore, Schwalbach, Germany), NO_3 was converted into NO_2 utilizing a commercial nitrate reductase kit (Cayman; Axxora, Lörrach, Germany). After adding Griess reagents, the content of NO_2 was determined by photometric measurement reading the absorbance at 540 nm on a microplate reader (Sunrise; Tecan, Männedorf, Switzerland) as previously described (40).

Confocal Microscopy of *Mtb* in Arg1- and NOS2-Expressing Cells

For fluorescence microscopy, deparaffinized formalin-fixed lung sections were boiled for 45 min in 0.01 M citrate buffer at pH 6.0 for antigen retrieval. Endogenous peroxidase activity was blocked by a 10-min incubation in 1% hydrogen peroxide, unspecific antibody binding was blocked by a 30 min incubation in 3% BSA and endogenous biotin or avidin/streptavidin binding proteins were blocked using the Avidin/Biotin blocking kit (Vector Laboratories). Sections were then incubated overnight at 4°C with goat anti-Arg1 antibody (1:50 dilution, Santa Cruz Biotechnologies) or rabbit anti-NOS2 antibody (1:200 dilution, Merck Millipore). Sections were subsequently incubated

with rabbit anti-goat IgG-biotin or goat anti-rabbit IgG-biotin (both Dianova), respectively, followed by an incubation with Streptavidin-Cy5 (Dianova). Finally, sections were co-stained with rabbit anti-*Mtb*-FITC (Biozol) and DAPI (Roche). Fluorescent stainings were analyzed using a TCS SP5 confocal microscope and LAS AF software (both from Leica, Wetzlar, Germany). Color images were produced by pasting each of the original grayscale images (shown in Figure S2 in Supplementary Material) into the red, the green, or the blue channels. Cross-reactivity of goat anti-Arg1 against *Mtb* could be excluded as goat anti-Arg1-dependent signals were absent in lung sections of *Mtb*-infected L-Nil-treated *Arg1*$^{flox/flox}$*Tie2cre* mice, which are deficient for *Arg1* in all macrophage populations.

Preparation of Single-Cell Suspensions from Infected Lungs

For antigen-specific restimulation and flow cytometric analysis, single-cell suspensions of lungs were prepared from *Mtb*-infected mice at different time points. Lungs were perfused through the right ventricle with warm PBS. Once lungs appeared white, they were removed and sectioned. Dissected lung tissue was then incubated in collagenase A (0.7 mg/ml; Roche Diagnostics, Mannheim, Germany) and DNase (30 µg/ml; Sigma) at 37°C for 2 h. Digested lung tissue was gently disrupted by subsequent passage through a 100 µm pore size nylon cell strainer. Suspensions were depleted of remaining erythrocytes using hypotonic red cell lysis buffer, containing NH_4Cl and $NaHCO_3$. Recovered vital lung cells were counted using an automatic cell counter (ViCell®; Beckman Coulter, Krefeld, Germany), diluted in RPMI 1640 medium (Sigma) supplemented with 10% FCS (Life Technologies), 0.05 mM β-mercaptoethanol (Sigma), and penicillin and streptomycin (100 U/ml and 100 µg/ml; Life Technologies) and used for further experiments.

Flow Cytometric Analysis

For flow cytometric analysis of surface markers, single-cell suspensions of lungs were incubated with an anti-FcγRIII/II monoclonal antibody (clone 2.4.G2) and stained with optimal concentrations of the following specific antibodies: anti-CD11b-eFluor450 (Ebioscience, Frankfurt, Germany), anti-CD11b-V500 (clone M1/70; BD Bioscience), anti-F4/80-Alexa-647 (clone BM8; Invitrogen), anti-F4/80-Pacific Blue (clone BM8; Biolegend), anti-Ly6G-PerCp-Cy5.5 (clone1A8; BD Bioscience), and anti-IL-4Rα-PE (clone mIL-4R-M1; BD Biosciences). For intracellular staining of NOS2 and Arg1, single-cell suspensions of lungs were stained for surface markers before permeabilization with Cytofix/Cytoperm® (BD Bioscience). Staining of NOS2 and Arg1 was performed using optimal concentrations of the following specific antibodies: NOS2-FITC (clone 6/iNOS/NOS type II; BD Bioscience), goat-anti mouse Arg1 (clone V-20; Santa Cruz Biotechnology) and polyclonal donkey-anti-goat IgG-Dylight 650 (Abcam, Cambridge, UK). Appropriate isotype controls were used. Fluorescence intensity was measured using a FACSCanto® II flowcytometer (BD Biosciences). Analysis was performed utilizing the FCS Express® program (*De Novo* Software, Los Angeles, CA, USA).

ESAT6$_{1-20}$-Specific ELISPOT Assays

Detection of antigen-specific IFN-γ-producing cells from infected lungs was conducted using an ELISPOT assay kit (BD Biosciences). To enrich CD4$^+$ T cells, single-cell suspensions were incubated with magnetic CD4 microbeads (Miltenyi, Bergisch Gladbach, Germany) and separated from other cells on a MACS separation unit (Miltenyi). Separated CD4$^+$ T cells were collected in Iscoves-modified Dulbeccos medium (IMDM; Life Technologies) supplemented with 10% FCS (Life Technologies), 0.05 mM β-mercaptoethanol (Sigma), and penicillin, and streptomycin (100 U/ml and 100 µg/ml; Life Technologies), counted using a cell counter (ViCell®; Beckman Coulter), diluted in IMDM and used for further experiments. For measuring the antigen-specific IFN-γ response in lungs from infected mice, single-cell suspensions or purified CD4$^+$ T cells from lungs were seeded in wells of anti-mouse IFN-γ-coated and blocked 96-well multitestplates at an initial concentration of 1×10^5 cells/well in IMDM. After doubling dilutions of these cells were made, mitomycin-D (Sigma)-inactivated splenocytes from uninfected control mice were used as APCs at a concentration of 1×10^6 cells/well. Cells were stimulated with the *Mtb* ESAT6$_{1-20}$ (Research Center Borstel, Germany) at a concentration of 10 µg/ml in the presence of 10 U/ml recombinant mouse IL-2 (Peprotech, Hamburg, Germany). After 20 h of incubation in 5% CO_2 at 37°C, plates were washed, and biotinylated anti-mouse IFN-γ was used to detect the captured cytokine. Spots were visualized using streptavidin-HRP as substrate. Spots were automatically enumerated using an ELISPOT reader (EliSpot 04 XL; AID, Straßberg, Germany). The frequency of responding cells was determined.

Neutralization of Endogenous IL-6

To neutralize endogenous IL-6 during experimental TB, 250 µg of a monoclonal rat IgG1, kappa anti-IL-6 antibody (clone MP5-20F3, *InVivo* BioTechServives, Henningsdorf, Germany) were injected i.p. at days −1, 2, 6, 9, 13, 16, 20, and 23 after infection with *Mtb*.

Statistical Analysis

Statistical analysis was performed using GraphPad Prism version 4.03 (GraphPad Software, San Diego, CA, USA). Quantifiable data are expressed as means of individual determinations and SD. After analyzing for Gaussian distribution, unpaired Student's *t*-test or the Mann–Whitney test was applied defining different error probabilities (*$p \leq 0.05$; **$p \leq 0.01$; ***$p \leq 0.001$). ANOVA was performed using the Bonferroni multiple comparison test different error probabilities (*$p \leq 0.05$; **$p \leq 0.01$; ***$p \leq 0.001$). Statistical survival analysis was performed using the Log-rank test.

AUTHOR CONTRIBUTIONS

ES: designed the study, performed experiments, analyzed the results, and drafted figures and manuscript. MD, JB, and HE: performed experiments, analyzed the results, and drafted figures. DR, TE, LH, and MH: performed experiments. AY, JS, SR-J,

and US: provided material. SE and RL: designed the study. CH: designed the study, drafted figures and manuscript.

ACKNOWLEDGMENTS

The authors thank Johanna Volz, Alexandra Hölscher, Tanja Sonntag, Gabriele Röver, Kerstin Traxel, Angela Servatius, Barbara Bodendorfer, and Manfred Richter for excellent technical assistance. We are also grateful to Ilka Monath, Jeanette Hein, and Klaus Möller for organizing the animal facility and taking care of the mice. We are also indebted to Tanya Parish for providing the *Mtb*^{mCherry}, respectively. This work was supported by grants from the Deutsche Forschungsgemeinschaft to RL (LA1262/4-1) and CH (HO2145/4-1) and by the Cluster of Excellence "Inflammation at Interface."

SUPPLEMENTARY MATERIAL

The Supplementary Material for this article can be found online at http://www.frontiersin.org/article/10.3389/fimmu.2017.01537/full#supplementary-material.

REFERENCES

1. WHO. *Global Tuberculosis Report – 2015*. Geneva, Switzerland: WHO (2015).
2. O'Shea JJ, Murray PJ. Cytokine signaling modules in inflammatory responses. *Immunity* (2008) 28:477–87. doi:10.1016/j.immuni.2008.03.002
3. Croker BA, Krebs DL, Zhang JG, Wormald S, Willson TA, Stanley EG, et al. SOCS3 negatively regulates IL-6 signaling in vivo. *Nat Immunol* (2003) 4:540–5. doi:10.1038/ni931
4. Lang R, Pauleau AL, Parganas E, Takahashi Y, Mages J, Ihle JN, et al. SOCS3 regulates the plasticity of gp130 signaling. *Nat Immunol* (2003) 4:546–50. doi:10.1038/ni932
5. Yasukawa H, Ohishi M, Mori H, Murakami M, Chinen T, Aki D, et al. IL-6 induces an anti-inflammatory response in the absence of SOCS3 in macrophages. *Nat Immunol* (2003) 4:551–6. doi:10.1038/ni938
6. Silver JS, Hunter CA. gp130 at the nexus of inflammation, autoimmunity, and cancer. *J Leukoc Biol* (2010) 88:1145–56. doi:10.1189/jlb.0410217
7. Scheller J, Chalaris A, Schmidt-Arras D, Rose-John S. The pro- and anti-inflammatory properties of the cytokine interleukin-6. *Biochim Biophys Acta* (2011) 1813:878–88. doi:10.1016/j.bbamcr.2011.01.034
8. Liu Y, Stewart KN, Bishop E, Marek CJ, Kluth DC, Rees AJ, et al. Unique expression of suppressor of cytokine signaling 3 is essential for classical macrophage activation in rodents in vitro and in vivo. *J Immunol* (2008) 180:6270–8. doi:10.4049/jimmunol.180.9.6270
9. North RJ, Jung Y-J. Immunity to tuberculosis. *Annu Rev Immunol* (2004) 22:599–623. doi:10.1146/annurev.immunol.22.012703.104635
10. MacMicking JD, North RJ, Lacourse R, Mudgett JS, Shah SK, Nathan CF. Identification of nitric oxide synthase as a protective locus against tuberculosis. *Proc Natl Acad Sci U S A* (1997) 94:5243–8. doi:10.1073/pnas.94.10.5243
11. MacMicking JD, Taylor GA, Mckinney JD. Immune control of tuberculosis by IFN-gamma-inducible LRG-47. *Science* (2003) 302:654–9. doi:10.1126/science.1088063
12. El Kasmi KC, Qualls JE, Pesce JT, Smith AM, Thompson RW, Henao-Tamayo M, et al. Toll-like receptor-induced arginase 1 in macrophages thwarts effective immunity against intracellular pathogens. *Nat Immunol* (2008) 9:1399–406. doi:10.1038/ni.1671
13. Schreiber T, Ehlers S, Heitmann L, Rausch A, Mages J, Murray PJ, et al. Autocrine IL-10 induces hallmarks of alternative activation in macrophages and suppresses antituberculosis effector mechanisms without compromising T cell immunity. *J Immunol* (2009) 183:1301–12. doi:10.4049/jimmunol.0803567
14. Heitmann L, Abad Dar M, Schreiber T, Erdmann H, Behrends J, Mckenzie AN, et al. The IL-13/IL-4Ralpha axis is involved in tuberculosis-associated pathology. *J Pathol* (2014) 234:338–50. doi:10.1002/path.4399
15. Carow B, Reuschl AK, Gavier-Widen D, Jenkins BJ, Ernst M, Yoshimura A, et al. Critical and independent role for SOCS3 in either myeloid or T cells in resistance to *Mycobacterium tuberculosis*. *PLoS Pathog* (2013) 9:e1003442. doi:10.1371/journal.ppat.1003442
16. Whitmarsh RJ, Gray CM, Gregg B, Christian DA, May MJ, Murray PJ, et al. A critical role for SOCS3 in innate resistance to *Toxoplasma gondii*. *Cell Host Microbe* (2011) 10:224–36. doi:10.1016/j.chom.2011.07.009
17. Hölscher C, Atkinson RA, Arendse B, Brown N, Myburgh E, Alber G, et al. A protective and agonistic function of IL-12p40 in mycobacterial infection. *J Immunol* (2001) 167:6957–66. doi:10.4049/jimmunol.167.12.6957
18. Rutschman R, Lang R, Hesse M, Ihle JN, Wynn TA, Murray PJ. Cutting edge: Stat6-dependent substrate depletion regulates nitric oxide production. *J Immunol* (2001) 166:2173–7. doi:10.4049/jimmunol.166.4.2173
19. Hölscher C, Arendse B, Schwegmann A, Myburgh E, Brombacher F. Impairment of alternative macrophage activation delays cutaneous leishmaniasis in nonhealing BALB/c mice. *J Immunol* (2006) 176:1115–21. doi:10.4049/jimmunol.176.2.1115
20. Hesse M, Modolell M, La Flamme AC, Schito M, Fuentes JM, Cheever AW, et al. Differential regulation of nitric oxide synthase-2 and arginase-1 by type 1/type 2 cytokines in vivo: granulomatous pathology is shaped by the pattern of L-arginine metabolism. *J Immunol* (2001) 167:6533–44. doi:10.4049/jimmunol.167.11.6533
21. Kropf P, Fuentes JM, Fahnrich E, Arpa L, Herath S, Weber V, et al. Arginase and polyamine synthesis are key factors in the regulation of experimental leishmaniasis in vivo. *FASEB J* (2005) 19:1000–2. doi:10.1096/fj.04-3416fje
22. Gordon S. Alternative activation of macrophages. *Nat Rev Immunol* (2003) 3:23–35. doi:10.1038/nri978
23. Peters W, Cyster JG, Mack M, Schlondorff D, Wolf AJ, Ernst JD, et al. CCR2-dependent trafficking of F4/80dim macrophages and CD11cdim/intermediate dendritic cells is crucial for T cell recruitment to lungs infected with *Mycobacterium tuberculosis*. *J Immunol* (2004) 172:7647–53. doi:10.4049/jimmunol.172.12.7647
24. Mistry R, Cliff JM, Clayton CL, Beyers N, Mohamed YS, Wilson PA, et al. Gene-expression patterns in whole blood identify subjects at risk for recurrent tuberculosis. *J Infect Dis* (2007) 195:357–65. doi:10.1086/510397
25. Masood KI, Rottenberg ME, Salahuddin N, Irfan M, Rao N, Carow B, et al. Expression of *M. tuberculosis*-induced suppressor of cytokine signaling (SOCS) 1, SOCS3, FoxP3 and secretion of IL-6 associates with differing clinical severity of tuberculosis. *BMC Infect Dis* (2013) 13:13. doi:10.1186/1471-2334-13-13
26. Schmitz J, Weissenbach M, Haan S, Heinrich PC, Schaper F. SOCS3 exerts its inhibitory function on interleukin-6 signal transduction through the SHP2 recruitment site of gp130. *J Biol Chem* (2000) 275:12848–56. doi:10.1074/jbc.275.17.12848
27. Dalpke AH, Opper S, Zimmermann S, Heeg K. Suppressors of cytokine signaling (SOCS)-1 and SOCS-3 are induced by CpG-DNA and modulate cytokine responses in APCs. *J Immunol* (2001) 166:7082–9. doi:10.4049/jimmunol.166.12.7082
28. Shouda T, Yoshida T, Hanada T, Wakioka T, Oishi M, Miyoshi K, et al. Induction of the cytokine signal regulator SOCS3/CIS3 as a therapeutic strategy for treating inflammatory arthritis. *J Clin Invest* (2001) 108:1781–8. doi:10.1172/JCI13568
29. Suzuki A, Hanada T, Mitsuyama K, Yoshida T, Kamizono S, Hoshino T, et al. CIS3/SOCS3/SSI3 plays a negative regulatory role in STAT3 activation and intestinal inflammation. *J Exp Med* (2001) 193:471–81. doi:10.1084/jem.193.4.471
30. Berlato C, Cassatella MA, Kinjyo I, Gatto L, Yoshimura A, Bazzoni F. Involvement of suppressor of cytokine signaling-3 as a mediator of the inhibitory effects of IL-10 on lipopolysaccharide-induced macrophage activation. *J Immunol* (2002) 168:6404–11. doi:10.4049/jimmunol.168.12.6404
31. Martin E, Nathan C, Xie QW. Role of interferon regulatory factor 1 in induction of nitric oxide synthase. *J Exp Med* (1994) 180:977–84. doi:10.1084/jem.180.3.977

32. Munder M, Eichmann K, Modolell M. Alternative metabolic states in murine macrophages reflected by the nitric oxide synthase/arginase balance: competitive regulation by CD4+ T cells correlates with Th1/Th2 phenotype. *J Immunol* (1998) 160:5347–54.
33. Lang R, Patel D, Morris JJ, Rutschman RL, Murray PJ. Shaping gene expression in activated and resting primary macrophages by IL-10. *J Immunol* (2002) 169:2253–63. doi:10.4049/jimmunol.169.5.2253
34. Keller C, Hoffmann R, Lang R, Brandau S, Hermann C, Ehlers S. Genetically determined susceptibility to tuberculosis in mice causally involves accelerated and enhanced recruitment of granulocytes. *Infect Immun* (2006) 74:4295–309. doi:10.1128/IAI.00057-06
35. Chan J, Xing Y, Magliozzo RS, Bloom BR. Killing of virulent *Mycobacterium tuberculosis* by reactive nitrogen intermediates produced by activated murine macrophages. *J Exp Med* (1992) 175:1111–22. doi:10.1084/jem.175.4.1111
36. Whyte CS, Bishop ET, Rückerl D, Gaspar-Pereira S, Barker RN, Allen JE, et al. Suppressor of cytokine signaling (SOCS)1 is a key determinant of differential macrophage activation and function. *J Leukoc Biol* (2011) 90:845–54. doi:10.1189/jlb.1110644
37. Dewals BG, Marillier RG, Hoving JC, Leeto M, Schwegmann A, Brombacher F. IL-4Ralpha-independent expression of mannose receptor and Ym1 by macrophages depends on their IL-10 responsiveness. *PLoS Negl Trop Dis* (2010) 4:e689. doi:10.1371/journal.pntd.0000689
38. Qualls JE, Neale G, Smith AM, Koo M-S, Defreitas AA, Zhang H, et al. Arginine usage in mycobacteria-infected macrophages depends on autocrine-paracrine cytokine signaling. *Sci Signal* (2010) 3:ra62. doi:10.1126/scisignal.2000955
39. Carroll P, Schreuder LJ, Muwanguzi-Karugaba J, Wiles S, Robertson BD, Ripoll J, et al. Sensitive detection of gene expression in mycobacteria under replicating and non-replicating conditions using optimized far-red reporters. *PLoS One* (2010) 5:e9823. doi:10.1371/journal.pone.0009823
40. Hölscher C, Reiling N, Schaible UE, Hölscher A, Bathmann C, Korbel D, et al. Containment of aerogenic *Mycobacterium tuberculosis* infection in mice does not require MyD88 adaptor function for TLR2, -4 and -9. *Eur J Immunol* (2008) 38:680–94. doi:10.1002/eji.200736458

Conflict of Interest Statement: The authors declare that the research was conducted in the absence of any commercial or financial relationships that could be construed as a potential conflict of interest.

Copyright © 2017 Schmok, Abad Dar, Behrends, Erdmann, Rückerl, Endermann, Heitmann, Hessmann, Yoshimura, Rose-John, Scheller, Schaible, Ehlers, Lang and Hölscher. This is an open-access article distributed under the terms of the Creative Commons Attribution License (CC BY). The use, distribution or reproduction in other forums is permitted, provided the original author(s) or licensor are credited and that the original publication in this journal is cited, in accordance with accepted academic practice. No use, distribution or reproduction is permitted which does not comply with these terms.

frontiers in Microbiology

MINI REVIEW
published: 23 November 2017
doi: 10.3389/fmicb.2017.02284

The Macrophage: A Disputed Fortress in the Battle against *Mycobacterium tuberculosis*

*Christophe J. Queval†, Roland Brosch and Roxane Simeone**

Unit for Integrated Mycobacterial Pathogenomics, Institut Pasteur, Paris, France

Mycobacterium tuberculosis (*Mtb*), the etiological agent of human tuberculosis (TB), has plagued humans for thousands of years. TB still remains a major public health problem in our era, causing more than 4,400 deaths worldwide every day and killing more people than HIV. After inhaling *Mtb*-contaminated aerosols, TB primo-infection starts in the terminal lung airways, where *Mtb* is taken up by alveolar macrophages. Although macrophages are known as professional killers for pathogens, *Mtb* has adopted remarkable strategies to circumvent host defenses, building suitable conditions to survive and proliferate. Within macrophages, *Mtb* initially resides inside phagosomes, where its survival mostly depends on its ability to take control of phagosomal processing, through inhibition of phagolysosome biogenesis and acidification processes, and by progressively getting access to the cytosol. Bacterial access to the cytosolic space is determinant for specific immune responses and cell death programs, both required for the replication and the dissemination of *Mtb*. Comprehension of the molecular events governing *Mtb* survival within macrophages is fundamental for the improvement of vaccine-based and therapeutic strategies in order to help the host to better defend itself in the battle against the fierce invader *Mtb*. In this mini-review, we discuss recent research exploring how *Mtb* conquers and transforms the macrophage into a strategic base for its survival and dissemination as well as the associated defense strategies mounted by host.

Keywords: ***Mycobacterium tuberculosis*, macrophages, phagosome maturation, cell death, cytosolic access**

OPEN ACCESS

Edited by:
Céline Cougoule,
Centre National de la Recherche Scientifique (CNRS), France

Reviewed by:
Roland Lang,
Universitätsklinikum Erlangen, Germany
Shashank Gupta,
Brown University, United States

****Correspondence:***
Roxane Simeone
roxane.simeone@pasteur.fr

†Present address:
Christophe J. Queval,
Host-Pathogen Interactions in Tuberculosis Laboratory, The Francis Crick Institute, London, United Kingdom

Specialty section:
This article was submitted to Microbial Immunology, a section of the journal Frontiers in Microbiology

Received: *21 September 2017*
Accepted: *06 November 2017*
Published: *23 November 2017*

Citation:
Queval CJ, Brosch R and Simeone R (2017) The Macrophage: A Disputed Fortress in the Battle against Mycobacterium tuberculosis. Front. Microbiol. 8:2284. doi: 10.3389/fmicb.2017.02284

INTRODUCTION

With over a billion deaths in the past 200 years, tuberculosis (TB) caused by *Mycobacterium tuberculosis* (*Mtb*) likely killed more people than any other infectious disease in the history of humanity (Paulson, 2013) and remains a major cause of death also in our era. *Mtb* is responsible for about 10 millions of new TB cases and 1.8 million deaths in 2015 (WHO, 2016). Estimations based on immunological tests suggest that about 2 billion people might be latently infected by *Mtb*. Statistically, 5–10% of latently infected individuals might then further develop active TB during their lifetime (Barry et al., 2009). TB primary infection occurs through inhalation of *Mtb*-containing aerosol droplets released by contagious individuals. After inhalation, *Mtb* rapidly reaches the lung's alveolar space where it is preferentially taken up by alveolar macrophages (Armstrong and Hart, 1971; Warner and Mizrahi, 2007). Following macrophage phagocytosis,

mycobacterial invaders deploy an army of factors, which circumvent macrophage defenses, to escape from macrophage killing and to replicate within these phagocytes (Ehrt and Schnappinger, 2009; Cambier et al., 2014). Manipulation of intracellular macrophage signaling also impacts the cytokine environment modifying the potency of protective immune response, setting up a *Mtb* tolerance by the host and favoring the intracellular survival of *Mtb* over time (BoseDasgupta and Pieters, 2014; Orme et al., 2015). Innate immune responses are essential for the outcome of TB infection as well as for the establishment of adaptive immunity (Torrado and Cooper, 2013; Orme et al., 2015). In lungs, the progressive establishment of an immune response during *Mtb* infection notably contributes to the aggregation of immune cells, forming an organized structure harboring macrophages at the center, surrounded by giant cells, T-lymphocytes, neutrophils, fibroblast, which is called a granuloma. A hallmark feature of the bacillus is its ability to remain concealed within host cells or/and within the granulomatous caseous necrotic centers, where it can persist during the long phase of TB latency (Barry et al., 2009). Establishment of an immune balance, orchestrated by both mycobacteria and host cells, is decisive for the outcome of the granuloma, which may either constrain the infection or promote its systemic dissemination (Ulrichs and Kaufmann, 2006; Davis and Ramakrishnan, 2009). The development of active pulmonary TB is tightly linked with a disordered immune balance, resulting in host's inability to keep the infection under control (O'Garra et al., 2013).

The current TB drug regimen generally requires 2-months of treatment with four first-line drugs: isoniazid, rifampicin, ethambutol, and pyrazinamide followed by 4 months of treatment with isoniazid and rifampicin (WHO, 2016). However, the protracted nature of the TB treatment and an inappropriate patient compliance favor the selection of multidrug resistant strains (MDR-TB). The more recent emergence of extensively drug resistant strains (XDR-TB) represents, nowadays, a major threat (Van Rie and Enarson, 2006; WHO, 2016). Therefore, new and alternative means to control *Mtb* are urgently needed. A better understanding of the fundamental biology of this complex interaction of the bacterium and the host cell represents a challenge for the design of new strategies to improve control of TB.

This mini-review focuses on selected aspects of this host-pathogen interaction, which shows quite some resemblance to medieval battlegrounds, where fierce warriors tried to invade well-equipped fortresses with their weapons and ruses.

MYCOBACTERIAL ARTILLERY

Mycobacterium tuberculosis belongs to the phylum *Actinobacteria* and is coated by a unique cell envelope, which represents a remarkably impermeable and hydrophobic armor (Brennan and Nikaido, 1995) that is composed of a capsule, an outer membrane, also termed mycomembrane, a peptidoglycan layer, an arabinogalactan layer, and an inner plasma membrane. The mycomembrane consists of mycolic acids and selected extractible lipids, including phthiocerol dimycocerosates (abbreviated DIM or PDIM), diacyltrehalose (DAT), and polyacyltrehalose (PAT) (Chalut, 2016). Additionally, Mannosyl-phosphatidyl-*myo*-inositol-based glycolipids (PIM) and related lipoglycans such as lipomannan (LM) and lipoarabinomannan (LAM) are also abundantly present in the *Mtb* cell envelope as well as in the inner and outer membranes (Daffe et al., 2014). To ensure protein transport across this unusual cell envelope *Mtb* uses different secretion systems, some of which are also widely present in other bacteria, such as the general Sec systems and the Twin Arginine Translocation (TAT) pathway, whereas others are exclusively present in mycobacteria and in some distantly related versions in other species within the phyla *Actinobacteria* and *Firmicutes*. These latter systems are called ESX secretion systems (Gröschel et al., 2016) and are also known as Type VII secretion (T7S) systems (Abdallah et al., 2007). The *Mtb* genome carries 5 *esx* loci, which encode for 5 distinct systems (ESX-1-ESX-5). The molecular architecture of a representative ESX model (ESX-5 of *Mycobacterium xenopi*) was recently determined at 13Å resolution by electron microscopy (Beckham et al., 2017). This work showed four core proteins of the ESX-5 complex (EccB5, EccC5, EccD5, and EccE5), which assembled with equimolar stoichiometry into an oligomeric complex that displays sixfold symmetry (Beckham et al., 2017). Among the ESX systems, the *esx-1* locus is probably the most studied as it encodes the 6 kDa Early Secretory Antigenic Target (ESAT-6; EsxA) and the 10 kDa Culture Filtrate Protein (CFP-10; EsxB), considered as key virulence determinants of *Mtb* as well as strong T-cell antigens (Gröschel et al., 2016). Recent work has shown a concerted action of the ESX-1 secretion system of *Mtb* with DIM/PDIM in phagosomal rupture, leading to access of *Mtb* to the cytosol of the host macrophage (Augenstreich et al., 2017), a phenomenon recently discussed from different perspectives (Russell, 2016; Simeone et al., 2016) and described further below.

DOORWAYS OF *Mtb* TO ENTER INTO MACROPHAGES

Interaction of *Mtb* with phagocytic cells mostly occurs through the recognition of Pathogen-Associated Molecular Patterns (PAMP) present at the bacterial surface by Pattern Recognition Receptors (PRRs) of the host cell such as Toll-Like Receptors (TLR), C-type Lectin Receptors (abbreviated as CLR or CTL), Fc Receptors (FcR), Scavenger Receptors (SR), and cytosolic DNA sensors (Satoh and Akira, 2016). Stimulation of PRRs leads to bacterial phagocytosis, the initiation of immune responses as well as the activation of numerous cellular processes such as apoptosis, antigen processing/presentation, inflammasome activation, phagosome maturation, and autophagy (Lugo-Villarino et al., 2011; Mortaz et al., 2015). The interaction between TLR and *Mtb* leads to phagocyte activation without immediate ingestion of mycobacteria. Recognition of specific mycobacterial structures, such as lipoproteins 19 kDa, LM, LAM, and PIM was reported to be established by TLR2 (Quesniaux et al., 2004), which is consistent with observations that TLR2-mediated recognition is diminished by the presence

of Lipooligosaccharide (LOS) in *Mycobacterium canettii*, the smooth variant of tubercle bacilli (Boritsch et al., 2016). It is noteworthy that loss of LOS production during the evolution of tuberculosis-causing mycobacteria has resulted in the rough colony morphology of *Mtb* strains, which apparently contributed to stronger recognition of *Mtb* by TLR2 (Boritsch et al., 2016). Moreover, unmethylated CpG motifs in bacterial DNA were reported to be recognized by TLR9 (Bafica et al., 2005). These events induce a signaling cascade by stimulation of Myeloid Differentiation primary response protein 88 (MyD88) leading to activation and nuclear translocation of transcription factors, such as the Nuclear transcription Factor NF-κB and activation of the innate host defense such as the production of pro-inflammatory cytokines.

CLR/CTL are a family of membrane-bound calcium-dependent receptors that recognize carbohydrate-rich molecules. Among the CLR family, one of the most well-known receptors is the Mannose Receptor (MR), which recognizes mannose molecules/glycolipids present on *Mtb*'s surface such as LAM, ManLAM, and PIM. Stimulation through MR induces production of anti-inflammatory cytokines and fails to activate oxidative responses (Nigou et al., 2001). Previous studies have shown that phagocytosis of mannosylated beads and/or MR-ManLAM interferes with phagosome maturation, highlighting the potential role of glycolipids in the intracellular survival of mycobacteria (Astarie-Dequeker et al., 1999; Kang et al., 2005). A recent analysis of SNPs in the *MRC1* gene within a Chinese population has suggested a possible association of selected SNPs and the susceptibility of individuals to pulmonary TB (Zhang et al., 2012). Moreover, Mincle, Dectin-1 and -2, and Dendritic Cell immunoActivating Receptor (DCAR) also belong to the CLR sub-family and represent probably the most well-known CLR expressed on macrophages. The Mincle receptor specifically recognizes mycobacterial cord factor Trehalose-6,6-dimycolate (TDM), which likely represents the most abundant glycolipid in the mycobacterial cell wall (Ishikawa et al., 2009). Ligation of TDM to Mincle induces several responses such as production of pro-inflammatory cytokines, generation of Th1/Th17 immune responses and induction of granuloma-genesis (Ishikawa et al., 2009; Mishra et al., 2017). It is known that Dectin-1 recognizes β-glucans in fungal pathogens but the precise *Mtb*'s PAMP is not known (Dinadayala et al., 2004). It has been showed that Dectin-1 is important for the innate immunity recognition of *Mtb* and for inducing Th1 and Th17 responses, independently of TLR2 recognition (van de Veerdonk et al., 2010). Dectin-2 has been recently shown to induce host immune responses against *Mtb* infection through the recognition of ManLAM (Yonekawa et al., 2014). DCAR recognizes PIM to induce Th1 responses during *Mtb* infection (Toyonaga et al., 2016). One other particular CRL/CTL, named DCSIGN/CD209, expressed by dendritic cells and macrophages recognizes conserved sugar motifs in a number of viruses, parasites, and bacteria, including *Mtb* (Tailleux et al., 2003; Tanne and Neyrolles, 2010).

Fc receptors and Complement Receptor (CR) are strongly expressed on surface of macrophages. CR3 plays a key role in the phagocytosis of *Mtb* by macrophages with recognition of *Mtb* polysaccharides or PIM (Villeneuve et al., 2005).

Scavenger Receptors are expressed on the cell surface of mammalian monocytes and macrophages and recognized oxidized or acetylated lipoproteins. During *Mtb* infections, the Macrophage Receptor with Collagenous (MARCO) structure is the most studied. MARCO recognizes TDM and cooperates with TLR2 to induce the activation of the transcriptional factor NF-κB and secretion of pro-inflammatory cytokines (Bowdish et al., 2009).

Finally, cytosolic DNA sensors have also been described as PRR, which can recognize the presence of mycobacterial DNA in the cytosol (Manzanillo et al., 2012). This process is dependent on phagosomal rupture induced by ESX-1 and is mediated via the cytosolic sensors cGAS or AIM2 (Collins et al., 2015; Majlessi and Brosch, 2015; Wassermann et al., 2015; Watson et al., 2015; **Figure 1**).

Mtb STRATEGIES TO CONQUER MACROPHAGES

Strategy 1: Interference with Phagosome Maturation

Macrophages are acting as the first line of defense against pathogenic invaders. After internalization, pathogens are trapped in a vacuole called phagosome, which immediately undergoes sequential fusion events to acquire microbicidal and degrading characteristics by a process called maturation. The dynamic of phagosome maturation is actively regulated by the network of Rab GTPases, proteins that sequentially drive the phagosome progression from early to later stages of maturation. Rab GTPases (Rab) contribute to the identity of the endosomal organelle (e.g., Rab5, early endosomes; Rab7, late endosome), regulating membrane-fusion events but also the sorting of protein and lipids through the recycling pathway (Gruenberg and van der Goot, 2006; Gutierrez, 2013; Prashar et al., 2017). Thus, all along the usual maturation process, biological changes of the phagosome are characterized by the specific recruitment of Rab GTPase until the final fusion with lysosomes, which carry a set of hydrolytic enzymes that contribute to pathogen clearance. Recently other regulators of the phagosomal maturation, Rab34, Rab20, and the proneurotropin receptor sortilin, have been described as important for control and elimination of intracellular *Mtb* (Kasmapour et al., 2012; Vazquez et al., 2016; Schnettger et al., 2017). Concurrently with the maturation process, the pH of phagosomes quickly drops from neutral to 5, through a high activity of a vesicular proton-pump ATPase (H+ V-ATPase) (Russell et al., 2009). Phagosomal acidification is a prerequisite for intracellular bacterial clearance, as acidic pH is essential for the optimal activity of lysosomal digestive enzymes and for reactive oxygen species production (Vieira et al., 2002; Sun-Wada et al., 2009). All along common trafficking pathways within macrophages, pathogens have to face multiple dangers such as exposure to cytosolic pattern recognition or danger receptors. The cytosolic lectin, Galectin8, notably recognizes damaged pathogen-containing vacuoles (including *Mtb* damaged phagosomes), and promotes their elimination by activating

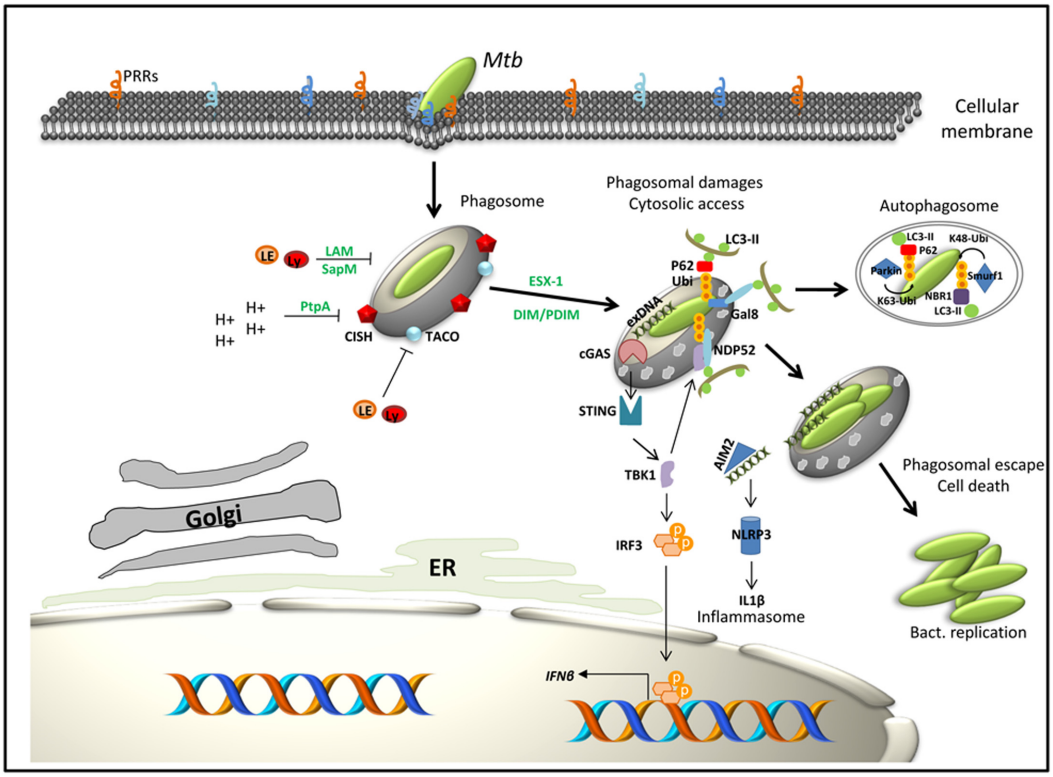


FIGURE 1 | Working model for selected components intervening in the immune subversion strategies of *Mtb* as well as macrophage factors that contribute to host defense. In green: bacterial factors; in black: macrophage factors. Interaction of *Mtb* with macrophage PRRs triggers bacteria internalization. The first strategy of *Mtb* to conquer macrophages is to inhibit phagosome maturation and acidification through the expression or secretion of bacterial factors (LAM, SapM, PtpA) or by subverting host pathways such as TACO or CISH signaling. Bacteria then progressively access to the cytosol through the action of the ESX-1 secretion system and DIM/PDIM. When in contact with the cytosol, bacteria get targeted by ubiquitin ligases (Parkin, Smurf1) and/or activate specific cytosolic recognition pathways (gal8, cGAS, or AIM2). This latter step induces expression of type I IFN, activation of the NRLP3 inflammasome and initiation of autophagy. Lastly, cytosolic *Mtb* induces host cell death programs (apoptosis and necrosis) to enhance its dissemination.

anti-bacterial autophagy (Thurston et al., 2012; **Figure 1**). Additionally, Ubiquitin ligases Parkin, Ubiquilin1, and Smurf1 recognize intracellular *Mtb* and enhance its clearance through an ubiquitin-mediated autophagy pathway (Manzanillo et al., 2013; Sakowski et al., 2015; **Figure 1**).

To survive in this harsh environment, *Mtb* developed a wide range of strategies to counteract macrophages defenses. *Mtb* indeed triggers rapid interferences in phagosome functions by inhibiting the phagolysosome biogenesis. Unless the macrophage is activated by inflammatory cytokines, the mycobacterial vacuole fails to mature along the normal endocytic pathway, and retains features typical of an immature endosome. Just after macrophage uptake, mycobacterial phagosome transitory recruits early endosomal markers Rab5 and remains accessible to the marker of recycling endosome Rab11 (Via et al., 1997; Tailleux et al., 2003; Vergne et al., 2004). In addition, Coronin1, also called TACO, is reported to be recruited and retained at the phagosomal surface where it activates calcium–calcineurin signaling to block the fusion of lysosomes with mycobacterial phagosomes (Jayachandran et al., 2007; **Figure 1**). Consistent with these immature characteristics, this organelle lacks the late endosomal and lysosomal markers Rab7 and CD63, as well as mature and active forms of various lysosomal hydrolases, including cathepsin D (Clemens and Horwitz, 1995; Via et al., 1997; Ullrich et al., 1999). Both bacterial ManLAM and the secreted phosphatase SapM have been shown to inhibit the activity of membrane trafficking regulatory lipid phosphatidylinositol 3-phosphate (PI3P), impairing the phagosomal acquisition of the lysosomal cargo and the delivery of hydrolytic enzyme from the Golgi network (Fratti et al., 2001, 2003; Vergne et al., 2005; **Figure 1**).

Blockade of phagosomal acidification is also a key feature for the intracellular survival of pathogens. Consistently, *Mtb* has developed at least three different strategies aiming to inhibit H+ V-ATPase complex assembly and its subsequent fusion with the phagosomal membrane in order to stabilize the phagosomal pH between 6.2 and 6.5 (Sturgill-Koszycki et al., 1994). Indeed, the phosphatase PtpA secreted by *Mtb* inhibits the assembly of H+ V-ATPase machinery by direct interaction with the subunits H of this complex (Wong et al., 2011). Additionally, interaction of TDM with C-type lectin receptor Mincle has been shown to delay phagosomal maturation and acidification (Axelrod et al.,

2008; Patin et al., 2017). As parallel mechanism, we recently reported that *Mtb* depletes H+ V-ATPase from its phagosome by co-opting the function of a host immune regulator, i.e., cytokine-inducible SH2 containing protein (CISH), which selectively targets the H+ V-ATPase subunit A for ubiquitination and degradation by the proteasome (Queval et al., 2017; **Figure 1**). The control of the pH is decisive not only for the survival of *Mtb* but also for the further processing of the mycobacterial phagosome. Indeed, early blockade of the acidification process is a pre-requisite for the ESX-1 dependent phagosomal rupture and the access of *Mtb* to the cytosol of the macrophage (Simeone et al., 2015).

Strategy 2: Getting Access to the Cytosol

The intracellular localization of *Mtb* inside host cells has been studied since the 1970s. The seminal work of Armstrong and Hart (1971) showed in mouse peritoneal macrophages that were infected with viable or non-viable *Mtb* and BCG strains that mycobacteria can be observed by electron microscopy (EM) inside phagosomes that have blocked the phagosome–lysosome fusion (Armstrong and Hart, 1971). In following years, further EM studies also observed *Mtb* outside the phagosome under certain conditions (Leake et al., 1984; Myrvik et al., 1984; McDonough et al., 1993), whereas others could not observe mycobacteria in the cytosol by EM (Xu et al., 1994). Some of these disparities were thought to have been caused by differences in the EM conditions and protocols used. More recently, using sophisticated cryo-immunogold EM, van der Wel et al. (2007) have challenged the dogma of the exclusive intracellular localization of *Mtb* and have described the existence of cytosolic *Mtb* in THP-1 human macrophage-like cells at 4 days post-infection whereas the BCG strain did not show such a distribution (van der Wel et al., 2007; Houben et al., 2012). This result has been correlated with the function of the ESX/T7S system in *Mtb*, which is absent from BCG due to the ESX-1 deletion. However, given the situation that the suggested paradigm shift was entirely based on ultrastructural observations generated by electron microscopy, the presence of *Mtb* in the cytosol has remained controversial for some time. The development of a Fluorescent Resonance Energy Transfer (FRET) for detection of mycobacteria that have ruptured the phagosome and have established cytosolic contact has been an important advance to study this delicate and fascinating question (Simeone et al., 2012, 2015). For that purpose, host cells are loaded with a chemical probe that is sensitive to FRET changes based on β-lactamase activity present on the surface of bacteria. The use of this FRET-based technology combined with automated fluorescent microscopy (Simeone et al., 2012) and multicolor quantitative cytofluorometry allowed to explore the role of ESX-1 in the induction of phagosomal rupture and more recently to show that *Mtb* induces phagosomal rupture *in vivo* (Simeone et al., 2015; **Figure 1**).

Based on the results from different groups using independent techniques, it thus became clear that the ESX-1/T7S system plays a primordial role for establishing cytosolic access of selected mycobacteria in host cells (van der Wel et al., 2007; Houben et al., 2012; Simeone et al., 2012, 2015). However, very recently, in independent studies, additional mycobacterial factors have been identified that favor the access of *Mtb* to the cytosol. Indeed, it was found that cytosolic access of *Mtb* only occurs when the production and the export of the outer membrane lipids (DIM/PDIM) are intact (Augenstreich et al., 2017). DIM/PDIM are key virulent lipids and play important roles in host-pathogen interaction. Their presence favors intracellular bacterial replication through arrest of phagosomal acidification by excluding the vacuolar proton-ATPase from the phagosomal membrane (Astarie-Dequeker et al., 2009) and they are also involved in the death of macrophages (Passemar et al., 2014). The use of monoclonal antibodies against Galectin-3 and ubiquitinated proteins for identification of damaged phagosomal-membranes (Wong and Jacobs, 2011), in parallel to a FRET-based cytofluorometric approach for detection of phagosomal rupture, demonstrated the implication of DIM/PDIM in phagosomal rupture (**Figure 1**). This study showed that both the ESX-1 system and a functional DIM/PDIM production were required to cause phagosomal damage and rupture, which ultimately leads to host cell death (Augenstreich et al., 2017). The implication of DIM/PDIM in this phenomenon has independently been confirmed by a study that investigated the DNA interaction and the regulon of a transcriptional repressor (Rv3167c), which was found to control the DIM/PDIM operon and to impact phagosomal escape (Quigley et al., 2017). Additional confirmation came from a third study that carried out a multiparametric analysis, combining pathogen and host phenotypes, and found similar profiles for ESX-1 and DIM/PDIM loss-of-function mutants (Barczak et al., 2017). Phospholipases have been described to play a role in the escape of the bacteria from phagosome to cytosol by acting together with pore-forming proteins such as listeriolysin from *Listeria monocytogenes* (Cossart, 2011). The *Mtb* genome presents four phospholipases PlcA-D, whereby in the reference strain *Mtb* H37Rv PlcD has already been naturally inactivated by an IS*6110*-mediated deletion (Cole et al., 1998). The use of FRET-based cytofluorometry, however, showed that Plcs of *Mtb* do not seem to play a role in the phagosomal rupture as triple/quadruple Plc deletion mutants continued to generate positive signals in the phagosomal rupture assay, similar to wild-type strains (Le Chevalier et al., 2015).

Few studies report data on the implication of host factors involved in the induction of phagosomal rupture. A first result was obtained by the use of the FRET-cytofluorometry approach for the study of *Mtb* infection in macrophages carrying a non-functional *nramp* gene, encoding the Natural Resistance-Associated Macrophage Protein (Nramp-1), a phagosomal bivalent cation transporter implicated in phagosomal acidification and pH regulation (Simeone et al., 2015). This approach showed that initial blockage of the acidification of the phagosome is necessary to allow bacteria to survive and to induce phagosomal rupture (Simeone et al., 2015). Another host element that has been suggested in this context is the cytosolic phospholipase A2 (cPLA2). This enzyme plays a critical role in both phagosomal trafficking and export of cargo from the various endocytic comportments and permeabilizes the

endosomal membrane in *Mtb*-infected macrophages (Lee et al., 2011). Treatment of *Mtb*-infected macrophages with an inhibitor of this enzyme induces a marked reduction of cytosolic bacteria as observed by EM (Jamwal et al., 2016).

Cytosolic contact of *Mtb* thus seems to be fundamental in mycobacterial host-pathogen interaction, influencing both the fate of the host cell and the bacteria. Indeed, the recognition of mycobacteria-associated patterns by the cytosolic receptors of the innate immunity determines innate and adaptive immune responses (Gröschel et al., 2016). Following steps exist: (i) DNA is sensed by cGAS, which synthesizes the second messenger cGAMP from ATP and GTP. cGAMP activates the Endoplasmic Reticulum (ER) associates Stimulator of IFN Genes (STING) and downstream TBK-1-IRF-3-IFN-β signaling axis (**Figure 1**). This effect leads to the expression of type I IFNs, such as IFN-α/β, which are thought to be disadvantageous to the host during *Mtb* infection, (ii) the cytosolic *Mtb* DNA may be sensed by AIM-2, which contributes partially to the activation of the NRLP3 inflammasome axis and release of mature IL-1β and IL-18 (Collins et al., 2015; Wassermann et al., 2015; Watson et al., 2015; Kupz et al., 2016), and (iii) the ESX-1-mediated cytosolic translocation of mycobacterial DNA results in the activation of TBK-1 which initiates the recruitment of LC3-II involved in autophagic activity (Romagnoli et al., 2012; Watson et al., 2012; **Figure 1**). The last two points, in contrast to the first one, might be considered as more beneficial for the host. Thus, during infection, different and sometimes opposite responses govern the balance between the benefit for the mycobacteria and for the host. Nonetheless, during the infectious process mycobacteria are not necessarily constrained within the host cells, and may escape from the microbicidal environment of macrophages by disseminating inside the organism. It has been notably reported in the Zebra fish model that *Mycobacterium marinum* membrane Phenolic Glycolipids (PGL) trigger a STING-dependent secretion of monocyte chemoattractant protein 1 (MCP1; also called CCL2) by infected-resident macrophages, resulting in the recruitment of circulating monocytes and a subsequent transfer of the bacteria from tissue resident- to circulating macrophages (Cambier et al., 2017).

Finally, in the context of vaccination, the induction of ESX-1-mediated cytosolic responses seems to be beneficial for increased protective efficacy provided by recombinant BCG strains over parental BCG strains (Kupz et al., 2016; Groschel et al., 2017).

Strategy 3: The Control of Host Cell Death

The control of host cell death allows *Mtb* to escape host defenses and to take the power on the pathogenesis control. For decades, host cell death upon *Mtb*-infection has been controversial and apoptosis cell death was considered as the only programmed cell death. Two main types of cell death are known for elimination of infected cells: (i) apoptosis or programmed cell death and (ii) necrosis.

(i) From a morphological point of view, apoptosis is defined by plasma membrane bleeding, cell body shrinkage, nuclear condensation and fragmentation, and formation of apoptotic bodies, which are membrane-bound cell fragments rapidly phagocytosed by neighboring cells and resident phagocytes (Lamkanfi and Dixit, 2010). From a biochemical point of view, apoptosis induces a decrease in mitochondrial inner transmembrane potential, activation of selective proteases, cleavage of chromosomal DNA, and various cellular proteins and translocation of phosphatidylserine from the inner to the outer plasma membrane (Behar et al., 2011). Apoptosis does occur via TNF-α activation and caspase 3 and 8 activation. Suppression of inflammation allows to limit tissue damage. Apoptosis of infected cells is considered as a benefit for the host. Indeed, it allows elimination of a favorable environment for replication of the pathogen, and provides an important source of bacterial antigens that can stimulate *Mtb*-specific T-cell immunity (Behar et al., 2011). Apoptosis has been directly linked to an increase CD8+ T-cell response via cross-presentation and enhances class II MHC-restricted antigen presentation (Behar et al., 2011). Some *Mtb* genes have been reported to play a role in the inhibition or induction of host cell death, as for example *sodA*, encoding superoxide dismutase A, or *nuoG*, encoding the NADH dehydrogenase 1 subunit G (Velmurugan et al., 2007; Gengenbacher et al., 2016). An *Mtb* gene well known for inducing host cell death is *esxA*, encoding EsxA, which has been described as a pro-apoptotic (Aguilo et al., 2013). The exact role of EsxA in this process remains unclear, but most probably it is the contribution to the access of *Mtb* to the host cytosol, which plays a main role. However, while the biological role of the ESX-1 system in the process remains fully valid, the function of recombinant EsxA as a putative membranolytic molecule was recently questioned, as the lytic activity of EsxA preparations expressed and purified from *Escherichia coli* lysates on red blood cells continued even after digestion with proteinase K, suggesting that some of the previously described pore-forming activity might be simply caused by a selected detergent used during the protein purification process (Conrad et al., 2017). Further studies are needed to clarify the role of EsxA in the process.

(ii) In contrast to apoptosis, necrosis is characterized by loss of plasma membrane integrity, cytoplasmic organelles swelling such as mitochondria and cell nuclei, release of cytoplasmic and nuclear contents to the extracellular space, hydrolysis of chromatin and DNA and is caspase-independent cell death (Lamkanfi and Dixit, 2010). It was previously thought that virulent *Mtb* inhibits apoptosis and triggers necrosis to evade innate immunity and thus to delay the initiation of adaptive immunity. On the contrary, attenuated *Mtb* induces macrophage apoptosis, which reduces bacterial viability (Behar et al., 2010). However, from different recent studies, it can be hypothesized that apoptosis induced by virulent *Mtb* favors dissemination of bacilli (Aguilo et al., 2013; Augenstreich et al., 2017), while necrosis tends to enhance bacterial replication (Dallenga et al., 2017; Lerner et al., 2017).

Colonization of macrophages by *Mtb* is a highly disputed process that depends on the ability of the pathogen to escape from macrophage killing and the capacity of the macrophages to control the bacterial proliferation.

PERSPECTIVES

It is clear that the interaction of *Mtb* with the macrophage has major impact on the outcome of infection, whereby both mycobacterial and host factors play important roles. The accumulated vast knowledge in recent years on this process might also turn out as important for developing potential new strategies in the fight against TB, concerning vaccines and host-directed therapies. For example, BCG complemented with the functional ESX-1 system of *Mtb* showed better efficacy to protect against disseminated TB in mice and guinea pigs (Pym et al., 2003; Kupz et al., 2016). However, this recombinant strain named BCG::RD1 has also been shown to be more virulent than the wild-type BCG strain (Pym et al., 2002). As one possibility to reduce this enhanced virulence, introduction of selected mutations in the *esxA* gene of the cloned ESX-1 locus have shown some effect (Bottai et al., 2015). Alternatively, the use of an ESX-1 secretion system taken from a less virulent mycobacterium than *Mtb* for the complementation of BCG seems also promising. Indeed, recombinant BCG expressing the ESX-1 system from *Mycobacterium marinum*, BCG::ESX-1^{Mmar}, has been recently shown to be low virulent and more protective than parental BCG strains in different murine models of infection (Groschel et al., 2017). This strain enhances NLRP3 inflammasome activation and induces type I IFN production and stronger $CD8^+$ and $CD4^+$ T-cell responses (Groschel et al., 2017).

Using attenuated live *Mtb* strains as vaccines is another alternative approach, presenting the advantage that these strains naturally carry genetic regions encoding for important immunodominant antigens that might be absent from BCG in combination with sufficient safety, provided by the introduction of deletions in virulence genes. The live-attenuated MTBVAC is a good example (Aguilo et al., 2017). MTBVAC attenuation is based on two independent stable genetic deletions, without antibiotic resistance markers, introduced into *phoP* and *fadD26*, affecting the production and secretion of selected lipidic and proteic virulence factors of *Mtb*. MTBVAC presents promising features in preclinical animal models and is presently being evaluated in a phase I clinical trial in newborns in South Africa (Marinova et al., 2017). Other attenuated *Mtb* strain, presently in preclinical development with promising results in murine infection models, is the *Mtb*Δppe25-pe19 strain, in which selected PE and PPE proteins of the ESX-5 secretion system have been deleted, but which retains an intact ESX-1 secretion system (Bottai et al., 2012; Sayes et al., 2012, 2016).

Concerning drug treatment of TB, most of the drugs used today date from the 1950s to 1960s, with a few exceptions, such as bedaquiline, a recently discovered ATP synthase inhibitor (Andries et al., 2005) that is currently used successfully in drug regimens against MDR-TB (Diacon et al., 2009). However, additional identification of new active anti-TB drugs is urgently needed. In this perspective, it should be mentioned that remarkable progress has been made in developing new screening approaches that can simultaneously evaluate the anti-bacterial potency and the non-cytotoxic properties of small molecule inhibitors in the intracellular environment of *Mtb*-infected macrophages (Christophe et al., 2009; Pethe et al., 2013; VanderVen et al., 2015). Moreover, targeting of mycobacterial virulence factors might also be a possibility to find alternative treatment approaches (Chen et al., 2010; Bottai et al., 2014). As one example, screening of a compound library recently allowed molecules to be identified that target the ESX-1 secretion system of *Mtb* (Rybniker et al., 2014) and/or the global two-component regulator PhoP/R which among many other virulence factors also regulates ESX-1-mediated secretion (Johnson et al., 2015).

Host-directed therapy (HDT) to treat TB is a relatively new and promising concept that starts to arouse a great interest from the scientific community. Instead of targeting *Mtb* compounds directly, HDT targets the host response, such as the modulation of host inflammatory pathways to reduce inflammation and lungs tissue damages, augmenting cellular anti-microbial mechanisms. In the case of TB-HIV co-infection, HDT may reduce the risk of interaction with antiretroviral drugs. In the case of MDR or XDR-TB, HDT could be added to anti-TB treatment to increase the capacity of the host system to eliminate mycobacteria or to limit tissue damage due to the infection (Wallis and Hafner, 2015; Zumla et al., 2015). For instance, in association with anti-TB drugs, statins, a family of inhibitors of HMG-CoA reductase, originally used to lower cholesterol levels in patients, drastically enhance the efficacy of first-line TB treatments in macrophages and *in vivo* models (Lobato et al., 2014; Parihar et al., 2014; Skerry et al., 2014). Moreover, Vitamin D treatment has been suggested to promote the expression anti-microbial peptide Cathelicidin by macrophages, and thus lowering of the intracellular survival of *Mtb* (Liu et al., 2006; Wheelwright et al., 2014).

Some HDTs are in clinical human trials or preclinical animal studies, such as anti-inflammatory therapies, modulation of inflammation by phosphodiesterase inhibitors, eicosanoid modulation, non-steroidal anti-inflammatory drugs, high-dose vitamin D application, alteration of lipid metabolism, as well as new HDT that targets autophagy (Tobin, 2015). Autophagy appears to be a promising pathway to target for the development of drugs. Interestingly, anti-mycobacterial activities of both statins and Cathelicidin have been correlated with their ability to enhance the autophagy pathway (Yuk et al., 2009; Hoyer-Hansen et al., 2010; Parihar et al., 2014). As such, HDT opens new avenues for individualized TB therapies.

CONCLUSION

We have discussed a selection of amazing strategies of *Mtb* and host cells in their battle about survival and death in host-pathogen interaction that remains a highly interesting research domain. Driven by an advancing technical progress, many new insights were obtained in recent years and have often led to changes in long-lasting hypotheses and theories, a finding which

gives hope that in the upcoming years more progress will further contribute to the knowledge how to better fight *Mtb* and reduce the burden of TB in the world.

AUTHOR CONTRIBUTIONS

All authors listed have made a substantial, direct and intellectual contribution to the work, and approved it for publication.

ACKNOWLEDGMENTS

We thank our colleagues who were involved in the various research projects that are reviewed in this article. We are grateful for support of our TB research by the European Union (Grant 643381 – TBVAC2020), the Agence National de Recherche (Grants ANR-14-JAMR-001-02, ANR-10-LABX-62-IBEID, and ANR-16-CE15-0003), and the Fondation pour la Recherche Médicale (DEQ20130326471).

REFERENCES

Abdallah, A. M., Gey Van Pittius, N. C., Champion, P. A., Cox, J., Luirink, J., Vandenbroucke-Grauls, C. M., et al. (2007). Type VII secretion system of mycobacteria show the way. *Nat. Rev. Microbiol.* 5, 883–891. doi: 10.1038/nrmicro1773

Aguilo, J., Alonso, H., Uranga, S., Marinova, D., Arbues, A., De Martino, A., et al. (2013). ESX-1-induced apoptosis is involved in cell-to-cell spread of *Mycobacterium tuberculosis*. *Cell Microbiol* 15, 1994–2005. doi: 10.1111/cmi.12169

Aguilo, N., Gonzalo-Asensio, J., Alvarez-Arguedas, S., Marinova, D., Gomez, A. B., Uranga, S., et al. (2017). Reactogenicity to major tuberculosis antigens absent in BCG is linked to improved protection against *Mycobacterium tuberculosis*. *Nat. Commun.* 8:16085. doi: 10.1038/ncomms16085

Andries, K., Verhasselt, P., Guillemont, J., Gohlmann, H. W., Neefs, J. M., Winkler, H., et al. (2005). A diarylquinoline drug active on the ATP synthase of *Mycobacterium tuberculosis*. *Science* 307, 223–227. doi: 10.1126/science.1106753

Armstrong, J. A., and Hart, P. D. (1971). Response of cultured macrophages to *Mycobacterium tuberculosis*, with observations on fusion of lysosomes with phagosomes. *J. Exp. Med.* 134, 713–740. doi: 10.1084/jem.134.3.713

Astarie-Dequeker, C., Le Guyader, L., Malaga, W., Seaphanh, F. K., Chalut, C., Lopez, A., et al. (2009). Phthiocerol dimycocerosates of *M. tuberculosis* participate in macrophage invasion by inducing changes in the organization of plasma membrane lipids. *PLOS Pathog.* 5:e1000289. doi: 10.1371/journal.ppat.1000289

Astarie-Dequeker, C., N'diaye, E. N., Le Cabec, V., Rittig, M. G., Prandi, J., and Maridonneau-Parini, I. (1999). The mannose receptor mediates uptake of pathogenic and nonpathogenic mycobacteria and bypasses bactericidal responses in human macrophages. *Infect. Immun.* 67, 469–477.

Augenstreich, J., Arbues, A., Simeone, R., Haanappel, E., Wegener, A., Sayes, F., et al. (2017). ESX-1 and phthiocerol dimycocerosates of *Mycobacterium tuberculosis* act in concert to cause phagosomal rupture and host cell apoptosis. *Cell Microbiol.* 19:e12726. doi: 10.1111/cmi.12726

Axelrod, S., Oschkinat, H., Enders, J., Schlegel, B., Brinkmann, V., Kaufmann, S. H., et al. (2008). Delay of phagosome maturation by a mycobacterial lipid is reversed by nitric oxide. *Cell Microbiol.* 10, 1530–1545. doi: 10.1111/j.1462-5822.2008.01147.x

Bafica, A., Scanga, C. A., Feng, C. G., Leifer, C., Cheever, A., and Sher, A. (2005). TLR9 regulates Th1 responses and cooperates with TLR2 in mediating optimal resistance to *Mycobacterium tuberculosis*. *J. Exp. Med.* 202, 1715–1724. doi: 10.1084/jem.20051782

Barczak, A. K., Avraham, R., Singh, S., Luo, S. S., Zhang, W. R., Bray, M. A., et al. (2017). Systematic, multiparametric analysis of *Mycobacterium tuberculosis* intracellular infection offers insight into coordinated virulence. *PLOS Pathog.* 13:e1006363. doi: 10.1371/journal.ppat.1006363

Barry, C. E. III, Boshoff, H. I., Dartois, V., Dick, T., Ehrt, S., Flynn, J., et al. (2009). The spectrum of latent tuberculosis: rethinking the biology and intervention strategies. *Nat. Rev. Microbiol.* 7, 845–855. doi: 10.1038/nrmicro2236

Beckham, K. S., Ciccarelli, L., Bunduc, C. M., Mertens, H. D., Ummels, R., Lugmayr, W., et al. (2017). Structure of the mycobacterial ESX-5 type VII secretion system membrane complex by single-particle analysis. *Nat. Microbiol.* 2:17047. doi: 10.1038/nmicrobiol.2017.1047

Behar, S. M., Divangahi, M., and Remold, H. G. (2010). Evasion of innate immunity by *Mycobacterium tuberculosis*: is death an exit strategy? *Nat. Rev. Microbiol.* 8, 668–674. doi: 10.1038/nrmicro2387

Behar, S. M., Martin, C. J., Booty, M. G., Nishimura, T., Zhao, X., Gan, H. X., et al. (2011). Apoptosis is an innate defense function of macrophages against *Mycobacterium tuberculosis*. *Mucosal Immunol.* 4, 279–287. doi: 10.1038/mi.2011.3

Boritsch, E. C., Frigui, W., Cascioferro, A., Malaga, W., Etienne, G., Laval, F., et al. (2016). pks5-recombination-mediated surface remodelling in *Mycobacterium tuberculosis* emergence. *Nat. Microbiol.* 1:15019. doi: 10.1038/nmicrobiol.2015.19

BoseDasgupta, S., and Pieters, J. (2014). Striking the right balance determines TB or not TB. *Front. Immunol.* 5:455. doi: 10.3389/fimmu.2014.00455

Bottai, D., Di Luca, M., Majlessi, L., Frigui, W., Simeone, R., Sayes, F., et al. (2012). Disruption of the ESX-5 system of *Mycobacterium tuberculosis* causes loss of PPE protein secretion, reduction of cell wall integrity and strong attenuation. *Mol. Microbiol.* 83, 1195–1209. doi: 10.1111/j.1365-2958.2012.08001.x

Bottai, D., Frigui, W., Clark, S., Rayner, E., Zelmer, A., Andreu, N., et al. (2015). Increased protective efficacy of recombinant BCG strains expressing virulence-neutral proteins of the ESX-1 secretion system. *Vaccine* 33, 2710–2718. doi: 10.1016/j.vaccine.2015.03.083

Bottai, D., Serafini, A., Cascioferro, A., Brosch, R., and Manganelli, R. (2014). Targeting type VII/ESX secretion systems for development of novel antimycobacterial drugs. *Curr. Pharm. Des* 20, 4346–4356. doi: 10.2174/1381612819666131118170717

Bowdish, D. M., Sakamoto, K., Kim, M. J., Kroos, M., Mukhopadhyay, S., Leifer, C. A., et al. (2009). MARCO, TLR2, and CD14 are required for macrophage cytokine responses to mycobacterial trehalose dimycolate and *Mycobacterium tuberculosis*. *PLOS Pathog.* 5:e1000474. doi: 10.1371/journal.ppat.1000474

Brennan, P. J., and Nikaido, H. (1995). The envelope of mycobacteria. *Annu. Rev. Biochem.* 64, 29–63. doi: 10.1146/annurev.bi.64.070195.000333

Cambier, C. J., Falkow, S., and Ramakrishnan, L. (2014). Host evasion and exploitation schemes of *Mycobacterium tuberculosis*. *Cell* 159, 1497–1509. doi: 10.1016/j.cell.2014.11.024

Cambier, C. J., O'leary, S. M., O'sullivan, M. P., Keane, J., and Ramakrishnan, L. (2017). Phenolic glycolipid facilitates mycobacterial escape from microbicidal tissue-resident macrophages. *Immunity* 47, 552.e–565.e. doi: 10.1016/j.immuni.2017.08.003

Chalut, C. (2016). MmpL transporter-mediated export of cell-wall associated lipids and siderophores in mycobacteria. *Tuberculosis* 100, 32–45. doi: 10.1016/j.tube.2016.1006.1004

Chen, J. M., Pojer, F., Blasco, B., and Cole, S. T. (2010). Towards anti-virulence drugs targeting ESX-1 mediated pathogenesis of *Mycobacterium tuberculosis*. *Drug Discov. Today* 7, e25–e31. doi: 10.1016/j.ddmec.2010.09.002

Christophe, T., Jackson, M., Jeon, H. K., Fenistein, D., Contreras-Dominguez, M., Kim, J., et al. (2009). High content screening identifies decaprenyl-phosphoribose 2' epimerase as a target for intracellular antimycobacterial inhibitors. *PLOS Pathog.* 5:e1000645. doi: 10.1371/journal.ppat.1000645

Clemens, D. L., and Horwitz, M. A. (1995). Characterization of the *Mycobacterium tuberculosis* phagosome and evidence that phagosomal maturation is inhibited. *J. Exp. Med.* 181, 257–270. doi: 10.1084/jem.181.1.257

Cole, S. T., Brosch, R., Parkhill, J., Garnier, T., Churcher, C., Harris, D., et al. (1998). Deciphering the biology of *Mycobacterium tuberculosis* from the complete genome sequence. *Nature* 393, 537–544. doi: 10.1038/31159

Collins, A. C., Cai, H., Li, T., Franco, L. H., Li, X. D., Nair, V. R., et al. (2015). Cyclic GMP-AMP synthase is an innate immune DNA sensor for *Mycobacterium tuberculosis*. *Cell Host Microbe* 17, 820–828. doi: 10.1016/j.chom.2015.05.005

Conrad, W. H., Osman, M. M., Shanahan, J. K., Chu, F., Takaki, K. K., Cameron, J., et al. (2017). Mycobacterial ESX-1 secretion system mediates host cell lysis through bacterium contact-dependent gross membrane disruptions. *Proc. Natl. Acad. Sci. U.S.A.* 114, 1371–1376. doi: 10.1073/pnas.1620133114

Cossart, P. (2011). Illuminating the landscape of host-pathogen interactions with the bacterium Listeria monocytogenes. *Proc. Natl. Acad. Sci. U.S.A.* 108, 19484–19491. doi: 10.1073/pnas.1112371108

Daffe, M., Crick, D. C., and Jackson, M. (2014). Genetics of capsular polysaccharides and cell envelope (Glyco)lipids. *Microbiol. Spectr.* 2, 14. doi: 10.1128/microbiolspec.MGM2-0021-2013

Dallenga, T., Repnik, U., Corleis, B., Eich, J., Reimer, R., Griffiths, G. W., et al. (2017). *M. tuberculosis*-induced necrosis of infected neutrophils promotes bacterial growth following phagocytosis by macrophages. *Cell Host Microbe* 22, 519–530.e3. doi: 10.1016/j.chom.2017.09.003

Davis, J. M., and Ramakrishnan, L. (2009). The role of the granuloma in expansion and dissemination of early tuberculous infection. *Cell* 136, 37–49. doi: 10.1016/j.cell.2008.11.014

Diacon, A. H., Pym, A., Grobusch, M., Patientia, R., Rustomjee, R., Page-Shipp, L., et al. (2009). The diarylquinoline TMC207 for multidrug-resistant tuberculosis. *N. Engl. J. Med.* 360, 2397–2405. doi: 10.1056/NEJMoa0808427

Dinadayala, P., Lemassu, A., Granovski, P., Cerantola, S., Winter, N., and Daffe, M. (2004). Revisiting the structure of the anti-neoplastic glucans of *Mycobacterium bovis* Bacille Calmette-Guerin. Structural analysis of the extracellular and boiling water extract-derived glucans of the vaccine substrains. *J. Biol. Chem.* 279, 12369–12378. doi: 10.1074/jbc.M308908200

Ehrt, S., and Schnappinger, D. (2009). Mycobacterial survival strategies in the phagosome: defence against host stresses. *Cell Microbiol.* 11, 1170–1178. doi: 10.1111/j.1462-5822.2009.01335.x

Fratti, R. A., Backer, J. M., Gruenberg, J., Corvera, S., and Deretic, V. (2001). Role of phosphatidylinositol 3-kinase and Rab5 effectors in phagosomal biogenesis and mycobacterial phagosome maturation arrest. *J. Cell Biol.* 154, 631–644. doi: 10.1083/jcb.200106049

Fratti, R. A., Chua, J., Vergne, I., and Deretic, V. (2003). *Mycobacterium tuberculosis* glycosylated phosphatidylinositol causes phagosome maturation arrest. *Proc. Natl. Acad. Sci. U.S.A.* 100, 5437–5442. doi: 10.1073/pnas.0737613100

Gengenbacher, M., Nieuwenhuizen, N., Vogelzang, A., Liu, H., Kaiser, P., Schuerer, S., et al. (2016). Deletion of nuoG from the vaccine candidate *Mycobacterium bovis* BCG DeltaureC::hly improves protection against tuberculosis. *mBio* 7:e00679-16. doi: 10.1128/mBio.00679-16

Groschel, M. I., Sayes, F., Shin, S. J., Frigui, W., Pawlik, A., Orgeur, M., et al. (2017). Recombinant BCG expressing ESX-1 of *Mycobacterium marinum* combines low virulence with cytosolic immune signaling and improved TB protection. *Cell Rep.* 18, 2752–2765. doi: 10.1016/j.celrep.2017.02.057

Gröschel, M. I., Sayes, F., Simeone, R., Majlessi, L., and Brosch, R. (2016). ESX secretion systems: mycobacterial evolution to counter host immunity. *Nat. Rev. Microbiol.* 14, 677–691. doi: 10.1038/nrmicro.2016.131

Gruenberg, J., and van der Goot, F. G. (2006). Mechanisms of pathogen entry through the endosomal compartments. *Nat. Rev. Mol. Cell Biol.* 7, 495–504. doi: 10.1038/nrm1959

Gutierrez, M. G. (2013). Functional role(s) of phagosomal Rab GTPases. *Small GTPases* 4, 148–158. doi: 10.4161/sgtp.25604

Houben, D., Demangel, C., Van Ingen, J., Perez, J., Baldeon, L., Abdallah, A. M., et al. (2012). ESX-1-mediated translocation to the cytosol controls virulence of mycobacteria. *Cell Microbiol.* 14, 1287–1298. doi: 10.1111/j.1462-5822.2012.01799.x

Hoyer-Hansen, M., Nordbrandt, S. P., and Jaattela, M. (2010). Autophagy as a basis for the health-promoting effects of vitamin D. *Trends Mol. Med.* 16, 295–302. doi: 10.1016/j.molmed.2010.04.005

Ishikawa, E., Ishikawa, T., Morita, Y. S., Toyonaga, K., Yamada, H., Takeuchi, O., et al. (2009). Direct recognition of the mycobacterial glycolipid, trehalose dimycolate, by C-type lectin Mincle. *J. Exp. Med.* 206, 2879–2888. doi: 10.1084/jem.20091750

Jamwal, S. V., Mehrotra, P., Singh, A., Siddiqui, Z., Basu, A., and Rao, K. V. (2016). Mycobacterial escape from macrophage phagosomes to the cytoplasm represents an alternate adaptation mechanism. *Sci. Rep.* 6:23089. doi: 10.1038/srep23089

Jayachandran, R., Sundaramurthy, V., Combaluzier, B., Mueller, P., Korf, H., Huygen, K., et al. (2007). Survival of mycobacteria in macrophages is mediated by coronin 1-dependent activation of calcineurin. *Cell* 130, 37–50. doi: 10.1016/j.cell.2007.04.043

Johnson, B. K., Colvin, C. J., Needle, D. B., Mba Medie, F., Champion, P. A., and Abramovitch, R. B. (2015). The carbonic anhydrase inhibitor ethoxzolamide inhibits the *Mycobacterium tuberculosis* PhoPR regulon and Esx-1 secretion and attenuates virulence. *Antimicrob. Agents Chemother.* 59, 4436–4445. doi: 10.1128/AAC.00719-15

Kang, P. B., Azad, A. K., Torrelles, J. B., Kaufman, T. M., Beharka, A., Tibesar, E., et al. (2005). The human macrophage mannose receptor directs *Mycobacterium tuberculosis* lipoarabinomannan-mediated phagosome biogenesis. *J. Exp. Med.* 202, 987–999. doi: 10.1084/jem.20051239

Kasmapour, B., Gronow, A., Bleck, C. K., Hong, W., and Gutierrez, M. G. (2012). Size-dependent mechanism of cargo sorting during lysosome-phagosome fusion is controlled by Rab34. *Proc. Natl. Acad. Sci. U.S.A.* 109, 20485–20490. doi: 10.1073/pnas.1206811109

Kupz, A., Zedler, U., Staber, M., Perdomo, C., Dorhoi, A., Brosch, R., et al. (2016). ESAT-6-dependent cytosolic pattern recognition drives noncognate tuberculosis control in vivo. *J. Clin. Invest.* 126, 2109–2122. doi: 10.1172/JCI84978

Lamkanfi, M., and Dixit, V. M. (2010). Manipulation of host cell death pathways during microbial infections. *Cell Host Microbe.* 8, 44–54. doi: 10.1016/j.chom.2010.1006.1007

Le Chevalier, F., Cascioferro, A., Frigui, W., Pawlik, A., Boritsch, E. C., Bottai, D., et al. (2015). Revisiting the role of phospholipases C in the virulence of *Mycobacterium tuberculosis*. *Sci. Rep.* 5:16918. doi: 10.1038/srep16918

Leake, E. S., Myrvik, Q. N., and Wright, M. J. (1984). Phagosomal membranes of *Mycobacterium bovis* BCG-immune alveolar macrophages are resistant to disruption by *Mycobacterium tuberculosis* H37Rv. *Infect. Immun.* 45, 443–446.

Lee, J., Repasy, T., Papavinasasundaram, K., Sassetti, C., and Kornfeld, H. (2011). *Mycobacterium tuberculosis* induces an atypical cell death mode to escape from infected macrophages. *PLOS ONE* 6:e18367. doi: 10.1371/journal.pone.0018367

Lerner, T. R., Borel, S., Greenwood, D. J., Repnik, U., Russell, M. R., Herbst, S., et al. (2017). *Mycobacterium tuberculosis* replicates within necrotic human macrophages. *J. Cell Biol.* 216, 583–594. doi: 10.1083/jcb.201603040

Liu, P. T., Stenger, S., Li, H., Wenzel, L., Tan, B. H., Krutzik, S. R., et al. (2006). Toll-like receptor triggering of a vitamin D-mediated human antimicrobial response. *Science* 311, 1770–1773. doi: 10.1126/science.1123933

Lobato, L. S., Rosa, P. S., Ferreira Jda, S., Neumann Ada, S., Da Silva, M. G., Do Nascimento, D. C., et al. (2014). Statins increase rifampin mycobactericidal effect. *Antimicrob. Agents Chemother.* 58, 5766–5774. doi: 10.1128/AAC.01826-13

Lugo-Villarino, G., Hudrisier, D., Tanne, A., and Neyrolles, O. (2011). C-type lectins with a sweet spot for *Mycobacterium tuberculosis*. *Eur. J. Microbiol. Immunol.* 1, 25–40. doi: 10.1556/EuJMI.1551.2011.1551.1556

Majlessi, L., and Brosch, R. (2015). *Mycobacterium tuberculosis* meets the cytosol: the role of cGAS in anti-mycobacterial immunity. *Cell Host Microbe.* 17, 733–735. doi: 10.1016/j.chom.2015.05.017

Manzanillo, P. S., Ayres, J. S., Watson, R. O., Collins, A. C., Souza, G., Rae, C. S., et al. (2013). The ubiquitin ligase parkin mediates resistance to intracellular pathogens. *Nature* 501, 512–516. doi: 10.1038/nature12566

Manzanillo, P. S., Shiloh, M. U., Portnoy, D. A., and Cox, J. S. (2012). *Mycobacterium tuberculosis* activates the DNA-dependent cytosolic surveillance pathway within macrophages. *Cell Host Microbe* 11, 469–480. doi: 10.1016/j.chom.2012.03.007

Marinova, D., Gonzalo-Asensio, J., Aguilo, N., and Martin, C. (2017). MTBVAC from discovery to clinical trials in tuberculosis-endemic countries. *Expert Rev. Vaccines* 16, 565–576. doi: 10.1080/14760584.2017.1324303

McDonough, K. A., Kress, Y., and Bloom, B. R. (1993). Pathogenesis of tuberculosis: interaction of *Mycobacterium tuberculosis* with macrophages. *Infect. Immun.* 61, 2763–2773.

Mishra, A., Akhtar, S., Jagannath, C., and Khan, A. (2017). Pattern recognition receptors and coordinated cellular pathways involved in tuberculosis immunopathogenesis: emerging concepts and perspectives. *Mol. Immunol.* 87, 240–248. doi: 10.1016/j.molimm.2017.1005.1001

Mortaz, E., Adcock, I. M., Tabarsi, P., Masjedi, M. R., Mansouri, D., Velayati, A. A., et al. (2015). Interaction of pattern recognition receptors with *Mycobacterium tuberculosis*. *J. Clin. Immunol.* 35, 1–10. doi: 10.1007/s10875-014-0103-7

Myrvik, Q. N., Leake, E. S., and Wright, M. J. (1984). Disruption of phagosomal membranes of normal alveolar macrophages by the H37Rv strain of *Mycobacterium tuberculos*is. A correlate of virulence. *Am. Rev. Respir. Dis.* 129, 322–328.

Nigou, J., Zelle-Rieser, C., Gilleron, M., Thurnher, M., and Puzo, G. (2001). Mannosylated lipoarabinomannans inhibit IL-12 production by human dendritic cells: evidence for a negative signal delivered through the mannose receptor. *J. Immunol.* 166, 7477–7485. doi: 10.4049/jimmunol.166.12.7477

O'Garra, A., Redford, P. S., Mcnab, F. W., Bloom, C. I., Wilkinson, R. J., and Berry, M. P. (2013). The immune response in tuberculosis. *Annu. Rev. Immunol.* 31, 475–527. doi: 10.1146/annurev-immunol-032712-095939

Orme, I. M., Robinson, R. T., and Cooper, A. M. (2015). The balance between protective and pathogenic immune responses in the TB-infected lung. *Nat. Immunol.* 16, 57–63. doi: 10.1038/ni.3048

Parihar, S. P., Guler, R., Khutlang, R., Lang, D. M., Hurdayal, R., Mhlanga, M. M., et al. (2014). Statin therapy reduces the *Mycobacterium tuberculosis* burden in human macrophages and in mice by enhancing autophagy and phagosome maturation. *J. Infect. Dis.* 209, 754–763. doi: 10.1093/infdis/jit550

Passemar, C., Arbues, A., Malaga, W., Mercier, I., Moreau, F., Lepourry, L., et al. (2014). Multiple deletions in the polyketide synthase gene repertoire of *Mycobacterium tuberculosis* reveal functional overlap of cell envelope lipids in host-pathogen interactions. *Cell Microbiol.* 16, 195–213. doi: 10.1111/cmi.12214

Patin, E. C., Geffken, A. C., Willcocks, S., Leschczyk, C., Haas, A., Nimmerjahn, F., et al. (2017). Trehalose dimycolate interferes with FcgammaR-mediated phagosome maturation through Mincle, SHP-1 and FcgammaRIIB signalling. *PLOS ONE* 12:e0174973. doi: 10.1371/journal.pone.0174973

Paulson, T. (2013). Epidemiology: a mortal foe. *Nature* 502, S2–S3. doi: 10.1038/1502S1032a

Pethe, K., Bifani, P., Jang, J., Kang, S., Park, S., Ahn, S., et al. (2013). Discovery of Q203, a potent clinical candidate for the treatment of tuberculosis. *Nat. Med.* 19, 1157–1160. doi: 10.1038/nm.3262

Prashar, A., Schnettger, L., Bernard, E. M., and Gutierrez, M. G. (2017). Rab GTPases in immunity and inflammation. *Front. Cell Infect. Microbiol.* 7:435. doi: 10.3389/fcimb.2017.00435

Pym, A. S., Brodin, P., Brosch, R., Huerre, M., and Cole, S. T. (2002). Loss of RD1 contributed to the attenuation of the live tuberculosis vaccines *Mycobacterium bovis* BCG and *Mycobacterium microti*. *Mol. Microbiol.* 46, 709–717. doi: 10.1046/j.1365-2958.2002.03237.x

Pym, A. S., Brodin, P., Majlessi, L., Brosch, R., Demangel, C., Williams, A., et al. (2003). Recombinant BCG exporting ESAT-6 confers enhanced protection against tuberculosis. *Nat. Med.* 9, 533–539. doi: 10.1038/nm859

Quesniaux, V., Fremond, C., Jacobs, M., Parida, S., Nicolle, D., Yeremeev, V., et al. (2004). Toll-like receptor pathways in the immune responses to mycobacteria. *Microbes Infect.* 6, 946–959. doi: 10.1016/j.micinf.2004.04.016

Queval, C. J., Song, O. R., Carralot, J. P., Saliou, J. M., Bongiovanni, A., Deloison, G., et al. (2017). *Mycobacterium tuberculosis* controls phagosomal acidification by targeting CISH-mediated signalling. *Cell Rep.* 20, 3188–3198. doi: 10.1016/j.celrep.2017.08.101

Quigley, J., Hughitt, V. K., Velikovsky, C. A., Mariuzza, R. A., El-Sayed, N. M., and Briken, V. (2017). The cell wall lipid PDIM contributes to phagosomal escape and host cell exit of *Mycobacterium tuberculosis*. *mBio* 8:e00148-17. doi: 10.1128/mBio.00148-17

Romagnoli, A., Etna, M. P., Giacomini, E., Pardini, M., Remoli, M. E., Corazzari, M., et al. (2012). ESX-1 dependent impairment of autophagic flux by *Mycobacterium tuberculosis* in human dendritic cells. *Autophagy* 8, 1357–1370. doi: 10.4161/auto.20881

Russell, D. G. (2016). The ins and outs of the *Mycobacterium tuberculosis*-containing vacuole. *Cell Microbiol.* 18, 1065–1069. doi: 10.1111/cmi.12623

Russell, D. G., Cardona, P. J., Kim, M. J., Allain, S., and Altare, F. (2009). Foamy macrophages and the progression of the human tuberculosis granuloma. *Nat. Immunol.* 10, 943–948. doi: 10.1038/ni.1781

Rybniker, J., Chen, J. M., Sala, C., Hartkoorn, R. C., Vocat, A., Benjak, A., et al. (2014). Anticytolytic screen identifies inhibitors of mycobacterial virulence protein secretion. *Cell Host Microbe.* 16, 538–548. doi: 10.1016/j.chom.2014.09.008

Sakowski, E. T., Koster, S., Portal Celhay, C., Park, H. S., Shrestha, E., Hetzenecker, S. E., et al. (2015). Ubiquilin 1 promotes IFN-gamma-induced xenophagy of *Mycobacterium tuberculosis*. *PLOS Pathog.* 11:e1005076. doi: 10.1371/journal.ppat.1005076

Satoh, T., and Akira, S. (2016). Toll-like receptor signaling and its inducible proteins. *Microbiol. Spectr.* 4:MCHD-0040-2016. doi: 10.1128/microbiolspec.MCHD-0040-2016

Sayes, F., Pawlik, A., Frigui, W., Groschel, M. I., Crommelynck, S., Fayolle, C., et al. (2016). CD4+ T cells recognizing PE/PPE antigens directly or via cross reactivity are protective against pulmonary *Mycobacterium tuberculosis* infection. *PLOS Pathog.* 12:e1005770. doi: 10.1371/journal.ppat.1005770

Sayes, F., Sun, L., Di Luca, M., Simeone, R., Degaiffier, N., Fiette, L., et al. (2012). Strong immunogenicity and cross-reactivity of *Mycobacterium tuberculosis* ESX-5 Type VII secretion- encoded PE-PPE proteins predicts vaccine potential. *Cell Host Microbe* 11, 352–363. doi: 10.1016/j.chom.2012.03.003

Schnettger, L., Rodgers, A., Repnik, U., Lai, R. P., Pei, G., Verdoes, M., et al. (2017). A Rab20-Dependent membrane trafficking pathway controls *M. tuberculosis* replication by regulating phagosome spaciousness and integrity. *Cell Host Microbe* 21, 619.e–628.e. doi: 10.1016/j.chom.2017.04.004

Simeone, R., Bobard, A., Lippmann, J., Bitter, W., Majlessi, L., Brosch, R., et al. (2012). Phagosomal rupture by *Mycobacterium tuberculosis* results in toxicity and host cell death. *PLOS Pathog.* 8:e1002507. doi: 10.1371/journal.ppat.1002507

Simeone, R., Majlessi, L., Enninga, J., and Brosch, R. (2016). Perspectives on mycobacterial vacuole-to-cytosol translocation: the importance of cytosolic access. *Cell Microbiol.* 18, 1070–1077. doi: 10.1111/cmi.12622

Simeone, R., Sayes, F., Song, O., Groschel, M. I., Brodin, P., Brosch, R., et al. (2015). Cytosolic Access of *Mycobacterium tuberculosis*: critical impact of phagosomal acidification control and demonstration of occurrence in vivo. *PLOS Pathog.* 11:e1004650. doi: 10.1371/journal.ppat.1004650

Skerry, C., Pinn, M. L., Bruiners, N., Pine, R., Gennaro, M. L., and Karakousis, P. C. (2014). Simvastatin increases the in vivo activity of the first-line tuberculosis regimen. *J. Antimicrob. Chemother.* 69, 2453–2457. doi: 10.1093/jac/dku166

Sturgill-Koszycki, S., Schlesinger, P. H., Chakraborty, P., Haddix, P. L., Collins, H. L., Fok, A. K., et al. (1994). Lack of acidification in *Mycobacterium* phagosomes produced by exclusion of the vesicular proton-ATPase. *Science* 263, 678–681. doi: 10.1126/science.8303277

Sun-Wada, G. H., Tabata, H., Kawamura, N., Aoyama, M., and Wada, Y. (2009). Direct recruitment of H+-ATPase from lysosomes for phagosomal acidification. *J. Cell Sci.* 122, 2504–2513. doi: 10.1242/jcs.050443

Tailleux, L., Maeda, N., Nigou, J., Gicquel, B., and Neyrolles, O. (2003). How is the phagocyte lectin keyboard played? Master class lesson by *Mycobacterium tuberculosis*. *Trends Microbiol.* 11, 259–263. doi: 10.1016/S0966-842X(03)00102-1

Tanne, A., and Neyrolles, O. (2010). C-type lectins in immune defense against pathogens: the murine DC-SIGN homologue SIGNR3 confers early protection against *Mycobacterium tuberculosis* infection. *Virulence* 1, 285–290. doi: 10.4161/viru.1.4.11967

Thurston, T. L., Wandel, M. P., Von Muhlinen, N., Foeglein, A., and Randow, F. (2012). Galectin 8 targets damaged vesicles for autophagy to defend cells against bacterial invasion. *Nature* 482, 414–418. doi: 10.1038/nature10744

Tobin, D. M. (2015). Host-directed therapies for tuberculosis. *Cold Spring Harb. Perspect. Med.* 5:a021196. doi: 10.1101/cshperspect.a021196

Torrado, E., and Cooper, A. M. (2013). Cytokines in the balance of protection and pathology during mycobacterial infections. *Adv. Exp. Med. Biol.* 783, 121–140. doi: 10.1007/1978-1001-4614-6111-1001_1007

Toyonaga, K., Torigoe, S., Motomura, Y., Kamichi, T., Hayashi, J. M., Morita, Y. S., et al. (2016). C-Type lectin receptor DCAR recognizes mycobacterial phosphatidyl-inositol mannosides to promote a Th1 response during infection. *Immunity* 45, 1245–1257. doi: 10.1016/j.immuni.2016.10.012

Ullrich, H. J., Beatty, W. L., and Russell, D. G. (1999). Direct delivery of procathepsin D to phagosomes: implications for phagosome biogenesis and parasitism by *Mycobacterium*. *Eur. J. Cell Biol.* 78, 739–748. doi: 10.1016/S0171-9335(99)80042-9

Ulrichs, T., and Kaufmann, S. H. (2006). New insights into the function of granulomas in human tuberculosis. *J. Pathol.* 208, 261–269. doi: 10.1002/path.1906

van de Veerdonk, F. L., Teirlinck, A. C., Kleinnijenhuis, J., Kullberg, B. J., Van Crevel, R., Van Der Meer, J. W., et al. (2010). *Mycobacterium tuberculosis* induces IL-17A responses through TLR4 and dectin-1 and is critically dependent on endogenous IL-1. *J. Leukoc. Biol.* 88, 227–232. doi: 10.1189/jlb.0809550

van der Wel, N., Hava, D., Houben, D., Fluitsma, D., Van Zon, M., Pierson, J., et al. (2007). *M. tuberculosis* and *M. leprae* translocate from the phagolysosome to the cytosol in myeloid cells. *Cell* 129, 1287–1298. doi: 10.1016/j.cell.2007.05.059

Van Rie, A., and Enarson, D. (2006). XDR tuberculosis: an indicator of public-health negligence. *Lancet* 368, 1554–1556. doi: 10.1016/S0140-6736(06)69575-5

VanderVen, B. C., Fahey, R. J., Lee, W., Liu, Y., Abramovitch, R. B., Memmott, C., et al. (2015). Novel inhibitors of cholesterol degradation in *Mycobacterium tuberculosis* reveal how the bacterium's metabolism is constrained by the intracellular environment. *PLOS Pathog.* 11:e1004679. doi: 10.1371/journal.ppat.1004679

Vazquez, C. L., Rodgers, A., Herbst, S., Coade, S., Gronow, A., Guzman, C. A., et al. (2016). The proneurotrophin receptor sortilin is required for *Mycobacterium tuberculosis* control by macrophages. *Sci. Rep.* 6:29332. doi: 10.1038/srep29332

Velmurugan, K., Chen, B., Miller, J. L., Azogue, S., Gurses, S., Hsu, T., et al. (2007). *Mycobacterium tuberculosis* nuoG is a virulence gene that inhibits apoptosis of infected host cells. *PLOS Pathog.* 3:e110. doi: 10.1371/journal.ppat.0030110

Vergne, I., Chua, J., Lee, H. H., Lucas, M., Belisle, J., and Deretic, V. (2005). Mechanism of phagolysosome biogenesis block by viable *Mycobacterium tuberculosis*. *Proc. Natl. Acad. Sci. U.S.A.* 102, 4033–4038. doi: 10.1073/pnas.0409716102

Vergne, I., Fratti, R. A., Hill, P. J., Chua, J., Belisle, J., and Deretic, V. (2004). *Mycobacterium tuberculosis* phagosome maturation arrest: mycobacterial phosphatidylinositol analog phosphatidylinositol mannoside stimulates early endosomal fusion. *Mol. Biol. Cell* 15, 751–760. doi: 10.1091/mbc.E03-05-0307

Via, L. E., Deretic, D., Ulmer, R. J., Hibler, N. S., Huber, L. A., and Deretic, V. (1997). Arrest of mycobacterial phagosome maturation is caused by a block in vesicle fusion between stages controlled by rab5 and rab7. *J. Biol. Chem.* 272, 13326–13331. doi: 10.1074/jbc.272.20.13326

Vieira, O. V., Botelho, R. J., and Grinstein, S. (2002). Phagosome maturation: aging gracefully. *Biochem. J.* 366, 689–704. doi: 10.1042/bj20020691

Villeneuve, C., Gilleron, M., Maridonneau-Parini, I., Daffe, M., Astarie-Dequeker, C., and Etienne, G. (2005). Mycobacteria use their surface-exposed glycolipids to infect human macrophages through a receptor-dependent process. *J. Lipid Res.* 46, 475–483. doi: 10.1194/jlr.M400308-JLR200

Wallis, R. S., and Hafner, R. (2015). Advancing host-directed therapy for tuberculosis. *Nat. Rev. Immunol.* 15, 255–263. doi: 10.1038/nri3813

Warner, D. F., and Mizrahi, V. (2007). The survival kit of *Mycobacterium tuberculosis*. *Nat. Med.* 13, 282–284. doi: 10.1038/nm0307-282

Wassermann, R., Gulen, M. F., Sala, C., Perin, S. G., Lou, Y., Rybniker, J., et al. (2015). *Mycobacterium tuberculosis* differentially activates cGAS- and inflammasome-dependent intracellular immune responses through ESX-1. *Cell Host Microbe* 17, 799–810. doi: 10.1016/j.chom.2015.05.003

Watson, R. O., Bell, S. L., Macduff, D. A., Kimmey, J. M., Diner, E. J., Olivas, J., et al. (2015). The cytosolic sensor cGAS Detects *Mycobacterium tuberculosis* DNA to induce type I interferons and activate autophagy. *Cell Host Microbe* 17, 811–819. doi: 10.1016/j.chom.2015.05.004

Watson, R. O., Manzanillo, P. S., and Cox, J. S. (2012). Extracellular *M. tuberculosis* DNA targets bacteria for autophagy by activating the host DNA-sensing pathway. *Cell* 150, 803–815. doi: 10.1016/j.cell.2012.06.040

Wheelwright, M., Kim, E. W., Inkeles, M. S., De Leon, A., Pellegrini, M., Krutzik, S. R., et al. (2014). All-trans retinoic acid-triggered antimicrobial activity against *Mycobacterium tuberculosis* is dependent on NPC2. *J. Immunol.* 192, 2280–2290. doi: 10.4049/jimmunol.1301686

WHO (2016). *Global Tuberculosis Report 2016*. Geneva: World Health Organization.

Wong, D., Bach, H., Sun, J., Hmama, Z., and Av-Gay, Y. (2011). *Mycobacterium tuberculosis* protein tyrosine phosphatase (PtpA) excludes host vacuolar-H+-ATPase to inhibit phagosome acidification. *Proc. Natl. Acad. Sci. U.S.A.* 108, 19371–19376. doi: 10.1073/pnas.1109201108

Wong, K. W., and Jacobs, W. R. Jr. (2011). Critical role for NLRP3 in necrotic death triggered by *Mycobacterium tuberculosis*. *Cell Microbiol.* 13, 1371–1384. doi: 10.1111/j.1462-5822.2011.01625.x

Xu, S., Cooper, A., Sturgill-Koszycki, S., Van Heyningen, T., Chatterjee, D., Orme, I., et al. (1994). Intracellular trafficking in *Mycobacterium tuberculosis* and *Mycobacterium avium*-infected macrophages. *J. Immunol.* 153, 2568–2578.

Yonekawa, A., Saijo, S., Hoshino, Y., Miyake, Y., Ishikawa, E., Suzukawa, M., et al. (2014). Dectin-2 is a direct receptor for mannose-capped lipoarabinomannan of mycobacteria. *Immunity* 41, 402–413. doi: 10.1016/j.immuni.2014.08.005

Yuk, J. M., Shin, D. M., Lee, H. M., Yang, C. S., Jin, H. S., Kim, K. K., et al. (2009). Vitamin D3 induces autophagy in human monocytes/macrophages via cathelicidin. *Cell Host Microbe* 6, 231–243. doi: 10.1016/j.chom.2009.08.004

Zhang, X., Jiang, F., Wei, L., Li, F., Liu, J., Wang, C., et al. (2012). Polymorphic allele of human MRC1 confer protection against tuberculosis in a Chinese population. *Int. J. Biol. Sci.* 8, 375–382. doi: 10.7150/ijbs.4047

Zumla, A., Maeurer, M., Chakaya, J., Hoelscher, M., Ntoumi, F., Rustomjee, R., et al. (2015). Towards host-directed therapies for tuberculosis. *Nat. Rev. Drug Discov.* 14, 511–512. doi: 10.1038/nrd4696

Conflict of Interest Statement: The authors declare that the research was conducted in the absence of any commercial or financial relationships that could be construed as a potential conflict of interest.

Copyright © 2017 Queval, Brosch and Simeone. This is an open-access article distributed under the terms of the Creative Commons Attribution License (CC BY). The use, distribution or reproduction in other forums is permitted, provided the original author(s) or licensor are credited and that the original publication in this journal is cited, in accordance with accepted academic practice. No use, distribution or reproduction is permitted which does not comply with these terms.

frontiers in Immunology

REVIEW
published: 20 December 2017
doi: 10.3389/fimmu.2017.01836

Macrophage–Bacteria Interactions—A Lipid-Centric Relationship

*Ooiean Teng, Candice Ke En Ang and Xue Li Guan**

Lee Kong Chian School of Medicine, Nanyang Technological University, Singapore, Singapore

Macrophages are professional phagocytes at the front line of immune defenses against foreign bodies and microbial pathogens. Various bacteria, which are responsible for deadly diseases including tuberculosis and salmonellosis, are capable of hijacking this important immune cell type and thrive intracellularly, either in the cytoplasm or in specialized vacuoles. Tight regulation of cellular metabolism is critical in shaping the macrophage polarization states and immune functions. Lipids, besides being the bulk component of biological membranes, serve as energy sources as well as signaling molecules during infection and inflammation. With the advent of systems-scale analyses of genes, transcripts, proteins, and metabolites, in combination with classical biology, it is increasingly evident that macrophages undergo extensive lipid remodeling during activation and infection. Each bacterium species has evolved its own tactics to manipulate host metabolism toward its own advantage. Furthermore, modulation of host lipid metabolism affects disease susceptibility and outcome of infections, highlighting the critical roles of lipids in infectious diseases. Here, we will review the emerging roles of lipids in the complex host–pathogen relationship and discuss recent methodologies employed to probe these versatile metabolites during the infection process. An improved understanding of the lipid-centric nature of infections can lead to the identification of the Achilles' heel of the pathogens and host-directed targets for therapeutic interventions. Currently, lipid-moderating drugs are clinically available for a range of non-communicable diseases, which we anticipate can potentially be tapped into for various infections.

Keywords: lipids, metabolism, macrophage, intracellular bacteria, infection, immunity, tuberculosis, salmonellosis

OPEN ACCESS

Edited by:
Céline Cougoule, Centre national de la recherche scientifique (CNRS), France

Reviewed by:
Thierry Soldati, Université de Genève, Switzerland
Ricardo Silvestre, Instituto de Pesquisa em Ciências da Vida e da Saúde (ICVS), Portugal

***Correspondence:**
Xue Li Guan
xueli.guan@ntu.edu.sg

Specialty section:
This article was submitted to Microbial Immunology, a section of the journal Frontiers in Immunology

Received: *20 October 2017*
Accepted: *05 December 2017*
Published: *20 December 2017*

Citation:
Teng O, Ang CKE and Guan XL (2017) Macrophage–Bacteria Interactions—A Lipid-Centric Relationship. Front. Immunol. 8:1836. doi: 10.3389/fimmu.2017.01836

INTRODUCTION

Macrophages play a key role as the front line of host defenses against foreign bodies. Complex scavenger receptors (SR), pattern recognition receptors, and other signaling receptors expressed by macrophages make them professional phagocytes and antigen-presenting cells. They are highly specialized in engulfment and digestion of the invading pathogen, followed by presentation of antigens to T cells. Under normal circumstances, cytokines and chemokines are secreted by macrophages once pathogens are detected, to recruit more immune cells to the area of infection for restriction of pathogen invasion. Traditionally, macrophages have been classified as inflammatory macrophages (also known as classically activated or M1 macrophages) or anti-inflammatory macrophages (also known as alternatively activated or M2 macrophages), based on their polarization states and physiological features (1, 2). However, it is increasingly appreciated that these cells

display remarkable plasticity and their identities may be far more complex, as described in a comprehensive review by Mosser and Edwards (3). The inflammatory and anti-inflammatory responses of macrophages are tightly regulated at different infection stages and are pathogen-specific. Disturbance in this equilibrium will lead to excessive inflammation, or failure to activate the immune response, and this is often exploited by pathogens through the hijack of host signaling mechanisms to evade clearance by professional phagocytes. In fact, various intracellular pathogens have evolved strategies to reside and thrive in macrophages, despite the bactericidal capacity of these host cells. For instance, *Mycobacterium tuberculosis*, *Legionella pneumophila*, and *Salmonella enterica* serovar Typhimurium enter macrophages and persist in vacuolar compartments by modifying the vacuolar maturation processes, while others, including *Listeria monocytogenes*, *Shigella flexneri*, *Rickettsia rickettsii*, and *Mycobacterium marinum* escape the phagosome and replicate in the cytosol. *M. tuberculosis* and *Mycobacterium leprae* can also escape the phagolysosomal compartment into the cytosol, and this process is mediated by secreted proteins, including culture filtrate protein 10 and early secreted antigenic target 6 kDa (ESAT-6) (4). From the host perspective, it is well established that macrophages make use of soluble proteins for communication with other immune cells for initiation of complex signaling cascades during the infection process. In addition, it is increasingly evident that lipids play an equally important role in macrophage functions, influencing the outcome of infections (5–9).

Lipids are fundamental building blocks of cells and play pivotal roles in diverse biological processes. They are key structural components for cellular membranes. With their hydrophobic and amphipathic properties, lipids are able to form a barrier between cells and their environments, as well as within the cells to produce distinct organelles. These cellular membranes have the ability to mediate cell–cell and intracellular communication by budding, fission, and fusion. Lipids also serve as energy stores in eukaryotic cells, in the form of triglyceride esters and steryl esters in lipid droplets. In addition, they play a key role as first and second messengers in signaling cascades. The functions of membrane lipids as well as the lipid composition of an average mammalian plasma membrane have been thoroughly examined and reviewed previously (7, 10, 11).

In the context of macrophage–intracellular bacteria interactions, the plasma membrane of immune cells will be the first barrier the invading pathogen encounters. To successfully infect the host, pathogens often evolve various strategies to target the lipid-enriched plasma membrane for entry and exit, or to hijack host lipid metabolism to promote their survival (12–14). By contrast, lipids can also provide protection to the host during microbial infections (15), demonstrating that lipids are functionally double-edged swords. Here, we review the confounding nature of lipids in the intimate macrophage–pathogen relationship (**Figure 1**), with a focus on intracellular bacteria, as well as recent techniques employed to probe the dynamics of lipid metabolism during infections. It should be noted that this is not exhaustive as many other pathogens, including eukaryotic parasites, viruses, and fungal pathogens are capable of manipulating host lipid metabolism as part of their survival strategies (8, 9, 16, 17).

DYNAMIC LIPID REMODELING DURING MACROPHAGE POLARIZATION

Macrophages undergo polarization when they encounter foreign bodies, and numerous lines of evidence point toward dynamic lipid remodeling during this defense process. Transcriptional profiling of human macrophage polarization in an *in vitro* experimental model revealed striking enrichment of genes involved in lipid metabolism as one of the most overrepresented categories of differentially modulated transcripts (29). For M1 macrophages, besides exhibiting preference for aerobic glycolysis, upregulation of cyclooxygenase (COX)-2 and downregulation of COX-1, leukotriene A4 hydrolase, thromboxane A synthase 1, and arachidonate 5-lipoxygenase (5-LO) were observed. On the other hand, M2 macrophages are skewed toward fatty acid oxidation and have upregulated expression of COX-1 and arachidonate 15-lipoxygenase (15-LO) (29–31). Interestingly, opposing regulation of sphingosine and ceramide kinases was observed in both M1 and M2 macrophages (29), highlighting the contrasting nature of lipid metabolism in these distinct macrophage populations.

Receptors involved in binding diverse lipid metabolism products, such as peroxisome proliferator-activated receptor α, β/δ and γ, liver X receptor α and β, CD36, and SR class A-I/II, have also been linked to the polarization of M2 macrophages (32–34). These receptors internalize oxidized and modified lipoproteins and are critical orchestrators of macrophage cholesterol and fatty acid homeostasis (33, 34). M2 macrophages increase oxidized low-density-lipoproteins cholesterol uptake but have similar cholesterol efflux as compared with M1 macrophages. This difference in cholesterol handling leads to increased cholesterol deposition in M2 macrophages (32). It has also been shown that the expression of SR such as CD36 or SR-A1 on M2 macrophages induces endocytosis of triglyceride-rich lipoproteins and generates fatty acids for β-oxidation (32, 35). This aspect of macrophage lipid metabolism is in fact, closely associated with the pathogenesis of atherosclerosis, and the burgeoning field of immunometabolism highlights the critical roles of the cross talk between metabolism and immunity (36).

The dynamics of lipid metabolism during polarization have been further demonstrated at the metabolite level in various studies (37, 38). A shift in the degree of saturation of fatty acids towards monounsaturated fatty acids was observed during human monocyte differentiation to M2 macrophages using macrophage colony stimulating factor (M-CSF), which is in agreement with the induction of sterol regulatory element-binding transcription factor 1c regulated genes, fatty acid synthase, elongation of very long-chain fatty acid-like family member 6 (ELOVL6), and stearoyl-CoA desaturase (37). These observations on the fatty acid composition of glycerophospholipids were further corroborated in a recent study by Zhang and coworkers (38). In addition, an increase in phosphatidylcholine and phosphatidylethanolamine, and a decrease in cholesterol, were observed

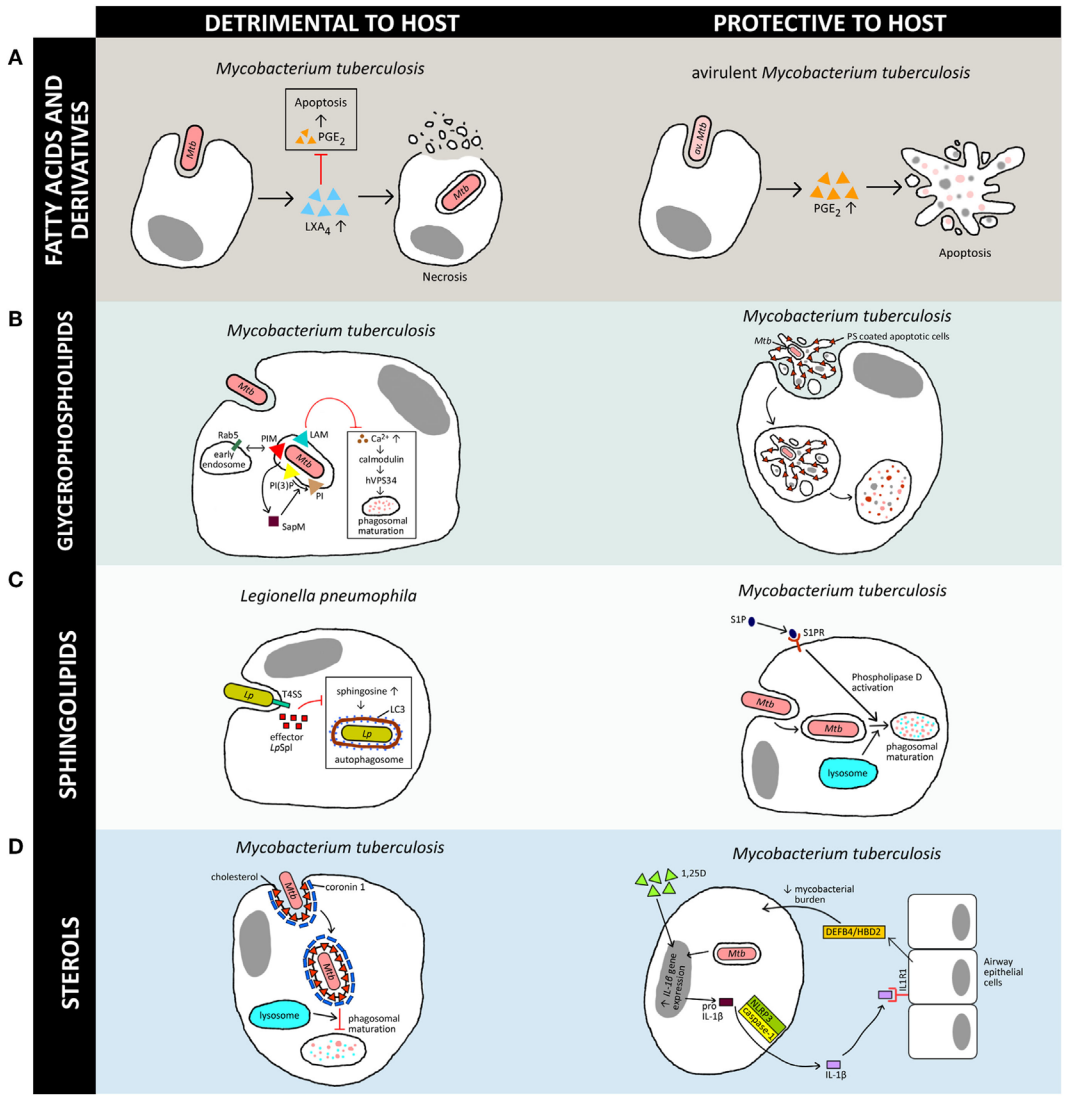


FIGURE 1 | Versatility of lipids in generation of host immune responses against various intracellular pathogens. The schematic diagram illustrates a simplified overview of how the four host-derived lipid classes discussed in this review can be a double-edged sword, either being exploited by the pathogen for its own survival or aiding the host in clearance of the bacteria. Note that there are multiple lipids involved in host–pathogen interactions but only a few representative examples are shown here, and further details can be found in the original works. [**(A)**, left] Induction of LXA_4 by virulent *M. tuberculosis* (*Mtb*) inhibits PGE_2 signaling and promotes necrosis in macrophages (18), whereas [**(A)**, right] induction of PGE_2 secretion by avirulent *M. tuberculosis* (av. *Mtb*)-infected macrophages leads to apoptosis and protects against mitochondrial inner membrane damage (19). [**(B)**, left] *Mtb* manipulates host phosphoinositides metabolism to promote their survival in macrophages *via* inhibition of phagosomal maturation. Mycobacterial phosphatidylinositol mannoside (PIM) stimulates early endosomal fusion by recruiting Rab5. Inhibition of Ca^{2+} increase by *Mycobacterium* lipoarabinomannan (LAM) further blocks phagosomal maturation as Ca^{2+} is required for calmodulin phosphatidylinositol 3-kinase hVPS34 signaling cascade activation. SapM secreted by *Mycobacterium* inhibits phagosomal-late endosome fusion by hydrolyzing phosphatidylinositol 3-phosphate (20–23). However, [**(B)**, right] redistribution of phosphatidylserine (PS) during apoptosis leads to efferocytosis and restricts the growth of *Mtb* (24). [**(C)**, left] Effector *Lp*Spl from *Legionella pneumophila* (*Lp*) mimics host sphingosine-1-phosphate (S1P) lyase and prevents an increase in sphingosine levels in infected macrophages, inhibiting autophagy (25). On the other hand, [**(C)**, right] S1P is essential for bacterial clearance as it promotes acidification of *Mycobacterium*-containing phagosomes *via* phospholipase D activation, which leads to phagosomal maturation and killing of *Mtb* (26). [**(D)**, left] Accumulation of cholesterol at the *Mtb* uptake site recruits coronin 1 protein, which inhibits phagosomal maturation (27). [**(D)**, right] The active metabolite of vitamin D (1,25D) controls *Mtb* infection *via* macrophage–epithelial paracrine signaling. IL-1β secreted through NLRP3/caspase-1 inflammasome signaling cascade stimulates epithelial cells to produce antimicrobial peptide DEFB4/HBD2, which reduces mycobacterial burden in macrophages (28). In this schematic diagram, triangles represent lipids whereas squares represent proteins.

during macrophage differentiation. Employing a combination of lipidomics, transcriptomics, and pharmacological and genetic manipulations, the direct connection between fatty acid and glycerophospholipid synthesis during the differentiation process was addressed. Furthermore, perturbation of macrophage lipid metabolism was also found to affect the ultrastructural and

phagocytic properties of these immune cells (37). These results corroborate earlier findings on the effects of fatty acid unsaturation on macrophage phagocytic activities (39).

Overall, these studies suggest that the polarization of macrophages *in vitro* is intimately linked to lipid metabolism, and perturbations of host lipid metabolism will affect immune and cellular functions. However, it should be noted that the spectrum of macrophage populations *in vivo* is more complex (3). This warrants more detailed analyses to determine the exact functions of lipids in the distinct populations and is dependent on environmental cues. We will next examine how macrophage lipids play critical functional roles in the intimate host–microbe relationship.

HOST LIPIDS—THE PROTAGONIST AND THE ANTAGONIST IN THE MACROPHAGE–MICROBE RELATIONSHIP

Fatty Acids and Derivatives

In macrophages, fatty acids can be synthesized *de novo* or be taken up by cells through lipolysis of triglyceride-rich lipoproteins particles such as low-density lipoproteins and very-low-density lipoproteins. This is achieved by the expression of SR such as CD36 (40) or SR-B1 (41). The function of fatty acids in various cellular components has a long history and has been extensively reviewed (42). Being the major component of triglycerides, glycerophospholipids, and other complex lipids, fatty acids play pivotal roles as membrane constituents and energy sources, and partake in regulation of signaling pathways as well as cell and tissue metabolism (43). Fatty acids are also substantially found in bacterial cell membranes (44) and serve as precursors for membrane biogenesis. Persistence of *M. tuberculosis*, an intracellular bacterium and the causative agent of tuberculosis, in mice, is facilitated by isocitrate lyase, an enzyme essential for fatty acid metabolism (45). This highlights the role of fatty acids for maintenance of mycobacterial survival during chronic infections. In fact, besides *de novo* synthesis, pathogens including *M. tuberculosis* have evolved multiple strategies to utilize fatty acids derived from their hosts. *M. tuberculosis* imports fatty acids from host triglycerides for synthesis of its own lipid inclusions and acquisition of dormancy traits in macrophages (46, 47). The mycobacterial protein, LucA, was found to form a complex with Mce1 and Mce4 fatty acid transporters to facilitate cholesterol and fatty acid uptake in infected macrophages (48). In dormant *M. tuberculosis*, the accumulation of triglycerides is modulated by fatty acid CoA ligase 6 (49), and during nutrient starvation, the bacterium is capable of hydrolyzing these stored triglycerides, owing to its lipase activity (50).

Interestingly, many intracellular pathogens also induce the formation of lipid droplets in the hosts during infections. This has previously been reviewed by Saka and Valdivia (51) and more recently by Barisch and Soldati (52). Besides serving as an energy reservoir, triglycerides found in lipid droplets are also producers of the mediator lipids, eicosanoids, in mammalian cells. Eicosanoids, which are oxidation products of arachidonic acid and other polyunsaturated fatty acids, have assumed a key role as mediators of the immune response during infections (53, 54), and as outlined above, have been shown to be differentially regulated during macrophage polarization. Broadly, it is noted that the effects of eicosanoids in host–pathogen interactions can be classified as pro-inflammatory (54) or anti-inflammatory (55), and they are closely interlinked with their protein counterparts, the cytokines, for orchestration of immune responses. Eicosanoids such as prostaglandin E2 (PGE_2) and lipoxin A4 (LXA_4) are highly active lipid mediators commonly described in bacterial infections. PGE_2 was found to be upregulated by various invasive bacteria, including *Mycobacterium bovis* bacillus Calmette–Guérin (BCG) (19), *L. monocytogenes*, *Yersinia enterocolitica*, *Shigella dysenteriae*, and the enteroinvasive *Escherichia coli* (56). These mediator lipids can benefit the host through various mechanisms. In avirulent *M. tuberculosis* infections, PGE_2 has been found to modulate host cell death pathways through the EP2 receptor, which promotes protection of the host against mitochondrial inner membrane perturbation and restricting the spread of bacterium caused by necrosis (57) (**Figure 1A**, right panel). Interestingly, PGE_2 is found to be involved in the repair of host plasma membranes by regulating synaptotagmin 7, the calcium sensing protein involved in lysosome-mediated membrane repair (58). Resealing of membrane lesions is crucial for preventing necrosis and promoting apoptosis, which benefits the host by increasing bacterial clearance.

By contrast, eicosanoids may also bring about detrimental effects to the host, which is to the pathogen's advantage. PGE_2, earlier discussed to be beneficial in mycobacterial infections, can compromise host immunity through inhibition of macrophage maturation (59) and reduction in the release of NAPDH oxidase (60). Upregulation of PGE_2 during infections is indeed beneficial for the survival of various pathogens, including *Salmonella enterica* (61) and *Burkholderia pseudomallei* (62). During *S. enterica* serovar Typhimurium infections, the *Salmonella* pathogenicity island (SPI)-2-encoded SpiC protein activates the ERK1/2 signaling pathway, leading to induction of COX-2 and increased production of PGE_2 levels (61). PGE_2 impairs killing of *Salmonella* species in macrophages by inducing IL-10 expression *via* the protein kinase A pathway (63). During *B. pseudomallei* infection in macrophages, PGE_2 mRNA was rapidly upregulated by over 400-fold at as early as 2h postinfection and promoted *B. pseudomallei* intracellular survival (62). The suppression of the bactericidal activity of macrophages was associated with decreased nitric oxide production through enhancing the expression of enzyme arginase 2 (62).

LXA_4 is another prominent mediator with anti-inflammatory effects (64) generated by 5-LO and 15-LO activities (65). Upregulation of LXA_4 levels during mycobacterial infections can lead to inhibition of PGE_2, and consequently mitochondrial inner membrane perturbation and macrophage necrosis (57). Unlike PGE_2 that protects the host during mycobacterial infections, 5-LO promotes the growth of the bacterium *in vivo* (66). Virulent *M. tuberculosis* induces LXA_4 and inhibits PGE_2 production (18). By inhibiting the production of PGE_2, LXA_4 impairs apoptotic signaling (67) and promotes necrosis of infected macrophages

(18) (**Figure 1A**, left panel). Furthermore, 5-LO-deficient mice exhibited enhanced expression of IL-12, IFN-γ, and nitrogen oxide synthase 2 in the lungs as compared with wild-type mice, indicating negative regulation of Th1 response by 5-LO during *M. tuberculosis* infections (66). Similar findings on the negative regulation of Th1 response by 5-LO were observed in *Brucella abortus* infections in mice (68). Activation of the 5-LO pathway was further demonstrated to impair host T cell immunity by preventing cross-presentation of *M. tuberculosis* antigen by dendritic cells (18). Interestingly, at the human population level, single nucleotide polymorphisms in eicosanoid receptor gene, EP2, and heterozygosity for leukotriene A4 hydrolase polymorphisms have been reported to modulate host susceptibility to tuberculosis, highlighting the critical roles of eicosanoids in mediating infections (69, 70).

Clearly, as exemplified by the multifaceted functions of eicosanoids, each lipid entity can be a man's meat and another man's poison. The type of eicosanoids and the fine balance between the pro-inflammatory and anti-inflammatory mediators are critical determinants of infection outcomes. Should this balance be disrupted, the host will be detrimentally affected either by high pathogen loads due to decreased clearance, or uncontrolled, non-specific inflammation (cytokine storms) leading to poor host outcomes (71). A more refined understanding of the functions of eicosanoids during interactions between specific pathogens and their hosts may potentially pave the future of host-directed therapy against these infections. In fact, a range of drugs (for instance, aspirin) that target eicosanoid biosynthesis are clinically available and can be further evaluated for their effects on bacterial infections.

Glycerophospholipids

As one of the main constituents of the mammalian membrane bilayer, glycerophospholipids have been demonstrated to be used by pathogens to evade host defenses. Choline-containing glycerophospholipids such as phosphatidylcholine are predominantly localized to the outer membrane leaflet of eukaryotic cells, while amino-containing glycerophospholipids such as PS and phosphatidylethanolamine are predominantly maintained in the inner membrane leaflet (72). Redistribution of PS to the external surface of the plasma membrane is a key event during apoptosis and has been known as one of the emblematic signals leading to tagging of cells for efferocytosis, a phagocytic process for removal of dead cells (24, 73). This signaling pathway has been shown to be manipulated by *L. monocytogenes* to ensure their own survival in the infected host (74). The pore-forming toxin listeriolysin O from *L. monocytogenes* promotes the release of bacteria-containing protrusions from host cell membranes, generating PS-coated vesicles that mimic apoptotic cells. This subsequently promotes efferocytosis by binding to the PS-binding receptor TIM-4 expressed on uninfected macrophages, and eventually facilitates cell-to-cell spread in macrophages *in vitro* (74). While efferocytosis promotes the spread of infection by *L. monocytogenes*, this mechanism of cellular clearance appears to be protective to the host for other intracellular bacteria. Notably, efferocytosis has been shown to effectively restrict the growth of *M. tuberculosis* (75), as the bacteria-infected macrophages are engulfed and killed by uninfected macrophages following apoptosis (75) (**Figure 1B**, right panel). This process is also effective in limiting the growth of *M. marinum* in infected macrophages by neutrophils (76).

Phosphoinositides, which are phosphorylated forms of the membrane glycerophospholipid, phosphatidylinositol, are extensively characterized mediators of intracellular signaling and play critical roles during infection. Phosphoinositides can be phosphorylated at the hydroxyl residues at positions 3, 4, or 5 of the inositol ring to produce different phosphoinositide species. These include phosphatidylinositol 3-phosphate [PI(3)P], phosphatidylinositol 4,5-biphosphate, and phosphatidylinositol 3,4,5-triphosphate, which are involved in endocytosis and phagocytosis (77, 78). In fact, different phosphoinositide species exhibit distinct characteristic subcellular distribution patterns due to the organelle-specific phosphoinositide kinases and phosphatases (78). These phosphoinositide species interact with actin-binding proteins through recognition of its head group by PH, PX, ENTH, ANTH, or FYVE domains (20). Many pathogens are able to manipulate host phosphoinositides metabolism to trigger their uptake into macrophages or non-phagocytic cells (21). *M. tuberculosis* escape phagocytic killing by macrophages through blocking phagosomal maturation *via* interference of phosphatidylinositol 3-kinase [PI(3)K] signaling (22). *M. tuberculosis* lipoarabinomannan acts as a phosphatidylinositol analog and inhibits cytosolic calcium increase, leading to the blocking of the Ca^{2+}/calmodulin PI(3)K hVPS34 cascade. This signaling pathway is needed to produce PI(3)P on liposomes or phagosomes and trigger downstream calmodulin kinase II-mediated EEA1 recruitment to phagosomal membranes, which are ultimately required for phagosome maturation (23). In addition, the lipid phosphatase, SapM, which is secreted by the bacterium, is responsible for the inhibition of phagosome-late endosome fusion by hydrolyzing PI(3)P and thus blocking phagosomal maturation (79). Concurrently, mycobacterial phosphatidylinositol mannoside stimulates early endosomal fusion by early recruitment of Rab5, which blocks the acquisition of late endosomal/lysosomal constituents (80) (**Figure 1B**, left panel). The orchestration of these intracellular signaling events mediated by lipids favors the intracellular persistence of *M. tuberculosis*, leading to chronic infections.

Similar to *M. tuberculosis*, *Salmonella* can infect macrophages and escape killing by these phagocytes to survive and replicate within host cells (81). More extensive research on salmonellosis has been carried out in non-immune epithelial cells since *Salmonella* initiates its infection *via* invasion of the intestinal epithelium. Invasion of host cells is dependent on two type III secretion systems (T3SSs) encoded on the SPI-1 and SPI-2 (82–84). One of the effector proteins of the T3SS of *Salmonella*, SopB (also known as SigD), is a phosphoinositide phosphatase which shows sequence homology to mammalian inositol polyphosphate 4-phosphatases (85) and type II inositol 5-phosphatase synaptojanin (86). The activity of SopB is required for invasion, formation, and maintenance of *Salmonella*-containing vacuoles (SCVs) in epithelial cells and macrophages (87, 88).

Manipulation of host glycerophospholipid metabolism by bacterial effector proteins is not unique to *Salmonella*. The *Legionella* Dot/Icm type IVB secretion system effector protein, VipD, is a

phospholipase A1 which binds to and is activated by the endosomal regulator Rab5. The resultant removal of PI(3)P mediated by the bacterial phospholipase blocks endosomal fusion with *Legionella*-containing vacuoles, shielding the intracellular pathogen from the microbicidal endosomal compartment (89). Besides VipD, two other *Legionella* effectors, LecE and LpdA, which are localized to *Legionella*-containing vacuoles, are also capable of manipulating biosynthesis of host glycerophospholipids. Indeed, bacterial phospholipases are well-characterized virulence factors, notably the alpha-toxin from *Clostridium perfringens* (90). The function of phospholipase C from *M. tuberculosis*, on the other hand, remains less clear. Originally proposed to promote *M. tuberculosis* growth in the late stage of infection in mice (91), the role of phospholipase C in mycobacterial virulence has been recently challenged by the works of Le Chevalier and coworkers. In contrast to the works by Raynaud et al. which demonstrated a 1.5-log growth reduction in the phospholipase C mutant (91), the latter study did not detect significant differences between the wild-type and mutant bacteria (92). Clinical *M. tuberculosis* strains with interruptions of all four mycobacterial phospholipase genes have been isolated in patients with active tuberculosis, supporting a less crucial role of this enzyme in the infectious cycle *in vivo* (93).

While bacterial phospholipases can be detrimental to the host, conversely, host phospholipase activities can antagonize the survival of intracellular pathogens. In the context of mycobacterial infections, host phospholipase D and lysosomal phospholipase A2 have been implicated in the cells' ability to control intracellular mycobacterial growth (94, 95). It should be noted that these studies were focused on the enzymes, and the exact lipid mediators remain to be identified. Nonetheless, the cumulative evidence of the involvement of both host and microbial glycerophospholipids metabolizing enzymes in the regulation of the infection process highlights the complexity of interplay of the metabolic networks of two organisms. This intricacy is not restricted to glycerophospholipids and will be reflected in the following subsections on two other major eukaryotic lipid classes, sphingolipids and sterols.

Sphingolipids

Sphingolipids are another key component of eukaryotic cell membranes. They comprise of a long-chain amino alcohol (also known as a sphingoid base or long-chain base) to which a fatty acid can be covalently linked to form ceramide. Structural variants arise from head group substitutions, as well as chain length differences and hydroxylation of the sphingoid bases and fatty acyl chains, giving rise to tens of thousands of different molecular species with diverse functions (96–98). Sphingolipids are partners with cholesterol in eukaryotic membranes, forming specialized domains (commonly termed as lipid rafts) and serve as signaling platforms and/or entry sites during pathogen invasion. The functions of lipid rafts in host–pathogen interactions have been extensively reviewed (99–102).

Beyond their structural functions, sphingolipids also serve as signaling molecules which mediate the infection process (103, 104). Sphingosine-1-phosphate (S1P) is an active metabolite formed by sphingosine kinases 1 and 2, and are involved in immune cell trafficking, through engagement with G-protein-coupled receptors (S1PR 1–5). S1PRs are expressed on different immune cells, and macrophages mostly express S1PR1 and S1PR2 (105). Recently, it has also been shown that human alveolar macrophages express high levels of S1PR3 and S1PR4, and lower levels of S1RP5 (26). Expression of S1PRs determines the function of an immune cell, as they play critical roles in lymphocyte trafficking, differentiation and triggering of inflammatory responses (106). During mycobacterial infections, phagocytosis is uncoupled from cytosolic calcium level elevation, mediated by the inhibition of macrophage sphingosine kinase activity and consequently, the downregulation of S1P levels. The blockade of phagosome–lysosome fusion allows the intracellular bacterium to avoid the bactericidal phagolysosomes to continue to persist within host cells (107). Stimulation of macrophages with S1P leads to increased killing of internalized *Mycobacterium* species through the acidification of phagosomes *via* host phospholipase D (108) (**Figure 1C**, right panel). Additionally, S1P modulates mycobacterial infections by promoting antigen processing and presentation (109). These studies, taken together, highlight the antimycobacterial properties of the mediator lipid S1P.

The phagolysosomal compartment is clearly crucial for defense against infection with intracellular pathogens. Besides S1P, phagosomal maturation is also regulated by other sphingolipids. Host acid sphingomyelinase (ASMase), which generates the signaling molecule ceramide, is required for the proper fusion of late phagosomes with lysosomes (110). Delivery of ASMase to mycobacteria-containing phagosomes is regulated by sortilin, which requires interactions with adaptor protein AP-1 and monomeric gamma-ear-containing ADP ribosylation factor-binding proteins (GGAs) (111). Sortilin knockout mice are more susceptible to *M. tuberculosis* infections. Moreover, treatment of mouse macrophages with desipramine, an ASMase inhibitor, resulted in increased mycobacterial survival, indicating that ASMase is required for restricting the growth of *M. tuberculosis*. The crucial role of this host enzyme in controlling intracellular bacteria can be further illustrated by the increased susceptibility of ASMase knockout mice to *L. monocytogenes* infections (112). Functional ASMase is also involved in the bactericidal activity of macrophages against *S. enterica* serovar Typhimurium (25). In contrast to the protective effects of ASMase, neutral sphingomyelinase is associated with superoxide production during *M. bovis* BCG infections *in vitro* and *in vivo*. The superoxide produced during infection inhibits autophagy and therefore reduces bacterial clearance (113).

Various intracellular pathogens have also evolved metabolic strategies to hijack host sphingolipids to promote their pathogenicity. This is evident from the presence of sphingolipid metabolizing genes in bacterial genomes (114), although sphingolipids are synthesized only in eukaryotes (with few exceptions in prokaryotes, such as *Sphingomonas* species). *M. tuberculosis* encodes a novel outer membrane protein, Rv0888, which possesses potent sphingomyelinase activity (115). The bacterial protein has been shown to promote intracellular infection in macrophages *in vitro*, but is not required for virulence of *M. tuberculosis* in mice (115). While the functions of Rv0888 in mycobacterial infections remain to be clarified, it is interesting

to note that a study conducted in as early as 1948 had already demonstrated that sphingomyelin supports the growth of the tubercle bacilli *in vitro* (116). Besides *M. tuberculosis*, a phospholipase C with sphingomyelinase activity has been characterized in *L. monocytogenes* (117). However, its function in *Listeria* infections has yet to be elucidated. By contrast, *L. pneumophila* produces an effector protein, *Lp*Spl, which shares structural and sequence homology to the eukaryotic counterpart sphingosine-1 phosphate lyase (118). Similar to the glycerophospholipid metabolizing enzymes, VipD, LecE, and LpdA, outlined above, *Lp*Spl is an effector protein of the Dot/Icm type IVB secretion system. It has been shown that *Lp*Spl activity prevents an increase of sphingosine levels in infected macrophages (**Figure 1C**, left panel). In addition, the bacterial sphingolipid metabolizing enzyme inhibits autophagy during macrophage infection and is required for efficient infection of mice. This represents a novel mechanism of inhibition of autophagy by an intracellular bacterium through perturbation of host sphingolipid biosynthesis. Strikingly, a similar strategy was observed in the facultative intracellular bacteria *B. pseudomallei* (119).

Evidently, the balance of host sphingolipids is another determinant of successful infections by intracellular bacteria. S1P is one of the most obvious sphingolipid metabolites which exhibit bactericidal activity. Various drugs which target the S1P axis are available and in fact used in clinical trials for various indications (120). With a deepened understanding of S1P and sphingolipids in inflammation and infection, the appropriate control of the S1P levels and potentially other sphingolipids may be targets for generation of novel drugs in treatment of various infections.

Sterols

Sterols are major components of many animals (zoosterols) and plants (phytosterols), but only a few bacteria are able to synthesize sterols. In bacterial membranes, hopanoids, a class of pentacyclic triterpenoids, execute the functions of sterols (121). The most well-known zoosterol, cholesterol, plays critical roles in modulating cellular functions. These include regulation of membrane fluidity, phagocytosis, cell signaling, and formation of lipid rafts with glycosphingolipids (27, 122–124). In addition, cholesterol also serves as precursors for bile salts, steroids, and vitamins (125). Cholesterol in mammalian cells can be obtained from exogenous sources such as low-density lipoproteins or endogenously synthesized. Cholesterol accumulation is commonly observed in the form of lipid droplets in infected cells as well as in biopsies, such as in lepromatous leprosy tissues and tuberculosis granulomas (126, 127). At the cellular level, it has been demonstrated that some pathogens utilize cholesterol on lipid rafts for invasion and intracellular replication (99–102). Plasma membrane cholesterol plays an essential role for host cell uptake of *M. tuberculosis*. In addition, the association of cholesterol with the coronin 1 protein in phagosomal membranes ensures the intracellular survival of *Mycobacterium* in coronin 1-coated phagosomes by preventing degradation of the tubercle bacilli in lysosomes (128) (**Figure 1D**, left panel). The need for cholesterol in mycobacterial infections and survival is best emphasized by the presence of multiple genes involved in cholesterol transport and catabolism, although the bacterium does not synthesize cholesterol *de novo*. These genes include the cholesterol transporter, Mce4 and the transcriptional regulator KstR, which control the expression of bacterial genes involved in sterol catabolism (129–132). Furthermore, mutants lacking genes in cholesterol utilization fail to establish infection in macrophages (133).

Besides *Mycobacterium*, *Listeria* species and *Salmonella* species are also capable of utilizing host cholesterol to promote their survival in macrophages. The cholesterol-binding cytolysin, listeriolysin O, secreted by *L. monocytogenes* binds to cholesterol embedded in the lipid bilayer of eukaryotic cell cytoplasmic membranes to facilitate bacterial escape from the phagosomal compartment into host cell cytosol (134–136). Listeriolysin O also performs other functions, including modulation of inflammatory responses through activation of caspase-1, leading to IL-18 secretion from the infected macrophages (137). In fact, cholesterol-binding cytolysins are also produced by other pathogens, including perfringolysin O from *C. perfringens*, and facilitate bacterial escape from phagosomes and survival in macrophages (90). *Salmonella*, which reside in vacuoles, take a distinct approach. During *Salmonella* infections, cholesterol accumulates in the SCV (138). SseJ, another effector protein of the T3SS, has been reported to be involved in cholesterol esterification and stabilization of the SCV (139). Interestingly, the modulation of macrophage cholesterol levels with statins has been shown to augment host protection against various intracellular pathogens including *M. tuberculosis*, *M. leprae*, *S. enterica* serovar Typhimurium, and *L. monocytogenes* (28, 126, 140, 141).

While it has been extensively proven that cholesterol supports the survival of intracellular pathogens within infected macrophages, cholesterol can also exert protective effects on the host during infection by specific intracellular bacteria. The protective role of cholesterol for the host has been shown recently during infection by *Coxiella burnetii*, the causative agent for Q fever. Mulye et al. (142) reported that increased cholesterol levels in the parasitophorous vacuole by cholesterol supplementation or treatment with U18666A inhibited the growth of intracellular bacteria. Cholesterol induces acidification of the parasitophorous vacuole and eventually, killing of the intracellular bacteria (142). Although this study was performed on mouse embryonic fibroblasts, earlier works on *C. burnetii*-infected THP-1 macrophage-like cells had also demonstrated inhibition of intracellular *C. burnetii* growth by U18666A (143), suggesting that alterations in cholesterol levels can affect the survival of this pathogen in immune cells. The biosynthetic intermediates as well as metabolites of cholesterol can also improve resistance of the host cells to infection. During *Listeria* infection of macrophages, lanosterol, an intermediate of cholesterol biosynthesis, accumulates due to type I IFN-dependent histone deacetylase 1 transcriptional repression of lanosterol-14α-demethylase, the gene product of Cyp51A1. Besides the modulation of IFN-β-stimulated gene expression and the effects on cytokine production, accumulation of lanosterol also leads to an increase of membrane fluidity and ROS production, thus potentiating phagocytosis and the destruction of bacteria (144).

Cholesterol also serves as a precursor for vitamins, including the fat-soluble vitamin D. Interestingly, vitamin D can have protective effects against bacterial infections (145). In the context of mycobacterial infections, 1,25-dihydroxy-vitamin D_3 (1,25D), the active metabolite of vitamin D, promotes maturation and activation of human monocytes and macrophages and reduces bacillary replication. In a macrophage–epithelial cell coculture system, 1,25D enhanced IL-1β expression and induced secretion of the cytokine from *M. tuberculosis*-infected macrophages *via* the NLRP3/caspase-1 inflammasome pathway. IL-1β secreted from macrophages reduced mycobacterial burden by stimulating the epithelial production of the antimicrobial peptide DEFB4/HBD2. This suggests that the control of *M. tuberculosis* infection by vitamin D is modulated by macrophage–epithelial paracrine signaling (146) (**Figure 1D**, right panel). In fact, vitamin D deficiency and vitamin D receptor polymorphism (147) have shown to affect human susceptibility to tuberculosis, and vitamin D-based oxysterols can promote clinical improvements in tuberculosis patients (148). Interestingly, the vitamin D metabolite $25(OH)D_3$ has also been found to act synergistically with the bacteriostatic antituberculosis drug phenylbutyrate, providing a potential indication of adjunct therapy for tuberculosis through resolution of inflammation and enhancement of bacterial clearance (149).

The possibility of using vitamin D, and potentially sunlight, to fortify antituberculosis resistance is an exciting and straightforward approach for tuberculosis interventions. Definitely, it will be of interest to extend such studies of vitamin D to other microbial infections. However, specifically for cholesterol, with its mixed roles of being both protective and harmful to the host during infection, as well as its central roles in diverse cellular processes, targeting cholesterol metabolism alone may cause undesired complications. Combination treatment or targeting of specific downstream products of cholesterol-induced signaling may be explored as an alternative.

MICROBIAL LIPIDS—MANIPULATORS OF MACROPHAGE METABOLISM

Glycolipids—Lipopolysaccharides (LPS)

Besides protein-based bacterial virulence factors which are capable of manipulating host lipid metabolism during infection, foreign lipid structures expressed on bacteria surfaces can also act as pathogen-associated molecular patterns which induce immune responses as well as remodeling of lipid metabolism in macrophages. LPS, a major component of the outer membrane of Gram-negative bacteria, is made up of a conserved lipid A, core oligosaccharide regions and a long polysaccharide chain with variable carbohydrate subunits (150). LPS is well known as a ligand for toll-like receptor 4 (TLR4) (151–153) and toll-like receptor 2 (TLR2) (154, 155). Signals triggered by TLR4 upon activation by LPS have been extensively studied and reviewed (151, 156–158). Briefly, this signaling cascade is initiated by LPS binding protein which binds directly with LPS and is transferred to CD14. This then dissociates LPS aggregates into monomeric forms and presents them to the TLR4–MD-2 complex. Binding of LPS to TLR4–MD-2 complex eventually activates NF-κB and IRF3, leading to the production of pro-inflammatory cytokines (*via* MyD88-dependent pathway) or type-1 interferon (MyD88-independent pathway) (159). In 2013, two independent studies demonstrated that LPS activates inflammasomes *via* murine caspase-11, independent of TLR4 (160, 161). Following that, Shi and coworkers showed that human caspase-4 and -5 [orthologs of murine caspase-11 (162)] served as intracellular sensors for LPS and lipid A. The binding of LPS to caspase-4 leads to pyroptosis in human monocytes and non-immune cells (163). Due to its ability to trigger strong immune responses, LPS has always been linked to a variety of pathologies such as septic shock and death, while inhibition of LPS-induced signaling pathways often favors the hosts (161, 164–166).

The impact of LPS on host lipid metabolism has been fairly well characterized. Very early studies demonstrated that LPS administration produced hypertriglyceridemia, with increased lipoprotein production and decreased lipoprotein clearance (167, 168). The effect of lipogenesis and lipolysis seemed to be affected by the dosage of LPS, as Feingold and coworkers showed that low doses (10 ng/100 g body weight) induced hepatic secretion of triglyceride, while high doses (50 μg/100 g body weight) decreased the clearance of triglyceride-rich lipoprotein (169). LPS also increased lipid body formation in human macrophages, through increasing the fatty acid uptake and reducing lipolysis, hence increasing triglyceride retention in the cells (170). Furthermore, turnover of glycerophospholipids during LPS stimulation has been observed, which is mediated by induction of acyl-CoA synthetase 1 (171). Accumulation of lipid droplets in non-adipocytic cells has also been reported as a pathological feature in infectious diseases, and it has been demonstrated to be an important site for PGE_2 synthesis (172, 173). Lipid body formation is largely dependent on TLRs, especially TLR2 and TLR4, as TLR2-deficient and TLR4-mutated mice both failed to form lipid droplets triggered by LPS (172, 173). When induced by LPS, lipid droplets are formed *via* the p38 α/β and PI(3)K/Akt pathways (174), and drugs blocking these pathways have been proven to inhibit their formation (174, 175).

A combined lipidomics and transcriptomics study on mouse macrophages upon LPS stimulation by Dennis and coworkers has brought together a system-based overview of the temporal and subcellular dynamics of macrophage lipid remodeling elicited by LPS (176). Treating RAW264.7 cells with Kdo_2-lipid A, a chemically defined substructure of LPS, increased COX-2 related lipid metabolites immediately after the stimulation, followed by sterols, sphingolipids, glycerophospholipids, and glycerolipids (176). Based on the reported findings on LPS-induced changes in sphingolipids, Köberlin and coworkers recently examined the lipid metabolic network of RAW264.7 cells during TLR signaling and showed that genes involving sphingolipids metabolism are tightly modulated upon TLR4 and TLR9 stimulation. Intriguingly, this study revealed that innate immune responses are modulated by a circular network co-regulating sphingolipids and glycerophospholipids (177). These studies have contributed to our current understanding on the complexity of the macrophage lipid metabolic networks during inflammation, and it

will be of interest to identify novel small molecules which can target lipid metabolism for immune protection.

Glycolipids—Trehalose-6, 6′-Dimycolate (TDM)

Besides the Gram-negative bacteria-specific LPS, lipids produced by other bacteria also possess host immune- and metabolism-modulating functions. *M. tuberculosis* and *M. leprae* are notorious for their fat-loving nature as well as their cell walls which are dominated by lipids (178, 179). TDM, also known as cord factor, is a glycolipid abundantly expressed on the cell wall of mycolic acid-containing bacteria such as *Mycobacterium*, *Nocardia*, *Tsukamurella*, *Gordona*, *Rhodococcus*, and *Corynebacterium* species and has previously been identified as a virulence factor (180). The TDM molecule consists of sugar trehalose esterified to two mycolic acid residues, and the length range of residues varies from 20 to 80 carbons depending on the bacterial species. TDM is responsible for the characteristic colony morphology observed in virulent *M. tuberculosis* due to its hydrophobic nature (181). In addition, at the gene expression level, TDM from *M. tuberculosis* H37Rv upregulates multiple cytokines (TNF-α, IL-1β, IL-1m, IL-10, and MCSF-1) and chemokines (CCL3, CCL4, CCL7, CCL12, CCR12, CXCL1, CXCL2, and CXCL10) (182), proving the ability of TDM to initiate the macrophage immune responses *in vitro* (183). Strikingly, TDM alone is sufficient to induce activated foreign body- and hypersensitivity-type granulomas in mice, as well as extensive foam cell formation, illustrating its importance in pathogenesis (127, 184–186). TDM also promotes *Mycobacterium* survival *in vivo* by inhibiting phagosome–lysosome fusion and protects the bacteria from destruction within macrophages (187, 188).

Besides its effects on the immune functions of macrophages, TDM has been shown to induce formation of caseating granulomas and foamy macrophages in the absence of *Mycobacterium* itself (127). The toxicity of TDM is greatly dependent on its surface crystalline structure. This can be enhanced by the presence of oil, as administration of TDM in oil-in-water emulsion has shown to induce higher mortality rates in mice, whereas administration of TDM without oil has no effect (189–193). Interestingly, *M. tuberculosis* preferentially associates with the lipid droplets in pulmonary lesions to increase the toxicity of TDM and initiation of necrosis (192). Separately, free mycolic acids have also been shown to induce macrophage lipid droplet formation (194). Keto-mycolic acid, the oxygenated form of mycolic acid, was found to transactivate the host orphan lipid-sensing nuclear receptor, testicular receptor 4 (TR4), and induce foamy macrophage formation *in vitro* and *in vivo* (195). TR4 is also involved in the polarization of macrophages toward a less microbicidal and an immunomodulatory M2 phenotype, which aids in the survival of *M. tuberculosis*. With more in-depth understanding of microbial lipid–host receptor interactions, guided designs of structural analogs of lipids to interfere with ligand–receptor binding holds promise as a combinatorial adjunct therapy.

Another mycobacterial lipid virulence factor that is capable of moderating macrophage functions, but differs in function from TDM, is phthiocerol dimycocerosates (PDIM) (196–199). PDIM has been proven to mediate phagosomal escape of *M. tuberculosis* by enhancing the membrane permeabilizing activity of ESAT-6, increasing phagosomal membrane destabilization and subsequent induction of apoptosis (200, 201). While PDIM and ESAT-6 are known to cause phagosomal membrane rupture, whether this process involves alterations in host lipid metabolism requires further investigation. Probing changes in host lipid metabolism is increasingly possible with the availability of a range of techniques, which we will cover in the next section.

PROBING LIPID DYNAMICS DURING THE HOST–MICROBE RELATIONSHIP

Despite the appreciation of the important roles lipids play in infectious diseases, it is not as well studied as compared with genes and proteins, due to chemical complexity of lipids and the limited availability of tools required. Most of our knowledge on the roles of lipids in the intimate host–pathogen relationship has been gained through genetic and cellular investigations, and only in recent years have sensitive and high resolution technologies for lipid analyses become available for revelation of novel insights of lipid functions during infections.

Traditional methods of lipid analysis include enzyme immunoassays (EIAs) and thin layer chromatography (TLC). EIAs, an established method particularly for cytokine and chemokine measurements in both infection and immunity research, have been commonly used to monitor the levels of various eicosanoids (202, 203). The underlying mechanism of EIA lies in the immunocomplexes formed between the lipids of interest and their antibodies. These assays serve as a fairly rapid method for lipid analyses, provided that the lipids of interest are well defined. Another restriction of EIAs is its limited availability, because lipids generally have poor immunogenicity, and the generation of high affinity anti-lipid antibodies is challenging using traditional hybridoma techniques (204). Furthermore, these assays have limited resolution (i.e., may not be able to separate between lipid molecular species) and sensitivity, and hence are not well suited for very low abundant signaling molecules. The use of TLC for the separation and detection of lipids have been described as early as the 1960s (205) and continues to be commonly used (127, 206, 207). Despite its low sensitivity and resolution, TLC offers the possibility to study the turnover of lipids and capture the temporal dynamics of lipid remodeling when used with radioisotopes labeling (46, 47).

Recently, more advanced methods including gas chromatography–mass spectrometry, liquid chromatography–mass spectrometry (LC–MS), nuclear magnetic resonance (NMR) spectroscopy, and mass spectrometry (MS)-based imaging techniques have revolutionized the fields of metabolomics and lipidomics. These technologies allow for more efficient analysis of the diverse metabolites and lipids in biological samples, with deeper and more sensitive coverage at the lipid molecular species level. Notably, the LC–MS analyses of the monocyte/macrophage lipidome spanning membrane lipids (sterols, glycerophospholipids, and sphingolipids), and mediator and signaling lipids

(phosphoinositides, eicosanoids, and phosphorylated sphingoid bases), have contributed to the revelation of the complex metabolic networks during macrophage differentiation (37, 38), TLR activation and signaling (176, 177, 208) as well as the complex host–pathogen interactions (8, 118, 209, 210). In the last 10–15 years, the lipidomes of various other host cell types including epithelial cells (211), platelets (212), and pathogens, including *M. tuberculosis* (213–215), *Clostridium novyi* (216), *E. coli* (217), *Enterococcus faecalis* (218), and *Pseudomonas aeruginosa* (219) have been established. The possibility to analyze both host and microbial lipids with high resolution structural information (**Figure 2**) has opened up new avenues to study the dynamics of lipid metabolism during the complex host–pathogen relationship.

While LC–MS- and NMR-based lipidomics approaches are extremely powerful, they lack the spatial resolution needed for determining the localization of lipids during the infection process (220), and, importantly, the source of the metabolites in the host–pathogen relationship. MS-based imaging has now offered a new dimension by providing spatial resolution of the metabolites during the infection process by various pathogens (221–223). Alternative novel imaging techniques involve the

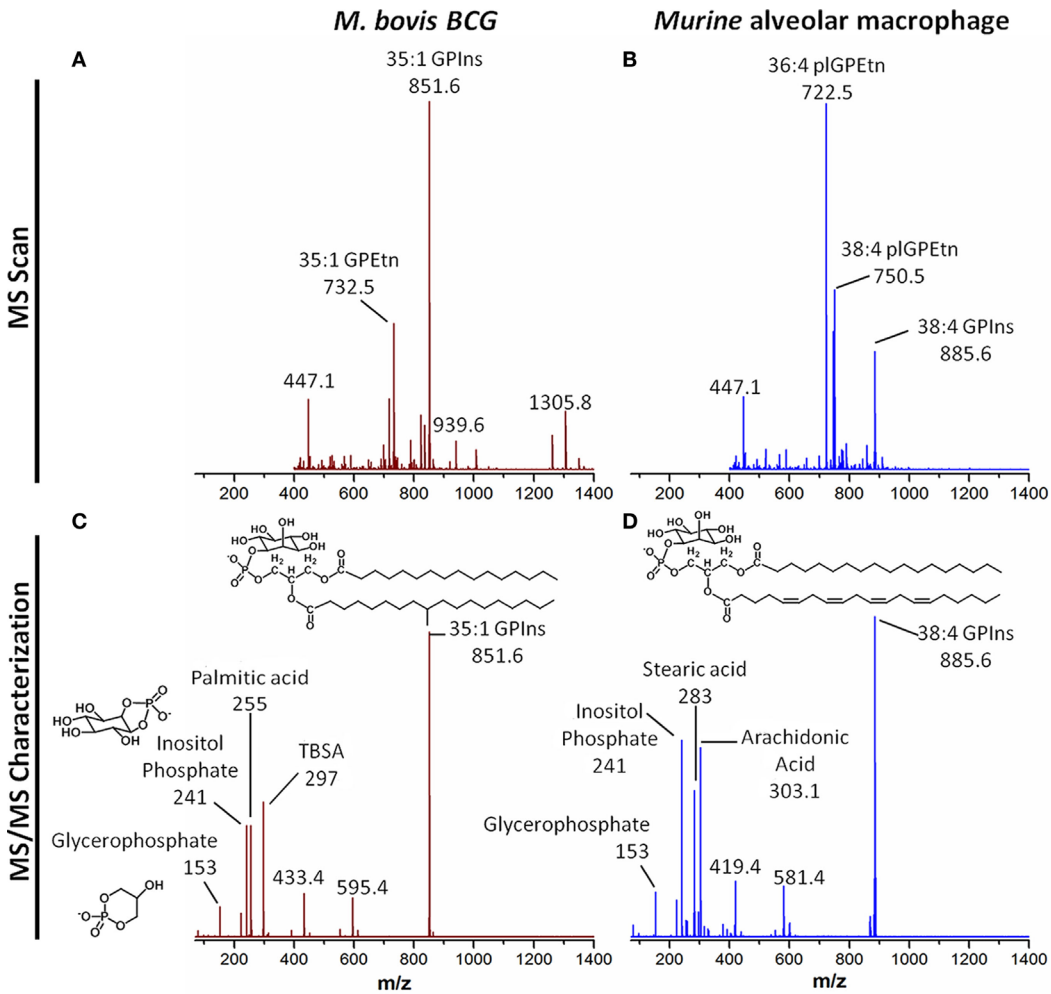


FIGURE 2 | Resolving host and microbial (polar) lipid molecular species by mass spectrometry (MS), a tool for probing host–pathogen interactions. With advances in technologies particularly MS, it is now possible to profile, characterize, and quantify lipids from both microbes and macrophages as well as other host cells and tissues. **(A)** Single stage MS scan to generate the "lipid profiles" of *M. bovis* BCG, an experimental surrogate for *M. tuberculosis*. **(B)** Single stage MS scan to generate the "lipid profiles" of murine alveolar macrophages. **(C)** MS/MS of the major phosphatidylinositol from *M. bovis* BCG, with mass-to-charge ratio (*m/z*) of 851.6. Collision-induced dissociation reveals the ion contains palmitic acid (*m/z* 255) and TBSA (*m/z* 297), as well as the phosphoinositol (*m/z* 241) and glycerophosphate (*m/z* 153) headgroups. This confirms the sum composition of fatty acyls to be 35:1 (35 carbons, 1 double bond). **(D)** MS/MS of the major phosphatidylinositol from murine alveolar macrophages, with *m/z* of 885.6. Collision-induced dissociation reveals the ion contains stearic acid (*m/z* 283) and arachidonic acid (*m/z* 303.1), as well as the phosphoinositol (*m/z* 241) and glycerophosphate (*m/z* 153) headgroups. This confirms the sum composite of fatty acyls to be 38:4 (38 carbons, 4 double bonds). The bioanalytical tool can be applied to probe the dynamic changes in levels of thousands of species of lipids from both the host and the pathogens, leading to the identification of novel pathways involved in infection and inflammation. Abbreviations: GPEtn, phosphatidylethanolamine; GPIns, phosphatidylinositol; MS, mass spectrometry; MS/MS, tandem mass spectrometry; *m/z*: mass-to-charge ratio; plGPEtn, plasmalogen phosphatidylethanolamine; TBSA, tuberculostearic acid.

use of immunofluorescent lipids, isotopic labeling, or lipid-binding probes and microscopy for the spatial resolution and real-time analysis of the host–pathogen interaction, providing extensive information regarding the roles of lipids in pathogenesis and the immune responses. In the study by Barisch and Soldati, pulse-chase experiments using fluorophore-labeled compounds coupled with electron microscopy has provided novel insights about the translocation of host-derived fatty acids in *M. marinum* to serve as an energy source for the bacteria (224, 225). Metabolic labeling of lipid droplets has also been used for the exploration of the carbon flux within pathogen metabolic networks (47). The lipid-binding properties of bacterial toxins, including perfringolysin O and aerolysin, have also been harnessed as tools to probe lipid localization and signaling (226, 227). In recent years, the specificities of lipid probes have vastly improved, with the recent possibility to study single lipid species in living cells (228).

The current availability and upcoming developments in technologies which provide temporal and/or spatial information of lipids at the single lipid species level are extremely powerful, especially when used in combination with cell and chemical biology, genetics and other systems biology approaches, including proteomics and genomics. Together, these will provide new insights into the complexity of host–pathogen interactions, disease pathogenesis as well as identification of novel markers of inflammation and infection.

CONCLUSION

Pathogenic infection of macrophages is an intricate process involving numerous sequences of events, during which lipids are clearly instrumental players. Each pathogen has evolved its own strategy to thrive in or kill the host cells, and it is not surprising to find that a single lipid class or species can display contrasting functions during bacterial infections, depending on the bacterial species and even cell types. A single lipid, such as cholesterol, can be utilized by a specific pathogen to promote its own survival in the macrophage and on the other hand, it can also be used by the host to assist in clearance of another bacterial species, making lipids a double-edge sword in the complex host–pathogen relationship. Adding on to the complexity is alterations in the fine chemistry of lipids. For instance, the oxidation of fatty acids can switch its function from being benign to bioactive, or from acting as the protagonist to the antagonist (and *vice versa*) in this complex interplay between host and pathogen. While we have described in this review how different lipid classes are involved in the infection process, it should be stressed that the system acts as a whole, and multiple components, including different lipid classes and proteins, act in concert to achieve the outcome of an infection. Hence, it is critical to undertake systems-level approaches to dissect the host–pathogen networks. Such in-depth analyses of the complex and interconnected lipid metabolic networks in infection and immunity will contribute to identification of potential lipids or metabolic pathways which can be potentially developed into therapeutics for treatment of infectious diseases or for boosting of immune functions.

AUTHOR CONTRIBUTIONS

OT, CKEA, and XLG contributed to the writing and review of the manuscript.

FUNDING

The research performed in XLG's group was funded by the Ministry of Education, Singapore (MOE) Tier 1 grant (Reference number: 2015-T1-001-092) and the Nanyang Assistant Professorship (awarded to XLG).

REFERENCES

1. Biswas SK, Mantovani A. Macrophage plasticity and interaction with lymphocyte subsets: cancer as a paradigm. *Nat Immunol* (2010) 11(10):889–96. doi:10.1038/ni.1937
2. Martinez FO, Gordon S. The M1 and M2 paradigm of macrophage activation: time for reassessment. *F1000Prime Rep* (2014) 6:13. doi:10.12703/P6-13
3. Mosser DM, Edwards JP. Exploring the full spectrum of macrophage activation. *Nat Rev Immunol* (2008) 8(12):958–69. doi:10.1038/nri2448
4. van der Wel N, Hava D, Houben D, Fluitsma D, van Zon M, Pierson J, et al. *M. tuberculosis* and *M. leprae* translocate from the phagolysosome to the cytosol in myeloid cells. *Cell* (2007) 129(7):1287–98. doi:10.1016/j.cell.2007.05.059
5. Boyce JA. Mast cells and eicosanoid mediators: a system of reciprocal paracrine and autocrine regulation. *Immunol Rev* (2007) 217:168–85. doi:10.1111/j.1600-065X.2007.00512.x
6. Engelman JA, Luo J, Cantley LC. The evolution of phosphatidylinositol 3-kinases as regulators of growth and metabolism. *Nat Rev Genet* (2006) 7(8):606–19. doi:10.1038/nrg1879
7. Wymann MP, Schneiter R. Lipid signalling in disease. *Nat Rev Mol Cell Biol* (2008) 9(2):162–76. doi:10.1038/nrm2335
8. Wenk MR. Lipidomics of host-pathogen interactions. *FEBS Lett* (2006) 580(23):5541–51. doi:10.1016/j.febslet.2006.07.007
9. Helms B. Host-pathogen interactions: lipids grease the way. *Eur J Lipid Sci Technol* (2006) 108(11):895–7. doi:10.1002/ejlt.200600194
10. van Meer G, Voelker DR, Feigenson GW. Membrane lipids: where they are and how they behave. *Nat Rev Mol Cell Biol* (2008) 9(2):112–24. doi:10.1038/nrm2330
11. Ingolfsson HI, Melo MN, van Eerden FJ, Arnarez C, Lopez CA, Wassenaar TA, et al. Lipid organization of the plasma membrane. *J Am Chem Soc* (2014) 136(41):14554–9. doi:10.1021/ja507832e
12. Queiroz A, Riley LW. Bacterial immunostat: *Mycobacterium tuberculosis* lipids and their role in the host immune response. *Rev Soc Bras Med Trop* (2017) 50(1):9–18. doi:10.1590/0037-8682-0230-2016
13. Zaas DW, Duncan M, Rae Wright J, Abraham SN. The role of lipid rafts in the pathogenesis of bacterial infections. *Biochim Biophys Acta* (2005) 1746(3):305–13. doi:10.1016/j.bbamcr.2005.10.003
14. Feingold KR, Grunfeld C. Lipids: a key player in the battle between the host and microorganisms. *J Lipid Res* (2012) 53(12):2487–9. doi:10.1194/jlr.E033407
15. Ravnskov U. High cholesterol may protect against infections and atherosclerosis. *QJM* (2003) 96(12):927–34. doi:10.1093/qjmed/hcg150
16. van der Meer-Janssen YP, van Galen J, Batenburg JJ, Helms JB. Lipids in host-pathogen interactions: pathogens exploit the complexity of the host cell lipidome. *Prog Lipid Res* (2010) 49(1):1–26. doi:10.1016/j.plipres.2009.07.003
17. Herker E, Ott M. Emerging role of lipid droplets in host/pathogen interactions. *J Biol Chem* (2012) 287(4):2280–7. doi:10.1074/jbc.R111.300202
18. Divangahi M, Desjardins D, Nunes-Alves C, Remold HG, Behar SM. Eicosanoid pathways regulate adaptive immunity to *Mycobacterium tuberculosis*. *Nat Immunol* (2010) 11(8):751–8. doi:10.1038/ni.1904

19. Bansal K, Narayana Y, Patil SA, Balaji KN. *M. bovis* BCG induced expression of COX-2 involves nitric oxide-dependent and -independent signaling pathways. *J Leukoc Biol* (2009) 85(5):804–16. doi:10.1189/jlb.0908561
20. Lemmon MA. Phosphoinositide recognition domains. *Traffic* (2003) 4(4): 201–13. doi:10.1034/j.1600-0854.2004.00071.x
21. Ireton K, Payrastre B, Chap H, Ogawa W, Sakaue H, Kasuga M, et al. A role for phosphoinositide 3-kinase in bacterial invasion. *Science* (1996) 274(5288):780–2. doi:10.1126/science.274.5288.780
22. Fratti RA, Backer JM, Gruenberg J, Corvera S, Deretic V. Role of phosphatidylinositol 3-kinase and Rab5 effectors in phagosomal biogenesis and mycobacterial phagosome maturation arrest. *J Cell Biol* (2001) 154(3):631–44. doi:10.1083/jcb.200106049
23. Vergne I, Chua J, Deretic V. Tuberculosis toxin blocking phagosome maturation inhibits a novel Ca2+/calmodulin-PI3K hVPS34 cascade. *J Exp Med* (2003) 198(4):653–9. doi:10.1084/jem.20030527
24. Callahan MK, Williamson P, Schlegel RA. Surface expression of phosphatidylserine on macrophages is required for phagocytosis of apoptotic thymocytes. *Cell Death Differ* (2000) 7(7):645–53. doi:10.1038/sj.cdd.4400690
25. McCollister BD, Myers JT, Jones-Carson J, Voelker DR, Vazquez-Torres A. Constitutive acid sphingomyelinase enhances early and late macrophage killing of *Salmonella enterica* serovar Typhimurium. *Infect Immun* (2007) 75(11):5346–52. doi:10.1128/IAI.00689-07
26. Barnawi J, Tran H, Jersmann H, Pitson S, Roscioli E, Hodge G, et al. Potential link between the sphingosine-1-phosphate (S1P) system and defective alveolar macrophage phagocytic function in chronic obstructive pulmonary disease (COPD). *PLoS One* (2015) 10(10):e0122771. doi:10.1371/journal.pone.0122771
27. Simons K, Ikonen E. Functional rafts in cell membranes. *Nature* (1997) 387(6633):569–72. doi:10.1038/42408
28. Parihar SP, Guler R, Lang DM, Suzuki H, Marais AD, Brombacher F. Simvastatin enhances protection against *Listeria monocytogenes* infection in mice by counteracting *Listeria*-induced phagosomal escape. *PLoS One* (2013) 8(9):e75490. doi:10.1371/journal.pone.0075490
29. Martinez FO, Gordon S, Locati M, Mantovani A. Transcriptional profiling of the human monocyte-to-macrophage differentiation and polarization: new molecules and patterns of gene expression. *J Immunol* (2006) 177(10): 7303–11. doi:10.4049/jimmunol.177.10.7303
30. Rodriguez-Prados JC, Traves PG, Cuenca J, Rico D, Aragones J, Martin-Sanz P, et al. Substrate fate in activated macrophages: a comparison between innate, classic, and alternative activation. *J Immunol* (2010) 185(1):605–14. doi:10.4049/jimmunol.0901698
31. Vats D, Mukundan L, Odegaard JI, Zhang L, Smith KL, Morel CR, et al. Oxidative metabolism and PGC-1beta attenuate macrophage-mediated inflammation. *Cell Metab* (2006) 4(1):13–24. doi:10.1016/j.cmet.2006.08.006
32. Oh J, Riek AE, Weng S, Petty M, Kim D, Colonna M, et al. Endoplasmic reticulum stress controls M2 macrophage differentiation and foam cell formation. *J Biol Chem* (2012) 287(15):11629–41. doi:10.1074/jbc.M111.338673
33. Kunjathoor VV, Febbraio M, Podrez EA, Moore KJ, Andersson L, Koehn S, et al. Scavenger receptors class A-I/II and CD36 are the principal receptors responsible for the uptake of modified low density lipoprotein leading to lipid loading in macrophages. *J Biol Chem* (2002) 277(51):49982–8. doi:10.1074/jbc.M209649200
34. Chinetti-Gbaguidi G, Baron M, Bouhlel MA, Vanhoutte J, Copin C, Sebti Y, et al. Human atherosclerotic plaque alternative macrophages display low cholesterol handling but high phagocytosis because of distinct activities of the PPARgamma and LXRalpha pathways. *Circ Res* (2011) 108(8):985–95. doi:10.1161/CIRCRESAHA.110.233775
35. Huang SC, Everts B, Ivanova Y, O'Sullivan D, Nascimento M, Smith AM, et al. Cell-intrinsic lysosomal lipolysis is essential for alternative activation of macrophages. *Nat Immunol* (2014) 15(9):846–55. doi:10.1038/ni.2956
36. Mathis D, Shoelson SE. Immunometabolism: an emerging frontier. *Nat Rev Immunol* (2011) 11(2):81. doi:10.1038/nri2922
37. Ecker J, Liebisch G, Englmaier M, Grandl M, Robenek H, Schmitz G. Induction of fatty acid synthesis is a key requirement for phagocytic differentiation of human monocytes. *Proc Natl Acad Sci U S A* (2010) 107(17):7817–22. doi:10.1073/pnas.0912059107
38. Zhang C, Wang Y, Wang F, Wang Z, Lu Y, Xu Y, et al. Quantitative profiling of glycerophospholipids during mouse and human macrophage differentiation using targeted mass spectrometry. *Sci Rep* (2017) 7(1):412. doi:10.1038/s41598-017-00341-2
39. Schroit AJ, Gallily R. Macrophage fatty acid composition and phagocytosis: effect of unsaturation on cellular phagocytic activity. *Immunology* (1979) 36(2):199–205.
40. Endemann G, Stanton LW, Madden KS, Bryant CM, White RT, Protter AA. CD36 is a receptor for oxidized low density lipoprotein. *J Biol Chem* (1993) 268(16):11811–6.
41. Spady DK, Kearney DM, Hobbs HH. Polyunsaturated fatty acids upregulate hepatic scavenger receptor B1 (SR-BI) expression and HDL cholesteryl ester uptake in the hamster. *J Lipid Res* (1999) 40(8):1384–94.
42. Alvarez-Curto E, Milligan G. Metabolism meets immunity: the role of free fatty acid receptors in the immune system. *Biochem Pharmacol* (2016) 114:3–13. doi:10.1016/j.bcp.2016.03.017
43. Calder PC. Functional roles of fatty acids and their effects on human health. *JPEN J Parenter Enteral Nutr* (2015) 39(1 Suppl):18S–32S. doi:10.1177/0148607115595980
44. Cho KY, Salton MR. Fatty acid composition of bacterial membrane and wall lipids. *Biochim Biophys Acta* (1966) 116(1):73–9. doi:10.1016/0005-2760(66)90093-2
45. McKinney JD, Honer zu Bentrup K, Munoz-Elias EJ, Miczak A, Chen B, Chan WT, et al. Persistence of *Mycobacterium tuberculosis* in macrophages and mice requires the glyoxylate shunt enzyme isocitrate lyase. *Nature* (2000) 406(6797):735–8. doi:10.1038/35021074
46. Daniel J, Maamar H, Deb C, Sirakova TD, Kolattukudy PE. *Mycobacterium tuberculosis* uses host triacylglycerol to accumulate lipid droplets and acquires a dormancy-like phenotype in lipid-loaded macrophages. *PLoS Pathog* (2011) 7(6):e1002093. doi:10.1371/journal.ppat.1002093
47. Lee W, VanderVen BC, Fahey RJ, Russell DG. Intracellular *Mycobacterium tuberculosis* exploits host-derived fatty acids to limit metabolic stress. *J Biol Chem* (2013) 288(10):6788–800. doi:10.1074/jbc.M112.445056
48. Nazarova EV, Montague CR, La T, Wilburn KM, Sukumar N, Lee W, et al. Rv3723/LucA coordinates fatty acid and cholesterol uptake in *Mycobacterium tuberculosis*. *Elife* (2017) 6:e26969. doi:10.7554/eLife.26969
49. Daniel J, Sirakova T, Kolattukudy P. An acyl-CoA synthetase in *Mycobacterium tuberculosis* involved in triacylglycerol accumulation during dormancy. *PLoS One* (2014) 9(12):e114877. doi:10.1371/journal.pone.0114877
50. Deb C, Daniel J, Sirakova TD, Abomoelak B, Dubey VS, Kolattukudy PE. A novel lipase belonging to the hormone-sensitive lipase family induced under starvation to utilize stored triacylglycerol in *Mycobacterium tuberculosis*. *J Biol Chem* (2006) 281(7):3866–75. doi:10.1074/jbc.M505556200
51. Saka HA, Valdivia R. Emerging roles for lipid droplets in immunity and host-pathogen interactions. *Annu Rev Cell Dev Biol* (2012) 28:411–37. doi:10.1146/annurev-cellbio-092910-153958
52. Barisch C, Soldati T. Breaking fat! How mycobacteria and other intracellular pathogens manipulate host lipid droplets. *Biochimie* (2017) 141:54–61. doi:10.1016/j.biochi.2017.06.001
53. Harizi H, Corcuff JB, Gualde N. Arachidonic-acid-derived eicosanoids: roles in biology and immunopathology. *Trends Mol Med* (2008) 14(10):461–9. doi:10.1016/j.molmed.2008.08.005
54. Dennis EA, Norris PC. Eicosanoid storm in infection and inflammation. *Nat Rev Immunol* (2015) 15(8):511–23. doi:10.1038/nri3859
55. Serhan CN, Chiang N, Van Dyke TE. Resolving inflammation: dual anti-inflammatory and pro-resolution lipid mediators. *Nat Rev Immunol* (2008) 8(5):349–61. doi:10.1038/nri2294
56. Eckmann L, Stenson WF, Savidge TC, Lowe DC, Barrett KE, Fierer J, et al. Role of intestinal epithelial cells in the host secretory response to infection by invasive bacteria. Bacterial entry induces epithelial prostaglandin H synthase-2 expression and prostaglandin E2 and F2alpha production. *J Clin Invest* (1997) 100(2):296–309. doi:10.1172/JCI119535
57. Chen M, Divangahi M, Gan H, Shin DS, Hong S, Lee DM, et al. Lipid mediators in innate immunity against tuberculosis: opposing roles of PGE2 and LXA4 in the induction of macrophage death. *J Exp Med* (2008) 205(12):2791–801. doi:10.1084/jem.20080767
58. Divangahi M, Chen M, Gan H, Desjardins D, Hickman TT, Lee DM, et al. *Mycobacterium tuberculosis* evades macrophage defenses by inhibiting

plasma membrane repair. *Nat Immunol* (2009) 10(8):899–906. doi:10.1038/ni.1758
59. Zaslona Z, Serezani CH, Okunishi K, Aronoff DM, Peters-Golden M. Prostaglandin E2 restrains macrophage maturation via E prostanoid receptor 2/protein kinase A signaling. *Blood* (2012) 119(10):2358–67. doi:10.1182/blood-2011-08-374207
60. Serezani CH, Chung J, Ballinger MN, Moore BB, Aronoff DM, Peters-Golden M. Prostaglandin E2 suppresses bacterial killing in alveolar macrophages by inhibiting NADPH oxidase. *Am J Respir Cell Mol Biol* (2007) 37(5):562–70. doi:10.1165/rcmb.2007-0153OC
61. Uchiya K, Nikai T. *Salmonella enterica* serovar Typhimurium infection induces cyclooxygenase 2 expression in macrophages: involvement of *Salmonella* pathogenicity island 2. *Infect Immun* (2004) 72(12):6860–9. doi:10.1128/IAI.72.12.6860-6869.2004
62. Asakrah S, Nieves W, Mahdi Z, Agard M, Zea AH, Roy CJ, et al. Post-exposure therapeutic efficacy of COX-2 inhibition against *Burkholderia pseudomallei*. *PLoS Negl Trop Dis* (2013) 7(5):e2212. doi:10.1371/journal.pntd.0002212
63. Uchiya K, Groisman EA, Nikai T. Involvement of *Salmonella* pathogenicity island 2 in the up-regulation of interleukin-10 expression in macrophages: role of protein kinase A signal pathway. *Infect Immun* (2004) 72(4):1964–73. doi:10.1128/IAI.72.4.1964-1973.2004
64. Kieran NE, Maderna P, Godson C. Lipoxins: potential anti-inflammatory, proresolution, and antifibrotic mediators in renal disease. *Kidney Int* (2004) 65(4):1145–54. doi:10.1111/j.1523-1755.2004.00487.x
65. Serhan CN, Hamberg M, Samuelsson B. Lipoxins: novel series of biologically active compounds formed from arachidonic acid in human leukocytes. *Proc Natl Acad Sci U S A* (1984) 81(17):5335–9. doi:10.1073/pnas.81.17.5335
66. Bafica A, Scanga CA, Serhan C, Machado F, White S, Sher A, et al. Host control of *Mycobacterium tuberculosis* is regulated by 5-lipoxygenase-dependent lipoxin production. *J Clin Invest* (2005) 115(6):1601–6. doi:10.1172/JCI23949
67. Prieto P, Cuenca J, Traves PG, Fernandez-Velasco M, Martin-Sanz P, Bosca L. Lipoxin A4 impairment of apoptotic signaling in macrophages: implication of the PI3K/Akt and the ERK/Nrf-2 defense pathways. *Cell Death Differ* (2010) 17(7):1179–88. doi:10.1038/cdd.2009.220
68. Fahel JS, de Souza MB, Gomes MT, Corsetti PP, Carvalho NB, Marinho FA, et al. 5-Lipoxygenase negatively regulates Th1 response during *Brucella abortus* infection in mice. *Infect Immun* (2015) 83(3):1210–6. doi:10.1128/IAI.02592-14
69. Liang L, Zhang Q, Luo LL, Yue J, Zhao YL, Han M, et al. Polymorphisms in the prostaglandin receptor EP2 gene confers susceptibility to tuberculosis. *Infect Genet Evol* (2016) 46:23–7. doi:10.1016/j.meegid.2016.10.016
70. Tobin DM, Vary JC Jr, Ray JP, Walsh GS, Dunstan SJ, Bang ND, et al. The lta4h locus modulates susceptibility to mycobacterial infection in zebrafish and humans. *Cell* (2010) 140(5):717–30. doi:10.1016/j.cell.2010.02.013
71. Tobin DM, Roca FJ, Oh SF, McFarland R, Vickery TW, Ray JP, et al. Host genotype-specific therapies can optimize the inflammatory response to mycobacterial infections. *Cell* (2012) 148(3):434–46. doi:10.1016/j.cell.2011.12.023
72. Leventis PA, Grinstein S. The distribution and function of phosphatidylserine in cellular membranes. *Annu Rev Biophys* (2010) 39:407–27. doi:10.1146/annurev.biophys.093008.131234
73. Schroit AJ, Madsen JW, Tanaka Y. In vivo recognition and clearance of red blood cells containing phosphatidylserine in their plasma membranes. *J Biol Chem* (1985) 260(8):5131–8.
74. Czuczman MA, Fattouh R, van Rijn JM, Canadien V, Osborne S, Muise AM, et al. *Listeria monocytogenes* exploits efferocytosis to promote cell-to-cell spread. *Nature* (2014) 509(7499):230–4. doi:10.1038/nature13168
75. Martin CJ, Booty MG, Rosebrock TR, Nunes-Alves C, Desjardins DM, Keren I, et al. Efferocytosis is an innate antibacterial mechanism. *Cell Host Microbe* (2012) 12(3):289–300. doi:10.1016/j.chom.2012.06.010
76. Yang CT, Cambier CJ, Davis JM, Hall CJ, Crosier PS, Ramakrishnan L. Neutrophils exert protection in the early tuberculous granuloma by oxidative killing of mycobacteria phagocytosed from infected macrophages. *Cell Host Microbe* (2012) 12(3):301–12. doi:10.1016/j.chom.2012.07.009
77. Defacque H, Bos E, Garvalov B, Barret C, Roy C, Mangeat P, et al. Phosphoinositides regulate membrane-dependent actin assembly by latex bead phagosomes. *Mol Biol Cell* (2002) 13(4):1190–202. doi:10.1091/mbc.01-06-0314
78. De Matteis MA, Godi A. PI-loting membrane traffic. *Nat Cell Biol* (2004) 6(6):487–92. doi:10.1038/ncb0604-487
79. Vergne I, Chua J, Lee HH, Lucas M, Belisle J, Deretic V. Mechanism of phagolysosome biogenesis block by viable *Mycobacterium tuberculosis*. *Proc Natl Acad Sci U S A* (2005) 102(11):4033–8. doi:10.1073/pnas.0409716102
80. Vergne I, Fratti RA, Hill PJ, Chua J, Belisle J, Deretic V. *Mycobacterium tuberculosis* phagosome maturation arrest: mycobacterial phosphatidylinositol analog phosphatidylinositol mannoside stimulates early endosomal fusion. *Mol Biol Cell* (2004) 15(2):751–60. doi:10.1091/mbc.E03-05-0307
81. Alpuche-Aranda CM, Racoosin EL, Swanson JA, Miller SI. *Salmonella* stimulate macrophage macropinocytosis and persist within spacious phagosomes. *J Exp Med* (1994) 179(2):601–8. doi:10.1084/jem.179.2.601
82. Drecktrah D, Knodler LA, Galbraith K, Steele-Mortimer O. The *Salmonella* SPI1 effector SopB stimulates nitric oxide production long after invasion. *Cell Microbiol* (2005) 7(1):105–13. doi:10.1111/j.1462-5822.2004.00436.x
83. Ochman H, Soncini FC, Solomon F, Groisman EA. Identification of a pathogenicity island required for *Salmonella* survival in host cells. *Proc Natl Acad Sci U S A* (1996) 93(15):7800–4. doi:10.1073/pnas.93.15.7800
84. Shea JE, Hensel M, Gleeson C, Holden DW. Identification of a virulence locus encoding a second type III secretion system in *Salmonella typhimurium*. *Proc Natl Acad Sci U S A* (1996) 93(6):2593–7. doi:10.1073/pnas.93.6.2593
85. Norris FA, Wilson MP, Wallis TS, Galyov EE, Majerus PW. SopB, a protein required for virulence of *Salmonella dublin*, is an inositol phosphate phosphatase. *Proc Natl Acad Sci U S A* (1998) 95(24):14057–9. doi:10.1073/pnas.95.24.14057
86. Marcus SL, Wenk MR, Steele-Mortimer O, Finlay BB. A synaptojanin-homologous region of *Salmonella typhimurium* SigD is essential for inositol phosphatase activity and Akt activation. *FEBS Lett* (2001) 494(3):201–7. doi:10.1016/S0014-5793(01)02356-0
87. Terebiznik MR, Vieira OV, Marcus SL, Slade A, Yip CM, Trimble WS, et al. Elimination of host cell PtdIns(4,5)P(2) by bacterial SigD promotes membrane fission during invasion by *Salmonella*. *Nat Cell Biol* (2002) 4(10):766–73. doi:10.1038/ncb854
88. Hernandez LD, Hueffer K, Wenk MR, Galan JE. *Salmonella* modulates vesicular traffic by altering phosphoinositide metabolism. *Science* (2004) 304(5678):1805–7. doi:10.1126/science.1098188
89. Gaspar AH, Machner MP. VipD is a Rab5-activated phospholipase A1 that protects *Legionella pneumophila* from endosomal fusion. *Proc Natl Acad Sci U S A* (2014) 111(12):4560–5. doi:10.1073/pnas.1316376111
90. O'Brien DK, Melville SB. Effects of *Clostridium perfringens* alpha-toxin (PLC) and perfringolysin O (PFO) on cytotoxicity to macrophages, on escape from the phagosomes of macrophages, and on persistence of *C. perfringens* in host tissues. *Infect Immun* (2004) 72(9):5204–15. doi:10.1128/IAI.72.9.5204-5215.2004
91. Raynaud C, Guilhot C, Rauzier J, Bordat Y, Pelicic V, Manganelli R, et al. Phospholipases C are involved in the virulence of *Mycobacterium tuberculosis*. *Mol Microbiol* (2002) 45(1):203–17. doi:10.1046/j.1365-2958.2002.03009.x
92. Le Chevalier F, Cascioferro A, Frigui W, Pawlik A, Boritsch EC, Bottai D, et al. Revisiting the role of phospholipases C in virulence and the lifecycle of *Mycobacterium tuberculosis*. *Sci Rep* (2015) 5:16918. doi:10.1038/srep16918
93. Viana-Niero C, de Haas PE, van Soolingen D, Leao SC. Analysis of genetic polymorphisms affecting the four phospholipase C (plc) genes in *Mycobacterium tuberculosis* complex clinical isolates. *Microbiology* (2004) 150(Pt 4):967–78. doi:10.1099/mic.0.26778-0
94. Auricchio G, Garg SK, Martino A, Volpe E, Ciaramella A, De Vito P, et al. Role of macrophage phospholipase D in natural and CpG-induced antimycobacterial activity. *Cell Microbiol* (2003) 5(12):913–20. doi:10.1046/j.1462-5822.2003.00330.x
95. Schneider BE, Behrends J, Hagens K, Harmel N, Shayman JA, Schaible UE. Lysosomal phospholipase A2: a novel player in host immunity to *Mycobacterium tuberculosis*. *Eur J Immunol* (2014) 44(8):2394–404. doi:10.1002/eji.201344383

96. Spiegel S, Milstien S. Sphingosine-1-phosphate: an enigmatic signalling lipid. *Nat Rev Mol Cell Biol* (2003) 4(5):397–407. doi:10.1038/nrm1103
97. Luberto C, Hannun YA. Sphingolipid metabolism in the regulation of bioactive molecules. *Lipids* (1999) 34(Suppl):S5–11. doi:10.1007/BF02562221
98. Merrill AH Jr, Schmelz EM, Dillehay DL, Spiegel S, Shayman JA, Schroeder JJ, et al. Sphingolipids – the enigmatic lipid class: biochemistry, physiology, and pathophysiology. *Toxicol Appl Pharmacol* (1997) 142(1):208–25. doi:10.1006/taap.1996.8029
99. van der Goot FG, Harder T. Raft membrane domains: from a liquid-ordered membrane phase to a site of pathogen attack. *Semin Immunol* (2001) 13(2):89–97. doi:10.1006/smim.2000.0300
100. Manes S, del Real G, Martinez AC. Pathogens: raft hijackers. *Nat Rev Immunol* (2003) 3(7):557–68. doi:10.1038/nri1129
101. Rosenberger CM, Brumell JH, Finlay BB. Microbial pathogenesis: lipid rafts as pathogen portals. *Curr Biol* (2000) 10(22):R823–5. doi:10.1016/S0960-9822(00)00788-0
102. Riethmuller J, Riehle A, Grassme H, Gulbins E. Membrane rafts in host-pathogen interactions. *Biochim Biophys Acta* (2006) 1758(12):2139–47. doi:10.1016/j.bbamem.2006.07.017
103. Hanada K. Sphingolipids in infectious diseases. *Jpn J Infect Dis* (2005) 58(3):131–48.
104. Heung LJ, Luberto C, Del Poeta M. Role of sphingolipids in microbial pathogenesis. *Infect Immun* (2006) 74(1):28–39. doi:10.1128/IAI.74.1.28-39.2006
105. Fueller M, Wang DA, Tigyi G, Siess W. Activation of human monocytic cells by lysophosphatidic acid and sphingosine-1-phosphate. *Cell Signal* (2003) 15(4):367–75. doi:10.1016/S0898-6568(02)00117-1
106. Rivera J, Proia RL, Olivera A. The alliance of sphingosine-1-phosphate and its receptors in immunity. *Nat Rev Immunol* (2008) 8(10):753–63. doi:10.1038/nri2400
107. Malik ZA, Thompson CR, Hashimi S, Porter B, Iyer SS, Kusner DJ. Cutting edge: *Mycobacterium tuberculosis* blocks Ca2+ signaling and phagosome maturation in human macrophages via specific inhibition of sphingosine kinase. *J Immunol* (2003) 170(6):2811–5. doi:10.4049/jimmunol.170.6.2811
108. Garg SK, Volpe E, Palmieri G, Mattei M, Galati D, Martino A, et al. Sphingosine 1-phosphate induces antimicrobial activity both in vitro and in vivo. *J Infect Dis* (2004) 189(11):2129–38. doi:10.1086/386286
109. Santucci MB, Greco E, De Spirito M, Arcovito G, De Angelis G, Cauda R, et al. Sphingosine 1-phosphate promotes antigen processing and presentation to CD4+ T cells in *Mycobacterium tuberculosis*-infected monocytes. *Biochem Biophys Res Commun* (2007) 361(3):687–93. doi:10.1016/j.bbrc.2007.07.087
110. Utermohlen O, Herz J, Schramm M, Kronke M. Fusogenicity of membranes: the impact of acid sphingomyelinase on innate immune responses. *Immunobiology* (2008) 213(3–4):307–14. doi:10.1016/j.imbio.2007.10.016
111. Vazquez CL, Rodgers A, Herbst S, Coade S, Gronow A, Guzman CA, et al. The proneurotrophin receptor sortilin is required for *Mycobacterium tuberculosis* control by macrophages. *Sci Rep* (2016) 6:29332. doi:10.1038/srep29332
112. Utermohlen O, Karow U, Lohler J, Kronke M. Severe impairment in early host defense against *Listeria monocytogenes* in mice deficient in acid sphingomyelinase. *J Immunol* (2003) 170(5):2621–8. doi:10.4049/jimmunol.170.5.2621
113. Li C, Peng H, Japtok L, Seitz A, Riehle A, Wilker B, et al. Inhibition of neutral sphingomyelinase protects mice against systemic tuberculosis. *Front Biosci (Elite Ed)* (2016) 8:311–25. doi:10.2741/e769
114. Flores-Diaz M, Monturiol-Gross L, Naylor C, Alape-Giron A, Flieger A. Bacterial sphingomyelinases and phospholipases as virulence factors. *Microbiol Mol Biol Rev* (2016) 80(3):597–628. doi:10.1128/MMBR.00082-15
115. Speer A, Sun J, Danilchanka O, Meikle V, Rowland JL, Walter K, et al. Surface hydrolysis of sphingomyelin by the outer membrane protein Rv0888 supports replication of *Mycobacterium tuberculosis* in macrophages. *Mol Microbiol* (2015) 97(5):881–97. doi:10.1111/mmi.13073
116. Dubos RJ. The effect of sphingomyelin on the growth of tubercle bacilli. *J Exp Med* (1948) 88(1):73–9. doi:10.1084/jem.88.1.73
117. Montes LR, Goni FM, Johnston NC, Goldfine H, Alonso A. Membrane fusion induced by the catalytic activity of a phospholipase C/sphingomyelinase from *Listeria monocytogenes*. *Biochemistry* (2004) 43(12):3688–95. doi:10.1021/bi0352522
118. Rolando M, Escoll P, Nora T, Botti J, Boitez V, Bedia C, et al. *Legionella pneumophila* S1P-lyase targets host sphingolipid metabolism and restrains autophagy. *Proc Natl Acad Sci U S A* (2016) 113(7):1901–6. doi:10.1073/pnas.1522067113
119. McLean CJ, Marles-Wright J, Custodio R, Lowther J, Kennedy AJ, Pollock J, et al. Characterization of homologous sphingosine-1-phosphate lyase isoforms in the bacterial pathogen *Burkholderia pseudomallei*. *J Lipid Res* (2017) 58(1):137–50. doi:10.1194/jlr.M071258
120. Kunkel GT, Maceyka M, Milstien S, Spiegel S. Targeting the sphingosine-1-phosphate axis in cancer, inflammation and beyond. *Nat Rev Drug Discov* (2013) 12(9):688–702. doi:10.1038/nrd4099
121. Poralla K, Kannenberg E. Hopanoids: sterol equivalents in bacteria. In: Fuller G, Nes WD, editors. *Ecology and Metabolism of Plant Lipids. ACS Symposium Series*. (Vol. 325). Washington, DC: American Chemical Society (1987). p. 239–51.
122. Riobo NA. Cholesterol and its derivatives in Sonic Hedgehog signaling and cancer. *Curr Opin Pharmacol* (2012) 12(6):736–41. doi:10.1016/j.coph.2012.07.002
123. Haines TH. Do sterols reduce proton and sodium leaks through lipid bilayers? *Prog Lipid Res* (2001) 40(4):299–324. doi:10.1016/S0163-7827(01)00009-1
124. Yeagle PL. Cholesterol and the cell membrane. *Biochim Biophys Acta* (1985) 822(3–4):267–87. doi:10.1016/0304-4157(85)90011-5
125. Berg J, Tymoczko J, Stryer L. Important derivatives of cholesterol include bile salts and steroid hormones. 5th ed. *Biochemistry*. New York: W. H. Freeman (2002).
126. Mattos KA, Oliveira VC, Berredo-Pinho M, Amaral JJ, Antunes LC, Melo RC, et al. *Mycobacterium leprae* intracellular survival relies on cholesterol accumulation in infected macrophages: a potential target for new drugs for leprosy treatment. *Cell Microbiol* (2014) 16(6):797–815. doi:10.1111/cmi.12279
127. Kim MJ, Wainwright HC, Locketz M, Bekker LG, Walther GB, Dittrich C, et al. Caseation of human tuberculosis granulomas correlates with elevated host lipid metabolism. *EMBO Mol Med* (2010) 2(7):258–74. doi:10.1002/emmm.201000079
128. Gatfield J, Pieters J. Essential role for cholesterol in entry of mycobacteria into macrophages. *Science* (2000) 288(5471):1647–50. doi:10.1126/science.288.5471.1647
129. Kendall SL, Withers M, Soffair CN, Moreland NJ, Gurcha S, Sidders B, et al. A highly conserved transcriptional repressor controls a large regulon involved in lipid degradation in *Mycobacterium smegmatis* and *Mycobacterium tuberculosis*. *Mol Microbiol* (2007) 65(3):684–99. doi:10.1111/j.1365-2958.2007.05827.x
130. Kendall SL, Burgess P, Balhana R, Withers M, Ten Bokum A, Lott JS, et al. Cholesterol utilization in mycobacteria is controlled by two TetR-type transcriptional regulators: kstR and kstR2. *Microbiology* (2010) 156(Pt 5):1362–71. doi:10.1099/mic.0.034538-0
131. Pandey AK, Sassetti CM. Mycobacterial persistence requires the utilization of host cholesterol. *Proc Natl Acad Sci U S A* (2008) 105(11):4376–80. doi:10.1073/pnas.0711159105
132. Griffin JE, Pandey AK, Gilmore SA, Mizrahi V, McKinney JD, Bertozzi CR, et al. Cholesterol catabolism by *Mycobacterium tuberculosis* requires transcriptional and metabolic adaptations. *Chem Biol* (2012) 19(2):218–27. doi:10.1016/j.chembiol.2012.08.012
133. Chang JC, Miner MD, Pandey AK, Gill WP, Harik NS, Sassetti CM, et al. igr Genes and *Mycobacterium tuberculosis* cholesterol metabolism. *J Bacteriol* (2009) 191(16):5232–9. doi:10.1128/JB.00452-09
134. Portnoy DA, Jacks PS, Hinrichs DJ. Role of hemolysin for the intracellular growth of *Listeria monocytogenes*. *J Exp Med* (1988) 167(4):1459–71. doi:10.1084/jem.167.4.1459
135. Birmingham CL, Canadien V, Kaniuk NA, Steinberg BE, Higgins DE, Brumell JH. Listeriolysin O allows *Listeria monocytogenes* replication in macrophage vacuoles. *Nature* (2008) 451(7176):350–4. doi:10.1038/nature06479
136. Bhakdi S, Tranum-Jensen J, Sziegoleit A. Mechanism of membrane damage by streptolysin-O. *Infect Immun* (1985) 47(1):52–60.
137. Hara H, Tsuchiya K, Nomura T, Kawamura I, Shoma S, Mitsuyama M. Dependency of caspase-1 activation induced in macrophages by *Listeria monocytogenes* on cytolysin, listeriolysin O, after evasion from phagosome

into the cytoplasm. *J Immunol* (2008) 180(12):7859–68. doi:10.4049/jimmunol.180.12.7859
138. Catron DM, Sylvester MD, Lange Y, Kadekoppala M, Jones BD, Monack DM, et al. The *Salmonella*-containing vacuole is a major site of intracellular cholesterol accumulation and recruits the GPI-anchored protein CD55. *Cell Microbiol* (2002) 4(6):315–28. doi:10.1046/j.1462-5822.2002.00198.x
139. Nawabi P, Catron DM, Haldar K. Esterification of cholesterol by a type III secretion effector during intracellular *Salmonella* infection. *Mol Microbiol* (2008) 68(1):173–85. doi:10.1111/j.1365-2958.2008.06142.x
140. Parihar SP, Guler R, Khutlang R, Lang DM, Hurdayal R, Mhlanga MM, et al. Statin therapy reduces the *Mycobacterium tuberculosis* burden in human macrophages and in mice by enhancing autophagy and phagosome maturation. *J Infect Dis* (2014) 209(5):754–63. doi:10.1093/infdis/jit550
141. Catron DM, Lange Y, Borensztajn J, Sylvester MD, Jones BD, Haldar K. *Salmonella enterica* serovar Typhimurium requires nonsterol precursors of the cholesterol biosynthetic pathway for intracellular proliferation. *Infect Immun* (2004) 72(2):1036–42. doi:10.1128/IAI.72.2.1036-1042.2004
142. Mulye M, Samanta D, Winfree S, Heinzen RA, Gilk SD. Elevated cholesterol in the *Coxiella burnetii* intracellular niche is bacteriolytic. *mBio* (2017) 8(1):e02313–16. doi:10.1128/mBio.02313-16
143. Czyz DM, Potluri LP, Jain-Gupta N, Riley SP, Martinez JJ, Steck TL, et al. Host-directed antimicrobial drugs with broad-spectrum efficacy against intracellular bacterial pathogens. *mBio* (2014) 5(4):e01534–14. doi:10.1128/mBio.01534-14
144. Araldi E, Fernandez-Fuertes M, Canfran-Duque A, Tang W, Cline GW, Madrigal-Matute J, et al. Lanosterol modulates TLR4-mediated innate immune responses in macrophages. *Cell Rep* (2017) 19(13):2743–55. doi:10.1016/j.celrep.2017.05.093
145. Bikle DD. Vitamin D and the immune system: role in protection against bacterial infection. *Curr Opin Nephrol Hypertens* (2008) 17(4):348–52. doi:10.1097/MNH.0b013e3282ff64a3
146. Verway M, Bouttier M, Wang TT, Carrier M, Calderon M, An BS, et al. Vitamin D induces interleukin-1beta expression: paracrine macrophage epithelial signaling controls *M. tuberculosis* infection. *PLoS Pathog* (2013) 9(6):e1003407. doi:10.1371/journal.ppat.1003407
147. Wilkinson RJ, Llewelyn M, Toossi Z, Patel P, Pasvol G, Lalvani A, et al. Influence of vitamin D deficiency and vitamin D receptor polymorphisms on tuberculosis among Gujarati Asians in west London: a case-control study. *Lancet* (2000) 355(9204):618–21. doi:10.1016/S0140-6736(99)02301-6
148. Salahuddin N, Ali F, Hasan Z, Rao N, Aqeel M, Mahmood F. Vitamin D accelerates clinical recovery from tuberculosis: results of the SUCCINCT study [supplementary cholecalciferol in recovery from tuberculosis]. A randomized, placebo-controlled, clinical trial of vitamin D supplementation in patients with pulmonary tuberculosis'. *BMC Infect Dis* (2013) 13:22. doi:10.1186/1471-2334-13-22
149. Coussens AK, Wilkinson RJ, Martineau AR. Phenylbutyrate is bacteriostatic against *Mycobacterium tuberculosis* and regulates the macrophage response to infection, synergistically with 25-hydroxy-vitamin D3. *PLoS Pathog* (2015) 11(7):e1005007. doi:10.1371/journal.ppat.1005007
150. Raetz CR, Reynolds CM, Trent MS, Bishop RE. Lipid A modification systems in Gram-negative bacteria. *Annu Rev Biochem* (2007) 76:295–329. doi:10.1146/annurev.biochem.76.010307.145803
151. Medzhitov R, Preston-Hurlburt P, Janeway CA Jr. A human homologue of the *Drosophila* toll protein signals activation of adaptive immunity. *Nature* (1997) 388(6640):394–7. doi:10.1038/41131
152. Poltorak A, He X, Smirnova I, Liu MY, Van Huffel C, Du X, et al. Defective LPS signaling in C3H/HeJ and C57BL/10ScCr mice: mutations in Tlr4 gene. *Science* (1998) 282(5396):2085–8. doi:10.1126/science.282.5396.2085
153. Akashi S, Saitoh S, Wakabayashi Y, Kikuchi T, Takamura N, Nagai Y, et al. Lipopolysaccharide interaction with cell surface toll-like receptor 4-MD-2: higher affinity than that with MD-2 or CD14. *J Exp Med* (2003) 198(7):1035–42. doi:10.1084/jem.20031076
154. Yang RB, Mark MR, Gray A, Huang A, Xie MH, Zhang M, et al. Toll-like receptor-2 mediates lipopolysaccharide-induced cellular signalling. *Nature* (1998) 395(6699):284–8. doi:10.1038/26239
155. Kirschning CJ, Wesche H, Merrill Ayres T, Rothe M. Human toll-like receptor 2 confers responsiveness to bacterial lipopolysaccharide. *J Exp Med* (1998) 188(11):2091–7. doi:10.1084/jem.188.11.2091
156. Akira S, Takeda K. Toll-like receptor signalling. *Nat Rev Immunol* (2004) 4(7):499–511. doi:10.1038/nri1391
157. Raetz CR, Whitfield C. Lipopolysaccharide endotoxins. *Annu Rev Biochem* (2002) 71:635–700. doi:10.1146/annurev.biochem.71.110601.135414
158. Park BS, Lee JO. Recognition of lipopolysaccharide pattern by TLR4 complexes. *Exp Mol Med* (2013) 45:e66. doi:10.1038/emm.2013.97
159. Kawai T, Takeuchi O, Fujita T, Inoue J, Muhlradt PF, Sato S, et al. Lipopolysaccharide stimulates the MyD88-independent pathway and results in activation of IFN-regulatory factor 3 and the expression of a subset of lipopolysaccharide-inducible genes. *J Immunol* (2001) 167(10):5887–94. doi:10.4049/jimmunol.167.10.5887
160. Hagar JA, Powell DA, Aachoui Y, Ernst RK, Miao EA. Cytoplasmic LPS activates caspase-11: implications in TLR4-independent endotoxic shock. *Science* (2013) 341(6151):1250–3. doi:10.1126/science.1240988
161. Kayagaki N, Wong MT, Stowe IB, Ramani SR, Gonzalez LC, Akashi-Takamura S, et al. Noncanonical inflammasome activation by intracellular LPS independent of TLR4. *Science* (2013) 341(6151):1246–9. doi:10.1126/science.1240248
162. Ng TM, Monack DM. Revisiting caspase-11 function in host defense. *Cell Host Microbe* (2013) 14(1):9–14. doi:10.1016/j.chom.2013.06.009
163. Shi J, Zhao Y, Wang Y, Gao W, Ding J, Li P, et al. Inflammatory caspases are innate immune receptors for intracellular LPS. *Nature* (2014) 514(7521):187–92. doi:10.1038/nature13683
164. Suzuki N, Suzuki S, Duncan GS, Millar DG, Wada T, Mirtsos C, et al. Severe impairment of interleukin-1 and toll-like receptor signalling in mice lacking IRAK-4. *Nature* (2002) 416(6882):750–6. doi:10.1038/nature736
165. Hoshino K, Takeuchi O, Kawai T, Sanjo H, Ogawa T, Takeda Y, et al. Cutting edge: toll-like receptor 4 (TLR4)-deficient mice are hyporesponsive to lipopolysaccharide: evidence for TLR4 as the Lps gene product. *J Immunol* (1999) 162(7):3749–52.
166. Knuefermann P, Nemoto S, Misra A, Nozaki N, Defreitas G, Goyert SM, et al. CD14-deficient mice are protected against lipopolysaccharide-induced cardiac inflammation and left ventricular dysfunction. *Circulation* (2002) 106(20):2608–15. doi:10.1161/01.CIR.0000038110.69369.4C
167. Lequire VS, Hutcherson JD, Hamilton RL, Gray ME. The effects of bacterial endotoxin on lipide metabolism. I. The responses of the serum lipides of rabbits to single and repeated injections of Shear's polysaccharide. *J Exp Med* (1959) 110(2):293–309. doi:10.1084/jem.110.2.293
168. Kaufmann RL, Matson CF, Beisel WR. Hypertriglyceridemia produced by endotoxin: role of impaired triglyceride disposal mechanisms. *J Infect Dis* (1976) 133(5):548–55. doi:10.1093/infdis/133.5.548
169. Feingold KR, Staprans I, Memon RA, Moser AH, Shigenaga JK, Doerrler W, et al. Endotoxin rapidly induces changes in lipid metabolism that produce hypertriglyceridemia: low doses stimulate hepatic triglyceride production while high doses inhibit clearance. *J Lipid Res* (1992) 33(12):1765–76.
170. Huang YL, Morales-Rosado J, Ray J, Myers TG, Kho T, Lu M, et al. Toll-like receptor agonists promote prolonged triglyceride storage in macrophages. *J Biol Chem* (2014) 289(5):3001–12. doi:10.1074/jbc.M113.524587
171. Rubinow KB, Wall VZ, Nelson J, Mar D, Bomsztyk K, Askari B, et al. Acyl-CoA synthetase 1 is induced by Gram-negative bacteria and lipopolysaccharide and is required for phospholipid turnover in stimulated macrophages. *J Biol Chem* (2013) 288(14):9957–70. doi:10.1074/jbc.M113.458372
172. D'Avila H, Melo RC, Parreira GG, Werneck-Barroso E, Castro-Faria-Neto HC, Bozza PT. *Mycobacterium bovis* bacillus Calmette-Guerin induces TLR2-mediated formation of lipid bodies: intracellular domains for eicosanoid synthesis in vivo. *J Immunol* (2006) 176(5):3087–97. doi:10.4049/jimmunol.176.5.3087
173. Pacheco P, Bozza FA, Gomes RN, Bozza M, Weller PF, Castro-Faria-Neto HC, et al. Lipopolysaccharide-induced leukocyte lipid body formation in vivo: innate immunity elicited intracellular loci involved in eicosanoid metabolism. *J Immunol* (2002) 169(11):6498–506. doi:10.4049/jimmunol.169.11.6498
174. Khatchadourian A, Bourque SD, Richard VR, Titorenko VI, Maysinger D. Dynamics and regulation of lipid droplet formation in lipopolysaccharide (LPS)-stimulated microglia. *Biochim Biophys Acta* (2012) 1821(4):607–17. doi:10.1016/j.bbalip.2012.01.007

175. Maya-Monteiro CM, Almeida PE, D'Avila H, Martins AS, Rezende AP, Castro-Faria-Neto H, et al. Leptin induces macrophage lipid body formation by a phosphatidylinositol 3-kinase- and mammalian target of rapamycin-dependent mechanism. *J Biol Chem* (2008) 283(4):2203–10. doi:10.1074/jbc.M706706200
176. Dennis EA, Deems RA, Harkewicz R, Quehenberger O, Brown HA, Milne SB, et al. A mouse macrophage lipidome. *J Biol Chem* (2010) 285(51):39976–85. doi:10.1074/jbc.M110.182915
177. Koberlin MS, Snijder B, Heinz LX, Baumann CL, Fauster A, Vladimer GI, et al. A conserved circular network of coregulated lipids modulates innate immune responses. *Cell* (2015) 162(1):170–83. doi:10.1016/j.cell.2015.05.051
178. Jankute M, Cox JA, Harrison J, Besra GS. Assembly of the mycobacterial cell wall. *Annu Rev Microbiol* (2015) 69:405–23. doi:10.1146/annurev-micro-091014-104121
179. Kaur G, Kaur J. Multifaceted role of lipids in *Mycobacterium leprae*. *Future Microbiol* (2017) 12:315–35. doi:10.2217/fmb-2016-0173
180. Bloch H, Sorkin E, Erlenmeyer H. A toxic lipid component of the tubercle bacillus (cord factor). I. Isolation from petroleum ether extracts of young bacterial cultures. *Am Rev Tuberc* (1953) 67(5):629–43.
181. Hunter RL, Venkataprasad N, Olsen MR. The role of trehalose dimycolate (cord factor) on morphology of virulent *M. tuberculosis* in vitro. *Tuberculosis* (2006) 86(5):349–56. doi:10.1016/j.tube.2005.08.017
182. Sakamoto K, Kim MJ, Rhoades ER, Allavena RE, Ehrt S, Wainwright HC, et al. Mycobacterial trehalose dimycolate reprograms macrophage global gene expression and activates matrix metalloproteinases. *Infect Immun* (2013) 81(3):764–76. doi:10.1128/IAI.00906-12
183. Geisel RE, Sakamoto K, Russell DG, Rhoades ER. In vivo activity of released cell wall lipids of *Mycobacterium bovis* bacillus Calmette-Guerin is due principally to trehalose mycolates. *J Immunol* (2005) 174(8):5007–15. doi:10.4049/jimmunol.174.8.5007
184. Yamagami H, Matsumoto T, Fujiwara N, Arakawa T, Kaneda K, Yano I, et al. Trehalose 6,6'-dimycolate (cord factor) of *Mycobacterium tuberculosis* induces foreign-body- and hypersensitivity-type granulomas in mice. *Infect Immun* (2001) 69(2):810–5. doi:10.1128/IAI.69.2.810-815.2001
185. Perez RL, Roman J, Roser S, Little C, Olsen M, Indrigo J, et al. Cytokine message and protein expression during lung granuloma formation and resolution induced by the mycobacterial cord factor trehalose-6,6'-dimycolate. *J Interferon Cytokine Res* (2000) 20(9):795–804. doi:10.1089/10799900050151067
186. Bekierkunst A, Yarkoni E. Granulomatous hypersensitivity to trehalose-6,6'-dimycolate (cord factor) in mice infected with BCG. *Infect Immun* (1973) 7(4):631–8.
187. Silva CL, Ekizlerian SM, Fazioli RA. Role of cord factor in the modulation of infection caused by mycobacteria. *Am J Pathol* (1985) 118(2):238–47.
188. Indrigo J, Hunter RL Jr, Actor JK. Cord factor trehalose 6,6'-dimycolate (TDM) mediates trafficking events during mycobacterial infection of murine macrophages. *Microbiology* (2003) 149(Pt 8):2049–59. doi:10.1099/mic.0.26226-0
189. Bloch H, Noll H. Studies on the virulence of tubercle bacilli; the effect of cord factor on murine tuberculosis. *Br J Exp Pathol* (1955) 36(1):8–17.
190. Retzinger GS, Meredith SC, Hunter RL, Takayama K, Kezdy FJ. Identification of the physiologically active state of the mycobacterial glycolipid trehalose 6,6'-dimycolate and the role of fibrinogen in the biologic activities of trehalose 6,6'-dimycolate monolayers. *J Immunol* (1982) 129(2):735–44.
191. Yarkoni E, Rapp HJ. Toxicity of emulsified trehalose-6,6'-dimycolate (cord factor) in mice depends on size distribution of mineral oil droplets. *Infect Immun* (1978) 20(3):856–60.
192. Hunter RL, Olsen M, Jagannath C, Actor JK. Trehalose 6,6'-dimycolate and lipid in the pathogenesis of caseating granulomas of tuberculosis in mice. *Am J Pathol* (2006) 168(4):1249–61. doi:10.2353/ajpath.2006.050848
193. Yarkoni E, Rapp HJ. Influence of oil and Tween concentrations on enhanced endotoxin lethality in mice pretreated with emulsified trehalose-6,6'-dimycolate (cord factor). *Infect Immun* (1979) 24(2):571–2.
194. Korf J, Stoltz A, Verschoor J, De Baetselier P, Grooten J. The *Mycobacterium tuberculosis* cell wall component mycolic acid elicits pathogen-associated host innate immune responses. *Eur J Immunol* (2005) 35(3):890–900. doi:10.1002/eji.200425332
195. Dkhar HK, Nanduri R, Mahajan S, Dave S, Saini A, Somavarapu AK, et al. *Mycobacterium tuberculosis* keto-mycolic acid and macrophage nuclear receptor TR4 modulate foamy biogenesis in granulomas: a case of a heterologous and noncanonical ligand-receptor pair. *J Immunol* (2014) 193(1):295–305. doi:10.4049/jimmunol.1400092
196. Astarie-Dequeker C, Le Guyader L, Malaga W, Seaphanh FK, Chalut C, Lopez A, et al. Phthiocerol dimycocerosates of *M. tuberculosis* participate in macrophage invasion by inducing changes in the organization of plasma membrane lipids. *PLoS Pathog* (2009) 5(2):e1000289. doi:10.1371/journal.ppat.1000289
197. Rousseau C, Winter N, Pivert E, Bordat Y, Neyrolles O, Ave P, et al. Production of phthiocerol dimycocerosates protects *Mycobacterium tuberculosis* from the cidal activity of reactive nitrogen intermediates produced by macrophages and modulates the early immune response to infection. *Cell Microbiol* (2004) 6(3):277–87. doi:10.1046/j.1462-5822.2004.00368.x
198. Cambier CJ, Takaki KK, Larson RP, Hernandez RE, Tobin DM, Urdahl KB, et al. Mycobacteria manipulate macrophage recruitment through coordinated use of membrane lipids. *Nature* (2014) 505(7482):218–22. doi:10.1038/nature12799
199. Barry CE III. Interpreting cell wall 'virulence factors' of *Mycobacterium tuberculosis*. *Trends Microbiol* (2001) 9(5):237–41. doi:10.1016/S0966-842X(01)02018-2
200. Berg JM, Tymoczko JL, Stryer L. Section 26.4, important derivatives of cholesterol include bile salts and steroid hormones. *Biochemistry*. 5th ed. New York: W. H. Freeman (2002). Available from: https://www.ncbi.nlm.nih.gov/books/NBK22339//
201. Quigley J, Hughitt VK, Velikovsky CA, Mariuzza RA, El-Sayed NM, Briken V. The cell wall lipid PDIM contributes to phagosomal escape and host cell exit of *Mycobacterium tuberculosis*. *mBio* (2017) 8(2):e00148–17. doi:10.1128/mBio.00148-17
202. Wenk MR. Lipidomics: new tools and applications. *Cell* (2010) 143(6):888–95. doi:10.1016/j.cell.2010.11.033
203. Peres CM, de Paula L, Medeiros AI, Sorgi CA, Soares EG, Carlos D, et al. Inhibition of leukotriene biosynthesis abrogates the host control of *Mycobacterium tuberculosis*. *Microbes Infect* (2007) 9(4):483–9. doi:10.1016/j.micinf.2007.01.006
204. Singh KV, Kaur J, Varshney GC, Raje M, Suri CR. Synthesis and characterization of hapten-protein conjugates for antibody production against small molecules. *Bioconjug Chem* (2004) 15(1):168–73. doi:10.1021/bc034158v
205. Brieskorn CH, Wenger E. [Analysis of ethereal sage oils by means of gas and thin layer chromatography. Part II. On the constituents of *Salvia off.* L]. *Arch Pharm Ber Dtsch Pharm Ges* (1960) 29(3/65):21–6. doi:10.1002/ardp.19602930105
206. Tashiro Y, Inagaki A, Shimizu M, Ichikawa S, Takaya N, Nakajima-Kambe T, et al. Characterization of phospholipids in membrane vesicles derived from *Pseudomonas aeruginosa*. *Biosci Biotechnol Biochem* (2011) 75(3):605–7. doi:10.1271/bbb.100754
207. Henderson JC, O'Brien JP, Brodbelt JS, Trent MS. Isolation and chemical characterization of lipid A from Gram-negative bacteria. *J Vis Exp* (2013) 79:e50623. doi:10.3791/50623
208. Buczynski MW, Stephens DL, Bowers-Gentry RC, Grkovich A, Deems RA, Dennis EA. TLR-4 and sustained calcium agonists synergistically produce eicosanoids independent of protein synthesis in RAW264.7 cells. *J Biol Chem* (2007) 282(31):22834–47. doi:10.1074/jbc.M701831200
209. Blaho VA, Buczynski MW, Brown CR, Dennis EA. Lipidomic analysis of dynamic eicosanoid responses during the induction and resolution of Lyme arthritis. *J Biol Chem* (2009) 284(32):21599–612. doi:10.1074/jbc.M109.003822
210. Tam VC. Lipidomic profiling of bioactive lipids by mass spectrometry during microbial infections. *Semin Immunol* (2013) 25(3):240–8. doi:10.1016/j.smim.2013.08.006
211. Sampaio JL, Gerl MJ, Klose C, Ejsing CS, Beug H, Simons K, et al. Membrane lipidome of an epithelial cell line. *Proc Natl Acad Sci U S A* (2011) 108(5):1903–7. doi:10.1073/pnas.1019267108
212. Slatter DA, Aldrovandi M, O'Connor A, Allen SM, Brasher CJ, Murphy RC, et al. Mapping the human platelet lipidome reveals cytosolic phospholipase A2 as a regulator of mitochondrial bioenergetics during activation. *Cell Metab* (2016) 23(5):930–44. doi:10.1016/j.cmet.2016.04.001

213. Sartain MJ, Dick DL, Rithner CD, Crick DC, Belisle JT. Lipidomic analyses of *Mycobacterium tuberculosis* based on accurate mass measurements and the novel "Mtb LipidDB". *J Lipid Res* (2011) 52(5):861–72. doi:10.1194/jlr.M010363
214. Crick PJ, Guan XL. Lipid metabolism in mycobacteria – insights using mass spectrometry-based lipidomics. *Biochim Biophys Acta* (2016) 1861(1):60–7. doi:10.1016/j.bbalip.2015.10.007
215. Mahrous EA, Lee RB, Lee RE. A rapid approach to lipid profiling of mycobacteria using 2D HSQC NMR maps. *J Lipid Res* (2008) 49(2):455–63. doi:10.1194/jlr.M700440-JLR200
216. Guan Z, Johnston NC, Aygun-Sunar S, Daldal F, Raetz CR, Goldfine H. Structural characterization of the polar lipids of *Clostridium novyi* NT. Further evidence for a novel anaerobic biosynthetic pathway to plasmalogens. *Biochim Biophys Acta* (2011) 1811(3):186–93. doi:10.1016/j.bbalip.2010.12.010
217. Oursel D, Loutelier-Bourhis C, Orange N, Chevalier S, Norris V, Lange CM. Lipid composition of membranes of *Escherichia coli* by liquid chromatography/tandem mass spectrometry using negative electrospray ionization. *Rapid Commun Mass Spectrom* (2007) 21(11):1721–8. doi:10.1002/rcm.3013
218. Rashid R, Cazenave-Gassiot A, Gao IH, Nair ZJ, Kumar JK, Gao L, et al. Comprehensive analysis of phospholipids and glycolipids in the opportunistic pathogen *Enterococcus faecalis*. *PLoS One* (2017) 12(4):e0175886. doi:10.1371/journal.pone.0175886
219. Benamara H, Rihouey C, Abbes I, Ben Mlouka MA, Hardouin J, Jouenne T, et al. Characterization of membrane lipidome changes in *Pseudomonas aeruginosa* during biofilm growth on glass wool. *PLoS One* (2014) 9(9):e108478. doi:10.1371/journal.pone.0108478
220. Barcelo-Coblijn G, Fernandez JA. Mass spectrometry coupled to imaging techniques: the better the view the greater the challenge. *Front Physiol* (2015) 6:3. doi:10.3389/fphys.2015.00003
221. Golf O, Strittmatter N, Karancsi T, Pringle SD, Speller AV, Mroz A, et al. Rapid evaporative ionization mass spectrometry imaging platform for direct mapping from bulk tissue and bacterial growth media. *Anal Chem* (2015) 87(5):2527–34. doi:10.1021/ac5046752
222. Hulme HE, Meikle LM, Wessel H, Strittmatter N, Swales J, Thomson C, et al. Mass spectrometry imaging identifies palmitoylcarnitine as an immunological mediator during *Salmonella* Typhimurium infection. *Sci Rep* (2017) 7(1):2786. doi:10.1038/s41598-017-03100-5
223. Desbenoit N, Saussereau E, Bich C, Bourderioux M, Fritsch J, Edelman A, et al. Localized lipidomics in cystic fibrosis: TOF-SIMS imaging of lungs from *Pseudomonas aeruginosa*-infected mice. *Int J Biochem Cell Biol* (2014) 52:77–82. doi:10.1016/j.biocel.2014.01.026
224. Barisch C, Paschke P, Hagedorn M, Maniak M, Soldati T. Lipid droplet dynamics at early stages of *Mycobacterium marinum* infection in *Dictyostelium*. *Cell Microbiol* (2015) 17(9):1332–49. doi:10.1111/cmi.12437
225. Barisch C, Soldati T. *Mycobacterium marinum* degrades both triacylglycerols and phospholipids from its *Dictyostelium* host to synthesise its own triacylglycerols and generate lipid inclusions. *PLoS Pathog* (2017) 13(1):e1006095. doi:10.1371/journal.ppat.1006095
226. Maekawa M, Yang Y, Fairn GD. Perfringolysin O theta toxin as a tool to monitor the distribution and inhomogeneity of cholesterol in cellular membranes. *Toxins (Basel)* (2016) 8(3):67. doi:10.3390/toxins8030067
227. Diep DB, Nelson KL, Raja SM, Pleshak EN, Buckley JT. Glycosylphosphatidylinositol anchors of membrane glycoproteins are binding determinants for the channel-forming toxin aerolysin. *J Biol Chem* (1998) 273(4):2355–60. doi:10.1074/jbc.273.4.2355
228. Hoglinger D, Nadler A, Haberkant P, Kirkpatrick J, Schifferer M, Stein F, et al. Trifunctional lipid probes for comprehensive studies of single lipid species in living cells. *Proc Natl Acad Sci U S A* (2017) 114(7):1566–71. doi:10.1073/pnas.1611096114

Conflict of Interest Statement: The authors declare that the research was conducted in the absence of any commercial or financial relationships that could be construed as a potential conflict of interest.

Copyright © 2017 Teng, Ang and Guan. This is an open-access article distributed under the terms of the Creative Commons Attribution License (CC BY). The use, distribution or reproduction in other forums is permitted, provided the original author(s) or licensor are credited and that the original publication in this journal is cited, in accordance with accepted academic practice. No use, distribution or reproduction is permitted which does not comply with these terms.

frontiers in Immunology

ORIGINAL RESEARCH
published: 19 January 2018
doi: 10.3389/fimmu.2018.00002

Mycobacterial Phenolic Glycolipids Selectively Disable TRIF-Dependent TLR4 Signaling in Macrophages

*Reid Oldenburg[1,2], Veronique Mayau[1], Jacques Prandi[3], Ainhoa Arbues[3], Catherine Astarie-Dequeker[3], Christophe Guilhot[3], Catherine Werts[4], Nathalie Winter[5,6] and Caroline Demangel[1]**

[1] Unité d'Immunobiologie de l'Infection, INSERM U1221, Institut Pasteur, Paris, France, [2] Université Paris Diderot, Paris, France, [3] Institut de Pharmacologie et de Biologie Structurale (IPBS), Université de Toulouse, CNRS, UPS, Toulouse, France, [4] Unité de Biologie et Génétique de la Paroi Bactérienne, Institut Pasteur, Paris, France, [5] INRA, UMR 1282 Infectiologie et Santé Publique, Nouzilly, France, [6] Université François Rabelais, Tours, France

Phenolic glycolipids (PGLs) are cell wall components of a subset of pathogenic mycobacteria, with immunomodulatory properties. Here, we show that in addition, PGLs exert antibactericidal activity by limiting the production of nitric oxide synthase (iNOS) in mycobacteria-infected macrophages. PGL-mediated downregulation of iNOS was complement receptor 3-dependent and comparably induced by bacterial and purified PGLs. Using *Mycobacterium leprae* PGL-1 as a model, we found that PGLs dampen the toll-like receptor (TLR)4 signaling pathway, with macrophage exposure to PGLs leading to significant reduction in TIR-domain-containing adapter-inducing interferon-β (TRIF) protein level. PGL-driven decrease in TRIF operated posttranscriptionally and independently of Src-family tyrosine kinases, lysosomal and proteasomal degradation. It resulted in the defective production of TRIF-dependent IFN-β and CXCL10 in TLR4-stimulated macrophages, in addition to iNOS. Our results unravel a mechanism by which PGLs hijack both the bactericidal and inflammatory responses of host macrophages. Moreover, they identify TRIF as a critical node in the crosstalk between CR3 and TLR4.

Keywords: mycobacteria, phenolic glycolipids, macrophages, TRIF, TLR4, iNOS

OPEN ACCESS

Edited by:
Christoph Hölscher, Forschungszentrum Borstel (LG), Germany

Reviewed by:
Roland Lang, Universitätsklinikum Erlangen, Germany
John T. Belisle, Colorado State University, United States

****Correspondence:***
Caroline Demangel
caroline.demangel@pasteur.fr

Specialty section:
This article was submitted to Microbial Immunology, a section of the journal Frontiers in Immunology

Received: *03 September 2017*
Accepted: *03 January 2018*
Published: *19 January 2018*

Citation:
Oldenburg R, Mayau V, Prandi J, Arbues A, Astarie-Dequeker C, Guilhot C, Werts C, Winter N and Demangel C (2018) Mycobacterial Phenolic Glycolipids Selectively Disable TRIF-Dependent TLR4 Signaling in Macrophages. Front. Immunol. 9:2. doi: 10.3389/fimmu.2018.00002

INTRODUCTION

Phenolic glycolipids (PGLs) are polyketide synthase products that are only synthesized by a subset of pathogenic mycobacteria, including the W-Beijing family of *Mycobacterium tuberculosis* strains and *Mycobacterium leprae* (1–3). In structure, these phenolphtiocerol dimycocerosates (DIMs) share a common phenolic lipid backbone that is decorated with species-specific oligosaccharide moieties (Figure S1 in Supplementary Material). PGL from *M. tuberculosis* (PGL-tb) inhibited the inflammatory cytokine responses of mycobacteria-infected macrophages, suggesting that it mediates the virulence of W-Beijing strains by suppressing host innate immune responses (4). While the association between PGL-tb and mycobacterial virulence later appeared more complex, the anti-inflammatory activity of PGL-tb was confirmed, using naturally deficient *M. tuberculosis* strains that were genetically engineered to express PGL-tb (5). In line with these results, synthetic analogs of PGL-tb and *M. leprae* PGL-1 inhibited toll-like receptor (TLR)2-driven production of inflammatory cytokines and nitric oxide (NO) by macrophages (2, 6, 7). Since PGL-1 bound to immobilized TLR2 in solid-phase assays, it was proposed that PGL-1 and PGL-tb can act as TLR2 antagonists (2).

Whether this mechanism is sufficient to explain the cytokine production defects of macrophages infected with PGL-expressing mycobacteria was not addressed.

In parallel, it was reported that recombinant *Mycobacterium bovis* BCG (rBCG) expressing PGL-1 instead of its native PGL (PGL-bov) exploit complement receptor (CR)3 for invasion of macrophages (2, 8). CR3, also known as Mac-1, CD11b/CD18, and αMβ2 integrin, is a widely expressed heterodimeric surface receptor, which in macrophages contributes to microbial pattern recognition and phagocytosis. CR3 is known to mediate the opsonic and non-opsonic uptake of *M. tuberculosis* and *M. leprae* by macrophages (9–11), *via* its complement-binding I-domain and its carbohydrate-binding lectin domain, respectively (12, 13). Based on biochemical evidence, the increased infectivity of PGL-1-expressing BCG was attributed to a selective interaction between its trisaccharide moiety and the lectin domain of CR3 (2). Of note, PGL-1-mediated phagocytosis required the Src-family kinase Lyn, a known mediator of β_2-integrin signal transduction in macrophages (2, 14). In addition to promote macrophage invasion, PGL-1 increased the long-term survival of BCG within macrophages by a mechanism that remained unclear (8).

In the present work, we sought to determine if and how PGLs interfere with the bactericidal functions of macrophages. We found that PGLs limit the capacity of activated macrophages to induce nitric oxide synthase (iNOS) and generate NO upon mycobacterial infection, by downregulating the TLR4 adapter TIR-domain-containing adapter-inducing interferon-β (TRIF). In addition to suppressing iNOS production, PGLs decreased the TLR4-induced production of TRIF-dependent cytokines and chemokines. Our results thus provide a mechanism for both the immunomodulatory and virulence properties of PGLs. They support the general concept that PGL production was evolved by pathogenic mycobacteria to enhance intracellular survival and immune evasion.

MATERIALS AND METHODS

Reagents

PGL-bov and DIMs were purified from bacterial cell pellets of *M. bovis* BCG and *Mycobacterium canettii*, respectively, as previously described (2). PGL-tb from *M. canettii* (#NR-36510) and PGL-1 from *M. leprae*-infected armadillos (#NR-19342) were obtained from BEI resources (https://www.beiresources.org/). Working solutions of lipids were prepared as follows: PGLs were dissolved in ethanol; DIMs were first recovered in a small volume of chloroform, before being added to water, then sonicated until complete suspension. These solutions were diluted >200 times in cell culture medium for cellular assays and compared to equivalent volumes of vehicle. Ultrapure LPS from *E. coli*, serotype O55:B5, TLR grade (#ALX-581-013-L001) was purchased from Enzo Life Sciences. Recombinant mouse IFN-γ (#PMC4031) and TNF-α (#PMC3014) were purchased from ThermoFisher Scientific. InSolution™ PP2 Src inhibitor (#529576) and ALLN (#208719) were from Calbiochem Merck Millipore, and chloroquine diphosphate salt (#C6628) from Sigma.

Cell Cultures

Bone marrow-derived macrophage (BMDM) progenitors were obtained by flushing mouse femurs and tibias, followed by erythrocyte lysis with red blood cell lysis buffer (#B00003, Roche). BMDMs were obtained by a 7-day differentiation of progenitors in RPMI 1640 GlutaMAX™ medium (#61870-010, ThermoFisher Scientific) supplemented with 10% heat-inactivated fetal calf serum (#A15-102, PAA) and 10% L929-conditioned medium as a source of M-CSF [hereafter called complete medium (CM)]. THP-1 human monocytes (ATCC, TIB-202) were cultured in RPMI supplemented with 10% heat-inactivated fetal calf serum, penicillin, and streptomycin (#15140122, ThermoFisher Scientific). They were differentiated into macrophages by addition of 2 ng/ml phorbol 12-myristate 13-acetate (#P8139, Sigma) for 3 days.

Mycobacteria Cultures and Cell Infection

Methods used to generate the PGL-expressing rBCGs used in this study and experimental validation that they grow comparably and express equivalent amounts of heterologous PGLs were reported previously (2, 8). Bacteria were grown at 37°C in suspension in Middlebrook 7H9 broth (#M0178) supplemented with ADC (#M0553) and 40 µg/ml kanamycin (#K0254), all from Sigma. Mycobacterial suspensions destined to infect BMDMs were pelleted at (3,200 × *g*) for 7 min, washed twice with phosphate-buffered saline (PBS), suspended in 5 ml of PBS before dissociation in M-tubes using the gentleMACS Dissociator (Miltenyi Biotec), then diluted in RPMI to the appropriate concentration. Before infection, BMDMs were washed twice with warm RPMI, followed by a 2 h infection in RPMI. BMDMs were washed twice again with warm RPMI, then incubated in complete CM.

NO Quantification

Bone marrow-derived macrophages were cultured at 2×10^5 cells per well in black clear-bottomed cell culture microplates (Greiner Bio-One International) for 24 h and infected or treated as indicated. Cells were washed once with warm PBS before addition of 5 µM 4,5-diaminofluorescein diacetate (#D225, Sigma), a cell permeable fluorescent dye for NO detection (15, 16), and incubation at 37°C in the dark. Fluorescence was measured using a fixed gain setting each hour for 5 h using a BMG FLUOstar OPTIMA Microplate reader (BMG Labtech) with emission and excitation wavelengths of 485 and 520 nm, respectively. In order to normalize cell number, BMDMs were subsequently stained with 0.05% crystal violet (#C0775, Sigma) in 2% ethanol for 15 min followed by four washes with PBS. Dye was then dissolved in methanol and absorbance was measured at 550 nm. All values were set as a fold change ratio to averaged value of unstimulated group.

Flow Cytometry

Adherent mouse BMDMs were detached with accutase (#A6964, Sigma) for 20 min at 37°C and blocked with FcR Blocking reagent (#130-092-575, Miltenyi Biotec) for 15 min at 4°C. Antibodies used in flow cytometry were anti-CD11b (M1/70), anti-CD11c (HL3), anti-CD86 (GL1), anti-CD40 (HM40-3) from BD Biosciences; anti-TLR4 (MTS510) from Biolegend; anti-IFNGR1

(2E2) from eBioscience; anti-iNOS (M-19) from SCT and anti-goat AlexaFluor 647 Donkey (polyclonal IgG H&L) from Abcam (#ab150131). For intracellular staining of iNOS, macrophages were fixed with BD Lyse/Fix solution (#558049) for 10 min at 37°C, then permeabilized with BD Perm Buffer III (#558050) for 20 min at 4°C prior to antibody staining. Flow cytometric acquisitions were performed on a BD FACS Accuri C6 and data were analyzed using FlowJo software.

Immunoblot Analysis and ELISA

Bone marrow-derived macrophages ($1–3 \times 10^6$) were washed and scraped in cold PBS, centrifuged, and then lysed in ice cold lysis buffer (20 mM Tris, 150 mM NaCl, 1mM EGTA, 1mM $MgCl_2$, 1% *n*-Dodecyl-(β)-D-maltoside (#D4641), 4 mM sodium orthovanadate (#S6508), 50 mM NaF (#S6776), 10 µg/ml leupeptin (#L2884), 10 µg/ml aprotinin (#10820), 1 mM Pefabloc-sc (A8456)), all purchased from Sigma, for 15 min. Protein concentration was quantified with NanoDrop Light SpectroPhotometer (Thermo Fisher Scientific). Cell lysates were resolved on NuPAGE Bis-Tris gels and transferred to nitrocellulose membranes (ThermoFisher Scientific). Protein detections used the following antibodies: MyD88 (#3699), Phospho-Src (Tyr416, #2101), GAPDH (#2118), all from CST, and Ticam-1 (TRIF, #657102, Biolegend). Detection of pSrc (MW 60 kDa), MyD88 (MW 33 kDa), TRIF (MW 98 kDa), and GAPDH (MW 37 kDa) was performed in a single Western blot assay using multiple antibodies. Before using this technique, we verified that our antibodies were specific (data not shown). When only TRIF and GAPDH were analyzed, blots were sliced horizontally after transfer, then stained separately in order to capture images at optimal exposure times. Protein complexes were revealed with the ECL Prime detection reagent (GE Healthcare) and chemiluminescence reading on a Fuji LAS-4000 Luminescent Image Analyzer. IFN-β and TNF-α concentrations in BMDM culture supernatants were measured by ELISA (Biolegend, #439407 and #430901), following the manufacturer's protocol.

RNA Extraction and Real-time Quantitative RT-PCR

Qiagen RNeasy Mini Kit (#74104) was used to extract total RNA from BMDMs. cDNA was amplified from 1 µg of total RNA using the high-capacity cDNA reverse transcription kit with added RNAse inhibitor (#4374966, Applied Biosystems). Relative mRNA levels were quantified by qRT-PCR using power SYBR green and with gene-specific primers (**Table 1**). Amplification conditions and dissociation step were as follows: 50°C for 2 min, 95°C for 10 min followed by 40 cycles (95°C for 15 s and 60°C for 1 min). ABI 7300 Sequence Detection System (Applied Biosystems) was used for data acquisition. Fold increase values were calculated for each gene transcript using the $2^{-\Delta\Delta Ct}$ method, using RPL19 as a house-keeping gene.

Mice

C57BL/6J (JAX™) and Itgam$^{-/-}$ (B6.129S4-Itgamtm1Myd/J) mice were obtained from Charles River and Jackson Laboratories, respectively. TRIF$^{LPS2/LPS2}$ mice [C57BL/6J—Ticam1^{Lps2} (22)] were originally from B. Beutler et al. (The Scripps Research Institute, CA, USA) and back-crossed into the C57BL/6J background at Institut Pasteur. TLR2$^{-/-}$ [B6.Cg-Tlr2^{tm1Aki} (23)] and MyD88$^{-/-}$ [B6.129-Myd88^{tm1Aki} (24)] mice were obtained from S. Akira (Osaka University, Japan). All animals were bred and housed under pathogen-free conditions in our animal facilities with food and water *ad libitum*. Transgenic mice were used between 6 and 10 weeks of age, with age and sex-matched wild-type controls. Since we only used mice as a source of bone marrow, the described experiments did not require approval from the French Ministry of Higher Education and Research. They were performed in compliance with the European Communities Council Directive of 22 September 2010 on the approximation of laws, regulations, and administrative provisions of the Member States regarding the protection of animals used for scientific purposes.

TABLE 1 | Primers used in the qRT-PCR analysis.

Gene	Primers (5′–3′)
Nos2 (17)	ACATCGACCCGTCCACAGTAT
	CAGAGGGGTAGGCTTGTCTC
Arg1 (17)	CTCCAAGCCAAAGTCCTTAGAG
	AGGAGCTGTCATTAGGGACATC
Cxcl10 (18)	GGATCCCTCTCGCAAGGA
	ATCGTGGCAATGATCTCAACA
Ifnb1 (19)	CCCTATGGAGATGACGGAGA
	ACCCAGTGCTGGAGAAATTG
Il6 (20)	AGTTGCCTTCTTGGGACTGA
	TCCACGATTTCCCAGAGAAC
Cebpb (21)	GGAGACGCAGCACAAGGT
	AGCTGCTTGAACAAGTTCCG
Tnf (17)	CTGGGACAGTGACCTGGACT
	GCACCTCAGGGAAGAGTCTG

Statistical Analysis

Statistical analyses were performed with the *StatView*® 5 software (SAS Institute, Inc.). The Prism software (5.0d) was used for graphical representation.

RESULTS

PGLs Inhibit Infection-Induced Production of iNOS and NO in Activated Macrophages

Following infection with mycobacteria and the early activation of innate immunity, T cells are stimulated to produce IFN-γ. This cytokine induces the expression of iNOS in infected macrophages, with subsequent production of NO efficiently controlling the growth of intracellular bacteria (25–28). To see if PGLs affect NO production in activated macrophages, we compared intracellular levels of iNOS in BMDMs infected with recombinant BCG expressing PGLs (rBCG:PGLs), or PGL-deficient BCGs (rBCG:no PGL) as control, in the presence of IFN-γ. **Figure 1A** shows that rBCG:bov, rBCG:PGL-1, and rBCG:PGL-tb all elicited less iNOS than rBCG:no PGL in infected macrophages. Consistently, the production of NO was lower in cells infected with any of the PGL-expressing strains, compared to those infected with PGL-deficient rBCG (**Figure 1B**). Importantly, addition of soluble

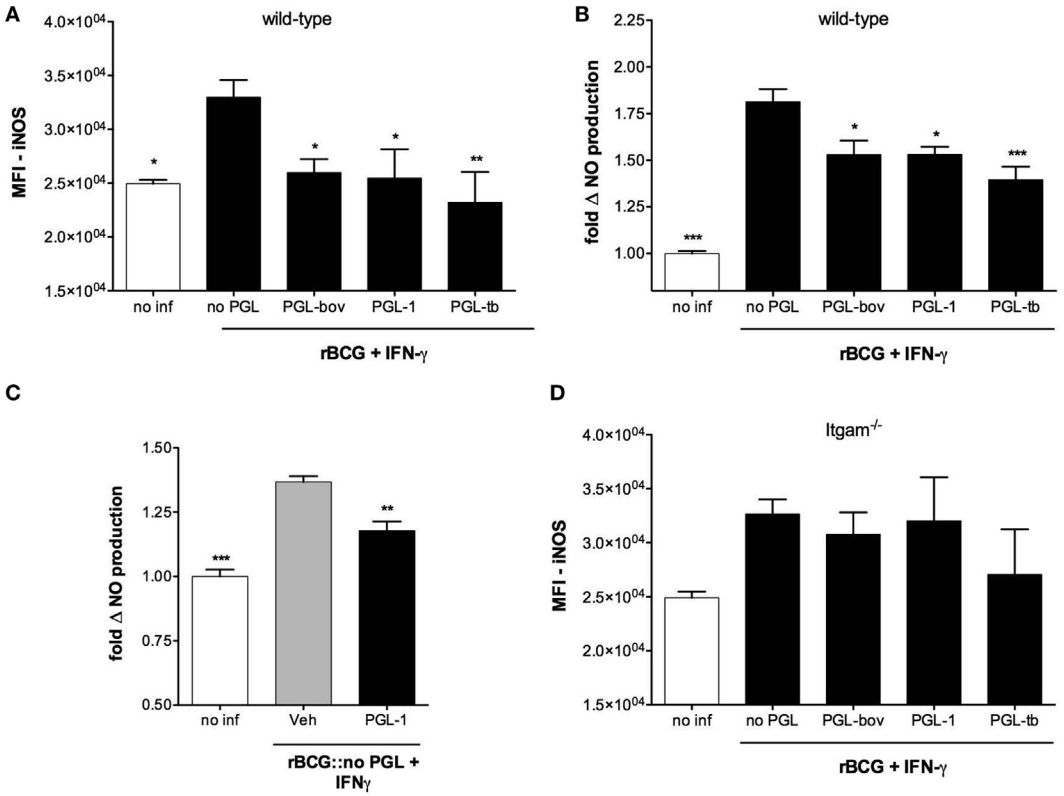


FIGURE 1 | Phenolic glycolipids (PGLs) inhibit infection-induced production of iNOS and NO in activated macrophages. **(A)** Differential induction of iNOS in bone marrow-derived macrophage (BMDMs) infected with rBCG:no PGL, rBCG:PGL-bov, rBCG:PGL-1 or rBCG:PGL-tb, or non-infected BMDMs (no inf), as determined by intracellular detection of iNOS using flow cytometry. BMDMs were infected for 2 h at a MOI of 1:1, then washed and cultivated in the presence of 100 U/ml IFN-γ for 48 h. Data are mean fluorescence intensities (MFI) ± SEM ($n = 3$). **(B)** Differential production of NO in the same conditions as in **(A)**. Data are mean NO levels ± SEM ($n = 8$), expressed as fold changes relative to non-infected controls (no inf). **(C)** NO production by BMDMs pretreated with 25 μM PGL-1 or ethanol vehicle (Veh) for 24 h prior to 48 h of infection with rBCG:no PGL at a MOI of 1:1 in the presence of 100 U/ml IFN-γ. **(D)** as in **(A)** in Itgam$^{-/-}$ BMDMs. Data shown are from one experiment repeated twice with similar results. *$P < 0.05$, **$P < 0.01$, ***$P < 0.001$, following statistical comparison by repeated measures ANOVA with Tukey *post hoc* test, relative to rBCG:no PGL.

PGL-1 to BMDMs was sufficient to reduce the cell production of NO upon infection with PGL-deficient rBCG (**Figure 1C**).

Since PGL-1 was previously reported to interact with CR3, we tested the potential involvement of this receptor in PGL-mediated inhibition of iNOS and NO production, using CD11b-deficient (Itgam$^{-/-}$) macrophages. PGL-expressing rBCGs induced comparable production of iNOS as PGL-deficient BCG in Itgam$^{-/-}$ macrophages, implying that CR3 is involved (**Figure 1D**). Together, these data suggested that PGLs have the intrinsic capacity to suppress the infection-induced production of NO in activated macrophages, by a mechanism involving CR3.

PGLs Reduce the LPS/IFN-γ-Induced Production of iNOS in a CR3-Dependent Manner

Induction of iNOS requires the cooperative activation of the JAK–STAT and pattern recognition receptor signaling pathways (29). To gain insight into the mechanism by which PGLs down-regulate iNOS in mycobacteria-infected macrophages, we next tested if PGLs affected NO production in BMDMs stimulated with IFN-γ and the TLR4 agonist LPS. PGL-1 added to macrophages at a concentration superior to 12 μM prior to stimulation with LPS/IFN-γ indeed caused a dose-dependent reduction in NO production (**Figure 2A**). Notably, NO decrease was not observed if cells were treated with PGL-1 at the time of LPS/IFN-γ stimulation, and required a preincubation with PGL-1 of at least 6 h (Figure S2A in Supplementary Material). PGL-tb was equivalent to PGL-1 in its capacity to decrease the LPS/IFN-γ-stimulated production of iNOS by BMDMs (**Figure 2B**). In contrast, phthiocerol DIMs, which correspond to PGLs devoid of phenol ring and oligosaccharide domains (Figure S1 in Supplementary Material) had no inhibitory effect on NO production in the same conditions of cell pretreatment and stimulation (**Figure 2C**). This indicated that the lipid backbone of PGLs is not sufficient to inhibit the LPS/IFN-γ-induced production of iNOS.

Consistent with our data in **Figure 1**, the inhibitory activity of PGL-1 on LPS/IFN-γ-mediated production of NO correlated with a significant decrease in iNOS (**Figure 2D**) and required BMDM expression of CR3 (**Figure 2E**). Since PGL-1 binds to TLR2 *in vitro* and decreases the TLR2-induced production of cytokines and NO by human macrophages (2, 6, 7, 30), we next

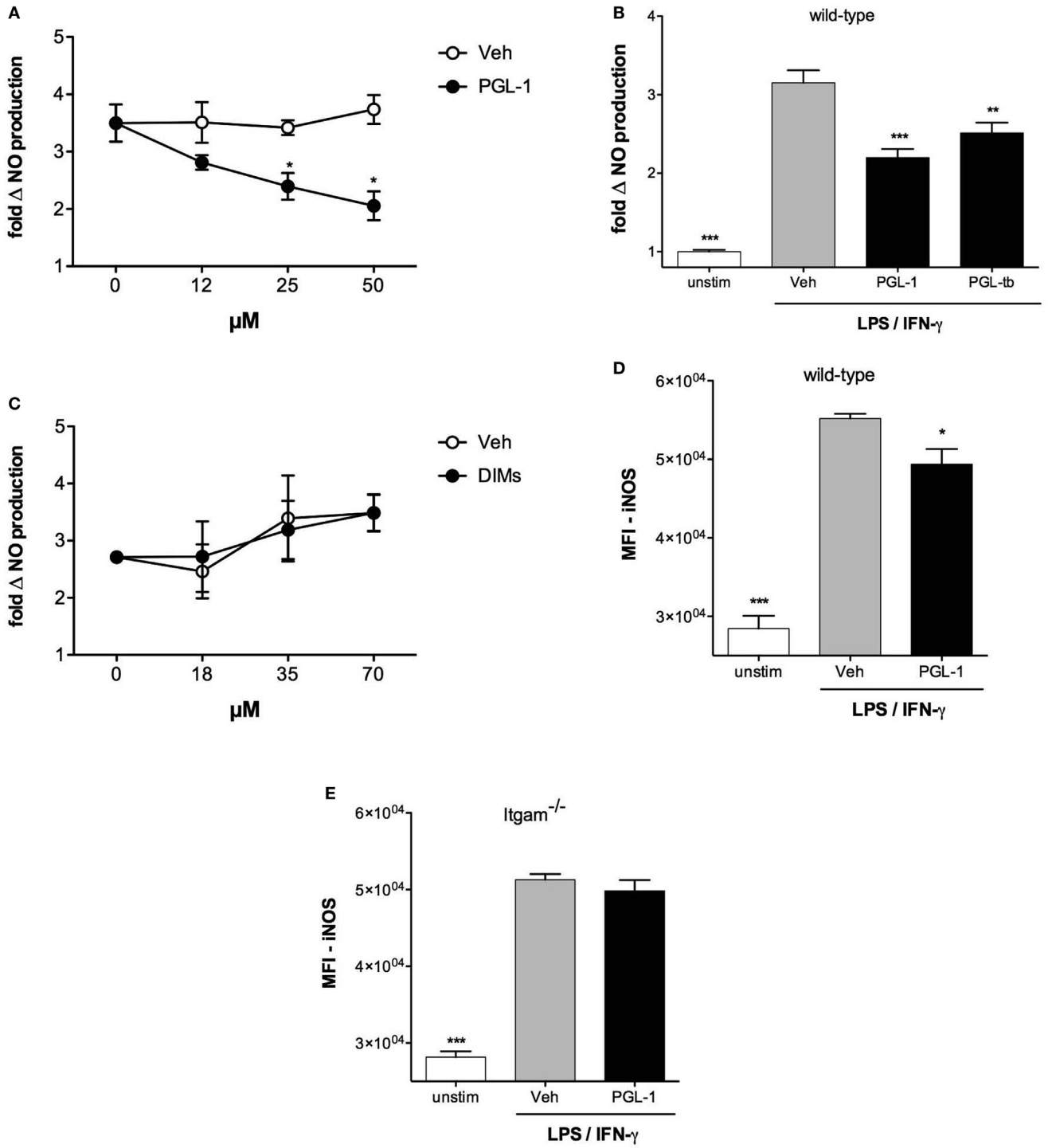


FIGURE 2 | Phenolic glycolipids (PGLs) reduce LPS/IFN-γ-induced production of iNOS in a CR3-dependent manner. **(A)** Differential production of NO by bone marrow-derived macrophages (BMDMs) pretreated with increasing concentrations of PGL-1 or vehicle (Veh) for 24 h prior to a 24 h stimulation with 1 μg/ml LPS and 100 U/ml IFN-γ. Data are mean NO levels ± SEM ($n = 4$), expressed as fold changes relative to non-treated, stimulated controls. *$P < 0.05$, Mann–Whitney test comparing PGL-1-treated to vehicle controls at each concentration. **(B)** As in **(A)** with 25 μM PGL-1 or 25 μM PGL-tb; unstim: non-treated, non-stimulated controls. **(C)** As in **(A)**, with increasing concentrations of dimycocerosates (DIMs). **(D)** Differential induction of iNOS in BMDMs exposed to 25 μM PGL-1 or vehicle (Veh) for 24 h prior to a 24 h stimulation with LPS/IFN-γ. Controls are non-treated, non-stimulated cells (unstim). Data are mean fluorescence intensities (MFI) ± SEM ($n = 3$). **(E)** As in **(D)** in Itgam$^{-/-}$ BMDMs. Data shown are from one experiment repeated twice with similar results. Statistical comparisons in **(B,D,E)** were performed with repeated measures ANOVA with Tukey *post hoc* test, relative to the vehicle-treated, LPS/IFN-γ-stimulated group. *$P < 0.05$, **$P < 0.01$, ***$P < 0.001$.

tested if TLR2 was involved in the observed effects. Decreased production of iNOS and NO was maintained in PGL-1-treated, LPS/IFN-γ-stimulated TLR2-deficient BMDMs (Figures S2B,C in Supplementary Material), ruling out this possibility. We concluded that PGLs suppress the LPS/IFN-γ-induced induction of iNOS in a CR3-dependent and TLR2-independent manner.

PGLs Impair TLR4-Mediated Downstream Signaling Pathways

We next sought to determine which of the TLR4 and IFN-γ receptor (IFNGR) signaling pathways was targeted by PGLs. BMDMs were stimulated with LPS/IFN-γ or TNF-α/IFN-γ, two combinations of reagents leading to significant production of NO. **Figure 3A** shows that PGL-1 only decreased the NO production of LPS/IFN-γ-stimulated cells, suggesting that PGLs interfere with TLR4 signaling independently of IFN-γ. Consistently, PGL-1 treatment did not alter the levels of total and Tyr701-phosporylated Stat1 in BMDMs stimulated with IFN-γ (data not shown). Surface expression of TLR4, IFN-γ receptor 1, or CD11b was not altered by PGL-1 treatment of BMDMs (Figure S3 in Supplementary Material), implying that PGL-1 interferes with signaling events downstream of TLR4. Since TLR4 uses two adaptor proteins (MyD88 and TRIF), we examined if they equally contribute to TLR4-induced production of NO. We used BMDMs generated from MyD88$^{-/-}$, TRIF$^{Lps2/Lps2}$, or double knock-out (DKO) mice. **Figure 3B** shows that LPS/IFN-γ-stimulated production of NO was strictly mediated by TRIF. Notably, PGL-1-mediated inhibition of LPS/IFN-γ-stimulated production of NO was lost in MyD88$^{-/-}$ BMDMs (**Figure 3B**). Comparable findings were

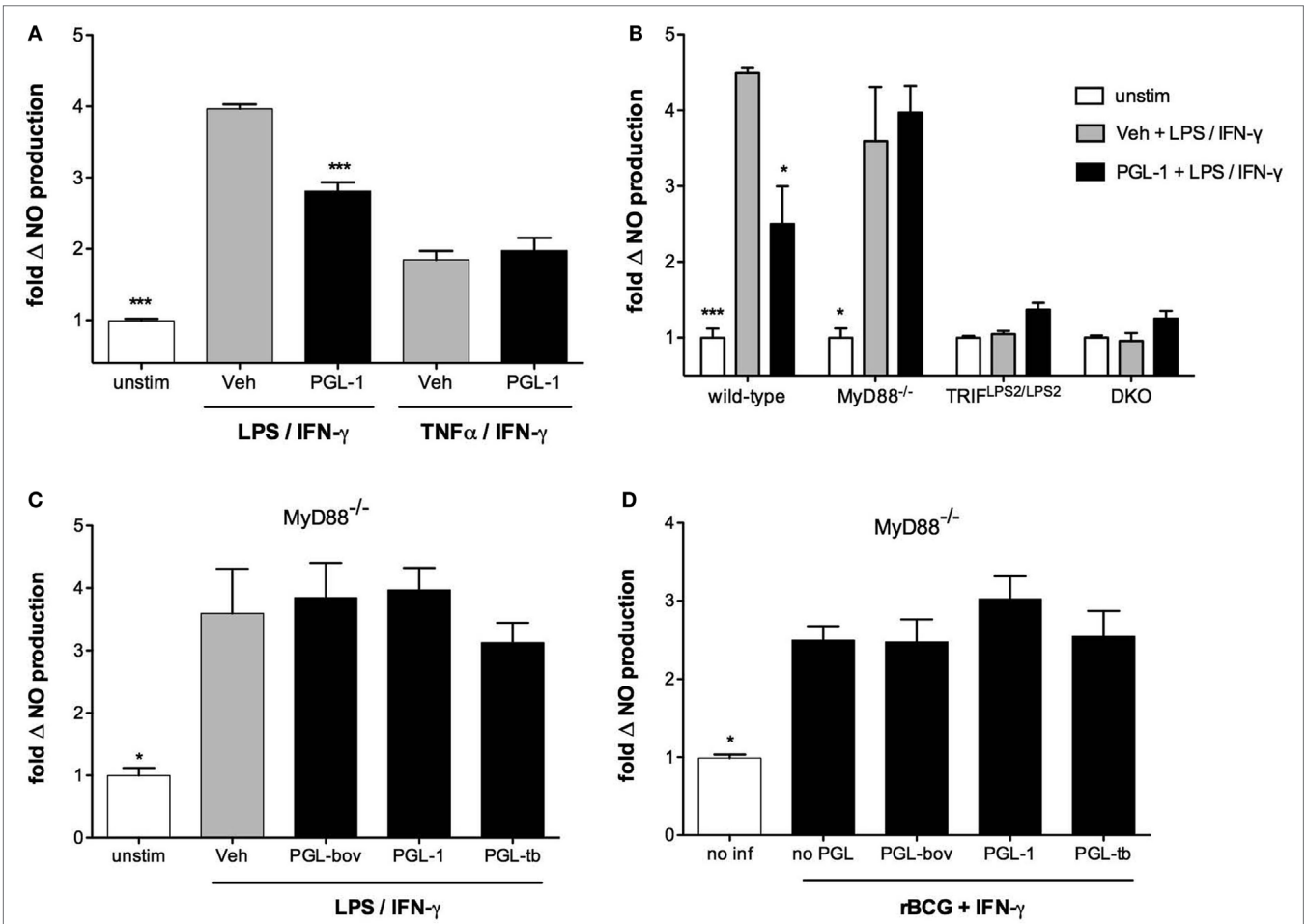


FIGURE 3 | Phenolic glycolipids (PGLs) impair TLR4-mediated downstream signaling pathways. **(A)** Differential production of NO by bone marrow-derived macrophages (BMDMs) pretreated with 25 μM PGL-1 or vehicle (Veh) for 24 h prior to a 24 h stimulation with 1 μg/ml LPS + 100 U/ml IFN-γ, or 10 ng/ml TNF-α + 100 U/ml IFN-γ. ***$P < 0.001$, Mann–Whitney test, comparing PGL-1-treated to vehicle controls in each condition of cell stimulation. **(B)** Differential production of NO by wild-type, MyD88$^{-/-}$, TRIF$^{Lps2/Lps2}$, or DKO BMDMs treated with 25 μM PGL-1 or vehicle (Veh) for 24 h prior to a 24 h stimulation with 1 μg/ml LPS + 100 U/ml IFN-γ. Controls include non-treated, non-stimulated cells (unstim). **(C)** Differential production of NO by MyD88$^{-/-}$ BMDMs treated with 25 μM PGL-bov, 25 μM PGL-1, 25 μM PGL-tb, or vehicle (Veh) for 24 h prior to a 24 h stimulation with LPS/IFN-γ. **(D)** Differential production of NO by MyD88$^{-/-}$ BMDMs infected with rBCG:no PGL, rBCG:PGL-bov, rBCG:PGL-tb, or rBCG:PGL-1 at a MOI of 5:1, or non-infected (no inf). In **(B–D)**, data are mean NO levels ± SEM ($n \geq 3$), expressed as fold changes relative to non-stimulated (unstim) or non-infected (no inf) controls. Data shown are from one experiment repeated twice with similar results. *$P < 0.05$, **$P < 0.01$, ***$P < 0.001$, repeated measures ANOVA with Tukey *post hoc* test, relative to vehicle or no PGL controls.

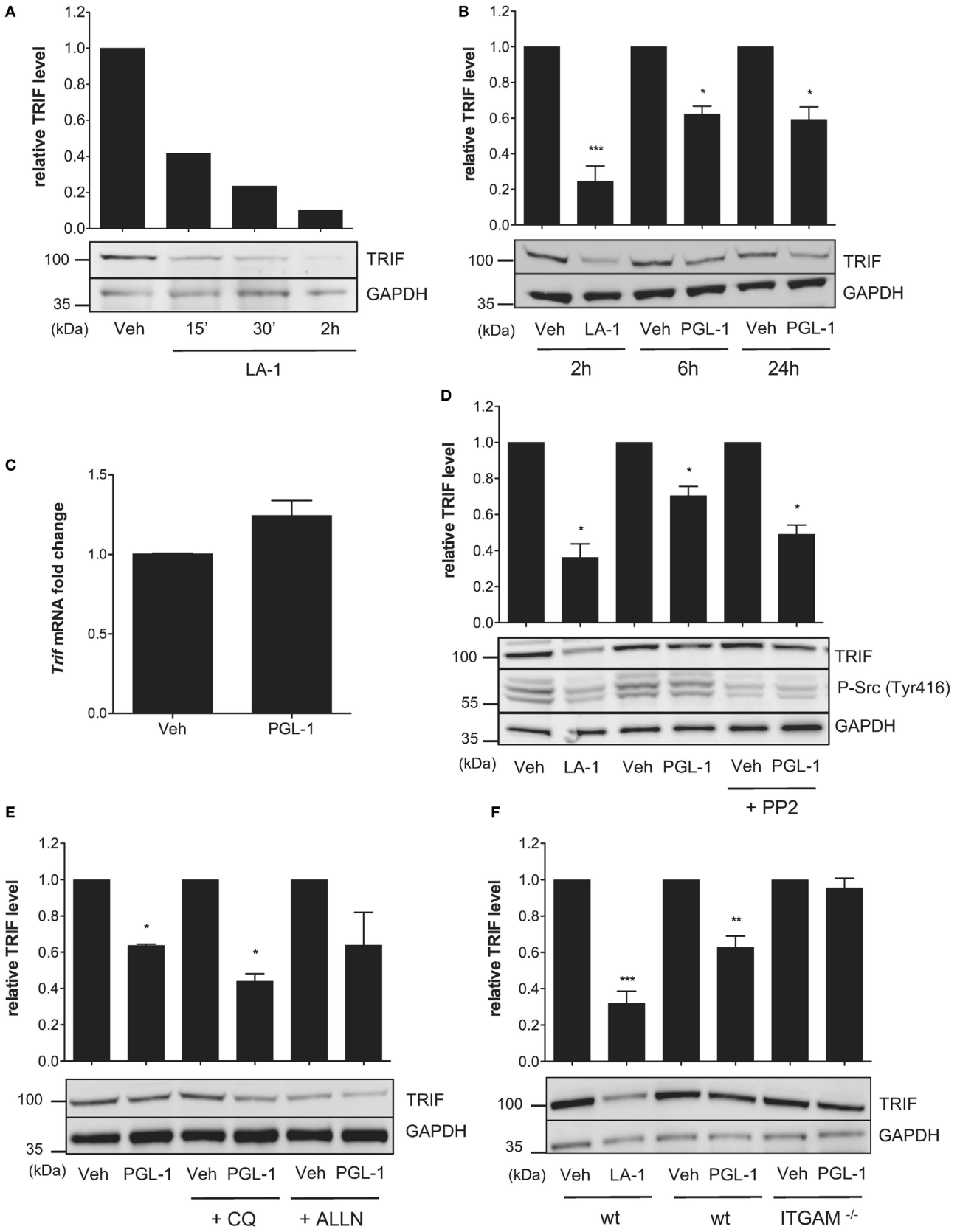


FIGURE 4 | Continued

FIGURE 4 | Phenolic glycolipid (PGL)-1 binding to CR3 downregulates TRIF protein levels. **(A)** Western blot analysis of TRIF with GAPDH as loading control, in bone marrow-derived macrophages (BMDMs) treated with 15 μM leukadherin (LA)-1 or DMSO vehicle (Veh) for the indicated times with relative quantification of TRIF levels. **(B)** Same as in **(A)**, for BMDMs treated for the indicated times with 15 μM LA-1 or 25 μM PGL-1, or their respective solvents (Veh). **(C)** Quantitation of *TRIF* mRNAs in BMDMs treated with 25 μM PGL-1 or vehicle (Veh) for 6 h. Data are mean transcript levels ± SEM ($n = 4$), expressed as fold changes relative to vehicle controls. They are representative from three independent experiments with similar results. **(D)** Relative TRIF levels in BMDMs treated with 15 μM LA-1 for 2 h, or 25 μM PGL-1 for 6 h in the presence or absence of 10 μM PP2 (Veh); **(E)** in BMDMs pretreated with 50 μM chloroquine (CQ) or calpain inhibitor (ALLN) for 2 h prior to a 24 h exposure to 25 μM PGL-1; **(F)** in wild-type (wt) or ITGAM$^{-/-}$ BMDMs treated with 15 μM LA-1 for 2 h, or 25 μM PGL-1 for 24 h. Data in **(B,D,E,F)** are mean band intensities ± SEM from two to five independent experiments, with one representative blot picture.

obtained with PGL-tb and PGL-bov (**Figure 3C**). In contrast to wild-type BMDMs (**Figure 1A**), infection of MyD88$^{-/-}$ BMDMs with PGL-expressing rBCGs did not alter their relative production of NO (**Figure 3D**). Together, these data in **Figure 3** thus suggest that PGLs decrease TRIF-dependent production of NO in a MyD88-dependent manner.

PGL-1 Downregulates TRIF Protein Levels

TLR4-driven inside–out activation of CR3 was previously shown to dampen TLR4 signaling in BMDMs through a negative feedback mechanism involving Src-mediated degradation of MyD88 and TRIF by the ubiquitin:proteasome system (31). In parallel, it was reported that Leukadherin (LA)-1, a CR3 agonist, downregulates MyD88 protein levels in TLR7/8-stimulated THP-1 macrophages (32). We hypothesized that CR3 engagement by PGLs may affect TLR4 signaling in macrophages by interfering with endogenous levels of MyD88 and/or TRIF. Consistent with previous work, MyD88 levels were decreased in BMDMs treated with LA-1 (Figure S4A in Supplementary Material). Notably, the inhibitory activity of LA-1 on MyD88 levels was modest in comparison to that on TRIF. A 2 h treatment of BMDMs with 15 μM LA-1 indeed provoked >90% reduction in TRIF protein levels (**Figure 4A**). A comparable decrease was seen in human THP-1 macrophages treated with LA-1 (Figure S4B in Supplementary Material). Exposing BMDMs or THP-1 cells to 25 μM PGL-1 for >6 h led to similar effects, although maximal downregulation of TRIF by PGL-1 reached a plateau at 50% (**Figure 4B**; Figure S4B in Supplementary Material). In contrast, PGL-1 had no major effects on MyD88 levels (Figure S4C in Supplementary Material).

PGL-1 treatment did not alter the level of TRIF transcripts in BMDMs, indicating that PGL-1-mediated decrease in TRIF protein levels operates at a posttranscriptional level (**Figure 4C**). It was maintained in the presence of the Src family tyrosine kinase inhibitor PP2 (**Figure 4D**), suggesting that PGL-1 operates independently of Src activation. We tested if PGL-1-driven reduction in TRIF depended on lysosomal or proteasomal degradation using chemical inhibitors of these pathways, but no significant restoration of TRIF levels could be observed (**Figure 4E**). Notably, PGL-1-mediated decrease in TRIF was not detected in Itgam$^{-/-}$ BMDMs, further illustrating the involvement of CR3 in this process (**Figure 4F**).

PGL-1-Mediated Decrease in TRIF Impairs Downstream Signaling Events

We next investigated to what extent PGL-1-driven decrease in TRIF protein level altered TLR4 signaling events in activated macrophages. Consistent with our data in **Figures 1** and **2**, pretreating BMDMs with PGL-1 for 24 h prior to LPS/IFN-γ stimulation durably suppressed *Nos2* transcription (**Figure 5A**). Expression of Arginase 1 (*Arg1*), which competes with iNOS for arginine, does not depend on TRIF. **Figure 5B** shows that contrary to *Nos2*, the LPS/IFN-γ-induced transcription of *Arg1* was not modified by PGL-1 pretreatment. Similarly, expression of MyD88-dependent IL-6 (*Il6*) and M2-inducer CEBPB (*Cebpb*) in LPS/IFN-γ-stimulated BMDMs were not impacted by pre-exposure to PGL-1 (as shown for IL-6 in **Figure 5C**). In contrast, the level of CXL10 (*Cxcl10*) transcripts, which relies on TRIF-IRF3 signaling, was significantly reduced by PGL-1 pretreatment in BMDMs stimulated with LPS/IFN-γ for 6 h (**Figure 5D**). Although statistical significance was not reached, a similar trend was observed with the expression of the TRIF-dependent cytokine IFN-β (*Ifnb1*) (**Figure 5E**). By measuring IFN-β concentration in culture supernatants, we could confirm that PGL-1 pretreatment reduces significantly the ability of BMDMs to produce IFN-β in response to TLR4 stimulation (**Figure 5G**). In comparison, gene and protein expression of TNF-α (*Tnf*), which depend on both the MyD88 and TRIF pathways, were minimally affected (**Figures 5F–H**).

DISCUSSION

We report in the present work that exposure of macrophages to mycobacterial PGLs affects the integrity of their TLR4 signaling pathway. Using PGL-1 as a model, we show that PGLs operate by selectively downregulating the TLR4 adaptor TRIF. Since TRIF mediates the production of iNOS and selected cytokines and chemokines in macrophages, PGL production endows mycobacteria with the capacity to alter both the bactericidal and inflammatory responses of the host during chronic infection.

This property adds to the previously reported inhibitory activity of PGL-1 and PGL-tb on TLR2 signaling, which was evidenced by a lower induction of NF-κB and associated production of TNF-α in macrophages stimulated with Pam3CSK4 in the presence of PGLs (2, 6, 7). Notably, PGL-mediated inhibition of TLR2 signaling operated immediately and independently of CR3-mediated phagocytosis. This is in stark contrast with the observed effects of PGLs on TRIF-dependent TLR4 signaling, which required that macrophages express CR3 and are exposed to PGLs for >6 h. Using TLR2-deficient BMDMs, we excluded the possibility that TLR2 contributes to PGL-mediated inhibition of TLR4 signaling. Unlike TRIF, MyD88 was not impacted by macrophage pretreatment with PGL-1. Together, these data thus suggest that PGLs affect TRIF independently of their effect on TLR2 signaling. Pretreating macrophages with PGL-1 prior to

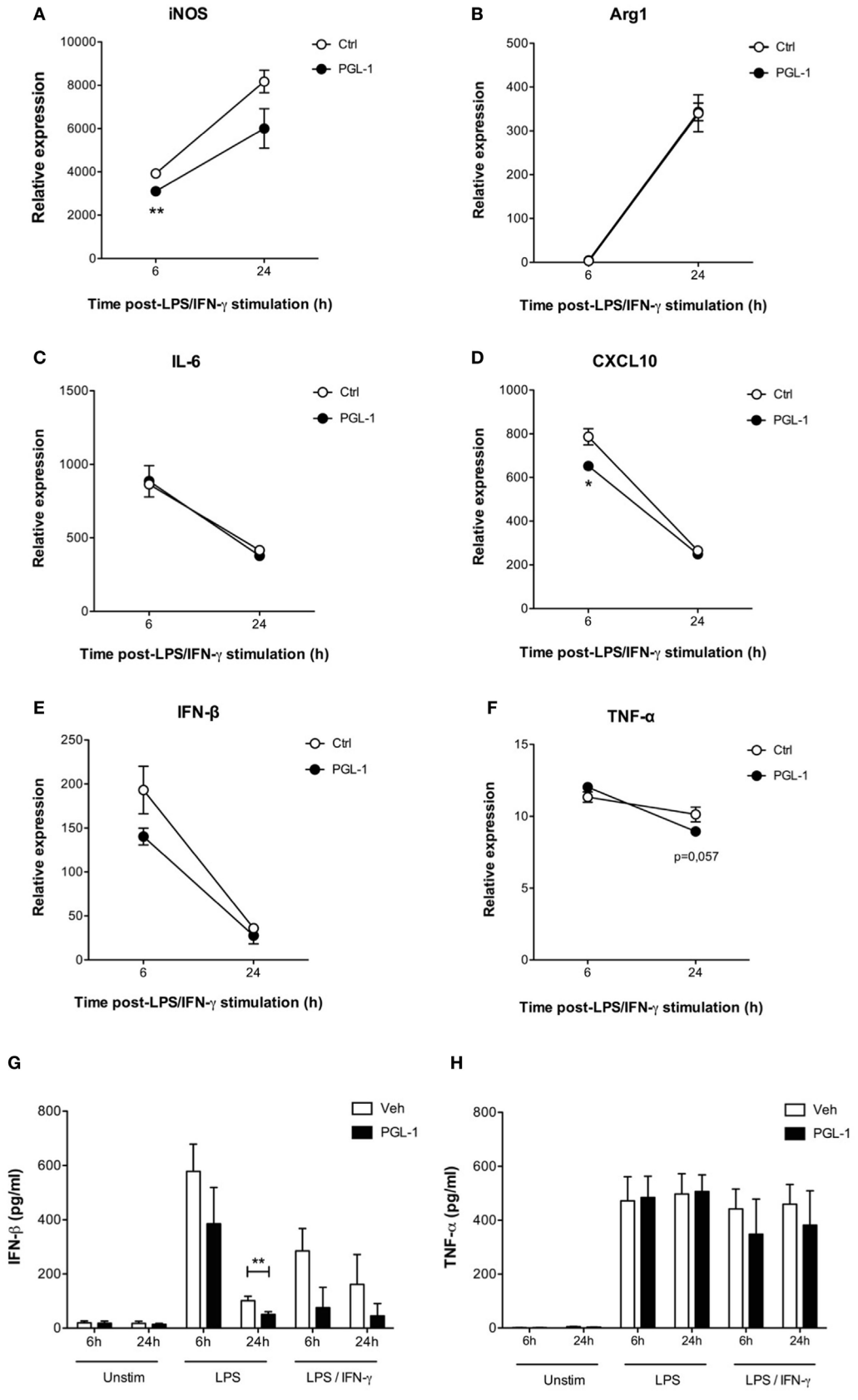


FIGURE 5 | Continued

FIGURE 5 | Phenolic glycolipid (PGL)-1-mediated decrease in TRIF impairs downstream signaling events. Quantitation of mRNAs in bone marrow-derived macrophages (BMDMs) treated with 25 μM PGL-1 or vehicle (Veh) for 24 h prior to 6–24 h of stimulation with LPS/IFN-γ: **(A)** *Nos2* (iNOS); **(B)** *Arg1* (Arginase 1); **(C)** *IL6* (IL-6); **(D)** *CXCL10* (CXCL10); **(E)** *Ifnb1* (IFN-β); **(F)** *Tnf* (TNF-α). Data are relative mean transcript levels ($n > 3$) ± SEM. $^{*}P < 0.05$, $^{**}P < 0.01$, Student's *t*-test, relative to RPL19 house-keeping gene. They are representative of at least two independent experiments with similar results. Production of IFN-β **(G)** and TNF-α **(H)** by BMDMs pretreated with 25 μM PGL-1 for 24 h prior to 6–24 h of stimulation with LPS ($n = 6$) or LPS/IFN-γ ($n = 2$). Data in **(G,H)** are mean cytokine concentrations from biological replicates ± SEM. $^{**}P < 0.01$, Mann–Whitney test comparing PGL-1-treated cells to vehicle controls.

stimulation with TLR3 ligand poly(I:C) did not alter their IFN-β production (Figure S5 in Supplementary Material), thus limiting the functional relevance of PGL-1-mediated decrease in TRIF to TLR4 signaling.

Mycobacteria display multiple TLR2 and TLR4 agonists, and studies using TLR knock-out animals have shown the importance of TLR2/4 signals in host responses to chronic mycobacterial infection, *via* production of bactericidal molecules and pro-inflammatory mediators (3, 33, 34). By inhibiting TLR2 signaling (previous work) and TRIF-dependent TLR4 signaling (present study) in macrophages, PGL production is thus likely to alter the immune control of *M. tuberculosis* and *M. leprae* infection *in vivo*. Interestingly, several strains of *M. tuberculosis* belonging to the W-Beijing lineage were shown to be potent activators of TLR4 and inducers of Type I IFNs in BMDMs (35). Production of Type I IFNs during infection with *M. tuberculosis* [reviewed in Ref. (36)] and *M. leprae* (37) is believed to promote rather than limit disease progression, through diverse autocrine and paracrine mechanisms contributing to suppress IFN-γ production and IFN-γ-induced microbicidal responses. However, recent studies have indicated that in conditions where IFN-γ signaling is absent, Type I IFNs confer protection against *M. tuberculosis* infection (38, 39). Our observation that PGLs limit the ability of macrophages to produce IFN-β upon TLR4 activation, irrespective of IFN-γ stimulation, is, therefore, particularly interesting to consider in the context of early immune responses to infection.

We excluded the possibility that PGLs suppress TRIF gene transcription or promote TRIF proteasomal or lysosomal degradation, but failed to identify a mechanism linking CR3 with TRIF protein loss. PGL-mediated inhibition of NO production was lost in MyD88$^{-/-}$ macrophages, suggesting that TRIF degradation requires MyD88. Previous studies have shown that PGL-1 differs from other PGLs in capacity to promote the CR3-dependent uptake of mycobacteria by macrophages (2). Consistently, PGL-1 binding to CR3 was not displaced by oligosaccharides from other PGLs in solid-phase assays (2). Whether all PGLs can bind to a distinct region of the CR3 receptor, without activating downstream Src signaling, is unknown. Our observation that PGL-1, PGL-tb, and PGL-bov comparably suppress TLR4-induced induction of iNOS, in a CR3-dependent manner, supports this possibility. Alternatively, PGLs may bind to a distinct macrophage receptor, secondarily interfering with CR3. Incubation of BMDMs with PGL-1 did not alter their surface expression of TLR4 (Figure S3 in Supplementary Material) nor basal production of IFN-β (**Figure 5G**), arguing against a direct interaction between PGLs and TLR4. Further work will be needed to determine how CR3 and MyD88 connect with PGL-driven TRIF downregulation, and whether TRIF production is altered at the translational level, or if other mechanisms are at play. Recently, it was reported that PGL-1 expressed by recombinant *Mycobacterium marinum* induces BMDMs to produce enhanced levels of iNOS transcripts after 6 h of infection (40). It would be interesting to see if the production of NO is augmented in macrophages infected *M. marinum*:PGL-1, and if the stimulatory effect of PGL-1 persists beyond 6 h postinfection in this system. If so, this would suggest that the mycobacterial strain expressing PGL-1 influences its effect on iNOS production by infected macrophages.

Aside from macrophages, CR3 is expressed by monocytes, dendritic cells, neutrophils, NK cells, basophils, eosinophils, and platelets. Interestingly, CD11b was reported to regulate TLR4-induced signaling pathways in a positive manner in dendritic cells (41). The authors proposed that, in these cells, but not in macrophages, CD11b facilitates TLR4 endocytosis and subsequent TRIF-mediated signaling in endosomes. Our preliminary investigations in the mouse MutuDC line showed that pretreatment with PGL-1 inhibits the LPS-stimulated upregulation of CD86 at the cell surface (data not shown), which suggests that PGL-1 comparably affects TRIF-dependent TLR4 signaling in dendritic cells. In all, our findings expand the list of subtle functional alterations caused by mycobacterial PGLs in the biology of host macrophages, namely hijacking the CR3 receptor for increased infectivity and directly interacting with surface-displayed TLR2. In addition to improve our understanding of how PGLs manipulate innate immunity receptor signaling and communication, our findings reveal a novel element of crosstalk between TLR and the complement system that is exploited by pathogens to improve persistence in infected hosts (42).

AUTHOR CONTRIBUTIONS

RO, VM, CW, NW, and CD conceived the experiments. RO and VM conducted the experiments. JP, AA, CA-D, CG, and CW provided essential materials. All authors analyzed the results and revised the manuscript.

ACKNOWLEDGMENTS

We are grateful to NIAID BEI Resources repository for providing *M. leprae* PGL-1, and *M. canettii* PGL-tb. We would also like to thank Emilie Doz-Deblauwe, Florence Carreras, and Mathieu Epardaud (INRA UMR1282, Nouzilly) for independently validating our findings in BMDMs, and our colleagues from the Pasteur Institute Molly Ingersoll and Philippe Bousso for providing MyD88$^{-/-}$ mice; Yongzheng Wu and Agathe Subtil for providing TLR2$^{-/-}$ mice, Eric Prina and Thibault Rosazza for help

with qRT-PCR, and Françoise Vuillier for thoughtful comments and discussion.

FUNDING

This study was supported by the "Marie Skłodowska-Curie Actions" of the European Union's Seventh Framework Programme FP7/2007-2013, REA grant agreement no. 317057; the French National Research Agency (ANR-11-BSV3-001); Institut Pasteur and Institut National de la Santé et de la Recherche Médicale (INSERM).

SUPPLEMENTARY MATERIAL

The Supplementary Material for this article can be found online at http://www.frontiersin.org/articles/10.3389/fimmu.2018.00002/full#supplementary-material.

REFERENCES

1. Quadri LE. Biosynthesis of mycobacterial lipids by polyketide synthases and beyond. *Crit Rev Biochem Mol Biol* (2014) 49(3):179–211. doi:10.3109/10409238.2014.896859
2. Arbues A, Malaga W, Constant P, Guilhot C, Prandi J, Astarie-Dequeker C. Trisaccharides of phenolic glycolipids confer advantages to pathogenic mycobacteria through manipulation of host-cell pattern-recognition receptors. *ACS Chem Biol* (2016) 11(10):2865–75. doi:10.1021/acschembio.6b00568
3. Oldenburg R, Demangel C. Pathogenic and immunosuppressive properties of mycobacterial phenolic glycolipids. *Biochimie* (2017) 141:3–8. doi:10.1016/j.biochi.2017.03.012
4. Reed MB, Domenech P, Manca C, Su H, Barczak AK, Kreiswirth BN, et al. A glycolipid of hypervirulent tuberculosis strains that inhibits the innate immune response. *Nature* (2004) 431(7004):84–7. doi:10.1038/nature02837
5. Sinsimer D, Huet G, Manca C, Tsenova L, Koo MS, Kurepina N, et al. The phenolic glycolipid of *Mycobacterium tuberculosis* differentially modulates the early host cytokine response but does not in itself confer hypervirulence. *Infect Immun* (2008) 76(7):3027–36. doi:10.1128/IAI.01663-07
6. Elsaidi HR, Barreda DR, Cairo CW, Lowary TL. Mycobacterial phenolic glycolipids with a simplified lipid aglycone modulate cytokine levels through toll-like receptor 2. *Chembiochem* (2013) 14(16):2153–9. doi:10.1002/cbic.201300505
7. Elsaidi HR, Lowary TL. Inhibition of cytokine release by *Mycobacterium tuberculosis* phenolic glycolipid analogues. *Chembiochem* (2014) 15(8):1176–82. doi:10.1002/cbic.201402001
8. Tabouret G, Astarie-Dequeker C, Demangel C, Malaga W, Constant P, Ray A, et al. *Mycobacterium leprae* phenolglycolipid-1 expressed by engineered *M. bovis* BCG modulates early interaction with human phagocytes. *PLoS Pathog* (2010) 6(10):e1001159. doi:10.1371/journal.ppat.1001159
9. Schlesinger LS, Horwitz MA. Phagocytosis of *Mycobacterium leprae* by human monocyte-derived macrophages is mediated by complement receptors CR1 (CD35), CR3 (CD11b/CD18), and CR4 (CD11c/CD18) and IFN-gamma activation inhibits complement receptor function and phagocytosis of this bacterium. *J Immunol* (1991) 147(6):1983–94.
10. Melo MD, Catchpole IR, Haggar G, Stokes RW. Utilization of CD11b knockout mice to characterize the role of complement receptor 3 (CR3, CD11b/CD18) in the growth of *Mycobacterium tuberculosis* in macrophages. *Cell Immunol* (2000) 205(1):13–23. doi:10.1006/cimm.2000.1710
11. Le Cabec V, Carreno S, Moisand A, Bordier C, Maridonneau-Parini I. Complement receptor 3 (CD11b/CD18) mediates type I and type II phagocytosis during nonopsonic and opsonic phagocytosis, respectively. *J Immunol* (2002) 169(4):2003–9. doi:10.4049/jimmunol.169.4.2003
12. Diamond MS, Garcia-Aguilar J, Bickford JK, Corbi AL, Springer TA. The I domain is a major recognition site on the leukocyte integrin Mac-1 (CD11b/CD18) for four distinct adhesion ligands. *J Cell Biol* (1993) 120(4):1031–43. doi:10.1083/jcb.120.4.1031
13. O'Brien XM, Heflin KE, Lavigne LM, Yu K, Kim M, Salomon AR, et al. Lectin site ligation of CR3 induces conformational changes and signaling. *J Biol Chem* (2012) 287(5):3337–48. doi:10.1074/jbc.M111.298307
14. Adachi R, Suzuki K. Lyn, one of the Src-family tyrosine kinases expressed in phagocytes, plays an important role in beta2 integrin-signalling pathways in opsonized zymosan-activated macrophage-like U937 cells. *Cell Biochem Funct* (2007) 25(3):323–33. doi:10.1002/cbf.1393
15. Kojima H, Nakatsubo N, Kikuchi K, Kawahara S, Kirino Y, Nagoshi H, et al. Detection and imaging of nitric oxide with novel fluorescent indicators: diaminofluoresceins. *Anal Chem* (1998) 70(13):2446–53. doi:10.1021/ac9801723
16. Bryan NS, Grisham MB. Methods to detect nitric oxide and its metabolites in biological samples. *Free Radic Biol Med* (2007) 43(5):645–57. doi:10.1016/j.freeradbiomed.2007.04.026
17. Alboni S, Poggini S, Garofalo S, Milior G, El Hajj H, Lecours C, et al. Fluoxetine treatment affects the inflammatory response and microglial function according to the quality of the living environment. *Brain Behav Immun* (2016) 58:261–71. doi:10.1016/j.bbi.2016.07.155
18. Bandow K, Kusuyama J, Shamoto M, Kakimoto K, Ohnishi T, Matsuguchi T. LPS-induced chemokine expression in both MyD88-dependent and -independent manners is regulated by Cot/Tpl2-ERK axis in macrophages. *FEBS Lett* (2012) 586(10):1540–6. doi:10.1016/j.febslet.2012.04.018
19. Yen JH, Ganea D. Interferon beta induces mature dendritic cell apoptosis through caspase-11/caspase-3 activation. *Blood* (2009) 114(7):1344–54. doi:10.1182/blood-2008-12-196592
20. Huelsenbeck J, Henninger C, Schad A, Lackner KJ, Kaina B, Fritz G. Inhibition of Rac1 signaling by lovastatin protects against anthracycline-induced cardiac toxicity. *Cell Death Dis* (2011) 2:e190. doi:10.1038/cddis.2011.65
21. Ruffell D, Mourkioti F, Gambardella A, Kirstetter P, Lopez RG, Rosenthal N, et al. A CREB-C/EBPbeta cascade induces M2 macrophage-specific gene expression and promotes muscle injury repair. *Proc Natl Acad Sci U S A* (2009) 106(41):17475–80. doi:10.1073/pnas.0908641106
22. Hoebe K, Du X, Georgel P, Janssen E, Tabeta K, Kim SO, et al. Identification of Lps2 as a key transducer of MyD88-independent TIR signalling. *Nature* (2003) 424(6950):743–8. doi:10.1038/nature01889
23. Takeuchi O, Hoshino K, Kawai T, Sanjo H, Takada H, Ogawa T, et al. Differential roles of TLR2 and TLR4 in recognition of Gram-negative and Gram-positive bacterial cell wall components. *Immunity* (1999) 11(4):443–51. doi:10.1016/S1074-7613(00)80119-3
24. Adachi O, Kawai T, Takeda K, Matsumoto M, Tsutsui H, Sakagami M, et al. Targeted disruption of the MyD88 gene results in loss of IL-1- and IL-18-mediated function. *Immunity* (1998) 9(1):143–50. doi:10.1016/S1074-7613(00)80596-8
25. Nozaki Y, Hasegawa Y, Ichiyama S, Nakashima I, Shimokata K. Mechanism of nitric oxide-dependent killing of *Mycobacterium bovis* BCG in human alveolar macrophages. *Infect Immun* (1997) 65(9):3644–7.
26. Jagannath C, Actor JK, Hunter RL Jr. Induction of nitric oxide in human monocytes and monocyte cell lines by *Mycobacterium tuberculosis*. *Nitric Oxide* (1998) 2(3):174–86. doi:10.1006/niox.1998.9999
27. Garcia I, Guler R, Vesin D, Olleros ML, Vassalli P, Chvatchko Y, et al. Lethal *Mycobacterium bovis* bacillus Calmette Guerin infection in nitric oxide synthase 2-deficient mice: cell-mediated immunity requires nitric oxide synthase 2. *Lab Invest* (2000) 80(9):1385–97. doi:10.1038/labinvest.3780146
28. Pautz A, Art J, Hahn S, Nowag S, Voss C, Kleinert H. Regulation of the expression of inducible nitric oxide synthase. *Nitric Oxide* (2010) 23(2):75–93. doi:10.1016/j.niox.2010.04.007
29. Farlik M, Reutterer B, Schindler C, Greten F, Vogl C, Muller M, et al. Nonconventional initiation complex assembly by STAT and NF-kappaB transcription factors regulates nitric oxide synthase expression. *Immunity* (2010) 33(1):25–34. doi:10.1016/j.immuni.2010.07.001
30. Fallows D, Peixoto B, Kaplan G, Manca C. *Mycobacterium leprae* alters classical activation of human monocytes in vitro. *J Inflamm (Lond)* (2016) 13:8. doi:10.1186/s12950-016-0117-4

31. Awua AK, Doe ED, Gyamfi OK. Evaluation of cost-effective total nucleic acids extraction protocols for cultured *Mycobacterium tuberculosis*; a comparison by PCR amplification of genes associated with drug resistance. *BMC Res Notes* (2010) 3:48. doi:10.1186/1756-0500-3-48
32. Reed JH, Jain M, Lee K, Kandimalla ER, Faridi MH, Buyon JP, et al. Complement receptor 3 influences toll-like receptor 7/8-dependent inflammation: implications for autoimmune diseases characterized by antibody reactivity to ribonucleoproteins. *J Biol Chem* (2013) 288(13):9077–83. doi:10.1074/jbc.M112.403303
33. Abel B, Thieblemont N, Quesniaux VJ, Brown N, Mpagi J, Miyake K, et al. Toll-like receptor 4 expression is required to control chronic *Mycobacterium tuberculosis* infection in mice. *J Immunol* (2002) 169(6):3155–62. doi:10.4049/jimmunol.169.6.3155
34. Drennan MB, Nicolle D, Quesniaux VJ, Jacobs M, Allie N, Mpagi J, et al. Toll-like receptor 2-deficient mice succumb to *Mycobacterium tuberculosis* infection. *Am J Pathol* (2004) 164(1):49–57. doi:10.1016/S0002-9440(10)63095-7
35. Carmona J, Cruz A, Moreira-Teixeira L, Sousa C, Sousa J, Osorio NS, et al. *Mycobacterium tuberculosis* strains are differentially recognized by TLRs with an impact on the immune response. *PLoS One* (2013) 8(6):e67277. doi:10.1371/journal.pone.0067277
36. O'Garra A, Redford PS, McNab FW, Bloom CI, Wilkinson RJ, Berry MP. The immune response in tuberculosis. *Annu Rev Immunol* (2013) 31:475–527. doi:10.1146/annurev-immunol-032712-095939
37. Teles RM, Graeber TG, Krutzik SR, Montoya D, Schenk M, Lee DJ, et al. Type I interferon suppresses type II interferon-triggered human anti-mycobacterial responses. *Science* (2013) 339(6126):1448–53. doi:10.1126/science.1233665
38. Desvignes L, Wolf AJ, Ernst JD. Dynamic roles of type I and type II IFNs in early infection with *Mycobacterium tuberculosis*. *J Immunol* (2012) 188(12):6205–15. doi:10.4049/jimmunol.1200255
39. Moreira-Teixeira L, Sousa J, McNab FW, Torrado E, Cardoso F, Machado H, et al. Type I IFN inhibits alternative macrophage activation during *Mycobacterium tuberculosis* infection and leads to enhanced protection in the absence of IFN-gamma signaling. *J Immunol* (2016) 197(12):4714–26. doi:10.4049/jimmunol.1600584
40. Madigan CA, Cambier CJ, Kelly-Scumpia KM, Scumpia PO, Cheng TY, Zailaa J, et al. A macrophage response to *Mycobacterium leprae* phenolic glycolipid initiates nerve damage in leprosy. *Cell* (2017) 170(5):973–985e910. doi:10.1016/j.cell.2017.07.030
41. Ling GS, Bennett J, Woollard KJ, Szajna M, Fossati-Jimack L, Taylor PR, et al. Integrin CD11b positively regulates TLR4-induced signalling pathways in dendritic cells but not in macrophages. *Nat Commun* (2014) 5:3039. doi:10.1038/ncomms4039
42. Hajishengallis G, Lambris JD. Crosstalk pathways between toll-like receptors and the complement system. *Trends Immunol* (2010) 31(4):154–63. doi:10.1016/j.it.2010.01.002

Conflict of Interest Statement: The authors declare that the research was conducted in the absence of any commercial or financial relationships that could be construed as a potential conflict of interest.

Copyright © 2018 Oldenburg, Mayau, Prandi, Arbues, Astarie-Dequeker, Guilhot, Werts, Winter and Demangel. This is an open-access article distributed under the terms of the Creative Commons Attribution License (CC BY). The use, distribution or reproduction in other forums is permitted, provided the original author(s) or licensor are credited and that the original publication in this journal is cited, in accordance with accepted academic practice. No use, distribution or reproduction is permitted which does not comply with these terms.

frontiers in Immunology

ORIGINAL RESEARCH
published: 27 November 2017
doi: 10.3389/fimmu.2017.01659

Lipoarabinomannan Decreases Galectin-9 Expression and Tumor Necrosis Factor Pathway in Macrophages Favoring *Mycobacterium tuberculosis* Intracellular Growth

Leslie Chávez-Galán[1]†, Lucero Ramon-Luing[1†], Claudia Carranza[2], Irene Garcia[3] and Isabel Sada-Ovalle[1]*

[1] Laboratory of Integrative Immunology, National Institute of Respiratory Diseases Ismael Cosio Villegas, Mexico City, Mexico, [2] Department of Microbiology, National Institute of Respiratory Diseases Ismael Cosio Villegas, Mexico City, Mexico, [3] Department of Pathology and Immunology, Centre Medical Universitaire, Faculty of Medicine, University of Geneva, Geneva, Switzerland

OPEN ACCESS

Edited by:
Yoann Rombouts,
UMR5089 Institut de Pharmacologie et de Biologie Structurale (IPBS), France

Reviewed by:
Shashank Gupta,
Brown University, United States
Jieliang Li,
Temple University, United States

***Correspondence:**
Leslie Chávez-Galán
lchavez_galan@iner.gob.mx

†These authors have contributed equally to this work.

Specialty section:
This article was submitted to Microbial Immunology, a section of the journal Frontiers in Immunology

Received: 11 July 2017
Accepted: 13 November 2017
Published: 27 November 2017

Citation:
Chávez-Galán L, Ramon-Luing L, Carranza C, Garcia I and Sada-Ovalle I (2017) Lipoarabinomannan Decreases Galectin-9 Expression and Tumor Necrosis Factor Pathway in Macrophages Favoring Mycobacterium tuberculosis Intracellular Growth. Front. Immunol. 8:1659. doi: 10.3389/fimmu.2017.01659

Lipoarabinomannan (LAM) is a lipid virulent factor secreted by *Mycobacterium tuberculosis* (*Mtb*). LAM can be found in the sputum and urine of patients with active tuberculosis. When human monocytes are differentiated into macrophages [monocyte-derived macrophages (MDM)] in the presence of LAM, MDM are poorly functional which may limit the immune response to *Mtb* infection. Our previous studies have shown that TIM3 and galectin (GAL)9 interaction induces anti-mycobacterial activity, and the expression levels of TIM3 and GAL9 are downregulated during *Mtb* infection. We postulated that LAM affects GAL9/TIM3 pathway, and, in consequence, the ability of the macrophage to control bacterial growth could be affected. In this work, we have generated MDM in the presence of LAM and observed that the expression of TIM3 was not affected; in contrast, GAL9 expression was downregulated at the transcriptional and protein levels. We observed that the cell surface and the soluble form of tumor necrosis factor (TNF) receptor 2 were decreased. We also found that when LAM-exposed MDM were activated with LPS, they produced less TNF, and the transcription factor proteinase-activated receptor-2 (PAR2), which is involved in host immune responses to infection, was not induced. Our data show that LAM-exposed MDM were deficient in the control of intracellular growth of *Mtb*. In conclusion, LAM-exposed MDM leads to MDM with impaired intracellular signal activation affecting GAL9, TNF, and PAR2 pathways, which are important to restrict *Mtb* growth.

Keywords: macrophage, *Mycobacterium tuberculosis*, lipoarabinomannan, galectin-9, tumor necrosis factor pathway

INTRODUCTION

Mycobacterium tuberculosis (*Mtb*) is the infectious agent of tuberculosis (TB), which is one of the leading causes of morbidity and mortality around the world. World Health Organization reported that in 2014, there were 9 million new cases of TB and 1.5 million deaths globally (1).

Mycobacterium tuberculosis is an intracellular pathogen whose cell wall has low permeability, which confers resistance to therapeutic agents. *Mtb* cell wall is rich in lipids (30–60% of dry weight)

that are strategically located and contribute to its virulence (2). Lipoarabinomannan (LAM) is a major lipoglycan found in the mycobacterial cell wall. Slow growing mycobacteria, as *Mtb*, have a LAM that structurally possess mannosyl caps (hereafter LAM), which is constantly released from the cell wall of *Mtb* (3). LAM is considered as an important virulence factor that can be identified in the sputum and urine of patients with TB (TB patients). In fact, LAM has an amphiphilic nature favoring its association with host lipid carriers, which suggests that peripheral blood mononuclear cells (PMBCs) from patients with TB might be exposed to LAM during the natural history of TB (4, 5). Consequently, LAM could be employed as a biomarker to predict outcomes during anti-TB therapy.

Macrophage is a professional antigen-presenting cell that has as origin the monocyte and plays a critical role in the pathogenesis of TB. It has been described that *Mtb* downregulates the macrophage activation in order to facilitate their persistence (6). In particular, LAM has been studied for its immunomodulatory properties in macrophage (7, 8). Using an *in vitro* model where monocytes were stimulated with LAM, we have shown that LAM exposure influenced monocyte differentiation generating poorly functional macrophage, a phenomenon that could limit the quality of immune response to *Mtb* infection (9).

The molecule T-cell immunoglobulin and mucin domain 3 (TIM3) is a receptor initially identified as a specific marker for Th1-type immune cells. Nowadays, there is evidence that TIM3 is expressed in diverse myeloid and lymphoid cells and that its failure or absence is associated with the development of several diseases including infectious diseases (10). The interaction of TIM3 with galectin (GAL)9, which is one of the TIM3 ligands, has been shown to induce macrophage activation for bactericidal functions and to control TB infection using a murine model of *Mtb* infection (11). However, TB patients have a lower frequency of $CD14^+TIM3^+$ cells in peripheral blood, suggesting that this downregulation could be a mechanism to disturb the immune response in the host (12).

Mycobacterium tuberculosis infection activates cellular pathways in macrophages to initiate immune response, which involves the production of cytokines playing a critical role to regulate host defense. Tumor necrosis factor (TNF) is a proinflammatory cytokine, which orchestrates a wide range of functions. It is synthesized as a transmembrane TNF (tmTNF) that is proteolytically processed by the metalloprotease TNF-α-converting enzyme (TACE) to generate the soluble TNF (solTNF). Both tmTNF and solTNF isoforms exert their bioactivities via binding of two different receptors, TNF receptor 1 (TNFR1) and TNF receptor 2 (TNFR2) (13). In animal models, TNF pathway has been shown to be crucial for the activation of host protective immune responses against mycobacterial infection (14, 15). In human, TNF inhibition, used for the treatment of autoimmune-inflammatory diseases, has been associated with an increased risk of opportunistic infections including TB (16, 17).

Considering the reported information on the relevance of TIM3/GAL9 pathway in the defense against mycobacterial infections, it is still not clear whether LAM may modify TIM3/GAL9 pathway and impair host defense mechanisms. In this study, we explore possible modifications of TIM3/GAL9 pathway due to LAM exposure that could reduce macrophage responses and compromise bacterial elimination. We have characterized the expression profile of TIM3 and GAL9 on human monocyte-derived macrophages (MDM) exposed to LAM during their differentiation process. We have evaluated the capacity of these MDM to produce cytokines, to activate transcription factors, and to control *Mtb* growth. Our findings indicate that LAM exposure induces MDM with reduced GAL9 expression, which in response to an activation stimulus leads to weak cytokine and intracellular signals affecting the control of *Mtb* survival.

MATERIALS AND METHODS

Ethics Statement

Peripheral blood mononuclear cells were obtained from buffy coats by the blood bank at the National Institute of Respiratory Diseases Ismael Cosio Villegas, Mexico City. The study was approved by the Institutional Review Board (IRB# B04-12) and was conducted following the principles stipulated in the Declaration of Helsinki.

LAM from *Mtb*-H37Rv

Purified LAM was obtained from Colorado State University (NR-14848). The lipid was then reconstituted in distilled water as recommended.

Preparation of PBMC and Magnetic Cell Sorting

Peripheral blood mononuclear cells were isolated from buffy coats by standard Lymphoprep™ (Accurate Chemical-Scientific, Westbury, NY, USA) gradient centrifugation. Monocytes were isolated by positive selection using anti-CD14-coated magnetic microbeads (Miltenyi Biotec). Enrichment of the $CD14^+$ fraction was routinely >95%, as analyzed by flow cytometry. $CD14^+$ cells were plated at 1×10^6 cells/well in 24-well plates (Costar, ON, Canada) with RPMI 1640 medium (GIBCO, Grand Island, NY, USA), supplemented with L-glutamine (2 mM; GIBCO, Grand Island, NY, USA), streptomycin, penicillin, and 10% heat-inactivated fetal bovine serum (GIBCO, Grand Island, NY, USA). $CD14^+$ cells were cultured for 7 days at 37°C in a humidified atmosphere containing 5% CO_2. After 7 days, viable cells were considered to be MDM based on their expression profile of differentiation molecules as previously reported (9).

Differentiation and Stimulation of MDM with LAM

$CD14^+$ cells were cultured to differentiate into MDM in the presence of LAM using an *in vitro* model that we have previously reported (9). Briefly, $CD14^+$ (1×10^6) cells were seeded in a 24-well plate and stimulated or not with LAM (1 μg/mL), for 1, 2, 3, 4, or 5 days. Every day, culture medium was replaced by medium without LAM and cells recovered at the 7th or 8th day of culture. Two control conditions were used: first, medium without LAM during the 7 or 8 days of culture and, second, cells were

left for differentiation without LAM for 6 days, and then, LAM was added and maintained until day 7 or 8 of culture. At day 7 of culture, we established two different protocols, the first consisted in recovering cells for FACS analysis, RNA extraction (real-time PCR), cellular lysis (western blot assays), for *in vitro* infection and mycobacterial quantification [colony-forming units (CFUs)], and the supernatants were for ELISA. In the second protocol, LPS (1 μg/mL) was added at day 7 for 24 h (day 8) to perform RNA extraction (real-time PCR) and the supernatants recovered for ELISA (**Diagram 1**).

Flow Cytometry

Cells were stained for 20 min at 4°C with fluorochrome-conjugated mAb against CD14, TIM3, GAL9, TNF, and interleukin-1 receptor (IL-1R) (BioLegend, San Diego, CA, USA). Both TNFR1 and TNFR2 (R&D Systems, Minneapolis, MN, USA). After incubation, cells were washed and re-suspended in staining buffer (BD Biosciences, San Jose, CA, USA) prior to FACS analysis. Data were collected using a FACS Aria II flow cytometer (Becton Dickinson, San Jose, CA, USA) and FACS Diva software (V.8.01). Cells were then analyzed with FlowJo (Tree Star, Inc., Ashland, OR, USA). Typically, 20,000 events were acquired.

Western Blot

After incubation, cells were washed twice with PBS and lysed in Laemmli buffer. Equal amounts of protein were subjected to Mini-protean TGK 4–15% gels and transferred to a 0.2-μm pore size Trans-Blot Turbo TM PVDF membrane (Bio-Rad Laboratories, Hercules, CA, USA). Western blot was performed using the following antibodies: c-Jun N-terminal kinase (JNK) 1/2 and poly(ADP-ribose) polymerase (PARP) (R&D Systems). Protein bands were detected by incubating with horseradish peroxidase-labeled antibodies and developed with enhanced chemoluminiscence reagent (Thermo Scientific, Pierce Biotech., Rockford, IL, USA) and ChemiDoc MP Imaging System (Bio-Rad). Band densities were analyzed by densitometry using online IMAGEJ software provided by the NIH (http://rsb.info.nih.gov/ij/index.html), as described by Luke Miller (http://www.lukemiller.org/journal/2007/08/quantifying-western-blots-without.html). Each sample was normalized using glyceraldehyde 3-phosphate dehydrogenase as a loading control.

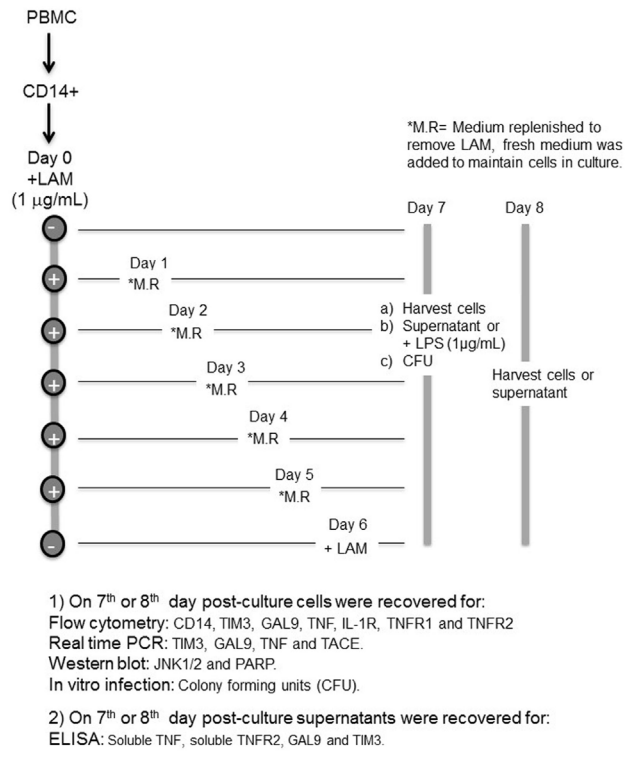


DIAGRAM 1 | Design of the experimental strategy.

Real-time PCR for TIM3, GAL9, TNF, TACE, RAB33A and Proteinase-Activated Receptor-2 (PAR2) Gene Expression

For the analysis of TIM3, GAL9, TNF, TACE, RAB33A, and PAR2 gene expressions, MDM exposed to LAM were generated as described in the previous section. Total RNA from 1×10^6 cells was isolated using RNeasy Mini Kit (Qiagen, Hilden, Germany) following the manufacturer's protocol. DNA genome was eliminated with RNase-Free DNase Set (Qiagen). RNA was eluted in 30 μL of nuclease-free water and the quantity of extracted RNA was evaluated by Qubit™ assay kit with the Qubit 2.0 Fluorometer (Life Technologies, Carlsbad, CA, USA). A total of 67.5 ng of total RNA was converted to cDNA using High Capacity cDNA Reverse Transcription Kit (Applied Biosystems, Foster City, CA, USA) as per the manufacturer's guidelines. Gene expression analyses was performed with the StepOnePlus™ Real-Time PCR Systems (Applied Biosystems) using standard thermal cycling conditions and Taqman assays specific for TIM3 (Hs00958618_m1), GAL9 (Hs01088490_m1), TNF (Hs01113624_g1), TACE (Hs01041915_m1), RAB33A (Hs00191243_m1), and PAR2 (Hs00608346_m1). Data were normalized to two endogenous controls, ACTB (β-actin) (Hs01060665_g1) and 18S (18S ribosomal RNA gene) (Hs03928990_g1). Before gene expression analysis, cDNA samples were serially diluted to 1:5 or 1:2 and 2.5 μL were used as template for the quantitative real-time PCR (qPCR) to perform the validation of the delta-delta CT method. Same cDNA dilutions were used for the all qPCR assays, and relative gene expression values of all different gene targets were calculated using the 2-DDCT formula. The expression of each target gene is presented as the "fold change" relative to that of control condition (MDM without LAM). All the qPCRs were run in duplicate along with no-template controls.

ELISA

Culture supernatants from MDM exposed to LAM (±LPS) were recovered and stored at −80°C for future analysis. We used the standard sandwich ELISA for GAL9, TIM3, and TNFR2 (R&D Systems) and TNF (BioLegend, Inc.) following

the manufacturer's instruction. All proteins in the culture supernatants were quantified by comparison with the appropriated recombinant standard.

Bacteria

Mycobacterium tuberculosis strain H37Ra (*Mtb*-H37Ra) (ATCC-25177) was grown for 21 days in Middlebrook 7H9 broth. Mycobacteria were harvested and clumps were disrupted with sterile 3 mm glass beads and vortexed for 5 min. The concentration of disaggregated mycobacteria was determined by counting CFUs on 7H10 agar plates in triplicate serial dilutions and after 21 days of incubation. Bacterial stock was stored at −70°C until use.

Intracellular Growth of *Mtb*

To evaluate mycobacterial intracellular growth, MDM were plated in duplicated wells at a concentration of 2×10^5 cells/well 96-well plates. MDM were infected with H37Ra at MOI of 1. After 1 h infection at 37°C in 5% CO_2 incubator, plates were washed three times to remove any extracellular mycobacteria. Cells were lysed with 0.1% sodium dodecyl sulfate in 7H9 Milddlebrook medium and neutralized with 20% bovine serum albumin on days 0 ($CFU_{day\ 0}$), 3 ($CFU_{day\ 3}$), and 7 ($CFU_{day\ 7}$) post-infection. Serial dilutions of the lysates from duplicate wells were plated on Middlebrook 7H10 agar by triplicate and CFU was determined after 21 days of incubation at 37°C and 5% CO_2. Average CFU numbers were from duplicate assessments to obtain the percentage of change. % CFU was calculated as follows: $CFU_{day\ 0}$ number per condition was considered as 100%, posteriorly the CFU number at day 3 or day 7 was obtained and calculated the percentage in relation to $CFU_{day\ 0}$ from each individual condition experiment.

Statistical Analysis

Data are shown as median ± interquartile range or median ± SD. Mann–Whitney *U* test was used to compare two groups, and a Kruskal–Wallis test with Dunn's *post hoc* test when more than two groups were compared. Values of $P < .05$ were considered statistically significant (GraphPad Software, Inc., San Diego, CA, USA).

RESULTS

TIM3 Expression in Macrophages Is Not Affected When Monocytes Are Exposed to LAM

Our previous results have shown that monocyte exposure to LAM promotes their differentiation into immature macrophages (9). This differentiation is not associated with an increased in cell death of MDM generated under LAM exposure compared to unexposed cells (Figure S1 in Supplementary Material). During MDM differentiation process, a low percentage of MDM lose or reduce CD14 expression (18). As differentiation markers can vary during MDM differentiation process, in this article, we are reporting the expression of TIM3 and other molecules on the total MDM population comprising $CD14^-$ and $CD14^+$ MDM and only on $CD14^+$ MDM subpopulations.

To determine if TIM3 expression is affected by the exposure of monocyte to LAM, we measured TIM3 expression on MDM that did not reveal changes of the percentage and intensity of $TIM3^+$ MDM (**Figure 1A**) (data not shown). Total MDM or $CD14^+$ MDM derived from monocytes exposed to LAM for 2 days showed a decrease of 50% compared to unexposed MDM, but the difference was not statically significant (**Figures 1B,C**). In order to evaluate LAM effect on TIM3 expression at the transcription level, we performed gene expression analysis by real-time PCR and observed that TIM3 gene expression was similar for the different MDM groups, independently of LAM exposure time (**Figure 1D**). Finally, the level of soluble TIM3 was measured by ELISA and protein levels correlated with gene expression (**Figure 1E**). These data indicate that previous monocyte exposure to LAM generates MDM with a normal expression of TIM3.

GAL9 Expression in Mature Macrophages Is Altered When Monocytes Are Exposed to LAM

Next, we address the question of whether LAM stimulus modulates the surface expression of GAL9, the ligand of TIM3. Flow cytometry analyses showed that when monocytes were exposed to LAM for 4 days, the frequency of $GAL9^+$ MDM was reduced (**Figure 2A**). This lower frequency was independent of coexpresion with CD14 molecule on MDM surface (**Figures 2B,C**). To further define this effect, we evaluated GAL9 gene expression. Interestingly, we observed a significant decrease of GAL9 gene expression in MDM when monocytes were exposed to LAM. In MDM generated after 4 and 5 days of LAM exposure, GAL9 was decreased of 25 and 30%, respectively, in comparison to MDM without LAM stimulus (**Figure 2D**). Finally, the level of soluble GAL9 was measured by ELISA and protein levels correlated with gene expression (**Figure 2E**). These findings suggest that monocytes exposed during a long time (4–5 days) to LAM stimulus generated MDM exhibiting modified GAL9 expression.

IL-1R Expression Is Not Affected in Mature Macrophages When Monocytes Are Exposed to LAM

Previously, it has been shown that the autocrine proinflamatory cytokine IL-1β signaling via IL-1R is an important mechanism by which TIM3–GAL9 interaction induces control of *Mtb* replication (11). To analyze if GAL9 downregulation observed after LAM monocyte exposure affects IL-1R pathway, we evaluated IL-1R expression on the cell surface of MDM generated under LAM stimulus (**Figure 3A**). Our flow cytometry data showed that LAM stimulus did not affect IL-1R expression on MDM as the frequency of MDM $IL\text{-}1R^+$ was similar in MDM generated under different times of LAM exposure, and it was similar independently of co-expression with CD14 (**Figures 3B,C**). This suggests that even if LAM affects GAL9 expression on MDM, the IL-1β pathway dependent on IL-1R is probably not affected by LAM exposure.

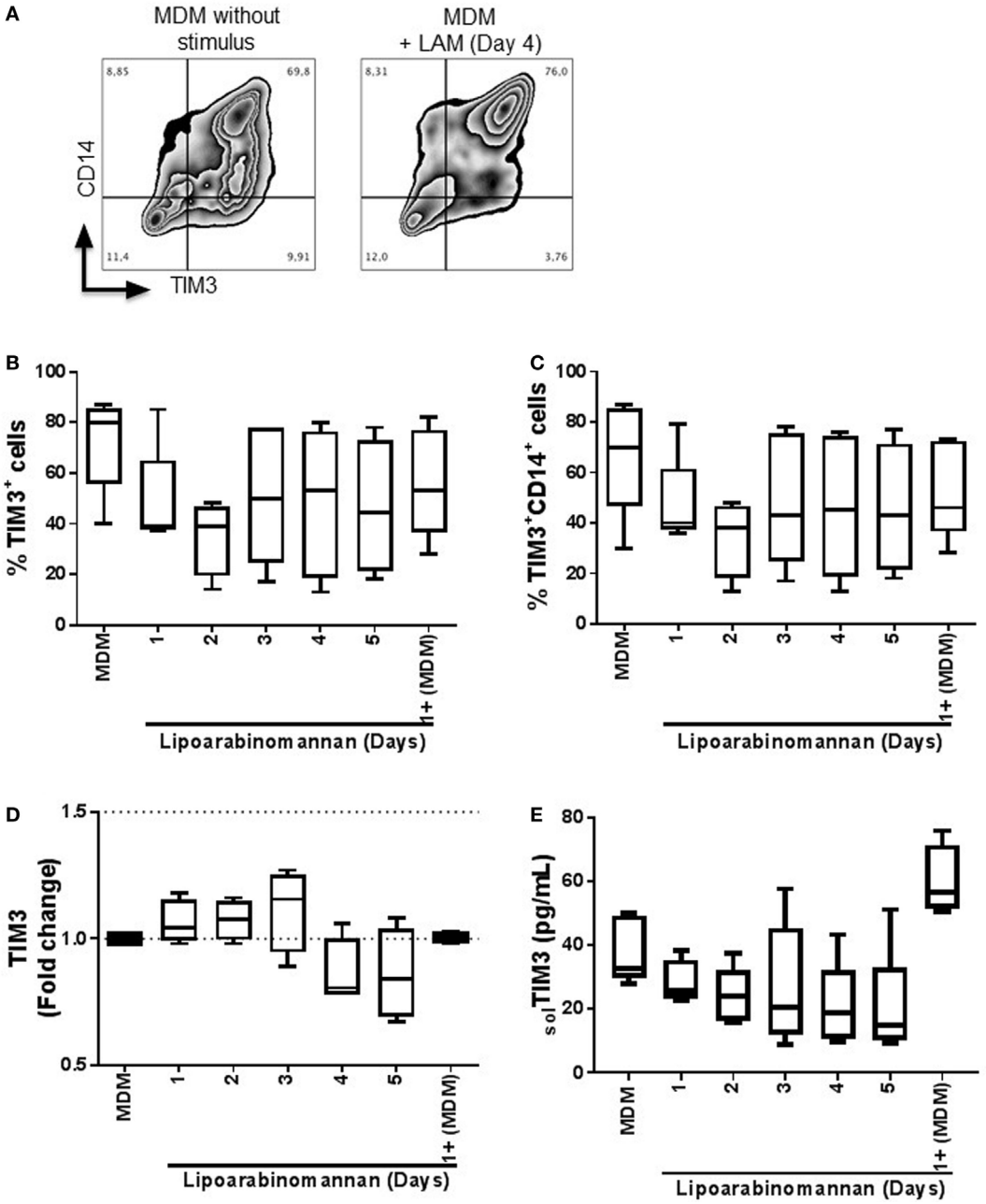


FIGURE 1 | Expression and frequency of TIM3+ MDM is not modified when monocytes are exposed to LAM. Pure monocytes were exposed to LAM for 1, 2 3, 4, or 5 days and at day 7 cells were recovered to perform flow cytometry or qPCR. Flow cytometry representative zebra plot of MDM without stimulus or exposed to LAM for 4 days (left and right, respectively) **(A)**. Expression of TIM3 was analyzed by flow cytometry independent or dependent of CD14 co-expression (**B** and **C**). TIM3 relative gene expression was measured by real-time PCR **(D)**. Soluble form of TIM3 was measured in supernatant by ELISA **(E)**. Data are representative of five independent experiments. Box plot indicates median ± IQR (5-95). Kruskal-Wallis and Dunn *post-hoc* tests compared to unexposed MDM.

TNF Is Regulated in MDM When Monocytes Are Exposed to LAM, but They Are Unable to Produce TNF after LPS Activation

It has been reported that secretion of IL-1β induced by TIM3–GAL9 interaction increased TNF signaling through the upregulation of TNF secretion and TNFR1 cell surface expression, which improved caspase-dependent restriction of intracellular *Mtb* growth (19). In contrast, we have reported that MDM generated under LAM stimulus for 3–5 days are less able to release solTNF after LPS stimulus (9). MDM expressing tmTNF form were measured by flow cytometry (**Figures 4A–C**). The frequency and the mean intensity of tmTNF+ MDM were

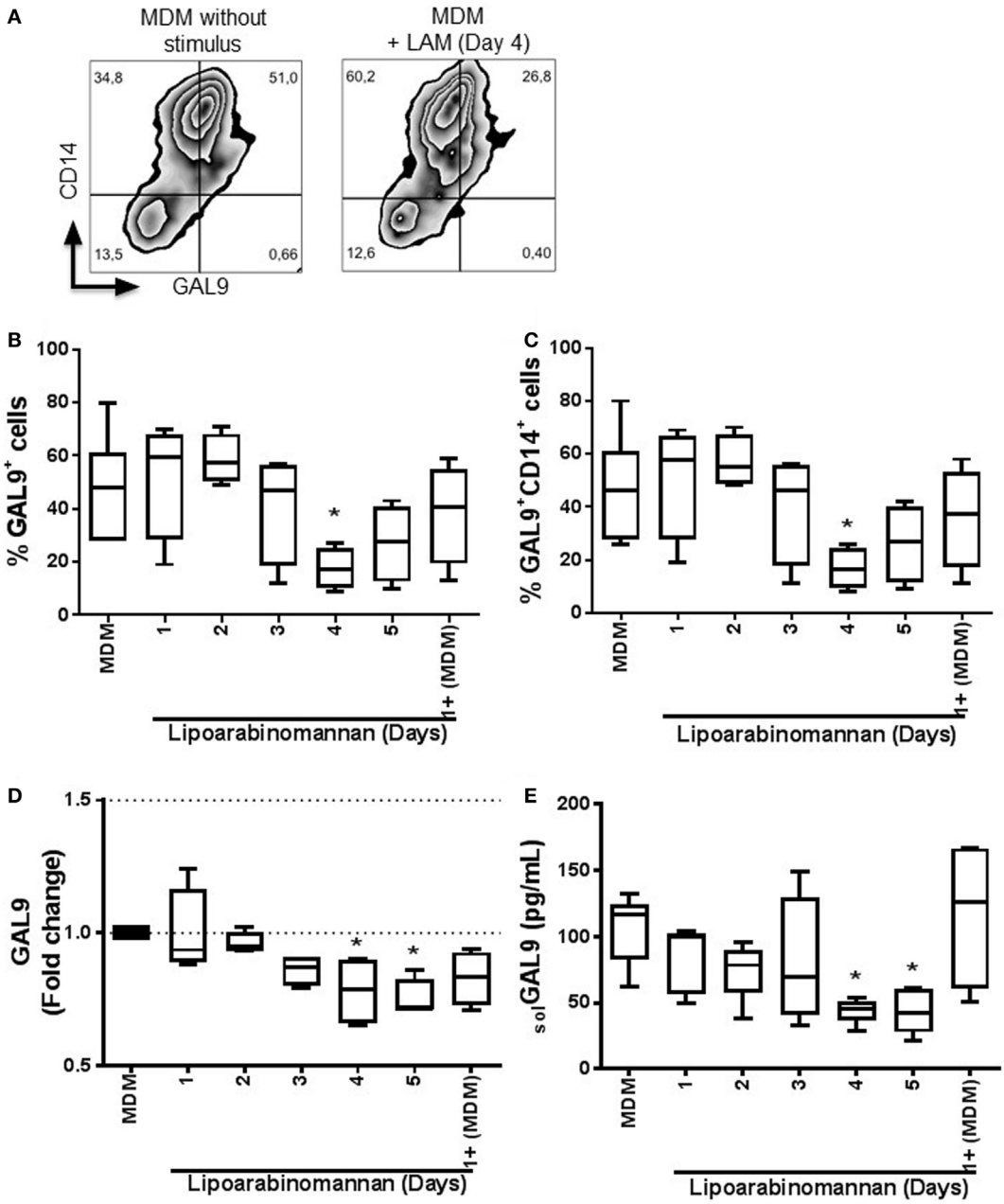


FIGURE 2 | Expression and frequency of GAL9+ monocyte-derived macrophages (MDM) decrease when monocytes are exposed to lipoarabinomannan (LAM). Pure monocytes were exposed to LAM for 1, 2, 3, 4, or 5 days, and at day 7, cells and supernatants were recovered to perform flow cytometry, qPCR, and ELISA. Representative zebra plot of MDM without stimulus or exposed to LAM for 4 days (left and right, respectively) **(A)**. Flow cytometry analysis of the expression of galectin (GAL)9 independent or dependent of CD14 co-expression **(B,C)**. GAL9 relative gene expression was evaluated by real-time PCR **(D)**. Soluble form of GAL9 was measured in supernatant by ELISA **(E)**. Data are representative of five independent experiments. Box plot indicates median ± interquartile range (5–95). *$P < 0.05$, Kruskal–Wallis and Dunn's *post hoc* tests compared to unexposed MDM.

increased in MDM generated under LAM stimulus for 4–5 days (**Figures 4B,D**).

To verify the inability of MDM exposed to LAM (3–5 days) to produce solTNF in response to LPS stimulus, we measured solTNF by ELISA and observed a downregulation of solTNF, confirming our previous reported data (9) (**Figure 5A**). To clarify this point, we measured TACE at the transcriptional level. Our data showed that TACE gene expression was not changed in MDM generated under LAM stimulus and also after a LPS stimulus (**Figure 5B**).

However, in concordance with the **Figures 4** and **5A**, TNF gene expression, measured also by qPCR, was increased in MDM derived from LAM exposed monocytes (for 4–5 days); but when MDM were activated with LPS, TNF gene expression

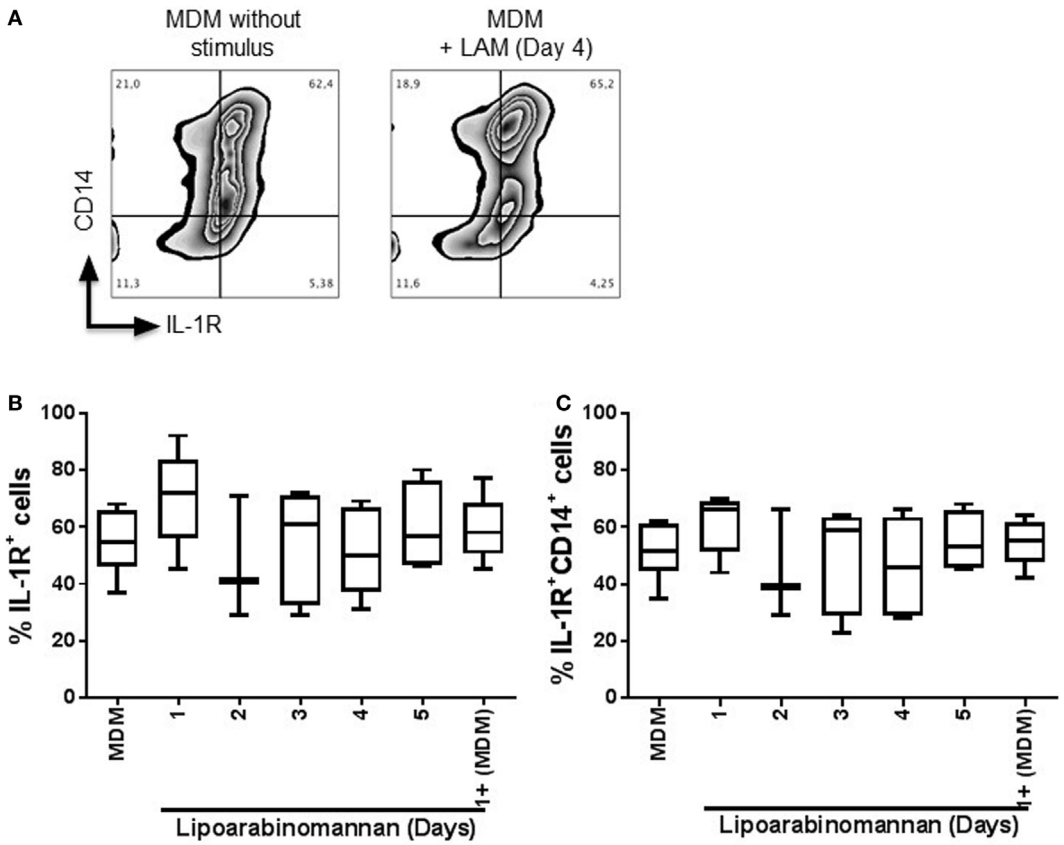


FIGURE 3 | Frequency of interleukin-1 receptor (IL-1R$^+$) monocyte-derived macrophages (MDM) is not modified when monocytes are exposed to lipoarabinomannan (LAM). Pure monocytes were exposed to LAM for 1, 2, 3, 4, or 5, and at day 7, cells were recovered. Flow cytometry representative zebra plot of MDM without stimulus or exposed to LAM for 4 days (left and right, respectively) **(A)**. Analysis of IL-1R$^+$ MDM was done independent or dependent of CD14 co-expression **(B,C)**. Data are representative of 3–5 independent experiments. Box plot indicates median ± interquartile range (5–95). Kruskal–Wallis and Dunn's *post hoc* tests compared to unexposed MDM.

was decreased (**Figure 5C**), as previously reported (9). Together, these data demonstrate that TNF is activated in response to LAM stimulus. However, mature MDM derived from monocytes exposed to LAM (4–5 days) were impaired in the capacity to produce TNF when activated with LPS, suggesting that these MDM are not able to efficiently activate intracellular pathways.

TNFR2 but No TNFR1 Is Downregulated in MDM Exposed to LAM

Next, we evaluated the expression of TNFR1 and TNFR2 (**Figures 6** and **7**, respectively), to explore if LAM stimulus *per se* can affect the TNF pathway. We found that TNFR1 expression is not affected on MDM cell surface, independently of the length of exposure to LAM stimulus, and the frequency of TNFR1$^+$ is not dependent of the CD14 co-expression (**Figures 6B,C**). In contrast, TNFR2 frequency is downregulated on MDM as a consequence of LAM exposure during a long time (**Figures 7B,C**). To validate our result, the solTNFR2 form was measured by ELISA. The LPS stimulus was included in order to verify if an activation process can potentiate the effect regarding TNFR2 expression similar to TNF. Our data confirmed that MDM exposed to LAM for 4–5 days released less solTNFR2 than MDM not exposed to LAM or exposed for a short time; however, those MDM maintained the same low level of solTNFR2 even after stimulation with LPS (**Figure 7D**).

PARP and JNK Pathways Are Not Affected in Mature Macrophages When Monocytes Are Exposed to LAM

The interaction of TNF with either TNFR1 or TNFR2 induces a different activation pathway, even if both receptors can activate the canonical NF-κB pathway and the JNK MAP kinase pathway. TNFR1 generates an anti-apoptotic and pro-inflammatory response; however, TNFR2 also can activate the no-canonical NF-κB pathway to induce differentiation and survival process (20). PARP is a nuclear protein that can regulate key cellular process such as DNA repair and cell death. It has been described that TNF is involved in caspase-8 and PARP activations, and JNK1 is required for PARP-induced mitochondrial dysfunction (21, 22). To verify if TNF activation by LAM stimulus (4–5 days) affects PARP, JNK1, and JNK2 pathways to induce cell damage, these molecules were evaluated by western blot assay (**Figure 8A**).

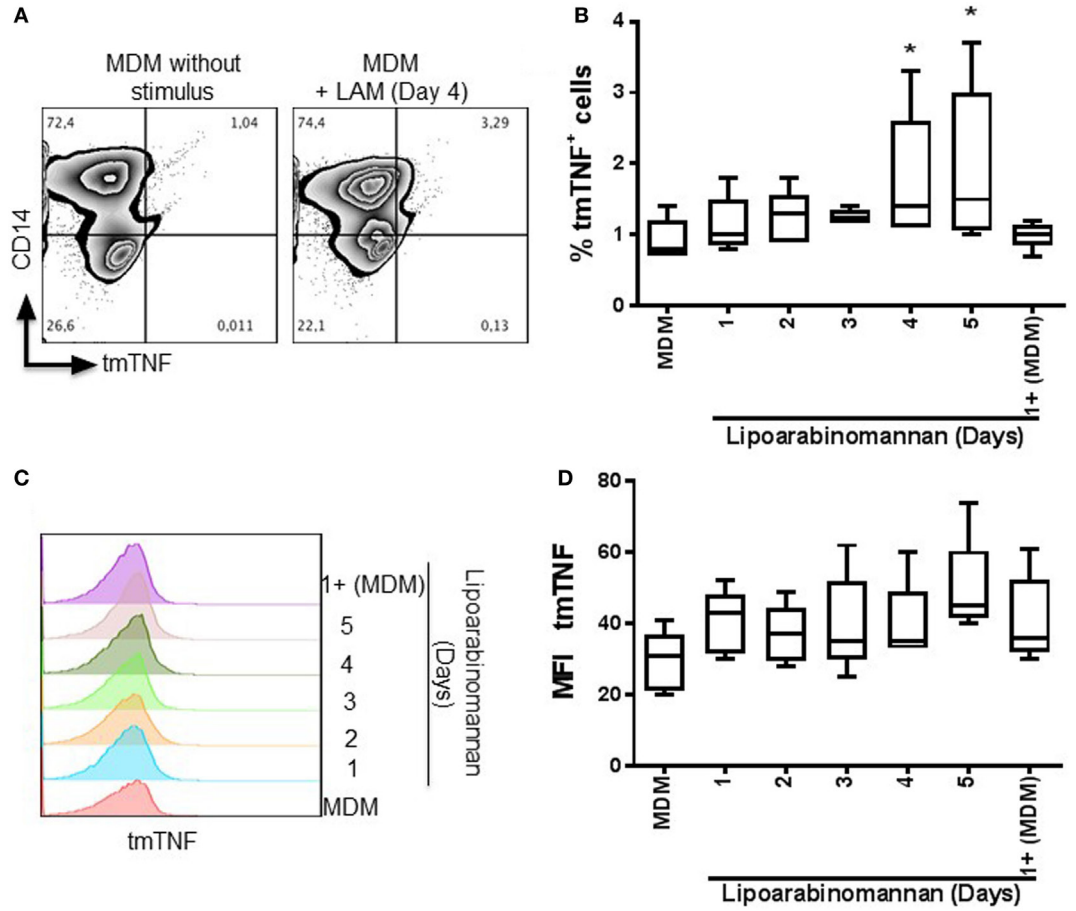


FIGURE 4 | Transmembrane tumor necrosis factor (tmTNF) is increased when monocytes are exposed to lipoarabinomannan (LAM). Pure monocytes were exposed to LAM for 1, 2, 3, 4, or 5 days, and at day 7, cells were analyzed for tmTNF and CD14 expression by flow cytometry. Representative zebra plot of monocyte-derived macrophages (MDM) without stimulus or exposed to LAM for 4 days (left and right, respectively) **(A)**. Analysis of the percentage of tmTNF$^+$ cells **(B)**. Histogram displays the median fluorescence intensity of tmTNF expression and its respective analysis [**(C,D)**, respectively]. Data are representative of four independent experiments. Box plot indicates median ± interquartile range (5–95). *$P < 0.05$, Kruskal–Wallis and Dunn's *post hoc* tests compared to unexposed MDM.

The detected full-length or fragment PARP (116 and 89 kDa, respectively) were not affected on MDM derived from monocytes exposed for short or long time to LAM (**Figure 8B**). We observed that the PARP cleaved fragment (89 kDa) was present in a double concentration in MDM exposed for a long time to LAM (96–120 h) compared to MDM not exposed to LAM, but these difference were not statistically significant (**Figure 8C**). Regarding JNK1 and JNK2, they were increased twice on MDM derived from 2 days LAM-exposed monocytes in comparison to MDM generated in absence of LAM stimulus; but this was not statistical different (**Figures 8D,E**). These data suggest that although LAM-exposed MDM affects TNF and TNFR2, the PARP and JNK pathways are not affected.

LAM Stimulus Affects PAR2 Level and the Ability to Control *Mtb* Intracellular Growth

To investigate whether LAM stimulus on MDM affects the presence of molecules necessary to control *Mtb* intracellular growth, we evaluated the presence of RAB33A, a small GTP-binding protein whose transcription is reduced in active TB (23). Our data showed that RAB33A transcription level is not affected in MDM when monocytes were exposed to LAM, although 24 h LAM-exposed monocyte MDM were activated by LPS and able to produce higher levels of RAB33A compared with not activated MDM (**Figure 9A**). We also measured the PAR2, a receptor activated by serine proteinases. It has been reported that PAR2 activation alters the macrophage phenotype toward a pro-inflammatory-like profile associated with high levels of TNF (24). PAR2 transcriptional level was increased in MDM when monocytes were exposed for a long time (4–5 days) in comparison with MDM without LAM stimulus. Interestingly, when MDM under a long-time exposure to LAM were activated with LPS, PAR2 gene expression was decreased (**Figure 9B**).

Finally, we evaluated the anti-microbial activity of MDM exposed to LAM. We infected MDM with *Mtb*-H37Ra at MOI 1, and CFU was evaluated at days 0, 3, and 7 post-infection.To

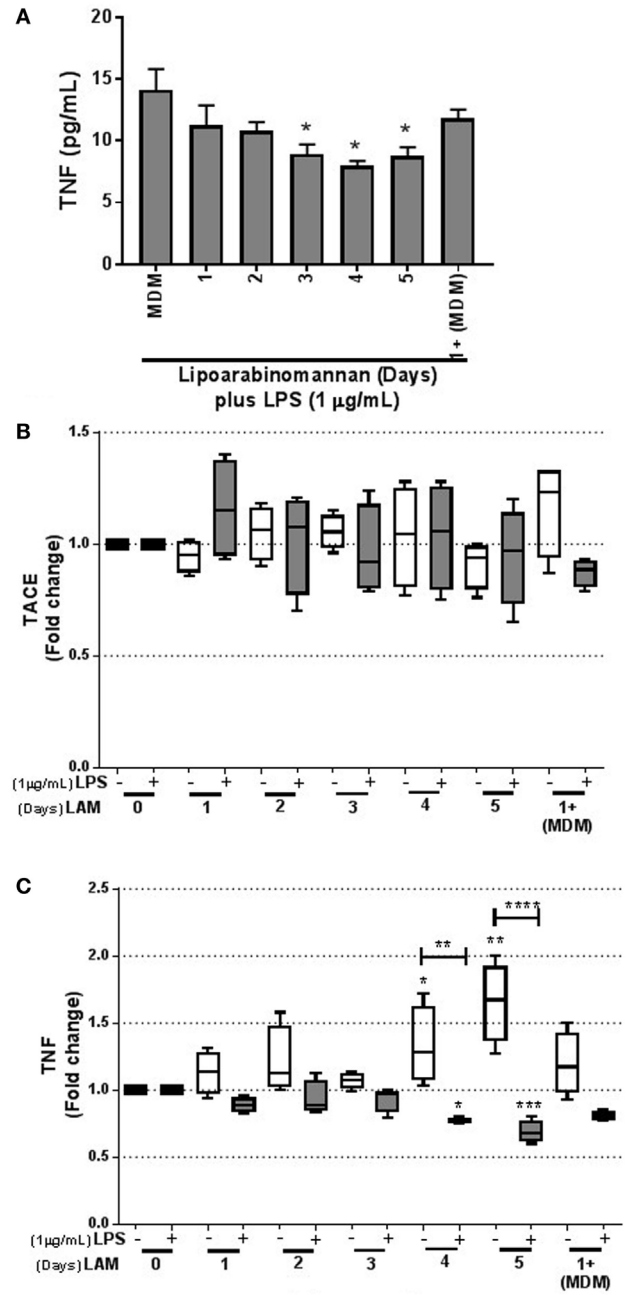


FIGURE 5 | Tumor necrosis factor (TNF) synthesis is downregulated following LPS activation when monocytes are previously exposed to lipoarabinomannan (LAM). Pure monocytes were exposed to LAM for 1, 2, 3, 4, or 5 days, and at day 7, cells were stimulated or not with LPS (1 µg/mL) for 24 h and recovered at day 8 for RT-PCR. Soluble TNF in supernatant was measured by ELISA **(A)**. TACE and TNF relative expression was measured by real-time PCR [**(B,C)**, respectively]. Data are representative of 4–5 independent experiments. Box plot indicates median ± interquartile range (5–95), and bars represent median ± SD. $^{*}P < 0.05$, $^{**}P < 0.01$, $^{***}P < 0.001$, $^{****}P < 0.0001$. Kruskal–Wallis and Dunn's *post hoc* tests. Monocyte-derived macrophages (MDM) exposed to LAM (white box) were compared with unexposed MDM, and MDM exposed to LAM plus LPS (gray box) were compared with unexposed MDM plus LPS.

evaluate bacterial intracellular growth, the percentage of CFU in relation to the number of bacteria engulfed by MDM generated under different LAM exposure times was obtained. The percentage of CFU was calculated by considering CFU at day 0 ($CFU_{day\,0}$) per individual experimental condition (**Figure 9C**) as 100% CFU in relation to CFU at day 3 ($CFU_{day\,3}$) and day 5 ($CFU_{day\,5}$) post-infection. We found that MDM with a short- or long-time exposure to LAM maintained similar ability of mycobacterial phagocytosis, even if MDM generated under LAM stimuli for 48–96 h showed increased CFU, but this was not statistically different at day 0 (**Figure 9C**). CFU measured at day 3 post-infection showed similar CFU counts for MDM generated under LAM stimulus or not exposed to LAM (**Figure 9D**); however, MDM exposed during differentiation to LAM for a longer time (4–5 days) showed a strong increase of CFU count at day 7 post-infection (**Figure 9E**). Using the absolute number of CFU also confirmed the increased of CFU at day 7 post-infection and showed that MDN exposed for 4–5 days to LAM contained the highest CFU at day 7 post-infection (**Figure 9F**). Together, these data suggest that longer LAM stimulus results in an increased expression of molecules such as PAR2 to activate anti-mycobacterial pathways. However, MDM whose monocytes were exposed to LAM for long time were not able to respond to activation stimulus such as LPS and mycobacteria. This suggests that these MDM are not efficient to control *Mtb* intracellular growth.

DISCUSSION

In this study, we found that LAM exposure of monocytes during differentiation toward macrophages modifies the expression of GAL9 and leads to MDM with reduced capacity to respond to an inflammatory stimulus and to eliminate intracellular mycobacteria. Our previous studies have shown that maturation and expression of Toll-like receptors are altered in MDM generated under LAM exposure (9). We now show that MDM dysfunction caused by LAM exposure affects TNF and PAR2 pathways and the control of intracellular mycobacterial growth.

Previous reports have shown that the expression of GAL9 and TIM3 molecules was downregulated during an *Mtb* infection and that GAL9/TIM3 pathway was necessary to activate bactericidal mechanisms to control intracellular bacterial growth (11, 12). However, it was unknown if the decrease of GAL9 and TIM3 expression on MDM surface could be induced only by the infection with the whole mycobacteria or if only LAM exposure could also affect the expression of these molecules. We postulated that LAM, which is an important virulent factor of *Mtb*, could affect the control of intracellular bacterial replication and explored at the molecular level several molecules involved in this process. Indeed, monocytes are in contact with mycobacterial glycolipids in the blood circulation and this can affect their maturation toward functional macrophages (5, 9). In fact, it is known that LAM can incorporate itself into the membrane of T cells to inhibit phosphorylation of TCR-dependent molecules in order to inhibit T-cell activation (25, 26). However, the molecular mechanisms affecting the macrophage differentiation are not

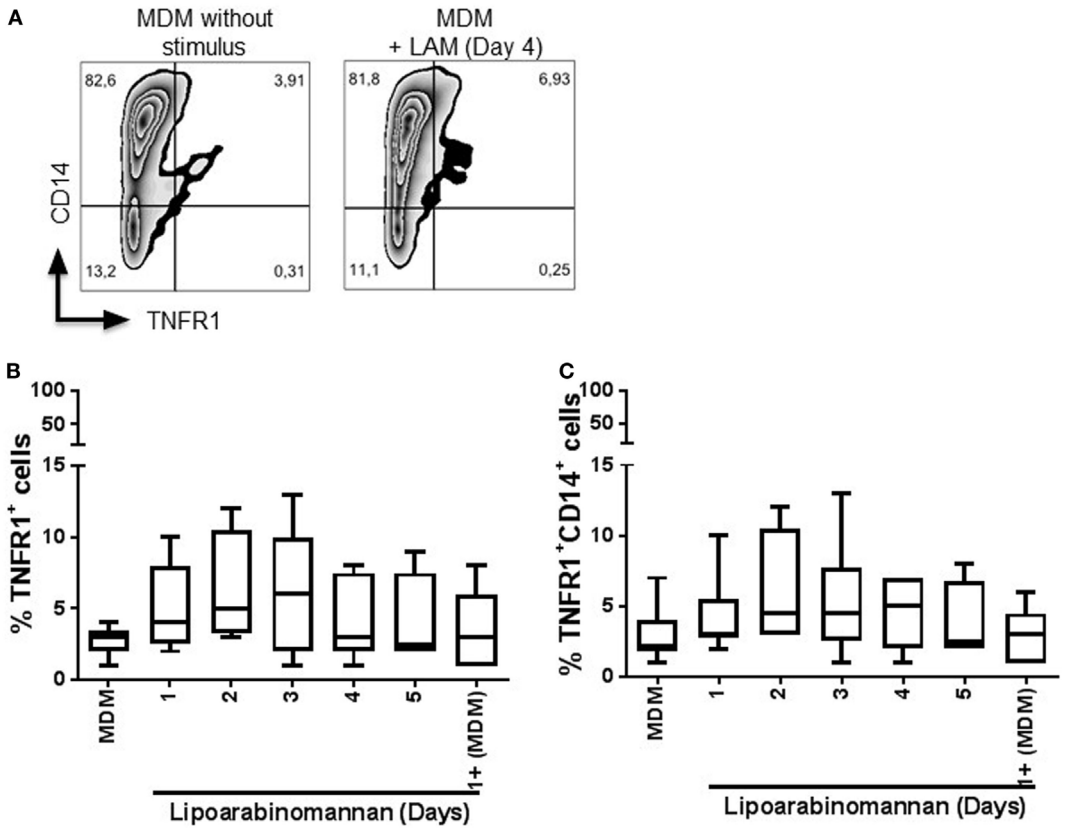


FIGURE 6 | Frequency of tumor necrosis factor receptor 1 (TNFR1$^+$) monocyte-derived macrophages (MDM) is not affected by lipoarabinomannan (LAM) exposure. Pure monocytes were exposed to LAM for 1, 2, 3, 4, or 5 days, and at day 7, cells were recovered to perform flow cytometry analyses. Representative zebra plot of MDM unexposed or exposed to LAM for 4 days (left and right, respectively) **(A)**. Flow cytometry analysis of TNFR1 independent or dependent of CD14 co-expression **(B,C)**. Data are representative of five independent experiments. Box plot indicates median ± interquartile range (5–95).

defined. In addition, as it can be expected, LAM exposure of monocytes can modify molecules that are involved in the control of microbial immunity in macrophages such as the TNF pathway (11, 19).

Our results show that TIM3 expression is not affected by LAM exposure during MDM differentiation. It has been shown that patients with pulmonary TB have low numbers of TIM3$^+$ monocytes in peripheral blood, and using an *in vitro* infection model, it has been observed that both pathogenic and no pathogenic strains of *Mtb* decreased the frequency of MDM TIM3$^+$ and GAL9$^+$ MDM (12). It is possible that TIM3 expression on MDM could be regulated trough a more complex signal than that induced by only one glycolipid such as LAM. Another possibility could be that LAM stimulus induces a downregulation of TLR molecules on the cell surface, and consequently, TIM3 expression is not changed. Previous reports have shown that TLR-dependent activation induces a significant reduction of TIM3 expression in the macrophage (27).

We then studied GAL9 expression, one of the best studied natural ligands of TIM3, and observed that it was clearly downregulated by LAM stimulus independently of CD14 co-expression on MDM. We noticed that monocytes required long exposure time (4–5 days) with LAM to generate a low frequency of GAL9$^+$ MDM. GAL9 regulation was also affected at the transcriptional level, and consequentially, the solGAL9 form was decreased. Thus, even if *Mtb* infection decreases both GAL9 and TIM3 expressions, it is now clear that the mechanism regulating their expression is different from exposure to LAM only, as LAM stimulus was enough to decrease GAL9 levels but not TIM3. It has been reported that the role of monocyte-derived GAL9 is important to induce the activation of other cells such as natural killer cells (28). A study analyzing GAL9 has proposed that plasma levels could reflect the status of inflammation and disease severity in malaria infection (29). Therefore, it is possible that this downregulation of GAL9 is used by *Mtb* as first step to manipulate the activation of pro-inflammatory responses in macrophage.

Jayaraman et al. have reported that GAL9/TIM3 pathways induced IL-1β, which allows downstream TNF production and therefore caspase-dependent restriction of intracellular bacterial growth (19). Based on these data, these pathways were evaluated in the present study. We found that the frequency of IL-1R$^+$ MDM was not modified by LAM stimulus, which is in agreement with previous data suggesting that viable *Mtb* total bacteria are required to induce IL-1β secretion by macrophage (30).

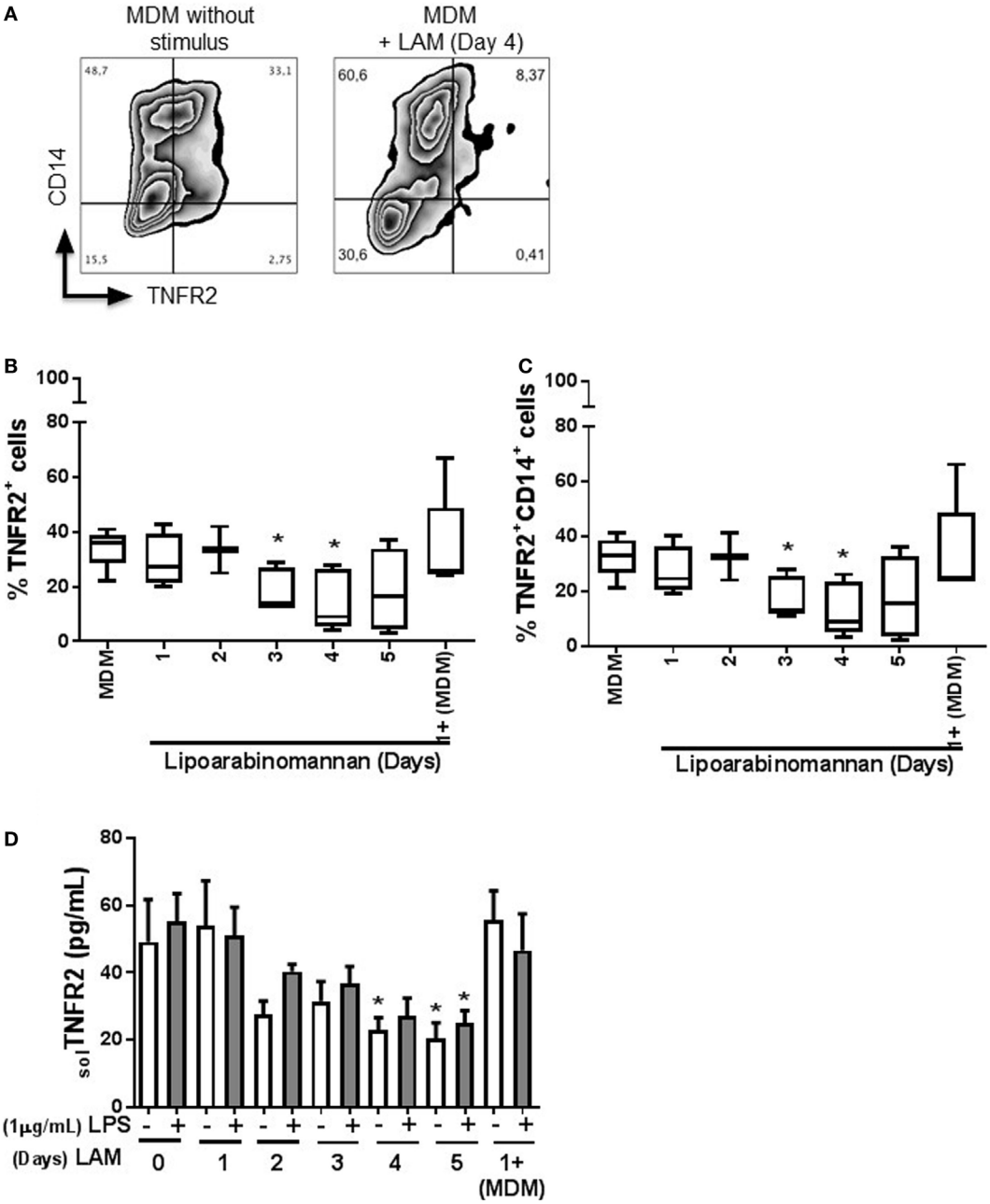


FIGURE 7 | Frequency of tumor necrosis factor receptor 2 (TNFR2+) monocyte-derived macrophages (MDM) and soluble TNFR2 are decreased when monocytes are exposed to lipoarabinomannan (LAM). Pure monocytes were exposed to LAM for 1, 2, 3, 4, or 5 days, and at day 7, cells were stimulated or not with LPS (1 μg/mL) for 24 h and then recovered at day 8. Flow cytometry zebra plot of MDM without stimulus or exposed for 4 days to LAM (left and right, respectively) **(A)**. Flow cytometry analysis of MDM expressing TNFR2 independent or dependent of CD14 co-expression **(B,C)**. Soluble form of TNFR2 was measured in supernatants by ELISA **(D)**. Data are representative of five independent experiments. Box plot indicates median ± interquartile range (5–95), and bars represent median ± SD. *$P < 0.05$, Kruskal–Wallis and Dunn's *post hoc* tests compared to unexposed MDM.

However, when TNF was measured, our data showed that the frequency of MDM expressing tmTNF was increased after monocyte exposure to LAM for 4–5 days. We also found that TNF was upregulated in MDM exposed to LAM at the transcriptional level and as previously reported, the presence of solTNF was decreased when LAM exposed MDM were activated with a second stimulus such as LPS (9). However, our results revealed that TACE expression, at the transcriptional level, was not affected in MDM generated under LAM stimulus. Our results confirmed that when LAM-exposed MDM received a stimulus (LPS), they were not able to produce TNF at the transcriptional and protein levels as we previously reported (9). An alternative hypothesis

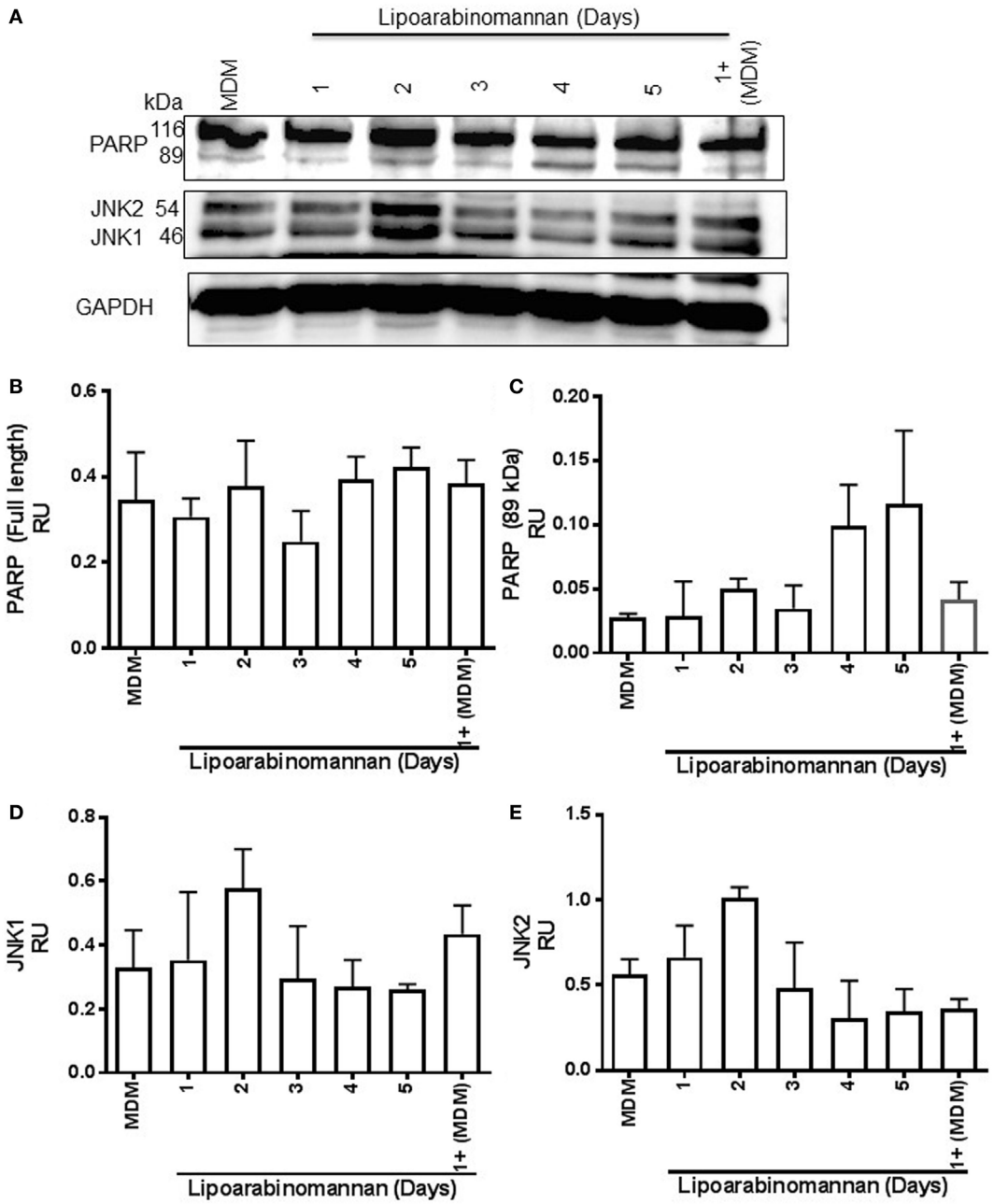


FIGURE 8 | Poly(ADP-ribose) polymerase (PARP) and Jun N-terminal kinase (JNK) pathways are not affected when monocytes are exposed to lipoarabinomannan (LAM). Pure monocytes were exposed to LAM for 1, 2, 3, 4, or 5 days, and at day 7, cells were recovered to perform Western blot assays. Representative Western blot of monocyte-derived macrophages (MDM) lysates for PARP, JNK, and glyceraldehyde 3-phosphate dehydrogenase (GAPDH) which was used as a loading control **(A)**. Band densities of full-length and fragmented PARP (116 and 89 kDa, respectively) **(B,C)** and JNK1 and JNK2 forms (46 and 54 kDa, respectively) **(D,E)** were normalized with GAPDH by densitometry. Results are shown in relative units of concentration using the ImageJ 1.39c software. Data are representative of two independent experiments. Each bar indicates mean ± SD.

to explain TNF levels as consequence of LAM stimulus was that LAM exposure can also induce an increase of TNFR level. This hypothesis was discarded because the expression of TNFR1 was not modified and TNFR2 was decreased when monocytes were exposed 3–5 days to LAM. TNFR2 was downregulated on the cell surface as well as its soluble TNFR2. Furthermore, the soluble TNFR2 was still downregulated when MDM were activated by LPS. Together data show that LAM exposure of monocytes during MDM differentiation affects TNF pathway and subsequent responses of MDM can be impaired. TNF pathway is involved in anti-bacterial activity of human macrophages, which could be affected in LAM-exposed MDM.

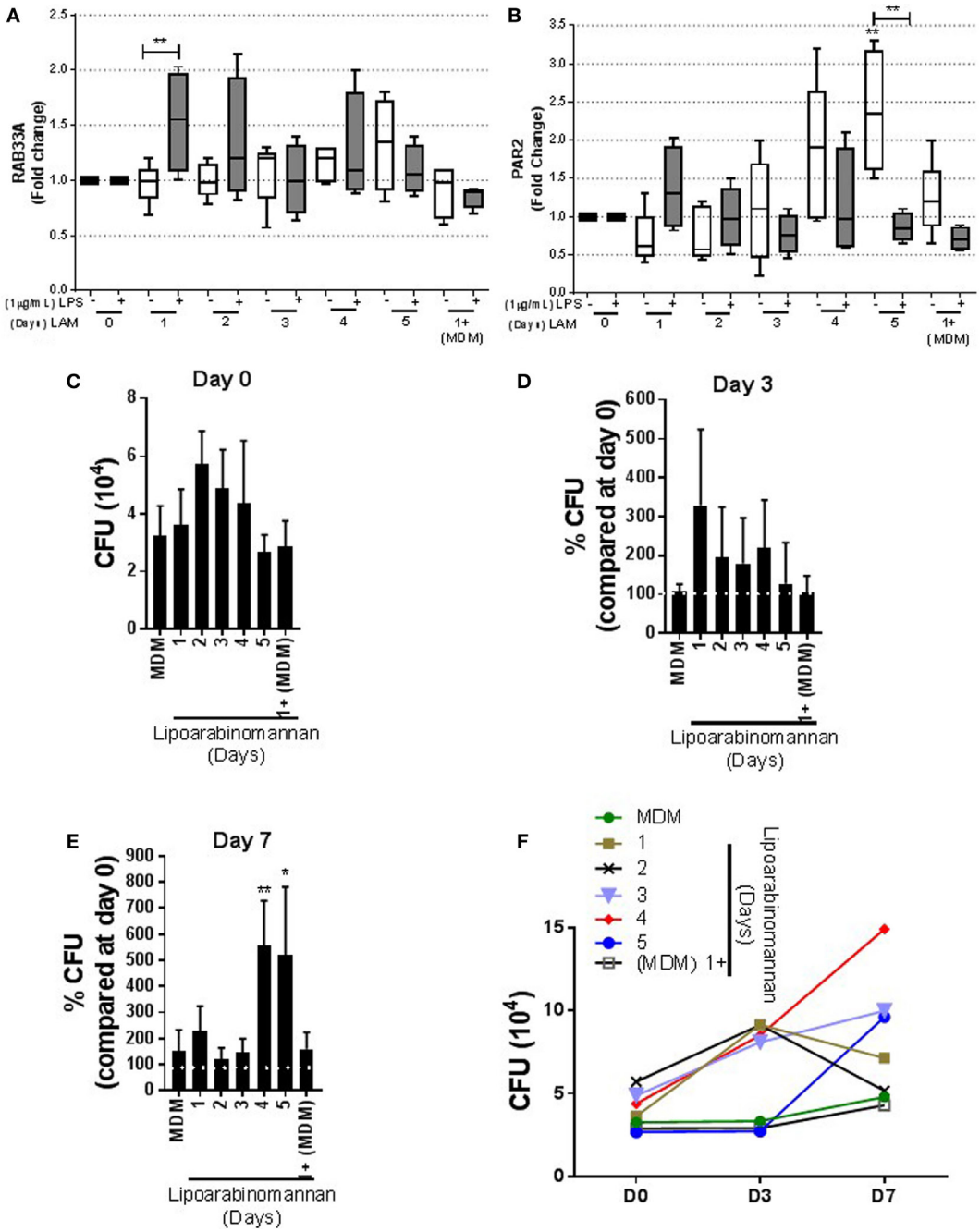


FIGURE 9 | Proteinase-activated receptor-2 (PAR2) production and bacterial growth are affected in monocyte-derived macrophages (MDM) when monocytes are exposed to lipoarabinomannan (LAM) for long time. Pure monocytes were exposed to LAM for 1, 2, 3, 4, or 5 days, and at day 7, cells were infected with *Mycobacterium tuberculosis* (*Mtb*)-H37Ra (MOI 1) or cells were stimulated or not with LPS (1 μg/mL) for 24 h and at day 8 recovered for RT-PCR. RAB33A and PAR2 relative expressions were measured by real-time PCR [**(A,B)**, respectively]. Colony-forming unit (CFU) assay measuring living *Mtb*-H37Ra bacteria in infected MDM on days 0, 3, and 7 post-infection. Day 0 was considered the basal living *Mtb*-H37Ra that has been engulfed by MDM **(C)**. Using as 100% the bacteria uptake at day 0 per individual experimental condition (white line), the percentage of CFU change was calculated at days 3 and 7 [**(D,E)**, respectively]. Summary of absolute number of CFU counted at days 0, 3, and 7 post-infection **(F)**. Data are representative of 4–5 independent experiments. Box plot indicates median ± interquartile range (5–95), and bars indicate mean ± SD. $^{*}P < 0.05$, $^{**}P < 0.01$. Kruskal–Wallis and Dunn's *post hoc* tests, MDM exposed to LAM were compared to unexposed MDM.

Proteinase-activated receptor-2 has been shown to be a modulator of innate and adaptive immunity during infections, helping macrophage differentiation toward a pro-inflammatory phenotype, favoring mainly TNF production (24, 31). Our result showed that PAR2 has an expression pattern similar to TNF. The PAR2 gene expression was increased in MDM when

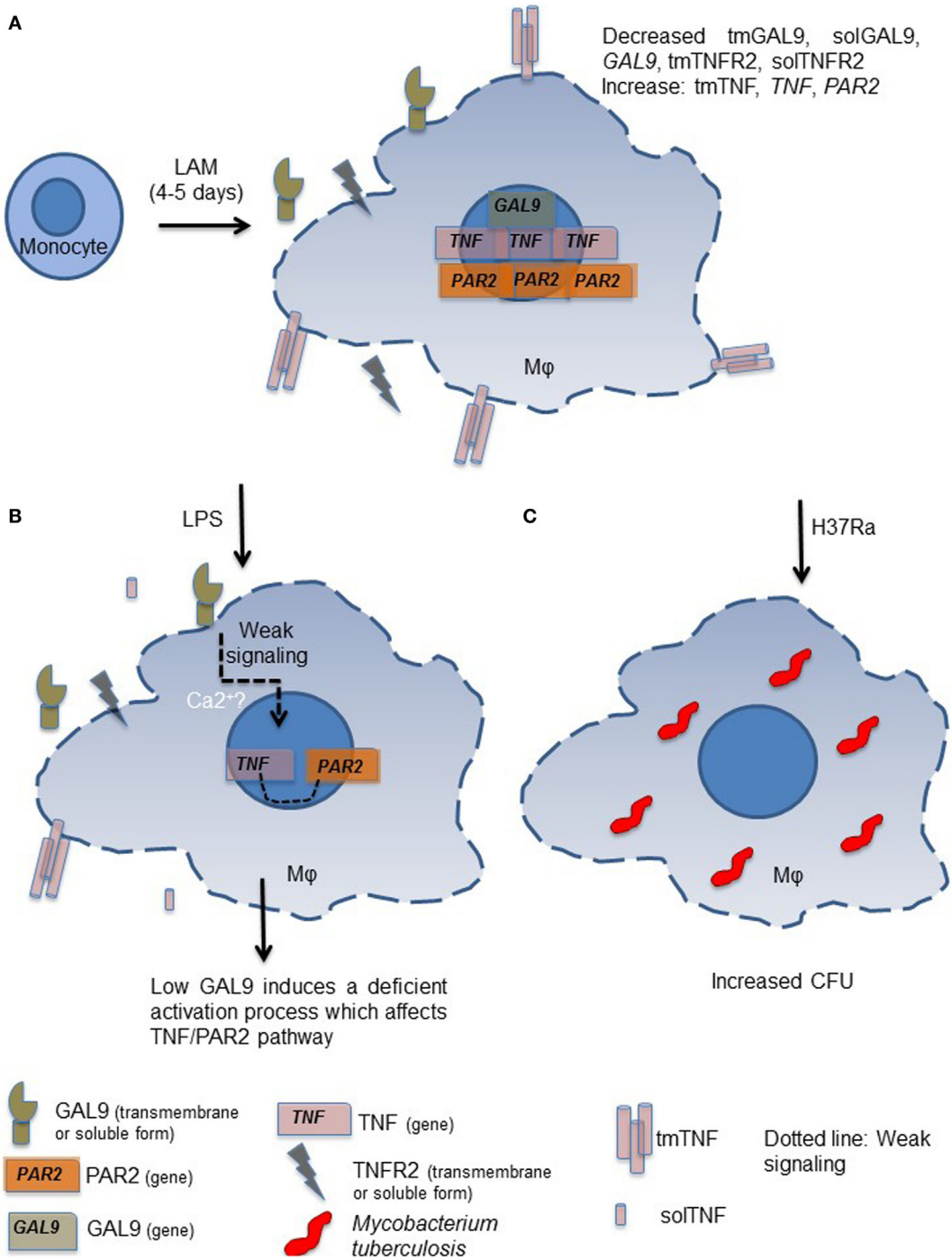


FIGURE 10 | Proposed model to explain the inability to control intracellular *Mycobacterium tuberculosis* growth by monocyte-derived macrophages (MDM) generated under exposure to lipoarabinomannan (LAM). Monocytes exposed for long time to LAM (4–5 days) differentiate into MDM that are characterized by deficiency in galectin (GAL)9 and TNFR2 but high tumor necrosis factor (TNF) and proteinase-activated receptor-2 (PAR2) expressions **(A)**. When altered LAM-exposed MDM are in contact with a second stimulus such as LPS only week signal are triggered and consequently the activation of crucial pathways such as TNF and PAR2 are affected **(B)**. The GAL9/TNF/PAR2 axis is crucial for the activation of microbicidal mechanism necessary to eliminate intracellular mycobacteria, as it is expected. MDM generated under LAM exposure are not able to efficiently eliminate intracellular bacteria **(C)**.

monocytes were exposed for a longer time to LAM but when those MDM were again activated, PAR2 production was blocked. We cannot know if this downregulation is a consequence of the TNF downregulation or the contrary. Since long exposition to LAM generates MDM unable to produce TNF and PAR2 in response to LPS stimulus, we thought that LAM exposed

MDM deficiencies may persist when other additional stimuli are encountered including mycobacterial infection. MDM exposed to LAM during their differentiation showed impaired capacity to control the intracellular growth of *Mtb*-H37Ra at day 7 post-infection. This shows that long-term LAM exposure is detrimental for the anti-microbial capacity of MDM resulting in the lack of control of intracellular bacterial growth.

In conclusion, our study shows that when monocytes are exposed for long time (4–5 days) to a microenvironment in which LAM is present, generated macrophages exhibit a different phenotype characterized by a decreased expression of GAL9 (**Figure 10A**). Although our knowledge of the signaling events triggered by GAL9 pathway on macrophages remains limited, we are aware that in human lymphocytes, this pathway increases cytosolic calcium (Ca^{2+}) mobilization, which in turn is required for the production of pro-inflammatory cytokines (**Figure 10B**) (32). When LAM-exposed MDM are subsequently activated by other stimuli such as *Mtb* infection, they are not able to respond and eliminate intracellular bacterial as unexposed MDM (**Figure 10C**) (32).

AUTHOR CONTRIBUTIONS

LC-G conceived and designed the experiments. LR-L, CC, and LC-G performed the experiments. LR-L, IS-O, IG, and LC-G analyzed and discussed the data. CC and IS-O contributed reagents/materials/analysis tools. LR-L, IG, and LC-G wrote the paper.

ACKNOWLEDGMENTS

Financial support: Novartis and FNS (310030_166662) (IG). The following reagent was obtained through BEI Resource, NIAID, NIH: purified Lipoarabinomannan (LAM) from *Mycobacterium tuberculosis*, Strain H37Rv, NR-14848.

SUPPLEMENTARY MATERIAL

The Supplementary Material for this article can be found online at http://www.frontiersin.org/article/10.3389/fimmu.2017.01659/full#supplementary-material.

REFERENCES

1. WHO. *Global Tuberculosis Report 2014*. Geneva: WHO (2014).
2. Guenin-Mace L, Simeone R, Demangel C. Lipids of pathogenic mycobacteria: contributions to virulence and host immune suppression. *Transbound Emerg Dis* (2009) 56(6–7):255–68. doi:10.1111/j.1865-1682.2009.01072.x
3. Fukuda T, Matsumura T, Ato M, Hamasaki M, Nishiuchi Y, Murakami Y, et al. Critical roles for lipomannan and lipoarabinomannan in cell wall integrity of mycobacteria and pathogenesis of tuberculosis. *MBio* (2013) 4(1):e00472–12. doi:10.1128/mBio.00472-12
4. Drain PK, Gounder L, Sahid F, Moosa MY. Rapid urine LAM testing improves diagnosis of expectorated smear-negative pulmonary tuberculosis in an HIV-endemic region. *Sci Rep* (2016) 6:19992. doi:10.1038/srep19992
5. Sakamuri RM, Price DN, Lee M, Cho SN, Barry CE III, Via LE, et al. Association of lipoarabinomannan with high density lipoprotein in blood: implications for diagnostics. *Tuberculosis* (2013) 93(3):301–7. doi:10.1016/j.tube.2013.02.015
6. Korb VC, Chuturgoon AA, Moodley D. *Mycobacterium tuberculosis*: manipulator of protective immunity. *Int J Mol Sci* (2016) 17(3):131. doi:10.3390/ijms17030131
7. Welin A, Winberg ME, Abdalla H, Sarndahl E, Rasmusson B, Stendahl O, et al. Incorporation of *Mycobacterium tuberculosis* lipoarabinomannan into macrophage membrane rafts is a prerequisite for the phagosomal maturation block. *Infect Immun* (2008) 76(7):2882–7. doi:10.1128/IAI.01549-07
8. Majumder N, Bhattacharjee S, Bhattacharyya Majumdar S, Dey R, Guha P, Pal NK, et al. Restoration of impaired free radical generation and proinflammatory cytokines by MCP-1 in mycobacterial pathogenesis. *Scand J Immunol* (2008) 67(4):329–39. doi:10.1111/j.1365-3083.2008.02070.x
9. Chavez-Galan L, Ocana-Guzman R, Torre-Bouscoulet L, Garcia-de-Alba C, Sada-Ovalle I. Exposure of monocytes to lipoarabinomannan promotes their differentiation into functionally and phenotypically immature macrophages. *J Immunol Res* (2015) 2015:984973. doi:10.1155/2015/984973
10. Ocana-Guzman R, Torre-Bouscoulet L, Sada-Ovalle I. TIM-3 regulates distinct functions in macrophages. *Front Immunol* (2016) 7:229. doi:10.3389/fimmu.2016.00229
11. Jayaraman P, Sada-Ovalle I, Beladi S, Anderson AC, Dardalhon V, Hotta C, et al. Tim3 binding to galectin-9 stimulates antimicrobial immunity. *J Exp Med* (2010) 207(11):2343–54. doi:10.1084/jem.20100687
12. Sada-Ovalle I, Chavez-Galan L, Torre-Bouscoulet L, Nava-Gamino L, Barrera L, Jayaraman P, et al. The Tim3-galectin 9 pathway induces antibacterial activity in human macrophages infected with *Mycobacterium tuberculosis*. *J Immunol* (2012) 189(12):5896–902. doi:10.4049/jimmunol.1200990
13. Wallach D. The cybernetics of TNF: old views and newer ones. *Semin Cell Dev Biol* (2016) 50:105–14. doi:10.1016/j.semcdb.2015.10.014
14. Chavez-Galan L, Vesin D, Segueni N, Prasad P, Buser-Llinares R, Blaser G, et al. Tumor necrosis factor and its receptors are crucial to control *Mycobacterium bovis* bacillus calmette-guerin pleural infection in a murine model. *Am J Pathol* (2016) 186(9):2364–77. doi:10.1016/j.ajpath.2016.05.015
15. Olleros ML, Guler R, Corazza N, Vesin D, Eugster HP, Marchal G, et al. Transmembrane TNF induces an efficient cell-mediated immunity and resistance to *Mycobacterium bovis* bacillus Calmette-Guerin infection in the absence of secreted TNF and lymphotoxin-alpha. *J Immunol* (2002) 168(7):3394–401. doi:10.4049/jimmunol.168.7.3394
16. Garcia I, Olleros ML, Quesniaux VF, Jacobs M, Allie N, Nedospasov SA, et al. Roles of soluble and membrane TNF and related ligands in mycobacterial infections: effects of selective and non-selective TNF inhibitors during infection. *Adv Exp Med Biol* (2011) 691:187–201. doi:10.1007/978-1-4419-6612-4_20
17. Quesniaux VF, Jacobs M, Allie N, Grivennikov S, Nedospasov SA, Garcia I, et al. TNF in host resistance to tuberculosis infection. *Curr Dir Autoimmun* (2010) 11:157–79. doi:10.1159/000289204
18. Ohradanova-Repic A, Machacek C, Fischer MB, Stockinger H. Differentiation of human monocytes and derived subsets of macrophages and dendritic cells by the HLDA10 monoclonal antibody panel. *Clin Transl Immunology* (2016) 5(1):e55. doi:10.1038/cti.2015.39
19. Jayaraman P, Sada-Ovalle I, Nishimura T, Anderson AC, Kuchroo VK, Remold HG, et al. IL-1beta promotes antimicrobial immunity in macrophages by regulating TNFR signaling and caspase-3 activation. *J Immunol* (2013) 190(8):4196–204. doi:10.4049/jimmunol.1202688
20. Borghi A, Verstrepen L, Beyaert R. TRAF2 multitasking in TNF receptor-induced signaling to NF-kappaB, MAP kinases and cell death. *Biochem Pharmacol* (2016) 116:1–10. doi:10.1016/j.bcp.2016.03.009
21. Roberge S, Roussel J, Andersson DC, Meli AC, Vidal B, Blandel F, et al. TNF-alpha-mediated caspase-8 activation induces ROS production and TRPM2 activation in adult ventricular myocytes. *Cardiovasc Res* (2014) 103(1):90–9. doi:10.1093/cvr/cvu112
22. Xu Y, Huang S, Liu ZG, Han J. Poly(ADP-ribose) polymerase-1 signaling to mitochondria in necrotic cell death requires RIP1/TRAF2-mediated JNK1 activation. *J Biol Chem* (2006) 281(13):8788–95. doi:10.1074/jbc.M508135200
23. Dhanasekaran S, Jenum S, Stavrum R, Ritz C, Faurholt-Jepsen D, Kenneth J, et al. Identification of biomarkers for *Mycobacterium tuberculosis* infection and disease in BCG-vaccinated young children in Southern India. *Genes Immun* (2013) 14(6):356–64. doi:10.1038/gene.2013.26
24. Steven R, Crilly A, Lockhart JC, Ferrell WR, McInnes IB. Proteinase-activated receptor-2 modulates human macrophage differentiation and effector function. *Innate Immun* (2013) 19(6):663–72. doi:10.1177/1753425913479984
25. Shabaana AK, Kulangara K, Semac I, Parel Y, Ilangumaran S, Dharmalingam K, et al. Mycobacterial lipoarabinomannans modulate cytokine production in

human T helper cells by interfering with raft/microdomain signalling. *Cell Mol Life Sci* (2005) 62(2):179–87. doi:10.1007/s00018-004-4404-5
26. Sande OJ, Karim AF, Li Q, Ding X, Harding CV, Rojas RE, et al. Mannose-capped lipoarabinomannan from *Mycobacterium tuberculosis* induces CD4+ T cell anergy via GRAIL. *J Immunol* (2016) 196(2):691–702. doi:10.4049/jimmunol.1500710
27. Zhang Y, Ma CJ, Wang JM, Ji XJ, Wu XY, Jia ZS, et al. Tim-3 negatively regulates IL-12 expression by monocytes in HCV infection. *PLoS One* (2011) 6(5):e19664. doi:10.1371/journal.pone.0019664
28. Nishio A, Tatsumi T, Nawa T, Suda T, Yoshioka T, Onishi Y, et al. CD14+ monocyte-derived galectin-9 induces natural killer cell cytotoxicity in chronic hepatitis C. *Hepatology* (2017) 65(1):18–31. doi:10.1002/hep.28847
29. Dembele BP, Chagan-Yasutan H, Niki T, Ashino Y, Tangpukdee N, Shinichi E, et al. Plasma levels of Galectin-9 reflect disease severity in malaria infection. *Malar J* (2016) 15(1):403. doi:10.1186/s12936-016-1471-7
30. Krishnan N, Robertson BD, Thwaites G. Pathways of IL-1beta secretion by macrophages infected with clinical *Mycobacterium tuberculosis* strains. *Tuberculosis* (2013) 93(5):538–47. doi:10.1016/j.tube.2013.05.002
31. Nakayama M, Niki Y, Kawasaki T, Takeda Y, Ikegami H, Toyama Y, et al. IL-32-PAR2 axis is an innate immunity sensor providing alternative signaling for LPS-TRIF axis. *Sci Rep* (2013) 3:2960. doi:10.1038/srep02960
32. Lhuillier C, Barjon C, Niki T, Gelin A, Praz F, Morales O, et al. Impact of exogenous galectin-9 on human T cells: contribution of the T cell receptor complex to antigen-independent activation but not to apoptosis induction. *J Biol Chem* (2015) 290(27):16797–811. doi:10.1074/jbc.M115.661272

Conflict of Interest Statement: The authors declare that the research was conducted in the absence of any commercial or financial relationships that could be construed as a potential conflict of interest.

Copyright © 2017 Chávez-Galán, Ramon-Luing, Carranza, Garcia and Sada-Ovalle. This is an open-access article distributed under the terms of the Creative Commons Attribution License (CC BY). The use, distribution or reproduction in other forums is permitted, provided the original author(s) or licensor are credited and that the original publication in this journal is cited, in accordance with accepted academic practice. No use, distribution or reproduction is permitted which does not comply with these terms.

frontiers in Immunology

ORIGINAL RESEARCH
published: 18 December 2017
doi: 10.3389/fimmu.2017.01819

Mycobacterium tuberculosis Modulates miR-106b-5p to Control Cathepsin S Expression Resulting in Higher Pathogen Survival and Poor T-Cell Activation

*David Pires[1‡], Elliott M. Bernard[2], João Palma Pombo[1], Nuno Carmo[1], Catarina Fialho[1], Maximiliano Gabriel Gutierrez[2], Paulo Bettencourt[1‡†] and Elsa Anes[1]**

[1] Host-Pathogen Interactions Unit, Faculty of Pharmacy, Research Institute for Medicines, iMed-ULisboa, Universidade de Lisboa, Lisboa, Portugal, [2] Host-Pathogen Interactions in Tuberculosis Laboratory, The Francis Crick Institute, London, United Kingdom

The success of tuberculosis (TB) bacillus, *Mycobacterium tuberculosis* (Mtb), relies on the ability to survive in host cells and escape to immune surveillance and activation. We recently demonstrated that Mtb manipulation of host lysosomal cathepsins in macrophages leads to decreased enzymatic activity and pathogen survival. In addition, while searching for microRNAs (miRNAs) involved in posttranscriptional gene regulation during mycobacteria infection of human macrophages, we found that selected miRNAs such as miR-106b-5p were specifically upregulated by pathogenic mycobacteria. Here, we show that miR-106b-5p is actively manipulated by Mtb to ensure its survival in macrophages. Using an *in silico* prediction approach, we identified miR-106b-5p with a potential binding to the 3′-untranslated region of cathepsin S (CtsS) mRNA. We demonstrated by luminescence-based methods that miR-106b-5p indeed targets CTSS mRNA resulting in protein translation silencing. Moreover, miR-106b-5p gain-of-function experiments lead to a decreased CtsS expression favoring Mtb intracellular survival. By contrast, miR-106b-5p loss-of-function in infected cells was concomitant with increased CtsS expression, with significant intracellular killing of Mtb and T-cell activation. Modulation of miR-106b-5p did not impact necrosis, apoptosis or autophagy arguing that miR-106b-5p directly targeted CtsS expression as a way for Mtb to avoid exposure to degradative enzymes in the endocytic pathway. Altogether, our data suggest that manipulation of miR-106b-5p as a potential target for host-directed therapy for Mtb infection.

Keywords: tuberculosis, host-directed therapies, microRNAs, cathepsin S, antigen presentation, lysosomal enzymes

OPEN ACCESS

Edited by:
Geanncarlo Lugo-Villarino, UMR5089 Institut de Pharmacologie et de Biologie Structurale (IPBS), France

Reviewed by:
Kithiganahalli Balaji, Indian Institute of Science, India
Sahana Holla, National Cancer Institute (NIH), United States
Venkat Laxmi Yeruva, University of Arkansas for Medical Sciences, United States

****Correspondence:***
Elsa Anes
eanes@ff.ulisboa.pt

†Present address:
Paulo Bettencourt, The Jenner Institute, University of Oxford, Oxford, United Kingdom

‡These authors have shared First authorship.

Specialty section:
This article was submitted to Microbial Immunology, a section of the journal Frontiers in Immunology

Received: *20 September 2017*
Accepted: *04 December 2017*
Published: *18 December 2017*

Citation:
Pires D, Bernard EM, Pombo JP, Carmo N, Fialho C, Gutierrez MG, Bettencourt P and Anes E (2017) Mycobacterium tuberculosis Modulates miR-106b-5p to Control Cathepsin S Expression Resulting in Higher Pathogen Survival and Poor T-Cell Activation. Front. Immunol. 8:1819. doi: 10.3389/fimmu.2017.01819

INTRODUCTION

Mycobacterium tuberculosis (Mtb) has succeeded in infecting about one third of the human population by evading innate and adaptive immune responses. Approximately 10% of chronically infected people will manifest the tuberculosis (TB) disease as age, HIV and other illnesses compromise their immune systems (1). From the past 30 years, the greatest threat evolving from this

infection was the emergence of drug-resistant strains resulting in multidrug-resistant TB, which accounts for approximately 4% of the new cases of disease. This lead us to search for host targets that may be manipulated during infection to boost the immune responses blocked by Mtb as alternative therapeutic to current antimicrobials.

One of the hallmarks of Mtb pathogenesis is the ability to persist in host professional phagocytes such as macrophages (Mø) (2). This persistence is enabled by the control of host cells functions, particularly those involved in phagosome maturation and fusion with lysosomes (2–5). Usually these processes lead to the acidification of the phagosome and activation of lysosomal enzymes such as proteases and lipases but during Mtb infection these events are halted and the bacteria persist in a less degradative environment (3, 6). An important group of degradative lysosomal enzymes for bacterial clearance includes cysteine cathepsin proteases. Cathepsin activity is optimized for the low pH of the lysosome, which helps to restrict it to this compartment under normal conditions. They are integrated into most processes associated with the lysosome as protein processing or degradation, autophagy, direct pathogen killing, antigen presentation, cellular stress signaling and lysosome-mediated cell death (7). These enzymes can also be secreted, in some circumstances which results in the degradation of extracellular targets such as ECM and granulomas (8).

However, it is yet to decipher how Mtb interferes with cathepsins (Cts) regulation and activity. We recently demonstrated that some Cts are downregulated during Mtb infection and that Mtb controls cathepsins and their inhibitors cystatins at the level of gene expression and proteolytic activity (9). Among the most differentially regulated cathepsins during Mtb infection when compared to *Mycobacterium smegmatis*, a non-pathogenic mycobacteria that is cleared within Mø, was CtsS. CtsS possesses a broad pH profile of activity and the maintenance of a significant endoproteolytic activity at neutral pH, suggesting that this enzyme may have important function along all endocytic pathway (10). Accordingly, our previous results indicated that pathogenic mycobacteria could be killed to some extent in early phagosomes within a pH 6.4–5.5 environment (6). CtsS constitutive expression is restricted primarily to antigen presenting cells and its mRNA expression and protein levels are upregulated by IFNγ [as their promoter responds to interferon-related factor 1 (IRF-1) transcription factor] (11). We found that in IFNγ-activated Mø, CtsS gene expression was highly inhibited during Mtb infection when comparing to non-infected cells (9). In addition, IRF-1 responding promoter and therefore CtsS, influence several important biological processes, including maturation and trafficking of MHC class II molecules required for antigen presentation (12, 13). Mtb has indeed ability to block antigen presentation by affecting the intracellular trafficking of MHC class II molecules *via* cathepsin S (CtsS) (14–16). Moreover, inhibition of CtsS activity has been implicated in autophagy (17) and IFN-γ induces autophagy during mycobacteria infection (18) leading to increased intracellular bacterial killing.

To address how Mtb manipulates CtsS downregulation and, in one attempt to restore the control over CtsS in Mø infected with Mtb, we investigated the potential involvement of microRNAs (miRNAs). miRNAs are predictable intermediates in this process due to their wide regulatory role. These molecules are small, non-coding regulator RNAs with 19–22 nucleotides long that are involved in posttranscriptional gene expression control (19). They silence their targets expression by forming complexes with the RNA-induced silencing complex and then binding their 7 nucleotide-long "seed region" with a complementary region of mRNA, leading to termination of translation and/or mRNA degradation (20, 21). There are already several studies proposing modulation of miRNAs by mycobacteria in order to increase the success of their infection by impairing the release of proinflammatory cytokines (22), controlling phagocytosis (23), preventing cell recruitment to the locus of infection (24) and miRNAs are also proposed as biomarkers of TB disease [recently reviewed by Ref. (25)].

Here, we show miR-106b-5p isoform as another miRNA strongly upregulated during Mtb infection in contrast to challenge with non-pathogenic *M. smegmatis*. Using *in silico* prediction approach, we found that miR-106b-5p has a high probability of binding to CtsS mRNA. Interestingly, miR-106b was described as the posttranscriptional target of the autophagy-related gene 16L1 (ATG16L1) regulating autophagy in the context of epithelial cells and Crohn's disease (26). Our data indicates that the consequence of miR-106b-5p manipulation by Mtb is a decrease of CtsS activity concomitant with an increase of the intracellular survival of the bacteria and decreased human leukocyte antigen (HLA)-DR class II surface expression in human macrophages, similar to what occurs during siRNA silencing of CtsS. Interestingly, the function of miR-106b-5p on CtsS activity in the context of infection was independent of autophagy. By using inhibitors of this miR, we were able to overcome the Mtb manipulation of the Mø anti-mycobacterial activity. Altogether, our data suggest that manipulation of miR-106b-5p as a potential target for host-directed therapy (HDT) for Mtb infection.

MATERIALS AND METHODS

Cell Lines and Culture Conditions

Human monocyte-derived Mø and CD4 lymphocytes were obtained by, respectively, isolating $CD14^+$ monocytes and $CD4^+$ lymphocytes from buffy coats of healthy PPD^+ blood donors provided by the national blood institute (Instituto Português do Sangue e da Transplantação, Lisbon, Portugal) following a protocol established between Dr. Anes and the Portuguese Institute for Blood, allowing access to buffy coats from healthy blood donors, for scientific research with academic purposes only. No personal details from the donors were provided by the supplier. The cells were separated using MACS cell separation system (Miltenyi Biotec). Differentiation of the monocytes into macrophages proceeded as previously described (27). When required, Mø were stimulated with 100 IU/ml IFNγ, overnight, prior to infection.

Bacterial Cultures

The strain *M. smegmatis* mc^2155, containing a p19 (long lived) EGFP plasmid was kindly provided by Dr. Douglas Young (The

Francis Crick Institute, London, UK), and the green fluorescent protein-expressing strain of Mtb (H37Rv-pEGFP) plasmid was a kind gift from G. R. Stewart (University of Surrey, United Kingdom). *M. smegmatis* was grown in medium containing Middlebrook's 7H9 Medium (Difco), nutrient broth (Difco) supplemented with 0.5% glucose and 0.05% tyloxapol at 37°C on a shaker at 200 rpm (23). Mtb H37Rv was grown in Middlebrook's 7H9 medium and supplemented with 10% OADC enrichment (Difco) (28). All experimental procedures using live Mtb were performed in the Biosafety Level 3 laboratory at the Faculty of Pharmacy of the University of Lisbon, respecting the national and European academic containment level 3, laboratory management and biosecurity standards, based on applicable EU Directives. All procedures have been approved by the faculty's biological safety committee.

Infection of Macrophages

Bacterial cultures on exponential grown phase were centrifuged, washed in phosphate-buffered saline (PBS). Bacteria were then resuspended in the desired culture medium without antibiotics. In order to dismantle bacterial clumps, the bacterial suspension was subjected to 5 min of ultrasonic bath. Residual clumps were removed by 1 min centrifugation at 500 *g*. Single-cell suspension was verified by fluorescence microscopy. Macrophages were infected with an MOI of 1 for 3 h at 37°C with 5% CO_2. Following internalization, cells were washed with PBS and resuspended in appropriate culture medium without antibiotics.

RT-qPCR

Mø were seeded in six-well plates at a density of 2×10^6 cells per well. RNA was isolated and purified from infected cells using Trizol reagent (Invitrogen) and following the manufacturer's protocol. The relative quantification of miRNAs in total RNA samples was performed by Exiqon (DK) miRNA qPCR services on RNA purified samples in triplicate. The specific quantification of miR-106b-5p in total RNA samples was performed in our laboratory using miRCURY LNA™ Universal RT miRNA PCR system (Exiqon) according to the manufacturer protocol and using the Exiqon LNA™ PCR primer sets: hsa-miR-106b-5p (205884), hsa-miR-23a-3p (204772), hsa-miR-23b-3p (204790), and hsa-miR-24-3p (204260). The qPCR was performed using an ABI 7300 Real Time PCR. The reaction proceeded as follows: 1 cycle of 95°C for 10 min, followed by 40 cycles of 95°C for 10 s and 60°C for 1 min. The miRNA expression profiles were normalized to the average obtained between miR-23a, miR-23b, and miR-24, whose expression levels were stable under the experimental conditions applied in this study (23).

Transfection

Transfection with anti-CtsS siRNA or with miR-106b-5p mimics and inhibitors was performed with Biontex K2® Transfection System. Macrophages were first incubated for 2 h with 4 µl/ml of K2 Multiplier reagent in culture medium. Then, they were incubated for 24 h with the transfection reagent and 100 nM of SMARTpool ON-TARGETplus human CTSS siRNA or with miRIDIAN miRNA human hsa-miR-106b-5p mimics or hairpin inhibitors and the respective siRNA or miRNA non-targeting controls (GE Dharmacon) in a ratio of 5 $\mu l_{reagent}$:1 μg_{siRNA} in antibiotic-free medium. Following that, transfection medium was removed and the cells were incubated for 3 days in fresh medium prior to any experiment in order to achieve maximum silencing. The transfection efficiency achieved was approximately 95%, as evaluated by flow cytometry using siGLO Green Transfection Indicator (GE Dharmacon).

miR-106b-5p Target Validation

A 413 bp fragment of the 3′-untranslated region (3′-UTR) of the human CtsS gene (CTSS) containing a sequence complementary to the seed region of miR-106b-5p, was amplified by PCR using the Phusion® HotStartII DNA Polymerase (New England BioLabs®, MA, USA), following the manufacturer's instructions (forward primer: 5′-GCGAGCTCCAAGAAATATGAAGCACTTTCTC-3′, reverse primer: 5′-CCCTCGAGTTTTTTGAAACAGAGTCTCCACT-3′). The fragment was inserted into the pmirGLO Dual Luciferase miRNA Target Expression Vector (Promega Corporation), between the *Sac*I and *Xho*I restriction sites, to originate a recombinant plasmid expressing the 3′-UTR fragment of the human CtsS gene. Mutant plasmids were constructed bearing a single point mutation on the primer that includes the seed sequence, thus incorporating this mutation on the amplicon during the PCR amplification. The forward primer 5′-GCGAGCT CCAAGAAATATGAAGCAT<u>T</u>TTTCTC-3′ for CTSS 3′-UTR plasmid was used. Pointmutation is underlined. All restriction enzymes and the DNA ligase used were from New England BioLabs®. PCR products and restriction products were purified using the illustra™ GFX™ PCR DNA and Gel Band Purification Kit (GE Healthcare). Recombinant plasmids were stored and propagated inside JM109 *E. coli* cells. The constructed plasmid, miR-106b-5p mimics and miRNA negative controls were transfected into HEK 293 T-cells using ScreenFect®A Transfection Reagent (ScreenFect GmbH), following the manufacturer's instructions. After transfection, the dual luciferase assay was initiated using the Dual-Luciferase® Reporter (DLR™) Assay System kit (Promega Corporation), following all the manufacturer's instructions.

Western Blotting

Mø were seeded in six-well plates at a density of 2×10^6 cells per well. Total proteins were recovered with 200 µl of Laemmli buffer (Sigma-Aldrich). Protein extracts were subjected to electrophoresis in 12% SDS-PAGE gels, transferred to a nitrocellulose membrane and blocked in Tris-buffered saline with 0.1% Tween 20, 5% of bovine serum albumin (BSA). The nitrocellulose membranes were incubated with primary antibodies specific for human CtsS and β-tubulin (Abcam, 92780 and 6046, respectively), overnight at 4°C. All membranes were washed and incubated with secondary HRP-conjugated antibodies (Biorad). The bands were visualized with Luminata Crescendo Western HRP substrate (Merck Millipore) and quantified using ImageJ (29).

Enzymatic Activity

Mø were seeded in six-well plates at a density of 2×10^6 cells per well, and were recovered with a 5 mM EDTA/PBS solution. Cell

lysis and measurement of the enzymatic activity was performed using the Cathepsin Activity Fluorometric Assay kits (Biovision) specific for each cathepsin and following the manufacturer's instructions. Essay specificity was verified by treating the cell lysates with specific inhibitors for each cathepsin, provided in the kit. The fluorescence intensity was measured by the Tecan M200 spectrofluorometer.

Immunofluorescence

Mø were seeded in 24-well plates at a density of 3×10^5 cells per well. Following the experiments, the samples were fixed with 4% paraformaldehyde in PBS for 1 h and quenched by incubating with PBS 50 mM NH_4Cl. Macrophages were permeabilized with 0.1% Triton in PBS for 5 min and subsequently washed and blocked with 1% BSA in PBS. Cells were stained with anti-LC3b antibody (Cell Signaling, 2775) in 1% BSA/PBS overnight at room temperature. Following that, the cell nuclei were stained with 5 µg/ml of hoechst dye (Thermo Scientific) for 10 min. Samples were mounted with ProLong™ Gold antifade mountant and analyzed by confocal microscopy (Leica AOBS SP5).

Flow Cytometry

Mø were seeded in 24-well plates at a density of 3×10^5 cells per well. Following the experiment, macrophages were recovered with 5 mM EDTA/PBS solution and fixed with 4% paraformaldehyde for 1 h. Following that, cells were stained for 30 min with antibodies specific for human HLA-DR (clone L243, Biolegend), CD14, CD4 (BD Biosciences), or Annexin V and propidium iodide (Immonotools, GmbH) for the quantification of apoptotic and necrotic cells. Samples were analyzed in Guava easyCyte™ 5HT flow cytometer.

Assays for CD4 Proliferation

Mø were seeded in 48-well plates at a density of 1.5×10^5 cells per well. Following 24 h of infection CD4 lymphocytes were added to the culture at a ratio of 5 lymphocytes per Mø. CD4 lymphocytes were recovered after 5 days of coculture and quantified using Guava easyCyte™ 5HT flow cytometer.

Assays for Bacteria Intracellular Survival

Mø were seeded in 96-well plates at a density of 5×10^4 cells per well. When required, infected cells were lysed in 0.05% Igepal solution. Serial dilutions of the resulting bacterial suspension were plated in Middlebrook 7H10 with 10% OADC (Difco) and incubated for 2–3 weeks at 37°C before colonies were observable.

Statistical Analysis

Data are presented as mean ± SE except if stated otherwise. Statistical analysis was made using SigmaPlot 12. Multiple group comparisons were made using ANOVA one parameter tests followed by pairwise comparisons of the groups using Holm-Sidak test. Two group comparisons were made using Student's *t*-test. All the prerequisites of the tests were verified. The considered nominal alpha criterion level was 0.05 below which differences between samples were deemed significant.

RESULTS

Mtb Induces the Expression of miR-106b-5p in Human Mø

We previously performed studies to assess the involvement of miRNAs in posttranscriptional regulation of phagocytosis in the context of a murine model of mycobacterial infection (23). A global transcriptomic analysis of Mø infected with *M. smegmatis*, revealed among the most differentially regulated miRNAs miR-142-3p; -5p; miR-32 (upregulated) and miR-106b-5p (downregulated). Here, we asked what would be the effect of human Mø in response to the infection of a pathogenic species, Mtb relatively to the non-virulent *M. smegmatis*, a species that is cleared in these phagocytic cells. Human primary Mø derived from blood monocytes of healthy donors were infected either with *M. smegmatis* or with Mtb and RNA samples were extracted for RT-qPCR analysis at 1, 4, and 24 h postinfection (p.i.). The Exiqon microarrays heat map generated diagram (**Figure 1A**) shows the result of the two-way hierarchical clustering of miRNAs and samples. Each row represents one miRNA and each column represents one sample. The miRNA clustering tree is shown on the left. The color scale shown at the bottom illustrates the relative expression level of a miRNA across all samples: red color represents an expression level above mean, blue color represents expression lower than the mean. miRNAs found common to all infection conditions are displayed. Notably, the results showed miR-106b-5p strongly upregulated during Mtb infection (**Figure 1A**). Our previous results indicated that miR-106b-5p was downregulated early upon *M. smegmatis* infection of the mouse Mø cell line J774 (23) while in the present study, using human cells, no effect was observed. These results emphasize the influence of the host cell species for the response to infection *in vitro*. Given these differences, we decided to use human primary Mø in our experiments to assess the response to Mtb infection.

For an accurate quantification of gene expression and in order to confirm that miR-106b-5p is being differentially regulated during infection with Mtb relatively to *M. smegmatis*, we independently validated the RT-qPCR analysis. Our results confirm those performed by Exiqon, i.e., a distinct phenotype between the two species (**Figure 1B**), with *M. smegmatis* infection having no effect in miR-106b-5p expression while the challenge with Mtb led to a 2-fold increase in miR-106b-5p RNA at 4 h which was maintained for the 24 h assay. Thus, Mtb infection upregulates miR-106b-5p in primary human Mø (**Figure 1**).

miR-106b-5p Targets CtsS mRNA

Using target prediction tools based on the miRanda (30), miRtaget2 (31), and miRmap (32) algorithms, we have identified several potential targets of miR-106b-5p, including CtsS mRNA (CTSS). Conversely, we then asked how many miRNAs are predicted to target CTSS. From the 1,054 potential targets generated by the miRmap algorithm the top 30 with highest score are shown in **Table 1** with miR-106b-5p at the 24th position with a score of

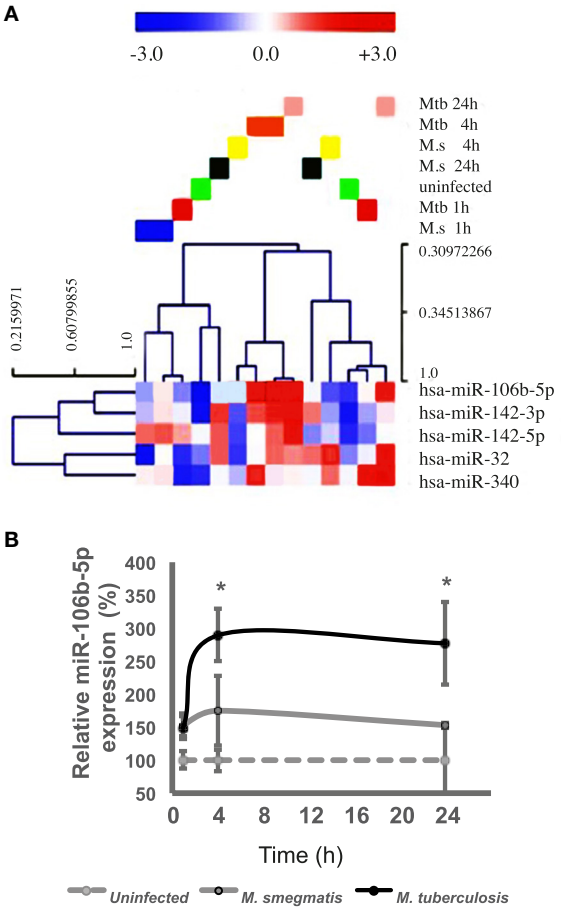


FIGURE 1 | miR-106b-5p is upregulated in human Mø during *Mycobacterium tuberculosis* (Mtb) infection. **(A)** Heat Map of human microRNA (miRNA) expression in Mø infected with *M. tuberculosis* and *Mycobacterium smegmatis* and Unsupervised Hierarchical Clustering performed by Exiqon. The clustering is performed on all samples and on the miRNAs detected in all samples. Each row represents one microRNA and each column represents one sample. The miRNA clustering tree is shown on the left. The color scale shown illustrates the relative expression level of a miRNA across all samples: red color represents an expression level above mean, blue color represents expression lower than the mean. The normalized (dCp) values have been used for the analysis. Normalizer microRNAs have been omitted from the analysis. **(B)** miR-106b-5p quantification by qt-RT-PCR along 48 h of infection. Values are relative to uninfected control cells and represent means of three biological replicates while error bars show the SE. Asterisks indicate statistical significance between samples (*$P < 0.01$).

TABLE 1 | Top 30 microRNAs predicted to bind to CTSS.

Rank	miRNA	Probability exact	miRmap score
1	hsa-miR-520c-3p	98.74	90.76
2	hsa-miR-520b	98.74	90.76
3	hsa-miR-520e	98.74	90.76
4	hsa-miR-520d-3p	98.74	90.73
5	hsa-miR-302c-3p	98.74	90.73
6	hsa-miR-302a-3p	98.74	90.73
7	hsa-miR-520a-3p	98.74	90.69
8	hsa-miR-373-3p	98.74	90.69
9	hsa-miR-526b-3p	99.00	90.67
10	hsa-miR-372	98.74	90.65
11	hsa-miR-302b-3p	98.74	90.63
12	hsa-miR-302d-3p	98.74	90.62
13	hsa-miR-302e	98.74	90.58
14	hsa-miR-93-5p	99.00	90.57
15	hsa-miR-586	97.13	90.51
16	hsa-miR-519d	99.00	90.50
17	hsa-miR-17-5p	99.00	90.49
18	hsa-miR-5787	99.74	90.49
19	hsa-miR-378g	99.78	90.49
20	hsa-miR-20b-5p	99.00	90.45
21	hsa-miR-106a-5p	99.00	90.44
22	hsa-miR-4674	99.62	90.43
23	hsa-miR-20a-5p	99.00	90.35
24	hsa-miR-106b-5p	99.00	90.35
25	hsa-miR-612	99.78	90.32
26	hsa-miR-4505	99.74	90.30
27	hsa-miR-651	98.01	90.27
28	hsa-miR-520f	87.32	90.24
29	hsa-miR-3619-5p	94.50	90.22
30	hsa-miR-939-3p	16.73	90.19

Based on the miRmap algorithm.

90.35. These results, combined with previous data from our group, establishing an important role of CtsS in Mtb infection (9), led us to generate the hypothesis of whether CtsS was a real target of miR-106b-5p, and if it has implications in bacterial survival, cell death as well as antigen presentation.

After screening the 3′-UTR of CTSS for potential miR-106b-5p interaction using RNAhybrid (33), we identified three different binding sites (**Figure 2A**). Our initial results portrayed an induction of miRNA-106b-5p in Mtb-infected Mø in agreement with our previous findings that CtsS is downregulated by Mtb infection (9). To confirm this interaction, we used a dual luciferase reporter vector system in which we inserted a fragment of the 3′-UTR sequence for CtsS into the pmirGLO dual-luciferase target expression vector. This fragment included one putative sequence complementary to the "seed region" of miR-106b-5p. Using this system, we were able to assess the specific interaction between the miRNA and the 3′-UTR sequence by analyzing the resulting decrease in luciferase expression in HEK 293 T-cells transfected with both the plasmid and the miRNA. The results showed a significant reduction in luciferase expression ($P < 0.05$, paired *t*-test) during cotransfection with miR-106b-5p and 3′-UTR CTSS plasmid relative to the control (cells transfected with a nonsense miR and the 3′-UTR CTSS reporter plasmid) (**Figure 2B**). On the contrary, when a plasmid bearing a mutation on the 3′-UTR CTSS seed sequence by one nucleotide substitution was tested, there was no decrease in luciferase activity detected.

Next, we tested whether we were able to modulate CtsS protein levels in non-infected cells by overexpressing or inhibiting miR-106b-5p. For this, we transfected primary human Mø with miR-106b-5p mimics or inhibitors and analyzed protein levels by Western blotting (**Figure 2C**). The resulted silencing of approximately 40% for CtsS using mimics was comparable to the reduction of luminescence in the luciferase assay. Conversely, when using inhibitors an increase of protein levels of around 40% was observed (**Figure 2C**). Altogether, the data indicate the

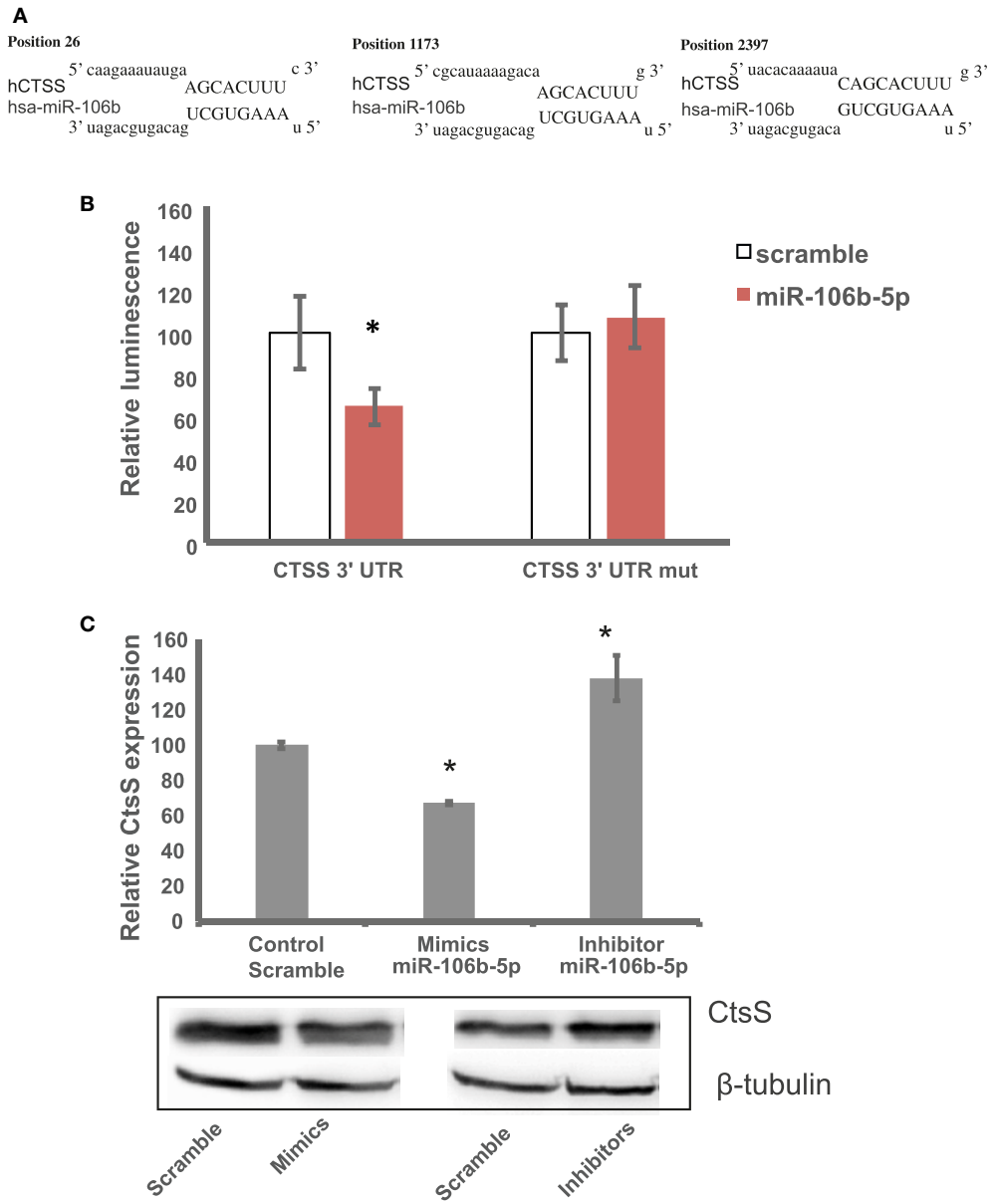


FIGURE 2 | miR-106b targets cathepsin S (CtsS). **(A)** Three different predicted sites were found after screening the 3′-untranslated region (3′-UTR) region of CTSS for potential miR-106b-5p binding sites using RNAhybrid. **(B)** The interaction was confirmed by means of relative luciferase activity measured in HEK 293 T-cell line transfected with CTSS 3′-UTR plasmid or CTSS 3′-UTR mut plasmid in combination with scramble control or miR-106b-5p mimic. Values are relative to the respective scramble control-transfected cells. The columns show means of three biological replicates each measured in triplicates while error bars show the SE. Asterisks indicate statistical significance relative to the respective scramble control-transfected cells (*$P < 0.05$). **(C)** CtsS protein expression in human Mø transfected with miR-106b-5p mimics or inhibitors. Values are relative to the scramble control and represent means of two biological replicates (*$P < 0.001$).

specificity of the interaction between CTSS 3′-UTR binding sites and miR-106b-5p leads to CtsS silencing.

The Modulation of miR-106b-5p Expression Regulates CtsS Protein Amounts in Mtb-Infected Mø

Our results showed an early Mtb-dependent upregulation of miR-106-5p and a specific interaction between this miRNA and CTSS. These findings are correlated with our previous results showing that Mtb induces the downregulation of CtsS at 24 h, suggesting that miR-106b-5p might be implicated in this regulation. To further test this hypothesis, we performed similar experiments, as described above, using mimics and inhibitors of miR-106b-5p in the context of Mtb infection. As shown in **Figure 3A** (right panel), transfecting cells with mimics of miR-106b-5p resulted in a decrease of CtsS protein levels in Mtb-infected cells, at all time points tested, relatively to scramble-infected cells (scramble:

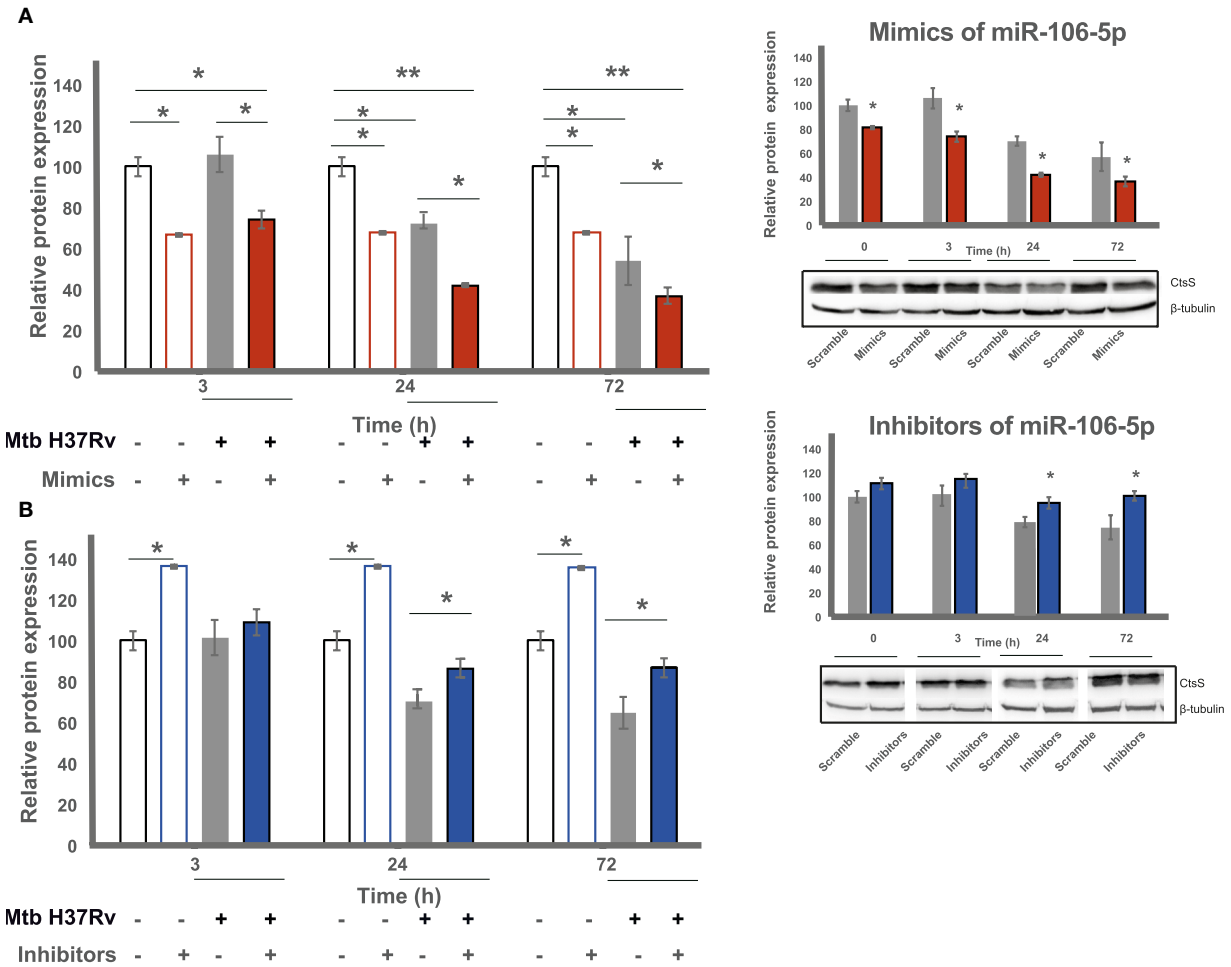


FIGURE 3 | miR-106b-5p regulates cathepsin S (CtsS) during infection with *Mycobacterium tuberculosis*. CtsS protein expression in human Mø transfected with miR-106b-5p mimics **(A)** or inhibitors **(B)** and subsequently infected with Mtb. Proteins were recovered from uninfected Mø (T0) and infected Mø after 3, 24, and 72 h postinfection. The right panels are a different representation of the same data including the protein gel bands (original Wester-blots in Figure S2). Values are relative to uninfected Mø transfected with the respective scramble control and represent means of two biological replicates with error bars depicting the SE. Asterisks indicate statistical significance between indicated samples or relative to the uninfected (T0) controls (*$P < 0.05$ or **$P < 0.001$).

infected and transfected with control nonsense RNA). The difference was even more significant when comparing cells treated with mimics after 3 days of infection relatively to control (scramble) non-infected cells (red bars to white bars in the left panel). When the inhibitors of miR-106b-5p were tested, significant effects were observed mostly later in the course of the infection, namely after 24 h p.i. In contrast to miR-106b-5p mimics, the transfection with inhibitors lead to an increase of CtsS levels in infected cells relatively to scramble-infected cells (**Figure 3B**, right panel). Altogether, miR-106b-5p modulates CtsS expression in human Mø during infection with Mtb.

miR-106b-5p Modulates the Intracellular Survival of Mtb

Given that Mtb manipulates miR-106b-5p expression resulting in reduced CtsS protein levels, we hypothesized that this regulation will affect the endolysosomal enzyme proteolytic activity and subsequently the ability of Mtb to survive inside host cells. To test this, we first analyzed the intracellular survival of Mtb during 5 days of infection in human Mø transfected with mimics or inhibitors. As expected, the mimics for miR-106b-5p gain-of-function, we observed an increase in Mtb survival, relative to the control (scramble transfected and infected cells) at day 3 p.i. (**Figure 4A**, left panel). In contrast, an exacerbated killing effect from day 3 p.i. was detected by using miR-106b-5p inhibitors in loss-of-function experiments (**Figure 4A**, right panel). The results were in agreement with a decrease in protein levels and hydrolytic activity for CtsS using mimics (**Figure 4B**, left panels) and a significant increase in protein and enzyme activity using miR-106-b-5p inhibitors (**Figure 4B**, right panels) calculated 3 days p.i. A similar trend on Mtb survival using mimics experiments was confirmed by CTSS siRNA (**Figure 4A**, top right).

Altogether, these results show that miR-106b-5p levels can impact intracellular survival of Mtb in human Mø.

To decipher whether the observed miR-106b-5p-dependent pathogen killing/survival was dependent on alternative activation pathways, we tested for the involvement of apoptosis, necrosis or autophagy, during gain- and loss-of-function experiments. We tested whether a decrease on CtsS due to miR-106b-5p gain-of-function will augment apoptosis in infected cells by using Annexin V staining to monitor the event. As shown in **Figure 4C** and Figure S1 in Supplementary Material, no increase on apoptosis was detected neither in mimic nor in inhibitors transfected Mtb-infected cells relatively to the control as quantified by flow cytometry. We next assessed necrosis also by flow cytometry using propidium iodide-labeled cells and observed

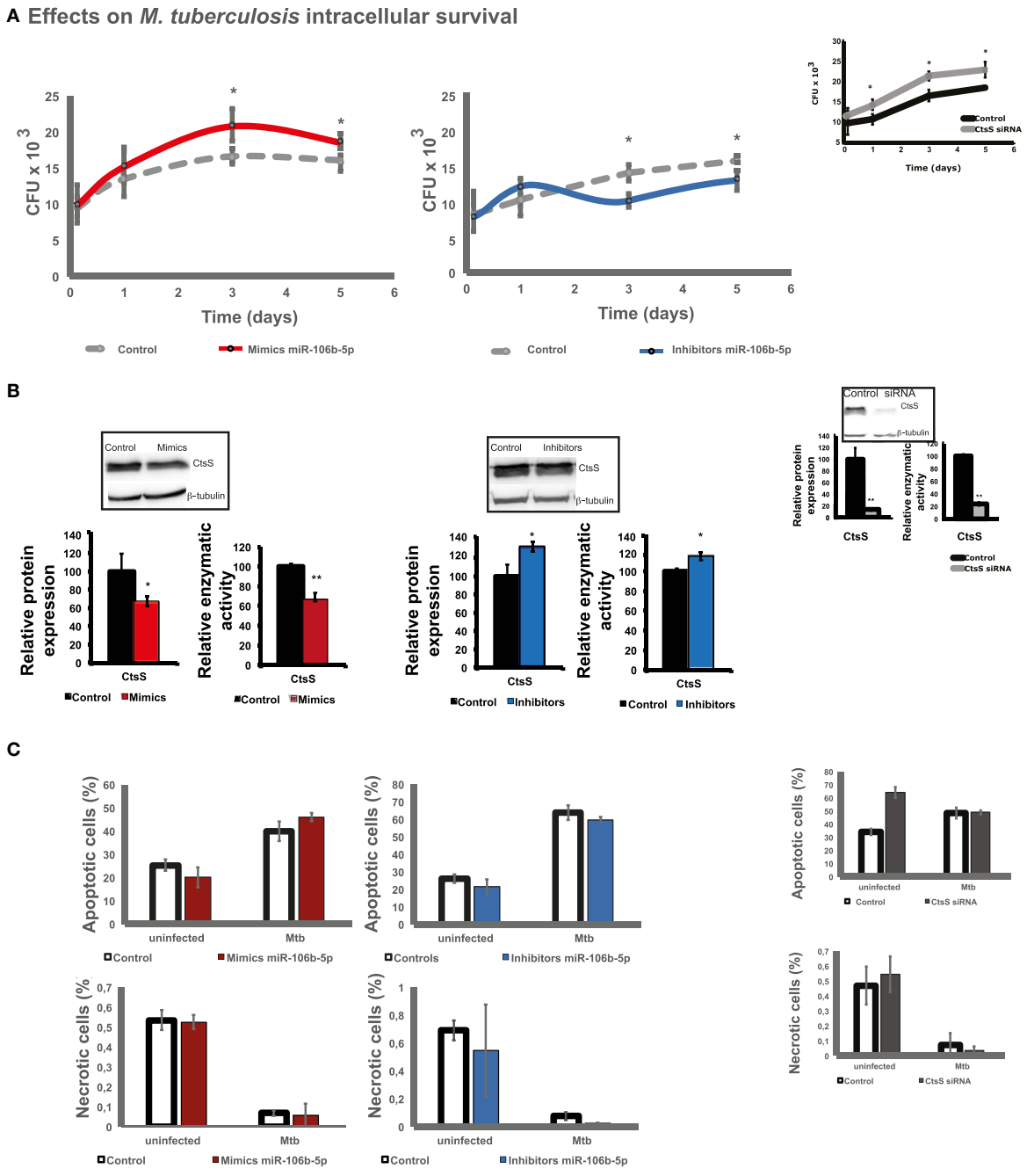


FIGURE 4 | Continued

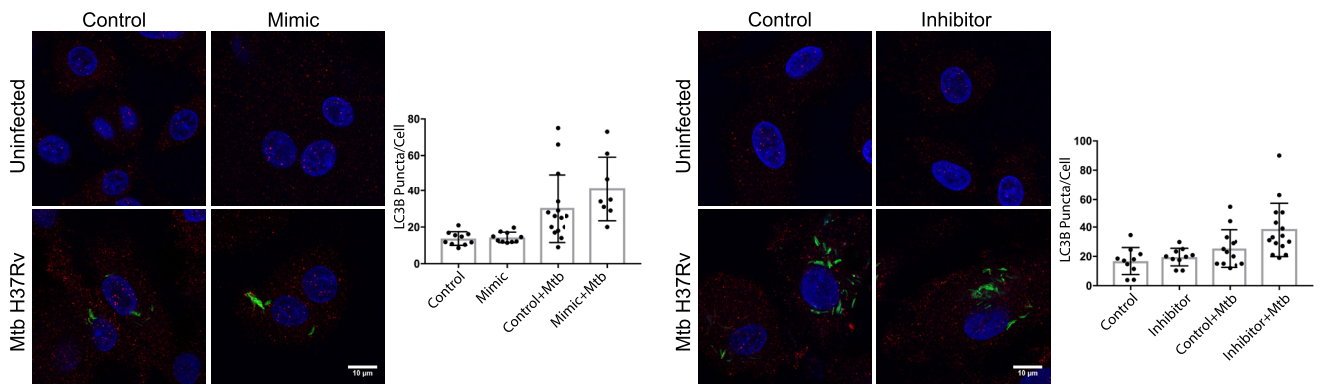


FIGURE 4 | Intracellular survival of *Mycobacterium tuberculosis* (Mtb) in Mø transfected with miR-106b-5p mimics or inhibitors. **(A)** Colony forming units of intracellular bacteria recovered from Mø transfected with miR-106b-5p mimics or inhibitors. CFUs were recovered after 3 h, 1, 3, and 5 days postinfection. Values depict mean colony-forming units representative of three biological replicates measured in duplicate while the error bars depict the SE. Asterisks indicate statistical significance between samples at the same time point (*$P < 0.05$). **(B)** Effects of mimics or inhibitors on cathepsin S (CtsS) protein levels and enzymatic activity. Values are relative to the scramble control and represent means of two biological replicates (for protein quantification) or means of three biological replicates (for enzymatic activity) (*$P < 0.05$ or **$P < 0.001$). **(C)** Effects of mimics or inhibitors on Mø cell death: apoptosis, necrosis. Cell death was measured by flow cytometry after 24 h of infection using fluorescent Annexin V antibodies and propidium iodide (see Figure S1 in Supplementary Material for the respective dot plots). Values show median fluorescence intensity from one representative experiment performed in triplicate while error bars depict SD. **(D)** Effects of mimics or inhibitors on autophagy. LC3 autophagy puncta were observed in uninfected Mø or 24 h postinfection with Mtb by confocal microscopy and quantified using ImageJ. Bar plots represent the mean values of at least eight analyzed microscopy fields (dots) from one representative experiment. Error bars depict the SD.

no effect on necrosis (**Figure 4C**-down panels; Figure S1 in Supplementary Material).

Finally, the process of autophagy was examined by immunofluorescence quantification of LC3A/B puncta (**Figure 4D**). A significant increase in LC3 puncta was observed after infection with Mtb-infected human Mø (**Figure 4D**). Surprisingly, there were no changes in LC3 puncta when comparing infected cells transfected with miR-106b-5p mimics or with inhibitors relatively to nonsense-scramble-transfected cells (**Figure 4D**). We concluded that the effect of miR-106b-5p was autophagy independent. Altogether, these results indicate that a knock-down of CtsS in the context of Mtb manipulation of miR-106b-5p is relevant for pathogen intracellular survival by interfering with proteolysis in the endolysosomal pathway and independently of autophagy and programed cell death activation.

miRNA-106b-5p Interferes with the Antigen Presentation Machinery and T-Cell Activation

According to the KEGG pathway database, CTSS is involved in several pathways such as (1) lysosomal, (2) phagosomal, and (3) antigen processing and presentation. CtsS has been implicated in endosomal antigen processing and antigen presentation (13, 34). We then hypothesized that Mtb modulation of miR-106b-5p for CtsS silencing might be linked to poor antigen processing and presentation compromising adaptive immunity response to infection. To test this, we performed miR-106b-5p gain- and loss-of-function experiments in Mtb-infected cells and analyzed changes in the surface expression of HLA-DR class II complexes using flow cytometry (**Figure 5**). Transfection of infected cells with miR inhibitors led to an increase expression of HLA-DR at the surface of Mø (**Figure 5**). No differences were observed relatively to HLA-DR surface expression of mimics and CtSS siRNA transfected cells relatively to control cells. Thus, we inferred that Mtb infection silencing of CtsS affect the antigen presentation machinery at a level that no more silencing of the enzyme either by mimics or by siRNA could revert the phenotype. To further evaluate the consequences of antigen presentation dependence on miR-106b-5p modulation, we performed cocultures of treated infected macrophages with CD4 + T-lymphocytes from the same blood samples and evaluated the ability to induce T-cell proliferation (**Figure 5B**). In order to test this, we used human Mø infected with Mtb from a donor population that is all vaccinated. It is expected in these cells a memory highly effective T-cell state that responds to Mtb infection. Following the same pattern of HLA surface expression, treatment with inhibitors in Mtb-infected cells induces a strong T-cell proliferation relatively to the control, after 5 days post-cocultures as evaluated by flow cytometry (**Figure 5B**). No changes were detected in all other conditions tested.

DISCUSSION

This study revealed that miR-106b-5p targets CTSS for protein silencing with consequences in Mtb persistence in human Mø obtained from healthy (BCG vaccinated) donors. Our results indicate that Mtb actively manipulates miR-106b-5p by upregulating their gene expression during infection in opposition to what it is observed with the non-pathogen *M. smegmatis*. We made use of algorithms such as the miRmap to predict miRNA targets

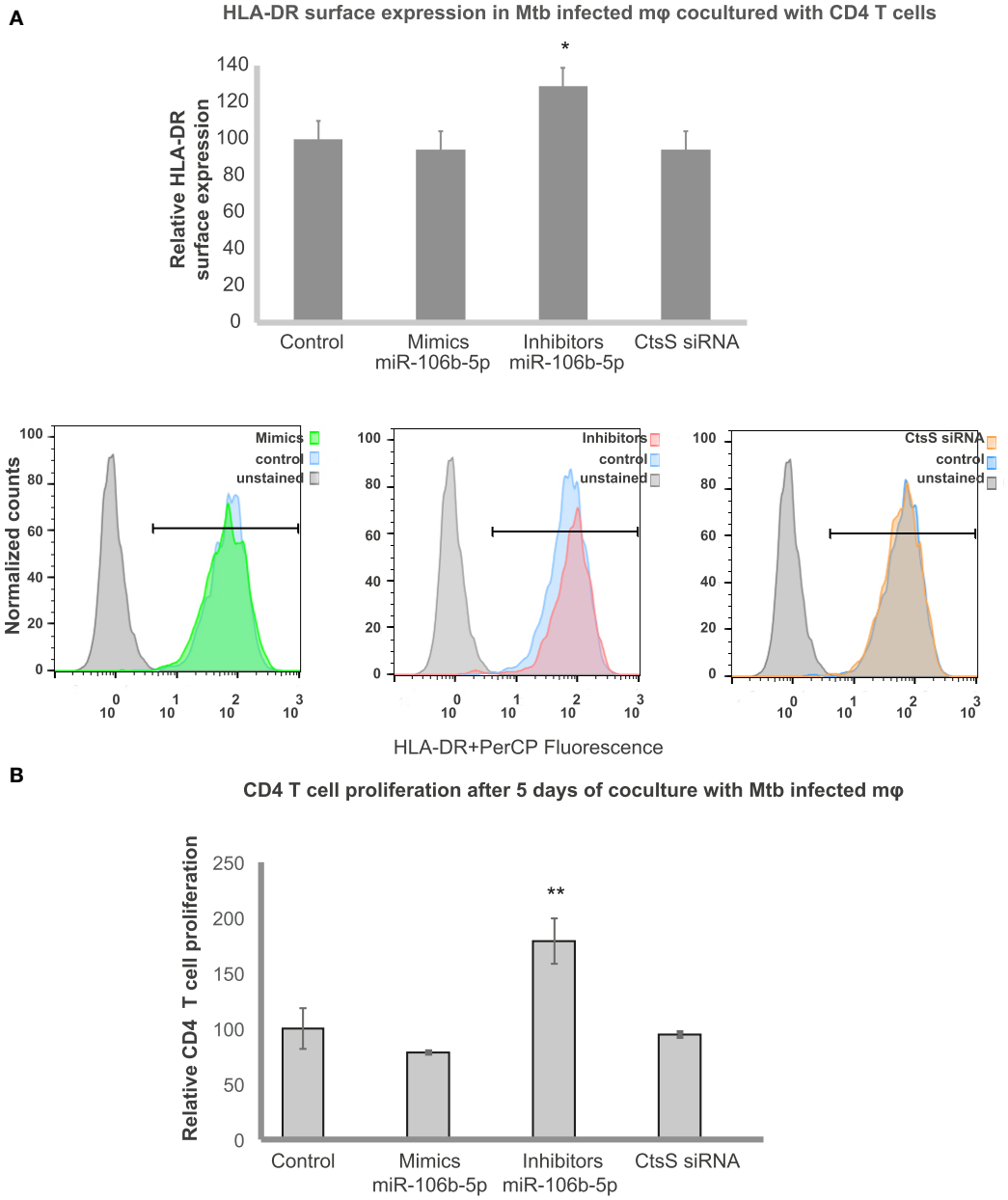


FIGURE 5 | Effects of miR-106b-5p on antigen presentation machinery and T-cell priming. **(A)** Surface expression of human leukocyte antigen (HLA)-DR on Mø transfected with miR-106b-5p mimics, inhibitors or by siRNA for CTSS and infected with *Mycobacterium tuberculosis*. HLA-DR was measured by flow cytometry after 24 h of infection. Values in bar plots represent median fluorescence intensity relative to the respective scramble controls from one representative experiment performed in triplicate while error bars depict SD (*$P < 0.05$). Raw values from one representative replicate are presented in the fluorescence intensity histograms. **(B)** CD4 T-cell proliferation after 5 days of coculture with Mtb-infected Mø. Following 24 h of the infection with Mtb, CD4 T-cells were added to the infected Mø culture. After 5 days of coculture, the number of CD4 T-cells comparatively to the non-infected controls was determined by flow cytometry. Values in bar plots represent the increase in CD4 T-cell number relative to each uninfected scramble control samples (**$P < 0.01$).

based on nucleic acid sequence, probabilistic, thermodynamic, or evolutionary features (32). Based on this and other's algorithms the mRNA for CtsS was revealed as a potential target. We then asked what would be the most probable miRNAs predicted to bind the 3′-UTR of CTSS. From the 1,054 targets generated by the miRmap algorithm, miRNA-106b-5p showed the 24th highest score (99.35) (**Table 1**). This score and probability to bind to CTSS is higher than that of miR-3619-5p (99.22), on the 29th position, that has been described and experimentally validated as a miRNA predicted to bind the 3′-UTR of CTSS (35). While both miRs target CTSS, contrary to miR-106b-5p that we found upregulated during Mtb infection, miR-3619-5p was downregulated in BCG-infected THP1 derived Mø. Importantly most members of the miR-17-92 cluster and all members of the

miR-17 cluster are present in the list: hsa-miR-17-5p, hsa-miR-20a-5p, hsa-miR-20b-5p, hsa-miR-106a-5p, hsa-miR-106b-5p, and hsa-miR-93-5p which have been implicated all in innate and adaptive immune responses (36). Therefore, we envisage that miR-106b-5p is actively manipulated by Mtb to ensure its survival in innate phagocytic cells and escape to immune surveillance and activation. Furthermore, from the above data we may foresee the relevance of CtsS regulation due to the observed numbers of distinct miRs that are predicted to target this mRNA.

The target was confirmed by luminescence-based methods and the miR-mRNA targeting resulted in about 40% in protein translation silencing. We made use of gain or loss-of-function experiments to modulate miR-106-b-5p during Mtb infection. The results indicated a decrease or increase of CtsS expression, respectively, concomitant with increased Mtb intracellular survival or killing, correspondingly. Altogether, this suggests that CtsS dependent Mtb intracellular survival *via* miR-106b-5p modulation resulted from a hydrolytic activity along the endocytic pathway upon phagocytosis. Mtb is known to block phagosome maturation, preventing its digestion in lysosomes (2–5). However, CtsS is a proteolytic enzyme that as a broad pH for activity along the endocytic pathway and not only into the acidic environment of the phagolysosome (10). Therefore, a modulation of mir-106b-5p to silence CtsS activity may be a pathogen strategy to survive along vesicles in this pathway.

Our results did not reveal significant changes in apoptosis after miR-106b-5p manipulation. Apoptosis has been associated with a mechanism for effective intracellular bacteria clearance (37, 38) therefore the results of miR in Mtb survival could not be attributed to control of apoptosis. Curiously, one of the miRs we showed to be more differentially regulated during mycobacteria infection, in addition to miR-106-b was miR-142-3p (**Figure 1A**). Both actually targets genes involved in phagocytosis as the endolysosomal enzyme CtsS and the actin binding protein N-WASP, respectively (23). Both are indeed targeting simultaneously the ATG16L1 (39, 40). We and other's identified miRs relevant during phagocytosis that simultaneously are predicted to manipulate autophagy (26, 35). Some studies suggest that inhibition of CtsS induces autophagy in different cells (17) while for others a silencing of CtsS is likely to affect degradation of autophagosomal contents leading to a block of autophagy in impaired LC3 vesicles (35). Indeed, the knock-down of CtsS was associated with mitophagy dysregulation leading to apoptosis and impairment and accumulation of autophagosomes (41).

Our data argue that the miR-106b-5p-dependent improved control of Mtb is independent of autophagy and more related to the process of phagosomal degradation. Autophagy is an important innate immune intracellular pathway that control mycobacteria in macrophages (18). In the context of CtsS, the downregulation of CtsS along with LAMP1 and CtsD lead to impaired autophagosome–lysosome fusion (42). The fact that miR-106b-5p, in addition to CtsS, also targets ATG16L1 may provide evidence for a double control of autophagy for bacteria survival and persistence. However, it has been recently shown that ATG5 but not ATG16L1 or others autophagy-related genes plays a key role in the host response to mycobacteria (43, 44). Moreover, the inhibition or impairment of ATG16L1 was associated with autophagy block and incapacity to control inflammasome proteolysis in autophagolysosomes resulting in exacerbated IL-1β secretion, inflammation and necrotic cell death in the context of epithelial cells and Crohn's disease (26, 45).

We neither found an increase on necrosis upon miR-106b-5p mimics or inhibitors treatment that could account for Mtb survival. Other studies associated a IFNγ knock-down leading to autophagy inhibition and therefore a low CtsS content in endolysosomal vesicles to an increase secretion of proinflammatory cytokine IL1β and programmed cell death by necrosis (46). The effect of necrotic programmed cell death as pyroptosis in control bacteria killing is unclear: some data show this process contributes to pathogen killing (47) whereas other data argues that it helps pathogen escaping and spread to non-infected cells (48).

Cathepsin S has been implicated in antigen processing and presentation (12, 13) and that Mtb has indeed ability to block antigen presentation *via* CtsS (14–16). Here, we show that modulation of miR-106b-5p during infection indeed modulates the surface expression of the MHC Class II antigen presentation machinery (HLA-DR). In the case of macrophages infected with Mtb, where HLA-DR antigen presentation was already blocked, the usage of mimics did not change this blockade, similar to what observed during CtsS silencing by conventional siRNA methods (**Figure 5B**). Importantly, in infected cells treated with inhibitors an increased CtsS activity was concomitant with an increase surface expression of the antigen presentation machinery. This was relevant to establish a bridge for the adaptive immunity as the inhibitors treated infected cells were more able to induce T-CD4 lymphocyte proliferation. A differential regulation of CtsS was already observed in previous published results when comparing the infection of the non-virulent species *M. smegmatis* with macrophage infection with Mtb (9). Indeed, Mtb was shown to induce lower MHC class II expression compared with *M. smegmatis* (49). Here, we show that the manipulation of MHC-II expression through the axis miR-106b-5p/CtsS may overcome the blockade induced during Mtb infection.

A recent study by Meng et al. (50) describes that miR-106b-5p is downregulated in samples from latently infected individuals, where Mtb is known to be not dividing and is enclosed within the phagosomes, avoiding the fusion with lysosomes containing cathepsins and other digestive enzymes. In our experiments, we describe that miR-106b-5p is upregulated in macrophages infected with Mtb which are dividing and producing an infection that mimics active TB, with increasing numbers of CFU overtime (**Figure 4A** control samples). Therefore, the work of Meng et al., combined with the present study might suggest that the miR-106b-5p is a good candidate to be used as a biomarker to distinguish between active and latent TB, although further experimental evidence would be required to formally validate this hypothesis.

Tuberculosis is a major worldwide public health concern among infectious diseases and the treatment remains a challenge. HDTs represent a new strategy for adjuvant TB therapy trying to potentiating key components of host antimycobacterial effector mechanisms, while restricting inflammation (51, 52). miRNAs are key players in controlling gene expression and are nucleic

acids feasible for targeted drug delivery to phagocytic cells (53). The present study reveals that Mtb blocks CtsS *via* miR-106b-5p for preventing innate and adaptive immune responses to persist in the host. We further provide means how to revert this process by manipulation of miR-106-5p helping to control the infection. Our study opens the door for future manipulation of miR-106b-5p to enhance the antimicrobial activity of innate immune cells.

AUTHOR CONTRIBUTIONS

Conceptualization: EA, DP, and PB. Methodology, acquisition, and analysis: DP, EB, NC, MG, PB, and EA. Investigation: DP, JP, NC, and CF. Writing: EA and DP. Supervision: EA. Read, commented, and approved the final version of the manuscript: all authors.

ACKNOWLEDGMENTS

We are thankful to the Instituto Português do Sangue for providing human blood samples; to BEI resources (and Colorado State University, USA) for proteins and strains; to the Centre for AIDS Reagents, NIBSC (United Kingdom) for providing IFN-γ donated by Genentech Inc.

FUNDING

This study was supported by the grants from National Foundation for Science, FCT, PTDC/BIA-BCM/102123/2008 and PTDC/Sau-MII/098024/2008 to EA. MG is supported by the Francis Crick Institute, which receives its core funding from Cancer Research UK (FC001092), the UK Medical Research Council (MC_UP_1202/11, FC001092), and the Wellcome Trust (FC001092).

SUPPLEMENTARY MATERIAL

The Supplementary Material for this article can be found online at http://www.frontiersin.org/articles/10.3389/fimmu.2017.01819/full#supplementary-material.

FIGURE S1 | Flow Cytometry generated dot-plots for necrosis and apoptosis effects of mimics and inhibitors of miR-106b-5p on *Mycobacterium tuberculosis* (Mtb)-infected cells and on non-infected cells. Cell death was measured by flow cytometry after 24 h of infection using fluorescent Annexin V antibodies and propidium iodide.

FIGURE S2 | Original Western blots from **Figure 3**. Cathepsin S protein expression in human Mø transfected with miR-106b-5p mimics or inhibitors and subsequently infected with *Mycobacterium tuberculosis* (Mtb). Proteins were recovered from uninfected Mø (T0) and infected Mø after 3, 24, and 72 h postinfection.

REFERENCES

1. World Health Organization. *Global Tuberculosis Report 2016*. Geneva: World Health Organization (2016).
2. Armstrong JA, Hart PD. Phagosome-lysosome interactions in cultured macrophages infected with virulent tubercle bacilli. Reversal of the usual nonfusion pattern and observations on bacterial survival. *J Exp Med* (1975) 142:1–16. doi:10.1084/jem.142.1.1
3. Clemens DL, Horwitz MA. Characterization of the *Mycobacterium tuberculosis* phagosome and evidence that phagosomal maturation is inhibited. *J Exp Med* (1995) 181:257–70. doi:10.1084/jem.181.1.257
4. Sturgill-Koszycki S, Schlesinger PH, Chakraborty P, Haddix PL, Collins HL, Fok AK, et al. Lack of acidification in *Mycobacterium* phagosomes produced by exclusion of the vesicular proton-ATPase. *Science* (1994) 263:678–81. doi:10.1126/science.8303277
5. Vergne I, Chua J, Singh SB, Deretic V. Cell biology of *Mycobacterium tuberculosis* phagosome. *Annu Rev Cell Dev Biol* (2004) 20:367–94. doi:10.1146/annurev.cellbio.20.010403.114015
6. Jordao L, Bleck CKE, Mayorga L, Griffiths G, Anes E. On the killing of mycobacteria by macrophages. *Cell Microbiol* (2008) 10:529–48. doi:10.1111/j.1462-5822.2007.01067.x
7. Olson OC, Joyce JA. Cysteine cathepsin proteases: regulators of cancer progression and therapeutic response. *Nat Rev Cancer* (2015) 15:712–29. doi:10.1038/nrc4027
8. de Martino M, Galli L, Chiappini E. Reflections on the immunology of tuberculosis: will we ever unravel the skein? *BMC Infect Dis* (2014) 14(Suppl 1):S1. doi:10.1186/1471-2334-14-S1-S1
9. Pires D, Marques J, Pombo JP, Carmo N, Bettencourt P, Neyrolles O, et al. Role of cathepsins in *Mycobacterium tuberculosis* survival in human macrophages. *Sci Rep* (2016) 6:32247. doi:10.1038/srep32247
10. Wilkinson RDA, Williams R, Scott CJ, Burden RE. Cathepsin S: therapeutic, diagnostic, and prognostic potential. *Biol Chem* (2015) 396:867–82. doi:10.1515/hsz-2015-0114
11. Storm van's Gravesande K, Layne MD, Ye Q, Le L, Baron RM, Perrella MA, et al. IFN regulatory factor-1 regulates IFN-γ-dependent cathepsin S expression. *J Immunol* (2002) 168:4488–94. doi:10.4049/jimmunol.168.9.4488
12. Costantino CM, Ploegh HL, Hafler DA. Cathepsin S regulates class II MHC processing in human CD4+ HLA-DR+ T cells. *J Immunol* (2009) 183:945–52. doi:10.4049/jimmunol.0900921
13. Driessen C, Bryant RA, Lennon-Duménil AM, Villadangos JA, Bryant PW, Shi GP, et al. Cathepsin S controls the trafficking and maturation of MHC class II molecules in dendritic cells. *J Cell Biol* (1999) 147:775–90. doi:10.1083/jcb.147.4.775
14. Baena A, Porcelli SA. Evasion and subversion of antigen presentation by *Mycobacterium tuberculosis*. *Tissue Antigens* (2009) 74:189–204. doi:10.1111/j.1399-0039.2009.01301.x
15. Pai RK, Convery M, Hamilton TA, Boom WH, Harding CV. Inhibition of IFNγ-induced class II transactivator expression by a 19-kDa lipoprotein from *Mycobacterium tuberculosis*: a potential mechanism for immune evasion. *J Immunol* (2003) 171:175–84. doi:10.4049/jimmunol.171.1.175
16. Sendide K, Deghmane AE, Pechkovsky D, Av-Gay Y, Talal A, Hmama Z. *Mycobacterium bovis* BCG attenuates surface expression of mature class II molecules through IL-10-dependent inhibition of cathepsin S. *J Immunol* (2005) 175:5324–32. doi:10.4049/jimmunol.175.8.5324
17. Chen K-L, Chang W-SW, Cheung CHA, Lin C-C, Huang C-C, Yang Y-N, et al. Targeting cathepsin S induces tumor cell autophagy via the EGFR-ERK signaling pathway. *Cancer Lett* (2012) 317:89–98. doi:10.1016/j.canlet.2011.11.015
18. Gutierrez MG, Master SS, Singh SB, Taylor GA, Colombo MI, Deretic V. Autophagy is a defense mechanism inhibiting BCG and *Mycobacterium tuberculosis* survival in infected macrophages. *Cell* (2004) 119:753–66. doi:10.1016/j.cell.2004.11.038
19. Bartel DP. MicroRNAs: genomics, biogenesis, mechanism, and function. *Cell* (2004) 116:281–97. doi:10.1016/S0092-8674(04)00045-5
20. Lu R, Maduro M, Li F, Li HW, Broitman-Maduro G, Li WX, et al. Animal virus replication and RNAi-mediated antiviral silencing in *Caenorhabditis elegans*. *Nature* (2005) 436:1040–3. doi:10.1038/nature03870
21. O'Donnell KA, Wentzel EA, Zeller KI, Dang CV, Mendell JT. c-Myc-regulated microRNAs modulate E2F1 expression. *Nature* (2005) 435:839–43. doi:10.1038/nature03677
22. Rajaram MV, Ni B, Morris JD, Brooks MN, Carlson TK, Bakthavachalu B, et al. *Mycobacterium tuberculosis* lipomannan blocks TNF biosynthesis by

regulating macrophage MAPK-activated protein kinase 2 (MK2) and microRNA miR-125b. *Proc Natl Acad Sci U S A* (2011) 108:17408–13. doi:10.1073/pnas.1112660108
23. Bettencourt P, Marion S, Pires D, Santos LF, Lastrucci C, Carmo N, et al. Actin-binding protein regulation by microRNAs as a novel microbial strategy to modulate phagocytosis by host cells: the case of N-Wasp and miR-142-3p. *Front Cell Infect Microbiol* (2013) 3:19. doi:10.3389/fcimb.2013.00019
24. Dorhoi A, Iannaccone M, Farinacci M, Faé KC, Schreiber J, Moura-Alves P, et al. MicroRNA-223 controls susceptibility to tuberculosis by regulating lung neutrophil recruitment. *J Clin Invest* (2013) 123:4836–48. doi:10.1172/JCI67604
25. Bettencourt P, Pires D, Anes E. Immunomodulating microRNAs of mycobacterial infections. *Tuberculosis* (2016) 97:1–7. doi:10.1016/j.tube.2015.12.004
26. Lu C, Chen J, Xu HG, Zhou X, He Q, Li YL, et al. MIR106B and MIR93 prevent removal of bacteria from epithelial cells by disrupting ATG16L1-mediated autophagy. *Gastroenterology* (2014) 146:188–99. doi:10.1053/j.gastro.2013.09.006
27. Wang C, Peyron P, Mestre O, Kaplan G, van Soolingen D, Gao Q, et al. Innate immune response to Mycobacterium tuberculosis Beijing and other genotypes. *PLoS ONE* (2010) 5:e13594. doi:10.1371/journal.pone.0013594
28. Anes E, Kuhnel M, Boss E, Moniz-Pereira J, Habermann A, Griffiths G. Selected lipids activate phagosome actin assembly and maturation resulting in killing of pathogenic mycobacteria. *Nat Cell Biol* (2003) 5:793–802. doi:10.1038/ncb1036
29. Schneider CA, Rasband WS, Eliceiri KW. NIH Image to ImageJ: 25 years of image analysis. *Nat Methods* (2012) 9:671–5. doi:10.1038/nmeth.2089
30. Betel D, Wilson M, Gabow A, Marks DS, Sander C. The microRNA.org resource: targets and expression. *Nucleic Acids Res* (2008) 36:D149–53. doi:10.1093/nar/gkm995
31. Wang X. miRDB: a microRNA target prediction and functional annotation database with a wiki interface. *RNA* (2008) 14:1012–7. doi:10.1261/rna.965408
32. Vejnar CE, Zdobnov EM. miRmap: comprehensive prediction of microRNA target repression strength. *Nucleic Acids Res* (2012) 40:11673–83. doi:10.1093/nar/gks901
33. Krüger J, Rehmsmeier M. RNAhybrid: microRNA target prediction easy, fast and flexible. *Nucleic Acids Res* (2006) 34:W451–4. doi:10.1093/nar/gkl243
34. Riese RJ, Mitchell RN, Villadangos JA, Shi GP, Palmer JT, Karp ER, et al. Cathepsin S activity regulates antigen presentation and immunity. *J Clin Invest* (1998) 101:2351–63. doi:10.1172/JCI1158
35. Pawar K, Sharbati J, Einspanier R, Sharbati S. *Mycobacterium bovis* BCG interferes with miR-3619-5p control of cathepsin S in the process of autophagy. *Front Cell Infect Microbiol* (2016) 6:27. doi:10.3389/fcimb.2016.00027
36. Mogilyansky E, Rigoutsos I. The miR-17/92 cluster: a comprehensive update on its genomics, genetics, functions and increasingly important and numerous roles in health and disease. *Cell Death Differ* (2013) 20:1603–14. doi:10.1038/cdd.2013.125
37. Behar SM, Divangahi M, Remold HG. Evasion of innate immunity by *Mycobacterium tuberculosis*: is death an exit strategy? *Nat Rev Microbiol* (2010) 8:668–74. doi:10.1038/nrmicro2387
38. Fairbairn IP. Macrophage apoptosis in host immunity to mycobacterial infections. *Biochem Soc Trans* (2004) 32:496–8. doi:10.1042/BST0320496
39. Zhai Z, Wu F, Chuang AY, Kwon JH. miR-106b fine tunes ATG16L1 expression and autophagic activity in intestinal epithelial HCT116 cells. *Inflamm Bowel Dis* (2013) 19:2295–301. doi:10.1097/MIB.0b013e31829e71cf
40. Zhai Z, Wu F, Dong F, Chuang AY, Messer JS, Boone DL, et al. Human autophagy gene ATG16L1 is post-transcriptionally regulated by MIR142-3p. *Autophagy* (2014) 10:468–79. doi:10.4161/auto.27553
41. Pan L, Li Y, Jia L, Qin Y, Qi G, Cheng J, et al. Cathepsin S deficiency results in abnormal accumulation of autophagosomes in macrophages and enhances Ang II-induced cardiac inflammation. *PLoS One* (2012) 7:e35315. doi:10.1371/journal.pone.0035315
42. Burgos-Portugal JA, Mitchell HM, Castaño-Rodríguez N, Kaakoush NO. The role of autophagy in the intracellular survival of *Campylobacter concisus*. *FEBS Open Bio* (2014) 4:301–9. doi:10.1016/j.fob.2014.03.008
43. Behar SM, Baehrecke EH. Tuberculosis: autophagy is not the answer. *Nature* (2015) 528:482–3. doi:10.1038/nature16324
44. Kimmey JM, Huynh JP, Weiss LA, Park S, Kambal A, Debnath J, et al. Unique role for ATG5 in neutrophil-mediated immunopathology during *M. tuberculosis* infection. *Nature* (2015) 528:565–9. doi:10.1038/nature16451
45. Saitoh T, Akira S. Regulation of inflammasomes by autophagy. *J Allergy Clin Immunol* (2016) 138:28–36. doi:10.1016/j.jaci.2016.05.009
46. Kleinnijenhuis J, Oosting M, Plantinga TS, van der Meer JWM, Joosten LAB, Crevel RV, et al. Autophagy modulates the *Mycobacterium tuberculosis*-induced cytokine response. *Immunology* (2011) 134:341–8. doi:10.1111/j.1365-2567.2011.03494.x
47. Bergsbaken T, Fink SL, Cookson BT. Pyroptosis: host cell death and inflammation. *Nat Rev Microbiol* (2009) 7:99–109. doi:10.1038/nrmicro2070
48. Simeone R, Bobard A, Lippmann J, Bitter W, Majlessi L, Brosch R, et al. Phagosomal rupture by *Mycobacterium tuberculosis* results in toxicity and host cell death. *PLoS Pathog* (2012) 8:e1002507. doi:10.1371/journal.ppat.1002507
49. Sengupta S, Naz S, Das I, Ahad A, Padhi A, Naik SK, et al. Mycobacterium tuberculosis EsxL inhibits MHC-II expression by promoting hypermethylation in class-II transactivator loci in macrophages. *J Biol Chem* (2017) 292:6855–68. doi:10.1074/jbc.M117.775205
50. Meng Q-L, Liu F, Yang X-Y, Liu X-M, Zhang X, Zhang C, et al. Identification of latent tuberculosis infection-related microRNAs in human U937 macrophages expressing *Mycobacterium tuberculosis* Hsp16.3. *BMC Microbiol* (2014) 14:37. doi:10.1186/1471-2180-14-37
51. Machelart A, Song O-R, Hoffmann E, Brodin P. Host-directed therapies offer novel opportunities for the fight against tuberculosis. *Drug Discov Today* (2017) 22:1250–7. doi:10.1016/j.drudis.2017.05.005
52. Yang C-S. Advancing host-directed therapy for tuberculosis. *Microb Cell* (2017) 4:105–7. doi:10.15698/mic2017.03.565
53. Jones AT, Sayers EJ. Cell entry of cell penetrating peptides: tales of tails wagging dogs. *J Control Release* (2012) 161:582–91. doi:10.1016/j.jconrel.2012.04.003

Conflict of Interest Statement: The authors declare that the research was conducted in the absence of any conflict of interest.

Copyright © 2017 Pires, Bernard, Pombo, Carmo, Fialho, Gutierrez, Bettencourt and Anes. This is an open-access article distributed under the terms of the Creative Commons Attribution License (CC BY). The use, distribution or reproduction in other forums is permitted, provided the original author(s) or licensor are credited and that the original publication in this journal is cited, in accordance with accepted academic practice. No use, distribution or reproduction is permitted which does not comply with these terms.

frontiers in Immunology

ORIGINAL RESEARCH
published: 01 May 2017
doi: 10.3389/fimmu.2017.00498

Iron- and Hepcidin-Independent Downregulation of the Iron Exporter Ferroportin in Macrophages during *Salmonella* Infection

*Alexandra Willemetz[1†], Sean Beatty[2,3†], Etienne Richer[2,3], Aude Rubio[4], Anne Auriac[1,4], Ruth J. Milkereit[2,3], Olivier Thibaudeau[5], Sophie Vaulont[6], Danielle Malo[2,3] and François Canonne-Hergaux[1,4]**

[1] Institut de Chimie des Substances Naturelles, Centre National de la Recherche Scientifique – UPR 2301, Gif-sur-Yvette, France, [2] Department of Human Genetics, McGill University, Montréal, QC, Canada, [3] McGill University Research Centre on Complex Traits, McGill University, Montréal, QC, Canada, [4] IRSD, Université de Toulouse, INSERM, INRA, ENVT, UPS, Toulouse, France, [5] Anatomie-Cytologie Pathologiques, CHU Bichat-Claude Bernard, Paris, France, [6] INSERM, U1016, Institut Cochin, Paris, France

OPEN ACCESS

Edited by:
Céline Cougoule, Centre national de la recherche scientifique (CNRS), France

Reviewed by:
Juliana Cassataro, Consejo Nacional de Investigaciones Científicas y Técnicas (CONICET), Argentina
Bruno Galy, Deutsches Krebsforschungszentrum (DKFZ), Germany

***Correspondence:**
François Canonne-Hergaux
francois.canonne-hergaux@inserm.fr

[†]These authors have contributed equally to this work.

Specialty section:
This article was submitted to Microbial Immunology, a section of the journal Frontiers in Immunology

Received: *01 March 2017*
Accepted: *11 April 2017*
Published: *01 May 2017*

Citation:
Willemetz A, Beatty S, Richer E, Rubio A, Auriac A, Milkereit RJ, Thibaudeau O, Vaulont S, Malo D and Canonne-Hergaux F (2017) Iron- and Hepcidin-Independent Downregulation of the Iron Exporter Ferroportin in Macrophages during Salmonella Infection. Front. Immunol. 8:498. doi: 10.3389/fimmu.2017.00498

Retention of iron in tissue macrophages *via* upregulation of hepcidin (HAMP) and downregulation of the iron exporter ferroportin (FPN) is thought to participate in the establishment of anemia of inflammation after infection. However, an upregulation of FPN has been proposed to limit macrophages iron access to intracellular pathogens. Therefore, we studied the iron homeostasis and in particular the regulation of FPN after infection with *Salmonella enterica* serovar Typhimurium in mice presenting tissue macrophages with high iron (AcB61), basal iron (A/J and wild-type mice), or low iron (*Hamp* knock out, *Hamp*$^{-/-}$) levels. The presence of iron in AcB61 macrophages due to extravascular hemolysis and strong erythrophagocytosis activity favored the proliferation of *Salmonella* in the spleen and liver with a concomitant decrease of FPN protein expression. Despite systemic iron overload, no or slight increase in *Salmonella* burden was observed in *Hamp*$^{-/-}$ mice compared to controls. Importantly, FPN expression at both mRNA and protein levels was strongly decreased during *Salmonella* infection in *Hamp*$^{-/-}$ mice. The repression of *Fpn* mRNA was also observed in *Salmonella*-infected cultured macrophages. In addition, the downregulation of FPN was associated with decreased iron stores in both the liver and spleen in infected mice. Our findings show that during *Salmonella* infection, FPN is repressed through an iron and hepcidin-independent mechanism. Such regulation likely provides the cellular iron indispensable for the growth of *Salmonella* inside the macrophages.

Keywords: *Salmonella* infection, anemia of inflammation, iron homeostasis, macrophage iron recycling, the iron regulatory hormone hepcidin, the iron exporter ferroportin

INTRODUCTION

Human infectious diseases are still a major public health problem in particular because of the development of antibiotic resistance, the lack of new products, and the demise of antibacterial drug discovery by pharmaceutical companies (1). Such context leads to the emergence and reemergence of infectious diseases, and it becomes critical to develop alternative approaches to identify new antibacterial drugs and to propose new treatments. Therefore, the natural host defense mechanisms against

invading microbes and the mechanisms regulating the virulence of microorganisms need to be better understood. An important host defense strategy against infection, known as "nutritional immunity," relies on the sequestration of essential molecules, such as iron, preventing the growth of pathogens (2). Iron is essential for both the host and the invading microbes and plays a critical role in host–pathogen interactions. In response to infection, patients commonly develop hypoferremia (i.e., a decrease of iron in the circulation), a host response to limit iron availability to invading pathogens (3). However, for the host, hypoferremia also contributes to the establishment of the so-called anemia of inflammation (AI) (4), an anemia difficult to treat and that can add substantially to the morbidity of the underlying infection.

Iron sequestration in macrophages is a described hallmark of the AI and is an efficient mechanism to quickly deplete iron in the serum to limit the growth of extracellular pathogens (5). Two molecules, namely hepcidin (HAMP) and ferroportin (FPN), have been identified to play key roles in decreasing systemic iron level by promoting macrophage iron sequestration during infection (5). FPN is the only known mammalian iron exporter and is expressed at the cell surface of macrophages (6, 7). FPN is quickly downregulated through endocytosis and degradation upon interaction with HAMP (6, 8). HAMP is produced mainly by hepatocytes in case of inflammation and also by infected macrophages (9). Therefore, decreasing the expression of FPN to retain iron inside the macrophages could limit serum iron access to extracellular pathogens.

On the other hand, macrophages are a common niche for the replication of numerous intracellular pathogens including *Salmonella*. Increased iron level inside macrophages might therefore represent either an advantage for the growth of intracellular microorganisms or a host strategy to fight against intracellular bacteria through the generation of highly toxic reactive oxygen species *via* Fenton's reaction (3). Recently, some studies have challenged these concepts and have suggested that macrophages infected with intracellular bacteria respond by decreasing their iron content *via* an upregulation of FPN to limit the growth of the invading microbes (10–12).

Therefore, the modulation of host iron homeostasis, in particular in macrophages, in response to infection with intracellular pathogens is currently a matter of debate, and the regulation of FPN is an important iron response to be evaluated in different intracellular bacterial infection settings. *Salmonella* is the most common bacterial cause of foodborne outbreaks, and many *Salmonella* strains are resistant to antibiotics. The main purpose of the current work was to explore the interplay between infection with *Salmonella* (*Salmonella enterica* serovar Typhimurium) and the systemic and macrophage iron homeostasis in different mouse models presenting distinct systemic and macrophages iron levels.

MATERIALS AND METHODS

Animals and *Salmonella* Infection *In Vivo*

The generation of AcB61 was reported previously (13). A/J mice were purchased from the Jackson Laboratory. Hamp^{tm1Svl} knockout mice [*Hamp*$^{-/-}$ (14)] were transferred onto a 129S6 background (129S6.B6*129S2-*Hamp*^{tm1Svl}). Both female and male aged between 8 and 12 weeks were used for the current study. The mice were fed with the diet Teklad 2920X, which contains 200 mg/kg of iron. All the experiments were done under the same housing conditions at McGill University (Montreal, QC, Canada). *In vivo* intravenous infections [~1,000 CFUs for A/J and AcB61 and ~5,000 CFUs for wild-type (WT) and *Hamp*$^{-/-}$] were performed with *S. enterica* serovar Typhimurium (strain Keller) as previously described (15).

Macrophage Cultures and *Salmonella* Infection *In Vitro*

Murine bone marrow-derived macrophages (BMDMs) from CD1 mice were cultured as previously described (16). *In vitro* infection of macrophages (MOI of 5–10) was performed for 1 h with *S. enterica* serovar Typhimurium (strain SL1344) (17). Extracellular bacteria were killed by incubation with 100 μg/ml gentamicin in fresh medium for 1 h. Cells were then washed and cultured in fresh medium containing 10 μg/ml gentamicin until the time points of RNA extraction.

Blood Parameters Analysis

Hematology profiles were performed at the McGill Comparative Medicine and Animal Resources Centre (Montréal, QC, Canada). Plasma iron, ferritin, transferrin, and bilirubin levels were measured with an Olympus AU400 automat at the Laboratory of Biochemistry at the Institut Fédératif de Recherche 02, CHU Bichat-Claude Bernard (Paris, France).

Tissues Iron Studies

Liver and spleen iron contents were determined by acid digestion (18) and measured with an Olympus AU400 automat. Tissue iron staining was done using Perls' Prussian blue solution and examined under a light microscope and photographed or digitized using a slide scanner (Pannoramic 250 from 3DHISTEC).

Immunohistofluorescence Studies

After blocking (1% BSA and 10% heat inactivated goat serum) for 30 min at room temperature, deparaffinized tissues sections were incubated with primary antibodies for 1 h: rabbit anti-FPN (7, 19): 1/50 to 1/100; rabbit anti-HMOX1 (Stressgen): 1/500; rat anti-F4/80 (AbDserotec): 1/500. After three washes with PBS/0.5% BSA, sections were incubated for 1 h at RT with Goat anti-rabbit-alexa488 (1/200) and Goat anti-rat-Alexa563 (1/200) (MolecularProbes). After mounting, sections were visualized using either an epifluorescence microscope LEICA DM-IRM or a Zeiss confocal fluorescent microscope. Images were acquired using either ARCHIMED-PRO (Microvision Instruments) or Zeiss LSM Image Browser softwares.

Western Blot Analysis

Crude membrane fractions (40 μg for spleen and 80 μg for liver) from mouse tissues were prepared and analyzed by western blotting as previously described (7). Antibodies were diluted in blocking solution as follows: anti-FPN (7, 19): 1/200 (liver) or

1/500 (spleen), anti-HMOX1 (Stressgen): 1/4,000, anti-LAMP1 (DSHB): 1/500, and anti-TfR1 (Zymed): 1/200.

RNA Studies

Complementary DNAs were synthesized from total RNA (Trizol) isolated from tissues or BMDM and using M-MLV reverse transcriptase (Invitrogen). Quantitative PCR was performed on Chromo4 Real-Time PCR Detection System (Bio-Rad Laboratories) or LightCycler 480 Instrument (Roche Diagnostics) using Brilliant SYBR Green QPCR Master Mix (Stratagene). Gene expression fold changes were calculated using the formula $2^{-\Delta\Delta Ct}$, in which $\Delta\Delta Ct^{A-B} = (Ct^{gene} - Ct^{Hprt})\ B - (Ct^{gene} - Ct^{Hprt})\ A$ and A = WT and B = *Hamp*$^{-/-}$. For tissues, data are presented as fold changes ($2^{-\Delta\Delta Ct}$) in infected mice relative to the mean value of A/J or WT (control) at each time point. For BMDM, the gene *Hprt* was used as a reference gene, and relative gene expression is expressed in −ΔCT (CT gene of interest − CT *Hprt*).

Statistical Analysis

Except for CFUs (unpaired two-tailed Student's *t*-test), data were analyzed by two-way ANOVA using Sidak's multiple comparisons test followed by unpaired *t*-tests. GraphPad Prism version 6 was used for statistical analysis (GraphPad Software, La Jolla, CA, USA).

RESULTS

Impact of *Salmonella* Infection on Anemia and Iron Homeostasis in A/J and AcB61 Mice

The recombinant congenic mouse strain AcB61 was generated from A/J and C57BL/6J mice and presents a deficiency in red blood cell pyruvate kinase activity (*de novo* mutation in *Pklr*). As a consequence of this mutation, AcB61 mice present chronic hemolytic anemia with tissue iron overload (20–22). AcB61 and their parental controls (A/J mice) were infected intravenously with *Salmonella* Typhimurium (*ST*), and samples were collected before (D0) and 5 day postinfection (D5). Hematocrit (A), plasma iron (B), and ferritin levels (C) in blood were analyzed (**Figure 1**). Consistent with previous reports (22), AcB61 mice showed a constitutive anemia at D0 with a lower hematocrit (35% in AcB61 versus 50% for A/J) that worsens during *Salmonella* infection (~20% in AcB61; **Figure 1A**). Signs of anemia occurred later during infection in A/J mice (data not shown). Compared to A/J, AcB61 mice presented hypoferremia (**Figure 1B**) and hyperferritinemia (**Figure 1C**). With *Salmonella* infection, both plasma iron and ferritin levels increase significantly in AcB61.

In the liver at D0, Perls staining of tissue sections (**Figure 1D**) and quantitative determination of iron (**Figure 1E**) indicated a strong iron accumulation in AcB61 liver when compared to A/J liver. We did not observe any significant changes in iron levels in the liver of both A/J and AcB61 after infection. Importantly, the bacterial load was significantly higher in the liver of AcB61 mice when compared to A/J (**Figure 1F**). In the AcB61 spleen, the iron level was significantly higher than the one detected in A/J and tended to slightly increase with infection (**Figure 1H**) with a marked iron accumulation in enlarged splenic macrophages (**Figure 1G**). On the other hand, the Perls staining of A/J spleen suggested a slight decrease in iron after infection (**Figure 1G**). As observed in the liver, the bacterial load was significantly higher in the spleen of AcB61 mice when compared to A/J (**Figure 1I**).

We next analyzed more precisely the localization of iron in both liver (**Figure 1J**) and spleen (**Figure 1K**) from AcB61 before and after infection. Histological examination of Perls staining indicated iron accumulation mostly in sinusoid zones and centrilobular (CL) area of the naïve AcB61 liver, whereas most periportal (PP) zones were not stained (**Figure 1J**). At the cellular level, iron strongly accumulated (deep blue) in Kupffer cells with some milder iron staining (light blue) in surrounding hepatocytes (**Figure 1J**, lower panels; Figure S1A in Supplementary Material). Signs of extramedullary erythropoiesis (clusters of nucleated cells surrounding or near iron loaded macrophages) were also observed at the vicinity of vessels in uninfected AcB61 (**Figure 1J**, arrowhead). With *Salmonella* infection, numerous and enlarged inflammatory foci were observed in iron-rich regions of the AcB61 liver (**Figure 1J**, arrows).

Histologic examination of the spleen of AcB61 mice before infection revealed a strong expansion of the red pulp (RP) and evidence of extramedullary erythropoiesis with numerous trapped RBC (**Figure 1K**, lower panel). Important accumulation of iron in the AcB61 spleen was clearly detected in enlarged splenic macrophage of the RP before and after infection (**Figure 1K**; Figure S1A in Supplementary Material).

Several observations in AcB61 mice including the presence of ingested RBC, the strong expression of the heme oxygenase 1 (heme catabolism enzyme), splenomegaly, and an high bilirubin level (marker of erythrophagocytosis and heme iron recycling) indicate that the macrophage iron overload of AcB61 mice is due to extravascular hemolysis and a strong erythrophagocytosis (EP) activity in tissue macrophages (Kupffer and splenic) (Figure S1 in Supplementary Material). FPN protein was also strongly expressed in AcB61 tissues (Figure S1E in Supplementary Material) and was localized at the cell surface of both hepatic (Figure S1F in Supplementary Material) and splenic (Figure S1G in Supplementary Material) AcB61 macrophages, presenting numerous engulfed RBC. Altogether our observation indicates a strong clearance of red blood cells and heme catabolism by macrophages in AcB61. As a consequence, such erythrophagocytosing AcB61 macrophages present large amount of iron and a strong expression of FPN.

FPN Expression in A/J and AcB61 after *Salmonella* Infection

During *Salmonella* infection, protein expression of HMOX1 increased in the liver (**Figures 2A,C**) of both of A/J and AcB61 mice and in the spleen (**Figures 2B,D**) of AcB61 mice. HMOX1 expression was maintained in spleen of infected A/J (**Figure 2B**). On the other hand, infection leads to a profound downregulation of FPN in the liver (**Figure 2A**, lower panels) and in the spleen (**Figure 2B**, lower panels) of AcB61. FPN downregulation was also observed in the spleen of A/J mice (**Figure 2B**, upper panels). Decreased expression of FPN in AcB61 organs was associated with the disappearance of FPN at the cell surface of tissue macrophages (**Figures 2C,D**). During infection, we also observed strong EP activity in the spleen of AcB61 as illustrated by the

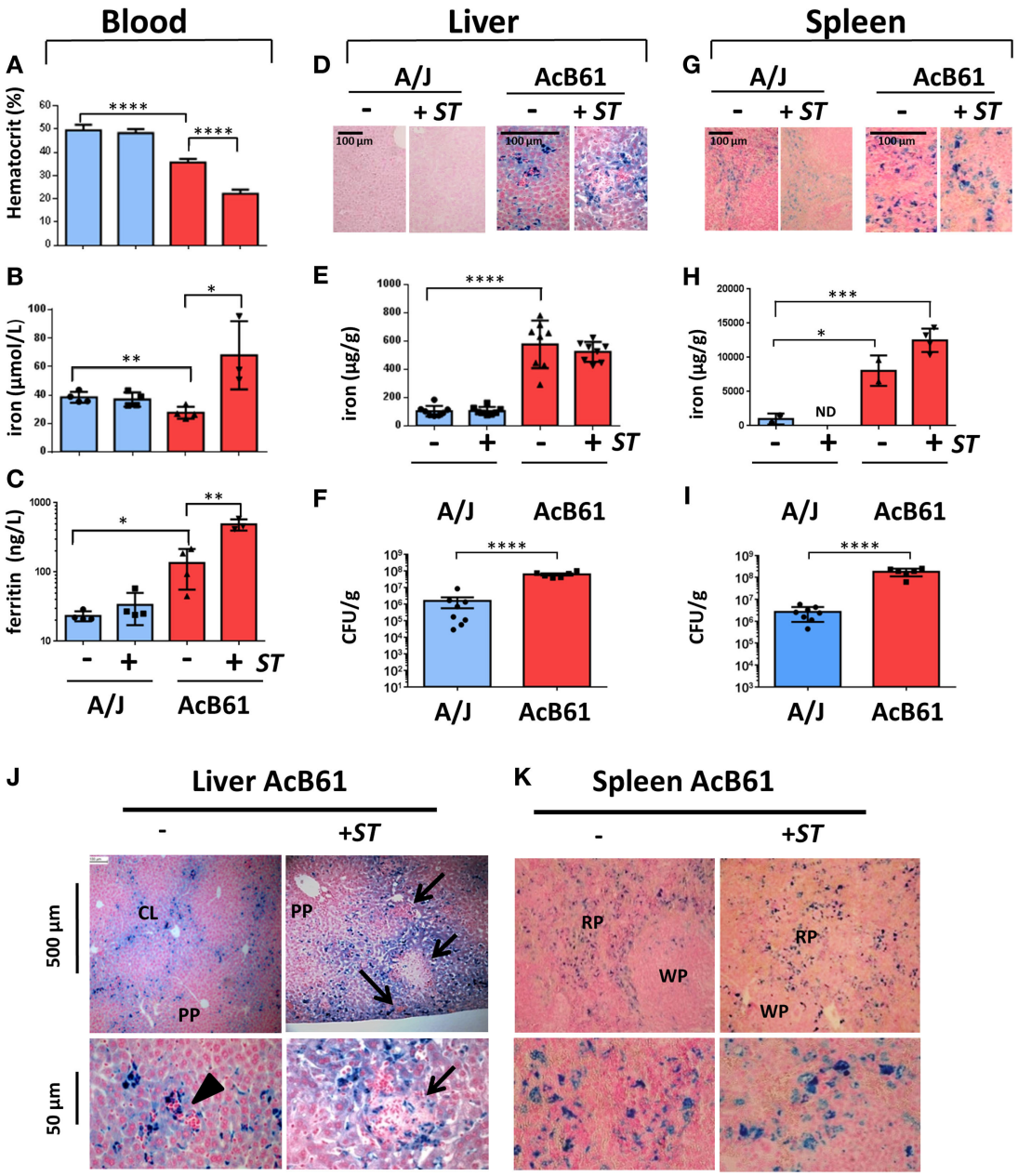


FIGURE 1 | Infectious, hematological and iron metabolism parameters in A/J and AcB61 mice following infection with *Salmonella* Typhimurium (*ST*). Blood parameters from A/J and AcB61 including hematocrit **(A)**, iron **(B)**, and ferritin **(C)** were analyzed before (–) or after 5 days of infection with *ST* (+*ST*). Iron levels were assessed by Perls staining **(D,G)** and dosage **(E,H)** on liver **(D,E)** or splenic **(G,H)** tissues. Bacterial load at day 5 of infection with *ST* was studied by measuring CFUs in liver **(F)** and spleen **(I)** of infected A/J and AcB61 mice. Statistical significance: $^{*}P < 0.05$, $^{**}P < 0.01$, $^{***}P < 0.001$, $^{****}P < 0.0001$. ND, not determined. Hepatic **(J)** and splenic **(K)** iron distribution in AcB61 mice before and after *Salmonella* infection. Liver and spleen sections from naive AcB61 mice (–) or AcB61 mice infected with *ST* (+*ST*, Day 5) were processed for Perls staining. Arrowhead indicates the presence of erythropoeitic islands in naïve AcB61 liver attesting of extramedullar erythropoiesis in these mice. After infections, numerous inflammatory foci and pathological lesions were observed in iron-rich region of the liver (arrows). Strong iron accumulation was seen in splenic macrophages of the RP before and after *Salmonella* infection. PP, periportal vessels; CL, centrilobular vessels; RP, red pulp; WP, white pulp. $n = 4$–8 mice per genotype used for the different measurements. The data are presented as mean ± SD.

high number of RBC (Hb autofluorescence) in large splenic macrophages (**Figure 2D**, enlargement).

At the hepatic mRNA levels (**Figure 2E**), in uninfected mice, *Fpn* and *Hmox1* were increased in AcB61 liver when compared to A/J tissues. *Hmox1* mRNA expression progressively increased during infection in both A/J and AcB61 liver. Contrasting with the strong protein downregulation, no major changes of *Fpn* mRNA expression were observed in AcB61 liver during *Salmonella* infection. In addition, *Hamp* expression did not change significantly during infection, suggesting that HAMP may not contribute to the anemia and downregulation of FPN during *ST* infection in AcB61 mice.

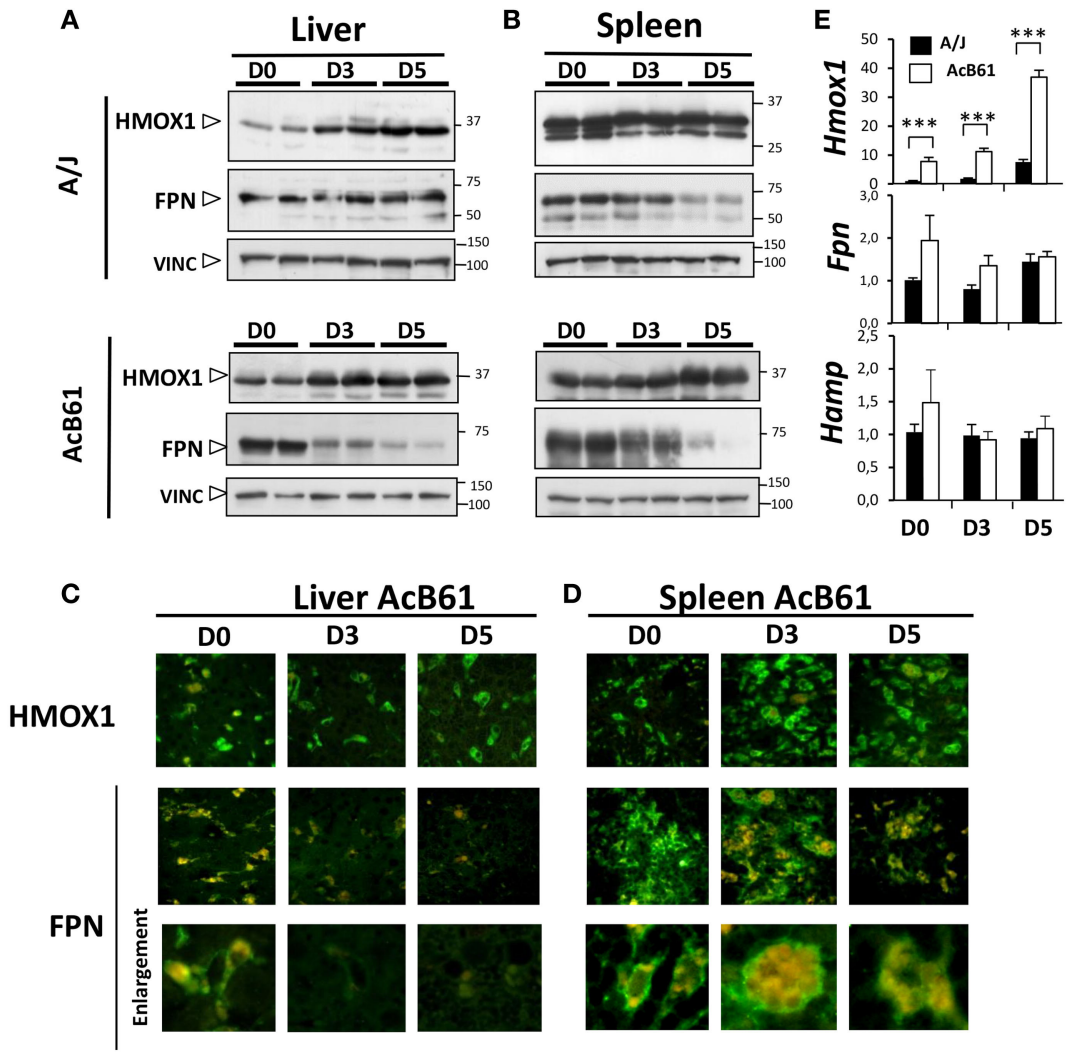


FIGURE 2 | **Ferroportin (FPN) and HMOX1 expression during *Salmonella* infection in A/J and AcB61 mice**. **(A,B)** Western blot analysis of HMOX1, FPN, and VINC (loading control) expression in liver **(A)** and spleen **(B)** during *Salmonella* Typhimurium (*ST*) infection in both A/J and AcB61. **(C,D)** Immunofluorescence labeling (green) of FPN or HMOX1 and autofluorescence (red) of RBC hemoglobin in liver of *Salmonella*-infected AcB61 mice. During *Salmonella* infection, HMOX1 expression was maintained, whereas FPN expression at the cell surface of tissue macrophages cells strongly decreased. **(E)** RT-qPCR analysis of *Fpn*, *Hmox1*, and *Hamp* mRNA expression in A/J ($n = 4$) and AcB61 ($n = 4$) liver before and after *ST* infection. Data are representative of three independent experiments. D0, uninfected; D3 and D5, 3 and 5 days postinfection, respectively. Statistical significance: $^{***}P < 0.001$. The data are presented as mean ± SD.

Impact of *Salmonella* Infection on Anemia and Iron Homeostasis in WT and *Hamp*$^{-/-}$ Mice

To understand better the role of HAMP during *Salmonella* infection, we next studied the impact of *Salmonella* infection in mice deficient in HAMP (*Hamp*$^{-/-}$) (14). *Hamp*$^{-/-}$ mice have been shown to develop a specific iron phenotype with high serum iron concentration, excess iron deposition in hepatocytes, and low iron levels in tissue macrophages (14).

Wild-type and *Hamp*$^{-/-}$ mice were intravenously infected with *ST* (+*ST*; **Figure 3**). After 10 days postinfection, WT mice present signs of anemia with hematocrit levels below 40% (**Figure 3A**) and decreased plasma iron levels (**Figure 3B**). As previously described (14), *Hamp*$^{-/-}$ mice present a higher hematocrit (60%) and a higher concentration of iron and ferritin in the blood when compared to WT (**Figures 3A–C**). During *Salmonella* infection in *Hamp*$^{-/-}$ mice, the hematocrit significantly decreased to 50% but was accompanied with a significant increase (around two times more) of plasma iron (**Figures 3A,B**).

With infection, no major changes in liver iron level were observed in WT mice (**Figures 3D,E**). On the other hand, iron was strongly detected in *Hamp*$^{-/-}$ liver (around 2,000 µg/g) and decreased significantly by more than 50% after infection (**Figure 3E**). In parallel to the hepatic iron overload phenotype of *Hamp*$^{-/-}$ mice, we did not observe significant changes in bacterial CFUs in the liver (**Figure 3F**) of *Hamp*$^{-/-}$ versus WT mice after *Salmonella* infection.

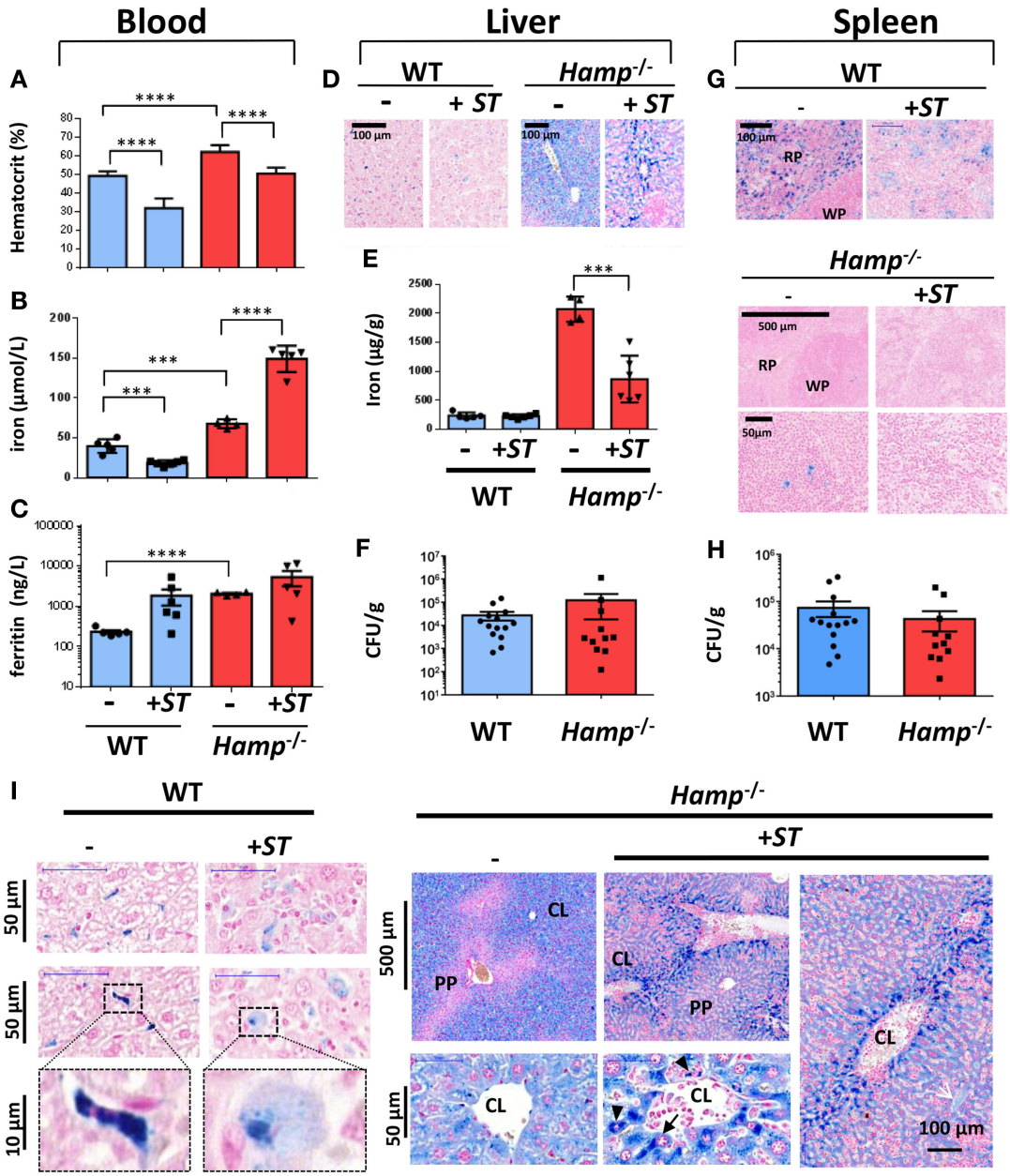


FIGURE 3 | Infectious, hematological and iron metabolism parameters in wild-type (WT) and hepcidin knockout (*Hamp*$^{-/-}$) mice following infection with *Salmonella* Typhimurium (*ST*). Blood parameters from WT and *hepcidin* knockout *Hamp*$^{-/-}$ including hematocrit **(A)**, iron **(B)**, and ferritin **(C)** were analyzed before (–) or after 10 days of infection with *ST* (+*ST*). Iron levels were assessed by Perls staining **(D,G)** and dosage **(E)** on liver **(D,E)** or splenic **(G)** tissues. Bacterial load at day 10 of infection with *ST* was studied by CFUs in the liver **(F)** and spleen **(H)** of infected WT and *Hamp*$^{-/-}$ mice. Statistical significance: ***$P < 0.001$; ****$P < 0.0001$. **(I)** Hepatic iron localization in WT and *Hamp*$^{-/-}$ mice before and after *Salmonella* infection. Perls staining of liver sections from naive (–) mice or mice infected with *ST* (+*ST*, Day 10). Lower panels in WT mice show high magnification of the cellular localization of iron in Kupffer cells. PP, periportal vessels; CL, centrilobular vessels. n = 4–15 mice per genotype. The data are presented as mean ± SD.

In the *Hamp*$^{-/-}$ spleen, iron was strongly depleted in the macrophages of the RP when compared with WT (**Figure 3G**) corroborating the described low iron level of *Hamp*$^{-/-}$ macrophages. In WT spleen, Perls staining indicated a decrease in macrophage iron after *Salmonella* infection (**Figure 3G**; Figure S2 in Supplementary Material). As observed in the liver, we did not detect significant changes in bacterial CFUs (**Figure 3H**) in *Hamp*$^{-/-}$ versus WT spleen. Together, these data suggest that the serum and parenchymal iron overload phenotype of *Hamp*$^{-/-}$ mice does not favor the growth of *Salmonella in vivo*.

Changes in Iron Localization in *Hamp*$^{-/-}$ Liver during *Salmonella* Infection

A careful microscopy analysis of Perls staining confirmed the presence of iron (deep blue staining) in WT Kupffer cells, which

tend to decrease (light blue staining) after *Salmonella* infection (**Figure 3I**). In the liver of uninfected *Hamp*$^{-/-}$ mice, iron accumulation was observed in hepatocytes of CL zones, whereas PP areas were not stained (**Figure 3I**). Interestingly, a change in the cellular localization of iron was observed after *Salmonella* infection with higher iron concentration in macrophages (**Figure 3I**, arrowheads) and hepatocytes (**Figure 3I**, arrows) lining the CL zones and the sinusoids walls. The decrease in liver iron content and its redistribution during infection suggest that *Salmonella* alter mechanisms of iron storage or export.

Downregulation of FPN during Infection by *Salmonella* Is Independent of Hepcidin

To determine whether FPN is involved in the redistribution of iron in the absence of *Hamp*, we measured FPN expression during *Salmonella* infection in *Hamp*$^{-/-}$ mice. As previously described, *Hamp*$^{-/-}$ mice expressed high levels of FPN protein in both spleen (Figure S3 in Supplementary Material) and liver (**Figure 4A**) compared to WT mice. FPN was mostly detected in Kupffer cells (F4/80+) in WT liver, whereas in *Hamp*$^{-/-}$ liver, FPN was strongly expressed by both Kupffer cells (F4/80^{+}) and hepatocytes (F4/80^{-}) (**Figure 4A**). After *ST* infection, in both WT and *Hamp*$^{-/-}$, the expression of FPN was strongly decreased in hepatocytes and Kupffer cells when compared to uninfected tissues (**Figure 4A**). Similarly, a decrease of FPN expression in macrophages of the RP in WT and *Hamp*$^{-/-}$ spleen was observed after *ST* infection (Figure S3 in Supplementary Material). Similar observation was made after *Salmonella* Enteritidis (*SE*) infection (Figure S4 in Supplementary Material). In some microscopy fields of the liver, despite a global decrease of FPN staining in most of the section area, some localized FPN- and F4/80-positive regions were detected after *ST* (Figure S5 in Supplementary Material) and *SE* (Figure S4 in Supplementary Material) infections. Panel B in Figure S5 in Supplementary Material clearly indicated, within infected liver, the presence of large resident Kupffer cells negative for FPN expression (F4/80^{+}; arrowhead) with smaller and round recruited monocytes both positive for FPN and F4/80 (arrow dot).

In parallel to the decrease of FPN protein expression, the level of *Fpn* mRNA was significantly downregulated in both WT and *Hamp*$^{-/-}$ liver after *ST* infection (**Figure 4B**). Previous reports (16, 23) suggest that the nitric oxide synthase 2 (NOS2) play a role in a positive regulation of FPN during *Salmonella* infection. However, concomitant with the decrease of *Fpn*, an increase in the mRNA expression of *Nos2* gene was observed with *ST* infection in both WT and *Hamp*$^{-/-}$ liver (**Figure 4B**).

A time-dependent downregulation of *Fpn* mRNA was also observed in BMDM cultures infected with *ST* (**Figure 4C**). Such negative regulation of *Fpn* was rapid occurring after 4 h of infection with no significant changes of *Hamp* level at that time. In contrast to *in vivo* infections, *Hamp* expression was slightly but significantly upregulated at 6 h in BMDM during *Salmonella*

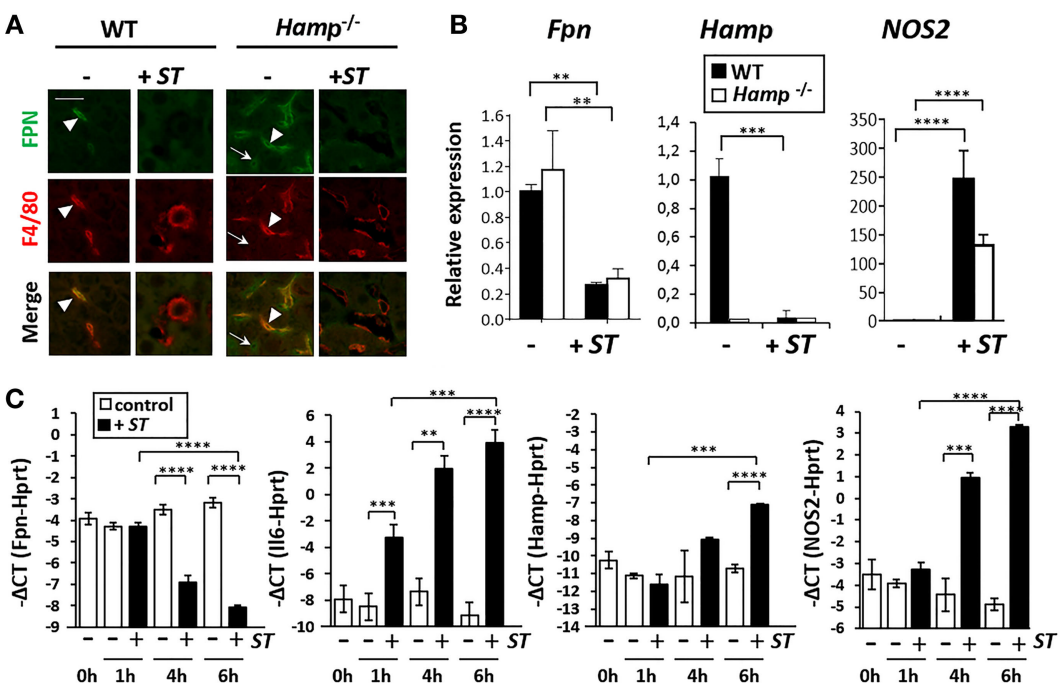


FIGURE 4 | Hepcidin-independent downregulation of ferroportin (FPN) expression in liver and macrophages after *Salmonella* infection.
(A) Immunohistofluorescence of FPN (green) and F4/80 (macrophage marker; red) expression in liver of naïve mice (–) or mice infected with *Salmonella* Typhimurium (*ST*) (+*ST*). **(B)** RT-qPCR analysis of *Fpn*, *Hamp*, and *nitric oxide synthase 2* (*NOS2*) mRNA expression in wild-type (WT) (black bars) and *Hamp*$^{-/-}$ (white bars) liver before (–) and after (+*ST*) *ST* infection. Data are presented as fold changes ($2^{-\Delta\Delta Ct}$) in infected mice relative to the mean value of WT (control) at each time point. **(C)** RT-qPCR analysis of *Fpn*, *IL6*, *Hamp*, and *NOS2* mRNA expression in bone marrow-derived macrophage (BMDM) at different time points after infection with *ST*. The relative gene expression is expressed as $-\Delta Ct$ ($Ct^{\text{gene of interest}} - Ct^{\text{Hprt}}$). White bars: uninfected BMDM (–); black bars: infected BMDM (+). Statistical significance: $^{**}P < 0.01$; $^{***}P < 0.001$; $^{****}P < 0.0001$. The data are presented as mean ± SD.

infection, suggesting that downregulation of *Hamp in vivo* most likely reflects a global repression in hepatocytes. As a control of BMDM infection, *Il6* expression strongly increased during *ST* infection (**Figure 4C**). As observed in liver, *Nos2* was also induced in BMDM after *Salmonella* infection. Overall these data are consistent with the conclusion that decreased expression of FPN during *Salmonella* infection is independent of HAMP.

DISCUSSION

In this article, we characterized the interplay between iron homeostasis and intracellular *Salmonella* infection, using different mouse models presenting distinct systemic and macrophages iron contents. Indeed two distinct models were used presenting either macrophage iron overload (AcB61) or macrophage iron deficiency but systemic iron overload (*Hamp*$^{-/-}$).

Among our models, the AcB61 mice were the most susceptible to *ST* infection. AcB61 mice harbor a mutation in the gene *Pklr* leading to PK deficiency and resulting in chronic hemolytic anemia and tissue iron overload (20–22). We observed intensive EP activity in AcB61 tissue macrophages *in vivo*, which is consistent with *in vitro* studies showing that *Pklr*-deficient erythrocytes were more vulnerable to phagocytosis by macrophages than control erythrocytes (24). As a consequence of enhanced EP activity in AcB61 macrophages, strong heme recycling is observed with increased bilirubinemia and enhanced expression of both HMOX1 and FPN. Heme is known to be a potent inducer of HMOX1 transcription (25), and both heme and iron positively regulate macrophage FPN at both transcriptional and posttranscriptional levels (23, 26). In addition, FPN was strongly detected *in vivo* at the cell surface of AcB61 hepatic and splenic macrophages, suggesting some export of the iron from the cytosol to circulation.

The important iron storage and iron fluxes in AcB61 macrophages likely represent an advantage for the growth of *Salmonella* and contribute to the high susceptibility of AcB61. Interestingly, AcB61 mice have been challenged for their response to infection with several intracellular bacteria including *Listeria monocytogenes* (D. Malo, unpublished), different strains of *Mycobacterium bovis* (22, 27), and *Legionella pneumophila* (13). For all these models of infection, the Pklr mutation in AcB61 did not contribute to the clinical phenotype, and no further studies focusing on iron metabolism were performed. Other observations (not shown) indicate that the exacerbated susceptibility of AcB61 mice to *Salmonella* infection is not the consequence of a blunted immune response or a defect in the expression of the iron-siderophore binding protein lipocalin 2 and therefore likely reflects the accessibility to intracellular iron by the bacteria. Iron is an indispensable metal for the spread of virtually all human pathogens (3). Of note, numerous *Salmonella*-induced granulomas, which represent infected foci containing the bacteria, were mostly localized in iron-rich regions in AcB61 mice. Importantly, there was a significant decrease of serum iron in AcB61 when compared to A/J, suggesting that despite the fact that *Salmonella* is a facultative intracellular bacterium, it takes more advantage of the intracellular macrophage iron sources rather than of the extracellular sources. Accordingly, in spite of a high iron level in blood and hepatocytes, we observed no change in *Salmonella* load in *Hamp*$^{-/-}$ mice when compared to WT mice. However, we previously showed that mice deficient in Hamp were significantly more susceptible to lethal infection than heterozygous or wild type littermates (28). Such observation indicates the involvement of Hamp during systemic model of *ST* infection. However, the exact mechanism underlying such differences remains obscure.

Iron deficiency, bone marrow suppression, and hemolysis are described to participate in the establishment of anemia in infectious diseases (4). Lower hematocrit levels after *Salmonella* infection were observed in AcB61 and *Hamp*$^{-/-}$ mice despite important levels of plasma iron, suggesting that these mice do not develop iron-restrictive anemia during infection. Our observations are concordant with literature, suggesting that the main driving force for the decrease of hematocrit during *Salmonella* infection is an accelerated clearance of RBC (29, 30). Indeed, during *Salmonella* infection, AcB61 spleens present signs of strong EP activity with numerous RBC per macrophages. *Salmonella* infection *via* the stimulation of Toll-like receptor 4 has been shown to stimulate macrophages to hemophagocytosis, a process that lead to the phagocytosis of red and white blood cells (29, 30).

In addition, our work suggests that the *Salmonella*-induced anemia is, at least in part, independent of HAMP. Indeed, either no changes (AcB61 mice) or a decrease (WT mice) of hepatic *Hamp* expression is associated with anemia after *ST* infection, and even in *Hamp*$^{-/-}$ mice, a decreased hematocrit is still observed. *In vivo*, the expression of *Hamp* in the hepatocyte is governed by stimulatory (iron overload and inflammation) and inhibitory factors (erythropoietic ERFE and hypoxia), the net effect of these factors defining the *Hamp* level in the organism (31). In uninfected AcB61 mice, the positive iron regulator is likely compensated by the negative erythropoietic regulator (ERFE) leading to normal but inadequately low level of *Hamp* for the degree of iron loading observed in these mice. Indeed, we observed extramedullary erythropoiesis and increase of *Erfe* mRNA levels (not shown) in the spleen of AcB61. As previously observed (28), in WT mice, *Hamp* expression was repressed after *ST* infection. In contrast, other studies have reported increased expression of *Hamp* during ST infection in mice (32) or *Salmonella* Typhi in humans (33). Interestingly, in a model of the AI using a heat-killed Gram-negative bacteria, *Brucella abortus*, *Hamp* was shown to be upregulated in an early phase associated with erythropoietic suppression but was downregulated in a second later phase in parallel with an increase in EPO and erythropoiesis (34, 35). In addition, *Salmonella* infection has been shown to initiate extramedullary erythropoiesis and splenomegaly with increases in RBC precursors and EPO production (36). These differences observed between studies in the regulation of *Hamp* during *Salmonella* infection may rely on differences in the degree of compensatory erythropoiesis at the infection time (negative regulation of *Hamp via* ERFE).

In this study, we observed a strong negative regulation of the iron exporter FPN at both the mRNA and the protein level in *Hamp*$^{-/-}$ mice, indicating that the repression of the iron exporter by *Salmonella* infection is independent of HAMP action. Recently, a strong HAMP-independent, negative regulation of FPN mRNA and protein was also documented in BMDM and liver and spleen of mice in response to acute inflammatory conditions induced by TLR2/6 agonists (37). In this study, the reduced expression

of FPN in macrophages was sufficient to rapidly induce hypoferremia in mice (37). Similarly, reduction of spleen *Fpn* mRNA level by TLR4 agonist was shown to be HAMP independent (38).

In WT mice, we also observed a concomitant decrease in both FPN expression and plasma iron with a decrease in *Hamp* expression. Together, such observations suggest that beside HAMP effect, other mechanisms exist to induce a pathogen-mediated hypoferremic response, contributing to the AI.

In vivo, the negative regulation of FPN protein was observed in tissue macrophages after *ST* infection. Similar observation was made after *SE* infection (Figure S4 in Supplementary Material). Of note, we did not observe a decrease in *Fpn* mRNA expression in infected AcB61 mice despite the strong loss of FPN protein expression at the cell surface of AcB61 macrophages. The strong positive regulation of *Fpn* mRNA expression by heme and iron in erythrophagocytic AcB61 macrophages likely counteracts the *Salmonella*-mediated negative regulation at the level of mRNA. Such observation suggests that posttranscriptional regulations may exist since FPN protein expression is diminished without any changes of *Fpn* and *Hamp* mRNA levels. Recently, iron regulatory proteins (IRPs) have been shown to play a role during *Salmonella* infection (39). FPN contains an iron-responsive element in its 5′ UTR, and its translation is repressed by the IRPs. Therefore, during *Salmonella* infection, IRPs could block the translation of *Fpn* and thereby contribute to the decrease of FPN protein levels despite no alteration at the levels of mRNA. However in the context of AcB61 mice, the high iron content observed in macrophages likely impairs the action of the IRPs. Since FPN protein expression decreased despite maintained level of *Fpn* mRNA in AcB61 mice during salmonella infection, other post-transcriptional mechanism(s) may occurred.

Interestingly, FPN- and F4/80-positive cluster of cells were detected only in the liver of *Hamp* KO mice after *Salmonella* infection. In these mice, our cellular analysis strongly suggests that such cellular aggregates correspond to the recruitment of uninfected circulating monocytes overexpressing FPN because of the lack of Hamp.

In vitro, the negative FPN regulation was directly observed at the level of mRNA in *ST*-infected cultured BMDM. Our data are consistent with previous observations showing decreased FPN mRNA expression *in vivo* (37, 40) and *ex vivo* in cultured murine and human macrophages treated with lipopolysaccharide (LPS) (16, 41–43). *ST* infection and LPS stimulation were shown to induce similar changes in macrophage gene expression (44). The molecular mechanism of *Fpn* mRNA repression in macrophages *via* LPS/TLR4 stimulation is still not known. Moreover, down-regulation of *Fpn* expression in macrophages was also reported with TLR2/6 (37, 45) expanding the FPN response to various pathogen-associated molecules.

In the context of intracellular pathogen infection, low levels of FPN in macrophages will favor cellular iron sequestration and bacterial growth inside the infected cells. This is consistent with *in vitro* studies showing that degradation of FPN resulted in increased macrophage bacterial growth in *Salmonella*-infected J774 macrophages (46). In opposition to this cellular scenario, other authors proposed that during infection with macrophage-tropic intracellular pathogens, macrophages respond by an upregulation of FPN to limit intracellular iron content (10, 12). Increases in FPN mRNA and protein expression in mouse macrophages cell lines RAW264.7 or thioglycollate-elicited peritoneal macrophages have been reported during *Salmonella* infection (10). The same authors have proposed that upregulation of FPN during *Salmonella* infection involves NO production by NOS2 (10, 12). However, in our *ST*-infected BMDM as well as in the liver of infected mice, the FPN gene repression occurred with a concomitant increase of the *NOS2* expression. The role of NOS2 and NO in the regulation of FPN needs further investigation. The discrepancy between studies regarding the regulation of FPN during intracellular infection is unclear and warrants continued effort to clarify this important regulation in the context of infectious diseases. The use of different antibodies against FPN, which are not all carefully characterized by appropriate controls of specificity, could contribute to the differences observed between different studies.

Despite FPN downregulation during *Salmonella* infection in our models, we observed a decrease in iron within infected spleen and liver. Such a decrease in tissues iron was strongly observed in $Hamp^{-/-}$ liver but was not seen in AcB61 tissues, likely masked by the exacerbated EP activity and heme iron uptake by macrophages in these tissues. During infection, macrophage iron could be consumed, at least in part, by the bacteria itself, dependent on this metal for its growth and dissemination. Alternatively, FPN-independent export of iron may occur in infected macrophages. A peculiar iron distribution was observed in *Salmonella* infected $Hamp^{-/-}$ liver, with some strong accumulation in CL hepatocytes and sinusoidal Kupffer cells. One possible explanation is the engulfment of iron-loaded apoptotic hepatocytes by liver macrophages. Indeed both iron overload and LPS/inflammation have been shown to induce apoptosis in hepatocytes (47, 48). Therefore, in $Hamp^{-/-}$ mice, the iron overloaded hepatocytes in the CL zone are likely more sensitive to apoptotic processes during *Salmonella* infection. Since macrophage FPN expression is repressed, an increase of phagocytosis of such apoptotic cells could lead to iron overload in sinusoidal and CL macrophages.

CONCLUSION

Our observations suggest that to promote its intracellular growth, *Salmonella* modulates macrophage iron homeostasis to favor its access to intracellular iron with the reduction of iron export *via* the downregulation of FPN. Importantly, such a macrophage cellular host response, which promotes infection, anemia, and hypoferremia, is independent of macrophage iron and HAMP levels. To fight against bacterial infectious diseases and to correct the anemia during chronic infection, effort has to be made to understand whether this HAMP-independent downregulation of FPN expression exists in different macrophages populations and is a general host response observed with other intracellular pathogens infection.

ETHICS STATEMENT

This study was carried out in accordance with the recommendations of the Canadian Council on Animal Care. The protocol was approved by the McGill University Animal Care Committee.

AUTHOR CONTRIBUTIONS

AW, SB, ER, and AR designed protocols and performed experiments. AA, RM, and OT performed experiments. SB reviewed data and provided statistical analysis and correction of the manuscript. SV provided *Hamp*$^{-/-}$ mice, reviewed the data, and provided comments and corrections of the manuscript. DM designed protocols, performed experiments, reviewed the data, and provided comments and corrections of the manuscript. FC-H designed protocols, performed experiments, reviewed the data, and wrote the paper.

ACKNOWLEDGMENTS

The authors wish to acknowledge the technical assistance of Ophélie Gourbeyre (IRSD, INSERM UMR 1220, CHU Purpan), Cécile Pouzet (CHU Bichat-Claude Bernard), and Line Larivière (McGill University, Montréal, QC, Canada).

FUNDING

This work was supported by the Canadian Institutes of Health Research (MOP-15461) to DM and by INSERM and "Agence Nationale de la Recherche," France (ANR-10-MIDI-004) to FC-H.

SUPPLEMENTARY MATERIAL

The Supplementary Material for this article can be found online at http://journal.frontiersin.org/article/10.3389/fimmu.2017.00498/full#supplementary-material.

REFERENCES

1. Piddock LJ. The crisis of no new antibiotics – what is the way forward? *Lancet Infect Dis* (2012) 12(3):249–53. doi:10.1016/S1473-3099(11)70316-4
2. Hood MI, Skaar EP. Nutritional immunity: transition metals at the pathogen-host interface. *Nat Rev Microbiol* (2012) 10(8):525–37. doi:10.1038/nrmicro2836
3. Cassat JE, Skaar EP. Iron in infection and immunity. *Cell Host Microbe* (2013) 13(5):509–19. doi:10.1016/j.chom.2013.04.010
4. Nemeth E, Ganz T. Anemia of inflammation. *Hematol Oncol Clin North Am* (2014) 28(4):671–681, vi. doi:10.1016/j.hoc.2014.04.005
5. Ganz T, Nemeth E. Iron sequestration and anemia of inflammation. *Semin Hematol* (2009) 46(4):387–93. doi:10.1053/j.seminhematol.2009.06.001
6. Delaby C, Pilard N, Goncalves AS, Beaumont C, Canonne-Hergaux F. Presence of the iron exporter ferroportin at the plasma membrane of macrophages is enhanced by iron loading and down-regulated by hepcidin. *Blood* (2005) 106(12):3979–84. doi:10.1182/blood-2005-06-2398
7. Canonne-Hergaux F, Donovan A, Delaby C, Wang HJ, Gros P. Comparative studies of duodenal and macrophage ferroportin proteins. *Am J Physiol Gastrointest Liver Physiol* (2006) 290(1):G156–63. doi:10.1152/ajpgi.00227.2005
8. Nemeth E, Tuttle MS, Powelson J, Vaughn MB, Donovan A, Ward DM, et al. Hepcidin regulates cellular iron efflux by binding to ferroportin and inducing its internalization. *Science* (2004) 306(5704):2090–3. doi:10.1126/science.1104742
9. Peyssonnaux C, Zinkernagel AS, Datta V, Lauth X, Johnson RS, Nizet V. TLR4-dependent hepcidin expression by myeloid cells in response to bacterial pathogens. *Blood* (2006) 107(9):3727–32. doi:10.1182/blood-2005-06-2259
10. Nairz M, Schleicher U, Schroll A, Sonnweber T, Theurl I, Ludwiczek S, et al. Nitric oxide-mediated regulation of ferroportin-1 controls macrophage iron homeostasis and immune function in *Salmonella* infection. *J Exp Med* (2013) 210(5):855–73. doi:10.1084/jem.20121946
11. Nairz M, Haschka D, Demetz E, Weiss G. Iron at the interface of immunity and infection. *Front Pharmacol* (2014) 5:152. doi:10.3389/fphar.2014.00152
12. Brown DE, Nick HJ, McCoy MW, Moreland SM, Stepanek AM, Benik R, et al. Increased ferroportin-1 expression and rapid splenic iron loss occur with anemia caused by *Salmonella enterica* serovar Typhimurium infection in mice. *Infect Immun* (2015) 83(6):2290–9. doi:10.1128/IAI.02863-14
13. Fortin A, Diez E, Rochefort D, Laroche L, Malo D, Rouleau GA, et al. Recombinant congenic strains derived from A/J and C57BL/6J: a tool for genetic dissection of complex traits. *Genomics* (2001) 74(1):21–35. doi:10.1006/geno.2001.6528
14. Lesbordes-Brion JC, Viatte L, Bennoun M, Lou DQ, Ramey G, Houbron C, et al. Targeted disruption of the hepcidin 1 gene results in severe hemochromatosis. *Blood* (2006) 108(4):1402–5. doi:10.1182/blood-2006-02-003376
15. Roy MF, Riendeau N, Loredo-Osti JC, Malo D. Complexity in the host response to *Salmonella typhimurium* infection in AcB and BcA recombinant congenic strains. *Genes Immun* (2006) 7(8):655–66. doi:10.1038/sj.gene.6364344
16. Delaby C, Pilard N, Hetet G, Driss F, Grandchamp B, Beaumont C, et al. A physiological model to study iron recycling in macrophages. *Exp Cell Res* (2005) 310(1):43–53. doi:10.1016/j.yexcr.2005.07.002
17. Hoiseth SK, Stocker BA. Aromatic-dependent *Salmonella typhimurium* are non-virulent and effective as live vaccines. *Nature* (1981) 291(5812):238–9. doi:10.1038/291238a0
18. Torrance JD, Bothwell TH. A simple technique for measuring storage iron concentrations in formalinised liver samples. *S Afr J Med Sci* (1968) 33(1):9–11.
19. Canonne-Hergaux F, Gruenheid S, Ponka P, Gros P. Cellular and subcellular localization of the Nramp2 iron transporter in the intestinal brush border and regulation by dietary iron. *Blood* (1999) 93(12):4406–17.
20. Min-Oo G, Fortin A, Tam MF, Nantel A, Stevenson MM, Gros P. Pyruvate kinase deficiency in mice protects against malaria. *Nat Genet* (2003) 35(4):357–62. doi:10.1038/ng1260
21. Min-Oo G, Fortin A, Tam MF, Gros P, Stevenson MM. Phenotypic expression of pyruvate kinase deficiency and protection against malaria in a mouse model. *Genes Immun* (2004) 5(3):168–75. doi:10.1038/sj.gene.6364069
22. Roy MF, Riendeau N, Bédard C, Hélie P, Min-Oo G, Turcotte K, et al. Pyruvate kinase deficiency confers susceptibility to *Salmonella typhimurium* infection in mice. *J Exp Med* (2007) 204(12):2949–61. doi:10.1084/jem.20062606
23. Delaby C, Pilard N, Puy H, Canonne-Hergaux F. Sequential regulation of ferroportin expression after erythrophagocytosis in murine macrophages: early mRNA induction by haem, followed by iron-dependent protein expression. *Biochem J* (2008) 411(1):123–31. doi:10.1042/BJ20071474
24. Ayi K, Liles WC, Gros P, Kain KC. Adenosine triphosphate depletion of erythrocytes simulates the phenotype associated with pyruvate kinase deficiency and confers protection against *Plasmodium falciparum* in vitro. *J Infect Dis* (2009) 200(8):1289–99. doi:10.1086/605843
25. Sun J, Brand M, Zenke Y, Tashiro S, Groudine M, Igarashi K. Heme regulates the dynamic exchange of Bach1 and NF-E2-related factors in the Maf transcription factor network. *Proc Natl Acad Sci U S A* (2004) 101(6):1461–6. doi:10.1073/pnas.0308083100
26. Marro S, Chiabrando D, Messana E, Stolte J, Turco E, Tolosano E, et al. Heme controls ferroportin1 (FPN1) transcription involving Bach1, Nrf2 and a MARE/ARE sequence motif at position -7007 of the FPN1 promoter. *Haematologica* (2010) 95(8):1261–8. doi:10.3324/haematol.2009.020123
27. Di Pietrantonio T, Hernandez C, Girard M, Verville A, Orlova M, Belley A, et al. Strain-specific differences in the genetic control of two closely related mycobacteria. *PLoS Pathog* (2010) 6(10):e1001169. doi:10.1371/journal.ppat.1001169
28. Yuki KE, Eva MM, Richer E, Chung D, Paquet M, Cellier M, et al. Suppression of hepcidin expression and iron overload mediate *Salmonella* susceptibility in ankyrin 1 ENU-induced mutant. *PLoS One* (2013) 8(2):e55331. doi:10.1371/journal.pone.0055331
29. Pilonieta MC, Moreland SM, English CN, Detweiler CS. *Salmonella enterica* infection stimulates macrophages to hemophagocytose. *MBio* (2014) 5(6):e02211. doi:10.1128/mBio.02211-14

30. McDonald EM, Pilonieta MC, Nick HJ, Detweiler CS. Bacterial stimulation of toll-like receptor 4 drives macrophages to hemophagocytose. *Infect Immun* (2015) 84(1):47–55. doi:10.1128/IAI.01149-15
31. Rishi G, Wallace DF, Subramaniam VN. Hepcidin: regulation of the master iron regulator. *Biosci Rep* (2015) 35(3):e00192. doi:10.1042/BSR20150014
32. Kim DK, Jeong JH, Lee JM, Kim KS, Park SH, Kim YD, et al. Inverse agonist of estrogen-related receptor gamma controls *Salmonella typhimurium* infection by modulating host iron homeostasis. *Nat Med* (2014) 20(4):419–24. doi:10.1038/nm.3483
33. Darton TC, Blohmke CJ, Giannoulatou E, Waddington CS, Jones C, Sturges P, et al. Rapidly escalating hepcidin and associated serum iron starvation are features of the acute response to typhoid infection in humans. *PLoS Negl Trop Dis* (2015) 9(9):e0004029. doi:10.1371/journal.pntd.0004029
34. Gardenghi S, Renaud TM, Meloni A, Casu C, Crielaard BJ, Bystrom LM, et al. Distinct roles for hepcidin and interleukin-6 in the recovery from anemia in mice injected with heat-killed *Brucella abortus*. *Blood* (2014) 123(8):1137–45. doi:10.1182/blood-2013-08-521625
35. Kim A, Fung E, Parikh SG, Valore EV, Gabayan V, Nemeth E, et al. A mouse model of anemia of inflammation: complex pathogenesis with partial dependence on hepcidin. *Blood* (2014) 123(8):1129–36. doi:10.1182/blood-2013-08-521419
36. Jackson A, Nanton MR, O'Donnell H, Akue AD, McSorley SJ. Innate immune activation during *Salmonella* infection initiates extramedullary erythropoiesis and splenomegaly. *J Immunol* (2010) 185(10):6198–204. doi:10.4049/jimmunol.1001198
37. Guida C, Altamura S, Klein FA, Galy B, Boutros M, Ulmer AJ, et al. A novel inflammatory pathway mediating rapid hepcidin-independent hypoferremia. *Blood* (2015) 125(14):2265–75. doi:10.1182/blood-2014-08-595256
38. Deschemin JC, Vaulont S. Role of hepcidin in the setting of hypoferremia during acute inflammation. *PLoS One* (2013) 8(4):e61050. doi:10.1371/journal.pone.0061050
39. Nairz M, Ferring-Appel D, Casarrubea D, Sonnweber T, Viatte L, Schroll A, et al. Iron regulatory proteins mediate host resistance to *Salmonella* infection. *Cell Host Microbe* (2015) 18(2):254–61. doi:10.1016/j.chom.2015.06.017
40. Yang F, Liu XB, Quinones M, Melby PC, Ghio A, Haile DJ. Regulation of reticuloendothelial iron transporter MTP1 (Slc11a3) by inflammation. *J Biol Chem* (2002) 277(42):39786–91. doi:10.1074/jbc.M201485200
41. Van Zandt KE, Sow FB, Florence WC, Zwilling BS, Satoskar AR, Schlesinger LS, et al. The iron export protein ferroportin 1 is differentially expressed in mouse macrophage populations and is present in the mycobacterial-containing phagosome. *J Leukoc Biol* (2008) 84(3):689–700. doi:10.1189/jlb.1107781
42. Layoun A, Huang H, Calve A, Santos MM. Toll-like receptor signal adaptor protein MyD88 is required for sustained endotoxin-induced acute hypoferremic response in mice. *Am J Pathol* (2012) 180(6):2340–50. doi:10.1016/j.ajpath.2012.01.046
43. Zughaier SM, Stauffer BB, McCarty NA. Inflammation and ER stress downregulate BDH2 expression and dysregulate intracellular iron in macrophages. *J Immunol Res* (2014) 2014:140728. doi:10.1155/2014/140728
44. Rosenberger CM, Scott MG, Gold MR, Hancock RE, Finlay BB. *Salmonella typhimurium* infection and lipopolysaccharide stimulation induce similar changes in macrophage gene expression. *J Immunol* (2000) 164(11):5894–904. doi:10.4049/jimmunol.164.11.5894
45. Ben-Othman R, Flannery AR, Miguel DC, Ward DM, Kaplan J, Andrews NW. *Leishmania*-mediated inhibition of iron export promotes parasite replication in macrophages. *PLoS Pathog* (2014) 10(1):e1003901. doi:10.1371/journal.ppat.1003901
46. Chlosta S, Fishman DS, Harrington L, Johnson EE, Knutson MD, Wessling-Resnick M, et al. The iron efflux protein ferroportin regulates the intracellular growth of *Salmonella enterica*. *Infect Immun* (2006) 74(5):3065–7. doi:10.1128/IAI.74.5.3065-3067.2006
47. Zhao M, Laissue JA, Zimmermann A. Hepatocyte apoptosis in hepatic iron overload diseases. *Histol Histopathol* (1997) 12(2):367–74.
48. Kudo H, Takahara T, Yata Y, Kawai K, Zhang W, Sugiyama T. Lipopolysaccharide triggered TNF-alpha-induced hepatocyte apoptosis in a murine non-alcoholic steatohepatitis model. *J Hepatol* (2009) 51(1):168–75. doi:10.1016/j.jhep.2009.02.032

Conflict of Interest Statement: The authors declare that the research was conducted in the absence of any commercial or financial relationships that could be construed as a potential conflict of interest.

The handling editor declared a shared affiliation, though no other collaboration, with several of the authors (AW, AA, and FC-H), and states that the process nevertheless met the standards of a fair and objective review.

Copyright © 2017 Willemetz, Beatty, Richer, Rubio, Auriac, Milkereit, Thibaudeau, Vaulont, Malo and Canonne-Hergaux. This is an open-access article distributed under the terms of the Creative Commons Attribution License (CC BY). The use, distribution or reproduction in other forums is permitted, provided the original author(s) or licensor are credited and that the original publication in this journal is cited, in accordance with accepted academic practice. No use, distribution or reproduction is permitted which does not comply with these terms.

frontiers in Immunology

REVIEW
published: 27 November 2017
doi: 10.3389/fimmu.2017.01633

Type I Interferons in the Pathogenesis of Tuberculosis: Molecular Drivers and Immunological Consequences

*Meg L. Donovan, Thomas E. Schultz, Taylor J. Duke and Antje Blumenthal**

The University of Queensland Diamantina Institute, The University of Queensland, Translational Research Institute, Brisbane, QLD, Australia

Tuberculosis (TB) remains a major global health threat. Urgent needs in the fight against TB include improved and innovative treatment options for drug-sensitive and -resistant TB as well as reliable biological indicators that discriminate active from latent disease and enable monitoring of treatment success or failure. Prominent interferon (IFN) inducible gene signatures in TB patients and animal models of *Mycobacterium tuberculosis* infection have drawn significant attention to the roles of type I IFNs in the host response to mycobacterial infections. Here, we review recent developments in the understanding of the innate immune pathways that drive type I IFN responses in mycobacteria-infected host cells and the functional consequences for the host defense against *M. tuberculosis*, with a view that such insights might be exploited for the development of targeted host-directed immunotherapies and development of reliable biomarkers.

Keywords: *Mycobacterium tuberculosis*, type I interferon, innate immune signaling, pattern recognition receptors, immune responses, cytokines, patients, mouse models

OPEN ACCESS

Edited by:
Geanncarlo Lugo-Villarino, UMR5089 Institut de Pharmacologie et de Biologie Structurale (IPBS), France

Reviewed by:
John R. Teijaro, The Scripps Research Institute, United States
Anca Dorhoi, Friedrich Loeffler Institute Greifswald, Germany

****Correspondence:***
Antje Blumenthal
a.blumenthal@uq.edu.au

Specialty section:
This article was submitted to Microbial Immunology, a section of the journal Frontiers in Immunology

Received: *15 September 2017*
Accepted: *09 November 2017*
Published: *27 November 2017*

Citation:
Donovan ML, Schultz TE, Duke TJ and Blumenthal A (2017) Type I Interferons in the Pathogenesis of Tuberculosis: Molecular Drivers and Immunological Consequences. Front. Immunol. 8:1633. doi: 10.3389/fimmu.2017.01633

INTRODUCTION

With an estimated 1.8 million TB-related annual deaths worldwide, approximately one-third of the global population harboring latent *Mycobacterium tuberculosis* infection, and significant numbers of drug-resistant cases, there is an urgent and compelling need for more sophisticated diagnostic and treatment options for tuberculosis (TB) (1). *M. tuberculosis* is an intracellular pathogen that mainly resides within macrophages. The multi-tiered immune response elicited upon *M. tuberculosis* infection is complex, and our understanding of the requirements for protective immunity remain incomplete (2). Observations in humans and mouse models have firmly established essential roles for interleukin-12 (IL-12) and interferon gamma (IFN-γ)-mediated T cell functions in the control of *M. tuberculosis* infection. Inflammatory cytokines such as tumor necrosis factor alpha (TNF-α) and IL-1 are critical contributors to the immune defense against *M. tuberculosis* (2). Recently described gene signatures in blood of patients with active TB disease (3–9) are being explored extensively for their utility as biomarkers for the reliable diagnosis of active TB, tracking of at-risk individuals, and monitoring of treatment outcome. Additionally, the discovery of IFN-related gene signatures in patients with active TB disease (3–9) has created significant momentum behind investigation of the innate immune pathways and pathophysiological consequences of type I IFN expression during *M. tuberculosis* infection. While IFN-γ is the sole type II IFN, type I IFNs in humans comprise several IFN-α subtypes, IFN-β, IFN-ω, IFN-ε, IFN-τ, and IFN-κ (10). All known type I IFNs signal through a common receptor, IFNAR, which consists of the low-affinity IFNAR1 and the high-affinity IFNAR2 (11, 12). It is increasingly appreciated

that type I IFNs not only play a significant role in the antiviral response but are also a central aspect of the host response to bacterial infections (13, 14). In this context, type I IFNs appear to promote or impair pathogen control and disease pathology depending on the infectious agent, acute or chronic state of the infection, and possibly also the model system studied (15). Evidence from human case reports and animal models suggests complex contributions of type I IFNs to the host response during *M. tuberculosis* infection as both protective and detrimental roles for the host have been described. The impact of type I IFNs and related immune response networks on pathology and pathogen control during *M. tuberculosis* infection are also assessed with an eye to host-directed interventions in TB. In this review, we highlight recent advances in the study of TB patient blood gene expression signatures, and the definition of innate immune drivers and immunological consequences of type I IFN expression in the context of *M. tuberculosis* infection.

BLOOD GENE EXPRESSION SIGNATURES IN THE QUEST FOR TB BIOMARKERS

There are increasing numbers of cross-sectional and longitudinal studies exploring whole blood gene expression in TB patients as a potential diagnostic indicator of disease status, manifestation, and responsiveness to treatment [reviewed in more detail elsewhere, e.g. (16–18)]. While the individual genes identified across the various studies are remarkably discordant (18), overall signatures returned from many of these studies have implicated IFN signaling (5, 16). However, independent meta-analyses of publicly available datasets have expressed different views on the dominance and robustness of IFN signatures in active TB (6, 19). An overarching goal of current studies is the identification of minimal gene signatures in global gene expression profiles that can be utilized as reliable TB diagnostic markers in clinical settings. Potential applications of this approach include distinguishing active TB from latent *M. tuberculosis* infection and other infections; monitoring of treatment success/failure; and predicting risk of developing active disease (6–9, 20–22). Some, but not all, of these proposed minimal marker combinations contain IFN-regulated genes. The "omics" approaches currently being pursued clearly indicate innate and adaptive immune response signatures that significantly enhance our current understanding of peripheral host responses during active and latent TB. Consideration of whether or not these molecular signatures are unique to TB is important when designing and interpreting global host response profiles for the derivation of reliable diagnostic markers. Consideration of potential confounding factors, as well as inclusion of unrelated disease controls cohorts, is also critical for success in these endeavors.

Human immunodeficiency virus (HIV) remains a major risk factor for development of active TB. Approximately 1/3 of HIV-positive individuals worldwide are latently infected with *M. tuberculosis* (1). Currently, 55% of notified TB cases are HIV-positive and approximately 22% of TB-related deaths occur in HIV-positive individuals (1). Due to significant virus-associated immunological alterations in HIV-positive individuals, the utility of minimal gene signatures in distinguishing active from latent TB may be compromised in these cases (9, 21). Encouragingly, signatures that distinguish active TB from latent TB in HIV-positive and -negative individuals are emerging (8, 23). Additionally, type II diabetes is being increasingly recognized as a significant comorbidity that adversely affects TB severity, treatment responsiveness, and outcome in high TB burden countries (24). Thus, exploration of molecular signatures to better understand the nature of the TB/type II diabetes interaction is an important upcoming challenge. Notably, a recent study that compared blood transcriptomics in South-Indian TB patients with and without type II diabetes concluded that the utility of blood gene expression markers in the diagnosis of TB might not be confounded by type II diabetes (25). Independent confirmation of these findings in populations where high type II diabetes and high TB burden intersect will be of great significance for the development of new molecular marker-based TB diagnostics.

Interferon-associated genes are present not only in blood gene expression signatures reported for active TB, but also in patients with the granulomatous diseases meliodosis and sarcoidosis (7, 26–29). This suggests that peripheral blood gene expression signatures may be shaped by responses to tissue pathology rather than a specific underlying cause. Moreover, Blankley et al. highlight that severity of clinical symptoms in TB patients is associated with the magnitude of gene expression, regardless of the site of infection (7). Nevertheless, comparisons of global response patterns in active and latent TB with other infectious or inflammatory conditions have yielded encouraging results, as they suggest that molecular signatures that reliably discriminate active TB can be identified (3, 21, 28, 30). Patient cohort-based profiling in search of reliable TB diagnostics calls for careful study design, inclusion of clinical metadata, and clear definition of patient and control cohorts (17). Continuing developments in the analysis of "omics" data, including statistical frameworks, machine learning, multi-platform integration, and network analyses, will be important assets in defining molecular markers that perform robustly independent of age, gender, ethnicity, and comorbidities.

MOLECULAR PATHWAYS THAT DRIVE TYPE I IFN PRODUCTION IN MYCOBACTERIA-INFECTED HOST CELLS

Mycobacterium tuberculosis infection induces type I IFN expression in human and mouse macrophages and myeloid dendritic cells (31–38). The serine/threonine kinase, TANK-binding kinase 1 (TBK1), is a central driver of type I IFN expression in *M. tuberculosis*-infected host cells (33). TBK1 facilitates phosphorylation of interferon regulatory factors (IRFs), and IRF3 and IRF5 have been reported to facilitate type I IFN expression in mycobacteria-infected host cells (39). IFN-β expression requires collaboration of IRFs with other transcription factors including NF-κB, ATF-2, and c-Jun (40), emphasizing the complexity of host signaling events that shape type I IFN expression. Pattern recognition receptors

(PRRs) that have been linked to TBK1 phosphorylation and type I IFN expression in response to mycobacterial infection include the Nod-like receptor NOD2, stimulator of interferon genes (STING) either directly or *via* activation of cyclic GMP-AMP synthase (cGAS), as well as Toll-like receptor (TLR) 4 (**Figure 1**).

The Mycobacterial Type VII Secretion System ESX-1 Facilitates Activation of Cytosolic Surveillance Pathways and Type I IFN Expression

Early studies established that induction of type I IFN responses by *M. tuberculosis* was greatly diminished if the genomic region of difference-1 (RD-1), the RD-1 encoded type VII ESAT-6 secretion system 1 (ESX-1), or its key components were deleted (33, 34, 39). The ESX-1 secretion system is a major virulence determinant of *M. tuberculosis* that mediates secretion of mycobacterial products that shape host responses to infection (41). ESX-1 may also directly affect phagosome membrane integrity (42). Co-localization studies with galectin-3, a marker of damaged membranes, and ubiquitin suggest that within 24 h of infection approximately 10% of *M. tuberculosis* bacteria are in contact with the cytoplasm and that this is dependent on ESX-1 (43). Compromised phagosomal membranes facilitate interactions of *M. tuberculosis* and its products with the cytosol fostering recognition by cytosolic surveillance pathways (33, 35, 39, 44, 45).

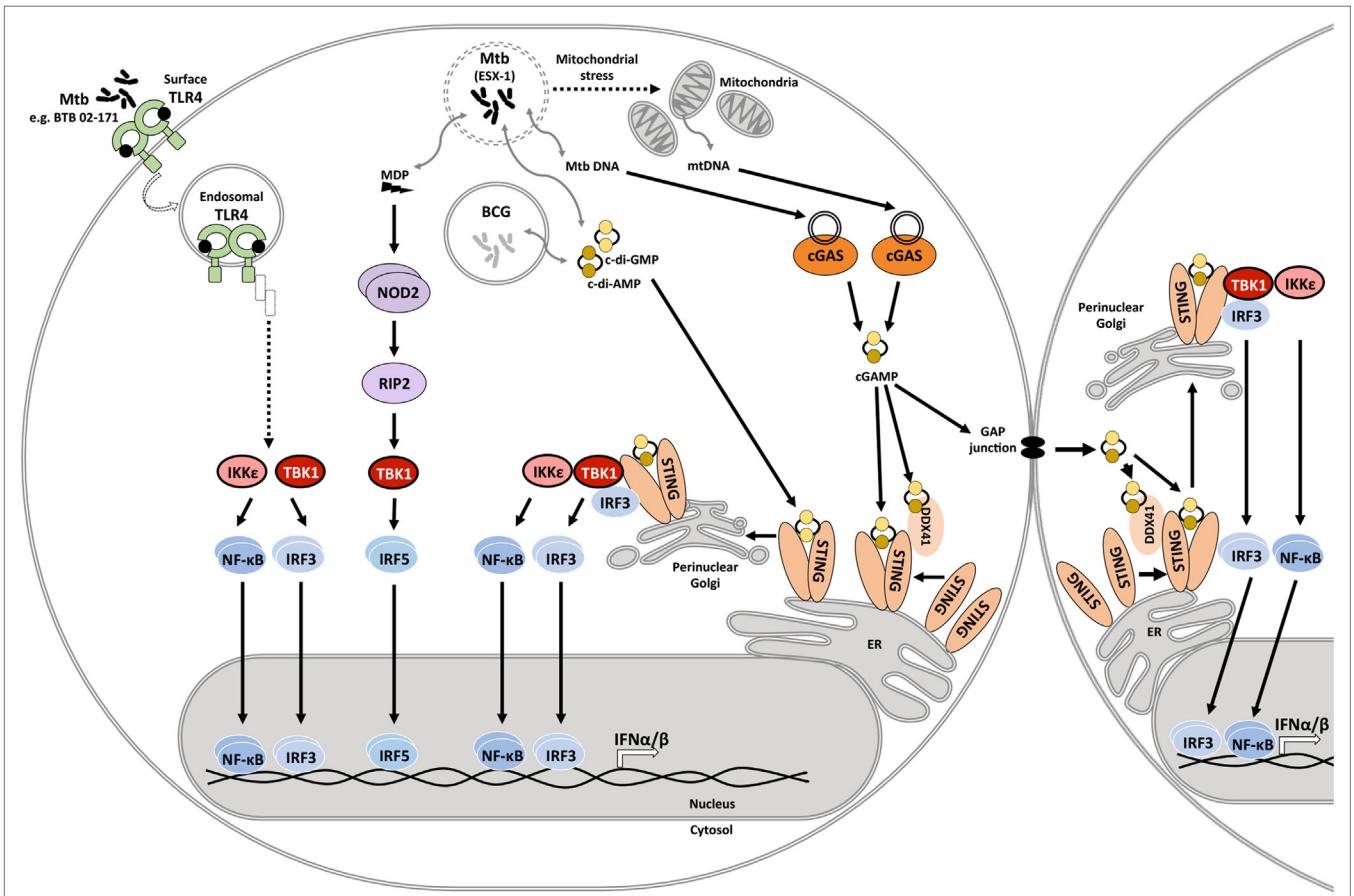


FIGURE 1 | Innate immune signaling pathways that drive type I IFN responses in mycobacteria-infected host cells. During infection, the *Mycobacterium tuberculosis* ESX-1 secretion system facilitates disruption of the phagosomal membrane contributing to mitochondrial stress and leakage of mycobacterial products into the cytosol. These products include the cyclic dinucleotides cyclic diadenosine monophosphate (c-di-AMP) and cyclic diguanosine monophosphate (c-di-GMP), DNA, and *N*-glycolylated muramyl dipeptide (MDP). Recognition of cytosolic mitochondrial and mycobacterial DNA by cyclic GMP-AMP synthase (cGAS) initiates formation of the second messenger cyclic-GMP-AMP (cGAMP). cGAMP and bacterial cyclic dinucleotides interact with dimeric STING on the endoplasmic reticulum or the STING-accessory molecule DDX41. STING activation and relocation to the perinuclear Golgi initiates recruitment and activation of TANK-binding kinase 1 (TBK1), and possibly also IKKε. Subsequent activation and nuclear translocation of the functionally active dimeric transcription factors interferon regulatory factor (IRF)3 and NF-κB drives expression of type I IFNs. cGAMP may also access uninfected cells *via* gap junctions, triggering STING activation and type I IFN expression in bystander cells. MDP is recognized by NOD2, which leads to RIP2-mediated activation of TBK1, culminating in IRF5 dimerization and nuclear translocation. *M. tuberculosis* isolate BTB 02-171 induces type I IFN expression dependent on TLR4. It is inferred that the induction pathway is similar to the known toll-like receptor (TLR)4 endosomal signaling pathway. However, this awaits experimental confirmation. *Mycobacterium bovis* Bacillus Calmette–Guérin (BCG) lacks ESX-1, yet, can elicit type I IFN expression. Cyclic dinucleotide-mediated STING activation independent of ESX-1 has been described.

NOD2 has been implicated as a cytosolic sensor of *M. tuberculosis* that drives IFN-α and IFN-β expression upon infection (39, 46). Polyubiquitination of the NOD2-effector RIP2 was significantly diminished upon infection with ESX-1-deficient *M. tuberculosis* when compared to wild-type bacteria, identifying RIP2 as a major downstream effector of NOD2 in the recognition of *M. tuberculosis*. The unusual mycobacterial *N*-glycolylated muramyl dipeptide is a driver of NOD2-mediated type I IFN responses *via* RIP2 and IRF5, but not IRF3 (39). Reports addressing the role of NOD2 in the host control of *M. tuberculosis* infection in the mouse model *in vivo* have returned varying results. Whereas NOD2-deficient (*Card15*$^{-/-}$) mice were not impaired in their ability to control infection with *M. tuberculosis* in two independent studies (47, 48), one study reported impaired T helper 1 (Th1) responses associated with slightly impaired survival and a modest increase in bacterial burden late during infection (48). Similarly, reports on human polymorphisms in the *NOD2* gene and susceptibility to, or protection from TB have returned varying results and will require further validation (49–53).

NOD2- and RIP2-deficiency only partially ablated *M. tuberculosis*-induced IFN-β and IFN-α expression (39), suggesting that additional molecular pathways of type I IFN induction exist. Several recent independent studies identified cGAS and STING as central drivers of IFN-β expression in human and murine macrophages during *M. tuberculosis* infection (35, 37, 38, 54). STING contains four transmembrane domains that anchor it into the endoplasmic reticulum membrane, as well as a large C-terminal domain involved in binding of TBK1 and IRF3. Binding of one molecule of cyclic di-nucleotide of either host or bacterial origin to STING dimers facilitates TBK1 and IRF3 activation (55). Endogenous 2′3′-cyclic GMP-AMP (cGAMP) is a second messenger generated by cGAS upon binding of cytoplasmic DNA. This cytoplasmic surveillance mechanism is a major driver of STING activation and type I IFN responses. Both cGAS- and STING-deficient human and mouse macrophages are impaired in their ability to express IFN-β in response to *M. tuberculosis* infection (35, 37, 38, 54). The underlying mechanisms that trigger this pathway are under intense investigation. It has been suggested that mycobacterial DNA gains access to the host cell cytoplasm and directly binds to cGAS, a process facilitated by ESX-1-dependent phagosome damage (37, 38). Others reported that the extent of macrophage IFN-β expression in response to different *M. tuberculosis* isolates correlated with mitochondrial stress, with no observable differences in the proportions of bacteria associated with damaged phagosomes (43). These observations suggest that the extent of mitochondrial DNA released during *M. tuberculosis* infection may contribute to cGAS-dependent activation of type I IFN expression by macrophages and determine the extent of the type I IFN response (43). Further amplification of STING-driven type I IFN expression may occur in uninfected bystander cells through shuttling of cGAMP through tight junction proteins (37, 56).

In addition, bacterial pathogens generate cyclic di-nucleotides that can activate STING independent of cGAS (55). The *M. tuberculosis* di-adenylate cyclase (disA or dacA) synthesizes c-di-AMP, which triggers IFN-β expression in macrophages and dendritic cells through STING activation, either through direct binding or *via* engagement of DEAD-box helicase 4 (DDX4) (35, 55, 57, 58). IFN-β expression in response to *M. tuberculosis disA* mutant bacteria was reduced compared to wild-type bacteria. Conversely, *disA* overexpression in *M. tuberculosis* CDC1551 and Erdman enhanced IFN-β expression (35). The discovery that *M. tuberculosis* expresses a phosphodiesterase, cdnP, that not only cleaves bacterial c-di-AMP and c-di-CMP but also the host-derived STING activator 2′3′-cGAMP (59, 60), is in keeping with the remarkable adaptation of this bacterium to its intracellular niche within the host. Accordingly, a *cdnP M. tuberculosis* transposon mutant induced elevated IFN-β, whereas *cdnP* overexpression impaired IFN-β expression by macrophages (60). Of note, the elevated IFN-β response elicited by *cdnP* deficient *M. tuberculosis* bacteria was independent of NOD2 (59), indicating that these cytoplasmic detection pathways are operating in parallel. Importantly, however, modulation of *disA* and *cdnP* expression did not only affect type I IFN expression but also pro-inflammatory cytokines like TNF, IL-6, and IL-1 (35, 60). These cytokines are important for the immune control of *M. tuberculosis* infection and can counter-regulate type I IFN expression (discussed below). This impact on the balance of key cytokines that are essential to control *M. tuberculosis* infection *in vivo* may account for the enhanced or attenuated virulence of the respective *M. tuberculosis* mutants *in vivo* (35, 59, 60). Moreover, the ability and extent of c-di-AMP production by *M. tuberculosis,* as well as cGAS and STING activation in *M. tuberculosis*-infected macrophages have been linked to autophagy (35, 38, 54). It will be valuable to further investigate molecular mechanisms of the engagement of pro-inflammatory cytokine responses and cell autonomous defense mechanisms by mycobacteria-derived c-di-AMP, which may involve other c-di-AMP-sensors such as DDX4 (35, 61) and RECON (62).

Despite the profound contributions of cGAS and STING to *M. tuberculosis*-induced type I IFN responses and autophagy activation reported by *in vitro* studies (35, 37, 38, 45, 54), bacterial burden in infected organs of mice deficient in cGAS or STING expression was comparable to wild-type controls (38, 54). One study reported impaired survival of cGAS- but not STING-deficient mice late during the chronic phase of infection (>100 days) (54). Whether this is linked to STING-independent functions of cGAS such as impaired autophagy (54, 63) remains to be established. Moreover, roles for DDX4 (61) and RECON (62) in regulating host responses and pathogen control during *M. tuberculosis* infection remain to be defined.

ESX-1-Independent Induction of Type I IFNs in Mycobacterial Infection

While the data discussed above support a central role for the ESX-1 secretion system in the induction of type I IFN expression in *M. tuberculosis*-infected host cells, there is compelling evidence for mycobacteria-induced type I IFN responses in the absence of ESX-1. Type I IFN expression in response to ESX-1-deficient *M. tuberculosis* strains is reduced but not ablated compared to WT mycobacteria (38, 39). Moreover, the attenuated *Mycobacterium bovis* strain Bacillus Calmette–Guérin (BCG) lacks the RD-1 region including the genes that encode

the ESX-1 secretion system (64). Yet, BCG induces type I IFN expression in both human and mouse primary macrophages, albeit to a significantly lesser degree than virulent *M. tuberculosis* (34, 35). IFN-β expression in BCG-infected macrophages was significantly reduced in *Sting*$^{-/-}$ cells, indicating STING-driven type I IFN expression. Moreover, overexpression of *disA* in BCG enhanced IFN-β expression compared to wild-type BCG (35). These data suggest that mycobacteria-derived dinucleotides may gain access to the cytosol in the absence of ESX-1 and induce IFN-β expression *via* activation of STING. It seems plausible that bacteria-derived dinucleotides may also activate STING and type I IFN expression in uninfected bystander cells by passing the cell membrane or through gap-junction *trans* signaling as proposed for cGAMP (37, 56). The extent to which mitochondrial stress responses may contribute to this STING-dependent type I IFN response (43) remains to be established.

Interactions of bacterial or viral components with specific TLRs can drive type I IFN expression. TLRs are type I transmembrane proteins that localize to the cell membrane or endosomal membranes. They sense microbial components in the extracellular environment or internalized materials in the "extracellular" space of intracellular trafficking compartments, but not in the cytoplasm (65). Dimerization of TLRs upon ligand binding facilitates recruitment of adaptor proteins and the initiation of intracellular signaling (66, 67). MyD88-dependent signaling from endosomal TLR7, TLR8, and TLR9 activates IRF-7 and results in the expression of type I IFNs (68). TLR4 internalization into endosomes upon stimulation with lipopolysaccharide engages TRIF and TRAM, facilitating IKKε and TBK-1 activation. Subsequent phosphorylation of IRF-3 leads to the expression of type I IFNs (69, 70). Recent data suggest that TLR2 may similarly induce TRIF- and TRAM-dependent signaling from endosomes (71). Initial studies concluded that TLRs are not a major driver of type I IFN responses during *M. tuberculosis* infection. *Ifnb1* expression by mouse macrophages infected with *M. tuberculosis* H37Rv was independent of TLR2, exhibited a minor defect in *Trif*$^{-/-}$ cells, and appeared to be negatively regulated by TLR4 (comparison of C3H/HeN versus C3H/HeJ) and MyD88 (33). A separate study showed that macrophage *Ifnb1* expression upon infection with the *M. tuberculosis* clinical isolate 1254 was equivalent between wild-type cells and macrophages deficient in *Tlr4*, *Tlr2*, *Tirap*, *Myd88*, or *Trif* (32). In contrast, TLR4-driven *Ifnb1* expression induced by the lineage 2 *M. tuberculosis* isolate BTB 02-171 was associated with TLR4-dependent enhanced virulence in mice (72, 73). While the TLR4 ligand in strain BTB 02-171 remains to be identified, these observations invite speculation that TLR4 signaling in this context may occur from maturing mycobacteria-containing phagosomes or endosomal compartments during infection. Whether such signaling engages TRIF, and/or also occurs downstream of other TLRs implicated in human susceptibility to *M. tuberculosis* infection, remains to be established. These findings encourage investigations into the TLR-activating properties of *M. tuberculosis* isolates dominant in populations or ethnic groups that show associations of TB susceptibility or severity with polymorphisms in TLR4 (74, 75), TLR2 and its co-receptors (76–81), as well as TLR8 (80, 82) and TLR9 (83). Comparisons with populations where such associations cannot be established (63, 84–87) will be of great value.

CONSEQUENCES OF TYPE I IFN SIGNALING DURING *M. tuberculosis* INFECTION

The IFN gene signatures reported by the landmark study by Berry et al. (3) and subsequently several other studies firmly establish that IFNs flavor the peripheral immune response in patients with active TB. It is important to note that both type I and type II IFNs are implicated in driving these IFN signatures, especially those attributable to STAT1 homodimerization-stimulated gamma-IFN activation sequence (GAS)-regulated gene expression, which occurs in response to both type I and type II IFNs (88).

Impact of Type I IFN Signaling in Mice and Humans on Pathogen Control and Disease Outcome

Mice

The functional consequences of type I IFN signaling in the context of *M. tuberculosis* infection are incompletely understood. The evidence so far suggests that the impact of type I IFN signaling on host resistance and disease severity are determined by the immune competence of the host, with contributions by the bacterial strain. The degree of *M. tuberculosis*-induced IFNα/β expression in mice has been correlated with the virulence of *M. tuberculosis* strains (43, 89). *Ifnar1*-deficiency in mice with a *M. tuberculosis*-susceptible genetic background (A129, 129S2) enhanced host survival upon infection with the high type I IFN-inducing hypervirulent HN878 strain but also the low IFN-inducing strain CDC1551 (90, 91). *Ifnar1*-deficiency also partially rescued accelerated mortality in the highly susceptible *Il1r*$^{-/-}$ mice infected with the moderate type I IFN-inducer, H37Rv (92). These data suggest that endogenous type I IFN signaling impairs host resistance to *M. tuberculosis* infection in susceptible hosts. A study in C57BL/6 mice, a mouse strain more resistant to *M. tuberculosis* infection, reported equivalent survival rates between *Ifnar1*$^{-/-}$ and C57BL/6 mice infected with the hypervirulent HN878 and other *M. tuberculosis* strains, despite diminished bacterial burden in the lungs of infected *Ifnar1*$^{-/-}$ mice (93). Other studies compared C57BL/6 and *Ifnar1*$^{-/-}$ mice during infection with H37Rv and the hypervirulent, high type I IFN-inducing BTB 02-171 strain for 70 and >200 days of infection. As neither C57BL/6 wild-type nor *Ifnar1*$^{-/-}$ mice succumbed to the infection during these time frames, the impact of *Ifnar1* single deficiency on survival upon infection with these *M. tuberculosis* strains remained unclear (73, 94). Of note, *Ifnar1*$^{-/-}$ mice on C57BL/6 background showed diminished bacterial burden and pathology as well as a minor survival advantage during long-term infection (>200 days) with *Mycobacterium africanum* (95). While *M. africanum* is a poor inducer of type I IFN responses (43), these data suggest that type I IFN signaling may subvert effective long-term host control of this infection in a relatively resistant host.

Administration of neutralizing anti-IFNα/β antibodies to resistant B6D2/F1 mice prior to and upon infection with

TABLE 1 | Perturbations of type I IFN signaling in mouse models and consequences for infection with bacteria of the *Mycobacterium tuberculosis* complex.

Mouse strain/Mtb susceptible (S) or resistant (R)	Type I IFN perturbation	Mycobacteria	Type I IFN response	Bacterial burden	Pathology	Survival	Reference
C57BL/6 (R)	*Ifnar1*$^{-/-}$	H37Rv	Reduced IFN-β in lung homogenate 18 and 25 days p.i.	Comparable to WT on days 18 and 25 p.i.	n.d.	No mortality in WT and *Ifnar1*$^{-/-}$ (day 70 p.i.)	(94)
	Ifnar1$^{-/-}$	BTB 02-171	n.d.	Comparable to WT on days 24 and 27 p.i.	Comparable to WT at day 27 p.i.	No mortality in WT and *Ifnar1*$^{-/-}$ (day 50 p.i.)	(73)
	Ifnar1$^{-/-}$	Erdman	n.d.	Comparable to WT on days 1, 10, and 21 p.i. in the lungs. Reduced bacterial burden in spleen on days 10 and 21 p.i.	n.d.	n.d.	(33)
	Ifnar1$^{-/-}$	*Mycobacterium africanum* GM041182	n.d.	Reduced bacterial burden in lungs on day 292 p.i. in *Ifnar1*$^{-/-}$ mice	Pathology diminished in *Ifnar1*$^{-/-}$ compared to WT mice	*Ifnar1*$^{-/-}$ mice survived 292 days p.i., small number of WT mice succumbed >200 days p.i.	(95)
	Poly-ICLC (i.n.) twice weekly for 28 days, starting (a) 1 day or (b) 4 months post infection	H37Rv	(b) Poly-ICLC increased *Ifnb* and *Ifna* expression in lungs of WT mice; levels equivalent between poly-ICLC and poly-ICLC+Mtb	(a) and (b) increased bacterial burden in lungs. Was prevented in *Ifnar*$^{-/-}$ mice	(a) and (b) increased lung pathology	(b) reduced survival	(97)
	Intranasal influenza A virus (a) 28 days before or (b) 1 and 14 days (2 different IVA subtypes) after Mtb infection	H37Rv	n.d.	Slightly elevated lung bacterial burden (a) 120 days (b) 27 days post Mtb infection (a) No effect on lung Mtb burden on days 28/31 and 63 post Mtb infection	(a) increased lung inflammation on day 120 post Mtb infection	(a) impaired survival of mice >160 days	(96)
B6D2/F_1 (R)	Purified mouse IFNα/β (5 days/weeks for 4 weeks) post infection	HN878	n.d.	Higher bacterial burden in lungs at day 28 for HN878 + IFNα/β compared to HN878 only mice	n.d.	IFNα/β administration significantly impaired survival	(89)
	Anti-IFNα/β (A1AB/5; i.p. every 48 h for 4 weeks starting 24 h prior to Mtb)	HN878	Lung IFN-α mRNA at d28 p.i. slightly elevated for anti-IFNα/β treated mice	Equal bacterial burden in lungs	n.d.	Enhanced survival of anti-IFNα/β treated mice	(90)
129 (S)	*Ifnar1*$^{-/-}$	H37Rv	n.d.	Slightly decreased lung bacterial burden in *Ifnar1*$^{-/-}$ mice 21 days p.i.	Diminished pathology in *Ifnar1*$^{-/-}$ mice in *Ifnar1*$^{-/-}$ mice 21 days p.i.	Most WT mice died within 40 days p.i., all *Ifnar1*$^{-/-}$ mice survived (d70)	(91)
	Ifnar1$^{-/-}$	HN878 CDC1551	n.d.	n.d.	n.d.	Small survival benefit for *Ifnar*$^{-/-}$ infected with HN878; *Ifnar*$^{-/-}$ survived significantly longer with CDC1551 infection compared to HN878	(90)

(*Continued*)

TABLE 1 | Continued

Mouse strain/Mtb susceptible (S) or resistant (R)	Type I IFN perturbation	Mycobacteria	Type I IFN response	Bacterial burden	Pathology	Survival	Reference
	Ifnar1$^{-/-}$	H37Rv HN878 CSU123 CDC1551 Erdman-KO1	n.d.	Reduced bacterial burden in lungs of *Ifnar1*$^{-/-}$ mice compared to WT mice (>25 days p.i.) for all Mtb strains	Increased lung pathology in WT mice infected with HN878 compared to H37Rv, CDC1551 or Erdman-KO1	Equivalent survival of *Ifnar1*$^{-/-}$ (129 background) and C57BL/6 WT mice during infection with HN878, CDC1551, and Erdman-KO1	(93)
C57BL/6/129 (S)	*Ifnar1*$^{-/-}$	Erdman	n.d.	Slightly increased lung bacterial burden at 10, 20, and 40 days p.i. compared to WT Comparable bacterial burden at 80 days p.i.	n.d.	n.d.	(101)
Il-1r$^{-/-}$ on C57BL/6 (S)	*Ifnar1*$^{-/-}$	H37Rv	n.d.	n.d.	n.d.	*Il-1r/Ifnar1*$^{-/-}$ partially rescued survival of highly susceptible *Il1r1*$^{-/-}$ mice but still impaired compared to WT and *Ifnar1*$^{-/-}$; no difference between WT and *Ifnar1*$^{-/-}$ until day 80 p.i.	(92)
Ifngr1$^{-/-}$ on C57BL/6 (S)	*Ifnαr1*$^{-/-}$	H37Rv	Slightly elevated IFN-β protein in lung homogenate of *Ifngr/Ifnar1*$^{-/-}$ compared to *Ifngr*$^{-/-}$ mice 25 days p.i.	Comparable bacterial burden in lung and MLN in *Ifngr/Ifnar1*$^{-/-}$ and *Ifngr*$^{-/-}$; both higher than WT and *Ifnar1*$^{-/-}$ 25 days p.i., no difference between WT and *Ifnar1*$^{-/-}$	Severe pathology in *Ifngr*$^{-/-}$ even more exacerbated in *Ifngr/Ifnar1*$^{-/-}$, both higher than WT	*Ifngr/Ifnar1*$^{-/-}$ succumbed approx. 7 days earlier than *Ifngr*$^{-/-}$	(94)
	Ifnar1$^{-/-}$	BTB 02-171	n.d.	Lung bacterial burden in *Ifngr/Ifnar1*$^{-/-}$ mice increased compared to *Ifngr*$^{-/-}$; both higher than WT and *Ifnar1*$^{-/-}$ 24 and 27 days p.i., no difference between WT and *Ifnar1*$^{-/-}$	Severe pathology in *Ifngr*$^{-/-}$ even more exacerbated in *Ifngr/Ifnar1*$^{-/-}$, both higher than WT and *Ifnar1*$^{-/-}$	*Ifngr/Ifnar1*$^{-/-}$ succumbed approx. 3 days earlier than *Ifngr*$^{-/-}$; no mortality in WT and *Ifnar1*$^{-/-}$ (until day 50 p.i.)	(73)

Ifnar1, interferon alpha receptor 1; Ifngr, interferon gamma receptor; Il-1r, interleukin 1 receptor; WT, wild-type; Mtb, M. tuberculosis; IFN, interferon; p.i., postinfection; i.n., intranasal; n.d., not determined; Poly-ICLC, polyinosinic-polycytidilic acid and poly-L-lysine double stranded RNA.

M. tuberculosis HN878 provided a long-term survival benefit, associated with lower IFN-α expression and STAT1 activation in lung tissue, albeit without significant effects on bacterial burden (90). This suggests that pre-existing type I IFN responses in the host at the time of exposure may influence the outcome of *M. tuberculosis* infection. This is supported by the observation that pre-infection of mice with influenza A virus accelerated host death (>160 days of *M. tuberculosis* infection). This was associated with exacerbated inflammation and some transient early and late elevation of bacterial burden, which was abrogated in *Ifnar1*$^{-/-}$ mice (96). Moreover, artificial exacerbation of type I IFN responses in *M. tuberculosis*-infected resistant mice, e.g., by intranasal administration of IFNα/β or the stabilized synthetic TLR3 agonist pICLC, significantly impaired host survival, exacerbated lung inflammation, and impaired the host's ability to restrict *M. tuberculosis* (89, 92, 97).

While the reasons for variable effects on bacterial burden and host survival in the abovementioned studies remain to be elucidated, the evidence gathered through genetic and exogenous modulation indicate detrimental effects of type I IFN signaling in mouse models of *M. tuberculosis* infection across a spectrum of host genetic backgrounds and mycobacterial strains (**Table 1**). However, there is evidence that type I IFN signaling exerts some protective effects in the absence of IFN-γ. Mice that lack the IFN-γ receptor are highly susceptible to *M. tuberculosis* infection, as reflected by poor host control of the bacteria, extensive pathology, and accelerated death. Additional *Ifnar1* deficiency in *Ifngr*$^{-/-}$ mice further impaired survival suggesting that type I IFN signaling played a non-redundant protective role relatively early during infection with *M. tuberculosis* H37Rv and BTB 02-171 that was only apparent in the absence of IFN-γ signaling (73, 94). These observations suggest that the relative balance of type I and type II IFN functions defines host control of *M. tuberculosis* and pathology during the infection. It is worth noting that in mice infected with *M. bovis* BCG, *Mycobacterium avium*, and *Mycobacterium smegmatis*, type I IFNs appear to have protective roles (98–100), encouraging further investigations into the functional contributions of type I IFNs to host protection across a wider spectrum of mycobacteria.

Humans

The evidence obtained from mouse models of *M. tuberculosis* infection suggests that in the immune competent host, type I IFN signaling impedes the host's ability to limit lung pathology and/or bacterial replication, to the benefit of the pathogen. However, there are several clinical case reports that inhaled or subcutaneous administration of IFN-α to tuberculosis patients, in conjunction with co-administration of antimycobacterial antibiotics, improved clinical symptoms (**Table 2**). It is important to note that these patients were selected due to failure of conventional treatment options and/or recurrent disease, and often received IFN-α late in their infection. Underlying unidentified immune deficiencies may thus have been a confounding factor. Moreover, reports of therapeutic effects of IFN-α administration to patients that presented with non-tuberculous mycobacterial infections suggest contributions of type I IFNs to the antimycobacterial defense in humans in the context of genetically manifested IFN-γ signaling deficiencies (102, 103). The clinical observations in IFN-γ signaling deficient patients are somewhat reminiscent of the studies in *Ifngr*$^{-/-}$*Ifnar1*$^{-/-}$ mice (73, 94). This encourages studies to enhance our understanding of the complex interplay between type I and type II IFN during mycobacterial infection and how this may be harnessed therapeutically in the context of compromised IFN-γ/IFNGR signaling. Recombinant IFN-α is commonly used in the treatment of chronic viral hepatitis. While some studies suggest that long-term administration of recombinant IFN-α does not bear a major risk for TB reactivation (104), case reports of TB reactivation associated with IFN-α therapy demand caution in the clinical management of co-infected individuals (105–109). Thus, detailed assessment of the direct and indirect roles of endogenous and therapeutically administered type I IFNs in the control of latent *M. tuberculosis* infection is an important area of future pursuit.

It is obvious that our understanding of the contributions of type I IFN signaling to host control of mycobacterial infections is incomplete. Parallels between mouse models and human patients are emerging, but remain limited. In-depth knowledge of type I IFN responses and their contributions to host control in other model systems may be required to bridge important gaps between human and mouse immune pathogenesis during *M. tuberculosis* infection. The non-human primate model where IFN signaling transcriptional signatures are also highly associated with active TB disease may offer valuable opportunities (115). Confounding factors that require careful consideration in future studies include the impact of host genetic susceptibility, the host's type I IFN status at the time of infection, the temporal contributions of type I IFNs in active and latent infection, the site of infection, and the infecting mycobacterial species. Detailed understanding of the timing and nature of the interactions between type I and type II IFNs may help to more clearly define intervention strategies and risk factors in the management of mycobacterial infections in patients with (known or unknown) underlying immune deficiencies and co-infections.

Mechanistic Insights into How Type I IFNs Regulate Immune Responses during *M. tuberculosis* Infection

In light of the potential implications for host-directed therapies in TB, the molecular and cellular mechanisms by which type I IFNs suppress, or in some contexts promote, effective immune control of *M. tuberculosis* are the subject of intense investigation and discussion (2, 116, 117) (**Figure 2**).

Myeloid Antimicrobial Defense

Independent studies in different mouse models suggest that type I IFN signaling during *M. tuberculosis* infection defines the nature of the early myeloid cell infiltrate into the lung, which may favor bacterial replication due to a diminished ability to restrict intracellular mycobacteria (91, 97, 118). Type I IFNs impair the IFN-γ-induced human and mouse macrophage control of *M. tuberculosis* and other mycobacteria (119–121). At least in human macrophages, this impaired ability to control intracellular mycobacteria is likely facilitated through the IL-10-mediated

TABLE 2 | Impact of type I IFNs in patients with mycobacterial infections.

Patients	TB MDR-TB, XDR-TB Non-tuberculous mycobacteria	Comorbidity	Treatment	Outcome	Reference
5 patients with advanced pulmonary cavitary disease, extensive drug resistance, chronic treatment failure	XDR-TB	–	Recombinant human IFN-α-2b subcutaneous injections weekly for 12 weeks in combination with anti-TB chemotherapy	2/5 clinical improvement, 1 year minimum six negative sputum cultures 1/5 transient clinical improvement, smear negative but culture positive 2/5 not responsive	(110)
7 patients non-responsive to second line chemotherapy after 6 months	MDR-TB	–	Aerosolized human IFN-α lymphoblastoid three times weekly for 9 weeks in combination with anti-TB chemotherapy	5/7 sputum smear negative but culture positive 2/7 reduced sputum burden and remained culture positive Bacterial burden increased in all after IFN-α treatment stopped	(111)
20 patients, drug-sensitive pulmonary TB	TB	–	10 patients with anti-TB chemotherapy vs. 10 patients with anti-TB chemotherapy + aerosolized IFN-α three times weekly for 2 months	Fever, bacterial load in sputum smears and high-resolution computer tomography abnormalities showed earlier resolution in IFN-α treated group	(112)
11 patients, pulmonary TB, isoniazid, and rifampin resistance	MDR-TB	–	6 patients with anti-TB chemotherapy vs. 6 patients with anti-TB chemotherapy + s.c. IFN-α three times weekly for 8 weeks	8 weeks: 5/5 sputum smear negative in IFN-α group 6 months: 2/5 sputum negative in IFN-α group 0/6 sputum negative in control group at both time points	(113)
48 years old male; previous treatment failure	TB	Diabetes mellitus	Co-administration of IFN-α-2a i.m. weekly for 8 months with anti-TB chemotherapy	Afebrile and body weight gain after 2 weeks, and radiological improvement after 2 months Radiological status stable and sputum cultures negative after 4 years	(114)
4 patients with disseminated disease; patients A–C had early childhood mycobacterial disease onset	Patient A: *Mycobacterium avium* complex (MAC), *Mycobacterium kansasii*, *Mycobacterium fortuitum*	Complete or partial IFNGR1 signaling deficiencies	Patient A: IFN-α2b three times weekly subcutaneously for 3 months	Patient A: reduction of pulmonary disease, lesions resolved after 1 year	(103)
Patient A: 22 years old female Patient B: 19 years old male Patient C: 7 years old male with Bacillus Calmette–Guérin (BCG) immunization at birth Patient D: 52 years old female	Patient B: MAC, *Mycobacterium abscessus* Patient C: *Mycobacterium bovis* BCG, MDR *M. bovis* Patient D: *M. fortuitum, MAC*	Patient B: B-cell lymphoma	Patient B: IFN-α2b 3 times weekly subcutaneously, then pegylated IFN-α Patient C and D: alternating doses of IFN-γ and IFN-α2b subcutaneously three times weekly; all in conjunction with individualized antibacterial treatment	Patient B: deceased at 20 years of age, but biopsies showed no mycobacteria Patient C: gained weight, lesion healed, pleural mass decreased Patient D: no new infections	
12 months old female disseminated disease	MAC	Complete IFNGR1 deficiency and complete loss of functional response to exogenous IFN-γ	Co-administration of IFN-α-2b subcutaneous injections three times weekly and antimycobacterials	Mycobacteremic but clinically stable with continuation of multi-drug regimen at 58 months of age	(102)

TB, tuberculosis; MDR, multi-drug resistant; XDR, extensively drug resistant; IFN, interferon; IFNGR1, interferon-gamma receptor 1; s.c., subcutaneous; i.m., intramuscular.

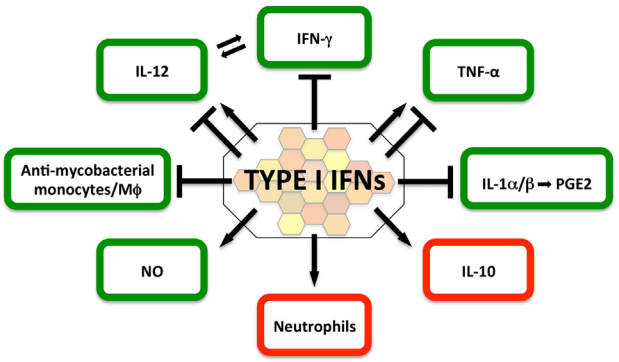


FIGURE 2 | Impact of type I IFNs on protective (green) and detrimental (red) host responses in the immune-competent *Mycobacterium tuberculosis*-infected host. The current literature suggests that in the immune-competent host, type I IFNs suppress host-protective IFN-γ and IL-1α/β responses, as well as the recruitment of mycobacteria-restricting monocytes/macrophages. In contrast, type I IFN signaling can directly induce NO production, a contributor to effective antimycobacterial host defense. The evidence for the contributions of type I IFNs to host-protective interleukin-12 and TNF responses is currently ambiguous and may be determined by timing, dose, and source of the type I IFN response. Type I IFNs are a driver of IL-10, a cytokine that impairs antimycobacterial immune responses during all stages of infection. Type I IFN signatures in patients have been associated with neutrophils and studies in mouse models of heightened *M. tuberculosis* susceptibility suggest that type I IFN signaling facilitates infection of permissive neutrophils, which have been associated with damaging tissue pathology.

inhibition of the IFN-γ-driven vitamin D3/cathelicidin/defensin beta 4A antimicrobial defense pathway (120). The interferon-stimulated gene (ISG) ISG-15 has recently been implicated in promotion of early intracellular *M. tuberculosis* replication in mice, but seems to have protective roles later during infection (122). This later role supports findings in ISG15-deficient patients with mycobacterial disease that suggest that secreted ISG15 promotes IFN-γ secretion (123). Of note, ISG15 expression was detectable in several human leukocyte subpopulations including T cells, NK cells, myeloid and plasmacytoid dendritic cells, monocytes, with the highest levels detected in granulocytes. Exogenous IFN-a enhanced *ISG15* expression most dramatically in granulocytes (123), which may provide a link for the functional importance of neutrophil-associated IFN-inducible gene signatures in humans with active disease (3). In contrast to the impaired IFN-γ-mediated macrophage control of mycobacteria, in the absence of IFN-γ signaling type I IFNs may facilitate the recruitment, differentiation and/or survival of myeloid cells that control *M. tuberculosis* to some extent. This may be due to type I IFN-mediated prevention of skewing of macrophages toward an alternatively activated phenotype (73, 94).

IL-12/IFN-γ and Th1 Response

High type I IFN responses in mice infected with hypervirulent HN878 are associated with diminished Th1 responses including lower IFN-γ production and proliferation by antigen-specific T cells (89, 90, 93). There is *in vitro* and *in vivo* evidence that type I IFNs exert these suppressive effects through impairment of myeloid-derived IL-12 production. In myeloid cells derived from *M. tuberculosis*-infected bone marrow chimeric mice, IFNAR-deficiency enhanced myeloid cell-derived IL-12p40 expression in response to re-stimulation with *M. tuberculosis* compared to wild-type cells (116). In murine *M. tuberculosis*-infected macrophages, exogenous addition of high concentrations of IFN-β suppressed IL-12 expression as well as IFN-γ-induced macrophage activation (121). Exogenously added type I IFNs also suppressed IFN-γ-induced cytokine responses in human monocytes (120, 124). Molecular mechanisms underlying type I IFN-mediated suppression of IL-12 responses include the induction of IL-10, downregulation of the IFN-γ receptor, and induction of protein arginine methyl transferase 1, a negative regulator of IFN signaling (120, 121, 124). However, diminished IL-12p40 release by *M. tuberculosis*-infected IFNAR$^{-/-}$ macrophages has been reported (121), suggesting that in isolated macrophage cultures, endogenous type I IFN signaling facilitates IL-12p40 responses. Future studies may need to address similarities and potential differences in the effects of endogenously produced versus exogenously added type I IFNs both in cell culture as well as *in vivo*.

Exogenous addition of recombinant IFN-α to *in vitro* cultured T cell clones from TB patients enhanced the number of clones that produced IFN-γ (125) in line with observations that IFN-α can promote IFN-γ production by human CD4$^+$ T cells (126). Thus, the overall impact of type I IFN signaling during mycobacterial infection may be a composite of differential effects on myeloid and lymphocyte cell functions. Mouse models that allow assessment of the impact of type I IFN signaling in specific cell subsets such as T cells (127) might prove valuable in dissecting the direct impact of type I IFNs on T cell functions during *M. tuberculosis* infection.

IL-10

Early studies associated higher virulence of *M. tuberculosis* isolates (defined by elevated bacterial burden and impaired survival of infected mice) with the capacity to elicit high type I IFN responses *in vivo*. This phenotype was accompanied by relatively lower pro-inflammatory cytokine responses (89, 90, 93). More recent data indicate that elevated virulence in the mouse model can be associated with induction of both high IFN-β and high pro-inflammatory cytokine responses (72). Association of elevated virulence with high type I IFN paired with high IL-10 levels may provide a more direct link between high type I IFN responses and impaired host control of the infection. Type I IFN signaling drives IL-10 expression by both *M. tuberculosis*-infected macrophages and CD4$^+$ T cells in infected mice (121, 128). While there is great variability between observations made in different mouse strains and between different labs, several studies in mice suggest that IL-10 significantly impairs host control of *M. tuberculosis* infection during active, chronic, and latent infection (2). Overexpression of IL-10 in macrophages driven by the CD86 promoter led to increased bacterial burden and impaired survival of *M. tuberculosis*-infected mice without noticeable effects on T cell functions (129). In contrast, a recent study that utilized cell-specific deletion of *Il10* expression *in vivo* suggests that a reduction of bacterial burden in lungs of IL-10-deficient mice

during the chronic phase of infection (day 60) is attributable to IL-10 produced by $CD4^+$ T cells rather than myeloid or B cells. However, while lung $CD4^+$ T cells from *M. tuberculosis*-infected *Ifnar1*$^{-/-}$ showed diminished *Il10* expression, lung bacterial burden in *Ifnar1*$^{-/-}$ mice was not decreased and did hence not mirror the reduction of lung bacterial load in *Il10*$^{-/-}$ and *Il10*$^{fl/fl}$ $CD4^{Cre+}$ mice (128). Instead, IL-27 receptor signaling was implicated to drive IL-10 expression by $CD4^+$ T cells, in parallel to type I IFNs, and *IL27ra*$^{-/-}$ mice exhibited diminished lung bacterial burden similar to *Il10*$^{-/-}$ and *Il10*$^{fl/fl}$ $CD4^{Cre+}$ mice (128). Thus, cell-specific targeting of the cellular source of IL-10 that impairs host control of *M. tuberculosis* replication may be of interest for host-directed intervention but requires detailed characterization of the functionalities and impact of IL-10-producing host cell populations.

TNF-α

The increased risk of TB reactivation in individuals undergoing TNF neutralizing therapies for chronic inflammatory diseases underpins the central role for this cytokine in the host control of *M. tuberculosis* infection, which is further supported by mouse studies (2, 130). Macrophages deficient for IFNAR signaling showed diminished TNF expression in response to *M. tuberculosis* infection, which was interpreted as a promoting role for endogenous type I IFN responses in the *M. tuberculosis*-induced TNF response (121). However, an independent study reported no differences between IFNAR-deficient and WT macrophages (131). In contrast, exogenously added IFN-β suppressed TNF release by *M. tuberculosis*-infected macrophages (121). The impact of type I IFN signaling on the TNF response *in vivo* remains to be clearly defined. WT and IFNAR-deficient mice infected with the high type I IFN-inducing *M. tuberculosis* strain BTB 02-171 displayed equivalent lung *Tnf* mRNA expression (day 20 p.i.) (73). In contrast, decreased TNF concentrations were observed in lung homogenates of *M. tuberculosis*-infected IFNAR-deficient 129 mice (day 21 p.i.) (91) and a small decrease in lung TNF concentrations was also reported in *M. africanum*-infected IFNAR-deficient C57BL/6 mice (day 292 p.i.) (95). The reasons for the apparent differences between individual studies are not immediately obvious, but may be attributable to the different time points analyzed postinfection and the different models systems studied. These observations may indicate, however, that the concentration, source, and timing of the type I IFN response direct TNF responses in the context of *M. tuberculosis* infection.

IL-1, Eicosanoids, Nitric Oxide (NO), and Neutrophils

IL-1 signaling is an important driver of host resistance against *M. tuberculosis* infection in humans and mice (132–135). The underlying molecular mechanisms are emerging and TNF-driven antimicrobial activity, autophagy, as well as eicosanoid signaling have been implicated (92, 134, 136). Type I IFN signaling suppressed IL-1α and β production by macrophages *in vitro* and *in vivo* mouse infection (34, 121, 137). The type I IFN-mediated regulation of IL-1 expression by human and mouse macrophages was shown to be dependent on NO synthase 2 and IL-10, and was associated with enhanced IL-1Ra expression (121, 137).

Thus, type I IFN signaling regulates IL-1 responses through inhibition of ligand expression as well as receptor signaling. A third potential mechanism may be inferred from the observation that NO interference with NLRP3 inflammasome assembly impairs IL-1β processing by *M. tuberculosis*-infected macrophages (138). As endogenous and exogenously added type I IFNs drive NO production by *M. tuberculosis*-infected macrophages (32, 73), type I IFN signaling may also interfere with IL-1 processing. It is interesting to note that NO-mediated thiol nitrosylation inhibited assembly and activation of the NLRP3 but not AIM2 inflammasome (138). AIM2 has been reported to be dispensable for IL-1β production by murine dendritic cells infected with virulent *M. tuberculosis in vitro*. In contrast, AIM2 was required for IL-1β release induced by *Mycobacterium smegmantis*, *Mycobacterium fortuitum*, *Mycobacterium kansasii* and, to a lesser extent, the attenuated *M. tuberculosis* H37Ra (139). Intriguingly, infection of DCs with virulent *M. tuberculosis* prior to infection with *M. smegmatis* reduced the IL-1β release, which was associated with an impaired IFN-β response. The authors concluded that virulent *M. tuberculosis* actively suppressed AIM2 activation by a mechanism that required *M. tuberculosis* ESX-1 (139). Yet, AIM2-deficient mice infected intratracheally with a high dose of *M. tuberculosis* H37Rv displayed elevated bacterial loads in the lung and liver 4 weeks postinfection accompanied by exacerbated pathology, impaired IL-18 and IL-10 production, as well as an impaired antigen-specific $CD4^+$ T cell-derived IFN-g response. The *Aim2*$^{-/-}$ mice succumbed to infection between 5 and 7 weeks postinoculation (140). It is important to note, however, that deficiency in caspase 1 and 11, inflammasome effector caspases that cleave pro-IL-1β, does not impair host control of *M. tuberculosis* infection *in vivo* (133, 141). This suggests that alternative mechanisms of pro-IL-1 processing during *M. tuberculosis* infection *in vivo* exist, and that AIM2 contributions to the host control of *M. tuberculosis* infection may exceed processing of pro-IL-1β.

An emerging pathway of type I IFN-mediated suppression of effective immune control of *M. tuberculosis* occurs *via* dysregulation of IL-1-controlled eicosanoid lipid mediators (116). In mice, IL-1 receptor signaling enhanced the ratio of host-protective prostaglandin E2 over host-detrimental 5-lipoxygenase products such as lipoxin A4 (116). Type I IFN signaling counter-regulates this IL-1-driven process, and conversely, IL-1 signaling impairs the type I IFN response (92). Poor control of *M. tuberculosis* infection in various mouse models is associated with an extensive neutrophil response in the lung. Pathogen control and host survival can be improved by neutrophil depletion and *Ifnar1*-deficiency in a susceptible mouse strain, which is associated with a shift of intracellular *M. tuberculosis* burden from permissive neutrophils toward monocytes (91, 142, 143). Recent findings suggest that in a permissive environment, 12/15-lipoxygenase products drive neutrophil infiltration into infected lungs, which is associated with poor host restriction of mycobacterial replication in a nutrient-rich environment (143). In the absence of NO production (*Nos2*$^{-/-}$ mice), this process was driven by inflammasome-dependent IL-1 production (143) linking back to the inhibitory effects of NO on inflammasome assembly (138).

Associations of IL-1, type I IFN, eicosanoids, neutrophil infiltration, and SNPs in associated genes with disease severity

and treatment responsiveness in human TB patients (92, 135, 143) underpin a dynamic cytokine network that balances the protective or detrimental roles of eicosanoid lipid mediators and neutrophil functions in *M. tuberculosis* infection. Pharmacologic targeting of eicosanoids has been proposed as a possible avenue for host-directed therapeutic intervention in TB (92).

CONCLUDING REMARKS

As we continue to gain mechanistic insight into the interactions between *M. tuberculosis* and innate immune sensors, it is evident that multiple independent extracellular and intracellular surveillance pathways converge to drive type I IFN expression in infected host cells. One of the main questions remaining is which cells are the key producers of type I IFNs during *M. tuberculosis* infection *in vivo*. *In vitro* evidence strongly suggests that host cells that harbor *M. tuberculosis* bacteria such as macrophages and myeloid DCs are sources of type I IFN during infection. In the context of the close interactions between infected and uninfected cells within granulomas, the concept of dinucleotide-mediated STING-activation in bystander cells warrants further exploration as it may allow for type I IFN expression not only in myeloid cells but also in T and B cells. Moreover, mice infected with hypervirulent, high type I IFN-inducing HN878 harbored elevated numbers of plasmacytoid DCs (pDCs) in their lungs (93). Human peripheral blood pDCs responded with high IFN-α production to stimulation with high concentrations of mycobacterial DNA (144). However, *in vitro* cultured pDCs expressed little to no type I IFNs when co-cultured with *M. tuberculosis*- or *M. bovis*-BCG-infected myeloid DCs (144, 145). Advanced single cell functional profiling in TB granulomas and the employment of sensitive IFN reporter animal models are just two approaches that may provide a better understanding of the dynamics and cellular sources of type I IFN expression during *M. tuberculosis* infection both at the site of infection and in the periphery. Individual type I IFNs exhibit distinct functions in various homeostatic and pathological contexts, which has at least in part been attributed to varying ligand affinity, stability of the receptor complex, and unique signaling capacity of IFN-β through IFNAR1 (146–148). Thus, insights into the spatial and temporal expression of individual members of the type I IFN family may hold the key to providing context for some of the apparent opposing roles of type I IFN signaling deduced from model systems and patient observations. As the discoveries around blood gene expression signatures in patients with active TB disease are being explored for suitable biomarkers, they also raise questions related to TB pathophysiology. For example: are IFN signatures related to neutrophils in the periphery (3, 149) a natural consequence of *M. tuberculosis* infection in humans, or an indication of disease susceptibility of the individual due to a propensity to mount a neutrophil response upon encounter with *M. tuberculosis*? How reflective is the peripheral gene expression profile of the response mounted locally at the site of infection or within the relevant secondary lymphoid organs? Longitudinal analyses and immune profiling in at-risk individuals (8) will provide valuable insights, and suitable animal models are key for functional context. While type I IFN signaling may contribute to some aspects of the host defense against *M. tuberculosis* infection, it is clear that extensive type I IFN responses, e.g. in the context of viral infections (150), promote pathology to the detriment of the host. Nevertheless, the reported therapeutic benefits of type I IFN administration in conjunction with antimycobacterial antibiotics warrants detailed exploration to establish whether this is reflective of a patient immune status permissive to potential antimycobacterial activities of type I IFN or whether IFNs facilitate mycobacterial replication rendering them more susceptible to antibiotics. Understanding whether and when type I IFNs are "friend or foe" in the context of mycobacterial infections will define their place in the quest for tailored host-directed therapeutic interventions in TB.

AUTHOR CONTRIBUTIONS

All authors contributed to the critical review of the literature and writing of the manuscript. MD and AB developed the figures and tables and edited the manuscript.

ACKNOWLEDGMENTS

We are grateful to Katharina Ronacher and Carl Feng for critical review and feedback on the manuscript.

FUNDING

AB acknowledges funding by the National Health and Medical Research Council of Australia (GNT1120230) and The University of Queensland Diamantina Institute. MD and TS gratefully acknowledge Research Higher Degree Scholarships by The University of Queensland and The University of Queensland Diamantina Institute.

REFERENCES

1. World Health Organisation. *Global Tuberculosis Report 2016*. Geneva (2016). p. 1–201.
2. O'Garra A, Redford PS, McNab FW, Bloom CI, Wilkinson RJ, Berry MP. The immune response in tuberculosis. *Annu Rev Immunol* (2013) 31:475–527. doi:10.1146/annurev-immunol-032712-095939
3. Berry MPR, Graham CM, McNab FW, Xu Z, Bloch SAA, Oni T, et al. An interferon-inducible neutrophil-driven blood transcriptional signature in human tuberculosis. *Nature* (2010) 466(7309):973–7. doi:10.1038/nature09247
4. Cliff JM, Lee JS, Constantinou N, Cho JE, Clark TG, Ronacher K, et al. Distinct phases of blood gene expression pattern through tuberculosis treatment reflect modulation of the humoral immune response. *J Infect Dis* (2013) 207(1):18–29. doi:10.1093/infdis/jis499
5. Blankley S, Berry MP, Graham CM, Bloom CI, Lipman M, O'Garra A. The application of transcriptional blood signatures to enhance our understanding of the host response to infection: the example of tuberculosis. *Philos Trans R Soc Lond B Biol Sci* (2014) 369(1645):20130427. doi:10.1098/rstb.2013.0427
6. Blankley S, Graham CM, Levin J, Turner J, Berry MP, Bloom CI, et al. A 380-gene meta-signature of active tuberculosis compared with healthy controls. *Eur Respir J* (2016) 47(6):1873–6. doi:10.1183/13993003.02121-2015
7. Blankley S, Graham CM, Turner J, Berry MP, Bloom CI, Xu Z, et al. The transcriptional signature of active tuberculosis reflects symptom status in extra-pulmonary and pulmonary tuberculosis. *PLoS One* (2016) 11(10):e0162220. doi:10.1371/journal.pone.0162220

8. Zak DE, Penn-Nicholson A, Scriba TJ, Thompson E, Suliman S, Amon LM, et al. A blood RNA signature for tuberculosis disease risk: a prospective cohort study. *Lancet* (2016) 387(10035):2312–22. doi:10.1016/s0140-6736(15)01316-1
9. Sambarey A, Devaprasad A, Mohan A, Ahmed A, Nayak S, Swaminathan S, et al. Unbiased identification of blood-based biomarkers for pulmonary tuberculosis by modeling and mining molecular interaction networks. *EBioMedicine* (2017) 15:112–26. doi:10.1016/j.ebiom.2016.12.009
10. Decker T, Muller M, Stockinger S. The yin and yang of type I interferon activity in bacterial infection. *Nat Rev Immunol* (2005) 5(9):675–87. doi:10.1038/nri1684
11. de Weerd NA, Nguyen T. The interferons and their receptors – distribution and regulation. *Immunol Cell Biol* (2012) 90(5):483–91. doi:10.1038/icb.2012.9
12. Schreiber G. The molecular basis for differential type I interferon signaling. *J Biol Chem* (2017) 292(18):7285–94. doi:10.1074/jbc.R116.774562
13. Kovarik P, Castiglia V, Ivin M, Ebner F. Type I interferons in bacterial infections: a balancing act. *Front Immunol* (2016) 7:652. doi:10.3389/fimmu.2016.00652
14. Snyder DT, Hedges JF, Jutila MA. Getting "inside" type I IFNs: type I IFNs in intracellular bacterial infections. *J Immunol Res* (2017) 2017:9361802. doi:10.1155/2017/9361802
15. Boxx GM, Cheng G. The roles of type I interferon in bacterial infection. *Cell Host Microbe* (2016) 19(6):760–9. doi:10.1016/j.chom.2016.05.016
16. Cliff JM, Kaufmann SHE, McShane H, van Helden P, O'Garra A. The human immune response to tuberculosis and its treatment: a view from the blood. *Immunol Rev* (2015) 264(1):88–102. doi:10.1111/imr.12269
17. Deffur A, Wilkinson RJ, Coussens AK. Tricks to translating TB transcriptomics. *Ann Transl Med* (2015) 3(Suppl 1):S43. doi:10.3978/j.issn.2305-5839.2015.04.12
18. Haas CT, Roe JK, Pollara G, Mehta M, Noursadeghi M. Diagnostic 'omics' for active tuberculosis. *BMC Med* (2016) 14:37. doi:10.1186/s12916-016-0583-9
19. Joosten SA, Fletcher HA, Ottenhoff TH. A helicopter perspective on TB biomarkers: pathway and process based analysis of gene expression data provides new insight into TB pathogenesis. *PLoS One* (2013) 8(9):e73230. doi:10.1371/journal.pone.0073230
20. Maertzdorf J, McEwen G, Weiner J III, Tian S, Lader E, Schriek U, et al. Concise gene signature for point-of-care classification of tuberculosis. *EMBO Mol Med* (2016) 8(2):86–95. doi:10.15252/emmm.201505790
21. Roe JK, Thomas N, Gil E, Best K, Tsaliki E, Morris-Jones S, et al. Blood transcriptomic diagnosis of pulmonary and extrapulmonary tuberculosis. *JCI Insight* (2016) 1(16):e87238. doi:10.1172/jci.insight.87238
22. Sweeney TE, Braviak L, Tato CM, Khatri P. Genome-wide expression for diagnosis of pulmonary tuberculosis: a multicohort analysis. *Lancet Respir Med* (2016) 4(3):213–24. doi:10.1016/s2213-2600(16)00048-5
23. Cattamanchi A, Walter ND, Metcalfe JZ, Davis JL. A transcriptional signature for active TB: have we found the needle in the haystack? *PLoS Med* (2013) 10(10):e1001539. doi:10.1371/journal.pmed.1001539
24. Harries AD, Lin Y, Satyanarayana S, Lonnroth K, Li L, Wilson N, et al. The looming epidemic of diabetes-associated tuberculosis: learning lessons from HIV-associated tuberculosis. *Int J Tuberc Lung Dis* (2011) 15(11):1436–44. doi:10.5588/ijtld.11.0503
25. Prada-Medina CA, Fukutani KF, Pavan Kumar N, Gil-Santana L, Babu S, Lichtenstein F, et al. Systems immunology of diabetes-tuberculosis comorbidity reveals signatures of disease complications. *Sci Rep* (2017) 7(1):1999. doi:10.1038/s41598-017-01767-4
26. Koth LL, Solberg OD, Peng JC, Bhakta NR, Nguyen CP, Woodruff PG. Sarcoidosis blood transcriptome reflects lung inflammation and overlaps with tuberculosis. *Am J Respir Crit Care Med* (2011) 184(10):1153–63. doi:10.1164/rccm.201106-1143OC
27. Maertzdorf J, Weiner J III, Mollenkopf HJ, Bauer T, Prasse A, Muller-Quernheim J, et al. Common patterns and disease-related signatures in tuberculosis and sarcoidosis. *Proc Natl Acad Sci U S A* (2012) 109(20):7853–8. doi:10.1073/pnas.1121072109
28. Bloom CI, Graham CM, Berry MP, Rozakeas F, Redford PS, Wang Y, et al. Transcriptional blood signatures distinguish pulmonary tuberculosis, pulmonary sarcoidosis, pneumonias and lung cancers. *PLoS One* (2013) 8(8):e70630. doi:10.1371/journal.pone.0070630
29. Koh GC, Schreiber MF, Bautista R, Maude RR, Dunachie S, Limmathurotsakul D, et al. Host responses to melioidosis and tuberculosis are both dominated by interferon-mediated signaling. *PLoS One* (2013) 8(1):e54961. doi:10.1371/journal.pone.0054961
30. Kaforou M, Wright VJ, Oni T, French N, Anderson ST, Bangani N, et al. Detection of tuberculosis in HIV-infected and -uninfected African adults using whole blood RNA expression signatures: a case-control study. *PLoS Med* (2013) 10(10):e1001538. doi:10.1371/journal.pmed.1001538
31. Remoli ME, Giacomini E, Lutfalla G, Dondi E, Orefici G, Battistini A, et al. Selective expression of type I IFN genes in human dendritic cells infected with *Mycobacterium tuberculosis*. *J Immunol* (2002) 169(1):366–74. doi:10.4049/jimmunol.169.1.366
32. Shi S, Blumenthal A, Hickey CM, Gandotra S, Levy D, Ehrt S. Expression of many immunologically important genes in *Mycobacterium tuberculosis*-infected macrophages is independent of both TLR2 and TLR4 but dependent on IFN-alphabeta receptor and STAT1. *J Immunol* (2005) 175(5):3318–28. doi:10.4049/jimmunol.175.5.3318
33. Stanley SA, Johndrow JE, Manzanillo P, Cox JS. The Type I IFN response to infection with *Mycobacterium tuberculosis* requires ESX-1-mediated secretion and contributes to pathogenesis. *J Immunol* (2007) 178(5):3143–52. doi:10.4049/jimmunol.178.5.3143
34. Novikov A, Cardone M, Thompson R, Shenderov K, Kirschman KD, Mayer-Barber KD, et al. *Mycobacterium tuberculosis* triggers host type I IFN signaling to regulate IL-1beta production in human macrophages. *J Immunol* (2011) 187(5):2540–7. doi:10.4049/jimmunol.1100926
35. Dey B, Dey RJ, Cheung LS, Pokkali S, Guo H, Lee JH, et al. A bacterial cyclic dinucleotide activates the cytosolic surveillance pathway and mediates innate resistance to tuberculosis. *Nat Med* (2015) 21(4):401–6. doi:10.1038/nm.3813
36. Etna MP, Giacomini E, Pardini M, Severa M, Bottai D, Cruciani M, et al. Impact of *Mycobacterium tuberculosis* RD1-locus on human primary dendritic cell immune functions. *Sci Rep* (2015) 5:17078. doi:10.1038/srep17078
37. Wassermann R, Gulen MF, Sala C, Perin SG, Lou Y, Rybniker J, et al. *Mycobacterium tuberculosis* differentially activates cGAS- and inflammasome-dependent intracellular immune responses through ESX-1. *Cell Host Microbe* (2015) 17(6):799–810. doi:10.1016/j.chom.2015.05.003
38. Watson RO, Bell SL, MacDuff DA, Kimmey JM, Diner EJ, Olivas J, et al. The cytosolic sensor cGAS detects *Mycobacterium tuberculosis* DNA to induce type I interferons and activate autophagy. *Cell Host Microbe* (2015) 17(6):811–9. doi:10.1016/j.chom.2015.05.004
39. Pandey AK, Yang Y, Jiang Z, Fortune SM, Coulombe F, Behr MA, et al. NOD2, RIP2 and IRF5 play a critical role in the type I interferon response to *Mycobacterium tuberculosis*. *PLoS Pathog* (2009) 5(7):e1000500. doi:10.1371/journal.ppat.1000500
40. Wathelet MG, Lin CH, Parekh BS, Ronco LV, Howley PM, Maniatis T. Virus infection induces the assembly of coordinately activated transcription factors on the IFN-beta enhancer in vivo. *Mol Cell* (1998) 1(4):507–18. doi:10.1016/S1097-2765(00)80051-9
41. Groschel MI, Sayes F, Simeone R, Majlessi L, Brosch R. ESX secretion systems: mycobacterial evolution to counter host immunity. *Nat Rev Microbiol* (2016) 14(11):677–91. doi:10.1038/nrmicro.2016.131
42. Conrad WH, Osman MM, Shanahan JK, Chu F, Takaki KK, Cameron J, et al. Mycobacterial ESX-1 secretion system mediates host cell lysis through bacterium contact-dependent gross membrane disruptions. *Proc Natl Acad Sci U S A* (2017) 114(6):1371–6. doi:10.1073/pnas.1620133114
43. Wiens KE, Ernst JD. The mechanism for type I interferon induction by *Mycobacterium tuberculosis* is bacterial strain-dependent. *PLoS Pathog* (2016) 12(8):e1005809. doi:10.1371/journal.ppat.1005809
44. Simeone R, Bobard A, Lippmann J, Bitter W, Majlessi L, Brosch R, et al. Phagosomal rupture by *Mycobacterium tuberculosis* results in toxicity and host cell death. *PLoS Pathog* (2012) 8(2):e1002507. doi:10.1371/journal.ppat.1002507
45. Watson RO, Manzanillo PS, Cox JS. Extracellular M. tuberculosis DNA targets bacteria for autophagy by activating the host DNA-sensing pathway. *Cell* (2012) 150(4):803–15. doi:10.1016/j.cell.2012.06.040
46. Leber JH, Crimmins GT, Raghavan S, Meyer-Morse NP, Cox JS, Portnoy DA. Distinct TLR- and NLR-mediated transcriptional responses to an intracellular pathogen. *PLoS Pathog* (2008) 4(1):e6. doi:10.1371/journal.ppat.0040006
47. Gandotra S, Jang S, Murray PJ, Salgame P, Ehrt S. Nucleotide-binding oligomerization domain protein 2-deficient mice control infection with *Mycobacterium tuberculosis*. *Infect Immun* (2007) 75(11):5127–34. doi:10.1128/iai.00458-07

48. Divangahi M, Mostowy S, Coulombe F, Kozak R, Guillot L, Veyrier F, et al. NOD2-deficient mice have impaired resistance to *Mycobacterium tuberculosis* infection through defective innate and adaptive immunity. *J Immunol* (2008) 181(10):7157–65. doi:10.4049/jimmunol.181.10.7157
49. Austin CM, Ma X, Graviss EA. Common nonsynonymous polymorphisms in the NOD2 gene are associated with resistance or susceptibility to tuberculosis disease in African Americans. *J Infect Dis* (2008) 197(12):1713–6. doi:10.1086/588384
50. Pan H, Dai Y, Tang S, Wang J. Polymorphisms of NOD2 and the risk of tuberculosis: a validation study in the Chinese population. *Int J Immunogenet* (2012) 39(3):233–40. doi:10.1111/j.1744-313X.2011.01079.x
51. Singh V, Gaur R, Mittal M, Biswas SK, Das R, Girdhar BK, et al. Absence of nucleotide-binding oligomerization domain-containing protein 2 variants in patients with leprosy and tuberculosis. *Int J Immunogenet* (2012) 39(4):353–6. doi:10.1111/j.1744-313X.2012.01085.x
52. Zhao M, Jiang F, Zhang W, Li F, Wei L, Liu J, et al. A novel single nucleotide polymorphism within the NOD2 gene is associated with pulmonary tuberculosis in the Chinese Han, Uygur and Kazak populations. *BMC Infect Dis* (2012) 12:91. doi:10.1186/1471-2334-12-91
53. Wang C, Chen ZL, Pan ZF, Wei LL, Xu DD, Jiang TT, et al. NOD2 polymorphisms and pulmonary tuberculosis susceptibility: a systematic review and meta-analysis. *Int J Biol Sci* (2013) 10(1):103–8. doi:10.7150/ijbs.7585
54. Collins AC, Cai H, Li T, Franco LH, Li XD, Nair VR, et al. Cyclic GMP-AMP synthase is an innate immune DNA sensor for *Mycobacterium tuberculosis*. *Cell Host Microbe* (2015) 17(6):820–8. doi:10.1016/j.chom.2015.05.005
55. Chen Q, Sun L, Chen ZJ. Regulation and function of the cGAS-STING pathway of cytosolic DNA sensing. *Nat Immunol* (2016) 17(10):1142–9. doi:10.1038/ni.3558
56. Ablasser A, Schmid-Burgk JL, Hemmerling I, Horvath GL, Schmidt T, Latz E, et al. Cell intrinsic immunity spreads to bystander cells via the intercellular transfer of cGAMP. *Nature* (2013) 503(7477):530–4. doi:10.1038/nature12640
57. Burdette DL, Monroe KM, Sotelo-Troha K, Iwig JS, Eckert B, Hyodo M, et al. STING is a direct innate immune sensor of cyclic di-GMP. *Nature* (2011) 478(7370):515–8. doi:10.1038/nature10429
58. Bai Y, Yang J, Zhou X, Ding X, Eisele LE, Bai G. *Mycobacterium tuberculosis* Rv3586 (DacA) is a diadenylate cyclase that converts ATP or ADP into c-di-AMP. *PLoS One* (2012) 7(4):e35206. doi:10.1371/journal.pone.0035206
59. Yang J, Bai Y, Zhang Y, Gabrielle VD, Jin L, Bai G. Deletion of the cyclic di-AMP phosphodiesterase gene (cnpB) in *Mycobacterium tuberculosis* leads to reduced virulence in a mouse model of infection. *Mol Microbiol* (2014) 93(1):65–79. doi:10.1111/mmi.12641
60. Dey RJ, Dey B, Zheng Y, Cheung LS, Zhou J, Sayre D, et al. Inhibition of innate immune cytosolic surveillance by an *M. tuberculosis* phosphodiesterase. *Nat Chem Biol* (2017) 13(2):210–7. doi:10.1038/nchembio.2254
61. Parvatiyar K, Zhang Z, Teles RM, Ouyang S, Jiang Y, Iyer SS, et al. The helicase DDX41 recognizes the bacterial secondary messengers cyclic di-GMP and cyclic di-AMP to activate a type I interferon immune response. *Nat Immunol* (2012) 13(12):1155–61. doi:10.1038/ni.2460
62. McFarland AP, Luo S, Ahmed-Qadri F, Zuck M, Thayer EF, Goo YA, et al. Sensing of bacterial cyclic dinucleotides by the oxidoreductase RECON promotes NF-kappaB activation and shapes a proinflammatory antibacterial state. *Immunity* (2017) 46(3):433–45. doi:10.1016/j.immuni.2017.02.014
63. Liang Q, Seo GJ, Choi YJ, Kwak MJ, Ge J, Rodgers MA, et al. Crosstalk between the cGAS DNA sensor and Beclin-1 autophagy protein shapes innate antimicrobial immune responses. *Cell Host Microbe* (2014) 15(2):228–38. doi:10.1016/j.chom.2014.01.009
64. Majlessi L, Prados-Rosales R, Casadevall A, Brosch R. Release of mycobacterial antigens. *Immunol Rev* (2015) 264(1):25–45. doi:10.1111/imr.12251
65. Kawai T, Akira S. Toll-like receptors and their crosstalk with other innate receptors in infection and immunity. *Immunity* (2011) 34(5):637–50. doi:10.1016/j.immuni.2011.05.006
66. Botos I, Segal DM, Davies DR. The structural biology of toll-like receptors. *Structure* (2011) 19(4):447–59. doi:10.1016/j.str.2011.02.004
67. Kang JY, Lee JO. Structural biology of the toll-like receptor family. *Annu Rev Biochem* (2011) 80:917–41. doi:10.1146/annurev-biochem-052909-141507
68. O'Neill LA, Golenbock D, Bowie AG. The history of toll-like receptors – redefining innate immunity. *Nat Rev Immunol* (2013) 13(6):453–60. doi:10.1038/nri3446
69. Kagan JC, Su T, Horng T, Chow A, Akira S, Medzhitov R. TRAM couples endocytosis of toll-like receptor 4 to the induction of interferon-beta. *Nat Immunol* (2008) 9(4):361–8. doi:10.1038/ni1569
70. Brown MG, McAlpine SM, Huang YY, Haidl ID, Al-Afif A, Marshall JS, et al. RNA sensors enable human mast cell anti-viral chemokine production and IFN-mediated protection in response to antibody-enhanced dengue virus infection. *PLoS One* (2012) 7(3):e34055. doi:10.1371/journal.pone.0034055
71. Nilsen NJ, Vladimer GI, Stenvik J, Orning MP, Zeid-Kilani MV, Bugge M, et al. A role for the adaptor proteins TRAM and TRIF in toll-like receptor 2 signaling. *J Biol Chem* (2015) 290(6):3209–22. doi:10.1074/jbc.M114.593426
72. Carmona J, Cruz A, Moreira-Teixeira L, Sousa C, Sousa J, Osorio NS, et al. *Mycobacterium tuberculosis* strains are differentially recognized by TLRs with an impact on the immune response. *PLoS One* (2013) 8(6):e67277. doi:10.1371/journal.pone.0067277
73. Moreira-Teixeira L, Sousa J, McNab FW, Torrado E, Cardoso F, Machado H, et al. Type I IFN inhibits alternative macrophage activation during *Mycobacterium tuberculosis* infection and leads to enhanced protection in the absence of IFN-gamma signaling. *J Immunol* (2016) 197(12):4714–26. doi:10.4049/jimmunol.1600584
74. Ferwerda G, Kullberg BJ, de Jong DJ, Girardin SE, Langenberg DM, van Crevel R, et al. *Mycobacterium paratuberculosis* is recognized by toll-like receptors and NOD2. *J Leukoc Biol* (2007) 82(4):1011–8. doi:10.1189/jlb.0307147
75. Pulido I, Leal M, Genebat M, Pacheco YM, Saez ME, Soriano-Sarabia N. The TLR4 ASP299GLY polymorphism is a risk factor for active tuberculosis in Caucasian HIV-infected patients. *Curr HIV Res* (2010) 8(3):253–8. doi:10.2174/157016210791111052
76. Ogus AC, Yoldas B, Ozdemir T, Uguz A, Olcen S, Keser I, et al. The Arg753GLn polymorphism of the human toll-like receptor 2 gene in tuberculosis disease. *Eur Respir J* (2004) 23(2):219–23. doi:10.1183/09031936.03.00061703
77. Ma X, Liu Y, Gowen BB, Graviss EA, Clark AG, Musser JM. Full-exon resequencing reveals toll-like receptor variants contribute to human susceptibility to tuberculosis disease. *PLoS One* (2007) 2(12):e1318. doi:10.1371/journal.pone.0001318
78. Etokebe GE, Skjeldal F, Nilsen N, Rodionov D, Knezevic J, Bulat-Kardum L, et al. Toll-like receptor 2 (P631H) mutant impairs membrane internalization and is a dominant negative allele. *Scand J Immunol* (2010) 71(5):369–81. doi:10.1111/j.1365-3083.2010.02379.x
79. Xue Y, Jin L, Li AZ, Wang HJ, Li M, Zhang YX, et al. Microsatellite polymorphisms in intron 2 of the toll-like receptor 2 gene and their association with susceptibility to pulmonary tuberculosis in Han Chinese. *Clin Chem Lab Med* (2010) 48(6):785–9. doi:10.1515/cclm.2010.154
80. Dalgic N, Tekin D, Kayaalti Z, Soylemezoglu T, Cakir E, Kilic B, et al. Arg753Gln polymorphism of the human toll-like receptor 2 gene from infection to disease in pediatric tuberculosis. *Hum Immunol* (2011) 72(5):440–5. doi:10.1016/j.humimm.2011.02.001
81. Wang JJ, Xia X, Tang SD, Wang J, Deng XZ, Zhang Y, et al. Meta-analysis on the associations of TLR2 gene polymorphisms with pulmonary tuberculosis susceptibility among Asian populations. *PLoS One* (2013) 8(10):e75090. doi:10.1371/journal.pone.0075090
82. Davila S, Hibberd ML, Hari Dass R, Wong HE, Sahiratmadja E, Bonnard C, et al. Genetic association and expression studies indicate a role of toll-like receptor 8 in pulmonary tuberculosis. *PLoS Genet* (2008) 4(10):e1000218. doi:10.1371/journal.pgen.1000218
83. Velez DR, Wejse C, Stryjewski ME, Abbate E, Hulme WF, Myers JL, et al. Variants in toll-like receptors 2 and 9 influence susceptibility to pulmonary tuberculosis in Caucasians, African-Americans, and West Africans. *Hum Genet* (2010) 127(1):65–73. doi:10.1007/s00439-009-0741-7
84. Xue Y, Zhao ZQ, Wang HJ, Jin L, Liu CP, Wang Y, et al. Toll-like receptors 2 and 4 gene polymorphisms in a southeastern Chinese population with tuberculosis. *Int J Immunogenet* (2010) 37(2):135–8. doi:10.1111/j.1744-313X.2009.00892.x
85. Kleinnijenhuis J, Oosting M, Joosten LA, Netea MG, Van Crevel R. Innate immune recognition of *Mycobacterium tuberculosis*. *Clin Dev Immunol* (2011) 2011:405310. doi:10.1155/2011/405310
86. Chen Z, Wang W, Liang J, Wang J, Feng S, Zhang G. Association between toll-like receptors 9 (TLR9) gene polymorphism and risk of pulmonary tuberculosis: meta-analysis. *BMC Pulm Med* (2015) 15:57. doi:10.1186/s12890-015-0049-4

87. Schurz H, Daya M, Moller M, Hoal EG, Salie M. TLR1, 2, 4, 6 and 9 variants associated with tuberculosis susceptibility: a systematic review and meta-analysis. *PLoS One* (2015) 10(10):e0139711. doi:10.1371/journal.pone.0139711
88. Schindler C, Levy DE, Decker T. JAK-STAT signaling: from interferons to cytokines. *J Biol Chem* (2007) 282(28):20059–63. doi:10.1074/jbc.R700016200
89. Manca C, Tsenova L, Bergtold A, Freeman S, Tovey M, Musser JM, et al. Virulence of a *Mycobacterium tuberculosis* clinical isolate in mice is determined by failure to induce Th1 type immunity and is associated with induction of IFN-alpha/beta. *Proc Natl Acad Sci U S A* (2001) 98(10):5752–7. doi:10.1073/pnas.091096998
90. Manca C, Tsenova L, Freeman S, Barczak AK, Tovey M, Murray PJ, et al. Hypervirulent M. tuberculosis W/Beijing strains upregulate type I IFNs and increase expression of negative regulators of the Jak-Stat pathway. *J Interferon Cytokine Res* (2005) 25(11):694–701. doi:10.1089/jir.2005.25.694
91. Dorhoi A, Yeremeev V, Nouailles G, Weiner J III, Jorg S, Heinemann E, et al. Type I IFN signaling triggers immunopathology in tuberculosis-susceptible mice by modulating lung phagocyte dynamics. *Eur J Immunol* (2014) 44(8):2380–93. doi:10.1002/eji.201344219
92. Mayer-Barber KD, Andrade BB, Oland SD, Amaral EP, Barber DL, Gonzales J, et al. Host-directed therapy of tuberculosis based on interleukin-1 and type I interferon crosstalk. *Nature* (2014) 511(7507):99–103. doi:10.1038/nature13489
93. Ordway D, Henao-Tamayo M, Harton M, Palanisamy G, Troudt J, Shanley C, et al. The hypervirulent *Mycobacterium tuberculosis* strain HN878 induces a potent TH1 response followed by rapid down-regulation. *J Immunol* (2007) 179(1):522–31. doi:10.4049/jimmunol.179.1.522
94. Desvignes L, Wolf AJ, Ernst JD. Dynamic roles of type I and type II IFNs in early infection with *Mycobacterium tuberculosis*. *J Immunol* (2012) 188(12):6205–15. doi:10.4049/jimmunol.1200255
95. Wiens KE, Ernst JD. Type I interferon is pathogenic during chronic *Mycobacterium africanum* Infection. *J Infect Dis* (2016) 214(12):1893–6. doi:10.1093/infdis/jiw519
96. Redford PS, Mayer-Barber KD, McNab FW, Stavropoulos E, Wack A, Sher A, et al. Influenza A virus impairs control of *Mycobacterium tuberculosis* coinfection through a type I interferon receptor-dependent pathway. *J Infect Dis* (2014) 209(2):270–4. doi:10.1093/infdis/jit424
97. Antonelli LR, Gigliotti Rothfuchs A, Goncalves R, Roffe E, Cheever AW, Bafica A, et al. Intranasal Poly-IC treatment exacerbates tuberculosis in mice through the pulmonary recruitment of a pathogen-permissive monocyte/macrophage population. *J Clin Invest* (2010) 120(5):1674–82. doi:10.1172/jci40817
98. Denis M. Recombinant murine beta interferon enhances resistance of mice to systemic *Mycobacterium avium* infection. *Infect Immun* (1991) 59(5):1857–9.
99. Kuchtey J, Fulton SA, Reba SM, Harding CV, Boom WH. Interferon-alphabeta mediates partial control of early pulmonary *Mycobacterium bovis* bacillus Calmette-Guerin infection. *Immunology* (2006) 118(1):39–49. doi:10.1111/j.1365-2567.2006.02337.x
100. Ruangkiattikul N, Nerlich A, Abdissa K, Lienenklaus S, Suwandi A, Janze N, et al. cGAS-STING-TBK1-IRF3/7 induced interferon-beta contributes to the clearing of non tuberculous mycobacterial infection in mice. *Virulence* (2017) 19:1–13. doi:10.1080/21505594.2017.1321191
101. Cooper AM, Pearl JE, Brooks JV, Ehlers S, Orme IM. Expression of the nitric oxide synthase 2 gene is not essential for early control of *Mycobacterium tuberculosis* in the murine lung. *Infect Immun* (2000) 68(12):6879–82. doi:10.1128/IAI.68.12.6879-6882.2000
102. Ward CM, Jyonouchi H, Kotenko SV, Smirnov SV, Patel R, Aguila H, et al. Adjunctive treatment of disseminated *Mycobacterium avium* complex infection with interferon alpha-2b in a patient with complete interferon-gamma receptor R1 deficiency. *Eur J Pediatr* (2007) 166(9):981–5. doi:10.1007/s00431-006-0339-1
103. Bax HI, Freeman AF, Ding L, Hsu AP, Marciano B, Kristosturyan E, et al. Interferon alpha treatment of patients with impaired interferon gamma signaling. *J Clin Immunol* (2013) 33(5):991–1001. doi:10.1007/s10875-013-9882-5
104. Lin SY, Chen TC, Lu PL, Lin CY, Lin WR, Yang YH, et al. Incidence rates of tuberculosis in chronic hepatitis C infected patients with or without interferon based therapy: a population-based cohort study in Taiwan. *BMC Infect Dis* (2014) 14:705. doi:10.1186/s12879-014-0705-y
105. Sabbatani S, Manfredi R, Marinacci G, Pavoni M, Cristoni L, Chiodo F. Reactivation of severe, acute pulmonary tuberculosis during treatment with pegylated interferon-alpha and ribavirin for chronic HCV hepatitis. *Scand J Infect Dis* (2006) 38(3):205–8. doi:10.1080/00365540500263268
106. Farah R, Awad J. The association of interferon with the development of pulmonary tuberculosis. *Int J Clin Pharmacol Ther* (2007) 45(11):598–600. doi:10.5414/CPP45598
107. Telesca C, Angelico M, Piccolo P, Nosotti L, Morrone A, Longhi C, et al. Interferon-alpha treatment of hepatitis D induces tuberculosis exacerbation in an immigrant. *J Infect* (2007) 54(4):e223–6. doi:10.1016/j.jinf.2006.12.009
108. Belkahla N, Kchir H, Maamouri N, Ouerghi H, Hariz FB, Chouaib S, et al. [Reactivation of tuberculosis during dual therapy with pegylated interferon and ribavirin for chronic hepatitis C]. *Rev Med Interne* (2010) 31(11):e1–3. doi:10.1016/j.revmed.2009.11.017
109. Guardigni V, Fabbri G, Grilli A, Contini C. Successful antiviral treatment of chronic hepatitis C in patients with rare comorbidities. Two case-reports. *Ann Hepatol* (2012) 11(3):404–8.
110. Palmero D, Eiguchi K, Rendo P, Castro Zorrilla L, Abbate E, Gonzalez Montaner LJ. Phase II trial of recombinant interferon-alpha2b in patients with advanced intractable multidrug-resistant pulmonary tuberculosis: long-term follow-up. *Int J Tuberc Lung Dis* (1999) 3(3):214–8.
111. Giosue S, Casarini M, Ameglio F, Zangrilli P, Palla M, Altieri AM, et al. Aerosolized interferon-alpha treatment in patients with multi-drug-resistant pulmonary tuberculosis. *Eur Cytokine Netw* (2000) 11(1):99–104.
112. Giosue S, Casarini M, Alemanno L, Galluccio G, Mattia P, Pedicelli G, et al. Effects of aerosolized interferon-alpha in patients with pulmonary tuberculosis. *Am J Respir Crit Care Med* (1998) 158(4):1156–62. doi:10.1164/ajrccm.158.4.9803065
113. Mansoori D, Tavana S, Mirsaeidi M, Yazdanpanah M, Sohrabpour H. The efficacy of interferon-α in the treatment of multidrug resistant tuberculosis. *Tanaffos* (2002) 1(3):29–34.
114. Zarogoulidis P, Kioumis I, Papanas N, Manika K, Kontakiotis T, Papagianis A, et al. The effect of combination IFN-alpha-2a with usual antituberculosis chemotherapy in non-responding tuberculosis and diabetes mellitus: a case report and review of the literature. *J Chemother* (2012) 24(3):173–7. doi:10.1179/1973947812y.0000000005
115. Gideon HP, Skinner JA, Baldwin N, Flynn JL, Lin PL. Early whole blood transcriptional signatures are associated with severity of lung inflammation in cynomolgus macaques with *Mycobacterium tuberculosis* infection. *J Immunol* (2016) 197(12):4817–28. doi:10.4049/jimmunol.1601138
116. Mayer-Barber KD, Sher A. Cytokine and lipid mediator networks in tuberculosis. *Immunol Rev* (2015) 264(1):264–75. doi:10.1111/imr.12249
117. Chin KL, Anis FZ, Sarmiento ME, Norazmi MN, Acosta A. Role of interferons in the development of diagnostics, vaccines, and therapy for tuberculosis. *J Immunol Res* (2017) 2017:5212910. doi:10.1155/2017/5212910
118. Mariotti S, Teloni R, Iona E, Fattorini L, Romagnoli G, Gagliardi MC, et al. *Mycobacterium tuberculosis* diverts alpha interferon-induced monocyte differentiation from dendritic cells into immunoprivileged macrophage-like host cells. *Infect Immun* (2004) 72(8):4385–92. doi:10.1128/iai.72.8.4385-4392.2004
119. Bouchonnet F, Boechat N, Bonay M, Hance AJ. Alpha/beta interferon impairs the ability of human macrophages to control growth of *Mycobacterium bovis* BCG. *Infect Immun* (2002) 70(6):3020–5. doi:10.1128/IAI.70.6.3020-3025.2002
120. Teles RM, Graeber TG, Krutzik SR, Montoya D, Schenk M, Lee DJ, et al. Type I interferon suppresses type II interferon-triggered human anti-mycobacterial responses. *Science* (2013) 339(6126):1448–53. doi:10.1126/science.1233665
121. McNab FW, Ewbank J, Howes A, Moreira-Teixeira L, Martirosyan A, Ghilardi N, et al. Type I IFN induces IL-10 production in an IL-27-independent manner and blocks responsiveness to IFN-gamma for production of IL-12 and bacterial killing in *Mycobacterium tuberculosis*-infected macrophages. *J Immunol* (2014) 193(7):3600–12. doi:10.4049/jimmunol.1401088
122. Kimmey JM, Campbell JA, Weiss LA, Monte KJ, Lenschow DJ, Stallings CL. The impact of ISGylation during *Mycobacterium tuberculosis* infection in mice. *Microbes Infect* (2017) 19(4–5):249–58. doi:10.1016/j.micinf.2016.12.006
123. Bogunovic D, Byun M, Durfee LA, Abhyankar A, Sanal O, Mansouri D, et al. Mycobacterial disease and impaired IFN-gamma immunity in humans with inherited ISG15 deficiency. *Science* (2012) 337(6102):1684–8. doi:10.1126/science.1224026

124. de Paus RA, van Wengen A, Schmidt I, Visser M, Verdegaal EM, van Dissel JT, et al. Inhibition of the type I immune responses of human monocytes by IFN-alpha and IFN-beta. *Cytokine* (2013) 61(2):645–55. doi:10.1016/j.cyto.2012.12.005
125. Marchant A, Amedei A, Azzurri A, Vekemans J, Benagiano M, Tamburini C, et al. Polarization of PPD-specific T-cell response of patients with tuberculosis from Th0 to Th1 profile after successful antimycobacterial therapy or in vitro conditioning with interferon-alpha or interleukin-12. *Am J Respir Cell Mol Biol* (2001) 24(2):187–94. doi:10.1165/ajrcmb.24.2.4274
126. Brinkmann V, Geiger T, Alkan S, Heusser CH. Interferon alpha increases the frequency of interferon gamma-producing human CD4+ T cells. *J Exp Med* (1993) 178(5):1655–63. doi:10.1084/jem.178.5.1655
127. Kavrochorianou N, Evangelidou M, Markogiannaki M, Tovey M, Thyphronitis G, Haralambous S. IFNAR signaling directly modulates T lymphocyte activity, resulting in milder experimental autoimmune encephalomyelitis development. *J Leukoc Biol* (2016) 99(1):175–88. doi:10.1189/jlb.3A1214-598R
128. Moreira-Teixeira L, Redford PS, Stavropoulos E, Ghilardi N, Maynard CL, Weaver CT, et al. T cell-derived IL-10 impairs host resistance to *Mycobacterium tuberculosis* infection. *J Immunol* (2017) 199(2):613–23. doi:10.4049/jimmunol.1601340
129. Schreiber T, Ehlers S, Heitmann L, Rausch A, Mages J, Murray PJ, et al. Autocrine IL-10 induces hallmarks of alternative activation in macrophages and suppresses antituberculosis effector mechanisms without compromising T cell immunity. *J Immunol* (2009) 183(2):1301–12. doi:10.4049/jimmunol.0803567
130. Domingo-Gonzalez R, Prince O, Cooper A, Khader SA. Cytokines and chemokines in *Mycobacterium tuberculosis* infection. *Microbiol Spectr* (2016) 4(5). doi:10.1128/microbiolspec.TBTB2-0018-2016
131. Lienard J, Movert E, Valfridsson C, Sturegard E, Carlsson F. ESX-1 exploits type I IFN-signalling to promote a regulatory macrophage phenotype refractory to IFNgamma-mediated autophagy and growth restriction of intracellular mycobacteria. *Cell Microbiol* (2016) 18(10):1471–85. doi:10.1111/cmi.12594
132. Fremond CM, Togbe D, Doz E, Rose S, Vasseur V, Maillet I, et al. IL-1 receptor-mediated signal is an essential component of MyD88-dependent innate response to *Mycobacterium tuberculosis* infection. *J Immunol* (2007) 179(2):1178–89. doi:10.4049/jimmunol.179.2.1178
133. Mayer-Barber KD, Barber DL, Shenderov K, White SD, Wilson MS, Cheever A, et al. Caspase-1 independent IL-1beta production is critical for host resistance to *Mycobacterium tuberculosis* and does not require TLR signaling in vivo. *J Immunol* (2010) 184(7):3326–30. doi:10.4049/jimmunol.0904189
134. Jayaraman P, Sada-Ovalle I, Nishimura T, Anderson AC, Kuchroo VK, Remold HG, et al. IL-1beta promotes antimicrobial immunity in macrophages by regulating TNFR signaling and caspase-3 activation. *J Immunol* (2013) 190(8):4196–204. doi:10.4049/jimmunol.1202688
135. Zhang G, Zhou B, Li S, Yue J, Yang H, Wen Y, et al. Allele-specific induction of IL-1beta expression by C/EBPbeta and PU.1 contributes to increased tuberculosis susceptibility. *PLoS Pathog* (2014) 10(10):e1004426. doi:10.1371/journal.ppat.1004426
136. Pilli M, Arko-Mensah J, Ponpuak M, Roberts E, Master S, Mandell MA, et al. TBK-1 promotes autophagy-mediated antimicrobial defense by controlling autophagosome maturation. *Immunity* (2012) 37(2):223–34. doi:10.1016/j.immuni.2012.04.015
137. Mayer-Barber KD, Andrade BB, Barber DL, Hieny S, Feng CG, Caspar P, et al. Innate and adaptive interferons suppress IL-1alpha and IL-1beta production by distinct pulmonary myeloid subsets during *Mycobacterium tuberculosis* infection. *Immunity* (2011) 35(6):1023–34. doi:10.1016/j.immuni.2011.12.002
138. Mishra BB, Rathinam VA, Martens GW, Martinot AJ, Kornfeld H, Fitzgerald KA, et al. Nitric oxide controls the immunopathology of tuberculosis by inhibiting NLRP3 inflammasome-dependent processing of IL-1beta. *Nat Immunol* (2013) 14(1):52–60. doi:10.1038/ni.2474
139. Shah S, Bohsali A, Ahlbrand SE, Srinivasan L, Rathinam VA, Vogel SN, et al. Cutting edge: *Mycobacterium tuberculosis* but not nonvirulent mycobacteria inhibits IFN-beta and AIM2 inflammasome-dependent IL-1beta production via its ESX-1 secretion system. *J Immunol* (2013) 191(7):3514–8. doi:10.4049/jimmunol.1301331
140. Saiga H, Kitada S, Shimada Y, Kamiyama N, Okuyama M, Makino M, et al. Critical role of AIM2 in *Mycobacterium tuberculosis* infection. *Int Immunol* (2012) 24(10):637–44. doi:10.1093/intimm/dxs062
141. McElvania Tekippe E, Allen IC, Hulseberg PD, Sullivan JT, McCann JR, Sandor M, et al. Granuloma formation and host defense in chronic *Mycobacterium tuberculosis* infection requires PYCARD/ASC but not NLRP3 or caspase-1. *PLoS One* (2010) 5(8):e12320. doi:10.1371/journal.pone.0012320
142. Keller C, Lauber J, Blumenthal A, Buer J, Ehlers S. Resistance and susceptibility to tuberculosis analysed at the transcriptome level: lessons from mouse macrophages. *Tuberculosis (Edinb)* (2004) 84(3–4):144–58. doi:10.1016/j.tube.2003.12.003
143. Mishra BB, Lovewell RR, Olive AJ, Zhang G, Wang W, Eugenin E, et al. Nitric oxide prevents a pathogen-permissive granulocytic inflammation during tuberculosis. *Nat Microbiol* (2017) 2:17072. doi:10.1038/nmicrobiol.2017.72
144. Lozza L, Farinacci M, Fae K, Bechtle M, Staber M, Dorhoi A, et al. Crosstalk between human DC subsets promotes antibacterial activity and CD8+ T-cell stimulation in response to bacille Calmette-Guerin. *Eur J Immunol* (2014) 44(1):80–92. doi:10.1002/eji.201343797
145. Lozza L, Farinacci M, Bechtle M, Staber M, Zedler U, Baiocchini A, et al. Communication between human dendritic cell subsets in tuberculosis: requirements for naive CD4(+) T cell stimulation. *Front Immunol* (2014) 5:324. doi:10.3389/fimmu.2014.00324
146. Kalie E, Jaitin DA, Podoplelova Y, Piehler J, Schreiber G. The stability of the ternary interferon-receptor complex rather than the affinity to the individual subunits dictates differential biological activities. *J Biol Chem* (2008) 283(47):32925–36. doi:10.1074/jbc.M806019200
147. Strunk JJ, Gregor I, Becker Y, Li Z, Gavutis M, Jaks E, et al. Ligand binding induces a conformational change in ifnar1 that is propagated to its membrane-proximal domain. *J Mol Biol* (2008) 377(3):725–39. doi:10.1016/j.jmb.2008.01.017
148. de Weerd NA, Vivian JP, Nguyen TK, Mangan NE, Gould JA, Braniff SJ, et al. Structural basis of a unique interferon-beta signaling axis mediated via the receptor IFNAR1. *Nat Immunol* (2013) 14(9):901–7. doi:10.1038/ni.2667
149. Wu K, Wong KW, Deng WL, Zhang H, Li J, Lowrie DB, et al. The numerical predominance and large transcriptome differences of neutrophils in peripheral blood together inevitably account for a reported pulmonary tuberculosis signature. *Int J Genomics* (2017) 2017:5830971. doi:10.1155/2017/5830971
150. Davidson S, Crotta S, McCabe TM, Wack A. Pathogenic potential of interferon alphabeta in acute influenza infection. *Nat Commun* (2014) 5:3864. doi:10.1038/ncomms4864

Conflict of Interest Statement: The authors declare that the research was conducted in the absence of any commercial or financial relationships that could be construed as a potential conflict of interest.

Copyright © 2017 Donovan, Schultz, Duke and Blumenthal. This is an open-access article distributed under the terms of the Creative Commons Attribution License (CC BY). The use, distribution or reproduction in other forums is permitted, provided the original author(s) or licensor are credited and that the original publication in this journal is cited, in accordance with accepted academic practice. No use, distribution or reproduction is permitted which does not comply with these terms.

frontiers in Immunology

ORIGINAL RESEARCH
published: 05 April 2018
doi: 10.3389/fimmu.2018.00495

De Novo Fatty Acid Synthesis During Mycobacterial Infection Is a Prerequisite for the Function of Highly Proliferative T Cells, But Not for Dendritic Cells or Macrophages

*Philipp Stüve[1†], Lucía Minarrieta[1†], Hanna Erdmann[2], Catharina Arnold-Schrauf[1], Maxine Swallow[1], Melanie Guderian[1], Freyja Krull[1], Alexandra Hölscher[2], Peyman Ghorbani[1], Jochen Behrends[3], Wolf-Rainer Abraham[4], Christoph Hölscher[2], Tim D. Sparwasser[1] and Luciana Berod[1]**

[1] Institute of Infection Immunology, TWINCORE, Centre for Experimental and Clinical Infection Research, A Joint Venture Between the Medical School Hannover (MHH) and the Helmholtz Centre for Infection Research (HZI), Hannover, Germany, [2] Infection Immunology, Research Center Borstel, Borstel, Germany, [3] Core Facility Fluorescence Cytometry, Research Center Borstel, Borstel, Germany, [4] Department of Chemical Microbiology, Helmholtz Centre for Infection Research, Braunschweig, Germany

OPEN ACCESS

Edited by:
Geanncarlo Lugo-Villarino, UMR5089 Institut de Pharmacologie et de Biologie Structurale (IPBS), France

Reviewed by:
Gerald Larrouy-Maumus, Imperial College London, United Kingdom
Maximiliano Gutierrez, Francis Crick Institute, United Kingdom
Roland Lang, Universitätsklinikum Erlangen, Germany

***Correspondence:**
Luciana Berod
luciana.berod@twincore.de

[†]These authors have contributed equally to this work.

Specialty section:
This article was submitted to Microbial Immunology, a section of the journal Frontiers in Immunology

Received: 25 October 2017
Accepted: 26 February 2018
Published: 05 April 2018

Citation:
Stüve P, Minarrieta L, Erdmann H, Arnold-Schrauf C, Swallow M, Guderian M, Krull F, Hölscher A, Ghorbani P, Behrends J, Abraham W-R, Hölscher C, Sparwasser TD and Berod L (2018) De Novo Fatty Acid Synthesis During Mycobacterial Infection Is a Prerequisite for the Function of Highly Proliferative T Cells, But Not for Dendritic Cells or Macrophages. Front. Immunol. 9:495. doi: 10.3389/fimmu.2018.00495

Mycobacterium tuberculosis (*Mtb*), the causative agent of human tuberculosis, is able to efficiently manipulate the host immune system establishing chronic infection, yet the underlying mechanisms of immune evasion are not fully understood. Evidence suggests that this pathogen interferes with host cell lipid metabolism to ensure its persistence. Fatty acid metabolism is regulated by acetyl-CoA carboxylase (ACC) 1 and 2; both isoforms catalyze the conversion of acetyl-CoA into malonyl-CoA, but have distinct roles. ACC1 is located in the cytosol, where it regulates *de novo* fatty acid synthesis (FAS), while ACC2 is associated with the outer mitochondrial membrane, regulating fatty acid oxidation (FAO). In macrophages, mycobacteria induce metabolic changes that lead to the cytosolic accumulation of lipids. This reprogramming impairs macrophage activation and contributes to chronic infection. In dendritic cells (DCs), FAS has been suggested to underlie optimal cytokine production and antigen presentation, but little is known about the metabolic changes occurring in DCs upon mycobacterial infection and how they affect the outcome of the immune response. We therefore determined the role of fatty acid metabolism in myeloid cells and T cells during *Mycobacterium bovis* BCG or *Mtb* infection, using novel genetic mouse models that allow cell-specific deletion of ACC1 and ACC2 in DCs, macrophages, or T cells. Our results demonstrate that *de novo* FAS is induced in DCs and macrophages upon *M. bovis* BCG infection. However, ACC1 expression in DCs and macrophages is not required to control mycobacteria. Similarly, absence of ACC2 did not influence the ability of DCs and macrophages to cope with infection. Furthermore, deletion of ACC1 in DCs or macrophages had no effect on systemic pro-inflammatory cytokine production or T cell priming, suggesting that FAS is dispensable for an intact innate response against mycobacteria. In contrast, mice with a

deletion of ACC1 specifically in T cells fail to generate efficient T helper 1 responses and succumb early to *Mtb* infection. In summary, our results reveal ACC1-dependent FAS as a crucial mechanism in T cells, but not DCs or macrophages, to fight against mycobacterial infection.

Keywords: dendritic cells, macrophages, acetyl-CoA carboxylase 1, acetyl-CoA carboxylase 2, *Mycobacterium tuberculosis*, *Mycobacterium bovis* BCG, fatty acid synthesis, fatty acid oxidation

INTRODUCTION

Mycobacterium tuberculosis (*Mtb*), the causative agent of tuberculosis (Tb), remains a major health problem worldwide, a situation that becomes aggravated by increasing cases of multidrug-resistant strains. One of the main obstacles for the eradication of Tb is the enormous reservoir of chronically infected patients, estimated as up to two billion people. Of them, 5–10% will develop active disease. Consequently, a better understanding of the basic mechanisms employed by the pathogen to persist within the host is of major importance to design therapeutic strategies aiming at completely eliminating the bacteria. *Mtb* is usually transmitted *via* aerosol droplets. Once in the lungs, mycobacteria are recognized and phagocytosed by alveolar macrophages (AMs) and patrolling dendritic cells (DCs). AMs serve as a niche for initial bacterial replication, until these cells die by apoptosis or necrosis and mycobacteria spread to the extracellular space where they can be detected by other mononuclear cells. This initiates an inflammatory response that leads to the formation of the granuloma and containment of bacterial growth. Macrophages exert a pivotal role in this process through different microbicidal mechanisms (1), including nutrient restriction, the production of reactive oxygen and nitrogen species (ROS; RNS), and the induction of autophagy (1–3). Despite this, *Mtb* has acquired the capacity to persist in macrophages for long periods of time, exploiting the host cell machinery for its own purposes.

Emerging evidence suggests that *Mtb* pathogenicity is related to the manipulation of core metabolic pathways in the host cell. Under normal physiological conditions, immune cells are relatively quiescent and rely on the process of oxidative phosphorylation (OXPHOS) in the mitochondria to obtain energy for their housekeeping functions. Infection with *Mtb* leads to an induction in aerobic glycolysis as evidenced by high lactate levels and increased expression of glycolytic enzymes in the lungs of infected mice (4). Additionally, genome-wide transcriptional profiling of lung granulomas from patients with active Tb revealed increased activity of the glycolytic pathway (5). Aerobic glycolysis was first described in the 1920s by the German Nobel laureate Otto Warburg for tumor cells and refers to the conversion of glucose to lactate in the presence of oxygen. Although this process has long been attributed to highly proliferative cells, it has recently become evident that macrophages also make use of this metabolic pathway to sustain specific functions. For example, augmented glycolytic flux is a signature of classically activated "M1" macrophages (6, 7) and has also been observed in bone marrow-derived macrophages (BMDMs) and AMs upon infection with different *Mtb* strains (8–10). Engagement of the glycolytic pathway by *Mtb* results in increased lipid metabolism, thus promoting lipid body (LB) formation and differentiation into "foamy" macrophages, a hallmark of granulomas in patients with Tb (11, 12). LBs, consisting of triacylglycerols and sterol esters, may serve as a source of nutrients and building blocks for *Mtb*, as suggested by the finding that *Mtb* resides closely associated to LBs within macrophages (12). Strikingly, *Mtb* survival depends on these host lipids. Lipid accumulation in macrophages diminishes their mycobacterial killing capacity through inhibition of autophagy and lysosome acidification (13, 14). However, how lipid metabolism affects other macrophage functions remains unknown. Furthermore, the mechanisms by which *Mtb* induces LB formation and foam cell differentiation are not fully understood. Recent studies suggested that accumulation of LBs relies on the induction of *de novo* cholesterol and fatty acid synthesis (FAS) and the generation of the ketone body D-3-hydroxybutyrate by the host cell (9, 14). Moreover, while early-secreted antigenic target (ESAT-6), the main virulence factor of *Mtb*, has been identified as a main factor contributing to LB formation (9, 15), LBs can also be found in macrophages infected with avirulent *Mycobacterium bovis* BCG, suggesting diverse mechanisms behind this phenomenon (16).

In contrast to macrophages, DCs are not specialized in the killing of mycobacteria (17, 18), but instead are essential for the induction of adaptive immunity by transporting antigens to the lung draining lymph nodes, secreting inflammatory IL-12, and subsequently priming naïve T cells to become T helper 1 (Th1) cells (19, 20). The control of mycobacterial infection largely depends on these Th1 cells that secrete IFN-γ, and thereby promote mycobacterial control by activating macrophages (21). In accordance, depletion of $CD11c^+$ DCs results in diminished generation of antigen-specific Th1 cells and increased bacterial burden (22). DCs are categorized into different subpopulations according to their function and localization, playing specific roles during mycobacterial infection. The involvement of certain DC subsets depends on the route of infection. Following intravenous (i.v.) infection, mycobacteria will be mostly encountered by $CD8^+$ DCs that are present in the spleen. These $CD8^+$ DCs mediate protective immunity by secreting IL-12 to induce IFN-γ production by Th1 cells (23–25) and by cross-presenting antigen to $CD8^+$ T cells. Conversely, upon aerosol infection, most bacteria reside in the lungs, which contain only $CD103^+$ DCs and $CD11b^+$ DCs, but no $CD8^+$ DCs (26). *Mtb*-resistant mouse strains (C57BL/6 and BALB/c) display higher numbers of $CD103^+$ DCs in the

Abbreviations: *Mtb*, *Mycobacterium tuberculosis*; BMDMs, bone marrow-derived macrophages; GM-CSF, granulocyte-macrophage colony-stimulating factor; Itgax, integrin alpha X; LysM, lysozyme M; p.i., post infection; FAS, fatty acid synthesis; FAO, fatty acid oxidation; ACC, acetyl-CoA carboxylase; CPT1, carnitine palmitoyltransferase 1.

lungs than the susceptible strain DBA/2 (27), suggesting that this subpopulation might be involved in mediating protection. However, the exact role of CD103$^+$ DCs during mycobacterial infection remains unclear.

We previously showed that activation of DCs *via* the toll-like receptor (TLR)/MyD88 pathway is crucial for mycobacterial protection (28). In granulocyte-macrophage colony-stimulating factor (GM-CSF)-derived DCs, TLR/MyD88 ligation leads to a rapid metabolic reprogramming from OXPHOS toward aerobic glycolysis (29, 30). This early increase in glycolytic flux was proposed to support *de novo* FAS for the expansion of membranes in the ER and Golgi apparatus (30). Pharmacological inhibition of *de novo* FAS impairs GM-CSF DC cytokine production and activation upon TLR stimulation (30). Consequently, it has been suggested that engagement of this metabolic pathway might be relevant for full DC function. In contrast, in tumor-bearing mice and cancer patients, high lipid content in DCs led to functional impairment and uncontrolled tumor growth (31). However, the importance of this pathway *in vivo* has not yet been investigated and no studies on the role of FAS for the function of DCs during mycobacterial infection have been conducted.

Acetyl-CoA carboxylase (ACC) 1 and 2 (ACC1 and ACC2) are the rate-limiting enzymes for FAS and fatty acid oxidation (FAO). Both enzymes catalyze the same biochemical reaction, the ATP-dependent carboxylation of acetyl-CoA to malonyl-CoA. While ACC1 is located in the cytoplasm, ACC2 is associated with the outer mitochondrial membrane, where it controls FAO by regulating import of long chain fatty acids into the mitochondria *via* the carnitine palmitoyltransferase 1 (CPT1) (32). We have previously shown that during autoimmunity, ACC1 expression and *de novo* FAS are essential for the differentiation of naïve T cells toward inflammatory T effector lineages (33–35). In this study, we investigated the importance of ACC1 and ACC2 for DC, macrophage and T cell activation and their capacity to induce protective immunity against mycobacterial infection. Our results suggest that while ACC1 and ACC2 expression in DCs and macrophages is dispensable for mycobacterial control, T cells greatly depend on ACC1 and *de novo* FAS to cope with infection.

MATERIALS AND METHODS

Mice

All mice were bred and kept under specific pathogen-free conditions at the animal facility of the Helmholtz Center for Infection Research (HZI, Braunschweig, Germany) or at TWINCORE (Hannover, Germany). C57BL/6 mice were purchased from Jackson Laboratories or bred in house. ACC1$^{flox/flox}$ mice (36), Acaca$^{flox/flox}$ (37), or ACC2$^{flox/flox}$ mice (38) were crossed to the following *cre*-expressing lines: CD4-*cre* mice (39) (TACC1), LysM-*cre* (40) (MΦ_ACC1 and MΦ_Acaca), or Itgax-*cre* (41) (DC_ACC1 and DC_Acaca) and maintained on a C57BL/6 genetic background. ACC2 knockout mice (42) were backcrossed to C57BL/6 background. Furthermore, P25ktk transgenic mice were used and bred in the same institutions (43). Sex- and age-matched littermates between 8 and 16 weeks of age were used for all experiments.

Mycobacterial Infections

Mycobacterium bovis BCG overexpressing Ag85B (*M. bovis* BCG Ag85B) was kindly provided by Dr. Joel Ernst (NYU School of Medicine, USA), *M. bovis* BCG GFP by Dr. Camille Locht (University of Lille), and *M. bovis* BCG RFP by Dr. Nathalie Winter (French National Institute for Agricultural Research). All strains were grown at 37°C in Middlebrook 7H9 broth (BD Biosciences) supplemented with 10% Middlebrook OADC enrichment medium (BD Biosciences), 0.002% glycerol (Roth), and 0.05% Tween 80 (Roth). Midlog phase cultures were harvested, aliquoted, and frozen at −80°C. For *in vitro* infections BCG strains were prepared as previously described (44) and cells infected with different multiplicities of infection (MOI). Bacteria for *in vivo* infections were prepared from frozen stocks by thawing at 37°C, washing with PBS 0.025% Tween 80 (PBS-T), and passaging through a 27 gauge needle. Mice were infected intravenously (i.v.) with 2×10^6 colony forming units (CFU). For *Mtb* infections, the *Mtb* strain H37Rv was grown and prepared as described previously (45). Mice were infected with a low (100 CFU) or a high dose (1,000 CFU) by aerosol exposure. *Mtb*-infected mice were scored according to Morton and Griffiths (46). According to the local animal welfare guidelines, mice that reached a score of >3.0 had to be euthanized.

Colony Enumeration Assay

To determine CFU, mice were sacrificed 21 days p.i. (for *M. bovis* BCG) or at different time points p.i. (for *Mtb*). Liver, spleen, and lungs were removed and organs were plated in serial dilutions as described previously (28, 45). CFU were enumerated after incubation at 37°C for 3 weeks. Data are presented as $\log_{10}$ CFU per organ.

Generation of iCD103 DCs, GM-CSF DCs, and BMDMs

Dendritic cell and macrophage cultures were started from BM cells, which were isolated from murine femurs and tibiae. iCD103 DCs were generated as described previously (47). In brief, BM cells were cultured in complete RPMI (cRPMI) 1640 GlutaMAX medium (Thermo Fisher Scientific), supplemented with 10% heat-inactivated FCS (Biochrom), 500 U penicillin-streptomycin (PAA laboratories), and 50 µM β-mercaptoethanol (Thermo Fisher Scientific) with a combination of GM-CSF and FLT3L (both self-made) for 9 days, followed by re-plating with both growth factors for additional 7 days at 37°C with 5% CO_2. For generating GM-CSF DCs, BM cells were cultured in cRPMI supplemented with 5% culture supernatant of a GM-CSF-producing cell line (48). For generating BMDMs, BM cells were incubated in cRPMI supplemented with L929 cell conditioned medium (LCCM; self-made) as a source of murine M-CSF for 7 days. After 3 days, half of the medium was replenished by fresh medium containing LCCM. Flt3-L-producing CHO Flt3-L FLAG cells were generated by Dr. Nicos Nicola and kindly provided by Dr. Karen Murphy (WEHI, Melbourne, VIC, Australia). The LCCM producing L929 cell line was kindly provided by Dr. Roland Lang (Universitätsklinikum Erlangen, Erlangen, Germany).

In Vitro Infection and Activation of iCD103 DCs and BMDMs

iCD103 DCs and BMDMs were harvested on day 16 or 7, respectively. A gradient with Optiprep (Progen Biotechnik) was performed to deplete the cell suspensions from dead cells. Cells were stimulated with CpG-B 1826 (1 μM; TIB MOLBIOL) or LPS (100 ng/mL, *E. coli* Serotype 055:B5; Sigma) or infected with the BCG strains mentioned above at different MOIs. Infection was monitored by evaluating the frequency of GFP^+ or RFP^+ cells by flow cytometry or confocal microscopy. As a positive control of complete blockade of ACC activity, cells were treated with SorA (1 μM; kindly provided by Dr. Rolf Müller, Helmholtz Institute for Pharmaceutical Research Saarland) or 5-(Tetradecyloxy)-2-furoic acid (TOFA) (20 μM; Enzo Life Sciences) during stimulation.

Flow Cytometry

The following monoclonal antibodies specific to mouse antigens and labeled with the indicated fluorescent markers were purchased from eBioscience/Thermo Fisher Scientific: CD3e eFluor450 (17A2), CD19 eFluor450 (eBio1D3), CD4 eFluor450 (RM4-5), CD4 Alexa488, CD4 eFluor660, CD4 PE-Cy7 (all GK1.5), CD8a (Ly-2) FITC, CD8a (Ly-2) eFluor450 (both 53-6.7), CD45.1 APC (A20) FoxP3 eFluor450, FoxP3 PE (both FJK-16s), CD62L PE-Cy7, CD62L PE, CD62L APC-eFluor780 (all MEL-14), IL-17A APC, IL-17A PE-Cy7 (both eBio17B7), IFN-γ FITC, IFN-γ PE, IFN-γ PE-Cy7 (all XMG1.2), CD11c (Integrin alpha chain) eFluor660, CD11c PE, CD11c APC-eFluor780 (all N418), CD11b PE, CD11b FITC (both M1/70), NK1.1 eFluor450 (PK136), CD45R/B220 PE-Cy7, CD45R/B220 PE (both RA3-6B2), CD86 (I-A/I-E) APC, CD86 (I-A/I-E) FITC (both GL1), MHC-II FITC, MHC-II eFluor450 (both M5/114.15.2), F4/80 eFluor450, F4/80 eFluor660 (both BM8), TCRbeta APC-eFluor780 (H57-597), CD90.2 APC-e780 (53-2.1), rat IgG1, κ isotype control FITC, rat IgG2a, κ isotype control FITC, rat IgG2b, and κ isotype control eFluor450. IL-10 PE (JES5-16E3), CD103 PB (2E7), CD44 FITC (IM7), and IFN-γ (XMG1.2) were purchased from Biolegend and CD4 V450 (RM4-5), CD25 APC (PC61), and CD62L PE (MEL-14) were purchased from BD. The $I\text{-}A^b$ ESAT-6 (4-17) APC tetramer was provided by the NIH Tetramer Core Facility, Emory University Vaccine Center, Atlanta, GA, USA. To analyze intracellular cytokine production by T cells *ex vivo*, cells were stimulated with phorbol 12-myristate 13-acetate (PMA, 100 ng/mL; Sigma-Aldrich) and ionomycin (1 μg/mL; Sigma-Aldrich) for 2 h followed by additional 2 h with Brefeldin A (5 μg/mL; eBioscience/Thermo Fisher Scientific). Where indicated, cells were alternatively stimulated with 5 μg/mL plate-bound anti-CD3/CD28 (clones 145-2C11 and 37.5, respectively; BD). To analyze intracellular cytokine production by iCD103 DCs and BMDMs, cells were stimulated or infected for a total of 6 h and incubated with Brefeldin A (5 μg/mL; eBioscience/Thermo Fisher Scientific) for the last 4 h. Intracellular staining was performed after fixation with paraformaldehyde (2%; Roth) and permeabilization with PBA-S buffer (0.5% Saponin and 0.25% BSA in PBS; both Roth). For FoxP3 staining, the FoxP3/Transcription Factor Fixation/Permeabilization Kit (eBioscience/Thermo Fisher Scientific) was used according to the manufacturer's instruction. For assessing DC activation *in vivo*, spleens were digested using Collagenase D (500 μg/mL; Roche) and DNase I (50 μg/mL; Roche) for 30 min at 37°C. The uptake of palmitate was determined by incubating cells in 100 μL PBS with 1 μg/mL Bodipy FL C_{16} (Thermo Fisher Scientific) at 37°C for 30 min.

The accumulation of lipids was evaluated using HCS LipidTOX™ Phospholipidosis and Steatosis Detection Kit (catalog number H34158; Thermo Fisher Scientific), which contains LipidTOX™ Red phospholipid stain and LipidTOX™ Green neutral lipid stain. For the detection of phospholipids, LipidTOX™ Red was added to the cells together with the stimuli or bacteria. For assessing the accumulation of neutral lipids, cells were stained with LipidTOX™ Green neutral lipid stain after treatment and PFA fixation according to the manufacturer's instructions. Data acquisition was conducted on a CyAn ADP (Beckman Coulter) or a LSR II (Becton Dickinson), and data were analyzed with FlowJo software (Tree Star).

In Vitro T Cell Proliferation Assay

iCD103 DCs or BMDMs were infected with different MOIs of *M. bovis* BCG Ag85B for 24 h in the presence or absence of SorA, washed four times and incubated at a 1:6 ratio (25,000 DCs/BMDMs:150,000 T cells) with naïve ($CD4^+CD25^-$) T cells obtained from spleen and lymph nodes of P25ktk mice. Naïve cells were enriched by negative magnetic cell sorting using the Dynal Mouse CD4 negative T cell isolation kit following the manufacturer's protocol (Thermo Fisher Scientific). $CD25^+$ cells were depleted by including an anti-CD25 functional grade antibody (clone PC61.5; eBioscience/Thermo Fisher Scientific) to the antibody cocktail for negative selection. After enrichment, cells were labeled with CellTrace Violet Cell Proliferation Kit (Thermo Fisher Scientific), as per manufacturer's instructions. For Th17 cell induction, cells were cultured in complete IMDM GlutaMAX medium (Thermo Fisher Scientific) containing rhTGF-β1 (2 ng/mL; Peprotech), anti-IFN-γ (5 μg/mL, clone XMG1.2; Bio X Cell), anti-IL-4 (5 μg/mL, clone 11B11; Bio X Cell), and anti-IL-12 (5 μg/mL, clone 17.8; Bio X Cell). For Th0 conditions, cells were cultured in plain cRPMI. Soluble CD3 (1 μg/mL, clone 145-2C11; Bio X Cell) or P25 peptide (10 μg/mL; Department of Chemical Biology, HZI Braunschweig) were used as positive controls. Co-cultures were performed for 4 days in 96-well round bottom (Th0) or flat bottom plates (Th17). Proliferation and cytokine production were determined by intracellular flow cytometry staining.

In Vivo T Cell Priming

WT or DC_ACC1 mice were infected with *M. bovis* BCG as described above. On day 9 p.i., $2–3 \times 10^6$ CellTrace Violet labeled $CD4^+$ T cells from P25ktk x CD45.1 mice were adoptively transferred i.v. After 5 days, mice were sacrificed and proliferation as well as cytokine production was determined upon PMA/ionomycin re-stimulation by intracellular flow cytometry staining.

$ESAT6_{1–20}$-Specific ELISPOT Assay

For measuring the frequency of antigen-specific $CD4^+$ T cells after *Mtb* infection, single cell suspensions from lungs were prepared and collected in complete IMDM. Lung cells were stimulated for 20 h with mitomycin-D (Sigma-Aldrich)-inactivated spleen cells from uninfected mice that had been pulsed with the MHC class

II peptide ESAT-6_{1-20} (Research Center Borstel). Detection of antigen-specific IFN-γ-producing $CD4^+$ T cells was conducted using ELISPOT assay kits as described by the manufacturer (BD Bioscience and R&D Systems, respectively). Spots were automatically enumerated using an ELISPOT reader (ELISPOT 04 XL; AID) and the frequency of cytokine-producing cells was determined.

Incorporation Assays

For ^{13}C incorporation analysis, [U-$^{13}C_6$] glucose (1 mM; Cambridge Isotope Laboratories) or [U-$^{13}C_{16}$] palmitate (1 μM; Cambridge Isotope Laboratories) was added at the onset of the *in vitro* infection experiments. To determine the incorporation of glucose- or palmitate-derived carbon into cellular fatty acids, cells were saponified [MeOH:NaOH (15%) 1:1, 1 h, 100°C], derivatized [MeOH:HCl 10:2, 10 min, 80°C] and then prepared for analysis on a gas chromatography-combustion-isotope ratio mass spectrometer (GC/C/IRMS) as described earlier (49). GC/C/IRMS measurements were performed in triplicate on a Finnigan MAT 253 isotope ratio mass spectrometer coupled with a Trace GC Ultra (Thermo Fisher Scientific) chromatograph *via* a combustion interface. The fatty acid methyl esters were separated with an Optima five column (5% phenyl, 95% dimethylpolysiloxane, 50 m, 0.32 mm inner diameter, and 0.25 μm film thickness). The oven program was 100°C for 2 min, increased to 290°C at 4°C min^{-1}, followed by an isothermal period of 8 min. The separated compounds were combusted on line in an oxidation oven. $^{13}C/^{12}C$ isotope ratios for the free fatty acids were calculated as described (49) and are presented as $\delta^{13}C$ in the figures.

Confocal Microscopy

iCD103 DCs and BMDMs were infected with *M. bovis* BCG GFP to check the infection rate. After 24 h, Hoechst 33342 was used to stain nuclei and cells were loaded in VI 0.5 μ-slides (Ibidi). Confocal microscopic images were taken on an Olympus FV1000 system using a 60× oil objective. All images were equally adjusted using Fiji software (NIH).

ELISA

Supernatants from iCD103 DCs and BMDM infected with different MOIs of *M. bovis* BCG were taken 4 or 24 h p.i. Serum samples from infected mice were collected by heart puncture on the day of analysis. The concentration of IL-12/23p40, IL-6, TNF-α, IL-10, IL-1β, and IFN-γ was determined by ELISA according to the manufacturer's instructions (Duo Set; R&D).

Nitrite Assay

Nitrite levels were determined in culture supernatants from iCD103 DCs and BMDMs after 24 h of stimulation as an indicator of nitric oxide (NO) production using the Griess reagent system (Promega), as per manufacturer's instructions.

Cell Sorting

Mice were euthanized by CO_2 inhalation. For alveolar macrophage isolation, mice were perfused with 5 mL PBS. Lung lobes were separated from the trachea, chopped, and incubated in digestion media, containing RPMI 1640 GlutaMAX medium (Thermo Fisher Scientific) supplemented with 5% FCS (Biochrom), containing 2.2 mg/mL collagenase D (Sigma-Aldrich) and 0.055 mg/mL DNase I (Roche) for 30 min at 37°C. For splenic DCs and macrophages, spleens were minced and incubated in digestion media for 30 min at 37°C. Digestion was stopped by addition of 10 mM ethylenediaminetetraacetic acid (EDTA), and the cell suspensions were passed through a 70 μm cell strainer. A gradient with Optiprep (Progen Biotechnik) was performed to deplete the cell suspensions of dead cells and erythrocytes. For isolation of peritoneal macrophages, 5 mL of PBS with 2% FCS (Biochrom) and 2 mM EDTA were injected into the peritoneal cavity and recovered. This process was repeated twice to obtain a final volume of 10 mL. For sorting of T cells, spleen and lymph nodes were isolated and homogenized. $CD4^+$ T cells were sorted after enrichment using the Dynal Mouse CD4 negative T cell isolation kit following the manufacturer's protocol (Thermo Fisher Scientific).

Cell suspensions were stained with the antibodies described above and the sorting strategy can be found in Figure S4 in Supplementary Material. For sorting myeloid cells from spleen and peritoneum, a lineage cocktail containing anti-CD3e, anti-CD19, and anti-NK1.1 conjugated to eFluor450 (eBioscience) was used. Dead cells were excluded using DAPI.

Targeting Efficiency

iCD103 DCs, GM-CSF DCs, and BMDMs were lysed in TRIzol reagent (Thermo Fisher Scientific) and RNA was isolated with Direct-zol RNA MiniPrep (Zymo Research). In order to assess the rate of ACC1 deletion *in vivo,* macrophages and DCs were sorted from MΦ_ACC1 or DC_ACC1 mice directly into RLT buffer (Qiagen). RNA was isolated with the RNeasy Micro Kit (Qiagen) following the manufacturer's instructions. RNA quality and concentration was determined with a 2100 Bioanalyzer (Agilent Technologies). RNA from *in vitro*-cultured and *ex vivo*-isolated cells was retrotranscribed into cDNA using SuperScript III Reverse Transcriptase Kit (Thermo Fisher Scientific). Real-time PCR reactions were carried out in a StepOne Real-time PCR system (Thermo Fisher Scientific) using Fast SYBR Green Master Mix (Thermo Fisher Scientific). *Acc1* mRNA levels were normalized to the housekeeping gene *Actb*.

Statistical Analysis

Data analyses were performed using GraphPad Prism Software version 6.0 (GraphPad Software) and statistics were calculated using Student's *t*-test, one-way ANOVA with Dunnett's correction or two-way ANOVA with Bonferroni correction. *P*-values were considered significant as follows: $^*P < 0.05$ and $^{**}P < 0.01$, $^{***}P < 0.001$, $^{****}P < 0.0001$.

RESULTS

iCD103 DCs Display Low Infection Rates but Become Highly Activated in Presence of Mycobacteria

Early studies investigating the role of DCs and macrophages during mycobacterial infection are mainly based on *in vitro*-generated macrophages and GM-CSF DCs derived from murine bone marrow

(BM) (17). Yet, GM-CSF DCs do not resemble the DC populations present in the lung which mainly consist of $CD11b^+$ and $CD103^+$ DCs. Recently, pulmonary $CD103^+$ DCs were shown to be important for the transport of mycobacteria to the lung-draining lymph nodes where they induce T cell responses (50). Thus, to explore the effect of mycobacteria on $CD103^+$ DCs, we made use of a novel method to generate large numbers of $CD103^+$ DCs (iCD103 DCs) *in vitro* functionally resembling lung $CD103^+$ DCs (47). By means of this system, we first determined the rate of infection in iCD103 DCs by flow cytometry using RFP-expressing *M. bovis* BCG and compared it to BMDMs. Our results show that the percentage of RFP^+ BMDMs increases rapidly after infection, with almost 50% of the cells being infected after 4 h (MOI 25). This rate further increased up to 80% after 24 h. In contrast, no RFP^+ iCD103 DCs could be detected after 4 h of infection and only 30% of them were RFP^+ 24 h post infection (p.i.) with the highest MOI tested (**Figure 1A**). Confocal analysis using GFP-expressing *M. bovis* BCG revealed that the majority of the bacteria were present within the cells, suggesting that BMDMs have a higher internalization capacity for mycobacteria than iCD103 DCs (**Figure 1B**). To rule out the contribution of microbicidal mechanisms to the low infection rates observed in iCD103 DCs, we measured the accumulation of nitrite (NO_2^-) in the culture supernatants as an indicator of NO production (**Figure 1C**). As expected, iCD103 DCs were not able to produce NO_2^- upon infection or TLR stimulation. In contrast, BMDMs produced high levels of NO_2^- upon infection with *M. bovis* BCG, which were dependent on the presence of IFN-γ. Thus, we could confirm that the low frequency of infection observed for iCD103 DCs is not a result of increased killing capacity.

Exposure of DCs and macrophages to mycobacteria or their products triggers TLR-signaling, which subsequently leads to their activation, upregulation of costimulatory molecules, and production of inflammatory cytokines required for bacterial containment (51). Therefore, we next evaluated the activation status of iCD103 DCs and BMDMs upon *M. bovis* BCG infection or stimulation with the TLR ligands CpG (TLR9) or LPS (TLR4) by assessing the expression of CD86 and MHC class II (MHCII). In iCD103 DCs, LPS and CpG led to a minor upregulation of CD86 and MHCII already 4 h after stimulation and this expression strongly increased after 24 h. The effect of *M. bovis* BCG was less pronounced and only observed after 24 h with a MOI ≥ 5 (**Figures 1D,E**). In contrast, BMDMs displayed no changes at 4 h in all conditions tested and only increased CD86 expression 24 h after stimulation with LPS or MOI 25 of *M. bovis* BCG (**Figure 1D**). Along the same line, MHCII expression on BMDMs increased only slightly upon infection with a MOI 25 of *M. bovis* BCG (**Figure 1E**). As expected with regards to their pivotal role in presenting antigens to T cells, the expression of MHCII and CD86 was in general much higher in iCD103 DCs than in BMDMs, even when the cells were not stimulated.

iCD103 DCs Produce High Levels of IL-12/23p40 and Have a Strong T Cell Priming Capacity Upon Mycobacterial Infection

We next determined the cytokine profile of iCD103 DCs and BMDMs infected with *M. bovis* BCG by ELISA (**Figure 2A**). Upon TLR stimulation, both iCD103 DCs and BMDMs produced IL-12/23p40, IL-6, and TNF-α already 4 h after stimulation, whereas induction of cytokines by *M. bovis* BCG did not occur until 24 h p.i. (**Figure 2A**). Of note, the production of IL-12/23p40 was much more pronounced in iCD103 DCs (**Figure 2A**), while TNF-α was mainly secreted by BMDMs. In addition, BMDMs but not iCD103 DCs produced IL-10 in response to TLR stimulation. Following a similar pattern, at 24 h p.i. *M. bovis* BCG strongly induced the production of IL-12/23p40 by iCD103 DCs, and to a lesser extent of IL-6 and TNF-α. In contrast, production of IL-10 and TNF-α in response to *M. bovis* BCG was more prominent in BMDMs than in iCD103 DCs. Altogether our data suggest that while BMDMs become preferentially infected with *M. bovis* BCG, iCD103 DCs mainly upregulate costimulatory molecules and secrete pro-inflammatory cytokines.

Activation of macrophages and DCs and production of inflammatory cytokines is a crucial step in the induction of adaptive immunity against mycobacterial infection. In addition to Th1 cells, Th17 cells were described to be important for protection against *Mtb*, especially against highly virulent *Mtb* strains and for the effectiveness of mucosal vaccines (52–54). Thus, we tested the capacity of iCD103 DCs and BMDMs to prime and polarize naïve $CD4^+$ T cells toward Th1 or Th17 cells. To this aim, iCD103 DCs and BMDMs from WT mice were infected with different MOI of *M. bovis* BCG overexpressing Ag85B (BCG Ag85B) for 24 h and subsequently co-cultured with naïve $CD4^+CD25^-$ P25ktk T cells, expressing a TCR that is specific for peptide P25 of Ag85B bound to $I\text{-}A^b$ (43). Under non-polarizing conditions, iCD103 DCs induced strong T cell proliferation and IFN-γ production, whereas BMDMs were unable to prime T cells (**Figure 2B**). Since IL-17 was only marginally induced (data not shown), we also performed co-cultures adding TGF-β and blocking IFN-γ, IL-12/23p40, and IL-4. Under these Th17-skewing conditions iCD103 DCs, but not BMDMs, were able to promote IL-17 production (**Figure 2B**). These results indicate that iCD103 DCs are highly efficient at priming anti-mycobacterial effector Th1/17 responses.

iCD103 DCs and BMDMs Upregulate Lipid Synthesis Upon Infection

Recently it was proposed that upon stimulation, immune cells undergo a metabolic switch from OXPHOS toward aerobic glycolysis, also known as the Warburg effect (55, 56). This metabolic reprogramming observed in macrophages upon infection with *Mtb*, subsequently induces *de novo* cholesterol and FAS, which results in lipid accumulation and so-called "foamy" macrophages (57). In DCs, commitment to aerobic glycolysis upon TLR stimulation was reported to be crucial for activation by supporting *de novo* FAS (30). Thus, we investigated whether DCs and macrophages upregulate the glycolytic-lipogenic pathway upon mycobacterial infection. To this aim, we cultured iCD103 DCs and BMDMs with *M. bovis* BCG or TLR stimuli in the presence of ^{13}C-glucose and tracked the incorporation of glucose-derived carbons into lipids (**Figure 3A**). Both iCD103 DCs and BMDMs increased the incorporation of ^{13}C-glucose-derived carbons into saturated fatty acids, such as palmitic acid (C16:0) and stearic acid (C18:0) as well as the unsaturated fatty acids palmitoleic acid (C16:1ω7) and vaccenic acid (C18:1ω7) upon infection (**Figure 3B**). In general, BMDMs showed lower incorporation of

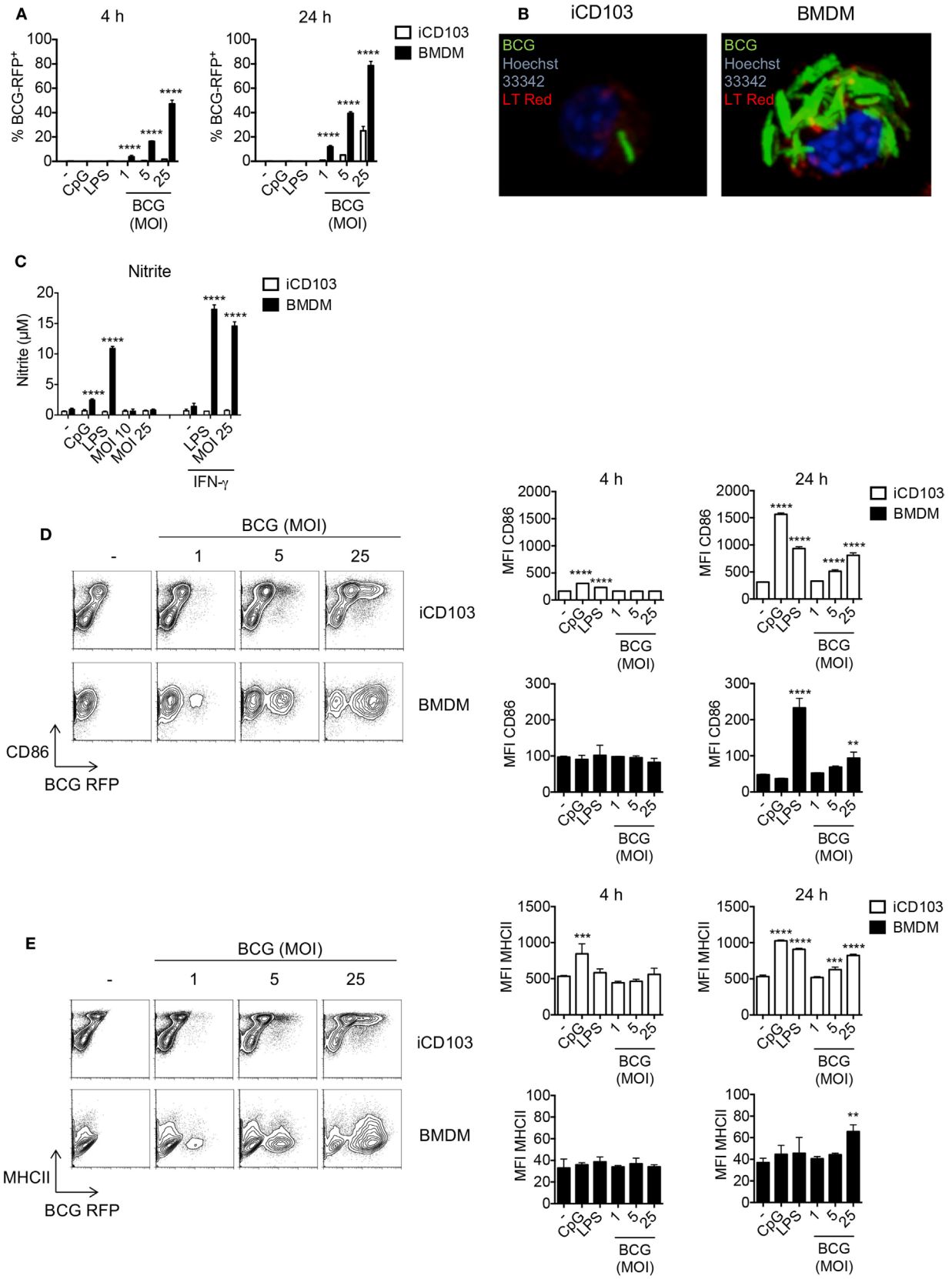


FIGURE 1 | Continued

FIGURE 1 | iCD103 dendritic cells (DCs) display low infection rates, but become highly activated in the presence of mycobacteria. iCD103 DCs and bone marrow-derived macrophages (BMDMs) were infected with different multiplicities of infection (MOIs) of *Mycobacterium bovis* BCG RFP or GFP and the infection rate, nitrite production, as well as activation status was analyzed after 4 and 24 h. LPS and CpG were used as stimulation controls. **(A)** Graphs show frequency of RFP$^+$ iCD103 DCs and BMDMs among live cells. **(B)** Confocal microscopy images of iCD103 DCs and BMDM at 24 h p.i. with MOI 10 of *M. bovis* BCG GFP (green) and stained for nuclei (Hoechst 33342; blue) and phospholipids (LT Red; red). **(C)** Bar graphs show nitrite levels in culture supernatants after 24 h determined by Griess reagent system. IFN-γ served as a positive control. **(D)** Representative flow cytometry plots display CD86 expression and *M. bovis* BCG RFP in iCD103 DCs and BMDMs at 24 h p.i. (left panel). Bar graphs show the MFI of CD86 expression at 4 and 24 h p.i. (right panel). **(E)** Representative flow cytometry plots display MHCII expression and *M. bovis* BCG RFP in iCD103 DCs and BMDMs at 24 h p.i. (left panel). Bar graphs show the MFI of MHCII expression at 4 and 24 h p.i. (right panel). Results are representative of two [**(B)**, BMDM], **(C)**, three [**(B)**, iCD103 DC], five **(D,E)**, or six **(A)** experiments. Error bars represent SD of triplicates. $^*P < 0.05$, $^{**}P < 0.01$, $^{***}P < 0.001$, $^{****}P < 0.0001$, two-way ANOVA with Bonferroni correction **(A,C)**, or one-way ANOVA with Dunnett's correction **(D,E)**.

^{13}C-glucose into fatty acids than iCD103 DCs in the basal state, but also upon infection or TLR stimulation (**Figure 3B**).

Lipids are important components of cellular membranes and they also participate in different signaling events within the cell. For DCs it was proposed that the induction of FAS upon TLR stimulation facilitates DC activation by generating membranes to promote Golgi and ER expansion and increased function (30). In line with this, infection with *M. bovis* BCG induced the accumulation of cellular phospholipids in iCD103 DCs as well as in BMDMs after 24 h, as evaluated by LipidTOX (LT) Red staining (**Figure 3C**). By confocal microscopy, we observed LT Red stained vesicle-shaped structures (**Figure 1B**), sometimes co-localizing with BCG, with variable levels of intensity between different cells, regardless of the degree of infection (data not shown). Therefore, in order to have a more quantitative and less biased analysis, we determined the phospholipid and neutral lipid content by flow cytometry. The MFI values for LT Red increased over time and were about 5–10-fold higher in BMDMs than iCD103 DCs, despite greater ^{13}C-glucose incorporation into fatty acids in iCD103 DCs (**Figure 3B**). Moreover, we assessed the accumulation of total neutral lipids by LT Green staining (**Figure 3D**). While the basal level of neutral lipids was comparable between iCD103 DCs and BMDMs, the accumulation of lipids upon TLR stimulation or *M. bovis* BCG infection at 24 h was more pronounced in BMDMs (**Figure 3D**). Altogether, these results demonstrate that not only BMDMs, as reported previously, but also DCs upregulate *de novo* FAS and accumulate lipids upon mycobacterial infection.

ACC1-Mediated *De Novo* FAS is Dispensable for the Function of BMDMs and iCD103 DCs

De novo FAS is controlled by the rate of malonyl-CoA production from acetyl-CoA *via* the enzyme ACC1 present in the cytosol. We therefore thought to address whether ACC1 deletion has an impact on DC and macrophage function upon mycobacterial infection. To this aim, we generated DC- and macrophage-specific ACC1-deficient mice (DC_ACC1 and MΦ_ACC1, respectively) by crossing mice carrying a loxP-flanked biotin carboxyl carrier protein domain in the *Acaca* gene (ACC1$^{flox/flox}$) (36) with mice expressing the *cre* recombinase under the control of the CD11c (Integrin alpha X) promoter (41) or the lysozyme M (LysM) promoter (40). We then cultured iCD103 DCs and BMDMs from BM of DC_ACC1 and MΦ_ACC1 mice, respectively, and analyzed their activation status and function after 24 h of infection with *M. bovis* BCG. ACC1-deficient iCD103 DCs behaved similarly to their WT counterparts in terms of CD86 and MHCII expression (**Figure 4A**, upper panel) and pro-inflammatory cytokine production (**Figure 4B**, upper panel; Figure S1A in Supplementary Material, upper panel). They also showed no defects in their ability to prime P25-specific CD4$^+$ T cells (**Figure 4C**). Likewise, BMDMs from MΦ_ACC1 mice had no defects in their expression of surface molecules (**Figure 4A**, lower panel) or their production of IL-10, TNF-α, IL-6, and IL-1β compared to WT controls (**Figure 4B**, lower panel; Figure S1A in Supplementary Material, lower panel).

Pharmacological inhibition of *de novo* FAS impairs the capacity of GM-CSF-derived DCs to produce cytokines and become activated in response to TLR ligation (30). Since we observed no effect of ACC1 deletion in iCD103 DCs, we next tested whether GM-CSF DCs from DC_ACC1 mice become properly activated upon TLR stimulation or infection with *M. bovis* BCG. However, compared to WT cells, we found no differences in the expression of the surface molecules CD86 and MHCII or the levels of IL-12/23p40 and TNF-α, when ACC1-deficient cells were stimulated (Figures S1B,C in Supplementary Material).

Subsequently, we addressed whether the deletion of ACC1 would result in lower rates of FAS. Thus, we evaluated the rate of ^{13}C-glucose incorporation into fatty acids. To our surprise, we observed only a slight reduction of *de novo* FAS in ACC1-deficient iCD103 DCs and BMDMs (Figure S2A in Supplementary Material). In order to determine if residual ACC activity was obscuring our results, we assessed the targeting efficiency of the CD11c *cre* and LysM *cre* promoters for ACC1 in these *in vitro*-generated cells. The rate of ACC1 deletion was around 50% for both iCD103 DCs and BMDMs, which could account for the small differences observed in *de novo* FAS rates between WT and transgenic cells (Figure S2B in Supplementary Material). In GM-CSF DCs generated from DC_ACC1 mice, the deletion rate was higher, averaging 70% (Figure S2B in Supplementary Material) and *de novo* FAS from glucose was halved upon ACC1 deletion (data not shown). Additionally, we assessed two pharmacological ACC inhibitors, Soraphen A (SorA) and TOFA in our experiments. Treatment with SorA, a natural compound derived from the myxobacterium *Sorangium cellulosum* (58–60) completely abrogated *de novo* FAS from glucose in iCD103 DCs and BMDMs (Figure S2A in Supplementary Material). However, it had no effect in TLR-driven induction of costimulatory molecules (**Figure 4A**) or pro-inflammatory cytokines (**Figure 4B**; Figure S1A in Supplementary Material). TOFA, a potent and widely characterized inhibitor that has been used in several studies (30, 33, 61, 62) also failed to inhibit iCD103 DC and

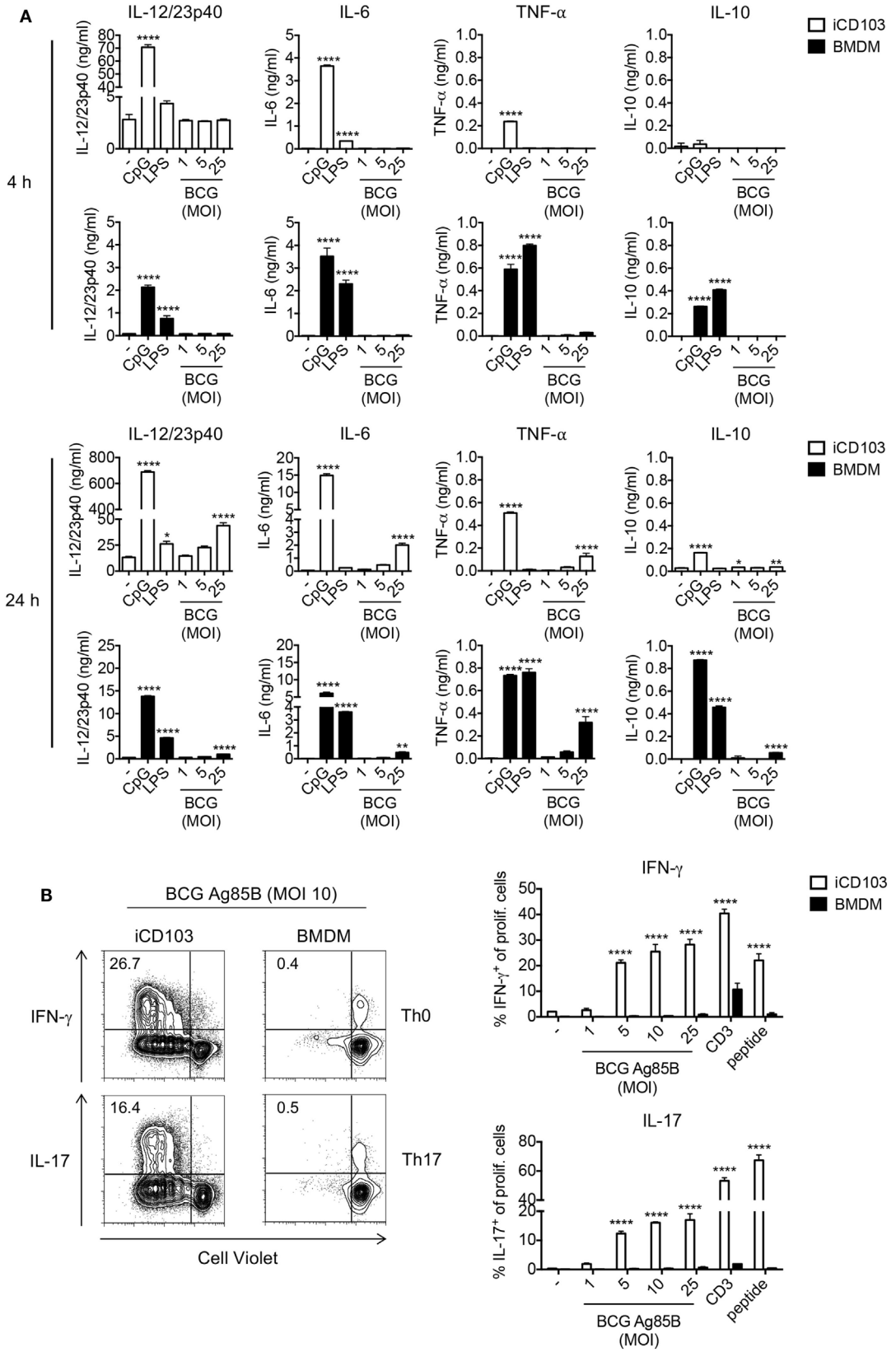


FIGURE 2 | Continued

FIGURE 2 | iCD103 dendritic cells (DCs) produce high levels of IL-12/23p40 and have a strong T cell priming capacity upon mycobacterial infection. **(A)** iCD103 DCs and bone marrow-derived macrophages (BMDMs) were infected with different multiplicities of infection (MOIs) of *Mycobacterium bovis* BCG RFP and levels of IL-12/23p40, IL-6, TNF-α, and IL-10 production were measured at 4 and 24 h p.i. by ELISA. LPS and CpG were used as stimulation controls. **(B)** iCD103 DCs or BMDMs were infected with *M. bovis* BCG overexpressing Ag85B and co-cultured with naïve $CD4^+CD25^-$ P25ktk T cells for 4 days under Th0 or Th17 polarizing conditions. Representative flow cytometry plots display proliferation and IFN-γ or IL-17 production of P25ktk cells upon infection of iCD103 DCs or BMDMs with MOI 10 of *M. bovis* BCG Ag85B (left panel). Bar graphs display the frequencies of $IFN\text{-}\gamma^+$ or $IL\text{-}17^+$ cells among total live $CD4^+$ T cells upon re-stimulation with PMA/ionomycin (right panel). Results are shown as a representative of two individual experiments **(A,B)**. Error bars represent SD of triplicates. $^*P < 0.05$, $^{**}P < 0.01$, $^{***}P < 0.001$, $^{****}P < 0.0001$, one-way ANOVA with Dunnett's correction **(A)**, or two-way ANOVA with Bonferroni correction **(B)**.

BMDM activation (**Figures 4A,B**; Figure S1A in Supplementary Material). Moreover, complete ACC inhibition by SorA did not affect the T cell priming capacity of iCD103 DCs (**Figure 4C**). In conclusion, our results suggest that the inhibition of ACC1-mediated FAS in DCs and macrophages does not compromise their ability to become efficiently activated or to prime effective anti-mycobacterial immune responses *in vitro*.

Interestingly, ^{13}C-palmitate and Bodipy-palmitate uptake assays (Figures S3A,B in Supplementary Material) revealed that ACC1 deletion or pharmacological inhibition in BMDMs, and more prominently in iCD103 DCs, results in increased fatty acid uptake. This implies that DCs and macrophages with impaired lipogenesis might exhibit compensatory mechanisms, i.e., augmented uptake of external lipids, to meet their biosynthetic requirements.

ACC1 Expression in DCs and Macrophages Is Not a Prerequisite for Inflammatory Cytokine Production or T Cell Priming *In Vivo*

To confirm the suitability of our mouse models to study the relevance of *de novo* FAS in myeloid cells *in vivo*, we next evaluated the targeting efficiency for ACC1 in *ex vivo*-isolated cells. We found it was over 90% for splenic $CD11c^+$ DCs from DC_ACC1 mice (Figure S4A in Supplementary Material), and about 40% for MΦ_ACC1 $F4/80^+$ splenic macrophages (Figure S4B in Supplementary Material). Importantly, in MΦ_ACC1 mice, peritoneal and AMs displayed deletion efficiencies between 90 and 100% (Figure S4B in Supplementary Material), thus suggesting that our mouse models are suitable to study the importance of *de novo* FAS in DCs and macrophages in the context of mycobacterial infection *in vivo*. To this aim, we infected DC_ACC1 and MΦ_ACC1 mice with *M. bovis* BCG *via* the i.v. route and analyzed the expression of CD86 in $CD11c^+$ or $F4/80^+$ cells in the spleen at day 21 p.i. In both DC_ACC1 and MΦ_ACC1 mice, CD86 was upregulated to the same extent as in their WT counterparts (**Figure 5A**). Next, we evaluated IL-12/23p40 and IL-1β production in the spleens of DC_ACC1 and MΦ_ACC1 at different time points after infection. Both cytokines increased over time, peaking at 21 days p.i. However, no differences were detected between DC_ACC1, MΦ_ACC1, and WT mice (**Figure 5B**). In accordance, IFN-γ and IL-12/23p40 levels in the serum were also not impaired upon ACC1 deletion on day 21 p.i. neither in DC_ACC1 nor in MΦ_ACC1 mice (Figure S5A in Supplementary Material). These results indicate that the overall production of inflammatory cytokines was not affected by the absence of ACC1 in myeloid cells. We also evaluated the requirement of *de novo* FAS in DCs and macrophages for priming protective T cell immunity during *M. bovis* BCG infection by analyzing T cell responses in the spleen at day 21 p.i. As shown in **Figure 5C**, the generation of endogenous IFN-γ-secreting Th1 cells was neither impaired in DC_ACC1 mice, nor in MΦ_ACC1 mice.

Finally, to further confirm that ACC1 expression in DCs is not required for T cell priming during infection, WT and DC_ACC1 mice were infected with 2×10^6 *M. bovis* BCG i.v. and on day 9 p.i. $CD4^+CD45.1^+$ T cells from P25ktk mice labeled with the proliferation dye CellTrace Violet were transferred, according to the experimental scheme shown in Figure S6A in Supplementary Material. After 5 days, the proliferation and cytokine production of transferred cells was analyzed in WT and DC_ACC1 mice. However, transferred P25ktk cells proliferated to the same extent in WT as in DC_ACC1 recipients and produced equal amounts of IFN-γ (Figure S6B in Supplementary Material).

Accordingly, 21 days after systemic *M. bovis* BCG infection, both DC_ACC1 and MΦ_ACC1 mice displayed comparable CFU in liver, spleen, and lungs compared to WT mice (**Figure 5D**). Moreover, we confirmed these results with another $ACC1^{flox/flox}$ mouse strain ($Acaca^{flox/flox}$), in which different exons are targeted for deletion (37). We crossed them with CD11c *cre* and LysM *cre* mice to generate DC_Acaca and MΦ_Acaca mice, which were also capable of controlling *M. bovis* BCG infection like WT mice (Figure S5B in Supplementary Material).

To evaluate if deletion of ACC1 in DCs or macrophages would impair the control of *Mtb* infection, we tested the susceptibility of DC_ACC1 and MΦ_ACC1 mice toward a high dose of *Mtb* aerosol infection. The lack of *de novo* FAS in myeloid cells had no impact on bacterial control as evidenced by the CFU counts in liver, spleen, and lungs at day 21 and 42 after infection, which were comparable to WT mice (**Figure 5E**; Figure S5C in Supplementary Material).

In addition to ACC1, ACC2 a second isoform of ACC can also convert acetyl-CoA to malonyl-CoA. However, ACC2 is present on the outer mitochondrial membrane and does not contribute to FAS, but instead regulates FAO by producing malonyl-CoA that inhibits the CPT1-dependent transport of long-chain fatty acids into the mitochondria (32). To investigate if ACC2 deletion would impact the outcome of mycobacterial infection, we generated mice with a cell-specific deletion of ACC2 in DCs or macrophages by crossing CD11c or LysM *cre* mice to $ACC2^{flox/flox}$ (38) mice and infected them with *M. bovis* BCG. Additionally, we used ACC2 complete knockout mice (42) and infected them with 100 CFU *Mtb via* the aerosol route. Still, the absence of ACC2 in DCs or macrophages did not affect mycobacterial control neither in the *M. bovis* BCG model, nor during *Mtb* infection (Figures S7A,B in Supplementary Material).

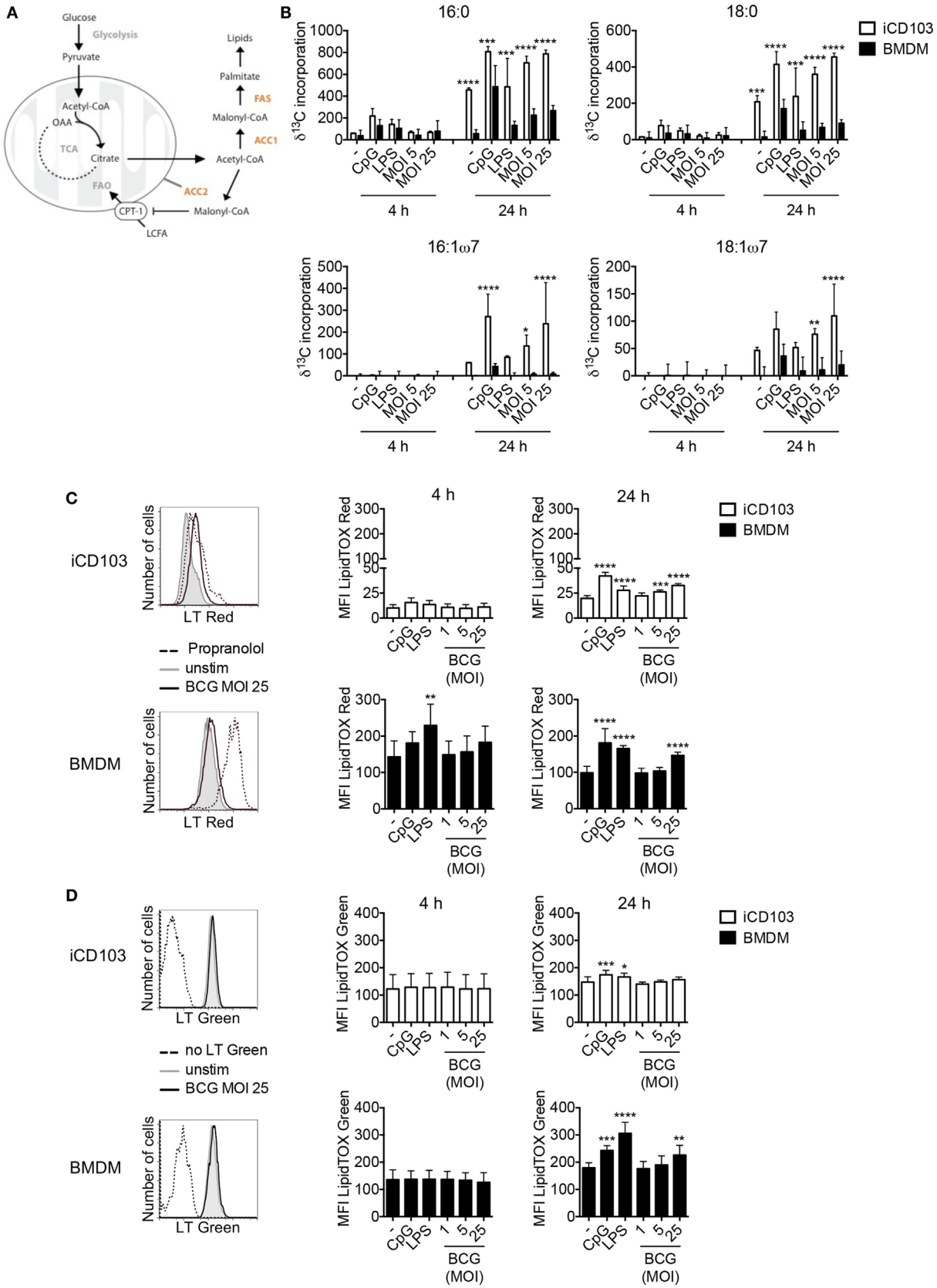


FIGURE 3 | Continued

FIGURE 3 | iCD103 dendritic cells (DCs) and macrophages upregulate lipid metabolism upon infection. iCD103 DCs and bone marrow-derived macrophages (BMDMs) were infected with *Mycobacterium bovis* BCG RFP and metabolic parameters were determined at 4 and 24 h p.i. LPS and CpG were used as stimulation controls. **(A)** Schematic overview depicting the glycolytic-lipogenic pathway regulated by acetyl-CoA carboxylase (ACC1) and ACC2. CPT1, carnithine palmitoyl transferase 1; LCFA, long chain fatty acids; FAO, fatty acid oxidation; FAS, fatty acid synthase; OAA, oxaloacetate; TCA, tricarboxylic acid cycle. **(B)** Incorporation (δ) of ^{13}C into fatty acids after 4 and 24 h of culture in the presence of [U-$^{13}C_6$] glucose. **(C,D)** Accumulation of phospholipids **(C)** and neutral lipids **(D)** in iCD103 DCs and BMDMs was assessed by LipidTox (LT) Red **(C)** or LT Green **(D)** staining, respectively. Representative histograms (left panel) depict LT Red/Green staining in unstimulated iCD103 DCs and BMDMs (gray) or cells infected with MOI 25 of *M. bovis* BCG (black) after 24 h. The dashed line represents the positive control Propranolol for LT Red staining **(C)** or an unstained control for LT Green staining **(D)**. Bar graphs show the MFI of LT Red/Green expression (right panel). Results are pooled from three **(B)** or five **(C,D)** experiments. Error bars represent SD of pooled data **(B–D)**. $^*P < 0.05$, $^{**}P < 0.01$, $^{***}P < 0.001$, $^{****}P < 0.0001$, one-way ANOVA with Dunnett's correction **(C,D)**, or two-way ANOVA with Bonferroni correction **(B)**.

ACC1 Deletion in T Cells Increases Susceptibility Toward *M. bovis* BCG Infection

Our previous work highlighted the critical dependency of T helper cell differentiation on the glycolytic-lipogenic pathway (33, 35). We therefore speculated that ACC1 deletion in T cells might impair anti-mycobacterial immunity. To test this hypothesis, we infected TACC1 mice that were generated by crossing CD4 *cre* mice to ACC1$^{flox/flox}$ mice with *M. bovis* BCG *via* the i.v. route. Indeed, mice lacking ACC1 in T cells exhibited elevated bacterial burden compared to WT littermates (**Figure 6A**). In TACC1 mice, almost 100% of CD4$^+$ T cells carry the targeted deletion (Figure S4C in Supplementary Material). In contrast to ACC1 deficiency, mice with a T cell-specific deletion of ACC2 showed bacterial burden comparable to WT mice (Figure S7C in Supplementary Material).

Analysis of the immune response during infection revealed that T cells from TACC1 mice exhibited reduced frequencies of IFN-γ$^+$ CD4 T cells indicating the importance of T cell-intrinsic FAS for mounting Th1 responses (**Figure 6B**). Additionally, we evaluated the production of IL-17 by CD4$^+$ T cells during infection. We did not observe differences in the production of IL-17A among the groups (data not shown). However, the Th17 response in our *M. bovis* BCG infection model was negligible, consisting of only about 0.3–1% IL-17A$^+$ cells within the live CD4$^+$ T cell compartment. Furthermore, while DC_ACC1 and MΦ_ACC1 mice showed comparable frequencies of CD62L^{low} cells among CD4$^+$ T cells compared to WT mice (data not shown), TACC1 displayed lower T cell activation levels (**Figure 6C**). Of note, in addition to CD4$^+$ T cells, also ACC1-deficient CD8$^+$ T cells showed a strong reduction in their production of IFN-γ (**Figure 6E**), suggesting that *de novo* lipid synthesis is also required in these cells to mount effective effector responses during infection.

Inflammatory immune responses are controlled by Tregs, which have been reported to expand in both mice (63) and humans (64–66) upon *Mtb* infection and might serve as a mechanism to establish chronic mycobacterial infection (67). As we have previously shown (45), the frequency of FoxP3$^+$ Tregs among live CD4$^+$ T cells during *M. bovis* BCG infection is transiently reduced compared to naïve mice (**Figure 6D**), which can be attributed to the expansion of T effector cells. Given our findings that interfering with *de novo* FAS blocks Th17 and favors Treg development, we speculated that ACC1 deficiency in T cells would lead to an expansion of Tregs during mycobacterial infection, as observed in the experimental autoimmune encephalomyelitis model for human multiple sclerosis (33). However, upon *M. bovis* BCG infection, TACC1 mice, like DC_ACC1 and MΦ_ACC1 mice (data not shown), did not show altered Treg frequencies compared to WT mice (**Figure 6D**). Taken together, our results highlight the importance of ACC1 expression in T cells to effectively generate an adaptive immunity against *M. bovis* BCG infection.

ACC1 Expression in T Cells Is Crucial for Immunity Against *Mtb* Infection

Finally, to determine the importance of *de novo* FAS in T cells for the control of Tb, we infected mice with a high dose (**Figures 7A,B**) or low dose aerosol (**Figures 7C–I**) of *Mtb*. TACC1 mice infected with a high dose reached a high disease score (>3.0) (**Figure 7A**) and had to be sacrificed at day 32 p.i. At this time point, they exhibited extremely high bacterial burden in all organs tested (**Figure 7B**). To gain further insights into the immune responses that could explain the susceptibility of TACC1 mice, we made use of the more physiological low dose infection model applying 100 CFU *Mtb via* the aerosol route. Interestingly, while CFU were comparable to WT mice at day 21 p.i., TACC1 mice displayed elevated bacterial burden at 42 days p.i. (**Figure 7C**). T cell activation, as measured by the downregulation of CD62L expression in CD44$^+$CD4$^+$ T cells, was reduced early during infection, and restored to WT levels at the later stage (**Figure 7D**).

Due to the pivotal role of Th1 cells for the protection against *Mtb* (21), we also determined the IFN-γ production by CD4$^+$ T cells. On day 21 p.i., we observed that IFN-γ production by CD44$^+$CD4$^+$ T cells in response to polyclonal CD3/CD28 re-stimulation was drastically impaired, but restored to WT levels at day 42 (**Figure 7E**). To evaluate whether TACC1 mice were able to generate antigen-specific T cell immunity, we stained lung cells with a tetramer of ESAT-6, a secreted virulence factor and highly immunodominant antigen of *Mtb*. Tetramer staining revealed that TACC1 mice display also a defect in the early generation of ESAT-specific CD4$^+$ T cells, which is slightly compensated at day 42, but still reduced compared to WT mice (**Figure 7F**). In accordance, TACC1 mice also exhibited a delay in the generation of antigen-specific T cells producing IFN-γ, as determined by ELISPOT upon re-stimulation with ESAT6$_{1-20}$-pulsed antigen presenting cells (**Figure 7G**). Interestingly, the presence of Tregs differed throughout the infection between WT and mice lacking ACC1 in T cells (**Figure 7H**). After 21 days TACC1 mice showed elevated Treg frequencies compared to

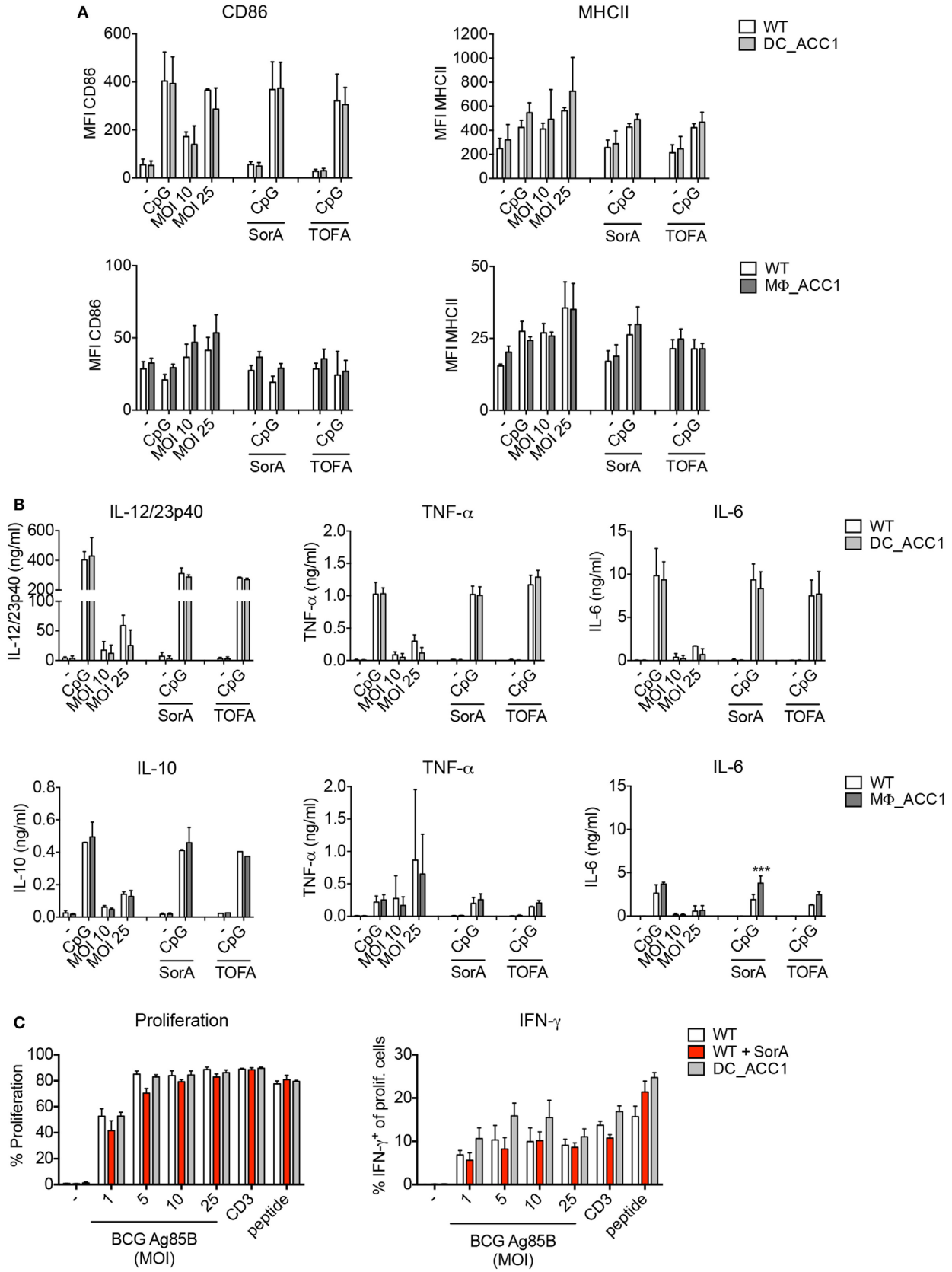


FIGURE 4 | Continued

FIGURE 4 | Acetyl-CoA carboxylase (ACC1)-mediated *de novo* fatty acid synthesis (FAS) is dispensable for the function of dendritic cells (DCs) and macrophages. **(A–C)** iCD103 DCs from WT and DC_ACC1 mice or bone marrow-derived macrophages (BMDMs) from WT and MΦ_ACC1 mice were infected with different multiplicities of infections (MOIs) of *Mycobacterium bovis* BCG and *de novo* FAS, activation and function were analyzed 24 h p.i. LPS and CpG served as stimulation controls and SorA and 5-(Tetradecyloxy)-2-furoic acid (TOFA) as inhibitors of ACC1. **(A)** Bar graphs show the MFI of CD86 and MHCII expression determined by flow cytometry. **(B)** Bar graphs display the cytokine levels of IL-12/23p40, TNF-α, IL-6, and IL-10 measured by ELISA. **(C)** iCD103 DCs from WT or DC_ACC1 mice were infected with *M. bovis* BCG overexpressing Ag85B in the presence or absence of SorA. After 24 h, cells were washed and co-cultured with naïve $CD4^+CD25^-$ P25ktk T cells for 4 days. Bar graphs display the proliferation rate and frequencies of IFN-γ^+ among total live $CD4^+$ T cells upon re-stimulation with PMA/ionomycin. Results are pooled from two [**(A)** BMDMs, **(B)** iCD103 DCs] or three [**(A)** iCD103 DCs, **(B)** BMDMs] experiments or shown as a representative of two **(C)** experiments. Each individual experiment had triplicates **(A,B)** or quadruplicates **(C)**. Bar graphs show mean with error bars of SD. $^*P < 0.05$ and $^{**}P < 0.01$, $^{***}P < 0.001$, $^{****}P < 0.0001$, n.s., non-significant, two-way ANOVA with Bonferroni correction **(A,B)**.

WT mice, which was reversed after 42 days. Since Tregs and IL-10 were postulated to limit the host immune response against mycobacteria, we measured the production of IL-10 by T cells in TACC1 during *Mtb* infection. We observed that at day 21 p.i., when Treg frequencies are higher in TACC1 mice, there were no significant differences in T cell-derived IL-10 between WT and transgenic mice (**Figure 7I**). However, at day 42 p.i., $CD4^+$ T cells from TACC1 mice produce more IL-10 than their WT counterparts. Therefore, we cannot definitely exclude that IL-10 dampens the control of mycobacterial growth and contributes to the increased bacterial loads at a later time point of infection. However, as the overall protective T cell response is impaired at earlier time points, we are convinced that this initially compromised reaction accounts for the increased CFUs observed at day 42 p.i. (**Figure 7C**) independently of Treg-derived IL-10.

Taken together, our data highlight the importance of T cell-intrinsic *de novo* FAS for the generation of protective Th1 immunity against *Mtb* infection. On the contrary, we observed that ACC1 and ACC2 expression in myeloid cells was not essential for the control of mycobacterial infection.

DISCUSSION

Macrophages and DCs possess distinct roles in the protection against mycobacterial infection. While macrophages control mycobacterial growth using several microbicidal mechanisms, DCs are essential for priming adaptive immunity. In several studies over the past years, these functional properties of immune cells were connected to specific metabolic pathways. Pathogens, such as mycobacteria, have evolved strategies to exploit these metabolic programs for their own survival and replication. In particular, the host cellular lipid metabolism was reported to be modulated by *Mtb*. However, how this metabolic reprogramming affects the function of macrophages and DCs during mycobacterial infection remains unknown. In this study, we demonstrate that in T cells, *de novo* FAS *via* ACC1 is essential to control mycobacterial infection. In contrast, engagement of *de novo* FAS is not a prerequisite for the optimal activation and function of macrophages and DCs.

Previous studies investigating the importance and contrasting roles of macrophages and DCs in generating protective immunity against mycobacteria were mainly performed using BM-derived GM-CSF DCs. GM-CSF DCs have been used in a wide range of studies, since they yield large numbers of cells and represent a useful tool to study certain properties of antigen presenting cells, such as their T cell priming capacity. However, it has recently become apparent that these cultures contain not only DCs, but also monocyte-derived macrophages, termed GM-DCs and GM-Macs, respectively (68). Since GM-CSF DCs represent a heterogeneous mixture of myeloid cells, it is difficult to draw conclusions out of this system on the different roles of DCs and macrophages upon mycobacterial infection. To overcome this, we here made use of a novel protocol developed in our laboratory to generate large numbers of $CD103^+$-like DCs (iCD103 DCs) *in vitro* (47). In mice, $CD103^+$ DCs are classified as conventional DCs that lack CD8α and express low levels of CD11b (69). They represent a rare population of DCs that survey non-lymphoid tissues and migrate to lymph nodes where they prime adaptive immunity. $CD103^+$ DCs were associated with protection against Tb, since they are found in higher numbers in the lungs of *Mtb*-resistant mice than in the susceptible DBA/2 strain (27). Additionally, $CD103^+$ DCs can migrate from the lungs to the draining-lymph nodes, where they contribute to the control of infection by initiating T cell responses (50). Here, we show that iCD103 DCs have a stronger upregulation of CD86 and MHCII as well as higher production of IL-12/23p40 and IL-6 in comparison to BMDMs. Consequently, only iCD103 DCs strongly promoted T cell proliferation and differentiation from naïve T cells into Th1 and Th17 cells *in vitro*. These data are in accordance with previous studies using GM-CSF DCs and BMDMs (17, 70) or DCs and macrophages from *M. bovis* BCG-infected mice (71). Additionally, it was described that the ability of DCs to kill mycobacteria is relatively low (17, 18), and, therefore, DCs can transport live bacteria to the lymph nodes (19). For this reason, it has been proposed that *Mtb* might use DCs as a "Trojan horse" to spread within the host and establish a persistent infection (72). Our data shows that iCD103 DCs become infected with mycobacteria, but at a lower rate than macrophages. Importantly, iCD103 DCs are unable to produce NO, in contrast to what was described for GM-CSF DCs (73, 74). NO production is one of the main microbicidal mechanisms required for mycobacterial killing (75). In this respect, iCD103 DCs might represent a good model to study how mycobacteria survive in DCs.

One of the main pathways required for DC activation and production of pro-inflammatory cytokines upon mycobacterial infection is the TLR/MyD88 pathway (28). Recently, it was proposed that TLR-driven activation and cytokine production in DCs is dependent on *de novo* FAS, which serves for the expansion of the ER and Golgi apparatus (30). Immune cells gain fatty acids by the glycolytic-lipogenic pathway, a process

by which carbons derived from glucose (and other substrates) are converted to acetyl-CoA, which is then used for the synthesis of fatty acids. Alternatively, fatty acids can be incorporated from the environment using transporters, such as the CD36 receptor or fatty acid binding proteins. Fatty acids can be further subjected to FAO in the mitochondria for the generation

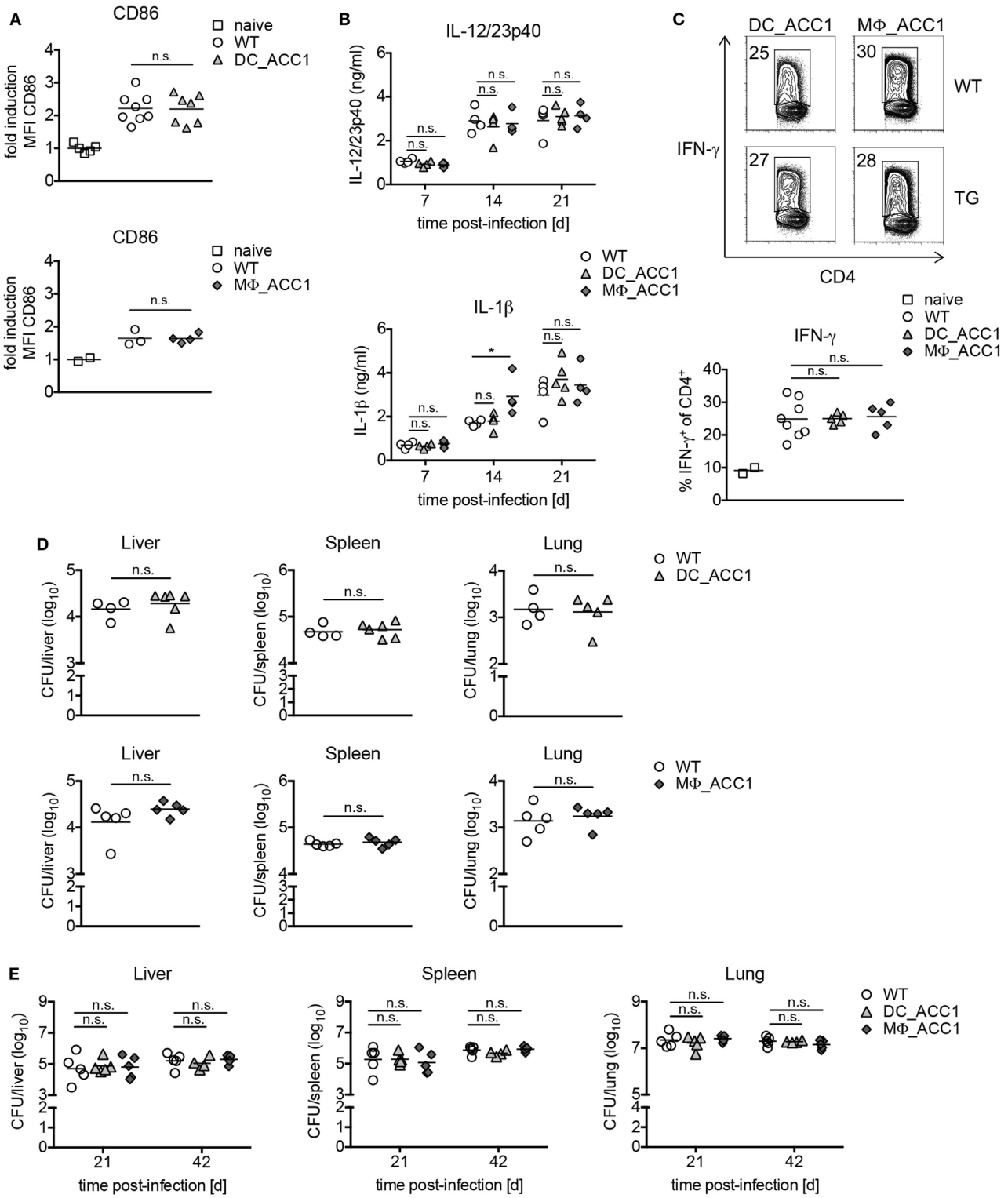


FIGURE 5 | Continued

FIGURE 5 | Acetyl-CoA carboxylase (ACC1) expression in dendritic cells (DCs) and macrophages is not a prerequisite for mycobacterial control. **(A–D)** WT, DC_ACC1, and MΦ_ACC1 mice were infected i.v. with 2×10^6 colony forming units (CFU) of *Mycobacterium bovis* BCG and analyzed on day 21 p.i. or also on day 7 and 14 p.i. **(B)**. **(A)** The expression of CD86 was analyzed in splenic $CD11c^{hi}$ $MHCII^{hi}$ DCs or $F4/80^+$ macrophages by flow cytometry. Graphs show fold induction of CD86 MFI in infected mice relative to naïve mice. **(B)** Graphs display levels of IL-12/23p40 and IL-1β in the spleen at different time points determined by ELISA. **(C)** Representative flow cytometry plots show the percentage of IFN-γ^+ cells within live $CD4^+$ T cells upon re-stimulation with PMA/ionomycin. Graph represents the frequency of IFN-γ^+ cells within live splenic $CD4^+$ T cells. **(D)** Graphs show bacterial burden in liver, spleen, and lung. **(E)** WT, DC_ACC1, and MΦ_ACC1 mice were infected with a high dose of 1,000 CFU *Mycobacterium tuberculosis* (*Mtb*) *via* the aerosol route and the bacterial burden was determined in liver, spleen, and lung on day 21 and 42 p.i. Each symbol represents an individual mouse. Results are pooled from two experiments [**(A)**, upper panel] with $n = 1$–4 mice per group, from one experiment with $n = 2$–4 mice per group [**(A)**, lower panel] or with $n = 4$–5 mice per group **(E)** or as a representative of four individual experiments with $n = 4$–5 mice per group **(C,D)**. $^*P < 0.05$ and $^{**}P < 0.01$, $^{***}P < 0.001$, $^{****}P < 0.0001$, n.s., non-significant, Student's *t*-test **(A,D)**, one-way ANOVA with Dunnett's correction **(C,E)** or two-way ANOVA with Bonferroni correction **(B)**.

of ATP or accumulated in the form of triglycerides within LBs. FAO and FAS are regulated by the enzymes ACC1 and ACC2, both catalyzing the conversion of acetyl-CoA to malonyl-CoA. The malonyl-CoA that is produced by ACC2 functions as an allosteric inhibitor of CPT1, the rate-limiting enzyme for the transport of long chain fatty acids into mitochondria for FAO. In contrast, ACC1 is located in the cytosol and represents the rate-limiting enzyme for *de novo* FAS. In the process of FAS, malonyl-CoA is condensed with acetyl-CoA by the fatty acid synthase (FASN) generating long-chain fatty acids which are further modified into lipids that are used for the synthesis of membranes or posttranslational modifications of proteins (34).

In this study, we demonstrate that iCD103 DCs strongly upregulate *de novo* FAS upon mycobacterial infection as shown by the incorporation of ^{13}C-labeled glucose into fatty acids. However, ACC1-deficient iCD103 DCs or GM-CSF DCs displayed normal maturation capacity, as demonstrated by CD86 and MHCII expression, and IL-12/23p40 and TNF-α secretion upon *M. bovis* BCG infection. Furthermore, even the stimulation with TLR agonists, such as LPS or CpG did not reveal any reduction in DC activation or cytokine production upon ACC1 deletion *in vitro*. Likewise, treatment of iCD103 DCs with SorA and TOFA, two different pharmacological inhibitors of ACCs, did not significantly influence iCD103 DC activation, cytokine production, or T cell priming capacity, despite completely blocking ACC-mediated *de novo* FAS. It is also important to mention that the concentrations of the inhibitors used in this study had no effect on cell viability. These results contrast those by Everts *et al.* who reported impaired activation of GM-CSF DCs upon TLR stimulation in the presence of TOFA or C75, an inhibitor of FASN (30). Although the reason for this discrepancy is not clear, it needs to be considered that pharmacological inhibitors often carry the risk of off-target effects [our own unpublished data and (76)]. For example, the previously employed FASN inhibitor C75 was shown to have toxic effects by attenuating cellular mitochondrial function (77). Whether the concentrations of C75 used in the study by Everts *et al.* also affect cell viability was not further addressed. In addition, C75 also promotes FAO by inducing CPT1 activity (78). Hence, it is possible that some of the properties attributed to FAS inhibition in DCs are a consequence of unspecific effects.

In vivo, FAS was implicated to be essential for the capacity of DCs to prime $CD8^+$ T cell responses (30). In contrast, our results demonstrate that deletion of ACC1 in DCs did not abrogate the cytokine production and maturation capacity of myeloid cells or their ability to prime anti-mycobacterial $CD8^+$ or $CD4^+$ T cell responses *in vivo*. Consequently, DC_ACC1 mice were able to control the infection with *M. bovis* BCG or *Mtb* to the same extent as WT mice. Likewise, DC_ACC1 mice control *Listeria monocytogenes* infection comparable to WT mice (data not shown). Our results also demonstrate that similar to DCs, macrophages upregulate lipid synthesis upon infection with *M. bovis* BCG *in vitro* as evidenced by incorporation of ^{13}C-labeled glucose into lipids and accumulation of phospholipids and neutral lipids. However, upon genetic ablation or pharmacological inhibition of ACC1, BMDMs were still able to upregulate costimulatory molecules and produce pro-inflammatory cytokines to the same extent as WT cells. Additionally, FAS was not required for production of IL-1β, IL-12/23p40, or IFN-γ, generation of protective IFN-γ-secreting $CD4^+$ T cells or the subsequent control of *M. bovis* BCG or *Mtb* infection. Together, our data clearly argues against a pivotal role of *de novo* FAS for DC or macrophage activation and function for priming protective immunity against mycobacterial infection.

Of note, the targeting efficiency in splenic DCs and AMs was higher than 90% in our transgenic mouse models, thus excluding the possibility of residual ACC1 expression due to incomplete targeting. Although we did not evaluate the deletion rate in lung $CD103^+$ DCs in this study, previous work from our laboratory indicates that CD11c *cre* targets about 80% of this cell subset (79). It is important to consider that this genetic approach also partially targets other cell populations. For example, CD11c *cre* also targets AMs in the lung, while LysM *cre* also targets neutrophils (79, 80), probably also excluding a broader role of FAS in other myeloid cell populations.

Mycobacterium tuberculosis survives within macrophages, where it leads to formation of LBs and differentiation into "foamy" macrophages (57). This process has been associated with the induction of *de novo* FAS and cholesterol synthesis in the host macrophage (9, 14). Our findings that bacterial burdens in the lung of WT and MΦ_ACC1 mice are comparable suggest that the *Mtb* strain H37Rv does not strictly depend on FAS within host macrophages. Yet, it needs to be considered that in mice, granulomas do not adequately resemble the fibrocaseous structures containing "foamy" macrophages found in humans (81). Therefore, it might be interesting to address the impact of ACC1 deletion in macrophages on the outcome of anti-mycobacterial immunity and *Mtb* survival in other models, such as in the post-primary tuberculosis model or in IL-13-overexpressing mice, where "foamy" macrophages are highly abundant (11, 82).

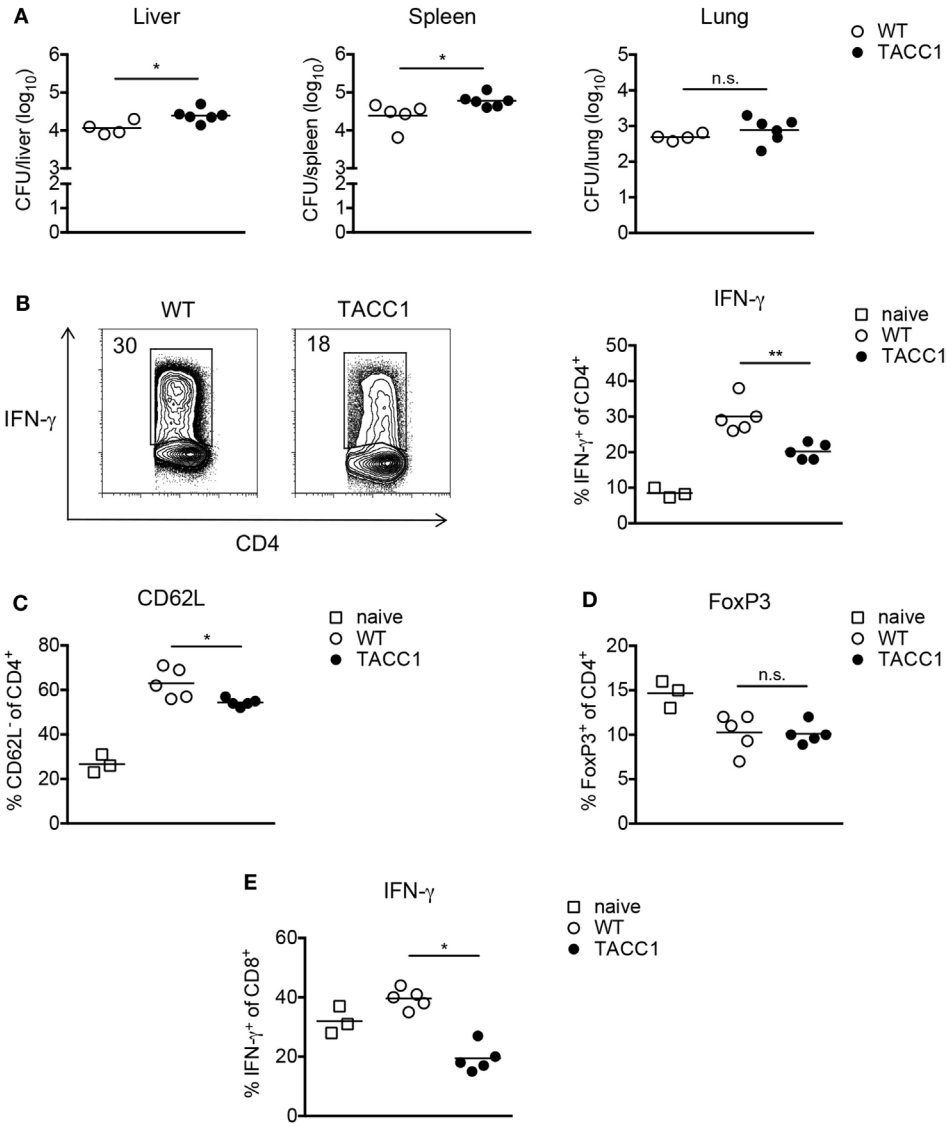


FIGURE 6 | Acetyl-CoA carboxylase (ACC1) deletion in T cells increases susceptibility toward *Mycobacterium bovis* BCG infection. WT and TACC1 mice were infected with 2×10^6 colony forming units (CFU) of *M. bovis* BCG and analyzed on day 21 p.i. **(A)** Bacterial burden in liver, spleen, and lung. **(B–E)** T cell responses were evaluated in spleen 21 days p.i. by flow cytometry. **(B)** Representative flow cytometry plots display the frequency of IFN-γ$^+$ cells within live CD4$^+$ T cells upon re-stimulation with PMA/ionomycin (left panel). Graph represents the frequency of IFN-γ$^+$ cells within live CD4$^+$ T cells (right panel). **(C)** Frequency of CD62L$^-$ cells within live CD4$^+$ T cells. **(D)** Expression of FoxP3 within live CD4$^+$ T cells. **(E)** Frequency of IFN-γ$^+$ cells within live CD8$^+$ T cells. Each symbol represents an individual mouse. Results are representative from three **(C)** or four **(A,B,D,E)** experiments with $n = 3$–6 mice per group. $^*P < 0.05$ and $^{**}P < 0.01$, $^{***}P < 0.001$, $^{****}P < 0.0001$, n.s., non-significant, Student's *t*-test.

"Foamy" macrophages have also been observed at later stages during classical aerosol *Mtb* infection.

The usage of FAS or FAO in myeloid cells has been implicated as a metabolic switch regulating immunity and tolerance. While inflammatory "M1" macrophages have been associated with glycolysis, "M2" macrophages were proposed to be committed to FAO and OXPHOS (55, 83, 84). These "M2" macrophages were reported to be immunomodulatory and poorly microbicidal (85, 86) resulting in impaired anti-mycobacterial function (87). This is supported by the finding that *Mtb* induces the production of IL-10 resulting in "M2" polarization and compromised macrophage function (88). In contrast, a recent study reported that *Mtb* induces the microRNAs miR-33 and miR-33* in macrophages, which suppressed autophagy, lysosomal function, and FAO (89). Thereby, *Mtb* facilitates the accumulation of LBs and promotes its survival, indicating that manipulation of FAO in macrophages might affect their anti-mycobacterial function. In line with the current thoughts about macrophages, FAO in DCs is connected to tolerogenicity. This is highlighted by studies showing that resveratrol or vitamin D3 and dexamethasone promote FAO and tolerogenic function of DCs (90–92). Moreover, FAO and CPT1 activity were reported recently to be crucial for

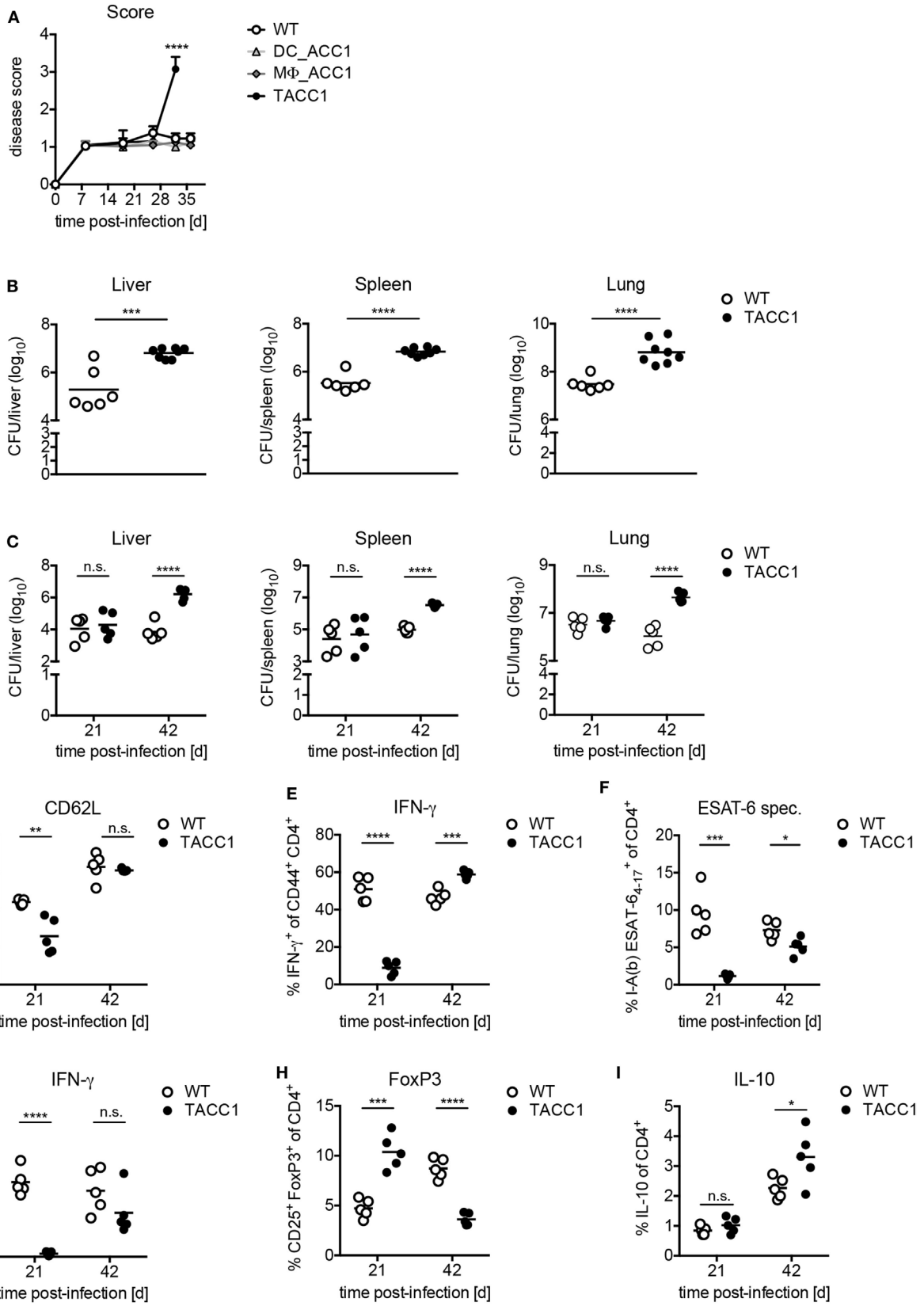


FIGURE 7 | Continued

FIGURE 7 | Acetyl-CoA carboxylase (ACC1) expression in T cells is crucial for immunity against *Mycobacterium tuberculosis* (*Mtb*) infection. **(A)** WT, DC_ACC1, MΦ_ACC1, and TACC1 mice were infected with a high dose of 1,000 colony forming units (CFU) *Mtb via* the aerosol route and the disease score was determined during the course of infection. **(B)** WT and TACC1 mice were infected with a high dose of 1,000 CFU *Mtb via* the aerosol route and the bacterial burden was determined in liver, spleen, and lung on day 32 p.i. **(C)** WT and TACC1 mice were infected with a low dose of 100 CFU *Mtb via* the aerosol route and the bacterial burden was determined in liver, spleen, and lung on day 21 and day 42 p.i. **(D–I)** T cell responses were analyzed in the lung of WT and TACC1 mice on day 21 and day 42 p.i. with a low dose of 100 CFU *Mtb via* aerosol route. **(D)** Frequency of $CD62L^-$ effector T cells among live $CD4^+CD44^+$ cells. **(E)** Frequency of IFN-γ^+ T helper 1 cells within live $CD4^+CD44^+$ T cells upon re-stimulation with anti-CD3/CD28. **(F)** Percentage of I-A^b *Mtb* $ESAT6_{4-17}$ tetramer$^+$ cells among live $CD4^+$ T cells. **(G)** Frequency of $ESAT6_{1-20}$-specific IFN-γ^+ $CD4^+$ T cells per 10^5 total lung cells determined by ELISPOT. **(H)** Frequency of $CD25^+FoxP3^+$ Tregs within live $CD4^+$ gate. **(I)** Frequency of IL-10-producing live $CD4^+$ T cells. Each symbol represents an individual mouse. Results are from one [**(A)**: DC_ACC1, MΦ_ACC1, **(C–H)**: day 42, **(I)**] experiment or as a representative of two [**(A)** WT, TACC1, **(B,C–H)** day 21] experiments with $n = 9–10$ **(A)** or $n = 6–8$ **(B)** or $n = 5$ **(C–I)** mice per group. $^*P < 0.05$ and $^{**}P < 0.01$, $^{***}P < 0.001$, $^{****}P < 0.0001$, n.s., non-significant, Student's *t*-test.

activation of plasmacytoid DCs upon virus infection (93). Yet, it remains unclear whether the rate of FAO affects the function of DCs and macrophages to cope with mycobacterial infection. Using cell-specific deletion of ACC2 in DCs or macrophages, we could demonstrate that these mice control mycobacterial infection to the same extent as WT mice. In addition, the paradigm that FAO is required for "M2" polarization was questioned recently (76, 94). In these studies, conditional deletion of CPT2 in macrophages, which functions together with CPT1 to transport long-chain fatty acids into the mitochondria for FAO, blocked β-oxidation of fatty acids, yet it did not affect "M2" polarization (76, 94). Furthermore, this study suggests that the previously observed block of "M2" polarization by using etomoxir as a pharmacological inhibitor for CPT1 (84, 95) might be due to off-target effects [our own unpublished data and (76)].

Metabolic reprogramming upon activation was not only associated with the activation and function of myeloid cells, but also shown to be crucial for the proliferation, differentiation, and function of T cells (34, 96, 97). Our previous work showed that the development of T helper cells requires *de novo* FAS (33). ACC1-deficient T cells (TACC1) are less pathogenic than WT T cells during autoimmune encephalomyelitis and in a lethal model of acute GVHD, where they permitted survival of recipient mice (35). Our current results indicate that ACC1 deletion diminished the generation of Th1 and $CD8^+$ T cell responses resulting in higher susceptibility against mycobacterial infection. Indeed, when infected with a high aerosol dose of *Mtb*, TACC1 mice succumb to infection as early as 4 weeks, highlighting the importance of *de novo* FAS for IFN-γ production by Th1 and $CD8^+$ T cells. These data are in line with previous publications that established Th1 cells as a prerequisite for the defense against mycobacteria, since mice deficient for Th1-inducing cytokines, as IL-12p40 or IFN-γ, succumb to *Mtb* infection due to high bacterial loads (98–101).

Inflammatory responses are controlled by patrolling Tregs that balance anti-mycobacterial immunity and pathology. Studies in human and mice showed that Tregs expand during *Mtb* infection which was associated with higher bacterial burdens and active Tb (63–65). Our recent data indicate that the deletion of ACC1 in T cells enhances iTreg differentiation [(33) and unpublished data]. Therefore, we speculated that elevated levels of Tregs upon ACC1 deletion might contribute to impaired mycobacterial control in TACC1 mice. Yet, we observed normal Treg frequencies upon *M. bovis* BCG infection and only an early increase during *Mtb* infection that was reversed at day 42. Thus, our results suggest that the lack of protection in TACC1 mice can preferentially be attributed to the impaired ability to generate Th1 cells and not to an increase in Treg development.

Interestingly, genetic ablation or pharmacological inhibition of ACC1 in DCs and macrophages results in higher fatty acid uptake. These results suggest that non-proliferating macrophages and DCs are able to compensate for impaired endogenous FAS by increasing the uptake of external fatty acids. We believe these findings support the notion that myeloid cells are flexible in their choice of substrate, being able to shape their metabolic pathways in order to meet their energetic and biosynthetic demands. Despite displaying a similar compensatory mechanism (data not shown), T cells from TACC1 mice show a strong functional defect upon mycobacterial infection. Together, our data suggest that intrinsic ACC1 expression in DCs and macrophages is dispensable for their activation and function to generate protective immunity against mycobacterial infection. In contrast, ACC1 in highly proliferative T cells constitutes a prerequisite to ensure mycobacterial control.

ETHICS STATEMENT

All animal experiments were performed in compliance with the German animal protection law (TierSchG BGBl. I S. 1105; 25.05.1998). The mice were housed and handled in accordance with good animal practice as defined by FELASA and the national animal welfare body GV-SOLAS. All animal experiments were approved by the Lower Saxony Committee on the Ethics of Animal Experiments as well as the responsible state office (Lower Saxony State Office of Consumer Protection and Food Safety) under the permit numbers 33.19-42502-04-17/2472 and 33.9-42502-04-12/0732 or the Animal Research Ethics Board of the Ministry of the Environment [Kiel, Germany—Permit number: V244-30074/2015 (46-4/15)] considering the German Animal Welfare Act.

AUTHOR CONTRIBUTIONS

Conceptualization: LB, TS. Investigation: PS, LM, HE, CA-S, MS, MG, FK, AH, PG, and JB. Writing and Visualization: PS, LM, CH, TS, and LB. Supervision and Project Administration: LB, TS, W-RA, and CH. Funding Acquisition: LB, TS.

ACKNOWLEDGMENTS

We thank S. J. Wakil (Baylor College of Medicine) for providing ACC1$^{flox/flox}$ and ACC2$^{ko/ko}$ mice, David E. James (University of Sydney) for providing Acaca$^{flox/flox}$ mice, Lis Velasquez for critical reading of the manuscript and all members of the Institute of Infection Immunology at TWINCORE for discussion and support. We would like to acknowledge the assistance of the Cell Sorting Core Facility of the Hannover Medical School. We thank E. Surges for excellent technical help with the ^{13}C incorporation analysis. This work was supported by the Deutsche Forschungsgemeinschaft (DFG; SFB900, project B7) to TS and HiLF to LB. LB was further funded by the Ellen-Schmidt Program from the Hannover Medical School. PS was supported by the International Research Training Group 1273 funded by the German Research Foundation (DFG) and LM by a PhD fellowship from the Boehringer Ingelheim Fonds, Foundation for Basic Research in Medicine.

SUPPLEMENTARY MATERIAL

The Supplementary Material for this article can be found online at https://www.frontiersin.org/articles/10.3389/fimmu.2018.00495/full#supplementary-material.

REFERENCES

1. Weiss G, Schaible UE. Macrophage defense mechanisms against intracellular bacteria. *Immunol Rev* (2015) 264(1):182–203. doi:10.1111/imr.12266
2. Deretic V, Delgado M, Vergne I, Master S, De Haro S, Ponpuak M, et al. Autophagy in immunity against *Mycobacterium tuberculosis*: a model system to dissect immunological roles of autophagy. *Curr Top Microbiol Immunol* (2009) 335:169–88. doi:10.1007/978-3-642-00302-8_8
3. Xu G, Wang J, Gao and GF, Liu CH. Insights into battles between *Mycobacterium tuberculosis* and macrophages. *Protein Cell* (2014) 5(10):728–36. doi:10.1007/s13238-014-0077-5
4. Shi L, Salamon H, Eugenin EA, Pine R, Cooperand A, Gennaro ML. Infection with *Mycobacterium tuberculosis* induces the Warburg effect in mouse lungs. *Sci Rep* (2015) 5:18176. doi:10.1038/srep18176
5. Subbian S, Tsenova L, Kim MJ, Wainwright HC, Visser A, Bandyopadhyay N, et al. Lesion-specific immune response in granulomas of patients with pulmonary tuberculosis: a pilot study. *PLoS One* (2015) 10(7):e0132249. doi:10.1371/journal.pone.0132249
6. Rodriguez-Prados JC, Traves PG, Cuenca J, Rico D, Aragones J, Martin-Sanz P, et al. Substrate fate in activated macrophages: a comparison between innate, classic, and alternative activation. *J Immunol* (2010) 185(1):605–14. doi:10.4049/jimmunol.0901698
7. Galvan-Pena S, O'Neill LA. Metabolic reprograming in macrophage polarization. *Front Immunol* (2014) 5:420. doi:10.3389/fimmu.2014.00420
8. Koo MS, Subbianand S, Kaplan G. Strain specific transcriptional response in *Mycobacterium tuberculosis* infected macrophages. *Cell Commun Signal* (2012) 10(1):2. doi:10.1186/1478-811X-10-2
9. Mehrotra P, Jamwal SV, Saquib N, Sinha N, Siddiqui Z, Manivel V, et al. Pathogenicity of *Mycobacterium tuberculosis* is expressed by regulating metabolic thresholds of the host macrophage. *PLoS Pathog* (2014) 10(7):e1004265. doi:10.1371/journal.ppat.1004265
10. Gleeson LE, Sheedy FJ, Palsson-McDermott EM, Triglia D, O'Leary SM, O'Sullivan MP, et al. Cutting edge: *Mycobacterium tuberculosis* induces aerobic glycolysis in human alveolar macrophages that is required for control of intracellular bacillary replication. *J Immunol* (2016) 196(6):2444–9. doi:10.4049/jimmunol.1501612
11. Hunter RL, Jagannathand C, Actor JK. Pathology of postprimary tuberculosis in humans and mice: contradiction of long-held beliefs. *Tuberculosis (Edinb)* (2007) 87(4):267–78. doi:10.1016/j.tube.2006.11.003
12. Peyron P, Vaubourgeix J, Poquet Y, Levillain F, Botanch C, Bardou F, et al. Foamy macrophages from tuberculous patients' granulomas constitute a nutrient-rich reservoir for *M. tuberculosis* persistence. *PLoS Pathog* (2008) 4(11):e1000204. doi:10.1371/journal.ppat.1000204
13. Gutierrez MG, Master SS, Singh SB, Taylor GA, Colomboand MI, Deretic V. Autophagy is a defense mechanism inhibiting BCG and *Mycobacterium tuberculosis* survival in infected macrophages. *Cell* (2004) 119(6):753–66. doi:10.1016/j.cell.2004.11.038
14. Singh V, Jamwal S, Jain R, Verma P, Gokhaleand R, Rao KV. *Mycobacterium tuberculosis*-driven targeted recalibration of macrophage lipid homeostasis promotes the foamy phenotype. *Cell Host Microbe* (2012) 12(5):669–81. doi:10.1016/j.chom.2012.09.012
15. Singh V, Kaur C, Chaudhary VK, Raoand KV, Chatterjee S. *M. tuberculosis* secretory protein ESAT-6 induces metabolic flux perturbations to drive foamy macrophage differentiation. *Sci Rep* (2015) 5:12906. doi:10.1038/srep12906
16. D'Avila H, Melo RC, Parreira GG, Werneck-Barroso E, Castro-Faria-Netoand HC, Bozza PT. *Mycobacterium bovis* bacillus Calmette-Guerin induces TLR2-mediated formation of lipid bodies: intracellular domains for eicosanoid synthesis in vivo. *J Immunol* (2006) 176(5):3087–97. doi:10.4049/jimmunol.176.5.3087
17. Bodnar KA, Serbinaand NV, Flynn JL. Fate of *Mycobacterium tuberculosis* within murine dendritic cells. *Infect Immun* (2001) 69(2):800–9. doi:10.1128/IAI.69.2.800-809.2001
18. Buettner M, Meinken C, Bastian M, Bhat R, Stossel E, Faller G, et al. Inverse correlation of maturity and antibacterial activity in human dendritic cells. *J Immunol* (2005) 174(7):4203–9. doi:10.4049/jimmunol.174.7.4203
19. Wolf AJ, Linas B, Trevejo-Nunez GJ, Kincaid E, Tamura T, Takatsu K, et al. *Mycobacterium tuberculosis* infects dendritic cells with high frequency and impairs their function in vivo. *J Immunol* (2007) 179(4):2509–19. doi:10.4049/jimmunol.179.4.2509
20. Wolf AJ, Desvignes L, Linas B, Banaiee N, Tamura T, Takatsu K, et al. Initiation of the adaptive immune response to *Mycobacterium tuberculosis* depends on antigen production in the local lymph node, not the lungs. *J Exp Med* (2008) 205(1):105–15. doi:10.1084/jem.20071367
21. Green AM, Difazioand R, Flynn JL. IFN-gamma from CD4 T cells is essential for host survival and enhances CD8 T cell function during *Mycobacterium tuberculosis* infection. *J Immunol* (2013) 190(1):270–7. doi:10.4049/jimmunol.1200061
22. Tian T, Woodworth J, Skoldand M, Behar SM. In vivo depletion of CD11c+ cells delays the CD4+ T cell response to *Mycobacterium tuberculosis* and exacerbates the outcome of infection. *J Immunol* (2005) 175(5):3268–72. doi:10.4049/jimmunol.175.5.3268
23. Maldonado MA, MacDonald GC, Kakkanaiah VN, Fecho K, Dransfield M, Sekiguchi D, et al. Differential control of autoantibodies and lymphoproliferation by Fas ligand expression on CD4+ and CD8+ T cells in vivo. *J Immunol* (1999) 163(6):3138–42.
24. Hochrein H, Shortman K, Vremec D, Scott B, Hertzogand P, O'Keeffe M. Differential production of IL-12, IFN-alpha, and IFN-gamma by mouse dendritic cell subsets. *J Immunol* (2001) 166(9):5448–55. doi:10.4049/jimmunol.166.9.5448
25. Shortman K, Heath WR. The CD8+ dendritic cell subset. *Immunol Rev* (2010) 234(1):18–31. doi:10.1111/j.0105-2896.2009.00870.x
26. Sung SS, Fu SM, Rose CE Jr, Gaskin F, Juand ST, Beaty SR. A major lung CD103 (alphaE)-beta7 integrin-positive epithelial dendritic cell population expressing Langerin and tight junction proteins. *J Immunol* (2006) 176(4):2161–72. doi:10.4049/jimmunol.176.4.2161
27. Leepiyasakulchai C, Ignatowicz L, Pawlowski A, Kalleniusand G, Skold M. Failure to recruit anti-inflammatory CD103+ dendritic cells and a diminished CD4+ Foxp3+ regulatory T cell pool in mice that display excessive lung inflammation and increased susceptibility to *Mycobacterium tuberculosis*. *Infect Immun* (2012) 80(3):1128–39. doi:10.1128/IAI.05552-11
28. Berod L, Stuve P, Swallow M, Arnold-Schrauf C, Kruse F, Gentilini MV, et al. MyD88 signalling in myeloid cells is sufficient to prevent chronic mycobacterial infection. *Eur J Immunol* (2014) 44(5):1399–409. doi:10.1002/eji.201344039
29. Krawczyk CM, Holowka T, Sun J, Blagih J, Amiel E, DeBerardinis RJ, et al. Toll-like receptor-induced changes in glycolytic metabolism regulate dendritic cell activation. *Blood* (2010) 115(23):4742–9. doi:10.1182/blood-2009-10-249540

30. Everts B, Amiel E, Huang SC, Smith AM, Chang CH, Lam WY, et al. TLR-driven early glycolytic reprogramming via the kinases TBK1-IKKvarepsilon supports the anabolic demands of dendritic cell activation. *Nat Immunol* (2014) 15(4):323–32. doi:10.1038/ni.2833
31. Herber DL, Cao W, Nefedova Y, Novitskiy SV, Nagaraj S, Tyurin VA, et al. Lipid accumulation and dendritic cell dysfunction in cancer. *Nat Med* (2010) 16(8):880–6. doi:10.1038/nm.2172
32. Wakil SJ, Abu-Elheiga LA. Fatty acid metabolism: target for metabolic syndrome. *J Lipid Res* (2009) 50(Suppl):S138–43. doi:10.1194/jlr.R800079-JLR200
33. Berod L, Friedrich C, Nandan A, Freitag J, Hagemann S, Harmrolfs K, et al. De novo fatty acid synthesis controls the fate between regulatory T and T helper 17 cells. *Nat Med* (2014) 20(11):1327–33. doi:10.1038/nm.3704
34. Lochner M, Berodand L, Sparwasser T. Fatty acid metabolism in the regulation of T cell function. *Trends Immunol* (2015) 36(2):81–91. doi:10.1016/j.it.2014.12.005
35. Raha S, Raud B, Oberdorfer L, Castro CN, Schreder A, Freitag J, et al. Disruption of de novo fatty acid synthesis via acetyl-CoA carboxylase 1 inhibition prevents acute graft-versus-host disease. *Eur J Immunol* (2016) 46(9):2233–8. doi:10.1002/eji.201546152
36. Mao J, DeMayo FJ, Li H, Abu-Elheiga L, Gu Z, Shaikenov TE, et al. Liver-specific deletion of acetyl-CoA carboxylase 1 reduces hepatic triglyceride accumulation without affecting glucose homeostasis. *Proc Natl Acad Sci U S A* (2006) 103(22):8552–7. doi:10.1073/pnas.0603115103
37. Lee J, Walsh MC, Hoehn KL, James DE, Wherryand EJ, Choi Y. Regulator of fatty acid metabolism, acetyl coenzyme a carboxylase 1, controls T cell immunity. *J Immunol* (2014) 192(7):3190–9. doi:10.4049/jimmunol.1302985
38. Olson DP, Pulinilkunnil T, Cline GW, Shulmanand GI, Lowell BB. Gene knockout of Acc2 has little effect on body weight, fat mass, or food intake. *Proc Natl Acad Sci U S A* (2010) 107(16):7598–603. doi:10.1073/pnas.0913492107
39. Lee PP, Fitzpatrick DR, Beard C, Jessup HK, Lehar S, Makar KW, et al. A critical role for Dnmt1 and DNA methylation in T cell development, function, and survival. *Immunity* (2001) 15(5):763–74. doi:10.1016/S1074-7613(01)00227-8
40. Clausen BE, Burkhardt C, Reith W, Renkawitzand R, Forster I. Conditional gene targeting in macrophages and granulocytes using LysMcre mice. *Transgenic Res* (1999) 8(4):265–77. doi:10.1023/A:1008942828960
41. Caton ML, Smith-Raskaand MR, Reizis B. Notch-RBP-J signaling controls the homeostasis of CD8- dendritic cells in the spleen. *J Exp Med* (2007) 204(7):1653–64. doi:10.1084/jem.20062648
42. Abu-Elheiga L, Matzuk MM, Abo-Hashemaand KA, Wakil SJ. Continuous fatty acid oxidation and reduced fat storage in mice lacking acetyl-CoA carboxylase 2. *Science* (2001) 291(5513):2613–6. doi:10.1126/science.1056843
43. Tamura T, Ariga H, Kinashi T, Uehara S, Kikuchi T, Nakada M, et al. The role of antigenic peptide in CD4+ T helper phenotype development in a T cell receptor transgenic model. *Int Immunol* (2004) 16(12):1691–9. doi:10.1093/intimm/dxh170
44. Schaefer M, Reiling N, Fessler C, Stephani J, Taniuchi I, Hatam F, et al. Decreased pathology and prolonged survival of human DC-SIGN transgenic mice during mycobacterial infection. *J Immunol* (2008) 180(10):6836–45. doi:10.4049/jimmunol.180.10.6836
45. Berod L, Stuve P, Varela F, Behrends J, Swallow M, Kruse F, et al. Rapid rebound of the Treg compartment in DEREG mice limits the impact of Treg depletion on mycobacterial burden, but prevents autoimmunity. *PLoS One* (2014) 9(7):e102804. doi:10.1371/journal.pone.0102804
46. Morton DB, Griffiths PH. Guidelines on the recognition of pain, distress and discomfort in experimental animals and an hypothesis for assessment. *Vet Rec* (1985) 116(16):431–6. doi:10.1136/vr.116.16.431
47. Mayer CT, Ghorbani P, Nandan A, Dudek M, Arnold-Schrauf C, Hesse C, et al. Selective and efficient generation of functional Batf3-dependent CD103+ dendritic cells from mouse bone marrow. *Blood* (2014) 124(20):3081–91. doi:10.1182/blood-2013-12-545772
48. Zal T, Volkmannand A, Stockinger B. Mechanisms of tolerance induction in major histocompatibility complex class II-restricted T cells specific for a blood-borne self-antigen. *J Exp Med* (1994) 180(6):2089–99. doi:10.1084/jem.180.6.2089
49. Abraham WR, Hesse C. Isotope fractionations in the biosynthesis of cell components by different fungi: a basis for environmental carbon flux studies. *FEMS Microbiol Ecol* (2003) 46(1):121–8. doi:10.1016/S0168-6496(03)00203-4
50. Koh VH, Ng SL, Ang ML, Lin W, Ruedland C, Alonso S. Role and contribution of pulmonary CD103+ dendritic cells in the adaptive immune response to *Mycobacterium tuberculosis*. *Tuberculosis (Edinb)* (2017) 102:34–46. doi:10.1016/j.tube.2016.12.003
51. von Meyenn FM, Schaefer H, Weighardt S, Bauer C, Kirschning J, Wagner H, et al. Toll-like receptor 9 contributes to recognition of *Mycobacterium bovis* bacillus Calmette-Guerin by Flt3-ligand generated dendritic cells. *Immunobiology* (2006) 211(6–8):557–65. doi:10.1016/j.imbio.2006.05.004
52. Khader SA, Bell GK, Pearl JE, Fountain JJ, Rangel-Moreno J, Cilley GE, et al. IL-23 and IL-17 in the establishment of protective pulmonary CD4+ T cell responses after vaccination and during *Mycobacterium tuberculosis* challenge. *Nat Immunol* (2007) 8(4):369–77. doi:10.1038/ni1449
53. Gopal R, Rangel-Moreno J, Slight S, Lin Y, Nawar HF, Fallert Junecko BA, et al. Interleukin-17-dependent CXCL13 mediates mucosal vaccine-induced immunity against tuberculosis. *Mucosal Immunol* (2013) 6(5):972–84. doi:10.1038/mi.2012.135
54. Gopal R, Monin L, Slight S, Uche U, Blanchard E, Fallert Junecko BA, et al. Unexpected role for IL-17 in protective immunity against hypervirulent *Mycobacterium tuberculosis* HN878 infection. *PLoS Pathog* (2014) 10(5):e1004099. doi:10.1371/journal.ppat.1004099
55. Pearce EL, Pearce EJ. Metabolic pathways in immune cell activation and quiescence. *Immunity* (2013) 38(4):633–43. doi:10.1016/j.immuni.2013.04.005
56. Ganeshan K, Chawla A. Metabolic regulation of immune responses. *Annu Rev Immunol* (2014) 32:609–34. doi:10.1146/annurev-immunol-032713-120236
57. Russell DG, Cardona PJ, Kim MJ, Allainand S, Altare F. Foamy macrophages and the progression of the human tuberculosis granuloma. *Nat Immunol* (2009) 10(9):943–8. doi:10.1038/ni.1781
58. Gerth K, Bedorf N, Irschik H, Hofleand G, Reichenbach H. The soraphens: a family of novel antifungal compounds from *Sorangium cellulosum* (Myxobacteria). I. Soraphen A1 alpha: fermentation, isolation, biological properties. *J Antibiot (Tokyo)* (1994) 47(1):23–31. doi:10.7164/antibiotics.47.23
59. Vahlensieck HF, Pridzun L, Reichenbachand H, Hinnen A. Identification of the yeast ACC1 gene product (acetyl-CoA carboxylase) as the target of the polyketide fungicide soraphen A. *Curr Genet* (1994) 25(2):95–100. doi:10.1007/BF00309532
60. Shen Y, Volrath SL, Weatherly SC, Elichand TD, Tong L. A mechanism for the potent inhibition of eukaryotic acetyl-coenzyme A carboxylase by soraphen A, a macrocyclic polyketide natural product. *Mol Cell* (2004) 16(6):881–91. doi:10.1016/j.molcel.2004.11.034
61. Endo Y, Asou HK, Matsugae N, Hirahara K, Shinoda K, Tumes DJ, et al. Obesity drives Th17 cell differentiation by inducing the lipid metabolic kinase, ACC1. *Cell Rep* (2015) 12(6):1042–55. doi:10.1016/j.celrep.2015.07.014
62. Angela M, Endo Y, Asou HK, Yamamoto T, Tumes DJ, Tokuyama H, et al. Fatty acid metabolic reprogramming via mTOR-mediated inductions of PPARgamma directs early activation of T cells. *Nat Commun* (2016) 7:13683. doi:10.1038/ncomms13683
63. Scott-Browne JP, Shafiani S, Tucker-Heard G, Ishida-Tsubota K, Fontenot JD, Rudensky AY, et al. Expansion and function of Foxp3-expressing T regulatory cells during tuberculosis. *J Exp Med* (2007) 204(9):2159–69. doi:10.1084/jem.20062105
64. Guyot-Revol V, Innes JA, Hackforth S, Hinksand T, Lalvani A. Regulatory T cells are expanded in blood and disease sites in patients with tuberculosis. *Am J Respir Crit Care Med* (2006) 173(7):803–10. doi:10.1164/rccm.200508-1294OC
65. Chen X, Zhou B, Li M, Deng Q, Wu X, Le X, et al. CD4(+)CD25(+)FoxP3(+) regulatory T cells suppress *Mycobacterium tuberculosis* immunity in patients with active disease. *Clin Immunol* (2007) 123(1):50–9. doi:10.1016/j.clim.2006.11.009
66. Hougardy JM, Verscheure V, Lochtand C, Mascart F. In vitro expansion of CD4+CD25highFOXP3+CD127low/- regulatory T cells from peripheral blood lymphocytes of healthy *Mycobacterium tuberculosis*-infected humans. *Microbes Infect* (2007) 9(11):1325–32. doi:10.1016/j.micinf.2007.06.004
67. Berod L, Puttur F, Huehnand J, Sparwasser T. Tregs in infection and vaccinology: heroes or traitors? *Microb Biotechnol* (2012) 5(2):260–9. doi:10.1111/j.1751-7915.2011.00299.x
68. Helft J, Bottcher J, Chakravarty P, Zelenay S, Huotari J, Schraml BU, et al. GM-CSF mouse bone marrow cultures comprise a heterogeneous population

of CD11c(+)MHCII(+) macrophages and dendritic cells. *Immunity* (2015) 42(6):1197–211. doi:10.1016/j.immuni.2015.05.018
69. Ginhoux F, Liu K, Helft J, Bogunovic M, Greter M, Hashimoto D, et al. The origin and development of nonlymphoid tissue CD103+ DCs. *J Exp Med* (2009) 206(13):3115–30. doi:10.1084/jem.20091756
70. Grace PS, Ernst JD. Suboptimal antigen presentation contributes to virulence of *Mycobacterium tuberculosis* in vivo. *J Immunol* (2016) 196(1):357–64. doi:10.4049/jimmunol.1501494
71. Jiao X, Lo-Man R, Guermonprez P, Fiette L, Deriaud E, Burgaud S, et al. Dendritic cells are host cells for mycobacteria in vivo that trigger innate and acquired immunity. *J Immunol* (2002) 168(3):1294–301. doi:10.4049/jimmunol.168.3.1294
72. Herrmann JL, Lagrange PH. Dendritic cells and *Mycobacterium tuberculosis*: which is the Trojan horse? *Pathol Biol (Paris)* (2005) 53(1):35–40. doi:10.1016/j.patbio.2004.01.004
73. Bonham CA, Lu L, Hoffman RA, Simmonsand RL, Thomson AW. Generation of nitric oxide by mouse dendritic cells and its implications for immune response regulation. *Adv Exp Med Biol* (1997) 417:283–90. doi:10.1007/978-1-4757-9966-8_46
74. Everts B, Amiel E, van der Windt GJ, Freitas TC, Chott R, Yarasheski KE, et al. Commitment to glycolysis sustains survival of NO-producing inflammatory dendritic cells. *Blood* (2012) 120(7):1422–31. doi:10.1182/blood-2012-03-419747
75. Adams LB, Dinauer MC, Morgensternand DE, Krahenbuhl JL. Comparison of the roles of reactive oxygen and nitrogen intermediates in the host response to *Mycobacterium tuberculosis* using transgenic mice. *Tuber Lung Dis* (1997) 78(5–6):237–46. doi:10.1016/S0962-8479(97)90004-6
76. Nomura M, Liu J, Rovira II, Gonzalez-Hurtado E, Lee J, Wolfgang MJ, et al. Fatty acid oxidation in macrophage polarization. *Nat Immunol* (2016) 17(3):216–7. doi:10.1038/ni.3366
77. Chen C, Han X, Zou X, Li Y, Yang L, Cao K, et al. 4-methylene-2-octyl-5-oxotetrahydrofuran-3-carboxylic acid (C75), an inhibitor of fatty-acid synthase, suppresses the mitochondrial fatty acid synthesis pathway and impairs mitochondrial function. *J Biol Chem* (2014) 289(24):17184–94. doi:10.1074/jbc.M114.550806
78. Thupari JN, Landree LE, Ronnettand GV, Kuhajda FP. C75 increases peripheral energy utilization and fatty acid oxidation in diet-induced obesity. *Proc Natl Acad Sci U S A* (2002) 99(14):9498–502. doi:10.1073/pnas.132128899
79. Dudek M, Puttur F, Arnold-Schrauf C, Kuhl AA, Holzmann B, Henriques-Normark B, et al. Lung epithelium and myeloid cells cooperate to clear acute pneumococcal infection. *Mucosal Immunol* (2016) 9(5):1288–302. doi:10.1038/mi.2015.128
80. Abram CL, Roberge GL, Huand Y, Lowell CA. Comparative analysis of the efficiency and specificity of myeloid-Cre deleting strains using ROSA-EYFP reporter mice. *J Immunol Methods* (2014) 408:89–100. doi:10.1016/j.jim.2014.05.009
81. Russell DG, Barry CE III, Flynn JL. Tuberculosis: what we don't know can, and does, hurt us. *Science* (2010) 328(5980):852–6. doi:10.1126/science.1184784
82. Heitmann L, Abad Dar M, Schreiber T, Erdmann H, Behrends J, McKenzie AN, et al. The IL-13/IL-4Ralpha axis is involved in tuberculosis-associated pathology. *J Pathol* (2014) 234(3):338–50. doi:10.1002/path.4399
83. Odegaard JI, Chawla A. The immune system as a sensor of the metabolic state. *Immunity* (2013) 38(4):644–54. doi:10.1016/j.immuni.2013.04.001
84. Huang SC, Everts B, Ivanova Y, O'Sullivan D, Nascimento M, Smith AM, et al. Cell-intrinsic lysosomal lipolysis is essential for alternative activation of macrophages. *Nat Immunol* (2014) 15(9):846–55. doi:10.1038/ni.2956
85. Raju B, Hoshino Y, Belitskaya-Lévy I, Dawson R, Ress S, Gold JA, et al. Gene expression profiles of bronchoalveolar cells in pulmonary TB. *Tuberculosis (Edinb)* (2008) 88(1):39–51. doi:10.1016/j.tube.2007.07.003
86. Martinez FO, Helmingand L, Gordon S. Alternative activation of macrophages: an immunologic functional perspective. *Annu Rev Immunol* (2009) 27:451–83. doi:10.1146/annurev.immunol.021908.132532
87. Kahnert A, Seiler P, Stein M, Bandermann S, Hahnke K, Mollenkopf H, et al. Alternative activation deprives macrophages of a coordinated defense program to *Mycobacterium tuberculosis*. *Eur J Immunol* (2006) 36(3):631–47. doi:10.1002/eji.200535496
88. Schreiber T, Ehlers S, Heitmann L, Rausch A, Mages J, Murray PJ, et al. Autocrine IL-10 induces hallmarks of alternative activation in macrophages and suppresses antituberculosis effector mechanisms without compromising T cell immunity. *J Immunol* (2009) 183(2):1301–12. doi:10.4049/jimmunol.0803567
89. Ouimet M, Koster S, Sakowski E, Ramkhelawon B, van Solingen C, Oldebeken S, et al. *Mycobacterium tuberculosis* induces the miR-33 locus to reprogram autophagy and host lipid metabolism. *Nat Immunol* (2016) 17(6):677–86. doi:10.1038/ni.3434
90. Svajger U, Obermajerand N, Jeras M. Dendritic cells treated with resveratrol during differentiation from monocytes gain substantial tolerogenic properties upon activation. *Immunology* (2010) 129(4):525–35. doi:10.1111/j.1365-2567.2009.03205.x
91. Ferreira GB, Vanherwegen AS, Eelen G, Gutierrez AC, Van Lommel L, Marchal K, et al. Vitamin D3 induces tolerance in human dendritic cells by activation of intracellular metabolic pathways. *Cell Rep* (2015) 10(5):711–25. doi:10.1016/j.celrep.2015.01.013
92. Malinarich F, Duan K, Hamid RA, Bijin A, Lin WX, Poidinger M, et al. High mitochondrial respiration and glycolytic capacity represent a metabolic phenotype of human tolerogenic dendritic cells. *J Immunol* (2015) 194(11):5174–86. doi:10.4049/jimmunol.1303316
93. Wu D, Sanin DE, Everts B, Chen Q, Qiu J, Buck MD, et al. Type 1 interferons induce changes in core metabolism that are critical for immune function. *Immunity* (2016) 44(6):1325–36. doi:10.1016/j.immuni.2016.06.006
94. Gonzalez-Hurtado E, Lee J, Choi J, Selen Alpergin ES, Collins SL, Horton MR, et al. Loss of macrophage fatty acid oxidation does not potentiate systemic metabolic dysfunction. *Am J Physiol Endocrinol Metab* (2017) 312(5):E381–93. doi:10.1152/ajpendo.00408.2016
95. Vats D, Mukundan L, Odegaard JI, Zhang L, Smith KL, Morel CR, et al. Oxidative metabolism and PGC-1beta attenuate macrophage-mediated inflammation. *Cell Metab* (2006) 4(1):13–24. doi:10.1016/j.cmet.2006.08.006
96. MacIver NJ, Michalekand RD, Rathmell JC. Metabolic regulation of T lymphocytes. *Annu Rev Immunol* (2013) 31:259–83. doi:10.1146/annurev-immunol-032712-095956
97. Almeida L, Lochner M, Berodand L, Sparwasser T. Metabolic pathways in T cell activation and lineage differentiation. *Semin Immunol* (2016) 28(5):514–24. doi:10.1016/j.smim.2016.10.009
98. Cooper AM, Dalton DK, Stewart TA, Griffin JP, Russelland DG, Orme IM. Disseminated tuberculosis in interferon gamma gene-disrupted mice. *J Exp Med* (1993) 178(6):2243–7. doi:10.1084/jem.178.6.2243
99. Cooper AM, Magram J, Ferranteand J, Orme IM. Interleukin 12 (IL-12) is crucial to the development of protective immunity in mice intravenously infected with *Mycobacterium tuberculosis*. *J Exp Med* (1997) 186(1):39–45. doi:10.1084/jem.186.1.39
100. Caruso AM, Serbina N, Klein E, Triebold K, Bloomand BR, Flynn JL. Mice deficient in CD4 T cells have only transiently diminished levels of IFN-gamma, yet succumb to tuberculosis. *J Immunol* (1999) 162(9):5407–16.
101. Mogues T, Goodrich ME, Ryan L, LaCourseand R, North RJ. The relative importance of T cell subsets in immunity and immunopathology of airborne *Mycobacterium tuberculosis* infection in mice. *J Exp Med* (2001) 193(3):271–80. doi:10.1084/jem.193.3.271

Conflict of Interest Statement: The authors declare that the research was conducted in the absence of any commercial or financial relationships that could be construed as a potential conflict of interest.

Copyright © 2018 Stüve, Minarrieta, Erdmann, Arnold-Schrauf, Swallow, Guderian, Krull, Hölscher, Ghorbani, Behrends, Abraham, Hölscher, Sparwasser and Berod. This is an open-access article distributed under the terms of the Creative Commons Attribution License (CC BY). The use, distribution or reproduction in other forums is permitted, provided the original author(s) and the copyright owner are credited and that the original publication in this journal is cited, in accordance with accepted academic practice. No use, distribution or reproduction is permitted which does not comply with these terms.

frontiers in Immunology

MINI REVIEW
published: 30 January 2018
doi: 10.3389/fimmu.2018.00086

Proteomics of *Mycobacterium* Infection: Moving towards a Better Understanding of Pathogen-Driven Immunomodulation

Eik Hoffmann, Arnaud Machelart, Ok-Ryul Song and Priscille Brodin*

CNRS, INSERM, CHU Lille, U1019, UMR8204, Centre d'Infection et d'Immunité de Lille (CIIL), Institut Pasteur de Lille, Université de Lille, Lille, France

Intracellular bacteria are responsible for many infectious diseases in humans and have developed diverse mechanisms to interfere with host defense pathways. In particular, intracellular vacuoles are an essential niche used by pathogens to alter cellular and organelle functions, which facilitate replication and survival. *Mycobacterium tuberculosis* (Mtb), the pathogen causing tuberculosis in humans, is not only able to modulate its intraphagosomal fate by blocking phagosome maturation but has also evolved strategies to successfully prevent clearance by immune cells and to establish long-term survival in the host. Mass spectrometry (MS)-based proteomics allows the identification and quantitative analysis of complex protein mixtures and is increasingly employed to investigate host–pathogen interactions. Major challenges are limited availability and purity of pathogen-containing compartments as well as the asymmetric ratio in protein abundance when comparing bacterial and host proteins during the infection. Recent advances in purification techniques and MS technology helped to overcome previous difficulties and enable the detailed proteomic characterization of infected host cells and their pathogen-containing vacuoles. Here, we summarize current findings of the proteomic analysis of *Mycobacterium*-infected host cells and highlight progress that has been made to study the protein composition of mycobacterial vacuoles. Current investigations focus on the pathogenicity during Mtb infection, which will allow to better understand pathogen-induced changes and immunomodulation of infected host cells. Consequently, future research in this field will have important implications on host response, pathogen survival, and persistence, induced adaptive immunity and metabolic changes of immune cells promoting the development of novel host-directed therapies in tuberculosis.

Keywords: host–pathogen interactions, immunometabolism, mass spectrometry, mycobacterial infection, *Mycobacterium tuberculosis*, phagocytosis, phagosome maturation, proteomics

OPEN ACCESS

Edited by:
Yoann Rombouts, UMR5089 Institut de Pharmacologie et de Biologie Structurale (IPBS), France

Reviewed by:
Roland Lang, Universitätsklinikum Erlangen, Germany
Shashank Gupta, Brown University, United States

****Correspondence:***
Eik Hoffmann
eik.hoffmann@ibl.cnrs.fr

Specialty section:
This article was submitted to Microbial Immunology, a section of the journal Frontiers in Immunology

Received: *02 November 2017*
Accepted: *11 January 2018*
Published: *30 January 2018*

Citation:
Hoffmann E, Machelart A, Song O-R and Brodin P (2018) Proteomics of Mycobacterium Infection: Moving towards a Better Understanding of Pathogen-Driven Immunomodulation. Front. Immunol. 9:86. doi: 10.3389/fimmu.2018.00086

INTRODUCTION

Phagocytic cells, such as macrophages, dendritic cells, and neutrophils, represent the first line of defense against invading pathogens, such as *Legionella pneumophila*, *Coxiella burnetti*, and *Leishmania donovani*, by engulfing and eliminating them by phagocytosis. Phagocytosis is a complex process divided in several steps, which is initiated by the innate recognition of microbial patterns,

leading to the formation of microbe-containing vesicles. These vesicles fuse successively with different endocytic compartments [early endosome (EE) and late endosome (LE), and lysosomes (LYSs)] to form a microbicidal organelle, the phagolysosome (1). This process results in the formation of an acidic, oxidative, and degradative environment, which is additionally influenced by immune signals inside and outside of the phagocyte that determine phagosomal fate (2). However, pathogen-containing vacuoles (PCVs) are also occupied and altered by intracellular pathogens providing a successful niche to survive and replicate within phagocytes. Therefore, it is not surprising that numerous microbes developed a wide variety of strategies to adapt and manipulate the phagocytic process (3).

Among these strategies induced by intracellular pathogens, the phagosome maturation arrest initiated by *Mycobacterium tuberculosis* (Mtb) infection allows the colonization of phagocytes and long-term survival within host cells (4). Mtb is causing tuberculosis (TB) in humans with more than 1.3 million deaths each year and an increasing incidence of drug-resistant strains (5). In addition to the lack of an efficient vaccine, tuberculosis remains together with malaria and HIV/AIDS one of the deadliest infectious diseases worldwide. The inter- and intracellular modifications of the host environment induced by Mtb infection are diverse and not fully understood (6). Briefly, after phagocytic uptake, mycobacteria-containing vacuoles (MCVs) are formed, which were shown to interact and exchange material with early endosomal compartments but are devoid of, or only interact transiently, with molecules of LEs and LYSs and are able to retain a pH at around 6.5 within MCVs. The lack of phagosomal acidification is mostly due to a defective retention of the vacuolar proton ATPase (V-ATPase) complex at the phagosome (7, 8). Moreover, it was also considered for long that MCVs are sealed, but recent findings demonstrated that Mtb is able to induce vacuolar rupture, thereby allowing direct interactions of bacterial components with host cytosolic proteins (9–11). Despite numerous studies analyzing the host machinery that controls spatiotemporal vacuolar acidification, progression of phagosome maturation, and intracellular survival of different *Mycobacterium* species, the Mtb-induced delay of phagosome maturation is not fully characterized. Furthermore, we also only begin to understand the impact of the different virulence factor secreted upon Mtb infection, which additionally interfere with host pathways to promote Mtb survival and growth (12). Together with the fact that the existing BCG vaccine is inefficient and needs further improvement and alternatives (13), it is clear that we need more knowledge of mycobacterial pathogenesis and the host factors manipulated by Mtb allowing to establish its intracellular niche. In particular, a better understanding of host immune responses and the involved mechanisms controlling the infection are needed, because they affect disease outcome as well as TB pathology. The possibility of modulating host immunity to maximize mycobacterial killing while minimizing inflammatory tissue damage has received increasing attention in recent years and is applied as novel host-directed therapy against drug-resistant Mtb strains (14).

The development of powerful and sensitive mass spectrometry (MS)-based methods during the past decade allows now the accurate, spatiotemporal identification, quantification, and modification of almost any expressed protein (15). These robust methodologies are increasingly applied to study host–pathogen interactions and to elucidate the proteome of the pathogen itself, of infected cells and of subcellular compartments. In the case of Mtb infection, protein profiling of different mycobacterial strains as well as of clinical, drug-resistant isolates increased tremendously our knowledge about their proteome (16, 17), while MS methods also helped to identify biomarkers of Mtb-infected patients (18). Many previous MS studies on host infection were carried out with non-pathogenic mycobacteria strains or were performed with beads coated with single mycobacterial virulence factors, while data on virulent Mtb strains were scarce. Here, we want to focus on the host side of mycobacterial infection and summarize current findings of the proteomic analysis of *Mycobacterium*-infected cells and the progress that has been made in the purification of PCVs that helped to overcome previous difficulties and will allow the detailed and reproducible proteomic characterization of MCVs to better understand Mtb pathogenicity. In this review, we aim to point out the potential of current MS technology to increase our knowledge of the host response during Mtb infection including pathogen-driven immunomodulation.

PROTEOME ANALYSIS OF MYCOBACTERIA-INFECTED CELLS

The intracellular niche protects mycobacteria from cellular and humoral component of the immune system. To overcome host cell defense mechanisms, Mtb subverts the normal passage through the endocytic pathway to form a distinct replicative membranous compartment. Furthermore, Mtb is also able to induce vacuolar rupture to reach nutrients in the host cytosol and to escape host defense pathways, both favoring Mtb growth. Therefore, several proteome studies of mycobacteria-infected cells were initiated to collect an inventory of host cell factors required to establish mycobacterial colonization at the cellular level. By using liquid chromatography–tandem MS (LC–MS/MS) approaches for proteome analysis, high identification rates were achieved, which also allow the measurement of the quantitative state of cellular proteomes at any given time of infection (19). In addition, the introduction of stable isotope labeling of proteins prior MS analysis further improved the relative quantification of complex proteomic samples (20). This approach has gained success due to its high proteome coverage, quantification reliability, and high-throughput format. Over the past years, a few MS studies addressed infection settings with virulent and avirulent strains of the Mtb complex, which we have summarized in **Table 1A** that gave insight on the host environment during mycobacterial colonization.

In one of the first studies, Shui et al. published a list of 166 murine macrophage proteins, which showed a differential expression after Mtb lipid exposure (21). Lipids of the mycobacterial cell wall represent approximately 60% of the total bacterial dry weight (37) and were shown to be actively trafficked out of the MCV (38). After both metabolic stable isotope labeling by amino acids in cell culture and chemical isobaric tagging (iTRAQ), the authors found that Mtb lipids act on diverse cellular processes, such as immune response, apoptosis, metabolism, vesicle transport, and signal transduction (21). In addition, also Fc gamma

TABLE 1 | List of host proteomic studies of mycobacterial infection performed (A) on total cellular extracts, (B) on isolated cell organelles of infected cells, and (C) specifically on mycobacteria-containing vacuoles (MCVs) and bead-containing phagosomes.

Reference	Type of sample	Experimental design	Peptide labeling	Proteins affected by infection	Main findings/pathways affected by mycobacterial infection
(A) Mass spectrometry (MS) data of total cellular host proteins					
Shui et al. (21)	Cellular extract	J774.A1 treated by *Mycobacterium tuberculosis* (Mtb) lipid extract	iTRAQ/SILAC	166	Immune response, oxidation and reduction, signal transduction, vesicle transport, metabolism, etc.
Yu et al. (22)	Lung tissue	Mtb-infected patient tissue, negative for HIV and HBV	Label-free	6 Mtb peptides	Identification of novel Mtb antigens from granuloma lesions, antigen-specific IFN-γ secretion, and functional CTL responses
Kaewseekhao et al. (23)	Cellular extract/ supernatant	THP-1 infected by Mtb H37Rv (MOI 1; 1–5 days)	Label-free	283	Cell cycle, antimicrobial and inflammatory responses, DNA replication, etc.
Li et al. (24)	Cellular extract	THP-1 infected by Mtb H37Rv/H37Ra or beads (MOI 35; 12 h)	TMT	235	Apoptosis, blood coagulation, and oxidative phosphorylation
Li et al. (25)	Cellular extract	THP-1 infected by BCG/*Mycobacterium bovis*/Mtb H37Rv (MOI 10; 24 h)	iTRAQ	61	Phagosome maturation and TNF signaling
(B) MS data of cell organelle proteins					
Wang et al. (26)	Cytoplasm and nucleus	RAW264.7 infected by *Mycobacterium marinum* (MOI 10; 4 h)	AACT/SILAC	1,429	Toll-like receptor 2-inflammatory responses, major histocompatibility complex-I processing and presentation, and transcriptional factors
Saquib et al. (27)	Endoplasmic reticulum	THP-1 infected by Mtb H37Rv/H37Ra (MOI 10; 12 h)	SILAC	133	Cytosolic Ca^{2+} levels, apoptosis, and cholesterol homeostasis
Diaz et al. (28)	Exosome	THP-1 infected by Mtb H37Rv (MOI 5; 24 h)	Biotinylated	41	Analysis of the exosome content
Kumar et al. (29)	Secretome	THP-1 infected by Mtb H37Rv/H37Ra/ BND433/JAL2287 (MOI 10; 6–26 h)	iTRAQ	n/a	Analysis of the secretome
Kuo et al. (30)	Cell and plasma membrane	THP-1 derived DCs treated by heat-killed Mtb powder (10 μg/ml; 3 days)	Deuterium	115	Aminopeptidase N (ANPEP, CD13)
Long et al. (31)	Plasma membrane	THP-1 infected by BCG (MOI 5; 4 h)	SILAC	559	Immune interactions and lipid metabolism
(C) MS data of MCVs and phagosomes					
Rao et al. (32)	Phagosome	BMA.A3 infected by Mtb H37Rv/H37Rv ΔfbpA/BCG (MOI 5; 18 h)	Label-free	322	Phagosome maturation and role of the ER in phagosome biogenesis
Lee et al. (33)	Phagosome	THP-1 infected by BCG or beads (MOI 80; 3 h–5 days)	SYPRO Ruby	447	Membrane trafficking and signal transduction
Shui et al. (34)	Phagosome	RAW264.7 incubated with beads coated with ManLAM/PILAM/LPS	iTRAQ	42	Vesicle trafficking, phagosome maturation, and autophagosome
Li et al. (35)	Phagosome	BMDM and BMDC infected by Mtb H37Rv (MOI 5; 18 h)	Label-free	41	Phagosome maturation and antigen presentation
Herweg et al. (36)	Phagosome	RAW264.7 incubated with Mtb or trehalose-dimycolate-coated beads for 30 min	Label-free	835	Mitochondria, cytoskeleton, plasma membrane, ER, endosome, and Golgi-associated proteins

receptor type IIb is upregulated upon Mtb lipid exposure, which is known to block calcium influx and to inhibit phagocytosis and inflammatory responses (39). Moreover, also three proteins implicated in the oxidative burst, which help macrophages to kill intracellular pathogens, were found upregulated upon Mtb lipid exposure: p67phox, p47phox (both subunits of NADPH oxidase), and macrophage migration inhibitory factor. At the cellular level, a recent work compared human THP-1 cells infected by either the BCG vaccine strain or two virulent strains (Mtb H37Rv and *Mycobacterium bovis*) (25). The authors identified 61 host proteins differentially regulated depending on the used infection model with seven of them specifically upregulated upon virulent strain exposure, including CCL20 and ICAM1 involved in TNF signaling. Mtb H37Rv infection also induced upregulation of two interferon-induced transmembrane proteins (Ifitm1 and Ifitm3), which is in agreement with previously published results (40). This study has shown the importance of using appropriate infection models to identify host factors influencing the establishment of a pathogen. In line with this, another recent study identified in human macrophages the downregulation of 235 host proteins, when they compared their profile between macrophages infected with the virulent Mtb H37Rv and the avirulent H37Ra strain (24). The main host cell processes found altered by Mtb infection were blood coagulation, apoptosis, and oxidative phosphorylation. Among these candidates, some proteins showed differential expression levels between both models of infection suggesting the existence of different immunity mechanisms that influence immune responses. For example, the expression of HLA class I, a major histocompatibility complex antigen chain specific to humans, was downregulated after Mtb H37Rv infection,

providing evidence that the cross-presentation pathway is affected by Mtb colonization. In another study, Mtb-specific antigens from granulomatous lesions of TB patients could be identified (22), demonstrating the potential of MS-based approaches to study pathogen-driven immune responses.

Although the proteome analysis performed on infected cells and tissue is able to give insight into the host defense mechanisms affected by Mtb colonization, it does not provide specific information about the occupied niche, the MCV, and how its composition and molecular function is altered by the pathogen to allow intracellular growth and replication. Therefore, several labs aim to purify intact cell organelles and PCVs, including those containing different mycobacteria species, to further analyze these compartments by quantitative MS approaches to better understand host–pathogen interactions.

CURRENT STATE AND PITFALLS OF PCV PURIFICATION

Traditional organelle enrichment techniques, such as differential centrifugation in (dis-)continuous density gradients and biochemical fractionation, often resulted in preparations of low purity and contained contaminants, such as other cell organelles and molecular constituents. In recent years, additional techniques have been developed, which allow better purification of PCVs enabling organelle proteomics at higher accuracy and reproducibility. The selective enrichment of PCVs is crucial to increase both specificity and quality of sample preparations and can be achieved by immuno-affinity purification, flow cytometry-based single organelle enrichment, and subcellular fractionation in regard of the physicochemical characteristics of the PCVs of interest. Hilbi and coworkers provide a comprehensive overview of different techniques developed to purify vacuoles containing *Legionella*, *Salmonella*, *Chlamydia*, *Simkania*, and a *Mycobacterium* trehalose-dimycolate (TDM) bead model (36). It is essential to control all experimental steps carefully to avoid the presence of contaminating cell organelles and remnants, which will result in the identification of artifacts during MS analysis. In particular, the use of immunomagnetic separation techniques combined with fractionation and density gradient centrifugation has been used successfully to purify vacuoles of intracellular pathogens that allowed the MS-based identification of host proteins recruited to PCVs, such as IRG1, a catalytic enzyme shown to regulate an antimicrobial host response against *Legionella pneumophila in vitro* and *in vivo* (41).

There is a long-standing interest in MCV isolation to identify and characterize pathogen-specific virulence and persistence mechanisms during infection. The first protocols of MCV purification were reported by the Russell laboratory (42, 43) and Pieters laboratory (44) more than 20 years ago and were based on sucrose and/or Ficoll gradient centrifugation. More recently, these approaches have been either modified, e.g., by combining them with iso-osmotic iodixanol density gradients (33), or were replaced by separation techniques, where mycobacteria are magnetically labeled prior infection (45, 46). Currently, the latter methods seem to be superior to purify MCVs since they allow the selective enrichment of pathogen-containing compartments. In all cases, homogenous MCV isolation with a high degree of purity remains technically challenging, especially if one aims to perform it on virulent Mtb strains at BSL3 conditions. However, in combination with methods developed for other intracellular pathogens, for example, the immunomagnetic separation of PCVs using antibodies against species-specific virulence factors (47), will further boost the efforts to unravel the Mtb-specific phagosomal proteome during different times of infection.

PROTEOME ANALYSIS OF MYCOBACTERIA-CONTAINING VACUOLES

During the last years, several MS studies were published that analyzed different cell organelles of mycobacteria-infected cells (48), such as cytoplasm and nucleus (26), the ER (27), secreted exosomes (28), plasma and cell organelle membranes (30, 31), as well as phagosomes (32–36), which provide detailed insight in the cellular mechanisms of mycobacterial infection. We have listed these findings in **Tables 1B,C**. For example, in a quantitative MS approach, Kuo et al. performed membrane profiling on human dendritic cells and identified 115 proteins that were upregulated in response to heat-killed Mtb (30). Among those host proteins, aminopeptidase N was found largely overexpressed, and the authors could demonstrate that membranous aminopeptidase N is capable of binding live bacteria and is involved in antigen presentation that impaired T cell activation to facilitate Mtb pathogenesis.

The different MS studies on the phagosomal proteome (**Table 1C**) were performed in immune cells infected by either Mtb H37Rv and *M. bovis* BCG or beads coated with Mtb cell wall components (ManLAM, PILAM, and TDM) and identified phagosomal host proteins that are altered during mycobacterial infection. Together with the findings of non-MS studies investigating MCVs at different time points postinfection, we start to better understand the phagosome maturation block and other features of Mtb infection, which we have illustrated in **Figure 1**. While molecules such as transferrin receptor and Rab5 (33–36) are commonly found in MCVs, suggesting fusion with EEs, other EE markers are not found or only at much lower quantities, such as phosphatidyl-inositol-3-phosphate and early endosomal antigen 1 (32), confirming previous findings on MCV biogenesis (49–51). The different MS studies (33–35) also confirm the notion that mycobacterial infection actively suppresses the recruitment of the V-ATPase to the MCV membrane (7) to avoid phagosomal acidification due to the secreted Mtb protein tyrosine phosphatase (8). A recent study from us has also shown that the V-ATPase is targeted for ubiquitination and proteasomal degradation during Mtb infection due to the activity of cytokine-inducible SH2-containing protein (Cish) (52). Moreover, Mtb infection also blocks fusion with late endosomal and lysosomal compartments, which excludes molecules such as cathepsin D and S and lysosome-associated membrane protein 2 from MCVs (33–35, 76). Only late endosomal proteins, such as Rab7 and Nramp-1, were shown to be acquired transiently to the MCV membrane (10, 53, 54), the latter being involved in vacuolar rupture and access of Mtb to the cytosol. Recently, the mannose receptor was found

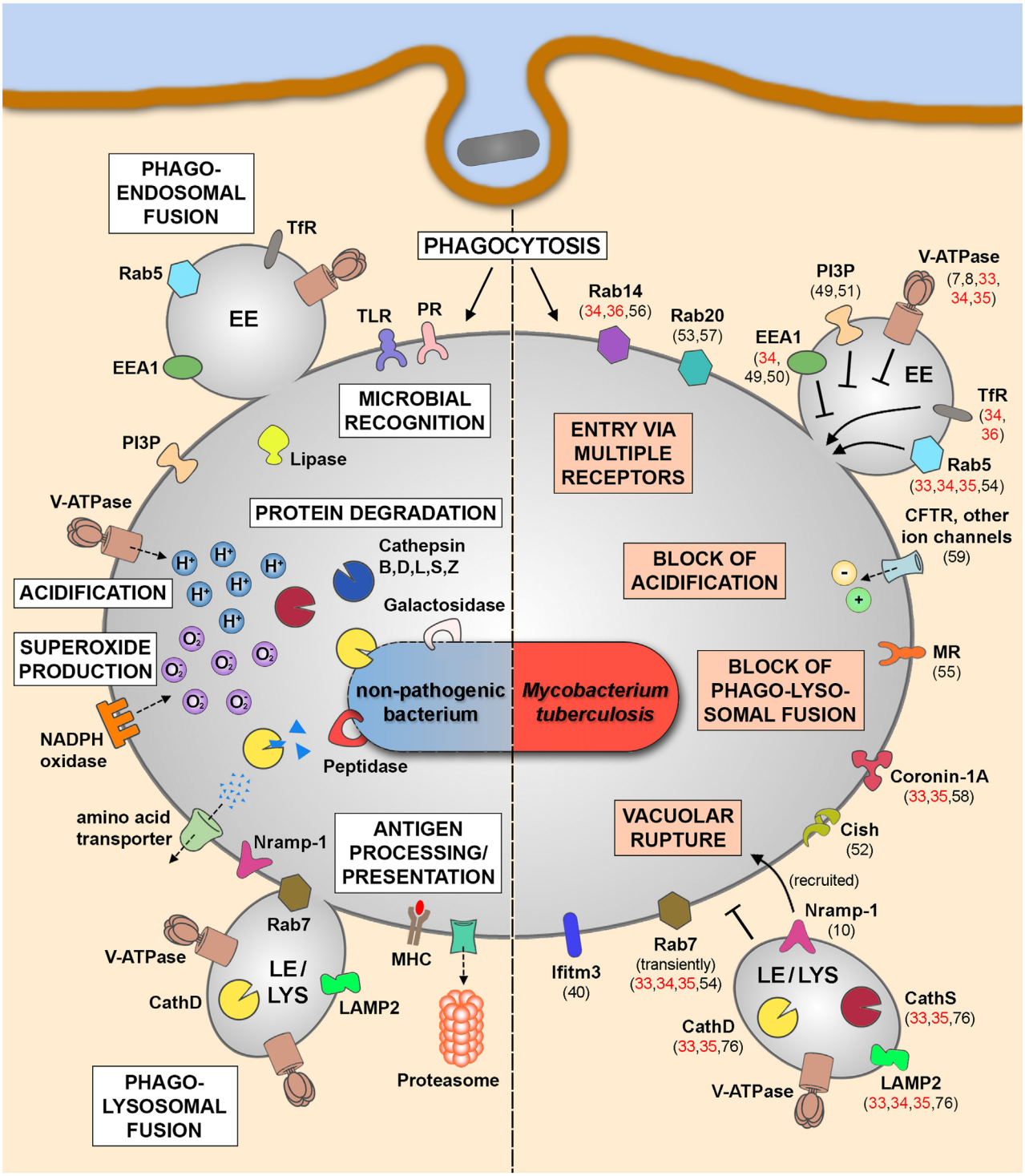


FIGURE 1 | Phagosomal functions after internalization of non-pathogenic bacteria (left panel) and in the context of Mtb infection (right panel). Schematic representation of the key players and main functional features after the uptake of non-pathogenic bacteria leading to the clearance of the internalized cargo (left panel). Upon Mtb infection, the pathogen is internalized into mycobacteria-containing vacuoles (MCVs), which are delayed in phagosome maturation (right panel). Some of the altered phagosomal functions are indicated here together with involved host molecules that were identified by MS approaches (references shown in red) or by non-MS techniques (references shown in black). Abbreviations: CathD, cathepsin D; CathS, cathepsin S; Cish, cytokine-inducible SH2-containing protein; EE, early endosome; EEA1, early endosomal antigen 1; Ifitm3, interferon-induced transmembrane protein 3; LAMP2, lysosome-associated membrane protein 2; LE, late endosome; LYS, lysosome; MHC, major histocompatibility complex; MR, mannose receptor; MS, mass spectrometry; Mtb, *Mycobacterium tuberculosis*; Nramp-1, natural resistance-associated macrophage protein 1; PI3P, phosphatidyl-inositol-3-phosphate; PR, phagocytic receptor; TfR, transferrin receptor; TLR, toll-like receptor; V-ATPase, vacuolar proton ATPase.

to be involved in blocking phagolysosomal fusion by its recruitment of SHP-1 (55). Also two other Rab GTPases, Rab14 and Rab20, were shown to play important roles in MCV biogenesis (34, 53, 56, 57), while other molecules, such as coronin-1A, are actively retained on MCVs containing live Mtb (58). The block of phagosomal acidification, and therefore hydrolase activity, is also supported by the activity of ion channels, such as CFTR (59) and others, which lead to, e.g., high levels of chloride ions in early MCVs (60–62). Finally, there are also other cellular mechanisms, such as autophagy, necrosis, apoptosis, and impairment of antigen presentation, involved in the outcome of mycobacterial infections, which is beyond the scope of this review. However, all these different findings demonstrate an impressive body of evidence, how Mtb interferes with host defense to survive and replicate in different cell types, and how MS analysis of infected cells and of MCVs provide a valuable tool to better understand host–pathogen interactions.

CONCLUSION AND OUTLOOK

Research on mycobacterial infections includes an increasing number of MS-based approaches, which refine our understanding of the molecular mechanisms underlying Mtb pathogenesis. Together with improvements on purity and reproducibility of sample preparations, in particular of MCVs containing virulent Mtb strains, it is now feasible to combine these methods with other techniques analyzing dynamics and impact of host–pathogen interactions. In addition, current advances in quantitative MS as well as recently emerging targeting MS-based techniques, such as selected reaction monitoring and SWATH MS (17), enable accurate and very sensitive protein measurements. Combined with systems biology-driven workflows, future studies on Mtb infection will allow a better understanding of pathogen-induced changes and immunomodulation of infected host cells.

Future research should focus on the diversity of innate immune cells and their distinct functions that cooperate to control Mtb infection, such as the contribution of myeloid cells and lymphocyte populations (63–65). MS approaches could help to uncover the underlying mechanisms by identifying the involved players. Effective immunity against Mtb requires balanced adaptive immune responses while avoiding damages by immune activation, which determines the persistence of chronic TB infection (66). We now begin to understand the different mechanisms of immune manipulation induced by Mtb infection that favor disease progression, and current interventions aim to reverse these effects by altering the frequency of specific immune cell populations (67). Therefore, novel immunotherapies include depletion strategies targeting regulatory T cells (68, 69) and myeloid-derived suppressor cells (70, 71) to restrict mycobacterial replication. Finally, current findings also demonstrate the importance of metabolic remodeling of immune cells during infection, and how these processes influence effector functions, inflammatory responses, and the outcome of disease (72). How precise changes in metabolites are beneficial for the host during Mtb infection and contribute to protection from TB remains to be uncovered, but the inflammatory state of certain immune cell populations appears to be crucial (73). Without doubt, current MS technology allows the identification of metabolic adaptation during Mtb infection (74) and will allow further insight how immune responses are regulated, for example, the role of different interferons in TB pathogenesis (75). Consequently, future research in these fields will have important implications on host response, pathogen survival, and TB persistence and will promote the development of novel host-directed therapies, particularly against emergent drug-resistant Mtb strains.

AUTHOR CONTRIBUTIONS

All the authors participated in the concept, preparation, and writing of the manuscript. EH conceived the content and edited the final version of the manuscript.

ACKNOWLEDGMENTS

The authors are grateful to Gareth Griffiths and Edouard Yeramian for their comments on the manuscript. The authors apologize to all colleagues whose work could not be cited due to space limitations. Financial support of our lab is provided by the European Research Council (ERC-STG INTRACELLTB Grant no. 260901, MM4TB Grant no. 260872, and CycloNHit no. 608407), the EMBO YIP program, the Agence Nationale de la Recherche (ANR-10-EQPX-04-01, ANR-14-CE14-0024, ANR-14-CE08-0017, and ANR-16-CE35-0009), the Projet Transversal de Recherche de l'Institut Pasteur (PTR441 and PTR22-16), the Feder [12001407 (D-AL) Equipex Imaginex BioMed], the Région Nord Pas de Calais (convention no. 12000080). AM is supported by a fellowship of the Fondation pour la Recherche Médicale (SPF20170938709).

REFERENCES

1. Levin R, Grinstein S, Canton J. The life cycle of phagosomes: formation, maturation, and resolution. *Immunol Rev* (2016) 273:156–79. doi:10.1111/imr.12439
2. Pauwels AM, Trost M, Beyaert R, Hoffmann E. Patterns, receptors, and signals: regulation of phagosome maturation. *Trends Immunol* (2017) 38:407–22. doi:10.1016/j.it.2017.03.006
3. Uribe-Querol E, Rosales C. Control of phagocytosis by microbial pathogens. *Front Immunol* (2017) 8:1368. doi:10.3389/fimmu.2017.01368
4. Stanley SA, Cox JS. Host-pathogen interactions during *Mycobacterium tuberculosis* infections. *Curr Top Microbiol Immunol* (2013) 374:211–41. doi:10.1007/82_2013_332
5. WHO. Global tuberculosis report. (2017).
6. Schorey JS, Schlesinger LS. Innate immune responses to tuberculosis. *Microbiol Spectr* (2016) 4:TBTB2-0010-2016. doi:10.1128/microbiolspec.TBTB2-0010-2016
7. Sturgill-Koszycki S, Schaible UE, Russell DG. *Mycobacterium*-containing phagosomes are accessible to early endosomes and reflect a transitional state in normal phagosome biogenesis. *EMBO J* (1996) 15:6960–8.
8. Wong D, Bach H, Sun J, Hmama Z, Av-Gay Y. *Mycobacterium tuberculosis* protein tyrosine phosphatase (PtpA) excludes host vacuolar-H+-ATPase to inhibit phagosome acidification. *Proc Natl Acad Sci U S A* (2011) 108:19371–6. doi:10.1073/pnas.1109201108
9. Simeone R, Bobard A, Lippmann J, Bitter W, Majlessi L, Brosch R, et al. Phagosomal rupture by *Mycobacterium tuberculosis* results in toxicity and host cell death. *PLoS Pathog* (2012) 8:e1002507. doi:10.1371/journal.ppat.1002507

10. Simeone R, Sayes F, Song O, Groschel MI, Brodin P, Brosch R, et al. Cytosolic access of *Mycobacterium tuberculosis*: critical impact of phagosomal acidification control and demonstration of occurrence in vivo. *PLoS Pathog* (2015) 11:e1004650. doi:10.1371/journal.ppat.1004650
11. van der Wel N, Hava D, Houben D, Fluitsma D, van Zon M, Pierson J, et al. M. tuberculosis and M. leprae translocate from the phagolysosome to the cytosol in myeloid cells. *Cell* (2007) 129:1287–98. doi:10.1016/j.cell.2007.05.059
12. Philips JA, Ernst JD. Tuberculosis pathogenesis and immunity. *Annu Rev Pathol* (2012) 7:353–84. doi:10.1146/annurev-pathol-011811-132458
13. Kaufmann SHE, Dockrell HM, Drager N, Ho MM, McShane H, Neyrolles O, et al. TBVAC2020: advancing tuberculosis vaccines from discovery to clinical development. *Front Immunol* (2017) 8:1203. doi:10.3389/fimmu.2017.01203
14. Tobin DM. Host-directed therapies for tuberculosis. *Cold Spring Harb Perspect Med* (2015) 5:a021196. doi:10.1101/cshperspect.a021196
15. Aebersold R, Mann M. Mass-spectrometric exploration of proteome structure and function. *Nature* (2016) 537:347–55. doi:10.1038/nature19949
16. Banaei-Esfahani A, Nicod C, Aebersold R, Collins BC. Systems proteomics approaches to study bacterial pathogens: application to *Mycobacterium tuberculosis*. *Curr Opin Microbiol* (2017) 39:64–72. doi:10.1016/j.mib.2017.09.013
17. Schubert OT, Aebersold R. Microbial proteome profiling and systems biology: applications to *Mycobacterium tuberculosis*. *Adv Exp Med Biol* (2015) 883:235–54. doi:10.1007/978-3-319-23603-2_13
18. Walzl G, Haks MC, Joosten SA, Kleynhans L, Ronacher K, Ottenhoff TH. Clinical immunology and multiplex biomarkers of human tuberculosis. *Cold Spring Harb Perspect Med* (2014) 5:a018515. doi:10.1101/cshperspect.a018515
19. Schubert OT, Rost HL, Collins BC, Rosenberger G, Aebersold R. Quantitative proteomics: challenges and opportunities in basic and applied research. *Nat Protoc* (2017) 12:1289–94. doi:10.1038/nprot.2017.040
20. Rauniyar N, Yates JR III. Isobaric labeling-based relative quantification in shotgun proteomics. *J Proteome Res* (2014) 13:5293–309. doi:10.1021/pr500880b
21. Shui W, Gilmore SA, Sheu L, Liu J, Keasling JD, Bertozzi CR. Quantitative proteomic profiling of host-pathogen interactions: the macrophage response to *Mycobacterium tuberculosis* lipids. *J Proteome Res* (2009) 8:282–9. doi:10.1021/pr800422e
22. Yu Y, Jin D, Hu S, Zhang Y, Zheng X, Zheng J, et al. A novel tuberculosis antigen identified from human tuberculosis granulomas. *Mol Cell Proteomics* (2015) 14:1093–103. doi:10.1074/mcp.M114.045237
23. Kaewseekhao B, Naranbhai V, Roytrakul S, Namwat W, Paemanee A, Lulitanond V, et al. Comparative proteomics of activated THP-1 cells infected with *Mycobacterium tuberculosis* identifies putative clearance biomarkers for tuberculosis treatment. *PLoS One* (2015) 10:e0134168. doi:10.1371/journal.pone.0134168
24. Li H, Wei S, Fang Y, Li M, Li X, Li Z, et al. Quantitative proteomic analysis of host responses triggered by *Mycobacterium tuberculosis* infection in human macrophage cells. *Acta Biochim Biophys* (2017) 49:835–44. doi:10.1093/abbs/gmx080
25. Li P, Wang R, Dong W, Hu L, Zong B, Zhang Y, et al. Comparative proteomics analysis of human macrophages infected with virulent *Mycobacterium bovis*. *Front Cell Infect Microbiol* (2017) 7:65. doi:10.3389/fcimb.2017.00065
26. Wang H, Dong D, Tang S, Chen X, Gao Q. PPE38 of *Mycobacterium marinum* triggers the cross-talk of multiple pathways involved in the host response, as revealed by subcellular quantitative proteomics. *J Proteome Res* (2013) 12:2055–66. doi:10.1021/pr301017e
27. Saquib NM, Jamwal S, Midha MK, Verma HN, Manivel V. Quantitative proteomics and lipidomics analysis of endoplasmic reticulum of macrophage infected with *Mycobacterium tuberculosis*. *Int J Proteomics* (2015) 2015:270438. doi:10.1155/2015/270438
28. Diaz G, Wolfe LM, Kruh-Garcia NA, Dobos KM. Changes in the membrane-associated proteins of exosomes released from human macrophages after *Mycobacterium tuberculosis* infection. *Sci Rep* (2016) 6:37975. doi:10.1038/srep37975
29. Kumar A, Jamwal S, Midha MK, Hamza B, Aggarwal S, Yadav AK, et al. Dataset generated using hyperplexing and click chemistry to monitor temporal dynamics of newly synthesized macrophage secretome post infection by mycobacterial strains. *Data Brief* (2016) 9:349–54. doi:10.1016/j.dib.2016.08.055
30. Kuo CP, Chang KS, Hsu JL, Tsai IF, Lin AB, Wei TY, et al. Analysis of the immune response of human dendritic cells to *Mycobacterium tuberculosis* by quantitative proteomics. *Proteome Sci* (2016) 14:5. doi:10.1186/s12953-016-0095-8
31. Long J, Basu Roy R, Zhang YJ, Antrobus R, Du Y, Smith DL, et al. Plasma membrane profiling reveals upregulation of ABCA1 by infected macrophages leading to restriction of mycobacterial growth. *Front Microbiol* (2016) 7:1086. doi:10.3389/fmicb.2016.01086
32. Rao PK, Singh CR, Jagannath C, Li Q. A systems biology approach to study the phagosomal proteome modulated by mycobacterial infections. *Int J Clin Exp Med* (2009) 2:233–47.
33. Lee BY, Jethwaney D, Schilling B, Clemens DL, Gibson BW, Horwitz MA. The *Mycobacterium bovis* bacille Calmette-Guerin phagosome proteome. *Mol Cell Proteomics* (2010) 9:32–53. doi:10.1074/mcp.M900396-MCP200
34. Shui W, Petzold CJ, Redding A, Liu J, Pitcher A, Sheu L, et al. Organelle membrane proteomics reveals differential influence of mycobacterial lipoglycans on macrophage phagosome maturation and autophagosome accumulation. *J Proteome Res* (2011) 10:339–48. doi:10.1021/pr100688h
35. Li Q, Singh CR, Ma S, Price ND, Jagannath C. Label-free proteomics and systems biology analysis of mycobacterial phagosomes in dendritic cells and macrophages. *J Proteome Res* (2011) 10:2425–39. doi:10.1021/pr101245u
36. Herweg JA, Hansmeier N, Otto A, Geffken AC, Subbarayal P, Prusty BK, et al. Purification and proteomics of pathogen-modified vacuoles and membranes. *Front Cell Infect Microbiol* (2015) 5:48. doi:10.3389/fcimb.2015.00048
37. Kolattukudy PE, Fernandes ND, Azad AK, Fitzmaurice AM, Sirakova TD. Biochemistry and molecular genetics of cell-wall lipid biosynthesis in mycobacteria. *Mol Microbiol* (1997) 24:263–70. doi:10.1046/j.1365-2958.1997.3361705.x
38. Beatty WL, Rhoades ER, Ullrich HJ, Chatterjee D, Heuser JE, Russell DG. Trafficking and release of mycobacterial lipids from infected macrophages. *Traffic* (2000) 1:235–47. doi:10.1034/j.1600-0854.2000.010306.x
39. Maglione PJ, Xu J, Casadevall A, Chan J. Fc gamma receptors regulate immune activation and susceptibility during *Mycobacterium tuberculosis* infection. *J Immunol* (2008) 180:3329–38. doi:10.4049/jimmunol.180.5.3329
40. Ranjbar S, Haridas V, Jasenosky LD, Falvo JV, Goldfeld AE. A role for IFITM proteins in restriction of *Mycobacterium tuberculosis* infection. *Cell Rep* (2015) 13:874–83. doi:10.1016/j.celrep.2015.09.048
41. Naujoks J, Tabeling C, Dill BD, Hoffmann C, Brown AS, Kunze M, et al. IFNs modify the proteome of legionella-containing vacuoles and restrict infection via IRG1-derived itaconic acid. *PLoS Pathog* (2016) 12:e1005408. doi:10.1371/journal.ppat.1005408
42. Chakraborty P, Sturgill-Koszycki S, Russell DG. Isolation and characterization of pathogen-containing phagosomes. *Methods Cell Biol* (1994) 45:261–76. doi:10.1016/S0091-679X(08)61856-7
43. Sturgill-Koszycki S, Schlesinger PH, Chakraborty P, Haddix PL, Collins HL, Fok AK, et al. Lack of acidification in *Mycobacterium* phagosomes produced by exclusion of the vesicular proton-ATPase. *Science* (1994) 263:678–81. doi:10.1126/science.8303277
44. Hasan Z, Schlax C, Kuhn L, Lefkovits I, Young D, Thole J, et al. Isolation and characterization of the mycobacterial phagosome: segregation from the endosomal/lysosomal pathway. *Mol Microbiol* (1997) 24:545–53. doi:10.1046/j.1365-2958.1997.3591731.x
45. Lönnbro P, Nordenfelt P, Tapper H. Isolation of bacteria-containing phagosomes by magnetic selection. *BMC Cell Biol* (2008) 9:35. doi:10.1186/1471-2121-9-35
46. Steinhäuser C, Dallenga T, Tchikov V, Schaible UE, Schütze S, Reiling N. Immunomagnetic isolation of pathogen-containing phagosomes and apoptotic blebs from primary phagocytes. *Curr Protoc Immunol* (2014) 105:14361–26. doi:10.1002/0471142735.im1436s105
47. Hoffmann C, Finsel I, Hilbi H. Pathogen vacuole purification from legionella-infected amoeba and macrophages. *Methods Mol Biol* (2013) 954:309–21. doi:10.1007/978-1-62703-161-5_18
48. He Y, Li W, Liao G, Xie J. *Mycobacterium tuberculosis*-specific phagosome proteome and underlying signaling pathways. *J Proteome Res* (2012) 11:2635–43. doi:10.1021/pr300125t
49. Fratti RA, Backer JM, Gruenberg J, Corvera S, Deretic V. Role of phosphatidylinositol 3-kinase and Rab5 effectors in phagosomal biogenesis and mycobacterial phagosome maturation arrest. *J Cell Biol* (2001) 154:631–44. doi:10.1083/jcb.200106049

50. Vergne I, Chua J, Deretic V. *Mycobacterium tuberculosis* phagosome maturation arrest: selective targeting of PI3P-dependent membrane trafficking. *Traffic* (2003) 4:600–6. doi:10.1034/j.1600-0854.2003.00120.x
51. Vergne I, Chua J, Lee HH, Lucas M, Belisle J, Deretic V. Mechanism of phagolysosome biogenesis block by viable *Mycobacterium tuberculosis*. *Proc Natl Acad Sci U S A* (2005) 102:4033–8. doi:10.1073/pnas.0409716102
52. Queval CJ, Song OR, Carralot JP, Saliou JM, Bongiovanni A, Deloison G, et al. *Mycobacterium tuberculosis* controls phagosomal acidification by targeting CISH-mediated signaling. *Cell Rep* (2017) 20:3188–98. doi:10.1016/j.celrep.2017.08.101
53. Schnettger L, Rodgers A, Repnik U, Lai RP, Pei G, Verdoes M, et al. A Rab20-dependent membrane trafficking pathway controls *M. tuberculosis* replication by regulating phagosome spaciousness and integrity. *Cell Host Microbe* (2017) 21:619–628e5. doi:10.1016/j.chom.2017.04.004
54. Via LE, Deretic D, Ulmer RJ, Hibler NS, Huber LA, Deretic V. Arrest of mycobacterial phagosome maturation is caused by a block in vesicle fusion between stages controlled by rab5 and rab7. *J Biol Chem* (1997) 272:13326–31. doi:10.1074/jbc.272.20.13326
55. Rajaram MVS, Arnett E, Azad AK, Guirado E, Ni B, Gerberick AD, et al. *M. tuberculosis*-initiated human mannose receptor signaling regulates macrophage recognition and vesicle trafficking by FcRgamma-Chain, Grb2, and SHP-1. *Cell Rep* (2017) 21:126–40. doi:10.1016/j.celrep.2017.09.034
56. Kyei GB, Vergne I, Chua J, Roberts E, Harris J, Junutula JR, et al. Rab14 is critical for maintenance of *Mycobacterium tuberculosis* phagosome maturation arrest. *EMBO J* (2006) 25:5250–9. doi:10.1038/sj.emboj.7601407
57. Seto S, Tsujimura K, Koide Y. Rab GTPases regulating phagosome maturation are differentially recruited to mycobacterial phagosomes. *Traffic* (2011) 12:407–20. doi:10.1111/j.1600-0854.2011.01165.x
58. Ferrari G, Langen H, Naito M, Pieters J. A coat protein on phagosomes involved in the intracellular survival of mycobacteria. *Cell* (1999) 97:435–47. doi:10.1016/S0092-8674(00)80754-0
59. Di A, Brown ME, Deriy LV, Li C, Szeto FL, Chen Y, et al. CFTR regulates phagosome acidification in macrophages and alters bactericidal activity. *Nat Cell Biol* (2006) 8:933–44. doi:10.1038/ncb1456
60. Neyrolles O, Wolschendorf F, Mitra A, Niederweis M. Mycobacteria, metals, and the macrophage. *Immunol Rev* (2015) 264:249–63. doi:10.1111/imr.12265
61. Soldati T, Neyrolles O. Mycobacteria and the intraphagosomal environment: take it with a pinch of salt(s)! *Traffic* (2012) 13:1042–52. doi:10.1111/j.1600-0854.2012.01358.x
62. Wagner D, Maser J, Lai B, Cai Z, Barry CE III, Honer Zu Bentrup K, et al. Elemental analysis of *Mycobacterium avium*-, *Mycobacterium tuberculosis*-, and *Mycobacterium smegmatis*-containing phagosomes indicates pathogen-induced microenvironments within the host cell's endosomal system. *J Immunol* (2005) 174:1491–500. doi:10.4049/jimmunol.174.3.1491
63. Mayer-Barber KD, Barber DL. Innate and adaptive cellular immune responses to *Mycobacterium tuberculosis* infection. *Cold Spring Harb Perspect Med* (2015) 5:a018424. doi:10.1101/cshperspect.a018424
64. Srivastava S, Grace PS, Ernst JD. Antigen export reduces antigen presentation and limits T cell control of *M. tuberculosis*. *Cell Host Microbe* (2016) 19:44–54. doi:10.1016/j.chom.2015.12.003
65. Bénard A, Sakwa I, Schierloh P, Colom A, Mercier I, Tailleux L, et al. B cells producing type I interferon modulate macrophage polarization in tuberculosis. *Am J Respir Crit Care Med* (2017). doi:10.1164/rccm.201707-1475OC
66. Brighenti S, Ordway DJ. Regulation of immunity to tuberculosis. *Microbiol Spectr* (2016) 4:TBTB2-0006-2016. doi:10.1128/microbiolspec.TBTB2-0006-2016
67. Jayashankar L, Hafner R. Adjunct strategies for tuberculosis vaccines: modulating key immune cell regulatory mechanisms to potentiate vaccination. *Front Immunol* (2016) 7:577. doi:10.3389/fimmu.2016.00577
68. Parkash O, Agrawal S, Madhan Kumar M. T regulatory cells: Achilles' heel of *Mycobacterium tuberculosis* infection? *Immunol Res* (2015) 62:386–98. doi:10.1007/s12026-015-8654-0
69. Bhattacharya D, Dwivedi VP, Kumar S, Reddy MC, Van Kaer L, Moodley P, et al. Simultaneous inhibition of T helper 2 and T regulatory cell differentiation by small molecules enhances bacillus Calmette-Guerin vaccine efficacy against tuberculosis. *J Biol Chem* (2014) 289:33404–11. doi:10.1074/jbc.M114.600452
70. Dorhoi A, Kaufmann SH. Versatile myeloid cell subsets contribute to tuberculosis-associated inflammation. *Eur J Immunol* (2015) 45:2191–202. doi:10.1002/eji.201545493
71. Gupta S, Cheung L, Pokkali S, Winglee K, Guo H, Murphy JR, et al. Suppressor cell-depleting immunotherapy with denileukin diftitox is an effective host-directed therapy for tuberculosis. *J Infect Dis* (2017) 215:1883–7. doi:10.1093/infdis/jix208
72. Olenchock BA, Rathmell JC, Vander Heiden MG. Biochemical underpinnings of immune cell metabolic phenotypes. *Immunity* (2017) 46:703–13. doi:10.1016/j.immuni.2017.04.013
73. Mishra BB, Lovewell RR, Olive AJ, Zhang G, Wang W, Eugenin E, et al. Nitric oxide prevents a pathogen-permissive granulocytic inflammation during tuberculosis. *Nat Microbiol* (2017) 2:17072. doi:10.1038/nmicrobiol.2017.72
74. Eoh H, Wang Z, Layre E, Rath P, Morris R, Moody DB, et al. Metabolic anticipation in *Mycobacterium tuberculosis*. *Nat Microbiol* (2017) 2:17084. doi:10.1038/nmicrobiol.2017.84
75. Travar M, Petkovic M, Verhaz A. Type I, II, and III Interferons: regulating immunity to *Mycobacterium tuberculosis* infection. *Arch Immunol Ther Exp* (2016) 64:19–31. doi:10.1007/s00005-015-0365-7
76. Clemens DL, Horwitz HA. Characterization of the *Mycobacterium tuberculosis* phagosome and evidence that phagosomal maturation is inhibited. *J Exp Med* (1995) 181(1):257–70. doi:10.1084/jem.181.1.257

Conflict of Interest Statement: The authors declare that the research was conducted in the absence of any commercial or financial relationships that could be construed as a potential conflict of interest.

Copyright © 2018 Hoffmann, Machelart, Song and Brodin. This is an open-access article distributed under the terms of the Creative Commons Attribution License (CC BY). The use, distribution or reproduction in other forums is permitted, provided the original author(s) and the copyright owner are credited and that the original publication in this journal is cited, in accordance with accepted academic practice. No use, distribution or reproduction is permitted which does not comply with these terms.

frontiers in Immunology

REVIEW
published: 09 February 2018
doi: 10.3389/fimmu.2018.00193

Reinforcing the Functionality of Mononuclear Phagocyte System to Control Tuberculosis

*Susanta Pahari, Gurpreet Kaur, Shikha Negi, Mohammad Aqdas, Deepjyoti K. Das, Hilal Bashir, Sanpreet Singh, Mukta Nagare, Junaid Khan and Javed N. Agrewala**

Immunology Laboratory, CSIR-Institute of Microbial Technology, Chandigarh, India

The mononuclear phagocyte system (MPS) constitutes dendritic cells, monocytes, and macrophages. This system contributes to various functions that are essential for maintaining homeostasis, activation of innate immunity, and bridging it with the adaptive immunity. Consequently, MPS is highly important in bolstering immunity against the pathogens. However, MPS is the frontline cells in destroying *Mycobacterium tuberculosis* (*Mtb*), yet the bacterium prefers to reside in the hostile environment of macrophages. Therefore, it may be very interesting to study the struggle between *Mtb* and MPS to understand the outcome of the disease. In an event when MPS predominates *Mtb*, the host remains protected. By contrast, the situation becomes devastating when the pathogen tames and tunes the host MPS, which ultimately culminates into tuberculosis (TB). Hence, it becomes extremely crucial to reinvigorate MPS functionality to overwhelm *Mtb* and eliminate it. In this article, we discuss the strategies to bolster the function of MPS by exploiting the molecules associated with the innate immunity and highlight the mechanisms involved to overcome the *Mtb*-induced suppression of host immunity. In future, such approaches may provide an insight to develop immunotherapeutics to treat TB.

Keywords: mononuclear phagocyte system, tuberculosis, monocyte, macrophage, dendritic cell, pattern recognition receptors, infection, immunotherapy

OPEN ACCESS

Edited by:
Geanncarlo Lugo-Villarino, UMR5089 Institut de Pharmacologie et de Biologie Structurale (IPBS), France

Reviewed by:
Niyaz Ahmed, International Centre for Diarrhoeal Disease Research, Bangladesh
Saurabh Aggarwal, University of Alabama at Birmingham, United States
Giampietro Sgaragli, University of Siena, Italy

***Correspondence:**
Javed N. Agrewala
javed@imtech.res.in

Specialty section:
This article was submitted to Microbial Immunology, a section of the journal Frontiers in Immunology

Received: *15 September 2017*
Accepted: *23 January 2018*
Published: *09 February 2018*

Citation:
Pahari S, Kaur G, Negi S, Aqdas M, Das DK, Bashir H, Singh S, Nagare M, Khan J and Agrewala JN (2018) Reinforcing the Functionality of Mononuclear Phagocyte System to Control Tuberculosis. Front. Immunol. 9:193. doi: 10.3389/fimmu.2018.00193

INTRODUCTION

Despite of the fact that efficient anti-tuberculosis (TB) drugs are available, TB remains to ruin public health globally. Reports suggest that one-third of the populace is infected with *Mycobacterium tuberculosis* (*Mtb*), almost 10.4 million active cases and around 1.8 million deaths in 2016 (1). The occurrence of threat is further complicated due to acquired immunodeficiency syndrome pandemic, the appearance of multidrug-resistant (MDR), extensively drug-resistant, as well as totally drug-resistant *Mtb* strains (2). Vaccines are the most effective strategy to control and eliminate any disease (3, 4). Ironically, bacillus Calmette–Guérin (BCG) is the most controversial vaccine because of its variable efficacy worldwide (5). Moreover, it protects only children but not adults (6). Therefore, an urgent necessity and the challenge for the scientific society are to improve the current drug regimen or develop alternative stratagems against TB.

Our immune system is quite complex and complicated, comprising of innate as well as adaptive branch of immunity. Innate immunity is the primary and foremost line of defense against intruding pathogens (7). Innate immunity was initially believed to be non-specific and considered to be of lesser importance for the immune function. On the other hand, adaptive immunity is allied with

the exclusion of intracellular pathogens in the subsequent stages of infection. It was considered as sentinel of the immune system owing to its specificity as well as immunological memory generation. Since the last few decades, innate immunity has gained enormous consideration due to the discovery of "germ line-encoded" pattern recognition receptors (PRRs), which makes the innate immunity capable of discriminating between self and an array of pathogens (8). PRRs are predominantly expressed by various antigen-presenting cells (APCs) such as monocytes, macrophages, and dendritic cells (DCs). These cells constitute the mononuclear phagocyte system (MPS). Mononuclear phagocyte cells (MPCs) are progenitors derived from bone marrow hematopoietic cell lineage (9). "Committed myeloid progenitor cells" can differentiate into blood monocytes, which then migrate to the bloodstream and subsequently enter in different tissues to develop into the resident tissue macrophages and DCs (10, 11). In the conventional sight of the MPS, cell division happens primarily in monoblasts and promonocytes. The expansion of mature macrophages provides the maintenance and number of resident tissue macrophages (10). MPCs mainly contribute in the recognition and eradication of pathogens and their related products. Furthermore, they contribute substantially in promoting innate immunity and subsequently stimulating, shaping, and expanding the adaptive immunity (12). Initiation of adaptive immunity not only depends on the direct detection of antigen by the receptors of MPCs but also relies on crucial signals delivered through costimulatory molecules, cytokines, and PRRs (13). Importantly, DCs contribute considerably in bridging innate and adaptive immunity (8, 14). DCs express a plentiful amount of costimulatory molecules and PRRs, which regulate several immune functions and signaling cascades that are crucial for the instigation of adaptive immune response (15). In addition, they successively alert other immune cells to accumulate at the infection site. Furthermore, they combat and resist *Mtb* in establishing infection and restrain them from becoming an active disease.

Based on the aforementioned investigations, MPS are considered as an important first line of defense against pathogen. Exploiting MPCs or their components, namely, PRRs, costimulatory molecules, cytokines, and chemokines as therapeutic agents may be an exciting line of study to control TB. Previously, our group has highlighted the importance of signaling through innate molecules in context with nasal and mucosal immunity to restrict *Mtb* entry and consequently prohibiting its infection. We discussed the role of several immunomodulators *in vitro*, *in vivo*, or in clinical studies to enhance the efficacy of anti-TB drugs in treating TB patients (16). Current review highlights the interaction between *Mtb* and MPS influencing the outcome of disease. Hence, as evidenced by published literature, we hypothesize a crucial strategy to reinvigorate MPS functionality to overwhelm *Mtb* and eliminate it. Furthermore, we discuss the strategies to bolster the function of MPS by exploiting the molecules associated with the innate immunity and highlight the mechanisms involved therein. It may be hypothesized that involving MPS in conjunction with drugs, as an adjunct therapy may lessen the dose as well as duration of ongoing drug regimen; and therefore, may reduce the chances of developing drug resistance by the pathogen.

VARIOUS MONONUCLEAR PHAGOCYTIC CELLS AND THEIR FUNCTION IN INNATE AND ADAPTIVE IMMUNITY

Mononuclear phagocyte cells located in various tissues differ in terms of their nomenclature and morphological appearance (17). For example, macrophages are called as histiocytes in subcutaneous tissues, Kupffer cells resides in liver, microglia present in nervous tissue, alveolar macrophages in lungs, osteoclasts in bones, etc. Besides phagocytosing pathogens and eliminating them from the blood, lymph, and tissues, MPS also clears the senescent cells and mounts immunity against the pathogens (18). MPS recognizes, captures, and internalizes the pathogenic determinants identified as pathogen-associated molecular patterns (PAMPs) through PRRs localized on their surface. This leads to the secretion of biologically active molecules such as free radicals, cytokines, and chemokines. The chemokines attract chiefly neutrophils from the bloodstream and initiate a pro-inflammatory response leading to the engulfment and destruction of *Mtb*.

Lung alveolar macrophages and myeloid DCs are some of the foremost cell types that get infected after aerosol challenge with *Mtb*. Subsequently, interstitial macrophages, monocytes, and neutrophils are recruited to infection site (19). MPCs capture *Mtb* and migrate to the local draining lymph nodes, then process and present antigens efficiently in context with MHCs to activate T cells (20). The intensity of MPCs and *Mtb* counterattack widely depends upon the host genetics as well as bacterial virulence factors. Accordingly, *Mtb* replicates within the host MPCs (21, 22) and manipulates function by impairing their ability to control infection (23, 24). *Mtb* can obstruct the antigen processing and presentation by MPCs to T cells (25–27). Macrophages and DCs that are not optimally activated cannot kill the intracellular *Mtb* and serve as a reservoir for the dissemination of the pathogen. In addition, due to their striking migratory potential, they play a key role in transmitting *Mtb* from the site of infection to other tissues (28).

EVASION STRATEGIES ADOPTED BY *Mtb* TO COUNTERACT HOST IMMUNITY

One of the major mechanisms through which *Mtb* obstructs MPS function is by inhibiting the fusion of phagosome with lysosome. Various mycobacterial lipids and glycolipids, proteins, and enzymes, namely, lipoarabinomannan (LAM) and trehalose-6,6'-dimycolate (TDM), protein tyrosine phosphatase A (PtpA), secretory acid phosphatase M, zinc-dependent metalloprotease 1, lipoamide dehydrogenase C, serine/threonine protein kinase G, and PEPGRS62 protein have been proved to play an important role in the capacity of *Mtb* to escape phagolysosome fusion (29–32).

Two signals are important for the optimal activation of T cells. Initial one is the engagement of TCR with MHC–peptide complex and subsequent upregulation of costimulatory molecules. Instead of getting activated, T cells get anergized ("a state of unresponsiveness") in the absence of costimulatory molecules (33). Interestingly, *Mtb* has the ability to successfully down modulate the expression of costimulatory molecules. Furthermore, after infecting MPCs, *Mtb* upregulates the expression of immunosuppressive markers

programmed cell death-1, Lymphocyte activation gene-3, and T-cell immunoglobulin mucin-domain containing-3, thus retaliating against the potential threat caused by T cells (34, 35).

Another mechanism is the deprivation of MPS nutrients by *Mtb.* The most common battle between host cells and the pathogen is for iron utilization. *Mtb* efficiently utilizes its siderophores for iron uptake and thus deprives host of its availability (36). Furthermore, carbon from various sugars and fatty acids are extracted by *Mtb* in host cells *via* its major enzymes, such as the polyphosphate glucokinase, isocitrate lyases (ICL1 and ICL2), and the phosphoenolpyruvate carboxykinase (37–39). *Mtb* favors the differentiation of macrophages toward M2 subtype (40). By contrast, it impairs the formation of M1 macrophages. M2 macrophages are responsible for suppression of inflammatory function. M1 subtype arises from type-1 inflammatory conditions and secretes pro-inflammatory cytokines and is endowed with microbicidal activity (41). Virulence factors of *Mtb* are known to preferably skew the generation of M2 macrophages (42). Therefore, *Mtb* is successful in creating an environment for its intracellular survival inside macrophages (43, 44). Furthermore, *Mtb* mainly skews the differentiation of CD4 T cells toward Th2 cells phenotype (45). Similarly, the generation of regulatory T cells that secrete TGF-β is promoted. Both Th2 cells and Tregs help in the TB progression. By contrast, the formation of Th1 cells and Th17 cells is suppressed by hijacked MPS, since they have potential to successfully control the *Mtb* infection (46).

MPS HELPS IN THE RESTORATION OF HOST IMMUNITY IMPAIRED BY *Mtb*

Mononuclear phagocyte system contributes significantly to the health and disease (47). One of the most imperative mechanism and early response of innate immunity is the generation of reactive oxygen species (ROS) by MPS, which not only destroys the pathogen but also plays a physiological role in maintaining and controlling the cellular functions. Clearance of colonized microorganisms and initiation of signaling pathways related to inflammation, cell proliferation, and induction of immunity is highly dependent on ROS (48). Two sources of ROS generation in the host upon microbial infection is membrane-bound NADPH oxidase complex as well as mitochondrial electron transport chain (49). Important PRRs associated with an intracellular pathogen is NOD-like receptors (NLRs), which makes cell attentive on pathogen interaction/invasion. Among many NLRs, NLRX1 moves to mitochondria and initiates the ROS production (50).

ROLE OF MPS TO OVERCOME THE MODULATION OF CELLULAR METABOLISM AND NUTRIENT ACQUISITION BY *Mtb*

Mycobacterium tuberculosis utilizes cholesterol for its survival and establishes infection in the host cells (43). This cholesterol is further converted into sterol, which is crucial for *Mtb* persistence in the host cells (51). Adenosine-5′-triphosphate (ATP) plays a decisive role in the host by acting directly on cell metabolism and signaling cascade. The ATP that comes out of the cell into the extracellular environment is known as extracellular ATP (eATP). It has been seen that eATP can activate the immune system by acting as a "danger signal" (52). Moreover, it is well known that eATP has a potential role in stimulating the release of pro-inflammatory cytokines. eATP induces IL-6 secretion from macrophages (53) and IL-1β production from LPS primed monocytes (54). Furthermore, it is noted that eATP signaling is not only implicated in the generation of ROS and pro-inflammatory cytokines but also plays a significant role in antigen presentation. Previous report demonstrated that eATP along with its putative receptor P2X7 on inflammasome activation induces the shedding of exosomes containing the MHC class II from macrophages (55). It is well-known fact that ROS signaling is involved in the inflammasome formation (56). Thus, it facilitates innate as well as adaptive immune response. *Mtb*-infected phagocytes release exosomes containing the MHC class II and *Mtb* Ag85B, which activates the T cells (57). The eATP–P2X7 receptor signaling plays an important role in clearing *Mtb* infection through multiple ways such as phospholipase-D (58), apoptosis (57), phagosome–lysosome fusion (59), and autophagy (60). Thus, MPS is recognized to play an appreciable role in neutralizing and eradication of *Mtb* from the host.

INVOLVEMENT OF PHAGOCYTIC CELLS TO BOOST IMMUNITY AGAINST *Mtb*

Both DCs and macrophages play crucial roles in protection against mycobacterium. The presence of *Mtb* at infection site is sensed by macrophages through chemokine-mediated migration, as these macrophages express surface receptor for these chemokines known as G-protein-coupled receptors (61). *Mtb* is efficiently phagocytosed by these professional phagocytic cells. Studies on human macrophages have shown that phagocytosis is significantly improved in the presence of anti-*Mtb* antibodies and complement factors (62). Once *Mtb* is phagocytosed by the macrophage or DCs, it encounters a number of defense mechanisms operated through the innate immunity of the host. These include the formation of free radicals, namely, ROS, reactive nitrogen intermediates (RNI), cytokines, and chemokines. Moreover, MPS helps in the differentiation of T cells; DCs secrete IL-12, which results in the generation of Th1 cells. Moreover, Th1 cells mainly secrete IFN-γ that activates macrophages to release TNF-α (63). Similarly, IL-6 and TGF-β secreted by MPS helps to differentiate naïve T cells into Th17 phenotype (64). Th1 cells and Th17 cells can reciprocally regulate the function of Th2 cells and Tregs, respectively. Both Th2 cells and Tregs promote the progression of TB.

Mononuclear phagocyte system employs factors that are involved in basic metabolism of the body to fight against intracellular pathogens. One such important molecule is vitamin D3, which enhances the phagocytosis of MPS by upregulating the expression of CD14 and CD206 receptors (65). Toll-like receptor (TLR)-2 signaling in macrophage upregulates the expression of vitamin-D–1-hydroxylase and surface vitamin-D receptor, which stimulates the generation of antimicrobial peptide cathelicidin and contributes to resistance to *Mtb* (66).

PRRs-MEDIATED BOLSTERING OF MPS ACTIVITY AGAINST *Mtb*

Mononuclear phagocyte cells are the key sensory cells that reinforce the innate immunity. They express the plethora of innate receptors such as TLRs, NLRs, and C-type lectin receptors (CLRs), which are collectively called as PRRs that are present either on the cell surface or endocytic vesicles. The PRRs including TLRs (TLR-2, -3, -4, and -9) and non-TLRs [CLRs, NLRs such as nucleotide-binding oligomerization domain (NOD)-2, mannose receptors (MRs), Dectin-1, and DC-SIGN] recognize conserved PAMPs that are present on *Mtb*. PRRs have the capacity to recognize a broad range of structural components of pathogens grouped as PAMPs and DAMPs, which includes lipopeptides, lipoproteins, lipoteichoic acid, peptidoglycans, ssRNA, dsRNA, siRNA, mRNA, DNA, LPS, heat shock proteins, and flagellin. The role of several PPRs in protecting against *Mtb* has been widely studied (16, 67–70). The interaction of PRRs with PAMPs triggers a series of signaling pathways inside the MPCs (**Table 1**). PRRs activated MPCs acquire augmented expression of MHC I, MHC II, and costimulatory molecules on their surface (63), which leads to the better presentation of *Mtb* antigens to naïve T cells followed by generation of efficient T cell response against this pathogen. *Mtb* loaded macrophages,

TABLE 1 | Activation of PRRs through PAMPs.

	PRRs (structure)	Adapters (structure)	PAMPs/activators	Species	Cell types	Location
TLR	TLR-1–TLR-2 (LRR-TIR)	MyD88 (TIR-DD) and TIRAP (TIR)	Triacyl lipopeptides	Bacteria	Granulocytes, macrophages, mDCs, monocytes, and B cells	Cell surface
	TLR-2–TLR-6 (LRR-TIR)	MyD88 and TIRAP	Diacyl lipopeptides LTA Zymosan	Mycoplasma Bacteria Fungus	Granulocytes, macrophages, mDCs, monocytes, and B cells	Cell surface
	TLR-2 (LRR-TIR)	MyD88 and TIRAP	PGN Lipoarabinomannan Porins tGPI-mucin HA protein	Bacteria Mycobacteria Bacteria (Neisseria) Parasites (Trypanosoma) Viruses (Measles virus)	Granulocytes, macrophages, mDCs, monocytes, mast cells, and neutrophils	Cell surface
	TLR-3 (LRR-TIR)	TRIF (TIR)	dsRNA	Viruses	DCs, macrophages, NK cells, and B cells	Endosome
	TLR-4 (LRR-TIR)	MyD88, TIRAP, TRIF. TRAM (TIR)	LPS Envelope proteins	Bacteria Viruses (RSV, MMTV)	DCs. macrophages, B cells, monocytes, neutrophils, granulocytes, and regulatory T cells	Cell surface
	TLR-5 (LRR-TIR)	MyD88	Flagellin	Bacteria	Monocytes, DCs, mast cells, epithelial cells, mast cells, and regulatory T cells	Cell surface
	TLR-7 (LRR-TIR)	MyD88	ssRNA	RNA viruses	B cells, DCs, macrophages, monocytes, and regulatory T cells	Endosome
	hTLR-8 (LRR-TIR)	MyD88	ssRNA	RNA viruses	Monocytes, DCs, mast cells, epithelial cells, mast cells, and regulatory T cells	Endosome
	TLR-9 (LRR-TIR)	MyD88	CpG DNA DNA Malaria hemozoin	Bacteria DNA viruses Parasites	DCs. macrophages, B cells, monocytes, and neutrophils	Endosome
	TLR-10	Unknown	Unknown	Unknown	B cells, monocytes, neutrophils, and pDCs	Cell surface
	mTLR-11 (LRR-TIR)	MyD88	Not determined Profilin-like molecule	Bacteria (uropathogenic bacteria) Parasites (*Toxoplasma gondii*)	Monocytes, macrophages, and epithelial cells	Endosome
	TLR-12	MyD88	Profilin-like molecule	Parasites (*Toxoplasma gondii*)	DCs, macrophages, and neurons	Unknown
	TLR-13	MyD88, TAK-1	Bacterial 23S ribosomal RNA (rRNA)	Virus, bacteria	Monocytes, macrophages, and DCs	Endosome
RLR	RIG-I (CARDx2-helicase)	IPS-1 (CARD)	RNA (5′-PPPssRNA, short dsRNA)	Viruses	cDCs, macrophages, and fibroblasts	Endosome
	MDA5 (CARDx2-helicase)	IPS-1	RNA (poly IC, long dsRNA)	Viruses	cDCs, macrophages, and fibroblasts	Endosome
	LGP2 (helicase)		RNA	Viruses	cDCs, macrophages, and fibroblasts	Endosome

(*Continued*)

TABLE 1 | Continued

	PRRs (structure)	Adapters (structure)	PAMPs/activators	Species	Cell types	Location
NLR	NOD-1/NLRC1 (CARD-NBD-LRR)	RICK (CARD), CARD9 (CARD)	iE-DAP	Bacteria	DCs, macrophages, and epithelial cells	Endosome
	NOD-2/NLRC2 (CARDx2-NBD-LRR)	RICK, CARD9	MDP	Bacteria	DCs, macrophages, and epithelial cells	Endosome
	NALP3/NLRP3 (PYD-NBD-LRR)	ASC (PYD-CARD) CARDINAL (PYD-FIND)	MDP RNA ATP Toxins Uric acid, CPPD, amyloid-β	Bacteria Bacteria and viruses Bacteria Host Bacteria Host	DCs, macrophages, epithelial cells, and T cells	Cytoplasm
	NALP1/NLRP1 (CARD-FIND-NBD-LRR-PYD)	ASC	Anthrax lethal toxin	Bacteria	Bone marrow blast cells, epithelial cells, Langerhans cells, and neurons	Cytoplasm
	IPAF/NLRC4 (CARD-NBD-LRR)		Flagellin	Bacteria	Hematopoietic cells, macrophages, and epithelial cells	Cytoplasm
	NAIP5 (BIRx3-NBD-LRR)		Flagellin	Bacteria	Hematopoietic cells, macrophages, and epithelial cells	Cytoplasm
CLR	Dectin-1 (lectin-ITAM)		β-Glucan	Fungi, bacteria	DCs, macrophages, monocytes, neutrophils, B cells, and NK cells	Cell surface
	Mincle (Clec4e)	ITAM-bearing adaptor FcRy	TDB and TDM	Mycobacteria and fungi	DCs, macrophages, B cells, and neutrophils	Cell surface

Distinct signaling cascades are triggered through PRRs against pathogen-associated moieties.

The PAMPs expressed on array of pathogens are recognized by the PRRs present on the cells of immune system. The PRRs are located either intracellularly or on the surface of the cells.

TLR, toll-like receptor; CLR, C-type lectin receptor; NLR, NOD-like receptor; NOD, nucleotide-binding oligomerization domain; RLR, RIG-like receptor; RIG-1, retinoic acid-inducible gene 1; LRR, leucine-rich repeat receptor; TIR, toll/interleukin-1 (IL-1) receptor; MDA5, melanoma differentiation-associated protein 5; LGP2, laboratory of genetics and physiology 2; NLRC, nuclear oligomerization domain proteins subfamily C; NLRP, NLR family pyrin domain; NBD, nucleotide-binding domains; PYD, pyrin domain; FIND, function to find domain; IPAF, IL-1β-converting enzyme protease-activating factor; NAIP5, neuronal apoptosis inhibitory protein 5; BIR, baculovirus inhibitor of apoptosis protein repeat; ITAM, immunoreceptor tyrosine-based activation motif; Mincle, macrophage-inducible C-type lectin receptor; Clec4e, C-type lectin domain family 4 member e; TIRAP, TIR-domain-containing adaptor protein; MyD88, myeloid differentiation primary response 88; TRIF, TIR-domain-containing adapter-inducing interferon-β; TRAM, TRIF-related adapter molecule; TAK-1, TGF-β-activated kinase 1; IPS-1, interferon promoter stimulator-1; RICK, RIP-like interacting CLARP kinase; CARD, caspase recruitment domain; ASC, apoptosis-associated speck-like protein containing a CARD; TUCAN, tumor-upregulated CARD-containing antagonist of caspase-nine; CARDINAL, CARD8, DACAR, NDPP1, and TUCAN; TDB, trehalose-6,6-dibehenate; TDM, trehalose-6,6′-dimycolate; CPPD, calcium pyrophosphate dihydrate crystals; LTA, lipoteichoic acid; PGN, peptidoglycan; tGPI-mucin, trypomastigote glycosylphosphatidylinositol mucins; HA protein, hemagglutinin protein; LPS, lipopolysaccharides; iE-DAP, D-glutamyl-meso-diaminopimelic acid; MDP, muramyl dipeptide; RSV, respiratory syncytial virus; MMTV, mouse mammary tumor virus; Mdc, myeloid dendritic cells; cDC, conventional dendritic cells; PAMP, pathogen-associated molecular pattern; PRR, pattern recognition receptor; ATP, adenosine-5′-triphosphate; DC, dendritic cell.

after activation, can mount bactericidal activities such as nitric oxide (NO) production, maturation of phagosomes toward phagolysosomes and autophagolysosomes (71). Recruitment and activation of many signaling molecules in cascade lead to nuclear translocation of NF-κB, which eventually causes the activation of MPCs. In a different setup, the activated macrophages have the capability to carry out macro-autophagy to take care of intracellular *Mtb* (72, 73). In a similar phenomenon known as "programmed necroptosis," MPCs controls the intracellular replication of *Mtb*. This process speeds up the recruitment of neutrophils and thereby enhances the killing of mycobacterium (74). MPS activation is evident by the release of pro-inflammatory cytokines such as IL-1β, IL-6, IL-12, and TNF-α; which help in phagocytosis of the bacterium followed by activation of *Mtb* reactive T cells. These T cells play a cardinal role in controlling the *Mtb* growth.

Importance of PRRs signaling in the activation of an immune response against *Mtb* can be accounted by the evidence that MyD88$^{-/-}$ mice were more prone to *Mtb* infection. TLR-2-knockout mice showed low IL-12 and TNF-α yield on *Mtb* infection and more granulomas formation in the lungs (75). The 19 kDa lipoprotein of *Mtb* activates MPCs through TLR-2 triggering and induces IL-12 and NO production, and subsequently killing of *Mtb* (76). In humans, the interaction of 19 kDa lipoprotein with TLR-2 induces apoptosis of *Mtb*-infected macrophages (77). TLR-4 senses HSP60/65 and 38-kDa *Mtb* antigen inducing protective TNF-α production (78). In addition, another *Mtb* small heat shock protein X also recognized as α-crystallin-1 can specifically modulate the function of DCs at different maturation stages (79, 80). TLR-4 activation is known to induce macro-autophagy by recruitment of Beclin-1. Recently, we showed that cumulative signaling of

DCs through TLR-4 and NOD-2 successfully inhibits the intracellular survival of *Mtb* through autophagy (70). Mycobacterial DNA interacts with TLR-9 and elicits macrophages to produce pro-inflammatory cytokines. Furthermore, TLR-9-knockout mice showed less release of IFN-γ and IL-12. *Mtb*-infected macrophages and DCs deficient in TLR-9 are less responsive to IL-12 (81). NLRs and CLRs can also influence the function of MPCs. NOD-2-deficient mice exhibit impairment in cytokine and NO release upon *Mtb* infection (82). Activation of *Mtb*-infected human macrophages through NOD-2 induces autophagy and restricts *Mtb* growth (83). Likewise, signaling of *Mtb*-infected DCs through Dectin-1 and macrophage-inducible C-type lectin (Mincle) influences the intracellular survival of the pathogen (84, 85). By contrast, DC-specific intercellular adhesion molecule-3-grabbing non-integrin (DC-SIGN) interaction with LAM of *Mtb* initiates the anti-inflammatory response by inducing the secretion of IL-10 (86). Overall, it signifies that the engagement of various PRRs on MPCs can differentially regulate their function toward *Mtb.*

CONTRIBUTION OF INFLAMMATORY RESPONSE IN CONTROLLING *Mtb* INFECTION

Inflammatory response generated by cytokines helps to control *Mtb* infection directing the pathogenesis of disease. Diverse cytokines produced on *Mtb* infection determines the fate of host response. Cells of MPS recruited at the infection site trigger cascade of events necessary for the release of various pro-inflammatory cytokines such as IL-1β, IL-6, IL-12, TNF-α, and IL-18. Furthermore, the protective function of IL-1 during *Mtb* infection was first demonstrated in mice dually deficient in IL-1α/β or IL-1R1 signaling (87). Several findings have reported enhanced *Mtb* load and less survival of mice with defect in IL-1R1 signaling. By contrast, IL-1β and IL-18 are synthesized after processing by caspases-1 of pro-IL-1β and pro-IL-18, respectively. Besides caspase-1, four more caspases, caspases-11 and -12 of mouse and caspases-4 and -5 of human regulate the inflammatory processing. Inflammasome plays a decisive role in host defense, as mice lacking IL-1β, IL-1 receptor, or IL-18 was more prone to *Mtb* infection. Furthermore, ASC protein deficiency led to the severe form of disease in the murine model of TB. IL-1β production is known to rely on the early secreted antigenic target of 6 kDa (ESAT-6) secretion system 1 (ESX-1) of *Mtb*, which contributes to the expression of virulence genes encoded by region of difference (RD-1). Inflammasome formation mediated by ESX-1 relies on the host NLR family pyrin domain containing-3 (NLRP3) along with ASC protein (88). Based on the above observations, it can be speculated that failure of BCG to induce optimum protection in TB is attributed to the lack of IL-1β and IL-18 mediated by RD-1 (89).

We, therefore, postulate that adjunct therapy of BCG with innate ligands that can regulate inflammasome formation and can enhance its efficacy as a potential vaccine against *Mtb*. In addition, inflammasome regulates *Mtb* infection during early phase by activating innate immunity and also plays a decisive role in augmenting the adaptive immunity against the bacterium.

ACTIVATION OF CD4 T CELLS AND CD8 T CELLS BY MPS IN RESTRICTING *Mtb* GROWTH

The onset of the adaptive immune response to *Mtb* generally takes 8–11 days subsequent to primary exposure of *Mtb*. This involves the transportation of the bacterium to the draining lymph nodes (90). Infected MPCs are involved in the priming and proliferation of *Mtb*-specific effector T cells and their subsequent migration to the lungs.

T cells play a fundamental role in conferring defense against *Mtb.* IL-12 secreted by MPS is a crucial regulator of the differentiation of naive CD4 T cells to Th1 cells. IL-6, TGF-β, and IL-1β released by MPCs help in the differentiation to Th17 cells (91). Inflammasome generated by MPS in synergy with IL-6 facilitates Th17 cells development *via* upregulation of IRF4 and RORγt. In absence of TGF-β signaling, IL-1β coordinates with IL-6 and IL-23 to generate pathogenic Th17 cells (92). A concerted action of both Th1 cells and Th17 cells is essential to control *Mtb* infection. IFN-γ released by Th1 cells plays a fundamental role in the activation of MPCs and the release of TNF-α, a cytokine responsible for inhibiting the growth of *Mtb* (93). Recent evidences highlight the role of Th17 cells producing IL-17 and IL-22 in restricting *Mtb* (93). Th17 cells mainly recruit monocytes and Th1 cells to the lungs that help to clear infection rapidly (93). Recent studies showed that Tregs can effectively diminish Th1 immunity (94) or hinder the effector T cells influx to the lungs during initial phase of *Mtb* infection (95). Similarly, Th2 cells that secrete mainly IL-4 and IL-13 significantly contribute to the progression of TB (96).

Although, CD8 T cells sufficiently provide immunity against *Mtb*, but their role is not adequately studied as has been done in the case of CD4 T cells. However, the importance of CD8 T cells has been established by the fact that their depletion leads to higher susceptibility toward *Mtb* in the experimental model of TB. Furthermore, β_2m-knockout mice died rapidly on exposure to *Mtb* (97). CD8 T cells released IFN-γ and granulysin lyse the *Mtb*-infected macrophages, as well as can induce perforin (Pfn)-mediated cytotoxicity to kill the *Mtb* (98, 99). Furthermore, CD8 T cells in lung can directly lyse *Mtb*-infected macrophages in a Pfn-dependent manner (100). In addition, the presence of CD8 T cells expressing granzyme B has been observed in the TB patients and latent infection (101). However, CD8 T cells secrete IL-17, TNF-α, IL-10, and IL-2 but IFN-γ is considered to be a key mediator in defense against *Mtb* (101). Furthermore, IFN-γ augments the production of various chemokines CXCL9, CXCL10, and CXCL11 and therefore helps in recruiting the cells toward granulomas. Recently, it has been shown that the *Mtb*-infected macrophages undergoing apoptosis releases several antigens in apoptotic vesicles, thus permitting the access of these apoptotic bodies to bystander cells to present antigen in context with MHC class I molecules. This can be confirmed by inhibiting the formation of blebbing in a plasma membrane by caspase inhibitors. Consequently, it may hamper the CD8 T cell activation. Furthermore, unconventional CD1-restricted γδ-TCR T cells can specifically respond to *Mtb* glycolipids (102). The γδ T cells are the less abundant type of T cells population, which differ from common αβ T cells in having gamma delta (γδ) glycoprotein

chains bearing TCR on T cells (102). Mycobacterial phosphoantigens are known as the potent activators of Vγ9Vδ2 T cell functions (103). These cells recognize *Mtb*-infected monocytes and alveolar macrophages in a non-MHC restricted manner (104). γδ T cells are responsible for initiating defense mechanism upon *Mtb* infection by generating cytotoxic function, cytokine secretion, and contact-dependent lysis of infected cells (105).

INVOLVEMENT OF REACTIVE OXYGEN AND NITROGEN SPECIES IN CONTROLLING *Mtb* INFECTION

Antimicrobial ROS and RNI are critical in controlling *Mtb* infection. RNI and NO produced by MPCs are considered potent antimicrobial agents. Human alveolar macrophages can kill *Mtb* in an iNOs dependent manner. Whereas, macrophages obtained from healthy individuals that are latently infected with *Mtb* prevent the growth of bacterium by secreting NO (106). These results were validated in the murine model of TB, where the abrogation of inducible NO synthase activity resulted in a dramatic increase in the microbial burden (107). Moreover, disruption of *Inos* gene increases *Mtb* dissemination and mortality of the mice. Indeed, NO released by macrophages is critically dependent on IFN-γ (108). Although effector T cells are the key producer of IFN-γ but it takes few weeks for these cells to release IFN-γ. Nevertheless, the NO production by macrophages is noticed within 3 h of *Mtb* infection (109). NK and γδ T cells are the first to reach the infection site. They secrete IFN-γ that stimulates macrophages to produce NO. The antimycobacterial function of NO secreted by MPS is well documented in the case of mice. However, there are evidences that depict that NO secretion by human alveolar epithelial cells and macrophages inhibits the growth of *Mtb*, but the role of NO still needs to be fully authenticated in humans (110). Furthermore, NOS and NO are highly evident in the macrophages obtained from bronchoalveolar lavages of TB patients. Apparently, MDR patients secrete lesser NO, as compared with TB patients (111). In addition, it has been reported that NOS2-deficient mice are immunocompetent to cure *Mtb* infection (112). It has been demonstrated that ciprofloxacin elicits the release of NO to eliminate *Mtb* (113). Furthermore, NO regulates the secretion of many pro-inflammatory cytokines such as IL-1β, IL-8, and TNF-α (114).

However, *Mtb* has successfully developed immune evasion strategies to resist the intracellular killing by ROS and RNI produced by MPS. *Mtb* has phenolic glycolipid I, cyclopropanated mycolic acids, and LAM rich thick cell wall that is the effective scavenger of oxygen radicals providing resistance to ROS (115). Besides, *Mtb* produces various ROS scavenging enzymes such as KatG, superoxide dismutases (Sod A and C), peroxidase along with peroxynitrite reductase complex consisting of AhpC, AhpD, SucB (DlaT), and Lpd (116, 117). Interestingly, Lsr2 bound to *Mtb* DNA protects the pathogen from ROS mediated destruction (118). Truncated hemoglobin in *M. smegmatis* protects the bacterium from aerobic respiration by inhibiting the NO production (119). Surprisingly, despite the strong killing potential of RNI, ROS, and cytokines, *Mtb* has successfully learned to prevail in the host environment.

MPS RESIST *Mtb* INFLICTED DEATH

The apoptosis (programmed cell death) is a well-known event, where a cell undergoing death still retains its cytoplasmic material within membranous vesicles called as apoptotic bodies. MPCs eliminate apoptotic bodies through the mechanism known as "efferocytosis," which critically contributes in boosting host immune response. The caspase family of serine proteases is the essential molecules that generate apoptosis in MPS. Apoptosis operates through several classical pathways. One of the essential pathways is the ligation of TNF receptor family-2, which activates caspases and subsequently induces the formation of apoptotic bodies. Primarily, apoptosis occurs due to the nutrients deprivation, oxidative stress, or intracellular stresses that ultimately alter the mitochondrial membrane permeability. Consequently, cytochrome *c* is translocated to cytosol, which leads to the caspases activation. Another pathway is interceded by the release of granzyme B from cytotoxic T cells as well as NK cells. Subsequent to *Mtb* infection, MPCs augment the production of TNF-α, which elicits apoptosis. This process confines the growth of *Mtb* by activating local MPS and insulating it into the apoptotic vesicles. Intriguingly, considerable inhibition in *Mtb* growth was demonstrated when cells undergoing apoptosis were cocultured with naïve macrophages. In addition, it has been demonstrated that antimicrobial effect performed by macrophages is through the involvement of IL-1 signaling and NO-dependent antimycobacterial activity (120). The level of apoptosis induced by virulent and avirulent *Mtb* is quite distinct (121). Few reports signify that virulent strain of *Mtb* triggers necrosis by avoiding host defensive strategy, while avirulent strain induces apoptosis (121, 122). Furthermore, the frequency of apoptosis is quite high in the macrophages infected with an attenuated strain of *Mtb* (123). Even though the production of TNF-α is commensurate, MPCs infected with non-virulent *Mtb* are found to be more susceptible to undergo apoptosis. The possible reasons suggested for the differences between virulent and avirulent *Mtb* may be the virulence factors, bacterial load and duration of exposure. H37Rv infected MPCs secretes IL-10, leading to the induction of TNFR. The soluble form of TNF-α and TNFR complex inhibits the apoptosis (124). Furthermore, ESAT-6 of *Mtb,* leads to apoptosis in THP-1 macrophages by diminishing the expression of antiapoptotic molecules (125).

Neutrophil plays an imperative role in preventing *Mtb* infection (126). These cells reach first at the infection site. Furthermore, neutrophils phagocytose *Mtb* and generate ROS and restrict *Mtb* growth. In addition, they help macrophages to eliminate the infection. *Mtb*-infected neutrophils can also undergo apoptosis. At the time of apoptosis, these cells display "eat-me or find-me" signal on their plasma membrane, which helps in recognizing the unwanted constituents of MPCs (127). Macrophages recognize "find-me" signals and then phagocytose these cells. Macrophages engulf neutrophils undergoing apoptosis and secrete TNF-α to control *Mtb* infection by granulomas formation (128). It will be an exciting line of investigation employing the concept of "eat-me" signal to develop a novel strategy for targeted delivery of immunomodulators along with anti-TB drugs for the clearance of *Mtb* hiding in a quiescent state inside the endosome (**Figure 1**).

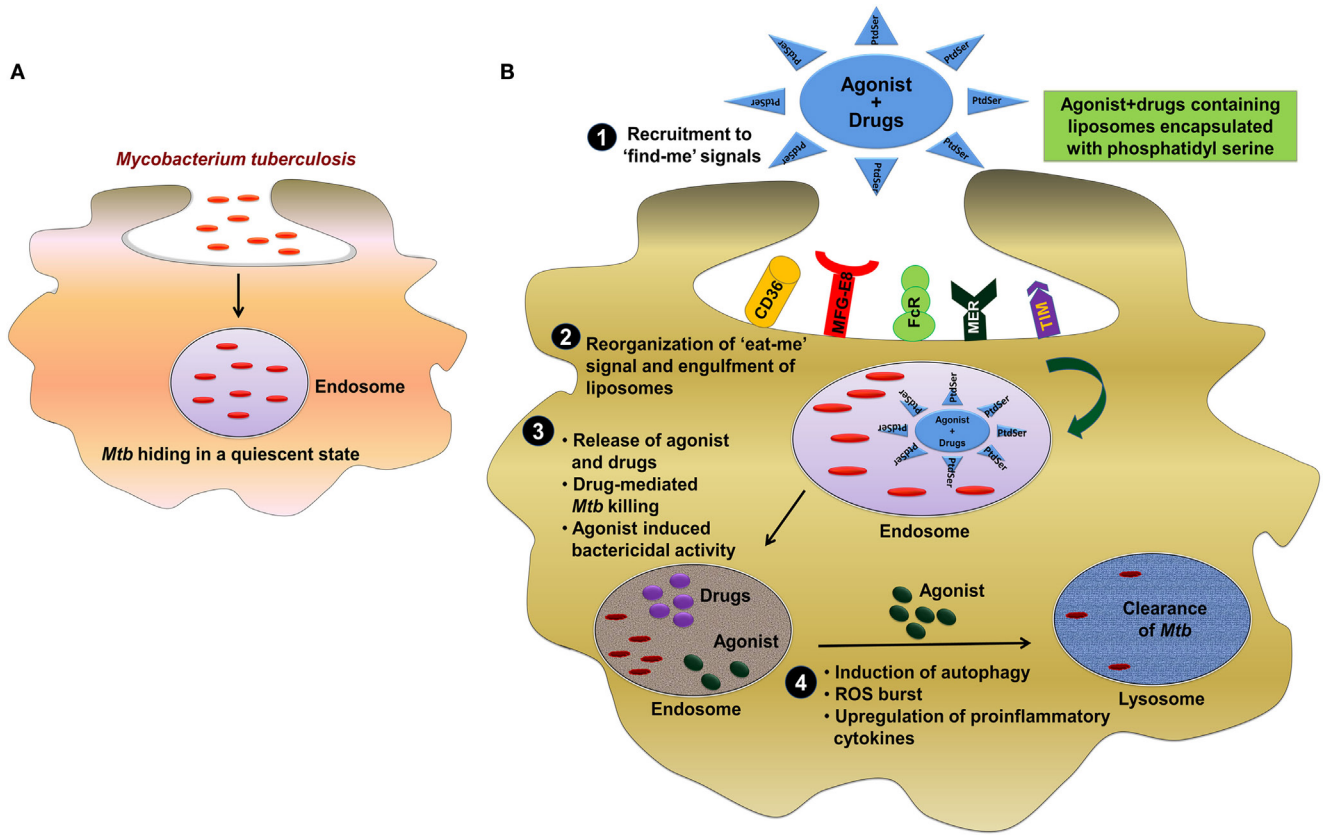


FIGURE 1 | Involvement of "eat-me" signal in targeted delivery of immunomodulators along with anti-TB drug for the clearance of *Mtb*. **(A)** *Mtb* employs elegant strategy to impair the function of host cells by residing inside the endosome of macrophages in a quiescent state. **(B)** The most effective strategy to control and eliminate *Mtb* can be through targeting of pathogen-bearing MPCs by exploiting "eat-me" signal. One of the possible approach could be the engagement of phosphatidylserine (PtdSer) as an "eat-me" signal to deliver PRRs agonist/drug in liposome to target *Mtb* in the endosomes. (1, 2) Primarily, mononuclear phagocytic cells recognize "find-me" signal by several receptors such as CD36, MFG-E8, FcR, MER, TIM, and then phagocytose the liposomes through receptor-mediated endocytosis. (3) The direct clearance of *Mtb* in the endosome can be achieved by delivering the drug (rifampicin/isoniazid) to the site of infection. (4) However, the majority of *Mtb* would be eliminated but the eradication of residual bacterial population can be achieved by the agonist of TLRs (TLR-2, TLR-4, and TLR-9), NLRs (NOD-1 and NOD-2), and CLRs (Mincle, Dectin-1, and Dectin-2) mediated bactericidal mechanism and subsequently clearance of *Mtb* from lysosomes.
Abbreviations: CD36, cluster of differentiation 36; MFG-E8, milk fat globule-EGF factor 8; FcR, Fc receptor; MER, membrane-bound receptor tyrosine kinase; TIM, T cell immunoglobulin and mucin domain; MPC, mononuclear phagocyte cell; NLR, NOD-like receptor; PtdSer, phosphatidylserine TLR, toll-like receptor; CLR, C-type lectin receptor; *Mtb*, *Mycobacterium tuberculosis*; TB, tuberculosis; NOD, nucleotide-binding oligomerization domain; Mincle, macrophage-inducible C-type lectin.

ROLE OF ER STRESS (ERS) IN THE REGULATION OF INNATE IMMUNITY DURING *Mtb* INFECTION

In humans, endoplasmic reticulum (ER) performs various functions such as metabolism of lipids, protein folding, and maintaining cellular homeostasis. Different factors such as accumulation of unfolded proteins, loss of oxygen or hypoxia, and bacterial infections are responsible for the unfolded protein response (UPR), which causes ERS. Uncontrolled ERS leads to apoptosis. Furthermore, UPR activates various innate signaling pathways, which result in the survival of intracellular pathogens such as *Mtb* (129, 130). Apoptosis of macrophages helps to prevent the spread of mycobacterial infection by activating innate immunity (131). However, growing number of findings suggest that *Mtb* has evolved various strategies to control the ERS for its survival in the host (132). *Mtb* can efficiently alter the structure of macrophage ER. It was shown that macrophages infected by virulent (H37Rv) along with avirulent (H37Ra) *Mtb* strains possess distinct ER phenotypes (133). Difference in the morphology of ER in macrophages targeted during *Mtb* infection is a crucial factor for initiation of apoptosis. Ca^{2+} is very important in different apoptotic pathways and is responsible for the phagosome–lysosome fusion. A smooth ER phenotype linked with avirulent *Mtb*-infected macrophages increases cytosolic Ca^{2+} levels and simultaneously increases the synthesis of phosphatidyl choline/phosphatidyl ethanolamine (PC/PE), which leads to apoptosis. However, H37Rv but not H37Ra manipulates rough ER of macrophages and disturbs the cholesterol homeostasis to inhibit the apoptosis and establishes its intracellular persistence.

Endoplasmic reticulum stress is already known to influence macrophages. It stimulates conversion of macrophages toward M1 phenotype and induces apoptosis, thereby aiding in *Mtb*

clearance. On the other hand, polarization of M2 phenotype by *Mtb* infection aids its escape by suppressing apoptosis (134). At the site of granuloma formation during *Mtb* infection, ERS markers such as activating transcription factor-3, pIre1α, and eukaryotic initiation factor 2α levels are increased (135). Depending on ERS, macrophage apoptosis is influenced by various *Mtb* proteins such as ESAT-6, 38-kDa antigen and PE-PGRS33. Henceforth, ERS is crucial in imparting protection against *Mtb* and restricting it to advanced granulomas (63, 136).

MPCs RESTRICT THE *Mtb*-INDUCED INHIBITION OF PHAGOSOME MATURATION

Mononuclear phagocyte cells have developed an array of strategies to control *Mtb* infection. MPCs recognize and phagocytose *Mtb* through PRRs such as C-type lectins, Dectin-1, Dectin-2, Mincle, macrophage C-type lectin, DC-SIGN, MR, scavenger receptors-A, and macrophage receptor with collagenous structure (MARCO) (scavenger receptors) (137). Consequently, activation through these receptors triggers various downstream signaling pathways mainly through Rac1–2, Cdc42, and most importantly GTPases. Arp2/3 is a key activator of actin polymerization. It is a primary step in instigating the process of phagocytosis and is triggered by the interaction of Wiskott–Aldrich syndrome protein with Rac1–2 and Cdc42 (43). Phagocytosis of *Mtb* triggers the formation and maturation of phagosome. During this process, a sequence of events occurs involving several molecules (25). Fc-gamma receptor along with MR is involved in the antigen trafficking to early phagosome. Early phagosome formation occurs upon interaction of MR with *Mtb* lipids such as PIMs and manLAM (138). The phosphorylation of immunoreceptor tyrosine-based activation motif by kinase of Src family, followed by downstream phosphorylation of Src homology region 2 domain-containing phosphatase-1 (SHP-1) and ras-related C3 botulinum toxin substrate (RAC) are critical for phagosome maturation (139). Membrane molecules exchange and deliver cargo either by "touch and run" or complete fusion with phagosome undergoing maturation. Motor proteins such as dynein and dynactin are key players to bring vesicles in an appropriate orientation for vesicular fusion, which is important for phagosome maturation. Many SNARE proteins such as vesicle-associated membrane proteins-7 and VAMP-8 are also involved in this event. During phagosome maturation, early endosome carrying *Mtb* undergo closure forming phagocytic cup by various coat proteins such as coronin or tryptophane aspartate-containing coat protein (140). Recruitment of proteins such as PX or FYVE motif proteins such as early endosome antigen 1 (EEA1) to early endosome for phagosome maturation is done through phosphotidylinositol-3-phosphate (PI(3)P) (141, 142). Endosome fusion to phagosome leads to oxidative and hydrolytic environment, which ultimately causes cargo degradation (143). Recruitment of lysosome-associated membrane proteins (LAMPs) 1 and 2 is a characteristic feature of late endosomal stage. Acidic pH of around 5 is an important marker of the late endosomal stage to control *Mtb* growth. This acidification process is controlled by Abl tyrosine kinase that functions as a negative regulator of phagosome maturation. Inhibition of this kinase by certain drugs such as imatinib results in controlling *Mtb* growth (144). The lipid body formation in the cell is induced by various bacterial infections such as *S. aureus*, *M. leprae*, and *Mtb*. The fusion of lipid compartments of the cells has been shown to be important for the maturation of phagosomes containing *Mtb* (145). However, *Mtb* resist this process of eradication by interfering in the maturation of phagosomes and subsequent fusion with lysosome (44). *Mtb* bearing phagosomes show reduced acidification due to halt H^+-ATPase (146). The lipids produced by *Mtb* inside the macrophages mimic the host lipids such as phosphatidylinositol (PI3P) giving rise to inhibition of PI3P trafficking (147). EEA1 is an important molecule that inhibits Rab5 and acts as a key player in membrane fusion (148). There is a reduced recruitment of EEA1 in *Mtb*-infected macrophages, which inhibits the maturation of phagosome (149). Ca^{2+} is an important molecule involved in the phagosome maturation. However, *Mtb* inhibits sphingosine kinase dependent Ca^{2+} increase, leading to reduced phagosome maturation (150).

Phagosome containing *Mtb* express abnormal early endosomal markers for instance small GTPase Rab5, transferrin along with its receptor and absence of late endosomal markers *viz* small GTPase Rab7 along with vacuolar proton transporter v-ATPase (146). Furthermore, there is a reduced level of PI3P, EEA1 along with hepatocyte growth factor–regulated tyrosine kinase substrate (HRS) onto the *Mtb* phagosome membrane. These molecules are implicated in the protein sorting and fusion of the phagosome with late endosome followed by lysosome (151). Recently, it has been demonstrated that protein tyrosine phosphatase A (PtpA) binds to one of the subunits of v-ATPase leading to dephosphorylation of vacuolar-sorting protein 33B (152). Furthermore, *Mtb* glycolipids such as LAM as well as TDM inhibit the phagolysosome fusion (153). *Mtb* employs its type VII secretion system by exporting effector proteins EsxH and EsxG to destroy endosomal sorting complex required for transport and thereby impairing the maturation of phagosome (154). Overall, this signifies that the modulation of phagosome maturation of MPS can ultimately lead to the eradication of *Mtb.* In future, it can be used as an important therapeutic platform to control TB (**Figure 2**).

REGULATORY ROLE OF MPCs IN INDUCING AUTOPHAGY AGAINST *Mtb*

Autophagy is an intracellular degradation phenomenon that is developed during the stress response. It allows cells to alter their biomass and turn over components during starvation. Autophagy specifically targets the cytoplasmic components, which include organelles, macromolecules, and cells undergoing unintended cell death to lysosomes for their degradation. It ultimately leads to a periodical cleaning of the cell interiors. Similarly, autophagy has an essential role in numerous diseases, which includes cancer, degenerative diseases, as well as aging. In addition, autophagy augments the ability of cells to engulf and eliminate microbes and thereby protects the host. Treatment with rapamycin or IFN-γ or starvation can initiate and enhance autophagy. Furthermore,

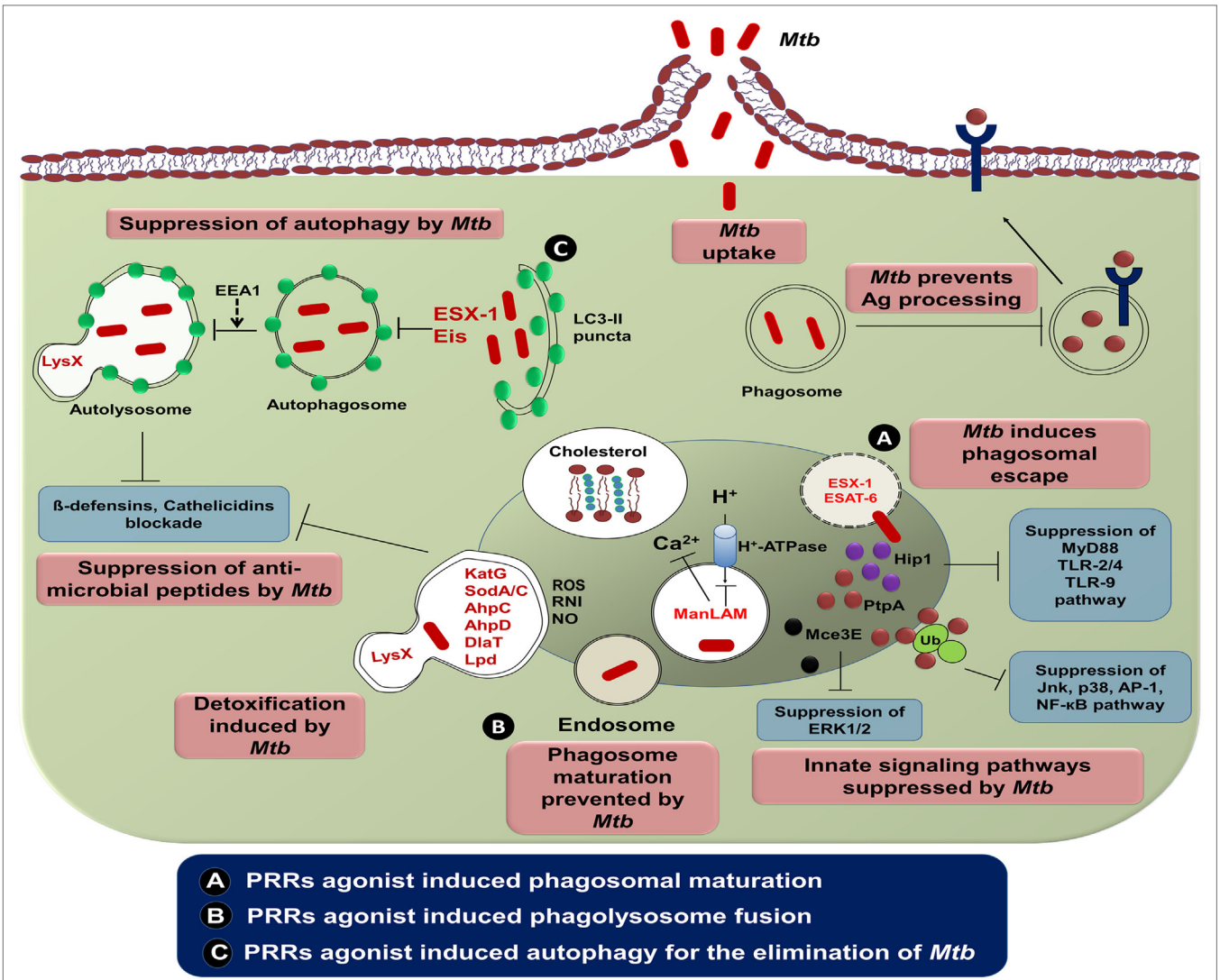


FIGURE 2 | The intracellular evasion strategies adopted by *Mycobacterium tuberculosis* (*Mtb*) and its counteraction through cellular defense mechanism. Phagocytosis of *Mtb* is promoted by diverse cell-surface receptors and cholesterol present in the mononuclear phagocytic cells. *Mtb* utilizes the host cholesterol for its survival and impedes antigen processing and presentation by its lipoproteins. Consequently, ESAT-6 and ESX-1 of *Mtb* alter phagosome maturation process. The potential virulence factors, namely, PtpA and Mce3E of *Mtb* ultimately restrain various signaling cascades of innate immunity by binding with host ubiquitin. Another virulent factor of *Mtb*, ManLAM arrests phagosomal maturation *via* interrupting the transport of host H^+-ATPase to phagosomes and blockading cytosolic Ca^{2+} release. *Mtb* enzymes such as KatG, SodA/C, NADH-dependent peroxidase, superoxide dismutases, and DlaT are involved in detoxification of ROI and RNI. Neutralization of antimicrobial peptides is accomplished through mycobacterial protein LysX. Suppression of autophagy in mononuclear cells is rendered by the *Mtb* encoded gene "enhanced intracellular survival (Eis)." **(A)** Several PRRs agonist such as TLRs (TLR-2, -4, and -9), NLRs (NOD-1 and NOD-2), and CLRs (Mincle, Dectin-1, and Dectin-2) induce phagosomal maturation and inhibit *Mtb* growth by membrane cholesterol reduction. **(B,C)** Involvement of these agonists triggers the phagolysosome fusion and subsequent process of autophagy. To monitor the effect of targeting various PRRs, a comprehensive investigation is required, before selecting the best combination of agonists to control *Mtb* infection. Abbreviations: Hip1, huntingtin-interacting protein 1; PtpA, protein tyrosine phosphatase A; Mce3E, mammalian cell entry operon 3E; ManLAM, mannose lipoarabinomannan; EEA1, early endosome antigen 1; ESAT-6, early secreted antigenic target of 6 kDa; ESX-1, ESTAT6 secretion system I; LysX, lysylphosphatidylglycerol biosynthesis bifunctional protein; KatG, catalase-peroxidase; SodA/C, superoxide dismutase A/C; AhpC/D, alkyl hydroperoxide reductase subunit C/D; DlaT, dihydrolipoamide acyltransferase; Lpd, lipoamide dehydrogenase; Ag, antigen; Ub, ubiquitin; MyD88, myeloid differentiation primary response gene 88; TLR, toll-like receptor; Jnk, c-Jun N-terminal kinase; AP-1, activator protein 1; NF-κB, nuclear factor-κB; ERK1/2, extracellular signal-regulated protein kinases 1 and 2; LC3, microtubule-associated protein 1A/1B-light chain 3; ROS, reactive oxygen species; RNI, reactive nitrogen intermediates; NO, nitric oxide; CLR, C-type lectin receptor; NOD, nucleotide-binding oligomerization domain; Mincle, macrophage-inducible C-type lectin.

signaling through PRRs has been reported to have direct association with the induction of autophagy. It has been well established that triggering through various agonists of TLR-3, TLR-4, and TLR-7 can promote autophagy (155).

Autophagy boosts bactericidal mechanism by sequestering of the process in "double membrane envelope" structure called autophagosome. These processes follow the fusion of autophagosome with lysosomes by forming autolysosome for the

subsequent elimination of the mycobacterium. Autophagy can be initiated within 30 min, as shown through the conversion of LC3-I to LC3-II, which is a fundamental indicator of this process. Autophagy helps in the clearance of *Mycobacterium bovis* BCG as well as *Mtb* by transporting them to the lysosome for their successive degradation (156). It has been reported that triggering infected macrophages through TLR-7 stimulates autophagy and can curb the intracellular growth of *Mtb* (155). Autophagy not only transports *Mtb* to lysosomes but also delivers bactericidal components to the *Mtb* degradation compartment. This

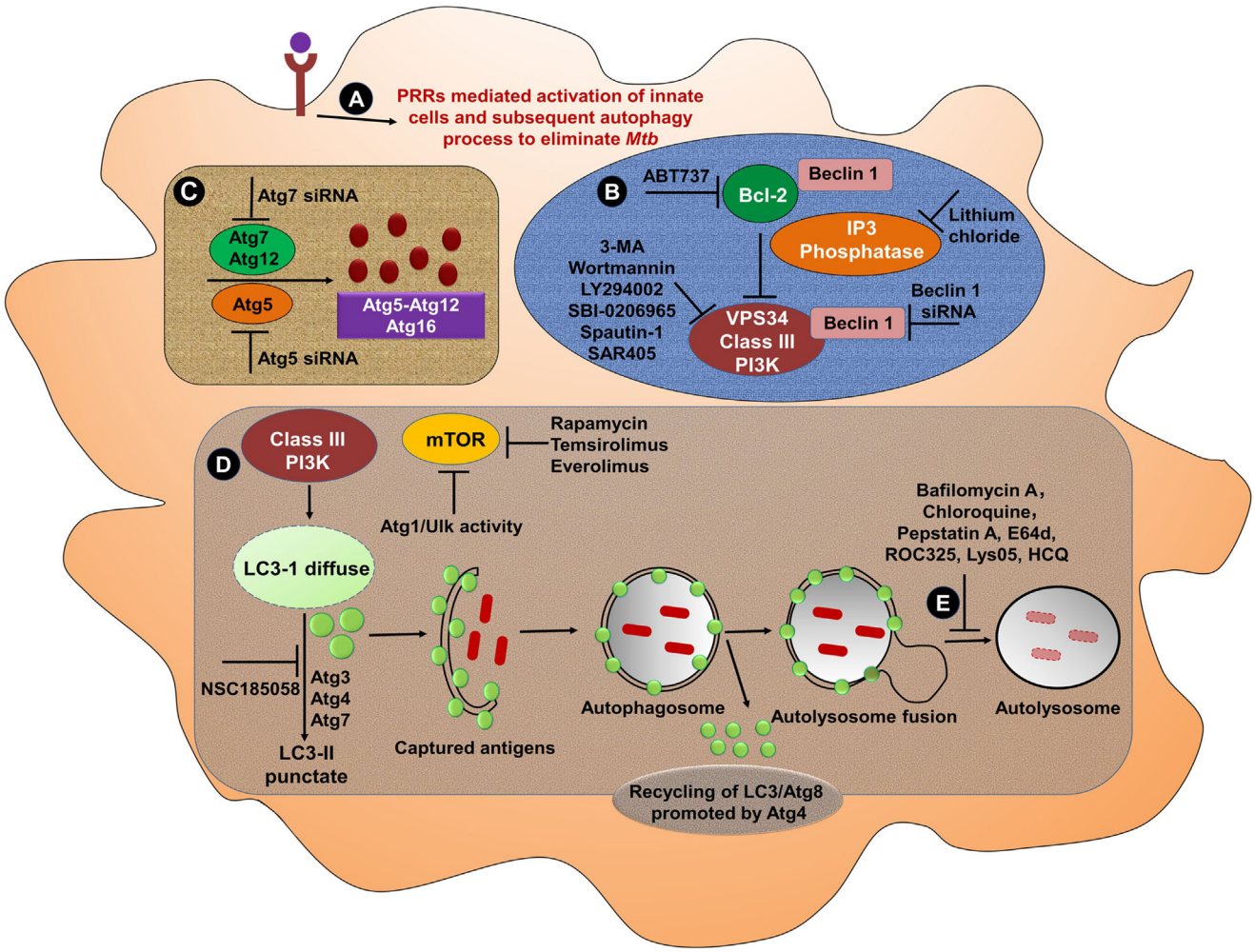


FIGURE 3 | Bolstering the functionality of mononuclear phagocytic cells through PRRs and induction of autophagy. **(A)** Several PRRs-mediated approaches can be used to activate MPS. Activated cells then undergo autophagy to eliminate *Mtb*. Various strategies can be employed to induce or block different steps of autophagy from phagosome maturation to lysosomal fusion. **(B)** At the initiation stage of autophagy, the phagophore formation or nucleation processes occur. One of the most frequently used genetic approaches to inhibit autophagy is knockdown or knockout of *Beclin 1* gene to demonstrate the specificity. The activation of *Beclin 1* gene induces autophagy. The instigation of autophagy can be originated through the activation of PI3 kinase pathway. Treatment of cells with 3-MA, wortmannin, LY294002, SBI-0206965, spautin-1, and SAR405 inhibits the activity of class III PI3K for instance Vps34, which abrogates autophagy process. Autophagy can be artificially induced using lithium chloride, which inhibits inositol phosphatase, leading to augmented intracellular PI3P levels. Other targeted peptides, such as ABT737 that obstruct the interaction of Beclin 1 with Bcl-2 have also been validated to promote autophagy (160). **(C)** Similarly, the knockdown of *Beclin 1* can effectively inhibit the autophagy, leading to the knockdown of *Atg5* (161). Therefore, the knockdown of *Beclin 1* may be the preferred approach to inhibit the autophagy. **(D)** The treatment with rapamycin induces the autophagy through its capacity to obstruct the inhibitory activity of mTOR. Subsequently, the conversion of LC3-I to LC3-II, capturing antigens and phagosome–lysosome fusion can effectively clear pathogens. **(E)** Several inhibitors such as bafilomycin A1 that inhibit the lysosomal Na^+H^+ ATPase are frequently used to reduce lysosomal turnover of autophagosomes. Other agents such as chloroquine, HCQ, Lys05, and ROC325 increase pH, lead to the prevention of the lysosomal acid proteases, as well as cause autophagosomes to accumulate in the lysosome (162, 163). The specific inhibitors of lysosomal proteases, for instance, pepstatin A or E64d abrogates the autophagy (164). Abbreviations: PRRs, pattern recognition receptors; Atg, autophagy-related protein; siRNA, small interfering RNA; Ulk, Unc-51-like kinase 1; ROC325, inhibitor of lysosomal-mediated autophagy; Lys05, dimeric chloroquine (lysosomal autophagy inhibitor); 3-MA, 3-methyl adenine; LC3, microtubule-associated protein 1A/1B-light chain 3; PIK3C3/Vps34, class III phosphatidylinositol-3-kinase; SAR405, selective ATP-competitive inhibitor of Vps34; HCQ, hydroxychloroquine; E64d, ethyl-ester of E64c; Bcl-2, B cell lymphoma-2; ABT-737, BH3 mimetic inhibitor of Bcl-2; NSC185058, inhibitor of Atg4B; mTOR, mammalian target of rapamycin; ATP, adenosine-5′-triphosphate; MPS, mononuclear phagocyte system; *Mtb*, *Mycobacterium tuberculosis*.

observation was further confirmed by blocking the autophagy through knockdown of *Atg5* and *Beclin 1*. Both these molecules are considered to be essential for autophagy. It may be an exciting line of study to identify the mechanism that triggers the autophagy-mediated clearance of *Mtb*. One of the possible mechanisms is an ubiquitination process, where the arrangement of "poly-ubiquitinylated protein aggregates" and contributes as an autophagy substrate. These protein aggregates are broken down into bactericidal peptides, which contribute in destroying *Mtb* (157).

Mycobacterium tuberculosis impedes MPCs bactericidal mechanism by deactivating the acidification of phagosome, lysosome and subsequently inhibiting the phagosome–lysosome fusion. Interestingly, autophagy directs the innate immunity to obstruct the evasion strategies adopted by *Mtb* by targeting the bacterium inhabiting inside, as well as outside the phagosome (156, 158). Similarly, BCG also hampers fusion of the phagosome with the lysosome, consequently resulting in the interference of antigen processing, presentation and therefore impairment in T cell response. This is considered as one of the possible reasons for BCG failure to safeguard people living in TB-endemic regions.

By contrast, autophagy in MPCs promotes both *Mtb* and BCG antigens processing and presentation. Mice adoptively transferred BCG infected APCs that were incubated with rapamycin, elicited Th1 cells that protected against *Mtb*. Rapamycin-induced autophagy with subsequent antigen processing and presentation was suppressed by treatment of cells with the autophagy inhibitors 3-MA or small interfering RNA against *Beclin 1* (159). Designing of a novel approach with an appropriate adjuvant to induce autophagy may be an alternative and effective strategy to make BCG an effective vaccine for people living in TB-endemic zones. To achieve a full pharmacological evidence of the importance of the phagocytotic process in TB, it will be of interest to ascertain whether several PRR agonists or certain autophagy inducers are capable of stimulating the formation of autophagolysosome in MPCs (**Figure 3**).

DEVELOPMENT OF THE POSSIBLE IMMUNOTHERAPEUTIC STRATEGIES TO ENHANCE ANTI-TB IMMUNITY

After the discovery of anti-TB drugs, it was assumed that the disease can be easily eliminated. Unfortunately, this could not be achieved due to the lengthy regimen, narrow therapeutic index and emergence of drug-resistant strains of *Mtb* (165). Currently, novel therapies are being explored for the treatment of numerous ailments such as cardiac diseases, cancer, and autoimmunity. In recent times, better information of host–pathogen interplay has given rise to a paradigm shift in remedial measures such as host-directed therapies, signaling pathway blockade, stem cells, signaling *via* receptors, adoptive transfer of antigen-loaded DCs to protect against cancers, treatment with immunomodulators and humanized Abs, probiotics as well as herbal remedies. In addition, Food and Drug Administration has permitted anti-cytotoxic T lymphocyte-associated antigen-4, CD80 as well as CD52 antibodies for treating cancer. Besides this, interferon-β is endorsed for the treatment of multiple sclerosis (166, 167). In spite of promising immunotherapies in diverse diseases, no thoughtful effort has been attempted in case of TB. Furthermore, immunotherapies with agonists of PRRs in conjunction with drugs have shown to improve the clinical outcome of the disease (168, 169). It will be of great interest to monitor the impact of drugs on *Mtb* in association with the immunomodulatory activity driven through PRRs. Such stratagem has dual advantage over the treatment with drugs alone. The drug will kill the bacterium residing in the MPCs, whereas immunomodulators will stimulate the host immunity to eliminate the pathogen, which had escaped the killing by the drug. Furthermore, this approach may not only reduce the dose as well as duration of the anti-TB drug regimen but can also curb the development of drug resistance in *Mtb*. Therefore, in future, immunotherapies may be the best choice to treat TB and its drug-resistant form.

The second most effective strategy to control and eliminate any disease is vaccine (3, 4). Presently, BCG is the only existing vaccine to treat TB. Ironically, BCG is the most controversial vaccine because of its highly variable efficacy worldwide. Moreover, it protects only children but not adults, as very categorically evident by 15 years follow-up study in India (170). The urgent necessity and challenge for the scientific communal is to improve the current drug regimen or develop alternative and innovative stratagems against TB. In essence, reinforcing the immunity against *Mtb* by triggering through the receptors of innate immunity might be a prudent idea to treat TB patients.

CONCLUSION AND FUTURE PROSPECTS

There is no iota of doubt that for several years TB is treated with potent drugs. Unfortunately, the disease is neither controlled nor eradicated by these drugs; rather the regime has contributed in gifting resistant strains of the *Mtb*. Consequently, it is an important to devise and discover innovative and alternative therapies to control TB. In this connection, understanding the struggle between the bacterium and the host cells such as MPS may have an important impact on the disease outcome. The safe survival heaven for *Mtb* is MPCs. Targeting molecules such as PRRs that can optimally elicit MPCs to eliminate *Mtb* will be an interesting strategy to employ as an adjunct therapy along with the anti-TB drugs. There may be a distinct possibility of such therapeutic measurement in controlling TB by decreasing the dose and duration of drugs and also curbing the emergence of mono and MDR strains of the bacterium. In this article, we have mentioned about a possible combination of various PRRs such as TLRs (TLR-2, TLR-4, and TLR-9), NLRs (NOD-1 and NOD-2), and CLRs (Mincle, Dectin-1, and Dectin-2) as suggested by several studies, to control *Mtb* infection. However, studies are still required to select the best possible combination of PRRs

to achieve complete elimination of *Mtb*. Exploration of this strategy may be an exciting line of future study to control TB.

AUTHOR CONTRIBUTIONS

In this manuscript, the concept and theme were generated by JA and SP. The writing of manuscript and figures were done by SP, GK, SN, MA, DD, HB, SS, MN, JK, and JA.

FUNDING

This work is funded by the Council of Scientific and Industrial Research (CSIR), New Delhi, India. SP, GK, HB, and JK are the Council of Scientific and Industrial Research fellowship recipient; SN, DD, and MN of Department of Biotechnology (DBT); MA of Department of Science and Technology (DST), and SS of Indian Council of Medical Research (ICMR).

REFERENCES

1. World Health Organization. *Global Tuberculosis Report 2017*. Geneva (2017).
2. Gandhi NR, Nunn P, Dheda K, Schaaf HS, Zignol M, van Soolingen D, et al. Multidrug-resistant and extensively drug-resistant tuberculosis: a threat to global control of tuberculosis. *Lancet* (2010) 375(9728):1830–43. doi:10.1016/S0140-6736(10)60410-2
3. Francis DP. Successes and failures: worldwide vaccine development and application. *Biologicals* (2010) 38(5):523–8. doi:10.1016/j.biologicals.2010.06.003
4. Smith R, Renaud RC. Vaccines of the future. *Nat Rev Drug Discov* (2003) 2(10):767–8. doi:10.1038/nrd1204
5. Gowthaman U, Rai PK, Khan N, Jackson DC, Agrewala JN. Lipidated promiscuous peptides vaccine for tuberculosis-endemic regions. *Trends Mol Med* (2012) 18(10):607–14. doi:10.1016/j.molmed.2012.07.008
6. Andersen P, Doherty TM. The success and failure of BCG – implications for a novel tuberculosis vaccine. *Nat Rev Microbiol* (2005) 3(8):656–62. doi:10.1038/nrmicro1211
7. Mogensen TH. Pathogen recognition and inflammatory signaling in innate immune defenses. *Clin Microbiol Rev* (2009) 22(2):240–73. doi:10.1128/CMR.00046-08
8. Hoebe K, Janssen E, Beutler B. The interface between innate and adaptive immunity. *Nat Immunol* (2004) 5(10):971–4. doi:10.1038/ni1004-971
9. Guilliams M, Ginhoux F, Jakubzick C, Naik SH, Onai N, Schraml BU, et al. Dendritic cells, monocytes and macrophages: a unified nomenclature based on ontogeny. *Nat Rev Immunol* (2014) 14(8):571–8. doi:10.1038/nri3712
10. Hume DA, Ross IL, Himes SR, Sasmono RT, Wells CA, Ravasi T. The mononuclear phagocyte system revisited. *J Leukoc Biol* (2002) 72(4):621–7.
11. Jenkins SJ, Hume DA. Homeostasis in the mononuclear phagocyte system. *Trends Immunol* (2014) 35(8):358–67. doi:10.1016/j.it.2014.06.006
12. Akira S, Takeda K, Kaisho T. Toll-like receptors: critical proteins linking innate and acquired immunity. *Nat Immunol* (2001) 2(8):675–80. doi:10.1038/9060990609
13. Schnare M, Barton GM, Holt AC, Takeda K, Akira S, Medzhitov R. Toll-like receptors control activation of adaptive immune responses. *Nat Immunol* (2001) 2(10):947–50. doi:10.1038/ni712
14. Steinman RM. Linking innate to adaptive immunity through dendritic cells. *Novartis Found Symp* (2006) 279:101–9; discussion 109–13, 216–9.
15. Steinman RM, Hemmi H. Dendritic cells: translating innate to adaptive immunity. *Curr Top Microbiol Immunol* (2006) 311:17–58.
16. Pahari S, Kaur G, Aqdas M, Negi S, Chatterjee D, Bashir H, et al. Bolstering immunity through pattern recognition receptors: a unique approach to control tuberculosis. *Front Immunol* (2017) 8:906. doi:10.3389/fimmu.2017.00906
17. McClean CM, Tobin DM. Macrophage form, function, and phenotype in mycobacterial infection: lessons from tuberculosis and other diseases. *Pathog Dis* (2016) 74(7). doi:10.1093/femspd/ftw068
18. van Furth R, Cohn ZA, Hirsch JG, Humphrey JH, Spector WG, Langevoort HL. The mononuclear phagocyte system: a new classification of macrophages, monocytes, and their precursor cells. *Bull World Health Organ* (1972) 46(6):845–52.
19. Wolf AJ, Linas B, Trevejo-Nunez GJ, Kincaid E, Tamura T, Takatsu K, et al. *Mycobacterium tuberculosis* infects dendritic cells with high frequency and impairs their function in vivo. *J Immunol* (2007) 179(4):2509–19. doi:10.4049/jimmunol.179.4.2509
20. Marino S, Pawar S, Fuller CL, Reinhart TA, Flynn JL, Kirschner DE. Dendritic cell trafficking and antigen presentation in the human immune response to *Mycobacterium tuberculosis*. *J Immunol* (2004) 173(1):494–506. doi:10.4049/jimmunol.173.1.494
21. Fortsch D, Rollinghoff M, Stenger S. IL-10 converts human dendritic cells into macrophage-like cells with increased antibacterial activity against virulent *Mycobacterium tuberculosis*. *J Immunol* (2000) 165(2):978–87. doi:10.4049/jimmunol.165.2.978
22. Srivastava S, Ernst JD, Desvignes L. Beyond macrophages: the diversity of mononuclear cells in tuberculosis. *Immunol Rev* (2014) 262(1):179–92. doi:10.1111/imr.12217
23. Hanekom WA, Mendillo M, Manca C, Haslett PA, Siddiqui MR, Barry C III, et al. *Mycobacterium tuberculosis* inhibits maturation of human monocyte-derived dendritic cells in vitro. *J Infect Dis* (2003) 188(2):257–66. doi:10.1086/376451
24. Saraav I, Singh S, Sharma S. Outcome of *Mycobacterium tuberculosis* and Toll-like receptor interaction: immune response or immune evasion? *Immunol Cell Biol* (2014) 92(9):741–6. doi:10.1038/icb.2014.52
25. Flannagan RS, Cosio G, Grinstein S. Antimicrobial mechanisms of phagocytes and bacterial evasion strategies. *Nat Rev Microbiol* (2009) 7(5):355–66. doi:10.1038/nrmicro2128
26. Goldberg MF, Saini NK, Porcelli SA. Evasion of innate and adaptive immunity by *Mycobacterium tuberculosis*. *Microbiol Spectr* (2014) 2(5). doi:10.1128/microbiolspec.MGM2-0005-2013
27. Poirier V, Av-Gay Y. *Mycobacterium tuberculosis* modulators of the macrophage's cellular events. *Microbes Infect* (2012) 14(13):1211–9. doi:10.1016/j.micinf.2012.07.001
28. Humphreys IR, Stewart GR, Turner DJ, Patel J, Karamanou D, Snelgrove RJ, et al. A role for dendritic cells in the dissemination of mycobacterial infection. *Microbes Infect* (2006) 8(5):1339–46. doi:10.1016/j.micinf.2005.12.023
29. Thi EP, Hong CJ, Sanghera G, Reiner NE. Identification of the *Mycobacterium tuberculosis* protein PE-PGRS62 as a novel effector that functions to block phagosome maturation and inhibit iNOS expression. *Cell Microbiol* (2013) 15(5):795–808. doi:10.1111/cmi.12073
30. Deghmane AE, Soualhine H, Bach H, Sendide K, Itoh S, Tam A, et al. Lipoamide dehydrogenase mediates retention of coronin-1 on BCG vacuoles, leading to arrest in phagosome maturation. *J Cell Sci* (2007) 120(Pt 16):2796–806. doi:10.1242/jcs.006221
31. Bach H, Papavinasasundaram KG, Wong D, Hmama Z, Av-Gay Y. *Mycobacterium tuberculosis* virulence is mediated by PtpA dephosphorylation of human vacuolar protein sorting 33B. *Cell Host Microbe* (2008) 3(5):316–22. doi:10.1016/j.chom.2008.03.008
32. Vergne I, Chua J, Lee HH, Lucas M, Belisle J, Deretic V. Mechanism of phagolysosome biogenesis block by viable *Mycobacterium tuberculosis*. *Proc Natl Acad Sci U S A* (2005) 102(11):4033–8. doi:10.1073/pnas.0409716102
33. Khan N, Gowthaman U, Pahari S, Agrewala JN. Manipulation of costimulatory molecules by intracellular pathogens: veni, vidi, vici!! *PLoS Pathog* (2012) 8(6):e1002676. doi:10.1371/journal.ppat.1002676
34. Jozefowski S, Sobota A, Kwiatkowska K. How *Mycobacterium tuberculosis* subverts host immune responses. *Bioessays* (2008) 30(10):943–54. doi:10.1002/bies.20815
35. Khan N, Vidyarthi A, Amir M, Mushtaq K, Agrewala JN. T-cell exhaustion in tuberculosis: pitfalls and prospects. *Crit Rev Microbiol* (2017) 43(2):133–41. doi:10.1080/1040841X.2016.1185603
36. Luo M, Fadeev EA, Groves JT. Mycobactin-mediated iron acquisition within macrophages. *Nat Chem Biol* (2005) 1(3):149–53. doi:10.1038/nchembio717

37. Munoz-Elias EJ, McKinney JD. *Mycobacterium tuberculosis* isocitrate lyases 1 and 2 are jointly required for in vivo growth and virulence. *Nat Med* (2005) 11(6):638–44. doi:10.1038/nm1252
38. Marrero J, Rhee KY, Schnappinger D, Pethe K, Ehrt S. Gluconeogenic carbon flow of tricarboxylic acid cycle intermediates is critical for *Mycobacterium tuberculosis* to establish and maintain infection. *Proc Natl Acad Sci U S A* (2010) 107(21):9819–24. doi:10.1073/pnas.1000715107
39. McKinney JD, Honer zu Bentrup K, Munoz-Elias EJ, Miczak A, Chen B, Chan WT, et al. Persistence of *Mycobacterium tuberculosis* in macrophages and mice requires the glyoxylate shunt enzyme isocitrate lyase. *Nature* (2000) 406(6797):735–8. doi:10.1038/35021074
40. Arkhipov SA, Shkurupy VA, Solomatina MV, Akhramenko ES, Iljine DA. Study of macrophages in BCG granulomas in different compartments of the mononuclear phagocyte system. *Bull Exp Biol Med* (2013) 154(4):467–70. doi:10.1007/s10517-013-1979-6
41. Martinez FO, Helming L, Gordon S. Alternative activation of macrophages: an immunologic functional perspective. *Annu Rev Immunol* (2009) 27: 451–83. doi:10.1146/annurev.immunol.021908.132532
42. Mege JL, Mehraj V, Capo C. Macrophage polarization and bacterial infections. *Curr Opin Infect Dis* (2011) 24(3):230–4. doi:10.1097/QCO.0b013e328344b73e
43. Cambier CJ, Takaki KK, Larson RP, Hernandez RE, Tobin DM, Urdahl KB, et al. Mycobacteria manipulate macrophage recruitment through coordinated use of membrane lipids. *Nature* (2014) 505(7482):218–22. doi:10.1038/nature12799
44. Lugo-Villarino G, Neyrolles O. Manipulation of the mononuclear phagocyte system by *Mycobacterium tuberculosis*. *Cold Spring Harb Perspect Med* (2014) 4(11):a018549. doi:10.1101/cshperspect.a018549
45. He XY, Xiao L, Chen HB, Hao J, Li J, Wang YJ, et al. T regulatory cells and Th1/Th2 cytokines in peripheral blood from tuberculosis patients. *Eur J Clin Microbiol Infect Dis* (2010) 29(6):643–50. doi:10.1007/s10096-010-0908-0
46. Lyadova IV, Panteleev AV. Th1 and Th17 cells in tuberculosis: protection, pathology, and biomarkers. *Mediators Inflamm* (2015) 2015:854507. doi:10.1155/2015/854507
47. Diebold J. [Mononuclear phagocyte system. Morphology and function of the principal constituting cells]. *Ann Pathol* (1986) 6(1):3–12.
48. Sareila O, Kelkka T, Pizzolla A, Hultqvist M, Holmdahl R. NOX2 complex-derived ROS as immune regulators. *Antioxid Redox Signal* (2011) 15(8):2197–208. doi:10.1089/ars.2010.3635
49. Koopman WJ, Nijtmans LG, Dieteren CE, Roestenberg P, Valsecchi F, Smeitink JA, et al. Mammalian mitochondrial complex I: biogenesis, regulation, and reactive oxygen species generation. *Antioxid Redox Signal* (2010) 12(12):1431–70. doi:10.1089/ars.2009.2743
50. Arnoult D, Soares F, Tattoli I, Castanier C, Philpott DJ, Girardin SE. An N-terminal addressing sequence targets NLRX1 to the mitochondrial matrix. *J Cell Sci* (2009) 122(Pt 17):3161–8. doi:10.1242/jcs.051193
51. Miner MD, Chang JC, Pandey AK, Sassetti CM, Sherman DR. Role of cholesterol in *Mycobacterium tuberculosis* infection. *Indian J Exp Biol* (2009) 47(6):407–11.
52. Trautmann A. Extracellular ATP in the immune system: more than just a "danger signal". *Sci Signal* (2009) 2(56):e6. doi:10.1126/scisignal.256pe6
53. Hanley PJ, Musset B, Renigunta V, Limberg SH, Dalpke AH, Sus R, et al. Extracellular ATP induces oscillations of intracellular Ca2+ and membrane potential and promotes transcription of IL-6 in macrophages. *Proc Natl Acad Sci U S A* (2004) 101(25):9479–84. doi:10.1073/pnas.0400733101
54. Grahames CB, Michel AD, Chessell IP, Humphrey PP. Pharmacological characterization of ATP- and LPS-induced IL-1beta release in human monocytes. *Br J Pharmacol* (1999) 127(8):1915–21. doi:10.1038/sj.bjp.0702732
55. Qu Y, Ramachandra L, Mohr S, Franchi L, Harding CV, Nunez G, et al. P2X7 receptor-stimulated secretion of MHC class II-containing exosomes requires the ASC/NLRP3 inflammasome but is independent of caspase-1. *J Immunol* (2009) 182(8):5052–62. doi:10.4049/jimmunol.0802968
56. Ramachandra L, Qu Y, Wang Y, Lewis CJ, Cobb BA, Takatsu K, et al. *Mycobacterium tuberculosis* synergizes with ATP to induce release of microvesicles and exosomes containing major histocompatibility complex class II molecules capable of antigen presentation. *Infect Immun* (2010) 78(12):5116–25. doi:10.1128/IAI.01089-09
57. Kusner DJ, Adams J. ATP-induced killing of virulent *Mycobacterium tuberculosis* within human macrophages requires phospholipase D. *J Immunol* (2000) 164(1). doi:10.4049/jimmunol.164.1.379
58. Lammas DA, Stober C, Harvey CJ, Kendrick N, Panchalingam S, Kumararatne DS. ATP-induced killing of mycobacteria by human macrophages is mediated by purinergic P2Z(P2X7) receptors. *Immunity* (1997) 7(3):433–44. doi:10.1016/S1074-7613(00)80364-7
59. Biswas D, Qureshi OS, Lee WY, Croudace JE, Mura M, Lammas DA. ATP-induced autophagy is associated with rapid killing of intracellular mycobacteria within human monocytes/macrophages. *BMC Immunol* (2008) 9:35. doi:10.1186/1471-2172-9-35
60. Fairbairn IP, Stober CB, Kumararatne DS, Lammas DA. ATP-mediated killing of intracellular mycobacteria by macrophages is a P2X(7)-dependent process inducing bacterial death by phagosome-lysosome fusion. *J Immunol* (2001) 167(6):3300–7. doi:10.4049/jimmunol.167.6.3300
61. Cotton M, Claing A. G protein-coupled receptors stimulation and the control of cell migration. *Cell Signal* (2009) 21(7):1045–53. doi:10.1016/j.cellsig.2009.02.008
62. Manivannan S, Rao NV, Ramanathan VD. Role of complement activation and antibody in the interaction between *Mycobacterium tuberculosis* and human macrophages. *Indian J Exp Biol* (2012) 50(8):542–50.
63. Weiss G, Schaible UE. Macrophage defense mechanisms against intracellular bacteria. *Immunol Rev* (2015) 264(1):182–203. doi:10.1111/imr.12266
64. Gutcher I, Donkor MK, Ma Q, Rudensky AY, Flavell RA, Li MO. Autocrine transforming growth factor-beta1 promotes in vivo Th17 cell differentiation. *Immunity* (2011) 34(3):396–408. doi:10.1016/j.immuni.2011.03.005
65. Hidaka M, Wakabayashi I, Takeda Y, Fukuzawa K. Vitamin D(3) derivatives increase soluble CD14 release through ERK1/2 activation and decrease IL-8 production in intestinal epithelial cells. *Eur J Pharmacol* (2013) 721(1–3):305–12. doi:10.1016/j.ejphar.2013.09.014
66. Liu PT, Stenger S, Li H, Wenzel L, Tan BH, Krutzik SR, et al. Toll-like receptor triggering of a vitamin D-mediated human antimicrobial response. *Science* (2006) 311(5768):1770–3. doi:10.1126/science.1123933
67. Mortaz E, Adcock IM, Tabarsi P, Masjedi MR, Mansouri D, Velayati AA, et al. Interaction of pattern recognition receptors with *Mycobacterium tuberculosis*. *J Clin Immunol* (2015) 35(1):1–10. doi:10.1007/s10875-014-0103-7
68. Khan N, Pahari S, Vidyarthi A, Aqdas M, Agrewala JN. Stimulation through CD40 and TLR-4 is an effective host directed therapy against *Mycobacterium tuberculosis*. *Front Immunol* (2016) 7:386. doi:10.3389/fimmu.2016.00386
69. Khan N, Aqdas M, Vidyarthi A, Negi S, Pahari S, Agnihotri T, et al. Triggering through NOD-2 differentiates bone marrow precursors to dendritic cells with potent bactericidal activity. *Sci Rep* (2016) 6:27263. doi:10.1038/srep27263
70. Khan N, Vidyarthi A, Pahari S, Negi S, Aqdas M, Nadeem S, et al. Signaling through NOD-2 and TLR-4 bolsters the T cell priming capability of dendritic cells by inducing autophagy. *Sci Rep* (2016) 6:19084. doi:10.1038/srep19084
71. Deretic V, Saitoh T, Akira S. Autophagy in infection, inflammation and immunity. *Nat Rev Immunol* (2013) 13(10):722–37. doi:10.1038/nri3532
72. Moraco AH, Kornfeld H. Cell death and autophagy in tuberculosis. *Semin Immunol* (2014) 26(6):497–511. doi:10.1016/j.smim.2014.10.001
73. Pahari S, Khan N, Aqdas M, Negi S, Kaur J, Agrewala JN. Infergen stimulated macrophages restrict *Mycobacterium tuberculosis* growth by autophagy and release of nitric oxide. *Sci Rep* (2016) 6:39492. doi:10.1038/srep39492
74. Cunha LD, Zamboni DS. Subversion of inflammasome activation and pyroptosis by pathogenic bacteria. *Front Cell Infect Microbiol* (2013) 3:76. doi:10.3389/fcimb.2013.00076
75. Drennan MB, Nicolle D, Quesniaux VJ, Jacobs M, Allie N, Mpagi J, et al. Toll-like receptor 2-deficient mice succumb to *Mycobacterium tuberculosis* infection. *Am J Pathol* (2004) 164(1):49–57. doi:10.1016/S0002-9440(10)63095-7
76. Shin DM, Yang CS, Lee JY, Lee SJ, Choi HH, Lee HM, et al. *Mycobacterium tuberculosis* lipoprotein-induced association of TLR2 with protein kinase C zeta in lipid rafts contributes to reactive oxygen species-dependent inflammatory signalling in macrophages. *Cell Microbiol* (2008) 10(9):1893–905. doi:10.1111/j.1462-5822.2008.01179.x
77. Lopez M, Sly LM, Luu Y, Young D, Cooper H, Reiner NE. The 19-kDa *Mycobacterium tuberculosis* protein induces macrophage apoptosis through

Toll-like receptor-2. *J Immunol* (2003) 170(5):2409–16. doi:10.4049/jimmunol.170.5.2409
78. Reiling N, Holscher C, Fehrenbach A, Kroger S, Kirschning CJ, Goyert S, et al. Cutting edge: toll-like receptor (TLR)2- and TLR4-mediated pathogen recognition in resistance to airborne infection with *Mycobacterium tuberculosis*. *J Immunol* (2002) 169(7):3480–4. doi:10.4049/jimmunol.169.7.3480
79. Amir M, Aqdas M, Nadeem S, Siddiqui KF, Khan N, Sheikh JA, et al. Diametric role of the latency-associated protein acr1 of *Mycobacterium tuberculosis* in modulating the functionality of pre- and post-maturational stages of dendritic cells. *Front Immunol* (2017) 8:624. doi:10.3389/fimmu.2017.00624
80. Siddiqui KF, Amir M, Gurram RK, Khan N, Arora A, Rajagopal K, et al. Latency-associated protein Acr1 impairs dendritic cell maturation and functionality: a possible mechanism of immune evasion by *Mycobacterium tuberculosis*. *J Infect Dis* (2014) 209(9):1436–45. doi:10.1093/infdis/jit595
81. Bafica A, Scanga CA, Feng CG, Leifer C, Cheever A, Sher A. TLR9 regulates Th1 responses and cooperates with TLR2 in mediating optimal resistance to *Mycobacterium tuberculosis*. *J Exp Med* (2005) 202(12):1715–24. doi:10.1084/jem.20051782
82. Ferwerda G, Girardin SE, Kullberg BJ, Le Bourhis L, de Jong DJ, Langenberg DM, et al. NOD2 and toll-like receptors are nonredundant recognition systems of *Mycobacterium tuberculosis*. *PLoS Pathog* (2005) 1(3):279–85. doi:10.1371/journal.ppat.0010034
83. Juarez E, Carranza C, Hernandez-Sanchez F, Leon-Contreras JC, Hernandez-Pando R, Escobedo D, et al. NOD2 enhances the innate response of alveolar macrophages to *Mycobacterium tuberculosis* in humans. *Eur J Immunol* (2012) 42(4):880–9. doi:10.1002/eji.201142105
84. Rothfuchs AG, Bafica A, Feng CG, Egen JG, Williams DL, Brown GD, et al. Dectin-1 interaction with *Mycobacterium tuberculosis* leads to enhanced IL-12p40 production by splenic dendritic cells. *J Immunol* (2007) 179(6):3463–71. doi:10.4049/jimmunol.179.6.3463
85. Schoenen H, Bodendorfer B, Hitchens K, Manzanero S, Werninghaus K, Nimmerjahn F, et al. Cutting edge: mincle is essential for recognition and adjuvanticity of the mycobacterial cord factor and its synthetic analog trehalose-dibehenate. *J Immunol* (2010) 184(6):2756–60. doi:10.4049/jimmunol.0904013
86. Wu T, Guo S, Wang J, Li L, Xu L, Liu P, et al. Interaction between mannosylated lipoarabinomannan and dendritic cell-specific intercellular adhesion molecule-3 grabbing nonintegrin influences dendritic cells maturation and T cell immunity. *Cell Immunol* (2011) 272(1):94–101. doi:10.1016/j.cellimm.2011.09.001
87. Sugawara I, Yamada H, Hua S, Mizuno S. Role of interleukin (IL)-1 type 1 receptor in mycobacterial infection. *Microbiol Immunol* (2001) 45(11):743–50. doi:10.1111/j.1348-0421.2001.tb01310.x
88. Mishra BB, Moura-Alves P, Sonawane A, Hacohen N, Griffiths G, Moita LF, et al. *Mycobacterium tuberculosis* protein ESAT-6 is a potent activator of the NLRP3/ASC inflammasome. *Cell Microbiol* (2010) 12(8):1046–63. doi:10.1111/j.1462-5822.2010.01450.x
89. Kurenuma T, Kawamura I, Hara H, Uchiyama R, Daim S, Dewamitta SR, et al. The RD1 locus in the *Mycobacterium tuberculosis* genome contributes to activation of caspase-1 via induction of potassium ion efflux in infected macrophages. *Infect Immun* (2009) 77(9):3992–4001. doi:10.1128/IAI.00015-09
90. Chackerian AA, Alt JM, Perera TV, Dascher CC, Behar SM. Dissemination of *Mycobacterium tuberculosis* is influenced by host factors and precedes the initiation of T-cell immunity. *Infect Immun* (2002) 70(8):4501–9. doi:10.1128/IAI.70.8.4501-4509.2002
91. Santarlasci V, Cosmi L, Maggi L, Liotta F, Annunziato F. IL-1 and T helper immune responses. *Front Immunol* (2013) 4:182. doi:10.3389/fimmu.2013.00182
92. Ghoreschi K, Laurence A, Yang XP, Tato CM, McGeachy MJ, Konkel JE, et al. Generation of pathogenic T(H)17 cells in the absence of TGF-beta signalling. *Nature* (2010) 467(7318):967–71. doi:10.1038/nature09447
93. Khader SA, Bell GK, Pearl JE, Fountain JJ, Rangel-Moreno J, Cilley GE, et al. IL-23 and IL-17 in the establishment of protective pulmonary CD4+ T cell responses after vaccination and during *Mycobacterium tuberculosis* challenge. *Nat Immunol* (2007) 8(4):369–77. doi:10.1038/ni1449
94. Kursar M, Koch M, Mittrucker HW, Nouailles G, Bonhagen K, Kamradt T, et al. Cutting edge: regulatory T cells prevent efficient clearance of *Mycobacterium tuberculosis*. *J Immunol* (2007) 178(5):2661–5. doi:10.4049/jimmunol.178.5.2661
95. Shafiani S, Tucker-Heard G, Kariyone A, Takatsu K, Urdahl KB. Pathogen-specific regulatory T cells delay the arrival of effector T cells in the lung during early tuberculosis. *J Exp Med* (2010) 207(7):1409–20. doi:10.1084/jem.20091885
96. Domingo-Gonzalez R, Prince O, Cooper A, Khader SA. Cytokines and chemokines in *Mycobacterium tuberculosis* infection. *Microbiol Spectr* (2016) 4(5). doi:10.1128/microbiolspec.TBTB2-0018-2016
97. Flynn JL, Goldstein MM, Triebold KJ, Koller B, Bloom BR. Major histocompatibility complex class I-restricted T cells are required for resistance to *Mycobacterium tuberculosis* infection. *Proc Natl Acad Sci U S A* (1992) 89(24):12013–7. doi:10.1073/pnas.89.24.12013
98. Woodworth JS, Wu Y, Behar SM. *Mycobacterium tuberculosis*-specific CD8+ T cells require perforin to kill target cells and provide protection in vivo. *J Immunol* (2008) 181(12):8595–603. doi:10.4049/jimmunol.181.12.8595
99. Stenger S, Hanson DA, Teitelbaum R, Dewan P, Niazi KR, Froelich CJ, et al. An antimicrobial activity of cytolytic T cells mediated by granulysin. *Science* (1998) 282(5386):121–5. doi:10.1126/science.282.5386.121
100. Serbina NV, Liu CC, Scanga CA, Flynn JL. CD8+ CTL from lungs of *Mycobacterium tuberculosis*-infected mice express perforin in vivo and lyse infected macrophages. *J Immunol* (2000) 165(1):353–63. doi:10.4049/jimmunol.165.1.353
101. Silva BDS, Trentini MM, da Costa AC, Kipnis A, Junqueira-Kipnis AP. Different phenotypes of CD8+ T cells associated with bacterial load in active tuberculosis. *Immunol Lett* (2014) 160(1):23–32. doi:10.1016/j.imlet.2014.03.009
102. D'Souza CD, Cooper AM, Frank AA, Mazzaccaro RJ, Bloom BR, Orme IM. An anti-inflammatory role for gamma delta T lymphocytes in acquired immunity to *Mycobacterium tuberculosis*. *J Immunol* (1997) 158(3):1217–21.
103. Tanaka Y, Sano S, Nieves E, De Libero G, Rosa D, Modlin RL, et al. Nonpeptide ligands for human gamma delta T cells. *Proc Natl Acad Sci U S A* (1994) 91(17):8175–9. doi:10.1073/pnas.91.17.8175
104. Boom WH, Chervenak KA, Mincek MA, Ellner JJ. Role of the mononuclear phagocyte as an antigen-presenting cell for human gamma delta T cells activated by live *Mycobacterium tuberculosis*. *Infect Immun* (1992) 60(9):3480–8.
105. Casetti R, Martino A. The plasticity of gamma delta T cells: innate immunity, antigen presentation and new immunotherapy. *Cell Mol Immunol* (2008) 5(3):161–70. doi:10.1038/cmi.2008.20
106. Yang CS, Yuk JM, Jo EK. The role of nitric oxide in mycobacterial infections. *Immune Netw* (2009) 9(2):46–52. doi:10.4110/in.2009.9.2.46
107. MacMicking JD, North RJ, LaCourse R, Mudgett JS, Shah SK, Nathan CF. Identification of nitric oxide synthase as a protective locus against tuberculosis. *Proc Natl Acad Sci U S A* (1997) 94(10):5243–8. doi:10.1073/pnas.94.10.5243
108. Flesch IE, Kaufmann SH. Mechanisms involved in mycobacterial growth inhibition by gamma interferon-activated bone marrow macrophages: role of reactive nitrogen intermediates. *Infect Immun* (1991) 59(9):3213–8.
109. Akaki T, Sato K, Shimizu T, Sano C, Kajitani H, Dekio S, et al. Effector molecules in expression of the antimicrobial activity of macrophages against *Mycobacterium avium* complex: roles of reactive nitrogen intermediates, reactive oxygen intermediates, and free fatty acids. *J Leukoc Biol* (1997) 62(6):795–804. doi:10.1002/jlb.62.6.795
110. Nicholson S, Bonecini-Almeida Mda G, Lapa e Silva JR, Nathan C, Xie QW, Mumford R, et al. Inducible nitric oxide synthase in pulmonary alveolar macrophages from patients with tuberculosis. *J Exp Med* (1996) 183(5):2293–302. doi:10.1084/jem.183.5.2293
111. Sharma S, Sharma M, Roy S, Kumar P, Bose M. *Mycobacterium tuberculosis* induces high production of nitric oxide in coordination with production of tumour necrosis factor-alpha in patients with fresh active tuberculosis but not in MDR tuberculosis. *Immunol Cell Biol* (2004) 82(4):377–82. doi:10.1111/j.0818-9641.2004.01245.x
112. Nathan C, Shiloh MU. Reactive oxygen and nitrogen intermediates in the relationship between mammalian hosts and microbial pathogens. *Proc Natl Acad Sci U S A* (2000) 97(16):8841–8. doi:10.1073/pnas.97.16.8841
113. Ciccone R, Mariani F, Cavone A, Persichini T, Venturini G, Ongini E, et al. Inhibitory effect of NO-releasing ciprofloxacin (NCX 976) on *Mycobacterium tuberculosis* survival. *Antimicrob Agents Chemother* (2003) 47(7):2299–302. doi:10.1128/AAC.47.7.2299-2302.2003
114. Kuo HP, Wang CH, Huang KS, Lin HC, Yu CT, Liu CY, et al. Nitric oxide modulates interleukin-1beta and tumor necrosis factor-alpha synthesis by

alveolar macrophages in pulmonary tuberculosis. *Am J Respir Crit Care Med* (2000) 161(1):192–9. doi:10.1164/ajrccm.161.1.9902113
115. Flynn JL, Chan J. Immunology of tuberculosis. *Annu Rev Immunol* (2001) 19:93–129. doi:10.1146/annurev.immunol.19.1.93
116. Piddington DL, Fang FC, Laessig T, Cooper AM, Orme IM, Buchmeier NA. Cu,Zn superoxide dismutase of *Mycobacterium tuberculosis* contributes to survival in activated macrophages that are generating an oxidative burst. *Infect Immun* (2001) 69(8):4980–7. doi:10.1128/IAI.69.8.4980-4987.2001
117. Bryk R, Lima CD, Erdjument-Bromage H, Tempst P, Nathan C. Metabolic enzymes of mycobacteria linked to antioxidant defense by a thioredoxin-like protein. *Science* (2002) 295(5557):1073–7. doi:10.1126/science.1067798
118. Colangeli R, Haq A, Arcus VL, Summers E, Magliozzo RS, McBride A, et al. The multifunctional histone-like protein Lsr2 protects mycobacteria against reactive oxygen intermediates. *Proc Natl Acad Sci U S A* (2009) 106(11):4414–8. doi:10.1073/pnas.0810126106
119. Pathania R, Navani NK, Gardner AM, Gardner PR, Dikshit KL. Nitric oxide scavenging and detoxification by the *Mycobacterium tuberculosis* haemoglobin, HbN in *Escherichia coli*. *Mol Microbiol* (2002) 45(5):1303–14. doi:10.1046/j.1365-2958.2002.03095.x
120. Hartman ML, Kornfeld H. Interactions between naive and infected macrophages reduce *Mycobacterium tuberculosis* viability. *PLoS One* (2011) 6(11):e27972. doi:10.1371/journal.pone.0027972
121. Chen M, Gan H, Remold HG. A mechanism of virulence: virulent *Mycobacterium tuberculosis* strain H37Rv, but not attenuated H37Ra, causes significant mitochondrial inner membrane disruption in macrophages leading to necrosis. *J Immunol* (2006) 176(6):3707–16. doi:10.4049/jimmunol.176.6.3707
122. Lerner TR, Borel S, Greenwood DJ, Repnik U, Russell MR, Herbst S, et al. *Mycobacterium tuberculosis* replicates within necrotic human macrophages. *J Cell Biol* (2017) 216(3):583–94. doi:10.1083/jcb.201603040
123. Keane J, Remold HG, Kornfeld H. Virulent *Mycobacterium tuberculosis* strains evade apoptosis of infected alveolar macrophages. *J Immunol* (2000) 164(4):2016–20. doi:10.4049/jimmunol.164.4.2016
124. Balcewicz-Sablinska MK, Keane J, Kornfeld H, Remold HG. Pathogenic *Mycobacterium tuberculosis* evades apoptosis of host macrophages by release of TNF-R2, resulting in inactivation of TNF-alpha. *J Immunol* (1998) 161(5):2636–41.
125. Riendeau CJ, Kornfeld H. THP-1 cell apoptosis in response to Mycobacterial infection. *Infect Immun* (2003) 71(1):254–9. doi:10.1128/IAI.71.1.254-259.2003
126. Andersson H, Andersson B, Eklund D, Ngoh E, Persson A, Svensson K, et al. Apoptotic neutrophils augment the inflammatory response to *Mycobacterium tuberculosis* infection in human macrophages. *PLoS One* (2014) 9(7):e101514. doi:10.1371/journal.pone.0101514
127. Behar SM, Martin CJ, Booty MG, Nishimura T, Zhao X, Gan HX, et al. Apoptosis is an innate defense function of macrophages against *Mycobacterium tuberculosis*. *Mucosal Immunol* (2011) 4(3):279–87. doi:10.1038/mi.2011.3
128. Perskvist N, Long M, Stendahl O, Zheng L. *Mycobacterium tuberculosis* promotes apoptosis in human neutrophils by activating caspase-3 and altering expression of Bax/Bcl-xL via an oxygen-dependent pathway. *J Immunol* (2002) 168(12):6358–65. doi:10.4049/jimmunol.168.12.6358
129. Lim YJ, Choi JA, Choi HH, Cho SN, Kim HJ, Jo EK, et al. Endoplasmic reticulum stress pathway-mediated apoptosis in macrophages contributes to the survival of *Mycobacterium tuberculosis*. *PLoS One* (2011) 6(12):e28531. doi:10.1371/journal.pone.0028531
130. Choi JA, Lim YJ, Cho SN, Lee JH, Jeong JA, Kim EJ, et al. Mycobacterial HBHA induces endoplasmic reticulum stress-mediated apoptosis through the generation of reactive oxygen species and cytosolic Ca2+ in murine macrophage RAW 264.7 cells. *Cell Death Dis* (2013) 4:e957. doi:10.1038/cddis.2013.489
131. Pan H, Yan BS, Rojas M, Shebzukhov YV, Zhou H, Kobzik L, et al. Ipr1 gene mediates innate immunity to tuberculosis. *Nature* (2005) 434(7034):767–72. doi:10.1038/nature03419
132. Lee J, Hartman M, Kornfeld H. Macrophage apoptosis in tuberculosis. *Yonsei Med J* (2009) 50(1):1–11. doi:10.3349/ymj.2009.50.1.1
133. Saquib NM, Jamwal S, Midha MK, Verma HN, Manivel V. Quantitative proteomics and lipidomics analysis of endoplasmic reticulum of macrophage infected with *Mycobacterium tuberculosis*. *Int J Proteomics* (2015) 2015:270438. doi:10.1155/2015/270438
134. Lim YJ, Yi MH, Choi JA, Lee J, Han JY, Jo SH, et al. Roles of endoplasmic reticulum stress-mediated apoptosis in M1-polarized macrophages during mycobacterial infections. *Sci Rep* (2016) 6:37211. doi:10.1038/srep37211
135. Seimon TA, Kim MJ, Blumenthal A, Koo J, Ehrt S, Wainwright H, et al. Induction of ER stress in macrophages of tuberculosis granulomas. *PLoS One* (2010) 5(9):e12772. doi:10.1371/journal.pone.0012772
136. Lam A, Prabhu R, Gross CM, Riesenberg LA, Singh V, Aggarwal S. Role of apoptosis and autophagy in tuberculosis. *Am J Physiol Lung Cell Mol Physiol* (2017) 313(2):L218–29. doi:10.1152/ajplung.00162.2017
137. Watson RO, Manzanillo PS, Cox JS. Extracellular *M. tuberculosis* DNA targets bacteria for autophagy by activating the host DNA-sensing pathway. *Cell* (2012) 150(4):803–15. doi:10.1016/j.cell.2012.06.040
138. Kang PB, Azad AK, Torrelles JB, Kaufman TM, Beharka A, Tibesar E, et al. The human macrophage mannose receptor directs *Mycobacterium tuberculosis* lipoarabinomannan-mediated phagosome biogenesis. *J Exp Med* (2005) 202(7):987–99. doi:10.1084/jem.20051239
139. Kant AM, De P, Peng X, Yi T, Rawlings DJ, Kim JS, et al. SHP-1 regulates Fcgamma receptor-mediated phagocytosis and the activation of RAC. *Blood* (2002) 100(5):1852–9.
140. Schuller S, Neefjes J, Ottenhoff T, Thole J, Young D. Coronin is involved in uptake of *Mycobacterium bovis* BCG in human macrophages but not in phagosome maintenance. *Cell Microbiol* (2001) 3(12):785–93. doi:10.1046/j.1462-5822.2001.00155.x
141. Gaullier JM, Simonsen A, D'Arrigo A, Bremnes B, Stenmark H, Aasland R. FYVE fingers bind PtdIns(3)P. *Nature* (1998) 394(6692):432–3. doi:10.1038/28767
142. Kanai F, Liu H, Field SJ, Akbary H, Matsuo T, Brown GE, et al. The PX domains of p47phox and p40phox bind to lipid products of PI(3)K. *Nat Cell Biol* (2001) 3(7):675–8. doi:10.1038/35083070
143. Johansson M, Rocha N, Zwart W, Jordens I, Janssen L, Kuijl C, et al. Activation of endosomal dynein motors by stepwise assembly of Rab7-RILP-p150Glued, ORP1L, and the receptor betalll spectrin. *J Cell Biol* (2007) 176(4):459–71. doi:10.1083/jcb.200606077
144. Bruns H, Stegelmann F, Fabri M, Dohner K, van Zandbergen G, Wagner M, et al. Abelson tyrosine kinase controls phagosomal acidification required for killing of *Mycobacterium tuberculosis* in human macrophages. *J Immunol* (2012) 189(8):4069–78. doi:10.4049/jimmunol.1201538
145. Melo RC, Dvorak AM. Lipid body-phagosome interaction in macrophages during infectious diseases: host defense or pathogen survival strategy? *PLoS Pathog* (2012) 8(7):e1002729. doi:10.1371/journal.ppat.1002729
146. Sturgill-Koszycki S, Schlesinger PH, Chakraborty P, Haddix PL, Collins HL, Fok AK, et al. Lack of acidification in Mycobacterium phagosomes produced by exclusion of the vesicular proton-ATPase. *Science* (1994) 263(5147):678–81. doi:10.1126/science.8303277
147. Vergne I, Chua J, Singh SB, Deretic V. Cell biology of *Mycobacterium tuberculosis* phagosome. *Annu Rev Cell Dev Biol* (2004) 20:367–94. doi:10.1146/annurev.cellbio.20.010403.114015
148. Simonsen A, Lippe R, Christoforidis S, Gaullier JM, Brech A, Callaghan J, et al. EEA1 links PI(3)K function to Rab5 regulation of endosome fusion. *Nature* (1998) 394(6692):494–8. doi:10.1038/28879
149. Fratti RA, Chua J, Vergne I, Deretic V. *Mycobacterium tuberculosis* glycosylated phosphatidylinositol causes phagosome maturation arrest. *Proc Natl Acad Sci U S A* (2003) 100(9):5437–42. doi:10.1073/pnas.0737613100
150. Malik ZA, Thompson CR, Hashimi S, Porter B, Iyer SS, Kusner DJ. Cutting edge: *Mycobacterium tuberculosis* blocks Ca2+ signaling and phagosome maturation in human macrophages via specific inhibition of sphingosine kinase. *J Immunol* (2003) 170(6):2811–5. doi:10.4049/jimmunol.170.6.2811
151. Philips JA. Mycobacterial manipulation of vacuolar sorting. *Cell Microbiol* (2008) 10(12):2408–15. doi:10.1111/j.1462-5822.2008.01239.x
152. Wong D, Bach H, Sun J, Hmama Z, Av-Gay Y. *Mycobacterium tuberculosis* protein tyrosine phosphatase (PtpA) excludes host vacuolar-H+-ATPase to inhibit phagosome acidification. *Proc Natl Acad Sci U S A* (2011) 108(48):19371–6. doi:10.1073/pnas.1109201108
153. Russell DG. *Mycobacterium tuberculosis* and the intimate discourse of a chronic infection. *Immunol Rev* (2011) 240(1):252–68. doi:10.1111/j.1600-065X.2010.00984.x

154. Mehra A, Zahra A, Thompson V, Sirisaengtaksin N, Wells A, Porto M, et al. *Mycobacterium tuberculosis* type VII secreted effector EsxH targets host ESCRT to impair trafficking. *PLoS Pathog* (2013) 9(10):e1003734. doi:10.1371/journal.ppat.1003734
155. Delgado MA, Elmaoued RA, Davis AS, Kyei G, Deretic V. Toll-like receptors control autophagy. *EMBO J* (2008) 27(7):1110–21. doi:10.1038/emboj.2008.31
156. Gutierrez MG, Master SS, Singh SB, Taylor GA, Colombo MI, Deretic V. Autophagy is a defense mechanism inhibiting BCG and *Mycobacterium tuberculosis* survival in infected macrophages. *Cell* (2004) 119(6):753–66. doi:10.1016/j.cell.2004.11.038
157. Alonso S, Pethe K, Russell DG, Purdy GE. Lysosomal killing of Mycobacterium mediated by ubiquitin-derived peptides is enhanced by autophagy. *Proc Natl Acad Sci U S A* (2007) 104(14):6031–6. doi:10.1073/pnas.0700036104
158. Bento CF, Empadinhas N, Mendes V. Autophagy in the fight against tuberculosis. *DNA Cell Biol* (2015) 34(4):228–42. doi:10.1089/dna.2014.2745
159. Jagannath C, Lindsey DR, Dhandayuthapani S, Xu Y, Hunter RL Jr, Eissa NT. Autophagy enhances the efficacy of BCG vaccine by increasing peptide presentation in mouse dendritic cells. *Nat Med* (2009) 15(3):267–76. doi:10.1038/nm.1928
160. Maiuri MC, Le Toumelin G, Criollo A, Rain JC, Gautier F, Juin P, et al. Functional and physical interaction between Bcl-X(L) and a BH3-like domain in Beclin-1. *EMBO J* (2007) 26(10):2527–39. doi:10.1038/sj.emboj.7601689
161. Lum JJ, Bauer DE, Kong M, Harris MH, Li C, Lindsten T, et al. Growth factor regulation of autophagy and cell survival in the absence of apoptosis. *Cell* (2005) 120(2):237–48. doi:10.1016/j.cell.2004.11.046
162. Amaravadi RK, Winkler JD. Lys05: a new lysosomal autophagy inhibitor. *Autophagy* (2012) 8(9):1383–4. doi:10.4161/auto.20958
163. Chude CI, Amaravadi RK. Targeting autophagy in cancer: update on clinical trials and novel inhibitors. *Int J Mol Sci* (2017) 18(6). doi:10.3390/ijms18061279
164. Barth S, Glick D, Macleod KF. Autophagy: assays and artifacts. *J Pathol* (2010) 221(2):117–24. doi:10.1002/path.2694
165. Forget EJ, Menzies D. Adverse reactions to first-line antituberculosis drugs. *Expert Opin Drug Saf* (2006) 5(2):231–49. doi:10.1517/14740338.5.2.231
166. Rech AJ, Mick R, Martin S, Recio A, Aqui NA, Powell DJ Jr, et al. CD25 blockade depletes and selectively reprograms regulatory T cells in concert with immunotherapy in cancer patients. *Sci Transl Med* (2012) 4(134):134ra62. doi:10.1126/scitranslmed.3003330
167. Weinstock-Guttman B, Ramanathan M, Zivadinov R. Interferon-beta treatment for relapsing multiple sclerosis. *Expert Opin Biol Ther* (2008) 8(9):1435–47. doi:10.1517/14712598.8.9.1435
168. Vanneman M, Dranoff G. Combining immunotherapy and targeted therapies in cancer treatment. *Nat Rev Cancer* (2012) 12(4):237–51. doi:10.1038/nrc3237
169. Khan N, Pahari S, Vidyarthi A, Aqdas M, Agrewala JN. NOD-2 and TLR-4 signaling reinforces the efficacy of dendritic cells and reduces the dose of TB drugs against *Mycobacterium tuberculosis*. *J Innate Immun* (2016) 8(3):228–42. doi:10.1159/000439591
170. Fifteen year follow up of trial of BCG vaccines in south India for tuberculosis prevention. Tuberculosis Research Centre (ICMR), Chennai. *Indian J Med Res* (1999) 110:56–69.

Conflict of Interest Statement: The authors declare that the research was conducted in the absence of any commercial or financial relationships that could be construed as a potential conflict of interest.

Copyright © 2018 Pahari, Kaur, Negi, Aqdas, Das, Bashir, Singh, Nagare, Khan and Agrewala. This is an open-access article distributed under the terms of the Creative Commons Attribution License (CC BY). The use, distribution or reproduction in other forums is permitted, provided the original author(s) and the copyright owner are credited and that the original publication in this journal is cited, in accordance with accepted academic practice. No use, distribution or reproduction is permitted which does not comply with these terms.

frontiers in Microbiology

ORIGINAL RESEARCH
published: 02 November 2017
doi: 10.3389/fmicb.2017.02142

Antimycobacterial and Anti-inflammatory Mechanisms of Baicalin via Induced Autophagy in Macrophages Infected with *Mycobacterium tuberculosis*

Qingwen Zhang[1†], Jinxia Sun[1†], Yuli Wang[1], Weigang He[1], Lixin Wang[1], Yuejuan Zheng[1], Jing Wu[2], Ying Zhang[3] and Xin Jiang[1*]*

[1] Department of Immunology and Microbiology, School of Basic Medical Sciences, Shanghai University of Traditional Chinese Medicine, Shanghai, China, [2] Department of Infectious Diseases, Institute of Infectious Diseases, Huashan Hospital, Fudan University, Shanghai, China, [3] Department of Molecular Microbiology and Immunology, Bloomberg School of Public Health, Johns Hopkins University, Baltimore, MD, United States

OPEN ACCESS

Edited by:
Luciana Balboa,
Consejo Nacional de Investigaciones Científicas y Técnicas (CONICET), Argentina

Reviewed by:
Anca Dorhoi,
Friedrich Loeffler Institute Greifswald, Germany
Elsa Anes,
Universidade de Lisboa, Portugal

***Correspondence:**
Ying Zhang
yzhang5@jhu.edu
Xin Jiang
jiangxingao@163.com

[†] *These authors have contributed equally to this work.*

Specialty section:
This article was submitted to Microbial Immunology, a section of the journal Frontiers in Microbiology

Received: *24 June 2017*
Accepted: *19 October 2017*
Published: *02 November 2017*

Citation:
Zhang Q, Sun J, Wang Y, He W, Wang L, Zheng Y, Wu J, Zhang Y and Jiang X (2017) Antimycobacterial and Anti-inflammatory Mechanisms of Baicalin via Induced Autophagy in Macrophages Infected with Mycobacterium tuberculosis. Front. Microbiol. 8:2142. doi: 10.3389/fmicb.2017.02142

Tuberculosis (TB) remains a leading killer worldwide among infectious diseases and the effective control of TB is still challenging. Autophagy is an intracellular self-digestion process which has been increasingly recognized as a major host immune defense mechanism against intracellular microorganisms like *Mycobacterium tuberculosis* (Mtb) and serves as a key negative regulator of inflammation. Clinically, chronic inflammation surrounding Mtb can persist for decades leading to lung injury that can remain even after successful treatment. Adjunct host-directed therapy (HDT) based on both antimycobacterial and anti-inflammatory interventions could be exploited to improve treatment efficacy and outcome. Autophagy occurring in the host macrophages represents a logical host target. Here, we show that herbal medicine, baicalin, could induce autophagy in macrophage cell line Raw264.7 and caused increased killing of intracellular Mtb. Further, baicalin inhibited Mtb-induced NLRP3 inflammasome activation and subsequent inflammasome-derived IL-1β. To investigate the molecular mechanisms of baicalin, the signaling pathways associated with autophagy were examined. Results indicated that baicalin decreased the levels of phosphorylated protein kinase B (p-Akt) and phosphorylated mammalian target of rapamycin (p-mTOR) at Ser473 and Ser2448, respectively, but did not alter the phosphorylation of p38, JNK, or ERK both in Raw264.7 and primary peritoneal macrophages. Moreover, baicalin exerted an obvious inhibitory effect on nuclear factor-kappa B (NF-κB) activity. Finally, immunofluorescence studies demonstrated that baicalin promoted the co-localization of inflammasome with autophagosome may serve as the underlying mechanism of autophagic degradative effect on reducing inflammasome activation. Together, baicalin definitely induces the activation of autophagy on the Mtb-infected macrophages through PI3K/Akt/mTOR pathway instead of MAPK pathway. Furthermore, baicalin inhibited the PI3K/Akt/NF-κB signal pathway, and both autophagy induction and NF-κB inhibition contribute to

limiting the NLRP3 inflammasome as well as subsequent production of pro-inflammatory cytokine IL-1β. Based on these results, we conclude that baicalin is a promising antimycobacterial and anti-inflammatory agent which can be a novel candidate for the development of new adjunct drugs targeting HDT for possible improved treatment.

Keywords: baicalin, *Mycobacterium tuberculosis*, host-directed therapy, autophagy, inflammasome

INTRODUCTION

Tuberculosis (TB) continues to be a major cause of significant morbidity and mortality world-wide. The latest World Health Organization (WHO) report indicates that TB remains a global emergency (WHO, 2016). New available anti-TB drugs are limited in number and activity and they mostly direct microbial targets and have faced many obstacles (Zumla et al., 2015) such as increasing drug resistance, complex drug regimens, lengthy, and toxic treatment durations. Recent work on host immunity, host-pathogen interactions and host-directed interventions have shown that supplementation anti-TB therapy with host modulators, such as imatinib and nitazoxanide may shorten the treatment times, reduce the lung damage caused by inflammation, and lower the risk of relapse or reinfection (Hawn et al., 2013). Host-directed therapy (HDT) is a new strategy for adjuvant therapy in fighting against TB, which focuses on potentiating key components of host antimycobacterial effector mechanisms, while restricting inflammation and pathological damage in the lung (Hawn et al., 2013; Zumla and Maeurer, 2016; Machelart et al., 2017; Yang, 2017).

Autophagy is a highly conserved and fundamental biological process in eukaryotic cells (Mizushima et al., 2008). Most of autophagic physiological effects, such as maintaining cell, tissue, and organism homeostasis, are the result of its degradative activities (Boya et al., 2013), while the unconventional function of autophagy such as biogenesis and secretory roles in protein processing are beginning to be recognized (Deretic et al., 2012; Boya et al., 2013). A cardinal structural and functional feature of autophagy is the formation of bilayer membrane organelles called autophagosomes. The generation of LC3-II is an emblematic event associated with autophagy and the reduction of p62, a specific substrate protein of autophagosome, signifies the generation of highly lytic degradative organelles, autolysosome, resulting from the fusion of autophagosome with lysosome. Increasing evidences have shown antimicrobial role of autophagy against *Mycobacterium tuberculosis* (Mtb) (Gutierrez et al., 2004; Singh et al., 2006; Bradfute et al., 2013). The mechanism of killing of intracellular mycobacteria by autophagy is based on the strong degradative and other antimicrobial properties unique to autolysosome (Ponpuak et al., 2010). Autophagy eliminates mycobacteria through several mechanisms. First, induction of autophagy indirectly promotes maturation of Mtb phagosomes into degradative organelles (Harris et al., 2007; Fabri et al., 2011), conquering the well-known Mtb-mediated phagosome maturation arrest. Second, autophagosomes directly capture a subset of intracellular Mtb that then progress into degradative autolysosomes (Gutierrez et al., 2004; Watson et al., 2012). Third, autophagy has a bactericidal effect relying on the classical antimicrobial peptides such as cathelicidin through fusion with lysosomes where cathelicidin is stored or neo-antimicrobial peptides produced through autophagic proteolysis of innocuous cytosolic proteins such as ubiquitin (Alonso et al., 2007) and ribosomal proteins (Yuk et al., 2009; Ponpuak et al., 2010; Fabri et al., 2011). Thus, autophagy can be triggered by immunological and physiological stimuli enabling macrophages to kill intracellular Mtb.

The activation of autophagy can be regulated by a wide variety of signals (He and Klionsky, 2009; Yang and Klionsky, 2009; Yin et al., 2016). The kinase mTOR is a major modulator of autophagy and it receives inputs from different signaling pathways, and is a downstream target of the phosphatidylinositol 3 kinase (PI3K)/protein kinase B (Akt) pathway. The PI3K/Akt/mTOR signaling pathway has been recognized to negatively regulate the activation of autophagy (Heras-Sandoval et al., 2014). Moreover, the activation of mitogen activated protein kinases (MAPK) pathway can induce autophagy (Krishna and Narang, 2008; Zhou et al., 2015). MAPK is a well-known serine/threonine protein kinase, the associated signal pathway is one of the most important regulatory mechanisms in eukaryotic cells, with p38, JNK, ERK1/2 being the key members of MAPK sub-families (Krishna and Narang, 2008). Additionally, PI3K/Akt pathway also contributes to the activation of NF-κB by inducing the phosphorylation level of IKKα/β and IκBα (Kang et al., 2012; Guo et al., 2016).

Macrophages infected with Mtb secrete proinflammatory cytokines, including IL-1β and IL-18 (Koo et al., 2008; Kleinnijenhuis et al., 2009). The increase of IL-1β could trigger other immunological and inflammatory cells to synthesize proinflammatory cytokines including TNF-α, IL-6 et al, causing subsequently inflammatory and immunological damage (Dinarello, 1996; Dorhoi and Kaufmann, 2016). Although the production of IL-1 and TNF-α, as well as other proinflammatory cytokines is designed to be protective, if left unchecked, their excessive or inappropriate production may lead to severe inflammatory diseases (Beutler and Cerami, 1988; Dorhoi and Kaufmann, 2014). Relevant to Mtb infection, IL-1-coated beads are capable of inducing large granulomas in lung tissue (Kasahara et al., 1988). Furthermore, production of elevated TNF-α could cause severe inflammation in vital organs (such as lungs and spleen) and leading to early death (Bekker et al., 2000). It has

Abbreviations: TB, tuberculosis; Mtb, *Mycobacterium tuberculosis*; WHO, World Health Organization; HDT, Host-directed therapy; ASC, apoptosis-associated speck-like protein containing a caspase recruitment domain; PI3K, phosphatidylinositol 3 kinase; Akt, protein kinase B; mTOR, mammalian target of rapamycin; MAPK, mitogen activated protein kinases; NF-κB, nuclear factor-kappa B; NLR, NOD-like receptor; DMEM, Dulbecco's Modified Eagle's Medium; CFU, Colony forming unit; BCA, bicinchoninic acid; PBS, phosphate-buffered saline; BSA, bovine serum albumin; CQ, chloroquine; Con, control; Lys, lysate; Sup, supernatant; rapa, rapamycin.

been shown that Mtb activates NLRP3 inflammasome and results in the production of mature IL-1β in infected macrophages (Mishra et al., 2010; Wong and Jacobs, 2011; Dorhoi et al., 2012). The inflammasome is a macromolecular protein complex consisting of at least three components: a NLR (NOD-like receptor) protein such as NLRP3, apoptosis-associated speck-like protein containing a caspase recruitment domain (ASC), and pro-caspase-1. Upon activation by agonists, the inflammasome processes pro-IL-1β into a mature, biologically active IL-1β for secretion extracellularly (Lamkanfi and Dixit, 2014; He et al., 2016). The NLRP3 inflammasome can be regulated by NF-κB pathway where synthesis of NLRP3 and pro-IL-1β provides the first signals for inflammasome activation (Ghonime et al., 2014; Patel et al., 2017). Interestingly, a number of consistent reports have unequivocally indicated that autophagy plays a negative role in the process of inflammation by inhibiting the releasing of IL-1β (Lupfer et al., 2013; Martins et al., 2015; Saitoh and Akira, 2016). Loss of autophagy (ATG16L1 deficiency) increases IL-1β levels which aggravates the degree of inflammation in a mouse gut inflammation model (Saitoh et al., 2008). Autophagy inhibits the production of IL-1β indirectly, by lowering the endogenous stimuli of inflammasome activation (Nakahira et al., 2011; Zhou et al., 2011) and may also directly, via autophagic degradation of inflammasome components (Harris et al., 2011; Shi et al., 2012). Consistently, there are studies which have shown that autophagy protects from excessive inflammation during Mtb infection (Castillo et al., 2012) and protects against Mtb pathogenesis *in vivo* (Castillo et al., 2012; Watson et al., 2012). Thus, autophagy plays an important role in fighting against TB by direct killing the pathogen while preventing excessive inflammatory injury as well. In fact, as an adjunctive therapy, it has been demonstrated that autophagy contributes to the efficacy of frontline anti-tuberculosis chemotherapeutics, such as isoniazid and pyrazinamide (Kim et al., 2012). Thus, pharmaceutical manipulation on autophagy could be potentially useful as new strategies in anti-tuberculosis chemotherapeutics.

Baicalin is a flavonoid isolated from the extracts of dried roots of Scutellaria baicalensis Georgi (Huang Qin), a plant that belongs to the labiatae family, and its chemical structure has been verified (de Oliveira et al., 2015). Baicalin possesses many biological activities such as antibacterial, anti-inflammatory, anti-allergic, anti-spasmodic, and anti-cancer (Srinivas, 2010; Yu et al., 2013). Furthermore, baicalin could induce autophay in cancer (Zhang et al., 2012; Lin et al., 2013) causing subsequent autophagic tumor cell death. The molecular mechanisms of bacalin-induced autophagy in cancer cells involves blocking of the Akt signaling (Lin et al., 2013) and downregulation of CD147 (Zhang et al., 2012). The present study was carried out to investigate the mechanism of the immunological protective effect of baicalin in macrophages infected with Mtb.

MATERIALS AND METHODS

Mice and Reagents

Female C57BL/6 J mice (4–8 weeks of age, weight 20 ± 3 g) were obtained from Vital River Laboratory Animal Technology Co., Ltd. (Beijing, China). All mice were acclimated for at least 1 week before the experiments and housed in a pathogen-free facility. Animal experiments were carried out in strict accordance with the National Institute of Health Guide for the Care and Use of Laboratory Animals, with the approval of the Scientific Investigation Board of Shanghai University of Traditional Chinese Medicine (Shanghai, China). DMSO, bovine serum albumin (BSA) and OPTI-MEM medium were purchased from Sigma (St. Louis, MO). RIPA lysis buffer, BCA Protein Assay Kit and Protein A/G agarose/sepharose beads were obtained from the Beyotime Institute of Biotechnology (Shanghai, China). The following antibodies were used: anti-NLRP3 (cat. #15101), anti-IL-1β (cat. #12507), anti-ASC (cat. #67824), anti-LC3 (cat. #2775), anti-p62 (cat. #5114), anti-Akt (cat. #4691), anti-phosphorylated Akt (Ser473) (cat. #4060), anti-mTOR (cat. #2972), anti-phosphorylated mTOR (Ser2448) (cat. #5536), anti-phosphorylated p38 (cat. #4511), anti-phosphorylated JNK (cat. #4668), and anti-phosphorylated ERK1/2 (cat. #4370) were purchased from Cell Signaling Technology, Inc. (CST, Danvers, MA, USA); rabbit anti-caspase-1 (cat. #sc-514), goat anti-rabbit (cat. #sc-2012), donkey anti-goat (cat. #sc-2094), and goat anti-mouse LC3 (cat. #sc-16755) were purchased from Santa Cruz Biotechnology, Inc. (Santa Cruz CA, USA); donkey anti-rabbit IgG H&L antibody (conjugated with Alexa Fluor® 488; ab150073) and donkey anti- goat IgG H&L antibody (conjugated with Alexa Fluor® 647; ab150131) were acquired from Abcam (Cambridge, UK); anti-β-actin (cat. #66009-1-lg) monoclonal antibody was from ProteinTech Group (Chicago, IL). Baicalin (Molecular Weight: 446.36, purity > 98%) was purchased from shanghai tauto biotech co., LTD. (shanghai, China). Dulbecco's Modified Eagle's Medium (DMEM) was obtained from HyClone

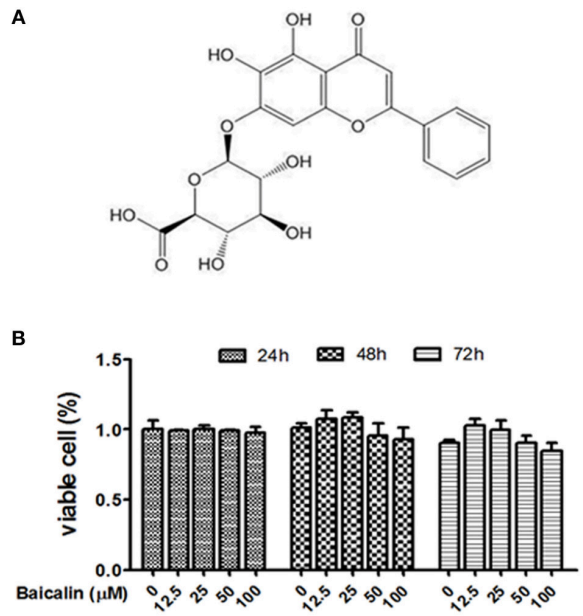


FIGURE 1 | Effect of baicalin on the viability of Raw264.7. **(A)** The chemical structure of baicalin; **(B)** Proliferation assay was conducted to assess the cytotoxic effect of baicalin on Raw264.7. Data are shown as means ± SD of three independent experiments.

Laboratories, Inc (Logan, UT, USA). Middlebrook 7H9 and 7H10 media were obtained from Difco (Detroit, MI, USA) and oleic acid-albumin-dextrose-catalase (OADC) supplements were from BD Biosciences (BD, Sparks, MD, USA).

Cell Culture

The Raw264.7 murine macrophage cell line was cultured in DMEM supplemented with 10% fetal bovine serum (FBS) in 5% CO2 at 37°C. Thioglycolate-elicited mouse primary peritoneal macrophages were prepared from female C57BL/6 J mice as described previously (Jiang et al., 2017). After 2 h, non-adherent cells were removed and the adherent cells were used as primary peritoneal macrophages.

CCK-8 Assay for Cell Viability

Raw264.7 (1×10^4 cells/100 μl) cells were seeded into 96-well culture plates overnight at 37°C and atmospheric conditions of 5% CO_2. The culture medium was then replaced with medium containing different concentrations of baicalin (0, 12.5, 25, 50, 100 μM) for 24, 48, 72 h. At the end of the culture, 10 μl of the CCK-8 reagent was added to each well. After 1–2 h of incubation at 37°C, the absorbance was determined at 450 nm using a Synergy 2 Microplate Reader (Bio-Tek, USA).

Bacterial Strains

The Mtb H37Ra was used in this study. H37Ra strain was grown in Middlebrook 7H9 or 7H10 broth supplemented with 0.2% glycerol, 0.05% Tween-80, and 10% Middlebrook OADC supplement.

Mtb Infection

The Raw264.7 or primary peritoneal macrophage cells were seeded at various specifications of the cell culture plates and grown at 37°C overnight. The cells (1×10^6, 1×10^5, or 5×10^5) were infected with Mtb H37Ra (MOI = 10). After 4 h of co-incubation at 37°C, cells were washed three times

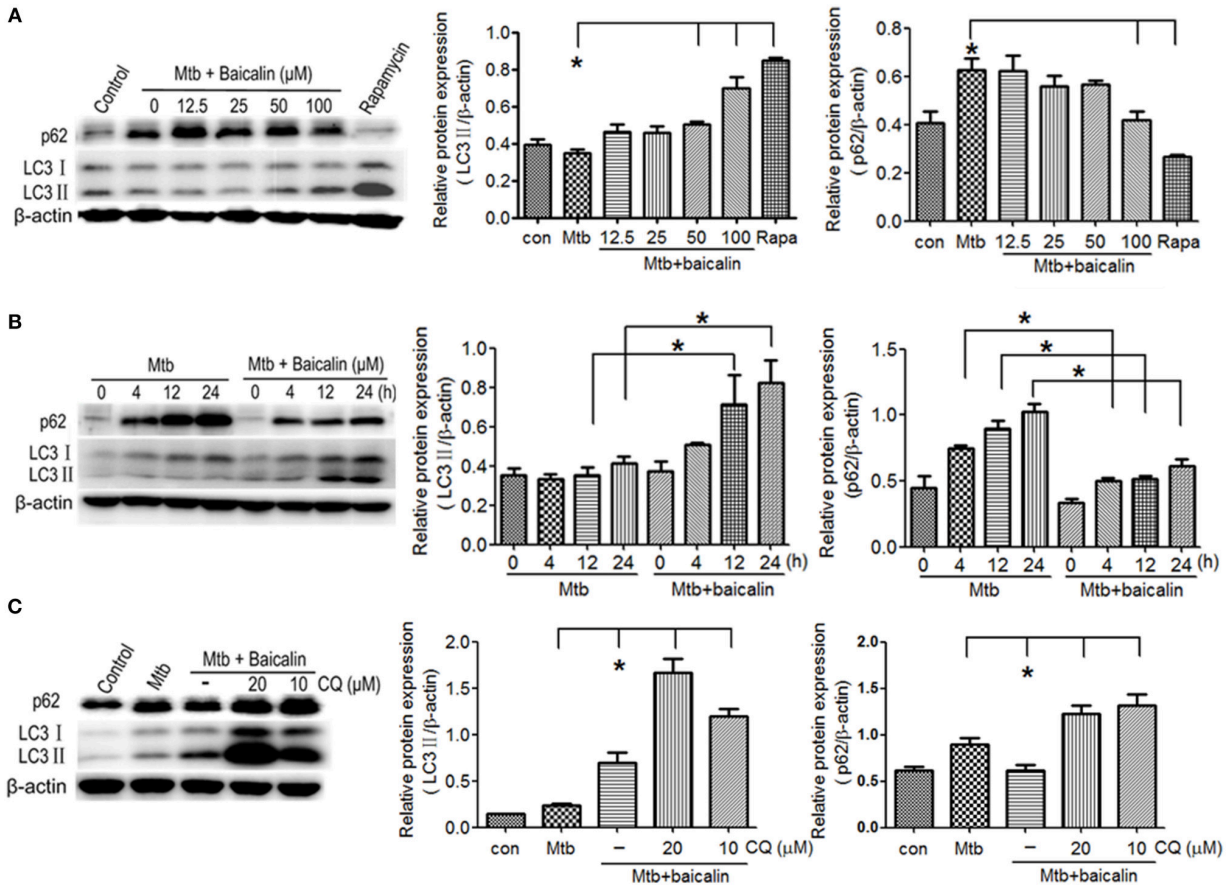


FIGURE 2 | Baicalin can promote the activation of autophagy in Mtb-infected macrophages. **(A)** Western blot analysis of LC3 I/II and p62 expression in Mtb-infected Raw264.7 cells after treatment with different concentrations of baicalin (0, 12.5, 25, 50, 100 μM) or rapamycin (1 μg/ml) for 12 h. The right bar graphs show the statistical results for the relative quantitative expression of LC3 II and p62. **(B)** Western blot analysis of LC3 I/II and p62 expression in Mtb-infected Raw264.7 cells. After different times of Mtb infection (0, 4, 12, 24 h), cells were treatment with or without baicalin (100 μM). The right bar graphs showed the statistical results for the relative quantitative expression of LC3 II and p62. **(C)** Western blot analysis of LC3 I/II and p62 expression in Mtb-infected Raw264.7 cells after treatment with baicalin (100 μM) or CQ (10, 20 μM) for 12 h. The right bar graphs showed the statistical results for the relative quantitative expression of LC3 II and p62 expression. Data are shown with the means ± *SD* of at least three independent experiments. *$p < 0.05$.

with sterile phosphate-buffered saline (PBS) and cultured with DMEM containing 10% FBS in the presence and absence of different concentrations of baicalin (0, 12.5, 25, 50, or 100 μM) for different times.

Colony Forming Unit (CFU)

Raw264.7 cells (5×10^5) were seeded in six-well plates, after infection for 4 h (MOI = 10), cells were washed with sterile PBS and added new complete medium (10% FBS) into the plates in the presence or absence of baicalin (100 μM). After 48 h, the cells were ruptured (0.1% Triton X-100) to release intracellular bacteria and diluted to appropriate dilutions with sterile PBS for CFU count on 7H10 agar plates.

Western Blot

Cells were collected and lysed in lysis buffer, and then the whole cell lysate was separated by SDS-PAGE and further transferred onto nitrocellulose membranes. After blocking with TBST (0.5% Tween-20) containing 5% (w/v) non-fat milk, the membranes were incubated with specific primary antibodies against NLRP3, IL-1β, caspase-1, ASC, mTOR, p-mTOR, Akt, p-Akt, p-p38, p-JNK, p-ERK, or p-p65 at 4°C overnight in blocking solution, all antibodies were diluted at 1:1,000. Following three times of washed with TBST, the membranes were incubated with HRP-conjugated secondary antibodies at room temperature for 1 h. The chemiluminescence was detected using the ECL-chemiluminescent kit (Thermo Scientific) with Protein Simple (USA).

Co-immunoprecipitation

Raw264.7 cells were lysed at 4°C in ice-cold cell lysis buffer and cell lysates were cleared by centrifugation (12,000 g, 10 min). Concentrations of proteins in the supernatant were determined by bicinchoninic acid (BCA) assay. Before immunoprecipitation, samples containing equal amounts of proteins were pre-cleared with various irrelevant IgG or specific antibodies (2–5 mg/ml) overnight at 4°C with gentle rotation and subsequently incubated with Protein A/G agarose/sepharose beads at 4°C with gentle rotation. Following 3 h incubation, agarose/sepharose beads were washed extensively with PBS for four times and proteins were eluted by boiling in 1×SDS sample buffer before SDS-PAGE electrophoresis.

Measurement of Mature IL-1β

Raw264.7 cells (1×10^6) were cultured in six-well plates which infected with H37Ra for 4 h. Then washed twice with sterile PBS and replaced with 1 ml OPTI-MEM medium containing different concentration of baicalin (0, 12.5, 25, 50, or 100 μM). After 12 h, the supernatant of each well were concentrated according to the literature and with slightly modification (Shi et al., 2012). Removing 0.8 ml of the medium collected from each well and mixed with 0.8 ml methanol and 0.2 ml chloroform,

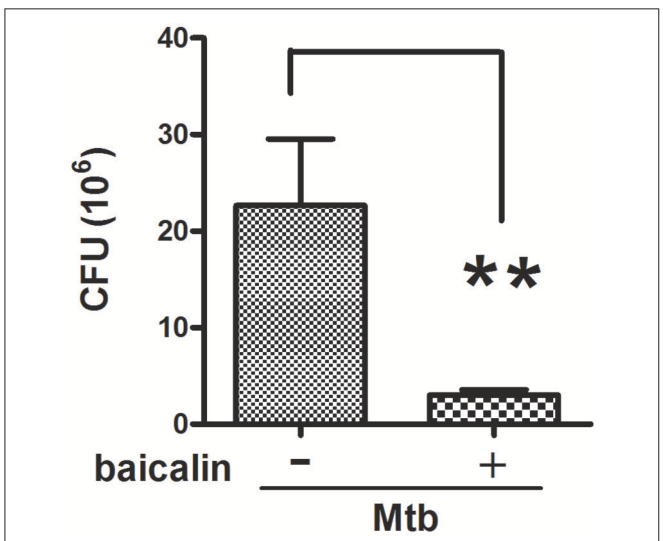


FIGURE 3 | Inhibitory effect of baicalin on bacillary loads. Bacterial CFUs were counted after baicalin treatment for 48 h. $^{**}p < 0.01$, Data are shown as mean ± *SD* of three independent experiments.

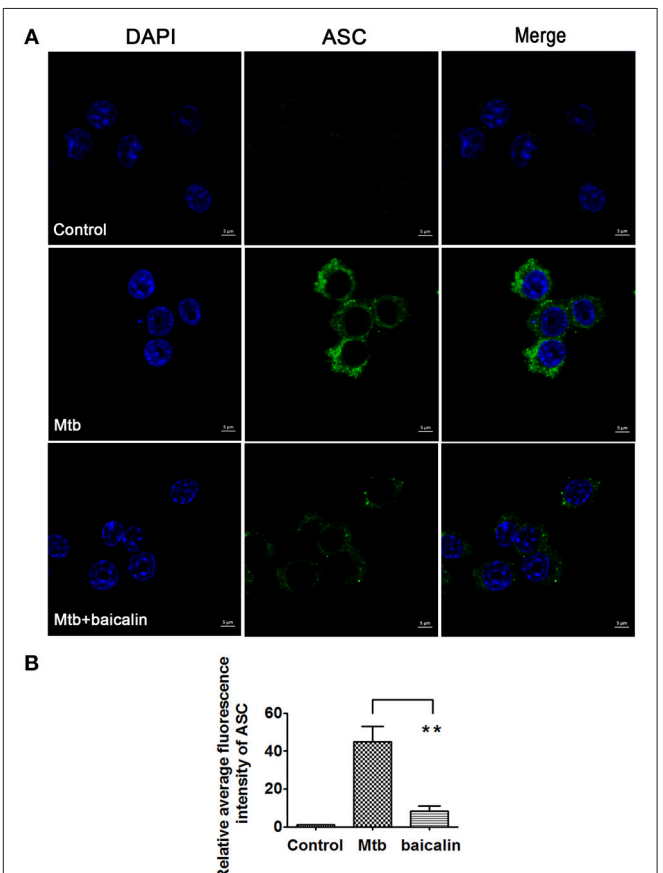


FIGURE 4 | Baicalin inhibits the aggregation of ASC. **(A)** Immunofluorescence assay was performed and rabbit anti-ASC (green) and DAPI (blue) were used for immunostaining. Images were obtained with laser scanning confocal microscopy. **(B)** Quantification of the confocal images about ASC. The confocal images about ASC were quantified with ZEN 2011 Blue Version. Data are shown with means ± *SD*. $^{*}p < 0.05$.

vortexed, and centrifuged at 12,000 g for 5 min. The upper phase from each sample was removed and 0.8 ml methanol added. The samples were centrifuged again for 5 min at 12,000 g to remove the supernatant, and the pellet was placed in room temperature for 10 min to volatilize the methanol. Seventy milliliters of 1×loading buffer was added to each sample followed by boiling for 10 min prior to SDS-PAGE and immunoblotting with antibodies to detect mature IL-1β (AB-400-NA, R&D Systems). The adherent cells from each well were lysed with the above-mentioned lysis buffer and quantified before immunoblot to determine the cellular content of the different proteins.

Immunofluorescence

Following the appropriate treatment, the cells were washed twice with PBS, fixed with 4% paraformaldehyde at room temperature for 10 min, and washed again with PBS. The cells were treated with penetrating reagents (0.2% of BSA, 2% of Triton X-100) for 10 min at 4°C and washed again with PBS, and then the cells were blocked with 5% bovine serum albumin for 30 min at room temperature. Rabbit anti-ASC, anti-LC3, anti-caspase-1, and anti-pp65 antibodies were used for immunofluorescence. Donkey anti-mouse IgG and goat anti-rabbit FITC conjugated antibodies were used as secondary antibodies. The nuclei were stained with DAPI at the concentration of 1 μg/ml for 10 min. In this experiment, confocal microscopy (LSM 880, Zeiss optics international trading co., LTD) was used for examination.

Statistical Analysis

Statistical analysis was performed by using SPSS 18.0 software (SPSS, Inc., Chicago, IL, USA). *P*-values were assessed by one-way analysis of variance (ANOVA), results were given as means ± standard deviations (SD). Data shown are representative of at least triplicate experiments. A value of $p < 0.05$ was considered to be statistically significant.

RESULTS

Effect of Baicalin on the Viability of Raw264.7

To optimize the concentration of baicalin, the cell viability assay was conducted to evaluate potential drug-induced toxicity. The proliferation of Raw264.7 cells was tested using the CCK-8 kit. As shown in **Figure 1**, baicalin (within 100 μM) did not affect the viability of Raw264.7 during observation periods (24, 48, or 72 h). Thus, the concentrations of baicalin within 100 μM were considered as safe for cells and could be used for the subsequent studies.

Baicalin Induces Autophagy in Mtb Infected Macrophages

Mtb is an intracellular pathogen which can proliferate within infected macrophages by preventing the maturation of the phagosome where the bacteria reside. Autophagy represents a recognized cell-autonomous defense against intracellular pathogens that can employ various mechanisms for elimination of invasive Mtb (Gutierrez et al., 2004; Singh et al., 2006; Ponpuak et al., 2010). To assess the effect of baicalin on autophagy induction, we examined the expression of LC3 II and p62 (the biomarker of autophagosome) after treatment

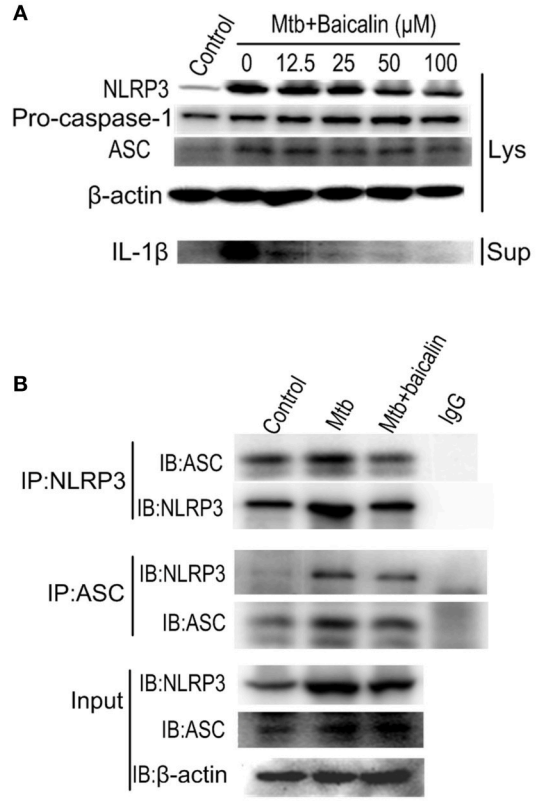


FIGURE 5 | Baicalin evidently inhibits the Mtb-induced NLRP3 inflammasome activation. **(A)** Levels of NLRP3, ASC and pro-caspase-1 expression in cell lysates and the mature IL-1β in the supernatant were determined by immunoblot. **(B)** ASC or NLRP3 immunoprecipitates from Raw264.7 cells were immunoblotted for NLRP3 or ASC respectively, and re-blotted for ASC or NLRP3 respectively. Experiment performed three times.

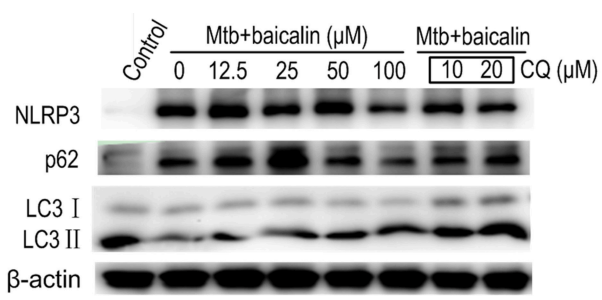


FIGURE 6 | Baicalin inhibits the expression of Mtb-induced NLRP3 in primary peritoneal macrophage cells and chloroquine (CQ) prevented this effect. The expression of NLRP3, LC3 I/II and p62 in Mtb-infected primary peritoneal macrophage cells after treatment with different concentrations of baicalin or CQ (10, 20 μM) was detected by Western blot. The concentration of baicalin when used in combination with CQ was 100 μM.

with different concentrations of baicalin (0, 12.5, 25, 50, or 100 μM). As shown in **Figure 2A**, baicalin induced the activation of autophagy in a dose-dependent manner and the concentration of 100 μM triggered most potent autophagy. The autophagy activation induced by baicalin (100 μM) was time-dependent (**Figure 2B**). To further validate the effect of baicalin on autophagy, we next evaluated the autophagic flux utilized with an autophagy inhibitor, chloroquine (CQ). As shown in **Figure 2C**, either 10 or 20 μM of CQ caused remarkable accumulation of LC3 and p62 compared to baicalin treatment. These data demonstrated that baicalin indeed induced the activation of autophagy in a concentration- and time-dependent manner.

Baicalin Has a Significant Killing Effect on Mtb in Macrophages

Mtb, as a well-known intracellular pathogen, has developed several schemes (e.g., dampening the antimicrobial activity of ROS and RNS, preventing the maturation of early phagosomes, inhibiting the fusion of phagosome with lysosome, interrupting autophagy process) to escape from the antimicrobial mechanisms of macrophages and thus survive intracellularly (Awuh and Flo, 2017). Studies have shown that autophagy possesses the ability to eliminate intracellular bacteria. Since we have confirmed the induction effect of baicalin on autophagy (**Figure 2**), to assess the antibacterial effect of baicalin on Mtb, we performed the colony forming unit (CFU) counting assay. As shown in **Figure 3**,

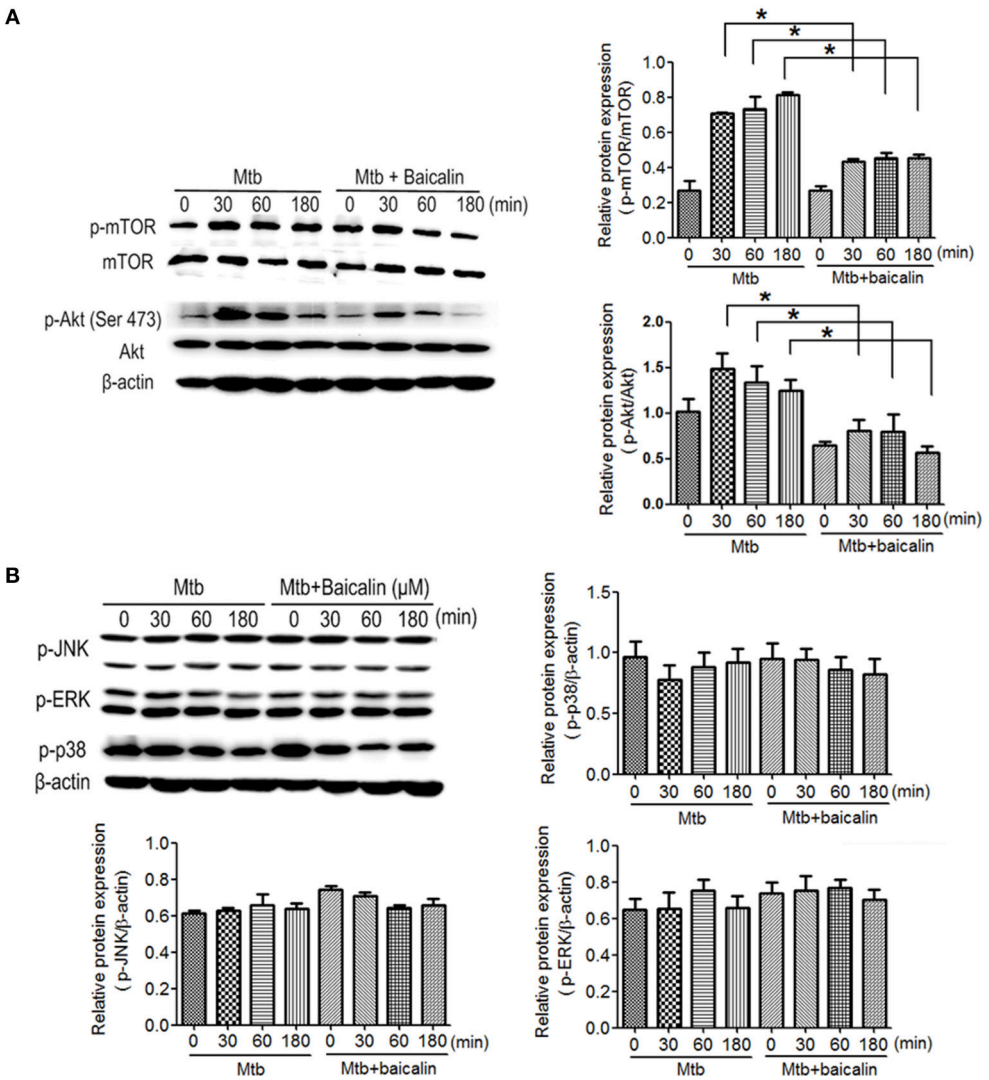


FIGURE 7 | Bacalin suppresses the PI3K/Akt/mTOR pathway but has no effect on the MAPK signaling in Raw264.7 cells. **(A)** Western blot analysis of mTOR, p-mTOR, Akt, and p-Akt expression in Raw264.7 cells. β-actin was used as a control. The right bar graphs show the statistical results for the relative quantitative expression of p-Akt and p-mTOR. **(B)** Western blot analysis of p-JNK, p-ERK, and p-p38 expression in Raw264.7 cells. The right and below bar graphs show the statistical results for the relative quantitative expression of p-p38, p-ERK, and p-JNK. Data are shown with the means ± *SD* of at least three independent experiments. $^*p < 0.05$.

baicalin exerted an obvious antibacterial effect (the bactericide rate of baicalin reached 86.7% compared to untreated control) and this ability most likely relied on the induction of autophagy that further facilitated the killing of Mtb, as baicalin had no bactericidal effect on within 2.24 mM (data not shown).

Baicalin Suppresses the Activation of NLRP3 Inflammasome

Activation of inflammasome is an important post-transcriptional event to facilitate IL-1β release. Uncontrolled activation of inflammasome is associated with several inflammatory diseases, including TB (Wong and Jacobs, 2011; Mishra et al., 2013). NLRP3 inflammasome has been reported to contribute to the inflammatory tissue damage during mycobacterial infection (Kasahara et al., 1988; Mishra et al., 2013). Consistently, our immunofluorescence assay (**Figure 4**) indicated that Mtb triggered the accumulation of ASC which is essential for the activation of NLRP3 inflammasome or AIM2 inflammasome (Bryan et al., 2009; Mishra et al., 2010). We found that AIM2 was unchanged in Mtb-infected Raw264.7 regardless of the presence or absence of baicalin (data not shown). Moreover, Western blot showed that Mtb induced the increase of NLRP3, ASC, pro-caspase-1 which are the components of NLRP3 inflammasome

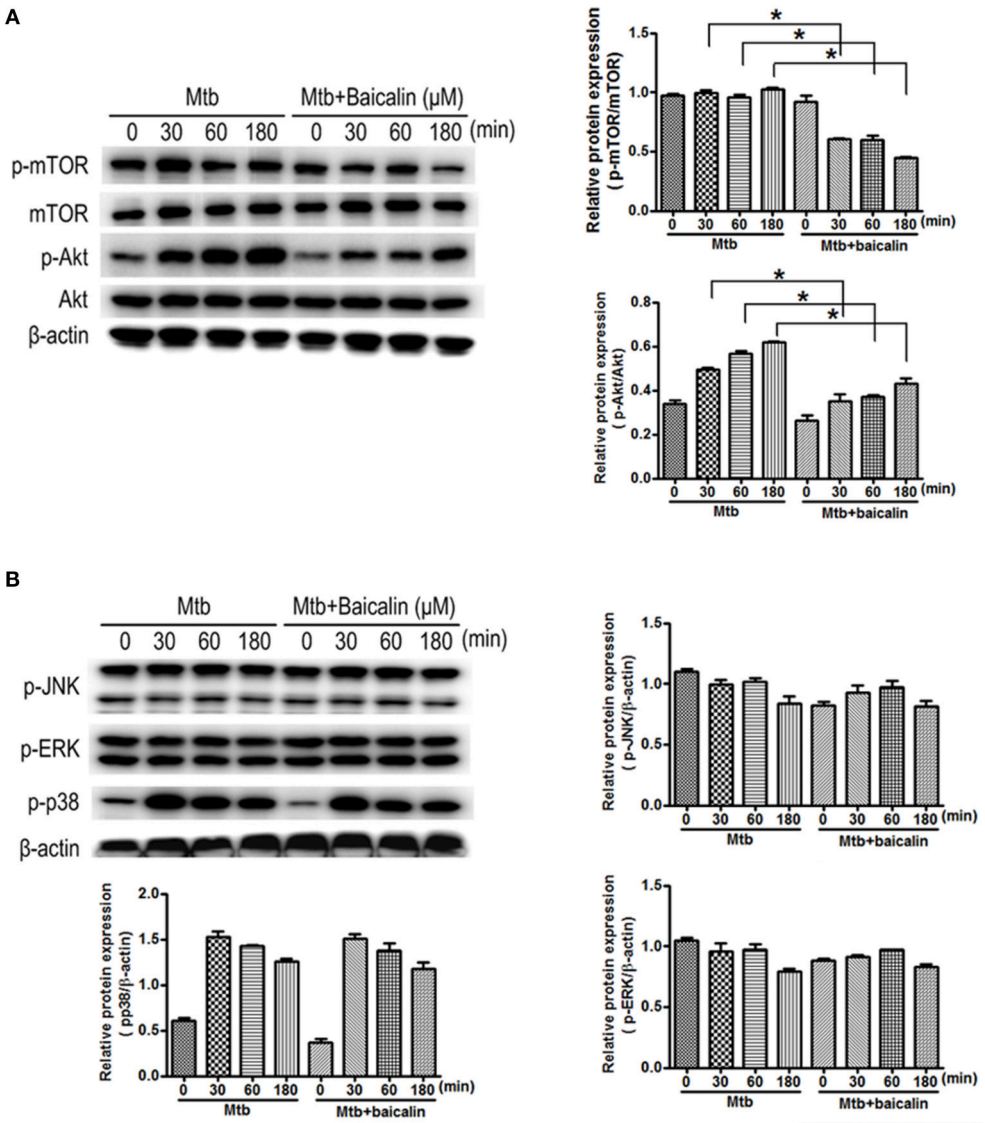


FIGURE 8 | Bacalin suppresses the PI3K/Akt/mTOR pathway but has no effect on the MAPK signaling in primary peritoneal macrophage cells. **(A)** Western blot analysis of mTOR, p-mTOR, Akt, and p-Akt expression in primary peritoneal macrophage cells. β-actin was used as a control. The right bar graphs show the statistical results for the relative quantitative expression of p-Akt and p-mTOR. **(B)** Western blot analysis of p-JNK, p-ERK, and p-p38 expression in peritoneal macrophage cells. The right and below bar graphs show the statistical results for the relative quantitative expression of p-p38, p-ERK, and p-JNK. Data are shown with the means ± *SD* of at least three independent experiments. *$p < 0.05$.

(**Figure 5A**). On the contrary, baicalin treatment could either inhibit the formation of ASC specks in immunofluorescence (**Figure 4**) or decrease the NLRP3, ASC, pro-caspase-1 in a dose-dependent manner (**Figure 5A**). In addition, the inflammasome-derived IL-1β in the supernatant in Mtb infected macrophages was inhibited by baicalin. Furthermore, co-immunoprecipitation (Co-IP) showed that baicalin treatment restrained the interaction of NLRP3 with ASC (**Figure 5B**). Besides, in primary peritoneal macrophages, baicalin also showed inhibitory effect on the expression of NLRP3 and this inhibition ability was remarkably weakened when autophagy activity was blocked by CQ (**Figure 6**). ESAT-6 has been demonstrated the essential element to activate NLRP3 inflammasome (Mishra et al., 2010), although intracellular concentrations of ESAT-6 are similar in both H37Rv and H37Ra, the H37Ra remains defective for ESAT-6 secretion as the phoP gene mutation (Fortune et al., 2005). We speculate the potential mechanism on the activation of H37Ra-induced NLRP3 inflammasome that may be the case that *in vitro* cultures of the strain with some lysed bacteria may release ESAT-6 and therefore activate the inflammasome as observed in **Figures 4–6**. Together, our data indicated that baicalin could suppress the Mtb-induced NLRP3 inflammasome activation.

Baicalin Activates Autophagy by Inhibiting PI3K/Akt/mTOR Signaling Pathway Instead of MAPK Pathway

The activation of autophagy can be modulated by a wide range of signals. Inhibition of PI3K/Akt/mTOR and activation of MAPK pathway are known to induce autophagy activation. Then, we analyzed the effect of baicalin on these two signaling pathways. Results indicated that baicalin treatment inhibited the phosphorylation of Akt (Ser473) and mTOR (Ser2448) in a time-dependent manner both in Raw264.7 (**Figure 7A**) and peritoneal macrophages (**Figure 8A**). In addition, we also assessed the MAPK pathway and our results showed that baicalin had no effect on the phosphorylation of p38, JNK or ERK (**Figures 7B**, **8B**). This is different with the reports that H37Rv could cause the activation of MAPK signaling pathway triggering secretion of inflammatory cytokines (Fietta et al., 2002; Jung et al., 2006). This difference is probably caused by the differences between the H37Ra and H37Rv strains (Jena et al., 2013). Although the H37Ra we used here is an attenuated strain which may cause lower toxic inflammatory reaction to host, but in terms of basic mechanism research, it is an irreplaceable good model for the study of intracellular TB as reported (Hart and Armstrong, 1974). Thus, our data revealed that baicalin inhibited the PI3K/Akt/mTOR signaling pathway instead of MAPK pathway to activate autophagy.

Baicalin Inhibits Mtb-Induced NF-κB Activation

NF-κB plays essential roles in the activation of NLRP3 inflammasome (Ghonime et al., 2014; Lamkanfi and Dixit, 2014; He et al., 2016) and the transcriptional induction of various genes involved in inflammation. As shown in **Figure 9**, Mtb

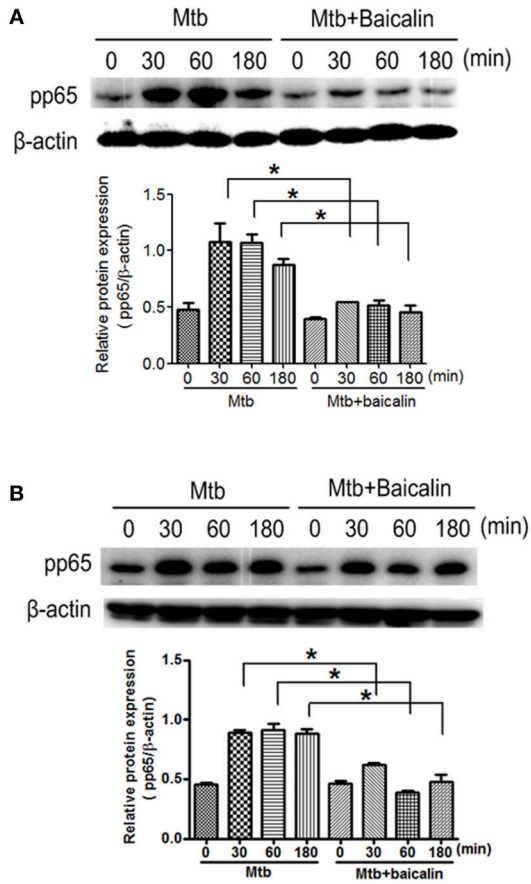


FIGURE 9 | Baicalin inhibits Mtb-induced NF-κB activation. **(A)** Western blot analysis of p-p65 expression in Raw264.7 cells. β-actin was used as a loading control. The below bar graph shows the statistical result for the relative quantitative expression of p-p65. **(B)** Western blot analysis of p-p65 expression in primary peritoneal macrophage cells. β-actin was used as a loading control. The below bar graph shows the statistical result for the relative quantitative expression of p-p65. Data are shown as the means ± *SD* of at least three independent experiments. $^*p < 0.05$.

infection caused the activation of NF-κB signaling as evidenced by the elevated p65 phosphorylation levels both in Raw264.7 (**Figure 9A**) and primary peritoneal macrophages (**Figure 9B**). Confocal images indicated that Mtb increased nuclear entry of phosphorylated p65, while baicalin treatment markedly reduced the production of phosphorylated protein and prevented it from entering into the nucleus (**Figure 10**).

Baicalin Can Induce Co-localization of Autophagosome and Inflammasome

Autophagy has been shown to play an important role in regulating inflammasome activation through the removal of inflammasome-activating endogenous signals or the sequestration and degradation of inflammasome components (Harris et al., 2011; Shi et al., 2012). We evaluated the relationship between them by means of immunofluorescence using confocal laser scanning microscope. As shown in

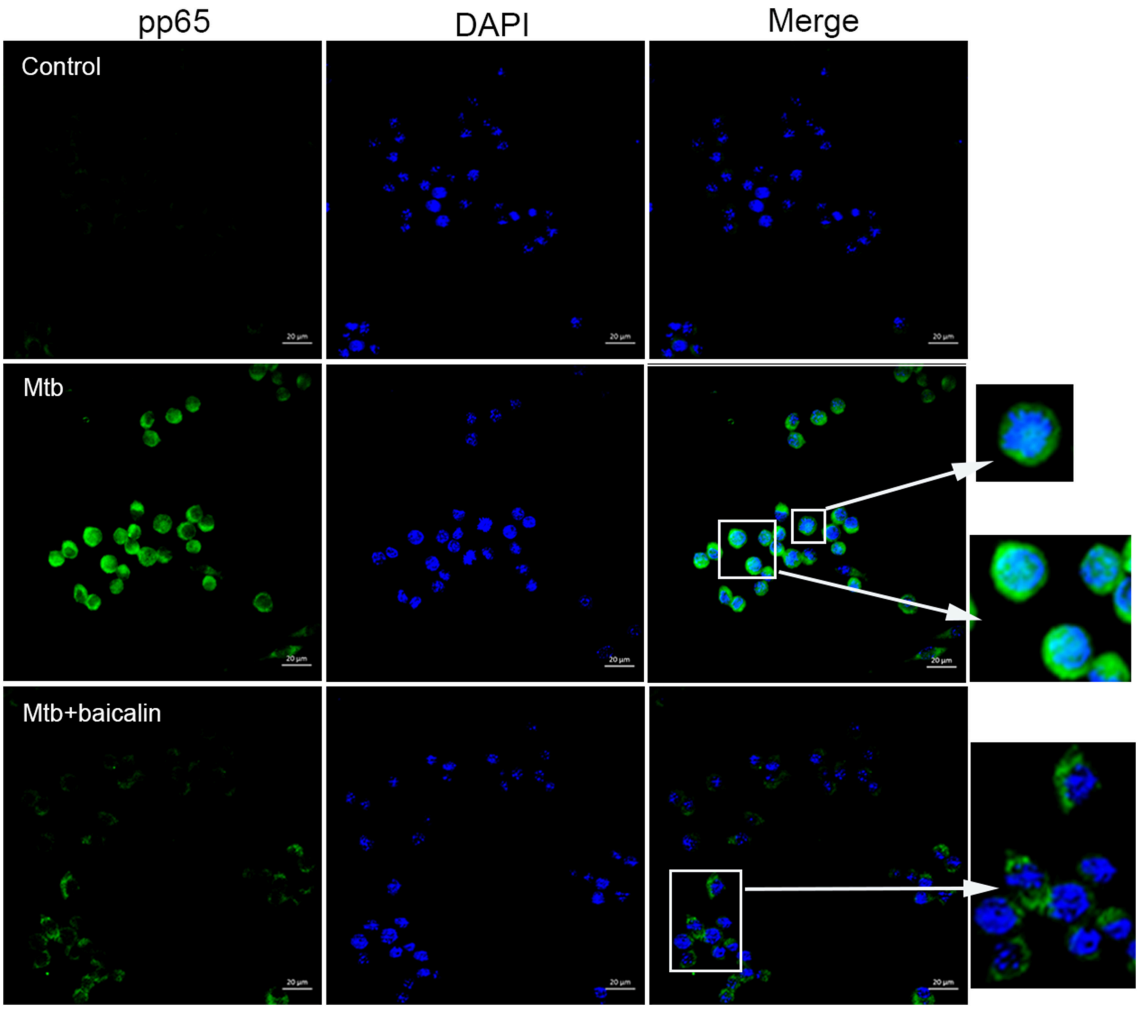


FIGURE 10 | Baicalin prevents the nuclear translocation of Mtb-induced NF-κB. Confocal microscopy of Raw264.7 cells with different treatments immunostained with anti-pp65 (green) and DAPI (blue). Scale bars shown are 20 μm.

Figure 11, Mtb induced the accumulation of ASC protein which represented the activation of NLRP3 inflammasome, and baicalin treatment decreased the ASC specks. Meanwhile, baicalin elevated the production of LC3 and induced the co-localization of LC3 and ASC, which is representative of autophagosome and inflammasome respectively. Thus, we conclude that baicalin induced autophagy activation, inhibited the activity of NLRP3 inflammasome through autophagic degradative mechanism, and restrained the secretion of IL-1β.

DISCUSSION

This study first reveals the roles of baicalin-mediated autophagy inducing effect in protection against Mtb infection. Our work demonstrated that baicalin inhibited the phosphorylation of Akt/mTOR thereby inducing autophagy to kill intracellular Mtb and showed suppressing effect on the activation of NLRP3 inflammasome and NF-κB signaling pathway triggered by Mtb (as shown in **Figure 12**). Baicalin is a safe, effective and widely available herb monomer which can be extracted from plants of genus Scutellaria (grown in Asian countries including China) or Oroxylum indicum (grown in other countries) (Dinda et al., 2017). The extracts from the roots of Scutellaria baicalensis are widely used in traditional Chinese medicines to treat various diseases such as hepatitis, atherosclerosis, dysentery, as well as common cold and other respiratory disorders (Li-Weber, 2009). Consistent with our work, previous studies have reported that baicalin was capable of inducing autophagy to cause cancer cell autophagic death (Zhang et al., 2012; Lin et al., 2013). Unlike the results of these publications and our research, there a study reported that baicalin inhibited influenza A virus induced autophagy (Zhu et al., 2015). As for TB, to our knowledge, this is the first demonstration that baicalin has antimycobacterial activity via induction of autophagy of host macrophages.

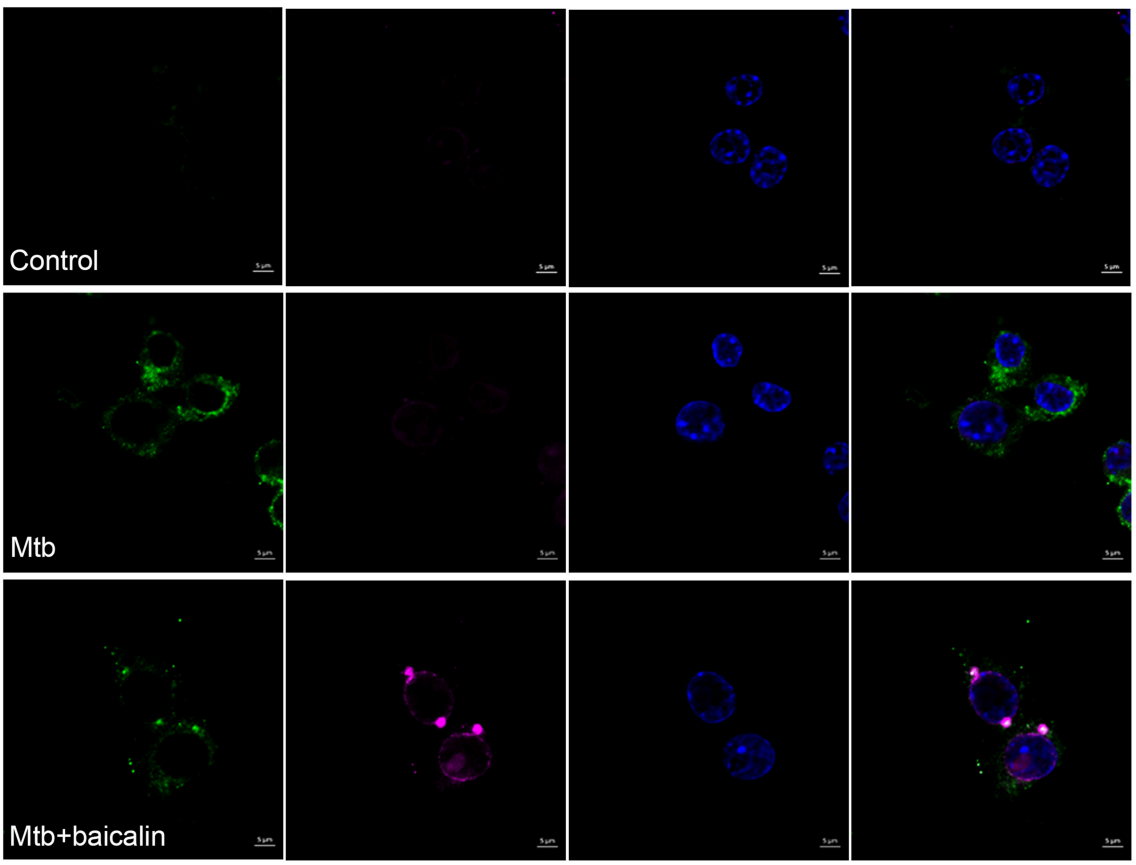


FIGURE 11 | Baicalin promotes co-localization of inflammasome with autophagosome. Confocal microscopy of Raw264.7 cells with different treatments immunostained with anti-LC3 antibody (pink), anti-ASC antibody (green), and DAPI (blue). Scale bars shown are 5 μm.

Induction of autophagy in Mtb-infected macrophages by several means (physiologically, immunologically, or pharmacologically) has been shown to kill Mtb (Gutierrez et al., 2004). Subsequent studies have extended the initial observation and established the key role of autophagy in defense against TB (Deretic, 2008; Harris et al., 2009; Jo, 2013). Consistent with these data, our results demonstrated that baicalin stimulated the activation of autophagy as evidenced by the upregulation of LC3II and downregulation of p62 and the unobstructed autophagic flux process after baicalin treatment. In addition, baicalin caused inhibition of intracellular Mtb replication. We attributed this killing effect to baicalin-stimulated autophagy effect because baicalin showed no direct impact on Mtb proliferation at 300 μM in our *in vitro* study. Autophagy has anti-inflammatory activity and protects the host from tissue necrosis and lung pathology (Castillo et al., 2012). The existing reports agree that autophagy negatively regulating inflammasome activation through a variety of mechanisms (Saitoh et al., 2008; Harris et al., 2011; Nakahira et al., 2011; Zhou et al., 2011; Shi et al., 2012; Lupfer et al., 2013; Martins et al., 2015; Saitoh and Akira, 2016). Inflammasome has been recognized to be involved in the pathological progress of Mtb infection (Carlsson et al., 2010; Wong and Jacobs, 2011; Castillo et al., 2012; Dorhoi et al., 2012; Mishra et al., 2013) causing granulomatous lung lesions and systemic inflammatory responses (Bekker et al., 2000). Although granulomas have long been considered to benefit the host by containing and restricting mycobacteria, recent studies have demonstrated that tuberculous granuloma provides a safety shelter for bacterial growth, persistence, and proliferation (Davis and Ramakrishnan, 2009; Silva Miranda et al., 2012; Cambier et al., 2014) and even caused lung damage (Bekker et al., 2000; Philips and Ernst, 2012). Our data indicated that baicalin inhibited the Mtb-induced inflammation process by restraining the NLRP3 inflammasome activation and subsequent production of inflammatory mediators triggered by Mtb infection. Complementing anti-TB drugs with anti-inflammation interventions could improve treatment efficiency and outcome evidenced by reports that patients treated with corticosteroids in conjunction with TB drugs contribute to a modest decrease in mortality and is helpful in extrapulmonary tuberculosis including meningitis and pleural disease (Critchley et al., 2013; Prasad et al., 2016).

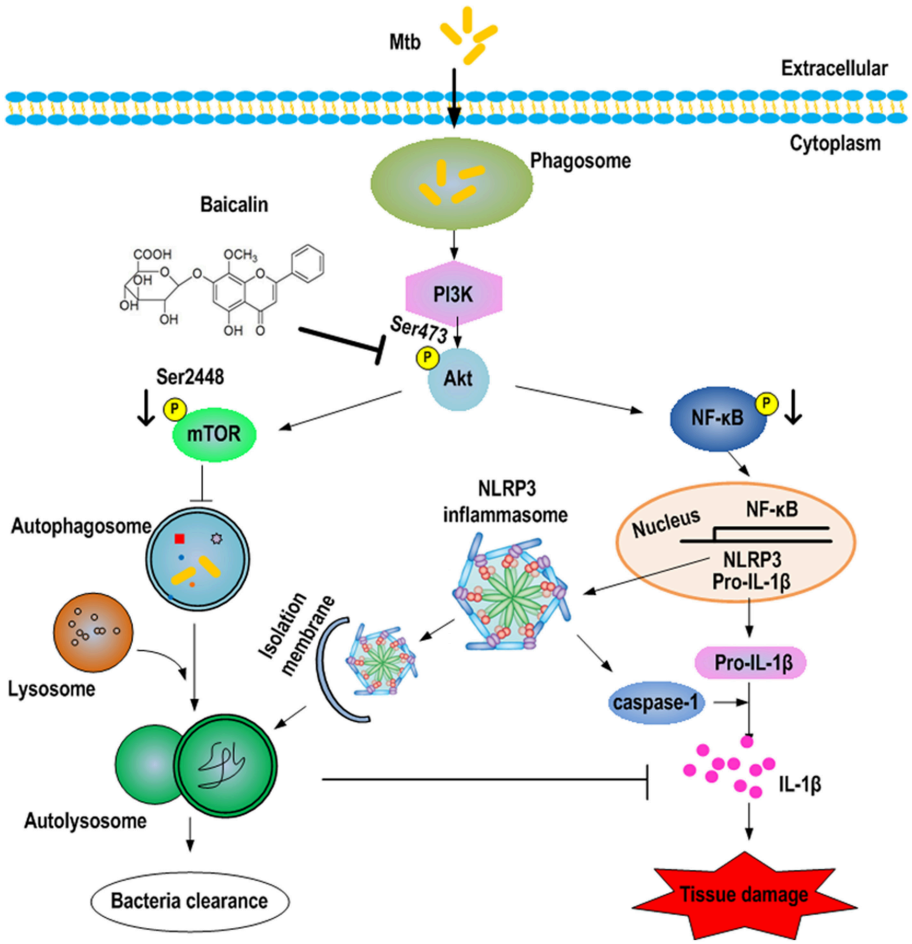


FIGURE 12 | Schematic summary of baicalin-driven regulation of autophagy and inflammation during Mtb infection. Baicalin inhibits the phosphorylation of Akt, thus inducing the activation of autophagy through PI3K/Akt/mTOR signaling pathways leading to bactericidal and inflammasome-inhibitory effect. Furthermore, baicalin inhibits the PI3K/Akt/NF-κB pathway contributing to the inhibitory effect on NLRP3 inflammasome activation.

Nevertheless, considering the strong immunosuppressive effects and many other side effects, caution is needed when applying corticosteroids in pulmonary TB. In contrast, baicalin possess the advantage over corticosteroids that has no side effects such as immunosuppression. Moreover, baicalin has been demonstrated to inhibit sterile (Wang et al., 2016) or bacterial inflammation (Guo et al., 2013; Liu et al., 2017) and showed immunoprotective effect in the sepsis model (Hu et al., 2015). Hence, baicalin could be a new candidate for the development of adjunctive anti-TB therapies.

Having confirmed the antimycobacterial and anti-inflammatory effects of baicalin, we next explored the functional mechanisms. Two classical autophagy related signaling pathways were assessed, the PI3K/Akt/mTOR signaling pathway which has been recognized as negatively regulating the activation of autophagy (Heras-Sandoval et al., 2014), and the MAPK pathway which acts as a positive regulator of autophagy (Krishna and Narang, 2008; Zhou et al., 2015). Data indicated that baicalin inhibited the phosphorylated Akt (Ser473) and mTOR (Ser2448) but without influencing phosphorylated JNK, ERK, or p38. Previous studies have suggested that baicalin showed evident inhibitory effect on NF-κB activation (Guo et al., 2013; Fu et al., 2016). Here, our data showed that baicalin significantly inhibited the phosphorylation of NF-κB and prevented its entry to the nucleus. Based on our findings, we conclude that baicalin actually targeted PI3K/Akt to restrain the NF-κB activity, which is consistent with previous studies (Kang et al., 2012; Guo et al., 2016).

Taken together, our data demonstrated that baicalin has both anti-inflammatory and antimycobacterial effects on Mtb-infected macrophages and this endows baicalin the great potential as a candidate of HDT for new anti-TB adjuvant therapy. Additionally, better understanding the basic biology of mycobacterial pathogenesis may guide the search for more effective and specific HDT targets. Drugs like baicalin that manipulate host cellular defense mechanisms such as autophagy could achieve bactericidal and anti-inflammatory effects may provide new opportunities to combat intracellular pathogens

like Mtb. Future studies are needed to evaluate baicalin in conjunction with TB drugs for improved treatment of TB in animal models and if promising in humans.

AUTHOR CONTRIBUTIONS

XJ and YiZ conceived and designed the experiments. QZ, JS, YW, WH, and JW performed the experiments. XJ, YiZ, QZ, JS, YuZ, and LW analyzed the data. QZ, JS, XJ, and YiZ wrote the paper. All authors have read and approved the final manuscript.

ACKNOWLEDGMENTS

This work was supported by Innovation Program of Shanghai Municipal Education Commission (15ZZ065), the National Natural Science Foundation of China (81102869).

REFERENCES

Alonso, S., Pethe, K., Russell, D. G., and Purdy, G. E. (2007). Lysosomal killing of mycobacterium mediated by ubiquitin-derived peptides is enhanced by autophagy. *Proc. Natl. Acad. Sci. U.S.A.* 104, 6031–6036. doi: 10.1073/pnas.0700036104

Awuh, J. A., and Flo, T. H. (2017). Molecular basis of mycobacterial survival in macrophages. *Cell Mol. Life Sci.* 74, 1625–1648. doi: 10.1007/s00018-016-2422-8

Bekker, L. G., Moreira, A. L., Bergtold, A., Freeman, S., Ryffel, B., and Kaplan, G. (2000). Immunopathologic effects of tumor necrosis factor alpha in murine mycobacterial infection are dose dependent. *Infect. Immun.* 68, 6954–6961. doi: 10.1128/IAI.68.12.6954-6961.2000

Beutler, B., and Cerami, A. (1988). Tumor necrosis, cachexia, shock, and inflammation: a common mediator. *Annu. Rev. Biochem.* 57, 505–518. doi: 10.1146/annurev.bi.57.070188.002445

Boya, P., Reggiori, F., and Codogno, P. (2013). Emerging regulation and functions of autophagy. *Nat. Cell Biol.* 15, 713–720. doi: 10.1038/ncb2788

Bradfute, S. B., Castillo, E. F., Arko-Mensah, J., Chauhan, S., Jiang, S., Mandell, M., et al. (2013). Autophagy as an immune effector against tuberculosis. *Curr. Opin. Microbiol.* 16, 355–365. doi: 10.1016/j.mib.2013.05.003

Bryan, N. B., Dorfleutner, A., Rojanasakul, Y., and Stehlik, C. (2009). Activation of inflammasomes requires intracellular redistribution of the apoptotic speck-like protein containing a caspase recruitment domain. *J. Immunol.* 182, 3173–3182. doi: 10.4049/jimmunol.0802367

Cambier, C. J., Falkow, S., and Ramakrishnan, L. (2014). Host evasion and exploitation schemes of *Mycobacterium tuberculosis*. *Cell* 159, 1497–1509. doi: 10.1016/j.cell.2014.11.024

Carlsson, F., Kim, J., Dumitru, C., Barck, K. H., Carano, R. A., Sun, M., et al. (2010). Host-detrimental role of Esx-1-mediated inflammasome activation in mycobacterial infection. *PLoS Pathog.* 6:e1000895. doi: 10.1371/journal.ppat.1000895

Castillo, E. F., Dekonenko, A., Arko-Mensah, J., Mandell, M. A., Dupont, N., Jiang, S., et al. (2012). Autophagy protects against active tuberculosis by suppressing bacterial burden and inflammation. *Proc. Natl. Acad. Sci. U.S.A.* 109, E3168–E3176. doi: 10.1073/pnas.1210500109

Critchley, J. A., Young, F., Orton, L., and Garner, P. (2013). Corticosteroids for prevention of mortality in people with tuberculosis: a systematic review and meta-analysis. *Lancet Infect. Dis.* 13, 223–237. doi: 10.1016/S1473-3099(12)70321-3

Davis, J. M., and Ramakrishnan, L. (2009). The role of the granuloma in expansion and dissemination of early tuberculous infection. *Cell* 136, 37–49. doi: 10.1016/j.cell.2008.11.014

de Oliveira, M. R., Nabavi, S. F., Habtemariam, S., Erdogan Orhan, I., Daglia, M., and Nabavi, S. M. (2015). The effects of baicalein and baicalin on mitochondrial function and dynamics: a review. *Pharmacol. Res.* 100, 296–308. doi: 10.1016/j.phrs.2015.08.021

Deretic, V. (2008). Autophagy, an immunologic magic bullet: *Mycobacterium tuberculosis* phagosome maturation block and how to bypass it. *Future Microbiol.* 3, 517–524. doi: 10.2217/17460913.3.5.517

Deretic, V., Jiang, S., and Dupont, N. (2012). Autophagy intersections with conventional and unconventional secretion in tissue development, remodeling and inflammation. *Trends Cell Biol.* 22, 397–406. doi: 10.1016/j.tcb.2012.04.008

Dinarello, C. A. (1996). Biologic basis for interleukin-1 in disease. *Blood* 87, 2095–2147.

Dinda, B., Dinda, S., DasSharma, S., Banik, R., Chakraborty, A., and Dinda, M. (2017). Therapeutic potentials of baicalin and its aglycone, baicalein against inflammatory disorders. *Eur. J. Med. Chem.* 131, 68–80. doi: 10.1016/j.ejmech.2017.03.004

Dorhoi, A., and Kaufmann, S. H. (2014). Perspectives on host adaptation in response to *Mycobacterium tuberculosis*: modulation of inflammation. *Semin. Immunol.* 26, 533–542. doi: 10.1016/j.smim.2014.10.002

Dorhoi, A., and Kaufmann, S. H. (2016). Pathology and immune reactivity: understanding multidimensionality in pulmonary tuberculosis. *Semin. Immunopathol.* 38, 153–166. doi: 10.1007/s00281-015-0531-3

Dorhoi, A., Nouailles, G., Jörg, S., Hagens, K., Heinemann, E., Pradl, L., et al. (2012). Activation of the NLRP3 inflammasome by *Mycobacterium tuberculosis* is uncoupled from susceptibility to active tuberculosis. *Eur. J. Immunol.* 42, 374–384. doi: 10.1002/eji.201141548

Fabri, M. 1., Stenger, S., Shin, D. M., Yuk, J. M., Liu, P. T., Realegeno, S., et al. (2011). Vitamin D is required for IFN-gamma-mediated antimicrobial activity of human macrophages. *Sci. Transl. Med.* 3, 104ra102. doi: 10.1126/scitranslmed.3003045

Fietta, A. M., Morosini, M., Meloni, F., Bianco, A. M., and Pozzi, E. (2002). Pharmacological analysis of signal transduction pathways required for *Mycobacterium tuberculosis*-induced IL-8 and MCP-1 production in human peripheral monocytes. *Cytokine* 19, 242–249. doi: 10.1006/cyto.2002.1968

Fortune, S., Jaeger, A., Sarracino, D. A., Chase, M. R., Sassetti, C., Sherman, D. R., et al. (2005). Mutually dependent secretion of proteins required for mycobacterial virulence. *Proc. Natl. Acad. Sci. U.S.A.* 102, 10676–10681. doi: 10.1073/pnas.0504922102

Fu, S., Xu, L., Li, S., Qiu, Y., Liu, Y., Wu, Z., et al. (2016). Baicalin suppresses NLRP3 inflammasome and nuclear factor-kappa B (NF-κB) signaling during *Haemophilus parasuis* infection. *Vet. Res.* 47:80. doi: 10.1186/s13567-016-0359-4

Ghonime, M. G., Shamaa, O. R., Das, S., Eldomany, R. A., Fernandes-Alnemri, T., Alnemri, E. S., et al. (2014). Inflammasome priming by lipopolysaccharide is dependent upon ERK signaling and proteasome function. *J. Immunol.* 192, 3881–3888. doi: 10.4049/jimmunol.1301974

Guo, C., Yang, L., Luo, J., Zhang, C., Xia, Y., Ma, T., et al. (2016). Sophoraflavanone G from Sophora alopecuroides inhibits lipopolysaccharide-induced inflammation in RAW264.7 cells by targeting PI3K/Akt, JAK/STAT and Nrf2/HO-1 pathways. *Int. Immunopharmacol.* 38, 349–356. doi: 10.1016/j.intimp.2016.06.021

Guo, M., Zhang, N., Li, D., Liang, D., Liu, Z., Li, F., et al. (2013). Baicalin plays an anti-inflammatory role through reducing nuclear factor-κB and p38 phosphorylation in *S. aureus*-induced mastitis. *Int. Immunopharmacol.* 16, 125–130. doi: 10.1016/j.intimp.2013.03.006

Gutierrez, M. G., Master, S. S., Singh, S. B., Taylor, G. A., Colombo, M. I., and Deretic, V. (2004). Autophagy is a defense mechanism inhibiting BCG and *Mycobacterium tuberculosis* survival in infected macrophages. *Cell* 119, 753–766. doi: 10.1016/j.cell.2004.11.038

Harris, J., De Haro, S. A., Master, S. S., Keane, J., Roberts, E. A., Delgado, M., et al. (2007). T helper 2 cytokines inhibit autophagic control of intracellular *Mycobacterium tuberculosis*. *Immunity* 27, 505–517. doi: 10.1016/j.immuni.2007.07.022

Harris, J., Hartman, M., Roche, C., Zeng, S. G., O'Shea, A., Sharp, F. A., et al. (2011). Autophagy controls IL-1beta secretion by targeting pro-IL-1beta for degradation. *J. Biol. Chem*. 286, 9587–9597. doi: 10.1074/jbc.M110.202911

Harris, J., Hope, J. C., and Lavelle, E. C. (2009). Autophagy and the immune response to TB. *Transbound Emerg. Dis*. 56, 248–254. doi: 10.1111/j.1865-1682.2009.01069.x

Hart, P. D., and Armstrong, J. A. (1974). Strain virulence and the lysosomal response in macrophages infected with *Mycobacterium tuberculosis*. *Infect. Immun*. 10, 742–746.

Hawn, T. R., Matheson, A. I., Maley, S. N., and Vandal, O. (2013). Host-directed therapeutics for tuberculosis: can we harness the host? *Microbiol. Mol. Biol. Rev*. 77, 608–627. doi: 10.1128/MMBR.00032-13

He, C., and Klionsky, D. J. (2009). Regulation mechanisms and signaling pathways of autophagy. *Annu. Rev. Genet*. 43, 67–93. doi: 10.1146/annurev-genet-102808-114910

He, Y.,Hara, H., and Nuez, G. (2016). Mechanism and regulation of NLRP3 inflammasome activation. *Trends Biochem. Sci*. 41, 1012–1021. doi: 10.1016/j.tibs.2016.09.002

Heras-Sandoval, D., Pérez-Rojas, J. M., Hernández-Damián, J., and Pedraza-Chaverri, J. (2014). The role of PI3K/AKT/mTOR pathway in the modulation of autophagy and the clearance of protein aggregates in neurodegeneration. *Cell Signal*. 26, 2694–2701. doi: 10.1016/j.cellsig.2014.08.019

Hu, X., Miao, P., Yu, R., and Zheng, H. (2015). The immunoprotective activity of baicalin in mouse model of cecal ligation and puncture-induced sepsis. *Cell Biochem. Biophys*. 71, 543–547. doi: 10.1007/s12013-014-0232-x

Jena, L., Kashikar, S., Kumar, S., and Harinath, B. C. (2013). Comparative proteomic analysis of *Mycobacterium tuberculosis* strain H37Rv versus H37Ra. *Int. J. Mycobacteriol*. 2, 220–226. doi: 10.1016/j.ijmyco.2013.10.004

Jiang, X., Wang, Y., Qin, Y., He, W., Benlahrech, A., Zhang, Q., et al. (2017). Micheliolide provides protection of mice against *Staphylococcus aureus* and MRSA infection by down-regulating inflammatory response. *Sci. Rep*. 7:41964. doi: 10.1038/srep41964

Jo, E. K. (2013). Autophagy as an innate defense against mycobacteria. *Pathog. Dis*. 67, 108–118. doi: 10.1111/2049-632X.12023

Jung, S. B., Yang, C. S., Lee, J. S., Shin, A. R., Jung, S. S., Son, J. W., et al. (2006). The mycobacterial 38-kilodalton glycolipoprotein antigen activates the mitogen-activated protein kinase pathway and release of proinflammatory cytokines through Toll-like receptors 2 and 4 in human monocytes. *Infect. Immun*. 74, 2686–2696. doi: 10.1128/IAI.74.5.2686-2696.2006

Kang, H. W., Kim, J. M., Cha, M. Y., Jung, H. C., Song, I. S., and Kim, J. S. (2012). Deguelin, an Akt inhibitor, down-regulates NF-κB signaling and induces apoptosis in colon cancer cells and inhibits tumor growth in mice. *Dig. Dis. Sci*. 57, 2873–2882. doi: 10.1007/s10620-012-2237-x

Kasahara, K., Kobayashi, K., Shikama, Y., Yoneya, I., Soezima, K., Ide, H., et al. (1988). Direct evidence for granuloma-inducing activity of interleukin-1. Induction of experimental pulmonary granuloma formation in mice by interleukin-1-coupled beads. *Am. J. Pathol*. 130, 629–638.

Kim, J. J., Lee, H. M., Shin, D. M., Kim, W., Yuk, J. M., Jin, H. S., et al. (2012). Host cell autophagy activated by antibiotics is required for their effective antimycobacterial drug action. *Cell Host Microbe* 11, 457–468. doi: 10.1016/j.chom.2012.03.008

Kleinnijenhuis, J., Joosten, L. A., van de Veerdonk, F. L., Savage, N., van Crevel, R., Kullberg, B. J., et al. (2009). Transcriptional and inflammasome-mediated pathways for the induction of IL-1beta production by *Mycobacterium tuberculosis*. *Eur. J. Immunol*. 39, 1914–1922. doi: 10.1002/eji.200839115

Koo, I. C., Wang, C., Raghavan, S., Morisaki, J. H., Cox, J. S., and Brown, E. J. (2008). ESX-1-dependent cytolysis in lysosome secretion and inflammasome activation during mycobacterial infection. *Cell Microbiol*. 10, 1866–1878. doi: 10.1111/j.1462-5822.2008.01177.x

Krishna, M., and Narang, H. (2008). The complexity of mitogen-activated protein kinases (MAPKs) made simple. *Cell Mol. Life Sci*. 65, 3525–3544. doi: 10.1007/s00018-008-8170-7

Lamkanfi, M., and Dixit, V. M. (2014). Mechanisms and functions of inflammasomes. *Cell* 157, 1013–1022. doi: 10.1016/j.cell.2014.04.007

Lin, C., Tsai, S. C., Tseng, M. T., Peng, S. F., Kuo, S. C., Lin, M. W., et al. (2013). AKT serine/threonine protein kinase modulates baicalin-triggered autophagy in human bladder cancer T24 cells. *Int. J. Oncol*. 42, 993–1000. doi: 10.3892/ijo.2013.1791

Liu, S., Liu, B., Luo, Z. Q., Qiu, J., Zhou, X., Li, G., et al. (2017). The combination of osthole with baicalin protects mice from *Staphylococcus aureus* pneumonia. *World J. Microbiol. Biotechnol*. 33:11. doi: 10.1007/s11274-016-2162-9

Li-Weber, M. (2009). New therapeutic aspects of flavones: the anticancer properties of Scutellaria and its main active constituents Wogonin, Baicalein and Baicalin. *Cancer Treat Rev*. 35, 57–68. doi: 10.1016/j.ctrv.2008.09.005

Lupfer, C., Thomas, P. G., Anand, P. K., Vogel, P., Milasta, S., Martinez, J., et al. (2013). Receptor interacting protein kinase 2-mediated mitophagy regulates inflammasome activation during virus infection. *Nat. Immunol*. 14, 480–488. doi: 10.1038/ni.2563

Machelart, A., Song, O. R., Hoffmann, E., and Brodin, P. (2017). Host-directed therapies offer novel opportunities for the fight against tuberculosis. *Drug Discov. Today* 22, 1250–1257. doi: 10.1016/j.drudis.2017.05.005

Martins, J. D., Liberal, J., Silva, A., Ferreira, I., Neves, B. M., and Cruz, M. T. (2015). Autophagy and inflammasome interplay. *DNA Cell Biol*. 34, 274–281. doi: 10.1089/dna.2014.2752

Mishra, B. B., Moura-Alves, P., Sonawane, A., Hacohen, N., Griffiths, G., Moita, L. F., et al. (2010). *Mycobacterium tuberculosis* protein ESAT-6 is a potent activator of the NLRP3/ASC inflammasome. *Cell Microbiol*. 12, 1046–1063. doi: 10.1111/j.1462-5822.2010.01450.x

Mishra, B. B., Rathinam, V. A., Martens, G. W., Martinot, A. J., Kornfeld, H., Fitzgerald, K. A., et al. (2013). Nitric oxide controls the immunopathology of tuberculosis by inhibiting NLRP3 inflammasome-dependent processing of IL-1β. *Nat. Immunol*. 14, 52–60. doi: 10.1038/ni.2474

Mizushima, N., Levine, B., Cuervo, A. M., and Klionsky, D. J. (2008). Autophagy fights disease through cellular self-digestion. *Nature* 451, 1069–1075. doi: 10.1038/nature06639

Nakahira, K., Haspel, J. A., Rathinam, V. A., Lee, S. J., Dolinay, T., Lam, H. C., et al. (2011). Autophagy proteins regulate innate immune responses by inhibiting the release of mitochondrial DNA mediated by the NALP3 inflammasome. *Nat. Immunol*. 12, 222–230. doi: 10.1038/ni.1980

Patel, M. N., Carroll, R. G., Galván-Pe-a, S., Mills, E. L., Olden, R., Triantafilou, M., et al. (2017). Inflammasome priming in sterile inflammatory disease. *Trends Mol. Med*. 23, 165–180. doi: 10.1016/j.molmed.2016.12.007

Philips, J. A., and Ernst, J. D. (2012). Tuberculosis pathogenesis and immunity. *Annu. Rev. Pathol*. 7, 353–384. doi: 10.1146/annurev-pathol-011811-132458

Ponpuak, M., Davis, A. S., Roberts, E. A., Delgado, M. A., Dinkins, C., Zhao, Z., et al. (2010). Delivery of cytosolic components by autophagic adaptor protein p62 endows autophagosomes with unique antimicrobial properties. *Immunity* 32, 329–341. doi: 10.1016/j.immuni.2010.02.009

Prasad, K., Singh, M. B., and Ryan, H. (2016). Corticosteroids for managing tuberculous meningitis. *Cochrane Database Syst. Rev*. 4:CD002244. doi: 10.1002/14651858.CD002244.pub4

Saitoh, T., and Akira, S. (2016). Regulation of inflammasomes by autophagy. *J. Allergy Clin. Immunol*. 138, 28–36. doi: 10.1016/j.jaci.2016.05.009

Saitoh, T., Fujita, N., Jang, M. H., Uematsu, S., Yang, B. G., Satoh, T., et al. (2008). Loss of the autophagy protein Atg16L1 enhances endotoxin-induced IL-1beta production. *Nature* 456, 264–268. doi: 10.1038/nature07383

Shi, C. S., Shenderov, K., Huang, N. N., Kabat, J., Abu-Asab, M., Fitzgerald, K. A., et al. (2012). Activation of autophagy by inflammatory signals limits IL-1β production by targeting ubiquitinated inflammasomes for destruction. *Nat. Immunol*. 13, 255–263. doi: 10.1038/ni.2215

Silva Miranda, M., Breiman, A., Allain, S., Deknuydt, F., and Altare, F. (2012). The tuberculous granuloma: an unsuccessful host defence mechanism providing a safety shelter for the bacteria? *Clin. Dev. Immunol*. 2012:139127. doi: 10.1155/2012/139127

Singh, S. B., Davis, A. S., Taylor, G. A., and Deretic, V. (2006). Human IRGM induces autophagy to eliminate intracellular mycobacteria. *Science* 313, 1438–1441. doi: 10.1126/science.1129577

Srinivas, N. R. (2010). Baicalin, an emerging multi-therapeutic agent: pharmacodynamics, pharmacokinetics, and considerations from drug development perspectives. *Xenobiotica* 40, 357–367. doi: 10.3109/00498251003663724

Wang, H., Zhang, Y., Bai, R., Wang, M., and Du, S. (2016). Baicalin attenuates alcoholic liver injury through modulation of hepatic oxidative stress,

inflammation and sonic Hedgehog pathway in rats. *Cell Physiol. Biochem*. 39, 1129–1140. doi: 10.1159/000447820

Watson, R. O., Manzanillo, P. S., and Cox, J. S. (2012). Extracellular *M. tuberculosis* DNA targets bacteria for autophagy by activating the host DNA-sensing pathway. *Cell* 150, 803–815. doi: 10.1016/j.cell.2012.06.040

WHO (2016). *Global Tuberculosis Report*. World Health Organization, Geneva.

Wong, K. W., and Jacobs, W. R. Jr. (2011). Critical role for NLRP3 in necrotic death triggered by *Mycobacterium tuberculosis*. *Cell Microbiol*. 13, 1371–1384. doi: 10.1111/j.1462-5822.2011.01625.x

Yang, C. S. (2017). Advancing host-directed therapy for tuberculosis. *Microb. Cell* 4, 105–107. doi: 10.15698/mic2017.03.565

Yang, Z., and Klionsky, D. J. (2009). An overview of the molecular mechanism of autophagy. *Curr. Top Microbiol. Immunol*. 335, 1–32. doi: 10.1007/978-3-642-00302-8_1

Yin, Z., Pascual, C., and Klionsky, D. J. (2016). Autophagy: machinery and regulation. *Microb. Cell* 3, 588–596. doi: 10.15698/mic2016.12.546

Yu, C., Zhang, Z., Zhang, H., Zhen, Z., Calway, T., Wang, Y., et al. (2013). Pretreatment of baicalin and wogonoside with glycoside hydrolase: a promising approach to enhance anticancer potential. *Oncol. Rep*. 30, 2411–2418. doi: 10.3892/or.2013.2726

Yuk, J. M., Shin, D. M., Lee, H. M., Yang, C. S., Jin, H. S., Kim, K. K., et al. (2009). Vitamin D3 induces autophagy in human monocytes/macrophages via cathelicidin. *Cell Host Microbe* 6, 231–243. doi: 10.1016/j.chom.2009.08.004

Zhang, X., Tang, X., Liu, H., Li, L., Hou, Q., and Gao, J. (2012). Autophagy induced by baicalin involves downregulation of CD147 in SMMC-7721 cells *in vitro*. *Oncol. Rep*. 27, 1128–1134. doi: 10.3892/or.2011.1599

Zhou, R., Yazdi, A. S., Menu, P., and Tschopp, J. (2011). A role for mitochondria in NLRP3 inflammasome activation. *Nature* 469, 221–225. doi: 10.1038/nature09663

Zhou, Y. Y., Li, Y., Jiang, W. Q., and Zhou, L. F. (2015). MAPK/JNK signalling: a potential autophagy regulation pathway. *Biosci. Rep*. 35:e00199. doi: 10.1042/BSR20140141

Zhu, H. Y., Han, L., Shi, X. L., Wang, B. L., Huang, H., Wang, X., et al. (2015). Baicalin inhibits autophagy induced by influenza A virus H3N2. *Antiviral Res*. 113, 62–70. doi: 10.1016/j.antiviral.2014.11.003

Zumla, A., and Maeurer, M. (2016). Host-directed therapies for multidrug resistant tuberculosis. *Int. J. Mycobacteriol*. 5(Suppl. 1), S21–S22. doi: 10.1016/j.ijmyco.2016.09.044

Zumla, A., Maeurer, M., Host-Directed Therapies Network, Chakaya, J., Hoelscher, M., Ntoumi, F., et al. (2015). Towards host-directed therapies for tuberculosis. *Nat. Rev. Drug Discov*. 14, 511–512. doi: 10.1038/nrd4696

Conflict of Interest Statement: The authors declare that the research was conducted in the absence of any commercial or financial relationships that could be construed as a potential conflict of interest.

Copyright © 2017 Zhang, Sun, Wang, He, Wang, Zheng, Wu, Zhang and Jiang. This is an open-access article distributed under the terms of the Creative Commons Attribution License (CC BY). The use, distribution or reproduction in other forums is permitted, provided the original author(s) or licensor are credited and that the original publication in this journal is cited, in accordance with accepted academic practice. No use, distribution or reproduction is permitted which does not comply with these terms.

frontiers in Microbiology

ORIGINAL RESEARCH
published: 21 February 2018
doi: 10.3389/fmicb.2018.00275

Cytokine Biomarkers Associated with Human Extra-Pulmonary Tuberculosis Clinical Strains and Symptoms

*Paulo Ranaivomanana[1], Mihaja Raberahona[2], Sedera Rabarioelina[1], Ysé Borella[1], Alice Machado[1], Mamy J. De Dieu Randria[2], Rivo A. Rakotoarivelo[2,3], Voahangy Rasolofo[1] and Niaina Rakotosamimanana[1]**

[1] Unité des Mycobactéries, Institut Pasteur de Madagascar, Antananarivo, Madagascar, [2] Infectious Diseases, Joseph Raseta Befelatanana University Hospital, Antananarivo, Madagascar, [3] Faculté de Médecine, University of Fianarantsoa, Fianarantsoa, Madagascar

Background: The primary site of infection for *Mycobacterium tuberculosis* (*Mtb*) is the alveolar macrophages. However, *Mtb* can disseminate into other organs and causes extrapulmonary tuberculosis (EPTB). The diagnosis of EPTB is challenging due to relatively inaccessible infectious sites that may be paucibacillary and with clinical symptoms varying by site that are similar to those seen in other diseases. Hence, we sought to identify the expression patterns of a variety of cytokines that may be specific to EPTB from *in vitro* infections and in the plasma of TB patients.

Methods: To define those cytokine secretions associated with EPTB, human THP-1 derived macrophages were first infected with *Mtb* clinical isolates from pulmonary and EPTB. Infected macrophages supernatants were harvested at different time points and cytokines known to play key roles in TB immune responses including TNF-α, IL-6, IL-10, IFN-γ, and VEGF-A were measured by ELISA. Those cytokines that were *in vitro* associated to EPTB were also measured in the plasma from patients with PTB, EPTB, non-EPTB-confirmed-like symptoms and healthy controls.

Results: While all of the studied cytokine secretions varied after *in vitro* infection, higher levels of TNF-α and VEGF secretions were observed *in vitro* in the infected macrophages respectively in the PTB and EPTB infecting clinical isolates. Similar trends were observed from the plasma of patients where patients with PTB showed significantly higher level of TNF-α compared to EPTB and healthy control groups. The patients with EPTB showed higher plasma level of VEGF compared to those patients with the non-EPTB ($p < 0.01$) and to healthy controls group ($p < 0.0001$). Using Receiver Operating Curves (ROC), we showed that TNF-α and VEGF concentrations could distinguish EPTB from non-confirmed EPTB with high sensitivity and specificity.

Conclusion: Pulmonary and extrapulmonary *Mtb* clinical isolates showed different cytokine induction pattern in human macrophages that is also found in the plasma level of the EPTB patients. Further investigations are needed to define cytokine secretions that can lead to the definition of bio-signatures to differentiate EPTB from other pathologies with confusing symptoms that hampered the diagnosis of TB.

Keywords: ***Mycobacterium tuberculosis*, extra-pulmonary tuberculosis, immune response, cytokine, biomarker**

OPEN ACCESS

Edited by:
Céline Cougoule, Centre National de la Recherche Scientifique (CNRS), France

Reviewed by:
Carmen Judith Serrano, Instituto Mexicano del Seguro Social (IMSS), Mexico
Irene Garcia, Université de Genève, Switzerland

***Correspondence:**
Niaina Rakotosamimanana
niaina@pasteur.mg

Specialty section:
This article was submitted to Microbial Immunology, a section of the journal Frontiers in Microbiology

Received: *31 October 2017*
Accepted: *07 February 2018*
Published: *21 February 2018*

Citation:
Ranaivomanana P, Raberahona M, Rabarioelina S, Borella Y, Machado A, Randria MJD, Rakotoarivelo RA, Rasolofo V and Rakotosamimanana N (2018) Cytokine Biomarkers Associated with Human Extra-Pulmonary Tuberculosis Clinical Strains and Symptoms. Front. Microbiol. 9:275. doi: 10.3389/fmicb.2018.00275

INTRODUCTION

With 10.4 million new cases and 1.5 million deaths in 2015 (World Health Organization [WHO], 2016), tuberculosis (TB) remains a major global public health problem. TB, an air transmitted infectious disease, is known to affect primarily the lungs; however, TB has also been described in virtually all tissues or organs (Alvarez and McCabe, 1984; Mazza-Stalder et al., 2012). Extrapulmonary TB (EPTB) represents about 20% of all TB cases in developing countries (Cagatay et al., 2004; Sharma and Mohan, 2004) and can be much higher in immune-compromised individuals. The diagnosis of EPTB is challenging due to the poor performance of conventional diagnostic techniques. Moreover, while the TB symptoms are constituted by local pain, weight loss, night sweat and fever (Golden and Vikram, 2005), there is no EPTB specific symptoms in any tissue or organ and the observed symptoms can be confused with those of other pathologies. This would further result in delayed diagnosis and treatment that can quickly lead to death depending on the severity of the affection (World Health Organization [WHO], 2016). Finding biomarkers to improve EPTB diagnosis can thus be important in the global control of TB.

The mechanism of *Mtb* dissemination from the pulmonary site to other organs is not well elucidated. Following entry of the bacillus in the lungs, alveolar macrophages invade the subtending epithelial layer and secrete several cytokines including the Th1 profile. These cytokines allow the recruitment and activation of inflammatory cells to form the granuloma that contains the pathogen (Orme and Basaraba, 2014; Gideon et al., 2015). The outcome of the infection will then depend on the imbalance of interactions between the host immune system response and the infecting bacteria (Ernst, 2012). Lymphohematogenous dissemination of *Mtb* is one of the key events in TB pathogenesis since it is involved in the development of protective T-cell mediated immune response but it also enables the bacteria to spread to new niches and therefore to establish alternative sites of infection (Krishnan et al., 2010). Genetic and host immune factors are suspected to be involved in extrapulmonary dissemination of *Mtb* and TB pathogenesis (Caws et al., 2008).

It was reported that the production of cytokines was different in persons healed from pulmonary TB when compared to those with EPTB (Hasan et al., 2009; Fiske et al., 2012). As development of EPTB seems to be the result of an immune host defects (Fiske et al., 2012), the discovery of factors that are associated to extrapulmonary disease will advance TB prevention efforts by identifying immune responses that could be boosted by TB vaccines.

The human host immune response against *Mtb* was shown to vary according to the genotype families of the infecting *Mtb* (Rakotosamimanana et al., 2010; Portevin et al., 2011) and studies using animal models identified some bacterial factors that were associated with extrapulmonary dissemination or colonization of specific organs (Pethe et al., 2001; Chawla et al., 2012). In a recent study using *Mtb* infected-macrophages and observations from TB patients, a correlation was found between *Mtb* infection and the production of angiogenesis factors (VEGF: Vascular endothelial growth factor) and subsequent vascularization during the bacterial dissemination into other organs (Polena et al., 2016). VEGF is a known major player in angiogenesis and lymphangiogenesis and is induced in response to tissue inflammation, hypoxia and pro-inflammatory cytokines (Ferrara et al., 2003; Koch et al., 2011).

Previous studied have reported cytokines TNF-α, IL-6, IL-1β, IL-10, IFN-γ, TGF-β and chemokine VEGF, levels to be significantly different in macrophage cells infected by mycobacteria compared to uninfected controls as well as in TB patients compared to healthy controls (Dlugovitzky et al., 1997; Morosini et al., 2003; Vankayalapati et al., 2003; Sahiratmadja et al., 2007; Dubois-Colas et al., 2014; Helguera-Repetto et al., 2014; Sousa-Vasconcelos Pda et al., 2015). However, there are few comparative studies describing the levels of cytokines and chemokines in patients with different clinical sites of TB, (PTB, EPTB) and EPTB-like pathologies. Moreover, studies which have investigated immune responses against EPTB have often combined patients without differentiating *Mtb* strains (Sharma et al., 2002; Jamil et al., 2007). It is important to consider the diversity associated with virulence capacity of these clinical isolates for inducing TB active disease and to evaluate the TB clinical forms (PTB or EPTB) and the immune response variations in relation to this bacterial diversity.

We propose here to identify human immune host signatures that could be involved in the dissemination of the pathogen and the colonization of other organs than the pulmonary sites that can be used for EPTB diagnosis by considering the genotype of infecting *Mtb*. In this study, we first determined the variations of cytokines TNF-α, IL-6, IL-10, IFN-γ and VEGF, in macrophages infected with different *Mtb* clinical isolates from patients with PTB and EPTB with *Mtb* strains belonging to the same Lineage 1 genotype known to enhance an elevated human pro-inflammatory responses (Rakotosamimanana et al., 2010; Portevin et al., 2011). Secondly, the variations of those cytokines productions presenting an *in vitro* difference between PTB and EPTB were measured in plasmas of patients and healthy controls to study their ability to distinguish the clinical groups of confirmed EPTB, EPTB-like symptoms and PTB patients.

MATERIALS AND METHODS

Ethics Statement

The study was approved by the National Ethics Committee of the Ministry of Health of Madagascar (N°072-MSANP/CE of 14/08/2014). All the patients that participated in the *ex vivo* part of the study gave their informed consents before any process was performed.

Mtb Clinical Isolates Selection and Mycobacteriology Procedures

The *Mtb* strains with EAI8_MDG spoligotype (shared-type 109) from the IPM-National Reference center for Mycobacteria clinical strains collection were used for the macrophage infections. PTB and EPTB isolated Mtb strains were matched by the same spoligotype, the gender/age/matched-patients. During the *in vitro* study, *Mtb* isolates from 7 different PTB and 7 other

EPTB patients were used to *in vitro* infect the macrophages. Supplementary Table S1 described the characteristic of those clinical isolates and the TB patients they were isolated from. The clinical sites where the EPTB isolates came were heterogeneous: lymph node (n = 1), pleural (n = 2), cerebrospinal (n = 1), urine (n = 2), pus (n = 1). *Mtb* was grown in Middlebrook7H9 broth supplemented with albumin-dextrose-catalase (M0178 Middlebrook 7H9 Broth Base).

Macrophages *in Vitro* Infection

The human monocyte–macrophage cell line THP-1 (Sigma) was maintained in culture medium containing RPMI-1640 medium supplemented with 200 mM L-glutamine, 10% inactivated foetal bovine serum(FBS), antibiotics (penicillin and streptomycin), and antifungal (fungizone) at 37°C, in a humidified 5% CO2 environment. The day before infection experiment, 100 nM phorbolmyristate acetate (Sigma) was added to differentiate cells into macrophages according to Spano et al. (2013) and distributed in 6-well plates (5×10^5 cells /well). The cells were cultured in RPMI-1640 medium, with 10% inactivated FBS and 200 mM L-glutamine, without antibiotics or antifungal.

THP1-derived macrophages were infected as previously described (Tailleux et al., 2003) at a multiplicity of infection of 1/1 bacteria/cell. Briefly, before infection, mid-log phase *Mtb* strains were washed two times with PBS, clumps were disassociated by 100 passages through a needle, followed by 5 min of sedimentation. The density of bacteria in the supernatant was checked at OD 600 nm and correlated to the numeration of the aliquot to allow 1-to-1 bacterium-per-cell infections. The infection was performed in a six-well plate with 5.10^5 cells/5.10^5 bacteria/well in 2 ml complete medium (without antibiotics). Non-infected cells were used as control for the experiments. All experiments were performed in duplicate. After 3 h of incubation at 37°C and 5% CO_2, infected cells were washed three times to remove extracellular bacteria and were incubated in fresh complete medium. Supernatants from control uninfected cells and *Mtb*–infected macrophages were harvested after 0 h (just after wash: 3 h post infection), 24, 48, and 120 h of macrophage infection, filtered using Millipore filter of 0.22 μm; and stored at −80°C for cytokine analysis.

Enumeration of intracellular bacteria was performed at 0 h (3 h post infection), 24, 48, and 120 h post-infection. Cell supernatant was removed and the wells were washed two times to remove extracellular bacteria and then lysed by cold distilled water with 0.05% Tween 20%. Cell lysates were diluted in 4 different dilutions and plated in triplicate on 7H11 solid medium complemented with OADC and incubated at 37°C. CFUs were scored after 3 weeks. CFUs were enumerated as previously described (Tailleux et al., 2003). All of the Mtb preparations and infections procedures were performed in a biosafety level 3 facility.

Study Population and TB Diagnostic Tests

All patients with suspected TB present or referred at the Infectious Diseases Unit of the Joseph Raseta Befelatanana Hospital (HUJRB), the EUSSPA/DAT (Etablissement Universitaire de Soins et de Santé Publique Analakely/Dispensaire antituberculeux) and at the IPM's anti-rabies center (healthy controls) were included in this study. Blood and specimens were harvested from the patients and plasma obtained through centrifugation. For suspected extrapulmonary TB patients, all clinical specimens (cerebrospinal fluid, pleural fluid, lymph node, ascitic fluid, pus) were considered and investigated for TB diagnosis. For PTB patients, sputum smear direct microscopy and LJ culture were performed. For all biological fluids samples for TB diagnosis by bacteriological detection of Mtb were beforehand decontaminated using the sodium lauryl-sulfate method. Then, one drop of previously decontaminated specimen was fixed on a slide, stained with auramine staining and examined under fluorescent microscopy. The remaining sample was cultured on standard Löwenstein-Jensen (LJ) medium.

The clinical criteria were: (1) EPTB: patients presenting suspected clinical symptoms of extrapulmonary TB regardless of the anatomic localization with positive smear acid-fast bacilli or *Mtb* positive on LJ culture; HIV positive patients and pregnant women were excluded from the study; (2) PTB: new TB cases with sputum smear AFB+ or *Mtb* positive on LJ culture; (3) Healthy control: healthy individual without any active TB symptoms after clinical investigation and chest X-ray, (4) non-EPTB: suspected-EPTB patients with negative *Mtb* in biological specimen culture.

Cytokine Quantification by Enzyme-Linked Immunosorbent Assay, ELISA

After the *in vitro* infections, the concentrations of IL-10, IL-6, TNF-α, IFN-γ and VEGF-A in the thawed supernatant were determined by ELISA as described by the assay kit manufacturers (Duoset kit, R&D Systems). The concentrations of cytokines in the plasma from the patients were measured in duplicate by specific sandwich ELISA as described by the manufacturers (R&D Systems).

Statistical Analysis

The normality of the each measures obtained was assessed with the D'Agostino & Pearson omnibus normality test. Multiple comparisons were performed using a two-way ANOVA adjusted by the Holm–Sidak post-test to assess the difference of CFU and cytokine concentrations according to the *in vitro* infection time points and the clinical groups. The one-way ANOVA test was used with multiple comparisons adjusted by the Tukey or the Dunn's post-tests respectively for parametric and non-parametric tests to assess the plasmatic cytokine concentrations differences amongst the clinical groups. Receiver Operating Characteristic (ROC) analysis was used to assess the diagnostic strength of the plasmatic concentration of cytokines to distinguish the clinical groups. Results were considered significant if the 95% confidence interval (CI) of the area under the curve (AUC) exceeded 0.70. A p value below 0.05 was considered as significant. The Prism GraphPad6 Software was used for the statistical analysis.

RESULTS

Similar Intra Macrophagic CFU Counts after *in Vitro* Infection with Isolates from Different Clinical Infectious Sites

The enumeration of intracellular bacteria was performed at 0 h (3 h post infection), 24, 48, and 120 h post-macrophage infection. Infecting *Mtb* strains isolated from PTB and EPTB patients showed similar growth rates in the macrophages from t0 to t120 post-infection (**Figure 1**). No significant difference was observed in bacterial count at any post infection time points between PTB and EPTB strains.

Different Level of Cytokine Secretions Depending on the Clinical Infectious Sites Origin of the Infecting Strains

After quantifying the concentration of the cytokines harvested from the infected macrophages supernatants, trends of increased productions of all the studied cytokines were observed in comparison to uninfected macrophages (**Figure 2**). Despite the observation from the other cytokines production, the secretions of both the TNF-α and VEGF trends increased over time (**Figures 2A,B**) after 24, 48, and 120 h post-infection. Surprisingly, unlike the others cytokines, a slight increase of the VEGF secretion was observed within the uninfected macrophages. The release of this chemokine by the control cells also increased over time with a higher level at 120 h post infection. We next compared the cytokine responses between PTB and EPTB infecting isolate strains at the different time points. Tendency in differences in the level of cytokines produced by the THP-1 derived macrophage depending on the clinical site origin of the *Mtb* infecting strains. Tendency of higher levels of TNF-α were observed when the PTB-isolated strains infected the macrophages compared to the EPTB-isolated strains infected macrophages depending on the infection time point. A statistically significant higher level of TNF-α was observed at 120 h (**Figure 2A**, $p < 0.001$). Unlike the TNF-α, after adjusting with the basal secretion observed in the uninfected macrophages, a trend of higher level of VEGF was observed with the EPTB-isolated strains compared to the PTB isolates at all time points, with a significant difference in the secretion levels after 120 h post infection ($p = 0.04$, **Figure 2B**).

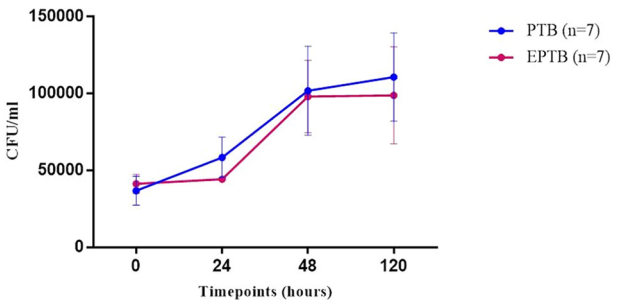


FIGURE 1 | Bacterial growth curve showing the intracellular CFU of *Mtb* in the infected macrophages at different timepoints post infection (hours) with EPTB-isolated strains (red line, $n = 7$) and PTB-isolated strains (blue line, $n = 7$). CFU, colony forming unit; PTB, pulmonary tuberculosis strains; EPTB, extrapulmonary tuberculosis strain; ctrl, non-infected cells. Each point corresponds to the average of three determinations ± SD. Statistical comparison was performed with a two-way ANOVA (p = ns).

Plasma Levels of TNF-α and VEGF Varied Depending on the Clinical Symptoms of the Patients

We measured the level of both cytokines that differed *in vitro* between PTB and EPTB in the plasmas collected from patients with different clinical symptoms. Eighty six (86) persons were included in the study. Fourty-four participants were suspected of EPTB with quite heterogeneous symptoms and included a large variety of clinical specimens; the most frequent were cerebrospinal fluid ($n = 18$, 39.06%) and pleural fluid ($n = 17$, 28.12%). Finally, according to the bacteriology, EPTB was confirmed in 16 patients, 13 had confirmed PTB, 28 had EPTB-like symptoms without bacteriological confirmation and 29 were healthy controls. **Table 1** described the characteristic of those TB patients.

After comparing the plasma level of the two different cytokines in the four clinical groups, PTB patients showed a significantly higher production of TNF-α compared to the EPTB patients, to the EPTB-like and to CTRL group, ($p = 0.004$, $p < 0.001$, and $p < 0.0001$ respectively) (**Figure 3A**). Differently from the observations in the *in vitro* infections, the plasma of EPTB patients showed a higher concentration of VEGF to the non-EPTB ($p = 0.022$) and to healthy controls group ($p < 0.0001$). No statistical differences were observed when comparing plasma level of VEGF in EPTB patients to PTB (**Figure 3B**).

Plasma Level of TNF-α and VEGF Concentrations Allowed to Respectively Distinguishing PTB and EPTB from the Other Patients Groups

We asked whether the plasmatic cytokines concentration could be useful for detecting a bacteriologically confirmed EPTB from the other clinical groups. Baseline levels of TNF-α and VEGF showed significant area under the curve (AUC) to respectively distinguish PTB and EPTB from the other clinical groups (**Tables 2**, **3** and **Figure 4**). The TNF-α showed more than 80% AUC yielded when distinguishing PTB from the other clinical groups ($p < 0.01$) (**Table 3** and **Figures 4D–F**). Moreover, the plasmatic VEGF concentration yielded an AUC of 73% ($p < 0.05$) when compared to PTB (**Table 2** and **Figure 4B**), 79 and 89% ($p < 0.01$) in distinguishing bacteriologically confirmed EPTB respectively from the other pathology with extrapulmonary symptoms and healthy control group (**Table 2** and **Figures 4A,C**)

DISCUSSIONS

The EPTB represents a non-negligible proportion of the TB active cases; however, its diagnosis that is lying firstly on

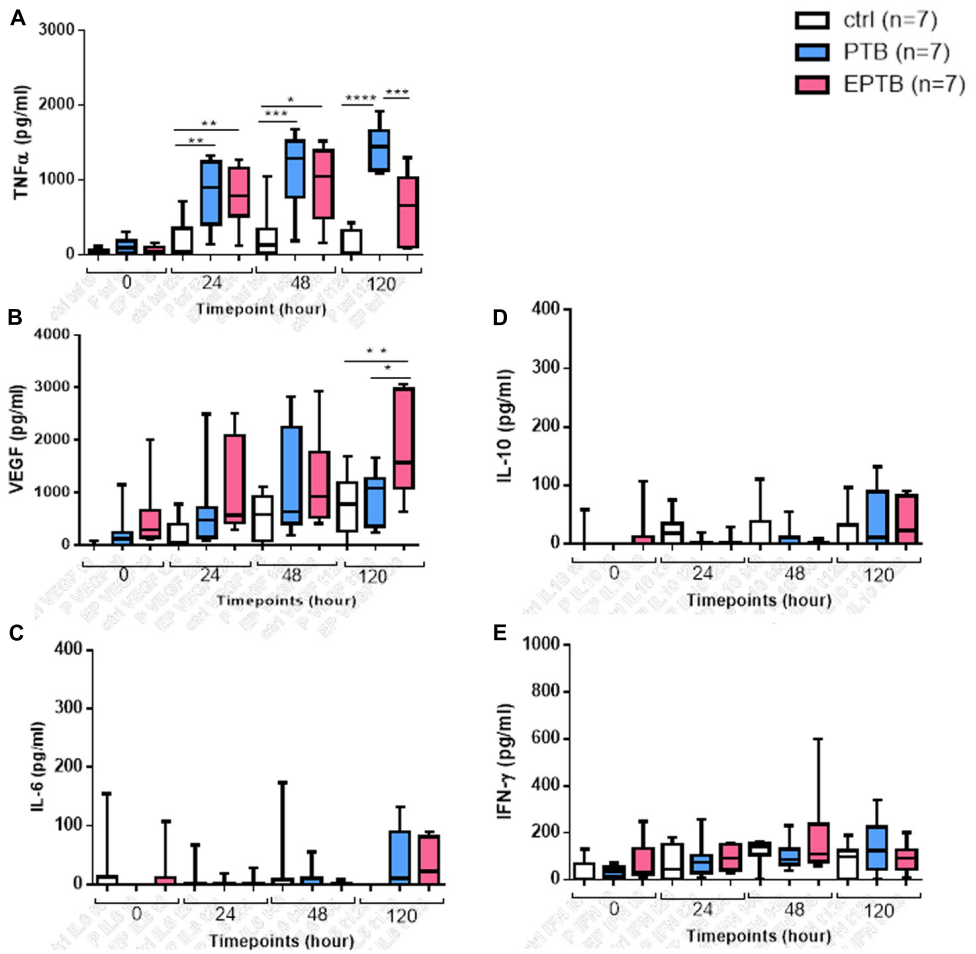


FIGURE 2 | Cytokine secretions by THP-1 derived macrophages infected with *Mtb* strains. **(A)** TNF-α, **(B)** VEGF, **(C)** IL-6, **(D)** IL-10, **(E)** IFN-γ concentrations. Multiple comparisons were assessed with a two-way ANOVA for the different timepoints and the clinical group with a Holm–Sidak post-test. $*P < 0.05$, $**P < 0.01$. PTB, pulmonary tuberculosis strains; EPTB, extrapulmonary tuberculosis strain; ctrl, non-infected cells.

TABLE 1 | Baseline characteristics of patients and type of specimen.

	EPTB *N* = 16	Non-EPTB *N* = 28	PTB *N* = 13	CTRL *N* = 29
Gender*: *n* (%)				
Female	10 (35.71)	10 (35.71)	4 (30.77)	15 (51.72)
Male	18 (64.29)	18 (64.29)	9 (69,23)	14 (48.28)
Age# : Mean (*SD*)	32 (12.18)	35 (15.92)	30 (7.76)	32 (10.62)
Sputum and blood harvested	Sputum/blood	Sputum/blood	Sputum/blood	blood
Specimen harvested: *n* (%)				
Pleural fluid	1 (6.25)	5 (17.86)		
Lymph nodes	3 (18.75)	2 (7.14)		
Ascitic fluid	1 (6.25)	10 (35.71)		
Cerebrospinal fluid	7 (43.75)	11 (39.26)		
Pus	1 (6.25)			
Miliary	3 (18.75)			

**A chi-square test to determine whether the gender distribution was equal in the clinical groups was not statistically significant $\chi^2(4, N = 86) = 2.23$, p-value < 0.527.*
#A one-way ANOVA with multiple comparisons adjusted by the Tukey post-test performed to assess the age differences amongst the clinical groups was not statistically significant ($p = 0.62$).

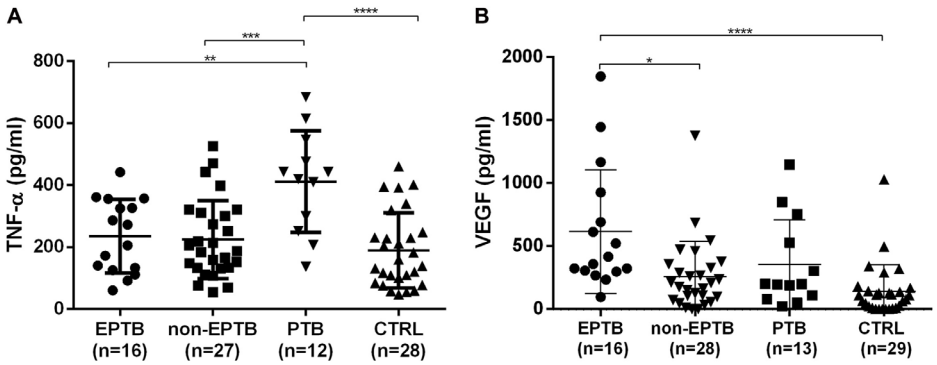


FIGURE 3 | Quantity of TNF-α **(A)** and VEGF **(B)** secreted in the plasma of EPTB, non-EPTB, PTB, and healthy controls group. Multiple comparisons were assessed with a one-way ANOVA for two clinical groups adjusted with Tukey post-test **(A)** or Dunn's post-test **(B)**: * $P < 0.05$, ** $P < 0.01$, *** $P < 0.001$, **** $P < 0.0001$. EPTB: bacteriologically confirmed extrapulmonary tuberculosis patients; non-EPTB, suspected-EPTB patients not bacteriologically confirmed; PTB, pulmonary tuberculosis patients; CTRL, healthy control group.

TABLE 2 | Area-under-the-curve (AUC) of VEGF as to distinguish confirmed EPTB from the other clinical groups.

Host cytokine	Clinics	AUC (95% CI)	*p*-value	Sensitivity % (95% CI)	Specificity % (95% CI)
VEGF					
	Non-EPTB	0.79 (0.65–0.92)	0.0015	57 (37–75)	93 (69–99)
	PTB	0.73 (0.53–0.92)	0.0353	61 (31–86)	93 (69–99)
	CTRL	0.89 (0.80–0.99)	<0.0001	82 (64–94)	93 (69–99)

TABLE 3 | Area-under-the-curve of TFN-α as to distinguish confirmed PTB from the other clinical groups.

Host cytokine	Clinics	AUC (95% CI)	*p*-value	Sensitivity % (95% CI)	Specificity % (95% CI)
TFN-α					
	Non-EPTB	0.81 (0.66–0.95)	0.002	51 (31–71)	91 (61–99)
	EPTB	0.81 (0.65–0.98)	0.0046	66 (34–90)	93 (69–99)
	CTRL	0.87 (0.75–0.99)	0.0002	60 (40–78)	91 (61–99)

clinical symptoms considerations is difficult due to the confusing symptoms with other pathologies as any human tissue or organ can be affected by EPTB while the traditional bacteriological tools to confirm TB were challenged by relatively inaccessible infectious sites that may be paucibacillary. In order to establish confirmation, invasive procedures are often necessary, making the diagnosis more difficult. The main objective of this study was to propose EPTB specific biomarkers deduced by the *in vitro* comparison of TB-associated cytokine response induced by different clinical isolates (PTB vs. EPTB) from human macrophages that were then assessed in human patients. Different cytokines known to be involved in the anti-tuberculosis immune response such as IFN-γ, TNF-α, IL-6, IL-10 and VEGF were first measured in human commercial cell-line derived infected macrophages to consider the host genetic effects on the immune response that was widely reported to be associated with EPTB (Caws et al., 2008). Although the THP-1 cell line was widely considered to be a good model of macrophages for *in vitro Mtb* infection studies (Riendeau and Kornfeld, 2003; Theus et al., 2005; Iona et al., 2012), it should not be forgotten that these are tumor cells and that certain functions remain poorly controlled. However, similar cytokine productions trends observed in this macrophage model were also observed *ex vivo* in human plasma in our study.

Moreover, the characterization of the determinants of *Mtb* virulence is an important process for understanding the pathogenesis of TB. The bacterial genetics effects on cytokine production were also considered here by infecting the macrophages with *Mtb* from similar bacterial lineages. Infecting the macrophages with the EAI-MDG8 (lineage 1) was preferred as the *Mtb*-lineage 1 strains were associated with an increased pro-inflammatory responses that would boost the cytokine levels we want to study (Rakotosamimanana et al., 2010; Portevin et al., 2011). Moreover, the *Mtb* EAI-MDG8 genotype was a predominant spoligotype profile in Madagascar where the study was performed (Rakotosamimanana et al., 2010).

The molecular and cellular mechanism of *Mtb* dissemination is not yet well understood. The cytokine network plays a central role in the inflammatory response and outcome of mycobacterial infections (van Crevel et al., 2002) and can be useful for a correct, specific and timely diagnosis is essential for EPTB. It has been reported that mycobacteria counteract the defense mechanisms deployed by the host immune system by altering the cytokine

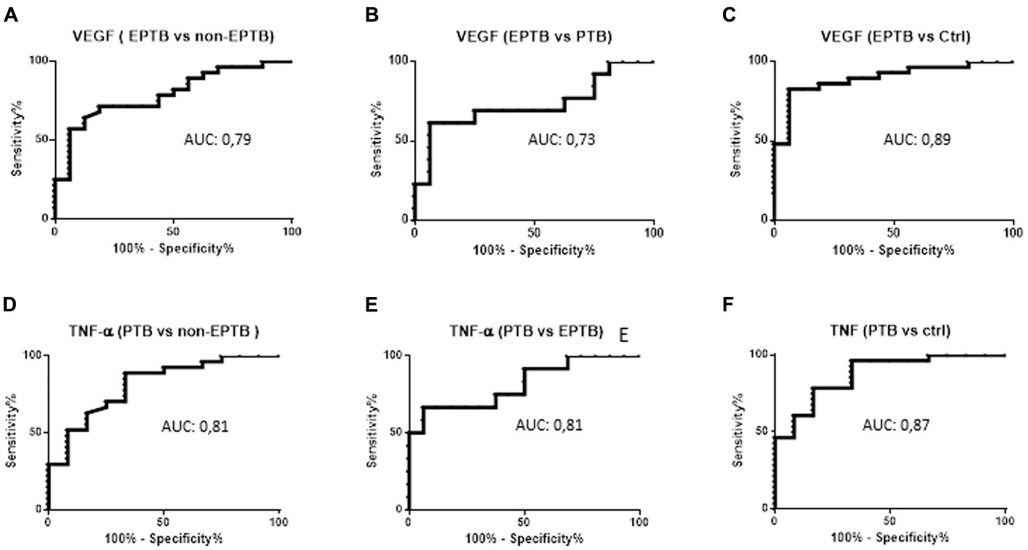


FIGURE 4 | Receiver operating curves (ROC) analysis of TNF-α and VEGF as markers to distinguish the differen clinical groups. VEGF ROC between EPTB and non-EPTB **(A)**, PTB **(B)**, Ctrl **(C)**, TNF-α ROC between PTB and non-EPTB **(D)**, EPTB **(E)**, Ctrl **(F)**. EPTB, bacteriologically confirmed extrapulmonary tuberculosis patients; non-EPTB, suspected-EPTB patients not bacteriologically confirmed; PTB, pulmonary tuberculosis patients; CTRL, healthy control group.

profile (van Crevel et al., 2002; Sousa-Vasconcelos Pda et al., 2015). TNF-α, IL-6, IL-10 IFN-γ, and VEGF play important roles in the immune response to the outcome of mycobacterial infections (van Crevel et al., 2002; Polena et al., 2016).

Our results indicate that EPTB strains elicit reduced TNF-α responses compared to the PTB strains indicating their ability to down-regulate one of the powerful pro-inflammatory response, which is crucial for controlling mycobacterial infections. The strongest evidence for the role of TNF-α to prevent TB pathogenesis was well reported in patients treated with TNF-α antagonist (Keane et al., 2001; Gardam et al., 2003; Askling et al., 2005; Wong et al., 2007a; Wallis, 2008; Martin-Mola and Balsa, 2009; Yasui, 2014). Moreover, it was shown that neutralization of TNF-α could induce dissemination of *Mtb* (Lin et al., 2010) but the mechanism was not well investigated. Previous study showed low TNF-α production by peripheral blood mononuclear cells from patients presenting EPTB but the mechanism has not been elucidated (Sterling et al., 2001; Fiske et al., 2012). The role of TNF-α in the control of bacilli in the latent stage has also been demonstrated by the reactivation of tuberculous infection (including miliary and extrapulmonary) in patients with Crohn's disease and rheumatoid arthritis, after treatment with monoclonal anti-TNF-α antibodies (Keane et al., 2001). Similar results were also reported in a study using mice unable to synthesize TNF-α, which has increased susceptibility to TB (Bean et al., 1999). Thus, in the present study, the ability of EPTB-isolated strains to down regulate TNF-α production may be associated with a lower immune response and then a mechanism that would allow dissemination. It has been shown that the neutralization of TNF-α can induce the spread of *Mtb* (Mayordomo et al., 2002; Lin et al., 2010). Our results are comparable with those observed in another study showing a significant reduction in the production of TNF-α in (*ex vivo*) macrophages infected by hypervirulent strains of *Mtb* isolated from patients with tuberculous meningitis and where the production of IL-10 and IL-12 was even undetectable (Wong et al., 2007b). Despite a relatively high level of TNF-α observed in the healthy controls that may be due to latent *Mtb* infection or exposure due to the fact that the study was performed in a TB high incidence area, the difference between PTB and EPTB was also observed in the plasma of the patients from the present study. This cytokine acts in synergy with IFN-γ to increase the production of metabolites of nitric oxide and to eliminate mycobacteria and is essential for the formation of granulomas for the confinement of a mycobacterial infection (Gomez-Reino et al., 2003; Bottasso et al., 2007). While some studies identified the IFN-γ or the type I interferons as biomarkers for EPTB when compared to healthy controls that was also observed in the present study (Goyal et al., 2016), no difference was observed when comparing the PTB vs EPTB for the IFN-γ *in vitro* response that would probe for an host genetic effects associated with the IFN responses differences observed in EPTB.

During the *in vitro* macrophage infection, unlike TNF-α, our results indicated that VEGF production is significantly induced by the EPTB-isolated strains compared to PTB strains. This chemokine was also significantly higher in the plasma of EPTB-confirmed patients compared to patients with EPTB-like symptoms, but we did not observe a statistic difference with PTB patients. The VEGF is best known for its role as an activator of angiogenesis. In cancer, the angiogenesis induces tumor progression and metastasis (Carmeliet, 2005). Angiogenesis would play a similar role in TB and may well be involved in extrapulmonary forms of the disease. Indeed, a recent study argues in favor of this hypothesis. In zebrafish model, the formation of new blood vessels facilitates the dissemination of *M. Marinum* (Oehlers et al., 2015). Moreover, high VEGF levels

were observed in tuberculous pleural effusion (Seiscento et al., 2010; Qama et al., 2012) and tuberculous meningitis (Matsuyama et al., 2001; van der Flier et al., 2004). Thus, other studies have used anti-VEGF agents in EPTB therapy to prevent bacteria from disseminating and inhibiting their growth (Invernizzi et al., 2015; Oehlers et al., 2015). Moreover, the results observed in the present study are in agreement with previous studies which have shown that the production of VEGF is positively stimulated in EPTB disease (Seiscento et al., 2010; Thayil et al., 2011; Misra et al., 2013; Zucchi et al., 2013). Similarly to the present study, Qama et al. (2012) reported an increase of both TNF-α and VEGF in EPTB patients compared to healthy controls from tuberculous pleural effusions with notably a 31-fold increase of the VEGF produced in the bronchoalveolar lavage fluids of patients with pleural TB compared to healthy control subjects (Qama et al., 2012). Thus, these observations confirm the crucial role of VEGF in the diffusion of *Mtb*. However, in other studies, VEGF was mostly considered as a biomarker of active PTB disease (Matsuyama et al., 2000; Abe et al., 2001; Alatas et al., 2004; Riou et al., 2012; Mihret et al., 2013; Ota et al., 2014). Further investigation is therefore needed to decipher the exact role of VEGF in TB, especially in its disseminated forms.

It is noteworthy to mention that our study has several limitations. First, despite our aim to propose tools that can be used in resources limited area the studied cytokine panel was only restricted to the well known TB-associated cytokines. The current observations could benefit from the proteomic or transcriptomic high-throughput tools that would target more and/or new cytokines (Blankley et al., 2016; Roe et al., 2016). Increasing the sample size would also strengthen the statistical differences observed to get a stronger distinction of EPTB with the other clinical symptoms depending on the cytokine quantification as well as getting enough biological materials to investigate the production of these cytokines in clinical sites other than blood. Moreover, as we were able to study the effects of the infecting strains during the *in vitro* infections, we did not study the genotypes of the strains infecting the confirmed EPTB patients even the cytokine variations were quite similar. Furthermore, despite the fact that we were able to distinguish the EPTB from the cytokine secretions, we did not obtained the final diagnostic of those suspected EPTB that were not confirmed bacteriologically that is cruelly lacking in most of low-resources countries. Finally, in future studies, it would be interesting to investigate other factors such as malnutrition (Edwards et al., 1971) or immunodeficiency (e.g., CD4 + depletion, Slutsker et al., 1993; Jones et al., 1997; Golden and Vikram, 2005) and other factors such as a history of renal insufficiency may be associated with an increased risk of TB and are therefore potential confounders for risk factors for EPTB (Gonzalez et al., 2003; Abdelrahman et al., 2006; Sen et al., 2008; Lin et al., 2009).

CONCLUSION

This study showed that *Mtb* PTB and EPTB strains have different cytokine/chemokine profile induction in macrophages. EPTB strains are characterized by strong VEGF induction/low TNF-α induction and inversely with PTB strains. We conclude that this ability to reduce TNF-α production and increase VEGF secretion can be considered as a specific biomarker in EPTB disease. Specifically, in this study the up-regulation of VEGF secretion could help in evaluating suspected EPTB compared to other affections in the body. These findings can be useful for understanding the immune response to *Mtb* infection and help to understand factors that may influence the progression to extrapulmonary disease. Although the exact mechanism leading to these differences is still poorly understood and the panel of cytokines limited, our observations may serve as a basis for future studies. Finally, the mechanisms of induction or inhibition of the secretion of these cytokines must be well elucidated in order to better anticipate the fight against severe forms of TB in particular disseminated TB such as meningitis and miliary TB which are often fatal.

AUTHOR CONTRIBUTIONS

Substantial contributions to the conception or design of the work, or the acquisition, analysis, or interpretation of data for the work: NR, VR, PR, MR, RR, MJDR, SR, AM, and YB. Drafting the work or revising it critically for important intellectual content: NR, VR, PR, MR, RR, MJDR, SR, AM, and YB. Final approval of the version to be published: NR, VR, PR, MR, RR, MJDR, SR, AM, and YB. Agreement to be accountable for all aspects of the work in ensuring that questions related to the accuracy or integrity of any part of the work are appropriately investigated and resolved: NR, VR, PR, MR, RR, MJDR, SR, AM, and YB.

FUNDING

The study was funded by the Dedonder Clayton Grant (Institut Pasteur International Network) and the Institut Pasteur de Madagascar.

ACKNOWLEDGMENTS

We would like to thank Ludovic Tailleux (Genetic Mycobacteria Unit, Institut Pasteur, Paris) for his contribution in technological help and setting up the study. We acknowledge the infectious disease department of the HUJRB hospital (Joseph Raseta Befelatanana University Hospital, Antananarivo, Madagascar), the EUSSPA/DAT (Etablissement Universitaire de Soins et de Santé Publique Analakely/Dispensaire antituberculeux) and the IPM antirabies center for their help in specimen collection, and also thank Mrs. Elie Vololonirina, and Sandratra Andriatsalama from the IPM for their contribution to the study experiment.

SUPPLEMENTARY MATERIAL

The Supplementary Material for this article can be found online at: https://www.frontiersin.org/articles/10.3389/fmicb.2018.00275/full#supplementary-material

REFERENCES

Abdelrahman, M., Sinha, A. K., and Karkar, A. (2006). Tuberculosis in end-stage renal disease patients on hemodialysis. *Hemodial. Int.* 10, 360–364. doi: 10.1111/j.1542-4758.2006.00130.x

Abe, Y., Nakamura, M., Oshika, Y., Hatanaka, H., Tokunaga, T., Ohkubo, Y., et al. (2001). Serum levels of vascular endothelial growth factor and cavity formation in active pulmonary tuberculosis. *Respiration* 68, 496–500. doi: 10.1159/000050557

Alatas, F., Alatas, O., Metintas, M., Ozarslan, A., Erginel, S., and Yildirim, H. (2004). Vascular endothelial growth factor levels in active pulmonary tuberculosis. *Chest* 125, 2156–2159. doi: 10.1378/chest.125.6.2156

Alvarez, S., and McCabe, W. R. (1984). Extrapulmonary tuberculosis revisited: a review of experience at Boston City and other hospitals. *Medicine* 63, 25–55. doi: 10.1097/00005792-198401000-00003

Askling, J., Fored, C. M., Brandt, L., Baecklund, E., Bertilsson, L., Coster, L., et al. (2005). Risk and case characteristics of tuberculosis in rheumatoid arthritis associated with tumor necrosis factor antagonists in Sweden. *Arthritis Rheum.* 52, 1986–1992. doi: 10.1002/art.21137

Bean, A. G., Roach, D. R., Briscoe, H., France, M. P., Korner, H., Sedgwick, J. D., et al. (1999). Structural deficiencies in granuloma formation in TNF gene-targeted mice underlie the heightened susceptibility to aerosol *Mycobacterium tuberculosis* infection, which is not compensated for by lymphotoxin. *J. Immunol.* 162, 3504–3511.

Blankley, S., Graham, C. M., Turner, J., Berry, M. P., Bloom, C. I., Xu, Z., et al. (2016). The transcriptional signature of active tuberculosis reflects symptom status in extra-pulmonary and pulmonary tuberculosis. *PLoS One* 11:e0162220. doi: 10.1371/journal.pone.0162220

Bottasso, O., Bay, M. L., Besedovsky, H., and Del Rey, A. (2007). The immuno-endocrine component in the pathogenesis of tuberculosis. *Scand. J. Immunol.* 66, 166–175. doi: 10.1111/j.1365-3083.2007.01962.x

Cagatay, A. A., Caliskan, Y., Aksoz, S., Gulec, L., Kucukoglu, S., Cagatay, Y., et al. (2004). Extrapulmonary tuberculosis in immunocompetent adults. *Scand. J. Infect. Dis.* 36, 799–806. doi: 10.1080/00365540410025339

Carmeliet, P. (2005). Angiogenesis in life, disease and medicine. *Nature* 438, 932–936. doi: 10.1038/nature04478

Caws, M., Thwaites, G., Dunstan, S., Hawn, T. R., Lan, N. T., Thuong, N. T., et al. (2008). The influence of host and bacterial genotype on the development of disseminated disease with *Mycobacterium tuberculosis*. *PLoS Pathog.* 4:e1000034. doi: 10.1371/journal.ppat.1000034

Chawla, M., Parikh, P., Saxena, A., Munshi, M., Mehta, M., Mai, D., et al. (2012). *Mycobacterium tuberculosis* WhiB4 regulates oxidative stress response to modulate survival and dissemination in vivo. *Mol. Microbiol.* 85, 1148–1165. doi: 10.1111/j.1365-2958.2012.08165.x

Dlugovitzky, D., Torres-Morales, A., Rateni, L., Farroni, M. A., Largacha, C., Molteni, O., et al. (1997). Circulating profile of Th1 and Th2 cytokines in tuberculosis patients with different degrees of pulmonary involvement. *FEMS Immunol. Med. Microbiol.* 18, 203–207. doi: 10.1111/j.1574-695X.1997.tb01046.x

Dubois-Colas, N., Petit-Jentreau, L., Barreiro, L. B., Durand, S. R., Soubigou, G., Lecointe, C. C., et al. (2014). Extracellular adenosine triphosphate affects the response of human macrophages infected with *Mycobacterium tuberculosis*. *J. Infect. Dis.* 210, 824–833. doi: 10.1093/infdis/jiu135

Edwards, L. B., Livesay, V. T., Acquaviva, F. A., and Palmer, C. E. (1971). Height, weight, tuberculous infection, and tuberculous disease. *Arch. Environ. Health Int. J.* 22, 106–112. doi: 10.1080/00039896.1971.10665820

Ernst, J. D. (2012). The immunological life cycle of tuberculosis. *Nat. Rev. Immunol.* 12, 581–591. doi: 10.1038/nri3259

Ferrara, N., Gerber, H.-P., and LeCouter, J. (2003). The biology of VEGF and its receptors. *Nat. Med.* 9, 669–676. doi: 10.1038/nm0603-669

Fiske, C. T., de Almeida, A. S., Shintani, A. K., Kalams, S. A., and Sterling, T. R. (2012). Abnormal immune responses in persons with previous extrapulmonary tuberculosis in an in vitro model that simulates in vivo infection with *Mycobacterium tuberculosis*. *Clin. Vaccine Immunol.* 19, 1142–1149. doi: 10.1128/CVI.00221-12

Gardam, M. A., Keystone, E. C., Menzies, R., Manners, S., Skamene, E., Long, R., et al. (2003). Anti-tumour necrosis factor agents and tuberculosis risk: mechanisms of action and clinical management. *Lancet Infect. Dis.* 3, 148–155. doi: 10.1016/S1473-3099(03)00545-0

Gideon, H. P., Phuah, J., Myers, A. J., Bryson, B. D., Rodgers, M. A., Coleman, M. T., et al. (2015). Variability in tuberculosis granuloma T cell responses exists, but a balance of pro-and anti-inflammatory cytokines is associated with sterilization. *PLoS Pathog.* 11:e1004603. doi: 10.1371/journal.ppat.1004603

Golden, M. P., and Vikram, H. R. (2005). Extrapulmonary tuberculosis: an overview. *Am. Fam. Phys.* 72, 1761–1768.

Gomez-Reino, J. J., Carmona, L., Valverde, V. R., Mola, E. M., and Montero, M. D. (2003). Treatment of rheumatoid arthritis with tumor necrosis factor inhibitors may predispose to significant increase in tuberculosis risk: a multicenter active-surveillance report. *Arthritis Rheum.* 48, 2122–2127. doi: 10.1002/art.11137

Gonzalez, O. Y., Adams, G., Teeter, L. D., Bui, T. T., Musser, J. M., and Graviss, E. A. (2003). Extra-pulmonary manifestations in a large metropolitan area with a low incidence of tuberculosis. *Int. J. Tuberc. Lung Dis.* 7, 1178–1185.

Goyal, N., Kashyap, B., and Kaur, I. R. (2016). Significance of IFNg/IL-2 ratio as a circulating diagnostic biomarker in extrapulmonary tuberculosis. *Scand. J. Immunol.* 83, 338–344. doi: 10.1111/sji.12424

Hasan, Z., Jamil, B., Ashraf, M., Islam, M., Yusuf, M. S., Khan, J. A., et al. (2009). ESAT6-induced IFNγ and CXCL9 can differentiate severity of tuberculosis. *PLoS One* 4:e5158. doi: 10.1371/journal.pone.0005158

Helguera-Repetto, A. C., Chacon-Salinas, R., Cerna-Cortes, J. F., Rivera-Gutierrez, S., Ortiz-Navarrete, V., Estrada-Garcia, I., et al. (2014). Differential macrophage response to slow-and fast-growing pathogenic mycobacteria. *Biomed Res. Int.* 2014:916521. doi: 10.1155/2014/916521

Invernizzi, A., Franzetti, F., Viola, F., Meroni, L., and Staurenghi, G. (2015). Optic nerve head tubercular granuloma successfully treated with anti-VEGF intravitreal injections in addition to systemic therapy. *Eur. J. Ophthalmol.* 25, 270–272. doi: 10.5301/ejo.5000528

Iona, E., Pardini, M., Gagliardi, M. C., Colone, M., Stringaro, A. R., Teloni, R., et al. (2012). Infection of human THP-1 cells with dormant *Mycobacterium tuberculosis*. *Microbes Infect.* 14, 959–967. doi: 10.1016/j.micinf.2012.04.003

Jamil, B., Shahid, F., Hasan, Z., Nasir, N., Razzaki, T., Dawood, G., et al. (2007). Interferon gamma/IL10 ratio defines the disease severity in pulmonary and extra pulmonary tuberculosis. *Tuberculosis* 87, 279–287. doi: 10.1016/j.tube.2007.03.004

Jones, B. E., Oo, M. M., Taikwel, E. K., Qian, D., Kumar, A., Maslow, E. R., et al. (1997). CD4 cell counts in human immunodeficiency virus-negative patients with tuberculosis. *Clin. Infect. Dis.* 24, 988–991. doi: 10.1093/clinids/24.5.988

Keane, J., Gershon, S., Wise, R. P., Mirabile-Levens, E., Kasznica, J., Schwieterman, W. D., et al. (2001). Tuberculosis associated with infliximab, a tumor necrosis factor alpha-neutralizing agent. *N. Engl. J. Med.* 345, 1098–1104. doi: 10.1056/NEJMoa011110

Koch, S., Tugues, S. N., Li, X., Gualandi, L., and Claesson-Welsh, L. (2011). Signal transduction by vascular endothelial growth factor receptors. *Biochem. J.* 437, 169–183. doi: 10.1042/BJ20110301

Krishnan, N., Robertson, B. D., and Thwaites, G. (2010). The mechanisms and consequences of the extra-pulmonary dissemination of *Mycobacterium tuberculosis*. *Tuberculosis* 90, 361–366. doi: 10.1016/j.tube.2010.08.005

Lin, J. N., Lai, C. H., Chen, Y. H., Lee, S. S. J., Tsai, S. S., Huang, C. K., et al. (2009). Risk factors for extra-pulmonary tuberculosis compared to pulmonary tuberculosis. *Int. J. Tuberc. Lung Dis.* 13, 620–625.

Lin, P. L., Myers, A., Smith, L., Bigbee, C., Bigbee, M., Fuhrman, C., et al. (2010). Tumor necrosis factor neutralization results in disseminated disease in acute and latent *Mycobacterium tuberculosis* infection with normal granuloma structure in a cynomolgus macaque model. *Arthritis Rheum.* 62, 340–350. doi: 10.1002/art.27271

Martin-Mola, E., and Balsa, A. (2009). Infectious complications of biologic agents. *Rheum. Dis. Clin. North Am.* 35, 183–199. doi: 10.1016/j.rdc.2009.03.009

Matsuyama, W., Hashiguchi, T., Matsumuro, K., Iwami, F., Hirotsu, Y., Kawabata, M., et al. (2000). Increased serum level of vascular endothelial growth factor in pulmonary tuberculosis. *Am. J. Respir. Crit. Care Med.* 162, 1120–1122. doi: 10.1164/ajrccm.162.3.9911010

Matsuyama, W., Hashiguchi, T., Umehara, F., Matsuura, E., Kawabata, M., Arimura, K., et al. (2001). Expression of vascular endothelial growth factor in tuberculous meningitis. *J. Neurol. Sci.* 186, 75–79. doi: 10.1016/S0022-510X(01)00515-9

Mayordomo, L., Marenco, J. L., Gomez-Mateos, J., and Rejon, E. (2002). Pulmonary miliary tuberculosis in a patient with anti-TNF-alpha treatment. *Scand. J. Rheumatol.* 31, 44–45. doi: 10.1080/030097402317255372

Mazza-Stalder, J., Nicod, L., and Janssens, J. P. (2012). Extrapulmonary tuberculosis. *Rev. Mal. Respir.* 29, 566–578. doi: 10.1016/j.rmr.2011.05.021

Mihret, A., Bekele, Y., Bobosha, K., Kidd, M., Aseffa, A., Howe, R., et al. (2013). Plasma cytokines and chemokines differentiate between active disease and non-active tuberculosis infection. *J. Infect.* 66, 357–365. doi: 10.1016/j.jinf.2012.11.005

Misra, U. K., Kalita, J., Singh, A. P., and Prasad, S. (2013). Vascular endothelial growth factor in tuberculous meningitis. *Int. J. Neurosci.* 123, 128–132. doi: 10.3109/00207454.2012.743127

Morosini, M., Meloni, F., Marone Bianco, A., Paschetto, E., Uccelli, M., Pozzi, E., et al. (2003). The assessment of IFN-gamma and its regulatory cytokines in the plasma and bronchoalveolar lavage fluid of patients with active pulmonary tuberculosis. *Int. J. Tuberc. Lung Dis.* 7, 994–1000.

Oehlers, S. H., Cronan, M. R., Scott, N. R., Thomas, M. I., Okuda, K. S., Walton, E. M., et al. (2015). Interception of host angiogenic signalling limits mycobacterial growth. *Nature* 517, 612–615. doi: 10.1038/nature13967

Orme, I. M., and Basaraba, R. J. (2014). The formation of the granuloma in tuberculosis infection. *Semin. Immunol.* 26, 601–609. doi: 10.1016/j.smim.2014.09.009

Ota, M. O., Mendy, J. F., Donkor, S., Togun, T., Daramy, M., Gomez, M. P., et al. (2014). Rapid diagnosis of tuberculosis using ex vivo host biomarkers in sputum. *Eur. Respir. J.* 44, 254–257. doi: 10.1183/09031936.00209913

Pethe, K., Alonso, S., Biet, F., Delogu, G., Brennan, M. J., Locht, C., et al. (2001). The heparin-binding haemagglutinin of *M. tuberculosis* is required for extrapulmonary dissemination. *Nature* 412, 190–194. doi: 10.1038/35084083

Polena, H., Boudou, F., Tilleul, S., Dubois-Colas, N., Lecointe, C., Rakotosamimanana, N., et al. (2016). *Mycobacterium tuberculosis* exploits the formation of new blood vessels for its dissemination. *Sci. Rep.* 6:33162. doi: 10.1038/srep33162

Portevin, D., Gagneux, S., Comas, I., and Young, D. (2011). Human macrophage responses to clinical isolates from the *Mycobacterium tuberculosis* complex discriminate between ancient and modern lineages. *PLoS Pathog.* 7:e1001307. doi: 10.1371/journal.ppat.1001307

Qama, D., Choi, W. I., and Kwon, K. Y. (2012). Immune responses in the lungs of patients with tuberculous pleural effusion without pulmonary tuberculosis. *BMC Immunol.* 13:45. doi: 10.1186/1471-2172-13-45

Rakotosamimanana, N., Raharimanga, V., Andriamandimby, S. F., Soares, J. L., Doherty, T. M., Ratsitorahina, M., et al. (2010). Variation in gamma interferon responses to different infecting strains of *Mycobacterium tuberculosis* in acid-fast bacillus smear-positive patients and household contacts in Antananarivo, Madagascar. *Clin. Vaccine Immunol.* 17, 1094–1103. doi: 10.1128/CVI.00049-10

Riendeau, C. J., and Kornfeld, H. (2003). THP-1 cell apoptosis in response to mycobacterial infection. *Infect. Immun.* 71, 254–259. doi: 10.1128/IAI.71.1.254-259.2003

Riou, C., Perez Peixoto, B., Roberts, L., Ronacher, K., Walzl, G., Manca, C., et al. (2012). Effect of standard tuberculosis treatment on plasma cytokine levels in patients with active pulmonary tuberculosis. *PLoS One* 7:e36886. doi: 10.1371/journal.pone.0036886

Roe, J. K., Thomas, N., Gil, E., Best, K., Tsaliki, E., Morris-Jones, S., et al. (2016). Blood transcriptomic diagnosis of pulmonary and extrapulmonary tuberculosis. *JCI Insight* 1:e87238. doi: 10.1172/jci.insight.87238

Sahiratmadja, E., Alisjahbana, B., de Boer, T., Adnan, I., Maya, A., Danusantoso, H., et al. (2007). Dynamic changes in pro- and anti-inflammatory cytokine profiles and gamma interferon receptor signaling integrity correlate with tuberculosis disease activity and response to curative treatment. *Infect. Immun.* 75, 820–829. doi: 10.1128/IAI.00602-06

Seiscento, M., Vargas, F. S., Acencio, M. M., Teixeira, L. R., Capelozzi, V. L., Sales, R. K., et al. (2010). Pleural fluid cytokines correlate with tissue inflammatory expression in tuberculosis. *Int. J. Tuberc. Lung Dis.* 14, 1153–1158.

Sen, N., Turunc, T., Karatasli, M., Sezer, S., Demiroglu, Y. Z., and Oner Eyuboglu, F. (2008). Tuberculosis in patients with end-stage renal disease undergoing dialysis in an endemic region of Turkey. *Transplant Proc.* 40, 81–84. doi: 10.1016/j.transproceed.2007.12.003

Sharma, S. K., Mitra, D. K., Balamurugan, A., Pandey, R. M., and Mehra, N. K. (2002). Cytokine polarization in miliary and pleural tuberculosis. *J. Clin. Immunol.* 22, 345–352. doi: 10.1023/A:1020604331886

Sharma, S. K., and Mohan, A. (2004). Extrapulmonary tuberculosis. *Indian J. Med. Res.* 120, 316–353.

Slutsker, L., Castro, K. G., Ward, J. W., and Dooley, S. W. Jr. (1993). Epidemiology of extrapulmonary tuberculosis among persons with AIDS in the United States. *Clin. Infect. Dis.* 16, 513–518. doi: 10.1093/clind/16.4.513

Sousa-Vasconcelos Pda, S., Seguins Wda, S., Luz Ede, S. S., and Pinho, R. T. (2015). Pattern of cytokine and chemokine production by THP-1 derived macrophages in response to live or heat-killed *Mycobacterium bovis* bacillus Calmette-Guerin Moreau strain. *Mem. Inst. Oswaldo Cruz* 110, 809–813. doi: 10.1590/0074-02760140420

Spano, A., Barni, S., and Sciola, L. (2013). PMA withdrawal in PMA-treated monocytic THP-1 cells and subsequent retinoic acid stimulation, modulate induction of apoptosis and appearance of dendritic cells. *Cell Prolif.* 46, 328–347. doi: 10.1111/cpr.12030

Sterling, T. R., Dorman, S. E., Chaisson, R. E., Ding, L., Hackman, J., Moore, K., et al. (2001). Human immunodeficiency virus-seronegative adults with extrapulmonary tuberculosis have abnormal innate immune responses. *Clin. Infect. Dis.* 33, 976–982. doi: 10.1086/322670

Tailleux, L., Schwartz, O., Herrmann, J. L., Pivert, E., Jackson, M., Amara, A., et al. (2003). DC-SIGN is the major *Mycobacterium tuberculosis* receptor on human dendritic cells. *J. Exp. Med.* 197, 121–127. doi: 10.1084/jem.20021468

Thayil, S. M., Albini, T. A., Nazari, H., Moshfeghi, A. A., Parel, J. M., Rao, N. A., et al. (2011). Local ischemia and increased expression of vascular endothelial growth factor following ocular dissemination of *Mycobacterium tuberculosis*. *PLoS One* 6:e28383. doi: 10.1371/journal.pone.0028383

Theus, S. A., Cave, M. D., and Eisenach, K. D. (2005). Intracellular macrophage growth rates and cytokine profiles of *Mycobacterium tuberculosis* strains with different transmission dynamics. *J. Infect. Dis.* 191, 453–460. doi: 10.1086/425936

van Crevel, R., Ottenhoff, T. H., and van der Meer, J. W. (2002). Innate immunity to *Mycobacterium tuberculosis*. *Clin. Microbiol. Rev.* 15, 294–309. doi: 10.1128/CMR.15.2.294-309.2002

van der Flier, M., Hoppenreijs, S., van Rensburg, A. J., Ruyken, M., Kolk, A. H., Springer, P., et al. (2004). Vascular endothelial growth factor and blood-brain barrier disruption in tuberculous meningitis. *Pediatr. Infect. Dis. J.* 23, 608–613. doi: 10.1097/01.inf.0000131634.57368.45

Vankayalapati, R., Wizel, B., Weis, S. E., Klucar, P., Shams, H., Samten, B., et al. (2003). Serum cytokine concentrations do not parallel *Mycobacterium tuberculosis*-induced cytokine production in patients with tuberculosis. *Clin. Infect. Dis.* 36, 24–28. doi: 10.1086/344903

Wallis, R. S. (2008). Mathematical modeling of the cause of tuberculosis during tumor necrosis factor blockade. *Arthritis Rheum.* 58, 947–952. doi: 10.1002/art.23285

Wong, C. K., Wong, B. C., Chan, K. C., Joynt, G. M., Yap, F. Y., Lam, C. W., et al. (2007a). Cytokine profile in fatal human immunodeficiency virus tuberculosis Epstein-Barr virus associated hemophagocytic syndrome. *Arch. Intern. Med.* 167, 1901–1903. doi: 10.1001/archinte.167.17.1901

Wong, K. C., Leong, W. M., Law, H. K., Ip, K. F., Lam, J. T., Yuen, K. Y., et al. (2007b). Molecular characterization of clinical isolates of *Mycobacterium*

tuberculosis and their association with phenotypic virulence in human macrophages. *Clin. Vaccine Immunol.* 14, 1279–1284.

World Health Organization [WHO] (2016). *Global Tuberculosis Report 2015*. Geneva: World Health Organization.

Yasui, K. (2014). Immunity against *Mycobacterium tuberculosis* and the risk of biologic anti-TNF-α reagents. *Pediatr. Rheumatol.* 12:45. doi: 10.1186/1546-0096-12-45

Zucchi, F. C., Tsanaclis, A. M., Moura-Dias, Q. Jr., Silva, C. L., Pelegrini-da-Silva, A., Neder, L., et al. (2013). Modulation of angiogenic factor VEGF by DNA-hsp65 vaccination in a murine CNS tuberculosis model. *Tuberculosis* 93, 373–380. doi: 10.1016/j.tube.2013.02.002

Conflict of Interest Statement: The authors declare that the research was conducted in the absence of any commercial or financial relationships that could be construed as a potential conflict of interest.

Copyright © 2018 Ranaivomanana, Raberahona, Rabarioelina, Borella, Machado, Randria, Rakotoarivelo, Rasolofo and Rakotosamimanana. This is an open-access article distributed under the terms of the Creative Commons Attribution License (CC BY). The use, distribution or reproduction in other forums is permitted, provided the original author(s) and the copyright owner are credited and that the original publication in this journal is cited, in accordance with accepted academic practice. No use, distribution or reproduction is permitted which does not comply with these terms.

frontiers in Immunology

ORIGINAL RESEARCH
published: 22 May 2017
doi: 10.3389/fimmu.2017.00534

Bovine WC1^{+} and WC1^{neg} γδ T Lymphocytes Influence Monocyte Differentiation and Monocyte-Derived Dendritic Cell Maturation during *In Vitro Mycobacterium avium* Subspecies *paratuberculosis* Infection

Monica M. Baquero and Brandon L. Plattner*

Department of Pathobiology, Ontario Veterinary College, University of Guelph, Guelph, ON, Canada

OPEN ACCESS

Edited by:
Geanncarlo Lugo-Villarino, UMR5089 Institut de Pharmacologie et de Biologie Structurale (IPBS), France

Reviewed by:
Paul M. Coussens, Michigan State University, USA
Jayne Hope, University of Edinburgh, UK

****Correspondence:***
Monica M. Baquero
mbaquero@uoguelph.ca

Specialty section:
This article was submitted to Microbial Immunology, a section of the journal Frontiers in Immunology

Received: *09 March 2017*
Accepted: *21 April 2017*
Published: *22 May 2017*

Citation:
Baquero MM and Plattner BL (2017) Bovine WC1+ and WC1^{neg} γδ T Lymphocytes Influence Monocyte Differentiation and Monocyte-Derived Dendritic Cell Maturation during In Vitro Mycobacterium avium Subspecies paratuberculosis Infection. Front. Immunol. 8:534. doi: 10.3389/fimmu.2017.00534

During early *Mycobacterium avium* subspecies *paratuberculosis* (*Map*) infection, complex interactions occur between the bacteria, cells from the mononuclear phagocyte system (MPS) including both resident (macrophages and dendritic cells) and recruited (monocytes) cells, and other mucosal sentinel cells such as γδ T lymphocytes. Though the details of early host–pathogen interactions in cattle remain largely underexplored, our hypothesis is that these significantly influence development of host immunity and ultimate success or failure of the host to respond to *Map* infection. The aims of the present study were to first characterize monocyte-derived MPS cells from young calves with respect to their immunophenotype and function. Then, we set out to investigate the effects of WC1^{+} and WC1^{neg} γδ T lymphocytes on (1) the differentiation of autologous monocytes and (2) the maturation of autologous monocyte-derived dendritic cells (MDDCs). To achieve this, peripheral blood WC1^{+} or WC1^{neg} γδ T lymphocytes were cocultured with either autologous freshly isolated peripheral blood-derived monocytes or autologous immature MDDCs (iMDDCs). We began by measuring several markers of interest on MPS cells. Useful markers to distinguish monocyte-derived macrophages (MDMs) from MDDCs include CD11b, CD163, and CD172a, which are expressed significantly higher on MDMs compared with MDDCs. Function, but not phenotype, was influenced by WC1^{neg} γδ T lymphocytes: viability of *Map* harvested from monocytes differentiated in the presence of WC1^{neg} γδ T lymphocytes (dMonWC1^{neg}) was significantly lower compared to MDMs and MDDCs. With respect to DC maturation, we first showed that mature MDDCs (mMDDCs) have significantly higher expression of CD11c, CD80, and CD86 compared with iMDDCs, and the phagocytic capacity of mMDDCs is significantly reduced compared to iMDDCs. We then showed that γδ T lymphocyte subsets induce functional (reduced phagocytosis) but not phenotypic (surface marker expression) iMDDC maturation. These data collectively show that γδ T lymphocytes influence differentiation, maturation, and ultimately the function of monocytes during

Map infection, which has significant implications on survival of *Map* and success of host defense during early *Map* infection.

Keywords: *Mycobacterium avium* subspecies *paratuberculosis*, γδ T lymphocytes, WC1, macrophages, monocytes, dendritic cells, mononuclear phagocyte system

INTRODUCTION

The mononuclear phagocyte system (MPS) comprises monocytes, macrophages, dendritic cells (DCs), and their precursors in the bone marrow (1). Myeloid progenitor cells give rise to circulating monocytes which migrate into various tissues where they function as resident tissue macrophages or DCs (2–4). A primary function of cells from the MPS under normal physiologic conditions is to maintain homeostasis in peripheral tissues (5). During inflammatory processes, they play a crucial role initiating and regulating immune responses by processing and presenting antigens to naïve T lymphocytes (6). Cells from the MPS share several surface markers and functions, making it difficult to clearly define the distinction between them (6). The phenotype of monocytes, macrophages, and DCs of humans and mice has been extensively studied and these cells have been classified according to the expression of specific markers [reviewed in Ref. (7)]. Classification of bovine DCs, including monocyte-derived dendritic cells (MDDCs) based on phenotype and function has been described [reviewed in Ref. (8)]; however, little is known about the phenotype and function of bovine monocytes, macrophages, and the expression of phenotypic surface markers after monocyte *in vitro* differentiation.

During initial exposure to pathogens at mucosal surfaces, cells from the MPS including tissue-resident macrophages and DCs interact with other immune cells, such as γδ T lymphocytes at mucosal surfaces. γδ T lymphocytes are considered to be a bridge between innate and adaptive immune systems. In cattle, γδ T lymphocytes are classified broadly as $WC1^+$ and $WC1^{neg}$ according to their expression of the workshop cluster 1 (WC1) molecule, which is a transmembrane glycoprotein belonging to the scavenger receptor cysteine-rich family (CD163) (9). $WC1^+$ γδ T lymphocytes are considered pro-inflammatory (9) and less is known about the function of $WC1^{neg}$ γδ T lymphocytes; however, it is believed that they are mucosal sentinel cells, given their presence at mucosal surfaces (10). Human and murine γδ T lymphocytes have been the most widely studied. In these species, γδ T lymphocytes recognize pathogen-associated molecular patterns (PAMPs) through pattern-recognition receptors (11), execute their effector functions without clonal expansion because they are not major histocompatibility complex (MHC)-restricted (12, 13), and present antigens to naïve αβ T lymphocytes (14). During adaptive immune responses, γδ T lymphocytes develop memory responses (15, 16), induce DC maturation (17), and polarize into T_H1-, T_H2-, T_H17-, T_{FH}-, or T_{REG}-effector functions based on the cytokine milieu in which γδ T lymphocytes encounter the antigen (17–20). In cattle, γδ T lymphocytes have shown to produce pro-inflammatory cytokines, such as IFN-γ and IL-17A (18–21), regulate granuloma development (22), have regulatory effects (23, 24), and modulate macrophage-effector functions (25, 26).

This work focuses on studying the specific interactions of bovine γδ T lymphocyte subsets with cells from the MPS in the context of *Mycobacterium avium* subspecies *paratuberculosis* (*Map*) infection *in vitro*. Macrophages and DCs are the primary host cells for *Map* (27, 28), an intracellular bacterium causing paratuberculosis, which is an important mycobacterial infection of ruminants. The disease is characterized by a long subclinical phase (>2 years) (27), followed by a clinical phase in which animals show diarrhea and weight loss caused by inadequate nutrient absorption as a result of progressive granulomatous enteritis (29).

Both γδ T lymphocytes and the MPS play critical roles during the early pathogenesis of *Map* infection in cattle: (1) macrophages are the preferred cell host and the main effector cell during *Map* infection (30); (2) *Map* also infects DCs (28); and (3) monocytes migrate into the intestinal tract during infection and differentiate into effector cells, presumably in the presence of both $WC1^+$ and $WC1^{neg}$ γδ T lymphocyte subsets (9, 31). Furthermore, we have previously shown that γδ T lymphocytes influence autologous monocyte-derived macrophage (MDM) effector functions of young calves and heifers during *Map* infection *in vitro* (25, 26). Therefore, the hypothesis for this study was that $WC1^+$ and $WC1^{neg}$ γδ T lymphocytes of young calves influence (1) monocyte differentiation and (2) DC maturation during *Map* infection *in vitro*. The specific aims of this study were to first characterize cells from MPS of young calves and then to understand how bovine $WC1^+$ or $WC1^{neg}$ γδ T lymphocytes influence autologous monocyte differentiation and DC maturation during *in vitro Map* infection.

MATERIALS AND METHODS

Animals and Blood Collection

All animal procedures in this study were approved by the Institutional Committee on Animal Care at the University of Guelph (Animal Utilization Protocol # 3373). All animals were randomly selected from the Elora Dairy Research Centre, where there is no official paratuberculosis herd certification program; however, the estimated prevalence is near zero in this herd, because it is under continual surveillance for *Map* infection by regular screening for *Map*-specific antibodies using ELISA. No positive antibody tests, clinical or suspect paratuberculosis cases have been diagnosed on this farm for several years. Approximately 120 mL of blood were collected *via* jugular venipuncture using EDTA vacutainer tubes (BD Biosciences, Mississauga, ON, Canada) from seven healthy Holstein calves between 30 and 40 days of age. Number of animals was selected based on sample power calculations. Additional 60 mL of blood from the same calves were collected in serum separator vacutainer tubes (BD Biosciences). Blood samples were stored at 4°C and promptly transferred to the laboratory.

Peripheral Blood Mononuclear Cells (PBMCs), MDMs, and MDDCs

Under sterile conditions, whole blood was diluted (1:1) with PBS containing 0.5% BSA. PBMCs were isolated from whole blood using Histopaque 1077 (Sigma Aldrich, Oakville, ON, Canada) density gradient centrifugation, counted using a Moxi Z cell counter (Orflo, Hailey, ID, USA), and resuspended in complete medium RPMI 1640 containing 2 mM of L-glutamine and 25 mM of HEPES (Gibco, Carlsbad, CA, USA) supplemented with 5×10^{-5} M 2-mercaptoethanol (Sigma Aldrich, Oakville, ON, Canada), with penicillin (1,000 U/mL), streptomycin sulfate (10 mg/mL), and amphotericin B (0.25 μg/mL) (Sigma Aldrich). Our source of serum was 10% autologous serum based on our previous findings that show that cells are not self-reactive to cytokines or other soluble mediators present in autologous serum (26). Cell suspensions were transferred to 175 cm^2 flasks (Corning, Tewksbury, MA, USA) at a concentration of 7.5×10^6/mL per flask. After 1 h of incubation at 37°C in 5% CO_2, non-adherent cells were collected by washing each flask 3× with PBS prior to lymphocyte staining and sorting. Adherent cells (monocytes) were detached from the flasks using TrypLE Express (Gibco), washed, counted, and resuspended in complete RPMI. 2×10^5 monocytes/well were cultured in 24-well flat-bottomed plates (Corning). To obtain MDMs, monocytes were incubated for 6 days in complete RPMI. To obtain iMDDCs, complete RPMI was supplemented with 200 ng/mL of recombinant bovine interleukin-4 (Kingfisher Biotech, MN, USA) and 100 ng/mL of recombinant bovine GM-CSF (Kingfisher Biotech). After 6 days of differentiation, cells were used in coculture assays as iMDDCs; some wells of iMDDCs were induced to maturity (mMDDCs) by adding 1 μL/mL of *Escherichia coli* LPS (Sigma Aldrich) to the cell culture for 48 h prior to use in coculture assays as previously described (32, 33).

γδ T Lymphocyte Sorting

Non-adherent cells collected from the original flasks were resuspended in PBS containing 0.5% BSA, incubated in the dark at 4°C for 15 min with WC1 γδ T lymphocyte monoclonal antibody (BAQ4A, N2 epitope, IgG1, Monoclonal Antibody Center, Washington State University) and γδ T cell receptor monoclonal antibody (GB21A, TCR1-N24 δ chain-specific, IgG2b, Washington State University), washed, and incubated in the dark at 4°C for 15 min with the secondary antibody PE-Cy7 (IgG1, Biolegend, San Diego, CA, USA) and DyLight 405 (IgG2b, Jackson ImmunoResearch, Suffolk, UK). After washing, stained cells were sorted by FACS (Aria IIu, BD Biosciences, Mississauga, ON, Canada). After sorting $WC1^+$ and $WC1^{neg}$ γδ T cell populations, cells were resuspended in complete RPMI. The purity of each subset was verified by FACS to be 85–95% and confirmation of a viability over 85% was assessed using the trypan blue exclusion assay described previously (34).

Cocultures

For monocyte differentiation assays, 1×10^6 sorted $WC1^+$ or $WC1^{neg}$ γδ T lymphocytes were added directly to wells containing 2×10^5 monocytes the same day of PBMC isolation (day 0). After 6 days, cultures of MDMs, iMDDC, monocytes differentiated in presence of $WC1^+$ (dMonWC1$^+$), or $WC1^{neg}$ (dMonWC1^{neg}) γδ T lymphocytes were obtained (**Figure 1**). For MDDC maturation assays, 1×10^6 sorted $WC1^+$ or $WC1^{neg}$ γδ T lymphocytes were added to wells containing 2×10^5 iMDDCs (day 6) for 48 h (iMDDC + $WC1^+$ and iMDDC + $WC1^{neg}$) (**Figure 4**).

Infection with *Map*

For monocyte differentiation assays on day six MDMs, iMDDC, dMonWC1$^+$, and dMonWC1^{neg} were infected. For MDDC maturation assays, γδ T lymphocyte subsets and bacterial suspensions of *Map* were added on day 6 to iMDDCs. Cell cultures were infected at a multiplicity of infection (MOI) of 10:1 for 48 h with an Ontario-derived clinical bovine *Map* strain (gc86). The *Map* strain was cultured in Middlebrook 7H9 broth supplemented with 10% OADC (oleic acid, albumin, dextrose, catalase) enrichment (BD Biosciences), 0.05% Tween 80 (Sigma Aldrich), and 2 mg/L of mycobactin J (Allied Monitor, Inc., Fayette, MO, USA) referred to below as 7H9-OADC-MJ-T. Optical density (OD) was measured with a spectrophotometer (Genesys 10S VIS, ThermoFisher Scientific, Waltham, MA, USA) at 540 nm wavelength and quantification of bacteria was performed using a standard growth curve. The bacterial suspension was briefly sonicated with a sonic dismembrator (Model 120, Fisher Scientific) at 60% amplitude during 2 s pulses to disperse bacterial clumps. Aliquots of *Map* with viability of 97.4% measured by fluorescein diacetate (Sigma Aldrich) as described previously (25) were kept at −80°C in saline to ensure that the same *Map* passage was used throughout this study.

Antibodies and Flow Cytometry

Antibodies used in this study are shown in **Table 1**. Cells were collected 48 h after *Map* infection into serum-free media before staining and assessment (FACSAria IIu, BD Biosciences). Viability was assessed using Zombie NIR fixable viability kit (Biolegend, CA, USA). The acquisition software used was FACS Diva II, and data were analyzed using FlowJo software (Treestar, Inc., San Carlos, CA, USA) (Figure S2 in Supplementary Material shows gating strategy).

DQ-Ovalbumin (DQ-OVA) Endocytosis Assay

DQ-ovalbumin was added at a concentration of 10 μg/mL to 60 μL of cell suspension (2×10^5 cells) of monocytes, MDMs, iMDDCs, mMDDCs, dMonWC1$^+$, dMonWC1^{neg}, iMDDC + $WC1^+$, or iMDDC + $WC1^{neg}$. Cells were incubated at 37°C for 45 min. After incubation, cells were washed with cold PBS and immediately analyzed by flow cytometry (FACSAria IIu, BD Biosciences) to measure the bright green fluorescence exhibited by the ovalbumin labeled with the pH-insensitive fluorescent dye, boron-dipyrromethene, upon proteolytic degradation after phagocytosis.

Map Viability

Forty-eight hours after *Map* infection of MDMs, iMDDCs, dMonWC1$^+$, or dMonWC1^{neg}, culture supernatants were collected and wells containing *Map*-infected cells were washed twice with

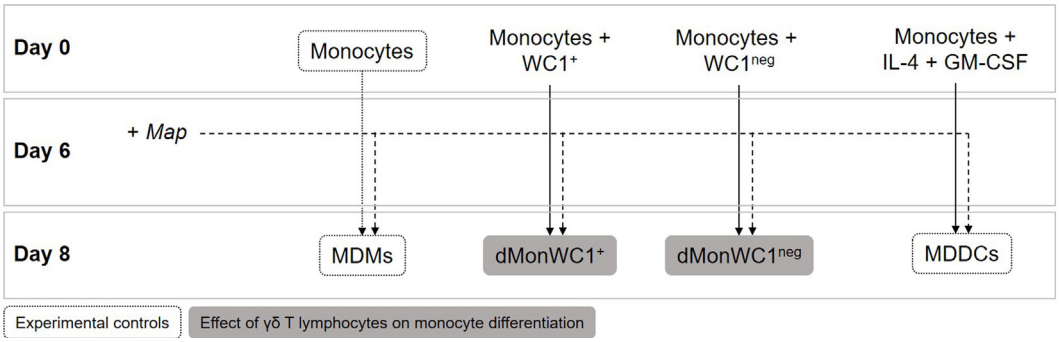


FIGURE 1 | Monocyte differentiation assays. 1×10^6 $WC1^+$ or $WC1^{neg}$ γδ T lymphocytes were added directly to wells containing 2×10^5 monocytes the same day of peripheral blood mononuclear cell isolation (day 0). After 6 days of differentiation, cultures of monocyte-derived macrophages (MDMs), monocyte-derived dendritic cells (MDDCs), monocytes differentiated in presence of $WC1^+$ (dMonWC1$^+$) or $WC1^{neg}$ (dMonWC1^{neg}) γδ T lymphocytes were obtained. On day 6, live *Map* was added at a multiplicity of infection of 10:1 to evaluate how it affected phenotype of MDMs, dMonWC1$^+$ and dMonWC1^{neg}; and MDDC after 48 h.

TABLE 1 | Anti-bovine monoclonal antibodies used for peripheral blood mononuclear cell immunophenotyping and coculture experiments.

Primary mAb	Clone	Isotype	Source	Secondary antibody	Source
Monocyte differentiation					
CD11c	BAQ153A	IgM	WSU[a]	PE/Cy7	Biolegend
CD163	LND68A	IgG1	WSU[a]	Pacific Orange	TFS[b]
CD11b	MM10A	IgG2b	WSU[a]	DyLight405	JIR[c]
CD14	CAM36A	IgG1	WSU[a]	AF647[d]	TFS[b]
R-PE-conjugated anti-CD1b	CC20	IgG2a	BioRad	–	–
R-PE/Cy5-conjugated anti-CD172a	CC149	IgG2b	BioRad	–	–
FITC-conjugated anti-CD205	CC98	IgG2b	BioRad	–	–
Monocyte-derived dendritic cell maturation					
Major histocompatibility complex (MHC)-I	B5C	IgG2b	WSU[a]	AF594	
MHC-II	H42A	IgG2a	WSU[a]	AF647	
R-PE-conjugated anti-CD86	ILA190	IgG1	LSBio	–	–
FITC-conjugated anti-CD80	ILA159	IgG1	BioRad	–	–

[a]*Washington State University, Monoclonal Antibody Center.*
[b]*ThermoFisher Scientific.*
[c]*Jackson ImmunoResearch.*
[d]*Zenon antibody labeling kit.*

warm PBS to remove free *Map*. Cells were then detached from the flasks using TrypLE Express (Gibco), centrifuged at 400 × *g* for 2 min, and resuspended in sterile saline solution. Cell suspensions were stored at −80°C until further analysis. After thawing, cell suspensions were vortexed vigorously for 10 s to lyse cells, centrifuged at 400 × *g* for 2 min, resuspended in 7H9-OADC-MJ-T, and incubated in 24-well plates for 24 h at 37°C in 5% CO_2. Contents of each well were centrifuged at 400 × *g* for 10 min and pellets were resuspended in 100 µL of saline solution in 5 mL conical tubes. One microliter of fluorescein diacetate at a concentration of 2 mg/mL (Sigma Aldrich) was added to each tube. After 30 min of incubation at 37°C, samples were analyzed by flow cytometry (Accuri C6, BD Biosciences). Standardization of the procedure and determination of gates were performed using a standard curve generated from known proportions of live and heat-killed *Map* as described previously (25).

Statistical Analysis

Statistical comparisons were performed using analysis of variance with SAS 9.4 software (SAS Institute, Cary, NC, USA) and GraphPad Prism 6.0 (GraphPad Software, La Jolla, CA, USA). The mean and SEM were calculated in experiments containing multiple data points. A *P* value of ≤0.05 was considered statistically significant.

RESULTS

Phenotypic and Functional Characterization of Bovine Cells from the MPS Show Clear Distinctions between MDMs and MDDCs

To determine the expression of MPS cell markers in this study, several cell types were defined: monocytes were freshly isolated by adherence; MDMs were collected from flasks after fresh adherent monocytes were cultured for 6 days; MDDCs were generated by adding IL-4 and GM-CSF to fresh adherent monocyte cultures (**Figure 1**). Monocytes display significantly lower expression ($p < 0.0001$) of CD14, CD11b, CD11c, and CD172a compared with MDMs or MDDCs (**Figure 2**). Fresh monocytes

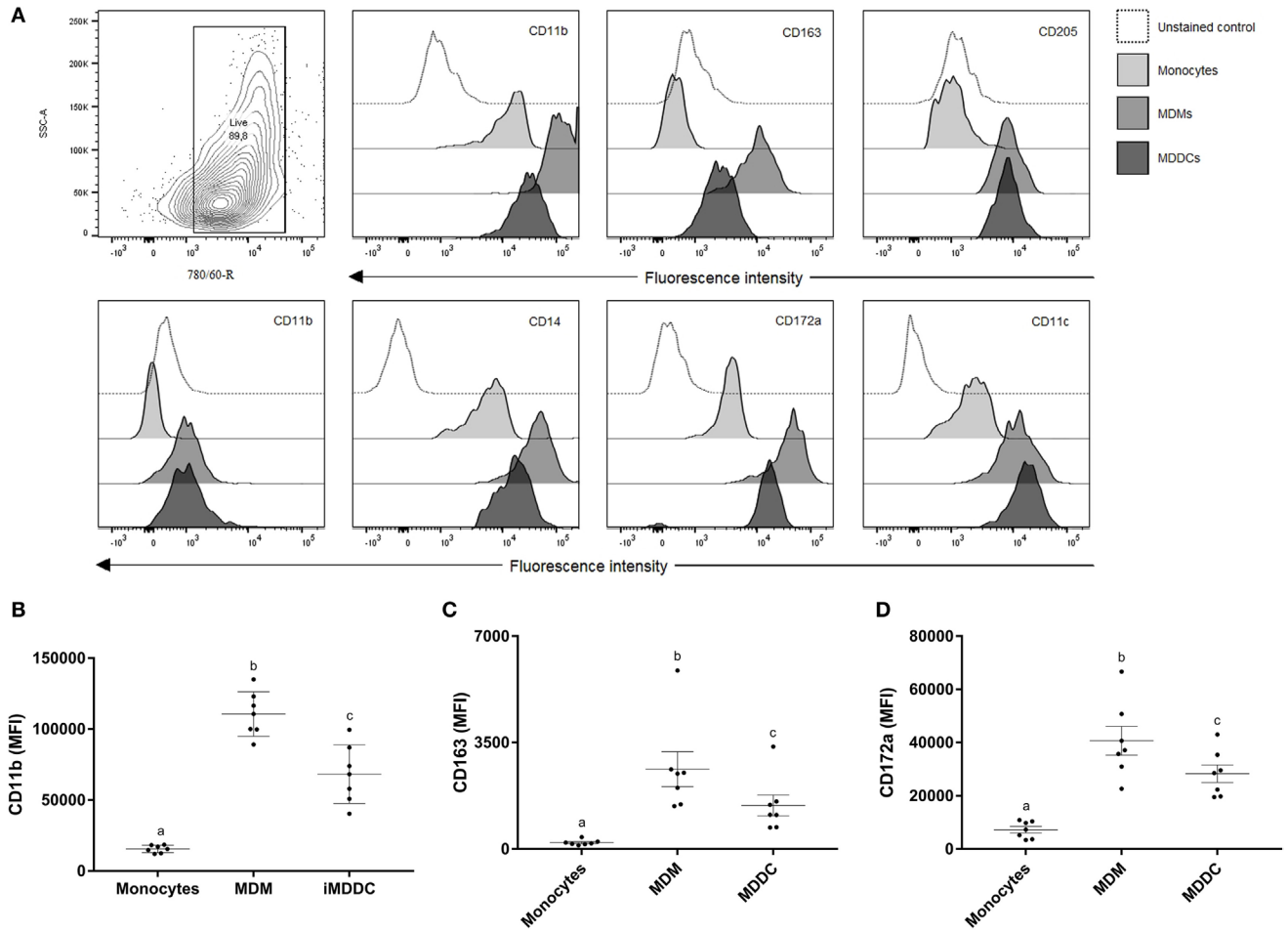


FIGURE 2 | Surface marker expression of cells from the MPS is heterogeneous. **(A)** Contour plot of live cell population and flow cytometry analysis of surface expression of CD11b, CD163, CD205, CD1b, CD14, CD172a, and CD11c on monocytes, monocyte-derived macrophages (MDMs), and monocyte-derived dendritic cells (MDDCs). CD11b, CD163, and CD172a are useful surface markers to distinguish MDMs from MDDCs **(B–D)**. Useful markers that distinguish MDMs from MDDCs include CD11b, CD163, and CD172a. Histograms of a representative animal are shown ($n = 7$). Different letters indicate statistically significant difference ($p < 0.05$).

lack expression of CD163, CD1b, and CD205. The markers that help to differentiate MDMs from MDDCs in our system are CD11b, CD163, and CD172a, which are each significantly higher on MDMs compared to MDDCs with p values of <0.0001, <0.0001, and 0.0333, respectively (**Figures 2B–D**). To establish the phagocytic capacity of MPS cells in our study, monocytes, MDMs, and MDDCs were assessed with the DQ-OVA endocytosis assay. As expected, our data show that MDMs had the highest phagocytic capacity followed by MDDC ($p = 0.0418$), while monocytes have minimal phagocytic activity compared with MDMs and MDDCs ($p < 0.0001$ and 0.0028, respectively) (**Figure 3A**). To compare the ability of MDMs and MDDCs to alter *Map* viability, the viability of *Map* recovered from MDMs and MDDCs 48 h after *in vitro* infection with live *Map* was evaluated by flow cytometry. No significant differences were found between the viability of *Map* harvested from MDMs and MDDCs ($p = 0.2929$) (**Figure 3B**).

The Presence of γδ T Lymphocytes during Monocyte Differentiation Does Not Affect Phenotype or Phagocytic Capacity; However, Viability of *Map* Recovered from dMonWC1^{neg} Was Significantly Lower

To analyze the effect of WC1^{+} or WC1^{neg} γδ T lymphocyte subsets on monocytes during differentiation, sorted WC1^{+} or WC1^{neg} γδ T lymphocytes were added to freshly isolated autologous monocytes, and the cells were left in direct contact for 6 days prior to assessment of MPS surface-marker expression (**Figure 1**). Our data show that the phenotype of monocytes differentiated after 6 days in presence of either WC1^{+} or WC1^{neg} γδ T lymphocytes (dMonWC1^{+} and dMonWC1^{neg}) was not significantly different from the phenotype of monocytes differentiated without γδ T lymphocytes (MDMs) in our system. The mean and SD median fluorescence intensity (MFI) of surface markers of MPS in this

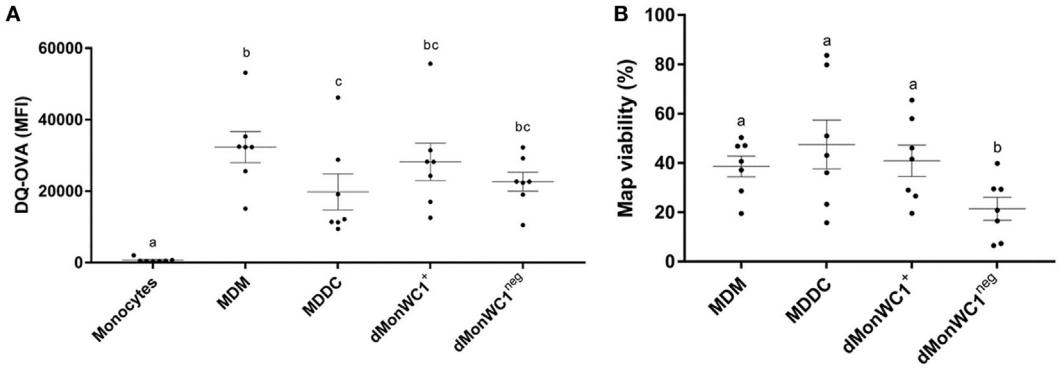


FIGURE 3 | Cells from the MPS have a heterogeneous phagocytic capacity and the presence of WC1^{neg} γδ T lymphocytes increase the ability of differentiated monocytes to alter *Mycobacterium avium* subspecies *paratuberculosis* (*Map*) viability. **(A)** Monocyte-derived macrophages (MDMs) had the highest phagocytic capacity, followed by monocyte-derived dendritic cell (MDDC). dMonWC1^{+} and dMonWC1^{neg} showed an intermediate phagocytic activity between MDMs and MDDC. **(B)** *Map* viability measured by flow cytometry after 48 h of infection of MDMs, MDDC, dMonWC1^{+}, and dMonWC1^{neg}. The viability of *Map* harvested from dMonWC1^{neg} was significantly lower compared to MDMs, MDDC, and dMonWC1^{+}. Results are individual animal data points and means ± SEM of seven animals. Different letters indicate statistically significant difference ($p < 0.05$).

study are shown in Table S1 in Supplementary Material. The phagocytic capacity of dMonWC1^{+} and dMonWC1^{neg} was assessed with the DQ-OVA endocytosis assay. dMonWC1^{+} and dMonWC-1^{neg} showed an intermediate phagocytic activity between MDMs ($p = 0.5403$ and 0.1582, respectively) and MDDC ($p = 0.3165$ and 0.8772, respectively) (**Figure 3A**). To determine the ability of dMonWC1^{+} and dMonWC1^{neg} to alter *Map* viability, the viability of *Map* recovered from these cells 48 h after live *Map* infection was evaluated by flow cytometry. The viability of *Map* harvested from dMonWC1^{neg} was significantly lower compared with the viability of *Map* harvested from either MDMs ($p = 0.0492$), MDDC ($p = 0.0044$), or dMonWC1^{+} ($p = 0.0277$) (**Figure 3B**).

Presence of Live *Map* Does Not Alter Phenotype or Functions of Cells from the MPS

To determine the effect of the presence of *Map* on the phenotype of MPS cells in this system, *Map* was added to cultures of MDMs, MDDC, dMonWC1^{+}, and dMonWC1^{neg} for 48 h (**Figure 1**). The effect of the presence of *Map* was examined by comparing the same cell type (i.e., uninfected MDMs vs. *Map*-infected MDMs). Our data show that infection of MDMs, MDDCs, dMonWC1^{+}, or dMonWC1^{neg} with *Map* did not significantly alter surface expression of CD163, CD1b, CD205, CD14, CD172a, CD11b, or CD11c at 48 h post infection (Table S1 in Supplementary Material).

MDDC Maturation Is Characterized by Upregulation of Surface Expression of MHC-I, CD80, and CD86, and Significant Reduction in Phagocytic Capacity

To examine the DC maturation process, iMDDCs were generated by adding IL-4 and GM-CSF to fresh peripheral blood-derived adherent monocyte cultures and their maturation was then induced by adding LPS for 48 h (**Figure 4**). As expected, our data showed that expression of MHC-I, CD80, and CD86 were significantly higher on mMDDCs compared with iMMDCs (**Figure 5**, $p = 0.0105$, <0.0001, and 0.0002, respectively); however, expression of MHC-II on mMDDCs was not significantly different from iMDDCs ($p = 0.0640$) (**Figure 5**). To study the effect of maturation of MDDCs on their phagocytic capacity, a DQ-OVA phagocytosis assay was performed on iMDDCs and mMDDCs using flow cytometry. Our data showed that the phagocytic capacity of mMDDCs was significantly reduced compared with iMDDCs ($p \leq 0.0001$, **Figure 6**).

WC1^{neg} γδ T Lymphocytes Increase MHC-II Expression on iMDDCs and Both γδ T Lymphocyte Subsets Reduce Phagocytic Capacity of iMDDCs

To determine the effect of WC1^{+} and WC1^{neg} γδ T lymphocytes on maturation of MDDCs, sorted γδ T lymphocyte subsets were added to iMDDCs for 48 h (**Figure 4**). iMDDC + WC1^{neg} had significantly increased expression of MHC-II compared with both iMDDC ($p = 0.0013$) and mMDDC ($p = 0.0046$) (**Figure 7**). Presence of γδ T lymphocytes did not affect the expression of CD80, CD86, and MHC-I on mMDDCs at 48 h post *Map* infection (data not shown). An interesting finding was increased individual variation of expression of MHC-II on mMDDCs compared with all iMDDCs, iMDDC + WC1^{+}, and iMDDC + WC1^{neg}, which may suggest that the DC maturation process varies widely between animals. To study the effects of WC1^{+} and WC1^{neg} γδ T lymphocytes on the maturation of MDDCs, γδ T lymphocytes were added to cultures of iMDDC for 48 h and then the DQ-OVA phagocytosis assay was performed using flow cytometry to measure changes in phagocytic ability. iMDDCs cultured in the presence of either WC1^{+} or WC1^{neg} γδ T lymphocytes had significantly reduced phagocytic ability compared to iMDDCs cultured without γδ T lymphocytes ($p = 0.0111$ and 0.0174, respectively) (**Figure 6**). These findings indicate that both γδ T lymphocyte subsets reduce phagocytosis by iMDDCs in our model.

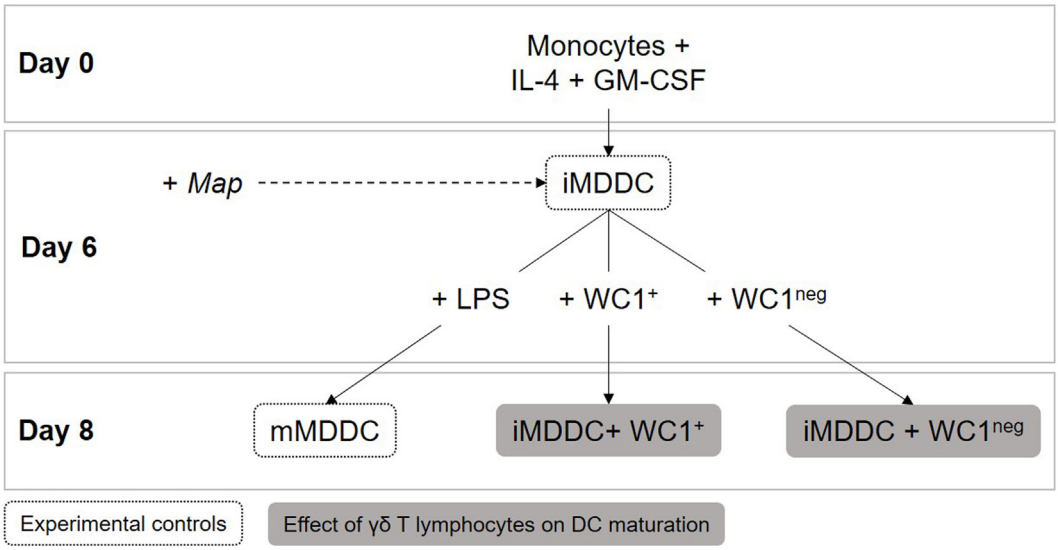


FIGURE 4 | **Dendritic cell maturation assays**. Immature monocyte-derived dendritic cells (iMDDCs) were generated by adding IL-4 and GM-CSF to fresh monocyte cultures. After 6 days of differentiation, 1×10^6 sorted γδ T lymphocytes were added to wells containing 2×10^5 iMDDCs for 48 h (iMDDC + WC1$^+$ and iMDDC + WC1^{neg}). On day 6, live *Mycobacterium avium* subspecies *paratuberculosis* was added at a multiplicity of infection of 10:1 to evaluate if it affected iMDDC maturation after 48 h.

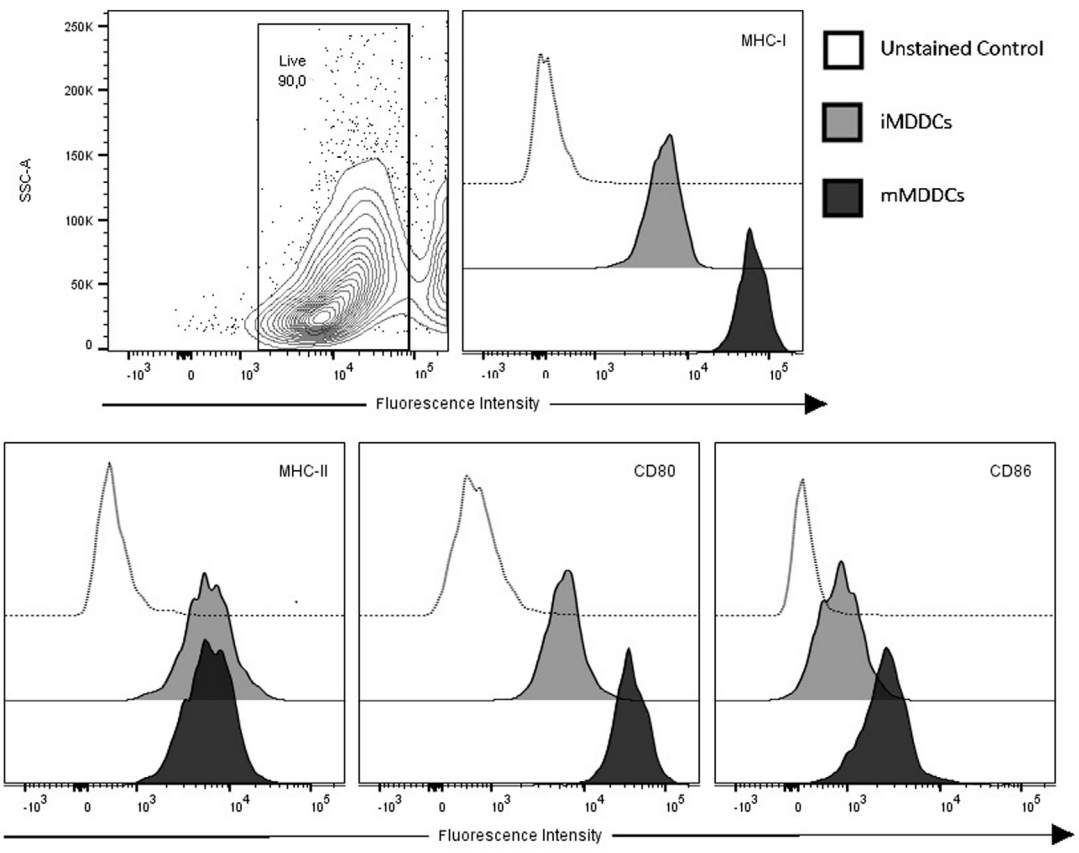


FIGURE 5 | **Monocyte-derived dendritic cells (MDDCs) upregulate surface expression of major histocompatibility complex (MHC)-I, CD80, and CD86 during maturation**. Contour plot of live cell population and flow cytometry analysis of surface expressions of MHC-I, MHC-II, CD80, and CD86 on immature MDDCs and mature MDDCs. Histograms of a representative animal are shown ($n = 7$).

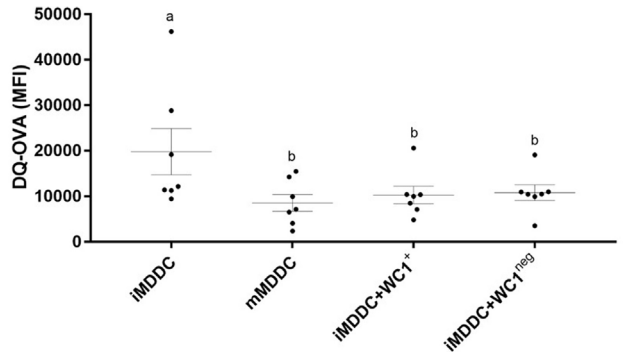


FIGURE 6 | γδ T lymphocytes induce monocyte-derived dendritic cell (MDDC) maturation. DQ-ovalbumin endocytosis assay on immature MDDC (iMDDC), mature MDDC (mMDDC), iMDDC + WC1+, and iMDDC + WC1neg. iMDDC + WC1+ and iMDDC + WC1neg had a reduction in their phagocytic ability in the same proportion as mMDDC. Results are individual animal data points and means ± SEM of seven animals. Different letters indicate statistically significant difference ($p < 0.05$).

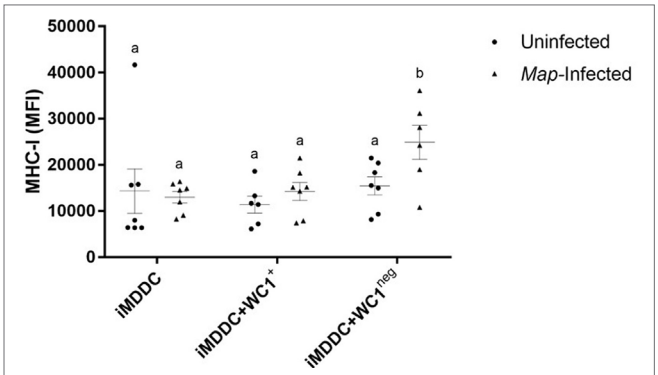


FIGURE 8 | Live *Mycobacterium avium* subspecies *paratuberculosis* (*Map*) was associated with significantly increased expression of major histocompatibility complex (MHC)-I on immature monocyte-derived dendritic cell (iMDDC) + WC1neg. Infection with live *Map* was associated with significantly increased expression of MHC-I on iMDDC + WC1neg. Median fluorescence intensity of MHC-I on iMDDCs, iMDDCs + WC1+, and iMDDCs + WC1neg. Results are individual animal data points and means ± SEM of seven animals. Different letters indicate statistically significant difference ($p < 0.05$).

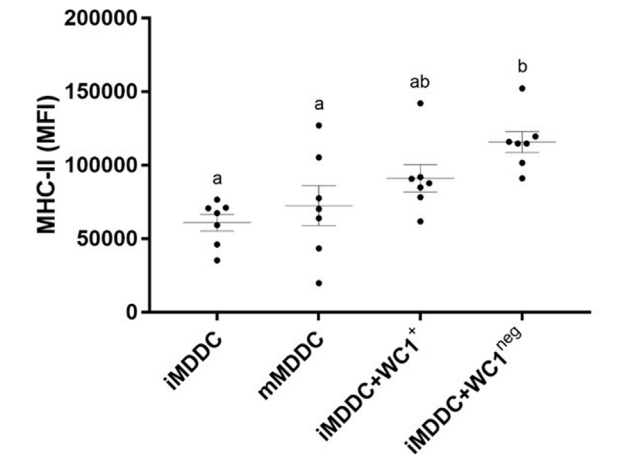


FIGURE 7 | WC1neg γδ T lymphocytes increase the antigen presenting ability of immature monocyte-derived dendritic cells (iMDDCs). Median fluorescence intensity of major histocompatibility complex-II on iMDDCs, mature MDDCs, iMDDCs + WC1+, and iMDDCs + WC1neg. Results are individual animal data points and means ± SEM of seven animals. Different letters indicate statistically significant difference ($p < 0.05$).

Live *Map* Was Associated with Significantly Increased Expression of MHC-I on iMDDC + WC1neg

To determine the effect of *Map* on maturation of MDDCs, live *Map* was added to cultures of iMDDC, iMDDC + WC1+, and iMDDC + WC1neg for 48 h (**Figure 4**). The presence of live *Map* was associated with significantly increased expression of MHC-I on iMDDC + WC1neg compared to iMDDC + WC1neg unexposed to *Map* ($p = 0.0090$) (**Figure 8**). The presence of live *Map* did not affect the expression of CD80, CD86, and MHC-II on MDDCs at 48 h post *Map* infection (data not shown).

DISCUSSION

During the development of host responses against pathogens, monocytes are recruited to the site of infection where they differentiate into effector cells amidst crosstalk with resident tissue immune cells (35, 36). After encountering an antigen, immature DCs begin their maturation process, migrate to local draining lymph nodes where they present antigen to naïve T lymphocytes to initiate, or perpetuate antigen-specific immune responses (37, 38). γδ T lymphocytes are resident sentinel cells in a variety of mucosal surfaces but especially in the ileum, where infection with *Map* is generally assumed to initially occur (39). In this study, we sought to first define and characterize MPS cells from young calves; using that information, we then set out to determine how WC1+ and WC1neg γδ T lymphocytes affect (1) monocyte differentiation and (2) DC maturation, both processes important to initiation and propagation of effective immune responses during infection by *Map* and other pathogens. For monocyte differentiation experiments, sorted peripheral blood derived WC1+ or WC1neg γδ T lymphocytes were cocultured with freshly isolated autologous monocytes for 6 days so that their phenotype and function could be compared with the experimental controls previously defined: monocytes, MDMs, and MDDCs. For DC maturation experiments, sorted peripheral blood WC1+ or WC1neg γδ T lymphocytes were cocultured for 48 h with iMDDCs and then compared with iMDDCs (without γδ T lymphocytes) and mMDDCs (obtained after stimulation of iMDDCs with LPS for 48 h).

Cells from the MPS share precursors as well as several surface markers and functions which makes it difficult to clearly distinguish between them (6). We show that freshly isolated peripheral blood monocytes express low levels of CD14, CD11b, CD11c, and CD172a and lack expression of CD163, CD1b, and CD205. These data are consistent with a recent review showing that bovine monocytes express CD172a but lack expression of CD1b and

CD205 [reviewed in Ref. (8)]. Other studies have defined three distinct phenotypic bovine monocyte subsets based on their variable surface expression of CD14 and CD16 among CD172a$^+$ cells (40). Expression of CD11c and CD172a is considered constitutive in bovine monocyte subsets, while expression of CD11b is variable (41). We did not find significant expression of CD163 on monocytes in our study; however, expression of CD163 has been described by others in bovine monocytes (41). A possible explanation for these contradictory findings is the utilization of different clones of the CD163 monoclonal antibody. We used a murine anti-bovine clone (LND68A) while Corripio-Miyar et al. (41) used human clone (EDHu-1); potential concerns regarding interspecies cross-reactivity of monoclonal antibodies have been published (42).

In our model CD1b, CD11c, CD14, and CD205 were all upregulated following *in vitro* differentiation of monocytes; however, these particular markers do not reliably distinguish MDMs from MDDCs. Our data do suggest that MDMs can be phenotypically distinguished from MDDCs because of significantly higher expression of CD11b, CD163, and CD172a on MDMs compared to MDDCs. Bovine MDDCs have been described as CD172a$^+$ while the expression of CD1b, CD11b, CD14, and CD205 vary depending on the subset of MDDC [reviewed in Ref. (8)]. MDMs have historically been classified by phenotype and function using surface-marker expression and cytokine-secretion profiles, respectively, but more recently classification of MDMs as either classically (M1) and alternatively activated (M2) macrophages using expression of CD163 has been described. M1 macrophages are CD163$^-$ and secrete pro-inflammatory cytokines while M2 macrophages are CD163$^+$ and secrete low levels of pro-inflammatory cytokines and high levels of IL-10 (43). In our *in vitro* model, we neither identified CD163$^-$ populations of MDMs nor assessed cytokine concentration in supernatants. Thus, further research is required to characterize and classify cells of the bovine MPS under different isolation (a.k.a. magnetic beads, FACS, adherence), culture conditions *in vitro* and evaluating other relevant surface markers such as CD209 (DC-SIGN) (44), CD16 (41), CD68 (45), and CD11a (46). Regardless, our data support the basic hypothesis that MPS cells comprise a complex network of distinct cell subsets that though they share some overlapping phenotypic and functional characteristics, they polarize depending on the local microenvironment for specific functions (47).

After coculturing freshly isolated blood monocytes with sorted WC1$^+$ and WC1^{neg} γδ T lymphocytes (dMonWC1$^+$ and dMonWC1^{neg}, respectively) during the differentiation process, our data indicate that the presence of γδ T lymphocytes has no phenotype-altering effect on monocyte differentiation. Viability of *Map* recovered from dMonWC1^{neg}, however, was significantly reduced suggesting that the presence of WC1^{neg} γδ T lymphocytes improves the ability of differentiated monocytes (dMonWC1^{neg}) to limit *Map* viability. In a previous study, we showed that the presence of either WC1$^+$ or WC1^{neg} γδ T lymphocytes cocultured with autologous *Map*-infected MDMs from 30- to 40-day-old calves was associated with reduced viability of *Map* recovered from MDMs (26). Taking into account that (1) in the previous study, MDMs were considered fully differentiated prior to the addition of γδ T lymphocytes into cocultures, (2) in the current study, significant differences were observed between the viability of *Map* recovered from dMonWC1$^+$ and dMonWC1^{neg}, and (3) when *Map* was introduced in the current study, WC1$^+$ and WC1^{neg} γδ T lymphocytes had been removed; we hypothesize that dMonWC1^{neg} are distinct from classical MDMs, and that WC1^{neg} γδ T lymphocytes alter the functional differentiation of peripheral blood monocytes. Based on these data, our hypothesis is that WC1^{neg} γδ T lymphocytes have a direct effect on transcription factor expression during monocyte differentiation resulting in a monocyte-derived cell with increased ability to limit *Map* viability. Because we have observed that the number of γδ T lymphocyte subsets within tissues of mucosal surfaces is variable between calves (unpublished data), we hypothesize that inter-animal variability also influences the different immune responses and disease outcomes that can be commonly observed within groups of calves (i.e., a herd with endemic *Map* infection). This inter-animal variability might explain why some animals (i.e., those with more WC1^{neg} γδ T lymphocytes or those that have more cognate γδ T lymphocyte/MPS cell interactions in the ileum) clear *Map* infection and do not progress to later stages of bovine paratuberculosis. Further studies are required to characterize the distribution and function of bovine γδ T lymphocytes in different mucosal and non-mucosal tissues.

To determine how γδ T lymphocyte subsets affect DC maturation, we first defined the characteristics of both iMDDC and mMDDC in our system by evaluating expression of specific maturation markers and co-stimulatory molecules. As expected and based on the current literature, our data confirm that MHC-I, CD80, and CD86 are useful markers to differentiate mMDDCs from iMDDCS because they are upregulated during the maturation process. Other bovine models have shown that *Salmonella typhimurium*-infected DCs had significantly increased expression of MHC-I, MHC-II, CD40, CD80, and CD86 (48). In our system, MHC-II was not upregulated on mMDDCs at 48 h post *Map* infection; however, the expression of MHC-II was highly variable between animals in our study. Inter-animal immune cell phenotypic variability has been well established in bovine studies of our lab and others (25, 26, 49), and the distinct pattern of high/low-effector functions and specific phenotypes in cattle is complex but probably explains an individual's unique ability to respond (or not) to infection. Timing may also have influenced our ability to detect early and transient changes in MHC-II expression. It is known that after stimulation of murine DC PAMPs receptors, MHC-II expression increases transiently but then decreases (50), though this phenomenon has not been shown in bovine DCs. Furthermore, it is known that MHC-II expression on bovine MDMs is downregulated between 24 and 48 h post *Map* infection (51) and because cells in this study were analyzed at only a single time point (48 h after *Map* infection), we may have thus been unable to detect early differences in the expression of MHC-II due to timing.

The presence of WC1^{neg} γδ T lymphocytes in our coculture experiment was associated with significantly increased expression of MHC-II on iMDDC + WC1^{neg} cells compared with iMDDCs and mMDDCs. Upregulation of MHC-II, along with CD86 and CD83 has also been induced by human Vγ9Vδ2 T lymphocytes on DCs, suggesting the ability of γδ T lymphocytes to specifically

promote DC maturation (17). Furthermore, human iMDDCs induce Vγ9Vδ2 T lymphocytes to secrete pro-inflammatory cytokines required for their own maturation (52). This reciprocal effect has not been definitively demonstrated in cattle, and further research is required to determine if bovine DCs could induce this effect on either $WC1^{+}$ and/or $WC1^{neg}$ γδ T lymphocytes.

A major functional change during MDDC maturation is reduced phagocytic capacity of MDDCs; this finding is supported by studies in adult cows (28). In our study, a reduced phagocytic capacity was observed in iMMDCs cocultured with either $WC1^{+}$ or $WC1^{neg}$ γδ T lymphocyte subsets, which suggests that $WC1^{+}$ or $WC1^{neg}$ γδ T lymphocytes induce "functional" MDDC maturation with respect to phagocytic capacity.

Our overall hypothesis was that early γδ T lymphocytes/MPS/*Map* interactions influence the initiation of early local host immunity and potentially the induction of adaptive immunity and progression or eventual outcome of *Map* infection. To test our hypothesis, we first needed to define the phenotype and effector functions of MPS cells specifically under *in vitro* conditions in our laboratory. We have shown that cells from the MPS can be distinguished by collective examination of phenotype and function: (1) monocytes lack the expression of CD1b, CD205, and CD163; (2) MDMs express higher levels of CD11b, CD163, and CD172a compared to MDDCs; (3) mMDDCs express higher levels of CD11c, CD80, and CD86 compared to iMDDC; mMDDCs have reduced phagocytic capacity compared to iMDDCs. In this study, the most significant findings related to the effect of γδ T lymphocytes include: (1) the presence of $WC1^{neg}$ γδ T lymphocytes contributes to differentiation of monocytes into cells with increased ability to limit *Map* viability and (2) both γδ T lymphocyte subsets induce functional MDDC maturation (reduced phagocytosis).

ETHICS STATEMENT

All animal procedures in this study were approved by the Institutional Committee on Animal Care at the University of Guelph (Animal Utilization Protocol # 3373).

AUTHOR CONTRIBUTIONS

MMB and BLP performed the experiments; designed the experiments; interpreted the data; drafted the manuscript; reviewed and approved the final version of the manuscript; agreed to be accountable for the content of the work.

ACKNOWLEDGMENTS

We thank John F. Prescott, Lucy Mutharia, Stefan Keller and Shayan Sharif for their scientific advice and Laura Wright for her collaboration during the blood collection.

FUNDING

This work was funded by The National Science and Engineering Research Council (NSERC) of Canada. We acknowledge The Vanier Canada Graduate Scholarship and the Colombian Administrative Department of Science, Technology and Innovation (Colciencias) for their financial assistance.

SUPPLEMENTARY MATERIAL

The Supplementary Material for this article can be found online at http://journal.frontiersin.org/article/10.3389/fimmu.2017.00534/full#supplementary-material.

REFERENCES

1. Hume DA. The mononuclear phagocyte system. *Curr Opin Immunol* (2006) 18:49–53. doi:10.1016/j.coi.2005.11.008
2. Hume DA, Ross IL, Himes SR, Sasmono RT, Wells CA, Ravasi T. The mononuclear phagocyte system revisited. *J Leukoc Biol* (2002) 72:621–7.
3. Wu L, Li CL, Shortman K. Thymic dendritic cell precursors: relationship to the T lymphocyte lineage and phenotype of the dendritic cell progeny. *J Exp Med* (1996) 184:903–11. doi:10.1084/jem.184.3.903
4. Manz MG, Traver D, Akashi K, Merad M, Miyamoto T, Engleman EG, et al. Dendritic cell development from common myeloid progenitors. *Ann N Y Acad Sci* (2001) 938:167–73; discussion 173–4. doi:10.1111/j.1749-6632.2001.tb03586.x
5. Jenkins SJ, Hume DA. Homeostasis in the mononuclear phagocyte system. *Trends Immunol* (2014) 35:358–67. doi:10.1016/j.it.2014.06.006
6. Strauss O, Dunbar PR, Bartlett A, Phillips A. The immunophenotype of antigen presenting cells of the mononuclear phagocyte system in normal human liver—a systematic review. *J Hepatol* (2015) 62:458–68. doi:10.1016/j.jhep.2014.10.006
7. Haniffa M, Bigley V, Collin M. Human mononuclear phagocyte system reunited. *Semin Cell Dev Biol* (2015) 41:59–69. doi:10.1016/j.semcdb.2015.05.004
8. Summerfield A, Auray G, Ricklin M. Comparative dendritic cell biology of veterinary mammals. *Annu Rev Anim Biosci* (2015) 3:533–57. doi:10.1146/annurev-animal-022114-111009
9. Rogers AN, Vanburen DG, Hedblom EE, Tilahun ME, Telfer JC, Baldwin CL. Gammadelta T cell function varies with the expressed WC1 coreceptor. *J Immunol* (2005) 174:3386–93. doi:10.4049/jimmunol.174.6.3386
10. Hedges JF, Cockrell D, Jackiw L, Meissner N, Jutila MA. Differential mRNA expression in circulating gammadelta T lymphocyte subsets defines unique tissue-specific functions. *J Leukoc Biol* (2003) 73:306–14. doi:10.1189/jlb.0902453
11. Hedges JF, Lubick KJ, Jutila MA. γδ T cells respond directly to pathogen-associated molecular patterns. *J Immunol* (2005) 174:6045–53. doi:10.4049/jimmunol.174.10.6045
12. Vantourout P, Hayday A. Six-of-the-best: unique contributions of γδ T cells to immunology. *Nat Rev Immunol* (2013) 13:88–100. doi:10.1038/nri3384
13. Tanaka Y, Morita CT, Tanaka Y, Nieves E, Brenner MB, Bloom BR. Natural and synthetic non-peptide antigens recognized by human γδ T cells. *Nature* (1995) 375:155–8. doi:10.1038/375155a0
14. Brandes M, Willimann K, Moser B. Professional antigen-presentation function by human gammadelta T cells. *Science* (2005) 309:264–8. doi:10.1126/science.1110267
15. Hartwig T, Pantelyushin S, Croxford AL, Kulig P, Becher B. Dermal IL-17-producing γδ T cells establish long-lived memory in the skin. *Eur J Immunol* (2015) 45:3022–33. doi:10.1002/eji.201545883
16. Murphy AG, O'Keeffe KM, Lalor SJ, Maher BM, Mills KHG, McLoughlin RM. *Staphylococcus aureus* infection of mice expands a population of memory γδ T cells that are protective against subsequent infection. *J Immunol* (2014) 192:3697–708. doi:10.4049/jimmunol.1303420
17. Ismaili J, Olislagers V, Poupot R, Fournié J-J, Goldman M. Human gamma delta T cells induce dendritic cell maturation. *Clin Immunol* (2002) 103:296–302. doi:10.1006/clim.2002.5218
18. Rhodes SG, Hewinson RG, Vordermeier HM. Antigen recognition and immunomodulation by gamma delta T cells in bovine tuberculosis. *J Immunol* (2001) 166:5604–10. doi:10.4049/JIMMUNOL.166.9.5604

19. Baldwin CL, Sathiyaseelan T, Rocchi M, McKeever D. Rapid changes occur in the percentage of circulating bovine WC1(+)gamma delta Th1 cells. *Res Vet Sci* (2000) 69:175–80. doi:10.1053/rvsc.2000.0410
20. Plattner BL, Huffman E, Jones DE, Hostetter JM. T lymphocyte responses during early enteric *Mycobacterium avium* subspecies paratuberculosis infection in cattle. *Vet Immunol Immunopathol* (2014) 157:12–9. doi:10.1016/j.vetimm.2013.11.001
21. Zarin P, Chen ELY, In TSH, Anderson MK, Zúñiga-Pflücker JC. Gamma delta T-cell differentiation and effector function programming, TCR signal strength, when and how much? *Cell Immunol* (2015) 296:70–5. doi:10.1016/j.cellimm.2015.03.007
22. Plattner BL, Doyle RT, Hostetter JM. Gamma–delta T cell subsets are differentially associated with granuloma development and organization in a bovine model of mycobacterial disease. *Int J Exp Pathol* (2009) 90:587–97. doi:10.1111/j.1365-2613.2009.00679.x
23. Hoek A, Rutten VP, Kool J, Arkesteijn GJ, Bouwstra RJ, Van Rhijn I, et al. Subpopulations of bovine WC1(+) gammadelta T cells rather than CD4(+) CD25(high) Foxp3(+) T cells act as immune regulatory cells ex vivo. *Vet Res* (2009) 40:6. doi:10.1051/vetres:2008044
24. Guzman E, Hope J, Taylor G, Smith AL, Cubillos-Zapata C, Charleston B. Bovine γδ T cells are a major regulatory T cell subset. *J Immunol* (2014) 193:208–22. doi:10.4049/jimmunol.1303398
25. Baquero MM, Plattner BL. Bovine WC1(+) γδ T lymphocytes modify monocyte-derived macrophage responses during early *Mycobacterium avium* subspecies paratuberculosis infection. *Vet Immunol Immunopathol* (2016) 170:65–72. doi:10.1016/j.vetimm.2015.12.002
26. Baquero MM, Plattner BL. Bovine peripheral blood WC1+ and WC1neg γδ T lymphocytes modulate monocyte-derived macrophage effector functions during in vitro *Mycobacterium avium* subspecies paratuberculosis infection. *Cell Immunol* (2017) 315:34–44. doi:10.1016/j.cellimm.2017.01.009
27. Subharat S, Shu D, Wedlock DN, Price-Carter M, de Lisle GW, Luo D, et al. Immune responses associated with progression and control of infection in calves experimentally challenged with *Mycobacterium avium* subsp. paratuberculosis. *Vet Immunol Immunopathol* (2012) 149:225–36. doi:10.1016/j.vetimm.2012.07.005
28. Lei L, Hostetter JM. Limited phenotypic and functional maturation of bovine monocyte-derived dendritic cells following *Mycobacterium avium* subspecies paratuberculosis infection in vitro. *Vet Immunol Immunopathol* (2007) 120:177–86. doi:10.1016/j.vetimm.2007.06.031
29. Fernández-Silva JA, Abdulmawjood A, Akineden Ö, Dräger K, Klawonn W, Bülte M. Molecular epidemiology of *Mycobacterium avium* subsp. paratuberculosis at a regional scale in Germany. *Res Vet Sci* (2012) 93:776–82. doi:10.1016/j.rvsc.2011.12.005
30. Mitchell RM, Gollnick NS, Sreevatsan S, Russell DG, Schukken YH. Quantification of *Mycobacterium avium* subsp. paratuberculosis (MAP) survival in monocyte-derived macrophages. *Vet Immunol Immunopathol* (2011) 139(1):73–8. doi:10.1016/j.vetimm.2010.08.003
31. Machugh ND, Mburu JK, Carol MJ, Wyatt CR, Orden JA, Davis WC. Identification of two distinct subsets of bovine gamma delta T cells with unique cell surface phenotype and tissue distribution. *Immunology* (1997) 92:340–5. doi:10.1046/j.1365-2567.1997.00350.x
32. Pinchuk L, Boyd B, Kruger E, Roditi I, Furger A. Bovine dendritic cells generated from monocytes and bone marrow progenitors regulate immunoglobulin production in peripheral blood B cells. *Comp Immunol Microbiol Infect Dis* (2003) 26:233–49. doi:10.1016/S0147-9571(02)00061-9
33. De Smedt T, Pajak B, Muraille E, Lespagnard L, Heinen E, De Baetselier P, et al. Regulation of dendritic cell numbers and maturation by lipopolysaccharide in vivo. *J Exp Med* (1996) 184:1413–24. doi:10.1084/jem.184.4.1413
34. Strober W. Trypan blue exclusion test of cell viability. *Curr Protoc Immunol* (2001) Appendix 3:Appendix 3B. doi:10.1002/0471142735.ima03bs21
35. Yoshihara K, Nagata R, Muneta Y, Inumaru S, Yokomizo Y, Mori Y. Generation of multinucleated giant cells in vitro from bovine monocytes and macrophages. *J Vet Med Sci* (2004) 66:1065–9. doi:10.1292/jvms.66.1065
36. Ingersoll MA, Platt AM, Potteaux S, Randolph GJ. Monocyte trafficking in acute and chronic inflammation. *Trends Immunol* (2011) 32:470–7. doi:10.1016/j.it.2011.05.001
37. Hope JC, Whelan AO, Hewinson R, Vordermeier M, Howard CJ. Maturation of bovine dendritic cells by lipopeptides. *Vet Immunol Immunopathol* (2003) 95:21–31. doi:10.1016/S0165-2427(03)00104-1
38. Alexis NE, Lay JC, Almond M, Bromberg PA, Patel DD, Peden DB. Acute LPS inhalation in healthy volunteers induces dendritic cell maturation in vivo. *J Allergy Clin Immunol* (2005) 115:345–50. doi:10.1016/j.jaci.2004.11.040
39. Koets A, Rutten V, Hoek A, van Mil F, Müller K, Bakker D, et al. Progressive bovine paratuberculosis is associated with local loss of CD4(+) T cells, increased frequency of gamma delta T cells, and related changes in T-cell function. *Infect Immun* (2002) 70:3856–64. doi:10.1128/IAI.70.7.3856-3864.2002
40. Hussen J, Düvel A, Sandra O, Smith D, Sheldon IM, Zieger P, et al. Phenotypic and functional heterogeneity of bovine blood monocytes. *PLoS One* (2013) 8:e71502. doi:10.1371/journal.pone.0071502
41. Corripio-Miyar Y, Hope J, McInnes CJ, Wattegedera SR, Jensen K, Pang Y, et al. Phenotypic and functional analysis of monocyte populations in cattle peripheral blood identifies a subset with high endocytic and allogeneic T-cell stimulatory capacity. *Vet Res* (2015) 46:112. doi:10.1186/s13567-015-0246-4
42. Cummings HS, Ploplis VA, Beals JM, Castellino FJ. Interspecies cross-reactivity of monoclonal antibodies to various epitopes of human plasminogen. *Arch Biochem Biophys* (1984) 230:306–15. doi:10.1016/0003-9861(84)90112-7
43. Verreck FAW, de Boer T, Langenberg DML, van der Zanden L,Ottenhoff THM. Phenotypic and functional profiling of human proinflammatory type-1 and anti-inflammatory type-2 macrophages in response to microbial antigens and IFN-gamma- and CD40L-mediated costimulation. *J Leukoc Biol* (2006) 79:285–93. doi:10.1189/jlb.0105015
44. Park KT, Burnett S, Davis WC. Development and characterization of a monoclonal antibody specific for bovine CD209. *Vet Immunol Immunopathol* (2015) 163(3):216–20. doi:10.1016/j.vetimm.2014.12.008
45. Kitani H, Yoshioka M, Takenouchi T, Sato M, Yamanaka N. Isolation and characterization of macrophages from a mixed primary culture of bovine liver cells. *Vet Immunol Immunopathol* (2011) 140(3):341–5. doi:10.1016/j.vetimm.2011.01.011
46. Hussen J, Koy M, Petzl W, Schuberth H-J. Neutrophil degranulation differentially modulates phenotype and function of bovine monocyte subsets. *Innate Immun* (2016) 22:124–37. doi:10.1177/1753425915620911
47. Mansouri-Attia N, Oliveira LJ, Forde N, Fahey AG, Browne JA, Roche JF, et al. Pivotal role for monocytes/macrophages and dendritic cells in maternal immune response to the developing embryo in cattle. *Biol Reprod* (2012) 87:123. doi:10.1095/biolreprod.112.101121
48. Norimatsu M, Harris J, Chance V, Dougan G, Howard CJ, Villarreal-Ramos B. Differential response of bovine monocyte-derived macrophages and dendritic cells to infection with *Salmonella typhimurium* in a low-dose model in vitro. *Immunology* (2003) 108:55–61. doi:10.1046/j.1365-2567.2003.01557.x
49. Umemura M, Yahagi A, Hamada S, Begum MD, Watanabe H, Kawakami K, et al. IL-17-mediated regulation of innate and acquired immune response against pulmonary *Mycobacterium bovis* bacille Calmette-Guerin infection. *J Immunol* (2007) 178:3786–96. doi:10.4049/jimmunol.178.6.3786
50. Casals C, Barrachina M, Serra M, Lloberas J, Celada A. Lipopolysaccharide up-regulates MHC class II expression on dendritic cells through an AP-1 enhancer without affecting the levels of CIITA. *J Immunol* (2007) 178:6307–15. doi:10.4049/JIMMUNOL.178.10.6307
51. Weiss DJ, Evanson OA, Mcclenahan DJ, Abrahamsen MS, Walcheck BK. Regulation of expression of major histocompatibility antigens by bovine macrophages infected with *Mycobacterium avium* subsp. paratuberculosis or *Mycobacterium avium* subsp. avium. *Infect Immun* (2001) 69:1002–8. doi:10.1128/IAI.69.2.1002-1008.2001
52. Devilder M-C, Maillet S, Bouyge-Moreau I, Donnadieu E, Bonneville M, Scotet E. Potentiation of antigen-stimulated V 9V 2 T cell cytokine production by immature dendritic cells (DC) and reciprocal effect on DC maturation. *J Immunol* (2006) 176:1386–93. doi:10.4049/jimmunol.176.3.1386

Conflict of Interest Statement: The authors declare that the research was conducted in the absence of any commercial or financial relationships that could be construed as a potential conflict of interest.

Copyright © 2017 Baquero and Plattner. This is an open-access article distributed under the terms of the Creative Commons Attribution License (CC BY). The use, distribution or reproduction in other forums is permitted, provided the original author(s) or licensor are credited and that the original publication in this journal is cited, in accordance with accepted academic practice. No use, distribution or reproduction is permitted which does not comply with these terms.

frontiers in Immunology

REVIEW
published: 30 November 2017
doi: 10.3389/fimmu.2017.01698

Myeloid Cell Interaction with HIV: A Complex Relationship

*Vasco Rodrigues[1], Nicolas Ruffin[1], Mabel San-Roman[2] and Philippe Benaroch[1]**

[1] Institut Curie, PSL Research University, INSERM U932, Paris, France, [2] Institut Curie, PSL Research University, UMR3216, Paris, France

Cells of the myeloid lineage, particularly macrophages, serve as primary hosts for HIV *in vivo*, along with CD4 T lymphocytes. Macrophages are present in virtually every tissue of the organism, including locations with negligible T cell colonization, such as the brain, where HIV-mediated inflammation may lead to pathological sequelae. Moreover, infected macrophages are present in multiple other tissues. Recent evidence obtained in humanized mice and macaque models highlighted the capacity of macrophages to sustain HIV replication *in vivo* in the absence of T cells. Combined with the known resistance of the macrophage to the cytopathic effects of HIV infection, such data bring a renewed interest in this cell type both as a vehicle for viral spread as well as a viral reservoir. While our understanding of key processes of HIV infection of macrophages is far from complete, recent years have nevertheless brought important insight into the uniqueness of the macrophage infection. Productive infection of macrophages by HIV can occur by different routes including from phagocytosis of infected T cells. In macrophages, HIV assembles and buds into a peculiar plasma membrane-connected compartment that preexists to the infection. While the function of such compartment remains elusive, it supposedly allows for the persistence of infectious viral particles over extended periods of time and may play a role on viral transmission. As cells of the innate immune system, macrophages have the capacity to detect and respond to viral components. Recent data suggest that such sensing may occur at multiple steps of the viral cycle and impact subsequent viral spread. We aim to provide an overview of the HIV–macrophage interaction along the multiple stages of the viral life cycle, extending when pertinent such observations to additional myeloid cell types such as dendritic cells or blood monocytes.

Keywords: macrophages, sensing, viral assembly, antiretroviral therapy, reservoir, virus-containing compartment, restriction factors

OPEN ACCESS

Edited by:
Christel Vérollet, Institut de Pharmacologie et de Biologie Structurale (IPBS), France

Reviewed by:
*Florent Ginhoux, Singapore Immunology Network (A*STAR), Singapore*
Quentin James Sattentau, University of Oxford, United Kingdom

****Correspondence:***
Philippe Benaroch
philippe.benaroch@curie.fr

Specialty section:
This article was submitted to Microbial Immunology, a section of the journal Frontiers in Immunology

Received: *05 October 2017*
Accepted: *17 November 2017*
Published: *30 November 2017*

Citation:
Rodrigues V, Ruffin N, San-Roman M and Benaroch P (2017) Myeloid Cell Interaction with HIV: A Complex Relationship. Front. Immunol. 8:1698. doi: 10.3389/fimmu.2017.01698

INTRODUCTION

The introduction of antiretroviral therapy (ART) to treat HIV infection in the mid 1990s was met with extraordinary success and dramatically improved the lives of patients, by turning a deadly infection into a manageable chronic disease. However, while able to prevent progression to AIDS, ART cannot eradicate HIV from the body, and a viral reservoir quickly rebounds after interruption of the therapy. In addition, HIV patients under suppressive therapy are at elevated risk of developing several non-AIDS related diseases, including cognitive impairment and cardiovascular problems.

HIV mainly replicates in CD4 T cells and macrophages in the body. Loss of CD4 T cells has long been known as the major pathological event leading to AIDS. In macrophages, HIV infection does not induce immediate cell death and viral replication proceeds for extended periods of time.

Macrophages maintain tissue homeostasis by performing crucial housekeeping tasks. Their ubiquitous distribution in the body allows HIV to disseminate into organs and tissues and establish compartmentalized infection. Macrophages are also an important effector arm of the innate immune system. These cells detect HIV infection and express cellular factors that severely restrain the capacity of the virus to replicate.

Here, we discuss the interplay between HIV and macrophages. We review recent work highlighting the unique interaction between HIV and macrophages, at the cellular level. We further discuss evidence pointing to a role for macrophages as cellular reservoirs of HIV during ART and how they participate in the pathological morbidities that prevail in patients under therapy.

MACROPHAGE ONTOGENY AND FUNCTION

Macrophages populate virtually all tissues of the body, where they perform a multitude of functions that are essential for tissue homeostasis, architecture, and protection (1). This wide range of macrophage action was described more than a century ago by Elie Metchnikoff. In his pioneering work, Metchnikoff observed the swarming and subsequent clearance of foreign objects by phagocytic cells in starfish larvae and water fleas (1). He correctly foresaw the importance of macrophages in the removal of obsolete cells, pathogen elimination, or sterile inflammation (2, 3).

Tissue macrophages have classically been considered as originating exclusively and in a continuous manner from bone marrow-derived monocytes, as part of the mononuclear–phagocyte system, a concept put forward by Van Furth in the 1970s (4). However, fate-mapping studies over the past decade have drastically changed our views on macrophage ontogeny. It is now widely accepted that many tissues are seeded with macrophages derived from the yolk sac or the fetal liver, during embryonic development [reviewed in Ref. (5)]. Once at their site of residency, macrophages proliferate locally to maintain a population size able to meet the requirements of the developing tissue or organ (6). The ability to self-renew suggests the existence of a subpopulation of tissue-resident macrophages with stem cell properties and capable of asymmetric cell division, but no such cell has yet been described in the tissues (6), with the possible exception of a subpopulation of epidermal Langerhans cells (7). Alternatively, the whole population of macrophages residing in a given tissue may be endowed with self-renewal potential, as suggested in studies with microglial cells or peritoneal macrophages (8–10). In some tissues, such as the brain or the liver, the resident macrophage population appears to be exclusively derived from embryonic cells throughout all adulthood (6). While monocytes may infiltrate these tissues under inflammatory or pathologic conditions, and differentiate into macrophages, they do not become part of the stable resident population (11). In stark contrast, embryonic macrophages that seed the gut prenatally appear to be completely replaced by monocyte-derived cells after birth (12). The factors that dictate this differential capacity of embryonically or monocyte-derived cells to stably engraft different tissues are not well understood and are an area of active research (6).

In their tissues of residency, macrophages perform a wide range of tasks. Some of these functions, such as apoptotic cell removal or extracellular matrix (MA) remodeling, are required in all tissues to different extents, indicating that macrophages are engaged in cross talks with their local microenvironment. The capacity to perform such general functions appears to be imprinted in the whole macrophage lineage and possibly involves the role of master transcription regulators such as PU (13). Other functions, by contrast, are specific to certain tissues. For instance, alveolar macrophages are specialized in clearing excessive surfactant, while macrophages of the red pulp of the spleen recycle iron from senescent erythrocytes (6). These site-specific functions are presumably imprinted on macrophages by tissue-specific signals and will induce transcriptional programs that define macrophage populations in different tissues (13).

Tissue macrophages are further subjected to environmental cues that occur in non-homeostatic conditions such as inflammation. Evolution has shaped macrophages as primary tissue sentinels (14). These cells are equipped with a broad range of receptors capable of detecting molecular patterns from all classes of microbes and multiple types of tissue damage, as well as receptors for chemokines and cytokines produced by immune cells (1). Integration of these multiple signals leads to what is commonly known as macrophage polarization (15). For instance, in an infected/inflamed tissue, macrophages may encounter microbial products such as LPS or be exposed to T cell-derived IFN-γ, leading to a polarized state known as M1, that is highly efficient in killing intracellular or ingested pathogens (15). Importantly, the majority of the knowledge gathered on macrophage polarization derives from well-defined *in vitro* experiments (16). These studies led to the M1 versus M2 model of macrophage polarization, which is unlikely to capture the complexity and the diversity of signals that macrophages can integrate *in vivo*. Furthermore, these polarizing stimuli act upon macrophages with previously imprinted tissue-specific programs. As such, similar polarizing signals probably lead to distinct phenotypes in macrophages from different tissues (13).

A wealth of information on the ontogeny, differentiation, and function of macrophages, derived from multiple studies in recent years, has profound implications in how we perceive the role of the macrophage in pathological settings, such as cancer, metabolic disease, or infections like HIV.

MACROPHAGES DURING ACUTE AND CHRONIC HIV INFECTION

The first description that tissue macrophages were permissive to HIV infection and capable of replicating the virus came in 1986, from the lab of Robert Gallo (17), amid the fast-paced period that characterized the early years of HIV/AIDS research. That very same pioneering study further provided the initial evidence that

macrophages produce HIV for extended periods of time, hence coping with viral-induced cytopathy (17). In addition, the study revealed that in macrophages, HIV accumulates in apparent intracellular compartments absent from T cells.

HIV can infect macrophages as these cells express both the viral entry receptor, CD4, and co-receptors, CCR5 and CXCR4, that bind the viral envelop protein, gp120. Macrophage infection by HIV requires initial adsorption of the virus to the cell surface, mediated by lectin-like receptors, integrins, and heparan sulfate proteoglycans (18). Entry then probably takes place following virion internalization into macropinosomes (19) or endosomes, where fusion between the viral envelope and the host cell appears to occur (20), as recently proposed by a study following the internalization of fluorescent quantum dots encapsulated by infectious HIV-1 particles in primary macrophages (21).

Classically, macrophage-tropic viruses (M-tropic) were thought to exclusively employ CCR5 for entry (R5 viruses), while CXCR4-using strains (X4 viruses) were viewed as unable to enter macrophages and establish productive infection (22). This simplified categorization of macrophage tropism based on co-receptor usage has been proven imperfect as many R5 viruses are unable to infect macrophages (23), whereas some X4 isolates can (24). While co-receptor usage may frequently predict macrophage tropism, categorizing a virus as M-tropic requires demonstration of its ability to replicate *in vitro* in macrophages, although, understandably, this may not be a practical approach to test every isolate (18).

Transmitted/founder (T/F) viruses are the viral variants that initiate infection in a new host, at genital or rectal mucosal surfaces. Their sequences can be inferred by the mathematical modeling of virus evolution after single-genome amplification analysis of the plasma viral population (25). These types of analyses, across multiple studies, support the idea that most infections are initiated by a single or a very limited number of founder viruses (26). Biological characterization of T/F viruses demonstrated that they are usually unable to replicate in macrophages (27, 28), possibly due to the lower densities of the CD4 molecule on the macrophage surface, as compared with CD4 T cells (29). This suggests that macrophages are not an important source of viral replication in the initial stages of infection, emerging only later, as the virus adapts to infect cells with a lower CD4 density at the surface. In agreement, studies with mucosal explants from the human reproductive tract (30–32), or in non-human primates (33) support the idea that $CD4^+$ T cells are the crucial targets at very early time points of infection.

Following migration from mucosal entry points into regional lymph nodes, *via* yet poorly described mechanisms, HIV rapidly disseminates systemically in the host. In SIV-infected rhesus macaques, viral spread to distal tissues such as the gastrointestinal (GI) tract or the spleen can be detected as early as 1 day after intravaginal inoculation and systemic distribution of SIV was observed by day 7 (34). This rapid but clinically silent spread is followed by the acute phase of HIV infection characterized by unrestrained viral replication in multiple tissues (35–37).

Macrophages are likely targets of HIV during the acute phase of infection, as viral nucleic acids have been detected in tissue macrophages from multiple organs in infected patients. These include Kupffer cells in the liver (38), microglial cells in the brain (39), alveolar macrophages in the lung (40), and intestinal macrophages obtained from several segments of the GI tract (41, 42). Importantly, replication-competent virus can be recovered from cultures of macrophages purified from lymphoid tissues of acutely infected rhesus macaques (43), implying that productive infection is taking place. It remains unclear how HIV disseminates to establish infection in these cells and tissues.

Monocytes can seed many tissues and differentiate locally into macrophages, turning this cell type into a potential vehicle for HIV dissemination across the myeloid compartment. Several reports claim indeed that replication of HIV-1 can take place *in vivo* in monocytes, even in patients under ART (44–46). Infected monocytes have been proposed to play a key role in viral dissemination to the brain due to their capacity to cross the blood–brain barrier (47), see Ref. (48).

At their sites of residency, macrophages constitutively patrol the tissues for danger signals, while also performing several housekeeping tasks. Interestingly, through the action of the viral accessory protein Nef, HIV is capable of reprogramming the migration of macrophages and selectively promotes a mesenchymal type of migration, while inhibiting the amoeboid type (49). The mesenchymal mode of migration is characterized by extensive extracellular MA remodeling, thus allowing the invasion of dense microenvironments, which may further promote viral dissemination and persistence. The relevance of these findings is supported by the increased accumulation of macrophages in the tissues of mice engineered to express the HIV Nef protein (49).

Alternatively, migratory, infected $CD4^+$ T cells may serve as vehicles for HIV systemic dissemination, as suggested by intravital microscopy in infected humanized mice (50), and possibly transmit the virus to tissue-resident macrophages. Interestingly, during the acute phase, SIV-DNA-positive myeloid cells present in lymphoid tissues also contain rearranged T cell receptor DNA (51). This suggests that phagocytosis of infected T cells allows macrophages to acquire viral DNA, which is presumably taken to the macrophage degradative compartments for destruction preventing potential infection of macrophages (51). However, at least *in vitro*, cultured macrophages become productively infected after ingesting infected T cells (52). This mode of direct T cell-to-macrophage HIV transmission results in more efficient macrophage infection than exposure to cell-free virus (52). While this mechanism has yet to be demonstrated *in vivo*, it seemingly represents a strategy employed by HIV to maximize its spread, by exploiting the extensive phagocytic capacity of macrophages (53).

Chronic untreated HIV infection leads to extensive depletion of the body's $CD4^+$ T cell pool and progression to AIDS (54). Concurrently, the viral population evolves to become more M-tropic (55), presumably because extensive $CD4^+$ T cell loss makes the macrophage the most abundant cell target in advanced disease. Rhesus macaques treated with an antibody depleting $CD4^+$ T cells before SIV infection mimic this advanced stage AIDS (56). In these animals, macrophages represent about 80% of the SIV-RNA^+ cells in the tissues with evidence of productive infection of macrophages from lymphoid tissues and the brain, frequently associated with activation markers. Remarkably, plasma viral loads were two logs higher in depleted animals as

compared with CD4+ T cell-sufficient controls, which led to rapid disease progression (56). Thus, in the context of CD4+ T cell depletion that might reflect the advanced AIDS status, extensive activation and viral replication in macrophages drives a precipitous progression of clinical disease.

MACROPHAGE SENSING OF HIV AND INTRINSIC RESTRICTIONS TO VIRAL REPLICATION

The macrophage paradox refers to the fact that macrophages represent both the first line of defense against many pathogens, including viruses, and yet are exploited by many of these pathogens as their favorite cellular niche for replication (57). Such is the case of HIV-1, which efficiently replicates in macrophages. However, as sentinel cells, macrophages are equipped with a range of sensors that detect ongoing infection at many steps of the viral cycle and trigger cellular responses that will activate antiviral immunity (58). A number of these induced antiviral effector genes, known as restrictions factors, will block infection at specific steps of the viral life cycle (59). Thus, from the viral perspective, the extent to which HIV-1 replicates in macrophages must be tightly regulated as to ensure viral transmission/dissemination, while avoiding significant antiviral responses. Such delicate balance is achieved by a combination of precise employment of viral accessory proteins and usurpation of the normal function of cellular factors. Complete reviews devoted to the various restriction factors are available (59), we will focus here on factors that play important roles in infected macrophages.

Studies examining the initial stages of the viral cycle, i.e., upon viral entry and retro-transcription (RT) of the viral RNA into cDNA in the cytosol, proposed that HIV-1 escapes early innate sensing in myeloid cells before viral DNA integration. This would result from a combination of shielding the newly synthesized cDNA by viral and cellular factors (60, 61), and maintenance of very low levels of cytosolic viral cDNA due to the action of the cellular nuclease TREX1 (62, 63). However, induction of a weak, yet detectable, interferon-stimulated gene (ISG) response after HIV-1 infection of macrophages has also been reported (64, 65), with type I IFNs levels remaining undetectable (64, 66).

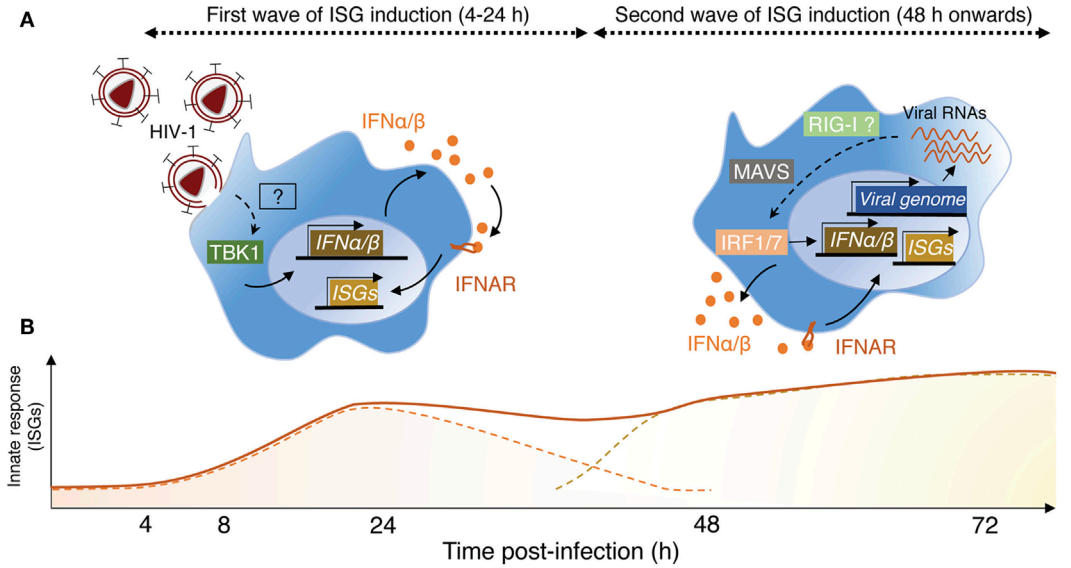
Examining these apparent discrepancies, we recently confirmed this transient response of monocyte-derived macrophages (MDMs) to HIV-1 infection, detectable as soon as 6 h postexposure and peaking at 24 h (67). Such response induces an ISG signature and depends on the induction of low levels of type I IFN. This sensing step is macrophage specific as it does not occur in monocyte-derived dendritic cells (MDDCs) exposed to HIV-1 (Decalf et al., unpublished results). The signal inducing the early ISG wave preceded reverse transcription but required viral fusion. Virus-like particles devoid of their genome, but capable of fusing, elicited a similar ISG response, indicating that viral nucleic acids were not implicated is this sensing step (67). Importantly, this early and transient ISG induction alone conferred partial protection to macrophages against subsequent HIV-1 infection. Different viruses carrying different envelopes and thus entering MDM although different receptors exhibited similar capacities to induce this response (67). The actual sensor of viral entry involved in this process remains to be identified. Membrane perturbations, such as fusion events, can elicit antiviral responses in macrophages, *via* the stimulator of IFN genes (STING)/tank-binding kinase-1 (TBK-1)/interferon-responsive factor-3 (IRF-3) pathway (68, 69). Thus, it is tempting to consider that the plasma membrane of the macrophage represents its first line of defense, and that sensing membrane perturbations, like viral entry, as soon as it occurs would be advantageous for the rapidity of the establishment of the antiviral response (**Figure 1**).

Retro-transcription represents a very specific and mandatory step for retroviral replication and is the target of SAM domain- and HD domain-containing protein 1 (SAMHD1), a major restriction factor for HIV-1 replication in macrophages and other cells of the myeloid lineage, such as DCs (71, 72). Upon fusion of the HIV envelope with the host cell membrane, the viral capsid (CA) is released into the cytoplasm and the viral reverse transcriptase initiates reverse transcription of the viral RNA genome. SAMHD1 restricts HIV infection by depleting the cytosolic pool of dNTPs available for reverse transcription, *via* its deoxynucleoside triphosphate triphosphohydrolase activity (73) and possibly also by directly attacking viral RNA *via* its ribonuclease activity (74). While HIV-1 has no known factor to counteract SAMHD1 restriction, HIV-2 and several SIV strains encode the accessory protein Vpx that targets SAMHD1 for degradation (71, 72). Yet, HIV-1 is capable of replicating in macrophages, suggesting alternative mechanisms to bypass restriction.

Cyclin-dependent kinases (CDKs) phosphorylate SAMHD1 in proliferating cells, halting its activity (75, 76). Interestingly, primary macrophages in culture spontaneously and temporarily enter a G1-like state, without progressing to actual cell division, leading to CDK1 induction that limits the levels of SAMHD1 in its active form (77). This provides HIV-1 with a window of opportunity, as the virus preferentially infects these G1-like phase macrophages (77). Importantly, microglial and peritoneal macrophages recovered from mouse tissues similarly exhibit spontaneous cycling between G0 and the G1 state, suggesting a relevance for this mechanism *in vivo* (77). Other recent studies reported elevated levels of different members of the cyclin family in macrophages, rendering them permissive to HIV-1 infection, further supporting an important role for cell cycle proteins in the mechanism through which HIV-1 bypasses SAMDH1 restriction (78, 79).

Packaging Vpx into HIV-1 virions leads to a strong increase in infection efficiency of macrophages and DCs (80). However, such increased infectivity comes at the cost of detection of the viral cDNA by the cytoplasmic DNA sensor cGAS and induction of antiviral type I IFN (63). This suggests that HIV-1, unlike HIV-2, adopts a strategy of co-habitation with SAMHD1 in myeloid cells to avoid triggering antiviral immunity (81).

There is, however, a second phase of ISG induction in macrophages, peaking around 96 h postinfection that requires retro-transcription (67) and viral integration (70). This response is induced by detection of newly transcribed viral RNA by the RNA sensor retinoic acid-inducible gene I, and it requires the activity of the trans-activating (tat) HIV-1 accessory protein, responsible for the elongation of HIV-1 transcripts (70). Together,



C

	First wave	Second wave
Viral Cycle Step	Unknown. Precedes reverse transcription. Possibly, viral fusion.	Post-integration. Requires transcription of the viral genome.
PAMP	Unknown. Does not require viral nucleic acids.	Viral RNAs (gRNA?).
PRR	Unknown. Possibly, perturbation of the plasma membrane as a result of viral fusion.	Not formally identified. Possibly RIG-I.
Downstream Signaling	TBK-1, induction of type I IFNs.	MAVS, IRF-1 and IRF-7, induction of type I IFNs.

FIGURE 1 | Schematic view of HIV-1 sensing by macrophages. **(A)** Macrophages sense HIV-1 at two independent steps of the viral cycle. *Left panel*—Early sensing of HIV-1 by macrophages requires viral fusion with the plasma membrane but precedes retro-transcription (RT). This sensing step is detectable by 4 h after cell exposure to the virus and declines after 24 h when RT is inhibited. While the actual sensor involved remains to be identified, it activates the kinase tank-binding kinase-1 (TBK1), leading to production of type I IFN, signaling *via* IFNAR, and triggering of interferon-stimulated genes (ISGs). *Right panel*—The second wave on HIV-1 sensing is measurable only 48 h after cell exposure to the virus. It requires integration of the viral genome in the host DNA and transcription of viral RNAs, which appear to be the viral component triggering the late ISG response. Here also, the actual sensor remains to be identified, but retinoic acid-inducible gene I (RIG-I) is a likely candidate as the signaling cascade involves the adaptor MAVS and IRF-1 and IRF-7, leading to type I IFN production. **(B)** Schematic representation of the two ISG waves induced by the sensing steps described in panel **(A)**. The full line represents the putative measurable ISG response, whereas the dashed lines indicate the contribution of the individual waves for the measurable response. **(C)** This table resumes the main characteristics associated with the two sensing mechanisms through which macrophages detect HIV-1 and was established based on Ref. (67, 70).

the two sensing steps confer an ISG signature in HIV-1-infected macrophages that may contribute to maintaining a low level of viral replication in this cell type (67, 70) (**Figure 1**).

Once viral proteins are produced, a key step in the assembly of new viral particles is the incorporation of the viral envelope. Two recently identified restriction factors, active in macrophages, target the viral envelope and thus reduce infectivity. Membrane-associated RING-CH 8 is highly expressed in myeloid cells where it retains the viral envelope glycoproteins intracellularly hence impairing their incorporation into the budding viral particles (82). The guanylate binding protein-5 (GBP5) is highly inducible by type I IFN and interferes with processing, trimming and incorporation of the HIV-1 envelope, rendering the produced virions less infectious (83). Interestingly, the viral genes encoding Env and the HIV-1 accessory protein Vpu are expressed from the same bicistronic RNA (84). Deletion of *Vpu* from the viral genome enhances Env expression and renders HIV-1 less susceptible to GBP5 restriction (83). These observations may explain the high frequencies of defective Vpu gene observed in M-tropic HIV-1 strains (85).

Not surprisingly, restriction also takes place during the late phase of HIV replication cycle in macrophages. Tetherin (or BST2) is an interferon-inducible transmembrane protein that restricts HIV-1 particle release by inserting its C-terminal end into the viral lipid bilayer (86). As a result, newly formed virions are unable to leave the surface of infected T cells; i.e., they stay tethered (87). Tetherin activity is counteracted by Vpu that mediates its surface downregulation and degradation (88). HIV-1 infection of macrophages upregulates tetherin in an apparently IFN-independent but Nef-dependent manner (89). However, despite the presence of Vpu, HIV-1-infected macrophages still express detectable levels of tetherin that appears to partially restrict viral particle release (89).

The interferon-induced transmembrane (IFITM) proteins belong to a small family of highly related proteins and act has

as broad restriction factors able to interfere with the replication of many viruses. These relatively short proteins (around 130 aa) were initially characterized for their capacity to protect IFITM expressing cells from HIV-1 infection (90, 91). In addition, viral particles produced by IFITM expressing cells exhibit a reduced infectivity due to their incorporation of IFITM into the viral envelope (92). Whether present in the membrane of the target cell or the viral particles, IFITM proteins appear to impair viral fusion. Of note, endogenous IFITM3 also inhibits cell-to-cell transmission, and its inhibitory effect is stronger when it is present in viral particles than when part of the target cell membrane (92). The mechanism of action of IFITM is still unclear but probably relies on their capacity to reduce the fluidity of the membranes where they insert, thereby preventing viral fusion (or hemifusion). The precise topology of IFITM proteins is probably key to understand how they work, but this aspect is still debated. Mutagenesis studies combined with secondary structure predictions indicate that IFITM3 is a type 2 transmembrane protein that possesses an amphipathic helix adjacent to two palmitoylated cysteines (93). Silencing of IFITM1, 2, and 3 in HIV-1 producing cells resulted in increased infectivity of the viruses released (94). Importantly, the impact of such silencing was more striking in MDM than in any other cell type (94), raising the possibility that IFITM expression induced early in HIV-1-exposed MDM, as we documented (67), reduces the infectivity of the viral progeny.

In conclusion, low-level sensing of HIV-1 by macrophages results in the induction of a panoply of restriction factors that severely restricts infection. This antiviral state still allows for a certain degree of replication-competent viral production and may explain why HIV-1-infected macrophages are so resistant to the cytopathic effects that the virus exhibits in other cell types. The net effect, however, is that macrophages produce HIV-1 for extended periods of time which may favor long-term viral persistence.

CELL BIOLOGY OF HIV ASSEMBLY IN MACROPHAGES: FROM GAG SYNTHESIS TO PARTICLE RELEASE

In $CD4^+$ T cells and model cell lines, HIV assembly and budding take place at the plasma membrane. By contrast, in infected macrophages HIV buds into an apparently intracellular compartment, known as the virus-containing compartment (VCC). The VCC is a unique compartment with topological and biochemical properties distinct from late endosomes or multivesicular bodies, see Ref. (95). Indeed, the VCC (i) lacks classical markers of endosomal and lysosomal compartments (96, 97); (ii) possesses a near neutral pH (97); and (iii) is connected to the extracellular milieu making its lumen accessible to small membrane-impermeable dies (96, 98–100). The compartment consists of a complex membranous system of interconnected tubules and vesicles enclosing immature and mature viral particles in its lumen as well as budding virions in its limiting membrane (99) (**Figure 2**). The limiting membrane of the VCC possesses specific biophysical properties due in part to the particular membrane topology of the proteins that are inserted and the presence of high levels of cholesterol (101).

Evidence supports the notion that the VCC originates from intracellular sequestration of domains of the plasma membrane with a specific protein and lipid composition (102, 103). Cell surface proteins found in the limiting membrane of the VCC include the tetraspanins CD9, CD53, CD81, and CD82 (96, 104) that provide membrane rigidity; the scavenger receptor CD36 (105) that contains two cytoplasmic tails; CD44 (98), a receptor with promiscuous capacity to bind numerous ligands; and MHC II complexes (106) (**Figure 2**). The restriction factors IFITM, with their peculiar topology of membrane insertion, are incorporated into viral membranes, especially in viruses produced by MDM (94), and may therefore also associate with the limiting membrane of the VCC, potentially contributing to a decreased membrane fluidity. As in T cells, the ESCRT complex is in charge of promoting the fission of nascent particles (107) and ESCRT III proteins that are key players in the late abscission process have been found at the VCC limiting membrane (108). Further supporting a surface origin for the VCC, fluorescence recovery after photobleaching (FRAP) experiments demonstrated that the VCC limiting membrane and the plasma membrane are in rapid equilibrium (102).

Given that newly formed particles bud away from the cytosol toward the lumen of the VCC, they become wrapped with VCC-derived membrane (**Figure 2**). The proteomic analysis of purified HIV-1 particles released by infected MDM published more than 10 years ago (109) thus reflects the protein composition of the VCC limiting membrane, and still represents a valuable source of information. Studies published thereafter indeed confirmed not only the presence of the given proteins at the VCC limiting membrane but also revealed their role in the viral assembly process [see, for instance, CD36 (105), IFITM (94), and CD18 or Filamin A (110)].

An issue debated since the initial characterization of the VCC is whether some degree of viral budding can also occur at the surface of the macrophage. Indeed, some studies claimed that budding at the surface occurs alongside budding at the VCC (99, 111). A recent study provided an exhaustive examination of the site of virion assembly in individual macrophages by using a viral mutant arrested at the budding stage (103). Although such arrested buds could potentially move toward the plasma membrane, the analysis indicated that only about 5–12% of budding events occur at the cell surface. Moreover, these events were concentrated in the region where the VCC connected with the surface (103). These observations confirm that the VCC is the primary site of HIV assembly in macrophages, while budding at the surface is, at best, rare.

Thus, the specific lipid and protein composition of the limiting membrane of the VCC seem to constitute an assembly platform (101, 112), and presumably possess specific properties required for assembly and budding. However, which cellular and viral determinants direct HIV assembly and budding in macrophages to the VCC, remain poorly elucidated. The Gag polyprotein precursor drives the multistep process of HIV assembly and coordinates the activity of the cellular players involved. Recent studies indicate that viral genomic RNA is an important player/cofactor in the viral assembly process. Using elegant cross-linking immunoprecipitation sequencing coupled to membrane flotations, Kutluay

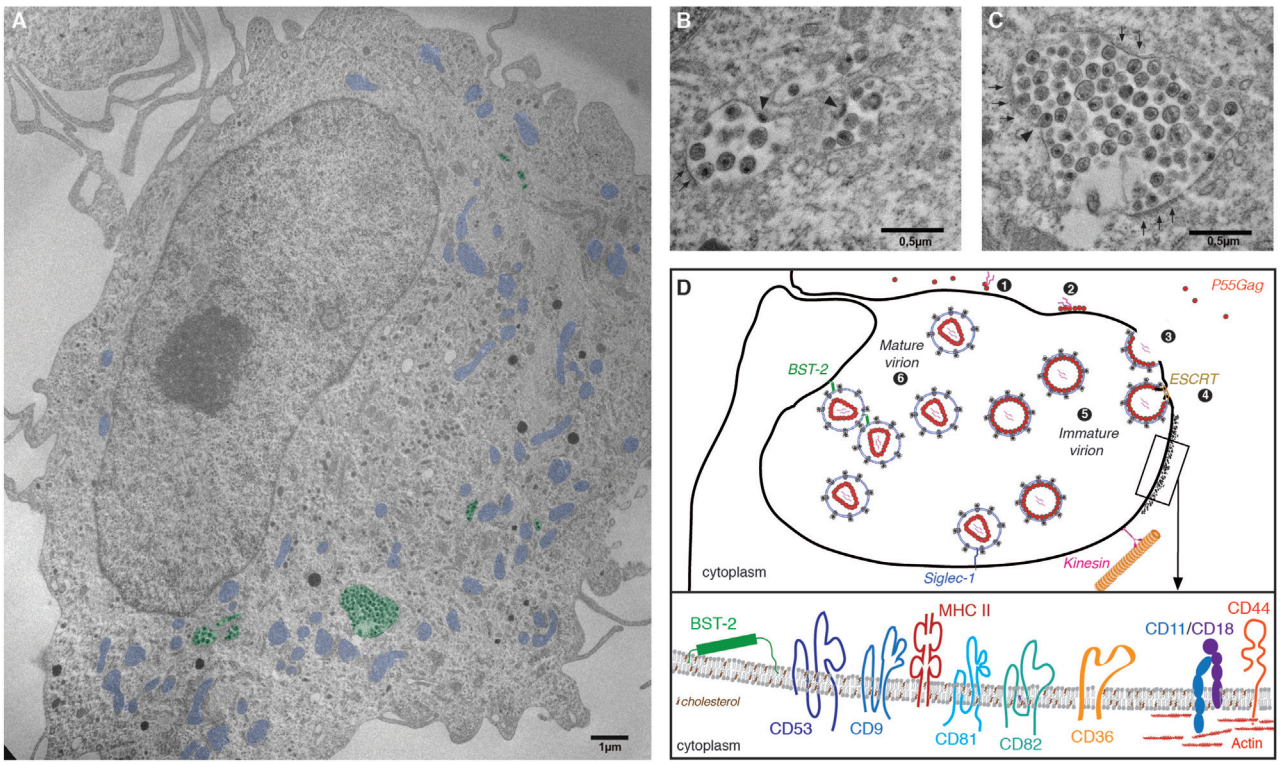


FIGURE 2 | The virus-containing compartment (VCC) in macrophages. **(A)** Electron micrograph depicting HIV-1-infected monocyte-derived macrophages (MDMs). MDMs were differentiated from monocytes purified from the peripheral blood of healthy human donors, by culture over 7 days in the presence of M-cerebrospinal fluid. Cells were then infected with HIV-1 NL-AD8 and fixed and embedded in epon 5 days postinfection. Ultrathin sections were processed for electron microscopy and imaged using a Philips 120 keV. For clarity, VCC is pseudo-colored in green and mitochondria in blue. **(B,C)** Magnifications of VCC present in the MDM depicted in panel **(A)**. Arrowheads indicate viral buds. A thick molecular coat, electron dense and often associated with the VCC limiting membrane of the VCC can be seen in panel **(C)**, see arrowheads. **(D)** Schematic representation of the late phases of the HIV life cycle in macrophages. (1) Gag monomers initiate oligomerization in the cytoplasm, forming dimers with the viral genomic RNA and (2) subsequently bind the plasma membrane *via* interactions with acidic phospholipids. (3) In macrophages, high-order Gag multimerization and formation of a viral bud only occurs at the limiting membrane of the VCC. (4) Gag subsequently recruits the components of the ESCRT complex that ensure fission of the budding viral particle into the lumen of the VCC. (5) Immature viral particles accumulate inside the VCC and (6) convert into mature viral particles *via* the activity of the viral protease. The restriction factor BST2/tetherin and Siglec-1/CD169 may contribute to the retention of viral particles within the lumen of the VCC. The limiting membrane of the VCC is tightly associated with the microtubule network on which kinesins may drive the transport of the VCC toward the cell periphery. *Inset*: Magnification of a region associated with a molecular coat: the VCC limiting membrane constitutes a platform for viral assembly where Gag oligomerization will lead to virus production. Therefore, the viral and VCC membranes share similar composition. They are enriched in particular lipids such as cholesterol and transmembrane proteins. These include the tetraspanins CD9, CD53, CD81, and CD82, the scavenger receptor CD36, the integrins CD18/CD11, or the surface glycoprotein CD44 (see text for details and references). The electron micrograph depicted in this figure panel results from original work performed in our lab and has not been published elsewhere previously.

et al. established that assembly starts in the cytoplasm where monomers and dimers of newly synthesized Gag bound to viral genome accumulate (113, 114). Oligomerization of Gag requires interactions with membrane enriched in cholesterol (115), *via* its MA domain that directly binds to membrane phosphatidylinositol 4,5-bisphosphate (PI(4,5)P2) (116) [see Ref. (112)]. The levels of PI(4,5)P2 in the VCC are similar to those at the surface (102) and hence should not be a determining factor that directs viral assembly to the VCC. Assembly of the viral particle at the membrane is coordinated *via* lateral interactions promoted by the CA and nucleocapsid (NC) domains of Gag, leading to a nascent virion that buds off the membrane (117). Gag possesses two RNA binding domains (NC and MA) with different specificities (115). In addition, the RNA binding specificities for the viral genome versus cellular RNA, i.e., mRNA and tRNA, present in the cytosol change during these processes finally promoting packaging of viral genomic RNA into the nascent viral particles (115).

Aiming to elucidate the role of the viral factors dictating the assembly site of HIV in macrophages, Inlora and colleagues evaluated the impact of targeted deletions or mutations in the different Gag domains, on virion assembly at the VCC (118). Viral mutants unable of high-order multimerization, due to NC substitutions, distributed equally between the VCC and the cell surface (118). This indicates that Gag initially binds the membrane arbitrarily at the surface membrane or the VCC and initiates low-order multimerization. However, in macrophages, high-order multimerization and complete virion assembly occur at the VCC but not at the surface.

Assembly of the polyprotein Gag precursor leads to the formation of a bud head and stalk. Gag further coordinates

the recruitment of important cellular factors. These include the ESCRT proteins; key players critically required for proper abscission of the nascent viral particles. Gag recruits components of the ESCRT complex through its late p6 C-ter domain, thus promoting severance of the viral stalk and particle release in the VCC. The precise molecular mechanisms involved in membrane abscission have stimulated numerous studies and corresponding excellent reviews [see, for instance, Ref. (107, 119)], and thus will not be discussed here.

The molecular players implicated in the establishment and maintenance of the VCC's intricate architecture remain poorly characterized. The cytoskeleton appears to play a key role in maintaining the integrity of the VCC. Indeed, a meshwork of filamentous actin surrounds the VCC and treating MDMs with actin-depolymerizing agents causes dispersion of the VCC throughout the cell (102). Moreover, the VCC limiting membrane is often surrounded by an electron dense and thick molecular coat visible by EM and containing CD18, a β2 integrin and its associated α integrins CD11b and CD11c (**Figure 2**) (120). Proteins known to interact with integrins are also associated with the molecular coat, including actin and focal adhesion scaffold/linker proteins such as talin, vinculin, and paxillin (120). These adherent complexes appear to be involved in the maintenance of the architecture of the VCC; however, CD18 silencing does not affect the amount of virus released nor its infectivity (120). Links between VCC and the autophagy machinery in HIV-1-infected macrophages have been investigated in a few studies that should be extended in the future (121).

The VCC limiting membrane appears tightly associated with the microtubule network and disruption of this network by nocodazole exposure leads to relocalization of the VCC into the perinuclear area (122). This suggested that kinesins, molecular motors associated with microtubules, could be involved in maintaining the correct positioning of the compartment. The kinesin II, KIF3A, is closely associated with VCCs in infected macrophages (122). Moreover, time-lapse microscopy in primary MDM showed paired movements of Gag and KIF3A. Importantly, KIF3A silencing in HIV-1-infected macrophages reduced viral particle release and increased intracellular Gag and the VCC volume. Overall, KIF3A is likely involved in the transport of the VCC along microtubules and toward the macrophage periphery or provides a force for particle release from the VCC (122). Other molecular motors are likely involved in the transport and positioning of the VCC but also in transport steps of viral components toward the assembly sites, i.e., the VCC (123). Future work will aim to establish at the molecular level how viral release from VCC is regulated.

While the VCC is defined by its viral content, the question of its induction by HIV or its existence in macrophages before infection was of interest. Analysis of primary MDMs by ultrastructural approaches suggested that indeed similar compartments are present in non-infected macrophages (96, 99, 120). Confocal microscopy confirmed the presence in non-infected MDMs of compartments sharing specific features with the VCC; i.e., containing CD36 and CD9, rapid accessibility to small dextran and therefore connected to the external medium (105). The direct proof of HIV capacity to highjack such compartments was obtained when transduced macrophages exhibiting CD36-GFP$^+$ compartments were subjected to time-lapse epifluorescent microscopy after infection with HIV-1 Gag-iCherry allowing the visualization in real time of Gag recruitment and accumulation only to preexisting CD36$^+$ compartments (105). Thus, in macrophages, HIV-1 hijacks these CD36$^+$ compartments for viral assembly (105), and expands them (96).

Viral particles accumulate in the VCC over time (100). Infected MDMs initially contain sparse, barely filled VCCs, but as the time after infection progresses the compartments become crowded with virions and Brownian-like movements of particles within the VCC become highly limited as shown by FRAP experiments (100). In parallel, viral release into the extracellular media decreases over time, suggesting that viral particles remain within the VCC (100). The restriction factor tetherin is concentrated in the VCC where it may connect viral particles to each other or to the VCC limiting membrane, hence apparently tethering virions to the compartment (89, 124). Indeed, silencing tetherin expression increases viral release and reduces the size of the compartment (89).

Whether HIV-1 release from the VCC is inducible remains indeed elusive. The connections between the VCC and the membrane appear too narrow to allow passive viral diffusion to the extracellular media (99). The release of HIV-1 from infected MDMs can be induced by exposure to extracellular ATP, *via* activation of the P2X7 purinergic receptor that triggers a drastic remodeling of the cytoskeleton and the VCC, accompanied by sudden release of the viral particles packed within the VCC (125). However, we also propose that the highly dynamic nature of the plasma membrane of macrophages, which is subjected to a very active flux of exocytosis and endocytosis/phagocytosis, may promote the temporary widening of the VCC connections to the plasma membrane and allow the release of viral particles to the extracellular media. Supporting this hypothesis, antibodies specific for VCC components, such as tetraspanins (96), gp120 (126), or CD36 (105) had access to the VCC only after several hours of incubation at 37°C and not at 4°C. These observations suggest that the access of extracellular molecules to the VCC depends on the dynamics of the macrophage's plasma membrane, which possibly promotes a frequent opening of the connections between the lumen of the compartment and the surface. Future insight into the role of the cytoskeleton and its associated proteins in regulating the dynamics of the VCC and its impact on viral release may open new avenues to pharmacologically target the VCC (123, 127).

Whether tissue macrophages *in vivo* possess VCCs remains poorly investigated. Indeed, our current view of the VCC results almost exclusively from studies *in vitro* with MDMs. Of note, former ultrastructural analysis of tissue macrophages from patient's organs confirmed the presence of mature and immature virions in intracellular compartments (128, 129). Accumulation of viral particles within VCC in macrophages *in vivo* could be advantageous for the virus to be less accessible to (i) soluble immune mediators such as neutralizing antibodies as observed *in vitro* (126), (ii) to innate sensors that are cytoplasmic or endosomal, and (iii) to anti-pathogen effector mechanisms such as reactive oxygen species or acidic pH.

Direct cell-to-cell transfer is more efficient for spreading HIV infection than the cell-free route (130). This process involves the formation of a stable interface between an infected and an uninfected cell, known as viral synapse. Interaction between the viral envelope present at the membrane of the infected cell and $CD4^+$ in the target cell initiates formation of the viral synapse, which is then maintained *via* additional interactions between cell adhesion molecules (131). Directed release leads to virion accumulation at the viral synapse and efficient infection of the target cell (132). Macrophages can transfer HIV directly to T cells (133), and the VCC appears to play a role in this process. Real-time imaging suggested a recruitment of the compartment to the proximity of viral synapses leading to subsequent T cell infection (134, 135), and the VCC markers CD9, CD18, and CD81 were found enriched at the macrophage to T cell interface (124). However, the precise mechanisms underlying viral transfer from infected macrophages to target cells (T cells or macrophages) remains incompletely understood as compared with T cell to T cell transfer and thus deserve further studies.

Despite their monocytic origin MDDCs are rather resistant to HIV-1 infection as compared with MDMs. Yet, MDDCs, when activated by LPS, can capture and retain vial particles in surface-connected compartments that bear some resemblance with the VCC. Although activated MDDCs are resistant to the infection and do not produce new viral progeny, they can efficiently transfer captured viruses to activated $CD4^+$ T cells that get then productively infected. This transfer mode known as infection *in trans* [see accompanying review by Izquierdo-Useros or Izquierdo-Useros et al. (136)] appears to be highly related to the virological synapse established between HIV-1-infected T cells and target cells (137). This process is thought to play an important role in viral dissemination at the early stages of HIV-1 infection at mucosal entry sites (138). Intravital microscopy revealed that subcapsular sinus macrophages from the peripheral lymph nodes can capture and transfer HIV-1 to target cells without getting productively infected in the process (139). Viral capture is mediated by the sialoadhesin CD169/SIGLEC1 that binds gangliosides embedded in the envelope glycoprotein (139). Interestingly, CD169-mediated capture of HIV-1 in macrophages leads to virion retention in the VCC and subsequent transfer to and productive infection of $CD4^+$ T cells (140). Remarkably, viral particles captured *via* CD169 intermingled with virions endogenously produced by the macrophage in the same VCCs (140), suggesting that the VCC is not only the site of HIV budding and assembly in macrophages but also a compartment of retention of particles captured from the extracellular media. Indeed, compartments with topologies resembling the VCC have been described in the past after exposure of macrophages to various particulate matter, including latex, cholesterol, or low-density lipoprotein (95).

MACROPHAGES AND THE HIV RESERVOIR IN THE POST-ART ERA

While ART can efficiently prevent AIDS by restoring $CD4^+$ T cell counts and suppressing viral load to undetectable levels, it fails to provide a sterilizing cure (141). A viral reservoir remains stable in HIV-infected patients under prolonged therapy (142, 143), and is responsible for the quick viral rebound observed within weeks after ART interruption (144). The cumulative toxicity and the cost associated with lifelong ART made it imperative to devise new strategies to eliminate or curb the viral reservoir (145). Unfortunately, such goal has remained elusive.

At the cellular level, the HIV reservoir during ART is mainly composed of resting memory $CD4^+$ T cells that are latently infected; i.e., cells bearing integrated, transcriptionally silent, but replication-competent proviruses (146). The mechanism behind HIV latency is not fully understood but likely results from multiple factors acting together, such as sequestration of cellular transcription factors in the cytoplasm, epigenetic regulation, or the action of transcriptional repressors [reviewed in Ref. (147)]. T cells with central memory (T_{CM}), transitional memory (T_{TM}), and effector memory (T_{EM}) phenotypes contain the highest levels of latent HIV-1 (148–150). A major breakthrough in the characterization of the latent $CD4^+$ reservoir is the recent identification of CD32a as a surface marker highly enriched in circulating cells harboring replication-competent quiescent proviruses (151). The HIV reservoir is seeded very early after infection (within 2–3 days) (152, 153), and its size remains stable even after years of suppressive therapy (154, 155).

Whether residual viral replication under ART, the so-called active reservoir, contributes to HIV persistence is a rather contentious issue in the field (156). Low-level viremia ("Blips") can be detected in patients under therapy (157, 158). However, HIV shows little sign of genetic evolution during ART (159, 160), and the emergence of drug-resistant virus is remarkably low (158, 161), suggesting that ongoing residual replication does not significantly influence long-term viral persistence. However, a recent high-depth temporal analysis of the phylogeny of viral sequences from the blood and lymph node of patients under ART revealed a constant replenishment of the circulating reservoir as a result of low-level viral replication in sanctuary sites within lymphoid tissues (162). Experimental evidence for the existence of such lymphoid sanctuaries has emerged in the last years. B cell follicles and more specifically germinal centers have long been known as primary sites of HIV replication (163), possibly due to lower antiretroviral drug penetration (164), exclusion of cytotoxic $CD8^+$ T cells (165, 166), and retention of infectious virions within immune complexes on the surface of follicular dendritic cells (167). In patients under treatment and with an aviremic status, $CD4^+$ T cells with a T follicular helper phenotype that reside within germinal centers are the major source of residual infectious virus and contain the highest levels of HIV DNA (168–170).

These recent advances highlight the importance of accurately defining the HIV reservoir, with respect to its cellular and anatomic composition (171). However, studies evaluating the importance of cellular reservoirs other than $CD4^+$ T lymphocytes have been scarce and, for the most part, non-conclusive. Analysis of the rebounding viral sequences in patients after therapy interruption revealed that they differ from proviral sequences integrated in resting CD4 T cells (172). Recovery of M-tropic sequences among the pool of rebounding virus has been recently

reported (173). However, there is no readily available method to measure viral rebound from macrophages or other cellular reservoirs, equivalent to the viral outgrowth assay (VOA) typically used to quantify the latent CD4$^+$ reservoir (171). Usually, VOAs require the culture of several million purified cells for accurate quantification of the CD4 reservoir, due to the rarity of latently infected cells (150), making an adaptation of the assay to tissue macrophages unfeasible. Alternatively, quantification of viral nucleic acids provides a more practical manner to evaluate the macrophage reservoir (174). In patients under ART, HIV DNA and/or RNA has been detected in alveolar (175) and duodenal (41) macrophages, microglia in the brain (39), as well as in liver Kupffer cells (176).

Evaluation of the HIV reservoir based on cell-associated DNA or RNA tends to largely overestimate the pool of replication-competent virus, as many defective viral genomes accumulate in patients (177, 178). Also, macrophages may acquire viral DNA *via* phagocytosis of infected T cells (51), as discussed previously. In the absence of a reliable outgrowth assay to measure the macrophage HIV reservoir from treated patients, animal models become a valuable alternative.

In a recent study with Asian macaques chronically infected with SIV, replication-competent virus could be recovered from macrophages purified from the spleen and mesenteric lymph nodes, using a modified version of the VOA (43). However, in macaques that had been under ART for 5 months, no replication-competent virus could be recovered after macrophage culture, from any of the animals under study and despite the presence of detectable SIV-DNA in macrophages in 40% of the animals (43). A possible limitation of this study is the small number of macrophages that could be purified for the viral outgrowth experiments. However, in parallel experiments, replicating virus could be recovered after culture of purified memory CD4$^+$ T cells from all animals under therapy (43). This suggests that, in the SIV model, the macrophage reservoir, if existent, is clearly smaller than the memory CD4 reservoir.

T cell-deficient humanized mice can be generated by transferring CD34$^+$ human hematopoietic cells into NOD/SCID mice. These mice are reconstituted with human myeloid cells and B cells, but completely devoid of T cells (179). As only macrophages can sustain HIV replication, these myeloid-only mice (MoM) provide a valuable model to test the HIV macrophage reservoir without the confounding effects conferred by the presence of the more abundant CD4$^+$ T cell compartment. When infected with macrophage-tropic HIV-1, MoM present sustained viremia, and viral nucleic acids were detected in macrophages of the liver, bone marrow, spleen, lungs, and brain (179). Initiation of ART in infected MoM leads to undetectable viremia within 2 weeks, and a drastic reduction in the levels of HIV DNA and RNA in the tissues. Importantly, ART interruption led to viral rebound about 7 weeks later, although only in three out of nine animals under study (180). This represents a significantly longer period of viral remission after treatment interruption when compared with T cell-sufficient humanized mice, where rebound occurs within 1–2 weeks after ART interruption (181). Due to the short life span of the MoM mice, the authors could not extend the study and evaluate whether the non-rebounding group of mice would eventually show signs of reactivation of the infection (180).

The absence of T cells in the MoM model of HIV infection, certainly constitute a large deviation from the regular course of HIV infection in humans. Nevertheless, these observations provide the first direct evidence for HIV persistence in macrophages, in the setting of suppressive therapy. Whether such persistence is due to latent infection or ongoing residual replication remains unclear from the data available, as both viral DNA and RNA dropped to undetectable levels in most treated mice (180). Efforts to purge the CD4$^+$ T cell reservoir have mostly employed the "shock and kill" approach (145); a latency-reversal agent (LRA) is initially administered to reactivate viral production in latently infected cells (shock), and followed by an immune-modulatory intervention that renders infected cells susceptible to destruction by the immune system (kill) (182). However, HIV latency in macrophages is not well understood (183), and LRAs that efficiently purge the CD4 reservoir may not have a similar effect in latently infected macrophages. Worse, if the macrophage reservoir is maintained mostly *via* residual ongoing replication or retention of infectious viral particles within VCCs then LRA therapy will be of negligible effect.

Definitive proof of the macrophage reservoir will require demonstration in human patients under therapy. This will likely require more sensitive methods of measuring the reservoir. A promising alternative is the recent report of an *in vivo* VOA, wherein cells from patients with undetectable viremia are transplanted into humanized mice (184). This method appears more sensitive than *in vitro* VOAs, although its widespread application will likely be hampered by the costs associated (185).

MACROPHAGES DURING CHRONIC DISEASE IN TREATED HIV-1 INFECTION

Introduction of ART effectively halted the AIDS pandemic, improved health, and prolonged the life of patients. However, a new group of problems, commonly known as "non-AIDS-related conditions," is emerging in HIV patients with long-term suppressed viremia (186). People living with HIV are at increased risk of developing, among others, cardiovascular and neurocognitive disease, osteoporosis, or cancer (187).

Persistent inflammation appears to lie at the origin of these pathologies, although its causes remain incompletely elucidated and may involve multiple factors. Microbial translocation across the gut mucosa is a well-established cause of systemic inflammation during HIV-1 (188, 189). Long-term suppressive therapy does not completely reconstitute the pool of CD4$^+$ T cells in the gut mucosa, particularly those of the Th17 subset (190). This leads to loss of integrity of the epithelial mucosa and translocation of bacterial products through the lamina propria to mesenteric lymph nodes and extranodal sites (189). These microbial products engage pattern-recognition receptors in cells of the innate immune system, particularly monocytes, macrophages and DCs, leading to widespread production of inflammatory mediators (191). Indeed, myeloid cell-derived biomarkers of microbial translocation, such as IL-6, soluble

CD14 (sCD14) or sCD163 are found elevated in ART-treated individuals, as compared with age-matched controls, and are strongly associated with premature mortality of HIV-infected individuals (191, 192). This persistent pro-inflammatory state appears to feedback on intestinal macrophages as they become unable to phagocyte microbial debris in the lamina propria and are thus unable to halt this inflammatory cycle (193). Importantly, persistent systemic inflammation drives the occurrence of non-AIDS comorbidities. For instance, inflammatory monocytes migrate to the heart and contribute to HIV-associated myocarditis (194).

Before the implementation of ART, more than half of HIV-infected patients exhibited HIV-1-associated dementia (HAD); a broad term used to described symptoms of cognitive impairment, including psychiatric disorders, loss of motor coordination, and in severe cases, HIV-1-associated encephalitis (195). The incidence of HAD has dramatically decreased with ART, but a set of milder cognitive problems have emerged and are collectively known as HIV-associated neurological disorders (HAND) that still affect about half of the HIV-1-infected population (196).

Residual viral replication in the CNS and neuronal death has been proposed has an explanation for the occurrence of HAND (197). This effect is probably indirect, as neurons and cells of the macroglia do not support productive HIV infection. Instead, residual viral replication in macrophages leads to the production of inflammatory mediators with neurotoxic action (196). While it is challenging to assess productive infection of brain-resident cells, macrophages are known to contain the highest levels of viral nucleic acids of all CNS cell populations (198). Both perivascular macrophages and microglial cells are targeted by HIV in the CNS (199) and HIV DNA has been detected in brain macrophages from patients under long-term therapy (39). HIV RNA persists in the cerebrospinal fluid (CSF) of ART-treated patients even after suppression of plasma viral RNA to undetectable levels (200), and genetic analysis revealed a significant compartmentalization between the CSF and plasma viral populations (201). Importantly, viruses isolated from the CSF are frequently M-tropic (202). Taken together, these studies suggest that the CNS is a tissue reservoir of HIV-1 during ART, likely maintained through low-level viral replication in resident macrophages (203).

Systemic inflammation is also likely to play a role in the progression of HAND. There is a strong association between circulating levels of sCD14 and the development of neurological disorders in HIV-1 infected individuals (204). It has been proposed that microbial products activate circulating monocytes, particularly those of the $CD16^+$ subset that subsequently cross the blood–brain barrier and differentiate into a pro-inflammatory macrophage population in the brain by producing chemokines, cytokines, and neurotoxic factors such as nitric oxide (48). Supporting this model, $CD14^+CD16^+$ cells accumulate in the white matter and perivascular space of brains from non-treated patients (205). Also, these $CD14^+CD16^+$ monocytes are capable of transmigrating across *in vitro* models of the blood–brain barrier in response to the chemokine CCL2 (206).

These selected examples highlight the pathological role played by macrophages and other myeloid cells in non-AIDS conditions that afflict HIV-1-infected patients with suppressed viremia. It is thus crucial to devise new therapies able to complement ART and capable of targeting the persistent inflammation that drives these morbidities.

CONCLUSION

Because of their localization in many tissues, their long life span and the unique nature of their interaction with HIV-1, macrophages play a key role in HIV-1 pathogenesis. The last decade of research brought new and exciting insight into the ontogeny and functional specialization of tissue-resident macrophages. Whether these recently described macrophage properties, such as their proliferative potential, are explored HIV for dissemination and persistence remains unknown, but this subject should deserve increased interest in future studies. Macrophages are susceptible to HIV-1 infection but also sense the virus and thus participate in the general immune activation observed in infected patients. However, initiation of the antiviral immune response relies on the DC population whose capacity to perform antigen presentation and deal with infection is highly organized in space and time. This dual function appears to be ensured by a division of labor between DC subsets (207). While cDC1 ($CD141^+$) are resistant to productive HIV-1 infection, they can cross-present viral antigens derived from cDC2 ($CD1c^+$) that are susceptible to HIV-1. Thus, this dissociation of the viral infection and the antigen presentation function provides to DC populations the capacity to elicit antiviral immune responses and prime T cell responses (207). How macrophages cross talk with DCs and contribute to the antiviral response remains obscure. Reciprocally, how HIV succeeds to cope with these immune cells specialized in antiviral immunity is similarly incompletely understood. Future work addressing these questions should keep on producing exciting results enlightening our general comprehension of the virus–immune system relationships.

AUTHOR CONTRIBUTIONS

VR and PB wrote the review. MS-R performed the electron microscopy. NR, PB, and VR designed the cartoon. All the authors edited the review.

ACKNOWLEDGMENTS

The authors would like to thank Nicolas Manel at the Institut Curie for critical reading of the manuscript.

FUNDING

This work was supported by grants from «Agence Nationale de Recherche contre le SIDA et les hépatites virales» (ANRS), «Ensemble contre le SIDA» (Sidaction), ANR-10-IDEX-0001-02 PSL and ANR-11-LABX-0043 to PB. VR and NR were supported by postdoctoral fellowships from ANRS.

REFERENCES

1. Davies LC, Jenkins SJ, Allen JE, Taylor PR. Tissue-resident macrophages. *Nat Immunol* (2013) 14:986–95. doi:10.1038/ni.2705
2. Cavaillon JM. The historical milestones in the understanding of leukocyte biology initiated by Elie Metchnikoff. *J Leukoc Biol* (2011) 90:413–24. doi:10.1189/jlb.0211094
3. Gordon S. Phagocytosis: the legacy of Metchnikoff. *Cell* (2016) 166:1065–8. doi:10.1016/j.cell.2016.08.017
4. Van Furth R, Cohn ZA, Hirsch JG, Humphrey JH, Spector WG, Langevoort HL. The mononuclear phagocyte system: a new classification of macrophages, monocytes, and their precursor cells. *Bull World Health Organ* (1972) 46:845–52.
5. Ginhoux F, Guilliams M. Tissue-resident macrophage ontogeny and homeostasis. *Immunity* (2016) 44:439–49. doi:10.1016/j.immuni.2016.02.024
6. Varol C, Mildner A, Jung S. Macrophages: development and tissue specialization. *Annu Rev Immunol* (2015) 33:643–75. doi:10.1146/annurev-immunol-032414-112220
7. Ghigo C, Mondor I, Jorquera A, Nowak J, Wienert S, Zahner SP, et al. Multicolor fate mapping of Langerhans cell homeostasis. *J Exp Med* (2013) 210: 1657–64. doi:10.1084/jem.20130403
8. Alliot F, Lecain E, Grima B, Pessac B. Microglial progenitors with a high proliferative potential in the embryonic and adult mouse brain. *Proc Natl Acad Sci U S A* (1991) 88:1541–5. doi:10.1073/pnas.88.4.1541
9. Ginhoux F, Greter M, Leboeuf M, Nandi S, See P, Gokhan S, et al. Fate mapping analysis reveals that adult microglia derive from primitive macrophages. *Science* (2010) 330:841–5. doi:10.1126/science.1194637
10. Hashimoto D, Chow A, Noizat C, Teo P, Beasley MB, Leboeuf M, et al. Tissue-resident macrophages self-maintain locally throughout adult life with minimal contribution from circulating monocytes. *Immunity* (2013) 38:792–804. doi:10.1016/j.immuni.2013.04.004
11. Ajami B, Bennett JL, Krieger C, Mcnagny KM, Rossi FM. Infiltrating monocytes trigger EAE progression, but do not contribute to the resident microglia pool. *Nat Neurosci* (2011) 14:1142–9. doi:10.1038/nn.2887
12. Bain CC, Bravo-Blas A, Scott CL, Perdiguero EG, Geissmann F, Henri S, et al. Constant replenishment from circulating monocytes maintains the macrophage pool in the intestine of adult mice. *Nat Immunol* (2014) 15:929–37. doi:10.1038/ni.2967
13. Okabe Y, Medzhitov R. Tissue biology perspective on macrophages. *Nat Immunol* (2016) 17:9–17. doi:10.1038/ni.3320
14. Franken L, Schiwon M, Kurts C. Macrophages: sentinels and regulators of the immune system. *Cell Microbiol* (2016) 18:475–87. doi:10.1111/cmi.12580
15. Murray PJ. Macrophage polarization. *Annu Rev Physiol* (2017) 79:541–66. doi:10.1146/annurev-physiol-022516-034339
16. Murray PJ, Wynn TA. Protective and pathogenic functions of macrophage subsets. *Nat Rev Immunol* (2011) 11:723–37. doi:10.1038/nri3073
17. Gartner S, Markovits P, Markovitz DM, Kaplan MH, Gallo RC, Popovic M. The role of mononuclear phagocytes in HTLV-III/LAV infection. *Science* (1986) 233:215–9. doi:10.1126/science.3014648
18. Duncan CJ, Sattentau QJ. Viral determinants of HIV-1 macrophage tropism. *Viruses* (2011) 3:2255–79. doi:10.3390/v3112255
19. Marechal V, Prevost MC, Petit C, Perret E, Heard JM, Schwartz O. Human immunodeficiency virus type 1 entry into macrophages mediated by macropinocytosis. *J Virol* (2001) 75:11166–77. doi:10.1128/JVI.75.22.11166-11177.2001
20. Van Wilgenburg B, Moore MD, James WS, Cowley SA. The productive entry pathway of HIV-1 in macrophages is dependent on endocytosis through lipid rafts containing CD4. *PLoS One* (2014) 9:e86071. doi:10.1371/journal.pone.0086071
21. Li Q, Li W, Yin W, Guo J, Zhang ZP, Zeng D, et al. Single-particle tracking of human immunodeficiency virus type 1 productive entry into human primary macrophages. *ACS Nano* (2017) 11:3890–903. doi:10.1021/acsnano.7b00275
22. Carter CA, Ehrlich LS. Cell biology of HIV-1 infection of macrophages. *Annu Rev Microbiol* (2008) 62:425–43. doi:10.1146/annurev.micro.62.081307.162758
23. Peters PJ, Sullivan WM, Duenas-Decamp MJ, Bhattacharya J, Ankghuambom C, Brown R, et al. Non-macrophage-tropic human immunodeficiency virus type 1 R5 envelopes predominate in blood, lymph nodes, and semen: implications for transmission and pathogenesis. *J Virol* (2006) 80:6324–32. doi:10.1128/JVI.02328-05
24. Jayakumar P, Berger I, Autschbach F, Weinstein M, Funke B, Verdin E, et al. Tissue-resident macrophages are productively infected ex vivo by primary X4 isolates of human immunodeficiency virus type 1. *J Virol* (2005) 79:5220–6. doi:10.1128/JVI.79.8.5220-5226.2005
25. Boltz VF, Rausch J, Shao W, Hattori J, Luke B, Maldarelli F, et al. Ultrasensitive single-genome sequencing: accurate, targeted, next generation sequencing of HIV-1 RNA. *Retrovirology* (2016) 13:87. doi:10.1186/s12977-016-0321-6
26. Joseph SB, Swanstrom R, Kashuba AD, Cohen MS. Bottlenecks in HIV-1 transmission: insights from the study of founder viruses. *Nat Rev Microbiol* (2015) 13:414–25. doi:10.1038/nrmicro3471
27. Salazar-Gonzalez JF, Salazar MG, Keele BF, Learn GH, Giorgi EE, Li H, et al. Genetic identity, biological phenotype, and evolutionary pathways of transmitted/founder viruses in acute and early HIV-1 infection. *J Exp Med* (2009) 206:1273–89. doi:10.1084/jem.20090378
28. Ochsenbauer C, Edmonds TG, Ding H, Keele BF, Decker J, Salazar MG, et al. Generation of transmitted/founder HIV-1 infectious molecular clones and characterization of their replication capacity in CD4 T lymphocytes and monocyte-derived macrophages. *J Virol* (2012) 86:2715–28. doi:10.1128/JVI.06157-11
29. Fackler OT, Murooka TT, Imle A, Mempel TR. Adding new dimensions: towards an integrative understanding of HIV-1 spread. *Nat Rev Microbiol* (2014) 12:563–74. doi:10.1038/nrmicro3309
30. Hladik F, Sakchalathorn P, Ballweber L, Lentz G, Fialkow M, Eschenbach D, et al. Initial events in establishing vaginal entry and infection by human immunodeficiency virus type-1. *Immunity* (2007) 26:257–70. doi:10.1016/j.immuni.2007.01.007
31. Saba E, Grivel JC, Vanpouille C, Brichacek B, Fitzgerald W, Margolis L, et al. HIV-1 sexual transmission: early events of HIV-1 infection of human cervico-vaginal tissue in an optimized ex vivo model. *Mucosal Immunol* (2010) 3:280–90. doi:10.1038/mi.2010.2
32. King DF, Siddiqui AA, Buffa V, Fischetti L, Gao Y, Stieh D, et al. Mucosal tissue tropism and dissemination of HIV-1 subtype B acute envelope-expressing chimeric virus. *J Virol* (2013) 87:890–9. doi:10.1128/JVI.02216-12
33. Spira AI, Marx PA, Patterson BK, Mahoney J, Koup RA, Wolinsky SM, et al. Cellular targets of infection and route of viral dissemination after an intravaginal inoculation of simian immunodeficiency virus into rhesus macaques. *J Exp Med* (1996) 183:215–25. doi:10.1084/jem.183.1.215
34. Barouch DH, Ghneim K, Bosche WJ, Li Y, Berkemeier B, Hull M, et al. Rapid inflammasome activation following mucosal SIV infection of rhesus monkeys. *Cell* (2016) 165:656–67. doi:10.1016/j.cell.2016.03.021
35. Brenchley JM, Schacker TW, Ruff LE, Price DA, Taylor JH, Beilman GJ, et al. CD4+ T cell depletion during all stages of HIV disease occurs predominantly in the gastrointestinal tract. *J Exp Med* (2004) 200:749–59. doi:10.1084/jem.20040874
36. Li Q, Duan L, Estes JD, Ma ZM, Rourke T, Wang Y, et al. Peak SIV replication in resting memory CD4+ T cells depletes gut lamina propria CD4+ T cells. *Nature* (2005) 434:1148–52. doi:10.1038/nature03513
37. Mattapallil JJ, Douek DC, Hill B, Nishimura Y, Martin M, Roederer M. Massive infection and loss of memory CD4+ T cells in multiple tissues during acute SIV infection. *Nature* (2005) 434:1093–7. doi:10.1038/nature03501
38. Hufert FT, Schmitz J, Schreiber M, Schmitz H, Racz P, Von Laer DD. Human Kupffer cells infected with HIV-1 in vivo. *J Acquir Immune Defic Syndr* (1993) 6:772–7.
39. Churchill MJ, Gorry PR, Cowley D, Lal L, Sonza S, Purcell DF, et al. Use of laser capture microdissection to detect integrated HIV-1 DNA in macrophages and astrocytes from autopsy brain tissues. *J Neurovirol* (2006) 12:146–52. doi:10.1080/13550280600748946
40. Jambo KC, Banda DH, Kankwatira AM, Sukumar N, Allain TJ, Heyderman RS, et al. Small alveolar macrophages are infected preferentially by HIV and exhibit impaired phagocytic function. *Mucosal Immunol* (2014) 7:1116–26. doi:10.1038/mi.2013.127
41. Zalar A, Figueroa MI, Ruibal-Ares B, Bare P, Cahn P, De Bracco MM, et al. Macrophage HIV-1 infection in duodenal tissue of patients on long term HAART. *Antiviral Res* (2010) 87:269–71. doi:10.1016/j.antiviral.2010.05.005
42. Yukl SA, Sinclair E, Somsouk M, Hunt PW, Epling L, Killian M, et al. A comparison of methods for measuring rectal HIV levels suggests that HIV DNA resides in cells other than CD4+ T cells, including myeloid cells. *AIDS* (2014) 28:439–42. doi:10.1097/QAD.0000000000000166

43. Dinapoli SR, Ortiz AM, Wu F, Matsuda K, Twigg HL III, Hirsch VM, et al. Tissue-resident macrophages can contain replication-competent virus in antiretroviral-naive, SIV-infected Asian macaques. *JCI Insight* (2017) 2:e91214. doi:10.1172/jci.insight.91214
44. Sonza S, Mutimer HP, Oelrichs R, Jardine D, Harvey K, Dunne A, et al. Monocytes harbour replication-competent, non-latent HIV-1 in patients on highly active antiretroviral therapy. *AIDS* (2001) 15:17–22. doi:10.1097/00002030-200101050-00005
45. Zhu T, Muthui D, Holte S, Nickle D, Feng F, Brodie S, et al. Evidence for human immunodeficiency virus type 1 replication in vivo in CD14(+) monocytes and its potential role as a source of virus in patients on highly active antiretroviral therapy. *J Virol* (2002) 76:707–16. doi:10.1128/JVI.76.2.707-716.2002
46. Ellery PJ, Tippett E, Chiu YL, Paukovics G, Cameron PU, Solomon A, et al. The CD16+ monocyte subset is more permissive to infection and preferentially harbors HIV-1 in vivo. *J Immunol* (2007) 178:6581–9. doi:10.4049/jimmunol.178.10.6581
47. Pulliam L, Gascon R, Stubblebine M, Mcguire D, Mcgrath MS. Unique monocyte subset in patients with AIDS dementia. *Lancet* (1997) 349:692–5. doi:10.1016/S0140-6736(96)10178-1
48. Williams DW, Veenstra M, Gaskill PJ, Morgello S, Calderon TM, Berman JW. Monocytes mediate HIV neuropathogenesis: mechanisms that contribute to HIV associated neurocognitive disorders. *Curr HIV Res* (2014) 12:85–96. doi:10.2174/1570162X12666140526114526
49. Verollet C, Souriant S, Bonnaud E, Jolicoeur P, Raynaud-Messina B, Kinnaer C, et al. HIV-1 reprograms the migration of macrophages. *Blood* (2015) 125:1611–22. doi:10.1182/blood-2014-08-596775
50. Murooka TT, Deruaz M, Marangoni F, Vrbanac VD, Seung E, Von Andrian UH, et al. HIV-infected T cells are migratory vehicles for viral dissemination. *Nature* (2012) 490:283–7. doi:10.1038/nature11398
51. Calantone N, Wu F, Klase Z, Deleage C, Perkins M, Matsuda K, et al. Tissue myeloid cells in SIV-infected primates acquire viral DNA through phagocytosis of infected T cells. *Immunity* (2014) 41:493–502. doi:10.1016/j.immuni.2014.08.014
52. Baxter AE, Russell RA, Duncan CJ, Moore MD, Willberg CB, Pablos JL, et al. Macrophage infection via selective capture of HIV-1-infected CD4+ T cells. *Cell Host Microbe* (2014) 16:711–21. doi:10.1016/j.chom.2014.10.010
53. Sattentau QJ, Stevenson M. Macrophages and HIV-1: an unhealthy constellation. *Cell Host Microbe* (2016) 19:304–10. doi:10.1016/j.chom.2016.02.013
54. Moir S, Chun TW, Fauci AS. Pathogenic mechanisms of HIV disease. *Annu Rev Pathol* (2011) 6:223–48. doi:10.1146/annurev-pathol-011110-130254
55. Richards KH, Aasa-Chapman MM, Mcknight A, Clapham PR. Modulation of HIV-1 macrophage-tropism among R5 envelopes occurs before detection of neutralizing antibodies. *Retrovirology* (2010) 7:48. doi:10.1186/1742-4690-7-48
56. Micci L, Alvarez X, Iriele RI, Ortiz AM, Ryan ES, Mcgary CS, et al. CD4 depletion in SIV-infected macaques results in macrophage and microglia infection with rapid turnover of infected cells. *PLoS Pathog* (2014) 10:e1004467. doi:10.1371/journal.ppat.1004467
57. Price JV, Vance RE. The macrophage paradox. *Immunity* (2014) 41:685–93. doi:10.1016/j.immuni.2014.10.015
58. Altfeld M, Gale M Jr. Innate immunity against HIV-1 infection. *Nat Immunol* (2015) 16:554–62. doi:10.1038/ni.3157
59. Simon V, Bloch N, Landau NR. Intrinsic host restrictions to HIV-1 and mechanisms of viral escape. *Nat Immunol* (2015) 16:546–53. doi:10.1038/ni.3156
60. Lahaye X, Satoh T, Gentili M, Cerboni S, Conrad C, Hurbain I, et al. The capsids of HIV-1 and HIV-2 determine immune detection of the viral cDNA by the innate sensor cGAS in dendritic cells. *Immunity* (2013) 39:1132–42. doi:10.1016/j.immuni.2013.11.002
61. Rasaiyaah J, Tan CP, Fletcher AJ, Price AJ, Blondeau C, Hilditch L, et al. HIV-1 evades innate immune recognition through specific cofactor recruitment. *Nature* (2013) 503:402–5. doi:10.1038/nature12769
62. Yan N, Regalado-Magdos AD, Stiggelbout B, Lee-Kirsch MA, Lieberman J. The cytosolic exonuclease TREX1 inhibits the innate immune response to human immunodeficiency virus type 1. *Nat Immunol* (2010) 11:1005–13. doi:10.1038/ni.1941
63. Gao D, Wu J, Wu YT, Du F, Aroh C, Yan N, et al. Cyclic GMP-AMP synthase is an innate immune sensor of HIV and other retroviruses. *Science* (2013) 341:903–6. doi:10.1126/science.1240933
64. Nasr N, Maddocks S, Turville SG, Harman AN, Woolger N, Helbig KJ, et al. HIV-1 infection of human macrophages directly induces viperin which inhibits viral production. *Blood* (2012) 120:778–88. doi:10.1182/blood-2012-01-407395
65. Diget EA, Zuwala K, Berg RK, Laursen RR, Soby S, Ostergaard L, et al. Characterization of HIV-1 infection and innate sensing in different types of primary human monocyte-derived macrophages. *Mediators Inflamm* (2013) 2013:208412. doi:10.1155/2013/208412
66. Woelk CH, Ottones F, Plotkin CR, Du P, Royer CD, Rought SE, et al. Interferon gene expression following HIV type 1 infection of monocyte-derived macrophages. *AIDS Res Hum Retroviruses* (2004) 20:1210–22. doi:10.1089/aid.2004.20.1210
67. Decalf J, Desdouits M, Rodrigues V, Gobert FX, Gentili M, Marques-Ladeira S, et al. Sensing of HIV-1 entry triggers a type I interferon response in human primary macrophages. *J Virol* (2017) 91:e147–117. doi:10.1128/JVI.00147-17
68. Noyce RS, Taylor K, Ciechonska M, Collins SE, Duncan R, Mossman KL. Membrane perturbation elicits an IRF3-dependent, interferon-independent antiviral response. *J Virol* (2011) 85:10926–31. doi:10.1128/JVI.00862-11
69. Holm CK, Jensen SB, Jakobsen MR, Cheshenko N, Horan KA, Moeller HB, et al. Virus-cell fusion as a trigger of innate immunity dependent on the adaptor STING. *Nat Immunol* (2012) 13:737–43. doi:10.1038/ni.2350
70. Nasr N, Alshehri AA, Wright TK, Shahid M, Heiner BM, Harman AN, et al. Mechanism of interferon-stimulated gene induction in HIV-1-infected macrophages. *J Virol* (2017) 91:e744–717. doi:10.1128/JVI.00744-17
71. Hrecka K, Hao C, Gierszewska M, Swanson SK, Kesik-Brodacka M, Srivastava S, et al. Vpx relieves inhibition of HIV-1 infection of macrophages mediated by the SAMHD1 protein. *Nature* (2011) 474:658–61. doi:10.1038/nature10195
72. Laguette N, Sobhian B, Casartelli N, Ringeard M, Chable-Bessia C, Segeral E, et al. SAMHD1 is the dendritic- and myeloid-cell-specific HIV-1 restriction factor counteracted by Vpx. *Nature* (2011) 474:654–7. doi:10.1038/nature10117
73. Lahouassa H, Daddacha W, Hofmann H, Ayinde D, Logue EC, Dragin L, et al. SAMHD1 restricts the replication of human immunodeficiency virus type 1 by depleting the intracellular pool of deoxynucleoside triphosphates. *Nat Immunol* (2012) 13:223–8. doi:10.1038/ni0612-621c
74. Ryoo J, Choi J, Oh C, Kim S, Seo M, Kim SY, et al. The ribonuclease activity of SAMHD1 is required for HIV-1 restriction. *Nat Med* (2014) 20:936–41. doi:10.1038/nm.3626
75. Cribier A, Descours B, Valadao AL, Laguette N, Benkirane M. Phosphorylation of SAMHD1 by cyclin A2/CDK1 regulates its restriction activity toward HIV-1. *Cell Rep* (2013) 3:1036–43. doi:10.1016/j.celrep.2013.03.017
76. Pauls E, Ruiz A, Badia R, Permanyer M, Gubern A, Riveira-Munoz E, et al. Cell cycle control and HIV-1 susceptibility are linked by CDK6-dependent CDK2 phosphorylation of SAMHD1 in myeloid and lymphoid cells. *J Immunol* (2014) 193:1988–97. doi:10.4049/jimmunol.1400873
77. Mlcochova P, Sutherland KA, Watters SA, Bertoli C, De Bruin RA, Rehwinkel J, et al. A G1-like state allows HIV-1 to bypass SAMHD1 restriction in macrophages. *EMBO J* (2017) 36:604–16. doi:10.15252/embj.201696025
78. Kyei GB, Cheng X, Ramani R, Ratner L. Cyclin L2 is a critical HIV dependency factor in macrophages that controls SAMHD1 abundance. *Cell Host Microbe* (2015) 17:98–106. doi:10.1016/j.chom.2014.11.009
79. Badia R, Pujantell M, Riveira-Munoz E, Puig T, Torres-Torronteras J, Marti R, et al. The G1/S specific cyclin D2 is a regulator of HIV-1 restriction in non-proliferating cells. *PLoS Pathog* (2016) 12:e1005829. doi:10.1371/journal.ppat.1005829
80. Sunseri N, O'Brien M, Bhardwaj N, Landau NR. Human immunodeficiency virus type 1 modified to package Simian immunodeficiency virus Vpx efficiently infects macrophages and dendritic cells. *J Virol* (2011) 85:6263–74. doi:10.1128/JVI.00346-11
81. Lahaye X, Manel N. Viral and cellular mechanisms of the innate immune sensing of HIV. *Curr Opin Virol* (2015) 11:55–62. doi:10.1016/j.coviro.2015.01.013
82. Tada T, Zhang Y, Koyama T, Tobiume M, Tsunetsugu-Yokota Y, Yamaoka S, et al. MARCH8 inhibits HIV-1 infection by reducing virion incorporation of envelope glycoproteins. *Nat Med* (2015) 21:1502–7. doi:10.1038/nm.3956
83. Krapp C, Hotter D, Gawanbacht A, Mclaren PJ, Kluge SF, Sturzel CM, et al. Guanylate binding protein (GBP) 5 is an interferon-inducible inhibitor of HIV-1 infectivity. *Cell Host Microbe* (2016) 19:504–14. doi:10.1016/j.chom.2016.02.019
84. Schwartz S, Felber BK, Fenyo EM, Pavlakis GN. Env and Vpu proteins of human immunodeficiency virus type 1 are produced from multiple bicistronic mRNAs. *J Virol* (1990) 64:5448–56.

85. Thomas ER, Dunfee RL, Stanton J, Bogdan D, Kunstman K, Wolinsky SM, et al. High frequency of defective vpu compared with tat and rev genes in brain from patients with HIV type 1-associated dementia. *AIDS Res Hum Retroviruses* (2007) 23:575–80. doi:10.1089/aid.2006.0246
86. Neil SJ, Zang T, Bieniasz PD. Tetherin inhibits retrovirus release and is antagonized by HIV-1 Vpu. *Nature* (2008) 451:425–30. doi:10.1038/nature06553
87. Perez-Caballero D, Zang T, Ebrahimi A, Mcnatt MW, Gregory DA, Johnson MC, et al. Tetherin inhibits HIV-1 release by directly tethering virions to cells. *Cell* (2009) 139:499–511. doi:10.1016/j.cell.2009.08.039
88. Van Damme N, Goff D, Katsura C, Jorgenson RL, Mitchell R, Johnson MC, et al. The interferon-induced protein BST-2 restricts HIV-1 release and is downregulated from the cell surface by the viral Vpu protein. *Cell Host Microbe* (2008) 3:245–52. doi:10.1016/j.chom.2008.03.001
89. Chu H, Wang JJ, Qi M, Yoon JJ, Chen X, Wen X, et al. Tetherin/BST-2 is essential for the formation of the intracellular virus-containing compartment in HIV-infected macrophages. *Cell Host Microbe* (2012) 12:360–72. doi:10.1016/j.chom.2012.07.011
90. Lu J, Pan Q, Rong L, He W, Liu SL, Liang C. The IFITM proteins inhibit HIV-1 infection. *J Virol* (2011) 85:2126–37. doi:10.1128/JVI.01531-10
91. Jia R, Pan Q, Ding S, Rong L, Liu SL, Geng Y, et al. The N-terminal region of IFITM3 modulates its antiviral activity by regulating IFITM3 cellular localization. *J Virol* (2012) 86:13697–707. doi:10.1128/JVI.01828-12
92. Compton AA, Bruel T, Porrot F, Mallet A, Sachse M, Euvrard M, et al. IFITM proteins incorporated into HIV-1 virions impair viral fusion and spread. *Cell Host Microbe* (2014) 16:736–47. doi:10.1016/j.chom.2014.11.001
93. Chesarino NM, Compton AA, Mcmichael TM, Kenney AD, Zhang L, Soewarna V, et al. IFITM3 requires an amphipathic helix for antiviral activity. *EMBO Rep* (2017) 18:1740–51. doi:10.15252/embr.201744100
94. Tartour K, Appourchaux R, Gaillard J, Nguyen XN, Durand S, Turpin J, et al. IFITM proteins are incorporated onto HIV-1 virion particles and negatively imprint their infectivity. *Retrovirology* (2014) 11:103. doi:10.1186/s12977-014-0103-y
95. Tan J, Sattentau QJ. The HIV-1-containing macrophage compartment: a perfect cellular niche? *Trends Microbiol* (2013) 21:405–12. doi:10.1016/j.tim.2013.05.001
96. Deneka M, Pelchen-Matthews A, Byland R, Ruiz-Mateos E, Marsh M. In macrophages, HIV-1 assembles into an intracellular plasma membrane domain containing the tetraspanins CD81, CD9, and CD53. *J Cell Biol* (2007) 177:329–41. doi:10.1083/jcb.200609050
97. Jouve M, Sol-Foulon N, Watson S, Schwartz O, Benaroch P. HIV-1 buds and accumulates in "nonacidic" endosomes of macrophages. *Cell Host Microbe* (2007) 2:85–95. doi:10.1016/j.chom.2007.06.011
98. Welsch S, Keppler OT, Habermann A, Allespach I, Krijnse-Locker J, Krausslich HG. HIV-1 buds predominantly at the plasma membrane of primary human macrophages. *PLoS Pathog* (2007) 3:e36. doi:10.1371/journal.ppat.0030036
99. Welsch S, Groot F, Krausslich HG, Keppler OT, Sattentau QJ. Architecture and regulation of the HIV-1 assembly and holding compartment in macrophages. *J Virol* (2011) 85:7922–7. doi:10.1128/JVI.00834-11
100. Gaudin R, Berre S, Cunha De Alencar B, Decalf J, Schindler M, Gobert FX, et al. Dynamics of HIV-containing compartments in macrophages reveal sequestration of virions and transient surface connections. *PLoS One* (2013) 8:e69450. doi:10.1371/journal.pone.0069450
101. Waheed AA, Freed EO. Lipids and membrane microdomains in HIV-1 replication. *Virus Res* (2009) 143:162–76. doi:10.1016/j.virusres.2009.04.007
102. Mlcochova P, Pelchen-Matthews A, Marsh M. Organization and regulation of intracellular plasma membrane-connected HIV-1 assembly compartments in macrophages. *BMC Biol* (2013) 11:89. doi:10.1186/1741-7007-11-89
103. Nkwe DO, Pelchen-Matthews A, Burden JJ, Collinson LM, Marsh M. The intracellular plasma membrane-connected compartment in the assembly of HIV-1 in human macrophages. *BMC Biol* (2016) 14:50. doi:10.1186/s12915-016-0272-3
104. Pelchen-Matthews A, Kramer B, Marsh M. Infectious HIV-1 assembles in late endosomes in primary macrophages. *J Cell Biol* (2003) 162:443–55. doi:10.1083/jcb.200304008
105. Berre S, Gaudin R, Cunha De Alencar B, Desdouits M, Chabaud M, Naffakh N, et al. CD36-specific antibodies block release of HIV-1 from infected primary macrophages and its transmission to T cells. *J Exp Med* (2013) 210:2523–38. doi:10.1084/jem.20130566
106. Raposo G, Moore M, Innes D, Leijendekker R, Leigh-Brown A, Benaroch P, et al. Human macrophages accumulate HIV-1 particles in MHC II compartments. *Traffic* (2002) 3:718–29. doi:10.1034/j.1600-0854.2002.31004.x
107. Lippincott-Schwartz J, Freed EO, Van Engelenburg SB. A consensus view of ESCRT-mediated human immunodeficiency virus type 1 abscission. *Annu Rev Virol* (2017) 4:309–25. doi:10.1146/annurev-virology-101416-041840
108. Welsch S, Habermann A, Jager S, Muller B, Krijnse-Locker J, Krausslich HG. Ultrastructural analysis of ESCRT proteins suggests a role for endosome-associated tubular-vesicular membranes in ESCRT function. *Traffic* (2006) 7:1551–66. doi:10.1111/j.1600-0854.2006.00489.x
109. Chertova E, Chertov O, Coren LV, Roser JD, Trubey CM, Bess JW Jr, et al. Proteomic and biochemical analysis of purified human immunodeficiency virus type 1 produced from infected monocyte-derived macrophages. *J Virol* (2006) 80:9039–52. doi:10.1128/JVI.01013-06
110. Dotson D, Woodruff EA, Villalta F, Dong X. Filamin A is involved in HIV-1 Vpu-mediated evasion of host restriction by modulating tetherin expression. *J Biol Chem* (2016) 291:4236–46. doi:10.1074/jbc.M115.708123
111. Bennett AE, Narayan K, Shi D, Hartnell LM, Gousset K, He H, et al. Ion-abrasion scanning electron microscopy reveals surface-connected tubular conduits in HIV-infected macrophages. *PLoS Pathog* (2009) 5:e1000591. doi:10.1371/journal.ppat.1000591
112. Mariani C, Desdouits M, Favard C, Benaroch P, Muriaux DM. Role of Gag and lipids during HIV-1 assembly in CD4(+) T cells and macrophages. *Front Microbiol* (2014) 5:312. doi:10.3389/fmicb.2014.00312
113. Kutluay SB, Bieniasz PD. Analysis of the initiating events in HIV-1 particle assembly and genome packaging. *PLoS Pathog* (2010) 6:e1001200. doi:10.1371/journal.ppat.1001200
114. Kutluay SB, Zang T, Blanco-Melo D, Powell C, Jannain D, Errando M, et al. Global changes in the RNA binding specificity of HIV-1 gag regulate virion genesis. *Cell* (2014) 159:1096–109. doi:10.1016/j.cell.2014.09.057
115. Ono A, Waheed AA, Freed EO. Depletion of cellular cholesterol inhibits membrane binding and higher-order multimerization of human immunodeficiency virus type 1 Gag. *Virology* (2007) 360:27–35. doi:10.1016/j.virol.2006.10.011
116. Chukkapalli V, Hogue IB, Boyko V, Hu WS, Ono A. Interaction between the human immunodeficiency virus type 1 Gag matrix domain and phosphatidylinositol-(4,5)-bisphosphate is essential for efficient gag membrane binding. *J Virol* (2008) 82:2405–17. doi:10.1128/JVI.01614-07
117. Balasubramaniam M, Freed EO. New insights into HIV assembly and trafficking. *Physiology (Bethesda)* (2011) 26:236–51. doi:10.1152/physiol.00051.2010
118. Inlora J, Chukkapalli V, Bedi S, Ono A. Molecular determinants directing HIV-1 Gag assembly to virus-containing compartments in primary macrophages. *J Virol* (2016) 90:8509–19. doi:10.1128/JVI.01004-16
119. Schoneberg J, Lee IH, Iwasa JH, Hurley JH. Reverse-topology membrane scission by the ESCRT proteins. *Nat Rev Mol Cell Biol* (2017) 18:5–17. doi:10.1038/nrm.2016.121
120. Pelchen-Matthews A, Giese S, Mlcochova P, Turner J, Marsh M. beta2 Integrin adhesion complexes maintain the integrity of HIV-1 assembly compartments in primary macrophages. *Traffic* (2012) 13:273–91. doi:10.1111/j.1600-0854.2011.01306.x
121. Dinkins C, Pilli M, Kehrl JH. Roles of autophagy in HIV infection. *Immunol Cell Biol* (2015) 93:11–7. doi:10.1038/icb.2014.88
122. Gaudin R, De Alencar BC, Jouve M, Berre S, Le Bouder E, Schindler M, et al. Critical role for the kinesin KIF3A in the HIV life cycle in primary human macrophages. *J Cell Biol* (2012) 199:467–79. doi:10.1083/jcb.201201144
123. Gaudin R, De Alencar BC, Arhel N, Benaroch P. HIV trafficking in host cells: motors wanted! *Trends Cell Biol* (2013) 23:652–62. doi:10.1016/j.tcb.2013.09.004
124. Giese S, Marsh M. Tetherin can restrict cell-free and cell-cell transmission of HIV from primary macrophages to T cells. *PLoS Pathog* (2014) 10:e1004189. doi:10.1371/journal.ppat.1004189
125. Graziano F, Desdouits M, Garzetti L, Podini P, Alfano M, Rubartelli A, et al. Extracellular ATP induces the rapid release of HIV-1 from virus containing compartments of human macrophages. *Proc Natl Acad Sci U S A* (2015) 112:E3265–73. doi:10.1073/pnas.1500656112
126. Koppensteiner H, Banning C, Schneider C, Hohenberg H, Schindler M. Macrophage internal HIV-1 is protected from neutralizing antibodies. *J Virol* (2012) 86:2826–36. doi:10.1128/JVI.05915-11

127. Graziano F, Vicenzi E, Poli G. Immuno-pharmacological targeting of virus-containing compartments in HIV-1-infected macrophages. *Trends Microbiol* (2016) 24:558–67. doi:10.1016/j.tim.2016.02.018
128. Orenstein JM, Meltzer MS, Phipps T, Gendelman HE. Cytoplasmic assembly and accumulation of human immunodeficiency virus types 1 and 2 in recombinant human colony-stimulating factor-1-treated human monocytes: an ultrastructural study. *J Virol* (1988) 62:2578–86.
129. Orenstein JM. Replication of HIV-1 in vivo and in vitro. *Ultrastruct Pathol* (2007) 31:151–67. doi:10.1080/01913120701344343
130. Sattentau Q. Avoiding the void: cell-to-cell spread of human viruses. *Nat Rev Microbiol* (2008) 6:815–26. doi:10.1038/nrmicro1972
131. Law KM, Satija N, Esposito AM, Chen BK. Cell-to-cell spread of HIV and viral pathogenesis. *Adv Virus Res* (2016) 95:43–85. doi:10.1016/bs.aivir.2016.03.001
132. Agosto LM, Uchil PD, Mothes W. HIV cell-to-cell transmission: effects on pathogenesis and antiretroviral therapy. *Trends Microbiol* (2015) 23:289–95. doi:10.1016/j.tim.2015.02.003
133. Groot F, Welsch S, Sattentau QJ. Efficient HIV-1 transmission from macrophages to T cells across transient virological synapses. *Blood* (2008) 111:4660–3. doi:10.1182/blood-2007-12-130070
134. Gousset K, Ablan SD, Coren LV, Ono A, Soheilian F, Nagashima K, et al. Real-time visualization of HIV-1 GAG trafficking in infected macrophages. *PLoS Pathog* (2008) 4:e1000015. doi:10.1371/journal.ppat.1000015
135. Duncan CJ, Williams JP, Schiffner T, Gartner K, Ochsenbauer C, Kappes J, et al. High-multiplicity HIV-1 infection and neutralizing antibody evasion mediated by the macrophage-T cell virological synapse. *J Virol* (2014) 88:2025–34. doi:10.1128/JVI.03245-13
136. Izquierdo-Useros N, Lorizate M, Mclaren PJ, Telenti A, Krausslich HG, Martinez-Picado J. HIV-1 capture and transmission by dendritic cells: the role of viral glycolipids and the cellular receptor Siglec-1. *PLoS Pathog* (2014) 10:e1004146. doi:10.1371/journal.ppat.1004146
137. Piguet V, Sattentau Q. Dangerous liaisons at the virological synapse. *J Clin Invest* (2004) 114:605–10. doi:10.1172/JCI22812
138. Coleman CM, Gelais CS, Wu L. Cellular and viral mechanisms of HIV-1 transmission mediated by dendritic cells. *Adv Exp Med Biol* (2013) 762:109–30. doi:10.1007/978-1-4614-4433-6_4
139. Sewald X, Ladinsky MS, Uchil PD, Beloor J, Pi R, Herrmann C, et al. Retroviruses use CD169-mediated trans-infection of permissive lymphocytes to establish infection. *Science* (2015) 350:563–7. doi:10.1126/science.aab2749
140. Hammonds JE, Beeman N, Ding L, Takushi S, Francis AC, Wang JJ, et al. Siglec-1 initiates formation of the virus-containing compartment and enhances macrophage-to-T cell transmission of HIV-1. *PLoS Pathog* (2017) 13:e1006181. doi:10.1371/journal.ppat.1006181
141. Chun TW, Moir S, Fauci AS. HIV reservoirs as obstacles and opportunities for an HIV cure. *Nat Immunol* (2015) 16:584–9. doi:10.1038/ni.3152
142. Finzi D, Hermankova M, Pierson T, Carruth LM, Buck C, Chaisson RE, et al. Identification of a reservoir for HIV-1 in patients on highly active antiretroviral therapy. *Science* (1997) 278:1295–300. doi:10.1126/science.278.5341.1295
143. Wong JK, Hezareh M, Gunthard HF, Havlir DV, Ignacio CC, Spina CA, et al. Recovery of replication-competent HIV despite prolonged suppression of plasma viremia. *Science* (1997) 278:1291–5. doi:10.1126/science.278.5341.1291
144. Davey RT Jr, Bhat N, Yoder C, Chun TW, Metcalf JA, Dewar R, et al. HIV-1 and T cell dynamics after interruption of highly active antiretroviral therapy (HAART) in patients with a history of sustained viral suppression. *Proc Natl Acad Sci U S A* (1999) 96:15109–14. doi:10.1073/pnas.96.26.15109
145. Margolis DM, Garcia JV, Hazuda DJ, Haynes BF. Latency reversal and viral clearance to cure HIV-1. *Science* (2016) 353:aaf6517. doi:10.1126/science.aaf6517
146. Barton K, Winckelmann A, Palmer S. HIV-1 reservoirs during suppressive therapy. *Trends Microbiol* (2016) 24:345–55. doi:10.1016/j.tim.2016.01.006
147. Dahabieh MS, Battivelli E, Verdin E. Understanding HIV latency: the road to an HIV cure. *Annu Rev Med* (2015) 66:407–21. doi:10.1146/annurev-med-092112-152941
148. Chomont N, El-Far M, Ancuta P, Trautmann L, Procopio FA, Yassine-Diab B, et al. HIV reservoir size and persistence are driven by T cell survival and homeostatic proliferation. *Nat Med* (2009) 15:893–900. doi:10.1038/nm.1972
149. Buzon MJ, Sun H, Li C, Shaw A, Seiss K, Ouyang Z, et al. HIV-1 persistence in CD4+ T cells with stem cell-like properties. *Nat Med* (2014) 20:139–42. doi:10.1038/nm.3445
150. Soriano-Sarabia N, Bateson RE, Dahl NP, Crooks AM, Kuruc JD, Margolis DM, et al. Quantitation of replication-competent HIV-1 in populations of resting CD4+ T cells. *J Virol* (2014) 88:14070–7. doi:10.1128/JVI.01900-14
151. Descours B, Petitjean G, Lopez-Zaragoza JL, Bruel T, Raffel R, Psomas C, et al. CD32a is a marker of a CD4 T-cell HIV reservoir harbouring replication-competent proviruses. *Nature* (2017) 543:564–7. doi:10.1038/nature21710
152. Chun TW, Engel D, Berrey MM, Shea T, Corey L, Fauci AS. Early establishment of a pool of latently infected, resting CD4(+) T cells during primary HIV-1 infection. *Proc Natl Acad Sci U S A* (1998) 95:8869–73. doi:10.1073/pnas.95.15.8869
153. Whitney JB, Hill AL, Sanisetty S, Penaloza-Macmaster P, Liu J, Shetty M, et al. Rapid seeding of the viral reservoir prior to SIV viraemia in rhesus monkeys. *Nature* (2014) 512:74–7. doi:10.1038/nature13594
154. Siliciano JD, Kajdas J, Finzi D, Quinn TC, Chadwick K, Margolick JB, et al. Long-term follow-up studies confirm the stability of the latent reservoir for HIV-1 in resting CD4+ T cells. *Nat Med* (2003) 9:727–8. doi:10.1038/nm880
155. Crooks AM, Bateson R, Cope AB, Dahl NP, Griggs MK, Kuruc JD, et al. Precise quantitation of the latent HIV-1 reservoir: implications for eradication strategies. *J Infect Dis* (2015) 212:1361–5. doi:10.1093/infdis/jiv218
156. Churchill MJ, Deeks SG, Margolis DM, Siliciano RF, Swanstrom R. HIV reservoirs: what, where and how to target them. *Nat Rev Microbiol* (2016) 14:55–60. doi:10.1038/nrmicro.2015.5
157. Dornadula G, Zhang H, Vanuitert B, Stern J, Livornese L Jr, Ingerman MJ, et al. Residual HIV-1 RNA in blood plasma of patients taking suppressive highly active antiretroviral therapy. *JAMA* (1999) 282:1627–32. doi:10.1001/jama.282.17.1627
158. Nettles RE, Kieffer TL, Kwon P, Monie D, Han Y, Parsons T, et al. Intermittent HIV-1 viremia (Blips) and drug resistance in patients receiving HAART. *JAMA* (2005) 293:817–29. doi:10.1001/jama.293.7.817
159. Josefsson L, Von Stockenstrom S, Faria NR, Sinclair E, Bacchetti P, Killian M, et al. The HIV-1 reservoir in eight patients on long-term suppressive antiretroviral therapy is stable with few genetic changes over time. *Proc Natl Acad Sci U S A* (2013) 110:E4987–96. doi:10.1073/pnas.1308313110
160. Kearney MF, Spindler J, Shao W, Yu S, Anderson EM, O'Shea A, et al. Lack of detectable HIV-1 molecular evolution during suppressive antiretroviral therapy. *PLoS Pathog* (2014) 10:e1004010. doi:10.1371/journal.ppat.1004010
161. Siliciano JD, Siliciano RF. Recent trends in HIV-1 drug resistance. *Curr Opin Virol* (2013) 3:487–94. doi:10.1016/j.coviro.2013.08.007
162. Lorenzo-Redondo R, Fryer HR, Bedford T, Kim EY, Archer J, Pond SLK, et al. Persistent HIV-1 replication maintains the tissue reservoir during therapy. *Nature* (2016) 530:51–6. doi:10.1038/nature16933
163. Fox CH, Tenner-Racz K, Racz P, Firpo A, Pizzo PA, Fauci AS. Lymphoid germinal centers are reservoirs of human immunodeficiency virus type 1 RNA. *J Infect Dis* (1991) 164:1051–7. doi:10.1093/infdis/164.6.1051
164. Fletcher CV, Staskus K, Wietgrefe SW, Rothenberger M, Reilly C, Chipman JG, et al. Persistent HIV-1 replication is associated with lower antiretroviral drug concentrations in lymphatic tissues. *Proc Natl Acad Sci U S A* (2014) 111:2307–12. doi:10.1073/pnas.1318249111
165. Connick E, Mattila T, Folkvord JM, Schlichtemeier R, Meditz AL, Ray MG, et al. CTL fail to accumulate at sites of HIV-1 replication in lymphoid tissue. *J Immunol* (2007) 178:6975–83. doi:10.4049/jimmunol.178.11.6975
166. Mylvaganam GH, Rios D, Abdelaal HM, Iyer S, Tharp G, Mavinger M, et al. Dynamics of SIV-specific CXCR5+ CD8 T cells during chronic SIV infection. *Proc Natl Acad Sci U S A* (2017) 114:1976–81. doi:10.1073/pnas.1621418114
167. Keele BF, Tazi L, Gartner S, Liu Y, Burgon TB, Estes JD, et al. Characterization of the follicular dendritic cell reservoir of human immunodeficiency virus type 1. *J Virol* (2008) 82:5548–61. doi:10.1128/JVI.00124-08
168. Perreau M, Savoye AL, De Crignis E, Corpataux JM, Cubas R, Haddad EK, et al. Follicular helper T cells serve as the major CD4 T cell compartment for HIV-1 infection, replication, and production. *J Exp Med* (2013) 210:143–56. doi:10.1084/jem.20121932
169. Banga R, Procopio FA, Noto A, Pollakis G, Cavassini M, Ohmiti K, et al. PD-1(+) and follicular helper T cells are responsible for persistent HIV-1 transcription in treated aviremic individuals. *Nat Med* (2016) 22:754–61. doi:10.1038/nm.4113
170. Moukambi F, Rodrigues V, Fortier Y, Rabezanahary H, Borde C, Krust B, et al. CD4 T follicular helper cells and HIV infection: friends or enemies? *Front Immunol* (2017) 8:135. doi:10.3389/fimmu.2017.00135

171. Kandathil AJ, Sugawara S, Balagopal A. Are T cells the only HIV-1 reservoir? *Retrovirology* (2016) 13:86. doi:10.1186/s12977-016-0323-4
172. Chun TW, Davey RT Jr, Ostrowski M, Shawn Justement J, Engel D, Mullins JI, et al. Relationship between pre-existing viral reservoirs and the re-emergence of plasma viremia after discontinuation of highly active anti-retroviral therapy. *Nat Med* (2000) 6:757–61. doi:10.1038/77481
173. Clayton KL, Garcia JV, Clements JE, Walker BD. HIV infection of macrophages: implications for pathogenesis and cure. *Pathog Immun* (2017) 2:179–92. doi:10.20411/pai.v2i2.204
174. Eriksson S, Graf EH, Dahl V, Strain MC, Yukl SA, Lysenko ES, et al. Comparative analysis of measures of viral reservoirs in HIV-1 eradication studies. *PLoS Pathog* (2013) 9:e1003174. doi:10.1371/journal.ppat.1003174
175. Cribbs SK, Lennox J, Caliendo AM, Brown LA, Guidot DM. Healthy HIV-1-infected individuals on highly active antiretroviral therapy harbor HIV-1 in their alveolar macrophages. *AIDS Res Hum Retroviruses* (2015) 31:64–70. doi:10.1089/AID.2014.0133
176. Kandathil AJ, Durand CM, Quinn J, Cameron AM, Thomas DL, Balagopal A. Liver macrophages and HIV persistence. *Conference on Retroviruses and Opportunistic Infections*. Seattle, WA (2015).
177. Sanchez G, Xu X, Chermann JC, Hirsch I. Accumulation of defective viral genomes in peripheral blood mononuclear cells of human immunodeficiency virus type 1-infected individuals. *J Virol* (1997) 71:2233–40.
178. Bruner KM, Murray AJ, Pollack RA, Soliman MG, Laskey SB, Capoferri AA, et al. Defective proviruses rapidly accumulate during acute HIV-1 infection. *Nat Med* (2016) 22:1043–9. doi:10.1038/nm.4156
179. Honeycutt JB, Wahl A, Baker C, Spagnuolo RA, Foster J, Zakharova O, et al. Macrophages sustain HIV replication in vivo independently of T cells. *J Clin Invest* (2016) 126:1353–66. doi:10.1172/JCI84456
180. Honeycutt JB, Thayer WO, Baker CE, Ribeiro RM, Lada SM, Cao Y, et al. HIV persistence in tissue macrophages of humanized myeloid-only mice during antiretroviral therapy. *Nat Med* (2017) 23:638–43. doi:10.1038/nm.4319
181. Honeycutt JB, Wahl A, Archin N, Choudhary S, Margolis D, Garcia JV. HIV-1 infection, response to treatment and establishment of viral latency in a novel humanized T cell-only mouse (TOM) model. *Retrovirology* (2013) 10:121. doi:10.1186/1742-4690-10-121
182. Archin NM, Sung JM, Garrido C, Soriano-Sarabia N, Margolis DM. Eradicating HIV-1 infection: seeking to clear a persistent pathogen. *Nat Rev Microbiol* (2014) 12:750–64. doi:10.1038/nrmicro3352
183. Kumar A, Abbas W, Herbein G. HIV-1 latency in monocytes/macrophages. *Viruses* (2014) 6:1837–60. doi:10.3390/v6041837
184. Metcalf Pate KA, Pohlmeyer CW, Walker-Sperling VE, Foote JB, Najarro KM, Cryer CG, et al. A murine viral outgrowth assay to detect residual HIV type 1 in patients with undetectable viral loads. *J Infect Dis* (2015) 212:1387–96. doi:10.1093/infdis/jiv230
185. Henrich TJ, Deeks SG, Pillai SK. Measuring the size of the latent human immunodeficiency virus reservoir: the present and future of evaluating eradication strategies. *J Infect Dis* (2017) 215:S134–41. doi:10.1093/infdis/jiw648
186. Deeks SG, Lewin SR, Havlir DV. The end of AIDS: HIV infection as a chronic disease. *Lancet* (2013) 382:1525–33. doi:10.1016/S0140-6736(13)61809-7
187. Guaraldi G, Orlando G, Zona S, Menozzi M, Carli F, Garlassi E, et al. Premature age-related comorbidities among HIV-infected persons compared with the general population. *Clin Infect Dis* (2011) 53:1120–6. doi:10.1093/cid/cir627
188. Brenchley JM, Price DA, Schacker TW, Asher TE, Silvestri G, Rao S, et al. Microbial translocation is a cause of systemic immune activation in chronic HIV infection. *Nat Med* (2006) 12:1365–71. doi:10.1038/nm1511
189. Marchetti G, Tincati C, Silvestri G. Microbial translocation in the pathogenesis of HIV infection and AIDS. *Clin Microbiol Rev* (2013) 26:2–18. doi:10.1128/CMR.00050-12
190. Hunt PW. Th17, gut, and HIV: therapeutic implications. *Curr Opin HIV AIDS* (2010) 5:189–93. doi:10.1097/COH.0b013e32833647d9
191. Marchetti G, Bellistri GM, Borghi E, Tincati C, Ferramosca S, La Francesca M, et al. Microbial translocation is associated with sustained failure in CD4+ T-cell reconstitution in HIV-infected patients on long-term highly active antiretroviral therapy. *AIDS* (2008) 22:2035–8. doi:10.1097/QAD.0b013e3283112d29
192. Sandler NG, Wand H, Roque A, Law M, Nason MC, Nixon DE, et al. Plasma levels of soluble CD14 independently predict mortality in HIV infection. *J Infect Dis* (2011) 203:780–90. doi:10.1093/infdis/jiq118
193. Estes JD, Gordon SN, Zeng M, Chahroudi AM, Dunham RM, Staprans SI, et al. Early resolution of acute immune activation and induction of PD-1 in SIV-infected sooty mangabeys distinguishes nonpathogenic from pathogenic infection in rhesus macaques. *J Immunol* (2008) 180:6798–807. doi:10.4049/jimmunol.180.10.6798
194. Walker JA, Beck GA, Campbell JH, Miller AD, Burdo TH, Williams KC. Anti-alpha4 integrin antibody blocks monocyte/macrophage traffic to the heart and decreases cardiac pathology in a SIV infection model of AIDS. *J Am Heart Assoc* (2015) 4:e001932. doi:10.1161/JAHA.115.001932
195. Dinapoli SR, Hirsch VM, Brenchley JM. Macrophages in progressive human immunodeficiency virus/simian immunodeficiency virus infections. *J Virol* (2016) 90:7596–606. doi:10.1128/JVI.00672-16
196. Saylor D, Dickens AM, Sacktor N, Haughey N, Slusher B, Pletnikov M, et al. HIV-associated neurocognitive disorder – pathogenesis and prospects for treatment. *Nat Rev Neurol* (2016) 12:309. doi:10.1038/nrneurol.2016.53
197. Heaton RK, Franklin DR Jr, Deutsch R, Letendre S, Ellis RJ, Casaletto K, et al. Neurocognitive change in the era of HIV combination antiretroviral therapy: the longitudinal CHARTER study. *Clin Infect Dis* (2015) 60:473–80. doi:10.1093/cid/ciu862
198. Cosenza MA, Zhao ML, Si Q, Lee SC. Human brain parenchymal microglia express CD14 and CD45 and are productively infected by HIV-1 in HIV-1 encephalitis. *Brain Pathol* (2002) 12:442–55. doi:10.1111/j.1750-3639.2002.tb00461.x
199. Thompson KA, Cherry CL, Bell JE, Mclean CA. Brain cell reservoirs of latent virus in presymptomatic HIV-infected individuals. *Am J Pathol* (2011) 179:1623–9. doi:10.1016/j.ajpath.2011.06.039
200. Eden A, Fuchs D, Hagberg L, Nilsson S, Spudich S, Svennerholm B, et al. HIV-1 viral escape in cerebrospinal fluid of subjects on suppressive antiretroviral treatment. *J Infect Dis* (2010) 202:1819–25. doi:10.1086/657342
201. Dahl V, Gisslen M, Hagberg L, Peterson J, Shao W, Spudich S, et al. An example of genetically distinct HIV type 1 variants in cerebrospinal fluid and plasma during suppressive therapy. *J Infect Dis* (2014) 209:1618–22. doi:10.1093/infdis/jit805
202. Sturdevant CB, Joseph SB, Schnell G, Price RW, Swanstrom R, Spudich S. Compartmentalized replication of R5 T cell-tropic HIV-1 in the central nervous system early in the course of infection. *PLoS Pathog* (2015) 11:e1004720. doi:10.1371/journal.ppat.1004720
203. Fois AF, Brew BJ. The potential of the CNS as a reservoir for HIV-1 infection: implications for HIV eradication. *Curr HIV/AIDS Rep* (2015) 12:299–303. doi:10.1007/s11904-015-0257-9
204. Ancuta P, Kamat A, Kunstman KJ, Kim EY, Autissier P, Wurcel A, et al. Microbial translocation is associated with increased monocyte activation and dementia in AIDS patients. *PLoS One* (2008) 3:e2516. doi:10.1371/journal.pone.0002516
205. Fischer-Smith T, Croul S, Sverstiuk AE, Capini C, L'Heureux D, Regulier EG, et al. CNS invasion by CD14+/CD16+ peripheral blood-derived monocytes in HIV dementia: perivascular accumulation and reservoir of HIV infection. *J Neurovirol* (2001) 7:528–41. doi:10.1080/13550280175324811 4
206. Buckner CM, Calderon TM, Willams DW, Belbin TJ, Berman JW. Characterization of monocyte maturation/differentiation that facilitates their transmigration across the blood-brain barrier and infection by HIV: implications for NeuroAIDS. *Cell Immunol* (2011) 267:109–23. doi:10.1016/j.cellimm.2010.12.004
207. Silvin A, Yu CI, Lahaye X, Imperatore F, Brault JB, Cardinaud S, et al. Constitutive resistance to viral infection in human CD141+ dendritic cells. *Sci Immunol* (2017) 2:eaai8071. doi:10.1126/sciimmunol.aai8071

Conflict of Interest Statement: The authors declare that the research was conducted in the absence of any commercial or financial relationships that could be construed as a potential conflict of interest.

Copyright © 2017 Rodrigues, Ruffin, San-Roman and Benaroch. This is an open-access article distributed under the terms of the Creative Commons Attribution License (CC BY). The use, distribution or reproduction in other forums is permitted, provided the original author(s) or licensor are credited and that the original publication in this journal is cited, in accordance with accepted academic practice. No use, distribution or reproduction is permitted which does not comply with these terms.

frontiers in Immunology

REVIEW
published: 05 December 2017
doi: 10.3389/fimmu.2017.01693

Role of Monocyte/Macrophages during HIV/SIV Infection in Adult and Pediatric Acquired Immune Deficiency Syndrome

*Kristen M. Merino[1], Carolina Allers[1], Elizabeth S. Didier[2] and Marcelo J. Kuroda[1]**

[1] Division of Immunology, Tulane National Primate Research Center, Covington LA, United States, [2] Division of Microbiology, Tulane National Primate Research Center, Covington LA, United States

Monocytes/macrophages are a diverse group of cells that act as first responders in innate immunity and then as mediators for adaptive immunity to help clear infections. In performing these functions, however, the macrophage inflammatory responses can also contribute to pathogenesis. Various monocyte and tissue macrophage subsets have been associated with inflammatory disorders and tissue pathogeneses such as occur during HIV infection. Non-human primate research of simian immunodeficiency virus (SIV) has been invaluable in better understanding the pathogenesis of HIV infection. The question of HIV/SIV-infected macrophages serving as a viral reservoir has become significant for achieving a cure. In the rhesus macaque model, SIV-infected macrophages have been shown to promote pathogenesis in several tissues resulting in cardiovascular, metabolic, and neurological diseases. Results from human studies illustrated that alveolar macrophages could be an important HIV reservoir and humanized myeloid-only mice supported productive HIV infection and viral persistence in macrophages during ART treatment. Depletion of CD4+ T cells is considered the primary cause for terminal progression, but it was reported that increasing monocyte turnover was a significantly better predictor in SIV-infected adult macaques. Notably, pediatric cases of HIV/SIV exhibit faster and more severe disease progression than adults, yet neonates have fewer target T cells and generally lack the hallmark CD4+ T cell depletion typical of adult infections. Current data show that the baseline blood monocyte turnover rate was significantly higher in neonatal macaques compared to adults and this remained high with disease progression. In this review, we discuss recent data exploring the contribution of monocytes and macrophages to HIV/SIV infection and progression. Furthermore, we highlight the need to further investigate their role in pediatric cases of infection.

Keywords: HIV, SIV, macrophages, monocytes, pediatrics, Acquired Immune Deficiency Syndrome

OPEN ACCESS

Edited by:
Geanncarlo Lugo-Villarino, UMR5089 Institut de Pharmacologie et de Biologie Structurale (IPBS), France

Reviewed by:
Masaaki Miyazawa, Kindai University, Japan
Nina Derby, Population Council, United States
Donald Sodora, Center for Infectious Disease Research, United States

***Correspondence:**
Marcelo J. Kuroda
mkuroda@tulane.edu

Specialty section:
This article was submitted to Microbial Immunology, a section of the journal Frontiers in Immunology

Received: *14 August 2017*
Accepted: *16 November 2017*
Published: *05 December 2017*

Citation:
Merino KM, Allers C, Didier ES and Kuroda MJ (2017) Role of Monocyte/Macrophages during HIV/SIV Infection in Adult and Pediatric Acquired Immune Deficiency Syndrome. Front. Immunol. 8:1693. doi: 10.3389/fimmu.2017.01693

INTRODUCTION

A cure for HIV infection continues to be elusive, despite the use of antiretroviral therapy (ART). Studies using non-human primate (NHPs) models of simian immunodeficiency virus (SIV) have been invaluable in better understanding the pathogenesis of this infection. Declining numbers of CD4+ T cells during HIV/SIV infections have long been attributed as the primary cause of

immune-deficiency, progression to acquired immune deficiency syndrome (AIDS), and sites of virus reservoirs established during ART. While it is likely that various other immune cells influence disease progression and viral seeding, the purpose of this review is to focus on the contribution of monocytes and macrophages to HIV/SIV infection. Although in adult macaques, monocyte levels in blood remain constant during infection, the monocyte turnover rate increases during the onset of simian AIDS (SAIDS) and reflects damage to short-lived tissue macrophages. Interestingly, physiological monocyte turnover rate in neonates (<1 month old) is higher than in adults and appears to be associated with the more rapid disease progression that occurs in pediatric HIV/SIV infections. As infants became older (<1 year old), they exhibited a biphasic pattern of monocyte turnover and disease progression, with some animals presenting with rapid disease such as seen in neonates, while others progressed similarly as adult macaques. We theorize that the magnitude of infected macrophages influences disease outcome, and susceptibility of macrophages to infection is impacted by age. Our data suggest shorter-lived macrophages are more easily destroyed by virus while longer-lived macrophages appear more resistant to destruction and may contribute to the viral reservoir. This review discusses the possible contributions of macrophages to HIV/SIV infection and pathogenesis. It is important to consider that macrophages also may need to be targeted to achieve cure.

MACROPHAGES IN HEALTH AND DISEASE

The immune system is essential for maintaining health and combatting infectious disease (1). Innate immune responses typically act immediately to produce inflammation and are performed directly by immune surveillance by effector cells such as neutrophils, natural killer (NK) cells, and macrophages. The innate immune cells work en masse to detect and clear pathogens and this is thought to limit the initial infection and thus buys time for adaptive immune responses to mount. Adaptive immune responses generally require weeks-to-months to develop and rely heavily on antigen-presenting cells (e.g., dendritic cells, macrophages, B cells) and T cells to clear infection and establish immunologic memory.

Macrophages are a diverse group of cells that play important roles in both innate and adaptive immune responses. During innate immune responses, macrophages sense and promote inflammation and recruit effector cells for clearance of pathogens. In adaptive immune responses, they function in antigen presentation and secretion of immune modulators for recruitment of lymphocytes (1). In addition, macrophages are imperative for tissue modeling during fetal development, maintaining homeostasis, and wound healing (2–4). Conversely, dysfunctional macrophages and unregulated inflammation are devastating to homeostasis and may instead contribute to pathogenesis in specific disease settings, such as pulmonary tissue injury during asthma (5), islet cell destruction in diabetes (6), and neurological damage, lymphoma and cardiovascular disease during human immunodeficiency virus (HIV) infection [reviewed in Ref. (7)].

Macrophages are derived from multiple sources during development, with earliest generation from the yolk sac during embryogenesis, and later generation from the fetal liver and bone marrow. In human and rhesus macaque adults, replenishment of tissue macrophages lost from death due to infection or injury occurs mainly from monocytes generated by hematopoietic stem cells in the bone marrow, which then circulate through the blood stream, deposit into the tissues, and differentiate into various types of macrophages (8–10). Macrophages in the mouse model have been shown to self-renew rather than being replaced with emigrating monocytes from the periphery (11–13). Based on published reports in murine models, tissue-resident macrophages can originate from two sources, with the self-renewing subset derived from the fetal liver during embryonic development and from the bone marrow after birth [reviewed in Ref. (10, 14)]. Studies have yet to identify self-renewing macrophages in primates, with possible exception of the brain (15). As summarized in **Figure 1**, there exist at least two types of macrophages in the tissues; the short-lived macrophages that are continuously replenished by circulating classical monocytes arising from the bone marrow and the long-lived macrophages. These two types of macrophages appear to differ in their phenotypes and functions, so it is critical to better understand their unique roles during development, immune responses, disease pathogenesis, and maintaining homeostasis.

Historically, subsets of macrophages have largely been classified as pro-inflammatory (M1) or anti-inflammatory (M2) on the basis of expressing various markers, secreting cytokines, and phagocytic and antigen-presenting functions. Results from more recent research has suggested that the polarization of macrophage phenotypes is more fluid and less dichotomous than originally thought, based on the ability of macrophages to change phenotypes in response to changes in the surrounding environment within the tissues and vasculature (16). Generally, tissue-resident macrophages appear more M2-like with functions supporting an anti-inflammatory environment such as phagocytosing debris and promoting healing and growth. These tissue-resident macrophages are considered longer-lived as illustrated in the lung with alveolar macrophages (17). Macrophages recruited from circulating monocytes, in contrast, largely constitute the interstitial macrophages (IM) in the lung and subsets of perivascular macrophages in the brain and are thought to be shorter-lived. These have been classified as both M1-like and M2-like depending on immune homeostasis, infection events, and expression of MAC387 and CD163 differentiation markers, respectively (16). CD163, a hemoglobin/haptoglobin scavenger receptor associated with anti-inflammatory responses, is expressed on subsets of tissue macrophages as well as on monocyte populations, which are thought to derive from CD14+CD16− monocytes (18). Soluble CD163 shed from monocyte populations exerts anti-inflammatory functions, and studies showed that increased levels are associated with infectious and autoimmune diseases [reviewed in Ref. (19)]. MAC387 recognizes the L1 or Calprotectin molecule, and has been used to identify recently infiltrated macrophages associated with acute inflammation (20, 21). During infections, particularly in the case of HIV/SIV disease progression, increased monocyte turnover occurs in association with an accumulation

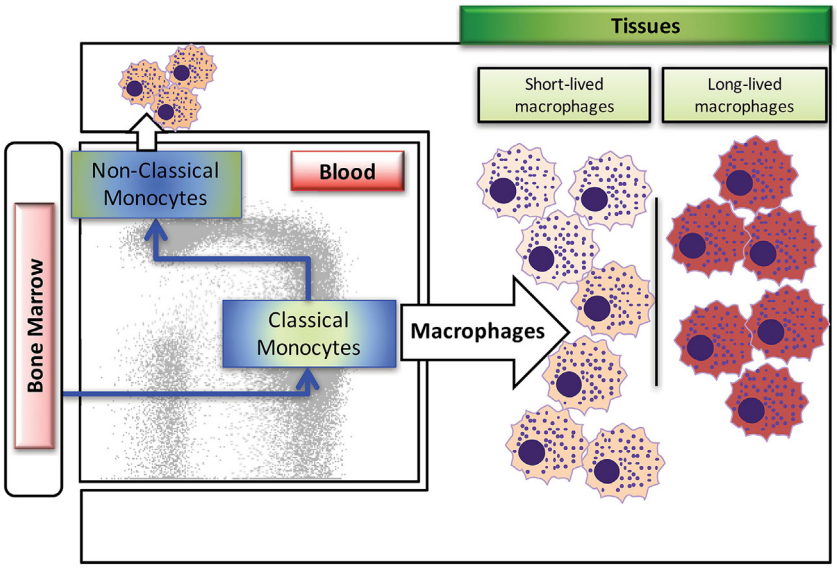


FIGURE 1 | Summary of blood monocyte and dendritic cells (DC) differentiation in rhesus macaques. Myeloid precursor cells in the bone marrow migrate into blood and give rise to $CD14^{+}CD16^{-}$ classical monocytes. A large proportion of these classical monocytes rapidly disappear from the circulation to become tissue macrophages. A fraction of the classical monocytes differentiate into $CD14^{+}CD16^{+}$ intermediate monocytes and then into $CD14^{-}CD16^{+}$ non-classical monocytes in the circulation. The populations of mDCs, pDCs, and perhaps other unidentified DCs appear to differentiate from various DC precursors directly in the bone marrow prior entering the blood circulation. Figure modified from Ref. (8). Copyright 2015. The American Association of Immunologists, Inc.

of these various short-lived macrophage subsets in the tissues. This macrophage deposition seems to primarily occur in classical sites of AIDS pathology, including the brain, heart, lung, and gut tissues (15, 22–24). One study proposes that during acute infection M1-like macrophages are recruited into tissues to help fight infection, while M2-like macrophages accumulate later during chronic disease to dampen inflammation and repair tissues. The accumulation of both macrophage subsets seems to promote cardiovascular disease (16). Thus, the characterization of monocyte and macrophage subsets in relation to their number, phenotype, and function becomes increasingly important for predicting disease outcomes and subsequently attempting to ameliorate or reverse pathogenesis.

HIV INFECTION

Human immunodeficiency virus is the etiological agent of AIDS and, since the beginning of this pandemic in the early 1980s, has caused the loss of over 40 million lives (25). HIV infection in humans follows a distinct pattern (26) starting with an eclipse phase during the first 1–2 weeks of infection, which constitutes a time when the virus replicates and disseminates while the immune response is developing and not yet effective at clearing the virus. HIV preferentially targets T cells for infection, using the CD4 receptor in combination with the CCR5 chemokine receptor to gain entry. Effector CD4+ T cells express the highest level of CCR5 and are depleted drastically early after infection (27) in what is known as the acute phase. This particular phase follows 2–4 weeks post-infection (pi) and is evident by high viral RNA loads in the plasma, and a reduction in peripheral CD4+ T cells. During the acute phase, there is a stark increase in detectable immune responses, most notably with higher levels of virus-specific effector CD8+ T cells and antibodies. The end of the acute phase and transition to the chronic stages of infection is characterized by a marked reduction in plasma viral load (VL) and establishment of a viral "set point" that appears to result from incomplete control of viral replication by adaptive immune responses with concurrent loss of target CD4+ T cells available for new infection. The chronic phase of HIV infection is accompanied by clinical latency that may last from 1 to 20 years in untreated individuals. Eventually CD4+ T cells decline to levels below 200 cells/μl in blood and infected individuals become susceptible to opportunistic infections such as *Pneumocystis jiroveci* (earlier named *P. carinii*), cytomegalovirus, *Cryptosporidium* spp., and *Mycobacterium tuberculosis,* and cancers such as Kaposi's sarcoma [reviewed in Ref. (28, 29)]. These late-stage infections and cancers associated with a loss of CD4+ T cells define the onset of AIDS that ultimately leads to death (30). With the development and application of combination ART (cART), survival in HIV-infected adults has been extended by suppression of virus to undetectable levels and restoration of CD4+ T cell numbers to normal levels, thus preventing onset of AIDS (31). Instead, longer-surviving HIV-infected individuals administered cART may experience inflammation-associated chronic diseases referred to as HIV-associated non-AIDS (HANA) conditions (32).

Despite the large success of ART treatment for lifespan and clinical symptoms, it does not completely eliminate the virus, which persists in reservoirs. In general terms, a viral reservoir is defined as a virus-infected cell that persists despite treatment.

A reservoir can be described as active or latent. Active reservoirs continue to produce virus, such as HIV or SIV, and in this case the virus actively produces virons using the cells machinery for transcription and translation. This could result from an infected cell being refractory to ART treatment because the drugs may not penetrate the cell membrane or intracellular drugs may be ineffective at inhibiting the reverse transcriptase or integrase enzymes. In such cases, viral RNA or protein should be detected if expressed above threshold limits of the assay used. Alternatively latent virus reservoirs develop after insertion of viral DNA into a host cell genome. Here, virus is not actively being transcribed and effectively remains dormant. In this case, viral DNA should be detectable with sensitive assays. Cellular activation and some chemical compounds (latency reversal agents) can stimulate the active transcription and translation of the dormant virus, wherby viral RNA and protein will then be produced. Resting CD4+ T cells are thought to serve as latent reservoirs of HIV and SIV during ART treatment, and some latency reversal agents have produced successful reactivation of those reservoirs in attempt to eliminate the infection with continued long-term ART treatment. This is a fascinating and growing area of study that we will not review here but is described in depth in other reviews (33, 34).

Interestingly, in human and macaques, macrophages and dendritic cells (DC) are also capable of expressing the CD4 and CCR5 receptors required for HIV/SIV infection (35–39) and earlier work shows that macrophages can be targeted by HIV (40, 41) and SIV *in vivo* (42). Initially, virus tropism for the T cell and macrophage CCR5 receptor was used to delineate specific strains of these lentiviruses (43). It was largely accepted that while macrophages were capable of being infected by HIV, they were second to infection of CD4+ T cells, and possibly only targeted after significant loss of CD4+ T cells in the host (44). This evoked some persisting controversies regarding macrophage infection by HIV/SIV. *In vitro* studies showed that macrophages can be infected productively (45–47), and several strains of virus were considered macrophage-tropic yet *in vivo*, these same strains predominantly infected CD4+ T cells. *In vivo* data revealed that alveolar macrophages collected from bronchoalveolar lavage (BAL) in ART-treated human patients were positive for HIV DNA, indicating they are likely an important macrophage reservoir (48). Contradicting reports have indicated that while HIV DNA could be found in ART-treated human alveolar macrophages, subsequent outgrowth assays failed to detect any replication-competent virus, attributing positive DNA results to macrophage engulfment of infected CD4+ T cells (42). Work performed with rapidly progressing adult macaques (SAIDS progression occurring in months compared to years) reported detectable SIV RNA in macrophages of the lung and lymph nodes (LNs) (49). For example, Avalos and colleagues recently found that in virus-suppressed ART-treated macaques, macrophages isolated from the brain harbored replication-competent virus. These macrophages were designated as latently infected given that viral DNA was detectable, while *in situ* hybridization and qPCR of brain tissue showed no detectable viral RNA. These infected macrophages were found after 2 years of ART treatment, supporting the notion that they constituted a long-lived macrophage reservoir (50). Alternatively, Dinapoli and others detected SIV DNA and replication-competent virus in lymphoid macrophages isolated from ART-naïve macaques, but they were unable to detect viral outgrowth from similar macrophage populations in ART-treated animals. They suggested that infected macrophages were short-lived and were lost after longer treatment periods (42). In the humanized mouse model, results showed productive infection of macrophages as well as viral rebound after successful ART treatment in myeloid-only mice (MoM), which lacked human T cells (51). The viral rebound in the MoM study supports infection of long-lived tissue macrophage populations because short-lived macrophages have a half-life of 1 day and viral rebound occurred 7 weeks after withdrawal of ART (52). Additional studies in macaques have also reported infection of long-lived tissue macrophages and together these findings support the theory that macrophages can contribute to the viral reservoir (53, 54).

There is increasing attention on the characterization of macrophage phenotypes and functions during active HIV/SIV infections to better understand their roles in immune responses and tissue pathogenesis. For example, Burdo and colleagues found that an increase of MAC387+ macrophages in the central nervous system (CNS) was associated with more damage to the dorsal root ganglia, which is related to neurological complications in HIV infection (55). They also found that while MAC387+ macrophages were within brain lesions during acute SIV encephalitis (SIVE), higher numbers of CD163+ macrophages were associated with severe SIV encephalitic lesions during chronic infection. Additionally, an increase in CD163+CD16+ monocytes was found in HIV-infected patients with detectable viral loads despite ART treatment. The numbers of these cells were inversely correlated with numbers of CD4+ T cells among patients with <450 CD4 T cells/μl, suggesting that the CD163+CD16+ monocytes were contributing to viral replication (18). Another study reported increasing CD163 expression on monocytes in HIV-infected, ART-treated patients that inversely correlated with CD4 T cell number, however, this did not correlate with viral load (VL) and the use of protease inhibitors during treatment resulted in reduced shedding of CD163 on monocyte populations (56). In addition, increased monocyte turnover in the periphery was associated with increased trafficking of CD16+ macrophages into the gut tissue of chronic SIV-infected, progressing rhesus macaques (24). These gut macrophages were skewed functionally for anti-inflammatory responses and exhibited impaired phagocytic ability, which in turn was associated with increased disease of the gut. In *ex vivo* studies, monocytes expressing CD16 were preferentially infected by HIV over CD16-negative populations, and HIV DNA was detected in this cell subset sampled from ART-treated patients, also suggesting that these monocytes may serve as a viral reservoir (57).

Importantly, in contrast to T cells, macrophages and DC are described as more resistant to the cytopathic effects of the virus infection (47, 58, 59) and are not cleared by antigen-specific cytotoxic CD8+ T cells (60). Thus, in theory, infection of long-lived macrophages would allow the virus to rapidly evade CD8+ T cell immunity and replicate to produce "escape" mutations that then preferentially infect CD4+ T cells. As CD4+ T cells

are depleted, B cell responses for antibody production may become less effective. These events would then promote widespread activation and infection of macrophages that survive and enable continued virus replication and release for long periods of time. Macrophages are clearly capable of contributing to disease progression, treatment failure, and viral rebound. Thus, our studies are currently devoted to depleting macrophages during various stages of SIV infection to develop a clearer understanding about their role in disease, with and without concomitant T-cell depletion.

Despite recent advances in antiretroviral therapies for treatment of HIV, the question of an HIV-infected macrophage reservoir has become significant as efforts are aimed at developing a cure. It has been shown that nucleoside reverse transcriptase inhibitors and/or protease inhibitors were less effective at targeting infected macrophages while being more effective against virus-infected T lymphocytes in SIV-infected rhesus macaques (61, 62). Also, macrophages may be productively infected by mechanisms different from CD4+ T cells such as by phagocytosis of infected cells (63) or by direct spread of infection between monocyte-derived macrophages using nanotubes (64). Macrophages can also harbor cell-free virus and spread infection to lymphocytes *in trans* using lectin receptors (e.g., CD169) (65). In addition, the mean half-life of HIV DNA was found to be longer in monocyte populations compared to CD4+ T cells (66). Together, these findings highlight the need to characterize macrophages in relation to disease pathogenesis and for developing effective treatments to eliminate this population as a viral reservoir.

RHESUS MACAQUE MODEL FOR HIV

Non-human primates experimentally infected with SIV, primarily Indian and Chinese rhesus macaques, have been used to study the pathogenesis, immunology, and therapeutic interventions. They display a similar course of infection and disease progression pattern as seen in persons infected with HIV but at a faster rate. Rhesus macaques inoculated with SIV typically exhibit a high initial viral load, significant depletion of CCR5+CD4+T cells in the gut, and rapid seeding of virus in the tissues followed by establishment of the viral set point and gradual loss of CD4+ T cells in the periphery. After a few years, SIV-infected macaques develop SAIDS and succumb to opportunistic infections and wasting (67, 68).

Compared to HIV in humans, SIV in rhesus macaques uses the same cellular targets and anatomical sites, displays similar persistence, latency and viral loads, and is similarly responsive, though to a lesser degree, to the cART regimen used in human patients (69). The SIV-infected macaque model has enabled more detailed studies about cART therapy, viral seeding of reservoir cells, immune cell depletion effects, administration or generation of neutralizing antibodies, viral rebound, vaccine therapies and latency reversal agents [reviewed in Ref. (69)], much of which could not be examined to the same degree in human patients. Most importantly, animal studies have assisted in the development of effective drug treatments, advanced to producing undetectable viral loads and prolonged maintenance of normal levels of CD4+ T cells to thereby extend a long asymptomatic lifespan to HIV-infected individuals. However, even with strict adherence to cART therapy, drug treatment does not completely eliminate latent virus or virus production from long-lived host cells, and disruption of treatment consistently results in HIV viral rebound from a cellular reservoir [reviewed in Ref. (70)]. Viral seeding studies in macaques showed that even with ART initiation 3 days pi, prior to detectable VL or antigen-specific immune responses, viral rebound occurred when treatment was stopped. While this observed viral rebound was delayed, the post-rebound set points were similar to those observed in animals with ART initiation 2 weeks pi (71). Notably, studies performed in NHPs have found that viral reservoir seeding can be accomplished within 24 h of infection, and ART initiated as soon as 4 h pi, while beneficial in reduction of viral load, dissemination and reservoir seeding, was still not curative (72, 73). Taken together these studies highlight the difficulty and necessity of defining the viral reservoir and for eliminating long-lived or proliferating reservoirs to achieve cure. Much work has been devoted to investigating the role of memory CD4+T cell populations as a reservoir but other host cells, particularly long-lived macrophages, require attention as well due to their being refractory to ART and their potential to harbor virus for years.

SIV INFECTION AND DISEASE PROGRESSION IN ADULT RHESUS MACAQUES

The typical course of SIV infection in rhesus macaques varies with age of the host as depicted in **Figure 2**. Early after infection, adult macaques produce a high initial viral load at ~10^8 RNA copies per ml followed by a set point at ~10^5 viral copies per ml that corresponds to a loss in CD4+ T cell numbers in the blood, all of which resemble HIV infection kinetics in adult human patients (74, 75). Disease progression and onset of AIDS/SAIDS is described typically using parameters such as CD4+ T cell count <200/μl with significant increase in viral load, and presentation with opportunistic infections, weight loss, anemia, pneumonia, fatigue, diarrhea, thymic atrophy, lymphoid atrophy, bone marrow hyperplasia, encephalitis, and colitis. Common reported opportunistic infections with SAIDS include cytomegalovirus, adenovirus, *Cryptosporidium, Pneumocystis*, *Mycobacterium, Shigella*, and *Campylobacter* (76, 77).

One of the many focal points in HIV/SIV research has been to characterize the physiological "flashpoint" and reliable prognostic markers that define onset of AIDS. Depletion of CD4+ T cells has been described as the primary cause for terminal progression to AIDS. Interestingly, however, CD4+ T cells can be depleted or remain at stable low levels for years before SAIDS onset occurs in rhesus macaques (78–80). In addition, CD4+ T-cell depletion or turnover has proven to not be the best predictive value for onset of terminal disease progression (80, 81). A recent working theory is that the depletion of CD4+ T cells occurs in three stages during the chronic stages of infection prior to AIDS onset such that initially effector memory (EM) T cells with high expression of CCR5 are depleted. This is

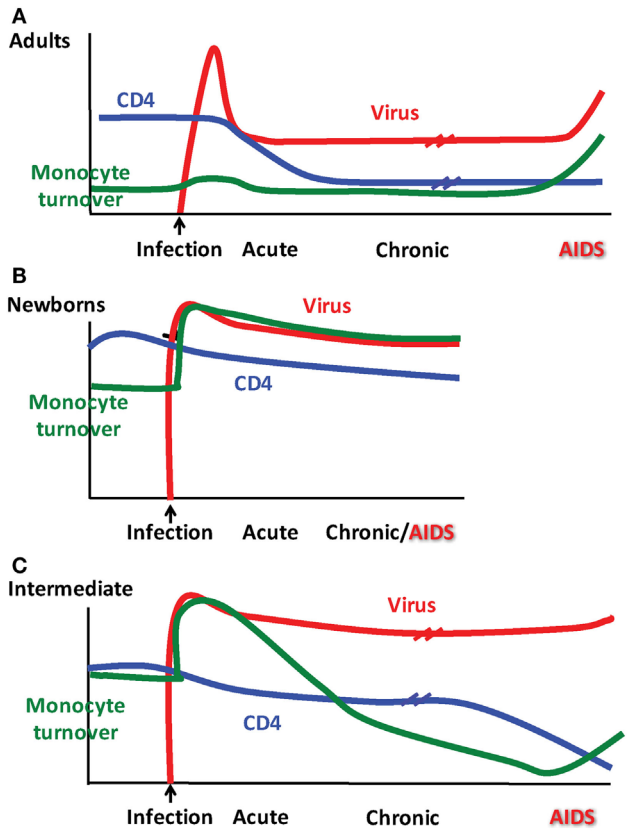


FIGURE 2 | Patterns observed for monocyte turnover, CD4 T cell counts and simian immunodeficiency virus (SIV) infection differ depending on age at infection. Results from Kuroda and colleagues showing monocyte turnover determined by quantification of bromodeoxyuridine (BrdU) incorporation by flow cytometry in monocytes at 24 h post-BrdU intravenous injection, CD4 T cell count obtained by peripheral blood cellular immunophenotyping *via* flow cytometry in conjunction with complete blood count (CBC), and SIV RNA plasma viremia as determined by quantitative PCR. Distinct patterns emerged for clinical progression of SIV in rhesus macaques illustrated in **(A)** adults, **(B)** newborns, and **(C)** as what we refer to as an "intermediate" phenotype in older infants infected at ~3–4 months of age.

followed by immune reconstitution of this population by CCR5-negative central memory (CM) cells and then ultimately leads to progressive loss of both effector and CM T cell pools over time with repeating cycles of reconstitution and depletion (27). It is thought that the loss of CM T cells leads to dysregulation of the immune network as a whole and immunodeficiency allowing for opportunistic infections that define the onset of AIDS (27).

During studies to further define biomarkers for the onset of SAIDS, we reported that increasing monocyte turnover with corresponding destruction of tissue macrophages was a significantly better predictor than declining CD4+ T cell counts or increasing plasma viral load (81), as diagrammed in **Figure 2A**. This suggested that in untreated adult rhesus macaques, macrophages play important roles in HIV/SIV pathogenesis and persistence. Additional studies show that they do so, in a tissue–specific manner as elaborated further in the next section.

THE ROLE OF MACROPHAGES IN ADULT SAIDS

Increases in peripheral CD16+ monocyte subsets have been associated with inflammatory disorders such as cardiac disease (82), lesions within the kidney vasculature during systemic lupus erythematosus (83), rheumatoid arthritis (84) and intestinal pathology (85). A subset of CD14+ macrophages has been linked to greater inflammatory damage in intestinal tissues, impacted by Crohn's disease (86, 87). To also characterize the relationship between macrophages and SIV pathogenesis, we measured turnover rates of monocytes during steady-state homeostasis in uninfected macaques in comparison to SIV-infected rhesus macaques. Monocyte turnover was followed by measuring uptake of the thymidine analog, bromodeoxyuridine (BrdU), into dividing cells followed by immunofluorescent antibody staining and flow cytometry. The homeostatic baseline monocyte turnover in the blood of uninfected adult rhesus macaques was ~5% across several study groups, while the turnover of monocytes increased up to 50% prior to onset of terminal SAIDS (81). This agrees with data in a study where increased turnover of monocyte populations in the blood was predictive of more severe disease progression, in particular the development of SIVE (88). This was also related to an increase in macrophage populations deposited in the brain tissue, leading to localized pathology. Our study showed that an increase in monocyte turnover kinetics was associated with a loss of tissue macrophages by SIV infection in the LNs, and that this was not accompanied by changes in the absolute count of monocytes in peripheral blood (23, 54, 81). Interestingly, the shift in monocyte turnover was also not linked to numbers of CD4+ T cells or lymphocyte activation, similar to results reported by Burdo et al. (88), suggesting an independent mechanism of disease pathogenesis relating specifically to monocyte/macrophage infection (81). Further evaluations found that increased trafficking of monocytes from the bone marrow during SIV infection did occur with successive recruitment to the LN, CNS, and lung (23, 54, 88). In fact, increased rates of monocyte turnover and recruitment to become tissue macrophages were linked to rate of progression to SAIDS, severity of lung tissue pathology, and SIV encephalitis.

The lung, followed by the brain, appears to be among the organs most affected by HIV in the post-ART era (89, 90) with macrophages thought to play an important role in the chronic immune activation required for lung and brain lesions associated with chronic HIV/SIV infection. The accrual of CD163+ macrophages has also been observed in the hearts of rhesus macaques infected with SIV, which positively associated with cardiac disease (22). Given that respiratory infections such as *Pneumocystis* pneumonia and tuberculosis are among the most common AIDS-defining diseases and involve direct bacterial infections of macrophages, we focused further on characterizing macrophages of the lung. At least two different populations of macrophages were identified in the lung tissue of rhesus macaques; namely IM (23) and macrophages located in the alveolar spaces (AM) (91). BAL macrophages did not entirely represent macrophage-mediated innate immune responses of the lung, so we examined macrophages in whole lung tissues and observed that IM and

alveolar macrophages (AM) exhibited different turnover kinetics and phenotypes in adult rhesus macaque lung tissue. IM were smaller, located exclusively in the interstitium, and phenotypically resembled blood monocytes. *In vivo* BrdU incorporation by dividing cells demonstrated higher turnover rates for blood monocytes and lung IM compared to AM during steady state (91). The relatively higher TUNEL-staining IM also suggested a continuous transition of blood monocytes replacing apoptotic IM in an effort to maintain homeostasis in the lung. These data led us to believe that IMs are a short-lived population of macrophages in the lung. AM on the other hand, were larger, expressed CD206 (not expressed on IM), and were located in the alveolar spaces. AM turnover was negligible during steady state indicating that these are longer-lived cells. In addition, *in vivo* BrdU labeling suggested that IM can differentiate into AM when AMs are depleted (91). These findings suggest that AM and IM possess different functions.

Investigations of BAL collected from HIV-infected patients have produced some conflicting data and merited some interesting questions about whether AMS are productively infected and contribute to the viral reservoir. Results from several studies have found viral DNA and RNA in AMs (92–95) and some work has even defined a specific subset of HIV-specific CD8+ T cells whose function is thought to target HIV-infected alveolar macrophages (92, 96). There remains, however, a persisting argument that these results reflect macrophages engulfing infected CD4+T cells rather than true infection and replication within macrophages. In one study, viral DNA was found in AMS collected from a patient after 3 years of ART treatment, but the levels of rearranged TCR DNA supported their interpretation that viral DNA was present due to phagocytosis of infected CD4 T cells rather than macrophage infection (42). We thus investigated the effects of SIV infection on lung macrophage populations in ART-naïve macaques. Confocal imaging techniques were applied and lung macrophages were identified containing SIV RNA **Figure 3A**. This strongly supports the prospect that viral replication can occur in tissue macrophages. Furthermore, data showed that increasing blood monocyte turnover significantly correlated with turnover and apoptosis of IM but not with turnover of AM in SIV-infected macaques during terminal disease progression as shown in **Figure 3B** (54, 91). Interestingly, virus DNA copies increased in IM and AM after monocyte turnover increased in SIV-infected macaques but remained at the same levels in CD4+ T cells regardless of monocyte turnover (**Figure 3B**). The low turnover rate of AM despite their being infected with SIV strongly suggested that if infected with replication-competent virus, this macrophage subset could constitute an important long-lived virus reservoir (23, 91). Our interpretation is that the increased monocyte turnover was due to a compensatory mechanism to replace the short-lived macrophages (IM), which were destroyed by SIV in the tissues. This increase in turnover of both monocytes and IMs corresponds to greater infection of long-lived AMs, however mechanisms for this relationship are unclear. Based on these studies we proposed a working model as shown in **Figure 4** that (a) There exist at least two types of macrophages in the lung including the shorter-lived IM exhibiting relatively higher turnover during homeostasis suggesting a critical role for daily protection, and longer-lived AM that exhibit lower turnover rate; (b) Increased SIV infection of both IM and AM correlates with AIDS disease progression; (c) SIV-induced IM apoptosis promotes further increases in IM (and monocyte) turnover rate in contrast to AM that become infected with SIV but exhibit far lower rates of apoptosis and turnover. This further suggested that similarly longer-lived macrophage populations in other tissues/organs also may become infected, and because they appear to be resistant to apoptosis, are likely also to support viral infection for extended periods of time to serve as a virus reservoir and source of chronic inflammation. Together, these

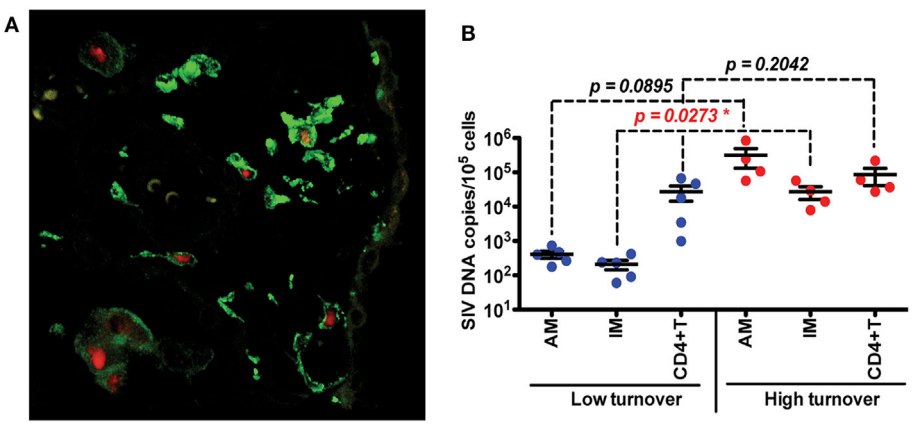


FIGURE 3 | Infection and replication of simian immunodeficiency virus (SIV) in interstitial macrophages (IM) and AM contribute to the viral load in lung tissues and higher death rate of lung IM correlates with increased blood monocyte turnover rate in adult SIV-infected rhesus macaques. **(A)** Confocal microscopy was performed on lung tissues obtained from SIV-infected monkeys with higher (>30%) blood monocyte turnover levels ($n = 6$). Anti-CD163 (Green) antibody was used to identify macrophages, and SIV RNA (Red) was detected with anti-sense riboprobes. **(B)** IM, AM and CD4+ T cells were sorted *via* FACS from single-cell suspensions of lung tissues from SIV-infected monkeys with low ($n = 5$) and high ($n = 4$) blood monocyte turnover, and SIV DNA levels were quantitated and standardized against RNase P levels. Figure modified from Ref. (54). Copyright 2015. The American Association of Immunologists, Inc.

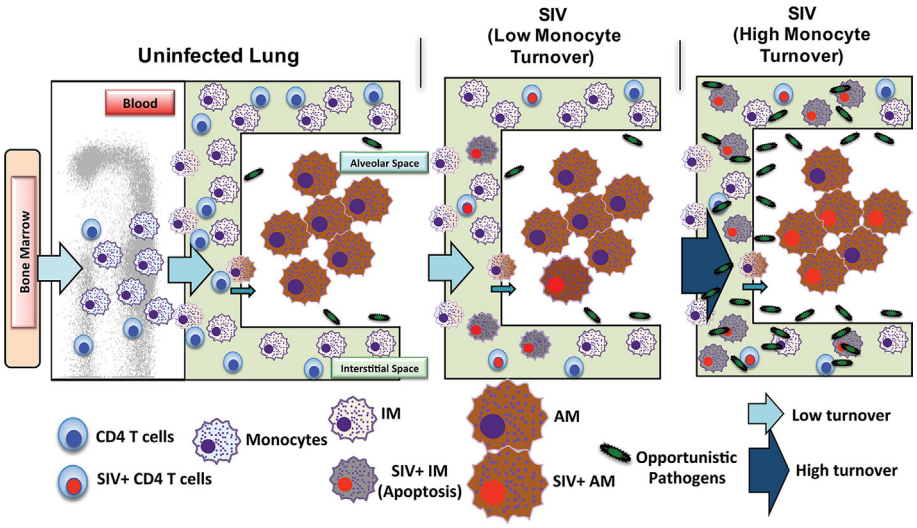


FIGURE 4 | Proposed mechanism of simian immunodeficiency virus (SIV) reservoir establishment in the lung of SIV-infected macaques. The lung contains at least two types of macrophages: short-lived interstitial macrophages (IM) and longer-lived alveolar macrophages (AM). IM become massively infected with SIV and undergo a high rate of apoptosis that correlates with increased blood monocyte turnover in SIV-infected newborn macaques from the beginning of infection (Acute). This is in contrast to SIV-infected adults where massive infection of macrophages occurs later during disease progression. Conversely, SIV infection of the longer-lived AM does not lead to a high rate of apoptosis compared to that of IM. Elimination of SIV-infected longer-lived AM, and CD4+ T cells, is crucial for reducing SIV/HIV reservoirs and consequently reducing lung tissue damage.

studies illustrate the rationale for our proposed macrophage depletion strategies.

Simian immunodeficiency virus-infected macrophages have appeared to promote pathogenesis in various tissues resulting in cardiovascular, metabolic and neurological diseases. Research on the CNS has shown that HIV/SIV infection in the brain was associated with accumulation of perivascular macrophages and microglia associated with lesions and encephalitis (15, 97–99). Attention is also being given to adipose tissues, which are capable of influencing systemic immune responses and are thought to contribute to chronic inflammation seen in aging and with some infections (100–102). Adipose tissue macrophages were found to be associated with increased inflammation and lipodystrophies during HIV/SIV infection (103). Infection with SIV resulted in phenotypic and functional changes in resident cells of adipose tissue, with overall increased immune activation. SIV-infected macrophages and memory CD4+ T cells were observed in the stromal vascular fraction of the adipose tissue studied and have been proposed as potential reservoirs during ART treatment, particularly as adipose may be a site not fully permissive to ART drugs (104, 105). In addition, virus-infected macrophages identified in bone marrow also correlated with hematologic abnormalities, anemia, and bone marrow hyperplasia in SIV-infected macaques (106) and may migrate to the CNS causing HIV-1-associated dementia in humans (107). Other studies on the gut mucosa in humans showed that infected macrophages accumulating in the ileum exhibited increased inflammatory profiles, and thus likely contributed to intestinal dysregulation associated with AIDS onset (108). Furthermore, HIV/SIV infection produced changes in splenic architecture associated with significant shifts in macrophage populations expressing CD68, CD163, and Mac387 in this organ (109). A recent study in humanized mice determined that longer-lived splenic macrophages could harbor latent HIV during ART treatment (110), which would not only account for viral persistence, but also conceivably contribute to macrophage dysfunction and chronic immune activation. Thus, a better understanding about different outcomes of HIV/SIV infections in short- and long-lived macrophages will be critical to fully characterize mechanisms of HIV pathogenesis and establishment of virus reservoir to ultimately achieve a cure for AIDS. Although the molecular mechanisms are yet unclear, data from our rhesus macaque model demonstrated that SIV infection and reduced half-life of the short-lived macrophages appears to contribute to pathogenesis and AIDS disease progression. By contrast, long-lived macrophages that also are susceptible to SIV infection, do not exhibit a reduction in half-life because they survive infection. The long-lived macrophages could, therefore, be the perfect site of a long-term virus reservoir and a source of chronic inflammation observed in HIV-infected individuals.

SIV INFECTION AND DISEASE PROGRESSION IN PEDIATRIC RHESUS MACAQUES

HIV/SIV infections produce rapid rates of disease in infants compared to adults and infants also exhibit an immune system that is overwhelmingly biased toward immunosuppression or anti-inflammatory responses [reviewed in Ref. (111)]. Pediatric immunity is often referred to as "impaired" due to minimal or absent Th1 responses that have not yet fully developed. *In utero,* babies are protected in a semi-sterile environment and must

remain immunologically tolerant to maternal antigens (112). After birth, neonates are bombarded with new foreign substances and organisms, many of which are considered harmless, or even beneficial. Prior to and during maturation of the immune system, neonates are partially protected by maternal immunity through transplacental transfer of antibodies and via breast feeding which allows for passive transfer of antibodies, lymphocytes, immune factors, as well as by seeding the neonate's gut with commensal bacteria that ultimately help regulate responses to infections and avoid deleterious inflammatory responses [reviewed in Ref. (113)]. Tolerance to many benign antigens early in life would be beneficial for the infants survival, coupled with a gradual recognition and ability to immunologically discriminate self from non-self antigens. The transition from tolerance to expression of mature effector immune responses occurs over several years and occurs asynchronously between immune compartments, with full immune-competence achieved at adolescence (114). However, it is important to consider that the initial lack of inflammation in a newborn and the slow maturation with development could also favor an infection to spread freely and reproduce exponentially, highlighting the important balance between initial tolerance mechanisms and eventual maturation of a Th1-capable immune responses. This also highlights the influence of age at infection, which could dictate severity of disease, depending on the pathogen and the immune-competence of the child at time of infection. Studies using infant macaques have proven vital for examining immune ontogeny during fetal and postnatal development due to their physiological similarities to humans and because they present with similar infection and disease outcomes after SIV infection compared to pediatric HIV infections (115). Unanswered questions remain, however, regarding pediatric development of competent immune responses in the context of the infection and time course of disease.

The rapid disease and higher mortality rates, which occur in pediatric cases, suggest that HIV and SIV are able to exploit the immature immune system in infants. As shown in **Figure 5**, total CD4+ T cell numbers are significantly higher in infants than adults (116, 117). The primary target cells of the virus are the CCR5+ fraction of CD4+ T cells, but these cells are lacking in the blood and LNs of infants (118). In humans, a biphasic pattern of disease progression occurs in untreated, HIV-infected children, with half reaching terminal AIDS by the age of two (119, 120), while the other half present with slower onset of disease, and survival through adolescence (121). In both groups of HIV-infected children however, acute plasma viremia generally increases 10-fold above levels seen in adults, and RNA levels do not decline to reach a viral set point until ~5 years of age (122) (**Figure 5**). This suggests that CD4+ T-cell depletion and/or degree of immune activation do not consistently correlate with or promote disease progression to AIDS as has been shown with adult infections (123, 124). Based on our earlier results that higher monocyte turnover and macrophage destruction predicted onset of SAIDS in adult macaques (23, 54, 81), we hypothesized that similarly, the destruction and increased turnover of monocytes/macrophages, would be all the more illustrated in the setting of severe pediatric infection. Rhesus infants, similar to human children, have an increased number of CD4+ T cells systemically, compared to adults. Previous pediatric macaque work has shown

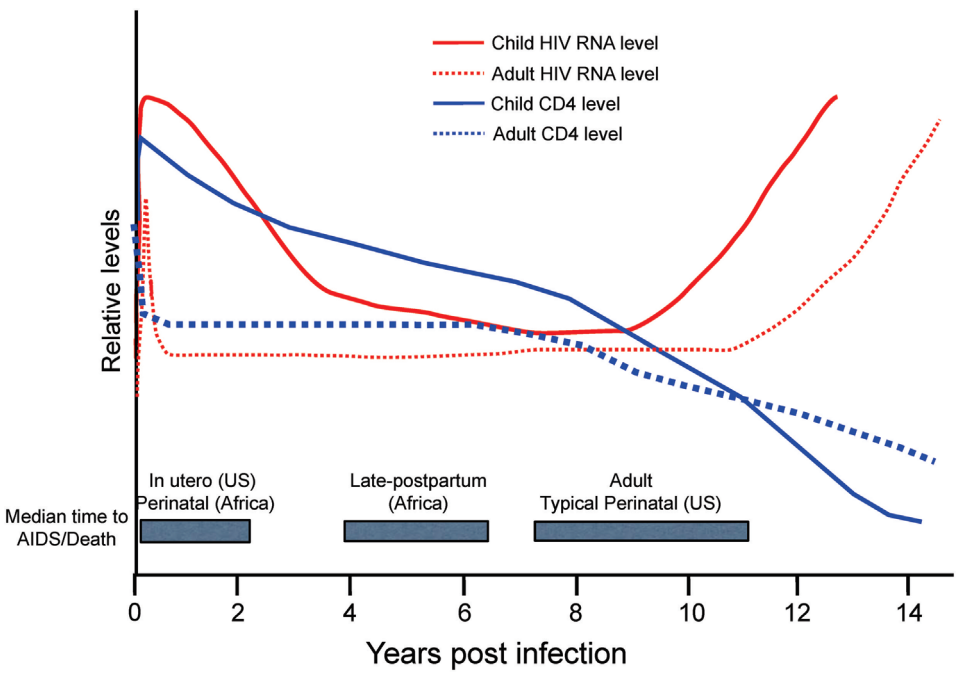


FIGURE 5 | Relative levels of human immunodeficiency virus (HIV) RNA (red) and CD4 cells (blue) in adults (dotted lines) and children (solid lines) in the years following acquisition of HIV-1. Gray boxes highlight the median time to AIDS/Death for infants by region and route of infection in comparison to adults. US, United States. Figure from Ref. (114) © 2013 John Wiley & Sons A/S. Published by John Wiley & Sons Ltd. Immunological Reviews 254/2013.

that intestinal CCR5+ CD4+ T cells are preferentially infected by SIV and subsequently depleted (118, 125, 126). However, while these CCR5+ CD4+ T cell subsets have been observed in pediatric gut tissue, the vast majority of CD4+ T cells found in neonates, are known to express a naïve phenotype and are functionally biased for immune tolerance (125, 127–130).

These phenotypic and functional differences of CD4+ T cells in children, in addition to reported age-related declines of CD4+ T cells (131–133), further complicate interpretations about the impact of CD4+ T cell infection in pediatric cases that progress more rapidly to AIDS. Considering that neonates have fewer target CCR5+ T cells, and largely lack that hallmark CD4+ T cell depletion typical of adult infection (114, 117, 134), our attention turned toward studies on macrophages to better understand their contribution to exacerbated disease progression found in pediatric cases.

MACROPHAGES IN PEDIATRIC SAIDS

Since increasing monocyte turnover and tissue macrophage destruction by SIV predicted onset of AIDS in infected adult macaques, we sought to determine if monocytes/macrophages also influenced the more rapid and severe disease observed in SIV-infected infants. Currently, there is a distinct lack of published studies for role of macrophages in pediatric HIV/SIV infections. Baseline studies recently published demonstrated that naïve, uninfected neonate, and infant macaques aged 4 months or less inherently exhibited higher monocyte turnover rates (median of 15.9%) than observed in uninfected adult rhesus macaques (median of 2.9%) (135) (**Figure 6A**). By approximately 4–6 months of age, the rates of monocyte turnover declined to levels seen in adults (**Figure 6B**). This observation suggested that monocytes were undergoing maturation in function or physiology during the first few months of life in the rhesus macaques. This may have affected the findings that in animals infected with SIV at birth, monocyte turnover rates increased even further and remained high through their progression to SAIDS, without an intervening chronic stage as seen in adult infection (**Figures 2A,B** and **6C**).

The physiologically higher monocyte turnover rates in the neonates appeared to reflect a developing, immature immune system that may pose a higher risk for macrophage infection by

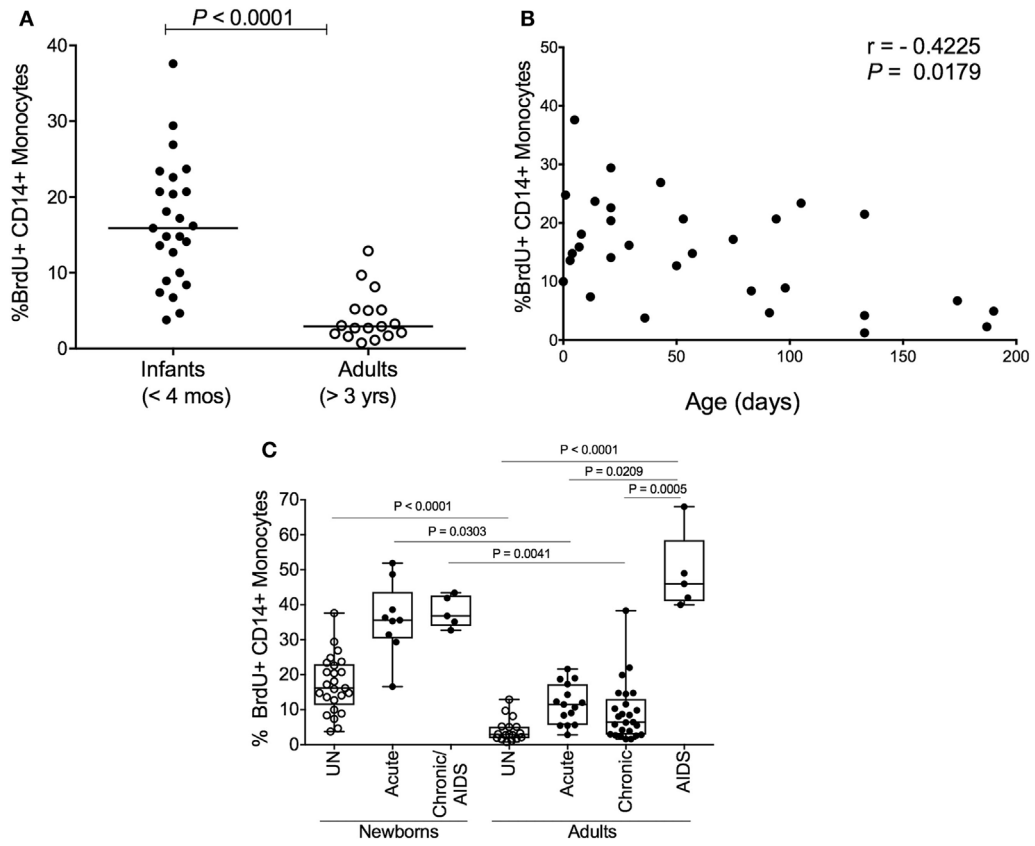


FIGURE 6 | High monocyte turnover in uninfected infant rhesus macaques is further increased with simian immunodeficiency virus (SIV) infection. Bromodeoxyuridine (BrdU) incorporation was analyzed at 24 h by multicolor flow cytometry to determine the percent of BrdU+ monocytes (HLA–DR+ CD3– CD8– CD20– CD14+). Monocyte turnover rates were **(A)** compared between infant rhesus macaques and adult rhesus macaques and **(B)** examined in 20 uninfected macaques ranging from 3 to 190 days of age. **(C)** Statistical significance of comparisons between monocyte turnover rates of newborn and adult rhesus macaques before infections (UN = uninfected) and during acute, chronic and SAIDS stages of SIV-infected macaques were determined by Kruskal–Wallis test corrected for multiple comparisons using Dunn's post-test; $P < 0.05$*, $P < 0.01$**, $P < 0.001$***. Figure modified from Ref. (135).

HIV/SIV. To examine this, we applied terminal deoxynucleotidyl transferase dUTP nick-end label (TUNEL) staining and observed apoptotic TUNEL-positive macrophages in LNs and intestine in SIV-infected neonates, which corresponded with increased trafficking of macrophages recently derived from circulating monocytes (BrdU+ CD163+). This was similar to observations in infected adult macaques progressing to SAIDS and suggested that the increased rate of monocyte turnover was necessary for reseeding tissue macrophages that were destroyed by the virus infection (135). Furthermore, immunofluorescence analysis of LN, gut and lung tissue demonstrated that a large proportion of the virus-producing cells were in fact macrophages (135). Taken together, the higher monocyte turnover in infants in concordance with damage to macrophages by SIV infection, may illuminate reasons for more rapid disease progression in SIV-infants as depicted in **Figure 2B**.

Despite similar levels of CD4+ T cells and plasma viremia between infected children, the age of the patient significantly influences the rate of terminal disease progression, with the youngest patients typically showing the highest mortality rates, as noted in **Figure 5** with shorter median time to death found for *in utero* and perinatal cases of HIV infection. The rapid HIV disease progression in children begins to shift toward rates more similar to those seen in adult infections at about 5 years of age. This parallels the observations that in persons over 5 years old, predictive biomarkers of CD4+ T cell levels and plasma viremia measures also transition toward levels observed in adults (114) that likely signify maturation of the immune system. In pediatric studies, age-related differences were reported in innate immune responses (136, 137) as well as in lymphocyte populations comprising the blood and mucosal immune responses, including CD4+ T cells, CD8+ T cells, B cells, and NK cells [reviewed in Ref. (111, 138–140)]. Also, plasma molecules vary in concentration as a function of age (141–143).

To further assess the transition from pediatric to adult disease progression patterns, we experimentally infected slightly older pediatric animals aged 3–4 months of age when physiological monocyte turnover rate was transitioning to rates comparable to healthy adults. Of the four animals infected in this age group, two presented with viral load dynamics similar to animals infected as newborns, and they progressed rapidly with SAIDS diagnosis by 20 weeks pi. The SIV plasma viral loads in the remaining two infants were more comparable to levels seen in adults, and they exhibited a typical infection course, with acute to chronic phase similar to adult infections, rather than progressing directly to overt SAIDS as occurs in infected neonates (135). For these animals infected at 3–4 months of age, monocyte turnover increased dramatically during the acute phase, which was similar to that seen in the infected newborns (**Figure 7A**). However, instead of continuing to increase throughout infection, the monocyte turnover rates in the older infants declined to similar levels as adults (**Figure 7B**) at 8 weeks pi (albeit slightly higher) and were without changes in absolute number of monocytes in the periphery. Chronic phase was not only visible in the older infected infants but exhibited monocyte turnover rates more similar to adults before progressing to SAIDS. As clinical signs associated with SAIDS began to be observed, monocyte turnover increased again in the older infants, thus exhibiting what we consider an "intermediate" phenotype for monocyte turnover, plasma viral load, and risk for onset of terminal SAIDS progression in relation to divergent disease course progression rates seen in neonate and adult infections (135) (**Figure 2C**). This intermediate phenotype helps explain the biphasic disease patterns observed in HIV-infected children such that varying immune parameters at different stages of maturation at the time of infection appear to impact the rates of effective immune responses, disease progression, and survival outcomes.

These observations highlight the importance of using appropriate age-matched controls when studying pediatric infections and provide a foundation to continue work relating maturation of immune responses with changes in pathogenesis, immune activation, and dynamics in tissue macrophage populations in infants infected at various ages. To our knowledge little to no published work is available to compare and contrast our

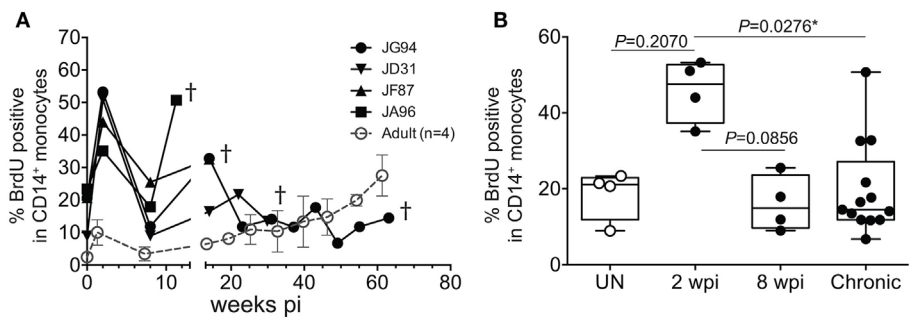


FIGURE 7 | Longitudinal course of changes observed during progression to simian AIDS (SAIDS) in infant macaques infected with SIVmac251 at 3–4 months of age. **(A)** Bromodeoxyuridine (BrdU) incorporation was evaluated for monocyte turnover at 24 h. Blood monocyte turnover rates were measured every 4–6 weeks during the course of infection until progression to SAIDS or at indicated time-points (†). Mean monocyte turnover rates (i.e., %BrdU+ CD14+ monocytes) of the four infected adults are shown for comparison (dotted line). **(B)** Statistical analysis of monocyte turnover rates in infant macaques was performed by Kruskal–Wallis test corrected for multiple comparisons using Dunn's post-test; $P < 0.05$*. UN; pre-infection, wpi; weeks post-infection. Chronic; all infant time-points after 8 wpi. Figure modified from Ref. (135).

pediatric macrophage studies with, particularly in the case of HIV/SIV infection and AIDS progression. Additional considerations are required to better understand age-related immune responses and pathogenesis in patients undergoing ART that are routinely used in human and experimental macaque HIV/SIV infections. In general, ART is less effective at suppressing viral load in HIV-infected children compared to adults (144, 145). Typical outcome measures for treatment efficacy in children are viral RNA loads and CD4+ T cell counts, which have been highly variable compared to outcomes from similar drug protocols in adults, and especially when comparing different combination drug treatments (146). In addition, the definition of virologic suppression varies between studies that may show up to 30% failure rate after first line treatment (which does not include protease inhibitors) (146). The measures of percentage failures also are reported independent of death outcomes. Unlike in human studies, it is common to use more similar dosing regimens in rhesus macaque neonates and adults based on weight, which allows for more direct comparison between treatment efficacy and survival outcomes after experimental infections initiated at varying ages. Adults are often treated with a tri-regimen of emtricitabine, tenofovir and dolutegravir, and successful control of viral replication is routinely reported (69). Interestingly in pediatric macaques, drug therapies appear less effective than in adults, and the animals exhibit sustained high viral loads and undergo disease progression despite treatment (147). This is possibly associated with the accumulation of specific drug-resistant mutations in addition to a suppressed immune system. Our lab is currently evaluating the persistence of virus in tissue macrophages and T cells in pediatric animals treated with ART that integrate with monocyte/macrophage phenotype shifts to identify biomarkers of ART efficacy.

CONCLUSION AND PERSPECTIVES

Results from many studies have shown productive infection in macrophages, but their role as a latent reservoir is still highly controversial. In some studies, viral DNA is not detected in tissue macrophage populations after successful ART therapy. This could be due to the shorter half-lives of some macrophage subsets, small sample sizes, and/or threshold detection limitations in assays employed for detecting virus. It is often difficult to identify infected macrophages, especially in tissues that test negative by PCR or *in situ* hybridization, but viral outgrowth assays have exposed tissue macrophages as capable, latently infected reservoirs. Assay limitations in addition to limitations of HIV research in human tissues, encourages a continued debate. Our studies in rhesus macaques, however, show that short-lived macrophages contribute to active infection and then die, thereby inducing increases in monocyte turnover, which serves as a physiological biomarker to predict onset of SAIDS. Our correlate hypothesis then follows that long-lived macrophages become infected, do not die, and instead serve as a reservoir, refractory to ART. Susceptibility of the macrophage populations to virus infection is likely to be different between individuals, and is probably influenced by time of ART initiation, magnitude of VLs at ART initiation, viral strain, immune status, and age at infection. These variables could result in the debated inconsistencies found in the literature regarding the contribution of infected macrophages to viral reservoirs. It is important to note that while this review focused primarily on the role of monocyte/macrophages in HIV/SIV infection, other cells of the immune system may also be important influences on infection and pathology. Clearly, further investigations are necessary to identify and remove all viral reservoirs for development of therapeutic cures.

In summary, we have shown that increase in blood monocyte turnover, which results from death of short-lived macrophages in the tissue, predicts disease progression in SIV-infected rhesus macaques. Baseline monocyte turnover rates observed in uninfected neonates are higher than observed in uninfected adults. In animals infected with SIV at birth, monocyte turnover increased further and remained higher than in SIV-infected adults, and this was associated with a more rapid disease progression.

Our current studies are directed to study the connection between higher monocyte turnover and rapid progression in infants, as well as the contribution of SIV-infected macrophages as a viral reservoir. Work is in progress to evaluate the persistence of virus in tissue macrophages and T cells in pediatric animals treated with ART. We hypothesize that early and high infection of neonatal macrophages results in establishment of viral reservoir in long-lived subsets of macrophages, contributing to uncontrolled viral load despite ART and perhaps explaining failures of first line treatment in children.

Together, we review some important aspects of macrophages in SIV infection and progression, and highlight the need to further investigate their role in pediatric cases.

NOTES

Data presented from our own studies was carried out in accordance with the standards of the National Institutes of Health (NIH), Guide for the Care and Use of Laboratory Animals. The Institutional Animal Care and Use Committee of Tulane University approved protocols used. Permission has been obtained for use of copyrighted material from other sources.

AUTHOR CONTRIBUTIONS

All authors participated in the concept, preparation, and editing of the manuscript. KM wrote the manuscript and developed the figures.

FUNDING

Research work from our own lab, referred to in this manuscript, was supported by NIH grants for MK, including RO1AI097059, R21AI091501, RO1HL125054, R21AI116198, R21AI110163, and R33AI110163.

REFERENCES

1. Iwasaki A, Foxman EF, Molony RD. Early local immune defences in the respiratory tract. *Nat Rev Immunol* (2017) 17(1):7–20. doi:10.1038/nri.2016.117
2. Gordon S, Taylor PR. Monocyte and macrophage heterogeneity. *Nat Rev Immunol* (2005) 5(12):953–64. doi:10.1038/nri1733
3. Gordon S. The macrophage: past, present and future. *Eur J Immunol* (2007) 37(Suppl 1):S9–17. doi:10.1002/eji.200737638
4. Stefater JA III, Ren S, Lang RA, Duffield JS. Metchnikoff's policemen: macrophages in development, homeostasis and regeneration. *Trends Mol Med* (2011) 17(12):743–52. doi:10.1016/j.molmed.2011.07.009
5. Boorsma CE, Draijer C, Melgert BN. Macrophage heterogeneity in respiratory diseases. *Mediators Inflamm* (2013) 2013:769214. doi:10.1155/2013/769214
6. Van Gassen N, Staels W, Van Overmeire E, De Groef S, Sojoodi M, Heremans Y, et al. Concise review: macrophages: versatile gatekeepers during pancreatic β-cell development, injury, and regeneration. *Stem Cells Transl Med* (2015) 4(6):555–63. doi:10.5966/sctm.2014-0272
7. Lamers SL, Fogel GB, Singer EJ, Salemi M, Nolan DJ, Huysentruyt LC, et al. HIV-1 Nef in macrophage-mediated disease pathogenesis. *Int Rev Immunol* (2012) 31(6):432–50. doi:10.3109/08830185.2012.737073
8. Sugimoto C, Hasegawa A, Saito Y, Fukuyo Y, Chiu KB, Cai Y, et al. Differentiation kinetics of blood monocytes and dendritic cells in macaques: insights to understanding human myeloid cell development. *J Immunol* (2015) 195(4): 1774–81. doi:10.4049/jimmunol.1500522
9. Wynn TA, Vannella KM. Macrophages in tissue repair, regeneration, and fibrosis. *Immunity* (2016) 44(3):450–62. doi:10.1016/j.immuni.2016.02.015
10. Epelman S, Lavine KJ, Randolph GJ. Origin and functions of tissue macrophages. *Immunity* (2014) 41(1):21–35. doi:10.1016/j.immuni.2014.06.013
11. Merad M, Manz MG, Karsunky H, Wagers A, Peters W, Charo I, et al. Langerhans cells renew in the skin throughout life under steady-state conditions. *Nat Immunol* (2002) 3(12):1135–41. doi:10.1038/ni852
12. Bouwens L, Baekeland M, De Zanger R, Wisse E. Quantitation, tissue distribution and proliferation kinetics of Kupffer cells in normal rat liver. *Hepatology* (1986) 6(4):718–22. doi:10.1002/hep.1840060430
13. Lawson LJ, Perry VH, Gordon S. Turnover of resident microglia in the normal adult mouse brain. *Neuroscience* (1992) 48(2):405–15. doi:10.1016/0306-4522(92)90500-2
14. Perdiguero EG, Geissmann F. The development and maintenance of resident macrophages. *Nat Immunol* (2016) 17(1):2–8. doi:10.1038/ni.3341
15. Filipowicz AR, McGary CM, Holder GE, Lindgren AA, Johnson EM, Sugimoto C, et al. Proliferation of perivascular macrophages contributes to the development of encephalitic lesions in HIV-infected humans and in SIV-infected macaques. *Sci Rep* (2016) 6:32900. doi:10.1038/srep32900
16. Burdo TH, Walker J, Williams KC. Macrophage polarization in AIDS: dynamic interface between anti-viral and anti-inflammatory macrophages during acute and chronic infection. *J Clin Cell Immunol* (2015) 6(3):333. doi:10.4172/2155-9899.1000333
17. Guilliams M, De Kleer I, Henri S, Post S, Vanhoutte L, De Prijck S, et al. Alveolar macrophages develop from fetal monocytes that differentiate into long-lived cells in the first week of life via GM-CSF. *J Exp Med* (2013) 210(10): 1977–92. doi:10.1084/jem.20131199
18. Fischer-Smith T, Tedaldi EM, Rappaport J. CD163/CD16 coexpression by circulating monocytes/macrophages in HIV: potential biomarkers for HIV infection and AIDS progression. *AIDS Res Hum Retroviruses* (2008) 24(3): 417–21. doi:10.1089/aid.2007.0193
19. Møller HJ. Soluble CD163. *Scand J Clin Lab Invest* (2012) 72(1):1–13. doi:10.3109/00365513.2011.626868
20. Soulas C, Conerly C, Kim WK, Burdo TH, Alvarez X, Lackner AA, et al. Recently infiltrating MAC387(+) monocytes/macrophages a third macrophage population involved in SIV and HIV encephalitic lesion formation. *Am J Pathol* (2011) 178(5):2121–35. doi:10.1016/j.ajpath.2011.01.023
21. Odink K, Cerletti N, Brüggen J, Clerc RG, Tarcsay L, Zwadlo G, et al. Two calcium-binding proteins in infiltrate macrophages of rheumatoid arthritis. *Nature* (1987) 330(6143):80–2. doi:10.1038/330080a0
22. Walker JA, Sulciner ML, Nowicki KD, Miller AD, Burdo TH, Williams KC. Elevated numbers of CD163+ macrophages in hearts of simian immunodeficiency virus-infected monkeys correlate with cardiac pathology and fibrosis. *AIDS Res Hum Retroviruses* (2014) 30(7):685–94. doi:10.1089/aid.2013.0268
23. Cai Y, Sugimoto C, Liu DX, Midkiff CC, Alvarez X, Lackner AA, et al. Increased monocyte turnover is associated with interstitial macrophage accumulation and pulmonary tissue damage in SIV-infected rhesus macaques. *J Leukoc Biol* (2015) 97(6):1147–53. doi:10.1189/jlb.4A0914-441R
24. Swan ZD, Bouwer AL, Wonderlich ER, Barratt-Boyes SM. Persistent accumulation of gut macrophages with impaired phagocytic function correlates with SIV disease progression in macaques. *Eur J Immunol* (2017) 47(11):1925–35. doi:10.1002/eji.201646904
25. Becerra JC, Bildstein LS, Gach JS. Recent Insights into the HIV/AIDS pandemic. *Microb Cell* (2016) 3(9):451–75. doi:10.15698/mic2016.09.529
26. Pantaleo G, Graziosi C, Fauci AS. The immunopathogenesis of human immunodeficiency virus infection. *N Engl J Med* (1993) 328(5):327–35. doi:10.1056/NEJM199302043280508
27. Okoye AA, Picker LJ. CD4(+) T-cell depletion in HIV infection: mechanisms of immunological failure. *Immunol Rev* (2013) 254(1):54–64. doi:10.1111/imr.12066
28. Carmichael C. Prevention and treatment of common HIV-associated opportunistic complications. *Prim Care* (1997) 24(3):561–74.
29. Lloyd A. HIV infection and AIDS. *P N G Med J* (1996) 39(3):174–80.
30. Centers for Disease Control and Prevention (CDC). Revised surveillance case definition for HIV infection – United States, 2014. *MMWR Recomm Rep* (2014) 63(RR-03):1–10.
31. Cihlar T, Fordyce M. Current status and prospects of HIV treatment. *Curr Opin Virol* (2016) 18:50–6. doi:10.1016/j.coviro.2016.03.004
32. Deeks SG, Lewin SR, Havlir DV. The end of AIDS: HIV infection as a chronic disease. *Lancet* (2013) 382(9903):1525–33. doi:10.1016/S0140-6736(13)61809-7
33. Margolis DM, Archin NM. Proviral latency, persistent human immunodeficiency virus infection, and the development of latency reversing agents. *J Infect Dis* (2017) 215(Suppl_3):S111–8. doi:10.1093/infdis/jiw618
34. Shang HT, Ding JW, Yu SY, Wu T, Zhang QL, Liang FJ. Progress and challenges in the use of latent HIV-1 reactivating agents. *Acta Pharmacol Sin* (2015) 36(8):908–16. doi:10.1038/aps.2015.22
35. Bannert N, Schenten D, Craig S, Sodroski J. The level of CD4 expression limits infection of primary rhesus monkey macrophages by a T-tropic simian immunodeficiency virus and macrophagetropic human immunodeficiency viruses. *J Virol* (2000) 74(23):10984–93. doi:10.1128/JVI.74.23.10984-10993.2000
36. Lee B, Sharron M, Montaner LJ, Weissman D, Doms RW. Quantification of CD4, CCR5, and CXCR4 levels on lymphocyte subsets, dendritic cells, and differentially conditioned monocyte-derived macrophages. *Proc Natl Acad Sci U S A* (1999) 96(9):5215–20. doi:10.1073/pnas.96.9.5215
37. Bergamini A, Bolacchi F, Pesce CD, Carbone M, Cepparulo M, Demin F, et al. Increased CD4 and CCR5 expression and human immunodeficiency virus type 1 entry in CD40 ligand-stimulated macrophages. *J Infect Dis* (2002) 185(11):1567–77. doi:10.1086/340413
38. Mori K, Rosenzweig M, Desrosiers RC. Mechanisms for adaptation of simian immunodeficiency virus to replication in alveolar macrophages. *J Virol* (2000) 74(22):10852–9. doi:10.1128/JVI.74.22.10852-10859.2000
39. Tuttle DL, Harrison JK, Anders C, Sleasman JW, Goodenow MM. Expression of CCR5 increases during monocyte differentiation and directly mediates macrophage susceptibility to infection by human immunodeficiency virus type 1. *J Virol* (1998) 72(6):4962–9.
40. Embretson J, Zupancic M, Ribas JL, Burke A, Racz P, Tenner-Racz K, et al. Massive covert infection of helper T lymphocytes and macrophages by HIV during the incubation period of AIDS. *Nature* (1993) 362(6418):359–62. doi:10.1038/362359a0
41. Gartner S. HIV infection and dementia. *Science* (2000) 287(5453):602–4. doi:10.1126/science.287.5453.602
42. DiNapoli SR, Ortiz AM, Wu F, Matsuda K, Twigg HL 3rd, Hirsch VM, et al. Tissue-resident macrophages can contain replication-competent virus in antiretroviral-naive, SIV-infected Asian macaques. *JCI Insight* (2017) 2(4):e91214. doi:10.1172/jci.insight.91214
43. Arrildt KT, LaBranche CC, Joseph SB, Dukhovlinova EN, Graham WD, Ping LH, et al. Phenotypic correlates of HIV-1 macrophage tropism. *J Virol* (2015) 89(22):11294–311. doi:10.1128/JVI.00946-15
44. Micci L, Alvarez X, Iriele RI, Ortiz AM, Ryan ES, McGary CS, et al. CD4 depletion in SIV-infected macaques results in macrophage and microglia infection with rapid turnover of infected cells. *PLoS Pathog* (2014) 10(10):e1004467. doi:10.1371/journal.ppat.1004467

45. Ho DD, Rota TR, Hirsch MS. Infection of monocyte/macrophages by human T lymphotropic virus type III. *J Clin Invest* (1986) 77(5):1712–5. doi:10.1172/JCI112491
46. Nicholson JK, Cross GD, Callaway CS, McDougal JS. In vitro infection of human monocytes with human T lymphotropic virus type III/lymphadenopathy-associated virus (HTLV-III/LAV). *J Immunol* (1986) 137(1):323–9.
47. Gendelman HE, Orenstein JM, Martin MA, Ferrua C, Mitra R, Phipps T, et al. Efficient isolation and propagation of human immunodeficiency virus on recombinant colony-stimulating factor 1-treated monocytes. *J Exp Med* (1988) 167(4):1428–41. doi:10.1084/jem.167.4.1428
48. Cribbs SK, Lennox J, Caliendo AM, Brown LA, Guidot DM. Healthy HIV-1-infected individuals on highly active antiretroviral therapy harbor HIV-1 in their alveolar macrophages. *AIDS Res Hum Retroviruses* (2015) 31(1):64–70. doi:10.1089/AID.2014.0133
49. Brown CR, Czapiga M, Kabat J, Dang Q, Ourmanov I, Nishimura Y, et al. Unique pathology in simian immunodeficiency virus-infected rapid progressor macaques is consistent with a pathogenesis distinct from that of classical AIDS. *J Virol* (2007) 81(11):5594–606. doi:10.1128/JVI.00202-07
50. Avalos CR, Abreu CM, Queen SE, Li M, Price S, Shirk EN, et al. Brain macrophages in simian immunodeficiency virus-infected, antiretroviral-suppressed macaques: a functional latent reservoir. *MBio* (2017) 8(4):e01186-17. doi:10.1128/mBio.01186-17
51. Honeycutt JB, Thayer WO, Baker CE, Ribeiro RM, Lada SM, Cao Y, et al. HIV persistence in tissue macrophages of humanized myeloid-only mice during antiretroviral therapy. *Nat Med* (2017) 23(5):638–43. doi:10.1038/nm.4319
52. Stevenson M. HIV persistence in macrophages. *Nat Med* (2017) 23(5):538–9. doi:10.1038/nm.4337
53. Igarashi T, Brown CR, Endo Y, Buckler-White A, Plishka R, Bischofberger N, et al. Macrophage are the principal reservoir and sustain high virus loads in rhesus macaques after the depletion of CD4+ T cells by a highly pathogenic simian immunodeficiency virus/HIV type 1 chimera (SHIV): implications for HIV-1 infections of humans. *Proc Natl Acad Sci U S A* (2001) 98(2):658–63. doi:10.1073/pnas.98.2.658
54. Cai Y, Sugimoto C, Arainga M, Midkiff CC, Liu DX, Alvarez X, et al. Preferential destruction of interstitial macrophages over alveolar macrophages as a cause of pulmonary disease in simian immunodeficiency virus-infected rhesus macaques. *J Immunol* (2015) 195(10):4884–91. doi:10.4049/jimmunol.1501194
55. Lakritz JR, Bodair A, Shah N, O'Donnell R, Polydefkis MJ, Miller AD, et al. Monocyte traffic, dorsal root ganglion histopathology, and loss of intraepidermal nerve fiber density in SIV peripheral neuropathy. *Am J Pathol* (2015) 185(7):1912–23. doi:10.1016/j.ajpath.2015.03.007
56. Tippett E, Cheng WJ, Westhorpe C, Cameron PU, Brew BJ, Lewin SR, et al. Differential expression of CD163 on monocyte subsets in healthy and HIV-1 infected individuals. *PLoS One* (2011) 6(5):e19968. doi:10.1371/journal.pone.0019968
57. Ellery PJ, Tippett E, Chiu YL, Paukovics G, Cameron PU, Solomon A, et al. The CD16+ monocyte subset is more permissive to infection and preferentially harbors HIV-1 in vivo. *J Immunol* (2007) 178(10):6581–9. doi:10.4049/jimmunol.178.10.6581
58. Orenstein JM, Fox C, Wahl SM. Macrophages as a source of HIV during opportunistic infections. *Science* (1997) 276(5320):1857–61. doi:10.1126/science.276.5320.1857
59. Carter CA, Ehrlich LS. Cell biology of HIV-1 infection of macrophages. *Annu Rev Microbiol* (2008) 62:425–43. doi:10.1146/annurev.micro.62.081307.162758
60. Vojnov L, Martins MA, Bean AT, Veloso de Santana MG, Sacha JB, Wilson NA, et al. The majority of freshly sorted simian immunodeficiency virus (SIV)-specific CD8(+) T cells cannot suppress viral replication in SIV-infected macrophages. *J Virol* (2012) 86(8):4682–7. doi:10.1128/JVI.06324-11
61. Aquaro S, Calió R, Balzarini J, Bellocchi MC, Garaci E, Perno CF. Macrophages and HIV infection: therapeutical approaches toward this strategic virus reservoir. *Antiviral Res* (2002) 55(2):209–25. doi:10.1016/S0166-3542(02)00052-9
62. Perno CF, Newcomb FM, Davis DA, Aquaro S, Humphrey RW, Calió R, et al. Relative potency of protease inhibitors in monocytes/macrophages acutely and chronically infected with human immunodeficiency virus. *J Infect Dis* (1998) 178(2):413–22. doi:10.1086/515642
63. Baxter AE, Russell RA, Duncan CJ, Moore MD, Willberg CB, Pablos JL, et al. Macrophage infection via selective capture of HIV-1-infected CD4+ T cells. *Cell Host Microbe* (2014) 16(6):711–21. doi:10.1016/j.chom.2014.10.010
64. Eugenin EA, Gaskill PJ, Berman JW. Tunneling nanotubes (TNT) are induced by HIV-infection of macrophages: a potential mechanism for intercellular HIV trafficking. *Cell Immunol* (2009) 254(2):142–8. doi:10.1016/j.cellimm.2008.08.005
65. Sewald X, Ladinsky MS, Uchil PD, Beloor J, Pi R, Herrmann C, et al. Retroviruses use CD169-mediated trans-infection of permissive lymphocytes to establish infection. *Science* (2015) 350(6260):563–7. doi:10.1126/science.aab2749
66. Zhu T, Muthui D, Holte S, Nickle D, Feng F, Brodie S, et al. Evidence for human immunodeficiency virus type 1 replication in vivo in CD14(+) monocytes and its potential role as a source of virus in patients on highly active antiretroviral therapy. *J Virol* (2002) 76(2):707–16. doi:10.1128/JVI.76.2.707-716.2002
67. Hu SL. Non-human primate models for AIDS vaccine research. *Curr Drug Targets Infect Disord* (2005) 5(2):193–201. doi:10.2174/1568005054201508
68. Garcia-Tellez T, Huot N, Ploquin MJ, Rascle P, Jacquelin B, Müller-Trutwin M. Non-human primates in HIV research: achievements, limits and alternatives. *Infect Genet Evol* (2016) 46:324–32. doi:10.1016/j.meegid.2016.07.012
69. Policicchio BB, Pandrea I, Apetrei C. Animal models for HIV cure research. *Front Immunol* (2016) 7:12. doi:10.3389/fimmu.2016.00012
70. Hong FF, Mellors JW. Impact of antiretroviral therapy on HIV-1 persistence: the case for early initiation. *AIDS Rev* (2015) 17(2):71–82.
71. Whitney JB, Hill AL, Sanisetty S, Penaloza-MacMaster P, Liu J, Shetty M, et al. Rapid seeding of the viral reservoir prior to SIV viraemia in rhesus monkeys. *Nature* (2014) 512(7512):74–7. doi:10.1038/nature13594
72. Sellier P, Mannioui A, Bourry O, Dereuddre-Bosquet N, Delache B, Brochard P, et al. Antiretroviral treatment start-time during primary SIV(mac) infection in macaques exerts a different impact on early viral replication and dissemination. *PLoS One* (2010) 5(5):e10570. doi:10.1371/journal.pone.0010570
73. Bourry O, Mannioui A, Sellier P, Roucairol C, Durand-Gasselin L, Dereuddre-Bosquet N, et al. Effect of a short-term HAART on SIV load in macaque tissues is dependent on time of initiation and antiviral diffusion. *Retrovirology* (2010) 7:78. doi:10.1186/1742-4690-7-78
74. Sui Y, Gordon S, Franchini G, Berzofsky JA. Nonhuman primate models for HIV/AIDS vaccine development. *Curr Protoc Immunol* (2013) 102:Unit12.14. doi:10.1002/0471142735.im1214s102
75. Lifson JD, Haigwood NL. Lessons in nonhuman primate models for AIDS vaccine research: from minefields to milestones. *Cold Spring Harb Perspect Med* (2012) 2(6):a007310. doi:10.1101/cshperspect.a007310
76. Baskin GB, Murphey-Corb M, Watson EA, Martin LN. Necropsy findings in rhesus monkeys experimentally infected with cultured simian immunodeficiency virus (SIV)/delta. *Vet Pathol* (1988) 25(6):456–67. doi:10.1177/030098588802500609
77. Henrickson RV, Maul DH, Lerche NW, Osborn KG, Lowenstine LJ, Prahalada S, et al. Clinical features of simian acquired immunodeficiency syndrome (SAIDS) in rhesus monkeys. *Lab Anim Sci* (1984) 34(2):140–5.
78. Brenchley JM, Schacker TW, Ruff LE, Price DA, Taylor JH, Beilman GJ, et al. CD4+ T cell depletion during all stages of HIV disease occurs predominantly in the gastrointestinal tract. *J Exp Med* (2004) 200(6):749–59. doi:10.1084/jem.20040874
79. Grivel JC, Malkevitch N, Margolis L. Human immunodeficiency virus type 1 induces apoptosis in CD4(+) but not in CD8(+) T cells in ex vivo-infected human lymphoid tissue. *J Virol* (2000) 74(17):8077–84. doi:10.1128/JVI.74.17.8077-8084.2000
80. Picker LJ, Hagen SI, Lum R, Reed-Inderbitzin EF, Daly LM, Sylwester AW, et al. Insufficient production and tissue delivery of CD4+ memory T cells in rapidly progressive simian immunodeficiency virus infection. *J Exp Med* (2004) 200(10):1299–314. doi:10.1084/jem.20041049
81. Hasegawa A, Liu H, Ling B, Borda JT, Alvarez X, Sugimoto C, et al. The level of monocyte turnover predicts disease progression in the macaque model of AIDS. *Blood* (2009) 114(14):2917–25. doi:10.1182/blood-2009-02-204263
82. Huang Y, Yin H, Wang J, Ma X, Zhang Y, Chen K. The significant increase of FcγRIIIA (CD16), a sensitive marker, in patients with coronary heart disease. *Gene* (2012) 504(2):284–7. doi:10.1016/j.gene.2012.05.017

83. Yoshimoto S, Nakatani K, Iwano M, Asai O, Samejima K, Sakan H, et al. Elevated levels of fractalkine expression and accumulation of CD16+ monocytes in glomeruli of active lupus nephritis. *Am J Kidney Dis* (2007) 50(1):47–58. doi:10.1053/j.ajkd.2007.04.012
84. Rossol M, Kraus S, Pierer M, Baerwald C, Wagner U. The CD14(bright) CD16+ monocyte subset is expanded in rheumatoid arthritis and promotes expansion of the Th17 cell population. *Arthritis Rheum* (2012) 64(3):671–7. doi:10.1002/art.33418
85. Grip O, Bredberg A, Lindgren S, Henriksson G. Increased subpopulations of CD16(+) and CD56(+) blood monocytes in patients with active Crohn's disease. *Inflamm Bowel Dis* (2007) 13(5):566–72. doi:10.1002/ibd.20025
86. Kamada N, Hisamatsu T, Okamoto S, Chinen H, Kobayashi T, Sato T, et al. Unique CD14 intestinal macrophages contribute to the pathogenesis of Crohn disease via IL-23/IFN-gamma axis. *J Clin Invest* (2008) 118(6): 2269–80. doi:10.1172/JCI34610
87. Thiesen S, Janciauskiene S, Uronen-Hansson H, Agace W, Högerkorp CM, Spee P, et al. CD14(hi)HLA-DR(dim) macrophages, with a resemblance to classical blood monocytes, dominate inflamed mucosa in Crohn's disease. *J Leukoc Biol* (2014) 95(3):531–41. doi:10.1189/jlb.0113021
88. Burdo TH, Soulas C, Orzechowski K, Button J, Krishnan A, Sugimoto C, et al. Increased monocyte turnover from bone marrow correlates with severity of SIV encephalitis and CD163 levels in plasma. *PLoS Pathog* (2010) 6(4):e1000842. doi:10.1371/journal.ppat.1000842
89. Jellinger KA, Setinek U, Drlicek M, Böhm G, Steurer A, Lintner F. Neuropathology and general autopsy findings in AIDS during the last 15 years. *Acta Neuropathol* (2000) 100(2):213–20. doi:10.1007/s004010000245
90. Masliah E, DeTeresa RM, Mallory ME, Hansen LA. Changes in pathological findings at autopsy in AIDS cases for the last 15 years. *AIDS* (2000) 14(1):69–74. doi:10.1097/00002030-200001070-00008
91. Cai Y, Sugimoto C, Arainga M, Alvarez X, Didier ES, Kuroda MJ. In vivo characterization of alveolar and interstitial lung macrophages in rhesus macaques: implications for understanding lung disease in humans. *J Immunol* (2014) 192(6):2821–9. doi:10.4049/jimmunol.1302269
92. Plata F, Autran B, Martins LP, Wain-Hobson S, Raphaël M, Mayaud C, et al. AIDS virus-specific cytotoxic T lymphocytes in lung disorders. *Nature* (1987) 328(6128):348–51. doi:10.1038/328348a0
93. Clarke JR, Krishnan V, Bennett J, Mitchell D, Jeffries DJ. Detection of HIV-1 in human lung macrophages using the polymerase chain reaction. *AIDS* (1990) 4(11):1133–6. doi:10.1097/00002030-199011000-00012
94. Nakata K, Weiden M, Harkin T, Ho D, Rom WN. Low copy number and limited variability of proviral DNA in alveolar macrophages from HIV-1-infected patients: evidence for genetic differences in HIV-1 between lung and blood macrophage populations. *Mol Med* (1995) 1(7):744–57.
95. Lewin SR, Kirihara J, Sonza S, Irving L, Mills J, Crowe SM. HIV-1 DNA and mRNA concentrations are similar in peripheral blood monocytes and alveolar macrophages in HIV-1-infected individuals. *AIDS* (1998) 12(7):719–27. doi:10.1097/00002030-199807000-00008
96. Autran B, Plata F, Guillon JM, Joly P, Mayaud C, Debré P. HIV-specific cytotoxic T lymphocytes directed against alveolar macrophages in HIV-infected patients. *Res Virol* (1990) 141(2):131–6. doi:10.1016/0923-2516(90)90014-A
97. Fischer-Smith T, Croul S, Adeniyi A, Rybicka K, Morgello S, Khalili K, et al. Macrophage/microglial accumulation and proliferating cell nuclear antigen expression in the central nervous system in human immunodeficiency virus encephalopathy. *Am J Pathol* (2004) 164(6):2089–99. doi:10.1016/S0002-9440(10)63767-4
98. Kim WK, Alvarez X, Fisher J, Bronfin B, Westmoreland S, McLaurin J, et al. CD163 identifies perivascular macrophages in normal and viral encephalitic brains and potential precursors to perivascular macrophages in blood. *Am J Pathol* (2006) 168(3):822–34. doi:10.2353/ajpath.2006.050215
99. Nowlin BT, Burdo TH, Midkiff CC, Salemi M, Alvarez X, Williams KC. SIV encephalitis lesions are composed of CD163(+) macrophages present in the central nervous system during early SIV infection and SIV-positive macrophages recruited terminally with AIDS. *Am J Pathol* (2015) 185(6):1649–65. doi:10.1016/j.ajpath.2015.01.033
100. Palmer AK, Kirkland JL. Aging and adipose tissue: potential interventions for diabetes and regenerative medicine. *Exp Gerontol* (2016) 86:97–105. doi:10.1016/j.exger.2016.02.013
101. Karlsson EA, Beck MA. The burden of obesity on infectious disease. *Exp Biol Med (Maywood)* (2010) 235(12):1412–24. doi:10.1258/ebm.2010.010227
102. Frasca D, Blomberg BB. Adipose tissue inflammation induces B cell inflammation and decreases B cell function in aging. *Front Immunol* (2017) 8:1003. doi:10.3389/fimmu.2017.01003
103. Shikuma CM, Gangcuangco LM, Killebrew DA, Libutti DE, Chow DC, Nakamoto BK, et al. The role of HIV and monocytes/macrophages in adipose tissue biology. *J Acquir Immune Defic Syndr* (2014) 65(2):151–9. doi:10.1097/01.qai.0000435599.27727.6c
104. Damouche A, Lazure T, Avettand-Fènoël V, Huot N, Dejucq-Rainsford N, Satie AP, et al. Adipose tissue is a neglected viral reservoir and an inflammatory site during chronic HIV and SIV infection. *PLoS Pathog* (2015) 11(9):e1005153. doi:10.1371/journal.ppat.1005153
105. Pallikkuth S, Mohan M. Adipose tissue: sanctuary for HIV/SIV persistence and replication. *Trends Microbiol* (2015) 23(12):748–50. doi:10.1016/j.tim.2015.11.001
106. Kitagawa M, Lackner AA, Martfeld DJ, Gardner MB, Dandekar S. Simian immunodeficiency virus infection of macaque bone marrow macrophages correlates with disease progression in vivo. *Am J Pathol* (1991) 138(4):921–30.
107. Alexaki A, Wigdahl B. HIV-1 infection of bone marrow hematopoietic progenitor cells and their role in trafficking and viral dissemination. *PLoS Pathog* (2008) 4(12):e1000215. doi:10.1371/journal.ppat.1000215
108. Swan ZD, Wonderlich ER, Barratt-Boyes SM. Macrophage accumulation in gut mucosa differentiates AIDS from chronic SIV infection in rhesus macaques. *Eur J Immunol* (2016) 46(2):446–54. doi:10.1002/eji.201545738
109. Williams DW, Engle EL, Shirk EN, Queen SE, Gama L, Mankowski JL, et al. Splenic damage during SIV infection: role of T-cell depletion and macrophage polarization and infection. *Am J Pathol* (2016) 186(8):2068–87. doi:10.1016/j.ajpath.2016.03.019
110. Araínga M, Edagwa B, Mosley RL, Poluektova LY, Gorantla S, Gendelman HE. A mature macrophage is a principal HIV-1 cellular reservoir in humanized mice after treatment with long acting antiretroviral therapy. *Retrovirology* (2017) 14(1):17. doi:10.1186/s12977-017-0344-7
111. Basha S, Surendran N, Pichichero M. Immune responses in neonates. *Expert Rev Clin Immunol* (2014) 10(9):1171–84. doi:10.1586/1744666X.2014.942288
112. Wassenaar TM, Panigrahi P. Is a foetus developing in a sterile environment? *Lett Appl Microbiol* (2014) 59(6):572–9. doi:10.1111/lam.12334
113. Palmeira P, Carneiro-Sampaio M. Immunology of breast milk. *Rev Assoc Med Bras (1992)* (2016) 62(6):584–93. doi:10.1590/1806-9282.62.06.584
114. Tobin NH, Aldrovandi GM. Immunology of pediatric HIV infection. *Immunol Rev* (2013) 254(1):143–69. doi:10.1111/imr.12074
115. Dey A, Allen J, Hankey-Giblin PA. Ontogeny and polarization of macrophages in inflammation: blood monocytes versus tissue macrophages. *Front Immunol* (2014) 5:683. doi:10.3389/fimmu.2014.00683
116. Shearer WT, Rosenblatt HM, Gelman RS, Oyomopito R, Plaeger S, Stiehm ER, et al. Lymphocyte subsets in healthy children from birth through 18 years of age: the Pediatric AIDS Clinical Trials Group P1009 study. *J Allergy Clin Immunol* (2003) 112(5):973–80. doi:10.1016/j.jaci.2003.07.003
117. Rich KC, Brambilla D, Pitt J, Moye J, Cooper E, Hillyer G, et al. Lymphocyte phenotyping in infants: maturation of lymphocyte subpopulations and the effects of HIV infection. *Clin Immunol Immunopathol* (1997) 85(3): 273–81. doi:10.1006/clin.1997.4439
118. Bunders MJ, van der Loos CM, Klarenbeek PL, van Hamme JL, Boer K, Wilde JC, et al. Memory CD4(+)CCR5(+) T cells are abundantly present in the gut of newborn infants to facilitate mother-to-child transmission of HIV-1. *Blood* (2012) 120(22):4383–90. doi:10.1182/blood-2012-06-437566
119. Newell ML, Coovadia H, Cortina-Borja M, Rollins N, Gaillard P, Dabis F, et al. Mortality of infected and uninfected infants born to HIV-infected mothers in Africa: a pooled analysis. *Lancet* (2004) 364(9441):1236–43. doi:10.1016/S0140-6736(04)17140-7
120. Goulder PJ, Lewin SR, Leitman EM. Paediatric HIV infection: the potential for cure. *Nat Rev Immunol* (2016) 16(4):259–71. doi:10.1038/nri.2016.19
121. Tovo PA, de Martino M, Gabiano C, Cappello N, D'Elia R, Loy A, et al. Prognostic factors and survival in children with perinatal HIV-1 infection. The Italian register for HIV infections in children. *Lancet* (1992) 339(8804):1249–53. doi:10.1016/0140-6736(92)91592-V
122. McIntosh K, Shevitz A, Zaknun D, Kornegay J, Chatis P, Karthas N, et al. Age- and time-related changes in extracellular viral load in children vertically

infected by human immunodeficiency virus. *Pediatr Infect Dis J* (1996) 15(12):1087–91. doi:10.1097/00006454-199612000-00006
123. Moir S, Chun TW, Fauci AS. Pathogenic mechanisms of HIV disease. *Annu Rev Pathol* (2011) 6:223–48. doi:10.1146/annurev-pathol-011110-130254
124. Milush JM, Reeves JD, Gordon SN, Zhou D, Muthukumar A, Kosub DA, et al. Virally induced CD4+ T cell depletion is not sufficient to induce AIDS in a natural host. *J Immunol* (2007) 179(5):3047–56. doi:10.4049/jimmunol.179.5.3047
125. Veazey RS, Lifson JD, Pandrea I, Purcell J, Piatak M Jr, Lackner AA. Simian immunodeficiency virus infection in neonatal macaques. *J Virol* (2003) 77(16):8783–92. doi:10.1128/JVI.77.16.8783-8792.2003
126. Wang X, Xu H, Pahar B, Alvarez X, Green LC, Dufour J, et al. Simian immunodeficiency virus selectively infects proliferating CD4+ T cells in neonatal rhesus macaques. *Blood* (2010) 116(20):4168–74. doi:10.1182/blood-2010-03-273482
127. Torow N, Yu K, Hassani K, Freitag J, Schulz O, Basic M, et al. Active suppression of intestinal CD4(+)TCRalphabeta(+) T-lymphocyte maturation during the postnatal period. *Nat Commun* (2015) 6:7725. doi:10.1038/ncomms8725
128. Thome JJ, Bickham KL, Ohmura Y, Kubota M, Matsuoka N, Gordon C, et al. Early-life compartmentalization of human T cell differentiation and regulatory function in mucosal and lymphoid tissues. *Nat Med* (2016) 22(1):72–7. doi:10.1038/nm.4008
129. D'Arena G, Musto P, Cascavilla N, Di Giorgio G, Fusilli S, Zendoli F, et al. Flow cytometric characterization of human umbilical cord blood lymphocytes: immunophenotypic features. *Haematologica* (1998) 83(3):197–203.
130. Peoples JD, Cheung S, Nesin M, Lin H, Tatad AM, Hoang D, et al. Neonatal cord blood subsets and cytokine response to bacterial antigens. *Am J Perinatol* (2009) 26(9):647–57. doi:10.1055/s-0029-1220788
131. Waecker NJ Jr, Ascher DP, Robb ML, Moriarty R, Krober M, Rickman WJ, et al. Age-adjusted CD4+ lymphocyte parameters in healthy children at risk for infection with the human immunodeficiency virus. The Military Pediatric HIV Consortium. *Clin Infect Dis* (1993) 17(1):123–5. doi:10.1093/clinids/17.1.123
132. Gesner M, Papaevangelou V, Kim M, Chen SH, Moore T, Krasinski K, et al. Alteration in the proportion of CD4 T lymphocytes in a subgroup of human immunodeficiency virus-exposed-uninfected children. *Pediatrics* (1994) 93(4):624–30.
133. Age-related standards for T lymphocyte subsets based on uninfected children born to human immunodeficiency virus 1-infected women. The European Collaborative Study. *Pediatr Infect Dis J* (1992) 11(12):1018–26. doi:10.1097/00006454-199211120-00006
134. Plaeger-Marshall S, Hultin P, Bertolli J, O'Rourke S, Kobayashi R, Kobayashi AL, et al. Activation and differentiation antigens on T cells of healthy, at-risk, and HIV-infected children. *J Acquir Immune Defic Syndr* (1993) 6(9):984–93.
135. Sugimoto C, Merino KM, Hasegawa A, Wang X, Alvarez XA, Wakao H, et al. A critical role for monocytes/macrophages in the rapid progression to AIDS in pediatric SIV-infected rhesus macaques. *J Virol* (2017) 91(22):e01346-17. doi:10.1128/JVI.01346-17
136. Burl S, Townend J, Njie-Jobe J, Cox M, Adetifa UJ, Touray E, et al. Age-dependent maturation of Toll-like receptor-mediated cytokine responses in Gambian infants. *PLoS One* (2011) 6(4):e18185. doi:10.1371/journal.pone.0018185
137. Asquith M, Haberthur K, Brown M, Engelmann F, Murphy A, Al-Mahdi Z, et al. Age-dependent changes in innate immune phenotype and function in rhesus macaques (Macaca mulatta). *Pathobiol Aging Age Relat Dis* (2012) 2. doi:10.3402/pba.v2i0.18052
138. Le Garff-Tavernier M, Béziat V, Decocq J, Siguret V, Gandjbakhch F, Pautas E, et al. Human NK cells display major phenotypic and functional changes over the life span. *Aging Cell* (2010) 9(4):527–35. doi:10.1111/j.1474-9726.2010.00584.x
139. Torow N, Marsland BJ, Hornef MW, Gollwitzer ES. Neonatal mucosal immunology. *Mucosal Immunol* (2017) 10(1):5–17. doi:10.1038/mi.2016.81
140. Fulde M, Hornef MW. Maturation of the enteric mucosal innate immune system during the postnatal period. *Immunol Rev* (2014) 260(1):21–34. doi:10.1111/imr.12190
141. Lusyati S, Hulzebos CV, Zandvoort J, Sauer PJ. Levels of 25 cytokines in the first seven days of life in newborn infants. *BMC Res Notes* (2013) 6:547. doi:10.1186/1756-0500-6-547
142. Belderbos ME, Levy O, Meyaard L, Bont L. Plasma-mediated immune suppression: a neonatal perspective. *Pediatr Allergy Immunol* (2013) 24(2):102–13. doi:10.1111/pai.12023
143. Pettengill MA, van Haren SD, Levy O. Soluble mediators regulating immunity in early life. *Front Immunol* (2014) 5:457. doi:10.3389/fimmu.2014.00457
144. De Rossi A. Virological and immunological response to antiretroviral therapy in HIV-1 infected children: genotypic and phenotypic assays in monitoring virological failure. *New Microbiol* (2004) 27(2 Suppl 1):45–50.
145. Paintsil E. Monitoring antiretroviral therapy in HIV-infected children in resource-limited countries: a tale of two epidemics. *AIDS Res Treat* (2011) 2011:280901. doi:10.1155/2011/280901
146. van Rossum AM, Fraaij PL, de Groot R. Efficacy of highly active antiretroviral therapy in HIV-1 infected children. *Lancet Infect Dis* (2002) 2(2):93–102. doi:10.1016/S1473-3099(02)00183-4
147. Van Rompay KK, Matthews TB, Higgins J, Canfield DR, Tarara RP, Wainberg MA, et al. Virulence and reduced fitness of simian immunodeficiency virus with the M184V mutation in reverse transcriptase. *J Virol* (2002) 76(12):6083–92. doi:10.1128/JVI.76.12.6083-6092.2002

Conflict of Interest Statement: The authors declare that the research was conducted in the absence of any commercial or financial relationships that could be construed as a potential conflict of interest.

Copyright © 2017 Merino, Allers, Didier and Kuroda. This is an open-access article distributed under the terms of the Creative Commons Attribution License (CC BY). The use, distribution or reproduction in other forums is permitted, provided the original author(s) or licensor are credited and that the original publication in this journal is cited, in accordance with accepted academic practice. No use, distribution or reproduction is permitted which does not comply with these terms.

frontiers in Immunology

ORIGINAL RESEARCH
published: 27 June 2018
doi: 10.3389/fimmu.2018.01494

Interaction Between Macrophage Migration Inhibitory Factor and CD74 in Human Immunodeficiency Virus Type I Infected Primary Monocyte-Derived Macrophages Triggers the Production of Proinflammatory Mediators and Enhances Infection of Unactivated CD4+ T Cells

*César Trifone[1], Jimena Salido[1], María Julia Ruiz[1†], Lin Leng[2], María Florencia Quiroga[1], Horacio Salomón[1], Richard Bucala[2], Yanina Ghiglione[1] and Gabriela Turk[1]**

[1] CONICET-Universidad de Buenos Aires, Instituto de Investigaciones Biomédicas en Retrovirus y Sida (INBIRS), Buenos Aires, Argentina, [2] Department of Medicine, Yale University School of Medicine, New Haven, CT, United States

OPEN ACCESS

Edited by:
Christel Vérollet, UMR5089 Institut de Pharmacologie et de Biologie Structurale (IPBS), France

Reviewed by:
Arnaud Moris, INSERM U1135 Centre d'Immunologie et de Maladies Infectieuses, France
Bin Su, Capital Medical University, China

***Correspondence:**
Gabriela Turk
gturk@fmed.uba.ar

†Present address:
María Julia Ruiz, Centre de Recherche du Centre Hospitalier de l'Université de Montréal (CRCHUM), Montréal, QC, Canada

Specialty section:
This article was submitted to Microbial Immunology, a section of the journal Frontiers in Immunology

Received: 14 September 2017
Accepted: 15 June 2018
Published: 27 June 2018

Citation:
Trifone C, Salido J, Ruiz MJ, Leng L, Quiroga MF, Salomón H, Bucala R, Ghiglione Y and Turk G (2018) Interaction Between Macrophage Migration Inhibitory Factor and CD74 in Human Immunodeficiency Virus Type I Infected Primary Monocyte-Derived Macrophages Triggers the Production of Proinflammatory Mediators and Enhances Infection of Unactivated CD4+ T Cells. Front. Immunol. 9:1494. doi: 10.3389/fimmu.2018.01494

Understanding the mechanisms of human immunodeficiency virus type I (HIV-1) pathogenesis would facilitate the identification of new therapeutic targets to control the infection in face of current antiretroviral therapy limitations. CD74 membrane expression is upregulated in HIV-1-infected cells and the magnitude of its modulation correlates with immune hyperactivation in HIV-infected individuals. In addition, plasma level of the CD74 activating ligand macrophage migration inhibitory factor (MIF) is increased in infected subjects. However, the role played by MIF/CD74 interaction in HIV pathogenesis remains unexplored. Here, we studied the effect of MIF/CD74 interaction on primary HIV-infected monocyte-derived macrophages (MDMs) and its implications for HIV immunopathogenesis. Confocal immunofluorescence analysis of CD74 and CD44 (the MIF signal transduction co-receptor) expression indicated that both molecules colocalized at the plasma membrane specifically in wild-type HIV-infected MDMs. Treatment of infected MDMs with MIF resulted in an MIF-dependent increase in TLR4 expression. Similarly, there was a dose-dependent increase in the production of IL-6, IL-8, TNFα, IL-1β, and sICAM compared to the no-MIF condition, specifically from infected MDMs. Importantly, the effect observed on IL-6, IL-8, TNFα, and IL-1β was abrogated by impeding MIF interaction with CD74. Moreover, the use of a neutralizing αMIF antibody or an MIF antagonist reverted these effects, supporting the specificity of the results. Treatment of unactivated CD4+ T-cells with MIF-treated HIV-infected MDM-derived culture supernatants led to enhanced permissiveness to HIV-1 infection. This effect was lost when CD4+ T-cells were treated with supernatants derived from infected MDMs in which CD74/MIF interaction had been blocked. Moreover, the enhanced permissiveness of unactivated CD4+ T-cells was recapitulated by exogenous addition of IL-6, IL-8, IL-1β,

and TNFα, or abrogated by neutralizing its biological activity using specific antibodies. Results obtained with BAL and NL4-3 HIV laboratory strains were reproduced using transmitted/founder primary isolates. This evidence indicated that MIF/CD74 interaction resulted in a higher production of proinflammatory cytokines from HIV-infected MDMs. This caused the generation of an inflammatory microenvironment which predisposed unactivated CD4+ T-cells to HIV-1 infection, which might contribute to viral spreading and reservoir seeding. Overall, these results support a novel role of the MIF/CD74 axis in HIV pathogenesis that deserves further investigation.

Keywords: human immunodeficiency virus, CD74, macrophage migration inhibitory factor, primary monocyte-derived macrophages, CD4+ T-cells, immunopathogenesis

INTRODUCTION

The pandemic of human immunodeficiency virus/acquired immunodeficiency syndrome (HIV/AIDS) is still a major public health concern worldwide. Combined antiretroviral therapy (cART) can diminish the viral load (VL) to undetectable levels, reducing not only morbidity and mortality but also transmission risks, with the subsequent impact on the dynamic of the global epidemic (1). However, cART has several limitations like the need of daily doses, the development of viral resistance, and toxicity. More importantly, the rebound of VL levels in patients who discontinue cART suggests the presence of long-lived viral reservoirs that are resistant to cART, hampering the cure of the infection. In addition, it is being increasingly clear that even effectively treated HIV-infected individuals have a greater risk of experiencing non-AIDS related morbidity and mortality events than age-matched HIV-uninfected adults, indicating that even effective cART cannot fully restore health. Most of these complications are related to immune dysfunction and inflammation and include gut-associated mucosal disruption, lymphoid tissue damage, liver dysfunction, and monocyte/macrophage activation which ultimately lead to the development of coagulopathies, atherosclerosis, vascular dysfunction, and frailty, among other effects (2). Thus, understanding the mechanisms underlying HIV persistence and irreversible immune damage is extremely important to fight the infection and its consequences.

CD4+ T-cells are the major targets of HIV infection followed by macrophages. Productive viral replication is supported mostly in activated CD4+ T-cells, which culminates in cell apoptosis. Conversely, macrophages are less permissive to HIV-1 infection albeit more resistant to virus-mediated cell killing, thus viral replication proceeds for a longer time compared to T cells (3, 4). Both cell types play an important role since the onset of infection to the development of chronic inflammation regardless of the different viral replication strategies maintained in each cell type.

CD74 (also known as invariant chain or Ii) is a non-polymorphic type II integral membrane protein expressed by antigen-presenting cells. It was first described to act as a major histocompatibility class II-associated chaperone; but now, it is increasingly understood as a versatile protein with multiple roles (5–7). In the context of HIV-1 infection, surface CD74 expression is upregulated by Nef (8, 9) and Vpu (10) viral proteins. Moreover, accumulated data suggest that Nef-mediated CD74 upregulation might play an important role in HIV immunopathogenesis as: (i) this activity is conserved among *nef* alleles from HIV-1 primary isolates, HIV-2, and SIV (9, 11) as well as HIV-1 BF inter-subtype recombinant forms (12), (ii) it has been documented in *in vitro* infected cell lines [HeLa-CIITA, MelJuSo, and THP-1 (8, 13)] and also in primary CD4+ T-cells and monocyte-derived macrophages (MDMs) (13, 14), and (iii) modulation levels differ among progressive versus non-progressive infected individuals, both in adult (9) and pediatric populations (13). Moreover, our group has demonstrated that CD74 upregulation occurs on naturally infected MDMs obtained directly from HIV+ subjects and that the magnitude of this upregulation correlates with the level of immune activation in those subjects, providing evidence for the contribution of the HIV-mediated CD74 upregulation to immune damage during the course of infection (15).

One of the alternative activities described for CD74 is its ability to serve as the high-affinity binding component of the heteromeric receptor for macrophage migration inhibitory factor (MIF) (16–18). MIF is a proinflammatory cytokine that plays a key role in anti-stress and anti-microbial responses. It is secreted by different immune cells including T and B lymphocytes, macrophages, monocytes, and dendritic cells among others (19). MIF has been related to the pathogenesis of diverse inflammatory, infectious, autoimmune, and metabolic diseases as well as different types of cancer (20–33). During HIV infection, increased MIF plasma levels have been observed during the acute phase of infection and remained elevated (34, 35). On the other hand, it has been demonstrated that MIF was heavily produced by *in vitro* infected peripheral blood mononuclear cells (PBMCs) and also by uninfected gp120-stimulated PBMCs. Moreover, the addition of exogenous recombinant MIF to *in vitro* infected PBMCs increased viral replication (34).

Despite the fact that MIF is a key component of the inflammatory immune response, that it is elevated in plasma from HIV-infected subjects, and that the virus itself modulates the surface expression of its receptor, no reports have explored the role of the MIF/CD74 axis in HIV immunopathogenesis. Thus, the aim of this work was to study the effect of MIF/CD74 interaction on the phenotype and the function of primary HIV-infected MDMs, and how this axis determines the environment to modulate CD4+ T-cell permissiveness to infection.

MATERIALS AND METHODS

Primary Human MDM and CD4+ T-Cell Purification and Culture

Buffy coats from healthy donors were used to obtain PBMCs by Ficoll-Hypaque (GE Healthcare Life Sciences, USA) density gradient centrifugation. Monocytes were then separated from PBMCs by Percoll (GE Healthcare Life Sciences, USA) gradient technique. Isolated monocytes (purity >80% measured by flow cytometry) were further purified by adherence to plastic plates in RPMI 1640 medium (HyClone, GE Healthcare Life Sciences, USA). Non-adherent cells were removed after 2 h plating by means of extensive washes. Adherent cells were allowed to differentiate into MDMs in RPMI 1640 medium supplemented with 10% fetal bovine serum (FBS, Gibco, Thermo Fischer Corporation, USA), 2 mM L-glutamine (Sigma-Aldrich, USA), 100 U/ml penicillin (Sigma-Aldrich USA), 100 µg/ml streptomycin (Sigma-Aldrich, USA), and 10 mM HEPES (Sigma-Aldrich) (from now on complete RPMI medium) plus 20 ng/ml recombinant granulocyte monocyte-colony stimulating factor (GM-CSF, Miltenyi, Germany) for 4 days. After differentiation, MDM purity was analyzed by flow cytometry and only donors with >90% purity were used in subsequent assays.

CD4+ T-cells were isolated from buffy coats by negative selection using the RosetteSep kit (Stem cell, Canada). Purified cells (>95% purity by flow cytometry) were cultured in complete RPMI medium plus 25 ng/ml IL-2 (BioLegend, USA). Culture plates were incubated at 37°C in a humidified atmosphere with 5% CO_2.

Virus Production and Infections

GFP-expressing X4-tropic HIV-1 virus stock was produced by transfecting 293 T cells using the X-tremeGENE 9 DNA transfection reagent (Roche, Switzerland) with the pBR43IeG-nef+plasmid (kindly provided by Dr. Michael Schindler). This plasmid encodes the full-length HIV genome plus the reporter protein GFP (pBR-NL4-3 nef-IRES-eGFP, NefWT virus). Similarly, a Nef-defective virus (ΔNef) was produced using the pBR43IeG-nefSTOP plasmid. When stated, a pseudotyped X4-tropic virus, generated by adding a plasmid encoding the vesicular stomatitis virus (VSV) protein G to the transfection solution, was used. Also, an R5-tropic HIV-1 viral stock was produced by infecting primary MDMs from healthy donors with the HIV-1 BAL strain. Finally, an R5- and a dual (R5X4)-tropic transmitted/founder (T/F) infectious molecular clones (IMCs) were selected from the full panel of T/F IMCs available at the NIH AIDS Reagent program [Division of AIDS, NIAID, NIH: Cat #11746 and 11744, respectively, from Dr. John Kappes (36–39)]. Both T/F viral stocks were produced by transfecting 293 T cells using the X-tremeGENE 9 DNA transfection reagent. Culture supernatants were harvested 48 h post-transfection (for the NL4-3 and T/F viruses) or 14 days post-infection (for the BAL R5-tropic stock). In all cases, culture supernatants were clarified by centrifugation at 600 *g* for 15 min at 4°C, fractioned and stored at −80°C until use. Viral titer was estimated by p24 antigen quantitation by ELISA (Sino Biological Inc., China).

Monocyte-derived macrophages were infected with the R5-tropic viruses (either with the BAL or the R5-tropic T/F strain) using a ratio of 1 ng p24/10^6 cells. MDMs to be evaluated by immunofluorescence microscopy were infected with the VSV-G pseudotyped X4-virus and CD4+ T-cells were infected using the X4-tropic virus (either the NL4-3 or the dual-tropic T/F strain) by spinoculation (1,200 *g* for 1.5 h at 37°C) using a ratio of 150 ng p24/10^6 cells in both cases. After adsorption, the inoculum was removed and cells were washed twice in RPMI medium.

Human Samples

Plasma from 13 HIV seronegative healthy donors (HIV−) and 13 individuals with recent HIV-1 infection (HIV+) were obtained. Samples from HD were obtained from eligible voluntary blood donors >18 years old who completed a survey on blood donation which particularly excludes persons who had been exposed to HIV; and were screened for serological markers before being accepted as donors. HIV-infected subjects were enrolled as part of an ongoing acute/early primary HIV infection cohort from Argentina (40–45). This study was reviewed and approved by two institutional review boards: *Comité de Ética Humana, Facultad de Medicina, Universidad de Buenos Aires* and *Comité de Bioética, Fundación Huésped (Buenos Aires, Argentina)*. Both HIV-infected participants and HD provided written informed consents accepting to participate in this study in accordance with the Declaration of Helsinki.

Immunofluorescence Microscopy

Monocyte-derived macrophages obtained as mentioned above were cultured over coverslips and infected either with the pseudotyped GFP-expressing Nef wild type (WT) virus or the pseudotyped GFP-expressing Nef-defective (ΔNef) virus. Uninfected cells were used as controls. Three days post-infection, MDMs were fixed and permeabilized with Cytofix-Cytoperm buffer (BD Biosciences) following the manufacturer's instructions and blocked with Cytoperm wash buffer plus 2% FBS. MDMs were subsequently stained overnight with an anti-CD44 antibody (BioLegend). The following day, cells were washed three times and stained with an Alexa546-conjugated anti-mouse antibody (Jackson, MS, USA) during 1 h. Finally, cells were washed three times, treated again with cytofix-cytoperm buffer, blocked, and stained overnight with an APC-conjugated anti-CD74 antibody (BioLegend, USA). After three final washes, cells were fixed and mounted with DAPI-Fluoromount-G (Thermo Fisher Scientific) and analyzed in an Olympus FV-1000 (Olympus, Tokyo, Japan) microscope with a Plapon 60×/1.42 NA oil immersion objective and using FV10-ASW v.01.07.03.00 software. Cross-sectional quantitation of mean fluorescence intensity (mFI) was performed using Image J software. Single stained controls were performed in order to exclude channel spillover (cells stained only with APC-conjugated anti-CD74 antibody or the anti-CD44 antibody followed by Alexa546-conjugated anti-mouse antibody staining). Also, individual isotype controls were performed in order to exclude unspecific antibody binding and cross-reactivity with the secondary antibody.

Evaluation of CD74 Modulation

After infection with the WT or ΔNef GFP-expressing viruses, MDMs were detached with trypsin (Gibco) and stained with an anti-CD74-PE (Santa Cruz Biotechnology, USA). Cells were washed and analyzed in a BD FACSCanto flow cytometer (BD Biosciences) using the FACSDiva v8.0.1 software (BD Biosciences) or FlowJO v10 (Data Analysis Software, LLC). HIV-mediated CD74 upregulation was calculated as the ratio between the FL2 median fluorescence intensity (MFI) of infected (GFP^+) versus uninfected (GFP^-) cells.

Recombinant Cytokines and Antibodies

Recombinant human MIF (rhMIF) was prepared as described elsewhere (46) (endotoxin content < 0.1 EU/ml). MIF antagonist MIF098 [3-(3-hydroxybenzyl)-5-methylbenzooxazol-2-one] was dissolved in DMSO at a concentration of 149 μM (47). The neutralizing anti-MIF monoclonal antibody (clone NIHlllD.9) was obtained from ascites after purification using protein A/G spin column and resuspended at 5.15 mg/ml (48, 49). A CD74 blocking antibody (BD Pharmingen, clone LN2), the recombinant human cytokines IL-6, IL-8, IL-1β (BioLegend), and TNFα (MiltenyiBiotec), and the cytokine neutralizing antibodies anti-IL-8 (R&D Systems), anti-IL-6, anti-IL-1β, and anti-TNFα (BioLegend) were obtained.

MDM Stimuli

Monocyte-derived macrophages were infected with the R5-tropic HIV and the infection was left to progress. At day 11, infection percentage was evaluated by p24 intracellular staining as described in the following paragraph (Figure S1 in Supplementary Material). After that, MDMs were washed twice with PBS 1× (Sigma) and rhMIF was added to a final concentration of 1, 10, or 25 ng/ml. Cells were incubated at 37°C for 8 h until the supernatant was collected. When denoted, pretreatment with the αCD74 blocking antibody (or the appropriate isotype control) was performed at 5 ng/ml for 30 min. In some experiments (TLR4 expression), Fc receptors were blocked for 10 min before the addition of the αCD74 blocking antibody (or its isotype-matched control) with an Fc blocking reagent from BD Biosciences.

Evaluation of TLR4 Expression

After MIF stimulation, infected and uninfected MDMs were harvested and stained with a PE-conjugated anti-TLR4 antibody (BioLegend) for 30 min at 4°C. Following incubation, cells were washed, fixed, and permeabilized using the Cytofix/Cytoperm kit (BD Biosciences) following the instructions provided by the manufacturer. Then, intracellular p24 antigen was stained using an anti-p24-FITC antibody (KC57-FITC, Coulter-clone, Beckman Coulter, USA) for 30 min at 4°C. Cells were then washed, fixed, and acquired in a BD FACSCanto flow cytometer. Data acquisition was performed using the BD FACSDiva software and analyzed subsequently with FlowJO v10 software (Data Analysis Software, LLC). An isotype-matched FITC-conjugated non-specific antibody was used to set the p24-negative population accurately.

First, single cells were gated in a forward scatter (FSC)-height (FSC-H) versus an FSC-area (FSC-A) plot. Then, gating was performed on living MDMs in an FSC versus a side scatter (SSC) plot. Infected cells were identified in an SSC versus FL-1 (FITC) plot as p24 positive events (Figure S1 in Supplementary Material). Bystander cells were identified as the p24-negative population on the same plot. TLR4 median fluorescence intensity (MFI) was determined for uninfected, infected, and bystander cells. Modulation of TLR4 expression was calculated as the ratio between MFI corresponding to infected or bystander versus uninfected cells.

Cytokine Quantitation

The levels of the following cytokines were evaluated in MDM supernatants using commercially available ELISA sets: IL-8, IL-6, IL-1β, TNFα, IL-10 (ELISA MAX Deluxe kits, BioLegend) and sICAM (DouSet ELISA, R&D Systems). MIF plasma levels were evaluated using an in-house ELISA constructed with an anti-human MIF antibody pair and an MIF standard obtained from BioLegend.

Permissiveness Induction in Unactivated $CD4^+$ T-Cells

Unactivated $CD4^+$ T-cells were incubated with supernatants (1/2,000 dilution) from MIF-treated or untreated MDMs, for 72 h at 37°C. Before incubation, supernatants were clarified for 15 min at 600 *g* and UV-inactivated for 30 min (253.7 nm, 15 cm away from the light source). After that, cells were washed and infected with an X4-tropic HIV. Supernatants were collected daily for p24 antigen quantitation till day 7 post-infection. Phytohemagglutinin- (PHA, 2.5 ng/ml, Sigma-Aldrich, USA) and RPMI-treated $CD4^+$ T-cells were used as positive and negative controls, respectively.

Alternatively, unactivated $CD4^+$ T-cells were stimulated with recombinant IL-1β, IL-6, IL-8, and TNF-α, either alone or in combination, for 72 h prior to infection.

$CD4^+$ T-Cell Phenotype, Viability, and Infection Percentage

The expression of CD38, CD69, HLA-DR, CD25, PD-1, and CD28 surface molecules were analyzed by flow cytometry after $CD4^+$ T-cell stimulation with MDMs-derived supernatants for 72 h. Percentages of cells expressing the markers mentioned above as well as their MFI were recorded. Initial gating was performed on lymphocytes followed by gating on $CD4^+$ events. Isotype-matched non-specific antibodies were used in each sample to set the corresponding negative populations accurately.

In addition, $CD4^+$ T-cells were harvested from day 1 to 7 post-infection and both cell viability and infection percentages were evaluated by flow cytometry. First, single cells were gated in an FSC-H versus an FSH-A plot. Then, living lymphocytes were gated an FSC versus an SSC plot (%viability). Subsequently, infected cells were identified in an FSC-H versus GFP plot (Figure S1 in Supplementary Material). Data acquisition was performed in a BD FACSCanto flow cytometer using the BD FACSDiva software and analyzed subsequently with FlowJO v10 software (Data Analysis Software, LLC).

Data Analysis

Experiments were performed at least three independent times and analyzed using parametric tests, unless otherwise stated (see exact number of independent experiments in each figure legend). Data normality was assessed using the Shapiro–Wilk test. All tests were considered significant when $p < 0.05$ (GraphPad Prism 7 Software).

RESULTS

CD74 Is Upregulated in *In Vitro* HIV-Infected MDMs and This Effect Is Accompanied by Higher MIF Plasma Levels in HIV-Infected Subjects, Compared to HIV-Negative Donors

Nef-mediated CD74 upregulation is a well-described phenomenon. More specifically, this was shown to occur in *in vitro* HIV-infected primary MDMs (13) and in an *ex vivo* model of MDMs obtained from HIV-infected subjects (15). **Figure 1A** depicts surface CD74 expression in one representative MDM donor. CD74 expression was monitored in uninfected cells (UN, left panel) as well as in cells infected with a Nef-defective virus (ΔNef, middle panel) or a Nef-expressing virus (WT, right panel). In the cultures infected with the WT virus, CD74 MFI was significantly higher in GFP-expressing cells (i.e., infected) when compared to GFP-negative cells (i.e., uninfected). On the contrary, no differences were observed in cultures infected with the Nef-defective virus when comparing infected versus uninfected cells. **Figure 1B** compiles the upregulation magnitude from three different donors (relative to the Nef-defective virus). On the other hand, it has been reported that the plasma levels of the CD74 ligand MIF were elevated during HIV infection (34, 35). To confirm this, MIF concentration was evaluated in plasma from recently HIV-infected subjects enrolled as part of the *Grupo Argentino de Seroconversión* study group. In line with the previous reports, our results indicated that the MIF plasma level during the acute HIV infection (<6-month post-infection) was 30-fold higher when compared to uninfected individuals (**Figure 1C**).

Plasma Membrane Expression of CD74 and CD44, the Signaling Component of the MIF Receptor Complex, Are Increased in WT HIV-Infected MDMs

We hypothesized that the increased CD74 expression found in HIV-1 infected MDMs may translate into enhanced MIF

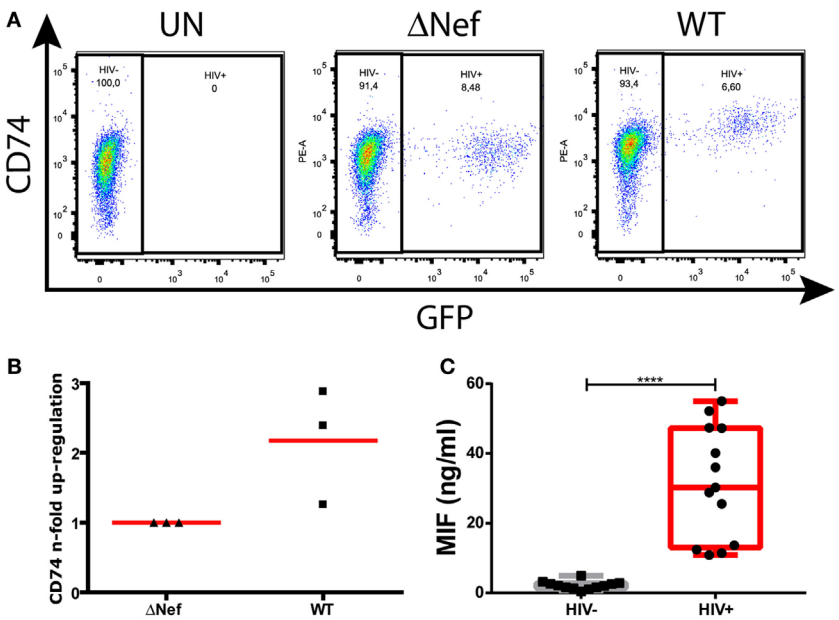


FIGURE 1 | CD74 upregulation in human immunodeficiency virus (HIV)-infected monocyte-derived macrophages (MDMs) and macrophage migration inhibitory factor (MIF) plasma levels in HIV+ subjects. **(A)** Flow cytometry analysis of CD74 surface expression in primary uninfected MDMs (left panel); infected MDMs with a Nef-defective virus expressing the reporter molecule GFP (ΔNef HIV-1, middle panel); and infected with a wild type (WT) HIV-1 also expressing the reporter molecule GFP (WT HIV, right panel). The plots show CD74 versus GFP expression (HIV-1 infection) on MDMs [gated previously in a forward scatter (FSC) versus side scatter plot]. In each dot plot, two different populations were gated: the HIV-1 negative population (GFP negative) and the HIV-1 positive population (GFP positive). One representative healthy donor, out of three donors, is shown. **(B)** Quantitation of Nef-mediated upregulation of CD74, calculated as the ratio between FL-2 MFI obtained for cells infected with the WT virus and the FL-2 MFI obtained for cells infected with the ΔNef virus. Each black dot represents one out of three independent experiments (donors). Horizontal red bars stand for the mean value. **(C)** MIF concentration in plasma obtained from HIV-negative (HIV−, $N = 13$) and HIV-positive (HIV+, $N = 13$) donors. Each plasma was evaluated in duplicate. Dots represent the average of duplicates for each donor. Data were normally distributed and analyzed by two-tailed unpaired Student's *t*-test. Horizontal lines within boxes represent the median and whiskers extend from min to max. ****$p < 0.0001$.

receptor availability and signal transduction. Thus, the cellular localization of CD74 and the CD44 signaling co-receptor was evaluated in infected primary MDMs by confocal immunofluorescence microscopy. In consonance with previous reports on HeLa-CIITA cells (8, 50), CD74 staining was observed mainly in intracellularly both in uninfected cells and in cells infected with the Nef-defective virus (**Figure 2A**). More specifically, CD74 staining was mostly located in membranous compartments within the cytoplasm. This could be visualized in the images but it also could be inferred from cross-sectional quantitation of mean fluorescence intensity (mFI) by image processing (**Figure 2B**) where an uneven mFI profile characterized by different cytoplasmic peaks was obtained. Conversely, an intense CD74 signal comprising the plasma membrane was observed in MDMs infected with the WT virus (**Figures 2A,B**, lower panels). This is consistent with the ability of Nef to reduce the rate of CD74 internalization (12, 51). Surprisingly, CD44 distribution mirrored that of CD74 in all conditions. Particularly, both CD44 and CD74 were strongly co-expressed at the plasma membrane of WT HIV-infected cells.

In order to quantitate CD44 and CD74 expression at different subcellular localization across all conditions, MFI cross-sectional quantifications corresponding to the regions encompassing only the plasma membrane (**Figure 2C**) or the cytoplasm (**Figure 2D**), both for CD74 and CD44, were performed in all infection conditions. Results again indicated that there is a substantial overlap between both molecules in all conditions but that the staining pattern was significantly different in WT-infected cells compared both to uninfected and ΔNef-infected cells, being the expression of both molecules concentrated at the plasma membrane. These

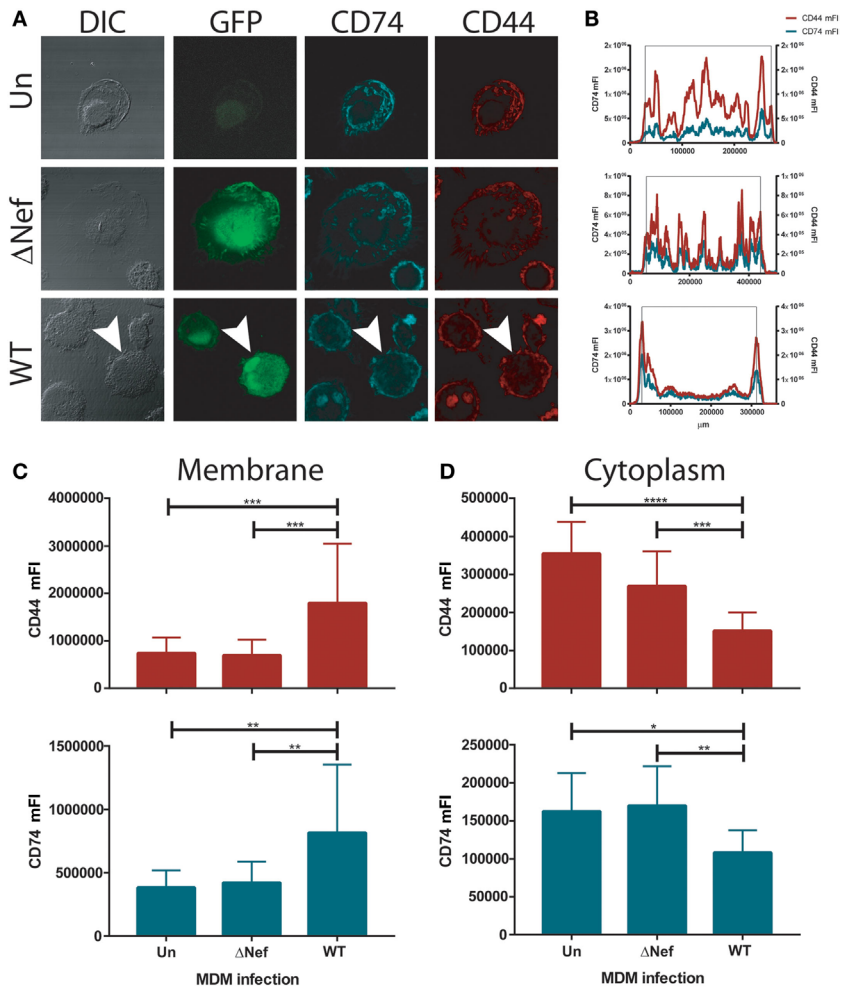


FIGURE 2 | CD74 and CD44 expression in uninfected and infected monocyte-derived macrophages (MDMs). **(A)** Confocal immunofluorescence microscopy of primary uninfected MDMs (UN, upper panels); primary ΔNef human immunodeficiency virus (HIV)-infected MDMs (ΔNef, middle panels); and primary wild type (WT) HIV-infected MDMs (WT, lower panels). From left to right: bright field, GFP (HIV-1 infection), CD74 staining and CD44 staining are shown, in one representative cell for each condition. **(B)** Plots show cross-sectional mean fluorescence intensity (mFI) for CD74 (left axis, cyan line) and CD44 (right axis, red line) corresponding to the depicted cells (in the lower panel, cross-sectional mFI was evaluated in the cell pointed with an arrow). The black lines indicate the area comprising the cell according to the DIC. **(C,D)** Cross-sectional mFI quantification for CD44 (upper panel) and CD74 (lower panel) intensity at plasma membrane **(C)** and cytoplasm **(D)**. Quantifications were performed in 15 individual cells for each condition. Bars represent mean ± SD. Data were analyzed by one-way ANOVA followed by Dunnett's post-test. *$p < 0.05$, **$p < 0.01$, ***$p < 0.001$, ****$p < 0.0001$.

data support the notion that the expression of the components of the main MIF receptor might be enhanced in Nef-expressing HIV-infected cells which in turn would be translated into higher responsiveness to MIF by HIV-infected cells.

MIF Modulates TLR4 Expression in HIV-Infected MDMs in a CD74-Independent Fashion

We next investigated the well-documented action of MIF to upregulate TLR4 expression in MDMs. To elucidate if this activity was affected by HIV infection, and if it was dependent of CD74 engagement, MDMs were infected with the R5-tropic HIV strain. Uninfected cells were used as controls. At day 11, cells were treated with 1, 10, or 25 ng/ml of MIF. These concentrations were chosen as reported previously to represent those observed in plasma from healthy volunteers, pathophysiological fluids, or plasma from HIV^+ individuals, respectively (34, 52). In this model, cell viability at day 11 was $83 \pm 3.7\%$ in uninfected wells and $66.8 \pm 2.5\%$ in infected wells post-treatment. Percentage of infection was $48.48 \pm 16.8\%$, and p24 production in culture supernatant was 20.53 ± 12.7 ng/ml. These parameters did not differed significantly across the different MIF concentrations evaluated here (not shown). To study the expression of TLR4 in uninfected (UN), bystander (By), and productively infected (IN) cells, the gating strategy shown in Figure S1 in Supplementary Material and **Figure 3A** was used. Representative results from one donor can be observed in **Figure 3B**. There, it can be observed that TLR4 expression was not modified by MIF treatment either in uninfected of bystander cells. However, TLR4 expression increased with increasing MIF concentration in productively infected cells. When results from four independent donors were expressed relative to their corresponding UN condition and then combined (**Figure 3C**) it could be observed that TLR4 expression peaked at 25 ng/ml MIF specifically in HIV-infected cells, almost doubling in magnitude when compared to the "no-MIF" condition. This can also be observed in the overlaid histograms shown in **Figure 3D**, where the MFI for the "IN plus 25 ng/ml MIF" condition is the highest. In order to elucidate whether an interaction between CD74 and MIF was responsible for a higher TLR4 expression, cells were pre-incubated with a neutralizing anti-CD74 antibody (or an isotype-matched control antibody), prior to MIF treatment at peak effect concentration (25 ng/ml MIF). TLR4 expression was significantly reduced both in the CD74-blocked condition but also in the control condition (**Figure 3C**, gray box). As MDMs may constitutively release MIF in low levels (53), this result may reflect the saturating action of autocrine/paracrine stimulation by endogenously released MIF or, alternatively, a non-specific action of Fc receptor engagement. To test the latter hypothesis, Fc receptors were blocked in this model (**Figure 3E**). When the FcR block was applied prior to the treatment with the anti-CD74 blocking antibody or the isotype-matched control and the cells were treated with 25 ng/ml MIF, the TLR4 expression reverted to the levels detected in cells only treated with MIF. Moreover, no differences were observed between the CD74 blocked and isotype control conditions. This indicates that the reduction found in TLR4 expression when cells were treated with the anti-CD74 blocking antibody or the isotype-matched control represented a non-specific response to Fc engagement. Collectively, these results indicate that exogenous MIF had an effect on TLR4 up-modulation, which was only evident in IN cells (not UN or By cells) but this effect could not be blocked by interfering MIF binding to CD74.

Interaction Between CD74 and MIF Triggers the Production of Proinflammatory Mediators Specifically From HIV-Infected MDMs

Next, we aimed at investigating the requirement of CD74/MIF interaction in the production of proinflammatory cytokines from HIV-infected versus uninfected MDMs following treatment with MIF. MDMs were infected with the R5-tropic HIV strain and uninfected cells were used as controls. At day 11 (peak infection), cells were treated with different MIF concentrations. Cell viability, infection percentages, and culture supernatant p24 production were as described in the previous section. **Figures 4A,B** show the raw data from one representative donor and the compiled data from six donors, respectively. Except for IL-10, most supernatants obtained from infected MDMs showed higher production of cytokines when treated with MIF, compared to the uninfected MIF-treated counterpart. While no-MIF effect was observed in uninfected cultures, an MIF-dependent production of IL-8, IL-6, IL-1β, TNF-α, and sICAM was detected in infected cells. Compiled results ($N = 6$) indicated that the greatest effect of MIF on IL-8 production occurred at 10 ng/ml (twofold increase). Similar observations were found for IL-6 (a peak fold increase of 2 and 2.5 at 10 and 25 ng/ml MIF, respectively), IL-1β (a peak fold increase of 8 at 25 ng/ml MIF), TNF-α (a peak fold increase of 26 at 1 ng/ml MIF), and sICAM (a peak fold increase of 2 at 1 ng/ml MIF). By contrast, no-MIF effect was observed in IL-10 production. These results suggest that MIF drive the production of proinflammatory mediators and that this effect is specific for HIV-infected cells. In order to elucidate whether an interaction between CD74 and MIF was responsible for the higher production of these cytokines, cells were pre-incubated with an anti-CD74 blocking antibody prior to MIF treatment at the peak effect concentrations (e.g., 25 ng/ml MIF for IL-8, IL-6, and IL-1β and 1 ng/ml MIF for TNF-α and sICAM; **Figures 4A,B**, gray boxes). In all cases, except for sICAM, CD74 blockade resulted in diminished levels of cytokine production similar to those observed in the no-MIF condition. Conversely, this effect was not observed when cells were pre-incubated with the corresponding isotype control antibody. Thus, CD74/MIF interaction was a necessary condition for the higher production of the studied cytokines in infected cells. Of note, this result was not recapitulated for sICAM, suggesting an alternative mechanism for this mediator.

Altogether, these results reveal that MIF favors the production of proinflammatory mediators specifically from HIV-infected cells and demonstrate that the interaction with CD74 is needed to achieve this effect. Moreover, they suggest a joint contribution of MDM infection, HIV-mediated upregulation of

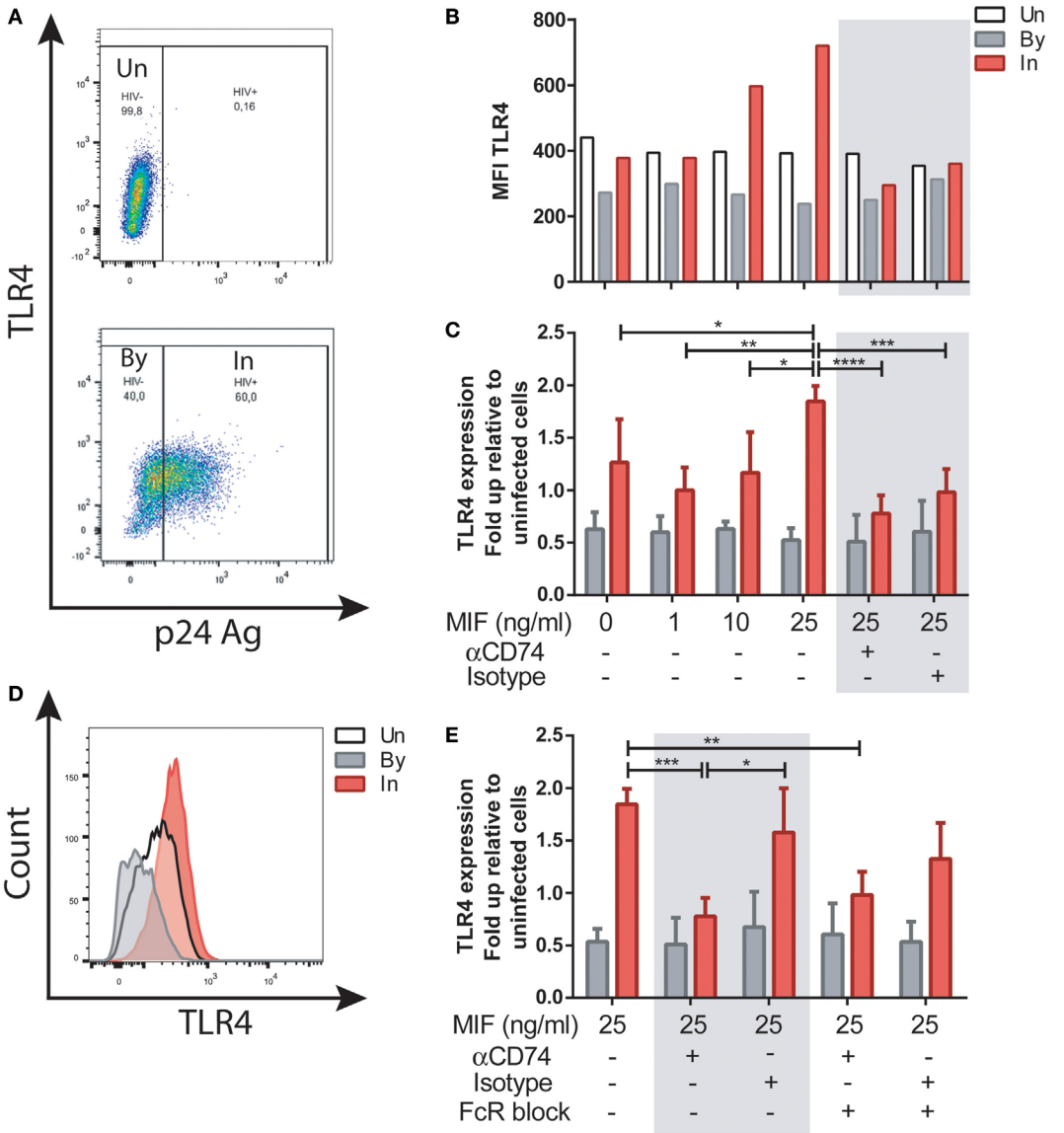


FIGURE 3 | TLR4 expression after macrophage migration inhibitory factor (MIF) stimulation in primary human immunodeficiency virus (HIV)-infected monocyte-derived macrophages (MDMs). **(A)** TLR4 expression in uninfected (UN, upper panel), bystander (By, lower panel), and productively infected cells identified on the bases of intracellular p24 staining (In, lower panel). Living MDMs were gated previously on a forward scatter versus side scatter dot plot. An isotype-matched FITC-conjugated antibody was used to accurately set the p24-negative population. **(B)** TLR4 MFI in uninfected MDMs (Un), in productively infected MDMs (p24 positive population within the well inoculated with the virus, In) and in the bystander uninfected MDMs (p24-negative population within the well inoculated with the virus, By) after MIF treatment. These data represent the results obtained from one representative donor. **(C)** Ratio between the TLR4 MFI of the infected (or bystander population) and the TLR4 MFI of the uninfected cells after treatment with MIF, with or without CD74 blockade with an anti-CD74 antibody. Fold up from four independent donors, evaluated in duplicate are shown collectively. Data represent the mean ± SD. **(D)** Flow cytometry histogram overlay for TLR4 expression on Un, By, and In MDMs all treated with 25 ng/ml MIF **(E)** Ratio between the TLR4 MFI of the infected (or by-stander population) and the TLR4 MFI of the uninfected cells using the different CD74-blocking conditions represented in the *x*-axis. Data were analyzed by two-way ANOVA followed by Tukey's post-test. $^{*}p < 0.05$, $^{**}p < 0.01$, $^{***}p < 0.001$, $^{****}p < 0.0001$.

surface CD74, and MIF stimulation to promote the production of a proinflammatory environment.

To provide further insight into the role of MIF in these observations, infected and uninfected MDMs from three independent donors were treated with 25 ng/ml of MIF plus different concentrations of an anti-MIF neutralizing monoclonal antibody (range 3.125–100 ng/ml, **Figure 5A**) or the MIF antagonist MIF098 (range 5–100 nM, **Figure 5B**). Neither the anti-MIF neutralizing monoclonal antibody nor the MIF antagonist affected cell viability in the concentration range tested. After incubation, production of IL-8, IL-6, IL-1β, and IL-10 was monitored. As expected, a significant reduction in IL-8, IL-6, and IL-1β production was

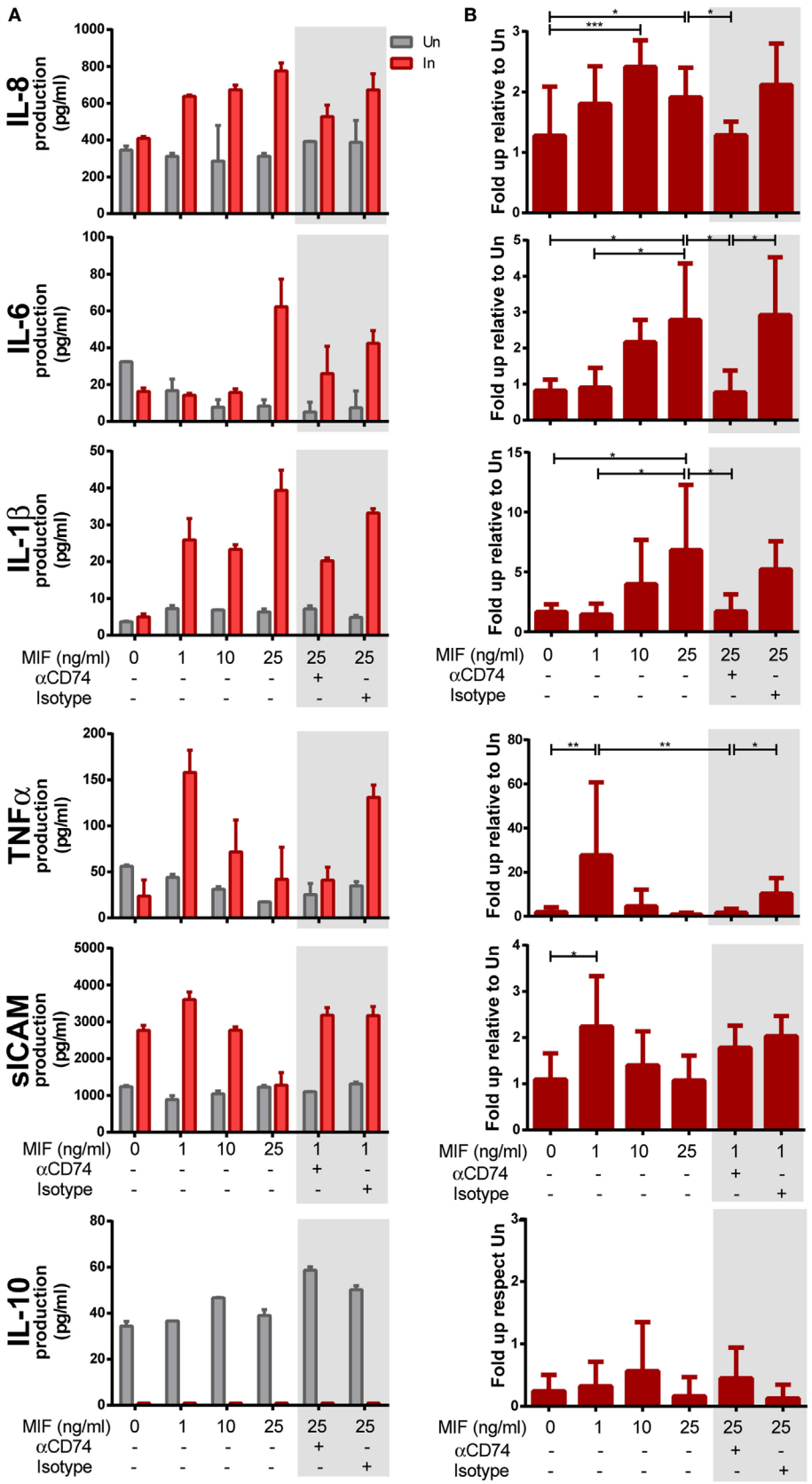


FIGURE 4 | Continued

FIGURE 4 | Expression of cytokines after macrophage migration inhibitory factor (MIF) stimulation in primary human immunodeficiency virus (HIV)-infected and uninfected monocyte-derived macrophages (MDMs). **(A)** Expression of IL-8, IL-6, IL-1β, TNF-α, sICAM, and IL-10 in supernatants from HIV-infected (In) and uninfected (Un) MDMs obtained from one representative healthy donor. **(B)** Data combined from six independent experiments (donors), each evaluated in triplicate. Here, data are shown as the ratio between cytokine concentrations found under the infection condition versus the uninfected counterpart. Cells were stimulated with MIF as follows: 0, 1, 10, or 25 ng/ml. Data shown in the gray boxes depict CD74 blocking (10 ng/ml of αCD74 or the corresponding isotype control) followed by MIF stimulation (1 or 25 ng/ml as denoted). Data represent the mean ± SD. Data were analyzed by one-way ANOVA followed by Tukey's post-test. $^{*}p < 0.05$, $^{**}p < 0.01$, $^{***}p < 0.001$.

observed upon MIF inhibition when using either the neutralizing antibody or the small molecule MIF antagonist. Serial dilution of both of these CD74/MIF interaction inhibitors reconstituted cytokine expression. Indeed, significant dose-dependent effects were observed, further supporting a role for MIF in promoting the production of proinflammatory mediators specifically from HIV-infected cells. No significant MIF or anti-MIF effects were observed on uninfected cells. Similarly, no changes were observed in IL-10 production.

CD74/MIF-Dependent Production of Proinflammatory Factors From HIV-Infected MDMs Enhances Viral Production From Unactivated CD4⁺ T-Cells

Then, we reasoned that conditioned media (supernatants) from MIF-treated HIV-infected MDMs could have an enhancing effect on the permissiveness of unactivated CD4⁺ T-cells to HIV infection, which are mostly naturally resistant to HIV. To test this hypothesis, supernatants obtained from infected and uninfected MDMs, treated or not with MIF, were UV inactivated and used to stimulate purified unactivated CD4⁺ T-cells. RPMI- or PHA-treated CD4⁺ T-cells were used as negative and positive controls, respectively. At 72 h post-treatment, CD4⁺ T-cells were infected with an X4-tropic GFP-expressing viral strain, and infection was monitored during 7 days by flow cytometry to evaluate % of infected cells (GFP+, see Figure S1 in Supplementary Material) and by ELISA (p24 antigen) to evaluate viral production. **Figures 6A,B** depict the viral production kinetics observed in CD4⁺ T-cells treated with supernatants derived from uninfected and HIV-infected MDMs, respectively, treated with 0, 1, and 25 ng/ml MIF (the 10 ng/ml condition was not evaluated). Viral production was very low when CD4⁺ T-cells were pre-incubated with supernatants derived from uninfected MDMs and it was independent of MDM MIF treatment (**Figure 6A**). A similar kinetic was observed in CD4⁺ T-cells pre-incubated with supernatants from infected MDMs treated with 0 MIF (**Figure 6B**, pink line). Conversely, viral production from CD4⁺ T-cells pre-incubated with supernatants from infected MDMs treated with 1 ng/ml MIF (**Figure 6B**, red line) and 25 ng/ml MIF (**Figure 6B**, dark red line) tended to increase over time reaching maximal viral production at day 7 for the 1 ng/ml MIF condition and at day 4 for the 25 ng/ml MIF condition. This can be better observed in **Figures 6C,D**. Here, viral production from CD4⁺ T-cells pre-incubated with supernatants from infected MDMs treated with 1 ng/ml (**Figure 6C**) and 25 ng/ml (**Figure 6D**) is shown relative to the viral production from CD4⁺ T-cells pre-incubated with supernatants from uninfected MDMs treated with the corresponding MIF concentration. Overall, results indicate that, at 7 days post-infection, viral production from initially unactivated CD4⁺ T-cells is significantly higher upon exposure to supernatants derived from infected MDMs treated with 1 ng/ml MIF, compared to exposure to supernatants derived from uninfected MDMs. Similarly, unactivated CD4⁺ T-cells sensitized with supernatants from infected MDMs treated with 25 ng/ml MIF showed a significant, albeit transient, increase in viral production at day 4 post-infection, compared to the uninfected condition, which was later downmodulated.

Despite sustained viral production is observed from CD4⁺ T-cells treated with supernatants derived from the 25 ng/ml MIF-treated infected MDMs (see **Figure 6B**, dark red line), the peak effect observed at day 4 in **Figure 6D** is lost at later time points. This might be indicating that the supernatant from infected MDMs treated with 25 ng/ml might be enhancing cell permissiveness and/or favoring an earlier viral production from these unactivated cells.

In order to rule out the possibility of inefficient viral inactivation by UV of MDM-derived supernatants, CD4⁺ T-cells were incubated with the UV-inactivated supernatants and left to proceed as described previously but without infecting them. At days 4 and 7, p24 antigen was quantified, and no viral production was detected under either condition. This indicates that no viral carry-on from infected MDMs occurred. We also explored whether CD4⁺ T-cell viability and infection percentages were affected by the addition of supernatants derived from MDMs treated under the different MIF conditions. No differences in cell viability (**Figure 6E**) was observed along time for CD4⁺ T-cell treated with supernatants obtained from uninfected MDMs treated with the different MIF concentrations (black, dark gray, and light gray lines). As expected, CD4⁺ T-cell treated with supernatants obtained from infected MDMs showed a reduction in cell viability, compared to the uninfected condition, no differences were observed across the different MIF concentrations (pink, red, and dark red lines). This indicates that cell viability most likely does not account for the differences observed in viral production. On the other hand, the infection percentage was higher after PHA treatment (**Figure 6F**). All other conditions, including the RPMI control, showed infection percentages <2% and no significant differences across treatments were observed. This might be indicating that the treatments with the MDM-derived supernatant might enhance viral production from those few infected cells rather than promoting infection. Then, the effect of blocking CD74/MIF interaction in MDMs on the observed results was studied. For this, unactivated CD4⁺ T-cells were incubated with supernatants derived from MDMs in which the interaction between CD74 and MIF had been blocked with

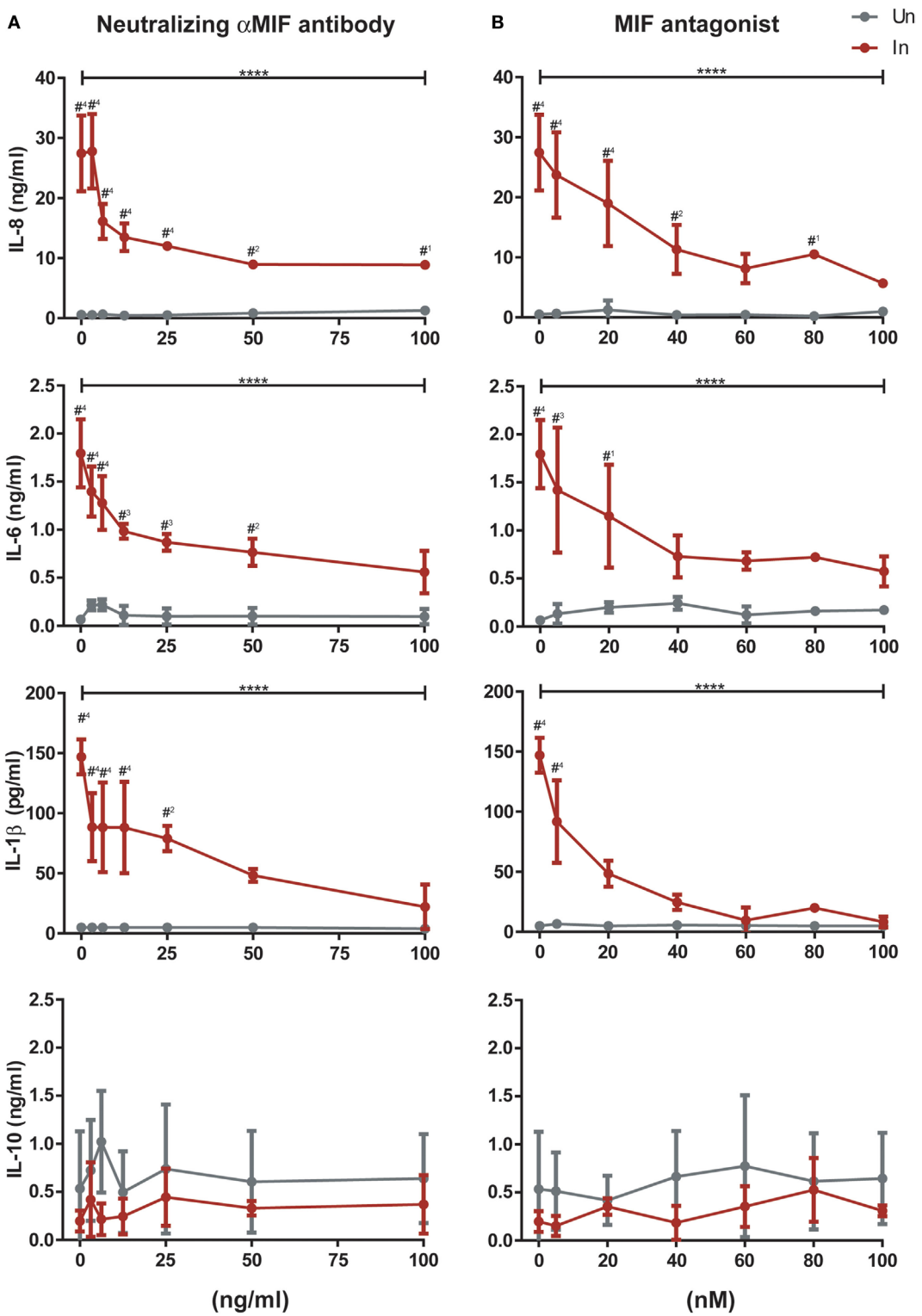


FIGURE 5 | Effect of macrophage migration inhibitory factor (MIF) neutralization in the expression of cytokines from primary human immunodeficiency virus-infected and uninfected monocyte-derived macrophages (MDMs). Serial dilutions of a neutralizing αMIF antibody (clone NIHIIIID.9) **(A)**, and the MIF antagonist MIF098 **(B)** were used to inhibit MIF activity in infected (In, red lines) and uninfected (Un, gray lines) MDMs at a constant concentration of this cytokine (25 ng/ml). Data represent three independent experiments (donors), each evaluated in duplicate. Data represent the mean ± SD. Data were analyzed by two-way ANOVA followed by Tukey's post-test (intragroup analysis, In group only; $^{****}p < 0.0001$) or by Sidak's post-test (intergroup, In versus Un; $^{\#1}p < 0.05$, $^{\#2}p < 0.01$, $^{\#3}p < 0.001$, $^{\#4}p < 0.0001$). Asterisks corresponding to the intragroup analysis are shown above the horizontal bars, and those from the intergroup analysis are shown above points corresponding to each antagonist or antibody dilution.

an anti-CD74 neutralizing antibody (**Figure 6G**). This assay was performed using supernatants from MDMs treated with the 25 ng/ml condition and viral production was evaluated at day 4 to reproduce the peak result observed in **Figure 6D**. Notably, unactivated CD4+ T-cells treated with supernatants derived from "CD74-blocked" MDMs were not able to recapitulate the increase

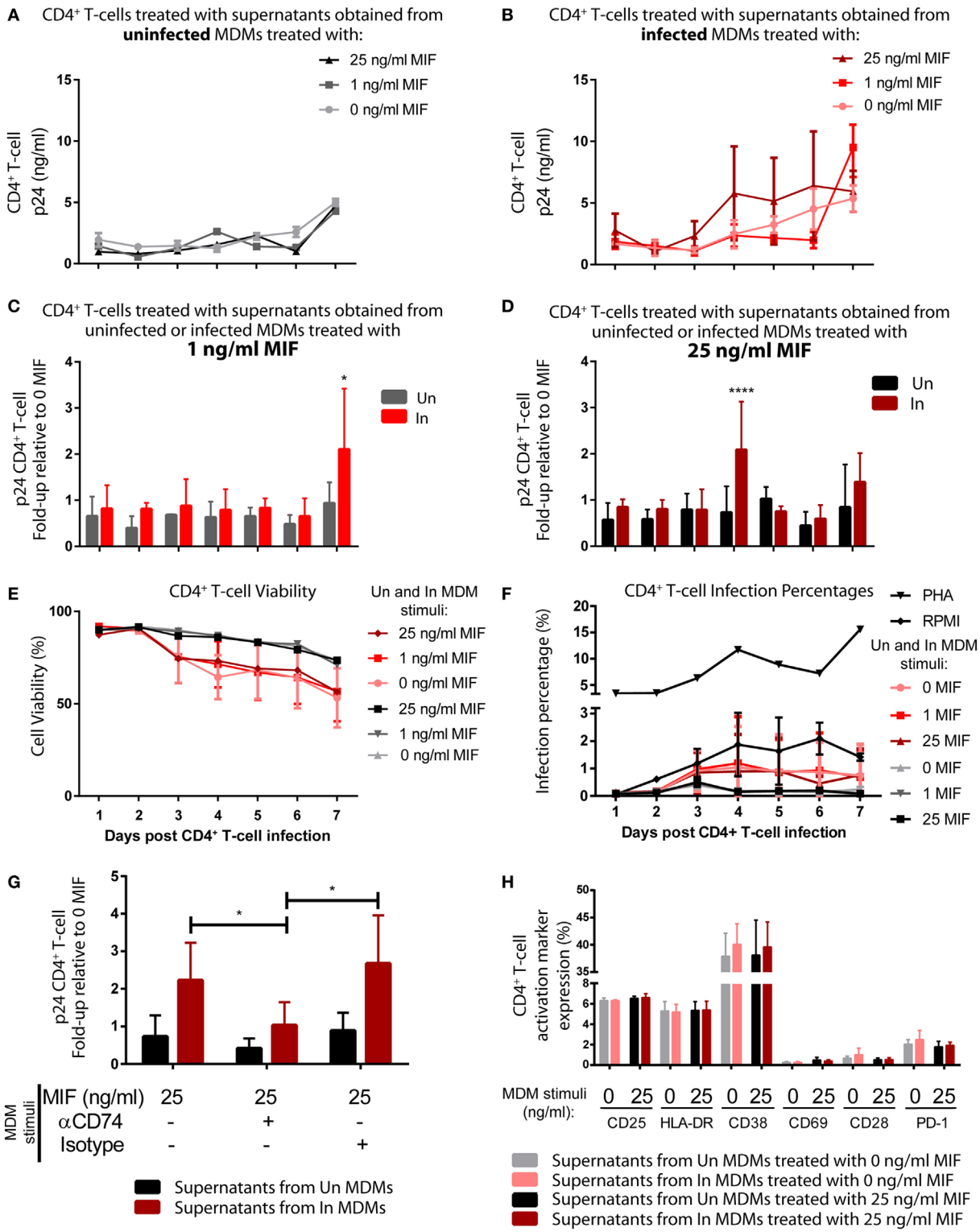


FIGURE 6 | Continued

FIGURE 6 | Induction of permissiveness to human immunodeficiency virus type I (HIV-1) infection in primary CD4+ T-cells after stimulation with macrophage migration inhibitory factor (MIF)-treated monocyte-derived macrophages (MDMs)-derived supernatants. **(A,B)** Seven-day kinetics of HIV p24 antigen production from primary unactivated CD4+ T-cell incubated with supernatants from uninfected **(A)** and infected **(B)** MDMs treated with 0, 1, or 25 ng/ml MIF. **(C,D)** Ratio of p24 production from unactivated CD4+ T-cell incubated with supernatants from uninfected MDMs and infected MDMs treated with 1 ng/ml MIF **(C)** or 25 ng/ml MIF **(D)** over the no-MIF condition. **(E)** Percentage of living CD4+ T-cells stimulated with supernatants derived from uninfected (black, dark gray, and light gray lines) and infected (pink, red, and dark red lines) MDMs. **(F)** Percentage of infected (GFP+) CD4+ T-cells after stimulation with MDM-derived supernatants obtained from MIF-treated uninfected MDMs (black, dark gray, and light gray lines), infected (pink, red, and dark red lines) MDMs, RPMI (negative control, black line with diamonds), or PHA (positive control, black line with triangles). **(G)** Ratio of p24 production from unactivated CD4+ T-cell incubated with supernatants from uninfected MDMs and infected MDMs treated with 25 ng/ml MIF, with or without CD74 blockade with an anti-CD74 antibody. **(H)** Expression of surface markers on CD4+ T-cells subjected to 72 h stimulation with supernatants derived from infected and uninfected MDMs and exposed or not to MIF treatment (0 and 25 ng/ml MIF). Data represent the mean ± SD from six independent donors evaluated in duplicate. In **(C,D)**, data were analyzed by two-way ANOVA followed by Sidak's post-test. In **(G)**, data were analyzed by two-way ANOVA followed by Tukey's post-test. *$p < 0.05$, ****$p < 0.0001$.

in viral production observed in the "non-blocked" condition. In summary, these results suggested that soluble factors released after MIF treatment in infected MDMs enhanced permissiveness of unactivated CD4+ T cell. Moreover, the production of these factors appears to be dependent on CD74/MIF interaction as the effect was abrogated by immunoneutralization of CD74.

Finally, we investigated if preincubation with the supernatants derived from MDMs induced CD4+ T-cell activation differentially as it is known that the level of cell activation correlates with HIV-1 infection efficiency. To assess this, the phenotype of CD4+ T-cells was studied after stimulation with MDMs-derived supernatants. The expression of CD38, CD69, HLA-DR, CD25, PD-1, and CD28 markers was evaluated by flow cytometry after 72 h. Supernatants from infected or uninfected MDMs treated (25 ng/ml) or not with MIF were used. No differences were detected in the percentage of cells expressing the different membrane markers (**Figure 6H**) or their MFI (not shown) among treatments. In sum, the improved viral production observed in CD4+ T-cells after treatment with supernatants derived from 25 ng/ml MIF-treated infected MDMs could not to be explained by differential cell viability, infection percentage, or cell activation (measured by surface markers).

In summary, we identified that the production of TNFα, IL-6, IL-8, and IL-1β increased significantly after CD74/MIF interaction in infected MDMs. Moreover, conditioned media from MIF-treated infected MDMs significantly enhanced viral production from unactivated CD4+ T-cells. Thus, the next step was to study a possible link between cytokines secreted by infected MDMs in an MIF-dependent manner and viral production from unactivated CD4+ T-cells. To do this analysis, recombinant IL-1β, IL-6, IL-8, and TNFα were used to stimulate primary unactivated CD4+ T-cells in the absence of any other stimuli at concentrations that resemble those found in MDM supernatants stimulated with 25 ng/ml MIF (peak effect). RPMI alone and PHA-supplemented RPMI were used as negative and positive controls, respectively. After 72 h, cells were infected, and viral p24 antigen was quantified. CD4+ T-cells treated with single cytokines or dual combinations did not alter viral production, regardless of the cytokines involved (data not shown). Only when treating CD4+ T-cells with three or four cytokines simultaneously viral production increased significantly compared to the RPMI control (**Figure 7A**). No differences in cell viability and infection percentages were observed across treatments (except for PHA) (**Figures 7B,C**). Finally, MDMs-derived supernatants were incubated with anti-IL-8, -IL-6, -IL-1β, and -TNFα neutralizing antibodies and used as CD4+ T-cells activation stimuli. In line with our hypothesis, a significant reduction in viral production was observed under this condition, compared to the non-neutralized and isotype control supplemented supernatants (**Figure 7D**).

Overall, IL-1β, IL-6, IL-8, and TNFα were identified as factors secreted from MIF-treated HIV-infected MDMs that, in combination, exerted a transient enhancing effect on viral production from unactivated CD4+ T-cells.

In Vitro Infections With Transmitted/Founder (T/F) HIV Strains Reproduced Both the Effect of MIF on the Production of Proinflammatory Mediators From HIV-Infected MDMs and Also the Enhanced Viral Production From Unactivated CD4+ T-Cells Stimulated With Conditioned Media Derived From MIF-Treated HIV-Infected MDMs

To examine whether the findings reported here could be extended to other HIV-1 strains, we generated viral stocks from selected transmitted/founder (T/F) IMCs. These clones were derived from full-length transmitted HIV-1 genomes and represent viruses actually responsible for productive clinical infection. Thus, these are instrumental tools for studying different aspects of HIV pathogenesis (36–39).

First, MDMs were infected with the R5 T/F virus. At day 11, both infected and uninfected cells were treated with 0, 1, or 25 ng/ml MIF and the production of cytokines was evaluated in cell supernatants. As observed for the HIV BAL strain, an MIF-dependent effect was observed for IL-1β, IL-6, and IL-8, which was significantly marked in infected cells while the production of IL-10 was unaltered across conditions (**Figure 8A**). In particular, peak IL-6 and IL-8 effects were observed at 25 ng/ml MIF while for IL-1β, the effect was already evident at 1 ng/ml MIF. Contrary to our initial observations using the BAL strain, the production of TNF-α and sICAM was not affected by MIF (not shown).

Then, the effect of MDM supernatants on viral production from unactivated CD4+ T-cells was again tested but using the dual-tropic T/F virus to infect the CD4+ T-cells. Thus, supernatants

from MIF-treated BAL-infected and uninfected MDMs were used to stimulate unactivated CD4+ T-cells during 72 h. Viral production was evaluated at 4 and 7 days post-infection. Results indicated that production of a dual-tropic T/F virus from unactivated CD4+ T-cells sensitized with supernatants derived from 25 ng/ml MIF-treated infected MDMs was significantly higher compared to the uninfected counterpart (**Figure 8B**, right panel). Contrary, no effect was observed when using supernatants derived from 1 ng/ml MIF-treated MDMs (**Figure 8B**, left panel). These results partially recapitulated those obtained when infecting unactivated CD4+ T-cells with the X4-tropic NL4-3 laboratory strain: an enhancing effect on viral production was observed when sensitizing cells with MIF-treated infected MDM-derived supernatants although the kinetics seems to be different for the T/F strain.

Overall, MIF effect on the production of proinflammatory mediators from HIV-infected MDMs and also the enhancing effect of the conditioned media (derived from MIF-treated HIV-infected MDMs) on viral production from unactivated CD4+ T-cells could be reproduced when using T/F viral strains. This provides further support to the notions presented in this work pointing toward a relevant role of the MIF/CD74 axis in HIV pathogenesis.

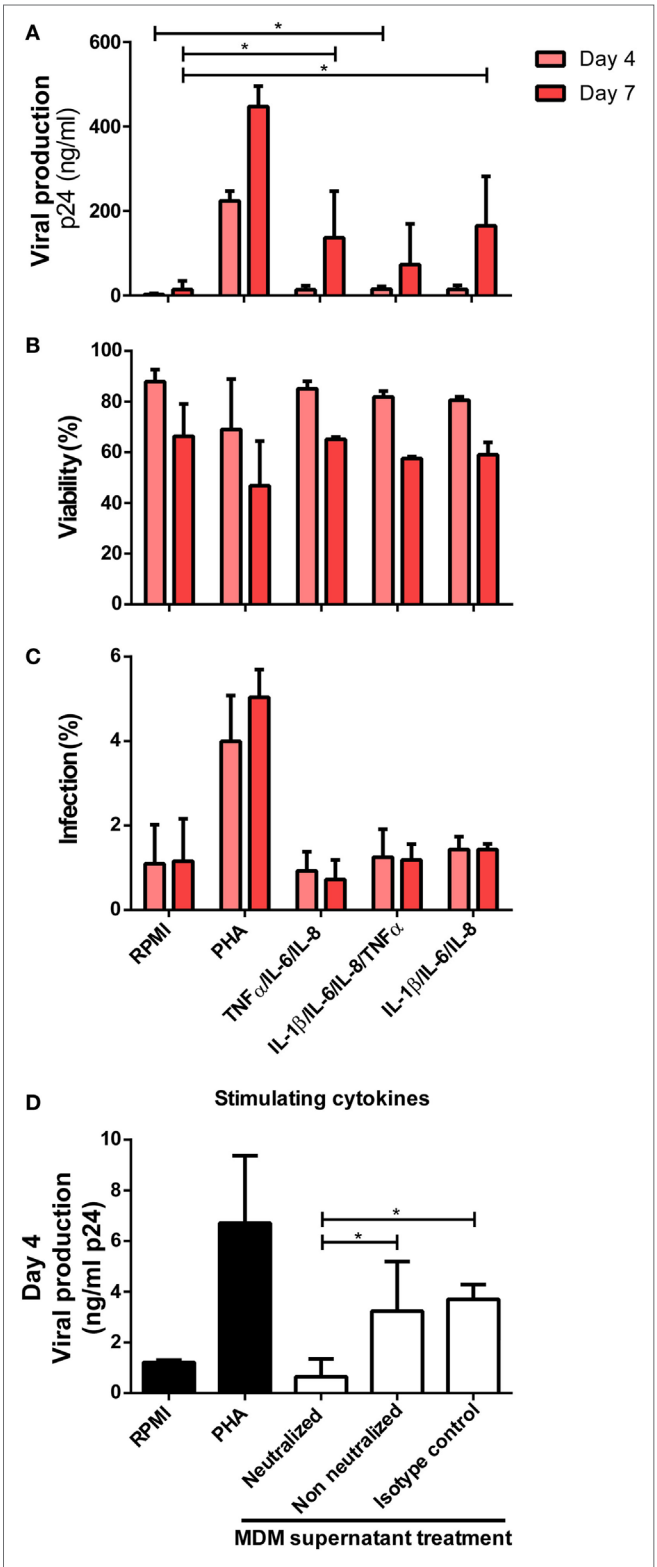


FIGURE 7 | Continued

FIGURE 7 | Identification of cytokines as responsible for enhancing human immunodeficiency virus type I (HIV-1) infection in unactivated CD4+ T-cells. **(A)** Unactivated CD4+ T-cells were stimulated with different combinations of cytokines for 72 h. Then, cells were infected and p24 antigen production was evaluated at days 4 and 7 post-infection. Each condition was compared with the corresponding RPMI condition (negative control). As a positive control, PHA stimulation was used. Percentage of living CD4+ T-cells **(B)** and percentage of infected (GFP+) CD4+ T-cells **(C)** after stimulation with the denoted treatments are shown. Data represent mean ± SD from four independent donors evaluated in duplicate. Concentrations of cytokines used in these experiments corresponded to the average concentrations found in monocyte-derived macrophage (MDM) supernatants stimulated with 25 ng/ml macrophage migration inhibitory factor (MIF) (peak effect) as follows: 250 pg/ml IL-6, 9,000 pg/ml IL-8, 1,400 pg/ml TNF-α, and 20 pg/ml IL-1β. **(D)** Neutralization of IL-8, IL-6, IL-1 β, and TNFα biological activity with monoclonal neutralizing antibodies. Primary CD4+ T-cells were incubated with supernatants derived from the 25 ng/ml MIF-treated HIV-infected MDM neutralized previously with 18 μg/ml anti-IL-8, 20 ng/ml anti-IL-6, 2 μg/ml anti-IL-1β, and 2 μg/ml anti-TNFα antibodies. Non-neutralized and isotype control antibody conditions were tested for comparison. Also, RPMI and PHA controls were included. Viral production was evaluated at day 4 post-infection. Data were analyzed by one-way ANOVA followed by Dunnett's post-test (all conditions versus the corresponding RMPI control) in **(A)** and Tukey's post-test in **(D)**. *$p < 0.05$.

DISCUSSION

It has become increasingly clear that signaling events downstream of MIF/CD74 interaction are key components in the regulation of immune responses that are involved in the pathogenesis of different inflammatory and immune-mediated diseases. However, whether this axis participates in HIV-mediated immune dysfunction has not been elucidated yet. Several lines of evidence suggest that this might be the case, based on the fact that CD74 expression is modulated in HIV-infected cells and that MIF plasma levels are elevated throughout the course of infection in HIV-infected subjects. Results depicted in this study provide support to this hypothesis by showing

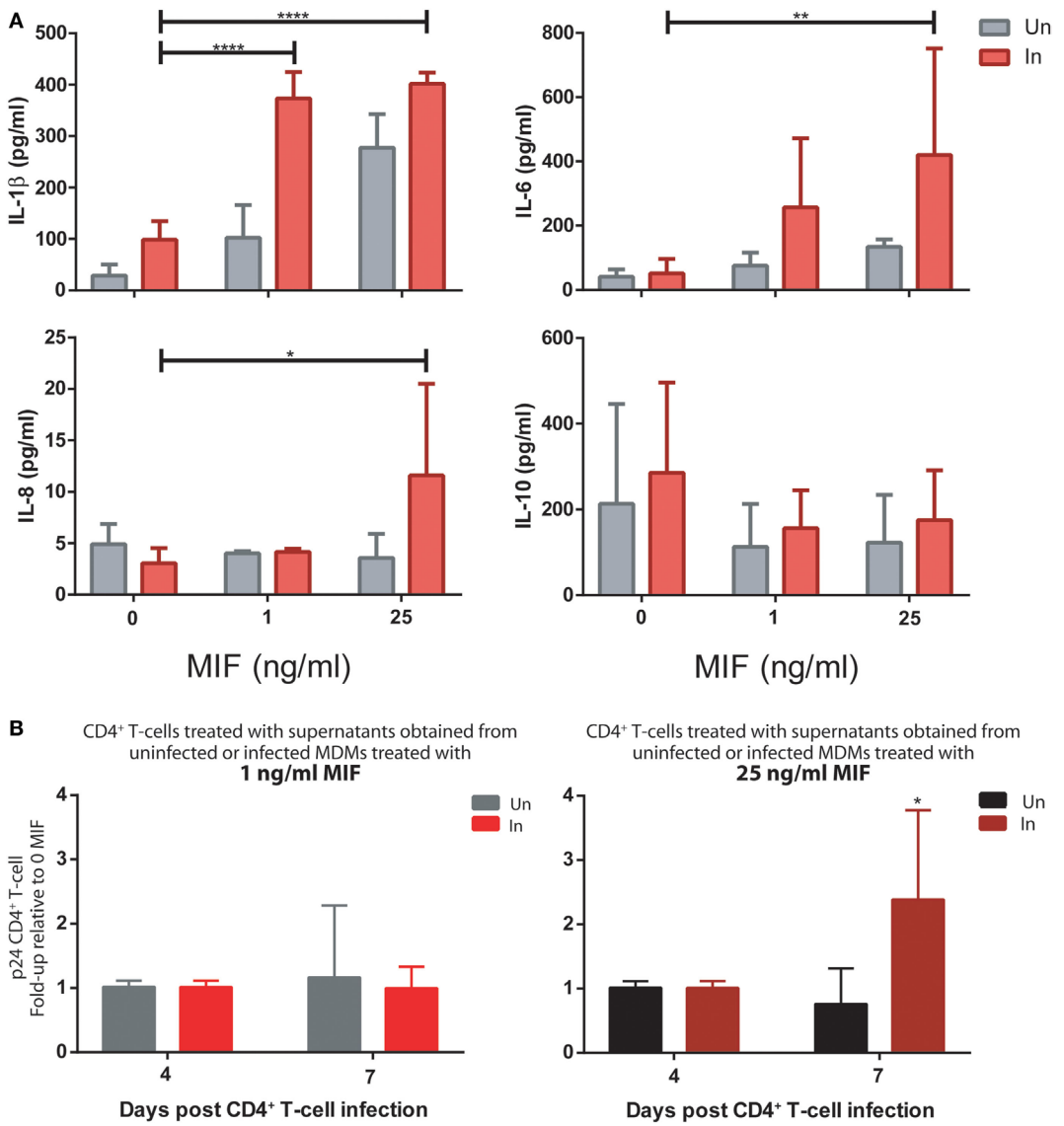


FIGURE 8 | Infection of monocyte-derived macrophages (MDMs) and unactivated CD4+ T-cells with T/F viruses reproduce the results obtained with the R5-tropic (BAL) and the X4-tropic (NL4-3) laboratory strains. **(A)** Expression of IL-1β, IL-8, IL-6, and IL-10 in supernatants from uninfected (Un) and R5-tropic T/F-infected (In) MDMs. Data represent mean ± SD from three independent donors. Data were analyzed by two-way ANOVA followed by Tukey's post-test. *$p < 0.05$, **$p < 0.01$, ****$p < 0.0001$. **(B)** Human immunodeficiency virus (HIV) p24 antigen production from primary unactivated CD4+ T-cells incubated with supernatants from uninfected and infected MDMs treated with 1 ng/ml (left panel) or 25 ng/ml (right panel) macrophage migration inhibitory factor (MIF). Treated CD4+ T-cells were infected with a dual-tropic T/F virus and viral production was evaluated at 4 and 7 days post-infection. Data represent mean ± SD from five independent donors. Data were analyzed by two-way ANOVA followed by Sidak's post-test. *$p < 0.05$.

that production of soluble inflammatory factors by primary HIV-infected MDMs was increased in an MIF dose-dependent manner and that CD74/MIF interaction was necessary for this effect. Moreover, the conditioned environment generated by MIF/CD74 interaction in infected MDMs promotes CD4+ T-cell permissiveness to infection.

In an initial report, CD74 was described as the central component of the MIF cell surface receptor (54). However, whereas the CD74 intracellular domain was shown to undergo intracellular phosphorylation upon engagement of the CD74 ectodomain by MIF, its short non-canonical structure suggested the involvement of a recruited co-receptor. A subsequent study demonstrated that CD44 was a necessary component for MIF signaling (16). CD74 surface expression has been shown to be upregulated in HIV-infected cells, and we show herein that this was also accompanied by surface CD44 upregulation which translated into an overlapping cell surface expression pattern observed specifically in WT HIV-infected cells. This allowed us to hypothesize that this phenomenon may translate into higher MIF receptor availability and enhanced receptor activation by MIF in these cells.

It is worth highlighting that only few reports describe the effect of HIV infection in CD44 expression in myeloid cells (55–57). Other molecules proposed to act as MIF coreceptors together with CD74, including CXCR2, CXCR4, and CXCR7 (17, 18, 58), were not analyzed here.

This evidence led us to study the MIF/CD74 interaction in HIV infection. First, we decided to study MIF-mediated modulation of TLR4 in infected cells. This was based on the observation that detectable plasma LPS levels are common in HIV infection (2, 59), thus modulation of one of the components of LPS receptor complex, TLR4, might contribute to disease progression. Also, endogenous MIF has been shown to modulate TLR4 expression in murine macrophages (60, 61). Here, the effect of exogenously added MIF was studied to unravel how its interaction with CD74 might have an impact on TLR4 modulation. In our system, a modest effect was observed particularly in infected cells at 25 ng/ml MIF with no evidence of CD74 participation. A more recent report indicated that exogenously added MIF could modulate TLR4 in murine fibroblasts but only at 375 ng/ml MIF (15-fold higher concentration than in our system) (62). Regardless MIF stimuli, it is also worth pointing that TLR4 expression was lower in bystander cells, compared to the uninfected condition. We speculate that this might be the consequence of factors produced by productively infected cells that affect, directly or indirectly, the phenotype and/or function of the neighboring non-productively infected cells (63).

The capability of HIV-infected MDMs to secrete different proinflammatory cytokines in response to MIF treatment was examined later. The fact that MIF is able to stimulate the secretion of proinflammatory cytokines in different settings is a phenomenon well-documented (19, 64–66). Moreover, many of these events have been reported to occur after CD74 engagement and by activating multiple intracellular signaling pathways (7, 29, 67–69). We add new evidence on the role of MIF in the clinically important HIV infection scenario. Quantitation of IL-1β, IL-6, IL-8, TNFα, and sICAM in MDMs supernatants demonstrated that MIF stimulation led to an augmented production of the proinflammatory cytokines studied. The first three cases showed a dose dependence with the MIF stimuli with maximum expression when using the highest MIF concentration tested. On the other hand, TNFα and sICAM production peaked at the lowest MIF concentration tested. Even more, enhanced production of IL-1β, IL-6, and IL-8 was also observed in MIF-treated MDMs infected with a T/F virus, indicating that this effect could be reproduced with clinically relevant viral strains. These results led to a direct link between the secretion of proinflammatory cytokines and MDM exposure to MIF. Even more relevant, the effect was maximum in infected cells compared to uninfected cells, pointing to a differential effect on HIV-infected cells. According to our hypothesis, this outcome could be explained by the higher availability of membrane CD74 molecules in HIV-infected cells that translate into greater MIF binding and signal transduction. To confirm that the MIF/CD74 axis was required for these effects, the interaction was blocked with a αCD74 immunoglobulin. The production of most mediators (all but sICAM) was inhibited by this treatment. In sum, our results provide support to the hypothesis that links the MIF/CD74 interaction and the differential production of proinflammatory molecules such as IL-1β, IL-6, IL-8, and TNFα expression from HIV-infected cells. Of note, sICAM was proposed to promote interactions between B and T cells that ultimately render resting T-cells permissive to HIV infection (70). Thus, the finding regarding MIF-mediated induction of sICAM production was of special interest. Results indicated that sICAM response peaked at 1 ng/ml MIF and was then downmodulated at higher exogenous MIF concentrations. Again, this result might be reflecting the saturating action of autocrine/paracrine stimulation by endogenously produced MIF or the involvement of alternative mechanisms yet to be elucidated.

During the last years, the concept of macrophage polarization has gained special focus, thus distinguishing different MDM subsets with different functionalities (71). Here, unpolarized (i.e., differentiated from blood monocytes only in the presence of GM-CSF) MDMs were used throughout the study. This was based on bibliography indicating that M1 and M2 polarized MDMs are less efficient to support productive HIV infection compared to unpolarized cells due to different blocks imposed at different levels of the replicative cycle (72–74). On the other hand, it has been reported that MDM infection with HIV results in polarization toward an M1-like phenotype. Moreover, infection sensitized macrophage responses to TLR ligands (75). Despite TLR ligands were not assayed here, a parallelism between these and our findings can be proposed since, according to our results, HIV infection renders MDMs more reactive to a proinflammatory stimuli such as MIF.

The hallmarks of HIV infection include the gradual decline in the number of $CD4^+$ T-lymphocytes and the chronic and persistent inflammation and immune activation. HIV-mediated immunopathogenesis is a complex process involving a dynamic interplay between viral and host molecules. Activation of T cells is driven directly by HIV replication but also by indirect mechanisms such as the breakdown in the gut mucosa and dysfunction of immunoregulatory factors, among others (2). Concomitantly, immune activation plays a key role in the systemic spread of the infection. HIV efficiently infects activated $CD4^+$ T-cells leading to a productive infection state. However, it has been recently documented that the infection of unactivated $CD4^+$ T-cells also occurs, resulting mostly in a latent infection (76). We therefore raised the question of whether MIF-treated MDM-derived supernatants could promote the infection of unactivated primary $CD4^+$ T-cells in the absence of other stimuli. Results indicated that viral production was significantly enhanced by conditioned media obtained from MIF-treated HIV-infected MDMs (compared to MIF-treated uninfected MDMs). The effect was highest as early as 4 days post-infection when using the 25 ng/ml MIF-stimulated MDMs while it occurred at day 7 post-infection for the 1 ng/ml MIF condition. This pattern in viral production mirrors the MIF-dependent cytokine production from infected MDMs: a peak production of IL-1β, IL-6, and IL-8 was observed with 25 ng/ml MIF and a peak in TNFα with 1 ng/ml. Particularly, TNFα showed the highest modulation magnitude when infected MDMs were compared with those uninfected but at

the lowest MIF concentration tested. In line with the dependence on CD74/MIF interaction for MDM cytokine production, blockade of MIF/CD74 engagement in infected MDMs abrogated the effect observed in $CD4^+$ T cells. In order to better support the impact of cytokines produced from infected MDMs downstream of the MIF/CD74 interaction on the permissiveness of unactivated $CD4^+$ T-cells, recombinant cytokines were used as direct stimuli. When a combined treatment with IL-1β, IL-6, IL-8, and/or TNFα was attempted, viral production increased. In the same line, neutralizing the biological activity of these cytokines in MDM-derived supernatants resulted in diminished $CD4^+$ T-cell permissiveness, resembling the same scenario obtained in the negative control. Finally, supernatants from MIF-treated HIV-infected MDMs could enhance viral production from unactivated $CD4^+$ T-cells infected with a T/F virus suggesting that the proposed mechanism extends not only to laboratory strains but also to primary viral isolates.

The fact that cytokines enhance viral replication but, more importantly, promote the infection of resting $CD4^+$ T-cells is not new (77). CCL19, CCL21, IL-7, and IL-15 are known to promote latent infection in resting $CD4^+$ T-cells (78–80). Also, IL-6 and TNFα has been shown to facilitate infection of resting $CD4^+$ T-cells and to induce productive infection (77, 81). In a particularly relevant report, soluble factors (sCD23 and sICAM) released by infected MDMs promoted the efficient infection of resting lymphocytes although the presence of B cells was a requisite for this effect (70). Nevertheless, it resulted interesting that the effect on resting $CD4^+$ T-cell permissiveness mediated by sCD23 and sICAM, occurred without promoting cell activation and proliferation, which is in line with the observations described in this work. In a recent report, Morris et al. (81) described that IL-6 produced from endothelial cells increased productive HIV infection in resting $CD4^+$ T-cells. Even more, this effect was not accompanied by an increase in the expression of T cell activation markers, mirroring our own results. Although the mechanism underlying this phenomenon was not studied by the authors, it could be associated with the capacity of IL-6 to favor $CD4^+$ T-cell cycling and survival (82). On the other hand, IL-8 and TNFα have been reported to directly enhance the rate of productive infection in activated T cells (82, 83). In particular, binding of TNFα to its receptor triggers several signaling cascades, including NF-κB, MAPK, ERK, and JNK pathways, which directly enhances transcription from the LTR promoter both on models of productive HIV infection and also in latently infected cells [reviewed in Ref. (82)].

Thus, in our model we suggest that IL-6, IL-8, TNFα, and IL-1β might be acting synergistically at different levels (i.e., modifying the cellular environment and/or by enhancing transcriptional and/or post-transcriptional mechanisms) to promote, at least transiently, the productive infection of unactivated $CD4^+$ T cells. This could explain that no effect was observed when cells were treated with a single or a dual combination of the cytokines studied. It will be a matter of subsequent studies to investigate if this also results in a higher rate of latent infection in these cells. Finally, the role of IL-1β is less clear since there is no definite report suggesting a direct mechanism of IL-1β-mediated modulation of HIV replication in T-cells.

Taken together, we postulate that modulation of CD74 by HIV infection in MDMs leads to the enhanced susceptibility of these cells to MIF stimulation, which may have an impact on the spread of HIV infection and the enhancement of viral-mediated pathogenesis. The current results indicate that the expression of proinflammatory cytokines was significantly higher in MIF-stimulated infected MDMs compared to MIF-stimulated uninfected MDMs. In addition, this proinflammatory microenvironment, conditioned positively primary unactivated $CD4^+$ T cells to HIV-1 infection. The methodological strengths of this work include the exclusive use of primary cells, emphasizing that treatment effects can be observed despite interdonor variability, the use of both laboratory and T/F viral strains, and the employment of physiological MIF concentrations as stimuli. On the other hand, interdonor variability and the use of a limited number of donors might have masked differences across conditions, representing an important limitation of the study. Also, macrophages exhibit significant heterogeneity *in vivo*, as already discussed and this fact should not be overlooked. Thus, results might not be extended to polarized MDMs, tissue macrophages, or other HIV susceptible myeloid cells such as dendritic cells. For instance, it would be very interesting to evaluate CD74/MIF axis in microglial cells. If a similar hypothesis was confirmed in this model, this mechanism could be associated with the development of HIV-related neurological complications.

Overall, this work provides further insights in the role of macrophages in HIV infection, not only as a cell type which supports viral replication itself but also as a source of soluble factors that facilitate viral dissemination. Evidence gathered here suggests that CD74/MIF interaction could be implicated in modulating viral reservoir seeding, persistent viremia and inflammation—all key aspects of HIV immunophatogenesis. Data presented here support further studies to fully understand how this mechanism operates in HIV infection and to explore the possibility to target CD74/MIF axis as a therapy aimed at reducing inflammation and reservoir size during HIV infection.

ETHICS STATEMENT

Samples from HIV-infected subjects used in this study were enrolled as part of an ongoing acute/early primary HIV infection cohort from Argentina (Grupo Argentino de Seroconversión study group). This study was reviewed and approved by two institutional review boards (IRB): Comité de Ética Humana, Facultad de Medicina, Universidad de Buenos Aires and Comité de Bioética, Fundación Huésped (Buenos Aires, Argentina). Both HIV-infected participants and HD provided written informed consents accepting to participate in this study in accordance with the Declaration of Helsinki.

AUTHOR CONTRIBUTIONS

YG and GT conceived the study and designed the experiments; CT, JS, MR, and YG performed experiments; LL and RB contributed with reagents; CT, RB, MQ, HS, YG, and GT analyzed and interpreted the data; CT and GT wrote the manuscript. All authors read and approved the final version of this manuscript.

ACKNOWLEDGMENTS

We would like to acknowledge Dr. Philippe Benaroch (Institut Curie, INSERM U932, Paris, France) and Dr. Michael Schindler (University Hospital Tübingen, Tübingen, and German Research Center for Environmental Health, Neuherberg, Germany) for providing reagents to perform the study and for intellectual input. We also thank María Noé García and Daniel Grasso [Instituto de Bioquímica y Medicina Molecular (IBIMOL), Universidad de Buenos Aires/CONICET, Argentina] for technical assistance with fluorescence microscopy image analysis; Matías Ostrowski (INBIRS) and María Victoria Delpino (Instituto de Inmunología, Genética y Metabolismo (INIGEM), Universidad de Buenos Aires/CONICET, Argentina) for helpful suggestions during the course of the study; and *Grupo Argentino de Seroconversión* study group for providing plasma samples. Finally, we thank Mr. Sergio Mazzini for language assistance during manuscript preparation.

FUNDING

This work was supported by grants from the Agencia Nacional de Promoción Científica y Tecnológica (ANPCyT) and GlaxoSmithKline (PICT2012, Grant #0475 and PICTO-GSK2013, Grant #0006), from Fundación Alberto J. Roemmers (2013/2015) and from the Universidad de Buenos Aires (UBACyT 2013–2016, Grant #20020120200263BA) to GT; by a grant from ANPCyT to MQ (PICT2012, Grant #0549), and by the US NIH NIAID (RB and LL). The funders had no role in study design, data collection and interpretation, or the decision to submit the manuscript for publication.

SUPPLEMENTARY MATERIAL

The Supplementary Material for this article can be found online at https://www.frontiersin.org/articles/10.3389/fimmu.2018.01494/full#supplementary-material.

FIGURE S1 | Gating strategy used for flow cytometry analysis of monocyte-derived macrophages (MDMs) **(A)** and CD4+ T-cells **(B)**. First, doublets were excluded in a forward scatter (FSC)-height (FSC-H) versus an FSH-area (FSH-A) plot. Then, living cells were gated an FSC-A versus a side scatter (SSC) plot. Subsequently, infected cells were identified in an FSC-H versus FITC plot (MDMs) or versus GFP plot (CD4+ T-cells). Data acquisition was performed in a BD FACSCanto flow cytometer using the BD FACSDiva software and analyzed subsequently with FlowJO v10 software (Data Analysis Software, LLC).

REFERENCES

1. Hull M, Lange J, Montaner JS. Treatment as prevention – where next? *Curr HIV/AIDS Rep* (2014) 11(4):496–504. doi:10.1007/s11904-014-0237-5
2. Deeks SG, Tracy R, Douek DC. Systemic effects of inflammation on health during chronic HIV infection. *Immunity* (2013) 39(4):633–45. doi:10.1016/j.immuni.2013.10.001
3. Sattentau QJ, Stevenson M. Macrophages and HIV-1: an unhealthy constellation. *Cell Host Microbe* (2016) 19(3):304–10. doi:10.1016/j.chom.2016.02.013
4. Rodrigues V, Ruffin N, San-Roman M, Benaroch P. Myeloid cell interaction with HIV: a complex relationship. *Front Immunol* (2017) 8:1698. doi:10.3389/fimmu.2017.01698
5. Stumptner-Cuvelette P, Benaroch P. Multiple roles of the invariant chain in MHC class II function. *Biochim Biophys Acta* (2002) 1542(1–3):1–13. doi:10.1016/S0167-4889(01)00166-5
6. Borghese F, Clanchy FI. CD74: an emerging opportunity as a therapeutic target in cancer and autoimmune disease. *Expert Opin Ther Targets* (2011) 15(3):237–51. doi:10.1517/14728222.2011.550879
7. Bucala R, Shachar I. The integral role of CD74 in antigen presentation, MIF signal transduction, and B cell survival and homeostasis. *Mini Rev Med Chem* (2014) 14(14):1132–8. doi:10.2174/1389557515666150203144111
8. Stumptner-Cuvelette P, Morchoisne S, Dugast M, Le Gall S, Raposo G, Schwartz O, et al. HIV-1 Nef impairs MHC class II antigen presentation and surface expression. *Proc Natl Acad Sci U S A* (2001) 98(21):12144–9. doi:10.1073/pnas.221256498
9. Schindler M, Wurfl S, Benaroch P, Greenough TC, Daniels R, Easterbrook P, et al. Down-modulation of mature histocompatibility complex class II and up-regulation of invariant chain cell surface expression are well-conserved functions of human and simian immunodeficiency virus Nef alleles. *J Virol* (2003) 77(19):10548–56. doi:10.1128/JVI.77.19.10548-10556.2003
10. Hussain A, Wesley C, Khalid M, Chaudhry A, Jameel S. Human immunodeficiency virus type 1 Vpu protein interacts with CD74 and modulates major histocompatibility complex class II presentation. *J Virol* (2008) 82(2):893–902. doi:10.1128/JVI.01373-07
11. Schmokel J, Li H, Bailes E, Schindler M, Silvestri G, Hahn BH, et al. Conservation of Nef function across highly diverse lineages of SIVsmm. *Retrovirology* (2009) 6:36. doi:10.1186/1742-4690-6-36
12. Turk G, Gundlach S, Carobene M, Schindler M, Salomon H, Benaroch P. Single Nef proteins from HIV type 1 subtypes C and F fail to upregulate invariant chain cell surface expression but are active for other functions. *AIDS Res Hum Retroviruses* (2009) 25(3):285–96. doi:10.1089/aid.2008.0132
13. Schindler M, Wildum S, Casartelli N, Doria M, Kirchhoff F. Nef alleles from children with non-progressive HIV-1 infection modulate MHC-II expression more efficiently than those from rapid progressors. *AIDS* (2007) 21(9):1103–7. doi:10.1097/QAD.0b013e32816aa37c
14. Keppler OT, Tibroni N, Venzke S, Rauch S, Fackler OT. Modulation of specific surface receptors and activation sensitization in primary resting CD4+ T lymphocytes by the Nef protein of HIV-1. *J Leukoc Biol* (2006) 79(3):616–27. doi:10.1189/jlb.0805461
15. Ghiglione Y, Rodriguez AM, De Candia C, Carobene M, Benaroch P, Schindler M, et al. HIV-mediated up-regulation of invariant chain (CD74) correlates with generalized immune activation in HIV+ subjects. *Virus Res* (2012) 163(1):380–4. doi:10.1016/j.virusres.2011.09.011
16. Shi X, Leng L, Wang T, Wang W, Du X, Li J, et al. CD44 is the signaling component of the macrophage migration inhibitory factor-CD74 receptor complex. *Immunity* (2006) 25(4):595–606. doi:10.1016/j.immuni.2006.08.020
17. Bernhagen J, Krohn R, Lue H, Gregory JL, Zernecke A, Koenen RR, et al. MIF is a noncognate ligand of CXC chemokine receptors in inflammatory and atherogenic cell recruitment. *Nat Med* (2007) 13(5):587–96. doi:10.1038/nm1567
18. Tarnowski M, Grymula K, Liu R, Tarnowska J, Drukala J, Ratajczak J, et al. Macrophage migration inhibitory factor is secreted by rhabdomyosarcoma cells, modulates tumor metastasis by binding to CXCR4 and CXCR7 receptors and inhibits recruitment of cancer-associated fibroblasts. *Mol Cancer Res* (2010) 8(10):1328–43. doi:10.1158/1541-7786.MCR-10-0288
19. Calandra T, Roger T. Macrophage migration inhibitory factor: a regulator of innate immunity. *Nat Rev Immunol* (2003) 3(10):791–800. doi:10.1038/nri1200
20. Leech M, Metz C, Hall P, Hutchinson P, Gianis K, Smith M, et al. Macrophage migration inhibitory factor in rheumatoid arthritis: evidence of proinflammatory function and regulation by glucocorticoids. *Arthritis Rheum* (1999) 42(8):1601–8. doi:10.1002/1529-0131(199908)42:8<1601::AID-ANR6>3.0.CO;2-B
21. Yamaguchi E, Nishihira J, Shimizu T, Takahashi T, Kitashiro N, Hizawa N, et al. Macrophage migration inhibitory factor (MIF) in bronchial asthma. *Clin Exp Allergy* (2000) 30(9):1244–9. doi:10.1046/j.1365-2222.2000.00888.x
22. Burger-Kentischer A, Goebel H, Seiler R, Fraedrich G, Schaefer HE, Dimmeler S, et al. Expression of macrophage migration inhibitory factor in

different stages of human atherosclerosis. *Circulation* (2002) 105(13):1561–6. doi:10.1161/01.CIR.0000012942.49244.82
23. Lai KN, Leung JC, Metz CN, Lai FM, Bucala R, Lan HY. Role for macrophage migration inhibitory factor in acute respiratory distress syndrome. *J Pathol* (2003) 199(4):496–508. doi:10.1002/path.1291
24. Awandare GA, Martinson JJ, Were T, Ouma C, Davenport GC, Ong'echa JM, et al. MIF (macrophage migration inhibitory factor) promoter polymorphisms and susceptibility to severe malarial anemia. *J Infect Dis* (2009) 200(4):629–37. doi:10.1086/600894
25. He XX, Chen K, Yang J, Li XY, Gan HY, Liu CY, et al. Macrophage migration inhibitory factor promotes colorectal cancer. *Mol Med* (2009) 15(1–2):1–10. doi:10.2119/molmed.2008.00107
26. Conroy H, Mawhinney L, Donnelly SC. Inflammation and cancer: macrophage migration inhibitory factor (MIF) – the potential missing link. *QJM* (2010) 103(11):831–6. doi:10.1093/qjmed/hcq148
27. Grieb G, Merk M, Bernhagen J, Bucala R. Macrophage migration inhibitory factor (MIF): a promising biomarker. *Drug News Perspect* (2010) 23(4):257–64. doi:10.1358/dnp.2010.23.4.1453629
28. Bozza MT, Martins YC, Carneiro LA, Paiva CN. Macrophage migration inhibitory factor in protozoan infections. *J Parasitol Res* (2012) 2012:413052. doi:10.1155/2012/413052
29. Herrero LJ, Sheng KC, Jian P, Taylor A, Her Z, Herring BL, et al. Macrophage migration inhibitory factor receptor CD74 mediates alphavirus-induced arthritis and myositis in murine models of alphavirus infection. *Arthritis Rheum* (2013) 65(10):2724–36. doi:10.1002/art.38090
30. Kindt N, Laurent G, Nonclercq D, Journe F, Ghanem G, Duvillier H, et al. Pharmacological inhibition of macrophage migration inhibitory factor interferes with the proliferation and invasiveness of squamous carcinoma cells. *Int J Oncol* (2013) 43(1):185–93. doi:10.3892/ijo.2013.1944
31. Zhang L, Ye SB, Ma G, Tang XF, Chen SP, He J, et al. The expressions of MIF and CXCR4 protein in tumor microenvironment are adverse prognostic factors in patients with esophageal squamous cell carcinoma. *J Transl Med* (2013) 11:60. doi:10.1186/1479-5876-11-60
32. Chuang YC, Chen HR, Yeh TM. Pathogenic roles of macrophage migration inhibitory factor during dengue virus infection. *Mediators Inflamm* (2015) 2015:547094. doi:10.1155/2015/547094
33. Subbannayya T, Leal-Rojas P, Barbhuiya MA, Raja R, Renuse S, Sathe G, et al. Macrophage migration inhibitory factor – a therapeutic target in gallbladder cancer. *BMC Cancer* (2015) 15:843. doi:10.1186/s12885-015-1855-z
34. Regis EG, Barreto-de-Souza V, Morgado MG, Bozza MT, Leng L, Bucala R, et al. Elevated levels of macrophage migration inhibitory factor (MIF) in the plasma of HIV-1-infected patients and in HIV-1-infected cell cultures: a relevant role on viral replication. *Virology* (2010) 399(1):31–8. doi:10.1016/j.virol.2009.12.018
35. Delaloye J, De Bruin IJ, Darling KE, Reymond MK, Sweep FC, Roger T, et al. Increased macrophage migration inhibitory factor (MIF) plasma levels in acute HIV-1 infection. *Cytokine* (2012) 60(2):338–40. doi:10.1016/j.cyto.2012.07.027
36. Keele BF, Giorgi EE, Salazar-Gonzalez JF, Decker JM, Pham KT, Salazar MG, et al. Identification and characterization of transmitted and early founder virus envelopes in primary HIV-1 infection. *Proc Natl Acad Sci U S A* (2008) 105(21):7552–7. doi:10.1073/pnas.0802203105
37. Salazar-Gonzalez JF, Bailes E, Pham KT, Salazar MG, Guffey MB, Keele BF, et al. Deciphering human immunodeficiency virus type 1 transmission and early envelope diversification by single-genome amplification and sequencing. *J Virol* (2008) 82(8):3952–70. doi:10.1128/JVI.02660-07
38. Lee HY, Giorgi EE, Keele BF, Gaschen B, Athreya GS, Salazar-Gonzalez JF, et al. Modeling sequence evolution in acute HIV-1 infection. *J Theor Biol* (2009) 261(2):341–60. doi:10.1016/j.jtbi.2009.07.038
39. Salazar-Gonzalez JF, Salazar MG, Keele BF, Learn GH, Giorgi EE, Li H, et al. Genetic identity, biological phenotype, and evolutionary pathways of transmitted/founder viruses in acute and early HIV-1 infection. *J Exp Med* (2009) 206(6):1273–89. doi:10.1084/jem.20090378
40. Socias ME, Sued O, Laufer N, Lazaro ME, Mingrone H, Pryluka D, et al. Acute retroviral syndrome and high baseline viral load are predictors of rapid HIV progression among untreated Argentinean seroconverters. *J Int AIDS Soc* (2011) 14:40. doi:10.1186/1758-2652-14-40
41. Turk G, Ghiglione Y, Falivene J, Socias ME, Laufer N, Coloccini RS, et al. Early Gag immunodominance of the HIV-specific T-cell response during acute/early infection is associated with higher CD8+ T-cell antiviral activity and correlates with preservation of the CD4+ T-cell compartment. *J Virol* (2013) 87(13):7445–62. doi:10.1128/JVI.00865-13
42. Coloccini RS, Dilernia D, Ghiglione Y, Turk G, Laufer N, Rubio A, et al. Host genetic factors associated with symptomatic primary HIV infection and disease progression among Argentinean seroconverters. *PLoS One* (2014) 9(11):e113146. doi:10.1371/journal.pone.0113146
43. Ghiglione Y, Falivene J, Ruiz MJ, Laufer N, Socias ME, Cahn P, et al. Early skewed distribution of total and HIV-specific CD8+ T-cell memory phenotypes during primary HIV infection is related to reduced antiviral activity and faster disease progression. *PLoS One* (2014) 9(8):e104235. doi:10.1371/journal.pone.0104235
44. Falivene J, Ghiglione Y, Laufer N, Socias ME, Holgado MP, Ruiz MJ, et al. Th17 and Th17/Treg ratio at early HIV infection associate with protective HIV-specific CD8(+) T-cell responses and disease progression. *Sci Rep* (2015) 5:11511. doi:10.1038/srep11511
45. Ruiz MJ, Ghiglione Y, Falivene J, Laufer N, Holgado MP, Socias ME, et al. Env-specific IgA from viremic HIV-infected subjects compromises antibody-dependent cellular cytotoxicity. *J Virol* (2016) 90(2):670–81. doi:10.1128/JVI.02363-15
46. Bernhagen J, Mitchell RA, Calandra T, Voelter W, Cerami A, Bucala R. Purification, bioactivity, and secondary structure analysis of mouse and human macrophage migration inhibitory factor (MIF). *Biochemistry* (1994) 33(47):14144–55. doi:10.1021/bi00251a025
47. Hare AA, Leng L, Gandavadi S, Du X, Cournia Z, Bucala R, et al. Optimization of N-benzyl-benzoxazol-2-ones as receptor antagonists of macrophage migration inhibitory factor (MIF). *Bioorg Med Chem Lett* (2010) 20(19):5811–4. doi:10.1016/j.bmcl.2010.07.129
48. Leng L, Chen L, Fan J, Greven D, Arjona A, Du X, et al. A small-molecule macrophage migration inhibitory factor antagonist protects against glomerulonephritis in lupus-prone NZB/NZW F1 and MRL/lpr mice. *J Immunol* (2011) 186(1):527–38. doi:10.4049/jimmunol.1001767
49. Rowe MA, Harper LR, McNulty MA, Lau AG, Carlson CS, Leng L, et al. Reduced osteoarthritis severity in aged mice with deletion of macrophage migration inhibitory factor. *Arthritis Rheumatol* (2017) 69(2):352–61. doi:10.1002/art.39844
50. Stumptner-Cuvelette P, Jouve M, Helft J, Dugast M, Glouzman AS, Jooss K, et al. Human immunodeficiency virus-1 Nef expression induces intracellular accumulation of multivesicular bodies and major histocompatibility complex class II complexes: potential role of phosphatidylinositol 3-kinase. *Mol Biol Cell* (2003) 14(12):4857–70. doi:10.1091/mbc.e03-04-0211
51. Toussaint H, Gobert FX, Schindler M, Banning C, Kozik P, Jouve M, et al. Human immunodeficiency virus type 1 nef expression prevents AP-2-mediated internalization of the major histocompatibility complex class II-associated invariant chain. *J Virol* (2008) 82(17):8373–82. doi:10.1128/JVI.00670-08
52. Verjans E, Noetzel E, Bektas N, Schutz AK, Lue H, Lennartz B, et al. Dual role of macrophage migration inhibitory factor (MIF) in human breast cancer. *BMC Cancer* (2009) 9:230. doi:10.1186/1471-2407-9-230
53. Calandra T, Bernhagen J, Mitchell RA, Bucala R. The macrophage is an important and previously unrecognized source of macrophage migration inhibitory factor. *J Exp Med* (1994) 179(6):1895–902. doi:10.1084/jem.179.6.1895
54. Leng L, Metz CN, Fang Y, Xu J, Donnelly S, Baugh J, et al. MIF signal transduction initiated by binding to CD74. *J Exp Med* (2003) 197(11):1467–76. doi:10.1084/jem.20030286
55. Giordanengo V, Limouse M, Doglio A, Lesimple J, Lefebvre JC. Alteration of CD44 expression in HIV type 1-infected T cell lines. *AIDS Res Hum Retroviruses* (1996) 12(17):1615–22. doi:10.1089/aid.1996.12.1615
56. Zembala M, Bach S, Szczepanek A, Mancino G, Colizzi V. Phenotypic changes of monocytes induced by HIV-1 gp120 molecule and its fragments. *Immunobiology* (1997) 197(1):110–21. doi:10.1016/S0171-2985(97)80061-7
57. Suyama M, Daikoku E, Goto T, Sano K, Morikawa Y. Reactivation from latency displays HIV particle budding at plasma membrane, accompanying CD44 upregulation and recruitment. *Retrovirology* (2009) 6:63. doi:10.1186/1742-4690-6-63
58. Alampour-Rajabi S, El Bounkari O, Rot A, Muller-Newen G, Bachelerie F, Gawaz M, et al. MIF interacts with CXCR7 to promote receptor internalization,

ERK1/2 and ZAP-70 signaling, and lymphocyte chemotaxis. *FASEB J* (2015) 29(11):4497–511. doi:10.1096/fj.15-273904
59. Brenchley JM, Price DA, Schacker TW, Asher TE, Silvestri G, Rao S, et al. Microbial translocation is a cause of systemic immune activation in chronic HIV infection. *Nat Med* (2006) 12(12):1365–71. doi:10.1038/nm1511
60. Roger T, David J, Glauser MP, Calandra T. MIF regulates innate immune responses through modulation of Toll-like receptor 4. *Nature* (2001) 414 (6866):920–4. doi:10.1038/414920a
61. Roger T, Froidevaux C, Martin C, Calandra T. Macrophage migration inhibitory factor (MIF) regulates host responses to endotoxin through modulation of toll-like receptor 4 (TLR4). *J Endotoxin Res* (2003) 9(2):119–23. doi:10.1179/096805103125001513
62. Xi ZD, Xie CY, Xi YB. Macrophage migration inhibitory factor enhances lipopolysaccharide-induced fibroblast proliferation by inducing toll-like receptor 4. *BMC Musculoskelet Disord* (2016) 17:43. doi:10.1186/s12891-016-0895-0
63. Deshiere A, Joly-Beauparlant C, Breton Y, Ouellet M, Raymond F, Lodge R, et al. Global mapping of the macrophage-HIV-1 transcriptome reveals that productive infection induces remodeling of host cell DNA and chromatin. *Sci Rep* (2017) 7(1):5238. doi:10.1038/s41598-017-05566-9
64. Mitchell RA, Liao H, Chesney J, Fingerle-Rowson G, Baugh J, David J, et al. Macrophage migration inhibitory factor (MIF) sustains macrophage proinflammatory function by inhibiting p53: regulatory role in the innate immune response. *Proc Natl Acad Sci U S A* (2002) 99(1):345–50. doi:10.1073/pnas.012511599
65. Assuncao-Miranda I, Bozza MT, Da Poian AT. Pro-inflammatory response resulting from sindbis virus infection of human macrophages: implications for the pathogenesis of viral arthritis. *J Med Virol* (2010) 82(1):164–74. doi:10.1002/jmv.21649
66. Chuang CC, Chuang YC, Chang WT, Chen CC, Hor LI, Huang AM, et al. Macrophage migration inhibitory factor regulates interleukin-6 production by facilitating nuclear factor-kappa B activation during Vibrio vulnificus infection. *BMC Immunol* (2010) 11:50. doi:10.1186/1471-2172-11-50
67. Benedek G, Meza-Romero R, Andrew S, Leng L, Burrows GG, Bourdette D, et al. Partial MHC class II constructs inhibit MIF/CD74 binding and downstream effects. *Eur J Immunol* (2013) 43(5):1309–21. doi:10.1002/eji.201243162
68. Tanese K, Hashimoto Y, Berkova Z, Wang Y, Samaniego F, Lee JE, et al. Cell surface CD74-MIF interactions drive melanoma survival in response to interferon-gamma. *J Invest Dermatol* (2015) 135(11):2901. doi:10.1038/jid.2015.204
69. Su H, Na N, Zhang X, Zhao Y. The biological function and significance of CD74 in immune diseases. *Inflamm Res* (2017) 66(3):209–16. doi:10.1007/s00011-016-0995-1
70. Swingler S, Brichacek B, Jacque JM, Ulich C, Zhou J, Stevenson M. HIV-1 Nef intersects the macrophage CD40L signalling pathway to promote resting-cell infection. *Nature* (2003) 424(6945):213–9. doi:10.1038/nature01749
71. Mills CD. Anatomy of a discovery: m1 and m2 macrophages. *Front Immunol* (2015) 6:212. doi:10.3389/fimmu.2015.00212
72. Cassol E, Cassetta L, Rizzi C, Alfano M, Poli G. M1 and M2a polarization of human monocyte-derived macrophages inhibits HIV-1 replication by distinct mechanisms. *J Immunol* (2009) 182(10):6237–46. doi:10.4049/jimmunol.0803447
73. Herbein G, Varin A. The macrophage in HIV-1 infection: from activation to deactivation? *Retrovirology* (2010) 7:33. doi:10.1186/1742-4690-7-33
74. Alfano M, Graziano F, Genovese L, Poli G. Macrophage polarization at the crossroad between HIV-1 infection and cancer development. *Arterioscler Thromb Vasc Biol* (2013) 33(6):1145–52. doi:10.1161/ATVBAHA.112.300171
75. Brown JN, Kohler JJ, Coberley CR, Sleasman JW, Goodenow MM. HIV-1 activates macrophages independent of toll-like receptors. *PLoS One* (2008) 3(12):e3664. doi:10.1371/journal.pone.0003664
76. Chavez L, Calvanese V, Verdin E. HIV latency is established directly and early in both resting and activated primary CD4 T cells. *PLoS Pathog* (2015) 11(6):e1004955. doi:10.1371/journal.ppat.1004955
77. Chun TW, Engel D, Mizell SB, Ehler LA, Fauci AS. Induction of HIV-1 replication in latently infected CD4+ T cells using a combination of cytokines. *J Exp Med* (1998) 188(1):83–91. doi:10.1084/jem.188.1.83
78. Unutmaz D, KewalRamani VN, Marmon S, Littman DR. Cytokine signals are sufficient for HIV-1 infection of resting human T lymphocytes. *J Exp Med* (1999) 189(11):1735–46. doi:10.1084/jem.189.11.1735
79. Ducrey-Rundquist O, Guyader M, Trono D. Modalities of interleukin-7-induced human immunodeficiency virus permissiveness in quiescent T lymphocytes. *J Virol* (2002) 76(18):9103–11. doi:10.1128/JVI.76.18.9103-9111.2002
80. Saleh S, Solomon A, Wightman F, Xhilaga M, Cameron PU, Lewin SR. CCR7 ligands CCL19 and CCL21 increase permissiveness of resting memory CD4+ T cells to HIV-1 infection: a novel model of HIV-1 latency. *Blood* (2007) 110(13):4161–4. doi:10.1182/blood-2007-06-097907
81. Morris JH III, Nguyen T, Nwadike A, Geels ML, Kamp DL, Kim BR, et al. Soluble factors secreted by endothelial cells allow for productive and latent HIV-1 infection in resting CD4+ T cells. *AIDS Res Hum Retroviruses* (2017) 33(2):110–20. doi:10.1089/AID.2016.0058
82. Freeman ML, Shive CL, Nguyen TP, Younes SA, Panigrahi S, Lederman MM. Cytokines and T-cell homeostasis in HIV infection. *J Infect Dis* (2016) 214 (Suppl 2):S51–7. doi:10.1093/infdis/jiw287
83. Lane BR, Lore K, Bock PJ, Andersson J, Coffey MJ, Strieter RM, et al. Interleukin-8 stimulates human immunodeficiency virus type 1 replication and is a potential new target for antiretroviral therapy. *J Virol* (2001) 75(17):8195–202. doi:10.1128/JVI.75.17.8195-8202.2001

Conflict of Interest Statement: The authors declare that the research was conducted in the absence of any commercial or financial relationships that could be construed as a potential conflict of interest.

Copyright © 2018 Trifone, Salido, Ruiz, Leng, Quiroga, Salomón, Bucala, Ghiglione and Turk. This is an open-access article distributed under the terms of the Creative Commons Attribution License (CC BY). The use, distribution or reproduction in other forums is permitted, provided the original author(s) and the copyright owner are credited and that the original publication in this journal is cited, in accordance with accepted academic practice. No use, distribution or reproduction is permitted which does not comply with these terms.

frontiers in Immunology

REVIEW
published: 19 February 2018
doi: 10.3389/fimmu.2018.00260

Mechanisms for Cell-to-Cell Transmission of HIV-1

Lucie Bracq[1,2,3,4,5], Maorong Xie[1,2,3,5], Serge Benichou[1,2,3,4,5] and Jérôme Bouchet[1,2,3,5]**

[1] Inserm U1016, Institut Cochin, Paris, France, [2] CNRS, UMR8104, Paris, France, [3] Université Paris-Descartes, Sorbonne Paris-Cité, Paris, France, [4] International Associated Laboratory (LIA VirHost), Institut Pasteur Shanghai-Chinese Academy of Sciences, Shanghai, China, [5] International Associated Laboratory (LIA VirHost), CNRS, Université Paris-Descartes, Institut Pasteur, Paris, France

While HIV-1 infection of target cells with cell-free viral particles has been largely documented, intercellular transmission through direct cell-to-cell contact may be a predominant mode of propagation in host. To spread, HIV-1 infects cells of the immune system and takes advantage of their specific particularities and functions. Subversion of intercellular communication allows to improve HIV-1 replication through a multiplicity of intercellular structures and membrane protrusions, like tunneling nanotubes, filopodia, or lamellipodia-like structures involved in the formation of the virological synapse. Other features of immune cells, like the immunological synapse or the phagocytosis of infected cells are hijacked by HIV-1 and used as gateways to infect target cells. Finally, HIV-1 reuses its fusogenic capacity to provoke fusion between infected donor cells and target cells, and to form infected syncytia with high capacity of viral production and improved capacities of motility or survival. All these modes of cell-to-cell transfer are now considered as viral mechanisms to escape immune system and antiretroviral therapies, and could be involved in the establishment of persistent virus reservoirs in different host tissues.

Keywords: HIV-1, cell-to-cell transfer, macrophages, dendritic cells, T cells

OPEN ACCESS

Edited by:
Céline Cougoule, Centre national de la recherche scientifique (CNRS), France

Reviewed by:
Nuria Izquierdo-Useros, IrsiCaixa, Spain
Marina Cella, Washington University in St. Louis, United States

***Correspondence:**
Serge Benichou
serge.benichou@inserm.fr;
Jérôme Bouchet
jerome.bouchet@inserm.fr

Specialty section:
This article was submitted to Viral Immunology, a section of the journal Frontiers in Immunology

Received: *19 December 2017*
Accepted: *30 January 2018*
Published: *19 February 2018*

Citation:
Bracq L, Xie M, Benichou S and Bouchet J (2018) Mechanisms for Cell-to-Cell Transmission of HIV-1. Front. Immunol. 9:260. doi: 10.3389/fimmu.2018.00260

CELL-FREE AND CELL-TO-CELL INFECTION

The worldwide pandemic of HIV-1 infection is a global and major public health problem, and sexual transmission is the major route of infection of the newly HIV-1-infected adults. Even though the use of antiretroviral therapies led to a net decrease of morbidity and mortality of HIV-1-infected patients, a better understanding of the cellular mechanisms involved in the sexual transmission and early dissemination of the virus is still required in order to rationally design more specific and potent strategies for HIV-1 prevention. A research priority for HIV-1 eradication is then the elucidation of the events involved in the mucosal viral transmission through the mucosa of the male and female rectal and genital tracts. While both cell-free and cell-associated HIV-1 are present in the semen, vaginal secretions, and anal mucus, and are thought to contribute to the virus sexual transmission, the cell-associated HIV-1 mucosal transmission has been largely understudied. Cell-to-cell transmission of HIV-1 involves various cell types of the immune system, including T lymphocytes, macrophages, and dendritic cells (DCs). Whereas the infection of T lymphocytes *via* cell-to-cell transfer was broadly investigated *in vitro*, there is a paucity in knowledge of the mechanisms that control infection and virus dissemination in macrophages and DCs by cell-to-cell transfer. Yet, macrophages and DCs play crucial roles in the physiopathology of infection, with macrophages being involved in the establishment of persistent virus reservoirs in different host tissues

while DCs participate in the early stages of virus transmission and dissemination after primo-infection at the level of genital and rectal mucosa. Specific therapies blocking HIV-1 mucosal transmission to these target cells should therefore be designed.

While HIV-1 infection of target cells with cell-free viral particles has been largely documented, pioneer studies from early 1990s showed that HIV-1 dissemination was largely increased through the establishment of direct cell-to-cell contacts between infected donor CD4+ T cells and target T cells [for review: Ref. (1)]. At least *in vitro*, cell-to-cell transfer of HIV-1 between T cells leads to a massive and very efficient infection that may be 100–1,000-fold more efficient than infection carried out by cell-free viral particles (1–5). The efficiency of cell-to-cell infection between CD4+ T cells has been related to a high-multiplicity of infection at the site of the cell–cell contact, probably leading to the integration, and accelerated viral gene expression of multiple proviruses in the target cell (6–10). While some reports suggest that cell-to-cell infection could be the main route of HIV-1 infection *in vivo* (10, 11), the specific contribution of cell-free and cell-to-cell infection by HIV-1 in infected hosts is still a matter of debate. Using multiphoton intravital microscopy in HIV-1-infected "humanized" mice, Murooka et al. showed that HIV-1-infected T cells establish interaction with surrounding cells and can even form syncytia with other lymph node-resident cells. The potency of infected T cells in lymph nodes to migrate may facilitate virus cell-to-cell transmission and spreading *in vivo* (12). Interestingly, exposure of human or macaque mucosal explants to HIV-1- or SIV-infected cells, allows more efficient viral transmission and infection than cell-free viruses (13, 14), suggesting the potency of HIV-1- or SIV-infected T cells to transmit viruses and propagate infection in host tissues. The high efficiency of cell-to-cell infection was also proposed to be a mechanism for HIV-1 to escape to antiretroviral therapy and neutralizing antibodies (15) but these results are still controversial and will be discussed below (4, 6, 16).

Different modes of infection through different cellular structures enabling close contacts between virus-donor cells and recipient target cells have been described over the past years for cell-to-cell transmission of HIV-1 *in vitro*. Intercellular transfer of viral material has been described mainly through establishment of the infectious or virological synapses, but also using membrane protrusions such as filopodia and tunneling nanotubes (TNTs), and cell fusion or cell engulfment processes. The implication of these different structures and processes for cell-to-cell transfer and dissemination of HIV will be discussed in this review.

NANOTUBES, FILOPODIA

The role of membrane protrusions in intercellular communications has been widely explored [for review: Ref. (17)]. A large diversity of membrane protrusions have been described, both *in vitro* (18, 19) and *in vivo* (20–22), and play important roles in the transmission of information between cells from different physiological systems, such as neurons (18, 23, 24), myeloid cells (25–29), or T cells (30).

Among the described membrane protrusions, two different types of nanotubes have been reported, corresponding to close-ended nanotubes and open-ended nanotubes (also known as TNTs) (27, 31, 32). Intercellular communications involving TNTs were first observed in 2004 as F-actin-containing membrane extensions able to connect distant cells during minutes to hours (18). TNTs are fragile and dynamic structures extended up to 100 μm in length with diameters ranging from 50 to 200 nm, and are not attached to the substratum (18, 30). They can mediate and facilitate the transfer, between several cell types, of cytoplasmic, and plasma membrane molecules, Ca2+ (29, 33), cargos including vesicles derived from various organelles such as early endosomes, endoplasmic reticulum, Golgi complex, and lysosomes (24, 33, 34), and even bigger cellular organelles like mitochondria and endosome-related structures (18, 32), but also pathogens such as bacteria (28).

Several studies showed that HIV-1 utilizes TNT networks to move from one cell to another leading to virus cell-to-cell transfer (25, 30, 34, 35) (**Figure 1A**). The frequency of TNT formation is not affected by HIV-1 in T cells but these structures could allow rapid spread of virus between T cells (30). Virus particles can thus be transferred by surfing along the surface of TNTs between T cells (30). Virus dissemination through TNTs was also reported between macrophages, in which HIV-1 particles can be transferred through intracellular vesicles derived from the endosomal reticulum or the Golgi apparatus (34, 35). Furthermore, in macrophages, HIV-1 increases the number of these intercellular structures to infect new cells (25). The HIV-1 Nef auxiliary protein has been reported to be responsible for the formation of TNTs in the THP-1 macrophage-like cell line (36) as well as in primary monocyte-derived macrophages, in which Nef alters the localization of the scaffolding protein M-Sec (37), which is a key regulator of TNT formation by a still undefined mechanism (26).

Another route of viral cell-to-cell transmission through membrane extension involving formation of filopodia has been first described for transmission of the retroviral murine leukemia virus (MLV) (19). Filopodia are F-actin-rich thin plasma membrane extensions that are involved in several cellular functions, such as chemo-migration, adhesion to the extracellular matrix, or formation of cell–cell contacts [for review: Ref. (38)]. In DCs, after engagement of the lectin DC-SIGN, HIV-1 mediates the activation of the small GTPase CDC42 and the remodeling of actin cytoskeleton to promote filopodia extension that allows virus transmission to neighboring CD4+ T cells (39) (**Figure 1B**). By budding at the tip of filopodia in DCs, HIV-1 could be able to tether concomitantly several neighboring CD4+ T cells, leading to viral transfer and infection of the target T cells (40) (**Figure 1C**).

THE VIROLOGICAL SYNAPSES

The formation of the so-called virological synapse is the major and well-established route for viral cell-to-cell transmission, and was first described in the context of human T-lympho-tropic virus infection as a close and organized cell-to-cell contact structure between an infected donor cell and a target cell, enabling the transfer of viral material between the two cells (41) (**Figure 1D**). The virological synapse has been named after its homologies with

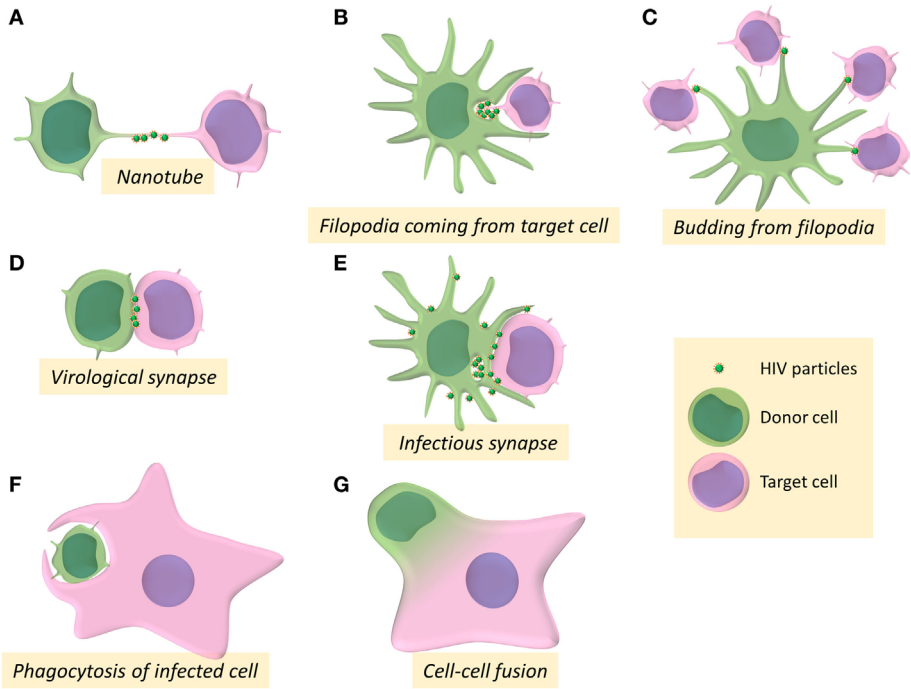


FIGURE 1 | Intercellular structures and processes involved in cell-to-cell transmission of HIV-1. **(A–G)** Schemes represent the different pathways for HIV-1 cell-to-cell transfer between donor cells (in green) and target cells (in pink).

the immunological synapse formed between antigen-presenting cells (APCs) and T cells for antigen presentation. During the formation of the immunological synapse, binding of the T-cell receptor (TCR) to the MHC-peptide complex expressed at the surface of APCs ensures T-cell activation by transducing signals that cause transcriptional upregulation of numerous genes, polarized secretion of cytokines or cytotoxic granules, and cell-proliferation (42, 43). Microtubules and actin cytoskeleton, together with adhesion molecules (LFA-1 and its ligand ICAM-1), participate in the stabilization of the immunological synapse.

Whilst virus cell-to-cell transmission was defined, from the early 1990s, to be more efficient than cell-free virus infection (1, 44–46), the concept of "virological synapse" between HIV-1-infected donor cells and target cells was defined by the group of Quentin Sattentau as a "cytoskeleton-dependent, stable adhesive junction, across which virus is transmitted by directed transfer" (47). The virological synapse shares several common features with the immunological synapse. Indeed, formation of both virological and immunological synapses involves the recruitment of receptors and cell adhesion molecules to an adhesive interface in an actin-dependent manner (48, 49). We focus here on the structure of the virological synapse established between a donor infected CD4+ T-cell and a CD4+ T-cell target which has been the best documented (48, 50, 51). The specific synapses formed between DCs or macrophages and target CD4+ T cells will be described below.

The virological synapse is a dynamic structure initiated by the recognition of the target T-cell surface receptor CD4 by the viral surface envelope glycoprotein gp120 expressed at the surface of the infected donor T cell (**Figure 2**). This interaction allows the recruitment of the viral Gag polyprotein precursor to the intercellular interface (52) and triggers the recruitment of co-receptors, CXCR4 or CCR5, adhesion molecules LFA-1, ICAM-1, and other cell surface proteins such as tetraspanins to the site of intercellular contact, for stabilization of the virological synapse and efficient viral transfer (48, 52, 53). The interaction between HIV-1 envelope glycoprotein and the receptor CD4 is the major determinant for virus transfer across the virological synapse (54). In addition to CD4, the implication of the co-receptors CCR5 and CXCR4 has been investigated by several groups. Some initial studies suggested that the formation of the virological synapse could be independent of the co-receptor usage since the inhibition of these co-receptors did not affect the number of cellular conjugates between cells (55) or HIV-1 transfer (4, 56). However, other reports showed that expression of these co-receptors was necessary for productive infection of the target cells downstream of the formation of the virological synapse (57–60). Therefore, the use of the co-receptor could be dispensable for the formation of the virological synapse but could be required for efficient infection of the target cell after viral transfer through the virological synapse.

Similarly, the role of the adhesion molecules LFA-1 and ICAM-1 in the formation of the virological synapse was debated. Initially, interaction between LFA-1 and ICAM-1 has been proposed to stabilize the virological synapse for efficient viral transfer. Jolly et al. first showed that antibodies against LFA-1 and ICAM-1 were able to partially block viral transfer through the virological synapse (48, 52). However, the percentages of inhibition were

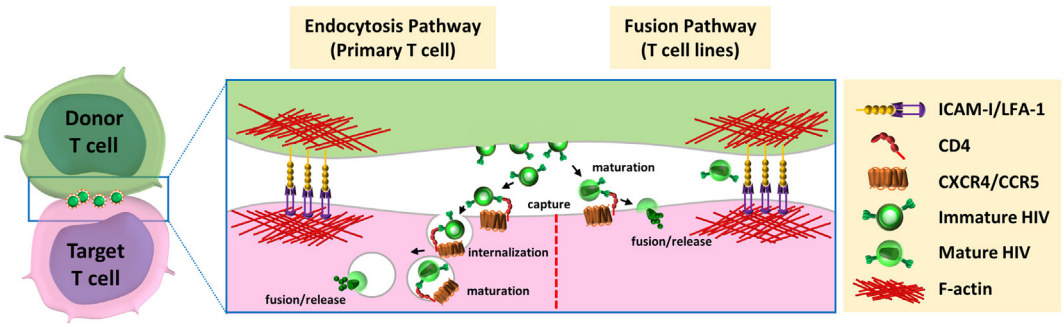


FIGURE 2 | Models for HIV-1 entry downstream of the virological synapse. After budding and release from infected donor cells, HIV could be able to enter the target cells *via* two distinct pathways. (left) Entry through endocytic pathway: immature virions interact with the CD4 receptor at cell surface of target cell, are internalized by endocytosis, mature in endocytic compartments, and fuse with the luminal membrane of endosomes. (right) Fusion with plasma membrane: mature viruses are captured by CD4, at the surface of target cells, and directly fuse with plasma membrane for release of viral material in the cytoplasm of the target cells.

very different depending on the antibody used (40–90% inhibition using LFA-1 antibodies and 30% inhibition with ICAM-1 antibodies). The role of adhesion molecules for the formation of the virological synapse and virus transfer was then confirmed, showing a significant threefold inhibition in virus transfer using a Jurkat T-cell line lacking the α subunit of LFA-1 (61). However, a third group obtained opposite results showing that virus transfer through the virological synapse between T cells did not require LFA-1 binding to ICAM-1 (55). Using antibodies blocking adhesion molecules such as LFA-1, ICAM-1, and ICAM-3 in MOLT or primary T cells, or 293 T cells lacking LFA-1, no inhibition of viral transfer through the virological synapse was observed in this study. The different assays used to analyze viral transfer and viral production could explain this divergence. In these studies, antibodies targeting different epitopes were used to block adhesion molecules and could have differential effects on virological synapse formation and HIV-1 transfer. The discrepancy in the results obtained by several groups could also be explained by the different cell models used in these experiments. Indeed, the level of adhesion molecule expression (i.e., ICAMs and Integrins) largely differs from T-cell lines to primary T cells (52, 55). To conclude, while the recruitment of adhesion molecules to the virological synapse is well established (52, 53), their specific role and requirement for cell-to-cell transmission of HIV-1 remains to be determined.

Finally, specific rearrangements of the cytoskeleton are required for the formation of the virological synapse and efficient viral transfer. Engagement of the CD4 receptor by the gp120 viral envelope glycoprotein triggers actin cytoskeleton remodeling and microtubule polarization toward the virological synapse (51). These cytoskeleton modifications are needed for polarization of the Gag precursor and envelope glycoproteins to the site of cell–cell contact (61, 62). By comparison, engagement of the TCR by MHC-antigen complex expressed at the surface of APC induces a polarization of the T cell toward the immunological synapse that triggers a cascade of intracellular signals leading to cytoskeleton remodeling, cytokine gene expression, proliferation, and execution of the T-cell effector functions. Similarly, polarization of the microtubule-organizing center (MTOC) of infected donor T cells toward the virological synapse has been observed in 30–60% of the conjugated formed with target T cells (54, 63, 64). Viral envelope glycoproteins are also reoriented to the virological synapse through their interaction with an intracellular compartment associated with the polarized MTOC. This suggests an active role of the microtubule network in the recruitment of the viral envelope to the virological synapse (4, 53, 54, 59, 63). Electron microscopy analyses with tomography reconstruction revealed the polarization of organelles such as mitochondria, lysosomes at the site of cell–cell contact in around 75% of the virological synapse formed. The colocalization of viral material with secretory lysosomal compartments and the relocalization of these vesicular compartments toward the cell–cell interface indicates that HIV-1 could take advantage of intracellular traffic and secretory pathways to disseminate through the virological synapse (63). Some molecules involved in T-cell signaling also participate in cell-to-cell transmission of HIV-1. Accordingly, polarization of the cells can be mediated by ICAM-1/LFA-1 signaling, which in addition to its effect on stabilizing virological synapse formation, induces a ZAP70-dependant signaling pathway for cytoskeleton remodeling, T cells polarization, and efficient HIV-1 transfer at the virological synapse (53, 64). In target T cells, CD4 engagement by viral gp120 induces phosphorylation of the T-cell specific Src kinase Lck allowing the recruitment of several TCR signaling molecules such as ZAP70, LAT, SLP76, or PLCγ in their active phosphorylated form. This unusual signaling does not trigger regular T-cell activation nor proliferation, but could induce a local depletion of F-actin at the center of the virological synapse that could facilitate viral transfer to target cells (54).

The first observation of the virological synapse by electron microscopy by Jolly et al. showed that mature HIV-1 particles were clustered in the synaptic space (48), but they did not show evidence of endocytosis of viral particles by target cells, suggesting that mature viruses released from the donor T cells at the virological synapse space could fuse directly with the plasma membrane of the target T cells (48). Another group also observed HIV-1 particles in the synaptic space by electron microscopy, but suggested that these particles could be internalized by target

cells into trypsin-resistant large intracellular vesicles containing several virus particles. This internalization of viruses could occur using an actin-dependent mechanism through lamellipodia-like structures (56). Several groups confirmed that HIV-1 can be internalized by endocytosis at the virological synapse. Therefore, immature HIV-1 particles have been shown to be transferred across the virological synapse through dynamin- and clathrin-dependent endocytosis leading to productive infection of the target T cells (59, 65–67). After internalization, the HIV-1 particles were found in intracellular compartments that co-localized with the early-endosomal marker EEA1 but not with the lysosomal-associated membrane protein LAMP1, indicating that viruses are internalized in endosomal compartments but are not addressed to lysosomal degradation (68). In accordance with these results, Dale et al. demonstrated that after endocytosis of immature virions by the target T cells, the cleavage of the Gag polyprotein precursor by the viral protease induced the maturation of the viral particle in some endosomal compartments (57). This cleavage restored the membrane fusion activity of the viral envelope and led to viral-cell membrane fusion into these endosomal compartments.

However, the group of Quentin Sattentau, who first described the formation of the virological synapse for HIV-1 cell-to-cell transfer, failed to observe endocytosis of viral particles at the virological synapse using confocal microscopy, electron microscopy, or electron microscopy coupled with tomography (47, 60). Puigdomenech et al. hypothesized that these different results could be explained by the different experimental systems used and the use of primary T cells or immortalized T-cell lines (69). They suggest that these differences may be associated with the different kinetics of the fusion events observed between primary CD4+ T cells and T-cell lines. Delayed fusion at the plasma membrane of the target cell may increase virus endocytosis in primary cells (**Figure 2**, left). In contrast, a rapid fusion at the cell membrane in T-cell lines may favor HIV-1 transmission without need for endocytosis (**Figure 2**, right). From this hypothesis, these authors suggest that endocytosis of virus particles is the main mechanism used by HIV-1 for cell-to-cell transfer and infection of primary CD4+ T cells. Remarkable differences between virological synapses formed with Jurkat cells or primary CD4+ T cells have been indeed reported (70). Scanning electron microscopy experiments revealed strong differences in spatial distribution of virions at the intercellular interface and important differences in the architecture of the contacts between T cells. These differences could be due to the increase deformability of primary T cells compared with the immortalized Jurkat cells, and questioned the relevance of cell line models used so far for studying virological synapse formation and cell-to-cell transmission of HIV-1.

It is noteworthy to mention that cell-to-cell transfer of HIV-1 between T cells is associated to an increase mortality of the target cells, when compared with cell-free infection of T cells. First, the massive entry of viral particles into target cells across the virological synapse has been shown to be responsible for caspase-1-mediated pyropoptosis of target T cells (71). In addition, while the formation of the virological synapse is triggered by gp120/CD4 interaction, it has been reported that upon cell-to-cell contact, the gp41 transmembrane viral glycoprotein was able to trigger hemifusion but not fusion events responsible for rapid CD4+ T-cell death (72, 73).

Viral Transfer and Resistance to Neutralizing Antibodies and Antiretroviral Drugs

Like some other viruses (Herpesviruses, poxviruses, and Hepatitis C virus), it has been proposed that HIV-1 could escape, at least partially, to neutralization by specific antibodies targeting the viral envelope when it is transferred across the virological synapse. Failure of inhibition of HIV-1 cell-to-cell infection by neutralizing antibodies was first suggested in 1995 in a study showing that antibodies against the glycan V3-loop of gp120 were unable to block cell-to-cell viral transfer (74). However, after characterization of the virological synapse for HIV-1 cell-to-cell transfer in 2004, several different groups tried to elucidate the mechanisms of neutralizing antibody escape in the virological synapse-mediated viral transfer. There is a general agreement that the potency of neutralizing antibodies is reduced during cell-to-cell transmission compared with cell-free infection and that only a subset of neutralizing antibodies can efficiently inhibit cell-to-cell transmission (47, 56, 75–77). For example, it was reported that several specific anti-gp120 antibodies targeting the CD4 binding site lost considerable potency (10- to 100-fold decrease) when HIV-1 was transferred by cell-to-cell transmission (75). Though some antibodies are still able to block cell-to-cell viral transmission at high concentration, VRC01, which is one of the most potent antibody for inhibition of cell-free infection, is particularly ineffective for blocking cell-to-cell viral transfer (75). While most anti-gp120-directed antibodies, and in particular those directed against the gp120 CD4 binding site displayed a reduced activity during viral cell-to-cell transmission, the same group reported that the T20 fusion inhibitor targeting the gp41 transmembrane glycoprotein as well as neutralizing antibodies directed against gp41 maintained their activity and were thus able to block both cell-free and cell-to-cell infection with the same efficiency. However, other groups showed that some anti-gp41 neutralizing antibodies failed to inhibit cell-to-cell transmission (4, 56, 77). Globally, the efficiency of neutralizing antibodies for neutralization of the virological synape-mediated viral transfer is variable and some epitopes of the viral envelope glycoproteins seem more susceptible than others to neutralization of the viral cell-to-cell transfer between T cells.

Similarly, the activity of the T20 peptide entry inhibitor of the Env-mediated membrane fusion on HIV-1 transmission through the virological synapse is still a matter of debate, and a lot of contradictory results have been published regarding the effect of this inhibitor. Whereas it was initially reported that T20 was unable to block virological synapse-mediated viral transfer using flow cytometry analysis (4), Martin et al. then showed that cell-free and cell-to-cell infection across the virological synapse were equivalently susceptible to T20, using qPCR for detection of infection in the target T cells

(60). These different results can be explained by the different experimental approaches used since the first study was looking for viral transfer of viral material when the other study analyzed *de novo* synthesized viral DNA after viral transfer. We can hypothesize that the T20 fusion inhibitor does not affect viral transfer across the virological synapse, but inhibits HIV-1 infection in the target cell after the viral transfer mediated through the virological synapse. The fusion inhibitors T20 and C34, targeting gp41, could also have no effect on capture and endocytosis of virus particles for viral cell-to-cell transfer, but would rather block subsequent viral fusion in the endosomal compartments leading to inhibition of productive infection (65).

While it is usually accepted that HIV-1 could escape or is less sensitive to the inhibitory activity of antiviral drugs used in clinic when T cells are infected by virus transfer through the virological synapse, only a few studies have reported rational analyses of the effects of antiretroviral drugs such as anti-protease or anti-reverse transcriptase inhibitors on viral cell-to-cell transfer. Some studies indeed reported that HIV-1 virological synapse-mediated infection and cell-free infection were similarly inhibited by anti-protease drugs (15, 78). Regarding reverse transcriptase inhibitors, it seems that non-nucleoside-analog inhibitors of the reverse transcriptase could block virological synapse-mediated infection of T-cell targets (15, 78), whereas nucleoside-analog reverse transcriptase inhibitors (NRTI) were unable to do it. However, it was also reported that cell-to-cell infection was blocked efficiently when these NRTIs were used in combination even if the level of inhibition is lower than for cell-free infection (15, 78, 79). Usage of HIV-1 protease inhibitors Lopinavir and Darunavir has been reported as an efficient way to inhibit cell-to-cell transmission as efficiently as cell-free infection (79). This effect of protease inhibitors compared with reverse transcriptase inhibitors is suspected to be due to their ability to target immature virions and blocking their maturation in fully infectious viruses.

In conclusion, it seems from the data reported in the literature that the idea that the cell-to-cell viral transfer through the virological synapse can escape from neutralizing antibodies and antiretroviral drugs is not so evident and is probably dependent on the inhibitors used. Further systematic investigations with standardized assays to evaluate and compare activities of neutralizing antibodies and antiretroviral drugs in both cell-free and cell-to-cell infections are absolutely needed to address this important point.

HETEROGENEITY OF THE VIROLOGICAL SYNAPSES

HIV-1 transmission through the virological synapse established between an infected donor T cell and a recipient target T cell have been extensively studied. Nonetheless, DCs and macrophages can also transmit HIV-1 to target CD4+ T cells through the formation of a related virological synapse (80–82). If virus cell-to-cell transfer between DCs and T cells, as well as between macrophages and T cells, presents some similarities with the virological synapse observed between T cells, they also showed some specific differences.

The DC Infectious Synapse

Regarding DCs as virus-donor cells, two types of cell-to-cell viral transfer and infection of T-cell targets have been proposed: in *cis*-infection, DCs are productively infected and can then transfer viruses to CD4+ T cells, whereas in *trans*-infection, DCs are able to capture HIV-1 independently of CD4 and then transfer viruses to CD4+ T cells through the formation of the so-called "infectious synapse" (39, 83–85) (**Figure 1E**). HIV-1 *cis*-infection and *trans*-infection of CD4+ T target cells from DCs have been proposed to be mediated by distinct processes (86). However, because DCs highly express antiviral cellular restriction factors (APOBEC3G, TRIM5α, BST-2, and SAMHD-I), HIV-1 replicates poorly in this cell type. That is probably the reason why most of the studies of cell-to-cell transmission of HIV-1 from infected DCs to T cells developed *cis*-infection models of DCs using massive quantities of VSV-G-pseudotyped HIV-1 particles to infect DCs *in vitro*, thus questioning the validity of these models of *cis*-infection.

Regarding the *trans*-infection cell-to-cell process from DCs, several studies showed that DCs can capture HIV-1 through binding of the viral envelope glycoproteins to the mannose specific C-type lectin receptor (DC-SIGN) and store viruses into tetraspanin-enriched compartments, in continuity with the plasma membrane without viral replication in recipient DCs (58, 83, 84, 87). More recently, it has been reported that the immunoglobulin(I)-type lectin Siglec-1 (or CD169) can also bind to HIV-1 particles carrying sialyl-lactose gangliosides on their envelope (88–90). After capture, viruses remain at the cell surface or are internalized in vesicular containing compartments (see below). Then, DCs are able to transfer these viruses to CD4+ T cells independently of viral replication through the formation of an "infectious" synapse (91–94), thus decreasing the efficiency of broadly neutralizing antibodies on HIV-1 infection of target T cells (95).

While the formation of the virological synapse depends on the interaction between the viral gp120 envelope glycoprotein and the CD4 receptor, the infectious synapse formed during *trans*-infection does not rely upon CD4/gp120 interaction since Rodriguez-Plata et al. showed that the number of cell-to-cell conjugates formed between DCs and CD4+ T cells was not increased in the presence of HIV-1 (85). However, they also reported that the formation of the infectious synapse was decreased by 60% when the interaction between the adhesion molecules ICAM-1 and LFA-1 was disrupted. Furthermore, recognition of MHC-superantigen complexes presented at the surface of DCs by the TCR significantly enhanced virus transfer across the infectious synapse (85, 91). These authors suggest that the formation of the infectious synapse is not triggered by the virus but is more related to a hijacking of the immunological synapse by HIV-1. However, their experiments do not prove formally the formation of a canonical immunological synapse in their system as TCR or signaling molecules recruitment at the interface was not verified. Moreover, a previous study failed to detect any MHC-II or TCR recruitment at

the interface between DCs carrying viruses and target CD4+ T cells, thus excluding the identification of this structure as a *bone fide* immunological synapse (87).

While the formation of the infectious synapse does not rely on CD4/gp120 interaction, this interaction is still required for efficient productive infection of CD4+ T cells following formation of cell-to-cell conjugates with DCs carrying HIV-1. After the formation of conjugates, the CD4 receptor and CXCR4 or CCR5 co-receptors are recruited at the site of the cell–cell contact (96). Furthermore, intercellular transfer to CD4+ T cells of virus particles captured by DCs can be blocked using high concentrations of broadly neutralizing antibodies targeting the gp120 and gp41 envelope glycoproteins (97).

Rearrangements of the actin cytoskeleton also play a key role in HIV-1 transfer across the infectious synapse. A recent screening shows that tetraspanin 7 and dynamin-2 control nucleation and cortical stabilization of actin to maintain viruses onto dendrites for efficient cell-to-cell transfer from DCs to CD4+ T cells when cells are cocultured, and simultaneously infected with HIV-1 (98). Furthermore, it has been shown that large sheet-like membrane structures derived from DCs carrying HIV-1 wrap around T cells leading to a large interface at the infectious synapse (58). Within this interface, filopodia extensions from T cells are able to interact with the virus-containing compartments (VCCs) in continuity with the plasma membrane of DCs for efficient cell-to-cell transmission (58). Together, these results show that in DCs, HIV-1 can be efficiently transferred by hijacking the immunological synapse without productive infection of DCs.

As specialized DCs present in cervico-vaginal and rectal mucosa, Langerhans cells have been proposed to be the first targets of HIV-1 after sexual exposure. However, these cells were proposed to capture and degrade captured virions through expression of the DC-SIGN-related lectin Langerin at their surface, avoiding virus transmission from Langerhans cells to CD4+ T cells (99). More recently, in an *ex vivo* human tissue explant model, Ballweber et al. showed that vaginal Langerhans cells were able to transmit HIV-1 to CD4+ T cells, without being productively infected, rendering HIV-1 particles insensitive to inhibition by reverse transcriptase inhibitors in this context (100).

Of note, some studies suggest that the expression of Siglec-1 in macrophages mediates the internalization of HIV-1 particles in a VCC. As for DCs-to-T-cell transmission, the presence of these storage compartments in macrophages allows for the transfer of virions to CD4+ T cells (3, 101). Interestingly, the role of Siglec-1 for viral capture by macrophages has been evidenced *in vivo* in lymph node from HIV-1 or MLV infected mice (90). By showing subsequent transfer of MLV from macrophages to B cells, Sewald et al. proposed that this mechanism could be transposed to HIV-1 macrophage-to-T-cell transmission (90).

HIV-1 Transfer through Conjugates Formed with Macrophages

Compared with the cell-to-cell transmission mechanisms of HIV-1 involving T cells or DCs as infected donor cells, little is known about the formation of conjugates between HIV-1-infected macrophages and target CD4+ T cells. As evidenced by the presence of infected macrophages in different tissues in infected patients, macrophages are cellular targets of HIV-1 and probably play an important role in HIV-1 pathogenesis (102–108). Like other infected cells, they participate in cell-to-cell transmission of HIV-1 and are essential for HIV-1 spread in tissues of infected patients. One major feature of HIV-1-infected macrophages is related to the assembly and budding steps of the new viral particles. While in T cells viral assembly takes place at the plasma membrane, *de novo* formed viral particles accumulate both at the plasma membrane and in tetraspanin-enriched compartments called VCCs in productively infected macrophages (109–112). These VCCs, which do not exhibit the same characteristics than endosomes or multivesicular bodies, but are characterized by the presence of the tetraspanins CD63 and CD81 (113–116), and are connected to the extracellular space by thin channels in continuity with the plasma membrane (110, 117, 118). Viruses thus assemble in macrophages in a protected compartment and are then released in the extracellular environment.

Infected macrophages can efficiently transfer viruses to uninfected CD4+ T cells across the formation of a virological synapse but the mechanisms involved in the formation of this macrophage/T-cell virological synapse are not completely characterized (3, 119). During the formation of the conjugates between infected macrophages and target T cells, VCCs could rapidly move to the virological synapse (82) through an actin cytoskeleton-dependent mechanism (81). Similarly to the virological synapse formed between T cells, the virological synapse involving virus-donor macrophages leads to the recruitment of CD4, CCR5, LFA-1, and ICAM-1, as well as the viral Gag precursor and envelope glycoproteins at the site of cell–cell contact (81, 119). In contrast to the virological synapse formed between T cells, which is dependent of CD4, the formation of conjugates between infected macrophages and CD4+ T cells appears to be independent of gp120 (82), while the viral transfer is dependent of gp120/CD4 and LFA-1/ICAM-1 interactions (81). Through the formation of the virological synapse, infected macrophages can transfer a high multiplicity of HIV-1 to CD4+ T cells, promoting reduced viral sensitivity to reverse transcriptase inhibitors as well as to a panel of neutralizing antibodies (81, 82). While the virological synapse between infected macrophage and T-cell targets show several differences with the virological synapse between T cells (82, 119, 120), no similar structure has been described so far, to our knowledge, between infected T cells and uninfected macrophages for virus cell-to-cell transfer in these HIV-1 target cells.

ENGULFMENT OF INFECTED T CELLS BY MACROPHAGES AND ENTOSIS

Despite the fact that HIV-1 infection of T cells by cell-to-cell transfer has been largely documented, cell-to-cell infection of macrophages remains poorly investigated. Recently, the

group of Quentin Sattentau pointed out for the first time a new mechanism of specific cell-to-cell transfer of HIV-1 from infected CD4+ T cells to macrophage targets (121) (**Figure 1F**). The authors showed that macrophages could engulf HIV-1-infected T cells leading to productive infection of the macrophage targets. The engulfment of infected healthy but rather dying T cells was significantly higher compared with uninfected healthy T cells, indicating that the cell death and infection of virus-donor T cells might independently promotes T-cell engulfment by macrophages. This preferential uptake of infected dying T cells was independent of the interaction between gp120 and the CD4 receptor but was dependent of remodeling of the actin cytoskeleton. Since this engulfment/uptake of infected T cells by macrophages was dependent of actin remodeling and was not inhibited by amiloride, an inhibitor of macropinocytosis, the authors suggested that this engulfment process likely results from phagocytosis mechanisms.

While the uptake of infected T cell by macrophages was independent of the Env/CD4 interaction, the productive infection of macrophages following uptake of T cells would be dependent of this interaction, and also depended of the tropism of the viruses. The uptake of infected T cells was evidenced by a concentrated localization of the viral Gag precursor in the macrophage target observed in association with the CD3 T-cell specific marker. The engulfment of T cells infected with CCR5-tropic viruses led to productive infection of the macrophage targets able to produce infectious virus particles in the cell-culture supernatant. In contrast, after engulfment of T cells infected with CXCR4-tropic viruses, no productive infection of the macrophage targets was observed (121). From these data, it appears evident that macrophages can be productively infected by phagocytosis of HIV-1-infected T cells, but the mechanisms for virus entry in macrophages from intracellular phagocytosed T cells remains to be defined. Nonetheless, the dependency of co-receptor usage by HIV-1 particles for productive infection could indicate a fusion of viral particles with the phagosome membrane.

Phagocytosis of SIV-infected T cells by myeloid cells *in vivo* was also suggested by the group of Jason Brenchley in SIV-infected macaque models (122, 123). Their studies point out the presence of viral RNA and DNA originating from T cells in myeloid cells from spleen and lymph nodes of infected monkeys, but do not formally prove that this presence of specific markers was related to a phagocytosis mechanism of SIV-infected T cells by myeloid cells, since no *per se* phagocytosis experiment was carried out in these studies.

Of note, another type of engulfment of HIV-1-infected CD4+ T cells by epithelial cells *via* an entosis mechanism has been observed. Entosis refers to the invasion of non-apoptotic cells into another live cell and then induces the formation of cell-in-cell structures (124, 125). Using infected cells from an immortalized T-cell line, Ni et al. reported that epithelial cells could internalize infected T cells *in vitro*, as well as *in vivo* in sigmoid colon explants from HIV-1-infected patients showing the formation of cell-in-cell structures (126). Through this entosis process, the epithelial cells could be productively infected, as evidenced by the diffuse intracytoplasmic staining of the viral capsid protein.

CELL–CELL FUSION

Formation of T-Cell Syncytia

Cell-to-cell fusion between infected CD4+ T cells, or between infected and uninfected CD4+ T cells, has been initially proposed to be another mechanism for HIV-1 infection and dissemination between T cells (127–131). Early studies suggested that infected T cells could fuse with uninfected T cells to form giant syncytia, 5–100 times bigger than individual cells (131, 132). In this context, cell-to-cell fusion occurs through actin cytoskeleton rearrangements, is dependent of LFA-1/ICAM-1 interaction and is mediated through interaction between envelope glycoproteins expressed at the cell surface of infected cells and CD4 expressed on the target cells (127, 129, 131, 133). Yet, these T-cell syncytia, initially observed only *in vitro* with infected immortalized T-cell lines, have been shown to die rapidly by a mitochondrion-dependent apoptosis mechanism (134, 135). The formation of HIV-1 T cell syncytia leads to activation of the serine-threonine kinase, mTOR, which mediates phosphorylation of the transcription factor p53. Thus, p53 induces upregulation of the pro-apoptotic regulator Bax leading to mitochondrial permeabilization and release of pro-apoptotic mitochondrial proteins (136, 137). Several groups thus proposed that this cytopathic effect related to the formation of T-cell syncytia could be the mechanism of the CD4+ T cells loss observed during infection in HIV-1-infected patients (127, 128, 132).

However, formation of T-cell syncytia has been a controversial subject since other studies did not observed formation of T-cell syncytia using HIV-1-infected primary CD4+ T cells (3, 4, 11). Because no evidence of the formation of such T-cell syncytia was reported *in vivo*, it has been suggested that these giant syncytia could be *in vitro* artifacts only observed with immortalized cell lines and restricted to CXCR4-viruses (138). Viral strains were indeed initially classified as syncytia-inducing or non-syncytia inducing (NSI) strains, referring to their capacity to induce syncytia *in vitro*, and then to their ability to use either CXCR4 or CCR5 for virus entry, respectively (139). However, cells infected with NSI viruses can readily form syncytia with CCR5-positive cells, and a new classification of viral strains based on CXCR4 or CCR5-usage was adopted (140).

Interestingly, small T-cell syncytia, containing no more than five nuclei, have been then observed *in vivo* in lymph nodes from HIV-1-infected patients (141). In addition, some more recent studies using HIV-1-infected "humanized mouse models" reported the presence of motile infected syncytia in lymph nodes, smaller than those observed *in vitro* (12). These motile small T-cell syncytia can establish tethering interactions with uninfected T cells that may facilitate cell-to-cell transmission through the formation of a virological synapse (12, 142). Interestingly, these interactions between infected small syncytia and uninfected T cells do not lead to cell-to-cell fusion suggesting that this mechanism of cell fusion is finely regulated (12).

Inhibition of T-Cell Fusion at the Virological Synapse

The numerous studies describing the formation of conjugates between infected and uninfected T cells for viral transfer across the virological synapse do not present observations of cell–cell fusion between the virus-donor T cells expressing the viral envelope glycoproteins and the target T cells expressing the CD4 receptor and CXCR4 and CCR5 co-receptors, confirming that this process is finely regulated during the formation of the virological synapse between T cells.

Since HIV-1 is a highly fusogenic virus that is preferentially transmitted by direct contact between two cells, the mechanisms inhibiting the fusion between an infected cell and a target cell deserves to be questioned. Indeed, in most of the T cell-to-T-cell transmission of HIV-1, a very few syncytia are observed compared with the formation of virological synapses (3, 4, 11). Moreover, large syncytia formed with T cells were characterized as rapid-dying cells (134, 136), which might indicate that HIV-1 has developed some mechanisms to inhibit the formation of these large T-cell syncytia to survive in infected host. As usually, it was proposed that HIV-1 took advantage of the intracellular systems displayed by its host, and used molecular mechanism to inhibit cell–cell fusion.

For example, the CD81 tetraspanin membrane protein is recruited at the site of cell–cell contact during HIV-1 cell-to-cell transmission and was proposed to be involved in the regulation of fusion (143). CD81 knockdown or inhibition with a specific antibody dramatically increased the capacity of infected T cells to fuse with surrounding non-infected cells, indicating that CD81 is a negative regulator of T cell–T cell fusion during virological synapse formation. CD81 expression at the virological synapse seems to be regulated by the actin/plasma membrane connector, ezrin. Accordingly, reduction of ezrin expression in T cells decreased the level of CD81 localized at virological synapses, thus increasing cell–cell fusion between infected T cells (144). Other tetraspanin proteins such as CD9, CD63, or CD82, have been also studied for their role in HIV-1-mediated cell–cell fusion (144, 145). In addition, it has been shown that CD63 may interact with the CXCR4 co-receptor and induces downregulation of CXCR4 expression at the cell surface, resulting in the inhibition of HIV-1 infection (146, 147). Like CD81, these molecules may act as regulators of cell fusion, but most of the experiments have been performed using HeLa or HEK293T non-lymphoid cell lines. Therefore, experiments need to be performed in more relevant cell models to precisely define the molecular requirement of these tetraspanins in the regulation of syncytia formation between HIV-1-infected T cells.

Presence of Multinucleated Giant Cells (MGCs) in Infected Tissues

The mechanism of T-cell syncytia formation has been largely documented *in vitro* and discussed for its *in vivo* relevance. Nonetheless, processes of cell–cell fusion for HIV-1 infection and dissemination are not restricted to T cells. Some studies showed that infected multinucleated macrophages, as well as multinucleated DCs, could be found in different tissues *in vivo* in HIV-1-infected patients (148, 149). The presence of HIV-1-infected multinucleated syncytia expressing specific DC markers was found at the surface of the nasopharyngeal tonsils of HIV-1-infected patients and reported 20 years ago (148). The same group reported that infected T cells could fuse *in vitro* with skin-derived DCs (94), thus leading to multinucleated cell formation between T cells and DCs. Similarly, multinucleated giant HIV-1-infected macrophages have been found *in vivo* during infection in several different tissues, including lymph nodes, spleen, lungs, genital, and digestive tracts, and the central nervous system (CNS) (102–106, 108, 148, 150–153). While several groups showed the presence of infected multinucleated macrophages in tissues, and more specifically in the brain of HIV-1-infected patients and SIV-infected monkeys, the cellular and molecular mechanisms related to their formation remained poorly investigated, with only one *in vitro* study demonstrating a role for the HIV-1 auxiliary protein Nef in the formation of multinucleated macrophages (154).

We recently reported *in vitro* original results and proposed a model for the formation of HIV-1-infected MGCs related to a two-step cell–cell fusion process for HIV-1 cell-to-cell transfer from infected T cells and viral dissemination in macrophage targets (155) (**Figure 1G**). First, a heterotypic fusion occurs between HIV-1-infected T cells and macrophage targets for virus transfer. Then the newly formed lymphocyte/macrophage infected fused cells acquire the ability to fuse with surrounding uninfected macrophages for virus dissemination. As evidenced by cell imaging analyses, the first step is related to the establishment of contacts with infected T cells leading to the fusion of the infected T cells with macrophages. This cell fusion, dependent of the viral envelope/CD4 receptor interaction and restricted to CCR5-tropic viral strains, has been evidenced by a massive and fast transfer of Gag + material, as well as the presence of specific T cells markers (CD3, CD2, and Lck) in the cytoplasm and at the plasma membrane of the macrophage targets. The newly formed lymphocyte/macrophage fused cells (LMFCs) are then able to fuse with surrounding uninfected macrophages. These two sequential cell fusion processes are dependent on the viral envelope and lead to the formation of highly virus-productive MGCs that could survive for a long time in host tissues to produce infectious virus particles as shown *in vivo* in lymphoid organs and the CNS of HIV-1-infected patients and SIV-infected macaques (103, 106, 108, 152, 156). Similarly, the first step related to the initial T cell-to-macrophage fusion agrees with results showing that myeloid cells from lymphoid tissues of SIV-infected macaques contain T-cell markers and viral RNA and DNA originating from infected T cells (122, 123). This route of infection may be a major determinant *in vivo* for virus dissemination and establishment of macrophage virus reservoirs in host tissues.

CONCLUSION

Since the HIV-1 discovery, a lot of works have been accomplished to decipher its life cycle, in order to counteract virus

transmission and dissemination. Counteraction of host defenses is a major feature of HIV-1, since it is able to infect a large panel of immune cells and to largely decrease their effector functions. During the past years, several entry pathways for virus dissemination have been discovered but still need further investigations. While HIV-1 was initially suspected to enter its target cells only through fusion of viral particles with host T-cell membranes, it appears more and more evident that it can use a large diversity of cellular features to infect target cells, especially through direct cell-to-cell transmission by close contacts between an infected virus-donor cell and a target cell. Cell-to-cell transfer of HIV-1 indeed allows a massive release of viral material toward the target cell inducing a strong increase of viral infectivity, compared with infection with cell-free viruses. Depending on the infected donor cells as well as the target cell lineages, HIV-1 can take advantage of their specific physiology and features to infect its host. In T cell-to-T-cell transmission, HIV-1 provokes the formation of contacts, through Env–CD4 interactions, to allow a massive transfer of viruses between the two cells, thus improving its ability to enter the host cell. This intercellular structure, called virological synapse, is strongly similar to another but physiological one, the immunological synapse, indicating the HIV-1 ability to hijack T-cell pathways to spread. During trans-infection from DCs to target T cells, HIV-1 is even able to re-use at its advantage the interaction between APCs and T cells to cross the intercellular space for infection of target T cells. Through the interface formed between donor and target cells, filopodia coming from target T cells penetrate some VCCs in donor DCs to capture virions.

Therefore, intercellular communication pathways seem to be a road of choice for HIV-1 spreading. By increasing the frequency of filopodia formation in host infected cells, HIV-1 also enhances the surface of contacts of infected cells with the environment, thus improving its efficiency to be transferred to a non-infected neighboring target cell. In addition, HIV-1 can also create real bridges between cells, the so-called TNTs, which resemble to highways for virus transmission and dissemination. Moreover, when infected T cells are engulfed by specialized-phagocytic cells such macrophages, instead of being destroyed, HIV-1 is still able to infect the phagocyte.

Finally, HIV-1 uses its own ability to fuse with host cell membranes to provoke fusion between an infected donor cell and a target cell. By this way, HIV-1 is totally hidden form extracellular milieu since the sharing of the cytosol between the two cells appears to be sufficient for viral material dissemination and productive infection the new-formed fused cell able to produce new fully infectious virus particles. While fusion between T cells has been observed since a long time but was controverted as an *in vitro* artifact, more recent studies have pointed out the presence of small T-cell syncytia *in vivo* in lymph nodes from infected patients and proposed that these syncytia are fully able to transmit viral particles by cell-to-cell transfer to other cell targets. Multinucleated macrophages or DCs have also been observed *in vivo* in different tissues from HIV-1-infected patients, indicating the cell-to-cell fusogenicity of HIV-1 for different cell types. We have recently discovered a new mechanism of cell fusion between HIV-1-infected T cells and target macrophages. Heterotypic fusion between these cells appears, at least *in vitro*, to be a massive and very fast process allowing the formation of LMFCs that acquire the ability to fuse rapidly with neighboring non-infected macrophages, thus forming MGCs. The new-formed MGCs can survive for a long period *in vitro* and are highly productive of fully infectious viral particles. This important process could explain the presence of MGCs observed in several tissues of infected patients. Because of their long-time survival capacity, infected MGCs could participate in virus dissemination and establishment of persistent virus reservoirs in host tissues.

To conclude, while cell-associated HIV-1 transmission is believed to contribute to sexual transmission or viral spreading as well as to the formation of latent virus reservoirs, only few studies address the importance of cell-to-cell transfer of HIV-1 *in vivo*, and further investigations are needed to decipher the role of all the intercellular structures and processes described *in vitro* for pathogenesis in HIV-1-infected patients.

AUTHOR CONTRIBUTIONS

All authors listed, have made a substantial, direct, and intellectual contribution to the work, and approved it for publication.

ACKNOWLEDGMENTS

Financial support is provided by INSERM, the CNRS, and the University Paris-Descartes. The team is also funded by Grants from the *Agence Nationale de Recherche sur le SIDA et les Hépatites virales* (ANRS) and Sidaction. LB is supported by grants from the Institut Pasteur International Network and the Chinese Academy of Sciences. MX is supported by a grant from the China Scholarship Council. JB is supported by a grant from Sidaction. The team is part of the International Associated Laboratory (LIA) VIRHOST between CNRS, Institut Pasteur, Université Paris-Descartes, and the Institut Pasteur Shanghai—Chinese Academy of Sciences.

FUNDING

Financial support is provided by INSERM, the CNRS, and the University Paris-Descartes. The team is also funded by Grants from the Agence Nationale de Recherche sur le SIDA et les Hépatites virales (ANRS) and Sidaction. LB is supported by grants from the Institut Pasteur International Network and the Chinese Academy of Sciences. MX is supported by a grant from the China Scholarship Council. JB is supported by a grant from Sidaction. The team is part of the International Associated Laboratory (LIA) VIRHOST between CNRS, Institut Pasteur, Université Paris-Descartes, and the Institut Pasteur Shanghai—Chinese Academy of Sciences.

REFERENCES

1. Phillips DM. The role of cell-to-cell transmission in HIV infection. *AIDS* (1994) 8:719–31. doi:10.1097/00002030-199406000-00001
2. Dimitrov DS, Broder CC, Berger EA, Blumenthal R. Calcium ions are required for cell fusion mediated by the CD4-human immunodeficiency virus type 1 envelope glycoprotein interaction. *J Virol* (1993) 67:1647–52.
3. Carr JM, Hocking H, Li P, Burrell CJ. Rapid and efficient cell-to-cell transmission of human immunodeficiency virus infection from monocyte-derived macrophages to peripheral blood lymphocytes. *Virology* (1999) 265:319–29. doi:10.1006/viro.1999.0047
4. Chen P, Hübner W, Spinelli MA, Chen BK. Predominant mode of human immunodeficiency virus transfer between T cells is mediated by sustained Env-dependent neutralization-resistant virological synapses. *J Virol* (2007) 81:12582–95. doi:10.1128/JVI.00381-07
5. Martin N, Sattentau Q. Cell-to-cell HIV-1 spread and its implications for immune evasion. *Curr Opin HIV AIDS* (2009) 4:143–9. doi:10.1097/COH.0b013e328322f94a
6. Agosto LM, Uchil PD, Mothes W. HIV cell-to-cell transmission: effects on pathogenesis and antiretroviral therapy. *Trends Microbiol* (2015) 23:289–95. doi:10.1016/j.tim.2015.02.003
7. Boullé M, Müller TG, Dähling S, Ganga Y, Jackson L, Mahamed D, et al. HIV cell-to-cell spread results in earlier onset of viral gene expression by multiple infections per cell. *PLoS Pathog* (2016) 12:e1005964. doi:10.1371/journal.ppat.1005964
8. Del Portillo A, Tripodi J, Najfeld V, Wodarz D, Levy DN, Chen BK. Multiploid inheritance of HIV-1 during cell-to-cell infection. *J Virol* (2011) 85:7169–76. doi:10.1128/JVI.00231-11
9. Russell RA, Martin N, Mitar I, Jones E, Sattentau QJ. Multiple proviral integration events after virological synapse-mediated HIV-1 spread. *Virology* (2013) 443:143–9. doi:10.1016/j.virol.2013.05.005
10. Zhong P, Agosto LM, Munro JB, Mothes W. Cell-to-cell transmission of viruses. *Curr Opin Virol* (2013) 3:44–50. doi:10.1016/j.coviro.2012.11.004
11. Sourisseau M, Sol-Foulon N, Porrot F, Blanchet F, Schwartz O. Inefficient human immunodeficiency virus replication in mobile lymphocytes. *J Virol* (2007) 81:1000–12. doi:10.1128/JVI.01629-06
12. Murooka TT, Deruaz M, Marangoni F, Vrbanac VD, Seung E, von Andrian UH, et al. HIV-infected T cells are migratory vehicles for viral dissemination. *Nature* (2012) 490:283–7. doi:10.1038/nature11398
13. Sallé B, Brochard P, Bourry O, Mannioui A, Andrieu T, Prevot S, et al. Infection of macaques after vaginal exposure to cell-associated simian immunodeficiency virus. *J Infect Dis* (2010) 202:337–44. doi:10.1086/653619
14. Kolodkin-Gal D, Hulot SL, Korioth-Schmitz B, Gombos RB, Zheng Y, Owuor J, et al. Efficiency of cell-free and cell-associated virus in mucosal transmission of human immunodeficiency virus type 1 and simian immunodeficiency virus. *J Virol* (2013) 87:13589–97. doi:10.1128/JVI.03108-12
15. Sigal A, Kim JT, Balazs AB, Dekel E, Mayo A, Milo R, et al. Cell-to-cell spread of HIV permits ongoing replication despite antiretroviral therapy. *Nature* (2011) 477:95–8. doi:10.1038/nature10347
16. Permanyer M, Ballana E, Ruiz A, Badia R, Riveira-Munoz E, Gonzalo E, et al. Antiretroviral agents effectively block HIV replication after cell-to-cell transfer. *J Virol* (2012) 86:8773–80. doi:10.1128/JVI.01044-12
17. Buszczak M, Inaba M, Yamashita YM. Signaling by cellular protrusions: keeping the conversation private. *Trends Cell Biol* (2016) 26:526–34. doi:10.1016/j.tcb.2016.03.003
18. Rustom A, Saffrich R, Markovic I, Walther P, Gerdes H-H. Nanotubular highways for intercellular organelle transport. *Science* (2004) 303:1007–10. doi:10.1126/science.1093133
19. Sherer NM, Lehmann MJ, Jimenez-Soto LF, Horensavitz C, Pypaert M, Mothes W. Retroviruses can establish filopodial bridges for efficient cell-to-cell transmission. *Nat Cell Biol* (2007) 9:310. doi:10.1038/ncb1544
20. Chinnery HR, Pearlman E, McMenamin PG. Cutting edge: membrane nanotubes in vivo: a feature of MHC class II+ cells in the mouse cornea. *J Immunol* (2008) 180:5779–83. doi:10.4049/jimmunol.180.9.5779
21. Lou E, Fujisawa S, Morozov A, Barlas A, Romin Y, Dogan Y, et al. Tunneling nanotubes provide a unique conduit for intercellular transfer of cellular contents in human malignant pleural mesothelioma. *PLoS One* (2012) 7:e33093. doi:10.1371/journal.pone.0033093
22. Seyed-Razavi Y, Hickey MJ, Kuffová L, McMenamin PG, Chinnery HR. Membrane nanotubes in myeloid cells in the adult mouse cornea represent a novel mode of immune cell interaction. *Immunol Cell Biol* (2013) 91:89–95. doi:10.1038/icb.2012.52
23. Gousset K, Zurzolo C. Tunnelling nanotubes: a highway for prion spreading? *Prion* (2009) 3:94–8. doi:10.4161/pri.3.2.8917
24. Wang Y, Cui J, Sun X, Zhang Y. Tunneling-nanotube development in astrocytes depends on p53 activation. *Cell Death Differ* (2011) 18:732–42. doi:10.1038/cdd.2010.147
25. Eugenin EA, Gaskill PJ, Berman JW. Tunneling nanotubes (TNT) are induced by HIV-infection of macrophages: a potential mechanism for intercellular HIV trafficking. *Cell Immunol* (2009) 254:142–8. doi:10.1016/j.cellimm.2008.08.005
26. Hase K, Kimura S, Takatsu H, Ohmae M, Kawano S, Kitamura H, et al. M-Sec promotes membrane nanotube formation by interacting with Ral and the exocyst complex. *Nat Cell Biol* (2009) 11:1427–32. doi:10.1038/ncb1990
27. Onfelt B, Nedvetzki S, Yanagi K, Davis DM. Cutting edge: membrane nanotubes connect immune cells. *J Immunol* (2004) 173:1511–3. doi:10.4049/jimmunol.173.3.1511
28. Onfelt B, Nedvetzki S, Benninger RKP, Purbhoo MA, Sowinski S, Hume AN, et al. Structurally distinct membrane nanotubes between human macrophages support long-distance vesicular traffic or surfing of bacteria. *J Immunol* (2006) 177:8476–83. doi:10.4049/jimmunol.177.12.8476
29. Watkins SC, Salter RD. Functional connectivity between immune cells mediated by tunneling nanotubules. *Immunity* (2005) 23:309–18. doi:10.1016/j.immuni.2005.08.009
30. Sowinski S, Jolly C, Berninghausen O, Purbhoo MA, Chauveau A, Köhler K, et al. Membrane nanotubes physically connect T cells over long distances presenting a novel route for HIV-1 transmission. *Nat Cell Biol* (2008) 10:211–9. doi:10.1038/ncb1682
31. Kimura S, Hase K, Ohno H. The molecular basis of induction and formation of tunneling nanotubes. *Cell Tissue Res* (2013) 352:67–76. doi:10.1007/s00441-012-1518-1
32. Marzo L, Gousset K, Zurzolo C. Multifaceted roles of tunneling nanotubes in intercellular communication. *Front Physiol* (2012) 3:72. doi:10.3389/fphys.2012.00072
33. Smith IF, Shuai J, Parker I. Active generation and propagation of Ca2+ signals within tunneling membrane nanotubes. *Biophys J* (2011) 100:L37–9. doi:10.1016/j.bpj.2011.03.007
34. Kadiu I, Gendelman HE. Macrophage bridging conduit trafficking of HIV-1 through the endoplasmic reticulum and Golgi network. *J Proteome Res* (2011) 10:3225–38. doi:10.1021/pr200262q
35. Kadiu I, Gendelman HE. Human immunodeficiency virus type 1 endocytic trafficking through macrophage bridging conduits facilitates spread of infection. *J Neuroimmune Pharmacol* (2011) 6:658–75. doi:10.1007/s11481-011-9298-z
36. Xu W, Santini PA, Sullivan JS, He B, Shan M, Ball SC, et al. HIV-1 evades virus-specific IgG2 and IgA responses by targeting systemic and intestinal B cells via long-range intercellular conduits. *Nat Immunol* (2009) 10:1008–17. doi:10.1038/ni.1753
37. Hashimoto M, Bhuyan F, Hiyoshi M, Noyori O, Nasser H, Miyazaki M, et al. Potential role of the formation of tunneling nanotubes in HIV-1 spread in macrophages. *J Immunol* (2016) 196:1832–41. doi:10.4049/jimmunol.1500845
38. Mattila PK, Lappalainen P. Filopodia: molecular architecture and cellular functions. *Nat Rev Mol Cell Biol* (2008) 9:446–54. doi:10.1038/nrm2406
39. Nikolic DS, Lehmann M, Felts R, Garcia E, Blanchet FP, Subramaniam S, et al. HIV-1 activates Cdc42 and induces membrane extensions in immature dendritic cells to facilitate cell-to-cell virus propagation. *Blood* (2011) 118:4841–52. doi:10.1182/blood-2010-09-305417
40. Aggarwal A, Iemma TL, Shih I, Newsome TP, McAllery S, Cunningham AL, et al. Mobilization of HIV spread by diaphanous 2 dependent filopodia in infected dendritic cells. *PLoS Pathog* (2012) 8:e1002762. doi:10.1371/journal.ppat.1002762
41. Igakura T, Stinchcombe JC, Goon PKC, Taylor GP, Weber JN, Griffiths GM, et al. Spread of HTLV-I between lymphocytes by virus-induced polarization of the cytoskeleton. *Science* (2003) 299:1713–6. doi:10.1126/science.1080115

42. Agüera-Gonzalez S, Bouchet J, Alcover A. Immunological synapse. *eLS*. John Wiley & Sons, Ltd (2015). Available from: http://onlinelibrary.wiley.com/doi/10.1002/9780470015902.a0004027.pub2/abstract
43. Huppa JB, Davis MM. T-cell-antigen recognition and the immunological synapse. *Nat Rev Immunol* (2003) 3:973–83. doi:10.1038/nri1245
44. Cameron PU, Freudenthal PS, Barker JM, Gezelter S, Inaba K, Steinman RM. Dendritic cells exposed to human immunodeficiency virus type-1 transmit a vigorous cytopathic infection to CD4+ T cells. *Science* (1992) 257:383–7. doi:10.1126/science.1352913
45. Gupta P, Balachandran R, Ho M, Enrico A, Rinaldo C. Cell-to-cell transmission of human immunodeficiency virus type 1 in the presence of azidothymidine and neutralizing antibody. *J Virol* (1989) 63:2361–5.
46. Sato H, Orenstein J, Dimitrov D, Martin M. Cell-to-cell spread of HIV-1 occurs within minutes and may not involve the participation of virus particles. *Virology* (1992) 186:712–24. doi:10.1016/0042-6822(92)90038-Q
47. Jolly C, Sattentau QJ. Retroviral spread by induction of virological synapses. *Traffic* (2004) 5:643–50. doi:10.1111/j.1600-0854.2004.00209.x
48. Jolly C, Kashefi K, Hollinshead M, Sattentau QJ. HIV-1 cell to cell transfer across an Env-induced, actin-dependent synapse. *J Exp Med* (2004) 199: 283–93. doi:10.1084/jem.20030648
49. Vasiliver-Shamis G, Dustin ML, Hioe CE. HIV-1 virological synapse is not simply a copycat of the immunological synapse. *Viruses* (2010) 2:1239–60. doi:10.3390/v2051239
50. Alvarez RA, Barría MI, Chen BK. Unique features of HIV-1 spread through T cell virological synapses. *PLoS Pathog* (2014) 10:e1004513. doi:10.1371/journal.ppat.1004513
51. Jolly C, Mitar I, Sattentau QJ. Requirement for an intact T-cell actin and tubulin cytoskeleton for efficient assembly and spread of human immunodeficiency virus type 1. *J Virol* (2007) 81:5547–60. doi:10.1128/JVI.01469-06
52. Jolly C, Mitar I, Sattentau QJ. Adhesion molecule interactions facilitate human immunodeficiency virus type 1-induced virological synapse formation between T cells. *J Virol* (2007) 81:13916–21. doi:10.1128/JVI.01585-07
53. Starling S, Jolly C. LFA-1 engagement triggers T cell polarization at the HIV-1 virological synapse. *J Virol* (2016) 90:9841–54. doi:10.1128/JVI.01152-16
54. Vasiliver-Shamis G, Cho MW, Hioe CE, Dustin ML. Human immunodeficiency virus type 1 envelope gp120-induced partial T-cell receptor signaling creates an F-actin-depleted zone in the virological synapse. *J Virol* (2009) 83:11341–55. doi:10.1128/JVI.01440-09
55. Puigdomènech I, Massanella M, Izquierdo-Useros N, Ruiz-Hernandez R, Curriu M, Bofill M, et al. HIV transfer between CD4 T cells does not require LFA-1 binding to ICAM-1 and is governed by the interaction of HIV envelope glycoprotein with CD4. *Retrovirology* (2008) 5:32. doi:10.1186/1742-4690-5-32
56. Blanco J, Bosch B, Fernández-Figueras MT, Barretina J, Clotet B, Esté JA. High level of coreceptor-independent HIV transfer induced by contacts between primary CD4 T cells. *J Biol Chem* (2004) 279:51305–14. doi:10.1074/jbc.M408547200
57. Dale BM, McNerney GP, Thompson DL, Hubner W, de Los Reyes K, Chuang FYS, et al. Cell-to-cell transfer of HIV-1 via virological synapses leads to endosomal virion maturation that activates viral membrane fusion. *Cell Host Microbe* (2011) 10:551–62. doi:10.1016/j.chom.2011.10.015
58. Felts RL, Narayan K, Estes JD, Shi D, Trubey CM, Fu J, et al. 3D visualization of HIV transfer at the virological synapse between dendritic cells and T cells. *Proc Natl Acad Sci U S A* (2010) 107:13336–41. doi:10.1073/pnas.1003040107
59. Hübner W, McNerney GP, Chen P, Dale BM, Gordon RE, Chuang FYS, et al. Quantitative 3D video microscopy of HIV transfer across T cell virological synapses. *Science* (2009) 323:1743–7. doi:10.1126/science.1167525
60. Martin N, Welsch S, Jolly C, Briggs JAG, Vaux D, Sattentau QJ. Virological synapse-mediated spread of human immunodeficiency virus type 1 between T cells is sensitive to entry inhibition. *J Virol* (2010) 84:3516–27. doi:10.1128/JVI.02651-09
61. Rudnicka D, Feldmann J, Porrot F, Wietgrefe S, Guadagnini S, Prévost M-C, et al. Simultaneous cell-to-cell transmission of human immunodeficiency virus to multiple targets through polysynapses. *J Virol* (2009) 83:6234–46. doi:10.1128/JVI.00282-09
62. Jolly C, Sattentau QJ. Regulated secretion from CD4+ T cells. *Trends Immunol* (2007) 28:474–81. doi:10.1016/j.it.2007.08.008
63. Jolly C, Welsch S, Michor S, Sattentau QJ. The regulated secretory pathway in CD4(+) T cells contributes to human immunodeficiency virus type-1 cell-to-cell spread at the virological synapse. *PLoS Pathog* (2011) 7:e1002226. doi:10.1371/journal.ppat.1002226
64. Sol-Foulon N, Sourisseau M, Porrot F, Thoulouze M-I, Trouillet C, Nobile C, et al. ZAP-70 kinase regulates HIV cell-to-cell spread and virological synapse formation. *EMBO J* (2007) 26:516–26. doi:10.1038/sj.emboj.7601509
65. Miyauchi K, Kim Y, Latinovic O, Morozov V, Melikyan GB. HIV enters cells via endocytosis and dynamin-dependent fusion with endosomes. *Cell* (2009) 137:433–44. doi:10.1016/j.cell.2009.02.046
66. Ruggiero E, Bona R, Muratori C, Federico M. Virological consequences of early events following cell-cell contact between human immunodeficiency virus type 1-infected and uninfected CD4+ cells. *J Virol* (2008) 82:7773–89. doi:10.1128/JVI.00695-08
67. Sloan RD, Kuhl BD, Mesplède T, Münch J, Donahue DA, Wainberg MA. Productive entry of HIV-1 during cell-to-cell transmission via dynamin-dependent endocytosis. *J Virol* (2013) 87:8110–23. doi:10.1128/JVI.00815-13
68. Bosch B, Grigorov B, Senserrich J, Clotet B, Darlix J-L, Muriaux D, et al. A clathrin-dynamin-dependent endocytic pathway for the uptake of HIV-1 by direct T cell-T cell transmission. *Antiviral Res* (2008) 80:185–93. doi:10.1016/j.antiviral.2008.06.004
69. Puigdomènech I, Massanella M, Cabrera C, Clotet B, Blanco J. On the steps of cell-to-cell HIV transmission between CD4 T cells. *Retrovirology* (2009) 6:89. doi:10.1186/1742-4690-6-89
70. Do T, Murphy G, Earl LA, Del Prete GQ, Grandinetti G, Li G-H, et al. Three-dimensional imaging of HIV-1 virological synapses reveals membrane architectures involved in virus transmission. *J Virol* (2014) 88:10327–39. doi:10.1128/JVI.00788-14
71. Galloway NL, Doitsh G, Monroe KM, Yang Z, Muñoz-Arias I, Levy DN, et al. Cell-to-cell transmission of HIV-1 is required to trigger pyroptotic death of lymphoid tissue-derived CD4 T cells. *Cell Rep* (2015) 12:1555–63. doi:10.1016/j.celrep.2015.08.011
72. Denizot M, Varbanov M, Espert L, Robert-Hebmann V, Sagnier S, Garcia E, et al. HIV-1 gp41 fusogenic function triggers autophagy in uninfected cells. *Autophagy* (2008) 4:998–1008. doi:10.4161/auto.6880
73. Blanco J, Barretina J, Ferri KF, Jacotot E, Gutiérrez A, Armand-Ugón M, et al. Cell-surface-expressed HIV-1 envelope induces the death of CD4 T cells during GP41-mediated hemifusion-like events. *Virology* (2003) 305:318–29. doi:10.1006/viro.2002.1764
74. Pantaleo G, Demarest JF, Vaccarezza M, Graziosi C, Bansal GP, Koenig S, et al. Effect of anti-V3 antibodies on cell-free and cell-to-cell human immunodeficiency virus transmission. *Eur J Immunol* (1995) 25:226–31. doi:10.1002/eji.1830250137
75. Abela IA, Berlinger L, Schanz M, Reynell L, Günthard HF, Rusert P, et al. Cell-cell transmission enables HIV-1 to evade inhibition by potent CD4bs directed antibodies. *PLoS Pathog* (2012) 8:e1002634. doi:10.1371/journal.ppat.1002634
76. Malbec M, Sourisseau M, Guivel-Benhassine F, Porrot F, Blanchet F, Schwartz O, et al. HIV-1 Nef promotes the localization of Gag to the cell membrane and facilitates viral cell-to-cell transfer. *Retrovirology* (2013) 10:80. doi:10.1186/1742-4690-10-80
77. Massanella M, Puigdomènech I, Cabrera C, Fernandez-Figueras MT, Aucher A, Gaibelet G, et al. Antigp41 antibodies fail to block early events of virological synapses but inhibit HIV spread between T cells. *AIDS* (2009) 23:183–8. doi:10.1097/QAD.0b013e32831ef1a3
78. Agosto LM, Zhong P, Munro J, Mothes W. Highly active antiretroviral therapies are effective against HIV-1 cell-to-cell transmission. *PLoS Pathog* (2014) 10:e1003982. doi:10.1371/journal.ppat.1003982
79. Titanji BK, Aasa-Chapman M, Pillay D, Jolly C. Protease inhibitors effectively block cell-to-cell spread of HIV-1 between T cells. *Retrovirology* (2013) 10:161. doi:10.1186/1742-4690-10-161
80. Burleigh L, Lozach P-Y, Schiffer C, Staropoli I, Pezo V, Porrot F, et al. Infection of dendritic cells (DCs), not DC-SIGN-mediated internalization of human immunodeficiency virus, is required for long-term transfer of virus to T cells. *J Virol* (2006) 80:2949–57. doi:10.1128/JVI.80.6.2949-2957.2006
81. Duncan CJA, Williams JP, Schiffner T, Gärtner K, Ochsenbauer C, Kappes J, et al. High-multiplicity HIV-1 infection and neutralizing antibody evasion mediated by the macrophage-T cell virological synapse. *J Virol* (2014) 88:2025–34. doi:10.1128/JVI.03245-13
82. Gousset K, Ablan SD, Coren LV, Ono A, Soheilian F, Nagashima K, et al. Real-time visualization of HIV-1 GAG trafficking in infected

macrophages. *PLoS Pathog* (2008) 4:e1000015. doi:10.1371/journal.ppat.1000015
83. Arrighi J-F, Pion M, Garcia E, Escola J-M, van Kooyk Y, Geijtenbeek TB, et al. DC-SIGN-mediated infectious synapse formation enhances X4 HIV-1 transmission from dendritic cells to T cells. *J Exp Med* (2004) 200:1279–88. doi:10.1084/jem.20041356
84. Geijtenbeek TB, Kwon DS, Torensma R, van Vliet SJ, van Duijnhoven GC, Middel J, et al. DC-SIGN, a dendritic cell-specific HIV-1-binding protein that enhances trans-infection of T cells. *Cell* (2000) 100:587–97. doi:10.1016/S0092-8674(00)80694-7
85. Rodriguez-Plata MT, Puigdomènech I, Izquierdo-Useros N, Puertas MC, Carrillo J, Erkizia I, et al. The infectious synapse formed between mature dendritic cells and CD4(+) T cells is independent of the presence of the HIV-1 envelope glycoprotein. *Retrovirology* (2013) 10:42. doi:10.1186/1742-4690-10-42
86. Dong C, Janas AM, Wang J-H, Olson WJ, Wu L. Characterization of human immunodeficiency virus type 1 replication in immature and mature dendritic cells reveals dissociable cis- and trans-infection. *J Virol* (2007) 81:11352–62. doi:10.1128/JVI.01081-07
87. Garcia E, Pion M, Pelchen-Matthews A, Collinson L, Arrighi J-F, Blot G, et al. HIV-1 trafficking to the dendritic cell-T-cell infectious synapse uses a pathway of tetraspanin sorting to the immunological synapse. *Traffic* (2005) 6:488–501. doi:10.1111/j.1600-0854.2005.00293.x
88. Izquierdo-Useros N, Lorizate M, Contreras F-X, Rodriguez-Plata MT, Glass B, Erkizia I, et al. Sialyllactose in viral membrane gangliosides is a novel molecular recognition pattern for mature dendritic cell capture of HIV-1. *PLoS Biol* (2012) 10:e1001315. doi:10.1371/journal.pbio.1001315
89. Izquierdo-Useros N, Lorizate M, Puertas MC, Rodriguez-Plata MT, Zangger N, Erikson E, et al. Siglec-1 is a novel dendritic cell receptor that mediates HIV-1 trans-infection through recognition of viral membrane gangliosides. *PLoS Biol* (2012) 10:e1001448. doi:10.1371/journal.pbio.1001448
90. Sewald X, Ladinsky MS, Uchil PD, Beloor J, Pi R, Herrmann C, et al. Retroviruses use CD169-mediated trans-infection of permissive lymphocytes to establish infection. *Science* (2015) 350:563–7. doi:10.1126/science.aab2749
91. Dutartre H, Clavière M, Journo C, Mahieux R. Cell-free versus cell-to-cell infection by human immunodeficiency virus type 1 and human T-lymphotropic virus type 1: exploring the link among viral source, viral trafficking, and viral replication. *J Virol* (2016) 90:7607–17. doi:10.1128/JVI.00407-16
92. McDonald D. Dendritic cells and HIV-1 trans-infection. *Viruses* (2010) 2:1704–17. doi:10.3390/v2081704
93. Piguet V, Steinman RM. The interaction of HIV with dendritic cells: outcomes and pathways. *Trends Immunol* (2007) 28:503–10. doi:10.1016/j.it.2007.07.010
94. Pope M, Betjes MG, Romani N, Hirmand H, Cameron PU, Hoffman L, et al. Conjugates of dendritic cells and memory T lymphocytes from skin facilitate productive infection with HIV-1. *Cell* (1994) 78:389–98. doi:10.1016/0092-8674(94)90418-9
95. Akiyama H, Ramirez N-GP, Gudheti MV, Gummuluru S. CD169-mediated trafficking of HIV to plasma membrane invaginations in dendritic cells attenuates efficacy of anti-gp120 broadly neutralizing antibodies. *PLoS Pathog* (2015) 11:e1004751. doi:10.1371/journal.ppat.1004751
96. McDonald D, Wu L, Bohks SM, KewalRamani VN, Unutmaz D, Hope TJ. Recruitment of HIV and its receptors to dendritic cell-T cell junctions. *Science* (2003) 300:1295–7. doi:10.1126/science.1084238
97. Sagar M, Akiyama H, Etemad B, Ramirez N, Freitas I, Gummuluru S. Transmembrane domain membrane proximal external region but not surface unit-directed broadly neutralizing HIV-1 antibodies can restrict dendritic cell-mediated HIV-1 trans-infection. *J Infect Dis* (2012) 205:1248–57. doi:10.1093/infdis/jis183
98. Ménager MM, Littman DR. Actin dynamics regulates dendritic cell-mediated transfer of HIV-1 to T cells. *Cell* (2016) 164:695–709. doi:10.1016/j.cell.2015.12.036
99. de Witte L, Nabatov A, Pion M, Fluitsma D, de Jong MAWP, de Gruijl T, et al. Langerin is a natural barrier to HIV-1 transmission by Langerhans cells. *Nat Med* (2007) 13:367–71. doi:10.1038/nm1541
100. Ballweber L, Robinson B, Kreger A, Fialkow M, Lentz G, McElrath MJ, et al. Vaginal Langerhans cells nonproductively transporting HIV-1 mediate infection of T cells. *J Virol* (2011) 85:13443–7. doi:10.1128/JVI.05615-11
101. Hammonds JE, Beeman N, Ding L, Takushi S, Francis AC, Wang J-J, et al. Siglec-1 initiates formation of the virus-containing compartment and enhances macrophage-to-T cell transmission of HIV-1. *PLoS Pathog* (2017) 13:e1006181. doi:10.1371/journal.ppat.1006181
102. Costiniuk CT, Jenabian M-A. Cell-to-cell transfer of HIV infection: implications for HIV viral persistence. *J Gen Virol* (2014) 95:2346–55. doi:10.1099/vir.0.069641-0
103. Dargent JL, Lespagnard L, Kornreich A, Hermans P, Clumeck N, Verhest A. HIV-associated multinucleated giant cells in lymphoid tissue of the Waldeyer's ring: a detailed study. *Mod Pathol* (2000) 13:1293–9. doi:10.1038/modpathol.3880237
104. Fischer-Smith T, Bell C, Croul S, Lewis M, Rappaport J. Monocyte/macrophage trafficking in acquired immunodeficiency syndrome encephalitis: lessons from human and nonhuman primate studies. *J Neurovirol* (2008) 14:318–26. doi:10.1080/13550280802132857
105. Geny C, Gherardi R, Boudes P, Lionnet F, Cesaro P, Gray F. Multifocal multinucleated giant cell myelitis in an AIDS patient. *Neuropathol Appl Neurobiol* (1991) 17:157–62. doi:10.1111/j.1365-2990.1991.tb00707.x
106. Lewin-Smith M, Wahl SM, Orenstein JM. Human immunodeficiency virus-rich multinucleated giant cells in the colon: a case report with transmission electron microscopy, immunohistochemistry, and in situ hybridization. *Mod Pathol* (1999) 12:75–81.
107. Orenstein JM. The macrophage in HIV infection. *Immunobiology* (2001) 204:598–602. doi:10.1078/0171-2985-00098
108. Vicandi B, Jiménez-Heffernan JA, López-Ferrer P, Patrón M, Gamallo C, Colmenero C, et al. HIV-1 (p24)-positive multinucleated giant cells in HIV-associated lymphoepithelial lesion of the parotid gland. A report of two cases. *Acta Cytol* (1999) 43:247–51. doi:10.1159/000330987
109. Carter CA, Ehrlich LS. Cell biology of HIV-1 infection of macrophages. *Annu Rev Microbiol* (2008) 62:425–43. doi:10.1146/annurev.micro.62.081307.162758
110. Deneka M, Pelchen-Matthews A, Byland R, Ruiz-Mateos E, Marsh M. In macrophages, HIV-1 assembles into an intracellular plasma membrane domain containing the tetraspanins CD81, CD9, and CD53. *J Cell Biol* (2007) 177:329–41. doi:10.1083/jcb.200609050
111. Mlcochova P, Pelchen-Matthews A, Marsh M. Organization and regulation of intracellular plasma membrane-connected HIV-1 assembly compartments in macrophages. *BMC Biol* (2013) 11:89. doi:10.1186/1741-7007-11-89
112. Nkwe DO, Pelchen-Matthews A, Burden JJ, Collinson LM, Marsh M. The intracellular plasma membrane-connected compartment in the assembly of HIV-1 in human macrophages. *BMC Biol* (2016) 14:50. doi:10.1186/s12915-016-0272-3
113. Jouve M, Sol-Foulon N, Watson S, Schwartz O, Benaroch P. HIV-1 buds and accumulates in "nonacidic" endosomes of macrophages. *Cell Host Microbe* (2007) 2:85–95. doi:10.1016/j.chom.2007.06.011
114. Ono A, Freed EO. Cell-type-dependent targeting of human immunodeficiency virus type 1 assembly to the plasma membrane and the multivesicular body. *J Virol* (2004) 78:1552–63. doi:10.1128/JVI.78.3.1552-1563.2004
115. Orenstein JM, Meltzer MS, Phipps T, Gendelman HE. Cytoplasmic assembly and accumulation of human immunodeficiency virus types 1 and 2 in recombinant human colony-stimulating factor-1-treated human monocytes: an ultrastructural study. *J Virol* (1988) 62:2578–86.
116. Pelchen-Matthews A, Kramer B, Marsh M. Infectious HIV-1 assembles in late endosomes in primary macrophages. *J Cell Biol* (2003) 162:443–55. doi:10.1083/jcb.200304008
117. Bennett AE, Narayan K, Shi D, Hartnell LM, Gousset K, He H, et al. Ion-abrasion scanning electron microscopy reveals surface-connected tubular conduits in HIV-infected macrophages. *PLoS Pathog* (2009) 5:e1000591. doi:10.1371/journal.ppat.1000591
118. Welsch S, Keppler OT, Habermann A, Allespach I, Krijnse-Locker J, Kräusslich H-G. HIV-1 buds predominantly at the plasma membrane of primary human macrophages. *PLoS Pathog* (2007) 3:e36. doi:10.1371/journal.ppat.0030036
119. Groot F, Welsch S, Sattentau QJ. Efficient HIV-1 transmission from macrophages to T cells across transient virological synapses. *Blood* (2008) 111:4660–3. doi:10.1182/blood-2007-12-130070

120. Waki K, Freed EO. Macrophages and cell-cell spread of HIV-1. *Viruses* (2010) 2:1603–20. doi:10.3390/v2081603
121. Baxter AE, Russell RA, Duncan CJA, Moore MD, Willberg CB, Pablos JL, et al. Macrophage infection via selective capture of HIV-1-infected CD4+ T cells. *Cell Host Microbe* (2014) 16:711–21. doi:10.1016/j.chom.2014.10.010
122. Calantone N, Wu F, Klase Z, Deleage C, Perkins M, Matsuda K, et al. Tissue myeloid cells in SIV-infected primates acquire viral DNA through phagocytosis of infected T cells. *Immunity* (2014) 41:493–502. doi:10.1016/j.immuni.2014.08.014
123. DiNapoli SR, Ortiz AM, Wu F, Matsuda K, Twigg HL, Hirsch VM, et al. Tissue-resident macrophages can contain replication-competent virus in antiretroviral-naive, SIV-infected Asian macaques. *JCI Insight* (2017) 2:e91214. doi:10.1172/jci.insight.91214
124. Overholtzer M, Mailleux AA, Mouneimne G, Normand G, Schnitt SJ, King RW, et al. A nonapoptotic cell death process, entosis, that occurs by cell-in-cell invasion. *Cell* (2007) 131:966–79. doi:10.1016/j.cell.2007.10.040
125. Overholtzer M, Brugge JS. The cell biology of cell-in-cell structures. *Nat Rev Mol Cell Biol* (2008) 9:796–809. doi:10.1038/nrm2504
126. Ni C, Huang L, Chen Y, He M, Hu Y, Liu S, et al. Implication of cell-in-cell structures in the transmission of HIV to epithelial cells. *Cell Res* (2015) 25:1265–8. doi:10.1038/cr.2015.119
127. Hildreth JE, Orentas RJ. Involvement of a leukocyte adhesion receptor (LFA-1) in HIV-induced syncytium formation. *Science* (1989) 244:1075–8. doi:10.1126/science.2543075
128. Lifson JD, Feinberg MB, Reyes GR, Rabin L, Banapour B, Chakrabarti S, et al. Induction of CD4-dependent cell fusion by the HTLV-III/LAV envelope glycoprotein. *Nature* (1986) 323:725–8. doi:10.1038/323725a0
129. Schols D, Pauwels R, Baba M, Desmyter J, De Clercq E. Syncytium formation and destruction of bystander CD4+ cells cocultured with T cells persistently infected with human immunodeficiency virus as demonstrated by flow cytometry. *J Gen Virol* (1989) 70(Pt 9):2397–408. doi:10.1099/0022-1317-70-9-2397
130. Sodroski J, Goh WC, Rosen C, Campbell K, Haseltine WA. Role of the HTLV-III/LAV envelope in syncytium formation and cytopathicity. *Nature* (1986) 322:470–4. doi:10.1038/322470a0
131. Sylwester A, Wessels D, Anderson SA, Warren RQ, Shutt DC, Kennedy RC, et al. HIV-induced syncytia of a T cell line form single giant pseudopods and are motile. *J Cell Sci* (1993) 106(Pt 3):941–53.
132. Sylwester A, Murphy S, Shutt D, Soll DR. HIV-induced T cell syncytia are self-perpetuating and the primary cause of T cell death in culture. *J Immunol* (1997) 158:3996–4007.
133. Soll DR, Kennedy RC. The role of T cell motility and cytoskeletal reorganization in HIV-induced syncytium formation. *AIDS Res Hum Retroviruses* (1994) 10:325–7. doi:10.1089/aid.1994.10.325
134. Roumier T, Castedo M, Perfettini J-L, Andreau K, Métivier D, Zamzami N, et al. Mitochondrion-dependent caspase activation by the HIV-1 envelope. *Biochem Pharmacol* (2003) 66:1321–9. doi:10.1016/S0006-2952(03)00480-5
135. Ferri KF, Jacotot E, Blanco J, Esté JA, Zamzami N, Susin SA, et al. Apoptosis control in syncytia induced by the HIV type 1–envelope glycoprotein complex: role of mitochondria and caspases. *J Exp Med* (2000) 192:1081–92. doi:10.1084/jem.192.8.1081
136. Ahr B, Robert-Hebmann V, Devaux C, Biard-Piechaczyk M. Apoptosis of uninfected cells induced by HIV envelope glycoproteins. *Retrovirology* (2004) 1:12. doi:10.1186/1742-4690-1-12
137. Nardacci R, Perfettini J-L, Grieco L, Thieffry D, Kroemer G, Piacentini M. Syncytial apoptosis signaling network induced by the HIV-1 envelope glycoprotein complex: an overview. *Cell Death Dis* (2015) 6:e1846. doi:10.1038/cddis.2015.204
138. Moore JP, Ho DD. HIV-1 neutralization: the consequences of viral adaptation to growth on transformed T cells. *AIDS* (1995) 9(Suppl A):S117–36.
139. Schuitemaker H, Kootstra NA, Groenink M, De Goede RE, Miedema F, Tersmette M. Differential tropism of clinical HIV-1 isolates for primary monocytes and promonocytic cell lines. *AIDS Res Hum Retroviruses* (1992) 8:1679–82. doi:10.1089/aid.1992.8.1679
140. Berger EA, Doms RW, Fenyo E-M, Korber BTM, Littman DR, Moore JP, et al. A new classification for HIV-1. *Nature* (1998) 391:240. doi:10.1038/34571
141. Orenstein JM. In vivo cytolysis and fusion of human immunodeficiency virus type 1-infected lymphocytes in lymphoid tissue. *J Infect Dis* (2000) 182:338–42. doi:10.1086/315640
142. Symeonides M, Murooka T, Bellfy L, Roy N, Mempel T, Thali M. HIV-1-induced small t cell syncytia can transfer virus particles to target cells through transient contacts. *Viruses* (2015) 7:6590–603. doi:10.3390/v7122959
143. Gordón-Alonso M, Yañez-Mó M, Barreiro O, Alvarez S, Muñoz-Fernández MA, Valenzuela-Fernández A, et al. Tetraspanins CD9 and CD81 modulate HIV-1-induced membrane fusion. *J Immunol* (2006) 177:5129–37.
144. Roy NH, Lambelé M, Chan J, Symeonides M, Thali M. Ezrin is a component of the HIV-1 virological presynapse and contributes to the inhibition of cell-cell fusion. *J Virol* (2014) 88:7645–58. doi:10.1128/JVI.00550-14
145. Weng J, Krementsov DN, Khurana S, Roy NH, Thali M. Formation of syncytia is repressed by tetraspanins in human immunodeficiency virus type 1-producing cells. *J Virol* (2009) 83:7467–74. doi:10.1128/JVI.00163-09
146. Yoshida T, Kawano Y, Sato K, Ando Y, Aoki J, Miura Y, et al. A CD63 mutant inhibits T-cell tropic human immunodeficiency virus type 1 entry by disrupting CXCR4 trafficking to the plasma membrane. *Traffic* (2008) 9:540–58. doi:10.1111/j.1600-0854.2008.00700.x
147. Yoshida T, Ebina H, Koyanagi Y. N-linked glycan-dependent interaction of CD63 with CXCR4 at the Golgi apparatus induces downregulation of CXCR4. *Microbiol Immunol* (2009) 53:629–35. doi:10.1111/j.1348-0421.2009.00167.x
148. Frankel SS, Wenig BM, Burke AP, Mannan P, Thompson LD, Abbondanzo SL, et al. Replication of HIV-1 in dendritic cell-derived syncytia at the mucosal surface of the adenoid. *Science* (1996) 272:115–7. doi:10.1126/science.272.5258.115
149. Granelli-Piperno A, Pope M, Inaba K, Steinman RM. Coexpression of NF-kappa B/Rel and Sp1 transcription factors in human immunodeficiency virus 1-induced, dendritic cell-T-cell syncytia. *Proc Natl Acad Sci U S A* (1995) 92:10944–8. doi:10.1073/pnas.92.24.10944
150. Koenig S, Gendelman HE, Orenstein JM, Dal Canto MC, Pezeshkpour GH, Yungbluth M, et al. Detection of AIDS virus in macrophages in brain tissue from AIDS patients with encephalopathy. *Science* (1986) 233:1089–93. doi:10.1126/science.3016903
151. Orenstein JM, Wahl SM. The macrophage origin of the HIV-expressing multinucleated giant cells in hyperplastic tonsils and adenoids. *Ultrastruct Pathol* (1999) 23:79–91. doi:10.1080/019131299281734
152. Teo I, Veryard C, Barnes H, An SF, Jones M, Lantos PL, et al. Circular forms of unintegrated human immunodeficiency virus type 1 DNA and high levels of viral protein expression: association with dementia and multinucleated giant cells in the brains of patients with AIDS. *J Virol* (1997) 71:2928–33.
153. Ward JM, O'Leary TJ, Baskin GB, Benveniste R, Harris CA, Nara PL, et al. Immunohistochemical localization of human and simian immunodeficiency viral antigens in fixed tissue sections. *Am J Pathol* (1987) 127:199–205.
154. Vérollet C, Zhang YM, Le Cabec V, Mazzolini J, Charrière G, Labrousse A, et al. HIV-1 Nef triggers macrophage fusion in a p61Hck- and protease-dependent manner. *J Immunol* (2010) 184:7030–9. doi:10.4049/jimmunol.0903345
155. Bracq L, Xie M, Lambelé M, Vu L-T, Matz J, Schmitt A, et al. T cell-macrophage fusion triggers multinucleated giant cell formation for HIV-1 spreading. *J Virol* (2017) 91:e1237–1217. doi:10.1128/JVI.01237-17
156. Harbison C, Zhuang K, Gettie A, Blanchard J, Knight H, Didier P, et al. Giant cell encephalitis and microglial infection with mucosally transmitted simian-human immunodeficiency virus SHIVSF162P3N in rhesus macaques. *J Neurovirol* (2014) 20:62–72. doi:10.1007/s13365-013-0229-z

Conflict of Interest Statement: The authors declare that the research was conducted in the absence of any commercial or financial relationships that could be construed as a potential conflict of interest.

Copyright © 2018 Bracq, Xie, Benichou and Bouchet. This is an open-access article distributed under the terms of the Creative Commons Attribution License (CC BY). The use, distribution or reproduction in other forums is permitted, provided the original author(s) and the copyright owner are credited and that the original publication in this journal is cited, in accordance with accepted academic practice. No use, distribution or reproduction is permitted which does not comply with these terms.

frontiers in Immunology

MINI REVIEW
published: 25 January 2018
doi: 10.3389/fimmu.2018.00043

Tunneling Nanotubes: Intimate Communication between Myeloid Cells

Maeva Dupont[1,2†], Shanti Souriant[1,2†], Geanncarlo Lugo-Villarino[1,2], Isabelle Maridonneau-Parini[1,2] and Christel Vérollet[1,2*]*

[1] Institut de Pharmacologie et de Biologie Structurale, Université de Toulouse, CNRS, Université Toulouse III Paul Sabatier, Toulouse, France, [2] Research Program "IM-TB/HIV" (1167), International Associated Laboratory (LIA), CNRS, Toulouse, France

Tunneling nanotubes (TNT) are dynamic connections between cells, which represent a novel route for cell-to-cell communication. A growing body of evidence points TNT towards a role for intercellular exchanges of signals, molecules, organelles, and pathogens, involving them in a diverse array of functions. TNT form among several cell types, including neuronal cells, epithelial cells, and almost all immune cells. In myeloid cells (e.g., macrophages, dendritic cells, and osteoclasts), intercellular communication *via* TNT contributes to their differentiation and immune functions. Importantly, TNT enable myeloid cells to communicate with a targeted neighboring or distant cell, as well as with other cell types, therefore creating a complex variety of cellular exchanges. TNT also contribute to pathogen spread as they serve as "corridors" from a cell to another. Herein, we addressed the complexity of the definition and *in vitro* characterization of TNT in innate immune cells, the different processes involved in their formation, and their relevance *in vivo*. We also assess our current understanding of how TNT participate in immune surveillance and the spread of pathogens, with a particular interest for HIV-1. Overall, despite recent progress in this growing research field, we highlight that further investigation is needed to better unveil the role of TNT in both physiological and pathological conditions.

Keywords: tunneling nanotubes, myeloid cells, innate immunity, pathogens, HIV-1

OPEN ACCESS

Edited by:
Christoph Hölscher, Forschungszentrum Borstel (LG), Germany

Reviewed by:
Christian Bogdan, University of Erlangen-Nuremberg, Germany
Mario M. D'Elios, University of Florence, Italy

***Correspondence:**
Isabelle Maridonneau-Parini
maridono@ipbs.fr;
Christel Vérollet
verollet@ipbs.fr

†These authors have contributed equally to this work.

Specialty section:
This article was submitted to Microbial Immunology, a section of the journal Frontiers in Immunology

Received: *17 October 2017*
Accepted: *08 January 2018*
Published: *25 January 2018*

Citation:
Dupont M, Souriant S, Lugo-Villarino G, Maridonneau-Parini I and Vérollet C (2018) Tunneling Nanotubes: Intimate Communication between Myeloid Cells. Front. Immunol. 9:43. doi: 10.3389/fimmu.2018.00043

INTRODUCTION

Tunneling nanotubes (TNT) represent a novel type of intercellular communication machinery, which differs from the secretion of signaling molecules and the signal transmission through gap or synaptic junctions between adjacent cells. Along with exosomes, TNT mediate long-range communication, independent of soluble factors. They are membranous structures displaying a remarkable capacity to communicate with selected neighbor or distant cells. There are recent reviews covering the broad biological role of TNT, which are able to form in multiple cell types (1–3). Here, our focus is exclusively on TNT formed by myeloid cells, including macrophages, osteoclasts, and dendritic cells (DC). Based on the nascent literature on TNT in these cells, we will discuss the definition of TNT, their mechanisms of formation, and their role in physiological and pathological contexts. We will also address the need of further investigation of these structures to better understand their

functions and improve their potential as therapeutic targets in pathological conditions.

DEFINITION AND FUNCTION OF TNT

The main obstacle in reviewing the emerging TNT field is the different names given to these structures: TNT, cellular and membrane nanotubes, filopodia bridges, conduits or tubes, and nanotubules. Also, the huge number of publications on carbon nanotubes impedes the track of developments on TNT. Unifying terminology for nanotubes would thus be beneficial. In this mini-review, the term TNT will be used as done previously (2, 4). TNT are membranous channels connecting two or more cells over short to long distances. Actually, these structures can extend up to 200 µm in length in macrophages (5). To define TNT, we adopted the three phenotypic criteria proposed in a recent elegant review: (i) they connect at least two cells, (ii) they contain F-actin, and (iii) they do not touch the substrate (2). This definition allows the discrimination of TNT with any other F-actin-rich structures, such as filopodia. Regarding their functional properties, TNT transfer cytoplasmic molecules from one cell to another such as calcium, proteins or miRNA, mitochondria, several vesicles (e.g., lysosomes), pathogens, and cell-surface molecules; this ability constitutes the main functional criterion for TNT definition (6). The end of the structure can form a junctional border with the targeted cell (close-ended TNT) or the cytoplasm of the two connected cells can be mixed (open-ended TNT). On the one hand, the transfer of large molecules such as the lipophilic dye DiO is used to identify open-ended TNT (7). On the other hand, close-ended TNT form a junction at their end which are visualized by scanning electron microscopy (8). To avoid the past arguments on the need of cytoplasmic interactions for TNT, we shall consider in this review both close-ended and open-ended TNT (**Figure 1A**). As close-ended TNT mediate signal transfer through distant gap junctions (8, 9), they meet the functional criterion to be considered as TNT. Also, close-ended TNT could represent an intermediary status in the process of open-ended TNT formation. Finally, the group of Davis demonstrated that one particularity of macrophages is their ability to form different classes of TNT: thin ones (<0.7 µm in diameter), containing only F-actin; and thick ones (>0.7 µm), containing F-actin and microtubules (7). These two types of TNT could have different functions, as large material (e.g., lysosomes, mitochondria) can only travel between macrophages *via* thick TNT on microtubules (7).

DISCOVERY OF TNT

The first description of functional TNT *in vitro* was made in rat kidney cells (PC12 cells) and human cell lines (10), followed immediately by the identification of similar structures in human monocytes and macrophages (11). It is now clear that TNT can form in several cell types, including cancer cells and most leukocytes. However, to our knowledge, TNT were not described in granulocytes. In DC, TNT appeared to be similar to those made by monocytes-derived macrophages (6, 12). However, unlike DC exposed to anti-inflammatory conditions, only those activated by pro-inflammatory conditions form complex network of TNT able to transfer soluble molecules and pathogens (13). Likewise, macrophages undergo different activation programs within the broad spectrum of pro- (M1) and anti-inflammatory (M2) polarization. Yet, their activation state has not been linked to the formation of TNT. The only available data concern the early HIV-1 infection of macrophages, driving them toward M1 polarization (14) and inducing a significant increase in TNT formation (5, 15–18).

While the majority of studies in TNT biology has been performed in one cell type (homotypic TNT) at a time, TNT formation between different cell types (heterotypic TNT) is not rare. In fact, TNT frequently form between macrophages or DC with another cell type, enabling the exchange of lysosomes, mitochondria, or viral proteins (16, 19–21).

The reason why TNT were discovered quite recently could be attributed to their fragility. Indeed, they are poorly resistant to the existing shearing forces in culture media, as well as light exposure and classical fixation methods. Thus, an appropriate way of performing live imaging is necessary to study TNT. When working on fixed cells, gentle fixation (e.g., glutaraldehyde-based fixation) should help preserve these highly delicate structures (22, 23).

FORMATION OF TNT

Mechanisms of Formation

Cell examination by time-lapse microscopy suggested two mechanisms of TNT formation could exist. The first one proposes that two cells initially in contact separate from each other, remaining connected through a thin thread of membrane, which will be elongated upon cell separation (**Figure 1A**, right). The second puts forward that a cell would first bulge filopodia and extend them until reaching a neighboring cell, then converting towards TNT after making contact (24, 25) (**Figure 1A**, left). While the former is the prevailing mechanism in lymphoid cells, the latter one is observed in DC as TNT were reported to develop mainly from conversion of their filopodia (13, 19). In the case of macrophages, while they can use both mechanisms (6), the murine macrophage cell line (RAW 264.7 cells) mainly forms TNT from actin-driven protrusions, also called TNT-precursors (26). Of note, these two processes are not necessarily exclusive and could both occur between a given pair of cells. In either case, the requirement of F-actin is not questioned since treatment with latrunculin or cytochalasin D is often used to abolish TNT formation (2, 27, 28).

Regarding the opening of the conduit, and the potential transition between close-ended and open-ended TNT (**Figure 1A**), there is no proposed mechanism available. It is likely that the formation of open-ended TNT involves a step similar to what occurs during virus-to-cell membrane fusion or cell-to-cell fusion (29, 30), eventually leading to the generation of multinucleated giant cells (MGC) (**Figure 1A**).

Molecular Actors

Few data are available to describe TNT at the molecular level. M-Sec, also known as tumor necrosis factor-α-induced protein, is one of the best characterized protein involved in TNT formation

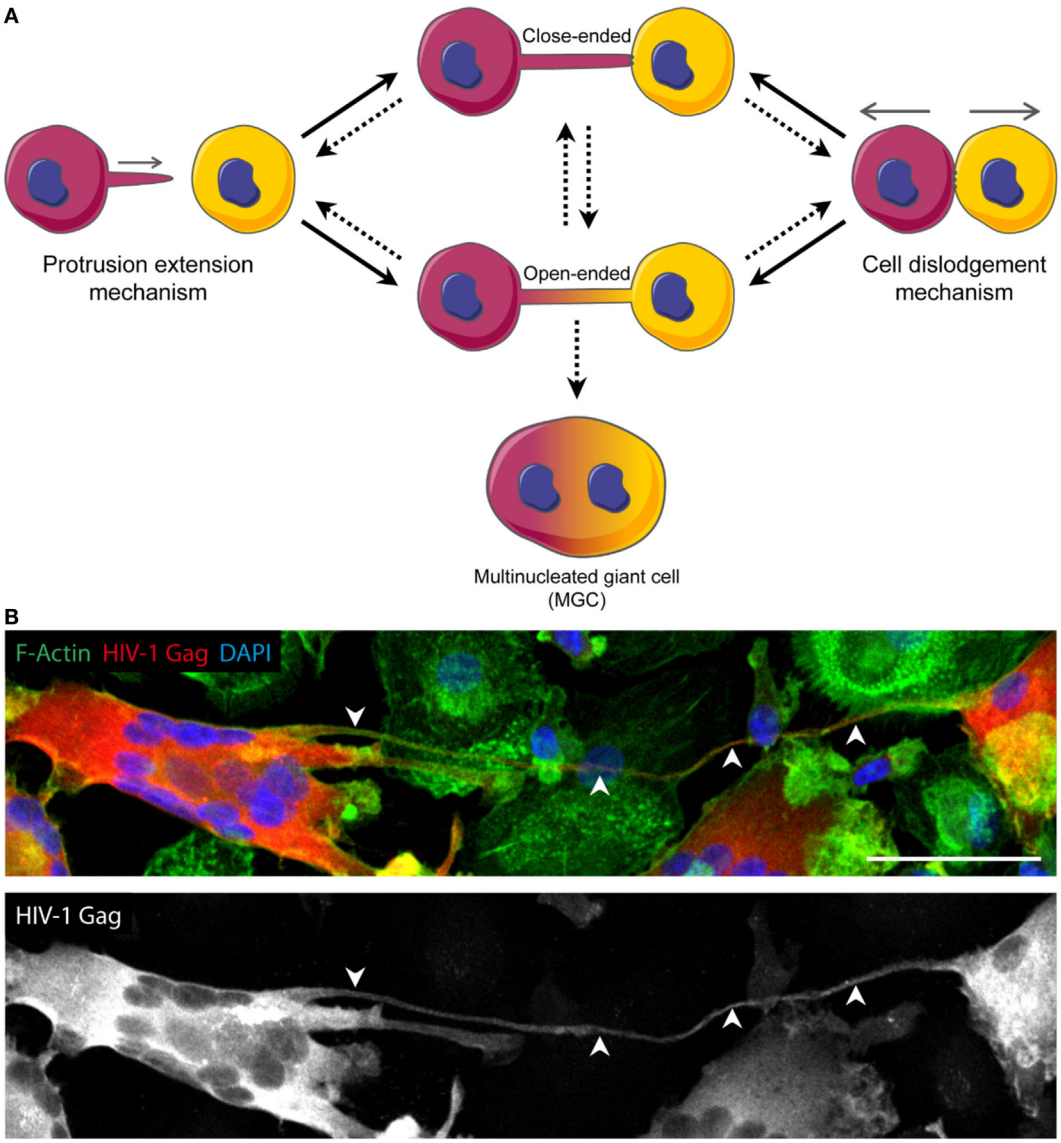


FIGURE 1 | Models of tunneling nanotube (TNT) formation and putative role in the generation of multinucleated giant cells (MGC). **(A)** TNT can form according to two mechanisms: the "protrusion elongation" mechanism where the cell extends filopodia-like protrusion toward a specific target cell (left), and the "cell dislodgement" mechanism for which two cells initially in contact separate from each other, stuck by a thread of membrane that gives rise to a TNT (right). Each of these mechanisms can lead to either close-ended or open-ended TNT, the last one allowing cytoplasmic continuity between interconnected cells. The dynamics of close-ended and open-ended TNT formation is still not understood. In addition, TNT could either disconnect cells and thus abrogate their communication or could lead to MGC. **(B)** Confocal image of day 13 HIV-1-infected human monocyte-derived macrophages and MGC interconnected through a TNT. Arrowheads show a TNT. HIV-1 Gag (red), F-actin (green), DAPI (blue). Scale bar, 50 μm.

in macrophages. Its depletion in Raw264.7 cells reduces the formation of *de novo* TNT and their associated function (transfer of calcium flux) (22). Using the same macrophage cell line, the group of D. Cox recently showed that actin polymerization factors including the Rho GTPases family Rac1 and Cdc42, and their downstream effectors WAVE and WASP, participate in TNT formation (26). In addition, functional TNT are induced by the expression of the leukocyte specific transcript 1 (LST1) protein in HeLa and HEK cell lines. LST1 recruits the actin cross-linking protein filamin and the small GTPase RalA to the plasma membrane where it promotes RalA interaction with the exocyst complex, M-Sec, and myosin; these interactions trigger TNT formation (22, 23). Whether the mechanisms that operate in cell lines derived often from tumor origin apply to primary cells remains to be confirmed.

IN VIVO RELEVANCE OF TNT

A remaining question is to determine to what extent the *in vitro* data available in the literature are relevant *in vivo*. One of the

problems is to apply *in vivo* the criteria of *bona fide* TNT (see above), in particular the requirement not to touch the substrate, which seems unlikely in 3D environments. In addition, testing the functionality of TNT in the context of tissues is challenging. Therefore, the structures observed *in vivo* should be carefully indicated as "TNT-like structures." Key evidence for TNT-like structures *in vivo* comes from the immunology field providing the first images of thick TNT connecting DC in inflamed mouse corneas (31). To our knowledge, macrophage TNT have not been observed *in vivo* yet. The identification of specific molecular markers for TNT would be a great tool to confirm the existence of these structures *in vivo*. M-Sec, which is involved in TNT formation, cannot be considered as a specific marker since this ubiquitous protein is expressed all over the cytoplasm (5, 18, 28, 32, 33). Thus, one of the priority to progress in the TNT field is to characterize markers allowing unambiguous identification of cell-to-cell tubular connections as TNT.

ROLE OF TNT IN PHYSIOLOGICAL CONTEXTS

One of the most studied functions of TNT is the propagation of calcium flux. Calcium signaling through TNT helps regulate cell metabolism and communication between neurons (34). Interestingly, DC present the ability to establish calcium fluxes *via* TNT transmitted within seconds to other DC as far as 500 µm away from the donor cell (12). When TNT are disturbed by M-Sec knockdown, this calcium flux is inhibited (12, 22). DC have also the particularity to form TNT networks allowing the intercellular exchange of antigens (13), including in the context of MHC molecules as described between Hela cells (19, 27). Therefore, TNT could contribute to a higher efficiency in the antigen presentation process to activate adaptive immunity (19).

Another physiological role for TNT concerns the differentiation of osteoclasts (5, 18, 28, 32, 33). Osteoclasts are MGC derived from a myeloid precursor that present the unique ability to degrade the bone matrix, and thus to regulate bone homeostasis. Inhibition of TNT either by latrunculin B or by M-Sec depletion significantly suppresses osteoclastogenesis, and the M-Sec expression level increases during osteoclastogenesis (28, 35). Dendritic cell-specific transmembrane protein, a receptor involved in cell-to-cell fusion, has been shown to be transferred *via* TNT. The authors proposed that this process could participate in cell fusion among osteoclast precursors (28, 35). Moreover, nuclei are found inside large TNT-like structures (36), inferring that they participate in cell-cell fusion to generate OC. Elucidating the role of TNT in differentiation of MGC such as placental trophoblast, myotubes, and osteoclasts could be a new research area.

ROLE OF TNT IN PATHOLOGICAL CONTEXTS

Tunneling nanotubes not only contribute to cell-to-cell communication in physiological conditions but also in pathological processes. For example, the transfer of lysosomes from macrophages to fibroblasts, and of mitochondria from mesenchymal stromal cells to macrophages, are mediated by TNT and have important consequences in cystinosis and acute respiratory distress syndrome, respectively (20, 21).

Without the shadow of doubt, the most studied consequence of TNT in diseases is the transfer of pathogens, including prions, bacteria, and viruses [for review, see Ref. (1)]. One of the well-known example concerns the role of TNT in neurological diseases, especially when caused by prions (34). Actually, in addition to the TNT-dependent transfer of the infectious form of the prion protein (PrP^{Sc}) between neuronal cells, TNT support PrP^{Sc} transfer from DC to the neurons in which PrP^{Sc} is further synthetized and transferred to the rest of the central nervous system (37). Regarding bacteria and viruses, some publications propose that they "surf" along TNT to spread from one cell to another (7, 13, 38–41). For example, in macrophages, live experiments show that *Mycobacterium bovis* bacillus Calmette–Guerin can travel along the surface of thin TNT, toward another macrophage, which will ingest it (7).

Viruses, including HIV-1, are well known to hijack the cytoskeleton in order to enter and travel inside their host cell, as well as towards bystander neighbor cells (5, 33, 39, 41, 42). For example, HIV-1 can actively induce the generation of filopodia in DC to propel virus particles towards neighboring cells. As one of the mechanism of TNT formation starts with membrane extension, filopodia formed upon HIV-1 infection could lead to TNT formation (2), especially in DC that develop networks of TNT from elongation of their dendrites (13, 19). Importantly, the formation of TNT by DC favors trans-infection of targeted $CD4^+$ T lymphocytes at a relatively long distance, similar to what happens between two distant $CD4^+$ T lymphocytes (8).

In macrophages, HIV-1 induces TNT formation and potentially uses them to spread (18). Whether thin or thick TNT are formed is unknown. Assuming that thick TNT are induced, HIV-1 could travel inside these structures by using a microtubule-dependent movement, in addition to the described "surfing" of HIV-1 at the surface of TNT. Despite the fact that Gag and Nef proteins and HIV-1-containing vesicles have been detected inside TNT, there are no convincing experiments in living cells available to prove that HIV-1 travels inside TNT and infects the targeted cell (5, 15, 17, 18). Pushing live imaging to super-resolution microscopy techniques would be of great help to study how HIV-1 traffics using TNT.

In light of the importance of macrophages in HIV-1 pathogenesis (43–45), it is crucial to bridge the several gaps that blur our understanding of the role of TNT in macrophages during HIV-1 infection. First, it is important to determine whether HIV-1-induced TNT in macrophages are close- or open-ended to better understand how HIV-1 traffics *via* TNT. Second, whether TNT from a HIV-infected cell could target non-infected cells remains to be elucidated. It would be an efficient way for the virus to spread around without being detected. Finally, the molecular regulation of HIV-1-induced TNT in macrophages has only started to be elucidated. The HIV-1 Nef protein could play a central role in TNT formation by interacting with members of the exocyst complex (16, 18, 46, 47). Moreover, Nef modulates F-actin and cell migration (48), two effects which could participate in TNT

generation. Finally, a hallmark of HIV-1 infection is the formation of MGC, a process that can be driven by TNT in order to persist during late infection stages, when most infected macrophages are MGC (**Figure 1B**) (32, 33). Interestingly, both HIV-1-induced TNT and MGC are reduced when macrophages are infected with *nef*-deleted viruses (18, 32, 33).

Importantly, while TNT spread the virus among HIV-1 target cells (T lymphocytes, macrophages, and DC), TNT also affects the nature of infection by circumventing the need for classical receptor-mediated virus entry or transfer viral components to cells that are not susceptible to infection. As a matter of fact, the transfer of Nef *via* TNT between infected macrophages and B cells induces drastic B cell abnormalities at the systemic and mucosal level (16).

CONCLUSION

The TNT field requires the unification of the terminology and definition of TNT, as well as the development of new tools adapted for the detection and monitoring of these particular structures. The main challenge so far is to discover molecular markers to specifically identify TNT, especially *in vivo*. To this end, an automated siRNA-based screen could be used in *in vitro* conditions for which TNT formation is controlled, as performed for the virological synapse (49). Another issue is the fragility of TNT which complicates their manipulation. Thus, the use of specific experimental conditions or devices, such as microfluidic systems (50), is needed. Moreover, it would be helpful to study the opening of close-ended TNT in terms of molecular components and dynamics. Likewise, it is imperative to determine whether TNT formation and regulation can be influenced by extracellular stimulti and/or tissue microenvironment in pertinent *in vivo* physiological and pathological contexts. For example, during HIV-1 infection, TNT represent a new way for viral spread. However, the literature remains scarce, rising far more questions than answers. Interestingly, HIV-1 and other microbes can serve as efficient tools to better understand TNT structure and function. Furthermore, TNT-based studies in the HIV-1 field are needed to better understand viral dissemination and pathogenesis. The particularity of TNT to perform "intimate" communication with a specific partner is probably key in HIV-1 spread. A tempting hypothesis is that infected cells could direct their TNT towards uninfected cells. This way, the virus could spread without being detected by the surveilling immune system. Finally, new insights into the mechanisms of TNT formation and regulation would be of high relevance to design novel therapeutics for several diseases, including viral infections.

AUTHOR CONTRIBUTIONS

MD, SS, IM-P, and CV wrote the manuscript. SS created the figure. GL-V edited the manuscript.

FUNDING

We are grateful to the TRI imaging facility, in particular Renaud Poincloux and Stéphanie Dauvillier. We thank A. Labrousse, C. A. Spinner, N. Roullet, and B. Raynaud-Messina for critical reading of the manuscript and helpful comments. This work was supported by the Centre National de la Recherche Scientifique, the Agence Nationale de la Recherche (ANR 2010-01301, ANR14-CE11-0020-02, ANR16-CE13-0005-01, ANR-11-EQUIPEX-0003), the Agence Nationale de Recherche sur le Sida et les hépatites virales (ANRS2014-CI-2, ANRS2014-049), the ECOS-Sud program (A14S01), the Fondation pour la Recherche Médicale (DEQ2016 0334894; DEQ2016 0334902), and the Fondation Bettencourt-Schueller. MD is supported by Paul Sabatier University, Toulouse, France, and SS by Sidaction.

REFERENCES

1. Sisakhtnezhad S, Khosravi L. Emerging physiological and pathological implications of tunneling nanotubes formation between cells. *Eur J Cell Biol* (2015) 94:429–43. doi:10.1016/j.ejcb.2015.06.010
2. McCoy-Simandle K, Hanna SJ, Cox D. Exosomes and nanotubes: control of immune cell communication. *Int J Biochem Cell Biol* (2016) 71:44–54. doi:10.1016/j.biocel.2015.12.006
3. Zaccard CR, Rinaldo CR, Mailliard RB. Linked in: immunologic membrane nanotube networks. *J Leukoc Biol* (2016) 100:81–94. doi:10.1189/jlb.4VMR0915-395R
4. Baker M. How the Internet of cells has biologists buzzing. *Nature* (2017) 549:322–4. doi:10.1038/549322a
5. Eugenin EA, Gaskill PJ, Berman JW. Tunneling nanotubes (TNT) are induced by HIV-infection of macrophages: a potential mechanism for intercellular HIV trafficking. *Cell Immunol* (2009) 254:142–8. doi:10.1016/j.cellimm.2008.08.005
6. Gerdes HH, Carvalho RN. Intercellular transfer mediated by tunneling nanotubes. *Curr Opin Cell Biol* (2008) 20:470–5. doi:10.1016/j.ceb.2008.03.005
7. Onfelt B, Nedvetzki S, Benninger RK, Purbhoo MA, Sowinski S, Hume AN, et al. Structurally distinct membrane nanotubes between human macrophages support long-distance vesicular traffic or surfing of bacteria. *J Immunol* (2006) 177:8476–83. doi:10.4049/jimmunol.177.12.8476
8. Sowinski S, Jolly C, Berninghausen O, Purbhoo MA, Chauveau A, Kohler K, et al. Membrane nanotubes physically connect T cells over long distances presenting a novel route for HIV-1 transmission. *Nat Cell Biol* (2008) 10:211–9. doi:10.1038/ncb1682
9. Wang X, Veruki ML, Bukoreshtliev NV, Hartveit E, Gerdes HH. Animal cells connected by nanotubes can be electrically coupled through interposed gap-junction channels. *Proc Natl Acad Sci U S A* (2010) 107:17194–9. doi:10.1073/pnas.1006785107
10. Rustom A, Saffrich R, Markovic I, Walther P, Gerdes HH. Nanotubular highways for intercellular organelle transport. *Science* (2004) 303:1007–10. doi:10.1126/science.1093133
11. Onfelt B, Nedvetzki S, Yanagi K, Davis DM. Cutting edge: membrane nanotubes connect immune cells. *J Immunol* (2004) 173:1511–3. doi:10.4049/jimmunol.173.3.1511
12. Watkins SC, Salter RD. Functional connectivity between immune cells mediated by tunneling nanotubules. *Immunity* (2005) 23:309–18. doi:10.1016/j.immuni.2005.08.009
13. Zaccard CR, Watkins SC, Kalinski P, Fecek RJ, Yates AL, Salter RD, et al. CD40L induces functional tunneling nanotube networks exclusively in dendritic cells programmed by mediators of type 1 immunity. *J Immunol* (2015) 194:1047–56. doi:10.4049/jimmunol.1401832
14. Lugo-Villarino G, Verollet C, Maridonneau-Parini I, Neyrolles O. Macrophage polarization: convergence point targeted by mycobacterium tuberculosis and HIV. *Front Immunol* (2011) 2:43. doi:10.3389/fimmu.2011.00043
15. Kadiu I, Ricardo-Dukelow M, Ciborowski P, Gendelman HE. Cytoskeletal protein transformation in HIV-1-infected macrophage giant cells. *J Immunol* (2007) 178:6404–15. doi:10.4049/jimmunol.178.10.6404

16. Xu W, Santini PA, Sullivan JS, He B, Shan M, Ball SC, et al. HIV-1 evades virus-specific IgG2 and IgA responses by targeting systemic and intestinal B cells via long-range intercellular conduits. *Nat Immunol* (2009) 10:1008–17. doi:10.1038/ni.1753
17. Kadiu I, Gendelman HE. Human immunodeficiency virus type 1 endocytic trafficking through macrophage bridging conduits facilitates spread of infection. *J Neuroimmune Pharmacol* (2011) 6:658–75. doi:10.1007/s11481-011-9298-z
18. Hashimoto M, Bhuyan F, Hiyoshi M, Noyori O, Nasser H, Miyazaki M, et al. Potential role of the formation of tunneling nanotubes in HIV-1 spread in macrophages. *J Immunol* (2016) 196:1832–41. doi:10.4049/jimmunol.1500845
19. Campana S, De Pasquale C, Carrega P, Ferlazzo G, Bonaccorsi I. Cross-dressing: an alternative mechanism for antigen presentation. *Immunol Lett* (2015) 168:349–54. doi:10.1016/j.imlet.2015.11.002
20. Naphade S, Sharma J, Gaide Chevronnay HP, Shook MA, Yeagy BA, Rocca CJ, et al. Brief reports: lysosomal cross-correction by hematopoietic stem cell-derived macrophages via tunneling nanotubes. *Stem Cells* (2015) 33:301–9. doi:10.1002/stem.1835
21. Jackson MV, Morrison TJ, Doherty DF, Mcauley DF, Matthay MA, Kissenpfennig A, et al. Mitochondrial transfer via tunneling nanotubes is an important mechanism by which mesenchymal stem cells enhance macrophage phagocytosis in the in vitro and in vivo models of ARDS. *Stem Cells* (2016) 34:2210–23. doi:10.1002/stem.2372
22. Hase K, Kimura S, Takatsu H, Ohmae M, Kawano S, Kitamura H, et al. M-Sec promotes membrane nanotube formation by interacting with Ral and the exocyst complex. *Nat Cell Biol* (2009) 11:1427–32. doi:10.1038/ncb1990
23. Schiller C, Diakopoulos KN, Rohwedder I, Kremmer E, Von Toerne C, Ueffing M, et al. LST1 promotes the assembly of a molecular machinery responsible for tunneling nanotube formation. *J Cell Sci* (2013) 126:767–77. doi:10.1242/jcs.114033
24. Kimura S, Hase K, Ohno H. Tunneling nanotubes: emerging view of their molecular components and formation mechanisms. *Exp Cell Res* (2012) 318:1699–706. doi:10.1016/j.yexcr.2012.05.013
25. Gerdes HH, Rustom A, Wang X. Tunneling nanotubes, an emerging intercellular communication route in development. *Mech Dev* (2013) 130:381–7. doi:10.1016/j.mod.2012.11.006
26. Hanna SJ, Mccoy-Simandle K, Miskolci V, Guo P, Cammer M, Hodgson L, et al. The role of Rho-GTPases and actin polymerization during macrophage tunneling nanotube biogenesis. *Sci Rep* (2017) 7:8547. doi:10.1038/s41598-017-08950-7
27. Schiller C, Huber JE, Diakopoulos KN, Weiss EH. Tunneling nanotubes enable intercellular transfer of MHC class I molecules. *Hum Immunol* (2013) 74:412–6. doi:10.1016/j.humimm.2012.11.026
28. Takahashi A, Kukita A, Li YJ, Zhang JQ, Nomiyama H, Yamaza T, et al. Tunneling nanotube formation is essential for the regulation of osteoclastogenesis. *J Cell Biochem* (2013) 114:1238–47. doi:10.1002/jcb.24433
29. Chen EH, Olson EN. Unveiling the mechanisms of cell-cell fusion. *Science* (2005) 308:369–73. doi:10.1126/science.1104799
30. Chen EH, Grote E, Mohler W, Vignery A. Cell-cell fusion. *FEBS Lett* (2007) 581:2181–93. doi:10.1016/j.febslet.2007.03.033
31. Chinnery HR, Pearlman E, Mcmenamin PG. Cutting edge: membrane nanotubes in vivo: a feature of MHC class II+ cells in the mouse cornea. *J Immunol* (2008) 180:5779–83. doi:10.4049/jimmunol.180.9.5779
32. Verollet C, Zhang YM, Le Cabec V, Mazzolini J, Charriere G, Labrousse A, et al. HIV-1 Nef triggers macrophage fusion in a p61Hck- and protease-dependent manner. *J Immunol* (2010) 184:7030–9. doi:10.4049/jimmunol.0903345
33. Verollet C, Souriant S, Bonnaud E, Jolicoeur P, Raynaud-Messina B, Kinnaer C, et al. HIV-1 reprograms the migration of macrophages. *Blood* (2015) 125:1611–22. doi:10.1182/blood-2014-08-596775
34. Victoria GS, Zurzolo C. The spread of prion-like proteins by lysosomes and tunneling nanotubes: Implications for neurodegenerative diseases. *J Cell Biol* (2017) 216(9):2633–44. doi:10.1083/jcb.201701047
35. Kukita T, Takahashi A, Zhang JQ, Kukita A. Membrane nanotube formation in osteoclastogenesis. *Methods Mol Biol* (2015) 1313:193–202. doi:10.1007/978-1-4939-2703-6_14
36. Pennanen P, Alanne MH, Fazeli E, Deguchi T, Nareoja T, Peltonen S, et al. Diversity of actin architecture in human osteoclasts: network of curved and branched actin supporting cell shape and intercellular micrometer-level tubes. *Mol Cell Biochem* (2017) 432:131–9. doi:10.1007/s11010-017-3004-2
37. Gousset K, Schiff E, Langevin C, Marijanovic Z, Caputo A, Browman DT, et al. Prions hijack tunnelling nanotubes for intercellular spread. *Nat Cell Biol* (2009) 11:328–36. doi:10.1038/ncb1841
38. Hope TJ. Bridging efficient viral infection. *Nat Cell Biol* (2007) 9:243–4. doi:10.1038/ncb0307-243
39. Sherer NM, Lehmann MJ, Jimenez-Soto LF, Horensavitz C, Pypaert M, Mothes W. Retroviruses can establish filopodial bridges for efficient cell-to-cell transmission. *Nat Cell Biol* (2007) 9:310–5. doi:10.1038/ncb1544
40. Davis DM, Sowinski S. Membrane nanotubes: dynamic long-distance connections between animal cells. *Nat Rev Mol Cell Biol* (2008) 9:431–6. doi:10.1038/nrm2399
41. Sherer NM, Mothes W. Cytonemes and tunneling nanotubules in cell-cell communication and viral pathogenesis. *Trends Cell Biol* (2008) 18:414–20. doi:10.1016/j.tcb.2008.07.003
42. Nikolic DS, Lehmann M, Felts R, Garcia E, Blanchet FP, Subramaniam S, et al. HIV-1 activates Cdc42 and induces membrane extensions in immature dendritic cells to facilitate cell-to-cell virus propagation. *Blood* (2011) 118:4841–52. doi:10.1182/blood-2010-09-305417
43. Honeycutt JB, Wahl A, Baker C, Spagnuolo RA, Foster J, Zakharova O, et al. Macrophages sustain HIV replication in vivo independently of T cells. *J Clin Invest* (2016) 126:1353–66. doi:10.1172/JCI84456
44. Sattentau QJ, Stevenson M. Macrophages and HIV-1: an unhealthy constellation. *Cell Host Microbe* (2016) 19:304–10. doi:10.1016/j.chom.2016.02.013
45. Honeycutt JB, Thayer WO, Baker CE, Ribeiro RM, Lada SM, Cao Y, et al. HIV persistence in tissue macrophages of humanized myeloid-only mice during antiretroviral therapy. *Nat Med* (2017) 23(5):638–43. doi:10.1038/nm.4319
46. Mukerji J, Olivieri KC, Misra V, Agopian KA, Gabuzda D. Proteomic analysis of HIV-1 Nef cellular binding partners reveals a role for exocyst complex proteins in mediating enhancement of intercellular nanotube formation. *Retrovirology* (2012) 9:33. doi:10.1186/1742-4690-9-33
47. Imle A, Abraham L, Tsopoulidis N, Hoflack B, Saksela K, Fackler OT. Association with PAK2 enables functional interactions of lentiviral Nef proteins with the exocyst complex. *MBio* (2015) 6:e1309–15. doi:10.1128/mBio.01309-15
48. Verollet C, Le Cabec V, Maridonneau-Parini I. HIV-1 infection of T lymphocytes and macrophages affects their migration via Nef. *Front Immunol* (2015) 6:514. doi:10.3389/fimmu.2015.00514
49. Menager MM, Littman DR. Actin dynamics regulates dendritic cell-mediated transfer of HIV-1 to T cells. *Cell* (2016) 164:695–709. doi:10.1016/j.cell.2015.12.036
50. Xiao M, Xu N, Wang C, Pang DW, Zhang ZL. Dynamic monitoring of membrane nanotubes formation induced by vaccinia virus on a high throughput microfluidic chip. *Sci Rep* (2017) 7:44835. doi:10.1038/srep44835

Conflict of Interest Statement: The authors declare that the research was conducted in the absence of any commercial or financial relationships that could be construed as a potential conflict of interest.

Copyright © 2018 Dupont, Souriant, Lugo-Villarino, Maridonneau-Parini and Vérollet. This is an open-access article distributed under the terms of the Creative Commons Attribution License (CC BY). The use, distribution or reproduction in other forums is permitted, provided the original author(s) or licensor are credited and that the original publication in this journal is cited, in accordance with accepted academic practice. No use, distribution or reproduction is permitted which does not comply with these terms.

frontiers in Immunology

PERSPECTIVE
published: 21 November 2017
doi: 10.3389/fimmu.2017.01593

Retroviruses As Myeloid Cell Riders: What Natural Human Siglec-1 "Knockouts" Tell Us About Pathogenesis

Javier Martinez-Picado[1,2,3†], Paul J. McLaren[4,5†], Amalio Telenti[6] and Nuria Izquierdo-Useros[1]*

[1] IrsiCaixa AIDS Research Institute, Badalona, Spain, [2] Institució Catalana de Recerca i Estudis Avançats (ICREA), Barcelona, Spain, [3] University of Vic-Central University of Catalonia (UVic-UCC), Vic, Spain, [4] National HIV and Retrovirology Laboratory, Public Health Agency of Canada, Winnipeg, MB, Canada, [5] Department of Medical Microbiology and Infectious Diseases, University of Manitoba, Winnipeg, MB, Canada, [6] Genomic Medicine, J. Craig Venter Institute, La Jolla, CA, United States

OPEN ACCESS

Edited by:
Christel Vérollet, UMR5089 Institut de Pharmacologie et de Biologie Structurale (IPBS), France

Reviewed by:
Paul Spearman, Cincinnati Children's Hospital Medical Center, United States
Masaaki Miyazawa, Kindai University, Japan

***Correspondence:**
Nuria Izquierdo-Useros
nizquierdo@irsicaixa.es

[†]These authors have contributed equally to this work.

Specialty section:
This article was submitted to Microbial Immunology, a section of the journal Frontiers in Immunology

Received: 14 August 2017
Accepted: 06 November 2017
Published: 21 November 2017

Citation:
Martinez-Picado J, McLaren PJ, Telenti A and Izquierdo-Useros N (2017) Retroviruses As Myeloid Cell Riders: What Natural Human Siglec-1 "Knockouts" Tell Us About Pathogenesis. Front. Immunol. 8:1593. doi: 10.3389/fimmu.2017.01593

Myeloid cells initiate immune responses and are crucial to control infections. In the case of retroviruses, however, myeloid cells also promote pathogenesis by enabling viral dissemination; a process extensively studied *in vitro* using human immunodeficiency virus type 1 (HIV-1). This viral hijacking mechanism does not rely on productive myeloid cell infection but requires HIV-1 capture *via* Siglec-1/CD169, a receptor expressed on myeloid cells that facilitates the infection of bystander target cells. Murine retroviruses are also recognized by Siglec-1, and this interaction is required for robust retroviral infection *in vivo*. Yet, the relative contribution of Siglec-1-mediated viral dissemination to HIV-1 disease progression remains unclear. The identification of human null individuals lacking working copies of a particular gene enables studying how this loss affects disease progression. Moreover, it can reveal novel antiviral targets whose blockade might be therapeutically effective and safe, since finding null individuals *in natura* uncovers dispensable functions. We previously described a loss-of-function variant in *SIGLEC*-1. Analysis of a large cohort of HIV-1-infected individuals identified homozygous and heterozygous subjects, whose cells were functionally null or partially defective for Siglec-1 activity in HIV-1 capture and transmission *ex vivo*. Nonetheless, analysis of the effect of Siglec-1 truncation on progression to AIDS was not conclusive due to the limited cohort size, the lack of complete clinical records, and the restriction to study only off-therapy periods. Here, we review how the study of loss-of-function variants might serve to illuminate the role of myeloid cells in viral pathogenesis *in vivo* and the challenges ahead.

Keywords: antigen-presenting cell, human immunodeficiency virus type 1, Siglec-1, knockout, genome, human

Antigen-presenting cells (APCs) of the myeloid lineage trigger innate and adaptive immune responses against invading viruses, thus modulating the outcome, progression, and clearance of infections (1, 2). Yet, chronic viral infections counteract several defenses orchestrated by APCs and exploit immunity to favor persistence. Infection caused by the human immunodeficiency virus type

Abbreviations: APCs, antigen-presenting cells; HIV-1, human immunodeficiency virus type 1; MLV, murine leukemia virus.

I (HIV-1) is one of the best-studied examples to illustrate this paradox, where APCs act as a double-edged sword throughout the course of infection. Myeloid APCs (such as dendritic cells, monocytes, and macrophages) are not as susceptible to HIV-1 infection as activated CD4+ T cells (3). This is likely due to host restriction factors such as SAMHD1 (4, 5) that restrict viral infection and decreases myeloid cell capacity for immune sensing (6), limiting the onset of antiviral responses. However, HIV-1 can exploit myeloid APC biology to reach and infect new target cells through a mechanism that does not rely on the productive infection of myeloid cells. This process was described *in vitro* at the early nineties by the laboratory of Dr. Ralph Steinman (7), who received the Nobel Prize for discovering dendritic cells. Despite decades of research though, there is no convincing *in vivo* evidence that demonstrates whether myeloid APCs play a critical role in HIV-1 disease progression.

Upon cellular activation, myeloid APCs can capture and store large numbers of HIV-1 particles (8–10), which are then efficiently transferred to bystander CD4+ T cells (7, 11, 12) *via* cell-to-cell interactions established as part of their immune surveillance routine. Throughout this process of retention and release of virus, HIV-1 exploits a mechanism by which APCs acquire antigens transported by extracellular secreted microvesicles termed exosomes (13). The acquisition of exosomes by activated myeloid APCs contributes to antigen presentation to CD4+ T cells (14). This step helps to amplify adaptive immunity without the need for myeloid APCs to be in direct contact with the pathogen (15, 16). Retention of exosomes within intracellular compartments might serve as an antigen depot to control and sustain adaptive immune responses. However, in the case of HIV-1, this internalization route retains infectious particles within protected dynamic compartments (17–19) from where viruses are efficiently transmitted across infectious synapses to susceptible lymphocytes (7, 11, 12).

This particular mode of HIV-1 transmission is known as *trans*-infection; a route that favors *de novo* infection of target cells under circumstances where the same dose of cell-free-viruses do not establish productive infection (11). *Trans*-infection is largely dependent on the expression of the sialic-acid binding I-type lectin receptor Siglec-1 (CD169 or Sialoadhesin) (20–22). Siglec-1 is an interferon inducible receptor constitutively expressed on myeloid cells (23), that is highly upregulated upon myeloid APC exposure to antiviral type I interferons (24, 25). Siglec-1 is a trans-membrane receptor with a long neck that protrudes beyond the glycocalyx of the cell and a terminal V-set domain with the ability to interact with sialylated ligands. While the affinity of Siglec-1 for sialic acid-containing molecules is low, avidity for clusters of sialylated molecules is high (23), allowing for the specific recognition of packaged gangliosides that expose sialyllactose moieties on the viral membrane (26, 27). Likewise, Siglec-1 captures exosomes *via* recognition of sialylated gangliosides packaged on the microvesicle membrane (21), which assemble and bud from cellular membranes. Murine studies have also confirmed the capacity of Siglec-1 expressed on lymphoid tissues to capture exosomes *in vivo* (28). Pioneering reports suggested that DC-SIGN, a C-type lectin expressed on immature DCs that patrol peripheral mucosae in search of invading pathogens, could capture HIV-1 early after viral invasion, travel to lymphoid tissues, and establish productive CD4+ T cell infection *via trans*-infection (11). While C-type lectins such as DC-SIGN recognize the viral envelope glycoprotein (11), capture of HIV-1 *via* Siglec-1 is independent of this interaction (10, 21). Siglec-1 viral uptake largely exceeds the capacity of C-type lectin receptors for HIV-1 capture (21), making this process much more infectious and underscoring novel scenarios within secondary lymphoid tissues in which Siglec-1 *trans*-infection could fuel viral dissemination.

The molecular pathways governing HIV-1 *trans*-infection *via* Siglec-1 on APCs have been described *in vitro* using both monocyte-derived APCs (20–22) and primary myeloid cells directly isolated from human tissues (25) (**Figure 1**). Another retrovirus, the murine leukemia virus (MLV), also contains sialylated gangliosides and is captured *via* Siglec-1 *in vitro* (29). MLV exploits Siglec-1-mediated *trans*-infection of permissive lymphocytes to establish infection within secondary lymphoid tissues in mice (30) (**Figure 1**). However, the *in vivo*

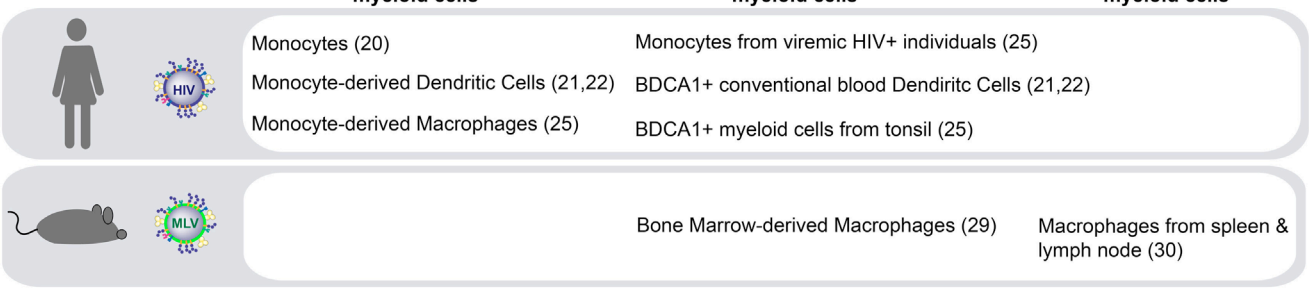


FIGURE 1 | Siglec-1-mediated retroviral *trans*-infection on distinct myeloid antigen-presenting cells (APCs). Human immunodeficiency virus type 1 (HIV-1) capture *via* Siglec-1 and subsequent transfer to target cells has been reported not only in human APCs derived *in vitro* but also in activated primary myeloid cells isolated *ex vivo*. In murine models, Siglec-1 retroviral *trans*-infection has been reported *ex vivo*, and most importantly, due to the extraordinary ability of Siglec-1 positive APCs to capture cell-free viruses from the lymphatic vessels at the edges of the lymphoid tissue and their capacity to transfer that infectivity to permissive lymphocytes, this mechanism has also been observed *in vivo*.

contribution of Siglec-1 to HIV-1 disease progression remains largely unknown.

The lack of available animal models to study HIV-1 infection makes it challenging to investigate the role of Siglec-1 on HIV-1 pathogenesis *in vivo*. Humanized mouse models susceptible to HIV-1 infection are only established in a few laboratories, and how disease progression in these animals correlates with human pathogenesis needs further investigation. Primate models are also restricted to specific facilities and rely on the use of primate retroviruses that may not directly reflect the biology of HIV-1. Under these circumstances, finding naturally occurring human knockouts could be a good alternative to address the role of key receptors such as Siglec-1 under physiological settings of infection. A deletion in the gene that codes for the HIV-1 co-receptor CCR5, which is needed for acquisition of CCR5-tropic HIV-1, is one of the best-known examples of how a genetic variant alters the phenotype of infection (31). These types of variants have been observed for decades and have also been confirmed by large-scale genomic analysis (32). However, these large-scale analyses have not uncovered novel candidates that might influence HIV-1 disease progression because the available sample sizes are not adequate to assess all possible classes of genetic variation, such as rare and low frequency polymorphisms.

The identification of individuals harboring rare, loss-of-function genetic variants provides an opportunity to study gene function *in vivo*. Recently, large catalogs of sequenced human genomes have demonstrated that individuals carrying homozygous loss-of-function variants, or natural human knockouts, can provide insight into genetic causes of disease and holds tremendous potential for identifying drug targets (33). However, given their generally low frequency, such variants have gone largely undetected in large-scale genomic analyses. As an alternative strategy to identify genes involved in HIV-1 progression, we conducted a search for individuals lacking the expression of Siglec-1 receptor to study the natural course of HIV-1 infection in the absence of this particular receptor (34). We focused on two well-established cohorts of HIV-1 infected individuals that had been longitudinally followed for decades and had extensive clinical records. We identified two homozygous and almost a 100 heterozygous subjects for a particular stop codon variant in the *SIGLEC1* gene. This stop-gain allele is found at highest frequency in individuals of European and South Asian ancestry (1.3%) and is rare or absent in African and East Asian populations (0.5%). *Ex vivo* experiments confirmed that cells from these individuals were functionally null or partially defective for Siglec-1 expression and, consequently, lost their activity in HIV-1 capture and transmission *in vitro*. While the lack of Siglec-1 is likely to abrogate *trans*-infection, the classical HIV-1 infection routes, including cell-free virus infection or cell-to-cell HIV-1 transmission still operate in the absence of Siglec-1, explaining the observation of Siglec-1 null individuals that are HIV-1 infected. However, despite the lack of impact on susceptibility, HIV-1 dissemination and disease progression in infected individuals with null or diminished Siglec-1 expression could be delayed compared with wild type individuals. Nonetheless, we did not observe an effect of Siglec-1 truncation on progression to AIDS.

Several challenges explain the lack of conclusive results in the study of Siglec-1 genetic variants (**Figure 2**). Power simulations indicate that analysis of a rare variant such as the Siglec-1 allele would require more than 10,000 individuals to detect a relative risk of 5 at $P < 0.05$ under a recessive model—an effect that would be similar to the beneficial outcome of B*57:01 on HIV-1 control (32, 35–37). This sample size far exceeds even the largest genome-wide studies of HIV-1 progression that comprises ~6,000 patients (38), which does not genotype the Siglec-1 stop variant and cannot be used to impute the presence of this rare allele. Given that the proposed effect requires long-term follow-up off therapy, it is extremely unlikely that a sufficient sample size could be reached to assess the long-term consequences of the Siglec-1 stop variant on HIV-1 disease. Another limitation faced was the lack of seroconversion date for most of the individuals screened; a clinical record that is normally missing in most cohorts of HIV-1 infected individuals. Thus, disease progression was only followed from the date of diagnosis, which may differ between individuals, especially if they are protected by beneficial phenotypes. Moreover, additional clinical data were missing from key individuals, even though we had focused on cohorts with exhaustive follow-up. Indeed, one of the homozygous individuals found had no clinical records for nine years, and information only resumed after antiretroviral treatment initiation, when viral suppression abrogated any potential effect that the Siglec-1 variant might have had on disease progression. Since current clinical guidelines recommend treatment introduction early after HIV-1 diagnosis (39), in the near future this type of analyses will be restricted to retrospective cohorts, which followed old recommendations and started treatment when CD4 counts dropped below a certain threshold, offering a window of opportunity to monitor the natural course of infection. Finally, complexity also arises from the analysis of phenotypes that can be influenced by the infection of several pathogens at the same time. Indeed, one of the homozygous individuals for the rare Siglec-1 allele had a high $CD4^+$ T cell count that dramatically dropped when tuberculosis was diagnosed. Lack of Siglec-1 could have had a negative impact on the immune control of the mycobacterial infection, masking any putative beneficial effects caused during HIV-1 progression. Previous studies indicate that Siglec-1 expression on myeloid APCs has a role in combating sialylated bacteria (40, 41). Although sialylation of *Mycobacteria* has not been documented to our knowledge, direct interaction between Siglec-1 and *Mycobacteria* might not be required to impact antibacterial immunity. Alternatively, the lack of Siglec-1 on myeloid APCs could compromise antigen capture *via* exosome or microvesicle transfer and affect the control of the bacterial infection (42–45).

Overall, difficulties and questions faced throughout the study of Siglec-1 null individuals infected with HIV-1 illustrate the major challenges of the field of human knockout genetics applied to infectious diseases. We need to address the biological function of knockout genes of interest *in vivo* and the effect of a particular variant on health-related phenotypes (46). Variability in the observed phenotypes arises not only from the effect that other genetic variants might have on the gene of interest, but also from the exposure to particular environmental conditions,

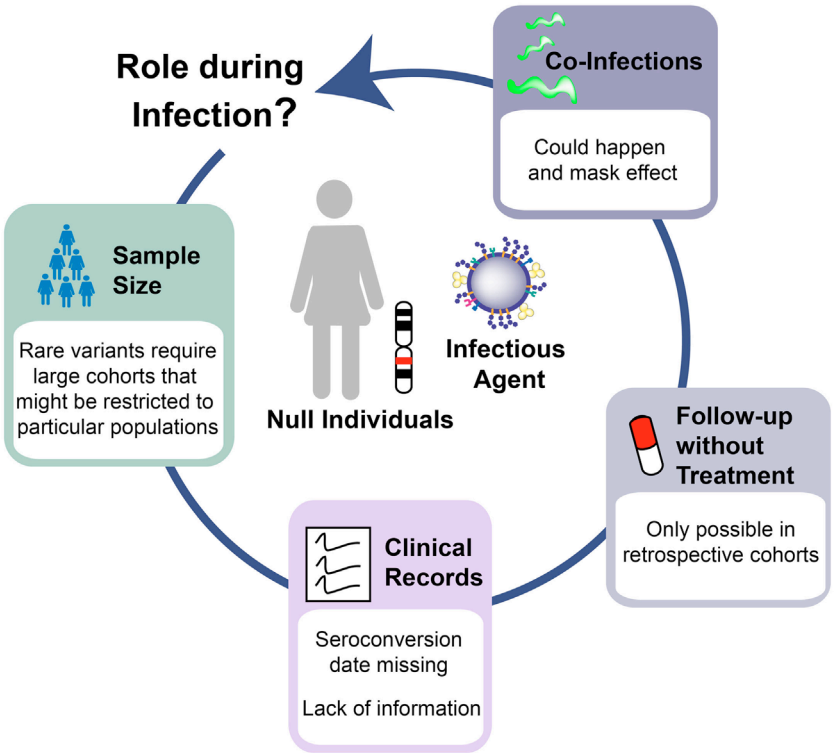


FIGURE 2 | Challenges to interpret human knockout genetics in infectious diseases. The study of Siglec-1 null individuals infected with human immunodeficiency virus type 1 highlights the barriers to understand the *in vivo* role of human knockout genes. Limitations arises from: the need to study large cohorts that can be restricted to specific populations where the variant of interest has the highest frequency; the lack of critical clinical information even in cohorts with good follow-up; the introduction of therapies that unmask any putative effect of the studied variant; and the co-infection with additional pathogens that might influence the observed phenotype in the opposite direction from what is expected.

including the co-occurrence of infections. Animal studies could help to dissect the contribution of these factors by creating the same genetic background and similar environmental conditions in pathogen-free facilities, where co-infections could be experimentally controlled. Working with adequate animal models is, however, complex in the case of HIV-1. An interesting alternative to unambiguously test the potential contribution of myeloid APCs *via* Siglec-1 to HIV-1 disease progression could be to develop antiviral therapeutic agents against Siglec-1. The identification of Siglec-1 null individuals demonstrates that this protein is dispensable, and its therapeutic blockade is therefore expected not to cause serious side effects. Future work targeting Siglec-1 could provide conclusive evidence of the real contribution of myeloid APC to HIV-1 pathogenesis *in vivo*. If proven effective, this new family of antiviral agents against HIV-1 could also offer protection against other retroviral infections by mimicking the loss-of-function mutation found in *SIGLEC1*.

AUTHOR CONTRIBUTIONS

JM-P, PM, AT, and NI-U designed the work, prepared the figures, reviewed bibliography, and prepared the manuscript. All the authors approved the final version.

ACKNOWLEDGMENTS

The authors are grateful to Dr. M. C. Puertas for critical reading of the manuscript. The authors would like to apologize to all those researchers whose work and contributions were not cited due to space limitations.

FUNDING

JM-P and NI-U are supported by the Spanish Secretariat of Science and Innovation through Grant SAF2016-80033-R.

REFERENCES

1. Banchereau J, Steinman RM. Dendritic cells and the control of immunity. *Nature* (1998) 392:245–52. doi:10.1038/32588
2. Steinman RM, Banchereau J. Taking dendritic cells into medicine. *Nature* (2007) 449:419–26. doi:10.1038/nature06175
3. Wu L, KewalRamani VN. Dendritic-cell interactions with HIV: infection and viral dissemination. *Nat Rev Immunol* (2006) 6:859–68. doi:10.1038/nri1960
4. Hrecka K, Hao C, Gierszewska M, Swanson SK, Kesik-Brodacka M, Srivastava S, et al. Vpx relieves inhibition of HIV-1 infection of macrophages mediated by the SAMHD1 protein. *Nature* (2011) 474:658–61. doi:10.1038/nature10195

5. Laguette N, Sobhian B, Casartelli N, Ringeard M, Chable-Bessia C, Ségéral E, et al. SAMHD1 is the dendritic- and myeloid-cell-specific HIV-1 restriction factor counteracted by Vpx. *Nature* (2011) 474:654–7. doi:10.1038/nature10117
6. Manel N, Hogstad B, Wang Y, Levy DE, Unutmaz D, Littman DR. A cryptic sensor for HIV-1 activates antiviral innate immunity in dendritic cells. *Nature* (2010) 467:214–7. doi:10.1038/nature09337
7. Cameron PU, Freudenthal PS, Barker JM, Gezelter S, Inaba K, Steinman RM. Dendritic cells exposed to human immunodeficiency virus type-1 transmit a vigorous cytopathic infection to CD4+ T cells. *Science* (1992) 257:383–7. doi:10.1126/science.1352913
8. Sanders RW, de Jong EC, Baldwin CE, Schuitemaker JHN, Kapsenberg ML, Berkhout B. Differential transmission of human immunodeficiency virus type 1 by distinct subsets of effector dendritic cells. *J Virol* (2002) 76:7812–21. doi:10.1128/JVI.76.15.7812-7821.2002
9. Wang JH, Janas AM, Olson WJ, Wu L. Functionally distinct transmission of human immunodeficiency virus type 1 mediated by immature and mature dendritic cells. *J Virol* (2007) 81:8933–43. doi:10.1128/JVI.00878-07
10. Izquierdo-Useros N, Blanco J, Erkizia I, Fernández-Figueras MT, Borràs FE, Naranjo-Gómez M, et al. Maturation of blood-derived dendritic cells enhances human immunodeficiency virus type 1 capture and transmission. *J Virol* (2007) 81:7559–70. doi:10.1128/JVI.02572-06
11. Geijtenbeek TB, Kwon DS, Torensma R, van Vliet SJ, van Duijnhoven GC, Middel J, et al. DC-SIGN, a dendritic cell-specific HIV-1-binding protein that enhances trans-infection of T cells. *Cell* (2000) 100:587–97. doi:10.1016/S0092-8674(00)80694-7
12. McDonald D, Wu L, Bohks SM, KewalRamani VN, Unutmaz D, Hope TJ. Recruitment of HIV and its receptors to dendritic cell-T cell junctions. *Science* (2003) 300:1295–7. doi:10.1126/science.1084238
13. Izquierdo-Useros N, Naranjo-Gómez M, Archer J, Hatch SC, Erkizia I, Blanco J, et al. Capture and transfer of HIV-1 particles by mature dendritic cells converges with the exosome-dissemination pathway. *Blood* (2009) 113:2732–41. doi:10.1182/blood-2008-05-158642
14. Théry C, Duban L, Segura E, Véron P, Lantz O, Amigorena S. Indirect activation of naïve CD4+ T cells by dendritic cell-derived exosomes. *Nat Immunol* (2002) 3:1156–62. doi:10.1038/ni854
15. Théry C, Zitvogel L, Amigorena S. Exosomes: composition, biogenesis and function. *Nat Rev Immunol* (2002) 2:569–79. doi:10.1038/nri855
16. Théry C, Ostrowski M, Segura E. Membrane vesicles as conveyors of immune responses. *Nat Rev Immunol* (2009) 9:581–93. doi:10.1038/nri2567
17. Yu HJ, Reuter MA, McDonald D. HIV traffics through a specialized, surface-accessible intracellular compartment during trans-infection of T cells by mature dendritic cells. *PLoS Pathog* (2008) 4:e1000134. doi:10.1371/journal.ppat.1000134
18. Izquierdo-Useros N, Esteban O, Rodriguez-Plata MT, Erkizia I, Prado JG, Blanco J, et al. Dynamic imaging of cell-free and cell-associated viral capture in mature dendritic cells. *Traffic* (2011) 12:1702–13. doi:10.1111/j.1600-0854.2011.01281.x
19. Akiyama H, Ramirez NG, Gudheti MV, Gummuluru S. CD169-mediated trafficking of HIV to plasma membrane invaginations in dendritic cells attenuates efficacy of anti-gp120 broadly neutralizing antibodies. *PLoS Pathog* (2015) 11:e1004751. doi:10.1371/journal.ppat.1004751
20. Rempel H, Calosing C, Sun B, Pulliam L. Sialoadhesin expressed on IFN-induced monocytes binds HIV-1 and enhances infectivity. *PLoS One* (2008) 3:e1967. doi:10.1371/journal.pone.0001967
21. Izquierdo-Useros N, Lorizate M, Puertas MC, Rodriguez-Plata MT, Zangger N, Erikson E, et al. Siglec-1 is a novel dendritic cell receptor that mediates HIV-1 trans-infection through recognition of viral membrane gangliosides. *PLoS Biol* (2012) 10:e1001448. doi:10.1371/journal.pbio.1001448
22. Puryear WB, Akiyama H, Geer SD, Ramirez NP, Yu X, Reinhard BM, et al. Interferon-inducible mechanism of dendritic cell-mediated HIV-1 dissemination is dependent on Siglec-1/CD169. *PLoS Pathog* (2013) 9:e1003291. doi:10.1371/journal.ppat.1003291
23. Crocker PR, Paulson JC, Varki A. Siglecs and their roles in the immune system. *Nat Rev Immunol* (2007) 7:255–66. doi:10.1038/nri2056
24. van der Kuyl AC, van den Burg R, Zorgdrager F, Groot F, Berkhout B, Cornelissen M. Sialoadhesin (CD169) expression in CD14+ cells is upregulated early after HIV-1 infection and increases during disease progression. *PLoS One* (2007) 2:e257. doi:10.1371/journal.pone.0000257
25. Pino M, Erkizia I, Benet S, Erikson E, Fernández-Figueras MT, Guerrero D, et al. HIV-1 immune activation induces Siglec-1 expression and enhances viral trans-infection in blood and tissue myeloid cells. *Retrovirology* (2015) 12:37. doi:10.1186/s12977-015-0160-x
26. Izquierdo-Useros N, Lorizate M, Contreras F-X, Rodriguez-Plata MT, Glass B, Erkizia I, et al. Sialyllactose in viral membrane gangliosides is a novel molecular recognition pattern for mature dendritic cell capture of HIV-1. *PLoS Biol* (2012) 10:e1001315. doi:10.1371/journal.pbio.1001315
27. Puryear WB, Yu X, Ramirez NP, Reinhard BM, Gummuluru S. HIV-1 incorporation of host-cell-derived glycosphingolipid GM3 allows for capture by mature dendritic cells. *Proc Natl Acad Sci U S A* (2012) 109:7475–80. doi:10.1073/pnas.1201104109
28. Saunderson SC, Dunn AC, Crocker PR, McLellan AD. CD169 mediates the capture of exosomes in spleen and lymph node. *Blood* (2013) 123:208–16. doi:10.1182/blood-2013-03-489732
29. Erikson E, Wratil PR, Frank M, Ambiel I, Pahnke K, Claveria MP, et al. Mouse Siglec-1 mediates trans-infection of surface-bound murine leukemia virus in a sialic acid N-acyl side chain-dependent manner. *J Biol Chem* (2015) 290:27345–59. doi:10.1074/jbc.M115.681338
30. Sewald X, Ladinsky MS, Uchil PD, Beloor J, Pi R, Herrmann C, et al. Retroviruses use CD169-mediated trans-infection of permissive lymphocytes to establish infection. *Science* (2015) 350:563–7. doi:10.1126/science.aab2749
31. Dean M, Carrington M, Winkler C, Huttley GA, Smith MW, Allikmets R, et al. Genetic restriction of HIV-1 infection and progression to AIDS by a deletion allele of the CKR5 structural gene. Hemophilia growth and development study, multicenter AIDS cohort study, multicenter hemophilia cohort study, San Francisco city cohort, ALIVE study. *Science* (1996) 273:1856–62.
32. Fellay J, Shianna KV, Ge D, Colombo S, Ledergerber B, Weale M, et al. A whole-genome association study of major determinants for host control of HIV-1. *Science* (2007) 317:944–7. doi:10.1126/science.1143767
33. István B, di Iulio J, Venter JC, Telenti A. Human gene essentiality. *Nat Rev Genet* (2017). doi:10.1038/nrg.2017.75
34. Martinez-Picado J, McLaren PJ, Erkizia I, Martin MP, Benet S, Rotger M, et al. Identification of Siglec-1 null individuals infected with HIV-1. *Nat Commun* (2016) 7:12412. doi:10.1038/ncomms12412
35. Kaslow RA, Carrington M, Apple R, Park L, Muñoz A, Saah AJ, et al. Influence of combinations of human major histocompatibility complex genes on the course of HIV-1 infection. *Nat Med* (1996) 2:405–11. doi:10.1038/nm0496-405
36. Fellay J, Ge D, Shianna KV, Colombo S, Ledergerber B, Cirulli ET, et al. Common genetic variation and the control of HIV-1 in humans. *PLoS Genet* (2009) 5:e1000791. doi:10.1371/journal.pgen.1000791
37. International HIV Controllers Study, Pereyra F, Jia X, McLaren PJ, Telenti A, de Bakker PI, et al. The major genetic determinants of HIV-1 control affect HLA class I peptide presentation. *Science* (2010) 330:1551–7. doi:10.1126/science.1195271
38. McLaren PJ, Coulonges C, Bartha I, Lenz TL, Deutsch AJ, Bashirova A, et al. Polymorphisms of large effect explain the majority of the host genetic contribution to variation of HIV-1 virus load. *Proc Natl Acad Sci U S A* (2015) 112:14658–63. doi:10.1073/pnas.1514867112
39. World Health Organization. *Guidelines for Managing Advanced HIV Disease and Rapid Initiation of Antiretroviral Therapy*. Geneva: World Health Organization (2017).
40. Klaas M, Oetke C, Lewis LE, Erwig LP, Heikema AP, Easton A, et al. Sialoadhesin promotes rapid proinflammatory and type I IFN responses to a sialylated pathogen, *Campylobacter jejuni*. *J Immunol* (2012) 189:2414–22. doi:10.4049/jimmunol.1200776
41. Jones C, Virji M, Crocker PR. Recognition of sialylated meningococcal lipopolysaccharide by siglecs expressed on myeloid cells leads to enhanced bacterial uptake. *Mol Microbiol* (2003) 49:1213–25. doi:10.1046/j.1365-2958.2003.03634.x
42. Bhatnagar S, Shinagawa K, Castellino FJ, Schorey JS. Exosomes released from macrophages infected with intracellular pathogens stimulate a proinflammatory response in vitro and in vivo. *Blood* (2007) 110:3234–44. doi:10.1182/blood-2007-03-079152
43. Ramachandra L, Qu Y, Wang Y, Lewis CJ, Cobb BA, Takatsu K, et al. *Mycobacterium tuberculosis* synergizes with ATP to induce release of microvesicles and exosomes containing major histocompatibility complex class II molecules capable of antigen presentation. *Infect Immun* (2010) 78:5116–25. doi:10.1128/IAI.01089-09

44. Singh PP, Smith VL, Karakousis PC, Schorey JS. Exosomes isolated from mycobacteria-infected mice or cultured macrophages can recruit and activate immune cells in vitro and in vivo. *J Immunol* (2012) 189:777–85. doi:10.4049/jimmunol.1103638
45. Cheng Y, Schorey JS. Exosomes carrying mycobacterial antigens can protect mice against *Mycobacterium tuberculosis* infection. *Eur J Immunol* (2013) 43:3279–90. doi:10.1002/eji.201343727
46. Narasimhan VM, Xue Y, Tyler-Smith C. Human knockout carriers: dead, diseased, healthy, or improved? *Trends Mol Med* (2016) 22:341–51. doi:10.1016/j.molmed.2016.02.006

Conflict of Interest Statement: The authors declare that the research was conducted in the absence of any commercial or financial relationships that could be construed as a potential conflict of interest.

Copyright © 2017 Martinez-Picado, McLaren, Telenti and Izquierdo-Useros. This is an open-access article distributed under the terms of the Creative Commons Attribution License (CC BY). The use, distribution or reproduction in other forums is permitted, provided the original author(s) or licensor are credited and that the original publication in this journal is cited, in accordance with accepted academic practice. No use, distribution or reproduction is permitted which does not comply with these terms.

frontiers in Immunology

METHODS
published: 28 September 2017
doi: 10.3389/fimmu.2017.01222

Functional Analysis of Phagocyte Activity in Whole Blood from HIV/Tuberculosis-Infected Individuals Using a Novel Flow Cytometry-Based Assay

Ankur Gupta-Wright[1,2†], Dumizulu Tembo[3†], Kondwani C. Jambo[1,4], Elizabeth Chimbayo[1], Leonard Mvaya[1], Shannon Caldwell[3], David G. Russell[3*] and Henry C. Mwandumba[1,4]*

[1] College of Medicine, Malawi-Liverpool-Wellcome Trust Clinical Research Programme, Blantyre, Malawi, [2] Clinical Research Department, London School of Hygiene and Tropical Medicine, London, United Kingdom, [3] Department of Microbiology and Immunology, College of Veterinary Medicine, Cornell University, Ithaca, NY, United States, [4] Department of Clinical Sciences, Liverpool School of Tropical Medicine, Liverpool, United Kingdom

OPEN ACCESS

Edited by:
Christel Vérollet,
UMR5089 Institut de Pharmacologie et de Biologie Structurale (IPBS), France

Reviewed by:
Anca Dorhoi,
Friedrich Loeffler Institute Greifswald, Germany
Roberta Olmo Pinheiro,
Oswaldo Cruz Foundation, Brazil

***Correspondence:**
Ankur Gupta-Wright
ankurgw@outlook.com;
David G. Russell
dgr8@cornell.edu

†These authors have contributed equally to this work.

Specialty section:
This article was submitted to Microbial Immunology, a section of the journal Frontiers in Immunology

Received: 11 August 2017
Accepted: 15 September 2017
Published: 28 September 2017

Citation:
Gupta-Wright A, Tembo D, Jambo KC, Chimbayo E, Mvaya L, Caldwell S, Russell DG and Mwandumba HC (2017) Functional Analysis of Phagocyte Activity in Whole Blood from HIV/Tuberculosis-Infected Individuals Using a Novel Flow Cytometry-Based Assay. Front. Immunol. 8:1222. doi: 10.3389/fimmu.2017.01222

The accurate assessment of immune competence through *ex vivo* analysis is paramount to our understanding of those immune mechanisms that lead to protection or susceptibility against a broad range of human pathogens. We have developed a flow cytometry-based, whole blood phagocyte functional assay that utilizes the inflammatory inducer zymosan, coupled to OxyBURST-SE, a fluorescent reporter of phagosomal oxidase activity. The assay measures both phagocytic uptake and the superoxide burst in the phagocyte populations in whole blood. We utilized this assay to demonstrate impaired superoxide burst activity in the phagocytes of hospitalized HIV-positive patients with laboratory-confirmed tuberculosis. These data validate the use of the assay to assess the immune competence of patients in a clinical setting. The method is highly reproducible with minimal intraindividual variation and opens opportunities for the rapid assessment of cellular immune competence in peripheral blood in a disease setting.

Keywords: phagocytosis, zymosan, inflammation, monocytes, neutrophils, HIV, tuberculosis, whole blood assay

INTRODUCTION

Bacterial killing assays in whole blood are well established and allow *ex vivo* assessment of immune function in patients, particularly in the context of assessing response to vaccines or evaluating new bactericidal therapies (1–4). The main read out of these assays is microbial killing measured *via* culture and colony counting, or fluorescence if reporter strain organisms are used.

Potential problems of these microbiological killing assays include difficulties in standardizing the number of microbes and their multiplication rate. The tendency of the microbes to aggregate inconsistently during assays may also result in misrepresentation of the actual numbers of microbes measured at the end of the assay. In addition, there are other factors that can result in microbial loss that are not dependent on the host immune response or antimicrobial therapy (5). Finally, because the read out is simply bacterial survival, these assays lack the ability to differentiate mechanisms of killing and the relative contributions of the different phagocyte lineages present in the blood.

Phagocytosis is an important mechanism in the microbial killing pathway of phagocytes. Deficiencies in phagocyte function likely predispose individuals to acquire or succumb to infectious diseases. An extensive range of dynamic assays of phagosome function have been developed that are capable of providing a broad range of physiological readouts from the phagosome (6, 7).

These assays have mostly utilized inert beads derivatized with different fluorescent reporters and focused on human alveolar macrophages or murine bone marrow-derived macrophages in culture (8–10). By removing cells from whole blood or their usual tissue fluid, we are unable to assess the potentially important influence of soluble proteins such as cytokines, chemokines, or antibodies on phagocytosis and phagosomal behavior. We therefore sought to develop an assay using a reporter particle more suitable for probing phagocyte biology in whole blood. The assay is designed to provide reproducible, unbiased, real-time analysis of phagosomal function of immune cells and potentially identify patients with impaired immune responses.

We utilized zymosan derivatized with the oxidation-sensitive fluorescent reporter, OxyBURST-SE, to quantify phagosomal oxidase activity in peripheral blood phagocytes *in situ*. Zymosan is a preparation of a cell wall glucan from *Saccharomyces cerevisiae* that has been used as a model microbial particle in immune assays for over half a century (11). Zymosan is highly mannosylated and linked to β-glucan, making it susceptible to phagocytosis by monocytes, polymorphonuclear leukocytes, and macrophages through various receptors, including C-type lectin receptors such as dectin-1 and mannose receptors (12, 13). Phagocytosis of zymosan can occur independent of opsonization, of which complement factor 3 (C3) predominates with immunoglobulin G (IgG) being of minor importance (14). Zymosan also stimulates an inflammatory cytokine response *via* toll-like receptors (TLR) 2 and 6, although activation of these receptors is not required for internalization by phagocytes (12). We had demonstrated previously how inert particles coupled to OxyBURST-SE can be used to quantify the superoxide bust of murine macrophages *in vitro* (15).

Superoxide burst is one of the key enzymatic activities involved in killing microbes during the process of phagocytosis. The generation of oxygen radicals *via* nicotinamide adenine dinucleotide phosphate (NADPH) oxidase leads to the production of noxious compounds such as hydrogen peroxide with potent antimicrobial activity (16, 17). Superoxide burst's importance is clearly demonstrated by the greatly increased risk of bacterial, fungal, and mycobacterial infection in patient with chronic granulomatous disease due to mutations in NADPH oxidase (18). It has also been shown to be suppressed in individuals with HIV infection (19) and by *Mycobacterium tuberculosis* (TB) infection *in vitro* (20).

In this study, we report the application of this novel reporter platform to quantify the phagocytic and superoxide burst functions of phagocytes in whole blood obtained from individuals in a clinical setting. First, we detail the information generated by application of the assay in whole blood from healthy controls. We then present data showing the utility of this assay in demonstrating the perturbation of phagocyte function in the blood from HIV- and TB-coinfected patients in Malawi.

MATERIALS AND METHODS

Study Population

Adult patients with HIV and tuberculosis coinfection (HIV-TB) were recruited as part of a sub-study examining immune responses in the Malawi arm of the rapid urine-based screening for TB to reduce AIDS-related mortality in hospitalized patients in Africa (STAMP) (21). Healthy HIV-negative adults with no evidence of active TB were also recruited as controls. 5 ml of blood was collected from both patients and controls in sodium heparin tubes. All samples were processed and analyzed by flow cytometry at the Malawi-Liverpool-Wellcome Trust Clinical Research Programme in Blantyre, Malawi within 2 h of blood draw. The study has been approved by the London School of Hygiene & Tropical Medicine Research Ethics Committee and the College of Medicine Research Ethics Committee, Malawi.

Zymosan Reporter Particles

To quantify both phagocytic activity and the magnitude of the superoxide burst we utilized zymosan particles coupled to both a calibration fluorochrome (Alexa Fluor 405-SE, Invitrogen) and an oxidation-sensitive fluorescent reporter (OxyBURST® Green H_2DCFDA-SE, Invitrogen). Zymosan reporter particles were prepared by washing 6 mg of zymosan (Sigma-Aldrich) three times in 1× phosphate-buffered saline (PBS) by centrifugation at 10,000 rpm for 1 min. Particles were resuspended in 950 µl coupling buffer (0.1 M boric acid to pH 8.0 with NaOH) containing 10 µl of 25 mg/ml OxyBURST-SE/DMSO stock solution and 5 µl of 5 mg/ml Alexa Fluor 405-SE/DMSO solution. The particles were mixed well and incubated on a tube rocker in the dark for 1 h at room temperature and washed with 1 ml of coupling buffer. The 1 h coupling with OxyBURST-SE and calibration fluorochrome was repeated twice. Finally, particles were washed three times with PBS and stored in 1 ml of PBS containing 0.01% sodium azide in the dark at 4°C generating a final stock concentration of approximately 5×10^6 particles/ml.

Whole Blood Assay

Zymosan reporter particles were prepared for the whole blood assay by washing 50 µl of stock Zymosan particle suspensions three times with 1 ml of RPMI-1640 to remove sodium azide and resuspended in 250 µl RPMI-1640 to give a 1:6 dilution and a final concentration of approximately 8×10^5 particles/ml.

Whole blood was diluted 1:1 with warm RPMI-1640. 20 µl of washed and diluted reporter particles (containing approximately 2×10^4 particles) were added to 1 ml of diluted blood and incubated at 37°C with rocking to ensure particles and cells remain in suspension. Diluted blood without zymosan reporter particles was also processed in parallel as control. Phagocytosis of zymosan reporter particles and superoxide burst was assessed at 10, 30, 60, 90, and 180 min after the addition of reporter particles.

100 µl of diluted blood was harvested from the zymosan reporter and biological control tubes 10 min before each time point for cell surface staining (as phagocytosis continues during cell surface staining of live cells). Once harvested, the diluted blood was stained with appropriately titrated concentrations of antibodies (anti-CD45 PerCP 1:33, anti-CD66b APC 1:50, and anti-CD14 PE-Cy7 1:100; all from BioLegend) for 10 min. Biological activity was arrested, red blood cells were lysed, and leukocytes fixed by adding 3 ml of BD FACS lysing solution (BD Biosciences), containing formaldehyde and diethylene glycol, to each tube and incubating at room temperature for 10 min.

The cells were washed once with 1× PBS by centrifugation at 500 *g* for 10 min then resuspended in 500 µl 1× PBS. Counting beads (Countbright, Life Technologies) were added per the manufacturer's instruction before acquisition on a CyAn ADP flow cytometer (Beckman Coulter, USA). The phagocytosis assay was performed in triplicate on the whole blood samples from healthy, HIV-negative adults. Data were analyzed using FlowJo version 10 (Treestar, USA).

In addition to the zymosan reporter assay, for HIV/TB-coinfected patients, immunophenotyping of monocytes in fresh whole blood was undertaken to investigate the association between monocyte phenotype and phagocytosis. In brief, 100 µl of fresh whole blood was stained with anti-CD45 Pacific Orange (Invitrogen), anti-HLA-DR PE-Cy7, anti-CD14 PE, and anti-CD16 FITC (all from BioLegend) for 10 min. Red blood cells were lysed, and leukocytes fixed with BD FACS lysing solution, washed once with 1× PBS by centrifugation at 500 *g* for 10 min then resuspended in 300 µl PBS for flow cytometry acquisition.

Electron Microscopy (EM)

In parallel, 2 ml of whole blood from a healthy HIV-negative control was incubated with approximately 8×10^4 zymosan reporter particles to confirm the zymosan particles were internalized by whole blood phagocytes. White blood cells were harvested after 10, 60, and 180 min by centrifugation at 500 *g* for 10 min and carefully pipetting out the buffy coat layer in buffered glutaraldehyde fixative solution (2.5% glutaraldehyde in 0.1 M sodium cacodylate, 5 mM $CaCl_2$, 5 mM $MgCl_2$, 0.1 M sucrose, pH 7.2). The samples were processed and stained for EM as described previously (22).

Calculations and Statistical Analysis

The proportion of cells that had phagocytosed reporter particles was calculated based on expression of calibration fluorochrome, and absolute cell numbers calculated using counting beads. An "activity index" of phagocytosis and superoxide burst was calculated by subtracting the median fluorescence intensity of the negative cells from the positive cells, and dividing this by two times the robust SD of the negative cells (23). This method accounted for variations in auto fluorescence between cells from different individuals.

Statistical analysis was performed using GraphPad Prism 7 (GraphPad Software, USA) and Stata 11 (StataCorp, USA). Peak activity index (AI) was calculated and mean AI was compared between groups. The AI at each time point was also used to calculate the area under the curve. Means were compared using paired *t*-tests and median using Wilcoxon rank-sum.

RESULTS/DISCUSSION

Zymosan Uptake by Whole Blood Phagocytes

We used whole blood from four healthy HIV-negative controls to measure phagocytosis and superoxide burst of phagocytes *ex vivo* using zymosan-reporter particles. We first sought to determine the kinetics of zymosan uptake by whole blood phagocytes. The flow cytometry gating strategy to identify neutrophils and monocytes is outlined in **Figure 1**. Cells that had phagocytosed zymosan-reporter particles were identified and quantified through measurement of the calibration fluor, Alexa Fluor 405.

Zymosan particles were avidly internalized by both neutrophils and monocytes in blood from healthy controls. Uptake was rapid, with a mean of 26% of neutrophils phagocytosing the particles compared with 12% of monocytes by 30 min (**Figure 2A**). The proportion of neutrophils phagocytosing zymosan did not increase substantially between 30 and 180 min, whereas the percentage of monocytes associated with zymosan-reporter particles increased gradually during the assay. This pattern of uptake was consistent across all healthy controls.

The uptake of zymosan reporter particles by both monocytes and neutrophils is dose dependent as shown in the dose–response curve generated for 0.5×10^4–8×10^4 zymosan particles/ml (**Figure 2B**). The abundance of the phagocytic cells in whole blood also influences the overall proportion of cells phagocytosing zymosan particles (**Figure 2C**). The higher the concentration of cells, the lower the proportion of cells carrying the zymosan-reporter signal, shown for both neutrophils and monocytes (**Figures 2D,E**). This relationship persists throughout the assay and demonstrates the importance of the phagocyte to particle ratio in the kinetics of phagocytosis. Relying solely on internalization of particles to assess phagocytic function is a potential limitation of the assay, as the magnitude of phagocytosis may be influenced by a function of cell concentration and/or cell to particle ratio, rather than cellular deficiencies in phagocytic capacity.

Electron microscopy of white blood cells from a healthy control whole blood incubated with zymosan particles demonstrates phagocytosis of zymosan particles by peripheral blood phagocytes (**Figure 3**). The EM images support the assumption that the zymosan reporter signal detected by flow cytometry originates from phagocytosis rather than the association of zymosan particles with the phagocyte surface. Almost without exception, the zymosan particles were observed inside the phagocyte.

Cell Loss Associated With Zymosan

To examine the effect of the zymosan particles on cell loss, we compared the samples containing zymosan reporter particles and control samples from the same healthy individuals. The mean concentration of neutrophils and monocytes declined during the assay more rapidly in the presence of zymosan than in control samples, with the largest decline occurring between 90 and 180 min (**Figures 4A,B**).

Furthermore, the concentration of neutrophils associated with zymosan-reporter signal peaked at 60 min, followed by a decline (**Figure 4A**). By contrast, the concentration of zymosan-associated monocytes plateaus at 30 min (**Figure 4B**). However, in both cell types the peak in zymosan uptake coincided with cell loss, suggesting that zymosan plays a role in inducing cell death. This is also supported by increased cell loss at higher concentrations of zymosan in the assay (**Figure 2B**).

These observations are consistent with neutrophil and monocyte biology. Neutrophils are known to have a short half-life *in vitro*, estimated to be 6–12 h, and do not proliferate (24). Programmed cell death of neutrophils occurs rapidly following

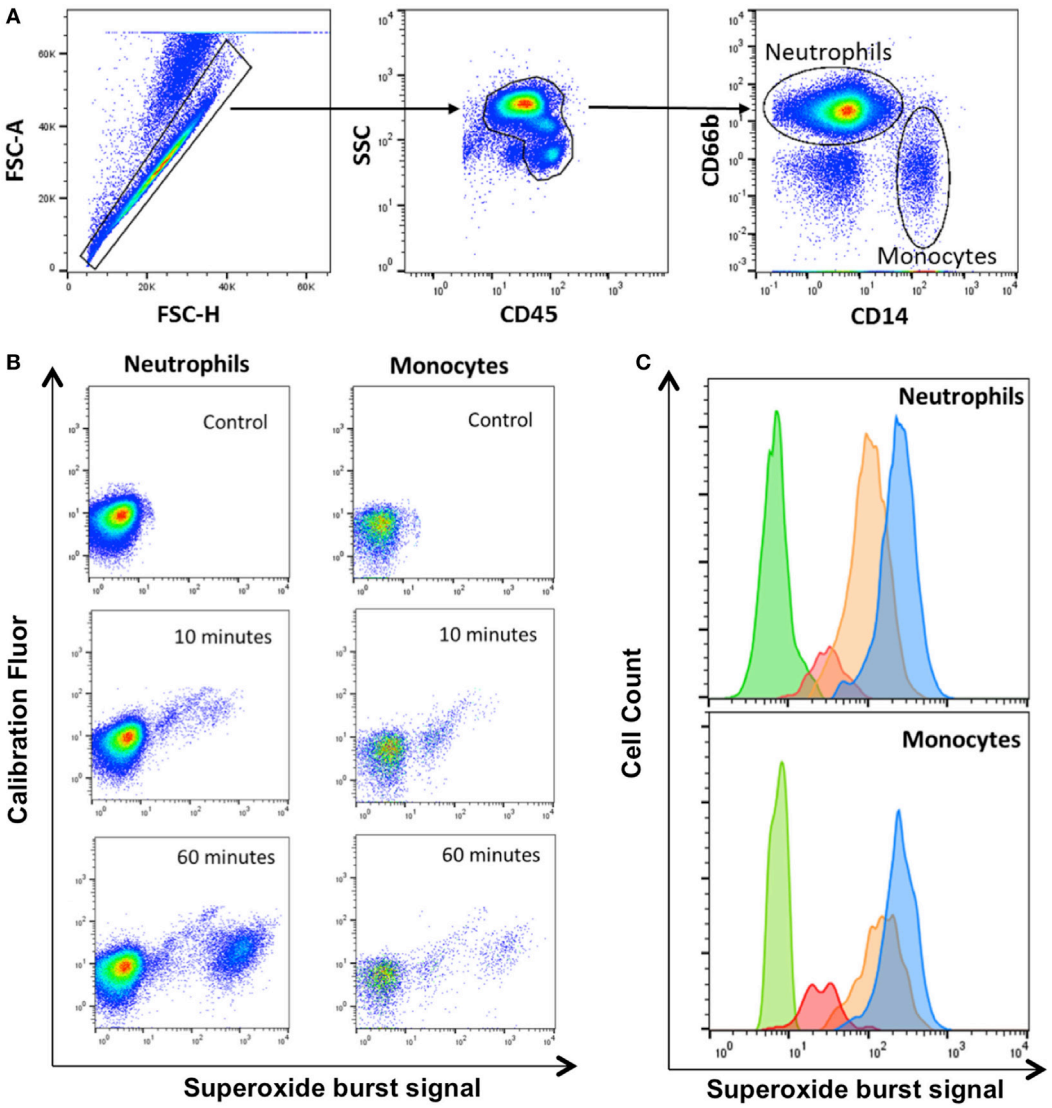


FIGURE 1 | Gating strategy for identification of phagocytes with zymosan reporter particles and quantitation of intraphagosomal oxidation. **(A)** Gating strategy displaying forward scatter (FSC), side scatter (SSC), CD45 PerCP, CD66b APC, and CD14 PE-Cy7 to identify neutrophils and monocytes. The gating strategy illustrated is from one representative healthy volunteer. **(B)** Zymosan-induced superoxide burst activity in neutrophils and monocytes in a healthy control. The OxyBURST fluorescence increases after intraphagosomal oxidation of the zymosan-reporter particles (Alexa Fluor 405-labeled) after 10 and 60 min compared with control sample with no zymosan-reporter particles. **(C)** Overlay histogram demonstrating the shift in fluorescence of cells with zymosan reporter particles due to oxidation after 10 min (red), 30 min (orange), and 60 min (blue) compared with cells without zymosan-reporter particles (green) for both neutrophils and monocytes.

phagocytosis of inflammatory particles, and reactive oxygen species may be important triggers for induction of apoptosis (20). In neutrophils that have not phagocytosed zymosan particles, activation *via* direct binding of zymosan to TLR2 and TLR6 or in response to inflammatory cytokine and chemokine production may also contribute to cell death (12). By contrast, monocytes have an estimated half-life of <20 h *in vivo*, although this may be shorter *ex vivo* (25). Monocytes also undergo programmed cell death, unless they migrate to tissues and undergo differentiation into tissue macrophages (26). However, in contrast to neutrophils, inflammatory cytokine production and stimulation *via* TLR2 can promote survival by blocking programmed cell death (27). This may explain why monocytes that had phagocytosed zymosan reporter particles did not substantially decrease in number during the assay.

Phagocytosis and Superoxide Burst

Superoxide burst activity was measured at 10, 30, 60, 90, and 180 min by comparing fluorescence of cells that had internalized zymosan reporter particles (calibration fluor-positive cells) with the cell population without zymosan (calibration fluor-negative cells) through measurement of the OxyBURST, superoxide sensor signal. The proportion of cells and intensity of superoxide reporter fluorescence increased over the time course of the assay in both

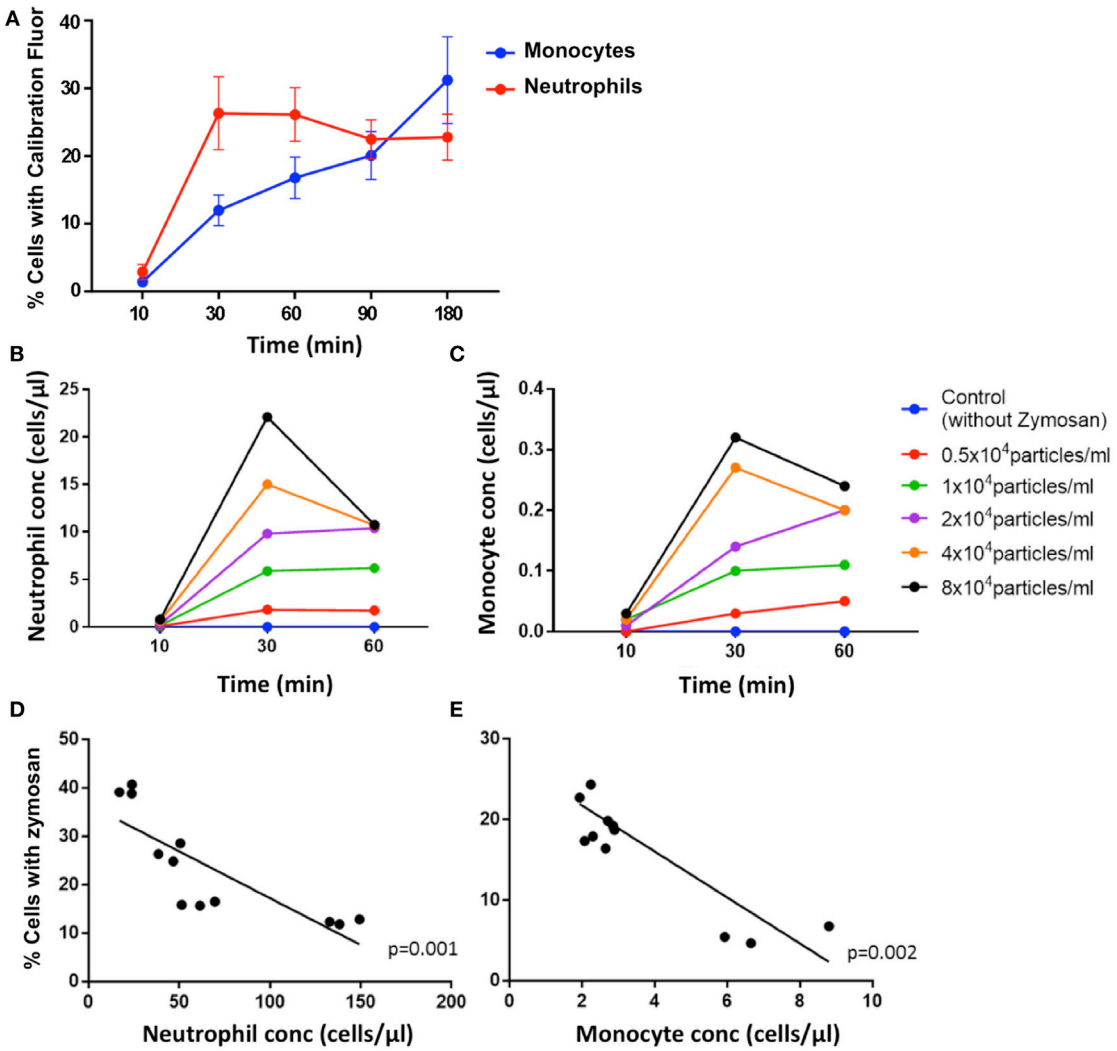


FIGURE 2 | Phagocytosis of zymosan reporter particles by monocytes and neutrophils. **(A)** Proportion of cells that have phagocytosed zymosan over time using blood from healthy individuals incubated with approximately 2 × 10^4 zymosan particles/ml. Data represent mean values, and the error bars indicate SEM. Concentration of neutrophils **(B)** and monocytes **(C)** that have internalized zymosan reporter particles over time, with varying concentrations of particles. Relationship between the proportion of cells internalizing zymosan reporter particles (at an approximate concentration of 2 × 10^4 zymosan particles/ml) and absolute cell concentration for neutrophils **(D)** and monocytes **(E)** after 60 min. Each data point represents one sample from each individual done in triplicate. Four healthy volunteers in triplicate are shown in panels **(A,D,E)**, and one health volunteer is shown in panels **(B,C)**.

monocytes and neutrophils (**Figures 1B,C**). The intensity of the calibration fluorochrome signal did not increase over time, suggesting the increase in superoxide reporter signal was not due to cells internalizing greater numbers of zymosan-reporter particles but was specific to the oxidase activity (**Figure 1B**).

Both peripheral blood monocytes and neutrophils showed rapid oxidation within 30–60 min (**Figures 4C,D**). The kinetics of oxidation in neutrophils and monocytes were similar to macrophages in other studies, with rapid oxidation before an equilibrium being reached, which likely represents cessation of NADPH oxidase activity (6, 15).

When the concentration of zymosan reporter particles was varied, the AI remained constant despite the concentration and proportion of cells taking up zymosan changing. This indicates the assay is able to measure physiological changes in the intensity and duration of phagocytosis and superoxide burst within the phagosome at an individual cell level. This is a significant advance over existing assays, which measure the extracellular accumulation of products of oxidation that is dependent on the summation of phagocytosis and superoxide burst (28). Moreover, because this assay has cellular resolution, the relative contribution of the different phagocyte subsets can be accurately measured. We have also demonstrated that the assay is reproducible with minimal intraindividual variation.

Assays using OxyBURST coupled to IgG coated beads have previously been used to investigate oxidation within macrophage phagosomes (6, 15), and more recently in whole blood (29). The current assay exploiting zymosan as a reporter particle is an

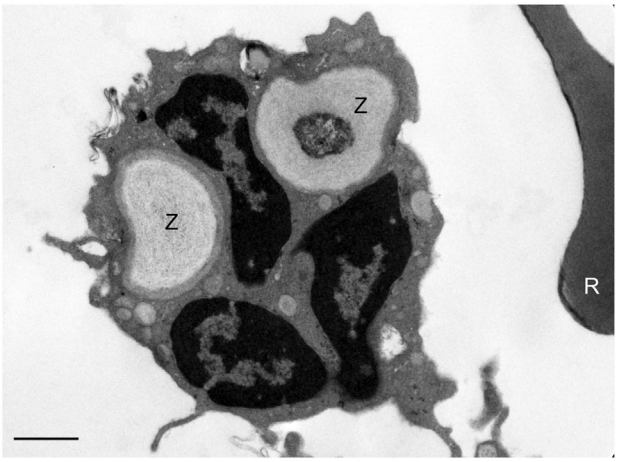


FIGURE 3 | Assessment of phagocytosis of zymosan reporter particles by electron microscopy. An electron micrograph illustrating zymosan particles (Z) inside a neutrophil 60 min post incubation of the reporter particles with whole blood. A red blood cell (R) can be seen to the right of the neutrophil. This image is representative and indicates that the zymosan particles are effectively internalized by cells in suspension. The scale bar = 1 μm.

important addition to the range of phagocyte functional assays and offers considerable practical and technical advantages in the functional interrogation of whole blood direct from human subjects of interest.

Assessment of Whole Blood Phagocyte Function in Patients with HIV/TB Coinfection

The zymosan reporter assay was performed on blood samples obtained from 18 hospitalized HIV-positive patients with laboratory confirmed TB disease to compare phagocytic and superoxide respiratory burst activity in the phagosome between patients and healthy, HIV-negative, controls. The HIV/TB patients had a mean age of 41.4 years, a median CD4 cell count of 108.5 cells/mm^3 and 13/18 were taking antiretroviral therapy at the point of hospital admission. The HIV/TB-coinfected patients demonstrated marked variation in phagosomal oxidation activity compared with healthy controls. The kinetics were similar to healthy controls with peak activity occurring at 30 min, although overall mean intensity of superoxide burst was significantly reduced throughout the assay (paired t-test, all $p < 0.0001$) (**Figure 5A**).

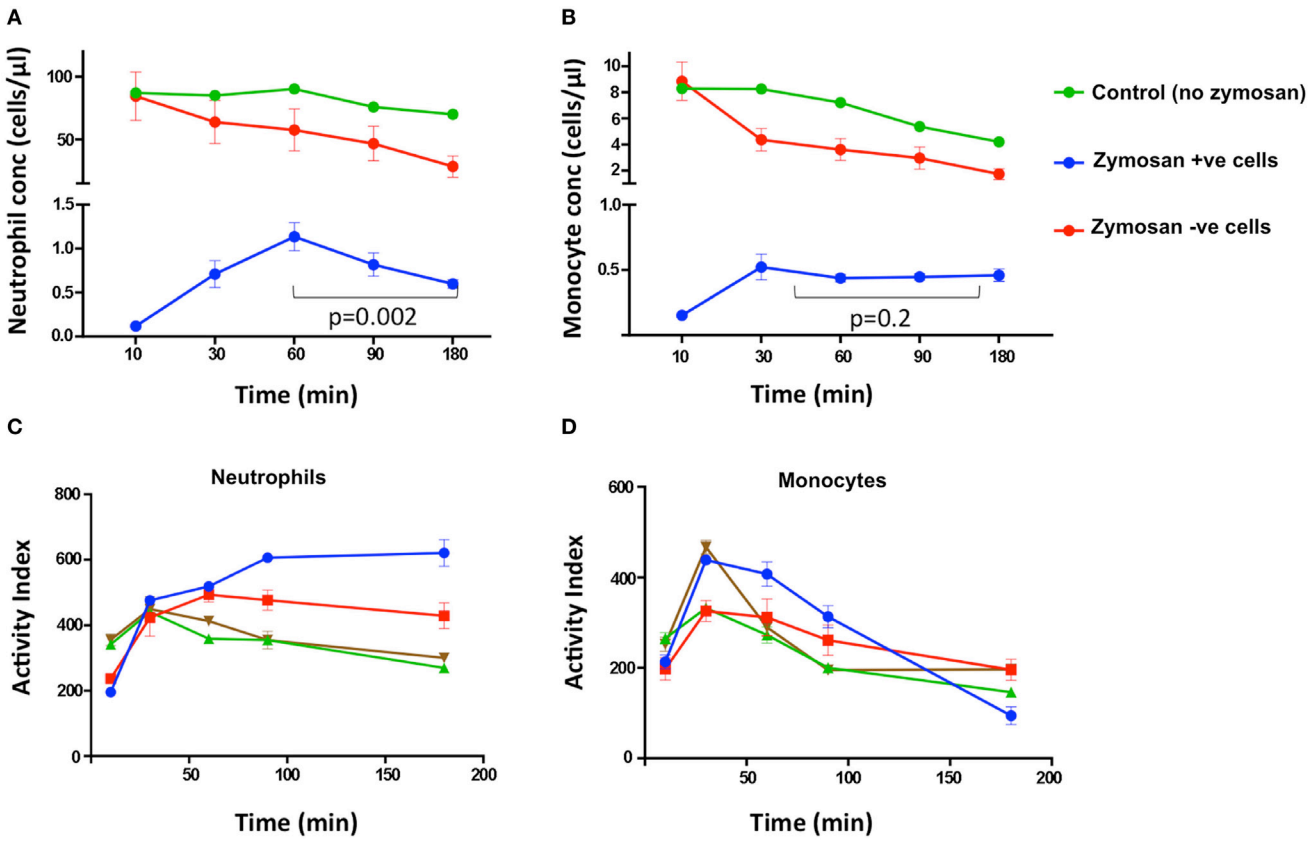


FIGURE 4 | Cell concentrations and activity index (AI) of superoxide burst over time. The concentration of neutrophils **(A)** and monocytes **(B)** at different time points from HIV-negative control samples without zymosan (green), and samples incubated with zymosan reporter beads that had internalized zymosan (blue) or did not internalize zymosan (red). In **(C)** neutrophils and **(D)** monocytes, each color represents the superoxide AI data from different individuals. The AIs are from four healthy, HIV-negative individuals, each performed in triplicate.

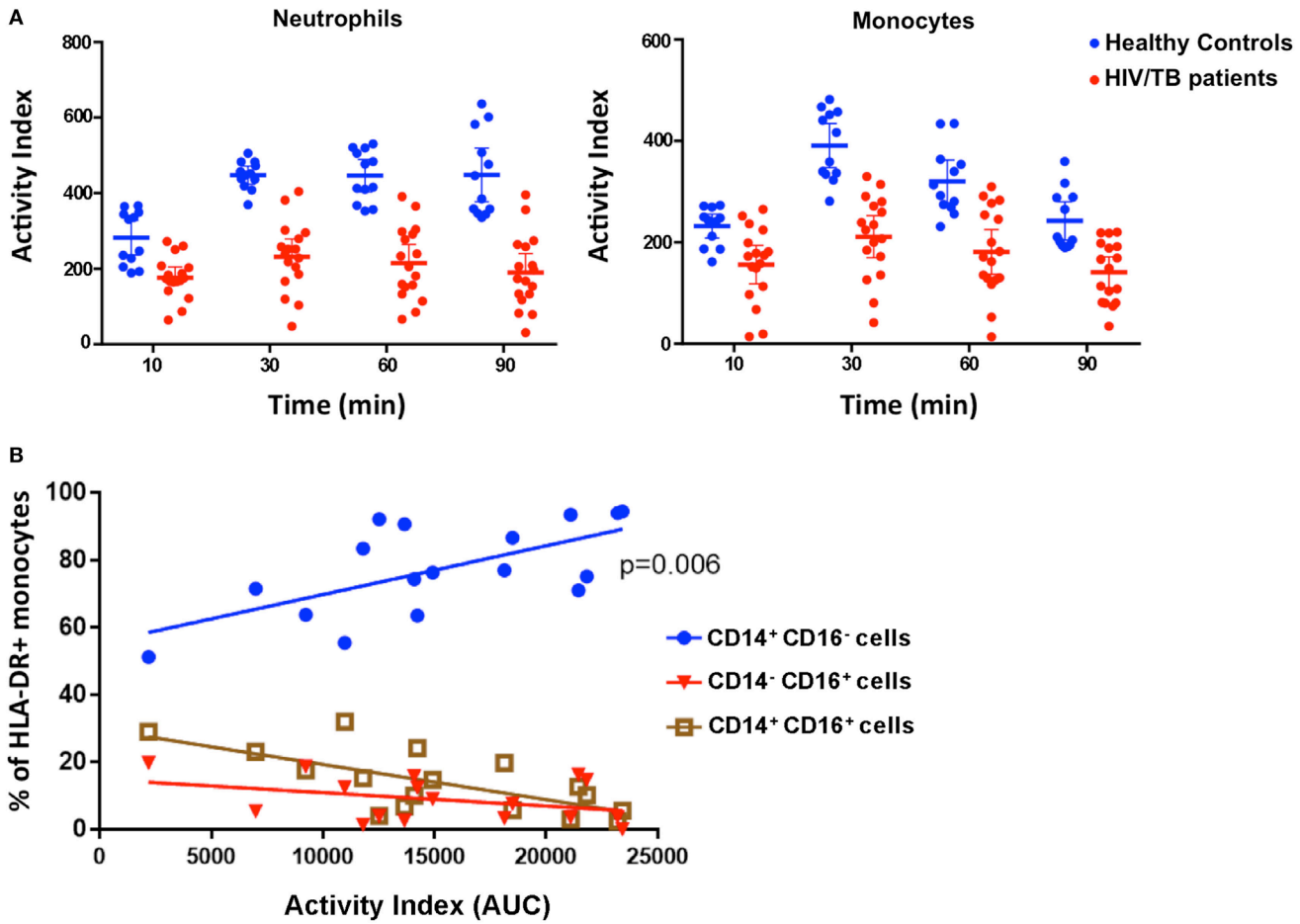


FIGURE 5 | Phagocytosis, superoxide burst, and monocyte phenotypes in peripheral blood phagocytes of HIV/tuberculosis (TB)-coinfected patients. **(A)** The superoxide burst activity index (AI) over time comparing cells from healthy individuals (blue) with cells from HIV/TB-coinfected patients (red). Lines represent means, and error bars are 95% CI. Mean AIs were lower in the HIV/TB patients at all time points analyzed (paired *t*-tests, all $p < 0.0001$). **(B)** The association between the proportion of HLA-DR$^+$ monocytes that are CD14^{++}CD16$^-$ (classical), CD14$^+$CD16$^+$ (intermediate), and CD14$^-$CD16$^+$ (non-classical), and monocyte phagocytosis and superoxide burst AI (measured as "area under the curve"). There is a strong association between higher proportions of classical monocytes and increased AI ($p = 0.006$) ($n = 18$). The data in panel **(A)** are from four health volunteers in triplicate, and the data in panel **(B)** are from 18 HIV/TB patients.

There was also a strong association between increased monocyte superoxide burst activity and the presence of a higher proportion of "classical" CD14^{++}CD16$^-$ monocytes (**Figure 5B**, linear regression coefficient 0.0014, 95% CI 0.0005–0.0024, $p = 0.006$). This association is consistent with the suggestion that classical monocytes are thought to specialize in phagocytosis compared with other monocyte subsets (30). However, the superoxide activity in monocytes was not related to the overall concentration of monocytes in patient's blood (linear regression slope 0.0002, 95% CI −0.0002 to 0.0005, $p = 0.19$), supporting the contention that the superoxide AI was not simply a function of phagocyte abundance.

These data demonstrate that the whole blood assay with zymosan reporter particles is a robust tool for assessing phagocyte function in a clinical setting. The time required to run the assay once the reporter particles have been made is minimal, with the processing of the sample through to acquisition by flow cytometry taking less than 4 h. We also demonstrated this assay can show marked differences between individuals and groups of patients based on clinical phenotype. It is interesting to note that the reduced superoxide burst in the phagocytes from HIV/TB-coinfected individuals observed in this study is consistent with a recent report of impaired innate immune function of monocytes from HIV/TB-coinfected patient cohort in South Africa (31).

CONCLUDING REMARKS

We present a new method for studying whole blood phagocyte functional capacity *ex vivo*. This technique uses fluorescent-tagged zymosan-reporter particles and whole blood, preserving, at least in part, the physiological *in vivo* conditions. It offers several advantages over standard microbiological killing assays because of its speed and simplicity, and its increased resolution whereby

cellular responses such as phagocytic capacity and superoxide burst, can be quantified at the level of the individual cell.

We have demonstrated that the assay can be used to characterize immune function and to detect perturbation of cellular function in patients with severe immunological impairment (in HIV/TB-coinfected individuals). This assay is easily adaptable to standard immunological assays based on cell surface marker expression measured by flow cytometry and has the capacity to provide direct functional readouts of immune cell activities. Previously, we have used inert reporter particles to measure rates of phagosomal acidification, intraphagosomal proteolytic and lipolytic activities, as well as superoxide burst in tissue macrophages in culture. These activities are differentially modulated by immune status and infection (7–9). The use of zymosan as an alternative, biologically active carrier particle for whole blood-based assays brings these complex biological readouts into a clinical setting for functional interrogation of patient-derived samples linked to disease status.

ETHICS STATEMENT

The study was carried out in accordance with the recommendations from the London School of Hygiene & Tropical Medicine Research Ethics Committee and the College of Medicine Research Ethics Committee, Malawi, with written informed consent from all subjects. All subjects gave written informed consent in accordance with the Declaration of Helsinki.

AUTHOR CONTRIBUTIONS

All the authors contributed to the analysis and interpretation of data and preparation of the manuscript. All the authors have approved the final article.

FUNDING

This work was supported by the Royal College of Physicians London JMGP fellowship and the Joint Global Health Trials Scheme (grant number MR/M007375/1) to AG-W, the Wellcome Trust (088696/Z/09/Z) to HCM and (105831/Z/14/Z) to KCJ, the Bill and Melinda Gates Foundation awards (OPP1125279) to HCM and (OPP1156451) to DGR, and the US National Institutes of Health awards AI118582, AI089683, and AI134183 to DGR. A Strategic award from the Wellcome Trust supports the MLW Programme.

REFERENCES

1. Kampmann B, Tena GN, Mzazi S, Young DB, Levin M, Eley B. Novel human in vitro system for evaluating antimycobacterial vaccines. *Infect Immun* (2004) 72:6401–7. doi:10.1128/IAI.72.11.6401
2. Pattanapanyasat K, Sukapirom K, Tachavanich K, Kaewmoon S. Flow cytometric quantitation of opsonophagocytosis and intracellular killing of *Candida albicans* using a whole blood microassay. *Cytometry A* (2007) 71:1027–33. doi:10.1002/cyto.a.20475
3. Wallis RS, Palaci M, Vinhas S, Hise AG, Ribeiro FC, Landen K, et al. A whole blood bactericidal assay for tuberculosis. *J Infect Dis* (2001) 183:1300–3. doi:10.1086/319679
4. DeForge LE, Billeci KL, Kramer SM. Effect of IFN-γ on the killing of *S. aureus* in human whole blood: assessment of bacterial viability by CFU determination and by a new method using alamarBlue. *J Immunol Methods* (2000) 245: 79–89. doi:10.1016/S0022-1759(00)00279-9
5. Hampton MB, Winterbourn CC. Methods for quantifying phagocytosis and bacterial killing by human neutrophils. *J Immunol Methods* (1999) 232:15–22. doi:10.1016/S0022-1759(99)00147-7
6. Podinovskaia M, VanderVen BC, Yates RM, Glennie S, Fullerton D, Mwandumba HC, et al. Dynamic, quantitative assays of phagosomal function. *Curr Protoc Immunol* (2014) 102:14.34.1–14. doi:10.1002/0471142735.im1434s102
7. Russell DG, Vanderven BC, Glennie S, Mwandumba H, Heyderman RS. The macrophage marches on its phagosome: dynamic assays of phagosome function. *Nat Rev Immunol* (2009) 9:594–600. doi:10.1038/nri2591
8. Yates RM, Hermetter A, Taylor GA, Russell DG. Macrophage activation downregulates the degradative capacity of the phagosome. *Traffic* (2007) 8:241–50. doi:10.1111/j.1600-0854.2006.00528.x
9. Podinovskaia M, Lee W, Caldwell S, Russell DG. Infection of macrophages with *Mycobacterium tuberculosis* induces global modifications to phagosomal function. *Cell Microbiol* (2013) 15:843–59. doi:10.1111/cmi.12092
10. Jambo KC, Banda DH, Afran L, Kankwatira AM, Malamba RD, Allain TJ, et al. Asymptomatic HIV-infected individuals on antiretroviral therapy exhibit impaired lung CD4(+) T-cell responses to mycobacteria. *Am J Respir Crit Care Med* (2014) 190:938–47. doi:10.1164/rccm.201405-0864OC
11. Di Carlo FJ, Fiore JV. On the composition of zymosan. *Science* (1958) 127:756–7. doi:10.1126/science.127.3301.756-a
12. Underhill DM. Macrophage recognition of zymosan particles. *J Endotoxin Res* (2003) 9:176–80. doi:10.1179/096805103125001586
13. Crespo MS, Alvarez Y, Valera I, Municio C, Hugo E, Padrn F, et al. Eicosanoids in the innate immune response: TLR and non-TLR routes. *Mediators Inflamm* (2010) 2010. doi:10.1155/2010/201929
14. Lindena J, Burkhardt H, Dwenger A. Mechanisms of non-opsonized zymosan-induced and luminol-enhanced chemiluminescence in whole blood and isolated phagocytes. *Clin Chem Lab Med* (1987) 25:765–78. doi:10.1515/cclm.1987.25.11.765
15. Vanderven BC, Yates RM, Russell DG. Intraphagosomal measurement of the magnitude and duration of the oxidative burst. *Traffic* (2009) 10:372–8. doi:10.1111/j.1600-0854.2009.00877.x.Intraphagosomal
16. Nauseef WM. How human neutrophils kill and degrade microbes: an integrated view. *Immunol Rev* (2007) 219:88–102. doi:10.1111/j.1600-065X.2007.00550.x
17. Fang FC. Antimicrobial reactive oxygen and nitrogen species: concepts and controversies. *Nat Rev Microbiol* (2004) 2:820–32. doi:10.1038/nrmicro1004
18. Segal AW. The NADPH oxidase and chronic granulomatous disease. *Mol Med Today* (1996) 2:129–35. doi:10.1016/1357-4310(96)88723-5
19. Koziel H, Li X, Armstrong MY, Richards FF, Rose RM. Alveolar macrophages from human immunodeficiency virus-infected persons demonstrate impaired oxidative burst response to *Pneumocystis carinii* in vitro. *Am J Respir Cell Mol Biol* (2000) 23:452–9. doi:10.1165/ajrcmb.23.4.4084
20. Corleis B, Korbel D, Wilson R, Bylund J, Chee R, Schaible UE. Escape of *Mycobacterium tuberculosis* from oxidative killing by neutrophils. *Cell Microbiol* (2012) 14:1109–21. doi:10.1111/j.1462-5822.2012.01783.x
21. Gupta-Wright A, Fielding KL, van Oosterhout JJ, Wilson DK, Corbett EL, Flach C, et al. Rapid urine-based screening for tuberculosis to reduce AIDS-related mortality in hospitalized patients in Africa (the STAMP trial): study protocol for a randomised controlled trial. *BMC Infect Dis* (2016) 16:501. doi:10.1186/s12879-016-1837-z
22. Rohde KH, Veiga DFT, Caldwell S, Balázsi G, Russell DG. Linking the transcriptional profiles and the physiological states of *Mycobacterium tuberculosis* during an extended intracellular infection. *PLoS Pathog* (2012) 8:e1002769. doi:10.1371/journal.ppat.1002769
23. Maecker HT, Frey T, Nomura LE, Trotter J. Selecting fluorochrome conjugates for maximum sensitivity. *Cytometry A* (2004) 62:169–73. doi:10.1002/cyto.a.20092

24. Summers C, Rankin SM, Condliffe AM, Singh N, Peters AM, Chilvers ER. Neutrophil kinetics in health and disease. *Trends Immunol* (2010) 31:318–24. doi:10.1016/j.it.2010.05.006
25. van Furth R, Cohn ZA. The origin and kinetics of mononuclear phagocytes. *J Exp Med* (1968) 128:415–35. doi:10.1084/jem.128.3.415
26. Fahy RJ, Doseff AI, Wewers MD. Spontaneous human monocyte apoptosis utilizes a caspase-3-dependent pathway that is blocked by endotoxin and is independent of caspase-1. *J Immunol* (1999) 163:1755–62.
27. Mangan DF, Wahl SM. Differential regulation of human monocyte programmed cell death (apoptosis) by chemotactic factors and pro-inflammatory cytokines. *J Immunol* (1991) 147:3408–12.
28. Seitz PM, Cooper R, Gatto GJ, Ramon F, Sweitzer TD, Johns DG, et al. Development of a high-throughput cell-based assay for superoxide production in HL-60 cells. *J Biomol Screen* (2010) 15:388–97. doi:10.1177/1087057109359687
29. Morton B, Mitsi E, Pennington SH, Reiné J, Wright AD, Parker R, et al. Augmented passive immunotherapy with P4 peptide improves phagocyte activity in severe sepsis. *Shock* (2016) 46:635–41. doi:10.1097/SHK.0000000000000715
30. Wong KL, Yeap WH, Tai JJY, Ong SM, Dang TM, Wong SC. The three human monocyte subsets: implications for health and disease. *Immunol Res* (2012) 53:41–57. doi:10.1007/s12026-012-8297-3
31. Janssen S, Schutz C, Ward A, Nemes E, Wilkinson KA, Scriven J, et al. Mortality in severe human immunodeficiency virus-tuberculosis associates with innate immune activation and dysfunction of monocytes. *Clin Infect Dis* (2017) 65:73–82. doi:10.1093/cid/cix254

Conflict of Interest Statement: The authors declare that the research was conducted in the absence of any commercial or financial relationships that could be construed as a potential conflict of interest.

Copyright © 2017 Gupta-Wright, Tembo, Jambo, Chimbayo, Mvaya, Caldwell, Russell and Mwandumba. This is an open-access article distributed under the terms of the Creative Commons Attribution License (CC BY). The use, distribution or reproduction in other forums is permitted, provided the original author(s) or licensor are credited and that the original publication in this journal is cited, in accordance with accepted academic practice. No use, distribution or reproduction is permitted which does not comply with these terms.

frontiers in Immunology

REVIEW
published: 23 March 2018
doi: 10.3389/fimmu.2018.00531

Defective Phagocytic Properties of HIV-Infected Macrophages: How Might They Be Implicated in the Development of Invasive *Salmonella* Typhimurium?

Gabrielle Lê-Bury[1,2,3] *and Florence Niedergang*[1,2,3]*

[1] INSERM, U1016, Institut Cochin, Paris, France, [2] CNRS, UMR 8104, Paris, France, [3] Université Paris Descartes, Sorbonne Paris Cité, Paris, France

Human immunodeficiency virus type 1 (HIV-1) infects and kills T cells, profoundly damaging the host-specific immune response. The virus also integrates into memory T cells and long-lived macrophages, establishing chronic infections. HIV-1 infection impairs the functions of macrophages both *in vivo* and *in vitro*, which contributes to the development of opportunistic diseases. Non-typhoidal *Salmonella enterica* serovar Typhimurium has been identified as the most common cause of bacterial bloodstream infections in HIV-infected adults. In this review, we report how the functions of macrophages are impaired post HIV infection; introduce what makes invasive *Salmonella* Typhimurium specific for its pathogenesis; and finally, we discuss why these bacteria may be particularly adapted to the HIV-infected host.

Keywords: macrophages, HIV, *Salmonella*, phagocytosis, opportunistic diseases

OPEN ACCESS

Edited by:
Christel Vérollet, UMR5089 Institut de Pharmacologie et de Biologie Structurale (IPBS), France

Reviewed by:
Aldo Tagliabue, Istituto di Ricerca Genetica e Biomedica (CNR), Italy
Elsa Anes, Universidade de Lisboa, Portugal

***Correspondence:**
Florence Niedergang
florence.niedergang@inserm.fr

Specialty section:
This article was submitted to Microbial Immunology, a section of the journal Frontiers in Immunology

Received: *03 November 2017*
Accepted: *28 February 2018*
Published: *23 March 2018*

Citation:
Lê-Bury G and Niedergang F (2018) Defective Phagocytic Properties of HIV-Infected Macrophages: How Might They Be Implicated in the Development of Invasive Salmonella Typhimurium? Front. Immunol. 9:531. doi: 10.3389/fimmu.2018.00531

CLEARANCE AND ACTIVATION CAPACITY OF MACROPHAGES

Although macrophages are different in the different tissues and organs in which they reside, they can all be characterized by their strong capacity to internalize and degrade particles in phagolysosomes. Transcriptomic analysis has pointed to unique gene expression profiles in response to pathogens components (1). One obvious functional set of genes shared by all phagocytes encodes for the components of lysosomes, such as the vacuolar ATPase H^+ pump and lysosomal hydrolases. Subtle differences can be revealed when comparing the clearance capacities of polymorphonuclear neutrophils, macrophages or dendritic cells. Clearance is the hallmark of neutrophils and macrophages, while dendritic cells have been reported to be milder with internalized material, with some material remaining undegraded (2–5). In this review, we will focus on macrophages, as they are target cells for both the human immunodeficiency virus type 1 (HIV-1) and *Salmonella* pathogens.

Phagocytosis begins with the clustering of receptors that are engaged by ligands present on the surface of the target particle. Many types of receptors can be implicated in the recognition step, regulating the fate of the internalized material. Phagocytic receptors can be subdivided into receptors that bind to opsonins, like the immunoglobulins and complement, and receptors that bind to non-opsonins. The latter interact with molecular groups on the surface of the target particle or pathogen, including sugars, lipids, and polypeptides that are referred to as pathogen-associated molecular patterns (6, 7). Early signaling from surface receptors leads to the polymerization of actin that drives plasma membrane deformation and the formation of a closed phagosome (8, 9). For

large targets to be efficiently internalized, membrane remodeling is essential, relying on the focal delivery of intracellular compartments including recycling endosomes (10–12). The large GTPase dynamin2 is crucial for phagosome sealing (13).

Once closed, the phagosome evolves very much like smaller endocytic compartments, undergoing a series of fusion and fission events with the compartments of the endocytic pathway (14, 15). This process, called phagosome maturation, is accompanied by the dynein-mediated movement of the phagosome along microtubules (16, 17). The microtubule network is crucial for the phagosome to reach the lysosomes positioned at the center of the cell and to efficiently mature into a phagolysosome. Indeed, it has been demonstrated that the loading of dyneins at the plus ends of microtubules by the plus-end binding protein, EB1, is critical for phagosome maturation (18).

Early phagosomes harbor markers of the early endosomes such as Rab5 and its effector, the early endosome antigen 1 (EEA1) (19). Other effectors of Rab5 are the class III phosphatidylinositol 3 kinase human vacuolar protein-sorting 34 that generates phosphatidylinositol 3-phosphate [PI(3)P] (20). It has been demonstrated that PI(3)P is important after phagosome completion, for its maturation (21). EEA1 carries a FYVE domain that binds to PI(3)P, a zinc finger that binds to Rab5 and regions responsible for multimerization. EEA1 also binds to the t-SNARE Syntaxin-13, which is important for membrane fusion (22). Rab5 exchange factors, including Rabex-5, Rin1, and Gapex-5, coordinate Rab5 activation and microtubule dynamics (23).

Acquisition of Rab7 is still considered to be a hallmark of late phagosomes, although a choreography of Rab proteins has been shown to be recruited during phagocytosis (24). The products of PI3K are involved in the dissociation of Rab5, but are not essential for the recruitment of Rab7 on the phagosome (25). Data in yeast have shown that the proteins Mon1 and Ccz1 serve as a Rab7 exchange factor (26). Phagosomes undergo fusion with late endosomes and lysosomes *via* a Soluble NSF attachment protein receptor (SNARE) mediated process. It has been demonstrated that Syntaxin 7 and Syntaxin 8, with VAMP7 and VAMP8, are involved in phagosome-lysosome fusion (27). The vpsC–homotypic protein sorting (HOPS) complex that mediates the transition from Rab5 to Rab7 endosomes could play a similar function in phagosome maturation. The complex is composed of Vps11, Vps16, Vps18, Vps33, Vps39, and Vps41. In yeast, Rab7 is activated by Vps39. The Vps41 protein is a key component of the HOPS complex as it is required for the stabilization of the HOPS complex on the endosomal membrane before fusion with the vacuole. Regulation by the p38 MAP kinases of Vps41 has recently been highlighted as an explanation for the differential trafficking of virulent LPS of *Coxiella burnetii* (28). This type of regulation might also be implicated in phagosome maturation in macrophages. Rab7 and Arl8 orchestrate both microtubule-dependent transport of late endosomes/lysosomes and their fusion with endosomes, autophagosomes, and phagosomes. Both proteins are important for lysosome tubulation in macrophages (29). Rab7-interacting lysosomal protein and the long splice-variant of oxysterol-binding protein related-protein 1 (ORP1L) function together to link phagosomes to the microtubule motor dynein/dynactin (30, 31). Arl8 has been shown to control phagosome maturation and bacterial killing (32). It has also been demonstrated that Arl8 plays an important role in phagosome maturation in *Caenorhabditis elegans* (33). Arl8 connects lysosomes to kinesins through SifA and kinesin interacting protein (34), in particular, to kinesins 1 and 3, controlling lysosomal positioning (35). Some effectors, like PLEKHM1, act as dual effectors for Rab7 and Arl8 to promote cargo delivery to lysosomes (36) and may also play a role during phagosome maturation.

Acidification occurs gradually while the compartment matures into a phagolysosome, which is important for the optimal activity of hydrolytic enzymes delivered by late endosomes and lysosomes. Acidification reaches a pH of 5.5 in the late phagosome, due to the acquisition of proton pumping vATPases. Negatively charged chloride ions may enter the compartments to compensate for the proton influx, although this role has not been established experimentally. However, the depletion of luminal cations, Na^+ and K^+, during maturation has been established (37). Anion and luminal cation exchange may serve to maintain lysosome osmolarity and volume during the acidification steps.

Microbicidal activity in the phagolysosome depends both on hydrolases and on the generation of reactive oxygen and nitrogen species (ROS and RNS, respectively) (38). The NADPH oxidase is acquired at the early stages of phagosome maturation. Its activity is complemented by the inducible NO synthase, iron scavengers, and transporters, as well as lysozymes, lipases and proteases, such as the cathepsins. These species are delivered to phagosomes and directly contribute to killing. Their activities can be modulated by cell activation and the concomitant signaling pathways that are initiated downstream of surface receptors in complex regulatory loops. For instance, the interaction between the RUN domain Beclin-1 interacting cysteine-rich-containing (RUBICON) protein and the NADPH oxidase upon TLR stimulation forms a feedback loop with the cascade signaling to cytokine production (39).

Finally, when degradation is incomplete, antigens derived from the internalized material are presented on the major histocompatibility complex molecules (Class I or II), especially in dendritic cells. Signaling pathways are activated and the phagosome itself can be considered a signaling platform. Together, these events lead to the production of cytokines and inflammatory mediators, which can be modulated depending on the surface receptors engaged by the cargo (40, 41).

DYSREGULATION OF MACROPHAGE PHAGOCYTOSIS BY HIV INFECTION

The initial detection of the acquired immunodeficiency syndrome (AIDS) epidemic in 1981 began with reports of an unusual syndrome in which previously healthy young males were presenting with diseases such as Kaposi's sarcoma, cytomegalovirus pneumonia, and *Pneumocystis carinii* pneumonia, previously described in immunocompromised patients (42). The syndrome was then named AIDS. Indeed, the principal effect of the virus is to decrease the immune defenses of infected individuals, leading to the appearance of opportunistic diseases and tumors. Invasive pneumococcal and oral candidosis presented early in

HIV-infected patients, especially in Africa, together with non-typhoidal *Salmonella* infections, which will be the focus of the following section in this review.

The introduction of highly active antiretroviral therapy (HAART) has radically altered the incidence of AIDS, initially in developed countries, and later on, worldwide. However, even with HAART, which results in undetectable plasma HIV loads, HIV transcription persists in reservoirs, such as long-lived memory T cells, phagocytic cells, as well as other cell types in various tissues (43).

Already in the 1980s, Crowe et al. reported that macrophages are targets for HIV-1 and may act as major reservoirs of virus (44, 45). It has since been established that there is some specificity in the infection cycle of HIV-1 in macrophages (46–49) and see Ref. (50) for a recent review in the same topic.

The group of Crowe has performed pioneering work in analyzing the phagocytic capacity of blood monocytes from a small sample of the Sydney Blood Bank Cohort or *in vitro* differentiated and infected macrophages. They studied phagocytosis of apoptotic neutrophils, a *Mycobacterium avium* complex, *Candida albicans*, *Toxoplasma gondii*, and IgG- or complement-opsonized targets (51–55). The data suggested that phagocytosis by monocytes from WT HIV-1-infected individuals was impaired, whereas the phagocytic capacity of the phagocytes from the Δ*nef* HIV-1-infected subjects was not. Interestingly, no correlation was found between the level of inhibition of phagocytosis and the viral load or the CD4 counts (52). The authors reported an increased level of basal F-actin in HIV-infected cells, which could account for a defective capacity of the actin cytoskeleton to efficiently remodel during phagosome formation (**Figure 1A**).

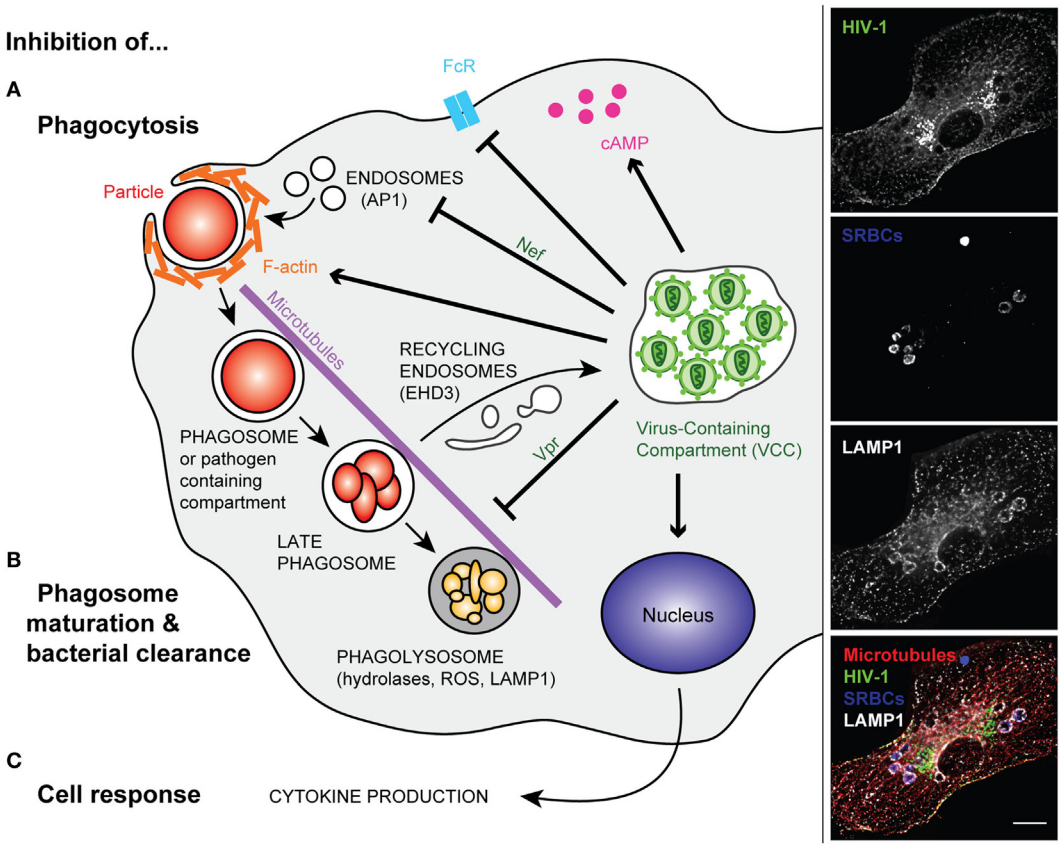


FIGURE 1 | Modified phagocytosis in HIV-infected macrophages. Left panel—Once HIV infection of a macrophage is established, intracellular trafficking is rerouted to the virus-containing compartment (VCC). In non-infected macrophages, phagocytosis is initiated by the binding of phagocyte surface receptors to ligands present on the microorganism or to the opsonizing molecules that coat the target particle. In HIV-infected cells, surface receptors (e.g., FcR) can be downregulated **(A)**. After binding, a cascade of signaling events leads to actin polymerization and engulfment of the particulate material in a closed compartment termed, the phagosome. The inhibition of phagocytosis in HIV-infected macrophages was related to perturbation of F-actin and cAMP production. The viral factor Nef further reduces the efficiency of phagosome formation *via* its interaction with the AP1 adaptor protein, reducing the focal delivery of intracellular compartments **(A)**. In non-infected macrophages, the phagosome matures into a degradative compartment called phagolysosome. This occurs after fusion and fission with various endocytic compartments, and the phagolysosome migrates along microtubules. However, in HIV-infected macrophages, the viral factor Vpr inhibits phagosome maturation and centripetal movement of the phagolysosome toward the nucleus. Part of the intracellular trafficking, such as the EHD3 recycling machinery, is rerouted to the VCC **(B)**. In addition, viral infection inhibits macrophage late events and responses such as cytokine production **(C)**. Right panel—Primary human macrophages were infected with HIV-1_{ADA} for 8 days before incubation with IgG-opsonized sheep red blood cells (SRBCs) for 60 min at 37°C. They were fixed, permeabilized, and labeled with anti-p24 followed by Alexa488-anti-goat IgG (upper line), AMCA-anti-rabbit IgG to detect the total SRBCs (second line), anti-LAMP1 followed by Cy3-anti-mouse IgG (third line), and anti-tubulin followed by Cy5-anti-human IgG (not shown). Merged images (lower line) show p24 in green, SRBCs in blue, LAMP1 in white, and microtubules in red. Z stacks of wide field fluorescent images were acquired, deconvoluted, and treated with ImageJ. Bar, 10 μm.

Some HIV-1 induced receptor downregulation was observed in primary human macrophages (56), as in alveolar macrophages for mannose receptors (57). The group of Crowe also pointed to a crucial role of the Nef viral protein in impairing phagocytosis in infected blood monocytes *in vivo*, a phenotype that they did not observe in monocyte-derived macrophages-infected *in vitro*. Nef was reported to downregulate many surface receptors and markers from the surface of treated model cells (58, 59), as well as CD36 on macrophages, which may be related to defective phagocytosis of inert particles and killed bacteria in Nef-treated cells (60). Other reports showed that HIV-1 infection did not induce any decrease in the surface expression of phagocytic receptors (52, 61). The impact of *in vitro* infection of macrophages with HIV-1 on various types of phagocytosis was analyzed. The focal delivery of endosomal compartments at the site of phagocytosis was impaired in a Nef-dependent manner, probably due to Nef interaction with the adaptor complex, AP1, on endosomes (61) (**Figure 1A**). This endosomal delivery was shown to be required for efficient phagocytosis of large particulate material (11, 62), and interestingly, to be controlled by the NF-κB signaling protein Bcl10 (63). Other molecular defects reported in HIV-infected macrophages include elevated intracellular cAMP levels (64) and decreased expression of the common gamma chain (65) (**Figure 1**). Of particular significance, defective phagocytosis was also reported in the population of small alveolar macrophages in the lung of HIV-infected patients (66).

The later steps of phagosome maturation were also reported to be impaired in HIV-infected macrophages, with early reports showing that the intracellular replication of live *T. gondii* was enhanced in HIV-infected macrophages. Interestingly, treatment of macrophages with interferon gamma, a known activator of these cells, decreased parasite replication, but did not control parasite levels (53). An assay developed in the laboratory of Russell to monitor the superoxide burst in phagocytes by flow cytometry was used to analyze whole blood samples of HIV/tuberculosis-infected individuals (67). The authors were able to demonstrate an impaired superoxide burst activity in the phagocytes of coinfected patients. Using similar tools together with other assays, it was determined that Nef was not crucial to the *in vitro* mediation of the phagosome maturation defect in HIV-infected macrophages, while, unexpectedly, the viral protein Vpr, was (**Figure 1B**) (18). Vpr perturbs the microtubule dynamics, the localization of the plus-end microtubule binding protein EB1 and therefore, the positioning of the dynein motors necessary for driving phagosomes to the cell center. In addition, the viral infection of macrophages relies on the budding of newly enveloped viral particles in virus-containing compartments (VCCs), which presumably requires the recruitment of large amounts of membrane. Part of the intracellular endocytic machineries are de-routed toward the VCCs in HIV-1-infected macrophages, as is the case for the EHD3 sorting protein (18). It is therefore probable that many of the intracellular trafficking pathways are altered in virus-infected cells, as a side effect of viral particle production. This may benefit many opportunistic pathogens in a non-specific manner.

Similarly, signaling to initiate cell activation and cytokine production is altered in HIV-infected cells (**Figure 1C**). Placental blood mononuclear cells purified from HIV-infected mothers constitutively secrete more IL-1β and IL-6 and have more IL6, IL1β, and TNF-α mRNA; however, the high basal rates of secretion were associated with a lower response to stimulation with LPS (68). Reduced cytokine production was also observed in HIV-infected macrophages that were triggered for receptor-mediated phagocytosis or infected with bacteria (18). Many pro-inflammatory cytokine signaling pathways rely on the activation of the NF-κB pathway. The latter is transiently activated during the activation of transcription *via* the HIV promoter or the long terminal repeats. This may result in inadequate subsequent activation when the cells are subjected to a secondary trigger. Reduced intracellular protein levels of FcRγ, the signaling adaptor protein and chaperone required for FcγRI and III expression and function, were reported (69). Inhibition of subsequent downstream phosphorylation of Hck and Syk tyrosine kinases was observed in HIV-infected monocyte-derived macrophages undergoing Fcγ receptor-mediated phagocytosis.

UNIQUE INTRINSIC PROPERTIES OF INVASIVE NON-TYPHOIDAL SALMONELLAE (iNTS)

In as early as 1990, non-typhoidal salmonellae (NTS) were confirmed as HIV-related pathogens in sub-Saharan African adults (70). Later, NTS bacteremia has become a common and recurrent illness among susceptible African children and HIV-infected adults (71). This bloodstream infection, in African, HIV-infected adults, was reported to have high mortality (47%) and recurrence (43%) rates (72), due to recrudescence and reinfection (73). The bacteremia may be due to both *Salmonella enterica* serovar Typhimurium and *Salmonella enterica* serovar Enteritidis (74).

Salmonella enterica is a Gram-negative bacterium that causes enteric diseases. The species, *S. enterica,* includes typhoidal and non-typhoidal *Salmonella* and comprises a large number of serovars. *S. enterica* serovars Typhi and Paratyphi cause typhoid and paratyphoid fevers, respectively. The pathogens penetrate through the intestinal mucosa, producing bacteremia and lodge in the macrophages of the reticuloendothelial system. The remaining serovars normally lead to a self-limiting diarrheal disease in healthy individuals, but some NTS, such as *Salmonella* Typhimurium, can cause bloodstream infection in immunocompromised adults (75). Thus, iNTS have emerged as a prominent cause of bacteremia in African individuals with an associated case fatality of 20–25% (76).

Multilocus sequence typing (MLST) analysis of numerous isolates of *Salmonella* Typhimurium from Malawi and Kenya revealed new sequence type variants of *S.* Typhimurium associated with iNTS in sub-Saharan Africa. This dominant regional genotype, MLST group ST313, presents several genetic differences compared with other strains of this serotype, such as NTS ST19 (77).

In addition, whole-genome sequence-based phylogenetic methods revealed that the majority of ST313 isolates fell within two closely related, clustered phylogenetic lineages: lineage I, with A130 as a hallmark strain; and lineage II, with D23580 as

a hallmark strain (78). These lineages are distinct from other *S.* Typhimurium lineages due to their distinct metabolic profiles (79) and antibiotic resistance (77). Indeed, Okoro et al. observed that isolates from lineage II appeared after the use of chloramphenicol for the treatment of iNTS disease, suggesting a clonal replacement of isolates from lineage I, by those from lineage II influenced by antibiotic usage. In addition, the authors estimated that lineage I and lineage II appeared independently, ~52 and ~35 years ago, respectively, and then developed with the HIV pandemic. Thus, Okoro et al. propose that iNTS disease, in sub-Saharan Africa, is caused by highly related *Salmonella* Typhimurium lineages that may have developed in immunosuppressed populations and following antibiotic treatment (78).

Host-adapted *Salmonella* serovars that cause invasive disease such as *S. enterica* Typhi and *S. enterica* Paratyphi display some similarities to ST313 isolates, in particular some genome degradation (80). Compared with non-iNTS *S.* Typhimurium isolates, ST313 isolates present numerous pseudogenes and deletions (77). In addition, whole-genome comparisons of a representative isolate of ST313, D23580 from Malawi, and ST19 strains (LT2, SL1344, and DT104) revealed a distinct repertoire of six prophage-like elements. These include five full-length prophages arbitrarily named Blantyre Prophage "BTP" 1 through 5, and one prophage remnant (77). Okoro et al. highlighted that this set of prophage sequences is present in all ST313 isolates belonging to lineage I and II (79). Among the five full-length prophages, three of them were already well-characterized, and commonly found in *S.* Typhimurium genomes: Gifsy-2^{D23580} (BTP2), $ST64B^{D23580}$ (BTP3), and Gifsy-1^{D23580} (BTP4) that are all defective in ST313. The two remaining, BTP1 and BTP5, are novel prophages that are found only in the ST313 genome. BTP1 contains three virulence-related genes: *st313-td*, *gtrCc*, and *gtrAc* (81). *st313-td* was reported to play a role in survival within murine macrophages and in virulence in a mouse model of bacterial infection (82). The *gtrAC* operon encodes an *O*-glycosyltransferase that modifies the composition and the length of O-antigen of the bacterial lipopolysaccharide (83). Further, the LPS of D23580 (ST313) present particular O-polysaccharide chains (84), which have been used to design glycoconjugate vaccines against invasive African *S. enterica* serovar Typhimurium (85, 86).

The D23580 isolate has four plasmids including one virulence-associated plasmid. This plasmid contains an insertion that resembles a composite *Tn21*-like mobile element encoding multiple drug resistance genes (77). Before the appearance of MDR *S.* Typhimurium, ST313 strains of lineage I were susceptible to chloramphenicol. The selection of this virulence-associated plasmid explains the emergence of MDR *S.* Typhimurium, such as D23580 (lineage II), associated with the epidemic increase in the incidence of iNTS in Malawi after chloramphenicol treatment (74).

After an analysis of 129 ST313 isolates, Yang et al. demonstrated that these exhibit a distinct metabolic signature compared with non-ST313 *S.* Typhimurium. For instance, D23580 seems to be more resistant to acid stress than non-ST313 *S.* Typhimurium (87). Among the differences in metabolic pathways, ST313 strains present two loss-of-function mutations that impair multicellular stress resistance associated with survival outside the host. Hence, ST313 bacteria are less resistant to oxidative stress than ST19 (87, 88), due to mutations causing inactivation of KatE catalase in ST313. Catalase converts hydrogen peroxide (H_2O_2) to oxygen and water and this H_2O_2 detoxification protects high-density bacterial communities from oxidative stress. Another loss-of-function mutation in the *bcsG* gene in D23580 induces an inactivation of the BcsG cellulose biosynthetic enzyme required for the RDAR (red, dry, and rough) colonial phenotype (88). RDAR colonies represent a form of multicellular behavior that enhances *Salmonella* stress resistance in the environment and allows biofilm formation (89). A comparative analysis of biofilm-forming ability and long-term survival has shown that ST19 strains, that are strong biofilm producers, can survive desiccation better than ST313 that form weak biofilms and survive poorly following desiccation (90). In addition, several ST313 strains express less flagellin, a component of the flagellum appendage responsible for bacterial motility (91, 92). Indeed, ST313 strains (D65, Q55, S11, S12, D23580, and A130) were reported to be less motile than ST19 strains (I77, I89, I41, S52, and SL1344) (91, 93), although some variability among the strains was observed (87). These data suggest that, like *Salmonella* Typhi, *Salmonella* Typhimurium ST313 lack some of the mechanisms that allow transmission and/or survival in the environment.

SALMONELLA TYPHIMURIUM AND HOST INTERACTIONS

Salmonella Typhimurium were reported to be quickly taken up by $CD18^+$ cells in the blood after oral infection (94). *Salmonella* Typhimurium are also taken up by $CCR6^+$ phagocytes located in the subepithelium dome of Peyer's patches in the intestine, then carried to the mesenteric lymph node (95). In addition, dendritic cells were shown to be able to extend dendrites toward the intestinal lumen, without perturbing the tight junctions of epithelial cells, to capture bacteria (96). *Salmonella* Typhimurium persist within macrophages in the mesenteric lymph nodes of chronically infected Nramp1 (natural resistance associated macrophage protein 1)$^{+/+}$ mice (97). *S.* Typhimurium may be killed by the cell (98) or can hijack the host cell defenses to survive inside the cell (99–101). More recently, it has been recognized that macrophage polarization can influence bacterial infection. A macrophage population is heterogeneous in its susceptibility to the infection, potentially due to a mixture of type 1 and type 2 macrophages, as shown *in vitro* with mouse bone marrow-derived macrophages (102). *S.* Typhimurium cannot replicate in primary human monocyte-derived macrophages polarized into inflammatory M1 macrophages, while M2 and M0 macrophages allowed bacterial replication (103). The tissue source of macrophages further determines the degree of growth or survival of bacteria. For example, *S.* Typhimurium seems to survive better in splenic macrophages than in peritoneal macrophages (104). This is consistent with the main reported site of *Salmonella* infection (105).

At the cellular level, *S.* Typhimurium can enter in macrophages by SPI1 (*Salmonella* pathogenicity island-1)-dependent invasion (106) or by host cell-mediated phagocytosis or macropinocytosis, which occurs through either SPI-1-dependent or SPI-1-independent mechanisms (107). After invasion, *S.* Typhimurium

resides in a spacious phagosomal compartment that evolves to form a specific compartment called *Salmonella*-containing vacuole (SCV) (108). It is important to note that *Salmonella* finely regulate virulence gene expression while replicating inside a macrophage (109). Thus, bacteria can survive within the SCV, despite partial fusion with the lysosomal compartment (110). Acidification of the compartment induces the transcription of virulence genes of *S.* Typhimurium to inhibit macrophage phagosome acidification (111). In addition, the *Salmonella* pathogenicity island-2 encodes proteins required for bacterial replication (112, 113) but does not have a major influence on resistance to killing (114). Intracellular bacteria can exhibit large heterogeneity in growth rate inside the vacuolar environment of host cells. A segment of the bacterial population does not replicate inside the cell but instead appears to enter a dormant-like state, perhaps providing a reservoir for relapsing infection (114, 115). Recent transcriptomic analysis demonstrated that macrophages containing non-growing bacteria are in a pro-inflammatory state of polarization. By contrast, macrophages containing growing bacteria exist in an anti-inflammatory, M2-like state. Thus, the growth arrest of *Salmonella* seems to facilitate immune evasion and the establishment of a long-term niche, while macrophages with replicating bacteria allow *Salmonella* to escape intracellular antimicrobial activity and proliferate (116). The heterogeneous activity of bacterial factors in individual infecting bacteria determines the heterogeneity of immune responses of individual-infected host cells (117). Macrophage infection induces the production of pro-inflammatory mediators (118) but also leads to macrophage cell death (119), an essential virulence mechanism of *Salmonella* Typhimurium (120). One form of cell death, pyroptosis, occurs either *via* a rapid caspase-1-mediated SPI-1-dependent pathway or a delayed SPI-2-dependent caspase-1-mediated pathway. Caspase-1, a central effector of pyroptosis, is activated in the inflammasome complex during *Salmonella* infection and has a protective role during *Salmonella* infection *in vivo* (121).

HOST–PATHOGEN INTERACTION OF iNTS

In several studies, gentamicin protection assays were used to assess the invasion properties of the ST19 and ST313 strains

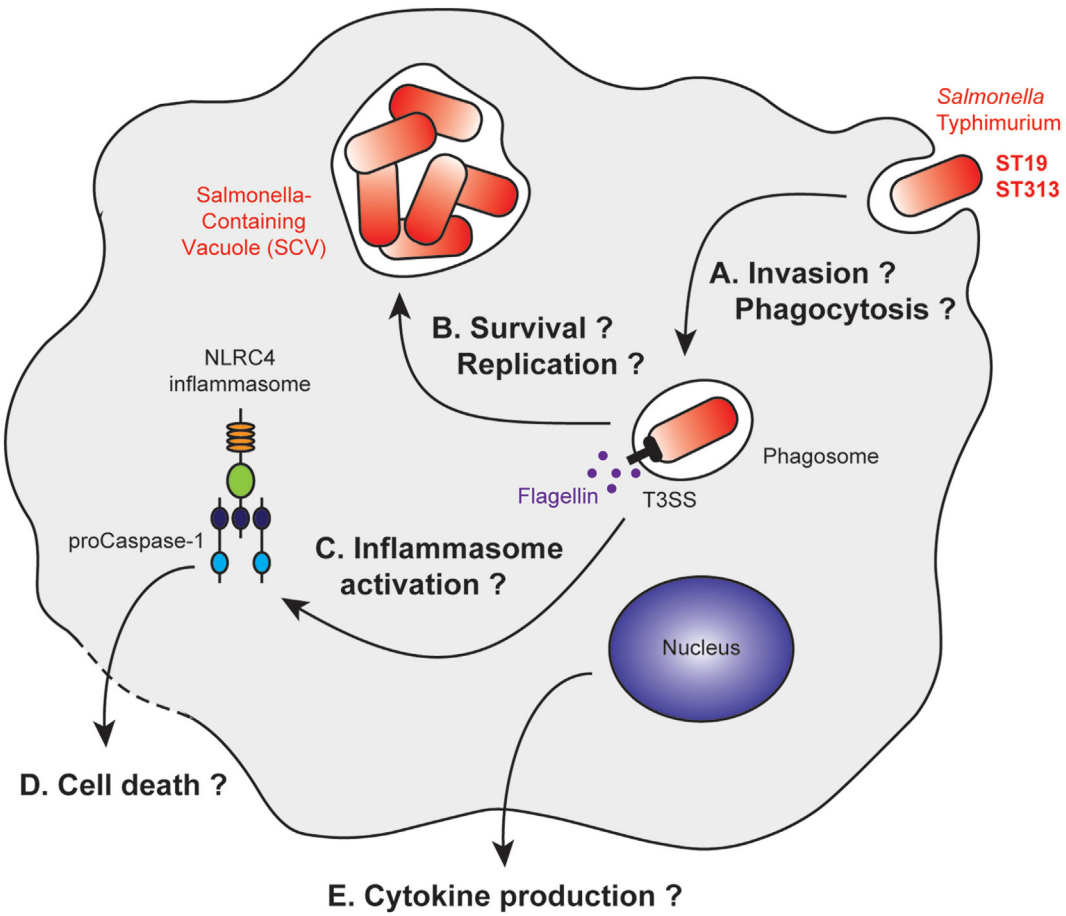


FIGURE 2 | Stages of *Salmonella* Typhimurium infection with differential macrophage response to ST19 or ST313 infection. After macrophage invasion **(A)**, *Salmonella* Typhimurium resides in vacuoles called *Salmonella*-containing vacuoles (SCV). The bacteria form this vacuole to prevent maturation of the phagosome into a phagolysosome **(B)**. Bacterial products, such as flagellin, are released after membrane rupture, or secreted into the cytosol. This leads to inflammasome activation **(C)** and IL1β production, which are associated or not with cell death pathways **(D)**. Other cytokines are released by the macrophage, and their secretions could be differentially regulated **(E)**.

in vitro (**Figure 2A**). Two studies found that ST313 invades less Hep2 and HeLa cells than ST19 (79, 92). By contrast, Herrero-Fresno et al. observed no difference in invasion of another human cell line (human epithelial Int407 cells) with ST19 (4/74) and ST313 (02-03/002) (82). In the final study, ST313 (D23580) was shown to be more invasive than ST19 (14028) in HeLa cells (88). Studies pertaining to macrophages have also generated conflicting data. J774 mouse macrophages phagocytose ST313 (D65, Q55, S11, S12, and A13) more efficiently than ST19 (I77, I41, S52, and I89) (91). Bone marrow-derived C57BL/6 macrophages are highly phagocytic of both ST19 (SL1344 and DT104) and ST313 (D23580, A130, 5597, and 5579) (92). Taken together, these results do not indicate major differences in the invasive capacity of the two strains.

The intracellular survival of the ST19 and ST313 strains was analyzed in various model systems, resulting in variable and contradictory data (**Figure 2B**). Ramachandran et al. demonstrated that ST313 (D65, Q55, S11, S12, and A13) survives better than ST19 (I77, I41, S52, and I89) within macrophages using several cell lines and primary cells (U937 cells, THP-1 cells, peritoneal macrophages from BALB/c mice and CD-1 mice, human peripheral blood mononuclear cells) (91). Two other studies in murine cell lines (J774 mouse macrophages, RAW264.7 murine macrophages-like cells), however, have shown that there are no differences in survival between the two strains (82, 88). These differences could be due to the opsonization of the bacteria, their growth phase at the time of infection, and the degradative properties of the infected cells (82, 88, 91). To date, no precise characterization of the SCV has been performed to understand whether there is a difference in the intracellular survivability of two strains.

Initially, it was observed that both strains, ST19 (4/74) and ST313 (02-03/002) induce the same cytotoxicity toward J774 mouse macrophages (82). By contrast, two studies on bone marrow-derived C57BL/6 macrophages (92) and THP-1 cells (91) have shown that ST313 (D65, D23580, A130, 5597, and 5579) induces less macrophage death than ST19 (I77, SL1344, and DT104). Cytotoxicity appears to be dependent on the NLRC4 inflammasome (92). However, a more recent study has suggested that ST313 (D23580) is more cytotoxic than ST19 (14028) toward the RAW264.7 murine macrophage cell line (88) (**Figures 2C,D**).

Cell activation was also compared in terms of cytokine production. ST313 (D65, D23580, A130, 5597, and 5579) induced less cytokine production by macrophages compared with ST19 (I77, SL1344, and DT104) for IL1β (91, 92), IL8, and TNFα (91). These studies were performed with the human THP-1 (91) and U937 cell lines (92), as well as with bone marrow-derived C57BL/6 macrophages (92) (**Figure 2E**).

To better understand NTS pathogenesis, different animal models can be used. The non-human primates, such as rhesus macaques, are especially useful for investigating coinfection with simian immunodeficiency virus (122). Calves can be used as infection models as their infection with *S.* Typhimurium results in a pathology similar to humans. Furthermore, *S.* Typhimurium is a natural pathogen of cattle, and beef is a common reservoir for human infection (123, 124). Poultry products are well known as a source of human infections (125). Interestingly, ST313 was reported to be more invasive than ST19 in experimentally infected chicken (126). Mice are not typically suitable as an adapted model for S. Typhimurium, as these bacteria induce a typhoid-like systemic illness that leads to death of the animals. Although the 50% lethal dose (LD_{50}) was not reported to be significantly different between ST313- and ST19-infected mice (87, 93). Further, there was no consistent difference in the inflammatory response (79, 88, 93, 126) or in the ability of the bacteria to colonize the intestinal tract and to disseminate in the body (79, 87, 88, 92, 93, 126).

WHAT IS KNOWN ABOUT THE COINFECTIONS WITH HIV AND *SALMONELLA*

Non-typhoidal salmonellae have been identified early as HIV-related pathogens in both adults and children in sub-Saharan Africa. Although HIV and *Salmonella* coinfections have been the focus of several studies, most of these aimed to characterize the intrinsic properties of the invasive *Salmonella* compared with reference strains, rather than study the co-evolution of the bacteria with the HIV epidemy. Some reports have pointed to the dysregulation of inflammation induced by HIV. During non-typhoid *Salmonella* and HIV coinfection, human blood displays attenuated NFkB-mediated inflammation (127) (**Figure 3**). Cytokine changes in acute iNTS disease are correlated with cytokine signatures associated with macrophage functions and with sepsis. HIV–*Salmonella* coinfection had no major impact on the blood cytokines of patients (128). In one study, primary human alveolar macrophages from a small number of HIV-infected adults did not display any differential internalization and killing of bacteria but showed a dysregulation of cytokine responses to *Salmonella*. Increased quantities of TNF, IL10, and IL12 were released in the HIV-positive samples in response to the bacterial challenge. This may underlie the susceptibility to severe salmonellosis of patients with AIDS (129). It is worth noting, however, that cytokine read-outs might represent the "tip of the iceberg" for other profoundly modified cell phenotypes that have recently received new attention, like imbalanced metabolic status, cell death, or survival pathway. All of these pathways should be further studied by global analysis of gene expression profiles in infected and coinfected cells.

The intracellular relationship between the VCC and the SCV could be also studied with high-resolution microscopy to determine if there are structural connections between the two types of compartments and to ascertain whether one strain of bacteria is better at exploiting the mechanisms described in **Figure 1**. For example (and as cited above), the analysis of phagocytic function in HIV-*Salmonella* coinfected individuals could be aided by novel assays such as the detection of defective superoxide burst by flow cytometry on whole blood samples, as for HIV/tuberculosis-infected individuals (67).

Importantly, the dysregulated humoral immunity in HIV-infected individuals is characterized by high titers of inhibitory antibodies against *Salmonella* LPS. This is associated with defective killing of the bacteria, which relies more on antibodies against the outer membrane proteins (130). Therefore, the HIV infection prevents efficient humoral immunity without blocking bacteria

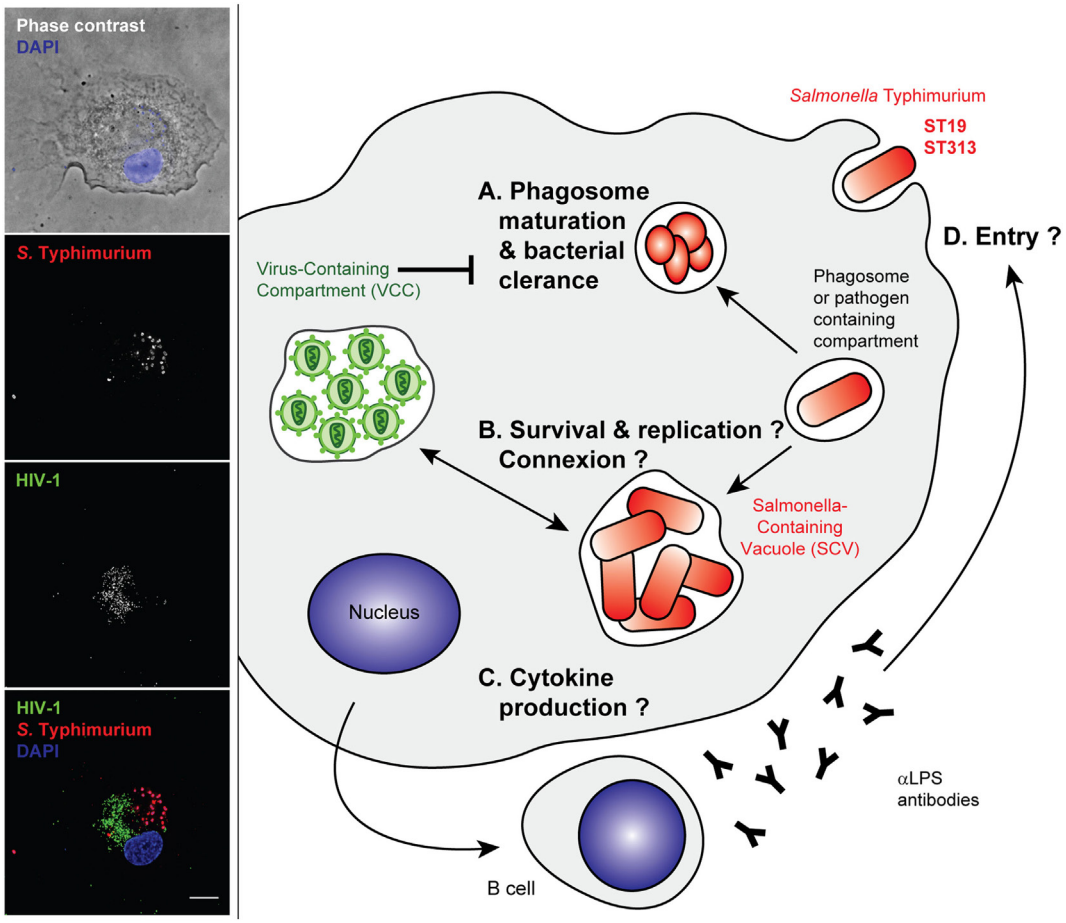


FIGURE 3 | Stages of *Salmonella* Typhimurium infection that may benefit from an established human immunodeficiency virus type 1 (HIV-1)-infection of the host cell. Left panel—Primary human macrophages were infected with HIV-1_{ADA} for 8 days before incubation with invasive *Salmonella* Typhimurium for 6 h at 37°C. They were fixed, permeabilized, and labeled with anti-p24 followed by Alexa488-anti-goat IgG (third line), anti-LPS followed by Cy5-anti-rabbit IgG (second line), and DAPI. Phase contrast image with DAPI (blue) is shown in the upper panel. Merged images (lower panel) show p24 in green (third line in gray), *S.* Typhimurium in red (second line in gray), and DAPI in blue. Z stacks of wide field fluorescent images were acquired, deconvoluted, and treated with ImageJ. Bar, 10 µm. Right panel—Intracellular bacteria may take advantage of arrested phagosome maturation in HIV-infected host cells, either **(A)** indirectly due to changes in intracellular trafficking or gene expression programs or **(B)** directly, through intracellular connections between *Salmonella*-containing vacuoles (SCV) and virus-containing compartment (VCC) that have neutral pH. The cell activation pathways and cytokine production were reported to be different between ST19 and ST313, although gene expression profiles are yet to be sufficiently dissected in the context of an HIV-infected host macrophage **(C)**. The humoral immune responses are biased, and anti-LPS antibodies are produced that are non-neutralizing and do not appear to block entry of bacteria **(D)**.

from invading host cells. The bacteria can then remain hidden within host cells to disseminate throughout the body (**Figure 3**).

CONCLUSION

The initial observation that macrophages are permissive to HIV infection was reported as early as in 1986. However, the effects of the viral infection on those phagocytic functions of macrophages and the emergence of opportunistic pathogens have been somewhat overlooked. One reason for that is that the reciprocal impact of the virus and the opportunistic pathogens on their common host is difficult to assess experimentally. Studying the cell biology of the *Salmonella* vacuole in HIV-infected hosts using tools developed recently for host–pathogen analysis, such as flow cytometry or advanced microscopy, may provide valuable information. In addition, the recent development of gene expression analysis, of both the bacteria and the host, in conjunction with single-cell analytical approaches, offers unprecedented opportunities for future studies to generate better understanding of the unique relationship between iNTS and the HIV-infected host. A better understanding of the interplay between HIV and these bacteria will have implications not only for treatment and management of *Salmonella* but also of other opportunistic pathogens.

AUTHOR CONTRIBUTIONS

Both authors have made a substantial, direct, and intellectual contribution to the work and approved it for publication.

ACKNOWLEDGMENTS

We thank Dr. Anna Mularski for reading the manuscript, Dr. Olivia Steele-Mortimer for advising us to work on *Salmonella* in the context of HIV-1, and Drs. Melita Gordon and Jay Hinton for their input. Work in the FN laboratory was supported by INSERM, CNRS, and Université Paris Descartes and grants from Agence Nationale de la Recherche, Fondation pour la Recherche Médicale ("Equipe FRM," DEQ20130326518), Sidaction, and ANRS (France Recherche Nord & Sud SIDA HIV Hepatites). FRM and ANRS contributed to support the PhD salary of GL-B.

REFERENCES

1. Hume DA, Wells CA, Ravasi T. Transcriptional regulatory networks in macrophages. *Novartis Found Symp* (2007) 281:2–18; discussion 24, 50–3, 208–9.
2. Delamarre L, Pack M, Chang H, Mellman I, Trombetta ES. Differential lysosomal proteolysis in antigen-presenting cells determines antigen fate. *Science* (2005) 307(5715):1630–4. doi:10.1126/science.1108003
3. Le Roux D, Le Bon A, Dumas A, Taleb K, Sachse M, Sikora R, et al. Antigen stored in dendritic cells after macropinocytosis is released unprocessed from late endosomes to target B cells. *Blood* (2012) 119(1):95–105. doi:10.1182/blood-2011-02-336123
4. Amigorena S, Savina A. Intracellular mechanisms of antigen cross presentation in dendritic cells. *Curr Opin Immunol* (2010) 22(1):109–17. doi:10.1016/j.coi.2010.01.022
5. Trombetta ES, Ebersold M, Garrett W, Pypaert M, Mellman I. Activation of lysosomal function during dendritic cell maturation. *Science* (2003) 299(5611):1400–3. doi:10.1126/science.1080106
6. Flannagan RS, Jaumouille V, Grinstein S. The cell biology of phagocytosis. *Annu Rev Pathol* (2012) 7:61–98. doi:10.1146/annurev-pathol-011811-132445
7. Prabhudas M, Bowdish D, Drickamer K, Febbraio M, Herz J, Kobzik L, et al. Standardizing scavenger receptor nomenclature. *J Immunol* (2014) 192(5):1997–2006. doi:10.4049/jimmunol.1490003
8. Mularski A, Niedergang F. Chapter 4: Phagosome formation and sealing: a physical point of view. *Phagocytosis: Overview, History and Role in Human Health and Disease*. Nova Science Publishers (2018). p. 111–34.
9. Niedergang F, Di Bartolo V, Alcover A. Comparative anatomy of phagocytic and immunological synapses. *Front Immunol* (2016) 7:18. doi:10.3389/fimmu.2016.00018
10. Bajno L, Peng X-R, Schreiber AD, Moore H-P, Trimble WS, Grinstein S. Focal exocytosis of VAMP3-containing vesicles at sites of phagosome formation. *J Cell Biol* (2000) 149:697–705. doi:10.1083/jcb.149.3.697
11. Braun V, Deschamps C, Raposo G, Benaroch P, Benmerah A, Chavrier P, et al. AP-1 and ARF1 control endosomal dynamics at sites of FcR mediated phagocytosis. *Mol Biol Cell* (2007) 18(12):4921–31. doi:10.1091/mbc.E07-04-0392
12. Niedergang F, Colucci-Guyon E, Dubois T, Raposo G, Chavrier P. ADP ribosylation factor 6 is activated and controls membrane delivery during phagocytosis in macrophages. *J Cell Biol* (2003) 161(6):1143–50. doi:10.1083/jcb.200210069
13. Marie-Anais F, Mazzolini J, Herit F, Niedergang F. Dynamin-actin cross talk contributes to phagosome formation and closure. *Traffic* (2016) 17(5):487–99. doi:10.1111/tra.12386
14. Desjardins M. Biogenesis of phagolysosomes: the 'kiss and run' hypothesis. *Trends Cell Biol* (1995) 5(5):183–6. doi:10.1016/S0962-8924(00)88989-8
15. Fairn GD, Grinstein S. How nascent phagosomes mature to become phagolysosomes. *Trends Immunol* (2012) 33(8):397–405. doi:10.1016/j.it.2012.03.003
16. Blocker A, Griffiths G, Olivo JC, Hyman AA, Severin FF. A role for microtubule dynamics in phagosome movement. *J Cell Sci* (1998) 111(Pt 3):303–12.
17. Blocker A, Severin FF, Burkhardt JK, Bingham JB, Yu H, Olivo JC, et al. Molecular requirements for bi-directional movement of phagosomes along microtubules. *J Cell Biol* (1997) 137(1):113–29. doi:10.1083/jcb.137.1.113
18. Dumas A, Le-Bury G, Marie-Anais F, Herit F, Mazzolini J, Guilbert T, et al. The HIV-1 protein Vpr impairs phagosome maturation by controlling microtubule-dependent trafficking. *J Cell Biol* (2015) 211(2):359–72. doi:10.1083/jcb.201503124
19. Christoforidis S, McBride HM, Burgoyne RD, Zerial M. The Rab5 effector EEA1 is a core component of endosome docking. *Nature* (1999) 397(6720):621–5. doi:10.1038/17618
20. Christoforidis S, Miaczynska M, Ashman K, Wilm M, Zhao L, Yip SC, et al. Phosphatidylinositol-3-OH kinases are Rab5 effectors. *Nat Cell Biol* (1999) 1(4):249–52. doi:10.1038/12075
21. Vieira OV, Botelho RJ, Rameh L, Brachmann SM, Matsuo T, Davidson HW, et al. Distinct roles of class I and class III phosphatidylinositol 3-kinases in phagosome formation and maturation. *J Cell Biol* (2001) 155(1):19–25. doi:10.1083/jcb.200107069
22. McBride HM, Rybin V, Murphy C, Giner A, Teasdale R, Zerial M. Oligomeric complexes link Rab5 effectors with NSF and drive membrane fusion via interactions between EEA1 and syntaxin 13. *Cell* (1999) 98(3):377–86. doi:10.1016/S0092-8674(00)81966-2
23. Kitano M, Nakaya M, Nakamura T, Nagata S, Matsuda M. Imaging of Rab5 activity identifies essential regulators for phagosome maturation. *Nature* (2008) 453(7192):241–5. doi:10.1038/nature06857
24. Yeo JC, Wall AA, Luo L, Stow JL. Sequential recruitment of Rab GTPases during early stages of phagocytosis. *Cell Logist* (2016) 6(1):e1140615. doi:10.1080/21592799.2016.1140615
25. Vieira OV, Bucci C, Harrison RE, Trimble WS, Lanzetti L, Gruenberg J, et al. Modulation of Rab5 and Rab7 recruitment to phagosomes by phosphatidylinositol 3-kinase. *Mol Cell Biol* (2003) 23(7):2501–14. doi:10.1128/MCB.23.7.2501-2514.2003
26. Nordmann M, Cabrera M, Perz A, Brocker C, Ostrowicz C, Engelbrecht-Vandre S, et al. The Mon1-Ccz1 complex is the GEF of the late endosomal Rab7 homolog Ypt7. *Curr Biol* (2010) 20(18):1654–9. doi:10.1016/j.cub.2010.08.002
27. Becken U, Jeschke A, Veltman K, Haas A. Cell-free fusion of bacteria-containing phagosomes with endocytic compartments. *Proc Natl Acad Sci U S A* (2010) 107(48):20726–31. doi:10.1073/pnas.1007295107
28. Barry AO, Boucherit N, Mottola G, Vadovic P, Trouplin V, Soubeyran P, et al. Impaired stimulation of p38alpha-MAPK/Vps41-HOPS by LPS from pathogenic *Coxiella burnetii* prevents trafficking to microbicidal phagolysosomes. *Cell Host Microbe* (2012) 12(6):751–63. doi:10.1016/j.chom.2012.10.015
29. Mrakovic A, Kay JG, Furuya W, Brumell JH, Botelho RJ. Rab7 and Arl8 GTPases are necessary for lysosome tubulation in macrophages. *Traffic* (2012) 13(12):1667–79. doi:10.1111/tra.12003
30. Harrison RE, Bucci C, Vieira OV, Schroer TA, Grinstein S. Phagosomes fuse with late endosomes and/or lysosomes by extension of membrane protrusions along microtubules: role of Rab7 and RILP. *Mol Cell Biol* (2003) 23(18):6494–506. doi:10.1128/MCB.23.18.6494-6506.2003
31. Johansson M, Rocha N, Zwart W, Jordens I, Janssen L, Kuijl C, et al. Activation of endosomal dynein motors by stepwise assembly of Rab7-RILP-p150Glued, ORP1L, and the receptor betalll spectrin. *J Cell Biol* (2007) 176(4):459–71. doi:10.1083/jcb.200606077
32. Garg S, Sharma M, Ung C, Tuli A, Barral DC, Hava DL, et al. Lysosomal trafficking, antigen presentation, and microbial killing are controlled by the Arf-like GTPase Arl8b. *Immunity* (2011) 35(2):182–93. doi:10.1016/j.immuni.2011.06.009
33. Sasaki A, Nakae I, Nagasawa M, Hashimoto K, Abe F, Saito K, et al. Arl8/ARL-8 functions in apoptotic cell removal by mediating phagolysosome formation in *Caenorhabditis elegans*. *Mol Biol Cell* (2013) 24(10):1584–92. doi:10.1091/mbc.E12-08-0628
34. Rosa-Ferreira C, Munro S. Arl8 and SKIP act together to link lysosomes to kinesin-1. *Dev Cell* (2011) 21(6):1171–8. doi:10.1016/j.devcel.2011.10.007
35. Guardia CM, Farias GG, Jia R, Pu J, Bonifacino JS. BORC functions upstream of kinesins 1 and 3 to coordinate regional movement of lysosomes along different microtubule tracks. *Cell Rep* (2016) 17(8):1950–61. doi:10.1016/j.celrep.2016.10.062

36. Marwaha R, Arya SB, Jagga D, Kaur H, Tuli A, Sharma M. The Rab7 effector PLEKHM1 binds Arl8b to promote cargo traffic to lysosomes. *J Cell Biol* (2017) 216(4):1051–70. doi:10.1083/jcb.201607085
37. Steinberg BE, Huynh KK, Brodovitch A, Jabs S, Stauber T, Jentsch TJ, et al. A cation counterflux supports lysosomal acidification. *J Cell Biol* (2010) 189(7):1171–86. doi:10.1083/jcb.200911083
38. Flannagan RS, Cosio G, Grinstein S. Antimicrobial mechanisms of phagocytes and bacterial evasion strategies. *Nat Rev Microbiol* (2009) 7(5):355–66. doi:10.1038/nrmicro2128
39. Yang CS, Rodgers M, Min CK, Lee JS, Kingeter L, Lee JY, et al. The autophagy regulator Rubicon is a feedback inhibitor of CARD9-mediated host innate immunity. *Cell Host Microbe* (2012) 11(3):277–89. doi:10.1016/j.chom.2012.01.019
40. Savina A, Amigorena S. Phagocytosis and antigen presentation in dendritic cells. *Immunol Rev* (2007) 219:143–56. doi:10.1111/j.1600-065X.2007.00552.x
41. Pauwels AM, Trost M, Beyaert R, Hoffmann E. Patterns, receptors, and signals: regulation of phagosome maturation. *Trends Immunol* (2017) 38(6):407–22. doi:10.1016/j.it.2017.03.006
42. Centers for Disease Control. Kaposi's sarcoma and *Pneumocystis* pneumonia among homosexual men – New York City and California. *MMWR Morb Mortal Wkly Rep* (1981) 30(25):305–8.
43. Lewin SR, Crowe SM. AIDS pathogenesis. *AIDS* (1994) 8(Suppl 2):S3–11.
44. Crowe S, Mills J, McGrath MS. Quantitative immunocytofluorographic analysis of CD4 surface antigen expression and HIV infection of human peripheral blood monocyte/macrophages. *AIDS Res Hum Retroviruses* (1987) 3(2):135–45. doi:10.1089/aid.1987.3.135
45. Sonza S, Kiernan RE, Maerz AL, Deacon NJ, McPhee DA, Crowe SM. Accumulation of unintegrated circular viral DNA in monocytes and growth-arrested T cells following infection with HIV-1. *J Leukoc Biol* (1994) 56(3):289–93. doi:10.1002/jlb.56.3.289
46. Carter CA, Ehrlich LS. Cell biology of HIV-1 infection of macrophages. *Annu Rev Microbiol* (2008) 62:425–43. doi:10.1146/annurev.micro.62.081307.162758
47. Gartner S. The macrophage and HIV: basic concepts and methodologies. *Methods Mol Biol* (2014) 1087:207–20. doi:10.1007/978-1-62703-670-2_17
48. Coleman CM, Wu L. HIV interactions with monocytes and dendritic cells: viral latency and reservoirs. *Retrovirology* (2009) 6:51. doi:10.1186/1742-4690-6-51
49. Cobos-Jimenez V, Booiman T, Hamann J, Kootstra NA. Macrophages and HIV-1. *Curr Opin HIV AIDS* (2011) 6(5):385–90. doi:10.1097/COH.0b013e3283497203
50. Rodrigues V, Ruffin N, San-Roman M, Benaroch P. Myeloid cell interaction with HIV: a complex relationship. *Front Immunol* (2017) 8:1698. doi:10.3389/fimmu.2017.01698
51. Crowe SM, Vardaxis NJ, Kent SJ, Maerz AL, Hewish MJ, McGrath MS, et al. HIV infection of monocyte-derived macrophages in vitro reduces phagocytosis of *Candida albicans*. *J Leukoc Biol* (1994) 56(3):318–27. doi:10.1002/jlb.56.3.318
52. Kedzierska K, Mak J, Jaworowski A, Greenway A, Violo A, Chan HT, et al. nef-deleted HIV-1 inhibits phagocytosis by monocyte-derived macrophages in vitro but not by peripheral blood monocytes in vivo. *AIDS* (2001) 15(8):945–55. doi:10.1097/00002030-200105250-00002
53. Biggs BA, Hewish M, Kent S, Hayes K, Crowe SM. HIV-1 infection of human macrophages impairs phagocytosis and killing of *Toxoplasma gondii*. *J Immunol* (1995) 154(11):6132–9.
54. Torre D, Gennero L, Baccino FM, Speranza F, Biondi G, Pugliese A. Impaired macrophage phagocytosis of apoptotic neutrophils in patients with human immunodeficiency virus type 1 infection. *Clin Diagn Lab Immunol* (2002) 9(5):983–6. doi:10.1128/CDLI.9.5.983–986.2002
55. Kedzierska K, Azzam R, Ellery P, Mak J, Jaworowski A, Crowe SM. Defective phagocytosis by human monocyte/macrophages following HIV-1 infection: underlying mechanisms and modulation by adjunctive cytokine therapy. *J Clin Virol* (2003) 26(2):247–63. doi:10.1016/S1386-6532(02)00123-3
56. Kent SJ, Stent G, Sonza S, Hunter SD, Crowe SM. HIV-1 infection of monocyte-derived macrophages reduces Fc and complement receptor expression. *Clin Exp Immunol* (1994) 95(3):450–4. doi:10.1111/j.1365-2249.1994.tb07017.x
57. Koziel H, Eichbaum Q, Kruskal BA, Pinkston P, Rogers RA, Armstrong MY, et al. Reduced binding and phagocytosis of *Pneumocystis carinii* by alveolar macrophages from persons infected with HIV-1 correlates with mannose receptor downregulation. *J Clin Invest* (1998) 102(7):1332–44. doi:10.1172/JCI560
58. Foster JL, Garcia JV. HIV-1 Nef: at the crossroads. *Retrovirology* (2008) 5:84. doi:10.1186/1742-4690-5-84
59. Witkowski W, Verhasselt B. Contributions of HIV-1 Nef to immune dysregulation in HIV-infected patients: a therapeutic target? *Expert Opin Ther Targets* (2013) 17(11):1345–56. doi:10.1517/14728222.2013.830712
60. Olivetta E, Tirelli V, Chiozzini C, Scazzocchio B, Romano I, Arenaccio C, et al. HIV-1 Nef impairs key functional activities in human macrophages through CD36 downregulation. *PLoS One* (2014) 9(4):e93699. doi:10.1371/journal.pone.0093699
61. Mazzolini J, Herit F, Bouchet J, Benmerah A, Benichou S, Niedergang F. Inhibition of phagocytosis in HIV-1-infected macrophages relies on Nef-dependent alteration of focal delivery of recycling compartments. *Blood* (2010) 115(21):4226–36. doi:10.1182/blood-2009-12-259473
62. Lefkir Y, Malbouyres M, Gotthardt D, Ozinsky A, Cornillon S, Bruckert F, et al. Involvement of the AP-1 adaptor complex in early steps of phagocytosis and macropinocytosis. *Mol Biol Cell* (2004) 15(2):861–9. doi:10.1091/mbc.E03-06-0365
63. Marion S, Mazzolini J, Herit F, Bourdoncle P, Kambou-Pene N, Hailfinger S, et al. The NF-kappaB signaling protein Bcl10 regulates actin dynamics by controlling AP1 and OCRL-bearing vesicles. *Dev Cell* (2012) 23(5):954–67. doi:10.1016/j.devcel.2012.09.021
64. Azzam R, Kedzierska K, Leeansyah E, Chan H, Doischer D, Gorry PR, et al. Impaired complement-mediated phagocytosis by HIV type-1-infected human monocyte-derived macrophages involves a cAMP-dependent mechanism. *AIDS Res Hum Retroviruses* (2006) 22(7):619–29. doi:10.1089/aid.2006.22.619
65. Leeansyah E, Wines BD, Crowe SM, Jaworowski A. The mechanism underlying defective Fcgamma receptor-mediated phagocytosis by HIV-1-infected human monocyte-derived macrophages. *J Immunol* (2007) 178(2):1096–104. doi:10.4049/jimmunol.178.2.1096
66. Jambo KC, Banda DH, Kankwatira AM, Sukumar N, Allain TJ, Heyderman RS, et al. Small alveolar macrophages are infected preferentially by HIV and exhibit impaired phagocytic function. *Mucosal Immunol* (2014) 7(5):1116–26. doi:10.1038/mi.2013.127
67. Gupta-Wright A, Tembo D, Jambo KC, Chimbayo E, Mvaya L, Caldwell S, et al. Functional analysis of phagocyte activity in whole blood from HIV/tuberculosis-infected individuals using a novel flow cytometry-based assay. *Front Immunol* (2017) 8:1222. doi:10.3389/fimmu.2017.01222
68. Reuben JM, Turpin JA, Lee BN, Doyle M, Gonik B, Jacobson R, et al. Induction of inflammatory cytokines in placental monocytes of gravidae infected with the human immunodeficiency virus type 1. *J Interferon Cytokine Res* (1996) 16(11):963–71. doi:10.1089/jir.1996.16.963
69. Kedzierska K, Ellery P, Mak J, Lewin SR, Crowe SM, Jaworowski A. HIV-1 down-modulates gamma signaling chain of Fc gamma R in human macrophages: a possible mechanism for inhibition of phagocytosis. *J Immunol* (2002) 168(6):2895–903. doi:10.4049/jimmunol.168.6.2895
70. Gilks CF, Brindle RJ, Otieno LS, Simani PM, Newnham RS, Bhatt SM, et al. Life-threatening bacteraemia in HIV-1 seropositive adults admitted to hospital in Nairobi, Kenya. *Lancet* (1990) 336(8714):545–9. doi:10.1016/0140-6736(90)92096-Z
71. Gordon MA, Walsh AL, Chaponda M, Soko D, Mbvwinji M, Molyneux ME, et al. Bacteraemia and mortality among adult medical admissions in Malawi – predominance of non-typhi salmonellae and *Streptococcus* pneumoniae. *J Infect* (2001) 42(1):44–9. doi:10.1053/jinf.2000.0779
72. Gordon MA, Banda HT, Gondwe M, Gordon SB, Boeree MJ, Walsh AL, et al. Non-typhoidal *Salmonella* bacteraemia among HIV-infected Malawian adults: high mortality and frequent recrudescence. *AIDS* (2002) 16(12):1633–41. doi:10.1097/00002030-200208160-00009
73. Okoro CK, Kingsley RA, Quail MA, Kankwatira AM, Feasey NA, Parkhill J, et al. High-resolution single nucleotide polymorphism analysis distinguishes recrudescence and reinfection in recurrent invasive nontyphoidal *Salmonella typhimurium* disease. *Clin Infect Dis* (2012) 54(7):955–63. doi:10.1093/cid/cir1032

74. Gordon MA, Graham SM, Walsh AL, Wilson L, Phiri A, Molyneux E, et al. Epidemics of invasive *Salmonella enterica* serovar enteritidis and *S. enterica* serovar typhimurium infection associated with multidrug resistance among adults and children in Malawi. *Clin Infect Dis* (2008) 46(7):963–9. doi:10.1086/529146
75. Gordon MA. *Salmonella* infections in immunocompromised adults. *J Infect* (2008) 56(6):413–22. doi:10.1016/j.jinf.2008.03.012
76. Feasey NA, Dougan G, Kingsley RA, Heyderman RS, Gordon MA. Invasive non-typhoidal *Salmonella* disease: an emerging and neglected tropical disease in Africa. *Lancet* (2012) 379(9835):2489–99. doi:10.1016/S0140-6736(11)61752-2
77. Kingsley RA, Msefula CL, Thomson NR, Kariuki S, Holt KE, Gordon MA, et al. Epidemic multiple drug resistant *Salmonella* Typhimurium causing invasive disease in sub-Saharan Africa have a distinct genotype. *Genome Res* (2009) 19(12):2279–87. doi:10.1101/gr.091017.109
78. Okoro CK, Kingsley RA, Connor TR, Harris SR, Parry CM, Al-Mashhadani MN, et al. Intracontinental spread of human invasive *Salmonella* Typhimurium pathovariants in sub-Saharan Africa. *Nat Genet* (2012) 44(11):1215–21. doi:10.1038/ng.2423
79. Okoro CK, Barquist L, Connor TR, Harris SR, Clare S, Stevens MP, et al. Signatures of adaptation in human invasive *Salmonella* Typhimurium ST313 populations from sub-Saharan Africa. *PLoS Negl Trop Dis* (2015) 9(3):e0003611. doi:10.1371/journal.pntd.0003611
80. McClelland M, Sanderson KE, Clifton SW, Latreille P, Porwollik S, Sabo A, et al. Comparison of genome degradation in Paratyphi A and Typhi, human-restricted serovars of *Salmonella enterica* that cause typhoid. *Nat Genet* (2004) 36(12):1268–74. doi:10.1038/ng1470
81. Owen SV, Wenner N, Canals R, Makumi A, Hammarlof DL, Gordon MA, et al. Characterization of the prophage repertoire of African *Salmonella* Typhimurium ST313 reveals high levels of spontaneous induction of novel phage BTP1. *Front Microbiol* (2017) 8:235. doi:10.3389/fmicb.2017.00235
82. Herrero-Fresno A, Wallrodt I, Leekitcharoenphon P, Olsen JE, Aarestrup FM, Hendriksen RS. The role of the st313-td gene in virulence of *Salmonella* Typhimurium ST313. *PLoS One* (2014) 9(1):e84566. doi:10.1371/journal.pone.0084566
83. Kintz E, Davies MR, Hammarlof DL, Canals R, Hinton JC, van der Woude MWA. BTP1 prophage gene present in invasive non-typhoidal *Salmonella* determines composition and length of the O-antigen of the lipopolysaccharide. *Mol Microbiol* (2015) 96(2):263–75. doi:10.1111/mmi.12933
84. Micoli F, Ravenscroft N, Cescutti P, Stefanetti G, Londero S, Rondini S, et al. Structural analysis of O-polysaccharide chains extracted from different *Salmonella* Typhimurium strains. *Carbohydr Res* (2014) 385:1–8. doi:10.1016/j.carres.2013.12.003
85. Rondini S, Micoli F, Lanzilao L, Gavini M, Alfini R, Brandt C, et al. Design of glycoconjugate vaccines against invasive African *Salmonella* enterica serovar Typhimurium. *Infect Immun* (2015) 83(3):996–1007. doi:10.1128/IAI.03079-14
86. Goh YS, Clare S, Micoli F, Saul A, Mastroeni P, MacLennan CA. Monoclonal antibodies of a diverse isotype induced by an O-antigen glycoconjugate vaccine mediate in vitro and in vivo killing of African invasive nontyphoidal *Salmonella*. *Infect Immun* (2015) 83(9):3722–31. doi:10.1128/IAI.00547-15
87. Yang J, Barrila J, Roland KL, Kilbourne J, Ott CM, Forsyth RJ, et al. Characterization of the invasive, multidrug resistant non-typhoidal *Salmonella* strain d23580 in a murine model of infection. *PLoS Negl Trop Dis* (2015) 9(6):e0003839. doi:10.1371/journal.pntd.0003839
88. Singletary LA, Karlinsey JE, Libby SJ, Mooney JP, Lokken KL, Tsolis RM, et al. Loss of multicellular behavior in epidemic African nontyphoidal *Salmonella enterica* serovar Typhimurium ST313 strain D23580. *MBio* (2016) 7(2):e02265. doi:10.1128/mBio.02265-15
89. Simm R, Ahmad I, Rhen M, Le Guyon S, Romling U. Regulation of biofilm formation in *Salmonella enterica* serovar Typhimurium. *Future Microbiol* (2014) 9(11):1261–82. doi:10.2217/fmb.14.88
90. Ramachandran G, Aheto K, Shirtliff ME, Tennant SM. Poor biofilm-forming ability and long-term survival of invasive *Salmonella* Typhimurium ST313. *Pathog Dis* (2016) 74(5):ftw049. doi:10.1093/femspd/ftw049
91. Ramachandran G, Perkins DJ, Schmidlein PJ, Tulapurkar ME, Tennant SM. Invasive *Salmonella* Typhimurium ST313 with naturally attenuated flagellin elicits reduced inflammation and replicates within macrophages. *PLoS Negl Trop Dis* (2015) 9(1):e3394. doi:10.1371/journal.pntd.0003394
92. Carden S, Okoro C, Dougan G, Monack D. Non-typhoidal *Salmonella* Typhimurium ST313 isolates that cause bacteremia in humans stimulate less inflammasome activation than ST19 isolates associated with gastroenteritis. *Pathog Dis* (2015) 73(4):ftu023. doi:10.1093/femspd/ftu023
93. Ramachandran G, Panda A, Higginson EE, Ateh E, Lipsky MM, Sen S, et al. Virulence of invasive *Salmonella* Typhimurium ST313 in animal models of infection. *PLoS Negl Trop Dis* (2017) 11(8):e0005697. doi:10.1371/journal.pntd.0005697
94. Vazquez-Torres A, Jones-Carson J, Baumler AJ, Falkow S, Valdivia R, Brown W, et al. Extraintestinal dissemination of *Salmonella* by CD18-expressing phagocytes. *Nature* (1999) 401(6755):804–8. doi:10.1038/44593
95. Hopkins S, Niedergang F, Corthésy-Theulaz I, Kraehenbuhl J-P. A recombinant *Salmonella typhimurium* vaccine strain is taken up and survives within murine Peyer's patch dendritic cells. *Cell Microbiol* (2000) 2:59–68. doi:10.1046/j.1462-5822.2000.00035.x
96. Rescigno M, Urbano M, Valzasina B, Francolini M, Rotta G, Bonasio R, et al. Dendritic cells express tight junction proteins and penetrate gut epithelial monolayers to sample bacteria. *Nat Immunol* (2001) 2(4):361–7. doi:10.1038/86373
97. Monack DM, Bouley DM, Falkow S. *Salmonella typhimurium* persists within macrophages in the mesenteric lymph nodes of chronically infected Nramp1+/+ mice and can be reactivated by IFNgamma neutralization. *J Exp Med* (2004) 199(2):231–41. doi:10.1084/jem.20031319
98. Vazquez-Torres A, Xu Y, Jones-Carson J, Holden DW, Lucia SM, Dinauer MC, et al. *Salmonella* pathogenicity island 2-dependent evasion of the phagocyte NADPH oxidase. *Science* (2000) 287(5458):1655–8. doi:10.1126/science.287.5458.1655
99. Fields PI, Groisman EA, Heffron FA. *Salmonella* locus that controls resistance to microbicidal proteins from phagocytic cells. *Science* (1989) 243(4894 Pt 1):1059–62. doi:10.1126/science.2646710
100. Fields PI, Swanson RV, Haidaris CG, Heffron F. Mutants of *Salmonella typhimurium* that cannot survive within the macrophage are avirulent. *Proc Natl Acad Sci U S A* (1986) 83:5189–93. doi:10.1073/pnas.83.14.5189
101. Miller SI, Mekalanos JJ. Constitutive expression of the *phoP* regulon attenuates *Salmonella* virulence and survival within macrophages. *J Bacteriol* (1990) 172:2485–90. doi:10.1128/jb.172.5.2485-2490.1990
102. Gog JR, Murcia A, Osterman N, Restif O, McKinley TJ, Sheppard M, et al. Dynamics of *Salmonella* infection of macrophages at the single cell level. *J R Soc Interface* (2012) 9(75):2696–707. doi:10.1098/rsif.2012.0163
103. Lathrop SK, Binder KA, Starr T, Cooper KG, Chong A, Carmody AB, et al. Replication of *Salmonella* enterica serovar Typhimurium in human monocyte-derived macrophages. *Infect Immun* (2015) 83(7):2661–71. doi:10.1128/IAI.00033-15
104. Buchmeier NA, Heffron F. Intracellular survival of wild-type *Salmonella typhimurium* and macrophage-sensitive mutants in diverse populations of macrophages. *Infect Immun* (1989) 57(1):1–7.
105. Akeda H, Mitsuyama M, Tatsukawa K, Nomoto K, Takeya K. The synergistic contribution of macrophages and antibody to protection against *Salmonella typhimurium* during the early phase of infection. *J Gen Microbiol* (1981) 123(2):209–14. doi:10.1099/00221287-123-2-209
106. Drecktrah D, Knodler LA, Ireland R, Steele-Mortimer O. The mechanism of *Salmonella* entry determines the vacuolar environment and intracellular gene expression. *Traffic* (2006) 7(1):39–51. doi:10.1111/j.1600-0854.2005.00360.x
107. Alpuche-Aranda CM, Racoosin EL, Swanson JA, Miller SI. *Salmonella* stimulate macrophage macropinocytosis and persist within spacious phagosomes. *J Exp Med* (1994) 179:601–8. doi:10.1084/jem.179.2.601
108. Oh Y-K, Alpuche-Aranda C, Berthiaume E, Jinks T, Miller SI, Swanson JA. Rapid and complete fusion of macrophage lysosomes with phagosomes containing *Salmonella typhimurium*. *Infect Immun* (1996) 64:3877–83.
109. Srikumar S, Kröger C, Hébrard M, Colgan A, Beckett M, Luque-Sastre L, et al. The intra-macrophage transcriptome of *Salmonella* Typhimurium identifies a genus-specific sRNA required for virulence. *PLoS Pathog* (2015) 11(11):e1005262. doi:10.1371/journal.ppat.1005262
110. Eswarappa SM, Negi VD, Chakraborty S, Chandrasekhar Sagar BK, Chakravortty D. Division of the *Salmonella*-containing vacuole and depletion

of acidic lysosomes in *Salmonella*-infected host cells are novel strategies of *Salmonella* enterica to avoid lysosomes. *Infect Immun* (2010) 78(1):68–79. doi:10.1128/IAI.00668-09

111. Alpuche Aranda CM, Swanson JA, Loomis WP, Miller SI. *Salmonella typhimurium* activates virulence gene transcription within acidified macrophage phagosomes. *Proc Natl Acad Sci U S A* (1992) 89(21):10079–83. doi:10.1073/pnas.89.21.10079
112. Cirillo DM, Valdivia RH, Monack DM, Falkow S. Macrophage-dependent induction of the *Salmonella* pathogenicity island 2 type III secretion system and its role in intracellular survival. *Mol Microbiol* (1998) 30(1):175–88. doi:10.1046/j.1365-2958.1998.01048.x
113. Salcedo SP, Noursadeghi M, Cohen J, Holden DW. Intracellular replication of *Salmonella typhimurium* strains in specific subsets of splenic macrophages in vivo. *Cell Microbiol* (2001) 3(9):587–97. doi:10.1046/j.1462-5822.2001.00137.x
114. Helaine S, Thompson JA, Watson KG, Liu M, Boyle C, Holden DW. Dynamics of intracellular bacterial replication at the single cell level. *Proc Natl Acad Sci U S A* (2010) 107(8):3746–51. doi:10.1073/pnas.1000041107
115. Helaine S, Cheverton AM, Watson KG, Faure LM, Matthews SA, Holden DW. Internalization of *Salmonella* by macrophages induces formation of nonreplicating persisters. *Science* (2014) 343(6167):204–8. doi:10.1126/science.1244705
116. Saliba AE, Li L, Westermann AJ, Appenzeller S, Stapels DA, Schulte LN, et al. Single-cell RNA-seq ties macrophage polarization to growth rate of intracellular *Salmonella*. *Nat Microbiol* (2016) 2:16206. doi:10.1038/nmicrobiol.2016.206
117. Avraham R, Haseley N, Brown D, Penaranda C, Jijon HB, Trombetta JJ, et al. Pathogen cell-to-cell variability drives heterogeneity in host immune responses. *Cell* (2015) 162(6):1309–21. doi:10.1016/j.cell.2015.08.027
118. Royle MC, Totemeyer S, Alldridge LC, Maskell DJ, Bryant CE. Stimulation of Toll-like receptor 4 by lipopolysaccharide during cellular invasion by live *Salmonella typhimurium* is a critical but not exclusive event leading to macrophage responses. *J Immunol* (2003) 170(11):5445–54. doi:10.4049/jimmunol.170.11.5445
119. Monack DM, Raupach B, Hromockyj AE, Falkow S. *Salmonella typhimurium* invasion induces apoptosis in infected macrophages. *Proc Natl Acad Sci U S A* (1996) 93:9833–8. doi:10.1073/pnas.93.18.9833
120. Lindgren SW, Stojiljkovic I, Heffron F. Macrophage killing is an essential virulence mechanism of *Salmonella typhimurium*. *Proc Natl Acad Sci U S A* (1996) 93:4197–201. doi:10.1073/pnas.93.9.4197
121. Fink SL, Cookson BT. Pyroptosis and host cell death responses during *Salmonella* infection. *Cell Microbiol* (2007) 9(11):2562–70. doi:10.1111/j.1462-5822.2007.01036.x
122. Raffatellu M, Santos RL, Verhoeven DE, George MD, Wilson RP, Winter SE, et al. Simian immunodeficiency virus-induced mucosal interleukin-17 deficiency promotes *Salmonella* dissemination from the gut. *Nat Med* (2008) 14(4):421–8. doi:10.1038/nm1743
123. Santos RL, Zhang S, Tsolis RM, Kingsley RA, Adams LG, Baumler AJ. Animal models of *Salmonella* infections: enteritis versus typhoid fever. *Microbes Infect.* (2001) 3(14–15):1335–44. doi:10.1016/S1286-4579(01)01495-2
124. Costa LF, Paixao TA, Tsolis RM, Baumler AJ, Santos RL. Salmonellosis in cattle: advantages of being an experimental model. *Res Vet Sci* (2012) 93(1):1–6. doi:10.1016/j.rvsc.2012.03.002
125. Barrow PA, Jones MA, Smith AL, Wigley P. The long view: *Salmonella* – the last forty years. *Avian Pathol* (2012) 41(5):413–20. doi:10.1080/03079457.2012.718071
126. Parsons BN, Humphrey S, Salisbury AM, Mikoleit J, Hinton JC, Gordon MA, et al. Invasive non-typhoidal *Salmonella typhimurium* ST313 are not host-restricted and have an invasive phenotype in experimentally infected chickens. *PLoS Negl Trop Dis* (2013) 7(10):e2487. doi:10.1371/journal.pntd.0002487
127. Schreiber F, Lynn DJ, Houston A, Peters J, Mwafulirwa G, Finlay BB, et al. The human transcriptome during nontyphoid *Salmonella* and HIV coinfection reveals attenuated NFkappaB-mediated inflammation and persistent cell cycle disruption. *J Infect Dis* (2011) 204(8):1237–45. doi:10.1093/infdis/jir512
128. Gilchrist JJ, Heath JN, Msefula CL, Gondwe EN, Naranbhai V, Mandala W, et al. Cytokine profiles during invasive nontyphoidal *Salmonella* disease predict outcome in African children. *Clin Vaccine Immunol* (2016) 23(7):601–9. doi:10.1128/CVI.00128-16
129. Gordon MA, Gordon SB, Musaya L, Zijlstra EE, Molyneux ME, Read RC. Primary macrophages from HIV-infected adults show dysregulated cytokine responses to *Salmonella*, but normal internalization and killing. *AIDS* (2007) 21(18):2399–408. doi:10.1097/QAD.0b013e3282f25107
130. MacLennan CA, Gilchrist JJ, Gordon MA, Cunningham AF, Cobbold M, Goodall M, et al. Dysregulated humoral immunity to nontyphoidal *Salmonella* in HIV-infected African adults. *Science* (2010) 328(5977):508–12. doi:10.1126/science.1180346

Conflict of Interest Statement: The authors declare that the research was conducted in the absence of any commercial or financial relationships that could be construed as a potential conflict of interest.

Copyright © 2018 Lê-Bury and Niedergang. This is an open-access article distributed under the terms of the Creative Commons Attribution License (CC BY). The use, distribution or reproduction in other forums is permitted, provided the original author(s) and the copyright owner are credited and that the original publication in this journal is cited, in accordance with accepted academic practice. No use, distribution or reproduction is permitted which does not comply with these terms.

frontiers in Immunology

MINI REVIEW
published: 04 June 2018
doi: 10.3389/fimmu.2018.01276

Perturbation of Intracellular Cholesterol and Fatty Acid Homeostasis During Flavivirus Infections

Joao Palma Pombo[1] *and Sumana Sanyal*[1,2]*

[1] HKU-Pasteur Research Pole, School of Public Health, The University of Hong Kong, Hong Kong, Hong Kong,
[2] School of Biomedical Sciences, Li Ka Shing Faculty of Medicine, The University of Hong Kong, Hong Kong, Hong Kong

Cellular lipid homeostasis is maintained through an intricately linked array of anabolic and catabolic pathways. Upon flavivirus infections, these are significantly altered: on the one hand, these viruses can co-opt lipid metabolic pathways to generate ATP to facilitate replication, or to synthesize membrane components to generate replication sites; on the other hand, more recent evidence suggests counter strategies employed by host cells, which actively modulate several of these networks in response to infection, enhancing interferon signaling by doing so, and thus creating an antiviral environment. In this review, we discuss recent data on mechanisms of alteration of lipid metabolic pathways during infection by flaviviruses, with a focus on cholesterol and fatty acid biosynthesis, which can be manipulated by the invading viruses to support replication, but can also be modulated by the host immune system itself, as a means to fight infection.

Keywords: cholesterol, lipid metabolism, virus, innate immunity, fatty acid

OPEN ACCESS

Edited by:
Geanncarlo Lugo-Villarino, UMR5089 Institut de Pharmacologie et de Biologie Structurale (IPBS), France

Reviewed by:
Benjamin Jennings Renquist, University of Arizona, United States
Mario Antonio Bianchet, Johns Hopkins University, United States

***Correspondence:**
Sumana Sanyal
sanyal@hku.hk

Specialty section:
This article was submitted to Microbial Immunology, a section of the journal Frontiers in Immunology

Received: *28 November 2017*
Accepted: *22 May 2018*
Published: *04 June 2018*

Citation:
Pombo JP and Sanyal S (2018) Perturbation of Intracellular Cholesterol and Fatty Acid Homeostasis During Flavivirus Infections. Front. Immunol. 9:1276. doi: 10.3389/fimmu.2018.01276

INTRODUCTION

Metabolic reprogramming in immune cells is a recurrent phenomenon when exposed to pro-inflammatory stimulants in the form of pathogens or cytokines. Macrophages and dendritic cells in particular are well-equipped to sense and respond to impending danger by pathogens, thus establishing the frontline of host defenses. Recent studies have highlighted the extraordinary contribution that multiple host metabolic pathways confer toward the ability of innate immune cells to respond to infections (1). Not surprisingly, some of the very same pathways that function to eradicate infection are often rewired by the invading pathogen.

Most viruses are known to induce aerobic glycolysis akin to the Warburg effect (2, 3). More recently, perturbation in lipid metabolic pathways has also been reported for several classes of pathogens (4, 5). Intracellular lipid homeostasis is achieved through a balance in biosynthetic, transport, and degradation processes. Current evidence increasingly points toward an intricate relationship between host lipid metabolism and intracellular pathogens, including bacteria, viruses, and parasites. While the mechanistic details are yet to be unraveled, it is hypothesized that these pathogens, on account of their limited genome sizes, co-opt the host metabolic network to meet the energy demands and procure precursors for their anabolic processes including replication and intracellular transport. In addition, viruses alter lipid metabolism to facilitate amplification and evade the host immune response. This has been decidedly observed in cases of positive strand RNA virus infections, such as dengue, West Nile, Hepatitis C, and several coronaviruses (6–10). Marked alterations in cholesterol and fatty acid biosynthesis occur upon infection, accompanied by the

appearance of distinctive compartments, believed to be their replication sites (11–14).

Despite diversity in their genome organization, many viruses share certain salient features, primary of which is their dependence on host factors to undergo replication, assembly, intracellular transport, and release (15–20). The intracellular life cycle of positive strand RNA viruses is largely confined to the cytosol, within or on the surface of virus-induced organelle-like structures regarded as replication compartments (21–26). Notwithstanding differences in transmission, host cell tropism, and pathogenesis, these viruses employ similar strategies for replication and assembly, often accompanied by reorganization of the host secretory pathway (13, 24, 25, 27, 28). The replication sites serve multiple purposes that function in a concerted fashion to facilitate efficient virus propagation. Primarily, they offer spatial segregation of the different steps in the intracellular life cycle, such as RNA translation, replication, and packaging of the viral genome into virions during assembly. Viral replication compartments also enable a high local concentration of the necessary components—both viral and host—in a physically constrained space, ensuring efficient RNA amplification. An equally important feature of these replication sites is to limit exposure of viral RNA to the hostile cytoplasmic environment that contains cellular nucleases and sensors of the innate immune surveillance. Degradation of dsRNA replication intermediates is minimized by protection in membrane-delimited compartments.

Although lipid metabolism has received particular attention with Gram-negative bacterial infection, several recent reports highlight their function in viral infections (29). Analogous to lipopolysaccharide (LPS)-mediated downregulation of sterol synthesis in case of viral infections, limiting cholesterol biosynthesis in human macrophages and fibroblasts *via* genetic knockdown of sterol regulatory element-binding proteins [sterol-regulatory element-binding proteins (SREBPs), discussed in a later section], was reported to spontaneously engage type I IFN signaling and restrict infection (30–33). Initiation of anti-viral immunity thus displays a clear link with intracellular cholesterol biosynthesis, in a way that the induction of cholesterol synthesis would allow subversion of host immune responses and facilitate viral multiplication.

With the advent of omics-based studies, it is increasingly becoming obvious that viruses induce large-scale alterations in host cellular metabolism (3, 34–37). Among other examples are the induction of fatty acid synthesis by hepatitis C virus (HCV) in human hepatocytes, and the utilization of cellular lipid stores of hepatocytes by dengue virus. The effects of these events have been experimentally demonstrated by genetic and pharmacological inhibition of lipid biosynthetic pathways that attenuate viral pathogenesis (5, 38). These viral adaptation strategies can effectively increase available energy for virus replication and assembly, provide specific components for progeny particles, and for creating replication sites while suppressing antiviral signaling cascades. These reports highlight the intricate link between viruses and lipid metabolism. In the following sections, we discuss emerging data on fatty acid and cholesterol biosynthetic pathways that are upregulated by certain viruses to facilitate infection.

UPREGULATION OF CHOLESTEROL AND FATTY ACID SYNTHESES DURING VIRUS INFECTIONS

Fatty Acid Synthase (FASN)

Intracellular contents of fatty acids and cholesterol contribute to fuel storage as well as a source of components necessary for increased membrane production. The core reaction of fatty acid synthesis is catalyzed by FASN starting from acetyl CoA and malonyl CoA. Once synthesized, palmitate can have several different fates, including further elongation to long chain fatty acids, which can be used for membrane production or storage in lipid droplets (LDs) in the form of triacylglycerols and esterified cholesterol. LDs are storage organelles consisting of triacylglycerols and steryl esters, and function as inert storage depots of excess cellular lipids. Abundance and size of LDs could be indicative of increased fatty acid synthesis, which might poise the cell for rapid membrane generation if needed and also maintains energy reserves (39). According to cellular states and their corresponding energy demands, fatty acids undergo β-oxidation to generate acetyl CoA and NADH and $FADH_2$ molecules in the mitochondrial matrix, for ATP production *via* oxidative phosphorylation. Viruses induce and require availability of fatty acids at several stages of their lifecycle—either to supplement energy requirements for their anabolic processes or to generate viral replication compartments, most notably observed during infection by positive strand RNA viruses (40, 41). This is primarily due to the process of replication—confined to the cytoplasm—where such viruses alter the host intracellular lipid composition to create a beneficial environment. This phenomenon is exemplified by HCV, where all aspects of the viral lifecycle, including entry, replication, assembly, and release are host lipid associated (8). HCV requires low density lipoprotein receptor as a co-factor for entry into target cells (42). Its replication occurs in membranous web-like compartments referred to as double membrane vesicles (13, 43) and they assemble using LDs as platforms (18, 44). To generate replication sites, HCV triggers synthesis of fatty acids, cholesterol, and LDs (45–48). Another member of the Flaviviridae family, dengue, has also been reported to induce production of fatty acids (49, 50). FASN and ACC1 were identified through a targeted siRNA screen as necessary factors for efficient dengue virus replication (38, 51). Drugs that inhibited FASN activity resulted in a significant attenuation in virus replication (49). Infection with dengue virus does not affect FASN expression levels, but rather its redistribution to virus-triggered structures referred to as convoluted membranes (50). This phenomenon appears to be Rab18-mediated, a member of the GTPase family that typically resides in the ER and LDs. Upon infection dengue NS3 was found to interact with Rab18, which allowed recruitment of FASN to viral replication sites, thus promoting fatty acid biosynthesis to increase their local concentration (51, 52). Inhibiting FASN activity has a similar effect in mosquito cells with loss of infectious progeny virion production (53).

3-Hydroxy-3-Methylglutaryl-CoA Reductase (HMGCR)

3-hydroxy-3-methylglutaryl-CoA reductase is the rate-limiting enzyme for cholesterol biosynthesis and is regulated *via* a negative

feedback mechanism mediated by products of the mevalonate pathway. In mammalian cells, HMGCR activity is suppressed by cholesterol imported through receptor-mediated endocytosis of low density lipoproteins (54). Dengue infection inhibits phosphorylation of HMGCR at an inactivating site, generating a cholesterol-rich environment in the process (55, 56). This was further corroborated through inactivation of AMPK and a subsequent increase in HMGCR activity, respectively (56). In comparison, West Nile virus infection has a more direct impact on intracellular cholesterol distribution. Infection was accompanied by redirecting cholesterol from the plasma membrane to virus replication sites (12). In mammalian cells cholesterol homeostasis is tightly regulated in a feedback mechanism *via* transcription factors that sense intracellular cholesterol levels (57, 58). These transcription factors are termed SREBPs that associate tightly with the sterol-sensing SREBP cleavage-activating protein (SCAP) within the ER membrane, *via* an additional interaction with the ER-resident protein Insig, which functions as an inhibitor of SREBP (59, 60). SCAP has an additional role as a chaperone that mediates transport of the SREBP–SCAP complex to the Golgi network, where SREBP is proteolytically cleaved by two resident Golgi proteases (S1P and S2P) to release the transcriptionally active fragment of SREBP from the membrane. The released forms of SREBPs are transported to the nucleus and activate transcription of target genes required for cholesterol and fatty acid biosynthesis, including HMGCR and FASN, respectively. When cholesterol levels are high, SCAP binds to cholesterol in the ER, promoting an association with Insig, and retains the complex within the ER, thus reducing the synthesis of cholesterol. Conversely, when cholesterol levels are low, binding of SCAP to Insig is disrupted, and cholesterol synthesis is initiated (61–63). The authors of these studies postulated that de-enrichment of cholesterol from sites harboring sensory molecules, such as the SCAP–SREBP–Insig complex, results in activation of this signaling pathway, enabling the host cell to increase cholesterol levels to accommodate proliferation of intracellular membranes.

MODULATION OF LDs DURING VIRUS INFECTIONS

Lipid droplets are multifunctional organelles present in most organisms from bacteria to eukaryotes (64–66). These structures are particularly abundant in mammalian adipocytes and insect fat body cells. LDs are mainly composed of a phospholipid monolayer and structural proteins, such as Perilipins, which are involved in LD biogenesis and degradation. Despite previous notions on a rather static role of LDs in the maintenance of lipid homeostasis, more recently, it has become evident that LDs are also present in immune cells, such as neutrophils and macrophages, where they regulate inflammatory or infectious processes (65, 67). Upon stimulation with different challenges, they display an increase in abundance and thereby serve as reliable markers of immune cell activation. Autophagy dependent degradation of LDs has been reported for dengue virus infection in human hepatocytes (38). A similar activation of the autophagy pathway was recently described for Zika virus infection as well (68). Our own data (accepted, queued for publication) support a drastic upregulation of LD consumption through induction of autophagy upon both dengue and Zika virus infections. This pathway appears to operate in an ancient ubiquitous protein 1 (Aup1)-dependent manner, and is dictated by its ubiquitylation status. Unmodified Aup1 enabled dispersion of LDs, which underwent lipophagy upon infection. This virus-triggered pathway is essential for assembly and production of newly synthesized progeny virions (in press). Current consensus, therefore, supports a model where mobilization of LDs in combination with increased synthesis of fatty acids and cholesterol provides a proviral environment for production of progeny virions (53) (**Figure 1**).

RECONFIGURING CHOLESTEROL METABOLISM AS HOST RESPONSE TO INFECTION

The interdependence of innate immune signaling processes and the regulation of sterols and fatty acid metabolism is increasingly being consolidated through emerging data (30). Their role in production of inflammatory mediators has been reported by several groups (69–71). Interferons (IFNs) modulate the expression of a multitude of IFN-stimulated genes including viperin, which has been observed to be highly upregulated in response to bacterial LPS, double-stranded DNA, and RNA analogs, and also possesses antiviral activity against a range of viruses including HCV and dengue virus (72). In a similar vein, inhibition of cholesterol biosynthesis also exerts an antiviral effect (12, 73, 74). SREBPs are involved in coordinating the regulation of the sterol and fatty acid biosynthesis pathways; IFNs effectively inhibit SREBP2 at both mRNA and protein levels. Interestingly, WNV-induced redistribution of cellular cholesterol was found to downregulate IFN-stimulated JAK–STAT antiviral signaling response to infection, potentially by removing cholesterol from their usual microenvironment.

Recent evidence suggests that alterations to cellular lipid metabolism have a more direct role in host defense, through positive regulation of the type I IFN-mediated antiviral response: for example, activation of type I IFN signaling can induce upregulation of β-oxidation and inhibition of cholesterol synthesis, in order to create a hostile cellular environment for viruses (31, 75). Intracellular pathogens are known to stimulate *de novo* lipid and cholesterol biosynthesis to ensure their own survival. Accordingly, repressing these anabolic pathways can inhibit the evolution of intracellular infections. Activation of type I interferon receptors has been correlated to inhibition of cholesterol biosynthesis; however, repression of lipid metabolism in this manner is accompanied by an increase in the influx of environmental lipids, which maintain intracellular lipids and cholesterol at normal levels. Thus, type I IFN signals reprogram cellular lipid metabolism, but this does not function to limit lipid availability to pathogens. It, therefore, remains unclear whether IFN-I linked repression of cholesterol biosynthesis, in the context of intracellular infection, is meant to limit nutrient availability to pathogens, or if it serves a different purpose.

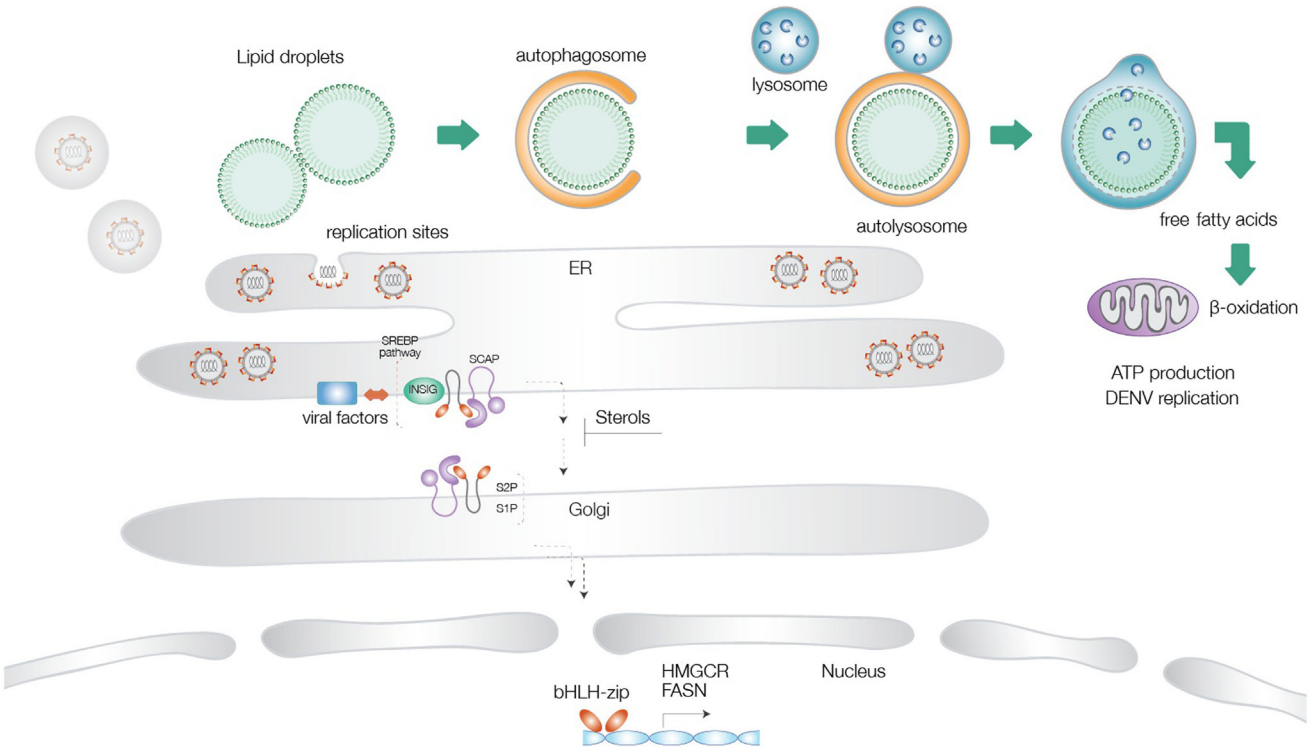


FIGURE 1 | Schematic illustration of the different lipid metabolic pathways exploited during flavivirus infections. Virus-triggered activation of lipophagy results in generation of cholesterol and free fatty acids, which undergo β-oxidation in the mitochondrial matrix to increase cellular energy levels. Activation of the sterol-regulatory element-binding proteins (SREBP) pathway at the endoplasmic reticulum is followed by transport of the SREBP cleavage-activating protein-SREBP complex to the Golgi network, proteolysis, and translocation of the transcription factor to the nucleus, where it turns on genes for cholesterol and fatty acid biosynthesis. Several flaviviral factors have been implicated in exploitation of this pathway. Increased FA production provides energy supplies necessary for virus replication and components necessary for generation of replication sites.

Type I Interferon Response and Lipid Homeostasis During Infection

Bone marrow-derived macrophages (BMDMs), when challenged with IFN-β, poly:IC, or viral infection, showed decreased intracellular synthesis of fatty acids and cholesterol, as well as increased uptake of extracellular lipids and cholesterol. This was also demonstrated by a lower expression of genes related to cholesterol and fatty acid metabolism and an enhanced expression of genes related to cholesterol and lipid import, post viral challenge. Suppressing interferon alpha/beta signaling, while infecting BMDMs with virus, nullified all changes in lipid and cholesterol intracellular balance, including the gene expression level, which proves that type I IFNs can shift lipid homeostasis from biosynthesis to import, despite not significantly altering the intracellular levels of cholesterol and fatty acids (31).

Crosstalk Between Lipid Metabolism and the Type I Interferon Pathway

The SCAP protein acts as a sterol-sensing element, as well as a chaperone, which associates with immature SREBP transcription factors in the ER membrane. By knocking out or knocking down SCAP in macrophages, SREBP activity is lowered, as well as expression of genes involved in lipid metabolism. As anticipated, *de novo* synthesis of cholesterol and fatty acids went down in the absence of SCAP, but total intracellular lipid levels remained unchanged. Loss of SCAP also correlated with heightened resistance to viral infection in *in vitro* and *in vivo* models, confirming the functional equivalence between activation of type I interferon pathway and inhibition of lipid metabolism. Culture medium supernatants from $SCAP^{-/-}$ macrophage cultures were enough to markedly increase resistance to viral challenge, when supplied to wild-type BMDMs, suggesting that the higher type I interferon-mediated viral resistance was a causal effect of a secreted effector molecule, such as interferon-beta (IFNβ). In light of this, qPCR analysis revealed that both $SCAP^{-/-}$ BMDMs and alveolar macrophages extracted from $SCAP^{-/-}$ mice constitutively express higher levels of IFNβ and interferon-stimulated genes (ISGs), compared to wild-type macrophages. Finally, blocking the interferon alpha/beta receptor (IFNAR) was enough to restore interferon and ISGs expression back to normal levels, as well as losing resistance to viral infection. These data strongly suggested that the absence of SCAP activity spontaneously triggers type I interferon production, which translates into a constitutive state of higher resistance to viral infection in macrophages (31).

Deficiency in Cholesterol Metabolism Triggers Type I Interferon Response

SREBP1 generally drives transcription of genes related to fatty acid metabolism, whereas SREBP2 activates transcription of genes linked to cholesterol biosynthesis. RNA-seq and qPCR analysis revealed that knockdown of SREBP1 in macrophages did not significantly impact IFNβ or ISG expression, whereas knockdown of SREBP2 caused a distinct increase in expression of IFNβ and several ISGs, not only in immune cells (macrophages) but also in non-immune cells (fibroblasts). Resistance to viral challenge was highly increased in SREBP2-deficient macrophages and SREBP2$^{-/-}$ mouse fibroblasts (31). Moreover, blocking IFNAR in SREBP2-deficient cells restored ISGs to normal expression levels, decreasing resistance to virus infection to wild-type levels as well. This suggests that a higher type I interferon response is specifically caused by an inhibition of cholesterol metabolism (31, 32). In support of this hypothesis, cells (immune and non-immune) with deficiency in the mevalonate pathway showed a constitutively exacerbated type I interferon response. Also, addition of free cholesterol to SREBP2-deficient cells, or to cells with genetically impaired cholesterol metabolism, causes the exaggerated type I interferon response to decrease to basal levels (31, 71).

Stimulator of interferon genes (STING) is an ER resident kinase, which activates interferon regulatory factor 3 (IRF3) through phosphorylation of Tank binding kinase-1 (TBK1) (76). STING kinase activity is stimulated by cyclic dinucleotides, which are synthesized by cyclic GMP-AMP synthase (cGAS). cGAS, STING, and phosphorylated TBK1 (pTBK1) exist in higher basal levels in SREBP2$^{-/-}$ cells compared to wild-type cells; in addition, knocking down either cGAS or STING in enough to drastically lower pTBK1 presence in SREBP2-deficient cells. Also, knockdown of cGAS, STING, or TBK1 in SREBP2$^{-/-}$ cells caused the expression of Ifnb1 and ISGs to decrease to levels similar to those in wild-type cells (31).

Addition of free cholesterol to SREBP2-knockout cells significantly decreased pTBK1, while blocking IFNAR had no effect on pTBK1 levels, reinforcing the idea that cholesterol directly influences STING-mediated activation of TBK1. These data support a model in which a lack of cholesterol in the cell makes STING more sensitive to cyclic dinucleotides, upregulating the STING-pTBK1-IRF3 signaling axis, and ultimately increasing expression of Ifnb1 and ISGs, conferring an intrinsic pro-inflammatory phenotype to cholesterol-deficient cells (77). Admittedly, most of these experiments used MHV68; however, these conclusions may very well be relevant in other virus infections.

TARGETING FATTY ACID AND CHOLESTEROL METABOLISM AS AN ANTIVIRAL STRATEGY

Repressing the cholesterol biosynthetic pathway through inhibitors of HMGCR is a common treatment for cardiovascular diseases (78). The clinical success of these inhibitors for human disorders provides strong support that targeting lipid metabolism can effective for human therapy. Elucidating the specific alterations incurred upon virus infections would allow novel therapeutic approaches to emerge through targeted inhibition of such metabolic pathways. IFNs or viral infections often result in induction of 25-hydroxycholesterol in macrophages—an antiviral effector, which broadly inhibits many enveloped viruses by interfering with membrane fusion (79). Whether it has an additional impact on activating the interferon signaling pathway is to be seen in future studies. Different strategies can be employed to interfere with virus infection, including those involving lipid utilization; notwithstanding, it is tempting to speculate that drugs already in clinical use against cholesterol and fatty acid metabolic pathways might be repurposed to boost antiviral immunity and provide resistance to infection.

AUTHOR CONTRIBUTIONS

JP and SS discussed and wrote the manuscript.

FUNDING

This work was funded by Research Grants Council (GRF grants 17117914 and 17113915), and partially supported by Health and Medical Research Funds (14131103 and 16150592), theme-based research grant from the Research Grants Council (Project No. T11-705/14N), and research funds from Institut Pasteur (PTR 546). SS is supported by the Croucher Foundation.

REFERENCES

1. Kelly B, O'Neill LAJ. Metabolic reprogramming in macrophages and dendritic cells in innate immunity. *Cell Res* (2015) 25:771–84. doi:10.1038/cr.2015.68
2. Kostic M. From glioblastoma to hepatitis C: it's a metabolism thing. *Cell Chem Biol* (2016) 23:1315–6. doi:10.1016/j.chembiol.2016.11.005
3. Levy G, Habib N, Guzzardi MA, Kitsberg D, Bomze D, Ezra E, et al. Nuclear receptors control pro-viral and antiviral metabolic responses to hepatitis C virus infection. *Nat Chem Biol* (2016) 12:1037–45. doi:10.1038/nchembio.2193
4. Herker E, Ott M. Emerging role of lipid droplets in host/pathogen interactions. *J Biol Chem* (2012) 287:2280–7. doi:10.1074/jbc.R111.300202
5. David R. Enabling HCV's need for fat. *Nat Rev Microbiol* (2013) 11:432. doi:10.1038/nrmicro3054
6. Strating JR, van Kuppeveld FJ. Viral rewiring of cellular lipid metabolism to create membranous replication compartments. *Curr Opin Cell Biol* (2017) 47:24–33. doi:10.1016/j.ceb.2017.02.005
7. Heaton NS, Randall G. Multifaceted roles for lipids in viral infection. *Trends Microbiol* (2011) 19:368–75. doi:10.1016/j.tim.2011.03.007
8. Alvisi G, Madan V, Bartenschlager R. Hepatitis C virus and host cell lipids: an intimate connection. *RNA Biol* (2011) 8:258–69. doi:10.4161/rna.8.2.15011
9. Morita M, Kuba K, Ichikawa A, Nakayama M, Katahira J, Iwamoto R, et al. The lipid mediator protectin D1 inhibits influenza virus replication and improves severe influenza. *Cell* (2013) 153:112–25. doi:10.1016/j.cell.2013.02.027
10. Zhang J, Zhang Z, Chukkapalli V, Nchoutmboube JA, Li J, Randall G, et al. Positive-strand RNA viruses stimulate host phosphatidylcholine synthesis at viral replication sites. *Proc Natl Acad Sci U S A* (2016) 113:E1064–73. doi:10.1073/pnas.1519730113
11. Keller P, Simons K. Cholesterol is required for surface transport of influenza virus hemagglutinin. *J Cell Biol* (1998) 140:1357–67. doi:10.1083/jcb.140.6.1357
12. Mackenzie JM, Khromykh AA, Parton RG. Cholesterol manipulation by West Nile virus perturbs the cellular immune response. *Cell Host Microbe* (2007) 2:229–39. doi:10.1016/j.chom.2007.09.003
13. Paul D, Bartenschlager R. Flaviviridae replication organelles: oh, what a tangled web we weave. *Annu Rev Virol* (2015) 2:289–310. doi:10.1146/annurev-virology-100114-055007

14. Filipe A, McLauchlan J. Hepatitis C virus and lipid droplets: finding a niche. *Trends Mol Med* (2015) 21:34–42. doi:10.1016/j.molmed.2014.11.003
15. Ramage H, Cherry S. Virus-host interactions: from unbiased genetic screens to function. *Annu Rev Virol* (2015) 2:497–524. doi:10.1146/annurev-virology-100114-055238
16. Marceau CD, Puschnik AS, Majzoub K, Ooi YS, Brewer SM, Fuchs G, et al. Genetic dissection of Flaviviridae host factors through genome-scale CRISPR screens. *Nature* (2016) 535:159–63. doi:10.1038/nature18631
17. Sessions OM, Barrows NJ, Souza-Neto JA, Robinson TJ, Hershey CL, Rodgers MA, et al. Discovery of insect and human dengue virus host factors. *Nature* (2009) 458:1047–50. doi:10.1038/nature07967
18. Li Q, Brass AL, Ng A, Hu Z, Xavier RJ, Liang TJ, et al. A genome-wide genetic screen for host factors required for hepatitis C virus propagation. *Proc Natl Acad Sci U S A* (2009) 106:16410–5. doi:10.1073/pnas.0907439106
19. Sanyal S, Ashour J, Maruyama T, Altenburg AF, Cragnolini JJ, Bilate A, et al. Type I interferon imposes a TSG101/ISG15 checkpoint at the Golgi for glycoprotein trafficking during influenza virus infection. *Cell Host Microbe* (2013) 14:510–21. doi:10.1016/j.chom.2013.10.011
20. Shapira SD, Gat-Viks I, Shum BOV, Dricot A, de Grace MM, Wu L, et al. A physical and regulatory map of host-influenza interactions reveals pathways in H1N1 infection. *Cell* (2009) 139:1255–67. doi:10.1016/j.cell.2009.12.018
21. Gillespie LK, Hoenen A, Morgan G, Mackenzie JM. The endoplasmic reticulum provides the membrane platform for biogenesis of the flavivirus replication complex. *J Virol* (2010) 84:10438–47. doi:10.1128/JVI.00986-10
22. Apte-Sengupta S, Sirohi D, Kuhn RJ. ScienceDirectCoupling of replication and assembly in flaviviruses. *Curr Opin Virol* (2014) 9:134–42. doi:10.1016/j.coviro.2014.09.020
23. Fernandez-Garcia M-D, Mazzon M, Jacobs M, Amara A. Pathogenesis of flavivirus infections: using and abusing the host cell. *Cell Host Microbe* (2009) 5:318–28. doi:10.1016/j.chom.2009.04.001
24. Salonen A, Ahola T, Kääriäinen L. Viral RNA replication in association with cellular membranes. *Curr Top Microbiol Immunol* (2005) 285:139–73. doi:10.1007/3-540-26764-6_5
25. Welsch S, Miller S, Romero-Brey I, Merz A, Bleck CKE, Walther P, et al. Composition and three-dimensional architecture of the dengue virus replication and assembly sites. *Cell Host Microbe* (2009) 5:365–75. doi:10.1016/j.chom.2009.03.007
26. Mackenzie JM, Westaway EG. Assembly and maturation of the flavivirus Kunjin virus appear to occur in the rough endoplasmic reticulum and along the secretory pathway, respectively. *J Virol* (2001) 75:10787–99. doi:10.1128/JVI.75.22.10787-10799.2001
27. Hsu N-Y, Ilnytska O, Belov G, Santiana M, Chen Y-H, Takvorian PM, et al. Viral reorganization of the secretory pathway generates distinct organelles for RNA replication. *Cell* (2010) 141:799–811. doi:10.1016/j.cell.2010.03.050
28. Peña J, Harris E. Early dengue virus protein synthesis induces extensive rearrangement of the endoplasmic reticulum independent of the UPR and SREBP-2 pathway. *PLoS One* (2012) 7:e38202. doi:10.1371/journal.pone.0038202
29. Cronan JE. Bacterial membrane lipids: where do we stand? *Annu Rev Microbiol* (2003) 57:203–24. doi:10.1146/annurev.micro.57.030502.090851
30. Azzam KM, Fessler MB. Crosstalk between reverse cholesterol transport and innate immunity. *Trends Endocrinol Metab* (2012) 23:169–78. doi:10.1016/j.tem.2012.02.001
31. York AG, Williams KJ, Argus JP, Zhou QD, Brar G, Vergnes L, et al. Limiting cholesterol biosynthetic flux spontaneously engages type I IFN signaling. *Cell* (2015) 163:1716–29. doi:10.1016/j.cell.2015.11.045
32. O'Neill LAJ. How low cholesterol is good for anti-viral immunity. *Cell* (2015) 163:1572–4. doi:10.1016/j.cell.2015.12.004
33. Josset L, Menachery VD, Gralinski LE, Agnihothram S, Sova P, Carter VS, et al. Cell host response to infection with novel human coronavirus EMC predicts potential antivirals and important differences with SARS coronavirus. *MBio* (2013) 4:e165–113. doi:10.1128/mBio.00165-13
34. Lin S, Liu N, Yang Z, Song W, Wang P, Chen H, et al. GC/MS-based metabolomics reveals fatty acid biosynthesis and cholesterol metabolism in cell lines infected with influenza A virus. *Talanta* (2010) 83:262–8. doi:10.1016/j.talanta.2010.09.019
35. Matheson NJ, Sumner J, Wals K, Rapiteanu R, Weekes MP, Vigan R, et al. Cell surface proteomic map of HIV infection reveals antagonism of amino acid metabolism by Vpu and Nef. *Cell Host Microbe* (2015) 18:409–23. doi:10.1016/j.chom.2015.09.003
36. Law GL, Korth MJ, Benecke AG, Katze MG. Systems virology: host-directed approaches to viral pathogenesis and drug targeting. *Nat Rev Microbiol* (2013) 11:455–66. doi:10.1038/nrmicro3036
37. Zitvogel L, Galluzzi L, Kepp O, Smyth MJ, Kroemer G. Type I interferons in anticancer immunity. *Nat Rev Immunol* (2015) 15:405–14. doi:10.1038/nri3845
38. Heaton NS, Randall G. Dengue virus-induced autophagy regulates lipid metabolism. *Cell Host Microbe* (2010) 8:422–32. doi:10.1016/j.chom.2010.10.006
39. Shi X, Li J, Zou X, Greggain J, Rodkaer SV, Faergeman NJ, et al. Regulation of lipid droplet size and phospholipid composition by stearoyl-CoA desaturase. *J Lipid Res* (2013) 54:2504–14. doi:10.1194/jlr.M039669
40. Carneiro FA, Lapido-Loureiro PA, Cordo SM, Stauffer F, Weissmuller G, Bianconi ML, et al. Probing the interaction between vesicular stomatitis virus and phosphatidylserine. *Eur Biophys J* (2006) 35:145–54. doi:10.1007/s00249-006-0056-8
41. Shavinskaya A, Boulant S, Penin F, Mclauchlan J, Bartenschlager R. The lipid droplet binding domain of hepatitis C virus core protein is a major determinant for efficient virus assembly. *J Biol Chem* (2007) 282:37158–69. doi:10.1074/jbc.M707329200
42. Nakamuta M, Fujino T, Yada R, Aoyagi Y, Yasutake K, Kohjima M, et al. Expression profiles of genes associated with viral entry in HCV-infected human liver. *J Med Virol* (2011) 83:921–7. doi:10.1002/jmv.22042
43. Miller S, Krijnse-Locker J. Modification of intracellular membrane structures for virus replication. *Nat Rev Microbiol* (2008) 6:363–74. doi:10.1038/nrmicro1890
44. Miyanari Y, Atsuzawa K, Usuda N, Watashi K, Hishiki T, Zayas M, et al. The lipid droplet is an important organelle for hepatitis C virus production. *Nat Cell Biol* (2007) 9:1089–97. doi:10.1038/ncb1631
45. Oem JK, Jackel-Cram C, Li YP, Zhou Y, Zhong J, Shimano H, et al. Activation of sterol regulatory element-binding protein 1c and fatty acid synthase transcription by hepatitis C virus non-structural protein 2. *J Gen Virol* (2008) 89:1225–30. doi:10.1099/vir.0.83491-0
46. Park CY, Jun HJ, Wakita T, Cheong JH, Hwang SB. Hepatitis C virus nonstructural 4B protein modulates sterol regulatory element-binding protein signaling via the AKT pathway. *J Biol Chem* (2009) 284:9237–46. doi:10.1074/jbc.M808773200
47. Waris G, Felmlee DJ, Negro F, Siddiqui A. Hepatitis C virus induces proteolytic cleavage of sterol regulatory element binding proteins and stimulates their phosphorylation via oxidative stress. *J Virol* (2007) 81:8122–30. doi:10.1128/JVI.00125-07
48. Moriya K, Yotsuyanagi H, Shintani Y, Fujie H, Ishibashi K, Matsuura Y, et al. Hepatitis C virus core protein induces hepatic steatosis in transgenic mice. *J Gen Virol* (1997) 78(Pt 7):1527–31. doi:10.1099/0022-1317-78-7-1527
49. Samsa MM, Mondotte JA, Iglesias NG, Assunção-Miranda I, Barbosa-Lima G, Da Poian AT, et al. PLOS pathogens: dengue virus capsid protein usurps lipid droplets for viral particle formation. *PLoS Pathog* (2009) 5:e1000632. doi:10.1371/journal.ppat.1000632
50. Heaton NS, Perera R, Berger KL, Khadka S, Lacount DJ, Kuhn RJ, et al. Dengue virus nonstructural protein 3 redistributes fatty acid synthase to sites of viral replication and increases cellular fatty acid synthesis. *Proc Natl Acad Sci U S A* (2010) 107:17345–50. doi:10.1073/pnas.1010811107
51. Tongluan N, Ramphan S, Wintachai P, Jaresitthikunchai J, Khongwichit S, Wikan N, et al. Involvement of fatty acid synthase in dengue virus infection. *Virol J* (2017) 14:28. doi:10.1186/s12985-017-0685-9
52. Tang W-C, Lin R-J, Liao C-L, Lin Y-L. Rab18 facilitates dengue virus infection by targeting fatty acid synthase to sites of viral replication. *J Virol* (2014) 88:6793–804. doi:10.1128/JVI.00045-14
53. Perera R, Riley C, Isaac G, Hopf-Jannasch AS, Moore RJ, Weitz KW, et al. Dengue virus infection perturbs lipid homeostasis in infected mosquito cells. *PLoS Pathog* (2012) 8:e1002584. doi:10.1371/journal.ppat.1002584
54. Brown MS, Dana SE, Goldstein JL. Regulation of 3-hydroxy-3-methylglutaryl coenzyme A reductase activity in cultured human fibroblasts. Comparison of cells from a normal subject and from a patient with homozygous familial hypercholesterolemia. *J Biol Chem* (1974) 249:789–96.
55. Soto-Acosta R, Mosso C, Cervantes-Salazar M, Puerta-Guardo H, Medina F, Favari L, et al. The increase in cholesterol levels at early stages after dengue virus infection correlates with an augment in LDL particle uptake and

HMG-CoA reductase activity. *Virology* (2013) 442:132–47. doi:10.1016/j.virol.2013.04.003
56. Soto-Acosta R, Bautista-Carbajal P, Cervantes-Salazar M, Angel-Ambrocio AH, del Angel RM. DENV up-regulates the HMG-CoA reductase activity through the impairment of AMPK phosphorylation: a potential antiviral target. *PLoS Pathog* (2017) 13:e1006257. doi:10.1371/journal.ppat.1006257
57. Amemiya-Kudo M, Shimano H, Hasty AH, Yahagi N, Yoshikawa T, Matsuzaka T, et al. Transcriptional activities of nuclear SREBP-1a, -1c, and -2 to different target promoters of lipogenic and cholesterogenic genes. *J Lipid Res* (2002) 43:1220–35. doi:10.1194/jlr.M100417-JLR200
58. Sun LP, Seemann J, Goldstein JL, Brown MS. Sterol-regulated transport of SREBPs from endoplasmic reticulum to Golgi: Insig renders sorting signal in Scap inaccessible to COPII proteins. *Proc Natl Acad Sci U S A* (2007) 104:6519–26. doi:10.1073/pnas.0700907104
59. Lee J, Ye J. Proteolytic activation of sterol regulatory element-binding protein induced by cellular stress through depletion of Insig-1. *J Biol Chem* (2004) 279:45257–65. doi:10.1074/jbc.M408235200
60. Ikeda Y, Demartino GN, Brown MS, Lee JN, Goldstein JL, Ye J. Regulated endoplasmic reticulum-associated degradation of a polytopic protein: p97 recruits proteasomes to Insig-1 before extraction from membranes. *J Biol Chem* (2009) 284:34889–900. doi:10.1074/jbc.M109.044875
61. Sakai J, Nohturfft A, Cheng D, Ho YK, Brown MS, Goldstein JL. Identification of complexes between the COOH-terminal domains of sterol regulatory element-binding proteins (SREBPs) and SREBP cleavage-activating protein. *J Biol Chem* (1997) 272:20213–21. doi:10.1074/jbc.272.32.20213
62. Sakai J, Nohturfft A, Goldstein JL, Brown MS. Cleavage of sterol regulatory element-binding proteins (SREBPs) at site-1 requires interaction with SREBP cleavage-activating protein. Evidence from in vivo competition studies. *J Biol Chem* (1998) 273:5785–93. doi:10.1074/jbc.273.10.5785
63. Sun LP, Li L, Goldstein JL, Brown MS. Insig required for sterol-mediated inhibition of Scap/SREBP binding to COPII proteins in vitro. *J Biol Chem* (2005) 280:26483–90. doi:10.1074/jbc.M504041200
64. Murphy DJ. The biogenesis and functions of lipid bodies in animals, plants and microorganisms. *Prog Lipid Res* (2001) 40:325–438. doi:10.1016/S0163-7827(01)00013-3
65. Saka HA, Valdivia R. Emerging roles for lipid droplets in immunity and host-pathogen interactions. *Annu Rev Cell Dev Biol* (2012) 28:411–37. doi:10.1146/annurev-cellbio-092910-153958
66. Walther TC, Farese RV. The life of lipid droplets. *Biochim Biophys Acta* (2009) 1791:459–66. doi:10.1016/j.bbalip.2008.10.009
67. Li Q, Pène V, Krishnamurthy S, Cha H, Liang TJ. Hepatitis C virus infection activates an innate pathway involving IKK. *Nat Med* (2013) 19:722–9. doi:10.1038/nm.3190
68. Liang Q, Luo Z, Zeng J, Chen W, Foo SS, Lee SA, et al. Zika virus NS4A and NS4B proteins deregulate Akt-mTOR signaling in human fetal neural stem cells to inhibit neurogenesis and induce autophagy. *Cell Stem Cell* (2016) 19(5):663–71. doi:10.1016/j.stem.2016.07.019
69. Gold ES, Diercks AH, Podolsky I, Podyminogin RL, Askovich PS, Treuting PM, et al. 25-Hydroxycholesterol acts as an amplifier of inflammatory signaling. *Proc Natl Acad Sci U S A* (2014) 111:10666–71. doi:10.1073/pnas.1404271111
70. Namgaladze D, Brune B. Macrophage fatty acid oxidation and its roles in macrophage polarization and fatty acid-induced inflammation. *Biochim Biophys Acta* (2016) 1861:1796–807. doi:10.1016/j.bbalip.2016.09.002
71. Akula MK, Shi M, Jiang Z, Foster CE, Miao D, Li AS, et al. Control of the innate immune response by the mevalonate pathway. *Nat Immunol* (2016) 17:922–9. doi:10.1038/ni.3487
72. Wang X, Hinson ER, Cresswell P. The interferon-inducible protein viperin inhibits influenza virus release by perturbing lipid rafts. *Cell Host Microbe* (2007) 2:96–105. doi:10.1016/j.chom.2007.06.009
73. Tanner LB, Lee B. The greasy response to virus infections. *Cell Host Microbe* (2013) 13(4):375–7. doi:10.1016/j.chom.2013.04.002
74. Amini-Bavil-Olyaee S, Choi YJ, Lee JH, Shi M, Huang I-C, Farzan M, et al. The antiviral effector IFITM3 disrupts intracellular cholesterol homeostasis to block viral entry. *Cell Host Microbe* (2013) 13:452–64. doi:10.1016/j.chom.2013.03.006
75. Wu D, Sanin DE, Everts B, Chen Q, Qiu J, Buck MD, et al. Type 1 interferons induce changes in core metabolism that are critical for immune function. *Immunity* (2016) 44:1325–36. doi:10.1016/j.immuni.2016.06.006
76. Liu S, Cai X, Wu J, Cong Q, Chen X, Li T, et al. Phosphorylation of innate immune adaptor proteins MAVS, STING, and TRIF induces IRF3 activation. *Science* (2015) 347:aaa2630. doi:10.1126/science.aaa2630
77. Ma F, Li B, Liu S-Y, Iyer SS, Yu Y, Wu A, et al. Positive feedback regulation of type I IFN production by the IFN-inducible DNA sensor cGAS. *J Immunol* (2015) 194:1545–54. doi:10.4049/jimmunol.1402066
78. Sharpe LJ, Brown AJ. Controlling cholesterol synthesis beyond 3-hydroxy-3-methylglutaryl-CoA reductase (HMGCR). *J Biol Chem* (2013) 288:18707–15. doi:10.1074/jbc.R113.479808
79. Cyster JG, Dang EV, Reboldi A, Yi T. 25-Hydroxycholesterols in innate and adaptive immunity. *Nat Rev Immunol* (2014) 14:731–43. doi:10.1038/nri3755

Conflict of Interest Statement: The authors declare that the research was conducted in the absence of any commercial or financial relationships that could be construed as a potential conflict of interest.

Copyright © 2018 Pombo and Sanyal. This is an open-access article distributed under the terms of the Creative Commons Attribution License (CC BY). The use, distribution or reproduction in other forums is permitted, provided the original author(s) and the copyright owner are credited and that the original publication in this journal is cited, in accordance with accepted academic practice. No use, distribution or reproduction is permitted which does not comply with these terms.

frontiers in Immunology

REVIEW
published: 27 November 2017
doi: 10.3389/fimmu.2017.01643

Functional Impairment of Mononuclear Phagocyte System by the Human Respiratory Syncytial Virus

*Karen Bohmwald[1], Janyra A. Espinoza[1], Raúl A. Pulgar[1], Evelyn L. Jara[1] and Alexis M. Kalergis[1,2]**

[1] *Millennium Institute on Immunology and Immunotherapy, Departamento de Genética Molecular y Microbiología, Facultad de Ciencias Biológicas, Pontificia Universidad Católica de Chile, Santiago, Chile,* [2] *Departamento de Endocrinología, Facultad de Medicina, Escuela de Medicina, Pontificia Universidad Católica de Chile, Santiago, Chile*

The mononuclear phagocyte system (MPS) comprises of monocytes, macrophages (MΦ), and dendritic cells (DCs). MPS is part of the first line of immune defense against a wide range of pathogens, including viruses, such as the human respiratory syncytial virus (hRSV). The hRSV is an enveloped virus that belongs to the *Pneumoviridae* family, *Orthopneumovirus* genus. This virus is the main etiological agent causing severe acute lower respiratory tract infection, especially in infants, children and the elderly. Human RSV can cause bronchiolitis and pneumonia and it has also been implicated in the development of recurrent wheezing and asthma. Monocytes, MΦ, and DCs significantly contribute to acute inflammation during hRSV-induced bronchiolitis and asthma exacerbation. Furthermore, these cells seem to be an important component for the association between hRSV and reactive airway disease. After hRSV infection, the first cells encountered by the virus are respiratory epithelial cells, alveolar macrophages (AMs), DCs, and monocytes in the airways. Because AMs constitute the predominant cell population at the alveolar space in healthy subjects, these cells work as major innate sentinels for the recognition of pathogens. Although adaptive immunity is crucial for viral clearance, AMs are required for the early immune response against hRSV, promoting viral clearance and controlling immunopathology. Furthermore, exposure to hRSV may affect the phagocytic and microbicidal capacity of monocytes and MΦs against other infectious agents. Finally, different studies have addressed the roles of different DC subsets during infection by hRSV. In this review article, we discuss the role of the lung MPS during hRSV infection and their involvement in the development of bronchiolitis.

Keywords: human respiratory syncytial virus, dendritic cells, macrophages, infection, immunity

OPEN ACCESS

Edited by:
Luciana Balboa, Consejo Nacional de Investigaciones Científicas y Técnicas (CONICET), Argentina

Reviewed by:
Robert Braidwood Sim, University of Leicester, United Kingdom
Silvia Beatriz Boscardin, University of São Paulo, Brazil

****Correspondence:***
Alexis M. Kalergis
akalergis@bio.puc.cl

Specialty section:
This article was submitted to Microbial Immunology, a section of the journal Frontiers in Immunology

Received: *14 August 2017*
Accepted: *10 November 2017*
Published: *27 November 2017*

Citation:
Bohmwald K, Espinoza JA, Pulgar RA, Jara EL and Kalergis AM (2017) Functional Impairment of Mononuclear Phagocyte System by the Human Respiratory Syncytial Virus. Front. Immunol. 8:1643. doi: 10.3389/fimmu.2017.01643

INTRODUCTION

Mononuclear Phagocyte System (MPS): Background

Since the 1960s, the term MPS was defined as a family of cells differentiated from a common committed progenitor derived from the bone marrow (1–3). The MPS is composed of three major cell types, including monocytes, macrophages (MΦs), and dendritic cells (DCs) (2, 4). These cells share common morphologic and functional features, such as stellated form and the endocytic capacity (2).

In addition, MPS cells express a heterogeneity of cell surface markers based on the tissue where they are located (3, 5, 6).

In the lungs, the cells of the MPS play a key role during host defense and homeostasis (7, 8). MΦs are found mostly in the alveolus adjacent to the epithelium and less frequently in the terminal airways and interstitial space, while most DCs are located in the pulmonary interstitium (7). Finally, this cellular system play critical roles in pulmonary host defense against viral pathogens, such as human respiratory syncytial virus (hRSV), which will be discussed in detail below.

Monocytes

Monocytes originate in the bone marrow from a common myeloid progenitor that is shared with granulocytes and macrophages (9). Furthermore, recruitment of monocytes is critical for an effective control and clearance of viral infections (10). It has been described that, in the bone marrow, the earliest monocytic precursor needs between two or three generations before becoming a mature monocyte that can be released into the peripheral blood. Once in the blood, these cells circulate for several days before entering the tissues and replenishing tissue macrophage populations (10). In the absence of an inflammatory process, it is thought that migration of monocytes into tissues is a random phenomenon (10). Once there, monocytes are able to differentiate into tissue-specific-resident phagocytes (8, 10). Monocytes can differentiate *in vivo* and *in vitro* into other myeloid cells, such as MΦs or DCs in response to cytokines including granulocyte-macrophage colony-stimulating factor and macrophage colony-stimulating factor (11–13).

In humans, monocytes can be classified into three groups according to molecular markers and their function: (1) classical ($CD14^{++}CD16^{-}$); (2) intermediate ($CD14^{++}CD16^{+}$); and (3) non-classical ($CD14^{+}CD16^{+}$) (12, 14). While classical monocytes exert a high myeloperoxidase and intermediate phagocytic activity, non-classical monocytes are important during inflammatory and antiviral responses (12, 15). On the other hand, murine monocytes are classified into two groups: (1) $LyC6^{low}$ and (2) $LyC6^{High}$ (12). While the $LyC6^{High}$ subpopulation is responsible for the inflammatory and antimicrobial response (11, 12), $LyC6^{low}$ monocytes contribute mainly to immune surveillance and to tissue repair (12).

Macrophages (MΦs)

Macrophages are characterized by their phagocytic capacity, which is required for the removal of cellular debris during tissue repair processes (16). MΦs are present in different tissues, such as the brain, bone marrow, lung, and liver, among others. During an inflammatory response, MΦs can migrate into various tissues from the peripheral blood (16).

Macrophages can be activated both by a microbial infection or by endogenous stimuli, which include inflammatory cytokines, such as IFN-γ, IL-4, and IL-13 (16). These cells can display two different activation profiles known as M1 (classic) and M2 (alternative) (17). The M1 MΦ subset displays higher antimicrobial, inflammatory and antigen-presenting capacity (17). Meanwhile, the M2 MΦ subset mainly displays anti-inflammatory activity (16–18). In addition, M1 MΦs are stimulated by IFN-γ, while the activation of M2 MΦs requires IL-4 and IL-13 (17, 19). Importantly, M1 and M2 polarization can be modulated by viral infections (20). The role of these cells during hRSV infection will be discussed below.

Dendritic Cells

Dendritic cells are specialized cells whose main function is to modulate the communication between the innate and acquired immune responses (21). These cells are considered as professional antigen-presenting cells (APCs) with a low phagocytic capacity, as compared to other cells of the MPS (7). In mice, two major subsets of DCs have been identified: (1) conventional DCs (cDCs) or "myeloid" DCs and (2) plasmacytoid DCs (pDCs) (**Table 1**). While cDCs locate mainly in lymphoid and non-lymphoid tissues, pDCs can be found in blood, lymph nodes (LN), and lymphoid tissues (22). Additionally, murine cDCs can be divided in two subtypes: $CD103^{+}$ cDCs and $CD11b^{+}$ cDCs (**Table 1**) (22, 23). Further,

TABLE 1 | Dendritic cell (DC) subsets, location, and their surface markers.

DC subset	Location	Surface markers	Reference
Mouse conventional DC (cDC) $CD103^{+}$	Lymphoid organs and non-lymphoid organs	$CD11c^{+}$ MHC-II^{+} F4/80^{-} $CD11b^{-}$ $CD103^{+}$	(22)
Mouse cDC $CD11b^{+}$	Lymphoid organs	$CD11c^{+}$ MHC-II^{+-} $CD103^{-}$ F4/80^{-} integrin αEβ7^{+} $CD11b^{+}$	(22)
Mouse cDC $CD8\alpha^{+}$	Lymphoid organs	$CD11c^{+}$ $CD205^{+}$ MHC-II^{+} $CD11b^{-}$ $CD8\alpha^{+}$	(22, 24)
Human myeloid DC $CD1c^{+}$	Lymphoid organs	$CD1c^{+}$ $CD11b^{+}$ $CD11c^{high}$ BDCA-1^{+} $CD206^{+}$ $CD207^{+}$	(14, 25, 26)
Human myeloid DC $CD141^{+}$	Lymphoid organs	$CD141^{+}$ $CD11c^{+}$ $CD11b^{-}$ BDCA-3^{+} CLEC9A^{+} XCR1^{+} $CD123^{+}$	(14, 25, 26)
Plasmacytoid DC (pDC)	Blood, lymph nodes, and lymphoid tissues	$CD11c^{low}$ mPDCA-1^{+}	(22)
Human pDC	Blood and bone marrow	Lin^{-} MHC-II^{+} $CD123^{+}$ $CD4^{+}$ $CD303^{+}$ $CD304^{+}$	(14, 25, 26)

cDCs can be separated in lymphoid tissues in two subsets: $CD8^+$ and $CD11b^+$ cDCs. $CD8^+$ cDCs express the CD8α transcript and protein, but not CD8αβ heterodimer, which is most commonly expressed by $CD8^+$ T cells (**Table 1**) (22).

As for the case of human DCs, these cells can be divided into pDCs and myeloid DCs. These latter cells are additionally classified into two subsets: $CD1c^+$ and $CD141^+$ (**Table 1**) (14, 26). Here, $CD1c^+$ and $CD141^+$ are analogous to the mouse tissue-resident $CD11b^+$ and $CD103^+$ DCs, respectively (27).

With respect to the function of the various DCs subsets, cDCs display an increased ability of sensing tissue damage independent of their role in the capture, processing, and presentation of antigens (22). Equivalent to other MPS members, DCs are found in the lungs as is the case for $CD103^+$ cDCs, $CD11b^+$ cDCs, and pDCs subsets, which are distributed in the lamina propria (28). Furthermore, both subsets of cDCs ($CD103^+$ and $CD11b^+$) are found in the alveoli, allowing their migration to the mediastinal LNs (28). Consistent with this notion, it is known that lung DCs play an active role in the pulmonary pathogenesis caused by viral infection and asthma (28).

On the other hand, pDCs are able to secrete large amounts of type I IFN during viral infections and contribute to the maintenance of immune tolerance (22). The latter activity of pDCs is achieved through the expression of molecules, such as the inducible tolerogenic enzyme indoleamine 2,3-dioxygenase (IDO), the inducible costimulator ligand, and/or the programmed death 1 ligand. These molecules promote the expansion of regulatory T cell (Treg) and the suppression of self-specific and alloreactive lymphocytes (28–31).

EPIDEMIOLOGY FEATURES OF hRSV INFECTION

Viral infections are the most important cause of acute lower respiratory tract infection (ALTRI), affecting mainly young children and the elderly (32, 33). Up to date, the main agent causing this pathology is the hRSV (33–37). Human RSV produces a broad spectrum of clinical manifestations, ranging from mild, such as rhinitis, to more serious symptoms that include bronchiolitis and pneumonia (38, 39). Clinical symptoms not only are due hRSV but also involve host risk factors, such as preterm birth, immunosuppression, congenital heart disease, and chronic lung disease (40–43). Importantly, it is known that almost 100% of children have been infected with hRSV before 2 years old, due to the fact that this virus is highly contagious and efficient at disseminating from one individual to the next (44, 45). Up to date, infections due to hRSV remain still as one of the most important global public health burdens affecting humans in all countries (45). Annually, approximately 33 millions new cases worldwide are associated to ALTRI caused by hRSV infection alone, affecting mainly children under 5 years old (33, 46). Moreover, hospitalization events due to a severe bronchiolitis or pneumonia caused by hRSV infection have increased and reached about a 10% of the total number of cases (46). Importantly, the annual cost of hospitalizations due to hRSV outbreaks is about 394 million USD, a situation that repeats every year (33, 47).

In young children, the immune system fails to establish a protective response against hRSV, which leads to frequent reinfections (33, 47–49). Lack of protective immunity is explained by an impaired induction of cellular and humoral immune memory after the primary exposure to hRSV (34, 39, 50). Furthermore, hRSV is capable of modulating phagocytic cell function, leading to the respiratory immunopathology that is a characteristic of the infection by this virus (44).

The most severe clinical manifestation caused by hRSV is bronchiolitis (51), which is mainly characterized by a distal bronchiole inflammation and obstruction, which reduces the airflow into small airways and impairs the exhalation capacity (52). All these alterations promote an abnormal lung function that is manifested as airway hyperexpansion, increased mucus production, atelectasis, and wheezing (52, 53). The bronchiolitis caused by hRSV infection also can produce long-term pathologies and sequelae, such as asthma and respiratory hyperreactivity (54).

After that hRSV encounters the airway epithelial cells (AECs), this virus gets in contact with innate immune cells, such as monocytes, MΦ, and DCs located at the lung tissue (10). These immune cells produce significant amounts of pro- inflammatory cytokines after a viral infection that is involved in controlling adaptive immunity by their interaction with helper T cells (10, 55). In addition to contributing to the clearance of microbial pathogens, monocytes and MΦs also play an important role as APCs to prime T lymphocytes (56). Consistently with this notion, monocytes, MΦs and DCs not only are involved during the acute inflammatory phase of hRSV-induced bronchiolitis but also contribute to the promotion of reactive airway disease caused by this virus (57–59).

MONOCYTES ARE REQUIRED TO INITIATE THE IMMUNE RESPONSE AGAINST hRSV

Monocytes are part of the first line of the host immune defense against viral pathogens (60). In response to infection with hRSV, human AEC-derived cell lines secrete cytokines and chemokines *in vitro*, including IL-6, IL-8, CCL2, CCL3, and CCL5 that promote the recruitment of monocytes and eosinophils to the site of infection (**Figure 1**) (60, 61). In addition, infection of BEAS2B cells (human lung epithelial cell line) with hRSV kept them from inhibiting the secretion of pro-inflammatory cytokines by monocytes, such as TNFα (62). During homeostasis, AECs are able to inhibit the function of inflammatory monocytes, a feature that is impaired in hRSV-infected AECs (62). Interestingly, monocytes can be directly infected by hRSV, reducing the expression of the intercellular adhesion molecule 1 and its ligand, the lymphocyte function-associated antigen 1, which alters the collaboration between monocytes and other immune cells (10, 63). These observations suggest that monocytes infected with hRSV can display a reduced capacity to induce a protective immune response against hRSV (10).

Patients infected with hRSV show a frequency increase for $CD14^+CD16^+$ monocytes in the blood (37). Furthermore, an

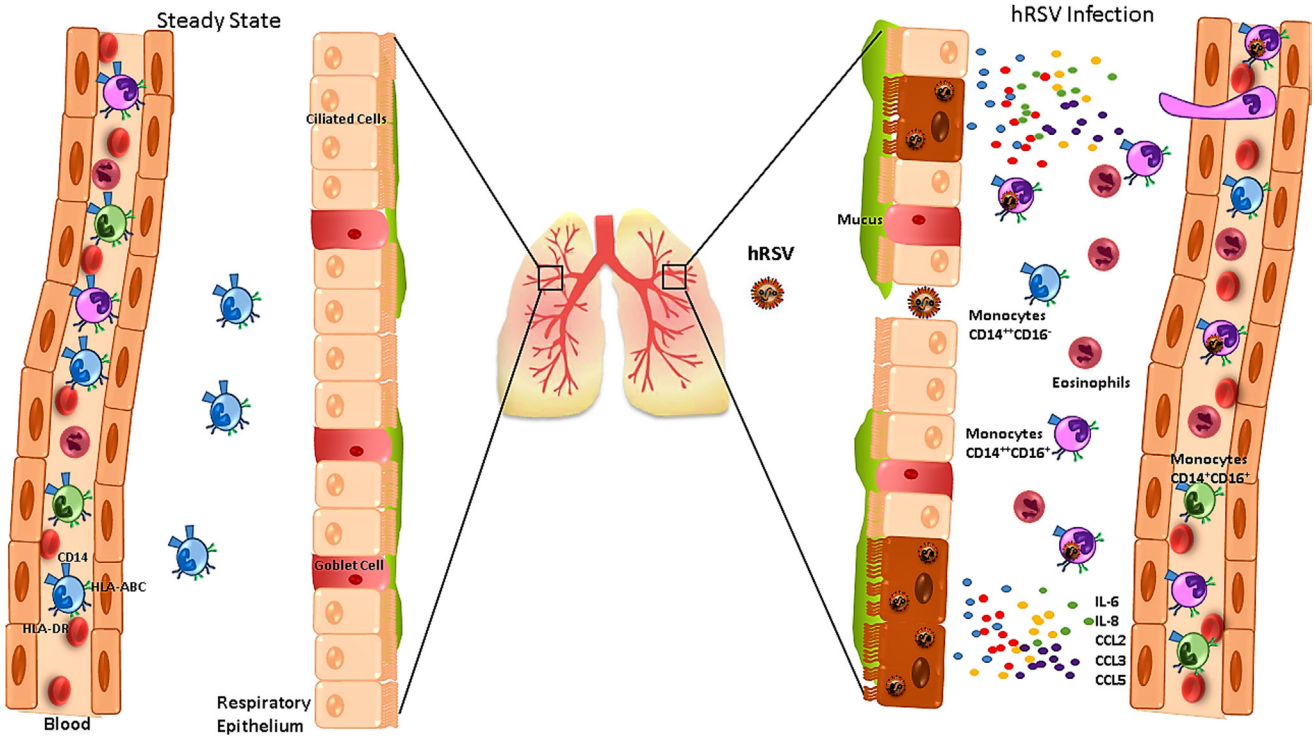


FIGURE 1 | Human respiratory syncytial virus (hRSV) infection alters the function of monocytes and promotes their infiltration into the lungs. During the steady state (left), the main monocytes subset found in lungs are $CD14^{+}CD16^{-}$. During hRSV infection (right), infected airway epithelial cells secrete IL-6, IL-8, CCL2, CCL3, and CCL5, which promote monocytes and eosinophils infiltration into the airways. In addition, blood monocytes express increased levels of CD14 and HLA-ABC and reduced levels of HLA-DR, which is associated with severe bronchiolitis.

increase of CD14 expression has been observed for all the monocyte subsets (**Figure 1**) (37, 64), suggesting that these cells can display an enhanced capacity to secrete cytokines and to migrate into the airways, probably to replace alveolar MΦ during hRSV infection (37, 64). Moreover, monocytes from hRSV-infected patients show a diminished expression of HLA-DR (**Figure 1**), correlating with disease severity (37, 65).

As mentioned above, hRSV infection causes bronchiolitis in children under 2 years old (66). Moreover, the pathology is worsened by some cytokines produced by monocytes during the early state of hRSV infection (67). Monocytes from of hRSV-infected patients presenting bronchiolitis in the convalescent stage of the infection secreted large amounts of IL-10 in response to stimulation with LPS and IFN-γ *in vitro* (67). Furthermore, authors showed a significant correlation between the monocyte-produced IL-10 and the number of wheezing episodes (10, 67).

Similar to MΦ and DCs, monocytes express TLR8 that promotes endosomal activation and IL-12p70 release upon binding to viral RNA (68). Monocytes derived from hRSV-infected infants displayed reduced expression of TLR8 during the acute phase of infection (68). Additionally, this study showed that monocytes from hRSV-infected infants produced reduced levels of TNF-α as compared to monocytes from healthy controls (68). Taken together, these results suggest that hRSV infection interferes with the normal expression of TLR8 and perhaps with the cytokines production that are important to initiate the immune response against hRSV (68).

The data relative to the role of monocytes during the immune response induced by the hRSV infection suggest that these cells are important to initiate the immunity against this pathogen. Further, monocytes are also involved in the development of bronchiolitis and the recurrent wheezing. Thus, it is likely that these cells could contribute to chronic respiratory sequelae caused by hRSV, such as asthma and airway hyperreactivity.

ALVEOLAR MACROPHAGES (AMs) ARE CRUCIAL TO CONTROL hRSV-CAUSED DISEASE

Lung-resident macrophages consist of two distinct populations namely (1) AMs and (2) interstitial macrophages (IMs) (69). AMs locate in the luminal surface, while IMs reside in the interstitial space of the lung parenchyma (70). AMs are the most abundant phagocytic resident cells in the lungs, which uptake foreign particles, remove cellular debris, initiate immune responses against pathogens and contribute to restoring homeostasis in the lung epithelium (70). During the steady state (**Figure 2**), AMs can display an immunosuppressive effect by directly inhibiting

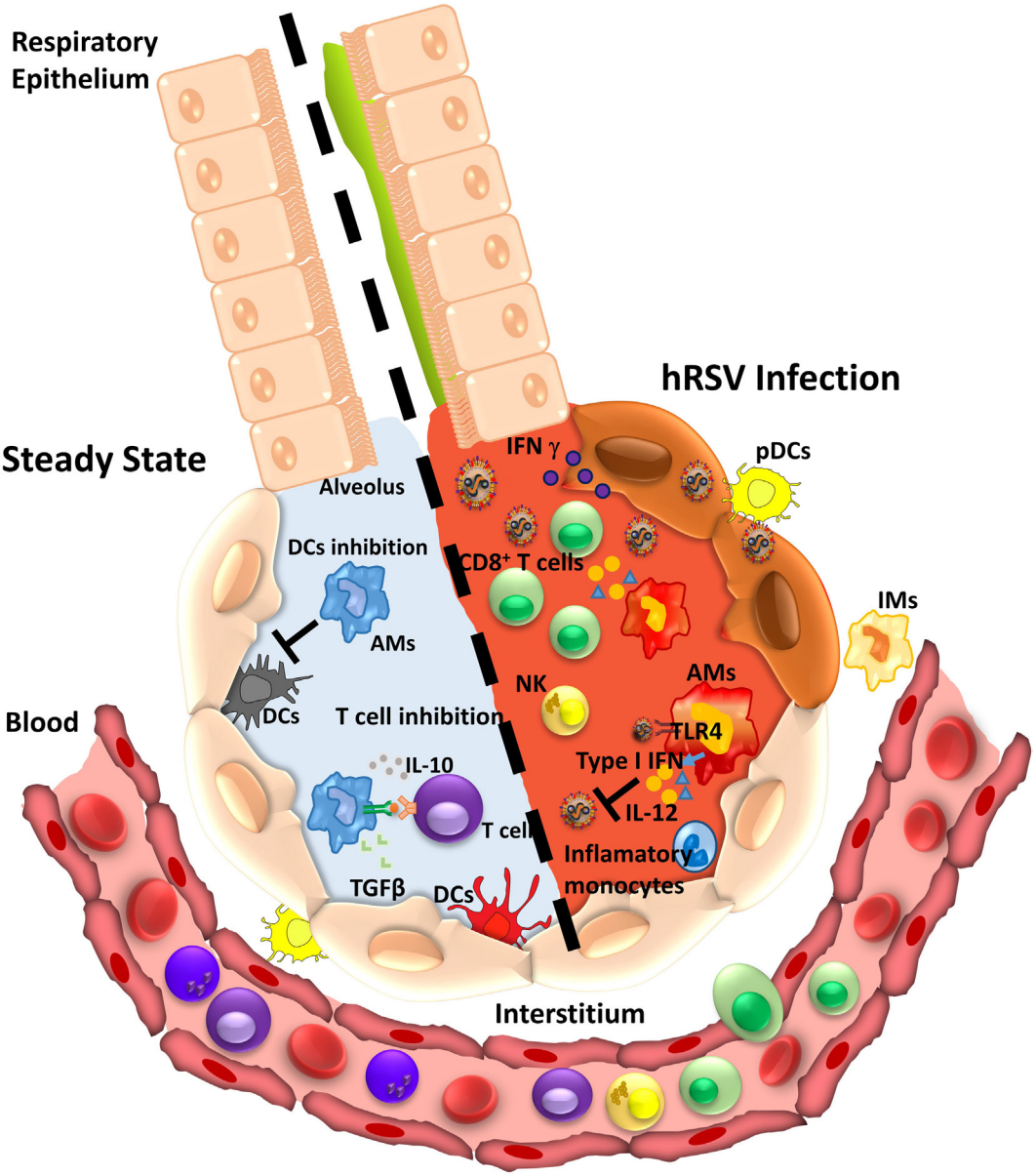


FIGURE 2 | Alveolar macrophage (AM) function during homeostasis or infection by human respiratory syncytial virus (hRSV). During the steady state (left), AMs perform an anti-inflammatory function leading to immune tolerance. AM suppresses the response of T cell in an antigen-dependent manner and secretes cytokines as IL-10 and transforming growth factor-β (TGFβ). Also, AMs impair dendritic cells (DCs) activity inhibiting T cell presentation. Under hRSV infection (right), AMs can recognize the virus by TLR4 and respond by secreting type I IFNs that induce an antiviral state in epithelial cells. In addition, the secretion of pro-inflammatory cytokines promotes recruitment of inflammatory monocytes, $CD8^+$ T cells, and NK cells that contribute with viral clearance.

the antigen-presenting function of lung DCs (71) or by inducing $CD4^+$ T cell unresponsiveness in an antigen-specific manner (72). Furthermore, AMs can secrete several immunomodulatory molecules, such as IL-10, nitric oxide, prostaglandins, and transforming growth factor-β (**Figure 2**), which reduce inflammation in the lungs (73).

The role of AMs during hRSV infection has been characterized in murine models by depleting these cells through the administration of liposomes containing clodronate, a molecule that promotes the apoptosis of AMs (70, 74, 75). It was shown that AMs are crucial for the clearance of hRSV and for the control of lung inflammation (70). The depletion of AMs during hRSV infection leads to an increased viral replication and an exacerbated lung immunopathology (70). These results were consistent with a dramatic increase of neutrophils and inflammatory DCs recruitment to the lungs (70, 74). Then, in mice, AMs display a protective function during hRSV infection and contribute to attenuating lung inflammation and bronchiolitis

triggered by this pathogen (76). Similar results were obtained in New Zealand Black (NZB) mice, which lack normal macrophage function and show an enhanced lung immunopathology upon hRSV exposure (76). Although the mechanisms responsible for the beneficial effect of AMs to control hRSV infection remain unknown, the available data suggest that the phagocytic and microbicidal capacity of AMs together with the secretion of type I IFN are the main elements contributing to the protection against this virus (76).

Alveolar macrophages are the main producers of type I IFNs in the airways during hRSV infection, even more than other cells, such as epithelial cells and pDCs (75). Type I IFN production by AMs is triggered by hRSV recognition and mediated by cytosolic mitochondrial antiviral signaling protein-coupled retinoic acid-inducible gene 1 (RIG-I)-like receptors (RLRs) (77). The type I IFN production promotes the monocytes-derived inflammatory cells recruitment (**Figure 2**), which further contributes to controlling hRSV infection and reducing lung pathology (77).

On the other hand, *ex vivo* experiments showed that hRSV infects both murine and human AMs (78). However, in both cases, the infection failed to lead to an increase of viral particle production (70, 79). These results suggest that the infection of AMs by hRSV might be abortive, allowing that AMs maintain a sentinel activity. Further, it is thought that abortive replication may allow AMs to resist the effects of hRSV NS protein, which inhibits the activity of RIG-I-like receptors (RLR) (77). Along these lines, AMs can restrict hRSV replication even in the absence of type I IFNs (75). However, the exposure of AMs to hRSV can result in a reduced phagocytic capacity during subsequent infections (79).

Moreover, AMs are essential for the activation of the early immune response against hRSV (70). Infection of human AMs by hRSV leads to the secretion of several pro-inflammatory cytokines, such as IL-6, TNF-α, IL-1β, and IL-8 (78, 80, 81). Conversely, similar experiments have described the secretion of IL-10 by these cells (82). The AMs response to hRSV is mediated mainly by the activation of NF-κB through recognition of non-replicative viral particles and surface viral proteins by TLR4 at early times postinfection (**Figure 2**) (83). Based on the available data about the role of TLR4 in the infection with hRSV, it has been hypothesized that in the beginning, surfactant protein A-opsonized hRSV can bind to TLR4 expressed on the surface of alveolar epithelial cells and AMs (84). Next, additional TLR4 and CX3CR1 molecules are recruited to the virus attachment site (84). Then, the hRSV F and G proteins interact with TLR4 and CX3CR1, respectively. Furthermore, both proteins interact with heparan sulfate structures (84), an interaction that is followed by the recruitment of caveolin-1 and the formation of caveolae with the subsequently recruitment of RhoA to the binding site (84). Moreover, it has been suggested that the binding of the hRSV F protein to TLR4 may activate the signaling pathway for this receptor and NF-κB translocation (84, 85). However, the role of TLR4 during the hRSV entry into target cells remains controversial, as well as the interaction with viral proteins that trigger the activation of the NF-κB pathway (86). A study performed in TLR4-positive cells (HEK 293 reporter cell lines) showed that infection with hRSV does not activate the NF-κB signaling pathway through the TLR4/MD-2/CD14 complex (87). However, in the context of the AM-directed immune response, studies have shown that in the absence of TLR4, the NF-κB signaling pathway is not activated (83) and that the latter is required for the polarization of MΦ toward the M2 phenotype (88). On the other hand, the establishment of this initial condition allows an effective lymphocyte recruitment and proper antiviral activity. Along these lines, human neonatal AMs infected with hRSV showed an impairment in the IFN-γ and IL-12 production (81). An inefficient secretion of IFN-γ has been associated with an increase of severe illness in infants (89). Considering that IFN-γ is necessary for the activation of AMs, a reduced production of IFN-γ in neonates has been observed to impair AMs activation, affecting the phagocytic capacity of these cells and exacerbating the hRSV-mediated bronchiolitis (90, 91). Also, an impaired AMs function reduces the T and NKT cells recruitment to the lungs, contributing to higher viral loads (91).

According with the data described above, AMs are important for the elicitation of an early immune response against hRSV, contributing to the viral clearance mainly mediated by the type I IFN secretion and the coordination of the adaptive response against this pathogen. Thus, an impaired function or absence of AMs can increase hRSV-induced bronchiolitis, both in mouse models and infants.

In contrast to the significant research efforts to understand the role of AMs during the infection with hRSV, the participation of IMs has only been poorly studied (92). Qi et al. evaluated the role of AMs and IMs in the production of IL-33 during hRSV infection (93). This study showed that the absolute number of IMs in lungs of hRSV-infected mice remained constant during the hRSV infection, in contrast to the increase observed for the absolute number of AMs (93). Furthermore, IMs from lungs of hRSV-infected mice showed an increase in the expression of both TLR3 and TLR7 mRNA (93). Considering that the number of IL-33-producing IMs in the lungs of mice was affected by hRSV infection, authors concluded that the IMs may not be the source of IL-33 during hRSV infection (93).

Therefore, additional studies are required to better understand the contribution of IMs to hRSV infection and pathogenesis.

DCs AS COMMANDERS OF THE IMMUNE RESPONSE DURING hRSV INFECTION

The infection with hRSV can induce different immune responses depending on the type of DC subset infected (94). According to this notion, it has been described that hRSV infection promotes CDs maturation by increasing the expression of CD80, CD86, CD40, and MHC-II in the lungs, which leads to a decrease of phagocyte function (95). Moreover, some studies in mice have reported that during the acute phase of hRSV infection, the frequency of mature DCs in the lungs is increased (95). On the other hand, it has been shown that hRSV has the capacity to infect and replicate inside DCs but in a non-productive manner (96–98). Importantly, it has been described that toll-like receptors expressed by DCs can interact with hRSV proteins. TLR-2 interacts with the viral fusion glycoprotein (F) and TLR-4 with

both the F and the attachment G protein (99, 100). TLR4 activation promotes the secretion of IL-6 and TNF-α, as well as antigen cross-presentation *in vivo* and *in vitro* (101). Additionally, hRSV G glycoprotein interacts with DC- and L-SIGN, inducing both DC/L-SIGN-dependent and -independent phosphorylation of ERK1 and ERK2. As a result, DCs activation is impaired (102). This mechanism can be considered as a possible explanation for the reduced immunity induced by hRSV reinfections.

To understand as to how DCs become infected with hRSV, *in vitro* and *in vivo* experiments were performed in mouse models, which showed the contribution of Fcγ receptors (FcγRs), mainly FcγRIII, to infection by this virus (103). Human RSV-infected FcγRIII KO mice showed reduced airway inflammation as compared to infected wild-type mice, suggesting that FcγRIII plays a pro-inflammatory role during hRSV infection (103). On the other hand, it is known that hRSV infection induces only weak immune memory in the host (50). To understand this phenomenon, a possible impairment of the immunological synapsis between hRSV-infected DCs and T cells was evaluated *in vitro*. It was observed that hRSV infection of DCs not only impaired the assembly of the immunological synapsis with T cells but also the activation of naïve antigen-specific T cells (50, 104). The hRSV virulence factor that seems responsible for the inhibition of immunological synapse assembly is the nucleoprotein (N) (104). The N protein was found on the DCs membrane and by itself could interfere with the assembly of the immunological synapsis (104). Further, the N protein was located nearby to the TCR–pMHC complexes at the DC-T cell synapse interface (50, 104).

On the other hand, it has been reported that the mTOR protein on bone marrow-derived dendritic cells (BMDCs) plays an important role during hRSV infection (105). According to this notion, mTOR inhibition by rapamycin in hRSV-infected BMDCs decreased the number of $CD8^+CD44^{high}$ T cells, suggesting that mTOR is necessary for the proliferation of the T cell memory subset (105). Moreover, the treatment of the hRSV-infected BMDCs with rapamycin did not affect maturation and increased the survival when DCs were cocultured with T cells, suggesting that this phenomenon requires the contact of both cell types (105).

$CD103^+$ cDCs are the most prevalent population of DCs in the lungs, which locate directly underneath the airway epithelium (14). $CD103^+$ cDCs express the integrin $\alpha_E\beta_7$ and are found mainly at the lamina basal of the bronchial epithelia and arterioles (106). This DCs subset efficiently loads virus-derived peptides onto MHC-I molecules, inducing a potent proliferation of naïve $CD8^+$ T cells (**Figure 3**) (107). Therefore, $CD103^+$ cDCs work as key mediators of immunity to intracellular pathogens infecting the lungs (108, 109). In several studies with hRSV, neonatal mice have been used to better compare the human clinical features with mouse models of the disease (110). $CD103^+$ DCs from neonatal mice infected with hRSV showed lower expression of co-stimulatory molecules, CD80 and CD86, as compared to the

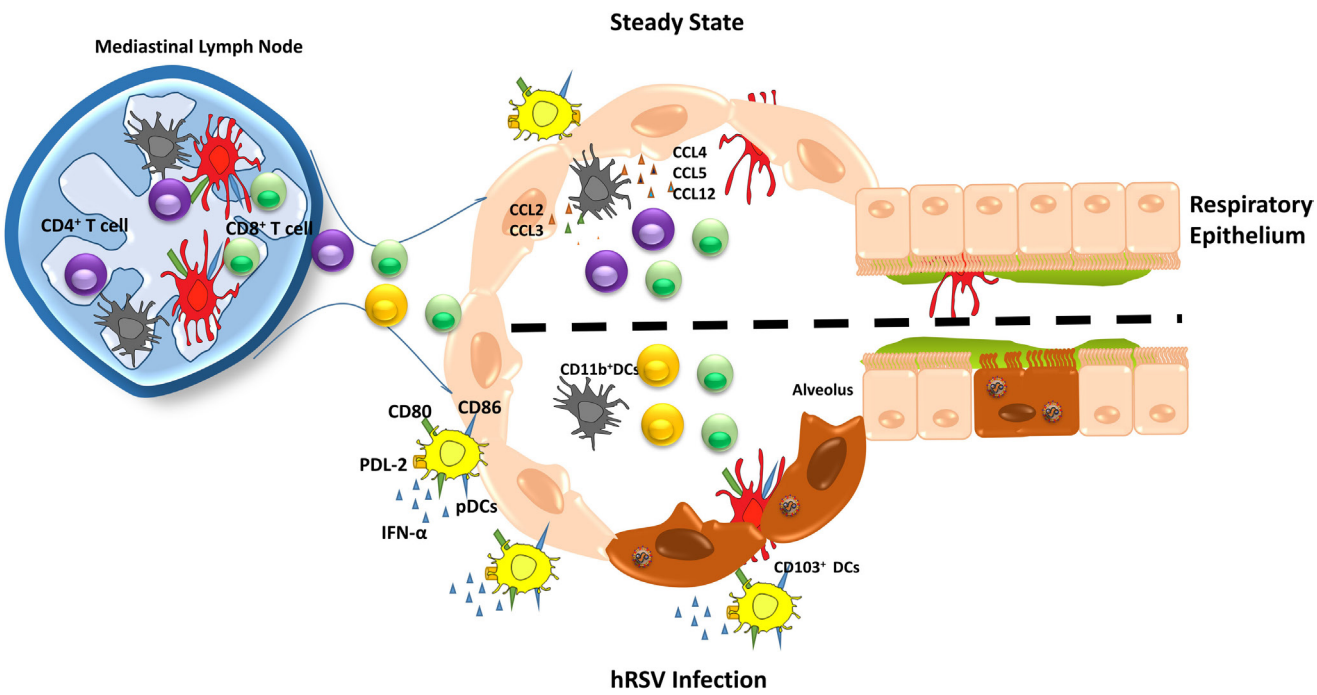


FIGURE 3 | Different roles of dendritic cells (DCs) subsets during human respiratory syncytial virus (hRSV) infection. During the steady state (upper), DCs subset maintain the lung homeostasis and when an infection occurs, they are capable to migrate to mediastinal lymph node to present antigens to T cells, promoting an immune response. Upon hRSV infection, plasmacytoid DCs (pDCs) increase in numbers, as well as the expression of co-stimulatory molecules, such as CD80, CD86. In addition, pDCs secretes high levels of IFN-α and PDL-2 expression is reduced. Moreover, in response to hRSV infection, $CD11b^+$ DCs fail to activate $CD4^+$ T cells leading a poor response against the virus. On the other hand, $CD103^+$ DCs show a lower expression of CD80 and CD86, which are required for an appropriate antiviral immune response.

adult counterparts, affecting the T cell synapsis quality (110). For this reason, neonatal mice infected with hRSV generated a distinct $CD8^+$ T cell response as compared to adult mice, suggesting a key role of $CD103^+$ DCs (110). Furthermore, the immunization with F virus-like particles (VLP) of hRSV-infected mice showed high levels of $CD103^+$ DCs in bronchoalveolar lavage fluids (BALFs) and lungs (23). Moreover, the mediastinal LN from F VLP-immunized mice showed higher levels of $CD103^+$ DCs and resident $CD8\alpha^+$ DCs (23). It is known that after hRSV infection is resolved, is possible to develop subsequent asthma during childhood (111, 112). Here, $CD103^+$ DCs play a protective role during asthma/allergic-related symptoms by producing IL-12 (113).

As mentioned above, another DCs cell subset, $CD11b^+$ cDCs locate in the lung parenchyma (114, 115). In addition to the uptake of extracellular pathogens, the main function of these cells is to present antigens to $CD4^+$ T cells (116). Studies were carried out in mice to understand the role of $CD11b^+$ DCs during hRSV infection. In lungs from mice infected with hRSV, an increase was observed for the frequency of $CD11b^+$ DCs (114). Moreover, it was determined that the ability of $CD11b^+$ DCs to migrate to LN remained intact (114). One of the mechanisms proposed for the accumulation of $CD11b^+$ DCs in the airways is that during hRSV infection, the high levels detected for CCL20 in the lungs can attract $CD11b^+$ $CCR6^+$ DCs (117, 118). To evaluate the role of $CD11b^+$ $CCR6^+$ DCs during hRSV infection, studies were performed in CCR6-deficient mice, showing an increase of viral clearance, lower levels of Th2 pro-inflammatory cytokines, as well as reduced mucus production (117, 118). Overall, these findings suggest that the $CD11b^+$ $CCR6^+$ DCs promote a Th2 immune response upon hRSV infection (117, 118). Additional studies performed in the neonatal murine model described that lung $CD11b^+$ DCs express higher levels of the IL-4 α receptor (IL-4Rα) as compared to adult mice (119). *In vitro* experiments using neonatal murine $CD11b^+$ DCs showed that IL-4Rα promotes the differentiation of T cells into a Th2 phenotype (119). Furthermore, when the IL-4Rα was deleted, maturation of these cells increased, suggesting that neonatal $CD11b^+$ DCs are less prone to maturation. This feature of neonatal DCs could impair their capacity to induce a protective hRSV-specific immune response (119). Similar results were observed *in vivo* experiments; however, the deletion of IL-4Rα could be observed in several cells types including AMs, $CD11b^+$ DCs, and $CD103^+$ DCs (119).

Plasmacytoid DCs are the other prominent subset present in the lungs, which are an important source of IFN-α/β, fundamental antiviral cytokines during an infection, both in humans and mice (120, 121). The role of this DCs subset was elucidated by performing experiments with hRSV-infected bone marrow-derived pDCs, which expressed high levels of IFN-α, CD80, and CD86 and lower PD-L2 levels (**Figure 3**) (122). Moreover, in the same study, authors showed that the number of pDCs was increased early after infection and then decreased with the resolution of the disease, suggesting that pDCs are required during early stages of infection by hRSV (122). Also, it has been demonstrated that when pDCs are depleted using a 120G8 antibody, the lungs of hRSV-infected mice displayed an enhanced inflammation consisting mainly of mononuclear cells and lymphocytes, together an increase of viral loads (123). Consistently with these findings, it was observed that BALFs from hRSV-infected preterm born children showed reduced recruitment of pDCs into the lungs. These data are in agreement with the notion that low numbers of pDCs could work as a risk factor for severe bronchiolitis (124).

Additionally, three pDCs subsets have been characterized that include $CD8\alpha^-\beta^-$, $CD8\alpha^+\beta^-$, and $CD8\alpha^+\beta^+$ (125). The frequency of these subsets is 61, 22, and 6% in the lungs of healthy mice, respectively (125). However, beside all the current knowledge about the role of the different subset of DCs during hRSV infection, there are no data about the contribution of these cells to the hRSV-induced pathology.

In summary, all DCs subsets seem to be important for an antiviral immune response. However, hRSV is able to modulate the function of these cells by promoting an imbalance between these subsets, which could be critical for the resolution of the disease caused by this virus.

CONCLUDING REMARKS

The MPS consists of a family of cells that include monocytes, MΦ, and DCs, among others (1–3). These cells are characterized by their high mobility, phagocytic capacity, and ability to secrete a broad spectrum of immunomodulatory molecules (2). MPS exerts several functions in health and disease in several tissues (2). In the lungs, MPS plays an important role in the maintenance of homeostasis during steady state. During an infection, the MPS works as the first line of immune response against pathogens (2). Among the respiratory pathogens, hRSV is considered the most important cause of respiratory illness in infants and young children (33). The main severe clinical manifestation due to the hRSV infection is bronchiolitis (33). In this context, the MPS can contribute to the development of the immunopathology induced by hRSV (10). This viral pathogen is able to infect the MPS cells, altering the proper immune response required for viral clearance and the later acquisition of an antiviral immune memory (10). During the acute phase of the hRSV infection, monocytes are important to initiate the innate immune response, secreting cytokines and chemokines that recruit other immune cells, such as MΦ, eosinophils, and neutrophils (126). The normal function of monocytes during hRSV infection can be impaired not only by the pathogen itself but also by the contact with virus-infected AECs, contributing to the development of severe bronchiolitis (62).

During hRSV infection, MΦs play a protective role against infection and, finally, these cells are required for proper virus clearance (77). This notion is supported by experimental data obtained from various experimental models, such as neonatal mice and MΦ-depleted animals.

One of the effector mechanisms of MΦs is the secretion of IFN-γ and IL-12, which are reduced in human neonates infected by hRSV, contributing to development of bronchiolitis (81). Also, the inefficient recruitment of T and NKT cells into the airways (91) contributes to the development of bronchiolitis. As a consequence, there is a significant decrease of the protective capacity of the immune response triggered by hRSV and promoting virus spreading (91).

The ability of hRSV to infect DCs seems to be a major virulence mechanism used by this pathogen. The hRSV-infection of DCs impairs the correct immunological synapsis, which is required for T cell activation (104). These findings may contribute to explaining the lack of an effective immunological memory against hRSV, which allow subsequent reinfections throughout life. Moreover, pDCs are the major source of type I IFNs, cytokines necessary to induce an appropriate antiviral immune response (122). Consistently with a lack of protective immunity to hRSV, DCs infected by this virus show an impaired capacity to produce type I IFNs (122). Based on the current knowledge relative to the role of DCs in the hRSV-infection, these cells could be important for the promotion of an exacerbation of the inflammation during bronchiolitis. Besides the actual knowledge about the MPS in the hRSV immunopathology, is still necessary to further understand the mechanisms involved in the impairment of MPS function by hRSV virulence factors.

AUTHOR CONTRIBUTIONS

AK wrote, revised, and edited the article and figures. KB, JE, RP, and EJ wrote the article and drew the figures.

FUNDING

The grants are Millennium Institute in Immunology and Immunotherapy and Comisión Nacional de Investigación Científica y Tecnológica (CONICYT) CONICYT/FONDECYT POSTDOCTORADO No. 3150559.

REFERENCES

1. van Furth R, Cohn ZA. The origin and kinetics of mononuclear phagocytes. *J Exp Med* (1968) 128(3):415–35. doi:10.1084/jem.128.3.415
2. Hume DA. The mononuclear phagocyte system. *Curr Opin Immunol* (2006) 18(1):49–53. doi:10.1016/j.coi.2005.11.008
3. Hume DA. Differentiation and heterogeneity in the mononuclear phagocyte system. *Mucosal Immunol* (2008) 1(6):432–41. doi:10.1038/mi.2008.36
4. Geissmann F, Jung S, Littman DR. Blood monocytes consist of two principal subsets with distinct migratory properties. *Immunity* (2003) 19(1):71–82. doi:10.1016/S1074-7613(03)00174-2
5. Chow A, Brown BD, Merad M. Studying the mononuclear phagocyte system in the molecular age. *Nat Rev Immunol* (2011) 11(11):788–98. doi:10.1038/nri3087
6. Hull TD, Agarwal A, George JF. The mononuclear phagocyte system in homeostasis and disease: a role for heme oxygenase-1. *Antioxid Redox Signal* (2014) 20(11):1770–88. doi:10.1089/ars.2013.5673
7. Zaslona Z, Wilhelm J, Cakarova L, Marsh LM, Seeger W, Lohmeyer J, et al. Transcriptome profiling of primary murine monocytes, lung macrophages and lung dendritic cells reveals a distinct expression of genes involved in cell trafficking. *Respir Res* (2009) 10:2. doi:10.1186/1465-9921-10-2
8. Rodero MP, Poupel L, Loyher PL, Hamon P, Licata F, Pessel C, et al. Immune surveillance of the lung by migrating tissue monocytes. *Elife* (2015) 4:e07847. doi:10.7554/eLife.07847
9. Hettinger J, Richards DM, Hansson J, Barra MM, Joschko AC, Krijgsveld J, et al. Origin of monocytes and macrophages in a committed progenitor. *Nat Immunol* (2013) 14(8):821–30. doi:10.1038/ni.2638
10. Kimpen JL. Respiratory syncytial virus and asthma. The role of monocytes. *Am J Respir Crit Care Med* (2001) 163(3 Pt 2):S7–9. doi:10.1164/ajrccm.163.supplement_1.2011110
11. Sunderkotter C, Nikolic T, Dillon MJ, Van Rooijen N, Stehling M, Drevets DA, et al. Subpopulations of mouse blood monocytes differ in maturation stage and inflammatory response. *J Immunol* (2004) 172(7):4410–7. doi:10.4049/jimmunol.172.7.4410
12. Shi C, Pamer EG. Monocyte recruitment during infection and inflammation. *Nat Rev Immunol* (2011) 11(11):762–74. doi:10.1038/nri3070
13. Qu C, Brinck-Jensen NS, Zang M, Chen K. Monocyte-derived dendritic cells: targets as potent antigen-presenting cells for the design of vaccines against infectious diseases. *Int J Infect Dis* (2014) 19:1–5. doi:10.1016/j.ijid.2013.09.023
14. Baharom F, Rankin G, Blomberg A, Smed-Sorensen A. Human lung mononuclear phagocytes in health and disease. *Front Immunol* (2017) 8:499. doi:10.3389/fimmu.2017.00499
15. Idzkowska E, Eljaszewicz A, Miklasz P, Musial WJ, Tycinska AM, Moniuszko M. The role of different monocyte subsets in the pathogenesis of atherosclerosis and acute coronary syndromes. *Scand J Immunol* (2015) 82(3):163–73. doi:10.1111/sji.12314
16. Mosser DM, Edwards JP. Exploring the full spectrum of macrophage activation. *Nat Rev Immunol* (2008) 8(12):958–69. doi:10.1038/nri2448
17. Gordon S. Alternative activation of macrophages. *Nat Rev Immunol* (2003) 3(1):23–35. doi:10.1038/nri978
18. Gordon S, Pluddemann A. Tissue macrophages: heterogeneity and functions. *BMC Biol* (2017) 15(1):53. doi:10.1186/s12915-017-0392-4
19. Martinez FO, Gordon S. The M1 and M2 paradigm of macrophage activation: time for reassessment. *F1000Prime Rep* (2014) 6:13. doi:10.12703/P6-13
20. Sang Y, Miller LC, Blecha F. Macrophage polarization in virus-host interactions. *J Clin Cell Immunol* (2015) 6(2):311. doi:10.4172/2155-9899.1000311
21. Stockwin LH, McGonagle D, Martin IG, Blair GE. Dendritic cells: immunological sentinels with a central role in health and disease. *Immunol Cell Biol* (2000) 78(2):91–102. doi:10.1046/j.1440-1711.2000.00888.x
22. Merad M, Sathe P, Helft J, Miller J, Mortha A. The dendritic cell lineage: ontogeny and function of dendritic cells and their subsets in the steady state and the inflamed setting. *Annu Rev Immunol* (2013) 31:563–604. doi:10.1146/annurev-immunol-020711-074950
23. Kim KH, Lee YT, Hwang HS, Kwon YM, Kim MC, Ko EJ, et al. Virus-like particle vaccine containing the F protein of respiratory syncytial virus confers protection without pulmonary disease by modulating specific subsets of dendritic cells and effector T cells. *J Virol* (2015) 89(22):11692–705. doi:10.1128/JVI.02018-15
24. Mildner A, Jung S. Development and function of dendritic cell subsets. *Immunity* (2014) 40(5):642–56. doi:10.1016/j.immuni.2014.04.016
25. Sato K, Fujita S. Dendritic cells: nature and classification. *Allergol Int* (2007) 56(3):183–91. doi:10.2332/allergolint.R-06-139
26. Boltjes A, van Wijk F. Human dendritic cell functional specialization in steady-state and inflammation. *Front Immunol* (2014) 5:131. doi:10.3389/fimmu.2014.00131
27. Schlitzer A, McGovern N, Teo P, Zelante T, Atarashi K, Low D, et al. IRF4 transcription factor-dependent CD11b(+) dendritic cells in human and mouse control mucosal IL-17 cytokine responses. *Immunity* (2013) 38(5):970–83. doi:10.1016/j.immuni.2013.04.011
28. Condon TV, Sawyer RT, Fenton MJ, Riches DW. Lung dendritic cells at the innate-adaptive immune interface. *J Leukoc Biol* (2011) 90(5):883–95. doi:10.1189/jlb.0311134
29. Gehrie E, Van der Touw W, Bromberg JS, Ochando JC. Plasmacytoid dendritic cells in tolerance. *Methods Mol Biol* (2011) 677:127–47. doi:10.1007/978-1-60761-869-0_9
30. Reizis B, Bunin A, Ghosh HS, Lewis KL, Sisirak V. Plasmacytoid dendritic cells: recent progress and open questions. *Annu Rev Immunol* (2011) 29:163–83. doi:10.1146/annurev-immunol-031210-101345
31. Swiecki M, Colonna M. The multifaceted biology of plasmacytoid dendritic cells. *Nat Rev Immunol* (2015) 15(8):471–85. doi:10.1038/nri3865
32. Calvo C, Garcia-Garcia ML, Blanco C, Vazquez MC, Frias ME, Perez-Brena P, et al. Multiple simultaneous viral infections in infants with acute respiratory tract infections in Spain. *J Clin Virol* (2008) 42(3):268–72. doi:10.1016/j.jcv.2008.03.012
33. Bohmwald K, Espinoza JA, Rey-Jurado E, Gomez RS, Gonzalez PA, Bueno SM, et al. Human respiratory syncytial virus: infection and pathology. *Semin Respir Crit Care Med* (2016) 37(4):522–37. doi:10.1055/s-0036-1584799

34. Bueno SM, Gonzalez PA, Pacheco R, Leiva ED, Cautivo KM, Tobar HE, et al. Host immunity during RSV pathogenesis. *Int Immunopharmacol* (2008) 8(10):1320–9. doi:10.1016/j.intimp.2008.03.012
35. Espinoza JA, Bohmwald K, Cespedes PF, Riedel CA, Bueno SM, Kalergis AM. Modulation of host adaptive immunity by hRSV proteins. *Virulence* (2014) 5(7):740–51. doi:10.4161/viru.32225
36. Bohmwald K, Espinoza JA, Becerra D, Rivera K, Lay MK, Bueno SM, et al. Inflammatory damage on respiratory and nervous systems due to hRSV infection. *Curr Opin Immunol* (2015) 36:14–21. doi:10.1016/j.coi.2015.05.003
37. Ahout IM, Jans J, Haroutiounian L, Simonetti ER, van der Gaast-de Jongh C, Diavatopoulos DA, et al. Reduced expression of HLA-DR on monocytes during severe respiratory syncytial virus infections. *Pediatr Infect Dis J* (2016) 35(3):e89–96. doi:10.1097/INF.0000000000001007
38. Sweetman LL, Ng YT, Butler IJ, Bodensteiner JB. Neurologic complications associated with respiratory syncytial virus. *Pediatr Neurol* (2005) 32(5):307–10. doi:10.1016/j.pediatrneurol.2005.01.010
39. van Drunen Littel-van den Hurk S, Watkiss ER. Pathogenesis of respiratory syncytial virus. *Curr Opin Virol* (2012) 2(3):300–5. doi:10.1016/j.coviro.2012.01.008
40. Navas L, Wang E, de Carvalho V, Robinson J. Improved outcome of respiratory syncytial virus infection in a high-risk hospitalized population of Canadian children. Pediatric investigators collaborative network on infections in Canada. *J Pediatr* (1992) 121(3):348–54. doi:10.1016/S0022-3476(05)90000-0
41. Wang EE, Law BJ, Boucher FD, Stephens D, Robinson JL, Dobson S, et al. Pediatric Investigators Collaborative Network on Infections in Canada (PICNIC) study of admission and management variation in patients hospitalized with respiratory syncytial viral lower respiratory tract infection. *J Pediatr* (1996) 129(3):390–5. doi:10.1016/S0022-3476(96)70071-9
42. Boyce TG, Mellen BG, Mitchel EF Jr, Wright PF, Griffin MR. Rates of hospitalization for respiratory syncytial virus infection among children in medicaid. *J Pediatr* (2000) 137(6):865–70. doi:10.1067/mpd.2000.110531
43. Aujard Y, Fauroux B. Risk factors for severe respiratory syncytial virus infection in infants. *Respir Med* (2002) 96(Suppl B):S9–14. doi:10.1053/rmed.2002.1295
44. Collins PL, Graham BS. Viral and host factors in human respiratory syncytial virus pathogenesis. *J Virol* (2008) 82(5):2040–55. doi:10.1128/JVI.01625-07
45. Shi T, McAllister DA, O'Brien KL, Simoes EAF, Madhi SA, Gessner BD, et al. Global, regional, and national disease burden estimates of acute lower respiratory infections due to respiratory syncytial virus in young children in 2015: a systematic review and modelling study. *Lancet* (2017) 390(10098):946–58. doi:10.1016/S0140-6736(17)30938-8
46. Nair H, Simoes EA, Rudan I, Gessner BD, Azziz-Baumgartner E, Zhang JS, et al. Global and regional burden of hospital admissions for severe acute lower respiratory infections in young children in 2010: a systematic analysis. *Lancet* (2013) 381(9875):1380–90. doi:10.1016/S0140-6736(12)61901-1
47. Paramore LC, Ciuryla V, Ciesla G, Liu L. Economic impact of respiratory syncytial virus-related illness in the US: an analysis of national databases. *Pharmacoeconomics* (2004) 22(5):275–84. doi:10.2165/00019053-200422050-00001
48. Dudas RA, Karron RA. Respiratory syncytial virus vaccines. *Clin Microbiol Rev* (1998) 11(3):430–9.
49. Storey S. Respiratory syncytial virus market. *Nat Rev Drug Discov* (2010) 9(1):15–6. doi:10.1038/nrd3075
50. Gonzalez PA, Prado CE, Leiva ED, Carreno LJ, Bueno SM, Riedel CA, et al. Respiratory syncytial virus impairs T cell activation by preventing synapse assembly with dendritic cells. *Proc Natl Acad Sci U S A* (2008) 105(39):14999–5004. doi:10.1073/pnas.0802555105
51. Rossi GA, Colin AA. Respiratory syncytial virus-Host interaction in the pathogenesis of bronchiolitis and its impact on respiratory morbidity in later life. *Pediatr Allergy Immunol* (2017) 28(4):320–31. doi:10.1111/pai.12716
52. Pickles RJ, DeVincenzo JP. Respiratory syncytial virus (RSV) and its propensity for causing bronchiolitis. *J Pathol* (2015) 235(2):266–76. doi:10.1002/path.4462
53. Guo-Parke H, Canning P, Douglas I, Villenave R, Heaney LG, Coyle PV, et al. Relative respiratory syncytial virus cytopathogenesis in upper and lower respiratory tract epithelium. *Am J Respir Crit Care Med* (2013) 188(7):842–51. doi:10.1164/rccm.201304-0750OC
54. Barreira ER, Precioso AR, Bousso A. Pulmonary surfactant in respiratory syncytial virus bronchiolitis: the role in pathogenesis and clinical implications. *Pediatr Pulmonol* (2011) 46(5):415–20. doi:10.1002/ppul.21395
55. Newton AH, Cardani A, Braciale TJ. The host immune response in respiratory virus infection: balancing virus clearance and immunopathology. *Semin Immunopathol* (2016) 38(4):471–82. doi:10.1007/s00281-016-0558-0
56. Randolph GJ, Jakubzick C, Qu C. Antigen presentation by monocytes and monocyte-derived cells. *Curr Opin Immunol* (2008) 20(1):52–60. doi:10.1016/j.coi.2007.10.010
57. Cherrie AH, Anderson K, Wertz GW, Openshaw PJ. Human cytotoxic T cells stimulated by antigen on dendritic cells recognize the N, SH, F, M, 22K, and 1b proteins of respiratory syncytial virus. *J Virol* (1992) 66(4):2102–10.
58. Werling D, Hope JC, Chaplin P, Collins RA, Taylor G, Howard CJ. Involvement of caveolae in the uptake of respiratory syncytial virus antigen by dendritic cells. *J Leukoc Biol* (1999) 66(1):50–8.
59. Masten BJ, Lipscomb MF. Dendritic cells: pulmonary immune regulation and asthma. *Monaldi Arch Chest Dis* (2000) 55(3):225–30.
60. Becker S, Soukup JM. Airway epithelial cell-induced activation of monocytes and eosinophils in respiratory syncytial viral infection. *Immunobiology* (1999) 201(1):88–106. doi:10.1016/S0171-2985(99)80049-7
61. Soukup JM, Becker S. Role of monocytes and eosinophils in human respiratory syncytial virus infection in vitro. *Clin Immunol* (2003) 107(3):178–85. doi:10.1016/S1521-6616(03)00038-X
62. Oumouna M, Weitnauer M, Mijosek V, Schmidt LM, Eigenbrod T, Dalpke AH. Cell-contact dependent inhibition of monocytes by airway epithelial cells and reversion by infection with respiratory syncytial virus. *Immunobiology* (2015) 220(11):1240–5. doi:10.1016/j.imbio.2015.06.017
63. Salkind AR, Nichols JE, Roberts NJ Jr. Suppressed expression of ICAM-1 and LFA-1 and abrogation of leukocyte collaboration after exposure of human mononuclear leukocytes to respiratory syncytial virus in vitro. Comparison with exposure to influenza virus. *J Clin Invest* (1991) 88(2):505–11. doi:10.1172/JCI115332
64. Maus U, Herold S, Muth H, Maus R, Ermert L, Ermert M, et al. Monocytes recruited into the alveolar air space of mice show a monocytic phenotype but upregulate CD14. *Am J Physiol Lung Cell Mol Physiol* (2001) 280(1):L58–68.
65. Maus UA, Janzen S, Wall G, Srivastava M, Blackwell TS, Christman JW, et al. Resident alveolar macrophages are replaced by recruited monocytes in response to endotoxin-induced lung inflammation. *Am J Respir Cell Mol Biol* (2006) 35(2):227–35. doi:10.1165/rcmb.2005-0241OC
66. Collins CL, Pollard AJ. Respiratory syncytial virus infections in children and adults. *J Infect* (2002) 45(1):10–7. doi:10.1053/jinf.2001.1016
67. Bont L, Heijnen CJ, Kavelaars A, van Aalderen WM, Brus F, Draaisma JT, et al. Monocyte IL-10 production during respiratory syncytial virus bronchiolitis is associated with recurrent wheezing in a one-year follow-up study. *Am J Respir Crit Care Med* (2000) 161(5):1518–23. doi:10.1164/ajrccm.161.5.9904078
68. Bendelja K, Vojvoda V, Aberle N, Cepin-Bogovic J, Gagro A, Mlinaric-Galinovic G, et al. Decreased toll-like receptor 8 expression and lower TNF-alpha synthesis in infants with acute RSV infection. *Respir Res* (2010) 11:143. doi:10.1186/1465-9921-11-143
69. Byrne AJ, Maher TM, Lloyd CM. Pulmonary macrophages: a new therapeutic pathway in fibrosing lung disease? *Trends Mol Med* (2016) 22(4):303–16. doi:10.1016/j.molmed.2016.02.004
70. Kolli D, Gupta MR, Sbrana E, Velayutham TS, Chao H, Casola A, et al. Alveolar macrophages contribute to the pathogenesis of human metapneumovirus infection while protecting against respiratory syncytial virus infection. *Am J Respir Cell Mol Biol* (2014) 51(4):502–15. doi:10.1165/rcmb.2013-0414OC
71. Rivera R, Hutchens M, Luker KE, Sonstein J, Curtis JL, Luker GD. Murine alveolar macrophages limit replication of vaccinia virus. *Virology* (2007) 363(1):48–58. doi:10.1016/j.virol.2007.01.033
72. Blumenthal RL, Campbell DE, Hwang P, DeKruyff RH, Frankel LR, Umetsu DT. Human alveolar macrophages induce functional inactivation in antigen-specific CD4 T cells. *J Allergy Clin Immunol* (2001) 107(2):258–64. doi:10.1067/mai.2001.112845

73. Empey KM, Orend JG, Peebles RS Jr, Egana L, Norris KA, Oury TD, et al. Stimulation of immature lung macrophages with intranasal interferon gamma in a novel neonatal mouse model of respiratory syncytial virus infection. *PLoS One* (2012) 7(7):e40499. doi:10.1371/journal.pone.0040499
74. Benoit A, Huang Y, Proctor J, Rowden G, Anderson R. Effects of alveolar macrophage depletion on liposomal vaccine protection against respiratory syncytial virus (RSV). *Clin Exp Immunol* (2006) 145(1):147–54. doi:10.1111/j.1365-2249.2006.03114.x
75. Makris S, Bajorek M, Culley FJ, Goritzka M, Johansson C. Alveolar macrophages can control respiratory syncytial virus infection in the absence of type I interferons. *J Innate Immun* (2016) 8(5):452–63. doi:10.1159/000446824
76. Reed JL, Brewah YA, Delaney T, Welliver T, Burwell T, Benjamin E, et al. Macrophage impairment underlies airway occlusion in primary respiratory syncytial virus bronchiolitis. *J Infect Dis* (2008) 198(12):1783–93. doi:10.1086/593173
77. Goritzka M, Makris S, Kausar F, Durant LR, Pereira C, Kumagai Y, et al. Alveolar macrophage-derived type I interferons orchestrate innate immunity to RSV through recruitment of antiviral monocytes. *J Exp Med* (2015) 212(5):699–714. doi:10.1084/jem.20140825
78. Becker S, Quay J, Soukup J. Cytokine (tumor necrosis factor, IL-6, and IL-8) production by respiratory syncytial virus-infected human alveolar macrophages. *J Immunol* (1991) 147(12):4307–12.
79. Franke-Ullmann G, Pfortner C, Walter P, Steinmuller C, Lohmann-Matthes ML, Kobzik L, et al. Alteration of pulmonary macrophage function by respiratory syncytial virus infection in vitro. *J Immunol* (1995) 154(1):268–80.
80. Roberts NJ Jr, Prill AH, Mann TN. Interleukin 1 and interleukin 1 inhibitor production by human macrophages exposed to influenza virus or respiratory syncytial virus. Respiratory syncytial virus is a potent inducer of inhibitor activity. *J Exp Med* (1986) 163(3):511–9. doi:10.1084/jem.163.3.511
81. Tsutsumi H, Matsuda K, Sone S, Takeuchi R, Chiba S. Respiratory syncytial virus-induced cytokine production by neonatal macrophages. *Clin Exp Immunol* (1996) 106(3):442–6. doi:10.1046/j.1365-2249.1996.d01-874.x
82. Panuska JR, Merolla R, Rebert NA, Hoffmann SP, Tsivitse P, Cirino NM, et al. Respiratory syncytial virus induces interleukin-10 by human alveolar macrophages. Suppression of early cytokine production and implications for incomplete immunity. *J Clin Invest* (1995) 96(5):2445–53. doi:10.1172/JCI118302
83. Haeberle HA, Takizawa R, Casola A, Brasier AR, Dieterich HJ, Van Rooijen N, et al. Respiratory syncytial virus-induced activation of nuclear factor-kappaB in the lung involves alveolar macrophages and toll-like receptor 4-dependent pathways. *J Infect Dis* (2002) 186(9):1199–206. doi:10.1086/344644
84. Harris J, Werling D. Binding and entry of respiratory syncytial virus into host cells and initiation of the innate immune response. *Cell Microbiol* (2003) 5(10):671–80. doi:10.1046/j.1462-5822.2003.00313.x
85. Haynes LM, Moore DD, Kurt-Jones EA, Finberg RW, Anderson LJ, Tripp RA. Involvement of toll-like receptor 4 in innate immunity to respiratory syncytial virus. *J Virol* (2001) 75(22):10730–7. doi:10.1128/JVI.75.22.10730-10737.2001
86. Schijf MA, Lukens MV, Kruijsen D, van Uden NO, Garssen J, Coenjaerts FE, et al. Respiratory syncytial virus induced type I IFN production by pDC is regulated by RSV-infected airway epithelial cells, RSV-exposed monocytes and virus specific antibodies. *PLoS One* (2013) 8(11):e81695. doi:10.1371/journal.pone.0081695
87. Marr N, Turvey SE. Role of human TLR4 in respiratory syncytial virus-induced NF-kappaB activation, viral entry and replication. *Innate Immun* (2012) 18(6):856–65. doi:10.1177/1753425912444479
88. Shirey KA, Pletneva LM, Puche AC, Keegan AD, Prince GA, Blanco JC, et al. Control of RSV-induced lung injury by alternatively activated macrophages is IL-4R alpha-, TLR4-, and IFN-beta-dependent. *Mucosal Immunol* (2010) 3(3):291–300. doi:10.1038/mi.2010.6
89. Schultz C, Richter N, Moller JC, Bucsky P. IFN-gamma response and IL-8 plasma levels in neonates with respiratory syncytial virus bronchiolitis. *Eur Respir J* (2001) 17(2):321–4. doi:10.1183/09031936.01.17203210
90. Harker JA, Yamaguchi Y, Culley FJ, Tregoning JS, Openshaw PJ. Delayed sequelae of neonatal respiratory syncytial virus infection are dependent on cells of the innate immune system. *J Virol* (2014) 88(1):604–11. doi:10.1128/JVI.02620-13
91. Eichinger KM, Egana L, Orend JG, Resetar E, Anderson KB, Patel R, et al. Alveolar macrophages support interferon gamma-mediated viral clearance in RSV-infected neonatal mice. *Respir Res* (2015) 16:122. doi:10.1186/s12931-015-0282-7
92. Guilliams M, Lambrecht BN, Hammad H. Division of labor between lung dendritic cells and macrophages in the defense against pulmonary infections. *Mucosal Immunol* (2013) 6(3):464–73. doi:10.1038/mi.2013.14
93. Qi F, Wang D, Liu J, Zeng S, Xu L, Hu H, et al. Respiratory macrophages and dendritic cells mediate respiratory syncytial virus-induced IL-33 production in TLR3- or TLR7-dependent manner. *Int Immunopharmacol* (2015) 29(2):408–15. doi:10.1016/j.intimp.2015.10.022
94. Johnson TR, Johnson CN, Corbett KS, Edwards GC, Graham BS. Primary human mDC1, mDC2, and pDC dendritic cells are differentially infected and activated by respiratory syncytial virus. *PLoS One* (2011) 6(1):e16458. doi:10.1371/journal.pone.0016458
95. Schwarze J. Lung dendritic cells in respiratory syncytial virus bronchiolitis. *Pediatr Infect Dis J* (2008) 27(10 Suppl):S89–91. doi:10.1097/INF.0b013e318168b6f0
96. Kondo Y, Matsuse H, Machida I, Kawano T, Saeki S, Tomari S, et al. Regulation of mite allergen-pulsed murine dendritic cells by respiratory syncytial virus. *Am J Respir Crit Care Med* (2004) 169(4):494–8. doi:10.1164/rccm.200305-663OC
97. de Graaff PM, de Jong EC, van Capel TM, van Dijk ME, Roholl PJ, Boes J, et al. Respiratory syncytial virus infection of monocyte-derived dendritic cells decreases their capacity to activate CD4 T cells. *J Immunol* (2005) 175(9):5904–11. doi:10.4049/jimmunol.175.9.5904
98. Guerrero-Plata A, Casola A, Suarez G, Yu X, Spetch L, Peeples ME, et al. Differential response of dendritic cells to human metapneumovirus and respiratory syncytial virus. *Am J Respir Cell Mol Biol* (2006) 34(3):320–9. doi:10.1165/rcmb.2005-0287OC
99. Kurt-Jones EA, Popova L, Kwinn L, Haynes LM, Jones LP, Tripp RA, et al. Pattern recognition receptors TLR4 and CD14 mediate response to respiratory syncytial virus. *Nat Immunol* (2000) 1(5):398–401. doi:10.1038/80833
100. Murawski MR, Bowen GN, Cerny AM, Anderson LJ, Haynes LM, Tripp RA, et al. Respiratory syncytial virus activates innate immunity through toll-like receptor 2. *J Virol* (2009) 83(3):1492–500. doi:10.1128/JVI.00671-08
101. Alloatti A, Kotsias F, Pauwels AM, Carpier JM, Jouve M, Timmerman E, et al. Toll-like receptor 4 engagement on dendritic cells restrains phago-lysosome fusion and promotes cross-presentation of antigens. *Immunity* (2015) 43(6):1087–100. doi:10.1016/j.immuni.2015.11.006
102. Johnson TR, McLellan JS, Graham BS. Respiratory syncytial virus glycoprotein G interacts with DC-SIGN and L-SIGN to activate ERK1 and ERK2. *J Virol* (2012) 86(3):1339–47. doi:10.1128/JVI.06096-11
103. Gomez RS, Ramirez BA, Cespedes PF, Cautivo KM, Riquelme SA, Prado CE, et al. Contribution of Fcgamma receptors to human respiratory syncytial virus pathogenesis and the impairment of T-cell activation by dendritic cells. *Immunology* (2016) 147(1):55–72. doi:10.1111/imm.12541
104. Cespedes PF, Bueno SM, Ramirez BA, Gomez RS, Riquelme SA, Palavecino CE, et al. Surface expression of the hRSV nucleoprotein impairs immunological synapse formation with T cells. *Proc Natl Acad Sci U S A* (2014) 111(31):E3214–23. doi:10.1073/pnas.1400760111
105. do Nascimento de Freitas D, Gassen RB, Fazolo T, Souza APD. Rapamycin increases RSV RNA levels and survival of RSV-infected dendritic cell depending on T cell contact. *Toxicol In Vitro* (2016) 36:114–9. doi:10.1016/j.tiv.2016.07.016
106. Sung SS, Fu SM, Rose CE Jr, Gaskin F, Ju ST, Beaty SR. A major lung CD103 (alphaE)-beta7 integrin-positive epithelial dendritic cell population expressing Langerin and tight junction proteins. *J Immunol* (2006) 176(4):2161–72. doi:10.4049/jimmunol.176.4.2161
107. Ho AW, Prabhu N, Betts RJ, Ge MQ, Dai X, Hutchinson PE, et al. Lung CD103+ dendritic cells efficiently transport influenza virus to the lymph node and load viral antigen onto MHC class I for presentation to CD8 T cells. *J Immunol* (2011) 187(11):6011–21. doi:10.4049/jimmunol.1100987
108. Hildner K, Edelson BT, Purtha WE, Diamond M, Matsushita H, Kohyama M, et al. Batf3 deficiency reveals a critical role for CD8α+ dendritic cells in cytotoxic T cell immunity. *Science* (2008) 322(5904):1097–100. doi:10.1126/science.1164206

109. Helft J, Manicassamy B, Guermonprez P, Hashimoto D, Silvin A, Agudo J, et al. Cross-presenting CD103+ dendritic cells are protected from influenza virus infection. *J Clin Invest* (2012) 122(11):4037–47. doi:10.1172/JCI60659
110. Ruckwardt TJ, Malloy AM, Morabito KM, Graham BS. Quantitative and qualitative deficits in neonatal lung-migratory dendritic cells impact the generation of the CD8+ T cell response. *PLoS Pathog* (2014) 10(2):e1003934. doi:10.1371/journal.ppat.1003934
111. Wu P, Hartert TV. Evidence for a causal relationship between respiratory syncytial virus infection and asthma. *Expert Rev Anti Infect Ther* (2011) 9(9):731–45. doi:10.1586/eri.11.92
112. Knudson CJ, Varga SM. The relationship between respiratory syncytial virus and asthma. *Vet Pathol* (2015) 52(1):97–106. doi:10.1177/0300985814520639
113. Conejero L, Khouili SC, Martinez-Cano S, Izquierdo HM, Brandi P, Sancho D. Lung CD103+ dendritic cells restrain allergic airway inflammation through IL-12 production. *JCI Insight* (2017) 2(10):90420. doi:10.1172/jci.insight.90420
114. Lukens MV, Kruijsen D, Coenjaerts FE, Kimpen JL, van Bleek GM. Respiratory syncytial virus-induced activation and migration of respiratory dendritic cells and subsequent antigen presentation in the lung-draining lymph node. *J Virol* (2009) 83(14):7235–43. doi:10.1128/JVI.00452-09
115. Persson EK, Uronen-Hansson H, Semmrich M, Rivollier A, Hagerbrand K, Marsal J, et al. IRF4 transcription-factor-dependent CD103(+)CD11b(+) dendritic cells drive mucosal T helper 17 cell differentiation. *Immunity* (2013) 38(5):958–69. doi:10.1016/j.immuni.2013.03.009
116. Plantinga M, Guilliams M, Vanheerswynghels M, Deswarte K, Branco-Madeira F, Toussaint W, et al. Conventional and monocyte-derived CD11b(+) dendritic cells initiate and maintain T helper 2 cell-mediated immunity to house dust mite allergen. *Immunity* (2013) 38(2):322–35. doi:10.1016/j.immuni.2012.10.016
117. Kallal LE, Schaller MA, Lindell DM, Lira SA, Lukacs NW. CCL20/CCR6 blockade enhances immunity to RSV by impairing recruitment of DC. *Eur J Immunol* (2010) 40(4):1042–52. doi:10.1002/eji.200939778
118. McDermott DS, Weiss KA, Knudson CJ, Varga SM. Central role of dendritic cells in shaping the adaptive immune response during respiratory syncytial virus infection. *Future Virol* (2011) 6(8):963–73. doi:10.2217/fvl.11.62
119. Shrestha B, You D, Saravia J, Siefker DT, Jaligama S, Lee GI, et al. IL-4Ralpha on dendritic cells in neonates and Th2 immunopathology in respiratory syncytial virus infection. *J Leukoc Biol* (2017) 102(1):153–61. doi:10.1189/jlb.4A1216-536R
120. Hornung V, Schlender J, Guenthner-Biller M, Rothenfusser S, Endres S, Conzelmann KK, et al. Replication-dependent potent IFN-alpha induction in human plasmacytoid dendritic cells by a single-stranded RNA virus. *J Immunol* (2004) 173(10):5935–43. doi:10.4049/jimmunol.173.10.5935
121. Smit JJ, Lindell DM, Boon L, Kool M, Lambrecht BN, Lukacs NW. The balance between plasmacytoid DC versus conventional DC determines pulmonary immunity to virus infections. *PLoS One* (2008) 3(3):e1720. doi:10.1371/journal.pone.0001720
122. Wang H, Peters N, Schwarze J. Plasmacytoid dendritic cells limit viral replication, pulmonary inflammation, and airway hyperresponsiveness in respiratory syncytial virus infection. *J Immunol* (2006) 177(9):6263–70. doi:10.4049/jimmunol.177.9.6263
123. Smit JJ, Rudd BD, Lukacs NW. Plasmacytoid dendritic cells inhibit pulmonary immunopathology and promote clearance of respiratory syncytial virus. *J Exp Med* (2006) 203(5):1153–9. doi:10.1084/jem.20052359
124. Kerrin A, Fitch P, Errington C, Kerr D, Waxman L, Riding K, et al. Differential lower airway dendritic cell patterns may reveal distinct endotypes of RSV bronchiolitis. *Thorax* (2017) 72(7):620–7. doi:10.1136/thoraxjnl-2015-207358
125. Lombardi V, Speak AO, Kerzerho J, Szely N, Akbari O. CD8alpha(+)beta(-) and CD8alpha(+)beta(+) plasmacytoid dendritic cells induce Foxp3(+) regulatory T cells and prevent the induction of airway hyper-reactivity. *Mucosal Immunol* (2012) 5(4):432–43. doi:10.1038/mi.2012.20
126. Kimpen JL, Garofalo R, Welliver RC, Fujihara K, Ogra PL. An ultrastructural study of the interaction of human eosinophils with respiratory syncytial virus. *Pediatr Allergy Immunol* (1996) 7(1):48–53. doi:10.1111/j.1399-3038.1996.tb00105.x

Conflict of Interest Statement: The authors declare that the research was conducted in the absence of any commercial or financial relationships that could be construed as a potential conflict of interest.

Copyright © 2017 Bohmwald, Espinoza, Pulgar, Jara and Kalergis. This is an open-access article distributed under the terms of the Creative Commons Attribution License (CC BY). The use, distribution or reproduction in other forums is permitted, provided the original author(s) or licensor are credited and that the original publication in this journal is cited, in accordance with accepted academic practice. No use, distribution or reproduction is permitted which does not comply with these terms.

frontiers in Immunology

ORIGINAL RESEARCH
published: 30 November 2017
doi: 10.3389/fimmu.2017.01629

M(IL-4) Tissue Macrophages Support Efficient Interferon-Gamma Production in Antigen-Specific CD8+ T Cells with Reduced Proliferative Capacity

*Rylend Mulder, Andra Banete, Kyle Seaver and Sameh Basta**

Department of Biomedical and Molecular Sciences, Queen's University, Kingston, ON, Canada

CD8+ cytotoxic T cell (CTL) responses are necessary for the lysis of virally infected cells and control of infection. CTLs are activated when their TCRs bind a major histocompatibility complex (MHC)-I/peptide complex on the surface of antigen presenting cells such as macrophages (MΦ). It is now apparent that MΦ display remarkable plasticity in response to environmental signals to polarize into classically activated M(LPS + IFN-γ) or alternatively activated M(IL-4). However, little is known about how MΦ activation status influences their antigen presentation function to CD8+ T cell in models of virus infection. Consequently, we tested how polarization of spleen-derived (Sp)-MΦ impacts direct presentation of viral antigens to influence effector and proliferative CD8+ T-cell responses. We show that M(IL-4) Sp-MΦ retain MHC-I surface expression and the ability to stimulate IFN-γ production by CTL following peptide stimulation and lymphocytic choriomeningitis virus infection to levels similar to M0 and M(LPS + IFN-γ) MΦ. However, memory CD8+ T cells cultured in the presence of M(IL-4) MΦ underwent significantly reduced proliferation and produced similar IFN-γ levels as coculturing with M0 or M(LPS + IFN-γ) cells. Thus, these results show a novel ability of polarized MΦ to regulate CD8+ T-cell proliferation and effector functions during virus infection.

Keywords: polarized macrophages, major histocompatibility complex, interleukin-4, interferon-gamma, T cells, lymphocytic choriomeningitis virus infection

OPEN ACCESS

Edited by:
Geanncarlo Lugo-Villarino, UMR5089 Institut de Pharmacologie et de Biologie Structurale (IPBS), France

Reviewed by:
Oberdan Leo, Free University of Brussels, Belgium
Guillaume Tabouret, Institut National de la Recherche Agronomique (INRA), France

****Correspondence:***
Sameh Basta
bastas@queensu.ca

Specialty section:
This article was submitted to Microbial Immunology, a section of the journal Frontiers in Immunology

Received: *14 July 2017*
Accepted: *09 November 2017*
Published: *30 November 2017*

Citation:
Mulder R, Banete A, Seaver K and Basta S (2017) M(IL-4) Tissue Macrophages Support Efficient Interferon-Gamma Production in Antigen-Specific CD8+ T Cells with Reduced Proliferative Capacity. Front. Immunol. 8:1629. doi: 10.3389/fimmu.2017.01629

INTRODUCTION

Tissue macrophages (MΦ) comprise an important member of the mononuclear phagocyte system where they regulate inflammation, cancer, and autoimmunity (1). They are involved in innate and adaptive immune responses to invading pathogens (2), and adapt their phenotype and function in accordance with their environment through a process termed MΦ polarization (3–5). It is now understood that both tissue MΦ and bone marrow (BM)-MΦ can develop into pro-inflammatory (M1) or anti-inflammatory (M2) (6–8).

M1 or M(LPS + IFN-γ) activation occurs in response to interferon-gamma (IFN-γ) in combination with bacterial moieties, such as lipopolysaccharide (LPS) (9, 10). M(LPS + IFN-γ) MΦ exhibit elevated secretion levels of nitric oxide (NO), and pro-inflammatory cytokines including tumor necrosis factor (TNF)-α, and IL-1β (11). Phenotypically, M(LPS + IFN-γ) cells express major

histocompatibility complex (MHC)-II, and the costimulatory molecules CD80 and CD86 (6) to stimulate $CD4^+$ T-cell proliferation (6, 12). M(LPS + IFN-γ) cells have been studied for their anti-bacterial, anti-viral immunity (13–17).

On the other hand, M2 cells are subdivided into M2a, M2b, M2c, and M2d depending on their environmental stimulus. The most studied subclass, M2a, is induced with interleukin IL-4 or IL-13 (9, 10). M2a or M(IL-4) MΦ upregulate Arginase-1 expression (11), and express high levels of mannose receptor (CD206) and chitinase-3-like protein 3 (Chi3l3) (6, 18). As such, M(IL-4) MΦ are widely considered regulatory and reparative cells (19). However, unchecked expansion of M2 MΦ can cause severe pathologies (19). For example, during chronic hepatitis C virus (HCV) infection, circulating and liver monocytes convert to an M2-like state resulting in fibrosis development (20). It is therefore important to study MΦ polarization during virus infection as a strategy to unlock MΦ targeting therapeutics to limit virus-associated damage (17).

During lymphocytic choriomeningitis virus infection (LCMV), MΦ support viral replication, process, and present viral antigens to activate $CD8^+$ T cells (21–26). Activated $CD8^+$ T cells proliferate, gradually acquire cytotoxic T lymphocyte (CTL) effector function and home to the site of infection to secrete IFN-γ and lyse virally infected upon recognition of viral epitopes on MHC-I (27). It is known that M(IL-4) peritoneal MΦ and BM-MΦ inhibit OT-II proliferation in a signal transducer and activator of transcription (STAT)-6-dependent fashion (28). Moreover, in a murine norovirus infection model, helminth-induced M2 cells inhibit $CD8^+$ T-cell proliferation (29). Yet, how polarized MΦ engage $CD8^+$ T cells to control proliferation and functions during RNA virus infection remains unexplored. Here, we report on a novel finding supporting a dichotomized regulatory role of M(IL-4) tissue MΦ where they can inhibit $CD8^+$ T-cell proliferation without affecting their IFN-γ production after peptide-specific antigen presentation.

RESULTS

Phenotypic and Functional Characterization of Activated Spleen-Derived (Sp)-MΦ

Nitrite and urea production are known to be effective functional measures of M(LPS + IFN-γ) and M(IL-4) polarization, respectively (6, 8). Therefore, to demonstrate plasticity of Sp-MΦ, we characterized the biochemical properties profiles of polarized BM-MΦ and Sp-MΦ following IFN-γ (16 h) + LPS (8 h) or IL-4 stimulation (24 h). In agreement with previous publications, BM-MΦ and Sp-MΦ induce significant nitrite production after M(LPS + IFN-γ) stimulating conditions (**Figure 1A**: left panel), while producing urea following IL-4 treatment (**Figure 1A**: right panel) confirming previous published data (6, 8). Thus, both BM-MΦ and tissue-derived Sp-MΦ show similar biochemical profiles when polarized into M(LPS + IFN-γ) and M(IL-4) status as reported previously (8).

Professional antigen presenting cells (pAPC) such as MΦ are needed for the activation of adaptive immune cells (30), as they are involved in antigen presentation *via* both MHC-I and MHC-II as well as their expression of costimulatory molecules (31). Nevertheless, LCMV has evolved mechanisms to interrupt APC activation and costimulatory molecule expression (32). Therefore, in order to assess the ability of polarized Sp-MΦ to engage $CD8^+$ T-cell receptors, we characterized surface expression of activated Sp-MΦ markers following 24 h of LCMV infection (**Figure 1B**). With regard to CD80 expression, M0 and M(LPS + IFN-γ) cells increased surface levels following viral infection, while M(IL-4) cells expression of CD80 remained largely unchanged (column 1). Interestingly, M0 cells slightly decreased CD86 expression following LCMV infection compared with M(LPS + IFN-γ) and M(IL-4) cells where no change was detected (column 2). M0 cells exhibited slight MHC-I reduction but not M(LPS + IFN-γ) or M(IL-4) Sp-MΦ (column 3). In addition, we also assessed expression of the inhibitory molecule PD-L1 (column 4). We observed that M(LPS + IFN-γ) cells expressed the greatest levels of PD-L1, while M0 and M(IL-4) had similar expression levels, which confirmed data in BM-MΦ published by another group (33). LCMV infection increased expression of PD-L1 in M0 and M(IL-4), while reduced expression in M(LPS + IFN-γ) Sp-MΦ. These data demonstrate that polarized cells are not negatively affected by LCMV infection when considering CD80/86 or MHC-I expression, while LCMV increases inhibitory molecule PD-L1 expression in M2 and M0 cells, but not M(LPS + IFN-γ).

To characterize further the functional profile of polarized cells, we investigated the release of pro- and anti-inflammatory cytokines in uninfected and LCMV-infected (24 h) Sp-MΦ. As expected, for the secretion of the cytokines TNF-α and IL-6 (**Figure 1C**), M0 and M(IL-4) cells were poor, while M(LPS + IFN-γ) stimulation produced substantial levels agreeing with what has been described previously (34). Interestingly, 24 h post-LCMV infection, M0 and M(IL-4) cells both significantly increased production of TNF-α and IL-6. Moreover, M(LPS + IFN-γ) cells had reduced production of TNF-α after infection but were still producing significantly higher amounts than M0 and M(IL-4). No changes in IL-6 secretion were observed with M(LPS + IFN-γ) after the infection.

Lymphocytic choriomeningitis virus infection significantly decreased production of IL-12p40, in M0 and M(LPS + IFN-γ) cells while the opposite is true for M(IL-4), where production levels increased. Collectively, these data point to LCMV-promoting M(IL-4) cells to acquire a mixed M(LPS + IFN-γ)/M(IL-4) phenotype considering the ability to produce pro-inflammatory cytokines post-infection. For the anti-inflammatory cytokine IL-10, LCMV infection increased secretion in all subsets; however, M(LPS + IFN-γ) and M(IL-4) produced substantially less amounts than M0 infected cells (**Figure 1C**).

M(IL-4) Sp-MΦ Present SIINFEKL Peptide Bound to MHC-I at Lower Levels Compared with M(LPS + IFN-γ)

Having observed substantial levels of MHC-I expression on all MΦ, we questioned to what extent polarized MΦ can bind and present MHC-I peptides. For this, we utilized the 25-D1.16

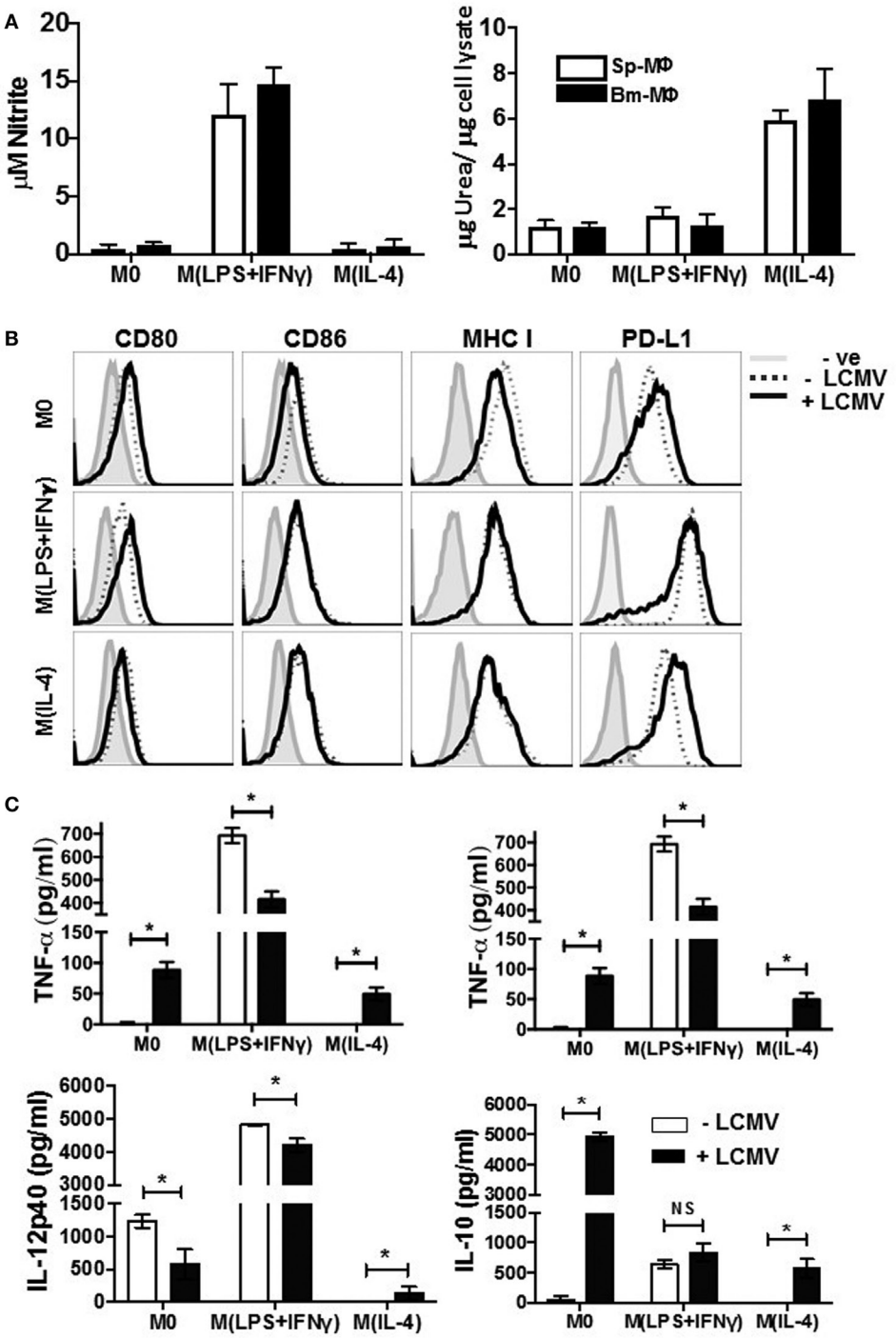


FIGURE 1 | Immunophenotyping of polarized macrophages. Activated BM-MΦ or Sp-MΦ populations were polarized into M(LPS + IFN-γ) (25 ng/mL IFN-γ + 100 ng/mL LPS), or M(IL-4) (20 ng/mL IL4) or left unstimulated. **(A)** Nitrite detection after BM-MΦ or Sp-MΦ were polarized into M(LPS + IFN-γ) or M(IL-4), or left unstimulated (left panel). Supernatants were collected before testing them for nitrite production using the Greiss reaction. The OD was measured using Varioskan plate reader to quantify nitrite production after comparing the values to the standard curve. In the right panel, urea production was measured in polarized BM-MΦ and Sp-MΦ samples to monitor arginase activity indicative of M(IL-4) polarization. Values are represented as μg urea corrected to μg cell lysate. Data shown and error bars are the mean ± SD from one representative experiment out of three. **(B)** Staining profiles of activated polarized BM-MΦ and Sp-MΦ populations that were either controls or infected with LCMV-WE (MOI 5 for 24 h). Histograms show surface staining for CD80, MHC-86, MHC-I, or PD-L1 in the various MΦ populations compared with the isotype control (−ve). Data shown are representative from one of two experiments. **(C)** Cell supernatants from LCMV-uninfected or LCMV-infected (24 h) polarized Sp-MΦ were subjected to ELISA for quantification of TNF-α, IL-12p40, IL-6, and IL-10. Graphical data show mean ± SD from two independent experiments containing two experimental replicates. BM, bone marrow; MHC, major histocompatibility complex; LCMV, lymphocytic choriomeningitis virus infection; LPS, lipopolysaccharide.

monoclonal antibody, which recognizes the SIINFEKL peptide only when bound to H2-K^b MHC-I (p:MHC) (35). Representative staining of unpulsed and SIINFEKL-pulsed all MΦ (1 h) histograms depicted in **Figure 2A** demonstrate that each population of Sp-MΦ are able to display p:MHC on their surface. Measuring the fold change in mean fluorescent intensity (MFI) over unpulsed controls revealed M(LPS + IFN-γ) were best at binding and presenting the peptide and that Sp-M(IL-4) cells were the least efficient (**Figure 2B**). This suggests that the polarized all MΦ subsets should be able to present H2-K^b restricted epitopes to CD8$^+$ T cells to varying degrees.

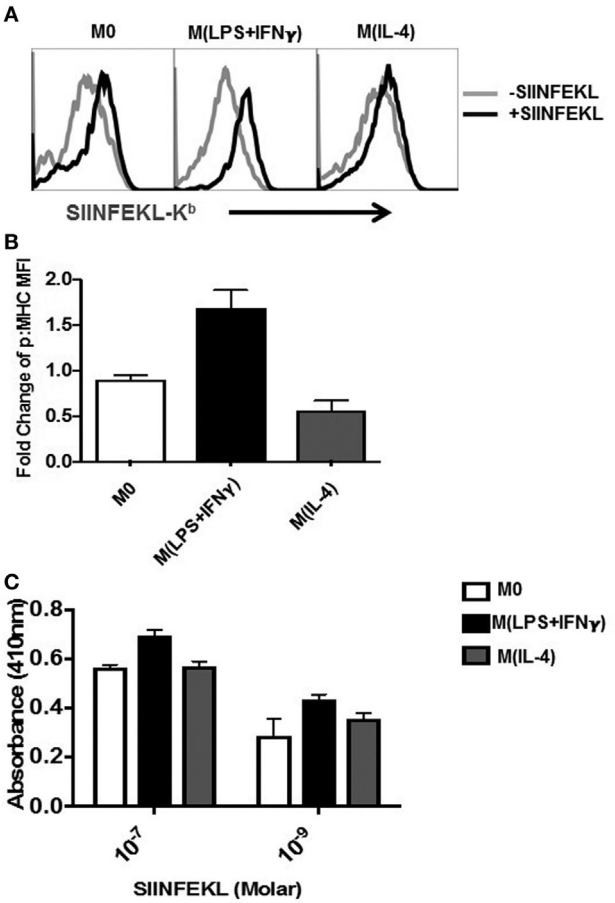


FIGURE 2 | Detection of SIINFEKL peptide bound to MHC-I on MΦ. Sp-MΦ were polarized into either M(LPS + IFN-γ), M(IL-4) or left untreated (M0) and pulsed with SIINFEKL (10^{-7}M) for 2 h at 37°C. **(A)** Cells were stained with 25-D1.16 monoclonal antibody, which detects SIINFEKL bound to H2-K^b MHC-I (p:MHC) before acquisition using FCM. The data are demonstrative histograms from one of three representative experiments. **(B)** Fold change in MFI of detected ab staining was calculated by comparing 25D staining in SIINFEKL pulsed versus unpulsed controls. Graphical data show mean ± SD from three independent experiments. **(C)** Cells were pulsed 10^{-7} or 10^{-9} M SIINFEKL for 2 h at 37°C before coincubation with the T-cell B3Z hybridoma for 18 h (1:1 ratio). The detection assay was carried out as described in Section "Materials and Methods" and OD was measured at 415 nm. Graphs depicting mean ± SD from three experimental replicates. MFI, mean fluorescent intensity; MHC, major histocompatibility complex.

Based on the above observations (**Figures 2A,B**), we reasoned that this would translate to differential abilities to activate CD8$^+$ T cells by the MΦ population. To test this, we employed the CD8$^+$ T-cell hybridoma system for which inducible *Lac-Z* is under the NFAT enhancer that binds the IL-2 promoter (36, 37). In this system, SIINFEKL-K^b-specific TCR ligation results in binding to the IL-2 promotor and expression of downstream *Lac-Z* that can be detected by colorimetric changes (38). Using two different concentrations of the SIINFEKL peptide (10^{-7} and 10^{-9} M), we observed that M(LPS + IFN-γ) MΦ populations elicited B3Z activation better than M0 and M(IL-4) (**Figure 2C**). Yet, M(IL-4) were still very proficient in activating B3Z T cells indicating that M(IL-4) cells retain sufficient antigen presentation capabilities that was close to M0 cells.

M(IL-4) MΦ Effectively Stimulate Epitope-Specific CD8$^+$ T Cells to Synthesize IFN-γ

Recently, it was shown that splenic marginal zone MΦ are responsible for activating an LCMV-specific CD8$^+$ T cells when left unprimed by DC (39). Therefore, we extended our testing into the LCMV system, which includes H2-K^b and H2-D^b binding epitopes in H-2^b mice (40). Polarized Sp-MΦ were pulsed with either GP33-41 or NP396-404 then cocultured with splenocytes isolated from LCMV-infected mice (2×10^5 pfu i.p.), 8 days post-infection. The ability of virus-specific CD8$^+$ T cells to produce IFN-γ after *in vitro* re-stimulation with the ICS assay was used to assess the polarized Sp-MΦ antigen presentation functions (**Figure 3**).

We found that the percentage of IFN-γ antigen-specific CD8$^+$ T cells remained constant irrespective of MΦ activation status (**Figures 3A,B**). Moreover, in agreement with immunodominance hierarchy reported for this model (41), there was a greater percentage of IFN-γ-secreting GP33-41-specific CD8$^+$ T cells than NP396-404 T cells (**Figures 3A,B**). This finding was identical irrespective of the activation MΦ state even at low-peptide concentrations of 10^{-9} M. We further tested IFN-γ induction in LCMV-memory-specific CD8$^+$ T cells using the LCMV GP33-41 peptide. After *ex vivo* stimulation by GP33-41 pulsed MΦ, we found that M(IL-4) cells were able to elicit similar activation of the memory T cells compared with M0 (data not shown). Therefore, we were able to demonstrate that M(IL-4)-MΦ polarization does not negatively influence their ability to stimulate activation and release of IFN-γ from antigen-specific effector or memory CD8$^+$ T cells after virus infection.

Evaluating the Ability of Activated MΦ to Present Viral Antigens after Infection

To assess whether the functional abilities with regard to antigen presentation were retained by the MΦ during viral infection, we infected Sp-MΦ with LCMV (MOI 5), and assessed their ability to present LCMV antigens to epitope-specific CTL. It was clear from the data (**Figure 4A**) that LCMV was to infect the polarized MΦ *in vitro* and initiate its replication cycle as evident by LCMV-NP detection 24 h post-infection (**Figure 4A**). This protein was not detected immediately during the first hour

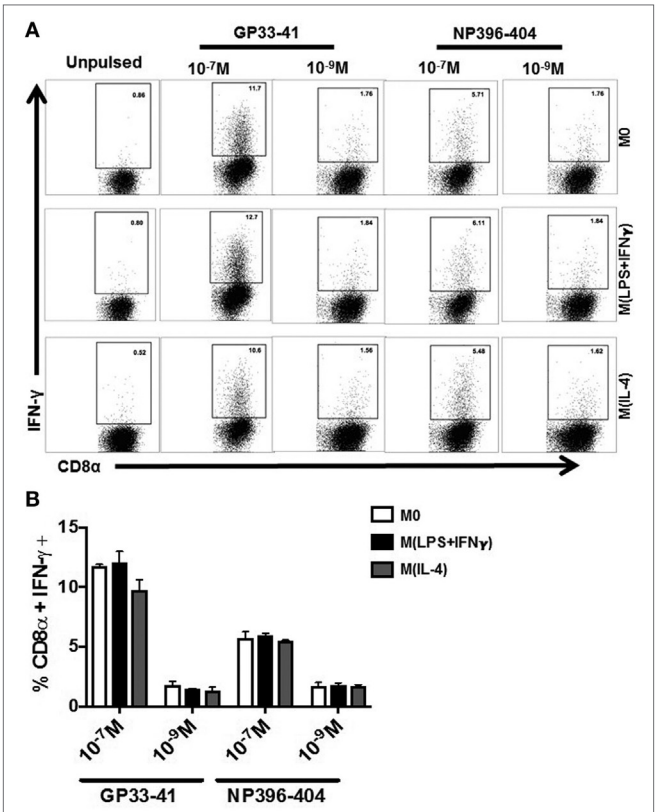


FIGURE 3 | Stimulation of epitope-specific CD8+ T cells by polarized MΦ *via* antigen presentation. Sp-MΦ were polarized into either M(LPS + IFN-γ), M(IL-4) or left untreated (M0) and were pulsed with GP33-41 or NP396-404 (10^{-7} or 10^{-9} M) for 1 h in serum free medium. Cells 1×10^5 were washed and cocultured with splenocytes from LCMV-infected mouse (20,000 pfu; day 8 p.i). Sp-MΦ were cocultured at a ratio of 10 (splenocytes): 1 Sp-MΦ for 6 h at 37° followed before CD8α and IFN-γ on CD3+ gated cells. As a negative control, unpulsed polarized Sp-MΦ were cocultured with splenocytes as described above. The percentage of CD8α+ IFN-γ+ from the dot plots in **(A)** were grouped in **(B)** where the data shown are the mean ± SD from three experimental replicates. LCMV, lymphocytic choriomeningitis virus infection.

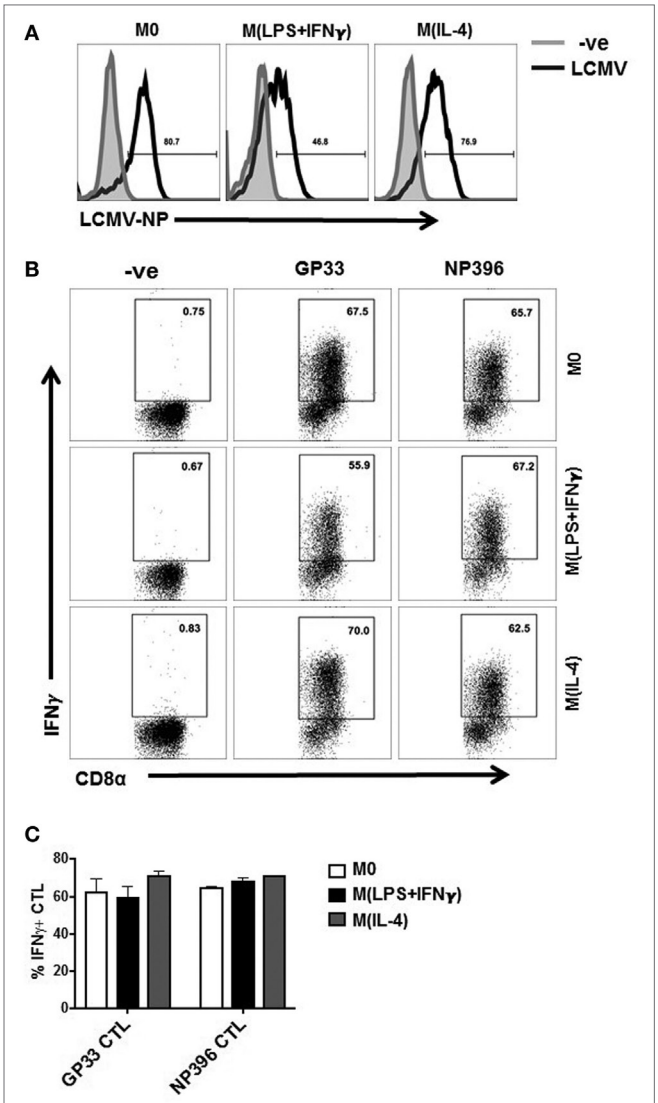


FIGURE 4 | Presentation of viral epitopes to CD8 T cells by LCMV-infected MΦ. **(A)** Polarized Sp-MΦ were infected with LCMV-WE (MOI 5) before testing for expression of LCMV-NP 24 h later. **(B)** In parallel, the same infected Sp-MΦ or uninfected negative controls were tested for their ability to directly present the LCMV GP33-41 or NP396-404 epitopes to their specific CTL cultures by assaying for IFN-γ production after *in vitro* stimulation by ICS. **(C)** Graphical representation of dot plots from B showing mean ± SD from three repeats. CTL, cytotoxic T lymphocyte; LCMV, lymphocytic choriomeningitis virus infection.

of infection and needed to accumulate for approximately 8 h post-infection to be detected at significant levels due to the increased number of copies as a result of viral replication (data not shown), confirming our previous published data (42). Notably, we detected a reduction in LCMV-NP expression in M(LPS + IFN-γ) polarized cells compared with M0 and M2 (**Figure 4A**) indicating that M(LPS + IFN-γ) cells were likely inhibiting viral replication as described elsewhere.

After 24 h of LCMV infection, we assessed the antigen presenting capacity of polarized MΦ compared with M0 to epitope-specific CTLs. From the data shown in (**Figures 4B,C**), M(LPS + IFN-γ) cells activated GP33-41- and NP396-404-specific CTLs to levels similar to M0 and M(IL-4) cells. Thus, to our surprise M(IL-4) cells were very potent stimulators IFN-γ release from both GP33-41- and NP396-404-specific CD8+ T cells following viral infection. Thus, despite the prevailing dogma of M(IL-4) MΦ perceived to be poor antigen presenting cells when interacting with CD8+ T cells, we discovered that they were proficient in presenting either peptides or processing viral antigens in different model systems.

M(IL-4) Sp-MΦ Poorly Support Epitope-Specific CD8+ T-Cell Proliferation When IL-2 Levels are Limiting

Upon successful activation, naïve CD8+ T cells undergo an estimated 10^4- to 10^5-fold expansion at their peak proliferation during activation (43). Other groups have demonstrated that

M(IL-4) MΦ inhibit antigen-specific T-cell proliferation (28, 29). These publications utilized culture systems with M(IL-4) BM-MΦ and naïve P14 CD8+ T cells (specific for GP33-41) or anti-TCR and anti-CD28 antibodies to artificially stimulate naïve CD8+ T-cell proliferation in an antigen-independent fashion proliferation (28, 29). However, how M(IL-4) cells direct memory recall responses is unknown. Therefore, we asked how CD8 T cells from LCMV memory, non-transgenic mice would respond to antigen presentation by polarized Sp-MΦ. To assess this, we cultured peptide-pulsed either polarized or unstimulated Sp-MΦ with carboxyfluorescein succinimidyl ester (CFSE) labeled splenocytes from LCMV immune WT mice in the absence or presence of IL-2 (**Figures 5A,B**). Without exogenous IL-2 added to cultures, all the three MΦ populations failed to induce recall proliferation *in vitro* (data not shown), confirming previously published data by other groups (44). We then increased IL-2 culture concentrations to determine the minimum threshold of exogenous IL-2 required for T-cell expansion. At 5 U/mL, M0 and M(LPS + IFN-γ) MΦ induced 40 and 60% CD8+ T-cell proliferation, respectively (**Figures 5A,B**). In contrast, M(IL-4) induced the lowest proliferation (20%) by antigen-specific CD8+ T cells (**Figures 5A,B**).

We were able to restore the deficit in the stimulation ability of M(IL-4) cells by increasing the IL-2 levels in the culture system to 20 U/mL. This finding was not restricted to a single specificity of epitope-specific T cells, as both GP33-41- and NP396-404-specific T cells proliferated to similar levels when comparing M(IL-4) with either M(LPS + IFN-γ) or M0 (**Figures 5C,D**). Collectively, the data from **Figures 2–5** demonstrate that although M(IL-4) cells are proficient at presenting antigens to CD8+ T cell and stimulate them to elicit IFN-γ release either as effector, memory cells, M(IL-4)-MΦ were poor inducers of their if IL-2 is not present at sufficient quantities in the environment.

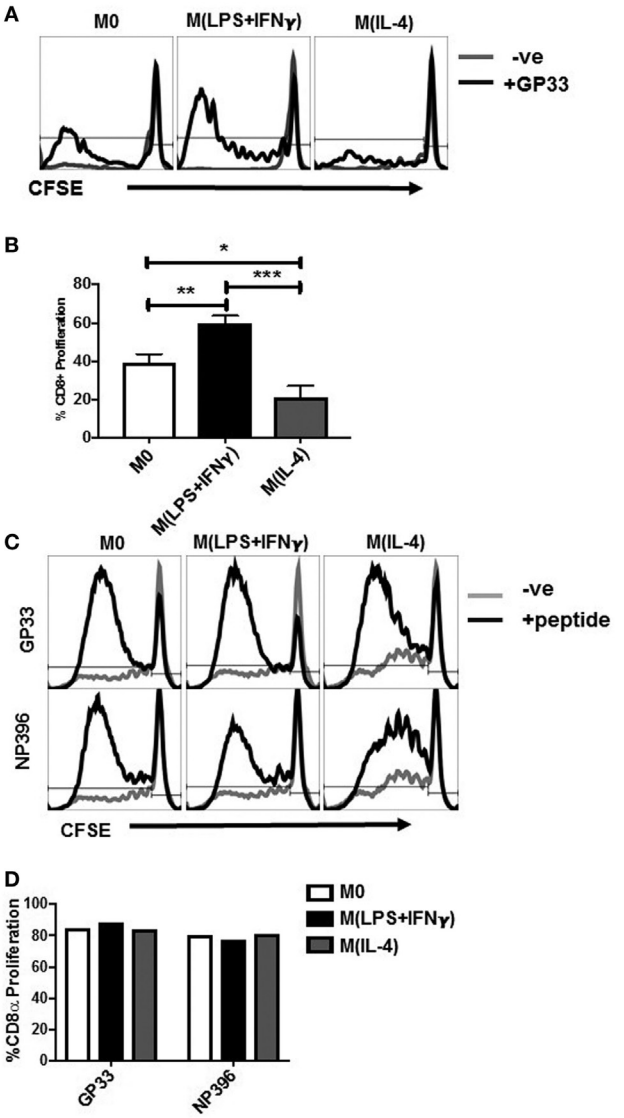


FIGURE 5 | M(IL-4) Sp-MΦ poorly support epitope-specific CD8+ T-cell proliferation. Polarized Sp-MΦ were pulsed with the LCMV GP33-41 peptide and cultured with CFSE labeled splenocytes from LCMV immune mice (10:1 ratio) for 4 days in the presence of 5 U/mL IL-2. **(A)** Representative histograms showing CFSE dilution in CD8+ T cells. **(B)** Graphical representation of % CFSE low, CD8+ T cells of three replicates from one representative experiment. *$P < 0.05$, **$P < 0.0005$, and ***$P < 0.0005$. **(C)** When the CD8+ T-cell proliferation experiments were carried out in culture supernatant containing 20 U/mL IL-2, no differences were observed in the ability of M(IL-4) Sp-MΦ to induce CD8+ T-cell proliferation when compared with either M0 or M(LPS + IFN-γ) cells. **(D)** Graphical representation of % CFSE low, CD8+ T cells from one of four independent experiments. CFSE, carboxyfluorescein succinimidyl ester; LCMV, lymphocytic choriomeningitis virus infection.

CD8+ T Cells Expanded for 6 Days by M(IL-4) Stimulators Exhibit Attenuated IFN-γ Secretion Compared with M0 or M(LPS + IFN-γ) Cells

From our observations above, we noted that although CD8+ T-cell proliferation was impaired compared with M0 and M(IL-4), approximately 20–30% of CD8+ T cell were still proliferating after peptide antigen presentation with M(IL-4) MΦ (**Figure 5B**). As CD8+ T cells proliferate, they progressively acquire CTL functions (45). To test whether the epitope-specific CD8+ T cells were fully functional after the expansion period, we restimulated the expanded T cells using a common (BMA) MΦ cell line as antigen presenting cells so that the only variable factor in the assay would be the expansion difference of the Sp-MΦ (23, 42, 46).

Consequently, we cocultured the cells *in vitro* for 6 days using 5 U/mL IL-2 because this was the concentration at which we observed minimal M(IL-4)-induced CTL expansion (**Figure 5A**). We then tested for IFN-γ production by ICS as described earlier, but this time using the BMA cell line as APC to present the LCMV peptide to T cells (**Figure 6A**).

M0 and M(LPS + IFN-γ)-expanded CTL were ~60% IFN-γ positive, whereas M(IL-4)-expanded CTL displayed lower level of ~30%. This indicates that in addition to M(IL-4) cells being poor expanders of CD8+ T cells, the CTLs that were able to expand were not potent effector cells. Upon increasing culture conditions to 10 U/mL of IL-2 (**Figure 6B**), we noted a partial restoration (an increase of approximately 10%) of IFN-γ production by CD8+

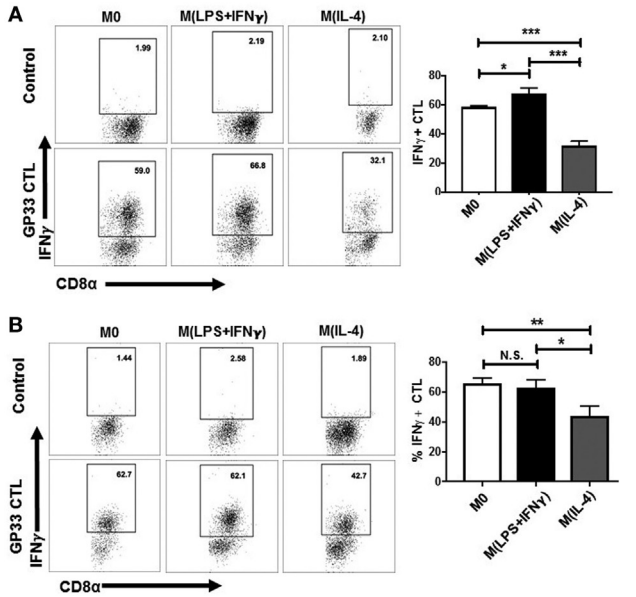


FIGURE 6 | CD8+ T cells expanded by M(IL-4) stimulators exhibiting attenuated IFN-γ secretion. Sp-MΦ [M0, M(LPS + IFN-γ) or M(IL-4) cells] were pulsed with LCMV GP33-41 and cultured with CFSE-labeled splenocytes from LCMV immune mice (10:1 ratio) for 6 days in the presence of 5 U/mL IL-2 **(A)** or 10 U/mL IL-2 **(B)**. Expanded cells were restimulated with GP33-41 pulsed BMA or unpulsed controls for detection of IFN-γ production by ICS in a restimulation assay to detect their epitope-specific activation. Graphs show mean ± SD from three replicates where $^{*}P < 0.05$ and $^{***}P < 0.0005$. CFSE, carboxyfluorescein succinimidyl ester; LCMV, lymphocytic choriomeningitis virus infection.

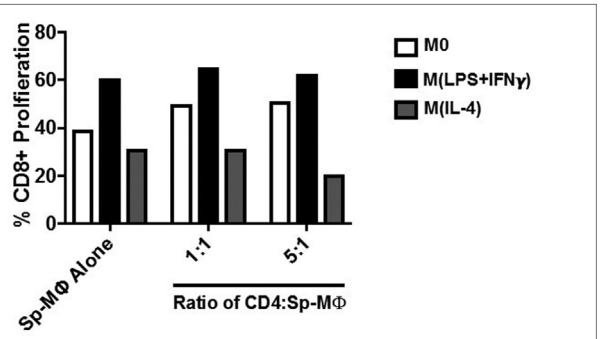


FIGURE 7 | Activated CD4+ T cells from LCMV immune mice fail to enhance the M(IL-4) expansion of CD8+ T-cell proliferation to levels obtained with the M(LPS + IFN-γ) cells. CD4+ T cells were negatively sorted from LCMV-infected mice (20,000 pfu) on day 4 post-infection as described in Section "Materials and Methods." The CD4+ T cells were added in different ratios to a polarized, GP33-41 pulsed Sp-MΦ mixed with splenocytes in culture containing 5 U/mL IL-2. As in **Figure 5B**, after 4 days of coculturing, the CD8+ T cells were tested for CFSE dilution as described before. CFSE, carboxyfluorescein succinimidyl ester; LCMV, lymphocytic choriomeningitis virus infection.

T cells cocultured with the M(IL-4) stimulators. This finding suggests that exogenous IL-2 can overcome stimulatory deficits in M(IL-4) cells, implying that M(IL-4) cells can dampen the proliferation and subsequent cytokine synthesis in CD8+ T cells through antigen presentation when IL-2 levels are low or limiting in the environment.

Activated CD4+ T Cells from LCMV Immune Mice are Not Sufficient to Enhance the M(IL-4) Expansion of CD8+ T-Cell Proliferation

CD4+ T helper cells play an important role in shaping efficient CTL, CD8+ T-cell memory, and recall responses (47). Evidence suggests that for efficient CD8+ T-cell responses to occur, the APC must be helped by CD4+ T cells (48). In particular, direct engagement between CD40 and CD40L activates APC to enable IL-2 production for memory CD8+ T-cell proliferation (49). Given that IL-2 rescued CD8+ T-cell proliferation in M(IL-4) MΦ cultures in our experimental model, we reasoned that activated CD4+ T from an *in vivo* LCMV infection would compensate for the M(IL-4) ability to support CD8+ T cells in our model when the exogenous IL-2 levels are limiting in culture.

To test this hypothesis, we sorted CD4+ T cells from LCMV-infected mice on day 4 because it has been shown that CD69 expression levels are near their peak after virus infection *in vivo* (50). We cocultured the sorted CD4+ T cells with the MΦ plus CD8+ T cells during the CFSE proliferation assays in our model, when exogenous IL-2 levels are limiting. Although we observed that addition of CD4+ T cells enhanced the ability of M0 cells to increase CD8+ T-cell proliferation (from 38 to 50%), there was no positive influence in the M(IL-4) cultures (**Figure 7**) possibly because they may require additional help. Interestingly, no further proliferation (60%) was noted with M(LPS + IFN-γ) cells when we included the helper cells, indicating that a possible maximum proliferation had already been reached at such IL-2 levels without the CD4+ T cells present in the culture.

DISCUSSION

It is now understood that polarized MΦ can modulate the outcome of infection and play a role in exacerbating or combating multiple diseases (4, 10). We previously reported that M-CSF induces *in vitro* differentiation of Sp-MΦ into cells that resemble splenic red pulp MΦ (23, 51). Further characterization revealed that Sp-MΦ are effective antigen presenting cells capable of direct and cross presentation (23). Additionally, mature Sp-MΦ remain plastic and can be induced to M(LPS + IFN-γ) and M(IL-4) phenotypes, similar to BM-MΦ (8).

Several groups have reported on the ability of M(IL-4) polarized cells to negatively regulate CD4+ T cells (6, 9, 28, 52–54). In addition, M(IL-4)-polarized BM cells were shown to inhibit CD3/CD28-activated naïve CD8+ T-cell proliferation, and impair proliferation of naïve LCMV-specific transgenic (P14) CD8+ T cells in a helminth/norovirus coinfection model (28, 29). However, not much is known regarding how polarized MΦ influence antigen-specific CD8+ T-cell IFN-γ secretion and memory CD8+ T-cell recall responses after antigen presentation has ensued, particularly during viral infection. To this end, using the well-defined LCMV model, our study uncovers a dichotomous

effect of M(IL-4) MΦ on CD8+ T-cell proliferation and effector molecule release.

We demonstrate that polarized M(IL-4) MΦ present MHC-I-restricted peptides to activate CD8+ T cells and stimulate IFN-γ expression. LCMV infected all three subsets of MΦ as detected by LCMV-NP expression 24 h post-infection. However, we observed a substantial reduction of LCMV-NP in M(LPS + IFN-γ) cells. This is likely owing to the upregulation IFN-γ-induced anti-viral genes inhibiting the replication of capacity of LCMV described (55). M(IL-4) cells effectively processed and presented *de novo* synthesized antigens to activate GP33-41- and NP396-404-specific CTL. However, when polarized cells were cultured with splenocytes cells from LCMV-immune mice, M(IL-4) cells stimulated the lowest level of CD8+ T-cell proliferation, a deficit that was overridden by increasing the levels of exogenous IL-2 added to the culture system. Collectively, these observations highlight how polarized MΦ modify CD8+ T-cell function and are of particular importance to the design of cell-based immunotherapies.

The suppressive effects of M(IL-4) MΦ on T-cell proliferation have been reported in the literature where M(IL-4) cells prevented proliferation of EL4 and D10.G4 T cells through an undefined cell-contact-dependent mechanism during nematode infection (52). Subsequent gene analysis revealed several M(IL-4)-specific markers including program death ligand (PD-L2), resistin like molecule (RELM)-α and YM-1, regulating CD4+ T-cell and CD8+ T-cell proliferation (28, 29, 54). Moreover, *in vitro* M(IL-4) MΦ express high levels of Arginase-1 and can also interrupt TCR signaling through L-arginine deprivation (56). For instance, coculture of M(IL-4) MΦ with Jurkat T cells or spleen T cells for 24 h resulted in the downregulation of CD3ζ T-cell surface expression and inhibition of CD4+ T-cell proliferation (56–58). Moreover, L-arginine deprivation yields a G_0–G_1 arrest by preventing increases of cyclin D3 and cyclin-dependent kinase 4 (CDK4) levels (58). Thus, M(IL-4) cells have the ability to modulate T-cell proliferation by contact-dependent and contact-independent mechanisms.

In our system, we observed a significant reduction of antigen-specific memory CD8+ T-cell proliferation when stimulated with M(IL-4) cells compared with M0 or M(LPS + IFN-γ) when employing IL-2 at limiting concentrations. Interestingly, supplementing the coculture medium with additional IL-2 restored CD8+ T-cell proliferation and subsequent IFN-γ secretion upon restimulation. The most likely explanation for this finding is likely due to the ability of IL-2 to tune TCR sensitivity and regulate cell-cycle progression. With regard to TCR sensitivity, exogenous IL-2 restores basally depressed CD3ζ expression in patients with chronic myeloid leukemia (59). Moreover, it was recently demonstrated that IL-2 reduces the threshold of activation in CD8+ T cells promoting responsiveness to low antigen levels (60). Therefore, by adding IL-2 we ostensibly improved the TCR sensitivity to antigen. In terms of cell cycle, IL-2 enhances expression of cyclin D3 and CDK4, and activates CDK2 promoting cell-cycle progression into S phase (61, 62). Therefore, it is plausible that additional IL-2 overrides the M(IL-4) cell-induced CD8+ T-cell impairments by increasing CD3ζ expression and promoting entrance into cell cycle. In agreement with this notion, delivery of IL-2 complexed to anti-IL-2 monoclonal antibody breaks established CD8+ T-cell tolerance in an FBL model of murine leukemia (63). As such, future research into the biological mechanisms of our reported novel finding that IL-2 can overcome M(IL-4) stimulatory deficits CD8+ T cell is of immense interest to the immunotherapy field.

Another novel finding that is reported here is the ability of the polarized MΦ to elicit IFN-γ production by antigen-specific CTL following peptide stimulation or LCMV infection. Given the impairment of CD8+ T-cell TCR signaling described above following M(IL-4) coculture, we anticipated M(IL-4) cells to poorly induce IFN-γ secretion from CTL (57, 59). A limitation of these studies was that they did not address the consequence of short-term (<24 h) M(IL-4) MΦ–T-cell interactions on CD3ζ expression (57, 59). However, the duration of our cytokine detection assays (approximately 6 h) allows us to separate the short-term and long-term impacts of M(IL-4) cells on CD8+ T-cell effector function and memory CD8+ T-cell proliferative response.

In our system, the observed ability of M(IL-4) cells to stimulate CTL IFN-γ release is likely attributed to the lower threshold of CTL activation for cytokine production compared with proliferation (64). It was previously demonstrated that low concentrations of TCR ligands result in IFN-γ, but not IL-2 production nor proliferation in CD4+ T cells (64). However, as ligand concentration increases, so does the diversity of cytokine response and proliferation levels (64, 65). This implies that additional characteristic of polyfunctional CD8+ T cells requires a successive increase in signaling threshold. Conceptually, this might serve as a safeguard to control against unwanted CD8+ T-cell effector activity and cytokine production.

In summary, our results uncover a previously unknown ability of M(IL-4) cells to induce IFN-γ secretion by CTL and yet negatively regulate memory CD8+ T-cell proliferation compared with other forms of MΦ employed in this study. Thus, it is plausible that M(IL-4) cells possess novel undefined characteristics that need to be uncovered regarding how they may regulate immunity during infections.

MATERIALS AND METHODS

Animals, Cell Lines, and Virus

C57BL/6 (H-2^b) mice (6–8 weeks) were purchased from (Jackson Laboratories) and were kept under specific pathogen-free conditions. Animal experiments were carried out in accordance with the guidelines of the Canadian Council of Animal Use and with approval from Queen's University Animal Care Committee. The BMA cell line BMA3.1A7 (a gift from Dr. K. Rock, University of Massachusetts Medical School, Worcester, MA, USA) is an adherent murine MΦ cell line generated from the BM of female C57BL/6 mice by overexpressing *myc* and *raf* oncogenes and has recently been characterized by our group to be a good model to study MΦ polarization (66, 67). For viral infections, mice were injected at indicated plaque forming units (PFUs) or LCMV-WE intraperitoneal in 200 μL of sterile PBS.

Macrophage Generation and Activation

Bone marrow-MΦ and Sp-MΦ were generated as previously described (8, 23, 51). Briefly, cells (for both BM-MΦ and

Sp-MΦ) were cultured in 6 well plates (Corning) with conditioned RPMI 1640 (Gibco) medium (CM) supplemented with 10% fetal calf serum (Fisher Scientific), M-CSF media and 50 μg/mL gentamycin. On days 3 and 5 of culturing, non-adherent cells were removed and fresh CM was added. Sp-MΦ and BM-MΦ were cultured for 6–7 days in total before activation and testing for their functions as described below. For M(LPS + IFN-γ) MΦ: cells were primed with IFN-γ (25 ng/mL for 16–18 h; Shenandoah Biotechnology) followed by *Escherichia coli* LPS (O55:B5, 100 ng/mL for 6 h; Sigma-Aldrich). To induce M(IL-4) MΦ, polarization cells were treated with rIL-4 (20 ng/mL for 18–24 h; Shenandoah Biotechnology). Unstimulated control MΦ (M0) were placed in RPMI 10% FCS for 18–24 h.

Assessment of Arginase and Inducible Nitric Oxide Activity

M(LPS + IFN-γ) polarization was determined by assessing NO production using Griess reagent as published previously (8, 24). MΦ (200,000 cells/well) were seeded in a round-bottom 96-well plate and activated in phenol-red free RPMI, where nitrite concentration was determined by measuring OD at 540 nm using the Varioskan microplate reader. Sodium nitrite was used for the standard graph (0–100 μM) to calculate nitrite concentrations in the test samples and was purchased from Fisher Scientific (Whitby, ON, Canada).

M(IL-4) polarization was assessed by arginase activity as described (8, 68). Activated MΦ were resuspended in lysis buffer (0.1% Triton-X, 25-mM Tris–Cl, pH 8.0) purchased from Sigma (Oakville, ON, Canada) and incubated for 30 min at 4°C followed by centrifugation at 10,000× *g* for 20 min at 4°C. Protein content in supernatant was determined using Bradford reagent (Bioshop) and sample concentrations were equalized to 100 μg/mL. For the reaction, 100 μL of sample was added to 1.5-mL eppendorfs followed by 10 μL of 10-mM $MnCl_2$ an incubation at a 55°C for 10 min. 100 μL 0.5-M L-arginine solution (pH 9.7) was then added before incubation for 1 h at 37°C. To stop the reaction, 800 μL of acid solution (7:3:1; H_2O:H_2PO_4, 85%: H_2SO_4, 95%) and 40 μL of α-isonitrosopropiophenone (ISPF) (9% w/v in absolute ethanol) were added. Samples were heated at 100°C for 30 min and urea concentration was determined with the help of a urea standard graph (0–25 M) by measuring OD at 550 nm using a Varioskan spectrophotometric microplate reader.

Cytokine ELISA Assay

Uninfected or LCMV-infected (MOI 3: 24 h) were seeded at 2–3 × 10^6 cells/mL into 6-well plates and incubated at 37°C for 24 h. After incubation, ELISAs were performed on collected supernatants. The levels of IL-6, IL-10, IL-12p40, and TNF-α were measured in accordance with R&D systems manufacturer's instructions.

Reverse-Transcriptase Polymerase Chain Reaction (RT-PCR)

Total RNA was extracted from primary, LCMV-infected cells using TRI reagent (Molecular Research Center Inc.). RT reaction was carried out using RT master mix with reagents obtained from Froggabio (North York, ON, Canada). PCR was performed using Taq 5X Master Mix (Froggabio) and the following primers (Forward and Reverse) obtained from Integrated DNA Technologies (Coraville, IA, USA) for LCMV Nucleoprotein (F: 5′-TCC ATG AGA GCA CAG TGC GGG GTG AT-3′, R: 5′-GCA TGG GAG AAC ACG ACA ATT GAC C-3′) and 18S control (F:5′-AAACGGCTACCACATCCAAG-3′, R: 5′-CCTCCAATGGATCCTCGTTA-3′).

Flow Cytometry

Cells were stained with a combination of surface marker antibodies detailed below. Primary direct staining was performed with antibodies purchased from Biolegend: FITC anti-CD86, clone RMMP-2; FITC anti-MHC-II (I-A/I-E), clone M5/114.15.2; FITC anti-CD25, clone 3C7; PE anti-MHC-I, clone AF6-88.5; PE Biotin anti-CD80, clone 1610A1; PE anti-PDL1, clone 10F.9G2; PE anti-CD137, clone 17B5; APC/Cy7 anti-CD69, clone H1.2F3. For indirect staining antibodies were purchased from Biolegend: Biotin anti-IFN-γ, clone XMG1.2; from eBioscience: Biotin anti-SIINFEKL/H2-K^b, clone 25-D1.16. Here, applicable cells were stained with secondary Streptavidin-FITC (Invitrogen) or FITC anti-rat IgG, clone Poly4054 (Biolegend). Staining was carried out for 20–30 min at 4°C in FACS buffer containing 0.5% sodium azide in PBS. Samples were acquired using the Epics XL-MCL flow cytometer (Beckman Coulter, Miami, FL, USA) and analyzed using FlowJo software. Fold change in MFI was calculated by using the following formula: fold change = [(SIINFEKL MFI − Negative MFI)/Negative MFI], where "SIINFEKL" refers to cells that were pulsed with SIINFEKL peptide and "Negative" refers to unpulsed cells.

Induction of LCMV-Specific $CD8^+$ T Cells

Peptide-specific short-term T-cell lines were generated as previously described (23, 24, 42, 46). Splenocytes isolated from LCMV immune mice (30 days post-infection) were subjected to ficoll-gradient lymphocyte enrichment. Enriched T cells were cocultured with γ-irradiated peptide-loaded (GP33-41, NP396-404; 10^{-7}M) BMA at a ratio of 10:1 in RPMI (10% FCS, 50-μM β-mercaptoethanol, 20 U/mL rIL-2, 50-μg/mL gentamycin). After 5 days, medium was isolated and ficolled to remove dead APC and enriched cells were re-seeded in a new 6-well plate with fresh medium for 2–3 days before use.

Antigen Presentation Assays

In order to compare direct antigen presentation by activated MΦ, we utilized LCMV-specific T cells, either *in vitro* generated LCMV CTL or the B3Z hybridoma T cells. For *ex vivo* stimulation of LCMV-specific $CD8^+$ T cells by polarized MΦ, splenocytes isolated from an LCMV-infected mouse on day 8 and were restimulated with GP33-41 or NP396-404 (10^{-7} M) peptide-pulsed MΦ (ratio of 10 splenocytes: 1 APC) for 2 h. ICS for IFN-γ production was then performed as described below. LCMV-specific CTL were cultured with activated MΦ (1:1) that were pulsed with decreased peptide molarity (GP33-41/NP396-404: 10^{-7} to 10^{-9} M) or infected with LCMV-WE (MOI 3 or 5) for

various time points for 4 h in the presence of Brefeldin A (10 μg/mL; Sigma-Aldrich).

B3Z Assay

B3Z CD8$^+$ T-cell hybridoma cell line specific for OVA residues 257–264 (SIINFEKL) presented on murine MHC-I (H2-K^b) was also used (36, 69). Cells were cultured in IMDM medium containing 500 μg/mL G418 to ensure positive selection of reporter cells until time of experiment. For antigen presentation assays, APC were pulsed with SIINFEKL peptide (10^{-7} or 10^{-9}M) at 37°C for 2 h before extensive washing in warm PBS. Thereafter, the APC were cocultured with B3Z in a 96-well round-bottom plate (Thermo Scientific) at a ratio of 1:1 for 18 h in IMDM medium (5% FCS) at 37°C. For Laz-Z detection, Z Buffer (150 μL), containing 0.125% NP-40, 9-mM $MgCl_2$, 100 mM of β-mercaptoethanol, and 5-mM ONPG, was added to the B3Z:APC cell pellets and incubated at 37°C for 4 h to allow for colorimetric change. Thereafter, 100 μL of buffer was transferred to a flat-bottom 96-well plate for absorbance measurement at 410 nm using a Varioskan plate reader.

Detection of LCMV-NP

For LCMV-NP detection, infected cells were fixed and permeabilized with PBS containing 4% paraformaldehyde and 0.5% saponin for 20 min at room temperature. Cells were washed in PBS with 0.25% saponin and incubated for 1 h with rat anti-LCMV-NP Ab (clone VL4) supernatants (a gift from Dr. M. Groettrup, University of Constance, Germany) to detect NP expression (70). After washing twice, FITC-conjugated goat anti-rat IgG Ab (Invitrogen) was incubated with the cells overnight at 4°C. In separate experiments, propidium idodide (1 μg/mL; Sigma Aldrich, Oakville, ON, Canada) was added to uninfected and LCMV-infected samples for assessment of cell death. Data were acquired with the Epics XL MCL (Beckman) and analyzed with the FlowJo software.

In Vitro CD8$^+$ Proliferation Assay

Splenocytes were harvested from LCMV-WE immune (30 days post-infection) and lymphocytes were purified by ficoll-gradient centrifugation with lymphocytes separation medium (Fisher, Whitby, ON, Canada). Purified cells were labeled with CFSE (0.4 μM) for 15 min at 37°C then washed twice in warm PBS. Lymphocytes were cultured in a 96-well flat-bottomed plate with GP33-41 or NP396-41 peptide pulsed polarized MΦ for 3–6 days (at decreasing concentrations of recombinant IL-2) before staining for CD3 and CD8α expression and assessed for CFSE staining by FCM. Percent proliferation was determined by calculating the % of CD8$^+$ CFSE^{Low} cells compared with unstimulated CFSE labeled controls (CFSE^{Hi}). For the CD4$^+$ T-cell coculture experiment: CD4$^+$ T cells were negatively selected for by gating out B220$^+$, CD11b$^+$, F480$^+$, and CD8$^+$ cells from the spleen using a BD FACS Aria III sorter (Beckman-Dickinson). CD4$^+$ T cells were added to MΦ$^+$ CFSE labeled splenocyte at the indicated ratio and incubated for 4 days.

Statistical Analysis

Statistical analysis was performed using Prism 7.0 (La Jolla, CA, USA) with unpaired (Student's) *t*-test.

ETHICS STATEMENT

Mice were used according to Canadian Council of Animal Care guidelines to isolate primary cells and the protocol for this work was approved by the Office of University Animal Care Committee at Queen's University (Protocol no. 1536).

AUTHOR CONTRIBUTIONS

SB and RM contributed to the design of the project and writing of the paper. RM, AB and KS performed experiments.

FUNDING

This work was funded by grants from the Canadian Institutes of Health Research and Natural Sciences and Engineering Research Council of Canada to SB.

SUPPLEMENTARY MATERIAL

The Supplementary Material for this article can be found online at http://www.frontiersin.org/article/10.3389/fimmu.2017.01629/full#supplementary-material.

REFERENCES

1. Chow A, Brown BD, Merad M. Studying the mononuclear phagocyte system in the molecular age. *Nat Rev Immunol* (2011) 11:788–98. doi:10.1038/nri3087
2. Davies LC, Jenkins SJ, Allen JE, Taylor PR. Tissue-resident macrophages. *Nat Immunol* (2013) 14:986–95. doi:10.1038/ni.2705
3. Dey A, Allen J, Hankey-Giblin PA. Ontogeny and polarization of macrophages in inflammation: blood monocytes versus tissue macrophages. *Front Immunol* (2014) 5:683. doi:10.3389/fimmu.2014.00683
4. Labonte AC, Tosello-Trampont AC, Hahn YS. The role of macrophage polarization in infectious and inflammatory diseases. *Mol Cells* (2014) 37:275–85. doi:10.14348/molcells.2014.2374
5. Liu YC, Zou XB, Chai YF, Yao YM. Macrophage polarization in inflammatory diseases. *Int J Biol Sci* (2014) 10:520–9. doi:10.7150/ijbs.8879
6. Edwards JP, Zhang X, Frauwirth KA, Mosser DM. Biochemical and functional characterization of three activated macrophage populations. *J Leukoc Biol* (2006) 80:1298–307. doi:10.1189/jlb.0406249
7. Wang C, Yu X, Cao Q, Wang Y, Zheng G, Tan TK, et al. Characterization of murine macrophages from bone marrow, spleen and peritoneum. *BMC Immunol* (2013) 14:6. doi:10.1186/1471-2172-14-6
8. Mulder R, Banete A, Basta S. Spleen-derived macrophages are readily polarized into classically activated (M1) or alternatively activated (M2) states. *Immunobiology* (2014) 219:737–45. doi:10.1016/j.imbio.2014.05.005
9. Cassetta L, Cassol E, Poli G. Macrophage polarization in health and disease. *ScientificWorldJournal* (2011) 11:2391–402. doi:10.1100/2011/213962
10. Biswas SK, Chittezhath M, Shalova IN, Lim JY. Macrophage polarization and plasticity in health and disease. *Immunol Res* (2012) 53:11–24. doi:10.1007/s12026-012-8291-9
11. Mantovani A, Sica A, Sozzani S, Allavena P, Vecchi A, Locati M. The chemokine system in diverse forms of macrophage activation and polarization. *Trends Immunol* (2004) 25:677–86. doi:10.1016/j.it.2004.09.015
12. Arnold CE, Gordon P, Barker RN, Wilson HM. The activation status of human macrophages presenting antigen determines the efficiency of Th17 responses. *Immunobiology* (2015) 220:10–9. doi:10.1016/j.imbio.2014.09.022

13. Benoit M, Desnues B, Mege JL. Macrophage polarization in bacterial infections. *J Immunol* (2008) 181:3733–9. doi:10.4049/jimmunol.181.6.3733
14. Cassol E, Cassetta L, Alfano M, Poli G. Macrophage polarization and HIV-1 infection. *J Leukoc Biol* (2010) 87:599–608. doi:10.1189/jlb.1009673
15. Mege JL, Mehraj V, Capo C. Macrophage polarization and bacterial infections. *Curr Opin Infect Dis* (2011) 24:230–4. doi:10.1097/QCO.0b013e328344b73e
16. Pan XQ. The mechanism of the anticancer function of M1 macrophages and their use in the clinic. *Chin J Cancer* (2012) 31:557–63. doi:10.5732/cjc.012.10046
17. Sang Y, Miller LC, Blecha F. Macrophage polarization in virus-host interactions. *J Clin Cell Immunol* (2015) 6:311. doi:10.4172/2155-9899.1000311
18. Raes G, De Baetselier P, Noel W, Beschin A, Brombacher F, Hassanzadeh Gh G. Differential expression of FIZZ1 and Ym1 in alternatively versus classically activated macrophages. *J Leukoc Biol* (2002) 71:597–602.
19. Roszer T. Understanding the mysterious M2 macrophage through activation markers and effector mechanisms. *Mediators Inflamm* (2015) 2015:816460. doi:10.1155/2015/816460
20. Saha B, Kodys K, Szabo G. Hepatitis C virus-induced monocyte differentiation into polarized M2 macrophages promotes stellate cell activation via TGF-beta. *Cell Mol Gastroenterol Hepatol* (2016) 2:302–16.e8. doi:10.1016/j.jcmgh.2015.12.005
21. Butz EA, Hostager BS, Southern PJ. Macrophages in mice acutely infected with lymphocytic choriomeningitis virus are primed for nitric oxide synthesis. *Microb Pathog* (1994) 16:283–95. doi:10.1006/mpat.1994.1029
22. Pozzi LA, Maciaszek JW, Rock KL. Both dendritic cells and macrophages can stimulate naive CD8 T cells in vivo to proliferate, develop effector function, and differentiate into memory cells. *J Immunol* (2005) 175:2071–81. doi:10.4049/jimmunol.175.4.2071
23. Alatery A, Siddiqui S, Chan M, Kus A, Petrof EO, Basta S. Cross, but not direct, presentation of cell-associated virus antigens by spleen macrophages is influenced by their differentiation state. *Immunol Cell Biol* (2010) 88:3–12. doi:10.1038/icb.2009.90
24. Siddiqui S, Alatery A, Kus A, Basta S. TLR engagement prior to virus infection influences MHC-I antigen presentation in an epitope-dependent manner as a result of nitric oxide release. *J Leukoc Biol* (2011) 89:457–68. doi:10.1189/jlb.0610357
25. Siddiqui S, Basta S. CD8+ T cell immunodominance in lymphocytic choriomeningitis virus infection is modified in the presence of toll-like receptor agonists. *J Virol* (2011) 85:13224–33. doi:10.1128/JVI.05996-11
26. Zhou X, Ramachandran S, Mann M, Popkin DL. Role of lymphocytic choriomeningitis virus (LCMV) in understanding viral immunology: past, present and future. *Viruses* (2012) 4:2650–69. doi:10.3390/v4112650
27. Cox MA, Kahan SM, Zajac AJ. Anti-viral CD8 T cells and the cytokines that they love. *Virology* (2013) 435:157–69. doi:10.1016/j.virol.2012.09.012
28. Huber S, Hoffmann R, Muskens F, Voehringer D. Alternatively activated macrophages inhibit T-cell proliferation by Stat6-dependent expression of PD-L2. *Blood* (2010) 116:3311–20. doi:10.1182/blood-2010-02-271981
29. Osborne LC, Monticelli LA, Nice TJ, Sutherland TE, Siracusa MC, Hepworth MR, et al. Coinfection. Virus-helminth coinfection reveals a microbiota-independent mechanism of immunomodulation. *Science* (2014) 345:578–82. doi:10.1126/science.1256942
30. Kaiko GE, Horvat JC, Beagley KW, Hansbro PM. Immunological decision-making: how does the immune system decide to mount a helper T-cell response? *Immunology* (2008) 123:326–38. doi:10.1111/j.1365-2567.2007.02719.x
31. Grakoui A, Bromley SK, Sumen C, Davis MM, Shaw AS, Allen PM, et al. Pillars article: the immunological synapse: a molecular machine controlling T cell activation. Science. 1999.285: 221-227. *J Immunol* (2015) 194(9):4066–72. doi:10.1126/science.285.5425.221
32. Xing J, Chai Z, Ly H, Liang Y. Differential inhibition of macrophage activation by lymphocytic choriomeningitis virus and pichinde virus is mediated by the Z protein N-terminal domain. *J Virol* (2015) 89:12513–7. doi:10.1128/JVI.01674-15
33. Parsa R, Andresen P, Gillett A, Mia S, Zhang XM, Mayans S, et al. Adoptive transfer of immunomodulatory M2 macrophages prevents type 1 diabetes in NOD mice. *Diabetes* (2012) 61:2881–92. doi:10.2337/db11-1635
34. Davis MJ, Tsang TM, Qiu Y, Dayrit JK, Freij JB, Huffnagle GB, et al. Macrophage M1/M2 polarization dynamically adapts to changes in cytokine microenvironments in *Cryptococcus neoformans* infection. *MBio* (2013) 4:e264–213. doi:10.1128/mBio.00264-13
35. Mareeva T, Lebedeva T, Anikeeva N, Manser T, Sykulev Y. Antibody specific for the peptide.major histocompatibility complex. Is it T cell receptor-like? *J Biol Chem* (2004) 279:44243–9. doi:10.1074/jbc.M407021200
36. Shastri N, Gonzalez F. Endogenous generation and presentation of the ovalbumin peptide/Kb complex to T cells. *J Immunol* (1993) 150:2724–36.
37. Shen SS, Yang YW. Antigen delivery for cross priming via the emulsion vaccine adjuvants. *Vaccine* (2012) 30:1560–71. doi:10.1016/j.vaccine.2011.12.120
38. Macian F. NFAT proteins: key regulators of T-cell development and function. *Nat Rev Immunol* (2005) 5:472–84. doi:10.1038/nri1632
39. Bernhard CA, Ried C, Kochanek S, Brocker T. CD169+ macrophages are sufficient for priming of CTLs with specificities left out by cross-priming dendritic cells. *Proc Natl Acad Sci U S A* (2015) 112:5461–6. doi:10.1073/pnas.1423356112
40. Kotturi MF, Scott I, Wolfe T, Peters B, Sidney J, Cheroutre H, et al. Naive precursor frequencies and MHC binding rather than the degree of epitope diversity shape CD8+ T cell immunodominance. *J Immunol* (2008) 181:2124–33. doi:10.4049/jimmunol.181.3.2124
41. Tewari K, Sacha J, Gao X, Suresh M. Effect of chronic viral infection on epitope selection, cytokine production, and surface phenotype of CD8 T cells and the role of IFN-gamma receptor in immune regulation. *J Immunol* (2004) 172:1491–500. doi:10.4049/jimmunol.172.3.1491
42. Alatery A, Tarrab E, Lamarre A, Basta S. The outcome of cross-priming during virus infection is not directly linked to the ability of the antigen to be cross-presented. *Eur J Immunol* (2010) 40:2190–9. doi:10.1002/eji.200939973
43. Wherry EJ, Ahmed R. Memory CD8 T-cell differentiation during viral infection. *J Virol* (2004) 78:5535–45. doi:10.1128/JVI.78.11.5535-5545.2004
44. Manjunath N, Shankar P, Wan J, Weninger W, Crowley MA, Hieshima K, et al. Effector differentiation is not prerequisite for generation of memory cytotoxic T lymphocytes. *J Clin Invest* (2001) 108:871–8. doi:10.1172/JCI13296
45. Oehen S, Brduscha-Riem K. Differentiation of naive CTL to effector and memory CTL: correlation of effector function with phenotype and cell division. *J Immunol* (1998) 161:5338–46.
46. Basta S, Stoessel R, Basler M, Van Den Broek M, Groettrup M. Cross-presentation of the long-lived lymphocytic choriomeningitis virus nucleoprotein does not require neosynthesis and is enhanced via heat shock proteins. *J Immunol* (2005) 175:796–805. doi:10.4049/jimmunol.175.2.796
47. Boyman O, Sprent J. The role of interleukin-2 during homeostasis and activation of the immune system. *Nat Rev Immunol* (2012) 12:180–90. doi:10.1038/nri3156
48. Behrens G, Li M, Smith CM, Belz GT, Mintern J, Carbone FR, et al. Helper T cells, dendritic cells and CTL Immunity. *Immunol Cell Biol* (2004) 82:84–90. doi:10.1111/j.1440-1711.2004.01211.x
49. Feau S, Arens R, Togher S, Schoenberger SP. Autocrine IL-2 is required for secondary population expansion of CD8(+) memory T cells. *Nat Immunol* (2011) 12:908–13. doi:10.1038/ni.2079
50. Anghelina D, Pewe L, Perlman S. Pathogenic role for virus-specific CD4 T cells in mice with coronavirus-induced acute encephalitis. *Am J Pathol* (2006) 169:209–22. doi:10.2353/ajpath.2006.051308
51. Alatery A, Basta S. An efficient culture method for generating large quantities of mature mouse splenic macrophages. *J Immunol Methods* (2008) 338:47–57. doi:10.1016/j.jim.2008.07.009
52. Loke P, Macdonald AS, Robb A, Maizels RM, Allen JE. Alternatively activated macrophages induced by nematode infection inhibit proliferation via cell-to-cell contact. *Eur J Immunol* (2000) 30:2669–78. doi:10.1002/1521-4141(200009)30:9<2669::AID-IMMU2669>3.0.CO;2-1
53. Taylor MD, Harris A, Nair MG, Maizels RM, Allen JE. F4/80+ alternatively activated macrophages control CD4+ T cell hyporesponsiveness at sites peripheral to filarial infection. *J Immunol* (2006) 176:6918–27. doi:10.4049/jimmunol.176.11.6918
54. Cook PC, Jones LH, Jenkins SJ, Wynn TA, Allen JE, Macdonald AS. Alternatively activated dendritic cells regulate CD4+ T-cell polarization in vitro and in vivo. *Proc Natl Acad Sci U S A* (2012) 109:9977–82. doi:10.1073/pnas.1121231109
55. Gunthner R, Anders HJ. Interferon-regulatory factors determine macrophage phenotype polarization. *Mediators Inflamm* (2013) 2013:731023. doi:10.1155/2013/731023
56. Rodriguez PC, Zea AH, Desalvo J, Culotta KS, Zabaleta J, Quiceno DG, et al. L-arginine consumption by macrophages modulates the expression of CD3

zeta chain in T lymphocytes. *J Immunol* (2003) 171:1232–9. doi:10.4049/jimmunol.171.3.1232
57. Rodriguez PC, Zea AH, Culotta KS, Zabaleta J, Ochoa JB, Ochoa AC. Regulation of T cell receptor CD3zeta chain expression by L-arginine. *J Biol Chem* (2002) 277:21123–9. doi:10.1074/jbc.M110675200
58. Rodriguez PC, Quiceno DG, Ochoa AC. L-arginine availability regulates T-lymphocyte cell-cycle progression. *Blood* (2007) 109:1568–73. doi:10.1182/blood-2006-06-031856
59. Chen X, Woiciechowsky A, Raffegerst S, Schendel D, Kolb HJ, Roskrow M. Impaired expression of the CD3-zeta chain in peripheral blood T cells of patients with chronic myeloid leukaemia results in an increased susceptibility to apoptosis. *Br J Haematol* (2000) 111:817–25. doi:10.1111/j.1365-2141.2000.02415.x
60. Au-Yeung BB, Smith GA, Mueller JL, Heyn CS, Jaszczak RG, Weiss A, et al. IL-2 modulates the TCR signaling threshold for CD8 but not CD4 T cell proliferation on a single-cell level. *J Immunol* (2017) 198:2445–56. doi:10.4049/jimmunol.1601453
61. Firpo EJ, Koff A, Solomon MJ, Roberts JM. Inactivation of a Cdk2 inhibitor during interleukin 2-induced proliferation of human T lymphocytes. *Mol Cell Biol* (1994) 14:4889–901. doi:10.1128/MCB.14.7.4889
62. Siwicki JK, Hedberg Y, Nowak R, Loden M, Zhao J, Landberg G, et al. Long-term cultured IL-2-dependent T cell lines demonstrate p16(INK4a) overexpression, normal pRb/p53, and upregulation of cyclins E or D2. *Exp Gerontol* (2000) 35:375–88. doi:10.1016/S0531-5565(00)00088-7
63. Klevorn LE, Berrien-Elliott MM, Yuan J, Kuehm LM, Felock GD, Crowe SA, et al. Rescue of tolerant CD8+ T cells during cancer immunotherapy with IL2:antibody complexes. *Cancer Immunol Res* (2016) 4:1016–26. doi:10.1158/2326-6066.CIR-16-0159
64. Itoh Y, Germain RN. Single cell analysis reveals regulated hierarchical T cell antigen receptor signaling thresholds and intraclonal heterogeneity for individual cytokine responses of CD4+ T cells. *J Exp Med* (1997) 186:757–66. doi:10.1084/jem.186.5.757
65. Auphan-Anezin N, Verdeil G, Schmitt-Verhulst AM. Distinct thresholds for CD8 T cell activation lead to functional heterogeneity: CD8 T cell priming can occur independently of cell division. *J Immunol* (2003) 170:2442–8. doi:10.4049/jimmunol.170.5.2442
66. Kovacsovics-Bankowski M, Rock KL. Presentation of exogenous antigens by macrophages: analysis of major histocompatibility complex class I and II presentation and regulation by cytokines. *Eur J Immunol* (1994) 24:2421–8. doi:10.1002/eji.1830241024
67. Banete A, Achita P, Harding K, Mulder R, Basta S. Immortalized murine macrophage cell line as a model for macrophage polarization into classically activated M(IFNgamma+LPS) or alternatively activated M(IL-4) macrophages. *J Clin Cell Immunol* (2015) 6:318. doi:10.4172/2155-9899.1000318
68. Ho VW, Sly LM. Derivation and characterization of murine alternatively activated (M2) macrophages. *Methods Mol Biol* (2009) 531:173–85. doi:10.1007/978-1-59745-396-7_12
69. Sanderson S, Shastri N. LacZ inducible, antigen/MHC-specific T cell hybrids. *Int Immunol* (1994) 6:369–76. doi:10.1093/intimm/6.3.369
70. Korns Johnson D, Homann D. Accelerated and improved quantification of lymphocytic choriomeningitis virus (LCMV) titers by flow cytometry. *PLoS One* (2012) 7:e37337. doi:10.1371/journal.pone.0037337

Conflict of Interest Statement: The authors declare that the research was conducted in the absence of any commercial or financial relationships that could be construed as a potential conflict of interest.

Copyright © 2017 Mulder, Banete, Seaver and Basta. This is an open-access article distributed under the terms of the Creative Commons Attribution License (CC BY). The use, distribution or reproduction in other forums is permitted, provided the original author(s) or licensor are credited and that the original publication in this journal is cited, in accordance with accepted academic practice. No use, distribution or reproduction is permitted which does not comply with these terms.

frontiers in Immunology

ORIGINAL RESEARCH
published: 04 April 2018
doi: 10.3389/fimmu.2018.00366

Enhanced Replication of Virulent Newcastle Disease Virus in Chicken Macrophages Is due to Polarized Activation of Cells by Inhibition of TLR7

*Pingze Zhang[1], Zhuang Ding[1], Xinxin Liu[2], Yanyu Chen[1], Junjiao Li[1], Zhi Tao[1], Yidong Fei[1], Cong Xue[1], Jing Qian[1], Xueli Wang[3], Qingmei Li[4], Tobias Stoeger[5], Jianjun Chen[6], Yuhai Bi[7] and Renfu Yin[1]**

[1] Department of Veterinary Preventive Medicine, College of Veterinary Medicine, Jilin University, Changchun, China, [2] College of Food Science and Engineering, Jilin University, Changchun, China, [3] College of Animal Science and Technology, Inner Mongolia University for Nationalities, Tongliao, China, [4] Laboratory of Animal Immunology, Henan Academy of Agricultural Sciences, Zhengzhou, China, [5] Comprehensive Pneumology Center, Institute of Lung Biology and Disease (iLBD), Helmholtz Zentrum Muenchen, Munich, Germany, [6] CAS Key Laboratory of Special Pathogens and Biosafety, Wuhan Institute of Virology, Chinese Academy of Sciences, Hubei, China, [7] CAS Key Laboratory of Pathogenic Microbiology and Immunology, Institute of Microbiology, Chinese Academy of Sciences, Beijing, China*

OPEN ACCESS

Edited by:
Geanncarlo Lugo-Villarino, UMR5089 Institut de Pharmacologie et de Biologie Structurale (IPBS), France

Reviewed by:
Mohammad Heidari, Agricultural Research Service (USDA), United States
Mohamed Faizal Abdul-Careem, University of Calgary, Canada
Christine Jansen, Utrecht University, Netherlands

***Correspondence:**
Renfu Yin
yin@jlu.edu.cn

Specialty section:
This article was submitted to Microbial Immunology, a section of the journal Frontiers in Immunology

Received: *15 August 2017*
Accepted: *09 February 2018*
Published: *04 April 2018*

Citation:
Zhang P, Ding Z, Liu X, Chen Y, Li J, Tao Z, Fei Y, Xue C, Qian J, Wang X, Li Q, Stoeger T, Chen J, Bi Y and Yin R (2018) Enhanced Replication of Virulent Newcastle Disease Virus in Chicken Macrophages Is due to Polarized Activation of Cells by Inhibition of TLR7. Front. Immunol. 9:366. doi: 10.3389/fimmu.2018.00366

Newcastle disease (ND), caused by infections with virulent strains of Newcastle disease virus (NDV), is one of the most important infectious disease affecting wild, peridomestic, and domestic birds worldwide. Vaccines constructed from live, low-virulence (lentogenic) viruses are the most accepted prevention and control strategies for combating ND in poultry across the globe. Avian macrophages are one of the first cell lines of defense against microbial infection, responding to signals in the microenvironment. Although macrophages are considered to be one of the main target cells for NDV infection *in vivo*, very little is known about the ability of NDV to infect chicken macrophages, and virulence mechanisms of NDV as well as the polarized activation patterns of macrophages and correlation with viral infection and replication. In the present study, a cell culture model (chicken bone marrow macrophage cell line HD11) and three different virulence and genotypes of NDV (including class II virulent NA-1, class II lentogenic LaSota, and class I lentogenic F55) were used to solve the above underlying questions. Our data indicated that all three NDV strains had similar replication rates during the early stages of infection. Virulent NDV titers were shown to increase compared to the other lentogenic strains, and this growth was associated with a strong upregulation of both pro-inflammatory M1-like markers/cytokines and anti-inflammatory M2-like markers/cytokines in chicken macrophages. Virulent NDV was found to block toll-like receptor (TLR) 7 expression, inducing higher expression of type I interferons in chicken macrophages at the late stage of viral infection. Only virulent NDV replication can be inhibited by pretreatment with TLR7 ligand. Overall, this study demonstrated that virulent NDV activates a M1-/M2-like mixed polarized activation of chicken macrophages by inhibition of TLR7, resulting in enhanced replication compared to lentogenic viruses.

Keywords: chicken macrophages, newcastle disease virus, toll-like receptor 7, macrophage polarized activation, virus growth, immune response

INTRODUCTION

Newcastle disease (ND), caused by the virulent Newcastle disease virus (NDV), is a highly contagious and fatal viral infectious disease in birds and can have devastating economic effects on global domestic poultry production. ND is listed by the World Health Organization for Animals (OIE) as a vitally important pathogen for avian species and products, in which NDV detection in a specific geographical location often leads to trade restrictions and embargoes (1). NDV was previously synonymous with avian paramyxovirus type 1 (2); however, due to changes in taxonomy is now referred to as avian avulavirus (3). NDV is an enveloped virus containing a single-stranded, negative-sense, non-segmented RNA genome that is approximately 15,000 nucleotides in length. Six structural proteins are encoded, including the nucleocapsid (N) protein, phosphoprotein (P), matrix (M) protein, fusion (F) protein, hemagglutinin-neuraminidase (HN) protein, large (L) protein, and two non-structural V and W proteins (2). Strains of NDV are grouped into virulent (velogenic), intermediate (mesogenic), and non-virulent or low virulent (lentogenic) on the basis of the clinical signs seen in infected chickens (2).

Newcastle disease virus is categorized genetically into two classes with 18 genotypes in class II and only one genotype in class I, according to phylogenetic relationships of the F gene (4). Class I NDV isolates are distributed worldwide and are isolated frequently from waterfowl, shorebirds, wild birds, and live bird markets (LBMs). All reported strains are thought to be low virulence except for one strain, chicken/Ireland/1990 (5–11). Class II NDVs are further divided into 18 genotypes (I –XVIII) (12), contain viruses that have been isolated from multiple birds. Most Class II NDV are virulent and cause devastating economic losses to the poultry production worldwide (4), while lentogenic strains may be used as vaccines.

Newcastle disease virus infection *in vivo* results in various reactions and clinical symptoms based on its pathogenicity. Even though all strains of NDV belong to one serotype and cause similar humoral immune responses, differences in host innate immune responses play a role in the resistance to ND due to genetic variation of host, virulence, and genotypes of virus (13).

The host innate immune response to virus infection is designed to limit virus replication, growth, and spread in order to give the host time to develop the virus-specific adaptive immune responses (14). The primary components of innate immunity of birds are (a) physical and chemical barriers, such as skin, epithelia, and feathers; (b) phagocytic cells, including dendritic cells, macrophages, and natural killer cells; (c) inflammatory mediators, cytokines, and complement proteins (13). Macrophages, as one of the first lines of defense against microbial infection, exert numerous biological functions across a broad spectrum of acute and chronic inflammatory conditions *via* secreting high amounts of chemokines and cytokines, orchestrating host innate and adaptive immune responses, and clearing infected and dying cells to aid recovery (15).

In response to microenvironmental signals, mammalian macrophages polarize into dynamic specialized functional pro-inflammatory M1 (classically activated macrophages) and anti-inflammatory M2 (alternatively activated macrophages, TAM) phenotypes (16–21). M1 macrophages play a vital role in virus clearance and host immune responses, but excess inflammation is harmful to tissues and organs (22). By contrast, M2 cells contribute a major role in protecting tissues and organs. The M1/M2 responses from virus infection must be balanced by inhibitory and regulatory effector mechanisms to protect bystander cell, tissue and organ damage from the effects of excess inflammation, preserve oxygenation, and promote host tissue and organ repair after viral clearance (22–25). As their mammalian counterpart, plasticity also is a hallmark of chicken macrophages, and in response to microenvironment signals, including microbial infection and pathogenesis of infectious diseases (26–36), these cells undergo different forms of polarized activation, the extremes of which may called pro-inflammatory M1-like macrophages and anti-inflammatory M2-like macrophages.

Macrophages, including chicken macrophages, partly rely on the detection of characteristics of viral nucleic acids in response to virus infection (28, 37, 38). Recognition of viral nucleic acids triggers the induction of type I interferons (IFNs) that induce macrophages into an antiviral state and activate immunoregulatory functions in nearby cells. A subset of pattern recognition receptors includes toll-like receptors (TLRs), which recognize different pathogen-associated molecular patterns (PAMPs) and induces intracellular signals responsible for the activation of genes that encode for pro-/anti- (M1-/M2-like) inflammatory chemokines and cytokines, anti-microbial peptides, and anti-apoptotic factors (28, 37, 39). There is a total of 13 known TLRs in mammals (TLR1–13), with each TLR recognizing and responding to different pathogen components (40). In birds, a total of 10 TLRs have been identified and include two isoforms each of TLR1 and TLR2, which detect triacylated, and diacylated lipopeptides. TLR3, 4, 5, and 7 detect dsRNA, LPS, flagellin, and ssRNA, respectively. TLR15 has been shown to recognize yeast proteases while TLR21, a functional homolog of mammalian TLR9, detects dsDNA (41). TLR3, 7, and 21 are located in the cytoplasm, while TLR1, 2, 4, 5, and 15 are located on the cell surface (42). Previous data demonstrated that chicken origin TLR7 can exert specific abilities against viral and bacterial infectious diseases of birds, such as avian influenza (37) and Salmonella (43).

To date, NDV-induced macrophage polarized activation and its role in anti-tumor cytotoxicity, cytokine release, and immunoregulation have been widely investigated in mice and humans (44–47). Although most reliable markers for mammalian macrophage polarized activation are not available for chicken macrophages, chicken macrophages are similar to their mammalian counterparts since they have the capacity to change their phenotype in response to the microenvironmental signals (35, 48). However, whether NDV has the capacity to change chicken macrophage phenotype during viral infection mainly depends on the virulence and genotypes of virus. The specifics of this phenomenon and underlying molecular mechanisms are still unclear.

In the present work, we explored the polarized activation patterns of chicken macrophages and correlation with infection and replication using three different NDV genotypes of varying virulence. Levels of M1- and M2-like polarized activation-related genes and proteins in chicken macrophage cell line HD11 were used for presentation of different forms of NDV-induced chicken macrophage polarized activation. In addition, we

explored the role of chicken origin TLR7 on virus replication and chicken macrophage polarized activation caused by different virulence and genotypes NDV strains.

MATERIALS AND METHODS

Ethical Statement

All experiments performed at the Jilin University were reviewed and approved by the Jilin University Experimental Animal Care and Use Committee.

Cell and Viruses

Chicken origin HD11 cell (permanent chicken bone marrow macrophages cell line) was kindly provided by Prof. Daxin Peng, College of Veterinary Medicine, Yangzhou University (49). NDV commercial vaccine strain LaSota (lentogenic, genotype II within class II, GenBank: AF077761.1) was obtained from ATCC. NDV virulent strain NA-1 (genotype VII within class II, GenBank: DQ659677.1) was isolated from a goose farm in Nong'an of Jilin province, China in 1999 (50). NDV lentogenic strain F55 (Chicken/CH/JL/CC05/2015, genotype Ib within class I, GenBank: KT892749.1) was isolated from chicken in LBMs of Changchun, Jilin, China in 2015 (51). HD11 cell was cultured in DMEM/F-12 (Dulbecco's Modified Eagle Medium/Nutrient Mixture F-12) supplemented with 10% fetal bovine serum (FBS) (Gibco, Shanghai, China), 100 μg/ml streptomycin and 100 U/ml penicillin (Gibco, Shanghai, China) at 37°C under 5% CO_2. All NDV strains were grew in the allantoic cavity of 9- to 10-day-old specific pathogen-free (SPF) chicken embryonated eggs (MERIAL, Beijing, China) and purified directly from the allantoic fluid as described in a previous study (52).

NDV Infection of Cells

HD11 cells were planted into a 24-well cell culture plate at a viable cell density (determined by Trypan blue exclusion, Sigma, Shanghai, China) of 3×10^5 cells per well in complete DMEM/F12 containing 10% FBS, 100 μg/ml streptomycin, and 100 U/ml penicillin at 37°C under 5% CO_2 for 8 h. Cells then were washed three times with phosphate-buffered saline (PBS), and supernatant was changed into fresh DMEM/F12 supplemented with 100 μg/ml streptomycin and 100 U/ml penicillin without FBS. Thereafter, cells were absorbed with virus at 2 multiplicity of infection (MOI) for 1 h and fresh medium was added into the well and then incubated with 4, 12, 24, 48, and 72 h post infection (hpi), respectively. Subsequent to infection, viral genome load and genes of target expression levels in the cells were detected by qPCR, as well as the virus titer in the supernatants was measured using a micro-HA method. For viral infection efficiency detection, HD11 cells were planted into a 6-well cell culture plate containing sterile coverslips at a viable cell density of 1×10^6 cells per cell for 8 h. Cells then were rinsed three times with PBS and supernatant was changed into fresh incomplete DMEM/F12 without FBS. Thereafter, cells were absorbed with virus at 2 MOI for 1 h and fresh medium was added into the well and then incubated with 24 hpi. Subsequent to infection, cells were acetone fixed (5 min), permeabilized with 0.1% Triton X-100 for 5 min, and then incubated in 10% FBS in 0.1% PBS-Tween for 0.5 h to block non-specific protein–protein interactions. The cells were then incubated with the primary polyclonal antibody for NDV prepared by our lab (Mouse anti-NDV, 1:200) overnight at +4°C. Then cells were incubated with secondary Goat Anti-Mouse IgG H&L (Alexa Fluor® 488) (ab150113) (abcom, Shanghai, Beijing) at 2 μg/ml for 1 h. 4′,6-diamidino-2-phenylindole (DAPI) was used to stain the cell nuclei (blue) at a concentration of 1.43 μM. Coverslips were inverted onto glass slides for immunofluorescence detection. Positive staining was evaluated using a laser confocal microscope (Leica, TCS SP5 Confocal Spectral Microscope Imaging System, Taipei, Taiwan). In a preliminary study, three different MOI (0.1, 2, and 10) were tested and it was verified that 2 MOI was ideal for all three NDV strains used (the infection efficiency rate of all three NDV strains ranged from 85 to 95% at 24 hpi and non-cytotoxic to cells when treated with virulent strain NA-1 early after infection from 4 to 24 hpi, data as shown in **Figure 1** and Figure S1 in Supplementary Material). The negative control (100 μg/ml streptomycin and 100 U/ml penicillin but no virus was added into the same volume of NDV culture medium) were harvested following the same process.

Macrophage Treatment with TLR7 Agonist and Cell Infection with NDV

To determine the roles of TLR7 on the replication of NDV strains in chicken macrophages *in vitro* and the status of chicken

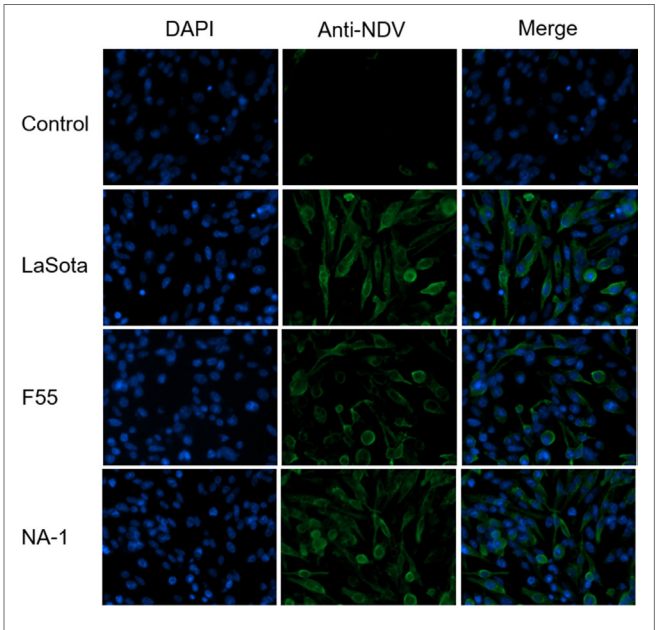


FIGURE 1 | Characteristics and infection efficiency of three different virulence and genotypes Newcastle disease virus strains in chicken macrophages analysis by immunofluorescence. HD11 cells were infected with three different virulence and genotypes NDV strains (including virulent class II genotype VII strain NA-1, lentogenic class II strain genotype III strain LaSota, and lentogenic class I genotype I strain F55) at a MOI of 2 for 24 h, then viral infection efficiency was determined by immunofluorescence. Primary Mouse anti-NDV polyclonal antibody for NDV and secondary Goat Anti-Mouse IgG H&L (Alexa Fluor® 488) antibody were used for immunofluorescence, and 4′,6-diamidino-2-phenylindole was used for labeling DNA to define the nuclear compartment.

macrophage polarized activation caused by NDV infection, a TLR7 agonist loxoribine (7-allyl-7,8-dihydro-8-oxoguanosine; InvivoGen, San Diego, CA, USA) was used. Loxoribine was dissolved in DMSO at a stock concentration of 100 mM. HD11 cells were planted into a 24-well cell culture plate at a viable cell density (determined by Trypan blue exclusion, Sigma, Shanghai, China) of 3×10^5 cells per well in complete DMEM/F12 containing 10% FBS, 100 μg/ml streptomycin and 100 U/ml penicillin at 37°C under 5% CO_2 for 8 h. Subsequently, cells were pretreated with 1 mM TLR7 agonist loxoribine for 6 h and followed by infection of different genotype NDV strains at a MOI of 2 for 48 h; thereafter, both viral genome load and genes of target expression levels in the cells and the virus titer in the supernatants were measured.

Total RNA Isolation, cDNA Synthesis, PCR, and qPCR Data Analysis

Total RNA from cells was extracted by Eastep Super Total RNA Extraction Kit (Promega, Fitchburg, MA, USA) according to the manual's recommendations. RNA concentration and purity were evaluated by A260 and A280 measurements using a NanoDrop ND-1000 spectrophotometer. A260/A280 ratio for all RNA samples extracted spanned between 1.90 and 2.15, reflecting RNA high purity. RNA integrity was determined by the ratio of 28S/18S rRNA bands after electrophoresis in denaturing 1% agarose gel. To ensure the quality necessary for gene expression analysis, all samples extracted had a 28S/18S rRNA ratio more than 1.7.

One thousand nanograms of total RNA was reverse transcribed using Moloney murine leukemia virus reverse transcriptase (Promega, Fitchburg, MA, USA) for first strand cDNA synthesis with 5 μM random hexamer primer and 5 μg oligo-dT according to the manufacturer's instructions. Briefly, primer and RNA were mixed and incubated at 70°C for 5 min and then cooled on ice for 5 min and followed by room temperature for 5–10 min. Then cDNA synthesis was started after adding tran-scription mixture prepared previously at 42°C lasting 1 h for reverse transcription. Finally, the reverse transcription was stopped at 70°C for 15 min. All cDNA samples were diluted 1:5 with DNase/RNase-free water and stored at −20°C for further studies.

PCR was conducted using the ABI StepOne Real-Time PCR system (Applied Biosystems, CA, USA), based on Fast Start Universal SYBR Green Master kit (Roche, Basel, Switzerland) and TransStart Probe qPCR SuperMix (TransGen, Beijing, China). The PCR mixture contained 1 μl cDNA (10 ng), 1 μl (5 μM) of each primer, 10 μl PCR mix, and DNase/RNase-free water up to a total volume of 20 μl. First, one cycle at 50°C for 2 min and 95°C for 10 min, followed by 40 cycles at 95°C for 15 s and 60°C for 90 s. PCR were performed in 48-well optical reaction plates (Sangon, Shanghai, China). To evaluate that the used primers produced only a single PCR product, a melt curve stage was added after thermocycling from 60 to 95°C by increasing 0.5°C per cycle in the SYBR Green qPCR. The primers and probe are listed in **Table 1**.

qPCR data analysis was performed in this work has been descri-bed previously (54). Briefly, relative expression of the gene of interest was analyzed by the ΔC_t method, where $\Delta Ct = (C_t$ target gene, test sample—C_t housekeeping genes, test sample). Relative quantities of target gene was calculated as $2^{-\Delta Ct} \pm$ SEM and normalized to the geometric mean of β-actin and hydroxymethyl-bilane synthase housekeeping genes in this work.

TABLE 1 | Primers and probe of qPCR were used in the work.

Primers	Sequences (5′–3′)	Length (bp)	Reference
NDV-I	F: ACTTCGATTCTGCCTTACCAT R: TTCCTCACTCCCGACCTG	188	This study
NDV-II	F: AGTGATGTGCTCGGACCTTC Probe: TTCTCTAGCAGTGGGACAGCCTGC R: CCTGAGGAGAGGCATTTGCTA	121	(53)
β-actin	F: CAGACATCAGGGTGTGATGG R: TCAGGGGCTACTCTCAGCTC	183	(54)
HMBS	F: GGCGGCTTTGGTGACTCTAG R: ATCGAACCCTGATTCCCCGT	131	(54)
iNOS	F: GGCAGCAGCGTCTCTATGACTTG R: GACTTTAGGCTGCCCAGGTTG	185	(55)
IL-1β	F: TGGGCATCAAGGGCTACA R: TCGGGTTGGTTGGTGATG	244	(56)
IL-10	F: GCTGCGCTTCTACACAGATG R: TCCCGTTCTCATCCATCTTC	202	(57)
PPAR-γ	F: GGGCGATCTTGACAGGAA R: GCCTCCACAGAGCGAAAC	175	(58)
TLR7	F: AGAGACTGGCTTCCAGGACA R: CAGCTGAACATACCGGGACT	218	(57)
IFN-α	F: GACATGGCTCCCACACTACC R: AGGCGCTGTAATCGTTGTCT	348	(57)
IFN-β	F: GCTCACCTCAGCATCAACAA R: GGGTGTTGAGACGTTTGGAT	186	(57)

Virus Titer Measurement

The ability of three different NDV strains (including class II virulent genotype VII strain NA-1, class II lentogenic strain genotype III strain LaSota, and class I lentogenic genotype I strain F55) to replicate and grow in chicken macrophages was investigated *in vitro*. Replication and growth kinetics of three different virulence and genotypes of NDV were assessed by multi-step growth curves in HD11 cells. Cells were seeded into 24-well cell culture plates at a viable cell density of 3×10^5 cells/well and inoculated with each virus at a 2 MOI; thereafter, the viral genomic RNA load in the cell and infectious virus titer in the supernatants were determined by qPCR and micro-HA method at specific hpi, respectively.

The virus titer in the supernatants was quantified by the micro-HA method as described previously (52). Briefly, after adding an aliquot of 100 μl medium to each well, twofold dilutions of culture supernatants or virus prepared previously were transferred to the 96-well cell culture plate. Each dilution was distributed to 8 wells. Supernatants and virus were transferred in a descending manner, from the higher (2^{-9}) to the lower (2^{-1}) dilutions using one cell culture plate. An aliquot of 50 μl of a chicken embryo fibroblast suspension containing 10^6 cells/mL was then added to very well and 96-well cell culture plates was incubated at 37°C under 5% CO2 for 48 h. A medium control, cell control, and virus control were also included in every cell culture plate. The virus titer was measured by the traditional HA method using a 0.5% chicken red blood cell suspension at 4°C and reading in a vertical position after 5–10 min.

Nitrite Assay

Nitrite (a stable metabolite of nitric oxide, produced from polarized activation M1-like chicken macrophages) concentration in the cell culture supernatants was measured by the Griess assay as described previously (35). Briefly, 100 microliters of supernatants from each tested well was transferred to the 96-well ELISA plate and mixed with 50 µl of 0.1% naphthalenediamine and 50 µl of 1% sulfanilamide (both were prepared in 2.5% phosphoric acid solution). After incubation at 25°C for 10 min, the nitrite concentration was determined by measuring absorbance at 595 nm of each well in a microplate reader (Molecular Devices, Sunnyvale, CA, USA). Sodium nitrite standard solution (Sigma, Shanghai, China) also including in every ELISA plate.

Lactate Dehydrogenase (LDH) Assay

For detection of the cytosolic enzyme LDH concentration (U/ml) in HD11 cell upon three different genotypes NDV strains infection, characteristic for membrane damaging effects, the colorimetric LDH assay kit (Nanjing Jiancheng Bioenginering Institute, Nanjing, China) was used according to the manufacturer's instructions. Briefly, HD11 were pretreated with TLR7 agonist for 6 h and then infected with each of three different NDV strains at MOI of 2 for 48 hpi; thereafter, LDH concentration in the 30 µl undiluted cell culture supernatant was determined using an ELISA reader (Labsystems iEMS Reader, Helsinki, Finland) at a 492 nm wavelength by monitoring the reduction of NAD^+ in the presence of lactate.

Statistical Analysis

The results are indicated as the mean ± SEM of at least four individual samples per group (n = 4–6). We used analysis of variance, as calculated by Prism 5 (GraphPad Software, Inc., CA, USA), to establish the statistical significance of differences between the experimental groups. Two-tailed unpaired t-test with Welch's correction was used to analyze the comparisons of individual inter-group. Differences were significantly considered at $^*P < 0.05$, $^{**}P < 0.01$, and $^{***}P < 0.001$ as compared with the respective control or vehicle groups.

RESULTS

Virulent NDV Replicates Rapidly than Lentogenic Viruses in Chicken Macrophages

Consistent with previous studies (59, 60), the amount of viral RNA in the cell and infectious virus titers in the supernatant significantly increased from 12 to 72 hpi in HD11 cells after infection with NDV strains (**Figures 2A,B**), although no infectious virus was detected in the supernatant at 4 hpi. While no differences in replication kinetics were observed between the two lentogenic NDV strains from 24 to 72 hpi, NDV strain LaSota presented a reduced ability to replicate in chicken macrophages (HD11) at 4 and 12 hpi, as evidenced by lower viral genomic RNA loads, when compared with the lentogenic NDV strain F55 (**Figure 2A**). In contrast with two lentogenic viruses, virulent NDV strain NA-1 presented a marked decrease in the viral RNA amount in macrophages by 12 hpi (**Figure 2A**), followed by a sharp increase from 24 hpi to a peak at 72 hpi, as evidenced by significant differences in replication kinetics between the virulent strain and lentogenic strains (**Figure 2**). Together, these results indicate that virulent NDV replicates more rapidly than lentogenic viruses in chicken macrophages *in vitro*.

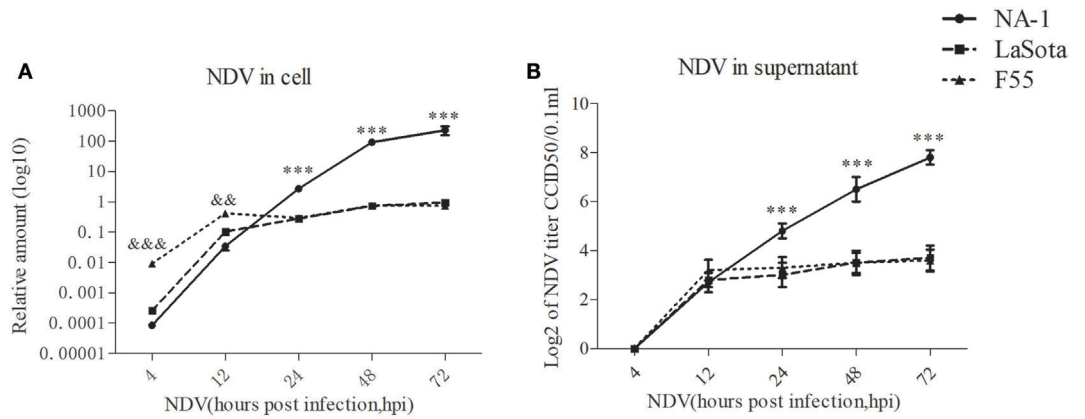


FIGURE 2 | Virulent Newcastle disease virus (NDV) replicates rapidly than lentogenic viruses in chicken macrophages. The relative viral genome load in HD11 cells infected with three different virulence and genotypes NDV strains (including virulent class II genotype VII strain NA-1, lentogenic class II strain genotype III strain LaSota, and lentogenic class I genotype I strain F55) at a MOI of 2 for 4–72 h post infection (hpi) was measured by qPCR **(A)**. The virus titer in the supernatants was quantified by the micro-HA method **(B)**. The relative virus genome amount was normalized to the geometric mean of cellular endogenous genes β-actin and hydroxymethylbilane synthase and qPCR data were calculated using the $2^{-\Delta Ct}$ method. Furthermore, viral RNA genome in cells and infectious virus titer in supernatants were undetected in all uninfected cells. All values are shown as mean ± SEM (n = 4–6) and differences were considered significant if $^*P < 0.05$, $^{**}P < 0.01$, and $^{***}P < 0.001$ as compared to the two lentogenic virus LaSota and F55 strains infected cells, $^{\&\&\&}P < 0.001$ as compared to the virulent virus NA-1 strain infected cells. All data are representative of at least three independent experiments.

Dynamic Polarized Activation of Chicken Macrophages Induced by Virulent and Lentogenic Viruses

Compared with uninfected cells, expression of the prototypic M1- and M2-like associated genes were significantly upregulated in HD11 cells after virulent strain NA-1 infection at 48 hpi, whereas a significant change was not seen in cells infected with lentogenic viruses (**Figure 3A**). However, the expression pattern of these M1- and M2-like associated genes was found to be different between cells infected with the two lentogenic viruses. Specifically, M1-like associated gene IL-1β was significantly increased in cells after class II strain LaSota infection, whereas M2-like associated gene IL-10 was only upregulated in class I strain F55-infected cells (**Figure 3A**). Furthermore, a higher concentration of nitrite in the supernatant was only found in virulent strain NA-1-infected cells (**Figure 3B**). Therefore, virulent NDV infection can polarize chicken macrophages into the M1-/M2-like mixed phenotype, but the lentogenic viruses induced much more moderate polarized activation status according to their genotypes: lentogenic class II NDV infection induces a mild M1-like phenotype and lentogenic class I NDV infection causes a mild M2-like phenotype.

Virulent NDV Blocks TLR7 Expression but Induces Higher Expression of Type I IFNs in Chicken Macrophages at the Late Stage of Viral Infection

Newcastle disease virus did not significantly alter the TLR7 expression level in HD11 cells compared to uninfected cells at 24 hpi (**Figure 4A**). However, at 4 and 12 hpi, both class II lentogenic strain LaSota and class I lentogenic strain F55 significantly inhibited TLR7 expression in HD11 cells. By contrast, the TLR7 expression level was dramatically downregulated in cells infected with virulent NA-1 strain at 48 and 72 hpi.

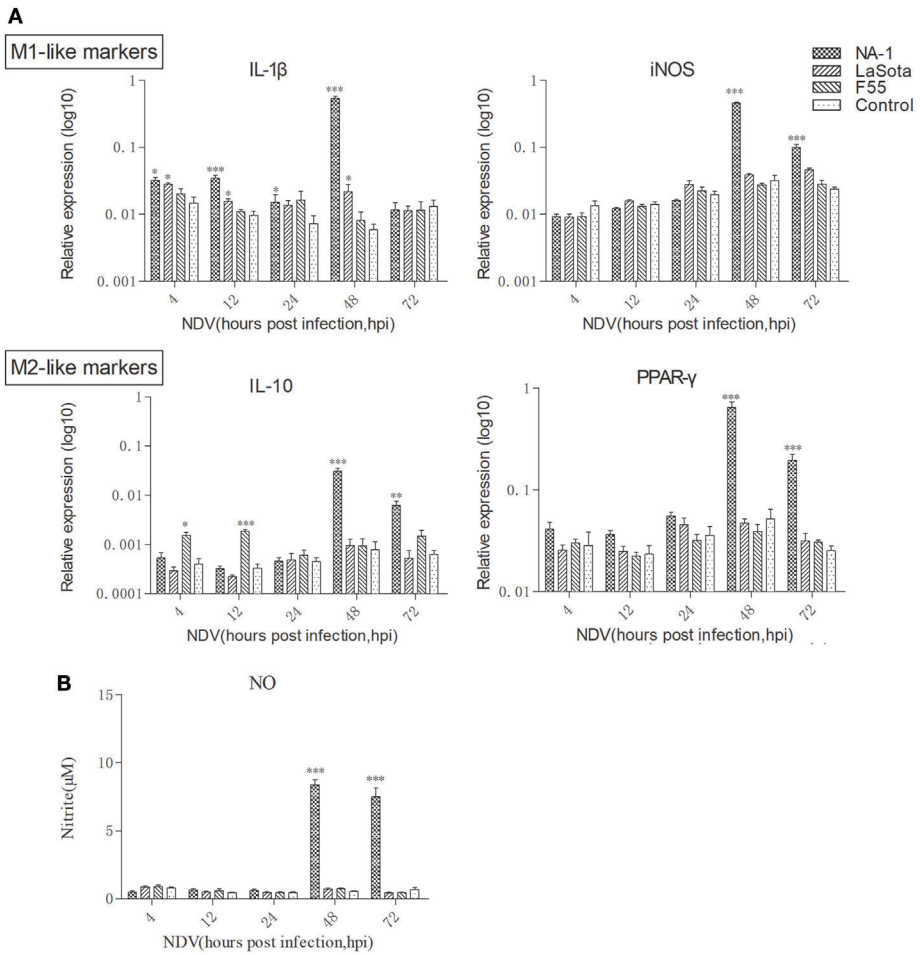


FIGURE 3 | Dynamic polarized activation of chicken macrophages induced by virulent and lentogenic viruses. Expression levels of M1-like (IL-1β and iNOS) and M2 (IL-10 and PPAR-γ) genes in HD cells infected with three different virulence and genotypes Newcastle disease virus (NDV) strains at a multiplicity of infection of 2 for 4–72 h was analyzed by qPCR method **(A)**. Nitrite, a stable metabolite of nitric oxide, produced by activated M1-like macrophages was measured by the Griess assay **(B)**. All qPCR data were normalized to the geometric mean of cellular endogenous genes β-actin and hydroxymethylbilane synthase and calculated using the $2^{-\Delta Ct}$ method. All values are shown as mean ± SEM (n = 4–6) and differences were considered significant if $^{*}P < 0.05$, $^{**}P < 0.01$, and $^{***}P < 0.001$ as compared to the respective control (uninfected) cells. All data are representative of at least three independent experiments.

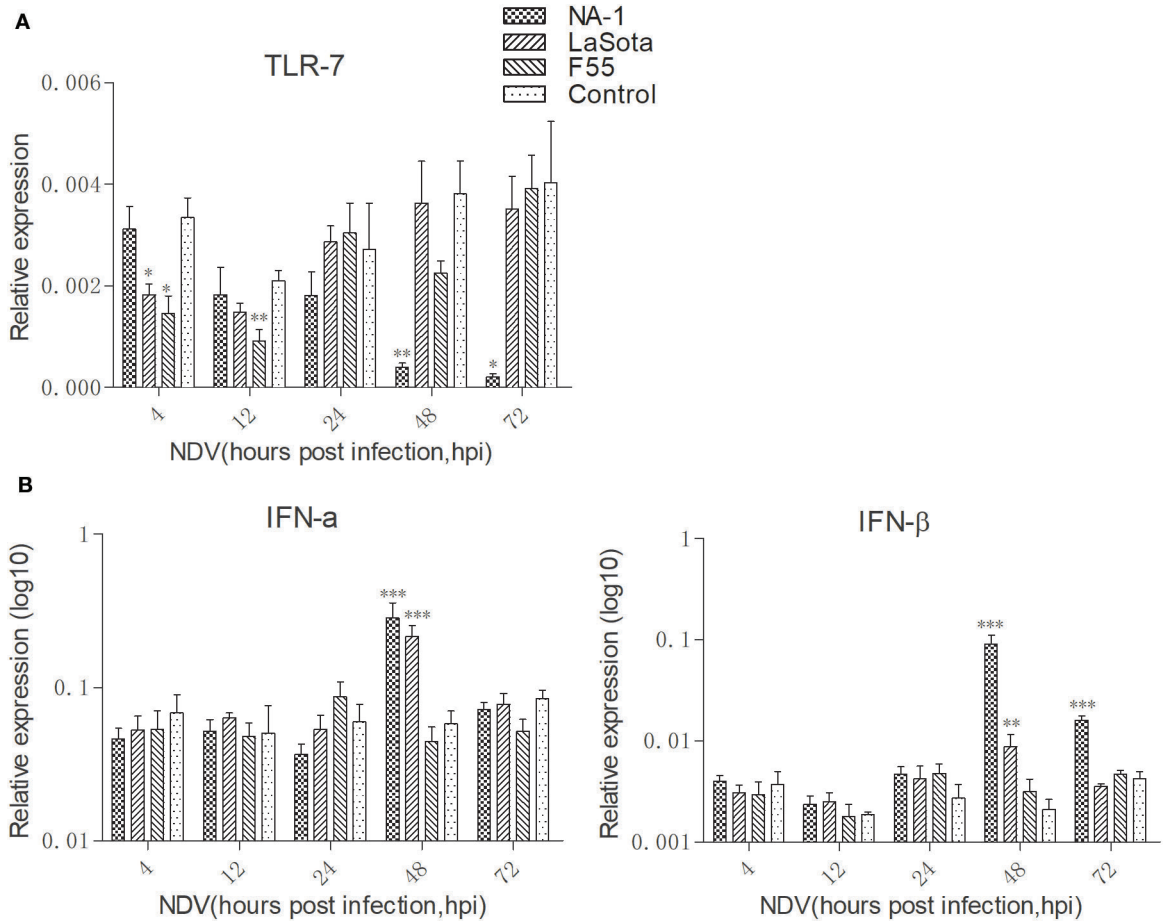


FIGURE 4 | Virulent Newcastle disease virus (NDV) inhibit TLR7 expression but induce higher expression of type I interferons (IFNs) in chicken macrophages at the late stage of viral infection. Expression levels of TLR7 **(A)** and type I IFNs [IFN-α and IFN-β, **(B)**] in HD11 cells upon three different virulence and genotypes viruses for 4 to 72 h was quantified by qPCR. All qPCR data were normalized to the geometric mean of cellular endogenous genes β-actin and hydroxymethylbilane synthase and calculated using the $2^{-\Delta Ct}$ method. All values are shown as mean ± SEM (n = 4–6) and differences were considered significant if $^{*}P < 0.05$, $^{**}P < 0.01$, $^{***}P < 0.001$ as compared to the respective control (uninfected) cells. All data are representative of at least three independent experiments.

The kinetics of IFN-α and IFN-β expression were then evaluated in HD11 cells after NDV infection from 4 to 72 hpi (**Figure 4B**). Our data clearly indicated that while class I NDV (F55) infection does not result in changes to IFN-α and IFN-β expression, class II NDV strains (LaSota and NA-1) resulted in significant increase of type I IFN expression at 48 hpi. In addition, a higher level of IFN-β expression was observed in cells infected with virulent NA-1 the late stage of virus infection (48 and 72 hpi) compared with lentogenic LaSota. Together, these results indicate that virulent NDV blocks TLR7 expression but induces higher expression of type I IFNs in chicken macrophages at the late stage of viral infection.

TLR7-Mediated Macrophage Activation Inhibits Virulent NDV Replication and Restores Virulent Virus Induced Macrophage Polarized Activation

Consistent with previous studies (37, 43, 61), pretreatment with 1 mM loxoribine for 6 h significantly reduced the growth of virulent NDV in HD11cells as compared to the vehicle and control cells; however, such reduction was not seen in cells infected with two lentogenic viruses (**Figure 5**). However, cellular viability was not decreased in HD11 cells treated with 1 mM loxoribine for 6 h, as compared with untreated control cells (data as shown in Figure S2 in Supplementary Material).

To further examine the effects of TLR7 agonist loxoribine on NDV-induced chicken macrophage polarized activation, HD11 cells were pretreated with 1 mM loxoribine for 6 h and then infected with three different virulence and genotypes NDV strains for 48 h. As depicted in **Figure 6A**, loxoribine pretreatment induced a significant increase in M1-like gene (iNOS, except IL-1β) and M2-like genes (IL-10 and PPAR-γ) in two lentogenic NDV-infected and -uninfected cells compared to the respective untreated cells. By contrast, loxoribine pretreatment resulted in a sharp decline in both M1- and M2-like genes in virulent NDV-infected cells compared to the respective untreated cells (**Figure 6A**), as evidenced by the concentration of nitrite in the supernatants (**Figure 6B**). Next, we determined that loxoribine pretreatment whether resulted in a sharp decrease in the growth

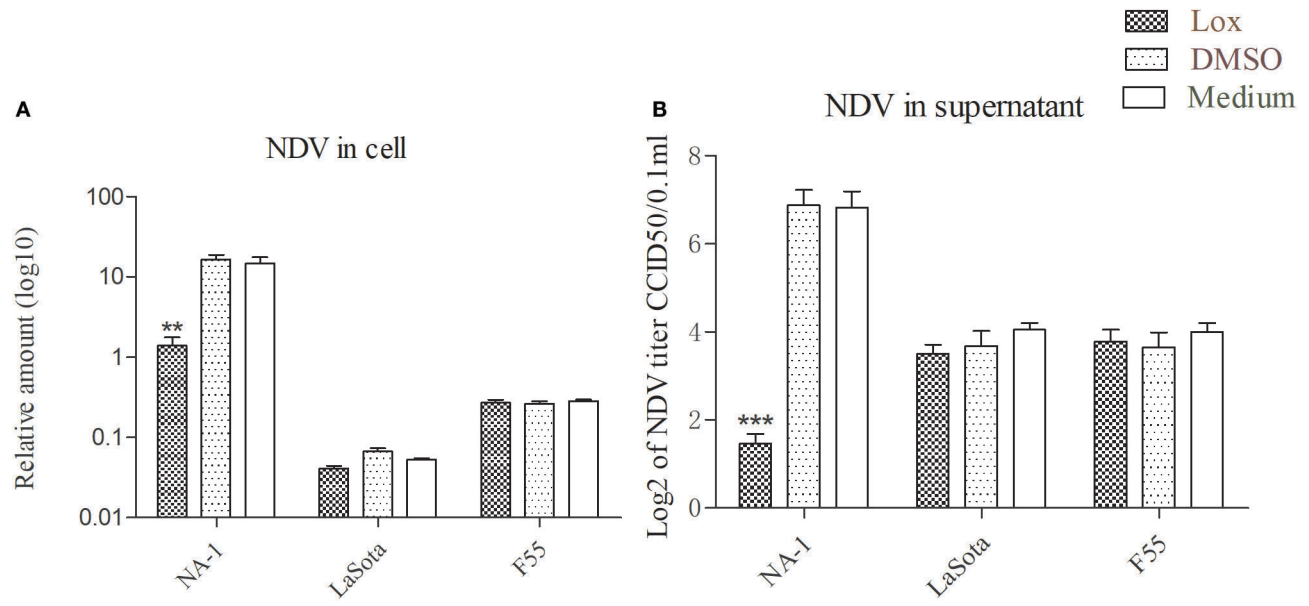


FIGURE 5 | TLR7 agonist inhibit virulent Newcastle disease virus (NDV) rather than lentogenic virus replication in chicken macrophages. HD11 cells were pretreated with 1 mM loxoribine for 6 h and followed treated with three different virulence and genotypes NDV strains at 2 multiplicity of infection for 48 h; thereafter, viral genome amount in the cells and virus titer in the supernatants were measured by qPCR and micro-HA method, respectively **(A,B)**. All qPCR data were normalized to the geometric mean of cellular endogenous genes β-actin and hydroxymethylbilane synthase and calculated using the $2^{-\Delta Ct}$ method. All values are shown as mean ± SEM (n = 4–6) and differences were considered significant if $^{*}P < 0.05$, $^{**}P < 0.01$, $^{***}P < 0.001$ as compared to the respective control (untreated) cells. All data are representative of at least two independent experiments.

of the virulent strain rather than the two lentogenic strains through inhibition of IFN-α and IFN-β. As expected, after pretreatment of HD11 cells with 1 mM loxoribine for 6 h, the expression levels of type I IFNs (IFN-α and IFN-β) were significantly decreased in cells infected with virulent virus rather than two lentogenic viruses (**Figure 7A**). Finally, we evaluated the cell injury caused by different genotypes NDV infection by LDH assay. As depicted in **Figure 7B**, pretreatment with 1 mM loxoribine for 6 h significantly decreased the virulent NDV strain NA-1 induced cell damage. Taken together, TLR7-mediated macrophage polarized activation inhibits virulent NDV replication and restores virulent virus-induced macrophage polarized activation and cell damage.

DISCUSSION

Macrophages play a critical role in the regulation and induction of innate and adaptive immune responses and protection of the host against pathogens (15, 62), especially viruses (19, 20, 37, 38, 63). However, recent findings demonstrated that macrophages could be a double-edged sword in virus clearance and pathology: they not only help fight against virus infection, but may also contribute to virus production and dissemination during viral infections (26, 64). In mammal models, a number of viruses have been found target macrophages and impair the function of these cells (65–67). By contrast, limited information is known about the interaction between chicken viruses and chicken macrophages. For example, previous studies showed that macrophages may be acting as a main target cell for some avian viruses infection and dissemination from the respiratory tract to nearby tissues and organs, which are necessary for continuation of the virus growth cycle (27, 68–70). Although macrophages are considered to be one of the main target cells for NDV infection and growth *in vivo* (59), very little is known about the ability of NDV to infect macrophage and the mechanisms of consequent macrophage responses to virus infections. The cell culture results in the present work indicated that chicken macrophages support the replication and growth of NDV strains of varying virulence and genotypes, and the results are in agreement with previous studies (59, 71–73).

Strains of NDV are categorized into virulent (velogenic), intermediate (mesogenic), and low virulent or non-virulent (lentogenic) on the basis of their pathogenicity in SPF chickens. However, the underlying mechanisms of virulent and lentogenic NDV strains infection as well as host responses to infections of different virulence and genotypes of NDV are still largely unknown. Although all NDV strains can infect and replicate in macrophages, it remains unclear how productive infection of macrophage by different virulence and genotypes NDV strains is impaired. In this study, we selected three different virulence and genotypes of NDV (including class II virulent genotype VII strain NA-1, class II lentogenic strain genotype III strain LaSota, and class I lentogenic genotype I strain F55), processed a preliminary experiment, and found that MOI 2 was ideal for all three NDV strains used, and no cytopathic effect to cells when treated with virulent strain NA-1 during the early stage of infection (from 4 to 12 hpi).

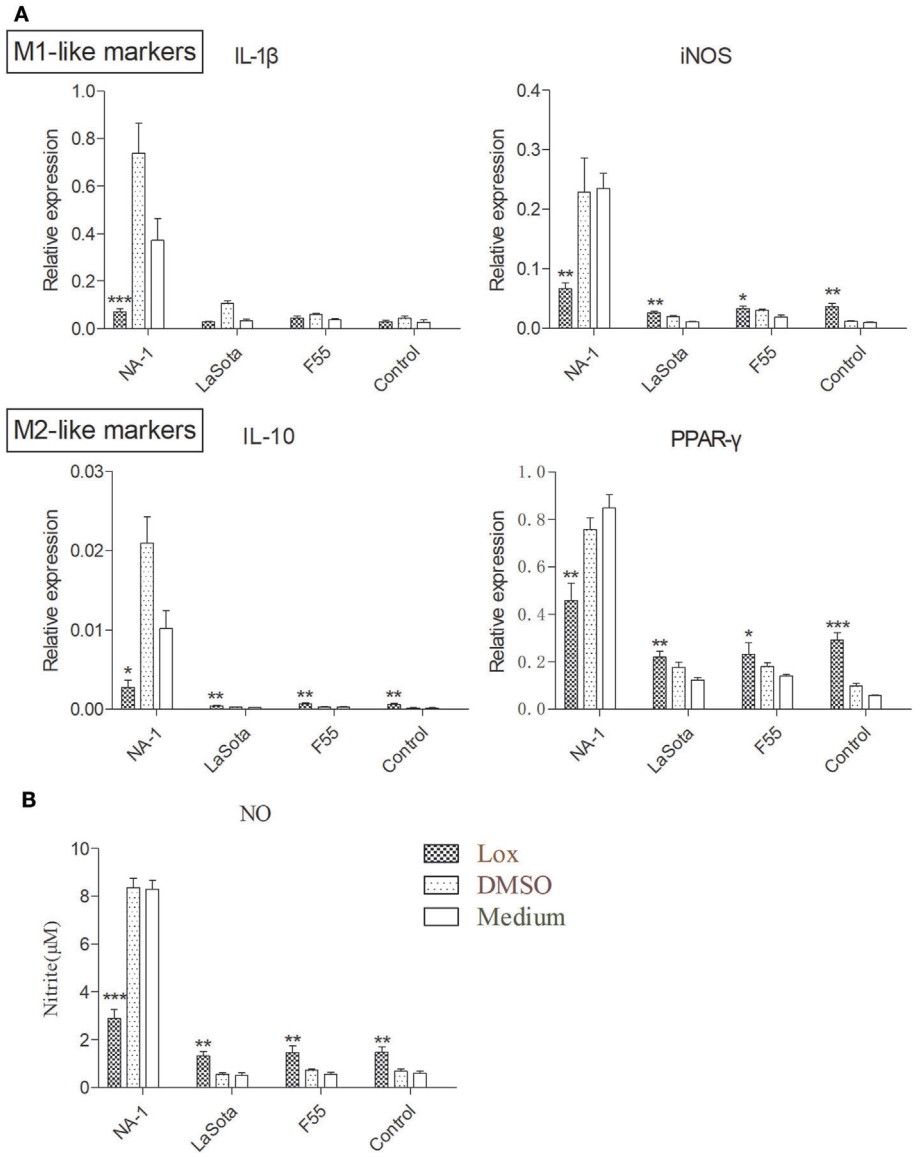


FIGURE 6 | TLR7 agonist decreases macrophage polarized activation markers in cells infected virulent virus rather than lentogenic virus. HD11 cells were pretreated with 1 mM loxoribine for 6 h and subsequently infected with three different virulence and genotypes Newcastle disease virus (NDV) strains at 2 multiplicity of infection for 48 h; thereafter, expression levels of M1-like (IL-1β and iNOS) and M2 (IL-10 and PPAR-γ) genes in HD cells **(A)** and M1-like protein nitrite concentration in the supernatants **(B)** were measured by qPCR and Griess assay, respectively. All qPCR data were normalized to the geometric mean of cellular endogenous genes β-actin and hydroxymethylbilane synthase and calculated using the $2^{-\Delta Ct}$ method. All values are shown as mean ± SEM (n = 4–6) and differences were considered significant if $^{*}P < 0.05$, $^{**}P < 0.01$, and $^{***}P < 0.001$ as compared to the respective control (untreated) cells. All data are representative of at least three independent experiments.

Our study demonstrated the replication and growth rate of three different virulence and genotypes viruses in chicken macrophages and the chicken macrophages polarized activation patterns which were induced by. Results indicated that all three NDV strains had similar replication and growth rate during the early stage of infection (from 4 to 12 hpi). However, virulent NDV replication and growth rate was shown to increase sharply from 24 hpi to a peak at 72 hpi compared to two lentogenic viruses (**Figure 2**), and this growth was associated with a strong upregulation of both pro-inflammatory M1-like markers/cytokines and anti-inflammatory M2-like markers/cytokines in chicken macrophages (**Figure 3**). Therefore, such M1-/M2-like mixed macrophages polarized activation may contribute to virulent NDV replication and growth sharply during the later stage of infection. Although two lentogenic strains did not elicit stronger M1-like or M2-like markers/cytokines production, the expression pattern of these M1- and M2-like associated genes was found to be different between cells infected with the two lentogenic viruses. In details, class I lentogenic F55 induces a mild M2-like macrophage polarized activation and class II lentogenic

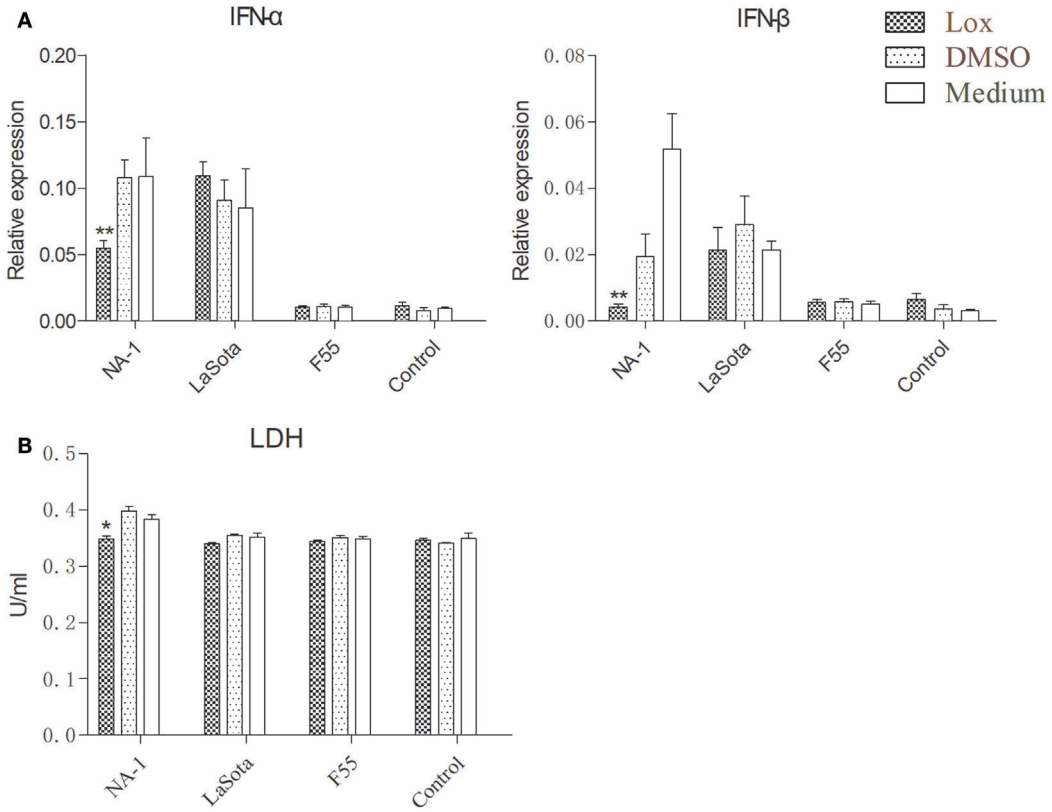


FIGURE 7 | TLR7 agonist notably reduces type I interferons (IFNs) expression and alleviates cell damaging effects in chicken macrophages caused by virulent virus rather than lentogenic virus infection. HD11 cells were pretreated with 1 mM loxoribine for 6 h and subsequently infected with three different virulence and genotypes Newcastle disease virus strains at 2 multiplicity of infection for 48 h; thereafter, expression levels of type I IFNs (IFN-α and IFN-β) genes in HD cells **(A)** and lactate dehydrogenase (LDH) concentration in the supernatants **(B)** were measured by qPCR and cytotoxicity detection method, respectively. All qPCR data were normalized to the geometric mean of cellular endogenous genes β-actin and hydroxymethylbilane synthase and calculated using the $2^{-\Delta Ct}$ method. All values are shown as mean ± SEM (n = 4–6) and differences were considered significant if $^{*}P < 0.05$, $^{**}P < 0.01$, and $^{***}P < 0.001$ as compared to the respective control (untreated) cells. All data are representative of at least three independent experiments.

LaSota induces a mild M1-like macrophage polarized activation (**Figure 3A**).

Chicken macrophages express a number of receptors for recognition of pathogens, including TLRs. TLRs bind to PAMPs derived from viral or bacterial pathogens leading to the polarized activation of macrophages (37). Although chicken origin TLR7 functions as same as mammalian TLR7 and encodes a 1047-amino-acid protein with only 62% identity to human TLR7 (74, 75). Previous results have been indicated that chicken origin TLR7 can be recognized by viral ssRNA (75, 76), which is largely released during the infections with chicken influenza virus (61). However, the inhibition of TLR7 expression levels and higher expression of type I (IFN-α and IFN-β) IFNs were observed in chicken macrophages when treated with virulent strain NA-1 during the later stage of infection (from 48 to 72 hpi) (**Figure 4**). This phenomenon was not observed in lentogenic viruses infected cells.

We supposed that inhibition of TLR7 may contribute to a M1-/M2-like mixed macrophages polarized activation caused by virulent strain NDV at the later stages of viral infection. Therefore, the TLR7 ligand 7-allyl-8-oxoguanosine (loxoribine) was used for determination of TLR7 roles in chicken macrophage upon NDV infections. Like as an antiviral compound against others chicken pathogens (37, 43, 61), pretreatment of HD11 cell with 1 mM loxoribine for 6 h inhibited virulent strain replication and restored virulent virus induced M1-/M2-like mixed macrophage polarized activation (**Figures 5** and **6**). Furthermore, TLR7 ligand loxoribine is a stimulator for M1-/M2-like mixed chicken macrophage polarized activation (**Figure 6**).

It has been reported that V protein of virulent strains exhibits IFNs antagonistic activity, which contributes to the viral virulence, tissue tropism, and host range (77, 78). Interestingly, in the present study, the expression of antiviral type I IFNs was significantly enhanced, rather than weakened, in chicken macrophages following the infection with virulent NDV and it was associated with the rapid replication of virus (**Figures 2** and **4**). However, some virus, such as virulent strain NA-1 used in this work, is a stronger stimulator for upregulated mRNA expression of type I IFNs, that means reduction in mRNA expression of type I IFNs because of reduced viral replication and growth (**Figures 5** and **7**). Meanwhile, pretreatment of HD11 cell with loxoribine for decreased virulent NDV caused type-I IFNs responses and alleviated virulent NDV-induced cell damage (**Figure 7**).

Overall, this study demonstrated that enhanced replication and growth of virulent NDV in chicken macrophages is due to M1-/M2-like mixed macrophages polarized activation of cells by inhibition of TLR7. Although no differences in replication and growth kinetics of two lentogenic NDV strains were observed *in vitro*, the lentogenic viruses induced much more moderate macrophages polarized activation status according to their genotypes. In addition, these results with the use of TLR7 ligand 7-allyl-8-oxoguanosine (loxoribine) suggest that TLR7 could be used as an antiviral potential target against the enzootic virulent NDV infection in birds.

AUTHOR CONTRIBUTIONS

RY, ZD and PZ designed the study, drafted the manuscript and analyzed the data. PZ, ZD, XL, YC, JL, ZT, YF, CX, JQ, XW, QL, TS, JC, YB and RY carried out experiments. All authors read and approved the final manuscript.

FUNDING

This study was partly financed by two grants from the National Science Foundation of China (31402195, 31472195), one grant from the Key Project of Chinese National Programs for Research and Development (2017YFD0500800), one grant from the Natural Science Foundation of Jilin Province (20160414029GH), one grant from the Chinese Special Fund for Agri-scientific Research in the public interest (201303033). None of the authors of this manuscript has a personal or financial relationship with other organizations or people that could inappropriately bias or influence the content of the manuscript.

SUPPLEMENTARY MATERIAL

The Supplementary Material for this article can be found online at https://www.frontiersin.org/articles/10.3389/fimmu.2018.00366/full#supplementary-material.

REFERENCES

1. Brown VR, Bevins SN. A review of virulent Newcastle disease viruses in the United States and the role of wild birds in viral persistence and spread. *Vet Res* (2017) 48(1):68. doi:10.1186/s13567-017-0475-9
2. Swayne DE, Glisson JR, McDougald LR, Nolan LK, Suarez DL, Nair VL. *Diseases of Poultry*. Ames: John Wiley & Sons (2013).
3. Amarasinghe GK, Bao Y, Basler CF, Bavari S, Beer M, Bejerman N, et al. Taxonomy of the order Mononegavirales: update 2017. *Arch Virol* (2017) 162(8):2493–504. doi:10.1007/s00705-017-3311-7
4. Czeglédi A, Ujvári D, Somogyi E, Wehmann E, Werner O, Lomniczi B. Third genome size category of avian paramyxovirus serotype 1 (Newcastle disease virus) and evolutionary implications. *Virus Res* (2006) 120(1):36–48. doi:10.1016/j.virusres.2005.11.009
5. Kim LM, King DJ, Curry PE, Suarez DL, Swayne DE, Stallknecht DE, et al. Phylogenetic diversity among low-virulence newcastle disease viruses from waterfowl and shorebirds and comparison of genotype distributions to those of poultry-origin isolates. *J Virol* (2007) 81(22):12641–53. doi:10.1128/JVI.00843-07
6. Kim LM, King DJ, Suarez DL, Wong CW, Afonso CL. Characterization of class I Newcastle disease virus isolates from Hong Kong live bird markets and detection using real-time reverse transcription-PCR. *J Clin Microbiol* (2007) 45(4):1310–4. doi:10.1128/JCM.02594-06
7. Lee EK, Jeon WJ, Kwon JH, Yang CB, Choi KS. Molecular epidemiological investigation of Newcastle disease virus from domestic ducks in Korea. *Vet Microbiol* (2009) 134(3–4):241–8. doi:10.1016/j.vetmic.2008.08.020
8. Liu X, Wang X, Wu S, Hu S, Peng Y, Xue F, et al. Surveillance for avirulent Newcastle disease viruses in domestic ducks (*Anas platyrhynchos* and *Cairina moschata*) at live bird markets in Eastern China and characterization of the viruses isolated. *Avian Pathol* (2009) 38(5):377–91. doi:10.1080/03079450903183637
9. Wu S, Wang W, Yao C, Wang X, Hu S, Cao J, et al. Genetic diversity of Newcastle disease viruses isolated from domestic poultry species in Eastern China during 2005-2008. *Arch Virol* (2011) 156(2):253–61. doi:10.1007/s00705-010-0851-5
10. Lindh E, Ek-Kommonen C, Vaananen VM, Alasaari J, Vaheri A, Vapalahti O, et al. Molecular epidemiology of outbreak-associated and wild-waterfowl-derived newcastle disease virus strains in Finland, including a novel class I genotype. *J Clin Microbiol* (2012) 50(11):3664–73. doi:10.1128/JCM.01427-12
11. Alexander DJ, Campbell G, Manvell RJ, Collins MS, Parsons G, McNulty MS. Characterisation of an antigenically unusual virus responsible for two outbreaks of Newcastle disease in the republic of Ireland in 1990. *Vet Rec* (1992) 130(4):65–8. doi:10.1136/vr.130.4.65
12. Diel DG, da Silva LH, Liu H, Wang Z, Miller PJ, Afonso CL. Genetic diversity of avian paramyxovirus type 1: proposal for a unified nomenclature and classification system of Newcastle disease virus genotypes. *Infect Genet Evol* (2012) 12(8):1770–9. doi:10.1016/j.meegid.2012.07.012
13. Kapczynski DR, Afonso CL, Miller PJ. Immune responses of poultry to Newcastle disease virus. *Dev Comp Immunol* (2013) 41(3):447–53. doi:10.1016/j.dci.2013.04.012
14. Rue CA, Susta L, Cornax I, Brown CC, Kapczynski DR, Suarez DL, et al. Virulent Newcastle disease virus elicits a strong innate immune response in chickens. *J Gen Virol* (2011) 92(Pt 4):931–9. doi:10.1099/vir.0.025486-0
15. Murray PJ, Wynn TA. Protective and pathogenic functions of macrophage subsets. *Nat Rev Immunol* (2011) 11(11):723–37. doi:10.1038/nri3073
16. Murray PJ, Allen JE, Biswas SK, Fisher EA, Gilroy DW, Goerdt S, et al. Macrophage activation and polarization: nomenclature and experimental guidelines. *Immunity* (2014) 41(1):14–20. doi:10.1016/j.immuni.2014.06.008
17. Martinez FO, Gordon S. The M1 and M2 paradigm of macrophage activation: time for reassessment. *F1000Prime Rep* (2014) 6:13. doi:10.12703/P6-13
18. Martinez FO, Sica A, Mantovani A, Locati M. Macrophage activation and polarization. *Front Biosci* (2008) 13:453–61. doi:10.2741/2692
19. Zhao X, Dai J, Xiao X, Wu L, Zeng J, Sheng J, et al. PI3K/Akt signaling pathway modulates influenza virus induced mouse alveolar macrophage polarization to M1/M2b. *PLoS One* (2014) 9(8):e104506. doi:10.1371/journal.pone.0104506
20. Shirey KA, Pletneva LM, Puche AC, Keegan AD, Prince GA, Blanco JC, et al. Control of RSV-induced lung injury by alternatively activated macrophages is IL-4R alpha-, TLR4-, and IFN-beta-dependent. *Mucosal Immunol* (2010) 3(3):291–300. doi:10.1038/mi.2010.6
21. Chawla A. Control of macrophage activation and function by PPARs. *Circ Res* (2010) 106(10):1559–69. doi:10.1161/CIRCRESAHA.110.216523
22. Kobasa D, Jones SM, Shinya K, Kash JC, Copps J, Ebihara H, et al. Aberrant innate immune response in lethal infection of macaques with the 1918 influenza virus. *Nature* (2007) 445(7125):319–23. doi:10.1038/nature05495
23. Cheung C, Poon L, Lau A, Luk W, Lau Y, Shortridge K, et al. Induction of proinflammatory cytokines in human macrophages by influenza A (H5N1) viruses: a mechanism for the unusual severity of human disease? *Lancet* (2002) 360(9348):1831–7. doi:10.1016/S0140-6736(02)11772-7
24. Lambrecht BN. Alveolar macrophage in the driver's seat. *Immunity* (2006) 24(4):366–8. doi:10.1016/j.immuni.2006.03.008
25. Snelgrove RJ, Godlee A, Hussell T. Airway immune homeostasis and implications for influenza-induced inflammation. *Trends Immunol* (2011) 32(7):328–34. doi:10.1016/j.it.2011.04.006
26. Cline TD, Beck D, Bianchini E. Influenza virus replication in macrophages: balancing protection and pathogenesis. *J Gen Virol* (2017) 98(10):2401–12. doi:10.1099/jgv.0.000922
27. Amarasinghe A, Abdul-Cader MS, Nazir S, De Silva Senapathi U, van der Meer F, Cork SC, et al. Infectious bronchitis corona virus establishes productive infection in avian macrophages interfering with selected antimicrobial

functions. *PLoS One* (2017) 12(8):e0181801. doi:10.1371/journal.pone.0181801
28. Abdul-Cader MS, Ahmed-Hassan H, Amarasinghe A, Nagy E, Sharif S, Abdul-Careem MF. Toll-like receptor (TLR)21 signalling-mediated antiviral response against avian influenza virus infection correlates with macrophage recruitment and nitric oxide production. *J Gen Virol* (2017) 98(6):1209–23. doi:10.1099/jgv.0.000787
29. Reese S, Dalamani G, Kaspers B. The avian lung-associated immune system: a review. *Vet Res* (2006) 37(3):311–24. doi:10.1051/vetres:2006003
30. Djeraba A, Musset E, van Rooijen N, Quere P. Resistance and susceptibility to Marek's disease: nitric oxide synthase/arginase activity balance. *Vet Microbiol* (2002) 86(3):229–44. doi:10.1016/S0378-1135(02)00010-X
31. Babu US, Gaines DW, Lillehoj H, Raybourne RB. Differential reactive oxygen and nitrogen production and clearance of *Salmonella* serovars by chicken and mouse macrophages. *Dev Comp Immunol* (2006) 30(10):942–53. doi:10.1016/j.dci.2005.12.001
32. Jarvis NA, Donaldson JR, O'Bryan CA, Ricke SC, Crandall PG. *Listeria monocytogenes* infection of HD11, chicken macrophage-like cells. *Poult Sci* (2017) 96(4):950–6. doi:10.3382/ps/pew358
33. Malkwitz I, Berndt A, Zhang R, Daugschies A, Bangoura B. Replication of *Toxoplasma gondii* in chicken erythrocytes and thrombocytes compared to macrophages. *Parasitol Res* (2017) 116(1):123–31. doi:10.1007/s00436-016-5268-y
34. Kim WH, Jeong J, Park AR, Yim D, Kim S, Chang HH, et al. Downregulation of chicken interleukin-17 receptor A during *Eimeria* infection. *Infect Immun* (2014) 82(9):3845–54. doi:10.1128/IAI.02141-14
35. He H, Genovese KJ, Kogut MH. Modulation of chicken macrophage effector function by T(H)1/T(H)2 cytokines. *Cytokine* (2011) 53(3):363–9. doi:10.1016/j.cyto.2010.12.009
36. Degen WG, Daal N, Rothwell L, Kaiser P, Schijns VE. Th1/Th2 polarization by viral and helminth infection in birds. *Vet Microbiol* (2005) 105(3–4):163–7. doi:10.1016/j.vetmic.2004.12.001
37. Barjesteh N, Behboudi S, Brisbin JT, Villanueva AI, Nagy E, Sharif S. TLR ligands induce antiviral responses in chicken macrophages. *PLoS One* (2014) 9(8):e105713. doi:10.1371/journal.pone.0105713
38. Haddadi S, Kim DS, Jasmine H, van der Meer F, Czub M, Abdul-Careem MF. Induction of toll-like receptor 4 signaling in avian macrophages inhibits infectious laryngotracheitis virus replication in a nitric oxide dependent way. *Vet Immunol Immunopathol* (2013) 155(4):270–5. doi:10.1016/j.vetimm.2013.08.005
39. Haddadi S, Thapa S, Kameka AM, Hui J, Czub M, Nagy E, et al. Toll-like receptor 2 ligand, lipoteichoic acid is inhibitory against infectious laryngotracheitis virus infection in vitro and in vivo. *Dev Comp Immunol* (2015) 48(1):22–32. doi:10.1016/j.dci.2014.08.011
40. Shi ZC, Cai ZY, Sanchez A, Zhang TT, Wen S, Wang J, et al. A novel toll-like receptor that recognizes vesicular stomatitis virus. *J Biol Chem* (2011) 286(6):4517–24. doi:10.1074/jbc.M110.159590
41. Gupta SK, Deb R, Dey S, Chellappa MM. Toll-like receptor-based adjuvants: enhancing the immune response to vaccines against infectious diseases of chicken. *Expert Rev Vaccines* (2014) 13(7):909–25. doi:10.1586/14760584.2014.920236
42. Brownlie R, Allan B. Avian toll-like receptors. *Cell Tissue Res* (2011) 343(1):121–30. doi:10.1007/s00441-010-1026-0
43. Swaggerty CL, He H, Genovese KJ, Duke SE, Kogut MH. Loxoribine pretreatment reduces *Salmonella* enteritidis organ invasion in 1-day-old chickens. *Poult Sci* (2012) 91(4):1038–42. doi:10.3382/ps.2011-01939
44. Schirrmacher V, Bai LH, Umansky V, Yu LH, Xing Y, Qian ZC. Newcastle disease virus activates macrophages for anti-tumor activity. *Int J Oncol* (2000) 16(2):363–73.
45. Umansky V, Shatrov VA, Lehmann V, Schirrmacher V. Induction of NO synthesis in macrophages by Newcastle disease virus is associated with activation of nuclear factor-kappa B. *Int Immunol* (1996) 8(4):491–8. doi:10.1093/intimm/8.4.491
46. Wilden H, Fournier P, Zawatzky R, Schirrmacher V. Expression of RIG-I, IRF3, IFN-β and IRF7 determines resistance or susceptibility of cells to infection by Newcastle disease virus. *Int J Oncol* (2009) 34(4):971–82. doi:10.3892/ijo.16.2.363
47. Washburn B, Weigand MA, Grosse-Wilde A, Janke M, Stahl H, Rieser E, et al. TNF-related apoptosis-inducing ligand mediates tumoricidal activity of human monocytes stimulated by Newcastle disease virus. *J Immunol* (2003) 170(4):1814–21. doi:10.4049/jimmunol.170.4.1814
48. Wen-Ko C. *Basic and Applied Aspects of Chicken Macrophage Biology*. Texas: Texas A&M University (2013). doi:10.3892/ijo_00000223
49. El Hag M, Feng Z, Su Y, Wang X, Yassin A, Chen S, et al. Contribution of the csgA and bcsA genes to *Salmonella* enterica serovar pullorum biofilm formation and virulence. *Avian Pathol* (2017) 46(5):541–7. doi:10.1080/03079457.2017.1324198
50. Xu M, Chang S, Ding Z, Gao HW, Wan JY, Liu WS, et al. Genomic analysis of Newcastle disease virus strain NA-1 isolated from geese in China. *Arch Virol* (2008) 153(7):1281–9. doi:10.1007/s00705-008-0115-9
51. Zhang P, Xie G, Liu X, Ai L, Chen Y, Meng X, et al. High genetic diversity of Newcastle disease virus in wild and domestic birds in Northeastern China from 2013 to 2015 reveals potential epidemic trends. *Appl Environ Microbiol* (2016) 82(5):1530–6. doi:10.1128/AEM.03402-15
52. Yin R, Ding Z, Liu X, Mu L, Cong Y, Stoeger T. Inhibition of Newcastle disease virus replication by RNA interference targeting the matrix protein gene in chicken embryo fibroblasts. *J Virol Methods* (2010) 167(1):107–11. doi:10.1016/j.jviromet.2010.02.014
53. Kim LM, Suarez DL, Afonso CL. Detection of a broad range of class I and II Newcastle disease viruses using a multiplex real-time reverse transcription polymerase chain reaction assay. *J Vet Diagn Invest* (2008) 20(4):414–25. doi:10.1177/104063870802000402
54. Yin R, Liu X, Liu C, Ding Z, Zhang X, Tian F, et al. Systematic selection of housekeeping genes for gene expression normalization in chicken embryo fibroblasts infected with Newcastle disease virus. *Biochem Biophys Res Commun* (2011) 413(4):537–40. doi:10.1016/j.bbrc.2011.08.131
55. St Paul M, Paolucci S, Barjesteh N, Wood RD, Schat KA, Sharif S. Characterization of chicken thrombocyte responses to toll-like receptor ligands. *PLoS One* (2012) 7(8):e43381. doi:10.1371/journal.pone.0043381
56. Hong YH, Lillehoj HS, Lee SH, Dalloul RA, Lillehoj EP. Analysis of chicken cytokine and chemokine gene expression following *Eimeria acervulina* and *Eimeria tenella* infections. *Vet Immunol Immunopathol* (2006) 114(3–4):209–23. doi:10.1016/j.vetimm.2006.07.007
57. Nang NT, Lee JS, Song BM, Kang YM, Kim HS, Seo SH. Induction of inflammatory cytokines and toll-like receptors in chickens infected with avian H9N2 influenza virus. *Vet Res* (2011) 42:64. doi:10.1186/1297-9716-42-64
58. Selvaraj RK, Klasing KC. Lutein and eicosapentaenoic acid interact to modify iNOS mRNA levels through the PPARgamma/RXR pathway in chickens and HD11 cell lines. *J Nutr* (2006) 136(6):1610–6. doi:10.1093/jn/136.6.1610
59. Cornax I, Diel DG, Rue CA, Estevez C, Yu Q, Miller PJ, et al. Newcastle disease virus fusion and haemagglutinin-neuraminidase proteins contribute to its macrophage host range. *J Gen Virol* (2013) 94(Pt 6):1189–94. doi:10.1099/vir.0.048579-0
60. Yin R, Liu X, Bi Y, Xie G, Zhang P, Meng X, et al. Expression of Raf kinase inhibitor protein is downregulated in response to Newcastle disease virus infection to promote viral replication. *J Gen Virol* (2015) 96(9):2579–86. doi:10.1099/jgv.0.000228
61. Stewart CR, Bagnaud-Baule A, Karpala AJ, Lowther S, Mohr PG, Wise TG, et al. Toll-like receptor 7 ligands inhibit influenza A infection in chickens. *J Interferon Cytokine Res* (2012) 32(1):46–51. doi:10.1089/jir.2011.0036
62. Wynn TA, Chawla A, Pollard JW. Macrophage biology in development, homeostasis and disease. *Nature* (2013) 496(7446):445–55. doi:10.1038/nature12034
63. Schneider C, Nobs SP, Heer AK, Kurrer M, Klinke G, van Rooijen N, et al. Alveolar macrophages are essential for protection from respiratory failure and associated morbidity following influenza virus infection. *PLoS Pathog* (2014) 10(4):e1004053. doi:10.1371/journal.ppat.1004053
64. Pawelek KA, Dor D Jr, Salmeron C, Handel A. Within-host models of high and low pathogenic influenza virus infections: the role of macrophages. *PLoS One* (2016) 11(2):e0150568. doi:10.1371/journal.pone.0150568
65. Coleman JR. The PB1-F2 protein of influenza A virus: increasing pathogenicity by disrupting alveolar macrophages. *Virol J* (2007) 4:9. doi:10.1186/1743-422X-4-9
66. Jia D, Rahbar R, Chan RW, Lee SM, Chan MC, Wang BX, et al. Influenza virus non-structural protein 1 (NS1) disrupts interferon signaling. *PLoS One* (2010) 5(11):e13927. doi:10.1371/journal.pone.0013927

67. Welsh MD, Adair BM, Foster JC. Effect of BVD virus infection on alveolar macrophage functions. *Vet Immunol Immunopathol* (1995) 46(3–4):195–210. doi:10.1016/0165-2427(94)05366-Z
68. Barrow AD, Burgess SC, Baigent SJ, Howes K, Nair VK. Infection of macrophages by a lymphotropic herpesvirus: a new tropism for Marek's disease virus. *J Gen Virol* (2003) 84(Pt 10):2635–45. doi:10.1099/vir.0.19206-0
69. Abdul-Careem MF, Haq K, Shanmuganathan S, Read LR, Schat KA, Heidari M, et al. Induction of innate host responses in the lungs of chickens following infection with a very virulent strain of Marek's disease virus. *Virology* (2009) 393(2):250–7. doi:10.1016/j.virol.2009.08.001
70. Chhabra R, Chantrey J, Ganapathy K. Immune responses to virulent and vaccine strains of infectious bronchitis viruses in chickens. *Viral Immunol* (2015) 28(9):478–88. doi:10.1089/vim.2015.0027
71. Lam KM. Growth of Newcastle disease virus in chicken macrophages. *J Comp Pathol* (1996) 115(3):253–63. doi:10.1016/S0021-9975(96)80083-1
72. Brown C, King DJ, Seal B. Detection of a macrophage-specific antigen and the production of interferon gamma in chickens infected with Newcastle disease virus. *Avian Dis* (1999) 43(4):696–703. doi:10.2307/1592739
73. Rasoli M, Yeap SK, Tan SW, Moeini H, Ideris A, Bejo MH, et al. Alteration in lymphocyte responses, cytokine and chemokine profiles in chickens infected with genotype VII and VIII velogenic Newcastle disease virus. *Comp Immunol Microbiol Infect Dis* (2014) 37(1):11–21. doi:10.1016/j.cimid.2013.10.003
74. Yilmaz A, Shen S, Adelson DL, Xavier S, Zhu JJ. Identification and sequence analysis of chicken toll-like receptors. *Immunogenetics* (2005) 56(10):743–53. doi:10.1007/s00251-004-0740-8
75. Philbin VJ, Iqbal M, Boyd Y, Goodchild MJ, Beal RK, Bumstead N, et al. Identification and characterization of a functional, alternatively spliced toll-like receptor 7 (TLR7) and genomic disruption of TLR8 in chickens. *Immunology* (2005) 114(4):507–21. doi:10.1111/j.1365-2567.2005.02125.x
76. Annamalai A, Ramakrishnan S, Sachan S, Kumar BSA, Sharma BK, Kumar V, et al. Prophylactic potential of resiquimod against very virulent infectious bursal disease virus (vvIBDV) challenge in the chicken. *Vet Microbiol* (2016) 187:21–30. doi:10.1016/j.vetmic.2016.03.005
77. Alamares JG, Elankumaran S, Samal SK, Iorio RM. The interferon antagonistic activities of the V proteins from two strains of Newcastle disease virus correlate with their known virulence properties. *Virus Res* (2010) 147(1):153–7. doi:10.1016/j.virusres.2009.10.020
78. Jang J, Hong SH, Choi D, Choi KS, Kang S, Kim IH. Overexpression of Newcastle disease virus (NDV) V protein enhances NDV production kinetics in chicken embryo fibroblasts. *Appl Microbiol Biotechnol* (2010) 85(5):1509–20. doi:10.1007/s00253-009-2189-z

Conflict of Interest Statement: The authors declare that the research was conducted in the absence of any commercial or financial relationships that could be construed as a potential conflict of interest.

Copyright © 2018 Zhang, Ding, Liu, Chen, Li, Tao, Fei, Xue, Qian, Wang, Li, Stoeger, Chen, Bi and Yin. This is an open-access article distributed under the terms of the Creative Commons Attribution License (CC BY). The use, distribution or reproduction in other forums is permitted, provided the original author(s) and the copyright owner are credited and that the original publication in this journal is cited, in accordance with accepted academic practice. No use, distribution or reproduction is permitted which does not comply with these terms.

frontiers in Immunology

REVIEW
published: 04 April 2018
doi: 10.3389/fimmu.2018.00664

Helminth Infections: Recognition and Modulation of the Immune Response by Innate Immune Cells

Claudia Cristina Motran[1,2], Leonardo Silvane[1,2], Laura Silvina Chiapello[1,2], Martin Gustavo Theumer[1,2], Laura Fernanda Ambrosio[1,2], Ximena Volpini[1,2], Daiana Pamela Celias[1,2] and Laura Cervi[1,2]**

[1] Departamento de Bioquímica Clínica, Facultad de Ciencias Químicas, Universidad Nacional de Córdoba, Córdoba, Argentina, [2] Centro de Investigaciones en Bioquímica Clínica e Inmunología (CIBICI), Consejo Nacional de Investigaciones Científicas y Tecnológicas (CONICET), Córdoba, Argentina

OPEN ACCESS

Edited by:
Geanncarlo Lugo-Villarino, UMR5089 Institut de Pharmacologie et de Biologie Structurale (IPBS), France

Reviewed by:
Marcela Freitas Lopes, Institute of Biophysics Carlos Chagas Filho (IBCCF), Brazil
Keke Celeste Fairfax, Purdue University, United States
Amélia Ribeiro De Jesus, Federal University of Sergipe, Brazil

***Correspondence:**
Claudia Cristina Motran
cmotran@fcq.unc.edu.ar;
Laura Cervi
lcervi@fcq.unc.edu.ar

Specialty section:
This article was submitted to Microbial Immunology, a section of the journal Frontiers in Immunology

Received: 11 January 2018
Accepted: 19 March 2018
Published: 04 April 2018

Citation:
Motran CC, Silvane L, Chiapello LS, Theumer MG, Ambrosio LF, Volpini X, Celias DP and Cervi L (2018) Helminth Infections: Recognition and Modulation of the Immune Response by Innate Immune Cells. Front. Immunol. 9:664. doi: 10.3389/fimmu.2018.00664

The survival of helminths in the host over long periods of time is the result of a process of adaptation or dynamic co-evolution between the host and the parasite. However, infection with helminth parasites causes damage to the host tissues producing the release of danger signals that induce the recruitment of various cells, including innate immune cells such as macrophages (Mo), dendritic cells (DCs), eosinophils, basophils, and mast cells. In this scenario, these cells are able to secrete soluble factors, which orchestrate immune effector mechanisms that depend on the different niches these parasites inhabit. Here, we focus on recent advances in the knowledge of excretory-secretory products (ESP), resulting from helminth recognition by DCs and Mo. Phagocytes and other cells types such as innate lymphocyte T cells 2 (ILC2), when activated by ESP, participate in an intricate cytokine network to generate innate and adaptive Th2 responses. In this review, we also discuss the mechanisms of innate immune cell-induced parasite killing and the tissue repair necessary to assure helminth survival over long periods of time.

Keywords: helminths, excretory-secretory products, phagocytes, M2 macrophages, dendritic cells, effector mechanisms, tissue repair

INTRODUCTION

Helminths, or worms, are invertebrate animals that comprise a broad spectrum of different pathogens able to affect human health. Among these parasites, there are two major phyla: the nematodes (or roundworms) and the platyhelminthes (also known as flatworms), with the latter in turn being subdivided into trematodes (flukes) and cestodes (tapeworms). The helminths infect a vast number of people all over the world, and it is estimated that soil-transmitted helminths cause infection in more than 1.5 billion people, or 24% of the entire human population. The main species that infect people are the nematodes *Ascaris lumbricoides*, *Trichuris trichiura*, *Necator americanus,* and *Ancylostoma duodenale,* with some of these producing chronic infections that can last up to 20 years (1).

The course of infection can vary greatly depending on the helminth. For example, certain filarial nematodes are transmitted by mosquitoes and can occupy and obstruct lymphatic vessels, which produces a chronic infection that causes lymphatic filariasis or elephantiasis (2), while other parasitic nematodes such as *T. trichiura* are strictly enteric and reside in the epithelium. In the case of schistosomiasis, an acute and chronic disease produced by different species of the trematodes worm *Schistosoma,* the pathology is caused by the inflammatory reaction of the host to the eggs deposited

in the tissues. This triggers the development of granulomas constituted by an inflammatory infiltrate and fibrosis around the eggs. During the evolution of the granulomas, the excessive fibrosis can cause periportal hypertension and even occasionally strokes when its location is cerebral or spinal (3).

The survival of helminths in the host for long periods of time is the result of a process of adaptation or dynamic co-evolution between the host and the parasite. In the case of these pathogens, it is necessary for them to locate a niche suitable for maturation and propagation without killing or damaging the host. Otherwise, the host would be able to generate an effective immune response to expel the parasite or at least limit the negative fitness effects of a given parasite load by inducing tolerance without sacrificing its ability to respond effectively to other pathogens.

This review is focused on the mechanisms by which phagocytes, in particular macrophages (Mo) and dendritic cells (DCs), recognize helminth parasites, become activated and induce effector immune responses. We also discuss recent advances in the knowledge about how Mo, DCs, and other phagocytes, such as mast cells, Eos, and basophils, are involved in the shaping of the innate and adaptive immune responses. We analyze the protective immune mechanisms generated against helminths, with a particular emphasis being placed on the trematodes *Fasciola hepatica*.

HELMINTH RECOGNITION BY PHAGOCYTES: MODULATION OF THE IMMUNE RESPONSE BY SECRETED PRODUCTS

Unlike other parasites, helminths are macropathogens, a condition that prevents them from being ingested by phagocytic cells. Thus, during infection by helminths, the products secreted by these parasites play a fundamental role as modulators of phagocyte activation by modifying the microenvironment in which these cells participate in the induction and instruction of the innate and adaptive immune responses.

The term "excretory/secretory antigens" (ES) refers to the parasite molecules that are released at the interface between the parasite and the cells of the immune system by various mechanisms, such as active secretion and diffusion from parasitic soma. These molecules are originated from adult worms intestinal content as well as female worms uterine content released during egg or larval deposition (4, 5). The development of systematic proteomic analysis has allowed many of the main ES helminth products to be characterized (6). These studies have revealed a common set of proteins that are secreted by helminths, including protease enzymes, glycolytic enzymes, protease enzyme inhibitors, antigens homologous to allergens, and lectins. However, as ES composition varies in different parasites and is affected by the stage of their life cycles, the reported different effects of ES on phagocytic cells may just be reflecting the complexity of their composition (5, 7).

Dendritic cells are mediators between innate and adaptive immunity, consequently, they play the principal role in the recognition, capture, processing, and presentation of helminth ES to T cells. A predominant Th2 response during helminth infections has been widely reported, although the precise mechanism initiating this response has not been fully elucidated (8). Nevertheless, it is clear that DCs are involved in the recognition of helminths or their products and the subsequent promotion of Th2 development. In fact, DCs are able to detect multiple ES by expressing the different innate immune receptors involved in the recognition of molecular patterns highly conserved in pathogens or PAMPs. Toll-like receptors (TLRs), C-type lectin receptors (CLRs), and nucleotide binding domain leucine-rich repeat (LRR)-containing (or NOD-like) receptors (NLRs) are the most studied of those involved in the interaction with helminth-derived molecules. DCs have been shown to recognize the *Schistosoma mansoni* lipid antigen containing phosphatidyl serine through TLR2, while lacto-N-fucopentaose III (LNFPIII) from *S. mansoni* and glycoprotein ES-62 of filaria are recognized through TLR4 (9, 10). In all cases, signaling through TLR2 or TLR4 reduces the ability of DCs to produce IL-12 and promotes a polarization toward a Th2-type response. This association between TLR signaling and polarization toward Th2-type response is surprising, as this signaling has been mostly associated with the development of a Th1-type response. However, it is important to highlight that the signaling cascade initiated in DCs downstream from TLRs, after their ligation by molecules derived from helminths, differs from that exerted by Th1 stimuli (such as LPS). Thus, the ligation of DC TLR4 by bacterial LPS strongly activates the mitogen-activated MAP kinases (MAPK) p38, JNK, and ERK, whereas the recognition of LNFPIII of *Schistosoma* by TLR4 present in DCs only induces phosphorylation of ERK (9). Similarly, the ES-62 protein of filaria and LNFPIII activate TLR4, but unlike LPS, they drive the response toward a Th2-type profile, suppressing the activation of p38 and JNK and inhibiting the production of IL-12 in an ERK-dependent manner. In the same way, the recognition of ES from eggs of *S. mansoni* through TLR2 is associated with the stabilization of the MAPK ERK, which promotes polarization to Th2 through the stabilization of the transcription factor c-Fos (which in turn suppresses the production of IL-12) (11). One possible explanation for these differences could be the association of the TLRs with different co-receptors, which may interfere with the downstream signaling cascade under TLRs. An example of this situation is the case of zymosan (an insoluble carbohydrate obtained from a yeast cell walls), which induces the production of the anti-inflammatory cytokine IL-10 by simultaneously signaling through the carbohydrate receptors dectin-1 and TLR2 (12). In fact, this mechanism of pattern-recognition receptors crosstalk could be occurring in the identification of carbohydrate helminths by the CLR. Consequently, it has recently been shown that the omega-1 molecule, a glycoprotein with ribonuclease activity secreted by *S. mansoni* eggs, signals *via* the mannose receptor (MR) through its carbohydrate domain. This recognition allows the internalization of omega-1 in DCs, with its RNAse activity being essential for inducing the Th2-type response (13). Other glycans derived from helminths, such as a Lewis^X-containing glycan secreted by both the eggs and the schistosomula of *S. mansoni*, are recognized by DC-SIGN and MR receptors on DCs, while carbohydrates rich in N-acetyl galactosamine are recognized by the macrophage galactose-type lectin (4).

It is well known that for Th2 differentiation, the early production of IL-4 is essential. However, DC activation by helminth products fails to induce IL-4 secretion. Therefore, it can be assumed that the modulation of DCs to promote Th2 polarization is dependent not only on a direct effect of helminths or their products on these cells but also on cell interaction with tissue-derived factors, such as the "alarmins," thymic stromal lymphopoietin (TSLP), matrix metalloproteinase 2 (MMP-2), IL-33, IL-25, and Eos-derived neurotoxin (EDN), among others, which also have an impact on DC activation [reviewed in Ref. (14)].

In contrast, to what was observed on DCs, the basophils and Eos have been reported to be involved in the development and amplification of the Th2 response, because of their ability to produce and secrete IL-4. Moreover, in addition to being key cells in the link between innate immunity and the development of the Th2 response, basophils, and Eos are phagocytes that are able to sense PAMPS as well as to process and present helminth antigens to naive T cells (15). Eos from healthy humans either treated with extracts from *Brugia malayi* or isolated from mice infected with this parasite have shown maturation signals with increasing MHC class II and some co-stimulatory molecule expression (16). In a similar way, *Strongyloides stercoralis* antigen-pulsed Eos induce Th2-type responses when injected into mice (17). Accordingly, Eos from MHC II-deficient mice fail to induce this type response, thereby highlighting the crucial role of these cells as antigen-presenting cells (APCs) in the induction of the Th2 adaptive immune response.

Basophils are granulocytes which represent about 1% of the circulating white blood cells. They are phagocytic cells able to induce inflammatory responses and share many characteristics with mast cells, such as the expression of the high-affinity Fc receptor for IgE (FcεRI) and the TLRs, TLR2 and TLR4. Basophils can also release mediators (including leukotrienes, prostaglandins, and histamine) that promote luminal fluid flow, nerve stimulation, and intestine contractility upon activation and IL-4 secretion (18). Although basophils are an important source of IL-4 and IL-13, they have been shown to be dispensable in the generation of the Th2 response in some helminth infections [e.g., during *Nippostrongylus brasiliensis* infection in basophil-deficient mice (Mcpt8-cre)]. Th2 polarization occurs even in the absence of these cells (19). By contrast, injection of mice with IPSE/alpha-1 protein derived from *S. mansoni* eggs induces IL-4 production by basophils, which contributes to initiating a Th2-type response, emphasizing the importance of basophils IL-4 in the linking of innate immunity and Th2 development (20). Recent studies have proposed that basophils can act as APCs, and, in this regard, the ability of basophils as APCs to promote the Th2-type response against helminth parasites might be dependent on MHC II expression. However, two controversial points arise from different studies proposing basophils as APCs: first, the low expression levels of the H-2M invariant chain, crucial in the regulation of the MHC-II peptide loading and, second, the low levels of MHC II expression in these cells compared to professional APCs. These issues have been clarified recently, since basophils can obtain peptide–MHC-II complexes from DCs by trogocytosis, allowing these cells to function as APCs, promoting a Th2-type response (21).

Mast cells originated from bone marrow, enter the peripheral blood, and complete their differentiation in tissues such as the skin or gut. A relevant study from Hepworth et al. demonstrated the involvement of mast cells in the development of the innate and adaptive Th2 responses during helminth infection (22). This study showed that in the absence of mast cells, mice infected with *Heligmosomoides polygyrus bakeri* or *Trichuris muris* revealed a deficiency in the production of the alarmins IL-25, IL-33, and TSLP derived from tissues. This led to an impaired innate and adaptive Th2-type responses; thus, showing the relevance of mast cell-induced responses during the early stages of gastrointestinal helminth infection.

Interestingly, Eos, basophils, and mast cells can also modulate and instruct the adaptive immune response after their stimulation through the release of the granules' content, as will be described below.

MODULATION OF PHAGOCYTE ACTIVATION BY *F. HEPATICA*

Fasciola hepatica is a causative agent of fasciolosis, which is a neglected disease that affects a vast number of cattle and sheep throughout the world and now is becoming an emerging disease in humans (23). During its migration through the host tissues, the parasite excretes and/or secretes many products capable of modulating the immune response. Soon after infection, the larval stage of *F. hepatica* crosses the intestinal wall and reaches the peritoneum. At the same time, the recruitment of alternatively activated Mo occurs, with upregulation in the expression of Fizz, Ym1, and arginase-1.

Many investigations have shown the ability of *F. hepatica* ES (24), *F. hepatica* tegumental antigens (FhTeg) (25), and ES-derived enzymes [such as thioredoxin peroxidase (26), 2-Cys peroxiredoxin (27), fatty acid binding protein (28) and more recently heme-oxygenase-1 (29)] to modulate Mo phenotype toward an alternative activation. This profile promotes three fundamental effects: the secretion of anti-inflammatory factors, the driving toward a Th2-profile and an increase in the pro-fibrotic factors involved in wound healing (**Figure 1**) (30). These are essential steps to compensate for the damage caused by the migration of the parasite in the host tissues, thereby allowing its establishment in the liver during the chronic phase of the disease.

Interestingly, a secreted peptide from *F. hepatica* called helminth defense molecule 1 (FhHDM-1) has been shown to have the ability to destabilize lysosomal acidification, which impairs Mo NLRP3 activation and consequently inflammasome function, resulting in the downregulation of IL-1 β production. These authors propose that in the absence of a Th1-type inflammatory milieu, the Th2-type immune response and parasite survival is favored (**Figure 1**) (31).

In addition, a mechanism of inhibition of TLR-dependent Mo activation was described by Donnelly et al. In this study, the cysteine protease activity of *F. hepatica* Cathepsin L1 (FheCL1), has been involved in the degradation of TLR3 within the endosome upon TLR3 and TLR4 stimulation. The ability of FheCL1 to inhibit TRIF-dependent signaling is a strategy used by *F. hepatica*

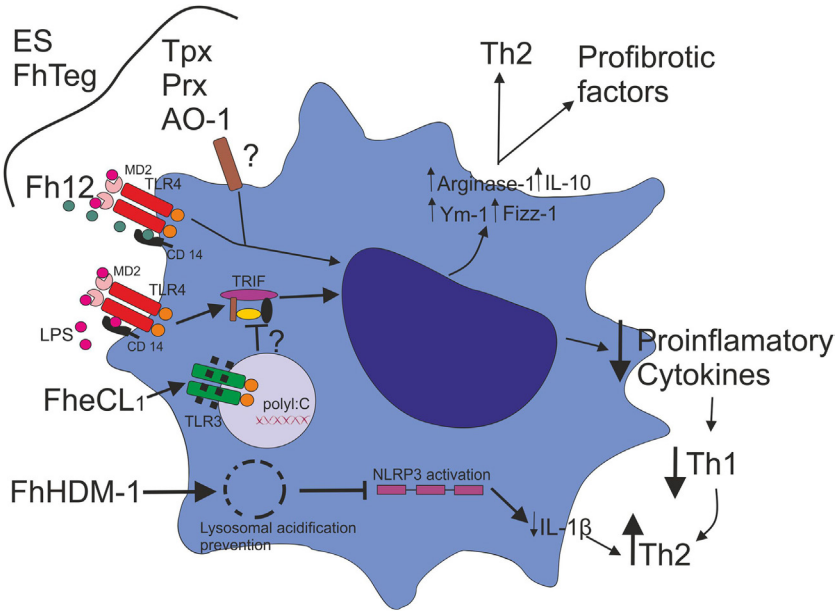


FIGURE 1 | *Fasciola hepatica* modulates macrophage activation. *F. hepatica* ES, *F. hepatica* tegumental antigens (FhTeg), and ES-derived enzymes, such as thioredoxin peroxidase (Tpx), 2-Cys peroxiredoxin (Prx), and heme-oxygenase-1 (AO-1) drive Mo phenotype toward an alternative activation profile. Fatty acid binding protein (Fh12) binds the co-receptor CD14 and inhibits LPS-induced TLR4 activation, suppressing the expression of IL-12, TNF, IL-6, and IL-1β. *F. hepatica* Cathepsin L1 (FheCL1) induces TLR3 degradation, which impairs LPS-induced TLR4–TRIF-dependent pathway with the consequent inhibition of inflammatory cytokine production. The decrease of an inflammatory cytokine milieu might promote the inhibition of a Th1 type response favoring a Th2 profile. *F. hepatica* defense molecule 1 (FhHDM-1) has been shown to have the ability to destabilize lysosomal acidification, which impairs Mo NLRP3 activation and consequently inflammasome function, resulting in the downregulation of IL-1 β production.

to control innate immune responses suppressing consequently Th1 development (**Figure 1**) (32).

Similarly, the exposure of DCs to *F. hepatica* products inhibits the ability of these cells to mature in response to inflammatory stimuli. Related to this, we have shown that *F. hepatica* ES inhibits TLR-activated DCs maturation and their ability to induce allogeneic responses (33). FhTeg, isolated from the coat of the parasite, has also been reported to downregulate inflammatory cytokine production and the expression of co-stimulatory molecules in response to TLR and non-TLR stimuli (34).

The relevance of the modulatory effect of *F. hepatica* antigens on DCs was demonstrated by the ability of these cells to inhibit inflammatory responses, such as those observed in the collagen-induced arthritis model (CIA). We evaluated the capacity of DCs treated with a total extract (TE) of *F. hepatica* together with CpG to modulate the inflammatory responses in CIA. The immunization of mice with collagen II-pulsed TE/CpG-conditioned DCs to diminish the severity and incidence of CIA symptoms induced anti-inflammatory cytokine production and promoted regulatory T cell (Treg) development (35). In addition, we have identified a protein Kunitz-type molecule that is present in TE as being able to inhibit TLR-induced DCs activation (36). Overall, these findings suggest that the modulation of DC activation might aid the chronic establishment of the parasite in the host.

In recent years, there has been an important advance in the knowledge about the receptors involved in the recognition of *F. hepatica* products. The role of CLRs, such as MR and dectin-1 in the interaction with *F. hepatica* ES has been reported. A partial inhibition of immunomodulatory factors such as arginase-1 expression, with TGF-β and IL-10 production has been observed when these receptors were blocked (24). In line with these findings, it was demonstrated that the recognition of FhTegs by MR-DCs is essential for the induction of Foxp3+ Treg cells and the CD4+ T cells anergy. This study showed that in the absence of MR, the ability of DCs to induce T cell anergy markers is downregulated (37). Finally, the participation of the CLR DC-SIGN, which recognizes *F. hepatica* glycans, has recently been demonstrated. In fact, DC-SIGN triggering is a critical event that induces some DC regulatory functions, such as the ability of these cells to induce anergic/Treg cells (38). Overall, all these results highlight the importance of improved knowledge about innate immunity receptors such as C-type lectins in the recognition and decoding of helminth molecular patterns, which are relevant to the induction of immunoregulatory responses.

KILLING OF HELMINTHS MEDIATED BY PHAGOCYTES AND ANTIBODIES

Among the cells that belong to the innate immune system, in the first line of defense against microorganisms, the phagocytic cells mediate the internalization and destruction of some pathogens, especially those that are opsonized by antibodies. As mentioned above, as helminth parasites are macropathogens, they cannot be ingested by phagocytic cells. Therefore, the immune system uses other mechanisms in order to eliminate them, such as

antibody-dependent cellular cytotoxicity (ADCC), which is also referred to as antibody-dependent cell-mediated cytotoxicity. The Fc-receptor-bearing effector cells can recognize and kill antibody-coated parasite worms by discharging their lysosomal or granular content (15) (**Figure 2**).

As stated above, helminth infections strongly induce Th2-skewed responses associated with cytokines (e.g., IL-4, IL-5, and IL-13), mastocytosis, eosinophilia, and antibody class-switching producing IgE [reviewed in Ref. (39)]. This antibody isotype is greatly elevated in helminth infection and mainly involved in ADCC. As a result, it is considered almost certain that the contribution of Eos to the host defense against helminth parasites is crucial (40). In agreement with this, *in vitro* studies have demonstrated that Eos use ADCC mechanisms to directly eliminate a variety of helminthic species through the action of Eos granule proteins. Furthermore, *in vivo* studies have shown that Eos can directly kill helminthic larvae (41, 42), exept for the adult forms of the parasites, which are more relevant to the infection (43).

Antibody-dependent cellular cytotoxicity by Eos degranulation occurs as a consequence of the interaction of Eos FcεRI with the Fc portion of specific-IgE bound to the parasite. The Eos granules mainly contain cytotoxic proteins such as the major basic proteins (MBP-1 and MBP-2), eosinophil peroxidase, eosinophil cationic protein (ECP) and EDN, which cause cytolysis of the parasite when released into the extracellular space (**Figure 2**) (15, 44). Mouse models of Eos depletion have demonstrated the protective role of these cells in secondary infections with helminths, with the depletion of Eos inducing an increase in the parasite burden of *N. brasiliensis* and *Trichinella spiralis* in murine models (45). Moreover, it has recently been reported

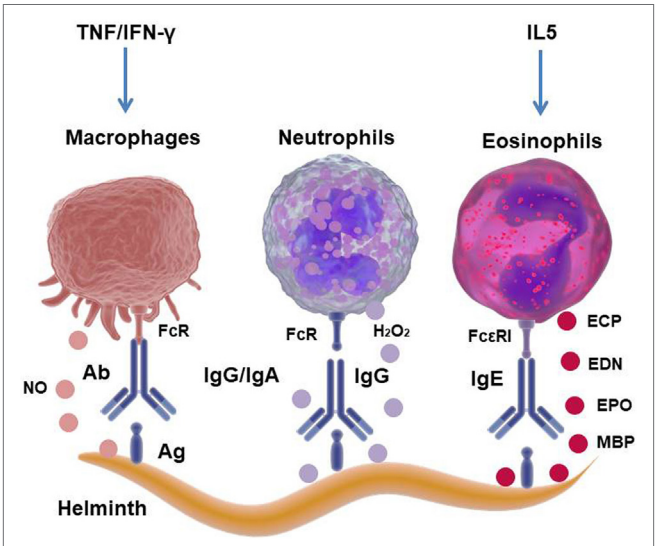


FIGURE 2 | Mechanism of cellular cytotoxicity mediated by antibodies against helminth parasites. The interaction of the antibodies that cover the parasite with the Fc receptors present in eosinophils (Eos), neutrophils, or macrophages (Mo) induces degranulation and the release of lysosomal/granular content, hydrogen peroxide (H_2O_2) or nitric oxide (NO), causing lysis of the helminth. Eos granules contain parasite toxic proteins, such as major basic protein (MBP), eosinophil peroxidase (EPO), eosinophil cationic protein (ECP), and eosinophil-derived neurotoxin (EDN).

that Eos are an important source of growth factors for plasma cell survival, suggesting an important role in the effector function to sustain antibody production (40). Eos produce cytokines and chemokines, such as IL-4, IL-5, IL-13, TGF-β, IL-10, IL-8, IL-12, IL-18, TNF, CCL11, and CCL5, with these cytokines being stored pre-formed in the granules to be rapidly released after Eos degranulation (46). Thus, these molecules can rapidly modulate innate and adaptive immune responses, and emerging data have demonstrated that during *T. spiralis* infection, Eos favors parasitic infection by inhibiting the Th1-type response (47). Therefore, it is questionable whether Eos contribute to anti-helminthic immunity. Furthermore, it is possible to conclude that eosinophilia is a sign of helminthic infection and that Eos are critically involved in immunoregulatory and/or host protective effects during parasitic worm infections.

Macrophages from rats have been involved in the *in vitro* ADCC of newly encysted juvenile (NEJ) worms of the trematodes *F. hepatica* through nitric oxide-dependent killing (**Figure 2**). Similarly, Mo and Eos from sheep have been shown to be able to eliminate juvenile larvae from *F. gigantica* through the release of superoxide radicals (48). However, this latter mechanism was shown to be ineffective when ovine peritoneal cells were cultured with *F. hepatica* NEJ, suggesting the ability of this parasite to resist elimination by reactive oxygen species, possibly through the release of antioxidant enzymes (48).

The predominant cell in the early response to schistosomula is the neutrophil, and the earliest histologic signs of parasite damage involve larval–neutrophil interactions (49). Besides, the killing of schistosomula by neutrophils (50, 51) or Mo (52, 53) has been reported. Also, ADCC by lung cells from rats infected with *T. spiralis* was demonstrated to be effective against newborn larva (NBL) with the FcεRI receptor present in Mo and neutrophils with Eos playing a critical role in cytotoxic attack (54). In addition, Bass and Szejda reported that neutrophils are at least as effective as Eos in the killing of NBL of *T. spiralis*, which appeared to be mediated by the generation of hydrogen peroxide (55).

Despite considerable pieces of evidence from *in vitro* assays showing the killing of helminth parasites by ADCC (15), there are few reports about whether this mechanism occurs *in vivo*. However, it has been demonstrated in helminth infections that the absence of antibodies or effector cells, crucial in ADCC, has a significant impact on the resistance to infection. In this regard, depletion of Eos, neutrophils, or Mo in studies of mice infected by helminths has revealed the importance of these cells in controlling infection levels (44, 56). In a similar way, antibody production was shown to correlate with protection in mice helminth infections (57, 58). In agreement with this, mice lacking antibodies ($J_H^{-/-}$) or activating Fc receptors (FcRγ$^{-/-}$) have shown increased numbers of larvae when infected with *Heligmosomoides polygyrus bakeri*, highlighting the relevant role of antibodies in the protective mechanism against helminth parasites (59).

Some mechanisms identified in helminth infections to prevent the immune system attack have been reported. One example that shows an inefficient ADCC is the ability of *F. hepatica*, on the one hand, to cleave IgG and IgE through the release of cathepsin L-protease and, on the other hand, to induce apoptosis of Eos and Mo (60–62). Furthermore, the release of antioxidant enzymes

such as superoxide dismutase or glutathione transferase could inhibit the superoxide anion, which is potentially toxic for the parasite larvae (63). It has also been recently demonstrated that a TGF-β-like molecule from *F. hepatica* called FhTLM, which is expressed by the NEJ stage of the parasite, inhibits the ability of Mo-dependent ADCC by using the TGF-β receptor (64). In this way, the parasite is able to inhibit each of the different components of the ADCC mechanism (such as effector cells, antibodies, and toxic molecules), resulting in its escape from the immune system and allowing its survival in the host.

Early studies by James et al. and Moser and Sher, have shown the ability of different granulocytes such as Mo, Eos, and neutrophils to kill the schistosomula. These granulocytes play a critical role in the antigen-antibody specific interaction on the surface of the larvae with the resulting death of these parasites (65, 66). In line with these findings, CBA mice immunized with an irradiated cercariae showed subdermal inflammatory foci around the dead *Schistosoma* larvae, with eosinophils and mononuclear cells the main infiltrating cells (67).

Mast cells are inflammatory cells that respond to different signals from innate and adaptive immunity by the release of inflammatory mediators. Thus, the phenotype and function of mast cells is modified by Th2-type cytokines, such as IL-4 and IL-5. Activation of mast cells is associated with the aggregation of FcεR1 by the antigens recognized by bound IgE. The density of FcεR1 on these cells is upregulated by higher levels of free IgE or the presence of IL-4 (49). Moreover, mast cells are activated by TLR ligands through damage-associated molecular patterns and the binding of IgG to FcγR1 and C3a and C5a through CD88. An example of the effector function of mast cells against helminths is their participation in IgE-mediated immediate hypersensitivity reactions, for example, against enteropathogens (49), thereby contributing to diarrhea production and at the same time assisting in parasite expulsion. The immediate hypersensitivity is a consequence of the presence of high levels of non-specific IgE generated by the Th2-type cytokine milieu as a result of worm infection. This cytokine binds FcεRI on mast cells, inducing degranulation (anaphylactic degranulation) and the release of inflammatory factors when they are cross-linked by cross-reactive antigens on the surface of the larva or adult worms (49, 68). Intriguingly, ES-62, a molecule secreted by filarial helminths, is able to inhibit the FcεRI-induced release of allergy mediators by selectively blocking key signal transduction events in mast cells, thus protecting the mice from cell-dependent hypersensitivity (69).

MO IN HELMINTH INFECTIONS: RECRUITMENT, ACTIVATION, AND CONTROL OF TISSUE DAMAGE

A subject of recent controversy is related to the origin of the Mo that expand during helminth infections. In the case of viral, bacterial, or fungal infections and even protozoa, the Mo of tissues have been reported to be derived from monocytes. However, it is not that clear this is the case during helminth infections. As regards the origin of the Mo, there is a report showing that in infections by nematodes, such as *Litomosoides sigmodontis,* an inflammatory infiltrate rich in Mo in the pleural cavity appears because of the proliferation of these cells due to the effect of IL-4, rather than by a recruitment of monocytes (70). By contrast, during *S. mansoni* infection in mice, the majority of Mo in the liver was demonstrated to be monocyte-derived, with CCL2 being involved in the recruitment process (71). A possible explanation for this difference could be the fact that in the schistosomiasis model, the classical inflammation due to TLR activation can occur due to the leakage of bacterial ligands from the intestinal lumen to the circulation, with the resulting passage of the eggs from the vasculature to the lumen. In contrast, in infection with *L. sigmodontis,* which resides in sterile tissues such as lung, the recruitment of Mo to the pleural cavity is mainly a consequence of local Mo proliferation (70).

Tissue damage caused by the migration of helminth parasites through different organs of the host triggers a "type-2" inflammatory response characterized by the recruitment of cells, including basophils, Eos, and Th2-type CD4 lymphocytes. The secretion of cytokines IL-4 together with IL-13 from these cells promotes the accumulation and activation of Mo toward an M2 (also known as alternatively activated phenotype). Numerous examples of murine models of helminth infection (*S. mansoni, H. polygyrus, N. brasiliensis, Tenia crassiceps, T. spiralis, L. sigmodontis, F. hepatica, Ascaris suum,* and the filarial parasite *B. malayi*) show the recruitment of M2 Mo after a few days of infection (30).

Interestingly, it has recently been demonstrated that alternative activation of Mo could be induced in an antibody-dependent and an IL-4Rα-independent way. Thus, during infection with the murine parasite *H. polygyrus bakeri*, helminth antigens can develop a new type of Mo called helminth-antibody activated macrophages, which are involved in the resistance mechanism against the helminth and in the avoidance of tissue damage (59).

Different markers such as IL-4Rα, MR (CD206), and arginase-1 activity together with its metabolic products (such as urea and proline) are characteristic of M2 Mo (30). In addition, soon after infection with helminth parasites, the M2 Mo produce high levels of the proteins Ym1 and Fizz, which are both secreted after the activation of these cells by Th2 cytokines (72). Ym1, a lectin with an affinity for chitin, is a member of mammalian proteins that share homology with chitinase family proteins and has been described as an Eos chemotactic factor (73, 74). A role in cell-to-cell and cell-to-extracellular matrix (ECM) interactions has been attributed to Ym1 due to its ability to bind heparin (75), and deposit ECM involved in the wound healing process (73).

Another abundant protein secreted after a nematode infection, Fizz1 (also known as resistin-like molecule α) has also been implicated in the process of deposition of ECM (76), which has angiogenic properties and the capacity to stimulate actin and collagen synthesis. M2 Mo also promote increased levels of vascular endothelial growth factor, insulin-like growth factor 1 (IGF-1), and MMPs, and trigger receptor expression on the myeloid cells 2 (TREM2), TGF-β and growth factors such as platelet-derived growth factor (PDGF). All these factors have been shown to be involved in different stages of the wound healing responses. Also increased levels of these mediators

have been reported in helminth infections, suggesting that they might contribute to the control of the tissue damage induced by these parasites (77–79).

The early stage of tissue repairing (up to hours or few days after tissue damage occurs) involves events including bleeding and inflammation with the recruitment of mast cells, neutrophils, platelets, as well as monocytes, which play a role in the control of bleeding. Different events of tissue damage and hemorrhages take place during the life cycle of *S. mansoni* as follows:

1. The cercariae penetrate the skin of the host by means of the secreted proteases.
2. Immature schistosomula can cross capillaries to enter the arterial flow.
3. Adult parasites mate in the mesenteric veins and the female lays eggs.
4. The eggs from the veins enter the gut wall and some reach lumen.
5. Some eggs are dragged by the blood flow into the liver where they are trapped in the small sinusoidal vessels, inducing a strong granulomatous response.

Thus, all stages of the parasite produce relevant tissue damage and hemorrhages in the host (78). Another example of tissue damage occurs during the life cycle of *F. hepatica,* where NEJ cross the intestinal wall, fall into the peritoneum and then go through the liver parenchyma leaving tunnels that cause necrosis (80). Among the nematodes, *A. lumbricoides* and *N. brasiliensis* cause damage to the lung tissue during their migration through the host (15).

In the healing process after tissue damage, the proliferation of fibroblasts and remodeling takes place. In particular, neutrophils and Mo are important cells because of their phagocytic capacity to help in debris removal. In addition, Mo and fibroblast induce fibroblast proliferation and promote fibrogenesis and collagen production through the release of different molecules, such as TGF-β and PDGF (81, 82). Interestingly, an opposing role can be attributed to Mo during an inflammatory process after tissue damage. On the one hand, these cells are able to activate a pro-fibrotic process by promoting the recruitment of inflammatory cells, which stimulate the activity of fibroblasts and the deposition of ECM (83). On the other hand, Mo are able to terminate the inflammation by the elimination of the debris coming from the rupture of tissue including dead inflammatory cells (82).

Tissue damage can cause upregulation of the alarmin IL-33. This is a strong positive stimulus for innate lymphocyte T cell 2 (ILC2) accumulation and cytokine production, which can support tissue-protective M2 Mo differentiation. Recent data suggest the possibility that ILC2, M2 Mo, amphiregulin (AREG), and IGF-1 may collaborate in promoting wound healing at the mucosal barrier surfaces.

Interestingly, Mo are also involved in the immunopathology of schistosomiasis, since in both mice and humans infected with *S. mansoni* many of these cells are recruited to the granulome in response to trapped eggs in the liver, intestinal or bladder tissues. In a mouse model of *S. mansoni,* it was demonstrated that Mo are the predominant cell population in gut granulomas, in contrast to what was observed in the liver, where Eos are the majority of the cells recruited (15).

In addition to promoting tissue repair, M2 Mo also play a role in the inhibition of the pro-inflammatory responses mediated by M1 Mo and Th1 and Th17 responses, which in turn can exacerbate tissue damage if not controlled. A demonstrative study from Ref. (84) shows that IL-4Rα signaling in Mo is essential for mice survival during acute schistosomiasis. Thus, the absence of IL4R-α in Mo was responsible for the death of mice due to increased levels of Th1 cytokines, NOS-2 activity and immunopathology in the liver and gut as well as increased egg expulsion. These results highlight the key role played by M2 Mo in protection against tissue damage. In the same line, results from a human study show the importance of the Th2 response to down modulate the inflammatory response in acute schistosomiasis (85). In addition, an Arg-1 Mo-dependent suppressive mechanism to control excessive fibrosis (characteristic of the severe human disease) has been recently reported. However, this is a surprising finding, considering that Arg-1 is involved in the synthesis of proline (amino acid precursor of collagen), and therefore in the promotion of fibrosis and tissue repair. At the same time, Arg-1-derived M2 Mo help in the resolution of Th2-type-dependent inflammation and fibrosis by acting as suppressor cells (86).

ROLE OF PHAGOCYTES DURING ORCHESTRATION OF THE INTESTINAL IMMUNE RESPONSE IN HELMINTH INFECTIONS

Intestinal helminth parasites interact with the host intestinal barrier producing damage related to different causes, such as the attachment of the parasite to epithelial cells, migration through the host tissue, worm feeding events, or secondary opportunistic bacterial infections (87). Damage to host tissues induces the release of alarmins including the cytokines IL-33, IL-25, and TSLP by intestinal epithelial cells (IECs), among others. Furthermore, helminth infection promotes the early recruitment of the phagocytes Eos, mast cells, and basophils at the site of infections, which provide the rapid secretion of the Th2-type cytokines IL-4, IL-13, and TSLP (88). In addition to IECs, Mo, Eos, neutrophils, and mast cells can also secrete endogenous inflammatory mediators or alarmins, which can function as chemotactic factors or induce DC maturation (88, 89). These alarmins include EDN, cathelicidins, defensins, and high-mobility group box protein 1 with a suggested role of EDN in the initiation and maintenance of the Th2-type response (90). However, the mice models using anti-IL-5 or anti-CCR3 antibodies for Eos depletion have shown the dispensable role of these cells in the promotion of the Th2 response against helminth parasites (91).

A dominant Th2-type cytokine response in infected hosts influences the development of intestinal and systemic immune and immunopathological changes. These include strong peripheral and intestinal IgE-type responses, eosinophilia, goblet cell (GC) hyperplasia, villous atrophy and crypt hyperplasia, increased muscle contractility, and mastocyte hyperplasia in the intestinal mucosa. In addition, profound changes in the

function of the IECs have been observed, including alterations in permeability, proliferation, and differentiation (92). All these mechanisms together contribute to the expulsion of the parasite from the intestinal lumen.

The hypercontractility of the intestinal smooth muscle in an IL-4/IL-13-dependent manner is a characteristic of nematode infections. Furthermore, the involvement of M2 Mo in the regulation of intestinal contractility has been demonstrated. The expulsion of worms from the lumen appears to be mediated by the expression of Arg-1 in M2 Mo, as a regulator of this function (93). By contrast, innate lymphoid cells (ILCs) perform crucial functions in different tissues, particularly at the mucosa surface of the intestine and lung, where they are important regulators of the innate immune response. Among these, the ILC2s are localized mainly in mucosa-associated tissues with IL-25 together with IL-33. These innate immune responses contribute to the elimination of parasites such as *N. brasilienses* (a gastrointestinal nematode that infects mice and has a life cycle similar to that of hookworms in humans) (94). In line with this, it has also been reported that IL-33 has a crucial role in resistance against other nematodes including *S. venezuelensis* in mice (95) and *T. muris* (96). After being activated by IL-33, the ILC2s increase their IL-13 production, which in turn mediates two mechanisms that contribute to the rodent hookworm *N. brasiliensis* being expelled from the intestinal lumen:

(1) The induction of the anti-nematode protein resistin-like molecule beta or Fizz2 (RELMβ) expression, a protein released by GCs which are able to inhibit worm nutrition (97).
(2) Eos recruitment, a key cell for eliminating intestinal nematodes from infected hosts.

Interestingly, after *N. brasiliensis* infection, the activation of ILC2s induces the hyperplasia of tuft cells (a secretory intestinal cell type), which in turn are capable of secreting IL-25, and together with IL-33 promotes the secretion of IL-13 by ILC2 cells (**Figure 3**). In this circuit, the Th2 cytokines IL-4 and IL-13 are also capable of inducing tuft cell hyperplasia (98). In fact, IL-13 produced by activated ILC2s and Th2 cells has been shown to promote an active renewal of IECs, a process that acts as an "epithelial escalator" and helps to expel parasites from the intestine (99). In addition, IL-13 induces GC differentiation, which results in the secretion of mucus and anti-helminthic molecules, such as RELMβ (97).

Zaiss et al. have reported the involvement of AREG, originally described as an epithelial cell-derived factor, which has a critical role in helminth resistance and shows its relevance in the expulsion of the nematodes *T. muris* through the promotion of IEC replacement. Although non-lymphoid gut cells might produce AREG, the exact cellular sources of this molecule are still unknown (100).

Considering a scenario where helminth infection causes the recruitment of different cell populations, it is logical to speculate how ILC2s interplay with phagocytes. In this way, Bouchery et al. (101) reported that ILC2s and T cells cooperate with M2 Mo in the lung during infection with *N. brasiliensis*, thereby trapping and killing the larvae in re-infected mice. Furthermore, they showed that IL-33- or IL-2-dependent ILC2 activation stimulates M2 Mo to reduce worm burden in the lung of re-infected mice. Nevertheless, it is important to emphasize the role of mast cells in the immunity against intestinal helminths, since the accumulation of these cells or mastocytosis is a feature of infections caused by these parasites. The proteases of mast cells promote the breakdown of the narrow joints of the IECs, allowing the discharge of fluids into the intestinal lumen. In line with this, mast cell-deficient mice (by a mutation in the c-kit gene) have been demonstrated to have difficulty in eliminating the *T. spiralis* nematode (102). In addition, a crucial role of mast cells has been

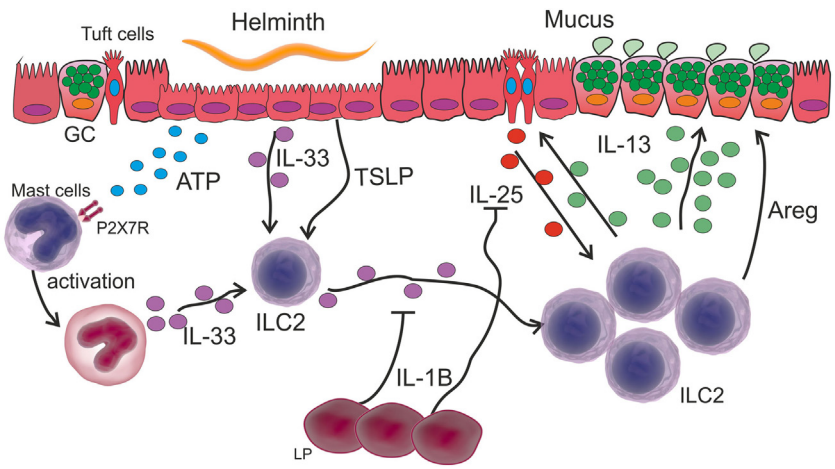


FIGURE 3 | Innate immune response in intestinal helminth infection. Tissue damage caused by intestinal helminths induces an ATP increase that is recognized by P2X7R on the surface of mast cells, which in turn are activated secreting IL-33. This cytokine together with other alarmins such as stromal lymphopoietin (TSLP) activate ILC2 and induce their proliferation. Activated ILC2 cells secrete IL-13 thereby increasing mucus secretion in goblet cells (GC). The activation of ILC2s induces the hyperplasia of tuft cells and the release of IL-25, which together with IL-33 promotes the secretion of IL-13 by ILC2 cells. IL-1β produced by lamina propria (LP) cells inhibits IL-25 and IL-33, thereby controlling the expansion of the Th2-type response.

recently demonstrated in eradicating *H. polygyrus* in the early stage of infection. These cells secrete IL-33 that activates an ILC2 response after the recognition of tissue damage-derived ATP through the P2X7 receptor (103) (**Figure 3**).

Finally, a recent mechanism for Th2 immunity constriction has been demonstrated. Early post-infection with *H. polygyrus bakeri,* intestinal lamina propria (LP) cells secrete IL-1β, which inhibits the helminth-induced IL-25 and IL-33 and results in a reduced Th2 protective immune response, thus allowing the parasite chronicity (104) (**Figure 3**).

CONCLUSION

In the last decade, there have been important advances in the knowledge about how helminth parasites are recognized by DCs and also regarding the capacity of these cells to induce a Th2-type response. However, other phagocytes are necessary to generate an intricate network of cytokines, soluble factors, and danger signals arising from the damage produced by parasite migration, which promotes a Th2-type response. This response in turn drives the alternative activation of Mo, and the activation of Eos, basophils, and mast cells, which contribute to the expulsion of intestinal nematodes. Among the phagocytes, M2 Mo play a key role in providing factors for rapid and efficient tissue repair and to complete the process of wound healing.

Although an undeniable involvement of phagocytes, such as Mo, neutrophils, Eos, basophils, mast cells, and antibodies in *in vitro* death mechanisms against helminths, have been demonstrated, it is not clear whether these mechanisms occur *in vivo*. However, there is growing evidence showing the importance of these cells in the mechanisms of protection against parasitic helminths in different settings of cell depletion or vaccination in mice.

Some interactions between phagocytes with other cell types (e.g., ILC2) during helminth infection have been demonstrated. However, further studies are still required to elucidate the factors that modulate the maturation of DCs to promote the Th2 response in naive T cells and possible interaction between other phagocytic cells such as Mo, neutrophils, basophils, and mast cells during infection by helminth parasites.

AUTHOR CONTRIBUTIONS

CM and LC wrote the manuscript, LS and DC designed the figures, LSC and MT critically revised the manuscript, and LA and XV revised the manuscript.

ACKNOWLEDGMENTS

This work was supported by grants from the Consejo Nacional de Investigaciones Científicas y Técnicas of Argentina (CONICET) PIP 2015-2017 GI, 112201 501002 60CO, Agencia Nacional de Promoción Científica y Técnica (PICT-2015-1179 and 2488), and Secretaría de Ciencia y Técnica-Universidad Nacional de Córdoba (grants to CM and LC). CM, LC, LSC, and MT are members of the Scientific Career of CONICET. DC, LA, and XV thank CONICET for the fellowships granted.

REFERENCES

1. Brooker S. Estimating the global distribution and disease burden of intestinal nematode infections: adding up the numbers – a review. *Int J Parasitol* (2010) 40(10):1137–44. doi:10.1016/j.ijpara.2010.04.004
2. Chakraborty S, Gurusamy M, Zawieja DC, Muthuchamy M. Lymphatic filariasis: perspectives on lymphatic remodeling and contractile dysfunction in filarial disease pathogenesis. *Microcirculation* (2013) 20(5):349–64. doi:10.1111/micc.12031
3. Pearce EJ, MacDonald AS. The immunobiology of schistosomiasis. *Nat Rev Immunol* (2002) 2(7):499–511. doi:10.1038/nri843
4. White RR, Artavanis-Tsakonas K. How helminths use excretory secretory fractions to modulate dendritic cells. *Virulence* (2012) 3(7):668–77. doi:10.4161/viru.22832
5. Hewitson JP, Grainger JR, Maizels RM. Helminth immunoregulation: the role of parasite secreted proteins in modulating host immunity. *Mol Biochem Parasitol* (2009) 167(1):1–11. doi:10.1016/j.molbiopara.2009.04.008
6. Robinson MW, Tort JF, Lowther J, Donnelly SM, Wong E, Xu W, et al. Proteomics and phylogenetic analysis of the Cathepsin L protease family of the helminth pathogen *Fasciola hepatica* expansion of a repertoire of virulence-associated factors. *Mol Cell Proteomics* (2008) 7(6):1111–23. doi:10.1074/mcp.M700560-MCP200
7. Harnett W. Secretory products of helminth parasites as immunomodulators. *Mol Biochem Parasitol* (2014) 195(2):130–6. doi:10.1016/j.molbiopara.2014.03.007
8. Everts B, Smits HH, Hokke CH, Yazdanbakhsh M. Helminths and dendritic cells: sensing and regulating via pattern recognition receptors, Th2 and Treg responses. *Eur J Immunol* (2010) 40(6):1525–37. doi:10.1002/eji.200940109
9. Thomas PG, Carter MR, Atochina O, Da'Dara AA, Piskorska D, McGuire E, et al. Maturation of dendritic cell 2 phenotype by a helminth glycan uses a toll-like receptor 4-dependent mechanism. *J Immunol* (2003) 171(11): 5837–41. doi:10.4049/jimmunol.171.11.5837
10. Goodridge HS, Marshall FA, Else KJ, Houston KM, Egan C, Al-Riyami L, et al. Immunomodulation via novel use of TLR4 by the filarial nematode phosphorylcholine-containing secreted product, ES-62. *J Immunol* (2005) 174(1):284–93. doi:10.4049/jimmunol.174.1.284
11. Agrawal S, Agrawal A, Doughty B, Gerwitz A, Blenis J, Van Dyke T, et al. Cutting edge: different toll-like receptor agonists instruct dendritic cells to induce distinct Th responses via differential modulation of extracellular signal-regulated kinase-mitogen-activated protein kinase and c-Fos. *J Immunol* (2003) 171(10):4984–9. doi:10.4049/jimmunol.171.10.4984
12. Gantner BN, Simmons RM, Canavera SJ, Akira S, Underhill DM. Collaborative induction of inflammatory responses by dectin-1 and toll-like receptor 2. *J Exp Med* (2003) 197(9):1107–17. doi:10.1084/jem.20021787
13. Everts B, Perona-Wright G, Smits HH, Hokke CH, van der Ham AJ, Fitzsimmons CM, et al. Omega-1, a glycoprotein secreted by *Schistosoma mansoni* eggs, drives Th2 responses. *J Exp Med* (2009) 206(8):1673–80. doi:10.1084/jem.20082460
14. Motran CC, Ambrosio LF, Volpini X, Celias DP, Cervi L. Dendritic cells and parasites: from recognition and activation to immune response instruction. *Semin Immunopathol* (2017) 39(2):199–213. doi:10.1007/s00281-016-0588-7
15. Makepeace BL, Martin C, Turner JD, Specht S. Granulocytes in helminth infection – who is calling the shots? *Curr Med Chem* (2012) 19(10):1567–86. doi:10.2174/092986712799828337
16. Mawhorter SD, Kazura JW, Boom WH. Human eosinophils as antigen-presenting cells: relative efficiency for superantigen- and antigen-induced CD4+ T-cell proliferation. *Immunology* (1994) 81(4):584–91.
17. Padigel UM, Hess JA, Lee JJ, Lok JB, Nolan TJ, Schad GA, et al. Eosinophils act as antigen-presenting cells to induce immunity to *Strongyloides stercoralis* in mice. *J Infect Dis* (2007) 196(12):1844–51. doi:10.1086/522968
18. Arinobu Y, Iwasaki H, Gurish MF, Mizuno S, Shigematsu H, Ozawa H, et al. Developmental checkpoints of the basophil/mast cell lineages in adult murine hematopoiesis. *Proc Natl Acad Sci U S A* (2005) 102(50):18105–10. doi:10.1073/pnas.0509148102

19. Ohnmacht C, Schwartz C, Panzer M, Schiedewitz I, Naumann R, Voehringer D. Basophils orchestrate chronic allergic dermatitis and protective immunity against helminths. *Immunity* (2010) 33(3):364–74. doi:10.1016/j.immuni.2010.08.011
20. Schramm G, Mohrs K, Wodrich M, Doenhoff MJ, Pearce EJ, Haas H, et al. Cutting edge: IPSE/alpha-1, a glycoprotein from *Schistosoma mansoni* eggs, induces IgE-dependent, antigen-independent IL-4 production by murine basophils in vivo. *J Immunol* (2007) 178(10):6023–7. doi:10.4049/jimmunol.178.10.6023
21. Miyake K, Shiozawa N, Nagao T, Yoshikawa S, Yamanishi Y, Karasuyama H. Trogocytosis of peptide–MHC class II complexes from dendritic cells confers antigen-presenting ability on basophils. *Proc Natl Acad Sci U S A* (2017) 114(5):1111–6. doi:10.1073/pnas.1615973114
22. Hepworth MR, Daniłowicz-Luebert E, Rausch S, Metz M, Klotz C, Maurer M, et al. Mast cells orchestrate type 2 immunity to helminths through regulation of tissue-derived cytokines. *Proc Natl Acad Sci U S A* (2012) 109(17):6644–9. doi:10.1073/pnas.1112268109
23. Cwiklinski K, O'Neill SM, Donnelly S, Dalton JP. A prospective view of animal and human fasciolosis. *Parasite Immunol* (2016) 38(9):558–68. doi:10.1111/pim.12343
24. Guasconi L, Serradell MC, Garro AP, Iacobelli L, Masih DT. C-type lectins on macrophages participate in the immunomodulatory response to *Fasciola hepatica* products. *Immunology* (2011) 133(3):386–96. doi:10.1111/j.1365-2567.2011.03449.x
25. Haçarız O, Sayers G, Mulcahy G. A preliminary study to understand the effect of *Fasciola hepatica* tegument on naïve macrophages and humoral responses in an ovine model. *Vet Immunol Immunopathol* (2011) 139(2):245–9. doi:10.1016/j.vetimm.2010.08.007
26. Donnelly S, O'Neill SM, Sekiya M, Mulcahy G, Dalton JP. Thioredoxin peroxidase secreted by *Fasciola hepatica* induces the alternative activation of macrophages. *Infect Immun* (2005) 73(1):166–73. doi:10.1128/IAI.73.1.166-173.2005
27. Donnelly S, Stack CM, O'Neill SM, Sayed AA, Williams DL, Dalton JP. Helminth 2-Cys peroxiredoxin drives Th2 responses through a mechanism involving alternatively activated macrophages. *FASEB J* (2008) 22(11):4022–32. doi:10.1096/fj.08-106278
28. Figueroa-Santiago O, Espino AM. *Fasciola hepatica* fatty acid binding protein induces the alternative activation of human macrophages. *Infect Immun* (2014) 82(12):5005–12. doi:10.1128/IAI.02541-14
29. Carasi P, Rodríguez E, da Costa V, Frigerio S, Brossard N, Noya V, et al. Heme-oxygenase-1 expression contributes to the immunoregulation induced by *Fasciola hepatica* and promotes infection. *Front Immunol* (2017) 8:883. doi:10.3389/fimmu.2017.00883
30. Kreider T, Anthony RM, Urban JF, Gause WC. Alternatively activated macrophages in helminth infections. *Curr Opin Immunol* (2007) 19(4):448–53. doi:10.1016/j.coi.2007.07.002
31. Alvarado R, To J, Lund ME, Pinar A, Mansell A, Robinson MW, et al. The immune modulatory peptide FhHDM-1 secreted by the helminth *Fasciola hepatica* prevents NLRP3 inflammasome activation by inhibiting endolysosomal acidification in macrophages. *FASEB J* (2017) 31(1):85–95. doi:10.1096/fj.201500093R
32. Donnelly S, O'Neill SM, Stack CM, Robinson MW, Turnbull L, Whitchurch C, et al. Helminth cysteine proteases inhibit TRIF-dependent activation of macrophages via degradation of TLR3. *J Biol Chem* (2010) 285(5):3383–92. doi:10.1074/jbc.M109.060368
33. Falcon C, Carranza F, Martinez FF, Knubel CP, Masih DT, Motran CC, et al. Excretory-secretory products (ESP) from *Fasciola hepatica* induce tolerogenic properties in myeloid dendritic cells. *Vet Immunol Immunopathol* (2010) 137(1–2):36–46. doi:10.1016/j.vetimm.2010.04.007
34. Hamilton CM, Dowling DJ, Loscher CE, Morphew RM, Brophy PM, O'Neill SM. The *Fasciola hepatica* tegumental antigen suppresses dendritic cell maturation and function. *Infect Immun* (2009) 77(6):2488–98. doi:10.1128/IAI.00919-08
35. Carranza F, Falcón C, Nuñez N, Knubel C, Correa S, Bianco I, et al. Helminth antigens enable CpG-activated dendritic cells to inhibit the symptoms of collagen-induced arthritis through Foxp3+ regulatory T cells. *PLoS One* (2012) 7(7):e40356. doi:10.1371/journal.pone.0040356
36. Falcon CR, Masih D, Gatti G, Sanchez MC, Motran CC, Cervi L. *Fasciola hepatica* Kunitz type molecule decreases dendritic cell activation and their ability to induce inflammatory responses. *PLoS One* (2014) 9(12):e114505. doi:10.1371/journal.pone.0114505
37. Aldridge A, O'Neill SM. *Fasciola hepatica* tegumental antigens induce anergic-like T cells via dendritic cells in a mannose receptor-dependent manner. *Eur J Immunol* (2016) 46(5):1180–92. doi:10.1002/eji.201545905
38. Rodríguez E, Kalay H, Noya V, Brossard N, Giacomini C, Van Kooyk Y, et al. *Fasciola hepatica* glycoconjugates immuneregulate dendritic cells through the dendritic cell-specific intercellular adhesion molecule-3-Grabbing Non-integrin inducing T cell anergy. *Sci Rep* (2017) 7:46748. doi:10.1038/srep46748
39. Allen JE, Maizels RM. Diversity and dialogue in immunity to helminths. *Nat Rev Immunol* (2011) 11(6):375–88. doi:10.1038/nri2992
40. Huang L, Appleton JA. Eosinophils in helminth infection: defenders and dupes. *Trends Parasitol* (2016) 32(10):798–807. doi:10.1016/j.pt.2016.05.004
41. Rotman HL, Yutanawiboonchai W, Brigandi RA, Leon O, Gleich GJ, Nolan TJ, et al. *Strongyloides stercoralis*: eosinophil-dependent immune-mediated killing of third stage larvae in BALB/cByJ mice. *Exp Parasitol* (1996) 82(3):267–78. doi:10.1006/expr.1996.0034
42. Lange AM, Yutanawiboonchai W, Scott P, Abraham D. IL-4-and IL-5-dependent protective immunity to *Onchocerca volvulus* infective larvae in BALB/cBYJ mice. *J Immunol* (1994) 153(1):205–11.
43. Meeusen E, Balic A. Do eosinophils have a role in the killing of helminth parasites? *Parasitol Today* (2000) 16(3):95–101. doi:10.1016/S0169-4758(99)01607-5
44. Shamri R, Xenakis JJ, Spencer LA. Eosinophils in innate immunity: an evolving story. *Cell Tissue Res* (2011) 343(1):57–83. doi:10.1007/s00441-010-1049-6
45. Huang L, Gebreselassie NG, Gagliardo LF, Ruyechan MC, Luber KL, Lee NA, et al. Eosinophils mediate protective immunity against secondary nematode infection. *J Immunol* (2015) 194(1):283–90. doi:10.4049/jimmunol.1402219
46. Stone KD, Prussin C, Metcalfe DD. IgE, mast cells, basophils, and eosinophils. *J Allergy Clin Immunol* (2010) 125(2 Suppl 2):S73–80. doi:10.1016/j.jaci.2009.11.017
47. Fabre V, Beiting DP, Bliss SK, Gebreselassie NG, Gagliardo LF, Lee NA, et al. Eosinophil deficiency compromises parasite survival in chronic nematode infection. *J Immunol* (2009) 182(3):1577–83. doi:10.4049/jimmunol.182.3.1577
48. Raadsma H, Kingsford N, Spithill T, Piedrafita D. Host responses during experimental infection with *Fasciola gigantica* or *Fasciola hepatica* in Merino sheep: I. Comparative immunological and plasma biochemical changes during early infection. *Vet Parasitol* (2007) 143(3):275–86. doi:10.1016/j.vetpar.2006.09.008
49. Moreau E, Chauvin A. Immunity against helminths: interactions with the host and the intercurrent infections. *Biomed Res Int* (2010) 2010:428593. doi:10.1155/2010/428593
50. Dean DA, Wistar R, Murrell KD. Combined in vitro effects of rat antibody and neutrophilic leukocytes on schistosomula of *Schistosoma mansoni*. *Am J Trop Med Hyg* (1974) 23(3):420–8. doi:10.4269/ajtmh.1974.23.420
51. Hsü S, Hsü H, Isacson P, Cheng H. In vitro schistosomulicidal effect of immune serum and eosinophils, neutrophils and lymphocytes. *J Reticuloendothel Soc* (1977) 21(3):153.
52. Kassis AI, Aikawa M, Mahmoud AA. Mouse antibody-dependent eosinophil and macrophage adherence and damage to schistosomula of *Schistosoma mansoni*. *J Immunol* (1979) 122(2):398–405.
53. Capron A, Dessaint J-P, Capron M, BAZIN H. Specific IgE antibodies in immune adherence of normal macrophages to *Schistosoma mansoni* schistosomules. *Nature* (1975) 253(5491):474. doi:10.1038/253474a0
54. Falduto GH, Vila CC, Saracino MP, Calcagno MA, Venturiello SM. *Trichinella spiralis*: killing of newborn larvae by lung cells. *Parasitol Res* (2015) 114(2):679–85. doi:10.1007/s00436-014-4233-x
55. Bass DA, Szejda P. Eosinophils versus neutrophils in host defense. Killing of newborn larvae of *Trichinella spiralis* by human granulocytes in vitro. *J Clin Invest* (1979) 64(5):1415–22. doi:10.1172/jci109599
56. Chen F, Wu W, Millman A, Craft JF, Chen E, Patel N, et al. Neutrophils prime a long-lived effector macrophage phenotype that mediates accelerated helminth expulsion. *Nat Immunol* (2014) 15(10):938–46. doi:10.1038/ni.2984
57. Blackwell NM, Else KJ. B cells and antibodies are required for resistance to the parasitic gastrointestinal nematode *Trichuris muris*. *Infect Immun* (2001) 69(6):3860–8. doi:10.1128/iai.69.6.3860-3868.2001

58. Gurish MF, Bryce PJ, Tao H, Kisselgof AB, Thornton EM, Miller HR, et al. IgE enhances parasite clearance and regulates mast cell responses in mice infected with *Trichinella spiralis*. *J Immunol* (2004) 172(2):1139–45. doi:10.4049/jimmunol.172.2.1139
59. Esser-von Bieren J, Mosconi I, Guiet R, Piersgilli A, Volpe B, Chen F, et al. Antibodies trap tissue migrating helminth larvae and prevent tissue damage by driving IL-4Ralpha-independent alternative differentiation of macrophages. *PLoS Pathog* (2013) 9(11):e1003771. doi:10.1371/journal.ppat.1003771
60. Berasain P, Carmona C, Frangione B, Dalton JP, Goni F. *Fasciola hepatica*: parasite-secreted proteinases degrade all human IgG subclasses: determination of the specific cleavage sites and identification of the immunoglobulin fragments produced. *Exp Parasitol* (2000) 94(2):99–110. doi:10.1006/expr.1999.4479
61. Guasconi L, Serradell MC, Masih DT. *Fasciola hepatica* products induce apoptosis of peritoneal macrophages. *Vet Immunol Immunopathol* (2012) 148(3–4):359–63. doi:10.1016/j.vetimm.2012.06.022
62. Serradell MC, Guasconi L, Cervi L, Chiapello LS, Masih DT. Excretory-secretory products from *Fasciola hepatica* induce eosinophil apoptosis by a caspase-dependent mechanism. *Vet Immunol Immunopathol* (2007) 117(3–4):197–208. doi:10.1016/j.vetimm.2007.03.007
63. Piedrafita D, Estuningsih E, Pleasance J, Prowse R, Raadsma HW, Meeusen EN, et al. Peritoneal lavage cells of Indonesian thin-tail sheep mediate antibody-dependent superoxide radical cytotoxicity in vitro against newly excysted juvenile *Fasciola gigantica* but not juvenile *Fasciola hepatica*. *Infect Immun* (2007) 75(4):1954–63. doi:10.1128/iai.01034-06
64. Sulaiman AA, Zolnierczyk K, Japa O, Owen JP, Maddison BC, Emes RD, et al. A trematode parasite derived growth factor binds and exerts influences on host immune functions via host cytokine receptor complexes. *PLoS Pathog* (2016) 12(11):e1005991. doi:10.1371/journal.ppat.1005991
65. James SL, Sher A, Lazdins JK, Meltzer MS. Macrophages as effector cells of protective immunity in murine schistosomiasis. II. Killing of newly transformed schistosomula in vitro by macrophages activated as a consequence of *Schistosoma mansoni* infection. *J Immunol* (1982) 128(4):1535–40.
66. Moser G, Sher A. Studies of the antibody-dependent killing of schistosomula of *Schistosoma mansoni* employing haptenic target antigens. II. In vitro killing of TNP-schistosomula by human eosinophils and neutrophils. *J Immunol* (1981) 126(3):1025–9.
67. Ward RE, McLaren DJ. *Schistosoma mansoni*: evidence that eosinophils and/or macrophages contribute to skin-phase challenge attrition in vaccinated CBA/Ca mice. *Parasitology* (1988) 96(Pt 1):63–84. doi:10.1017/S003118200008166X
68. Farthing MJ. Immune response-mediated pathology in human intestinal parasitic infection. *Parasite Immunol* (2003) 25(5):247–57. doi:10.1046/j.1365-3024.2003.00633.x
69. Melendez AJ, Harnett MM, Pushparaj PN, Wong WF, Tay HK, McSharry CP, et al. Inhibition of FcεRI-mediated mast cell responses by ES-62, a product of parasitic filarial nematodes. *Nat Med* (2007) 13(11):1375–81. doi:10.1038/nm1654
70. Jenkins SJ, Ruckerl D, Cook PC, Jones LH, Finkelman FD, van Rooijen N, et al. Local macrophage proliferation, rather than recruitment from the blood, is a signature of Th2 inflammation. *Science* (2011) 332(6035):1284–8. doi:10.1126/science.1204351
71. Nascimento M, Huang SC, Smith A, Everts B, Lam W, Bassity E, et al. Ly6Chi monocyte recruitment is responsible for Th2 associated host-protective macrophage accumulation in liver inflammation due to schistosomiasis. *PLoS Pathog* (2014) 10(8):e1004282. doi:10.1371/journal.ppat.1004282
72. Nair MG, Gallagher IJ, Taylor MD, Loke P, Coulson PS, Wilson RA, et al. Chitinase and Fizz family members are a generalized feature of nematode infection with selective upregulation of Ym1 and Fizz1 by antigen-presenting cells. *Infect Immun* (2005) 73(1):385–94. doi:10.1128/iai.73.1.385-394.2005
73. Chang N-CA, Hung S-I, Hwa K-Y, Kato I, Chen J-E, Liu C-H, et al. A macrophage protein, Ym1, transiently expressed during inflammation is a novel mammalian lectin. *J Biol Chem* (2001) 276(20):17497–506. doi:10.1074/jbc.M010417200
74. Owhashi M, Arita H, Hayai N. Identification of a novel eosinophil chemotactic cytokine (ECF-L) as a chitinase family protein. *J Biol Chem* (2000) 275(2):1279–86. doi:10.1074/jbc.275.2.1279
75. Sun YJ, Chang NC, Hung SI, Chang AC, Chou CC, Hsiao CD. The crystal structure of a novel mammalian lectin, Ym1, suggests a saccharide binding site. *J Biol Chem* (2001) 276(20):17507–14. doi:10.1074/jbc.M010416200
76. Liu T, Dhanasekaran SM, Jin H, Hu B, Tomlins SA, Chinnaiyan AM, et al. FIZZ1 stimulation of myofibroblast differentiation. *Am J Pathol* (2004) 164(4):1315–26. doi:10.1016/s0002-9440(10)63218-x
77. Gause WC, Wynn TA, Allen JE. Type 2 immunity and wound healing: evolutionary refinement of adaptive immunity by helminths. *Nat Rev Immunol* (2013) 13(8):607–14. doi:10.1038/nri3476
78. Allen JE, Wynn TA. Evolution of Th2 immunity: a rapid repair response to tissue destructive pathogens. *PLoS Pathog* (2011) 7(5):e1002003. doi:10.1371/journal.ppat.1002003
79. Sandler NG, Mentink-Kane MM, Cheever AW, Wynn TA. Global gene expression profiles during acute pathogen-induced pulmonary inflammation reveal divergent roles for Th1 and Th2 responses in tissue repair. *J Immunol* (2003) 171(7):3655–67. doi:10.4049/jimmunol.171.7.3655
80. Cervi L, Cejas H, Masih DT. Cytokines involved in the immunosuppressor period in experimental fasciolosis in rats. *Int J Parasitol* (2001) 31(13):1467–73. doi:10.1016/S0020-7519(01)00275-2
81. Song E, Ouyang N, Horbelt M, Antus B, Wang M, Exton MS. Influence of alternatively and classically activated macrophages on fibrogenic activities of human fibroblasts. *Cell Immunol* (2000) 204(1):19–28. doi:10.1006/cimm.2000.1687
82. Wynn TA, Barron L. Macrophages: master regulators of inflammation and fibrosis. *Semin Liver Dis* (2010) 30(3):245–57. doi:10.1055/s-0030-1255354
83. Lech M, Anders HJ. Macrophages and fibrosis: how resident and infiltrating mononuclear phagocytes orchestrate all phases of tissue injury and repair. *Biochim Biophys Acta* (2013) 1832(7):989–97. doi:10.1016/j.bbadis.2012.12.001
84. Herbert DR, Holscher C, Mohrs M, Arendse B, Schwegmann A, Radwanska M, et al. Alternative macrophage activation is essential for survival during schistosomiasis and downmodulates T helper 1 responses and immunopathology. *Immunity* (2004) 20(5):623–35. doi:10.1016/S1074-7613(04)00107-4
85. de Jesus AR, Silva A, Santana LB, Magalhaes A, de Jesus AA, de Almeida RP, et al. Clinical and immunologic evaluation of 31 patients with acute schistosomiasis mansoni. *J Infect Dis* (2002) 185(1):98–105. doi:10.1086/324668
86. Pesce JT, Ramalingam TR, Mentink-Kane MM, Wilson MS, El Kasmi KC, Smith AM, et al. Arginase-1-expressing macrophages suppress Th2 cytokine-driven inflammation and fibrosis. *PLoS Pathog* (2009) 5(4):e1000371. doi:10.1371/journal.ppat.1000371
87. Garside P, Kennedy MW, Wakelin D, Lawrence CE. Immunopathology of intestinal helminth infection. *Parasite Immunol* (2000) 22(12):605–12. doi:10.1046/j.1365-3024.2000.00344.x
88. Perrigoue JG, Marshall FA, Artis D. On the hunt for helminths: innate immune cells in the recognition and response to helminth parasites. *Cell Microbiol* (2008) 10(9):1757–64. doi:10.1111/j.1462-5822.2008.01174.x
89. Oppenheim JJ, Yang D. Alarmins: chemotactic activators of immune responses. *Curr Opin Immunol* (2005) 17(4):359–65. doi:10.1016/j.coi.2005.06.002
90. Yang D, Chen Q, Su SB, Zhang P, Kurosaka K, Caspi RR, et al. Eosinophil-derived neurotoxin acts as an alarmin to activate the TLR2-MyD88 signal pathway in dendritic cells and enhances Th2 immune responses. *J Exp Med* (2008) 205(1):79–90. doi:10.1084/jem.20062027
91. Anthony RM, Rutitzky LI, Urban JF Jr, Stadecker MJ, Gause WC. Protective immune mechanisms in helminth infection. *Nat Rev Immunol* (2007) 7(12):975–87. doi:10.1038/nri2199
92. Artis D, Grencis RK. The intestinal epithelium: sensors to effectors in nematode infection. *Mucosal Immunol* (2008) 1(4):252–64. doi:10.1038/mi.2008.21
93. Zhao A, Urban JF Jr, Anthony RM, Sun R, Stiltz J, van Rooijen N, et al. Th2 cytokine-induced alterations in intestinal smooth muscle function depend on alternatively activated macrophages. *Gastroenterology* (2008) 135(1):217–25.e1. doi:10.1053/j.gastro.2008.03.077
94. Klose CS, Artis D. Innate lymphoid cells as regulators of immunity, inflammation and tissue homeostasis. *Nat Immunol* (2016) 17(7):765–74. doi:10.1038/ni.3489

95. Yasuda K, Muto T, Kawagoe T, Matsumoto M, Sasaki Y, Matsushita K, et al. Contribution of IL-33-activated type II innate lymphoid cells to pulmonary eosinophilia in intestinal nematode-infected mice. *Proc Natl Acad Sci U S A* (2012) 109(9):3451–6. doi:10.1073/pnas.1201042109
96. Humphreys NE, Xu D, Hepworth MR, Liew FY, Grencis RK. IL-33, a potent inducer of adaptive immunity to intestinal nematodes. *J Immunol* (2008) 180(4):2443–9. doi:10.4049/jimmunol.180.4.2443
97. Artis D, Wang ML, Keilbaugh SA, He W, Brenes M, Swain GP, et al. RELMbeta/FIZZ2 is a goblet cell-specific immune-effector molecule in the gastrointestinal tract. *Proc Natl Acad Sci U S A* (2004) 101(37):13596–600. doi:10.1073/pnas.0404034101
98. von Moltke J, Ji M, Liang HE, Locksley RM. Tuft-cell-derived IL-25 regulates an intestinal ILC2-epithelial response circuit. *Nature* (2016) 529(7585):221–5. doi:10.1038/nature16161
99. Cliffe LJ, Humphreys NE, Lane TE, Potten CS, Booth C, Grencis RK. Accelerated intestinal epithelial cell turnover: a new mechanism of parasite expulsion. *Science* (2005) 308(5727):1463–5. doi:10.1126/science.1108661
100. Zaiss DM, Yang L, Shah PR, Kobie JJ, Urban JF, Mosmann TR. Amphiregulin, a TH2 cytokine enhancing resistance to nematodes. *Science* (2006) 314(5806):1746. doi:10.1126/science.1133715
101. Bouchery T, Kyle R, Camberis M, Shepherd A, Filbey K, Smith A, et al. ILC2s and T cells cooperate to ensure maintenance of M2 macrophages for lung immunity against hookworms. *Nat Commun* (2015) 6:6970. doi:10.1038/ncomms7970
102. McDermott JR, Bartram RE, Knight PA, Miller HR, Garrod DR, Grencis RK. Mast cells disrupt epithelial barrier function during enteric nematode infection. *Proc Natl Acad Sci U S A* (2003) 100(13):7761–6. doi:10.1073/pnas.1231488100
103. Shimokawa C, Kanaya T, Hachisuka M, Ishiwata K, Hisaeda H, Kurashima Y, et al. Mast cells are crucial for induction of group 2 innate lymphoid cells and clearance of helminth infections. *Immunity* (2017) 46(5):863–74.e4. doi:10.1016/j.immuni.2017.04.017
104. Zaiss MM, Maslowski KM, Mosconi I, Guenat N, Marsland BJ, Harris NL. IL-1beta suppresses innate IL-25 and IL-33 production and maintains helminth chronicity. *PLoS Pathog* (2013) 9(8):e1003531. doi:10.1371/journal.ppat.1003531

Conflict of Interest Statement: The authors declare that the research was conducted in the absence of any commercial or financial relationships that could be construed as a potential conflict of interest.

Copyright © 2018 Motran, Silvane, Chiapello, Theumer, Ambrosio, Volpini, Celias and Cervi. This is an open-access article distributed under the terms of the Creative Commons Attribution License (CC BY). The use, distribution or reproduction in other forums is permitted, provided the original author(s) and the copyright owner are credited and that the original publication in this journal is cited, in accordance with accepted academic practice. No use, distribution or reproduction is permitted which does not comply with these terms.

frontiers in Immunology

REVIEW
published: 29 November 2017
doi: 10.3389/fimmu.2017.01677

The Mannose Receptor in Regulation of Helminth-Mediated Host Immunity

Irma van Die[1]* *and Richard D. Cummings*[2]

[1] Department of Molecular Cell Biology and Immunology, VU University Medical Center, Amsterdam, Netherlands,
[2] Department of Surgery, Beth Israel Deaconess Medical Center, Harvard Medical School, Boston, MA, United States

Infection with parasitic helminths affects humanity and animal welfare. Parasitic helminths have the capacity to modulate host immune responses to promote their survival in infected hosts, often for a long time leading to chronic infections. In contrast to many infectious microbes, however, the helminths are able to induce immune responses that show positive bystander effects such as the protection to several immune disorders, including multiple sclerosis, inflammatory bowel disease, and allergies. They generally promote the generation of a tolerogenic immune microenvironment including the induction of type 2 (Th2) responses and a sub-population of alternatively activated macrophages. It is proposed that this anti-inflammatory response enables helminths to survive in their hosts and protects the host from excessive pathology arising from infection with these large pathogens. In any case, there is an urgent need to enhance understanding of how helminths beneficially modulate inflammatory reactions, to identify the molecules involved and to promote approaches to exploit this knowledge for future therapeutic interventions. Evidence is increasing that C-type lectins play an important role in driving helminth-mediated immune responses. C-type lectins belong to a large family of calcium-dependent receptors with broad glycan specificity. They are abundantly present on immune cells, such as dendritic cells and macrophages, which are essential in shaping host immune responses. Here, we will focus on the role of the C-type lectin macrophage mannose receptor (MR) in helminth–host interactions, which is a critically understudied area in the field of helminth immunobiology. We give an overview of the structural aspects of the MR including its glycan specificity, and the functional implications of the MR in helminth–host interactions focusing on a few selected helminth species.

Keywords: C-type lectin, mannose receptor, helminth, schistosoma, trichuris, immune regulation

OPEN ACCESS

Edited by:
Yoann Rombouts,
UMR5089 Institut de Pharmacologie et de Biologie Structurale (IPBS), France

Reviewed by:
Keke Celeste Fairfax,
Purdue University, United States
Alan L. Scott,
Johns Hopkins University, United States

***Correspondence:**
Irma van Die
im.vandie@vumc.nl

Specialty section:
This article was submitted to Microbial Immunology, a section of the journal Frontiers in Immunology

Received: *14 September 2017*
Accepted: *15 November 2017*
Published: *29 November 2017*

Citation:
van Die I and Cummings RD (2017) The Mannose Receptor in Regulation of Helminth-Mediated Host Immunity. Front. Immunol. 8:1677. doi: 10.3389/fimmu.2017.01677

INTRODUCTION

Parasites have been a great burden to human health throughout many centuries. Parasitic helminths (worms) are a large and important group of parasites that cause diseases, such as ascariasis, filariasis, and schistosomiasis, which are often endemic in tropical areas.

Over the past 20–30 years it has been observed in the Western world that a correlation exists between an effective hygiene and the increase in atopic, autoimmune, and inflammatory diseases. These findings are reflected in the "hygiene hypothesis" (1, 2), and led to the concept that in the developed world the reduction in exposure to helminths affects the immunoregulatory mechanisms of our immune system (3, 4). The existence of a long and close association between helminths and

their hosts is proposed to have been the driving force of the co-evolution of helminth and host mechanisms that ameliorate harmful inflammatory responses. These enable helminths to survive and protect the host from excessive pathology arising from infection with these large pathogens (5).

The anti-inflammatory consequences of helminth infections are further supported by the observations that either infection with parasitic helminths or systemic treatment with helminth extracts can reduce the symptoms of allergic diseases (6) and inflammation associated with autoimmune diseases. The latter include inflammatory bowel diseases (7, 8), multiple sclerosis (9–12), or rheumatoid arthritis (13, 14), as well as metabolic disorders such as obesities (15–17), diabetes (18, 19), or atherosclerosis (20). From this perspective, there is some rationale in regarding parasitic helminths, as long as they do not induce obvious pathology, as potentially beneficial commensals rather than dangerous pathogens that need to be expelled. Along this way, infection with helminth parasites is being explored as a potential therapy for a variety of diseases in clinical trials (21).

Increased understanding of the nature of helminth effects on the immune system could enable new treatment options for parasitic diseases, or beneficially modulate inflammatory reactions. Such studies could lead to identification of the molecules involved and promote approaches to exploit this knowledge for future therapeutic interventions. In this regard, there is increasing evidence that carbohydrate-binding proteins, and specifically C-type lectins, play an important role in driving helminth-mediated immune responses (22, 23). C-type lectins are a large family of calcium-dependent receptors and each member has a relatively unique carbohydrate (glycan)-binding specificity. These lectins are abundantly present on immune cells that shape host immune responses and collectively they can recognize a wide variety of glycans.

HELMINTH INFECTION AND HELMINTH-INDUCED IMMUNE REACTIONS

Infection with parasitic helminths typically induces a type 2 (Th2) immune response and promotes the generation of alternatively activated macrophages (AAMs) and eosinophils. Soon after infection, innate responses are initiated by many different cell types [including antigen-presenting cells such as dendritic cells (DCs) and macrophages], which, upon encountering the invading parasites, promote the suppression of T-cell-driven protective immune responses and a shift to Th2 responses. The helminth-driven Th1/Th2 immune responses are controlled through the generation of regulatory networks, which can include FoxP3+ regulatory T cells (Treg), anergic/hyporesponsive T cells, regulatory monocytes/macrophages, and/or B cells.

It is possible that evolution of different types of helminths has resulted in relatively similar pattern of immune responses in infected hosts. Many different molecules, receptors, and host cells cooperate and interact, generating mechanisms that have evolved to achieve a balance between host and parasite, dependent on the living environment and biology of the parasites. To dissect the different molecular mechanisms and signaling pathways involved, experimental data with isolated soluble products are essential. Several of such helminth products have been purified and studied in animal models and *in vitro* assays with antigen-presenting cells (24–29). These parasite-derived molecules include secreted glycoconjugates, e.g., glycoproteins and glycolipids, which play important roles in host immune modulation. The helminth-derived glycans can interact with immune cell-expressed C-type lectins [termed C-type lectin receptors (CLRs)] and other glycan-binding proteins, such as galectins, and these interactions help to shape the innate and adaptive immune responses (22, 23, 30). Because helminths do not express sialic acid, they do not appear to interact with the Siglec family of sialic acid-binding lectins on immune cells. Dendritic cells express many different CLRs, including DC-SIGN, Dectin-1, MGL, and the mannose receptor (MR); their expression can vary within distinct DC subsets. CLRs can act as endocytic and/or signaling receptors, and play major roles in both innate and adaptive immune responses often in concerted action with other CLRs and/or toll-like receptors (TLRs) (31–33). One of the best studied CLRs is the human DC-SIGN (31, 34), which typically binds glycans containing terminal fucose or mannose residues (35), such as fucosylated glycans of *Schistosoma mansoni*, including Lewis-X [Galβ1-4(Fucα1-3)GlcNAc-], LDNF [GalNAcβ1-4(Fucα1-3)GlcNAc-], and the schistosome-specific pseudo-LeY ligand [Fucα1-3Galβ1-4(Fucα1-3)GlcNAc-] (35–38). Remarkably, DC-SIGN induces distinct signaling pathways dependent on the type of glycan that is recognized (39, 40). Similar to DC-SIGN, the MR typically recognizes mannose- and fucose-containing glycans in both trematode and nematode parasites, but its glycan specificity and functions are less well understood.

THE MANNOSE RECEPTOR

Structural Properties of the MR

The MR is expressed by a selected population of myeloid cells and non-vascular endothelium and has been implicated in helminth-induced modulation of host immune responses. The MR is a type I membrane glycoprotein of 165 kDa that is comprised of a cytoplasmic domain of 45 amino acids and three types of extracellular domains as shown in **Figure 1**. These domains are an N-terminal cysteine-rich domain, followed by a fibronectin type II repeat (FNII), and eight consecutive C-type lectin-like

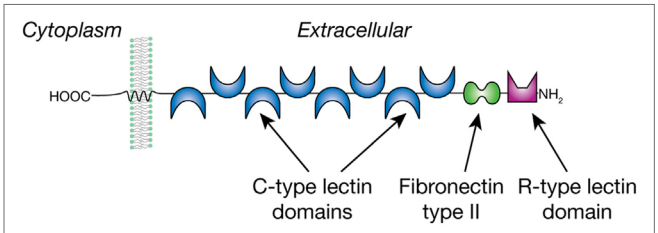


FIGURE 1 | The mannose receptor is a type 1 membrane glycoprotein with multiple C-type lectin domains that can bind mannose- and fucose-containing glycans and an R-type lectin domain that binds sulfated Gal/GalNAc residues.

domains (CRDs) (41). The MR was originally described as an endocytic receptor with a broad binding specificity for both microbial and endogenous ligands and constantly cycles from the cell surface to the cytoplasm (42, 43). More recently, there is evidence that the MR is also involved in cellular activation and signaling. However, the signaling activity of the MR is unusual, since the receptor does not have clear signaling motifs in its cytoplasmic domain; thus, the mechanisms and potential signaling pathways may involve the action of co-receptor(s) and are poorly understood (44).

Glycan Specificity of the MR

The MR is unique among the CLRs in that it consists of multiple carbohydrate-recognition domains (CRDs) (**Figure 1**). The N-terminal domain is an R-type domain that binds in a calcium-independent manner to glycans that have a non-reducing terminal 3-*O*-sulfated galactose or 3/4-*O*-sulfated-*N*-acetylgalactosamine (45). The FN II domain is involved in binding collagens (46). The MR was eponymously named by its property of binding to mannose, which is mediated within the C-type lectin domains 4–8. Fibroblast expression studies showed that CRD 4 has the major affinity for carbohydrate, whereas CRDs 5 and 7 appear to contribute to the binding capacity of mannose-containing glycans. Removal of CRDs 1–3 did not affect affinity for the ligands tested (47), and their roles, if any, in glycan binding is unknown. *In vitro* binding studies with the MR showed its preferential but weak interaction with both the monosaccharides Man and Fuc above other monosaccharides (48). With more complex glycans the MR shows a preference for Manα1-6Man-R and Manα1-3Man-R compared to α1-2/4-linked Man residues, whereas the branched mannotrioside Manα1-6(Manα1-3) Man-R showed the highest affinity to the MR. Of the fucosylated ligands tested, Fucα1-6GlcNAc-R showed a similar affinity as the branched mannotrioside, whereas binding to Fucα1-2Gal-R was lower and α1-3/4-linked Fuc was not tested. The latter linkage is found in the Lewis antigens to which the MR does not bind (49), in contrast to the C-type lectin DC-SIGN (37), which is also expressed by DCs and shares with the MR a preference for mannose/fucose/GlcNAc. The MR selectivity for Manα1-3/6Man corresponds well to its function as a pathogen receptor, considering the abundance of these termini in yeast mannans, and the presence in helminths of paucimannose-*N*-glycans such as $Man_3GlcNAc_2$-Asn (23). It is likely that the multivalent nature of the MR facilitates high avidity interactions with multivalent or repetitive glycan-ligands, which occur in many microorganisms, fungi, and parasites (48). Whereas multivalent binding by most CLRs is mediated by multimer-forming of lectin molecules, the presence of multiple CRDs in the MR is thought to promote its multivalent binding within a single MR molecule. This implies that the binding affinity of the MR highly depends both on valency and structural characteristics of a particular glycoconjugate (47).

The glycosylation of the MR may further fine-tune its binding to ligands (50). The MR contains many Asn-linked N-glycans, and their structures in the mouse appear to be tissue specific (51). Terminal sialylation of glycans on the MR is of special interest, since it has been suggested that this may affect the MR binding properties to mannosylated glycans, whereas non-sialylated or neutral glycans might affect the avidity for sulfated carbohydrate ligands (50). Such differential glycosylation of the MR might not only influence its binding properties to exogenous ligands but might also influence its interactions with other receptors on the cell membrane, thereby possibly modulating MR functions.

Expression of the MR on Immune Cells

The MR is primarily expressed on human and mouse DCs and macrophages (MF), but it is also found on other cells, such as non-vascular endothelial cells (44). Interestingly, the MR is largely found intracellularly in membranous structures, and only 10–30% is expressed at the cell surface under steady state conditions (43); this is consistent with the recycling and internalization nature of the receptor. The Th2 cytokines interleukin (IL)-4, IL-13, and IL-10 (52–54) as well as prostaglandins PGE1 and PGE2 (55) upregulate MR expression on murine macrophages; in human macrophages generated *in vitro* culture with human serum, activation by treatment with IL-4 results in significantly increased MR expression (56). The MR is expressed at low levels on naïve monocytes. Monocytes constitute around 10% of total leukocytes in blood and are key players of the human innate immune response. Blood-derived monocytes are an independent cell lineage that has the ability to differentiate into specific DC and macrophage populations, which often constitutively express the MR. In monocytes, the expression of the MR is induced upon maturation (44), and specific (pro-inflammatory) subsets of monocytes have been reported to be MR positive (57). Interestingly, a sub-population of monocytes with an enhanced expression of the MR has been identified in patients with asymptomatic filarial infection; such expression is correlated with enhanced expression of the suppressor of cytokine signaling-1 (SOCS-1) and the cytokines IL-10 and transforming growth factor β (TGFβ) (58). We recently observed a similar monocyte phenotype in helminth-infected Ethiopian individuals (unpublished observation). Furthermore, human monocytes treated *in vitro* with soluble components (SPs) of the whipworm *Trichuris suis* induce a sub-population of anti-inflammatory patrolling monocytes with enhanced CD16, IL-10, and MR protein expression (59). These data indicate that interaction with helminth components, either directly or indirectly *via* the induction of Th2 cytokines, can induce expression of the MR on monocytes. Such modulated monocytes may differentiate to AAMs, as are known to be induced by helminths (60). Indeed, human monocytes treated *in vitro* with *T. suis* SPs differentiate into a subset of macrophages with enhanced AAM properties, including elevated MR expression and IL-10 production (61). An interesting possibility is that the helminth-induced MR expression on AAMs may be relevant for the known role of AAMs in wound healing. A common property of helminths is that they need to migrate in the hosts as part of their life cycles, and this causes extensive tissue damage. The ability of helminths to thus limit host-damage may promote their survival in the hosts. In summary, these data indicate that helminths modulate the phenotype of human blood monocytes, which in turn may lead to the generation of AAMs expressing the MR.

THE MR IN HELMINTH-MEDIATED IMMUNE RESPONSES

Whereas enhanced expression of the MR is observed upon contact with helminths as described above, the role of the MR in modulating immune responses is still unclear. The MR interacts with and internalizes components of several helminth species, and this is often associated with the induction of anti-inflammatory or Th2 responses (**Table 1**).

Flatworm Trematodes Interacting with the MR

The interaction of the MR has been reported both with the bloodfluke *S. mansoni* and with the liver fluke *Fasciola hepatica* (**Table 1**). *S. mansoni* is a human parasite causing schistosomiasis (bilharzia), affecting millions of individuals especially in tropical areas (72). *S. mansoni* can also infect rodents, which are often used as model system to study the immunobiology of the disease. *F. hepatica* primarily infects sheep and cattle causing fascioliasis, but is also an important emerging pathogen of humans (73).

Schistosoma mansoni—Th2 polarization by infection with *S. mansoni* and exposure to *S. mansoni* antigens involves the induction of tolerogenic DCs and the expansion of regulatory cell populations (including IL-10 secreting and Foxp3-expressing Tregs) (74–76). The immune response against *S. mansoni* infection begins at the earliest stage of infection, when cercaria gain entry to the mammalian host *via* the skin, which initially stimulates the innate immune response. During transformation from cercariae to schistosomula within 72 h after infection, the parasite secretes large amounts of highly glycosylated components, termed excretory/secretory (E/S) products. Mononuclear phagocytic cells in the skin internalize E/S products released by the schistosomula *via* the MR (66). In addition, it was shown that the ligation of the MR by *S. mansoni* larval E/S products has a major role in limiting the production of pro-inflammatory cytokines (66), which may prime the immune system for the subsequent development of a Th2 response.

After maturation of the larvae to adult worm pairs of female/male, eggs are deposited that secrete soluble egg components. One of these components is Omega-1, a major secreted egg glycoprotein RNase, which is capable of inducing a Th2 response (25, 77, 78). It has been proposed that the MR on DCs is essential for internalization of Omega-1, which subsequently acts as an RNase to degrade RNA thereby impairing protein synthesis (25, 64). Intraperitoneal injection of obese mice with Omega-1 resulted in a Th2 immune response in the white adipose tissue, improving glucose tolerance and induction of a transient delay in weight gain (79). Whereas IL-33 release from cells in the adipose tissue was mediated by the RNase activity of Omega-1, its ability to improve metabolic status was shown to be dependent upon effective binding to the MR (79).

We recently showed that SEA, both untreated and heat-treated (in which RNases and thus Omega-1 activity were eliminated), potently suppressed LPS-induced TNF and IL12 production and upregulated SOCS-1, SHP-1, and OX40L expression in human DCs (65); these are phenotypic and functional changes in DCs associated with Th2 polarization. Remarkably, treatment of SEA with periodate (PI) (in which glycans are oxidized and lose their recognition potential), causes a loss of the inducing activity, suggesting an important role of SEA glycans in regulating DC function. Similarly, CD4+ T cell proliferation was suppressed by the addition of DCs primed with either untreated or heat-treated SEA, but suppression was not observed by using PI-treated SEA (65). The SEA-induced upregulation of expression of SOCS-1 and SHP-1 appeared to be MR-dependent. These data indicate that RNase activities within SEA are not essential to induce Th2 polarizing DCs in the human system; however, it is possible that glycans linked to Omega-1 and/or other MR-ligands trigger the MR to induce inhibition of pro-inflammatory responses, perhaps similar to the larval E/S products (66).

Many reports have described a potential role of parasite-derived glycans in modulation of schistosome-mediated immune responses (39, 66, 80–82). The observation that PI-treated SEA has a strongly decreased ability to modulate DC function, compared to heat-treated and untreated SEA, also indicates that

TABLE 1 | Interaction of the mannose receptor (MR) with helminth components, and immunological parameters.

Helminth	Components	Effects	Reference
Schistosoma mansoni	SEA	Interaction with MR (h, m), internalization in dendritic cells (DCs) (h)	(62, 63)
	Omega-1	Internalization of Omega-1 by MR in DCs (h)	(64)
	SEA	MR-dependent expression of suppressor of cytokine signaling-1 and SHP1 on DCs (h)	(65)
	Larval E/S	Binding Larval E/S products by MR; reduction INF production, stimulation Th2 responses (m)	(66)
Fasciola hepatica	E/S products	Induction high levels of transforming growth factor β and interleukin (IL)-10 in macrophages (m)	(67)
	Tegumental coat proteins	Binding to BMDCs (m)	(68)
Trichuris suis	SWP	Inducing enhanced motility of monocytes (h)	(59)
	SWP	Enhancing IL-10 and reducing CCR2 expression on monocytes (h)	(59)
Trichuris muris		Binding of BMDM and production of IL-6 (m)	(69)
Trichinella spiralis	SP L1 larvae	Binding to macrophages, stimulation of NO secretion (m)	(70)
Ascaris suum	High MW SWP	Inhibition LPS-induced BMDCs maturation and *in vitro* T cell proliferation (m)	(71)

h, human; m, mouse; SEA, soluble egg proteins; SWP, soluble worm products; E/S, excretory secretory products; MW, molecular weight.

glycans within SEA play an important role in polarization of DC-mediated immune responses (65). The observation that Omega-1, in contrast to SEA, has no potential to inhibit T-cell proliferation (83) suggests that SEA contains additional components that contribute to modulation of the host's immune response; thus, it will be important to identify the SEA components that are responsible for these properties. One possibility is that the lipid mediator prostaglandinE_2 (PGE_2) contributes to SEA-induced immune responses. SEA preparations have been shown to contain the lipid mediator PGE_2 (27, 84), and PGE_2 has been shown to have the potential to induce Th2 responses (27, 85). Remarkably, it appears that the activity of PGE_2 is PI-sensitive (27), which shows that deducing a role for glycans based only on PI sensitivity of the putative compounds should be regarded with caution. In conclusion, there may be several pathways and multiple schistosome components mechanistically involved in the suppression of inflammatory responses and Th2 polarization, some of which essentially involve a role of the MR.

Fasciola hepatica—As observed with many other helminths, infection with *F. hepatica* leads to downregulation of Th1 immune responses and the generation of Th2 immune responses in mice (29, 86). During infection, the parasites release a myriad of different products (E/S products and tegumental antigens) that downregulate Th1 responses and promote Th2 responses, including development of AAMs with immunomodulatory potential (29, 87). Macrophages stimulated with *F. hepatica* E/S products show enhanced MR, Arg-1, TGF-β, IL-10, and PD-L1 expression and a reduced potential to respond to LPS activation (67, 88). Furthermore, blocking the MR with the mannan hapten or an anti-MR blocking antibody resulted in a partial loss of the macrophages' inflammatory phenotype. Interestingly, similar effects were observed when mice were intraperitoneally injected with mannan before being infected (67).

Fasciola hepatica tegumental antigens (FhTeg) enhance expression of the negative regulator SOCS3 (89) and the MR (90) on BMDCs, which may contribute to its immune modulatory properties, such as the induction of T-cell anergy or T-cell hyporesponsiveness (90). Interaction of FhTeg, which contains glycoproteins with oligo-mannose-type glycans, with BMDCs was partly MR-dependent (68). On the other hand, the ability of FhTeg to induce SOCS3 or suppress cytokine secretion from LPS activated BMDCs appeared not to be MR-dependent, as was demonstrated by the use of MR-deficient BMDCs (68), indicating that other mechanistic pathways are involved. The enhanced MR expression on the FhTeg-treated BMDCs has been suggested to be involved in induction of T-cell anergy. DC-CD4+ T-cell communication appeared to be MR-dependent, as was deduced from a reduced ability of MR-deficient BMDCs to enhance expression of the anergic markers GRAIL and CTLA4 on CD4+ T-cells, and a reversal of the suppression of IL-2 and IFN-γ compared to mock-treated BMDCs (90). These data illustrate a role for the MR in the immunoregulatory properties of both murine macrophages and BMDCs upon interaction with *F. hepatica* components.

Whipworms Interacting with the MR

Parasitic nematodes of the order Trichocephalida (whipworms) contain several genera of medical importance including *Trichuris* and *Trichinella* species. Human infection with *Trichuris trichuria* and *Trichinella spiralis* typically occurs after ingestion of contaminated food. *Trichuris muris* is often used as a natural mouse model of *T. trichiura*. The pig whipworm *T. suis* has strong anti-inflammatory properties (27, 91, 92) and transient infection with these parasites, which are not able to reproduce and lack long-term survival in non-pig mammals, are being investigated as a natural treatment for human inflammatory diseases, such as inflammatory bowel disease and multiple sclerosis (21). Studies with *T. muris* in different mouse models and *T. suis* infection in pigs have shown that a Th2-dominated immune response is required for worm expulsion (93, 94), whereas the development of a Th1 response leads to host susceptibility (94).

A Th2-dominated response includes the generation of AAMs which typically express the MR. *T. muris* E/S products contain components that bind to the MR; however, a functional role *in vivo* for the MR in worm expulsion could not be demonstrated (69). Knockdown of the MR revealed a role of the MR in the production of IL-6 by the AAMs, but no effect on the expulsion of the parasite (69). This suggests that either the MR may not be involved in expulsion of the parasite or alternative pathways compensate for the loss of the MR. Interaction of *T. spiralis* L1 larvae with the MR expressed on the surface of peritoneal macrophages did not mediate IL-6 secretion, but resulted in an enhanced NO production, suggesting that the MR contributes to macrophage activation.

Human DCs bind soluble components of *T. suis via* C-type lectins including the MR (59, 91). To date, no clear role for the MR has been demonstrated upon interaction of *T. suis* components with DCs (unpublished observations). However, monocytes showed an enhanced expression of the MR upon treatment with *T. suis* components associated with the generation of a non-classical phenotype (59). In addition, treatment of endothelial cells with *T. suis* resulted in an enhanced motility and reduced trans-endothelial migration in an *in vitro* model of the blood–brain barrier. The presence of MR blocking antibody significantly inhibited the *T. suis*-induced patrolling behavior of monocytes and rescued the *T. suis*-induced reduction in monocyte trans-endothelial migration. In addition, the MR can induce these properties in monocytes *via* downstream signaling including the action of protein kinase C (PKC) (59). This indicates that the MR is critically involved in the monocyte modulation.

DISCUSSION AND FUTURE PROSPECTS

The MR is an important CLR that interacts with a number of products generated by a variety of helminths, and clearly plays a role in modulating host immune responses, but many questions remain about its functional mechanisms. Due to its presence on different cells in the immune system, ligation of the MR might lead to different signaling consequences, but whether the MR can signal alone or requires co-receptors is unknown. In addition, the presence of multiple carbohydrate-binding domains in the MR allows differential binding of natural glycan ligands and differential effects. Little is known about the MR binding specificity to natural ligands of pathogens including helminths, and this is an important aspect to address. The ambiguity of the

MR role is also illustrated by the observation that DCs, primed with some natural ligands of the MR, such as MUC III, biglycan, and *Mycobacterium tuberculosis* mannosylated lipoarabinomannan, inhibit the generation of Th1-polarized immune responses, whereas other ligands that also bind the MR, such as thyroglobulin, had no effect (95).

The observation that glycosylation of the MR itself influences its glycan-binding properties, suggests that the function of the MR can vary dependent on the cells that express the lectin and their activation status and ability to glycosylate the MR. It is known that in DCs, for example, their glycosylation dramatically changes during cellular activation (96), which may result in changes of the glycosylation state of the expressed MR, but this has not yet been demonstrated.

Since the cytoplasmic domain of the MR has no clear signaling motifs, it has been assumed that the MR cannot directly induce downstream signaling upon ligand binding. We recently demonstrated, however, that the MR is critically involved in PKC signaling in monocytes (59), and many of the effects observed for MR ligation imply its signaling potential. The most likely explanation is that the MR may be needed for concerted action with another receptor that may be more directly involved in signaling, and that the primary role of the MR may be in capturing and/or internalizing a ligand. For example, collaboration of the MR with Dectin-1 has been suggested to be important in inducing high levels of TGF-β and IL-10 in macrophages upon stimulation with *F. hepatica* E/S products (67). Furthermore, the MR and TLR2 are both critically involved in pro-inflammatory cytokine production by human monocytes in response to *Pseudomonas aeruginosa* infection (97). Thus, the MR may indirectly influence signaling cascades in immune cells, but the exact mechanism of how this collaboration takes place is unknown.

The MR is one of the most unique CLRs produced by animals. The ability of this receptor to bind a wide variety of mannose- and fucose-containing ligands puts it at the forefront of the innate immune response to pathogens rich in such glycan signatures. While there are many aspects of MR functioning and glycan recognition yet to be discovered, there are exciting translational opportunities as the glycan ligands that regulate MR activity are identified and allow us to exploit its anti-inflammatory and regulatory functions.

AUTHOR CONTRIBUTIONS

All authors listed have made a substantial, direct, and intellectual contribution to the work and approved it for publication.

ACKNOWLEDGMENTS

The work of the authors was partly supported by NIH Grant AI101982. The authors thank Jamie Heimburg-Molinaro for critical reading of the manuscript.

REFERENCES

1. Strachan DP. Hay fever, hygiene, and household size. *BMJ* (1989) 299:1259–60. doi:10.1136/bmj.299.6710.1259
2. Yazdanbakhsh M, Matricardi PM. Parasites and the hygiene hypothesis: regulating the immune system? *Clin Rev Allergy Immunol* (2004) 26:15–24. doi:10.1385/CRIAI:26:1:15
3. Kuijk LM, van Die I. Worms to the rescue: can worm glycans protect from autoimmune diseases? *IUBMB Life* (2010) 62:303–12. doi:10.1002/iub.304
4. Rook GA. Review series on helminths, immune modulation and the hygiene hypothesis: the broader implications of the hygiene hypothesis. *Immunology* (2009) 126:3–11. doi:10.1111/j.1365-2567.2008.03007.x
5. Maizels RM, Yazdanbakhsh M. Immune regulation by helminth parasites: cellular and molecular mechanisms. *Nat Rev Immunol* (2003) 3:733–44. doi:10.1038/nri1183
6. Godfrey RC. Asthma and IgE levels in rural and urban communities of The Gambia. *Clin Allergy* (1975) 5:201–7. doi:10.1111/j.1365-2222.1975.tb01853.x
7. Elliott DE, Li J, Blum A, Metwali A, Qadir K, Urban JF Jr, et al. Exposure to schistosome eggs protects mice from TNBS-induced colitis. *Am J Physiol Gastrointest Liver Physiol* (2003) 284:G385–91. doi:10.1152/ajpgi.00049.2002
8. Elliott DE, Weinstock JV. Helminthic therapy: using worms to treat immune-mediated disease. *Adv Exp Med Biol* (2009) 666:157–66. doi:10.1007/978-1-4419-1601-3_12
9. La Flamme AC, Ruddenklau K, Backstrom BT. Schistosomiasis decreases central nervous system inflammation and alters the progression of experimental autoimmune encephalomyelitis. *Infect Immun* (2003) 71:4996–5004. doi:10.1128/IAI.71.9.4996-5004.2003
10. Correale J, Farez M, Razzitte G. Helminth infections associated with multiple sclerosis induce regulatory B cells. *Ann Neurol* (2008) 64:187–99. doi:10.1002/ana.21438
11. Fleming JO. Helminth therapy and multiple sclerosis. *Int J Parasitol* (2013) 43:259–74. doi:10.1016/j.ijpara.2012.10.025
12. Kuijk LM, Klaver EJ, Kooij G, van der Pol SM, Heijnen P, Bruijns SC, et al. Soluble helminth products suppress clinical signs in murine experimental autoimmune encephalomyelitis and differentially modulate human dendritic cell activation. *Mol Immunol* (2012) 51:210–8. doi:10.1016/j.molimm.2012.03.020
13. McInnes IB, Leung BP, Harnett M, Gracie JA, Liew FY, Harnett W. A novel therapeutic approach targeting articular inflammation using the filarial nematode-derived phosphorylcholine-containing glycoprotein ES-62. *J Immunol* (2003) 171:2127–33. doi:10.4049/jimmunol.171.4.2127
14. Pearson DJ, Taylor G. The influence of the nematode *Syphacia oblevata* on adjuvant arthritis in the rat. *Immunology* (1975) 29:391–6.
15. Wu D, Molofsky AB, Liang HE, Ricardo-Gonzalez RR, Jouihan HA, Bando JK, et al. Eosinophils sustain adipose alternatively activated macrophages associated with glucose homeostasis. *Science* (2011) 332:243–7. doi:10.1126/science.1201475
16. Hussaarts L, Yazdanbakhsh M, Guigas B. Priming dendritic cells for th2 polarization: lessons learned from helminths and implications for metabolic disorders. *Front Immunol* (2014) 5:499. doi:10.3389/fimmu.2014.00499
17. van den Berg SM, van Dam AD, Kusters PJ, Beckers L, den Toom M, van der Velden S, et al. Helminth antigens counteract a rapid high-fat diet induced decrease in adipose tissue eosinophils. *J Mol Endocrinol* (2017) 59:245–55. doi:10.1530/JME-17-0112
18. Cooke A, Tonks P, Jones FM, O'Shea H, Hutchings P, Fulford AJ, et al. Infection with *Schistosoma mansoni* prevents insulin dependent diabetes mellitus in non-obese diabetic mice. *Parasite Immunol* (1999) 21:169–76. doi:10.1046/j.1365-3024.1999.00213.x
19. Zaccone P, Burton O, Miller N, Jones FM, Dunne DW, Cooke A. *Schistosoma mansoni* egg antigens induce Treg that participate in diabetes prevention in NOD mice. *Eur J Immunol* (2009) 39:1098–107. doi:10.1002/eji.200838871
20. Wolfs IM, Stoger JL, Goossens P, Pottgens C, Gijbels MJ, Wijnands E, et al. Reprogramming macrophages to an anti-inflammatory phenotype by helminth antigens reduces murine atherosclerosis. *FASEB J* (2014) 28:288–99. doi:10.1096/fj.13-235911
21. Fleming JO, Weinstock JV. Clinical trials of helminth therapy in autoimmune diseases: rationale and findings. *Parasite Immunol* (2015) 37:277–92. doi:10.1111/pim.12175
22. Meevissen MH, Yazdanbakhsh M, Hokke CH. *Schistosoma mansoni* egg glycoproteins and C-type lectins of host immune cells: molecular partners

that shape immune responses. *Exp Parasitol* (2012) 132:14–21. doi:10.1016/j.exppara.2011.05.005
23. van Die I, Cummings RD. Glycan gimmickry by parasitic helminths: a strategy for modulating the host immune response? *Glycobiology* (2010) 20:2–12. doi:10.1093/glycob/cwp140
24. Navarro S, Pickering DA, Ferreira IB, Jones L, Ryan S, Troy S, et al. Hookworm recombinant protein promotes regulatory T cell responses that suppress experimental asthma. *Sci Transl Med* (2016) 8:362ra143. doi:10.1126/scitranslmed.aaf8807
25. Everts B, Perona-Wright G, Smits HH, Hokke CH, van der Ham AJ, Fitzsimmons CM, et al. Omega-1, a glycoprotein secreted by *Schistosoma mansoni* eggs, drives Th2 responses. *J Exp Med* (2009) 206:1673–80. doi:10.1084/jem.20082460
26. Harnett W, Deehan MR, Houston KM, Harnett MM. Immunomodulatory properties of a phosphorylcholine-containing secreted filarial glycoprotein. *Parasite Immunol* (1999) 21:601–8. doi:10.1046/j.1365-3024.1999.00267.x
27. Laan LC, Williams AR, Stavenhagen K, Giera M, Kooij G, Vlasakov I, et al. The whipworm (*Trichuris suis*) secretes prostaglandin E2 to suppress proinflammatory properties in human dendritic cells. *FASEB J* (2017) 31:719–31. doi:10.1096/fj.201600841R
28. Schramm G, Mohrs K, Wodrich M, Doenhoff MJ, Pearce EJ, Haas H, et al. Cutting edge: IPSE/alpha-1, a glycoprotein from *Schistosoma mansoni* eggs, induces IgE-dependent, antigen-independent IL-4 production by murine basophils in vivo. *J Immunol* (2007) 178:6023–7. doi:10.4049/jimmunol.178.10.6023
29. Dalton JP, Robinson MW, Mulcahy G, O'Neill SM, Donnelly S. Immunomodulatory molecules of *Fasciola hepatica*: candidates for both vaccine and immunotherapeutic development. *Vet Parasitol* (2013) 195:272–85. doi:10.1016/j.vetpar.2013.04.008
30. Tundup S, Srivastava L, Harn DA Jr. Polarization of host immune responses by helminth-expressed glycans. *Ann N Y Acad Sci* (2012) 1253:E1–13. doi:10.1111/j.1749-6632.2012.06618.x
31. Geijtenbeek TB, Gringhuis SI. Signalling through C-type lectin receptors: shaping immune responses. *Nat Rev Immunol* (2009) 9:465–79. doi:10.1038/nri2569
32. van Kooyk Y, Engering A, Lekkerkerker AN, Ludwig IS, Geijtenbeek TB. Pathogens use carbohydrates to escape immunity induced by dendritic cells. *Curr Opin Immunol* (2004) 16:488–93. doi:10.1016/j.coi.2004.05.010
33. van Vliet SJ, Garcia-Vallejo JJ, van Kooyk Y. Dendritic cells and C-type lectin receptors: coupling innate to adaptive immune responses. *Immunol Cell Biol* (2008) 86:580–7. doi:10.1038/icb.2008.55
34. Geijtenbeek TB, Engering A, Van Kooyk Y. DC-SIGN, a C-type lectin on dendritic cells that unveils many aspects of dendritic cell biology. *J Leukoc Biol* (2002) 71:921–31.
35. van Liempt E, Bank CM, Mehta P, Garcia-Vallejo JJ, Kawar ZS, Geyer R, et al. Specificity of DC-SIGN for mannose- and fucose-containing glycans. *FEBS Lett* (2006) 580:6123–31. doi:10.1016/j.febslet.2006.10.009
36. Meyer S, van Liempt E, Imberty A, van Kooyk Y, Geyer H, Geyer R, et al. DC-SIGN mediates binding of dendritic cells to authentic pseudo-LewisY glycolipids of *Schistosoma mansoni* cercariae, the first parasite-specific ligand of DC-SIGN. *J Biol Chem* (2005) 280:37349–59. doi:10.1074/jbc.M507100200
37. van Die I, van Vliet SJ, Nyame AK, Cummings RD, Bank CM, Appelmelk B, et al. The dendritic cell-specific C-type lectin DC-SIGN is a receptor for *Schistosoma mansoni* egg antigens and recognizes the glycan antigen Lewis x. *Glycobiology* (2003) 13:471–8. doi:10.1093/glycob/cwg052
38. Van Liempt E, Imberty A, Bank CM, Van Vliet SJ, Van Kooyk Y, Geijtenbeek TB, et al. Molecular basis of the differences in binding properties of the highly related C-type lectins DC-SIGN and L-SIGN to Lewis X trisaccharide and *Schistosoma mansoni* egg antigens. *J Biol Chem* (2004) 279:33161–7. doi:10.1074/jbc.M404988200
39. Gringhuis SI, Kaptein TM, Wevers BA, van der Vlist M, Klaver EJ, van Die I, et al. Fucose-based PAMPs prime dendritic cells for follicular T helper cell polarization via DC-SIGN-dependent IL-27 production. *Nat Commun* (2014) 5:5074. doi:10.1038/ncomms6074
40. Gringhuis SI, den Dunnen J, Litjens M, van der Vlist M, Geijtenbeek TB. Carbohydrate-specific signaling through the DC-SIGN signalosome tailors immunity to *Mycobacterium tuberculosis*, HIV-1 and *Helicobacter pylori*. *Nat Immunol* (2009) 10:1081–8. doi:10.1038/ni.1778
41. Stahl PD, Ezekowitz RA. The mannose receptor is a pattern recognition receptor involved in host defense. *Curr Opin Immunol* (1998) 10:50–5. doi:10.1016/S0952-7915(98)80031-9
42. Ezekowitz RA, Sastry K, Bailly P, Warner A. Molecular characterization of the human macrophage mannose receptor: demonstration of multiple carbohydrate recognition-like domains and phagocytosis of yeasts in Cos-1 cells. *J Exp Med* (1990) 172:1785–94. doi:10.1084/jem.172.6.1785
43. Schweizer A, Stahl PD, Rohrer J. A di-aromatic motif in the cytosolic tail of the mannose receptor mediates endosomal sorting. *J Biol Chem* (2000) 275:29694–700. doi:10.1074/jbc.M000571200
44. Martinez-Pomares L. The mannose receptor. *J Leukoc Biol* (2012) 92:1177–86. doi:10.1189/jlb.0512231
45. Leteux C, Chai W, Loveless RW, Yuen CT, Uhlin-Hansen L, Combarnous Y, et al. The cysteine-rich domain of the macrophage mannose receptor is a multispecific lectin that recognizes chondroitin sulfates A and B and sulfated oligosaccharides of blood group Lewis(a) and Lewis(x) types in addition to the sulfated N-glycans of lutropin. *J Exp Med* (2000) 191:1117–26. doi:10.1084/jem.191.7.1117
46. Martinez-Pomares L, Wienke D, Stillion R, McKenzie EJ, Arnold JN, Harris J, et al. Carbohydrate-independent recognition of collagens by the macrophage mannose receptor. *Eur J Immunol* (2006) 36:1074–82. doi:10.1002/eji.200535685
47. Taylor ME, Drickamer K. Structural requirements for high affinity binding of complex ligands by the macrophage mannose receptor. *J Biol Chem* (1993) 268:399–404.
48. Kery V, Krepinsky JJ, Warren CD, Capek P, Stahl PD. Ligand recognition by purified human mannose receptor. *Arch Biochem Biophys* (1992) 298:49–55. doi:10.1016/0003-9861(92)90092-B
49. Lee RT, Hsu TL, Huang SK, Hsieh SL, Wong CH, Lee YC. Survey of immune-related, mannose/fucose-binding C-type lectin receptors reveals widely divergent sugar-binding specificities. *Glycobiology* (2011) 21:512–20. doi:10.1093/glycob/cwq193
50. Su Y, Bakker T, Harris J, Tsang C, Brown GD, Wormald MR, et al. Glycosylation influences the lectin activities of the macrophage mannose receptor. *J Biol Chem* (2005) 280:32811–20. doi:10.1074/jbc.M503457200
51. Su Y, Royle L, Radcliffe CM, Harvey DJ, Dwek RA, Martinez-Pomares L, et al. Detailed N-glycan analysis of mannose receptor purified from murine spleen indicates tissue specific sialylation. *Biochem Biophys Res Commun* (2009) 384:436–43. doi:10.1016/j.bbrc.2009.04.159
52. Martinez-Pomares L, Reid DM, Brown GD, Taylor PR, Stillion RJ, Linehan SA, et al. Analysis of mannose receptor regulation by IL-4, IL-10, and proteolytic processing using novel monoclonal antibodies. *J Leukoc Biol* (2003) 73:604–13. doi:10.1189/jlb.0902450
53. Stein M, Keshav S, Harris N, Gordon S. Interleukin 4 potently enhances murine macrophage mannose receptor activity: a marker of alternative immunologic macrophage activation. *J Exp Med* (1992) 176:287–92. doi:10.1084/jem.176.1.287
54. Doyle AG, Herbein G, Montaner LJ, Minty AJ, Caput D, Ferrara P, et al. Interleukin-13 alters the activation state of murine macrophages in vitro: comparison with interleukin-4 and interferon-gamma. *Eur J Immunol* (1994) 24:1441–5. doi:10.1002/eji.1830240630
55. Schreiber S, Blum JS, Chappel JC, Stenson WF, Stahl PD, Teitelbaum SL, et al. Prostaglandin E specifically upregulates the expression of the mannose-receptor on mouse bone marrow-derived macrophages. *Cell Regul* (1990) 1:403–13.
56. Vogel DY, Glim JE, Stavenuiter AW, Breur M, Heijnen P, Amor S, et al. Human macrophage polarization in vitro: maturation and activation methods compared. *Immunobiology* (2014) 219(9):695–703. doi:10.1016/j.imbio.2014.05.002
57. Smeekens SP, van de Veerdonk FL, Joosten LA, Jacobs L, Jansen T, Williams DL, et al. The classical CD14(+)(+) CD16(-) monocytes, but not the patrolling CD14(+) CD16(+) monocytes, promote Th17 responses to Candida albicans. *Eur J Immunol* (2011) 41:2915–24. doi:10.1002/eji.201141418
58. Babu S, Kumaraswami V, Nutman TB. Alternatively activated and immunoregulatory monocytes in human filarial infections. *J Infect Dis* (2009) 199:1827–37. doi:10.1086/599090
59. Kooij G, Braster R, Koning JJ, Laan LC, van Vliet SJ, Los T, et al. *Trichuris suis* induces human non-classical patrolling monocytes via the mannose receptor and PKC: implications for multiple sclerosis. *Acta Neuropathol Commun* (2015) 3:45. doi:10.1186/s40478-015-0223-1

60. Kreider T, Anthony RM, Urban JF Jr, Gause WC. Alternatively activated macrophages in helminth infections. *Curr Opin Immunol* (2007) 19:448–53. doi:10.1016/j.coi.2007.07.002
61. Hoeksema MA, Laan LC, Postma JJ, Cummings RD, de Winther MP, Dijkstra CD, et al. Treatment with *Trichuris suis* soluble products during monocyte-to-macrophage differentiation reduces inflammatory responses through epigenetic remodeling. *FASEB J* (2016) 30:2826–36. doi:10.1096/fj.201600343R
62. van Liempt E, van Vliet SJ, Engering A, Garcia Vallejo JJ, Bank CM, Sanchez-Hernandez M, et al. *Schistosoma mansoni* soluble egg antigens are internalized by human dendritic cells through multiple C-type lectins and suppress TLR-induced dendritic cell activation. *Mol Immunol* (2007) 44:2605–15. doi:10.1016/j.molimm.2006.12.012
63. Linehan SA, Coulson PS, Wilson RA, Mountford AP, Brombacher F, Martinez-Pomares L, et al. IL-4 receptor signaling is required for mannose receptor expression by macrophages recruited to granulomata but not resident cells in mice infected with *Schistosoma mansoni*. *Lab Invest* (2003) 83:1223–31. doi:10.1097/01.LAB.0000081392.93701.6F
64. Everts B, Hussaarts L, Driessen NN, Meevissen MH, Schramm G, van der Ham AJ, et al. Schistosome-derived omega-1 drives Th2 polarization by suppressing protein synthesis following internalization by the mannose receptor. *J Exp Med* (2012) 209:1753–67, S1. doi:10.1084/jem.20111381
65. Klaver EJ, Kuijk LM, Lindhorst TK, Cummings RD, van Die I. *Schistosoma mansoni* soluble egg antigens induce expression of the negative regulators SOCS1 and SHP1 in human dendritic cells via interaction with the mannose receptor. *PLoS One* (2015) 10:e0124089. doi:10.1371/journal.pone.0124089
66. Paveley RA, Aynsley SA, Turner JD, Bourke CD, Jenkins SJ, Cook PC, et al. The mannose receptor (CD206) is an important pattern recognition receptor (PRR) in the detection of the infective stage of the helminth *Schistosoma mansoni* and modulates IFNgamma production. *Int J Parasitol* (2011) 41:1335–45. doi:10.1016/j.ijpara.2011.08.005
67. Guasconi L, Serradell MC, Garro AP, Iacobelli L, Masih DT. C-type lectins on macrophages participate in the immunomodulatory response to *Fasciola hepatica* products. *Immunology* (2011) 133:386–96. doi:10.1111/j.1365-2567.2011.03449.x
68. Ravida A, Aldridge AM, Driessen NN, Heus FA, Hokke CH, O'Neill SM. *Fasciola hepatica* surface coat glycoproteins contain mannosylated and phosphorylated N-glycans and exhibit immune modulatory properties independent of the mannose receptor. *PLoS Negl Trop Dis* (2016) 10:e0004601. doi:10.1371/journal.pntd.0004601
69. deSchoolmeester ML, Martinez-Pomares L, Gordon S, Else KJ. The mannose receptor binds *Trichuris muris* excretory/secretory proteins but is not essential for protective immunity. *Immunology* (2009) 126:246–55. doi:10.1111/j.1365-2567.2008.02893.x
70. Gruden-Movsesijan A, Milosavljevic Lj S. The involvement of the macrophage mannose receptor in the innate immune response to infection with parasite *Trichinella spiralis*. *Vet Immunol Immunopathol* (2006) 109:57–67. doi:10.1016/j.vetimm.2005.07.022
71. Favoretto BC, Casabuono AAC, Portes-Junior JA, Jacysyn JF, Couto AS, Faquim-Mauro EL. High molecular weight components containing N-linked oligosaccharides of *Ascaris suum* extract inhibit the dendritic cells activation through DC-SIGN and MR. *Mol Immunol* (2017) 87:33–46. doi:10.1016/j.molimm.2017.03.015
72. Pearce EJ, MacDonald AS. The immunobiology of schistosomiasis. *Nat Rev Immunol* (2002) 2:499–511. doi:10.1038/nri843
73. Mas-Coma S, Valero MA, Bargues MD. Fascioliasis. *Adv Exp Med Biol* (2014) 766:77–114. doi:10.1007/978-1-4939-0915-5_4
74. Pearce EJ, Caspar P, Grzych JM, Lewis FA, Sher A. Downregulation of Th1 cytokine production accompanies induction of Th2 responses by a parasitic helminth, *Schistosoma mansoni*. *J Exp Med* (1991) 173:159–66. doi:10.1084/jem.173.1.159
75. Pearce EJ, M Kane C, Sun J, J Taylor J, McKee AS, Cervi L. Th2 response polarization during infection with the helminth parasite *Schistosoma mansoni*. *Immunol Rev* (2004) 201:117–26. doi:10.1111/j.0105-2896.2004.00187.x
76. de Jong EC, Vieira PL, Kalinski P, Schuitemaker JH, Tanaka Y, Wierenga EA, et al. Microbial compounds selectively induce Th1 cell-promoting or Th2 cell-promoting dendritic cells in vitro with diverse th cell-polarizing signals. *J Immunol* (2002) 168:1704–9. doi:10.4049/jimmunol.168.4.1704
77. Steinfelder S, Andersen JF, Cannons JL, Feng CG, Joshi M, Dwyer D, et al. The major component in schistosome eggs responsible for conditioning dendritic cells for Th2 polarization is a T2 ribonuclease (omega-1). *J Exp Med* (2009) 206:1681–90. doi:10.1084/jem.20082462
78. Zaccone P, Burton OT, Gibbs S, Miller N, Jones FM, Dunne DW, et al. Immune modulation by *Schistosoma mansoni* antigens in NOD mice: effects on both innate and adaptive immune systems. *J Biomed Biotechnol* (2010) 2010:795210. doi:10.1155/2010/795210
79. Hams E, Bermingham R, Wurlod FA, Hogan AE, O'Shea D, Preston RJ, et al. The helminth T2 RNase omega1 promotes metabolic homeostasis in an IL-33- and group 2 innate lymphoid cell-dependent mechanism. *FASEB J* (2016) 30:824–35. doi:10.1096/fj.15-277822
80. Thomas PG, Harn DA Jr. Immune biasing by helminth glycans. *Cell Microbiol* (2004) 6:13–22. doi:10.1046/j.1462-5822.2003.00337.x
81. van de Vijver KK, Hokke CH, van Remoortere A, Jacobs W, Deelder AM, Van Marck EA. Glycans of *Schistosoma mansoni* and keyhole limpet haemocyanin induce hepatic granulomas in vivo. *Int J Parasitol* (2004) 34:951–61. doi:10.1016/j.ijpara.2004.04.009
82. van den Berg TK, Honing H, Franke N, van Remoortere A, Schiphorst WE, Liu FT, et al. LacdiNAc-glycans constitute a parasite pattern for galectin-3-mediated immune recognition. *J Immunol* (2004) 173:1902–7. doi:10.4049/jimmunol.173.3.1902
83. Zaccone P, Burton OT, Gibbs SE, Miller N, Jones FM, Schramm G, et al. The *S. mansoni* glycoprotein omega-1 induces Foxp3 expression in NOD mouse CD4 T cells. *Eur J Immunol* (2011) 41:2709–18. doi:10.1002/eji.201141429
84. Belley A, Chadee K. Eicosanoid production by parasites: from pathogenesis to immunomodulation? *Parasitol Today* (1995) 11:327–34. doi:10.1016/0169-4758(95)80185-5
85. Kalinski P. Regulation of immune responses by prostaglandin E2. *J Immunol* (2012) 188:21–8. doi:10.4049/jimmunol.1101029
86. O'Neill SM, Brady MT, Callanan JJ, Mulcahy G, Joyce P, Mills KH, et al. *Fasciola hepatica* infection downregulates Th1 responses in mice. *Parasite Immunol* (2000) 22:147–55. doi:10.1046/j.1365-3024.2000.00290.x
87. Cervi L, Rubinstein H, Masih DT. Involvement of excretion-secretion products from *Fasciola hepatica* inducing suppression of the cellular immune responses. *Vet Parasitol* (1996) 61:97–111. doi:10.1016/0304-4017(95)00816-0
88. Lund ME, O'Brien BA, Hutchinson AT, Robinson MW, Simpson AM, Dalton JP, et al. Secreted proteins from the helminth *Fasciola hepatica* inhibit the initiation of autoreactive T cell responses and prevent diabetes in the NOD mouse. *PLoS One* (2014) 9:e86289. doi:10.1371/journal.pone.0086289
89. Vukman KV, Adams PN, O'Neill SM. *Fasciola hepatica* tegumental coat antigen suppresses MAPK signalling in dendritic cells and up-regulates the expression of SOCS3. *Parasite Immunol* (2013) 35:234–8. doi:10.1111/pim.12033
90. Aldridge A, O'Neill SM. *Fasciola hepatica* tegumental antigens induce anergic-like T cells via dendritic cells in a mannose receptor-dependent manner. *Eur J Immunol* (2016) 46:1180–92. doi:10.1002/eji.201545905
91. Klaver EJ, Kuijk LM, Laan LC, Kringel H, van Vliet SJ, Bouma G, et al. *Trichuris suis*-induced modulation of human dendritic cell function is glycan-mediated. *Int J Parasitol* (2013) 43:191–200. doi:10.1016/j.ijpara.2012.10.021
92. Klaver EJ, van der Pouw Kraan TC, Laan LC, Kringel H, Cummings RD, Bouma G, et al. *Trichuris suis* soluble products induce Rab7b expression and limit TLR4 responses in human dendritic cells. *Genes Immun* (2015) 16:378–87. doi:10.1038/gene.2015.18
93. Kringel H, Roepstorff A. *Trichuris suis* population dynamics following a primary experimental infection. *Vet Parasitol* (2006) 139:132–9. doi:10.1016/j.vetpar.2006.03.002
94. Else KJ, Hultner L, Grencis RK. Cellular immune responses to the murine nematode parasite *Trichuris muris*. II. Differential induction of TH-cell subsets in resistant versus susceptible mice. *Immunology* (1992) 75:232–7.
95. Chieppa M, Bianchi G, Doni A, Del Prete A, Sironi M, Laskarin G, et al. Cross-linking of the mannose receptor on monocyte-derived dendritic cells activates an anti-inflammatory immunosuppressive program. *J Immunol* (2003) 171:4552–60. doi:10.4049/jimmunol.171.9.4552
96. Bax M, Garcia-Vallejo JJ, Jang-Lee J, North SJ, Gilmartin TJ, Hernandez G, et al. Dendritic cell maturation results in pronounced changes in glycan expression affecting recognition by siglecs and galectins. *J Immunol* (2007) 179:8216–24. doi:10.4049/jimmunol.179.12.8216
97. Xaplanteri P, Lagoumintzis G, Dimitracopoulos G, Paliogianni F. Synergistic regulation of *Pseudomonas aeruginosa*-induced cytokine production in

human monocytes by mannose receptor and TLR2. *Eur J Immunol* (2009) 39:730–40. doi:10.1002/eji.200838872

Conflict of Interest Statement: The authors declare that the research was conducted in the absence of any commercial or financial relationships that could be construed as a potential conflict of interest.

Copyright © 2017 van Die and Cummings. This is an open-access article distributed under the terms of the Creative Commons Attribution License (CC BY). The use, distribution or reproduction in other forums is permitted, provided the original author(s) or licensor are credited and that the original publication in this journal is cited, in accordance with accepted academic practice. No use, distribution or reproduction is permitted which does not comply with these terms.

frontiers in Immunology

REVIEW
published: 15 February 2018
doi: 10.3389/fimmu.2018.00218

African Trypanosomiasis-Associated Anemia: The Contribution of the Interplay between Parasites and the Mononuclear Phagocyte System

Benoit Stijlemans[1,2†], Patrick De Baetselier[1,2†], Stefan Magez[1,3], Jo A. Van Ginderachter[1,2] and Carl De Trez[1]*

[1] Laboratory of Cellular and Molecular Immunology, Vrije Universiteit Brussel (VUB), Brussels, Belgium, [2] Myeloid Cell Immunology Laboratory, VIB Center for Inflammation Research, Brussels, Belgium, [3] Laboratory for Biomedical Research, Ghent University Global Campus, Incheon, South Korea

OPEN ACCESS

Edited by:
Geanncarlo Lugo-Villarino, UMR5089 Institut de Pharmacologie et de Biologie Structurale (IPBS), France

Reviewed by:
Alan L. Scott, Johns Hopkins University, United States
Joana Tavares, Instituto de Biologia Molecular e Celular (IBMC), Portugal

***Correspondence:**
Benoit Stijlemans
benoit.stijlemans@vub.be

†*Shared first authorship.*

Specialty section:
This article was submitted to Microbial Immunology, a section of the journal Frontiers in Immunology

Received: *30 September 2017*
Accepted: *25 January 2018*
Published: *15 February 2018*

Citation:
Stijlemans B, De Baetselier P, Magez S, Van Ginderachter JA and De Trez C (2018) African Trypanosomiasis-Associated Anemia: The Contribution of the Interplay between Parasites and the Mononuclear Phagocyte System. Front. Immunol. 9:218. doi: 10.3389/fimmu.2018.00218

African trypanosomosis (AT) is a chronically debilitating parasitic disease of medical and economic importance for the development of sub-Saharan Africa. The trypanosomes that cause this disease are extracellular protozoan parasites that have developed efficient immune escape mechanisms to manipulate the entire host immune response to allow parasite survival and transmission. During the early stage of infection, a profound pro-inflammatory type 1 activation of the mononuclear phagocyte system (MPS), involving classically activated macrophages (i.e., M1), is required for initial parasite control. Yet, the persistence of this M1-type MPS activation in trypanosusceptible animals causes immunopathology with anemia as the most prominent pathological feature. By contrast, in trypanotolerant animals, there is an induction of IL-10 that promotes the induction of alternatively activated macrophages (M2) and collectively dampens tissue damage. A comparative gene expression analysis between M1 and M2 cells identified galectin-3 (Gal-3) and macrophage migration inhibitory factor (MIF) as novel M1-promoting factors, possibly acting synergistically and in concert with TNF-α during anemia development. While Gal-3 enhances erythrophagocytosis, MIF promotes both myeloid cell recruitment and iron retention within the MPS, thereby depriving iron for erythropoiesis. Hence, the enhanced erythrophagocytosis and suppressed erythropoiesis lead to anemia. Moreover, a thorough investigation using MIF-deficient mice revealed that the underlying mechanisms in AT-associated anemia development in trypanosusceptible and tolerant animals are quite distinct. In trypanosusceptible animals, anemia resembles anemia of inflammation, while in trypanotolerant animals' hemodilution, mainly caused by hepatosplenomegaly, is an additional factor contributing to anemia. In this review, we give an overview of how trypanosome- and host-derived factors can contribute to trypanosomosis-associated anemia development with a focus on the MPS system. Finally, we will discuss potential intervention strategies to alleviate AT-associated anemia that might also have therapeutic potential.

Keywords: anemia, MPS, MIF, erythrophagocytosis, inflammation, hemodilution, IL-10, IFN-γ

INTRODUCTION

African trypanosomes are extracellular protozoan parasites causing debilitating diseases of medical, veterinary, and socio-economical importance that adversely affect the economic development of sub-Saharan Africa (1–3). The distribution of the disease coincides with the habitat of the tsetse fly vector (*Glossina* spp.), and is called the tsetse fly "belt" or is sometimes referred to as "green desert" due to the fact that ~10 million km^2 of potential fertile land is rendered unsuitable for cultivation (3). Within this area, the majority of the 39 tsetse-infested countries are underdeveloped, poor, heavily indebted, food-deficit countries due to the lack of productive animals as far as meat/milk production and draft power are concerned, resulting in an annual economic loss of about 5 billion US$ (4, 5). In addition, about 60 million people living in this belt are at potential risk of infection with an estimated mortality rate of about 10,000 per year (6). Due to the low incidence of African trypanosomiasis, it is also considered a neglected disease. The disease caused by these extracellular hemoflagellates in humans is known as "sleeping sickness" or human African trypanosomiasis (HAT), while in domestic animals it is called "nagana" or animal African trypanosomiasis (AAT) (7). As far as HAT is concerned, two distinct subspecies of *Trypanosoma brucei* are responsible for the disease: (i) *Trypanosoma brucei gambiense*, typically found in western and central Africa (representing 98% of all cases, with humans as main reservoir), causes a chronic form of HAT (a few months to over several years) and (ii) *Trypanosoma brucei rhodesiense*, found in eastern and southern Africa [representing about 2% of all HAT cases due to the fact it is a zoonosis form with animals as main reservoir and humans being occasionally infected (8, 9)], generally causes an acute form of HAT leading to death within a few months if left untreated (6, 10, 11). HAT is characterized by two successive stages: an early hemolymphatic stage, whereby the parasites are observed in the peripheral blood and the lymphatic system, and a later meningoencephalitic stage, where parasites cross the blood–brain barrier and proliferate in the cerebral spinal fluid resulting in neurological complications/cerebral pathology and death if left untreated (12, 13). As far as AAT is concerned, the strictly intravascular parasites *Trypanosoma congolense*, as well as *Trypanosoma vivax*, can be considered the most important causative agents (14). Yet, also *Trypanosoma brucei brucei* and *Trypanosoma evansi*, residing both in intravascular as well as extravascular spaces within their host, have been documented to contribute to livestock infections (14–16). In contrast to game animals, where these parasites cause only mild infections, the disease in domestic animals is severe and often fatal (5, 17, 18).

Various methods have been implemented to control African trypanosomiasis (19); including (i) vector control (20), (ii) reducing the proximity of livestock to reservoir hosts, (iii) development op trypanotolerant livestock (disease-resistant breeds) (5, 21), and (iv) using trypanocidal drugs (22). Yet, their success is limited due to the fact that these techniques are often used locally and not necessarily in a coordinated fashion (23), game animals function as parasite reservoir without exhibiting pathological signs (24), and the rapid emergence of drug-resistant trypanosomes, thereby undermining their efficacy and leading to the widespread outbreaks of trypanosomiasis (19, 25, 26).

The main factor hampering control over African trypanosomiasis is the fact that these parasites have evolved very efficient immune escape mechanisms and are able to manipulate the entire host immune response to avoid elimination [reviewed in Ref. (27)]. Accordingly, an alternative approach to tackle African trypanosomiasis is targeting the infection-associated immunopathology. For example, in HAT patients neurological complications are the major pathological feature, yet, an additional complication observed during the hemolymphatic stage is anemia (28, 29). In AAT, anemia is considered the most prominent immunopathological disease-related feature and the major cause of death due to Nagana (30). Importantly, in cattle, trypanotolerance has been referred to as the capacity of an animal to control severe anemia development which is assumed to be independent of parasitemia levels (21, 30). Moreover, Naessens et al. (31) showed using chimeric studies between trypanotolerant N'Dama (i.e., ancient cattle breeds/West African longhorn, *Bos taurus*) and trypanosusceptible Boran (more recently introduced cattle breeds, *Bos indicus*) that trypanotolerance is composed of two traits, (i) a better capacity to control parasitemia which is independent of the genetic origin of the hematopoietic tissue and (ii) a better ability to control anemia which is dependent on hematopoietic cells and thus a tolerant hematopoietic tissue genotype. Moreover, the capacity to control anemia is considered as the most important trait of the more resistant/trypanotolerant cattle (32). Yet, not only the genetic background (N'Dama versus Boran) but also other factors such as the age of the host, type of trypanosome spp. infecting, and nutrition can contribute to bovine trypanotolerance (33–38).

Tsetse fly mediated (i.e., natural infection mode) and experimental (i.e., using clonal parasites) murine models have been developed to allow a more detailed unraveling of the underlying mechanisms of trypanosomiasis-associated anemia development. Although most trypanosomes cannot be considered natural pathogens for rodents, experimental infections in mice may offer good models to identify the molecular pathways that mediate particular traits or pathological features such as anemia (39). Moreover, the genetic background of the mice was also found to contribute to susceptibility or tolerance as far as anemia is concerned, whereby during *T. brucei* and *T. congolense* infection C57BL/6 mice exhibited severe anemia (yet low parasitemia) while BALB/c mice exhibited greatly reduced anemia (yet higher parasitemia) (40, 41). However, there are some differences in the phenotype. Indeed, even the most tolerant mouse strains eventually succumb to the infection, while in the absence of other stress factors, tolerant cattle survive such challenge. So far, studies in murine models focusing mainly on "clonal or natural (tsetse transmitted)" *T. congolense* and *T. brucei* parasites have shown that similar as in the bovine system, chronic anemia does not seem to correlate with parasitemia or survival, but rather is a result of infection-elicited host responses, where B-cells do not seem to play a major role (40, 42). By contrast, cells of the mononuclear phagocyte system (MPS, i.e., tissue resident myeloid cells and inflammation-elicited/inflammatory myeloid cells derived from circulating monocytes) have been shown to play a key role

in infection-associated pathogenicity/anemia development (43). Moreover, due to their sensing ability towards pathogen- and host-derived signals in the environment, their phagocytic capacity and functional plasticity in response to these signals, cells of the MPS are considered as a crucial immune population in both health and disease. A large number of studies, including our work, have begun to establish how the ontogeny/differentiation of these cells is tailored during the course of African trypanosome infections. In this review, we aim at (i) giving an overview of how trypanosome-derived and host-derived factors can affect the MPS and contribute to trypanosomosis-associated anemia development and (ii) discussing on potential intervention strategies to alleviate African trypanosomosis (AT)-associated anemia that might also have therapeutic potential.

ANEMIA DEVELOPMENT DURING AFRICAN TRYPANOSOME INFECTIONS

Myeloid Cells As Key Players in the Parasite–Host Interaction and Trypanosomiasis-Associated Acute Anemia Development

The interaction between African trypanosomes and their mammalian host elicits the sequential activation of innate and adaptive immune responses. Being extracellular parasites, they are continuously confronted with the host's immune system. However, through co-evolution, a well-balanced growth regulation system developed that allows sufficiently long parasite survival without killing its host to ensure transmission (44). This intricate balance consists of (i) a potent type 1 cellular/pro-inflammatory immune response and (ii) a strong humoral antiparasite B-cell response during the most prominent first peak parasitemia which collectively allows parasite control and temporary host resistance (42, 45). However, to avoid complete elimination, these extracellular parasites have developed various immune evasion mechanisms (consisting of antigenic variation, immunosuppression and B-cell depletion/loss of B-cell memory) to ensure progression/chronicity and transmission (46–50). Moreover, the early "beneficial" pro-inflammatory immune response mediated by the activated MPS, can culminate into severe collateral damage to the host if persistent. In this context, the level of the inflammatory immune response triggered and the capacity of the host to control this response determines whether immunopathology (i.e., anemia and tissue damage) develops and allows discriminating between trypanosusceptible and trypanotolerant animals (see **Figure 1**).

Experimental murine models, using gene-specific-deficient animals, have been very crucial in trying to unravel the mechanisms implicated in trypanosomiasis-associated pathogenicity and anemia in particular. In general, anemia occurs during all stages of a typical African trypanosome infection and can be divided into distinct phases (see **Figure 1**), (i) an early/acute stage whereby following/coinciding peak parasitemia clearance there is occurrence of a drastic drop in red blood cells (RBCs) numbers (i.e., acute or consumptive anemia) which is followed by a recovery phase and (ii) a more late/chronic phase coinciding with progressive anemia development. Accumulating evidence points to a pivotal role of myeloid cells in anemia development (see **Figure 1**). Hereby, their plasticity toward environmental triggers allows discriminating between classically activated macrophages (i.e., M1) and alternatively activated macrophages (i.e., M2). Moreover, the prevalence of M1 or M2 during the course of infection correlates with the severity of anemia (43). Consequently, both pro- and anti-inflammatory cytokines have been shown to be implicated in anemia onset and progression (51). In this section, different parasite- and host-derived factors contributing to both myeloid cell activation and to acute and chronic anemia development will be discussed. To this end, two different murine African trypanosome models, i.e., the *T. brucei* and *T. congolense* infection model, will be compared. It is important to mention that within the murine African trypanosomiasis model, *T. brucei* infections are associated with severe anemia (i.e., a more susceptible model) and *T. congolense* infections with reduced anemia (i.e., a more tolerant model). Emphasis will be put on the more thoroughly investigated murine *T. brucei* infection model. However, over the years more and more research has been conducted using the murine *T. congolense* infection model. Hence, we will also discuss, if possible, the common or distinct features underlying anemia development in both models.

Trypanosome-Derived Factors That Affect Myeloid Cell Activation during the Early/Acute Stage of Trypanosome Infection

Upon the bite of a trypanosome-infected tsetse fly, metacyclic parasites expressing a heterologous variant surface glycoprotein (VSG) coat (i.e., metacyclic VSG) that prevents early detection/elimination (52), are inoculated. Already during the early stage of infection, trypanosomes release factors that alone or in concert with saliva components can dampen/impair the activation of the host's immune response, to generate a privileged "micro"-environment to allow infection establishment [reviewed in Ref. (27) and shown in **Figure 2**, left panel]. Of note, with respect to parasite-released factors that could modulate the host MPS, most research so far has been performed using the model parasite *T. brucei* and remain to be determined for the *T. congolense* model. For instance, studies using the *T. brucei* model parasite revealed that they harbor a kinesin heavy chain 1 (TbKHC1), which induces IL-10 and arginase-1, signals through SIGN-R1 in myeloid cells and downregulates inducible nitric oxide synthase activity (53). In turn, this stimulates the production by the host of L-ornithine and hereby the synthesis of polyamines, which promotes early parasite growth (54). Consequently, IL-10/arginase-1-producing immune cells are impaired in their capacity to destroy the parasite, favoring parasite settlement. Another factor trypanosomes use to establish infection is the *T. brucei* adenylate cyclase, which converts ATP into cyclic adenosine monophosphate (cAMP) and is upregulated upon phagocytosis by M1 cells (55). This phenomenon leads to the inhibition/suppression of macrophage activation and consequently to an impaired production of parasite controlling molecules (56–59). Hence, it seems that trypanosomes have developed a system, where altruistic phagocytosed parasites can "temporarily" tempering/disabling

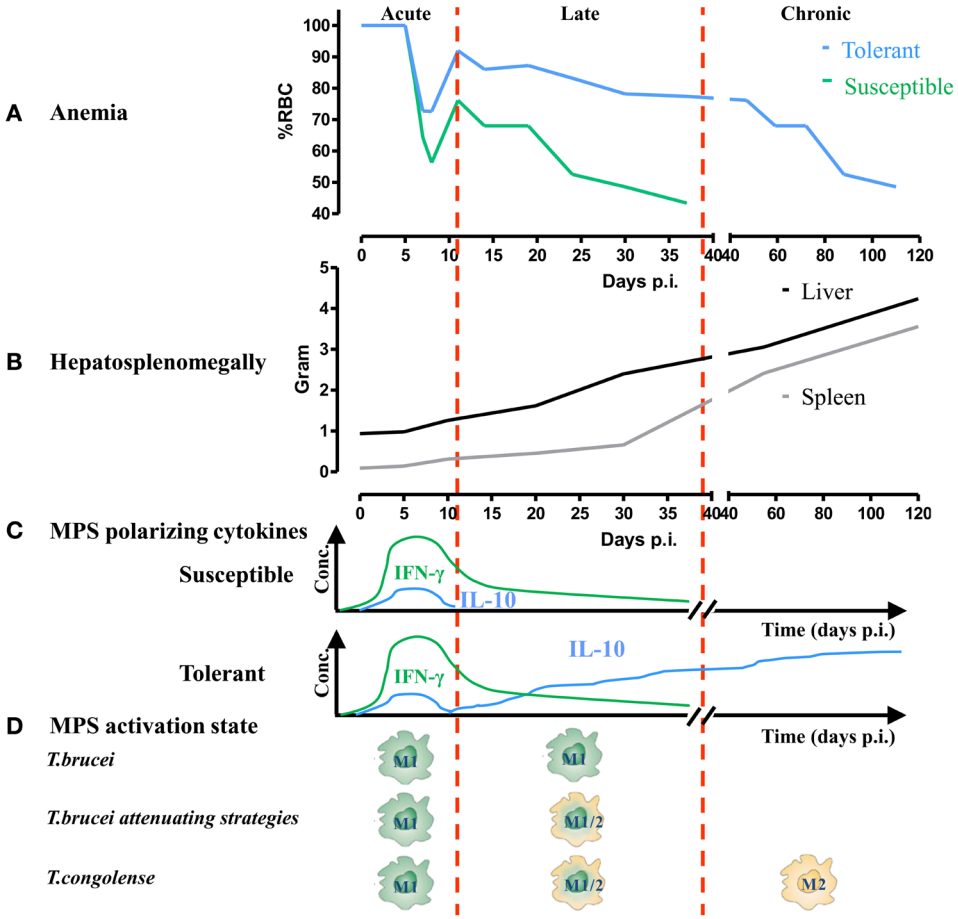


FIGURE 1 | The activation state of myeloid cells correlates with anemia development during trypanosome infections in trypanosusceptible and trypanotolerant animals. **(A)** Anemia development in trypanosusceptible (green) and trypanotolerant (blue) animals during the course of infection. Anemia progression can be divided into (i) an acute phase characterized by a rapid drop in red blood cell (RBC) numbers (i.e., consumptive anemia) followed by a partial recovery phase, (ii) a late stage characterized in the susceptible model by a progressive decline in RBC numbers (below that of the acute phase) and host death. In the tolerant model, this decline is less pronounced and leads to (iii) a chronic phase (i.e., progressive anemia), whereby RBC numbers keep on declining till finally reaching levels of that of the acute phase. **(B)** Throughout the course of infection progressive hepatosplenomegaly occurs, whereby the onset of splenomegaly precedes hepatomegaly. At the late/chronic stage of infection, splenomegaly is more pronounced than hepatomegaly. **(C)** During the different stages of infection, the host produces different mononuclear phagocyte system (MPS) polarizing molecules. During the early/acute stage, both trypanosusceptible (upper, green) and trypanotolerant (lower, blue) animals produce IFN-γ (green line) required to trigger the induction of classically activated macrophages (M1), which is followed by a moderate induction of IL-10 (blue line) to dampen the pathogenic effects of the M1. Only in the trypanotolerant model, there is a second progressive increase in IL-10 during the late/chronic phase of infection, which is required to induce alternatively activated macrophages (M2). **(D)** Occurrence of M1 and M2 during the course of aggressive *Trypanosoma brucei* or *T. brucei* attenuating strategies (GPI-based strategy or AAV-10/anti-CD28) or less virulent *T. brucei* PLC$^{-/-}$/*Trypanosoma congolense* infection.

the M1-mediated innate immune response required for parasite control (see **Figure 2**). In turn, this favors the induction of M2 and paves the way for initiation and establishment of the first wave of parasitemia.

Following initial infection, trypanosomes also "deliberately" trigger in a well-timed manner host cellular responses, whereby myeloid cells get activated *via* the combined exposure of (i) parasite-released components (i.e., pathogen-associated molecular patterns) such as the soluble and membrane-bound/glycosylphosphatidylinositol (GPI)-anchored VSG (sVSG and mfVSG, respectively) and CpG-DNA and (ii) NK/NKT/T-cell released IFN-γ, which most likely is mediated *via* a trypanosome-lymphocyte-triggering-factor (TLTF) (see **Figure 2**, right panel) (45, 60–64). This combination triggers the activation of M1 cells, which in turn release pro-inflammatory molecules such as tumor necrosis factor (TNF-α) and nitric oxide (NO). However, the timing of exposure of these (parasite- and host-derived) components is pivotal in the development of the immune response toward the parasites. These key events controlling host resistance occur within a short time period following initial exposure to the parasite-derived components. Indeed, trypanosomes can cleave their GPI-anchored VSG molecules from the membrane by the trypanosome GPI-phospholipase-C, which results in the release of soluble glycosylinositolphosphate VSG (GIP-sVSG) and the retention of the dimyristoylglycerol (DMG) moiety in the parasites' membrane (65–68). Both components (DMG and GIP-VSG) exhibit a distinct macrophage-activating

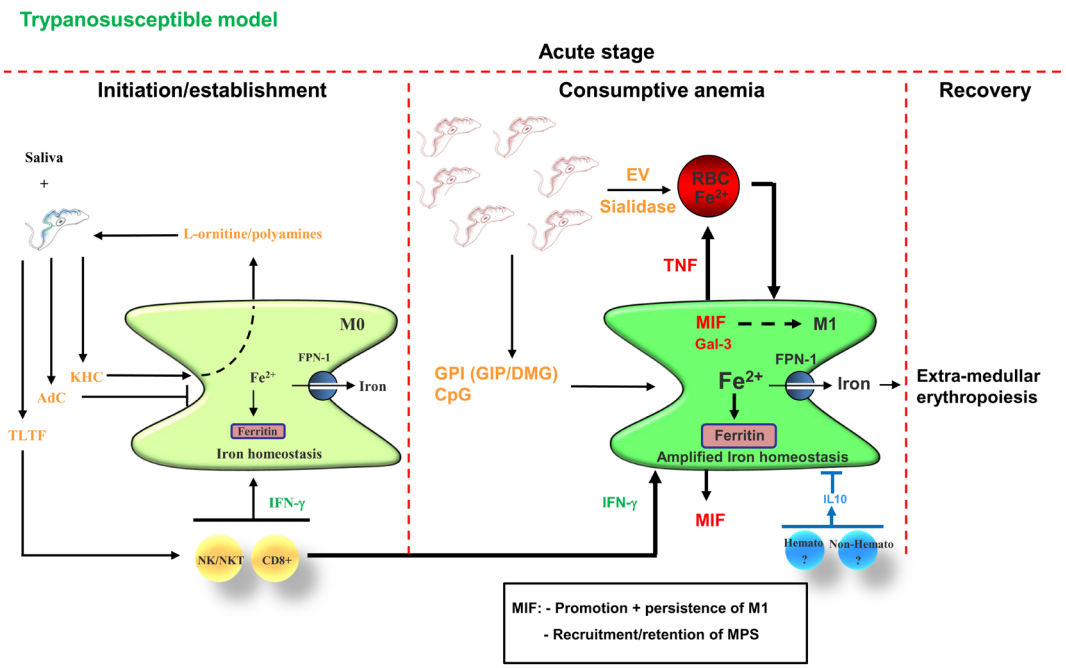


FIGURE 2 | Proposed model for acute anemia development during trypanosome infections in trypanosusceptible animals (i.e., *Trypanosoma brucei*). During the early stage of infection, saliva components in concert with parasite-derived factors such as KHC [fueling parasite nutrient production (i.e., polyamines)] and AdC (dampening the potential of M1), temporarily disable/attenuate the M1-mediated innate immune response, thereby allowing parasite initiation/establishment. In addition, parasites release TLTF to trigger IFN-γ production by NK/NKT and CD8$^+$ T cells, which will promote M1 cell activation. At the peak of parasitemia, these IFN-γ-primed M1 in concert with parasite-derived factors such as GPI-VSG (GIP/DMG) and CpG fuel M1 to produce pro-inflammatory molecules such as TNF, MIF, and Gal-3. In turn, TNF in concert with parasite-released extracellular vesicles (EVs) and/or sialidase trigger/enhance RBC senescence and hence erythrophagocytosis by M1 cells, leading to the development of acute anemia (i.e., hemophagocytic/consumptive anemia). Both MIF and Gal-3 promote M1 polarization and at this stage, there is an amplification of the iron homeostasis [i.e., increased iron storage (ferritin) and export (FPN-1)], which triggers extramedullary erythropoiesis. MIF also promotes recruitment/retention of mononuclear phagocytes and neutrophils, which in turn fuel the pathogenic effects of M1. At this stage, the host transiently produces IL-10, which is required to dampen the pathogenic effects of the M1 and in concert with the extramedullary erythropoiesis results in a partial recovery from acute anemia. Abbreviations: TLTF, T-lymphocyte triggering factor; KHC, kinesin heavy chain; AdC, adenylate cyclase; GPI, glycosylphosphatidylinositol; GIP, glycosylinosytolphosphate; RBC, red blood cell; MIF, macrophage migration inhibitory factor; Gal-3, galectin-3; FPN-1, ferroportin-1; Hemato, hematopoietic; Non-Hemato, non-hematopoietic; DMG, dimyristoylglycerol; VSG, variant surface glycoprotein.

potential (60, 62). For example, the GIP-VSG moiety is recognized by a type A scavenger receptor (SR-A) expressed mainly on mononuclear cells (e.g., macrophages and dendritic cells) leading to the concentration-dependent activation of NF-κB and MAPK pathways and expression of pro-inflammatory genes such as (TNF-α, IL-6, IL12p40, and granulocyte-macrophage colony-stimulating factor) in a MyD88 dependent manner (61, 63). However, the fluctuating levels of parasite (e.g., GIP-sVSG) and host (e.g., IFN-γ) factors during infection act to control macrophage activity in a complex and subtle way, with the outcome determined by the concentration of each mediator, the sequential pattern of its production, and the microenvironment of the target macrophage (69). For instance, during the early/initial stage of infection, the GIP-sVSG released before a high level of IFN-γ production prevents a prominent strong pro-inflammatory immune response and hence favors parasite establishment. Yet, if the IFN-γ levels increase this will prime macrophages to respond stronger toward the parasite-derived GIP-sVSG, which in turn will fuel M1 cells to mount a prominent pro-inflammatory immune response.

Host-Derived Factors That Affect Myeloid Cell Activation during the Early/Acute Stage of Trypanosome Infection

Using gene-deficient mice or neutralizing antibodies it was shown that the sequential production of IFN-γ by NK, NKT, as well as CD8$^+$ and CD4$^+$ T cells during the early stage of trypanosome infection seems to be crucial to initiate acute inflammation-associated anemia (70), also termed consumptive anemia (71, 72) (see **Figure 2**, left panel). In this scenario, IFN-γ activates M1 cells, which in turn allows parasite elimination/removal, but at the same time also promotes the M1-mediated enhanced uptake of RBCs resulting in a first rapid drop in RBC numbers. Indeed, IFN-γ receptor-deficient mice were found to exhibit greatly reduced acute anemia levels (73), coinciding with a reduced influx of myeloid-derived cells, e.g., neutrophils and M1, within the liver that exhibit an impaired erythrophagocytosis capacity (70). Increased levels of host-derived IFN-γ furthermore induce splenomegaly (71), which is typically observed during the acute stage. Recently, Stijlemans et al. (74) demonstrated using a

pHrodo-based assay that during the early stage of *T. brucei* infection, $CD11b^+Ly6G^+$ neutrophils, $CD11b^+Ly6C^{high}$ monocytic cells, as well as splenic $CD11b^+F4/80^+$ myeloid cells exhibit an enhanced erythrophagocytosis capacity that might account for the occurrence of severe acute-stage non-hemolytic anemia. Interestingly, it was shown by others that enhanced erythrophagocytosis is associated with the mobilization of $Ly6C^{high}$ monocytes in a CCR2-dependent manner from the bone marrow into the blood (75), which accumulate mainly within the liver and subsequently ingest stressed/senescent erythrocytes. These cells differentiate into iron-recycling/ferroportin-1 (FPN-1, sole iron exporting molecule)-expressing tissue macrophages and subsequently into iron-recycling Kupffer-like cells, which is a natural mechanism to preserve homeostasis during fluctuations of erythrocyte integrity (76).

Host- and Parasite-Derived Factors That Contribute to Acute Anemia

It was shown that RBCs from infected (i.e., day 6 postinfection) wild-type (WT) mice exhibited an enhanced osmotic fragility and an altered fatty acid membrane composition compared with RBCs from non-infected WT mice (70). This change in RBC fragility was not due to IFN-γ but might be due to host-derived factors such as TNF-α produced by M1 cells (77–80). Indeed, TNF-α could be a driving force for the observed changes in RBC fragility given that it was shown that it can decrease the RBC half-life and thereby fuel RBC senescence/elimination (81). The importance of host-derived factors such as TNF-α in acute anemia development was further substantiated by the observation that *T. brucei*-infected TNF-α-deficient ($TNF\text{-}\alpha^{-/-}$) mice exhibited greatly reduced acute anemia levels compared with control WT mice (see **Table 1**). Thereafter, RBC levels in $TNF\text{-}\alpha^{-/-}$ mice remained elevated. By contrast, in the *T. congolense* model, $TNF\text{-}\alpha^{-/-}$ mice exhibited similar acute anemia (and chronic) levels as control WT mice (82, 83), suggesting that in this model the underlying mechanisms of anemia development are different. Besides TNF-α produced by activated myeloid cells, NO was also found to be an important factor affecting *T. brucei*-associated acute anemia development. Indeed, treating C57BL/6 mice with L-NAME (a typical inhibitor of NO synthase) alleviated acute anemia development (coinciding with reduced peak parasitemia) and was proposed to affect proliferation of immature erythrocytes or hematopoietic stem cells (73, 84). In line with these observations, mice treated with corticosteroids (which downregulates NO synthesis) exhibited an alleviated anemia development (85). However, more research is required to unravel at which level NO affects *T. brucei*-associated acute anemia development.

Also parasite-derived factors such as sialidases in the case of *T. congolense* or extracellular vesicles (EVs) in the case of *T. brucei* infections could contribute to modifications of RBCs and thereby promote elimination (77–80). Indeed, it was proposed at least for the murine *T. brucei* model that during the acute stage, trypanosomes release EVs (filled with intracellular parasite cargo as well as VSG) that can fuse with RBCs. This causes a change in the physical properties of the RBC membrane, which enhances erythrophagocytosis and thereby fuels anemia development. In this context, it could be that binding of mfVSG (present in the EVs) to the RBC surface sensitizes erythrocytes to anti-VSG antibody-mediated complement lysis (86). In addition, this observation might also explain how active adenylate cyclase, playing a key role in increasing cAMP in host cells resulting in the activation of protein kinase A and downregulation of TNF-α, could be transferred from the parasite to the mammalian host (see above). Indeed, the highly fusogenic EVs containing this enzyme might be transferred to recipient host cells, thereby increasing the intracellular levels of cAMP. Given that these EVs are mainly produced at the peak of parasitemia, they might in one way stimulate RBC elimination and at the same time dampen subsequent inflammatory reactions, thereby allowing the next wave of parasites to escape. Also for the murine and bovine *T. congolense* model, factors such as congopain and sialidases were suggested to contribute directly/indirectly to anemia development, by damaging RBCs that results in the exposure of erythrophagocytosis promoting targets (phosphatidylserine) on the RBC membrane (78, 87, 88).

Different factors might account for the occurrence of acute anemia in both the *T. brucei* as well as the *T. congolense* murine infection model. Hence, the acute stage of anemia could be due to a "natural" reaction of the host following infection as well as to parasite-derived factors resulting in a rapid drop in RBC numbers due to enhanced erythrophagocytosis (89). At this stage of infection, due to the enhance erythrophagocytosis, there is an amplification of the iron-homeostasis metabolism (90), resulting in an increased release of iron to fuel the enhanced demand for erythropoiesis (**Figure 2**, right panel).

TABLE 1 | Overview of acute and chronic anemia development in different *Trypanosoma brucei*-infected mouse strains.

Mouse model	Acute anemia	Late/chronic anemia	Reference
BALB/c	+	+	(41, 42)
C57BL/6 (WT)	+++	+++	(41, 42, 74, 83, 90)
[a]B-cell$^{-/-}$	+++	+++	(42)
[a]Nu/Nu	+	+	(70)
[a]IFN-γ$^{-/-}$ or IFN-γR$^{-/-}$	+	+	(70, 73)
[a]CD8$^{-/-}$	+	++	(70)
[a]CD4$^{-/-}$	+++	+ to ++	(70)
C57BL/6 + anti-NK1.1	+	+++	(70)
C57BL/6 + anti-CD28 superagonist	+	+++	(130)
C57BL/6 + AAV-IL-10	ND	+	(131)
C57BL/6 + GPI-based strategy	+	+	(95, 132)
[a]IL-10$^{-/-}$	+++	ND	(131)
[a]TNF$^{-/-}$	+	+	(59, 83, 118)
[a]TNF-R1$^{-/-}$	+++	+++	(41)
[a]TNF-R2$^{-/-}$	++	+	(41)
[a]LT-α$^{-/-}$	++	+ to +++	(118)
C57BL/6 + L-NAME	+	ND	(84)
[a]MIF$^{-/-}$	+	+	(93)
[a]Gal-3$^{-/-}$	+	+	(133)

+, Mild anemia (<25% drop in RBCs); ++, moderate anemia (25–35% drop in RBCs); +++, severe anemia (>35% drop in RBCs); ND, not determined; RBC, red blood cell; AAV-IL-10, alternatively, adenoviral delivery of IL-10; Gal-3, galectin-3; MIF, macrophage migration inhibitory factor; WT, wild-type; LT-α, lymphotoxin-alpha.
[a]Gene-deficient mice in C57BL/6 background.

Transition from Acute to Chronic Anemia: The Recovery Phase

Following this acute anemia phase, there is a transient recovery phase in both the *T. brucei* as well as the *T. congolense* infection model (see **Figure 1**), as a natural response of the host to control/alleviate acute anemia development. Of note, within the *T. brucei* infection model, this recovery was more pronounced in the IFN-γR$^{-/-}$, CD8$^{-/-}$, TNF-α$^{-/-}$, and TNF-R2$^{-/-}$ mice, suggesting that a reduced early pro-inflammatory response/insult allows better recovery from acute anemia. However, so far, the exact mechanism(s) involved are not well characterized. From other experimental models of acute anemia (phenylhydrazine-induced injection or bleeding), it could be inferred that this is most likely due to an enhanced extramedullary erythropoiesis occurring mainly in the spleen and to a lesser extent in the liver and coincides with the occurrence of hepatosplenomegaly. In this context, both in the *T. brucei* and *T. congolense* infection model, hepatosplenomegaly has been documented starting already during the early stages of infection, and coincided with an increase in immature RBC numbers within the splenic compartment (91–95). It is generally known that anemia induces tissue hypoxia, which in turn triggers the activation of a physiological stress response (i.e., stress erythropoiesis) designed to increase oxygen delivery to tissues by rapidly generating large numbers of erythrocytes (96). Moreover, tissue hypoxia triggers the induction of erythropoietin (EPO) in the kidney (97), which drives the expansion and differentiation of erythroid progenitors. Of note, during murine and bovine trypanosome infections, serum EPO levels are increased during both the acute and chronic stage of infection (83, 98). Subsequently, the bone marrow progenitor cells migrating into the spleen or stress erythroid progenitors resident in the spleen expand and differentiate in response to bone morphogenetic protein 4 (BMP4) and Hedgehog, which act in concert with signals previously associated with stress erythropoiesis, such as EPO, stem cell factor and hypoxia, to replenish the pool of stress erythroid progenitors (96, 99, 100). Whether macrophages play also a role at the level of erythropoiesis within the African trypanosome model remains to be further investigated. However, it was shown that upon anemia or stress, macrophage-dependent erythropoiesis (within erythroblastic islands) is needed to adequately respond to produce enough erythrocytes to alleviate the shortage (101, 102). Interestingly, in experimental *T. congolense* infections in rats, erythroblastic islands were found to expand already during the early stages of infection within the bone marrow (103). It is important to mention that following this prominent pro-inflammatory immune response and coinciding with the partial recovery of acute anemia, the host is able to trigger a "transient" anti-inflammatory immune response, whereby IL-10 was shown to play a key role (104, 105). At this stage, CD4$^+$ T cells were shown to be important IL-10-producing cells to dampen the pathogenic effects of the IFN-γ-induced M1 (106). Yet, it can not be excluded that other cells (hematopoietic or non-hematopoietic) might also contribute (see **Figure 2**, right panel). Recently, it was also suggested that IL-27 can play a key role in dampening the pathogenic effects of T cell-mediated IFN-γ during *T. brucei* and *T. congolense* infection without affecting IL-10 levels (107).

Myeloid Cells As Key Players during the Late/Chronic/Progressive Stage of Trypanosomiasis-Associated Anemia Development

Following partial recovery from acute anemia, there is a new equilibrium established, which is different from the steady-state situation (see **Figure 1**). At this stage, the capacity of the host to keep the balance between erythrophagocytosis and erythropoiesis determines whether anemia persists. This also allows discriminating between susceptible and tolerant animals as far as anemia is concerned, whereby the activation stage of the myeloid cells determines the degree of anemia. Indeed, on one hand, trypanosusceptible animals maintain a prominent/polarized M1 activation state and exhibit progressive anemia (i.e., *T. b. brucei* model), which resembles anemia of chronic disease or anemia of inflammation (90). This is characterized by an enhanced erythrophagocytosis and impaired/reduced erythropoiesis that is linked to a perturbed iron homeostasis including altered iron recycling by macrophages and iron sequestration (**Figure 2**). Therefore, the iron-processing pathway is skewed toward iron sequestration (40, 90), as evidenced by increased ferritin expression (main iron storage molecule) and reduced FPN-1 (sole iron exporter), while enhanced uptake of RBC/iron-containing compounds is maintained (see **Figure 3**, left panel). Moreover, iron sequestration by cells of the MPS can fuel their M1-type activation status and limit iron availability for erythropoiesis (108–111), thereby contributing to the persistence of anemia.

In this context, it was shown that pro-inflammatory cytokines such as IFN-γ, TNF, IL-1, and IL-6 can affect iron-homeostasis regulation as well as erythropoiesis. Indeed, during homeostasis, there is a balance between RBC destruction and production, where the iron availability is adequate to accommodate the host's erythropoietic demand (112). Yet, during inflammation this balance is shifted toward an enhanced RBC destruction and impaired/insufficient production or RBCs, leading to anemia. These pro-inflammatory cytokines trigger (i) the upregulation of the divalent metal transporter-1, which increases iron uptake by the reticuloendothelial cells, (ii) an enhanced ferritin expression (i.e., iron storage molecule), and (iii) a downregulation of FPN-1 expression thereby promoting iron retention within the MPS (113, 114). This will cause a deprivation of iron from erythropoiesis. At the same time, these pro-inflammatory cytokines inhibit erythropoiesis by (i) downregulating EPO receptors thereby impairing the EPO-mediated effects, (ii) increasing erythroid apoptosis, and (iii) antagonizing pro-hematopoietic factors (115, 116).

On the other hand, trypanotolerant animals are able to switch to a protective anti-inflammatory response (induced *via* IL-10), which is reflected by the occurrence of M2 cells that in concert with IL-10 are able to dampen the pathological effects of the M1 cells, and exhibit an alleviated anemia development [i.e., *T. brucei* attenuation strategies, phospholipase-C-deficient (*PLC*$^{-/-}$) *T. brucei* and *T. congolense* model]. Moreover, trypanotolerant animals in contrast to trypanosusceptible animals exhibit a restored iron homeostasis (i.e., an enhanced FPN-1 and reduced ferritin expression) and increased iron availability for erythropoiesis (95). In addition, M2 cells exhibit a reduced erythrophagocytosis

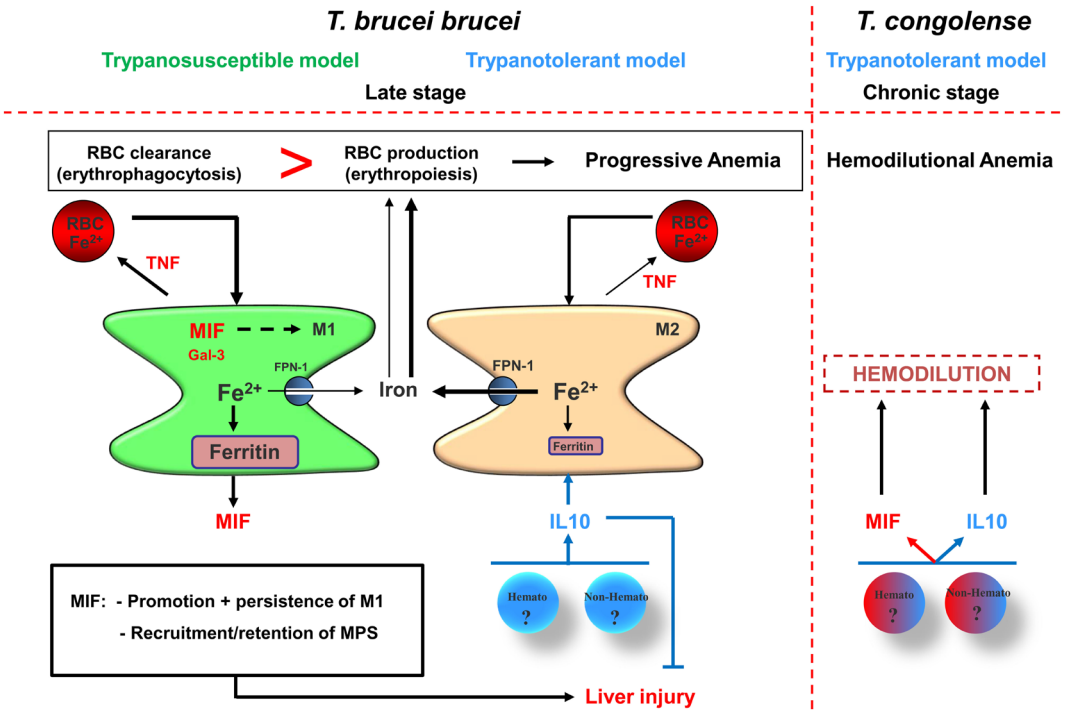


FIGURE 3 | Proposed model for pathogenicity development during the late/chronic stage of infection in trypanosusceptible and trypanotolerant animals. (Left panel) Following recovery from acute anemia (see **Figure 2**), trypanosusceptible animals are unable to trigger a second wave of IL-10 production resulting in persistence of M1, which is most likely promoted *via* macrophage migration inhibitory factor (MIF) and galectin-3. These M1 produce TNF that further promotes erythrophagocytosis and exhibit iron accumulation [increased ferritin and reduced ferroportin-1 (FPN-1) expression], resulting in iron deprivation from erythropoiesis and collectively leading to progressive anemia development. MIF also promotes myeloid cell recruitment/retention leading to liver injury. By contrast, in trypanotolerant animals, following the acute stage of infection, hematopoietic (hemato) or non-hematopoietic (non-hemato) cells produce IL-10, which dampens the pathogenic effects of the M1 by triggering the induction of M2. These M2 exhibit reduced erythrophagocytosis and reduced iron retention, leading to a more efficient erythropoiesis and in turn to reduced progressive anemia development. IL-10 also reduces liver injury by dampening the pathogenic effects of the M1. (Right panel) However, the chronic production of MIF by M1 and persistent IL-10 production can collectively promote progressive hemodilution, which is most likely due to enhanced (hepato)-splenomegaly. In turn, the hemodilution will cause an apparent anemia development in trypanotolerant animals, resulting in thrombocytopenia and impaired coagulation in infected mice. The heme catabolism following the chronically induced erythrophagocytosis leads to iron accumulation in myeloid cells and to hyperbilirubinemia. The combination of liver injury and hemodilution leads to declined serum albumin levels, thereby preventing efficient removal of toxic molecules from the circulation, including bilirubin, and cause multiple organ failure that culminates in reduced survival of the infected host.

capacity, whereby iron homeostasis is skewed toward export (117). It is important to mention that in both the *T. brucei* and *T. congolense* infection model, the host is able to produce IL-10 during the acute stage of anemia to dampen the pathogenic effects mediated *via* the pronounced pro-inflammatory response, which is linked to the first wave of parasitemia control. However, it seems that in the *T. brucei* (susceptible) model the host is unable to retrigger IL-10 induction to dampen the second wave of inflammation, while in the *PLC*$^{-/-}$ *T. brucei*/*T. congolense* (tolerant) model the host is able to mount a second progressive IL-10 response, which is sufficient to dampen the lower level of inflammation. This difference in ability to trigger a second wave of IL-10 (or alternatively, maintain an IL-10 triggering potential) is also reflected at the level of differences in M1 and M2 between susceptible and tolerant animals.

Myeloid Cell Activation in the *T. brucei* (Susceptible) versus *T. congolense* (Tolerant) Model

As far as the *T. brucei* model (using AnTat1.1E) is concerned, there is a persistent M1 activation contributing to severe anemia and tissue injury (see **Figures 1** and **3**). It was shown that the TNF-family members [TNF-α and lymphotoxin-alpha (LT-α)] play a key role in chronic/progressive anemia development by signaling *via* their dedicated receptors [TNF-R1 or p55 (CD120a), TNF-R2, or p75 (CD120b)] (see **Table 1**) (118). Thus, TNF-α-deficient (TNF-α$^{-/-}$) or TNF-R2-deficient (TNF-R2$^{-/-}$) mice exhibited greatly reduced chronic anemia compared with WT or TNF-R1-deficient (TNF-R1$^{-/-}$) mice (41, 59), suggesting that TNF-R2 signaling mediates infection-associated pathology, whereas TNF-R1 signaling has little or no impact on the *T. brucei* infection. Moreover, the serum levels of soluble TNF-R2 after shedding, which impaired TNF-α-signaling pathways in myeloid cells, correlated with the inhibition of TNF-mediated immunopathology. Moreover, the low ratio of total TNF-α to soluble TNF-R2 observed in BALB/c mice may account for the lack of TNF-mediated pathology, whereas an increased ratio in C57BL/6 mice coincided with the severe pathology/anemia. Using LT-α$^{-/-}$ mice, it was shown that the TIP sequence (i.e., lectin-like domain) of TNF-α does not seem to play a role in anemia development (118). Importantly, TNF-α and LT-α

have high amino acid sequence homology and both bind to the TNF-α p55 and p75 receptors (TNF-R1 and -R2, respectively) as soluble homotrimers (119), yet they exhibit alterations in the TIP sequences (120). For example, TNF-α exerts a lectin-like affinity for several carbohydrate sequences while LT-α does not (121). These LT-$\alpha^{-/-}$ mice were shown to exhibit during the middle stage of infection (days 10–28) a greatly reduced anemia compared with WT mice, which coincided with reduced TNF-α induction in LT-$\alpha^{-/-}$ mice during this stage. However, during the final stage of infection, serum TNF-α reaches the same levels in both LT-$\alpha^{-/-}$ and WT mice, concomitant with similar anemia levels in both mice groups. A possible explanation for this might be that TNF-α is also an important negative regulator of erythropoiesis and this aspect might predominate at later stages of infection (51, 122). Hence, strategies to reduce TNF signaling or allowing switching from M1 toward M2 might also be valuable to alleviate chronic anemia development. Different factors were found to contribute to the ability of the host to switch from M1 to M2 and the ability to maintain/trigger IL-10 during the later stages was shown to be detrimental to attenuate anemia.

Collectively, it seems that the mechanisms underlying trypanosomiasis-associated anemia are multifactorial and the relative contribution of each mechanism will differ according to the host–parasite model, the phase of anemia development and the severity of infection and is probably caused by massive extravascular erythrophagocytosis by an expanded MPS in concert with an inadequate erythropoiesis.

POTENTIAL INTERVENTION STRATEGIES TO ALLEVIATE AT-ASSOCIATED ANEMIA

The Parasite Strain Used Determines the MPS Activation State and Anemia Development

Typically, in the experimental *T. brucei* C57BL/6 model, the myeloid cells are polarized into an M1 state, which is promoted due to the inability of the host to sustain a strong anti-inflammatory immune response. By contrast, in the less aggressive model experimental *PLC*$^{-/-}$ *T. brucei* C57BL/6 model, there is a switch from M1 toward M2 mediated *via* IL-10, coinciding with reduced pathology (anemia/tissue injury) and prolonged survival. A possible explanation for this switch toward M2 in the *PLC*$^{-/-}$ *T. brucei* model and not in the WT *T. brucei* model might rely in the fact that the PLC is required to sustain M1 by (i) allowing the release of GPI-anchored proteins (encompassing the GIP) to stimulate macrophages to secrete pro-inflammatory molecules (TNF-α, IL-1, IL-6, and NO) and/or (ii) trigger CD1d-restricted NKT cells to secrete IFN-γ thereby triggering a very strong type 1 immune response (60, 123). Indeed, it was shown that in the *PLC*$^{-/-}$ *T. brucei* C57BL/6 model the lower parasitemia coincided with reduced early IFN-γ production and subsequent attenuated MPS-derived pro-inflammatory cytokine production, reflecting a reduced type 1 immune response mounted (124–126). The crucial role of IFN-γ and IL-10 during infection was further substantiated using gene-deficient mice, where the absence of IL-10 coincided with high pathology and early mortality. Although the source of IL-10 was not thoroughly investigated within the *PLC*$^{-/-}$ *T. brucei* model, some data suggest the involvement of $CD4^+$ T cells (124). Interestingly, infections of *PLC*$^{-/-}$ *T. brucei* parasites using C57BL/6 x BALB/c (B6B-F1) mice were found to exhibit striking similarities with that of the trypanotolerant N'Dama cattle naturally infected with *T. congolense*. These latter include (i) lower parasitemia, (ii) prolonged survival, (iii) increased type II and decreased type I immune responses, and (iv) reduced pathology and minimal clinical symptoms during the course of infection (127, 128). Therefore, *PLC*$^{-/-}$ *T. brucei*-infected B6B-F1 mice represent a suitable model to study the immune responses during bovine *T. congolense* infections. Within the *T. congolense* model in C57BL/6 mice, it was shown that spleen and liver regulatory T cells ($Foxp3^+$ Tregs) were an important source of IL-10, thereby limiting the production of early IFN-γ by T cells and in that way lowering pathology. Besides Tregs, also myeloid-derived IL-10 was shown to play an important role in limiting the production of pathogenic TNF-α by M1 cells (characterized as $CD11b^+Ly6C^+$) through induction of nuclear translocation of the NF-κB p50 member (129). However, it cannot be excluded that other hematopoietic and non-hematopoietic cells can be potential sources of IL-10 during the course of *T. congolense* infection (**Figure 3**).

IL-10-Inducing Strategies to Modulate the MPS Activation State and Anemia Development

As mentioned before, the capacity of the host to induce IL-10 immediately after the induction of a prominent pro-inflammatory immune response mediated *via* M1 cells determines whether pathology/anemia develops/is alleviated or not. This opens perspectives for potential IL-10 triggering/promoting intervention strategies aiming at triggering an M1 toward M2 switch, thereby reducing pathology development. So far, several strategies have been used to demonstrate/strengthen the pivotal role of IL-10 in reducing trypanosomiasis-associated pathogenicity using the susceptible *T. brucei* model. For instance, transient anti-CD28 superagonist antibody treatment (inducing regulatory T cells and M2) in the *T. brucei* model attenuated acute anemia development (130). Given that this treatment was not continued during the chronic phase of infection its effects during this stage remain to be determined. Alternatively, adenoviral delivery of IL-10 in the *T. brucei* model coincided with an alleviated pathology/anemia development (131), during the chronic phase of infection (see **Table 1**). Also a GPI-based treatment strategy, where the parasite-derived GPI moiety (i.e., most potent parasite-derived TNF-inducing molecule involved in M1 triggering) was used to reprogram macrophages toward an anti-inflammatory state (i.e., reflected by a reduced inflammatory cytokine production and increased IL-10 production), was shown to alleviate anemia in both clonal as well as natural/non-clonal *T. brucei* infections (132). This strategy allowed reducing RBC destruction, normalizing iron homeostasis (i.e., a shift in increased liver expression of iron storage toward iron export genes) and restoring

erythropoiesis [i.e., increased erythropoiesis in the bone marrow and extramedullary sites (spleen)] (95). Interestingly, this GPI-based treatment also alleviated "chronic" anemia development during experimental *T. congolense* as well as *T. evansi* infections suggesting a wide applicability.

M1-Promoting Factors Are Prime Targets to Attenuate Anemia

Given that M1 cells are major contributors to anemia development, identification of M1-derived pathological factors might open perspectives to attenuate the pathology. An approach to identify potential M1-derived pathology inducing/promoting factors consisted of scrutinizing a GPI-based strategy, which enabled a straightforward comparison between trypanotolerance and trypanosusceptibility in *T. brucei*-infected C57BL/6 mice, independent of the genetic background of the host (95). A resulting comparative gene expression analysis of M1-polarizing molecules and/or molecules involved in enhancing erythrophagocytosis identified galectin-3 (Gal-3) and macrophage migration inhibitory factor (MIF) as potential candidates. Both molecules were indeed found to contribute to anemia development during *T. brucei* infections by affecting/regulating different aspects of the host's immune response. As far as Gal-3 (i.e., a family member of beta-galactoside-binding animal lectins) is concerned, it was shown that *Gal-3*$^{-/-}$ mice manifested higher IL-10 levels that can exert an influence on iron uptake and counteract the effects of IFN-γ (133). Hence, Gal-3 can promote persistence of M1 and regulate the expression of iron-homeostasis genes, favoring iron storage, which ultimately culminates in iron shortage for erythropoiesis and exacerbate inflammation-associated anemia development (**Figures 2** and **3**) (133, 134). In addition, given the negative effect of Gal-3 on the induction of IL-10, a persistent inflammatory response is ensured in presence of Gal-3. As far as MIF is concerned, this "early response" cytokine is expressed by numerous cell types, including myeloid cells, plays a key role in innate and adaptive immunity and was shown to be involved in many protozoan infections (135–137). Using *Mif*$^{-/-}$ mice it was shown that this upstream regulator of the inflammatory cascade contributed to inflammation-associated pathogenicity by (i) sustaining a persistent pro-inflammatory type I immune response (impairing IL-10 production) and (ii) maintaining/enhancing the recruitment of pathogenic monocytic cells and neutrophils in the liver whereby neutrophil-derived MIF contributed significantly to enhanced TNF production and liver damage (**Figures 2** and **3**) (93). The pivotal role of MIF within the African trypanosomiasis model regarding the persistence of inflammation might be multifactorial. For instance, endogenous MIF has been shown to (i) promote macrophage-mediated inflammatory responses *via* induction of CC chemokine ligand 2 expression, thereby promoting the recruitment of monocytes into affected areas and (ii) exert a regulatory role in cellular responsiveness to key pro-inflammatory cytokines TNF and IL-1 *via* upregulation of cytokine receptor-dependent MAPK signaling (i.e., upregulation of TNF-R1 and IL-1R expression, respectively) independent of NF-κB (138, 139). Hence, by both attracting and activating monocyte/macrophages, MIF may contribute to the initiation and perpetuation of detrimental inflammation associated with diseases such as African trypanosomiasis. In addition, MIF importantly contributed to anemia development by (i) promoting iron accumulation in liver myeloid cells, (ii) enhancing RBC clearance, and (iii) suppressing erythropoiesis at later stages of erythroblast differentiation (**Figure 3**) (93). Interestingly, MIF was also shown to be a potential pathogenic molecule playing a key role in chronic anemia development during *T. congolense* infections by (i) promoting erythrophagocytosis, (ii) blocking extramedullary erythropoiesis and RBC maturation, and (iii) triggering hemodilution (**Figure 3**) (94).

Overall, it seems that during murine *T. brucei* and *T. congolense* infections anemia is mainly due to enhanced erythrophagocytosis combined with enhanced but inadequate extramedullary erythropoiesis. Yet, during *T. congolense* but not *T. brucei* infections, hemodilution (involving massive hepatosplenomegaly) seems to be an additional factor contributing to chronic anemia development (93, 94). However, it might be that within the *T. brucei* model the contribution of hepatosplenomegaly to hemodilution is minor or not reached within this "short" time period. This notion is strengthened by the fact that there was no correlation between anemia and hemodilution (involving hepatosplenomegaly) in *T. brucei* and *T. congolense*-infected rats within the same time window (92). However, a different *T. brucei* parasite strain (TREU 667 strain) causing a more chronic infection involving also revealed that the hepatosplenomegaly could contribute to hemodilution (140). Of note, also in HAT patients exhibiting anemia during later stages of the disease, hepatosplenomegaly has been recorded and this might therefore contribute to the observed "apparent" anemia (28). In this particular model, it seems that the virulence of the parasites determines whether hemodilution occurs. Interestingly, these observations correlate nicely with experimental *T. brucei* and *T. congolense* infections in domestic animals (cattle and sheep, respectively) (141, 142). Importantly, it was shown that MIF can also be present in erythrocytes and upon (hemo)lysis, due to oxidative stress, this factor can be released to further fuel inflammation (143). Given that hemolysis was shown to occur during *T. congolense* infections (40, 144), the increased levels of MIF observed during both the acute and chronic stage might mainly be due to parasite-inflicted rather that host-mediated damage of RBCs, which could also fuel a chronic (low-grade) anemia profile. Therefore, MIF might be an "important" player (upstream regulator) in African trypanosomiasis-associated anemia, mainly during the chronic stage of anemia development by fueling/promoting pathogenic M1 and could be considered as a prime anti-disease target.

GENERAL CONCLUSION AND PERSPECTIVES

African trypanosomes are very proficient in sculpturing a temporal environment to allow a gradual parasite establishment (27). Hereby, the host's response at different stages of the

infection determines whether pathogenicity/anemia develops. The mechanisms underlying African trypanosomiasis-associated anemia are multifactorial, whereby various molecules influence differentially the progression/development of anemia at distinct stages of infection. Initially, acute anemia seems to develop as part of the innate immune response upon infection, where parasite-derived factors, such as parasite-derived EVs, as well as host-derived (parasite-induced) IFN-γ trigger M1 cell differentiation that in turn produce pro-inflammatory molecules to control the infection. In this context, IFN-γ produced at the acute stage is the driving factor leading to acute/hemophagocytic anemia (30). In addition, the release of parasite-derived EVs in concert with host-derived TNF-α affect RBC survival and thereby fuels RBC elimination trough erythrophagocytosis (**Figure 2**). This is followed by a partial recovery, mediated most likely *via* extramedullary erythropoiesis, as a homeostatic reaction and a transient IL-10 production to dampen the pathogenic effects of the M1. Depending on the level of insult (i.e., M1-induced damage) and the capacity of the host to trigger and subsequently maintain IL-10 production, anemia is either alleviated (i.e., trypanotolerant animals) or sustained (i.e., trypanosusceptible animals). At this stage, MIF is an important host-derived factor determining/regulating the progression of anemia by promoting a persistent pro-inflammatory immune response and suppressing erythropoiesis. In addition, IFN-γ, TNF-α, and MIF are important molecules exerting a negative effect on erythropoiesis and at the same time at promoting erythrophagocytosis. By contrast, IL-10 was shown to positively affect erythropoiesis by down-regulating the effects of the pro-inflammatory cytokines (145). Therefore, the balance between these pro- and anti-inflammatory cytokines during the course of infection determines the course of anemia development (51). In other words, the ability of the host to mount an efficient erythropoietic response (stress-induced response) to compensate for the enhanced erythrophagocytosis determines whether anemia persists. In the murine model, but also in cattle, the erythropoietic potential determines the level of anemia (33, 40, 94, 122). However, it seems that chronic anemia is most likely host-inflicted and due to a disproportional immune response (30). In summary, the mechanisms underlying/promoting chronic anemia development during *T. brucei* and *T. congolense* infections seem to be different. In the *T. brucei* infection model the main driving forces for anemia development are (i) the persistence of M1 that promote enhanced RBC elimination and iron retention and (ii) an insufficient erythropoiesis due to iron deprivation and the presence of pro-inflammatory cytokines that suppress RBC differentiation/maturation (**Figure 3**). By contrast, in the *T. congolense* infection model these aspects seem to play a main role only during the acute stage, as once M2 are induced and expanding they can in concert with IL-10 dampen to a certain extent the pathogenic effects of the M1. Given that *T. congolense*-infected animals still exhibited chronic anemia despite the presence of M2 and IL-10 suggests that the underlying mechanisms of chronic anemia in this model might be different and might rely on the hematopoietic potential of the animals (40). It was proposed that the month-lasting low-grade inflammatory response can also drive erythrophagocytosis, where the ensuing catabolism of hemoglobin resulted in iron accumulation mainly in the spleen and is followed by the enhanced release of bilirubin in the blood circulation (94). The resulting hyperbilirubinemia could favor the externalization of phosphatidylserine on RBCs and thus further contribute to erythrophagocytosis or eryptosis during *T. congolense* infection (146). However, at this stage the persistence of IL-10 might be a double-edged sword by on one hand dampening tissue injury and reduce the suppression on erythropoiesis mediated by the M1-released pro-inflammatory mediators and on the other promoting (i) ferritin expression thereby indirectly affecting iron availability, (ii) thrombocytopenia, and (iii) splenomegaly, leading to hemodilution (147, 148). The latter might in turn culminate into the occurrence of apparent anemia development, despite an enhanced erythropoiesis activity. In this context, it was shown that sustained secretion of IL-10 from transduced muscle leads to thrombocytopenia and splenomegaly in mice injected with rAAV1-IL-10 (147). Interestingly, thrombocytopenia was also documented for *T. congolense*-infected animals (149, 150). The splenomegaly observed in both susceptible and tolerant animals is required to accommodate the increased demand for erythropoiesis (93–95). However, it seems that this excessive accumulation of immature RBCs is most likely due to an inefficient erythropoietic potential (e.g., iron retention or unresponsiveness toward EPO or inefficient functioning of erythroblastic islands). Indeed, it was shown that most genes involved in erythropoiesis were found to be significantly modulated during the course of both *T. brucei* and *T. congolense* infection (40, 93, 94). However, so far information regarding erythropoiesis during African trypanosomiasis is limited and requires more attention. Also, a possible involvement of macrophages (functionality) within erythroblastic islands requires consideration. Within the era of genomics/proteomics (151–154), we can assume that novel pathways, mechanisms and molecular target molecules will be identified in various mouse models (155, 156). These discoveries will help us to refine our understanding of the mechanisms underlying anemia development and could even pave the way to develop new intervention strategies to alleviate it.

AUTHOR CONTRIBUTIONS

All authors listed have made a substantial, direct, and intellectual contribution to the work and approved it for publication.

FUNDING

The authors acknowledge the financial support of the Inter-university Attraction Pole Program (PAI-IAP N. P7/41, http://www.belspo.be/belspo/iap/index_en.stm) and grants from the FWO (FWO G015016N and G.0.028.10.N.10). BS is a research fellow supported by the Strategic Research Program (SRP3, VUB): targeting inflammation linked to infectious diseases and cancer (Nanobodies for Health). The funders had no role in study design, data collection and analysis, decision to publish, or preparation of the manuscript.

REFERENCES

1. Aksoy S, Buscher P, Lehane M, Solano P, Van Den Abbeele J. Human African trypanosomiasis control: achievements and challenges. *PLoS Negl Trop Dis* (2017) 11(4):e0005454. doi:10.1371/journal.pntd.0005454
2. Sutherland CS, Yukich J, Goeree R, Tediosi F. A literature review of economic evaluations for a neglected tropical disease: human African trypanosomiasis ("sleeping sickness"). *PLoS Negl Trop Dis* (2015) 9:e0003397. doi:10.1371/journal.pntd.0003397
3. Shaw AP, Cecchi G, Wint GR, Mattioli RC, Robinson TP. Mapping the economic benefits to livestock keepers from intervening against bovine trypanosomosis in Eastern Africa. *Prev Vet Med* (2014) 113:197–210. doi:10.1016/j.prevetmed.2013.10.024
4. Giordani F, Morrison LJ, Rowan TG, De Koning HP, Barrett MP. The animal trypanosomiases and their chemotherapy: a review. *Parasitology* (2016) 143(14):1862–89. doi:10.1017/S0031182016001268
5. Yaro M, Munyard KA, Stear MJ, Groth DM. Combatting African animal trypanosomiasis (AAT) in livestock: the potential role of trypanotolerance. *Vet Parasitol* (2016) 225:43–52. doi:10.1016/j.vetpar.2016.05.003
6. Franco JR, Simarro PP, Diarra A, Jannin JG. Epidemiology of human African trypanosomiasis. *Clin Epidemiol* (2014) 6:257–75. doi:10.2147/CLEP.S39728
7. Courtin D, Berthier D, Thevenon S, Dayo G-K, Garcia A, Bucheton B. Host genetics in African trypanosomiasis. *Infect Genet Evol* (2008) 8:229–38. doi:10.1016/j.meegid.2008.02.007
8. Waiswa C, Olaho-Mukani W, Katunguka-Rwakishaya E. Domestic animals as reservoirs for sleeping sickness in three endemic foci in south-eastern Uganda. *Ann Trop Med Parasitol* (2003) 97:149–55. doi:10.1179/000349803235001688
9. Ruiz JP, Nyingilili HS, Mbata GH, Malele II. The role of domestic animals in the epidemiology of human African trypanosomiasis in Ngorongoro conservation area, Tanzania. *Parasit Vectors* (2015) 8:510. doi:10.1186/s13071-015-1125-6
10. Büscher P, Cecchi G, Jamonneau V, Priotto G. Human African trypanosomiasis. *Lancet* (2017) 390(10110):2397–409. doi:10.1016/S0140-6736(17)31510-6
11. Kennedy PG. The continuing problem of human African trypanosomiasis (sleeping sickness). *Ann Neurol* (2008) 64:116–26. doi:10.1002/ana.21429
12. MacLean L, Reiber H, Kennedy PGE, Sternberg JM. Stage progression and neurological symptoms in *Trypanosoma brucei* rhodesiense sleeping sickness: role of the CNS inflammatory response. *PLoS Negl Trop Dis* (2012) 6:e1857. doi:10.1371/journal.pntd.0001857
13. Kennedy PG. Clinical features, diagnosis, and treatment of human African trypanosomiasis (sleeping sickness). *Lancet Neurol* (2013) 12:186–94. doi:10.1016/S1474-4422(12)70296-X
14. Morrison LJ, Vezza L, Rowan T, Hope JC. Animal African trypanosomiasis: time to increase focus on clinically relevant parasite and host species. *Trends Parasitol* (2016) 32:599–607. doi:10.1016/j.pt.2016.04.012
15. Losos GJ, Ikede BO. Review of pathology of diseases in domestic and laboratory animals caused by *Trypanosoma congolense*, *T. vivax*, *T. brucei*, *T. rhodesiense* and *T. gambiense*. *Vet Pathol* (1972) 9:1–79. doi:10.1177/030098587200901s01
16. Kieft R, Capewell P, Turner CM, Veitch NJ, MacLeod A, Hajduk S. Mechanism of *Trypanosoma brucei* gambiense (group 1) resistance to human trypanosome lytic factor. *Proc Natl Acad Sci U S A* (2010) 107:16137–41. doi:10.1073/pnas.1007074107
17. Chitanga S, Namangala B, De Deken R, Marcotty T. Shifting from wild to domestic hosts: the effect on the transmission of *Trypanosoma congolense* to tsetse flies. *Acta Trop* (2013) 125:32–6. doi:10.1016/j.actatropica.2012.08.019
18. Connor RJ. The impact of nagana. *Onderstepoort J Vet Res* (1994) 61:379–83.
19. World Health Organization. Control and surveillance of human African trypanosomiasis. *World Health Organ Tech Rep Ser* (2013) 984:1–237.
20. Lehane M, Alfaroukh I, Bucheton B, Camara M, Harris A, Kaba D, et al. Tsetse control and the elimination of Gambian sleeping sickness. *PLoS Negl Trop Dis* (2016) 10(4):e0004437. doi:10.1371/journal.pntd.0004437
21. Berthier D, Brenière SF, Bras-Gonçalves R, Lemesre JL, Jamonneau V, Solano P, et al. Tolerance to trypanosomatids: a threat, or a key for disease elimination? *Trends Parasitol* (2016) 32:157–68. doi:10.1016/j.pt.2015.11.001
22. Field MC, Horn D, Fairlamb AH, Ferguson MAJ, Gray DW, Read KD, et al. Anti-trypanosomatid drug discovery: an ongoing challenge and a continuing need. *Nat Rev Microbiol* (2017) 15:217–31. doi:10.1038/nrmicro.2016.193
23. Bouyer J, Bouyer F, Donadeu M, Rowan T, Napier G. Community- and farmer-based management of animal African trypanosomosis in cattle. *Trends Parasitol* (2013) 29:519–22. doi:10.1016/j.pt.2013.08.003
24. Mbaya AW, Aliyu MM, Ibrahim UI. The clinico-pathology and mechanisms of trypanosomosis in captive and free-living wild animals: a review. *Vet Res Commun* (2009) 33:793–809. doi:10.1007/s11259-009-9214-7
25. Mäser P, Lüscher A, Kaminsky R. Drug transport and drug resistance in African trypanosomes. *Drug Resist Updat* (2003) 6:281–90. doi:10.1016/j.drup.2003.09.001
26. Baker N, de Koning HP, Maser P, Horn D. Drug resistance in African trypanosomiasis: the melarsoprol and pentamidine story. *Trends Parasitol* (2013) 29:110–8. doi:10.1016/j.pt.2012.12.005
27. Stijlemans B, Caljon G, Van Den Abbeele J, Van Ginderachter JA, Magez S, De Trez C. Immune evasion strategies of *Trypanosoma brucei* within the mammalian host: progression to pathogenicity. *Front Immunol* (2016) 7:233. doi:10.3389/fimmu.2016.00233
28. Chisi JE, Misiri H, Zverev Y, Nkhoma A, Sternberg JM. Anaemia in human African trypanosomiasis caused by *Trypanosoma brucei* rhodesiense. *East Afr Med J* (2004) 81:505–8. doi:10.4314/eamj.v81i10.9232
29. Jamonneau V, Garcia A, Ravel S, Cuny G, Oury B, Solano P, et al. Genetic characterization of *Trypanosoma brucei* gambiense and clinical evolution of human African trypanosomiasis in Cote d'Ivoire. *Trop Med Int Health* (2002) 7:610–21. doi:10.1046/j.1365-3156.2002.00905.x
30. Naessens J. Bovine trypanotolerance: a natural ability to prevent severe anaemia and haemophagocytic syndrome? *Int J Parasitol* (2006) 36:521–8. doi:10.1016/j.ijpara.2006.02.012
31. Naessens J, Leak SG, Kennedy DJ, Kemp SJ, Teale AJ. Responses of bovine chimaeras combining trypanosomosis resistant and susceptible genotypes to experimental infection with *Trypanosoma congolense*. *Vet Parasitol* (2003) 111:125–42. doi:10.1016/S0304-4017(02)00360-6
32. Trail JCM, d'Ieteren GDM, Maille JC, Yangari G. Genetic aspects of control of anaemia development in trypanotolerant N'Dama cattle. *Acta Trop* (1991) 48:285–91. doi:10.1016/0001-706X(91)90016-D
33. Andrianarivo AG, Muiya P, Logan-Henfrey LL. *Trypanosoma congolense*: high erythropoietic potential in infected yearling cattle during the acute phase of the anemia. *Exp Parasitol* (1996) 82:104–11. doi:10.1006/expr.1996.0014
34. Van Den Bossche P, Rowlands GJ. The relationship between the parasitological prevalence of trypanosomal infections in cattle and herd average packed cell volume. *Acta Trop* (2001) 78(2):163–70. doi:10.1016/S0001-706X(00)00182-0
35. Faye D, Fall A, Leak S, Losson B, Geerts S. Influence of an experimental *Trypanosoma congolense* infection and plane of nutrition on milk production and some biochemical parameters in West African Dwarf goats. *Acta Trop* (2005) 93:247–57. doi:10.1016/j.actatropica.2004.10.008
36. Katunguka-Rwakishaya E, Murray M, Holmes PH. The influence of energy intake on some blood biochemical parameters in Scottish Blackface sheep infected with *Trypanosoma congolense*. *Vet Parasitol* (1999) 84:1–11. doi:10.1016/S0304-4017(99)00088-6
37. Nnadi PA, Ezeh IO, Kalu KC, Ngene AA. The impact of dietary protein on the pathophysiology of porcine trypanosome infection. *Vet Parasitol* (2010) 173:193–9. doi:10.1016/j.vetpar.2010.07.004
38. Osaer S, Goossens B, Jeffcoate I, Holmes P. Effects of *Trypanosoma congolense* and nutritional supplements in Djallonke ewes on live weight during pregnancy, post partum weight, haematology parameters and lamb performance. *Res Vet Sci* (1998) 65:65–9. doi:10.1016/S0034-5288(98)90029-7
39. Magez S, Caljon G. Mouse models for pathogenic African trypanosomes: unravelling the immunology of host-parasite-vector interactions. *Parasite Immunol* (2011) 33:423–9. doi:10.1111/j.1365-3024.2011.01293.x
40. Noyes HA, Alimohammadian MH, Agaba M, Brass A, Fuchs H, Gailus-Durner V, et al. Mechanisms controlling anaemia in *Trypanosoma congolense* infected mice. *PLoS One* (2009) 4:e5170. doi:10.1371/journal.pone.0005170
41. Magez S, Truyens C, Merimi M, Radwanska M, Stijlemans B, Brouckaert P, et al. P75 tumor necrosis factor-receptor shedding occurs as a protective host response during African trypanosomiasis. *J Infect Dis* (2004) 189:527–39. doi:10.1086/381151
42. Magez S, Schwegmann A, Atkinson R, Claes F, Drennan M, De Baetselier P, et al. The role of B-cells and IgM antibodies in parasitemia, anemia, and VSG switching in *Trypanosoma brucei*-infected mice. *PLoS Pathog* (2008) 4:e1000122. doi:10.1371/journal.ppat.1000122

43. Stijlemans B, Vankrunkelsven A, Caljon G, Bockstal V, Guilliams M, Bosschaerts T, et al. The central role of macrophages in trypanosomiasis-associated anemia: rationale for therapeutical approaches. *Endocr Metab Immune Disord Drug Targets* (2010) 10:71–82. doi:10.2174/187153010790827966
44. Paulnock DM, Freeman BE, Mansfield JM. Modulation of innate immunity by African trypanosomes. *Parasitology* (2010) 137:2051–63. doi:10.1017/S0031182010001460
45. Mansfield JM, Paulnock DM. Regulation of innate and acquired immunity in African trypanosomiasis. *Parasite Immunol* (2005) 27:361–71. doi:10.1111/j.1365-3024.2005.00791.x
46. Jackson AP, Berry A, Aslett M, Allison HC, Burton P, Vavrova-Anderson J, et al. Antigenic diversity is generated by distinct evolutionary mechanisms in African trypanosome species. *Proc Natl Acad Sci U S A* (2012) 109:3416–21. doi:10.1073/pnas.1117313109
47. Morrison LJ, Marcello L, McCulloch R. Antigenic variation in the African trypanosome: molecular mechanisms and phenotypic complexity. *Cell Microbiol* (2009) 11:1724–34. doi:10.1111/j.1462-5822.2009.01383.x
48. Darji A, Lucas R, Magez S, Torreele E, Palacios J, Sileghem M, et al. Mechanisms underlying trypanosome-elicited immunosuppression. *Ann Soc Belg Med Trop* (1992) 72(Suppl 1):27–38.
49. Radwanska M, Guirnalda P, De Trez C, Ryffel B, Black S, Magez S. Trypanosomiasis-induced B cell apoptosis results in loss of protective anti-parasite antibody responses and abolishment of vaccine-induced memory responses. *PLoS Pathog* (2008) 4:e1000078. doi:10.1371/journal.ppat.1000078
50. Stijlemans B, Radwanska M, De Trez C, Magez S. African trypanosomes undermine humoral responses and vaccine development: link with inflammatory responses? *Front Immunol* (2017) 8:582. doi:10.3389/fimmu.2017.00582
51. Musaya J, Matovu E, Nyirenda M, Chisi J. Role of cytokines in *Trypanosoma brucei*-induced anaemia: a review of the literature. *Malawi Med J* (2015) 27:45–50. doi:10.4314/mmj.v27i2.3
52. Dubois ME, Demick KP, Mansfield JM. Trypanosomes expressing a mosaic variant surface glycoprotein coat escape early detection by the immune system. *Infect Immun* (2005) 73:2690–7. doi:10.1128/IAI.73.5.2690-2697.2005
53. De Muylder G, Daulouede S, Lecordier L, Uzureau P, Morias Y, Van Den Abbeele J, et al. A *Trypanosoma brucei* kinesin heavy chain promotes parasite growth by triggering host arginase activity. *PLoS Pathog* (2013) 9:e1003731. doi:10.1371/journal.ppat.1003731
54. Willert E, Phillips MA. Regulation and function of polyamines in African trypanosomes. *Trends Parasitol* (2012) 28:66–72. doi:10.1016/j.pt.2011.11.001
55. Salmon D, Vanwalleghem G, Morias Y, Denoeud J, Krumbholz C, Lhomme F, et al. Adenylate cyclases of *Trypanosoma brucei* inhibit the innate immune response of the host. *Science* (2012) 337:463–6. doi:10.1126/science.1222753
56. Wall EA, Zavzavadjian JR, Chang MS, Zhu X, Hsueh RC, Liu J, et al. Suppression of LPS-induced TNF-alpha production in macrophages by cAMP is mediated by PKA-AKAP95-p105. *Sci Signal* (2009) 2:ra28. doi:10.1126/scisignal.2000202.Suppression
57. McDonough KA, Rodriguez A. The myriad roles of cyclic AMP in microbial pathogens: from signal to sword. *Nat Rev Microbiol* (2011) 10(1):27–38. doi:10.1038/nrmicro2688
58. Gobert AP, Daulouede S, Lepoivre M, Boucher JL, Bouteille B, Buguet A, et al. L-arginine availability modulates local nitric oxide production and parasite killing in experimental trypanosomiasis. *Infect Immun* (2000) 68:4653–7. doi:10.1128/IAI.68.8.4653-4657.2000
59. Magez S, Radwanska M, Beschin A, Sekikawa K, De Baetselier P. Tumor necrosis factor alpha is a key mediator in the regulation of experimental *Trypanosoma brucei* infections. *Infect Immun* (1999) 67:3128–32.
60. Magez S, Stijlemans B, Radwanska M, Pays E, Ferguson MAJ, De Baetselier P. The glycosyl-inositol-phosphate and dimyristoylglycerol moieties of the glycosylphosphatidylinositol anchor of the trypanosome variant-specific surface glycoprotein are distinct macrophage-activating factors. *J Immunol* (1998) 160:1949–56.
61. Leppert BJ, Mansfield JM, Paulnock DM. The soluble variant surface glycoprotein of African trypanosomes is recognized by a macrophage scavenger receptor and induces I kappa B alpha degradation independently of TRAF6-mediated TLR signaling. *J Immunol* (2007) 179:548–56. doi:10.4049/jimmunol.179.1.548
62. Magez S, Stijlemans B, Baral T, De Baetselier P. VSG-GPI anchors of African trypanosomes: their role in macrophage activation and induction of infection-associated immunopathology. *Microbes Infect* (2002) 4:999–1006. doi:10.1016/S1286-4579(02)01617-9
63. Drennan MB, Stijlemans B, Van den Abbeele J, Quesniaux VJ, Barkhuizen M, Brombacher F, et al. The induction of a type 1 immune response following a *Trypanosoma brucei* infection is MyD88 dependent. *J Immunol* (2005) 175:2501–9. doi:10.4049/jimmunol.175.4.2501
64. Hamadien M, Lycke N, Bakhiet M. Induction of the trypanosome lymphocyte-triggering factor (TLTF) and neutralizing antibodies to the TLTF in experimental African trypanosomiasis. *Immunology* (1999) 96:606–11. doi:10.1046/j.1365-2567.1999.00730.x
65. Webb H, Carnall N, Vanhamme L, Rolin S, Van Den Abbeele J, Welburn S, et al. The GPI-phospholipase C of *Trypanosoma brucei* is nonessential but influences parasitemia in mice. *J Cell Biol* (1997) 139:103–14. doi:10.1083/jcb.139.1.103
66. Hereld D, Krakow JL, Bangs JD, Hart GW, Englund PT. A phospholipase C from *Trypanosoma brucei* which selectively cleaves the glycolipid on the variant surface glycoprotein. *J Biol Chem* (1986) 261:13813–9.
67. Cardoso de Almeida ML, Turner MJ. The membrane form of variant surface glycoproteins of *Trypanosoma brucei*. *Nature* (1983) 302:349–52. doi:10.1038/302349a0
68. Ferguson MAJ, Haldar K, Cross GAM. *Trypanosoma brucei* variant surface glycoprotein has a sn-1,2-dimyristyl glycerol membrane anchor at its COOH terminus. *J Biol Chem* (1985) 260:4963–8.
69. Coller SP, Mansfield JM, Paulnock DM. Glycosylinositolphosphate soluble variant surface glycoprotein inhibits IFN-gamma-induced nitric oxide production via reduction in STAT1 phosphorylation in African trypanosomiasis. *J Immunol* (2003) 171:1466–72. doi:10.4049/jimmunol.171.3.1466
70. Cnops J, De Trez C, Stijlemans B, Keirsse J, Kauffmann F, Barkhuizen M, et al. NK-, NKT- and CD8-derived IFNγ drives myeloid cell activation and erythrophagocytosis, resulting in trypanosomosis-associated acute anemia. *PLoS Pathog* (2015) 11(6):e1004964. doi:10.1371/journal.ppat.1004964
71. Zoller EE, Lykens JE, Terrell CE, Aliberti J, Filipovich AH, Henson PM, et al. Hemophagocytosis causes a consumptive anemia of inflammation. *J Exp Med* (2011) 208:1203–14. doi:10.1084/jem.20102538
72. Nemeth E, Ganz T. Anemia of inflammation. *Hematol Oncol Clin North Am* (2014) 28:671–81, vi. doi:10.1016/j.hoc.2014.04.005
73. Mabbott NA, Coulson PS, Smythies LE, Wilson RA, Sternberg JM. African trypanosome infections in mice that lack the interferon-gamma receptor gene: nitric oxide-dependent and -independent suppression of T-cell proliferative responses and the development of anaemia. *Immunology* (1998) 94:476–80. doi:10.1046/j.1365-2567.1998.00541.x
74. Stijlemans B, Cnops J, Naniima P, Vaast A, Bockstal V, De Baetselier P, et al. Development of a pHrodo-based assay for the assessment of in vitro and in vivo erythrophagocytosis during experimental trypanosomosis. *PLoS Negl Trop Dis* (2015) 9:e0003561. doi:10.1371/journal.pntd.0003561
75. Bosschaerts T, Guilliams M, Stijlemans B, Morias Y, Engel D, Tacke F, et al. Tip-DC development during parasitic infection is regulated by IL-10 and requires CCL2/CCR2, IFN-gamma and MyD88 signaling. *PLoS Pathog* (2010) 6:e1001045. doi:10.1371/journal.ppat.1001045
76. Theurl I, Hilgendorf I, Nairz M, Tymoszuk P, Haschka D, Asshoff M, et al. On-demand erythrocyte disposal and iron recycling requires transient macrophages in the liver. *Nat Med* (2016) 22:945–51. doi:10.1038/nm.4146
77. Balogun EO, Balogun JB, Yusuf S, Inuwa HM, Ndams IS, Sheridan P, et al. Anemia amelioration by lactose infusion during trypanosomosis could be associated with erythrocytes membrane de-galactosylation. *Vet Parasitol* (2014) 199:259–63. doi:10.1016/j.vetpar.2013.10.013
78. Coustou V, Plazolles N, Guegan F, Baltz T. Sialidases play a key role in infection and anaemia in *Trypanosoma congolense* animal trypanosomiasis. *Cell Microbiol* (2012) 14:431–45. doi:10.1111/j.1462-5822.2011.01730.x
79. Nok AJ, Balogun EO. A bloodstream *Trypanosoma congolense* sialidase could be involved in anemia during experimental trypanosomiasis. *J Biochem* (2003) 133:725–30. doi:10.1093/jb/mvg093
80. Szempruch AJ, Sykes SE, Kieft R, Dennison L, Becker AC, Gartrell A, et al. Extracellular vesicles from *Trypanosoma brucei* mediate virulence factor transfer and cause host anemia. *Cell* (2016) 164:246–57. doi:10.1016/j.cell.2015.11.051

81. Moldawer LL, Marano MA, Wei H, Fong Y, Silen ML, Kuo G, et al. Cachectin/tumor necrosis factor-alpha alters red blood cell kinetics and induces anemia in vivo. *FASEB J* (1989) 3:1637–43. doi:10.1096/fasebj.3.5.2784116
82. Magez S, Radwanska M, Drennan M, Fick L, Baral TN, Allie N, et al. Tumor necrosis factor (TNF) receptor-1 (TNFp55) signal transduction and macrophage-derived soluble TNF are crucial for nitric oxide-mediated *Trypanosoma congolense* parasite killing. *J Infect Dis* (2007) 196:954–62. doi:10.1086/520815
83. Naessens J, Kitani H, Nakamura Y, Yagi Y, Sekikawa K, Iraqi F. TNF-alpha mediates the development of anaemia in a murine *Trypanosoma brucei* rhodesiense infection, but not the anaemia associated with a murine *Trypanosoma congolense* infection. *Clin Exp Immunol* (2005) 139:405–10. doi:10.1111/j.1365-2249.2004.02717.x
84. Mabbott N, Sternberg J. Bone marrow nitric oxide production and development of anemia in *Trypanosoma brucei*-infected mice. *Infect Immun* (1995) 63:1563–6.
85. Balber AE. *Trypanosoma brucei*: attenuation by corticosteroids of the anemia of infected mice. *Exp Parasitol* (1974) 35:209–18. doi:10.1016/0014-4894(74)90024-1
86. Rifkin MR, Landsberger FR. Trypanosome variant surface glycoprotein transfer to target membranes: a model for the pathogenesis of trypanosomiasis. *Proc Natl Acad Sci U S A* (1990) 87:801–5. doi:10.1073/pnas.87.2.801
87. Authie E, Boulange A, Muteti D, Lalmanach G, Gauthier F, Musoke AJ. Immunisation of cattle with cysteine proteinases of *Trypanosoma congolense*: targetting the disease rather than the parasite. *Int J Parasitol* (2001) 31:1429–33. doi:10.1016/S0020-7519(01)00266-1
88. Bratosin D, Mazurier J, Tissier JP, Estaquier J, Huart JJ, Ameisen JC, et al. Cellular and molecular mechanisms of senescent erythrocyte phagocytosis by macrophages. A review. *Biochimie* (1998) 80:173–95. doi:10.1016/S0300-9084(98)80024-2
89. Witola WH, Lovelace CE. Demonstration of erythrophagocytosis in *Trypanosoma congolense*-infected goats. *Vet Parasitol* (2001) 96:115–26. doi:10.1016/S0304-4017(00)00430-1
90. Stijlemans B, Vankrunkelsven A, Brys L, Magez S, De Baetselier P. Role of iron homeostasis in trypanosomiasis-associated anemia. *Immunobiology* (2008) 213:823–35. doi:10.1016/j.imbio.2008.07.023
91. Anosa VO, Kaneko JJ. Pathogenesis of *Trypanosoma brucei* infection in deer mice (*Peromyscus maniculatus*). Ultrastructural pathology of the spleen, liver, heart, and kidney. *Vet Pathol* (1984) 21:229–37. doi:10.1177/030098588402100216
92. Igbokwe IO, Nwosu CO. Lack of correlation of anaemia with splenomegaly and hepatomegaly in *Trypanosoma brucei* and *Trypanosoma congolense* infections of rats. *J Comp Pathol* (1997) 117:261–5. doi:10.1016/S0021-9975(97)80020-5
93. Stijlemans B, Leng L, Brys L, Sparkes A, Vansintjan L, Caljon G, et al. MIF contributes to *Trypanosoma brucei* associated immunopathogenicity development. *PLoS Pathog* (2014) 10:e1004414. doi:10.1371/journal.ppat.1004414
94. Stijlemans B, Brys L, Korf H, Bieniasz-Krzywiec P, Sparkes A, Vansintjan L, et al. MIF-mediated hemodilution promotes pathogenic anemia in experimental African trypanosomosis. *PLoS Pathog* (2016) 12:e1005862. doi:10.1371/journal.ppat.1005862
95. Stijlemans B, Vankrunkelsven A, Brys L, Raes G, Magez S, De Baetselier P. Scrutinizing the mechanisms underlying the induction of anemia of inflammation through GPI-mediated modulation of macrophage activation in a model of African trypanosomiasis. *Microbes Infect* (2010) 12:389–99. doi:10.1016/j.micinf.2010.02.006
96. Lenox LE, Perry JM, Paulson RF. BMP4 and Madh5 regulate the erythroid response to acute anemia. *Blood* (2005) 105:2741–8. doi:10.1182/blood-2004-02-0703
97. Wang GL, Semenza GL. Molecular basis of hypoxia-induced erythropoietin expression. *Curr Opin Hematol* (1996) 3:156–62. doi:10.1097/00062752-199603020-00009
98. Suliman HB, Logan-Henfrey L, Majiwa PAO, Ole-Moiyoi O, Feldman BF. Analysis of erythropoietin and erythropoietin receptor genes expression in cattle during acute infection with *Trypanosoma congolense*. *Exp Hematol* (1999) 27:37–45. doi:10.1016/S0301-472X(98)00019-8
99. Socolovsky M. Molecular insights into stress erythropoiesis. *Curr Opin Hematol* (2007) 14:215–24. doi:10.1097/MOH.0b013e3280de2bf1
100. Paulson RF, Shi L, Wu D-C. Stress erythropoiesis: new signals and new stress progenitor cells. *Curr Opin Hematol* (2011) 18:139–45. doi:10.1097/MOH.0b013e32834521c8
101. Heideveld E, van den Akker E. Digesting the role of bone marrow macrophages on hematopoiesis. *Immunobiology* (2017) 222:814–22. doi:10.1016/j.imbio.2016.11.007
102. Rhodes MM, Kopsombut P, Bondurant MC, Price JO, Koury MJ. Adherence to macrophages in erythroblastic islands enhances erythroblast proliferation and increases erythrocyte production by a different mechanism than erythropoietin. *Blood* (2008) 111:1700–8. doi:10.1182/blood-2007-06-098178
103. Ojok L, Kaeufer-Weiss I, Weiss E. Bone marrow response to acute and chronic *Trypanosoma congolense* infection in multimammate rats (*Mastomys coucha*). *J Comp Pathol* (2001) 124:149–58. doi:10.1053/jcpa.2000.0445
104. Shi M, Wei G, Pan W, Tabel H. Experimental African trypanosomiasis: a subset of pathogenic, IFN-gamma-producing, MHC class II-restricted CD4+ T cells mediates early mortality in highly susceptible mice. *J Immunol* (2006) 176:1724–32. doi:10.4049/jimmunol.176.3.1724
105. Liu G, Sun D, Wu H, Zhang M, Huan H, Xu J, et al. Distinct contributions of CD4+ and CD8+ T cells to pathogenesis of *Trypanosoma brucei* infection in the context of gamma interferon and interleukin-10. *Infect Immun* (2015) 83:2785–95. doi:10.1128/IAI.00357-15
106. Guilliams M, Oldenhove G, Noel W, Herin M, Brys L, Loi P, et al. African trypanosomiasis: naturally occurring regulatory T cells favor trypanotolerance by limiting pathology associated with sustained type 1 inflammation. *J Immunol* (2007) 179:2748–57. doi:10.4049/jimmunol.179.5.2748
107. Liu G, Xu J, Wu H, Sun D, Zhang X, Zhu X, et al. IL-27 signaling is crucial for survival of mice infected with African trypanosomes via preventing lethal effects of CD4+ T cells and IFN-gamma. *PLoS Pathog* (2015) 11:e1005065. doi:10.1371/journal.ppat.1005065
108. Sindrilaru A, Peters T, Wieschalka S, Baican C, Baican A, Peter H, et al. An unrestrained proinflammatory M1 macrophage population induced by iron impairs wound healing in humans and mice. *J Clin Invest* (2011) 121:985–97. doi:10.1172/JCI44490
109. Cairo G, Recalcati S, Mantovani A, Locati M. Iron trafficking and metabolism in macrophages: contribution to the polarized phenotype. *Trends Immunol* (2011) 32:241–7. doi:10.1016/j.it.2011.03.007
110. Recalcati S, Locati M, Gammella E, Invernizzi P, Cairo G. Iron levels in polarized macrophages: regulation of immunity and autoimmunity. *Autoimmun Rev* (2012) 11:883–9. doi:10.1016/j.autrev.2012.03.003
111. Sica A, Invernizzi P, Mantovani A. Macrophage plasticity and polarization in liver homeostasis and pathology. *Hepatology* (2014) 59:2034–42. doi:10.1002/hep.26754
112. Sankaran VG, Weiss MJ. Anemia: progress in molecular mechanisms and therapies. *Nat Med* (2015) 21:221–30. doi:10.1038/nm.3814
113. Weiss G, Goodnough LT. Anemia of chronic disease. *N Engl J Med* (2005) 352:1011–23. doi:10.1056/NEJMra041809
114. Ludwiczek S, Aigner E, Theurl I, Weiss G. Cytokine-mediated regulation of iron transport in human monocytic cells. *Blood* (2003) 101:4148–54. doi:10.1182/blood-2002-08-2459
115. Macdougall IC, Cooper AC. Erythropoietin resistance: the role of inflammation and pro-inflammatory cytokines. *Nephrol Dial Transplant* (2002) 17(Suppl 1):39–43. doi:10.1093/ndt/17.suppl_11.39
116. Fraenkel PG. Anemia of inflammation: a review. *Med Clin North Am* (2017) 101:285–96. doi:10.1016/j.mcna.2016.09.005
117. Recalcati S, Locati M, Marini A, Santambrogio P, Zaninotto F, De Pizzol M, et al. Differential regulation of iron homeostasis during human macrophage polarized activation. *Eur J Immunol* (2010) 40:824–35. doi:10.1002/eji.200939889
118. Magez S, Stijlemans B, Caljon G, Eugster HP, De Baetselier P. Control of experimental *Trypanosoma brucei* infections occurs independently of lymphotoxin-alpha induction. *Infect Immun* (2002) 70:1342–51. doi:10.1128/IAI.70.3.1342-1351.2002
119. Tartaglia LA, Goeddel DV. Two TNF receptors. *Immunol Today* (1992) 13:151–3. doi:10.1016/0167-5699(92)90116-O
120. Nedwin GE, Naylor SL, Sakaguchi AY, Smith D, Jarrett-Nedwin J, Pennica D, et al. Human lymphotoxin and tumor necrosis factor genes: structure, homology and chromosomal localization. *Nucleic Acids Res* (1985) 13:6361–73. doi:10.1093/nar/13.17.6361

121. Lucas R, Magez S, De Leys R, Fransen L, Scheerlinck JP, Rampelberg M, et al. Mapping the lectin-like activity of tumor necrosis factor. *Science* (1994) 263:814–7. doi:10.1126/science.8303299
122. Nishimura K, Nakaya H, Nakagawa H, Matsuo S, Ohnishi Y, Yamasaki S. Effect of *Trypanosoma brucei* brucei on erythropoiesis in infected rats. *J Parasitol* (2011) 97:88–93. doi:10.1645/GE-2522.1
123. Schofield L, McConville MJ, Hansen D, Campbell AS, Fraser-Reid B, Grusby MJ, et al. CD1d-restricted immunoglobulin G formation to GPI-anchored antigens mediated by NKT cells. *Science* (1999) 283:225–9. doi:10.1126/science.283.5399.225
124. Baetselier PD, Namangala B, Noel W, Brys L, Pays E, Beschin A. Alternative versus classical macrophage activation during experimental African trypanosomosis. *Int J Parasitol* (2001) 31:575–87. doi:10.1016/S0020-7519(01)00170-9
125. Namangala B, De Baetselier P, Noel W, Brys L, Beschin A. Alternative versus classical macrophage activation during experimental African trypanosomosis. *J Leukoc Biol* (2001) 69:387–96. doi:10.1189/jlb.69.3.387
126. Namangala B, De Baetselier P, Brijs L, Stijlemans B, Noël W, Pays E, et al. Attenuation of *Trypanosoma brucei* is associated with reduced immunosuppression and concomitant production of Th2 lymphokines. *J Infect Dis* (2000) 181:1110–20. doi:10.1086/315322
127. Namangala B, De Baetselier P, Beschin A. Both type-I and type-II responses contribute to murine trypanotolerance. *J Vet Med Sci* (2009) 71:313–8. doi:10.1292/jvms.71.313
128. Taylor KA. Immune responses of cattle to African trypanosomes: protective or pathogenic? *Int J Parasitol* (1998) 28:219–40. doi:10.1016/S0020-7519(97)00154-9
129. Bosschaerts T, Morias Y, Stijlemans B, Hérin M, Porta C, Sica A, et al. IL-10 limits production of pathogenic TNF by M1 myeloid cells through induction of nuclear NF-κB p50 member in *Trypanosoma congolense* infection-resistant C57BL/6 mice. *Eur J Immunol* (2011) 41:3270–80. doi:10.1002/eji.201041307
130. Guilliams M, Bosschaerts T, Herin M, Hunig T, Loi P, Flamand V, et al. Experimental expansion of the regulatory T cell population increases resistance to African trypanosomiasis. *J Infect Dis* (2008) 198:781–91. doi:10.1086/590439
131. Guilliams M, Movahedi K, Bosschaerts T, VandenDriessche T, Chuah MK, Herin M, et al. IL-10 dampens TNF/inducible nitric oxide synthase-producing dendritic cell-mediated pathogenicity during parasitic infection. *J Immunol* (2009) 182:1107–18. doi:10.4049/jimmunol.182.2.1107
132. Stijlemans B, Baral TN, Guilliams M, Brys L, Korf J, Drennan M, et al. A glycosylphosphatidylinositol-based treatment alleviates trypanosomiasis-associated immunopathology. *J Immunol* (2007) 179:4003–14. doi:10.4049/jimmunol.179.6.4003
133. Ann V, Kris DC, Daniel H, Fu-Tong L, Patrick DB, Benoît S. Lack of galectin-3 alleviates trypanosomiasis-associated anemia of inflammation. *Immunobiology* (2010) 215:833–41. doi:10.1016/j.imbio.2010.05.028
134. Liu F-T, Hsu DK. The role of galectin-3 in promotion of the inflammatory response. *Drug News Perspect* (2007) 20:455–60. doi:10.1358/dnp.2007.20.7.1149628
135. Calandra T, Roger T. Macrophage migration inhibitory factor: a regulator of innate immunity. *Nat Rev Immunol* (2003) 3:791–800. doi:10.1038/nri1200
136. Larson DF, Horak K. Macrophage migration inhibitory factor: controller of systemic inflammation. *Crit Care* (2006) 10:138–40. doi:10.1186/cc4899
137. Rosado Jde D, Rodriguez-Sosa M. Macrophage migration inhibitory factor (MIF): a key player in protozoan infections. *Int J Biol Sci* (2011) 7:1239–56. doi:10.7150/ijbs.7.1239
138. Gregory JL, Morand EF, McKeown SJ, Ralph JA, Hall P, Yang YH, et al. Macrophage migration inhibitory factor induces macrophage recruitment via CC chemokine ligand 2. *J Immunol* (2006) 177:8072–9. doi:10.4049/jimmunol.177.11.8072
139. Toh M-L, Aeberli D, Lacey D, Yang Y, Santos LL, Clarkson M, et al. Regulation of IL-1 and TNF receptor expression and function by endogenous macrophage migration inhibitory factor. *J Immunol* (2006) 177:4818–25. doi:10.4049/jimmunol.177.7.4818
140. Amole BO, Clarkson AB Jr, Shear HL. Pathogenesis of anemia in *Trypanosoma brucei*-infected mice. *Infect Immun* (1982) 36:1060–8.
141. Dargie JD, Murray PK, Murray M, McIntyre WI. The blood volumes and erythrokinetics of Ndama and Zebu cattle experimentally infected with *Trypanosoma brucei*. *Res Vet Sci* (1979) 26:245–7.
142. Katunguka-Rwakishaya E, Murray M, Holmes PH. Pathophysiology of ovine trypanosomiasis: ferrokinetics and erythrocyte survival studies. *Res Vet Sci* (1992) 53:80–6. doi:10.1016/0034-5288(92)90089-K
143. Mizue Y, Nishihira J, Miyazaki T, Fujiwara S, Chida M, Nakamura K, et al. Quantitation of macrophage migration inhibitory factor (MIF) using the one-step sandwich enzyme immunosorbent assay: elevated serum MIF concentrations in patients with autoimmune diseases and identification of MIF in erythrocytes. *Int J Mol Med* (2000) 5:397–403. doi:10.3892/ijmm.5.4.397
144. Murray M, Dexter TM. Anaemia in bovine African trypanosomiasis. A review. *Acta Trop* (1988) 45:389–432.
145. Wang CQ, Udupa KB, Lipschitz DA. Evidence suggesting a stimulatory role for interleukin-10 in erythropoiesis in vitro. *J Cell Physiol* (1996) 166:305–10. doi:10.1002/(SICI)1097-4652(199602)166:2<305::AID-JCP8>3.0.CO;2-T
146. Brito MA, Silva RF, Brites D. Bilirubin induces loss of membrane lipids and exposure of phosphatidylserine in human erythrocytes. *Cell Biol Toxicol* (2002) 18:181–92. doi:10.1023/A:1015563704551
147. Mueller C, Braag SA, Martino AT, Tang Q, Campbell-Thompson M, Flotte TR. The pros and cons of immunomodulatory IL-10 gene therapy with recombinant AAV in a Cftr-/- -dependent allergy mouse model. *Gene Ther* (2009) 16:172–83. doi:10.1038/gt.2008.156
148. Tilg H, Ulmer H, Kaser A, Weiss G. Role of IL-10 for induction of anemia during inflammation. *J Immunol* (2002) 169:2204–9. doi:10.4049/jimmunol.169.4.2204
149. Wellde BT, Kovatch RM, Chumo DA, Wykoff DE. *Trypanosoma congolense*: thrombocytopenia in experimentally infected cattle. *Exp Parasitol* (1978) 45:26–33. doi:10.1016/0014-4894(78)90041-3
150. Katunguka-Rwakishaya E, Murray M, Holmes PH. Pathophysiology of *Trypanosoma congolense* infection in two breeds of sheep, Scottish blackface and Finn Dorset. *Vet Parasitol* (1997) 68:215–25. doi:10.1016/S0304-4017(96)01075-8
151. O'Gorman GM, Park SD, Hill EW, Meade KG, Coussens PM, Agaba M, et al. Transcriptional profiling of cattle infected with *Trypanosoma congolense* highlights gene expression signatures underlying trypanotolerance and trypanosusceptibility. *BMC Genomics* (2009) 10:207. doi:10.1186/1471-2164-10-207
152. Kierstein S, Noyes H, Naessens J, Nakamura Y, Pritchard C, Gibson J, et al. Gene expression profiling in a mouse model for African trypanosomiasis. *Genes Immun* (2006) 7:667–79. doi:10.1038/sj.gene.6364345
153. Hill EW, O'Gorman GM, Agaba M, Gibson JP, Hanotte O, Kemp SJ, et al. Understanding bovine trypanosomiasis and trypanotolerance: the promise of functional genomics. *Vet Immunol Immunopathol* (2005) 105:247–58. doi:10.1016/j.vetimm.2005.02.004
154. Berthier D, Chantal I, Thevenon S, Sakande H, Maillard JC, Bengaly Z, et al. Study of bovine trypanotolerance by whole transcriptome analysis. *Ann N Y Acad Sci* (2008) 1149:71–6. doi:10.1196/annals.1428.062
155. Kemp SJ, Hanotte O, Agaba M, Noyes HA, Gibson J, Archibald A, et al. Genomics approaches to study the biology underlying resistance to trypanosomiasis – some unexpected lessons. *Dev Biol* (2008) 132:89–91. doi:10.1159/000317147
156. Rathkolb B, Noyes HA, Brass A, Dark P, Fuchs H, Gailus-Durner V, et al. Clinical chemistry of congenic mice with quantitative trait loci for predicted responses to *Trypanosoma congolense* infection. *Infect Immun* (2009) 77:3948–57. doi:10.1128/IAI.00658-09

Conflict of Interest Statement: The authors declare that the research was conducted in the absence of any commercial or financial relationships that could be construed as a potential conflict of interest.

Copyright © 2018 Stijlemans, De Baetselier, Magez, Van Ginderachter and De Trez. This is an open-access article distributed under the terms of the Creative Commons Attribution License (CC BY). The use, distribution or reproduction in other forums is permitted, provided the original author(s) and the copyright owner are credited and that the original publication in this journal is cited, in accordance with accepted academic practice. No use, distribution or reproduction is permitted which does not comply with these terms.

frontiers in Immunology

REVIEW
published: 20 April 2018
doi: 10.3389/fimmu.2018.00778

Trypanosomatid Infections: How Do Parasites and Their Excreted–Secreted Factors Modulate the Inducible Metabolism of L-Arginine in Macrophages?

Philippe Holzmuller[1,2], Anne Geiger[3], Romaric Nzoumbou-Boko[3,4,5], Joana Pissarra[3], Sarra Hamrouni[3], Valérie Rodrigues[1,2], Frédéric-Antoine Dauchy[3,4,6], Jean-Loup Lemesre[3], Philippe Vincendeau[3,4,5] and Rachel Bras-Gonçalves[3]*

[1] CIRAD, Montpellier, France, [2] UMR 117 ASTRE "Animal, Santé, Territoire, Risques et Ecosystèmes", Univ. Montpellier (I-MUSE), CIRAD, INRA, Montpellier, France, [3] UMR 177 INTERTRYP "Interactions Hôte-Vecteur-Parasite-Environnement dans les maladies tropicales négligées dues aux Trypanosomatidae", Univ. Montpellier (I-MUSE), CIRAD, IRD, Univ. Bordeaux 2, Univ. Lyon 1, Montpellier, France, [4] Univ. Bordeaux, UMR 177 INTERTRYP, Bordeaux, France, [5] CHU Bordeaux, Laboratoire de Parasitologie-Mycologie, Bordeaux, France, [6] CHU Bordeaux, Département des Maladies Infectieuses et Tropicales, Bordeaux, France

OPEN ACCESS

Edited by:
Luciana Balboa, Academia Nacional de Medicina (CONICET), Argentina

Reviewed by:
Joao Luiz Mendes Wanderley, Universidade Federal do Rio de Janeiro, Brazil
Debora Decote-Ricardo, Universidade Federal Rural do Rio de Janeiro, Brazil
Pradeep Das, RMRIMS (ICMR), India

***Correspondence:**
Philippe Holzmuller
philippe.holzmuller@cirad.fr

Specialty section:
This article was submitted to Microbial Immunology, a section of the journal Frontiers in Immunology

Received: *12 November 2017*
Accepted: *28 March 2018*
Published: *20 April 2018*

Citation:
Holzmuller P, Geiger A, Nzoumbou-Boko R, Pissarra J, Hamrouni S, Rodrigues V, Dauchy F-A, Lemesre J-L, Vincendeau P and Bras-Gonçalves R (2018) Trypanosomatid Infections: How Do Parasites and Their Excreted–Secreted Factors Modulate the Inducible Metabolism of L-Arginine in Macrophages? Front. Immunol. 9:778. doi: 10.3389/fimmu.2018.00778

Mononuclear phagocytes (monocytes, dendritic cells, and macrophages) are among the first host cells to face intra- and extracellular protozoan parasites such as trypanosomatids, and significant expansion of macrophages has been observed in infected hosts. They play essential roles in the outcome of infections caused by trypanosomatids, as they can not only exert a powerful antimicrobial activity but also promote parasite proliferation. These varied functions, linked to their phenotypic and metabolic plasticity, are exerted *via* distinct activation states, in which L-arginine metabolism plays a pivotal role. Depending on the environmental factors and immune response elements, L-arginine metabolites contribute to parasite elimination, mainly through nitric oxide (NO) synthesis, or to parasite proliferation, through L-ornithine and polyamine production. To survive and adapt to their hosts, parasites such as trypanosomatids developed mechanisms of interaction to modulate macrophage activation in their favor, by manipulating several cellular metabolic pathways. Recent reports emphasize that some excreted–secreted (ES) molecules from parasites and sugar-binding host receptors play a major role in this dialog, particularly in the modulation of the macrophage's inducible L-arginine metabolism. Preventing L-arginine dysregulation by drugs or by immunization against trypanosomatid ES molecules or by blocking partner host molecules may control early infection and is a promising way to tackle neglected diseases including Chagas disease, leishmaniases, and African trypanosomiases. The present review summarizes recent knowledge on trypanosomatids and their ES factors with regard to their influence on macrophage activation pathways, mainly the NO synthase/arginase balance. The review ends with prospects for the use of biological knowledge to develop new strategies of interference in the infectious processes used by trypanosomatids, in particular for the development of vaccines or immunotherapeutic approaches.

Keywords: macrophage activation, L-arginine metabolism, arginase, secretome, trypanosomatids

TRYPANOSOMATID INFECTIOUS DISEASES AND MACROPHAGE ACTIVATION PATHWAYS

Infections Caused by Trypanosomatids

Trypanosomes and *Leishmania* parasites cause important but neglected infectious diseases in both humans and animals worldwide.

Sleeping sickness or human African trypanosomiasis (HAT) is an endemic parasitic disease exclusively located in intertropical Africa, caused by *Trypanosoma brucei gambiense* (*Tbg*, 95% of cases) and *T. b. rhodesiense*, transmitted by the tsetse fly (1). Related parasites, including *T. b. brucei* (*Tbb*), *T. congolense*, *T. vivax*, *T. evansi*, and *T. equiperdum*, cause wasting diseases in livestock, termed animal African trypanosomosis (AAT) or nagana, and are the cause of a few atypical cases in humans (2). HAT is a severe burden for poor rural populations (3, 4). The real number of infected people is most probably underestimated as published maps are the result of mathematical extrapolation of data recorded in only partial epidemiological surveys, a situation aggravated by wars and social conflicts (5–7). After a painful tsetse bite, the first clinical sign of HAT is the chancre at the bite site, which disappears within 2 or 3 weeks (1). The disease evolves in two distinct pathological stages. Within a few days after the tsetse bite, the patient enters the stage I also called hemolymphatic stage. Intermittent fever develops because of the successive waves of parasite replication in the blood. Adenopathies, splenomegaly, or even hepatological signs are frequent. The stage II or meningoencephalitis stage emerges slowly and insidiously over a period of months or years when the parasites invade the nervous system. The general signs of the hemolymphatic stage do not completely disappear, and the neurological symptoms develop progressively in parallel. A wide variety of neurological symptoms are encountered. The main symptoms after which sleeping sickness was named are daytime somnolence and nocturnal insomnia. Staging relies on white cell counts and detection of trypanosomes in the cerebrospinal fluid and is indispensable as the treatment of stages I and II differs (8), and it was recently demonstrated that the parasite could persist in adipose tissue (9).

American trypanosomiasis, named Chagas disease in recognition of Carlos Chagas, who first discovered it in 1909, is mostly encountered in South and Central America. Infection primarily affects poor rural populations in Latin America and has serious consequences for public health. The disease develops following infection by the protozoan parasite *Trypanosoma cruzi*. The parasite is mainly transmitted by the Triatomine vector also known as the "kissing bug" (10). The disease has two clinical stages. The initial acute stage lasts for about 2 months after infection, parasites circulate in the blood, but in most cases symptoms are mild or even absent. In less than 50% of people bitten by a bug, early characteristic clinical signs can be observed, such as skin lesion (chagoma) or unilateral edema in the eyelid (the sign of Romaña). *T. cruzi* proliferates actively in the infected individual and invades many types of host cell. The host immune response leads to a dramatic reduction in the parasite load. People then enter the chronic stage of the disease and remain asymptomatic for years. The patient shows evidence of immunity (antibodies to specific antigens of *T. cruzi*) but remains infected, and the immune system does not prevent disease progression to the chronic stage. Up to 30% of patients suffer from cardiac disorders and up to 10% suffer from digestive (typically enlargement of the esophagus or colon), neurological, or mixed alterations (11). In later years, the infection can cause sudden death due to cardiac arrhythmias or progressive heart failure caused by the destruction of the heart muscle and its nervous system. Chagas disease can also be reactivated if patients in the chronic phase are immune compromised as in the case of coinfection with HIV or due to chemotherapy (10).

Leishmaniases are vector-borne neglected tropical diseases caused by different species of the *Leishmania* protozoan parasite. They represent a major public health problem worldwide, as they are present in 98 endemic countries. Besides humans, several mammals, often domesticated or wild canids, provide an additional zoonotic reservoir of infection, especially of *L. infantum* (12). Although most people infected by *Leishmania* sp. develop no symptoms, the clinical features include a wide range of symptoms depending on the species of *Leishmania* concerned and the immune response of each host. Cutaneous leishmaniasis, the most common form of the disease causes skin sores on the exposed parts of the body (13). The sores may start out as papules or nodules and end up as ulcers with a raised edge. When the ulcers heal, they leave permanent scars, often the cause of serious social stigma. In mucocutaneous leishmaniasis, the parasite spreads from the skin and causes ulcers in the mucous membranes of the nose (most common location), mouth, or throat, which can lead to partial or total tissue destruction (14). Visceral leishmaniasis, also known as kala-azar, is characterized by irregular fever, weight loss, anemia, and enlargement of the spleen and liver and results in death if untreated (12). Severe pancytopenia is observed, and parasites are found in bone marrow. HIV/AIDS patients are much more likely to develop VL, and once infected, VL accelerates AIDS (15).

Recent investigations report an increase in arginase activity in trypanosomatid-infected patients (16–19), and for instance, arginase activity is considerably higher in the blood of VL/HIV coinfected patients than in VL patients (20) or its age-related alteration impacts on disease severity (21).

Excreted–Secreted (ES) Factors of Trypanosomatids and Macrophage Targeting

The excretory–secretory component is the primary interface between the parasite and its host and induces strong molecular crosstalk with its environment. Studies of naturally ES factors by microorganisms have dramatically increased in recent years, including viruses, bacteria, and parasites. The ES factors or secretome of trypanosomatids is a complex mixture of proteins, carbohydrates, and lipids excreted from the surface of the parasite or secreted through the flagellar pocket of the parasite and *via* exocytosis vesicles (22). The composition of this complex mixture is still largely unknown, despite the recent definition of an experimental approach for the identification of conserved secreted proteins in trypanosomatids (23), but it has long been suspected of being important for the parasitic lifestyle (24).

For example, the whole secretome of *Tbg* was shown to be able to inhibit the maturation of dendritic cells (DCs) and the induction of lymphocytic allogenic responses (25). In addition, there is evidence for the involvement of diverse enzyme families, such as proteases and hydrolases, in different aspects of the pathogenesis in human hosts (26–28). Regarding HAT, the whole secretome of three different bloodstream strains of *Tbg* were analyzed using a proteomics-based approach, which enabled the identification of over 440 proteins, several of which were described for the first time (29). Moreover, the secretome molecular profile was associated with the virulence of the parasite *in vivo* (30). Similar studies were conducted in species responsible for animal trypanosomoses, particularly *T. congolense* and *T. evansi* (31, 32). They evidenced a core secretome and specificities in African trypanosomes affecting humans and those affecting animals. In addition, results obtained with *Tbg* were compared with both the glycosome and with the total proteome of a *Tbb* strain, highlighting the importance of protein isoforms between the parasite cellular metabolism and its corresponding ES molecules (29). Interestingly, a large proportion of the secreted proteins were found in vesicles displaying active exocytosis beyond the flagellar pocket. Trypanosomes of the *brucei* group produce nanotubes coming from the flagelle, which dissociate into vesicles. Vesicles from *T. b. rhodesiense* contain the serum resistance-associated protein, which can be transferred to *Tbb* leading to evasion to human innate immunity (33, 34). This new type of secretion could be crucial for the survival strategy of *Trypanosoma* by allowing them to exchange proteins at least between parasites and/or to manipulate the host immune system.

For *T. cruzi*, it was also evidenced that proteins are released *via* vesicles formed by at least two different mechanisms, larger ectosomes budding from the plasma membrane and smaller exosomes within the flagellar pocket (35). Proteomics enabled the identification of proteins involved in metabolism, signaling, nucleic acid binding, and parasite survival and virulence. The authors concluded that *T. cruzi* uses different secretion pathways to excrete/secrete proteins and that infective forms of the parasite may use the extracellular vesicles to deliver cargo to the host cells (35). A recent comparative proteomic analysis demonstrated both common and specific proteins in the secretomes from two different *T. cruzi* strains, highlighting, similar to African trypanosomes, a plasticity probably associated with the parasite virulence (36).

Exosome-like microvesicles were also evidenced in *L. donovani*. Proteomics revealed a large majority of known eukaryotic exosomal proteins in the conditioned medium of cultured parasites (37). These proteomics results were extended to *L. braziliensis*, for which only 5% of the identified secreted proteins presented a classical secretion signal (38). Interestingly, these exosome-like vesicles were further shown to be involved in the communication with macrophages and immune modulation (39) and could be involved in immune evasion (40). Of importance, *Leishmania* exosomes presented mainly pro-parasitic activities, both *in vitro* and *in vivo*, functionally priming host cells in the first moments of the infection (41) or in the establishment of the disease (42). Moreover, *L. infantum* secretes various molecules that modulate human DC differentiation and functions (43).

Among the functional classes of ES factors, the group of unfolding and degradation proteins, mainly proteases, deserves the most attention. They cover a large panel of physiological and pathological functions, and representatives of this group are known to be virulence factors, to favor parasite invasion and its growth in the hostile host environment, to make it possible to escape the host immune defenses, and/or, finally, to produce nutrients by hydrolyzing host proteins (44–47). In addition, trypanosomatids can use at least four secretory systems to sequentially deliver factors to modulate macrophage response and consequently the response of the immune system as a whole; the classical signal peptide-mediated system as well as bacterial-type secretion systems that export proteins directly into the host environment, and two vesicular systems, including ectosomes and exosomes. These extracellular vesicles are specifically released by trypanosomatids to deliver signals to the target cells. Aside from considerable differences in content and morphology, with some ubiquitously assembled and released from the plasma membrane while others are released during exocytosis of the multivesicular bodies, the functions of ectosomes are largely analogous to those of exosomes (48). The study of these extracellular vesicles and their importance in biological communication is in full swing (49, 50), even using a philosophical approach (51), which could be appropriate in the case of parasites such as trypanosomatids (33, 34, 52). Interestingly, the different modes of secretion can also interact in different ways with the macrophage: *via* receptor–ligand interactions (free proteins and ectosomes), endocytosis (free proteins and ectosomes), phagocytosis (exosomes), or by direct fusion with the plasma membrane (**Figure 1**).

Macrophage Activation Pathways

Classical Versus Alternative Activation Pathway

The main function of macrophages is to react to external stimuli, including pathogens and particularly their ES factors, to inform the host's immune system, and to modulate the corresponding response. The functional properties of macrophages make it possible to distinguish different phenotypes of subpopulations (53). Depending on the type of cell, the cytokines and pathogens

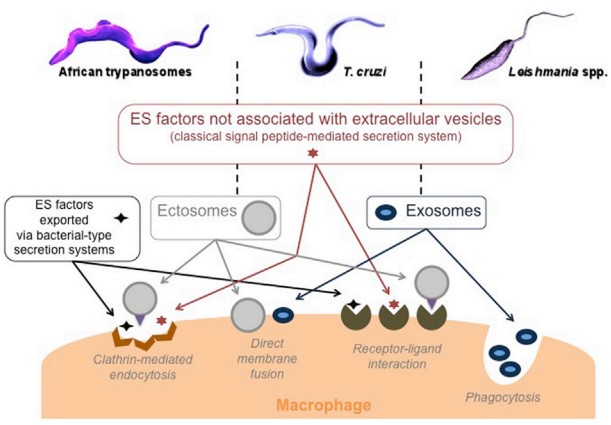


FIGURE 1 | Trypanosomatid modes of secretion and macrophage targeting. ES, excreted–secreted, ectosomes: ubiquitous microvesicles assembled at and released from the plasma membrane, and exosomes: nanovesicles released on the exocytosis of multivesicular bodies.

present at the infection site, unpolarized macrophages (M0) can differentiate into classically activated M1 macrophages or alternative activated M2 macrophages. The two macrophage subpopulations express different surface receptors and produce specific sets of cytokines or chemokines (54, 55). M1 are potent pro-inflammatory cells, with high microbicidal activity [e.g., expression of antigen presentation molecules (MHC II) and co-stimulation molecules (CD40 and CD80/86), secretion of tumor necrosis factor (TNF)-α, interleukin (IL)-12, and activation of nitric oxide synthase (NOS) 2], while M2, which have moderate anti-inflammatory properties (e.g., secretion of IL-10 and high levels of arginase-1), are poorly microbicidal and are involved in tissue repair (56, 57). Although it is difficult to find specific phenotypical markers to delineate M0, M1, and M2 macrophages, recent findings in mouse provide evidence that some surface markers can be considered as representative of each subtype of macrophage, such as CD38 for M1 and early growth response protein 2 for M2 (58). Taken together, the cytokine pathways, nitric oxide (NO) and polyamine levels, may explain why there is more than a simple duality of microbicidal/pro-inflammatory properties versus cell growth/anti-inflammatory properties in the macrophage subpopulations (59, 60). Actually, M1 and M2 phenotypes often coexist, and other terms have emerged to identify non-classical activation phenotypes such as M2a or M2b, the latter representing alternative activated macrophages that express small amounts of arginase 1 (56). The resulting mixed phenotype then depends on the balance between activator and inhibitor activities and the tissue environment, thereby determining the outcome of the infection (61, 62), particularly during trypanosomatid infections (**Figure 2**). Thus, the role of macrophage activation stimuli needs to be considered in the dynamic complexity driven by trypanosomatid parasites and particularly their ES factors (**Figures 2** and **3**), as well as a function of the host (63).

L-Arginine Metabolism Balance and T-Helper Subsets

Mammalian arginine metabolism is complex as this semi-essential amino acid is a substrate for many enzymes that may compete with each other (64). The dual role of L-arginine metabolism, its regulation by T cells, and alterations of L-arginine metabolism by pathogens were recently reviewed (65). Parasites and particularly *Leishmania* and trypanosomes are highly sensitive to the L-arginine-NO pathway (**Figure 3**). For instance, *L. major* infection in mice established the paradigm of Th1 and Th2 subset roles (66), a Th1 response being associated with IFN-γ production and NOS 2 expression, whereas a Th2 response being associated with IL-4 production and arginase 1 expression (67, 68). Interestingly, it has been demonstrated that a deprivation in L-arginine impairs *L. major*-specific T-cell responses (69). T-cell deficiency associated with L-arginine depletion has been evidenced in cancer and in infectious diseases including *T. cruzi* infection. A decrease in cyclin-dependent kinases essential for the cell cycle, the downregulation of T-cell receptor z chain, has been shown to be implicated in T-cell anergy (70).

The low levels of L-arginine and NO in macrophages lead to various RNI, such as peroxynitrites that can not only diffuse around macrophages and kill extracellular infectious agents and intracellular pathogens in adjacent cells but also induce the nitration of various proteins and are involved in the pathogenesis of various infections including leishmaniasis and trypanosomiasis (71–73). Products of NOS and NAPH oxidase in classically activated macrophages can react, leading to S-nitrosylation in protein resulting in the death of extracellular parasites and

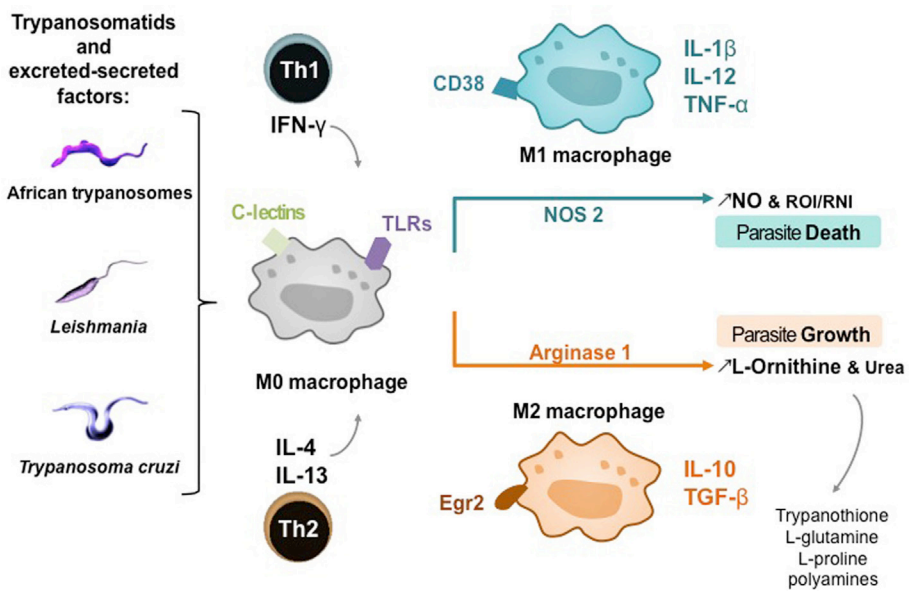


FIGURE 2 | Macrophage activation pathways in trypanosomatid infections. T-cell subsets potentiating M0 macrophage differentiation into M1 or M2 subtype; Th, helper T lymphocyte; IFN-γ, interferon-γ; IL, interleukin. Host cell receptors involved in trypanosomatid detection: C-lectins and toll-like receptors (TLRs). Phenotypic markers and cytokines of macrophage polarization: cluster of differentiation (CD) 38, Egr2, early growth response protein 2; TNF-α, tumor necrosis factor; TGF-β, transforming growth factor. Products of macrophage polarization influencing the death or growth of trypanosomatids; NO, nitric oxide.

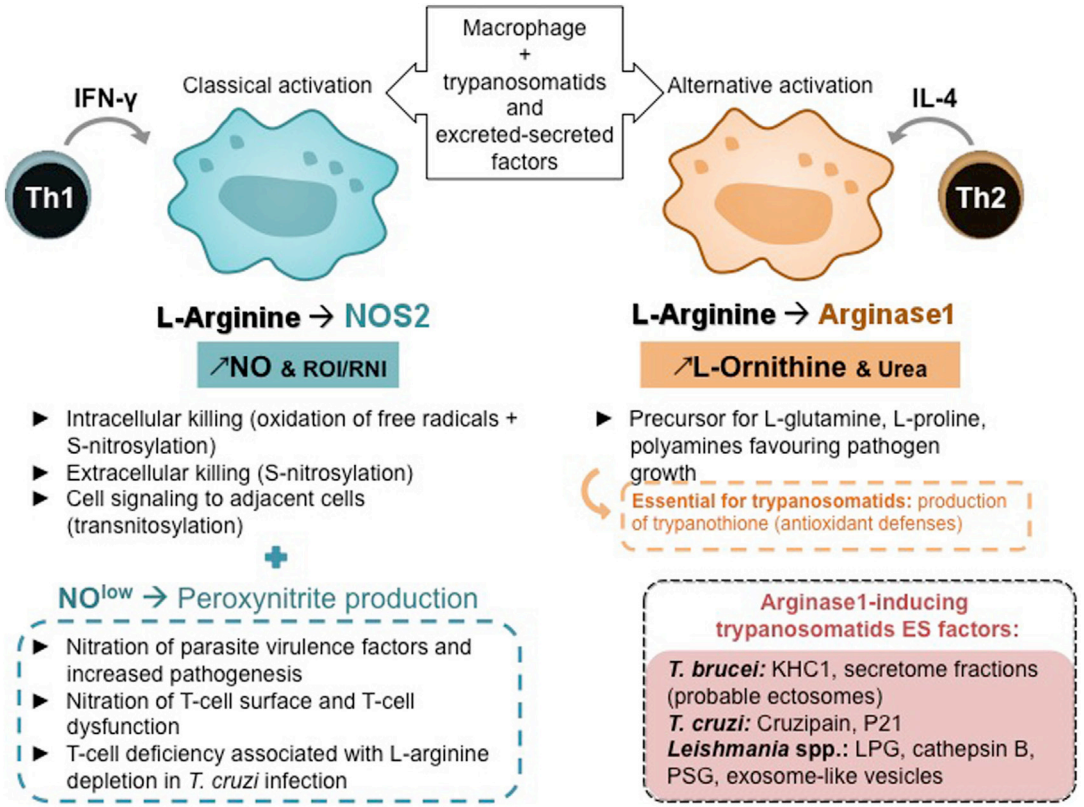


FIGURE 3 | Macrophage polarization, T-helper subsets, and L-arginine metabolism. Th, helper T lymphocyte; IFN-γ, interferon; IL, interleukin; NO, nitric oxide; ROI, reactive oxygen species; RNI, reactive nitrogen species.

through transnitrosylation can affect various targets in host cells, mainly molecules with Fe–S clusters, activating or inactivating various cell functions (74, 75). Arginase modulates NO production in activated macrophages (76), what is essential in infections by trypanosomatids, as arginase activity may be involved in NOS activity impairment by competing for L-arginine and reducing macrophage microbicidal activity (77). Moreover, arginase hydrolyzes L-arginine to L-ornithine that favors parasite growth and is a precursor for the synthesis of L-glutamine, L-proline, and polyamines. Polyamines are key regulators of cell growth and differentiation (78) and essential in trypanosomatids' antioxidant defense, which rely on trypanothione, an unusual spermidine–glutathione conjugate (**Figures 2** and **3**).

MACROPHAGE L-ARGININE METABOLISM DYSREGULATION DURING TRYPANOSOMATID INFECTIONS

NOS/Arginase Imbalance Induced by Trypanosomatids

Parasite Infection in the Dysregulation of the NOS/Arginase Balance

Several pathways regulate L-arginine metabolism, of which three are of interest in the context of trypanosomatids: first, in response to infection cleavage into citrulline and NO by the enzyme NOS, which is harmful since the produced NO is toxic for these parasites. Second, cleavage of arginine into ornithine and urea catalyzed by arginase, which favors trypanosome development as ornithine is a nutrient for trypanosomatids, and third, phosphorylation, in the presence of ATP, into Nω-phospho L-arginine by the arginine kinase, which allows storage of energy that can be delivered on demand, thanks to the reversibility of the reaction (arginine + ATP ↔ phospho-arginine + ADP), thus regulating energy homeostasis and contributing to trypanosomatids survival (79–81). Escaping toxic NO production requires either prevention of the activity of the NOS or a reduction in the availability of L-arginine, which may occur when several enzymes compete for this common substrate (77, 82).

Two arginase isoforms (arginase 1 and 2) have been identified in mammalian hosts so far, with a differential expression depending on tissues and cells (83, 84). Arginase activity of pathogens themselves interferes and competes in host L-arginine pathways. For instance, arginase from *Helicobacter pylori* inhibits NO production by eukaryotic cells (85). Arginase 1 and ornithine decarboxylase (ODC) are both located in the cytosol, facilitating polyamine synthesis from L-ornithine. Arginase 2 is a mitochondrial enzyme that could preferentially enhance L-proline or L-glutamate synthesis from L-ornithine because ornithine aminotransferase is also located in the mitochondria. However, it

has been shown that L-proline can be converted into L-ornithine, which can be transported from the mitochondria to the cytosol (86). Both arginases 1 and 2 have been reported to regulate polyamine synthesis (87).

Trypanosomes belonging to the *brucei* group were the first parasites in which the role of host arginase induction favoring infection was evidenced (77). Considerable expansion of macrophages has been reported in the liver, spleen, and bone marrow of infected mice (88), and the presence of NOS 2 has been demonstrated in these cells. However, in infected mice, parasites proliferate in the vicinity of macrophages in the peritoneal cavity, suggesting that the efficiency of NO-dependent cytotoxicity is limited *in vivo* even though NOS 2 was active *in vitro*. Actually, a decrease in plasmatic L-arginine was measured in *Tbb*-infected mice compared to controls. An increase in arginase activity was observed in peritoneal macrophages from the first days of *Tbb* infection. Intraperitoneal NO production and NO-dependent parasite killing were restored by intraperitoneal injection of L-arginine. The early increase in arginase production in trypanosomiasis is a way for parasites to avoid the antimicrobial effect of RNI and to benefit from the larger quantities of L-ornithine that are necessary for parasite growth (77). As expected, arginase activity and arginase 1 and arginase 2 mRNA expression were demonstrated to be higher in macrophages in "trypanosusceptible"-infected BALB/c compared with those in "trypanoresistant" C57BL/6 mice (89). The high level of arginase activity in *Tbb*-infected BALB/c macrophages strongly inhibited macrophage NO production, which in turn resulted in less trypanosome killing compared with C57BL/6 macrophages. NO generation and parasite killing were restored when arginase was specifically inhibited (89). Similarly, *Tbg* field stocks isolated from patients, which did not display apparent genetic variability but marked differences in virulence (capacity to multiply inside a host) and pathogenicity (ability of producing mortality), were observed in experimental murine infections. Two strains exhibiting opposite pathogenic and virulence properties in mouse were further investigated through their host–parasite interactions. *In vitro*, bloodstream forms and corresponding secretomes from both strains induced macrophage arginase as a function of their virulence (30). Moreover, infection of mice with *T. musculi* expressing *Nippostrongylus brasiliensis* acetylcholinesterase resulted in early parasite blood clearance. It was associated with elevated NO production and lowered arginase activity, a characteristic of a modified NOS2/arginase balance (90).

Arginase 1 induction in macrophages is used by *Leishmania* species to spread inside the host, as polyamines are key elements of parasite growth (91). The proliferation of amastigotes is triggered by IL-4, IL-10, and transforming growth factor (TGF)-β *via* arginase 1 induction in macrophages leading to the generation of the polyamines required for parasite replication. On the contrary, the cytokine IL-12 plays an essential role in the initiation of adaptive responses and production of IFN-γ, which is required to eliminate *Leishmania* parasites. Interestingly, it has been reported that *L. mexicana* promastigotes can activate an MAP kinase through a toll-like receptor (TLR)-4-dependent mechanism, to induce COX-2 and NOS 2 expression thereby downregulating IL-12 production (92). High splenic arginase 1 expression has been measured in an experimental model of visceral leishmaniasis caused by *L. donovani*. This detrimental activation pathway depended on the parasite-induced activation of the transcription factor STAT6, but in contrast to the previously accepted paradigm, did not require (but was amplified by) the presence of polarized Th2 cells or type 2 cytokines (93). Inhibition of arginase reduced the number of parasites and delayed disease outcome in BALB/c mice, while treatment with L-ornithine increased the susceptibility of C57BL/6 mice (94). The treatment of *L. major*-infected macrophages with Th2 cytokines (IL-4 and IL-10) or with TGF-β, which are all inducers of arginase 1, led to a proportional increase in the number of intracellular amastigotes, supporting the hypothesis that host arginase activity favors the spread of the parasite. Cell division of the parasite depends crucially on the level of L-ornithine available in the host (95).

T. cruzi killing by classically activated macrophages is counteracted by alternative activation, which enhances B7.2 expression, IL-10 and TGF-β production, and arginase induction (96). Macrophages are insufficiently activated in an inflammatory phenotype in response to *T. cruzi* infection, because *T. cruzi* inhibits the activation of the glycolytic pathway and the oxidative/nitrosative response in macrophage. Both arginase 1 and 2 were induced in heart tissues from *T. cruzi*-infected mice, and NOS 2 and arginase 2 were expressed by cardiomyocytes. Interestingly, heart-infiltrated CD68+ macrophages were the main cell type that expressed arginase 1 (97). Cruzipain, a major parasite antigen, was shown to induce arginase 1 expression in J774 cells, and the pretreatment of cruzipain-treated cells with N-omega-hydroxy-L-arginine (an arginase inhibitor) led to a dramatic reduction in amastigote growth. Macrophages with elevated arginase 1 activity, induced by either IL-4 or the *T. cruzi* component cruzipain, favored parasite replication and blocking arginase 1 restricted parasite growth (98).

Trypanosomatid Parasites ES Factors in Arginase Induction

T. b. brucei parasites were found to induce arginase activity in myeloid cells from non-infected mice, and activity was maintained when myeloid cells and trypanosomes were separated by a cell-retaining insert, indicating that soluble components from trypanosomes were involved. *Tbb* ES, prepared under conditions leading to no detectable trypanosome death, triggered arginase activity, but the effect was stopped by ES heat treatment. Monoclonal antibodies were raised against *Tbb* secretome and, interestingly, inhibited arginase activity induced by ES. The ES fraction, eluted after affinity chromatography, retained full arginase-inducing activity, confirming that this activity was directly targeted by an ES-specific antibody. The antibody was used to screen a cDNA expression library and identified the *Tbb* arginase-inducing protein: a kinesin heavy chain isoform (TbKHC1) (99). The secretome from TbKHC1 KO parasites did not trigger arginase activity in myeloid cells from non-infected mice, but the recombinant (r)TbKHC1 mimicked the arginase-inducing effect of secretome. Coincident with the induction of arginase activity, the secretome caused myeloid cells to express the regulatory cytokine IL-10. The arginase activity induced by ES was inhibited by a neutralizing anti-IL-10 antibody. The first

peak of parasitemia in mice infected by TbKHC1 KO trypanosomes was reduced by >70% compared to wild-type parasites. A reduced TbKHC1 KO parasite load has also been observed under natural infection conditions in which infected tsetse flies were allowed to feed on mice (99).

Host mammalian macrophages are not only the main host cells but are also the main effector cells for *Leishmania* parasite killing and can be activated *via* two major pathways resulting in classical and alternative activated macrophages. *Leishmania* parasites partly activate arginase and inactivate the NO production by the host cells and enhance parasite survival *via* depletion of the NOS 2 substrate (L-arginine) and reduce NO levels. LPG, the main promastigote glycoconjugate, plays an essential role in promastigote adhesion to macrophages, rapidly fusing with lysosomes, transiently inhibiting phagosome maturation and generating a parasitophorous vacuole that maintains an acidic pH and hydrolytic activity, what provides enough time for promastigotes to differentiate into more hydrolase-resistant amastigotes (100). The replicating amastigotes produce glycoconjugates that are secreted or linked to the cell surface, such as GIPLS and proteophosphoglycan (PPG), and protect parasites from proteolytic damage (101). In parallel, it was reported that *Leishmania* parasites release increased amounts of exosomes following a shift in temperature, which strongly affect macrophage cell signaling and functions in a pro-inflammatory way to recruit neutrophils that exacerbate the pathology (42). PPG and lipophosphoglycan can facilitate the parasite survival inside the macrophages by inhibiting NOS 2 and enhancing arginase expression. During the infection, cathepsin B exported in *L. donovani* exosomes could activate TGF-β1, leading to macrophage alternative activation and enhanced parasite survival, in an arginase 1-mediated way. To regulate parasite population, *L. infantum* eukaryotic initiation factor, an exosomal protein, inhibits parasite growth through the production of TNF-α, which induces microbicidal activity by stimulating NO and reactive oxygen species (ROS) production (102). Infected sand flies regurgitate a proteophosphoglycan gel (PSG) synthesized by the parasites in the sand fly midgut, which can exacerbate cutaneous leishmaniasis. PSG was shown to rapidly recruit macrophages to the dermal site of infection and to enhance alternative activation and arginase activity of recruited macrophages, thereby increasing L-arginine catabolism and the synthesis of polyamines essential for the parasite (103).

In Chagas disease, an induction of the arginase pathway could be used by *T. cruzi* to spread inside the host (104). Interestingly, different proteins related to similar functions have been evidenced in the exoproteome of *T. cruzi*, suggesting that the invasive strategy of the parasite is based on enhanced mechanisms dedicated to interaction, invasion, and dysregulation of host target cells, especially macrophages (105). Among the proteins secreted, cruzipain, the primary secreted lysosomal peptidase in *T. cruzi*, has been shown to induce a Th2 response and to stimulate activation of the macrophage arginase metabolic pathway, associated with a decrease in macrophage NO production (98, 106). P21 is a secreted protein expressed in all the developmental stages in the *T. cruzi* lifecycle and may play an important role in parasite internalization (107). Interestingly, recombinant P21 upregulated phagocytosis of different trypanosomatids in macrophages in a CXCR4-binding-dependent manner (108) and triggered the PI3K-AKT-mTORC1 signaling pathway that has been shown to mediate polarization into M2 macrophages (109). Actually, all factors ES by *T. cruzi* appear to have convergent effects toward arginase activation to prevent aggression and promote parasite growth (110).

Trypanosomatid Parasites' Own L-Arginine Metabolism Enzymes

Interestingly, in addition to ES that influence the host's NOS/arginase balance, trypanosomatids also have several enzymes related to L-arginine metabolism, including arginase. However, *Leishmania* arginase alone is insufficient for parasite growth (111), despite it has been shown to be active in parasites isolated from patients (112) and seems to be associated with pathogenicity of the species (113). These enzymes have been shown to consume host L-arginine thereby directing host metabolism to the arginase pathway, which favors parasite development (**Figure 4**). Curiously, the role played by trypanosomatids' arginase has only recently been considered to be involved in the establishment of infection in macrophages and in the immune response of the host (114). L-Arginine is an essential amino acid for *Leishmania* (115), as L-arginine deprivation or uptake determines parasite death or survival (116, 117). Induction of L-arginine transport is crucial, and to respond to L-arginine depletion in macrophage, among other transporters, *L. donovani* upregulates the expression and activity of a high affinity arginase specific transporter (118). Furthermore, in *L. amazonensis*-infected macrophages, parasite arginase downregulates NOS expression and favors *Leishmania* growth (119). Moreover, *Leishmania* parasites can modulate their own NOS-like/arginase balance (120), for instance by sensing available L-arginine and regulating its uptake (121). In *T. cruzi*, formiminoglutamase has been characterized as an arginase-like enzyme (122), and in *Leishmania* the crucial role of arginase depends on the developmental stage of the parasite (123), which adds to the complexity of modulating L-arginine metabolism by trypanosomatids. In African trypanosomes, arginase has only been identified in proteome, whereas arginine kinase has been detected as soluble and constitutive isoforms (29, 124). In addition, an arginine *N*-methyl transferase has been detected and reported to play an important biological role as it is involved in the methylation of over 800 proteins in *Tbb* (125, 126). Interestingly, arginine kinase and arginine *N*-methyl transferase genes were overexpressed in *Tbg* isolated from tsetse flies (127), as if targeting L-arginine were a metabolic key in the developmental life cycle of African trypanosomes. L-Arginine transporters were also defined as essential for trypanosomes (128). Differences in arginase subcellular locations between *Tbb* and in *T. cruzi* have been reported (129, 130), but their biological significance remains to be determined. Finally, besides arginase, two other enzymes from trypanosomatids compete with host enzymes for the same substrate, L-arginine.

Another crucial pathway deserves to be mentioned: the polyamine–trypanothione pathway, which is also connected to L-arginine metabolism and is unique to trypanosomatids (131). The biosynthetic sequence includes the following major

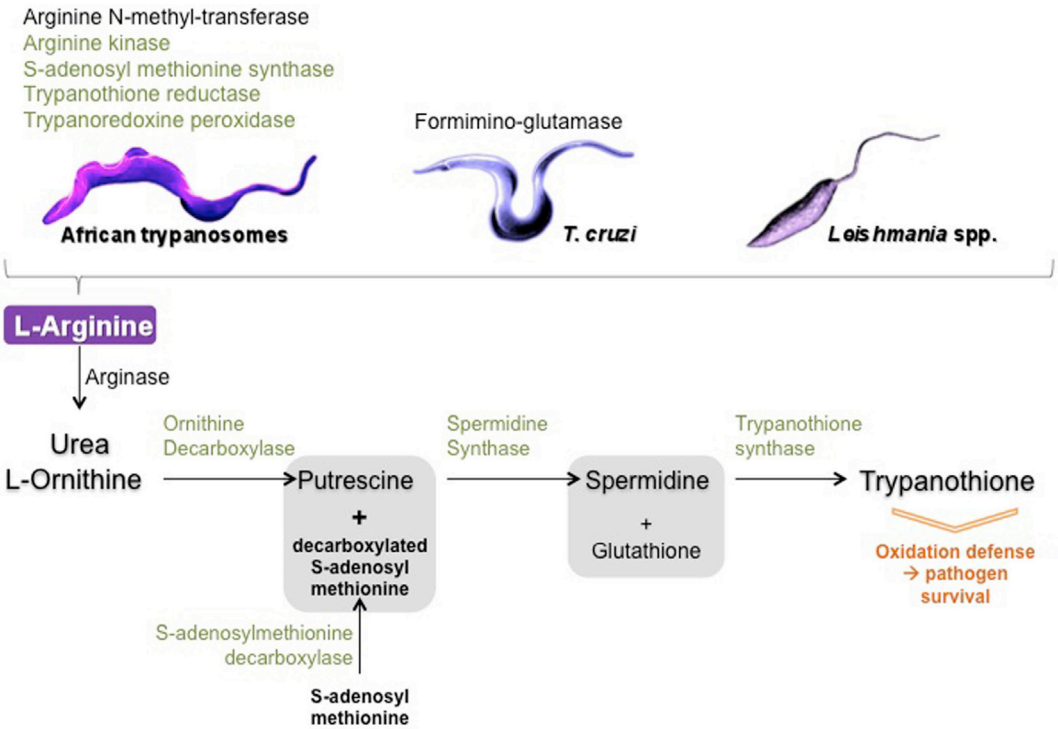


FIGURE 4 | Schematic view of trypanosomatid arginase and arginine metabolism enzymes. In black: enzymes only identified in the proteome of trypanosomatids and in green: enzymes identified in the secretome of trypanosomatids.

catalyzing steps: arginase (L-arginine ⇒ urea + L-ornithine), ODC (L-ornithine ⇒ putrescine), spermidine synthase [decarboxylated S-adenosyl methionine (produced by the S-adenosylmethionine decarboxylase) + putrescine ⇒ spermidine], and as a final step, the trypanothione synthase catalyzes the biosynthesis of trypanothione from glutathione and spermidine (131–134). Trypanothione is of crucial importance as this compound, which is specific of trypanosomatids, is mainly involved in detoxifying ROS, free radicals, and, more generally, in combating various kinds of stress that occur during the parasite's lifespan. Thus, for example, parasites lacking trypanothione reductase were shown to be avirulent and susceptible to oxidative stress (135). Of interest is the fact that most of the enzymes involved in trypanothione metabolism were identified in ES of *Tbg*: S-adenosyl-methionine synthase, spermidine synthase, trypanothione synthase-amidase, trypanothione reductase, and tryparedoxin peroxidase. The total proteome was shown to contain, in addition to the enzymes cited above, ornithine carboxylase that together with the arginase also identified in the total proteome insures the connection between the strict arginine pathway and the trypanothione pathway (29). In *T. cruzi*, some of the enzymes involved in trypanothione metabolism were also identified in the secretome (36). In *Leishmania*, enzymes secreted in the trypanothione pathways were shown to directly participate in parasite virulence and in modulating macrophage response (136).

All the abovementioned enzymes have already been described in a very large panel of reports, but only a few reported they could be ES by the parasites. Some of them, including arginase and ODC, seem to be only intracellular, but their reaction products (as well as those possible secreted by the parasite hosts—either insects or mammals) could be excreted and become the substrate of the excreted enzymes (**Figure 4**). How they work and their real effectiveness *in vivo* presents a large field for further investigations.

Host Receptors in Arginase Signaling

Current research has focused on modification of host cell signaling by pathogens. For instance, C-type lectin receptors (CLRs), expressed in large quantities by DCs and macrophages, play important roles in various aspects of the immune response to pathogens (137). Upon infection, a plethora of host macrophage receptors actively respond to the invading trypanosomatids by activating several signal cascades (**Figure 5**).

The *in vitro* induction of arginase activity by *Tbb*, ES, and rTbKHC1 was inhibited by D-mannose (99). Parasite load and arginase activity decreased in specific intercellular adhesion molecule grabbing non-integrin receptor 1 (SIGN-R1) (CD209) KO but not in macrophage mannose receptor (MMR) KO (CD206)-infected mice. In myeloid cells from SIGN-R1 KO mice rTbKHC1 did not stimulate IL-10 and arginase 1 activity, contrary to myeloid cells from MMR KO mice. Treatment with mannose also reduced parasitemia in mice infected by *T. musculi*. However, whereas TbKHC1 facilitates *Tbb* parasitemia *via* the SIGN-R1 receptor, the MMR receptor was apparently the main target of *T. musculi* ES (138). This suggests that kinesin heavy chain-related proteins play similar roles in promoting infection in two genetically distant trypanosomes, *via* macrophage arginase induction,

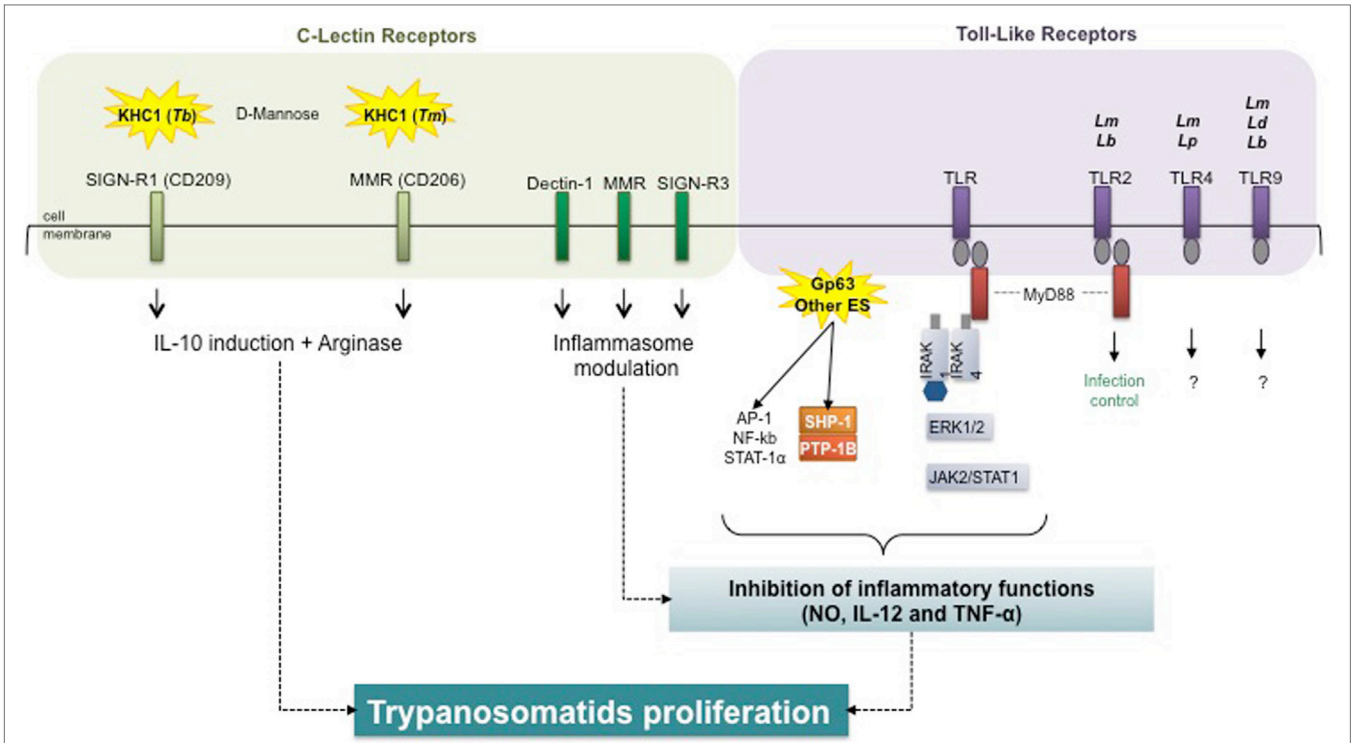


FIGURE 5 | Host receptors in trypanosomatid-mediated arginase modulation. Trypanosomatids and virulence factors: *Tb*, *Trypanosoma brucei; Tm, T. musculi; Lm*, *Leishmania major*; *Lb, L. braziliensis; Lp, L. pifanoi*; *Ld, L. donovani*; Gp, glycoprotein; ES, excreted–secreted. Macrophage receptors: SIGN-R1, specific intercellular adhesion molecule grabbing non-integrin receptor 1; MMR, macrophage mannose receptor; TLR, toll-like receptor. Signal transduction molecules: MyD88, myeloid differentiation primary response 88; IRAK, interleukin-1 receptor-associated kinase; AP, activator protein; NF-κB, nuclear factor-kappa B; STAT, signal transducers and activators of transcription; SHP, Src homology region 2 domain-containing phosphatase; PTB, protein tyrosine phosphatase; ERK, extracellular signal-regulated kinase; JAK, Janus kinase (or just another kinase). Inflammatory markers: NO, nitric oxide; IL, interleukin; TNF, tumor necrosis factor.

following distinct CLR targeting. Kinesins with close structures might act on distinct membrane receptors by recognizing related carbohydrate structures.

The initial binding and internalization of *Leishmania* promastigotes implicate the receptor-mediated classical endocytic pathway (139). This pathway involves a wide diversity of opsonic or pattern-recognition receptors, such as CR3, CR1, Fc receptors, or lectin receptors, such as the mannose fucose receptor (mannan-binding protein) and the integrin family (140, 141). The macrophage response against *L. infantum in vivo* is characterized by an M2b-like phenotype and CLR signature composed of dectin-1, MMR, and the DC-SIGN homolog SIGNR3 expression. Signals downstream from SIGNR3 shift macrophages toward a permissive state best reflected by the lower rate of parasitic proliferation in SIGNR3-deficient macrophages, suggesting that SIGNR3 modulates inflammasome activation for the benefit of the parasite (142). An important step in this immune evasion process is activation of the host protein tyrosine phosphatase SHP-1 by *Leishmania*, which directly inactivates JAK2 and Erk1/2 and contributes to the inactivation of critical macrophage inflammatory functions (e.g., NO, IL-12, and TNF-α production). SHP-1 is also involved in the inhibition of TLR-induced macrophage activation by binding to and inactivating IL-1-receptor-associated kinase 1 (143).

Toll-like receptors have been shown to impair macrophage effective immunity against intracellular pathogens through arginase 1 induction (144). TLRs were identified as determining the outcome of *L. major* (145, 146) and *L. braziliensis* (147) infections, with TLR-2 ligation and myeloid differentiation primary response 88 play an important role in infection control. Additionally, TLR-4 was demonstrated to be important in *L. major* (148, 149) and *L. pifanoi* (150) infections; TLR-9 in *L. donovani*, *L. major*, and *L. braziliensis* infections (151, 152), but knowledge concerning subsequent intracellular signaling is lacking. TLRs are involved in initial interactions and in downstream activation of NOS 2 and COX-2, making them key players in subsequent macrophage activation, all the more so, since TLR4 may be involved in arginase 1 induction (92).

In *T. cruzi* infection, MMR expression was upregulated in macrophages and cruzipain enhanced mannose receptor recycling, thereby favoring arginase induction and parasite survival. Moreover, receptor blockade decreased arginase activity and parasite growth in *T. cruzi*-infected mice (153).

CONCLUDING REMARKS

Trypanosomatids insure their survival and propagation within their host by altering the signaling pathways involved in the ability of macrophages to kill pathogens or to activate the adaptive immune system. All the data presented here underline the importance of arginase induction for extra- and intracellular trypanosomatids and confirm the identity of the parasite molecules and

host receptors involved. The advance in our understanding of the evasion mechanisms used by trypanosomatids enabled by these data should help to develop more efficient anti-trypanosomatids therapies in the near future. A illustrated here, the dysregulation of host L-arginine inducible metabolism by trypanosomatids ES is an effective mechanism used by the parasite to hamper host immune response and to modify host molecule production to favor parasite invasion and growth. Therefore, preventing this host metabolism dysregulation through drugs or immunization against ES active components or by blocking partner host molecules is a promising way to tackle trypanosomatid-mediated diseases.

Nevertheless, arginase triggering should be addressed with caution, as the urea cycle is essential in hosts. NOHA, a stable intermediate in NO synthesis and also an arginase inhibitor, has been shown to limit both lesion size and the parasite load in *L. major*-infected mice (94). New arginase inhibitors targeting macrophage arginase is a promising approach (154). Likewise, siRNA systems have been developed to knock down arginase 1-specific gene expression (155). Signaling is also a potential target, as inhibition of STAT3 signaling reduced arginase activity in myeloid derived suppressor cells from cancer patients (156). Blocking arginase induction, for instance by CLR-specific targeting, is another possible strategy (157, 158). On the other hand, more specific inhibition of the parasite molecules that induce host arginase activity could be an effective strategy with no side effects.

Interestingly, ES from *L. infantum* elicited a protective immune response in dogs, their natural hosts, by triggering a Th1-dominant immune response and an appropriate specific antibody response, thereby countering the parasite-induced arginase metabolism early on, and leading to the first anti-Leishmania vaccine commercially available in Europe (159–161). More recently, a secreted promastigote surface antigen, one of the main constituents and the highly immunogenic antigen of *Leishmania*, was shown to confer high levels of protection in naive dogs (162).

Trypanosoma cruzi secretes proteins that promote host cell invasion, and several studies have focused on the characterization of *T. cruzi* excretory–secretory antigens that are possible candidates for a vaccine. The most promising candidate appears to be the primary secreted lysosomal peptidase cruzipain, which plays vital roles in the *T. cruzi* life cycle, including triggering host arginase (163). Deleting a C-terminal domain in cruzipain led to an efficient immune response against N-terminal domain, which reduced the parasite load after a *T. cruzi* challenge (164). In addition, a new trans-sialidase-based immunogen was able to confer protection in a later *T. cruzi* challenge, by influencing populations of cells related to immune control, particularly in reducing splenic myeloid suppressor cells (165).

Like for *T. cruzi*, a sialidase-based vaccine provided partial protection in *T. b. brucei*-infected mice (107). Various approaches to vaccination against African trypanosomiasis have been investigated [reviewed in the study by LaGreca and Magez (166)]. A monoclonal antibody directed to TbKHC1 reduced arginase activity and parasite load in *T. musculi*-infected mice, and bioinformatics analysis revealed TbKHC1 homologs in other trypanosomes, including human pathogens (138). This trypanosome-specific invariant antigen is a promising candidate for a pan-trypanosome vaccine, by helping the host immune system to efficiently counter the parasite-induced arginase pathway.

The biological knowledge on how trypanosomatids and their ES factors modulate the inducible macrophage L-arginine metabolism deserves further sustained investigations to keep on prospecting for new strategies of interference in the infectious processes, whether through vaccine development or immunotherapeutic treatments.

AUTHOR CONTRIBUTIONS

PH, AG, RN-B, JP, SH, VR, F-AD, J-LL, PV, and RB-G defined the conception of the review, wrote the review, approved the version to be published, and agreed to be accountable for all aspects of the review.

FUNDING

This work was supported by CIRAD, IRD, and Bordeaux University, France. This project received specific funding from the European Union's Horizon 2020 research and innovation programme under the Marie Sklodowska-Curie Grant Agreement No. 642609. We also acknowledge the support of Laboratoire d'Excellence (Labex) Parafrap N8ANR-11-LABX-0024, the *Service de coopération et d'action culturelle de l'Ambassade de France à Bangui*, and the *Association pour le développement de la recherche en parasitologie et santé tropicale*.

REFERENCES

1. Lejon V, Bentivoglio M, Franco JR. Human African trypanosomiasis. *Handb Clin Neurol* (2013) 114:169–81. doi:10.1016/B978-0-444-53490-3.00011-X
2. Truc P, Büscher P, Cuny G, Gonzatti MI, Jannin J, Joshi P, et al. Atypical human infections by animal trypanosomes. *PLoS Negl Trop Dis* (2013) 7:e2256. doi:10.1371/journal.pntd.0002256
3. Odiit M, Shaw A, Welburn SC, Fèvre EM, Coleman PG, McDermott JJ. Assessing the patterns of health-seeking behaviour and awareness among sleeping-sickness patients in eastern Uganda. *Ann Trop Med Parasitol* (2004) 98:339–48. doi:10.1179/000349804225003389
4. Geiger A, Ponton F, Simo G. Adult blood-feeding tsetse flies, trypanosomes, microbiota and the fluctuating environment in sub-Saharan Africa. *ISME J* (2014) 9:1496–507. doi:10.1038/ismej.2014.236
5. Simarro PP, Diarra A, Ruiz Postigo JA, Franco JR, Jannin JG. The human African trypanosomiasis control and surveillance programme of the World Health Organization 2000–2009: the way forward. *PLoS Negl Trop Dis* (2011) 5:e1007. doi:10.1371/journal.pntd.0001007
6. Chappuis F, Lima MA, Flevaud L, Ritmeijer K. Human African trypanosomiasis in areas without surveillance. *Emerg Infect Dis* (2010) 16:354–6. doi:10.3201/eid1602.090967
7. Berrang-Ford L, Lundine J, Breau S. Conflict and human African trypanosomiasis. *Soc Sci Med* (2011) 72:398–407. doi:10.1016/j.socscimed.2010.06.006
8. Dumas M, Bouteille B. Current status of trypanosomiasis. *Med Trop* (1997) 57:65–9.
9. Trindade S, Rijo-Ferreira F, Carvalho T, Pinto-Neves D, Guegan F, Aresta-Branco F, et al. *Trypanosoma brucei* parasites occupy and functionally adapt to the adipose tissue in mice. *Cell Host Microbe* (2016) 19:837–48. doi:10.1016/j.chom.2016.05.002
10. Pérez-Molina JA, Molina I. Chagas disease. *Lancet* (2018) 391:82–94. doi:10.1016/S0140-6736(17)31612-4
11. Bern C. Chagas' disease. *N Engl J Med* (2015) 373:1882. doi:10.1056/NEJMra1410150

12. Murray HW, Berman JD, Davies CR, Saravia NG. Advances in leishmaniasis. *Lancet* (2005) 366:1561–77. doi:10.1016/S0140-6736(05)67629-5
13. Reithinger R, Dujardin JC, Louzir H, Pirmez C, Alexander B, Brooker S. Cutaneous leishmaniasis. *Lancet Infect Dis* (2007) 7:581–96. doi:10.1016/S1473-3099(07)70209-8
14. Handler MZ, Patel PA, Kapila R, Al-Qubati Y, Schwartz RA. Cutaneous and mucocutaneous leishmaniasis: clinical perspectives. *J Am Acad Dermatol* (2015) 73:897–908. doi:10.1016/j.jaad.2014.08.051
15. van Griensven J, Carrillo E, López-Vélez R, Lynen L, Moreno J. Leishmaniasis in immunosuppressed individuals. *Clin Microbiol Infect* (2014) 20:286–99. doi:10.1111/1469-0691.12556
16. Mortazavi H, Sadeghipour P, Taslimi Y, Habibzadeh S, Zali F, Zahedifard F, et al. Comparing acute and chronic human cutaneous leishmaniasis caused by *Leishmania major* and *Leishmania tropica* focusing on arginase activity. *J Eur Acad Dermatol Venereol* (2016) 30:2118–21. doi:10.1111/jdv.13838
17. Abebe T, Hailu A, Woldeyes M, Mekonen W, Bilcha K, Cloke T, et al. Local increase of arginase activity in lesions of patients with cutaneous leishmaniasis in Ethiopia. *PLoS Negl Trop Dis* (2012) 6:e1684. doi:10.1371/journal.pntd.0001684
18. Nzoumbou-Boko R, Dethoua M, Gabriel F, Buguet A, Cespuglio R, Courtois P, et al. Serum arginase, a biomarker of treatment efficacy in human African trypanosomiasis. *J Clin Microbiol* (2013) 51:2379–81. doi:10.1128/JCM.03371-12
19. Yizengaw E, Getahun M, Tajebe F, Cruz Cervera E, Adem E, Mesfin G, et al. Visceral leishmaniasis patients display altered composition and maturity of neutrophils as well as impaired neutrophil effector functions. *Front Immunol* (2016) 7:517. doi:10.3389/fimmu.2016.00517
20. Takele Y, Abebe T, Weldegebreal T, Hailu A, Hailu W, Hurissa Z, et al. Arginase activity in the blood of patients with visceral leishmaniasis and HIV infection. *PLoS Negl Trop Dis* (2013) 7:e1977. doi:10.1371/journal.pntd.0001977
21. Müller I, Hailu A, Choi BS, Abebe T, Fuentes JM, Munder M, et al. Age-related alteration of arginase activity impacts on severity of leishmaniasis. *PLoS Negl Trop Dis* (2008) 2:e235. doi:10.1371/journal.pntd.0000235
22. Chenik M, Lakhal S, Ben Khalef N, Zribi L, Louzir H, Dellagi K. Approaches for the identification of potential excreted/secreted proteins of *Leishmania major* parasites. *Parasitology* (2006) 132:493–509. doi:10.1017/S0031182005009546
23. Corrales RM, Mathieu-Daudé F, Garcia D, Brenière SF, Sereno D. An experimental approach for the identification of conserved secreted proteins in trypanosomatids. *J Biomed Biotechnol* (2010) 2010:752698. doi:10.1155/2010/752698
24. Hernández AG. Leishmanial excreted factors and their possible biological role. *Ciba Found Symp* (1983) 99:138–56.
25. Garzón E, Holzmuller P, Bras-Gonçalves R, Vincendeau P, Cuny G, Lemesre JL, et al. The *Trypanosoma brucei gambiense* secretome impairs lipopolysaccharide-induced maturation, cytokine production, and allostimulatory capacity of dendritic cells. *Infect Immun* (2013) 81:3300–8. doi:10.1128/IAI.00125-13
26. Okenu DMN, Opara KN, Nwuba RI, Nwagwu M. Purification and characterisation of an extracellular released protease of *Trypanosoma brucei*. *Parasitol Res* (1999) 85:424–8. doi:10.1007/s004360050571
27. Lonsdale-Eccles JD, Grab DJ. Trypanosome hydrolase and the blood-brain barrier. *Trends Parasitol* (2002) 18:17–9. doi:10.1016/S1471-4922(01)02120-1
28. Girard M, Bisser S, Courtioux B, Vermot-Desroches C, Bouteille B, Wijdenes J, et al. In vitro induction of microglial and endothelial cell apoptosis by cerebrospinal fluids from patients with human African trypanosomiasis. *Int J Parasitol* (2003) 33:713–20. doi:10.1016/S0020-7519(03)00033-X
29. Geiger A, Hirtz C, Bécue T, Bellard E, Centeno D, Gargani D, et al. Exocytosis and protein secretion in *Trypanosoma*. *BMC Microbiol* (2010) 10:20. doi:10.1186/1471-2180-10-20
30. Holzmuller P, Biron DG, Courtois P, Koffi M, Bras-Gonçalves R, Daulouède S, et al. Virulence and pathogenicity patterns of *Trypanosoma brucei gambiense* field isolates in experimentally infected mouse: differences in host immune response modulation by secretome and proteomics. *Microbes Infect* (2008) 10:79–86. doi:10.1016/j.micinf.2007.10.008
31. Holzmuller P, Grébaut P, Peltier JB, Brizard JP, Perrone T, Gonzatti M, et al. Secretome of animal trypanosomes. *Ann N Y Acad Sci* (2008) 1149:337–42. doi:10.1196/annals.1428.097
32. Grébaut P, Chuchana P, Brizard JP, Demettre E, Seveno M, Bossard G, et al. Identification of total and differentially expressed excreted-secreted proteins from *Trypanosoma congolense* strains exhibiting different virulence and pathogenicity. *Int J Parasitol* (2009) 39:1137–50. doi:10.1016/j.ijpara.2009.02.018
33. Szempruch AJ, Dennison L, Kieft R, Harrington JM, Hajduk SL. Sending a message: extracellular vesicles of pathogenic protozoan parasites. *Nat Rev Microbiol* (2016) 14:669–75. doi:10.1038/nrmicro.2016.110
34. Szempruch AJ, Sykes SE, Kieft R, Dennison L, Becker AC, Gartrell A, et al. Extracellular vesicles from *Trypanosoma brucei* mediate virulence factor transfer and cause host anemia. *Cell* (2016) 164:246–57. doi:10.1016/j.cell.2015.11.051
35. Bayer-Santos E, Aguilar-Bonavides C, Rodrigues SP, Cordero EM, Marques AF, Varela-Ramirez A, et al. Proteomic analysis of *Trypanosoma cruzi* secretome: characterization of two populations of extracellular vesicles and soluble proteins. *J Proteome Res* (2013) 12:883–97. doi:10.1021/pr300947g
36. Brossas JY, Gulin JEN, Bisio MMC, Chapelle M, Marinach-Patrice C, Bordessoules M, et al. Secretome analysis of *Trypanosoma cruzi* by proteomics studies. *PLoS One* (2017) 12:e0185504. doi:10.1371/journal.pone.0185504
37. Silverman JM, Chan SK, Robinson DP, Dwyer DM, Nandan D, Foster LJ, et al. Proteomic analysis of the secretome of *Leishmania donovani*. *Genome Biol* (2008) 9:R35. doi:10.1186/gb-2008-9-2-r35
38. Cuervo P, De Jesus JB, Saboia-Vahia L, Mendonça-Lima L, Domont GB, Cupolillo E. Proteomic characterization of the released/secreted proteins of *Leishmania* (Viannia) *braziliensis* promastigotes. *J Proteomics* (2009) 73:79–92. doi:10.1016/j.jprot.2009.08.006
39. Silverman JM, Clos J, Horakova E, Wang AY, Wiesgigl M, Kelly I, et al. *Leishmania* exosomes modulate innate and adaptive immune responses through effects on monocytes and dendritic cells. *J Immunol* (2010) 185:5011–22. doi:10.4049/jimmunol.1000541
40. Lambertz U, Silverman JM, Nandan D, McMaster WR, Clos J, Foster LJ, et al. Secreted virulence factors and immune evasion in visceral leishmaniasis. *J Leukoc Biol* (2012) 91:887–99. doi:10.1189/jlb.0611326
41. Silverman JM, Reiner NE. *Leishmania* exosomes deliver preemptive strikes to create an environment permissive for early infection. *Front Cell Infect Microbiol* (2012) 1:26. doi:10.3389/fcimb.2011.00026
42. Atayde VD, Hassani K, da Silva Lira Filho A, Borges AR, Adhikari A, Martel C, et al. *Leishmania* exosomes and other virulence factors: impact on innate immune response and macrophage functions. *Cell Immunol* (2016) 309:7–18. doi:10.1016/j.cellimm.2016.07.013
43. Markikou-Ouni W, Drini S, Bahi-Jaber N, Chenik M, Meddeb-Garnaoui A. Immunomodulatory effects of four *Leishmania infantum* potentially excreted/secreted proteins on human dendritic cells differentiation and maturation. *PLoS One* (2015) 10:e0143063. doi:10.1371/journal.pone.0143063
44. McKerrow JH, Sun E, Rosenthal PJ, Bouvier J. The proteases and pathogenicity of parasitic protozoa. *Annu Rev Microbiol* (1993) 47:821–53. doi:10.1146/annurev.mi.47.100193.004133
45. Alexander J, Coombs GH, Mottram JC. *Leishmania mexicana* cysteine proteinase-deficient mutants have attenuated virulence for mice and potentiate a Th1 response. *J Immunol* (1998) 161:6794–801.
46. Klemba M, Goldberg DE. Biological roles of proteases in parasitic protozoa. *Annu Rev Biochem* (2002) 71:275–305. doi:10.1146/annurev.biochem.71.090501.145453
47. McKerrow JH, Caffrey C, Kelly B, Loke P, Sajid M. Proteases in parasitic diseases. *Annu Rev Pathol* (2006) 1:497–536. doi:10.1146/annurev.pathol.1.110304.100151
48. Cocucci E, Meldolesi J. Ectosomes and exosomes: shedding the confusion between extracellular vesicles. *Trends Cell Biol* (2015) 25:364–72. doi:10.1016/j.tcb.2015.01.004
49. Lawson C, Kovacs D, Finding E, Ulfelder E, Luis-Fuentes V. Extracellular vesicles: evolutionarily conserved mediators of intercellular communication. *Yale J Biol Med* (2017) 90:481–91.
50. van Niel G, D'Angelo G, Raposo G. Shedding light on the cell biology of extracellular vesicles. *Nat Rev Mol Cell Biol* (2018) 19(4):213–28. doi:10.1038/nrm.2017.125

51. Tkach M, Kowal J, Théry C. Why the need and how to approach the functional diversity of extracellular vesicles. *Philos Trans R Soc Lond B Biol Sci* (2018) 373:1737. doi:10.1098/rstb.2016.0479
52. Marti M, Johnson PJ. Emerging roles for extracellular vesicles in parasitic infections. *Curr Opin Microbiol* (2016) 32:66–70. doi:10.1016/j.mib.2016.04.008
53. Mills CD, Kincaid K, Alt JM, Heilman MJ, Hill AM. M-1/M-2 macrophages and the Th1/Th2 paradigm. *J Immunol* (2000) 164:6166–73. doi:10.4049/jimmunol.164.12.6166
54. Benoit M, Desnues B, Mege JL. Macrophage polarization in bacterial infections. *J Immunol* (2008) 181:3733–9. doi:10.4049/jimmunol.181.6.3733
55. Mosser DM, Edwards JP. Exploring the full spectrum of macrophage activation. *Nat Rev Immunol* (2008) 8:958–69. doi:10.1038/nri2448
56. Martinez FO, Sica A, Mantovani A, Locati M. Macrophage activation and polarization. *Front Biosci* (2008) 13:453–61. doi:10.2741/2692
57. Varin A, Gordon S. Alternative activation of macrophages: immune function and cellular biology. *Immunobiology* (2009) 214:630–41. doi:10.1016/j.imbio.2008.11.009
58. Jablonski KA, Amici SA, Webb LM, Ruiz-Rosado Jde D, Popovich PG, Partida-Sanchez S, et al. Novel markers to delineate murine M1 and M2 macrophages. *PLoS One* (2015) 10:e0145342. doi:10.1371/journal.pone.0145342
59. Murray PJ, Allen JE, Biswas SK, Fisher EA, Gilroy DW, Goerdt S, et al. Macrophage activation and polarization: nomenclature and experimental guidelines. *Immunity* (2014) 41:14–20. doi:10.1016/j.immuni.2014.06.008
60. Lee M, Rey K, Besler K, Wang C, Choy J. Immunobiology of nitric oxide and regulation of inducible nitric oxide synthase. *Results Probl Cell Differ* (2017) 62:181–207. doi:10.1007/978-3-319-54090-0_8
61. Davis MJ, Tsang TM, Qiu Y, Dayrit JK, Freij JB, Huffnagle GB, et al. Macrophage M1/M2 polarization dynamically adapts to changes in cytokine microenvironments in *Cryptococcus neoformans* infection. *MBio* (2013) 4:e264–213. doi:10.1128/mBio.00264-13
62. Martinez FO, Gordon S. The M1 and M2 paradigm of macrophage activation: time for reassessment. *F1000Prime Rep* (2014) 6:13. doi:10.12703/P6-13
63. Holzmuller P, Nirdé P, Vezilier F, Chuchana P. The transcriptomic analytical level determines the human monocyte-derived macrophage response toward either the infectious agent or the host. *Infect Genet Evol* (2016) 45:426–33. doi:10.1016/j.meegid.2016.10.002
64. Morris SM Jr. Arginine metabolism revisited. *J Nutr* (2016) 146:2579S–86S. doi:10.3945/jn.115.226621
65. Gogoi M, Datey A, Wilson KT, Chakravortty D. Dual role of arginine metabolism in establishing pathogenesis. *Curr Opin Microbiol* (2016) 29:43–8. doi:10.1016/j.mib.2015.10.005
66. Locksley RM, Heinzel FP, Sadick MD, Holaday BJ, Gardner KD Jr. Murine cutaneous leishmaniasis: susceptibility correlates with differential expansion of helper T-cell subsets. *Ann Inst Pasteur Immunol* (1987) 138:744–9. doi:10.1016/S0769-2625(87)80030-2
67. Mosmann TR, Cherwinski HM, Bond MW, Giedlin MA, Coofman RL. Two types of murine helper T cell clone. I. Definition according to profiles of lymphokine activities and secreted proteins. *J Immunol* (1986) 136:2348–57.
68. Mosmann TR, Sad S. The expanding universe of T-cell subsets: Th1, Th2 and more. *Immunol Today* (1996) 17:138–46. doi:10.1016/0167-5699(96)80606-2
69. Munder M, Choi BS, Rogers M, Kropf P. L-Arginine deprivation impairs *Leishmania major*-specific T-cell responses. *Eur J Immunol* (2009) 39:2161–72. doi:10.1002/eji.200839041
70. Mondanelli G, Ugel S, Grohmann U, Bronte V. The immune regulation in cancer by the amino acid metabolizing enzymes ARG and IDO. *Curr Opin Pharmacol* (2017) 35:30–9. doi:10.1016/j.coph.2017.05.002
71. Giorgio S, Linares E, Capurro Mde L, de Bianchi AG, Augusto O. Formation of nitrosyl hemoglobin and nitrotyrosine during murine leishmaniasis. *Photochem Photobiol* (1996) 63:750–4. doi:10.1111/j.1751-1097.1996.tb09626.x
72. Keita M, Vincendeau P, Buguet A, Cespuglio R, Vallat JM, Dumas M, et al. Inducible nitric oxide synthase and nitrotyrosine in the central nervous system of mice chronically infected with *Trypanosoma brucei brucei*. *Exp Parasitol* (2000) 95:19–27. doi:10.1006/expr.2000.4505
73. Rodriguez PC, Ochoa AC, Al-Khami AA. Arginine metabolism in myeloid cells shapes innate and adaptive immunity. *Front Immunol* (2017) 8:93. doi:10.3389/fimmu.2017.00093
74. Monteiro HP, Costa PE, Reis AK, Stern A. Nitric oxide: protein tyrosine phosphorylation and protein S-nitrosylation in cancer. *Biomed J* (2015) 38:380–8. doi:10.4103/2319-4170.158624
75. Mnaimneh S, Geffard M, Veyret B, Vincendeau P. Albumin nitrosylated by activated macrophages possesses antiparasitic effects neutralized by anti-NO-acetylated-cysteine antibodies. *J Immunol* (1997) 158:308–14.
76. Chang CI, Liao JC, Kuo L. Arginase modulates nitric oxide production in activated macrophages. *Am J Physiol* (1998) 274:H342–8.
77. Gobert AP, Daulouede S, Lepoivre M, Boucher JL, Bouteille B, Buguet A, et al. L-Arginine availability modulates local nitric oxide production and parasite killing in experimental trypanosomiasis. *Infect Immun* (2000) 68:4653–7. doi:10.1128/IAI.68.8.4653-4657.2000
78. Igarashi K, Kashiwagi K. Polyamines: mysterious modulators of cellular functions. *Biochem Biophys Res Commun* (2000) 271:559–64. doi:10.1006/bbrc.2000.2601
79. Pereira CA, Alonso GD, Ivaldi S, Silber AM, Alves MJ, Torres HN, et al. Arginine kinase overexpression improves *Trypanosoma cruzi* survival capability. *FEBS Lett* (2003) 554:201–5. doi:10.1016/S0014-5793(03)01171-2
80. Valera Vera EA, Sayé M, Reigada C, Damasceno FS, Silber AM, Miranda MR, et al. Resveratrol inhibits *Trypanosoma cruzi* arginine kinase and exerts a trypanocidal activity. *Int J Biol Macromol* (2016) 87:498–503. doi:10.1016/j.ijbiomac.2016.03.014
81. Pereira CA. Arginine kinase: a potential pharmacological target in trypanosomiasis. *Infect Disord Drug Targets* (2014) 14:30–6. doi:10.2174/1871526514666140713144103
82. Boucher JL, Moali C, Tenu JP. Nitric oxide biosynthesis, nitric oxide synthase inhibitors and arginase competition for L-arginine utilization. *Cell Mol Life Sci* (1999) 55:1015–28. doi:10.1007/s000180050352
83. Mori M, Gotoh T. Regulation of nitric oxide production by arginine metabolic enzymes. *Biochem Biophys Res Commun* (2000) 275:715–9. doi:10.1006/bbrc.2000.3169
84. Morris SM Jr. Recent advances in arginine metabolism: roles and regulation of the arginases. *Br J Pharmacol* (2009) 157:922–30. doi:10.1111/j.1476-5381.2009.00278.x
85. Gobert AP, McGee DJ, Akhtar M, Mendz GL, Newton JC, Cheng Y, et al. *Helicobacter pylori* arginase inhibits nitric oxide production by eukaryotic cells: a strategy for bacterial survival. *Proc Natl Acad Sci U S A* (2001) 98:13844–9. doi:10.1073/pnas.241443798
86. Wu G, Morris SM Jr. Arginine metabolism: nitric oxide and beyond. *Biochem J* (1998) 336:1–17. doi:10.1042/bj3360001
87. Li H, Meininger CJ, Hawker JR Jr, Haynes TE, Kepka-Lenhart D, Mistry SK, et al. Regulatory role of arginase I and II in nitric oxide, polyamine, and proline syntheses in endothelial cells. *Am J Physiol Endocrinol Metab* (2001) 280:E75–82. doi:10.1152/ajpendo.2001.280.1.E75
88. Murray PK, Jennings W, Murray M, Urquhart GM. The nature of immunosuppression in *Trypanosoma brucei* infections in mice. The role of the macrophage. *Immunology* (1974) 27:815–24.
89. Duleu S, Vincendeau P, Courtois P, Semballa S, Lagroye I, Daulouède S, et al. Mouse strain susceptibility to trypanosome infection: an arginase-dependent effect. *J Immunol* (2004) 172:6298–303. doi:10.4049/jimmunol.172.10.6298
90. Vaux R, Schnoeller C, Berkachy R, Roberts LB, Hagen J, Gounaris K, et al. Modulation of the immune response by nematode secreted acetylcholinesterase revealed by heterologous expression in *Trypanosoma musculi*. *PLoS Pathog* (2016) 12:e1005998. doi:10.1371/journal.ppat.1005998
91. Muxel SM, Aoki JI, Fernandes JCR, Laranjeira-Silva MF, Zampieri RA, Acuña SM, et al. Arginine and polyamines fate in *Leishmania* infection. *Front Microbiol* (2018) 8:2682. doi:10.3389/fmicb.2017.02682
92. Shweash M, Adrienne McGachy H, Schroeder J, Neamatallah T, Bryant CE, Millington O, et al. *Leishmania mexicana* promastigotes inhibit macrophage IL-12 production via TLR-4 dependent COX-2, NOS 2 and arginase-1 expression. *Mol Immunol* (2011) 48:1800–8. doi:10.1016/j.molimm.2011.05.013
93. Osorio EY, Zhao W, Espitia C, Saldarriaga O, Hawel L, Byus CV, et al. Progressive visceral leishmaniasis is driven by dominant parasite-induced STAT6 activation and STAT6-dependent host arginase 1 expression. *PLoS Pathog* (2012) 8:e1002417. doi:10.1371/journal.ppat.1002417
94. Iniesta V, Carcelén J, Molano I, Peixoto PM, Redondo E, Parra P, et al. Arginase I induction during *Leishmania major* infection mediates the

development of disease. *Infect Immun* (2005) 73:6085–90. doi:10.1128/IAI.73.9.6085-6090.2005
95. Iniesta V, Gomez-Nieto LC, Molano I, Mohedano A, Carcelen J, Miron C, et al. Arginase I induction in macrophages, triggered by Th2-type cytokines, supports the growth of intracellular *Leishmania* parasites. *Parasite Immunol* (2002) 24:113. doi:10.1046/j.1365-3024.2002.00444.x
96. Stempin C, Giordanengo L, Gea S, Cerbán F. Alternative activation and increase of *Trypanosoma cruzi* survival in murine macrophages stimulated by cruzipain, a parasite antigen. *J Leukoc Biol* (2002) 72:727–34. doi:10.1189/jlb.72.4.727
97. Cuervo H, Pineda MA, Aoki MP, Gea S, Fresno M, Gironès N. Inducible nitric oxide synthase and arginase expression in heart tissue during acute *Trypanosoma cruzi* infection in mice: arginase I is expressed in infiltrating CD68+ macrophages. *Infect Dis* (2008) 197:1772–82. doi:10.1086/529527
98. Stempin CC, Tanos TB, Coso OA, Cerbán FM. Arginase induction promotes *Trypanosoma cruzi* intracellular replication in Cruzipain-treated J774 cells through the activation of multiple signaling pathways. *Eur J Immunol* (2004) 34:200–9. doi:10.1002/eji.200324313
99. De Muylder G, Daulouède S, Lecordier L, Uzureau P, Morias Y, Van Den Abbeele J, et al. A *Trypanosoma brucei* kinesin heavy chain promotes parasite growth by triggering host arginase activity. *PLoS Pathog* (2013) 9:e1003731. doi:10.1371/journal.ppat.1003731
100. Courret N, Fréhel C, Gouhier N, Pouchelet M, Prina E, Roux P, et al. Biogenesis of *Leishmania*-harbouring parasitophorous vacuoles following phagocytosis of the metacyclic promastigote or amastigote stages of the parasites. *J Cell Sci* (2002) 115:2303–16.
101. Freitas-Teixeira PM, Silveira-Lemos D, Giunchetti RC, Baratta-Masini A, Mayrink W, Peruhype-Magalhães V, et al. Distinct pattern of immunophenotypic features of innate and adaptive immunity as a putative signature of clinical and laboratorial status of patients with localized cutaneous leishmaniasis. *Scand J Immunol* (2012) 76:421–32. doi:10.1111/j.1365-3083.2012.02748.x
102. Koutsoni O, Barhoumi M, Guizani I, Dotsika E. *Leishmania* eukaryotic initiation factor (LeIF) inhibits parasite growth in murine macrophages. *PLoS One* (2014) 9:e97319. doi:10.1371/journal.pone.0097319
103. Rogers M, Kropf P, Choi BS, Dillon R, Podinovskaia M, Bates P, et al. Proteophosophoglycans regurgitated by *Leishmania*-infected sand flies target the L-arginine metabolism of host macrophages to promote parasite survival. *PLoS Pathog* (2009) 5:e1000555. doi:10.1371/journal.ppat.1000555
104. Stempin CC, Cerban FM. Macrophages and arginase induction as a mechanism for parasite escape. *Medicina (B Aires)* (2007) 67:737–46.
105. Queiroz RM, Ricart CA, Machado MO, Bastos IM, de Santana JM, de Sousa MV, et al. Insight into the exoproteome of the tissue-derived trypomastigote form of *Trypanosoma cruzi*. *Front Chem* (2016) 4:42. doi:10.3389/fchem.2016.00042
106. Doyle PS, Zhou YM, Hsieh I, Greenbaum DC, McKerrow JH, Engel JC. The *Trypanosoma cruzi* protease cruzain mediates immune evasion. *PLoS Pathog* (2011) 7:e1002139. doi:10.1371/journal.ppat.1002139
107. da Silva CV, Kawashita SY, Probst CM, Dallagiovanna B, Cruz MC, da Silva EA, et al. Characterization of a 21kDa protein from *Trypanosoma cruzi* associated with mammalian cell invasion. *Microbes Infect* (2009) 11:563–70. doi:10.1016/j.micinf.2009.03.007
108. Rodrigues AA, Clemente TM, Dos Santos MA, Machado FC, Gomes RG, Moreira HH, et al. A recombinant protein based on *Trypanosoma cruzi* P21 enhances phagocytosis. *PLoS One* (2012) 7:e51384. doi:10.1371/journal.pone.0051384
109. Rocher C, Singla DK. SMAD-PI3K-Akt-mTOR pathway mediates BMP-7 polarization of monocytes into M2 macrophages. *PLoS One* (2013) 8:e84009. doi:10.1371/journal.pone.0084009
110. Watanabe Costa R, da Silveira JF, Bahia D. Interactions between *Trypanosoma cruzi* secreted proteins and host cell signaling pathways. *Front Microbiol* (2016) 7:388. doi:10.3389/fmicb.2016.00388
111. da Silva MF, Floeter-Winter LM. Arginase in *Leishmania*. *Subcell Biochem* (2014) 74:103–17. doi:10.1007/978-94-007-7305-9_4
112. Badirzadeh A, Taheri T, Abedi-Astaneh F, Taslimi Y, Abdossamadi Z, Montakhab-Yeganeh H, et al. Arginase activity of *Leishmania* isolated from patients with cutaneous leishmaniasis. *Parasite Immunol* (2017) 39:e12454. doi:10.1111/pim.12454
113. Badirzadeh A, Taheri T, Taslimi Y, Abdossamadi Z, Heidari-Kharaji M, Gholami E, et al. Arginase activity in pathogenic and non-pathogenic species of *Leishmania* parasites. *PLoS Negl Trop Dis* (2017) 11:e0005774. doi:10.1371/journal.pntd.0005774
114. Balaña-Fouce R, Calvo-Álvarez E, Álvarez-Velilla R, Prada CF, Pérez-Pertejo Y, Reguera RM. Role of trypanosomatid's arginase in polyamine biosynthesis and pathogenesis. *Mol Biochem Parasitol* (2012) 181:85–93. doi:10.1016/j.molbiopara.2011.10.007
115. Darlyuk I, Goldman A, Roberts SC, Ullman B, Rentsch D, Zilberstein D. Arginine homeostasis and transport in the human pathogen *Leishmania donovani*. *J Biol Chem* (2009) 284:19800–7. doi:10.1074/jbc.M901066200
116. Mandal A, Das S, Roy S, Ghosh AK, Sardar AH, Verma S, et al. Deprivation of L-arginine induces oxidative stress mediated apoptosis in *Leishmania donovani* promastigotes: contribution of the polyamine pathway. *PLoS Negl Trop Dis* (2016) 10:e0004373. doi:10.1371/journal.pntd.0004373
117. Mandal A, Das S, Kumar A, Roy S, Verma S, Ghosh AK, et al. L-Arginine uptake by cationic amino acid transporter promotes intra-macrophage survival of *Leishmania donovani* by enhancing arginase-mediated polyamine synthesis. *Front Immunol* (2017) 8:839. doi:10.3389/fimmu.2017.00839
118. Goldman-Pinkovich A, Balno C, Strasser R, Zeituni-Molad M, Bendelak K, Rentsch D, et al. An arginine deprivation response pathway is induced in *Leishmania* during macrophage invasion. *PLoS Pathog* (2016) 12:e1005494. doi:10.1371/journal.ppat.1005494
119. Muxel SM, Laranjeira-Silva MF, Zampieri RA, Floeter-Winter LM. *Leishmania* (*Leishmania*) *amazonensis* induces macrophage miR-294 and miR-721 expression and modulates infection by targeting NOS2 and L-arginine metabolism. *Sci Rep* (2017) 7:44141. doi:10.1038/srep44141
120. Acuña SM, Aoki JI, Laranjeira-Silva MF, Zampieri RA, Fernandes JCR, Muxel SM, et al. Arginase expression modulates nitric oxide production in *Leishmania* (*Leishmania*) *amazonensis*. *PLoS One* (2017) 12:e0187186. doi:10.1371/journal.pone.0187186
121. Aoki JI, Muxel SM, Zampieri RA, Acuña SM, Fernandes JCR, Vanderlinde RH, et al. L-arginine availability and arginase activity: characterization of amino acid permease 3 in *Leishmania amazonensis*. *PLoS Negl Trop Dis* (2017) 11:e0006025. doi:10.1371/journal.pntd.0006025
122. Hai Y, Dugery RJ, Healy D, Christianson DW. Formiminoglutamase from *Trypanosoma cruzi* is an arginase-like manganese metalloenzyme. *Biochemistry* (2013) 52:9294–309. doi:10.1021/bi401352h
123. Boitz JM, Gilroy CA, Olenyik TD, Paradis D, Perdeh J, Dearman K, et al. Arginase is essential for survival of *Leishmania donovani* promastigotes but not intracellular amastigotes. *Infect Immun* (2016) 85:e00554–16. doi:10.1128/IAI.00554-16
124. Atyame Nten CM, Sommerer N, Rofidal V, Hirtz C, Rossignol M, Cuny G, et al. Excreted/secreted proteins from trypanosome procyclic strains. *J Biomed Biotechnol* (2010) 2010:212817. doi:10.1155/2010/212817
125. Pelletier M, Xu Y, Wang X, Zahariev S, Pongor S, Aletta JM, et al. Arginine methylation of a mitochondrial guide RNA binding protein from *Trypanosoma brucei*. *Mol Biochem Parasitol* (2001) 118:49–59. doi:10.1016/S0166-6851(01)00367-X
126. Lott K, Zhu L, Fisk JC, Tomasello DL, Read LK. Functional interplay between protein arginine methyltransferases in *Trypanosoma brucei*. *Microbiologyopen* (2014) 3:595–609. doi:10.1002/mbo3.191
127. Hamidou Soumana I, Klopp C, Ravel S, Nabihoudine I, Tchicaya B, Parrinello H, et al. RNA-seq de novo assembly reveals differential gene expression in *Glossina palpalis gambiensis* infected with *Trypanosoma brucei gambiense* vs. non-infected and self-cured flies. *Front Microbiol* (2015) 6:1259. doi:10.3389/fmicb.2015.01259
128. Mathieu C, Macêdo JP, Hürlimann D, Wirdnam C, Haindrich AC, Suter Grotemeyer M, et al. Arginine and lysine transporters are essential for *Trypanosoma brucei*. *PLoS One* (2017) 12:e0168775. doi:10.1371/journal.pone.0168775
129. Voncken F, Gao F, Wadforth C, Harley M, Colasante C. The phosphoarginine energy-buffering system of *trypanosoma brucei* involves multiple arginine kinase isoforms with different subcellular locations. *PLoS One* (2013) 8:e65908. doi:10.1371/journal.pone.0065908
130. Miranda MR, Bouvier LA, Canepa GE, Pereira CA. Subcellular localization of Trypanosoma cruzi arginine kinase. *Parasitology* (2009) 136:1201–7. doi:10.1017/S0031182009990448

131. Ilari A, Fiorillo A, Genovese I, Colotti G. Polyamine-trypanothione pathway: an update. *Future Med Chem* (2017) 9:61–77. doi:10.4155/fmc-2016-0180
132. Colotti G, Ilari A. Polyamine metabolism in *Leishmania*: from arginine to trypanothione. *Amino Acids* (2011) 40:269–85. doi:10.1007/s00726-010-0630-3
133. Oza SL, Shaw MP, Wyllie S, Fairlamb AH. Trypanothione biosynthesis in *Leishmania major*. *Mol Biochem Parasitol* (2005) 139:107–16. doi:10.1016/j.molbiopara.2004.10.004
134. Krauth-Siegel RL, Meiering SK, Schmidt H. The parasite-specific trypanothione metabolism of *Trypanosoma* and *Leishmania*. *Biol Chem* (2003) 384:539–49. doi:10.1515/BC.2003.062
135. Krieger S, Schwarz W, Ariyanayagam MR, Fairlamb AH, Krauth-Siegel RL, Clayton C. Trypanosomes lacking trypanothione reductase are avirulent and show increased sensitivity to oxidative stress. *Mol Microbiol* (2000) 35:542–52. doi:10.1046/j.1365-2958.2000.01721.x
136. Gerbaba TK, Gedamu L. Cathepsin B gene disruption induced *Leishmania donovani* proteome remodeling implies cathepsin B role in secretome regulation. *PLoS One* (2013) 8:e79951. doi:10.1371/journal.pone.0079951
137. Mayer S, Raulf MK, Lepenies B. C-type lectins: their network and roles in pathogen recognition and immunity. *Histochem Cell Biol* (2017) 147:223–37. doi:10.1007/s00418-016-1523-7
138. Nzoumbou-Boko R, De Muylder G, Semballa S, Lecordier L, Dauchy FA, Gobert AP, et al. *Trypanosoma musculi* infection in mice critically relies on mannose receptor-mediated arginase induction by a TbKHC1 kinesin H chain homolog. *J Immunol* (2017) 199:1762–71. doi:10.4049/jimmunol.1700179
139. Walker DM, Oghumu S, Gupta G, McGwire BS, Drew ME, Satoskar AR. Mechanisms of cellular invasion by intracellular parasites. *Cell Mol Life Sci* (2014) 71:1245–63. doi:10.1007/s00018-013-1491-1
140. Vannier-Santos MA, Martiny A, de Souza W. Cell biology of *Leishmania* spp.: invading and evading. *Curr Pharm Des* (2002) 8:297–318. doi:10.2174/1381612023396230
141. Alexander J, Russell DG. The interaction of *Leishmania* species with macrophages. *Adv Parasitol* (1992) 31:175–254. doi:10.1016/S0065-308X(08)60022-6
142. Lefèvre L, Lugo-Villarino G, Meunier E, Valentin A, Olagnier D, Authier H, et al. The C-type lectin receptors dectin-1, MR, and SIGNR3 contribute both positively and negatively to the macrophage response to *Leishmania infantum*. *Immunity* (2013) 38:1038–49. doi:10.1016/j.immuni.2013.04.010
143. Shio MT, Hassani K, Isnard A, Ralph B, Contreras I, Gomez MA, et al. Host cell signalling and *Leishmania* mechanisms of evasion. *J Trop Med* (2012) 2012:819512. doi:10.1155/2012/819512
144. El Kasmi KC, Qualls JE, Pesce JT, Smith AM, Thompson RW, Henao-Tamayo M, et al. Toll-like receptor-induced arginase 1 in macrophages thwarts effective immunity against intracellular pathogens. *Nat Immunol* (2008) 9:1399–406. doi:10.1038/ni.1671
145. de Veer MJ, Curtis JM, Baldwin TM, DiDonato JA, Sexton A, McConville MJ, et al. MyD88 is essential for clearance of *Leishmania major*: possible role for lipophosphoglycan and toll-like receptor 2 signaling. *Eur J Immunol* (2003) 33:2822–31. doi:10.1002/eji.200324128
146. Kavoosi G, Ardestani SK, Kariminia A, Alimohammadian MH. *Leishmania major* lipophosphoglycan: discrepancy in toll-like receptor signaling. *Exp Parasitol* (2010) 124:214–8. doi:10.1016/j.exppara.2009.09.017
147. Vargas-Inchaustegui DA, Tai W, Xin L, Hogg AE, Corry DB, Soong L. Distinct roles for MyD88 and toll-like receptor 2 during *Leishmania braziliensis* infection in mice. *Infect Immun* (2009) 77:2948–56. doi:10.1128/IAI.00154-09
148. Kropf P, Freudenberg MA, Modolell M, Price HP, Herath S, Antoniazi S, et al. Toll-like receptor 4 contributes to efficient control of infection with the protozoan parasite *Leishmania major*. *Infect Immun* (2004) 72(4):1920–8. doi:10.1128/IAI.72.4.1920-1928.2004
149. Kropf P, Freudenberg N, Kalis C, Modolell M, Herath S, Galanos C, et al. Infection of C57BL/10ScCr and C57BL/10ScNCr mice with *Leishmania major* reveals a role for toll-like receptor 4 in the control of parasite replication. *J Leukoc Biol* (2004) 76:48–57. doi:10.1189/jlb.1003484
150. Whitaker SM, Colmenares M, Pestana KG, McMahon-Pratt D. *Leishmania pifanoi* proteoglycolipid complex P8 induces macrophage cytokine production through toll-like receptor 4. *Infect Immun* (2008) 76:2149–56. doi:10.1128/IAI.01528-07
151. Liese J, Schleicher U, Bogdan C. TLR9 signaling is essential for the innate NK cell response in murine cutaneous leishmaniasis. *Eur J Immunol* (2007) 37:3424–34. doi:10.1002/eji.200737182
152. Schleicher U, Liese J, Knippertz I, Kurzmann C, Hesse A, Heit A, et al. NK cell activation in visceral leishmaniasis requires TLR9, myeloid DCs, and IL-12, but is independent of plasmacytoid DCs. *J Exp Med* (2007) 204:893–906. doi:10.1084/jem.20061293
153. Garrido VV, Dulgerian LR, Stempin CC, Cerbán FM. The increase in mannose receptor recycling favors arginase induction and *Trypanosoma cruzi* survival in macrophages. *Int J Biol Sci* (2011) 7:1257–72. doi:10.7150/ijbs.7.1257
154. Steppan J, Nyhan D, Berkowitz DE. Development of novel arginase inhibitors for therapy of endothelial dysfunction. *Front Immunol* (2013) 4:278. doi:10.3389/fimmu.2013.00278
155. Guo Z, Bucher BT, Shao L, Geller DA. Development of siRNA systems to knock-down arginase I-specific or NOS 2-specific gene expression. *FASEB J* (2008) 22:1120.1.
156. Vasquez-Dunddel D, Pan F, Zeng Q, Gorbounov M, Albesiano E, Fu J, et al. STAT3 regulates arginase-I in myeloid-derived suppressor cells from cancer patients. *J Clin Invest* (2013) 123:1580–9. doi:10.1172/JCI60083
157. Lepenies B, Lee J, Sonkaria S. Targeting C-type lectin receptors with multivalent carbohydrate ligands. *Adv Drug Deliv Rev* (2013) 65:1271–81. doi:10.1016/j.addr.2013.05.007
158. Azad AK, Rajaram MV, Metz WL, Cope FO, Blue MS, Vera DR, et al. γ-Tilmanocept, a new radiopharmaceutical tracer for cancer sentinel lymph nodes, binds to the mannose receptor (CD206). *J Immunol* (2015) 195:2019–29. doi:10.4049/jimmunol.1402005
159. Lemesre JL, Holzmuller P, Cavaleyra M, Gonçalves RB, Hottin G, Papierok G. Protection against experimental visceral leishmaniasis infection in dogs immunized with purified excreted secreted antigens of *Leishmania infantum* promastigotes. *Vaccine* (2005) 23:2825–40. doi:10.1016/j.vaccine.2004.11.061
160. Lemesre JL, Holzmuller P, Gonçalves RB, Bourdoiseau G, Hugnet C, Cavaleyra M, et al. Long-lasting protection against canine visceral leishmaniasis using the LiESAp-MDP vaccine in endemic areas of France: double-blind randomised efficacy field trial. *Vaccine* (2007) 25:4223–34. doi:10.1016/j.vaccine.2007.02.083
161. Bourdoiseau G, Hugnet C, Gonçalves RB, Vézilier F, Petit-Didier E, Papierok G, et al. Effective humoral and cellular immunoprotective responses in Li ESAp-MDP vaccinated protected dogs. *Vet Immunol Immunopathol* (2009) 128:71–8. doi:10.1016/j.vetimm.2008.10.309
162. Petitdidier E, Pagniez J, Papierok G, Vincendeau P, Lemesre JL, Bras-Gonçalves R. Recombinant forms of *Leishmania amazonensis* excreted/secreted promastigote surface antigen (PSA) induce protective immune responses in dogs. *PLoS Negl Trop Dis* (2016) 10:e0004614. doi:10.1371/journal.pntd.0004614
163. Rodríguez-Morales O, Monteón-Padilla V, Carrillo-Sánchez SC, Rios-Castro M, Martínez-Cruz M, Carabarin-Lima A, et al. Experimental vaccines against chagas disease: a journey through history. *J Immunol Res* (2015) 2015:489758. doi:10.1155/2015/489758
164. Cazorla SI, Frank FM, Becker PD, Arnaiz M, Mirkin GA, Corral RS, et al. Redirection of the immune response to the functional catalytic domain of the cysteine proteinase cruzipain improves protective immunity against *Trypanosoma cruzi* infection. *J Infect Dis* (2010) 202:136–44. doi:10.1086/652872
165. Prochetto E, Roldán C, Bontempi IA, Bertona D, Peverengo L, Vicco MH, et al. Trans-sialidase-based vaccine candidate protects against *Trypanosoma cruzi* infection, not only inducing an effector immune response but also affecting cells with regulatory/suppressor phenotype. *Oncotarget* (2017) 8:58003–20. doi:10.18632/oncotarget.18217
166. LaGreca F, Magez S. Vaccination against trypanosomiasis: can it be done or is the trypanosome truly the ultimate immune destroyer and escape artist? *Hum Vaccin* (2011) 7:1225–33. doi:10.4161/hv.7.11.18203

Conflict of Interest Statement: The authors declare that the research was conducted in the absence of any commercial or financial relationships that could be construed as a potential conflict of interest.

Copyright © 2018 Holzmuller, Geiger, Nzoumbou-Boko, Pissarra, Hamrouni, Rodrigues, Dauchy, Lemesre, Vincendeau and Bras-Gonçalves. This is an open-access article distributed under the terms of the Creative Commons Attribution License (CC BY). The use, distribution or reproduction in other forums is permitted, provided the original author(s) and the copyright owner are credited and that the original publication in this journal is cited, in accordance with accepted academic practice. No use, distribution or reproduction is permitted which does not comply with these terms.

frontiers in Immunology

ORIGINAL RESEARCH
published: 20 February 2018
doi: 10.3389/fimmu.2018.00313

Mammalian Target of Rapamycin Inhibition in *Trypanosoma cruzi*-Infected Macrophages Leads to an Intracellular Profile That Is Detrimental for Infection

*Jorge David Rojas Márquez, Yamile Ana, Ruth Eliana Baigorrí, Cinthia Carolina Stempin and Fabio Marcelo Cerban**

Facultad de Ciencias Químicas, Universidad Nacional de Córdoba (UNC), Centro de Investigaciones en Bioquímica Clínica e Inmunología (CIBICI), Consejo Nacional de Investigaciones Científicas y Técnicas (CONICET), Córdoba, Argentina

The causative agent of Chagas' disease, *Trypanosoma cruzi*, affects approximately 10 million people living mainly in Latin America, with macrophages being one of the first cellular actors confronting the invasion during *T. cruzi* infection and their function depending on their proper activation and polarization into distinct M1 and M2 subtypes. Macrophage polarization is thought to be regulated not only by cytokines and growth factors but also by environmental signals. The metabolic checkpoint kinase mammalian target of rapamycin (mTOR)-mediated sensing of environmental and metabolic cues influences macrophage polarization in a complex and as of yet incompletely understood manner. Here, we studied the role of the mTOR pathway in macrophages during *T. cruzi* infection. We demonstrated that the parasite activated mTOR, which was beneficial for its replication since inhibition of mTOR in macrophages by different inhibitors decreased parasite replication. Moreover, in rapamycin pretreated and infected macrophages, we observed a decreased arginase activity and expression, reduced IL-10 and increased interleukin-12 production, compared to control infected macrophages treated with DMSO. Surprisingly, we also found a reduced iNOS activity and expression in these macrophages. Therefore, we investigated possible alternative mechanisms involved in controlling parasite replication in rapamycin pretreated and infected macrophages. Although, cytoplasmic ROS and the enzyme indoleamine 2, 3-dioxygenase (IDO) were not involved, we observed a significant increase in IL-6, TNF-α, and IL-1β production. Taking into account that IL-1β is produced by activation of the cytoplasmic receptor NLRP3, which is one of the main components of the inflammasome, we evaluated NLRP3 expression during mTOR inhibition and *T. cruzi* infection. We observed that rapamycin-pretreated and infected macrophages showed a significant increase in NLRP3 expression and produced higher levels of mitochondrial ROS (mtROS) compared with control cells. Moreover, inhibition of mtROS production partially reversed the effect of rapamycin on parasite replication, with there being a significant increase in parasite load in rapamycin pretreated and infected macrophages from NLRP3 KO mice compared to wild-type control cells. Our findings strongly suggest that mTOR inhibition during *T. cruzi* infection induces NLRP3 inflammasome activation and mtROS production, resulting in an inflammatory-like macrophage profile that controls *T. cruzi* replication.

Keywords: mammalian target of rapamycin, macrophage, *Trypanosoma cruzi*, reactive oxygen species, NLRP3

OPEN ACCESS

Edited by:
Luciana Balboa, Academia Nacional de Medicina (CONICET), Argentina

Reviewed by:
K. Sandeep Prabhu, Pennsylvania State University, United States
Derek Nolan, Trinity College, Dublin, Ireland

****Correspondence:***
Fabio Marcelo Cerban
fmcerban@hotmail.com

Specialty section:
This article was submitted to Microbial Immunology, a section of the journal Frontiers in Immunology

Received: *29 September 2017*
Accepted: *05 February 2018*
Published: *20 February 2018*

Citation:
Rojas Márquez JD, Ana Y, Baigorrí RE, Stempin CC and Cerban FM (2018) Mammalian Target of Rapamycin Inhibition in Trypanosoma cruzi-Infected Macrophages Leads to an Intracellular Profile That Is Detrimental for Infection. Front. Immunol. 9:313. doi: 10.3389/fimmu.2018.00313

INTRODUCTION

Trypanosoma cruzi, which is an intracellular protozoan parasite, is the etiologic agent of Chagas disease. This is a chronic condition affecting in the region of 10 million people worldwide who mostly reside in Latin America (1). Although, many of the mechanisms involved in the pathogenesis of Chagas disease are not well understood, the development and severity of American trypanosomiasis depends on immune-mediated mechanisms. The pathogen-associated molecular patterns (PAMPs) present in *T. cruzi* can be recognized by pattern recognition receptors, which is a crucial event in host resistance (2), with the capability of *T. cruzi* to infect and replicate within of different cells, among them macrophages (3), being an critical feature in its cycle (4).

Macrophages are key effector cells that participate in different stages of immune responses, such as antigen presentation, phagocytosis, and the secretion of bioactive molecules. Macrophages may either suppress *T. cruzi* replication or afford a favorable environment where it can reproduce and be distributed to other area within the body (3–6). Furthermore, macrophages are indispensible in tissue homeostasis and have a significant effect on protective immunity and pathological immune-mediated damage (7–9). Macrophages are generally thought to represent a range of activated phenotypes instead of stable subpopulations. Normally, these are separated into two specific phenotypes, classically activated macrophages (M1) and alternatively activated ones (M2) (10–14). The M1 types are considered effector cells when responding to microbial products or interferon-gamma (IFN-γ), and are characterized by a large antigen presenting ability and yielding pro-inflammatory cytokines, including interleukin-12 (IL-12), tumor necrosis factor alpha (TNF-α), nitric oxide (NO), and reactive oxygen species (ROS) (13, 15, 16). Consequently, M1 macrophages stimulate a polarized type I immune response that mediates host defense against infections of bacteria, viruses, and protozoa as well as tumor cells. On the other hand, M2 macrophages are induced by IL-13, IL-4, glucocorticoids, and IL-10, and they display an anti-inflammatory function, as well as promoting adaptive Th2 immunity and regulating angiogenesis, wound healing, and tissue remodeling (11–13).

Despite it being well known that the transcriptional response triggered by PAMP recognition of the surrounding microenvironments (including cytokines and growth factors) determines the phenotype and function of macrophages (13, 15–17), the intrinsic molecular mechanisms driving macrophage polarization are not yet been fully understood. Related to this, macrophage polarization is also thought to be regulated by environmental signals with the metabolic checkpoint kinase mammalian target of rapamycin (mTOR) mediating the sensing of the environmental and metabolic cues influencing macrophage polarization in a complex but still incompletely understood manner (18).

The mTOR protein is a conserved serine–threonine kinase which is known to influence multiple cellular functions, such as cell growth, proliferation, and survival by integrating signals from nutrients, energy status, growth factors, cytokines, and TLRs (19, 20). These signals are recognized by the PI3-K–Akt axis, and depending on the context, can activate mTORC1 or mTORC2 complexes (20). Immediately downstream of Akt is the tuberous sclerosis complex (TSC), which consists of the TSC tumor suppressors TSC1 and TSC2, and also Tre2-TBC1D7. These control the Ras homolog enriched in the brain (RHEB), which is a crucial GTPase regulator of mTORC1. On this complex being phosphorylated by Akt or ERK1/2, it becomes inhibited and RHEB is activated, resulting in the activation of mTORC1 (20). In a general context, protein synthesis is the best characterized process controlled by mTORC1, with this kinase directly phosphorylating the translational regulator eukaryotic translation initiation factor 4E (eIF4E)-binding protein1 (4EBP1) and S6 kinase (S6K), which in turn, promote protein synthesis (21).

The activation of mTOR has been shown to downregulate IL-12p70 and IL-23 production in LPS-stimulated human macrophages (22). Futhermore, IL-12 was enhanced, but IL-10 was blocked, following mTOR inhibition in mouse bone marrow-derived macrophages (BMDMs) and myeloid dendritic cells (23). These results suggest that mTOR activation might limit the pro-inflammatory responses. However, other studies have demonstrated that TSC1-deficient macrophages produce certain pro-inflammatory cytokines, including TNF-α, IL-6, and IL-12p40 as a response to multiple TLR ligands (18, 19, 23). Related to this, TSC1-deficient BMDMs treated with LPS led to an increased pro-inflammatory cytokine production, such as IL-6 and TNF-α, but showed a reduction in anti-inflammatory cytokine IL-10 secretion (17, 24, 25). Despite the increasing number of investigations examining the effects of mTOR on the immune system, little emphasis has been placed on the function of this pathway in macrophages during infection.

Inflammasomes are nucleotide-binding oligomerization domain like receptors (NLRs) expressed on macrophages and activated in *T. cruzi* infection. When the inflammasome complex is activated, the pro-IL-1β is cleaved in an IL-1β active form (26, 27). In this study, we investigated the role of mTOR on macrophage polarization and parasite growth during *T. cruzi* infection. We demonstrated that *T. cruzi* can activate mTOR, with this molecule being important for its survival since mTOR inhibition decreased the parasite load in macrophages. We also showed that mTOR inhibition in *T. cruzi*-infected macrophages activates NLRP3 inflammasome, upregulates IL-12, IL-6, TNF-α, IL-1β, and mitochondrial ROS (mtROS), but downregulates IL-10 and NO production as well as reducing arginase and iNOS activity and expression. These results indicate that mTOR activation induced by the parasite may be important in inducing a M2 phenotype which favors parasite replication. In contrast, mTOR inhibition in *T. cruzi*-infected macrophages induces an inflammatory M1-like phenotype which was able to limit parasite replication.

MATERIALS AND METHODS

Mice

The BALB/c mice used were obtained from the Comisión Nacional de Energía Atómica (Buenos Aires, Argentina). Male TNFα-RKO (B6.129-Tnfrsf1a^{tm1Mak}), IL6KO (B6.129S2-Il6/^{Jtm1Copf}), and NLRP3 KO (B6.129S6-Nlrp3/J^{tm1Bhk}) mice were purchased

from the Jackson Laboratory. Male C57BL/6J mice were from Universidad Nacional de La Plata (Argentina). All mice were inbred and housed according to institutional guidelines (28).

Trypanosoma cruzi Infection

The *T. cruzi* infection protocols were performed as described (29). Briefly, the infection was maintained through intraperitoneal inoculations every 11 days. Then, blood-derived trypomastigotes were used to infect monolayers of Vero cells. After 7 days, supernatants were collected and stored at −80°C.

BMDMs and Peritoneal Macrophages (PM)

To obtain the BMDMs, the femur and tibia bones from different mice strains were flushed with cold RPMI 1640 containing 40 μg/mL gentamycin, following standard procedures (30). These recovered bone marrow progenitor cells were cultured in 100-mm bacteriologic plastic Petri dishes containing RPMI1640 supplemented with 10% FBS, 40 μg/mL gentamycin, 2 mM L-glutamine, and 30% L929-cell-conditioned medium (31) for 4 days. Then, bone marrow progenitors were supplemented with RPMI-LCM 30%. At day 6, BMDM were used as mentioned below, with a flow cytometric analysis of BMDM (Figure S1 in Supplementary Material) revealing that these cells were CD11b+ and F4/80+.

BALB/c mice underwent intraperitoneal infection as described previously (29), then PM were extracted and processed using several techniques. Non-infected animals were processed in parallel as control.

Chemical Reagents

DMSO, LY294002, diphenyleneiodonium chloride (DPI), 1-methyl-DL-tryptophan, ATP, Griess reagent assay, DAPI, and phosphatase inhibitor (PhosphoStop) were obtained from Sigma-Aldrich (St. Louis, MO, USA); rapamycin and Fluorsave were purchased from Calbiochem (Darmstadt, Germany) and PP242 from Cayman Chemical (Ann Arbor, MI, USA); Recombinant mouse IFNγ, anti-F4/80+ (PE) and anti-CD11b+ (APC) FACS antibodies, recombinant mouse IL-4, ELISA Kits Assay IL-10, IL-12p70, TNFα, IL-6, and IL-1β were obtained from BioLegend (San Diego, CA, USA); LPS (from *E. coli* 0111:B4 strain) was from InvivoGen with DAF-FM, H2DCFDA, and MitoSOX TM Red probes and protein ladders being obtained from Thermo Fisher Scientifics (Waltham, MA, USA). Western blot (WB) antibodies anti-phospho-mTOR, anti-phospho-p70S6K, anti-phospho-4EBP1, anti-ATP-cytrate lyase, anti-β-actin, anti-NLRP3, and anti-IL-1β were acquired from Cell Signaling Technology (Danvers, MA, USA) and anti-Arginase I and anti-iNOS antibodies were obtained from Santa Cruz Biotechnology (Palo Alto, CA, USA). The Odyssey antibodies IRDye® 680RD Donkey anti-Rabbit and IRDye® 680RD Donkey anti-Mouse IgG were obtained from Li-Cor Biosciences (Lincoln, NE, USA). Finally, antibody anti-IgGh was from Biocientifica and protease inhibitor cocktail from Roche (Basilea, Switzerland).

Inhibitors and Stimulus Treatments

Bone marrow-derived macrophage from Balb/c or C57BL6 mice at day 6 of differentiation were cultured for 3 h in RPMI-2%FBS for their adhesion. After that, cells were pretreated with DMSO as control; or pretreated with different inhibitors: 1-methyl-DL-tryptophan (1-MT, 100 μM, during 24 h, 37°C); diphenyleneiodonium chloride (DPI, 20 μM, during 3 h, 37°C), PP242 (40 or 80 nM, for 90 min., 37°C), LY294002 (10 or 50 nM, for 90 min.), rapamycin (50 or 100 nM, for 90 min.). After pretreatment, the BMDM were washed three times and then infected with *T. cruzi* (1:5, cell:parasites ratio). In addition, BMDM without inhibitor pretreatment were stimulated with LPS (1 μg/mL, as positive control of mTOR activation), LPS (1 μg/mL) + IFNγ (100 ng/mL), as positive control of M1 polarization, IL-4 (80 ng/mL), as positive control of M2 polarization, LPS (1 μg/mL) + ATP (5 mM) positive control of inflammasome. Then, cells and supernatants were collected for performing different techniques at 1, 3, 6, 12, 24, 48, and 72 p.i. The number of cells used for the different techniques was: 6×10^6 cells/well for WB and ELISA, 3×10^6 cells for Flow Cytometry, and 3×10^5 cells for Immunofluorescence.

Flow Cytometry

For the assessment of intracellular NO, cytoplasmic ROS (cROS), and mtROS, BMDM from each experimental condition were collected at 4°C and washed with PBS 2% FBS. First, cells were stained with APC labeled anti-CD11b and with FITC labeled anti-F4/80 for 20 min at 4°C. After that, BMDM were incubated with 20 μM DAF-FM diacetate probe for 30 min at 37°C for NO detection; 20 μM H2DCFDA probe for 20 min at 37°C for cROS detection; or 5 μM of a MitoSOX TM Red probe 20 min at 37°C for mtROS detection. Finally, these cells were analyzed by FACS as described previously (29).

Cytokine Determination

IL-10, IL-12p70, TNFα, IL-6, and IL-1β were measured in culture supernatants by ELISA sandwich following the manufacturer's guidelines.

Western Blot

Cells were processed as previously described (29). Lysates were prepared by protein measurement using the Bradford microtechnique (32). Membranes were incubated overnight at 4°C with primary rabbit and mouse monoclonal antibodies anti-phospho-mTOR, anti-phospho-p70S6K, anti-phospho-4EBP1, anti-Arginase-I, anti-iNOS, anti-NLRP3, anti-IL-1β, anti-β-actin, or anti-ATP-cytrate lyase. Then, sheets were incubated with antibodies anti-Rabbit (IRDye® 680RD Donkey anti-Rabbit) and anti-Mouse (IRDye® 680RD Donkey anti-Mouse IgG) for 1 h, at room temperature and in darkness. An Odyssey CLx Infrared Imaging System (LI-COR, Inc.) was used to detect the bands.

Immunofluorescence

Bone marrow-derived macrophages were treated as described in the Section "Inhibitors and Stimulus Treatments," and non-internalized parasites were eliminated by performing washes with RPMI 24 h later. Parasite growth in BMDM was determined by counting the number of intracellular amastigotes using immunofluorescence assays as described (33). For nuclear staining, coverslips were incubated with DAPI, before being washed and incubated in mounting media FluorSave overnight. The slides

were observed using an Olympus BX41 microscope (Olympus Corporation, Tokyo, Japan) and a Leica DMi8 microscope (Leica Microsystems). Images were processed with ImageJ software.

Griess Assay

Nitric oxide levels were obtained by measuring those of the stable end product (nitrites) with Griess reagent assay (34). Absorbance at 540 nm was measured by the Bio Rad microplate reader and optical density was converted to micro molar of nitrites using a standard curve of sodium nitrite.

Arginase Reaction

Arginase activity was measured in macrophage lysates as previously described (33, 35, 36). Cells were lysed with 100 µL of 1% Triton X-100 containing protease inhibitor cocktail and phosphatase inhibitor. Then after 30 min, lysates were prepared for protein measurement by using the Bradford micro-technique (32). The urea (produced by arginine hidrolysis) was measured at 540 nm. The results were expressed as micrograms of urea per microgram of protein.

Statistics

Statistical analyses were performed using the Student's *t*-test of GraphPad Prism software version 6.0 (GraphPad Software). Discrepancies with a value of $p < 0.05$ were considered significant.

RESULTS

T. cruzi Infection Induces mTOR Activation in Macrophages

It has been previously demonstrated that the invasion of trypomastigotes is reduced in HeLa cells treated with the mTOR inhibitor rapamycin (37). However, this has not yet been explored for mTOR function in macrophages during *T. cruzi* infection (38). Therefore, we infected BMDM with *T. cruzi* trypomastigotes and evaluated mTOR activation by WB through phosphorylation of its substrates 4EBP1 and P70S6K. The mTOR activation was observed at 6 and 24 h postinfection (**Figure 1A**), and in addition, we evaluated mTOR activation in peritoneal cells from mice at 15 days postinfection. The peritoneal cells from infected mice revealed an increase in 4EBP1 and P70S6K phosphorylation compared to control cells from uninfected mice (**Figure 1B**), with these results indicating that mTOR is an important pathway induced by the parasite in macrophages.

mTOR Activation in Macrophages Is Essential for Parasite Replication

To determine if mTOR activation is important for parasite survival, we performed experiments by targeting this pathway at different levels. First, BMDM were treated with the mTOR inhibitors rapamycin or PP242, or with Ly249002 (a PI3K inhibitor) or DMSO as control and incubated 90 min. Then, cells were washed and infected with *T. cruzi* trypomastigotes. The number of intracellular parasites was evaluated 72 h later by immunofluorescence. It was observed that pretreatment with rapamycin, PP242, and Ly294002 significantly reduced the number of parasites in BMDM (**Figures 2A,C**) and also in peritoneal infected cells compared to DMSO-treated and infected cells (**Figure 2B**). However, the number of parasites increased in IL-4 stimulated and infected cells, used as positive control of parasite replication (**Figures 2A,B**).

None of these treatments produced any cytotoxic effect on the cells according to cell viability measured by the release of LDH in the supernatants of these cultures (data not shown). The inhibitory effect of the drugs was not a consequence of its action on the trypomastigotes, since inhibitors were removed before incubation with parasites. In addition, it has been reported that pretreatment of parasites with rapamycin does not alter their infectivity in HeLa cells, even for high drug concentrations (37). Thus, our results indicate that the *T. cruzi* parasite activates the mTOR pathway in macrophages in order to promote its survival, since mTOR inhibitors control parasite replication.

Modulation of *T. cruzi*-Induced Macrophage Polarization by Rapamycin

It has been suggested that mTOR in macrophages enhances the expression of M2-associated cytokines (38–40). Moreover, the pharmacological inhibition of mTOR with rapamycin resulted in an inhibition of LPS induction of IL-10 mRNA and protein, but enhanced the pro-inflammatory cytokine TNFα production (41). Thus, to determine the role of mTOR in *T. cruzi*-induced cytokines and whether this could influence the survival of the parasite in macrophages, we performed experiments by incubating BMDM with rapamycin or DMSO as control for 90 min, then, cells were washed and infected with *T. cruzi* trypomastigotes. On evaluating IL-10 and IL-12 production 24 h later by ELISA, it was found that rapamycin pretreatment induced a switch in cytokine production in infected macrophages. Moreover, a rise in IL-12 but a reduction in IL-10 production were observed in rapamycin-pretreated and infected macrophages compared to DMSO control macrophages (**Figures 3A,B**). To achieve a better understanding about the mechanisms implicated in controlling the parasite in rapamycin-treated macrophages, we evaluated Arginase I and iNOS, which are hallmarks of the M1 or M2 activation profiles, respectively. BMDM were pretreated for 90 min with rapamycin or DMSO as control, after which, the cells were washed and infected with *T. cruzi* trypomastigotes and Arginase I and iNOS expression and activities were measured 24 h later. Arginase was slightly induced by the parasite whereas rapamycin pretreatment reduced its expression and activity (**Figures 3C,D**), correlating with a decreased IL-10 production (**Figure 3A**). Surprisingly iNOS expression was also reduced in rapamycin pretreated and infected macrophages (**Figure 3E**), as well as the nitrite production in culture supernatants (**Figure 3F**) and the frequency of NO producing cells (**Figure 3G**).

Cytoplasmic ROS Production and IDO Activity Are Not Involved in Parasite Control in Rapamycin-Treated and Infected Macrophages

It has been previously shown that the ROS resulting from the respiratory burst have an important role in *T. cruzi* control

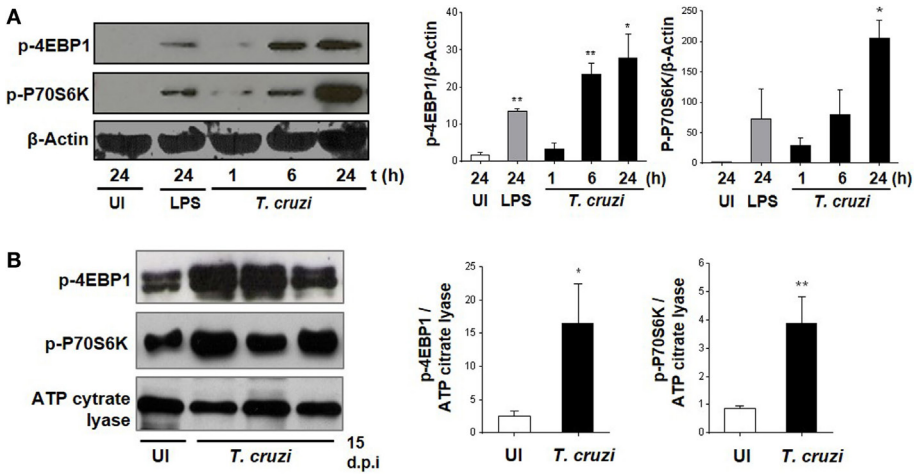


FIGURE 1 | *Trypanosoma cruzi* infection induces mammalian target of rapamycin (mTOR) activation in macrophages. mTOR activation was determined by phosphorylation of mTORC1 substrates, p-4EBP1, and p-P70S6K using Western blot assays (WB). **(A)** Bone marrow-derived macrophage (BMDM) cultured in RPMI without stimulus and without infection were used as control (UI), and BMDM stimulated with LPS 1 μg/mL were used as positive control (LPS). BMDM were infected by adding *T. cruzi* trypomastigotes (1:5, cell:parasite ratio). Infected BMDM were obtained and analyzed at different times (1, 6, and 24 h). Left panel shows a representative experiment and right panel shown densitometry analysis using ImageJ software. Bars represent mean ± SD from three independent experiments. Protein loading was evaluated by β-Actin expression, $^{*}p < 0.05$ and $^{**}p < 0.005$ vs. UI. **(B)** Peritoneal macrophages (PM) from *T. cruzi*-infected Balb/c mice were obtained at 15 days postinfection (d.p.i.) and PM from uninfected Balb/c mice were used as control (UI). Left panel shows a representative experiment and right panel shows densitometry analysis using ImageJ software. Bars represent mean ± SD of three independent experiments. The protein loading was evaluated by ATP citrate lyase expression ($^{*}p < 0.05$ and $^{**}p < 0.005$ vs. UI).

(42–44), but ROS may be involved in cellular signaling and proliferation of this parasite (45). Nevertheless, on evaluating cROS production in rapamycin-treated and infected macrophages at different points after infection by FACS (using H2DCFDA, which measures cROS and mainly detects H_2O_2), we did not observe any differences in the frequency of the cROS producing macrophages between rapamycin-treated and infected macrophages and DMSO-treated and infected macrophages at 6 or 24 h p.i. (**Figure 4A**) or 24 h p.i. (**Figure 4B**). However macrophages stimulated with LPS plus IFN-γ, used as a positive control of ROS production, revealed a high frequency of cROS producing cells (**Figure 4A**).

On the other hand, the enzyme indoleamine 2,3-dioxigenase (IDO) of the tryptophan catabolism is involved in inhibiting intracellular pathogen replication (46, 47); moreover, IDO activity is induced by inflammatory cytokines and is essential for limiting the parasite's reproduction in macrophages since *T. cruzi* amastigotes are sensitive to the L-kynurenine downstream metabolites (48). In order to examine the effect of IDO activity on the regulation of parasite growth *in vitro* in our experimental system, BMDM were cultured in the presence or absence of 1-methyl-D-tryptophan (1-MT), an IDO inhibitor, for 24 h, before being treated with rapamycin for 90 min and then infected with *T. cruzi*. After 24 h, the non-internalized parasites were eliminated through washes, and the intracellular parasites were counted by immunofluorescence 72 h later. IDO blockade with 1-MT was demonstrated to cause a strong stimulatory effect on intracellular parasite growth, as previously reported (48). However, 1-MT treatment did not reverse the effect of rapamycin (**Figures 4B,C**), indicating that IDO is not involved in limiting parasite growth in rapamycin-pretreated and infected macrophages.

mTOR Inhibition Alters the Cytokine Balance of Macrophages toward a Pro-inflammatory Phenotype upon *T. cruzi* Infection

We have shown that rapamycin pretreatment induced an increase in IL-12 and a corresponding reduction in IL-10 production in infected macrophages (**Figures 3A,B**). It has been reported that rapamycin differentially modulates both pro- and anti-inflammatory cytokine production in macrophages in response to LPS such as TNF-α, IL-6, and IL-1β, among others (24, 25, 49). BMDM were pretreated for 90 min with rapamycin or DMSO as control. Then, cells were washed and infected with *T. cruzi* trypomastigotes and cytokine production was evaluated at different time points after infection. mTOR inhibition by rapamycin in BMDM infected with *T. cruzi* led to a strong upregulation of IL-12 production (**Figures 3B** and **5B**). At the same time, the anti-inflammatory cytokine IL-10 was remarkably suppressed (**Figures 3A** and **5A**), whereas, importantly, mTOR inhibition increased the production of the pro-inflammatory cytokines IL-6, TNF-α, and IL-1β (**Figures 5C–E** respectively). These results indicate that mTOR inhibition alters the cytokine balance of macrophages toward a pro-inflammatory phenotype upon *T. cruzi* infection.

Rapamycin Induces NLRP3 Expression in *T. cruzi*-Infected Macrophages, Which Is Relevant in the Control of Parasite Replication

It has been shown that NLRP3 is involved in the antiparasitic response against *T. cruzi*, but the mechanisms involved are

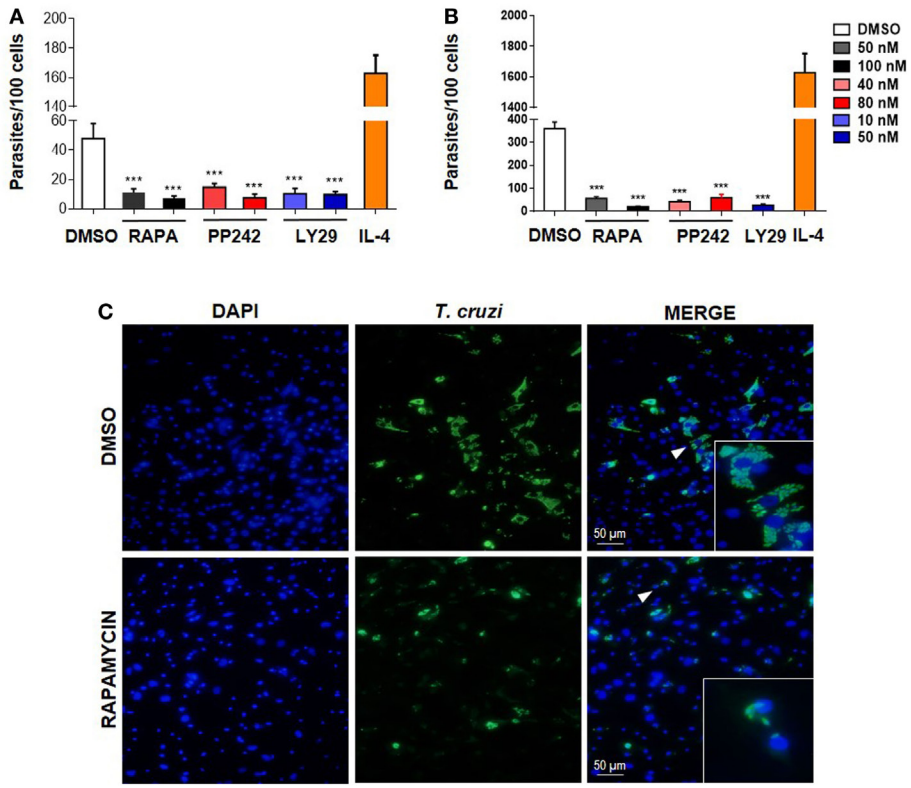


FIGURE 2 | Mammalian target of rapamycin (mTOR) activation in macrophages is essential for parasite replication. **(A)** Bone marrow-derived macrophage (BMDM) and **(B)** peritoneal macrophages (PM) from Balb/c mice were pretreated with DMSO as control or with different mTOR inhibitors: rapamycin (50 or 100 nM), PP242 (40 or 80 nM), and LY294002 (10 or 50 nM) during 90 min. Cells were washed and then were infected with *Trypanosoma cruzi* trypomastigotes (1:5, cell:parasite ratio) during 24 h. Besides, BMDM (A) or PM (B) without inhibitors pretreatment were stimulated with IL-4 (80 ng/mL) and infected with *T. cruzi* trypomastigotes (1:5, cell:parasite ratio) during 24 h as positive control of infection. After that, non-internalized parasites were removed and 72 h later intracellular amastigotes were counted by indirect immunofluorescence. Parasite replication was expressed as number of parasites per 100 cells, quantified by ImageJ software. Bars represent mean ± SD from three independent experiments (***$p < 0.001$ vs. DMSO). **(C)** A representative image from DMSO or rapamycin pretreated BMDM shown cell nucleus stained with DAPI and parasites in green. Inserts show an area from the image (arrowhead) at higher magnification, indicating infected macrophages.

known to depend on the experimental design employed (50). Here, we evaluated NLRP3 expression and IL-1β production in rapamycin pretreated and infected macrophages. Briefly, BMDM were pretreated for 90 min with rapamycin or DMSO as control and cells were washed and infected with *T. cruzi* trypomastigotes. Cell lysates and supernatants were collected 6 h p.i., and NLRP3 expression and IL-1β production were measured by wild type. We observed that mTOR inhibition by rapamycin in *T. cruzi*-infected BMDM led to a potent upregulation of NLRP3 and an increase in IL-lβ production (**Figure 6A**), with BMDM stimulated with ATP plus LPS serving as a positive control of inflammasome activation.

Then, to study the relevance of NLRP3 activation during mTOR inhibition in infected macrophages, we obtained BMDM from NLRP3 KO or wild-type (WT) mice and pretreated them with rapamycin or DMSO for 90 min. Then, cells were infected and *T. cruzi* intracellular replication was measured by immunofluorescence. In agreement with **Figure 2** and Figure S2 in Supplementary Material, a reduction in parasite growth in rapamycin pretreated and infected BMDM from WT was observed. However, rapamycin pretreated and infected BMDM from NLRP3 KO showed a strong increase in parasite replication, which was even more robust than that observed in IL-4 stimulated BMDM used as control (**Figure 6B**). Representative images from DMSO or rapamycin treated and infected WT BMDM (**Figures 6C**) and NLRP3 KO BMDM are shown in **Figure 6D**. In addition, in rapamycin pretreated and infected BMDM from TNFα-R KO and IL-6 KO mice there was an increase in parasite replication compared with rapamycin-pretreated and infected BMDM from WT mice. However, this effect was less evident than in the BMDM from NLRP3 KO mice (**Figure 6B** and Figure S3 in Supplementary Material).

mtROS Production Is Important in Controlling Parasite Replication during mTOR Inhibition in *T. cruzi*-Infected Macrophages

It has been previously shown that mitochondria participate in inflammasome activation (51). The NLRP3 inflammasome is the best characterized among various inflammasome complexes,

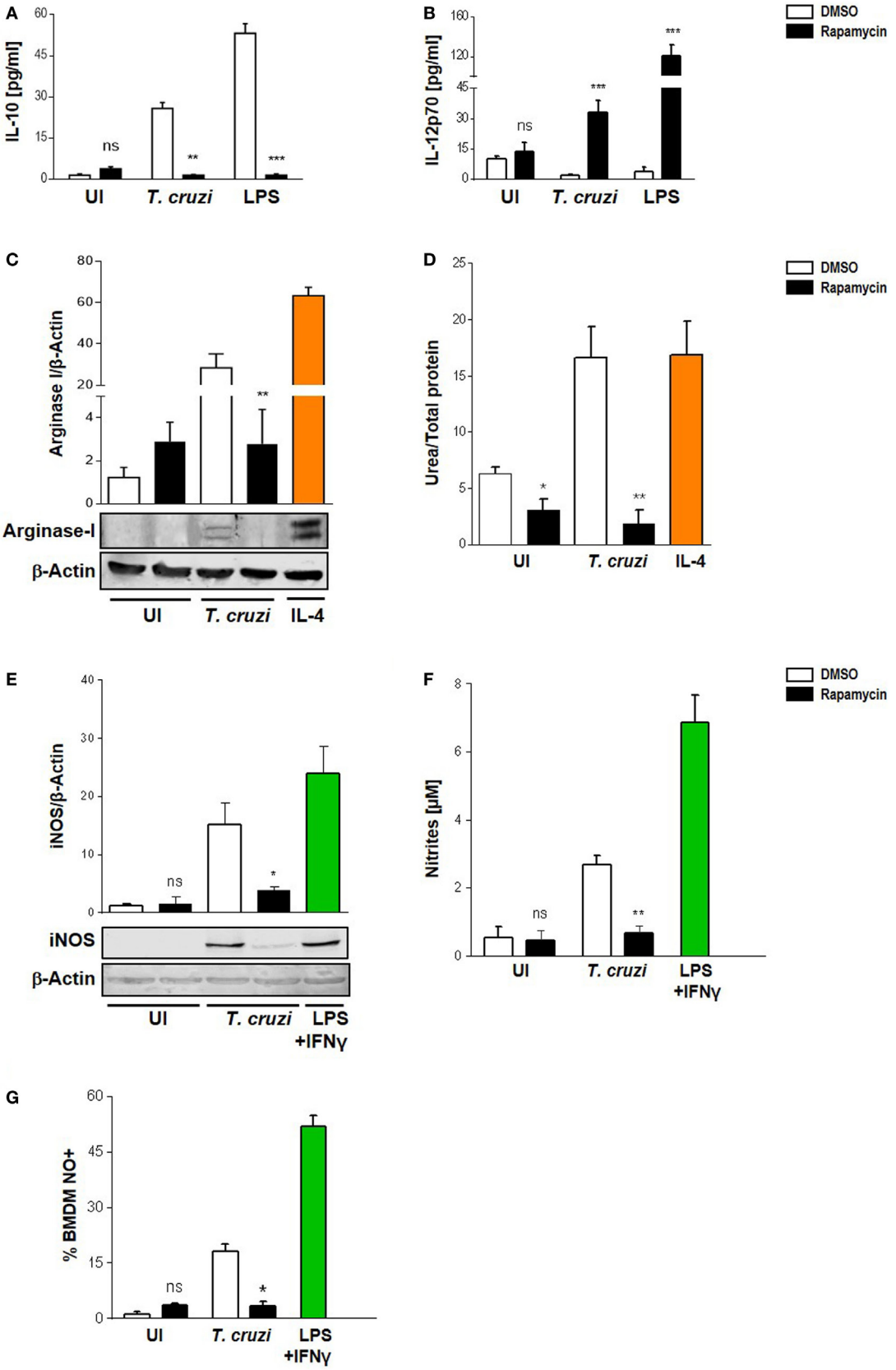


FIGURE 3 | Continued

FIGURE 3 | Modulation of *Trypanosoma cruzi*-induced macrophage polarization by rapamycin. Macrophage polarization was evaluated through cytokine production, Arginase I, and iNOS expression and activity. Bone marrow-derived macrophage (BMDM) from Balb/c mice were pretreated with DMSO as control, or with rapamycin (100 nM) during 90 min. After pretreatment cells were washed and uninfected (UI) or *T. cruzi*-infected (*T. cruzi*) (1:5, cell:parasite ratio) BMDM were cultured during 24 h and then processed for the different experiment. **(A)** IL-10 and **(B)** IL-12p70 production were measured by ELISA sandwich-assays. Besides, BMDM with or without rapamycin pretreatment were stimulated with LPS 1 μg/mL as positive control (LPS) during 24 h. Arginase I **(C)** and iNOS **(E)** expression from cellular lysates were performed by western blot at 24 h postinfection, using as loading control β-actin. Besides, BMDM were stimulated with IL-4 (80 ng/mL) or LPS (1 μg/mL) + IFNγ (100 ng/mL) during 24 h as positive controls for Arginase-I (C) or iNOS (E) expression, respectively. Upper panel shows densitometry analysis using ImageJ software. Bars represent mean ± SD from three independent experiments (***$p < 0.001$ vs. DMSO). Bottom panel shows a representative experiment. **(D)** Arginase activity was determined by urea production assay 24 h p.i. **(F)** iNOS activity was evaluate by Griess reaction on supernatants 24 h p.i. **(G)** Besides, iNOS activity was determined by FACS. BMDM were stained with anti-F480 (PE) and anti-CD11b (APC) and then incubated with DAF-FM-DA probe (20 μM, FITC), 30 min at 37°C for intracellular NO detection. Bars represent mean ± SD from three independent experiments (*$p < 0.05$, **$p < 0.005$, and ***$p < 0.001$ vs. DMSO; ns, no significant difference vs. DMSO).

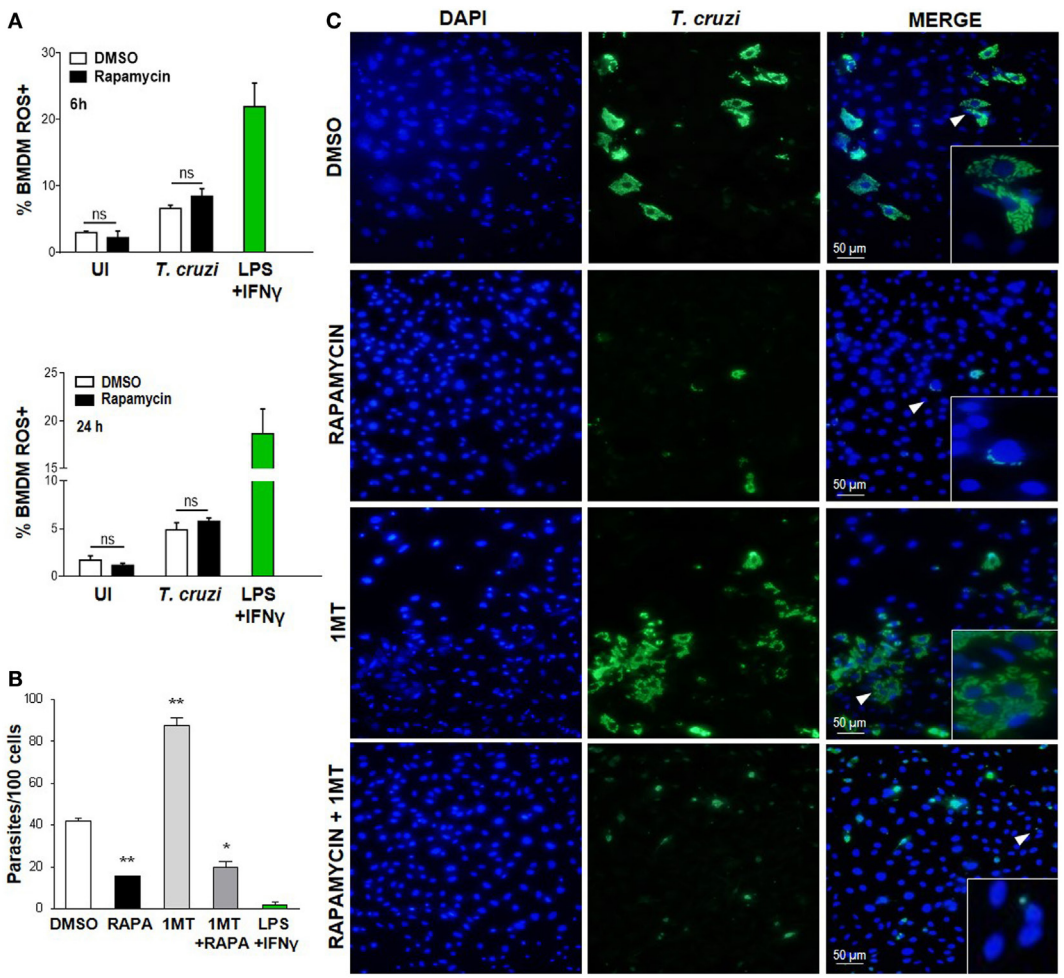


FIGURE 4 | Decreased *Trypanosoma cruzi* replication by mammalian target of rapamycin inhibition was independent of cytoplasmic ROS and IDO. **(A)** Bone marrow-derived macrophages (BMDM) from C57BL/6 mice were pretreated with DMSO as control or with rapamycin (100 nM) during 90 min. After pretreatment cells were washed and uninfected (UI) or *T. cruzi*-infected (*T. cruzi*) (1:5, cell:parasite ratio) were cultured at different times and then processed for the experiments. Besides, BMDM were stimulated with LPS + IFNγ (1 μg/mL + 100 ng/mL), during 24 h as positive control. BMDM at 6 and 24 h postinfection were stained with anti-F480 (PE) and anti-CD11b (APC) mAbs. Then, cells were incubated with 20 μM H2DCFDA probe, 20 min at 37°C for intracellular reactive oxygen species (ROS) detection. Bars represent mean ± SD of from three independent experiments (ns, no significant difference vs. DMSO). **(B–C)** Parasite replication in BMDM from C57BL6 mice pretreated with DMSO as control, or with Rapamycin (RAPA: 100 nM) during 90 min, or with 1-methyl tryptophan (1-MT: 100 μM; 24 h) or with 1-MT (24 h) + RAPA (90 min). After pretreatment BMDM were washed and then infected with *T. cruzi* trypomastigotes (1:5, cell:parasite ratio) during 24 h. Besides, BMDM without inhibitors pretreatment, were stimulated with LPS + IFNγ (1 μg/mL + 100 ng/mL), during 24 h as positive control. After that, non-internalized parasites were removed and 72 h later intracellular amastigotes were counted by indirect immunofluorescence. **(B)** Intracellular replication of *T. cruzi* is expressed as number of parasites per 100 cells, quantified by ImageJ software and represent mean ± SD from three independent experiments (*$p < 0.05$ and **$p < 0.005$, vs. DMSO). **(C)** A representative image shows cell nucleus stained with DAPI and parasites in green. Inserts show an area from the image (arrowhead) at higher magnification, indicating infected macrophages.

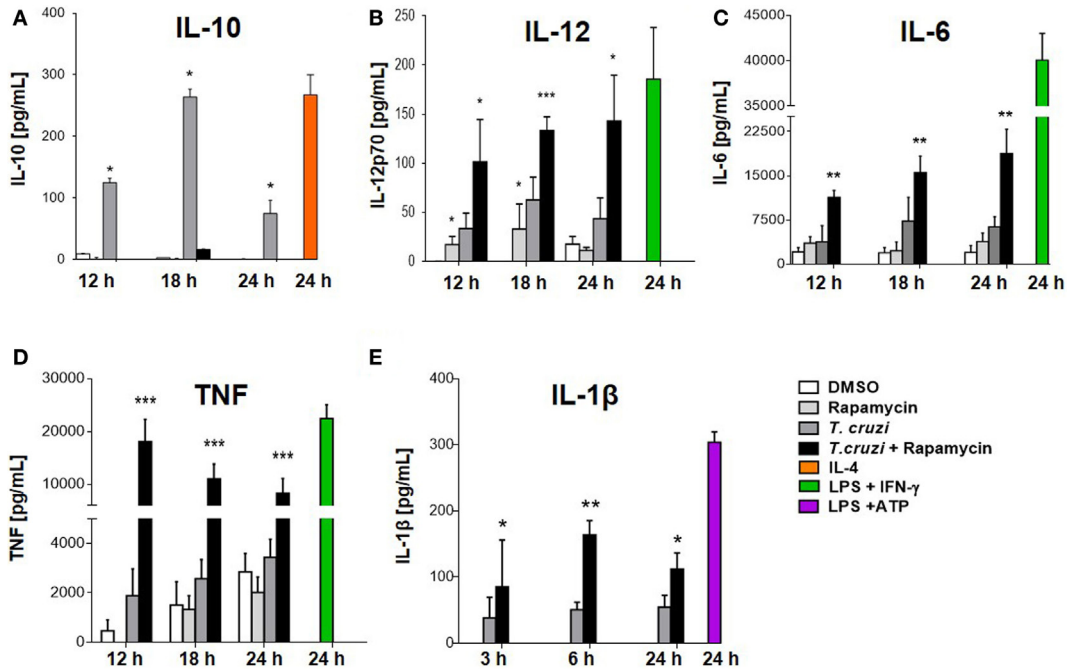


FIGURE 5 | Mammalian target of rapamycin inhibition alters cytokine balance in macrophages toward a pro-inflammatory phenotype upon *Trypanosoma cruzi* infection. Bone marrow-derived macrophages (BMDMs) from C57BL/6 mice were pretreated with DMSO as control or with rapamycin (100 nM) during 90 min. After pretreatment, BMDM uninfected or infected with *T. cruzi* trypomastigotes (1:5, cell:parasite ratio) were cultured at different times. At 12, 18, and 24 h postinfection, supernatants were collected and processed to determine the IL-10 **(A)**, IL-12p70 **(B)**, IL-6 **(C)**, TNFα **(D),** and IL-1β **(E)** production by ELISA Sandwich. Besides, supernatants from BMDM stimulated with IL-4 (80 ng/mL), or with LPS (1 μg/mL) + IFNγ (100 ng/mL), or with LPS (1 μg/mL) + ATP (5 mM) during 24 h were used as positive controls. Bars panels represent mean ± SD from three independent assays (*$p < 0.05$, **$p < 0.005$, and ***$p < 0.001$ vs. DMSO).

with its activation depending on different stress signals, including ROS production promoted by mitochondrial dysfunction (51). Thus, we evaluated mtROS production in rapamycin treated and infected BMDM at different points after infection using MitoSOX, which measures mtROS and mainly detects superoxide radical. We found a significant increase in mtROS production in rapamycin-pretreated and infected BMDM, with increased levels of mtROS being observed in ATP plus LPS-stimulated BMDM, used as positive control (**Figure 7A**). Then, to evaluate whether mtROS is relevant for controlling parasite replication, BMDM from WT mice were pretreated with rapamycin, DPI (NADPH oxidase inhibitor), rapamycin + DPI, or DMSO before being infected, and the parasite load was studied by immunofluorescence. It was observed that BMDM incubated with rapamycin plus DPI had a significantly higher parasite load compared to rapamycin-pretreated BMDM (**Figure 7B**), with a representative image from DMSO, rapamycin, DPI, and rapamycin plus DPI treated and infected BMDM being shown in **Figure 7C**. Additionally, we have observed that DPI inhibits mtROS production induced by rapamycin pretreatment and *T. cruzi* infection, Figure S4 in Supplementary Material. This may indicate that mtROS would participate in the control of *T. cruzi* replication. These findings strongly suggest that mTOR inhibition during *T. cruzi* infection in BMDM induces inflammasome NLRP3 activation and mtROS production, which controls parasite survival.

DISCUSSION

In order to control the *T. cruzi* infection, it is necessary that cytokine-mediated macrophage activation leads to intracellular killing of the parasite. Moreover, M1 polarization is closely related to parasite removal, whereas M2 polarization can be effective in countering the development of an oxidative and inflammatory pathology in Chagas disease (35, 36, 52).

As the protein mTOR is a critical regulator of the host cell metabolism, it is a logical target to be manipulated by invasive pathogens such as *T. cruzi*. In this investigation, we examined the role of the mTOR pathway in macrophage polarization induced by *T. cruzi* and we observed that mTOR is activated *in vitro* by the parasite in BMDM. In addition, peritoneal cells obtained from infected mice showed an increase in mTOR activation compared to those from uninfected mice. These results clearly indicate that mTOR is an important pathway induced by the parasite in macrophages considering that its inhibition during infection shifts these macrophages to an M1-like inflammatory profile by reducing IL-10 and arginase activity and expression. Rapamycin pretreated and infected macrophages revealed an activation of the NLRP3 inflammasome and an increased production of IL-12, IL-6, TNF-α, IL-1β, and mtROS. Thus, these macrophages have an increased ability to limit parasite replication, which was clearly demonstrated using three different inhibitors of the mTOR pathway (rapamycin, PP242, and LY249002).

The selective deletion of signals through mTORC1 in macrophages promotes M1 cytokines (53), whereas deletion of signals through mTORC2 inhibits the generation of M2 while maintaining intact the generation of M1 (54). In TLR-induced pro-inflammatory cytokine production, the role of the TSC-mTOR pathway is still unclear. It was reported that in TSC2-deficient

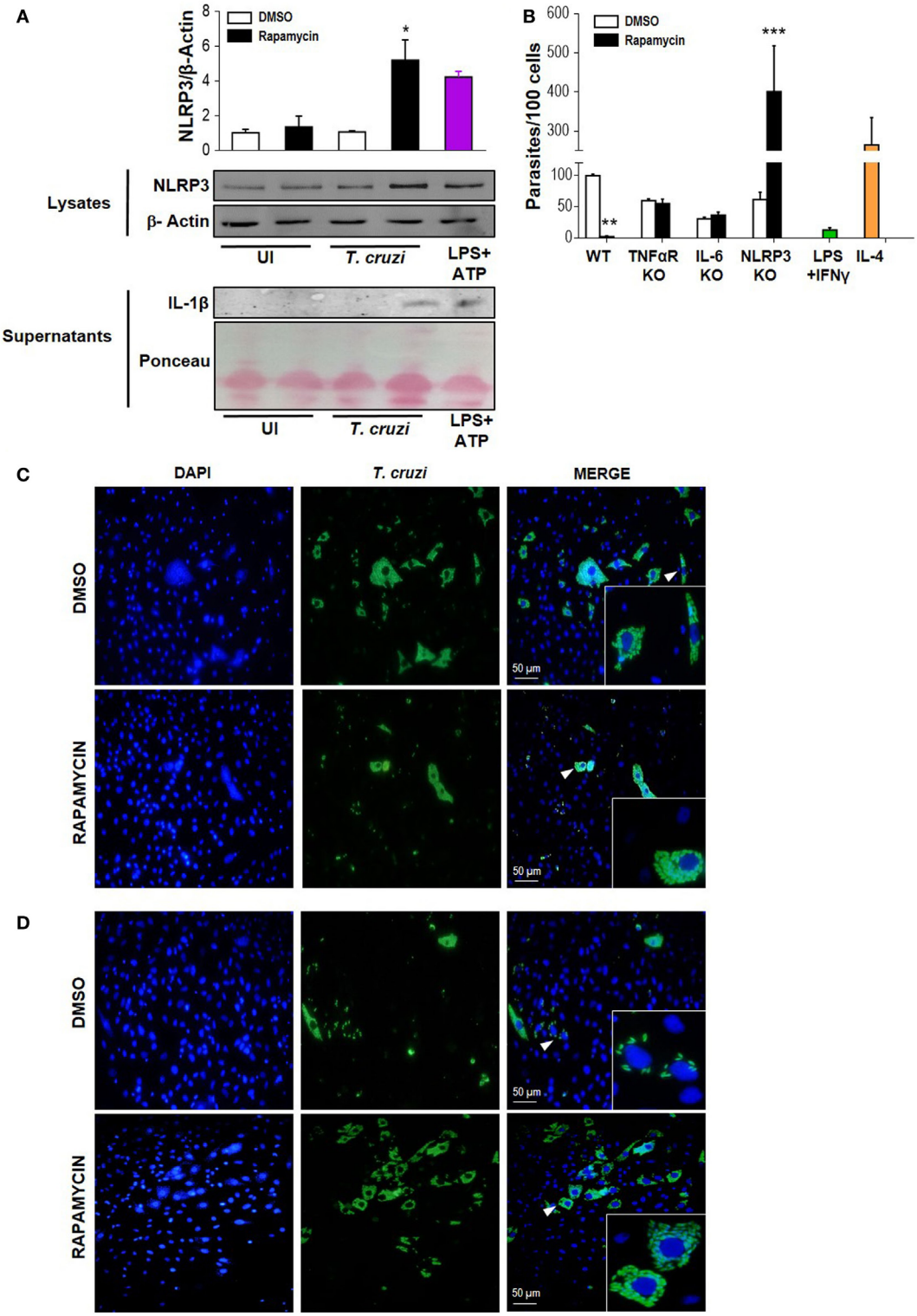


FIGURE 6 | Continued

FIGURE 6 | Rapamycin induces NLRP3 activation in *Trypanosoma cruzi*-infected macrophages, a relevant event to control parasite replication. **(A)** NLRP3 activation was determined by NLRP3 expression (upper panel) and cleaved IL-1β release (bottom panel) using western blot assays (WB). Bone marrow-derived macrophages (BMDMs) from C57BL/6 mice were pretreated with DMSO as control or with rapamycin (100 nM) during 90 min. After rapamycin pretreatment cells were washed and uninfected (UI) or *T. cruzi*-infected BMDM (*T. cruzi*) (1:5, cell:parasite ratio) were cultured during 6 h. Besides, BMDM were stimulated with LPS (1 μg/mL) + ATP (5 mM) as positive control. Then, cell lysates and supernatants were processed for WB. A representative experiment of three independent experiments is shown. The protein loading for NLRP3 and IL-1β was evaluated by β-Actin expression and by Ponceau staining, respectively. Densitometry analysis from cell lysates was performed by ImageJ software (*$p < 0.05$ and **$p < 0.005$ vs. DMSO). **(B)** Parasite replication in BMDM from wild-type (WT), TNFαR KO, IL-6 KO, and NLRP3 KO mice. BMDM were pretreated with DMSO as control or with rapamycin (100 nM) during 90 min. After pretreatment, cells were washed and infected with *T. cruzi* trypomastigotes (1:5, cell:parasite ratio) during 24 h. Besides, WT BMDM without rapamycin pretreatment were stimulated with LPS (1 μg/mL) + IFNγ (100 ng/mL) and infected with *T. cruzi* trypomastigotes (1:5, cell:parasite ratio) during 24 h as negative control of parasite replication. On the other hand, WT BMDM without rapamycin pretreatment were stimulated with IL-4 (80 ng/mL) and infected with *T. cruzi* trypomastigotes (1:5, cell:parasite ratio) during 24 h as positive control of parasite replication. After that, non-internalized parasite were removed, and 72 h later, intracellular amastigotes were counted by indirect immunofluorescence. Intracellular replication of *T. cruzi* is expressed as number of parasites per 100 cells, quantified by ImageJ software and represent mean ± SD from three independent experiments (*$p < 0.05$, **$p < 0.005$, and ***$p < 0.001$ vs. DMSO). A representative image from WT **(C)** and NLRP3 KO **(D)** BMDM show cell nucleus stained with DAPI and parasites in green. Insert show an area from the image (arrowhead) at higher magnification, indicating infected macrophages.

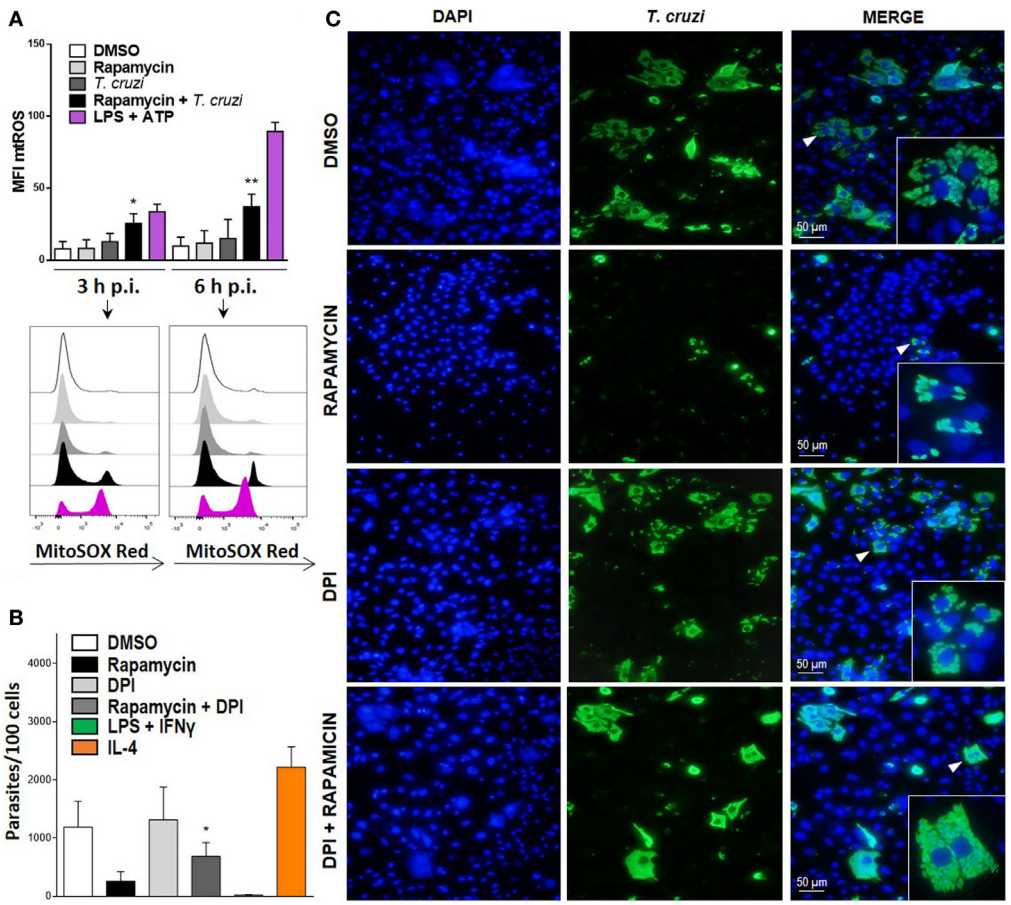


FIGURE 7 | Mitochondrial ROS (mtROS) production is important to control parasite replication during mammalian target of rapamycin (mTOR) inhibition in *Trypanosoma cruzi*-infected macrophages. **(A)** Bone marrow-derived macrophage (BMDM) from C57BL/6 mice pretreated with DMSO as control or with rapamycin (100 nM) during 90 min. After pretreatment cells were washed and uninfected or infected *T. cruzi* BMDM (1:5, cell:parasite ratio) were cultured at 3 and 6 h. Besides, BMDM without rapamycin pretreatment were stimulated with LPS + ATP (1 μg/mL and 5 mM) during 3 and 6 h. At indicates times postinfection (p.i.), BMDM were stained with anti-F480 (FITC) and anti-CD11b (APC) mAbs. Then, cells were incubated with 5 μM MitoSOX probe (PE) 15 min at 37°C and analyzed by Flow cytometry. Bars display mean fluorescence intensity (MFI) of mtROS on F4/80+ CD11b+ gated populations. Experiments were repeated three times with similar results being obtained and are expressed as mean ± SD (*$p < 0.05$ and **$p < 0.005$ vs. DMSO). A representative histogram of at least three independent experiments is shown. **(B)** Parasite replication in BMDM from C57BL6 mice pretreated with DMSO as control (24 h) rapamycin (100 nM, 90 min), with DPI (20 μm, 3 h) or with DPI + rapamycin. After pretreatment, cells were washed and infected with *T. cruzi* trypomastigotes (1:5, cell:parasite ratio) during 24 h. Besides, BMDM without inhibitors pretreatment, were stimulated with LPS (1 μg/mL) + IFNγ (100 ng/mL) or with IL-4 (80 ng/mL) and infected with *T. cruzi* trypomastigotes (1:5, cell:parasite ratio) during 24 h as controls. After that, non-internalized parasite were removed and 72 h later intracellular amastigotes were counted by indirect immunofluorescence. Intracellular replication of *T. cruzi* is expressed as number of parasites per 100 cells, quantified by ImageJ software and represent mean ± SD from three independent experiments (*$p < 0.05$; vs. rapamycin). **(C)** A representative image from DMSO, rapamycin, DPI, rapamycin + DPI pretreated BMDM, show cell nucleus stained with DAPI and parasites in green. Inserts show an area from the image (arrowhead) at higher magnification, indicating infected macrophages.

MEFs, the pro-inflammatory responses are reduced as a result of impaired IKK activation and NF-κB translation to the nuclei (54). Nevertheless, other studies have found that rapamycin treatment enhances the IL-12 production in myeloid DCs by stimulating NF-κB activation, but prevents IL-12 production in bone marrow-derived DCs and monocyte-derived ones (40, 55). Moreover, TSC1-deficient macrophages produce elevated pro-inflammatory cytokines in response to an LPS stimulation, such as TNF-α, IL-12, and IL-6 (18, 19, 24). The reason for this apparent inconsistency is still unknown, but possibly originates from the different cell types or the length of mTOR inhibition with rapamycin. Here, we found that mTOR inhibition by rapamycin (90 min) in BMDM infected with *T. cruzi* led to a potent upregulation of IL-12 production, whereas the anti-inflammatory cytokine IL-10 was notably suppressed. Furthermore, mTOR inhibition increased the production of the pro-inflammatory cytokines IL-6 and TNF-α. These results indicate that mTOR inhibition alters the cytokine balance of macrophages toward a pro-inflammatory phenotype upon *T. cruzi* infection.

The role of the mTOR pathway in the regulation of IL-1β expression has been examined in both mouse and human macrophages (38, 56). In addition, other authors have used TSC1-deficient macrophages and macrophage cell lines to study the involvement of TSC1 in pro-inflammatory cytokine IL-1β expression and investigated the associated molecular mechanism. They reported that at the level of both the mRNA and protein, the LPS-induced pro-IL-1β synthesis was significantly downregulated in TSC1-deficient macrophages, by extended rapamycin (48 h) treatment or mTOR deletion (18). In contrast, we found that mTOR inhibition by rapamycin (90 min) in *T. cruzi*-infected BMDM led to a potent upregulation of IL-1β production. However, it is possible that differences in exposure time of the macrophages to rapamycin, was crucial in determining the outcome.

Deletion of Akt1 promotes upregulation of inducible NO synthase and IL-12 (M1 activation) and enhances bacteria clearance (57, 58). We observed that pretreatment with mTOR inhibitors (rapamycin, PP242) and PI3K inhibitor (Ly294002) significantly reduced the number of parasites in BMDM and in peritoneal infected cells compared to DMSO-treated and infected cells. Also, we found that a short period of mTOR inhibition previous to infection induced an inflammatory profile in these macrophages similar to an M1 polarization without iNOS expression. It is also possible that mTOR inhibition also modifies *T. cruzi* invasion in BMDM, since this was demonstrated through the inhibition of PI3K (59, 60).

Importantly, macrophage alternative (or M2) activation is induced by signaling through the IL-4R *via* STAT6. Related to this, TSC1-deficient macrophages have been found to fail to alternatively activate in response to IL-4, reflecting the fact that pronounced mTORC1 signaling is a strong negative regulator of alternative activation (61, 62). This was not due to effects on STAT6 phosphorylation, but rather to feedback inhibition of Akt phosphorylation through effects on the insulin receptor substrate 2, which is also engaged by IL-4R signaling (18, 62). Interestingly, in TSC1-deficient macrophages, low-dose rapamycin (which preferentially inhibits mTORC1 but not mTORC2) allows an alternative activation in response to IL-4. However, recent work using higher concentrations of rapamycin (which also inhibits mTORC2), Torin (which inhibits both mTORC1 and mTORC2), and Rictor deficient macrophages has revealed that mTORC2 is critical for alternative activation (54, 63). Thus, mTORC2 acts in parallel with pSTAT6 to promote an alternative activation, in part by cooperating in events that lead to expression of IRF4 (63). In our present investigation, rapamycin induced not only a decrease in the activity and expression of arginase and IL-10 production in *T. cruzi*-infected BMDM but also produced a decrease in iNOS expression and activity. Moreover, although cROS was not induced, rapamycin induced mtROS and IL-1β production along with pro-inflammatory cytokines such as IL-12, IL-6, and TNF-α.

The NLRs are part of the response to *T. cruzi*, as first reported for NOD1 (27). Although KO animals for this receptor have a higher parasite burden and mortality than WT, they are still capable of producing cytokines at systemic level, suggesting that other NLRs may also contribute to resistance against this parasite. NLRP3 is activated in response to lysosomal damage generated by the escape of protozoan from the parasitophora vacuole, but this is independent of the K+ flow and ROS generation (26). These studies showed that NO production is eliminated in primary macrophages from NLRP3 KO *T. cruzi* Y strain-infected mice. However, some authors (64) argue that this phenomenon is dependent on both IL-1β and IL-1R, while others have postulated that this is independent of these molecules (50). Nevertheless, these results emphasize the complexity of the antiparasitic response orchestrated by the NLRP3 inflammasome together with other innate receptors and reflected in various microbicidal mechanisms assembled against *T. cruzi* (51, 65). In our study, rapamycin pretreatment in *T. cruzi*-infected BMDM induced NLRP3 expression, mtROS and IL-1β production, but not cROS or NO production.

Several studies have indicated that cROS is a necessary secondary messenger in order to achieve signaling caspase-1/ASC inflammasome activation (66, 67), but this was demonstrated for a feedback cycle of IL-1β signaling of cROS activation in *T. cruzi*-infected macrophages (50), with the molecular mechanisms involved in cROS production induced by IL-1β remaining to be clarified. In previous investigations, IL-1β was reported to promote phospholipase A2, thereby stimulating the release of arachidonic acid. However, since arachidonic acid is able to activate NADPH oxidase to afford superoxide, it is a possibility that this fatty acid serves as an intermediate in the IL-1β-induced activation of the enzymes, thus resulting in the production of ROS (67, 68). In our study, we demonstrated that rapamycin pretreatment in *T. cruzi*-infected macrophages induces mtROS production, which is involved in the control of *T. cruzi* replication, since an inhibitor of NADPH oxidase (DPI) partially reverses the effect of rapamycin. Certainly DPI is as potent as rotenone in inhibiting the production of superoxide and H_2O_2 by mitochondrial respiration.

It is important to emphasize that we cannot exclude the possible implication of mTOR inhibition in the limitation of some nutrients relevant for *T. cruzi* proliferation within BMDM,

thus potentiating microbicidal effect of mtROS. This would be supported by the effect of partial inhibition produced by DPI treatment. In addition, it would be interesting to study the mechanism of mtROS inhibition by DPI and its effect on *T. cruzi* replication. It would be possible that changes in macrophages metabolism lead them to a metabolic program mediated by oxidative phosphorylation in detriment of glycolysis that is characteristic of M1 macrophages (69), since DPI influences mitochondrial respiration. However, the relevance of mtROS in controlling the intracellular growth of a microorganism has already been demonstrated in macrophages treated with metformin and infected with *M. tuberculosis*. In fact, metformin is an activator of the AMP-activated protein kinase, which has an important role in cellular energy homeostasis. Subsequently, our results indicate that the modulation of macrophage metabolism may be a new therapeutic tool in the control of intracellular infections (70).

In summary, the relevance of this study lies in the fact that treatment with rapamycin prior to macrophage *T. cruzi* infection controlled the intracellular growth of the parasite through inflammasome NLRP3 expression and the production of mtROS. In contrast, the iNOS and IDO enzymes were not involved. Thus, induction of mtROS may be relevant in the control of pathogen infections residing in macrophages.

ETHICS STATEMENT

The Institutional Experimentation Animal Committee of the Chemical Sciences Faculty authorized the experimental protocols (no. 2016-213). This committee adopts the guidelines of the "Guide to the care and use of experimental animals" and those of the "Institutional Animal Care and Use Committee Guidebook."

AUTHOR CONTRIBUTIONS

The authors point out their participation in the conception, design, drafting, and revision of the investigation, which provided an important intellectual content. The study was directed, reviewed, and approved by FC and CS. The authors have agreed to be accountable for all aspects of this work, in terms of integrity, accuracy and all other related issues.

ACKNOWLEDGMENTS

The authors thank Belkys Maletto, Lilian Canavoso, Laura Gatica, Gabriela Furlan, Alejandra Romero, Pilar Crespo, Ximena Volpini, Jimena Leyria, Cecilia Ramello, Luisina Onofrio, Liliana Sanmarco, Augusto Paroli, Victoria Blanco, Diego Lutti, Fabricio Navarro, and Paula Abadie for their skillful technical assistance. JM also thanks CONICET, and YA and RB thank ANPCyT-FONCyT for the fellowships granted. The authors thank Dr. Paul Hobson, native speaker, for revision of the manuscript.

FUNDING

Our work has been supported by the Concejo Nacional de Investigaciones Cientificas y Tecnicas (CONICET), Secyt-UNC, Mincyt-Cba and Mincyt-Cba and Fondo para la Investigación Científica y Tecnológica (FONCyT). FMC and CCS are members of the Scientific Career of CONICET.

SUPPLEMENTARY MATERIAL

The Supplementary Material for this article can be found online at http://www.frontiersin.org/articles/10.3389/fimmu.2018.00313/full#supplementary-material.

REFERENCES

1. Organization WH. *Chagas Disease*. (2017). Available from: http://who.int/mediacentre/factsheets/fs340/en/
2. Campos MA, Closel M, Valente EP, Cardoso JE, Akira S, Alvarez-Leite JI, et al. Impaired production of proinflammatory cytokines and host resistance to acute infection with *Trypanosoma cruzi* in mice lacking functional myeloid differentiation factor 88. *J Immunol* (2004) 172(3):1711–8. doi:10.4049/jimmunol.172.3.1711
3. Tanowitz HB, Kirchhoff LV, Simon D, Morris SA, Weiss LM, Wittner M. Chagas' disease. *Clin Microbiol Rev* (1992) 5(4):400–19. doi:10.1128/CMR.5.4.400
4. Barrias ES, de Carvalho TM, De Souza W. *Trypanosoma cruzi*: entry into mammalian host cells and parasitophorous vacuole formation. *Front Immunol* (2013) 4:186. doi:10.3389/fimmu.2013.00186
5. Seljelid R, Eskeland T. The biology of macrophages: I. general principles and properties. *Eur J Haematol* (1993) 51(5):267–75. doi:10.1111/j.1600-0609.1993.tb01607.x
6. Seljelid R, Busund LT. The biology of macrophages: II. inflammation and tumors. *Eur J Haematol* (1994) 52(1):1–12. doi:10.1111/j.1600-0609.1994.tb01277.x
7. Gordon S, Taylor PR. Monocyte and macrophage heterogeneity. *Nat Rev Immunol* (2005) 5(12):953–64. doi:10.1038/nri1733
8. Mantovani A, Biswas SK, Galdiero MR, Sica A, Locati M. Macrophage plasticity and polarization in tissue repair and remodelling. *J Pathol* (2013) 229(2):176–85. doi:10.1002/path.4133
9. Biswas SK, Allavena P, Mantovani A. Tumor-associated macrophages: functional diversity, clinical significance, and open questions. *Semin Immunopathol* (2013) 35(5):585–600. doi:10.1007/s00281-013-0367-7
10. Zanluqui NGWP, Pinge-Filho P. Macrophage polarization in Chagas disease. *J Clin Cell Immunol* (2015) 6:317. doi:10.4172/2155-9899.1000317
11. Mantovani A, Sica A, Locati M. Macrophage polarization comes of age. *Immunity* (2005) 23(4):344–6. doi:10.1016/j.immuni.2005.10.001
12. Murray PJ, Allen JE, Biswas SK, Fisher EA, Gilroy DW, Goerdt S, et al. Macrophage activation and polarization: nomenclature and experimental guidelines. *Immunity* (2014) 41(1):14–20. doi:10.1016/j.immuni.2014.06.008
13. Gordon S. Alternative activation of macrophages. *Nat Rev Immunol* (2003) 3(1):23–35. doi:10.1038/nri978
14. Steevels TA, Meyaard L. Immune inhibitory receptors: essential regulators of phagocyte function. *Eur J Immunol* (2011) 41(3):575–87. doi:10.1002/eji.201041179
15. Sica A, Mantovani A. Macrophage plasticity and polarization: in vivo veritas. *J Clin Invest* (2012) 122(3):787–95. doi:10.1172/JCI59643
16. Novak ML, Koh TJ. Phenotypic transitions of macrophages orchestrate tissue repair. *Am J Pathol* (2013) 183(5):1352–63. doi:10.1016/j.ajpath.2013.06.034
17. Martinez FO. Regulators of macrophage activation. *Eur J Immunol* (2011) 41(6):1531–4. doi:10.1002/eji.201141670
18. Byles V, Covarrubias AJ, Ben-Sahra I, Lamming DW, Sabatini DM, Manning BD, et al. The TSC-mTOR pathway regulates macrophage polarization. *Nat Commun* (2013) 4:2834. doi:10.1038/ncomms3834

19. Pan H, O'Brien TF, Zhang P, Zhong XP. The role of tuberous sclerosis complex 1 in regulating innate immunity. *J Immunol* (2012) 188(8):3658–66. doi:10.4049/jimmunol.1102187
20. Dibble CC, Elis W, Menon S, Qin W, Klekota J, Asara JM, et al. TBC1D7 is a third subunit of the TSC1-TSC2 complex upstream of mTORC1. *Mol Cell* (2012) 47(4):535–46. doi:10.1016/j.molcel.2012.06.009
21. Laplante M, Sabatini DM. mTOR signaling in growth control and disease. *Cell* (2012) 149(2):274–93. doi:10.1016/j.cell.2012.03.017
22. Schmitz F, Heit A, Dreher S, Eisenacher K, Mages J, Haas T, et al. Mammalian target of rapamycin (mTOR) orchestrates the defense program of innate immune cells. *Eur J Immunol* (2008) 38(11):2981–92. doi:10.1002/eji.200838761
23. Ohtani M, Nagai S, Kondo S, Mizuno S, Nakamura K, Tanabe M, et al. Mammalian target of rapamycin and glycogen synthase kinase 3 differentially regulate lipopolysaccharide-induced interleukin-12 production in dendritic cells. *Blood* (2008) 112(3):635–43. doi:10.1182/blood-2008-02-137430
24. Zhu L, Yang T, Li L, Sun L, Hou Y, Hu X, et al. TSC1 controls macrophage polarization to prevent inflammatory disease. *Nat Commun* (2014) 5:4696. doi:10.1038/ncomms5696
25. Weichhart T, Saemann MD. The PI3K/Akt/mTOR pathway in innate immune cells: emerging therapeutic applications. *Ann Rheum Dis* (2008) 67(Suppl 3):iii70–4. doi:10.1136/ard.2008.098459
26. Dey N, Sinha M, Gupta S, Gonzalez MN, Fang R, Endsley JJ, et al. Caspase-1/ASC inflammasome-mediated activation of IL-1beta-ROS-NF-kappaB pathway for control of *Trypanosoma cruzi* replication and survival is dispensable in NLRP3-/- macrophages. *PLoS One* (2014) 9(11):e111539. doi:10.1371/journal.pone.0111539
27. Silva GK, Gutierrez FR, Guedes PM, Horta CV, Cunha LD, Mineo TW, et al. Cutting edge: nucleotide-binding oligomerization domain 1-dependent responses account for murine resistance against *Trypanosoma cruzi* infection. *J Immunol* (2010) 184(3):1148–52. doi:10.4049/jimmunol.0902254
28. Ministerio de Ciencia y Tecnología. *Sistemas Nacionales de Bioterios*. (2017). Available from: http://www.bioterios.mincyt.gob.ar/
29. Stempin CC, Rojas Marquez JD, Ana Y, Cerban FM. GRAIL and otubain-1 are related to T cell hyporesponsiveness during *Trypanosoma cruzi* infection. *PLoS Negl Trop Dis* (2017) 11(1):e0005307. doi:10.1371/journal.pntd.0005307
30. Zhang X, Goncalves R, Mosser DM. The isolation and characterization of murine macrophages. *Curr Protoc Immunol* (2008) Chapter 14:Unit 141. doi:10.1002/0471142735.im1401s83
31. Weischenfeldt J, Porse B. Bone marrow-derived macrophages (BMM): isolation and applications. *CSH Protoc* (2008) 2008:dbrot5080. doi:10.1101/pdb.prot5080
32. Bradford MM. A rapid and sensitive method for the quantitation of microgram quantities of protein utilizing the principle of protein-dye binding. *Anal Biochem* (1976) 72:248–54. doi:10.1016/0003-2697(76)90527-3
33. Stempin CC, Tanos TB, Coso OA, Cerban FM. Arginase induction promotes *Trypanosoma cruzi* intracellular replication in cruzipain-treated J774 cells through the activation of multiple signaling pathways. *Eur J Immunol* (2004) 34(1):200–9. doi:10.1002/eji.200324313
34. Green LC, Wagner DA, Glogowski J, Skipper PL, Wishnok JS, Tannenbaum SR. Analysis of nitrate, nitrite, and [15N]nitrate in biological fluids. *Anal Biochem* (1982) 126(1):131–8. doi:10.1016/0003-2697(82)90118-X
35. Stempin C, Giordanengo L, Gea S, Cerban F. Alternative activation and increase of *Trypanosoma cruzi* survival in murine macrophages stimulated by cruzipain, a parasite antigen. *J Leukoc Biol* (2002) 72(4):727–34. doi:10.1189/jlb.72.4.727
36. Stempin CC, Dulgerian LR, Garrido VV, Cerban FM. Arginase in parasitic infections: macrophage activation, immunosuppression, and intracellular signals. *J Biomed Biotechnol* (2010) 2010:683485. doi:10.1155/2010/683485
37. Martins RM, Alves RM, Macedo S, Yoshida N. Starvation and rapamycin differentially regulate host cell lysosome exocytosis and invasion by *Trypanosoma cruzi* metacyclic forms. *Cell Microbiol* (2011) 13(7):943–54. doi:10.1111/j.1462-5822.2011.01590.x
38. Weichhart T, Haidinger M, Katholnig K, Kopecky C, Poglitsch M, Lassnig C, et al. Inhibition of mTOR blocks the anti-inflammatory effects of glucocorticoids in myeloid immune cells. *Blood* (2011) 117(16):4273–83. doi:10.1182/blood-2010-09-310888
39. Bao W, Wang Y, Fu Y, Jia X, Li J, Vangan N, et al. mTORC1 regulates flagellin-induced inflammatory response in macrophages. *PLoS One* (2015) 10(5):e0125910. doi:10.1371/journal.pone.0125910
40. Weichhart T, Saemann MD. The multiple facets of mTOR in immunity. *Trends Immunol* (2009) 30(5):218–26. doi:10.1016/j.it.2009.02.002
41. Baker AK, Wang R, Mackman N, Luyendyk JP. Rapamycin enhances LPS induction of tissue factor and tumor necrosis factor-alpha expression in macrophages by reducing IL-10 expression. *Mol Immunol* (2009) 46(11–12):2249–55. doi:10.1016/j.molimm.2009.04.011
42. Alvarez MN, Peluffo G, Piacenza L, Radi R. Intraphagosomal peroxynitrite as a macrophage-derived cytotoxin against internalized *Trypanosoma cruzi*: consequences for oxidative killing and role of microbial peroxiredoxins in infectivity. *J Biol Chem* (2011) 286(8):6627–40. doi:10.1074/jbc.M110.167247
43. Cardoni RL, Antunez MI, Morales C, Nantes IR. Release of reactive oxygen species by phagocytic cells in response to live parasites in mice infected with *Trypanosoma cruzi*. *Am J Trop Med Hyg* (1997) 56(3):329–34. doi:10.4269/ajtmh.1997.56.329
44. Piacenza L, Alvarez MN, Peluffo G, Radi R. Fighting the oxidative assault: the *Trypanosoma cruzi* journey to infection. *Curr Opin Microbiol* (2009) 12(4):415–21. doi:10.1016/j.mib.2009.06.011
45. Paiva CN, Feijo DF, Dutra FF, Carneiro VC, Freitas GB, Alves LS, et al. Oxidative stress fuels *Trypanosoma cruzi* infection in mice. *J Clin Invest* (2012) 122(7):2531–42. doi:10.1172/JCI58525
46. Byrne GI, Lehmann LK, Kirschbaum JG, Borden EC, Lee CM, Brown RR. Induction of tryptophan degradation in vitro and in vivo: a gamma-interferon-stimulated activity. *J Interferon Res* (1986) 6(4):389–96. doi:10.1089/jir.1986.6.389
47. Pfefferkorn ER. Interferon gamma blocks the growth of *Toxoplasma gondii* in human fibroblasts by inducing the host cells to degrade tryptophan. *Proc Natl Acad Sci U S A* (1984) 81(3):908–12. doi:10.1073/pnas.81.3.908
48. Knubel CP, Martinez FF, Fretes RE, Diaz Lujan C, Theumer MG, Cervi L, et al. Indoleamine 2,3-dioxigenase (IDO) is critical for host resistance against *Trypanosoma cruzi*. *FASEB J* (2010) 24(8):2689–701. doi:10.1096/fj.09-150920
49. Yang T, Zhu L, Zhai Y, Zhao Q, Peng J, Zhang H, et al. TSC1 controls IL-1beta expression in macrophages via mTORC1-dependent C/EBPbeta pathway. *Cell Mol Immunol* (2016) 13(5):640–50. doi:10.1038/cmi.2015.43
50. Goncalves VM, Matteucci KC, Buzzo CL, Miollo BH, Ferrante D, Torrecilhas AC, et al. NLRP3 controls *Trypanosoma cruzi* infection through a caspase-1-dependent IL-1R-independent NO production. *PLoS Negl Trop Dis* (2013) 7(10):e2469. doi:10.1371/journal.pntd.0002469
51. Zhou R, Yazdi AS, Menu P, Tschopp J. A role for mitochondria in NLRP3 inflammasome activation. *Nature* (2011) 469(7329):221–5. doi:10.1038/nature09663
52. Stempin CC, Garrido VV, Dulgerian LR, Cerban FM. Cruzipain and SP600125 induce p38 activation, alter NO/arginase balance and favor the survival of *Trypanosoma cruzi* in macrophages. *Acta Trop* (2008) 106(2):119–27. doi:10.1016/j.actatropica.2008.02.004
53. Weichhart T, Costantino G, Poglitsch M, Rosner M, Zeyda M, Stuhlmeier KM, et al. The TSC-mTOR signaling pathway regulates the innate inflammatory response. *Immunity* (2008) 29(4):565–77. doi:10.1016/j.immuni.2008.08.012
54. Hallowell RW, Collins SL, Craig JM, Zhang Y, Oh M, Illei PB, et al. mTORC2 signalling regulates M2 macrophage differentiation in response to helminth infection and adaptive thermogenesis. *Nat Commun* (2017) 8:14208. doi:10.1038/ncomms14208
55. Haidinger M, Poglitsch M, Geyeregger R, Kasturi S, Zeyda M, Zlabinger GJ, et al. A versatile role of mammalian target of rapamycin in human dendritic cell function and differentiation. *J Immunol* (2010) 185(7):3919–31. doi:10.4049/jimmunol.1000296
56. Harris J, Hartman M, Roche C, Zeng SG, O'Shea A, Sharp FA, et al. Autophagy controls IL-1beta secretion by targeting pro-IL-1beta for degradation. *J Biol Chem* (2011) 286(11):9587–97. doi:10.1074/jbc.M110.202911
57. Arranz A, Doxaki C, Vergadi E, Martinez de la Torre Y, Vaporidi K, Lagoudaki ED, et al. Akt1 and Akt2 protein kinases differentially contribute to macrophage polarization. *Proc Natl Acad Sci U S A* (2012) 109(24):9517–22. doi:10.1073/pnas.1119038109
58. Kuijl CSN, Marsman M, Tuin AW, Janssen L, Egan DA, Ketema M, et al. Intracellular bacterial growth is controlled by a kinase network around PKB/AKT1. *Nature* (2007) 450(7170):725–30. doi:10.1038/nature06345

59. Maeda FY, Cortez C, Alves RM, Yoshida N. Mammalian cell invasion by closely related *Trypanosoma* species *T. dionisii* and *T. cruzi*. *Acta Trop* (2012) 121(2):141–7. doi:10.1016/j.actatropica.2011.10.017
60. Maeda FY, Cortez C, Yoshida N. Cell signaling during *Trypanosoma cruzi* invasion. *Front Immunol* (2012) 3:361. doi:10.3389/fimmu.2012.00361
61. Li K, Zhang Y, Liang KY, Xu S, Zhou XJ, Tan K, et al. Rheb1 deletion in myeloid cells aggravates OVA-induced allergic inflammation in mice. *Sci Rep* (2017) 7:42655. doi:10.1038/srep42655
62. Wills-Karp M, Finkelman FD. Untangling the complex web of IL-4- and IL-13-mediated signaling pathways. *Sci Signal* (2008) 1(51):e55. doi:10.1126/scisignal.1.51.pe55
63. Huang SC, Smith AM, Everts B, Colonna M, Pearce EL, Schilling JD, et al. Metabolic reprogramming mediated by the mTORC2-IRF4 signaling axis is essential for macrophage alternative activation. *Immunity* (2016) 45(4): 817–30. doi:10.1016/j.immuni.2016.09.016
64. Silva GK, Costa RS, Silveira TN, Caetano BC, Horta CV, Gutierrez FR, et al. Apoptosis-associated speck-like protein containing a caspase recruitment domain inflammasomes mediate IL-1beta response and host resistance to *Trypanosoma cruzi* infection. *J Immunol* (2013) 191(6):3373–83. doi:10.4049/jimmunol.1203293
65. Garg NJ. Inflammasomes in cardiovascular diseases. *Am J Cardiovasc Dis* (2011) 1(3):244–54.
66. Bauernfeind F, Bartok E, Rieger A, Franchi L, Nunez G, Hornung V. Cutting edge: reactive oxygen species inhibitors block priming, but not activation, of the NLRP3 inflammasome. *J Immunol* (2011) 187(2):613–7. doi:10.4049/jimmunol.1100613
67. Hwang YS, Jeong M, Park JS, Kim MH, Lee DB, Shin BA, et al. Interleukin-1beta stimulates IL-8 expression through MAP kinase and ROS signaling in human gastric carcinoma cells. *Oncogene* (2004) 23(39):6603–11. doi:10.1038/sj.onc.1207867
68. Lo YY, Conquer JA, Grinstein S, Cruz TF. Interleukin-1 beta induction of c-fos and collagenase expression in articular chondrocytes: involvement of reactive oxygen species. *J Cell Biochem* (1998) 69(1):19–29. doi:10.1002/(SICI)1097-4644(19980401)69:1<19::AID-JCB3>3.0.CO;2-Y
69. Galvan-Pena S, O'Neill LA. Metabolic reprograming in macrophage polarization. *Front Immunol* (2014) 5:420. doi:10.3389/fimmu.2014.00420
70. Singhal A, Jie L, Kumar P, Hong GS, Leow MK, Paleja B, et al. Metformin as adjunct antituberculosis therapy. *Sci Transl Med* (2014) 6(263):263ra159. doi:10.1126/scitranslmed.3009885

Conflict of Interest Statement: The authors declare that the research was conducted in the absence of any commercial or financial relationships that might be construed as a potential conflict of interest.

Copyright © 2018 Rojas Márquez, Ana, Baigorrí, Stempin and Cerban. This is an open-access article distributed under the terms of the Creative Commons Attribution License (CC BY). The use, distribution or reproduction in other forums is permitted, provided the original author(s) and the copyright owner are credited and that the original publication in this journal is cited, in accordance with accepted academic practice. No use, distribution or reproduction is permitted which does not comply with these terms.

frontiers in Immunology

ORIGINAL RESEARCH
published: 17 November 2017
doi: 10.3389/fimmu.2017.01560

All-*Trans* Retinoic Acid Promotes an M1- to M2-Phenotype Shift and Inhibits Macrophage-Mediated Immunity to *Leishmania major*

Natália S. Vellozo[1†], Sâmara T. Pereira-Marques[1†], Mariela P. Cabral-Piccin[1], Alessandra A. Filardy[1,2], Flávia L. Ribeiro-Gomes[1,3], Thaís S. Rigoni[1], George A. DosReis[1,4] and Marcela F. Lopes[1]*

[1] Instituto de Biofísica Carlos Chagas Filho, Universidade Federal do Rio de Janeiro, Rio de Janeiro, Brazil, [2] Instituto de Microbiologia Paulo de Góes, Universidade Federal do Rio de Janeiro, Rio de Janeiro, Brazil, [3] Instituto Oswaldo Cruz, Fundação Oswaldo Cruz, Rio de Janeiro, Brazil, [4] Instituto Nacional para Pesquisa Translacional em Saúde e Ambiente na Região Amazônica, Conselho Nacional de Desenvolvimento Científico e Tecnológico, Rio de Janeiro, Brazil

OPEN ACCESS

Edited by:
Etienne Meunier, UMR5089 Institut de Pharmacologie et de Biologie Structurale (IPBS), France

Reviewed by:
Phileno Pinge-Filho, Universidade Estadual de Londrina, Brazil
Ricardo Silvestre, Instituto de Pesquisa em Ciências da Vida e da Saúde (ICVS), Portugal

***Correspondence:**
Marcela F. Lopes
marcelal@biof.ufrj.br

†These authors have contributed equally to this work.

Specialty section:
This article was submitted to Microbial Immunology, a section of the journal Frontiers in Immunology

Received: *15 August 2017*
Accepted: *31 October 2017*
Published: *17 November 2017*

Citation:
Vellozo NS, Pereira-Marques ST, Cabral-Piccin MP, Filardy AA, Ribeiro-Gomes FL, Rigoni TS, DosReis GA and Lopes MF (2017) All-Trans Retinoic Acid Promotes an M1- to M2-Phenotype Shift and Inhibits Macrophage-Mediated Immunity to Leishmania major. Front. Immunol. 8:1560. doi: 10.3389/fimmu.2017.01560

As key cells, able to host and kill *Leishmania* parasites, inflammatory monocytes/macrophages are potential vaccine and therapeutic targets to improve immune responses in Leishmaniasis. Macrophage phenotypes range from M1, which express NO-mediated microbial killing, to M2 macrophages that might help infection. Resistance to Leishmaniasis depends on *Leishmania* species, mouse strain, and both innate and adaptive immunity. C57BL/6 (B6) mice are resistant and control infection, whereas *Leishmania* parasites thrive in BALB/c mice, which are susceptible to develop cutaneous lesions in the course of infection with *Leishmania major*, but not upon infection with *Leishmania braziliensis*. Here, we investigated whether a deficit in early maturation of inflammatory monocytes into macrophages in BALB/c mice underlies increased susceptibility to *L. major* versus *L. braziliensis* parasites. We show that, after infection with *L. braziliensis*, monocytes are recruited to peritoneum, differentiate into macrophages, and develop an M1 phenotype able to produce proinflammatory cytokines in both B6 and BALB/c mice. Nonetheless, more mature macrophages from B6 mice expressed inducible NO synthase (iNOS) and higher NO production in response to *L. braziliensis* parasites, whereas BALB/c mice developed macrophages expressing an incomplete M1 phenotype. By contrast, monocytes recruited upon *L. major* infection gave rise to immature macrophages that failed to induce an M1 response in BALB/c mice. Overall, these results are consistent with the idea that resistance to *Leishmania* infection correlates with improved maturation of macrophages in a mouse-strain and *Leishmania*-species dependent manner. All-*trans* retinoic acid (ATRA) has been proposed as a therapy to differentiate immature myeloid cells into macrophages and help immunity to tumors. To prompt monocyte to macrophage maturation upon *L. major* infection, we treated B6 and BALB/c mice with ATRA. Unexpectedly, treatment with ATRA reduced proinflammatory cytokines, iNOS expression, and parasite killing by macrophages. Moreover, ATRA promoted an M1 to M2 transition in bone marrow-derived macrophages from both strains. Therefore, ATRA uncouples

macrophage maturation and development of M1 phenotype and downmodulates macrophage-mediated immunity to *L. major* parasites. Cautions should be taken for the therapeutic use of ATRA, by considering direct effects on innate immunity to intracellular pathogens.

Keywords: all-*trans* retinoic acid, alternatively activated macrophage, classically activated macrophage, Leishmaniasis, nitric oxide, parasite infection, retinoic acid, vitamin A

INTRODUCTION

Leishmania parasites infect macrophages and cause Leishmaniasis, ranging from localized cutaneous or mucocutaneous to visceral or disseminated diseases. Monocytes/macrophages, as host and effector cells, play a major role to fight *Leishmania* infection in innate immunity, as well as an effector arm of adaptive immunity, upon activation by cytokines produced by T lymphocytes. IFN-γ-producing Th1 cells activate macrophages to express inducible NO synthase (iNOS/NOS2) and effect NO-mediated killing of *Leishmania* parasites. By contrast, Th2 cytokines, such as IL-4 and IL-10, inhibit macrophage activation, induce arginase expression, and promote parasite infection (1–6). By analogy to Th1 and Th2 lymphocytes, the functional phenotypes of macrophages are known as M1 and M2 or as classically activated and alternatively activated macrophages, with a range of intermediates between the extreme IFN/LPS and IL-4-induced phenotypes (7–11).

While Th1/M1 responses mediate immunity to *Leishmania* parasites in resistant C57BL/6 (B6) mice, Th2/M2 cells underlie susceptibility to *Leishmania major* infection in BALB/c mice, although the role of IL-4 on T cells and macrophages remains controversial (1, 5, 12–16). Equally important is the notion that exacerbated type-1 immune responses contribute for pathology in mucocutaneous Leishmaniasis, upon infection with *Leishmania braziliensis* (17, 18). In line with this, there are still unsolved issues, which once elucidated might help development of vaccines and therapies to improve immunity to *Leishmania* infection and/or prevent pathology. For instance, macrophages from resistant or susceptible strains can express features associated with M1 or M2 phenotypes even in the absence of adaptive immunity (7). Likewise, earlier differentiation kinetics of F4/80$^+$ monocytic cells in B6 mice versus a predominance of more immature cells in BALB/c mice may also contribute to development of resistance versus susceptibility to *L. major* infection (19–21). Moreover, *L. major* infection in B6 mice induces early inflammatory monocytes (CD11b$^+$Ly6C$^+$F4/80^{int} cells), which already express ROS or NO-mediated killing (22, 23). Therefore, the differentiation of immature monocytic cells into effector monocytes/macrophages is a promising vaccine/therapeutic target in Leishmaniasis.

All-*trans* retinoic acid (ATRA) is a vitamin A active metabolite, which binds to intracellular receptors in immune cells and may affect innate and adaptive immunity (24, 25). ATRA promotes differentiation of immature myeloid cells (IMCs) into macrophages and has been considered to promote anti-tumor immunity, by targeting IMC suppression of CD8 T-cell-mediated immunity (26). We have previously shown that inflammatory monocytes express features of IMCs upon *L. major* infection and that treatment with ATRA prevents NO-mediated suppression of T-cell proliferation in lymph nodes from infected B6 mice (23). However, ATRA-treated mice developed increased footpad lesions and parasite load in draining lymph nodes (23). We hypothesized that ATRA might directly affect macrophage phenotype and macrophage-mediated immunity to *L. major*. We also considered that treatment with ATRA could counteract the maturation deficit in monocytes/macrophages from BALB/c mice.

Here, we investigated whether a deficient maturation of inflammatory monocytes into macrophages may underlie increased susceptibility to *L. major* versus *L. braziliensis* parasites in BALB/c mice. *L. braziliensis*, but not *L. major* infection induced inflammatory monocytes that mature into macrophages and expressed an M1 phenotype. We also show that treatment with ATRA *in vivo* negatively affected the functional phenotype of inflammatory monocytes/macrophages and immunity to *L. major* infection. Furthermore, ATRA prevented induction of effector M1 macrophages, by promoting an M1- to M2-phenotype shift in bone marrow-derived macrophages (BMDMs) from both B6 and BALB/c mice.

MATERIALS AND METHODS

Animals and Parasites

C57BL/6 and BALB/c mice were obtained from the Oswaldo Cruz Foundation (FIOCRUZ, Rio de Janeiro, Brazil) and maintained in the animal facility at the Federal University of Rio de Janeiro (UFRJ). All experiments were approved and conducted in accordance with guidelines of the Ethics Committee for Use of Animals (UFRJ) (Protocol no. 078/16). We used the following parasite strains: the Venezuelan isolate Torres of *L. braziliensis* (27), *L. major* LV39 (MRHO/Sv/59/P), or a stable transfected line of *L. major* Friedlin FV1 (MHOM/IL/80/FN), which express a red fluorescent protein (*Lm*-RFP) (28). Parasites were isolated from popliteal lymph nodes of infected BALB/c mice and maintained up to 4 weeks at 28°C in Schneider's medium (Sigma, USA), supplemented with 2% of sterile human urine, 2 mM of L-glutamine, 10 μg/mL of gentamicin, and 10% of fetal bovine serum (FBS, Gibco BRL, South America). For infection, *Leishmania* parasites were cultured until stationary phase at 28°C in Schneider's medium. *L. braziliensis* parasites were then purified in a 10% ficoll gradient to obtain metacyclic forms (29).

Leishmania Infection

Female B6 and BALB/c mice, aging 6–8 weeks, were infected i.p. with 3×10^6 promastigote parasites of *L. major* LV39 or *Lm*-RFP or with 6×10^5 metacyclic forms of *L. braziliensis*.

Administration of ATRA *In Vivo*

C57BL/6 and BALB/c mice were infected i.p. with *L. major*. Upon 24 h, infected mice were injected i.p. with 100 µL of a 100-µM solution of ATRA (Sigma, St Louis, MO, USA) or control vehicle (0.2% dimethyl-sulfoxide, DMSO, Sigma). After 24 h, peritoneal exudates were collected for analysis and cultures.

Peritoneal Exudate Cells (PECs)

Peritoneal exudate cells were collected in 4 mL of DMEM (Invitrogen Life Technologies), supplemented with 2-mM glutamine, 5×10^5 M 2-ME, 10-µg/mL gentamicin, 1-mM sodium pyruvate, and 0.1-mM MEM non-essential amino acids (culture medium). Upon centrifugation, supernatants were collected for cytokine assays and NO production. PECs were processed for flow cytometry or cultured and infected, as bellow. After 72 h, culture supernatants were collected for cytokine and NO assays, and cultured cells were used to determine parasite burden.

Macrophage Infection and Parasite Load

Peritoneal exudate cells from control mice or from mice infected with *L. major* LV39, *Lm*-RFP, or *L. braziliensis* were cultured in triplicates at 5×10^5 cells/well in 48-well vessels or at 1×10^6/well in 24-well plates during 1 h, and then washed for removal of non-adherent cells. Adherent macrophages were reinfected (for 4 h) with 3×10^6 *L. major* or *Lm*-RFP promastigotes or with 4×10^4 metacyclic forms of *L. braziliensis*. Cultures were washed for removal of extracellular parasites and additional non-adherent cells. Infected macrophages were maintained in culture medium plus 10% FBS at 37°C and 7% CO_2 for 3–4 days. For evaluation of *Lm*-RFP infection, macrophages were detached from 24-well plates and analyzed by flow cytometry. In cultures established in 48-well vessels, supernatants were collected for cytokine analyses and replaced by Scheneider's medium. Macrophages were further cultured for at least 3 days at 28°C, in a BOD incubator (Cienlab) for determination of parasite load. Parasites released in culture supernatants were then counted in a Beckman Coulter (USA) within a range of 3–6 µm, for exclusion of cells.

BMDM Differentiation and Treatment with ATRA *In Vitro*

Tibiae from B6 and BALB/c mice (5–8 weeks) were removed and washed with HBSS (Gibco) plus 2% of FBS. Cells were collected, washed, and cultured at 5×10^4/well in 48-well plates or at 1×10^6/well in 24-well vessels for flow cytometry. Cultures were maintained for 7 days in culture medium plus 10% FBS, 20% of the L929 cell culture supernatant, as an M-CSF source, following a protocol adapted from Sutterwala et al. (30). After 7 days, cultures were treated with IFN-γ (0.5 ng/mL, R&D Systems) for 24 h. Then, cells were washed and cultured in the presence of IL-4 (5 ng/mL, R&D Systems), as before (31). DMSO (0.004%) or ATRA (2 µM) were also added to cultures. Three days later, cells were treated or not with 1 µg/mL of LPS from *Salmonella enterica* serovar Typhimurium (Sigma) and cultured for further 3 days. Culture supernatants were evaluated for cytokine and NO production and cells were prepared for flow cytometry.

Flow Cytometry

Peritoneal exudate cells or cultured cells were washed in FACS buffer (plus 2% FBS), followed by incubation with anti-CD16/CD32 (eBioscience, San Diego, CA, USA) for Fc blocking. We stained cells with anti-CD11b, anti-F4/80, and anti-Ly6C (HK1.4) labeled with PE, FITC or allophycocyanin (BD Biosciences, Chicago, IL, USA), or with Alexa Fluor 488-labeled anti-CD301 (MGL) mAb (AbD Serotec, Kidlington, UK), or control rat IgG2a mAb (R&D Systems, Minneapolis, MN, USA). For intracellular staining, we washed, permeabilized, and stained cells with PE-labeled anti-IL-12p35 or control murine IgG1 mAb (R&D Systems), anti-NOS2 or control rat IgG2a mAb (BD Bioscience), or with FITC-labeled anti-arginase 1 or control sheep IgG mAb. Cells were washed, fixed, and acquired with the CellQuest software, on a FACSCalibur system (BD Biosciences). For analysis, we used the FlowJo software (TreeStar, Ashland, OR, USA). For IL-12p35$^+$, NOS2$^+$ (M1), and CD301$^+$, arginase$^+$ (M2) subsets, gates were based on the exclusion of background staining with isotype control mAbs, as in **Figure 2B**. For evaluation of *Lm*-RFP infection, PECs or cultured macrophages were first stained with allophycocyanin-anti-F4/80 and then analyzed for *Lm*-RFP$^+$ cells within gated F4/80$^+$ macrophages.

Cytokine and Chemokine Assays

Supernatants from cultures or peritoneal exudates were used for detection of cytokines (IL-10, IL-12p70, G-CSF, TNF-α) and chemokines (CCL17, CXCL9, CXCL13) by ELISA assays. For that, we used pairs of specific mAbs (R&D Systems or eBioscience), one of which was labeled with biotin, and then developed with streptavidin-alkaline phosphatase (Invitrogen Life Technologies) and p-nitrophenyl phosphate (Thermo Scientific Pierce, Waltham, MA, USA) as substrate, according to manufacturer's guidelines.

Nitric Oxide

Production of NO was determined indirectly by quantification of nitrites. Peritoneal exudates or culture supernatants were mixed with Griess reagent (1% sulfanilamide, 0.1% naphthylethylenediamine dihydrochloride, 2% H3PO4; Sigma) in a 1:1 ratio. A standard curve with known concentrations of sodium nitrite ($NaNO_2$) was used and the results were expressed in µM. The optical density was determined at 540 nm on a plate spectrophotometer (VersaMax, Molecular Devices).

Statistics

All tests were performed by using the GraphPad Prism (v. 6.0). Results are expressed as mean and SEM in figures. The number (*N*) of animals per group is indicated in figure legends. For parasite load, data were transformed to log of parasites per mL for statistical analysis. Data were analyzed by Kolmogorov–Smirnov test for assessing normal distribution and by unpaired Student's two-tailed *t*-test or ANOVA, followed by Dunnett, Bonferroni, or Tukey post-test. Significant differences are indicated for $P < 0.05$ (*), $P < 0.01$ (**), $P < 0.001$ (***), and $P < 0.0001$ (****). For *in vitro* experiments, data are expressed as the mean of technical replicates per treatment and SEM. Significant differences in *t*-tests are indicated as above.

RESULTS

ATRA Induces a Shift from M1 to M2 Phenotype in BMDMs

To address how ATRA affects both M1- and M2-macrophage phenotypes, we cultured BMDMs from B6 and BALB/c mice with a mix of M1/M2-inducing reagents. BMDMs were generated and primed with IFN-γ: BMs from B6 and BALB/c render 90% of macrophages expressing F4/80 at higher levels (F4/80^{hi}) upon treatment with IFN-γ. Then, macrophages were cultured with IL-4, followed by LPS stimulation, as before (31), to give identical M1 and M2 conditions to B6 and BALB/c macrophages. BMDMs were first treated or not with ATRA during 3 days (concomitant with IL-4 and before stimulation with LPS) to address ATRA effects during the development of M1/M2 phenotypes, by mimicking stimuli from infection environment.

Under these M1/M2 mixed conditions, macrophages from B6 mice secreted M1 cytokines and chemokine, such as TNF-α, G-CSF, and CXCL9 (**Figure 1A**), and expressed IL-12p35 (not shown), but produced low levels of the M2 chemokines CCL17 and CXCL13. BMDMs from BALB/c mice (**Figure 1B**), however, produced both M1 and M2 cytokines and chemokines upon consecutive stimulation with IFN-γ, IL-4, and LPS. B6 or BALB/c macrophages did not produce IL-10 under these conditions (not shown). Treatment with ATRA prevented induction of M1 cytokines and CXCL9, but increased M2 chemokines, such as CCL17 in B6 macrophages, as well as CXCL13 in BALB/c macrophages (**Figures 1A,B**). These results indicate that ATRA promotes an M1- to M2-phenotype shift in BMDMs from mouse strains, either resistant or susceptible to *L. major* infection.

ATRA Reduces NO Production and NOS2 Expression by BMDMs

Next, we addressed whether ATRA directly affects M1 mechanisms of parasite killing. ATRA inhibited NO production by BMDMs from both B6 and BALB/c mice (**Figure 2A**). Moreover, treatment with ATRA reduced NOS2 expression and the ratio of NOS2/arginase 1 expression (**Figure 2B** and not shown) in BMDMs from B6 mice.

Earlier Monocyte Differentiation to Macrophages in B6 PECs

Before evaluating ATRA effects on the phenotype of inflammatory monocytes/macrophages recruited by *Leishmania* parasites, we investigated whether there is a differential kinetics of monocyte recruitment and differentiation in B6 versus BALB/c mice upon i.p. infection with *L. braziliensis* (Lb) or *L. major* (**Figure 3**; Figures S1 and S2 in Supplementary Material). To follow macrophage differentiation *in vivo*, we first infected mice with Lb (**Figure 3A**; Figure S1A in Supplementary Material). Lb infection in both B6 and BALB/c mice quickly recruited CD11b$^+$Ly6C$^+$F4/80$^+$ cells, which decreased thereafter (**Figure 3A**). Most of these Ly6C$^+$ immature monocytes/macrophages expressed intermediate levels of F4/80 (F4/80^{int}; not shown). By contrast, proportions (**Figure 3A**) and numbers (Figure S1A in Supplementary Material) of more mature macrophages, which do not express Ly6C, but are CD11b$^+$F4/80$^+$ (hi or int) cells, first decreased and then progressively increased in B6 and BALB/c mice. It is noteworthy that F4/80^{int} macrophages predominated over the more mature

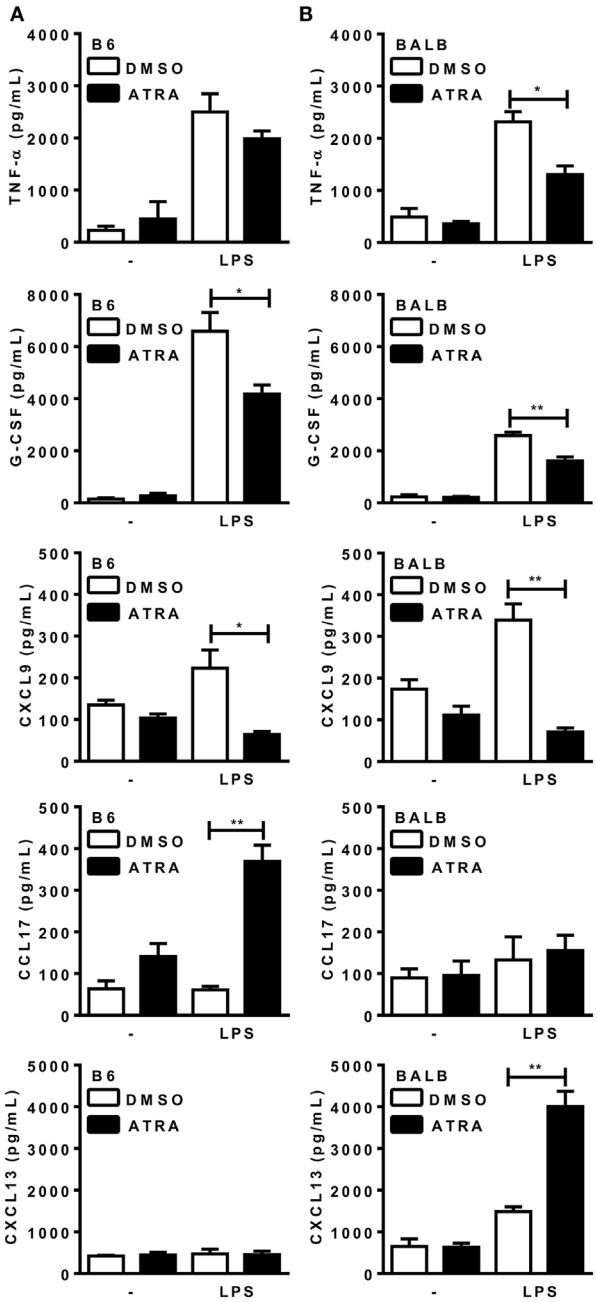


FIGURE 1 | All-*trans* retinoic acid (ATRA) induces bone marrow-derived macrophages (BMDMs) to shift from M1 to M2 macrophages. **(A,B)** BMDMs from B6 and BALB/c mice were primed with IFN-γ (for 24 h). Cells were then treated with IL-4 and ATRA or control vehicle (DMSO) during 3 days and cultured with or without LPS for further 3 days. Cytokines and chemokines in supernatants from **(A)** B6 and **(B)** BALB/c cultures were assayed by ELISA. Cultures were performed in triplicates. Results are expressed as mean and SEM. Significant differences between LPS-activated macrophages treated with or without ATRA were analyzed by *t*-test and indicated for $P < 0.05$ (*) and $P < 0.01$ (**). Data are representative of two independent experiments.

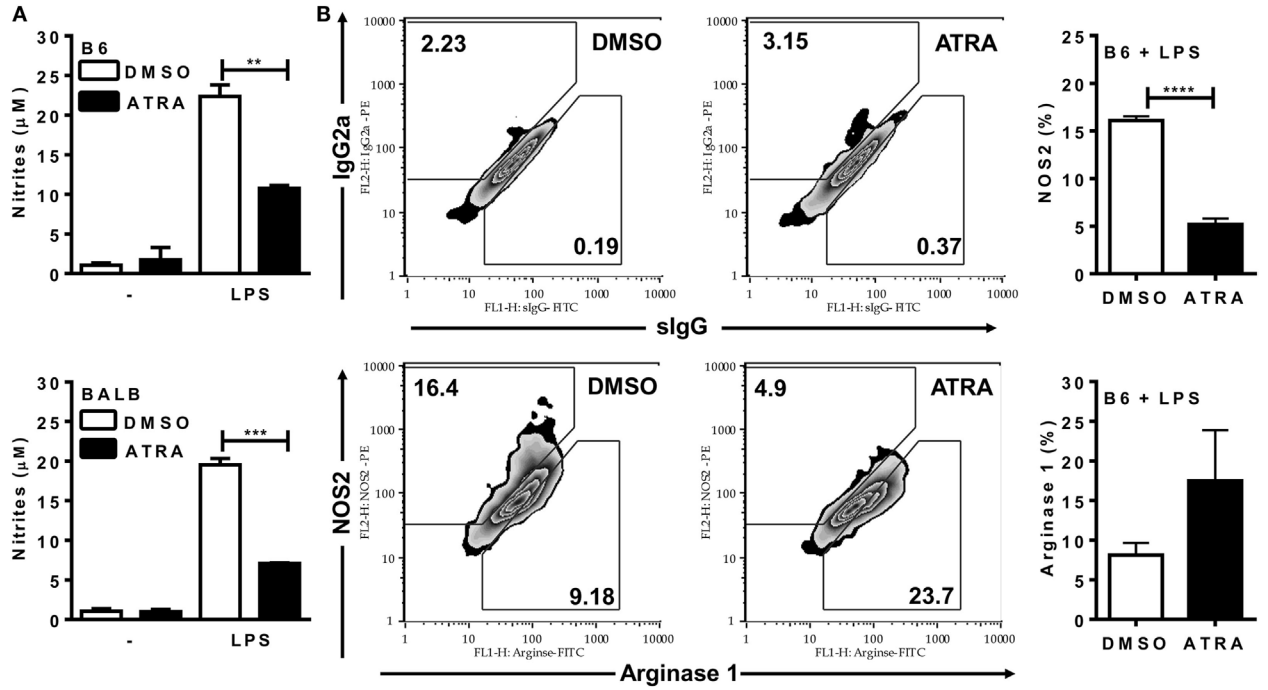


FIGURE 2 | All-*trans* retinoic acid (ATRA) reduces NO production and NOS2 expression by bone marrow-derived macrophages (BMDMs). **(A,B)** BMDMs from B6 and BALB/c mice were primed with IFN-γ (for 24 h). Cells were then treated with IL-4 and ATRA or control vehicle (DMSO) during 3 days and cultured with or without LPS for further 3 days. **(A)** Culture supernatants were collected and tested for NO production by the Griess method. **(B)** F4/80$^+$ macrophages from B6 mice were evaluated for NOS2 and arginase expression (lower panels), and for staining with the respective control mAbs (upper panels). Cultures were performed in triplicates. Results are expressed as mean and SEM. Significant differences between LPS-activated macrophages treated with or without ATRA were analyzed by *t*-test and indicated for $P < 0.01$ (**), $P < 0.001$ (***), and $P < 0.0001$ (****). Results depicted in **(A)** are representative of four independent experiments.

F4/80^{hi} macrophages in BALB/c, but not B6 mice. BALB/c and B6 mice also recruited CD11b$^+$Ly6C$^+$F4/80$^+$ macrophages upon i.p. infection with *L. major*, by peaking at 48 h (**Figure 3B**; Figures S1B and S2A in Supplementary Material). There was a decrease in resident F4/80^{int} or F4/80^{hi} macrophages upon 24 or 48 h (**Figure 3B**; Figure S2C in Supplementary Material), but mature macrophages expressing F4/80 at intermediate or high levels did not change in BALB/c mice thereafter (**Figure 3B**). These results indicate that more immature macrophages predominate in the peritoneum of BALB/c mice upon infection with *L. major* than after infection with *L. braziliensis*, and also corroborate a previously reported deficit in the differentiation of macrophages from BALB/c mice (19–21).

Mature Macrophages Express an M1 Phenotype upon Infection with *L. braziliensis*

Next we addressed the profile of cytokines produced by PECs from mice infected with Lb or *L. major* upon culture and stimulation with *Leishmania* parasites (**Figure 4**). At 72 h upon i.p. infection with Lb, macrophages from both B6 and BALB/c mice expressed an inflammatory phenotype, by producing TNF-α, G-CSF, and NO, but not IL-10 in Lb-stimulated cultures (**Figure 4A**). However, more mature macrophages from B6 mice (as in **Figure 3A**) showed increased NO production compared with less mature macrophages from BALB/c mice (**Figure 4A**). Interestingly, while Lb also elicited a strong M1 response by resident (d0) macrophages from both B6 and BALB/c mice (**Figure 4A**), peritoneal macrophages from BALB/c produced *L. major*-induced IL-10, but not inflammatory cytokines (**Figure 4B**). BALB/c macrophages recruited upon *L. major* infection also failed to produce M1 cytokines or NO upon stimulation with *L. major* (**Figure 4B**). We conducted parallel analyses to follow the development of M1/M2 phenotypes by flow cytometry upon i.p. infection with *Leishmania* parasites. CD11b$^+$ PECs from Lb-infected B6 and BALB/c mice expressed IL-12p35 and NOS2, but not the M2 marker CD301 (MGL) or arginase 1 (**Figures 5A,B**). Furthermore, expression of IL-12 and NOS2 by macrophages reached higher levels in Lb-infected B6 mice (**Figure 5**). In contrast to Lb, *L. major* infection did not induce expression of IL-12 or NOS2 in BALB/c macrophages (**Figures 6A,B**). Therefore, Lb infection induces a stronger M1 response (**Figures 4** and **5**) by more mature macrophages (**Figure 3**) from B6 versus BALB/c mice. These results also show that *L. major* is a weaker stimulus to induce monocyte-to-macrophage differentiation (**Figure 3**) and M1 responses (**Figures 4** and **6**) as compared with Lb parasites.

ATRA Reduces M1 Responses and Promotes *L. major* Infection

We used the *L. major* model to test how ATRA affects the functional phenotype of inflammatory monocytes/macrophages from BALB/c and B6 mice (**Figures 7A–E**). Mice were infected i.p. and

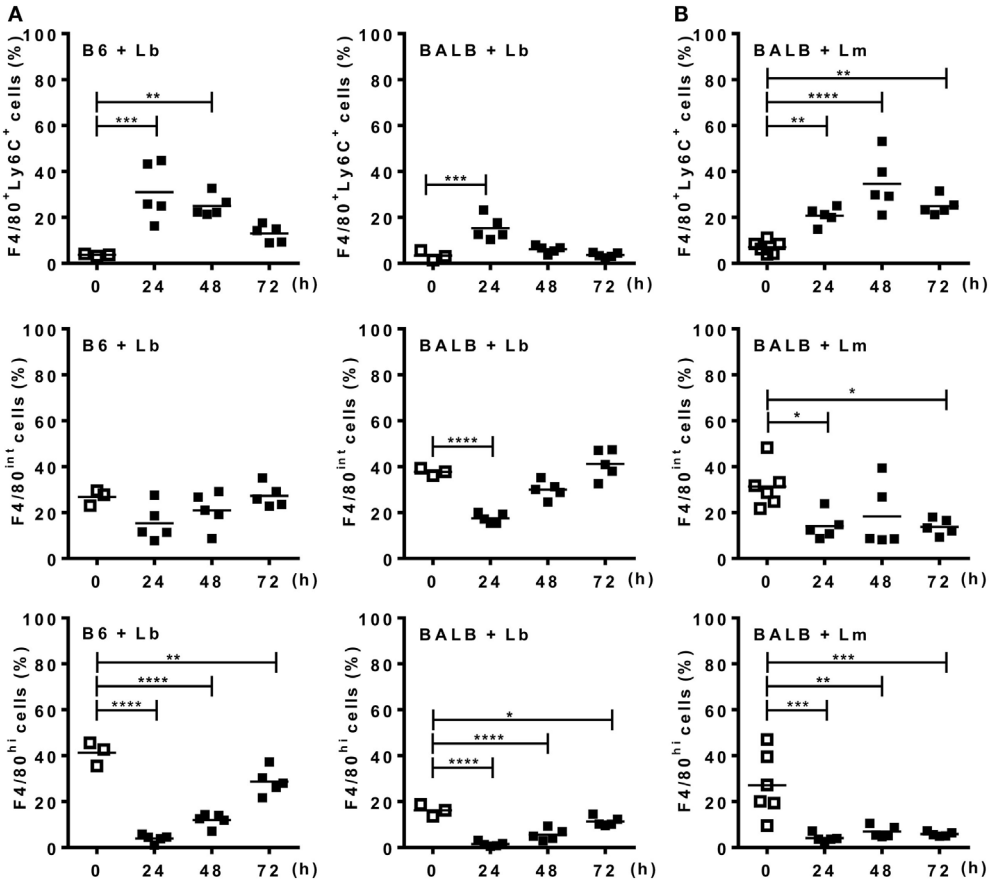


FIGURE 3 | Monocytes differentiate into macrophages upon *Leishmania* infection. Peritoneal exudate cells (PECs) from control [**(A)**, left panels] B6 or **(A,B)** BALB/c mice, as well as from mice infected with **(A)** *L. braziliensis* or **(B)** *L. major* were evaluated for expression of Ly6C and F4/80 within CD11b$^+$ gated cells. **(A,B)** Percentages of F4/80$^+$Ly6C$^+$, F4/80^{int}, and F4/80^{hi} cells from **(A)** *L. braziliensis*-infected B6 or BALB/c mice or **(B)** *L. major*-infected BALB/c mice compared with PECs from uninfected (d0) mice. Each symbol represents individual control (□, $N = 3$ or 6 mice/group) or infected mouse (■, $N = 5$ mice/group). Means are represented. Significant differences were analyzed by ANOVA with Dunnett post-test and indicated for $P < 0.05$ (*), $P < 0.01$ (**), $P < 0.001$ (***), and $P < 0.0001$ (****).

treated with ATRA 24 h upon infection. PECs were collected for analyses 24 h after treatment (48 h post-infection). Treatment with ATRA reduced the release of IL-12, TNF-α (**Figure 7A**), and NO (not shown) in the peritoneum. In addition, ATRA negatively affected NOS2 expression in F4/80$^+$ macrophages from B6 mice (**Figure 7C**). Next, we addressed how treatment with ATRA *in vivo* impacts on the rate of macrophage infection with Lm-RFP parasites (**Figure 7B**). Although only 1–2% of F4/80$^+$ macrophages show Lm-RFP infection (not shown), treatment with ATRA increased Lm-RFP-infected macrophages in both BALB/c and B6 mice (**Figure 7B**). Macrophages from *L. major*-infected and treated mice were also reinfected with *L. major in vitro* to test their ability to kill the parasites (**Figures 7D,E**). Upon *in vivo* treatment with ATRA, macrophages were less efficient to control *L. major* infection compared with macrophages from DMSO-treated mice, as evaluated by increased numbers of parasites released in culture supernatants (**Figure 7D**) or by Lm-RFP infection within macrophages (**Figure 7E**). Therefore, ATRA negatively affects M1 responses and undermines macrophage-mediated immunity to *L. major* in both resistant B6 and susceptible BALB/c mice.

DISCUSSION

Treatment with ATRA is considered as a promising therapy to improve immunity against tumors, by inducing differentiation of suppressor monocytes/IMCs into macrophages (26). Nonetheless, ATRA might also affect macrophage phenotype and ability to fight parasites and other pathogens.

It has been reported that inflammatory monocytes are major host and effector cells in *L. major* infection (22, 23, 32) and that delayed differentiation of monocytes into macrophages correlates with susceptibility to *L. major* infection in BALB/c versus B6 mice (19–21). Here, we addressed differentiation and functional phenotypes of inflammatory macrophages upon i.p. infection with *L. braziliensis* and *L. major* to investigate whether a maturation deficit reflects into an inability to develop protective M1 responses in BALB/c mice. We can summarize our results as follows:

1. Upon a transient recruitment of inflammatory monocytes by *L. braziliensis* infection, maturation into F4/80^{int} macrophages

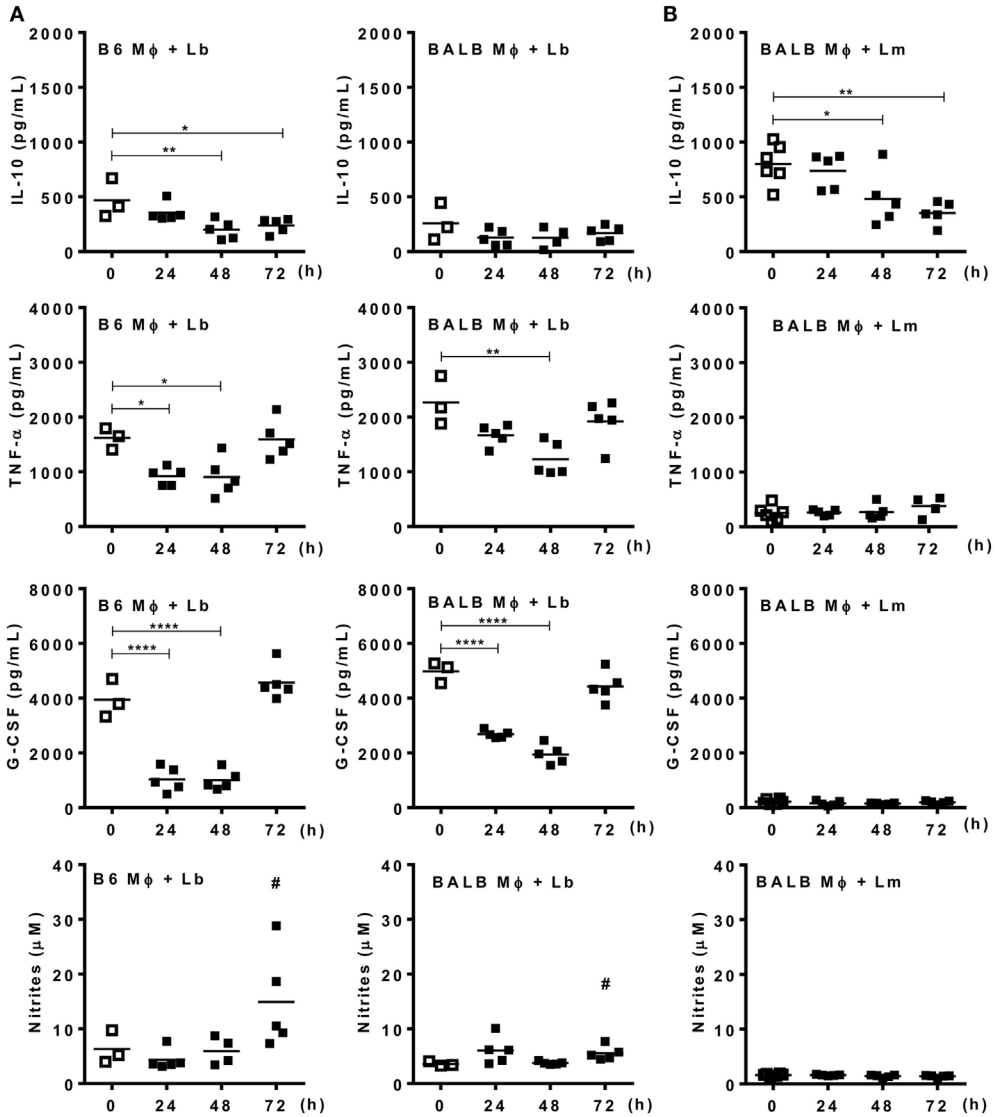


FIGURE 4 | Mature macrophages express an M1 phenotype upon infection with *Leishmania braziliensis*. B6 and BALB/c mice were infected i.p. with **(A)** *L. braziliensis* or **(B)** *L. major*. **(A,B)** Adherent peritoneal exudate cells were reinfected with *L. braziliensis* **(A)** or *L. major* **(B)**. **(A,B)** Culture supernatants were evaluated for the presence of type-1 (TNF-α and G-CSF) and type-2 (IL-10) cytokines by ELISA, and for NO by the Griess method. Each symbol represents individual control (□, $N = 3$ or 6 mice/group) or infected mouse (■, $N = 5$ mice/group). Means are represented. Significant differences were analyzed by ANOVA with Dunnett post-test and indicated for $P < 0.05$ (*), $P < 0.01$ (**), and $P < 0.0001$ (****). In **(A)**, # indicates a difference ($P < 0.05$) between Lb-infected B6 and BALB/c mice, as assessed by *t*-test.

overcomes recovery of more mature F480^{hi} macrophages in BALB/c, but not B6 mice.

2. Replacement of immature Ly6C^{+}F480^{int} monocytes by mature macrophages in B6 mice is accompanied by development of M1 macrophages, expressing more IL-12p35 and NOS2 and less arginase 1 than macrophages from BALB/c mice.
3. *L. braziliensis* infection increases macrophage maturation and induces a more robust M1 response in BALB/c mice than *L. major* parasites.

Altogether, these findings suggest that the development of protective M1 responses comes along with monocyte differentiation to mature macrophages and depends on both parasite infection and mouse strain.

More efficient induction of M1 responses by *L. braziliensis* might explain why unstimulated macrophages control better infection with *L. braziliensis in vitro*, whereas control of *L. major* infection requires activation by T-cell cytokines (33). Similarly, BALB/c mice control better cutaneous lesions upon *L. braziliensis* versus *L. major* infection (34). Moreover, a strong M1 response may underlie more severe clinical manifestations associated with inflammation in humans infected with *L. braziliensis* (17, 18). Finally, delayed and reduced macrophage maturation in BALB/c mice infected with *L. braziliensis* and *L. major*

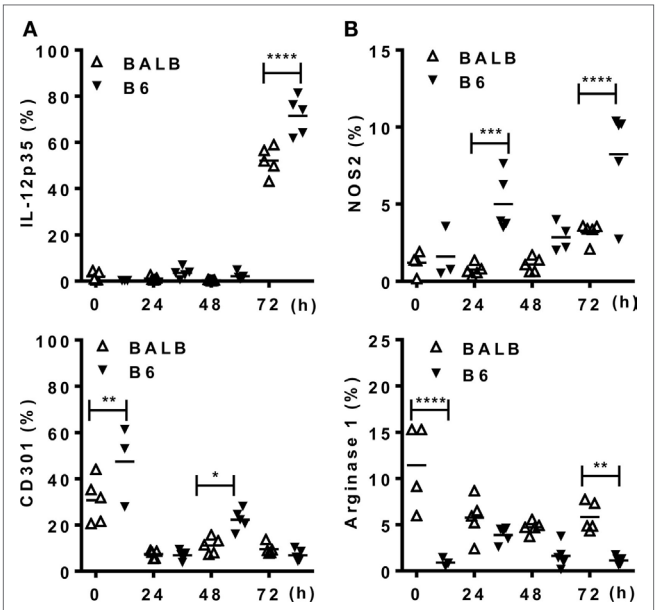


FIGURE 5 | Mature macrophages express M1, but not M2 markers upon infection with *Leishmania braziliensis*. B6 and BALB/c mice were infected i.p. with *L. braziliensis*. **(A,B)** CD11b$^+$ peritoneal exudate cells (PECs) were evaluated for the expression of **(A)** IL-12p35 and CD301 (MGL) or for **(B)** NOS2 and arginase 1. Symbols represent PECs from individual BALB/c (Δ) or B6 (▾) mice (N = 3–5/group of control mice and N = 5 mice/infected group). Means are represented. Significant differences were analyzed by ANOVA with Bonferroni post-test and indicated for $P < 0.05$ (*), $P < 0.01$ (**), $P < 0.001$ (***), and $P < 0.0001$ (****).

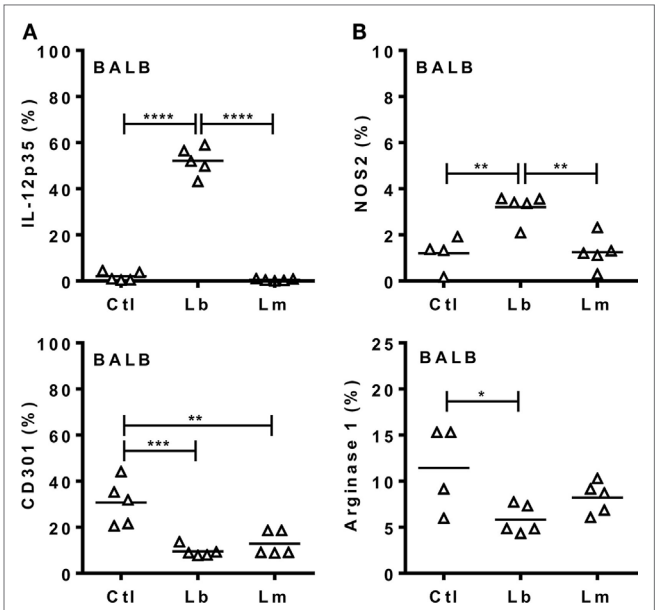


FIGURE 6 | *Leishmania braziliensis*, but not *L. major* induces an M1 response by macrophages from BALB/c mice. BALB/c mice were infected i.p. with *L. braziliensis* or *L. major*. **(A,B)** After 72 h, CD11b$^+$ peritoneal exudate cells (PECs) were evaluated for the expression of **(A)** IL-12p35 and CD301 (MGL) or for **(B)** NOS2 and arginase 1. Symbols represent PECs from individual BALB/c (Δ) mice (N = 4–5/group of control mice and N = 5 mice/infected group). Means are represented. Significant differences were analyzed by ANOVA with Tukey post-test and indicated for $P < 0.05$ (*), $P < 0.01$ (**), $P < 0.001$ (***), and $P < 0.0001$ (****).

corroborate previous results (19–21) and seems to be associated with defective development of M1 responses.

As inflammatory monocytes mature into M1 macrophages, we investigated whether treatment with ATRA short upon *L. major* infection could affect the functional phenotype and anticipate induction of M1 macrophages. Treatment *in vivo* with ATRA, however, did not help development of M1 responses in BALB/c mice and, therefore, it did not rescue BALB/c macrophages to express effective immune responses. Moreover, ATRA impaired NOS2 expression as well as secretion of M1 cytokines, such as IL-12 and TNF-α by macrophages from *L. major*-infected mice and increased parasite burden in macrophages from BALB/c and B6 mice. Previously, we found that ATRA promoted the differentiation of inflammatory monocytes into mature macrophages *in vitro*, but also enhanced *L. major* replication within macrophages (23). Moreover, subcutaneous injection of ATRA reduced NO-mediated suppression of T-cell responses in B6 mice, but paradoxically fostered the development of footpad lesions and parasite load in draining lymph nodes (23). Likewise, supplementation with vitamin A increased parasite burden in the hamster model of visceral Leishmaniasis (35). Collectively, these results indicate that ATRA uncouples maturation and microbicidal activity of macrophages.

Here, we show that the effects of ATRA go beyond control of parasite infection, by affecting induction of M1-inflammatory macrophages. We tested this idea in the absence of *Leishmania* infection, by culturing BALB/c and B6 BMDMs under M1 plus M2 conditions in the presence of ATRA. We show that ATRA promoted an M1 to M2 transition in macrophages from both strains, by preventing expression of proinflammatory cytokines, NOS2, and NO, but increasing secretion of M2 chemokines. We also found a non-significant increase in arginase expression, which further reduces NOS2/arginase ratio. Similarly, ATRA and IL-4 synergize to induce arginase activity in macrophages and DCs (36–38), whereas the presence of LPS in our model may have antagonized this effect (36). Furthermore, expression of retinal dehydrogenase to produce retinoic acid seems to be part of the differentiation program of M2 macrophages and regulatory DCs (38–40).

Treatment with ATRA has been proposed as an anti-inflammatory therapy (38, 41, 42), as well as a tissue repair promoter, by affecting M1 and M2 macrophages or regulatory DCs (37, 41). Some reports also show direct inhibitory effects of ATRA on proinflammatory cytokine production by activated monocytes/macrophages (43–45). More studies are necessary to elucidate how ATRA affects M1/M2 macrophage phenotypes. ATRA may interfere with a shared signaling pathway, such as activation of NF-κB, which is necessary for multiple inflammatory responses (42). These results indicate that, independent of potential direct effects on adaptive immunity (24, 25), by targeting macrophages, ATRA might alter the nature of inflammation and induction of T-cell responses. Moreover, depending on how ATRA affects macrophage phenotype, treatment may improve immunity to tumors (9, 46) and extracellular pathogens (39, 47). Otherwise,

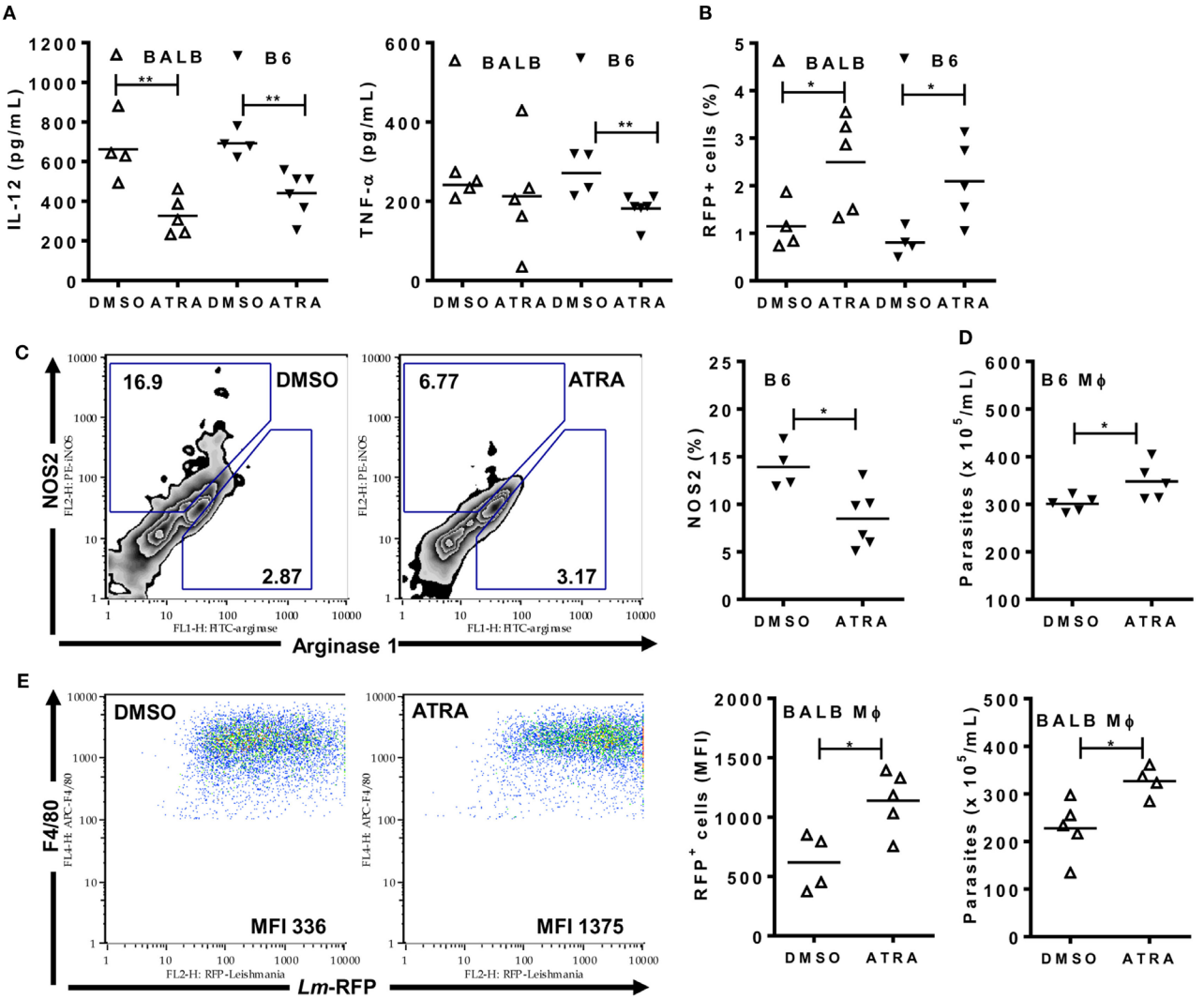


FIGURE 7 | All-*trans* retinoic acid (ATRA) reduces M1 responses and immunity to *Leishmania major* infection. BALB/c and B6 mice were first infected **(A,C,D)** with *L. major* LV39 strain or **(B,E)** with Lm-RFP and then treated with DMSO or ATRA after 24 h. **(A)** Peritoneal exudates were evaluated 48 h upon infection with *L. major* for type-1 cytokines (IL-12 and TNF-α) by ELISA. **(B)** F4/80$^+$ peritoneal exudate cells (PECs) were analyzed for the percentages of cells infected with Lm-RFP. **(C)** PECs from infected B6 mice were stained and analyzed for the expression of NOS2 and arginase 1 within F4/80$^+$ gated cells. **(D,E)** PECs from infected B6 and BALB/c mice were reinfected **(D)** with *L. major* LV39 or **(E)** with Lm-RFP and parasite burden was **(D)** counted in supernatants or **(E)** determined as Lm-RFP infection within F4/80$^+$ cells. MFI stands for median of fluorescence intensity of Lm-RFP-infected macrophages. Symbols represent individual infected (Δ) BALB/c and (▼) B6 mice treated with DMSO (N = 4–5 mice/group) or ATRA (N = 4–6 mice/group). Means are represented. Significant differences between mice treated with DMSO and ATRA were analyzed by t-test and indicated for $P < 0.05$ (*) and $P < 0.01$ (**). Data are representative of two independent experiments.

treatment with ATRA can be detrimental for immunity to tumors (9) and intracellular parasites, such as *L. major*, which take advantage of M2 macrophages to proliferate in the absence of effective M1 responses.

Here, we show that whereas parasite-induced maturation may promote M1 phenotype in *Leishmania* infection, treatment with ATRA prevents differentiation into M1 macrophages and immunity to *L. major*. Further studies are necessary to address whether a therapy with ATRA could target exacerbated inflammatory responses to ameliorate pathology in mucocutaneous Leishmaniasis. In light of current findings, therapies based on treatment with ATRA should be evaluated with caution.

ETHICS STATEMENT

All experiments were approved and conducted in accordance with guidelines of the Ethics Committee for Use of Animals, Federal University of Rio de Janeiro (UFRJ) (Protocol no. 078/16).

AUTHOR CONTRIBUTIONS

NV and SP-M performed and designed *in vivo* and *in vitro* experiments, analyzed data, and co-wrote the manuscript. NV, SP-M, MC-P, AF, FR-G, and TR performed cell culture, cytokine, and flow cytometry assays. GD contributed to interpretation of data

and critical revision of the manuscript. ML designed the research, supervised the experiments, analyzed data, and wrote the manuscript. All authors approved the final version of the manuscript.

ACKNOWLEDGMENTS

We thank Jorgete L. Oliveira and Lindomar M. da Silva (UFRJ) for technical assistance.

FUNDING

This work was supported by the Brazilian National Research Council (Conselho Nacional de Desenvolvimento Científico e Tecnológico, CNPq), the Rio de Janeiro State Science Foundation (Fundação Carlos Chagas Filho de Amparo à Pesquisa do Estado do Rio de Janeiro, FAPERJ), and the National Institute of Science and Technology (INCT-INPeTAm/CNPq/MCT). ML and GD are research fellows at CNPq, Brazil. We also received fellowships from CNPq (to NV and TR), FAPERJ (to MC-P and AF), and CAPES (to SP-M).

SUPPLEMENTARY MATERIAL

The Supplementary Material for this article can be found online at http://www.frontiersin.org/article/10.3389/fimmu.2017.01560/full#supplementary-material.

REFERENCES

1. Sacks D, Noben-Trauth N. The immunology of susceptibility and resistance to *Leishmania major* in mice. *Nat Rev Immunol* (2002) 2(11):845–58. doi:10.1038/nri933
2. Belkaid Y, Piccirillo CA, Mendez S, Shevach EM, Sacks DL. CD4+CD25+ regulatory T cells control *Leishmania major* persistence and immunity. *Nature* (2002) 420(6915):502–7. doi:10.1038/nature01152
3. Sacks D, Anderson C. Re-examination of the immunosuppressive mechanisms mediating non-cure of *Leishmania* infection in mice. *Immunol Rev* (2004) 201:225–38. doi:10.1111/j.0105-2896.2004.00185.x
4. McMahon-Pratt D, Alexander J. Does the *Leishmania major* paradigm of pathogenesis and protection hold for New World cutaneous leishmaniases or the visceral disease? *Immunol Rev* (2004) 201:206–24. doi:10.1111/j.0105-2896.2004.00190.x
5. Alexander J, Bryson K. T helper (h)1/Th2 and *Leishmania*: paradox rather than paradigm. *Immunol Lett* (2005) 99(1):17–23. doi:10.1016/j.imlet.2005.01.009
6. Kaye P, Scott P. Leishmaniasis: complexity at the host-pathogen interface. *Nat Rev Microbiol* (2011) 9(8):604–15. doi:10.1038/nrmicro2608
7. Mills CD, Kincaid K, Alt JM, Heilman MJ, Hill AM. M-1/M-2 macrophages and the Th1/Th2 paradigm. *J Immunol* (2000) 164(12):6166–73. doi:10.4049/jimmunol.164.12.6166
8. Mantovani A, Sozzani S, Locati M, Allavena P, Sica A. Macrophage polarization: tumor-associated macrophages as a paradigm for polarized M2 mononuclear phagocytes. *Trends Immunol* (2002) 23(11):549–55. doi:10.1016/S1471-4906(02)02302-5
9. Murray PJ, Wynn TA. Protective and pathogenic functions of macrophage subsets. *Nat Rev Immunol* (2011) 11(11):723–37. doi:10.1038/nri3073
10. Murray PJ, Allen JE, Biswas SK, Fisher EA, Gilroy DW, Goerdt S, et al. Macrophage activation and polarization: nomenclature and experimental guidelines. *Immunity* (2014) 41(1):14–20. doi:10.1016/j.immuni.2014.06.008
11. Italiani P, Boraschi D. From monocytes to M1/M2 macrophages: phenotypical vs. functional differentiation. *Front Immunol* (2014) 5:514. doi:10.3389/fimmu.2014.00514
12. Biedermann T, Zimmermann S, Himmelrich H, Gumy A, Egeter O, Sakrauski AK, et al. IL-4 instructs TH1 responses and resistance to *Leishmania major* in susceptible BALB/c mice. *Nat Immunol* (2001) 2(11):1054–60. doi:10.1038/ni725
13. Radwanska M, Cutler AJ, Hoving JC, Magez S, Holscher C, Bohms A, et al. Deletion of IL-4Ralpha on CD4 T cells renders BALB/c mice resistant to *Leishmania major* infection. *PLoS Pathog* (2007) 3(5):e68. doi:10.1371/journal.ppat.0030068
14. Hurdayal R, Nieuwenhuizen NE, Revaz-Breton M, Smith L, Hoving JC, Parihar SP, et al. Deletion of IL-4 receptor alpha on dendritic cells renders BALB/c mice hypersusceptible to *Leishmania major* infection. *PLoS Pathog* (2013) 9(10):e1003699. doi:10.1371/journal.ppat.1003699
15. Pereira-Manfro WF, Ribeiro-Gomes FL, Filardy AA, Vellozo NS, Guillermo LV, Silva EM, et al. Inhibition of caspase-8 activity promotes protective Th1- and Th2-mediated immunity to *Leishmania major* infection. *J Leukoc Biol* (2014) 95(2):347–55. doi:10.1189/jlb.0912463
16. Lopes MF, Costa-da-Silva AC, DosReis GA. Innate immunity to *Leishmania* infection: within phagocytes. *Mediators Inflamm* (2014) 2014:754965. doi:10.1155/2014/754965
17. Giudice A, Vendrame C, Bezerra C, Carvalho LP, Delavechia T, Carvalho EM, et al. Macrophages participate in host protection and the disease pathology associated with *Leishmania braziliensis* infection. *BMC Infect Dis* (2012) 12:75. doi:10.1186/1471-2334-12-75
18. Gaze ST, Dutra WO, Lessa M, Lessa H, Guimaraes LH, Jesus AR, et al. Mucosal leishmaniasis patients display an activated inflammatory T-cell phenotype associated with a nonbalanced monocyte population. *Scand J Immunol* (2006) 63(1):70–8. doi:10.1111/j.1365-3083.2005.01707.x
19. Beil WJ, Meinardus-Hager G, Neugebauer DC, Sorg C. Differences in the onset of the inflammatory response to cutaneous leishmaniasis in resistant and susceptible mice. *J Leukoc Biol* (1992) 52(2):135–42.
20. Sunderkotter C, Kunz M, Steinbrink K, Meinardus-Hager G, Goebeler M, Bildau H, et al. Resistance of mice to experimental leishmaniasis is associated with more rapid appearance of mature macrophages *in vitro* and *in vivo*. *J Immunol* (1993) 151(9):4891–901.
21. Steinbrink K, Schonlau F, Rescher U, Henseleit U, Vogel T, Sorg C, et al. Ineffective elimination of *Leishmania major* by inflammatory (MRP14-positive) subtype of monocytic cells. *Immunobiology* (2000) 202(5):442–59. doi:10.1016/S0171-2985(00)80103-5
22. Goncalves R, Zhang X, Cohen H, Debrabant A, Mosser DM. Platelet activation attracts a subpopulation of effector monocytes to sites of *Leishmania major* infection. *J Exp Med* (2011) 208(6):1253–65. doi:10.1084/jem.20101751
23. Pereira WF, Ribeiro-Gomes FL, Guillermo LV, Vellozo NS, Montalvao F, Dosreis GA, et al. Myeloid-derived suppressor cells help protective immunity to *Leishmania major* infection despite suppressed T cell responses. *J Leukoc Biol* (2011) 90(6):1191–7. doi:10.1189/jlb.1110608
24. Hall JA, Grainger JR, Spencer SP, Belkaid Y. The role of retinoic acid in tolerance and immunity. *Immunity* (2011) 35(1):13–22. doi:10.1016/j.immuni.2011.07.002
25. Pino-Lagos K, Guo Y, Noelle RJ. Retinoic acid: a key player in immunity. *Biofactors* (2010) 36(6):430–6. doi:10.1002/biof.117
26. Nefedova Y, Fishman M, Sherman S, Wang X, Beg AA, Gabrilovich DI. Mechanism of all-*trans* retinoic acid effect on tumor-associated myeloid-derived suppressor cells. *Cancer Res* (2007) 67(22):11021–8. doi:10.1158/0008-5472.CAN-07-2593
27. Bonfante-Garrido R, Melendez E, Barroeta S, de Alejos MA, Momen H, Cupolillo E, et al. Cutaneous leishmaniasis in western Venezuela caused by infection with *Leishmania venezuelensis* and *L. braziliensis* variants. *Trans R Soc Trop Med Hyg* (1992) 86(2):141–8. doi:10.1016/0035-9203(92)90544-M
28. Kimblin N, Peters N, Debrabant A, Secundino N, Egen J, Lawyer P, et al. Quantification of the infectious dose of *Leishmania major* transmitted to the skin by single sand flies. *Proc Natl Acad Sci U S A* (2008) 105(29):10125–30. doi:10.1073/pnas.0802331105
29. Spath GF, Beverley SM. A lipophosphoglycan-independent method for isolation of infective *Leishmania* metacyclic promastigotes by density gradient centrifugation. *Exp Parasitol* (2001) 99(2):97–103. doi:10.1006/expr.2001.4656

30. Sutterwala FS, Noel GJ, Clynes R, Mosser DM. Selective suppression of interleukin-12 induction after macrophage receptor ligation. *J Exp Med* (1997) 185(11):1977–85. doi:10.1084/jem.185.11.1977
31. Filardy AA, Pires DR, Nunes MP, Takiya CM, Freire-de-Lima CG, Ribeiro-Gomes FL, et al. Proinflammatory clearance of apoptotic neutrophils induces an IL-12(low)IL-10(high) regulatory phenotype in macrophages. *J Immunol* (2010) 185(4):2044–50. doi:10.4049/jimmunol.1000017
32. Romano A, Carneiro MBH, Doria NA, Roma EH, Ribeiro-Gomes FL, Inbar E, et al. Divergent roles for Ly6C+CCR2+CX3CR1+ inflammatory monocytes during primary or secondary infection of the skin with the intra-phagosomal pathogen *Leishmania major*. *PLoS Pathog* (2017) 13(6):e1006479. doi:10.1371/journal.ppat.1006479
33. Scott P, Sher A. A spectrum in the susceptibility of leishmanial strains to intracellular killing by murine macrophages. *J Immunol* (1986) 136(4):1461–6.
34. Rocha FJ, Schleicher U, Mattner J, Alber G, Bogdan C. Cytokines, signaling pathways, and effector molecules required for the control of *Leishmania* (*Viannia*) *braziliensis* in mice. *Infect Immun* (2007) 75(8):3823–32. doi:10.1128/IAI.01335-06
35. Garg R, Singh N, Dube A. Intake of nutrient supplements affects multiplication of *Leishmania donovani* in hamsters. *Parasitology* (2004) 129(Pt 6):685–91. doi:10.1017/S0031182004006055
36. Surace MJ, Li L. Potent suppression of arginase 1 expression in murine macrophages by low dose endotoxin. *Am J Clin Exp Immunol* (2013) 2(1):117–23.
37. Lee B, Wu CY, Lin YW, Park SW, Wei LN. Synergistic activation of Arg1 gene by retinoic acid and IL-4 involves chromatin remodeling for transcription initiation and elongation coupling. *Nucleic Acids Res* (2016) 44(16):7568–79. doi:10.1093/nar/gkw392
38. Zhu B, Buttrick T, Bassil R, Zhu C, Olah M, Wu C, et al. IL-4 and retinoic acid synergistically induce regulatory dendritic cells expressing Aldh1a2. *J Immunol* (2013) 191(6):3139–51. doi:10.4049/jimmunol.1300329
39. Broadhurst MJ, Leung JM, Lim KC, Girgis NM, Gundra UM, Fallon PG, et al. Upregulation of retinal dehydrogenase 2 in alternatively activated macrophages during retinoid-dependent type-2 immunity to helminth infection in mice. *PLoS Pathog* (2012) 8(8):e1002883. doi:10.1371/journal.ppat.1002883
40. Ouimet M, Ediriweera HN, Gundra UM, Sheedy FJ, Ramkhelawon B, Hutchison SB, et al. MicroRNA-33-dependent regulation of macrophage metabolism directs immune cell polarization in atherosclerosis. *J Clin Invest* (2015) 125(12):4334–48. doi:10.1172/JCI81676
41. Chiba T, Skrypnyk NI, Skvarca LB, Penchev R, Zhang KX, Rochon ER, et al. Retinoic acid signaling coordinates macrophage-dependent injury and repair after AKI. *J Am Soc Nephrol* (2016) 27(2):495–508. doi:10.1681/ASN.2014111108
42. Hong K, Zhang Y, Guo Y, Xie J, Wang J, He X, et al. All-*trans* retinoic acid attenuates experimental colitis through inhibition of NF-kappaB signaling. *Immunol Lett* (2014) 162(1 Pt A):34–40. doi:10.1016/j.imlet.2014.06.011
43. Dzhagalov I, Chambon P, He YW. Regulation of CD8+ T lymphocyte effector function and macrophage inflammatory cytokine production by retinoic acid receptor gamma. *J Immunol* (2007) 178(4):2113–21. doi:10.4049/jimmunol.178.4.2113
44. Mehta K, McQueen T, Tucker S, Pandita R, Aggarwal BB. Inhibition by all-*trans*-retinoic acid of tumor necrosis factor and nitric oxide production by peritoneal macrophages. *J Leukoc Biol* (1994) 55(3):336–42.
45. Wang X, Allen C, Ballow M. Retinoic acid enhances the production of IL-10 while reducing the synthesis of IL-12 and TNF-alpha from LPS-stimulated monocytes/macrophages. *J Clin Immunol* (2007) 27(2):193–200. doi:10.1007/s10875-006-9068-5
46. Zhou Q, Xian M, Xiang S, Xiang D, Shao X, Wang J, et al. All-*trans* retinoic acid prevents osteosarcoma metastasis by inhibiting M2 polarization of tumor-associated macrophages. *Cancer Immunol Res* (2017) 5(7):547–59. doi:10.1158/2326-6066.CIR-16-0259
47. Gundra UM, Girgis NM, Gonzalez MA, San Tang M, Van Der Zande HJP, Lin JD, et al. Vitamin A mediates conversion of monocyte-derived macrophages into tissue-resident macrophages during alternative activation. *Nat Immunol* (2017) 18(6):642–53. doi:10.1038/ni.3734

Conflict of Interest Statement: The authors declare that the research was conducted in the absence of any commercial or financial relationships that could be construed as a potential conflict of interest.

Copyright © 2017 Vellozo, Pereira-Marques, Cabral-Piccin, Filardy, Ribeiro-Gomes, Rigoni, DosReis and Lopes. This is an open-access article distributed under the terms of the Creative Commons Attribution License (CC BY). The use, distribution or reproduction in other forums is permitted, provided the original author(s) or licensor are credited and that the original publication in this journal is cited, in accordance with accepted academic practice. No use, distribution or reproduction is permitted which does not comply with these terms.

frontiers in Immunology

ORIGINAL RESEARCH
published: 11 January 2018
doi: 10.3389/fimmu.2017.01954

Infection of Human Macrophages by *Leishmania infantum* Is Influenced by Ecto-Nucleotidases

*Nalu Teixeira de Aguiar Peres[1,2†], Luana Celina Seraphim Cunha[1†], Meirielly Lima Almeida Barbosa[1], Márcio Bezerra Santos[1,3], Fabrícia Alvise de Oliveira[1], Amélia Maria Ribeiro de Jesus[1,4] and Roque Pacheco de Almeida[1,4]**

[1] Laboratory of Molecular Biology, Department of Medicine, University Hospital, Federal University of Sergipe, São Cristóvão, Brazil, [2] Department of Morphology, Biological and Health Sciences Centre, Federal University of Sergipe, Aracaju, Brazil, [3] Department of Health Science, Federal University of Sergipe, Aracaju, Brazil, [4] Instituto de Investigação em Imunologia, Institutos Nacionais de Ciência e Tecnologia, Conselho Nacional de Desenvolvimento Científico e Tecnológico (CNPq), Brasília, Brazil

Ecto-nucleotidase activity is involved in the infection process of *Leishmania* and various other parasites that enables modulation of host immune responses to promote disease progression. One of the enzymes responsible for this activity is the ecto-nucleoside triphosphate diphosphohydrolase (E-NTPDase). The enzyme hydrolyzes nucleotides tri- and/or di-phosphate into monophosphate products, which are subsequently hydrolyzed into adenosine. These nucleotides can serve as purinergic signaling molecules involved in diverse cellular processes that govern immune responses. Given the importance of the extracellular metabolism of these nucleotides during intracellular pathogen infections, this study evaluates the role of ecto-nucleotidase activity during *Leishmania infantum* (*L. infantum*) infection in human macrophages. E-NTPDase protein expression and activity was evaluated in *L. infantum* during purine starvation, adenosine-enriched medium, or in the presence of an inhibitor of ecto-nucleotidases. Results show that E-NTPDase is expressed in *L. infantum* parasites, including on the cell membrane. Furthermore, functional activity of the enzyme was modulated according to the availability of adenosine in the medium. Purine starvation increased the hydrolytic capacity of nucleotides leading to higher infectivity, while growth in adenosine-enriched medium led to lower infectivity. Moreover, inhibiting E-NTPDase function decreased *L. infantum* infection in macrophages, suggesting the enzyme may serve as a ligand. Taken together, the ability of *L. infantum* to hydrolyze nucleotides is directly associated with increased infectivity in macrophages.

Keywords: *Leishmania infantum*, macrophage, infection, ecto-nucleotidase, extracellular nucleotides

OPEN ACCESS

Edited by:
Etienne Meunier, UMR5089 Institut de Pharmacologie et de Biologie Structurale (IPBS), France

Reviewed by:
Joao Luiz Mendes Wanderley, Universidade Federal do Rio de Janeiro, Brazil
Debora Decote-Ricardo, Universidade Federal Rural do Rio de Janeiro, Brazil

***Correspondence:**
Roque Pacheco de Almeida
roquepachecoalmeida@gmail.com

†These authors share the first authorship.

Specialty section:
This article was submitted to Microbial Immunology, a section of the journal Frontiers in Immunology

Received: *15 September 2017*
Accepted: *18 December 2017*
Published: *11 January 2018*

Citation:
Peres NTA, Cunha LCS, Barbosa MLA, Santos MB, Oliveira FA, Jesus AMR and Almeida RP (2018) Infection of Human Macrophages by Leishmania infantum Is Influenced by Ecto-Nucleotidases. Front. Immunol. 8:1954. doi: 10.3389/fimmu.2017.01954

INTRODUCTION

Visceral leishmaniasis (VL) is a neglected parasitic disease caused by species of the genus *Leishmania*, which frequently leads to death if untreated (1, 2). It is estimated that about 200,000 new cases of VL occur yearly worldwide and that over 90% occur in Bangladesh, Brazil, Ethiopia, India, South Sudan, and Sudan (W.H.O. 2015). VL has a mortality rate of about 5% and has few clinical treatment options (3).

Several factors are determinant for the clinical outcome of VL. Disease severity can range between subclinical and different degree of severity. Several factors involved in early host–parasite interactions and innate immune responses can directly modulate VL severity. The release

of nucleotides, as well as the enzymes that participate in the degradation of these nucleotides and their receptors, into the extracellular environment can directly influence early events of host–parasite interactions (4). Extracellular adenosine triphosphate (ATPe) and its metabolites, ADP and adenosine, are important mediators of the immune response (5). Extracellular levels of ATP and adenosine are detected and transduced by the purinergic receptors of type P2 and P1, respectively. Most immune cells express P2 and P1 receptors. Depending on the concentration, ATPe can act as an immunostimulatory molecule, whereas adenosine often triggers immunosuppressive responses (6). Under normal physiological conditions, ATP is almost exclusively present inside the cells at high concentrations (in the millimolar range). In the extracellular environment, ATP concentration is negligible (at low nanomolar ranges) (7). ATP can serve as a potent signal of distress or damage. Cell damage often leads to ATP release, which can be detected by neighboring and surrounding cells. Detection leads to transmission of signals *via* ATP-conducting pathways to produce nucleotidases to degrade the ATPe (8). Interestingly, *Leishmania* sp. is able to modulate the concentration of extracellular nucleotides, thereby altering the balance of pro- and anti-inflammatory molecules to evade host immune responses (9).

Ecto-nucleoside triphosphate diphosphohydrolase (E-NTPDase) enzymes are another important element in the metabolism of nucleotides. The enzymes, also classified in the nucleoside triphosphate diphosphohydrolases family of ecto-nucleotidases or apyrases, are important for parasite nutrition by facilitating acquisition of extracellular purines. E-NTPDase has been suggested to play important roles in host–parasite interaction and has been identified as being a virulence factor that participates in adhesion and infection in trypanosomatides (10–13). Studies have further shown an association between ATP hydrolysis and the biological effects in host–parasite interaction (14–18).

The activity of ecto-nucleotidases has been demonstrated in *Leishmania tropica, Leishmania amazonensis*, and *L. infantum* (12, 19, 20). These enzymes play a role in virulence, cell adhesion, parasite release from infected cells, and in control of nucleotide concentrations inside cells and in the extracellular spaces (17, 21, 22). Moreover, these enzymes also plays a role in the immune response by favoring reduction of IFN -γ and increased IL-10 expression, thus dampening the host immune response to facilitate the parasite's survival (11, 22–24).

Purine starvation increases ecto-nucleotidase activity, thereby suggesting a major importance of these enzymes for parasite nutrition and survival. It is believed that the role of ecto-nucleotidases during infection is to degrade nucleotides molecules in the extracellular environment in support of parasitic infectivity and reproduction. However, the effect of purine starvation, as well as the supplementation of adenosine to the parasites during macrophage infection, has not been investigated. Furthermore, it is unknown whether these enzymes, present in the *Leishmania* membrane, can also facilitate parasite entry into host macrophages. Therefore, this study aimed to evaluate the influence of E-NTPDase activity during *L. infantum* infection in human macrophages. Moreover, as these early events of infection could influence the disease severity, we also aimed to compare the levels of E-NTPDase activity in different clinical isolates from VL patients.

MATERIALS AND METHODS

Parasites

Leishmania infantum strains LVHSE09, LVHSE17, LVHSE23, and LVHSE49 were obtained from bone marrow aspirates of visceral leishmaniasis patients, as previously reported (25). The promastigotes were cultured in Schneider's insect medium (Sigma Aldrich) pH 7.2, supplemented with 10% heat-inactivated fetal bovine serum (FBS) and 100 U/ml of penicillin/streptomycin.

Detection of *L. infantum* E-NTPDase-1 and E-NTPDase-2 by Confocal Microscopy

For the immunolocalization of E-NTPDase-1 and E-NTPDase-2 in *L. infantum,* promastigotes were washed in PBS and fixed in 0.1% glutaraldehyde and 2% paraformaldehyde in 0.1% cacodilate. The parasites were then placed onto glass slides containing 1% poly-L-lysine (Sigma Aldrich). Parasites were treated with 50 µM glycine for 30 min prior to blocking with 1% BSA containing 0.01% Tween 20 in PBS (PBS-T BSA). Samples were incubated with anti-human E-NTPDase 1 or 2 antibodies or respective isotype controls (Sigma Aldrich) in a 1:20 dilution for 12 h. Slides were then washed three times with PBS-T BSA, and incubated with secondary anti-rabbit IgG antibody conjugated to Alexa 488 (Santa Cruz Biotechnology) at a 1:100 dilution for 2 h. Slides were mounted and images acquired using Leica® SP8 confocal microscope.

Western Blot of the E-NTPDase-1 and 2 in Total Extract of *L. infantum*

Western blot studies were performed as previously described (12). Briefly, total extract of *L. infantum* was obtained after growth of 1×10^8 cells/ml until stationary phase. Cells were lysed using NP-40 lysis buffer supplemented with a protease inhibitor cocktail (2 mM AEBSF, 0.3 µM Aprotinina, 116 µM Bestatina, 14 µM E-64, 1 µM Leupeptina, and 1 mM EDTA; Sigma Adrich). After electrophoresis in a SDS-PAGE gel, samples were transferred to nitrocellulose membrane using the mini transblot electrophoretic transfer cell (Bio-Rad). Next, the membrane was blocked with 1% BSA prior to extensive washing in PBS Tween 0.1% (PBS-T). The blot was then incubated overnight with each respective primary antibody at a dilution of 1:250. Membranes were washed three times with PBS-T for 5 min and incubated with respective secondary antibodies conjugated to Alexa 488 (Santa Cruz Biotechnology). After washing three times with PBS-T for 5 min, the membranes were analyzed in the ChemiDoc MP (Bio-Rad).

Leishmania Culture Conditions and Pretreatments

Leishmania infantum promastigotes were grown to the stationary phase and then incubated for 1 h with 250 µM suramin (Sigma Aldrich), an inhibitor of the ecto-nucleotidase activity (20). After incubation, promastigotes were washed twice and resuspended in saline solution (0.9% NaCl). To demonstrate that suramin had

no effect on parasite growth, promastigotes at a concentration of 3×10^5 cells/ml were grown in the absence or presence of 500 μM suramin. Growth was estimated daily by standard cell counting using a Neubauer chamber. Analysis was performed by two independent observers.

In order to evaluate the activity of ecto-nucleotidases of the parasites under purine starvation, promastigotes were cultured for 48 h in Modified Eagle Medium depleted of purine (300 mg/L L-proline, 14.250 mg/L HEPES, 1 mg/L D-biotin, 0.2 mg/L ascorbic acid, 0.2 mg/L Vitamin B12, 15 mg/L bovine albumin, 10 mg/L phenol red, 0.4 mg/L lipolic acid 0.4 mg/L Menadione, 0.4 mg/L Vitamin A, 10 mg/L Hemin, and 11 mg/L folic acid; pH 7.4). In addition, to evaluate the ecto-nucleotidases activity in purine-enriched environment, promastigotes were grown in medium supplemented with 200 μM adenosine. After each culture condition, the ecto-nucleotidase activity was measured and the parasites were used to infect macrophages. To evaluate whether the human anti-E-NTPDase-1 blocking antibody inhibits E-NTPDase activity, promastigotes were incubated for 1 h in presence of the blocking antibody (diluted at 1:100) prior to measurement of E-NTPDase activity or for use in macrophage infection experiments.

Hydrolytic Activity of the Ecto-Nucleotidase

Four different strains of *L. infantum* were evaluated for E-NTPDase activity, but only strain LVHSE49 was used for infection studies. Hydrolysis of nucleotides were measured by incubation of *Leishmania* parasites for 1 h in the presence of 5 mM ATP, ADP, or AMP (Sigma Aldrich) in a solution containing 116 mM NaCl, 5.4 mM KCl, 5.5 mM D-glucose, 5 mM MgCl2, and 50 mM Hepes–Tris buffer, as previously described (21). The reaction was started by adding *L. infantum* promastigotes and terminated by the addition of ice cold 0.2 M HCl (10). Non-specific nucleotide hydrolysis was determined by adding the parasites after the reaction was terminated. The suspensions were pelleted and aliquots of the supernatant were used for the measurement of released inorganic phosphate (Pi) (26). Enzymatic activities were expressed as nmol of Pi released. Parasites viability and motility were assessed by trypan blue staining and microscopy (27).

Infection of Human Macrophages with *L. infantum*

Macrophages derived from peripheral blood mononuclear cells (PBMC) were obtained from healthy donor blood as previously described by Santos et al. (25). Briefly, heparinized venous blood was separated by Ficoll–Hypaque gradient (Sigma Aldrich) to isolate PBMC. The cells were washed twice, counted and resuspended in RPMI 1640 (Sigma Aldrich) supplemented with 10% fetal bovine serum (FBS) prior to plating on Lab-Tek glass plates (Thermo Scientific) at 3×10^5 cells/well. The cells were allowed to adhere for 3 h at 37°C in 5% CO_2. Non-adherent cells were removed by extensive washing with phosphate-buffered saline (PBS). Adherent monocytes were incubated in RPMI 1640 medium supplemented with 10% FBS at 37°C for 7 days to allow differentiation into macrophages. Next, these macrophages were infected with stationary-phase *L. infantum* promastigotes at ratio of 1:10, respectively. In some experiments, the culture of macrophages with *L. infantum* promastigotes was supplemented with 100 μM ATP to evaluate the role of nucleotide presence influencing infectivity. Extracellular parasites (that did not infect the macrophages) were removed after 2 h by extensive washing. Next, the culture was incubated for an additional 2 h at 37°C. The percentage of infected macrophages and the number of amastigotes per 100 macrophages was analyzed by microscopy. Each set of analyses was performed by two independent observers, with each counting different fields of the slide.

Statistical Analysis and Ethical Considerations

All experiments were performed in triplicate wells at a minimum of four independent experiments. Statistical analyses were performed using GraphPad Prism 5.0 software (La Jolla, CA, USA) and normality was analyzed by the D'Agostino & Pearson test. Non-parametric data were analyzed using the Mann–Whitney test. Data were considered statistically significant if p-value <0.05. Data were expressed as means ± SDs. This project was approved by the Ethical Committee of the Federal University of Sergipe (CONEP), CAAE-0151.0.107.000-07.

RESULTS

Ecto-Nucleotidase Activity Does Not Differ among *L. infantum* Isolates

Ecto-nucleoside triphosphate diphosphohydrolase activity was measured and compared among four *L. infantum* strains isolated from different patients. These strains displayed different susceptibility to Nitric Oxide, as previously shown by Santos et al. (25). However, the isolates LVHSE 09, 17, 23, and 49 each did not present significant differences in E-NTPDase activity (**Figure 1**). Microscopy studies showed that E-NTPDase was present on

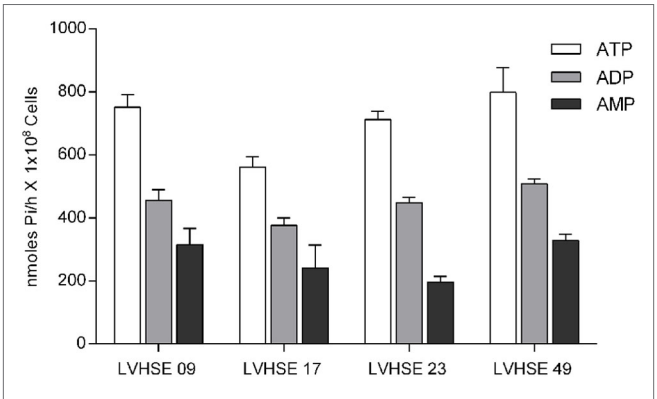


FIGURE 1 | Ecto-nucleoside triphosphate diphosphohydrolase activity of *L. infatum* isolates. Ecto-Nucleotidase activity of *L. infantum* strains LVHSE09, LVHSE17, LVHSE23, and LVHSE49 grown until stationary phase. Promastigotes (1×10^8) were incubated for 1 h at 37°C with ATP, ADP, or AMP, and enzymatic activity was evaluated by measuring inorganic phosphate (Pi) in the extracellular medium. Bars represent the mean ± SD of three independent experiments performed in triplicate.

L. infantum promastigotes, including in cellular membrane, as detected by immunostaining with the E-NTPDase 1 and E-NTPDase 2 antibodies (**Figure 2A**); isotype IgG antibody staining served as an internal control. Interestingly, a homogeneous distribution of E-NTPDase was found throughout the parasite, and also in the cellular membrane. Western blot analysis of the total extract of *L. infantum* promastigotes revealed the presence of two isoforms. A 70 kDa band represented E-NTPDase-1 and the 40 kDa was the E-NTPDase-2 (**Figure 2B**). The presence of a signal at just above the 70 kDa band was determined to be a non-specific auto-fluorescent signal, as detected in the internal controls (which used no antibodies).

Ecto-Nucleotidase Expression and Activity in *L. infantum* Influences Infectivity in Human Macrophages

The ecto-nucleotidase activity of the parasites in the presence of suramin, an inhibitor of protein tyrosine phosphatases, yielded a 70 and 53% reduction in ATP and AMP hydrolysis, respectively, compared to controls (**Figure 3A**). However, parasites grown under purine starvation resulted in increased hydrolytic capacity, with 65 and 63% for ATP and AMP, respectively (**Figure 3A**). Interestingly, there was no significant difference in the hydrolysis of ADP.

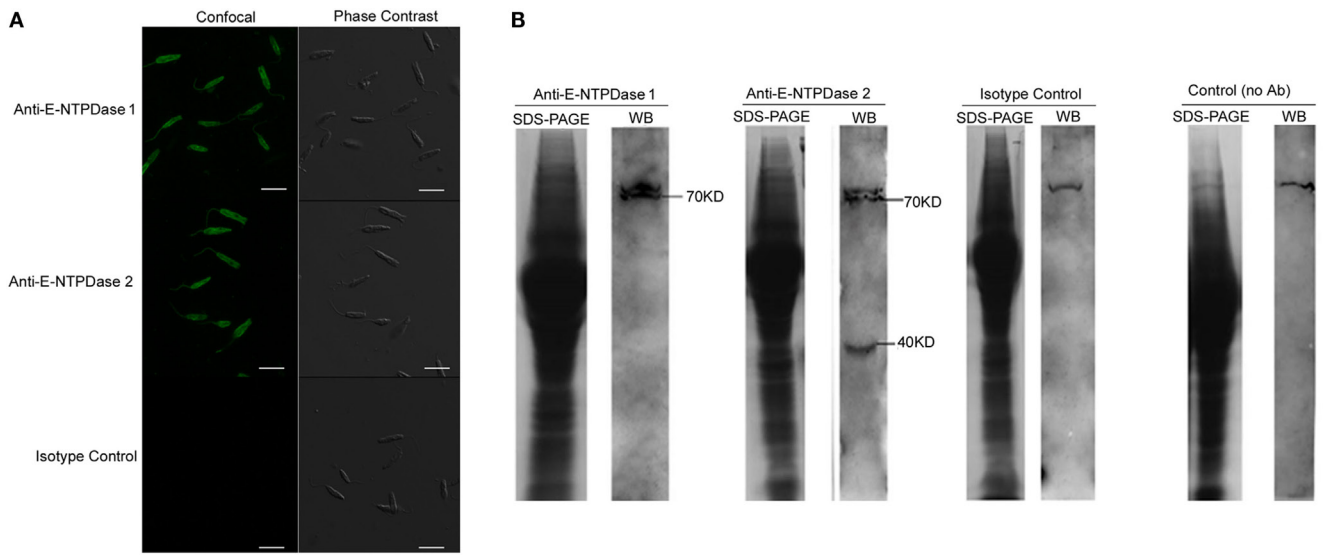


FIGURE 2 | Immunolocalization of ecto-nucleoside triphosphate diphosphohydrolase (E-NTPDase) in *Leishmania infantum*. **(A)** Confocal microscopy showing the presence of E-NTPDase 1 and E-NTPDase 2 in *L. infantum* promastigotes. Parasites were fixed and labeled with primary rabbit antibody IgG anti E-NTPDase 1, anti E -NTPDase 2, or respective isotype IgG controls, followed by secondary labeling with anti-rabbit IgG linked to Alexa 488. **(B)** Western blot of the total extract from *L. infantum* labeled with antibody anti E-NTPDase 1, anti E-NTPDase 2, isotype control, and without antibody. Bars represent 10 μm.

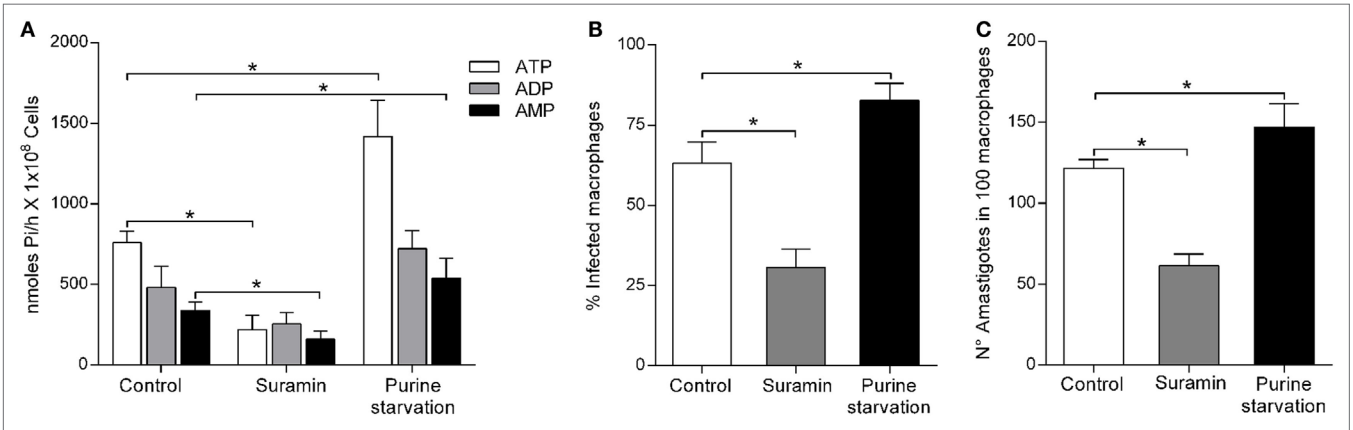


FIGURE 3 | *Leishmania infantum* ecto-nucleoside triphosphate diphosphohydrolase (E-NTPDase) activity and macrophage infection during purine starvation and inhibition by suramin. **(A)** *L. infantum* E-NTPDase activity was evaluated by measuring the inorganic phosphate (Pi) in the extracellular medium of *L. infantum* promastigotes incubated with suramin, or under purine starvation, for 1 h. **(B)** Percentage of infected macrophages after 48 h. **(C)** Number of amastigotes per 100 macrophages after 48 h of incubation. Bars represent the mean ± SD of four independent experiments performed in triplicate.

To assess whether nucleotide hydrolysis is related to the infectivity of *L. infantum*, macrophages infection studies were performed with parasites pretreated with suramin or, alternatively, grown under purine starvation. The infection rate of macrophages with parasites pretreated with suramin was 28.16 ± 3.75%, whereas it was 61.45 ± 5.1% for macrophages infected with untreated control parasites (**Figure 3B**). In the presence of suramin, the number of amastigotes/100 macrophages was 70.02 ± 4.2 compared to controls at 118.5 ± 5.03 (**Figure 3C**). No difference was observed in the *L. infantum* growth curve in the presence of suramin (data not shown). Promastigote integrity and viability were confirmed by performing cell motility assays. The number of macrophages infected with parasites treated with the E-NTPDase inhibitor was also about 50% lower in comparison to the control. In addition, the inhibitor treatment resulted in decreased number of intracellular parasites. However, for parasites cultured under purine starvation, the number of infected macrophages was significantly higher (82.75 ± 5.2%) compared to the control (63.16 ± 6.6%) (**Figure 3B**), as well as the number of amastigotes per 100 macrophages (**Figure 3C**).

When *L. infantum* parasites were cultured in the presence of E-NTPDase-1 neutralizing antibody, no inhibition of ecto-nucleotidase activity was measured (**Figure 4A**). However, blocking did reduce macrophage infection rate to 39.9 ± 6.0% compared to 61.4 ± 3.7% in the isotype and untreated controls (**Figure 4B**). The number of amastigotes per 100 macrophages was also decreased upon addition of the blocking antibody (78.2 ± 3.1) compared to isotype control (120.7 ± 5.0) and untreated control groups (**Figure 4C**).

Infection of Human Macrophages by *L. infantum* Is Enhanced by ATP Hydrolysis But Is Decreased When Adenosine Is Available to the Parasite

The purine adenosine is a source for trypanosomatids nutrition. Therefore, we evaluated whether supply of adenosine could alter the nucleotide hydrolysis capacity of *L. infantum* and its ability to infect macrophages. Culture of the *L. infantum* parasites with adenosine decreased ATP, ADP, and AMP hydrolytic capacities when compared to controls (**Figure 5A**). Moreover, decreased ecto-nucleotidase activity of the parasites resulted in a 30% decrease in the infection rate (43.51 ± 4.3%), compared to the control (61.45 ± 3.7%) (**Figure 5B**). The number of amastigotes per 100 macrophages was also significantly lower in parasites exposed to adenosine (75.83 ± 10.3) when compared to controls (123.16 ± 13.9) (**Figure 5C**). In turn, the presence of ATP during infection led to a 25% increase in the infection rate (83.72 ± 5.8%) compared to the control (60.71 ± 8.18%) (**Figure 5D**). In tandem, the number of amastigotes in 100 macrophages (146.81 ± 19.22) was also increased in the presence of ATP compared to the control (102.16 ± 10.63) (**Figure 5E**).

DISCUSSION

This study now shows that high ecto-nucleotidase activity in *L. infantum* parasites correlates directly with a high capacity to infect human macrophages. Furthermore, results revealed that the expression of the enzyme plays an important role in modulating infectivity, independently from the enzymatic activity. Moreover, parasites exposed to purine starvation enhanced nucleotidase activity and infectivity. However, while generation of adenosine by the parasite favors parasite infectivity, pre-exposure to adenosine during parasite growth resulted in increased nucleotidase activity. This demonstrates the importance of ecto-nucleotidase enzymes for the hydrolysis of extracellular nucleotides to modulate infectivity during host–parasite interactions.

The purinergic network signaling of immune cells senses small changes in the concentration of extracellular nucleotides. These responses play multiple roles in immunoregulation by stimulating lymphocytes proliferation, ROS and NO generation, and cytokines and chemokine secretion (9, 28, 29). This study

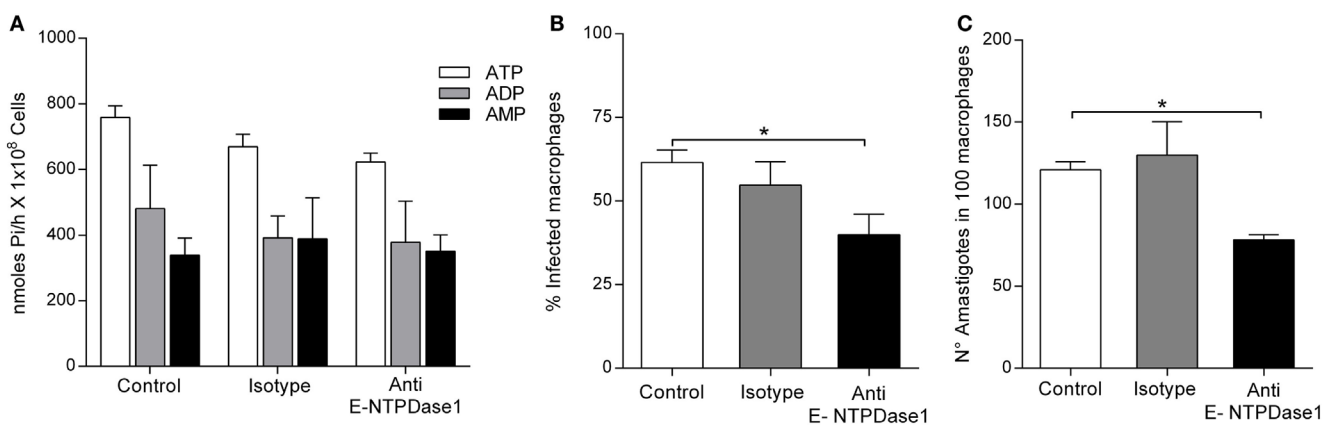


FIGURE 4 | Effect of the blockage of *Leishmania infantum* ecto-nucleoside triphosphate diphosphohydrolase (E-NTPDase) activity and in macrophage infection. **(A)** *L. infantum* E-NTPDase activity was evaluated by measuring the inorganic phosphate (Pi) in the extracellular medium of *L. infantum* promastigotes incubated with anti-human E-NTPDase 1 antibody, for 1 h. **(B)** Percentage of infected macrophages after 48 h. **(C)** Number of amastigotes in 100 macrophages after 48 h. Bars represent the mean ± SD of four independent experiments performed in triplicate, $^*p < 0.05$.

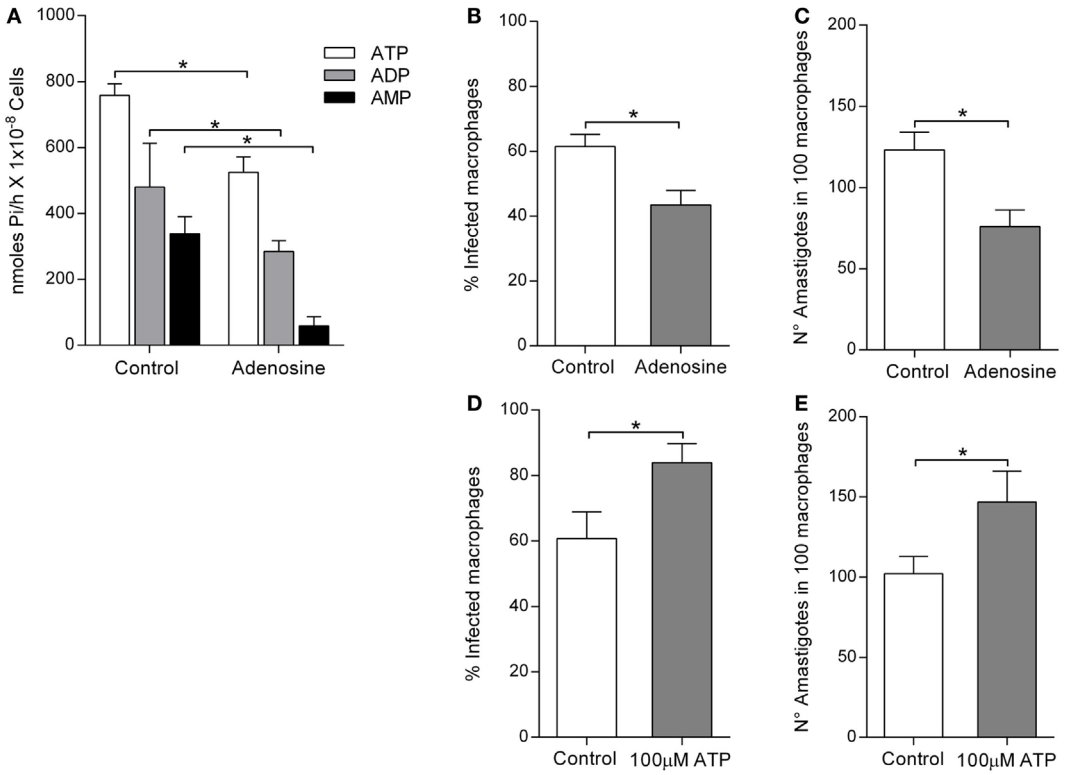


FIGURE 5 | *Leishmania infantum* ecto-nucleoside triphosphate diphosphohydrolase (E-NTPDase) activity and macrophage infection in the presence of adenosine or ATP. **(A)** *L. infantum* E-NTPDase activity was evaluated by measuring the inorganic phosphate (Pi) in the extracellular medium of *L. infantum* promastigotes incubated with adenosine, for 1 h. **(B)** Percentage of infected macrophages after 48 h in the presence of adenosine. **(C)** Number of amastigotes in 100 macrophages after 48 h in the presence of adenosine. **(D)** Percentage of infected macrophages after 48 h in the presence of ATP. **(E)** Number of amastigotes in 100 macrophages after 48 h in the presence of ATP. Bars represent the mean ± SD of four independent experiments performed in triplicate, $^*p < 0.05$.

now shows that *L. infantum* exerts NTPDase activity. Although different strains of *L. infantum* have different abilities to overcome NO responses in phagocytes, they do not have significant differences in their ecto-nucleotidase activity. Moreover, imaging studies revealed that these enzymes are present on *L. infantum* and western blot analyses revealed two different isoforms present at 40 and 70 kDa.

Incubation of parasites with suramin inhibited NTPDase activity for ATP, ADP, and AMP. Furthermore, this was followed by a 50% reduction in the infection rate and in the number of amastigote present within macrophages in the infection groups. These results support the notion that E-NTPDase plays an important role in the interaction between *L. infantum* and human macrophages. Previously published studies have shown that increased capacity to hydrolyze extracellular nucleotides is associated with virulence and infectivity of *Leishmania* sp. (22, 30, 31). Furthermore, similar to our findings, inhibition of NTPDase in *T. cruzi* led to a 50% reduction of *in vitro* infection (17). Recognition of *Leishmania* sp. by TLR in phagocytes may trigger the release of ATPe, which binds to the purinergic receptor P2X7. This then leads to activation of the NLRP3 inflammasome pathway and secretion of pro-inflammatory cytokines, such as interleukin-1β (18, 32).

Alternatively, purine starvation led to a higher capacity to hydrolyze adenine nucleotides by the parasites, which also resulted in an increased infection rate. Reports have shown that E-NTPDase activity generates adenosine in the extracellular medium, which allows binding to A2B receptors. This interaction then leads to decreased production of IL-12 and TNF-α by activated macrophages, thereby inhibiting NO production and favoring infection (24). Moreover, deprivation of purines upregulates the expression of enzymes involved in extracellular nucleotide metabolism in attempt to adapt to environmental changes (33–35). In addition, nucleosides can trigger metacyclogenesis in *L. amazonensis*, both *in vivo* and *in vitro* (36). Thus, it is possible that the higher infective capacity of *L. infantum* cultured in media depleted of purine leads to induced metacyclogenesis. However, additional studies are required to understand the effect of purine starvation in the parasites' life cycle.

In turn, supplementation of adenosine in the culture medium during the *L. infantum* growth significantly decreased NTPDase activity. This is possibly due to downregulation of enzyme expression, potentially because excess adenosine can facilitate the uptake of purines. Moreover, adenosine supplementation led to about 30% reduction in infectivity, corroborating the idea that ecto-nucleotidase activity plays an important role in

host–parasite interactions during infections. In *L. amazonensis*, there is a decrease in the E-NTPDase expression when parasites were grown in medium supplemented with adenosine. This led to a reduced survival rate in murine macrophages (24).

However, adenosine often triggers potent immunosuppressive responses by interaction with its P1 receptor on macrophages during infection (6), while ATPe can act in an immunostimulatory capacity. Therefore, *Leishmania* sp. is able to modulate the concentration of extracellular nucleotides, affecting the balance of pro- vs. anti-inflammatory molecules, and thus allowing evasion of host immune responses (9). For example, the blockage of the purinergic adenosine receptor causes decreased lesion size and parasitism in tegumentary leishmaniais (30).

Although the physiological roles of E-NTPDases are not fully understood, some functions have been postulated, such as participation in cell–cell adhesion (21, 37). The adherence of the parasite to host cells is an energy-dependent process (38). We demonstrated that E-NTPDase is expressed in *L. infantum*, including in the cell surface, and its activity promotes infection. The use of neutralizing antibodies to E-NTPDase did not alter the activity of the enzyme, but significantly decreased parasite infectivity in macrophages. This would suggest that not only is its activity important in establishing an infection, but also its localization on the surface of the parasites might favor adhesion to phagocytes. In *T. cruzi* infection, other studies have shown that adhesion and internalization rate is reduced when the NTPDase activity is inhibited by suramin (21). It has also been observed by others that reduction in the adhesion of *L. infantum* to murine macrophages previously treated with recombinant rLicE-2-NTPDase (12).

In conclusion, these studies demonstrate the presence of ecto-nucleotidase activity in human isolates of *L. infantum*. The enzyme is expressed in the parasite, including in the cell membrane, and its nucleotidase activity is increased by purine starvation, which suggests an essential role in parasite survival. Moreover, the ecto-nucleotidase activity of *L. infantum* was shown to be directly associated with infectivity in human macrophages. Antibodies that do not block the enzyme activity resulted in reduced human macrophage infection, suggesting expressed protein is used for infection. In this context, these enzymes, originally known for involvement in the metabolism of nucleotides, are crucial for both parasite nutrition and host–parasite interactions governing infectivity. Taken together, pharmaceutical agents targeting enzyme inhibition could represent novel therapeutic approaches against Leishmaniasis and other trypanosomatides infections.

ETHICS STATEMENT

This project was approved by the Ethical Committee of the Federal University of Sergipe (CONEP), CAAE-0151.0.107.000-07.

AUTHOR CONTRIBUTIONS

NP and LC share first authorship. Both performed the majority of the experiments, analyzed datasets, and wrote the manuscript. MA, MS, and FO helped with the macrophage infection experiments. AJ helped to design the experiments and write the manuscript. RA was responsible for experimental design, data analyses, and manuscript revisions.

ACKNOWLEDGMENTS

The authors would like to thank the blood donor volunteers and the microscope facility at the Instituto Gonçalo Muniz, Fiocruz in Bahia, Brazil for assistance with the imaging studies. LC received a fellowship from CAPES Parasitology, Process no. 23038.005304/2011-01.

FUNDING

This work was supported by the Fundação de Apoio à Pesquisa e à Inovação Tecnológica do Estado de Sergipe—FAPITEC/SE/Conselho Nacional de Desenvolvimento Científico e Tecnológico—CNPq, EDITAL FAPITEC/SE/FUNTEC/CNPq (Programa de Núcleos de Excelência—PRONEX), Process no. 019.203.02712/2009-8; CAPES Parasitology, Process no. 23038.005304/2011-01. CNPq Process no. 552721/2011-5.

REFERENCES

1. Collin S, Davidson R, Ritmeijer K, Keus K, Melaku Y, Kipngetich S, et al. Conflict and kala-azar: determinants of adverse outcomes of kala-azar among patients in southern Sudan. *Clin Infect Dis* (2004) 38(5):612–9. doi:10.1086/381203
2. Desjeux P. Leishmaniasis: current situation and new perspectives. *Comp Immunol Microbiol Infect Dis* (2004) 27(5):305–18. doi:10.1016/j.cimid.2004.03.004
3. Werneck GL. Geographic spread of visceral leishmaniasis in Brazil. *Cad Saude Publica* (2010) 26(4):644–5. doi:10.1590/S0102-311X2010000400001
4. Figueiredo AB, Souza-Testasicca MC, Afonso LC. Purinergic signaling and infection by *Leishmania*: a new approach to evasion of the immune response. *Biomed J* (2016) 39(4):244–50. doi:10.1016/j.bj.2016.08.004
5. Di Virgilio F. Purinergic mechanism in the immune system: a signal of danger for dendritic cells. *Purinergic Signal* (2005) 1(3):205–9. doi:10.1007/s11302-005-6312-z
6. Di Virgilio F, Vuerich M. Purinergic signaling in the immune system. *Auton Neurosci* (2015) 191:117–23. doi:10.1016/j.autneu.2015.04.011
7. Burnstock G. Physiology and pathophysiology of purinergic neurotransmission. *Physiol Rev* (2007) 87(2):659–797. doi:10.1152/physrev.00043.2006
8. Yegutkin GG. Enzymes involved in metabolism of extracellular nucleotides and nucleosides: functional implications and measurement of activities. *Crit Rev Biochem Mol Biol* (2014) 49(6):473–97. doi:10.3109/10409238.2014.953627
9. Chaves MM, Canetti C, Coutinho-Silva R. Crosstalk between purinergic receptors and lipid mediators in leishmaniasis. *Parasit Vectors* (2016) 9(1):489. doi:10.1186/s13071-016-1781-1
10. Fietto JL, DeMarco R, Nascimento IP, Castro IM, Carvalho TM, de Souza W, et al. Characterization and immunolocalization of an NTP diphosphohydrolase of *Trypanosoma cruzi*. *Biochem Biophys Res Commun* (2004) 316(2):454–60. doi:10.1016/j.bbrc.2004.02.071
11. Maioli TU, Takane E, Arantes RM, Fietto JL, Afonso LC. Immune response induced by New World *Leishmania* species in C57BL/6 mice. *Parasitol Res* (2004) 94(3):207–12. doi:10.1007/s00436-004-1193-6
12. Vasconcellos Rde S, Mariotini-Moura C, Gomes RS, Serafim TD, Firmino Rde C, Silva EBM, et al. *Leishmania infantum* ecto-nucleoside triphosphate diphosphohydrolase-2 is an apyrase involved in macrophage infection

and expressed in infected dogs. *PLoS Negl Trop Dis* (2014) 8(11):e3309. doi:10.1371/journal.pntd.0003309
13. Freitas-Mesquita AL, Meyer-Fernandes JR. 3'nucleotidase/nuclease in protozoan parasites: molecular and biochemical properties and physiological roles. *Exp Parasitol* (2017) 179:1–6. doi:10.1016/j.exppara.2017.06.001
14. Silverman JA, Qi H, Riehl A, Beckers C, Nakaar V, Joiner KA. Induced activation of the *Toxoplasma gondii* nucleoside triphosphate hydrolase leads to depletion of host cell ATP levels and rapid exit of intracellular parasites from infected cells. *J Biol Chem* (1998) 273(20):12352–9. doi:10.1074/jbc.273.20.12352
15. Sansom FM, Newton HJ, Crikis S, Cianciotto NP, Cowan PJ, d'Apice AJ, et al. A bacterial ecto-triphosphate diphosphohydrolase similar to human CD39 is essential for intracellular multiplication of *Legionella pneumophila*. *Cell Microbiol* (2007) 9(8):1922–35. doi:10.1111/j.1462-5822.2007.00924.x
16. Sansom FM, Robson SC, Hartland EL. Possible effects of microbial ecto-nucleoside triphosphate diphosphohydrolases on host-pathogen interactions. *Microbiol Mol Biol Rev* (2008) 72(4):765–781, Table of Contents. doi:10.1128/MMBR.00013-08
17. Santos RF, Possa MA, Bastos MS, Guedes PM, Almeida MR, Demarco R, et al. Influence of ecto-nucleoside triphosphate diphosphohydrolase activity on *Trypanosoma cruzi* infectivity and virulence. *PLoS Negl Trop Dis* (2009) 3(3):e387. doi:10.1371/journal.pntd.0000387
18. Marques-da-Silva C, Chaves MM, Rodrigues JC, Corte-Real S, Coutinho-Silva R, Persechini PM. Differential modulation of ATP-induced P2X7-associated permeabilities to cations and anions of macrophages by infection with *Leishmania amazonensis*. *PLoS One* (2011) 6(9):e25356. doi:10.1371/journal.pone.0025356
19. Meyer-Fernandes JR, Dutra PM, Rodrigues CO, Saad-Nehme J, Lopes AH. Mg-dependent ecto-ATPase activity in *Leishmania tropica*. *Arch Biochem Biophys* (1997) 341(1):40–6. doi:10.1006/abbi.1997.9933
20. Berredo-Pinho M, Peres-Sampaio CE, Chrispim PP, Belmont-Firpo R, Lemos AP, Martiny A, et al. A Mg-dependent ecto-ATPase in *Leishmania amazonensis* and its possible role in adenosine acquisition and virulence. *Arch Biochem Biophys* (2001) 391(1):16–24. doi:10.1006/abbi.2001.2384
21. Bisaggio DF, Peres-Sampaio CE, Meyer-Fernandes JR, Souto-Padron T. Ecto-ATPase activity on the surface of *Trypanosoma cruzi* and its possible role in the parasite-host cell interaction. *Parasitol Res* (2003) 91(4):273–82. doi:10.1007/s00436-003-0965-8
22. de Souza MC, de Assis EA, Gomes RS, Marques da Silva Ede A, Melo MN, Fietto JL, et al. The influence of ecto-nucleotidases on *Leishmania amazonensis* infection and immune response in C57B/6 mice. *Acta Trop* (2010) 115(3):262–9. doi:10.1016/j.actatropica.2010.04.007
23. DeMarco R, Kowaltowski AT, Mortara RA, Verjovski-Almeida S. Molecular characterization and immunolocalization of *Schistosoma mansoni* ATP-diphosphohydrolase. *Biochem Biophys Res Commun* (2003) 307(4):831–8. doi:10.1016/S0006-291X(03)01268-3
24. Gomes RS, de Carvalho LC, de Souza Vasconcellos R, Fietto JL, Afonso LC. E-NTPDase (ecto-nucleoside triphosphate diphosphohydrolase) of *Leishmania amazonensis* inhibits macrophage activation. *Microbes Infect* (2015) 17(4):295–303. doi:10.1016/j.micinf.2014.12.009
25. Santos PL, Costa RV, Braz JM, Santos LF, Batista AC, Vasconcelos CR, et al. *Leishmania chagasi* naturally resistant to nitric oxide isolated from humans and dogs with visceral leishmaniasis in Brazil. *Nitric Oxide* (2012) 27(1):67–71. doi:10.1016/j.niox.2012.04.004
26. Ekman P, Jager O. Quantification of subnanomolar amounts of phosphate bound to seryl and threonyl residues in phosphoproteins using alkaline hydrolysis and malachite green. *Anal Biochem* (1993) 214(1):138–41. doi:10.1006/abio.1993.1468
27. Dutra PM, Dias FA, Santos MA, Rodrigues CO, Romeiro A, Attias M, et al. Secreted phosphatase activities in trypanosomatid parasites of plants modulated by platelet-activating factor. *Phytopathology* (2001) 91(4):408–14. doi:10.1094/PHYTO.2001.91.4.408
28. Di Virgilio F. Purinergic signalling in the immune system. A brief update. *Purinergic Signal* (2007) 3(1–2):1–3. doi:10.1007/s11302-006-9048-5
29. Di Virgilio F, Boeynaems JM, Robson SC. Extracellular nucleotides as negative modulators of immunity. *Curr Opin Pharmacol* (2009) 9(4):507–13. doi:10.1016/j.coph.2009.06.021
30. de Almeida Marques-da-Silva E, de Oliveira JC, Figueiredo AB, de Souza Lima Junior D, Carneiro CM, Rangel Fietto JL, et al. Extracellular nucleotide metabolism in *Leishmania*: influence of adenosine in the establishment of infection. *Microbes Infect* (2008) 10(8):850–7. doi:10.1016/j.micinf.2008.04.016
31. de Souza RF, Dos Santos YL, de Souza Vasconcellos R, Borges-Pereira L, Caldas IS, de Almeida MR, et al. Recombinant *Leishmania* (*Leishmania*) *infantum* ecto-nucleoside triphosphate diphosphohydrolase NTPDase-2 as a new antigen in canine visceral leishmaniasis diagnosis. *Acta Trop* (2013) 125(1):60–6. doi:10.1016/j.actatropica.2012.09.011
32. Coutinho-Silva R, Ojcius DM. Role of extracellular nucleotides in the immune response against intracellular bacteria and protozoan parasites. *Microbes Infect* (2012) 14(14):1271–7. doi:10.1016/j.micinf.2012.05.009
33. Gottlieb M. Enzyme regulation in a trypanosomatid: effect of purine starvation on levels of 3'-nucleotidase activity. *Science* (1985) 227(4682):72–4. doi:10.1126/science.2981117
34. Carter NS, Yates PA, Gessford SK, Galagan SR, Landfear SM, Ullman B. Adaptive responses to purine starvation in *Leishmania donovani*. *Mol Microbiol* (2010) 78(1):92–107. doi:10.1111/j.1365-2958.2010.07327.x
35. Martin JL, Yates PA, Soysa R, Alfaro JF, Yang F, Burnum-Johnson KE, et al. Metabolic reprogramming during purine stress in the protozoan pathogen *Leishmania donovani*. *PLoS Pathog* (2014) 10(2):e1003938. doi:10.1371/journal.ppat.1003938
36. Serafim TD, Figueiredo AB, Costa PA, Marques-da-Silva EA, Goncalves R, de Moura SA, et al. *Leishmania* metacyclogenesis is promoted in the absence of purines. *PLoS Negl Trop Dis* (2012) 6(9):e1833. doi:10.1371/journal.pntd.0001833
37. Zimmermann H. Two novel families of ectonucleotidases: molecular structures, catalytic properties and a search for function. *Trends Pharmacol Sci* (1999) 20(6):231–6. doi:10.1016/S0165-6147(99)01293-6
38. Schenkman S, Robbins ES, Nussenzweig V. Attachment of *Trypanosoma cruzi* to mammalian cells requires parasite energy, and invasion can be independent of the target cell cytoskeleton. *Infect Immun* (1991) 59(2):645–54.

Conflict of Interest Statement: The authors declare that the research was conducted in the absence of any commercial or financial relationships that could be construed as a potential conflict of interest.

Copyright © 2018 Peres, Cunha, Barbosa, Santos, Oliveira, Jesus and de Almeida. This is an open-access article distributed under the terms of the Creative Commons Attribution License (CC BY). The use, distribution or reproduction in other forums is permitted, provided the original author(s) or licensor are credited and that the original publication in this journal is cited, in accordance with accepted academic practice. No use, distribution or reproduction is permitted which does not comply with these terms.

frontiers in Immunology

ORIGINAL RESEARCH
published: 26 July 2017
doi: 10.3389/fimmu.2017.00883

Heme-Oxygenase-1 Expression Contributes to the Immunoregulation Induced by *Fasciola hepatica* and Promotes Infection

*Paula Carasi[1], Ernesto Rodríguez[1], Valeria da Costa[1], Sofía Frigerio[1], Natalie Brossard[1], Verónica Noya[1], Carlos Robello[2,3], Ignacio Anegón[4,5] and Teresa Freire[1]**

[1] Laboratorio de Inmunomodulación y Desarrollo de Vacunas, Facultad de Medicina, Departamento de Inmunobiología, Universidad de República, Montevideo, Uruguay, [2] Departamento de Bioquimica, Facultad de Medicina, Universidad de la República, Montevideo, Uruguay, [3] Unidad de Biología Molecular, Institut Pasteur de Montevideo, Montevideo, Uruguay, [4] Centre de Recherche en Transplantation et Immunologie UMR1064, INSERM, Université de Nantes, CHU Nantes, Nantes, France, [5] Institut de Transplantation Urologie Néphrologie (ITUN), CHU Nantes, Nantes, France

Fasciola hepatica, also known as the liver fluke, is a trematode that infects livestock and humans causing fasciolosis, a zoonotic disease of increasing importance due to its worldwide distribution and high economic losses. This parasite immunoregulates the host immune system by inducing a strong Th2 and regulatory T immune response by immunomodulating dendritic cell (DC) maturation and alternative activation of macrophages. In this paper, we show that *F. hepatica* infection in mice induces the upregulation of heme-oxygenase-1 (HO-1), the rate-limiting enzyme in the catabolism of free heme that regulates the host inflammatory response. We show and characterize two different populations of antigen presenting cells that express HO-1 during infection in the peritoneum of infected animals. Cells that expressed high levels of HO-1 expressed intermediate levels of F4/80 but high expression of CD11c, CD38, TGFβ, and IL-10 suggesting that they correspond to regulatory DCs. On the other hand, cells expressing intermediate levels of HO-1 expressed high levels of F4/80, CD68, Ly6C, and FIZZ-1, indicating that they might correspond to alternatively activated macrophages. Furthermore, the pharmacological induction of HO-1 with the synthetic metalloporphyrin CoPP promoted *F. hepatica* infection increasing the clinical signs associated with the disease. In contrast, treatment with the HO-1 inhibitor SnPP protected mice from parasite infection, indicating that HO-1 plays an essential role during *F. hepatica* infection. Finally, HO-1 expression during *F. hepatica* infection was associated with TGFβ and IL-10 levels in liver and peritoneum, suggesting that HO-1 controls the expression of these immunoregulatory cytokines during infection favoring parasite survival in the host. These results contribute to the elucidation of the immunoregulatory mechanisms induced by *F. hepatica* in the host and provide alternative checkpoints to control fasciolosis.

Keywords: helminth, heme-oxigenase-1, immune regulation, dendritic cell, macrophage

OPEN ACCESS

Edited by:
Luciana Balboa, Consejo Nacional de Investigaciones Científicas y Técnicas (CONICET), Argentina

Reviewed by:
Grace Mulcahy, University College Dublin, Ireland
Beatrix Schumak, University of Bonn, Germany

***Correspondence:**
Teresa Freire
tfreire@fmed.edu.uy

Specialty section:
This article was submitted to Microbial Immunology, a section of the journal Frontiers in Immunology

Received: *29 May 2017*
Accepted: *11 July 2017*
Published: *26 July 2017*

Citation:
Carasi P, Rodríguez E, da Costa V, Frigerio S, Brossard N, Noya V, Robello C, Anegón I and Freire T (2017) Heme-Oxygenase-1 Expression Contributes to the Immunoregulation Induced by Fasciola hepatica and Promotes Infection. Front. Immunol. 8:883. doi: 10.3389/fimmu.2017.00883

INTRODUCTION

Fasciolosis, a helminth infection caused by *Fasciola hepatica*, is of paramount importance due to its wide spectrum of definitive hosts (1) and its worldwide distribution (2) affecting both livestock and human health. World Health Organization (WHO) estimates that at least 2.4 million people are infected in more than 70 countries worldwide, with several million at

risk. Several studies have independently demonstrated that *F. hepatica*-derived molecules inhibit or decrease dendritic cell (DC) activation, which results in the induction of a tolerogenic phenotype (3–7). Furthermore, we have demonstrated that DCs from mice infected with *F. hepatica* have a semi-mature phenotype that is characterized by low MHC II and CD40 expression, high secretion of the immunoregulatory cytokine IL-10, and the ability to differentiate and expand IL-10-producing CD4 T cells (8). In addition, different groups have reported that *F. hepatica*-derived molecules also modulate macrophage activation, inducing the alternative activation of IL-10-producing macrophages (9, 10) and inhibiting the production of pro-inflammatory cytokines, such as IL-1β (11), IL-10 (12), Arg-1, PDL-1 (13), and PDL-2 (14, 15). Thus, it has been hypothesized that *F. hepatica* may modulate both macrophages and DC function and fate as a mean to control its pathogenesis and survival in the infected hosts.

Heme-oxygenase-1 (HO-1), the rate-limiting enzyme in the catabolism of free heme, is involved in many physiological and pathophysiological processes, by affording cytoprotection (16) and regulating the host inflammatory response. Indeed, HO-1 is a stress-responsive enzyme important for defense against oxidant-induced injury during inflammatory processes and is highly inducible by a variety of stimuli, such as LPS, cytokines, heat shock, heavy metals, oxidants, and its substrate heme. Several works confirm that HO-1 plays a role in different infectious diseases, and can have both beneficial and detrimental consequences for the host immunity against pathogens (17). For instance, HO-1 is able to promote *Plasmodium* liver infection (18), whereas it plays a favorable role in the host during cerebral malaria (19). On the other hand, HO-1 controls a variety of infections in mice, including *Mycobacterium avium* (20), *Listeria monocytogenes* (21), *Plasmodium falciparum* (22), *Salmonella typhimurium* (23), *Toxoplasma gondii* (24), and respiratory syncytial virus (25).

Expression of HO-1 in monocyte-derived DC inhibits LPS-induced maturation and reactive oxygen species production (26). In addition, HO-1^{+} DCs express the anti-inflammatory cytokine IL-10 resulting in the inhibition of alloreactive T-cell proliferation (26). Also, IL-10-producing anti-inflammatory macrophages (M2) express HO-1 (27). Thus, HO-1 has been proposed to be key mediator of the anti-inflammatory effects of macrophages and DCs.

In the present study, we demonstrate that during infection with the trematode *F. hepatica*, HO-1 is upregulated by immune cells expressing F4/80 in the peritoneal cavity and liver. We also show that the pharmacological induction of HO-1 with the synthetic metalloporphyrin CoPP promotes *F. hepatica* infection increasing the clinical signs associated with the disease, such as liver damage. Moreover, treatment with the HO-1 inhibitor SnPP protected from parasite infection. The increase of HO-1 during *F. hepatica* infection was associated with the increase of TGFβ and IL-10 in liver and peritoneal exudate cells (PECs). Interestingly, we identified two different F4/80^{+} cell populations that expressed HO-1. HO-1^{hi} F4/80^{int} cells were characterized by the expression of CD11c, CD38, TGFβ, and IL-10 suggesting that they correspond to regulatory DCs. On the other hand, HO-1^{int} F4/80^{hi} cells expressed high levels of CD68, Ly6C, and FIZZ-1 indicating that they might be alternatively activated macrophages. Our results contribute to the elucidation of immunoregulatory mechanisms induced by *F. hepatica* in the host and could provide alternative checkpoints to control fasciolosis.

MATERIALS AND METHODS

Ethics Statement

Mouse experiments were carried out in accordance with strict guidelines from the National Committee on Animal Research (Comisión Nacional de Experimentación Animal, CNEA, National Law 18.611, Uruguay) according to the international statements on animal use in biomedical research from the Pan American Health Organization and WHO. The protocol was approved by the Uruguayan Committee on Animal Research. Cattle's livers were collected during the routine work of a local abattoir (Frigorífico Carrasco) in Montevideo (Uruguay).

Mice

Six- to eight-week-old female BALB/c mice were obtained from DILAVE Laboratories (Uruguay). Animals were kept in the animal house (URBE, Facultad de Medicina, UdelaR, Uruguay) with water and food supplied *ad libitum*. Mouse handling and experiments were carried out in accordance with strict guidelines from the National Committee on Animal Research (CNEA, Uruguay). All procedures involving animals were approved by the Universidad de la República's Committee on Animal Research (CHEA Protocol Number: 070153-000180-16).

Infections and Cell Cultures

BALB/c mice were orally infected with 10 *F. hepatica* metacercariae (Baldwin Aquatics, USA) per animal. After 1, 2, or 3 weeks post-infection (wpi) mice were bled and PECs, spleens, and livers were removed. In order to evaluate the severity of the infection, a disease severity score was developed (**Table 1**), which was applied in blinded experiments by two independent experimenters. Alanine aminotransferase (ALT) activity in sera was determined by using a commercial kit (Spinreact, Spain) according to the manufacturers' instructions. PECs from infected and non-infected mice were washed twice with PBS containing 2% FBS and 0.1% sodium azide. The following antibodies were used in these experiments anti-CD11c (N418), -I-A/I-E (2G9), CD40 (HM40-3), -F4/80 (BM8), -CD11b (M1/70), -CD172a (P84), -Ly6C (HK1.4), and -Siglec-F (E50-2440). Cells were then washed twice with PBS containing 2% FBS and 0.1% sodium azide and fixed with 1% formaldehyde. Cell populations were analyzed using a BD FACSCalibur (BD-Biosciences) or Cyan (Beckman Coulter). Expression of HO-1 (ab13248) and CD68 (FA-11) were analyzed by intracellular staining. Antibodies were obtained from Affymetrix (CA, USA), from BD-Biosciences (CA, USA), from Biolegend (CA, USA) or from Abcam.

TABLE 1 | Clinical score of *Fasciola hepatica*-infected mice.

Ascites		Spleen		Number of lesions/hepatic lobe		Liver lobes	
Score	Description	Score	Size	Score	Description	Score	Description
0	None (normal cell content)	0	Normal	0	None	0	Healthy
1	Mild (medium cell content)	1	Splenomegaly (<2×)	1	<3 lesions	1	1hepatic lobe affected
2	Moderate (high cell content)	2	Splenomegaly (>2×)	2	>3 lesions	2	>2 hepatic lobes affected
3	Severe (high cell and blood content)			3	Complete affection of lobes		

Maximal score is 10.

Pharmacological Induction or Inhibition of HO-1

In order to modulate HO-1 activity, mice infected with five metacercariae also received intraperitoneal injections of either vehicle (PBS, 100 μL), CoPP (20 mg/kg), SnPP (40 mg/kg), or CoPP plus SnPP. The doses of CoPP and SnPP were within a range of doses used in studies describing upregulation of HO-1 by CoPP and inhibition of the enzyme's activity by SnPP (28, 29). Mice were injected 1 day before infection, 1 day after infection and every 5 days until the end of the experimental protocol.

Quantitative Real-time RT-PCR

Total RNA was isolated by use of TRI-reagent (Sigma-Aldrich) from spleen, liver, PEC and purified F4/80^{int} and F4/80^{hi} cells from PEC. Samples were analyzed in an Eco real-time PCR System (Illumina) using Fast SYBR® Green Master Mix (Applied Biosystems). The reactions were performed according to the following settings: 95°C for 5 min for initial activation, followed by 40 thermal cycles of 10 s at 95°C and 30 s at 60°C. All reactions were performed with at least five biological replicates.

Microscopy Analyses

Livers from infected mice after 3 wpi or non-infected mice (control) were harvested, embedded in OCT, and snap frozen in nitrogen. Sections were cut at a thickness of 6 μm, fixed with cold acetone for 10 min and blocked with 5% BSA in 3% rat serum for 1 h at room temperature. Sections were then overnight incubated at 4°C with anti-HO-1 (ab13248) and -F4/80 (BM8), stained with DAPI and visualized in an epifluorencense microscope Olympus IX-81 and confocal microscope Leica TCS-SP5-II. The same procedure and the same antibody were used to evaluate HO-1 expression in bovine livers from naturally infected and non-infected cattle. In this case, livers were first examined by the veterinary inspector at the abattoir and determined to be infected by the presence of multiple parasites found in the bile ducts. Livers from non-infected animals were identified by absence of liver damage and flukes.

Statistical Analysis

Results were analyzed using GraphPad Prism software (GraphPad Software, San Diego, CA, USA). Normality distribution was evaluated using the D'Agostino-Pearson omnibus normality test followed by one-way ANOVA with Bonferroni Multiple Comparison test or a student's T test was used. Results were considered to be significantly different when $p < 0.05$ (*), 0.01 (**), or 0.001 (***).

RESULTS

HO-1 Expression Is Induced in *F. hepatica*-Infected Animals

We first evaluated whether HO-1 was expressed in *F. hepatica*-infected animals. To this end, mice were infected with 10 metacercariae and after 3 wpi, livers, spleens, and PECs were removed and HO-1 expression was analyzed by qRT-PCR, microscopy, and flow cytometry. Livers from infected mice expressed high levels of HO-1, both at the mRNA (**Figure 1A**) and protein levels (**Figure 1B**). Indeed, a 25-fold increase in the transcript levels was determined by qRT-PCR with respect to non-infected animals (**Figure 1A**). HO-1 expression was found both in the leukocyte infiltrates and the liver parenchyma (**Figure 1B**), while undetectable levels of HO-1 were found in control livers from naive mice (**Figure 1B**). HO-1 gene expression was also induced in PECs, revealing, similar to liver, a 25-fold increased in PECs from infected animals, comparing to control mice (**Figure 1C**). Moreover, HO-1$^+$ cells were detected in the peritoneum both by flow cytometry and microscopy (**Figures 1D–F**). On the contrary, we failed to detect an increase in HO-1 transcript levels and protein expression by flow cytometry in spleens from infected- with respect to control animals (Figure S1 in Supplementary Material).

The gene expression of HO-1 was also investigated in bovine livers (**Figure 2**) revealing an increase of HO-1 mRNA levels in livers from infected bovine with respect to non-infected animals (**Figure 2A**). This increase in HO-1 gene expression was confirmed at the protein level by microscopy (**Figure 2B**). HO-1 was expressed both in the hepatocytes (larger cells) and the infiltrated leukocytes (smaller cells) in livers from infected mice (**Figure 2B**). Altogether, these results indicate that HO-1 expression increases both in liver and PEC, but not in spleen, of *F. hepatica*-infected animals.

The Pharmacological Inhibition or Induction of HO-1 Affects Clinical Signs Associated to *F. hepatica* Infection

The use of pharmacological agents and genetic probes to manipulate HO-1 has been widely used as a tool to explore the role of HO-1 in infections and other pathological systems, as well as its

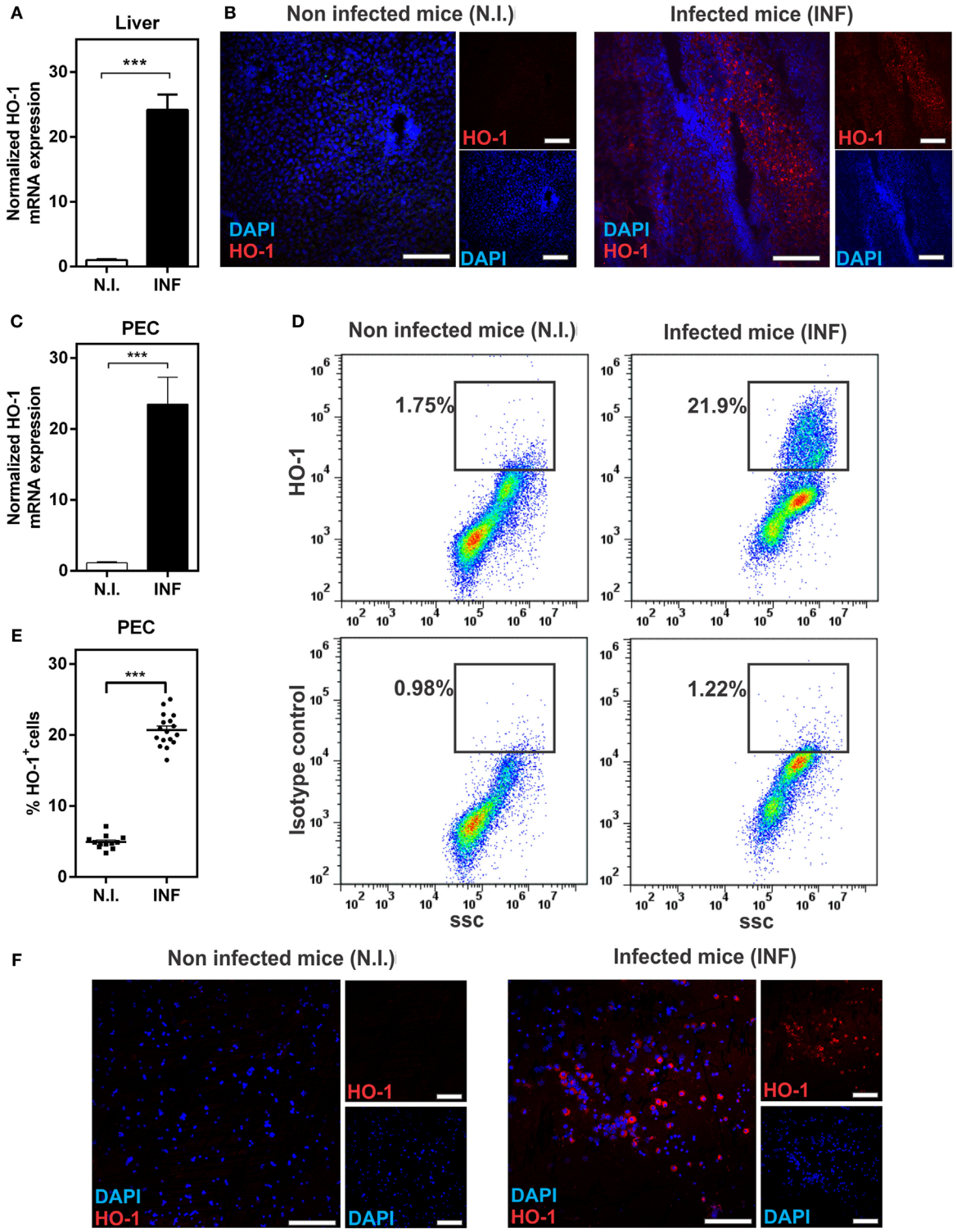


FIGURE 1 | Heme-oxygenase-1 (HO-1) is induced during *Fasciola hepatica* experimental infection in mice. **(A)** mRNA expression of HO-1 in the liver from control and *F. hepatica*-infected mice at 3 wpi. **(B)** HO-1 expression in the liver from control and infected mice at 3 wpi by confocal microscopy. **(C)** mRNA expression of HO-1 in peritoneal exudate cell (PECs) from control and infected mice at 3 wpi. **(D)** HO-1$^+$ cells in PECs from control and infected mice at 3 wpi by flow cytometry. **(E)** Percentage of HO-1$^+$ cells in PECs from control and infected mice at 3 wpi by flow cytometry. **(F)** HO-1 expression in PECs from control and infected mice at 3 wpi by confocal microscopy. **(F)** mRNA expression of HO-1 in the spleen from control and *F. hepatica*-infected mice at 3 wpi. The figures represent the results of three independent experiments (±SEM, indicated by error bars). Mice were analyzed individually: control mice $n = 12$ and infected mice $n = 17$. Asterisks indicate statistically significant differences (***$p < 0.001$). The bar represents 100 μm.

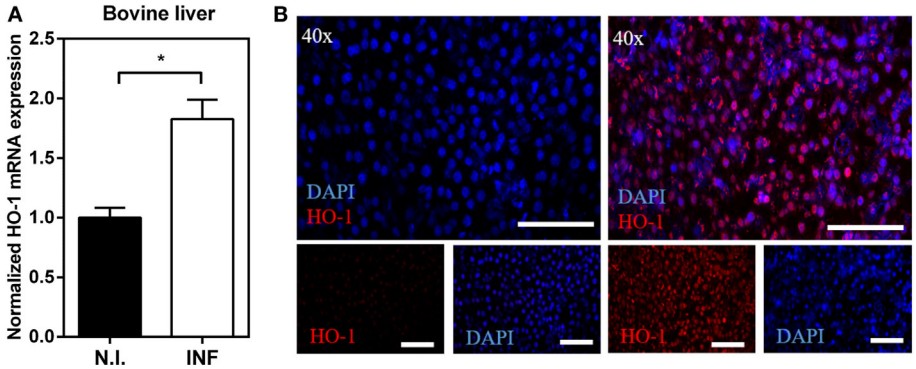


FIGURE 2 | Upregulation of heme-oxygenase-1 (HO-1) expression in liver from *Fasciola hepatica*-infected bovines. **(A)** mRNA expression of HO-1 in the liver from *F. hepatica*-infected ($n = 7$) and control ($n = 5$) animals. **(B)** HO-1 expression in the liver from infected and control animals by confocal microscopy. Asterisks indicate statistically significant differences (*$p < 0.05$). The bar represents 100 μm.

immune regulatory properties. Thus, we investigated whether the pharmacological induction or inhibition of HO-1, using cobalt (CoPP) and tin (SnPP) protoporphyrin IX, respectively, increased or ameliorated the clinical signs associated with by *F. hepatica* infection. The treatment consisted of five i.p. administrations of CoPP or SnPP at days −2, 2, 5, 12, and 17, with infection at day 0 (**Figure 3A**). Importantly, CoPP administration lead to a significant increase of HO-1 transcript levels, while SnPP administration did not change the HO-1 gene expression (Figures S2A,B in Supplementary Material) Clinical signs were determined by two different read outs: (i) hepatic damage followed by ALT activity in serum, a common marker to detect hepatic dysfunction (30), and (ii) general state of the animal by a defined clinical score (**Figure 3**). The clinical score was defined according the parameters described in **Table 1**. First, we evaluated the HO-1 transcript levels in livers and PECs from treated mice at 2 wpi, time were the highest differences in HO-1 expression were determined. Infected mice expressed high transcript levels of HO-1, both in liver (**Figure 3B**) and PEC (**Figure 3C**). Furthermore, when infected mice were treated with CoPP, they presented higher HO-1 transcript levels than infected mice in both biological samples, while SnPP-treatment dramatically reduced the gene expression of HO-1 in infected mice, both in liver (**Figure 3B**) and PEC (**Figure 3C**). Of note, when infected mice were treated with simultaneous administration of CoPP and SnPP, the HO-1 transcript levels both in PEC and liver were similar to those found for infected control mice (**Figures 3B,C**).

Importantly, the expression of HO-1 correlated with the ALT activity levels found in sera. Indeed, CoPP-treated infected mice presented higher ALT activity levels in serum at 2 and 3 wpi (**Figure 3D**). On the contrary, SnPP-treated infected mice, had a remarkable decrease in ALT activity levels at 3 wpi with levels comparable to those of non-infected mice, although they were slightly increased (**Figure 3D**). The hepatic damage determined as ALT activity in serum found in CoPP-treated infected mice correlated with other clinical signs, such as hemorrhage, splenomegaly and increase in ascites and cells in the peritoneum (**Figure 3E**). In contrast, SnPP-treated infected mice, presented a decreased clinical score as compared to controls. Importantly, control infected mice treated with a mix of SnPP and CoPP, presented the same clinical score as infected mice not treated with protoporfirins (**Figure 3E**). Importantly, non-infected mice treated with CoPP did not show either liver damage, changes in ALT activity in sera nor any clinical symptom related to the infection with respect to non-treated mice (Figure S2C,D in Supplementary Material). These results suggest that an increase of HO-1 expression augments the susceptibility of *F. hepatica* infection, while a decrease in this enzyme provides mice resistance to the infection.

It has been reported that HO-1 regulates the expression of multiple cytokines, and has essentially anti-inflammatory properties (26, 31–34). In order to further study the immune response induced in the group of mice treated with protoporphyrins, we evaluated the transcript levels of a panel of Th2/regulatory molecules that are highly expressed during *F hepatica* infection: FIZZ-1, IL-4, IL-10, and TGFβ. Indeed, at 2 wpi, livers from infected mice expressed high transcript levels of IL-10, TGFβ and FIZZ-1 (**Figure 4A**). Interestingly, IL-10 and TGFβ transcript levels were even higher in CoPP-treated infected mice, than control infected mice (**Figure 4B**). Moreover, SnPP-treated infected mice presented lower mRNA levels of IL-10 and FIZZ-1 than infected control mice (**Figure 4B**). Consistent with these results, simultaneous treatment with CoPP and SnPP did not induce any change in the mRNA levels of these molecules with respect to control infected mice (**Figure 4B**). Of note, IL-4 gene expression in liver was not modified either with *F. hepatica* infection nor the treatment with metal protoporphyrins.

Cells from the peritoneum of infected mice, on the other hand, expressed higher transcript levels of TGFβ, IL-4 and FIZZ-1 (**Figure 5A**), but not IL-10 as shown in liver. Surprisingly, PEC from CoPP- or SnPP-treated mice did not present any change in the expression of either TGFβ, IL-4, FIZZ-1 or IL-10, except for FIZZ-1 which was slightly decreased in SnPP-treated infected mice (**Figure 5B**), consistent with lower hepatic damage and clinical score.

In summary, these results show that the induction of HO-1 is associated with higher levels of the immunoregulatory molecules IL-10 and TGFβ and the reparatory molecule FIZZ-1 in liver, while the inhibition of HO-1correlated with lower

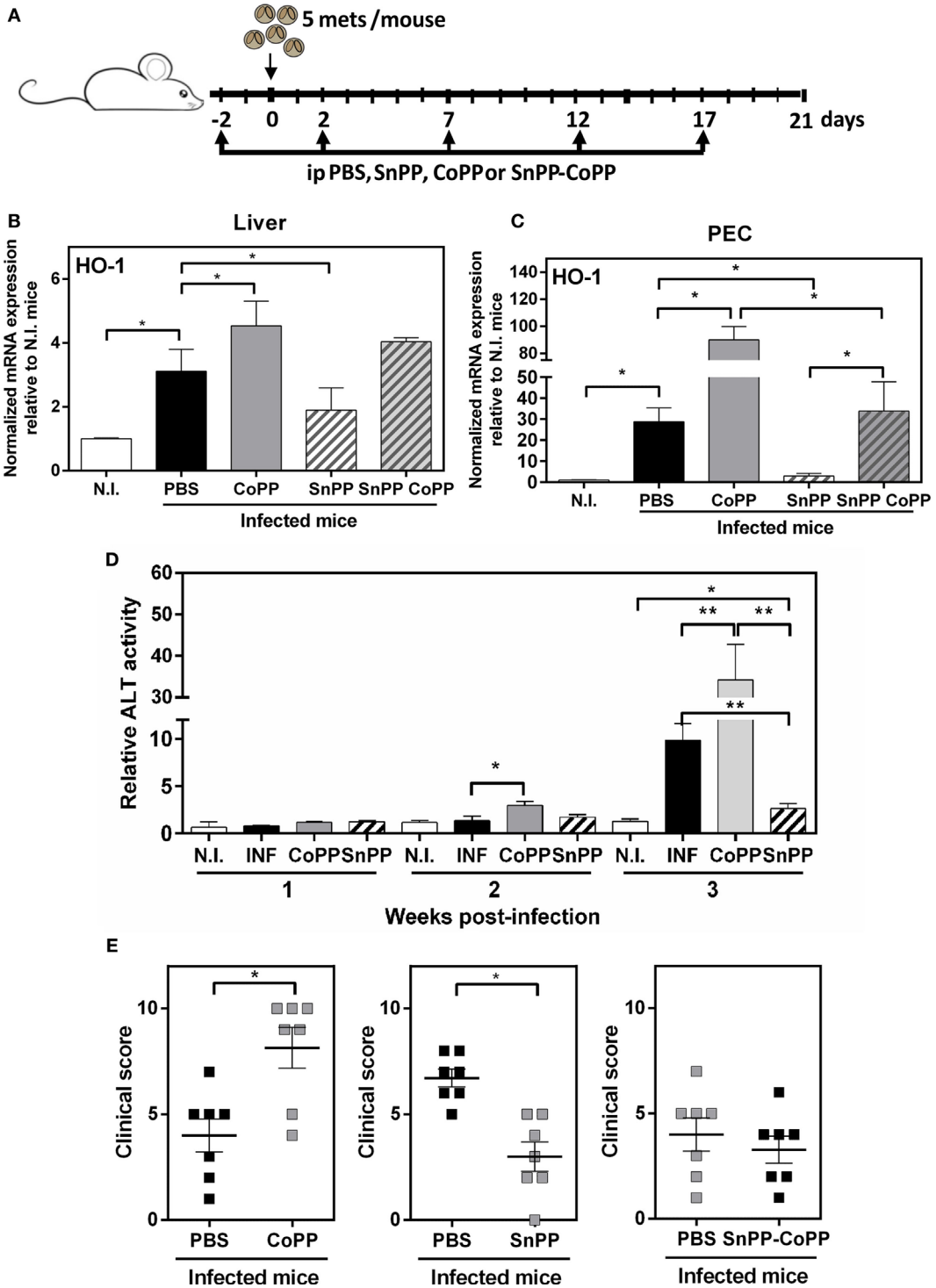


FIGURE 3 | Pharmacological induction and inhibition of heme-oxygenase-1 (HO-1) alters the clinical signs associated with *Fasciola hepatica* infection. **(A)** Treatment of infected mice with CoPP, SnPP, SnPP/CoPP, or PBS (control). **(B)** mRNA expression of HO-1 in liver from CoPP-, SnPP-, and SnPP/CoPP-treated *F. hepatica*-infected mice at 3 wpi. **(C)** mRNA expression of HO-1 in peritoneal exudate cells (PECs) from CoPP-, SnPP-, and SnPP/CoPP-treated *F. hepatica*-infected mice at 3 wpi. **(D)** Alanine aminotransferase (ALT) activity was measured in sera from CoPP- and SnPP-treated infected and control mice. **(E)** Clinical score of CoPP- and SnPP-treated *F. hepatica*-infected mice at 3 wpi, according to **Table 1**. The figures represent the results of three independent experiments (±SEM, indicated by error bars). Mice were analyzed individually: CoPP ($n = 7$), SnPP ($n = 7$), SnPP/CoPP ($n = 7$), or PBS ($n = 7$). Asterisks indicate statistically significant differences (*$p < 0.05$, **$p < 0.01$).

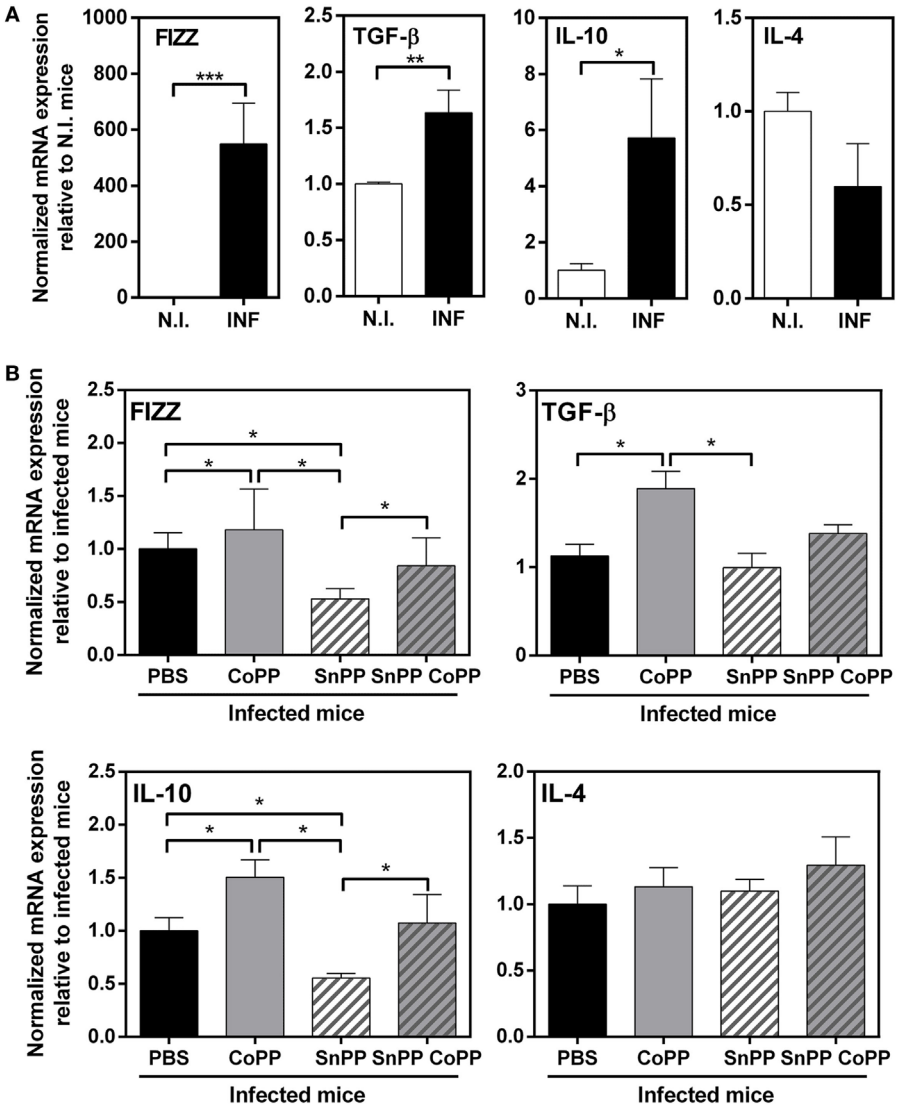


FIGURE 4 | Pharmacological induction of heme-oxygenase-1 expression correlates with IL-10, TGFβ, and FIZZ-1 transcript levels in liver of infected animals. **(A)** mRNA expression of IL-4, IL-10, TGFβ, and FIZZ-1 in the liver from control and *F. hepatica*-infected mice at 2 wpi. **(B)** mRNA expression of IL-4, IL-10, TGFβ, and FIZZ-1 in the liver from CoPP-, SnPP- and SnPP/CoPP-treated *F. hepatica*-infected mice at 2 wpi. The figures represent the results of three independent experiments (±SEM, indicated by error bars). Mice were analyzed individually: CoPP ($n = 7$), SnPP ($n = 7$), SnPP/CoPP ($n = 7$), or PBS ($n = 7$). Asterisks indicate statistically significant differences (*$p < 0.05$, **$p < 0.01$, ***$p < 0.001$).

expression of TGFβ and FIZZ-1 in the liver of infected animals. However, although infected animals presented increased levels of TGFβ, IL-4 and FIZZ-1 on peritoneal cells, we could not find significant changes associated with the modulation of HO-1. Considering that the peritoneum is essential for *F. hepatica* juvenile maturation, we studied in further detail peritoneal cells and the expression of HO-1.

HO-1 Is Induced in Two Different Peritoneal F4/80$^+$ Cell Populations

Considering previous reports demonstrating that: (i) *F. hepatica*-infected mice express high levels of IL-10 (8, 35), (ii) HO-1 expression is related to IL-10 signaling and viceversa (36, 37), (iii) alternatively activated macrophages are associated with *F. hepatica* infection (9, 38, 39), and (iv) HO-1 is highly expressed by M2 macrophages (40), we sought to evaluate whether the HO-1$^+$ cells identified in *F. hepatica*-infected mice expressed the molecule F4/80, traditionally used to identify macrophages. As seen in **Figure 6A**, HO-1$^+$ cells from PECs from infected animals expressed this surface marker. However, two HO-1$^+$ populations were identified according to the expression of HO-1 and F4/80: HO-1^{int} F4/80^{hi} and HO-1^{hi} F4/80^{int}, which significantly augmented upon infection (**Figure 6A**). Interestingly, although the F4/80^{hi} cell population was also detected in PECs from control mice (**Figure 6A**), the expression of HO-1 was induced upon infection (**Figure 6B**). On the contrary, the HO-1^{hi} F4/80^{int} cell

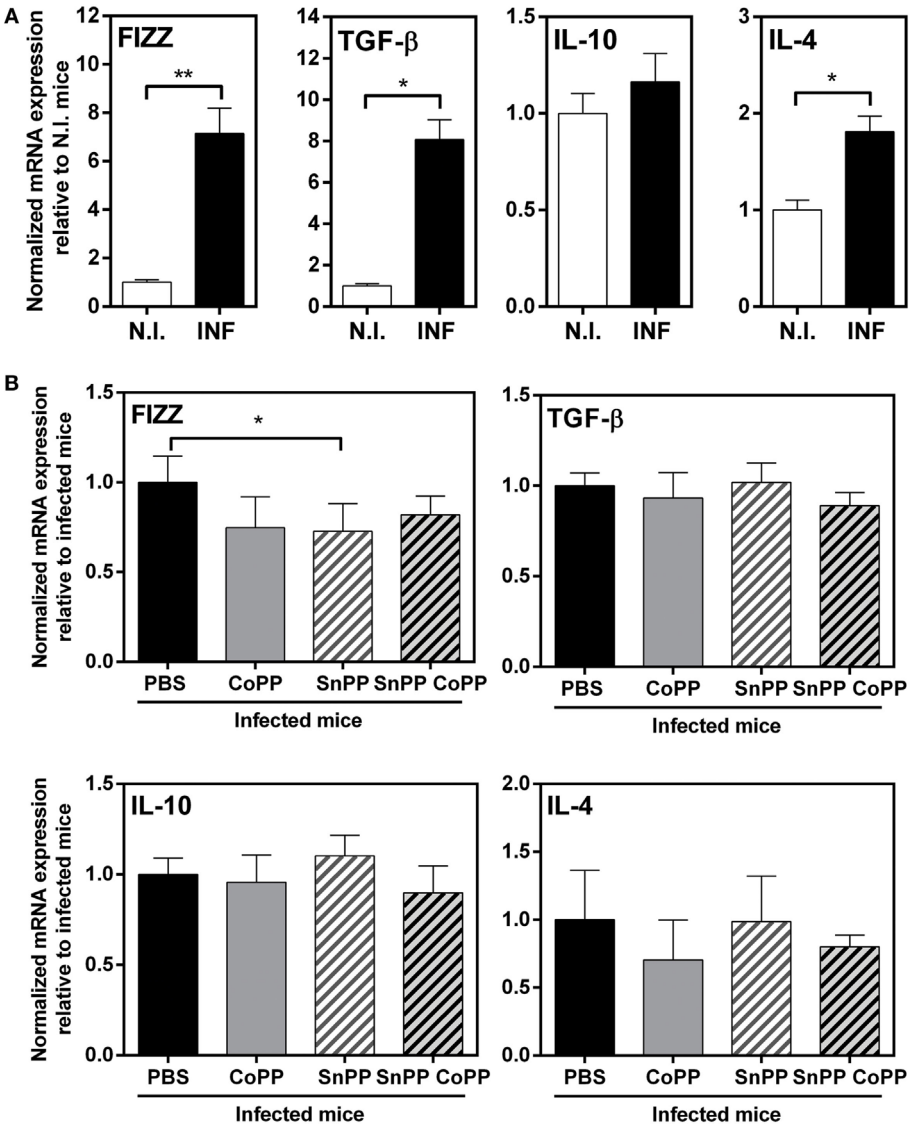


FIGURE 5 | IL-4, IL-10, TGFβ, and FIZZ-1 mRNA levels in peritoneal exudate cells (PECs) from CoPP-, SnPP-, and SnPP/CoPP-infected animals. **(A)** mRNA expression of IL-4, IL-10, TGFβ, and FIZZ-1 in PEC from control and *Fasciola hepatica*-infected mice at 2 wpi. **(B)** mRNA expression of IL-4, IL-10, TGFβ, and FIZZ-1 in PEC from CoPP-, SnPP- and SnPP/CoPP-treated *F. hepatica*-infected mice at 2 wpi. The figures represent the results of three independent experiments (±SEM, indicated by error bars). Mice were analyzed individually: CoPP ($n = 7$), SnPP ($n = 7$), SnPP/CoPP ($n = 7$), or PBS ($n = 7$). Asterisks indicate statistically significant differences (*$p < 0.05$, **$p < 0.01$).

population was absent in control mice (**Figure 6A**) and expressed higher HO-1 levels than HO-1^{int} F4/80^{hi} cells from infected mice (**Figure 6B**). Of note, the F4/80^{low} population identified in infected mice were Siglec-F$^+$ (could correspond to eosinophils) and did not express HO-1 as determined by the corresponding isotype staining (Figure S3 in Supplementary Material).

The presence of F4/80$^+$ cells in PECs expressing different levels of this surface marker was also confirmed by microscopy, revealing co-localization with HO-1 (**Figure 7A**). Furthermore, F4/80$^+$ HO-1$^+$ cells were also identified in the leukocyte infiltrate present in livers from infected mice (**Figure 7B**), while these cells were undetected in control livers (data not shown). HO-1 was also expressed by F4/80$^-$ hepatocytes (**Figure 7B**) as mentioned earlier (**Figure 1B**).

HO-1^{int} F4/80^{hi} and HO-1^{hi} F4/80^{int} Cells from Infected Mice Have Different Phenotype

In order to further characterize HO-1$^+$ cells, we evaluated both populations and HO-1 expression during the process of infection. To this end, PECs and livers were collected at 1, 2, and 3 wpi. Interestingly HO-1 transcript levels augmented progressively with the course of infection (**Figure 8A**). PECs from infected and control mice were labeled and analyzed by

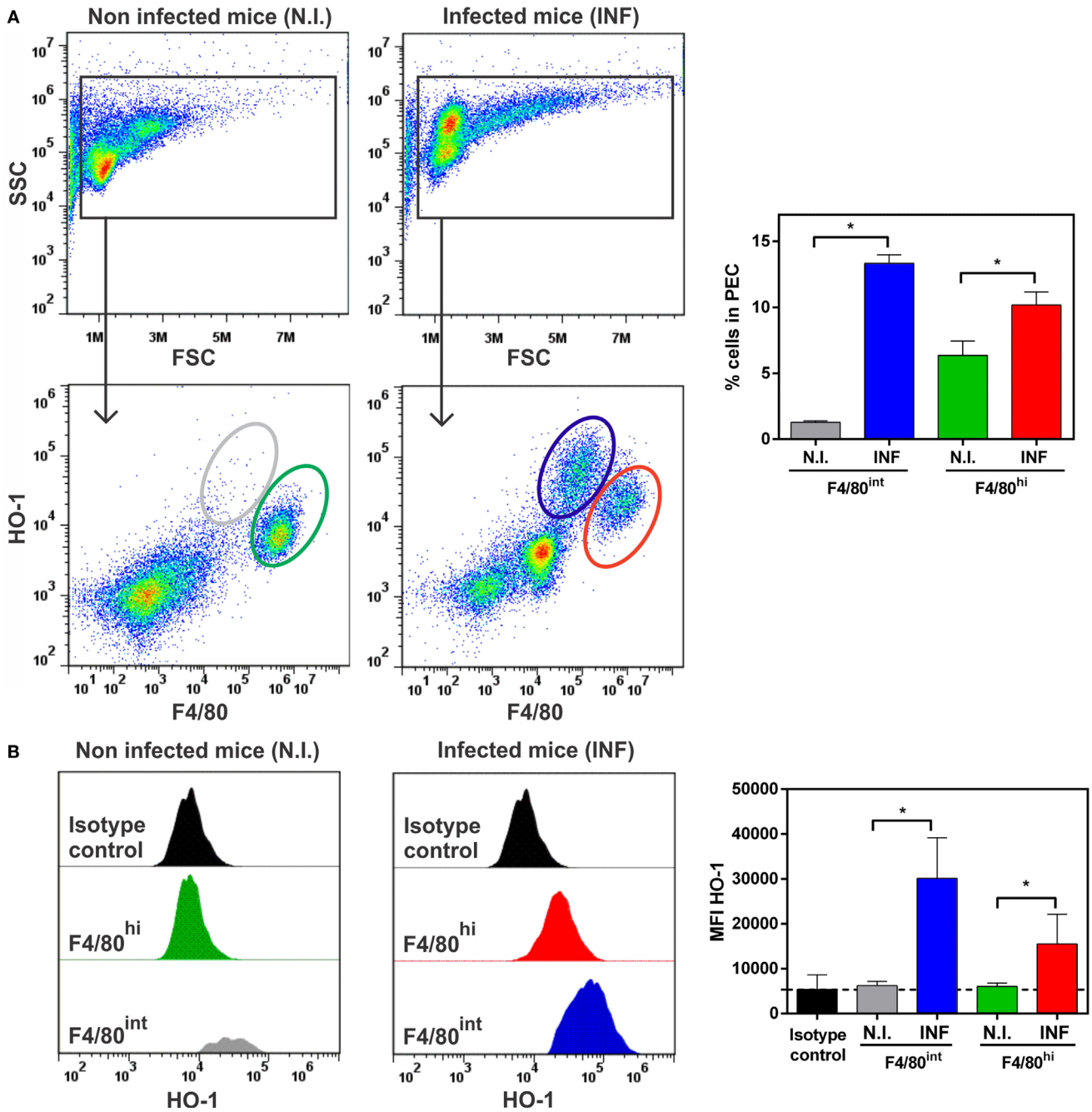


FIGURE 6 | HO-1$^+$ cells recruited in peritoneal exudate cell (PEC) during *Fasciola hepatica* infection are F4/80$^+$. **(A)** HO-1$^+$ and F4/80$^+$ cells in PEC from control and infected mice at 3 wpi by flow cytometry. Percentage of HO-1^{hi} F4/80^{int} and HO-1^{low} F4/80^{hi} cells in the peritoneum from control and infected mice at 3 wpi. **(B)** heme-oxygenase-1 (HO-1) expression in different cell populations from PEC from control and infected mice at 3 wpi. MFI (Mean Fluorescence Intensity) of HO-1 in HO-1^{hi} F4/80^{int} and HO-1^{low} F4/80^{hi} cells from PECs by flow cytometry. The figures represent the results from at least three independent experiments (±SEM, indicated by error bars). Mice were analyzed individually: CoPP (n = 7), SnPP (n = 7), SnPP/CoPP (n = 7), or PBS (n = 7). Asterisks indicate statistically significant differences (*p < 0.05).

flow cytometry in order to identify both HO-1$^+$ cell populations, HO-1^{hi} F4/80^{int} and HO-1^{int} F4/80^{hi}, and compare them with PECs from control mice. HO-1^{int} F4/80^{hi} cells were already present in control mice and its number doubled from the second week post infection (**Figure 8B**), time in which they presented increased levels of HO-1 expression (**Figure 8B**). On the other hand, HO-1^{hi} F4/80^{int} cells in PECs were detected as soon as 1 wpi, and remained constant up to 3 wpi (**Figure 8C**). The expression of HO-1 by these cells was induced from 2 wpi (**Figure 8C**). Both the cell number and the HO-1 expression

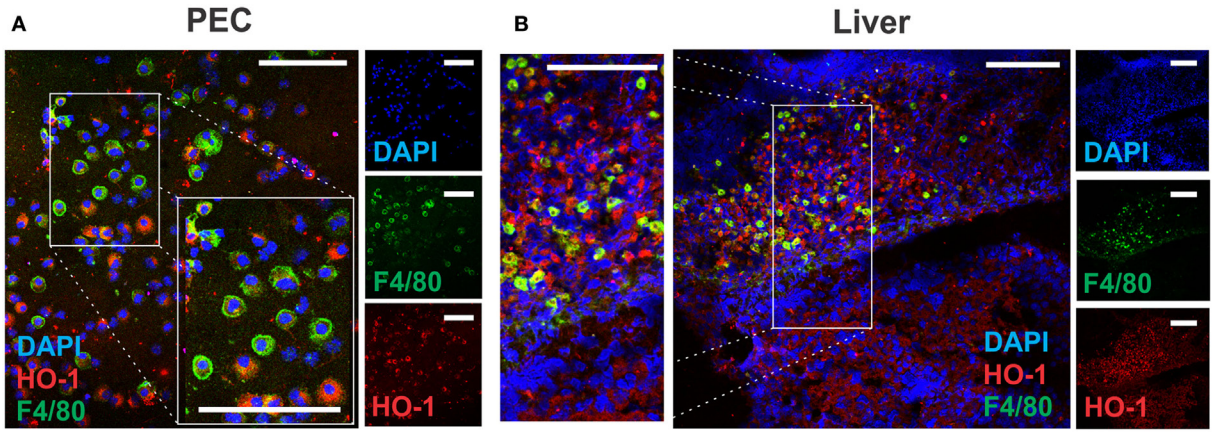


FIGURE 7 | Identification of HO-1$^+$ cells in peritoneal exudate cell (PEC) and liver by confocal microscopy. Heme-oxygenase-1 (HO-1) and F4/80 expression in PEC **(A)** and liver **(B)** from control (n = 5) and infected mice (n = 5) at 3 wpi by confocal microscopy. DAPI was used to stain cell nucleus. The bar represents 100 μm. The figures represent the results from at least three independent experiments.

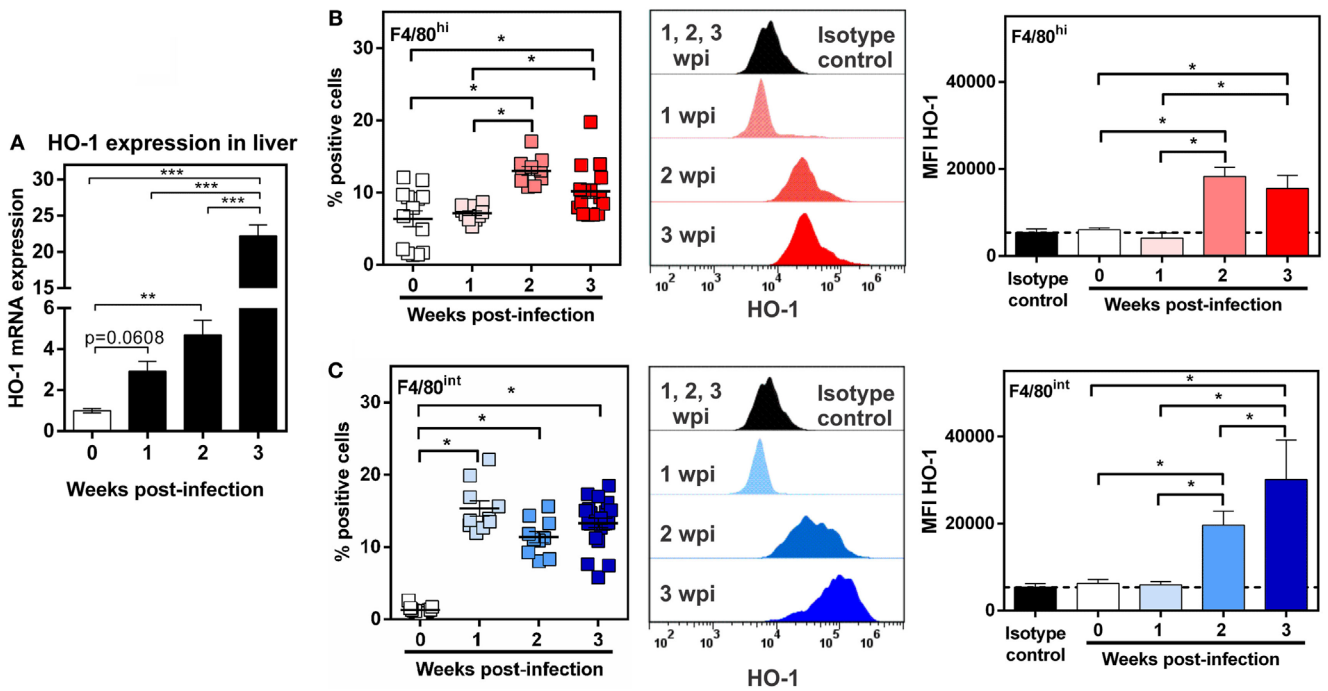


FIGURE 8 | Identification of HO-1$^+$ cells during *Fasciola hepatica*-infection. **(A)** mRNA expression of heme-oxygenase-1 (HO-1) in the liver from control (0 wpi) and infected mice (1, 2, and 3 wpi). **(B)** HO-1$^+$ F4/80^{hi} cells in peritoneal exudate cell (PEC) from control (0 wpi) and infected mice (1, 2, and 3 wpi) by flow cytometry. On the right the HO-1 expression as the MFI of HO-1$^+$ F4/80^{hi} cells is shown. **(C)** HO-1$^+$ F4/80^{int} cells in PEC from control (0 wpi) and infected mice (1, 2, and 3 wpi) by flow cytometry. On the right, the HO-1 expression as the MFI of HO-1$^+$ F4/80^{int} cells is shown. Mice were analyzed individually: control (n = 12), 1 wpi (n = 10), 2 wpi (n = 10) or 3 wpi (n = 16). Asterisks indicate statistically significant differences (*$p < 0.05$, **$p < 0.01$, ***$p < 0.001$).

by HO-1^{int} F4/80^{hi} cells remained constant or increased after 2 wpi (**Figure 8C**).

We then investigated the phenotype of HO-1$^+$ cells by evaluating the expression of different molecules by flow cytometry and compared them to F4/80$^+$ cells found in naïve mice (**Figure 9**; Figure S4 in Supplementary Material). HO-1^{int} F4/80^{hi} and HO-1^{hi} F4/80^{int} cells expressed CD11b, CD68 and CD172a (SIRPα, **Figure 9**), all molecules that are expressed by DCs or macrophages (41). However, HO-1^{int} F4/80^{hi} cells expressed higher levels of CD11b, CD68 and CD172a than HO-1^{hi} F4/80^{int} cells. Furthermore, HO-1^{hi} F4/80^{int} cells expressed CD11c while HO-1^{int} F4/80^{hi} expressed Ly6C (**Figure 9**). Finally, HO-1^{hi} F4/80^{int} cells expressed higher levels of MHC class II but lower expression of CD40 than HO-1^{int} F4/80^{hi} cells. Of note, both cells populations

expressed very low levels of Siglec-F (**Figure 9**). Interestingly, the phenotype described for HO-1^{int} F4/80^{hi} cells resembled to that of peritoneal macrophages from naïve mice (Figure S4 in Supplementary Material). Altogether, these results suggest that HO-1^{hi} F4/80^{int} cells could constitute DCs while HO-1^{int} F4/80^{hi} cells would correspond to monocytes or macrophages.

To further characterize these cells, we sorted them by flow cytometry and analyzed the gene expression of other molecules by qRT-PCR. In agreement with flow cytometry analyses, HO-1^{hi} F4/80^{int} cells expressed higher transcript levels of HO-1 than HO-1^{int} F4/80^{hi} cells (**Figure 10**). Interestingly, both cells populations were very different in the set of expressed genes. Indeed, HO-1^{hi} F4/80^{int} cells expressed CD38 and Arg-1, while HO-1^{int} F4/80^{hi} cells did not. On the contrary, HO-1^{int} F4/80^{hi} cells expressed FIZZ-1 and IL-10. Finally, HO-1^{hi} F4/80^{int} cells expressed TGFβ and IL-10 (**Figure 10**). According to the expression of these markers, these results suggest that HO-1^{hi} F4/80^{int} cells correspond to regulatory or tolerogenic DCs, while HO-1^{int} F4/80^{hi} cells could constitute alternatively activated macrophages.

DISCUSSION

In this work, we show that HO-1 is a key immunoregulatory molecule during *F. hepatica* infection and that promotes infection and liver damage. The role of HO-1 in infections by intracellular pathogens has been previously approached, demonstrating an upregulation of HO-1 mRNA and/or protein expression in response to viral (25), bacterial (23, 41–46), or protozoan parasitic (18, 19, 47) infections. Furthermore, overexpression or induction of HO-1 promotes persistence of other infectious agents, such as *Leishmania chagasi* and *Plasmodium* liver infection (18, 47). However, to our knowledge, this is the first report demonstrating the role of HO-1 in favoring a helminth infection.

The involvement of HO-1 in the anti-inflammatory immune response in *F. hepatica*-infected mice was confirmed using pharmacological approaches. We show that the pharmacological induction of HO-1 promoted clinical signs associated with *F. hepatica* infection, and it was correlated with an increase of IL-10 and TGFβ in liver, indicating that the induction of HO-1 is associated with the upregulation of these two immunoregulatory cytokines. The fact that the use of the enzymatic inhibitor of HO-1 SnPP significantly decreased the levels of IL-10, TGFβ, and FIZZ-1 in liver, even to lower levels to control infected mice (for IL-10 and FIZZ-1) strongly suggests that HO-1 is involved in the upregulation of IL-10, promoting parasite survival, and hence liver damage that leads to the upregulation of FIZZ-1 indicating liver fibrosis. Indeed, several studies have demonstrated that HO-1 mediates the anti-inflammatory effect of IL-10 (37, 48) showing that the use of competitive inhibitors or the knock down expression of HO-1 abrogated the suppressive effect of IL-10. In our model, this hypothesis is in agreement with the results obtained with the simultaneous administration of CoPP and SnPP, obtaining similar clinical signs and IL-10, TGFβ, and FIZZ-1 levels as non-treated mice. Further studies are needed to define which of the heme degradation products following the action of HO-1 activity iron, biliverdin, or CO, are responsible for these actions, as has been previously reported for other pathogens (23). Alternatively, cytokine induction may be due to direct interaction of HO-1 with other host molecules. Interestingly, HO-1 gene expression is regulated at the transcriptional level, by several transcriptional factors including activator protein-1 (49, 50), nuclear factor erythroid 2-related factor-2 (NRF2), nuclear factor-kappa B (50, 51), among others. Also, HO-1 expression is regulated by signaling cascades such as mitogen-activated protein kinase and phosphatidylinositol 3-kinase/Akt (49, 52). In our model, the identification of the molecular mechanisms that lead to HO-1 upregulation in *F. hepatica*-infected animals will eventually contribute to the development of molecular strategies to control the infection.

Apart from its immunoregulatory properties, HO-1 also plays a significant role in inhibiting oxidant-induced injury during inflammatory processes (53). In fact, an appropriate balance of the inflammatory and redox states is essential to resolve most infections and finally the infectious process (17). In this context, another possibility is that *F. hepatica* induces HO-1 expression not only to evade the host immune response, but also to inhibit oxidant production by macrophages or other cells. One immunologically relevant place in the host for *F. hepatica*, is the peritoneal cavity, where the production of oxygen or nitrogen derived molecules could limit and restrain juvenile parasites. Indeed, lower levels of liver damage have been suggested to be the consequence of effective killing of the invading parasites within the peritoneum or shortly after reaching the liver (54). In this context, *F. hepatica*-mediated HO-1 induction might support parasite survival, for instance by favoring its passage through the peritoneum to the liver.

Our data indicate that in the peritoneal cavity two different populations of antigen presenting cells express HO-1. Judged by the high expression of CD11c, CD38, MHCII and the immunoregulatory cytokines IL-10 and TGFβ, HO-1^{hi} F4/80^{int} cells could constitute tolerogenic myeloid-derived DCs (55) or regulatory DCs that potentially participate in the induction of specific regulatory or anergic T cells (8, 56). Indeed, DCs conditioned with parasite-derived molecules can induce T cell anergy (8, 14, 56, 57). It remains to be determined whether HO-1-expressing DCs can induce specific anergic or regulatory T cells in a HO-1 dependent mechanism. In contrast, HO-1^{int} F4/80^{hi} cells were characterized by the high expression of CD68, CD172a, Ly6C, CD11b, and FIZZ-1, as well as low levels of MHCII expression, indicating that they may correspond to alternatively activated macrophages (58). In this line, the alternative activation of macrophages by *F. hepatica* or its derived molecules has been previously described (10, 39, 59, 60). Macrophages play a central role in innate immune responses toward both extracellular and intracellular pathogens, particularly through the formation of reactive oxygen/nitrogen species (RO/NS) (61, 62). Indeed, oxidative stress can kill *F. hepatica* flukes by a mechanism that may involve oxidation of proteins or lipids from parasite tegument since peroxyntrite or superoxide radicals significantly diminished parasite viability *in vitro* (54, 63). Moreover, RO/NS can effectively target extracellular pathogens through the formation of extracellular traps (61). Taking into account that HO-1 in macrophages limits the production of reactive species (34) and induces IL-10 producing anti-inflammatory macrophages (64) and that *F. hepatica* favors

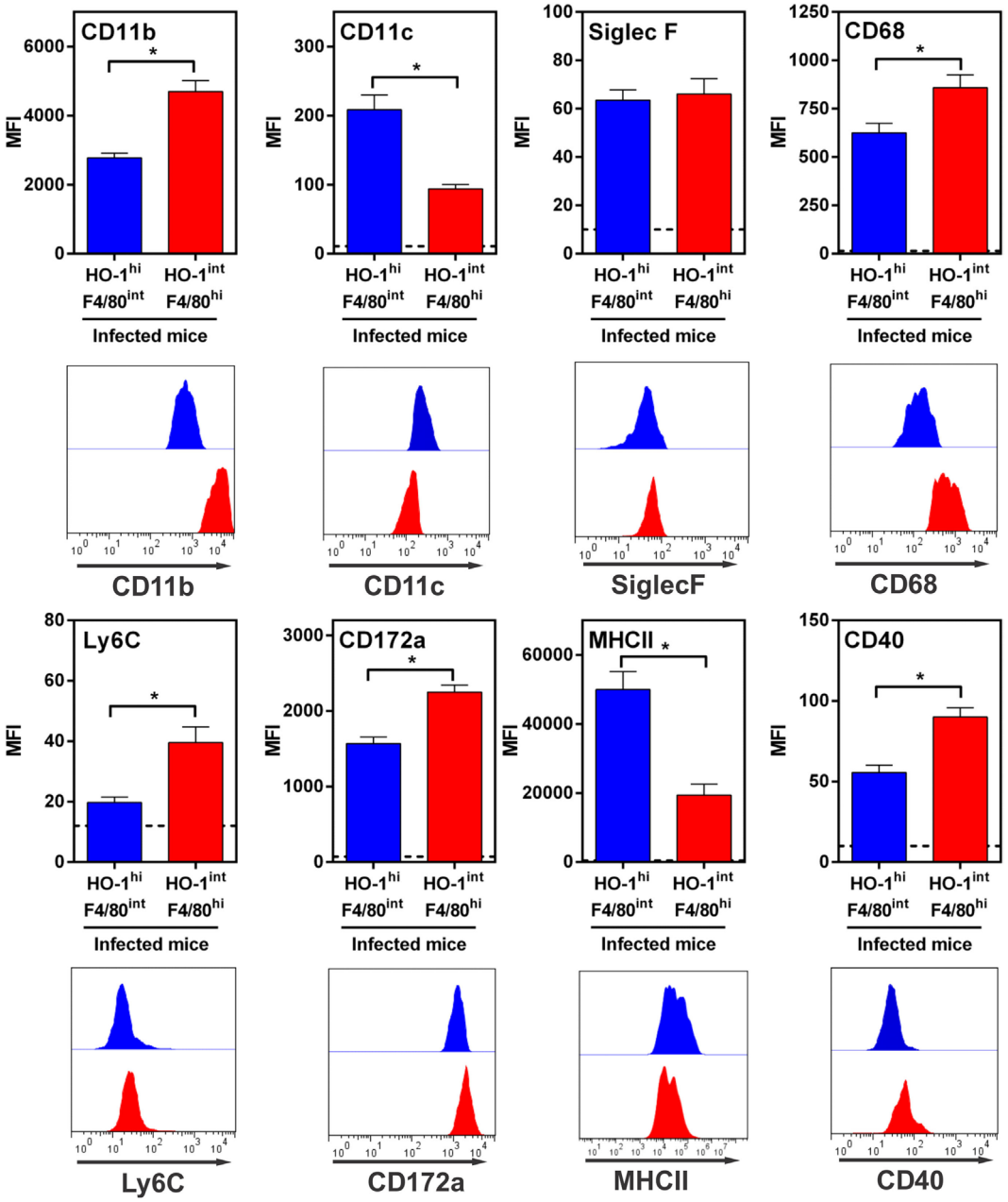


FIGURE 9 | Immunophenotyping of HO-1^{hi} F4/80^{int} and HO-1^{int} F4/80^{hi} in the peritoneum of *Fasciola hepatica*-infected animals. HO-1^{hi} F4/80^{int} cells (blue), HO-1^{int} F4/80^{hi} cells (red) from peritoneal exudate cells of infected mice at 3 wpi were evaluated for the expression of different cell markers by flow cytometry. Cells from the peritoneal cavity from infected mice were stained with CD11b- CD11c-, MHCII, CD40, SIRPα-, CD68-, Ly6C-, or Siglec-F- specific antibodies and evaluated by flow cytometry. A representative figure of three independent experiments is shown. Mice were analyzed individually: control mice $n = 5$ and *F. hepatica*-infected mice $n = 5$. Asterisks indicate statistically significant differences (*$p < 0.05$).

the alternative activation of macrophages (65, 66), it is likely that HO-1^{+} macrophages at early stages allow *F. hepatica* survival in the peritoneum through ineffective free radical production.

Finally, the role of HO-1 in favoring *F. hepatica* infection in the natural host (e.g., livestock, human) remains unknown. Although we show preliminary data demonstrating an increase in HO-1 expression in livers from naturally infected cattle, further studies are necessary to determine whether HO-1 expression correlates with a certain stage of the infection or if participates in the immunoregulatory or anti-oxidant mechanisms during the infection in these hosts.

In conclusion, HO-1 overexpression benefits *F. hepatica* infection increasing clinical signs and liver damage. Upregulation of HO-1 leads to an increase of IL-10 which could promote and benefit parasite transport from the peritoneum to the liver. On the other hand, an enzymatic inhibitor of HO-1 provided mice

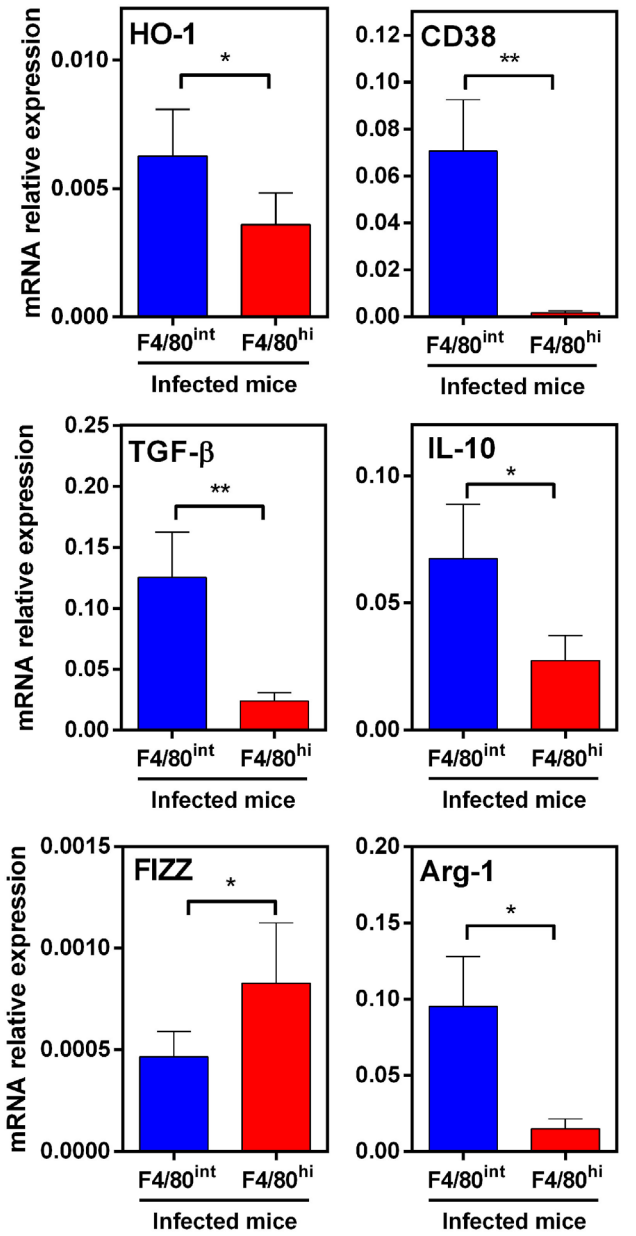


FIGURE 10 | Expression of immunoregulatory molecules in HO-1^{hi} F4/80^{int} and HO-1^{int} F4/80^{hi} in peritoneal exudate cells (PECs) from *Fasciola hepatica*-infected animals. HO-1^{hi} F4/80^{int} cells (blue), HO-1^{int} F4/80^{hi} cells (red) from PECs of infected mice at 3 wpi were first sorted. Then, the expression of heme-oxygenase-1 (HO-1), TGFβ, IL-10, FIZZ-1, Arg-1, and CD38 was evaluated by qRT-PCR. Gene expression relative to GAPDH transcript levels is shown. Mice were analyzed individually: control mice $n = 5$ and *F. hepatica*-infected mice $n = 5$. Asterisks indicate statistically significant differences (*$p < 0.05$, **$p < 0.01$).

with resistance to infection, decreasing IL-10 and FIZZ-1 transcript levels in liver. Although the mechanisms by which HO-1$^+$ DCs or macrophages regulate the expression of IL-10 or oxidative responses during *F. hepatica* infection remain to be elucidated, targeting HO-1 to control fasciolosis could constitute an interesting alternative strategy to drugs or vaccines against fasciolosis.

ETHICS STATEMENT

Mouse experiments were carried out in accordance with strict guidelines from the National Committee on Animal Research (Comisión Nacional de Experimentación Animal, CNEA, National Law 18.611, Uruguay) according to the international statements on animal use in biomedical research from the Pan American Health Organization (PAHO) and World Health Organization (WHO). The protocol was approved by the Uruguayan Committee on Animal Research. Cow's livers were collected during the routine work of a local abattoir (Frigorífico Carrasco) in Montevideo (Uruguay). All procedures involving animals were approved by the Universidad de la República's Committee on Animal Research (Comisión Honoraria de Experimentación Animal, CHEA Protocol Number: 070153-000180-16).

AUTHOR CONTRIBUTIONS

PC performed the experiments, analyzed data, and contributed with manuscript revision. ER, VC and SF contributed with mouse infections and flow cytometry experiments. VN and NB participated in obtention of flukes and extract preparation and detoxification. CR contributed with reactifs and participated in real-time RT-PCR experiments. IA contributed with reactifs, designed experiments with protoporphirn treatment and helped with manuscript revision. TF contributed to supervision and design of all experiments shown in this paper, analyzed data, and prepared the manuscript.

ACKNOWLEDGMENTS

We are particularly grateful to abattoir "Frigorífico Carrasco" for their help with the collection of flukes and cow's livers. We also thank Eduardo Osinaga and Marcelo Hill for their valuable advice.

FUNDING

PC was funded by "Agencia Nacional de Investigación e Innovación" (ANII) and "Asociación de Universidades Grupo Montevideo" from Uruguay. IA was funded by the Labex IGO project (no. ANR-11-LABX-0016-01) which is part of the «Investissements d'Avenir» French Government program managed by the ANR (ANR-11-LABX-0016-01) and by the IHU-Cesti project funded also by the «Investissements d'Avenir» French Government program, managed by the French ANR (ANR-10-IBHU-005). The IHU-Cesti project is also supported by Nantes Métropole and Région Pays de la Loire. TF received a grant from Comisión Sectorial de Investigación Científica (Uruguay), CSIC I+D 2016 ID114.

SUPPLEMENTARY MATERIAL

The Supplementary Material for this article can be found online at http://journal.frontiersin.org/article/10.3389/fimmu.2017.00883/full#supplementary-material.

REFERENCES

1. Rondelaud D, Vignoles P, Abrous M, Dreyfuss G. The definitive and intermediate hosts of *Fasciola hepatica* in the natural watercress beds in central France. *Parasitol Res* (2001) 87:475–8. doi:10.1007/s004360100385
2. Dietrich C, Kabaalioglu A, Brunetti E, Richter J. Fasciolosis. *Z Gastroenterol* (2015) 53:285–90. doi:10.1055/s-0034-1385728
3. Vukman KV, Adams PN, O'Neill SM. *Fasciola hepatica* tegumental coat antigen suppresses MAPK signalling in dendritic cells and up-regulates the expression of SOCS3. *Parasite Immunol* (2013) 35:234–8. doi:10.1111/pim.12033
4. Dowling DJ, Hamilton CM, Donnelly S, La Course J, Brophy PM, Dalton J, et al. Major secretory antigens of the helminth *Fasciola hepatica* activate a suppressive dendritic cell phenotype that attenuates Th17 cells but fails to activate Th2 immune responses. *Infect Immun* (2010) 78:793–801. doi:10.1128/IAI.00573-09
5. Falcón C, Carranza F, Martínez FF, Knubel CP, Masih DT, Motrán CC, et al. Excretory-secretory products (ESP) from *Fasciola hepatica* induce tolerogenic properties in myeloid dendritic cells. *Vet Immunol Immunopathol* (2010) 137:36–46. doi:10.1016/j.vetimm.2010.04.007
6. Falcon CR, Carranza FA, Aoki P, Motran CC, Cervi L. Adoptive transfer of dendritic cells pulsed with *Fasciola hepatica* antigens and lipopolysaccharides confers protection against fasciolosis in mice. *J Infect Dis* (2012) 205:506–14. doi:10.1093/infdis/jir606
7. Hamilton CM, Dowling DJ, Loscher CE, Morphew RM, Brophy PM, O'Neill SM. The *Fasciola hepatica* tegumental antigen suppresses dendritic cell maturation and function. *Infect Immun* (2009) 77:2488–98. doi:10.1128/IAI.00919-08
8. Rodriguez E, Carasi P, Frigerio S, da Costa V, van Vliet S, Noya V, et al. *Fasciola hepatica* immune regulates CD11c+ cells by interacting with the macrophage Gal/GalNAc lectin. *Front Immunol* (2017) 8:264. doi:10.3389/fimmu.2017.00264
9. Adams PN, Aldridge A, Vukman KV, Donnelly S, O'Neill SM. Fasciola hepatica tegumental antigens indirectly induce an M2 macrophage-like phenotype *in vivo*. *Parasite Immunol* (2014) 36:531–9. doi:10.1111/pim.12127
10. Figueroa-Santiago O, Espino AM. *Fasciola hepatica* fatty acid binding protein induces the alternative activation of human macrophages. *Infect Immun* (2014) 82:5005–12. doi:10.1128/IAI.02541-14
11. Alvarado R, To J, Lund ME, Pinar A, Mansell A, Robinson MW, et al. The immune modulatory peptide FhHDM-1 secreted by the helminth *Fasciola hepatica* prevents NLRP3 inflammasome activation by inhibiting endolysosomal acidification in macrophages. *FASEB J* (2017) 31:85–95. doi:10.1096/fj.201500093R
12. Sulaiman AA, Zolnierczyk K, Japa O, Owen JP, Maddison BC, Emes RD, et al. A trematode parasite derived growth factor binds and exerts influences on host immune functions via host cytokine receptor complexes. *PLoS Pathog* (2016) 12:e1005991. doi:10.1371/journal.ppat.1005991
13. Haçarız O, Akgün M, Kavak P, Yüksel B, Sağıroğlu MŞ. Comparative transcriptome profiling approach to glean virulence and immunomodulation-related genes of *Fasciola hepatica*. *BMC Genomics* (2015) 16:366. doi:10.1186/s12864-015-1539-8
14. Guasconi L, Chiapello LS, Masih DT. *Fasciola hepatica* excretory-secretory products induce CD4+T cell anergy via selective up-regulation of PD-L2 expression on macrophages in a Dectin-1 dependent way. *Immunobiology* (2015) 220:934–9. doi:10.1016/j.imbio.2015.02.001
15. Stempin CC, Motrán CC, Aoki MP, Falcón CR, Cerbán FM, Cervi L. PD-L2 negatively regulates Th1-mediated immunopathology during *Fasciola hepatica* infection. *Oncotarget* (2016) 7:77721–31. doi:10.18632/oncotarget.12790
16. Brouard S, Otterbein LE, Anrather J, Tobiasch E, Bach FH, Choi AMK, et al. Carbon monoxide generated by heme oxygenase 1 suppresses endothelial cell apoptosis. *J Exp Med* (2000) 192:1015–26. doi:10.1084/jem.192.7.1015
17. Chung SW, Hall SR, Perrella MA. Role of haem oxygenase-1 in microbial host defence. *Cell Microbiol* (2009) 11:199–207. doi:10.1111/j.1462-5822.2008.01261.x
18. Epiphanio S, Mikolajczak SA, Gonçalves LA, Pamplona A, Portugal S, Albuquerque S, et al. Heme oxygenase-1 is an anti-inflammatory host factor that promotes murine plasmodium liver infection. *Cell Host Microbe* (2008) 3:331–8. doi:10.1016/j.chom.2008.04.003
19. Pamplona A, Ferreira A, Balla J, Jeney V, Balla G, Epiphanio S, et al. Heme oxygenase-1 and carbon monoxide suppress the pathogenesis of experimental cerebral malaria. *Nat Med* (2007) 13:703–10. doi:10.1038/nm1586
20. Silva-Gomes S, Appelberg R, Larsen R, Soares MP, Gomes MS. Heme catabolism by heme oxygenase-1 confers host resistance to *Mycobacterium* infection. *Infect Immun* (2013) 81:2536–45. doi:10.1128/IAI.00251-13
21. Tachibana M, Hashino M, Nishida T, Shimizu T, Watarai M. Protective role of heme oxygenase-1 in *Listeria monocytogenes*-induced abortion. *PLoS One* (2011) 6(9):e25046. doi:10.1371/journal.pone.0025046
22. Seixas E, Gozzelino R, Chora A, Ferreira A, Silva G, Larsen R, et al. Heme oxygenase-1 affords protection against noncerebral forms of severe malaria. *Proc Natl Acad Sci U S A* (2009) 106:15837–42. doi:10.1073/pnas.0903419106
23. Onyiah JC, Sheikh SZ, Maharshak N, Steinbach EC, Russo SM, Kobayashi T, et al. Carbon monoxide and heme oxygenase-1 prevent intestinal inflammation in mice by promoting bacterial clearance. *Gastroenterology* (2013) 144:789–98. doi:10.1053/j.gastro.2012.12.025
24. Araujo ECB, Barbosa BF, Coutinho LB, Barenco PVC, Sousa LA, Milanezi CM, et al. Heme oxygenase-1 activity is involved in the control of *Toxoplasma gondii* infection in the lung of BALB/c and C57BL/6 and in the small intestine of C57BL/6 mice. *Vet Res* (2013) 44:89. doi:10.1186/1297-9716-44-89
25. Espinoza J, León M, Céspedes P, Gómez P, Canedo-Marroquín G, Riquelme S, et al. Heme oxygenase-1 modulates human respiratory syncytial virus replication and lung pathogenesis during infection. *J Immunol* (2017) 199(1):212–23. doi:10.4049/jimmunol.1601414
26. Chauveau C, Rémy S, Royer PJP, Hill M, Tanguy-royer S, Hubert F-X, et al. Heme oxygenase-1 expression inhibits dendritic cell maturation and proinflammatory function but conserves IL-10 expression. *Blood* (2005) 106:1694–702. doi:10.1182/blood-2005-02-0494
27. Sierra-Filardi E, Vega MA, Sánchez-Mateos P, Corbí AL, Puig-Kröger A. Heme oxygenase-1 expression in M-CSF-polarized M2 macrophages contributes to LPS-induced IL-10 release. *Immunobiology* (2010) 215:788–95. doi:10.1016/j.imbio.2010.05.020
28. Paul G, Bataille F, Obermeier F, Bock J, Klebl F, Strauch U, et al. Analysis of intestinal haem-oxygenase-1 (HO-1) in clinical and experimental colitis. *Clin Exp Immunol* (2005) 140:547–55. doi:10.1111/j.1365-2249.2005.02775.x
29. Sardana MK, Kappas A. Dual control mechanism for heme oxygenase: tin(IV)-protoporphyrin potently inhibits enzyme activity while markedly increasing content of enzyme protein in liver. *Proc Natl Acad Sci U S A* (1987) 84:2464–8. doi:10.1073/pnas.84.8.2464
30. Liu Z, Que S, Xu J, Peng T. Alanine aminotransferase-old biomarker and new concept: a review. *Int J Med Sci* (2014) 11:925–35. doi:10.7150/ijms.8951
31. Nitti M, Piras S, Marinari U, Moretta L, Pronzato M, Furfaro A. HO-1 induction in cancer progression: a matter of cell adaptation. *Antioxidants (Basel)* (2017) 6:29. doi:10.3390/antiox6020029
32. Espinoza JA, González PA, Kalergis AM. Modulation of antiviral immunity by heme oxygenase-1. *Am J Pathol* (2017) 187(3):487–93. doi:10.1016/j.ajpath.2016.11.011
33. Loboda A, Damulewicz M, Pyza E, Jozkowicz A, Dulak J. Role of Nrf2/HO-1 system in development, oxidative stress response and diseases : an evolutionarily conserved mechanism. *Cell Mol Life Sci* (2016) 73:3221–47. doi:10.1007/s00018-016-2223-0
34. Blancou P, Tardif V, Simon T, Rémy S, Carreño L, Kalergis A, et al. Immunoregulatory properties of heme oxygenase-1. In: Cuturi MC, Anegon I, editors. *Methods in Molecular Biology Methods in Molecular Biology*. Totowa, NJ: Humana Press (2010). p. 247–68.
35. Rodríguez E, Noya V, Cervi L, Chiribao ML, Brossard N, Chiale C, et al. Glycans from *Fasciola hepatica* modulate the host immune response and TLR-induced maturation of dendritic cells. *PLoS Negl Trop Dis* (2015) 9:e0004234. doi:10.1371/journal.pntd.0004234
36. Chen S, Kapturczak MH, Wasserfall C, Glushakova OY, Campbell-Thompson M, Deshane JS, et al. Interleukin 10 attenuates neointimal proliferation and inflammation in aortic allografts by a heme oxygenase-dependent pathway. *Proc Natl Acad Sci U S A* (2005) 102:7251–6. doi:10.1073/pnas.0502407102
37. Lee T-S, Chau L-Y. Heme oxygenase-1 mediates the anti-inflammatory effect of interleukin-10 in mice. *Nat Med* (2002) 8:240–6. doi:10.1038/nm0302-240

38. Flynn RJ, Mulcahy G. Possible role for Toll-like receptors in interaction of *Fasciola hepatica* excretory/secretory products with bovine macrophages. *Infect Immun* (2008) 76:678–84. doi:10.1128/IAI.00732-07
39. Flynn RJ, Irwin JA, Olivier M, Sekiya M, Dalton JP, Mulcahy G. Alternative activation of ruminant macrophages by *Fasciola hepatica*. *Vet Immunol Immunopathol* (2007) 120:31–40. doi:10.1016/j.vetimm.2007.07.003
40. Weis N, Weigert A, von Knethen A, Brüne B. Heme oxygenase-1 contributes to an alternative macrophage activation profile induced by apoptotic cell supernatants. *Mol Biol Cell* (2009) 20:1280–8. doi:10.1091/mbc.E08-10-1005
41. Athale J, Ulrich A, Chou MacGarvey N, Bartz RR, Welty-Wolf KE, Suliman HB, et al. Nrf2 promotes alveolar mitochondrial biogenesis and resolution of lung injury in *Staphylococcus aureus* pneumonia in mice. *Free Radic Biol Med* (2012) 53:1584–94. doi:10.1016/j.freeradbiomed.2012.08.009
42. Kumar A, Deshane JS, Crossman DK, Bolisetty S, Yan BS, Kramnik I, et al. Heme oxygenase-1-derived carbon monoxide induces the *Mycobacterium tuberculosis* dormancy regulon. *J Biol Chem* (2008) 283(26):18032–9. doi:10.1074/jbc.M802274200
43. MacGarvey NC, Suliman HB, Bartz RR, Fu P, Withers CM, Welty-Wolf KE, et al. Activation of mitochondrial biogenesis by heme oxygenase-1-mediated NF-E2-related factor-2 induction rescues mice from lethal *Staphylococcus aureus* sepsis. *Am J Respir Crit Care Med* (2012) 185(8):851–61. doi:10.1164/rccm.201106-1152OC
44. Regev D, Surolia R, Karki S, Zolak J, Montes-Worboys A, Oliva O, et al. Heme oxygenase-1 promotes granuloma development and protects against dissemination of mycobacteria. *Lab Investig* (2012) 93:868–79. doi:10.1038/labinvest.2012.125
45. Shiloh MU, Manzanillo P, Cox JS. *Mycobacterium tuberculosis* senses host-derived carbon monoxide during macrophage infection. *Cell Host Microbe* (2008) 3:323–30. doi:10.1016/j.chom.2008.03.007
46. Nairz M, Theurl I, Ludwiczek S, Theurl M, Mair SM, Fritsche G, et al. The co-ordinated regulation of iron homeostasis in murine macrophages limits the availability of iron for intracellular *Salmonella typhimurium*. *Cell Microbiol* (2007) 9:2126–40. doi:10.1111/j.1462-5822.2007.00942.x
47. Luz NF, Andrade BB, Feijó DF, Araújo-Santos T, Quintela GC, Andrade D, et al. Heme oxygenase-1 promotes the persistence of *Leishmania chagasi* infection. *J Immunol* (2012) 188(9):4460–7. doi:10.4049/jimmunol.1103072
48. Piantadosi CA, Withers CM, Bartz RR, MacGarvey NC, Fu P, Sweeney TE, et al. Heme oxygenase-1 couples activation of mitochondrial biogenesis to anti-inflammatory cytokine expression. *J Biol Chem* (2011) 286:16374–85. doi:10.1074/jbc.M110.207738
49. Lu C-Y, Yang Y-C, Li C-C, Liu K-L, Lii C-K, Chen H-W. Andrographolide inhibits TNFα-induced ICAM-1 expression via suppression of NADPH oxidase activation and induction of HO-1 and GCLM expression through the PI3K/Akt/Nrf2 and PI3K/Akt/AP-1 pathways in human endothelial cells. *Biochem Pharmacol* (2014) 91:40–50. doi:10.1016/j.bcp.2014.06.024
50. Lavrovsky Y, Schwartzman ML, Levere RD, Kappas A, Abraham NG. Identification of binding sites for transcription factors NF-kappa B and AP-2 in the promoter region of the human heme oxygenase 1 gene. *Proc Natl Acad Sci U S A* (1994) 91:5987–91. doi:10.1073/pnas.91.13.5987
51. Wardyn JD, Ponsford AH, Sanderson CM. Dissecting molecular cross-talk between Nrf2 and NF-κB response pathways. *Biochem Soc Trans* (2015) 43:621–6. doi:10.1042/BST20150014
52. Li W, Ma F, Zhang L, Huang Y, Li X, Zhang A, et al. Propargyl-cysteine exerts a novel protective effect on methionine and choline deficient diet-induced fatty liver via Akt/Nrf2/HO-1 pathway. *Oxid Med Cell Longev* (2016) 2016:1–17. doi:10.1155/2016/4690857
53. Chau L-Y. Heme oxygenase-1: emerging target of cancer therapy. *J Biomed Sci* (2015) 22:1–7. doi:10.1186/s12929-015-0128-0
54. Piedrafita D, Estuningsih E, Pleasance J, Prowse R, Raadsma HW, Meeusen ENT, et al. Peritoneal lavage cells of Indonesian thin-tail sheep mediate antibody-dependent superoxide radical cytotoxicity in vitro against newly excysted juvenile *Fasciola gigantica* but not juvenile *Fasciola hepatica*. *Infect Immun* (2007) 75:1954–63. doi:10.1128/IAI.01034-06
55. Simon T, Pogu J, Rémy S, Brau F, Pogu S, Maquigneau M, et al. Inhibition of effector antigen-specific T cells by intradermal administration of heme oxygenase-1 inducers. *J Autoimmun* (2017) 81:44–55. doi:10.1016/j.jaut.2017.03.005
56. Aldridge A, O'Neill SM. *Fasciola hepatica* tegumental antigens induce anergic-like T cells via dendritic cells in a mannose receptor-dependent manner. *Eur J Immunol* (2016) 46:1180–92. doi:10.1002/eji.201545905
57. Carranza F, Falcón CR, Nuñez N, Knubel C, Correa SG, Bianco I, et al. Helminth antigens enable CpG-activated dendritic cells to inhibit the symptoms of collagen-induced arthritis through Foxp3+ regulatory T cells. *PLoS One* (2012) 7:e40356. doi:10.1371/journal.pone.0040356
58. Gautier EL, Shay T, Miller J, Greter M, Jakubzick C, Ivanov S, et al. Gene-expression profiles and transcriptional regulatory pathways that underlie the identity and diversity of mouse tissue macrophages. *Nat Immunol* (2012) 13:1118–28. doi:10.1038/ni.2419
59. Donnelly S, O'Neill SM, Sekiya M, Mulcahy G, Dalton JP. Thioredoxin peroxidase secreted by *Fasciola hepatica* induces the alternative activation of macrophages. *Infect Immun* (2005) 73:166–73. doi:10.1128/IAI.73.1.166-173.2005
60. Donnelly S, Stack CM, Neill SMO, Sayed AA, Williams DL, Dalton JP. Helminth 2-Cys peroxiredoxin drives Th2 responses through a mechanism involving alternatively activated macrophages. *FASEB J* (2008) 22:4022–32. doi:10.1096/fj.08-106278
61. Gostner JM, Becker K, Fuchs D, Sucher R. Redox regulation of the immune response. *Redox Rep* (2013) 18:88–94. doi:10.1179/1351000213Y.0000000044
62. Singel KL, Segal BH. NOX2-dependent regulation of inflammation. *Clin Sci* (2016) 130:479–90. doi:10.1042/CS20150660
63. Sadeghi-Gashjin G, Naem S. Parasiticidal effects of peroxynitrite on ovine liver flukes in vitro. *J Helminthol* (2001) 75:73–6. doi:10.1079/JOH200032
64. Naito Y, Takagi T, Higashimura Y. Heme oxygenase-1 and anti-inflammatory M2 macrophages. *Arch Biochem Biophys* (2014) 564:83–8. doi:10.1016/j.abb.2014.09.005
65. Reyes JL, Terrazas LI. The divergent roles of alternatively activated macrophages in helminthic infections. *Parasite Immunol* (2007) 29:609–19. doi:10.1111/j.1365-3024.2007.00973.x
66. Jenkins SJ, Allen JE. Similarity and diversity in macrophage activation by nematodes, trematodes, and cestodes. *J Biomed Biotechnol* (2010) 2010:14. doi:10.1155/2010/262609

Conflict of Interest Statement: The authors declare that the research was conducted in the absence of any commercial or financial relationships that could be construed as a potential conflict of interest.

Copyright © 2017 Carasi, Rodríguez, da Costa, Frigerio, Brossard, Noya, Robello, Anegón and Freire. This is an open-access article distributed under the terms of the Creative Commons Attribution License (CC BY). The use, distribution or reproduction in other forums is permitted, provided the original author(s) or licensor are credited and that the original publication in this journal is cited, in accordance with accepted academic practice. No use, distribution or reproduction is permitted which does not comply with these terms.

frontiers in Immunology

ORIGINAL RESEARCH
published: 09 April 2018
doi: 10.3389/fimmu.2018.00710

Anaplasma phagocytophilum-Related Defects in CD8, NKT, and NK Lymphocyte Cytotoxicity

Diana G. Scorpio[1], Kyoung-Seong Choi[2] and J. Stephen Dumler[3]*

[1] *Vaccine Research Center, National Institutes of Allergy and Infectious Diseases, National Institutes of Health, Bethesda, MD, United States,* [2] *College of Ecology and Environmental Science, Kyungpook National University, Sangju, South Korea,* [3] *Department of Pathology, Uniformed Services University of the Health Sciences, Bethesda, MD, United States*

Human granulocytic anaplasmosis, caused by the tick-transmitted *Anaplasma phagocytophilum*, is not controlled by innate immunity, and induces a proinflammatory disease state with innate immune cell activation. In *A. phagocytophilum* murine infection models, hepatic injury occurs with production of IFNγ thought to be derived from NK, NKT cells, and CD8 T lymphocytes. Specific *A. phagocytophilum* ligands that drive inflammation and disease are not known, but suggest a clinical and pathophysiologic basis strikingly like macrophage activation syndrome (MAS) and hemophagocytic syndrome (HPS). We studied *in vivo* responses of NK, NKT, and CD8 T lymphocytes from infected animals for correlates of lymphocyte-mediated cytotoxicity and examined *in vitro* interactions with *A. phagocytophilum*-loaded antigen-presenting cells (APCs). Murine splenocytes were examined and found deficient in cytotoxicity as determined by CD107a expression *in vitro* for specific CTL effector subsets as determined by flow cytometry. Moreover, *A. phagocytophilum*-loaded APCs did not lead to IFNγ production among CTLs *in vitro*. These findings support the concept of impaired cytotoxicity with *A. phagocytophilum* presentation by APCs that express MHC class I and that interact with innate and adaptive immune cells with or after infection. The findings strengthen the concept of an enhanced proinflammatory phenotype, such as MAS and HPS disease states as the basis of disease and severity with *A. phagocytophilum* infection, and perhaps by other obligate intracellular bacteria.

Keywords: *Anaplasma phagocytophilum*, cytotoxic lymphocyte, CD107a, cytotoxicity, CD8 T cells, NKT cells, NK cells, MHCI

OPEN ACCESS

Edited by:
Geanncarlo Lugo-Villarino, UMR5089 Institut de Pharmacologie et de Biologie Structurale (IPBS), France

Reviewed by:
David H. Walker, University of Texas Medical Branch, United States
Krzysztof Tomasiewicz, Medical University of Lublin, Poland

****Correspondence:***
Diana G. Scorpio
diana.scorpio@nih.gov

Specialty section:
This article was submitted to Microbial Immunology, a section of the journal Frontiers in Immunology

Received: *06 October 2017*
Accepted: *22 March 2018*
Published: *09 April 2018*

Citation:
Scorpio DG, Choi KS and Dumler JS (2018) Anaplasma phagocytophilum-Related Defects in CD8, NKT, and NK Lymphocyte Cytotoxicity. Front. Immunol. 9:710. doi: 10.3389/fimmu.2018.00710

INTRODUCTION

Human granulocytic anaplasmosis, caused by the tick-transmitted *Anaplasma phagocytophilum*, is the third most common human vector-borne infection in the U.S., where 1% die and 7% require ICU admission (1–3). *A. phagocytophilum* is not controlled by innate immunity, but induction of a proinflammatory disease state occurs with innate immune cell activation *via* TLR2 and the inflammasome to achieve STAT1-mediated IFNγ and NF-κB-mediated proinflammatory gene transcription (4–8). As a result, infection in humans and in animal models leads to a macrophage activation syndrome (MAS) where severity is related to high serum levels of IFNγ, IL-10, IL-12, and ferritin (9–12).

In *A. phagocytophilum* murine infection models, inflammatory hepatic histopathologic injury is abrogated in *Ifng*$^{-/-}$ and enhanced in *Il10*$^{-/-}$ animals, confirming an important role for IFNγ in driving tissue injury (5, 6, 9, 10, 13). Key candidates for production of IFNγ include the innate immune NK and NKT cells, but also include CD8 T lymphocytes as adaptive immune responses mature. NK, NKT, and CD8 T lymphocytes react to fundamentally distinct ligands, microbe-associated molecules, or other signals (14–16). TLR2-activation implies a role for *A. phagocytophilum* lipoproteins as a ligand, and induction of the inflammasome *via* NLRC4 relates to endogenous host cell eicosanoid production following infection. However, the specific *A. phagocytophilum* ligands that drive inflammation and disease are not known (4, 17). Regardless, these observations secure an inflammatory basis for *A. phagocytophilum*-induced septic or toxic shock-like manifestations and imply that severity has its pathophysiologic basis in MAS and hemophagocytic syndrome (HPS) (11, 18).

MAS and HPS are related disorders that have either a genetic basis or an infectious trigger. Both are cytokine-driven diseases characterized by progressive fever, shock, organ failure, pancytopenia, liver dysfunction, and coagulopathy, and usually attributed to excessive IFNγ production (19, 20). Genetic forms of HPS result from mutations of genes encoding proteins involved in signaling perforin or granzyme delivery for cytolysis of target cells resulting in impaired cytotoxic lymphocyte (CTL) function, often among NK cells. Similarly, infection-associated HPS is characterized by defects in CTLs, either by NK cell lymphopenia, or NK cell defects in perforin delivery, although HPS has been observed in humans and animal models with defects in CD8 T cells as well (21). The explanation for the relentless progression with HPS and MAS is that the antigen-presenting cell (APC)-cytotoxic cell synapse through TCR–MHC class I interaction results in activation of the CTL and production of IL-12, IL-18, IL-15, and IL-2, resulting in lymphoproliferation and IFNγ generation (19, 20). IFNγ activates macrophage effector production (nitric oxide, reactive oxygen species, TNFα, phagocytosis). However, the inability of CTLs to deliver perforin to the APC presenting a cognate ligand frees the cascade from regulation, exacerbating disease due to unremitting cytokine stimulation (22).

Recent studies provide evidence that the signaling pathways generating the key functions for this response are distinct, providing a framework for understanding the dichotomy of hypercytokinemia without cytotoxicity (20, 23). To better understand the nature of MAS/HPS induced by *A. phagocytophilum* infection, we studied *in vivo* and *in vitro* responses of NK, NKT, and CD8 T lymphocytes from infected animals to determine if their interactions with *A. phagocytophilum*-loaded APCs results in delivery of cytotoxic cargo dissociated from intracellular production of IFNγ.

MATERIALS AND METHODS

In Vitro Cell Line and *A. phagocytophilum* Culture

The promyelocytic leukemia HL-60 cell line (ATCC CCL-240) was used as a host for *A. phagocytophilum* growth. HL-60 cells were grown in RPMI 1640 medium (Invitrogen, USA) containing 5–10% FBS in a humidified incubator at 37°C with 5% CO_2. Cell density was kept $<5 \times 10^5$ cells/mL by diluting with fresh medium every 3 days.

Animals and Immunophenotyping

Naïve C57BL/6 mice at 6–8 weeks of age (Jackson Labs, Bar Harbor, ME, USA) were inoculated IP with 10^6 *A. phagocytophilum* Webster strain-infected HL-60 cells. CD1d$^{-/-}$ animals on a C57BL/6 background used in the studies of NK cells were kind gifts from Albert Bendelac (University of Chicago) and Luc Van Kaer (Vanderbilt University). Mock-infected animals were inoculated with uninfected HL-60 cells. This inoculation reproducibly generates infection by days 2–4 and up to day 14, and IFNγ production peaks between days 4 and 10 p.i. To generate immune mice for CD8 T-cell experiments, mice were treated on day 14 with doxycycline (5 mg/kg PO q12h) for 7 days followed by 7 days with no treatment to allow drug clearance; on day 28, splenocytes were harvested and tested by PCR to exclude infection (24). Mice were euthanized following CO_2 exposure. All animal studies were reviewed and approved by the Johns Hopkins University Institutional Animal Care and Use committee. All mice were housed and cared for following the "Guide for the Care and Use of Laboratory Animals" (25).

Ex Vivo Experiments to Identify Cytotoxic CTL Activation

C57BL/6 mice were inoculated i.p. with *A. phagocytophilum*-infected HL-60 cells or mock-infected by uninfected HL-60 cells as described above. For evaluation of *in vivo* activation of cytotoxicity for CD8 T lymphocytes and NKT cells, splenocytes were harvested at 4 h, and days 4, 7, 10, and 14 p.i., and processed for flow cytometry. Spleens from individual mice were minced to obtain single-cell suspensions, washed and erythrocytes lysed in a hypotonic salt solution, and then resuspended in RPMI 1640 medium with 10% FBS and 1× penicillin/streptomycin. Single-cell suspensions were stained for 20 min on ice using antibodies to CD107a (BD Biosciences) and (i) for CD8 CTLs using anti-CD3ε (BD Biosciences) and R-PE-conjugated anti-CD8a (Ly-2) (BD Biosciences), or (ii) for NKT cells using α-galactosylceramide (αGC)-loaded CD1d:Ig dimers (Mouse DimerX, BD Biosciences). All studies also used isotype-matched control antibodies (BD Biosciences). The stained cells were washed twice with phosphate-buffered saline containing 0.5% bovine serum albumin (Sigma, St. Louis, MO, USA) and 0.02% NaN_3, washed again, and fixed. Cells were examined by multicolor flow cytometry comparing the proportion of splenocytes expressing each marker among infected and uninfected animals. Data were analyzed with FlowJo software (Tree Star, Ashland, OR, USA), and gates and fluorescent cutoffs were set based on isotype-matched control antibodies. Stained cells were initially gated to identify lymphocyte populations which were then quantified by flow cytometry per quadrant for 2 by 2 fluorescent cell markers.

Cell Preparations for *In Vitro* Determination of CTL Cytotoxicity by CD107a Expression

For these experiments, donor mice were used as source of splenic CD8 T, NKT, or NK lymphocytes; immune CD8 splenic T lymphocytes were harvested from immune animals prepared as described above and prepared as single-cell suspensions (26). Splenocytes were also obtained as sources of dendritic cells (DCs) and APCs, including from C57BL/6 and CD1d$^{-/-}$ mice as appropriate. DCs (Miltenyi Mouse DC Isolation, Auburn, CA, USA) or APCs from C57BL/6 mouse spleens (27) were loaded with viable cell-free *A. phagocytophilum* for 24–48 h; cell-free bacteria were removed by centrifugation and washing. Splenocytes that included unfractionated CTLs from naïve and immune animals were added to 96-well plates with *A. phagocytophilum*-loaded (or mock-loaded) DCs in effector: target ratios from 0.1:1 to 5:1 and anti-CD107a-FITC or isotype control antibodies (BD Biosciences) for 24–48 h. After multicolor flow cytometry to identify CD3$^+$/CD8$^+$, CD49b$^+$ (in CD1d$^{-/-}$ animals to preclude NKT cell responses), or CD3$^+$/Vα14$^+$ lymphocytes that also express the cytotoxicity marker CD107a, groups were compared to controls to demonstrate intact CTL functions.

Positive controls included concanavalin A (ConA), phorbol-12-myristate-13-acetate (PMA; CD8 T and NKT lymphocytes), α-galactosylceramide (αGalCer; NKT lymphocytes), or N-α-Palmitoyl-S-[2,3-bis(palmitoyloxy)-(2RS)-propyl]-L-cysteine (Pam_3Cys; NK cells); PMA/ionomycin were included in assays as positive control for intracellular IFNγ production, and negative controls received diluent vehicle only. For NKT analyses, controls included mock-loaded and αGalCer-loaded DCs, as well as stimulation by PMA/ionomycin. For NK cell analyses, controls included mock-loaded DCs, the TLR2 agonist Pam_3Cys, and PMA/ionomycin. Splenocyte cultures from naïve or immune animals were incubated with DCs for 1 h at 37°C, and then received brefeldin A to facilitate intracellular IFNγ detection. Cells were washed, saponin permeabilized, and stained with fluorescent anti-IFNγ, anti-CD3, anti-CD8, anti-CD49b (pan-NK cell marker), anti-Vα14 (NKT cell marker) or isotype-matched control antibodies, washed again, and fixed. The cells of interest were identified by multicolor flow cytometry, as previously described (8, 26). Expression of CD107a and intracellular IFNγ were examined and reported as a percentage of total cells analyzed for the subset examined (CD3$^+$/CD8$^+$, CD3$^+$/Vα14$^+$, CD3$^-$/CD49b$^+$). This allowed simultaneous evaluation of three cytotoxic cell subsets and their independent expression of cytokines and activation for cytotoxicity. Experiments were conducted in at least triplicate, and final data were also pooled for more detailed examination.

Statistical Analysis

Comparisons were performed across all groups within each CTL experiment. Expression of CD107a or IFNγ was examined and if not normally distributed, results were ranked (using percent rank) and examined by two-tailed Mann–Whitney tests with an α-value of 0.05. Results were analyzed individually in at least three repeated experiments for each condition, and the final ranked results were pooled for an overall statistical analysis using the same methods. Results reported reflect the relative cytotoxicity (CD107a expression) and intracellular IFNγ production comparing responses of CTLs to *A. phagocytophilum*-loaded or mock-loaded DCs. Results were considered significant if the *p*-value was less than 0.05.

RESULTS

A. phagocytophilum Infection Suppresses CD8 T Lymphocyte and NKT Lymphocyte Cytotoxicity *In Vivo*

We used expression of CD107a as a surrogate measure of degranulation and cytotoxicity after exposure to APCs presenting appropriate peptides or NKT-target glycolipids. When splenocytes were gated to identify the proportions of CD3$^+$/CD8$^+$ T lymphocytes also expressing CD107a, there was an increase from days 0 to 14 for both infected and mock-infected mice. For each of days 0–10, expression of CD107a on CD3$^+$/CD8$^+$ T cells from uninfected HL-60 cell (mock) controls was higher than that observed for cells from infected animals, although the results were not significant. However, on day 14 p.i., the increase in cytotoxicity (CD107a expression) among cells from mock-infected animals was more exaggerated but not significantly higher ($p = 0.056$, Mann–Whitney test) than observed among cells from infected animals (**Figure 1A**). Similarly, CD107a expression on NKT cells was generally unchanged among infected animals over the 14-day experiment, whereas control mice who received uninfected HL-60 cells, a xenogeneic cell line anticipated to stimulate cytotoxic responses, demonstrated a slow increase in CD8 and NK T lymphocyte cytotoxicity (CD107a expression) as early as day 7 p.i., peaking at day 14 at the experiment's conclusion by contrast, demonstrating significant suppression of responses in cells from infected animals at days 10 and 14 ($p = 0.048$ and 0.049, respectively; Mann–Whitney test) (**Figure 1B**).

In Vitro Suppression of CTL Expression of CD107a With Stimulation by *A. phagocytophilum*-Loaded DCs

Because the *in vivo* experiments suggested suppression of CTL responses by *A. phagocytophilum* infection, splenocytes, as sources of NK, NKT, and CD8 T lymphocytes from immune or naïve animals, were exposed to DCs preloaded with *A. phagocytophilum* (**Figure 2**). Compared to responses generated with exposure to mock-loaded DCs, CD3$^+$/CD8$^+$ splenic lymphocytes from immune animals stimulated by *A. phagocytophilum*-loaded DCs did not generate additional CD107a expression (**Figure 2A**), but demonstrated a suppressed response as compared to immune splenic CD3$^+$/CD8$^+$ lymphocytes exposed to ConA-stimulation ($p < 0.001$). CD107a expression to ionomycin was variable, but this treatment is established to render NK cells hyporesponsive (28). Thus, the CD3$^+$/CD8$^+$ immune lymphocytes retained functional capacity to degranulate but were suppressed in the presence of *A. phagocytophilum*-loaded DCs.

Similarly, splenocytes from naïve mice and from CD1d$^{-/-}$ mice were used to assess cytotoxicity responses to *A. phagocytophilum*-loaded DCs in NKT (**Figure 2B**) and NK (**Figure 2C**) cells, respectively. For both NKT and NK cells among the splenocyte populations, cytotoxicity responses (CD107a expression) were significantly higher than negative control mock-loaded DCs for positive controls [αGalCer-loaded DCs ($p < 0.001$) or Pam_3Cys ($p = 0.003$)]. By contrast, compared to the cytotoxicity responses of NKT and NK cells when exposed to positive control stimulants, exposure to *A. phagocytophilum*-loaded DCs suppressed cytotoxicity to levels not different than negative control mock-loaded DCs.

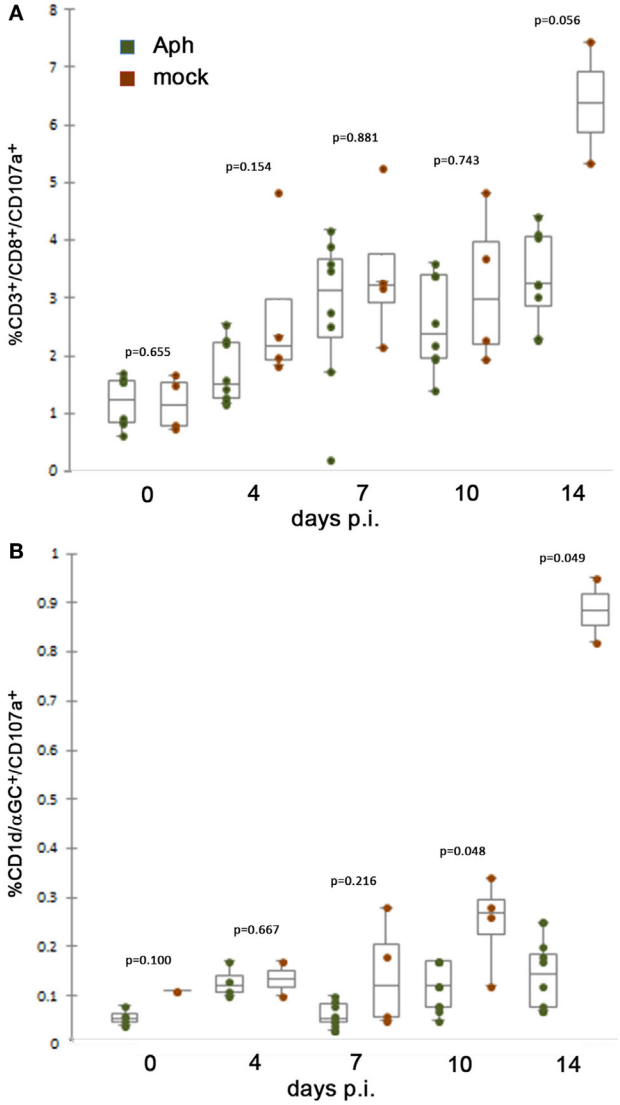


FIGURE 1 | At 10 days or later p.i., *in vivo* splenic CD8 and NKT cytotoxic lymphocyte CD107a expression is lower after infection by *A. phagocytophilum* in HL-60 cells compared to mock infection by uninfected HL-60 cells. **(A)** Splenic CD8 T lymphocytes from mock-infected (uninfected HL-60 cells) animals displayed mobilized cytotoxic responses as measured by surface CD107a expression at higher levels than with *A. phagocytophilum*-infected HL-60 at 14 days p.i. **(B)** Splenic NKT cells from infected animals demonstrate similar lack of significant cytotoxicity as measured by expression of CD107a compared to animals mock infected (uninfected HL-60 cells) at days 10 and 14 p.i. Individual points represent values from individual animals; box and whisker plots show median, first and second quartiles, and maximum and minimum values for each group. *p* Values are displayed comparing groups on individual days. Aph, *Anaplasma phagocytophilum*.

Intracellular IFNγ Production Is Impaired in Splenic CTLs

Given that *A. phagocytophilum*-loaded DCs suppressed cytotoxicity responses as measured by CD107a expression on splenic CTLs, we next examined whether these cells also were suppressed for the production of IFNγ, by examining the intracellular production of this key macrophage-activating cytokine (**Figure 3**). Surprisingly, *A. phagocytophilum*-immune CD8 T lymphocyte (**Figure 3A**), NKT cell (**Figure 3B**), and NK cell (**Figure 3C**) expression of IFNγ from splenocytes was suppressed when exposed to *A. phagocytophilum*-loaded DCs as compared with stimulation by PMA/ionomycin (CD8 T cells, NKT cells, and NK cells all $p<0.001$), ConA [immune ($p = 0.012$) and naïve CD8 T cells ($p = 0.413$)], and αGalCer-loaded DCs [NKT cells ($p = 0.004$)]. Pam_3Cys proved to be a poor stimulant for IFNγ production in NK cells. Of note, immune CD8 T lymphocytes exposed to *A. phagocytophilum*-loaded DCs did not stimulate IFNγ production more than either mock-loaded DCs or naïve CD8 T lymphocytes exposed to *A. phagocytophilum*-loaded DCs, and neither NK nor NKT cells generated more IFNγ when exposed to *A. phagocytophilum*-loaded DCs (wild type or CD1d$^{-/-}$ for NK cells) than for mock-loaded DCs. In summary, immune CD8 T, NKT, nor NK lymphocytes were unable to elicit IFNγ intracellular production when exposed to *A. phagocytophilum*-loaded DCs, despite the ready capacity of these cells to produce IFNγ with positive control stimulants.

DISCUSSION

Obligate intracellular bacteria such as *A. phagocytophilum* use their host cells as part of an extended environment and have evolved a capacity to interact with and manipulate host cells to improve microbial fitness, sometimes at the cost of damage to the host in the form of disease (18, 29, 30). Studies of *A. phagocytophilum*, therefore, focus on two important aspects of the unique bacterium, how it survives and propagates within the key host defense cell, the neutrophil, and how it causes disease, which increasingly is documented to involve inflammatory and immune induction (18, 31–33). Much has been studied regarding mechanisms by which the immune response resolves *A. phagocytophilum* infection, largely predicated on the development of CD4 T lymphocyte responses (5, 34). During investigations of immune pathways involved in resolving infection, it was discovered that although many innate and adaptive immune pathways are activated, few impact microbial burden (5). Of great interest was the discrepancy between bacterial load and inflammatory tissue injury or disease manifestations in humans and animal models (9, 10). It has increasingly become clear that infection of the neutrophil likely contributes to disease by induction of

proinflammatory responses and lack of antimicrobial killing (18, 33), but that key protective mechanisms are initiated *via* macrophages and other APCs that do not sustain infection, but contribute to the proinflammatory disease process and severity of infection (17, 35–37). In fact, aspects of granulocytic anaplasmosis in humans and animals mimic MASs and HPSs (10–12). We sought to discern whether *A. phagocytophilum* induces MAS or HPS driven by defective CTL delivery of perforin and granzyme while promoting hypercytokinemia primarily focused on IFNγ to further activate macrophages. Thus, we designed *in vivo* pilot studies and *in vitro* studies to examine the roles of immune CD8 T lymphocytes, NK cells, and NKT lymphocytes to interrogate both cytotoxicity responses and promotion of IFNγ production.

The findings from this investigation support the concept of impaired cytotoxicity of innate and adaptive immune CTLs that are, thus, unable to exert homeostatic control of APCs following antigen processing and MHC class I expression to these CTLs. While IFNγ is readily detected during *in vivo* infections, the relative lack of its expression in CTLs after exposure to APCs that should otherwise present microbial targets for activation suggests

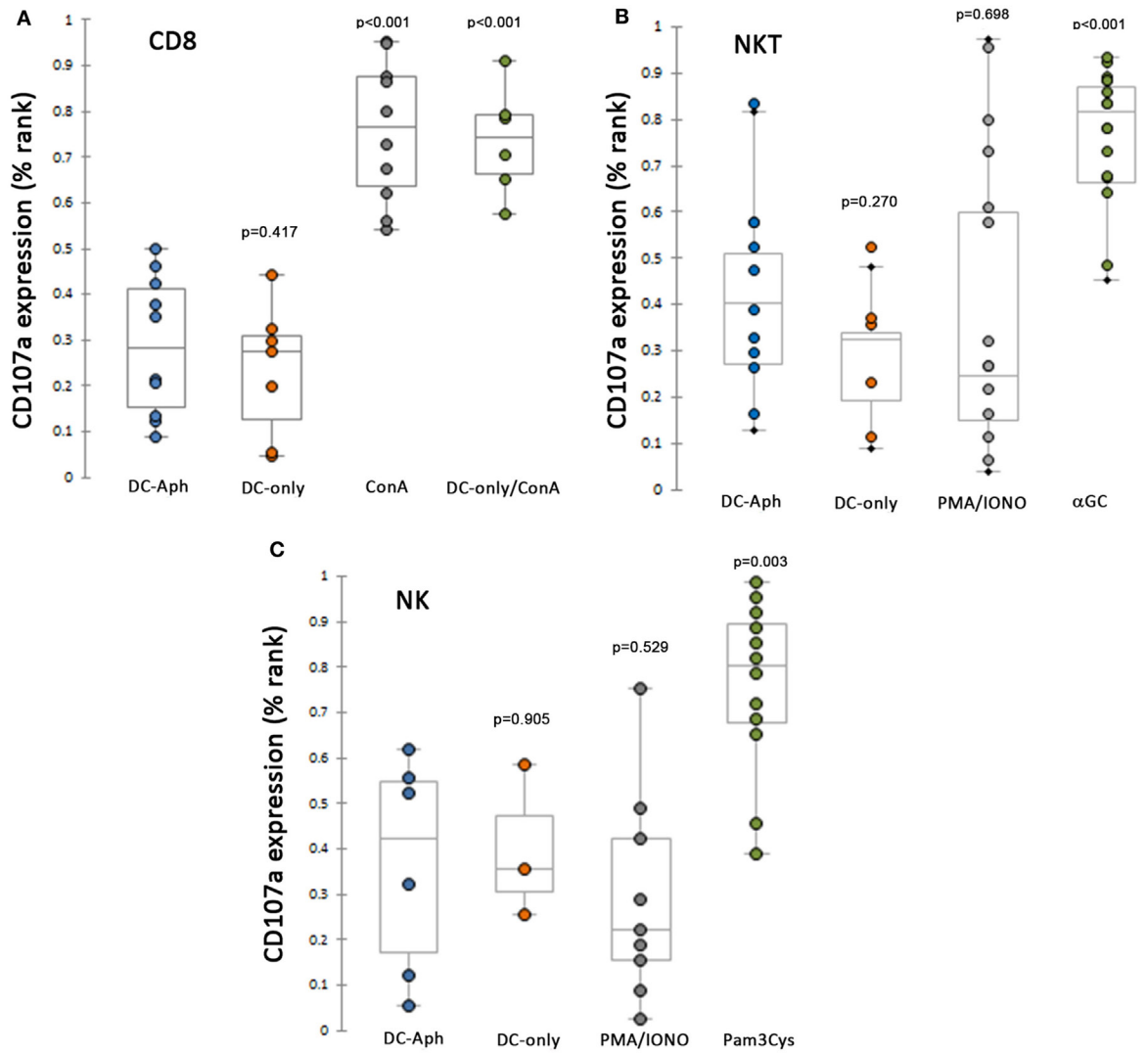


FIGURE 2 | CD8 immune T, NKT, and NK lymphocytes are suppressed from cytotoxicity (CD107a expression) when exposed to *A. phagocytophilum*-loaded dendritic cells (DCs). **(A)** Splenic CD8 T lymphocytes from immune animals are suppressed from expressing CD107a to a level observed with mock-loaded DCs, and significantly lower than when cells were stimulated by ConA. **(B)** As above, splenic NKT cells are unable to generate CD107a as a cytotoxic reporter when stimulated by *A. phagocytophilum*-loaded DCs more than mock stimulation, despite effective cytotoxic responses observed to control stimulus αGalCer-loaded DCs. **(C)** NK cells are suppressed from expression of CD107a under the same circumstances, except for the use of the control stimulus Pam_3Cys, a TLR2 agonist. DC-only, mock-loaded DCs; DC-Aph, *A. phagocytophilum*-loaded DCs; ConA, concanavalin A; αGC, α-galactosylceramide; PMA/IONO, phorbol-12-myristate-13-acetate/ionomycin C; Pam_3Cys, N-α-Palmitoyl-S-[2,3-bis(palmitoyloxy)-(2RS)-propyl]-L-cysteine. Variable results are shown for the use of PMA/ionomycin in generated cytotoxic responses. Responses are measured as the proportion of each gated cell population expressing CD107a divided by the total number of the gated cell population. Because the values were not normally distributed, the proportions were ranked by percentage and tested using Mann–Whitney tests for non-parametric significance, with a two-sided $\alpha = 0.05$. *p* Values are shown compared to DC-Aph for each condition. Aph, *Anaplasma phagocytophilum*.

that it originates from other sources and that the functional defect could instead reside within the APC. While these data do not support the classical paradigm toward development of MAS (19), the ongoing production of IFNγ by other cells coupled with the lack of effective feedback cytotoxicity by classical CTLs would be equivalent.

Anaplasma phagocytophilum can stimulate proinflammatory responses in macrophages *in vitro* through TLR2, presumably *via* a lipoprotein (4, 38). However, the recognition that intracellular pathogens are also sensed and controlled *via* intracellular pattern recognition receptors has triggered a line of investigations into nucleotide-binding domain and leucine-rich repeat containing proteins (NLRs) (37, 39). In fact, recent studies showed that *A. phagocytophilum* activates the inflammasome in macrophages by a novel process that involves NLRC4 and production of endogenous eicosanoids (17). Moreover, studies of inflammasome activation by this and other obligate intracellular bacteria that lack classical pathogen-associated molecular patterns (e.g., type III secretion system components or cell wall products) are now just being initiated.

Anaplasma phagocytophilum does not productively infect macrophages or presumably other APCs that could be involved in CTL engagement and activation of cytotoxicity (40). Therefore, how could its presence in APCs lead to dysfunctional recognition by immune CD8 T cells, NKT cells, and NK cells? The bacterium's lifestyle is obligatory intracellular, and it likely stimulates APCs in delivery of secreted effector proteins or molecules *via* type IV secretion or other methods to translocate such products into the

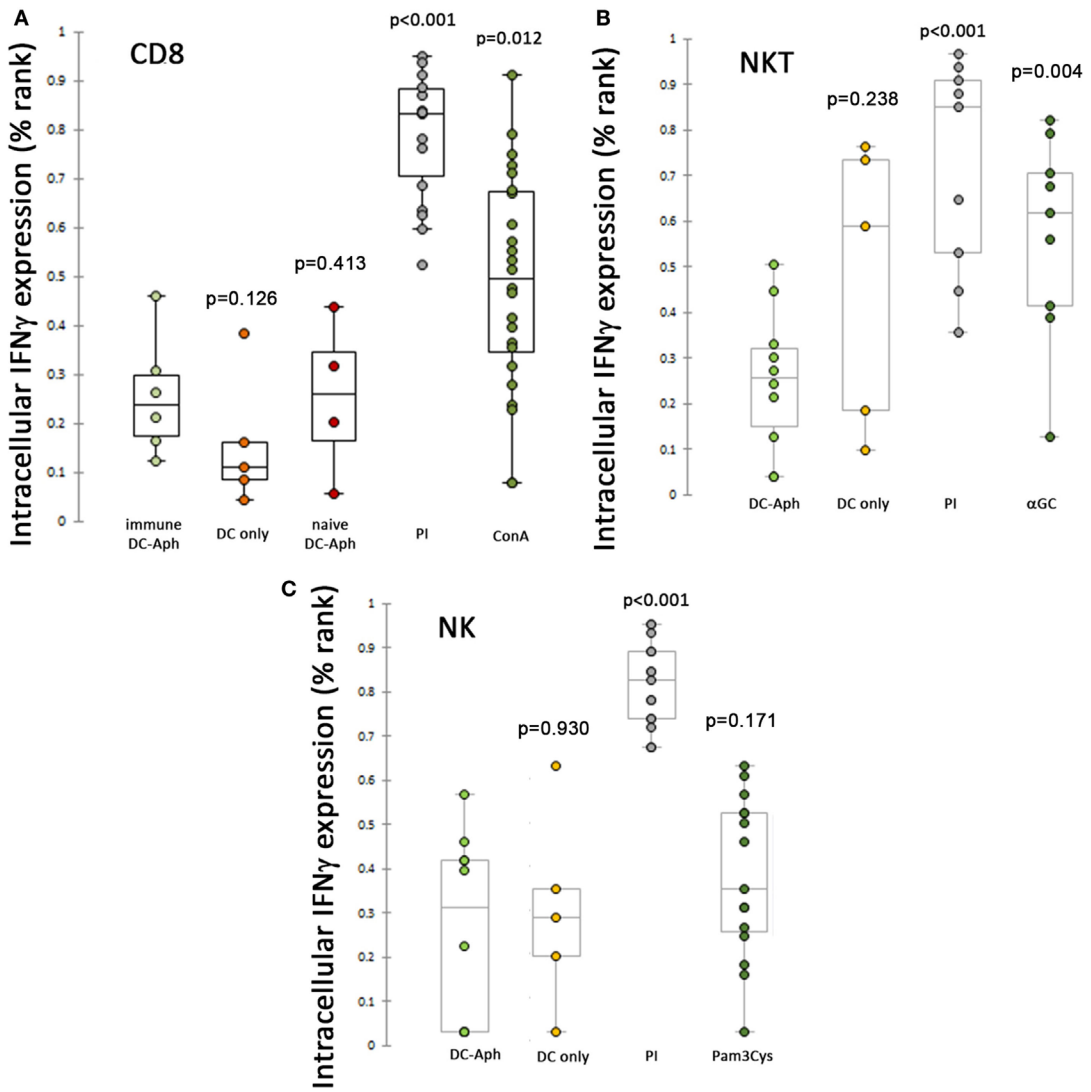


FIGURE 3 | Suppression of intracellular IFNγ production after stimulation of splenic cytotoxic lymphocytes (CTLs) by *A. phagocytophilum*-loaded dendritic cells (DCs). Intracellular production of IFNγ was measured as described in **Figure 2** and in the Section "Materials and Methods." Immune CD8 T **(A)**, NKT **(B)**, and NK **(C)** lymphocytes were suppressed from *A. phagocytophilum*-induced IFNγ expression as compared with positive control stimuli PMA/Ionomycin (all CTLs; **A–C**), ConA (CD8 T lymphocytes; **A**), and αGalCer (NKT lymphocytes; **B**). *P* values are generated from ranked data (as described in the Section "Materials and Methods" and **Figure 2**) and are displayed over each variable compared to the cells exposed to *A. phagocytophilum*-loaded DCs (DC-Aph). Aph, *Anaplasma phagocytophilum*.

cell's cytosol for MHC class I processing (41). By contrast, its ability to engage surfaces of myeloid and monocytic cells suggests effective endocytosis but ineffective remodeling of the newly formed vacuole for prolonged survival within monocyte-differentiated cells (32). It is likely that these vacuoles fuse with the degradative complexes that precede antigen processing and presentation, typically the domain of MHC class II presentation. Given the lack of the ability to generate effective cytotoxicity across three major CTL types (CD8, NKT, and NK cells) suggest a defect in processing for MHC class I presentation within APCs. Permutations for the MHC class I processing route could occur at delivery into or with proteasome degradation within the cytosol, delivery through transporter associated with antigen processing protein into the endoplasmic reticulum, proteolytic processing within the endoplasmic reticulum, loading of cargo onto MHC class I molecules, or delivery of the loaded MHC class I to the cell surface. While there are potential interactions that could be experimentally tested (32, 42, 43), little data currently exist to support most of these potential points of subversion.

Could *A. phagocytophilum* products derived *via* the processing for presentation by APCs impact its ability to present and activate CTLs? Among annotated NLRs, recent studies performed implicate NLRC5 as the key regulator of MHC class I gene expression (44–46). Regulation of NLRC5 expression is unclear, but likely linked in part to stimulation by type I and II interferons (47), Poly I:C (a mimic of double stranded RNA) (48), and possibly by bacterial porins, of which *A. phagocytophilum* expresses large quantities (49). Is it plausible that *A. phagocytophilum* impairs MHC class I expression *via* NLRC5, resulting in the observed failure to activate cytotoxicity and IFNγ generation in *A. phagocytophilum*-specific responses? We recently completed RNAseq transcriptional profiling of *A. phagocytophilum* infection in ATRA-differentiated HL-60 promyelocytic leukemia cells and examined splice variant transcripts (unpublished data). Although the studies were conducted in a cell differentiated toward myeloid maturity, within the transcriptome were identified 17 distinct alternative isoforms of NLRC5, all but one which were not differentially regulated by the infection; however, one nonsense-mediated decay isoform, *NLRC5*-010, was expressed at least ninefold greater with infection. Nonsense-mediated decay forms are now recognized as regulators of transcription in cell differentiation, in response to stress, and in development of disease (50). We suggest that additional studies to investigate whether this isoform transcript could affect NLRC5 and MHC class I expression should be conducted.

The results of this study will drive future investigations into the cellular and molecular mechanisms for the CTL functional dissociation of MASs. These data also provide another avenue to explore acquired or infectious MASs unrelated to this pathogen through the conduct of *in vivo* cytotoxicity studies. Such investigations should confirm *in vitro* studies and illustrate which cells possess *in vivo* cytotoxicity, and whether impaired cytotoxicity leads to an enhanced proinflammatory phenotype which would recapitulate MAS and HPS disease states, and whether approaches directed at MHC class I expression might be fruitful avenues for control of disease manifestations.

ETHICS STATEMENT

All animal studies were reviewed and approved by the Johns Hopkins University Institutional Animal Care and Use committee. All mice were housed and cared for following the "Guide for the Care and Use of Laboratory Animals" (25).

AUTHOR CONTRIBUTIONS

DS helped conceive the work, conduct experimentation, interpret results, and write the manuscript. KSC helped to conceive the work, conducted most of the research, interpreted results, and helped to edit the manuscript. JD helped conceived the work, interpret the results, and write the manuscript.

FUNDING

Supported by grants NIAID R21-AI096062 (DS and JD), NIAID R01-AI 044102 (JD) and a by Visiting Professors Program grant NRF-2011-013-E00055 (KSC) from the National Research Foundation of Korea.

REFERENCES

1. Chen SM, Dumler JS, Bakken JS, Walker DH. Identification of a granulocytotropic *Ehrlichia* species as the etiologic agent of human disease. *J Clin Microbiol* (1994) 32:589–95.
2. Bakken JS, Krueth J, Wilson-Nordskog C, Tilden RL, Asanovich K, Dumler JS. Clinical and laboratory characteristics of human granulocytic ehrlichiosis. *JAMA* (1996) 275:199–205. doi:10.1001/jama.1996.03530270039029
3. Bakken JS, Dumler JS. Human granulocytic anaplasmosis. *Infect Dis Clin North Am* (2015) 29:341–55. doi:10.1016/j.idc.2015.02.007
4. Choi KS, Scorpio DG, Dumler JS. *Anaplasma phagocytophilum* ligation to toll-like receptor (TLR) 2, but not to TLR4, activates macrophages for nuclear factor-kappa B nuclear translocation. *J Infect Dis* (2004) 189:1921–5. doi:10.1086/386284
5. von Loewenich FD, Scorpio DG, Reischl U, Dumler JS, Bogdan C. Frontline: control of *Anaplasma phagocytophilum*, an obligate intracellular pathogen, in the absence of inducible nitric oxide synthase, phagocyte NADPH oxidase, tumor necrosis factor, toll-like receptor (TLR)2 and TLR4, or the TLR adaptor molecule MyD88. *Eur J Immunol* (2004) 34:1789–97. doi:10.1002/eji.200425029
6. Scorpio DG, Von Loewenich FD, Gobel H, Bogdan C, Dumler JS. Innate immune response to *Anaplasma phagocytophilum* contributes to hepatic injury. *Clin Vaccine Immunol* (2006) 13:806–9. doi:10.1128/CVI.00092-06
7. Choi KS, Dumler JS. *Anaplasma phagocytophilum*, interferon gamma production and Stat1 signaling. *Microbiol Immunol* (2013) 57:207–12. doi:10.1111/1348-0421.12023
8. Choi KS, Scorpio DG, Dumler JS. Stat1 negatively regulates immune-mediated injury with *Anaplasma phagocytophilum* infection. *J Immunol* (2014) 193:5088–98. doi:10.4049/jimmunol.1401381
9. Martin ME, Bunnell JE, Dumler JS. Pathology, immunohistology, and cytokine responses in early phases of human granulocytic ehrlichiosis in a murine model. *J Infect Dis* (2000) 181:374–8. doi:10.1086/315206
10. Martin ME, Caspersen K, Dumler JS. Immunopathology and ehrlichial propagation are regulated by interferon-gamma and interleukin-10 in a murine model of human granulocytic ehrlichiosis. *Am J Pathol* (2001) 158:1881–8. doi:10.1016/S0002-9440(10)64145-4
11. Dumler JS, Barat NC, Barat CE, Bakken JS. Human granulocytic anaplasmosis and macrophage activation. *Clin Infect Dis* (2007) 45:199–204. doi:10.1086/518834
12. Davies RS, Madigan JE, Hodzic E, Borjesson DL, Dumler JS. Dexamethasone-induced cytokine changes associated with diminished disease severity in horses infected with *Anaplasma phagocytophilum*. *Clin Vaccine Immunol* (2011) 18:1962–8. doi:10.1128/CVI.05034-11

13. Browning MD, Garyu JW, Dumler JS, Scorpio DG. Role of reactive nitrogen species in development of hepatic injury in a C57BL/6 mouse model of human granulocytic anaplasmosis. *Comp Med* (2006) 56:55–62.
14. Kirschning CJ, Schumann RR. TLR2: cellular sensor for microbial and endogenous molecular patterns. *Curr Top Microbiol Immunol* (2002) 270:121–44. doi:10.1007/978-3-642-59430-4_8
15. Chalifour A, Jeannin P, Gauchat JF, Blaecke A, Malissard M, N'guyen T, et al. Direct bacterial protein PAMP recognition by human NK cells involves TLRs and triggers alpha-defensin production. *Blood* (2004) 104:1778–83. doi:10.1182/blood-2003-08-2820
16. Della Chiesa M, Sivori S, Castriconi R, Marcenaro E, Moretta A. Pathogen-induced private conversations between natural killer and dendritic cells. *Trends Microbiol* (2005) 13:128–36. doi:10.1016/j.tim.2005.01.006
17. Wang X, Shaw DK, Hammond HL, Sutterwala FS, Rayamajhi M, Shirey KA, et al. The prostaglandin E2-EP3 receptor axis regulates *Anaplasma phagocytophilum*-mediated NLRC4 inflammasome activation. *PLoS Pathog* (2016) 12:e1005803. doi:10.1371/journal.ppat.1005803
18. Dumler JS. The biological basis of severe outcomes in *Anaplasma phagocytophilum* infection. *FEMS Immunol Med Microbiol* (2012) 64:13–20. doi:10.1111/j.1574-695X.2011.00909.x
19. Grom AA, Horne A, De Benedetti F. Macrophage activation syndrome in the era of biologic therapy. *Nat Rev Rheumatol* (2016) 12:259–68. doi:10.1038/nrrheum.2015.179
20. Morimoto A, Nakazawa Y, Ishii E. Hemophagocytic lymphohistiocytosis: pathogenesis, diagnosis, and management. *Pediatr Int* (2016) 58:817–25. doi:10.1111/ped.13064
21. Humblet-Baron S, Franckaert D, Dooley J, Bornschein S, Cauwe B, Schonefeldt S, et al. IL-2 consumption by highly activated CD8 T cells induces regulatory T-cell dysfunction in patients with hemophagocytic lymphohistiocytosis. *J Allergy Clin Immunol* (2016) 138:200–9.e8. doi:10.1016/j.jaci.2015.12.1314
22. Sieni E, Cetica V, Mastrodicasa E, Pende D, Moretta L, Griffiths G, et al. Familial hemophagocytic lymphohistiocytosis: a model for understanding the human machinery of cellular cytotoxicity. *Cell Mol Life Sci* (2012) 69:29–40. doi:10.1007/s00018-011-0835-y
23. Gerbec ZJ, Thakar MS, Malarkannan S. The Fyn-ADAP axis: cytotoxicity versus cytokine production in killer cells. *Front Immunol* (2015) 6:472. doi:10.3389/fimmu.2015.00472
24. Scorpio DG, Caspersen K, Ogata H, Park J, Dumler JS. Restricted changes in major surface protein-2 (*msp2*) transcription after prolonged in vitro passage of *Anaplasma phagocytophilum*. *BMC Microbiol* (2004) 4:1. doi:10.1186/1471-2180-4-1
25. National Research Council (US) Committee for the Update of the Guide for the Care and Use of Laboratory Animals. *Guide for the Care and Use of Laboratory Animals*. 8th ed. Washington, DC: National Academies Press US (2011). Available from: https://www.ncbi.nlm.nih.gov/books/NBK54050
26. Choi KS, Webb T, Oelke M, Scorpio DG, Dumler JS. Differential innate immune cell activation and proinflammatory response in *Anaplasma phagocytophilum* infection. *Infect Immun* (2007) 75:3124–30. doi:10.1128/IAI.00098-07
27. Inaba K, Swiggard WJ, Steinman RM, Romani N, Schuler G, Brinster C. Isolation of dendritic cells. *Curr Protoc Immunol* (2009) Chapter 3:Unit 3.7. doi:10.1002/0471142735.im0307s86
28. Romera-Cardenas G, Thomas LM, Lopez-Cobo S, Garcia-Cuesta EM, Long EO, Reyburn HT. Ionomycin treatment renders NK cells hyporesponsive. *PLoS One* (2016) 11:e0150998. doi:10.1371/journal.pone.0150998
29. Mansueto P, Vitale G, Cascio A, Seidita A, Pepe I, Carroccio A, et al. New insight into immunity and immunopathology of Rickettsial diseases. *Clin Dev Immunol* (2012) 2012:967852. doi:10.1155/2012/967852
30. Hafner LM. Pathogenesis of fallopian tube damage caused by *Chlamydia trachomatis* infections. *Contraception* (2015) 92:108–15. doi:10.1016/j.contraception.2015.01.004
31. Carlyon JA, Fikrig E. Mechanisms of evasion of neutrophil killing by *Anaplasma phagocytophilum*. *Curr Opin Hematol* (2006) 13:28–33. doi:10.1097/01.moh.0000190109.00532.56
32. Truchan HK, Seidman D, Carlyon JA. Breaking in and grabbing a meal: *Anaplasma phagocytophilum* cellular invasion, nutrient acquisition, and promising tools for their study. *Microbes Infect* (2013) 15:1017–25. doi:10.1016/j.micinf.2013.10.010
33. Walker DH, Dumler JS. The role of CD8 T lymphocytes in rickettsial infections. *Semin Immunopathol* (2015) 37:289–99. doi:10.1007/s00281-015-0480-x
34. Rinkler C, Kern Y, Bogdan C, Von Loewenich FD. Mechanisms of immunological control of *Anaplasma phagocytophilum* in mice. *Ann N Y Acad Sci* (2005) 1063:411–2. doi:10.1196/annals.1355.073
35. Pedra JH, Sutterwala FS, Sukumaran B, Ogura Y, Qian F, Montgomery RR, et al. ASC/PYCARD and caspase-1 regulate the IL-18/IFN-gamma axis during *Anaplasma phagocytophilum* infection. *J Immunol* (2007) 179:4783–91. doi:10.4049/jimmunol.179.7.4783
36. Chen G, Severo MS, Sakhon OS, Choy A, Herron MJ, Felsheim RF, et al. *Anaplasma phagocytophilum* dihydrolipoamide dehydrogenase 1 affects host-derived immunopathology during microbial colonization. *Infect Immun* (2012) 80:3194–205. doi:10.1128/IAI.00532-12
37. Wang X, Shaw DK, Sakhon OS, Snyder GA, Sundberg EJ, Santambrogio L, et al. The tick protein sialostatin L2 binds to annexin A2 and inhibits NLRC4-mediated inflammasome activation. *Infect Immun* (2016) 84:1796–805. doi:10.1128/IAI.01526-15
38. Choi KS, Dumler JS. Mitogenic component in polar lipid-enriched *Anaplasma phagocytophilum* membranes. *Clin Vaccine Immunol* (2007) 14:1260–5. doi:10.1128/CVI.00204-07
39. Neerincx A, Castro W, Guarda G, Kufer TA. NLRC5, at the heart of antigen presentation. *Front Immunol* (2013) 4:397. doi:10.3389/fimmu.2013.00397
40. Heimer R, Van Andel A, Wormser GP, Wilson ML. Propagation of granulocytic *Ehrlichia* spp. from human and equine sources in HL-60 cells induced to differentiate into functional granulocytes. *J Clin Microbiol* (1997) 35:923–7.
41. Lin M, Den Dulk-Ras A, Hooykaas PJ, Rikihisa Y. *Anaplasma phagocytophilum* AnkA secreted by type IV secretion system is tyrosine phosphorylated by Abl-1 to facilitate infection. *Cell Microbiol* (2007) 9:2644–57. doi:10.1111/j.1462-5822.2007.00985.x
42. Rikihisa Y. Mechanisms of obligatory intracellular infection with *Anaplasma phagocytophilum*. *Clin Microbiol Rev* (2011) 24:469–89. doi:10.1128/CMR.00064-10
43. Truchan HK, Cockburn CL, Hebert KS, Magunda F, Noh SM, Carlyon JA. The pathogen-pccupied vacuoles of *Anaplasma phagocytophilum* and *Anaplasma marginale* interact with the endoplasmic reticulum. *Front Cell Infect Microbiol* (2016) 6:22. doi:10.3389/fcimb.2016.00022
44. Meissner TB, Li A, Biswas A, Lee KH, Liu YJ, Bayir E, et al. NLR family member NLRC5 is a transcriptional regulator of MHC class I genes. *Proc Natl Acad Sci U S A* (2010) 107:13794–9. doi:10.1073/pnas.1008684107
45. Yao Y, Wang Y, Chen F, Huang Y, Zhu S, Leng Q, et al. NLRC5 regulates MHC class I antigen presentation in host defense against intracellular pathogens. *Cell Res* (2012) 22:836–47. doi:10.1038/cr.2012.56
46. Chelbi ST, Dang AT, Guarda G. Emerging major histocompatibility complex class I-related functions of NLRC5. *Adv Immunol* (2017) 133:89–119. doi:10.1016/bs.ai.2016.11.003
47. Kuenzel S, Till A, Winkler M, Hasler R, Lipinski S, Jung S, et al. The nucleotide-binding oligomerization domain-like receptor NLRC5 is involved in IFN-dependent antiviral immune responses. *J Immunol* (2010) 184:1990–2000. doi:10.4049/jimmunol.0900557
48. Staehli F, Ludigs K, Heinz LX, Seguin-Estevez Q, Ferrero I, Braun M, et al. NLRC5 deficiency selectively impairs MHC class I-dependent lymphocyte killing by cytotoxic T cells. *J Immunol* (2012) 188:3820–8. doi:10.4049/jimmunol.1102671
49. Huang H, Wang X, Kikuchi T, Kumagai Y, Rikihisa Y. Porin activity of *Anaplasma phagocytophilum* outer membrane fraction and purified P44. *J Bacteriol* (2007) 189:1998–2006. doi:10.1128/JB.01548-06
50. Nickless A, Bailis JM, You Z. Control of gene expression through the nonsense-mediated RNA decay pathway. *Cell Biosci* (2017) 7:26. doi:10.1186/s13578-017-0153-7

Disclaimer: The opinions expressed herein are those of the author(s) and are not necessarily representative of those of the Uniformed Services University of the Health Sciences (USUHS), the Department of Defense (DOD); or, the United States Army, Navy, or Air Force.

Conflict of Interest Statement: The research was conducted in the absence of any commercial or financial relationships that could be construed as a potential conflict of interest.

Copyright © 2018 Scorpio, Choi and Dumler. This is an open-access article distributed under the terms of the Creative Commons Attribution License (CC BY). The use, distribution or reproduction in other forums is permitted, provided the original author(s) and the copyright owner are credited and that the original publication in this journal is cited, in accordance with accepted academic practice. No use, distribution or reproduction is permitted which does not comply with these terms.

frontiers in Immunology

REVIEW
published: 16 April 2018
doi: 10.3389/fimmu.2018.00673

The Complexity of Fungal β-Glucan in Health and Disease: Effects on the Mononuclear Phagocyte System

*Giorgio Camilli[1], Guillaume Tabouret[2] and Jessica Quintin[1]**

[1] *Immunology of Fungal Infections, Department of Mycology, Institut Pasteur, Paris, France,* [2] *Université de Toulouse, INRA, INP, ENVT, IHAP, Toulouse, France*

β-glucan, the most abundant fungal cell wall polysaccharide, has gained much attention from the scientific community in the last few decades for its fascinating but not yet fully understood immunobiology. Study of this molecule has been motivated by its importance as a pathogen-associated molecular pattern upon fungal infection as well as by its promising clinical utility as biological response modifier for the treatment of cancer and infectious diseases. Its immune effect is attributed to the ability to bind to different receptors expressed on the cell surface of phagocytic and cytotoxic innate immune cells, including monocytes, macrophages, neutrophils, and natural killer cells. The characteristics of the immune responses generated depend on the cell types and receptors involved. Size and biochemical composition of β-glucans isolated from different sources affect their immunomodulatory properties. The variety of studies using crude extracts of fungal cell wall rather than purified β-glucans renders data difficult to interpret. A better understanding of the mechanisms of purified fungal β-glucan recognition, downstream signaling pathways, and subsequent immune regulation activated, is, therefore, essential not only to develop new antifungal therapy but also to evaluate β-glucan as a putative anti-infective and antitumor mediator. Here, we briefly review the complexity of interactions between fungal β-glucans and mononuclear phagocytes during fungal infections. Furthermore, we discuss and present available studies suggesting how different fungal β-glucans exhibit antitumor and antimicrobial activities by modulating the biologic responses of mononuclear phagocytes, which make them potential candidates as therapeutic agents.

Keywords: fungal, β-glucan, mononuclear, phagocyte, health, disease

OPEN ACCESS

Edited by:
Yoann Rombouts, UMR5089 Institut de Pharmacologie et de Biologie Structurale (IPBS), France

Reviewed by:
Melissa Lodoen, University of California, Irvine, United States
Patricia Talamás-Rohana, Centro de Investigación y de Estudios Avanzados del Instituto Politécnico Nacional (CINVESTAV-IPN), Mexico

****Correspondence:***
Jessica Quintin
jessica.quintin@pasteur.fr

Specialty section:
This article was submitted to Microbial Immunology, a section of the journal Frontiers in Immunology

Received: *20 December 2017*
Accepted: *19 March 2018*
Published: *16 April 2018*

Citation:
Camilli G, Tabouret G and Quintin J (2018) The Complexity of Fungal β-Glucan in Health and Disease: Effects on the Mononuclear Phagocyte System. Front. Immunol. 9:673. doi: 10.3389/fimmu.2018.00673

INTRODUCTION

β-glucans are naturally occurring glucose polymers that are present in abundance in plants, bacteria, and fungi. For centuries, traditional Chinese medicine uses fungi for healing and currently, interests have focused on polysaccharides that are a crucial component of fungi cell walls (1). Within the multitude of polysaccharides present, β-glucans are a key reason fungi are used in cosmetics, as food additives, or as medicinal purposes (2); they have also shown beneficial effects in the outcome of various diseases (3). β-glucans, share a common structure consisting of a backbone of β(1,3)-linked β-D-glucopyranosyl units. However, they can strongly differ by their length and branching structure. Fungal β-glucans, that represent the most abundant polysaccharides found in the cell wall of fungi,

are mainly characterized by the presence of β(1,6)-linked branches coming off of the β(1,3) backbone. The structural diversity also depends on the fungal source (4). For example, β-glucans of mushrooms have short β(1,6)-linked branches whereas those of yeast have β(1,6)-side branches with additional β(1,3) regions (5). Of note, these structural differences may influence the immunogenic properties of β-glucans and many studies have suggested that a higher degree of structural complexity is associated with enhanced β-glucans-induced antimicrobial and anticancer activities (6).

β-glucans as the most abundant fungal cell wall polysaccharide in human fungal pathogens, is also a key pathogen-associated molecular pattern (PAMP) that is detected upon fungal infection to trigger the host immune responses in vertebrates and invertebrates (7). Different membrane-bound immune receptors can recognize β-glucans and receptor binding is also dependent on the structure and nature of the β-glucan (8). In fact, the cellular responses induced by mushroom or yeast β-glucans depend on their specific interactions with several cell surface receptors (PRRs), as scavenger receptors, lactosylceramide (LacCer), complement receptor 3 (CR3; CD11b/CD18), and dectin-1. Although the binding of β-glucan to LacCer (9) or scavenger receptors (10) on the cell surface of leukocytes has been described, the biological mechanisms that can result from these interactions and the effects on the immune responses are still lacking and need further investigations.

Complement receptor 3 is a heterodimeric transmembrane glycoprotein consisting of CD11b noncovalently associated with CD18 and mainly expressed on neutrophils, monocytes, and natural killer (NK) cells. Besides its first reported role in triggering phagocytosis and degranulation in response to yeast iC3b-opsonized yeast (11, 12), CR3 also has a β-glucans-specific binding site that map to a lectin-site C-terminal of the I-domain of the CD11b (13). β-glucan binding to the lectin site of the CR3 on phagocytes and NK cells primes the receptor to enhance the cytotoxicity against iC3b-opsonized target cells, including tumors, that are otherwise resistant to CR3-dependent cytotoxicity (14, 15). Recently, much attention has been focused on dectin-1, predominantly expressed on the cell surface of monocyte, macrophages, neutrophils, and dendritic cells (DCs), which has emerged as the primary β-glucan receptor (16–18). Interestingly, however, there has been some controversy about the relative importance of the various β-glucan receptors, and their activity seems to be tightly dependent on the cell context. In fact, while neutrophil modulation by β-glucan is predominantly CR3-dependent, dectin-1 is the most important β-glucan receptor on macrophages (19, 20).

Dectin-1 is a type II transmembrane protein characterized by the presence of an extracellular C-type lectin-like domain, a stalk, a transmembrane region, and an intracellular region with an immunoreceptor tyrosine-based activation motif (ITAM)-like motif containing a single tyrosine residue (21, 22). Binding of β-glucan to dectin-1 induces the phosphorylation of the hemi-ITAM, phosphorylation of Syk, and activation of the CARD9/Bcl10/MALT-1 (caspase recruitment domain/B cell CLL-lymphoma 10/mucosa associated lymphoid tissue lymphoma translocation gene 1) signaling complex, which in turn leads to the activation of the downstream signaling pathway (23). Moreover, Dectin-1 can also induce signaling *via* Raf-1 in a Syk-independent fashion as well as through the PI3K/Akt pathway (24, 25). As a consequence of these signaling activations, dectin-1 triggers phagocytosis, ROS generation, microbial killing, and cytokine production. Of note, β-glucan/dectin-1 interaction *per se* is sufficient to induce the phagocytosis and production of ROS. In contrast, the production of inflammatory cytokines seems to be dependent on the cooperation between dectin-1 and toll-like receptors (TLRs) (26–28).

The high structural variability, low purity, and the ability to bind to different receptors are probably the main limitations of current β-glucan research. Differences in the molecular weight, degree of branching, triple helical conformation, and solubility may affect the binding affinity of β-glucan to each receptor leading to activation of multiple and variable signaling pathways. A systematic investigation of the receptor binding, the signaling pathway, and the activated immune responses induced by pure β-glucans with known structure is, therefore, needed to better understand the fungal pathogenesis but also to effectively apply the use of the β-glucan for the treatment of cancer and infectious diseases.

The objectives of this review are to present the different functions triggered by mononuclear phagocytes upon an encounter with β-glucans covering the mechanisms of recognition and the importance of β-glucans structural diversity, as well as the interaction of the β-glucan with the host during an infection. We will also explore the effects of fungal β-glucan treatment on cancer and infectious diseases and finally discussed the recently described innate immune memory of monocytes associated with β-glucans training.

β-GLUCAN-MEDIATED INTERACTIONS OF FUNGAL PATHOGENS WITH MONONUCLEAR PHAGOCYTES

A diverse group of fungi is known to be pathogenic for humans, including *Candida* spp., *Cryptococcus neoformans*, *Aspergillus fumigatus*, and *Histoplasma capsulatum*. Fungal pathogenic organisms can cause diseases varying from mild infections of the skin and cutaneous tissues to severe invasive infections when tissue homeostasis is compromised. Of note, the prevalence of fungal infections registered a dramatic increase during the last decades due to a variety of factors, including AIDS epidemic and the use of immunosuppressive treatments in cancer and transplanted patients (29). An intact immune system is, therefore, essential to control fungal infections, and mononuclear phagocytes play a pivotal role in host defense against fungal invasion (30).

Since the discovery of specific PRRs for β-glucan on the cell surface of phagocytes (i.e., CR3 and dectin-1), this abundant cell wall polysaccharide has drawn increasingly more attention as a key PAMP in the host immune recognition of pathogenic fungi. However, some fungal species have developed surface structures to evade such immune control mechanism. For example, *H. capsulatum* can mask the recognition of the immunogenic β-(1,3)-glucan by phagocytic receptors through a less immunogenic outer layer of α-(1,3)-glucan (31). Similarly,

C. neoformans hides their surface immunogenic molecules, including β-(1,3)-glucan, behind a polysaccharide capsule thus inhibiting phagocytosis and cytokine production by macrophages (32). Pathogenicity of dimorphic fungi, such as the yeast *Candida albicans*, is known to be linked to their capacity to adapt and switch back and forth between the filamentous and yeast growth. Interestingly, β-glucan, which is normally masked by the mannan layer of the yeast cell wall, becomes exposed at the budding scar, but not during the filamentous growth. Thus, the process of the budding growth has been suggested as the target for dectin-1 recognition by macrophages (33). Moreover, β-glucan structure and activity differ between *C. albicans* yeast and hyphae (34). Interestingly, dectin-1, in contrast to other PRRs, discriminates between soluble and particulate β-glucans (35). Phagocytosis and cytokine production by macrophages are only induced when dectin-1 is bound to particulate β-glucan or live fungi through the formation of a "phagocytic synapse" and the exclusion of regulatory phosphatases (35). This process represents a unique mechanism to discriminate PAMPs associated with a microbial surface.

Recognition of the fungal PAMPs by phagocytes and the subsequent engulfment of the pathogen *via* phagocytosis represent the first steps to control fungal infections [as reviewed in Ref. (36)]. A series of signaling events are required to mediate phagocytosis when dectin-1 binds to the β-glucan-rich fungal cell wall. As mentioned above, clustering of dectin-1 with the concomitant exclusion of CD148 and CD45 phosphatases are essential steps to induce hemi-ITAM phosphorylation and recruitment of Syk kinase (35). However, the requirement of Syk in the phagocytic process is controversial, and its role is probably cell type dependent. In fact, the inactivation of Syk does not impair the phagocytosis of β-glucan-containing particles in genetically or pharmacologically inactivated macrophages (28, 37). On the opposite, Syk knockdown DCs are unable to phagocytose zymosan particles (38). Moreover, dectin-1 translocation to β-glucan-containing phagosomes and the subsequent Syk activation allow the acidification and maturation of *C. albicans* and β-glucan-containing phagosomes in macrophages (39). β-glucan binding to dectin-1 is, therefore, not only important to trigger phagocytosis but also to allow the lysosomal fusion and acidification of the phagocytic compartment. It is likely that other molecules can mediate a dectin-1-dependent phagocytosis through related or independent pathways besides the hemi-ITAM-mediated Syk activation. For instance, Vav1 and PI3K are required for dectin-1/β-glucan-dependent phagocytosis in microglial cells (25). Similarly, PI3K and the RhoGTPase inhibitors significantly reduce the internalization of zymosan particles in RAW2643.7 cells expressing dectin-1 (28).

Recognition of β-glucan by Dectin-1 triggers autophagy through an LC3-associated phagocytosis and directs LC3 recruitment to phagosomes containing fungi (40). Importantly, this mechanism regulates the subsequent immunological response. The association of LC3 to the β-glucan-containing phagosomes increases MHC II recruitment to phagosomes and presentation of fungal-derived antigens to CD4 T cells by DCs (41).

Besides the phagocytosis and the acidification of macrophage phagosome, the production of oxidative molecules is another important mechanism in killing fungal pathogens. β-glucan/Dectin-1 interaction followed by Syk activation is crucial for the generation of ROS in mononuclear phagocytes (37, 42, 43). However, whether dectin-1-mediated oxidative burst is a universal key mechanism in controlling fungal killing remains to be elucidated. As such, dectin-1 activation and ROS production in macrophages are essential for killing of *Pneumocystis carinii* but not *C. albicans*, suggesting that the mechanism is only required for immune responses to some fungal infection (44). Interestingly, form and structure of β-glucan impact on the type of oxidative burst triggered in human monocytes. More precisely, particulate and phagocytizable β-glucan activates the NADPH-dependent reaction *via* dectin-1 while immobilized and non-phagocytizable one triggers the reaction in a CR3-dependent fashion (45). Moreover, ROS production can affect the antifungal immune responses by regulating a multiplicity of other mechanisms, such as autophagy and inflammasome activation (46).

Although it is well known that purified β-glucan is able to activate phagocytosis and production of ROS, its ability to induce cytokine production is still debated. Production of inflammatory mediators by fungi or crude β-glucan preparation (i.e., zymosan) is mediated by a collaboration between dectin-1 and TLRs. For example, production of TNF-α and IL-12 in macrophages and DCs upon stimulation with β-glucan-containing particles is due to a synergism between dectin-1 and TLR2 (27). When the zymosan is hot alkali-treated to remove its TLR-stimulating properties, the particles are still internalized and induce dectin-1 activation and ROS production. On the opposite, the depleted zymosan fails to induce cytokine production, suggesting that dectin-1/β-glucan signaling is not enough *per se* to trigger a robust release of inflammatory cytokines (27). Similarly, the production of TNF-α in response to zymosan or live fungi requires activation of dectin-1 as well as TLR2 and Myd88 (26). In addition, TNF-α production is strongly decreased in dectin-1-knockout macrophages treated with *C. albicans* or zymosan (43). Therefore, high inflammatory signature of mononuclear phagocytes induced by β-glucan seems to be linked to a multiple receptor activation, but dectin-1 remains a crucial component in this network. Intriguingly, β-glucan binding to dectin-1 only, strongly induces the release of inflammatory molecules by mononuclear phagocytes when phagocytosis is impaired by actin polymerization inhibitors (47–49). Therefore, phagocytosis of β-glucan is also involved in the modulation of dectin-1 signaling and the weak mediated inflammatory response (47–49).

Many efforts have been recently made to examine the role of fungi and β-glucan in inflammasome activation and subsequent production of IL-1β. NLRP3 inflammasome plays a crucial role in regulating antifungal immune responses and host survival. Mice with impaired NLRP3 present increased fungal burden and decreased survival to *C. albicans*, *A. fumigatus*, or *C. neoformans* infections (50–53). β-glucan and fungi trigger the induction and processing of IL-1β in mouse DCs *via* dectin-1 and through the activation of a non-canonical caspase-8 inflammasome (54). The inflammasome is a multiprotein complex that regulates the processing and release of IL-1β and IL-18 but also triggers pyroptosis, a form of cell death of the infected cell that is distinct from classical apoptosis or necrosis and represents an efficient effector

mechanism to protect the host from infection (55). *C. albicans* causes macrophage cell death by pyroptosis (56) and mutant of *C. albicans* that is defective in triggering pyroptosis has reduced β-glucan exposure in hyphae (57). However, to date, there are no convincing evidences that β-glucan itself can trigger pyroptosis directly.

EFFECTS OF FUNGAL β-GLUCAN TREATMENT ON INFECTIOUS DISEASES AND CANCER: INVOLVEMENT OF THE MONOCYTE–MACROPHAGE AXIS

β-glucans are the key reason fungi are used in pharmacology and thought to positively impact cancer and infection evolution (3). *In vivo*, intramuscular administration of PGG-glucan, a highly purified soluble β-glucan isolated from *Saccharomyces cerevisiae*, results in an overall reduction in mortality and increase in absolute circulating numbers monocyte count in rats after a challenge with antibiotic-resistant *Staphylococcus aureus* (58). Monocytes isolated from untreated and β-glucan-treated mice show a different magnitude of cytokine response when stimulated *ex vivo* with either endotoxins or enterotoxins. Monocytes isolated from β-glucan-treated mice release a lower amount of pro-inflammatory cytokines involved in the pathogenesis of sepsis (i.e., TNF-α and IL-6) upon toxic stimulation, compared to cells isolated from control mice, suggesting a mechanism by which β-glucan treatment may reduce the host mortality during septicemia (59). Moreover, protection of glucan-treated mice from *Escherichia coli*-induced experimental peritonitis and bacteremia is due, in part, to an enhanced macrophage phagocytic function induced by the glucan (60). Lentinan, a (1,6)-branched (1,3)-β-glucan isolated from Japanese mushroom *Lentinus edodes* reduces *Mycobacterium tuberculosis* infection in mice and rats infected intraperitoneally and intranasally, respectively. Mouse peritoneal or rat alveolar macrophages show an increased acid phosphatase activity, free radicals production, and killing activity against *M. tuberculosis* (61, 62). In addition, *in vitro* stimulation of murine macrophages with Lentinan selectively attenuate AIM2 and non-canonical inflammasome activation. Accordingly, mice treated with Lentinan show a significant decrease in peritoneal IL-1β secretion after *Listeria monocytogenes* (AIM2 inflammasome trigger)-induced peritonitis (63). Lentinan administration also alleviates endotoxemic lethality of LPS-treated mice by inhibition of non-canonical inflammasome activation (63).

β-glucan has also been reported to have multiple antitumor properties and its effect may depend on the modulation of macrophage activity. The antitumor activity of GRN, a (1,6)-branched (1,3)-β-glucan obtained from mycelia of *Grifola frondosa*, is reduced when macrophage function are impaired with carrageean, suggesting a key role of macrophages in the antitumor-mediated mechanism (64). Peritoneal macrophages isolated from intraperitoneally lentinan-treated mice have a higher *in vitro* antitumor cytotoxic activity against murine or human target cells (65). Oral administration of *L. edodes* and *G. frondosa* counteract the inhibition of the chemotactic activity of macrophages induced by the carcinogen BBN (N-butyl-N-butanolnitrosoamine) (66). Blockage and inhibition in mice of dectin-1 expression on macrophages with mAbs, decrease the antitumor activity of SPG, a (1,6)-branched (1,3)-β-glucan from *S. commune* (67). Moreover, intravenous administration in mice of β-glucan isolated from *S. cerevisiae* strain reduces the colon 26-M3.1 carcinoma cell growth and increases the survival time of the tumor-bearing mice. These effects are associated with a higher production of pro-inflammatory cytokines and tumoricidal activity of peritoneal macrophages as well as an increased NK cell cytotoxicity (68). Orally administered β-glucan can enhance the tumoricidal activity of phagocytes toward iC3b-opsonized cancer cells. Schematically, the orally administered particulate yeast β-glucan is internalized by gastrointestinal macrophages and shuttles to the bone marrow where the glucan is degraded and released as a smaller size β-glucan fragments that are taken up by granulocytes *via* the CR3 receptor. The granulocytes with β-glucan-primed CR3 then kill iC3b/mAbs-coated tumor cells (69). Importantly, oral administration of β-glucan isolated either from mushrooms or yeast has the capacity to phenotypically convert the immunosuppressive M2 or tumor-associated macrophages into inflammatory M1 macrophages. In addition, the M2-to-M1 switch induced by β-glucan treatment leads to a reduced tumor burden (70, 71).

β-glucans also have potent hematopoietic activities by enhancing the production of hematopoietic factors, bone marrow recovery, as well as stem cell homing and engraftment. The hematopoiesis-stimulating properties of β-glucans are summarized in detail in the review by Hofer and Pospisil (72). Mice injected intraperitoneally with yeast β-glucan present macrophages with an altered morphology, increase in phosphatase activity as well as increased NO and superoxide production. These effects are especially observed when the animals are treated with β-glucan with a higher level of structural complexity in terms of molecular weight and degree of (1,6)-linkages (73). In addition, polysaccharides purified from the mycelium of *Ganoderma lucidum* (GL-PS), a medical mushroom commonly used in China, can impact immune cell proliferation and DCs maturation (74). GL-PS induces a proliferative response in human leukemia cell lines but also facilitates the maturation of DCs derived from THP1 monocytic leukemia cell line (75).

While animal studies seem promising, evidences for a human clinical application of the β-glucan are currently limited and does not fully support their recommendation. Most of the available clinical trials come from Eastern Countries and focused on the potential application of mushrooms in cancer therapy. A prospective clinical trial in patients with advanced breast cancer shows that administration of 10 mg capsules of soluble β-glucan from *S. cerevisiae* induces the proliferation and activation of peripheral blood monocytes with no clinical side effects (76). However, whether this can be clinically beneficial remains undisclosed. By contrast, the antimicrobial effect of β-glucan has been poorly investigated by clinical trials and results remain controversial. A phase I and II trials show that treatment with PGG-glucan reduces infection rates in high-risk surgery patients. However, while PGG-glucan administration lead to a reduction of serious infections and death, an increased incidence of adverse events is observed in patients receiving β-glucan treatment and phase III trial was terminated (77–79).

β-GLUCAN IMPRINTING OF MONONUCLEAR IMMUNE CELLS

As described above, direct administration of fungal β-glucans may positively impact the outcome of a number of infectious diseases. Interestingly, past few years of research have enlightened a protective phenomenon triggered by the pre-administration of β-glucans, a mechanism mediated by monocytes and coined trained immunity (80). The observation that fungi could trigger a protective innate immune memory was first made upon the inoculation of non-germinating attenuated strains of the opportunistic human fungal pathogen *C. albicans*. Inoculation with this strain not only protects the mice against a virulent *C. albicans* but also against bacteria (81). The protection is independent of T lymphocytes, as observed in athymic mice (82), but dependent on macrophages (81) and pro-inflammatory cytokines (83). Macrophages are highly plastic cells and the innate immune system presents some adaptive properties (84, 85). The protection mediated is not restrained to avirulent fungal strains. Mice defective in adaptive T and B lymphocytes can be protected against re-infection with *C. albicans* in a monocyte-dependent manner and using a virulent strain of fungi (86). These recent works shed light on the mechanisms behind the innate immune protection mediated. Within *C. albicans,* the β-glucan cell wall component of the yeast induces a functional reprogramming of monocytes leading to enhanced inflammatory responses *in vivo* in mice and *ex vivo* in humans (86). The β-glucan receptor dectin-1, as well as to a lesser extent the CR3 receptor, are mediating the signal and the non-canonical Raf-1 pathway, but not Syk pathway, are key components in the heightened immune status triggered in monocytes. Whole-genome transcriptional and epigenetic analyses have clearly demonstrated that in the process of β-glucans-induced training, many inflammatory genes are downregulated and others are not modified or even upregulated (87). β-glucans imprint the innate immune memory in monocytes through stable changes in histone methylation and acetylation, of promoters and enhancers (86, 87). More specifically, initial activation of gene transcription by the first β-glucans encounter is accompanied by the acquisition of specific chromatin marks, which are for some maintained even after the elimination of the stimulus. This enhanced epigenetic status of the mononuclear phagocytes, illustrated for example by the persistence of H3K4me1, characterizing "latent enhancers," results in a stronger response to secondary stimuli upon a non-specific (non-fungal-related) secondary challenge.

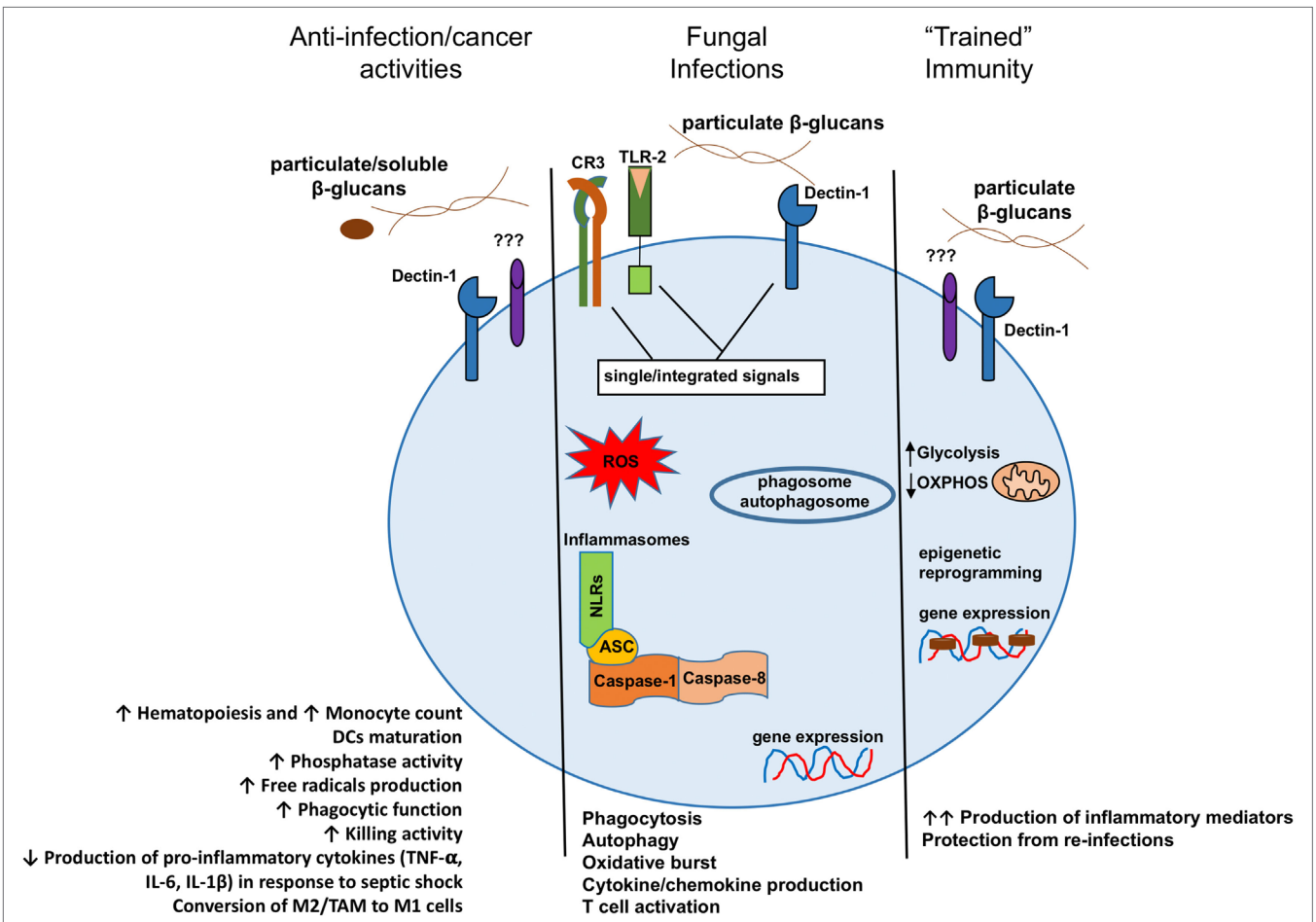


FIGURE 1 | Model presenting the different consequences of β-glucan recognition by mononuclear phagocytes in the context of antitumoral activities, fungal infection recognitions, or trained immunity. DCs, dendritic cells; M2, alternative macrophages; TAM, tumor-associated macrophages; M1, classical macrophages.

Pathway analysis of the different cluster of genes identified in the whole-genome transcriptional and epigenetic analyses highlight important immunological (cAMP-PKA activation) and metabolic (aerobic glycolysis) pathways (87, 88). These pathways play crucial roles in the induction and maintenance of trained immunity (87, 88). As such, β-glucans trained monocytes present a shift from oxidative phosphorylation toward glycolysis through an Akt/mTOR/HIF-1α-dependent pathway, a phenomenon reminiscent of the Warburg effect in cancer (88). Whether and how this shift influences epigenetic processes in trained immunity needs to be further investigated. However, glycolysis, glutaminolysis, and the cholesterol synthesis pathway are imperative for the induction of trained immunity by β-glucan in monocytes (89). Actually, fumarate accumulation through glutaminolysis integrates immune and metabolic circuits to induce monocyte epigenetic reprogramming by inhibiting KDM5 histone demethylases and fumarate itself induced an epigenetic program that mimics β-glucan-induced trained immunity (89).

Studies in patients and healthy volunteers have also helped understanding some of the crucial inflammatory effects required in trained immunity induced by β-glucan on monocytes. The immunological networks activated in trained monocytes depend on STAT1 activation, and defects in trained immunity have been reported in patients with chronic mucocutaneous candidiasis due to *STAT1* mutations (90). Finally, individuals with autophagy defects are unable to mount a full and potent trained immunity (91).

To our knowledge, only one trial has investigated the potential of β-glucan training effect in human circulating monocytes function (92). Oral β-glucan is inexpensive and well-tolerated and, therefore, thought to potentially represent a promising immunostimulatory compound for human use. In the randomized open-label intervention pilot-study, 15 healthy male volunteers absorbed a daily dose of 1,000 mg of β-glucan at once for 7 days (92). However, β-glucan is barely detectable in serum of volunteers at all time-points and neither cytokine production nor microbicidal activity of leukocytes are affected by orally administered β-glucan. The present study does not support the use of oral β-glucan to enhance innate immune responses in humans but does not preclude the use of a higher dosage of β-glucan to reach detectable level in the blood (92).

Regarding trained immunity in monocytes, it is important to consider the life span of these cells. Monocytes are cells with a short half-life in circulation, with studies suggesting it to be up to 1 day (93). Considering a long-lasting effect of the innate immune memory might, however, still be a valid hypothesis as orally administered β-glucans are taken up by macrophages and transported to some hematopoietic niches (69). Moreover, β-glucan administration to mice-induces expansion of hematopeitic progenitors in the bone marrow which is associated with cell metabolism and results in a beneficial response to chemotherapy-induced myelosuppression or secondary LPS challenge (94). Rather than a direct β-glucan contact with progenitors, modulation of hematopoietic progenitors is mediated by the immune mediators environment (IL-1, GM-CSF) (94).

CONCLUSION

Several experimental evidences have demonstrated a crucial role for β-glucan in the host–pathogen interaction during infections. Moreover, considerable efforts have been made to understand the cellular and molecular mechanisms of action of β-glucan in fungal pathogenesis as well as how it promotes a phagocytic-mediated immune response. Similarly, administration of fungal β-glucan is well known to stimulate the immune system and boost resistance to various infectious diseases and cancers, highlighting the multifaceted role of this molecule (**Figure 1**). However, although many *in vivo* studies have shown a beneficial effect of the β-glucans isolated from different sources, a comprehensive investigation of the mechanism of action is still lacking. In addition, the absence of detailed methodology on experimentation, β-glucan molecules source and purity reached render interpretation of the various results very complex. As such, discrepancies observed in the different studies are mainly related to the choice of purified components being used. In addition, unfortunately only few human studies are available and most of them have not been followed up with success. Hence, the possibility for clinical application of β-glucan should be considered with caution and will require further investigation. Future studies need to deeply characterize how β-glucans with different structure and molecular weight interact with each receptor and which specific signaling pathways are triggered. Moreover, providing details on the procedure and composition of the carbohydrate molecule under investigation remains crucial. An understanding should be made in the near future to use a common standardized β-glucan molecule with described biochemical properties. With such a common control, we might endeavor a rational use of this promising molecule in the future as an adjuvant or therapeutic agent.

AUTHOR CONTRIBUTIONS

GC, GT, and JQ jointly wrote the manuscript and approved it for publication.

FUNDING

GC and JQ were supported by the ANR JCJC grant ANR-16-CE15-0014-01 (to JQ). GT and JQ were supported by the Institut Carnot Pasteur MI and Institut Carnot Animal Health (F2E) grant ANR 11-CARN 017-01.

REFERENCES

1. Chang R. Bioactive polysaccharides from traditional Chinese medicine herbs as anticancer adjuvants. *J Altern Complement Med* (2002) 8:559–65. doi:10.1089/107555302320825066
2. Rop O, Mlcek J, Jurikova T. Beta-glucans in higher fungi and their health effects. *Nutr Rev* (2009) 67:624–31. doi:10.1111/j.1753-4887.2009.00230.x
3. Pelley RP, Strickland FM. Plants, polysaccharides, and the treatment and prevention of neoplasia. *Crit Rev Oncog* (2000) 11:189–225. doi:10.1615/CritRevOncog.v11.i34.10

4. Synytsya A, Novak M. Structural diversity of fungal glucans. *Carbohydr Polym* (2013) 92:792–809. doi:10.1016/j.carbpol.2012.09.077
5. Borchers AT, Keen CL, Gershwin ME. Mushrooms, tumors, and immunity: an update. *Exp Biol Med (Maywood)* (2004) 229:393–406. doi:10.1177/153537020422900507
6. Chen J, Seviour R. Medicinal importance of fungal beta-(1 – >3), (1 – >6)-glucans. *Mycol Res* (2007) 111:635–52. doi:10.1016/j.mycres.2007.02.011
7. Brown GD, Gordon S. Immune recognition of fungal beta-glucans. *Cell Microbiol* (2005) 7:471–9. doi:10.1111/j.1462-5822.2005.00505.x
8. Mueller A, Raptis J, Rice PJ, Kalbfleisch JH, Stout RD, Ensley HE, et al. The influence of glucan polymer structure and solution conformation on binding to (1 – >3)-beta-D-glucan receptors in a human monocyte-like cell line. *Glycobiology* (2000) 10:339–46. doi:10.1093/glycob/10.4.339
9. Zimmerman JW, Lindermuth J, Fish PA, Palace GP, Stevenson TT, DeMong DE. A novel carbohydrate-glycosphingolipid interaction between a beta-(1-3)-glucan immunomodulator, PGG-glucan, and lactosylceramide of human leukocytes. *J Biol Chem* (1998) 273:22014–20. doi:10.1074/jbc.273.34.22014
10. Rice PJ, Kelley JL, Kogan G, Ensley HE, Kalbfleisch JH, Browder IW, et al. Human monocyte scavenger receptors are pattern recognition receptors for (1 – >3)-beta-D-glucans. *J Leukoc Biol* (2002) 72:140–6. doi:10.1189/jlb.72.1.140
11. Cain JA, Newman SL, Ross GD. Role of complement receptor type three and serum opsonins in the neutrophil response to yeast. *Complement* (1987) 4:75–86. doi:10.1159/000463011
12. Ross GD, Cain JA, Myones BL, Newman SL, Lachmann PJ. Specificity of membrane complement receptor type three (CR3) for beta-glucans. *Complement* (1987) 4:61–74. doi:10.1159/000463010
13. Thornton BP, Vetvicka V, Pitman M, Goldman RC, Ross GD. Analysis of the sugar specificity and molecular location of the beta-glucan-binding lectin site of complement receptor type 3 (CD11b/CD18). *J Immunol* (1996) 156:1235–46.
14. Vetvicka V, Thornton BP, Ross GD. Soluble beta-glucan polysaccharide binding to the lectin site of neutrophil or natural killer cell complement receptor type 3 (CD11b/CD18) generates a primed state of the receptor capable of mediating cytotoxicity of iC3b-opsonized target cells. *J Clin Invest* (1996) 98:50–61. doi:10.1172/JCI118777
15. Ross GD, Vetvicka V, Yan J, Xia Y, Vetvickova J. Therapeutic intervention with complement and beta-glucan in cancer. *Immunopharmacology* (1999) 42:61–74. doi:10.1016/S0162-3109(99)00013-2
16. Ariizumi K, Shen GL, Shikano S, Xu S, Ritter R III, Kumamoto T, et al. Identification of a novel, dendritic cell-associated molecule, dectin-1, by subtractive cDNA cloning. *J Biol Chem* (2000) 275:20157–67. doi:10.1074/jbc.M909512199
17. Brown GD, Gordon S. Immune recognition. a new receptor for beta-glucans. *Nature* (2001) 413:36–7. doi:10.1038/35092620
18. Taylor PR, Brown GD, Reid DM, Willment JA, Martinez-Pomares L, Gordon S, et al. The beta-glucan receptor, dectin-1, is predominantly expressed on the surface of cells of the monocyte/macrophage and neutrophil lineages. *J Immunol* (2002) 169:3876–82. doi:10.4049/jimmunol.169.7.3876
19. van Bruggen R, Drewniak A, Jansen M, van Houdt M, Roos D, Chapel H, et al. Complement receptor 3, not Dectin-1, is the major receptor on human neutrophils for beta-glucan-bearing particles. *Mol Immunol* (2009) 47:575–81. doi:10.1016/j.molimm.2009.09.018
20. Brown GD, Taylor PR, Reid DM, Willment JA, Williams DL, Martinez-Pomares L, et al. Dectin-1 is a major beta-glucan receptor on macrophages. *J Exp Med* (2002) 196:407–12. doi:10.1084/jem.20020470
21. Huysamen C, Brown GD. The fungal pattern recognition receptor, dectin-1, and the associated cluster of C-type lectin-like receptors. *FEMS Microbiol Lett* (2009) 290:121–8. doi:10.1111/j.1574-6968.2008.01418.x
22. Brown GD. Dectin-1: a signalling non-TLR pattern-recognition receptor. *Nat Rev Immunol* (2006) 6:33–43. doi:10.1038/nri1745
23. Reid DM, Gow NA, Brown GD. Pattern recognition: recent insights from dectin-1. *Curr Opin Immunol* (2009) 21:30–7. doi:10.1016/j.coi.2009.01.003
24. Gringhuis SI, den Dunnen J, Litjens M, van der Vlist M, Wevers B, Bruijns SC, et al. Dectin-1 directs T helper cell differentiation by controlling noncanonical NF-kappaB activation through Raf-1 and Syk. *Nat Immunol* (2009) 10:203–13. doi:10.1038/ni.1692
25. Shah VB, Ozment-Skelton TR, Williams DL, Keshvara L. Vav1 and PI3K are required for phagocytosis of beta-glucan and subsequent superoxide generation by microglia. *Mol Immunol* (2009) 46:1845–53. doi:10.1016/j.molimm.2009.01.014
26. Brown GD, Herre J, Williams DL, Willment JA, Marshall AS, Gordon S. Dectin-1 mediates the biological effects of beta-glucans. *J Exp Med* (2003) 197:1119–24. doi:10.1084/jem.20021890
27. Gantner BN, Simmons RM, Canavera SJ, Akira S, Underhill DM. Collaborative induction of inflammatory responses by dectin-1 and toll-like receptor 2. *J Exp Med* (2003) 197:1107–17. doi:10.1084/jem.20021787
28. Herre J, Marshall AS, Caron E, Edwards AD, Williams DL, Schweighoffer E, et al. Dectin-1 uses novel mechanisms for yeast phagocytosis in macrophages. *Blood* (2004) 104:4038–45. doi:10.1182/blood-2004-03-1140
29. Brown GD, Denning DW, Gow NA, Levitz SM, Netea MG, White TC. Hidden killers: human fungal infections. *Sci Transl Med* (2012) 4:165rv13. doi:10.1126/scitranslmed.3004404
30. Swamydas M, Break TJ, Lionakis MS. Mononuclear phagocyte-mediated antifungal immunity: the role of chemotactic receptors and ligands. *Cell Mol Life Sci* (2015) 72:2157–75. doi:10.1007/s00018-015-1858-6
31. Rappleye CA, Eissenberg LG, Goldman WE. *Histoplasma capsulatum* alpha-(1,3)-glucan blocks innate immune recognition by the beta-glucan receptor. *Proc Natl Acad Sci U S A* (2007) 104:1366–70. doi:10.1073/pnas.0609848104
32. Cross CE, Bancroft GJ. Ingestion of acapsular *Cryptococcus neoformans* occurs via mannose and beta-glucan receptors, resulting in cytokine production and increased phagocytosis of the encapsulated form. *Infect Immun* (1995) 63:2604–11.
33. Gantner BN, Simmons RM, Underhill DM. Dectin-1 mediates macrophage recognition of *Candida albicans* yeast but not filaments. *EMBO J* (2005) 24:1277–86. doi:10.1038/sj.emboj.7600594
34. Lowman DW, Greene RR, Bearden DW, Kruppa MD, Pottier M, Monteiro MA, et al. Novel structural features in *Candida albicans* hyphal glucan provide a basis for differential innate immune recognition of hyphae versus yeast. *J Biol Chem* (2014) 289:3432–43. doi:10.1074/jbc.M113.529131
35. Goodridge HS, Reyes CN, Becker CA, Katsumoto TR, Ma J, Wolf AJ, et al. Activation of the innate immune receptor Dectin-1 upon formation of a 'phagocytic synapse'. *Nature* (2011) 472:471–5. doi:10.1038/nature10071
36. Erwig LP, Gow NA. Interactions of fungal pathogens with phagocytes. *Nat Rev Microbiol* (2016) 14:163–76. doi:10.1038/nrmicro.2015.21
37. Underhill DM, Rossnagle E, Lowell CA, Simmons RM. Dectin-1 activates Syk tyrosine kinase in a dynamic subset of macrophages for reactive oxygen production. *Blood* (2005) 106:2543–50. doi:10.1182/blood-2005-03-1239
38. Rogers NC, Slack EC, Edwards AD, Nolte MA, Schulz O, Schweighoffer E, et al. Syk-dependent cytokine induction by dectin-1 reveals a novel pattern recognition pathway for C type lectins. *Immunity* (2005) 22:507–17. doi:10.1016/j.immuni.2005.06.005
39. Mansour MK, Tam JM, Khan NS, Seward M, Davids PJ, Puranam S, et al. Dectin-1 activation controls maturation of beta-1,3-glucan-containing phagosomes. *J Biol Chem* (2013) 288:16043–54. doi:10.1074/jbc.M113.473223
40. Ma J, Underhill DM. Beta-glucan signaling connects phagocytosis to autophagy. *Glycobiology* (2013) 23:1047–51. doi:10.1093/glycob/cwt046
41. Ma J, Becker C, Lowell CA, Underhill DM. Dectin-1-triggered recruitment of light chain 3 protein to phagosomes facilitates major histocompatibility complex class II presentation of fungal-derived antigens. *J Biol Chem* (2012) 287:34149–56. doi:10.1074/jbc.M112.382812
42. Goodridge HS, Simmons RM, Underhill DM. Dectin-1 stimulation by *Candida albicans* yeast or zymosan triggers NFAT activation in macrophages and dendritic cells. *J Immunol* (2007) 178:3107–15. doi:10.4049/jimmunol.178.5.3107
43. Taylor PR, Tsoni SV, Willment JA, Dennehy KM, Rosas M, Findon H, et al. Dectin-1 is required for beta-glucan recognition and control of fungal infection. *Nat Immunol* (2007) 8:31–8. doi:10.1038/ni1408
44. Saijo S, Fujikado N, Furuta T, Chung SH, Kotaki H, Seki K, et al. Dectin-1 is required for host defense against *Pneumocystis carinii* but not against *Candida albicans*. *Nat Immunol* (2007) 8:39–46. doi:10.1038/ni1425
45. Bose N, Wurst LR, Chan AS, Dudney CM, LeRoux ML, Danielson ME, et al. Differential regulation of oxidative burst by distinct beta-glucan-binding receptors and signaling pathways in human peripheral blood mononuclear cells. *Glycobiology* (2014) 24:379–91. doi:10.1093/glycob/cwu005
46. Hogan D, Wheeler RT. The complex roles of NADPH oxidases in fungal infection. *Cell Microbiol* (2014) 16:1156–67. doi:10.1111/cmi.12320
47. Rosas M, Liddiard K, Kimberg M, Faro-Trindade I, McDonald JU, Williams DL, et al. The induction of inflammation by dectin-1 in vivo is dependent on

myeloid cell programming and the progression of phagocytosis. *J Immunol* (2008) 181:3549–57. doi:10.4049/jimmunol.181.5.3549
48. Hernanz-Falcon P, Joffre O, Williams DL, Reis e Sousa C. Internalization of dectin-1 terminates induction of inflammatory responses. *Eur J Immunol* (2009) 39:507–13. doi:10.1002/eji.200838687
49. Camilli G, Eren E, Williams DL, Aimanianda V, Meunier E, Quintin J. Impaired phagocytosis directs human monocyte activation in response to fungal derived beta-glucan particles. *Eur J Immunol* (2018). doi:10.1002/eji.201747224
50. Gross O, Poeck H, Bscheider M, Dostert C, Hannesschlager N, Endres S, et al. Syk kinase signalling couples to the Nlrp3 inflammasome for anti-fungal host defence. *Nature* (2009) 459:433–6. doi:10.1038/nature07965
51. Hise AG, Tomalka J, Ganesan S, Patel K, Hall BA, Brown GD, et al. An essential role for the NLRP3 inflammasome in host defense against the human fungal pathogen *Candida albicans*. *Cell Host Microbe* (2009) 5:487–97. doi:10.1016/j.chom.2009.05.002
52. Karki R, Man SM, Malireddi RK, Gurung P, Vogel P, Lamkanfi M, et al. Concerted activation of the AIM2 and NLRP3 inflammasomes orchestrates host protection against *Aspergillus* infection. *Cell Host Microbe* (2015) 17:357–68. doi:10.1016/j.chom.2015.01.006
53. Lei G, Chen M, Li H, Niu JL, Wu S, Mao L, et al. Biofilm from a clinical strain of *Cryptococcus neoformans* activates the NLRP3 inflammasome. *Cell Res* (2013) 23:965–8. doi:10.1038/cr.2013.49
54. Gringhuis SI, Kaptein TM, Wevers BA, Theelen B, van der Vlist M, Boekhout T, et al. Dectin-1 is an extracellular pathogen sensor for the induction and processing of IL-1beta via a noncanonical caspase-8 inflammasome. *Nat Immunol* (2012) 13:246–54. doi:10.1038/ni.2222
55. Brodsky IE, Medzhitov R. Pyroptosis: macrophage suicide exposes hidden invaders. *Curr Biol* (2011) 21:R72–5. doi:10.1016/j.cub.2010.12.008
56. Wellington M, Koselny K, Sutterwala FS, Krysan DJ. *Candida albicans* triggers NLRP3-mediated pyroptosis in macrophages. *Eukaryot Cell* (2014) 13:329–40. doi:10.1128/EC.00336-13
57. Uwamahoro N, Verma-Gaur J, Shen HH, Qu Y, Lewis R, Lu J, et al. The pathogen *Candida albicans* hijacks pyroptosis for escape from macrophages. *MBio* (2014) 5:e00003–14. doi:10.1128/mBio.00003-14
58. Liang J, Melican D, Cafro L, Palace G, Fisette L, Armstrong R, et al. Enhanced clearance of a multiple antibiotic resistant *Staphylococcus aureus* in rats treated with PGG-glucan is associated with increased leukocyte counts and increased neutrophil oxidative burst activity. *Int J Immunopharmacol* (1998) 20:595–614. doi:10.1016/S0192-0561(98)00007-1
59. Soltys J, Quinn MT. Modulation of endotoxin- and enterotoxin-induced cytokine release by in vivo treatment with beta-(1,6)-branched beta-(1,3)-glucan. *Infect Immun* (1999) 67:244–52.
60. Williams DL, Browder IW, Di Luzio NR. Immunotherapeutic modification of *Escherichia coli* – induced experimental peritonitis and bacteremia by glucan. *Surgery* (1983) 93:448–54.
61. Markova N, Kussovski V, Drandarska I, Nikolaeva S, Georgieva N, Radoucheva T. Protective activity of lentinan in experimental tuberculosis. *Int Immunopharmacol* (2003) 3:1557–62. doi:10.1016/S1567-5769(03)00178-4
62. Markova N, Michailova L, Kussovski V, Jourdanova M, Radoucheva T. Intranasal application of lentinan enhances bactericidal activity of rat alveolar macrophages against *Mycobacterium tuberculosis*. *Pharmazie* (2005) 60:42–8.
63. Ahn H, Jeon E, Kim JC, Kang SG, Yoon SI, Ko HJ, et al. Lentinan from shiitake selectively attenuates AIM2 and non-canonical inflammasome activation while inducing pro-inflammatory cytokine production. *Sci Rep* (2017) 7:1314. doi:10.1038/s41598-017-01462-4
64. Takeyama T, Suzuki I, Ohno N, Oikawa S, Sato K, Ohsawa M, et al. Host-mediated antitumor effect of grifolan NMF-5N, a polysaccharide obtained from *Grifola frondosa*. *J Pharmacobiodyn* (1987) 10:644–51. doi:10.1248/bpb1978.10.644
65. Ladanyi A, Timar J, Lapis K. Effect of lentinan on macrophage cytotoxicity against metastatic tumor cells. *Cancer Immunol Immunother* (1993) 36:123–6. doi:10.1007/BF01754412
66. Kurashige S, Akuzawa Y, Endo F. Effects of *Lentinus edodes*, *Grifola frondosa* and *Pleurotus ostreatus* administration on cancer outbreak, and activities of macrophages and lymphocytes in mice treated with a carcinogen, N-butyl-N-butanolnitrosoamine. *Immunopharmacol Immunotoxicol* (1997) 19:175–83. doi:10.3109/08923979709007657
67. Ikeda Y, Adachi Y, Ishii T, Tamura H, Aketagawa J, Tanaka S, et al. Blocking effect of anti-dectin-1 antibodies on the anti-tumor activity of 1,3-beta-glucan and the binding of dectin-1 to 1,3-beta-glucan. *Biol Pharm Bull* (2007) 30:1384–9. doi:10.1248/bpb.30.1384
68. Yoon TJ, Kim TJ, Lee H, Shin KS, Yun YP, Moon WK, et al. Anti-tumor metastatic activity of beta-glucan purified from mutated *Saccharomyces cerevisiae*. *Int Immunopharmacol* (2008) 8:36–42. doi:10.1016/j.intimp.2007.10.005
69. Hong F, Yan J, Baran JT, Allendorf DJ, Hansen RD, Ostroff GR, et al. Mechanism by which orally administered beta-1,3-glucans enhance the tumoricidal activity of antitumor monoclonal antibodies in murine tumor models. *J Immunol* (2004) 173:797–806. doi:10.4049/jimmunol.173.2.797
70. Wang WJ, Wu YS, Chen S, Liu CF, Chen SN. Mushroom beta-glucan may immunomodulate the tumor-associated macrophages in the Lewis lung carcinoma. *Biomed Res Int* (2015) 2015:604385. doi:10.1155/2015/604385
71. Liu M, Luo F, Ding C, Albeituni S, Hu X, Ma Y, et al. Dectin-1 activation by a natural product beta-glucan converts immunosuppressive macrophages into an M1-like phenotype. *J Immunol* (2015) 195:5055–65. doi:10.4049/jimmunol.1501158
72. Hofer M, Pospisil M. Modulation of animal and human hematopoiesis by beta-glucans: a review. *Molecules* (2011) 16:7969–79. doi:10.3390/molecules16097969
73. Cleary JA, Kelly GE, Husband AJ. The effect of molecular weight and beta-1,6-linkages on priming of macrophage function in mice by (1,3)-beta-D-glucan. *Immunol Cell Biol* (1999) 77:395–403. doi:10.1046/j.1440-1711.1999.00848.x
74. Chan WK, Law HK, Lin ZB, Lau YL, Chan GC. Response of human dendritic cells to different immunomodulatory polysaccharides derived from mushroom and barley. *Int Immunol* (2007) 19:891–9. doi:10.1093/intimm/dxm061
75. Chan WK, Cheung CC, Law HK, Lau YL, Chan GC. *Ganoderma lucidum* polysaccharides can induce human monocytic leukemia cells into dendritic cells with immuno-stimulatory function. *J Hematol Oncol* (2008) 1:9. doi:10.1186/1756-8722-1-9
76. Demir G, Klein HO, Mandel-Molinas N, Tuzuner N. Beta glucan induces proliferation and activation of monocytes in peripheral blood of patients with advanced breast cancer. *Int Immunopharmacol* (2007) 7:113–6. doi:10.1016/j.intimp.2006.08.011
77. Babineau TJ, Hackford A, Kenler A, Bistrian B, Forse RA, Fairchild PG, et al. A phase II multicenter, double-blind, randomized, placebo-controlled study of three dosages of an immunomodulator (PGG-glucan) in high-risk surgical patients. *Arch Surg* (1994) 129:1204–10. doi:10.1001/archsurg.1994.01420350102014
78. Babineau TJ, Marcello P, Swails W, Kenler A, Bistrian B, Forse RA. Randomized phase I/II trial of a macrophage-specific immunomodulator (PGG-glucan) in high-risk surgical patients. *Ann Surg* (1994) 220:601–9. doi:10.1097/00000658-199411000-00002
79. Dellinger EP, Babineau TJ, Bleicher P, Kaiser AB, Seibert GB, Postier RG, et al. Effect of PGG-glucan on the rate of serious postoperative infection or death observed after high-risk gastrointestinal operations. Betafectin Gastrointestinal Study Group. *Arch Surg* (1999) 134:977–83. doi:10.1001/archsurg.134.9.977
80. Netea MG, Quintin J, van der Meer JW. Trained immunity: a memory for innate host defense. *Cell Host Microbe* (2011) 9:355–61. doi:10.1016/j.chom.2011.04.006
81. Bistoni F, Vecchiarelli A, Cenci E, Puccetti P, Marconi P, Cassone A. Evidence for macrophage-mediated protection against lethal *Candida albicans* infection. *Infect Immun* (1986) 51:668–74.
82. Bistoni F, Verducci G, Perito S, Vecchiarelli A, Puccetti P, Marconi P, et al. Immunomodulation by a low-virulence, agerminative variant of *Candida albicans*. Further evidence for macrophage activation as one of the effector mechanisms of nonspecific anti-infectious protection. *J Med Vet Mycol* (1988) 26:285–99. doi:10.1080/02681218880000401
83. Vecchiarelli A, Cenci E, Puliti M, Blasi E, Puccetti P, Cassone A, et al. Protective immunity induced by low-virulence *Candida albicans*: cytokine production in the development of the anti-infectious state. *Cell Immunol* (1989) 124:334–44. doi:10.1016/0008-8749(89)90135-4
84. Biswas SK, Mantovani A. Macrophage plasticity and interaction with lymphocyte subsets: cancer as a paradigm. *Nat Immunol* (2010) 11:889–96. doi:10.1038/ni.1937

85. Bowdish DM, Loffredo MS, Mukhopadhyay S, Mantovani A, Gordon S. Macrophage receptors implicated in the "adaptive" form of innate immunity. *Microbes Infect* (2007) 9:1680–7. doi:10.1016/j.micinf.2007.09.002
86. Quintin J, Saeed S, Martens JH, Giamarellos-Bourboulis EJ, Ifrim DC, Logie C, et al. *Candida albicans* infection affords protection against reinfection via functional reprogramming of monocytes. *Cell Host Microbe* (2012) 12:223–32. doi:10.1016/j.chom.2012.06.006
87. Saeed S, Quintin J, Kerstens HH, Rao NA, Aghajanirefah A, Matarese F, et al. Epigenetic programming of monocyte-to-macrophage differentiation and trained innate immunity. *Science* (2014) 345:1251086. doi:10.1126/science.1251086
88. Cheng SC, Quintin J, Cramer RA, Shepardson KM, Saeed S, Kumar V, et al. mTOR- and HIF-1alpha-mediated aerobic glycolysis as metabolic basis for trained immunity. *Science* (2014) 345:1250684. doi:10.1126/science.1250684
89. Arts RJ, Novakovic B, Ter Horst R, Carvalho A, Bekkering S, Lachmandas E, et al. Glutaminolysis and fumarate accumulation integrate immunometabolic and epigenetic programs in trained immunity. *Cell Metab* (2016) 24:807–19. doi:10.1016/j.cmet.2016.10.008
90. Ifrim DC, Quintin J, Meerstein-Kessel L, Plantinga TS, Joosten LA, van der Meer JW, et al. Defective trained immunity in patients with STAT-1-dependent chronic mucocutaneaous candidiasis. *Clin Exp Immunol* (2015) 181:434–40. doi:10.1111/cei.12642
91. Buffen K, Oosting M, Quintin J, Ng A, Kleinnijenhuis J, Kumar V, et al. Autophagy controls BCG-induced trained immunity and the response to intravesical BCG therapy for bladder cancer. *PLoS Pathog* (2014) 10:e1004485. doi:10.1371/journal.ppat.1004485
92. Leentjens J, Quintin J, Gerretsen J, Kox M, Pickkers P, Netea MG. The effects of orally administered beta-glucan on innate immune responses in humans, a randomized open-label intervention pilot-study. *PLoS One* (2014) 9:e108794. doi:10.1371/journal.pone.0108794
93. Yona S, Kim KW, Wolf Y, Mildner A, Varol D, Breker M, et al. Fate mapping reveals origins and dynamics of monocytes and tissue macrophages under homeostasis. *Immunity* (2013) 38:79–91. doi:10.1016/j.immuni.2012.12.001
94. Mitroulis I, Ruppova K, Wang B, Chen LS, Grzybek M, Grinenko T, et al. Modulation of myelopoiesis progenitors is an integral component of trained immunity. *Cell* (2018) 172:147–61.e12. doi:10.1016/j.cell.2017.11.034

Conflict of Interest Statement: The authors declare that the research was conducted in the absence of any commercial or financial relationships that could be construed as a potential conflict of interest.

Copyright © 2018 Camilli, Tabouret and Quintin. This is an open-access article distributed under the terms of the Creative Commons Attribution License (CC BY). The use, distribution or reproduction in other forums is permitted, provided the original author(s) and the copyright owner are credited and that the original publication in this journal is cited, in accordance with accepted academic practice. No use, distribution or reproduction is permitted which does not comply with these terms.

frontiers in Microbiology

ORIGINAL RESEARCH
published: 29 November 2017
doi: 10.3389/fmicb.2017.02366

Combination of Classifiers Identifies Fungal-Specific Activation of Lysosome Genes in Human Monocytes

João P. Leonor Fernandes Saraiva[1,2†], Cristina Zubiria-Barrera[3†], Tilman E. Klassert[3], Maximilian J. Lautenbach[3], Markus Blaess[2], Ralf A. Claus[2], Hortense Slevogt[3] and Rainer König[1,2]*

[1] Network Modeling, Leibniz Institute for Natural Product Research and Infection Biology, Hans Knöll Institute, Jena, Germany,
[2] Integrated Research and Treatment Center, Center for Sepsis Control and Care, Jena University Hospital, Jena, Germany,
[3] Septomics Research Centre, Jena University Hospital, Jena, Germany

OPEN ACCESS

Edited by:
Geanncarlo Lugo-Villarino, UMR5089 Institut de Pharmacologie et de Biologie Structurale (IPBS), France

Reviewed by:
Anne Hosmalin, Institut National de la Santé et de la Recherche Médicale, France
Sumana Sanyal, University of Hong Kong, Hong Kong

***Correspondence:**
Rainer König
rainer.koenig@uni-jena.de

[†] These authors have contributed equally to this work.

Specialty section:
This article was submitted to Microbial Immunology, a section of the journal Frontiers in Microbiology

Received: *07 July 2017*
Accepted: *16 November 2017*
Published: *29 November 2017*

Citation:
Leonor Fernandes Saraiva JP, Zubiria-Barrera C, Klassert TE, Lautenbach MJ, Blaess M, Claus RA, Slevogt H and König R (2017) Combination of Classifiers Identifies Fungal-Specific Activation of Lysosome Genes in Human Monocytes. Front. Microbiol. 8:2366. doi: 10.3389/fmicb.2017.02366

Blood stream infections can be caused by several pathogens such as viruses, fungi and bacteria and can cause severe clinical complications including sepsis. Delivery of appropriate and quick treatment is mandatory. However, it requires a rapid identification of the invading pathogen. The current gold standard for pathogen identification relies on blood cultures and these methods require a long time to gain the needed diagnosis. The use of *in situ* experiments attempts to identify pathogen specific immune responses but these often lead to heterogeneous biomarkers due to the high variability in methods and materials used. Using gene expression profiles for machine learning is a developing approach to discriminate between types of infection, but also shows a high degree of inconsistency. To produce consistent gene signatures, capable of discriminating fungal from bacterial infection, we have employed Support Vector Machines (SVMs) based on Mixed Integer Linear Programming (MILP). Combining classifiers by joint optimization constraining them to the same set of discriminating features increased the consistency of our biomarker list independently of leukocyte-type or experimental setup. Our gene signature showed an enrichment of genes of the lysosome pathway which was not uncovered by the use of independent classifiers. Moreover, our results suggest that the lysosome genes are specifically induced in monocytes. Real time qPCR of the identified lysosome-related genes confirmed the distinct gene expression increase in monocytes during fungal infections. Concluding, our combined classifier approach presented increased consistency and was able to "unmask" signaling pathways of less-present immune cells in the used datasets.

Keywords: classification, feature selection, gene expression, machine learning, SVM

INTRODUCTION

A central goal of gene expression profiling studies is to identify key features that allow differentiation between specific clinical conditions of the patients of the corresponding samples (Ng et al., 2005). Several computational approaches have been developed to generate gene signatures with diagnostic potential: regression analyses, classification using decision trees, Random Forests

and Support Vector Machines (SVMs) (Saeys et al., 2007). Especially the latter is a powerful method in the discovery-based approach (linking differential expression to a disease state) in the field of diagnostic biomarkers (Golub et al., 1999; Brown et al., 2000; Furey et al., 2000; Noble, 2004; Lee, 2007). One of the greatest advantages of SVMs is their implicit optimization for generalization by maximizing the separating hyperplane (McDermott et al., 2012; Batuwita and Palade, 2013). In the case of gene biomarker discovery for pathogen discrimination, the SVM can be employed to find the distinctive gene expression pattern that distinguishes best the type of infection (Brown et al., 2000). However, the generated gene signatures from independent studies usually do not present a high degree of consistency even if the same discrimination problem was addressed. We previously showed that combining classifiers using a Mixed Integer Linear Programming (MILP) improved consistency of gene signatures even if generated from quite diverse settings (Saraiva et al., 2016). The gene signature produced by Saraiva et al. accurately discriminated infected from non-infected samples with an average accuracy of 92% and was proposed as a generic host immune response toward infections due to the heterogeneity of the expression datasets in terms of immune cell stimulation. Gene set enrichment analysis revealed that two pathways were significantly enriched (Toll-like and Nod-like receptor signaling; Saraiva et al., 2016).

Whilst knowing if an individual is infected or not, it is essential to determine the type of the infection for the administration of the accurate therapy in the least amount of time (Bloos and Reinhart, 2014). Discriminating between fungal and bacterial infections is of vital importance, especially in the context of systemic infection. The current "gold standard" for pathogen identification relies on blood cultures which require several days for a result (Kirn and Weinstein, 2013).

In this study, we followed up on our previous investigations. The human immune system is complex and composed of many players. The innate immunity is the first line of defense against pathogens in the body. The ability to mount an adequate and effective innate immune response relies on the efficient and proper activation of, but not exclusively, both neutrophils and monocytes. Monocytes not only fight infections but can also differentiate into other immune cells such as macrophages and dendritic cells (DCs) which, in turn, are capable of phagocytic activity and provide the necessary stimulus to the adaptive immune system cells (Shi and Pamer, 2011; Lauvau et al., 2015). Monocytes express most of the pattern recognition receptors (PRRs) involved in fungal (Netea et al., 2008) and bacterial infections (Hessle et al., 2005), and studies have shown that the type of infection influences monocyte differentiation and, consequently, trigger different signaling cascades (Shi and Pamer, 2011). Monocytes take a pivotal role in the early pathogen recognition during candidiasis (Netea et al., 2008; Klassert et al., 2014; Ngo et al., 2014) and have been suggested to be the most effective type of innate immune cells in the killing of *C. albicans* (Netea et al., 2008).

Considering the ratio of the different immune cells we hypothesized that the effect on specific pathways of a less abundant type of immune cells could be "masked" by the overwhelming effect of more numerous leukocytes such as neutrophils or lymphocytes. Studies have shown that the expression of several genes is immune cell type-specific (Wong et al., 2011; Allantaz et al., 2012; Gardinassi et al., 2016; Petryszak et al., 2016). Other studies have also shown that gene overexpression can activate distinct molecular pathways depending on the cell population (Liu et al., 2015; Didonna et al., 2016). Cell-type specific gene expression studies have also shown that the relative proportion of each leukocyte type invariably has an impact on the global gene expression profile (Palmer et al., 2006). In the same study, the set of genes with the highest relative expression in lymphoid cells presented the lowest relative expression in whole blood (e.g., *CD3G*, *LEF1*, *TCF7*, *CD3D*, *MAL*, and *CD2*). In our study, we employed the combined classifier approach we develop earlier (Saraiva et al., 2016) on datasets of similar leukocyte compositions and aimed to determine if these similarities also present specific signaling pathways not uncovered by the generic approach on the immune response in our previous study.

METHODS

Dataset Assembly

The normalized gene expression data from two datasets (accession numbers: GSE42606 and GSE69723) was obtained via Gene Expression Omnibus (GEO) (www.ncbi.nlm.nih.gov/geo/) from the National Center for Biotechnology Information (NCBI) database. RNA-Seq data was retrieved from NCBI's Sequence Read Archive (SRA). A study performed by Klassert et al. (Klassert et al., 2017; Riege et al., 2017), and hereon identified as "Klassert," generated RNA-Seq data (accession number SRP076532) which consisted of healthy human blood-derived monocytes stimulated with heat-killed *Aspergillus fumigatus* AF293, *Candida albicans* SC5314 yeast (both at a Multiplicity of infection (MOI) of 1), *Escherichia coli* serotype O18:K1:H7 (MOI of 10) or left untreated (control). Cells were stimulated for 3 and 6 h after which their RNA was extracted. On the raw reads a sequence quality analysis was performed using FastQC version 0.10.1 and a read trimming to 150 bp was performed using FASTX Toolkit 0.0.14 and adapter trimming using cutadapt version 1.3. Reads were mapped onto the reference genome GRCh38/hg38 from the UCSC server and counted for each gene across all samples using HTSeq-count. The read number per gene, total read number per sample and gene length was then used to calculate the Reads Per Kilobase of transcript per Million mapped reads (RPKM) values across all genes and samples. Genes with RPKM values of 0 across all samples were removed. Smeekens and co-workers (Smeekens et al., 2013) performed a study in which peripheral blood mononuclear cells (PBMCs), isolated from blood of healthy human donors, were stimulated with heat-killed *C. albicans* UC820 (1×10^6/mL), *Mycobacterium tuberculosis* (10 ng/mL) and LPS derived from *E. coli* (10 ng/mL). Cells grown in Roswell Park Memorial Institute Medium (RPMI) culture medium were used as controls (accession number GSE42606). Samples were taken at 4 and 24 h after infection. In this dataset, only the 4-h time point was considered for our studies since we were investigating the innate immune response

in the acute phase. For future reference, this dataset will be identified as "Smeekens." Transcriptomic data generated by Saraiva et al. (2016), and hereby identified as "Saraiva," was generated by challenging healthy human blood-derived PBMCs with either heat-killed *C. albicans* MYA-3573 yeast (MOI of 2) or LPS derived from *E. coli* 0111:B4 (10 ηg/mL) (InvivoGen). Four samples were extracted 4 h post-infection. RNA was extracted using RNAEasy Kit Qiagen and quantity and quality of the total RNA was analyzed using a Nanodrop ND-1000 spectrophotometer (Thermo Fischer Scientific, USA) and a Tape Station 2200 (Agilent Technologies, USA). Lastly, transcriptional data of human blood isolated monocytes challenged with *A. fumigatus* conidia (MOI of 2) and LPS (10 ng/mL) was downloaded from the European Molecular Biology Laboratory (EMBL) ArrayExpress database (E-MEXP-1103) (http://www.ebi.ac.uk/arrayexpress/experiments/E-MEXP-1103/) and is hereby identified as "Mattingsdal." A total of 5 and 6 samples were extracted 6 h post-challenge (*A. fumigatus* and LPS, respectively).

Data Preprocessing

Each dataset was controlled if prior normalization had been executed on the expression data. In the absence of normalization, the following was performed: RNA-Seq data was log2 transformed and a 1% quantile added onto all values, whilst microarray data was normalized by employing the functions "lumiN" and method "vsn" of the "lumi" R package (Du et al., 2008). Elimination of possible duplicate gene entries was carried out by use of the "avereps" function in the "limma" R package (Ritchie et al., 2015), which calculates the mean expression values for duplicate entries. Finally, z-scores were calculated for each gene. The gene list, to be used for feature selection and classification, consisted of the intersection of the gene lists from all datasets and amounted to 1,567 genes.

Classification

In each dataset, the samples were grouped into either fungal (class 1) or bacterial (class 2). The number of samples in each dataset for each analysis is shown in **Table 1**. For classification and feature selection, we employed Support Vector Machines (SVMs) implemented with Mixed Integer Linear Programming as previously described (Saraiva et al., 2016) and with the same parameters (number of cross-validations (runs) and number of features (genes) to be selected in each cross-validation) as explained in the following (full implementation procedure in the Text S1). This process was done for both single and combined classifiers to compare both approaches. Briefly, during each cross-validation, SVMs were constrained to n = 30 features (genes) and they selected these with which they best discriminated between fungal and bacterial infected samples on the training data. Two thirds of the samples were randomly selected for training whilst one third was used for testing. This procedure was repeated 100 times. To remove the possible imbalance between classes, a stratified approach was employed in which the maximum number of samples to be used in each class was determined by the class with the least number of samples.

TABLE 1 | Number of samples in each dataset divided into fungal and bacterial class.

Dataset	Cell type	Fungal class	Bacterial class
Smeekens	PBMC	24	49
Mattingsdal	Monocytes	5	6
Klassert	Monocytes	18	9
Saraiva	PBMC	4	4

To remove less frequently selected genes, further filtering of the gene lists was performed. Genes not selected in at least 20 runs (out of 100) in each classifier (both single and combined) were removed. The resulting gene lists were then merged into their respective group (either single or combined approach). Ascertaining the functional overview of the refined gene lists was achieved by performing literature analysis as well as using the functional annotation tools of the Database for Annotation, Visualization and Integrated Discovery (DAVID, version 6.7, https://david.ncifcrf.gov/home.jsp (Huang da et al., 2009) using *Homo sapiens* background. The full workflow is depicted in Figure S1.

Differential Gene Expression Analysis

In each dataset we calculated differentially expressed genes using Student's *t*-tests with multiple testing correction (Benjamini-Hochberg method, Benjamini and Hochberg, 1995). Genes were regarded as differentially expressed if their adjusted *p*-value was below 0.05. Intersection of differentially expressed genes was performed for all datasets and according to leukocyte composition (all datasets, PBMC specific and monocyte specific). Gene set enrichment analysis, for each list, was carried out as stated above.

EXPERIMENTAL VALIDATION

Monocyte Isolation

Buffy coats of healthy male donors for cell isolation were kindly provided by Dagmar Barz in anonymized form (Institute of Transfusional Medicine of the Jena University Hospital). Human monocytes were isolated from 50 ml buffy coats of four healthy male donors as previously described (Müller et al., 2017). Briefly, ficoll-density gradient centrifugation was used to isolate first peripheral blood mononuclear cells (PBMCs). After restoring the osmolarity of the cells with 0.45% NaCl, remaining erythrocytes were lysed using a hypotonic buffer. Where needed, 5×10^6 PBMCs were seeded in 6-well plates (VWR International, Germany) and allowed to equilibrate for 1 h at 37°C 5% CO_2. From the remaining PBMCs, monocytes were then isolated using quadro-MACS (Miltenyi Biotec, UK) by labeling the non-monocytic cells with a cocktail of Biotin-conjugated antibodies and Anti-Biotin Microbeads (Monocyte Isolation Kit II, Miltenyi Biotec, UK). Cell viability of >98% was assayed by Trypan blue staining. Monocyte concentration was adjusted to 2.5×10^6 cells/ml in RPMI 1640 GlutaMAX medium (Gibco, UK) supplemented with 10% fetal bovine serum (FBS,

Biochrom, Germany) and 1% Penicillin/Streptomycin (Thermo Fisher Scientific, USA), 5×10^6 cells were seeded in 6-well plates (VWR International, Germany) and allowed to equilibrate for 1 h at 37°C 5% CO_2.

Preparation of Fungi and Bacteria

Overnight culture from *Escherichia coli* (isolate 018:K1:H7) in LB medium was washed twice in PBS and resuspended in 1 ml RPMI 1640 GlutaMAX medium (Gibco, UK) supplemented with 10% FBS (Biochrom, Germany) at a concentration of 5×10^8 cfu/ml. *Aspergillus fumigatus (*AF293) was grown in Aspergillus Minimal Medium (AMM) Agar-plates for 6 days at 30°C. Conidiospores were harvested by rinsing the plates with sterile 0.05% Tween-20 (Sigma-Aldrich, Germany) and filtered through 70- and 30-μm pre-separation filters (Miltenyi Biotec, UK) to get rid of mycelium traces. Spores were washed twice in PBS and cell-concentration was adjusted to 10^7 conidia/ml in RPMI 1640 GlutaMAX medium supplemented with 10% FBS. Conidia were then incubated at 37°C under shaking for 7 h until cells turned to germ tubes. Germlings were centrifuged and resuspended at 1×10^8 cells/ml in RPMI 1640 GlutaMAX medium supplemented with 10% FBS. Overnight culture of *Candida albicans* (SC5314) in YPD medium was washed twice in PBS and cell concentration was adjusted to 5×10^7 cfu/ml in RPMI 1640 GlutaMAX medium supplemented with 10% FBS.

Monocyte Stimulation Assay

Pathogens were all heat-killed by incubation at 65°C for 30 min before infection. Monocytes were stimulated with heat-killed pathogens at a pathogen:host ratio of 10:1 for bacteria, 1:1 for *A. fumigatus* germ tubes and *C. albicans* yeasts. In addition, cells were stimulated with pathogen-derived cell wall components: LPS (50 ng/ml) and zymosan (1 μg/ml). After 3 h incubation at 37°C and 5% CO_2, monocytes were lysed for RNA isolation. To analyse the expression level of the genes of interest, total RNA was extracted from 5×10^6 Monocytes using the Qiagen RNeasy mini kit (Qiagen, Germany). Residual genomic DNA was removed by on-column incubation with DNaseI (Qiagen, Germany). A NanoDrop D-1000 Spectrophotometer (Thermo-Fisher Scientific, USA) was then used to assess the amount and quality of the isolated RNA samples. Complementary DNA (cDNA) was synthesized from 1.5 μg of RNA using the High Capacity cDNA Reverse Transcription Kit (Applied Biosystems, UK) following manufacturer's instructions. To detect the expression of the genes by PCR, specific primers for each target were designed using the online Primer-BLAST tool of the NCBI (http://www.ncbi.nlm.nih.gov/tools/primer-blast/). Possible secondary structures at the primer binding sites were taken into account by characterizing the nucleotide sequence of the regions of interest using the Mfold algorithm (Zuker, 2003). The sequences of all primers used for amplification are listed in Table S1. For quantification of the relative expression of each gene, we used a CAS-1200 pipetting robot (Qiagen) to set up the qPCR-reactions and a Corbett Rotor-Gene 6000 (Qiagen) as Real-Time qPCR apparatus. Each sample was analyzed in a total reaction volume of 20 μl containing 10 μl of 2 × SensiMix SYBR Master Mix (Bioline, UK) and 0.2 μM of each primer. The cycling conditions included an initial step of 95°C for 10 min followed by 40 cycles of 95°C for 15 s, 60°C for 20 s and 72°C for 20 s. For each experiment, an RT-negative sample was included as a control. Melting curve analysis and primer efficiency was used to confirm the specificity of the qPCR reactions. The relative expression of the target genes was analyzed using the Pfaffl method (Pfaffl et al., 2004; Rieu and Powers, 2009). To determine significant differences in the mRNA expression between different experimental conditions, the relative quantity (RQ) for each sample was calculated using the formula $1/E^{Ct}$, where E is the efficiency and Ct the threshold cycle. The RQ was then normalized to the housekeeping gene peptidylprolyl isomerase B (*PPIB*). The stability of the housekeeping gene was assessed using the BestKeeper algorithm (Pfaffl et al., 2004). The normalized RQ (NRQ) values were $\log_2$-transformed for further statistical analysis with GraphPad PRISM v7.02. Statistical analysis was performed using repeated measures one way ANOVA and Bonferroni correction.

RESULTS

Classification was performed on each individual dataset ("Klassert," "Smeekens," "Saraiva," and "Mattingsdal") using 100 randomly assigned training sets within a cross-validation scheme. A list of 30 genes was generated in each classification run which best discriminated samples infected with fungal from bacterial pathogens. Consistency of the gene signature was determined by calculating the pairwise overlap (POL) between cross-validations of each classifier. Briefly, the gene list ($n = 30$) of each cross-validation of one dataset was intersected with the gene list of each cross-validation of another, different dataset. This was done for each pair of single classifiers. To obtain better consistency (as we observed in our initial study identifying biomarkers for infection irrespective of the kind of infection, see Saraiva et al., 2016), we also combined classifiers of two datasets (e.g., Smeekens with Klassert) constrained to use the same feature selection. We intersected the 100 cross-validations between single classifiers, between single and combined classifiers and between only combined classifiers. An illustrative example of this procedure is depicted in Figure S2. The averaged POL of the 100 generated gene lists of single vs. single, single vs. combined and combined vs. combined classifiers returned values of 0.78 ($1\sigma = 0.41$), 1.09 ($1\sigma = 0.48$), and 1.64 ($1\sigma = 0.49$), respectively. The POL of combined vs. single already showed an increase in almost 40% when compared to single vs. single, increasing to more than 100% when calculating the POLs between combined classifiers.

Next, we aimed at determining which pathways were significantly enriched in both the single and combined classifier gene lists. In each classifier (single and combined approach), the genes not selected in at least 20% of the total number of runs ($k = 100$) were excluded from further analysis. A total of 175 and 164 genes, for single and combined classifiers, respectively, remained (Table S2). The enriched pathways of single and combined gene signatures are shown in **Tables 2**, **3**, respectively. Interestingly, one enriched gene set of the combined classifier

TABLE 2 | Enriched gene sets of the single classifier approach.

Gene set	*P*-value
Chemokine signaling	2.3E-17
Cytokine-cytokine receptor interaction	8.6E-15
Toll-like receptor signaling	2.7E-5
Jak-STAT signaling	7.2E-4
Chronic myeloid leukemia	0.0011
Leukocyte transendothelial migration	0.011
Natural killer cell mediated cytotoxicity	0.192
B cell receptor signaling	0.031
Fc epsilon RI signaling	0.035
Intestinal immune network for IgA production	0.042

TABLE 3 | Enriched gene sets of the combined classifier approach.

Gene set	*P*-value
Toll-like receptor signaling	2.2E-4
Cytokine-cytokine receptor interaction	3.1E-4
Lysosome	0.014
Chemokine signaling	0.027
Jak-STAT signaling	0.042

gene list was not present in that of the single classifier—Lysosome (KEGG pathway). Next, independent from the classifier results, for each dataset, differentially expressed genes in fungal vs. bacterial infected samples was calculated. The intersection of the differentially expressed genes across all datasets resulted in a list of 13 genes (*ST3GAL5*, *HMOX1*, *LGALS9*, *GLA*, *HAVCR2*, *TBC1D9*, *ACADVL*, *BCAR3*, *RHOU*, *MGAT2*, *CCL23*, *RGS1*, and *SPRY2*) and no enriched gene sets. Intersection of differentially expressed genes was performed not only for all datasets but now also based on the type of the immune cells to shape out the origin of these differences in gene expression.

As stated before, monocytes are vital players in the control of infection, by both promoting inflammation and differentiating into other immune cells. The processes that they influence, however, can be distinct to those of other more abundant immune cells such as lymphocytes and the expressed genes of monocytes may hence be "masked." To elucidate this masking phenomenon, we calculated the differentially expressed genes of the datasets of the PBMCs (datasets Saraiva, Smeekens), and of the monocytes (Klassert, Mattingsdal) separately. Intersecting differentially expressed genes, both up and down regulated, of the datasets encompassing solely monocytes resulted in 720 genes, whilst the intersection of datasets comprised of PBMCs resulted in a list of 57 genes. The enriched gene sets, for PBMC-specific and monocyte-specific differentially expressed genes are shown in **Table 4**. The enriched gene sets in all groups suggested that genes coding for the lysosome were specifically induced by monocytes during a fungal challenge. To note, the combined classifier-originated gene list also showed an enrichment of genes coding for the lysosome (lysosome gene set in the following). Additionally, we intersected the differentially expressed and up-regulated genes (in fungal vs. bacterial) from the monocyte datasets (Klassert and Mattingsdal) and performed gene set enrichment tests. Only two pathways were significantly enriched—the lysosome and Toll-like receptor signaling ($P =$ 3.2E-4 and 0.015, respectively). We believe that this strengthens our initial finding that cell type specific gene expression is still captured when combining classifiers, without the requirement of performing a cell type specific analysis beforehand. Performing gene set enrichment tests on differentially expressed genes from cell type specific datasets produced the same results.

TABLE 4 | Enriched gene sets of PBMC-specific and monocyte-specific differentially expressed genes in fungal vs. bacterial infection (both up and down regulated).

PBMC-specific		Monocyte-specific	
Gene set	***P*-value**	**Gene set**	***P*-value**
Jak-STAT signaling	0.0011	Toll-like receptor signaling	2.5E-5
Toll-like receptor signaling	0.0035	NOD-like receptor	3.5E-5
Cytokine-cytokine receptor interaction	0.046	Hematopoietic cell lineage	2.4E-4
		Cytokine-cytokine receptor interaction	3.9E-4
		Chemokine signaling	0.0018
		Jak-STAT signaling	0.0035
		Lysosome	0.0044
		Cytosolic DNA-sensing	0.0049
		MAPK signaling	0.0054
		Adipocytokine signaling	0.016

Gene set enrichment was also performed on the gene list that resulted in the intersection of differentially expressed and up regulated genes considering only the datasets of stimulated PBMCs, and comprised of Jak-STAT signaling, cytokine-cytokine receptor interaction and toll-like receptor signaling (Table S3).

In summary, we identified a few, well selected, distinct gene sets being enriched in differentially expressed genes discriminating fungal from bacterial infection, and when elucidating gene sets specifically expressed in monocytes by our combined classifier approach and a monocyte specific analysis, the lysosome gene set came out to be highly enriched in discriminative genes. Hence, in the following, we focused on the lysosomal gene set.

Experimental Validation

We reproduced the experimental settings of the studies herein considered focussing on monocytes, and stimulated human monocytes with the respective pathogens. The validation of the expression profiles observed for monocytes in the RNA-Seq data was performed using quantitative RT-PCR. For this purpose, we first tested the stability of the housekeeping gene used (*PPIB*). Using the algorithm BestKeeper (Pfaffl et al., 2004), the expression stability ($std\ dev \pm CP$) and coefficient of variation (CV) for the housekeeping gene was calculated for monocytes. On this basis, *PPIB* was proved as a highly stable housekeeping gene for relative expression analyses ($std\ dev \pm CP = 0.35$; $CP =$ 1.95 %).

Lysosome-Related Genes

Based on the results obtained using our combined classifier approach, 4 lysosome-related genes were selected for validation by real time RT-qPCR analysis. These were the genes encoding for Galactosidase A (*GLA*), Scavenger receptor class B member 2 (*SCARB2*), Niemann-Pick disease, type C1 (*NPC1*) and the *CD164* molecule (*CD164*). The real-time RT-qPCR plots are shown in **Figure 1** (The complete table of the RT-qPCR mean expression values across conditions and corresponding *p*-values are shown in Table S4). Almost all genes showed a significant increase in their expression when the fungi-stimulated group was compared to either the unstimulated controls and/or to the bacteria-challenged samples. *GLA* was significantly up-regulated by both fungal pathogens when compared to control and to *E. coli*-stimulated monocytes. *SCARB2* was up-regulated in a highly significant manner in *C. albicans*-stimulated monocytes when compared *to E. coli*-challenged monocytes. *SCARB2* also showed a significant increase in expression when compared to controls and *A. fumigatus*-challenged monocytes. In *E. coli* stimulated monocytes, *SCARB2* was significantly down-regulated when compared to controls. *NPC1* showed a significant increase in its expression in *A. fumigatus*-stimulated monocytes when compared to all other challenges. *C. albicans*-stimulated monocytes also showed significant increase of *NPC1* expression when compared to controls. Lastly, *CD164* was significantly up-regulated in both fungi when compared to *E. coli* and controls. In summary, we could validate the expression of the selected genes to be either specifically or significantly more up-regulated in monocytes stimulated by fungal pathogens when compared to monocytes stimulated by bacterial pathogens confirming them as potential biomarkers for fungal vs. bacterial induced systemic infection.

The fungi-specific pattern observed for lysosome-related genes in monocytes was less evident in PBMCs, as confirmed by an additional set of experiments in which monocytes and PBMCs from the same donors were stimulated in parallel with

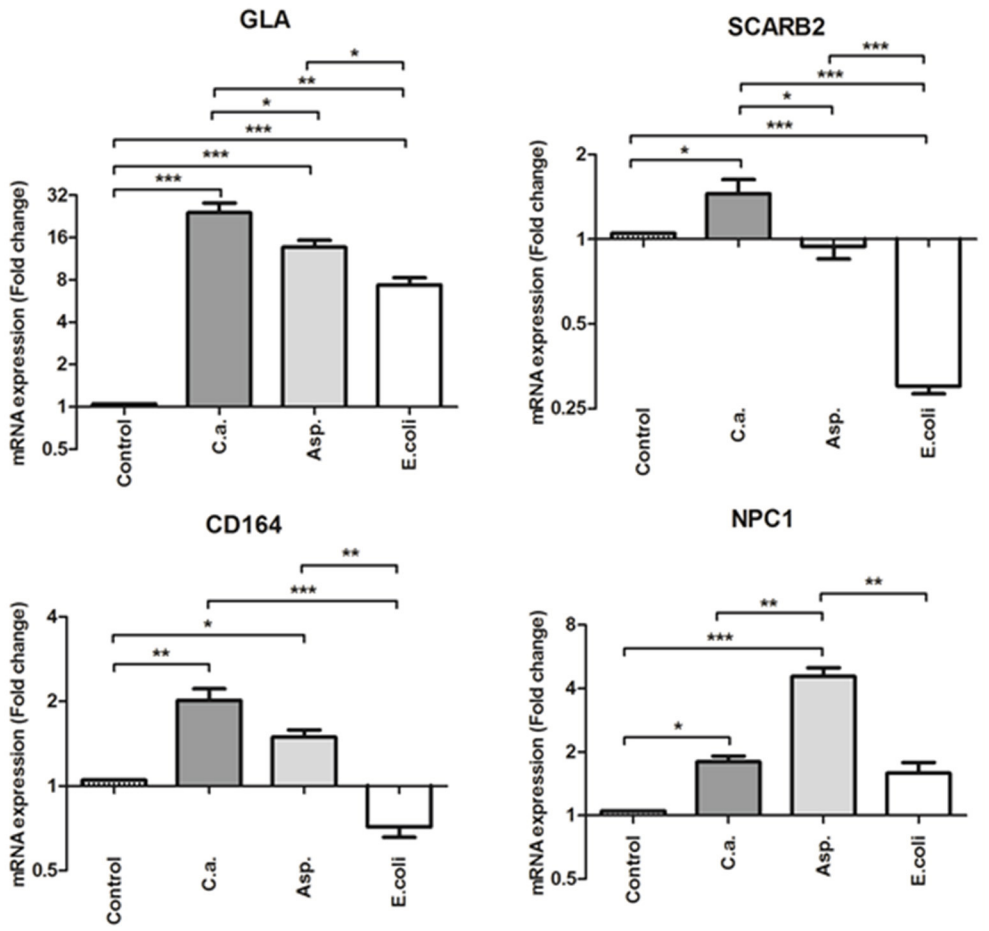


FIGURE 1 | Relative mRNA expression of *GLA, SCARB2, CD164*, and *NPC1* after stimulation with *Candida albicans* (C.a.), *Aspergillus fumigatus* (Asp.) and *Escherichia coli* (*E. coli*). Data were obtained from four independent experiments, each performed with cells from different donors. Results are presented as mean ± SE of the fold change relative to the control (unstimulated cells) according to (Pfaffl et al., 2004). (Please see also: Rieu and Powers, 2009. Real-Time Quantitative RT-PCR: Design, Calculations, and Statistics. The Plant Cell; Vol. 21: 1031–1033. Shown is also the statistical significance after repeated measures One-Way ANOVA after multiple testing correction (Bonferroni) (***$p < 0.001$; **$p < 0.01$; *$p < 0.05$).

C. albicans, A. fumigatus, and *E. coli* (Figure S3). These results are in accordance with the microarray and RNA-Seq readouts from the different datasets analyzed (Monocytes vs PBMCs), and might explain why the lysosome-pathway was significantly enriched only in the monocyte datasets.

Lysosome-Unrelated Genes

Our approach identified additional genes that showed a differential pattern in leukocytes upon fungal vs. bacterial infection but unrelated to the lysosome. These included the BAG family molecular chaperone regulator 3 (*BAG3*), the fatty acid binding protein 5 (*FABP5*), the peroxisome proliferator-activated receptor gamma (*PPARG*), the heme oxygenase 1 (*HMOX1*) and the C-C chemokine receptor type 1 (*CCR1*). Real-time qPCR of these genes showed a significant ($P \leq 0.05$) increased expression in fungal stimulated monocytes when compared to all other stimuli. Except for *BAG3*, all other genes were downregulated after *E. coli* stimulation, reaching statistical significance for two of the genes (*HMOX1* and *CCR1*) (Figure S4).

DISCUSSION

Accurate identification of key features that allow for differentiation between specific clinical conditions represents an important challenge with diagnostic potential for the clinical daily practice. As shown in our previous study (Saraiva et al., 2016), the consistency of differential gene signatures increases substantially after combining classifiers when compared to single classifiers. The application of the combined classifier approach limits the impact of many variables that exist when comparing datasets such as the pathogen strain, laboratory settings, time of sample extraction and stimulated cell-type (e.g., PBMCs or whole blood), amongst others. This is particularly important when trying to generate a generic gene signature capable of discriminating infections irrespective of the immune cell type. In the present work, we validated our method on specific populations of immune cells, and demonstrated its ability to identify cell-specific signatures that were masked in mixed populations if using classifiers without combining the datasets. As observed in our results, combining classifiers for discrimination between fungal and bacterial infections in different leukocyte-compositions, such as PBMCs and monocytes, generated a gene signature enriched for several immune signaling pathways, among which the lysosome gene set was observed which turned out to be specific for monocytes. This was ascertained by the comparison of the enriched signaling pathways of differentially expressed genes in cultures of monocytes against PBMCs, both challenged with fungal and bacterial pathogens. We validated our results experimentally employing qPCR, analyzing a set of lysosome-related genes that were either selected by the combined classifier or uniquely differentially expressed in the monocyte challenged datasets. As shown, all the lysosome-related genes (*GLA*, *SCARB2*, *NPC1,* and *CD164*) exhibited a significant increase in their expression after fungal challenge when compared to bacterial stimulation, indicating a fungal-specific response by monocytes (**Figure 1**). Similar results were also obtained for other, non-lysosome related genes that were part of the fungal-specific signature and also these genes could be validated by qPCR (Figure S4). These genes included *BAG3*, *PPARG*, *FABP5, HMOX1,* and *CCR1*.

Functional Relevance of the Differentially Expressed Lysosome-Related Genes

α-Galactosidase A (GLA) is a glycoside hydrolase enzyme encoded by the *GLA* gene. This enzyme hydrolyses the terminal α-galactosyl moieties (especially the α-1,6 linkage) of glycoproteins and glycolipids. Specifically, GLA is a lyososmal enzyme that degrades globotriaosylceramide (Gb3) to lactosylceramide, preventing its accumulation in this compartment (Darmoise et al., 2010). Deficiency of this enzyme (GLA) and accumulation of the glycolipid Gb3 in the lysosome of peripheral blood mononuclear cells (PBMCs) has been shown to contribute to diverse physiopathological alterations such as the continuous pro-oxidative and pro-inflammatory state of these cells (De Francesco et al., 2013). Moreover, a pro-inflammatory role of Gb3 could be demonstrated in that study, which was directly mediated by the TLR4-pro-inflammatory signaling pathway (De Francesco et al., 2013). *Candida albicans* yeast, among other fungi, binds to TLR4 that recognizes short linear O-bound mannan structures present in the fungal cell wall (Netea et al., 2008). Besides this, the GLA product lactosylceramide has been reported to be very abundant on plasma membranes of phagocytes, being involved in the phagocytosis, chemotaxis, and superoxide generation during fungal infection (Jimenez-Lucho et al., 1990; Iwabuchi et al., 2015). Our results show that *C. albicans* and *A. fumigatus* induce a significantly higher expression of the *GLA* gene than *E. coli*, suggesting the importance of this enzyme in monocytes during fungal infection. Among all the lysosome-related genes analyzed in this study, *GLA* showed the strongest up-regulation upon pathogen-challenge, particularly during fungal stimulation (24-fold for *C. albicans* and 14-fold for *A. fumigatus*). It might be speculated that GLA avoids the accumulation of the glycolipid Gb3 in the lysosome as an anti-inflammatory and protective mechanism in monocytes, which might be of special importance during fungal clearance. Moreover, the conversion of Gb3 to lactosylceramide, as a membrane microdomain of immune cells, may increase the phagocytosis and clearance of the fungi.

Scavenger receptor class B member 2 (*SCARB2*) is a gene whose encoded protein, the lysosomal integral membrane protein type-2 (LIMP-2/SCARB2), has been shown to be essential for the normal biogenesis and maintenance of lysosomes and endosomes (Gonzalez et al., 2014). As a lysosomal membrane protein, SCARB2 has been reported to act as an entry receptor for Enterovirus 71 (EV71) leading to its internalization to the lysosome (Yamayoshi et al., 2014). Other scavenger receptors, such as CD36 and SCARF1 (human homologs of the murine C03F11.3 and CED-1, respectively), have been shown to bind *C. neoformans* and *C. albicans* via ß-glucan structures, providing protection against these fungal pathogens in a mice model (Croze et al., 1989). Not much is known about the function of SCARB2 during fungal induced immune responses, but our results suggest that this scavenger receptor, like other similar members of

this protein family, may play an important role in fungal recognition and internalization to the lysosome. Moreover, we analyzed whether the most common fungal and bacterial cell wall components (the fungal ß-glucan and the bacterial lipopolysaccharide, respectively) could explain the differential regulation of this gene by the different pathogens. *E. coli*-derived LPS resembled the downregulation of *SCARB2* already observed after stimulation with *E. coli* cells. In contrast, the fungal ß-glucan component seems to have no effect on the regulation of this gene (Figure S5). From these results we could conclude that the bacterial liposaccharide seems to be responsible for the downregulation of *SCARB2*. In turn, the absence of regulation of this gene in the presence of zymosan, a representative of ß-glucan, suggests that other specific fungal epitopes might induce the expression of this gene during fungal infection, especially during *C. albicans* infection. In this study, other genes encoding lysosomal transmembrane proteins, *CD164* and *NPC1*, were analyzed. Croze et al. reported *CD164* encoding sialomucin protein (Endolyn-78) to be involved in the maturation of the endosomal-lysosomal compartment (Croze et al., 1989), while the Niemann-Pick disease type C1 (NPC1) protein encoded by the *NPC1* gene mediates intracellular cholesterol and sphingolipids trafficking into the late endosome and lysosome (Alam et al., 2012). *NPC1* is located in late endosomes and lysosomes and its encoded protein might promote the creation and/or movement of these compartments to and from the cell periphery (Ko et al., 2001). In our study, we have shown the up-regulation of *CD164* and *NPC1*in human monocytes specifically after fungal challenge, which again suggests the importance of biogenesis and functionality of the lysosome for fungal clearance in monocytes.

Functional Relevance of Differentially Expressed Non-lysosome-Related Genes

Most of the genes further analyzed in this study associated to the proper biosynthesis and functionality of the lysosome during fungal infection. In addition, other mechanisms, such as immune cells recruitment, phagocytosis and nutrient metabolism, are also known to be crucial for a successful fungal killing and clearance by the phagocytes. Thus, other genes identified in this study to be fungal-challenge specific are involved in those pathways and might play an important role during fungal infection. For instance, *BAG3* encodes the BAG family molecular chaperone regulator 3 (BAG3) protein which regulates macroautophagy for degradation of polyubiquitinated proteins (Gamerdinger et al., 2009). The peroxisome proliferator-activated receptor gamma (*PPARG*) is a gene expressed in macrophages and its encoding a protein that plays a central role in regulating fatty acid storage and glucose metabolism (Tyagi et al., 2011). Fatty Acid Binding Protein 5 (FABP5) is a protein encoded by *FABP5* gene and plays a role in the uptake of fatty acids, transport phenomena and fatty acid metabolism (Moore et al., 2015). The *HMOX1* gene, encoding heme oxygenase-1 (HO-1), has been shown to be required for immune cell protection against systemic infections (Silva-Gomes et al., 2013). Primarily, HO-1 degrades heme into biliverdin and carbon monoxide (CO). CO has shown different effects, it supports anti-inflammatory cytokine expression (Piantadosi et al., 2011) but may in turn increase the virulence of the infection (Navarathna and Roberts, 2010). The C-C Chemokine Receptor 1 (CCR1), encoded by the *CCR1* gene, has been shown to be widely expressed in immune cells and it was associated with the maintenance of chemokine gradients during infection (Lionakis et al., 2012).

In summary, by integrating our combined classifier approach with distinct differential gene expression analysis across well selected, different studies investigating diverse species of pathogens, we could identify genes that are up-regulated in monocytes during fungal infection, much more or exclusively in comparison to a bacterial infection. Once fungi are phagocytosed, monocytes display transcriptional and translational reprogramming, adapting their physiology and killing mechanisms to fungal-derived stressors. In our study, we show the up-regulation of fungi-specific genes, which seem to be important in the fungal-derived reprogramming. Moreover, the application of the combined classifier approach made it possible, for the first time, to identify lysosome-related gene expression as a monocyte-specific footprint of fungal infections. Determining whether loss of the candidate genes have any functional impact on infection is also of great importance. siRNA-mediated knock-down experiments, combined with pathogen-challenge should be performed in the future. The multiple readouts with possible effects on phagocytosis, killing, cytokine production and metabolism would represent an attractive target for follow-up studies.

AUTHOR CONTRIBUTIONS

JL and RK conceived and designed the study. MB and RC generated the Saraiva microarray dataset. CZ-B, ML, TK, and HS supported the analysis of the Klassert dataset and performed the RT-qPCR. JL performed all bioinformatics analysis. Analysis and interpretation of results was performed by JL, CZ-B, and TK. JL, CZ-B, TK, and RK wrote the manuscript. All authors have read and approved the final version of the manuscript.

FUNDING

This work has been supported by the Federal Ministry of Education and Research (BMBF), Germany, FKZ 01ZX1302B, 01ZX1602B (CancerTel-Sys), FKZ: 01EO1002, 01EO1502 (CSCC), and by the DFG within the graduate program Jena School for Microbial Communication and the framework of the Collaborative Research Center/Transregio 124 "Pathogenic fungi and their human host: Networks of Interaction," project A5.

SUPPLEMENTARY MATERIAL

The Supplementary Material for this article can be found online at: https://www.frontiersin.org/articles/10.3389/fmicb.2017.02366/full#supplementary-material

REFERENCES

Alam, M. S., Getz, M., Safeukui, I., Yi, S., Tamez, P., Shin, J., et al. (2012). Genomic expression analyses reveal lysosomal, innate immunity proteins, as disease correlates in murine models of a lysosomal storage disorder. *PLoS ONE* 7:e48273. doi: 10.1371/journal.pone.0048273

Allantaz, F., Cheng, D. T., Bergauer, T., Ravindran, P., Rossier, M. F., Ebeling, M., et al. (2012). Expression profiling of human immune cell subsets identifies miRNA-mRNA regulatory relationships correlated with cell type specific expression. *PLoS ONE* 7:e29979. doi: 10.1371/journal.pone.0029979

Batuwita, R., and Palade, V. (2013). "Class imbalance learning methods for support vector," in *Imbalanced Learning: Foundations, Algorithms, Applications*, eds H. He and Y. Ha (Hoboken, NJ: John Wiley & Sons, Inc.), 83–100.

Benjamini, Y., and Hochberg, Y. (1995). Controlling the false discovery rate - a practical and powerful approach to multiple testing. *J. R. Stat. Soc. Ser.B Stat. Methodol.* 57, 289–300.

Bloos, F., and Reinhart, K. (2014). Rapid diagnosis of sepsis. *Virulence* 5, 154–160. doi: 10.4161/viru.27393

Brown, M. P., Grundy, W. N., Lin, D., Cristianini, N., Sugnet, C. W., Furey, T. S., et al. (2000). Knowledge-based analysis of microarray gene expression data by using support vector machines. *Proc. Natl. Acad. Sci. U.S.A.* 97, 262–267. doi: 10.1073/pnas.97.1.262

Croze, E., Ivanov, I. E., Kreibich, G., Adesnik, M., Sabatini, D. D., and Rosenfeld, M. G. (1989). Endolyn-78, a membrane glycoprotein present in morphologically diverse components of the endosomal and lysosomal compartments: implications for lysosome biogenesis. *J. Cell Biol.* 108, 1597–1613.

Darmoise, A., Teneberg, S., Bouzonville, L., Brady, R. O., Beck, M., Kaufmann, S. H., et al. (2010). Lysosomal α-galactosidase controls the generation of self lipid antigens for natural killer T cells. *Immunity* 33, 216–228. doi: 10.1016/j.immuni.2010.08.003.

De Francesco, P. N., Mucci, J. M., Ceci, R., Fossati, C. A., and Rozenfeld, P. A. (2013). Fabry disease peripheral blood immune cells release inflammatory cytokines: role of globotriaosylceramide. *Mol Genet. Metabol.* 109, 93–99. doi: 10.1016/j.ymgme.2013.02.003

Didonna, A., Cekanaviciute, E., Oksenberg, J. R., and Baranzinia, S. E. (2016). Immune cell-specific transcriptional profiling highlights distinct molecular pathways controlled by Tob1 upon experimental autoimmune encephalomyelitis. *Sci. Rep.* 6:31603. doi: 10.1038/srep31603

Du, P., Kibbe, W. A., and Lin, S. M. (2008). lumi: a pipeline for processing illumina microarray. *Bioinformatics* 24, 1547–1548. doi: 10.1093/bioinformatics/btn224

Furey, T. S., Cristianini, N., Duffy, N., Bednarski, D. W., Schummer, M., and Haussler, D. (2000). Support vector machine classification and validation of cancer tissue samples using microarray expression data. *Bioinformatics* 16, 906–914. doi: 10.1093/bioinformatics/16.10.906

Gamerdinger, M., Hajieva, P., Kaya, A. M., Wolfrum, U., Hartl, F. U., and Behl, C. (2009). Protein quality control during aging involves recruitment of the macroautophagy pathway by BAG3. *EMBO J.* 28, 889–901. doi: 10.1038/emboj.2009.29

Gardinassi, L. G., Garcia, G. R., Costa, C. H. N., Silva, V. C., and de Miranda Santos, I. K. F. (2016). Blood transcriptional profiling reveals immunological signatures of distinct states of infection of humans with leishmania infantum. *PLOS Negl. Trop. Dis.* 10:e0005123. doi: 10.1371/journal.pntd.0005123

Golub, T. R., Slonim, D. K., Tamayo, P., Huard, C., Gaasenbeek, M., and Mesirov, J. P. (1999). Molecular classification of cancer: class discovery and class prediction by gene expression monitoring. *Science* 286, 531–537.

Gonzalez, A., Valeiras, M., Sidransky, E., and Tayebi, N. (2014). Lysosomal integral membrane protein-2: a new player in lysosome-related pathology. *Mol. Genet. Metabol.* 111, 84–91. doi: 10.1016/j.ymgme.2013.12.005

Hessle, C. C., Andersson, B., and Wold, A. E. (2005). Gram-positive and Gram-negative bacteria elicit different patterns of pro-inflammatory cytokines in human monocytes. *Cytokine* 30, 311–318. doi: 10.1016/j.cyto.2004.05.008

Huang da. W., Lempicki, R. A., and Sherman, B. T. (2009). Systematic and integrative analysis of large gene lists using DAVID bioinformatics resources. *Nat. Prot.* 4, 44–57. doi: 10.1038/nprot.2008.211.

Iwabuchi, K., Nakayama, H., Oizumi, A., Suga, Y., Ogawa, H., and Takamori, K. (2015). Role of ceramide from glycosphingolipids and its metabolites in immunological and inflammatory responses in humans. *Mediators Inflamm.* 2015:120748. doi: 10.1155/2015/120748

Jimenez-Lucho, V., Ginsburg, V., and Krivan, H. C. (1990). *Cryptococcus neoformans*, *Candida albicans*, and other fungi bind specifically to the glycosphingolipid lactosylceramide (GAl beta 1-4Glc beta 1-1Cer), a possible adhesion receptor for yeasts. *Infect. Immun.* 58, 2085–2090.

Kirn, T. J., and Weinstein, M. P. (2013). Update on blood cultures: how to obtain, process, report, and interpret. *Clin. Microbiol. Infect.* 19, 513–520. doi: 10.1111/1469-0691.12180

Klassert, T. E., Bräuer, J., Hölzer, M., Stock, M., Riege, K., Zubiría-Barrera, C., et al. (2017). Differential effects of vitamins A and D on the transcriptional landscape of human monocytes during infection. *Sci. Rep.* 7:40599. doi: 10.1038/srep40599.

Klassert, T. E., Hanisch, A., Bräuer, J., Klaile, E., Heyl, K. A., Mansour, M. K., et al. (2014). Modulatory role of vitamin A on the Candida albicans-induced immune response in human monocytes. *Med. Microbiol. Immunol.* 203, 415–424. doi: 10.1007/s00430-014-0351-4

Ko, D. C., Gordon, M. D., Jin, J. Y., and Scott, M. P. (2001). Dynamic movements of organelles containing Niemann-Pick C1 protein: NPC1 involvement in late endocytic events. *Mol. Biol. Cell.* 12, 601–614. doi: 10.1091/mbc.12.3.601

Lauvau, G., Loke, P., and Hohl, T. M. (2015). Monocyte-mediated defense against bacteria, fungi, and parasites. *Semin. Immunol.* 27, 397–409. doi: 10.1016/j.smim.2016.03.014

Lee, E. K. (2007). Large-scale optimization-based classification models in medicine and biology. *Ann. Biomed. Eng.* 35, 1095–1109. doi: 10.1007/s10439-007-9317-7

Lionakis, M. S., Fischer, B. G., Lim, J. K., Swamydas, M., Wan, W., Richard Lee, C. C., et al. (2012). Chemokine receptor Ccr1 drives neutrophil-mediated kidney immunopathology and mortality in invasive candidiasis. *PLoS Pathog.* 8:e1002865. doi: 10.1371/journal.ppat.1002865

Liu, Y., Shetty, A. C., Schwartz, J. A., Bradford, L. L., Xu, W., Phan, Q. T., et al. (2015). New signaling pathways govern the host response to *C. albicans* infection in various niches. *Genome Res.* 125, 679–689. doi: 10.1101/gr.187427.114

McDermott, J. E., Wang, J., Mitchell, H., Webb-Robertson, B. J., Hafen, R., Ramey, J., et al. (2012). Challenges in biomarker discovery: combining expert insights with statistical analysis of complex omics data. *Expert Opin. Med. Diagn.* 7, 1–15. doi: 10.1517/17530059.2012.718329

Moore, S. M., Holt, V. V., Malpass, L. R., Hines, I. N., and Wheeler, M. D. (2015). Fatty acid-binding protein 5 limits the anti-inflammatory response in murine macrophages. *Mol. Immunol.* 67, 265–275. doi: 10.1016/j.molimm.2015.06.001

Müller, M. M., Lehmann, R., Klassert, T. E., Reifenstein, S., Conrad, T., Moore, C., et al. (2017). Global analysis of glycoproteins identifies markers of endotoxin tolerant monocytes and GPR84 as a modulator of TNFα expression. *Sci. Rep.* 7:838. doi: 10.1038/s41598-017-00828-y

Navarathna, D. H., and Roberts, D. D. (2010). *Candida albicans* heme oxygenase and its product CO contribute to pathogenesis of candidemia and alter systemic chemokine and cytokine expression. *Free Radic. Biol. Med.* 49, 1561–1573. doi: 10.1016/j.freeradbiomed.2010.08.020

Netea, M. G., Brown, G. D., Kullberg, B. J., and Gow, N. A. (2008). An integrated model of the recognition of *Candida albicans* by the innate immune system. *Nat. Rev. Microbiol.* 6, 67–78. doi: 10.1038/nrmicro1815

Ng, H. H., Frantz, C. E., Rausch, L., Fairchild, D. C., Shimon,J., Riccio, E., et al. (2005). Gene expression profiling of mouse host response to Listeria monocytogenes infection. *Genomics* 86, 657–667. doi: 10.1016/j.ygeno.2005.07.005

Ngo, L. Y., Kasahara, S., Kumasaka, D. K., Knoblaugh, S. E., Jhingran, A., and Hohl, T. M. (2014). Inflammatory monocytes mediate early and organ-specific innate defense during systemic candidiasis. *J. Infect. Dis.* 209, 109–119. doi: 10.1093/infdis/jit413

Noble, W. S. (2004). "Support vector machine applications in computational biology,"in *Kernel Methods in Computational Biology,* eds B. Schölfkopf, K. Tsuda, and J. Vert (Cambridge, MA: MIT Press), 71–92.

Palmer, C., Diehn, M., Alizadeh, A. A., and Brown, P. O. (2006). Cell-type specific gene expression profiles of leukocytes in human peripheral blood. *BMC Genomics* 7:115. doi: 10.1186/1471-2164-7-115

Petryszak, R., Keays, M., Tang, Y. A., Fonseca, N. A., Barrera, E., Burdett, T., et al. (2016). Expression Atlas update - An integrated database of gene and protein expression in humans, animals and plants. *Nucleic Acids Res.* 44, D746–D752. doi: 10.1093/nar/gkv1045

Pfaffl, M. W., Tichopad, A., Prgomet, C., and Neuvians, T. P. (2004). Determination of stable housekeeping genes, differentially

regulated target genes and sample integrity: bestKeeper–excel-based tool using pair-wise correlations. *Biotechnol. Lett.* 26, 509–515. doi: 10.1023/B:BILE.0000019559.84305.47

Piantadosi, C. A., Withers, C. M., Bartz, R. R., MacGarvey, N. C., Fu, P., Sweeney, T. E., et al. (2011). Heme oxygenase-1 couples activation of mitochondrial biogenesis to anti-inflammatory cytokine expression. *J. Biol. Chem.* 286, 16374–16385. doi: 10.1074/jbc.M110.207738

Riege, K., Hölzer, M., Klassert, T. E., Barth, E., Bräuer, J., Collatz, M.,et al. (2017). Massive effect on LncRNAs in human monocytes during fungal and bacterial infections and in response to vitamins A and D. *Sci. Rep.* 7:40598. doi: 10.1038/srep40598

Rieu, I., and Powers, S. J. (2009). Real-time quantitative RT-PCR - design, calculations, and statistics. *Plant Cell* 21, 1031–1103. doi: 10.1105/tpc.109.066001

Ritchie, M. E., Phipson, B., Wu, D., Hu, Y., Law, C. W., Shi, W., et al. (2015). limma powers differential expression analyses for RNA-sequencing and microarray studies. *Nucleic Acids Res.* 43:e47. doi: 10.1093/nar/gkv007

Saeys, Y., Inza, I., and Larrañaga, P. (2007). A review of feature selection techniques in bioinformatics. *Bioinformatics* 23, 2507–2517. doi: 10.1093/bioinformatics/btm344

Saraiva, J. P., Marcus, O., Antje, B., Cora, A., Tilman, K., Markus, B., et al. (2016). Integrating classifiers across datasets improves consistency of biomarker predictions for sepsis. In *6th IFAC Conference on Foundations of Systems Biology in Engineering.* Magdeburg: Elsevier ScienceDirect.

Shi, C., and Pamer, E. G. (2011). Monocyte recruitment during infection and inflammation. *Nat. Rev. Immunol.* 11, 762–774. doi: 10.1038/nri3070.

Silva-Gomes, S., Appelberg, R., Larsen, R., Soares, M. P., and Gomes, M. S. (2013). Heme catabolism by heme oxygenase-1 confers host resistance to Mycobacterium infection. *Infect. Immun.* 81, 2536–2545. doi: 10.1128/IAI.00251-13

Smeekens, S. P., Ng, A., Kumar, V., Johnson, M. D., Plantinga, T. S., van Diemen, C., et al. (2013). Functional genomics identifies type I interferon pathway as central for host defense against *Candida albicans. Nat. Commun.* 4:1342. doi: 10.1038/ncomms2343

Tyagi, S., Gupta, P., Saini, A. S., Kaushal, C., and Sharma, S. (2011). The peroxisome proliferator-activated receptor: a family of nuclear receptors role in various diseases. *J. Adv. Pharmaceut. Technol. Res.* 2, 236–240. doi: 10.4103/2231-4040.90879

Wong, K. L., Tai, J. J., Wong, W. C., Han, H., Sem, X., Yeap, W. H., et al. (2011). Gene expression profiling reveals the defining features of the classical, intermediate, and nonclassical human monocyte subsets. *Blood* 118, e16–e31. doi: 10.1182/blood-2010-12-326355

Yamayoshi, S., Fujii, K., and Koike, S. (2014). Receptors for enterovirus 71. *Emerg. Microbes Infect.* 3:e53. doi: 10.1038/emi.2014.49

Zuker, M. (2003). Mfold web server for nucleic acid folding and hybridization prediction. *Nucleic Acids Res.* 31, 3406–3415. doi: 10.1093/nar/gkg595

Conflict of Interest Statement: The authors declare that the research was conducted in the absence of any commercial or financial relationships that could be construed as a potential conflict of interest.

Copyright © 2017 Leonor Fernandes Saraiva, Zubiria-Barrera, Klassert, Lautenbach, Blaess, Claus, Slevogt and König. This is an open-access article distributed under the terms of the Creative Commons Attribution License (CC BY). The use, distribution or reproduction in other forums is permitted, provided the original author(s) or licensor are credited and that the original publication in this journal is cited, in accordance with accepted academic practice. No use, distribution or reproduction is permitted which does not comply with these terms.

frontiers in Immunology

ORIGINAL RESEARCH
published: 30 November 2017
doi: 10.3389/fimmu.2017.01650

P17, an Original Host Defense Peptide from Ant Venom, Promotes Antifungal Activities of Macrophages through the Induction of C-Type Lectin Receptors Dependent on LTB4-Mediated PPARγ Activation

Khaddouj Benmoussa[1,2,3], Hélène Authier[1,2], Mélissa Prat[1,2], Mohammad AlaEddine[1,2], Lise Lefèvre[1,2], Mouna Chirine Rahabi[1,2], José Bernad[1,2], Agnès Aubouy[1,2], Elsa Bonnafé[3], Jérome Leprince[4], Bernard Pipy[1,2], Michel Treilhou[3†] and Agnès Coste[1,2†]*

[1] UMR 152 Pharma Dev, Université de Toulouse, IRD, UPS, Toulouse, France, [2] IRD, UMR 152, Toulouse, France, [3] EA7417 BTSB, Université Fédérale Toulouse Midi-Pyrénées, INU Champollion, Albi, France, [4] INSERM U982, PRIMACEN, IRIB, Université de Rouen, Mont-Saint-Aignan, France

Despite the growing knowledge with regard to the immunomodulatory properties of host defense peptides, their impact on macrophage differentiation and on its associated microbicidal functions is still poorly understood. Here, we demonstrated that the P17, a new cationic antimicrobial peptide from ant venom, induces an alternative phenotype of human monocyte-derived macrophages (h-MDMs). This phenotype is characterized by a C-type lectin receptors (CLRs) signature composed of mannose receptor (MR) and Dectin-1 expression. Concomitantly, this activation is associated to an inflammatory profile characterized by reactive oxygen species (ROS), interleukin (IL)-1β, and TNF-α release. P17-activated h-MDMs exhibit an improved capacity to recognize and to engulf *Candida albicans* through the overexpression both of MR and Dectin-1. This upregulation requires arachidonic acid (AA) mobilization and the activation of peroxisome proliferator-activated receptor gamma (PPARγ) nuclear receptor through the leukotriene B4 (LTB4) production. AA/LTB4/PPARγ/Dectin-1-MR signaling pathway is crucial for P17-mediated anti-fungal activity of h-MDMs, as indicated by the fact that the activation of this axis by P17 triggered ROS production and inflammasome-dependent IL-1β release. Moreover, we showed that the increased anti-fungal immune response of h-MDMs by P17 was dependent on intracellular calcium mobilization triggered by the interaction of P17 with pertussis toxin-sensitive G-protein-coupled receptors on h-MDMs. Finally, we also demonstrated that P17-treated mice infected with *C. albicans* develop less severe gastrointestinal infection related to a higher efficiency of their macrophages to engulf *Candida*, to produce ROS and IL-1β and to kill the yeasts. Altogether, these results identify P17 as an original activator of the fungicidal response of macrophages that acts upstream PPARγ/CLRs axis and offer new immunomodulatory therapeutic perspectives in the field of infectious diseases.

Keywords: Macrophages, host defense peptide, antimicrobial peptides, *Candida albicans*, C-type lectin receptors, arachidonic acid metabolism, PPARγ, inflammasome

OPEN ACCESS

Edited by:
Etienne Meunier, UMR5089 Institut de Pharmacologie et de Biologie Structurale (IPBS), France

Reviewed by:
Hridayesh Prakash, University of Hyderabad, India
Shashank Gupta, Brown University, United States

***Correspondence:**
Agnès Coste
agnes.coste@univ-tlse3.fr

†co-senior authors.

Specialty section:
This article was submitted to Microbial Immunology, a section of the journal Frontiers in Immunology

Received: *01 August 2017*
Accepted: *10 November 2017*
Published: *30 November 2017*

Citation:
Benmoussa K, Authier H, Prat M, AlaEddine M, Lefèvre L, Rahabi MC, Bernad J, Aubouy A, Bonnafé E, Leprince J, Pipy B, Treilhou M and Coste A (2017) P17, an Original Host Defense Peptide from Ant Venom, Promotes Antifungal Activities of Macrophages through the Induction of C-Type Lectin Receptors Dependent on LTB4-Mediated PPARγ Activation. Front. Immunol. 8:1650. doi: 10.3389/fimmu.2017.01650

INTRODUCTION

Antimicrobial peptides (AMPs), also called host defense peptides (HDPs), are small molecules produced by all living forms including bacteria, insects, plants and vertebrates. These peptides are especially found in skin and intestine; thus, they constitute the first line of organism immune defense (1). Although HDPs can be cationic or anionic, most of them are cationic molecules with an amphipatic structure (2).

Unlike antibiotics, cationic HDPs have a microbicidal activity against a broad spectrum of pathogens including bacteria, yeast, and viruses. They exercise their direct antimicrobial effect essentially by interacting with negatively charged membranes of target cells inducing membrane destabilization and cell death (1, 3, 4). These HDPs can also inhibit intracellular pathways critical for pathogen survival (5–7). Beside their microbicidal activity, most of cationic HDPs exhibit modulatory functions on immune cells. HDPs are produced by and act on several cell types including innate and adaptive immune cells (8–10). Their functions are multiples and depend on their structure, the microenvironment, and the target cell. In humans, the two main classes of HDPs are cathelicidins and defensins (11, 12). LL-37, the only member of the human cathelicidin AMP family, is well known to modulate innate and adaptive immune responses. Regarding adaptive immune response, this peptide induces T lymphocytes chemotaxis and regulates the activation of antigen-presenting cells and Th1 polarization of T cells (13). This AMP can also contribute to innate immune response by controlling the activation of monocytes, macrophages, and dendritic cells (13). Indeed, it was previously described that LL-37 regulates cytokine and chemokine genes expression and protein secretion in human monocytes and macrophages (14–16). Moreover, this AMP promotes directly microbicidal activities of monocytes, macrophages, and neutrophils by increasing pathogen phagocytosis and reactive oxygen species (ROS) release (14, 15, 17–19). This human cathelicidin is also involved in immune cells apoptosis, angiogenesis, and wound-healing regulation (20–24). Similar to LL-37, immunomodulatory effects on innate immunity were also described for defensins and several HDPs found in insect venom (25, 26). Usually, their effects on immune cells are mediated through G-protein-coupled receptors (GPCRs). Among the HDP-activated GPCRs, the *N*-formylmethionine-leucyl-phenylalanine receptors 1 and 2 (FPR1 and FPR2) and the chemokine receptors are the most involved (27–30).

Our laboratory has previously isolated two original HDPs from ant venom of *Tetramorium bicarinatum* (31). These peptides, named P16 (Bicarinalin) and P17, are cationic, C-terminal amidated, and adopt an α-helix conformation. In this previous study, the authors demonstrated a potent and broad antibacterial activity for the Bicarinalin (31). Although no microbicidal activity for P17 was demonstrated, this HDP could be a good candidate to modulate immune response because of its structural properties and its low toxicity on human cells.

Despite the growing knowledge with regard to the immunomodulatory properties of HDPs, little is known about how they control macrophage differentiation and its associated microbicidal functions. Emerging evidence indicates that the state of macrophage polarization plays a critical role in the host susceptibility against infections. The following two programs broadly classify polarized macrophages: classical (M1) and alternative (M2) (32, 33). The M1 program arises from type 1 inflammatory conditions (e.g., IFNγ) and is characterized by elevated levels of opsonic receptors. M1 macrophages highly produce pro-inflammatory effector molecules, such as reactive oxygen and nitrogen species, and pro-inflammatory cytokines [interleukin (IL)-1β, TNF-α, IL-6, and IL-12]. These macrophages contribute to inflammation and microbial killing. M2 alternative macrophages are characterized by abundant levels of the anti-inflammatory cytokine IL-10 and non-opsonic receptors, such as C-type lectin receptors (CLRs) and scavenger receptors. These alternative-activated macrophages can also efficiently participate to pathogen clearance through CLR-mediated recognition and phagocytosis (34–36).

Among the CLRs, Dectin-1 and mannose receptor (MR) of the phagocytic system have been described to be essential in anti-fungal functions of macrophages (34, 35, 37–42).

After binding of β-glucans and mannans, the major cell wall components of *Candida albicans*, these CLRs act in a cooperative manner to activate syk-p47^{phox} axis essential to ROS production and inflammasome-dependent signaling pathways for IL-1β release (35, 36, 43). Thus, the induction of these two CLRs at the surface of macrophages is critical for the fungicidal response.

The balance of macrophage differentiation toward an alternative phenotype, known to highly express MR and Dectin-1, is controlled by the nuclear receptor peroxisome proliferator-activated receptor gamma (PPARγ) activation (34, 35, 43). Among PPARγ ligands, lipids from the metabolism of arachidonic acid (AA) through the COX-1/COX-2 cyclooxygenases and 5- and 12/15-lipoxygenases (LOX), are considered to be critical for PPARγ endogenous activation (37, 44, 45). We have previously demonstrated that PPARγ activation in macrophages promotes the transcription of Dectin-1 and MR and its associated anti-fungal functions (34, 43, 46). Although the processes leading to PPARγ activation, such as AA release and its subsequent metabolic conversion, are important aspects of macrophage alternative polarization and CLR-dependent anti-fungal defense, the impact of HDPs on this signaling is not yet elucidated.

In the present study, we demonstrated that P17 promotes alternative activation of the human monocyte-derived macrophages (h-MDMs) characterized simultaneously by a CLRs signature composed of MR and Dectin-1 and a pro-inflammatory profile. Interestingly, this HDP also improves the recognition and the phagocytosis of *C. albicans* by h-MDMs through the overexpression of MR and Dectin-1. This upregulation requires AA release and the activation of PPARγ through the leukotriene B4 (LTB4) production. The activation of AA/LTB4/PPARγ/Dectin-1-MR axis by P17 triggers ROS production and inflammasome-dependent IL-1β release critical in the fungicidal activity of P17-activated h-MDMs. Finally, we validated the efficiency of P17 to eliminate *C. albicans in vivo*. Indeed, P17-treated mice infected with *C. albicans* develop less severe gastrointestinal infection related to a higher ability of their macrophages to engulf *Candida*, to produce ROS, IL-1β, and to kill *C. albicans* as compared to untreated mice. Altogether, these results identify P17 as an original activator of

the fungicidal response of macrophages and support that this novel HDP may constitute promising compound to restrain fungal infections.

MATERIALS AND METHODS

P17 AMP

The sequence of the P17 peptide (LFKEILEKIKAKL-NH2) was characterized by *de novo* sequencing using mass spectrometry and Edman degradation (31). P17 peptide and its randomly designed C-terminal amidated scrambled counterpart (KIKEEKFLLKLI-NH2) were synthesized on a Liberty microwave assisted automated peptide synthesizer (CEM, Saclay, France) at a purity grade higher than 99% as previously described (31, 47). The authenticity and the molecular identity of the synthetic peptides were controlled by MALDI-TOF-MS.

Preparation of h-MDMs

Human peripheral blood mononuclear cells were isolated from the blood of healthy volunteers by a density gradient centrifugation method on Lymphoprep (Abcys). Monocytes were isolated from mononuclear cells by adherence to plastic for 2 h in special macrophage serum-free medium (SFM; Life Technologies) with L-glutamine at 37°C in a humidified atmosphere containing 5% CO_2. Non-adherent cells were removed by washing with Hanks' balanced salt solution (HBSS) (Gibco, Invitrogen), and the remaining adherent cells (>85% monocytes) were incubated in SFM medium. The h-MDMs were obtained after 24 h of culture in SFM medium. Adherent h-MDMs were pre-incubated 30 min or not before the addition of P17 (200 µg/ml) with GW9662 (1 nM; Santa Cruz Biotechnology), MAFP (20 µM; Calbiochem), MK-886 (10 µM; Calbiochem), *N*-acetyl-cysteine (10 mM; Sigma), or Z-Vad-FMK (ZVAD) (50 µM; Calbiochem) for 30 min.

C. albicans Strains

The strain of *C. albicans* used throughout these experiments was isolated from a blood culture of a patient in the Toulouse-Rangueil University Hospital (98/26135). The isolate was identified as *C. albicans* based on common laboratory criteria and cultured on Sabouraud dextrose agar (SDA; Biorad, Hercules, CA, USA) plates containing gentamicin and chloramphenicol. *C. albicans* was maintained by transfers on SDA plates. Growth from an 18- to 24-h SDA culture of *C. albicans* was suspended in sterile saline buffer (HBSS; Life Technologies). In all experiments, the h-MDMs were challenged with blastospores.

Killing Assay

Human monocyte-derived macrophages were treated with P17 (200 µg/ml) for 24 h and were allowed to interact for 40 min at 37°C with *C. albicans* blastospores (at a ratio of 0.3 yeast per macrophage) as previously described (36, 40). Unbound yeasts were removed by four washes with medium. h-MDMs were then incubated at 37°C for 4 h. After incubation, the medium was removed and cells were lysed. The CFU of *C. albicans* were quantified after plating on Sabouraud plates for 24–48 h at 37°C.

In some experiments, monocyte-derived macrophages were incubated with 1 µg per well of MR siRNA (Santa Cruz Biotechnology sc-45360) and/or Dectin-1 siRNA (Santa Cruz Biotechnology sc-63276) for 6 h into siRNA transfection medium (siRNA reagent system, Santa Cruz Biotechnology sc-45064) according to the manufacturer's instructions before the addition of P17.

Binding and Phagocytosis Assay

Human monocyte-derived macrophages were treated with P17 (200 µg/ml) for 24 h and were then challenged with GFP-labeled yeasts at a ratio of 6 blastospores per macrophage. In some experiments, the monocyte-derived macrophages were incubated at 4°C for 20 min with 500 µg/ml of mannans and/or laminarins before the addition of the yeasts. The binding was performed at 4°C and the phagocytosis was initiated at 37°C. The number of *C. albicans* bound or engulfed by macrophages was determined by fluorescence quantification using the Envision fluorimetry-based approach (Perkin Elmer).

Assay for ROS Production

Human monocyte-derived macrophages were treated with P17 (200 µg/ml) for 24 h and ROS production was measured by chemiluminescence in the presence of 5-amino-2,3-dihydro-1, 4-phthalazinedione (luminol; Sigma) using a thermostatically (37°C) controlled luminometer (Envision; Perkin Elmer). The generation of chemiluminescence was monitored continuously for 1 h and 30 min after challenge or not with *C. albicans* blastospores (yeast-to-macrophage ratio: 3:1). Statistical analysis was performed using the area under the curve expressed in counts × seconds.

ELISA Cytokine Titration

Human monocyte-derived macrophages were treated with P17 (200 µg/ml) for 24 h and challenged with *C. albicans* blastospores at a ratio of 3 yeasts per macrophage for 8 h. The release of TNF-α, IL-1β, IL-12, and IL-10 in the cell supernatants was determined with a commercially available OptiEIA kit (BD Biosciences) according to the manufacturer's instructions.

Western Blot Analysis

Human monocyte-derived macrophages were treated with P17 (200 µg/ml) for 24 h and challenged for 8 h with *C. albicans* blastospores at a ratio of 3 yeasts per macrophage. h-MDMs were lysed with RIPA buffer (Sigma) and protein extracts were separated in SDS-PAGE as previously described (37). After protein transfer, membranes were incubated overnight at 4°C with a rabbit anti-phosphorylated $p47^{phox}$ (Assay biotechnology, A1171; 1/260), a rabbit anti-caspase-1 (Biovision, 3019-100; 1/100), or a goat anti-GAPDH antibody (Cell Signaling, #5174; 1/1,000) and then for 1 h at room temperature with a peroxidase conjugated secondary antibody. Membranes were washed, and proteins of interest were visualized with WesternBright™ ECL (Advansta) or the SuperSignal West Pico Chemiluminescent Substrate (ThermoScientific) for the GAPDH. Images have been cropped for presentation.

Flow Cytometry

Human monocyte-derived macrophages were treated with P17 (200 µg/ml) for 24 h and then incubated with ice-cold PBS and gently scraped. Collected cells were centrifuged at 1,500 rpm for 10 min, and the cell pellet was suspended in PBS medium supplemented with 1% fetal calf serum (FCS). Surface expressed MR, Dectin-1, DC-SIGN, CD16, or CD36 was detected, respectively, using PerCP-Dectin-1 monoclonal antibody (mAb; R&D FAB1859C-100, 1/40), PE-DC-SIGN (mAb; BD Biosciences 551 265, 1/20), FITC-CD16 (mAb; PNIM 0814, 1/20), or APC-CD36 monoclonal antibodies (mAb; BD Biociences 550 956, 1/40). To evaluate the MR surface expression, we have used MR-specific ligand conjugated with FITC (Sigma A7790, 1 mg/ml, 1/100). All staining were performed on $PBS^{-/-}$ 1% FCS medium. A population of 10,000 cells was analyzed for each data point. All analyses were carried out in a Becton Dickinson FACScalibur using the FACSDiva version 6.2 software.

Reverse Transcription and Real-time PCR

Human monocyte-derived macrophages were treated with P17 (200 µg/ml) and/or LTB4 (100 nM; Cayman Chemical Company) for 8 h.

The mRNA preparation was made using the EZ-10 Spin Column Total RNA Minipreps Super Kit (Bio Basic) using the manufacturer's protocol. Synthesis of cDNA was performed according to the manufacturer's recommendations (Thermo electron). RT-qPCR was performed on a LightCycler 480 system using LightCycler SYBR Green I Master (Roche Diagnostics). The primers (Eurogentec) were designed with the software Primer 3. GAPDH mRNA was used as the invariant control. Serially diluted samples of pooled cDNA were used as external standards in each run for the quantification. Primer sequences are listed in **Table 1**.

TABLE 1 | Human primer sequences used in qPCR analysis.

Gene	5′–3′ sequence	
Alox5	Antisense	ACT-GGA-AAC-ACG-GCA-AAA-AC
	Sense	TTT-CTC-AAA-GTC-GGC-GAA-GT
Itgam (CD11b)	Antisense	TTG-CAT-CCA-TCT-CAA-ATC-CA
	Sense	CTC-CCA-AAG-TGC-TGG-GAT-TA
Fcgr3 (CD16)	Antisense	TAC-AGC-GTG-CTT-GAG-AAG-GA
	Sense	GCA-CCT-GTA-CTC-TCC-ACT-GT
Fcgr2 (CD32)	Antisense	CCA-AAG-GCT-GTG-CTG-AAA-CT
	Sense	TAC-TCC-CCG-CTG-TCA-TTG-TT
Cd36	Antisense	TGA-TAG-GTG-CAG-CAA-AGC-AC
	Sense	TGT-AAC-CCA-GGA-CGC-TGA-GG
Clec7a (Dectin-1)	Antisense	CCA-AGC-ATA-GGA-TTC-CCA-AAA
	Sense	AAA-AGG-ATC-GTG-TGC-TGC-ATC
Ptgs2 (COX-2)	Antisense	TGA-GCA-TCT-ACG-GTT-TGC-TG
	Sense	TGC-TTG-TCT-GGA-ACA-ACT-GC
Pla2g4a (cPLA2)	Antisense	GCC-TTG-GTG-AGT-GAT-TCA-GCT
	Sense	AGA-TTC-AAG-CCC-AGC-ATG-AAG
Cd209 (DC-SIGN)	Antisense	GGG-CAT-GGA-GGC-TCC-AC
	Sense	CAA-CTT-AGA-AAC-AGC-CAA-ATG-GAA
Alox5ap (FLAP)	Antisense	ACC-CGC-TCA-AAG-GCA-ATG-G
	Sense	CAC-GAA-AGC-AGG-ACC-CAG-A
Gapdh	Antisense	AGG-TCG-GAG-TCA-ACG-GAT-TT
	Sense	ATC-TCG-CTC-CTG-GAA-GAT-GG
Il1b	Antisense	CAG-CCA-ATC-TTC-ATT-GCT-CA
	Sense	AGG-CAG-AGA-GGG-AAG-GAG-AG
Il6	Antisense	TAC-CCC-CAG-GAG-AAG-ATT-GT
	Sense	TTT-TCT-GCC-AGT-GCC-TCT-TT
Il12	Antisense	TGG-GTG-GGT-CAG-GTT-TGA-TG
	Sense	GCC-CAG-CTG-CTG-AGG-AGA-GT
Il10	Antisense	TGC-AAA-ACC-AAA-CCA-CAA-GA
	Sense	TCT-CGG-AGA-TCT-CGA-AGC-AT
Il1ra	Antisense	TGG-GAA-TCT-CAG-ATG-GGA-AG
	Sense	CTG-TGT-CCC-CCA-GAA-CTT-GT
Tgfb1	Antisense	ACT-GAG-GGG-AAG-GGA-CAA-CT
	Sense	TCG-GTA-CCA-GGT-GAG-GGT-AG
p47phox	Antisense	CCT-CAT-TGT-CCA-GTG-TGG-TG
	Sense	TCT-TCC-GTC-TCG-TCA-GGA-CT
Lta4h	Antisense	ACT-GCT-TGG-AGG-ACC-AGA-GA
	Sense	GGA-AAG-CAT-TAG-CAG-GCA-AG
Mrc1 (MR)	Antisense	GGC-GGT-GAC-CTC-ACA-AGT-AT
	Sense	ACG-AAG-CCA-TTT-GGT-AAA-CG
Ptges (PGES)	Antisense	CAT-GTG-AGT-CCC-TGT-GAT-GG
	Sense	GAC-TGC-AGC-AAA-GAC-ATC-CA
Pparg	Antisense	GCT-GTG-CAG-GAG-ATC-ACA-GA
	Sense	GGG-CTC-CAT-AAA-GTC-ACC-AA
Tnfα	Antisense	TCC-TTC-AGA-CAC-CCT-CAA-CC
	Sense	AGG-CCC-CAG-TTT-GAA-TTC-TT

AA Mobilization and EIA Lipid Quantification

Human monocyte-derived macrophages were pre-labeled with [^{3}H]AA. Briefly, h-MDMs (5×10^5 per well in 48-well plates) were cultured for 18 h at 37°C in the presence of P17 (200 µg/ml) and 1 µCi/ml [^{3}H]AA. The culture medium was then removed and pre-labeled macrophages were washed three times with 0.5 ml SFM. The cells were challenged with *C. albicans* blastospores at a ratio of 3 yeasts per macrophage for 2 h. The [^{3}H]AA metabolites released into the culture medium were quantified by measurement of the radioactivity by beta liquid scintillation counting using a 1217 Wallac Rackbeta LKB 1217, as previously described (37).

Determination of Intracellular Calcium Concentration

Intracellular calcium concentration was measured using the fluorescent probe Fluo 3-AM (Molecular Probe). Briefly, h-MDMs (1.5×10^5) were incubated with 11.5×10^{-6} M Fluo 3-AM for 30 min at 37°C. The time course of the intracytosolic Ca^{2+} level was recorded every 0.5 s for a total period of 3 min after the addition of P17 (200 µg/ml). In desensitization experiments, a second injection of bacterial *N*-formylmethionine-leucyl-phenylalanine peptide (fMLP) or P17 was performed at the end of fluorescence record and the time course of the intracytosolic Ca^{2+} level was recorded for supplemental 3 min. In some experiments, h-MDMs were pre-incubated with U73122 (2 µM) or with calcium-free HBSS for 10 min before the addition of P17. Fluorescence was quantified using the Envision fluorimetry-based approach (Perkin Elmer).

In Vivo Experiment

Male mice aged 12 weeks on C57BL/6 background were used for *in vivo* experiments. Mice were bred and handled by the protocols

approved by the Conseil Scientifique du Centre de Formation et de Recherche Experimental Medico Chirurgical and the ethics board of the Midi-Pyrénées ethic committee for animal experimentation (Approval no B3155503). All cages were changed twice weekly, and all manipulations of the animals were carried out in a laminal blow hood under aseptic conditions. The photoperiod was adjusted to 12 h light and 12 h dark. C57BL/6 mice were purchased from Janvier (France).

The gastrointestinal infection (GI) with the *C. albicans* was established by oral infection with 50×10^6 *C. albicans* per mouse. To establish esophageal and GI candidiasis in mice, we performed intra-esophageal infection with 5×10^7 viable cells of *C. albicans* in sterile saline solution. No antibiotic or immunosuppressive treatment was used to facilitate mucosal infection by *C. albicans* of the oral cavity and GI tract.

Mice were treated intraperitoneally with P17 (10 µg per mouse) 1 day before the day of the infection with *C. albicans* and then every 2 days (four injections). Control groups received saline solution. Therapeutic studies were performed on separate groups of six mice infected with *C. albicans* treated or not with P17.

The body weight of each mouse was recorded daily, and the condition of each mouse was assessed twice daily. Feces were collected on days 4 and 5 post-infections. At day 6 post-infection, all mice were euthanized using CO_2 asphyxia and the cecum and colon were aseptically removed to evaluate *C. albicans* colonization. To quantify the number of viable *C. albicans* in cecum, colon, and feces, each tissue sample removed was mechanically homogenized in 1 ml of saline with 100 U of penicillin/ml and 100 µg of streptomycin/ml. Serial dilutions of homogenate were plated onto SDA for quantitative determination of the number of *C. albicans* in the tissue samples. Plates were incubated at 37°C for 1–2 days and the number of colonies was counted.

After euthanasia, resident peritoneal cells were harvested by washing the peritoneal cavity with 5 ml of sterile 199 medium with Hanks' salts as previously described (6). Collected cells were centrifuged at $400 \times g$ for 8 min, and the cell pellet was suspended in SFM optimized for macrophage culture (Invitrogen Life Technologies). Cells were allowed to adhere for 2 h at 37 C and 5% CO_2. Non-adherent cells were then removed by washing with HBSS. The macrophage monolayers were used to investigate their capacity to bind, to engulf and to kill *C. albicans*, and to produce ROS and IL-1β in response to yeast challenge.

Statistical Analysis

For each experiment, the data were subjected to one-way analysis of variance followed by the means multiple comparison method of Bonferroni–Dunnett. $p < 0.05$ was considered as the level of statistical significance.

RESULTS

P17 Promotes Alternative Activation of h-MDMs Characterized by an Inflammatory Signature

In order to assess the impact of P17 in h-MDMs differentiation, we evaluated the expression of specific markers of classical and alternative activation in P17-treated h-MDMs. Overall, P17-treated h-MDMs displayed a downregulation of membrane receptors characteristics of classical M1 polarization, such as CD11b (*Itgam*), CD16 (*Fcgr3*), and CD32 (*Fcgr2*), which was mirrored by an upregulation of MR (*Mrc1*), Dectin-1 (*Clec7a*), DC-SIGN (*Cd209*), and CD36 (*Cd36*) alternative activation markers (**Figure 1A**). This finding was further supported by the reciprocal increase of anti-inflammatory IL-10 (*Il10*), IL-1 receptor antagonist (*Il1ra*), TGFβ (*Tgfb1*), CCL-17 (*Ccl17*), and CCR2 (*Ccr2*) and reduction of IL-12 (*Il12*) and CCL-2 (*Ccl2*) mRNA expression. Moreover, consistent with increased mRNA encoding alternative M2 activation markers, protein levels of MR, Dectin-1, and IL-10 were significantly increased (**Figures 1B,C**). The acquisition of this alternative phenotype upon P17 activation is reinforced by the strong decrease of IL-12 protein level (**Figure 1C**). We observed unaffected protein amounts for DC-SIGN, CD16, and CD36 (**Figure 1B**).

Surprisingly, the increase in alternative markers in P17-treated h-MDMs was accompanied by an inflammatory signature, as demonstrated by an augmentation in the mRNA level of the pro-inflammatory cytokines IL-1β (*Il1b*), TNF-α (*Tnf*α), and IL-6 (*Il6*). Consistently, the production of IL-1β and TNF-α was also induced in P17-treated h-MDMs (**Figure 1C**). In line with increased IL-1β production in P17-treated h-MDMs, the processing of pro-caspase-1 into its p20 subunit, which is a hallmark of caspase-1 activation, was significantly increased in P17-treated h-MDMs, demonstrating that the caspase-1-induced IL-1β release is activated by P17 (**Figure 1D**).

To further explore the pro-inflammatory impact of P17 on h-MDMs, we next assessed ROS production by P17-treated h-MDMs. We demonstrated that ROS release was strongly increased in P17-treated h-MDMs (**Figure 1E**). In line, the mRNA level and the amount of phosphorylated $p47^{phox}$, a cytosolic subunit of the NADPH oxidase complex whose activation is essential to ROS release, were significantly increased in h-MDMs activated by P17 (**Figures 1F,G**).

Taken together, these results indicated that P17 induces an alternative phenotype characterized simultaneously by a CLRs signature composed of MR and Dectin-1 and a pro-inflammatory profile.

P17 Induces MR and Dectin-1 Expression on h-MDMs through PPARγ Activation Dependent on LTB4 Production

The nuclear receptor PPARγ is a key component of the signaling pathway leading to alternative activation of macrophages and directly controls the expression of CLRs (34–36). To identify how P17 may have an impact on MR and Dectin-1 overexpression, we evaluated whether P17 can regulate PPARγ activation. The mRNA levels of PPARγ (*Pparg*) and of its target gene SRB1 (*Scarb1*) were significantly increased in P17-treated h-MDMs, suggesting that P17 improved PPARγ activation.

To further explore whether P17-induced PPARγ activation was involved in MR and Dectin-1 overexpression, we evaluated the gene expression of these two CLRs in the presence of GW9662, a selective PPARγ antagonist. The treatment

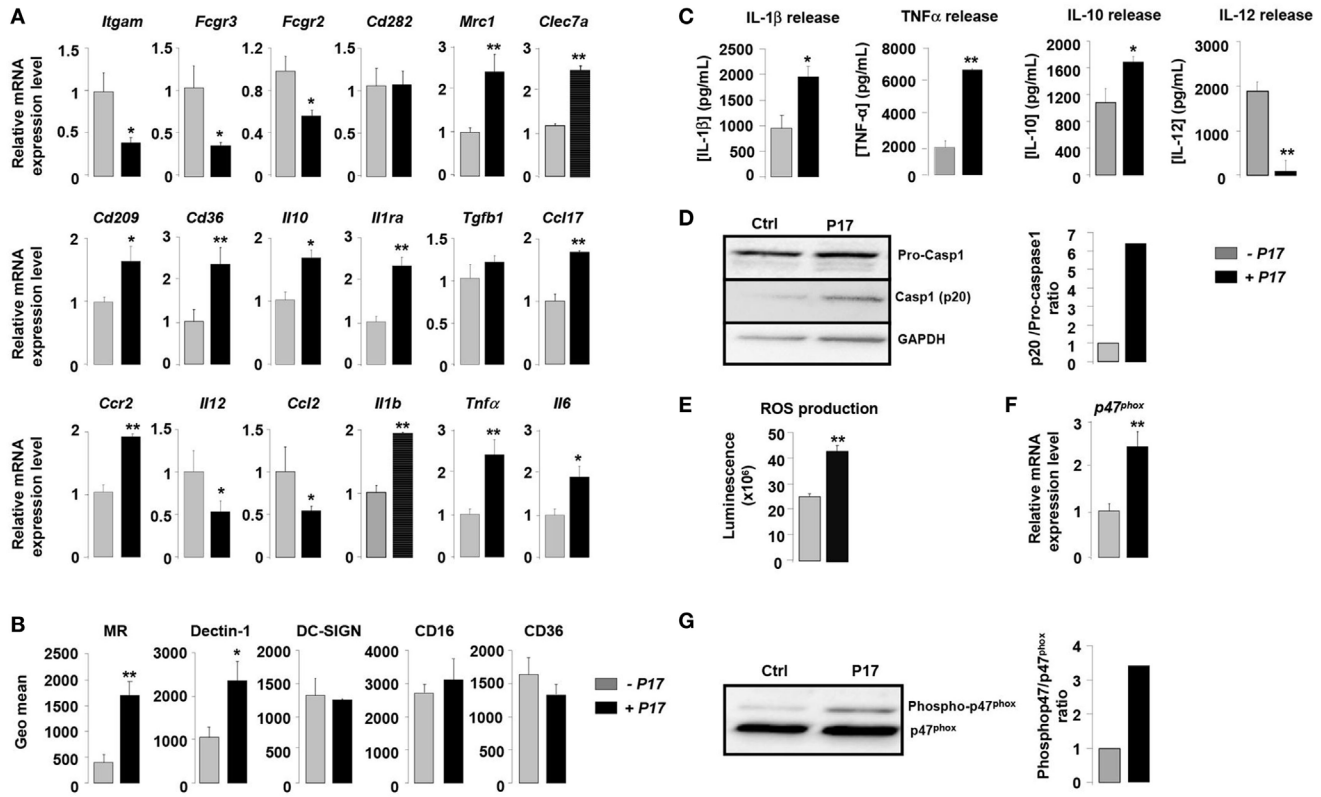


FIGURE 1 | P17 mediates an alternative phenotype of human monocyte-derived macrophages (h-MDMs) characterized by C-type lectin receptor (CLR) and inflammatory signatures. **(A)** Gene expression analysis of markers of classical and alternative polarization in h-MDMs treated or not with P17. The results were represented in fold induction relative to the untreated h-MDMs control. **(B)** Mannose receptor (MR), Dectin-1, DC-SIGN, CD16, and CD36 protein expressions in h-MDMs treated or not with P17. Graphs represent geomean fluorescence quantification for the indicated proteins. **(C)** TNF-α, interleukin (IL)-1β, IL-12, and IL-10 release by h-MDMs treated or not with P17 after challenge with *Candida albicans*. **(D)** Immunoblot analysis of caspase-1 p20 fragment cleavage in h-MDMs treated or not with P17 after *C. albicans* challenge. Band intensity was quantified using the ImageJ software and was represented as the ratio between the band intensities of p20 and of pro-caspase-1. **(E)** Reactive oxygen species production by h-MDMs treated or not with P17 after challenge with *C. albicans*. **(F)** Gene expression of $P47^{phox}$ in h-MDMs treated or not with P17. The results were represented in fold induction relative to the untreated h-MDMs control. **(G)** Phosphorylated $p47^{phox}$ immunoblot after *C. albicans* challenge in h-MDMs treated or not with P17. Band intensity was quantified using the ImageJ software and was represented as the ratio between the band intensities of phosphorylated $p47^{phox}$ and of $P47^{phox}$. Results correspond to mean ± SEM of triplicates. Data are representative of three independent experiments. $^{*}p < 0.05$, $^{**}p < 0.01$ compared to the respective untreated control.

of P17-activated h-MDMs with GW9662 inhibited Mrc1 and Clec7a gene overexpressions, demonstrating that PPARγ is critically required for P17-induced Dectin-1 and MR expression on human h-MDMs (**Figure 2A**).

Peroxisome proliferator-activated receptor gamma is activated by endogenous ligands derived from AA (34, 35, 43, 48). The COX-1/2 cyclooxygenase, 5- and 12/15-LOX are considered to be critical for the conversion of AA into endogenous PPARγ ligands. To assess whether P17 can coordinate PPARγ ligand availability, we evaluated the gene expression of enzymes involved in both COX and LOX signaling pathways. The mRNA levels of cPLA2 (*Pla2g4a*), enzyme needed for AA release from membrane phospholipids, 5-LOX (*Alox5*), FLAP (5-LOX activating enzyme) (*Alox5ap*), and LTA4 hydrolase (*Lta4h*), critical for LTB4 synthesis, were strongly increased in P17-treated h-MDM (**Figure 2B**). Moreover, the mRNA levels of COX-2 (*Ptgs2*), PGES (*Ptges*), and 15-LOX (*Alox15*) were not differentially expressed in untreated and P17-treated h-MDMs, supporting that P17 had no incidence on COX-2 and 12/15-LOX signaling pathways.

Then, we determined whether these effects on gene expression also translate into changes in ligand availability. Consistent with cPLA2 gene overexpression, the mobilization of AA was induced in P17-treated h-MDMs (**Figure 2C**). Furthermore, in line with LTA4 hydrolase expression in P17-treated h-MDMs, we observed strong increase of LTB4 release (**Figure 2D**). These data suggest that the generation of LTB4 metabolites by h-MDMs upon P17 treatment is dependent both on AA mobilization and metabolism.

To confirm that P17 positively regulates MR and Dectin-1 expressions through the AA metabolism, we determined Mrc1 and Clec7a gene expression in the presence of MAFP, a specific cPLA2 inhibitor, and MK-886, a FLAP inhibitor, which prevents 5-LOX activation. The increase of MR and Dectin-1 mRNA levels in P17-treated h-MDMs was completely lost in the presence of MAFP and MK-886 (**Figure 2E**), further supporting

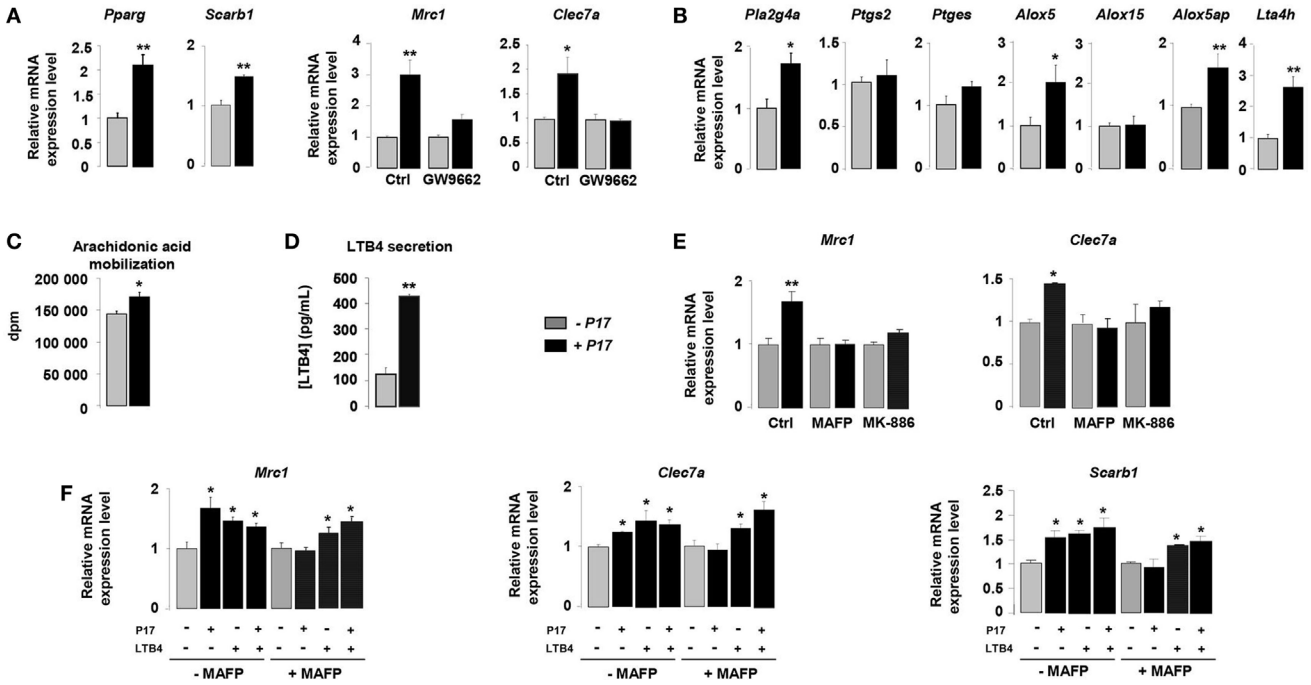


FIGURE 2 | P17 promotes C-type lectin receptor (CLR) expression on human monocyte-derived macrophages (h-MDMs) through leukotriene B4 (LTB4)-mediated peroxisome proliferator-activated receptor gamma (PPARγ) activation. **(A)** Gene expression analysis of PPARγ, SRB1, mannose receptor (MR), and Dectin-1 in h-MDMs treated or not with P17, in the presence of a selective PPARγ antagonist GW9662. The results were represented in fold induction relative to the untreated h-MDMs control. **(B)** Gene expression analysis of arachidonic acid metabolic enzymes in h-MDMs treated or not with P17. The results were represented in fold induction relative to the untreated h-MDMs control. **(C)** [^{3}H]AA mobilization in membrane phospholipids of h-MDMs treated or not with P17. **(D)** LTB4 production by h-MDMs treated or not with P17. **(E)** Gene expression analysis of MR and Dectin-1 in h-MDMs treated or not with P17, in the presence of MAFP, a specific cPLA2 inhibitor, and MK-886, a FLAP inhibitor, which prevents 5-LOX activation. The results were represented in fold induction relative to the untreated h-MDMs control. **(F)** Gene expression analysis of MR, Dectin-1, SRB1, and CD36 in h-MDMs treated or not with P17, in the presence of MAFP and/or LTB4. The results were represented in fold induction relative to the untreated h-MDMs control. Results correspond to mean ± SEM of triplicates. Data are representative of three independent experiments. $^*p < 0.05$, $^{**}p < 0.01$ compared to the respective untreated control.

that P17 controls MR and Dectin-1 expressions through AA metabolism.

Peroxisome proliferator-activated receptor gamma activity, as determinate by the induction of MR-, Dectin-1- and SRB1-specific PPARγ target genes, was increased similarly with P17 and LTB4 (**Figure 2F**). Furthermore, the addition of both P17 and LTB4 did not showed any additive effect, suggesting that P17 regulates MR and Dectin-1 surface expression by controlling PPARγ activation through the LTB4 production. Interestingly, the inhibition of P17-induced PPARγ target genes expression by MAFP was restored by the addition of LTB4, clearly establishing that P17-mediated PPARγ activation through LTB4 synthesis. Overall these data showed that P17 induces alternative activation of h-MDMs characterized by Dectin-1 and MR expressions through LTB4-mediated PPARγ activation.

P17 Improves Fungicidal Properties of h-MDM through AA/LTB4/PPARγ/MR-Dectin-1 Signaling

Previous works from our laboratory established the importance of alternative activation in the fungicidal functions of macrophages (34, 35, 43). On the basis of the current findings demonstrating an effect for P17 on alternative polarization, we next investigated whether P17-treated h-MDMs could have an impact on the *C. albicans* clearance. P17 did not exhibit an effective anti-fungal activity against *C. albicans* relative to the conventional amphotericin B anti-fungal agent. Furthermore, the association of P17 with amphotericin B did not improve the AMB anti-fungal activity, supporting that this peptide could not be used as a direct anti-fungal agent (Figure S1A in Supplementary Material). After P17 treatment, h-MDMs showed a robust increase in their ability to kill *C. albicans*, demonstrating that P17 promotes macrophage-intrinsic anti-fungal activity and supporting the use of P17 as a promising immunomodulatory compound to restrain fungal infections (**Figure 3A**). Consistent with our observation, P17-treated h-MDMs were more efficient to bind and to engulf *C. albicans* (**Figures 3B,C**). Interestingly, the induction of ROS production by P17 is essential in *in vitro* fungicidal activity of P17-activated h-MDMs, since the use of antioxidant *N*-acetyl cysteine (NAC) totally abolished the fungicidal effect of P17-treated h-MDMs against *C. albicans* (**Figure 3D**).

Then, we examined whether ROS production, which act as a common cellular signal upstream of the inflammasome activation (49), was responsible for IL-1β induction by P17 in response to *Candida*. While the antioxidant NAC suppressed

Candida-induced IL-1β secretion by P17-activated h-MDMs, the inhibition of caspase activation by the addition of ZVAD did not change ROS production by P17-activated h-MDMs after *Candida* challenge (**Figures 3E,F**). Therefore, these results showed that in response to *Candida*, ROS production occurred upstream of the caspase-1-induced IL-1β production.

To determine whether P17-mediated PPARγ activation dependently on LTB4 synthesis was involved in fungicidal activity of P17-treated h-MDMs, we evaluated their ability to kill *C. albicans* in the presence of a selective PPARγ antagonist GW9662, a specific inhibitor of AA mobilization MAFP, or an inhibitor of 5-LOX activation MK-886. The increased capacity of P17-treated h-MDMs to kill *C. albicans* was totally inhibited in presence of GW9662, MAFP, and MK-886 (**Figure 3G**). Consistent with these findings, the addition of these inhibitors abolished P17-mediated ROS, IL-1β release, and caspase-1 activation of h-MDMs in response to *C. albicans* (**Figures 3H–J**).

To explore whether the increased expression of Dectin-1 and MR on P17-treated h-MDMs has any functional consequence in *C. albicans* elimination, we assessed the ability of P17-treated h-MDMs deficient for Dectin-1 and/or MR to kill the yeast. The gene silencing for Dectin-1 and/or MR in P17-treated h-MDMs resulted in the abolition of the ability of these cells to kill more efficiently *C. albicans* (**Figure 3K**). In terms of recognition of *C. albicans*, the pre-treatment of P17-activated h-MDMs with soluble MR and Dectin-1-blocking agents (mannan and/or laminarin, respectively) abrogated the increased capacity for P17-treated h-MDMs to interact with the yeast (**Figure 3L**). Moreover, this pre-treatment totally abolished the induction of ROS production after *C. albicans* challenge (**Figure 3M**).

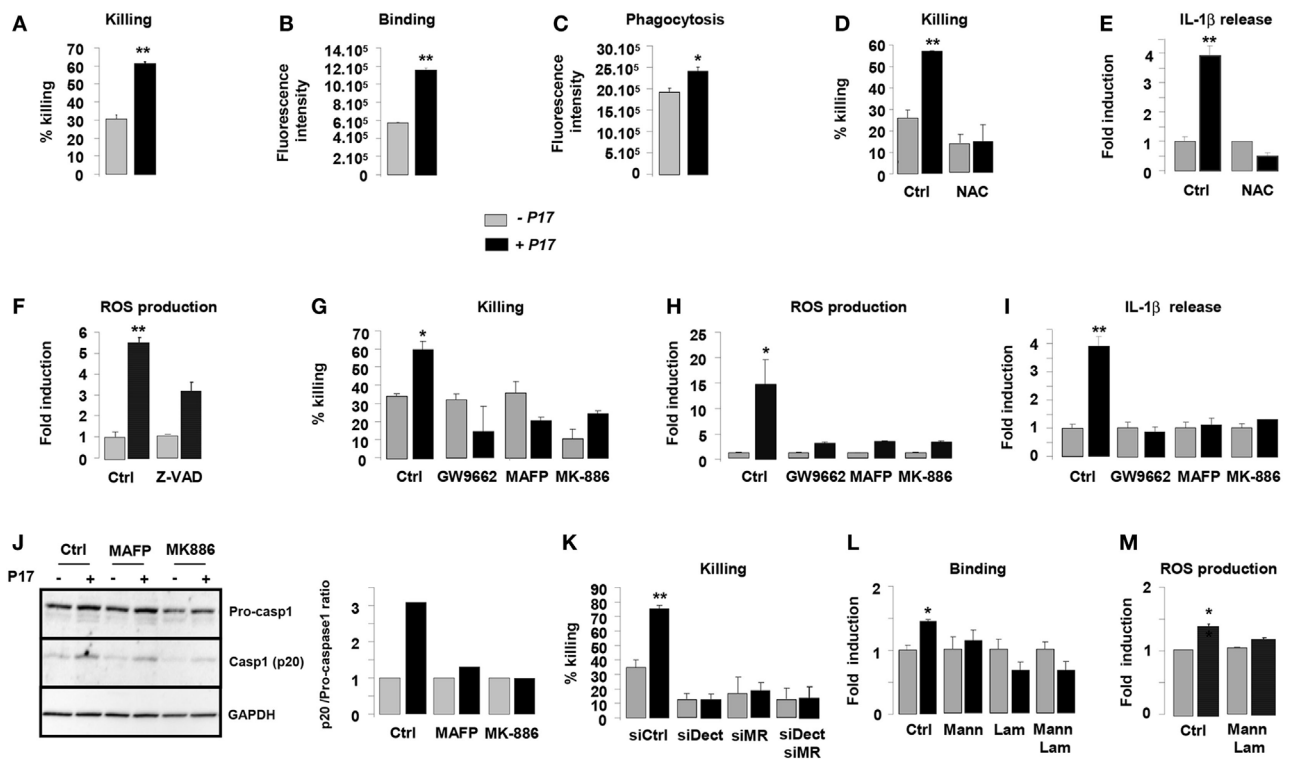


FIGURE 3 | P17 improves anti-fungal properties of human monocyte-derived macrophages (h-MDMs) through AA/LTB4/peroxisome proliferator-activated receptor gamma (PPARγ)/Dectin-1-MR signaling pathway. **(A)** Killing assay of h-MDMs treated or not with P17 incubated with *Candida albicans*. Binding **(B)** and phagocytosis **(C)** of *C. albicans* by h-MDMs treated or not with P17. **(D)** Killing assay of h-MDMs treated or not with P17 incubated with *C. albicans* in presence of antioxidant *N*-acetyl cysteine (NAC). **(E)** Interleukin (IL)-1β release by h-MDMs treated or not with P17 after *C. albicans* challenge in presence of antioxidant *N*-acetyl cysteine (NAC). The results were represented in fold induction relative to the respective untreated h-MDMs control. **(F)** Reactive oxygen species (ROS) production by h-MDMs treated or not with P17 after *C. albicans* challenge in presence of caspases inhibitor ZVAD. The results were represented in fold induction relative to the respective untreated h-MDMs control. **(G)** Killing assay of h-MDMs treated or not with P17 incubated with *C. albicans* in presence of a selective PPARγ antagonist (GW9662), a specific inhibitor of arachidonic acid (AA) mobilization (MAFP), or of an inhibitor of 5-LOX activation (MK-886). ROS **(H)** and IL-1β **(I)** production by h-MDMs treated or not with P17 after *C. albicans* challenge in presence of a selective PPARγ antagonist (GW9662), a specific inhibitor of AA mobilization (MAFP), or of an inhibitor of 5-LOX activation (MK-886). The results were represented in fold induction relative to the respective untreated h-MDMs control. **(J)** Immunoblot analysis of caspase-1 p20 fragment cleavage in h-MDMs treated or not with P17 after *C. albicans* challenge in presence of a specific inhibitor of AA mobilization (MAFP) or of 5-LOX activation inhibitor (MK-886). Band intensity was quantified with Image J software and was represented as the ratio between the band intensities of p20 and of pro-caspase-1. **(K)** Killing assay of h-MDMs silenced for Dectin-1 and/or mannose receptor (MR) treated or not with P17 after *C. albicans* challenge. **(L)** Binding of *C. albicans* by h-MDMs treated or not with P17 in presence of mannan and/or laminarin. The results were represented in fold induction relative to the respective untreated h-MDMs control. **(M)** ROS production by h-MDMs silenced for Dectin-1 and MR treated or not with P17 after *C. albicans* challenge. The results were represented in fold induction relative to the respective untreated h-MDMs control. Results correspond to mean ± SEM of triplicates. Data are representative of three independent experiments. $^{*}p < 0.05$, $^{**}p < 0.01$ compared to the respective untreated control.

Taken together, these data provided evidence that MR and dectin-1 are critical in fungicidal properties of h-MDMs mediated by P17 and support the importance of AA/LTB4/PPARγ/Dectin-1-MR axis in the strengthening of anti-fungal functions of h-MDMs by this HDP.

The Interaction between P17 and GPCR Controls Anti-Fungal Properties of h-MDM *via* the Induction of Intracellular Calcium Mobilization

Several studies demonstrated that HDPs induce intracellular calcium mobilization in immune cells (50–53). On this basis, we evaluated cytosolic calcium concentration in P17-activated h-MDMs. P17 treatment induced a significant augmentation of intracellular calcium concentration in h-MDMs, indicating that this HDP triggers intracellular calcium signal (**Figure 4A**). In order to determine the source of this calcium release, we assessed calcium mobilization in calcium-deprived medium to inhibit extracellular calcium influx (HBSS) and in the presence of U73122, an inhibitor of the intracellular pools calcium release. Interestingly, calcium mobilization was abolished both in presence of HBSS and U73122 (**Figure 4A**), suggesting that the P17-increase intracellular calcium concentration in h-MDMs was dependent on extracellular calcium influx and intracellular calcium stores mobilization.

Most of the HDPs immunomodulatory functions are mediated through GPCRs (27–29, 51). In order to evaluate the involvement of these receptors in the activation of h-MDMs mediated by P17, we used pertussis toxin (PTX), known to inhibit some GPCRs. PTX treatment totally inhibited the mobilization of calcium in P17-activated h-MDMs (**Figure 4B**), suggesting that P17 activity on h-MDMs was mediated by PTX-sensitive GPCR interaction. Interestingly, although PTX-sensitive fMLP receptors 1 and 2 (FPR1 and FPR2) are the main GPCRs involved in the modulation of immune response by HDPs, we demonstrated here that the desensitization of these receptors by the addition of fMLP did not affect P17-induced calcium mobilization (**Figure 4C**).

To investigate the role of P17-induced calcium mobilization in the fungicidal properties of P17-treated h-MDMs, we evaluated their capacity to kill the yeasts in the presence of an intracellular calcium chelator BAPTA-AM. The increase of ability to kill *C. albicans* of P17-activated h-MDMs was completely lost in the presence of BAPTA-AM (**Figure 4D**). These findings were consistent with the lack of induction of ROS and IL-1β production in BAPTA-AM pretreated h-MDMs activated with P17 (**Figures 4E,F**), further supporting that the intracellular mobilization of calcium is essential in fungicidal properties of P17-treated h-MDMs. Altogether, these data highlight that P17 modulates anti-fungal immune response of h-MDMs through PTX-sensitive GPCR-triggered intracellular calcium mobilization.

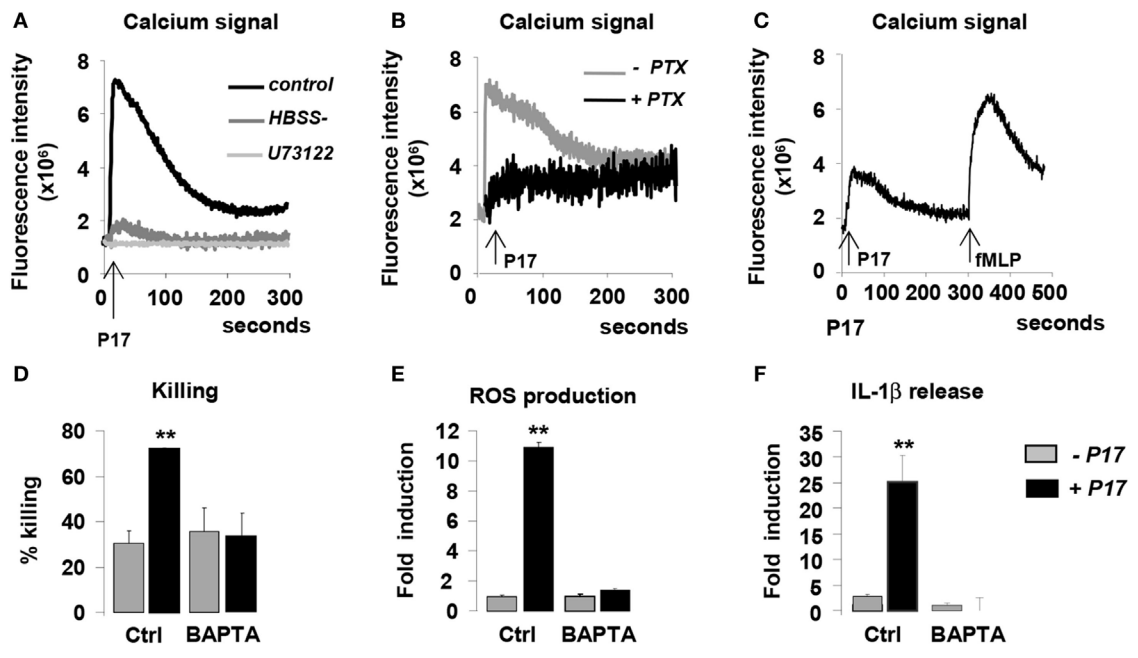


FIGURE 4 | P17 controls anti-fungal properties of human monocyte-derived macrophages (h-MDMs) *via* the induction of intracellular calcium mobilization dependent on pertussis toxin (PTX)-sensitive G-protein-coupled receptor interaction. Intracellular calcium concentration in h-MDMs treated or not with P17 using fluorescent probe Fluo 3-AM. **(A)** Calcium concentration in h-MDMs treated or not with P17 in the presence of calcium-deprived medium [Hank's balanced salt solution (HBSS-)] and an inhibitor of the intracellular pools calcium release (U73122). **(B)** Calcium concentration in h-MDM treated or not with P17 in the presence of PTX. **(C)** Calcium concentration in h-MDMs treated or not with P17 after desensitization of *N*-formylmethionine-leucyl-phenylalanine peptide receptors. **(D)** Killing assay of h-MDMs treated or not with P17 incubated with *Candida albicans* in the presence of calcium chelator (BAPTA-AM). Reactive oxygen species **(E)** and interleukin-1β **(F)** release by h-MDMs treated or not with P17 in the presence of calcium chelator (BAPTA-AM) after *C. albicans* challenge. The results were represented in fold induction relative to the respective untreated h-MDMs control. Results correspond to mean ± SEM of triplicates. Data are representative of three independent experiments. $^{*}p < 0.05$, $^{**}p < 0.01$ compared to the respective untreated control.

In Vivo P17 Treatment Induces Fungicidal Properties of Macrophages Hence Improving the Regression of Gastrointestinal Candidiasis

On the basis of the current findings demonstrating the microbicidal activity of P17-treated h-MDM against *C. albicans*, we next explored whether the P17 treatment could have an impact on the *in vivo* candidiasis outcome. In this context, we evaluated the fungal burden in the intestinal tract and the macrophage microbicidal functions in a murine experimental model of gastrointestinal candidiasis. P17-treated mice (P17) infected with *C. albicans* developed less severe gastrointestinal infection than untreated mice (NaCl), as demonstrated by lesser weight loss and by reduced fungal burden as reflected by a decreased number of CFU in the colon, cecum, and feces of mice treated with P17 (**Figures 5A,B**).

To investigate whether the effect of P17 on decreased *Candida* gastrointestinal colonization can be correlated to its impact on fungicidal functions of macrophages, we evaluated the capacity of macrophages from P17-treated mice to kill yeasts *in vitro*. Compared to macrophages from untreated mice, macrophages from P17-treated mice showed an increase in their ability to kill *C. albicans* (**Figure 5C**). Consistent with our observation, macrophages from P17-treated mice were more efficient in engulfing *C. albicans* and producing ROS and IL-1β (**Figures 5D–G**). Moreover, IL-12 release was similar in macrophages from untreated and P17-treated mice, demonstrating that P17 *in vivo* administration did not impact on IL-12 macrophage production (**Figure 5G**).

Taken together, these data provide *in vivo* evidence that P17 improves macrophage-intrinsic anti-fungal activity and support that P17 may constitute promising compound to restrain gastrointestinal fungal infection.

DISCUSSION

Although the majority of HDPs are currently known to exert antimicrobial activities against a broad spectrum of pathogenic microorganisms, they also can modulate the functions of immune cells (8). Among the two major groups of HDPs in humans, cathelicidins, and defensins, the LL-37 cathelicidin is the major AMP described for its immunomodulatory properties. Indeed, the LL-37 controls in several cells, particularly in human monocytes and murine macrophages, the transcription and the secretion of pro-inflammatory cytokines and chemokines (14–16, 18). Thus, the LL-37 participates to the immune cell differentiation, activation and chemotaxis (13, 54). Altogether these properties confer to LL-37 a strong microbicidal activity through its involvement in the control of inflammatory and anti-infectious signaling in macrophages. These immunomodulatory functions on human and murine cells are also described for HDPs from arthropods, such as apidaecin, bee venom AMP, and venom peptides 7.2 and 7.8, parabutoporin and opistoporin, isolated from scorpion venom (25, 26, 55). Our team has recently isolated a new short HDP from *T. bicarinatum* ant venom, called P17.

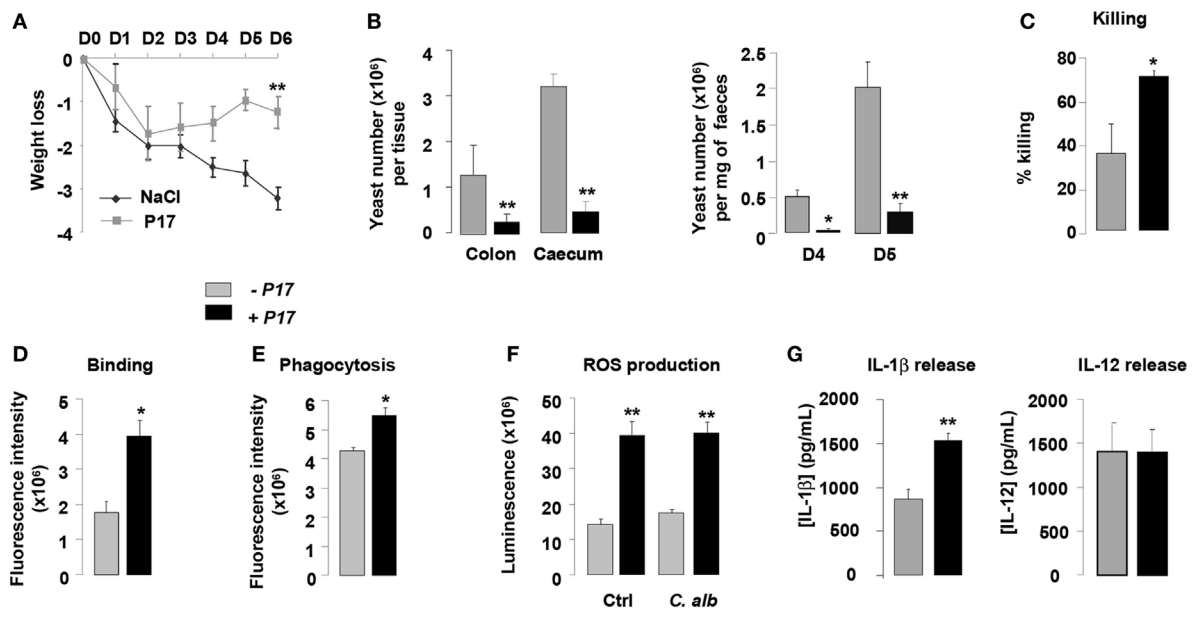


FIGURE 5 | P17 treatment of mice improves macrophage-intrinsic anti-fungal activities and restrains gastrointestinal fungal infection. **(A)** Body weight of untreated or P17-treated mice during *Candida albicans* gastrointestinal infection. **(B)** *C. albicans* GI colonization in cecum and colon of untreated or P17-treated mice determined on day 6 post-infection. *C. albicans* GI colonization in feces of untreated or P17-treated mice determined on days 4 and 5 post-infection. **(C)** Killing assay of peritoneal macrophages from untreated or P17-treated infected mice. Binding **(D)** and Phagocytosis **(E)** of *C. albicans* by peritoneal macrophages from untreated or P17-treated infected mice. Reactive oxygen species (ROS) **(F)** and interleukin (IL)-1β and IL-12 **(G)** production upon *Candida* challenge of peritoneal macrophages from untreated or P17-treated infected mice. Results correspond to mean ± SEM of triplicates. Data are representative of at least two independent experiments ($n = 6$ per group). *$p < 0.05$, **$p < 0.01$ compared to the respective untreated control.

Previous results demonstrated that this HDP shares common structural properties with LL-37. Indeed, structural studies of P17 revealed that this ant HDP, composed of 13 amino acids, is cationic, amphipatic, amidated in C-terminal position, and adopts an alpha helix conformation (31).

Here, we reported that the P17 influences phenotypic differentiation of h-MDMs toward an alternative phenotype characterized by a CLRs signature composed of MR and Dectin-1. Consistent with the key role of MR and Dectin-1 in yeast recognition, phagocytosis and clearance (35, 38, 56, 57), we demonstrated that the P17 increases the ability of h-MDMs to eliminate *C. albicans*. The involvement of MR and Dectin-1 in the P17-mediated anti-fungal activity of h-MDMs was further evidenced by the loss of *Candida* elimination in h-MDMs silenced for MR or Dectin-1. In line, the pre-treatment of P17-activated h-MDMs with soluble MR or Dectin-1 blocking agents, also severely compromised their capacity to bind and to kill *C. albicans*. Consistent with the cooperative role of MR and Dectin-1 in the induction of macrophage anti-fungal signaling pathways (34, 35, 37), we demonstrated that both MR and Dectin-1 are involved in the recognition of this yeast and in its subsequent elimination by P17-activated h-MDMs. Consistently, we showed that P17-activated h-MDMs is able to clear *Leishmania infantum* (Figures S1B,C in Supplementary Material), a parasite known to interact with macrophages through MR and Dectin-1 (36). These results reveal that the immunomodulatory activity of P17 presents a broader spectrum, as long as the pathogen expresses on its surface carbohydrates recognized by MR or Dectin-1.

This study also provided the mechanistic insight into the transcriptional control of MR and Dectin-1 by P17 in h-MDMs. On the basis of the established role of PPARγ in the alternative activation and in the control of CLRs expression (34, 58), these findings identify PPARγ as a critical component in the signaling cascade that drives P17-mediated MR and Dectin-1 overexpression.

In addition to the transcriptional increase of MR and Dectin-1 in h-MDM by P17 treatment, we demonstrated that this HDP positively regulates the transcription of cPLA2, enzyme needed for AA release from membrane phospholipids, of 5-LOX, FLAP, and LTA4 hydrolase, critical for LTB4 synthesis. Consistent with this observation, the mobilization of AA and the generation of LTB4 by h-MDMs upon P17 treatment are strongly increased. Interestingly, the impairment of LTB4 production by a specific inhibitor of 5-LOX activation, completely abolishes the induction of MR and Dectin-1 mediated by P17, suggesting that P17 controls MR and Dectin-1 expressions through the LTB4 release. Moreover, the fact that P17 increases MR-, Dectin-1-, and SRB1-specific PPARγ target genes, similar to LTB4, and that the addition of both P17 and LTB4 did not show any additive effect on these gene inductions supports that P17 regulates MR and Dectin-1 surface expressions by controlling PPARγ activation through the LTB4 production. This is reinforced by the finding showing that the inhibition of P17-induced MR, Dectin-1, and SRB1 PPARγ target gene expressions by MAFP, a specific inhibitor of AA release, was restored by the addition of LTB4. In agreement with the identification of LTB4 as PPARγ agonist in P17-mediated CLRs induction, numerous endogenous PPARγ ligands derived from the metabolism of AA are described (34, 35, 43, 48).

A significant contribution of this study was the identification of a novel signaling pathway triggered by an HDP involved in the antimicrobial response of macrophages. Indeed, the h-MDMs treated with PPARγ-specific antagonist, or with inhibitors of LTB4 synthesis, or silenced for MR or Dectin-1 failed to increase the killing of *C. albicans* in response to P17, establishing LTB4/PPARγ/Dectin-1-MR axis as crucial in the acquisition of anti-fungal properties of P17-treated h-MDMs.

Because ROS and pro-inflammatory cytokines are essentials *Candida*-killing components (35, 37, 39, 59, 60), we evaluated ROS and IL-1β release of h-MDMs upon P17 treatment and we investigated the signaling pathways involved in their production. Remarkably, the alternative phenotype of P17-treated h-MDMs is accompanied by an inflammatory signature characterized by IL-1β and ROS productions. In line, previous studies have highlighted the capacity of HDPs to simultaneously promote pro-inflammatory response while protecting host organism against exacerbated inflammatory response (18, 25, 26, 61–64). Consistent with the increased IL-1β production in P17-treated h-MDMs, the processing of pro-caspase-1 into its p20 subunit, which is a hallmark of caspase-1 activation (65), is augmented in P17-treated h-MDMs. Moreover, the involvement of P17 in ROS production is supported by large amounts of phosphorylated $p47^{phox}$, a cytosolic subunit of the NADPH oxidase complex whose activation is essential to ROS release (66), in h-MDMs activated by P17. We also established that this LTB4/PPARγ/Dectin-1-MR signaling drives ROS release in P17-treated h-MDMs, since the addition of GW9662, MAFP, and MK-886 or the pre-treatment of P17-activated h-MDMs with soluble MR- and Dectin-1-blocking agents abolishes P17-mediated ROS production by h-MDMs in response to *C. albicans*. This is supported by previous reports identifying Syk-dependent ROS production *via* Dectin-1 and MR receptors in fungal infection (67). Furthermore, we provided evidence for the major contribution of ROS production in IL-1β secretion by P17-activated h-MDMs in response to *Candida*. Consistent with these results, ROS production activates IL-1β processing *via* caspase-1-dependent activity (49). Thus, we identified both MR and Dectin-1 as extracellular sensors for *Candida* recognition by P17-activated h-MDMs and the subsequent activation of the pro-IL-1β synthesis and ROS production. These oxidant agents are essential in inflammasome-dependent IL-1β processing and hence in IL-1β production by P17-activated h-MDMs in response to *Candida* challenge. This is best supported by the fact that the induction of the Nlrp3 inflammasome complex activation is subjected to several events, such as the efflux of cellular potassium, the phagocytosis of particles, the generation of ROS, cathepsin B activation, and/or the vacuolar acidification (68–71).

Although we demonstrated with certitude that AA/LTB4/PPARγ/CLRs/ROS-IL-1β signaling pathway is involved in the anti-fungal activity of P17-activated h-MDMs, we also showed that P17 increases significantly the mRNA level of LL-37 (data not shown), the only human cathelicidin-related AMP known to promote a pro-inflammatory response (15, 16). Thus, LL-37, in addition to ROS and IL-1β, could be an important component of the

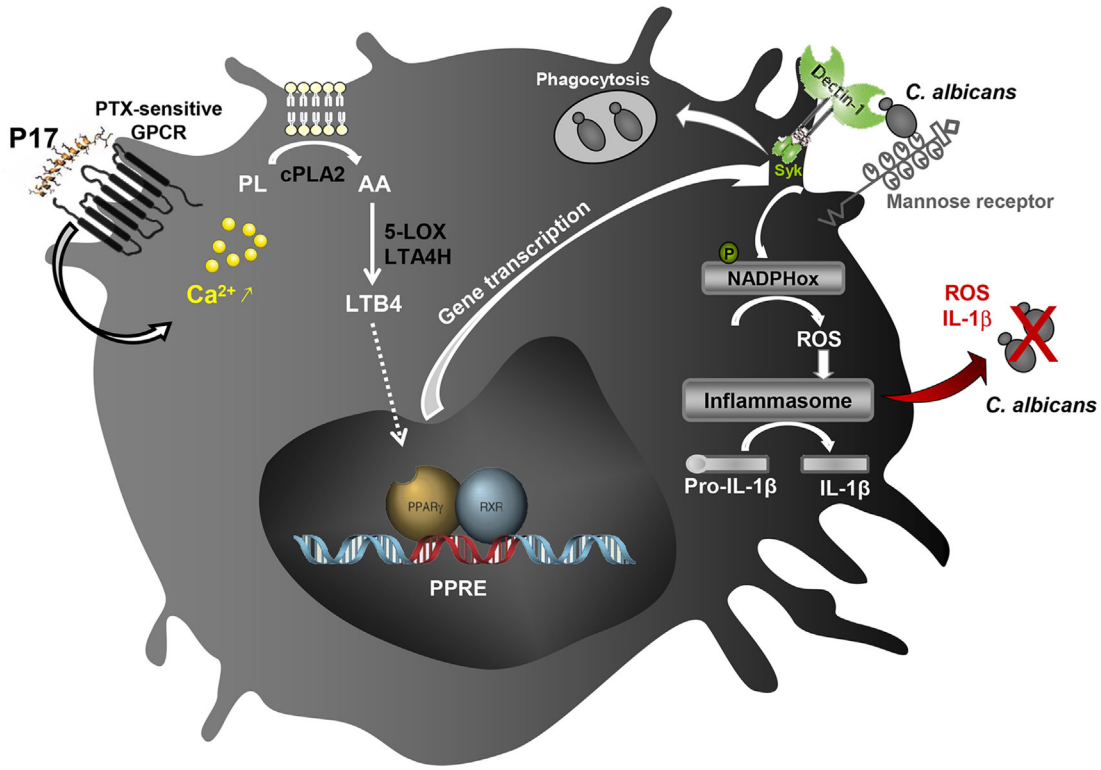


FIGURE 6 | Schematic illustration of the immunomodulatory activity of P17 on human macrophages. The identification of molecular mechanisms triggered by P17 reveals that this peptide modulates anti-fungal immune response of human monocyte-derived macrophages (h-MDMs) through pertussis toxin (PTX)-sensitive G-protein-coupled receptor (GPCR)-triggered intracellular calcium mobilization. The increased calcium mobilization in P17-activated h-MDMs is essential in cPLA2 activation and the subsequent arachidonic acid (AA) release. This AA mobilization and the promotion of AA metabolization to leukotriene B4 (LTB4) upon P17 treatment are responsible of the peroxisome proliferator-activated receptor gamma (PPARγ)-dependent mannose receptor and Dectin-1 overexpression. The activation of AA/leukotriene B4 (LTB4)/PPARγ/Dectin-1–mannose receptor axis by P17 triggers reactive oxygen species (ROS) production and inflammasome-dependent interleukin (IL)-1β release critical in fungicidal activity of P17-activated h-MDMs.

anti-fungal activity of P17-activated macrophages. Interestingly, several studies show that PPARγ agonists promote the induction of cationic AMP expression (72). These observations support that the AA/LTB4/PPARγ axis triggered by P17 could also be involved in the production of LL-37.

One main implication of our study was the validation *in vivo* of the ability of P17 to modulate fungicidal activity of macrophages on a murine model of gastrointestinal candidiasis. The P17 treatment rendered the mice less susceptible to gastrointestinal *C. albicans* infection by promoting macrophage-intrinsic anti-fungal activity. These data reveal the P17 as an effective immunomodulatory agent for anti-fungal functions of macrophages.

Finally, this study identified that the interaction between P17 and GPCR is crucial in the induction of anti-fungal properties of h-MDMs by P17. Consistently, most HDPs control immune cells responses in a GPCR-dependent manner, mainly through fMLP receptors, such as FPR1 and FPR2 (27–29, 51). Although we demonstrated that P17 did not interact with fMLP receptors, this HDP engages PTX-sensitive GPCR, which is currently under identification. Moreover, in agreement with the involvement of calcium release in immunomodulatory activity triggered by many HDPs (50–53, 73), P17 modulates anti-fungal immune response of h-MDMs through PTX-sensitive GPCR-triggered intracellular calcium mobilization. As calcium signaling is an essential factor of cPLA2 activation in monocytes and macrophages (74, 75), P17 could promote LTB4/PPARγ/Dectin-1-MR signaling pathway through the activation of cPLA2 and the subsequent AA release.

Taken together, all these data highlighted the immunomodulatory activity of P17 on h-MDMs differentiation and their associated anti-fungal response. The identification of molecular mechanisms triggered by P17 responsible of increased microbicidal response of h-MDMs against *C. albicans* revealed the importance of the AA/LTB4/PPARγ/Dectin-1-MR axis (**Figure 6**). Confronted to the emergence of many resistances to the usual anti-infectious agents, P17 could constitute a promising compound to fight against fungal infections. Thus, this work offers new therapeutic perspectives and supports the use of PAMs as immunomodulatory compounds to restrain infectious diseases.

ETHICS STATEMENT

Mononuclear cells were obtained from healthy blood donors (Etablissement Français du Sang, EFS Toulouse, France).

Written informed consents were obtained from the donors under EFS contract no 21/PLER/TOU/UPS4/2013–0106. All mice were bred and handled by the protocols approved by the Conseil Scientifique du Centre de Formation et de Recherche Experimental Medico Chirurgical and the ethics board of the Midi-Pyrénées ethic committee for animal experimentation (Approval no B3155503).

AUTHOR CONTRIBUTIONS

AC, KB, MT, and BP designed the study and analyzed the data. AC and KB wrote the manuscript. KB, HA, and MP did and analyzed experiments. MA, LL, and MR did research. JL, AA and EB for helpful discussions.

ACKNOWLEDGMENTS

We thank Philippe Batigne and Bénédicte Bertrand from Université Paul Sabatier for excellent technical support and Alexia Zakaroff-Girard and Christiane Pécher (TRI imaging platform, I2MC) for flow cytometry technical assistance. This work was supported by Région Midi-Pyrénées, Université de Toulouse, Institut de Recherche pour le Développement, and Institut National Universitaire Champollion (KB).

SUPPLEMENTARY MATERIAL

The Supplementary Material for this article can be found online at http://www.frontiersin.org/article/10.3389/fimmu.2017.01650/full#supplementary-material.

REFERENCES

1. Zasloff M. Antimicrobial peptides of multicellular organisms. *Nature* (2002) 415:389–95. doi:10.1038/415389a
2. Seo M-D, Won H-S, Kim J-H, Mishig-Ochir T, Lee B-J. Antimicrobial peptides for therapeutic applications: a review. *Molecules* (2012) 17:12276–86. doi:10.3390/molecules171012276
3. Matsuzaki K. Why and how are peptide-lipid interactions utilized for self-defense? Magainins and tachyplesins as archetypes. *Biochim Biophys Acta* (1999) 1462:1–10. doi:10.1016/S0005-2736(99)00197-2
4. Shai Y. Mechanism of the binding, insertion and destabilization of phospholipid bilayer membranes by alpha-helical antimicrobial and cell nonselective membrane-lytic peptides. *Biochim Biophys Acta* (1999) 1462:55–70. doi:10.1016/S0005-2736(99)00200-X
5. Brogden KA. Antimicrobial peptides: pore formers or metabolic inhibitors in bacteria? *Nat Rev Microbiol* (2005) 3:238–50. doi:10.1038/nrmicro1098
6. Brogden KA, Ackermann M, McCray PB, Tack BF. Antimicrobial peptides in animals and their role in host defences. *Int J Antimicrob Agents* (2003) 22:465–78. doi:10.1016/S0924-8579(03)00180-8
7. Jenssen H, Hamill P, Hancock REW. Peptide antimicrobial agents. *Clin Microbiol Rev* (2006) 19:491–511. doi:10.1128/CMR.00056-05
8. Hilchie AL, Wuerth K, Hancock REW. Immune modulation by multifaceted cationic host defense (antimicrobial) peptides. *Nat Chem Biol* (2013) 9:761–8. doi:10.1038/nchembio.1393
9. Mansour SC, Pena OM, Hancock REW. Host defense peptides: front-line immunomodulators. *Trends Immunol* (2014) 35:443–50. doi:10.1016/j.it.2014.07.004
10. Nijnik A, Hancock R. Host defence peptides: antimicrobial and immunomodulatory activity and potential applications for tackling antibiotic-resistant infections. *Emerg Health Threats J* (2009) 2:e1. doi:10.3134/ehtj.09.001
11. De Smet K, Contreras R. Human antimicrobial peptides: defensins, cathelicidins and histatins. *Biotechnol Lett* (2005) 27:1337–47. doi:10.1007/s10529-005-0936-5
12. Yang D, Chertov O, Oppenheim JJ. Participation of mammalian defensins and cathelicidins in anti-microbial immunity: receptors and activities of human defensins and cathelicidin (LL-37). *J Leukoc Biol* (2001) 69:691–7.
13. Nijnik A, Pistolic J, Wyatt A, Tam S, Hancock REW. Human cathelicidin peptide LL-37 modulates the effects of IFN-gamma on APCs. *J Immunol* (2009) 183:5788–98. doi:10.4049/jimmunol.0901491
14. Bowdish DME, Davidson DJ, Speert DP, Hancock REW. The human cationic peptide LL-37 induces activation of the extracellular signal-regulated kinase and p38 kinase pathways in primary human monocytes. *J Immunol* (2004) 172:3758–65. doi:10.1189/jlb.1005560
15. Elssner A, Duncan M, Gavrilin M, Wewers MD. A novel P2X7 receptor activator, the human cathelicidin-derived peptide LL37, induces IL-1 beta processing and release. *J Immunol* (2004) 172:4987–94. doi:10.4049/jimmunol.172.8.4987
16. Yu J, Mookherjee N, Wee K, Bowdish DME, Pistolic J, Li Y, et al. Host defense peptide LL-37, in synergy with inflammatory mediator IL-1beta, augments immune responses by multiple pathways. *J Immunol* (2007) 179:7684–91. doi:10.4049/jimmunol.179.11.7684
17. Alalwani SM, Sierigk J, Herr C, Pinkenburg O, Gallo R, Vogelmeier C, et al. The antimicrobial peptide LL-37 modulates the inflammatory and host defense response of human neutrophils. *Eur J Immunol* (2010) 40:1118–26. doi:10.1002/eji.200939275
18. Scott MG, Davidson DJ, Gold MR, Bowdish D, Hancock REW. The human antimicrobial peptide LL-37 is a multifunctional modulator of innate immune responses. *J Immunol* (2002) 169:3883–91. doi:10.4049/jimmunol.169.7.3883
19. Tang X, Basavarajappa D, Haeggstrom JZ, Wan M. P2X7 receptor regulates internalization of antimicrobial peptide LL-37 by human macrophages that promotes intracellular pathogen clearance. *J Immunol* (2015) 195:1191–201. doi:10.4049/jimmunol.1402845
20. Barlow PG, Li Y, Wilkinson TS, Bowdish DME, Lau YE, Cosseau C, et al. The human cationic host defense peptide LL-37 mediates contrasting effects on apoptotic pathways in different primary cells of the innate immune system. *J Leukoc Biol* (2006) 80:509–20. doi:10.1189/jlb.1005560
21. Barlow PG, Beaumont PE, Cosseau C, Mackellar A, Wilkinson TS, Hancock REW, et al. The human cathelicidin LL-37 preferentially promotes apoptosis of infected airway epithelium. *Am J Respir Cell Mol Biol* (2010) 43:692–702. doi:10.1165/rcmb.2009-0250OC
22. Carretero M, Escámez MJ, García M, Duarte B, Holguín A, Retamosa L, et al. In vitro and in vivo wound healing-promoting activities of human cathelicidin LL-37. *J Invest Dermatol* (2008) 128:223–36. doi:10.1038/sj.jid.5701043
23. Koczulla R, von Degenfeld G, Kupatt C, Krötz F, Zahler S, Gloe T, et al. An angiogenic role for the human peptide antibiotic LL-37/hCAP-18. *J Clin Invest* (2003) 111:1665–72. doi:10.1172/JCI17545
24. Salvado MD, Di Gennaro A, Lindbom L, Agerberth B, Haeggström JZ. Cathelicidin LL-37 induces angiogenesis via PGE2-EP3 signaling in endothelial cells, in vivo inhibition by aspirin. *Arterioscler Thromb Vasc Biol* (2013) 33:1965–72. doi:10.1161/ATVBAHA.113.301851
25. Pucca MB, Cerni FA, Pinheiro-Junior EL, Zoccal KF, de Bordon CF, Amorim FG, et al. Non-disulfide-bridged peptides from *Tityus serrulatus* venom: evidence for proline-free ACE-inhibitors. *Peptides* (2016) 82:44–51. doi:10.1016/j.peptides.2016.05.008
26. Tavano R, Segat D, Gobbo M, Papini E. The honeybee antimicrobial peptide apidaecin differentially immunomodulates human macrophages, monocytes and dendritic cells. *J Innate Immun* (2011) 3:614–22. doi:10.1159/000327839
27. Null DY, Chen Q, Schmidt AP, Anderson GM, Wang JM, Wooters J, et al. LL-37, the neutrophil granule- and epithelial cell-derived cathelicidin, utilizes formyl peptide receptor-like 1 (FPRL1) as a receptor to chemoattract human peripheral blood neutrophils, monocytes, and T cells. *J Exp Med* (2000) 192:1069–74. doi:10.1084/jem.192.7.1069
28. Smithrithee R, Niyonsaba F, Kiatsurayanon C, Ushio H, Ikeda S, Okumura K, et al. Human β-defensin-3 increases the expression of interleukin-37 through

CCR6 in human keratinocytes. *J Dermatol Sci* (2015) 77:46–53. doi:10.1016/j.jdermsci.2014.12.001
29. Wan M, Godson C, Guiry PJ, Agerberth B, Haeggström JZ. Leukotriene B4/antimicrobial peptide LL-37 proinflammatory circuits are mediated by BLT1 and FPR2/ALX and are counterregulated by lipoxin A4 and resolvin E1. *FASEB J* (2011) 25:1697–705. doi:10.1096/fj.10-175687
30. Wan M, van der Does AM, Tang X, Lindbom L, Agerberth B, Haeggström JZ. Antimicrobial peptide LL-37 promotes bacterial phagocytosis by human macrophages. *J Leukoc Biol* (2014) 95:971–81. doi:10.1189/jlb.0513304
31. Rifflet A, Gavalda S, Téné N, Orivel J, Leprince J, Guilhaudis L, et al. Identification and characterization of a novel antimicrobial peptide from the venom of the ant *Tetramorium bicarinatum*. *Peptides* (2012) 38:363–70. doi:10.1016/j.peptides.2012.08.018
32. Mantovani A, Sica A, Sozzani S, Allavena P, Vecchi A, Locati M. The chemokine system in diverse forms of macrophage activation and polarization. *Trends Immunol* (2004) 25:677–86. doi:10.1016/j.it.2004.09.015
33. Martinez FO, Sica A, Mantovani A, Locati M. Macrophage activation and polarization. *Front Biosci* (2008) 13:453–61. doi:10.2741/2692
34. Coste A, Dubourdeau M, Linas MD, Cassaing S, Lepert J-C, Balard P, et al. PPARgamma promotes mannose receptor gene expression in murine macrophages and contributes to the induction of this receptor by IL-13. *Immunity* (2003) 19:329–39. doi:10.1016/S1074-7613(03)00229-2
35. Galès A, Conduché A, Bernad J, Lefevre L, Olagnier D, Béraud M, et al. PPARγ controls dectin-1 expression required for host antifungal defense against *Candida albicans*. *PLoS Pathog* (2010) 6:e1000714. doi:10.1371/journal.ppat.1000714
36. Lefèvre L, Lugo-Villarino G, Meunier E, Valentin A, Olagnier D, Authier H, et al. The C-type lectin receptors dectin-1, MR, and SIGNR3 contribute both positively and negatively to the macrophage response to *Leishmania infantum*. *Immunity* (2013) 38:1038–49. doi:10.1016/j.immuni.2013.04.010
37. Lefèvre L, Authier H, Stein S, Majorel C, Couderc B, Dardenne C, et al. LRH-1 mediates anti-inflammatory and antifungal phenotype of IL-13-activated macrophages through the PPARγ ligand synthesis. *Nat Commun* (2015) 6:6801. doi:10.1038/ncomms7801
38. Netea MG, Gow NAR, Munro CA, Bates S, Collins C, Ferwerda G, et al. Immune sensing of *Candida albicans* requires cooperative recognition of mannans and glucans by lectin and Toll-like receptors. *J Clin Invest* (2006) 116:1642–50. doi:10.1172/JCI27114
39. Saijo S, Iwakura Y. Dectin-1 and dectin-2 in innate immunity against fungi. *Int Immunol* (2011) 23:467–72. doi:10.1093/intimm/dxr046
40. Taylor PR, Tsoni SV, Willment JA, Dennehy KM, Rosas M, Findon H, et al. Dectin-1 is required for β-glucan recognition and control of fungal infection. *Nat Immunol* (2007) 8:31–8. doi:10.1038/ni1408
41. van de Veerdonk FL, Joosten LAB, Devesa I, Mora-Montes HM, Kanneganti T-D, Dinarello CA, et al. Bypassing pathogen-induced inflammasome activation for the regulation of interleukin-1beta production by the fungal pathogen *Candida albicans*. *J Infect Dis* (2009) 199:1087–96. doi:10.1086/597274
42. Wevers BA, Geijtenbeek TBH, Gringhuis SI. C-type lectin receptors orchestrate antifungal immunity. *Future Microbiol* (2013) 8:839–54. doi:10.2217/fmb.13.56
43. Coste A, Lagane C, Filipe C, Authier H, Gales A, Bernad J, et al. IL-13 attenuates gastrointestinal candidiasis in normal and immunodeficient RAG-2-/- mice via peroxisome proliferator-activated receptor-activation. *J Immunol* (2008) 180:4939–47. doi:10.4049/jimmunol.180.7.4939
44. Daynes RA, Jones DC. Emerging roles of PPARS in inflammation and immunity. *Nat Rev Immunol* (2002) 2:748–59. doi:10.1038/nri912
45. Kliewer SA, Lenhard JM, Willson TM, Patel I, Morris DC, Lehmann JM. A prostaglandin J2 metabolite binds peroxisome proliferator-activated receptor gamma and promotes adipocyte differentiation. *Cell* (1995) 83:813–9. doi:10.1016/0092-8674(95)90194-9
46. Lefèvre L, Galès A, Olagnier D, Bernad J, Perez L, Burcelin R, et al. PPARγ ligands switched high fat diet-induced macrophage M2b polarization toward M2a thereby improving intestinal *Candida* elimination. *PLoS One* (2010) 5:e12828. doi:10.1371/journal.pone.0012828
47. Le Marec O, Neveu C, Lefranc B, Dubessy C, Boutin JA, Do-Régo J-C, et al. Structure-activity relationships of a series of analogues of the RFamide-related peptide 26RFa. *J Med Chem* (2011) 54:4806–14. doi:10.1021/jm200418c
48. Berry A, Balard P, Coste A, Olagnier D, Lagane C, Authier H, et al. IL-13 induces expression of CD36 in human monocytes through PPARgamma activation. *Eur J Immunol* (2007) 37:1642–52. doi:10.1002/eji.200636625
49. Gross O, Poeck H, Bscheider M, Dostert C, Hannesschläger N, Endres S, et al. Syk kinase signalling couples to the Nlrp3 inflammasome for anti-fungal host defence. *Nature* (2009) 459:433–6. doi:10.1038/nature07965
50. Gupta K, Subramanian H, Ali H. Modulation of host defense peptide-mediated human mast cell activation by LPS. *Innate Immun* (2016) 22:21–30. doi:10.1177/1753425915610643
51. Pundir P, Catalli A, Leggiadro C, Douglas SE, Kulka M. Pleurocidin, a novel antimicrobial peptide, induces human mast cell activation through the FPRL1 receptor. *Mucosal Immunol* (2014) 7:177–87. doi:10.1038/mi.2013.37
52. Wan M, Soehnlein O, Tang X, van der Does AM, Smedler E, Uhlén P, et al. Cathelicidin LL-37 induces time-resolved release of LTB4 and TXA2 by human macrophages and triggers eicosanoid generation in vivo. *FASEB J* (2014) 28:3456–67. doi:10.1096/fj.14-251306
53. Zhang Y-Y, Yu Y-Y, Zhang Y-R, Zhang W, Yu B. The modulatory effect of TLR2 on LL-37-induced human mast cells activation. *Biochem Biophys Res Commun* (2016) 470:368–74. doi:10.1016/j.bbrc.2016.01.037
54. van der Does AM, Beekhuizen H, Ravensbergen B, Vos T, Ottenhoff THM, van Dissel JT, et al. LL-37 directs macrophage differentiation toward macrophages with a proinflammatory signature. *J Immunol* (2010) 185:1442–9. doi:10.4049/jimmunol.1000376
55. Willems J, Noppe W, Moerman L, van der Walt J, Verdonck F. Cationic peptides from scorpion venom can stimulate and inhibit polymorphonuclear granulocytes. *Toxicon* (2002) 40:1679–83. doi:10.1016/S0041-0101(02)00183-6
56. Gantner BN, Simmons RM, Underhill DM. Dectin-1 mediates macrophage recognition of *Candida albicans* yeast but not filaments. *EMBO J* (2005) 24:1277–86. doi:10.1038/sj.emboj.7600594
57. Willment JA, Brown GD. C-type lectin receptors in antifungal immunity. *Trends Microbiol* (2008) 16:27–32. doi:10.1016/j.tim.2007.10.012
58. Odegaard JI, Ricardo-Gonzalez RR, Goforth MH, Morel CR, Subramanian V, Mukundan L, et al. Macrophage-specific PPARγ controls alternative activation and improves insulin resistance. *Nature* (2007) 447:1116–20. doi:10.1038/nature05894
59. Erwig LP, Gow NAR. Interactions of fungal pathogens with phagocytes. *Nat Rev Microbiol* (2016) 14:163–76. doi:10.1038/nrmicro.2015.21
60. Maródi L, Korchak HM, Johnston RB. Mechanisms of host defense against Candida species. I. Phagocytosis by monocytes and monocyte-derived macrophages. *J Immunol* (1991) 146:2783–9. doi:10.4049/jimmunol.176.4.2455
61. Bommineni YR, Pham GH, Sunkara LT, Achanta M, Zhang G. Immune regulatory activities of fowlicidin-1, a cathelicidin host defense peptide. *Mol Immunol* (2014) 59:55–63. doi:10.1016/j.molimm.2014.01.004
62. Mookherjee N, Brown KL, Bowdish DME, Doria S, Falsafi R, Hokamp K, et al. Modulation of the TLR-mediated inflammatory response by the endogenous human host defense peptide LL-37. *J Immunol* (2006) 176:2455–64.
63. Niyonsaba F, Madera L, Afacan N, Okumura K, Ogawa H, Hancock REW. The innate defense regulator peptides IDR-HH2, IDR-1002, and IDR-1018 modulate human neutrophil functions. *J Leukoc Biol* (2013) 94:159–70. doi:10.1189/jlb.1012497
64. Subramanian H, Gupta K, Guo Q, Price R, Ali H. Mas-related gene X2 (MrgX2) is a novel G protein-coupled receptor for the antimicrobial peptide LL-37 in human mast cells: resistance to receptor phosphorylation, desensitization, and internalization. *J Biol Chem* (2011) 286:44739–49. doi:10.1074/jbc.M111.277152
65. Yu HB, Finlay BB. The caspase-1 inflammasome: a pilot of innate immune responses. *Cell Host Microbe* (2008) 4:198–208. doi:10.1016/j.chom.2008.08.007
66. El-Benna J, Dang PM-C, Gougerot-Pocidalo M-A, Marie J-C, Braut-Boucher F. p47phox, the phagocyte NADPH oxidase/NOX2 organizer: structure, phosphorylation and implication in diseases. *Exp Mol Med* (2009) 41:217. doi:10.3858/emm.2009.41.4.058
67. Osorio F, Reis e Sousa C. Myeloid C-type lectin receptors in pathogen recognition and host defense. *Immunity* (2011) 34:651–64. doi:10.1016/j.immuni.2011.05.001

68. Martinon F, Mayor A, Tschopp J. The inflammasomes: guardians of the body. *Annu Rev Immunol* (2009) 27:229–65. doi:10.1146/annurev.immunol.021908.132715
69. Dostert C, Pétrilli V, Van Bruggen R, Steele C, Mossman BT, Tschopp J. Innate immune activation through Nalp3 inflammasome sensing of asbestos and silica. *Science* (2008) 320:674–7. doi:10.1126/science.1156995
70. Tschopp J, Schroder K. NLRP3 inflammasome activation: the convergence of multiple signalling pathways on ROS production? *Nat Rev Immunol* (2010) 10:210–5. doi:10.1038/nri2725
71. Zhou R, Yazdi AS, Menu P, Tschopp J. A role for mitochondria in NLRP3 inflammasome activation. *Nature* (2011) 469:221–5. doi:10.1038/nature09663
72. Kim JM. Antimicrobial proteins in intestine and inflammatory bowel diseases. *Intest Res* (2014) 12:20–33. doi:10.5217/ir.2014.12.1.20
73. Moerman L, Verdonck F, Willems J, Tytgat J, Bosteels S. Antimicrobial peptides from scorpion venom induce Ca(2+) signaling in HL-60 cells. *Biochem Biophys Res Commun* (2003) 311:90–7. doi:10.1016/j.bbrc.2003.09.175
74. Clark JD, Lin LL, Kriz RW, Ramesha CS, Sultzman LA, Lin AY, et al. A novel arachidonic acid-selective cytosolic PLA2 contains a Ca(2+)-dependent translocation domain with homology to PKC and GAP. *Cell* (1991) 65:1043–51. doi:10.1016/0092-8674(91)90556-E
75. Kramer RM, Roberts EF, Manetta J, Putnam JE. The Ca2(+)-sensitive cytosolic phospholipase A2 is a 100-kDa protein in human monoblast U937 cells. *J Biol Chem* (1991) 266:5268–72.

Conflict of Interest Statement: The authors declare that the research was conducted in the absence of any commercial or financial relationships that could be construed as a potential conflict of interest.

Copyright © 2017 Benmoussa, Authier, Prat, AlaEddine, Lefèvre, Rahabi, Bernad, Aubouy, Bonnafé, Leprince, Pipy, Treilhou and Coste. This is an open-access article distributed under the terms of the Creative Commons Attribution License (CC BY). The use, distribution or reproduction in other forums is permitted, provided the original author(s) or licensor are credited and that the original publication in this journal is cited, in accordance with accepted academic practice. No use, distribution or reproduction is permitted which does not comply with these terms.

frontiers in Immunology

MINI REVIEW
published: 01 December 2017
doi: 10.3389/fimmu.2017.01703

Macrophage–Microbe Interactions: Lessons from the Zebrafish Model

Nagisa Yoshida[1,2], Eva-Maria Frickel[1] and Serge Mostowy[2]**

[1] *Host-Toxoplasma Interaction Laboratory, The Francis Crick Institute, London, United Kingdom,* [2] *Section of Microbiology, MRC Centre for Molecular Bacteriology and Infection, Imperial College London, London, United Kingdom*

Macrophages provide front line defense against infections. The study of macrophage–microbe interplay is thus crucial for understanding pathogenesis and infection control. Zebrafish (*Danio rerio*) larvae provide a unique platform to study macrophage–microbe interactions *in vivo*, from the level of the single cell to the whole organism. Studies using zebrafish allow non-invasive, real-time visualization of macrophage recruitment and phagocytosis. Furthermore, the chemical and genetic tractability of zebrafish has been central to decipher the complex role of macrophages during infection. Here, we discuss the latest developments using zebrafish models of bacterial and fungal infection. We also review novel aspects of macrophage biology revealed by zebrafish, which can potentiate development of new therapeutic strategies for humans.

Keywords: host–pathogen interactions, infection, inflammation, macrophage, zebrafish

OPEN ACCESS

Edited by:
Etienne Meunier, UMR5089 Institut de Pharmacologie et de Biologie Structurale (IPBS), France

Reviewed by:
Jessica Lynn Humann, Florida A&M University, United States
Matthias Hauptmann, Research Center Borstel, Germany

****Correspondence:***
Eva-Maria Frickel
eva.frickel@crick.ac.uk;
Serge Mostowy
s.mostowy@imperial.ac.uk

Specialty section:
This article was submitted to Microbial Immunology, a section of the journal Frontiers in Immunology

Received: *19 October 2017*
Accepted: *20 November 2017*
Published: *01 December 2017*

Citation:
Yoshida N, Frickel E-M and Mostowy S (2017) Macrophage–Microbe Interactions: Lessons from the Zebrafish Model. Front. Immunol. 8:1703. doi: 10.3389/fimmu.2017.01703

INTRODUCTION

Macrophages are a major component of the innate immune system, responding efficiently to tissue damage and infection (1, 2). During infection, macrophages have diverse roles including phagocytosis of foreign bodies, release of cytotoxic factors, and coordination of the inflammatory response *via* the secretion of chemokines and cytokines (3, 4). Phagocytosis can involve the recognition of pathogen- and damage-associated molecular patterns (PAMPs and DAMPs, respectively) through pattern recognition receptors (PRRs) on the macrophage surface (5, 6). Further, the complement system can mark pathogens for phagocytosis by opsonization (7). Once internalized, the pathogen resides inside a vacuole known as a phagosome (8). Subsequent phagosome maturation involves acidification of the lumen, which leads to lysosomal fusion and degradation of the internalized microbe (9). Pathogen restriction is enhanced by the nutrient-limiting ability of the phagolysosome and the input of antimicrobial agents into the lumen, such as reactive oxygen/nitrogen species (ROS/RNS) (10). Although the majority of microbes succumb to the microbicidal environment within the phagolysosome, some pathogens (including *Mycobacterium tuberculosis* and *Salmonella Typhimurium*) can survive and replicate within this harsh environment (11, 12). In contrast, some bacterial pathogens (including *Listeria monocytogenes* and *Shigella flexneri*) have mechanisms to escape from the phagosome and proliferate in the cytosol (13).

Mechanisms of cell-autonomous immunity are crucial for protection of the host cell cytosol (14). Autophagy is an evolutionarily conserved process of intracellular degradation, recognized as an important defense mechanism against intracellular pathogens (15). Targeting of bacterial pathogens by the autophagy machinery is often mediated by ubiquitination, a posttranslational modification (16, 17). In this case, ubiquitinated substrates (such as bacterial components or damaged membrane) are recognized by autophagy receptors, including p62 and NDP52, which direct formation of the autophagic membrane around the targeted pathogen (18–20). Autophagy-related (ATG) proteins also direct immunity-related GTPases (IRGs) and guanylate-binding

proteins (GBPs) to pathogens (21). IRGs and GBPs belong to a family of GTPases that confer host cell resistance during infection by pathogens (22–24). IRGs cooperate with GBPs to target non-self vacuoles, trafficking nicotinamide adenine dinucleotide phosphate (NADPH) oxidase, ATG proteins, and inflammasome complex assembly for host defense (25–27). Intracellular pathogens are also detected *via* nucleotide-binding oligomerization domain-like receptors (NLRs), a class of PRRs that reside in the cytosol (28). An important example is NLRP3, which acts as a scaffold protein for inflammasome assembly, leading to caspase-1 activation and maturation of pro-inflammatory cytokines interleukin-1β (IL-1β) and IL-18 (29, 30). These cytokines enhance the immune response and induce pathways leading to pyroptosis, a highly inflammatory type of programmed cell death (31).

A variety of different animal models have made important contributions to the study of macrophage-microbe interplay *in vivo*. Originally used for studying development, the zebrafish has many similarities with higher vertebrates (including mammals), which has led to their use for studying infection and immunity (32, 33). During the first 4 weeks of development, zebrafish lack adaptive immunity and rely on the innate immune response for host defense (34). This, together with *ex utero* development of embryos, necessitates the rapid development of innate immune cells, progenitors of which can be observed as early as 20 h postfertilization (hpf). Although the precise sites of development and maturation differ between zebrafish and human phagocytes, zebrafish macrophages retain close morphological and functional similarities with their mammalian counterparts (35). Primitive macrophages, originally identified by Philippe Herbomel and colleagues, use phagocytosis to control infection by *Escherichia coli* and *Bacillus subtilis* (36). Optical accessibility during early life stages make zebrafish larvae highly suited for non-invasive live microscopy. Studies on the zebrafish immune system identified macrophage-specific genes (including *mpeg1* and *csf1ra*), discoveries that enabled the development of specific reporter lines (37, 38). By using transgenic lines that fluorescently label distinct leukocyte populations, studies have identified key roles for macrophages during infection control *in vivo* (6). Furthermore, the sequenced zebrafish genome and the ability to manipulate the immune system through chemical or genetic means (including morpholino oligonucleotides for transient depletion, or CRISPR/Cas9 for genome engineering) make the zebrafish a unique and powerful tool for studying host–pathogen interactions at the molecular, cellular, and whole-animal level (39–41).

In this review, we discuss novel aspects of host–pathogen interactions that have been recently revealed using bacterial (mycobacteria, Gram-positive, Gram-negative) and fungal zebrafish infection models, highlighting key roles for macrophages in host defense against a variety of important pathogens.

ZEBRAFISH MACROPHAGE–BACTERIA INTERACTIONS *IN VIVO*

Mycobacterium marinum is a natural pathogen of zebrafish, closely related to the causative agent of human tuberculosis (*M. tuberculosis*). Pioneering studies have shown that *M. marinum* infection leads to the aggregation of macrophages into granuloma-like structures that both contain and promote bacterial dissemination (**Figure 1A**) (42, 43). These structures are initiated by the ESX-1 secretion system, which induces expression of matrix metalloproteinase-9 in epithelial cells to recruit macrophages for bacterial phagocytosis (44, 45). Tissue-resident macrophages first responding to infection are microbicidal. Therefore, to create a replication niche, *M. marinum* induces chemokine (C-C motif) ligand 2 (CCL2) expression and recruits uninfected monocytes *via* the surface lipid phenolic glycolipid (PGL) (46). Moreover, *M. marinum* possess cell surface-associated phthiocerol dimycoceroserate lipids, which impede PAMP–TLR interactions and prevent the microbicidal response in newly recruited monocytes (47). Consistent with a protective niche, the granuloma supports bacterial growth, alteration of granuloma structure through disruption of E-cadherin increases immune cell accessibility, and reduces bacterial burden (48). Work has shown that macrophage deficiency leads to accelerated necrosis of the granuloma and increased susceptibility to infection (45). A balanced inflammatory response is crucial to prevent necrosis of the granuloma, as both low and high levels of tumor necrosis factor (TNF) can lead to increased bacterial replication (49). Supporting this, a forward genetic screen performed in zebrafish revealed that mutation of the *lta4h* locus (encoding leukotriene A_4 hydrolase) can modulate production of anti- and pro-inflammatory lipid mediators and susceptibility to mycobacterial infection (50). Angiogenesis has also been implicated in granuloma expansion and bacterial dissemination *via* a mechanism that requires hypoxia-induced vascular endothelial growth factor expression and C-X-C chemokine receptor type 4 (CXCR4) signaling (51, 52). Collectively, these studies highlight a complex role for macrophages in granuloma formation and in host defense against mycobacteria.

Infection by *Mycobacterium leprae,* an ancient pathogen that causes leprosy, is restricted to humans and nine-banded armadillos (*Dasypus novemcinctus*) (57). *M. leprae* infection causes demyelination of peripheral nerves and axonal damage, which can lead to symptoms such as muscle weakness and numbness. Remarkably, new work has shown that zebrafish can be used to study *M. leprae* pathogenesis *in vivo* (58). Although *M. leprae* replication is not observed in zebrafish due to its long doubling time of 12–15 days, the macrophage response to bacteria is comparable to that observed during *M. marinum* infection. In the case of *M. leprae*, PGL-1 is responsible for mediating structural changes in myelin by inducing macrophage RNS production, which subsequently causes mitochondrial swelling, demyelination, and axonal damage.

Listeria monocytogenes, a Gram-positive foodborne pathogen, can cause listeriosis and meningitis in immunocompromised individuals, and spontaneous abortions during pregnancy (59, 60). Inside macrophages, *L. monocytogenes* can escape from the phagosome and proliferate in the cytosol (**Figure 1B**) (61). Bacterial escape from the phagosome to the cytosol is linked to expression of listeriolysin O (LLO), a pore-forming toxin that targets the phagosomal membrane (62). ActA, another major

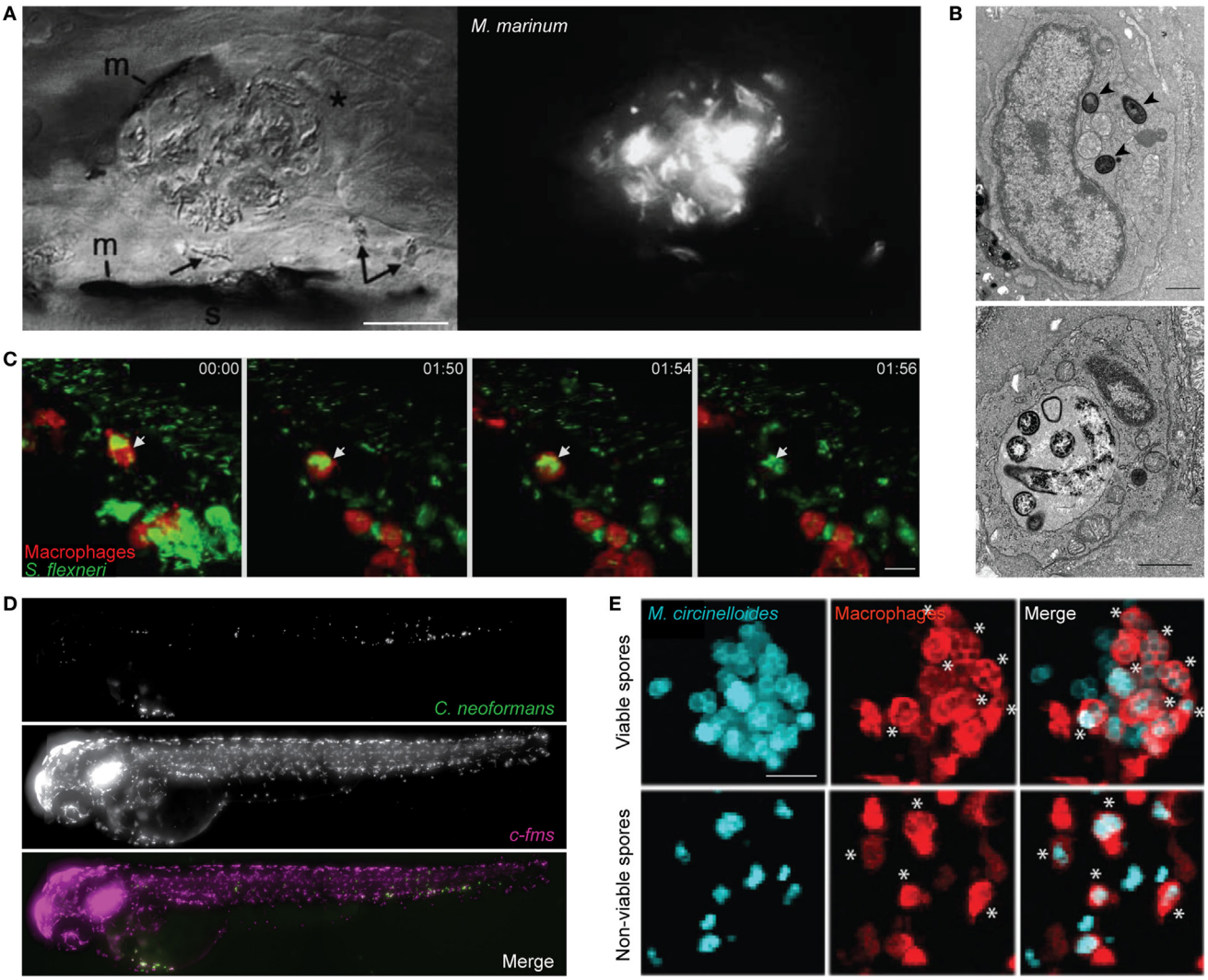


FIGURE 1 | Zebrafish macrophage-microbe interactions *in vivo*. **(A)** Differential interference contrast (left) and fluorescent microscopy (right) image of macrophage aggregation to *Mycobacterium marinum* in the tail of wild-type AB larvae. Asterisk (*) indicates an infected macrophage at the aggregate; arrows indicate infected macrophages near the aggregate. m, melanocyte; s, striated muscle; scale bar 25 µm. Image adapted from Ref. (42). **(B)** Electron microscopy images of the caudal hematopoietic tissue of wild-type AB larvae injected intravenously with *Listeria monocytogenes* 3 h postinfection (hpi). *Listeria* in a macrophage cytosol (arrowheads; top image), and *Listeria* in a macrophage phagosome (bottom image). Scale bar 1 µm. Images adapted from Ref. (53). **(C)** Confocal time-lapse images of *Tg(mpeg1:G/U:nfsb-mCherry)* larva (red macrophages) infected with *Shigella flexneri* (green) by caudal vein injection, first frame at 20 min postinjection (mpi). White arrow depicts GFP-*Shigella* phagocytosed by a red macrophage, with a loss of red fluorescence at frame 01:56 indicating macrophage cell death. Maximum intensity projection of six planes every 2 µm, scale bar 10 µm. Images adapted from Ref. (54). **(D)** High content imaging of *Tg(fms:Gal4.VP16)il86; Tg(UAS:nfsb.mCherry)il49* larvae harboring macrophages (middle) injected with *Cryptococcus neoformans* (top) into the yolk sac circulation valley; bottom panel showing a merged image of both macrophages (magenta) and *C. neoformans* (green). Maximum intensity projection of images obtained 2hpi. Images adapted from Ref. (55). **(E)** Hindbrain ventricle injection of viable (top row) or non-viable (bottom row) *Mucor circinelloides* spores (cyan) in *Tg(mpeg1:G/U:nfsb-mCherry/mpx:GFP)* larvae harboring red macrophages imaged at 10 h 45 min and 1 h 5 min, respectively. Asterisks (*) indicate spores inside macrophages (red). Z-stack of 15 sections every 7.3 µm; scale bar 20 µm. Images adapted from Ref. (56). All adapted images were used with the appropriate permissions from the copyright holders of this work.

virulence factor of *Listeria*, enables actin tail polymerization and autophagy escape (59, 63, 64). In agreement with studies performed *in vitro* using tissue culture cells, virulence of *Listeria* in zebrafish is dependent on LLO and ActA (53). More recent work using zebrafish has shown that bacterial dissemination (*via* necrosis of infected macrophages and release of bacterial-containing blebs) is LLO-dependent (65). To counteract this, Gp96 (an endoplasmic reticulum chaperone) can protect the integrity of the host cell plasma membrane against pore-forming toxins. In a separate study, zebrafish infection with a *Listeria* strain ectopically expressing flagellin (called *Lm*-pyro) was shown to activate the inflammasome in macrophage and reduce infection (66). These results highlight the inflammasome as crucial for protection against *Listeria*.

Staphylococcus aureus is an opportunistic pathogen, which latently resides in one-third of humans. Invasive surgery or lesions can increase the risk of infection, and considering the emergence of antibiotic-resistant strains, *S. aureus* is recognized as a major human threat. While systemic *S. aureus* infections are controlled, zebrafish are susceptible to yolk sac infection (i.e., a site inaccessible to leukocytes), underscoring the importance of leukocytes for infection control (67). Experiments performed using larvae depleted of myeloid cells demonstrate a role for macrophages in restriction of *S. aureus* proliferation in the blood (67). Interestingly, the incomplete clearance of bacteria by leukocytes can result in an "immunological bottleneck," viewed to select for persisting bacterial populations (68). The zebrafish can, therefore, be used to discover mechanisms used by *S. aureus* to evade destruction within leukocytes.

Colonization of humans by *Burkholderia cenocepacia* has severe consequences in cystic fibrosis (CF) patients and other immunocompromised individuals. Originally viewed to form a biofilm in CF patients, studies using clinical samples have shown that *B. cenocepacia* can reside in alveolar macrophages (69). More recently, a zebrafish infection model demonstrated that macrophages are crucial for *B. cenocepacia* replication (70). Consistent with this, depletion of macrophages from larvae restricts bacterial replication (71). During infection, macrophages express IL-1β and recruit uninfected cells to form cellular aggregates (70, 71). Paradoxically, the depletion of IL-1β (using morpholino oligonucleotide) during *B. cenocepacia* infection results in decreased survival, yet, inhibition of IL-1β signaling (using the IL-1 receptor antagonist anakinra) results in increased survival (71). Together, these experiments suggest the precise role of IL-1β during *B. cenocepacia* infection, and its manipulation for therapy, is complex.

Salmonella is a well-studied Gram-negative pathogen responsible for gastroenteritis, enteric fever, and bacteremia. Investigation of *S. Typhimurium* has made important contributions to macrophage biology (6, 11). During zebrafish infection, *S. Typhimurium* can replicate within macrophages and also extracellularly within the vasculature (72). A subpopulation of intracellular bacteria is lysed by mitochondrial-derived ROS produced by macrophages *via* a pathway dependent on immunoresponsive gene 1 (IRG1) (73). In addition, macrophages are responsible for the "fine-tuning" of the immune response to *S. Typhimurium via* secretion of granulocyte-colony stimulating factor (G-CSF), which in turn stimulates the transcription factor C/ebpβ and enhances neutrophil production by emergency granulopoiesis (74).

Shigella is a Gram-negative enteroinvasive pathogen classified by the WHO as a global threat due to its development of antibiotic resistance (75–77). Among the species of *Shigella*, *S. flexneri* is best recognized as a paradigm for studying macrophage cell death (78). In agreement with studies performed *in vitro*, *S. flexneri* can induce cell death in zebrafish macrophages *in vivo* (**Figure 1C**) (54). Despite this, macrophage-depleted transgenic zebrafish present increased mortality during infection (79). These results suggest that macrophages play an important role in the initial collection of injected bacteria, prior to the elimination of bacteria and cellular debris by neutrophils. The increasing risk of multidrug-resistant bacteria has driven the need for treatments that do not strictly rely on antibiotics. Injection of *Shigella*-infected zebrafish with predatory bacteria *Bdellovibrio bacteriovorus* revealed a synergy between predator–prey interactions with the host immune system to restrict multidrug-resistant infection (80). In this case, the reduction of *Shigella* burden by *Bdellovibrio* is beneficial for infection control by zebrafish leukocytes.

ZEBRAFISH MACROPHAGE–FUNGUS INTERACTIONS *IN VIVO*

Invasive fungal infections are a growing problem, causing significant morbidity and mortality in organ transplant patients. Immunosuppression using calcineurin inhibitors is a common strategy for the prevention of organ transplant rejection and increases the risk of infection by *Aspergillus fumigatus* (81). Alveolar macrophages and inflammatory monocytes in the murine lung have been described as critical for early antifungal immunity during *Aspergillus* infection (82). Real-time visualization using a zebrafish infection model revealed the inability of neutrophils to phagocytose fungal spores, and suggested macrophages as crucial for host defense against *A. fumigatus* (83, 84). In mouse models of *A. fumigatus* infection, treatment with calcineurin inhibitor FK506 leads to increased mortality (85). Consistent with this, studies using zebrafish infection showed a role for calcineurin in protection against *Aspergillus* (86). In this case, calcineurin activation leads to dephosphorylation of nuclear factor of activated T cells (NFAT), and FK506 treatment impairs neutrophil recruitment because of reduced TNF-α production by macrophages (86). A separate study revealed FK506 inhibits the calcineurin-dependent lateral transfer of *A. fumigatus* from necroptotic to naïve macrophages, allowing fungal escape and unrestricted growth (87). Collectively, these studies highlight the indispensable role of calcineurin in macrophages for *Aspergillus* control *in vivo*.

Candida albicans is an opportunistic fungal pathogen, which primarily affects immunocompromised individuals. Zebrafish infection models have been used to identify *C. albicans* virulence factors and indicate an important role for the filamentous (hyphal) form of *C. albicans* in pathogenesis (88–90). Strikingly, real-time microscopy of *C. albicans* infection showed the extrusion of hyphae from the zebrafish hindbrain (88). Fungal dissemination is observed by 24 h postinfection (hpi), followed by lethality resulting from uncontrolled hyphal growth (89). Here, macrophages can restrict germination (but not replication), and fungal killing by macrophages and neutrophils is a rare occurrence (89). Zebrafish infection has also demonstrated a new role for NADPH oxidase in controlling hyphal growth, helping to recruit macrophages through ROS and preventing germination (89, 91).

Another opportunistic fungal pathogen, *Cryptococcus neoformans* can be fatal in immunocompromised individuals and is responsible for over 600,000 deaths globally per annum (92). Although highly informative, mammalian and non-vertebrate infection models have limitations in visualizing fungus-leukocyte dynamics and the translatability to higher vertebrate models,

respectively. Live imaging of zebrafish during *Cryptococcus* infection revealed macrophages are required for pathogen control (**Figure 1D**) (55, 93). In agreement with this, macrophage depletion prior to infection leads to uncontrolled fungal replication and increased zebrafish mortality (55, 93). Macrophage-depletion postinfection also leads to increased fungal burden (55). The *Cryptococcus* capsule is made of polysaccharides contributing immunosuppressive functions, including the inhibition of phagocytosis. Consistent with this, capsule enlargement that occurs during infection of zebrafish can prevent phagocytosis, resulting in fungal proliferation and zebrafish mortality (55). By tracking individual macrophages over time, the first *in vivo* observation of vomocytosis (the controlled non-lytic expulsion of pathogens from phagocytes) was captured (55). The precise role of vomocytosis in host defense is not yet known.

Mucor circinelloides is an emerging fungal pathogen in which the incidence of infection is increasingly associated with aging populations (94). *M. circinelloides* causes mucormycosis, a disease with a wide range of symptoms including fever and gastrointestinal bleeding (95). Treatment of mucormycosis in humans remains costly and unsuccessful, and fatalities are often linked to corticosteroid treatment and immune defects (96, 97). In agreement with this, immunosuppression by corticosteroid treatment results in increased zebrafish mortality (56). Moreover, macrophage-depleted zebrafish succumb to infection, highlighting a key role for macrophages in *M. circinelloides* control. Remarkably, macrophages accumulate around viable spores in a manner similar to the granuloma structures described for *M. marinum* infection (**Figure 1E**) (56). While the role of macrophage clusters during *M. circinelloides* infection is not fully known, the zebrafish infection model can provide a novel platform to study macrophage–fungal interplay during mucormycosis.

DISCUSSION

Here, we describe recent mechanistic insights into the macrophage response to intracellular pathogens as revealed by zebrafish infection (**Table 1**). Although macrophage recruitment and phagocytosis is typically observed in response to infection, this is not always followed by pathogen restriction. Zebrafish infection has shown that, in some cases, macrophages can promote pathogenesis by shielding the pathogen from immune control or by providing a replicative niche. The zebrafish is a relatively new model for the study of human infectious disease. Therefore, a limitation of the system includes the lack of tools currently available, such as zebrafish antibodies and cell lines, which can impede in-depth mechanistic studies. On the other hand, the rapid development of transgenic zebrafish lines with fluorescently tagged proteins/cells, in combination with genome-editing technologies, compensate for these limitations. Considering advancements in RNAseq and high-resolution microscopy, we can expect that zebrafish infection will continue to illuminate fundamental aspects of host–pathogen interactions at the molecular, cellular, and whole animal level. The hope is that studying macrophage–microbe interactions *in vivo* using the zebrafish model can deliver therapeutic impact in humans.

TABLE 1 | The macrophage response/role during zebrafish infection.

Microbe			Macrophage response/role	Reference
Bacteria	Mycobacteria	*Mycobacterium marinum*	Recruitment, phagocytosis, intracellular niche for bacteria, accumulation in granuloma-like structures, restriction and promotion of bacterial dissemination	(42, 45, 47, 48, 51, 52)
		Mycobacterium leprae	Recruitment, phagocytosis, RNS production causing axonal damage	(58)
	Gram-positive	*Listeria monocytogenes*	Recruitment, phagocytosis, intracytosolic niche for bacteria, restriction of bacterial dissemination	(53, 65, 66)
		Staphylococcus aureus	Recruitment, phagocytosis, restriction of bacterial proliferation in blood	(67, 68)
	Gram-negative	*Burkholderia cenocepacia*	Recruitment, phagocytosis, intracellular niche for bacteria, source of inflammatory response	(70, 71)
		Salmonella Typhimurium	Recruitment, phagocytosis, intracellular niche for bacteria, IRG1-dependent ROS production, stimulates emergency granulopoiesis by G-CSF secretion	(72–74)
		Shigella flexneri	Recruitment, phagocytosis, scavenging of bacteria prior to neutrophil control	(54, 79, 80)
Fungi		*Apergillus fumigatus*	Recruitment, phagocytosis, production of TNFα for neutrophil recruitment, lateral transfer of *Aspergillus* from necroptotic to naïve macrophages	(83, 84, 86, 87)
		Candida albicans	Recruitment, phagocytosis, restriction of spore germination, rare fungal killing	(88, 89, 91)
		Cryptococcus neoformans	Recruitment, phagocytosis, expulsion of *Cryptococcus* by vomocytosis	(55, 93)
		Mucor circelloides	Recruitment, phagocytosis, accumulation around viable spores in granuloma-like structures	(56)

AUTHOR CONTRIBUTIONS

NY, E-MF, and SM jointly wrote the manuscript.

ACKNOWLEDGMENTS

The authors acknowledge Vincenzo Torraca, Gina Duggan, Alex Willis, and Joseph Wright for comments. NY is supported by the Joint Crick Ph.D. Programme with Imperial College London. Work in the Frickel laboratory is supported by the Francis Crick Institute, which receives its core funding from Cancer Research UK (FC001076), the UK Medical Research Council (FC001076), and the Wellcome Trust (FC001076). Work in the Mostowy laboratory is supported by a Wellcome Trust Senior Research Fellowship (206444/Z/17/Z), Wellcome Trust Research Career Development Fellowship (WT097411MA), and the Lister Institute of Preventive Medicine.

REFERENCES

1. Petrovski G, Zahuczky GB, Májai GN, Fésüs LS. Phagocytosis of cells dying through autophagy evokes a pro-inflammatory response in macrophages. *Autophagy* (2014) 3(5):508–10. doi:10.4161/auto.4731
2. Kapellos TS, Taylor L, Lee H, Cowley SA, James WS, Iqbal AJ, et al. A novel real time imaging platform to quantify macrophage phagocytosis. *Biochem Pharmacol* (2016) 116:107–19. doi:10.1016/j.bcp.2016.07.011
3. Murdoch C, Giannoudis A, Lewis CE. Mechanisms regulating the recruitment of macrophages into hypoxic areas of tumours and other ischemic tissues. *Blood* (2004) 104(8):2224–34. doi:10.1182/blood-2004-03-1109
4. Arango Duque G, Descoteaux A. Macrophage cytokines: involvement in immunity and infectious diseases. *Front Immunol* (2014) 5(11):491. doi:10.3389/fimmu.2014.00491
5. Aderem A. Phagocytosis and the inflammatory response. *J Infect Dis* (2003) 187(Suppl2):S340–5. doi:10.1086/374747
6. Torraca V, Masud S, Spaink HP, Meijer AH. Macrophage-pathogen interactions in infectious diseases: new therapeutic insights from the zebrafish host model. *Dis Model Mech* (2014) 7(7):785–97. doi:10.1242/dmm.015594
7. Dunkelberger JR, Song WC. Complement and its role in innate and adaptive immune responses. *Cell Res* (2010) 20(1):34–50. doi:10.1038/cr.2009.139
8. Yates RM, Hermetter A, Russell DG. The kinetics of phagosome maturation as a function of phagosome/lysosome fusion and acquisition of hydrolytic activity. *Traffic* (2005) 6(5):413–20. doi:10.1111/j.1600-0854.2005.00284.x
9. Kinchen JM, Ravichandran KS. Phagosome maturation: going through the acid test. *Nat Rev Mol Cell Biol* (2008) 9(10):781–95. doi:10.1038/nrm2515
10. Slauch JM. How does the oxidative burst of macrophages kill bacteria? Still an open question. *Mol Microbiol* (2011) 80(3):580–3. doi:10.1111/j.1365-2958.2011.07612.x
11. Aderem A, Underhill DM. Mechanisms of phagocytosis in macrophages. *Ann Rev Immunol* (1999) 17(1):593–623. doi:10.1146/annurev.immunol.17.1.593
12. Flannagan RS, Jaumouillé V, Grinstein S. The cell biology of phagocytosis. *Ann Rev Pathol* (2012) 7(1):61–98. doi:10.1146/annurev-pathol-011811-132445
13. Ray K, Marteyn B, Sansonetti PJ, Tang CM. Life on the inside: the intracellular lifestyle of cytosolic bacteria. *Nat Rev Microbiol* (2009) 7(5):333–40. doi:10.1038/nrmicro2112
14. Randow F, MacMicking JD, James LC. Cellular self-defense: how cell-autonomous immunity protects against pathogens. *Science* (2013) 340(6133):701–6. doi:10.1126/science.1233028
15. Levine B, Mizushima N, Virgin HW. Autophagy in immunity and inflammation. *Nature* (2011) 469(7330):323–35. doi:10.1038/nature09782
16. Deretic V, Saitoh T, Akira S. Autophagy in infection, inflammation and immunity. *Nat Rev Immunol* (2013) 13(10):722–37. doi:10.1038/nri3532
17. Dikic I. Proteasomal and autophagic degradation systems. *Ann Rev Biochem* (2017) 86(1):193–224. doi:10.1146/annurev-biochem-061516-044908
18. Ivanov S, Roy CR. NDP52: the missing link between ubiquitinated bacteria and autophagy. *Nat Immunol* (2009) 10(11):1137–9. doi:10.1038/ni1109-1137
19. Kirkin V, McEwan DG, Novak I, Dikic I. A role for ubiquitin in selective autophagy. *Mol Cell* (2009) 34(3):259–69. doi:10.1016/j.molcel.2009.04.026
20. Gomes LC, Dikic I. Autophagy in antimicrobial immunity. *Mol Cell* (2014) 54(2):224–33. doi:10.1016/j.molcel.2014.03.009
21. Clough B, Frickel E-M. The Toxoplasma parasitophorous vacuole: an evolving host-parasite frontier. *Trends Parasitol* (2017) 33(6):473–88. doi:10.1016/j.pt.2017.02.007
22. Meunier E, Broz P. Interferon-inducible GTPases in cell autonomous and innate immunity. *Cell Microbiol* (2015) 18(2):168–80. doi:10.1111/cmi.12546
23. Li P, Jiang W, Yu Q, Liu W, Zhou P, Li J, et al. Ubiquitination and degradation of GBPs by a *Shigella* effector to suppress host defence. *Nature* (2017) 551(7680):378–83. doi:10.1038/nature24467
24. Wandel MP, Pathe C, Werner EI, Ellison CJ, Boyle KB, von der Malsburg A, et al. GBPs inhibit motility of *Shigella flexneri* but are targeted for degradation by the bacterial ubiquitin ligase IpaH9.8. *Cell Host Microbe* (2017) 22(4):507–18.e5. doi:10.1016/j.chom.2017.09.007
25. Kim B-H, Shenoy AR, Kumar P, Das R, Tiwari S, MacMicking JD. A family of IFN-γ-inducible 65-kD GTPases protects against bacterial infection. *Science* (2011) 332(6030):717–21. doi:10.1126/science.1201711
26. Shenoy AR, Wellington DA, Kumar P, Kassa H, Booth CJ, Cresswell P, et al. GBP5 promotes NLRP3 inflammasome assembly and immunity in mammals. *Science* (2012) 336(6080):481–5. doi:10.1126/science.1217141
27. Haldar AK, Saka HA, Piro AS, Dunn JD, Henry SC, Taylor GA, et al. IRG and GBP host resistance factors target aberrant, "non-self" vacuoles characterized by the missing of "self" IRGM proteins. *PLoS Pathog* (2013) 9(6):e1003414. doi:10.1371/journal.ppat.1003414
28. Franchi L, Warner N, Viani K, Nuñez G. Function of NOD-like receptors in microbial recognition and host defense. *Immunol Rev* (2009) 227(1):106–28. doi:10.1111/j.1600-065X.2008.00734.x
29. Kanneganti T-D, Lamkanfi M, Nuñez G. Intracellular NOD-like receptors in host defense and disease. *Immunity* (2007) 27(4):549–59. doi:10.1016/j.immuni.2007.10.002
30. Geddes K, Magalhães JG, Girardin SE. Unleashing the therapeutic potential of NOD-like receptors. *Nat Rev Drug Discov* (2009) 8(6):465–79. doi:10.1038/nrd2783
31. Sahoo M, Ceballos-Olvera I, del Barrio L, Re F. Role of the inflammasome, IL-1β, and IL-18 in bacterial infections. *ScientificWorldJournal* (2011) 11(2):2037–50. doi:10.1100/2011/212680
32. Renshaw SA, Trede NS. A model 450 million years in the making: zebrafish and vertebrate immunity. *Dis Model Mech* (2012) 5(1):38–47. doi:10.1242/dmm.007138
33. Novoa B, Figueras A. Zebrafish: model for the study of inflammation and the innate immune response to infectious diseases. *Adv Exp Med Biol* (2012) 946:253–75. doi:10.1007/978-1-4614-0106-3_15
34. Masud S, Torraca V, Meijer AH. Modelling infectious diseases in the context of a developing immune system. *Curr Top Dev Biol* (2017) 124:277–329. doi:10.1016/bs.ctdb.2016.10.006
35. Meeker ND, Trede NS. Immunology and zebrafish: spawning new models of human disease. *Dev Comp Immunol* (2008) 32(7):745–57. doi:10.1016/j.dci.2007.11.011
36. Herbomel P, Thisse B, Thisse C. Ontogeny and behaviour of early macrophages in the zebrafish embryo. *Development* (1999) 126(17):3735–45.
37. Ellett F, Pase L, Hayman JW, Andrianopoulos A, Lieschke GJ. *mpeg1* promoter transgenes direct macrophage-lineage expression in zebrafish. *Blood* (2011) 117(4):e49–56. doi:10.1182/blood-2010-10-314120
38. Gray C, Loynes CA, Whyte MKB, Crossman DC, Renshaw SA, Chico TJA. Simultaneous intravital imaging of macrophage and neutrophil behaviour during inflammation using a novel transgenic zebrafish. *Thromb Haemost* (2011) 105(5):811–9. doi:10.1160/TH10-08-0525
39. Howe K, Clark MD, Torroja CF, Torrance J, Berthelot C, Muffato M, et al. The zebrafish reference genome sequence and its relationship to the human genome. *Nature* (2013) 496(7446):498–503. doi:10.1038/nature12111

40. Blum M, De Robertis EM, Wallingford JB, Niehrs C. Morpholinos: antisense and sensibility. *Dev Cell* (2015) 35(2):145–9. doi:10.1016/j.devcel.2015.09.017
41. Li M, Zhao L, Page-McCaw PS, Chen W. Zebrafish genome engineering using the CRISPR-Cas9 system. *Trends Genet* (2016) 32(12):815–27. doi:10.1016/j.tig.2016.10.005
42. Davis JM, Clay H, Lewis JL, Ghori N, Herbomel P, Ramakrishnan L. Real-time visualization of *mycobacterium*-macrophage interactions leading to initiation of granuloma formation in zebrafish embryos. *Immunity* (2002) 17(6):693–702. doi:10.1016/S1074-7613(02)00475-2
43. Davis JM, Ramakrishnan L. The role of the granuloma in expansion and dissemination of early tuberculous infection. *Cell* (2009) 136(1):37–49. doi:10.1016/j.cell.2008.11.014
44. Volkman HE, Pozos TC, Zheng J, Davis JM, Rawls JF, Ramakrishnan L. Tuberculous granuloma induction via interaction of a bacterial secreted protein with host epithelium. *Science* (2010) 327(5964):466–9. doi:10.1126/science.1179663
45. Pagán AJ, Yang CT, Cameron J, Swaim LE, Ellett F, Lieschke GJ, et al. Myeloid growth factors promote resistance to mycobacterial infection by curtailing granuloma necrosis through macrophage replenishment. *Cell Host Microbe* (2015) 18(1):15–26. doi:10.1016/j.chom.2015.06.008
46. Cambier CJ, O'Leary SM, O'Sullivan MP, Keane J, Ramakrishnan L. Phenolic glycolipid facilitates mycobacterial escape from microbicidal tissue-resident macrophages. *Immunity* (2017) 47(3):552–65.e4. doi:10.1016/j.immuni.2017.08.003
47. Cambier CJ, Takaki KK, Larson RP, Hernandez RE, Tobin DM, Urdahl KB, et al. Mycobacteria manipulate macrophage recruitment through coordinated use of membrane lipids. *Nature* (2013) 505(7482):218–22. doi:10.1038/nature12799
48. Cronan MR, Beerman RW, Rosenberg AF, Saelens JW, Johnson MG, Oehlers SH, et al. Macrophage epithelial reprogramming underlies mycobacterial granuloma formation and promotes infection. *Immunity* (2016) 45(4):861–76. doi:10.1016/j.immuni.2016.09.014
49. Roca FJ, Ramakrishnan L. TNF dually mediates resistance and susceptibility to mycobacteria via mitochondrial reactive oxygen species. *Cell* (2013) 153(3):521–34. doi:10.1016/j.cell.2013.03.022
50. Tobin DM, Vary JC, Ray JP, Walsh GS, Dunstan SJ, Bang ND, et al. The lta4h locus modulates susceptibility to mycobacterial infection in zebrafish and humans. *Cell* (2010) 140(5):717–30. doi:10.1016/j.cell.2010.02.013
51. Oehlers SH, Cronan MR, Scott NR, Thomas MI, Okuda KS, Walton EM, et al. Interception of host angiogenic signalling limits mycobacterial growth. *Nature* (2015) 517(7536):612–5. doi:10.1038/nature13967
52. Torraca V, Tulotta C, Snaar-Jagalska BE, Meijer AH. The chemokine receptor CXCR4 promotes granuloma formation by sustaining a mycobacteria-induced angiogenesis programme. *Sci Rep* (2017) 7:45061. doi:10.1038/srep45061
53. Levraud J-P, Disson O, Kissa K, Bonne I, Cossart P, Herbomel P, et al. Real-time observation of *Listeria monocytogenes*-phagocyte interactions in living zebrafish larvae. *Infect Immun* (2009) 77(9):3651–60. doi:10.1128/IAI.00408-09
54. Mostowy S, Boucontet L, Mazon Moya MJ, Sirianni A, Boudinot P, Hollinshead M, et al. The zebrafish as a new model for the *in vivo* study of *Shigella flexneri* interaction with phagocytes and bacterial autophagy. *PLoS Pathog* (2013) 9(9):e1003588. doi:10.1371/journal.ppat.1003588
55. Bojarczuk A, Miller KA, Hotham R, Lewis A, Ogryzko NV, Kamuyango AA, et al. *Cryptococcus neoformans* intracellular proliferation and capsule size determines early macrophage control of infection. *Sci Rep* (2016) 6:21489. doi:10.1038/srep21489
56. Voelz K, Gratacap RL, Wheeler RT. A zebrafish larval model reveals early tissue-specific innate immune responses to *Mucor circinelloides*. *Dis Model Mech* (2015) 8(11):1375–88. doi:10.1242/dmm.019992
57. Balamayooran G, Pena M, Sharma R, Truman RW. The armadillo as an animal model and reservoir host for *Mycobacterium leprae*. *Clin Dermatol* (2015) 33(1):108–15. doi:10.1016/j.clindermatol.2014.07.001
58. Madigan CA, Cambier CJ, Kelly-Scumpia KM, Scumpia PO, Cheng TY, Zailaa J, et al. A macrophage response to *Mycobacterium leprae* phenolic glycolipid initiates nerve damage in leprosy. *Cell* (2017) 170(5):973–85.e10. doi:10.1016/j.cell.2017.07.030
59. Cossart P. Illuminating the landscape of host-pathogen interactions with the bacterium *Listeria monocytogenes*. *Proc Natl Acad Sci U S A* (2011) 108(49):19484–91. doi:10.1073/pnas.1112371108
60. David DJV, Cossart P. Recent advances in understanding *Listeria monocytogenes* infection: the importance of subcellular and physiological context. *F1000Res* (2017) 6:1126. doi:10.12688/f1000research.11363.1
61. Chen GY, Pensinger DA, Sauer J-D. *Listeria monocytogenes* cytosolic metabolism promotes replication, survival and evasion of innate immunity. *Cell Microbiol* (2017) 19(10):e12762. doi:10.1111/cmi.12762
62. Seveau S. Multifaceted activity of listeriolysin O, the cholesterol-dependent cytolysin of *Listeria monocytogenes*. *Subcell Biochem* (2014) 80:161–95. doi:10.1007/978-94-017-8881-6_9
63. Birmingham CL, Higgins DE, Brumell JH. Avoiding death by autophagy: interactions of *Listeria monocytogenes* with the macrophage autophagy system. *Autophagy* (2008) 4(3):368–71. doi:10.4161/auto.5594
64. Yoshikawa Y, Ogawa M, Hain T, Yoshida M, Fukumatsu M, Kim M, et al. *Listeria monocytogenes* ActA-mediated escape from autophagic recognition. *Nat Cell Biol* (2009) 11(10):1233–40. doi:10.1038/ncb1967
65. Mesquita FS, Brito CU, Mazon Moya MJ, Pinheiro JC, Mostowy S, Cabanes D, et al. Endoplasmic reticulum chaperone Gp96 controls actomyosin dynamics and protects against pore-forming toxins. *EMBO Rep* (2017) 18(2):303–18. doi:10.15252/embr.201642833
66. Vincent WJB, Freisinger CM, Lam PY, Huttenlocher A, Sauer JD. Macrophages mediate flagellin induced inflammasome activation and host defense in zebrafish. *Cell Microbiol* (2015) 18(4):591–604. doi:10.1111/cmi.12536
67. Prajsnar TK, Cunliffe VT, Foster SJ, Renshaw SA. A novel vertebrate model of *Staphylococcus aureus* infection reveals phagocyte-dependent resistance of zebrafish to non-host specialized pathogens. *Cell Microbiol* (2008) 10(11):2312–25. doi:10.1111/j.1462-5822.2008.01213.x
68. Prajsnar TK, Hamilton R, Garcia-Lara J, McVicker G, Williams A, Boots M, et al. A privileged intraphagocyte niche is responsible for disseminated infection of *Staphylococcus aureus* in a zebrafish model. *Cell Microbiol* (2012) 14(10):1600–19. doi:10.1111/j.1462-5822.2012.01826.x
69. Sajjan U, Corey M, Humar A, Tullis E, Cutz E, Ackerley C, et al. Immunolocalisation of *Burkholderia cepacia* in the lungs of cystic fibrosis patients. *J Med Microbiol* (2001) 50(6):535–46. doi:10.1099/0022-1317-50-6-535
70. Vergunst AC, Meijer AH, Renshaw SA, O'Callaghan D. *Burkholderia cenocepacia* creates an intramacrophage replication niche in zebrafish embryos, followed by bacterial dissemination and establishment of systemic infection. *Infect Immun* (2010) 78(4):1495–508. doi:10.1128/IAI.00743-09
71. Mesureur J, Feliciano JR, Wagner N, Gomes MC, Zhang L, Blanco-Gonzalez M, et al. Macrophages, but not neutrophils, are critical for proliferation of *Burkholderia cenocepacia* and ensuing host-damaging inflammation. *PLoS Pathog* (2017) 13(6):e1006437. doi:10.1371/journal.ppat.1006437
72. van der Sar AM, Musters RJP, van Eeden FJM, Appelmelk BJ, Vandenbroucke-Grauls CMJE, Bitter W. Zebrafish embryos as a model host for the real time analysis of *Salmonella typhimurium* infections. *Cell Microbiol* (2003) 5(9):601–11. doi:10.1046/j.1462-5822.2003.00303.x
73. Hall CJ, Boyle RH, Astin JW, Flores MV, Oehlers SH, Sanderson LE, et al. Immunoresponsive gene 1 augments bactericidal activity of macrophage-lineage cells by regulating β-oxidation-dependent mitochondrial ROS production. *Cell Metab* (2013) 18(2):265–78. doi:10.1016/j.cmet.2013.06.018
74. Hall CJ, Flores MV, Oehlers SH, Sanderson LE, Lam EY, Crosier KE, et al. Infection-responsive expansion of the hematopoietic stem and progenitor cell compartment in zebrafish is dependent upon inducible nitric oxide. *Cell Stem Cell* (2012) 10(2):198–209. doi:10.1016/j.stem.2012.01.007
75. Kotloff KL, Winickoff JP, Ivanoff B, Clemens JD, Swerdlow DL, Sansonetti PJ, et al. Global burden of *Shigella* infections: implications for vaccine development and implementation of control strategies. *Bull World Health Organ* (1999) 77(8):651–66.
76. Jennison AV, Verma NK. *Shigella flexneri* infection: pathogenesis and vaccine development. *FEMS Microbiol Rev* (2004) 28(1):43–58. doi:10.1016/j.femsre.2003.07.002
77. Puzari M, Sharma M, Chetia P. Emergence of antibiotic resistant *Shigella* species: a matter of concern. *J Infect Public Health* (2017). doi:10.1016/j.jiph.2017.09.025
78. Zychlinsky A, Prevost MC, Sansonetti PJ. *Shigella flexneri* induces apoptosis in infected macrophages. *Nature* (1992) 358(6382):167–9. doi:10.1038/358167a0
79. Mazon Moya MJ, Willis AR, Torraca V, Boucontet L, Shenoy AR, Colucci-Guyon E, et al. Septins restrict inflammation and protect zebrafish larvae from *Shigella* infection. *PLoS Pathog* (2017) 13(6):e1006467. doi:10.1371/journal.ppat.1006467

80. Willis AR, Moore C, Mazon-Moya M, Krokowski S, Lambert C, Till R, et al. Injections of predatory bacteria work alongside host immune cells to treat *Shigella* infection in zebrafish larvae. *Curr Biol* (2016) 26(24):3343–51. doi:10.1016/j.cub.2016.09.067
81. Sugui JA, Kwon-Chung KJ, Juvvadi PR, Latgé J-P, Steinbach WJ. *Aspergillus fumigatus* and related species. *Cold Spring Harb Perspect Med* (2014) 5(2):a019786. doi:10.1101/cshperspect.a019786
82. Espinosa V, Jhingran A, Dutta O, Kasahara S, Donnelly R, Du P, et al. Inflammatory monocytes orchestrate innate antifungal immunity in the lung. *PLoS Pathog* (2014) 10(2):e1003940. doi:10.1371/journal.ppat.1003940
83. Knox BP, Deng Q, Rood M, Eickhoff JC, Keller NP, Huttenlocher A. Distinct innate immune phagocyte responses to *Aspergillus fumigatus* conidia and hyphae in zebrafish larvae. *Eukaryot Cell* (2014) 13(10):1266–77. doi:10.1128/EC.00080-14
84. Knox BP, Huttenlocher A, Keller NP. Real-time visualization of immune cell clearance of *Aspergillus fumigatus* spores and hyphae. *Fungal Genet Biol* (2017) 105:52–4. doi:10.1016/j.fgb.2017.05.005
85. Herbst S, Shah A, Carby M, Chusney G, Kikkeri N, Dorling A, et al. A new and clinically relevant murine model of solid-organ transplant aspergillosis. *Dis Model & Mech* (2013) 6(3):643–51. doi:10.1242/dmm.010330
86. Herbst S, Shah A, Mazon-Moya M, Marzola V, Jensen B, Reed A, et al. Phagocytosis-dependent activation of a TLR9-BTK-calcineurin-NFAT pathway co-ordinates innate immunity to *Aspergillus fumigatus*. *EMBO Mol Med* (2015) 7(3):240–58. doi:10.15252/emmm.201404556
87. Shah A, Kannambath S, Herbst S, Rogers A, Soresi S, Carby M, et al. Calcineurin orchestrates lateral transfer of *Aspergillus fumigatus* during macrophage cell death. *Am J Respir Crit Care Med* (2016) 194(9):1127–39. doi:10.1164/rccm.201601-0070OC
88. Chao CC, Hsu PC, Jen CF, Chen IH, Wang CH, Chan HC, et al. Zebrafish as a model host for *Candida albicans* infection. *Infect Immun* (2010) 78(6):2512–21. doi:10.1128/IAI.01293-09
89. Brothers KM, Newman ZR, Wheeler RT. Live imaging of disseminated candidiasis in zebrafish reveals role of phagocyte oxidase in limiting filamentous growth. *Eukaryot Cell* (2011) 10(7):932–44. doi:10.1128/EC.05005-11
90. Chen YZ, Yang YL, Chu WL, You MS, Lo HJ. Zebrafish egg infection model for studying *Candida albicans* adhesion factors. *PLoS One* (2015) 10(11):e0143048. doi:10.1371/journal.pone.0143048
91. Brothers KM, Gratacap RL, Barker SE, Newman ZR, Norum A, Wheeler RT. NADPH oxidase-driven phagocyte recruitment controls *Candida albicans* filamentous growth and prevents mortality. *PLoS Pathog* (2013) 9(10):e1003634. doi:10.1371/journal.ppat.1003634
92. Mada PK, Alam MU. *Cryptococcus (Cryptococcosis)*. Treasure Island, FL: StatPearls Publishing (2017).
93. Tenor JL, Oehlers SH, Yang JL, Tobin DM, Perfect JR. Live imaging of host-parasite interactions in a zebrafish infection model reveals cryptococcal determinants of virulence and central nervous system invasion. *MBio* (2015) 6(5):e01425–15. doi:10.1128/mBio.01425-15
94. Ibrahim AS, Kontoyiannis DP. Update on mucormycosis pathogenesis. *Curr Opin Infect Dis* (2013) 26(6):508–15. doi:10.1097/QCO.0000000000000008
95. Pak J, Tucci VT, Vincent AL, Sandin RL, Greene JN. Mucormycosis in immunochallenged patients. *J Emerg Trauma Shock* (2008) 1(2):106–13. doi:10.4103/0974-2700.42203
96. Waldorf AR, Levitz SM, Diamond RD. In vivo bronchoalveolar macrophage defense against *Rhizopus oryzae* and *Aspergillus fumigatus*. *J Infect Dis* (1984) 150(5):752–60. doi:10.1093/infdis/150.5.752
97. Ibrahim AS, Edwards JE Jr, Bryant R, Spellberg B. Economic burden of mucormycosis in the United States: can a vaccine be cost-effective? *Med Mycol* (2009) 47(6):592–600. doi:10.1080/13693780802326001

Conflict of Interest Statement: The authors declare that the research was conducted in the absence of any commercial or financial relationships that could be construed as a potential conflict of interest.

Copyright © 2017 Yoshida, Frickel and Mostowy. This is an open-access article distributed under the terms of the Creative Commons Attribution License (CC BY). The use, distribution or reproduction in other forums is permitted, provided the original author(s) or licensor are credited and that the original publication in this journal is cited, in accordance with accepted academic practice. No use, distribution or reproduction is permitted which does not comply with these terms.

frontiers in Immunology

ORIGINAL RESEARCH
published: 24 May 2018
doi: 10.3389/fimmu.2018.01084

A Model of Superinfection of Virus-Infected Zebrafish Larvae: Increased Susceptibility to Bacteria Associated With Neutrophil Death

Laurent Boucontet[1,2], Gabriella Passoni[1,2], Valéry Thiry[1,2], Ludovico Maggi[1,2], Philippe Herbomel[1,2], Jean-Pierre Levraud[1,2]† and Emma Colucci-Guyon[1,2]*†*

[1] Institut Pasteur, Unité Macrophages et Développement de l'Immunité, Paris, France, [2] CNRS UMR 3738, Paris, France

OPEN ACCESS

Edited by:
Geanncarlo Lugo-Villarino, UMR5089 Institut de Pharmacologie et de Biologie Structurale (IPBS), France

Reviewed by:
Robert T. Wheeler, University of Maine, United States
David Stachura, California State University, Chico, United States
Serge Mostowy, Imperial College London, United Kingdom

***Correspondence:**
Jean-Pierre Levraud
jean-pierre.levraud@pasteur.fr;
Emma Colucci-Guyon
emma.colucci@pasteur.fr

†These authors have contributed equally to this work.

Specialty section:
This article was submitted to Microbial Immunology, a section of the journal Frontiers in Immunology

Received: 15 February 2018
Accepted: 01 May 2018
Published: 24 May 2018

Citation:
Boucontet L, Passoni G, Thiry V, Maggi L, Herbomel P, Levraud J-P and Colucci-Guyon E (2018) A Model of Superinfection of Virus-Infected Zebrafish Larvae: Increased Susceptibility to Bacteria Associated With Neutrophil Death. Front. Immunol. 9:1084. doi: 10.3389/fimmu.2018.01084

Enhanced susceptibility to bacterial infection in the days following an acute virus infection such as flu is a major clinical problem. Mouse models have provided major advances in understanding viral-bacterial superinfections, yet interactions of the anti-viral and anti-bacterial responses remain elusive. Here, we have exploited the transparency of zebrafish to study how viral infections can pave the way for bacterial co-infections. We have set up a zebrafish model of sequential viral and bacterial infection, using sublethal doses of Sindbis virus and *Shigella flexneri* bacteria. This virus induces a strong type I interferons (IFN) response, while the bacterium induces a strong IL1β and TNFα-mediated inflammatory response. We found that virus-infected zebrafish larvae showed an increased susceptibility to bacterial infection. This resulted in the death with concomitant higher bacterial burden of the co-infected fish compared to the ones infected with bacteria only. By contrast, infecting with bacteria first and virus second did not lead to increased mortality or microbial burden. By high-resolution live imaging, we showed that neutrophil survival was impaired in Sindbis-then-*Shigella* co-infected fish. The two types of cytokine responses were strongly induced in co-infected fish. In addition to type I IFN, expression of the anti-inflammatory cytokine IL10 was induced by viral infection before bacterial superinfection. Collectively, these observations suggest the zebrafish larva as a useful animal model to address mechanisms underlying increased bacterial susceptibility upon viral infection.

Keywords: Sindbis virus, *Shigella flexneri*, co-infection, zebrafish, neutrophils, live imaging, innate immune response

INTRODUCTION

Despite steady progress in their diagnosis and treatment, viral and bacterial diseases continue to spread across the world and are causing a huge societal burden in terms of health and economical costs. Frequently, viruses and bacteria infect the same host, resulting in more severe illness compared to single infections. The best example is influenza-associated bacterial pneumonia, where bacterial superinfections have been documented as the major cause of death in major influenza pandemics but also during seasonal influenza epidemics (1, 2). *Staphylococcus aureus*, *Streptococcus pneumoniae*, and other bacteria commonly found even in healthy people have been identified to be associated in co-infections with influenza virus, causing severe and lethal pneumonias in influenza

virus-infected people. Other common viruses (e.g., rhinoviruses, enteroviruses, or rotaviruses) have been also associated in co-infection and have been reported causing increased susceptibility to a variety of bacteria (3). In general, polymicrobial infections result in a synergy among the various microbes, increasing the susceptibility and interfering with the immune response (4). To our knowledge, the only well-documented cases of increased resistance of the host to a second microbe, after a first infection with another microbe, occur after usage of vaccinal strains resulting in "trained immunity" (5).

Mammalian animal models are extensively used to address the mechanisms of increased bacterial susceptibility upon viral infection, using mostly influenza virus and bacteria found to be associated with co-infection during influenza episodes in humans (6). It has been shown that viruses could damage lung epithelium, favoring bacterial attachment and invasion (7, 8). However, immune interference is generally believed to be a more important factor than tissue damage (9). Several possible immunological mechanisms have been studied. Anti-bacterial and anti-viral innate immune responses are different as they involve the induction of largely distinct cytokines and signaling pathways, which could interfere with each other (10). Clear impact on myeloid cell recruitment or survival has been reported, but sometimes with conflicting results (11–15). Perturbed cytokine and chemokine induction (16, 17), as well as impaired bacterial killing (18, 19), have also been reported. Third, the crucial role of type I interferons (IFN) in modulating these aspects of antibacterial immunity has been demonstrated using IFNAR knockout mice models, that have been shown more resistant to bacterial superinfection (11, 12). However, modeling the antiviral immune response by injecting recombinant IFNs has also shown that IFN alone does not fully recapitulate the increased bacterial susceptibility upon viral infection (16). Thus, although mouse models have provided major advances in understanding viral–bacterial superinfections, the mechanisms of this hypersusceptibility remain an intense area of investigation.

The zebrafish (*Danio rerio*) has become a valuable non-mammalian vertebrate model to study infectious diseases. The zebrafish larva is an excellent system for live imaging, being transparent, small, and easy to anesthetize. With the availability of transgenic lines harboring fluorescent leukocytes coupled with diverse tools to manipulate immune cells and pathways, it offers the unique opportunity to study the immune response and leukocyte behavior *in vivo* upon infection in an entire vertebrate organism. As a vertebrate, it shares immune cell types and pathways with mammals, and it has been successfully used to study host-pathogen interactions using a variety of microbes causing disease in humans, including bacteria, fungi, and viruses (20–22).

Sindbis virus (SINV), the prototype species of the *Alphavirus* genus (positive strand RNA virus), is widely used as an experimental model in mice and can infect a broad range of vertebrates and insect cells (23). We recently established an infection model of this enveloped, single-stranded positive RNA virus in zebrafish (24). SINV infection in zebrafish is highly similar to that caused by its relative chikungunya virus (CHIKV) (25); both viruses replicate rapidly during the first day, then the viral burden stabilizes, correlating with the induction of a strong type I IFN response. Virus-infected cells visualized thanks to a GFP reporter in the virus genome, and present in many organs, then disappear progressively from most of the body, although infection persists longer in the central nervous system. CHIKV infection in zebrafish larvae causes an increase of the number of neutrophils, which are a major source of type I IFN. While zebrafish larvae normally survive CHIKV infection, lethality ensues after IFN receptors knockdown (25).

Shigella flexneri (hereafter simply designated as *Shigella*) are human-adapted Gram negative bacteria, close relatives of *Escherichia coli* that have gained the ability to invade the colonic mucosa, causing inflammation and diarrhea (26). We have previously established that *Shigella* is pathogenic for zebrafish larvae. We have shown that zebrafish survival is dose-dependent upon *Shigella* injection, where sublethal doses are cleared within 48 h post infection, and lethal doses causing the death of the infected larvae with concomitant high bacterial burden. Although both macrophages and neutrophil engulf the injected *Shigella*, we have highlighted a scavenger role for neutrophils in eliminating infected macrophages and non-immune cell types that have failed to control *Shigella* infection, thus playing a crucial role in anti-*Shigella* defense. However, both macrophages and neutrophils undergo cell death in larvae injected with high lethal *Shigella* inocula, and leukocyte depletion is associated with bacteremia preceding the death of the larvae (27).

The aim of this work was to test whether the zebrafish larva could be used to model viral-bacterial co-infections *in vivo*. Here, we have set up a zebrafish model of sequential viral and bacterial infection, using sublethal doses of SINV and *Shigella*. We have shown that larvae infected with SINV first display an increased susceptibility to *Shigella* infection, associated with death of the co-infected fish and increased bacterial burden. By contrast, larvae infected with *Shigella* first and SINV second do not show any difference in survival and pathogens dissemination compared to single viral and bacterial infection. We also observed that neutrophils, key players in anti *Shigella* defense, were severely depleted upon SINV + *Shigella* co-infection. By high-resolution live imaging, we documented the death of bacteria-engulfing neutrophils. We also measured the induction of the main cytokines genes. Co-infection did not blunt expression of typical antibacterial cytokines (*il1b* and *tnfa*); however, both type I IFN and the anti-inflammatory cytokine *il10* were induced by the viral infection prior to bacterial superinfection, suggesting a contribution to the observed phenotype.

These observations highlight the zebrafish model to study how viral infections can pave the way for bacterial co-infections. Moreover, this model could offer the opportunity to screen, in a live organism, libraries of anti-microbial, or immuno-modulating compounds.

MATERIALS AND METHODS

Ethic Statement

Animal experiments were performed according to European Union guidelines for handling of laboratory animals (http://ec.europa.eu/environment/chemicals/lab_animals/home_en.htm)

and were approved by the Institut Pasteur Animal Care and Use Committee.

Zebrafish Care and Maintenance

Wild-type AB fish, initially obtained from the Zebrafish International Resource Center (Eugene, OR, USA) and Tg(*mpx*:GFP)^{i114} (28), were raised in our facility. Eggs were obtained by marble-induced spawning, bleached according to standard protocols, and then kept in Petri dishes containing Volvic source water and, from 24 hours post fertilization (hpf) onward 0.003% 1-phenyl-2-thiourea (PTU) (Sigma-Aldrich) was added to prevent pigmentation. Embryos were reared at 28°C or 24°C according to the desired speed of development; infected larvae were always kept at 28°C. All timings in the text refer to the developmental stage at the reference temperature of 28.5°C (29). Larvae were anesthetized with 200 µg/ml tricaine (Sigma-Aldrich) during the injection procedure as well as during *in vivo* imaging.

Viruses

Sindbis viruses were produced on BHK cells [originally obtained from American Type Culture Collection (ATCC), #CC-L10], according to Ref. (30). Two SINV-GFP strains were used, both based on the hybrid TE12 strain backbone. SINV-3′GFP, the strain previously tested in zebrafish in Ref. (24), harbors a 3′ genomic insertion of the eGFP gene under the control of a second subgenomic promoter (31). The SINV-eGFP/2A harbors a self-cleavable eGFP inserted between the capsid and pE2 regions, based on (32). Briefly, the pTE-3′2 J GFP4-10 plasmid, which encodes for the SINV-3′GFP genome, was first modified to replace the region downstream of the structural genes (including the second subgenomic promoter and eGFP) with the 3′UTR from the AR339 strain. This region was amplified by PCR using pTR339-mCherry2A (Sun et al., 2014) as a template with primers SINV-E1-end-F (GACTAGCACACGAAGATGAc) and SINvec_Xho-R (AATTCCCCTCGAGGAATTCC), while PTE-3′2 J GFP4-10 was digested by ApaI and XhoI; purified fragments were then reassembled using In-Fusion® HD Cloning Kit Clontech/Takara (#639650), and after transformation in *E. coli*, plasmid pTE3′2J-3′UTR-339 was obtained. The eGFP-2A fragment, and some flanking regions (identical in TE12 and AR339 SINV strains) was then amplified by PCR from pTR339-EGFP2A using primers SINV-C-pml-F (GGTAATGAAACCTCTGcacg) and SIN-E3-stu-R (ATTGAGCAGGGTATCGTagg), and was then subcloned into pTE3′2J-3′UTR339 digested by PmlI and Stu I enzyme. This yielded the pTE3′2J-eGFP2A-3′UTR339, which was verified by sequencing and then used to produce the SINV-eGFP2A virus.

Virus Titration

Virus titer from concentrated BHK supernatants was measured on Vero-E6 cells (ATCC #CRL-1586) as described in Ref. (24). In addition, the infectivity of the virus in zebrafish cells was also measured by microinjection of serially diluted virus suspensions in the cell mass of dome stage AB zebrafish embryos), followed by observation of GFP expression one day later; the two methods yielded consistent titers.

Bacteria

Bacterial strains used in this study were wild-type invasive of *Shigella flexneri* serotype 5a M90T expressing DsRed (33). *Shigella* were plated from −80°C glycerol stock onto a Congo Red tryptic casein soy agar plate; a virulent clone was cultured overnight in trypticase soy complemented with ampicillin (50 µg/ml), and then diluted 80× in fresh trypticase soy, and cultured until $A_{600nm} = 0.6$. The bacterial exponential subculture was centrifuged at 1,000 × *g* for 5 min and the pellet washed with PBS and centrifuged at 1,000 × *g* for 5 min. The pellet was reconstituted with 60 µl of PBS for inoculation.

Zebrafish Infections

Titered viral suspensions were stored at −80°C as 10 µl aliquots, and one aliquot was used per experiment. The volume of injected suspension was deduced from the diameter of the drop obtained after mock microinjection, as described in Ref. (34); typically, ~3 nl of a 2.10^7 PFU/ml suspension was injected intravenously (iv) for a 60 PFU inoculum. Bacteria were recovered by centrifugation, washed, resuspended at the desired concentration in PBS. 72 or 96 hpf anesthetized zebrafish larvae were microinjected iv with 0.5–2 nl of bacterial suspension as described previously (27). Local bacterial infections were performed by injecting subcutaneously 0.5–1 nl of bacterial suspension to 96 hpf zebrafish larvae as previously described (35). The exact inoculum was checked *a posteriori* by injection in a water drop and plating onto LB agar. Infected larvae were transferred into individual wells (containing 1 ml of Volvic water + 0.003% PTU in 24-well culture plates), incubated at 28°C and regularly observed under a stereomicroscope.

Morpholino Injections

Morpholino antisense oligonucleotides (Gene Tools) were injected at the one to two cells stage as described (32). crfb1 splice morpholino (2 ng, CGCCAAGATCATACCTGTAAAGTAA) was injected together with crfb2 splice morpholino (2 ng, CTATGAA TCCTCACCTAGGGTAAAC), knocking down all type I IFN receptors (23). Control morphants were injected with 4 ng control morpholino, with no known target (GAAAGCATGGCATCTG GATCATCGA).

Measurement of Bacterial Burden

At the indicated times, animals were anesthetized, rinsed, and collected in 150 µl of sterile water. The animals were lysed and homogenized with a polypropylene piston (ten up-and-down sequences). Four serial 10-fold dilutions of the homogenates were plated onto LB agar, and CFU were enumerated after 24 h of incubation at 37°C; only colonies with the appropriate morphology and color were scored.

Live Imaging, Image Processing, and Analysis

Quantification of total neutrophils numbers on living transgenic reporter larvae was performed upon viral and bacterial infections as we previously described (27). Briefly, bright field, DsRed, and GFP images of whole living anesthetized larvae were taken using

a Leica Macrofluo™ Z16 APOA (zoom 16:1) equipped with a Leica PlanApo 2.0X lens, and a Photometrics® CoolSNAP™ *HQ*2 camera. Images were captured using the Metavue software version 7.5.6.0 (MDS Analytical Technologies). Using these settings, it was possible to discriminate between the GFP from the SINV-GFP infected cells (diffuse and weak) and the GFP signal from neutrophils (concentrated and bright). After capture of images, larvae were washed and transferred in a new 24-well plate filled with 1 ml of fresh water in each well, incubated at 28°C and imaged again under the same conditions the day after.

Then pictures were analyzed and neutrophils (*mpx:*GFP + bright cells) were manually counted using the ImageJ software version 10.2 (developed by the National Institute of Health). Counts shown in **Figures 3B** and **4B** are numbers of neutrophils per image.

High resolution confocal live imaging of infected larvae was performed as previously described (27, 35, 36). Briefly, the injected larvae were positioned in 35 mm glass-bottom dishes (Inagaki-Iwaki) and immobilized in the dish with a 1% low-melting-point agarose and then covered with 2 ml Volvic water containing tricaine. Confocal microscopy was performed at 23–26°C. A Leica SP8 confocal microscope equipped with two PMT and Hybrid detector, a 20X oil immersion objective (HC PL APO CS2 20X/0.75) and a X–Y motorized stage was used to live image SINV + *Shigella* co-infected and *Shigella* only infected larvae (represented in **Figure 4C**; Video S1 in Supplementary Material). To simultaneously acquire SINV + *Shigella* and *Shigella* infected larvae, the "mark and find" mode of acquisition was applied. A Leica SPE inverted microscope and a 40 × oil immersion objective (ACS APO 40 × 1.15 UV) was also used to live image SINV + *Shigella* co-infected larvae represented in **Figure 4F** and Video S2 in Supplementary Material. The 4D files generated by the time-lapse acquisitions were processed, cropped, analyzed, and annotated using the LAS-AF Leica software. Acquired Z-stacks were projected using maximum intensity projection and exported as AVI files. Frames were captured from the AVI files and handled with Photoshop software to mount figures. AVI files were also cropped and annotated with ImageJ software, then compressed and converted into QuickTime movies with the QuickTime Pro software. Neutrophils were manually counted and tracked over time from maximum intensity projection movies of infected larvae.

Cytokine Expression, Viral and Bacterial Burden Measurement by qRT-PCR

RNA was extracted from individual larvae using RNeasy® Mini Kit (Qiagen). cDNA was obtained using M-MLV H- reverse-transcriptase (Promega) with a dT_{17} primer or a random nonamer (for host and bacterial transcripts, respectively). Quantitative PCR was then performed on an ABI7300 thermocycler (Applied Biosystems) using Takyon™ ROX SYBR® 2× MasterMix (Eurogentec) in a final volume of 25 µl. The following pairs of primers were used:

ef1a (housekeeping gene used for normalization): GCTGATCGTTGGAGTCAACA and ACAGACTTGACCTCAGTGGT

ifnphi1 (secreted isoform): TGAGAACTCAAATGTGGACCT and GTCCTCCACCTTTGACTTGT

il1b: GAGACAGACGGTGCTGTTTA and GTAAGACGGCACTGAATCCA

il10: CATAACATAAACAGTCCCTATG and GTACCTCTTGCATTTCACCA

tnfa: TTCACGCTCCATAAGACCCA and CAGAGTTGTATCCACCTGTTA

mmp9: AACCACCGCAGACTATGACAAGGA and GTGCTTCATTGCTGTTCCCGTCAA

E1-SINV: GACAACATGCAATGCAGAATG and CTAGTCAGCATCATGCTGCA

il22: TGCAGAATCACTGTAAACACGA and CTCCCCGATTGCTTTGTTAC

cxcl8a: GTCGCTGCATTGAAACAGAAAGCC and CTTAACCCATGGAGCAGAGGGG

il23a: CTGAAAGTGCTTAAGGAATCGG and GAGAAGGAGTAGAGTCTTTCCAC

ifng1r: ACCAGCTGAATTCTAAGCCAA and TTTTCGCCTTGACTGAGTGAA

dram1: CCTGGTTATCTGGTCATCGA and CATGAATCCAAACACACAGCT

DsRed: CAAGGAGTTCATGCGCTTC and TACATCCGCTCGGTGGA

Statistical Analysis

Normal distributions were always analyzed with the Kolmogorov–Smirnov and the Shapiro–Wilk tests. To evaluate difference between means of normally distributed data (for neutrophil numbers and bacterial burdens) (**Figures 2D**, **3B**, **4B**, **4D** and **4F**; Figures S2C,D in Supplementary Material), an analysis of variance followed by Bonferroni's multiple comparison tests was used. For bacterial burdens (CFU counts), values were Log10 transformed. For cytokines expression and some bacterial burdens (**Figures 2C** and **5**; Figures S3–S5 in Supplementary Material), non-Gaussian data were analyzed with the Kruskal–Wallis test followed by Dunn's multiple comparison test. $P < 0.05$ was considered statistically significant (symbols: $^{***}P < 0.001$; $^{**}P < 0.01$; $^{*}P < 0.05$). Survival data were plotted using the Kaplan–Meier estimator and log-rank (Mantel–Cox) tests were performed to assess differences between groups. Statistical analyses were performed using GraphPad Prism® software.

RESULTS

Establishing Zebrafish as a Model for Viral Bacterial Co-Infections

To test whether the zebrafish larva could be a valuable model to address mechanisms of viral and bacterial co-infection *in vivo*, we decided to combine our well-characterized SINV and *Shigella* zebrafish infection models (**Figure 1**).

We used SINV-GFP viruses derived from the TE12 strain, which is moderately virulent in zebrafish (24). Unlike the strain used in our previous study (SINV-3′GFP), which bears an eGFP sequence in the 3′ region of the region preceded by an additional subgenomic promoter (31), the SINV-GFP2A virus bears an

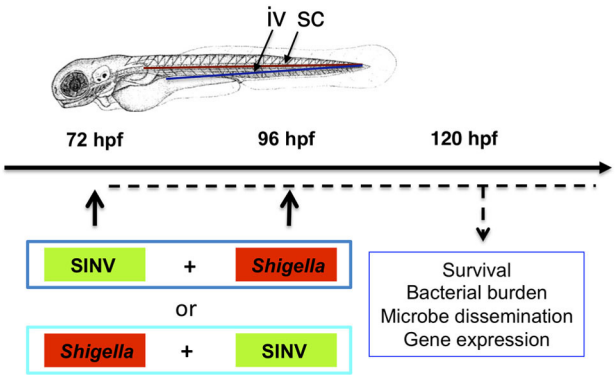


FIGURE 1 | Modeling viral-bacterial co-infection in zebrafish. Scheme of the experimental set up of viral bacterial co-infection using zebrafish. A 72 hpf zebrafish larva is shown. Microbes are injected in the bloodstream [intravenously (iv)] *via* the dorsal aorta (red line) or the ventral vein (blue line). Subcutaneous injections of the bacteria (sc) are performed over a somite, in the caudal region of the larva. Sindbis virus (SINV) and *Shigella flexneri* bacteria (*Shigella*) are sequentially injected in the bloodstream (iv) of zebrafish larvae at 72 and 96 hpf. Both SINV + *Shigella* and *Shigella* + SINV sequential co-infections are tested. Non-injected fish and fish injected with SINV or *Shigella* alone are used as a control. Single SINV or *Shigella* injections are performed at 72 or 96 hpf depending on the sequential co-infection tested. Survival, viral replication, bacterial burden, neutrophil behavior and expression of antiviral and antibacterial related genes are monitored over time as represented (dotted black line).

eGFP gene inserted in the structural ORF with a self-cleaving 2 A linker, thus being less prone to GFP loss upon replication (32). Both viruses led to a comparable amount of GFP signal in infected cells. Injecting 50–100 PFU of either virus into the bloodstream of 72 hpf zebrafish larvae results in infection of various cell types, easily observed thanks to the GFP gene inserted in the viral genome. The infection, however, remains sublethal, as viral burden quickly stabilizes after one day of rapid viral replication (24). However, upon type I IFN receptor knockdown, SINV infection is lethal (Figure S1 in Supplementary Material), showing that type IFN I plays a key protective role against SINV, similar to what has been described for the closely related CHIKV (25).

The M90T strain of *Shigella* causes a dose-dependent disease after inoculation to 72 hpf zebrafish larvae. An inoculum of up to 2,000 CFU is non-lethal and bacteria will be cleared in ~3 days, with phagocytes, and particularly neutrophils, playing a crucial role, while higher doses result in unbridled bacterial proliferation associated with macrophage and neutrophil depletion (27).

We combined SINV-GFP with *Shigella*-DsRed, allowing us to simultaneously monitor the dissemination of the two microbes. In the design of the sequential co-infection of zebrafish with virus and bacteria, we decided to inject one pathogen at 72 hpf, and the other 24 h later, when a robust response to the first one is established. We tested both SINV + *Shigella* or *Shigella* + SINV co-infection; single injections were used as controls. The scheme of the experimental set-up we designed is represented in **Figure 1**.

Increased Susceptibility to Co-Infection Is Only Observed When Virus Is Injected First

We tested the outcome of a sublethal (~60 PFU) SINV-GFP2A inoculation at 72 hpf followed by a sublethal (~2,000 CFU) *Shigella*-DsRed injection at 96 hpf (SINV + *Shigella*, **Figure 2A**), as well as the opposite combination, namely injecting *Shigella* at 72 hpf, followed the SINV injection at 96 hpf (*Shigella* + SINV, **Figure 2B**). We then assessed the survival of the infected fish at 28°C by regular observation using a stereomicroscope. As expected with these sublethal doses, single injections of bacteria or virus, performed at either 72 or 96 hpf, did not result in mortality; upon termination of the experiment at 144 hpf, these animals did not display any overt signs of disease. *Shigella* + SINV co-infection did not result in significant mortality (**Figure 2B**). In striking contrast, when *Shigella* was injected after SINV, we recorded the death of about 50% of the co-infected fish within 2 days (**Figure 2A**). This result was reproducibly observed in three independent experiments and was also observed with the SINV-3′GFP strain (Figure S2 in Supplementary Material).

We then assessed pathogen burden in co-infected larvae. Viable bacteria were quantified by plating serial dilution of homogenates of euthanized fish onto bacterial culture dishes over time. As shown in **Figures 2C,D**, survival of *Shigella*-infected larvae (either single-infected or *Shigella* + SINV sequentially infected) was associated with clearance of bacteria over time. In contrast, in larvae inoculated with SINV first followed by *Shigella* injection (SINV + *Shigella*), *Shigella* numbers dramatically increased during the first 24 h post *Shigella* injection in about half the larvae (**Figure 2C**). This fraction, consistent with the 50% survival rate observed previously (**Figure 2A**), suggested that these larvae were unable to restrict *Shigella* proliferation and succumbed to the bacterial infection. By contrast, when we measured SINV transcripts by qRT-PCR, we found that SINV replication was essentially unaffected by either previous or subsequent *Shigella* co-infection (**Figures 2E,F**).

In addition, we observed the co-infected fish under the fluorescence stereomicroscope to assess the distribution of virus-infected cells and of bacteria, revealed by green and red fluorescence, respectively. This immediately confirmed that SINV + *Shigella*-infected larvae displayed bacterial, but not viral, overgrowth (**Figure 2G**). By contrast, imaging of the reciprocally co-infected larvae did not suggest any interference of the two infections (not shown). In double- or single-infected larvae, SINV distribution patterns were similar, with frequent infection of the large yolk cell, and of many cells in the jaw, of muscle fibers close to the injection zone in the tail, with subsequent propagation to the spinal cord and/or the brain, as previously described (24). In all *Shigella*-infected animals, 4 h after *Shigella* injection (100 hpf), the fluorescent bacteria were visible as specks mostly localized in the caudal hematopoietic tissue as well as in the vein over the yolk, consistent with rapid capture of bacteria by blood-exposed phagocytes which are abundant in these areas (35), and as previously described (27). However, 1 day later, the infection course was radically different between the *Shigella*-only and the SINV + *Shigella*-infected animals.

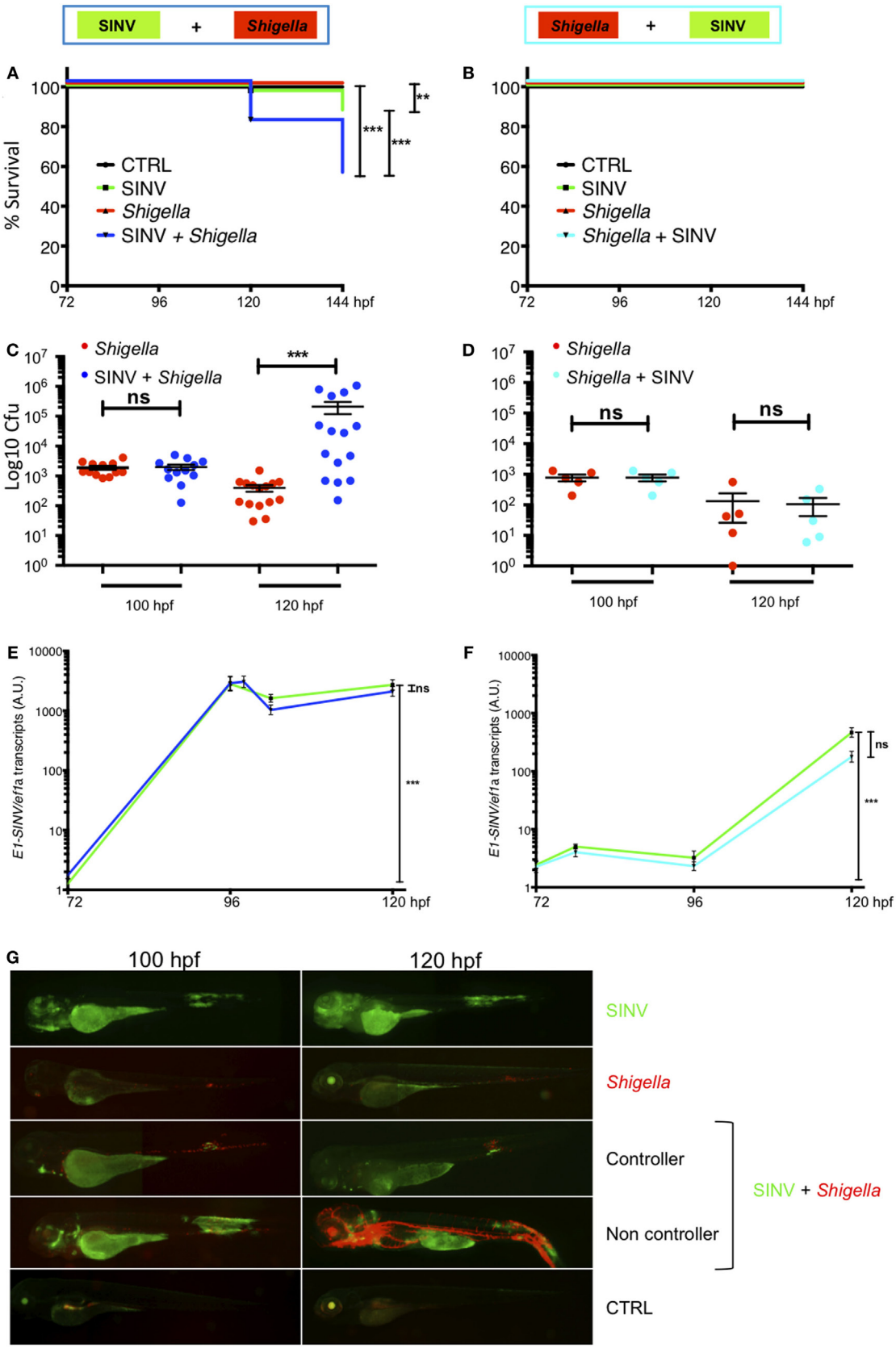


FIGURE 2 | Continued

FIGURE 2 | Increased susceptibility to co-infection is only observed when virus is injected first. Zebrafish larvae were sequentially injected in the bloodstream with Sindbis virus (SINV) and *Shigella* at 72 and 96 hpf and larvae injected with SINV or *Shigella* alone were used as a control as depicted in **Figure 1**. Survival, bacterial burden, and viral replication were evaluated over time in SINV + *Shigella* **(A,C,E)** and in *Shigella* + SINV **(B,D,E)** sequentially infected larvae settings. **(A,C,E)** Data pooled from three independent experiments; **(B,D,E)** data from one experiment; see also Figures S2A,B in Supplementary Material. Survival curves of zebrafish larvae injected with SINV + *Shigella* **(A)** (blue curve) or with *Shigella* + SINV **(B)** (cyan curve) and incubated at 28°C. For both sequential co-infection settings, fish injected with *Shigella* (red curves) or with SINV (green curves) alone at the appropriate time point, and non-injected fish (black curves) were used as controls. $n = 72$ **(A)** or 24 **(B)** fish for each condition. **(C,D)** Bacterial burden quantification by enumerating live bacteria in homogenates from individual larvae sequentially co-infected with SINV + *Shigella* **(C)** (blue symbols) or *Shigella* + SINV **(D)** (cyan symbols) or with *Shigella* alone (red symbols) measured by plating onto LB immediately after *Shigella* injection and 24 h post *Shigella* injection. $n = 15$ **(C)** or 5 **(D)** larvae for each condition. **(E,F)**. Viral replication measured by RT-qPCR from individual infected larvae in SINV-*Shigella* **(E)** (blue curve) or *Shigella*-SINV **(F)** (cyan curve) sequentially co-infected fish, or SINV (green curves). $n = 15$ **(E)** or 5 **(F)** larvae for each condition. **(G)** Representative images of virus (SINV-GFP) and bacteria (*Shigella*-DsRed) dissemination, determined by live imaging using a fluorescence stereomicroscope, of zebrafish larvae infected with SINV-GFP alone at 72 hpf, or with *Shigella* DsRed alone at 96 hpf, or sequentially co-infected with SINV-GFP first and *Shigella*-DsRed 1 day later. Non-infected larvae (CTRL) are also shown. The same infected larvae were live imaged 4 and 24 h post *Shigella* injection. Overlay of GFP and DsRed fluorescence is shown, except in SINV panels, where only GFP fluorescence was recorded.

At this time point, larvae that received *Shigella* only had almost all cleared the infection, showing few foci of *Shigella* mainly located near the injection point in the caudal part of the larvae. In contrast, half of the SINV + *Shigella*-infected larvae showed an uncontrolled *Shigella* proliferation, with dissemination in the bloodstream (bacteremia) and in the tissues near the site of injection. By daily observation of individual co-infected larvae under the fluorescent microscope to monitor bacterial dissemination, we observed that SINV + *Shigella* co-infected larvae that had controlled the bacterial proliferation at 120 hpf as suggested by the decreased level of bacterial fluorescence (e.g., 24 h post *Shigella* inoculation) usually survived; by contrast, SINV + *Shigella* co-infected larvae that exhibited high level of bacterial fluorescence at 120 hpf, usually were unable to control *Shigella* proliferation and died between 120 and 144 hpf (e.g., 24 and 48 h post *Shigella* inoculation). ($n = 24$ larvae scored for each condition; 100% survival for control and single infected larvae; 54% survival of SINV + *Shigella* co-infected larvae, 6/24 died at 120 hpf and 7/24 died at 144 hpf. All dead larvae were full of fluorescent bacteria.) This implies a critical time window early after *Shigella* inoculation.

Collectively, these observations show that SINV-infected zebrafish have an increased susceptibility to subsequent *Shigella* co-infection, establishing the zebrafish as a suitable model for the study of virus-induced hyper-susceptibility to bacterial superinfection.

Impaired Neutrophil Counts Upon *Shigella* Injection in SINV Infected Fish

In mammals, professional phagocytes play key roles in containing *Shigella* infection, especially neutrophils that efficiently kill the bacteria they engulf (37), while macrophages (but not monocytes) actually get invaded (38). Similarly, in zebrafish larvae, we have previously shown that professional phagocytes contain the bacteria immediately upon the injection; furthermore, if *Shigella* may persist and replicate inside macrophages, neutrophils that have engulfed similar amounts of bacteria efficiently kill them. Neutrophils play an essential scavenging role by immediately engulfing debris and bacteria released by dying infected macrophages on non-immune cells, thus preventing bacterial dissemination (27). Considering this crucial role of neutrophils, we addressed their status in our SINV + *Shigella* co-infection model.

First, we assessed the population of neutrophils at the whole body-level, using reporter transgenic zebrafish larvae harboring green neutrophils Tg(*mpx*:GFP)^{i114} (28), referred herein as *mpx*:GFP. While SINV-infected cells also expressed GFP, the fluorescence of individual *mpx*:GFP^{+} neutrophils was much stronger, the only exception being some dense clusters of SINV-infected cells in the brain, an organ which is devoid of neutrophils. Therefore, the identity of neutrophils under the fluorescence microscope was unambiguous (**Figure 3A**). We counted neutrophils from images of SINV + *Shigella* infected larvae, which we compared with uninfected larvae and larvae inoculated with SINV only at 72 hpf or *Shigella* only at 96 dpf (**Figure 3B**). Images were taken at 100 and 120 hpf, corresponding to 4 and 24 h after *Shigella* inoculation, respectively. As expected, in *Shigella* only infected larvae, neutrophil numbers did not change significantly, consistently with neutrophil quantification following sublethal *Shigella* inoculation at 72 hpf (27). Interesting, in SINV only infected animals, a significant increase of neutrophils was observed at 120 hpf, similarly to what had been described previously with CHIKV infection (25). Strikingly, neutrophil numbers decreased in SINV + *Shigella* co-infected larvae as soon as 4 h after *Shigella* infection ($p < 0.05$), and this reduction was even more pronounced the following day ($p < 0.001$).

Collectively, these observations show that a significant fraction of neutrophils undergo cell death *in vivo* when *Shigella* infection is preceded by SINV infection.

Impaired Neutrophil Recruitment and Survival in SINV + Local *Shigella* Co-Infection

To better observe the fate of neutrophils during SINV + *Shigella* co-infection, we replaced the bloodstream inoculation of *Shigella* by a subcutaneous inoculation in mid-trunk. The bacterial infection is thus essentially limited to the flat, thin space between the epidermis and 2 or 3 chevron-shaped somites, allowing detailed time-lapse imaging of phagocyte recruitment and of cell–cell and cell–bacteria interactions by confocal fluorescence microscopy (35).

We thus addressed the impact of SINV + *Shigella* co-infection on the ability of neutrophils to sense, migrate, and be recruited toward a local *Shigella* inoculum. We injected a sub lethal GFP-SINV inoculum in the bloodstream of 72 hpf *mpx*:GFP

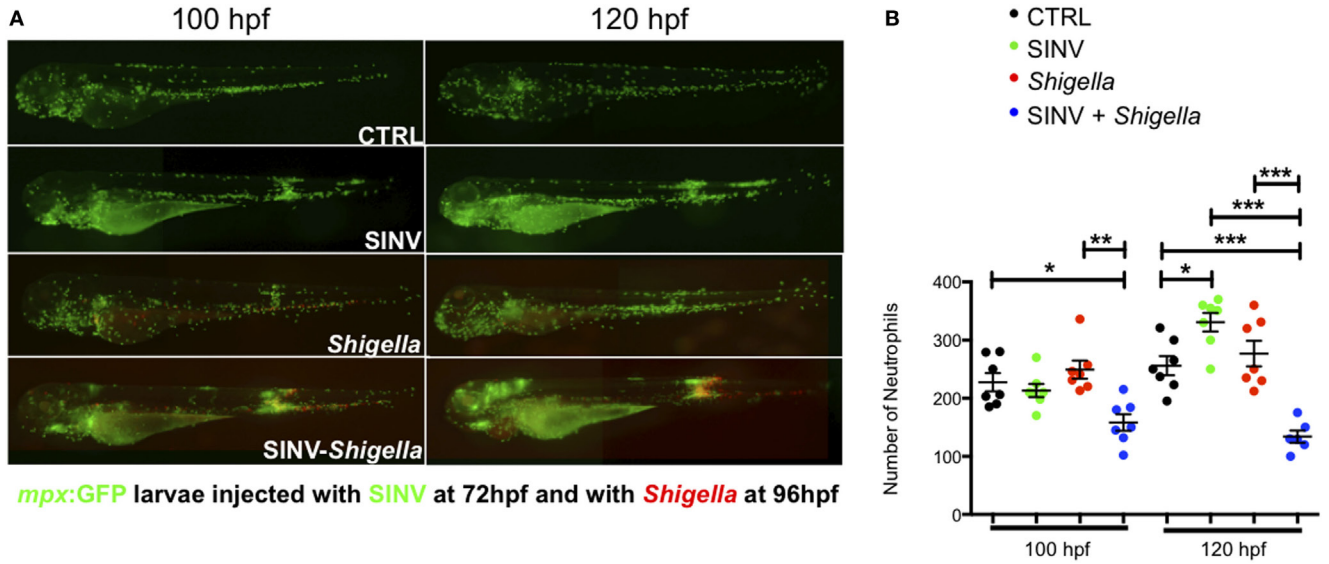


FIGURE 3 | Impaired neutrophil counts upon *Shigella* injection in Sindbis virus (SINV) infected fish. **(A)** *mpx*:GFP zebrafish larvae (green neutrophils) were sequentially injected intravenously with sublethal doses of SINV-GFP at 72 hpf and the day after with sublethal doses of *Shigella*-DsRed. As a control, similar doses of SINV-GFP only and *Shigella* DsRed only were injected in the blood of 72 and 96 hpf *mpx*:GFP larvae, respectively. The infected larvae were then imaged with a wild field fluorescent microscope over time at 100 hpf (4 h post *Shigella* injection) and at 120 hpf (24 h post *Shigella* injection) to monitor the impact of the co-infection on the neutrophil population at the level of the entire organism. Note that it was possible to discriminate under the microscope the GFP label of the SINV-GFP infected cells (diffuse and less bright) from the GFP label of the *mpx*:GFP neutrophils (brighter). The neutrophil numbers appeared to be decreased in SINV-*Shigella* co-infected larvae. Overlay of green (SINV and neutrophils) and red (*Shigella*) fluorescence from single or co-infected fish is shown. **(B)** Neutrophil counts in uninfected (CTRL, black symbols) or upon sublethal SINV-GFP (green symbols), *Shigella*-DsRed (red symbols) injection or sequential SINV + *Shigella* (blue symbol) injection. Neutrophils were counted from images taken on live infected larvae using ImageJ software, and plotted as specified in Section "Materials and Methods." Mean ± SEM are also shown (horizontal bars). Data plotted are from two pooled independent experiments ($n = 7$ larvae scored for each condition).

larvae, and the day after we injected about 2×10^3 *Shigella*-DsRed subcutaneously (a sublethal dose also by this route; not shown); as a control, we injected the same *Shigella* inoculum in previously uninfected fish (**Figure 4**). We first quantified neutrophil recruitment to the bacteria at 100 and 120 hpf, corresponding to 4 and 24 h post *Shigella* injection, using a wide field fluorescent microscope (**Figures 4A,B**). As expected, many neutrophils were already recruited by 4 h post *Shigella* injection, with co-localization of green and red fluorescence suggesting that neutrophils had started to engulf bacteria. The recruited neutrophils were still there 24 h post *Shigella* injection, and their numbers slightly increased, presumably due to bacterial invasion and proliferation in muscle fibers that die sporadically, releasing live bacteria quickly engulfed by neutrophils as we previously showed (27). Although recruitment occurred in both single- and co-infected larvae, the local neutrophil population was significantly decreased in the co-infected larvae at both time points (**Figure 4B**), indicating that the previous viral infection resulted in deficient recruitment and/or survival of neutrophils to the bacterial site.

To analyze the *Shigella*–neutrophil interactions in more detail, we recorded neutrophil behavior by live imaging at high resolution using a confocal microscope, documenting the early steps of neutrophil recruitment, between 30 min and 3 h post subcutaneous *Shigella* injection (**Figure 4C**; Video S1 in Supplementary Material). At the beginning of the acquisition, we found neutrophils already recruited to the bacteria, in comparable numbers in SINV + *Shigella* and *Shigella*-only injected animals. As expected, the number of recruited neutrophils progressively increased in *Shigella*-only injected larvae. However, the scenario was very different in the SINV + *Shigella*-injected animals, where the number on neutrophils did not increase, thus becoming significantly lower than in controls from 2 h post *Shigella* injection (**Figure 4D**).

Closer examination of the time-lapse movies revealed that these recruited neutrophils could undergo cell death upon *Shigella* engulfment in SINV + *Shigella*-injected animals (**Figure 4E**; Video S2 in Supplementary Material), something not previously observed in *Shigella*-only infected larvae. We thus quantified the number of neutrophils dying upon having engulfed the bacteria from 30 min to 4 h post *Shigella* injection by manually tracking neutrophils on live imaging acquisitions. This quantification confirmed that a significant number of *Shigella*-containing neutrophils died in co-infected fish, while none did in *Shigella*-only infected controls (**Figure 4F**; Videos S1 and S2 in Supplementary Material).

Collectively, these observations demonstrate that neutrophil anti-bacterial functions are perturbed in SINV + *Shigella* co-infected animals: neutrophil recruitment toward the bacteria is impaired, and phagocytosing neutrophils undergo cell death. Overall, they strongly suggest that the viral response initiated upon SINV injection interferes with the bacterial response

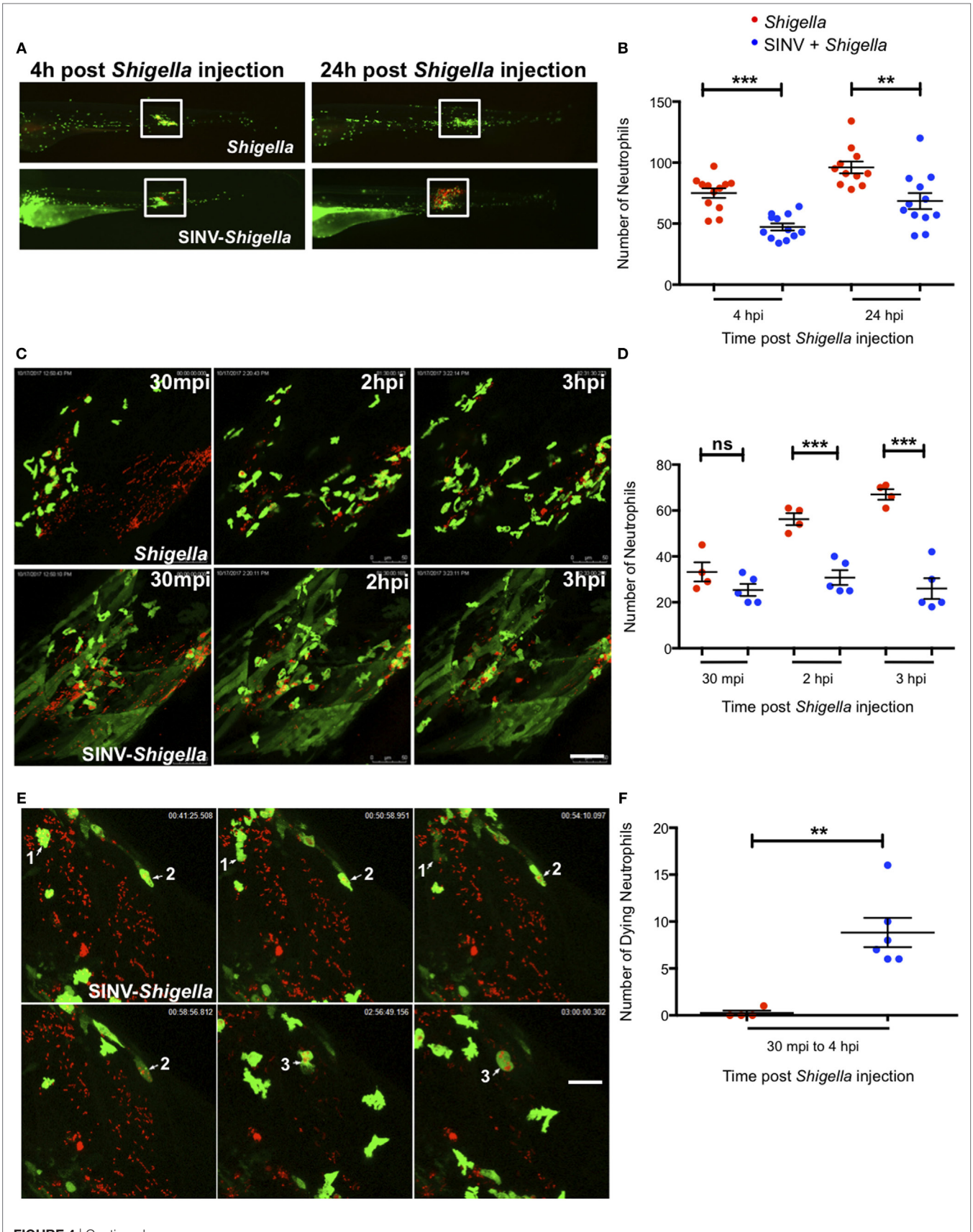


FIGURE 4 | Continued

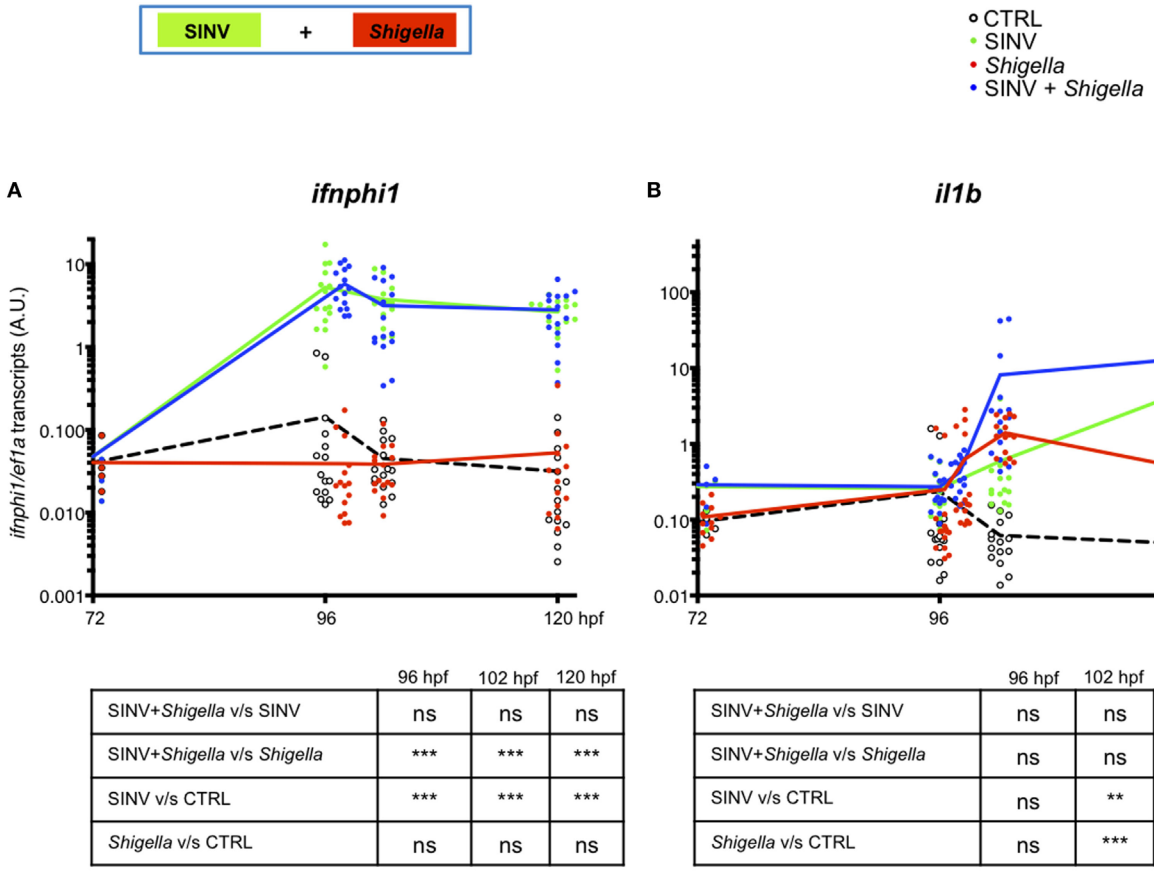
FIGURE 4 | Impaired neutrophil recruitment and survival in Sindbis virus (SINV)- > local *Shigella* co-infection. **(A)** 72 hpf *mpx*:GFP larvae were sequentially injected with SINV-GFP in the bloodstream then subcutaneously with *Shigella*-DsRed one day later (96 hpf). As control, *mpx*:GFP larvae were injected subcutaneously with *Shigella* only at 96 hpf. The infected larvae were imaged with a fluorescent stereomicroscope over time at 100 hpf (4 h post *Shigella* infection) and at 120 hpf (24 h post *Shigella* infection), to monitor neutrophil recruitment to the locally injected bacteria. Overlay of green (SINV and neutrophil) and red (*Shigella*) fluorescence is shown. The white box indicates the region chosen to count the recruited neutrophils. **(B)** Neutrophil recruitment quantification upon sublethal *Shigella*-DsRed (red symbol) injection or sequential SINV + *Shigella* (blue symbols) injection. Neutrophils were counted from images taken on live infected larvae [white box delimitated the region chosen to count the recruited neutrophils in **(A)**] using ImageJ software, and plotted as specified in Section "Materials and Methods." Data are from one experiment ($n = 12$ larvae scored for each condition). Mean ± SEM are also shown (horizontal bars). **(C)** Frames extracted from maximum intensity projection of *in vivo* time-lapse confocal imaging sessions of 96 hpf *mpx*:GFP larvae injected subcutaneously with *Shigella*-DsRed alone (top panel) or of SINV + *Shigella* co-infected larvae that had been injected one day before with SINV-GFP in the bloodstream (at 72 hpf) (bottom panel). Overlay of green (SINV and neutrophils) and red (*Shigella*) fluorescence of the caudal area of the larvae is shown. Time indicated on the frames is upon subcutaneously *Shigella* injection. See also Video S1 in Supplementary Material. Scale bar: 50 µm. **(D)** Neutrophil recruitment quantification upon subcutaneous *Shigella*-DsRed (red symbol) injection or sequential bloodstream SINV-GFP injection followed the day after by subcutaneous *Shigella*-DsRed (blue symbols) injection. Neutrophils were manually counted at 30 min, 2 and 3 h post *Shigella* injection from maximum intensity projections frames of confocal acquisitions of live infected larvae (to count the recruited neutrophils the region taken into consideration is shown in **(B)** and plotted as specified in Section "Materials and Methods." Data plotted are from $n = 4$ to 5 larvae scored for each condition. Mean ± SEM are also shown (horizontal bars). **(E)** Frames extracted from maximum intensity projection of confocal acquisition of SINV + *Shigella mpx*:GFP co-infected larvae. SINV-GFP was injected in the bloodstream at 72 hpf and *Shigella*-DsRed was subcutaneously injected the day after, at 96 hpf. The acquisition of the infected larvae was started about 30 min after *Shigella* injection. Three dying *Shigella* engulfing neutrophils are shown (annotated as 1, 2, and 3 on the frames). Overlay of green (SINV and neutrophils) and red (*Shigella*) fluorescence of the caudal area of the larvae is shown. Time indicated on the frames is upon subcutaneously *Shigella* injection. See also Video S2 in Supplementary Material. Scale bar: 20 µm. **(F)** Dying neutrophils quantitation upon subcutaneous *Shigella*-DsRed (red symbol) injection or sequential bloodstream SINV-GFP injection followed the day after by subcutaneous *Shigella*-DsRed (blue symbols) injection. Dying neutrophils were manually tracked and quantified from maximum intensity projections of confocal acquisitions and plotted as specified in Section "Materials and Methods." Data plotted are from $n = 4$ *Shigella*-infected larvae and $n = 6$ SINV + *Shigella*-infected larvae scored. Mean ± SEM are also shown (horizontal bars).

initiated upon *Shigella* injection, resulting in uncontrolled *Shigella* proliferation and dissemination in co-infected fish.

Immune Gene Modulation Upon SINV + *Shigella* Co-Infection

Finally, we measured cytokine gene expression by qRT-PCR in SINV + *Shigella* and corresponding single-infected fish. We first measured *ifnphi1* and *il1b*, two signature cytokines of anti-viral and anti-bacterial responses, respectively. As expected, a strong and sustained type I IFN response was detected in SINV-only infected fish, while *Shigella* only did not induce any detectable IFN induction (**Figure 5A**). IFN expression in co-infected fish was strictly similar to that of SINV-only infected fish, consistent with the fact that SINV burden is not affected by bacterial superinfection (**Figures 2E,F**). Reciprocally, a strong *il1b* response was rapidly induced in *Shigella*-only infected fish; SINV induced its expression much more slowly. However, while this response was transient in *Shigella*-only infected larvae, it was sustained in SINV + *Shigella* co-infected animal (**Figure 5B**). Of note, in *Shigella* + SINV co-infections, *ifnphi1* and *il1b* induction corresponded to the addition of those induced by single infections, again fitting with the absence of interference of the two responses when the two pathogens were administrated in that order (Figures S4A,B in Supplementary Material).

This increased expression of *il1b* in SINV + *Shigella* co-infections is mostly seen in late (24 h) but not early (6 h) time after *Shigella* injection, paralleling the increased bacterial burden of these animals (**Figure 2C**), making it unclear whether it is a cause or a consequence of higher bacterial loads. Since deficiency of neutrophil function is already observed a few hours after *Shigella* injection (**Figures 3** and **4**), we tested the expression of several other candidate genes at 6 h post *Shigella* injection (Figure S3 in Supplementary Material). Genes typically associated with bacterial, but not viral infection, such as *il8* (*cxcl8a*), *tnfa*, *il22*, were indeed not induced by SINV alone but were induced by *Shigella*, while *mmp9* was also induced by SINV, as previously observed with CHIKV (39). For other genes tested, no obvious interaction was revealed, as expression in dually infected fish was comparable to that of SINV or *Shigella* single-infected fish. Interestingly, the anti-inflammatory cytokine *il10* was induced by SINV only at this time point (6 h post *Shigella* injection). Thus, from these observations, we decided to measure the kinetics of induction of *tnfa* and *il10* over time comparing SINV or *Shigella* single injected fish to SINV + *Shigella* co-infected fish (**Figures 5C,D**). The induction of *tnfa* paralleled the induction of *il1b*, as expected (5 C). Strikingly, we found that *il10* was strongly induced by SINV only by 96 hpf, just before *Shigella* injection, and remained high over time in both SINV and SINV + *Shigella* co-injected fish (**Figure 5D**). We measured the induction of these genes in *Shigella* + SINV co-infected fish, showing no obvious interference between the antiviral and antibacterial induced genes when *Shigella* was injected first (Figures S4C,D in Supplementary Material). We also measured the kinetics of SINV dependent-*mmp9* (encoding for Matrix metalloproteinase 9) induction upon SINV + *Shigella* or *Shigella* + SINV co-infections, showing that *mmp9* was strongly induced only when SINV was injected before *Shigella*, again suggesting an interference between the antiviral and the antibacterial induced genes only when virus is injected first (Figures S5A,B in Supplementary Material). We also tested possible correlation of cytokine expression and bacterial burden (asses by qRT-PCR) at 120 hpf, to see if differences could be observed between controller and no-controllers SINV + *Shigella* co-infected fish. As reported on Figure S6 in Supplementary Material, no obvious correlation between bacterial burden and cytokine expression was observed, except for *il1b*, which is correlated with burden in co-infected but not in *Shigella*-only infected fish.



	96 hpf	102 hpf	120 hpf
SINV+*Shigella* v/s SINV	ns	ns	ns
SINV+*Shigella* v/s *Shigella*	***	***	***
SINV v/s CTRL	***	***	***
Shigella v/s CTRL	ns	ns	ns

	96 hpf	102 hpf	120 hpf
SINV+*Shigella* v/s SINV	ns	ns	*
SINV+*Shigella* v/s *Shigella*	ns	ns	***
SINV v/s CTRL	ns	**	ns
Shigella v/s CTRL	ns	***	***

	96 hpf	102 hpf	120 hpf
SINV+*Shigella* v/s SINV	ns	ns	ns
SINV+*Shigella* v/s *Shigella*	ns	ns	ns
SINV v/s CTRL	ns	ns	ns
Shigella v/s CTRL	ns	*	**

	96 hpf	102 hpf	120 hpf
SINV+*Shigella* v/s SINV	ns	ns	ns
SINV+*Shigella* v/s *Shigella*	***	ns	ns
SINV v/s CTRL	**	***	***
Shigella v/s CTRL	ns	***	ns

FIGURE 5 | Cytokine gene modulation upon Sindbis virus (SINV) + *Shigella* co-infection. **(A–D)** Cytokine (*ifnphi1*, *il1b*, *tnfa*, *il10*) induction was measured from individual zebrafish larvae sequentially co-injected with SINV + *Shigella* (blue) or from individual zebrafish larvae injected with SINV alone (green) or with *Shigella* alone (red), and non-injected fish as control (CTRL, black curves). Data plotted are from three independent experiments pooled (n = 15 larvae for each condition); individual values are shown and curves correspond to the means. Statistical analysis is shown as a table under each graph.

Overall, these observations suggest that, in addition to type I IFN, the SINV-dependent *il10* induction measured in SINV + *Shigella* co-infected fish, given the anti-inflammatory properties of this cytokine, could participate in the increased susceptibility to bacterial infection with the concomitant death and uncontrolled bacterial proliferation observed in SINV + *Shigella* co-infected fish.

DISCUSSION

Hyper-susceptibility to secondary bacterial infection following acute viral infections is a major clinical issue, for which animal models are indispensable to understand the underlying mechanisms and test therapeutic and prophylactic approaches (6). In that respect, mouse models have yielded remarkable insights, yet alternative models could also provide complementary information and valuable tools. The optically and genetically tractable swimming zebrafish larva constitutes a particularly attractive system. Here, using two infection models previously developed by our team with SINV (24) and *Shigella* (27), we describe the first instance of virus-induced bacterial hyper-susceptibility in zebrafish, and show that this susceptibility is associated with virus-induced defects in neutrophil function. Of note, another polymicrobial infection model, combining yeast and bacteria, has also been recently described in zebrafish (40).

To our knowledge, SINV and *Shigella* are not associated in co-infections in humans. This possibility is not excluded, since SINV infection has been largely neglected in humans, as it is considered to be mild (41). Interestingly, an outbreak of influenza virus H1N1 and *Shigella flexneri* co-infection was reported in a precarious and overcrowded gold miner camp in the tropical forest of French Guiana (42).

We do not think that the increased susceptibility to bacterial infection we observed in zebrafish larva upon SINV infection is specific to *Shigella flexneri*. We consider our model as a tool to address the possible interference of well-defined canonical anti-viral and anti-bacterial responses *in vivo*, beyond the specificities of SINV and *Shigella*. Other virus–bacterium combinations will be tested in zebrafish in the future to test this hypothesis.

This zebrafish viral–bacterial co-infection model offers great practical advantages. First, the timeframe of the experiments is quite short: less than a week from crossing breeding adults to final results. Second, microbe injections are performed at 72 and 96 hpf, late enough for the innate immune system of the larva to be operative, and yet early enough for use of many transient genetic manipulation approaches such as morpholino-mediated knockdown. Finally, the transparency, small size, and easy anesthesia of the zebrafish larva makes it quite easy to monitor the extant and spread of infections over time, and the combination of two different reporter fluorescent SINV and *Shigella* strains allow simultaneous observation of virus-infected cells and of bacteria dissemination. SINV and *Shigella* are both BSL2 pathogens, with many well-established genetic tools, and many other fluorescent colors are available beyond the GFP and DsRed used in this report. Thus, the various fluorescent zebrafish lines available, reporting immune cells or cytokine responses (25, 43, 44), can be combined in diverse ways with the fluorescent microbes, allowing the monitoring of the orchestration of the innate immune response and microbe-immune cell interactions in real time at the scale of the entire organism.

Timing is a key parameter when superinfection models are considered. In murine influenza-based models, hyper-susceptibility to bacteria is observed if 7 days elapse between the two infections, but not with a 3-day delay (16). In the zebrafish larva co-infection model described here, a 24-h time lapse between the two microbes was sufficient to detect a robust hyper-susceptibility to bacteria in virus infected animals. It would be worthwhile to more precisely determine the hyper-susceptibility time window in the zebrafish co-infection model in the future, by testing a range of delays, including simultaneous inoculation. Dosage of either microbe, predictably, is another key parameter, and we had to perform many tests (Table S1 in Supplementary Material) before finding the experimental conditions reported here.

Interestingly, while we found that virus-infected larvae were hyper-susceptible to bacteria, infecting with bacteria first and virus later did not result in increased mortality. Although one should certainly not derive any general conclusion from this observation, this appears remarkably similar to what has been observed in mouse models (45), and perhaps in humans as well, as hyper-susceptibility to viruses is not a notorious issue in bacteria-infected patients. The origin of this asymmetry would be worth investigating.

What are the molecular mechanisms that underlying the hypersensitivity we report here? Are they similar to those described in mice? Clearly, this will be our next line of investigation. The role of the type I IFN response, well-established in mouse, would be the first to address. Unfortunately, knocking down type I IFN receptor chains in zebrafish larvae results in death from the SINV dose used here (Figure S1 in Supplementary Material), requiring alternative approaches, such as injection of recombinant zebrafish type I IFNs, which will require extensive tests of IFN subtype, dosage, and timing.

Quite possibly, only one or a few of the hundreds of genes—mostly IFN-stimulated genes (ISGs)—induced by SINV infection could underlie the phenotype. In this context, it has been recently reported in a mouse model of influenza virus and *Streptococcus pneumoniae* co-infection, that the IFN-inducible methyltransferase Setdb2 mediates virus-induced susceptibility to bacterial infection, perturbing neutrophil functions by repressing the expression of genes encoding neutrophil attractant mediators like CXCL1 and other genes that are targets of the transcription factor NF-kB. Thus, Setdb2 could mediate the regulation of type I IFN and NF-kB pathways cross talk and could represent one of the mechanisms involved in virus induced susceptibility to bacterial superinfections (46). IFNs may even modify the phenotype of neutrophils independent of ISG induction, as recently shown for type III IFN and reactive oxygen species production (47).

We have shown that *il10* is induced upon SINV infection, and that its level remains high when *Shigella* is injected. Because of its known anti-inflammatory properties, IL-10 could be responsible of the increased bacterial susceptibility of viral infected fish, by impairing phagocyte anti-bacterial functions. In this context, it has been shown that IL-10 impairs neutrophil recruitment to

infected tissues in a neonatal mouse model of bacterial sepsis, and that perturbing IL10 induction resulted in the rescue of efficient neutrophil recruitment, bacterial clearance, and increased survival (48). Moreover, IL-10 expression prior to bacterial infection was shown to inhibit neutrophil recruitment, resulting in insufficient bacterial clearance and increased mortality in a mouse model of pneumonia (49). IL10 is thus an obvious candidate to test in our co-infection model.

We addressed the possible role of neutrophils in the hypersusceptibility phenotype and found that in co-infected animals, neutrophils frequently died after having engulfed bacteria. We cannot exclude that the death of other cell types also contribute to the phenotype, the most likely candidates being macrophages. However, as we have previously documented that, unlike neutrophils, some *Shigella*-infected macrophages already undergo cell death upon low dose *Shigella* infection (2,000 CFU, used in this study) (27), and therefore, we decided to focus on neutrophil behavior only. Interestingly, while found that even though viral infection increases the total neutrophil population (**Figure 3**), it also makes these cells less able to cope with bacteria. Intriguingly, in zebrafish, neutrophils themselves can be an important source of type I IFN (25), suggesting differentiation into virus-targeted cells to the detriment of their antibacterial function. IFN-dependent polarization of neutrophils into distinct "N1" and "N2" phenotypes has been proposed as an important mechanism in tumor rejection (50). In this context, our SINV-*Shigella* co infection model will allow to address if type I IFN-producing neutrophils are still able to sense, migrate to and engulf bacteria, or if they are a specialized neutrophil subset that have lost their antibacterial functions.

Expression of pro-inflammatory cytokine genes such as *il1b* and *tnfa* is rapidly induced by many bacterial infections, and *Shigella* is no exception (**Figure 5**; Figure S4 in Supplementary Material). These transcripts are more strongly upregulated in SINV + *Shigella* compared to *Shigella* only infected fish. These cytokines normally contribute to antibacterial defense, and this higher expression may be just a consequence of the higher bacterial burden of these animals, without leading to the hypersusceptibility phenotype. However, a causal (deleterious) role cannot be ruled out, perhaps linked to pyroptosis-mediated demise of myeloid cells. Pyroptosis of macrophages has been observed in zebrafish larvae infected with SVCV virus (51); however, the situation is quite different here as (i) unlike SINV, SVCV is a very poor IFN inducer (52) and (ii) unlike SVCV, SINV does not infect macrophages (24). A more detailed study of what cells express these cytokines during the co-infection using appropriate reporters (43, 44), and if they undergo inflammasome oligomerization (53), should illuminate this issue. To note, using a zebrafish model of local *Shigella* infection to perturb the cytoskeletal septins proteins expression, we recently reported deregulated inflammatory response and neutropenia and showed that too much IL1β-dependent inflammation resulted in the increased susceptibility of neutrophils to *Shigella* infection, with concomitant death of the engulfing neutrophils (36). It will be interesting to check if Anakinra, a IL1β receptor antagonist, that we have shown to rescue neutrophil death and host survival upon *Shigella* infection in septin depleted fish in this model (36), could also be able to rescue neutrophil functions and host survival in the SINV-*Shigella* co infection model we described here.

Although we still do not know if the mechanisms that lead to increased bacterial susceptibility upon a viral infection are shared by fish and mammals, the evolutionary conservation of this phenomenon is in itself remarkable. Since it is obviously counter-adaptive in some situations, one may infer that the immune modulation induced by the antiviral response provides a significant fitness advantage overall. This situation fits with the general concept of "immunity by equilibrium" (54), even if the aforementioned asymmetry of the virus-then-bacteria and bacteria-then-virus situations remain to be explained.

In conclusion, we describe here a new model of sequential infection of zebrafish larva with a virus (SINV) and a bacterium (*Shigella*), that uncovers the conservation of the virus-induced hyper-susceptibility to bacterial superinfection in this host. This opens up numerous avenues to unravel the mechanisms at play in this phenomenon. Importantly, the diminutive zebrafish larva, small enough to fit in microtitration plates, is highly suited to pharmacological screening (55). This system should therefore provide a valuable pre-clinical tool to test new candidate drugs to alleviate secondary bacterial superinfections—therapeutics that would restore the host immune system would be more desirable than current approaches, undermined by mounting antibiotics resistance.

ETHICS STATEMENT

Animal experiments were performed according to European Union guidelines for handling of laboratory animals (http://ec.europa.eu/environment/chemicals/lab_animals/home_en.htm) and were approved by the Institut Pasteur Animal Care and Use Committee.

AUTHOR CONTRIBUTIONS

LB generated most images and qPCR results, analyzed data, and made the figures. GP carried out most viral infections. VT analyzed the first co-infections experiments. LM performed infections in morphant larvae. PH contributed to funding acquisition. JPL and ECG conceived the study, performed infections, supervised the work, analyzed the data, and wrote the manuscript.

ACKNOWLEDGMENTS

The authors acknowledge Valérie Briolat for helping during the initial steps of this work, José Perez and Yohann Rolin for fish husbandry, and Bryan Mounce for SINV production.

FUNDING

This work was funded by Institut Pasteur and CNRS funding to PH, and by ANR grant Fish-RNAVAX (ANR-16-CE20-0002-03) to JPL. This project and LM have received funding from the European Union's Horizon 2020 research and innovation programme under the Marie Sklodowska-Curie grant agreement No 721537 "ImageInLife". GP was funded by a postdoctoral fellowship from Région Ile de France (DIM Malinf).

SUPPLEMENTARY MATERIAL

The Supplementary Material for this article can be found online at https://www.frontiersin.org/articles/10.3389/fimmu.2018.01084/full#supplementary-material.

FIGURE S1 | Dependence on type I interferons (IFN) response for survival to Sindbis virus (SINV) infection. Zebrafish embryos were injected with CRFB1 and CRFB2-specific morpholinos at the 1-cell stage to generate larvae deficient in type I IFN receptors, or with control morpholinos. At 72 hpf, they were infected with ~60 PFU of SINV-GFP2A (n = 8–10 per group), and survival was then assessed by daily observation.

FIGURE S2 | Sindbis virus (SINV)-GFP-3′UTR also causes susceptibility to co-infection when injected first. Same experiment and readout than for **Figure 2**, except that SINV-GFP-3′UTR was used instead of SINV-GFP2A. Two independent experiments pooled. **(A,B)** Survival curves; n = 48 fish for each condition. **(C,D)** Bacterial burden quantification; n = 8–10 larvae for each condition.

FIGURE S3 | qRT-PCR analysis of cytokine and inflammatory mediators induction, 6 h post *Shigella* injection. Gene expression was measured from individual zebrafish larvae sequentially co-injected with Sindbis virus (SINV) + *Shigella* (blue bars) or from individual zebrafish larvae injected with SINV alone (green bars) or with *Shigella* alone (red bars), and non-injected fish (CTRL, black bars) as control at 102 hpf (corresponding to 6 h post *Shigella* injection). N = 5 larvae per condition; note that these data were included among the values plotted on **Figure 5**.

FIGURE S4 | Cytokine expression upon *Shigella* + Sindbis virus (SINV) co-infection. Same settings and readout as for **Figure 5**, except that *Shigella* was injected first and SINV second (co-infected fish, cyan symbols). n = 5 larvae for each condition in total.

FIGURE S5 | Kinetics of *mmp9* induction upon Sindbis virus (SINV) + *Shigella* and *Shigella* + SINV co-infection. **(A,B)** *mmp9* induction was measured from individual zebrafish larvae sequentially co-injected with SINV-*Shigella* (blue curves) or *Shigella*-SINV (cyan curves), or from individual zebrafish larvae injected with SINV alone (green curves) or with *Shigella* alone (red curves), and non-injected fish (CTRL, black curves) as control.

FIGURE S6 | Possible correlation of cytokine expression levels and bacterial burden in Sindbis virus (SINV) + *Shigella* co-infected larvae. **(A–D)** Cytokine (*ifnphi1*, *il1b*, *tnfa*, *il10*) induction and bacterial content (*DsRed*) was measured from individual zebrafish larvae sequentially co-injected with SINV + *Shigella* (blue) or from individual zebrafish larvae injected with *Shigella* alone (red). Cytokine induction was correlated with bacterial content for each larva. Data plotted are from 3 independent experiments pooled (n = 15 larvae for each condition, same larvae showed in **Figure 5**); individual values are shown.

VIDEO S1 | (Related to **Figure 4C**) Impaired neutrophil recruitment upon Sindbis virus (SINV)-local *Shigella* co-infection. *Mpx*:GFP larvae were injected in the bloodstream with SINV-GFP at 72 hpf and subcutaneously with *Shigella*-DsRed at 96 hpf (panel on the right of the movie), or subcutaneously with *Shigella*-DsRed only at 96 hpf as a control (panel on the left of the movie), and live imaged in the trunk region (where the bacteria were injected) every 2 min from 30 mpi (t = 0 on the movie) to 3 h post infection (t = 2 h 33 on the movie) simultaneously by confocal fluorescence microscopy. Immediately after the starting of the acquisition, some neutrophils (GFP + bright cells) had already recruited to the bacteria in both conditions. In *Shigella*-only infected larvae (left), more neutrophils were progressively recruited to the bacteria (DsRed+), engulfing them quickly, and accumulating at the site of injection without any sign of cell death. In sequentially SINV + *Shigella*-injected larve (right), neutrophils poorly accumulated at the site of infection, and some underwent cell death upon engulfing bacteria. Note that SINV-GFP (GFP + diffuse signal) had replicated and invaded the muscle fibers of the trunk region. Maximum intensity projection is shown. Scale bar: 50 µm.

VIDEO S2 | (Related to **Figure 4E**) Impaired neutrophil survival upon Sindbis virus (SINV) + *Shigella* co-infection. A 72 hpf *mpx*:GFP larva was injected in the bloodstream with SINV-GFP and at 96 hpf subcutaneously with *Shigella*-DsRed, and live imaged immediately upon *Shigella* injection, every 1′30″ from 30 mpi (t = 0 on the movie) to 3 h 39 pi (t = 3 h 09 on the movie). Six engulfing neutrophils (GFP + bright cells, indicated by arrows on the movie) were manually tracked over time. Note the SINV-GFP infected cells (diffuse GFP signal, muscle fibers, and mesenchyme in the left bottom corner of the field). Injection site, maximum intensity projection. Scale bar: 20 µm.

REFERENCES

1. Bosch AATM, Biesbroek G, Trzcinski K, Sanders EAM, Bogaert D. Viral and bacterial interactions in the upper respiratory tract. *PLoS Pathog* (2013) 9:e1003057. doi:10.1371/journal.ppat.1003057
2. McCullers JA. The co-pathogenesis of influenza viruses with bacteria in the lung. *Nat Rev Microbiol* (2014) 12:252–62. doi:10.1038/nrmicro3231
3. Deng JC. Viral-bacterial interactions-therapeutic implications. *Influenza Other Respi Viruses* (2013) 7(Suppl 3):24–35. doi:10.1111/irv.12174
4. Almand EA, Moore MD, Jaykus LA. Virus-bacteria interactions: an emerging topic in human infection. *Viruses* (2017) 9:E58. doi:10.3390/v9030058
5. Arts RJW, Moorlag SJCFM, Novakovic B, Li Y, Wang S-Y, Oosting M, et al. BCG vaccination protects against experimental viral infection in humans through the induction of cytokines associated with trained immunity. *Cell Host Microbe* (2018) 23:89–100.e5. doi:10.1016/j.chom.2017.12.010
6. Hraiech S, Papazian L, Rolain J-M, Bregeon F. Animal models of polymicrobial pneumonia. *Drug Des Devel Ther* (2015) 9:3279. doi:10.2147/DDDT.S70993
7. McCullers JA, Bartmess KC. Role of neuraminidase in lethal synergism between influenza virus and *Streptococcus pneumoniae*. *J Infect Dis* (2003) 187:1000–9. doi:10.1086/368163
8. Ivanov S, Renneson J, Fontaine J, Barthelemy A, Paget C, Fernandez EM, et al. Interleukin-22 reduces lung inflammation during influenza A virus infection and protects against secondary bacterial infection. *J Virol* (2013) 87:6911–24. doi:10.1128/JVI.02943-12
9. Metzger DW, Sun K. Immune dysfunction and bacterial coinfections following influenza. *J Immunol* (2013) 191:2047–52. doi:10.4049/jimmunol.1301152
10. Guarda G, Braun M, Staehli F, Tardivel A, Mattmann C, Förster I, et al. Type I interferon inhibits interleukin-1 production and inflammasome activation. *Immunity* (2011) 34:213–23. doi:10.1016/j.immuni.2011.02.006
11. Navarini AA, Recher M, Lang KS, Georgiev P, Meury S, Bergthaler A, et al. Increased susceptibility to bacterial superinfection as a consequence of innate antiviral responses. *Proc Natl Acad Sci U S A* (2006) 103:15535–9. doi:10.1073/pnas.0607325103
12. Shahangian A, Chow EK, Tian X, Kang JR, Ghaffari A, Liu SY, et al. Type I IFNs mediate development of postinfluenza bacterial pneumonia in mice. *J Clin Invest* (2009) 119:1910–20. doi:10.1172/JCI35412
13. Nakamura S, Davis KM, Weiser JN. Synergistic stimulation of type I interferons during influenza virus coinfection promotes *Streptococcus pneumoniae* colonization in mice. *J Clin Invest* (2011) 121:3657–65. doi:10.1172/JCI57762
14. LeVine AM, Koeningsknecht V, Stark JM. Decreased pulmonary clearance of *S. pneumoniae* following influenza A infection in mice. *J Virol Methods* (2001) 94:173–86. doi:10.1016/S0166-0934(01)00287-7
15. Damjanovic D, Lai R, Jeyanathan M, Hogaboam CM, Xing Z. Marked improvement of severe lung immunopathology by influenza-associated pneumococcal superinfection requires the control of both bacterial replication and host immune responses. *Am J Pathol* (2013) 183:868–80. doi:10.1016/j.ajpath.2013.05.016
16. Rynda-Apple A, Robinson KM, Alcorn JF. Influenza and bacterial superinfection: illuminating the immunologic mechanisms of disease. *Infect Immun* (2015) 83:3764–70. doi:10.1128/IAI.00298-15
17. Mehta D, Petes C, Gee K, Basta S. The role of virus infection in deregulating the cytokine response to secondary bacterial infection. *J Interferon Cytokine Res* (2015) 35:925–34. doi:10.1089/jir.2015.0072
18. Robinson KM, McHugh KJ, Mandalapu S, Clay ME, Lee B, Scheller EV, et al. Influenza A virus exacerbates *Staphylococcus aureus* pneumonia in mice by attenuating antimicrobial peptide production. *J Infect Dis* (2014) 209:865–75. doi:10.1093/infdis/jit527
19. Sun K, Metzger DW. Influenza infection suppresses NADPH oxidase-dependent phagocytic bacterial clearance and enhances susceptibility to

secondary methicillin-resistant *Staphylococcus aureus* infection. *J Immunol* (2014) 192:3301–7. doi:10.4049/jimmunol.1303049
20. Levraud J-P, Palha N, Langevin C, Boudinot P. Through the looking glass: witnessing host-virus interplay in zebrafish. *Trends Microbiol* (2014) 22:490–7. doi:10.1016/j.tim.2014.04.014
21. Masud S, Torraca V, Meijer AH. Modeling infectious diseases in the context of a developing immune system. *Curr Top Dev Biol* (2017) 124:277–329. doi:10.1016/bs.ctdb.2016.10.006
22. Sullivan C, Matty MA, Jurczyszak D, Gabor KA, Millard PJ, Tobin DM, et al. Infectious disease models in zebrafish. *Methods Cell Biol* (2017) 138:101–36. doi:10.1016/bs.mcb.2016.10.005
23. Strauss JH, Strauss EG. The alphaviruses: gene expression, replication, and evolution. *Microbiol Rev* (1994) 58:491–562.
24. Passoni G, Langevin C, Palha N, Mounce BC, Briolat V, Affaticati P, et al. Imaging of viral neuroinvasion in the zebrafish reveals that Sindbis and chikungunya viruses favour different entry routes. *Dis Model Mech* (2017) 10(7):847–57. doi:10.1242/dmm.029231
25. Palha N, Guivel-Benhassine F, Briolat V, Lutfalla G, Sourisseau M, Ellett F, et al. Real-time whole-body visualization of chikungunya virus infection and host interferon response in zebrafish. *PLoS Pathog* (2013) 9:e1003619. doi:10.1371/journal.ppat.1003619
26. Anderson M, Sansonetti PJ, Marteyn BS. Shigella diversity and changing landscape: insights for the twenty-first century. *Front Cell Infect Microbiol* (2016) 6:45. doi:10.3389/fcimb.2016.00045
27. Mostowy S, Boucontet L, Mazon Moya MJ, Sirianni A, Boudinot P, Hollinshead M, et al. The zebrafish as a new model for the in vivo study of *Shigella flexneri* interaction with phagocytes and bacterial autophagy. *PLoS Pathog* (2013) 9:e1003588. doi:10.1371/journal.ppat.1003588
28. Renshaw SA, Loynes CA, Trushell DMI, Elworthy S, Ingham PW, Whyte MKB. A transgenic zebrafish model of neutrophilic inflammation. *Blood* (2006) 108:3976–8. doi:10.1182/blood-2006-05-024075
29. Kimmel CB, Ballard WW, Kimmel SR, Ullmann B, Schilling TF. Stages of embryonic development of the zebrafish. *Dev Dyn* (1995) 203:253–310. doi:10.1002/aja.1002030302
30. Hardwick JM, Levine B. Sindbis virus vector system for functional analysis of apoptosis regulators. *Methods Enzymol* (2000) 322:492–508. doi:10.1016/S0076-6879(00)22045-4
31. Hahn CS, Hahn YS, Braciale TJ, Rice CM. Infectious Sindbis virus transient expression vectors for studying antigen processing and presentation. *Proc Natl Acad Sci U S A* (1992) 89:2679–83. doi:10.1073/pnas.89.7.2679
32. Sun C, Gardner CL, Watson AM, Ryman KD, Klimstra WB. Stable, high-level expression of reporter proteins from improved alphavirus expression vectors to track replication and dissemination during encephalitic and arthritogenic disease. *J Virol* (2014) 88:2035–46. doi:10.1128/JVI.02990-13
33. Salgado-Pabon W, Celli S, Arena ET, Nothelfer K, Roux P, Sellge G, et al. *Shigella* impairs T lymphocyte dynamics in vivo. *Proc Natl Acad Sci U S A* (2013) 110:4458–63. doi:10.1073/pnas.1300981110
34. Levraud JP, Colucci-Guyon E, Redd MJ, Lutfalla G, Herbomel P. In vivo analysis of zebrafish innate immunity. *Methods Mol Biol* (2008) 415:337–63. doi:10.1007/978-1-59745-570-1_20
35. Colucci-Guyon E, Tinevez J-Y, Renshaw SA, Herbomel P. Strategies of professional phagocytes in vivo: unlike macrophages, neutrophils engulf only surface-associated microbes. *J Cell Sci* (2011) 124:3053–9. doi:10.1242/jcs.082792
36. Mazon-Moya MJ, Willis AR, Torraca V, Boucontet L, Shenoy AR, Colucci-Guyon E, et al. Septins restrict inflammation and protect zebrafish larvae from *Shigella* infection. *PLoS Pathog* (2017) 13:e1006467. doi:10.1371/journal.ppat.1006467
37. Mandic-Mulec I, Weiss J, Zychlinsky A. *Shigella flexneri* is trapped in polymorphonuclear leukocyte vacuoles and efficiently killed. *Infect Immun* (1997) 65:110–5.
38. Hathaway LJ, Griffin GE, Sansonetti PJ, Edgeworth JD. Human monocytes kill *Shigella flexneri* but then die by apoptosis associated with suppression of proinflammatory cytokine production. *Infect Immun* (2002) 70:3833–42. doi:10.1128/IAI.70.7.3833-3842.2002
39. Briolat V, Jouneau L, Carvalho R, Palha N, Langevin C, Herbomel P, et al. Contrasted innate responses to two viruses in zebrafish: insights into the ancestral repertoire of vertebrate IFN-stimulated genes. *J Immunol* (2014) 192:4328–41. doi:10.4049/jimmunol.1302611
40. Bergeron AC, Seman BG, Hammond JH, Archambault LS, Hogan DA, Wheeler RT. Candida and *Pseudomonas* interact to enhance virulence of mucosal infection in transparent zebrafish. *Infect Immun* (2017) 85:IAI.00475–17. doi:10.1128/IAI.00475-17
41. Storm N, Weyer J, Markotter W, Kemp A, Leman PA, Dermaux-Msimang V, et al. Human cases of Sindbis fever in South Africa, 2006-2010. *Epidemiol Infect* (2014) 142:234–8. doi:10.1017/S0950268813000964
42. Mosnier E, Ville M, Carvalho L, Mahamat A, Rousset D, Djossou F, Nacher M. *A Tree Hiding a Forest: An Outbreak of Influenza and Shigellosis in a Gold Miner Camp in the Tropical Forest of French Guiana, March 2013*. HAL: hal-01446818 (2015). Available from: https://hal.archives-ouvertes.fr/hal-01446818/document
43. Nguyen-Chi M, Phan QT, Gonzalez C, Dubremetz J-F, Levraud JP, Lutfalla G. Transient infection of the zebrafish notochord with *E. coli* induces chronic inflammation. *Dis Model Mech* (2014) 7:871–82. doi:10.1242/dmm.014498
44. Nguyen-Chi M, Laplace-Builhe B, Travnickova J, Luz-Crawford P, Tejedor G, Phan QT, et al. Identification of polarized macrophage subsets in zebrafish. *Elife* (2015) 4:e07288. doi:10.7554/eLife.07288
45. McCullers JA, Rehg JE. Lethal synergism between influenza virus and *Streptococcus pneumoniae*: characterization of a mouse model and the role of platelet-activating factor receptor. *J Infect Dis* (2002) 186:341–50. doi:10.1086/341462
46. Schliehe C, Flynn EK, Vilagos B, Richson U, Swaminanthan S, Bosnjak B, et al. The methyltransferase Setdb2 mediates virus-induced susceptibility to bacterial superinfection. *Nat Immunol* (2015) 16:67–74. doi:10.1038/ni.3046
47. Broggi A, Tan Y, Granucci F, Zanoni I. IFN-λ suppresses intestinal inflammation by non-translational regulation of neutrophil function. *Nat Immunol* (2017) 18:1084–93. doi:10.1038/ni.3821
48. Andrade EB, Alves J, Madureira P, Oliveira L, Ribeiro A, Cordeiro-da-Silva A, et al. TLR2-induced IL-10 production impairs neutrophil recruitment to infected tissues during neonatal bacterial sepsis. *J Immunol* (2013) 191:4759–68. doi:10.4049/jimmunol.1301752
49. Sun L, Guo RF, Newstead MW, Standiford TJ, Macariola DR, Shanley TP. Effect of IL-10 on neutrophil recruitment and survival after *Pseudomonas aeruginosa* challenge. *Am J Respir Cell Mol Biol* (2009) 41:76–84. doi:10.1165/rcmb.2008-0202OC
50. Pylaeva E, Lang S, Jablonska J. The essential role of type I interferons in differentiation and activation of tumor-associated neutrophils. *Front Immunol* (2016) 7:629. doi:10.3389/fimmu.2016.00629
51. Varela M, Romero A, Dios S, van der Vaart M, Figueras A, Meijer AH, et al. Cellular visualization of macrophage pyroptosis and interleukin-1β release in a viral hemorrhagic infection in zebrafish larvae. *J Virol* (2014) 88:12026–40. doi:10.1128/JVI.02056-14
52. López-Muñoz A, Roca FJ, Sepulcre MP, Meseguer J, Mulero V. Zebrafish larvae are unable to mount a protective antiviral response against waterborne infection by spring viremia of carp virus. *Dev Comp Immunol* (2010) 34:546–52. doi:10.1016/j.dci.2009.12.015
53. Kuri P, Schieber NL, Thumberger T, Wittbrodt J, Schwab Y, Leptin M. Dynamics of in vivo ASC speck formation. *J Cell Biol* (2017) 216:jcb.201703103. doi:10.1083/jcb.201703103
54. Eberl G. Immunity by equilibrium. *Nat Rev Immunol* (2016) 16:524–32. doi:10.1038/nri.2016.75
55. Wiley DS, Redfield SE, Zon LI. Chemical screening in zebrafish for novel biological and therapeutic discovery. *Methods Cell Biol* (2017) 138:651–79. doi:10.1016/bs.mcb.2016.10.004

Conflict of Interest Statement: The authors declare that the research was conducted in the absence of any commercial or financial relationships that could be construed as a potential conflict of interest.

The reviewer SM declared a past co-authorship with the authors to the handling Editor.

Copyright © 2018 Boucontet, Passoni, Thiry, Maggi, Herbomel, Levraud and Colucci-Guyon. This is an open-access article distributed under the terms of the Creative Commons Attribution License (CC BY). The use, distribution or reproduction in other forums is permitted, provided the original author(s) and the copyright owner are credited and that the original publication in this journal is cited, in accordance with accepted academic practice. No use, distribution or reproduction is permitted which does not comply with these terms.

frontiers in Immunology

REVIEW
published: 04 January 2018
doi: 10.3389/fimmu.2017.01906

Eat Prey, Live: *Dictyostelium discoideum* As a Model for Cell-Autonomous Defenses

Joe Dan Dunn, Cristina Bosmani, Caroline Barisch, Lyudmil Raykov, Louise H. Lefrançois, Elena Cardenal-Muñoz, Ana Teresa López-Jiménez and Thierry Soldati*

Faculty of Sciences, Department of Biochemistry, University of Geneva, Geneva, Switzerland

The soil-dwelling social amoeba *Dictyostelium discoideum* feeds on bacteria. Each meal is a potential infection because some bacteria have evolved mechanisms to resist predation. To survive such a hostile environment, *D. discoideum* has in turn evolved efficient antimicrobial responses that are intertwined with phagocytosis and autophagy, its nutrient acquisition pathways. The core machinery and antimicrobial functions of these pathways are conserved in the mononuclear phagocytes of mammals, which mediate the initial, innate-immune response to infection. In this review, we discuss the advantages and relevance of *D. discoideum* as a model phagocyte to study cell-autonomous defenses. We cover the antimicrobial functions of phagocytosis and autophagy and describe the processes that create a microbicidal phagosome: acidification and delivery of lytic enzymes, generation of reactive oxygen species, and the regulation of Zn^{2+}, Cu^{2+}, and Fe^{2+} availability. High concentrations of metals poison microbes while metal sequestration inhibits their metabolic activity. We also describe microbial interference with these defenses and highlight observations made first in *D. discoideum*. Finally, we discuss galectins, TNF receptor-associated factors, tripartite motif-containing proteins, and signal transducers and activators of transcription, microbial restriction factors initially characterized in mammalian phagocytes that have either homologs or functional analogs in *D. discoideum*.

Keywords: *Dictyostelium discoideum*, cell-autonomous defense, phagocytosis, autophagy, metal poisoning, nutritional immunity, mononuclear phagocyte system, host–pathogen interactions

OPEN ACCESS

Edited by:
Geanncarlo Lugo-Villarino, UMR5089 Institut de Pharmacologie et de Biologie Structurale (IPBS), France

Reviewed by:
Pierre Stallforth, Leibniz-Institut für Naturstoff-Forschung und Infektionsbiologie, Hans Knöll Institut, Germany
Christopher West, University of Georgia, United States
Salvatore Bozzaro, Università degli Studi di Torino, Italy

****Correspondence:***
Joe Dan Dunn
joedan.dunn@unige.ch

Specialty section:
This article was submitted to Microbial Immunology, a section of the journal Frontiers in Immunology

Received: *26 September 2017*
Accepted: *13 December 2017*
Published: *04 January 2018*

Citation:
Dunn JD, Bosmani C, Barisch C, Raykov L, Lefrançois LH, Cardenal-Muñoz E, López-Jiménez AT and Soldati T (2018) Eat Prey, Live: Dictyostelium discoideum As a Model for Cell-Autonomous Defenses. Front. Immunol. 8:1906. doi: 10.3389/fimmu.2017.01906

INTRODUCTION

The mononuclear phagocyte system (MPS), comprising monocytes, macrophages, and dendritic cells, is the first line of defense against infection. MPS cells monitor blood and tissue for the presence of microbes and respond to conserved molecules produced by and/or to damage caused by potential pathogens. These signals trigger innate-immune pathways that activate cell-autonomous defense mechanisms and secretion of intercellular signals that orchestrate inflammatory and subsequent adaptive immune responses.

Cell-autonomous defense mechanisms, which exist in MPS cells and also non-immune cells, provide a rapid antimicrobial response and evolved from the predator–prey relationship among the ancestors of current eukaryotes and prokaryotes (1, 2). In MPS cells, cell-autonomous defenses include phagocytosis and autophagy, processes that originated in ancient eukaryotes

for nutrient acquisition and reallocation. Indeed, the basic components of these pathways are conserved in immune cells of all metazoa and in bacterivorous and fungivorous single-celled eukaryotes such as amoebae. Microbial mechanisms to subvert cell-autonomous defenses predate metazoa and likely originated as resistance to predation by single-celled eukaryotes. Given this evolutionary context, amoebae are relevant surrogate phagocytes for the study of the conserved innate-immune responses of MPS cells and of microbial mechanisms to resist killing. Although the infection of amoebae cannot completely recapitulate the complexities of host–pathogen interactions in metazoa, the innate defenses of MPS cells establish the critical initial immune response to microbes, and MPS cells are often the physical interface of host and intracellular pathogens. Valuable insight can thus be gained by studying the interactions between microbes and amoebae that rely solely on cell-autonomous defenses for survival.

In this review, we focus on the use of the soil dwelling, social amoeba *Dictyostelium discoideum* as a model phagocyte to study the interactions between intracellular pathogens and cell-autonomous defense mechanisms of MPS cells. We cover phagocytosis with an emphasis on phagosome maturation and the mechanisms used to create an antimicrobial environment within the phagosome. These mechanisms include the delivery of lytic enzymes, the generation of reactive oxygen species (ROS), and the manipulation of the concentrations of divalent metals to either poison microbes or inhibit their metabolic activity. We describe autophagy as a defense pathway that responds when phagocytosis is insufficient to eliminate infection. We also highlight microbial interference with these defense responses first elucidated using *D. discoideum*. Finally, we discuss microbial restriction factors, initially characterized in MPS cells, that have either sequence homologs or potentially functional analogs in *D. discoideum*. Determining their contribution to cell-autonomous defense mechanisms in this amoeba will further strengthen its usefulness as a model for host–pathogen interactions.

PREDATION RESISTANCE, VIRULENCE, AND CELL-AUTONOMOUS DEFENSES

Given the complex interactions between pathogenic microorganisms and their metazoan hosts, it is difficult to pinpoint the origins of microbial virulence. How would a naïve bacterium encountering an elaborate immune response for the first time persist long enough to evolve mechanisms to counteract antimicrobial defenses? On the host side, why are such extensive immune responses in place? When did it all begin? An emerging concept in host–pathogen interactions is that microbial virulence evolved from selective forces in the environment such as the pressure to resist predation by amoebae and other protozoa (3–6).

In addition to competing for nutrients and adapting to variations in environmental conditions such as temperature and moisture, successful microbes avoid being a meal for predatory protozoa. These resistance mechanisms include avoidance of phagocytosis, e.g., masking of the microbial surface and biofilm formation, avoidance of digestion, e.g., inhibition of phagosome maturation, escape from the phagosome, the killing of the predator by toxin secretion pre- or post-phagocytosis, and the use of specialized secretion systems (3). On the predator side, the advent of resistance in turn selected for more robust strategies to kill bacteria and/or counteract this resistance. This ancient fight for survival among single-celled species with short generation times and large population sizes provided the context for the evolution of virulence and cell-autonomous defenses. As metazoa evolved and gained complexity, these defenses were conserved and also expanded (7, 8). Concurrently, some microbes evolved mechanisms not just to avoid killing but to survive inside hosts and exploit them for resources.

The coevolution of host and microbes beginning at the single-celled stage provides a plausible explanation for the conservation of cell-autonomous defenses. It is important to remember that single-celled eukaryotic predators continued to evolve and that successful cell-autonomous defense strategies are present in extant species such as *D. discoideum*. Bacteria must therefore contend with similar defense mechanisms in macrophages and amoebae; consequently, predation selects for bacterial survival strategies that are likely to resist killing by MPS cells (9–12). Another consequence of this conservation is that amoebae can select for and act as reservoirs of microbes that can infect humans, including *Mycobacterium* species, *Legionella pneumophila*, and *Vibrio cholera* (13–15). This evolutionary history makes amoebae ideal, relevant model phagocytes to study host–pathogen interactions (16–19).

Dictyostelium discoideum

Dictyostelium discoideum belongs to the Amoebozoa phylum, which diverged from the Opisthokonts, the phylum to which the animals belong, after sharing a common ancestor with plants. During its growth phase, the amoeba replicates by binary fission and employs phagocytosis to kill and extract nutrients from bacteria in the soil. Upon nutrient depletion, starvation induces amoebae to undergo a developmental cycle in which approximately 100,000 cells aggregate by chemotaxing toward cyclic AMP, differentiate into multiple cell types, and transition through several multicellular stages to ultimately produce the fruiting body that comprises a spore-containing sorus resting upon a stalk of dead cells (**Figure 1**) (20–22). Depending on environmental conditions, the early multicellular stage continues to develop in place or transitions to a motile slug that migrates away from ammonia and toward heat, light, and oxygen before fruiting body culmination (20–25). When development is initiated underground these cues guide the slug to the soil surface, where spore dispersion is more likely.

Due to its multicellular cycle, *D. discoideum*, referred to as a social amoeba, is used as a model to study aspects of development including intercellular signaling (27) [reviewed in Ref. (22)], quorum sensing (28), cell–cell recognition (29), cell fate determination (30), tissue patterning (31), and even societal concepts such as cooperativity and altruism (32). It is also an established model for basic cell biological processes, including phagocytosis (33), macropinocytosis (34), chemotaxis (35), autophagy (36), and

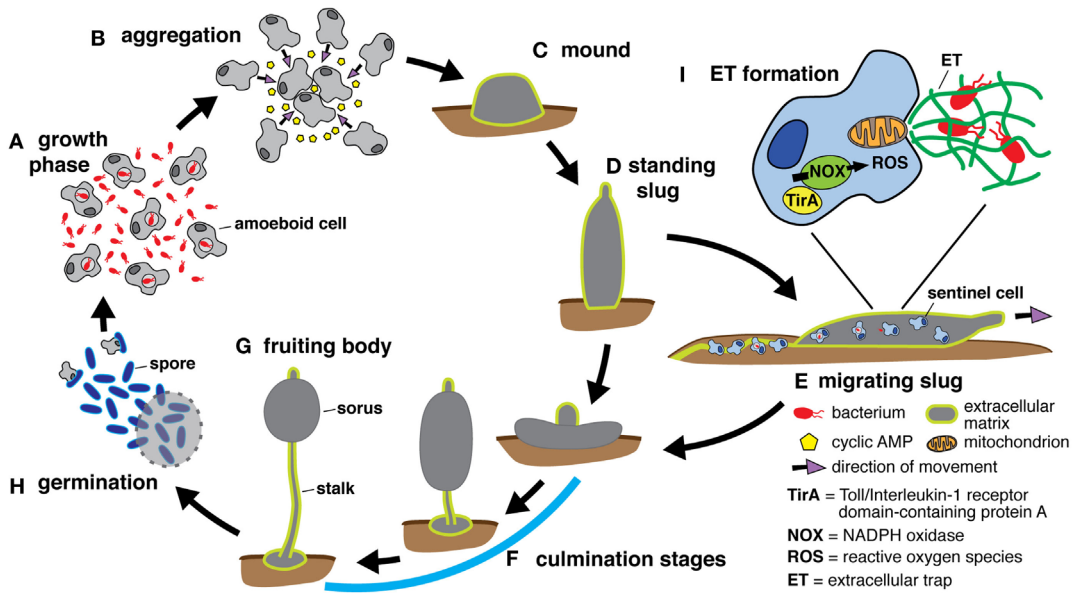


FIGURE 1 | The *Dictyostelium discoideum* life cycle includes multicellular stages. **(A)** During the growth phase of development, amoeboid cells feed on bacteria and replicate by binary fission. The development cycle is initiated upon resource depletion, and aggregation occurs when starving cells secrete cyclic AMP to recruit additional cells **(B)**. The aggregating cells organize to form the mound stage enclosed within an extracellular matrix composed of cellulose and mucopolysaccharide (26) **(C)** and continue to develop into the standing slug **(D)**. Depending on its environment, the standing slug either falls over to become a migrating slug that moves toward heat and light **(E)** or proceeds directly to the culmination stages **(F)** that ultimately produce the fruiting body, which consists of a spore-containing structure, the sorus, held aloft by a stalk of dead cells **(G)**. Spores are released from the sorus and germinate into growing cells **(H)**. Under optimal conditions, the developmental cycle takes around 24 h. If the slug forms underground, it migrates toward the surface to maximize spore dissemination. To protect itself from infection during migration, the slug possesses a rudimentary immune system comprising phagocytic sentinel cells. These cells move throughout the slug, take up bacteria and toxins, and are shed along with extracellular matrix as the slug moves **(E)**. In response to bacteria, sentinel cells release extracellular traps, derived from mitochondrial DNA, *via* an unknown mechanism involving NADPH oxidase (NOX)-generated reactive oxygen species (ROS) and TirA, a soluble protein containing a toll/interleukin 1 receptor domain **(I)**.

oxygen sensing (37), and the functions of proteins implicated in human diseases including Alzheimer's and Parkinson's (38–41). Indeed, this amoeba has proven to be a versatile model organism and is gaining traction as an attractive alternative to animal models (42, 43).

Dictyostelium discoideum has been used as a host cell for *L. pneumophila* (44–47), *Mycobacterium* species (48–51), *V. cholera* (17), *Francisella noatunensis* (52, 53), *Pseudomonas aeruginosa* (16), *Salmonella enterica* (54), and other intracellular pathogens (55). Moreover, its genome encodes numerous homologs of proteins and protein domains involved in sensing and responding to microbes by macrophages (5) (http://dictybase.org). The conservation of macropinocytosis, chemotaxis, phagocytosis, and autophagy pathways in *D. discoideum* make it a model MPS cell. Here we focus on phagocytosis and autophagy within the context of cell-autonomous defenses. Macropinocytosis and chemotaxis are beyond the scope of this review and have been covered extensively elsewhere [for reviews on chemotaxis (56, 57); for reviews on macropinocytosis (58, 59)].

From a practical standpoint, its amenability to experimentation also makes *D. discoideum* an ideal model organism. It is easily cultivatable and can be grown axenically in liquid media, which enables analysis of mutant strains defective for growth on bacteria. Cultures can be readily scaled up for biochemical and cell biological techniques (43) as well as high-throughput genetic and drug discovery screens (60–62). It is also well suited for microscopy including live-cell imaging (63). An extensive molecular genetic toolkit has been developed for the generation of mutants and ectopic gene expression (64). The haploid genome of multiple strains and closely related species have been sequenced (65–68), and numerous RNAseq and transcriptomic analyses have been performed (69, 70). The community's online resource, dictyBase, provides a central location to access sequence data, techniques, and available mutants and plasmids (71) (http://dictybase.org). Relevant its use as a model phagocyte, there are established protocols for infecting *D. discoideum* with various bacterial pathogens (63, 72, 73) and for monitoring and quantifying autophagy (74).

PHAGOCYTOSIS

Phagocytosis is the process that allows engulfment of particles larger than 200 nm and is used by MPS cells to ingest and kill pathogens as well as to activate the adaptive immune response through antigen presentation. The phagocytosis maturation pathway is highly conserved between MPS cells and *D. discoideum*, which uses the process for feeding (8). In a simplified view, the particle to ingest is recognized by surface receptors, and this interaction triggers a signaling cascade that stimulates polymerization of actin to deform the membrane around the

particle. After closure of the phagocytic cup, the newly formed phagosome undergoes maturation, a series of steps necessary to render the phagosome a highly acidic, degradative and oxidative compartment (**Figure 2**). Many pathogens, such as *L. pneumophila*, *S. enterica*, and *Mycobacterium* spp., have evolved ways to escape the phagosome or subvert its maturation to replicate within the host cell. In this section, we will briefly summarize the phagocytosis maturation steps in *D. discoideum* and how this model phagocyte has been used to extend our knowledge of several infectious diseases. It should be noted that studies using *D. discoideum* as a model phagocyte have mainly been performed with axenic laboratory strains. These strains are able to grow in the absence of bacteria due to a null mutation in the gene encoding the Ras-regulating neurofibromin, which results in enlarged macropinosomes that facilitate uptake of sufficient nutrients from liquid media to support growth and also enables the mutants to phagocytose larger particles than wild-type strains (75). Effects of this mutation on phagosome maturation have not been reported.

Particle Recognition and Phagocytosis Initiation

Innate-immune cells can recognize several pathogen-associated molecular patterns (PAMPs) secreted or present at the bacterial cell wall *via* specific pathogen recognition receptors (PRRs). In mammals, these include toll-like receptors (TLRs), integrins, scavenger receptors, and C-type lectins (76). TLRs monitor the cell surface and endocytic compartments and activate cell-autonomous defenses upon detection of PAMPs, while lectins, scavenger receptors, and integrins function as phagocytic receptors that bind to particles and are able to trigger uptake even in non-phagocytic cells (76). TLRs contain ligand-binding leucine-rich repeats (LRRs) in the luminal/extracellular domains and a toll/interleukin 1 receptor (TIR) domain in the cytoplasmic tail that mediates protein–protein interactions. *D. discoideum* does not have TLRs, but two cytosolic proteins with TIR domains, TirA and TirB, have been identified. Depletion of TirA inhibits growth on a laboratory strain of *Klebsiella* used as a food bacterium, but not in media (77). How TirA is involved in sensing and/or induction of phagocytic uptake remains to be studied. The *D. discoideum* genome encodes >150 LRR-containing proteins, but whether they function as PRRs remains to be determined (5).

In *D. discoideum*, only a few phagocytic receptors have been molecularly identified so far (5). The most studied are the integrin-like Sib (similar to integrin-β) family of proteins, comprising five members (SibA-E). Like human integrins, they contain a von Willebrand factor type A and a glycine-rich transmembrane domain and can interact with the actin-binding protein talin (78). Two members of the family, SibA and SibC, are directly involved in adhesion to substrate and to particles (78). Phg1a, a member of the TM9 family, and SadA were previously identified as phagocytic receptors (79, 80); however, recent findings show that these two proteins are instead involved in regulating surface levels of SibA (81).

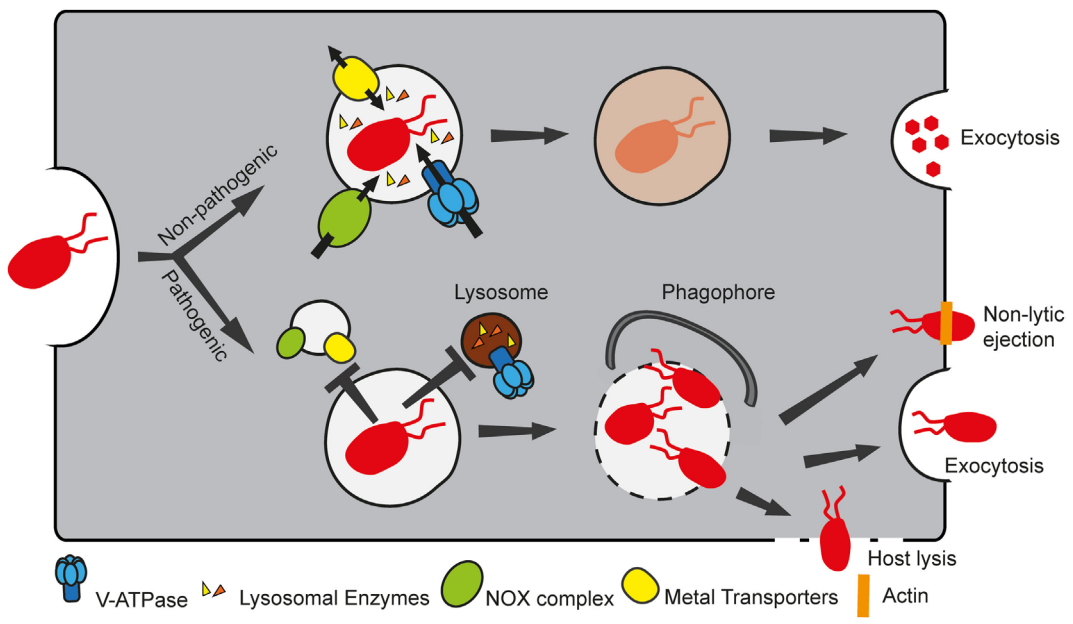


FIGURE 2 | Non-pathogenic and pathogenic bacteria follow different fates in *Dictyostelium discoideum*. *D. discoideum* takes up bacteria by phagocytosis. Non-pathogenic food bacteria follow the normal phagosomal maturation pathway, whereby the phagosome acquires several components, including the vacuolar ATPase (V-ATPase), lysosomal enzymes, the NADPH oxidase (NOX) complex, and several metal transporters to create a microbicidal compartment that digests and kills bacteria. Intracellular pathogens, however, are able to manipulate the maturation program, by preventing the phagosome from becoming bactericidal, thus ensuring proliferation in a "friendly" compartment. In addition, certain pathogens can eventually escape the compartment. In this case, they can either be recaptured by autophagy, or exit the host cell by exocytosis, or by lytic or non-lytic processes.

Lectins and scavenger receptors might also function as phagocytic receptors in *D. discoideum*. Three homologs of scavenger receptor class B proteins in mammals, LmpA, LmpB, and LmpC, are present in *D. discoideum*. LmpB is found on lipid rafts at the plasma membrane and in early phagocytic compartments and may function as a phagocytic receptor (82–84). It is thought that *D. discoideum* also possesses lectin-like receptors, as it was shown to be able to bind specifically to certain sugar derivatives (85, 86).

A well-studied chemoattractant and phagocytosis stimulator for *D. discoideum* is folate, a metabolite secreted by certain bacteria. Recently, Pan and colleagues identified fAR1, a G-protein coupled receptor for folic acid involved in signaling and initiation of uptake but not binding of bacteria (87). Presumably, the cytoskeletal rearrangements downstream of fAR1 that facilitate chemotaxis can also initiate phagocytosis when a burst of fAR1 activation occurs around a bacterium that is a concentrated source of folate. *D. discoideum* sensing of bacterial capsule independent of folate has also been described but not further characterized (88).

Actin Dynamics and Phosphatidylinositol Phosphates (PIPs)

After binding of ligands to their receptors, heterotrimeric G proteins are involved in downstream signaling to initiate phagocytosis through F-actin rearrangements. In *D. discoideum*, the G4αGβγ complex has been proposed to be activated by the fAR1 folate receptor, was shown to be implicated in particle uptake, and is therefore the most likely candidate involved in signaling from the phagocytic receptors to drive actin polymerization (87, 89). F-actin rearrangements occur at the uptake site to drive formation of pseudopods and the phagocytic cup. F-actin polymerization at the uptake site is driven by the Arp2/3 complex, an actin nucleation factor, and its activator, the SCAR/WAVE complex, in both macrophages and *D. discoideum* (90, 91). In addition, several other actin-binding proteins, such as profilins, cofilins, and Abp1, are present during the formation of the phagocytic cup [(92, 93), for a more detailed review on the phagocytic process in *D. discoideum*, see Ref. (94)]. Regulation of actin dynamics and subsequent trafficking events by Rho GTPases is also conserved in *D. discoideum,* with Rac1 homologs (RacA, B, C, and G) thought to be the main regulators of phagocytic uptake. Notably, Rac1 is involved in FcγR-mediated phagocytosis in macrophages [for a comprehensive review on Rho signaling, see Ref. (95)].

Phosphatidylinositol phosphates are important players during phagocytic uptake and maturation because they provide an identity to each compartment. PIP dynamics are well conserved between macrophages and *D. discoideum*. Briefly, phosphatidylinositol (4,5)-bisphosphate $PI(4,5)P_2$ is the predominant PIP of the plasma membrane and is involved in recruiting and activating actin-binding proteins and nucleation-promoting factors. After receptor engagement, $PI(4,5)P_2$ is phosphorylated into $PI(3,4,5,)P_3$ by phosphatidylinositol 3-kinase and hydrolyzed into diacylglycerol and inositol (1,4,5)-trisphosphate, second messengers involved in calcium release and activation of further signaling cascades, by the phospholipase C kinase. Decrease of $PI(4,5)P_2$ around the uptake site is necessary to then allow actin disassembly and closure of the phagocytic cup. In addition, closure of the phagocytic cup requires Dd5P4, the *D. discoideum* homolog of the phosphatase OCRL, which dephosphorylates $PI(3,4,5)P_3$ into $PI(3,4)P_2$ (96–98). Extensive recycling of plasma membrane components, including adhesion molecules, is a common feature shared by *D. discoideum* and macrophages in the early phases of phagosome formation, and in both organisms this step is regulated by the WASH complex, an Arp2/3 activator (99–101).

Phagosome Maturation

After closure of the phagocytic cup, the ingested particle is found in a closed compartment termed the phagosome. Extensive proteomic analyses as well as more recent live microscopy experiments have demonstrated the extraordinary plasticity of this organelle and the high degree of conservation of the phagosome maturation pathway between mammals and *D. discoideum* (8, 84). Phagosome maturation is a well-orchestrated series of events, which ensures killing and digestion of ingested bacteria (**Figure 3**). In a simplified view, Rab GTPases, notably Rab5 and Rab7, act as the masterminds of phagosome maturation by sequentially recruiting effectors involved in the various maturation steps [for an extensive review, see Ref. (102)]. In macrophages, Rab5 and its effectors are responsible for docking and fusion of endocytic compartments with the nascent phagosome and for acquisition of early phagosomal markers (103, 104). Subsequently, Rab7 ensures fusion with late-endosomal/lysosomal compartments and thus delivery of the lysosomal digestive content into the phagosome (104, 105). Rab GTPases are highly conserved at the protein sequence level between mammals and *D. discoideum*; indeed, this amoeba has homologs of most mammalian Rab GTPases that have been reported to be associated with phagosomes (102). *D. discoideum* Rab7 is recruited as early as 1–3 min after phagosome closure and regulates delivery of lysosomal proteins (106, 107). The localization and function of *D. discoideum* Rab5 have not been reported.

Recruited within minutes to the phagosome, the H^+-vacuolar ATPase (V-ATPase) is the main agent of acidification and pumps protons inside the phagosome thanks to ATP hydrolysis (108). By creating a proton gradient, the V-ATPase is a crucial complex not only for the killing and digestion of bacteria but also for the progression of the maturation program. Notably, the proton gradient is necessary for proper delivery and activity of lysosomal enzymes, as well as for the function of ion transporters, involved in poisoning by or deprivation of metals (detailed below). The V-ATPase has been shown to be delivered by fusion with lysosomal vesicles or tubules in *D. discoideum* and macrophages, respectively (108–110). Rapid acidification of the compartment ensues, with the lowest pH reached between 10 and 30 min after phagosome formation, depending on the measuring method (93, 111). In contrast to macrophages, whose phagosomes were reported to reach a pH of 4.5–5, *D. discoideum* phagosomes are more acidic, with a pH as low as 3.5–4 (111–113).

Although unprocessed antigens have been shown to be regurgitated from late-endosomal compartments in dendritic cells to

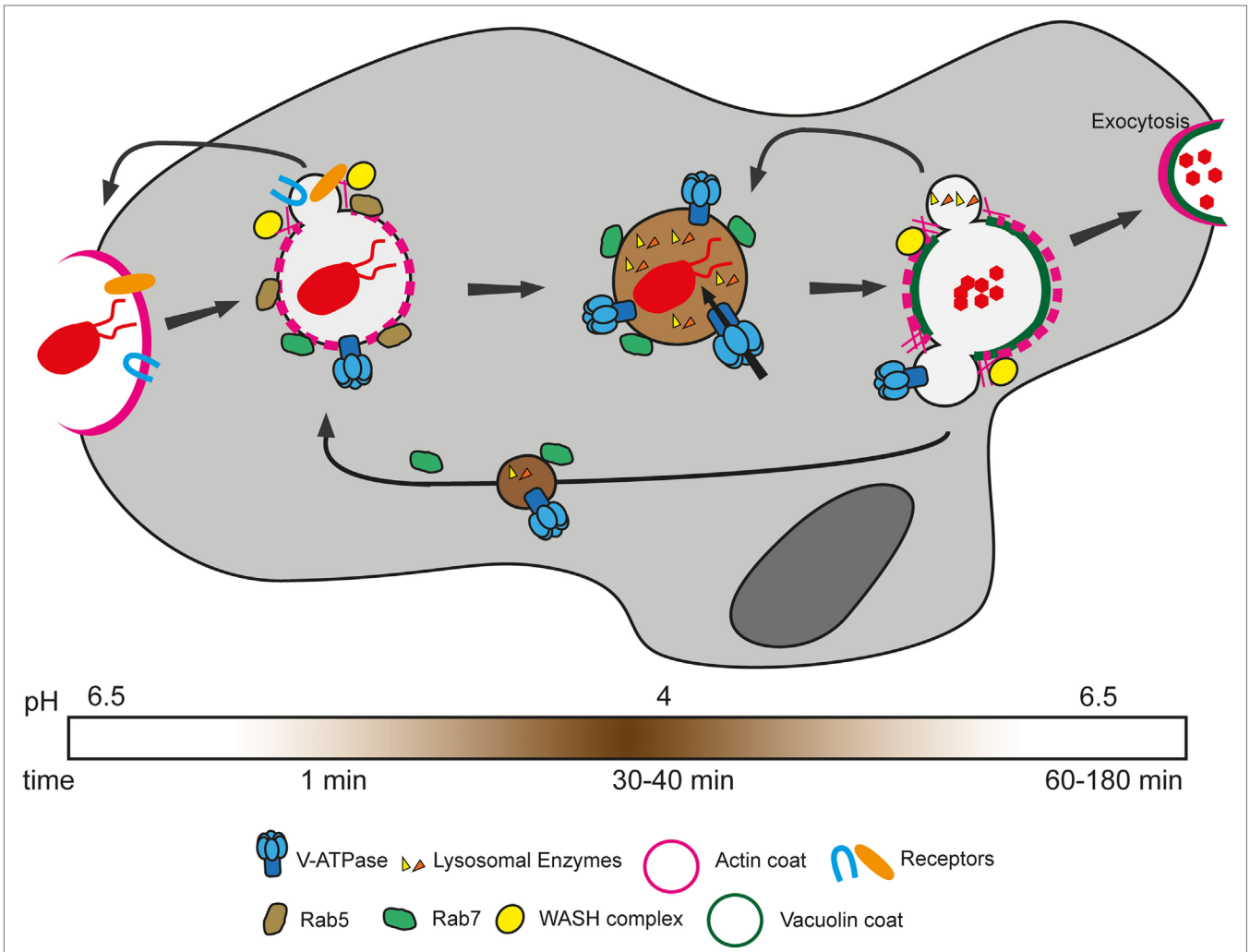


FIGURE 3 | Phagosome maturation in *Dictyostelium discoideum*. Bacteria are recognized and sensed by various phagocytic and/or signaling receptors. This triggers signaling cascades that allow actin polymerization and deformation of the membrane to engulf the particle. After closure of the phagosome, bacteria are enclosed in an early phagosome, which gradually loses its actin coat and is characterized by the presence of Rab5. As early as 1 min after uptake, Rab7 is recruited to the phagosome, enabling fusion with lysosomes. Meanwhile, phagocytic receptors and plasma membrane proteins are recycled to the cell surface through actin polymerization induced by the WASH complex through Arp2/3 activation. The proton pump vacuolar ATPase (V-ATPase) is also acquired early in the maturation, ensuring rapid decrease of the luminal pH. Lysosomal enzymes, comprising proteases, are acquired in subsequent waves of delivery and function at low pH to degrade bacterial components. After about 40 min, the V-ATPase and lysosomal enzymes are recycled by the WASH complex in separate waves of recycling. Finally, non-digested bacterial remnants are expelled by exocytosis.

allow antigen uptake by other MPS cells (114, 115), in general, the acidic phagosome of MPS cells is thought of as a dead-end for ingested bacteria. In contrast, the acidic *D. discoideum* phagosome matures into a postlysosome. The V-ATPase and lysosomal enzymes were shown to be retrieved in several subsequent waves of recycling mediated by the WASH complex, which drives local actin polymerization (116, 117). The WASH complex is a nucleation-promoting factor necessary for the activation of the Arp2/3 complex and actin polymerization in both mammals and *D. discoideum* (99, 100, 117). During retrieval of the V-ATPase, the phagosome reaches its neutral pH, and progressively acquires the postlysosomal markers vacuolin A and B, homologs of the mammalian lipid raft-associated flotillins (118–120). The postlysosome is also characterized by the presence of an actin coat and the actin-binding protein coronin (118). This compartment then fuses with the plasma membrane in a mechanism akin to exocytosis to expel its non-digested materials. Interestingly, this process is reminiscent of exocytosis of secretory lysosomes in mammalian cytotoxic cells of the immune system (121). In mammals, lysosomes were shown to fuse with the plasma membrane upon increase of cytosolic Ca^{2+} concentration. In *D. discoideum*, Ca^{2+} was also shown to be involved in exocytosis, with mucolipin, a Ca^{2+} transporter, involved in regulating this process. Mucolipin is thought to pump Ca^{2+} inside postlysosomes, thereby inhibiting fusion with the plasma membrane by decreasing local Ca^{2+} concentration (122).

Microbial Manipulation of *D. discoideum* Phagocytosis

Certain intracellular bacterial pathogens are known for subverting phagosome maturation to prevent the formation of an unfriendly bactericidal compartment and to enable replication within the host cell. *L. pneumophila*, a Gram-negative bacterium that causes Legionnaire's disease, is able to arrest early phagosomal maturation. In fact, the V-ATPase and other early endocytic markers are not delivered to the *Legionella*-containing vacuole (LCV) in either *D. discoideum* or macrophages (123). The endoplasmic reticulum (ER) is recruited in proximity to and fuses with the LCV, which becomes enriched in ER markers such as calnexin and calreticulin. This enrichment of ER markers is a consequence of a major strategy used by *L. pneumophila* to proliferate inside the host cell, which is termed identity theft and consists of changing the identity of its compartment to resemble the ER by recruiting different GTPases and PIPs (124, 125). For example, thanks to several bacterial effectors secreted through its type 4 secretion system, this pathogen is able to change the PIP composition of the phagosome by notably acquiring PI(4)P, a PIP normally associated with the *trans*-Golgi, ER, and plasma membrane (47). Other proteins involved in PIP dynamics and phagosome maturation, such as phosphatidylinositol 3-kinase and Dd5P4 have been shown to restrict *L. pneumophila* growth in *D. discoideum* (45, 46). *D. discoideum* has been used successfully to isolate and characterize the proteome of LCVs (44, 126). These studies have highlighted the importance of ER/Golgi small GTPases, such as Arf1 and Rab1, in gradually modifying the identity of the LCV. Rab8, a *trans*-Golgi-associated Rab GTPase, has also been detected at the LCV membrane and been shown to play a role in the association of SidC, a bacterial effector that mediates ER recruitment (44). Interestingly, Hoffmann and colleagues compared the LCV proteomes purified from murine macrophages and *D. discoideum* and uncovered that, if only considering proteins with conserved roles in these two organisms, about 50% of LCV-associated proteins were found in both organisms (126). These include the aforementioned Arf1, Rab8, and Rab1, as well as proteins involved in lipid metabolism, suggesting that *L. pneumophila* uses similar mechanisms to replicate in *D. discoideum* and macrophages and further corroborating the case that *D. discoideum* is an excellent model to study *L. pneumophila* infection.

Like *Legionella pneumophila*, albeit with completely different strategies, *Mycobacterium* spp. manipulate the phagosome maturation pathway. In fact, *Mycobacterium tuberculosis*, the causative agent of tuberculosis, and *Mycobacterium marinum*, a closely related mycobacterium that infects frogs and fish, prevent acquisition of the V-ATPase in macrophages (127). This was confirmed in *D. discoideum*, where it was shown that *M. marinum* is able to prevent accumulation of the V-ATPase and of cathepsin D (48). Recently, it was proposed that the WASH complex plays a role in preventing association of the V-ATPase with the mycobacteria-containing vacuole (MCV) by inducing polymerization of actin around the MCV, which probably prevents fusion with acidic vesicles. This mechanism was first studied in *D. discoideum*, but further confirmed in human macrophages with both *M. tuberculosis* and *M. marinum* (128). Of note, the mechanism of escape of cytosolic *M. marinum* from the host cell, termed ejection, and of cell-to-cell spreading has been well characterized and studied using *D. discoideum* as a host model [(49); reviewed in Ref. (129, 130)]. Interestingly, *D. discoideum* has also been extensively used as a model phagocyte to screen for new mycobacterial virulence factors (131–134).

MICROBICIDAL PHAGOSOME

Dictyostelium discoideum and macrophages employ conserved strategies to kill bacteria. As discussed previously, the V-ATPase has a central role in phagosome acidification; however, a low pH is not sufficient *per se* to kill bacteria. In fact, the phagosome acquires a series of proteases, hydrolases, lysozymes, and antimicrobial peptides necessary to breakdown several bacterial components or disrupt membrane integrity. Moreover, microbes can be poisoned and killed by transport of certain metals or by the production of ROS inside the compartment. Furthermore, metals can be pumped out of the phagosome to prevent bacterial growth. These bacterial-control strategies will be described in this section.

Lysozymes and Lysosomal Enzymes

Lysozymes, glycosidases that digest the peptidoglycan layer present in the cell wall of bacteria, belong to the Aly family in *D. discoideum* (135). Upregulation of lysozyme expression differs depending on the bacteria used as food. *D. discoideum* grown on Gram-positive bacteria upregulate AlyA, AlyB, AlyC, and AlyD whereas growth on Gram-negative bacteria leads to an increase in AlyL expression (136).

Lysosomal enzymes comprise several classes of enzymes involved in hydrolysis of sugar groups, such as mannosidases, or peptide bonds, such as proteases, and have been involved extensively in resistance to certain pathogens as well as bacterial killing in MPS cells. For instance, cysteine and serine cathepsins have been implicated in resistance to and killing of *Staphylococcus aureus* in neutrophils and macrophages (137, 138). More recently, *M. tuberculosis* was shown to downregulate expression and inhibit activity of cysteine proteases in macrophages, thus ensuring its replication (139). Cathepsin D, an aspartic protease, was also involved in resistance to *Listeria monocytogenes*, an intracellular food-borne pathogen (140).

Two main classes of lysosomal enzymes, bearing different posttranslational modifications, have been characterized in *D. discoideum*. The first class includes α-mannosidase, β-glucosidase, and cathepsins and is modified with mannose-6-phosphomethyldiester and/or mannose-6-sulfate, also known as common antigen-1 (141, 142). The second class of enzymes contains an *N*-acetylglucosamine-1-phosphate and comprises cysteine proteases (143). These different classes of enzymes reside in different vesicles at the steady state level and are recruited to phagosomes in a sequential manner, with first a wave of cysteine proteases followed by enzymes bearing the mannose-6-sulfate modification (84, 144).

Although lysosomal enzymes appear to be involved in bacterial killing in *D. discoideum* as in macrophages, direct evidence is lacking. Deletion of the cathepsin D gene is not sufficient to

abolish growth on the food bacterium *Klebsiella* (142). Several *D. discoideum* mutants impaired in lysosomal enzyme trafficking and/or activity have been characterized including strains lacking WshA, a subunit of the WASH complex involved in lysosomal enzyme recycling (117), LvsB, a protein involved in restricting heterotypic fusion of early endosomes with postlysosomal compartments (145), and TM9 protein A, which is involved in the sorting of glycosidases, cathepsins, and lysozymes (146). Interestingly, these mutants exhibit growth defects specific to certain subsets of bacterial species (117, 145–148). These data suggest that different classes of lysosomal enzymes might play redundant roles, that they are not the sole killing strategy employed by *D. discoideum*, and that specific mechanisms may be used depending on the encountered bacteria.

Reactive Oxygen Species

Reactive oxygen species are key components of cell-autonomous defenses of MPS cells and function as antimicrobial effectors (149) as well as signaling molecules that regulate NF-κB (150, 151), autophagy (152), cytokine secretion (153), inflammasome activation (154), and apoptosis (155). ROS are implicated in the regulation of pH within phagosomes and the production of antigenic peptides in dendritic cells (156–158). ROS have also been implicated in the regulation of cytoskeleton dynamics and chemotaxis (159, 160). The major source of ROS in MPS cells is the NADPH oxidase (NOX) 2. Depending on its localization, NOX2 generates superoxide by transferring an electron from cytosolic NADPH to O_2 in either the extracellular space or the lumen of the phagosome. Subsequent reactions convert superoxide into additional ROS. Superoxide dismutase catalyzes its conversion to hydrogen peroxide, which in turn reacts with Fe^{2+} in the Fenton reaction to generate hydroxyl radicals or with Cl^- to produce hypochlorous acid *via* myeloperoxidase (161–163).

NOX2 is a heterodimer comprising the transmembrane proteins gp91^{phox}/Nox2, the catalytic subunit, and p22^{phox}, the regulatory subunit. NOX2 activation occurs downstream of extracellular receptors including integrins and Fc receptors and is coupled with phagocytosis. Activation requires three additional subunits, p67^{phox}/neutrophil cytosol factor (Ncf) 2, p40^{phox}/Ncf4, and p47^{phox}/Ncf1, which form a ternary complex in the cytosol that is recruited to membrane-localized NOX2 by the small GTPases Rac1 and 2 (161–163). Mutations in NOX2 subunits cause chronic granulomatous disease (CGD), a condition that makes patients susceptible to recurring bacterial and fungal infections and demonstrates the importance of the NOX2-generated oxidative burst in the immune response (164, 165). Mitochondrial ROS production activated downstream of TLR signaling also contributes to antimicrobial mechanisms (166, 167).

Because ROS can damage host and microbe alike, ROS production and localization are tightly regulated, and MPS cells express ROS detoxifying enzymes such as superoxide dismutases (SODs), catalases, and peroxiredoxins to prevent self-damage. Microbes that persist inside the phagosome have mechanisms to minimize oxidative stress. These include expression of robust systems to maintain internal redox homeostasis (168), secretion of SODs and catalases to detoxify their compartment (149, 169), and deployment of effectors that inhibit NOX2 activation and/or delivery to the phagosome (170–173).

The *D. discoideum* genome encodes three catalytic NOX subunits: NoxA and NoxB, which are homologs of gp91^{phox}/Nox2, and NoxC, which is a homolog of Nox5 (174–176). It also encodes one homolog of p22^{phox}, CybA, and NcfA, a homolog of the cytosolic activating factor p67^{phox}/Ncf2 (174, 175). RNAseq data indicate that NoxA, CybA, and NcfA are expressed during growth while NoxB and NoxC are mainly expressed during development (69, 174). However, long-term growth on *Klebsiella* can cause upregulation of NoxB in growing cells (136). Interestingly, *D. discoideum* expresses multiple SOD and catalase homologs (177–179) and exhibits a high resistance to oxidative stress (180), which suggests that it encounters internally and/or externally generated ROS regularly.

Whether ROS contribute to cell-autonomous defenses during the growth phase of *D. discoideum* is not clear. Mutants lacking *noxA* or both *noxA* and *noxB* exhibit no growth or killing defects when grown on *Klebsiella* (148, 174). This lack of a defect might be a consequence of redundant killing mechanisms or of challenge with a bacterium that is easily killed. Intriguingly, a *D. discoideum* mutant lacking the Xpf nuclease, a component of DNA damage repair machinery, accumulates more mutations when grown on a range of bacteria including *Klebsiella* than when grown axenically in media (181). One possible explanation is that Xpf is required to repair DNA damaged by ROS generated in response to bacteria.

Excessive ROS production in growing cells due to a deletion of a surface-localized SOD causes defects in chemotaxis and cell motility *via* sustained Ras activation (182, 183). The authors hypothesize that the chemotaxis defect prevents the inclusion of the cell in the multicellular stage and thus prevents propagation of the potentially mutagenized genome. It is tempting to speculate that excessive ROS production in response to a resistant microbe causes the same effect and inhibits the inclusion of an infected cell in the multicellular stages. Although the context is different, this "self-sacrifice" might be analogous to ROS-induced apoptosis of infected macrophages (155, 184).

Reactive oxygen species have functions during development. Extracellular ROS scavengers inhibit aggregation (185), and mutations in the individual NOX subunit genes, *noxA*, *noxB*, *noxC*, or *cybA*, or in the development stage-specific catalase gene, *catB*, cause defects in fruiting body formation when developed under axenic conditions (174, 186). These results indicate a signaling role for ROS. When developed after feeding on bacteria, a *noxABC*$^-$ triple mutant exhibits increased bacterial contamination of fruiting bodies compared with wild type (187). Thus, ROS also have an immunity function.

One possible cause of the immunity defect in the *noxABC*$^-$ mutant is the abrogation of DNA extracellular trap (ET) formation (**Figure 1**). The slug stage can persist for multiple days, during which it migrates through a dangerous melange of infectious bacteria and fungi that could decrease and/or prevent spore production. Phagocytic flux is limited in non-feeding developed cells (188). Protection from infection and intoxication appears to be mediated in part by a subpopulation of cells (<1%) that retain the capacity for phagocytosis (77). These so-called sentinel cells

(S cells) are motile within the slug and phagocytose bacteria and toxins until they are eventually shed. Compared with the other cell types in slugs, S cells are enriched for *tirA* mRNA, and S cells from *tirA*$^-$ mutants have a decreased capacity to kill bacteria (77). In response to bacteria or LPS, S cells secrete mitochondrially derived ETs *via* a mechanism that requires both TirA and NOX-generated ROS, and increased contamination of fruiting bodies correlates with decreased ET production (187). Binding of the TLR2 TIR domain with Nox2 during *M. tuberculosis* infection of macrophages has been reported (189). How NOX and TirA fit into the pathway and whether they interact awaits further examination, as do the questions of whether S cells kill intracellular bacteria and, if so, whether TirA and NOX are involved. ET formation during the growth phase of the *D. discoideum* life cycle has not been observed.

First discovered in neutrophils and named neutrophil extracellular traps (NETs), ETs have been observed in numerous immune cell types including macrophages (190–193). ETs comprise antimicrobial peptides, proteases, and signaling molecules bound to a meshwork of DNA released from the nucleus or mitochondria [(190); reviewed in Ref. (194)]. The mechanisms by which ETs kill extracellular bacteria and/or prevent their dissemination are not well understood. Neutrophils from CGD patients fail to generate NETs (195), although NOX-independent mechanisms have also been described (196–199), some of which utilize ROS from mitochondria (200). ET production by S cells further illustrates the conservation of cell-autonomous defense mechanisms in *D. discoideum*, a precursor to the specialized phagocytes of the vertebrate immune system (201).

Divalent Metals

Maintaining the concentration of divalent trace metals such as iron, manganese, zinc, and copper is essential for every living organism to preserve metabolism and cell growth. Metalloproteins with trace metals as cofactors play a role in many important cellular functions such as signaling, respiration, transcription, translation, and cell division. Tight regulation of divalent metals is necessary: low levels of iron and manganese have detrimental metabolic effects, whereas zinc and copper are toxic at high concentrations.

For intracellular bacterial pathogens, trace metals are an important micronutrient resource with a role in many metabolic processes and are, as a consequence, essential for intracellular growth. Host cells such as macrophages have developed strategies to control growth of intracellular bacteria by sequestering metals such as iron and manganese (i.e., metal deprivation or nutritional immunity) or by pumping toxic metals inside the pathogen-containing compartment [i.e., metal poisoning; reviewed in Ref. (202–204)]. Bacteria have established ways to counteract metal deprivation or poisoning by expressing siderophores (i.e., small molecules with high affinity for the relevant metal) and uptake systems or by upregulating efflux systems such as P-type ATPases (203).

Consequently, the phagosomal concentration of essential trace metals varies during phagocytosis and infection with bacterial pathogens. Wagner et al. elegantly measured the metal concentration in the phagosome upon macrophage activation with inflammatory cytokines and upon infection with *M. tuberculosis* or *Mycobacterium avium* [(205); reviewed in Ref. (206)]. At 1-h post infection (hpi), the early phagosome was shown to be enriched in sulfur and chloride and depleted of calcium and potassium. At a later stage (24 hpi), the MCV harbored zinc, iron, and calcium at high concentrations. In addition, activation of infected macrophages with cytokines leads to a large increase in zinc and copper and a depletion of iron and chloride (205). Importantly, the metal concentration in the phagosome is very likely coupled to the proton gradient. Acidification of the phagosome is achieved by the combined actions of the V-ATPase and the Hv1 H^+-channel (207). To counter-balance the electrogenic H^+-gradient across the phagosomal membrane, Cl^- is imported into the phagosome by transporters of the CFTR (208) and CLC family [(209); reviewed in Ref. (210)], respectively [reviewed in Ref. (206)]. Lysosomal acidification is also facilitated by the efflux of cations (211).

Metal Poisoning

Zinc serves as a cofactor for more than 3,000 metalloproteins and is consequently the second most abundant trace element after iron. Zinc is redox neutral and has many roles in various biological processes as structural, catalytic and signaling component [reviewed in Ref. (212)]. It is essential for macrophage antimicrobial functions and controls among other processes monocyte chemotaxis, phagocytosis, and cytokine production [reviewed in Ref. (204)]. Intracellular zinc homeostasis is tightly regulated. 50% of zinc is present in the cytoplasm, whereas 30–40% can be found inside the nucleus and 10% is bound to membranes [reviewed in Ref. (212)]. To keep the cytosolic concentration of free zinc low (i.e., in the low nanomolar range), it is either bound to metalloproteins or metallothioneins or sequestered into membrane-bound organelles. Zinc is transported through biological membranes by various zinc transport proteins that are classified as zinc transporters (ZnTs, also cation diffusion facilitators) or Zrt-, Irt-related proteins (ZIPs) [reviewed in Ref. (212)]. Whereas ZnTs mediate the zinc transport from the cytosol to either organelles or the extracellular space, the ZIP family mediates transport into the cytosol from the extracellular space or organelles [reviewed in Ref. (212)]. Besides ZnT and ZIP transporters, various other proteins have been shown to mediate zinc transport, such as calcium channels (213), mucolipin-1 in interaction with TMEM163 (214), and members of the NRAMP family [reviewed in Ref. (215)].

Eleven putative zinc transporters have been previously identified in *D. discoideum* and categorized by functional analogy to mammalian zinc transporters into different subgroups (216). Three of the 11 were classified as members of a "ZIP subfamily" and 4 as members of an "LZT-like subfamily" (216). These two subfamilies correspond to the combined ZIP I and ZIP II subfamilies and the LIV-1 subfamily of mammalian ZIPs, respectively (212). Importantly, the members of the LZT-like family were named ZntA–ZntD even though they were classified as ZIP transporters, and four potential ZnT transporter homologs encoded in the *D. discoideum* genome were grouped by the authors as the "Cation efflux subfamily" (216).

To demonstrate that the proteins initially named ZntA–ZntD belong to the ZIP family of zinc transporters and are not ZnTs, we generated two simplified phylogenetic trees comparing the sequences of various *D. discoideum* zinc transport proteins with zinc transporters of other taxonomic groups such as amoebozoa, fungi, plantae, and metazoa. These taxonomic groups were chosen based on previously published phylogenetic studies (176, 217). According to our phylogenetic tree of ZIP transporters (**Figure 4**) an unequivocal classification of the seven *D. discoideum* ZIP-like proteins (Zpl) into ZIP I, ZIP II, and LIV-1 subgroups by analogy to the human classification, as was done previously (216), is not possible. Three of the seven ZIP transporters are more similar to each other and cluster in one group (ZplA–C) that is more related to the ZIP transporters of fungi and ZIP II transporters of mammals. The three proteins ZplD–ZplF are more similar to proteins of Amoebozoa, Stramenopiles, and Plantae. ZplG is more related to the human ZIP I subfamily.

Similarly, our phylogenetic tree of ZnT transporters clearly shows that the four proposed *D. discoideum* zinc transporters identified based on their homology to ZnTs indeed belong to this family (**Figure 5**). Consequently, we propose renaming the various transporters as outlined in **Table 1** according to their respective family names (Zpl or ZnT). The *D. discoideum* proteins ZntC and ZntD are likely homologs of the human proteins ZNT6 and ZNT7, which are located in the early secretory pathway and contribute to the activation of zinc-containing enzymes (220). Whereas ZntA does not have a close mammalian homolog, the closest human relatives of ZntB are the early endosomal protein ZNT10 and the plasma membrane protein ZNT1 (212).

At the host–pathogen interface, zinc deprivation (221) or zinc poisoning are strategies of mammalian professional phagocytes to restrict intracellular bacteria growth. Both processes are probably highly dependent on zinc transporter proteins (222, 223) During *M. tuberculosis* infection, it was proposed that free zinc is released from metallothioneins *via* the oxidative burst that is induced upon infection and, consequently, zinc poisoning was proposed as "a new chapter in the host–microbe arms race" (224). The contributions of zinc transporters to cell-autonomous defenses of macrophages and *D. discoideum* await elucidation.

In contrast to zinc, copper is redox active and cycles under physiological conditions between the two oxidative states Cu^{+} (i.e., cuprous) and Cu^{2+} (i.e., cupric). Consequently, copper serves as an ideal cofactor for electron transfer and redox reactions such as respiration and detoxification of free radicals [reviewed in Ref. (225)]. Proteins involved in copper uptake, sequestration, and trafficking regulate copper homeostasis in eukaryotic cells [reviewed in Ref. (226)]. Copper uptake into the cytosol is mediated by the copper permease CTR1 [reviewed in Ref. (227)]. Similar to zinc, copper belongs to the so-called "death metals" and is toxic at high concentrations. Therefore, by analogy to zinc, low copper concentrations in the cytosol are maintained by metallothioneins. Directly after its uptake, chaperones such as ATOX1, CCS, and COX17 are involved in copper trafficking inside the cytoplasm (228).

Copper is imported into the *trans*-Golgi network by the action of two P-type ATPases: ATP7A and ATP7B. ATP7A is also located at the plasma membrane, where it mediates copper efflux from the cytosol to the extracellular space, and at the phagosomal membrane, where it imports copper from the cytosol into the phagosomal lumen [reviewed in Ref. (226, 228)].

Copper has many antimicrobial properties. Its ability to switch between two oxidation states supports the production of hydroxyl radicals *via* the Fenton- and the Haber–Weiss reactions [reviewed in Ref. (229)]. In addition, copper is able to disrupt the structure of proteins, and Cu^{2+} might be able to disrupt Fe–S clusters. In macrophages, copper transport proteins such as ATP7A that mediate Cu^{2+} import into the phagosome are induced upon infection and stimulation with inflammatory cytokines (230). Bacteria have evolved strategies to overcome high copper concentrations. For instance, a multi-copper oxidase is required for copper resistance of *M. tuberculosis*, probably by oxidizing toxic Cu^{2+} in the periplasm (231).

The *D. discoideum* genome encodes one Ctr-type copper permease (i.e., p80) that, by analogy to mammalian cells, should mediate copper uptake into the cytosol, and three putative copper-translocating P-type ATPases that were annotated as *atp1* (DDB_G0273675), *atp2*, the ortholog of ATP7A (DDB_G0284141), and *atp3* (DDB_G0269590) (232, 233). ATP1 was induced upon incubation of *D. discoideum* with copper salts, leading to the conclusion that ATP1 is responsible for copper tolerance in *D. discoideum* (233). Expression of ATP7A and ATP3 was increased upon bacteria ingestion and decreased when bacteria and copper salts were added together, arguing for a possible role in copper trafficking during phagocytosis and killing of bacteria. The increased expression of p80 only upon incubation with bacteria suggests that copper is needed for bacterial killing (233).

Nutritional Immunity

In contrary to metal poisoning, nutritional immunity does not kill the bacteria but restricts its intracellular growth. During infection, pathogens need to acquire essential nutrients from the host such as amino acids, lipids, sugars, and, importantly, transition metals. Thus, to restrict their availability to the pathogen, these metals are depleted from the phagosome. The best studied metals that are sequestered by the host are iron and manganese (206, 234–236).

Nutritional immunity of transition metals is controlled in part by the Natural Resistance-Associated Macrophage Protein (i.e., NRAMP) family of divalent-metal transmembrane transporters (237–239). The NRAMP family is widely represented from bacteria to mammals (240, 241), as well as in plants (242) and yeast (243). The family members play an important role in intracellular metal-ion homeostasis and are able to transport a broad range of transition metals (215, 244).

In mammals, two NRAMP members have been identified: NRAMP1 [(SLC11A1) (237)] and NRAMP2 [(SLC11A2, DMT1, or DCT1) (241)]. Between these proteins, 63% of residues are identical and 15% are highly conservative substitutions, and they share very similar secondary structures with hydrophobic cores of 10 transmembrane segments (245). Regarding divalent-metal affinity, NRAMP1 has a clear preference for Mn^{2+}, Fe^{2+}, and Co^{2+} (246), whereas NRAMP2 transports those three metals and also Zn^{2+}, Cd^{2+}, Cu^{2+}, Ni^{2+}, and Pb^{2+} (241). NRAMP1 expression is restricted to late endocytic compartments (i.e., endo-lysosomes)

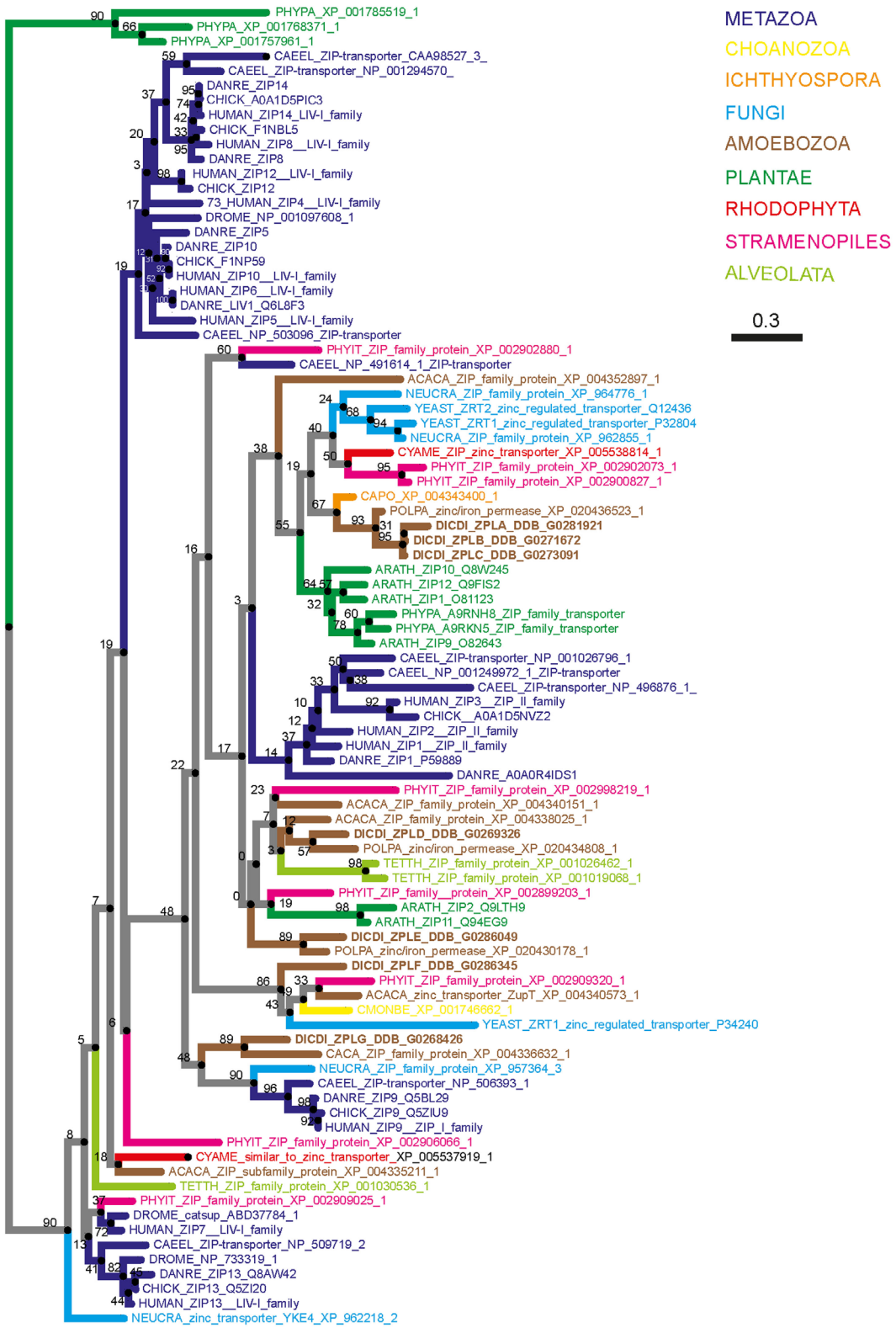


FIGURE 4 | Phylogenetic tree of the Zrt-, Irt-related protein (ZIP) family. The sequence of human ZIP7 was used to search for zinc transporters of the ZIP family among non-redundant sequences in selected organisms using NCBI PSI-BLAST. A score of 2×10^{-5} was used as a threshold. Sequences were aligned with the software AliView [(218); http://ormbunkar.se/aliview/] and curated manually, to remove divergent N- and C-terminus. Trees were built using MAFFT and the E-INS-i strategy (219).

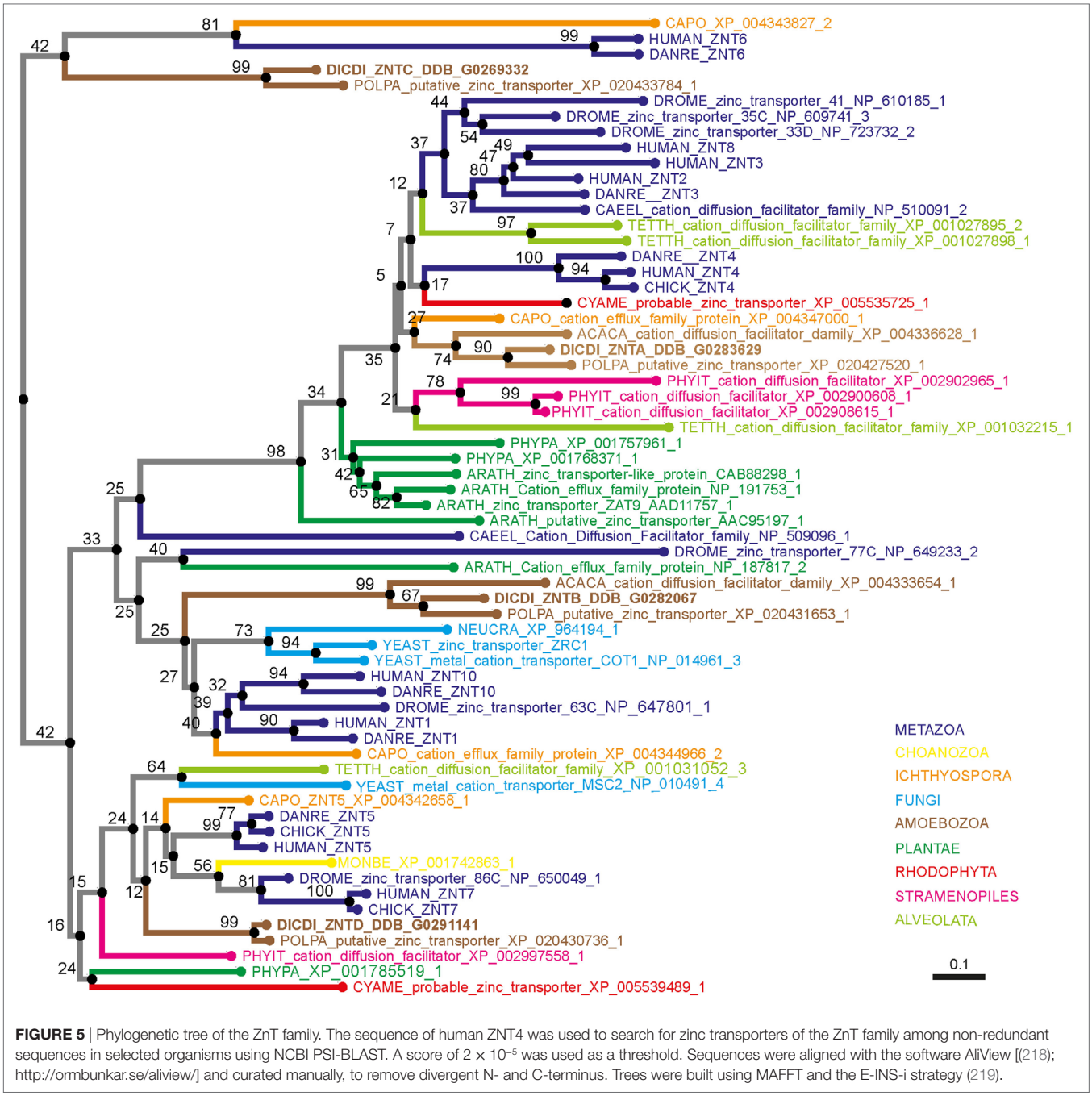


FIGURE 5 | Phylogenetic tree of the ZnT family. The sequence of human ZNT4 was used to search for zinc transporters of the ZnT family among non-redundant sequences in selected organisms using NCBI PSI-BLAST. A score of 2×10^{-5} was used as a threshold. Sequences were aligned with the software AliView [(218); http://ormbunkar.se/aliview/] and curated manually, to remove divergent N- and C-terminus. Trees were built using MAFFT and the E-INS-i strategy (219).

of professional phagocytes such as macrophages and neutrophils (247). NRAMP2 is ubiquitously expressed in all mammalian cells and is located at the plasma membrane (248). In addition, NRAMP2 was observed at the apical membrane of enterocytes as well in recycling endosomes (249). Mutations in *nramp2* lead to severe microcytic anemia related to an iron absorption deficiency (250, 251). Both NRAMP1 and NRAMP2 might be involved in neurodegenerative diseases such as Parkinson's (252, 253). NRAMP1 contributes to the resistance to intracellular bacterial infection. Indeed, depletion of NRAMP1 leads to an increased susceptibility of mice to several intracellular pathogens such as *Mycobacterium* species, *Leishmania donovani*, and *Salmonella* species (237, 254–259) by impairing phagosomal acidification and reducing fusion with the lysosomes (260). In human, *nramp1* polymorphic variants are associated with susceptibility to tuberculosis (261, 262) or leprosy (263).

Although it is accepted that NRAMPs depend on a V-ATPase-generated proton gradient to drive metal transport (264), the direction of metal transport at the phagosomal membrane remains controversial. Whether NRAMP1 is an antiporter or a symporter and whether NRAMP1 imports or depletes metals from the phagosome are unclear. On the one hand, some

TABLE 1 | Proposed nomenclature of zinc transporters in *Dictyostelium discoideum*.

Gene ID	Gene product	Proposed name
DDB_G0281921	Zrt-, Irt-related protein (ZIP) zinc transporter protein, zinc/iron permease	zplA (ZIP-like A)
DDB_G0271672	ZIP zinc transporter protein, zinc/iron permease	zplB
DDB_G0273091	ZIP zinc transporter protein, zinc/iron permease (there is a gene duplication in AX3 and AX4, but not in AX2)	zplC1 and 2
DDB_G0269326 (previously *zntD*)	Zinc/iron permease, zinc transporter	zplD
DDB_G0286049 (previously *zntC*)	Zinc/iron permease, zinc transporter	zplE
DDB_G0286345 (previously *zntB*)	Zinc/iron permease, zinc transporter	zplF
DDB_G0268426 (previously *zntA)*	Zinc/iron permease, zinc transporter	zplG
DDB_G0283629	Putative zinc transporter, cation diffusion facilitator (CDF) family protein	zntA (zinc transporter A)
DDB_G0282067	Putative zinc transporter, CDF family protein	zntB
DDB_G0269332	Putative zinc transporter, CDF family protein	zntC
DDB_G0291141	Putative zinc transporter, CDF family protein	zntD

authors suggest that NRAMP1 acts as an antiporter of protons and delivers cation metals into the phagosome, contributing to the generation and accumulation of toxic free radicals involved in bacteria killing (265–268). On the other hand, the hypothesis that NRAMP1 operates as a symporter of protons to efflux metals from the phagosome to the cytosol is better supported by the literature and is consistent with the function of its paralog NRAMP2. This is in line with the current hypothesis of nutritional immunity in which pathogen access to metals is restricted (246, 269). These two different scenarios are nicely described in previous reviews (215, 244, 270).

The *D. discoideum* genome encodes two NRAMP proteins called NRAMP1 (DDB_G0276973) and NRAMPB (DDB_G0275815, formerly NRAMP2). NRAMP1 is an archetypical NRAMP protein, orthologous to NRAMP1 in mammals, whereas NRAMPB is not the ortholog of NRAMP2 in mammals but rather is more closely related to the prototypical NRAMP from bacteria (271). Both transporters are in different subcellular compartments; however, they both co-localize with the V-ATPase. NRAMP1 localizes to macropinosomes and phagosomes with the V-ATPase, and NRAMP1 also localizes to the Golgi region (272). NRAMPB is exclusively found in the membrane of the contractile vacuole (CV) (273), which is enriched for the V-ATPase (108, 274) but has a neutral pH. Single *nramp1* or *B* null mutants exhibit slower growth than wild type under conditions of iron depletion while a double *nramp1* and *B* mutant, but not single mutants, is more resistant than wild type to iron overload (273). These results suggest that NRAMPB and NRAMP1 act non-redundantly to regulate iron homeostasis and that the CV serves as a transient storage compartment for metal cations (**Figure 6**). During infection, an *nramp1* mutant strain is more permissive for intracellular growth of *Mycobacterium* species and *L. pneumophila* (272), and *nrampB* null or *nramp1* and *B* double null mutants are more permissive for *L. pneumophila* growth (effects of *nrampB* deletion on the growth of *Mycobacterium* species have not been reported) (273). Moreover, *L. pneumophila* inhibits the recruitment of the V-ATPase, which attenuates the antimicrobial effects of NRAMP1 by preventing its proton-driven iron transport activity (46). A recent study demonstrates that, in addition to having an impact on phagosomal iron concentration, both NRAMP1 and NRAMPB influence the translocation efficiency of *F. noatunensis* from the bacteria-containing compartment into the cytosol, possibly due to alterations in phagosome maturation (53). This new insight into NRAMP function is in line with the results obtained for *M. tuberculosis* infection in macrophages, in which *nramp1* deletion induced a higher level of escape from its vacuole (275).

As described earlier, the directionality of the metal transport mediated by NRAMP1 is still poorly understood. Studies in *D. discoideum* suggest transport into the cytosol. In assays with purified phagosomes, iron export was NRAMP1- and ATP dependent (272). This observation is consistent with NRAMP1 acting as a symporter that uses a V-ATPase-generated proton gradient to transport iron out of the phagosome. Using the iron-chelating fluorochrome calcein, it was shown that NRAMP1 mediates iron efflux from macropinosomes *in vivo* (271). In addition, to obtain better insight into the ion selectivity of NRAMP1, the authors used *Xenopus* oocytes expressing NRAMP1, NRAMPB, or rat DMT1/NRAMP2 (used as an internal control). Interestingly, it was shown that NRAMP1 and DMT1 are able to transport Fe^{2+} and Mn^{2+} but not Fe^{3+} or Cu^{2+} in an electrogenic and proton-dependent manner, whereas NRAMPB transports only Fe^{2+}, and this in a non-electrogenic manner independently from protons (271) (**Figure 6**).

AUTOPHAGY

As described earlier, phagocytosis is the major mechanism by which *D. discoideum* digests intracellular bacteria with the purpose of nutrient acquisition. However, pathogenic microbes have evolved mechanisms to escape degradation within phagosomes (276). In *D. discoideum*, as in other eukaryotic phagocytes, bacterial escape from the phagosome triggers a more stringent catabolic pathway named autophagy, which serves as an additional defense mechanism for the infected amoeba [a comprehensive review on autophagy in *D. discoideum* can be found in Ref. (277)]. The autophagic process by which intracellular pathogens and/or their damaged phagosomes are specifically recognized and digested is termed xenophagy.

The autophagy pathway consists of the formation, upon induction by various stresses such as oxidation, nutrient starvation, or microbial infection, of a double-membrane cisterna, the phagophore, at multiple sites on the ER (36). During xenophagy, the membranes of the phagophore expand around the cytosolic bacterium and/or its damaged compartment to finally engulf them in a closed vacuole called the autophagosome, which, upon fusion with lysosomes, forms an acidic and degradative compartment, the autolysosome, where bacterium and membranes are digested (**Figure 7**). Many of the proteins involved in the process of autophagosome formation (for instance, proteins forming part of the TORC1, the ULK/Atg1 and the phosphatidylinositol

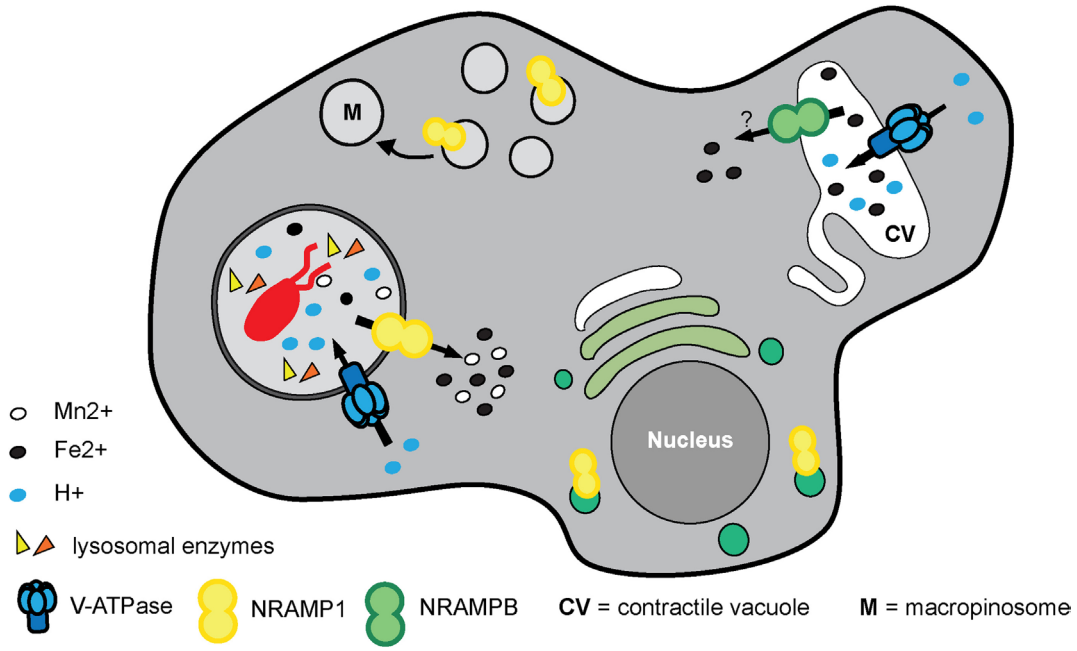


FIGURE 6 | "Nutritional immunity" and homeostasis of transitional metals orchestrated by NRAMP transporters in *Dictyostelium discoideum*. NRAMP1 is localized at macropinosomes, phagosomes, and the Golgi network whereas NRAMPB is exclusively found in the membrane of the contractile vacuole. Both co-localize with the vacuolar ATPase (V-ATPase), but only NRAMP1 is dependent on the H^+-gradient to efflux metals from the phagosome to the cytosol to restrict metal availability to the pathogen in the process referred to as "nutritional immunity." NRAMPB, together with NRAMP1, contributes to iron homeostasis and regulates osmolarity inside the cell independent of the H^+-gradient. Although the literature supports it as similar to the symporter NRAMP1, its role as symporter or antiporter still remains to be clearly defined.

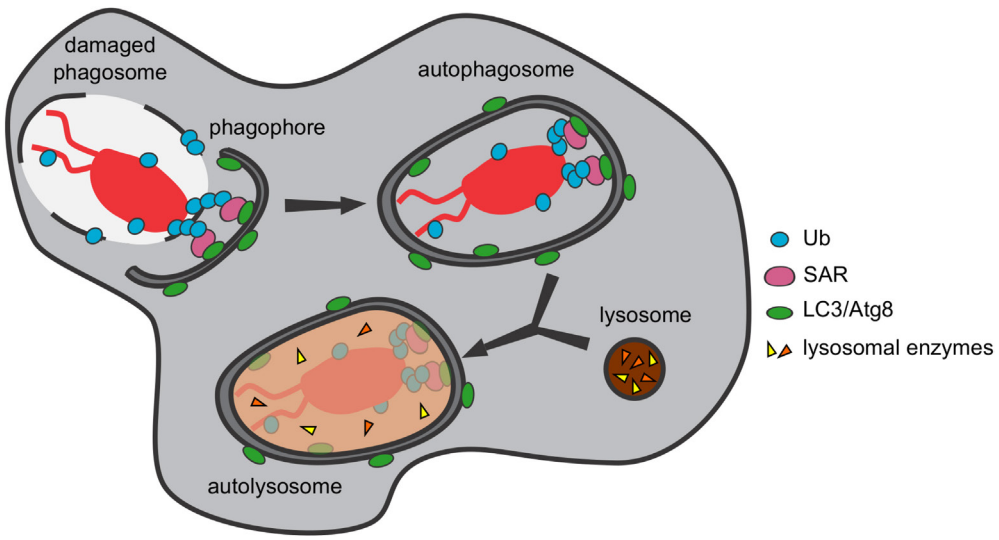


FIGURE 7 | Pathogenic bacteria are captured and digested by xenophagy. The autophagic machinery of *Dictyostelium discoideum* recognizes and captures cytosolic bacteria and/or their damaged phagosomes in autophagosomes, where they are digested upon fusion with lysosomes.

3-kinase complexes) are conserved between mammalian cells and *D. discoideum* (278). Interestingly, certain autophagy proteins conserved in both humans and *D. discoideum* are actually absent in *Saccharomyces cerevisiae*, making their study in this amoeba a perfect complement to those already performed in yeasts (279).

Specific receptor proteins are in charge of recruiting the phagophore membranes to the bacterial cargos or the remnants of the bacteria-containing compartment, which are tagged with ubiquitin for degradation. These receptors contain a ubiquitin-binding domain, which recognizes the ubiquitinated material,

and an LC3-interacting region, which binds the phagophore membrane through interaction with LC3/Atg8, the main autophagosomal marker (280). In *D. discoideum*, the only selective autophagy receptor identified so far is p62/SQSTM1 (278), which has been shown to recognize the intracellular pathogens *F. noatunensis* and *M. marinum* (51, 52, 130). In addition, the mRNA levels of *p62/sqstm1* increase upon infection of *D. discoideum* with both bacterial pathogens, which, in the case of *M. marinum,* has been demonstrated to be dependent on the membrane damage caused by the bacterium. However, *M. marinum* avoids its xenophagic killing by presumably blocking lysosomal fusion (51), a mechanism of intracellular mycobacterial survival that was previously proposed to occur in human dendritic cells during infection with *M. tuberculosis* (281). Other bacteria known to be captured and digested by xenophagy in this amoeba are *S. enterica* and *S. aureus* (54, 282).

In addition to pathogenic bacteria, *D. discoideum* xenophagy also fights against various *S. cerevisiae* strains (283). Mutant amoebae lacking the autophagy proteins Atg5, Atg6, Atg7, or Atg8 have a decreased capability of preying on this fungus. However, in *atg1*- amoebae, which cannot produce autophagosomes, *S. cerevisiae*, *Candida albicans*, and *Candida glabrata* are surprisingly killed more efficiently. Koller and collaborators suggest, among other hypotheses, that the autophagic machinery might be used by these yeasts to escape *D. discoideum* in a non-lytic manner, as already shown for *M. marinum*. During ejection from the *D. discoideum* cytosol, the wound generated by the egress of this bacterium through the plasma membrane is sealed with phagophores (130). One might speculate that the yeasts could egress from *D. discoideum* by autophagosome exocytosis, a process already shown to occur in this amoeba during secretion of the spore differentiation factor 2 precursor AcbA (284). During this unconventional exocytosis, yeasts would be engulfed by autophagic membranes, which would then fuse with multivesicular endosomes before fusing with the plasma membrane to release the yeast. Amoebae lacking Atg1 might be unable to exocytose the yeast efficiently, thus trapping them and facilitating their death. Further investigations are required to validate this hypothesis.

CONSERVED MICROBIAL RESTRICTION FACTORS: LESSONS FROM MPS CELLS

Studies conducted in MPS cells have identified numerous factors that are involved in the successful restriction of intracellular pathogens. Among these proteins are the glycan-binding galectins, TNF receptor-associated factors (TRAFs), and tripartite motif-containing proteins (TRIMs), which are E3 ubiquitin ligases, the guanylate-binding proteins (GBPs), a family of cytokine-induced large GTPases, and finally the signal transducers and activators of transcription (STAT) proteins. *D. discoideum* expresses a family of lectins, the discoidins, that might function analogously to galectins. Its genome also encodes homologs of TRAFs, TRIMs, GBPs, and STATs. Based on their counterparts in MPS cells, the *D. discoideum* versions of these restriction factors are likely to have immune functions (**Figure 8**).

Discoidins

The galectins compose a family of 15 mammalian lectins with affinity for β-galactoside sugars that share a characteristic carbohydrate recognition domain (285). They have been classified into three groups according to their overall structure: the "prototype," the "tandem-repeat," and the "chimera-type." Galectins are present in the cytosol (286) and nucleus (287) of cells but are also secreted extracellularly *via* an unconventional secretion mechanism that has remained elusive for decades (288). Galectins play a role in multiple biological processes, including angiogenesis (289), tumor growth (289), and inflammation (290), due to their ubiquitous localization as well as the high diversity of self and non-self glycoconjugates that they recognize [for a review, see Ref. (291)]. Importantly, extracellular lectins bind to the complex glycocalyx coat at the cell surface, which enables the formation of specific microdomains known as the galectin lattice (292). The galectin lattice restricts the mobility of glycoconjugates in the plasma membrane and has important functions in signaling and endocytosis (293). Some galectins recognize the surface of various pathogens (294–297) and have been proposed to have a direct antibacterial effect (298, 299). These interactions involve galectin binding to specific bacterial species or clades according to the carbohydrates displayed on their cell wall or capsules. In addition to their roles in the extracellular milieu, galectins have recently emerged as general innate-immune factors against a wide range of intracellular infections. This newly described function appears not to involve the binding of cytosolic galectins directly to the surface of intracellular pathogens but rather to result from the recognition of self glycans present on the luminal leaflet of pathogen-containing vacuoles. These glycans become accessible to the cytosolic lectins when membrane damage occurs, as shown during infection with *S. enterica*, *L. pneumophila*, and *Yersinia pseudotuberculosis* (300, 301). This process leads to the recruitment of the autophagy machinery (300) or of GBPs (301) to the compartment.

Although *D. discoideum* lacks galectin homologs, discoidins share molecular and biological characteristics with galectins. They form a family of four β-galactoside-binding and β-*N*-acetylgalactosamine-binding lectins with two carbohydrate binding domains (302, 303), and recent genome analyses identified three potential discoidin-like proteins in *D. discoideum* (http://dictybase.org). Discoidins are expressed throughout the *D. discoideum* life cycle (69, 70). They are highly abundant in the cytosol and are also secreted despite their lack of a signal peptide (304). Early reports suggested a possible role in self-recognition during the multicellular cycle of *D. discoideum* (305), but it was later observed that mutants with much reduced expression of discoidins (1–2% of wild type) were able to form apparently normal fruiting bodies (306). In addition, subsequent studies were unable to confirm surface localization of discoidins (307, 308). Consequently, the role of discoidins in self-recognition and adhesion during *D. discoideum* development has remained controversial for several decades. Whether discoidins bind bacteria and/or have a role in cell-autonomous defenses similar to that of galectins is currently under investigation.

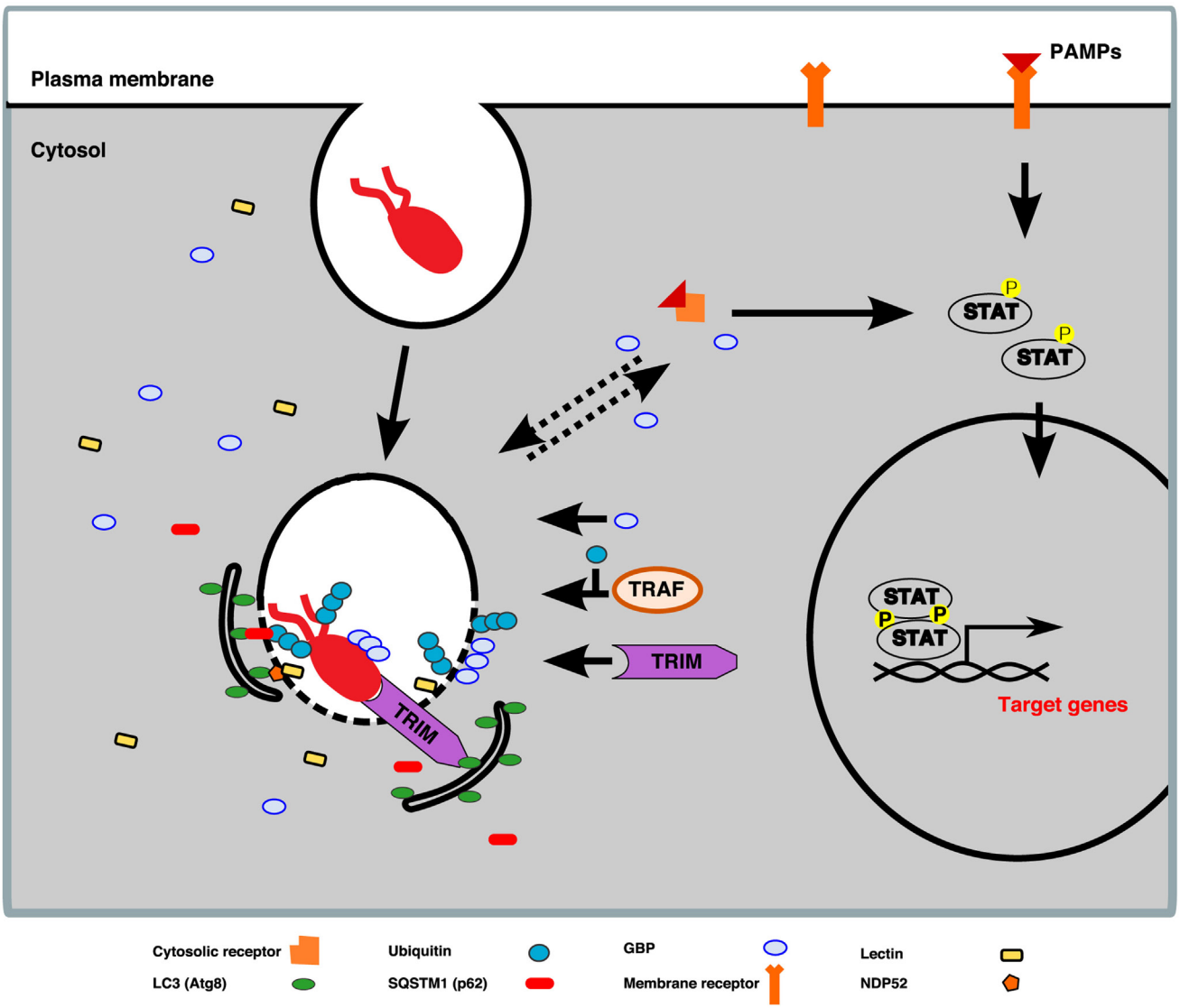


FIGURE 8 | Working model of TNF receptor-associated factor (TRAF), tripartite motif-containing protein (TRIM), guanylate-binding protein (GBP), and signal transducers and activators of transcription (STAT) proteins in *Dictyostelium discoideum*. Lessons learned from studies in macrophages allow us to envision a model according to which, upon bacterium uptake by *D. discoideum*, pathogen-associated molecular patterns (PAMPs), or danger-associated molecular patterns, shared by a broad range of microbes, are detected by membrane or cytosolic receptors. The perception of pathogens leads to the activation of transcription factors from the STAT family, which are translocated to the nucleus, where they bind the promoters of innate-immunity-related target genes encoding galectins, GBPs, NADPH oxidases, SQSTM1, TRIMs, and NDP52. In addition, membrane damage of the pathogen-containing vacuole (PCV) exposes pathogens to the cytosol and permits their decoration with K63-linked polyubiquitin chains deposited by members of the TRAF E3-ligase family. The K63-linked polyubiquitination chains serve as a cue for recruitment of the autophagy machinery *via* autophagy cargo receptors, for instance, SQSTM1 (p62 in *D. discoideum*). Moreover, K63 ubiquitin-tagged membranes also promote the recruitment of GBP oligomers to the pathogen surface and/or PCV membrane, which facilitates bacteria killing and clearance. Furthermore, members of the TRIM E3-ligase family are able to detect and bind directly to the invading pathogen and mediate its degradation by autophagy. The aforementioned factors are likely to function in an interrelated manner in human macrophages, and it remains to be explored whether the *D. discoideum* versions are involved in its cell-autonomous defenses.

Ubiquitination

The significance of ubiquitination in the regulation of various aspects of mammalian immunity has been increasingly recognized in recent years. Ubiquitination is an omnipresent posttranslational modification in which the 76-amino acid ubiquitin is covalently linked to lysine (K) residues of substrate proteins. The stepwise enzymatic cascade of ubiquitination involves following three proteins: ubiquitin-activating enzyme (E1), ubiquitin-conjugating enzyme (E2), and ubiquitin ligase (E3). Their activity results in the attachment of one ubiquitin to the substrate protein linked by an isopeptide bond between the ubiquitin C-terminus and the NH_2 group of the substrate K residue. This is referred to as monoubiquitination. Repeated ubiquitination leads to the generation of a polyubiquitin chain,

known also as polyubiquitination. Ubiquitin contains seven K residues (K6, K11, K27, K29, K33, K48, and K63). Typically, the attachment of K48-linked polyubiquitin chains to substrate proteins serves as a signal for their degradation by the proteasome. However, the other linkages and the C- or N-terminal linear linkage of ubiquitin moieties play roles in almost all aspects of plant and animal biology, such as growth, development, stress responses, and immunity. In mammals, K63-linked polyubiquitination has been associated with a broad range of immunity-related processes and particularly the activation of the NF-κB pathway, xenophagy and apoptosis (309). D. discoideum has 13 genes encoding ubiquitin, and the TRAFs and TRIMs responsible for K63-linked polyubiquitination are conserved from D. discoideum to mammals.

TNF Receptor-Associated Factors

TNF receptor-associated factors are a family of proteins primarily involved in the regulation of inflammation, antiviral responses, and apoptosis (309, 310). Currently, seven TRAF proteins have been characterized in humans: TRAF1–7. Typically, the TRAF proteins comprise an N-terminal RING domain that mediates the interaction between an E2 ligase and the substrate, followed by a zinc-finger domain, which may play a role in DNA, RNA, protein, and/or lipid binding, and a C-terminal TRAF homology (MATH) domain. The TRAF/MATH domain has an N-terminal TRAF region that mediates homo- and hetero-oligomerization between TRAF members and a C-terminal region that is important for interactions with receptors and adaptor proteins (310).

TNF receptor-associated factor 6, perhaps the most ancient mammalian TRAF, is a RING-type E3-ligase that ubiquitinates *via* the K63-linkage (311–313). It is required for mTORC1 translocation to the lysosome, and TRAF6-catalyzed K63 polyubiquitination modulates mTORC1 amino acid sensing capacity (314). Moreover, in macrophages, TRAF6 is responsible for the decoration of pathogens and pathogen-containing vacuoles with polyubiquitin chains, which serve as a cue for GBP recruitment and as a recognition signal for the autophagy cargo receptor p62 (313, 315).

BLAST analyses predict that TRAF-like proteins are also present in several social amoeba species. More than 40 TRAF-like proteins in *D. discoideum* are predicted, of which 16 contain the RING, zinc-finger and TRAF domains present in mammalian TRAF2, TRAF3, TRAF5, and TRAF6 (**Figure 9**; **Table 2**). Despite the fact that human and *D. discoideum* TRAF proteins show significant similarities with respect to their major domains, their evolutionary divergence precludes ortholog assignment. Determining whether *D. discoideum* TRAFs regulate nutrient sensing and/or ubiquitinate pathogens will expand our understanding of their roles in infection.

Tripartite Motif-Containing Proteins

The TRIM superfamily is remarkably conserved among metazoans and, perhaps as a result of an expansion during vertebrate evolution, is represented by more than 80 members in humans. TRIMs typically comprise an N-terminal RING domain, a B-box domain containing several zinc-binding motifs, a coiled-coil domain, and a considerably diverse C-terminal domain important for substrate binding (316).

Tripartite motif-containing proteins are important for many aspects of immunity resistance to pathogens. Recent studies in mouse macrophages demonstrate that various TRIM proteins are induced upon infection with influenza virus or activation of

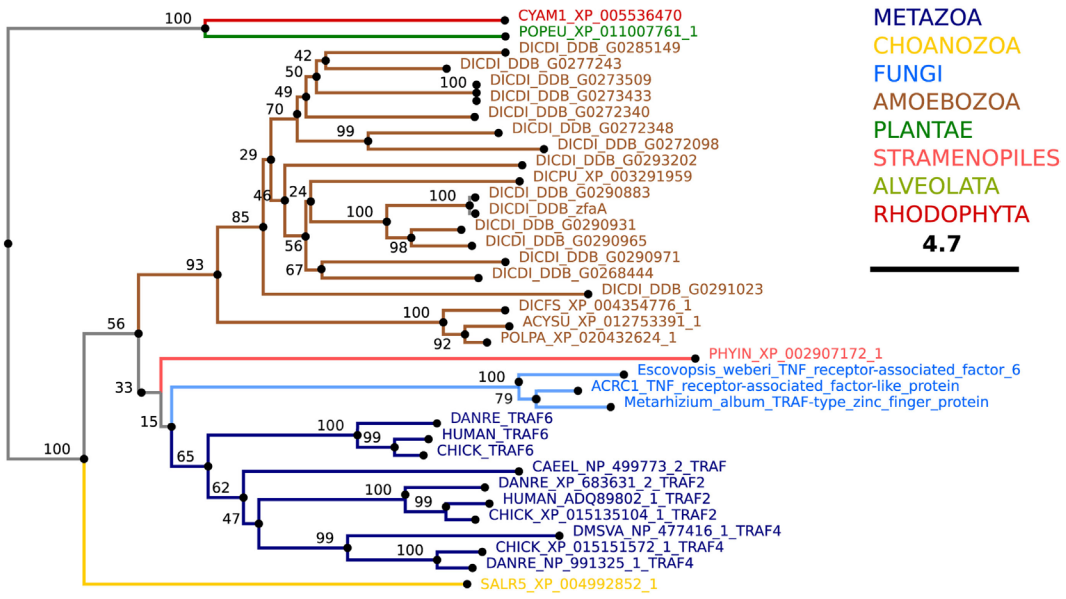


FIGURE 9 | Theoretical phylogenetic relations of TNF receptor-associated factor (TRAF) proteins. The sequence of human TRAF6 was used to search for TRAF homologs among the non-redundant sequences in selected organisms using NCBI PSI-BLAST. A score of 2×10^{-5} was used as a threshold. Similarities of the selected sequences were determined using BLOSUM62 matrix and E-INS-i strategy (219). Sequences were manually curated using AliView software [(218); http://ormbunkar.se/aliview/], and the resulting final alignment was used to generate a neighbor joining phylogenetic tree (NJ, bootstrap 1,000×).

TABLE 2 | Pairwise comparisons of the human TNF receptor-associated factor (TRAF) 6, tripartite motif-containing protein (TRIM) 37, guanylate-binding protein (GBP) 3, and signal transducers and activators of transcription (STAT) 2 with their putative *Dictyostelium discoideum* homologs.

D. discoideum	*Homo sapiens*	Bit score	*e*-Value	Identity (%)	Proposed name
dstD	STAT2	57.4	4e−12	26	NA
dstA	STAT2	77.4	4e−12	29	NA
dstC	STAT2	56.2	2e−11	25	NA
dstB	STAT2	71.6	1e−09	28	NA
DDB_G0281639	GBP3	137	3e−38	26	DdGBP
DDB_G0272454	TRAF6	152	1e−15	22	DdTRAFa
DDB_G0285149	TRAF6	79.7	1e−19	20	DdTRAFb
DDB_G0290883	TRAF6	70.1	2e−16	22	DdTRAFc
DDB_G0290961	TRAF6	75.9	2e−18	21	DdTRAFd
DDB_G0290971	TRAF6	73.5	9e−12	26	DdTRAFe
DDB_G0277243	TRAF6	84.7	1e−20	21	DdTRAFf
DDB_G0272340	TRAF6	80.1	4e−19	21	DdTRAFg
DDB_G0293202	TRAF6	72.0	1e−16	23	DdTRAFh
DDB_G0272348	TRAF6	92.8	1e−15	23	DdTRAFi
DDB_G0273433	TRAF6	68.6	2e−15	23	DdTRAFj
DDB_G0273509	TRAF6	68.6	2e−15	23	DdTRAFk
DDB_G0290931	TRAF6	97.0	2e−15	23	DdTRAFl
DDB_G0290965	TRAF6	65.5	2e−14	25	DdTRAFm
DDB_G0268444	TRAF6	61.6	3e−13	20	DdTRAFn
DDB_G0291023	TRAF6	79.7	2e−10	26	DdTRAFo
DDB_G0272098	TRAF6	70.1	7e−10	22	DdTRAFp
DDB_G0273381	TRIM37	188	1e−46	28	DdTRIM

The BLOSUM62 pairwise alignment was performed with NCBI BLASTp suite-2 sequences. This table shows the similarity scores with these D. discoideum homologs and their proposed name.

TLRs in a type-I-interferon (IFN)-dependent manner (317, 318). TRIMs are involved in restriction of HIV replication and activation of NF-κB downstream of TLRs (318). Moreover, they play a dual role as receptors and regulators of autophagy. As regulators, TRIMs serve as platforms for the assembly of the core autophagy initiators ULK1 (Atg1 in yeast and *D. discoideum*) and Beclin1 (Atg6 in yeast and *D. discoideum*) (319). In macrophages, autophagy cargo receptors recognize and bind K63-linked polyubiquitin chains and galectins, which serve as "eat-me" signals and mediate the binding of the cargo to phagophore-conjugated LC3. As receptors, TRIMs are able to recognize endogenous and exogenous (e.g., bacteria) cargo intended for autolysosomes *via* binding of their diverse C-terminal domains to the cargo in a ubiquitin-independent manner and mediate delivery to the phagophore by also binding LC3 (320, 321).

Tripartite motif-containing protein homologs are found in multiple social amoeba species, and a single TRIM has been identified in *D. discoideum*, DdTRIM, which is an ortholog of human TRIM37 (**Figure 10**; **Table 2**) (http://dictybase.org). According to an accumulating amount of evidence, human TRIMs are emerging as critical regulators of cell-autonomous defenses. Particularly, human TRIM37 has been shown to restrict HIV-1 replication (322). At present, the role of DdTRIM remains unknown, and the presence of a single member of the TRIM superfamily early in evolution makes *D. discoideum* an interesting model to explore the primordial role of TRIM proteins before their expansion.

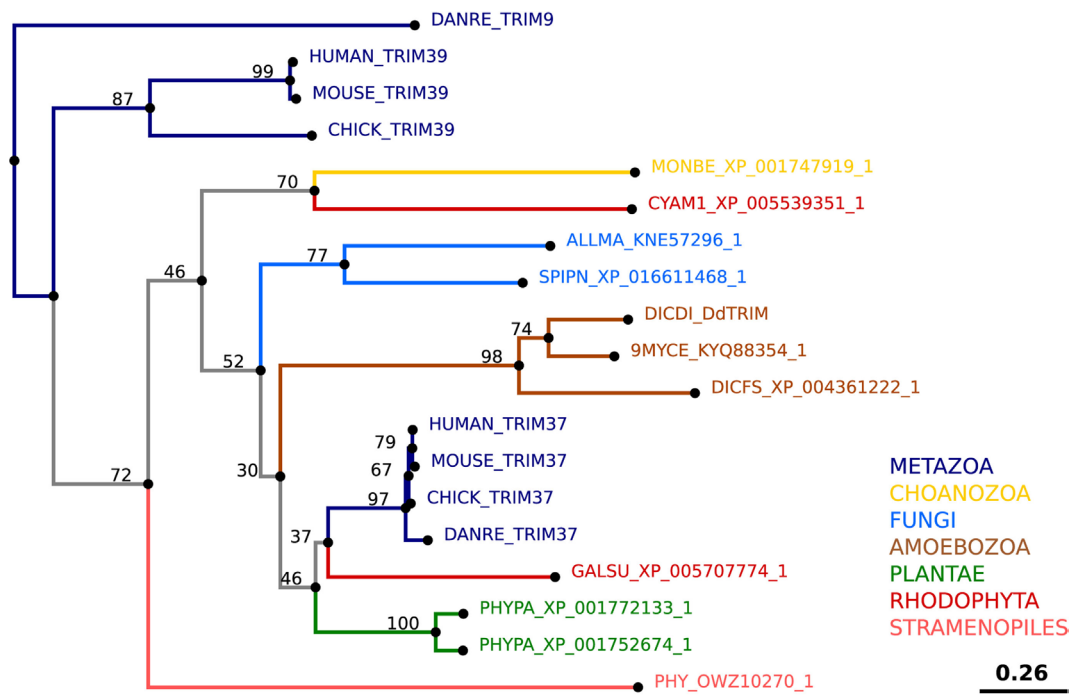


FIGURE 10 | Theoretical phylogenetic relations of tripartite motif-containing protein (TRIM) proteins. The sequence of human TRIM37 was used to search for TRIM homologs among the non-redundant sequences in selected organisms using NCBI PSI-BLAST. A score of 2×10^{-5} was used as a threshold. Similarities of the selected sequences were determined using BLOSUM62 matrix and E-INS-i strategy (219). Sequences were manually curated using AliView software [(218); http://ormbunkar.se/aliview/], and the resulting final alignment was used to generate a neighbor joining phylogenetic tree (NJ, bootstrap 1,000×). TRIM39 was used as an outgroup.

Guanylate-Binding Proteins

The GBP proteins are IFN-gamma-inducible, immunity-related GTPases. Generally, the GBP proteins comprise a globular N-terminal domain and a C-terminal alpha-helical baculovirus inhibitor of apoptosis repeat (BIR) domain. Both the globular N-terminal domain, which confers GTPase activity, and the C-terminal BIR domain mediate protein–protein and protein–lipid interactions and contribute to nucleotide-dependent homotypic and heterotypic GBP protein assembly (323). In addition, BIR domains have been reported to act as caspase regulators and mediators of homotypic interactions (324). GTP binding to the GTPase activity domain allows dimer formation, and its hydrolysis enables conformational changes resulting in GBP tetramer formation. In vertebrates, the GBPs proteins have been linked to a multitude of innate immunity-related responses such as inflammasome activation and xenophagy (325). Essential for their function is their ability to oligomerize and to bind target endomembranes (323, 326, 327). In mouse macrophages, GBP2 recruitment to *Chlamydia trachomatis*- and *Toxoplasma gondii*-containing vacuoles correlates with their host-mediated lysis, underlying the importance of these large GTPases in the successful immune response against intracellular invaders (313, 328).

Multiple social amoeba species have homologs of GBPs, and a single GBP homolog has been identified in *D. discoideum*, DdGBP (**Figure 11**; **Table 2**). Its role remains to be elucidated. As a single GBP representative, it may allow a better understanding of the primordial and conserved role that GBPs play in MPS cells.

Signal Transducers and Activators of Transcription

In humans, there are seven STATs, which have a unique N-terminus important for nuclear translocation and protein–protein interactions. This region is followed by a coiled-coil domain involved in nuclear export and regulation of tyrosine phosphorylation, a DNA-binding domain that mediates the recognition of sequences related to TTCN3–4GAA in the promoters of responsive genes, and an Src-homology (SH2) domain, which allows for specific recognition and docking to phosphotyrosines on cytokine receptors, Janus kinases (JAKs), and other STAT molecules. The C-terminus contains a divergent transactivator domain, which mediates STAT transcription factor transactivation *via* various cofactors (329).

Signal transducers and activators of transcription proteins are activated mainly by cytokines and growth factors. Binding of these signaling molecules to their receptors triggers receptor dimerization, allowing transphosphorylation and activation of receptor-associated JAKs. The JAKs also phosphorylate the cytoplasmic tails of the receptors, which promotes recruitment of the STAT proteins through their SH2 domain. The subsequent tyrosine phosphorylation of STATs results in the formation of homodimers and/or heterodimers and nuclear translocation, whereupon they bind to the promoter regions and initiate transcription of various immunity-related genes such as galectins, GBPs, NOXs, SQSTM1, TRIMs, and NDP52 (330). As part of their functional cycle, STATs shuttle between the cytosol and the nucleus (329). Mammalian STAT proteins act in a tissue-specific

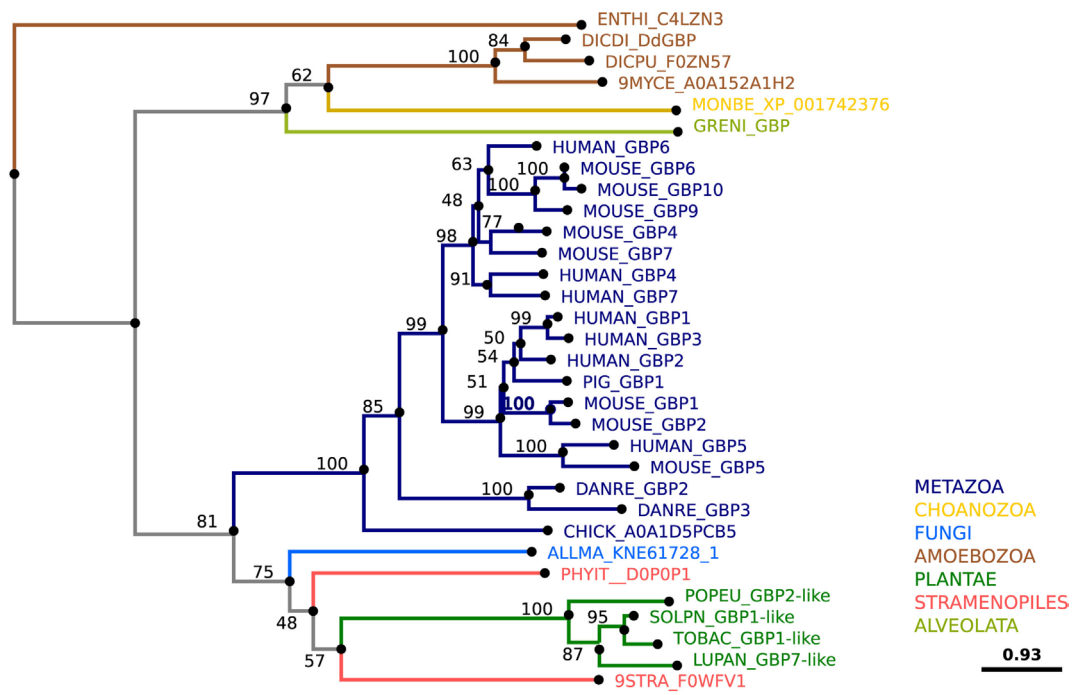


FIGURE 11 | Theoretical phylogenetic relations of guanylate-binding proteins (GBPs). The sequences of human GBPs were used to search for GBP homologs among the non-redundant sequences in selected organisms using NCBI PSI-BLAST. A score of 2×10^{-5} was used as a threshold. Similarities of the selected sequences were determined using BLOSUM62 matrix and E-INS-i strategy (219). Sequences were manually curated using AliView software [(218); http://ormbunkar.se/aliview/], and the resulting final alignment was used to generate a neighbor joining phylogenetic tree (NJ, bootstrap 1,000×).

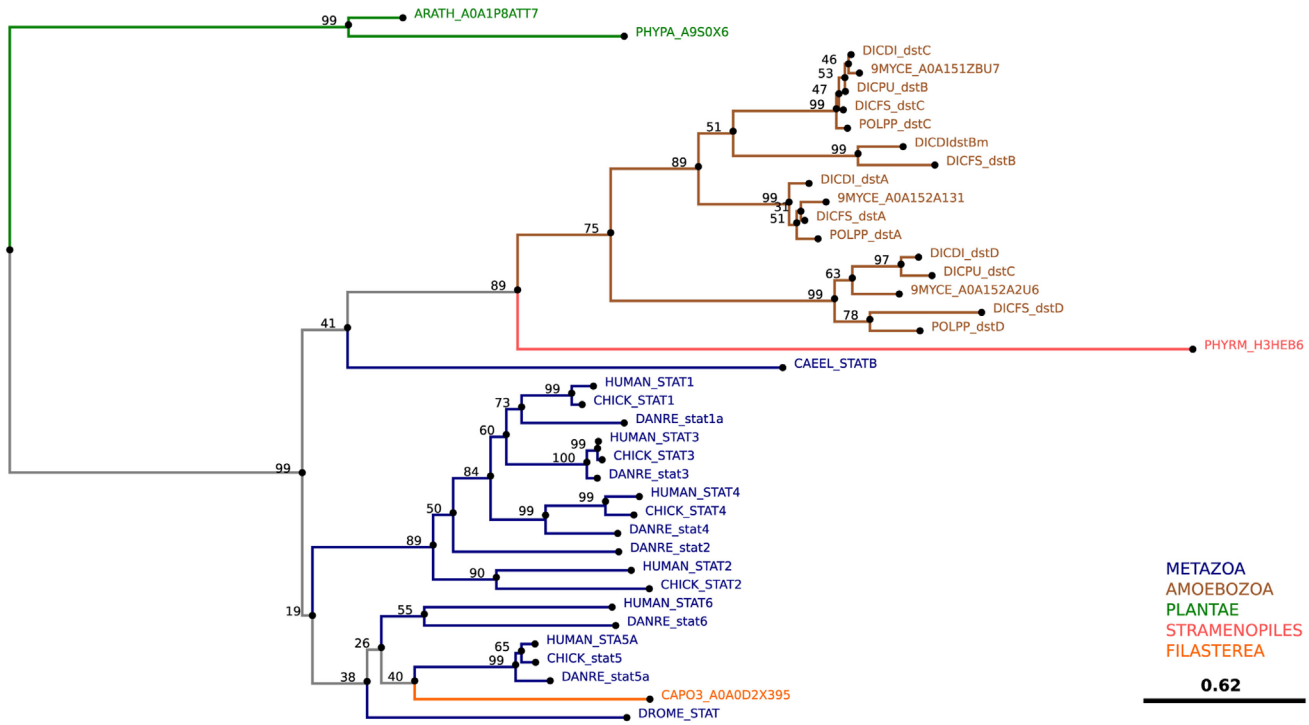


FIGURE 12 | Theoretical phylogenetic relations of signal transducers and activators of transcription (STAT) family proteins. The sequence of the human STAT3 was used to search for STAT homologs among the non-redundant sequences in selected organisms using NCBI PSI-BLAST. A score of 2×10^{-5} was used as a threshold. Similarities of the selected sequences were determined using BLOSUM62 matrix and E-INS-i strategy (219). Sequences were manually curated using AliView software [(218); http://ormbunkar.se/aliview/], and the resulting final alignment was used to generate a neighbor joining phylogenetic tree (NJ, bootstrap 1,000×).

manner to regulate growth and development, various immunity-related processes, and cellular stress responses (331, 332). Gain- or loss-of-function mutations in components of the JAK–STAT signaling pathway have been associated with a broad range of innate-immune deficiencies and autoimmune diseases (333).

Multiple social amoeba species have STAT homologs, and four *D. discoideum* homologs of STATs have been identified, DstA, DstB, DstC, and DstD [reviewed in Ref. (334)] (**Figure 12**; **Table 2**). These proteins have a predicted SH2 domain (335), and their activity is regulated in part by tyrosine kinases (336, 337) and phosphatases (338, 339). Like mammalian STATs, *D. discoideum* STATs regulate growth and development in response to extracellular signaling molecules (335, 340–342) and are activated by cellular stresses (339, 343). Whether they also contribute to antimicrobial responses in *D. discoideum* is unknown, and addressing this question will provide insight into their possible roles in cell-autonomous defenses.

CONCLUSION AND PERSPECTIVES

Dictyostelium discoideum is a natural predator of bacteria and must contend with the fact that every meal is a potential infection. To survive this situation, it has evolved multiple mechanisms to generate a microbicidal environment within phagosomes and thus, phagocytosis, its means of nutrient acquisition, is simultaneously a major component of its defenses against infection. Autophagy, a pathway of nutrient reallocation, has also been incorporated into its defenses and is activated when microbes disrupt the phagosome and/or escape into the cytosol. Importantly, core components of these pathways are conserved in the specialized phagocytes of metazoans such as MPS cells. Consequently, *D. discoideum* is a relevant model to study the role of cell-autonomous defenses in the response of MPS cells to infection. Indeed, it has been used successfully to identify bacterial virulence factors and mechanisms by which bacteria interfere with phagosome maturation and autophagy.

Although one might question the need for model organisms in the CRISPR era of genomic editing, the use of *D. discoideum* has many advantages and is far from over. The generation of unbiased *D. discoideum* mutant libraries requires fewer financial and technical resources than creating a library of CRISPR-edited macrophages, and cultivation of this amoeba requires no special growth factors or cytokines. Moreover, growing *D. discoideum* cells respond to and phagocytose microbes without the need for prior activation. High-throughput mutant screens are thus more feasible and more accessible to laboratories with fewer financial resources. Similarly, the functions of individual bacterial or host factors in infection can be more readily and thoroughly assessed in *D. discoideum* due to its amenability to numerous research techniques. The knowledge gained can then be used to pose specific questions that can be answered by targeted studies in MPS cells. Primary macrophages or dendritic cells are often

used to avoid the potential artifacts of immortalized cell lines. The use of *D. discoideum*, an organism compliant with the 3R initiative to reduce the use of animals (344), minimizes the need to sacrifice mice to procure these cells. Finally, given its lack of adaptive immunity, *D. discoideum* provides a context to study cell-autonomous defenses independent of other immune responses.

In addition to its importance as a model phagocyte, *D. discoideum* is also important from an ecological perspective. It is a key component of a complex network of bacteria, fungi, protists, and insects in the soil. The chemical language of this network is a potential source of natural products (345–348). Interactions between *D. discoideum* and bacteria can be symbiotic (349–351), and, as a reservoir and training ground for amoeba-resistant microbes, it can provide clues to understand and identify emerging pathogens. The structure of fruiting bodies appears to be evolutionarily optimized to be spread by insects (352), and insect-mediated transmission of fruiting bodies containing infectious *Bordetella bronchiseptica*, a respiratory pathogen of small mammals, has been demonstrated (353).

Many questions regarding interactions between intracellular pathogens and MPS cells remain unanswered, and *D. discoideum* still has much to teach us. For example, other than detecting disruption of the phagosome membrane, how *D. discoideum* "knows" it is infected is unknown. It might sense bacteria with PRRs, but, unless the bacteria are in the cytosol, this would not necessarily distinguish food bacteria that are readily killed from pathogenic bacteria. Given that its defense and nutrient pathways are intertwined, one possibility is that *D. discoideum* senses dysregulation of metabolism due to nutrient deprivation or imbalance. Another possibility is the recognition of DNA damage caused by bacterial toxins or excessive ROS production. Understanding how *D. discoideum* senses infection will open new avenues to explore in MPS cells. Other studies will continue to reveal the strategies used by microbes to resist being killed in the phagosome or by autophagy, to delineate the contributions of ROS to antimicrobial responses, and to elucidate the complexities of metal poisoning and nutritional immunity. Characterization of the *D. discoideum* versions of microbial restriction factors discovered in MPS cells will provide insight into their function and further establish the model. The future is bright for this fascinating and versatile amoeba.

AUTHOR CONTRIBUTIONS

JDD contributed ideas, wrote sections, created figures, edited, and compiled the manuscript. CBo, CBa, LR, LHL, EC-M, and ATL-J contributed ideas, wrote sections, and created figures. TS contributed ideas and edited.

ACKNOWLEDGMENTS

The authors gratefully acknowledge the collaboration of Dr. Petra Fey at http://dictybase.org and Dr. Takefumi Kawata for accepting and implementing the new nomenclature of Zinc transporters proposed here.

FUNDING

The TS laboratory is supported by multiple grants from the Swiss National Science Foundation, and TS is a member of iGE3 (www.ige3.unige.ch) as well as of the COST Actions BM1203 EU-ROS and CA15138 TRANSAUTOPHAGY.

SUPPLEMENTARY MATERIAL

The Supplementary Material for this article can be found online at http://www.frontiersin.org/articles/10.3389/fimmu.2017.01906/full#supplementary-material.

REFERENCES

1. Randow F, MacMicking JD, James LC. Cellular self-defense: how cell-autonomous immunity protects against pathogens. *Science* (2013) 340(6133): 701–6. doi:10.1126/science.1233028
2. Gaudet RG, Bradfield CJ, MacMicking JD. Evolution of cell-autonomous effector mechanisms in macrophages versus non-immune cells. *Microbiol Spectr* (2016) 4(6). doi:10.1128/microbiolspec.MCHD-0050-2016
3. Matz C, Kjelleberg S. Off the hook – how bacteria survive protozoan grazing. *Trends Microbiol* (2005) 13(7):302–7. doi:10.1016/j.tim.2005.05.009
4. Casadevall A, Pirofski L-A. Accidental virulence, cryptic pathogenesis, Martians, lost hosts, and the pathogenicity of environmental microbes. *Eukaryot Cell* (2007) 6(12):2169–74. doi:10.1128/EC.00308-07
5. Cosson P, Soldati T. Eat, kill or die: when amoeba meets bacteria. *Curr Opin Microbiol* (2008) 11(3):271–6. doi:10.1016/j.mib.2008.05.005
6. Erken M, Lutz C, McDougald D. The rise of pathogens: predation as a factor driving the evolution of human pathogens in the environment. *Microb Ecol* (2013) 65(4):860–8. doi:10.1007/s00248-013-0189-0
7. Desjardins M, Houde M, Gagnon E. Phagocytosis: the convoluted way from nutrition to adaptive immunity. *Immunol Rev* (2005) 207:158–65. doi:10.1111/j.0105-2896.2005.00319.x
8. Boulais J, Trost M, Landry CR, Dieckmann R, Levy ED, Soldati T, et al. Molecular characterization of the evolution of phagosomes. *Mol Syst Biol* (2010) 6:423. doi:10.1038/msb.2010.80
9. Matz C, Bergfeld T, Rice SA, Kjelleberg S. Microcolonies, quorum sensing and cytotoxicity determine the survival of *Pseudomonas aeruginosa* biofilms exposed to protozoan grazing. *Environ Microbiol* (2004) 6(3):218–26. doi:10.1038/nrmicro876
10. Matz C, McDougald D, Moreno AM, Yung PY, Yildiz FH, Kjelleberg S. Biofilm formation and phenotypic variation enhance predation-driven persistence of *Vibrio cholerae*. *Proc Natl Acad Sci U S A* (2005) 102(46):16819–24. doi:10.1073/pnas.0505350102
11. Adiba S, Nizak C, van Baalen M, Denamur E, Depaulis F. From grazing resistance to pathogenesis: the coincidental evolution of virulence factors. *PLoS One* (2010) 5(8):e11882. doi:10.1371/journal.pone.0011882
12. Amaro F, Wang W, Gilbert JA, Anderson OR, Shuman HA. Diverse protist grazers select for virulence-related traits in *Legionella*. *ISME J* (2015) 9(7):1607–18. doi:10.1038/ismej.2014.248
13. Salah IB, Ghigo E, Drancourt M. Free-living amoebae, a training field for macrophage resistance of mycobacteria. *Clin Microbiol Infect* (2009) 15(10):894–905. doi:10.1111/j.1469-0691.2009.03011.x
14. Drancourt M. Looking in amoebae as a source of mycobacteria. *Microb Pathog* (2014) 77:119–24. doi:10.1016/j.micpath.2014.07.001
15. Van der Henst C, Scrignari T, Maclachlan C, Blokesch M. An intracellular replication niche for *Vibrio cholerae* in the amoeba *Acanthamoeba castellanii*. *ISME J* (2016) 10(4):897–910. doi:10.1038/ismej.2015.165
16. Pukatzki S, Kessin RH, Mekalanos JJ. The human pathogen *Pseudomonas aeruginosa* utilizes conserved virulence pathways to infect the social amoeba

Dictyostelium discoideum. *Proc Natl Acad Sci U S A* (2002) 99(5):3159–64. doi:10.1073/pnas.052704399
17. Pukatzki S, Ma AT, Sturtevant D, Krastins B, Sarracino D, Nelson WC, et al. Identification of a conserved bacterial protein secretion system in *Vibrio cholerae* using the *Dictyostelium* host model system. *Proc Natl Acad Sci U S A* (2006) 103(5):1528–33. doi:10.1073/pnas.0510322103
18. Hilbi H, Weber SS, Ragaz C, Nyfeler Y, Urwyler S. Environmental predators as models for bacterial pathogenesis. *Environ Microbiol* (2007) 9(3):563–75. doi:10.1111/j.1462-2920.2007.01238.x
19. Pan Y-J, Lin T-L, Hsu C-R, Wang J-T. Use of a *Dictyostelium* model for isolation of genetic loci associated with phagocytosis and virulence in *Klebsiella pneumoniae*. *Infect Immun* (2011) 79(3):1006. doi:10.1128/IAI.00906-10
20. Kessin RH. *Dictyostelium: Evolution, Cell Biology, and the Development of Multicellularity*. Cambridge, UK; New York: Cambridge University Press (2001).
21. Schaap P. Evolutionary crossroads in developmental biology: *Dictyostelium discoideum*. *Development* (2011) 138(3):387–96. doi:10.1242/dev.048934
22. Loomis WF. Cell signaling during development of *Dictyostelium*. *Dev Biol* (2014) 391(1):1–16. doi:10.1016/j.ydbio.2014.04.001
23. Sternfeld J, David CN. Oxygen gradients cause pattern orientation in *Dictyostelium* cell clumps. *J Cell Sci* (1981) 50:9–17.
24. Feit IN, Medynski EJ, Rothrock MJ. Ammonia differentially suppresses the cAMP chemotaxis of anterior-like cells and prestalk cells in *Dictyostelium discoideum*. *J Biosci* (2001) 26(2):157–66. doi:10.1007/BF02703640
25. Bonner JT, Lamont DS. Behavior of cellular slime molds in the soil. *Mycologia* (2005) 97(1):178–84. doi:10.3852/mycologia.97.1.178
26. Huber RJ, O'Day DH. Extracellular matrix dynamics and functions in the social amoeba *Dictyostelium*: a critical review. *Biochim Biophys Acta* (2017) 1861(1 Pt A):2971–80. doi:10.1016/j.bbagen.2016.09.026
27. Suess PM, Watson J, Chen W, Gomer RH. Extracellular polyphosphate signals through Ras and Akt to prime *Dictyostelium discoideum* cells for development. *J Cell Sci* (2017) 130(14):2394–404. doi:10.1242/jcs.203372
28. Singh S, Mohamed W, Aguessy A, Dyett E, Shah S, Khan M, et al. Functional interaction of PkcA and PldB regulate aggregation and development in *Dictyostelium discoideum*. *Cell Signal* (2017) 34:47–54. doi:10.1016/j.cellsig.2017.02.022
29. Hirose S, Benabentos R, Ho HI, Kuspa A, Shaulsky G. Self-recognition in social amoebae is mediated by allelic pairs of tiger genes. *Science* (2011) 333(6041):467–70. doi:10.1126/science.1203903
30. Chattwood A, Nagayama K, Bolourani P, Harkin L, Kamjoo M, Weeks G, et al. Developmental lineage priming in *Dictyostelium* by heterogeneous Ras activation. *Elife* (2013) 2:e01067. doi:10.7554/eLife.01067
31. Hirose S, Santhanam B, Katoh-Kurosawa M, Shaulsky G, Kuspa A. Allorecognition, via TgrB1 and TgrC1, mediates the transition from unicellularity to multicellularity in the social amoeba *Dictyostelium discoideum*. *Development* (2015) 142(20):3561–70. doi:10.1242/dev.123281
32. Levin SR, Brock DA, Queller DC, Strassmann JE. Concurrent coevolution of intra-organismal cheaters and resisters. *J Evol Biol* (2015) 28(4):756–65. doi:10.1111/jeb.12618
33. Junemann A, Filic V, Winterhoff M, Nordholz B, Litschko C, Schwellenbach H, et al. A Diaphanous-related formin links Ras signaling directly to actin assembly in macropinocytosis and phagocytosis. *Proc Natl Acad Sci U S A* (2016) 113(47):E7464–73. doi:10.1073/pnas.1611024113
34. Veltman DM, Williams TD, Bloomfield G, Chen BC, Betzig E, Insall RH, et al. A plasma membrane template for macropinocytic cups. *Elife* (2016) 5:e20085. doi:10.7554/eLife.20085
35. Scavello M, Petlick AR, Ramesh R, Thompson VF, Lotfi P, Charest PG. Protein kinase A regulates the Ras, Rap1 and TORC2 pathways in response to the chemoattractant cAMP in *Dictyostelium*. *J Cell Sci* (2017) 130(9):1545–58. doi:10.1242/jcs.177170
36. Tabara LC, Escalante R. VMP1 establishes ER-microdomains that regulate membrane contact sites and autophagy. *PLoS One* (2016) 11(11):e0166499. doi:10.1371/journal.pone.0166499
37. West CM, Blader IJ. Oxygen sensing by protozoans: how they catch their breath. *Curr Opin Microbiol* (2015) 26:41–7. doi:10.1016/j.mib.2015.04.006
38. Gilsbach BK, Ho FY, Vetter IR, van Haastert PJ, Wittinghofer A, Kortholt A. Roco kinase structures give insights into the mechanism of Parkinson disease-related leucine-rich-repeat kinase 2 mutations. *Proc Natl Acad Sci U S A* (2012) 109(26):10322–7. doi:10.1073/pnas.1203223109
39. Ludtmann MH, Otto GP, Schilde C, Chen ZH, Allan CY, Brace S, et al. An ancestral non-proteolytic role for presenilin proteins in multicellular development of the social amoeba *Dictyostelium discoideum*. *J Cell Sci* (2014) 127(Pt 7):1576–84. doi:10.1242/jcs.140939
40. Chen S, Annesley SJ, Jasim RAF, Musco VJ, Sanislav O, Fisher PR. The Parkinson's disease-associated protein DJ-1 plays a positive nonmitochondrial role in endocytosis in *Dictyostelium* cells. *Dis Model Mech* (2017) 10(10):1261–71. doi:10.1242/dmm.028084
41. Frej AD, Otto GP, Williams RS. Tipping the scales: lessons from simple model systems on inositol imbalance in neurological disorders. *Eur J Cell Biol* (2017) 96(2):154–63. doi:10.1016/j.ejcb.2017.01.007
42. Bozzaro S. The model organism *Dictyostelium discoideum*. *Methods Mol Biol* (2013) 983:17–37. doi:10.1007/978-1-62703-302-2_2
43. Muller-Taubenberger A, Kortholt A, Eichinger L. Simple system – substantial share: the use of *Dictyostelium* in cell biology and molecular medicine. *Eur J Cell Biol* (2013) 92(2):45–53. doi:10.1016/j.ejcb.2012.10.003
44. Urwyler S, Nyfeler Y, Ragaz C, Lee H, Mueller LN, Aebersold R, et al. Proteome analysis of *Legionella* vacuoles purified by magnetic immunoseparation reveals secretory and endosomal GTPases. *Traffic* (2009) 10:76–87. doi:10.1111/j.1600-0854.2008.00851.x
45. Weber SS, Ragaz C, Hilbi H. The inositol polyphosphate 5-phosphatase OCRL1 restricts intracellular growth of *Legionella*, localizes to the replicative vacuole and binds to the bacterial effector LpnE. *Cell Microbiol* (2009) 11:442–60. doi:10.1111/j.1462-5822.2008.01266.x
46. Peracino B, Balest A, Bozzaro S. Phosphoinositides differentially regulate bacterial uptake and Nramp1-induced resistance to *Legionella* infection in *Dictyostelium*. *J Cell Sci* (2010) 123(Pt 23):4039–51. doi:10.1242/jcs.072124
47. Weber S, Wagner M, Hilbi H. Live-cell imaging of phosphoinositide dynamics and membrane architecture during *Legionella* infection. *MBio* (2014) 5:e00839–e813. doi:10.1128/mBio.00839-13
48. Hagedorn M, Soldati T. Flotillin and RacH modulate the intracellular immunity of *Dictyostelium* to *Mycobacterium marinum* infection. *Cell Microbiol* (2007) 9(11):2716–33. doi:10.1111/j.1462-5822.2007.00993.x
49. Hagedorn M, Rohde KH, Russell DG, Soldati T. Infection by tubercular mycobacteria is spread by nonlytic ejection from their amoeba hosts. *Science* (2009) 323(5922):1729–33. doi:10.1126/science.1169381
50. Barisch C, Soldati T. *Mycobacterium marinum* degrades both triacylglycerols and phospholipids from its *Dictyostelium* host to synthesise its own triacylglycerols and generate lipid inclusions. *PLoS Pathog* (2017) 13(1):e1006095. doi:10.1371/journal.ppat.1006095
51. Cardenal-Munoz E, Arafah S, Lopez-Jimenez AT, Kicka S, Falaise A, Bach F, et al. *Mycobacterium marinum* antagonistically induces an autophagic response while repressing the autophagic flux in a TORC1- and ESX-1-dependent manner. *PLoS Pathog* (2017) 13(4):e1006344. doi:10.1371/journal.ppat.1006344
52. Lampe EO, Brenz Y, Herrmann L, Repnik U, Griffiths G, Zingmark C, et al. Dissection of *Francisella*-host cell interactions in *Dictyostelium discoideum*. *Appl Environ Microbiol* (2016) 82(5):1586–98. doi:10.1128/AEM.02950-15
53. Brenz Y, Ohnezeit D, Winther-Larsen HC, Hagedorn M. Nramp1 and NrampB contribute to resistance against *Francisella* in *Dictyostelium*. *Front Cell Infect Microbiol* (2017) 7:282. doi:10.3389/fcimb.2017.00282
54. Jia K, Thomas C, Akbar M, Sun Q, Adams-Huet B, Gilpin C, et al. Autophagy genes protect against *Salmonella typhimurium* infection and mediate insulin signaling-regulated pathogen resistance. *Proc Natl Acad Sci U S A* (2009) 106(34):14564–9. doi:10.1073/pnas.0813319106
55. Bozzaro S, Eichinger L. The professional phagocyte *Dictyostelium discoideum* as a model host for bacterial pathogens. *Curr Drug Targets* (2011) 12:942–54. doi:10.2174/138945011795677782
56. Artemenko Y, Lampert TJ, Devreotes PN. Moving towards a paradigm: common mechanisms of chemotactic signaling in *Dictyostelium* and mammalian leukocytes. *Cell Mol Life Sci* (2014) 71(19):3711–47. doi:10.1007/s00018-014-1638-8
57. Nichols JM, Veltman D, Kay RR. Chemotaxis of a model organism: progress with *Dictyostelium*. *Curr Opin Cell Biol* (2015) 36:7–12. doi:10.1016/j.ceb.2015.06.005

58. Bloomfield G, Kay RR. Uses and abuses of macropinocytosis. *J Cell Sci* (2016) 129(14):2697–705. doi:10.1242/jcs.176149
59. Buckley CM, King JS. Drinking problems: mechanisms of macropinosome formation and maturation. *FEBS J* (2017) 284(22):3778–90. doi:10.1111/febs.14115
60. Kicka S, Trofimov V, Harrison C, Ouertatani-Sakouhi H, McKinney J, Scapozza L, et al. Establishment and validation of whole-cell based fluorescence assays to identify anti-mycobacterial compounds using the *Acanthamoeba castellanii-Mycobacterium marinum* host-pathogen system. *PLoS One* (2014) 9(1):e87834. doi:10.1371/journal.pone.0087834
61. Liao XH, Meena NP, Southall N, Liu L, Swaroop M, Zhang AL, et al. A high-throughput, multi-cell phenotype assay for the identification of novel inhibitors of chemotaxis/migration. *Sci Rep* (2016) 6:22273. doi:10.1038/srep22273
62. Ouertatani-Sakouhi H, Kicka S, Chiriano G, Harrison CF, Hilbi H, Scapozza L, et al. Inhibitors of *Mycobacterium marinum* virulence identified in a *Dictyostelium discoideum* host model. *PLoS One* (2017) 12(7):e0181121. doi:10.1371/journal.pone.0181121
63. Barisch C, Lopez-Jimenez AT, Soldati T. Live imaging of *Mycobacterium marinum* infection in *Dictyostelium discoideum*. *Methods Mol Biol* (2015) 1285:369–85. doi:10.1007/978-1-4939-2450-9_23
64. Eichinger L, Rivero-Crespo F, editors. *Dictyostelium discoideum Protocols*. Totowa, NJ: Humana Press (2013).
65. Eichinger L, Pachebat JA, Glockner G, Rajandream MA, Sucgang R, Berriman M, et al. The genome of the social amoeba *Dictyostelium discoideum*. *Nature* (2005) 435(7038):43–57. doi:10.1038/nature03481
66. Sucgang R, Kuo A, Tian X, Salerno W, Parikh A, Feasley CL, et al. Comparative genomics of the social amoebae *Dictyostelium discoideum* and *Dictyostelium purpureum*. *Genome Biol* (2011) 12(2):R20. doi:10.1186/gb-2011-12-2-r20
67. Basu S, Fey P, Pandit Y, Dodson R, Kibbe WA, Chisholm RL. DictyBase 2013: integrating multiple dictyostelid species. *Nucleic Acids Res* (2013) 41(Database issue):D676–83. doi:10.1093/nar/gks1064
68. Glockner G, Lawal HM, Felder M, Singh R, Singer G, Weijer CJ, et al. The multicellularity genes of dictyostelid social amoebas. *Nat Commun* (2016) 7:12085. doi:10.1038/ncomms12085
69. Rosengarten RD, Santhanam B, Fuller D, Katoh-Kurasawa M, Loomis WF, Zupan B, et al. Leaps and lulls in the developmental transcriptome of *Dictyostelium discoideum*. *BMC Genomics* (2015) 16:294. doi:10.1186/s12864-015-1491-7
70. Stajdohar M, Rosengarten RD, Kokosar J, Jeran L, Blenkus D, Shaulsky G, et al. dictyExpress: a web-based platform for sequence data management and analytics in *Dictyostelium* and beyond. *BMC Bioinformatics* (2017) 18(1):291. doi:10.1186/s12859-017-1706-9
71. Basu S, Fey P, Jimenez-Morales D, Dodson RJ, Chisholm RL. dictyBase 2015: expanding data and annotations in a new software environment. *Genesis* (2015) 53(8):523–34. doi:10.1002/dvg.22867
72. Arafah S, Kicka S, Trofimov V, Hagedorn M, Andreu N, Wiles S, et al. Setting up and monitoring an infection of *Dictyostelium discoideum* with mycobacteria. In: Eichinger L, Rivero F, editors. *Dictyostelium discoideum Protocols*. Totowa, NJ: Humana Press (2013). p. 403–17.
73. Weber S, Hilbi H. Live cell imaging of phosphoinositide dynamics during *Legionella* infection. *Methods Mol Biol* (2014) 1197:153–67. doi:10.1007/978-1-4939-1261-2_9
74. Dominguez-Martin E, Cardenal-Munoz E, King JS, Soldati T, Coria R, Escalante R. Methods to monitor and quantify autophagy in the social amoeba *Dictyostelium discoideum*. *Cells* (2017) 6(3):E18. doi:10.3390/cells6030018
75. Bloomfield G, Traynor D, Sander SP, Veltman DM, Pachebat JA, Kay RR. Neurofibromin controls macropinocytosis and phagocytosis in *Dictyostelium*. *Elife* (2015) 4. doi:10.7554/eLife.04940
76. Freeman SA, Grinstein S. Phagocytosis: receptors, signal integration, and the cytoskeleton. *Immunol Rev* (2014) 262:193–215. doi:10.1111/imr.12212
77. Chen G, Zhuchenko O, Kuspa A. Immune-like phagocyte activity in the social amoeba. *Science* (2007) 317(5838):678–81. doi:10.1126/science.1143991
78. Cornillon S, Gebbie L, Benghezal M, Nair P, Keller S, Wehrle-Haller B, et al. An adhesion molecule in free-living *Dictyostelium* amoebae with integrin β features. *EMBO Rep* (2006) 7:617–21. doi:10.1038/sj.embor.7400701
79. Cornillon S, Pech E, Benghezal M, Ravanel K, Gaynor E, Letourneur F, et al. Phg1p Is a nine-transmembrane protein superfamily member involved in *Dictyostelium* adhesion and phagocytosis. *J Biol Chem* (2000) 275:34287–92. doi:10.1074/jbc.M006725200
80. Fey P, Stephens S, Titus MA, Chisholm RL. SadA, a novel adhesion receptor in *Dictyostelium*. *J Cell Biol* (2002) 159:1109–19. doi:10.1083/jcb.200206067
81. Froquet R, Coadic M.l, Perrin J, Cherix N, Cornillon S, Cosson P. TM9/Phg1 and SadA proteins control surface expression and stability of SibA adhesion molecules in *Dictyostelium*. *Mol Biol Cell* (2012) 23:679–86. doi:10.1091/mbc.E11-04-0338
82. Harris TJ, Ravandi A, Siu CH. Assembly of glycoprotein-80 adhesion complexes in *Dictyostelium*. Receptor compartmentalization and oligomerization in membrane rafts. *J Biol Chem* (2001) 276(52):48764–74. doi:10.1074/jbc.M108030200
83. Janssen K-P, Rost R, Eichinger L, Schleicher M. Characterization of CD36/LIMPII homologues in *Dictyostelium discoideum*. *J Biol Chem* (2001) 276:38899–910. doi:10.1074/jbc.M103384200
84. Gotthardt D, Warnatz HJ, Henschel O, Brückert F, Schleicher M, Soldati T. High-resolution dissection of phagosome maturation reveals distinct membrane trafficking phases. *Mol Biol Cell* (2002) 13:3508–20. doi:10.1091/mbc.E02-04-0206
85. Vogel G, Thilo L, Schwarz H, Steinhart R. Mechanism of phagocytosis in *Dictyostelium discoideum*: phagocytosis is mediated by different recognition sites as disclosed by mutants with altered phagocytotic properties. *J Cell Biol* (1980) 86:456–65. doi:10.1083/jcb.86.2.456
86. Bozzaro S, Roseman S. Adhesion of *Dictyostelium discoideum* cells to carbohydrates immobilized in polyacrylamide gels. I. Evidence for three sugar-specific cell surface receptors. *J Biol Chem* (1983) 258:13882–9.
87. Pan M, Xu X, Chen Y, Jin T. Identification of a chemoattractant G-protein-coupled receptor for folic acid that controls both chemotaxis and phagocytosis. *Dev Cell* (2016) 36:428–39. doi:10.1016/j.devcel.2016.01.012
88. Lima WC, Balestrino D, Forestier C, Cosson P. Two distinct sensing pathways allow recognition of *Klebsiella pneumoniae* by *Dictyostelium* amoebae. *Cell Microbiol* (2014) 16(3):311–23. doi:10.1111/cmi.12226
89. Gotthardt D, Blancheteau V, Bosserhoff A, Ruppert T, Delorenzi M, Soldati T. Proteomics fingerprinting of phagosome maturation and evidence for the role of a Gα during uptake. *Mol Cell Proteom* (2006) 5:2228–43. doi:10.1074/mcp.M600113-MCP200
90. Insall R, Müller-Taubenberger A, Machesky L, Köhler J, Simmeth E, Atkinson SJ, et al. Dynamics of the *Dictyostelium* Arp2/3 complex in endocytosis, cytokinesis, and chemotaxis. *Cell Motil Cytoskeleton* (2001) 50:115–28. doi:10.1002/cm.10005
91. Seastone DJ, Harris E, Temesvari LA, Bear JE, Saxe CL, Cardelli J. The WASp-like protein Scar regulates macropinocytosis, phagocytosis and endosomal membrane flow in *Dictyostelium*. *J Cell Sci* (2001) 114:2673–83.
92. Dieckmann R, von Heyden Y, Kistler C, Gopaldass N, Hausherr S, Crawley SW, et al. A myosin IK-Abp1-PakB circuit acts as a switch to regulate phagocytosis efficiency. *Mol Biol Cell* (2010) 21(9):1505–18. doi:10.1091/mbc.E09-06-0485
93. Gopaldass N, Patel D, Kratzke R, Dieckmann R, Hausherr S, Hagedorn M, et al. Dynamin A, myosin IB and Abp1 couple phagosome maturation to F-actin binding. *Traffic* (2012) 13:120–30. doi:10.1111/j.1600-0854.2011.01296.x
94. Bozzaro S, Bucci C, Steinert M. Chapter 6 phagocytosis and host-pathogen interactions in *Dictyostelium* with a look at macrophages. In: Jeon KW, editor. *International Review of Cell and Molecular Biology*. Burlington: Academic Press (2008). p. 253–300.
95. Rivero F, Xiong H. Rho signaling in *Dictyostelium discoideum*. *Int Rev Cell Mol Biol* (2016) 322:61–181. doi:10.1016/bs.ircmb.2015.10.004
96. Dormann D, Weijer G, Dowler S, Weijer CJ. In vivo analysis of 3-phosphoinositide dynamics during *Dictyostelium* phagocytosis and chemotaxis. *J Cell Sci* (2004) 117(Pt 26):6497–509. doi:10.1242/jcs.01579
97. Blanc C, Charette S, Cherix N, Lefkir Y, Cosson P, Letourneur F. A novel phosphatidylinositol 4,5-bisphosphate-binding domain targeting the Phg2 kinase to the membrane in *Dictyostelium* cells. *Eur J Cell Biol* (2005) 84(12):951–60. doi:10.1016/j.ejcb.2005.09.014
98. Loovers HM, Kortholt A, de Groote H, Whitty L, Nussbaum RL, van Haastert PJM. Regulation of phagocytosis in *Dictyostelium* by the

inositol 5-phosphatase OCRL homolog Dd5P4. *Traffic* (2007) 8:618–28. doi:10.1111/j.1600-0854.2007.00546.x
99. Derivery E, Sousa C, Gautier JJ, Lombard B, Loew D, Gautreau A. The Arp2/3 activator WASH controls the fission of endosomes through a large multiprotein complex. *Dev Cell* (2009) 17:712–23. doi:10.1016/j.devcel.2009.09.010
100. Gomez TS, Billadeau DD. A FAM21-containing WASH complex regulates retromer-dependent sorting. *Dev Cell* (2009) 17:699–711. doi:10.1016/j.devcel.2009.09.009
101. Buckley CM, Gopaldass N, Bosmani C, Johnston SA, Soldati T, Insall RH, et al. WASH drives early recycling from macropinosomes and phagosomes to maintain surface phagocytic receptors. *Proc Natl Acad Sci U S A* (2016) 113(40):E5906–15. doi:10.1073/pnas.1524532113
102. Gutierrez MG. Functional role(s) of phagosomal Rab GTPases. *Small GTPases* (2013) 4:148–58. doi:10.4161/sgtp.25604
103. Gorvel JP, Chavrier P, Zerial M, Gruenberg J. rab5 controls early endosome fusion in vitro. *Cell* (1991) 64(5):915–25. doi:10.1016/0092-8674(91)90316-Q
104. Vieira OV, Bucci C, Harrison RE, Trimble WS, Lanzetti L, Gruenberg J, et al. Modulation of Rab5 and Rab7 recruitment to phagosomes by phosphatidylinositol 3-kinase. *Mol Cell Biol* (2003) 23(7):2501–14. doi:10.1128/MCB.23.7.2501-2514.2003
105. Harrison RE, Bucci C, Vieira OV, Schroer TA, Grinstein S. Phagosomes fuse with late endosomes and/or lysosomes by extension of membrane protrusions along microtubules: role of Rab7 and RILP. *Mol Cell Biol* (2003) 23(18):6494–506. doi:10.1128/MCB.23.18.6494-6506.2003
106. Buczynski G, Bush J, Zhang L, Rodriguez-Paris J, Cardelli J. Evidence for a recycling role for Rab7 in regulating a late step in endocytosis and in retention of lysosomal enzymes in *Dictyostelium discoideum*. *Mol Biol Cell* (1997) 8(7):1343–60. doi:10.1091/mbc.8.7.1343
107. Rupper A, Grove B, Cardelli J. Rab7 regulates phagosome maturation in *Dictyostelium*. *J Cell Sci* (2001) 114:2449–60.
108. Clarke M, Köhler J, Arana Q, Liu T, Heuser J, Gerisch G. Dynamics of the vacuolar H+-ATPase in the contractile vacuole complex and the endosomal pathway of *Dictyostelium* cells. *J Cell Sci* (2002) 115:2893–905.
109. Neuhaus EM, Almers W, Soldati T. Morphology and dynamics of the endocytic pathway in *Dictyostelium discoideum*. *Mol Biol Cell* (2002) 13(4):1390–407. doi:10.1091/mbc.01-08-0392
110. Sun-Wada G-H, Tabata H, Kawamura N, Aoyama M, Wada Y. Direct recruitment of H^+-ATPase from lysosomes for phagosomal acidification. *J Cell Sci* (2009) 122:2504–13. doi:10.1242/jcs.050443
111. Sattler N, Monroy R, Soldati T. Quantitative analysis of phagocytosis and phagosome maturation. *Methods Mol Biol* (2013) 983:383–402. doi:10.1007/978-1-62703-302-2_21
112. Yates RM, Hermetter A, Russell DG. The kinetics of phagosome maturation as a function of phagosome/lysosome fusion and acquisition of hydrolytic activity. *Traffic* (2005) 6:413–20. doi:10.1111/j.1600-0854.2005.00284.x
113. Marchetti A, Lelong E, Cosson P. A measure of endosomal pH by flow cytometry in *Dictyostelium*. *BMC Res Notes* (2009) 2:7. doi:10.1186/1756-0500-2-7
114. Le Roux D, Le Bon A, Dumas A, Taleb K, Sachse M, Sikora R, et al. Antigen stored in dendritic cells after macropinocytosis is released unprocessed from late endosomes to target B cells. *Blood* (2012) 119(1):95–105. doi:10.1182/blood-2011-02-336123
115. Le Roux D, Niedergang F. New insights into antigen encounter by B cells. *Immunobiology* (2012) 217(12):1285–91. doi:10.1016/j.imbio.2012.07.011
116. Carnell M, Zech T, Calaminus SD, Ura S, Hagedorn M, Johnston SA, et al. Actin polymerization driven by WASH causes V-ATPase retrieval and vesicle neutralization before exocytosis. *J Cell Biol* (2011) 193:831–9. doi:10.1083/jcb.201009119
117. King JS, Gueho A, Hagedorn M, Gopaldass N, Leuba F, Soldati T, et al. WASH is required for lysosomal recycling and efficient autophagic and phagocytic digestion. *Mol Biol Cell* (2013) 24(17):2714–26. doi:10.1091/mbc.E13-02-0092
118. Rauchenberger R, Hacker U, Murphy J, Niewöhner J, Maniak M. Coronin and vacuolin identify consecutive stages of a late, actin-coated endocytic compartment in *Dictyostelium*. *Curr Biol* (1997) 7:215–8. doi:10.1016/S0960-9822(97)70093-9
119. Jenne N, Rauchenberger R, Hacker U, Kast T, Maniak M. Targeted gene disruption reveals a role for vacuolin B in the late endocytic pathway and exocytosis. *J Cell Sci* (1998) 111:61–70.
120. Wienke D, Drengk A, Schmauch C, Jenne N, Maniak M. Vacuolin, a flotillin/reggie-related protein from *Dictyostelium* oligomerizes for endosome association. *Eur J Cell Biol* (2006) 85:991–1000. doi:10.1016/j.ejcb.2006.04.010
121. Holt OJ, Gallo F, Griffiths GM. Regulating secretory lysosomes. *J Biochem* (2006) 140:7–12. doi:10.1093/jb/mvj126
122. Lima WC, Leuba F, Soldati T, Cosson P. Mucolipin controls lysosome exocytosis in *Dictyostelium*. *J Cell Sci* (2012) 125(Pt 9):2315–22. doi:10.1242/jcs.100362
123. Lu H, Clarke M. Dynamic properties of *Legionella*-containing phagosomes in *Dictyostelium* amoebae. *Cell Microbiol* (2005) 7:995–1007. doi:10.1111/j.1462-5822.2005.00528.x
124. Hilbi H, Weber S, Finsel I. Anchors for effectors: subversion of phosphoinositide lipids by *Legionella*. *Front Microbiol* (2011) 2:91. doi:10.3389/fmicb.2011.00091
125. Simon S, Hilbi H. Subversion of cell-autonomous immunity and cell migration by *Legionella pneumophila* effectors. *Front Immunol* (2015) 6:447. doi:10.3389/fimmu.2015.00447
126. Hoffmann C, Finsel I, Otto A, Pfaffinger G, Rothmeier E, Hecker M, et al. Functional analysis of novel Rab GTPases identified in the proteome of purified *Legionella*-containing vacuoles from macrophages. *Cell Microbiol* (2014) 16:1034–52. doi:10.1111/cmi.12256
127. Vergne I, Chua J, Singh SB, Deretic V. Cell biology of *Mycobacterium tuberculosis* phagosome. *Annu Rev Cell Dev Biol* (2004) 20:367–94. doi:10.1146/annurev.cellbio.20.010403.114015
128. Kolonko M, Geffken AC, Blumer T, Hagens K, Schaible UE, Hagedorn M. WASH-driven actin polymerization is required for efficient mycobacterial phagosome maturation arrest. *Cell Microbiol* (2014) 16:232–46. doi:10.1111/cmi.12217
129. Friedrich N, Hagedorn M, Soldati-Favre D, Soldati T. Prison break: pathogens' strategies to egress from host cells. *Microbiol Mol Biol Rev* (2012) 76(4):707–20. doi:10.1128/MMBR.00024-12
130. Gerstenmaier L, Pilla R, Herrmann L, Herrmann H, Prado M, Villafano GJ, et al. The autophagic machinery ensures nonlytic transmission of mycobacteria. *Proc Natl Acad Sci U S A* (2015) 112(7):E687–92. doi:10.1073/pnas.1423318112
131. Alibaud L, Rombouts Y, Trivelli X, Burguière A, Cirillo SLG, Cirillo JD, et al. A *Mycobacterium marinum* TesA mutant defective for major cell wall-associated lipids is highly attenuated in *Dictyostelium discoideum* and zebrafish embryos. *Mol Microbiol* (2011) 80:919–34. doi:10.1111/j.1365-2958.2011.07618.x
132. Weerdenburg EM, Abdallah AM, Rangkuti F, Ghany MAE, Otto TD, Adroub SA, et al. Genome-wide transposon mutagenesis indicates that *Mycobacterium marinum* customizes its virulence mechanisms for survival and replication in different hosts. *Infect Immun* (2015) 83:1778–88. doi:10.1128/IAI.03050-14
133. Chen Y-Y, Yang F-L, Wu S-H, Lin T-L, Wang J-T. Mycobacterium marinum mmar_2318 and mmar_2319 are responsible for lipooligosaccharide biosynthesis and virulence toward *Dictyostelium*. *Front Microbiol* (2016) 6:1458. doi:10.3389/fmicb.2015.01458
134. Mohandas P, Budell WC, Mueller E, Au A, Bythrow GV, Quadri LEN. Pleiotropic consequences of gene knockouts in the phthiocerol dimycocerosate and phenolic glycolipid biosynthetic gene cluster of the opportunistic human pathogen *Mycobacterium marinum*. *FEMS Microbiol Lett* (2016) 363:fnw016. doi:10.1093/femsle/fnw016
135. Muller I, Subert N, Otto H, Herbst R, Ruhling H, Maniak M, et al. A *Dictyostelium* mutant with reduced lysozyme levels compensates by increased phagocytic activity. *J Biol Chem* (2005) 280(11):10435–43. doi:10.1074/jbc.M411445200
136. Nasser W, Santhanam B, Miranda ER, Parikh A, Juneja K, Rot G, et al. Bacterial discrimination by dictyostelid amoebae reveals the complexity of ancient interspecies interactions. *Curr Biol* (2013) 23:862–72. doi:10.1016/j.cub.2013.04.034
137. Reeves EP, Lu H, Jacobs HL, Messina CGM, Bolsover S, Gabella G, et al. Killing activity of neutrophils is mediated through activation of proteases by K+ flux. *Nature* (2002) 416:291–7. doi:10.1038/416291a

138. Müller S, Faulhaber A, Sieber C, Pfeifer D, Hochberg T, Gansz M, et al. The endolysosomal cysteine cathepsins L and K are involved in macrophage-mediated clearance of *Staphylococcus aureus* and the concomitant cytokine induction. *FASEB J* (2014) 28:162–75. doi:10.1096/fj.13-232272
139. Pires D, Marques J, Pombo JP, Carmo N, Bettencourt P, Neyrolles O, et al. Role of cathepsins in *Mycobacterium tuberculosis* survival in human macrophages. *Sci Rep* (2016) 6:sre32247. doi:10.1038/srep32247
140. del Cerro-Vadillo E, Madrazo-Toca F, Carrasco-Marín E, Fernandez-Prieto L, Beck C, Leyva-Cobián F, et al. Cutting edge: a novel nonoxidative phagosomal mechanism exerted by cathepsin-D controls *Listeria monocytogenes* intracellular growth. *J Immunol* (2006) 176:1321–5. doi:10.4049/jimmunol.176.3.1321
141. Freeze HH, Bush JM, Cardelli J. Biochemical and genetic analysis of an antigenic determinant found on N-linked oligosaccharides in *Dictyostelium*. *Dev Genet* (1990) 11:463–72. doi:10.1002/dvg.1020110523
142. Journet A, Chapel A, Jehan S, Adessi C, Freeze H, Klein G, et al. Characterization of *Dictyostelium discoideum* cathepsin D. *J Cell Sci* (1999) 112:3833–43.
143. Souza GM, Hirai J, Mehta DP, Freeze HH. Identification of two novel *Dictyostelium discoideum* cysteine proteinases that carry N-acetylglucosamine-1-P-modification. *J Biol Chem* (1995) 270:28938–45. doi:10.1074/jbc.270.48.28938
144. Souza GM, Mehta DP, Lammertz M, Rodriguez-Paris J, Wu R, Cardelli JA, et al. *Dictyostelium* lysosomal proteins with different sugar modifications sort to functionally distinct compartments. *J Cell Sci* (1997) 110:2239–48.
145. Kypri E, Schmauch C, Maniak M, Lozanne AD. The BEACH protein LvsB is localized on lysosomes and postlysosomes and limits their fusion with early endosomes. *Traffic* (2007) 8:774–83. doi:10.1111/j.1600-0854.2007.00567.x
146. Le Coadic M, Froquet R, Lima WC, Dias M, Marchetti A, Cosson P. Phg1/TM9 proteins control intracellular killing of bacteria by determining cellular levels of the Kil1 sulfotransferase in *Dictyostelium*. *PLoS One* (2013) 8(1):e53259. doi:10.1371/journal.pone.0053259
147. Harris E, Wang N, Wu W-L, Weatherford A, De Lozanne A, Cardelli J. *Dictyostelium* LvsB mutants model the lysosomal defects associated with Chediak-Higashi syndrome. *Mol Biol Cell* (2002) 13:656–69. doi:10.1091/mbc.01-09-0454
148. Benghezal M, Fauvarque MO, Tournebize R, Froquet R, Marchetti A, Bergeret E, et al. Specific host genes required for the killing of *Klebsiella* bacteria by phagocytes. *Cell Microbiol* (2006) 8(1):139–48. doi:10.1111/j.1462-5822.2005.00607.x
149. Fang FC. Antimicrobial actions of reactive oxygen species. *MBio* (2011) 2(5):e00141–111. doi:10.1128/mBio.00141-11
150. Li Q, Harraz MM, Zhou W, Zhang LN, Ding W, Zhang Y, et al. Nox2 and Rac1 regulate H2O2-dependent recruitment of TRAF6 to endosomal interleukin-1 receptor complexes. *Mol Cell Biol* (2006) 26(1):140–54. doi:10.1128/MCB.26.1.140-154.2006
151. Yang C-S, Kim J-J, Lee SJ, Hwang JH, Lee C-H, Lee M-S, et al. TLR3-triggered reactive oxygen species contribute to inflammatory responses by activating signal transducer and activator of transcription-1. *J Immunol* (2013) 190(12):6368–77. doi:10.4049/jimmunol.1202574
152. Huang J, Canadien V, Lam GY, Steinberg BE, Dinauer MC, Magalhaes MAO, et al. Activation of antibacterial autophagy by NADPH oxidases. *Proc Natl Acad Sci U S A* (2009) 106(15):6226–31. doi:10.1073/pnas.0811045106
153. Liu W, Peng Y, Yin Y, Zhou Z, Zhou W, Dai Y. The involvement of NADPH oxidase-mediated ROS in cytokine secretion from macrophages induced by *Mycobacterium tuberculosis* ESAT-6. *Inflammation* (2014) 37(3):880–92. doi:10.1007/s10753-013-9808-7
154. Cruz CM, Rinna A, Forman HJ, Ventura ALM, Persechini PM, Ojcius DM. ATP activates a reactive oxygen species-dependent oxidative stress response and secretion of proinflammatory cytokines in macrophages. *J Biol Chem* (2007) 282(5):2871–9. doi:10.1074/jbc.M608083200
155. Miller JL, Velmurugan K, Cowan MJ, Briken V. The type I NADH dehydrogenase of *Mycobacterium tuberculosis* counters phagosomal NOX2 activity to inhibit TNF-alpha-mediated host cell apoptosis. *PLoS Pathog* (2010) 6(4):e1000864. doi:10.1371/journal.ppat.1000864
156. Savina A, Jancic C, Hugues S, Guermonprez P, Vargas P, Moura IC, et al. NOX2 controls phagosomal pH to regulate antigen processing during crosspresentation by dendritic cells. *Cell* (2006) 126(1):205–18. doi:10.1016/j.cell.2006.05.035
157. Jancic C, Savina A, Wasmeier C, Tolmachova T, El-Benna J, Dang PM-C, et al. Rab27a regulates phagosomal pH and NADPH oxidase recruitment to dendritic cell phagosomes. *Nat Cell Biol* (2007) 9(4):367–78. doi:10.1038/ncb1552
158. Mantegazza AR, Savina A, Vermeulen M, Pérez L, Geffner J, Hermine O, et al. NADPH oxidase controls phagosomal pH and antigen cross-presentation in human dendritic cells. *Blood* (2008) 112(12):4712–22. doi:10.1182/blood-2008-01-134791
159. Kuiper JW, Sun C, Magalhaes MA, Glogauer M. Rac regulates PtdInsP(3) signaling and the chemotactic compass through a redox-mediated feedback loop. *Blood* (2011) 118(23):6164–71. doi:10.1182/blood-2010-09-310383
160. Stanley A, Thompson K, Hynes A, Brakebusch C, Quondamatteo F. NADPH oxidase complex-derived reactive oxygen species, the actin cytoskeleton, and Rho GTPases in cell migration. *Antioxid Redox Signal* (2014) 20(13):2026–42. doi:10.1089/ars.2013.5713
161. Minakami R, Sumimotoa H. Phagocytosis-coupled activation of the superoxide-producing phagocyte oxidase, a member of the NADPH oxidase (nox) family. *Int J Hematol* (2006) 84(3):193–8. doi:10.1532/IJH97.06133
162. Bedard K, Krause KH. The NOX family of ROS-generating NADPH oxidases: physiology and pathophysiology. *Physiol Rev* (2007) 87(1):245–313. doi:10.1152/physrev.00044.2005
163. Nguyen GT, Green ER, Mecsas J. Neutrophils to the ROScue: mechanisms of NADPH oxidase activation and bacterial resistance. *Front Cell Infect Microbiol* (2017) 7:373. doi:10.3389/fcimb.2017.00373
164. Goldblatt D, Thrasher AJ. Chronic granulomatous disease. *Clin Exp Immunol* (2000) 122(1):1–9. doi:10.1046/j.1365-2249.2000.01314.x
165. Ben-Ari J, Wolach O, Gavrieli R, Wolach B. Infections associated with chronic granulomatous disease: linking genetics to phenotypic expression. *Expert Rev Anti Infect Ther* (2012) 10(8):881–94. doi:10.1586/eri.12.77
166. West AP, Brodsky IE, Rahner C, Woo DK, Erdjument-Bromage H, Tempst P, et al. TLR signalling augments macrophage bactericidal activity through mitochondrial ROS. *Nature* (2011) 472(7344):476–80. doi:10.1038/nature09973
167. Hall CJ, Boyle RH, Astin JW, Flores MV, Oehlers SH, Sanderson LE, et al. Immunoresponsive gene 1 augments bactericidal activity of macrophage-lineage cells by regulating beta-oxidation-dependent mitochondrial ROS production. *Cell Metab* (2013) 18(2):265–78. doi:10.1016/j.cmet.2013.06.018
168. Nambi S, Long JE, Mishra BB, Baker R, Murphy KC, Olive AJ, et al. The oxidative stress network of *Mycobacterium tuberculosis* reveals coordination between radical detoxification systems. *Cell Host Microbe* (2015) 17(6):829–37. doi:10.1016/j.chom.2015.05.008
169. Broxton CN, Culotta VC. SOD enzymes and microbial pathogens: surviving the oxidative storm of infection. *PLoS Pathog* (2016) 12(1):e1005295. doi:10.1371/journal.ppat.1005295
170. Lodge R, Diallo TO, Descoteaux A. *Leishmania donovani* lipophosphoglycan blocks NADPH oxidase assembly at the phagosome membrane. *Cell Microbiol* (2006) 8(12):1922–31. doi:10.1111/j.1462-5822.2006.00758.x
171. Sun J, Singh V, Lau A, Stokes RW, Obregon-Henao A, Orme IM, et al. *Mycobacterium tuberculosis* nucleoside diphosphate kinase inactivates small GTPases leading to evasion of innate immunity. *PLoS Pathog* (2013) 9(7):e1003499. doi:10.1371/journal.ppat.1003499
172. de Souza Santos M, Salomon D, Orth K. T3SS effector VopL inhibits the host ROS response, promoting the intracellular survival of vibrio parahaemolyticus. *PLoS Pathog* (2017) 13(6):e1006438. doi:10.1371/journal.ppat.1006438
173. Vareechon C, Zmina SE, Karmakar M, Pearlman E, Rietsch A. *Pseudomonas aeruginosa* effector ExoS inhibits ROS production in human neutrophils. *Cell Host Microbe* (2017) 21(5): 611–8.e615. doi:10.1016/j.chom.2017.04.001
174. Lardy B, Bof M, Aubry L, Paclet MH, Morel F, Satre M, et al. NADPH oxidase homologs are required for normal cell differentiation and morphogenesis in *Dictyostelium discoideum*. *Biochim Biophys Acta* (2005) 1744(2):199–212. doi:10.1016/j.bbamcr.2005.02.004
175. Bedard K, Lardy B, Krause KH. NOX family NADPH oxidases: not just in mammals. *Biochimie* (2007) 89(9):1107–12. doi:10.1016/j.biochi.2007.01.012

176. Zhang X, Krause KH, Xenarios I, Soldati T, Boeckmann B. Evolution of the ferric reductase domain (FRD) superfamily: modularity, functional diversification, and signature motifs. *PLoS One* (2013) 8(3):e58126. doi:10.1371/journal.pone.0058126
177. Akaza Y, Tsuji A, Yasukawa H. Analysis of the gene encoding copper/zinc superoxide dismutase homolog in *Dictyostelium discoideum*. *Biol Pharm Bull* (2002) 25(12):1528–32. doi:10.1248/bpb.25.1528
178. Tsuji A, Akaza Y, Kodaira K, Yasukawa H. Copper/zinc superoxide dismutases in *Dictyostelium discoideum*: amino acid sequences and expression kinetics. *J Biochem Mol Biol Biophys* (2002) 6(3):215–20. doi:10.1080/10258140290018711
179. Tsuji A, Akaza Y, Nakamura S, Kodaira K, Yasukawa H. Multinucleation of the sodC-deficient *Dictyostelium discoideum*. *Biol Pharm Bull* (2003) 26(8):1174–7. doi:10.1248/bpb.26.1174
180. Katoch B, Begum R. Biochemical basis of the high resistance to oxidative stress in *Dictyostelium discoideum*. *J Biosci* (2003) 28(5):581–8. doi:10.1007/BF02703333
181. Pontel LB, Langenick J, Rosado IV, Zhang XY, Traynor D, Kay RR, et al. Xpf suppresses the mutagenic consequences of phagocytosis in *Dictyostelium*. *J Cell Sci* (2016) 129(24):4449–54. doi:10.1242/jcs.196337
182. Veeranki S, Kim B, Kim L. The GPI-anchored superoxide dismutase SodC is essential for regulating basal Ras activity and for chemotaxis of *Dictyostelium discoideum*. *J Cell Sci* (2008) 121(Pt 18):3099–108. doi:10.1242/jcs.030056
183. Castillo B, Kim SH, Sharief M, Sun T, Kim LW. SodC modulates ras and PKB signaling in *Dictyostelium*. *Eur J Cell Biol* (2017) 96(1):1–12. doi:10.1016/j.ejcb.2016.11.001
184. Velmurugan K, Chen B, Miller JL, Azogue S, Gurses S, Hsu T, et al. *Mycobacterium tuberculosis* nuoG is a virulence gene that inhibits apoptosis of infected host cells. *PLoS Pathog* (2007) 3(7):e110. doi:10.1371/journal.ppat.0030110
185. Bloomfield G, Pears C. Superoxide signalling required for multicellular development of *Dictyostelium*. *J Cell Sci* (2003) 116(Pt 16):3387–97. doi:10.1242/jcs.00649
186. Garcia MX, Alexander H, Mahadeo D, Cotter DA, Alexander S. The *Dictyostelium discoideum* prespore-specific catalase B functions to control late development and to protect spore viability. *Biochim Biophys Acta* (2003) 1641(1):55–64. doi:10.1016/S0167-4889(03)00064-8
187. Zhang X, Zhuchenko O, Kuspa A, Soldati T. Social amoebae trap and kill bacteria by casting DNA nets. *Nat Commun* (2016) 7:10938. doi:10.1038/ncomms10938
188. Smith EW, Lima WC, Charette SJ, Cosson P. Effect of starvation on the endocytic pathway in *Dictyostelium* cells. *Eukaryot Cell* (2010) 9(3):387–92. doi:10.1128/EC.00285-09
189. Yang CS, Shin DM, Kim KH, Lee ZW, Lee CH, Park SG, et al. NADPH oxidase 2 interaction with TLR2 is required for efficient innate immune responses to mycobacteria via cathelicidin expression. *J Immunol* (2009) 182(6):3696–705. doi:10.4049/jimmunol.0802217
190. Brinkmann V, Reichard U, Goosmann C, Fauler B, Uhlemann Y, Weiss DS, et al. Neutrophil extracellular traps kill bacteria. *Science* (2004) 303(5663):1532–5. doi:10.1126/science.1092385
191. Chow OA, von Köckritz-Blickwede M, Bright AT, Hensler ME, Zinkernagel AS, Cogen AL, et al. Statins enhance formation of phagocyte extracellular traps. *Cell Host Microbe* (2010) 8(5):445–54. doi:10.1016/j.chom.2010.10.005
192. Boe DM, Curtis BJ, Chen MM, Ippolito JA, Kovacs EJ. Extracellular traps and macrophages: new roles for the versatile phagocyte. *J Leukoc Biol* (2015) 97(6):1023–35. doi:10.1189/jlb.4RI1014-521R
193. Kalsum S, Braian C, Koeken VACM, Raffetseder J, Lindroth M, van Crevel R, et al. The cording phenotype of *Mycobacterium tuberculosis* induces the formation of extracellular traps in human macrophages. *Front Cell Infect Microbiol* (2017) 7:278. doi:10.3389/fcimb.2017.00278
194. Papayannopoulos V. Neutrophil extracellular traps in immunity and disease. *Nat Rev Immunol* (2017). doi:10.1038/nri.2017.105
195. Fuchs TA, Abed U, Goosmann C, Hurwitz R, Schulze I, Wahn V, et al. Novel cell death program leads to neutrophil extracellular traps. *J Cell Biol* (2007) 176(2):231–41. doi:10.1083/jcb.200606027
196. Parker H, Dragunow M, Hampton MB, Kettle AJ, Winterbourn CC. Requirements for NADPH oxidase and myeloperoxidase in neutrophil extracellular trap formation differ depending on the stimulus. *J Leukoc Biol* (2012) 92(4):841–9. doi:10.1189/jlb.1211601
197. Parker H, Winterbourn CC. Reactive oxidants and myeloperoxidase and their involvement in neutrophil extracellular traps. *Front Immunol* (2012) 3:424. doi:10.3389/fimmu.2012.00424
198. Arai Y, Nishinaka Y, Arai T, Morita M, Mizugishi K, Adachi S, et al. Uric acid induces NADPH oxidase-independent neutrophil extracellular trap formation. *Biochem Biophys Res Commun* (2014) 443(2):556–61. doi:10.1016/j.bbrc.2013.12.007
199. Bjornsdottir H, Dahlstrand Rudin A, Klose FP, Elmwall J, Welin A, Stylianou M, et al. Phenol-soluble modulin alpha peptide toxins from aggressive *Staphylococcus aureus* induce rapid formation of neutrophil extracellular traps through a reactive oxygen species-independent pathway. *Front Immunol* (2017) 8:257. doi:10.3389/fimmu.2017.00257
200. Douda DN, Khan MA, Grasemann H, Palaniyar N. SK3 channel and mitochondrial ROS mediate NADPH oxidase-independent NETosis induced by calcium influx. *Proc Natl Acad Sci U S A* (2015) 112(9):2817–22. doi:10.1073/pnas.1414055112
201. Zhang X, Soldati T. Of amoebae and men: extracellular DNA traps as an ancient cell-intrinsic defense mechanism. *Front Immunol* (2016) 7:269. doi:10.3389/fimmu.2016.00269
202. Botella H, Stadthagen G, Lugo-Villarino G, de Chastellier C, Neyrolles O. Metallobiology of host-pathogen interactions: an intoxicating new insight. *Trends Microbiol* (2012) 20(3):106–12. doi:10.1016/j.tim.2012.01.005
203. German N, Luthje F, Hao X, Ronn R, Rensing C. Microbial virulence and interactions with metals. *Prog Mol Biol Transl Sci* (2016) 142:27–49. doi:10.1016/bs.pmbts.2016.05.010
204. Subramanian Vignesh K, Deepe GS Jr. Immunological orchestration of zinc homeostasis: the battle between host mechanisms and pathogen defenses. *Arch Biochem Biophys* (2016) 611:66–78. doi:10.1016/j.abb.2016.02.020
205. Wagner D, Maser J, Lai B, Cai Z, Barry CE III, Honer Zu Bentrup K, et al. Elemental analysis of *Mycobacterium avium*-, *Mycobacterium tuberculosis*-, and *Mycobacterium smegmatis*-containing phagosomes indicates pathogen-induced microenvironments within the host cell's endosomal system. *J Immunol* (2005) 174(3):1491–500. doi:10.4049/jimmunol.174.3.1491
206. Soldati T, Neyrolles O. Mycobacteria and the intraphagosomal environment: take it with a pinch of salt(s)! *Traffic* (2012) 13(8):1042–52. doi:10.1111/j.1600-0854.2012.01358.x
207. El Chemaly A, Nunes P, Jimaja W, Castelbou C, Demaurex N. Hv1 proton channels differentially regulate the pH of neutrophil and macrophage phagosomes by sustaining the production of phagosomal ROS that inhibit the delivery of vacuolar ATPases. *J Leukoc Biol* (2014) 95(5):827–39. doi:10.1189/jlb.0513251
208. Di A, Brown ME, Deriy LV, Li C, Szeto FL, Chen Y, et al. CFTR regulates phagosome acidification in macrophages and alters bactericidal activity. *Nat Cell Biol* (2006) 8(9):933–44. doi:10.1038/ncb1456
209. Hara-Chikuma M, Yang B, Sonawane ND, Sasaki S, Uchida S, Verkman AS. ClC-3 chloride channels facilitate endosomal acidification and chloride accumulation. *J Biol Chem* (2005) 280(2):1241–7. doi:10.1074/jbc.M407030200
210. Jentsch TJ. Chloride and the endosomal-lysosomal pathway: emerging roles of CLC chloride transporters. *J Physiol* (2007) 578(Pt 3):633–40. doi:10.1113/jphysiol.2006.124719
211. Steinberg BE, Huynh KK, Brodovitch A, Jabs S, Stauber T, Jentsch TJ, et al. A cation counterflux supports lysosomal acidification. *J Cell Biol* (2010) 189(7):1171–86. doi:10.1083/jcb.200911083
212. Kambe T, Tsuji T, Hashimoto A, Itsumura N. The Physiological, biochemical, and molecular roles of zinc transporters in zinc homeostasis and metabolism. *Physiol Rev* (2015) 95(3):749–84. doi:10.1152/physrev.00035.2014
213. Bouron A, Oberwinkler J. Contribution of calcium-conducting channels to the transport of zinc ions. *Pflugers Arch* (2014) 466(3):381–7. doi:10.1007/s00424-013-1295-z
214. Cuajungco MP, Basilio LC, Silva J, Hart T, Tringali J, Chen CC, et al. Cellular zinc levels are modulated by TRPML1-TMEM163 interaction. *Traffic* (2014) 15(11):1247–65. doi:10.1111/tra.12205
215. Nevo Y, Nelson N. The NRAMP family of metal-ion transporters. *Biochim Biophys Acta* (2006) 1763(7):609–20. doi:10.1016/j.bbamcr.2006.05.007

216. Sunaga N, Monna M, Shimada N, Tsukamoto M, Kawata T. Expression of zinc transporter family genes in *Dictyostelium*. *Int J Dev Biol* (2008) 52(4):377–81. doi:10.1387/ijdb.072389ns
217. Sebe-Pedros A, Degnan BM, Ruiz-Trillo I. The origin of metazoa: a unicellular perspective. *Nat Rev Genet* (2017) 18(8):498–512. doi:10.1038/nrg.2017.21
218. Larsson A. AliView: a fast and lightweight alignment viewer and editor for large datasets. *Bioinformatics* (2014) 30(22):3276–8. doi:10.1093/bioinformatics/btu531
219. Katoh K, Kuma K, Toh H, Miyata T. MAFFT version 5: improvement in accuracy of multiple sequence alignment. *Nucleic Acids Res* (2005) 33(2):511–8. doi:10.1093/nar/gki198
220. Kambe T, Matsunaga M, Takeda TA. Understanding the contribution of zinc transporters in the function of the early secretory pathway. *Int J Mol Sci* (2017) 18(10):E2179. doi:10.3390/ijms18102179
221. Cassat JE, Skaar EP. Metal ion acquisition in *Staphylococcus aureus*: overcoming nutritional immunity. *Semin Immunopathol* (2012) 34(2):215–35. doi:10.1007/s00281-011-0294-4
222. Stafford SL, Bokil NJ, Achard ME, Kapetanovic R, Schembri MA, McEwan AG, et al. Metal ions in macrophage antimicrobial pathways: emerging roles for zinc and copper. *Biosci Rep* (2013) 33(4):e00049. doi:10.1042/BSR20130014
223. Flannagan RS, Heit B, Heinrichs DE. Antimicrobial mechanisms of macrophages and the immune evasion strategies of *Staphylococcus aureus*. *Pathogens* (2015) 4(4):826–68. doi:10.3390/pathogens4040826
224. Botella H, Peyron P, Levillain F, Poincloux R, Poquet Y, Brandli I, et al. Mycobacterial p(1)-type ATPases mediate resistance to zinc poisoning in human macrophages. *Cell Host Microbe* (2011) 10(3):248–59. doi:10.1016/j.chom.2011.08.006
225. Besold AN, Culbertson EM, Culotta VC. The Yin and Yang of copper during infection. *J Biol Inorg Chem* (2016) 21(2):137–44. doi:10.1007/s00775-016-1335-1
226. Neyrolles O, Wolschendorf F, Mitra A, Niederweis M. Mycobacteria, metals, and the macrophage. *Immunol Rev* (2015) 264(1):249–63. doi:10.1111/imr.12265
227. Inesi G. Molecular features of copper binding proteins involved in copper homeostasis. *IUBMB Life* (2017) 69(4):211–7. doi:10.1002/iub.1590
228. Wang Y, Hodgkinson V, Zhu S, Weisman GA, Petris MJ. Advances in the understanding of mammalian copper transporters. *Adv Nutr* (2011) 2(2):129–37. doi:10.3945/an.110.000273
229. Hodgkinson V, Petris MJ. Copper homeostasis at the host-pathogen interface. *J Biol Chem* (2012) 287(17):13549–55. doi:10.1074/jbc.R111.316406
230. White PJ, Broadley MR. Biofortification of crops with seven mineral elements often lacking in human diets – iron, zinc, copper, calcium, magnesium, selenium and iodine. *New Phytol* (2009) 182(1):49–84. doi:10.1111/j.1469-8137.2008.02738.x
231. Rowland JL, Niederweis M. A multicopper oxidase is required for copper resistance in *Mycobacterium tuberculosis*. *J Bacteriol* (2013) 195(16):3724–33. doi:10.1128/JB.00546-13
232. Burlando B, Evangelisti V, Dondero F, Pons G, Camakaris J, Viarengo A. Occurrence of Cu-ATPase in *Dictyostelium*: possible role in resistance to copper. *Biochem Biophys Res Commun* (2002) 291(3):476–83. doi:10.1006/bbrc.2002.6463
233. Hao X, Luthje F, Ronn R, German NA, Li X, Huang F, et al. A role for copper in protozoan grazing – two billion years selecting for bacterial copper resistance. *Mol Microbiol* (2016) 102(4):628–41. doi:10.1111/mmi.13483
234. Kehl-Fie TE, Skaar EP. Nutritional immunity beyond iron: a role for manganese and zinc. *Curr Opin Chem Biol* (2010) 14(2):218–24. doi:10.1016/j.cbpa.2009.11.008
235. Hood MI, Skaar EP. Nutritional immunity: transition metals at the pathogen-host interface. *Nat Rev Microbiol* (2012) 10(8):525–37. doi:10.1038/nrmicro2836
236. Morey JR, McDevitt CA, Kehl-Fie TE. Host-imposed manganese starvation of invading pathogens: two routes to the same destination. *Biometals* (2015) 28(3):509–19. doi:10.1007/s10534-015-9850-z
237. Vidal SM, Malo D, Vogan K, Skamene E, Gros P. Natural resistance to infection with intracellular parasites: isolation of a candidate for Bcg. *Cell* (1993) 73(3):469–85. doi:10.1016/0092-8674(93)90135-D
238. Cellier MF. Nramp: from sequence to structure and mechanism of divalent metal import. *Curr Top Membr* (2012) 69:249–93. doi:10.1016/B978-0-12-394390-3.00010-0
239. Wessling-Resnick M. Nramp1 and other transporters involved in metal withholding during infection. *J Biol Chem* (2015) 290(31):18984–90. doi:10.1074/jbc.R115.643973
240. Cellier M, Belouchi A, Gros P. Resistance to intracellular infections: comparative genomic analysis of Nramp. *Trends Genet* (1996) 12(6):201–4. doi:10.1016/0168-9525(96)30042-5
241. Gunshin H, Mackenzie B, Berger UV, Gunshin Y, Romero MF, Boron WF, et al. Cloning and characterization of a mammalian proton-coupled metal-ion transporter. *Nature* (1997) 388(6641):482–8. doi:10.1038/41343
242. Belouchi A, Kwan T, Gros P. Cloning and characterization of the OsNramp family from *Oryza sativa*, a new family of membrane proteins possibly implicated in the transport of metal ions. *Plant Mol Biol* (1997) 33(6):1085–92. doi:10.1023/A:1005723304911
243. Portnoy ME, Liu XF, Culotta VC. *Saccharomyces cerevisiae* expresses three functionally distinct homologues of the nramp family of metal transporters. *Mol Cell Biol* (2000) 20(21):7893–902. doi:10.1128/MCB.20.21.7893-7902.2000
244. Forbes JR, Gros P. Divalent-metal transport by NRAMP proteins at the interface of host-pathogen interactions. *Trends Microbiol* (2001) 9(8):397–403. doi:10.1016/S0966-842X(01)02098-4
245. Gruenheid S, Cellier M, Vidal S, Gros P. Identification and characterization of a second mouse Nramp gene. *Genomics* (1995) 25(2):514–25. doi:10.1016/0888-7543(95)80053-O
246. Forbes JR, Gros P. Iron, manganese, and cobalt transport by Nramp1 (Slc11a1) and Nramp2 (Slc11a2) expressed at the plasma membrane. *Blood* (2003) 102(5):1884–92. doi:10.1182/blood-2003-02-0425
247. Gruenheid S, Pinner E, Desjardins M, Gros P. Natural resistance to infection with intracellular pathogens: the Nramp1 protein is recruited to the membrane of the phagosome. *J Exp Med* (1997) 185(4):717–30. doi:10.1084/jem.185.4.717
248. Picard V, Govoni G, Jabado N, Gros P. Nramp 2 (DCT1/DMT1) expressed at the plasma membrane transports iron and other divalent cations into a calcein-accessible cytoplasmic pool. *J Biol Chem* (2000) 275(46):35738–45. doi:10.1074/jbc.M005387200
249. Gruenheid S, Canonne-Hergaux F, Gauthier S, Hackam DJ, Grinstein S, Gros P. The iron transport protein NRAMP2 is an integral membrane glycoprotein that colocalizes with transferrin in recycling endosomes. *J Exp Med* (1999) 189(5):831–41. doi:10.1084/jem.189.5.831
250. Fleming MD, Trenor CC III, Su MA, Foernzler D, Beier DR, Dietrich WF, et al. Microcytic anaemia mice have a mutation in Nramp2, a candidate iron transporter gene. *Nat Genet* (1997) 16(4):383–6. doi:10.1038/ng0897-383
251. Canonne-Hergaux F, Fleming MD, Levy JE, Gauthier S, Ralph T, Picard V, et al. The Nramp2/DMT1 iron transporter is induced in the duodenum of microcytic anemia MK mice but is not properly targeted to the intestinal brush border. *Blood* (2000) 96(12):3964–70.
252. Salazar J, Mena N, Hunot S, Prigent A, Alvarez-Fischer D, Arredondo M, et al. Divalent metal transporter 1 (DMT1) contributes to neurodegeneration in animal models of Parkinson's disease. *Proc Natl Acad Sci U S A* (2008) 105(47):18578–83. doi:10.1073/pnas.0804373105
253. Wu KC, Liou HH, Kao YH, Lee CY, Lin CJ. The critical role of Nramp1 in degrading alpha-synuclein oligomers in microglia under iron overload condition. *Neurobiol Dis* (2017) 104:61–72. doi:10.1016/j.nbd.2017.05.001
254. Gros P, Skamene E, Forget A. Genetic control of natural resistance to *Mycobacterium bovis* (BCG) in mice. *J Immunol* (1981) 127(6):2417–21.
255. Skamene E, Gros P, Forget A, Kongshavn PA, St Charles C, Taylor BA. Genetic regulation of resistance to intracellular pathogens. *Nature* (1982) 297(5866):506–9. doi:10.1038/297506a0
256. Lissner CR, Swanson RN, O'Brien AD. Genetic control of the innate resistance of mice to *Salmonella typhimurium*: expression of the Ity gene in peritoneal and splenic macrophages isolated in vitro. *J Immunol* (1983) 131(6):3006–13.
257. Vidal S, Gros P, Skamene E. Natural resistance to infection with intracellular parasites: molecular genetics identifies Nramp1 as the Bcg/Ity/Lsh locus. *J Leukoc Biol* (1995) 58(4):382–90.
258. Vidal S, Tremblay ML, Govoni G, Gauthier S, Sebastiani G, Malo D, et al. The Ity/Lsh/Bcg locus: natural resistance to infection with intracellular parasites is abrogated by disruption of the Nramp1 gene. *J Exp Med* (1995) 182(3):655–66. doi:10.1084/jem.182.3.655
259. Vidal SM, Pinner E, Lepage P, Gauthier S, Gros P. Natural resistance to intracellular infections: Nramp1 encodes a membrane phosphoglycoprotein

absent in macrophages from susceptible (Nramp1 D169) mouse strains. *J Immunol* (1996) 157(8):3559–68.
260. Hackam DJ, Rotstein OD, Zhang W, Gruenheid S, Gros P, Grinstein S. Host resistance to intracellular infection: mutation of natural resistance-associated macrophage protein 1 (Nramp1) impairs phagosomal acidification. *J Exp Med* (1998) 188(2):351–64. doi:10.1084/jem.188.2.351
261. Bellamy R, Ruwende C, Corrah T, McAdam KP, Whittle HC, Hill AV. Variations in the NRAMP1 gene and susceptibility to tuberculosis in West Africans. *N Engl J Med* (1998) 338(10):640–4. doi:10.1056/NEJM199803053381002
262. Medapati RV, Suvvari S, Godi S, Gangisetti P. NRAMP1 and VDR gene polymorphisms in susceptibility to pulmonary tuberculosis among Andhra Pradesh population in India: a case-control study. *BMC Pulm Med* (2017) 17(1):89. doi:10.1186/s12890-017-0431-5
263. Abel L, Sanchez FO, Oberti J, Thuc NV, Hoa LV, Lap VD, et al. Susceptibility to leprosy is linked to the human NRAMP1 gene. *J Infect Dis* (1998) 177(1):133–45. doi:10.1086/513830
264. Mackenzie B, Hediger MA. SLC11 family of H+-coupled metal-ion transporters NRAMP1 and DMT1. *Pflugers Arch* (2004) 447(5):571–9. doi:10.1007/s00424-003-1141-9
265. Kuhn DE, Baker BD, Lafuse WP, Zwilling BS. Differential iron transport into phagosomes isolated from the RAW264.7 macrophage cell lines transfected with Nramp1Gly169 or Nramp1Asp169. *J Leukoc Biol* (1999) 66(1):113–9.
266. Zwilling BS, Kuhn DE, Wikoff L, Brown D, Lafuse W. Role of iron in Nramp1-mediated inhibition of mycobacterial growth. *Infect Immun* (1999) 67(3):1386–92.
267. Goswami T, Bhattacharjee A, Babal P, Searle S, Moore E, Li M, et al. Natural-resistance-associated macrophage protein 1 is an H+/bivalent cation antiporter. *Biochem J* (2001) 354(Pt 3):511–9. doi:10.1042/bj3540511
268. Kuhn DE, Lafuse WP, Zwilling BS. Iron transport into *Mycobacterium avium*-containing phagosomes from an Nramp1(Gly169)-transfected RAW264.7 macrophage cell line. *J Leukoc Biol* (2001) 69(1):43–9.
269. Jabado N, Jankowski A, Dougaparsad S, Picard V, Grinstein S, Gros P. Natural resistance to intracellular infections: natural resistance-associated macrophage protein 1 (Nramp1) functions as a pH-dependent manganese transporter at the phagosomal membrane. *J Exp Med* (2000) 192(9):1237–48. doi:10.1084/jem.192.9.1237
270. Courville P, Chaloupka R, Cellier MF. Recent progress in structure-function analyses of Nramp proton-dependent metal-ion transporters. *Biochem Cell Biol* (2006) 84(6):960–78. doi:10.1139/o06-193
271. Buracco S, Peracino B, Cinquetti R, Signoretto E, Vollero A, Imperiali F, et al. *Dictyostelium* Nramp1, which is structurally and functionally similar to mammalian DMT1 transporter, mediates phagosomal iron efflux. *J Cell Sci* (2015) 128(17):3304–16. doi:10.1242/jcs.173153
272. Peracino B, Wagner C, Balest A, Balbo A, Pergolizzi B, Noegel AA, et al. Function and mechanism of action of *Dictyostelium* Nramp1 (Slc11a1) in bacterial infection. *Traffic* (2006) 7(1):22–38. doi:10.1111/j.1600-0854.2005.00356.x
273. Peracino B, Buracco S, Bozzaro S. The Nramp (Slc11) proteins regulate development, resistance to pathogenic bacteria and iron homeostasis in *Dictyostelium discoideum*. *J Cell Sci* (2013) 126(Pt 1):301–11. doi:10.1242/jcs.116210
274. Heuser J, Zhu Q, Clarke M. Proton pumps populate the contractile vacuoles of *Dictyostelium* amoebae. *J Cell Biol* (1993) 121(6):1311–27. doi:10.1083/jcb.121.6.1311
275. Simeone R, Sayes F, Song O, Groschel MI, Brodin P, Brosch R, et al. Cytosolic access of *Mycobacterium tuberculosis*: critical impact of phagosomal acidification control and demonstration of occurrence in vivo. *PLoS Pathog* (2015) 11(2):e1004650. doi:10.1371/journal.ppat.1004650
276. Hybiske K, Stephens RS. Exit strategies of intracellular pathogens. *Nat Rev Microbiol* (2008) 6(2):99–110. doi:10.1038/nrmicro1821
277. Mesquita A, Cardenal-Munoz E, Dominguez E, Munoz-Braceras S, Nunez-Corcuera B, Phillips BA, et al. Autophagy in *Dictyostelium*: mechanisms, regulation and disease in a simple biomedical model. *Autophagy* (2017) 13(1):24–40. doi:10.1080/15548627.2016.1226737
278. Calvo-Garrido J, Carilla-Latorre S, Kubohara Y, Santos-Rodrigo N, Mesquita A, Soldati T, et al. Autophagy in *Dictyostelium*: genes and pathways, cell death and infection. *Autophagy* (2010) 6(6):686–701. doi:10.4161/auto.6.6.12513
279. Reggiori F, Klionsky DJ. Autophagic processes in yeast: mechanism, machinery and regulation. *Genetics* (2013) 194(2):341–61. doi:10.1534/genetics.112.149013
280. Stolz A, Ernst A, Dikic I. Cargo recognition and trafficking in selective autophagy. *Nat Cell Biol* (2014) 16(6):495–501. doi:10.1038/ncb2979
281. Romagnoli A, Etna MP, Giacomini E, Pardini M, Remoli ME, Corazzari M, et al. ESX-1 dependent impairment of autophagic flux by *Mycobacterium tuberculosis* in human dendritic cells. *Autophagy* (2012) 8(9):1357–70. doi:10.4161/auto.20881
282. Pflaum K, Gerdes K, Yovo K, Callahan J, Snyder ML. Lipopolysaccharide induction of autophagy is associated with enhanced bactericidal activity in *Dictyostelium discoideum*. *Biochem Biophys Res Commun* (2012) 422(3):417–22. doi:10.1016/j.bbrc.2012.05.006
283. Koller B, Schramm C, Siebert S, Triebel J, Deland E, Pfefferkorn AM, et al. *Dictyostelium discoideum* as a novel host system to study the interaction between phagocytes and yeasts. *Front Microbiol* (2016) 7:1665. doi:10.3389/fmicb.2016.01665
284. Cabral M, Anjard C, Malhotra V, Loomis WF, Kuspa A. Unconventional secretion of AcbA in *Dictyostelium discoideum* through a vesicular intermediate. *Eukaryot Cell* (2010) 9(7):1009–17. doi:10.1128/ec.00337-09
285. Barondes SH, Castronovo V, Cooper DN, Cummings RD, Drickamer K, Feizi T, et al. Galectins: a family of animal beta-galactoside-binding lectins. *Cell* (1994) 76(4):597–8. doi:10.1016/0092-8674(94)90498-7
286. Briles EB, Gregory W, Fletcher P, Kornfeld S. Vertebrate lectins, comparison of properties of beta-galactoside-binding lectins from tissues of calf and chicken. *J Cell Biol* (1979) 81(3):528–37. doi:10.1083/jcb.81.3.528
287. Arnoys EJ, Ackerman CM, Wang JL. Nucleocytoplasmic shuttling of galectin-3. *Methods Mol Biol* (2015) 1207:465–83. doi:10.1007/978-1-4939-1396-1_30
288. Seelenmeyer C, Stegmayer C, Nickel W. Unconventional secretion of fibroblast growth factor 2 and galectin-1 does not require shedding of plasma membrane-derived vesicles. *FEBS Lett* (2008) 582(9):1362–8. doi:10.1016/j.febslet.2008.03.024
289. Griffioen AW, Thijssen VL. Galectins in tumor angiogenesis. *Ann Transl Med* (2014) 2(9):90. doi:10.3978/j.issn.2305-5839.2014.09.01
290. Liu FT, Yang RY, Hsu DK. Galectins in acute and chronic inflammation. *Ann N Y Acad Sci* (2012) 1253:80–91. doi:10.1111/j.1749-6632.2011.06386.x
291. Arthur CM, Baruffi MD, Cummings RD, Stowell SR. Evolving mechanistic insights into galectin functions. *Methods Mol Biol* (2015) 1207:1–35. doi:10.1007/978-1-4939-1396-1_1
292. Nabi IR, Shankar J, Dennis JW. The galectin lattice at a glance. *J Cell Sci* (2015) 128(13):2213–9. doi:10.1242/jcs.151159
293. Lakshminarayan R, Wunder C, Becken U, Howes MT, Benzing C, Arumugam S, et al. Galectin-3 drives glycosphingolipid-dependent biogenesis of clathrin-independent carriers. *Nat Cell Biol* (2014) 16(6):595–606. doi:10.1038/ncb2970
294. Mey A, Leffler H, Hmama Z, Normier G, Revillard JP. The animal lectin galectin-3 interacts with bacterial lipopolysaccharides via two independent sites. *J Immunol* (1996) 156(4):1572–7.
295. Kamhawi S. Phlebotomine sand flies and *Leishmania* parasites: friends or foes? *Trends Parasitol* (2006) 22(9):439–45. doi:10.1016/j.pt.2006.06.012
296. Lee B. Envelope-receptor interactions in Nipah virus pathobiology. *Ann N Y Acad Sci* (2007) 1102:51–65. doi:10.1196/annals.1408.004
297. Sato S, St-Pierre C, Bhaumik P, Nieminen J. Galectins in innate immunity: dual functions of host soluble beta-galactoside-binding lectins as damage-associated molecular patterns (DAMPs) and as receptors for pathogen-associated molecular patterns (PAMPs). *Immunol Rev* (2009) 230(1):172–87. doi:10.1111/j.1600-065X.2009.00790.x
298. Stowell SR, Arthur CM, Dias-Baruffi M, Rodrigues LC, Gourdine JP, Heimburg-Molinaro J, et al. Innate immune lectins kill bacteria expressing blood group antigen. *Nat Med* (2010) 16(3):295–301. doi:10.1038/nm.2103
299. Stowell SR, Arthur CM, McBride R, Berger O, Razi N, Heimburg-Molinaro J, et al. Microbial glycan microarrays define key features of host-microbial interactions. *Nat Chem Biol* (2014) 10(6):470–6. doi:10.1038/nchembio.1525

300. Thurston TL, Wandel MP, von Muhlinen N, Foeglein A, Randow F. Galectin 8 targets damaged vesicles for autophagy to defend cells against bacterial invasion. *Nature* (2012) 482(7385):414–8. doi:10.1038/nature10744
301. Feeley EM, Pilla-Moffett DM, Zwack EE, Piro AS, Finethy R, Kolb JP, et al. Galectin-3 directs antimicrobial guanylate binding proteins to vacuoles furnished with bacterial secretion systems. *Proc Natl Acad Sci U S A* (2017) 114(9):E1698–706. doi:10.1073/pnas.1615771114
302. Aragao KS, Satre M, Imberty A, Varrot A. Structure determination of discoidin II from *Dictyostelium discoideum* and carbohydrate binding properties of the lectin domain. *Proteins* (2008) 73(1):43–52. doi:10.1002/prot.22038
303. Mathieu SV, Aragao KS, Imberty A, Varrot A. Discoidin I from *Dictyostelium discoideum* and interactions with oligosaccharides: specificity, affinity, crystal structures, and comparison with discoidin II. *J Mol Biol* (2010) 400(3):540–54. doi:10.1016/j.jmb.2010.05.042
304. Barondes SH, Cooper DN, Haywood-Reid PL. Discoidin I and discoidin II are localized differently in developing *Dictyostelium discoideum*. *J Cell Biol* (1983) 96(1):291–6. doi:10.1083/jcb.96.1.291
305. Ray J, Shinnick T, Lerner R. A mutation altering the function of a carbohydrate binding protein blocks cell-cell cohesion in developing *Dictyostelium discoideum*. *Nature* (1979) 279(5710):215–21. doi:10.1038/279215a0
306. Alexander S, Shinnick TM, Lerner RA. Mutants of *Dictyostelium discoideum* blocked in expression of all members of the developmentally regulated discoidin multigene family. *Cell* (1983) 34(2):467–75. doi:10.1016/0092-8674(83)90380-X
307. Erdos GW, Whitaker D. Failure to detect immunocytochemically reactive endogenous lectin on the cell surface of *Dictyostelium discoideum*. *J Cell Biol* (1983) 97(4):993–1000. doi:10.1083/jcb.97.4.993
308. Stadler J, Bauer G, Westphal M, Gerisch G. Monoclonal antibody against cytoplasmic lectins of *Dictyostelium discoideum*: cross-reactivity with a membrane glycoprotein, contact site A, and with *E. coli* beta-galactosidase and lac repressor. *Hoppe Seylers Z Physiol Chem* (1984) 365(3):283–8. doi:10.1515/bchm2.1984.365.1.283
309. Xie P. TRAF molecules in cell signaling and in human diseases. *J Mol Signal* (2013) 8:7–7. doi:10.1186/1750-2187-8-7
310. Bradley JR, Pober JS. Tumor necrosis factor receptor-associated factors (TRAFs). *Oncogene* (2001) 20(44):6482–91. doi:10.1038/sj.onc.1204788
311. Grech A, Quinn R, Srinivasan D, Badoux X, Brink R. Complete structural characterisation of the mammalian and *Drosophila* TRAF genes: implications for TRAF evolution and the role of RING finger splice variants. *Mol Immunol* (2000) 37(12–13):721–34. doi:10.1016/S0161-5890(00)00098-5
312. Yin Q, Lin S-C, Lo Y-C, Damo SM, Wu H. Chapter 49 – tumor necrosis factor receptor-associated factors in immune receptor signal transduction A2 – Bradshaw, Ralph A. 2nd ed. In: Dennis EA, editor. *Handbook of Cell Signaling*. San Diego: Academic Press (2010). p. 339–45.
313. Haldar AK, Foltz C, Finethy R, Piro AS, Feeley EM, Pilla-Moffett DM, et al. Ubiquitin systems mark pathogen-containing vacuoles as targets for host defense by guanylate binding proteins. *Proc Natl Acad Sci U S A* (2015) 112(41):E5628–37. doi:10.1073/pnas.1515966112
314. Linares JF, Duran A, Yajima T, Pasparakis M, Moscat J, Diaz-Meco MT. K63 polyubiquitination and activation of mTOR by the p62-TRAF6 complex in nutrient-activated cells. *Mol Cell* (2013) 51(3):283–96. doi:10.1016/j.molcel.2013.06.020
315. Deretic V, Saitoh T, Akira S. Autophagy in infection, inflammation and immunity. *Nat Rev Immunol* (2013) 13(10):722–37. doi:10.1038/nri3532
316. Hatakeyama S. TRIM Family Proteins: Roles in Autophagy, Immunity, and Carcinogenesis. *Trends Biochem Sci* (2017) 42(4):297–311. doi:10.1016/j.tibs.2017.01.002
317. Reymond A, Meroni G, Fantozzi A, Merla G, Cairo S, Luzi L, et al. The tripartite motif family identifies cell compartments. *EMBO J* (2001) 20(9):2140–51. doi:10.1093/emboj/20.9.2140
318. Ozato K, Shin DM, Chang TH, Morse HC III. TRIM family proteins and their emerging roles in innate immunity. *Nat Rev Immunol* (2008) 8(11):849–60. doi:10.1038/nri2413
319. Kimura T, Jain A, Choi SW, Mandell MA, Schroder K, Johansen T, et al. TRIM-mediated precision autophagy targets cytoplasmic regulators of innate immunity. *J Cell Biol* (2015) 210(6):973–89. doi:10.1083/jcb.201503023
320. Mandell MA, Jain A, Arko-Mensah J, Chauhan S, Kimura T, Dinkins C, et al. TRIM proteins regulate autophagy and can target autophagic substrates by direct recognition. *Dev Cell* (2014) 30(4):394–409. doi:10.1016/j.devcel.2014.06.013
321. Kimura T, Mandell M, Deretic V. Precision autophagy directed by receptor regulators – emerging examples within the TRIM family. *J Cell Sci* (2016) 129(5):881–91. doi:10.1242/jcs.163758
322. Tabah AA, Tardif K, Mansky LM. Anti-HIV-1 activity of Trim 37. *J Gen Virol* (2014) 95(Pt 4):960–7. doi:10.1099/vir.0.057653-0
323. Kim BH, Shenoy AR, Kumar P, Bradfield CJ, MacMicking JD. IFN-inducible GTPases in host cell defense. *Cell Host Microbe* (2012) 12(4):432–44. doi:10.1016/j.chom.2012.09.007
324. Wu G, Chai J, Suber TL, Wu J-W, Du C, Wang X, et al. Structural basis of IAP recognition by Smac/DIABLO. *Nature* (2000) 408(6815):1008–12. doi:10.1038/35050012
325. Coers J, Haldar AK. Ubiquitination of pathogen-containing vacuoles promotes host defense to *Chlamydia trachomatis* and *Toxoplasma gondii*. *Commun Integr Biol* (2015) 8(6):e1115163. doi:10.1080/19420889.2015.1115163
326. MacMicking JD. Interferon-inducible effector mechanisms in cell-autonomous immunity. *Nat Rev Immunol* (2012) 12(5):367–82. doi:10.1038/nri3210
327. Meunier E, Broz P. Interferon-inducible GTPases in cell autonomous and innate immunity. *Cell Microbiol* (2016) 18(2):168–80. doi:10.1111/cmi.12546
328. Finethy R, Jorgensen I, Haldar AK, de Zoete MR, Strowig T, Flavell RA, et al. Guanylate binding proteins enable rapid activation of canonical and noncanonical inflammasomes in *Chlamydia*-infected macrophages. *Infect Immun* (2015) 83(12):4740–9. doi:10.1128/IAI.00856-15
329. Reich NC, Liu L. Tracking STAT nuclear traffic. *Nat Rev Immunol* (2006) 6(8):602–12. doi:10.1038/nri1885
330. Stark GR, Darnell JE Jr. The JAK-STAT pathway at twenty. *Immunity* (2012) 36(4):503–14. doi:10.1016/j.immuni.2012.03.013
331. Gatsios P, Terstegen L, Schliess F, Haussinger D, Kerr IM, Heinrich PC, et al. Activation of the Janus kinase/signal transducer and activator of transcription pathway by osmotic shock. *J Biol Chem* (1998) 273(36):22962–8. doi:10.1074/jbc.273.36.22962
332. Levy DE, Darnell JE Jr. Stats: transcriptional control and biological impact. *Nat Rev Mol Cell Biol* (2002) 3(9):651–62. doi:10.1038/nrm909
333. Casanova JL, Holland SM, Notarangelo LD. Inborn errors of human JAKs and STATs. *Immunity* (2012) 36(4):515–28. doi:10.1016/j.immuni.2012.03.016
334. Kawata T. STAT signaling in *Dictyostelium* development. *Dev Growth Differ* (2011) 53(4):548–57. doi:10.1111/j.1440-169X.2010.01243.x
335. Kawata T, Shevchenko A, Fukuzawa M, Jermyn KA, Totty NF, Zhukovskaya NV, et al. SH2 signaling in a lower eukaryote: a STAT protein that regulates stalk cell differentiation in *Dictyostelium*. *Cell* (1997) 89(6):909–16. doi:10.1016/S0092-8674(00)80276-7
336. Araki T, Kawata T, Williams JG. Identification of the kinase that activates a nonmetazoan STAT gives insights into the evolution of phosphotyrosine-SH2 domain signaling. *Proc Natl Acad Sci U S A* (2012) 109(28):E1931–7. doi:10.1073/pnas.1202715109
337. Araki T, Vu LH, Sasaki N, Kawata T, Eichinger L, Williams JG. Two *Dictyostelium* tyrosine kinase-like kinases function in parallel, stress-induced STAT activation pathways. *Mol Biol Cell* (2014) 25(20):3222–33. doi:10.1091/mbc.E14-07-1182
338. Early A, Gamper M, Moniakis J, Kim E, Hunter T, Williams JG, et al. Protein tyrosine phosphatase PTP1 negatively regulates *Dictyostelium* STATa and is required for proper cell-type proportioning. *Dev Biol* (2001) 232(1):233–45. doi:10.1006/dbio.2001.0171
339. Araki T, Langenick J, Gamper M, Firtel RA, Williams JG. Evidence that DIF-1 and hyper-osmotic stress activate a *Dictyostelium* STAT by inhibiting a specific protein tyrosine phosphatase. *Development* (2008) 135(7):1347–53. doi:10.1242/dev.009936
340. Araki T, Gamper M, Early A, Fukuzawa M, Abe T, Kawata T, et al. Developmentally and spatially regulated activation of a *Dictyostelium* STAT protein by a serpentine receptor. *EMBO J* (1998) 17(14):4018–28. doi:10.1093/emboj/17.14.4018

341. Fukuzawa M, Araki T, Adrian I, Williams JG. Tyrosine phosphorylation-independent nuclear translocation of a *Dictyostelium* STAT in response to DIF signaling. *Mol Cell* (2001) 7(4):779–88. doi:10.1016/S1097-2765(01)00222-2
342. Zhukovskaya NV, Fukuzawa M, Tsujioka M, Jermyn KA, Kawata T, Abe T, et al. Dd-STATb, a *Dictyostelium* STAT protein with a highly aberrant SH2 domain, functions as a regulator of gene expression during growth and early development. *Development* (2004) 131(2):447–58. doi:10.1242/dev.00927
343. Araki T, Tsujioka M, Abe T, Fukuzawa M, Meima M, Schaap P, et al. A STAT-regulated, stress-induced signalling pathway in *Dictyostelium*. *J Cell Sci* (2003) 116(Pt 14):2907–15. doi:10.1242/jcs.00501
344. Otto GP, Cocorocchio M, Munoz L, Tyson RA, Bretschneider T, Williams RS. Employing *Dictyostelium* as an advantageous 3Rs model for pharmacogenetic research. *Methods Mol Biol* (2016) 1407:123–30. doi:10.1007/978-1-4939-3480-5_9
345. Stallforth P, Brock DA, Cantley AM, Tian X, Queller DC, Strassmann JE, et al. A bacterial symbiont is converted from an inedible producer of beneficial molecules into food by a single mutation in the gacA gene. *Proc Natl Acad Sci U S A* (2013) 110(36):14528–33. doi:10.1073/pnas.1308199110
346. Chen X, Kollner TG, Jia Q, Norris A, Santhanam B, Rabe P, et al. Terpene synthase genes in eukaryotes beyond plants and fungi: occurrence in social amoebae. *Proc Natl Acad Sci U S A* (2016) 113(43):12132–7. doi:10.1073/pnas.1610379113
347. Klapper M, Gotze S, Barnett R, Willing K, Stallforth P. Bacterial alkaloids prevent amoebal predation. *Angew Chem Int Ed Engl* (2016) 55(31):8944–7. doi:10.1002/anie.201603312
348. Gotze S, Herbst-Irmer R, Klapper M, Gorls H, Schneider KRA, Barnett R, et al. Structure, biosynthesis, and biological activity of the cyclic lipopeptide anikasin. *ACS Chem Biol* (2017) 12(10):2498–502. doi:10.1021/acschembio.7b00589
349. Brock DA, Read S, Bozhchenko A, Queller DC, Strassmann JE. Social amoeba farmers carry defensive symbionts to protect and privatize their crops. *Nat Commun* (2013) 4:2385. doi:10.1038/ncomms3385
350. DiSalvo S, Haselkorn TS, Bashir U, Jimenez D, Brock DA, Queller DC, et al. Burkholderia bacteria infectiously induce the proto-farming symbiosis of *Dictyostelium* amoebae and food bacteria. *Proc Natl Acad Sci U S A* (2015) 112(36):E5029–37. doi:10.1073/pnas.1511878112
351. Brock DA, Callison WE, Strassmann JE, Queller DC. Sentinel cells, symbiotic bacteria and toxin resistance in the social amoeba *Dictyostelium discoideum*. *Proc Biol Sci* (2016) 283:1829. doi:10.1098/rspb.2015.2727
352. Smith J, Queller DC, Strassmann JE. Fruiting bodies of the social amoeba *Dictyostelium discoideum* increase spore transport by *Drosophila*. *BMC Evol Biol* (2014) 14:105. doi:10.1186/1471-2148-14-105
353. Taylor-Mulneix DL, Bendor L, Linz B, Rivera I, Ryman VE, Dewan KK, et al. Bordetella bronchiseptica exploits the complex life cycle of *Dictyostelium discoideum* as an amplifying transmission vector. *PLoS Biol* (2017) 15(4):e2000420. doi:10.1371/journal.pbio.2000420

Conflict of Interest Statement: The authors declare that the research was conducted in the absence of any commercial or financial relationships that could be construed as a potential conflict of interest.

Copyright © 2018 Dunn, Bosmani, Barisch, Raykov, Lefrançois, Cardenal-Muñoz, López-Jiménez and Soldati. This is an open-access article distributed under the terms of the Creative Commons Attribution License (CC BY). The use, distribution or reproduction in other forums is permitted, provided the original author(s) or licensor are credited and that the original publication in this journal is cited, in accordance with accepted academic practice. No use, distribution or reproduction is permitted which does not comply with these terms.

frontiers in Microbiology

PERSPECTIVE
published: 05 December 2017
doi: 10.3389/fmicb.2017.02402

Humans in a Dish: The Potential of Organoids in Modeling Immunity and Infectious Diseases

*Nino Iakobachvili and Peter J. Peters**

Division of Nanoscopy, Maastricht Multimodal Molecular Imaging Institute, Maastricht University, Maastricht, Netherlands

For many decades, human infectious diseases have been studied in immortalized cell lines, isolated primary cells from blood and a range of animal hosts. This research has been of fundamental importance in advancing our understanding of host and pathogen responses but remains limited by the absence of multicellular context and inherent differences in animal immune systems that result in altered immune responses. Recent developments in stem cell biology have led to the *in vitro* growth of organoids that faithfully recapitulate a variety of human tissues including lung, intestine and brain amongst many others. Organoids are derived from human stem cells and retain the genomic background, cellular organization and functionality of their tissue of origin. Thus they have been widely used to characterize stem cell development, numerous cancers and genetic diseases. We believe organoid technology can be harnessed to study host–pathogen interactions resulting in a more physiologically relevant model that yields more predictive data of human infectious diseases than current systems. Here, we highlight recent work and discuss the potential of human stem cell-derived organoids in studying infectious diseases and immunity.

Keywords: organoids, disease model, infection, macrophages, monocytes, dendritic cells, MPS, tuberculosis

OPEN ACCESS

Edited by:
Geanncarlo Lugo-Villarino, UMR5089 Institut de Pharmacologie et de Biologie Structurale (IPBS), France

Reviewed by:
Margarida Saraiva, Instituto de Biologia Molecular e Celular (IBMC), Portugal
Sina Bartfeld, University of Würzburg, Germany

***Correspondence:**
Peter J. Peters
peter.peters@maastrichtuniversity.nl

Specialty section:
This article was submitted to Microbial Immunology, a section of the journal Frontiers in Microbiology

Received: *02 October 2017*
Accepted: *20 November 2017*
Published: *05 December 2017*

Citation:
Iakobachvili N and Peters PJ (2017) Humans in a Dish: The Potential of Organoids in Modeling Immunity and Infectious Diseases. Front. Microbiol. 8:2402. doi: 10.3389/fmicb.2017.02402

INTRODUCTION

Lower respiratory infections, cancers (including those caused by infectious agents), diarrheal diseases and tuberculosis remain among the top 10 causes of death worldwide (WHO, 2017). Of crucial importance in sustaining organismal homeostasis, coordinating defenses against pathogenic attack and orchestrating the innate and adaptive immune responses is the mononuclear phagocyte system (MPS)- a key network of macrophages, dendritic cells and monocytes. The tissue resident macrophages function to clear cell debris, resolve inflammation and modulate immune responses (Davies et al., 2013); antigen-presenting dendritic cells initiate the adaptive immune response and prime the immune system to future attack (Mildner and Jung, 2014); and lastly, circulating monocytes migrate around the body where they can remain as monocytes, differentiate into macrophages in response to stimulatory signals or acquire antigen presenting abilities (Chow et al., 2011). The human MPS is part of the first line of immune defense, however, modeling this complex system in relation to infection, disease and development is difficult and is predominantly performed using three strategies:

(1) Purification of peripheral blood mononuclear cells (PBMC's) from human blood for short term *in vitro* culture (with the possibility to differentiate the monocytes to macrophages or dendritic cells); similarly, but in lower numbers, dendritic cells can be purified straight from blood or tissue resident macrophages from certain tissues, e.g., alveolar macrophages from lungs,
(2) Immortalized MPS-like single cell lines of human or animal origin, e.g., the human monocyte-like THP-1 cell line, the murine macrophage-like J774 cell line,
(3) Using animal organisms to study aspects of the system, e.g., non-human primates, zebrafish, mice, humanized mice, cell lineage depleted animals and extrapolating results to humans.

It is key to note that single cell culture and animal models are widely used and have been instrumental in many scientific advancements in fundamental research, drug and vaccine development, infectious, autoimmune and genetic diseases to name a few. Whilst their scientific importance cannot be underestimated, critical questions typically arise relating to the validity of these systems. This is a result of the inherent differences in cellular context (or the lack of it when using primary cells or cell lines), physiology and genetics of different species which influences disease outcome, progression and accurate prediction of human response. The severe effects of such matters become apparent in the fact that pre-clinical animal tests are still failing to predict human pharmacodynamics and toxicity as exemplified by the recent failure of the 2016 phase 1 clinical trial of BIA 10-2474 for neuropathic pain which resulted in the hospitalization of five participants and the death of one (Chaikin, 2017). With an estimated 90% of drugs that pass pre-clinical tests failing in human clinical trials (Mullard, 2016), it is not surprising that the scientific community is increasingly encouraging the development and exploitation of alternative approaches that may offer a more valid way of modeling diseases, disorders and drug interactions (Korch et al., 2011). In addition to the questionable validity of these non-human systems, the guiding principles of the '3 R's of animal research' have been increasingly implemented in new legislation where animals are being used for research (United States, Canada, United Kingdom, and Europe). The 3 R principles, a set of ethical guidelines first published in Russell and Burch (1959) aim to Replace the use of animals for scientific research, Reduce the number of animals used and Refine techniques to minimize the pain, suffering and distress caused to animals during scientific research. Consequently the need for human *in vitro* based systems is at a record high. We believe that the future of applied and fundamental research lies in the quickly expanding field of *in vitro* grown organoids that recapitulate human organs to varying degrees. Organoids bridge the gap between single cell culture and *in vivo* work, offering ethically obtained functional, multicellular tissue of human origin that provides a more similar *in vitro* system in which to study multiple components of host–pathogen interactions and drug response.

THE ORGANOID REVOLUTION

Recent advances in stem cell biology have allowed researchers to grow human tissues that resemble organs *in vitro*. These organoids are stem cell derived, self –organizing, multi-cellular aggregates that closely recapitulate the function, cellular components and architecture of human tissues. Organoids are cultured in 3D (in extracellular matrix) and reflect the cellular heterogeneity and cellular behavior of tissues *in vitro*. Unlike cell lines, organoids remain genetically stable for long periods (years) and do not show significant increases in the expression of stress-related genes during extended culture (Sato et al., 2009). In addition to their close resemblance to human tissues, organoids are amenable to the same analytical techniques as primary cells/cell lines including fluorescence labeling, live cell imaging, electron microscopy, mass spectrometry (Cristobal et al., 2017) and genetic manipulation including by CRISPR/Cas9 (Matano et al., 2015) making them particularly suitable for scientific research. Typically, organoids are derived from either embryonic or induced pluripotent stem cells (PSC's) or adult stem cells (ASC's) resected or biopsied from organs. Both cell types have the unique capacity to self-renew and differentiate- a defining feature of stem cells, and the absence of which in primary cells causes their quick death *in vitro* (Melton, 2014). Organoids derived from ASC's are grown from cell suspensions obtained from primary tissue biopsies or resected material that are immediately embedded in an extracellular matrix and grown in the presence of specific growth factors to direct cell differentiation (**Figure 1**). Organoids that can be cultured from human ASC's include colon (Sato et al., 2011), intestine (Sato et al., 2009), liver (Huch et al., 2013b), prostate (Karthaus et al., 2014), pancreas (Huch et al., 2013a), fallopian tube (Kessler et al., 2015), stomach (Barker et al., 2010), tongue (Hisha et al., 2013) and endometrium (Turco et al., 2017). Those derived from PSC's are generally grown from 2D cultures of stem cells that are matured into spheroids, committed to endoderm using Activin A (Takebe et al., 2013) and then cultured in 3D with specific differentiation signals that are dependent on the type of tissue that is ultimately required (**Figure 1**). Intestinal (Spence et al., 2011), liver (Takebe et al., 2013), lung (Dye et al., 2015), kidney (Takasato et al., 2015), pancreas (Huang et al., 2015), stomach (McCracken et al., 2014), and retinal (Völkner et al., 2016) organoids can all be cultured from PSC's. PSC-derived organoids that are not derived from endoderm can also be cultured with modifications to the above protocol as exemplified by cerebral (Lancaster et al., 2014), optic-cup (Eiraku et al., 2011) and kidney (Takasato et al., 2015) organoids.

The similarity of some organoids to their tissue of origin is exemplified in elegant research by the Clevers laboratory who first identified the Lgr5+ intestinal stem cell (Barker et al., 2007) and then characterized the signals (epidermal growth factor, Wnt-3, R-spondin and Noggin) required for maintaining these cells in culture and promoting their proliferation and cellular differentiation into intestinal epithelium (Sato and Clevers, 2013). This research established the first ASC-derived organoids, and has formed the basis for the growth cocktails used to culture a variety of different mouse and human tissues

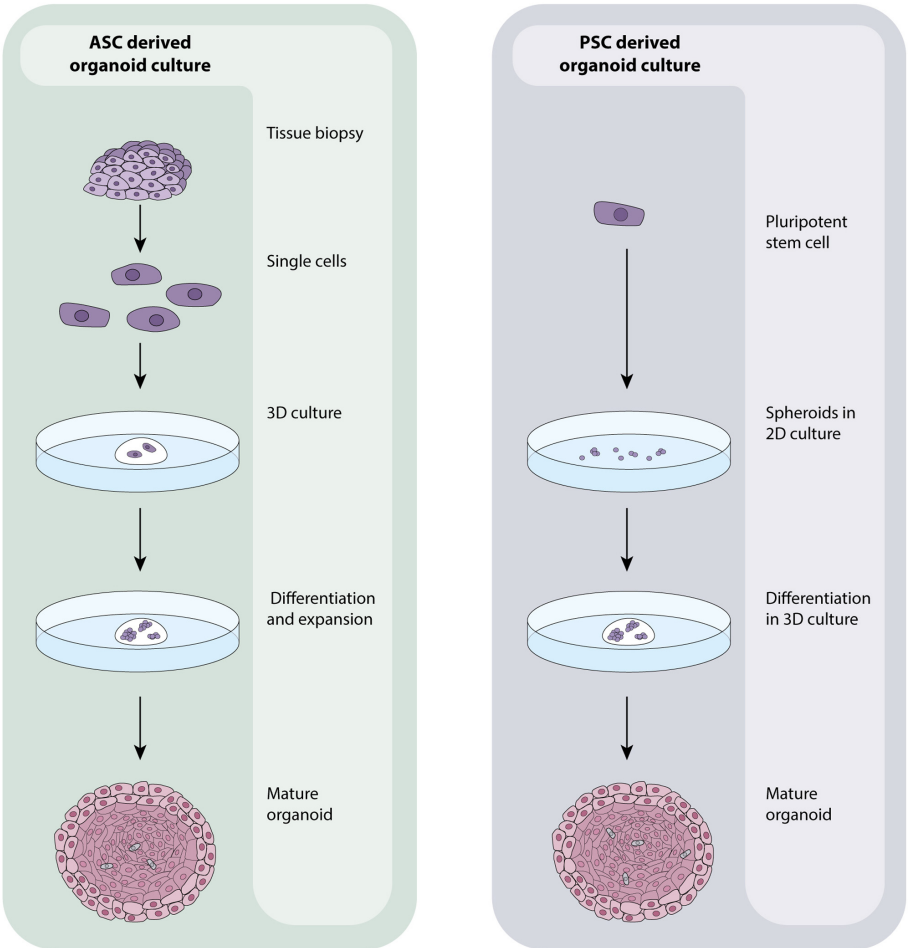


FIGURE 1 | ASC- and PSC-derived organoid culture protocols. ASC-derived organoids are grown from healthy or tumourous tissue biopsies. Tissues are processed into a single cell suspension which is directly embedded in an extracellular matrix. Media containing numerous growth factors, which vary dependent on the tissue being grown, is added and regularly changed until organoids have expanded. PSC-derived organoids originate with 2D cultures of PSC's that are grown into aggregates/spheroids. At this point, they may be embedded in an extracellular matrix and expanded to maturity using a a growth factor rich media that is again, specific to the tissue of interest. The composition and organization of cells within organoids is dictated by the identity of the tissue being grown which in turn affects the overall size and shape of the organoid.

including GFP expressing colonic mouse organoids. When GFP+ colon organoids are transplanted into mice treated with colitis-inducing dextran sulfate sodium, intestinal lesions show signs of recovery within 16 days of transplantation. Transplanted organoids were histologically indistinguishable from the surrounding epithelium, fully functional, contained all terminally differentiated cell types and recovered the body weight of diseased mice (Yui et al., 2012).

This pioneering method of tissue culture has thus unlocked an entirely new tool that can be harnessed in scientific research- one that provides a consistent, genetically stable source of multicellular human or animal tissue for experimental use. Additionally, whilst PSC-derived organoids typically recapitulate early stages of cellular proliferation that can be used to study development and foetal infections for example, ASC derived organoids can provide complimentary, adult epithelium to explore mature tissue responses to pathogenic attack or drugs. Thus developmental biologists have already begun to use organoids to study organogenesis (Shyer et al., 2015), lineage specification (Yin et al., 2014), stem cell niche and tissue homeostasis (Barker, 2013). Organoids can also be grown from healthy and tumorous human tissues (Van De Wetering et al., 2015)- in both cases, retaining some, if not most, of the features of the original tissue. Thus cancer biologists are extensively modeling *in vitro* patient heterogeneity (Weeber et al., 2015), metastatic potential (Nadauld et al., 2014) and drug screening. Due to their genetic and morphological similarities to the organ from which they are derived from, ASC organoids provide a novel approach to study stem cell and tissue transplantation. This feature is a key factor in making organoid-based personalized medicine a reality and which is exemplified by Beekman and colleagues who have applied intestinal organoids grown from cystic fibrosis (CF) patients to screen for drugs. Specifically for those that restore the function of mutant

CFTR (an anion channel called CF transmembrane conductance regulator that, when mutated, is responsible for causing CF in approximately 67% of cases worldwide) proteins (Dekkers et al., 2012). Considering the difficulties in predicting patient responses to drugs, and the expense of providing drugs that are ultimately inefficient, the development of this assay is an important step toward facilitating diagnosis, drug development and personalized treatment regimens. This discovery has been successfully translated to the clinical setting (Saini, 2016). It is clear that organoid systems have already begun to be widely and successfully used in a range of clinical and basic research environments and naturally, the infectious diseases community has also taken notice.

ORGANOIDS IN INFECTIOUS DISEASES

Zika virus infection (ZIKV) of humans was first identified in Dick et al. (1952); it is spread by mosquitoes and typically illness is mild with fever-like symptoms for 2–7 days. In 2016, ZIKV was declared a public health emergency by WHO based on epidemiological evidence that there was an association between babies born with neurological complications including microcephaly and ZIKV. At this point, no suitable model existed for studying this pathogen but microcephaly had been successfully modeled in induced PSC-derived cerebral organoids that develop discrete brain regions (Lancaster et al., 2014). ZIKV was modeled in such a system to great success; infection was found to cause neuronal cell death in the early stages of brain development (Garcez et al., 2016), to induce premature differentiation of preferentially infected neural progenitor cells resulting in mitotic defects (Gabriel et al., 2017), and to upregulate the innate immune receptor TLR3 (toll-like receptor 3) which resulted in dysregulation of neurogenesis and cell death (Dang et al., 2016). The organoid model of ZIKV has also been adapted to a large scale platform that can be used for modeling brain development, neurological diseases and drug screening by growing brain region specific organoids in miniaturized spinning bioreactors (Qian et al., 2016) further highlighting the power and success of using organoids for studying development, disease and treatment. Organoids have also proved themselves to be a robust, accurate and reproducible model to study Norovirus (Ettayebi et al., 2016), and clinical strains of Rotavirus (Finkbeiner et al., 2012; Zhu et al., 2017)- two viruses that were difficult to cultivate and study *in vitro* until organoids became available as a tool.

Bacterial pathogens are also being increasingly studied in organoids. Organoid based studies into *Salmonella enterica* serovar Typhi virulence provided the first evidence that infection with this bacteria is a causative agent of gallbladder carcinoma (Scanu et al., 2015). *S.* Typhimurium was found to alter the organoid transcriptome to activate the Akt and MapK kinase pathways which are often found to be elevated in human cancers (Manning and Cantley, 2007; Cseh et al., 2014). Similar features were presented in mouse gallbladder carcinomas and infected gallbladder organoids including loss of cellular polarity and enlarged nuclei. Interestingly, cells dissociated from organoids with previous *S.* Typhimurium infection were able to expand into new organoids in growth factor-diminished media, unlike those which had not been previously exposed to infection indicating a sustained alteration of host signaling pathways. PSC-derived intestinal organoids are being used to study shigatoxigenic serotypes of *Escherichia coli* for which no suitable animal models exist (Karve et al., 2017), whilst gastric organoids from ASC's are being developed as a model in which to study *Helicobacter pylori* infection (Bartfeld et al., 2015; Schlaermann et al., 2016) – with potential to extend the model to encompass the study of *H. pylori* associated gastric cancer. Our own laboratory is focused on modeling tuberculosis infection within ASC-derived lung organoids (**Figure 2**) to continue our research on unraveling the mechanisms behind ESX-1 dependent translocation and its

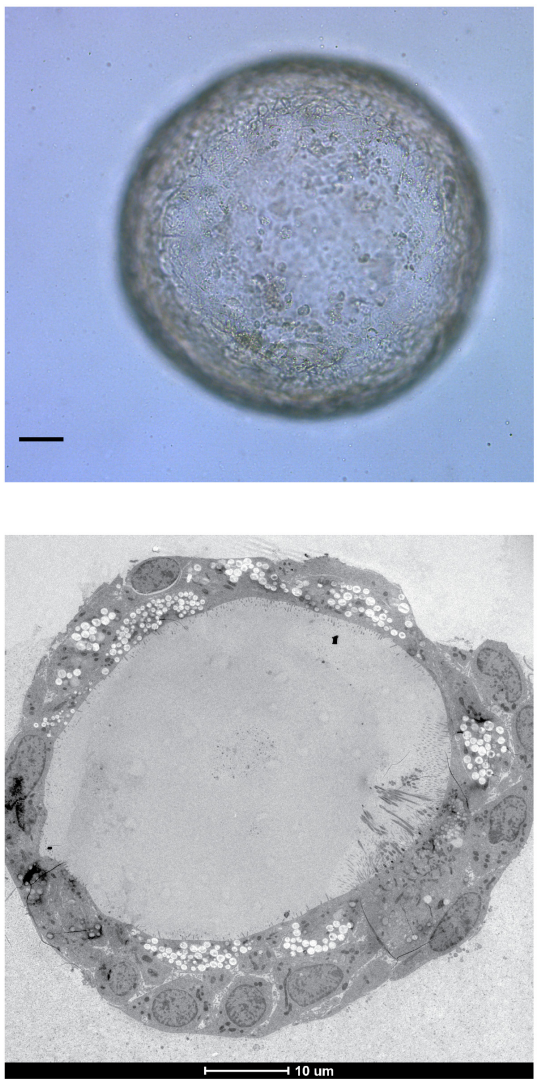


FIGURE 2 | *In vitro* grown ASC-derived lung organoid. **(A)** Mature lung organoid in extracellular matrix on day 25 of culture. Scale bar is 10 μm. **(B)** Electron microscope image of a mature lung organoid following high pressure freezing, freeze substitution, epon embedding and sectioning. Note self-organization of multiple differentiated cells. Both courtesy of Norman Sachs.

function during infection (van der Wel et al., 2007; Houben et al., 2012).

Studying interactions between human hosts and their protozoan parasites has been difficult due to a lack of appropriate animal models or due to the difficulty in culturing parasites with obligate human-host specificity. Currently, organoids have been limited to a supportive role to assay the role of tuft cells during infection with the helminth parasite *Nippostrongylus brasiliensis* (Gerbe et al., 2016). However, this field recognizes the ability of organoid technology in overcoming the experimental bottlenecks described above to model parasitic pathogens such as *Cyclospora* sp., *Cryptosporidium* sp. and *Giardia* sp. (Klotz et al., 2012).

INCREASING THE COMPLEXITY OF ORGANOID SYSTEMS

It is clear that organoids can represent tissue structure and function exceptionally well. Organoid technology is a significant and brilliant advancement in the tools available for scientific research across a wide range of different topics but they remain inherently incomplete- they lack the microenvironment of stroma, vasculature, immune cells and other organ systems that tissues interact with in the body during development and disease. It is also likely that not all developmental stages are currently being represented in a single organoid culture which is particularly relevant if fetal or adult infections are being modeled. Furthermore, certain cell types are not being maintained in organoid cultures due to incorrect signaling resulting in the growth of 'incomplete' tissues that compromise the validity of these systems in research.

Organoid culture techniques are thus in a constant state of evolution; culture conditions are constantly being improved to better support multiple cell types and drive proliferation. Current efforts are also guiding the development of designer matrices such as polyethylene glycol hydrogels that are mechanically more stable and whose composition is defined, unlike the inherently variable, animal sourced and traditionally used extracellular matrix (Gjorevski et al., 2016). Better defined culture conditions are more conducive to controlled modifications and will render organoids more accessible in clinical and basic research where reproducibility is important. Efforts are also being made to address the lack of vascularization in organoid cultures to improve nutrient availability, signaling and removal of toxins as would occur naturally in the body thus bringing organoids one step closer toward functional, *in vitro* grown organs. This is currently being accomplished by transplanting induced PSC-derived organoids grown with stromal populations and connecting the endothelial network to a mouse host (Takebe et al., 2013; Raikwar et al., 2015), however, it remains labor intensive and does not yet translate easily to standard tissue culture facilities.

Most important for studying the MPS in organoids, are advancements relating to co-culturing organoids with cell types that are absent in epithelial structures such as macrophages and dendritic cells. Though currently in its infancy, it is already possible to mix intestinal organoids cultured as normal, with purified cultures of intraepithelial lymphocytes in an extracellular matrix to study their migration against the basal side of the organoids via fluorescent imaging (Nozaki et al., 2016). It is also possible to microinject cells of interest into the lumen of organoids to ensure contact with the apical side if exogenously added cells are unable to migrate through organoid tissue. Such co-cultures are likely to be short term due to the current short life-span of primary purified immune cells but they lead the way toward creating organoid cultures with increased complexity that allow us to study human physiology *in vitro* at an unprecedented level and in a experimentally controllable environment. Immune cells are often the first point of contact during infection, and their response dictates disease outcome. It is thus important to use organoid systems to their full capacity. Therefore, to accurately model both the MPS and infectious disease, we must be sure to include missing but key cell types, even if they are not naturally present using current methods of organoid culture.

CONCLUDING REMARKS

The beauty of organoids in recapitulating human tissue and function *in vitro* has been described, and their use in stem cell development, cancer, infectious diseases, drug screening and transplantation demonstrated. As we get better insight into the culture conditions needed to maintain the multiple cell types and microenvironment associated with human tissues, we gain from being able to recapitulate more of human physiology *in vitro*. This in turn provides an increasingly suitable and better defined model system for modeling the role of MPS and other cells involved in infection, immunity and inflammation. Organoid systems are also exquisitely suitable for adaptation into diagnostic and screening platforms as they offer an excellent source of readily available human tissue that accurately reflects human responses. Whilst organoids are not without their caveats, we believe they will continue to significantly advance scientific attitudes, fundamental, therapeutic and clinical research for decades more.

AUTHOR CONTRIBUTIONS

NI conceived the idea, wrote and edited the manuscript. PP contributed ideas and discussion of the manuscript.

FUNDING

NI is supported by a grant from ZonMW (project number 114021005).

ACKNOWLEDGMENTS

The authors thank Norman Sachs for sharing his images of ASC-derived lung organoids. They kindly thank Hans Clevers for critical reading and discussion of the manuscript. They thank Raimond Ravelli and Carmen López-Iglesias for critical reading of the manuscript.

REFERENCES

Barker, N. (2013). Adult intestinal stem cells: critical drivers of epithelial homeostasis and regeneration. *Nat. Rev. Mol. Cell Biol.* 15, 19–33. doi: 10.1038/nrm3721

Barker, N., Huch, M., Kujala, P., van de Wetering, M., Snippert, H. J., van Es, J. H., et al. (2010). Lgr5^{+ve} stem cells drive self-renewal in the stomach and build long-lived gastric units in vitro. *Cell Stem Cell* 6, 25–36. doi: 10.1016/j.stem.2009.11.013

Barker, N., van Es, J. H., Kuipers, J., Kujala, P., van den Born, M., Cozijnsen, M., et al. (2007). Identification of stem cells in small intestine and colon by marker gene Lgr5. *Nature* 449, 1003–1007. doi: 10.1038/nature06196

Bartfeld, S., Bayram, T., Van De Wetering, M., Huch, M., Begthel, H., Kujala, P., et al. (2015). In vitro expansion of human gastric epithelial stem cells and their responses to bacterial infection. *Gastroenterology* 148, 126.e6–136.e6.

Chaikin, P. (2017). The Bial 10-2474 phase 1 study — a drug development perspective and recommendations for future first-in-human trials. *J. Clin. Pharmacol.* 57, 690–703. doi: 10.1002/jcph.889

Chow, A., Brown, B. D., and Merad, M. (2011). Studying the mononuclear phagocyte system in the molecular age. *Nat. Rev. Immunol.* 11, 788–798. doi: 10.1038/nri3087

Cristobal, A., van den Toorn, H. W. P., van de Wetering, M., Clevers, H., Heck, A. J. R., and Mohammed, S. (2017). Personalized proteome profiles of healthy and tumor human colon organoids reveal both individual diversity and basic features of colorectal cancer. *Cell Rep.* 18, 263–274. doi: 10.1016/j.celrep.2016.12.016

Cseh, B., Doma, E., and Baccarini, M. (2014). "RAF" neighborhood: protein – protein interaction in the Raf / Mek / Erk pathway. *FEBS Lett.* 588, 2398–2406. doi: 10.1016/j.febslet.2014.06.025

Dang, J., Tiwari, S. K., Lichinchi, G., Qin, Y., Patil, V. S., Eroshkin, A. M., et al. (2016). Zika virus depletes neural progenitors in human cerebral organoids through activation of the innate immune receptor TLR3. *Stem Cell* 19, 258–265. doi: 10.1016/j.stem.2016.04.014

Davies, L. C., Jenkins, S. J., Allen, J. E., and Taylor, P. R. (2013). Tissue-resident macrophages. *Nat. Immunol.* 14, 986–995. doi: 10.1038/ni.2705

Dekkers, J. F., Wiegerinck, C. L., de Jonge, H. R., Bronsveld, I., Janssens, H. M., de Winter-de Groot, J. F., et al. (2012). A functional CFTR assay using primary cystic fibrosis intestinal organoids. *Nat. Med.* 11, 939–947. doi: 10.1016/S1569-1993(12)60101-5

Dick, G. W. A., Kitchen, S. F., and Haddow, J. (1952). Zika virus (I). Isolation and serological specification. *Trans. R. Soc. Trop. Med. Hyg.* 46, 509–520. doi: 10.1016/0035-9203(52)90042-4

Dye, B. R., Hill, D. R., Ferguson, M. A., Tsai, Y.-H., Nagy, M. S., Dyal, R., et al. (2015). In vitro generation of human pluripotent stem cell derived lung organoids. *eLife* 4:e05098. doi: 10.7554/eLife.05098

Eiraku, M., Takata, N., Ishibashi, H., Kawada, M., Sakakura, E., Okuda, S., et al. (2011). Self-organizing optic-cup morphogenesis in three-dimensional culture. *Nature* 472, 51–56. doi: 10.1038/nature09941

Ettayebi, K., Crawford, S. E., Murakami, K., Broughman, J. R., Karandikar, U., Tenge, V. R., et al. (2016). Replication of human noroviruses in stem cell–derived human enteroid. *Science* 353, 1387–1394. doi: 10.1126/science.aaf5211

Finkbeiner, S. R., Zeng, X., Utama, B., Atmar, R. L., Shroyer, N. F., Estes, M. K., et al. (2012). Stem cell-derived human intestinal organoids as an infection model for rotaviruses. *mBio* 3:e00159-12. doi: 10.1128/mBio.00159-12.Editor

Gabriel, E., Ramani, A., Gottardo, M., Natarajan, K., Gooi, L. M., Goranci-Buzhala, G., et al. (2017). Zika virus isolates induce premature differentiation of neural progenitors in human brain organoids. *Cell Stem Cell* 20, 397–406. doi: 10.1016/j.stem.2016.12.005

Garcez, P. P., Loiola, E. C., Madeiro, da Costa, R., Higa, L. M., Trindade, P., et al. (2016). Zika virus impairs growth in human neurospheres and brain organoids. *Science* 352, 816–818. doi: 10.1086/429930

Gerbe, F., Sidot, E., Smyth, D. J., Ohmoto, M., Matsumoto, I., Dardalhon, V., et al. (2016). Intestinal epithelial tuft cells initiate type 2 mucosal immunity to helminth parasites. *Nature* 529, 226–230. doi: 10.1038/nature16527

Gjorevski, N., Sachs, N., Manfrin, A., Giger, S., Bragina, M. E., Ordonez-Moran, P., et al. (2016). Designer matrices for intestinal stem cell and organoid culture. *Nature* 539, 560–564. doi: 10.1038/nature20168

Hisha, H., Tanaka, T., Kanno, S., Tokuyama, Y., Komai, Y., Ohe, S., et al. (2013). Establishment of a novel lingual organoid culture system: generation of organoids having mature keratinized epithelium from adult epithelial stem cells. *Sci. Rep.* 3:3224. doi: 10.1038/srep03224

Houben, D., Demangel, C., van Ingen, J., Perez, J., Baldeón, L., Abdallah, A. M., et al. (2012). ESX-1-mediated translocation to the cytosol controls virulence of mycobacteria. *Cell. Microbiol.* 14, 1287–1298. doi: 10.1111/j.1462-5822.2012.01799.x

Huang, L., Holtzinger, A., Jagan, I., BeGora, M., Lohse, I., Ngai, N., et al. (2015). Ductal pancreatic cancer modeling and drug screening using human pluripotent stem cell– and patient-derived tumor organoids. *Nat. Med.* 21, 1364–1371. doi: 10.1038/nm.3973

Huch, M., Bonfanti, P., Boj, S. F., Sato, T., Loomans, C. J. M., van de Wetering, M., et al. (2013a). Unlimited in vitro expansion of adult bi-potent pancreas progenitors through the Lgr5/R-spondin axis. *EMBO J.* 32, 2708–2721. doi: 10.1038/emboj.2013.204

Huch, M., Dorrell, C., Boj, S. F., van Es, J. H., Li, V. S. W., van de Wetering, M., et al. (2013b). *In vitro* expansion of single Lgr5+ liver stem cells induced by Wnt-driven regeneration. *Nature* 494, 247–250. doi: 10.1038/nature11826

Karthaus, W. R., Iaquinta, P. J., Drost, J., Gracanin, A., Van Boxtel, R., Wongvipat, J., et al. (2014). Identification of multipotent luminal progenitor cells in human prostate organoid cultures. *Cell* 159, 163–175. doi: 10.1016/j.cell.2014.08.017

Karve, S. S., Pradhan, S., Ward, D. V., and Weiss, A. A. (2017). Intestinal organoids model human responses to infection by commensal and Shiga toxin producing *Escherichia coli*. *PLOS ONE* 12:e0178966. doi: 10.1371/journal.pone.0178966

Kessler, M., Hoffmann, K., Brinkmann, V., Thieck, O., Jackisch, S., Toelle, B., et al. (2015). The Notch and Wnt pathways regulate stemness and differentiation in human fallopian tube organoids. *Nat. Commun.* 6:8989. doi: 10.1038/ncomms9989

Klotz, C., Aebischer, T., and Seeber, F. (2012). Stem cell-derived cell cultures and organoids for protozoan parasite propagation and studying host-parasite interaction. *Int. J. Med. Microbiol.* 302, 203–209. doi: 10.1016/j.ijmm.2012.07.010

Korch, G. W., Niemi, S. M., Bergman, N. H., Carucci, D. J., Ehrlich, S. A., Gronvall, G. K., et al. (2011). *Animal Models for Assessing Countermeasures to Bioterrorism Agents*. Washington, DC: National Academies Press. doi: 10.17226/13233

Lancaster, M. A., Renner, M., Martin, C., Wenzel, D., Bicknell, L. S., Hurles, M. E., et al. (2014). Cerebral organoids model human brain development and microcephaly. *Nature* 501, 373–379. doi: 10.1038/nature12517.Cerebral

Manning, B. D., and Cantley, L. C. (2007). Review AKT / PKB signaling: navigating downstream. *Cell* 129, 1261–1274. doi: 10.1016/j.cell.2007.06.009

Matano, M., Date, S., Shimokawa, M., Takano, A., Fujii, M., Ohta, Y., et al. (2015). Modeling colorectal cancer using CRISPR-Cas9–mediated engineering of human intestinal organoids. *Nat. Med.* 21, 256–262. doi: 10.1038/nm.3802

McCracken, K. W., Catá, E. M., Crawford, C. M., Sinagoga, K. L., Schumacher, M., Rockich, B. E., et al. (2014). Modelling human development and disease in pluripotent stem-cell-derived gastric organoids. *Nature* 516, 400–404. doi: 10.1038/nature13863

Melton, D. (2014). "Stemness: definitions, criteria, and standards," in *Essentials of Stem Cell Biology*, eds R. Lanza and A. Atala (Amsterdam: Elsevier), 7–17.

Mildner, A., and Jung, S. (2014). Development and function of dendritic cell subsets. *Immunity* 40, 642–656. doi: 10.1016/j.immuni.2014.04.016

Mullard, A. (2016). Parsing clinical success rates. *Nat. Rev. Drug Discov.* 15, 447. doi: 10.1038/nrd.2016.136

Nadauld, L. D., Garcia, S., Natsoulis, G., Bell, J. M., Miotke, L., Hopmans, E. S., et al. (2014). Metastatic tumor evolution and organoid modeling implicate TGFBR2 as a cancer driver in diffuse gastric cancer. *Genome Biol.* 15, 428. doi: 10.1186/s13059-014-0428-9

Nozaki, K., Mochizuki, W., Matsumoto, Y., and Matsumoto, T. (2016). Co-culture with intestinal epithelial organoids allows efficient expansion and motility analysis of intraepithelial lymphocytes. *J. Gastroenterol.* 51, 206–213. doi: 10.1007/s00535-016-1170-8

Qian, X., Nguyen, H. N., Song, M. M., Hadiono, C., Ogden, S. C., Hammack, C., et al. (2016). Brain-region-specific organoids using mini- bioreactors for modeling ZIKV exposure. *Cell* 165, 1238–1254. doi: 10.1016/j.cell.2016.04.032

Raikwar, S. P., Kim, E., Sivitz, W. I., Allamargot, C., Thedens, D. R., and Zavazava, N. (2015). Human iPS cell-derived insulin producing cells form vascularized organoids under the kidney capsules of diabetic mice. *PLOS ONE* 10:e0116582. doi: 10.1371/journal.pone.0116582

Russell, W., and Burch, R. (1959). *The Principles of Humane Experimental Technique*. Available at: http://altweb.jhsph.edu/pubs/books/humane_exp/het-toc.

Saini, A. (2016). Cystic fibrosis patients benefit from mini guts. *Cell Stem Cell* 19, 425–427. doi: 10.1016/j.stem.2016.09.001

Sato, T., and Clevers, H. (2013). Growing self-organizing mini-guts from a single intestinal stem cell: mechanism and applications. *Science* 340, 1190–1194. doi: 10.1126/science.1234852

Sato, T., Stange, D. E., Ferrante, M., Vries, R. G. J., Van Es, J. H., Van Den Brink, S., et al. (2011). Long-term expansion of epithelial organoids from human colon, adenoma, adenocarcinoma, and Barrett's epithelium. *Gastroenterology* 141, 1762–1772. doi: 10.1053/j.gastro.2011.07.050

Sato, T., Vries, R. G., Snippert, H. J., van de Wetering, M., Barker, N., Stange, D. E., et al. (2009). Single Lgr5 stem cells build crypt-villus structures in vitro without a mesenchymal niche. *Nature* 459, 262–265. doi: 10.1038/nature07935

Scanu, T., Spaapen, R. M., Bakker, J. M., Holden, D. W., Nath, G., and Neefjes, J. (2015). *Salmonella* manipulation of host signaling pathways provokes cellular transformation associated with gallbladder carcinoma. *Cell Host Microbe* 17, 763–774. doi: 10.1016/j.chom.2015.05.002

Schlaermann, P., Toelle, B., Berger, H., Schmidt, S. C., Glanemann, M., Ordemann, J., et al. (2016). A novel human gastric primary cell culture system for modelling *Helicobacter pylori* infection in vitro. *Gut* 65, 202–213. doi: 10.1136/gutjnl-2014-307949

Shyer, A. E., Huycke, T. R., Lee, C., Mahadevan, L., and Tabin, C. J. (2015). Bending gradients: how the intestinal stem cell gets its home. *Cell* 161, 569–580. doi: 10.1016/j.cell.2015.03.041

Spence, J. R., Mayhew, C. N., Rankin, S. A., Kuhar, M. F., Vallance, J. E., Tolle, K., et al. (2011). Directed differentiation of human pluripotent stem cells into intestinal tissue in vitro. *Nature* 470, 105–109. doi: 10.1038/nature09691

Takasato, M., Er, P. X., Chiu, H. S., Maier, B., Baillie, G. J., Ferguson, C., et al. (2015). Kidney organoids from human iPS cells contain multiple lineages and model human nephrogenesis. *Nature* 526, 564–568. doi: 10.1038/nature15695

Takebe, T., Sekine, K., Enomura, M., Koike, H., Kimura, M., Ogaeri, T., et al. (2013). Vascularized and functional human liver from an iPSC-derived organ bud transplant. *Nature* 499, 481–484. doi: 10.1038/nature12271

Turco, M. Y., Gardner, L., Hughes, J., Cindrova-Davies, T., Gomez, M. J., Farrell, L., et al. (2017). Long-term, hormone-responsive organoid cultures of human endometrium in a chemically defined medium. *Nat. Cell Biol.* 19, 568–577. doi: 10.1038/ncb3516

Van De Wetering, M., Francies, H. E., Francis, J. M., Bounova, G., Iorio, F., Pronk, A., et al. (2015). Prospective derivation of a living organoid biobank of colorectal cancer patients. *Cell* 161, 933–945. doi: 10.1016/j.cell.2015.03.053

van der Wel, N., Hava, D., Houben, D., Fluitsma, D., van Zon, M., Pierson, J., et al. (2007). *M. tuberculosis* and *M. leprae* translocate from the phagolysosome to the cytosol in myeloid cells. *Cell* 129, 1287–1298. doi: 10.1016/j.cell.2007.05.059

Völkner, M., Zschätzsch, M., Rostovskaya, M., Overall, R. W., Busskamp, V., Anastassiadis, K., et al. (2016). Retinal organoids from pluripotent stem cells efficiently recapitulate retinogenesis. *Stem Cell Rep.* 6, 525–538. doi: 10.1016/j.stemcr.2016.03.001

Weeber, F., van de Wetering, M., Hoogstraat, M., Dijkstra, K. K., Krijgsman, O., Kuilman, T., et al. (2015). Preserved genetic diversity in organoids cultured from biopsies of human colorectal cancer metastases. *Proc. Natl. Acad. Sci. U.S.A.* 112, 13308–13311. doi: 10.1073/pnas.1516689112

WHO (2017). *The Top 10 Causes of Death*. Available at: http://www.who.int/mediacentre/factsheets/fs310/en/ [accessed November 2, 2017].

Yin, X., Farin, H. F., van Es, J. H., Clevers, H., Langer, R., and Karp, J. M. (2014). Niche-independent high-purity cultures of Lgr5+ intestinal stem cells and their progeny. *Nat. Methods* 11, 106–112. doi: 10.1038/nmeth.2737

Yui, S., Nakamura, T., Sato, T., Nemoto, Y., Mizutani, T., Zheng, X., et al. (2012). Functional engraftment of colon epithelium expanded in vitro from a single adult Lgr5+ stem cell. *Nat. Med.* 18, 618–623. doi: 10.1038/nm.2695

Zhu, S., Ding, S., Wang, P., Wei, Z., Pan, W., Palm, N. W., et al. (2017). Nlrp9b inflammasome restricts rotavirus infection in intestinal epithelial cells. *Nature* 546, 667–670. doi: 10.1038/nature22967

Conflict of Interest Statement: The authors declare that the research was conducted in the absence of any commercial or financial relationships that could be construed as a potential conflict of interest.

Copyright © 2017 Iakobachvili and Peters. This is an open-access article distributed under the terms of the Creative Commons Attribution License (CC BY). The use, distribution or reproduction in other forums is permitted, provided the original author(s) or licensor are credited and that the original publication in this journal is cited, in accordance with accepted academic practice. No use, distribution or reproduction is permitted which does not comply with these terms.

Advantages of publishing in Frontiers

OPEN ACCESS
Articles are free to read for greatest visibility and readership

FAST PUBLICATION
Around 90 days from submission to decision

HIGH QUALITY PEER-REVIEW
Rigorous, collaborative, and constructive peer-review

TRANSPARENT PEER-REVIEW
Editors and reviewers acknowledged by name on published articles

Frontiers
Avenue du Tribunal-Fédéral 34
1005 Lausanne | Switzerland

Visit us: www.frontiersin.org
Contact us: info@frontiersin.org | +41 21 510 17 00

REPRODUCIBILITY OF RESEARCH
Support open data and methods to enhance research reproducibility

DIGITAL PUBLISHING
Articles designed for optimal readership across devices

FOLLOW US
@frontiersin

IMPACT METRICS
Advanced article metrics track visibility across digital media

EXTENSIVE PROMOTION
Marketing and promotion of impactful research

LOOP RESEARCH NETWORK
Our network increases your article's readership